

NASA SP-7037 (261)

National Aeronautics and
Space Administration

Aeronautical Engineering Aeronaut
Engineering Aeronautical Engin
g Aeronautical Engineering Aer
cal Engineering Aeronautical En
onautical Engineering Aeronaut
ngineering Aeronautical Enginee
Aeronautical Engineering Aeror
Engineering Aeronautic Enginee
ing Aeronautical Engineering Ac
tical Engineering Aeronautical
g Aeronautical Engineering Aer

SUPPLEMENTS COVERED IN THIS ISSUE

<i>Document</i>	<i>Page Range</i>	<i>Date</i>	<i>Coverage</i>
NASA SP-7037(249)	1-80	February 1990	January 1990
NASA SP-7037(250)	81-142	March 1990	February 1990
NASA SP-7037(251)	143-220	April 1990	March 1990
NASA SP-7037(252)	221-284	May 1990	April 1990
NASA SP-7037(253)	285-380	June 1990	May 1990
NASA SP-7037(254)	381-466	July 1990	June 1990
NASA SP-7037(255)	467-550	August 1990	July 1990
NASA SP-7037(256)	551-616	September 1990	August 1990
NASA SP-7037(257)	617-700	October 1990	September 1990
NASA SP-7037(258)	701-784	November 1990	October 1990
NASA SP-7037(259)	785-900	December 1990	November 1990
NASA SP-7037(260)	901-968	January 1991	December 1990



**A CUMULATIVE INDEX
TO
A CONTINUING BIBLIOGRAPHY ON

AERONAUTICAL ENGINEERING**

This Cumulative Index supersedes the indexes contained in supplements [SP-7037(249) through SP-7037(260)] published by NASA during 1990.



National Aeronautics and Space Administration
Office of Management
Scientific and Technical Information Division
Washington, DC

1991

This index is available from the National Technical Information Service (NTIS), Springfield, Virginia 22161 on standing order subscription as PB90-914100 at the price of \$17.75 domestic; \$35.50 foreign.

INTRODUCTION

WHAT THIS CUMULATIVE INDEX IS

This publication is a cumulative index to the abstracts contained in NASA SP-7037(249) through NASA SP-7037(260) of *Aeronautical Engineering: A Continuing Bibliography*. NASA SP-7037, and its supplements have been compiled through the cooperative efforts of the American Institute of Aeronautics and Astronautics (AIAA), and the National Aeronautics and Space Administration (NASA). Entries prepared by the two contributing organizations are identified as follows:

1. NASA entries by their *STAR* accession numbers (N90-10000).
2. AIAA entries by their *IAA* accession numbers (A90-10000 series).

HOW THIS CUMULATIVE INDEX IS ORGANIZED

This Cumulative Index includes a subject, personal author, corporate source, foreign technology, contract number, report number, and accession number index.

HOW TO USE THE SUBJECT INDEX

Two types of cross-references appear in the subject index:

1. Use (U) references indicate that the subject term is not "postable," i.e., not a valid term, and that the following term or terms are used instead. For example:

AIRCRAFT PROTUBERANCES

U PROTUBERANCES

FLIGHT PERFORMANCE

U FLIGHT CHARACTERISTICS

2. Narrower Term (NT) references refer the user to more specific headings in the same subject area, under which additional material on the subject may be found. For example:

FLOW RESISTANCE

NT AERODYNAMIC DRAG

NT FRICTION DRAG

NT SUPERSONIC DRAG

In addition, a searcher may use the title or title and title extension in the index to narrow further his quest for particular items; this is because subject terms may include documents on different aspects of the same subject term. For example:

AIRLINE OPERATIONS

All-weather operations, including pilot role, instrument landing systems and guidance aids.

Airport congestion as constraint on air travel, considering runway capacity and adjusted demand.

HOW TO USE THE PERSONAL AUTHOR INDEX

All personal authors used in the abstract-section citations in the individual Supplements appear in the index. Differences in translation schemes may require multiple searching on the index for variants of an author's name. For example:

EMELIANOV, M. D.

and

YEMELYANOV, M. D.

HOW TO USE THE CORPORATE SOURCE INDEX

The corporate source index entries are abridged versions of the corporate sources used in the abstract-section citations in the individual Supplements. The corporate source supplementary (organizational component) does not appear in the index. For example:

BOEING CO., SEATTLE, WASH. MILITARY AIRCRAFT SYSTEMS DIV. (Source citation entry)

BOEING CO., SEATTLE, WASH. (Source index entry)

HOW TO USE THE FOREIGN TECHNOLOGY INDEX

The foreign technology index identifies research performed outside of the United States. Listings in this index are arranged alphabetically by country of intellectual origin. For example:

CHINA, PEOPLE'S REPUBLIC OF

HOW TO USE THE CONTRACT NUMBER INDEX

All contract numbers that are identified in the abstract-section citations in the individual Supplements appear in this index. Changes by agencies in the style in which contract numbers are presented may require multiple searching for variants. For example:

AF 33(615)-71-C-1758

F33615-71-C-1758

HOW TO USE THE REPORT/ACCESSION NUMBER INDEX

All report numbers that have been assigned by the corporate source, monitoring agency or cataloging activity appear in this index. Variations in cataloging may result in different report number series. For example:

TP-924

ONERA-TP-924

IDENTIFICATION OF DESIRED SUPPLEMENT

The abstract and descriptive cataloging for any accession number selected from the indexes may be found in the appropriate Supplement. The page-number range of each Supplement appears on the inside front cover of this index. Once the range of page numbers containing the selected accession number is located in the second column, the desired supplement number will be found in the first column. For example:

Page 150 will be found in Supplement 251

AVAILABILITY OF DOCUMENTS

Information concerning the availability of documents announced in *Aeronautical Engineering Supplements* is found in the Introduction to the most currently issued *Supplement*.

PUBLIC COLLECTIONS OF NASA DOCUMENTS

DOMESTIC: NASA and NASA-sponsored documents and a large number of aerospace publications are available to the public for reference purposes at the library maintained by the American Institute of Aeronautics and Astronautics, Technical Information Service, 555 West 57th Street, 12th Floor, New York, NY 10019.

EUROPEAN: An extensive collection of NASA and NASA-sponsored publications is maintained by the British Library Lending Division, Boston Spa, Wetherby, Yorkshire, England for public access. The British Library Lending Division also has available many of the non-NASA publications cited in *STAR*. European requesters may purchase facsimile copy or microfiche of NASA and NASA-sponsored documents, those identified by both the symbols # and * from ESA — Information Retrieval Service European Space Agency, 8-10 rue Mario-Nikis, 75738 CEDEX 15, France.

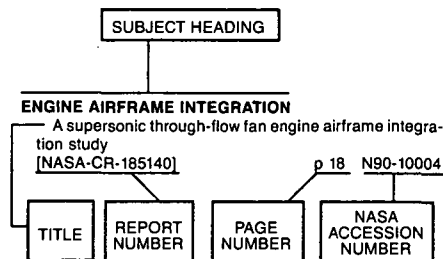
FEDERAL DEPOSITORY LIBRARY PROGRAM

In order to provide the general public with greater access to U.S. Government publications, Congress established the Federal Depository Library Program under the Government Printing Office (GPO), with 51 regional depositories responsible for permanent retention of material, inter-library loan, and reference services. At least one copy of nearly every NASA and NASA-sponsored publication, either in printed or microfiche format, is received and retained by the 51 regional depositories. A list of the regional GPO libraries, arranged alphabetically by state, appears on the inside back cover. These libraries are *not* sales outlets. A local library can contact a Regional Depository to help locate specific reports, or direct contact may be made by an individual.

TABLE OF CONTENTS

	<i>Page</i>
Subject Index	A-1
Personal Author Index	B-1
Corporate Source Index	C-1
Foreign Technology Index	D-1
Contract Number Index	E-1
Report Number Index	F-1
Accession Number Index	G-1

Typical Subject Index Listing



The subject heading is a key to the subject content of the document. The title is used to provide a description of the subject matter. When the title is insufficiently descriptive of document content, a title extension is added, separated from the title by three hyphens. The (NASA or AIAA) accession number and the page number are included in each entry to assist the user in locating the abstract in the abstract section. If applicable, a report number is also included as an aid in identifying the document. Under any one subject heading, the accession numbers are arranged in sequence with the AIAA accession numbers appearing first.

A

A-300 AIRCRAFT

- Comparison of the results of tests on A300 aircraft in the RAE 5 metre and ONERA F1 wind tunnels [RAE-TM-AERO-2130] p 122 N90-11768
- Simulation of transport aeroplanes [MBB-UT-007/89-PUB] p 723 N90-25089
- Study of the flow around the prototype of A300: Results of the third test campaign at F2 and comparison with calculations [CERT-33/5025-29-DERAT] p 817 N90-27663

A-310 AIRCRAFT

- Simulation of transport aeroplanes [MBB-UT-007/89-PUB] p 723 N90-25089

A-320 AIRCRAFT

- Determination of the ground effect on the characteristics of the A320 aircraft [ONERA, TP NO. 1989-188] p 245 A90-21048
- Cockpit evolution in Airbus p 247 A90-22434
- Design and fabrication of the carbon fiber/epoxy A-320 horizontal tailplane p 286 A90-25221
- After Habsheim p 401 A90-31388
- Airbus A320 CFRP-rudder structural requirements p 493 A90-33707
- A320 flight tests: Particularities and innovations p 34 N90-10864
- Determination of the ground effect on the characteristics of the A320 aircraft p 922 N90-28534

ABORT TRAJECTORIES

- Acceleration, gamma, and theta guidance for abort landing in a windshear p 98 A90-14733

ABRASION RESISTANCE

- Entrapment plating of abrasive particles for jet engine clearance control [SAE PAPER 890918] p 286 A90-24685
- Sliding and abrasive wear behaviour of an aluminum (2014)-SiC particle reinforced composite p 530 A90-33344

ABSORBERS (MATERIALS)

- Parametric studies of acoustic duct attenuation of perforated-plate-on-honeycomb absorber [NAL-TM-603] p 966 N90-30030

ABSORPTION

- The effect of jet fuel absorption on advanced aerospace thermoset and thermoplastic composites p 942 A90-50082

ABSTRACTS

- Advances in techniques and technologies for air vehicle navigation and guidance [AGARD-AR-276] p 243 N90-15899
- Noise and sonic boom impact technology. Effects of aircraft noise and sonic booms on structures: An assessment of the current state-of-knowledge [AD-A213919] p 378 N90-17409
- FAA Rotorcraft Research, Engineering, and Development Bibliography 1962-1989 [AD-A224256] p 902 N90-29299

ACCELERATED LIFE TESTS

- Validation of the accelerated equivalent testing of gas turbine engines for multivariant applications p 110 A90-14568
- Component behaviour and life management: The need for common AGARD approaches and actions p 856 N90-27710

ACCELERATION (PHYSICS)

- Lift development of delta wings undergoing constant acceleration from rest [AIAA PAPER 90-0310] p 164 A90-19789
- Unsteady lift development on a constantly accelerated rectangular wing [AIAA PAPER 90-1633] p 569 A90-38762
- Short time Force and moment measurement System for shock tubes (SFS) for measuring times less than 10 ms p 674 N90-24233

ACCELERATION PROTECTION

- Research in a high-fidelity acceleration environment p 439 A90-30734

ACCELERATION STRESSES (PHYSIOLOGY)

- Parachute opening shocks during high speed ejections: Normalization p 497 N90-20056

ACCELERATION TOLERANCE

- Accelerating hypersonic airplanes with ground-power p 586 A90-38186
- Parachute opening shocks during high speed ejections: Normalization p 497 N90-20056

ACCELERATORS

- Accelerators and decelerators for large, hypersonic aircraft [AIAA PAPER 90-1986] p 674 A90-40582
- Operation of the ram accelerator in the transdetonative velocity regime [AIAA PAPER 90-1985] p 741 A90-42712
- A study of the errors of a gyroscopic instrument for measuring linear accelerations p 771 A90-45133

ACCELEROMETERS

- Measurement of angles and angle characteristics with accelerometers and gyroscopes p 653 A90-41730
- In service life monitoring system using g-meter readings and mass configuration control [ETN-89-95218] p 134 N90-12035

ACCEPTABILITY

- En route noise of turboprop aircraft and their acceptability: Report of tests p 697 N90-24858

ACCIDENT INVESTIGATION

- Litigation and the National Weather Service [AIAA PAPER 90-0371] p 220 A90-19819
- Investigation and characteristics of major fire-related accidents in civil air transports over the past ten years p 324 N90-17582

ACCIDENT PREVENTION

- Underlying factors in air traffic control incidents p 401 A90-31335
- In the shadow of Aloha p 468 A90-33174
- Low-level windshear alert systems and Doppler radar in aircraft terminal operations p 574 A90-35758
- UK airmasses involving commercial air transport [CAA-2/88] p 96 N90-11718
- Improved lighting of taxiway/taxiway intersections for Instrument Flight Rules (IFR) operations [DOT/FAA/CT-TN89/64] p 243 N90-15089

- Results of TCAS-2 simulations in reconstructed dangerous encounters (Jul. 1986 to Jun. 1989) [ETN-90-96474] p 636 N90-23375

ACCIDENTS

- Peacetime replacement and crash damage factors for army aircraft [AD-A218544] p 636 N90-23372

ACCUMULATORS

- Hydraulic accumulators and high pressure bottles in composite material p 688 A90-42493

ACCURACY

- A high-order time-accurate scheme and its applications p 304 A90-25732

ACEE PROGRAM

- Energy Efficient Engine high pressure turbine component test performance report [NASA-CR-168289] p 929 N90-28553
- Energy Efficient Engine combustor test hardware detailed design report [NASA-CR-168301] p 929 N90-28554
- Energy Efficient Engine acoustic supporting technology report [NASA-CR-174834] p 930 N90-28557
- Energy Efficient Engine: Flight propulsion system final design and analysis [NASA-CR-168219] p 930 N90-28558
- Energy Efficient Engine core design and performance report [NASA-CR-168069] p 930 N90-28559
- Energy Efficient Engine integrated core/low spool design and performance report [NASA-CR-168211] p 931 N90-28561
- Energy Efficient Engine: Control system component performance report [NASA-CR-174651] p 931 N90-28562
- NASA/GE Energy Efficient Engine low pressure turbine scaled test vehicle performance report [NASA-CR-168290] p 931 N90-28563
- Energy efficient engine program technology benefit/cost study. Volume 1: Executive summary [NASA-CR-174766-VOL-1] p 931 N90-28564
- Energy efficient engine program technology benefit/cost study, volume 2 [NASA-CR-174766-VOL-2] p 931 N90-28565
- Energy efficient engine pin fin and ceramic composite segmented liner combustor sector rig test report [NASA-CR-179534] p 932 N90-28567
- Energy Efficient Engine: High-pressure compressor test hardware detailed design report [NASA-CR-180850] p 932 N90-28570

ACID RAIN

- Mesoscale acid deposition modeling studies [NASA-CR-4262] p 140 N90-13228

ACOUSTIC ATTENUATION

- Possibility of active propeller-noise suppression in piston-engine aircraft by changing the phase relation between the propeller and exhaust signals p 218 A90-18450

- Twin-jet screech suppression p 894 A90-48957
- The absorption of sound by perforated linings p 965 A90-51994

- Comparison between design and installed acoustic characteristics of NASA Lewis 9- by 15-foot low-speed wind tunnel acoustic treatment [NASA-TP-2996] p 440 N90-19242

- Parametric studies of acoustic duct attenuation of perforated-plate-on-honeycomb absorber [NAL-TM-603] p 966 N90-30030

ACOUSTIC COUPLING

- The sensitivity of near-field acoustics to the orientation of twin two-dimensional supersonic nozzles [AIAA PAPER 90-2149] p 625 A90-42045

ACOUSTIC DUCTS

- Optimization of the sound-absorption lining parameters of an ejector jet muffler p 378 A90-24117
- Parametric studies of acoustic duct attenuation of perforated-plate-on-honeycomb absorber [NAL-TM-603] p 966 N90-30030

ACOUSTIC EMISSION

- Some smart structures concepts p 503 A90-32858

Directivity of the noise radiation emitted from the inlet duct of a turboshaft helicopter engine
[ONERA, TP NO. 1990-26] p 695 A90-41205
Acoustic emission and signal analysis p 781 A90-43782

Characterisation of fatigue of aluminium alloys by acoustic emission. Part 2: Discrimination between primary and other emissions
[AERE-R-13303-PT-2] p 678 N90-23523
Acoustic emission detection of crack presence and crack advance during flight p 886 N90-28082
Use of acoustic emission for continuous surveillance of aircraft structures p 887 N90-28092

ACOUSTIC EXCITATION

Investigation of the flow structure behind the rotating blades in the elbow of a wind tunnel in the case of acoustic excitation p 297 A90-24124
The prediction and measurement of thermoacoustic response of plate structures
[AIAA PAPER 90-0988] p 451 A90-29400
Structure-borne noise transmission in cylindrical enclosures due to random excitation
[AIAA PAPER 90-0990] p 463 A90-29402
Acoustic excitation of boundary layer oscillations on a yawing wing p 805 A90-46567
Control of wall-separated flow by internal acoustic excitation p 809 A90-47314
Acoustic wave excitation during the aerodynamic interaction between a fan blade and a bluff obstacle p 965 A90-52289
Mobility power flow analysis of an L-shaped plate structure subjected to acoustic excitation
[NASA-CR-186130] p 214 N90-13817

ACOUSTIC FATIGUE

Application of localized active control to reduce propeller noise transmitted through fuselage surface p 78 A90-11884
An ultrasonic fatigue facility for HCF/LCF interactive tests p 363 A90-23900
A method for determining equivalents during the fatigue testing of structures in an acoustic field p 364 A90-24153
Twin jet screech suppression concepts tested for 4.7 percent axisymmetric and two-dimensional nozzle configurations
[AIAA PAPER 90-2150] p 696 A90-42046
Developments in the acoustic fatigue design process for composite aircraft structures p 882 A90-48047
Acoustic fatigue analysis by the finite element method p 954 A90-49886

ACOUSTIC FREQUENCIES

The acoustic phenomena of the stalling flutter p 78 A90-11801
The radiation of sound from a propeller at angle of attack
[NASA-CR-4264] p 548 N90-21602

ACOUSTIC MEASUREMENT

Supersonic jet noise reduction by a porous single expansion ramp nozzle
[AIAA PAPER 90-0366] p 219 A90-19815
Acoustic test and analysis of a counterrotating prop-fan model
[NASA-CR-179590] p 79 N90-10683
Comparison between design and installed acoustic characteristics of NASA Lewis 9- by 15-foot low-speed wind tunnel acoustic treatment
[NASA-TP-2996] p 440 N90-19242
Sandia National Laboratories' new high level acoustic test facility
[DE90-006810] p 464 N90-19820
Helicopter Airborne Laser Positioning System (HALPS)
[NASA-TM-102814] p 654 N90-23399
Preliminary thoughts on an acoustic metric for the wilderness aircraft overflight study p 697 N90-24862
Problems of internal acoustics in two and three dimensional cavities with deformable walls using the MSC/Nastran code
[DLC/STR-INT-TN-004] p 699 N90-24876
The acoustic results of a United Technologies scale model helicopter rotor tested at DNW
[NASA-TM-101879] p 896 N90-27471

ACOUSTIC PROPAGATION

Some processes of sound generation in a vortex-airfoil system with parallel axes p 218 A90-18448
Transport composite fuselage technology: Impact dynamics and acoustic transmission
[NASA-CR-4035] p 126 N90-11821
An investigation of the generation and radiation of aerodynamic noise in real piping systems p 614 N90-22368

ACOUSTIC PROPERTIES

Acoustic resonance in centrifugal compressors induced by interaction between rotor and stator p 78 A90-11803
Acoustic characteristics of counterrotating unducted fans from model scale tests p 378 A90-26138

Flow and acoustic features of a supersonic tapered nozzle
[AIAA PAPER 90-1599] p 567 A90-38731
Acoustic characteristics of a research step combustor
[AIAA PAPER 90-1851] p 655 A90-40530
A note on an acoustic response during an engine nacelle flight experiment
[NASA-TM-102585] p 464 N90-19821
Air Force Boom Event Analyzer Recorder (BEAR): System description
[AD-A218048] p 548 N90-20800
Relating flow between counter-rotating propellers to aerodynamic interaction noise p 479 N90-20944
Aerodynamic loads and blade vortex interaction noise prediction
[ISL-PU-310/89] p 719 N90-25942
Asymptotic modal analysis and statistical energy analysis
[NASA-CR-186732] p 782 N90-26634

ACOUSTIC RETROFITTING

Beech Starship interior noise experimental studies
[SAE PAPER 891082] p 101 A90-14374

ACOUSTIC SCATTERING

Free-field correction factor for spherical acoustic waves impinging on cylinders p 218 A90-17984
Fuselage boundary-layer effects on sound propagation and scattering p 695 A90-39781

ACOUSTIC SIMULATION

Acoustic-thermal environment for USB flap structure. Report 1: Ground simulation test results
[NAL-TM-567] p 88 N90-11697
Simulation of transport aeroplanes
[MBB-UT-007/89-PUB] p 723 N90-25089

ACOUSTIC SOUNDING

Acoustic recording systems for use in military aircraft
[RAE-TM-MM-11] p 140 N90-13207

ACOUSTIC VELOCITY

Summary of sonic boom rise times observed during FAA community response studies over a 6-month period in the Oklahoma City area
[NASA-CR-4277] p 696 N90-24852

ACOUSTICS

Reduction of blade-vortex interaction noise through higher harmonic pitch control p 377 A90-23937
Acoustic-vortical-combustion interaction in a solid fuel ramjet simulator p 194 N90-14234
An approximate model for the performance and acoustic predictions of counterrotating propeller configurations
[NASA-CR-180667] p 379 N90-18228
The validation and application of a rotor acoustic prediction computer program
[NASA-TM-101794] p 895 N90-27465
Air Force procedure for predicting aircraft noise around airbases: Noise Exposure Model (NOISEMAP). User's manual
[AD-A223162] p 895 N90-27467
Noise from tip vortex and bubble cavitation
[AD-A221962] p 896 N90-27468
Aviation acoustical noise measurement
[AD-A222014] p 896 N90-27469
The acoustic results of a United Technologies scale model helicopter rotor tested at DNW
[NASA-TM-101879] p 896 N90-27471
Entropy wave instability in compact ramjets p 858 N90-27932
Energy Efficient Engine acoustic supporting technology report
[NASA-CR-174834] p 930 N90-28557

ACTIVE CONTROL

Application of localized active control to reduce propeller noise transmitted through fuselage surface p 78 A90-11884
The active control of engine instabilities p 44 A90-12505
A simple active controller to suppress helicopter air resonance in hover and forward flight p 119 A90-16521
Flight-mechanics tasks in solving problems of active control p 257 A90-23358
A method for the active control of the boundary layer condition p 296 A90-24114
Active control of gust- and interference-induced vibration of tilt-rotor aircraft p 429 A90-28201
Exploratory design studies using an integrated multidisciplinary synthesis capability for actively controlled composite wings
[AIAA PAPER 90-0953] p 411 A90-29238
Rotary-wing aeroelasticity with application to VTOL vehicles
[AIAA PAPER 90-1115] p 392 A90-29387
Active flutter suppression for a wing model p 433 A90-31283
Practical techniques of modelling aeroelastic systems for active control applications p 545 A90-33402
Interactions of active controls and structural loads p 517 A90-33404

Application of active noise control to model propeller noise p 548 A90-34091
Investigation of several passive and active methods for turbulent flow separation control
[AIAA PAPER 90-1598] p 607 A90-38730
Experiments on the active control of the transmission of sound through a clamped rectangular plate p 695 A90-41109
ATHeS - A helicopter in-flight simulator for ACT testing p 643 A90-41727
Active control of helicopter cabin noise p 645 A90-42434
A model for active control of helicopter air resonance in hover and forward flight p 670 A90-42462
Active control of tiltrotor blade in-plane loads during maneuvers p 670 A90-42463
Active combustion control in a coaxial dump combustor p 743 A90-42806
Control of forebody flow asymmetry - A critical review
[AIAA PAPER 90-2833] p 711 A90-45164
Active flow control on low Reynolds number airfoils
[AIAA PAPER 90-3039] p 792 A90-45878
Active control of sound transmission through a cylindrical shell p 893 A90-46192
Active vibration control for flexible rotor by optimal direct-output feedback control p 879 A90-46222
Test and theory for piezoelectric actuator-active vibration control of rotating machinery p 879 A90-46226
Theoretical studies of the active control of propeller-induced cabin noise p 893 A90-46351
In-flight experiments on the active control of propeller-induced cabin noise p 893 A90-46352
Application of localized surface heating to actively control the boundary layer separation p 806 A90-46848

Comparison of active control on a servo flap rotor using fixed system and rotating system parameters p 862 A90-46976

Active control of propeller-induced noise fields inside a flexible cylinder p 833 A90-47306
Mechanisms of active control in cylindrical fuselage structures p 862 A90-47309
Active control of aerothermoelastic effects for a conceptual hypersonic aircraft
[AIAA PAPER 90-3337] p 863 A90-47597
Development and testing of methodology for evaluating the performance of multi-input/multi-output digital control systems
[AIAA PAPER 90-3501] p 867 A90-47747
Control law synthesis and optimization software for large order aeroservoelastic systems p 61 N90-10111
Combustion instabilities in liquid-fueled propulsion systems: An overview p 63 N90-10192
Application of formal optimization techniques in thermal/structural design of a heat-pipe-cooled panel for a hypersonic vehicle
[NASA-TM-89131] p 72 N90-10409

The active control of an unstable canard aircraft p 57 N90-10894

Active control of unsteady and separated flow structures
[AD-A212109] p 89 N90-11707

Effect of control surface mass unbalance on the stability of a closed-loop active control system
[NASA-TP-2952] p 134 N90-12042

Application of sound and temperature to control boundary-layer transition p 92 N90-12537

Active control system for gust load alleviation and structural damping p 259 N90-15056

Active stabilization of aeromechanical systems
[AD-A216629] p 454 N90-18672

The application of active controls technology to a generic hypersonic aircraft configuration
[NASA-TM-101689] p 497 N90-20071

Advances in optimal active control techniques for aerospace systems; application to aircraft active landing gear p 592 N90-21769

The Shock and Vibration Digest, volume 21, no. 6 p 614 N90-22363

Noise transmission into propeller-driven airplanes p 614 N90-22364

Elements of active vibration control for rotating machinery
[NASA-TM-102368] p 610 N90-22703

Active control of aerothermoelastic effects for a conceptual hypersonic aircraft
[NASA-TM-102713] p 869 N90-27725

Distributed control architecture for CNI preprocessors p 917 N90-29356

A digital controller for active aeroelastic controls
[NAL-TR-1014] p 936 N90-29402

ACTUATOR DISKS

A semi-actuator disk theory for prediction of stall flutter in axial flow compressors p 301 A90-25105

ACTUATORS

- Comparison of three concepts for a long stroke displacement transducer p 66 A90-11041
- Numerical simulation of the actuation system for the ALDF's propulsion control valve --- Aircraft Landing Dynamics Facility [AIAA PAPER 90-0079] p 211 A90-19674
- The selection of actuation devices for aircraft pneumatic valves in systems under computer control [SAE PAPER 891456] p 368 A90-27425
- Piezoelectric actuators for helicopter rotor control [AIAA PAPER 90-1076] p 411 A90-29384
- F/A-18 aileron smart servoactuator p 432 A90-30710
- Electric controls for a high-performance EHA using an interior permanent magnet motor drive p 452 A90-30711
- Implementation of comprehensive actuation system models in aerostochastic analysis p 517 A90-33406
- Development of high temperature actuation systems for advanced aircraft engines [AIAA PAPER 90-2031] p 660 A90-41990
- Use of smart actuators for the tail rotor collective pitch control p 688 A90-42483
- High-performance EHA controls using an interior permanent magnet motor --- electrohydraulic actuator for aircraft power systems p 730 A90-43152
- Rotary servohinge actuator [SAE PAPER 892261] p 733 A90-45458
- Lightweight, composite flight control actuators [SAE PAPER 892264] p 733 A90-45459
- Test and theory for piezoelectric actuator-active vibration control of rotating machinery p 879 A90-46226
- Adaptive flight control of CCV aircraft with limiting zeros [AIAA PAPER 90-3409] p 864 A90-47664
- Composite flight control actuators p 874 A90-48993
- Advanced actuation systems development, volume 1 [AD-A213334] p 121 N90-12624
- Advanced actuation systems development, volume 2 [AD-A213378] p 198 N90-13398
- Flexible heat pipe cold plate [AD-A216053] p 434 A90-18433
- Aerospace induction motor actuators driven from a 20-kHz power link [NASA-TM-102482] p 509 N90-20085
- Civil air transport: A fresh look at power-by-wire and fly-by-light [NASA-TM-102574] p 542 N90-21283
- Elements of active vibration control for rotating machinery [NASA-TM-102368] p 610 N90-22703
- Procedure for calibrating fly-by-wire control chains of the flying testbed ATLAS [DLR-MITT-90-02] p 936 N90-29401
- ADA (PROGRAMMING LANGUAGE)**
- RISC lifting off in avionics --- Reduced Instruction Set Computer [AIAA PAPER 89-2967] p 73 A90-10483
- An application of SQP and Ada to the structural optimization of aircraft wings p 216 A90-18444
- Evolution of Ada technology in the flight dynamics area: Implementation/testing phase analysis [NASA-TM-103310] p 546 N90-21539
- System testing of a production Ada (trademark) project: The GRODY study [NASA-TM-103308] p 546 N90-21541
- Evolution of Ada technology in the flight dynamics area: Design phase analysis [NASA-TM-103307] p 547 N90-21542
- Implementation of a production Ada project: The GRODY study [NASA-TM-103305] p 547 N90-21544
- National Airspace System (NAS) software life cycle management study [AD-A221180] p 729 N90-25122
- ADAPTATION**
- Advanced actuation systems development, volume 2 [AD-A213378] p 198 N90-13398
- Residual interference and wind tunnel wall adaption p 353 N90-17655
- High productivity testing p 871 N90-26843
- Adaptation for unsteady flow p 871 N90-26845
- ADAPTIVE CONTROL**
- Adaptive automatic control systems. Number 16 --- Russian book p 76 A90-10844
- An analysis of the possibility of expanding the information base of an adaptive control system for a flight vehicle surrounded by an ionized gas medium p 60 A90-10845
- Recursive real-time identification of step-response matrices of helicopters for adaptive digital flight control p 195 A90-17703
- The optimum control and adaptive control for airplane cabin pressure p 182 A90-18627

- An adaptive flight control system design for non-minimum phase CCV by relative order reduction p 196 A90-19428
- Three-dimensional adaptive grid generation on a composite-block grid p 374 A90-25289
- Application of a digital control theory for generating adaptive grids p 366 A90-25734
- Adaptive mesh generation for viscous flows using Delaunay triangulation p 310 A90-26531
- 2-D and 3-D unstructured mesh adaption relying on physical analogy p 310 A90-26534
- Multiple-block grid adaption for an airplane geometry p 311 A90-26547
- Adaptive elective fuel control test techniques p 421 A90-28168
- Flight testing of the Chandler Evans adaptive fuel control on the S-76A helicopter p 422 A90-28178
- Flight tests of Adaptive Fuel Control and decoupled rotor speed control systems p 422 A90-28183
- Mission effectiveness testing of an adaptive electronic fuel control on an S-76A p 422 A90-28199
- Design of adaptive digital controllers incorporating dynamic pole-assignment compensators for high-performance aircraft p 432 A90-30714
- Real-time adaptive control of knowledge based avionics tasks p 460 A90-30764
- Adaptive wind tunnel walls: Compendium of final report - AGARD FDP working group 12 [AIAA PAPER 90-1405] p 595 A90-37944
- Temporal-adaptive Euler/Navier-Stokes algorithm for unsteady aerodynamic analysis of airfoils using unstructured dynamic meshes [AIAA PAPER 90-1650] p 569 A90-38778
- Development of a mathematical model of an adaptive antilutler system p 769 A90-42911
- Adaptive flight control of CCV aircraft with limiting zeros [AIAA PAPER 90-3409] p 864 A90-47664
- Local adaptive maneuvering optimization for fighter aircraft [AIAA PAPER 90-3453] p 890 A90-47706
- Reconfigurable aircraft flight control system via robust direct adaptive control [AIAA PAPER 90-3226] p 868 A90-49111
- Adaptive control law design for model uncertainty compensation [AD-A211712] p 120 N90-11758
- Adaptive control of helicopter vibrations via the impulse response method [AD-A213728] p 260 N90-15113
- Discrete proportional Plus Integral (PI) multivariable control laws for the Control Reconfigurable Combat Aircraft (CRCA) [AD-A215664] p 433 N90-18431
- A rule-based paradigm for intelligent adaptive flight control p 434 N90-19238
- Rule-based mechanisms of learning for intelligent adaptive flight control p 521 N90-20939
- Design of a helicopter automatic flight control system using adaptive control p 522 N90-21040
- An adaptive human response mechanism controlling the V/STOL aircraft. Appendix 3: The adaptive control model of a pilot in V/STOL aircraft control loops [NASA-CR-186599] p 598 N90-21777
- A methodology for knowledge-based restructurable control to accommodate system failures p 609 N90-22058
- Adaptive control of a system with periodic dynamics: Application of an impulse response method to the helicopter vibration problem p 694 N90-23990
- An expert system to perform on-line controller restructuring for abrupt model changes [NASA-TM-103609] p 964 N90-29121
- ADAPTIVE FILTERS**
- Range obscuration mitigation by adaptive PRF selection for the TDWR system --- Pulse Repetition Frequency for Terminal Doppler Weather Radar p 456 A90-28617
- Fully vectorized implicit scheme for 2-D viscous hypersonic flow using adaptive finite element methods p 708 A90-44439
- Range determination in a multipath prone environment p 877 A90-45960
- Adaptive clutter rejection filters for airborne Doppler weather radar applied to the detection of low altitude windshear [NASA-CR-186211] p 214 N90-14453
- ADDITIONS**
- Micro separator and ball-on-cylinder lubricity evaluator tests or corrosion inhibitor/lubricity improver additives [AD-A221339] p 766 N90-25228
- ADHESION**
- The status of high temperature polymers for composites - Likely candidates p 528 A90-31516
- The effect of primer age on adhesion of polysulphide sealant p 269 N90-15909

- Fuel resistant coatings for metal and composite fuel tanks p 269 N90-15911
- Development of a mathematical model for the thermal decomposition of aviation fuels [AD-A221673] p 875 N90-26994
- ADHESION TESTS**
- Nondestructive analysis of aileron fatigue and aging in a Mirage F1 [REPT-M6-594000] p 184 N90-13378
- Criteria for coal tar seal coats on airport pavements. Volume 2: Laboratory and field studies [AD-A220167] p 674 N90-24277
- ADHESIVE BONDING**
- Repair adhesives - Development criteria for field level conditions p 528 A90-31575
- Adhesive-bonded composite-patching repair of cracked aircraft structure p 467 A90-31576
- Expert systems for design of battle damage repairs p 467 A90-33094
- Aluminum surface preparation for aircraft field repair p 764 A90-43204
- The surface pretreatment of aluminium-lithium alloys for structural bonding p 881 A90-47118
- Development of a high toughness heat resistant 177 C (350 F) curing film adhesive for aerospace bonding applications - FM 377 adhesive p 955 A90-50126
- Simple shear tests of the FMI 23.5.06 adhesive cured at low pressure (12 PSI) [INFORME-I-298/88] p 357 N90-17871
- Crack stoppers and ARALL laminates [PB90-166588] p 533 N90-21142
- Aircraft battle damage repair of transparencies [AD-A224168] p 925 N90-29387
- ADHESIVES**
- Sealing the future --- sealants and adhesives for military aircraft p 442 A90-29638
- Evaluation of various non-asbestos epoxy adhesives for aircraft repair p 529 A90-33078
- An investigation on boron used as a component of solid propellant p 765 A90-45708
- High temperature adhesives commercially available to be used for extended time with PMR15 laminates p 943 A90-50125
- Improved thermal performance using allylnadine-imides p 946 A90-50175
- The effect of matrix toughness in the development of improved structural adhesives p 955 A90-50183
- Effect of molecular weight and end group control on the adhesion behavior of thermoplastic polyimides and poly(imide siloxane) segmented copolymers p 947 A90-50199
- ADJUSTING**
- Geodetic network adjustment using GPS triple difference observations and a priori stochastic information [TR-1-1987] p 178 N90-13367
- ADVANCED LAUNCH SYSTEM (STS)**
- Recovery concepts for propulsion and avionics components --- for booster stage in launch vehicles [AIAA PAPER 90-1810] p 353 A90-25172
- Aerospace induction motor actuators driven from a 20-kHz power link [NASA-TM-102482] p 509 N90-20085
- ADVANCED SOLID ROCKET MOTOR (STS)**
- Review of the Aerospace Safety Advisory Panel report for NASA fiscal year 1990 authorization [GPO-24-234] p 177 N90-14213
- AERIAL PHOTOGRAPHY**
- A test of airborne kinematic GPS positioning for aerial photography - Methodology p 97 A90-13982
- A test of kinematic GPS combined with aerial photography - Organization, logistics and results p 97 A90-13983
- Final results of the NASA storm hazards program p 819 A90-49834
- Ice runways near the South Pole [AD-A211606] p 133 N90-11908
- AERIAL RECONNAISSANCE**
- The new light weight, high performance reconnaissance camera KRB 8/24 F p 847 A90-48607
- Applications for a small format airborne recorder p 847 A90-48620
- Cockpit display of hazardous wind shear information p 484 N90-20924
- AERIAL RUDDERS**
- Stability characteristics of a combat aircraft with control surface failure [AD-A216196] p 350 N90-17646
- Flutter investigations on a Transavia PL12/T-400 aircraft [AD-A219108] p 593 N90-22570
- AEROACOUSTICS**
- On unsteady surface forces, and sound produced by the normal chopping of a rectilinear vortex p 5 A90-11604
- Twenty-five years of rotorcraft aeroacoustics - Historical prospective and important issues p 78 A90-11878

Blade surface pressure measurement on a pusher propeller in flight
[SAE PAPER 891040] p 139 A90-14346

Finite element calculations of the interior noise of the Saab 340 aircraft
[SAE PAPER 891081] p 101 A90-14373

Noise prediction of a counter-rotation propfan
p 218 A90-17861

Prediction of transmission loss through an aircraft sidewall using statistical energy analysis --- study of cabin noise reduction
p 219 A90-18599

Rotor noise due to atmospheric turbulence ingestion. I
Fluid mechanics p 219 A90-19385

Rotor noise due to atmospheric turbulence ingestion. II - Aeroacoustic results
p 219 A90-19386

A kinematical/numerical analysis of rotor-stator interaction noise
[AIAA PAPER 90-0281] p 219 A90-19770

SARL noise measurements
[AIAA PAPER 90-0285] p 219 A90-19772

Acoustic noise emitted from vessels in an impulse-type wind tunnel
p 378 A90-24125

A method for determining equivalents during the fatigue testing of structures in an acoustic field
p 364 A90-24153

A panel method for arbitrary moving boundaries problems
p 302 A90-25284

An approximation model for the performance and acoustic predictions of counterrotating propeller configurations
[AIAA PAPER 90-0282] p 378 A90-26931

High resolution flow field prediction for tail rotor aerodynamics
p 463 A90-28158

Aeroacoustic flowfield and acoustics of a model helicopter tail rotor at high advance ratio
p 463 A90-28160

Tilt rotor aircraft aeroacoustics
p 409 A90-28238

Investigation of the near wake of a propfan
p 622 A90-40686

Interaction between a high-level steady acoustic field and a ducted turbulent flow
[ONERA, TP NO. 1990-27] p 695 A90-41206

Noise-source measurements by thin-film pressure transducers in a subsonic turbofan model
[ONERA, TP NO. 1990-36] p 659 A90-41212

A source of discrete noise components in the flow path of gas turbines and fans
p 894 A90-46506

Calculation of the rotation noise of a single propeller with blades of arbitrary shape
p 894 A90-46552

Mixer-ejector nozzle for jet noise suppression
[AIAA PAPER 90-1909] p 894 A90-47202

Noise generation by swept cascade
p 895 A90-49486

Large-scale Advanced Prop-fan (LAP) technology assessment report
[NASA-CR-182142] p 53 N90-10046

Measurement resolution of noise directivity patterns from acoustic flight tests
[NASA-TM-4134] p 79 N90-10679

An investigation of counterrotating tip vortex interaction
[NASA-CR-185135] p 79 N90-11549

Review and analysis of the DNW/Model 360 rotor acoustic data base
[NASA-TM-102253] p 81 N90-11692

Effects of acoustic sources
p 140 N90-12553

Acoustic design considerations: Review of rotor acoustic sources
p 106 N90-12585

NASA aerodynamics program
[NASA-TM-4175] p 373 N90-17235

Predicted and measured boundary layer refraction for advanced turboprop propeller noise
[NASA-TM-102365] p 379 N90-17413

Experimental performance and acoustic investigation of modern, counterrotating blade concepts
[NASA-CR-185158] p 649 N90-23393

PTA en route noise measurements
p 696 N90-24855

A review of instability and noise propagation in supersonic flows
[NASA-CR-186800] p 717 N90-25112

Aeroacoustics of advanced propellers
[NASA-TM-103137] p 782 N90-26635

The acoustic results of a United Technologies scale model helicopter rotor tested at DNW
[NASA-TM-101879] p 896 N90-27471

Development of a linearized unsteady aerodynamic analysis for cascade gust response predictions
[NASA-CR-4308] p 816 N90-27655

Cavity aeroacoustics
[AD-A223853] p 911 N90-29307

Generalized Advanced Propeller Analysis System (GAPAS). Volume 2: Computer program user manual
[NASA-CR-185277] p 933 N90-29394

AEROASSIST

Three dimensional Discrete Particle Simulation about the AFE geometry
[AIAA PAPER 90-1778] p 560 A90-38468

Guidance and Control strategies for aerospace vehicles
[NASA-CR-186195] p 199 N90-14243

Optimal trajectories for hypervelocity flight
p 918 N90-29378

AEROBRAKING

Airbrake design for base-line configuration of advanced jet trainers/light attack airplanes and military combat airplanes
p 810 A90-48081

AERODYNAMIC BALANCE

Higher harmonic and trim control of the X-wing circulation control wind tunnel model rotor
p 435 A90-28156

Rotor smoothing expert system
p 381 A90-28164

A fatigue study of electrical discharge machine (EDM) strain-gage balance materials
p 448 A90-28295

External 6-component wind tunnel balances for aerospace simulation facilities
p 438 A90-28296

Integrated structure/control concepts for oblique wing roll control and trim
p 433 A90-31282

Balance calibration and evaluation software --- in wind tunnel tests
p 523 A90-34237

Automatic calibration machine for internal cryogenic balances
p 524 A90-34247

Measurement of temperature gradients and assessment of balance performance using the RAE cryogenic test duct
p 525 A90-34252

Design of a three-component wall-mounted balance
[AIAA PAPER 90-1397] p 595 A90-37940

Wind tunnel testing techniques on aerodynamic effects with small asymmetry
[AIAA PAPER 90-1400] p 560 A90-38490

Drag measurements on a modified prolate spheroid using a magnetic suspension and balance system
p 672 A90-40684

Recent aerodynamic measurements with Magnetic Suspension Systems
p 759 A90-44399

Strain-gage applications in wind tunnel balances
p 957 A90-52037

Stability characteristics of a combat aircraft with control surface failure
[AD-A216196] p 350 N90-17646

Influence of forebody geometry on aerodynamic characteristics and a design guide for defining departure/spin resistant forebody configurations
[AD-A216714] p 414 N90-18388

Coupled rotor-body equations of motion hover flight
[NASA-CR-186710] p 717 N90-25111

AERODYNAMIC BRAKES

An analysis of the possibility of expanding the information base of an adaptive control system for a flight vehicle surrounded by an ionized gas medium
p 60 A90-10845

AERODYNAMIC CHARACTERISTICS

The effects of three centres of blade on flutter
p 42 A90-11800

Hypersonic flow past blunt edges at low Reynolds numbers
p 10 A90-12284

Aerodynamic and dynamic principles of helicopter flight --- Russian book
p 55 A90-12473

Helicopter dynamics: Limiting flight conditions --- Russian book
p 55 A90-12481

Influence of blade leaning on the flow field behind turbine rectangular cascades with different incidences and aspect ratios
p 11 A90-12519

Turbomachinery tip gap aerodynamics - A review
p 13 A90-12557

The development of a high response aerodynamic wedge probe and use on a high-speed research compressor
p 69 A90-12618

Turbulent separated flow over and downstream of a two-element airfoil
p 16 A90-12738

Surface roughness effect on the aerodynamic characteristics of a blunt body
p 16 A90-12740

Time domain parameter identification techniques applied to the UH-60A Black Hawk Helicopter
p 77 A90-12774

Closed-form solutions for nonlinear quasi-unsteady transonic aerodynamics
p 16 A90-12839

Airplane aerodynamics and performance --- Book
p 17 A90-12865

The effect of flow curvature on the aerodynamic characteristics of an ogive-cylinder body
p 82 A90-13785

Spanwise distribution of lift and drag at high angles of attack
[SAE PAPER 891019] p 83 A90-14331

Construction of a straight single-row airfoil lattice by the method of quasi-solutions for inverse boundary value problems
p 84 A90-14564

A numerical method for calculating supersonic nonisobaric jets
p 84 A90-14566

Effect of the inlet diameter and neck edge radius on the flow coefficient of straight-generatrix nozzles
p 84 A90-14577

Effect of the roughness of deposits in a compressor cascade on the flow lag angle
p 84 A90-14578

Calculation of cone drag
p 84 A90-14579

Symposium on Numerical and Physical Aspects of Aerodynamic Flows, 4th, California State University, Long Beach, Jan. 16-19, 1989, Proceedings
p 144 A90-16751

Experiments are telling you something (Stewartson Memorial Lecture) --- about aerodynamic flows
p 144 A90-16752

Computation of multi-element airfoil flows including confluence effects
p 144 A90-16755

On the effects of wind tunnel turbulence on steady and unsteady airfoil characteristics
p 147 A90-16777

Investigation of a nonlinear Kalman filter for estimating aircraft state variables
p 195 A90-16850

Direct search method to aeroelastic tailoring of a composite wing under multiple constraints
p 208 A90-17865

Application of the finite element method to the problem of rotational flow around wings
p 156 A90-18305

Aerodynamic design of an HP compressor stage using advanced computation codes
p 156 A90-18479

The aerodynamic behaviours of vortices for slender-wing
p 158 A90-18623

Rotational aerodynamics of elliptic bodies at high angles of attack
[AIAA PAPER 90-0068] p 161 A90-19664

Aerodynamic testing of a new semi-prone ejection seat design
[AIAA PAPER 90-0234] p 182 A90-19748

Results of aerodynamic testing of large-scale wing sections in a simulated natural rain environment
[AIAA PAPER 90-0486] p 167 A90-19874

The influence of a rotating leading edge on accelerating starting flow over an airfoil
[AIAA PAPER 90-0583] p 168 A90-19932

Numerical study of the effects of icing on finite wing aerodynamics
[AIAA PAPER 90-0757] p 169 A90-20010

Prediction of aerostat and airship mooring mast loads by nonlinear dynamic simulation
[AIAA PAPER 89-3172] p 245 A90-20587

Estimation of the flight dynamic characteristics of the YEZ-2A
[AIAA PAPER 89-3173] p 245 A90-20590

Conditional sampling --- technique for aerodynamic characteristics measurement from wind-tunnel experiments
[ONERA, TP NO. 1989-187] p 261 A90-21047

Determination of the ground effect on the characteristics of the A320 aircraft
[ONERA, TP NO. 1989-188] p 245 A90-21048

Effects of nonplanar outboard wing forms on a wing
p 232 A90-23279

Study of vortex breakdown of F-106B by Euler code
p 233 A90-23289

Measurements and calculations of the aerodynamic characteristics of the propeller sections series V3
p 233 A90-23355

Aerodynamic characteristics of an aircraft model at large angles of attack and large sideslip angles
p 233 A90-23361

Aerodynamic and torque characteristics of enclosed Co/counter rotating disks
[ASME PAPER 89-GT-177] p 361 A90-23858

Aerodynamic and heat transfer measurements on blading for a high rim-speed transonic turbine
[ASME PAPER 89-GT-228] p 293 A90-23883

Analytical approach to the induced flow of a helicopter rotor in vertical descent
p 293 A90-23938

Aerodynamic design methods for transonic wings
p 293 A90-23978

Some aspects of the numerical modeling of supersonic flow past flight vehicles
p 293 A90-24048

Nonsymmetric vortex breakdown and aerodynamic hysteresis in flow past a low-aspect-ratio wing/fuselage configuration
p 294 A90-24076

Model problems of continuous control law optimization for a tensometric aerodynamic experiment
p 295 A90-24086

Aeroelastic deformation of a crescent-shaped rigid support in the diffuser chamber of a wind tunnel
p 364 A90-24112

Multilevel method for calculating aerodynamic loads on a flight vehicle
p 296 A90-24122

An investigation of fillets in wing-fuselage joints at subsonic velocities
p 297 A90-24131

Aerodynamic characteristics of thin bodies moving in a gas with shock waves
p 297 A90-24140

Separation development and its effect on the aerodynamics of supercritical profiles at transonic velocities
p 297 A90-24142

SUBJECT INDEX

Advantages of flow variables in thin viscous shock layer problems p 364 A90-24145

Effect of similarity parameters on the aerodynamic quality and moment characteristics of a supersonic wing with blunt edges p 298 A90-24150

Jet flap theory p 298 A90-24154

Effect of a recess on the aerodynamic characteristics of very blunt bodies at supersonic velocities p 299 A90-24167

Practical aerodynamics of the Yak-42 aircraft --- Russian book p 334 A90-24218

Effects of compressibility on the characteristics of free shear layers p 302 A90-25285

Three-dimensional adaptive grid generation on a composite-block grid p 374 A90-25289

Navier-Stokes simulations around a high-speed propeller p 305 A90-25797

Transonic aerodynamics analysis of unconventional wing configurations by 3D-Euler code p 306 A90-25835

Prediction of tip-clearance effects on a wing by the panel method p 307 A90-25871

Experimental studies of 90 deg corner cascades in the National Full-Scale Aerodynamic Complex [AIAA PAPER 90-1826] p 307 A90-25935

The construction of component-adaptive grids for aerodynamic geometries p 309 A90-26513

Unsteady aerodynamic characteristics of a fighter model undergoing large-amplitude pitching motions at high angles of attack p 313 A90-26933

Operational considerations for aerodynamic testing of large-scale wing sections in a simulated natural rain environment [AIAA PAPER 90-0485] p 313 A90-26956

Development of the improved helicopter icing spray system (IHISS) p 400 A90-28182

A numerical analysis of the British Experimental Rotor Program blade p 384 A90-28194

The revolution continuous --- performance of military helicopters [MBB-UD-557-89-PUB] p 381 A90-28242

Aerodynamics of human-powered flight p 386 A90-28552

Comparison of calculated and experimental nonstationary aerodynamic characteristics of a delta wing pitching at large angles of attack p 387 A90-28988

Some characteristics of changes in the nonstationary aerodynamic characteristics of a wing profile with an aileron in transonic flow p 387 A90-28989

Aerodynamic quality of a plane delta wing with blunted edges at large supersonic flow velocities p 387 A90-28991

Using the lifting line theory for calculating straight wings of arbitrary profile p 387 A90-29004

Effect of the leading edge bluntness of a moderately swept wing on the aerodynamic characteristics of an aircraft model at subsonic and transonic velocities p 388 A90-29005

Wave rider volume distribution p 388 A90-29006

Combined effect of viscosity and bluntness on the aerodynamic efficiency of a delta wing in flow with a high supersonic velocity p 388 A90-29184

A study of approximately optimal cruising flight regimes of variable-mass aircraft p 430 A90-29187

Skin effect in flow of a disperse fluid past a wing profile p 395 A90-30334

Determination of the specific thrust in open regimes and design of a nonseparating convergent nozzle profile p 395 A90-30339

Aerodynamic characteristics of wave riders based on flows behind axisymmetric shock waves p 395 A90-30342

The numerical simulation of the low speed aerodynamic characteristics of a set of close-coupled canard configurations p 396 A90-31485

Flight test and numerical analysis of a half-scale Unmanned Air Vehicle [AIAA PAPER 90-1260] p 494 A90-33890

Equation decoupling - A new approach to the aerodynamic identification of unstable aircraft [AIAA PAPER 90-1276] p 518 A90-33900

Effect of vertical-ejector jet on the aerodynamics of delta wings p 553 A90-35755

Alternate table look-up routine for real-time digital flight simulation p 611 A90-35769

Comment on 'Improved thin-airfoil theory' p 554 A90-35772

Suppression of vortex asymmetry behind circular cones p 556 A90-36282

Measured aerodynamic performance of a swept wing with a simulated ice accretion [AIAA PAPER 90-0490] p 557 A90-37063

Results of wind tunnel ground effect measurements on Airbus A320 using turbine power simulation and moving tunnel floor techniques [AIAA PAPER 90-1427] p 559 A90-37964

Langley hypersonic aerodynamic/aerothermodynamic testing capabilities - Present and future [AIAA PAPER 90-1376] p 596 A90-38483

Direct simulation of low-density flow over airfoils [AIAA PAPER 90-1539] p 564 A90-38683

Computational study for passive control of supersonic asymmetric vortical flows around cones [AIAA PAPER 90-1581] p 566 A90-38718

Aerodynamic breakup of liquid jets - A review [AIAA PAPER 90-1616] p 607 A90-38746

Aerodynamic detuning for control of supersonic rotor forced response [AIAA PAPER 90-2018] p 621 A90-40596

Preliminary characterization of parachute wake recontact p 622 A90-40681

Numerical simulation of the growth of instabilities in supersonic free shear layers p 623 A90-40941

Aerodynamic work for Hermes spaceplane p 675 A90-41115

Investigations of the influence of slot blowing from the upper wing surface on the flow around the wing and its aerodynamic characteristics p 623 A90-41740

Application of a new adaptive grid for aerodynamic analysis of shock containing single jets [AIAA PAPER 90-2025] p 624 A90-41988

Quasi-3D viscous flow computations in subsonic and transonic turbomachinery bladings [AIAA PAPER 90-2126] p 625 A90-42033

The application of concentric vortex simulation to calculating the aerodynamic characteristics of bodies of revolution at high angles of attack p 627 A90-42357

Comparison with experiment of various computational methods of airflow on three helicopter fuselages p 630 A90-42436

Computation of viscous aerodynamic characteristics of 2-D airfoils for helicopter applications p 631 A90-42440

Improving helicopter aerodynamics - A step ahead p 631 A90-42443

Parametric evaluation of the aerodynamic performance of an annular combustor-diffuser system [AIAA PAPER 90-2163] p 742 A90-42741

Calculation of nonseparated flow past a wing profile at large Reynolds numbers p 706 A90-42995

Compressor aerodynamics --- Book p 706 A90-44052

Problems in the synthesis of advanced aircraft control systems p 751 A90-44723

Optimization of glides for constant wind fields and course headings p 731 A90-44734

Yaw damping of elliptic bodies at high angles of attack p 709 A90-44740

Aerodynamic drag of a pair of bodies in transonic and supersonic flow p 710 A90-44935

Aerodynamic effects of body roughness [AIAA PAPER 90-2850] p 712 A90-45168

A Volterra kernel identification scheme applied to aerodynamic reactions [AIAA PAPER 90-2803] p 712 A90-45178

Effects of unsteady blowing on the lift of a circulation controlled cylinder p 713 A90-45325

Forebody vortex manipulation for aerodynamic control of aircraft at high angles of attack [SAE PAPER 892220] p 756 A90-45437

Propulsion integration for military aircraft [SAE PAPER 892234] p 733 A90-45449

Application of divergent trailing-edge airfoil technology to the design of a derivative wing [SAE PAPER 892288] p 714 A90-45466

Low-speed aerodynamic characteristics of a powered NASP-like configuration in ground effect [SAE PAPER 892312] p 714 A90-45474

Vortical sources of aerodynamic force and moment [SAE PAPER 892346] p 715 A90-45498

Propulsive lift augmentation by side fences as applied to Japan's experimental STOL aircraft, ASKA [AIAA PAPER 90-3009] p 789 A90-45859

Effects of onset free-stream turbulence on the performance characteristics of an airfoil [AIAA PAPER 90-3025] p 790 A90-45867

The effect of separation on turbulent boundary layer characteristics over a smooth surface at Mach 6.0 [AIAA PAPER 90-3028] p 790 A90-45870

Thick airfoil designs for a HALE vehicle --- High Altitude Long Endurance [AIAA PAPER 90-3036] p 791 A90-45875

Aerodynamic characteristics of forward sweep [AIAA PAPER 90-3041] p 792 A90-45879

A laser sheet flow visualization and aerodynamic force data evaluation of a 3 percent YF-17 fighter aircraft model at high angles of attack [AIAA PAPER 90-3019] p 792 A90-45886

AERODYNAMIC CHARACTERISTICS

A review of low Reynolds number aerodynamic research at the University of Glasgow p 800 A90-46367

Experimental aerodynamic characteristics of the airfoils LA 5055 and DU 86-084/18 at low Reynolds numbers p 800 A90-46368

Control of low-Reynolds-number airfoils - A review p 801 A90-46376

Effect of a crescent-shaped rigid support on the aerodynamic characteristics of models in the presence of perforated boundaries p 869 A90-46537

A generalized relation for the aerodynamic efficiency of plane bodies p 804 A90-46559

Some possibilities of the vortex layer method for calculating the aerodynamic characteristics of an augmented airfoil interacting with the engine jet p 804 A90-46564

Analytical studies of the transonic flutter of aircraft p 860 A90-46577

Boundary-integral method for calculating aerodynamic sensitivities with illustration for lifting-surface theory p 806 A90-46841

Improvement to interactive two dimensional rotor section design p 808 A90-46943

Performance of an optimized rotor blade at off-design flight conditions p 830 A90-46946

Development of the Second Generation Comprehensive Helicopter Analysis System (2GCHAS) p 889 A90-46963

Airfoil design and data --- Book p 809 A90-47608

Flight test of a trajectory controller using linearizing transformations with measurement feedback [AIAA PAPER 90-3373] p 864 A90-47631

Winger - Computer code for aerodynamic analysis of wings p 810 A90-48077

Thick-wing spanloader all-freighter - A design concept for tomorrow's air cargo [AIAA PAPER 90-3198] p 834 A90-48831

The Bell X-22A V/STOL, Variable Stability Research Airplane - Lessons learned [AIAA PAPER 90-3207] p 834 A90-48835

Supersonic aerodynamic characteristics of a Mach 3 high-speed civil transport configuration [AIAA PAPER 90-3210] p 811 A90-48836

Design of a close-support aircraft [AIAA PAPER 90-3241] p 835 A90-48849

Method for simultaneous wing aerodynamic and structural load prediction p 838 A90-48955

Effects of transition on wind tunnel simulation of vehicle dynamics p 870 A90-49273

Aerodynamic losses in conventional fan blades of high by pass turbo engine p 854 A90-49487

Control of low-speed airfoil aerodynamics p 814 A90-49776

Effect of incoming flow turbulence on the aerodynamic characteristics of a smooth symmetric body at large angles of attack p 904 A90-50817

High temperature VSCF (Variable Speed Constant Frequency) generator system [AD-A210823] p 71 N90-10351

Low-speed, high-lift aerodynamic characteristics of slender, hypersonic accelerator-type configurations [NASA-TP-2945] p 20 N90-10830

An experimental investigation of the aerodynamic characteristics of slanted base ogive cylinders using magnetic suspension technology [NASA-CR-181708] p 21 N90-10834

P-180 AVANTI: Project and flight test program comprehensive overview p 34 N90-10863

The determination of the aerodynamic characteristics of an ogive-cylinder body in subsonic, curved, incompressible flow, and an assessment of the effect of flow curvature [REPT-87-13] p 89 N90-11712

Nacelle aerodynamic performance p 105 N90-12552

The development of a high response aerodynamic wedge probe and use on a high-speed research compressor [PNR90598] p 116 N90-12613

Large-scale Advanced Prop-fan (LAP) static rotor test report [NASA-CR-180848] p 117 N90-12617

Analysis of experimental data for CAST 10-2/DOA 2 supercritical airfoil at low Reynolds numbers and application to high Reynolds number flow [AD-A211654] p 170 N90-13326

Efficient methods for integrated structural-aerodynamic wing optimum design p 184 N90-13376

An in-flight investigation of ground effect on a forward-swept wing airplane [NASA-TM-101708] p 175 N90-14202

Concurrent processing adaptation of aeroplastic analysis of propfans [NASA-TM-102455] p 215 N90-14656

Flight and wind tunnel investigation of aerodynamic effects of aircraft ground deicing/anticing fluids

p 235 N90-15064

Serrated trailing edges for improving lift and drag characteristics of lifting surfaces

[NASA-CASE-LAR-13870-1] p 248 N90-15094

The US National Transonic Facility, NTF

p 262 N90-15942

NASA supercritical airfoils: A matrix of family-related airfoils

[NASA-TP-2969] p 315 N90-16710

Supersonic aerodynamic characteristics of a proposed Assured Crew Return Capability (ACRC) lifting-body configuration

[NASA-TM-4136] p 317 N90-17560

Analysis and numerical solution of flow over airfoil with control flap

p 318 N90-17564

Hypersonic nozzle/afterbody performance at low Mach numbers

[AD-A216223] p 319 N90-17575

CAST-10-2/DOA 2 Airfoil Studies Workshop Results

[NASA-CP-3052] p 352 N90-17647

High Reynolds number tests of the CAST-10-2/DOA 2 transonic airfoil at ambient and cryogenic temperature conditions

p 320 N90-17650

Main results of CAST-10 airfoil tested in T2 cryogenic wind tunnel

p 321 N90-17652

Investigation of CAST-10-2/DOA 2 airfoil in NAE high Reynolds number two-dimensional test facility

p 321 N90-17654

Modeling the wake as a continuous vortex sheet in a potential-flow solution using vortex panels

[AD-A216220] p 371 N90-18016

Prediction of rotor blade-vortex interaction noise from 2-D aerodynamic calculations and measurements

[ISL-CO-243/88] p 396 N90-18365

The effects of wind tunnel data uncertainty on aircraft point performance predictions

[AD-A216091] p 414 N90-18367

Computation of hypersonic unsteady viscous flow over a cylinder

p 397 N90-19194

Performance of an optimized rotor blade at off-design flight conditions

[NASA-CR-4288] p 416 N90-19226

Low-speed wind-tunnel investigation of the flight dynamic characteristics of an advanced turboprop business/commuter aircraft configuration

[NASA-TP-2982] p 434 N90-19239

Output model-following control synthesis for an oblique-wing aircraft

[NASA-TM-100454] p 435 N90-19241

Experimental and theoretical aerodynamic characteristics of a high-lift semispan wing model

[NASA-TP-2990] p 477 N90-20046

Unsteady free-wake viscous aerodynamic analysis of helicopter rotors

[AD-A217166] p 478 N90-20048

Windblast protection for advanced ejection seats

p 483 N90-20063

Measurement and prediction of propeller blade surface pressure distributions

p 481 N90-20961

Computational Methods for Aerodynamic Design (Inverse) and Optimization

p 500 N90-20976

Aerodynamic design techniques at DLR Institute for Design Aerodynamics

p 500 N90-20979

Aerodynamic design by optimization

p 502 N90-20996

Aerodynamic design via control theory

p 546 N90-20998

Optimization of aerodynamic designs using computational fluid dynamics

p 541 N90-20999

Prediction of forces and moments for flight vehicle control effectors. Part 1: Validation of methods for predicting hypersonic vehicle controls forces and moments

[NASA-CR-186571] p 571 N90-21734

Dynamic ground-effect measurements on the F-15 STOL and Maneuver Technology Demonstrator (S/MTD) configuration

[NASA-TP-3000] p 573 N90-22531

A computer code for the prediction of aerodynamic characteristics of lifting airfoils at transonic speed

[DLC-EST-TN-030] p 632 N90-23359

Experimental performance and acoustic investigation of modern, counterrotating blade concepts

[NASA-CR-185158] p 649 N90-23393

AVION: A detailed report on the preliminary design of a 79-passenger, high-efficiency, commercial transport aircraft

[NASA-CR-186663] p 649 N90-23395

Lateral-directional stability and control characteristics of the Quiet Short-Haul Research Aircraft (QSRA)

[NASA-TM-102250] p 671 N90-23413

Aerodynamic performance of a 0.27-scale model of an AH-64 helicopter with baseline and alternate rotor blade sets

[NASA-TM-4201] p 632 N90-24237

Aerodynamic characteristics of two rotorcraft airfoils designed for application to the inboard region of a main rotor blade

[NASA-TP-3009] p 633 N90-24239

Subsonic sting interference on the aerodynamic characteristics of a family of slanted-base ogive-cylinders

[NASA-CR-4299] p 633 N90-24242

Wind tunnel tests of a 20-gore disk-gap-band parachute

[AD-A221326] p 634 N90-24251

New transonic test sections for the NAE 5 ft x 5 ft trisonic wind tunnel

[AD-A220933] p 674 N90-24278

An analytic study of nonsteady two-phase laminar boundary layer around an airfoil

p 691 N90-25051

Design of a low cost short takeoff-vertical landing export fighter/attack aircraft

[NASA-CR-186658] p 734 N90-25132

A computational efficient modelling of laminar separation bubbles

[NASA-CR-186729] p 774 N90-25291

Prediction methodologies for nonlinear aerodynamic characteristics of control surfaces

[NIA-90-17] p 718 N90-25937

Effect of tail size reductions on longitudinal aerodynamic characteristics of a three surface F-15 model with nonaxisymmetric nozzles

[NASA-TP-3036] p 718 N90-25938

Identification of aerodynamic models for maneuvering aircraft

[NASA-CR-186630] p 719 N90-25943

Technical evaluation report on the Fluid Dynamics Panel Symposium on Computational Methods for Aerodynamic Design (Inverse) and Optimization

[AGARD-AR-267] p 720 N90-25947

Computation of viscous aerodynamic characteristics of 2-D airfoils for helicopter applications

[NLR-MP-88052-U] p 720 N90-25951

Effect of vortex generators on the aerodynamic wing characteristics and body of revolution

[AD-A222813] p 721 N90-25955

Turbulent reacting flows and supersonic combustion

[AD-A221793] p 875 N90-26933

The acoustic results of a United Technologies scale model helicopter rotor tested at DNW

[NASA-TM-101879] p 896 N90-27471

Development of a linearized unsteady aerodynamic analysis for cascade gust response predictions

[NASA-CR-4308] p 816 N90-27655

Active control of aerothermoelastic effects for a conceptual hypersonic aircraft

[NASA-TM-102713] p 869 N90-27725

Tests of an ultra-light tunnel in the anechoic wind tunnel facility CEPRA 19

[ONERA-RF-20/7294-PH] p 872 N90-27729

Prediction of subsonic vortex shedding from forebodies with chines

[NASA-CR-4323] p 909 N90-28494

Aerodynamics of Combat Aircraft Controls and of Ground Effects

[AGARD-CP-465] p 920 N90-28513

Effects of canard position on the aerodynamic characteristics of a close-coupled canard configuration at low speed

p 920 N90-28519

The steady and time-dependent aerodynamic characteristics of a combat aircraft with a delta or swept canard

p 921 N90-28526

Study of ground effects on flying scaled models

p 922 N90-28532

An in-flight investigation of ground effect on a forward-swept wing airplane

p 922 N90-28533

Determination of the ground effect on the characteristics of the A320 aircraft

p 922 N90-28534

Aerodynamic parameters of High-Angle-of attack Research Vehicle (HARV) estimated from flight data

[NASA-TM-102692] p 936 N90-28578

Transonic 3-D Euler analysis of flows around fanjet engine and TPS (Turbine Powered Simulator). Comparison with wind tunnel experiment, evaluation of TPS testing method and 3-D flow

[NAL-TR-1045] p 912 N90-29327

The DELTA MONSTER: An RPV designed to investigate the aerodynamics of a delta wing platform

[NASA-CR-186226] p 924 N90-29381

Fighter agility metrics

[NASA-CR-187289] p 925 N90-29389

Generalized Advanced Propeller Analysis System (GAPAS). Volume 2: Computer program user manual

[NASA-CR-185277] p 933 N90-29394

Numerical simulations of the structure of supersonic shear layers

[AD-A224164] p 960 N90-29587

The experimental investigation of flow in the core of a vortex structure

[BR114893] p 960 N90-29597

AERODYNAMIC COEFFICIENTS

Comparative cascade studies of some high diffusion compressor bladings

p 15 A90-12637

Wing-body mutual influence coefficients at angles-of-attack to 24 deg

p 151 A90-17693

New free-wake analysis of rotorcraft hover performance using influence coefficients

p 181 A90-17867

Fortified LEWICE with viscous effects --- Lewis Ice Accretion Prediction Code

[AIAA PAPER 90-0754] p 176 A90-20009

Computer-aided simulation of aircraft motion including nonlinearities in aerodynamic-coefficient relationships

p 257 A90-23359

External 6-component wind tunnel balances for aerospace simulation facilities

p 438 A90-28296

Numerical computations of transonic critical aerodynamic behavior

p 469 A90-32457

An implicit scheme with flow correction for the numerical solution of the Euler equation

p 477 A90-34674

Dynamic stall of a constant-rate pitching airfoil

p 553 A90-35754

Blockage corrections at high angles of attack in a wind tunnel

p 593 A90-35756

Connection between leading-edge sweep, vortex lift, and vortex strength for delta wings

p 554 A90-35770

Determination of aerodynamic sensitivity coefficients based on the transonic small perturbation formulation

p 622 A90-40682

Correlation of theory to wind-tunnel data at Reynolds numbers below 500,000

p 800 A90-46370

An orthogonal algorithm to the maximum likelihood estimation using an efficient method for computing sensitivities

[AIAA PAPER 90-3507] p 891 A90-47753

Exceptions to the $C(n, \beta, \gamma)$ criterion for aircraft stability at high angles of attack

p 867 A90-48515

Design and test of a natural laminar flow/large Reynolds number airfoil with a high design cruise lift coefficient

p 93 N90-12543

Effects of acoustic sources

p 140 N90-12553

Powered-lift aircraft technology

[NASA-SP-501] p 107 N90-12589

The maximum lift coefficient of plain wings at subsonic speeds

[ESDU-89034] p 236 N90-15082

Inclusion of nonlinear aerodynamics in the FLAP code

[DE89-009507] p 281 N90-15519

Main results of CAST-10 airfoil tested in T2 cryogenic wind tunnel

p 321 N90-17652

Comparison of NAE porous wall and NASA adaptive wall test results using the NAE CAST-10 airfoil model

p 353 N90-17656

An aerodynamic tradeoff study of the scissor wing configuration

[NASA-CR-186576] p 481 N90-20965

Slotted-wall research with disk and parachute models in a low-speed wind tunnel

[DE90-002989] p 572 N90-21737

Six-degree-of-freedom aircraft simulation with mixed-data structure using the applied dynamics simulation language, ADSIM

p 613 N90-23067

Aerodynamic characteristics of two rotorcraft airfoils designed for application to the inboard region of a main rotor blade

[NASA-TP-3009] p 633 N90-24239

An interactive boundary-layer method for unsteady airfoil flows. Part 1: Quasi-steady-state model

[AD-A221220] p 634 N90-24250

A flight dynamic model of aircraft spinning

[AR-005-600] p 935 N90-28576

Aerodynamic parameters of High-Angle-of attack Research Vehicle (HARV) estimated from flight data

[NASA-TM-102692] p 936 N90-28578

AERODYNAMIC CONFIGURATIONS

Aerodynamic and propulsive performance of hypersonic detonation wave ramjets

p 49 A90-12609

Construction of a straight single-row airfoil lattice by the method of quasi-solutions for inverse boundary value problems

p 84 A90-14564

Aircraft design: A conceptual approach --- Book

p 179 A90-17307

Optimization methods applied to aerodynamic design problems in computational fluid dynamics

p 156 A90-18308

Design optimization of natural laminar flow fuselages in compressible flow

[AIAA PAPER 90-0303] p 182 A90-19784

Aerodynamic control of NASP-type vehicles through vortex manipulation

[AIAA PAPER 90-0594] p 203 A90-19938

The local surface variation method in profile shape optimization problems p 297 A90-24136

Construction of a wing surface in a nonviscous transonic flow from a given pressure distribution p 298 A90-24149

The shape assumed by a soft conical shell in fluid flow p 300 A90-24752

B-2 aerodynamic design [AIAA PAPER 90-1802] p 334 A90-25174

Numerical study of three methods for solving reacting flows p 305 A90-25804

Techniques in multiblock domain decomposition and surface grid generation p 309 A90-26526

Grid generation for an aft-fuselage-mounted nacelle/pylon configuration p 311 A90-26543

Geometric modelling of complex aerodynamic surfaces and three-dimensional grid generation p 311 A90-26545

An approximation model for the performance and acoustic predictions of counterrotating propeller configurations [AIAA PAPER 90-0282] p 378 A90-26931

Using the method of symmetric singularities for calculating flow past subsonic flight vehicles p 386 A90-28979

Calculation of the drag of fuselage tail sections of different shapes in supersonic flow of a nonviscous gas p 388 A90-29182

Experimental transonic flutter characteristics of supersonic cruise configurations [AIAA PAPER 90-0979] p 390 A90-29369

Configuration aerodynamics p 557 A90-36540

A three-dimensional finite element Navier-Stokes solver with k-epsilon turbulence model for unstructured grids [AIAA PAPER 90-1652] p 570 A90-38780

Navier-Stokes solutions for vortical flows over a tangent-ogive cylinder p 620 A90-39780

Numerical simulation of vortical flows over a strake-delta wing and a close coupled delta-canard configuration [AIAA PAPER 90-3002] p 788 A90-45851

Design and experimental investigation of a laminar horizontal tail [AIAA PAPER 90-3042] p 798 A90-45934

A problem in the theory of optimal aerodynamic shapes p 803 A90-46503

Using the smoking-wire visualization method in the study of wing models at large angles of attack in subsonic wind tunnels p 881 A90-46561

Determination of the extreme values of the efficiency criteria for a flight vehicle control system in the probable scatter range of its characteristics p 859 A90-46569

CFD needs in conceptual design [AIAA PAPER 90-3209] p 813 A90-49106

A method for lifting surface design using nonlinear optimization [AIAA PAPER 90-3290] p 813 A90-49122

The aerodynamic design of the contraction for a subsonic wind tunnel p 907 A90-51545

US Navy principal site testing concept and the F-18 p 33 N90-10861

P-180 AVANTI: Project and flight test program comprehensive overview p 34 N90-10863

Study of the integration of wind tunnel and computational methods for aerodynamic configurations [NASA-TM-102196] p 170 N90-13332

Reduction of profile drag by modifying the structure next to the wake area [IMFL-88/35] p 172 N90-13356

A model suitable for predicting the noise associated with the ducted tail rotor of a helicopter [ECL-88-09] p 220 N90-14074

Application of the joined wing to tiltrotor aircraft [NASA-CR-177543] p 248 N90-15093

Models for cryogenic wind tunnels p 263 N90-15956

Preliminary design of a family of three close air support aircraft [NASA-CR-186070] p 336 N90-16751

An approximate model for the performance and acoustic predictions of counterrotating propeller configurations [NASA-CR-180667] p 379 N90-18228

Experimental and theoretical aerodynamic characteristics of a high-lift semispan wing model [NASA-TP-2990] p 477 N90-20046

An aerodynamic tradeoff study of the scissor wing configuration [NASA-CR-186576] p 481 N90-20965

An intensive procedure for the design of pressure-specified three-dimensional configurations at subsonic and supersonic speeds by means of a higher-order panel method p 500 N90-20982

Numerical optimization of wings in transonic flow p 502 N90-20997

Prediction of forces and moments for flight vehicle control effectors. Part 1: Validation of methods for predicting hypersonic vehicle controls forces and moments [NASA-CR-186571] p 571 N90-21734

Actuated forebody strakes [NASA-CASE-LAR-13983-1] p 648 N90-23390

Activities report in aerospace and aerodynamics [ETN-90-96774] p 699 N90-24224

Static wind-tunnel and radio-controlled flight test investigation of a remotely piloted vehicle having a delta wing planform [NASA-TM-4200] p 632 N90-24238

AM-X high incidence trials, development and results [ETN-90-97277] p 759 N90-26016

Combat aircraft control requirements for agility p 935 N90-28517

Energy Efficient Engine high pressure turbine component test performance report [NASA-CR-168289] p 929 N90-28553

Energy Efficient Engine program advanced turbofan nacelle definition study [NASA-CR-174942] p 930 N90-28560

Dynamic separation: Search for the cause of dynamic stall and search for its control [AD-A223412] p 911 N90-29305

AERODYNAMIC DRAG

Airplane design. Part 6 - Preliminary calculation of aerodynamic, thrust and power characteristics -- Book p 31 A90-12871

Leading edge flap influence on aerodynamic efficiency p 85 A90-15240

Design of axisymmetric bodies with minimum transonic drag p 154 A90-17997

Drag and propulsive efficiency of a light aircraft based on a new flight test technique [AIAA PAPER 90-0233] p 182 A90-19747

Inviscid drag prediction for transonic transport wings using a full-potential method [AIAA PAPER 90-0576] p 168 A90-19926

The distribution of normal-wash for minimum induced drag of non-planar wings p 226 A90-21983

Induced drag based on leading edge suction for a helicopter in forward flight p 232 A90-23102

Comment on 'Induced drag and the ideal wake of a lifting wing' p 233 A90-23291

The application of the discrete vortex method in aircraft design p 257 A90-23357

Experience with scale effects in non-airplane wind tunnel testing [AIAA PAPER 90-1822] p 350 A90-25165

Advanced rotor computations with a corrected potential method p 385 A90-28197

Instrumentation requirements for laminar flow research in the NLR high speed wind tunnel HST p 447 A90-28283

Induced drag of a wing of low aspect ratio p 387 A90-28987

Calculation of the induced drag of a wing with arbitrary deformation p 388 A90-29183

Hypersonic viscous shock-layer solutions over long slender bodies. II - Low Reynolds number flows p 393 A90-29695

Flight test and numerical analysis of a half-scale Unmanned Air Vehicle [AIAA PAPER 90-1260] p 494 A90-33890

A proposed automatic calibration facility for cryogenic balances p 524 A90-34246

Wall interference correction for three-dimensional transonic flows [AIAA PAPER 90-1408] p 558 A90-37947

Unsteady aerodynamic loading produced by a sinusoidally oscillating delta wing [AIAA PAPER 90-1536] p 564 A90-38680

On the use of external burning to reduce aerospace vehicle transonic drag [AIAA PAPER 90-1935] p 656 A90-40562

Minimum induced drag for wings with spanwise camber p 709 A90-44733

Development of a real-time aeroperformance analysis technique for the X-29A advanced technical demonstrator p 732 A90-44738

The effect of vibration-dissociation interaction on heat transfer and drag during the hypersonic flow past bodies p 710 A90-44934

Aerodynamic drag of a pair of bodies in transonic and supersonic flow p 710 A90-44935

Aerodynamic design considerations for aircraft radomes [AIAA PAPER 90-2843] p 711 A90-45163

Induced drag - Historical perspective [SAE PAPER 892341] p 715 A90-45495

Hypersonic forebody lift-induced drag [SAE PAPER 892345] p 715 A90-45497

Induced drag of wings with highly swept and tapered wing tips [AIAA PAPER 90-3062] p 794 A90-45896

A method for lifting surface design using nonlinear optimization [AIAA PAPER 90-3290] p 813 A90-49122

A closer look at the induced drag of crescent-shaped wings [AIAA PAPER 90-3063] p 903 A90-50638

Serrated trailing edges for improving lift and drag characteristics of lifting surfaces [NASA-CASE-LAR-13870-1] p 248 N90-15094

Effect of riblets on flow separation from a cylinder and an airfoil in subsonic flow [AD-A216197] p 319 N90-17574

Optimum spanwise camber for minimum induced drag [BU-403] p 397 N90-18369

Flight test investigation of certification issues pertaining to general-aviation-type aircraft with natural laminar flow [NASA-CR-181967] p 480 N90-20952

Constrained spanload optimization for minimum drag of multi-lifting-surface configurations p 501 N90-20992

Exhaust nozzles for propulsion systems with emphasis on supersonic cruise aircraft [NASA-RP-1235] p 516 N90-21037

On the use of external burning to reduce aerospace vehicle transonic drag [NASA-TM-103107] p 588 N90-21762

Preliminary airworthiness evaluation of the RC-12K [AD-A219545] p 648 N90-23387

Application of laminar flow control to supersonic transport configurations [NASA-CR-181917] p 719 N90-25944

Study of the compressibility effects on the turbulence of supersonic drags [ETN-90-97448] p 817 N90-27661

Study of the flow around the prototype of A300: Results of the third test campaign at F2 and comparison with calculations [CERT-33/5025-29-DERAT] p 817 N90-27663

Sting-support interference on afterbody drag at transonic speeds [NAL-TM-EA-8902] p 909 N90-28492

AERODYNAMIC FORCES

Finite element method for unsteady three-dimensional subsonic flows through a cascade oscillating with steady loading p 9 A90-11873

Numerical calculation of unsteady aerodynamic forces for two-dimensional supersonic oscillating cascades by finite element method p 9 A90-12238

Application of the double linearization theory to three-dimensional subsonic and supersonic cascade flutter p 50 A90-12638

Unsteady incompressible aerodynamics and forced response of detuned blade rows [AIAA PAPER 90-0340] p 191 A90-19805

Vortex dynamics of delta wings p 307 A90-26067

Measured forces and moments on a delta wing during pitch-up p 308 A90-26137

Circulation control tail boom aerodynamic prediction and validation p 385 A90-28243

Application of piezoelectric foils in experimental aerodynamics p 446 A90-28258

A novel technique for aerodynamic force measurement in shock tubes p 438 A90-28302

Static aeroelastic behavior of an adaptive laminated piezoelectric composite wing [AIAA PAPER 90-1078] p 412 A90-29386

The effect of structural variations on the dynamic characteristics of helicopter rotor blades [AIAA PAPER 90-1161] p 450 A90-29396

Aerodynamic characteristics of wave riders based on flows behind axisymmetric shock waves p 395 A90-30342

Flying qualities lessons learned - 1988 p 431 A90-30705

A calculation of the aerodynamic lift acting on cascade blades in a steady, viscous flow at high Reynolds number p 469 A90-32425

Unsteady lift and moment coefficients of an engine nacelle p 473 A90-33365

Inlet distortion generated periodic aerodynamic rotor response [ASME PAPER 89-GT-299] p 475 A90-33567

A technique for calculating nonlinear normal-force and pitching-moment coefficients for slender delta wings, accounting for wing thickness p 476 A90-34356

Counter-rotating propellant analysis using a frequency domain panel method p 623 A90-40937

Coupled aerodynamic forces due to unsteady stall on a high-aspect-ratio wing oscillating at high amplitude [ONERA, TP NO. 1990-24] p 623 A90-41203

Aerodynamics of store separation p 629 A90-42418

Measurements of aerodynamic forces on aircraft external stores in the NAE transonic blowdown wind-tunnel p 629 A90-42419

- Forced response on turbomachinery blades due to passing wakes
[AIAA PAPER 90-2353] p 705 A90-42781
Shaft flexibility effects on the forced response of a bladed-disk assembly p 744 A90-43218
Optimal plane change by low aerodynamic forces
[AIAA PAPER 90-2831] p 763 A90-45137
A laser sheet flow visualization and aerodynamic force data evaluation of a 3 percent YF-17 fighter aircraft model at high angles of attack
[AIAA PAPER 90-3019] p 792 A90-45886
Aerodynamic design of the Cal Poly Da Vinci Human-Powered Helicopter p 830 A90-46950
Improvement in turbine blade aerodynamic force in the tip region p 809 A90-47854
An integrated CFD/experimental analysis of aerodynamic forces and moments
[NASA-TM-102195] p 18 N90-10006
A scalar/vector potential solution for aerodynamic coefficients in wind shear p 21 N90-10838
Normal-force-curve and pitching-moment-curve slopes of forebody-cylinder combinations at zero angle of attack for Mach numbers up to 5
[ESDU-89008] p 89 N90-11709
In-plane forces and moments on installed inclined propellers at low forward speeds
[ESDU-89047] p 316 N90-16720
Windblast protection for advanced ejection seats p 483 N90-20063
Application of a dynamic stall model to rotor trim and aeroelastic response p 583 N90-22556
STARS: An integrated general-purpose finite element structural, aeroelastic, and aeroservoelastic analysis computer program
[NASA-TM-101709] p 689 N90-23768
Short time-dynamometer system for shock wave channels
[MBB-UT-115/89-PUB] p 773 N90-25084
Aerodynamic interferences of in-flight thrust reversers in ground effect p 921 N90-28529
Windshear estimation along the trajectory of an aircraft p 963 N90-29745
- AERODYNAMIC HEAT TRANSFER**
Infrared thermography in blowdown and intermittent hypersonic facilities p 440 A90-31302
Numerical study of heat transfer for unsteady viscous supersonic blunt body flows p 707 A90-44432
Heat transfer measurements from a NACA 0012 airfoil in flight and in the NASA Lewis icing research tunnel [NASA-CR-4278] p 399 N90-19203
- AERODYNAMIC HEATING**
Infrared radiation model for aircraft and reentry vehicle p 77 A90-10169
Thermostructural behavior of electromagnetic windows - Elaboration of a code package
[ONERA, TP NO. 1989-145] p 76 A90-11167
Aerodynamic heating in the interaction regions of shock waves and turbulent boundary layers induced by sharp fins p 9 A90-12220
Lee-side heating of a delta wing in supersonic flow p 10 A90-12281
Aerodynamic heating in shock wave/turbulent boundary layer interaction regions induced by blunt fins p 82 A90-13775
A model for the electrohydrodynamic flow in a constricted arc heater p 131 A90-15393
The critical role of aerodynamic heating effects in the design of hypersonic vehicles p 155 A90-18249
Thermal/structural analyses of several hydrogen-cooled leading-edge concepts for hypersonic flight vehicles
[AIAA PAPER 90-0053] p 274 A90-23702
Aerodynamic heat transfer testing in hypersonic wind tunnels using an infrared imaging system
[AIAA PAPER 90-0189] p 350 A90-25027
Liquid crystal thermography for aerodynamic heating measurements in short duration hypersonic facilities p 446 A90-28262
Generalized Transition Finite-Boundary Elements for high speed flight structures p 449 A90-29286
Thermal structures - Four decades of progress
[AIAA PAPER 90-0971] p 411 A90-29305
Particulate trajectories and impact characteristics in hypersonic flight involving gas coolant shielding p 476 A90-34583
Application of the LAURA code for slender-vehicle aerothermodynamics
[AIAA PAPER 90-1714] p 560 A90-38416
The ascending trajectories performance and control to minimize the heat load for the transatmospheric aero-space planes
[AIAA PAPER 90-2828] p 763 A90-45135
Effect of aerodynamic heating on deformation of composite cylindrical panels in a gas flow p 773 A90-45788
- Application of localized surface heating to actively control the boundary layer separation p 806 A90-46848
Active control of aerothermoelastic effects for a conceptual hypersonic aircraft p 863 A90-47597
Thermal management for a Mach 5 cruise aircraft using endothermic fuel p 853 A90-48871
Use of ECS-conditioned air for FLIR avionics thermal control - Fighter aircraft p 840 A90-49294
[SAE PAPER 901219]
Thermal protection systems for hypersonic transport vehicles p 882 A90-49358
[SAE PAPER 901306]
Optimum shape of a blunt forebody in hypersonic flow [NASA-CR-181955] p 171 N90-13351
Thermal/structural analyses of several hydrogen-cooled leading-edge concepts for hypersonic flight vehicles [NASA-TM-102391] p 215 N90-14511
A review of high-speed, convective, heat-transfer computation methods p 316 N90-17548
Analysis of flow-, thermal-, and structural-interaction of hypersonic structures subjected to severe aerodynamic heating
[AD-A217882] p 478 N90-20053
The application of active controls technology to a generic hypersonic aircraft configuration
[NASA-TM-101689] p 497 N90-20071
A brief review of some mechanisms causing boundary layer transition at high speeds p 720 N90-25945
[NASA-TM-102834]
Space plane model for visual measurement of aerodynamic heating p 720 N90-25949
[DE90-505514]
Real-time aerodynamic heating and surface temperature calculations for hypersonic flight simulation
[NASA-TM-4222] p 959 N90-28815
- AERODYNAMIC INTERFERENCE**
Experimental investigation on the interference effect of FL-23 wind tunnel wall on transonic flutter p 57 A90-10347
Simulations of propeller/airframe interference effects using an Euler correction method p 31 A90-13019
On the effects of wind tunnel turbulence on steady and unsteady airfoil characteristics p 147 A90-16777
Wing-body mutual influence coefficients at angles-of-attack to 24 deg p 151 A90-17693
Wall interference correction of high-lift multi-component airfoils p 158 A90-18604
Application of panel methods to wind-tunnel wall interference corrections p 200 A90-19629
[AIAA PAPER 90-0007]
Subsonic calculation of propeller/wing interference
[AIAA PAPER 90-0031] p 226 A90-22155
Aerodynamic interference of prismatic engine nacelles with the wing at supersonic velocities p 294 A90-24078
The performance and longitudinal stability and control of large receiver aircraft during air to air refueling p 346 A90-24338
Active control of gust- and interference-induced vibration of tilt-rotor aircraft p 429 A90-28201
Whirl flutter stability of a pusher configuration subject to a nonuniform flow p 393 A90-29397
[AIAA PAPER 90-1162]
Wall-interference corrections for parachutes in a closed wind tunnel p 440 A90-31281
Transonic Euler solutions on mutually interfering finned bodies p 555 A90-36256
Adaptive wind tunnel walls: Compendium of final report - AGARD FDP working group 12 p 595 A90-37944
[AIAA PAPER 90-1405]
Wall interference assessment/correction (WIAC) for transonic airfoil data from porous and shaped wall test sections p 595 A90-37945
[AIAA PAPER 90-1406]
Wall interference correction for three-dimensional transonic flows p 558 A90-37947
[AIAA PAPER 90-1408]
Evaluation of transonic wall interference assessment and correction for semi-span wing data p 597 A90-38487
[AIAA PAPER 90-1433]
Analysis of aeroelastic divergence for the slender flight vehicles p 680 A90-39298
Large receiver aircraft - The performance and longitudinal stability and control during air to air refueling p 669 A90-41767
The effect of constructive and destructive interference on the downstream development of twin jets in a crossflow. II - Interference effects of angularly displaced jets
[AIAA PAPER 90-2107] p 684 A90-42020
Wind tunnel wall interference investigations in NAE/NRC High Reynolds Number 2D Facility and NASA Langley 0.3m Transonic Cryogenic Tunnel p 628 A90-42404
- Wind tunnel studies of support strut interference on a 3 percent YF-17 fighter aircraft model at high angles of attack p 794 A90-45899
[AIAA PAPER 90-3083]
Interference between a vortex filament and shock waves in free flow and in nonisobaric jets p 804 A90-46550
Some characteristics of interference between shock waves and the aerodynamic wake behind a body p 804 A90-46551
An experimental study of instantaneous velocity perturbations over a rotor disk for low duty coefficients p 860 A90-46572
Comparisons of one- and two- interface methods for tunnel wall interference calculation p 870 A90-48961
A method for calculating the rotor-fuselage interference in helicopters p 919 A90-50246
[DGLR PAPER 88-060]
Wind tunnel support system effects on a fighter aircraft model at Mach numbers from 0.6 to 2.0 p 19 N90-10010
[AD-A210614]
Transonic Euler solutions on mutually interfering finned bodies p 170 N90-13331
[AD-A213395]
A wall interference assessment/correction interface measurement system for the NASA/ARC 12-ft PWT [NASA-CR-185474] p 200 N90-13401
A two-dimensional adaptive-wall test section with ventilated walls in the Ames 2- by 2-foot transonic wind tunnel p 201 N90-13407
[NASA-TM-102207]
An experimental investigation of wall-interference effects for parachutes in closed wind tunnels p 236 N90-15076
[DE90-001802]
Installed tailplane lift-curve slope at subsonic speeds p 236 N90-15081
[ESDU-89029]
Wind tunnel investigations on the configuration of the international vortex flow experiment p 277 N90-16181
Prediction methods for store separation p 317 N90-17549
CAST-10-2/DOA 2 Airfoil Studies Workshop Results [NASA-CP-3052] p 352 N90-17647
Nonlinear transonic Wall-Interference Assessment/Correction (WIAC) procedures and application to cast-10 airfoil results from the NASA 0.3-m TCT 8- by 24-inch Slotted Wall Test Section (SWTS) p 352 N90-17648
Comparison of conventional and adaptive wall wind tunnel results with regard to Reynolds number effects p 352 N90-17649
High Reynolds number tests of the CAST-10-2/DOA 2 transonic airfoil at ambient and cryogenic temperature conditions p 320 N90-17650
Investigation of CAST-10-2/DOA 2 airfoil in NAE high Reynolds number two-dimensional test facility p 321 N90-17654
Residual interference and wind tunnel wall adaption p 353 N90-17655
Comparison of NAE porous wall and NASA adaptive wall test results using the NAE CAST-10 airfoil model p 353 N90-17656
Experience with some repeat tests on the 9 inch chord CAST-10-2/DOA 2 airfoil model in the Langley 0.3-m TCT adaptive wall test section p 321 N90-17657
Comparison of two- and three-dimensional Navier-Stokes solutions with NASA experimental data for CAST-10 airfoil p 321 N90-17658
The MANTA: An RPV design to investigate forces and moments on a lifting surface p 499 N90-20971
[NASA-CR-186227]
An experimental investigation of support strut interference on a three-percent fighter model at high angles of attack p 631 N90-23353
[AD-A219793]
A contribution to the improvement of the accuracy in the parameter identification of nonlinear processes, by example of the aircraft motion p 736 N90-25974
[ETN-90-96961]
Limits of adaptation, residual interferences p 871 N90-26844
Adaptation for unsteady flow p 871 N90-26845
Sting-support interference on afterbody drag at transonic speeds p 909 N90-28492
[NAL-TM-EA-8902]
Unsteady aerodynamics of controls p 935 N90-28525
Aerodynamic interferences of in-flight thrust reversers in ground effect p 921 N90-28529
Three-dimensional model testing in the transonic self-streamlining wind tunnel p 938 N90-28583
- AERODYNAMIC LOADS**
An improved version of LTRAN2 p 2 A90-10350
Computation of aerodynamic blade loads due to wake influence and aerodynamic damping of turbine and compressor cascades p 7 A90-11791

- Improved double linearization method for prediction of mean loading effects on subsonic and supersonic cascade flutter p 41 A90-11795
- Structural optimization of lifting surfaces with divergence and control reversal constraints p 127 A90-13770
- Three-dimensional aerodynamics of an annular airfoil cascade including loading effects p 87 A90-15889
- A numerical method for computing the aerodynamic loads on wings with sharp-edge separations at large angles of attack in subcritical transonic flows p 150 A90-16852
- Investigation on the determination of airplane tail loads by flight tests p 178 A90-16853
- Analysis methods of tie-down loads and airframe stress for shipboard-helicopters p 199 A90-16855
- Low Reynolds number airfoils evaluation program p 151 A90-17692
- Numerical simulation of unsteady flow about cambered plates p 159 A90-19389
- Estimate of loads during wing-vortex interactions by Munk's transverse-flow method p 159 A90-19391
- Unsteady aerodynamic forces on rolling delta wings at high angle of attack p 159 A90-19426
- The fickle effect of nose microasymmetry on the high-alpha aerodynamics [AIAA PAPER 90-0067] p 161 A90-19663
- Aerodynamic loads computation on coaxial hingeless helicopter rotors [AIAA PAPER 90-0070] p 161 A90-19666
- Large-amplitude high-rate roll experiments on a delta and double delta wing [AIAA PAPER 90-0224] p 163 A90-19742
- Aerodynamic spike flowfields computed to select optimum configuration at Mach 2.5 with experimental validation [AIAA PAPER 90-0414] p 166 A90-19837
- Static aeroelastic analysis of fighter aircraft using a three-dimensional Navier-Stokes algorithm [AIAA PAPER 90-0435] p 166 A90-19845
- Prediction of aerostat and airship mooring mast loads by nonlinear dynamic simulation [AIAA PAPER 89-3172] p 245 A90-20587
- Estimation of the flight dynamic characteristics of the YEZ-2A [AIAA PAPER 89-3173] p 245 A90-20590
- Correlation of Puma airfoils - Evaluation of CFD prediction methods [ONERA, TP NO. 1989-185] p 224 A90-21045
- A hybrid method for prediction of propeller performance [AIAA PAPER 90-0440] p 229 A90-22219
- Analysis of extreme wind shear p 280 A90-23255
- The effect of uniform spanwise vorticity on the two-dimensional flow through cascades p 293 A90-23996
- Multilevel method for calculating aerodynamic loads on a flight vehicle p 296 A90-24122
- Unsteady Euler analysis of the flowfield of a propfan at an angle of attack [AIAA PAPER 90-0339] p 300 A90-25028
- Dynamics of spatial motion of an aeroplane after drop of loads p 346 A90-25189
- Nonlinear effects in helicopter rotor forward flight forced response p 347 A90-25420
- Wind tunnel testing of a helicopter model at HAL p 335 A90-26350
- Automated procedure for creating flight-by-flight spectra p 376 A90-26755
- Fatigue spectra development for airborne stores p 336 A90-26757
- Compilation of procedures for fatigue crack propagation testing under complex load sequences p 368 A90-26759
- Stochastic flutter of a panel subjected to random in-plane forces. I - Two mode interaction p 444 A90-27992
- A comprehensive hover test of the airloads and airflow of an extensively instrumented model helicopter rotor p 407 A90-28173
- Rotor loads validation utilizing a coupled aeroelastic analysis with refined aerodynamic modeling p 408 A90-28226
- V-22 aerodynamic loads analysis and development of loads alleviation flight control system p 410 A90-28239
- The prediction of loads on the Boeing Helicopters Model 360 rotor p 410 A90-28240
- Development of a dual strain gage balance system for measuring light loads p 437 A90-28289
- A fatigue study of electrical discharge machine (EDM) strain-gage balance materials p 448 A90-28295
- Aerodynamics of human-powered flight p 386 A90-28552
- Computation of steady and unsteady control surface loads in transonic flow [AIAA PAPER 90-0935] p 389 A90-29361
- Influence of joint fixity on the aeroelastic characteristics of a joined wing structure [AIAA PAPER 90-0980] p 390 A90-29370
- Aeroelastic analysis of helicopter rotor blades with advanced tip shapes [AIAA PAPER 90-1118] p 392 A90-29390
- Stochastic flutter of a panel subjected to random in-plane forces. II - Two and three mode non-Gaussian solutions [AIAA PAPER 90-0986] p 451 A90-29399
- State-space representation of unsteady airfoil behavior p 469 A90-32461
- Unsteady airloads due to separated flow on airfoils and wings p 471 A90-33311
- Unsteady aerodynamic forces of oscillating supersonic/hypersonic wings with attached shock waves p 473 A90-33363
- Numerical analysis of unsteady forces on oscillating ring airfoils and jet engines p 473 A90-33364
- Measurement of wind tunnel model deformation under airload p 522 A90-33370
- Aeroelastic analysis using finite element models p 492 A90-33388
- Practical techniques of modelling aeroelastic systems for active control applications p 545 A90-33402
- Advancements in rotor and airframe structural flight testing developed during the SH-60B G.W./C.G. expansion program [AIAA PAPER 90-1281] p 495 A90-33902
- A proposed automatic calibration facility for cryogenic balances p 524 A90-34246
- Blockage corrections at high angles of attack in a wind tunnel p 593 A90-35756
- A numerical method in aeroelasticity for wings with separation at large angle of attack p 557 A90-37209
- Aerodynamic loads and blade vortex interaction noise prediction p 614 A90-38520
- A survey of nonuniform inflow models for rotorcraft flight dynamics and control applications p 590 A90-38521
- Unsteady aerodynamic loading produced by a sinusoidally oscillating delta wing [AIAA PAPER 90-1536] p 564 A90-38680
- Lift response of a rectangular wing undergoing a step change in forward speed p 620 A90-39801
- Synthesis of optimal multidimensional digital systems for the simulation of the angular motions of a flight vehicle under random loading p 669 A90-41957
- SDOF dynamic loads on a jet vane [AIAA PAPER 90-2382] p 675 A90-42147
- A review of tilt rotor download research p 630 A90-42437
- Active control of tiltrotor blade in-plane loads during maneuvers p 670 A90-42463
- External nozzle flap dynamic load measurements on F-15 S/MTD model [AIAA PAPER 90-1910] p 740 A90-42692
- Structural and aerodynamic analysis of a large scale advanced propeller blade [AIAA PAPER 90-2401] p 743 A90-42793
- Development of a mathematical model of an adaptive antiflutter system p 769 A90-42911
- Iterative algorithm for correlation of strain gauge data with aerodynamic load p 709 A90-44739
- Delta wing surface pressures for high angle of attack maneuvers [AIAA PAPER 90-2813] p 711 A90-45153
- Steady and unsteady force testing of fighter aircraft models in a water tunnel [AIAA PAPER 90-2815] p 711 A90-45155
- Approach to side force alleviation through modification of the pointed forebody geometry [AIAA PAPER 90-2834] p 712 A90-45165
- A nonlinear transient formulation of UHB aeroelastic response and stability. I - Theoretical formulation [SAE PAPER 892322] p 715 A90-45481
- Vortical sources of aerodynamic force and moment [SAE PAPER 892346] p 715 A90-45498
- Performance measurements of an airfoil at low Reynolds numbers p 800 A90-46369
- Effect of the drag on the critical flutter velocity p 828 A90-46480
- Modeling of the buffeting of flight vehicles p 803 A90-46500
- Rotor loads computation using singularity methods and application to the noise prediction p 807 A90-46880
- Improvement to interactive two dimensional rotor section design p 808 A90-46943
- Experimental investigation of wingtip aerodynamic loading p 808 A90-46945
- Development of the Second Generation Comprehensive Helicopter Analysis System (2GCHAS) p 889 A90-46963
- Two and three dimensional indicial methods for rotor dynamic airloads p 808 A90-46973
- Method for simultaneous wing aerodynamic and structural load prediction p 838 A90-48955
- Assessment of service load experience p 901 A90-49877
- Acoustic wave excitation during the aerodynamic interaction between a fan blade and a bluff obstacle p 965 A90-52289
- Rotor blade structural design p 106 A90-12584
- Correlation of Puma airloads: Lifting-line and wake calculation [NASA-TM-102212] p 170 A90-13327
- Description of atmospheric turbulence p 280 A90-15043
- The interference of flightmechanical control laws with those of load alleviation and its influence on structural design p 258 A90-15054
- An examination of helicopter rotor load calculations [AD-A214295] p 249 A90-15098
- A survey of nonuniform inflow models for rotorcraft flight dynamics and control applications [NASA-TM-102219] p 260 A90-15938
- Cryogenic balances for the US NTF p 264 A90-15959
- The response of helicopter rotors to vibratory airload [AD-A215678] p 337 A90-16756
- Design guidance to minimize unsteady forces in turbomachines p 426 A90-18411
- Unsteady blade loads due to wake influence p 426 A90-18413
- Active stabilization of aeromechanical systems [AD-A216629] p 454 A90-18672
- Calculation of flight vibration levels of the AH-1G helicopter and correlation with existing flight vibration measurements [NASA-CR-181923] p 454 A90-18743
- X-29A aircraft structural loads flight testing [NASA-TM-101715] p 416 A90-19225
- Aeroelastic characteristics of aircraft with circulation control wings p 497 A90-20070
- The MANTA: An RPV design to investigate forces and moments on a lifting surface [NASA-CR-186227] p 499 A90-20971
- A computational design method for shock free transonic cascades and airfoils p 501 A90-20986
- The radiation of sound from a propeller at angle of attack [NASA-CR-4264] p 548 A90-21602
- Airloads, wakes, and aeroelasticity [NASA-CR-177551] p 572 A90-21738
- Aeroelastic simulation of higher harmonic control p 592 A90-21768
- Aerodynamic loads and blade vortex interaction noise prediction [ISL-PU-310/89] p 719 A90-25942
- Identification of aerodynamic models for maneuvering aircraft [NASA-CR-186630] p 719 A90-25943
- Formation of design envelope criterion in terms of deterministic spectral procedure [RAE-TM-SS-9] p 721 A90-25953
- An in-flight interaction of the X-29A canard and flight control system [NASA-TM-101718] p 736 A90-25973
- New inflight experiments to measure aerodynamics loads [ETN-90-97276] p 868 A90-26834
- NASA/GE Energy Efficient Engine low pressure turbine scaled test vehicle performance report [NASA-CR-168290] p 931 A90-28563
- The Second ARO Workshop on Rotorcraft Interactional Aerodynamics [AD-A223310] p 911 A90-29304
- Analysis of dynamic transient response and postflight behavior of super-maneuvering airplane [AD-A224126] p 925 A90-29386

AERODYNAMIC NOISE

- Wave cancellation properties of a splitter-plate porous wall configuration p 57 A90-11005
- The acoustic phenomena of the stalling flutter p 78 A90-11801
- Rotor noise due to atmospheric turbulence ingestion. I - Fluid mechanics p 219 A90-19385
- SARL noise measurements [AIAA PAPER 90-0285] p 219 A90-19772
- Simulation of sound propagation in axisymmetric jet p 378 A90-25872
- Structure-borne noise transmission in cylindrical enclosures due to random excitation [AIAA PAPER 90-0990] p 463 A90-29402
- Application of active noise control to model propeller noise p 548 A90-34091
- Broadband noise measurement in the transonic test section of the VTI T-38 wind tunnel [AIAA PAPER 90-1418] p 614 A90-37955
- An experimental evaluation of test section noise in transonic wind tunnels [AIAA PAPER 90-1419] p 614 A90-37956

- A new class of random processes with application to helicopter noise p 781 A90-42874
- Calculation of the rotation noise of a single propeller with blades of arbitrary shape p 894 A90-46552
- The ROTONET prediction system and initial comparisons with far-field acoustics measurements for the XV-15 tilt-rotor aircraft p 894 A90-46947
- Active control of propeller-induced noise fields inside a flexible cylinder p 833 A90-47306
- Acoustic design considerations: Review of rotor acoustic sources p 106 N90-12585
- Estimation of subsonic far-field jet-mixing noise from single-stream circular nozzles [ESDU-89041] p 316 N90-16721
- Direct numerical simulation of aerodynamic noise [AD-A214122] p 379 N90-18225
- Air Force Boom Event Analyzer Recorder (BEAR): System description p 548 N90-20800
- [AD-A218048] p 548 N90-20800
- Relating flow between counter-rotating propellers to aerodynamic interaction noise p 479 N90-20944
- An investigation of the generation and radiation of aerodynamic noise in real piping systems p 614 N90-22368
- Summary of sonic boom rise times observed during FAA community response studies over a 6-month period in the Oklahoma City area [NASA-CR-4277] p 696 N90-24852
- AERODYNAMIC STABILITY**
- Flutter of turbine blades p 41 A90-11794
- Advancements in frequency-domain methods for rotorcraft system identification p 56 A90-12771
- The application of linear maximum likelihood estimation of aerodynamic derivatives for the Bell-205 and Bell-206 p 30 A90-12773
- Aeroelastic detuning for stability enhancement of unstalled supersonic flutter p 189 A90-17462
- Effects of endwall suction and blowing on compressor stability enhancement [ASME PAPER 89-GT-64] p 290 A90-23787
- Dynamics of spatial motion of an aeroplane after drop of loads p 346 A90-25189
- Relative aeromechanical stability characteristics for hingeless and bearingless rotors p 409 A90-28230
- Whirl flutter stability of a pusher configuration subject to a nonuniform flow [AIAA PAPER 90-1162] p 393 A90-29397
- Investigation of cowl vent slots for supercritical stability enhancement in dual-mode ramjet inlets p 507 A90-32951
- A new simplification method for analysing the rapid rolling stability of aircraft p 669 A90-42367
- Stability characteristics of a conical aerospace plane concept [SAE PAPER 892313] p 757 A90-45475
- Rapid prediction of slender-wing aircraft dynamics [AIAA PAPER 90-3037] p 791 A90-45876
- Design for a natural laminar flow glove for a transport aircraft [AIAA PAPER 90-3043] p 792 A90-45880
- Effect of leading edge roundness on a delta wing in wing-rock motion [AIAA PAPER 90-3080] p 795 A90-45911
- BHTI's technical assessment of advanced rotor and control concepts p 861 A90-46949
- AHS National Specialists' Meeting on Rotorcraft Dynamics, Arlington, TX, Nov. 13, 14, 1989, Proceedings p 830 A90-46952
- Development of the Second Generation Comprehensive Helicopter Analysis System (2GCHAS) p 889 A90-46963
- New experimental results on the origin and structure of Fern and Dailey instabilities ('buzz') p 906 A90-51507
- Airworthiness and flight characteristics test of the UH-60A Black Hawk helicopter equipped with the XM-139 multiple mine dispensing system (VOLCANO) [AD-A210271] p 32 N90-10025
- Unsteady aerodynamics with applications to flight mechanics [AD-A211944] p 89 N90-11706
- Active control of unsteady and separated flow structures [AD-A212109] p 89 N90-11707
- Stability and control derivatives of the De Havilland DHC-2 BEAVER aircraft [PB89-217525] p 119 N90-11754
- Effect of control surface mass unbalance on the stability of a closed-loop active control system [NASA-TP-2952] p 134 N90-12042
- Rotor blade dynamic design p 106 N90-12583
- Airframe design considerations: Overview --- rotor design optimization p 106 N90-12586
- Applications of modern control theory synthesis to a super-augmented aircraft [AD-A215431] p 336 N90-16753

- Stability characteristics of a combat aircraft with control surface failure [AD-A216196] p 350 N90-17646
- The application of active controls technology to a generic hypersonic aircraft configuration [NASA-TM-101689] p 497 N90-20071
- Prediction of forces and moments for flight vehicle control effectors. Part 2: An analysis of delta wing aerodynamic control effectiveness in ground effect [NASA-CR-186572] p 571 N90-21735
- Actuated forebody strakes [NASA-CASE-LAR-13983-1] p 648 N90-23390
- Rotorcraft aeromechanical stability-methodology assessment. Phase 2: Workshop [NASA-TM-102272] p 816 N90-26800
- The SKY SHARK: An RPV designed to investigate the pressure distribution on a lifting surface [NASA-CR-186222] p 844 N90-26824
- The role of C(sub n beta dyn) in the aircraft stability at high angles of attack [AD-A221586] p 868 N90-26833
- Inflight thrust vectoring: A further degree of freedom in the aerodynamic/flight mechanical design of modern fighter aircraft p 921 N90-26528

AERODYNAMIC STALLING

- The study of the theoretical calculation method for power stall dynamic characteristics of multiple-engine propeller airplane p 29 A90-10349
- The effect of pitch location on dynamic stall p 2 A90-10641
- The acoustic phenomena of the stalling flutter p 78 A90-11801
- A study of flow structure in a contra-rotating axial compressor stage p 11 A90-12524
- An iterative non-linear lifting line model for wings with unsymmetrical stall [SAE PAPER 891020] p 83 A90-14332
- Development of a stall improvement package for the Gulfstream IV [SAE PAPER 891021] p 83 A90-14333
- A low cost stall/spin simulator [SAE PAPER 891022] p 117 A90-14334
- Prediction of post-stall flows on airfoils p 145 A90-16757
- Computational and experimental studies of compressible dynamic stall p 146 A90-16776
- Experimental and computational studies of dynamic stall p 147 A90-16780
- Dynamic stall of circulation control airfoils [AIAA PAPER 90-0573] p 167 A90-19923
- Amplitude effects on dynamic stall of an oscillating airfoil [AIAA PAPER 90-0575] p 167 A90-19925
- The influence of sweep on dynamic stall produced by a rapidly pitching wing [AIAA PAPER 90-0581] p 230 A90-22231
- A comparison between the design point and near-stall performance of an axial compressor [ASME PAPER 89-GT-70] p 254 A90-22667
- Stability of flow through multistage axial compressors [ASME PAPER 89-GT-311] p 231 A90-22668
- Stall inception in axial compressors [ASME PAPER 89-GT-63] p 290 A90-23786
- Navier-Stokes study of rotating stall in compressor cascades p 302 A90-25292
- Analysis of fully stalled compressor p 383 A90-27966
- Identification of retreating blade stall mechanisms using flight test pressure measurements p 384 A90-28172
- Design and development of a facility for compressible dynamic stall studies of a rapidly pitching airfoil p 436 A90-28255
- Nonlinear stall flutter and divergence analysis of cantilevered graphite/epoxy wings [AIAA PAPER 90-0983] p 450 A90-29373
- Computational prediction of stall flutter in cascaded airfoils [AIAA PAPER 90-1116] p 392 A90-29388
- Digital simulation of flight control systems for post-stall aircraft p 431 A90-30704
- Experimental investigation of the flow development of an airfoil at high angles of attack p 473 A90-33366
- Ten years of stall testing [AIAA PAPER 90-1268] p 518 A90-33895
- Differential equation modeling of dynamic stall p 476 A90-34325
- Thrust generation by an airfoil in hover modes [AD-A223602] p 552 A90-35137
- Dynamic stall experiments on the NACA 23012 airfoil p 552 A90-35140
- Dynamic stall of a constant-rate pitching airfoil p 553 A90-35754
- Air combat beyond the stall p 589 A90-35888
- Vortex generator jets - Means for flow separation control p 555 A90-36257

- Stall margin improvement in axial-flow compressors by circumferential variation of stationary blade setting angles [AIAA PAPER 90-1912] p 656 A90-40554
- Coupled aerodynamic forces due to unsteady stall on a high-aspect-ratio wing oscillating at high amplitude [ONERA, TP NO. 1990-24] p 623 A90-41203
- Expanding the B-1B flight envelope p 644 A90-41899
- Two dimensional post stall maneuver of a NACA 0015 airfoil at high pitching rates [AIAA PAPER 90-2810] p 710 A90-45150
- Helicopter trim with flap-lag-torsion and stall by an optimized controller p 755 A90-45332
- Schlieren studies of compressibility effects on dynamic stall of airfoils in transient pitching motion [AIAA PAPER 90-3038] p 791 A90-45877
- Finite wing lift prediction at high angles of attack [AIAA PAPER 90-3079] p 795 A90-45910
- Interactive boundary-layer method for unsteady airfoil flows - Quasisteady model p 812 A90-48953
- A method for predicting stall flutter under variable interblade phase angle along rotating direction p 813 A90-49455
- The interaction between distortion of inlet flow and blade stall flutter in axial-flow compressor p 854 A90-49466
- The calculation of incompressible separated turbulent boundary layers p 905 A90-51025
- Stall/spin/flight simulation [DOT/FAA/CT-88/28] p 122 N90-11765
- Some observations on transitory stall in conical diffusers [NASA-TM-102387] p 94 N90-12561
- Stall/spin aerodynamic data project [DOT/FAA/CT-88/29] p 185 N90-14222
- Schleicher ASK-21 glider (TG-9) stall and spin [AD-A213513] p 249 N90-15096
- Aircraft performance enhancement with active compressor stabilization [AD-A213652] p 249 N90-15097
- Dynamic derivatives of missiles and fighter-type configurations at high angles of attack p 337 N90-17554
- Measurement of velocity profiles and Reynolds stresses on an oscillating airfoil p 397 N90-18427
- Stall and recovery in multistage axial flow compressors p 428 N90-18429
- Active stabilization of aeromechanical systems [AD-A216629] p 454 N90-18672
- Application of a dynamic stall model to rotor trim and aeroelastic response p 583 N90-22556
- Flow visualization of dynamic stall on an oscillating airfoil [AD-A222202] p 815 N90-26797
- Control research in the NASA high-alpha technology program p 934 N90-28516
- Dynamic separation: Search for the cause of dynamic stall and search for its control [AD-A223412] p 911 N90-29305
- AERODYNAMICS**
- A class of implicit upwind schemes for Euler simulations with unstructured meshes p 5 A90-11597
- Unsteady aerodynamics and aeroelasticity of turbomachines and propellers; Proceedings of the Fourth International Symposium, Aachen, Federal Republic of Germany, Sept. 6-10, 1987 p 5 A90-11776
- The unsteady aerodynamics of an oscillating cascade in a compressible flow field p 7 A90-11789
- Airplane aerodynamics and performance --- Book p 17 A90-12865
- The characteristic decay region of a class of three-dimensional wall jets p 85 A90-15241
- Complementary field method for interferometric tomographic reconstruction of high speed aerodynamic flows [AD-A219698] p 131 A90-15900
- Recent developments in calculation methods for internal flows by solution of Euler or Navier-Stokes equations [ONERA, TP NO. 1989-167] p 223 A90-21033
- Multi-processing on supercomputers for computational aerodynamics [AIAA PAPER 90-0337] p 282 A90-22199
- Convergence of the method of discrete vortices when applied to steady-state aerodynamics problems p 231 A90-22816
- An approximate 3-D aerodynamic design method for centrifugal impeller blades [ASME PAPER 89-GT-73] p 291 A90-23794
- Design of a three dimensional Doppler anemometer for T2 transonic wind tunnel p 447 A90-28271
- A semiconductor laser-Doppler-anemometer for applications in aerodynamic research p 447 A90-28273
- Aerodynamic, thermal and mechanical problems in the aerospace field p 382 A90-29921

- Numerical modeling of separated turbulent flows
p 470 A90-32673
- Calculation of flow on a flat plate at angle of attack by numerical solution of Navier-Stokes equations
p 537 A90-33424
- Direct numerical simulations of transition in a compressible wake
p 553 A90-35212
- Boundary element method for solving direct aerodynamic problem of aerofoil cascades on an arbitrary stream surface of revolution
p 554 A90-35830
- Computational methods in design aerodynamics
p 557 A90-36539
- Boundary conditions for Euler equations at internal block faces of multi-block domains using local grid refinement [AIAA PAPER 90-1590]
p 607 A90-38725
- Three-dimensional flux-split Euler schemes involving unstructured dynamic meshes
p 569 A90-38777
- Annual General Meeting of the Canadian Aeronautics and Space Institute, 36th, Ottawa, Canada, May 15, 16, 1989, Proceedings
p 701 A90-42652
- AIAA Atmospheric Flight Mechanics Conference, Portland, OR, Aug. 20-22, 1990, Technical Papers
p 751 A90-45134
- AIAA Applied Aerodynamics Conference, 8th, Portland, OR, Aug. 20-22, 1990, Technical Papers, Parts 1 & 2
p 787 A90-45845
- CFD validation for aerodynamic flows - Challenge for the '90's
p 787 A90-45846
- Low Reynolds number aerodynamics; Proceedings of the Conference, University of Notre Dame, IN, June 5-7, 1989
p 799 A90-46358
- Wing theory --- Book
p 809 A90-47700
- National Conference on Aerodynamics, 5th, Poona, India, May 24, 25, 1990, Proceedings
p 809 A90-48076
- Airbus technologies - An evolutionary process
p 902 A90-52699
- The application of TSIM software to act design and analysis on flexible aircraft
p 60 N90-10086
- The spinning of aircraft: A discussion of spin prediction techniques including a chronological bibliography [ARL-AERO-R-177]
p 36 N90-10888
- Analytical study of mistuning/friction/aerodynamics interaction in a bladed disk assembly
p 55 N90-10893
- Computer simulation of aircraft aerodynamics [NASA-TM-102221]
p 88 N90-11699
- Effect of control surface mass unbalance on the stability of a closed-loop active control system [NASA-TP-2952]
p 134 N90-12042
- Development of a VSAERO (Vortex Separation Aerodynamics) model of the F/A-18
p 95 N90-12566
- Chordwise loading and camber for two-dimensional thin sections
p 95 N90-12568
- Block-structured solution of three-dimensional transonic flows using parallel processing [AD-A212851]
p 170 N90-13330
- Hypersonic aerodynamics
p 171 N90-13335
- A technique for the prediction of aerodynamics and aeroelasticity of rotor blades
p 184 N90-13377
- Multigrid and defect correction for the steady Navier-Stokes equations: Applications to aerodynamics [ETN-90-96011]
p 212 N90-13727
- An alternative derivation for an integral equation for linearized subsonic flow over a wing [AD-A214140]
p 236 N90-15079
- Aerodynamic and heat transfer measurements on blading for a high rim-speed transonic turbine [RAE-TM-P-1151]
p 256 N90-15920
- Aerodynamic and structural design challenges of a reusable single stage to orbit air-breathing launch vehicle
p 354 N90-16814
- A wind tunnel study of a sting-mounted circulation control wing [AD-A216248]
p 319 N90-17577
- Experimental investigation to suppress flow-induced pressure oscillations in open cavities [AD-A216285]
p 320 N90-17578
- Stability characteristics of a combat aircraft with control surface failure [AD-A216196]
p 350 N90-17646
- Nonlinear mechanics of unstable plasmas as related to high altitude aerodynamics [AD-A215126]
p 464 N90-19852
- Unsteady free-wake viscous aerodynamic analysis of helicopter rotors
p 478 N90-20048
- Aerodynamic analysis of a US Navy and Marine Corps unmanned air vehicle [AD-A218282]
p 498 N90-20077
- ETO (Earth-To-Orbit): A trajectory program for aerospace vehicles
p 528 N90-20103
- [AD-A218157]
p 540 N90-20325
- Analysis of small-scale rotor hover performance data [NASA-TM-102271]
p 482 N90-20977
- Progress in inverse design and optimization in aerodynamics
p 571 N90-21735
- Prediction of forces and moments for flight vehicle control effectors. Part 2: An analysis of delta wing aerodynamic control effectiveness in ground effect [NASA-CR-186572]
p 572 N90-21736
- Modeling of vortex-induced oscillations based on indicial response approach [NASA-CR-186560]
p 573 N90-22532
- Water-tunnel study results of a TF/A-18 and F/A-18 canopy flow visualization [NASA-TM-101705]
p 631 N90-23349
- A study of supermaneuver aerodynamics [AD-A218378]
p 637 N90-24260
- Aerodynamic development perspective for traffic aeroplanes [DGLR-89-141]
p 702 N90-25073
- Convex models of malfunction diagnosis in high performance aircraft [AD-A218514]
p 719 N90-25940
- An unsteady lifting surface method for single rotation propellers [NASA-CR-4302]
p 719 N90-25943
- Identification of aerodynamic models for maneuvering aircraft [NASA-CR-186630]
p 845 N90-26829
- Special essays for the 40th anniversary of the revolution: The chief designer discusses the F-8 2 and future fighter planes [AD-A221587]
p 816 N90-27653
- Advanced recovery systems wind tunnel test report [NASA-CR-177563]
p 817 N90-27657
- Aerodynamics of a linear oscillating cascade [NASA-TM-103250]
p 910 N90-28495
- Hypersonic Arbitrary-Body Aerodynamics (HABA) for conceptual design [DE90-014750]
p 910 N90-28496
- Aerodynamics of bodies in shear flow
p 910 N90-28496
- Aerodynamic and propulsive control development of the STOL and maneuver technology demonstrator
p 920 N90-28514
- Aerodynamic control design: Experience and results at Aermacchi
p 935 N90-28518
- Control of vortex aerodynamics at high angles of attack
p 921 N90-28523
- Study of the ground effects in the CEAT aerohydrodynamic tunnel: Using the results
p 922 N90-28530
- Numeric fluid mechanics
p 960 N90-29161
- Investigation of ATP blades, part 2: Validation of two-dimensional viscous flow simulation codes around thin airfoils [NAL-TR-1046]
p 912 N90-29326
- Some topics in computational transonic aerodynamics: Revision [NAL-TR-1018T]
p 912 N90-29332
- The DELTA MONSTER: An RPV designed to investigate the aerodynamics of a delta wing platform [NASA-CR-186226]
p 924 N90-29381
- ### AEROELASTICITY
- Wind tunnel tests of models of helicopter rotors
p 29 A90-10230
- Experimental investigation on the interference effect of FL-23 wind tunnel wall on transonic flutter
p 57 A90-10347
- Whirl-flutter investigation on an advanced turboprop configuration
p 40 A90-11008
- Unsteady aerodynamics and aeroelasticity of turbomachines and propellers; Proceedings of the Fourth International Symposium, Aachen, Federal Republic of Germany, Sept. 6-10, 1987
p 5 A90-11776
- Experimental investigation of the time-dependent flow in a vibrating annular cascade operating in the transonic flow regime
p 7 A90-11787
- Flutter of turbine blades
p 41 A90-11794
- Systematic study of flutter characteristics of two-dimensional cascades in incompressible flow
p 41 A90-11796
- Aircraft compressor flutter analysis
p 41 A90-11797
- The flutter characteristic analysis and optimization design of mistuning blade
p 42 A90-11799
- The acoustic phenomena of the stalling flutter
p 78 A90-11801
- Identification of a coupled body/coning/inflow model of Puma vertical response in the hover
p 56 A90-12765
- Flight simulation model validation procedure, a systematic approach
p 30 A90-12770
- Mach number effects on transonic aeroelastic forces and flutter characteristics
p 17 A90-13024
- Structural optimization of lifting surfaces with divergence and control reversal constraints
p 127 A90-13770
- The warping restraint effect in the critical and subcritical static aeroelastic behavior of swept forward composite wing structures [SAE PAPER 891056]
p 129 A90-14358
- Aeroelastic characteristics of wings in subsonic flow
p 102 A90-14615
- Shaft flexibility effects on aeroelastic stability of a rotating bladed disk
p 132 A90-16371
- Flutter analysis of composite panels using high-precision finite elements
p 207 A90-16725
- A synthetic research for aircraft active flutter suppression
p 195 A90-16827
- Aeroelastic detuning for stability enhancement of unstalled supersonic flutter
p 189 A90-17462
- Time-domain aeroservoelastic modeling using weighted unsteady aerodynamic forces
p 195 A90-17698
- Direct search method to aeroelastic tailoring of a composite wing under multiple constraints
p 208 A90-17865
- Response and hub loads sensitivity analysis of a helicopter rotor
p 181 A90-18145
- The static aeroelastic behavior of sweptforward composite wing structures taking into account their warping restraint effect
p 210 A90-18407
- Aeroelastic tailoring applied to composite wing
p 211 A90-18580
- Unsteady pressure and structural response measurements on an elastic supercritical wing
p 159 A90-19392
- Unsteady incompressible aerodynamics and forced response of detuned blade rows
p 191 A90-19805
- [AIAA PAPER 90-0340]
p 166 A90-19845
- Static aeroelastic analysis of fighter aircraft using a three-dimensional Navier-Stokes algorithm [AIAA PAPER 90-0435]
p 244 A90-20583
- A new type of non-rigid airship system [AIAA PAPER 89-3175]
p 225 A90-21593
- A parametric study of the flutter stability of two-dimensional turbine and compressor cascades in incompressible flow
p 226 A90-22153
- Application of an efficient hybrid scheme for aeroelastic analysis of advanced propellers [AIAA PAPER 90-0028]
p 343 A90-23896
- Blade mistuning coupled with shaft flexibility effects in rotor aeroelasticity [ASME PAPER 89-GT-330]
p 345 A90-24147
- Aeroelastic deformation of a crescent-shaped rigid support in the diffuser chamber of a wind tunnel
p 364 A90-24112
- A method for determining aileron efficiency and critical reversal and divergence rates at transonic velocities
p 345 A90-24147
- Tail rotor dynamics during the translational turn maneuver of a helicopter
p 334 A90-24148
- Calculation of the vibrations of aircraft with elastic suspended loads
p 345 A90-24171
- Aeroelastic tailoring of a wing with composite skin
p 366 A90-25108
- Unsteady aerodynamic and aeroelastic calculations for wings using Euler equations
p 302 A90-25288
- Helicopter rotor dynamics and aeroelasticity - Some key ideas and insights
p 335 A90-25425
- An in-flight interaction of the X-29A canard and flight control system [AIAA PAPER 90-1240]
p 348 A90-26820
- Stochastic flutter of a panel subjected to random in-plane forces. I - Two mode interaction
p 444 A90-27992
- Design, evaluation and proof-of-concept flights of a main rotor interblade viscoelastic damping system
p 406 A90-28152
- Helicopter ground/air resonance including rotor shaft flexibility and control coupling
p 406 A90-28153
- Examination of dynamic characteristics of UH-60A and EH-60A airframe structures
p 406 A90-28154
- A review of the V-22 dynamics validation program
p 406 A90-28155
- Higher harmonic and trim control of the X-wing circulation control wind tunnel model rotor
p 435 A90-28156
- Application of higher harmonic control (HHC) to rotors operating at high speed and maneuvering flight
p 429 A90-28157
- Rotor loads validation utilizing a coupled aeroelastic analysis with refined aerodynamic modeling
p 408 A90-28226
- The effect of an unsteady three-dimensional wake on elastic blade-flapping eigenvalues in hover
p 385 A90-28228
- Periodic response of thin-walled composite blades
p 408 A90-28229
- Relative aeromechanical stability characteristics for hingeless and bearingless rotors
p 409 A90-28230
- Tiltrotor aeroservoelastic design methodology at BHTI
p 410 A90-28244

Aeroelastic optimization of a helicopter rotor using an efficient sensitivity analysis
 [AIAA PAPER 90-0951] p 410 A90-29237

An application of structural optimization in wind tunnel model design
 [AIAA PAPER 90-0956] p 438 A90-29241

Applications of XTRAN3S and CAP-TSD to fighter aircraft
 [AIAA PAPER 90-1035] p 389 A90-29360

Unsteady flow computation of oscillating flexible wings
 [AIAA PAPER 90-0937] p 389 A90-29363

Navier-Stokes computations on swept-tapered wings, including flexibility
 [AIAA PAPER 90-1152] p 389 A90-29364

Time domain simulations of a flexible wing in subsonic, compressible flow
 [AIAA PAPER 90-1153] p 390 A90-29365

Reduced size first-order subsonic and supersonic aeroelastic modeling
 [AIAA PAPER 90-1154] p 390 A90-29366

A reduced cost rational-function approximation for unsteady aerodynamics
 [AIAA PAPER 90-1155] p 390 A90-29367

Fast calculation of root loci for aeroelastic systems and of response in time domain
 [AIAA PAPER 90-1156] p 390 A90-29368

Experimental transonic flutter characteristics of supersonic cruise configurations
 [AIAA PAPER 90-0979] p 390 A90-29369

Influence of joint fixity on the aeroelastic characteristics of a joined wing structure
 [AIAA PAPER 90-0980] p 390 A90-29370

Effects of spoiler surfaces on the aeroelastic behavior of a low-aspect-ratio rectangular wing
 [AIAA PAPER 90-0981] p 391 A90-29371

Nonlinear stall flutter and divergence analysis of cantilevered graphite/epoxy wings
 [AIAA PAPER 90-0983] p 450 A90-29373

Time domain flutter analysis of cascades using a full-potential solver
 [AIAA PAPER 90-0984] p 391 A90-29374

Nonlinear aeroelasticity
 [AIAA PAPER 90-1031] p 391 A90-29375

Aeroelastic analysis of wings using the Euler equations with a deforming mesh
 [AIAA PAPER 90-1032] p 391 A90-29376

Using transonic small disturbance theory for predicting the aeroelastic stability of a flexible wind-tunnel model
 [AIAA PAPER 90-1033] p 391 A90-29377

Chaotic response of aerosurfaces with structural nonlinearities (Status report)
 [AIAA PAPER 90-1034] p 392 A90-29378

Flutter analysis of composite panels in supersonic flow
 [AIAA PAPER 90-1180] p 450 A90-29379

Concurrent processing adaptation of aeroelastic analysis of propfans
 [AIAA PAPER 90-1036] p 450 A90-29380

Aeroservoelasticity
 [AIAA PAPER 90-1073] p 411 A90-29381

Simulation of static and dynamic aeroelastic behavior of a flexible wing with multiple control surfaces
 [AIAA PAPER 90-1075] p 392 A90-29383

Piezoelectric actuators for helicopter rotor control
 [AIAA PAPER 90-1076] p 411 A90-29384

ADAM 2.0 - An ASE analysis code for aircraft with digital flight control systems
 [AIAA PAPER 90-1077] p 431 A90-29385

Static aeroelastic behavior of an adaptive laminated piezoelectric composite wing
 [AIAA PAPER 90-1078] p 412 A90-29386

Rotary-wing aeroelasticity with application to VTOL vehicles
 [AIAA PAPER 90-1115] p 392 A90-29387

Hingeless rotor dynamics in coordinated turns
 [AIAA PAPER 90-1117] p 412 A90-29389

Aeroelastic analysis of helicopter rotor blades with advanced tip shapes
 [AIAA PAPER 90-1118] p 392 A90-29390

Rotor/airframe aeroelastic analyses using the transfer matrix approach
 [AIAA PAPER 90-1119] p 392 A90-29391

Three dimensional full potential method for the aeroelastic modeling of propfans
 [AIAA PAPER 90-1120] p 393 A90-29392

Aeroelastic problems in turbomachines
 [AIAA PAPER 90-1157] p 393 A90-29393

Dynamic analysis of rotor blades with rotor retention design variations
 [AIAA PAPER 90-1159] p 412 A90-29394

Aeroelastic tailoring analysis for preliminary design of advanced turbo propellers with composite blades
 p 412 A90-29395

Multi-output implementation of a modified sparse time domain technique for rotor stability testing
 [AIAA PAPER 90-0946] p 412 A90-29405

Experimental aeroelasticity - History, status and future in brief
 [AIAA PAPER 90-0978] p 382 A90-29598

Practical problems - Airplanes --- unsteady interactional aerodynamics, flutter characteristics, and active flight control
 p 394 A90-29885

Unsteady aerodynamics for turbomachinery aeroelastic applications
 p 394 A90-29888

Sensitivity derivatives of flutter characteristics and stability margins for aeroservoelastic design
 p 433 A90-31287

Numerical model of unsteady subsonic aeroelastic behavior
 p 535 A90-32471

Structural optimization with aeroelastic constraints of rotor blades with straight and swept tips
 p 535 A90-32475

Entry of a flexible airfoil into a vertical gust
 p 470 A90-32552

Aeroservoelastic tailoring for lateral control enhancement
 p 516 A90-33060

European Forum on Aeroelasticity and Structural Dynamics, Aachen, Federal Republic of Germany, Apr. 17-19, 1989, Proceedings
 [DGLR BERICHT 89-01] p 468 A90-33351

Review of active structural control systems and flight test techniques for dynamic stability investigations
 p 516 A90-33352

Unsteady aerodynamics methods for transonic aeroelastic analysis
 p 471 A90-33353

Application of the CAP-TSD unsteady transonic small disturbance program to wing flutter --- Computational Aeroelasticity Program
 p 491 A90-33354

A strong viscous-inviscid interaction method for computing unsteady transonic airloads for use in aerelastics
 p 471 A90-33355

Calculations of unsteady aerodynamics over oscillating wings
 p 472 A90-33362

On the prediction of the aeroelastic behaviour of lifting systems due to flow separation
 p 491 A90-33369

Ground vibration testing of aeroelanes with a sequence of single-point excitations - Simple and effective
 p 522 A90-33371

Whole helicopter aeroelasticity - Experience with a new approach
 p 492 A90-33380

Aeroelastic analysis using finite element models
 p 492 A90-33388

Aeroelastic tailoring validation by windtunnel model testing
 p 492 A90-33389

Aeroelastic analysis for a composite T-tailplane of a turboprop commuter aircraft
 p 492 A90-33390

Structural optimization in view of aeroelastic constraints
 p 536 A90-33391

Recent activities within the aeroservoelasticity branch at the NASA Langley Research Center
 p 492 A90-33400

Practical techniques of modelling aeroelastic systems for active control applications
 p 545 A90-33402

Flutter suppression control law synthesis for the active flexible wing model
 p 517 A90-33403

An analytical sensitivity method for use in integrated aeroservoelastic aircraft design
 p 517 A90-33405

Implementation of comprehensive actuation system models in aeroservoelastic analysis
 p 517 A90-33406

A review of aeroelasticity research at the flight dynamics laboratory
 p 493 A90-33409

Further studies of harmonic gradient method for supersonic aeroelastic applications
 p 473 A90-33410

Reduced-order aeroelastic models via dynamic residualization
 p 493 A90-33412

Fast calculation of root loci of aeroelastic systems and of gust response in time domain
 p 517 A90-33413

On dynamic stability boundaries for binary systems
 p 538 A90-33698

Analysis of perturbed longitudinal dynamics of an aircraft taking into consideration the stationary aeroelastic effects and the atmospheric perturbances
 p 520 A90-34822

A modern course in aeroelasticity (2nd revised and enlarged edition) --- Book
 p 497 A90-34968

Aeroelastic instabilities in aircraft engines - Application to a SNECMA fan stage
 p 584 A90-35174

Euler flutter analysis of airfoils using unstructured dynamic meshes
 p 602 A90-35760

Reduced-order aeroelastic models via dynamic residualization
 p 579 A90-35762

Exact solutions to the oscillations of composite aircraft wings with warping constraint and elastic coupling
 p 603 A90-36271

Stability sensitivity analysis of a helicopter rotor
 p 580 A90-36273

A numerical method in aeroelasticity for wings with separation at large angle of attack
 p 557 A90-37209

Aeroelastic tailoring of composite wing structures
 p 580 A90-37217

Non-conservative stability of a cracked thick rotating blade
 p 606 A90-38544

Aeroelastic analysis of a low aspect ratio wing
 p 619 A90-38915

Discrete Fourier transform with high resolution for low frequencies applied to the modal analysis of aircraft vibration
 p 679 A90-38975

The mechanisms and benefits of aeroelastic tailoring
 p 641 A90-39286

Analysis of aeroelastic divergence for the slender flight vehicles
 p 680 A90-39298

Parameter identification of aeroelastic modes of rotary wings from transient time histories
 p 642 A90-40166

Static aeroelastic tailoring for oblique wing lateral trim
 p 667 A90-40689

Supersonic flutter of shear deformable laminated composite flat panels
 p 683 A90-41104

Linearized unsteady aerodynamics for turbomachinery aeroelastic applications
 [AIAA PAPER 90-2355] p 626 A90-42137

Unsteady deformations of elastic rotor blades
 p 687 A90-42341

An experimental and analytical investigation of the buffet excitation parameter
 p 645 A90-42417

Aeroelastic response characteristics of a rotor executing arbitrary harmonic blade pitch variations
 p 646 A90-42464

Aeroelastic effects on stability and control of hingeless rotor helicopters
 p 647 A90-42473

Annual General Meeting of the Canadian Aeronautics and Space Institute, 36th, Ottawa, Canada, May 15, 16, 1989, Proceedings
 p 701 A90-42652

Shaft flexibility effects on the forced response of a bladed-disk assembly
 p 744 A90-43218

Parametric aeroelastic stability analysis of a generic X-wing aircraft
 p 731 A90-44737

A nonlinear transient formulation of UHB aeroelastic response and stability. I - Theoretical formulation
 [SAE PAPER 892322] p 715 A90-45481

Large-order modal analysis techniques in the Aeroelastic Design Optimization Program (ADOP)
 [SAE PAPER 892323] p 772 A90-45482

Active flow control on low Reynolds number airfoils
 [AIAA PAPER 90-3039] p 792 A90-45878

Application of a streamwise upwind algorithm for unsteady transonic computations over oscillating wings
 [AIAA PAPER 90-3103] p 796 A90-45915

Transient aeroelastic computations using multiple moving frames of reference
 [AIAA PAPER 90-3053] p 798 A90-45932

Multicriteria optimal layouts of aircraft and spacecraft structures
 p 889 A90-46046

Sensitivity analysis in the design of composite structures
 p 880 A90-46478

Analytical studies of the transonic flutter of aircraft
 p 860 A90-46577

Numerical analysis of natural vibrations of an aeroplane with symmetrically variable geometry wing
 p 860 A90-46715

Analysis of self-excited vibrations of stiffened covering panels of an aeroplane wing
 p 860 A90-46716

BHTI's technical assessment of advanced rotor and control concepts
 p 861 A90-46949

Evolution and test history of the V-22 0.2-scale aeroelastic model
 p 831 A90-46954

Theoretical and experimental investigation of the aeroelastic stability of an advanced bearingless rotor in hover and forward flight
 p 831 A90-46958

Development of the Second Generation Comprehensive Helicopter Analysis System (2GCHAS)
 p 889 A90-46963

A study of fundamental issues in higher harmonic control using aeroelastic simulation
 p 861 A90-46966

V-22 MSC/NASTRAN airframe vibration analysis and correlation
 p 832 A90-46969

An examination of helicopter rotor load calculations
 p 833 A90-46972

STOL Maneuver Technology Demonstrator aeroservoelasticity
 [AIAA PAPER 90-3336] p 863 A90-47596

Active control of aerothermoelastic effects for a conceptual hypersonic aircraft
 [AIAA PAPER 90-3337] p 863 A90-47597

Multivariable flight control synthesis and literal robustness analysis for an aeroelastic vehicle
 [AIAA PAPER 90-3446] p 890 A90-47699

Development and testing of methodology for evaluating the performance of multi-input/multi-output digital control systems
 [AIAA PAPER 90-3501] p 867 A90-47747

Longitudinal stability analysis for deformable aircraft
 p 867 A90-48514

Unsteady aerodynamics and aeroelasticity of turbomachines and propellers; Proceedings of the Fifth International Symposium, Beijing, People's Republic of China, Sept. 18-21, 1989
 p 853 A90-49451

A new method for high speed propeller flutter prediction
 p 854 A90-49454

- Aeroelastic vibrations of turbomachine blades and propellers p 854 A90-49482
- Static aeroelastic analysis for generic configuration aircraft [NASA-TM-89423] p 52 N90-10042
- Large-scale Advanced Prop-fan (LAP) technology assessment report [NASA-CR-182142] p 53 N90-10046
- The application of TSIM software to act design and analysis on flexible aircraft p 60 N90-10086
- Modifying high-order aeroelastic math model of a jet transport using maximum likelihood estimation p 61 N90-10106
- Control law synthesis and optimization software for large order aeroservoelastic systems p 61 N90-10111
- Flexible aircraft dynamic modeling for dynamic analysis and control synthesis p 61 N90-10112
- The active flexible wing aeroservoelastic wind-tunnel test program p 33 N90-10119
- Numerical simulation of unsteady rotational flow over propan configurations [NASA-CR-186037] p 90 N90-12500
- Application of an efficient hybrid scheme for aeroelastic analysis of advanced propellers [NASA-TM-102428] p 172 N90-13355
- A technique for the prediction of aerodynamics and aeroelasticity of rotor blades p 184 N90-13377
- Aeroelastic control of composite lifting surfaces: Integrated aeroelastic control optimization p 198 N90-13396
- Dynamic testing techniques and applications for an aeroelastic rotor test facility p 201 N90-13406
- Concurrent processing adaptation of aeroplastic analysis of propan [NASA-TM-102455] p 215 N90-14656
- Nonlinear phenomena in computational transonic aeroelasticity p 235 N90-15070
- Current status of the application of conventional aluminium-lithium alloys and the potential for future developments p 268 N90-15203
- Solution of potential flow past an elastic body using the boundary element technique [AD-A213843] p 275 N90-15390
- An iterative solution to aeroelastic effects in potential flow [AD-A216291] p 320 N90-17580
- A fractional calculus model of aeroelasticity [AD-A216244] p 377 N90-18212
- Aeroservoelasticity [NASA-TM-102620] p 416 N90-19227
- An experimental study of the aeroelastic behaviour of two parallel interfering circular cylinders p 455 N90-19609
- Using transonic small disturbance theory for predicting the aeroelastic stability of a flexible wind-tunnel model [NASA-TM-102617] p 478 N90-20047
- Aeroelastic characteristics of aircraft with circulation control wings p 497 N90-20070
- Static aeroelastic analysis of a three-dimensional generic wing [NASA-TM-102231] p 509 N90-20087
- Performance data from a wind-tunnel test of two main-rotor blade designs for a utility-class helicopter [NASA-TM-4183] p 499 N90-20974
- Experimental aeroelasticity history, status and future in brief [NASA-TM-102651] p 527 N90-21047
- Airloads, wakes, and aeroelasticity [NASA-CR-177551] p 572 N90-21738
- Identification of XV-15 aeroelastic modes using frequency-domain methods [NASA-TM-101021] p 582 N90-21756
- Aeroelastic simulation of higher harmonic control p 592 N90-21768
- Application of a dynamic stall model to rotor trim and aeroelastic response p 583 N90-22556
- Flutter investigations on a Transavia PL12/T-400 aircraft [AD-A219108] p 593 N90-22570
- STARS: An integrated general-purpose finite element structural, aeroelastic, and aeroservoelastic analysis computer program [NASA-TM-101709] p 689 N90-23768
- Calculation of the aeroelastic blade stabilization with linearized process [MITT-87-01] p 666 N90-24272
- Integral-equation methods in steady and unsteady subsonic, transonic and supersonic aerodynamics for interdisciplinary design [NASA-TM-102677] p 716 N90-25110
- Modeling flexible aircraft for flight control design [AD-A219123] p 757 N90-25140
- Structural dynamics branch research and accomplishments [NASA-TM-102488] p 778 N90-26373
- Adaptation for unsteady flow p 871 N90-26845
- Development and testing of methodology for evaluating the performance of multi-input/multi-output digital control systems [NASA-TM-102704] p 846 N90-27699
- Effects of spoiler surfaces on the aeroelastic behavior of a low-aspect-ratio rectangular wing [NASA-TM-102622] p 846 N90-27700
- Active control of aerothermoelastic effects for a conceptual hypersonic aircraft [NASA-TM-102713] p 869 N90-27725
- Multi-disciplinary optimization of aeroservoelastic systems [NASA-CR-185931] p 925 N90-29385
- A digital controller for active aeroelastic controls [NAL-TR-1014] p 936 N90-29402
- AEROLOGY**
- Meeting Review: Workshop on Airborne Instrumentation [PB89-174775] p 39 N90-10032
- AEROMANEUVERING**
- Application of a general-purpose mechanical systems analysis code to rotorcraft dynamics problems p 831 A90-46955
- AERONAUTICAL ENGINEERING**
- The birth of the airplane: The first designs and constructions --- Russian book p 79 A90-12478
- Aerospace coordinate systems and transformations --- Book p 282 A90-23372
- Eshbach's handbook of engineering fundamentals /4th edition/ p 448 A90-28825
- Aeronautical facility requirements into the 2,000's [AIAA PAPER 90-1375] p 594 A90-37926
- A review of Australian and New Zealand investigations on aeronautical fatigue during the period April 1987 to March 1989 [AD-A210373] p 32 N90-10026
- California air transportation study: A transportation system for the California Corridor of the year 2010 [NASA-CR-186219] p 176 N90-14212
- Profiles-aeronautical/astronautical engineering: Human resources and funding [PB90-103888] p 369 N90-16969
- Combustion in the gas turbine. Part 1: Combustor types and design [CIT/SME/VKI/RS/1] p 748 N90-25986
- Calculation of the combustion distribution in a liquid-fuel ramjet p 858 N90-27931
- AERONAUTICS**
- Ground aviation equipment: Handbook --- in Russian p 593 A90-36153
- The 21st century in space; Proceedings of the Thirty-fifth Annual AAS Conference, Saint Louis, MO, Oct. 24-26, 1988 p 762 A90-43460
- AEROSOLS**
- Aerosol effects on jet-engine IR radiation p 40 A90-10152
- Airborne aerosol inlet passing efficiency measurement p 927 A90-52077
- Aerosol separator for use in aircraft [PB90-142217] p 611 N90-22155
- AEROSPACE ENGINEERING**
- Interactive Videodisc training in aerospace applications [AIAA PAPER 89-3029] p 73 A90-10529
- A methodology for modeling, control design and simulation of aerospace mechanical systems [AIAA PAPER 89-3049] p 73 A90-10543
- Fiber optic smart structures and skins; Proceedings of the Meeting, Boston, MA, Sept. 8, 9, 1988 [SPIE-986] p 37 A90-11201
- Materials pace aerospace technology p 203 A90-17298
- Hypersonic airbreathing vehicle design - Focus on aero-space plane p 245 A90-21156
- Effects of thermochemistry, nonequilibrium, and surface catalysis on the design of hypersonic vehicles p 224 A90-21159
- Hypersonic flight testing p 245 A90-21171
- A methodology proposal to design and analyse counterrotating high speed propellers [ASME PAPER 89-GT-38] p 340 A90-23767
- Computers and the aerospace engineer p 375 A90-25719
- The design of supersonic aircraft and space vehicles by using global optimization techniques p 353 A90-25781
- Analysis of three-dimensional aerospace configurations using the Euler and Navier-Stokes equations p 305 A90-25798
- Smart structures with nerves of glass p 444 A90-27951
- Methodology of variable amplitude fatigue tests p 451 A90-29866
- Fundamentals of the design and development of parts and mechanisms for flight vehicles --- Russian book p 414 A90-30275
- Fluorosilicone sealants for aircraft fuel containment p 529 A90-31618
- Silicone sealants and adhesives for aerospace/defense applications p 529 A90-31619
- Design of an aero-engine thrust reverser blocker door p 467 A90-31651
- Eurofar - Status of the European tilt-rotor project p 645 A90-42441
- Evolution of flight commands in Aerialia design [ETN-89-95211] p 120 N90-11759
- Choice and characterization of new materials for aerospace applications [ETN-89-95219] p 126 N90-11819
- The evolution of light alloys in the aerospace industry [ETN-89-95216] p 126 N90-11872
- On the occasion of the 100th birthday of Ernst Heinkel [MBB/LW/3015/S/PUB/321] p 141 N90-12494
- Project, implementation, and utilization of composite structures [ETN-89-95209] p 127 N90-12665
- The microstructure and properties of aluminum-lithium alloys p 267 N90-15187
- Current status of the application of conventional aluminium-lithium alloys and the potential for future developments p 268 N90-15203
- Impact of composites in the aerospace industry [ETN-90-96231] p 443 N90-18527
- Langley aerospace test highlights, 1989 [NASA-TM-102631] p 699 N90-24221
- Materials and structures for 2000 and beyond: An attempted forecast by the DLR Materials and Structures Department [ESA-TT-1154-REV] p 775 N90-26173
- Control and estimation for aerospace applications with system time delays p 918 N90-29367
- Proceedings of damping '89. Volume 1: Pages AAB-1 through DCD-11 [AD-A223431] p 960 N90-29664
- AEROSPACE ENVIRONMENTS**
- High Voltage Design Guide summary p 605 A90-38097
- Proceedings of the 13th International Congress on Instrumentation in Aerospace Simulation Facilities [EOARD-LR-89-069] p 527 N90-21046
- AEROSPACE INDUSTRY**
- Placards, warning labels and operation manuals - An aircraft manufacturer's duty to warn p 79 A90-11396
- The advantages of automation in aerospace production p 130 A90-15357
- Cooking an aeroplane p 209 A90-17918
- Metal matrix composites - Ready for take-off? p 356 A90-26865
- Industry turns to ceramic composites p 356 A90-27597
- Materials get smarter p 356 A90-27598
- Coating turbine engine components p 451 A90-29893
- Resources - Supply and availability --- of superalloys for United States aerospace industry p 531 A90-34152
- Development of monolithic and composite ceramics at Allied-Signal Aerospace Company p 599 A90-35950
- Euromart - The European aviation research and technology program p 617 A90-41112
- A high performance aerospace resin for Resin Transfer Molding p 945 A90-50163
- Composites for aerospace application from Kevlar aramid reinforced PEKK thermoplastic p 946 A90-50176
- Assuring the future of civil aircraft industry in Germany [DGLR PAPER 88-004] p 902 A90-50232
- On the occasion of the 100th birthday of Ernst Heinkel [MBB/LW/3015/S/PUB/321] p 141 N90-12494
- Design and demonstration of heat pipe cooling for NASP and evaluation of heating methods at high heating rates [DE89-016995] p 186 N90-14227
- Impact of composites in the aerospace industry [ETN-90-96231] p 443 N90-18527
- NASA airframe structural integrity program [NASA-TM-102637] p 543 N90-21422
- AEROSPACE MEDICINE**
- Toxicology in aviation p 722 A90-44662
- Human centrifuge controller [NAL-TM-SE-8901] p 527 N90-21043
- AEROSPACE PLANES**
- Rockwell's simulator emulates NASP flight characteristics p 60 A90-11650
- Preliminary analysis of methodology for assessment of propulsion system for aerospace plane [IAF PAPER 89-307] p 123 A90-13442
- Development study of air turbo-ramjet for future space plane [IAF PAPER 89-311] p 109 A90-13445

- Keepers of the flame --- scramjet development programs p 141 A90-16300
- Advanced materials to fly high in NASP p 203 A90-17297
- Transonic Navier-Stokes solutions about a complex high-speed accelerator configuration [AIAA PAPER 90-0430] p 166 A90-19844
- Hypersonic airbreathing vehicle design - Focus on aero-space plane p 245 A90-21156
- The National Aero-Space Plane, the guidance and control engineer's dream or nightmare? [AAS PAPER 89-040] p 264 A90-21546
- Navier-Stokes computations for the investigation of flowfields about a Space-Plane p 306 A90-25836
- Hypersonic (T-D) 'pinch' and aerospaceplane propulsion [AIAA PAPER 90-2474] p 675 A90-42189
- Forebody design for the aerospaceplane [AIAA PAPER 90-2472] p 762 A90-42810
- The ascending trajectories performance and control to minimize the heat load for the transatmospheric aero-space planes p 763 A90-45135
- Flying qualities problems of aerospace craft [AIAA PAPER 90-2804] p 752 A90-45139
- Thrust law effects on the longitudinal stability of hypersonic cruise [AIAA PAPER 90-2820] p 763 A90-45149
- Stability characteristics of a conical aerospace plane concept [SAE PAPER 892313] p 757 A90-45475
- Project Falke - Performance of free flight tests in the supersonic, transonic, and subsonic regimes from balloons [DGLR PAPER 88-018] p 903 A90-50235
- Low-speed, high-lift aerodynamic characteristics of slender, hypersonic accelerator-type configurations [NASA-TP-2945] p 20 N90-10830
- Trajectory optimization and guidance for an aerospace plane [NASA-CR-185884] p 183 N90-13369
- Slush Hydrogen (SLH2) technology development for application to the National Aerospace Plane (NASP) [NASA-TM-102315] p 203 N90-14268
- HOTOL: A future launcher for Europe p 353 N90-16800
- National aero-spaceplane status and plans p 337 N90-16801
- A computational model for thickening boundary layers with mass addition for hypersonic engine inlet testing [AD-A216246] p 319 N90-17576
- HOTOL structures and materials at British Aerospace, Warton, UK [EOARD-LR-90-001] p 503 N90-21001
- Performance of an aero-space plane propulsion nozzle p 515 N90-21034
- Numerical simulation of hypersonic flow around a space plane. Part 2: Application to high angles of attack flow [NAL-TR-1011T] p 570 N90-21726
- Space plane model for visual measurement of aerodynamic heating [DE90-505514] p 720 N90-25949
- Background, current status, and prognosis of the ongoing slush hydrogen technology development program for the NASP [NASA-TM-103220] p 763 N90-26055
- Optimal trajectories for hypervelocity flight p 918 N90-29378
- AEROSPACE SYSTEMS**
- Development of finite element methods for compressible Navier-Stokes flow simulations in aerospace design [AIAA PAPER 90-0403] p 166 A90-19833
- Beyond the limits - Flight enters the computer age --- Book p 282 A90-20380
- Identification and diagnostics in the data processing and control systems of aerospace powerplants --- Russian book p 611 A90-36151
- Ground aviation equipment: Handbook --- in Russian p 593 A90-36153
- Supersonic flow computations over aerospace configurations using an Euler marching solver [NASA-CR-4085] p 19 N90-10012
- Advances in optimal active control techniques for aerospace systems; application to aircraft active landing gear p 592 N90-21769
- AEROSPACE TECHNOLOGY TRANSFER**
- Application of HOST technology to the SSME HPFTP blade [ASME PAPER 89-GT-130] p 360 A90-23828
- Technological preparations of civil aircraft programs p 617 A90-41110
- AEROSPACE VEHICLES**
- Overview of fiber optic smart structures for aerospace applications p 37 A90-11202
- Fiber optic sensor systems for smart aerospace structures p 38 A90-11208

- Optical fiber sensing considerations for a smart aerospace structure p 38 A90-11210
- On the use of external burning to reduce aerospace vehicle transonic drag [AIAA PAPER 90-1935] p 656 A90-40562
- Forebody design for the aerospaceplane [AIAA PAPER 90-2472] p 762 A90-42810
- Rapid prediction of slender-wing aircraft dynamics [AIAA PAPER 90-3037] p 791 A90-45876
- Hierarchical damage tolerant controllers for smart structures [AD-A209422] p 31 N90-10022
- Guidance and Control strategies for aerospace vehicles [NASA-CR-186195] p 199 N90-14243
- Effects of lightning on operations of aerospace vehicles p 239 N90-15065
- On the use of external burning to reduce aerospace vehicle transonic drag [NASA-TM-103107] p 588 N90-21762
- Conceptual design for aerospace vehicles p 651 N90-25043
- Model designation of military aerospace vehicles [PB90-206301] p 787 N90-27646
- Thermal structures: Four decades of progress [NASA-CR-186898] p 887 N90-28105
- AEROSTATICS**
- AIAA Lighter-Than-Air Systems Technology Conference, 8th, Jacksonville, FL, Oct. 5-7, 1989, Technical Papers p 221 A90-20576
- AEROTHERMOCHEMISTRY**
- Nonequilibrium recombination-dissociation boundary layer flows along arbitrarily-catalytic hypersonic vehicles [AIAA PAPER 90-0055] p 161 A90-19652
- Chemical and vibrational non-equilibrium nozzle flow calculation by an implicit upwind method [ONERA, TP NO. 1989-175] p 223 A90-21037
- Effects of thermochemistry, nonequilibrium, and surface catalysis on the design of hypersonic vehicles p 224 A90-21159
- Calculated chemical and vibrational nonequilibrium effects in hypersonic nozzles p 253 A90-21224
- New high-speed air transport system and stratospheric pollution [ONERA, TP NO. 1989-202] p 279 A90-22445
- The role of hydrogen/air chemistry in nozzle performance for a hypersonic propulsion system [AIAA PAPER 90-2492] p 658 A90-40637
- AEROTHERMODYNAMICS**
- Several problems posed by aerothermal calculations in machines [ONERA, TP NO. 1989-102] p 67 A90-11136
- Jet engine fault detection with differential gas path analysis at discrete operating points p 50 A90-12533
- Effect of the inertial nature of injection and temperature on the damping of body vibrations p 150 A90-17112
- Approximations for nonequilibrium hypervelocity aerodynamics p 154 A90-17990
- The critical role of aerodynamic heating effects in the design of hypersonic vehicles p 155 A90-18249
- Nonequilibrium recombination-dissociation boundary layer flows along arbitrarily-catalytic hypersonic vehicles [AIAA PAPER 90-0055] p 161 A90-19652
- A three-dimensional upwind parabolized Navier-Stokes code for chemically reacting flows [AIAA PAPER 90-0394] p 165 A90-19831
- Nonlinear stability of subsonic mixing layers with symmetric temperature variations p 223 A90-20501
- The application of infrared thermography to the measurement of heat fluxes in a wind tunnel [ONERA, TP NO. 1989-192] p 261 A90-21051
- Prediction of the aerodynamic environment and heat transfer for rotor-stator configurations [ASME PAPER 89-GT-89] p 359 A90-23807
- Experimental examination of the aerothermal performance of a gas turbine engine test facility [ASME PAPER 89-GT-94] p 341 A90-23810
- Many means to NASP p 285 A90-23917
- Design for hypersonic speed p 335 A90-26343
- Aerothermodynamics and transition in high-speed wind tunnels at NASA Langley p 386 A90-28555
- Thermal structures - Four decades of progress [AIAA PAPER 90-0971] p 411 A90-29305
- Finite element two-dimensional panel flutter at high supersonic speeds and elevated temperature [AIAA PAPER 90-0982] p 450 A90-29372
- Aerodynamic, thermal and mechanical problems in the aerospace field p 382 A90-29921
- Aerothermomechanical design of turbine-engine combustion chambers p 424 A90-29922
- Navier-Stokes analyses of the redistribution of inlet temperature distortions in a turbine p 471 A90-32959
- Computational aerothermodynamics p 476 A90-34380
- Pressure and heat-transfer investigation of a hypersonic configuration p 598 A90-35757

- The challenging process of validating CFD codes [AIAA PAPER 90-1402] p 558 A90-37943
- Langley hypersonic aerodynamic/aerothermodynamic testing capabilities - Present and future [AIAA PAPER 90-1376] p 596 A90-38483
- Enthalpy damping for high Mach number Euler solutions [AIAA PAPER 90-1585] p 566 A90-38720
- Experimental studies of combustor dilution zone aerodynamics. II - Jet development p 659 A90-40947
- The challenge of demonstrating the X-30 p 659 A90-41162
- CFD propels NASP propulsion progress p 683 A90-41163
- On and off-design performance prediction of single spool turbojets using gasdynamics [AIAA PAPER 90-2393] p 662 A90-42155
- Off-design performance of hypersonic waveriders p 763 A90-44735
- The effect of separation on turbulent boundary layer characteristics over a smooth surface at Mach 6.0 [AIAA PAPER 90-3028] p 790 A90-45870
- Wake interaction effects on the transition process on turbine blades [AD-A214492] p 343 N90-16759
- Verification of aerothermodynamic codes by means of a winged experimental re-entry vehicle p 354 N90-16842
- NASA aerodynamics program** p 373 N90-17235
- Shock-shock boundary layer interactions p 318 N90-17569
- Activities report in German aerospace [ISSN-0070-3966] p 465 N90-19189
- Heat transfer measurements from a NACA 0012 airfoil in flight and in the NASA Lewis icing research tunnel [NASA-CR-4278] p 399 N90-19203
- Probabilistic modeling for simulation of aerodynamic uncertainties in propulsion systems [NASA-TM-102472] p 515 N90-21036
- Navier-Stokes analysis of turbine blade heat transfer [NASA-TM-102496] p 542 N90-21300
- Infrared thermography at hypersonic channel H2K p 674 N90-24235
- Experimental aerothermodynamic research of hypersonic aircraft [NASA-CR-186903] p 721 N90-25954
- Computer modeling and data processing methods: An essential part of jet engine condition monitoring and fault diagnosis p 855 N90-27626
- Thermal structures: Four decades of progress [NASA-CR-186898] p 887 N90-28105
- AEROTHERMOELASTICITY**
- Computational prediction of stall flutter in cascaded airfoils [AIAA PAPER 90-1116] p 392 A90-29388
- The application of active controls technology to a generic hypersonic aircraft configuration [NASA-TM-101689] p 497 N90-20071
- Active control of aerothermoelastic effects for a conceptual hypersonic aircraft [NASA-TM-102713] p 869 N90-27725
- AFTERBODIES**
- Axisymmetric afterbody flow separation at transonic speeds in presence of jet exhaust p 13 A90-12576
- Underexpanded jet-freestream interactions on an axisymmetric afterbody configuration p 154 A90-18141
- Measurements, visualization and interpretation of 3-D flows - Application within base flows p 386 A90-28252
- Drag reduction by controlling flow separation using stepped afterbodies p 622 A90-40690
- Navier-Stokes simulation of transonic afterbody flows with jet exhaust [AIAA PAPER 90-3057] p 790 A90-45862
- Hypersonic nozzle/afterbody performance at low Mach numbers [AD-A216223] p 319 N90-17575
- Sting-support interference on afterbody drag at transonic speeds [NAL-TM-EA-8902] p 909 N90-28492
- AFTERBURNING**
- Combustion characteristics of a boron-fueled SFRJ with aft-burner p 62 A90-12514
- Simulation research on the afterburning dynamic characteristics of engine control system p 48 A90-12581
- Application of computational systems to aircraft engine components development p 188 A90-17448
- The establishment of mathematical model of engine control system and simulation research of afterburning dynamic characteristics p 190 A90-18613
- Simulation research on the afterburning dynamic characteristics of engine control system p 585 A90-35708

- Developmental tests on the M 88 engine are on track p 660 A90-41761
- Life estimation of a gas turbine afterburner spraybar p 739 A90-42662
- Spectral response of a UV flame sensor for a modern turbojet aircraft engine p 769 A90-43285
- Characteristics of combustion driven pressure oscillations in advanced turbo-fan engines with afterburner p 64 A90-10194
- Measurement effects on the calculation of in-flight thrust for an F404 turbofan engine [NASA-TM-4140] p 114 A90-11741
- Exhaust environment measurements of a turbofan engine equipped with an afterburner and 2D nozzle [NASA-CR-4289] p 588 A90-21760
- AGGREGATES**
- Development and testing of rapid repair methods for war damaged runways [AD-A223970] p 938 A90-28586
- AGING (MATERIALS)**
- The U.S. airline industry - Coping with an aging fleet p 221 A90-21702
- Aging and antioxidant surveillance studies on turbine fuel JP-5 and JP-10 p 442 A90-29492
- Douglas aging aircraft programs [SAE PAPER 892206] p 732 A90-45425
- Aging fleet Structures Working Group activities [AIAA PAPER 90-3219] p 786 A90-48840
- Aging jet transport structural evaluation programs p 901 A90-49889
- Nondestructive analysis of aileron fatigue and aging in a Mirage F1 [REPT-M6-594000] p 184 A90-13378
- Second Annual International Conference on Aging Aircraft [AD-A222715] p 724 A90-25961
- Applications of digital image processing in testing and evaluation of composite materials [AD-A222939] p 874 A90-26887
- AH-1G HELICOPTER**
- The Bell Helicopter AH-1 Cobra - Past, present, and future [AIAA PAPER 90-3271] p 836 A90-48862
- Investigation of difficult component effects on finite element model vibration prediction for the Bell AH-1G helicopter. Volume 1: Ground vibration test results [NASA-CR-181916-VOL-1] p 134 A90-12058
- Investigation of difficult component effects on finite element model vibration prediction for the Bell AG-1G helicopter. Volume 2: Correlation results [NASA-CR-181916-VOL-2] p 213 A90-13814
- Calculation of flight vibration levels of the AH-1G helicopter and correlation with existing flight vibration measurements [NASA-CR-181923] p 454 A90-18743
- Calculation of flight vibration levels of the AH-1G helicopter and correlation with existing flight vibration measurements [NASA-CR-182031] p 775 A90-25375
- AH-64 HELICOPTER**
- Flight simulation model validation procedure, a systematic approach p 30 A90-12770
- McDonnell Douglas Helicopter Company Apache telemetry antenna analysis p 403 A90-28839
- Aerodynamic performance of a 0.27-scale model of an AH-64 helicopter with baseline and alternate rotor blade sets [NASA-TM-4201] p 632 A90-24237
- Plan, execute, and discuss vibration measurements and correlations to evaluate a NASTRAN finite element model of the AH-64 helicopter airframe [NASA-CR-181973] p 960 A90-28866
- AILERONS**
- Analysis and design of sidestick controller systems for general aviation aircraft p 196 A90-19554
- A study of the stability of a wing aileron in supersonic flow p 222 A90-20442
- A method for determining aileron efficiency and critical reversal and divergence rates at transonic velocities p 345 A90-24147
- A method for calculating the stiffness characteristics of large-aspect-ratio wings with anisotropic panels in accordance with strength and aileron efficiency requirements p 334 A90-24161
- Flutter and aileron reversal safety factors p 345 A90-24164
- Some characteristics of changes in the nonstationary aerodynamic characteristics of a wing profile with an aileron in transonic flow p 387 A90-28989
- F/A-18 aileron smart servoactuator p 432 A90-30710
- Nondestructive analysis of aileron fatigue and aging in a Mirage F1 [REPT-M6-594000] p 184 A90-13378
- Prediction of forces and moments for flight vehicle control effectors. Part 1: Validation of methods for predicting hypersonic vehicle controls forces and moments [NASA-CR-186571] p 571 A90-21734
- AIR**
- WINCOF-I code for prediction of fan compressor unit with water ingestion [NASA-CR-185157] p 551 A90-21724
- AIR BREATHING ENGINES**
- International Symposium on Air Breathing Engines, 9th, Athens, Greece, Sept. 3-8, 1989, Proceedings. Volumes 1 & 2 p 43 A90-12501
- Swedish philosophy in aeroengine development p 44 A90-12504
- Application of three-dimensional methods for the calculation of gas dynamic and thermal processes at the design of gas turbines for air breathing engines p 46 A90-12552
- Advanced airbreathing powerplant for hypersonic vehicles p 49 A90-12607
- Inverse cycle engine for hypersonic air-breathing propulsion [ONERA, TP NO. 1989-121] p 50 A90-12611
- Hypersonic airbreathing vehicle design - Focus on aero-space plane p 245 A90-21156
- The next AIAA engine design competition - A commercial engine [AIAA PAPER 89-2258] p 550 A90-33675
- Large-scale structure in a supersonic slot-injected flowfield p 602 A90-36265
- Analysis of shock interactions and flow structure in high speed inlets [AIAA PAPER 90-2132] p 704 A90-42735
- Aircraft propulsion: Leading the way in aviation [LR-532] p 194 A90-13395
- A computational model for thickening boundary layers with mass addition for hypersonic engine inlet testing [AD-A216246] p 319 A90-17576
- AIR CARGO**
- The airship - An economical answer to air cargo [TABES PAPER 89-1203] p 238 A90-20390
- Fire hazards of aerosol cans in aircraft cargo compartments [DOT/FAA/CT-89/32] p 636 A90-23369
- AIR CONDITIONING**
- High-temperature bootstrap compared with F-15 growth air cycle air conditioning system [SAE PAPER 891436] p 336 A90-27407
- Starter systems and auxiliary power units p 660 A90-41760
- AIR CONDITIONING EQUIPMENT**
- Catalytic conversion of oil in bleed air - A maintenance tool [SAE PAPER 892214] p 732 A90-45431
- AIR COOLING**
- Advanced combustor liner cooling technology for gas turbines p 112 A90-16004
- A method for aerodynamic design calculation of axial gas turbine stages with cooling air mixing p 152 A90-17781
- An aerodynamic design and calculation method for gas turbine with cooling air mixing p 189 A90-17782
- Design and calculation of composite air-cooled blades in a highly-loaded transonic turbine p 189 A90-17790
- Calculation of coolant flow and heat transfer inside composite air-cooled turbine p 189 A90-17791
- Experimental investigation on composite air-cooled blades of highly-loaded transonic turbine p 189 A90-17793
- Design of an air-cooled metallic high-temperature radial turbine p 507 A90-32960
- Enhanced environmental control for the Harrier II Plus [SAE PAPER 901238] p 841 A90-49308
- Apparatus for cooling electronic components in aircraft [AD-D014207] p 183 A90-13373
- Transpiration cooling in hypersonic flight [NASA-CR-186435] p 478 A90-20052
- AIR CURRENTS**
- An electronic flight-recorder for a hang-glider p 39 A90-12234
- AIR DATA SYSTEMS**
- Preliminary results from a subsonic high-angle-of-attack flush airdata sensing (HI-FADS) system - Design, calibration, algorithm development, and flight test evaluation [AIAA PAPER 90-0232] p 187 A90-19746
- Preliminary results from a subsonic high angle-of-attack flush airdata sensing (HI-FADS) system: Design, calibration, and flight test evaluation [NASA-TM-101713] p 339 A90-16758
- Wind-tunnel investigation of a flush airdata system at Mach numbers from 0.7 to 1.4 [NASA-TM-101697] p 421 A90-18395
- Experimental characterization of the effects of pneumatic tubing on unsteady pressure measurements [NASA-TM-4171] p 850 A90-27703
- AIR DEFENSE**
- Stealth - Deception, evasion, and concealment in the air --- Book p 285 A90-24265
- The GE solid state air defence/ATC radar p 639 A90-41062
- Counterair situation awareness display for Army aviation p 964 A90-28982
- AIR DROP OPERATIONS**
- Dynamics of spatial motion of an aeroplane after drop of loads p 346 A90-25189
- Modeling the effects of the use of GPS (Global Positioning System) derived altitude indication in the C-17A airdrop system [AD-A215366] p 333 A90-16748
- AIR DUCTS**
- DB/SPF cooler outlet duct for aircraft application p 132 A90-16620
- AIR FILTERS**
- Airborne aerosol inlet passing efficiency measurement p 927 A90-52077
- Aerosol separator for use in aircraft [PB90-142217] p 611 A90-22155
- AIR FLOW**
- Numerical analysis of flow of an ideal fluid past an airfoil p 2 A90-10228
- Effect of primary air swirl on emissions formations in gas turbine combustors p 47 A90-12573
- Operation of a compressor with intermediate air bleed p 111 A90-14589
- A study of ground vortex p 158 A90-18590
- Mean flow measurements of heated supersonic slot injection into a high Reynolds number supersonic stream [AIAA PAPER 90-0180] p 163 A90-19722
- Development of a dual fuel injector for a gas turbine combustor [ASME PAPER 89-GT-25] p 340 A90-23764
- Effect of rib-angle orientation on local mass transfer distribution in a three-pass rib-roughened channel [ASME PAPER 89-GT-98] p 359 A90-23812
- Damping of the inlet vortex in a turbojet engine p 301 A90-25185
- Non-equilibrium hypersonic flows - Physics and numerics p 304 A90-25777
- Air/water two-phase flow test tunnel for airfoil studies p 352 A90-26842
- Wave formation on a liquid layer for de-icing airplane wings p 445 A90-28137
- A comprehensive hover test of the airloads and airflow of an extensively instrumented model helicopter rotor p 407 A90-28173
- Local convection heat transfer on a plane wall in the vicinity of strong streamwise accelerations p 535 A90-32174
- Nonlinear effects in the two-dimensional adaptive-wall outer-flow problem p 554 A90-35771
- Effect of condensation in a diffuser on the flow field p 603 A90-36784
- Gas turbine engine brush seal applications [AIAA PAPER 90-2142] p 685 A90-42041
- Navier-Stokes solutions of 2-D transonic flow over unconventional airfoils p 173 A90-14195
- Numerical modeling of supersonic turbulent reacting free shear layers p 174 A90-14197
- A wind tunnel study of a sting-mounted circulation control wing [AD-A216248] p 319 A90-17577
- Experimental investigation to suppress flow-induced pressure oscillations in open cavities [AD-A216285] p 320 A90-17578
- Passive venting technique for shallow cavities [NASA-CASE-LAR-14031-1] p 499 A90-20079
- The MANTA: An RPV design to investigate forces and moments on a lifting surface [NASA-CR-186227] p 499 A90-20971
- Aerosol separator for use in aircraft [PB90-142217] p 611 A90-22155
- Mechanical paint removal techniques for aircraft structures [IAR-89-23] p 773 A90-25254
- Modeling of supersonic reacting flow fields p 855 A90-26898
- Comparison of altitude test cell results p 856 A90-27715
- Comparison of ground-level test cells and ground-level to altitude test cells p 857 A90-27716
- General test plan p 857 A90-27721
- AIR INTAKES**
- Application of the hydrogen bubble visualization method to the water tunnels of ONERA [ONERA, TP NO. 1989-107] p 58 A90-11140

The inclusion of a similarity representation of compressor rotation in the modeling of the interaction of cannon firing with air intakes at incidence

[AAAF PAPER NT 88-18] p 4 A90-11435

Wind-tunnel test of the air intake of an unducted fan

[AAAF PAPER NT 88-19] p 4 A90-11436

A study of particle trajectories in a gas turbine intake

p 48 A90-12583

Icing test techniques for air intake screens on helicopters

functioning in temperatures around 0 C

p 23 A90-12619

Viscous flow analysis for advanced inlet particle separators

[AIAA PAPER 90-2136] p 661 A90-42038

Calculation of three-dimensional flow past a plane

supersonic air intake at angles of attack and sideslip

p 805 A90-46573

Airborne aerosol inlet passing-efficiency measurement

p 927 A90-52077

AIR JETS

Development process of turbulence in a round-nozzle

air jet p 87 A90-16101

AIR LAW

Recent cases and developments in aviation law

p 79 A90-11393

Placards, warning labels and operation manuals - An

aircraft manufacturer's duty to warn p 79 A90-11396

Litigation and the National Weather Service

[AIAA PAPER 90-0371] p 220 A90-19819

Aviation litigation - An ATC perspective

[AIAA PAPER 90-0372] p 175 A90-19820

Use of Computer-Aided Video Display technology in

aviation weather litigation

[AIAA PAPER 90-0373] p 216 A90-19821

From the DC-3 to hypersonic flight - ICAO in a changing

environment p 222 A90-23662

Recent developments in EEC aviation law - 'The second

phase' p 897 A90-46648

Considerations on the legal regulation of air transport

in the near future p 897 A90-46649

Latin American Conference on International Air

Transport and Activities in Outer Space, Mexico City,

Mexico, Aug. 14-18, 1988, Proceedings

p 897 A90-49613

Insurance aspects of airline liability

p 898 A90-49615

U.S. deregulation - Evidence from ten years of

experience p 898 A90-49619

AIR MASSES

Optimal control of an aircraft flying through a

downburst p 591 N90-21765

AIR NAVIGATION

Eurofix p 25 A90-10239

A precise flight reference system for evaluating airborne

navigation aids p 27 A90-12752

GPS monitor alarm limits for nonprecision approaches

p 98 A90-15315

Digital map for helicopter navigation and guidance

p 252 A90-21609

Status and potential of GPS-receiver development

p 265 A90-21717

From the DC-3 to hypersonic flight - ICAO in a changing

environment p 222 A90-23662

The disadvantages of GPS - Comparative study of

solutions adapted to civil aviation p 329 A90-23994

Performance study of an integrated NAVSTAR

GPS/SINS navigation system p 329 A90-24003

Aircraft interface with the future ATC system

p 331 A90-25574

Our future air navigation system embodies a global

concept p 402 A90-27922

Institutional stepping stones for FANS - Future Air

Navigation Systems p 403 A90-27923

Prospects are very good for using satellites for

aeronautical navigation p 403 A90-27924

Operating principles of a terrain-recognition air

navigation system p 403 A90-29655

Dual mode radar fusion based on morphological

processing p 459 A90-30249

Cognitive perspectives on map displays for helicopter

flight p 419 A90-31329

Basic areas of research in the development of a future

ATM system - air traffic management

p 551 A90-35685

Database management considerations for IFR certified

earth-referenced navigation systems

p 577 A90-36921

A surveillance 360 deg television orientation and ranging

system as an aid to collision avoidance

p 577 A90-36922

The multi-function RLG system comes of age - A

technical update p 578 A90-36931

Differential-geometrical technique of signal

transformation and estimation of position, rate and

acceleration parameters using supplementary data

sources p 638 A90-41004

Experiments on Mode S secondary surveillance radar

- The participation of the French Direction de la Navigation

Aerienne in the European effort p 639 A90-41057

The Canadian Airspace Systems Plan - Maintaining the

safety and efficiency of the air navigation system

p 725 A90-42655

Estimation of the efficiency of various operational modes

of a navigation complex p 725 A90-42924

Stability and controllability in proportional navigation

p 725 A90-42990

UK reference station for Navstar GPS

p 725 A90-43681

USCG HH-65A/SRR GPS integration and test results

p 726 A90-43705

A robust RAIM system using GPS/GLONASS

systems p 726 A90-43713

RAIM - An implementation study p 726 A90-43714

Omega coverage - Analytical and empirical methods and

solutions p 728 A90-45234

GPSNOTAM - A demonstration system for GPS status

notification p 728 A90-45238

AIAA Guidance, Navigation and Control Conference,

Portland, OR, Aug. 20-22, 1990, Technical Papers. Parts

1 & 2 p 862 A90-47576

The use of onboard sensor data in aerial triangulation

- GPS, pressure sensors, laser telemetry

p 822 A90-47901

The FAA gears up for Loran p 823 A90-49493

Certification impact of introducing G.P.S. into

commercial transport navigation systems

p 824 A90-49501

Operation of aviation radio and electronic equipment

(Handbook) - Russian book p 914 A90-50747

Military navigation - The fourth generation

p 914 A90-50775

Control outside of independent surveillance coverage

operational concept

[AD-A214163] p 243 N90-15090

Advances in Techniques and Technologies for Air

Vehicle Navigation and Guidance

[AGARD-CP-455] p 332 N90-16731

Interoperability issues in the use of satellite-based

navigation systems for civil aviation purposes

[AD-A217279] p 405 N90-19223

Joint University Program for Air Transportation

Research, 1988-1989

[NASA-CP-3063] p 468 N90-20921

Ridge regression processing p 489 N90-20931

Application of optimal tracking methods to aircraft terrain

following

[AD-A221099] p 641 N90-24264

Cognitive requirements for aircraft navigation

[NASA-CR-186933] p 824 N90-26804

FAA Loran early implementation project

[AD-A218866] p 824 N90-26805

Analysis, Design and Synthesis Methods for Guidance

and Control Systems

[AGARD-AG-314] p 916 N90-29338

GPS integrity requirements for use by civil aviation

p 916 N90-29339

An analysis of GPS as the sole means navigation system

in US Navy aircraft p 917 N90-29350

AIR PIRACY

Aviation security: Corrective actions underway, but better

inspection guidance still needed. Report to the

Chairwoman, Government Activities and Transportation

Subcommittee, Committee on Government Operations,

House of Representatives

[GAO/RCED-88-160] p 635 N90-23367

AIR POLLUTION

New high-speed air transport system and stratospheric

pollution

[ONERA, TP NO. 1989-202] p 279 A90-22445

Contamination of cabin air by synthetic oil and

breakdown products

[SAE PAPER 891455] p 323 A90-27424

Jet engines performance deterioration

p 852 A90-46871

Characterization of chemicals on engine exhaust

particles

[AD-A213566] p 256 N90-15106

Aerodynamic development perspective for traffic

aeroplanes

[DGLR-89-141] p 637 N90-24260

Source emission test of gas turbine engine test facility,

Kelly AFB, TX

[AD-A223869] p 932 N90-28571

AIR PURIFICATION

F-15 Environment Control System improvements

[SAE PAPER 901235] p 841 A90-49305

AIR QUALITY

Pollutants: Production and methods of reduction

[CIT/SME/VKI/RS/6] p 749 N90-25990

Source emission test of gas turbine engine test facility,

Kelly AFB, TX

[AD-A223869] p 932 N90-28571

AIR SAMPLING

Aerosol separator for use in aircraft

[PB90-142217] p 611 N90-22155

Feasibility study for a microwave-powered ozone sniffer

aircraft

[NASA-CR-186660] p 650 N90-23397

NASA/USRA high altitude reconnaissance aircraft

[NASA-CR-186685] p 650 N90-24266

AIR START

Restart characteristics of turbofan engines

p 50 A90-12627

In flight relight tests on AM-X single engine fly-by-wire

aircraft p 34 N90-10869

AIR TO AIR MISSILES

The Franco-German helicopter programme HAP,

PAH-2/HAC p 618 A90-42478

An autopilot design methodology for bank-to-turn

missiles

[AD-A213379] p 198 N90-13399

AIR TO AIR REFUELING

The performance and longitudinal stability and control

of large receiver aircraft during air to air refueling

p 346 A90-24338

Robotics for flightline servicing p 383 A90-30760

KC-135R low altitude air refueling flight test program

[AIAA PAPER 90-1265] p 494 A90-33893

Large receiver aircraft - The performance and

longitudinal stability and control during air to air

refuelling p 669 A90-41767

Visual servoing for autonomous aircraft refueling

[AD-A216042] p 414 N90-18386

AIR TRAFFIC

SST/HST air traffic - Challenge for the future

p 763 A90-44752

Conceptual design and feasibility study of very large

passenger aircraft

[AIAA PAPER 90-3220] p 834 A90-48841

A review of regulations - The Chicago Convention and

the bilateral network p 898 A90-49614

The integration of Latin American transport - Realities

and perspectives p 898 A90-49618

Anatomy of airline regulation - Towards a pluriform,

plurilateral, pluralistic, flexible world-wide regulatory

framework for air transport p 898 A90-49620

Safer skies with TCAS: Traffic Alert and Collision

Avoidance System

[PB89-169221] p 27 N90-10016

FAA air traffic activity: Fiscal year 1988

[AD-A211338] p 99 N90-12570

National Airspace System airspace management

operational concept

[DOT/FAA/DS-89/29] p 177 N90-13361

Preliminary design of four aircraft to service the California

Corridor in the year 2010: The California Condor, California

Sky-Hopper, high capacity short range transport tilt rotor

aircraft needed to simplify intercity transportation

[NASA-CR-186232] p 186 N90-14226

Turbulence spectral widths view angle independence

as observed by Doppler radar

[DOT/FAA/SA-89/2] p 281 N90-15566

Dallas/Fort Worth simulation. Volume 2: Appendixes D,

E, and F

[AD-A216613] p 405 N90-

- Applying artificial intelligence techniques to air traffic control automation p 282 A90-21389
- Using aircraft radar tracks to estimate wind aloft p 241 A90-21390
- Flight-path measurement p 242 A90-21721
- Ground navigation in airport traffic p 242 A90-21725
- TCAS - A lengthy but beneficial development effort p 339 A90-25494
- Prospects are good for using ATC radar to detect birds p 329 A90-25496
- The US air traffic control system architecture p 330 A90-25561
- National Airspace System demand and capacity modeling p 330 A90-25562
- Future ATC automation aids based upon AI technology p 375 A90-25563
- Advanced Traffic Management System automation p 330 A90-25565
- Advanced Automation System design p 375 A90-25566
- ATC ground communications system optimization techniques p 330 A90-25568
- Mode S system design and architecture p 330 A90-25569
- The use of satellite technology for oceanic air traffic control p 330 A90-25570
- Applicability of an augmented GPS for navigation in the National Airspace System p 331 A90-25571
- Development and operation of the Traffic Alert and Collision Avoidance System (TCAS) p 331 A90-25573
- Aircraft interface with the future ATC system p 331 A90-25574
- Rapsat - Application of onboard processing for communication and surveillance in air traffic control [AIAA PAPER 90-0883] p 331 A90-25702
- Avoiding a maneuvering aircraft with TCAS --- Traffic Alert and Collision Avoidance System p 347 A90-26222
- Array processor supercomputers p 376 A90-26626
- Our future air navigation system embodies a global concept p 402 A90-27922
- ARSR-4 long range radar will upgrade U.S. en-route surveillance p 403 A90-27925
- A microcomputer-based airspace control simulation and prototype human-machine interface p 461 A90-30800
- Underlying factors in air traffic control incidents p 401 A90-31335
- TCAS for commuter aircraft p 487 A90-33348
- Tests of automatic dependent surveillance (ADS) in Western Europe - Possible future developments p 574 A90-35353
- Mode S - A data link for future air traffic control p 576 A90-35684
- Basic areas of research in the development of a future ATM system --- air traffic management p 551 A90-35685
- Air traffic control --- Russian book p 638 A90-39581
- The TVD 900 - A modern signal processing applied to primary civilian ATC radar p 638 A90-41034
- Design of new Polish primary radars AVIA DM/CM p 638 A90-41035
- Performances and new surveillance possibilities in SSR - Mode S p 639 A90-41036
- Applications of Mode S secondary surveillance radar to civil air traffic control - Studies, experiments, and policy of the French Direction de la Navigation Aérienne p 639 A90-41056
- Experiments on Mode S secondary surveillance radar - The participation of the French Direction de la Navigation Aérienne in the European effort p 639 A90-41057
- The development result of SPEKTR automated air traffic control (ATC) system with extended grade of automation for terminal and hub areas p 639 A90-41058
- The GE solid state air defence/ATC radar p 639 A90-41062
- Monitoring and maintenance of automatic control systems in aviation --- Russian book p 778 A90-42524
- The planning of air transportation on airlines --- Russian book p 721 A90-42648
- The Canadian Airspace Systems Plan - Maintaining the safety and efficiency of the air navigation system p 725 A90-42655
- Aircraft Separation by Synchronized Transponder Interrogation (ASSTI) p 727 A90-43724
- More cruising levels expected at higher altitudes p 721 A90-44548
- Improved guidance and control of vehicles and personnel on the ground will benefit airport traffic capacity p 760 A90-44549
- Efforts continue to increase airport/airspace capacity p 722 A90-44550
- Multiple sensor data association and fusion in aerospace applications p 778 A90-44644
- Simulation of MLS-ATC procedures in the New York and San Francisco Terminal Control Areas [SAE PAPER 892217] p 728 A90-45434
- Radio Technical Commission for Aeronautics, Annual Assembly and Technical Symposium, Washington, DC, Dec. 4-6, 1989, Proceedings p 821 A90-46390
- Collision alert p 847 A90-48521
- Possibilities for improving traffic flows p 823 A90-49272
- Coordination strategies in a hierarchical air traffic control system with allowance for meteorological conditions p 914 A90-50779
- Organization of air traffic control --- Russian book p 915 A90-52415
- National airspace system approach and departure sequencing operational concept [NAS-SR-1322] p 27 N90-10017
- Design of a final approach spacing tool for TRACON air traffic control [NASA-TM-102229] p 24 N90-10841
- Ground and Obstacle Avoidance (GOA) concept of operations [DOT/FAA/DS-89/08] p 28 N90-10855
- A simulation study of landing time allocation procedures for use in computer-assisted air traffic management systems [AD-A212159] p 99 N90-11722
- On the generation of a variable structure airport surface traffic control system [AD-A211306] p 99 N90-11724
- The 1987 survey of track keeping and altitudes on Heathrow and Gatwick, standard instrument departure routes (DAY) [CAA-PAPER-88010] p 99 N90-11729
- FAA air traffic activity: Fiscal year 1988 [AD-A211338] p 99 N90-12570
- Development and evaluation at ATCEU of executive and support operations, phase 4A/3D --- ATCEU (Air Traffic Control Evaluation Unit) [CAA-PAPER-88017] p 99 N90-12572
- Operational trial of effect of raising minimum stack level in Heathrow stacks [CAA-PAPER-89003] p 99 N90-12573
- Parallel approach separation and controller performance: A study of the impact of two separation standards [DOT/FAA/CT-TN89/50] p 99 N90-12574
- Software fault tolerance [RSRE-MEMO-4237] p 99 N90-12575
- Aircraft Reply and Interference Environment Simulator (ARIES) hardware principles of operation, Volume 2: Appendixes [DOT/FAA/CT-TN88/4-2] p 135 N90-12781
- Aircraft Reply and Interference Environment Simulator (ARIES) hardware principles of operation, volume 1 [DOT/FAA/CT-TN88/4-1] p 135 N90-12782
- Assessment of voice coders for ATC/pilot voice communications via satellite digital communication channels [CAA-PAPER-89004] p 135 N90-12807
- Fine resolution errors in secondary surveillance radar altitude reporting amongst aircraft transmitting the conspicuity codes 4321 and 4322 [RSRE-88004] p 135 N90-12816
- National Airspace System airspace management operational concept [DOT/FAA/DS-89/29] p 177 N90-13361
- An update to the system safety study of TCAS 2 [DOT/FAA/SA-89/3] p 177 N90-13363
- Computer-based tools for assisting air traffic controllers with arrivals flow management [RSRE-88001] p 178 N90-13366
- Flight deck automation: Promises and realities [NASA-CP-10036] p 187 N90-13384
- National airspace system monitoring operational concept [NAS-SR-1330] p 178 N90-14214
- Adaptive clutter rejection filters for airborne Doppler weather radar applied to the detection of low altitude windshear [NASA-CR-186211] p 214 N90-14453
- Control outside of independent surveillance coverage operational concept [AD-A214163] p 243 N90-15090
- Piloted simulation of a ground-based time-control concept for air traffic control [NASA-TM-101085] p 240 N90-15898
- FAA air traffic control operations concepts, Volume 7: ATCT (Airport Traffic Control Towers) tower controllers [AD-A210455] p 332 N90-16730
- National airspace system plan: Facilities, equipment, associated development and other capital needs [AD-A215882] p 402 N90-18373
- Delivery performance of conventional aircraft by terminal-area, time-based air traffic control: A real-time simulation evaluation [NASA-TP-2978] p 404 N90-18378
- Dallas/Fort Worth simulation, Volume 2: Appendixes D, E, and F [AD-A216613] p 405 N90-18380
- Interoperability issues in the use of satellite-based navigation systems for civil aviation purposes [AD-A217279] p 405 N90-19223
- Operational evaluation of initial data link air traffic control services, volume 1 [DOT/FAA/CT-90/1-VOL-1] p 455 N90-19472
- Joint University Program for Air Transportation Research, 1988-1989 [NASA-CP-3063] p 468 N90-20921
- Investigation of air transportation technology at the Massachusetts Institute of Technology, 1988-1989 p 484 N90-20922
- Automatic speech recognition in air traffic control p 488 N90-20923
- Cockpit display of hazardous wind shear information p 484 N90-20924
- Investigation of air transportation technology at Princeton University, 1988-1989 p 486 N90-20935
- Plan for the FAA air traffic operational evaluation of the Automated Surface Observing System (ASOS) [DOT/FAA/CT-TN89/56] p 489 N90-20968
- Feasibility of using frequency offset on very high frequency air/ground voice channels [DOT/FAA/CT-TN89/71] p 542 N90-21248
- National airspace system air-ground communications operational concept [DOT/FAA/DS-90/2] p 542 N90-21249
- Meteorologist Weather Processor (MWP) integration test plan [DOT/FAA/CT-TN89/62] p 544 N90-21500
- Windshear case study: Denver, Colorado, July 11, 1988 [DOT/FAA/DS-89/19] p 544 N90-21509
- A conflict analysis of 4D descent strategies in a metered, multiple-arrival route environment [NASA-CR-182019] p 593 N90-21772
- FAA (Federal Aviation Administration) aviation forecasts, fiscal years 1990-2001 [AD-A219165] p 552 N90-22530
- Analysis of sequencing and scheduling methods for arrival traffic [NASA-TM-102795] p 636 N90-23373
- Simulator evaluation of the final approach spacing tool [NASA-TM-102807] p 636 N90-23374
- IFR aircraft handled forecast by air route traffic control center: Fiscal years 1990 to 2005 [AD-A220312] p 641 N90-24263
- Automatic speech recognition in air-ground data link p 690 N90-25037
- National Airspace System (NAS) software life cycle management study [AD-A221180] p 729 N90-25122
- The Federal Aviation Administration plan for research, engineering and development, Volume 2: Project descriptions [AD-A221264] p 783 N90-25931
- Aviation safety: Serious problems continue to trouble the air traffic control work force. Report to congressional requesters [GAO/RCED-89-112] p 724 N90-25959
- The disturbance processes on the data links of the mode-S air traffic control system [ETN-90-96960] p 729 N90-25965
- Mobile satellite communications for civil aviation [NLR-MP-8806-U] p 775 N90-26238
- Dallas/Fort Worth simulation, volume 1 [DOT/FAA/CT-TN89/28-VOL-1] p 824 N90-26802
- Data link test and analysis system/ATCRBS transponder test system technical reference [DOT/FAA/CT-TN90/7] p 824 N90-26803
- Atlanta tower simulation, volume 1 [DOT/FAA/CT-TN89/27-VOL-1] p 870 N90-26835
- Atlanta tower simulation, Volume 2: Appendixes [DOT/FAA/CT-TN89/27-VOL-2] p 870 N90-26836
- Real-time adaptive aircraft scheduling [NASA-CR-177558] p 820 N90-27669
- Flight service automation system, model 1 full capacity, NAS operational test and evaluation integration test plan [DOT/FAA/CT-TN90/4] p 825 N90-27672
- Integrated Air Traffic Management [DLR-MITT-89-23] p 825 N90-27676
- Air traffic management in Europe: Structure, tasks, potential p 825 N90-27677
- Airline requirements for a future air traffic management system p 825 N90-27678
- R and D aspects of the future operational concept of the BFS p 826 N90-27679

- Four-dimensional planner: A ground based planning system for time accurate approach guidance p 826 N90-27683
- Development of a COMPAS prototype for the ATC Centre at Frankfurt (Fed. Republic of Germany) p 826 N90-27684
- Safety net functions p 826 N90-27685
- Approach towards a future integrated airport surface traffic management p 827 N90-27686
- Experimental study towards a future airport ground movement simulator p 827 N90-27687
- Aspects of data link applications for ATC purposes p 827 N90-27688
- Application of a company data link at Lufthansa German Airlines p 827 N90-27689
- PHARE: Concept and programme p 827 N90-27690
- Integration of flight management and air traffic management systems p 827 N90-27693
- Dallas/Forth Worth simulation. Phase 2: Triple simultaneous parallel Instrument Landing System (ILS) approaches (turbojets) p 915 N90-28509
- Communications Interface Driver (CID) test plan [DOT/FAA/CT-TN89/35] p 958 N90-28762
- Analysis, Design and Synthesis Methods for Guidance and Control Systems [AGARD-AG-314] p 916 N90-29338
- Study improvement training facilities ground control air traffic controllers. Part 1: Alternative solutions and their consequences p 919 N90-29380
- Study improvement training facilities ground control air traffic controllers. Part 2: Functional analysis approach control trainer [FEL-89-A280-PT-2] p 939 N90-29409
- AIR TRAFFIC CONTROLLERS (PERSONNEL)**
- Air traffic control --- Russian book p 638 A90-39581
- Independent operations' on closely spaced runways p 821 A90-46393
- The mythology of first-come-first-serve landing order p 821 A90-46394
- FAA air traffic control operations concepts. Volume 7: ATCT (Airport Traffic Control Towers) tower controllers [AD-A210455] p 332 N90-16730
- Delivery performance of conventional aircraft by terminal-area, time-based air traffic control: A real-time simulation evaluation p 404 N90-18378
- Meteorologist Weather Processor (MWP) integration test plan [DOT/FAA/CT-TN89/62] p 544 N90-21500
- Aviation safety: Conditions within the air traffic control work force. Fact sheet for congressional requesters [GAO/RCEd-89-113FS] p 724 N90-25958
- Aviation safety: Serious problems continue to trouble the air traffic control work force. Report to congressional requesters [GAO/RCEd-89-112] p 724 N90-25959
- Atlanta tower simulation, volume 1 [DOT/FAA/CT-TN89/27-VOL-1] p 870 N90-26835
- Atlanta tower simulation. Volume 2: Appendixes [DOT/FAA/CT-TN89/27-VOL-2] p 870 N90-26836
- Airline requirements for a future air traffic management system p 825 N90-27678
- R and D aspects of the future operational concept of the BFS p 826 N90-27679
- Four-dimensional planner: A ground based planning system for time accurate approach guidance p 826 N90-27683
- Approach towards a future integrated airport surface traffic management p 827 N90-27686
- Study improvement training facilities ground control air traffic controllers. Part 2: Functional analysis approach control trainer [FEL-89-A280-PT-2] p 939 N90-29409
- AIR TRANSPORTATION**
- A new hybrid airship ('Heliship') for commuter transport p 29 A90-11875
- High-performance composite materials in air and space travel - State of the art and future perspectives [MBB-Z-0279/89] p 266 A90-22599
- From the DC-3 to hypersonic flight - ICAO in a changing environment p 222 A90-23662
- Probabilistic risk assessment and aviation system safety p 322 A90-26231
- Hydrogen in future energy and propulsion technology p 692 A90-41736
- The Airbus ... a challenge launched twenty years ago p 699 A90-41769
- The planning of air transportation on airlines --- Russian book p 721 A90-42648
- The McDonnell Douglas MD-11 ... or, how the DC-10 grew bigger p 730 A90-43766
- Civil supersonics - A less distant thunder p 731 A90-44223
- Improved guidance and control of vehicles and personnel on the ground will benefit airport traffic capacity p 760 A90-44549
- Air transportation in COMECON countries --- Russian book p 785 A90-46616
- Recent developments in EEC aviation law - 'The second phase' p 897 A90-46648
- Considerations on the legal regulation of air transport in the near future p 897 A90-46649
- Commercial aircraft DOC methods [AIAA PAPER 90-3224] p 897 A90-48843
- Latin American Conference on International Air Transport and Activities in Outer Space, Mexico City, Mexico, Aug. 14-18, 1988, Proceedings p 897 A90-49613
- A review of regulations - The Chicago Convention and the bilateral network p 898 A90-49614
- The integration of Latin American transport - Realities and perspectives p 898 A90-49618
- U.S. deregulation - Evidence from ten years of experience p 898 A90-49619
- Anatomy of airline regulation - Towards a pluriform, pluralistic, flexible world-wide regulatory framework for air transport p 898 A90-49620
- Airport technology international 1989/1990 --- Book p 937 A90-52857
- Study of high-speed civil transports [NASA-CR-4235] p 183 N90-13370
- Flight deck automation: Promises and realities [NASA-CP-10036] p 187 N90-13384
- California air transportation study: A transportation system for the California Corridor of the year 2010 [NASA-CR-186219] p 176 N90-14212
- UK airmisses involving commercial air transport, September to December 1988 [ISSN-0951-6301] p 240 N90-15897
- Fire hardening of aircraft through upgrades of materials and designs p 327 N90-17605
- Joint University Program for Air Transportation Research, 1988-1989 [NASA-CP-3063] p 468 N90-20921
- Investigation of air transportation technology at the Massachusetts Institute of Technology, 1988-1989 p 484 N90-20922
- Automatic speech recognition in air traffic control p 488 N90-20923
- Investigation of air transportation technology at Princeton University, 1988-1989 p 486 N90-20935
- FAA (Federal Aviation Administration) aviation forecasts, fiscal years 1990-2001 [AD-A219165] p 552 N90-22530
- The cost of air service fragmentation [JT-9010] p 913 N90-29334
- AIR WATER INTERACTIONS**
- Aircraft measurements of sea surface conditions and their relationship to marine boundary-layer dynamics p 888 A90-47572
- AIRBORNE EQUIPMENT**
- Electromagnetic characterization of lightning on aircraft [ONERA, TP NO. 1989-131] p 22 A90-11155
- Transall 88 - Lightning characterization program [ONERA, TP NO. 1989-142] p 22 A90-11164
- Testing facility and procedure of the ATTAS on-board data acquisition system p 39 A90-12202
- Holographic head-up displays for air and ground applications p 108 A90-13885
- A test of airborne kinematic GPS positioning for aerial photography - Methodology p 97 A90-13982
- Radio deviation of airborne goniometers --- Russian book p 242 A90-22733
- A waveform alignment approach to positioning airborne radar-sounding data p 332 A90-26651
- Fatigue spectra development for airborne stores p 336 A90-26757
- A ground simulation-inspection system for avionic devices p 594 A90-37232
- The Super Puma MKII automatic flight control system p 669 A90-42449
- Main characteristics of an integrated flight and display system for AS MKII Super-Puma p 653 A90-42450
- New systems for helicopter and aircraft vibration monitoring p 653 A90-42477
- Airborne early warning radar --- Book p 727 A90-45200
- Lightweight, composite flight control actuators [SAE PAPER 892264] p 733 A90-45459
- The airborne synthetic cartographic indicator p 822 A90-46671
- An airborne instrument for characterizing the 10,000 electromagnetic signals generated by one lightning flash p 848 A90-49830
- Operation of aviation radio and electronic equipment (Handbook) --- Russian book p 914 A90-50747
- Airborne aerosol inlet passing efficiency measurement p 927 A90-52077
- Meeting Review: Workshop on Airborne Instrumentation [PB89-174775] p 39 N90-10032
- The development of an airborne synthetic aperture radar motion compensation system p 333 N90-16745
- Feasibility study for a microwave-powered ozone sniffer aircraft [NASA-CR-186660] p 650 N90-23397
- NASA/USRA high altitude reconnaissance aircraft [NASA-CR-186685] p 650 N90-24266
- Description of the MARC measuring system [FEL-89-B170] p 963 N90-28887
- AIRBORNE LASERS**
- A laser obstacle avoidance and display system p 419 A90-30694
- China-built airborne synchronous laser ranger the new L-8 jet trainer aircraft [AD-A213835] p 275 N90-15422
- Helicopter Airborne Laser Positioning System (HALPS) [NASA-TM-102814] p 654 N90-23399
- AIRBORNE SURVEILLANCE RADAR**
- Antenna sidelobe requirements for the medium PRF mode of an airborne radar p 37 A90-10985
- Airborne Doppler radar detection of low-altitude wind shear p 252 A90-23284
- High resolution spectrum analysis for airborne pulse Doppler radars p 339 A90-24329
- Software architecture concepts for avionics p 461 A90-30806
- Clutter rejection and transmitter-receiver requirements in an airborne radar p 738 A90-45354
- Airborne Doppler radar flight experiments for the detection of microbursts p 542 N90-21243
- AIRBORNE/SPACEBORNE COMPUTERS**
- RISC lifting off in avionics --- Reduced Instruction Set Computer [AIAA PAPER 89-2967] p 73 A90-10483
- An experimental investigation of fault tolerant software structures in an avionics application [AIAA PAPER 89-3082] p 74 A90-10568
- A heterogeneous parallel processing architecture for avionic and aerospace applications [AIAA PAPER 89-3108] p 74 A90-10590
- A comfortable and universal data-acquisition-system for flight research p 39 A90-12204
- Beyond the limits - Flight enters the computer age --- Book p 282 A90-20380
- The selection of actuation devices for aircraft pneumatic valves in systems under computer control [SAE PAPER 891456] p 368 A90-27425
- Telemetry systems of the future p 458 A90-28829
- The Modular Flighttest Instrumentation/MFI 90 - A helicopter measuring system p 418 A90-28850
- Bubble memory applications for aircraft systems p 418 A90-30681
- The evolution of built-in test for an electrical power generating system (EPGS) p 424 A90-30699
- The airborne supercomputer p 538 A90-33775
- Thermal management of closed computer modules utilizing high density circuitry --- in Airborne Information Management System [AIAA PAPER 90-1748] p 583 A90-38441
- Correlation between vibration and computer operator response onboard a UH-1H helicopter p 737 A90-43727
- Software maintenance on the Airbus family [SAE PAPER 892326] p 738 A90-45484
- Use of Onboard Data Loaders [SAE PAPER 892327] p 738 A90-45485
- Fault tolerant architecture for a fly-by-light flight control computer p 860 A90-46931
- The Most Mounted Sight 771 processor upgrade program --- for helicopter p 926 A90-51058
- Airborne digital computers and systems --- Russian book p 927 A90-52410
- Software and hardware description of the helicopter motion equations for VAX computers [AD-A213248] p 184 N90-13375
- A knowledge-based system design/information tool for aircraft flight control systems [NASA-TM-101704] p 217 N90-13990
- A comparison of time-optimal interception trajectories for the F-8 and F-15 [NASA-CR-186300] p 581 N90-21753
- Preliminary development of an intelligent computer assistant for engine monitoring [NASA-TM-101702] p 612 N90-22322
- Aircraft condition monitoring system for future Airbus aircraft: New concept for programming and data recording p 848 N90-27619
- Start-up built-in test for the DISCUS fault tolerant, fly-by-wire computer system p 869 N90-27625

SUBJECT INDEX

- Integration of flight management and air traffic management systems [RAE-TM-FM-41] p 827 N90-27693
- AIRCRAFT**
- The FAA technical classification of aircraft and airports p 96 A90-15876
- AIRCRAFT ACCIDENT INVESTIGATION**
- The use of soot analysis as an investigative tool in aircraft fires p 22 A90-10269
- Safety management in aircraft testing and certification p 180 A90-17421
- After Habsheim p 401 A90-31388
- In the shadow of Aloha p 468 A90-33174
- Analyses of Arrow Air DC-8-63 accident of December 12, 1985 - Gander, Newfoundland p 635 A90-40687
- A comparison of emergency medical helicopter accident rates in the United States and the Federal Republic of Germany p 722 A90-44640
- Aircraft accident report: Aloha Airlines, Flight 243, Boeing 737-200, N73711, near Maui, Hawaii, April 28, 1988 [PB89-910404] p 24 N90-10013
- Post crash flight analysis: Visualizing flight recorder data [AD-A212063] p 96 N90-11715
- Aircraft accident report: Delta Air Lines, Inc., Boeing 727-232, N473DA, Dallas-Fort Worth International Airport, Texas, August 31, 1988 [PB89-910406] p 240 N90-15895
- RAAF Orion aircraft A9-300 oxygen fire [AD-A215496] p 323 N90-16725
- Aircraft accident report, United Airlines Flight 811, Boeing 747-122, N4713U, Honolulu, Hawaii, February 24, 1989 [PB90-910401] p 574 N90-21748
- UK airmisses involving commercial air transport: May - August 1989 [ISSN-0951-6301] p 913 N90-29335
- AIRCRAFT ACCIDENTS**
- Helicopter wire strike accident and high voltage electrocution - A case report p 22 A90-10265
- Fire deaths in aircraft without the crashworthy fuel system p 22 A90-10266
- Landing gear integrity - The bottom line of aircraft safety p 180 A90-17408
- Atmospheric conditions producing aircraft icing on 24-25 January 1989 - A case study utilizing combinations of surface and remote sensors [AIAA PAPER 90-0197] p 175 A90-19734
- Colorado mountain flying - Crashes and weather [AIAA PAPER 90-0369] p 175 A90-19818
- Aviation litigation - An ATC perspective [AIAA PAPER 90-0372] p 175 A90-19820
- Charging of aircraft - High-velocity collisions p 322 A90-26131
- The role of expert systems in aircraft safety management p 375 A90-26225
- Another look at aircraft accident statistics p 322 A90-26301
- Why birds kill - Cross-sectional analysis of U.S. Air Force bird strike data p 400 A90-30587
- After Habsheim p 401 A90-31388
- The importance of measured data as a contribution to reducing crew caused accidents [AIAA PAPER 89-3219] p 482 A90-31703
- Aviation meteorology - Panel report p 692 A90-39403
- Obstacle warning system for helicopters p 653 A90-41114
- Aircraft Ground Deicing Conference, Denver, CO, Sept. 20-22, 1988, Proceedings [SAE P-217] p 817 A90-46004
- Analysis of failures in aircraft structures p 882 A90-48998
- Insurance aspects of airline liability p 898 A90-49615
- Aircraft accident report: Aloha Airlines, Flight 243, Boeing 737-200, N73711, near Maui, Hawaii, April 28, 1988 [PB89-910404] p 24 N90-10013
- Classification and reduction of pilot error [NASA-CR-181867] p 24 N90-10014
- The human factors relating to escape and survival from helicopters ditching in water [AGARD-AG-305(E)] p 176 N90-13358
- Flight in Adverse Environmental Conditions [AGARD-CP-470] p 222 N90-15041
- The human element: The key to safe, civil operations in adverse weather p 248 N90-15042
- See and avoid/cockpit visibility [AD-A214214] p 239 N90-15084
- International Aircraft Occupant Safety Conference and Workshop proceedings [AD-A214452] p 239 N90-15085

- Aircraft accident report: Delta Air Lines, Inc., Boeing 727-232, N473DA, Dallas-Fort Worth International Airport, Texas, August 31, 1988 [PB89-910406] p 240 N90-15895
- RAAF Orion aircraft A9-300 oxygen fire [AD-A215496] p 323 N90-16725
- Aircraft Fire Safety [AGARD-CP-467] p 324 N90-17581
- Fire safety in civil aviation p 325 N90-17586
- Full scale study of a cabin fire in an A300 fuselage section p 326 N90-17592
- Aircraft fire safety in the Canadian Forces p 327 N90-17604
- A review of the analytical simulation of aircraft crash dynamics [NASA-TM-102595] p 484 N90-20068
- Annual review of aircraft accident data: US general aviation calendar year 1987 [PB90-138066] p 486 N90-20966
- Aircraft accident report, United Airlines Flight 811, Boeing 747-122, N4713U, Honolulu, Hawaii, February 24, 1989 [PB90-910401] p 574 N90-21748
- Optimal control of an aircraft flying through a downburst p 591 N90-21765
- UK airmisses involving commercial air transport, January - April 1989 [ISSN-0951-6301] p 575 N90-22544
- Aircraft crash survival design guide. Volume 1: Design criteria and checklists [AD-A218434] p 575 N90-22545
- Aircraft crash survival design guide. Volume 2: Aircraft design crash impact conditions and human tolerance [AD-A218435] p 575 N90-22546
- Aircraft crash survival design guide. Volume 4: Aircraft seats, restraints, litters, and cockpit/cabin dealthalization [AD-A218437] p 575 N90-22548
- Aircraft crash survival design guide. Volume 5: Aircraft postcrash survival [AD-A218438] p 575 N90-22549
- Aeronautical decisionmaking for air ambulance program administrators [DOT/FAA/DS-88/8] p 635 N90-23368
- Unique failure behavior of metal/composite aircraft structural components under crash type loads [NASA-TM-102679] p 690 N90-24660
- Computational crash dynamics. Project 1.2: Computational crash dynamics analysis [IAR-89-19] p 724 N90-25956
- Annual review of aircraft accident data: US general aviation, calendar year 1987 [PB90-138066] p 820 N90-27666
- A review of research and development in crashworthiness of general aviation aircraft: Seats, restraints and floor structures [AD-A221557] p 846 N90-27698
- AIRCRAFT ANTENNAS**
- Airborne array antennas for satellite communication p 265 A90-23202
- McDonnell Douglas Helicopter Company Apache telemetry antenna analysis p 403 A90-28839
- AIRCRAFT APPROACH SPACING**
- Experimental examination of the benefits of improved terminal air traffic control planning p 241 A90-21388
- Visual information for simulated landing approaches p 347 A90-26189
- Preliminary flight test investigation of an airborne wake vortex detection concept [AIAA PAPER 90-1282] p 495 A90-33903
- Aircraft Separation by Synchronized Transponder Interrogation (ASSTI) p 727 A90-43724
- National airspace system approach and departure sequencing operational concept [NAS-SR-1322] p 27 N90-10017
- Design of a final approach spacing tool for TRACON air traffic control [NASA-TM-102229] p 24 N90-10841
- UK airmisses involving commercial air transport, May-August 1988 [ISSN-0951-6301] p 96 N90-11717
- Parallel approach separation and controller performance: A study of the impact of two separation standards [DOT/FAA/CT-TN89/50] p 99 N90-12574
- Piloted simulation of a ground-based time-control concept for air traffic control [NASA-TM-101085] p 240 N90-15898
- Analysis of sequencing and scheduling methods for arrival traffic [NASA-TM-102795] p 636 N90-23373
- Four-dimensional navigation and Flight Management Systems p 826 N90-27681
- Dallas/Forth Worth simulation. Phase 2: Triple simultaneous parallel Instrument Landing System (ILS) approaches (turbojets) [DOT/FAA/CT-90/2] p 915 N90-28509

AIRCRAFT COMPARTMENTS

- AIRCRAFT BRAKES**
- Brake performance of the McDonnell Douglas DC-10-30/40 during high speed, high energy rejected takeoffs [PB90-917004] p 503 N90-21000
- AIRCRAFT CARRIERS**
- Supplemented visual cues for helicopter hovering above a moving ship deck p 195 A90-17704
- Census of US civil aircraft [PB90-120296] p 468 N90-20920
- AIRCRAFT COMMUNICATION**
- Laser communication system design p 26 A90-11813
- Research on transmission quality of telemetry system in flight test p 26 A90-12189
- Multiple channel frequency demodulator p 69 A90-12190
- Decommutation techniques and their integration into post flight analysis system p 26 A90-12191
- System identification - Multibus acquisition and simulation equipment p 26 A90-12192
- Acquisition and recording of AMX A/C Aeritalia experience and present trends p 26 A90-12194
- Prospects of onboard magnetic tape recording during flight tests p 39 A90-12198
- GPS monitor alarm limits for nonprecision approaches p 98 A90-15315
- A fiberoptic LAN for aircraft and other applications p 282 A90-23241
- Our future air navigation system embodies a global concept p 402 A90-27922
- Automated measurement of aircraft-level electromagnetic interference p 404 A90-30752
- A fiber optic headset compatible with power-by-light p 504 A90-32906
- Basic areas of research in the development of a future ATM system --- air traffic management p 551 A90-35685
- RAIM - An implementation study p 726 A90-43714
- Real time data collection and control in a distributed simulator system using Ethernet TCP/IP [SAE PAPER 892356] p 761 A90-45507
- The E-SAT 300A - A multichannel satellite communication system for aircraft p 914 A90-51339
- Fine resolution errors in secondary surveillance radar altitude reporting amongst aircraft transmitting the conspicuity codes 4321 and 4322 [RSRE-88004] p 135 N90-12816
- Data Link Processor (DLP) operational test and evaluation/integration test plan [DOT/FAA/CT-TN89/32] p 214 N90-14404
- The application of queueing theory to the modelling of CP-140 aircraft communications [AD-A213479] p 274 N90-15310
- AIRNET: A real-time communications network for aircraft [NASA-CR-186140] p 690 N90-24514
- AIRCRAFT COMPARTMENTS**
- Effect of an isolated shell on interior noise levels in a turboprop aircraft [SAE PAPER 891083] p 102 A90-14375
- The optimum control and adaptive control for airplane cabin pressure p 182 A90-18627
- Digital control of local sound fields in an aircraft passenger compartment p 247 A90-23113
- High-temperature bootstrap compared with F-15 growth air cycle air conditioning system [SAE PAPER 891436] p 336 A90-27407
- Embedded digital control for aircraft environmental control systems - A practical vehicle management system approach [SAE PAPER 891438] p 339 A90-27409
- Aircraft cabin interior systems meeting new FAA regulations p 482 A90-33710
- Analysis and improvement of cabin temperature control system p 580 A90-37241
- Active control of helicopter cabin noise p 645 A90-42434
- The all glass helicopter cockpit p 653 A90-42447
- Interior noise in the untreated Gulfstream II Propfan Test Assessment aircraft p 731 A90-44736
- Catalytic conversion of oil in bleed air - A maintenance tool [SAE PAPER 892214] p 732 A90-45431
- Active control of sound transmission through a cylindrical shell p 893 A90-46192
- Theoretical studies of the active control of propeller-induced cabin noise p 893 A90-46351
- In-flight experiments on the active control of propeller-induced cabin noise p 893 A90-46352
- UHB demonstrator interior noise control flight tests and analysis [NASA-CR-181897] p 140 N90-13198
- Objectives and results of cabin fire research in Germany p 325 N90-17588

- New aircraft cabin and cargo flammability standards for transport category aircraft p 325 A90-17589
- Fire prevention in transport airplane passenger cabins p 325 A90-17590
- Characteristics of transport, aircraft fires measured by full-scale tests p 325 A90-17591
- Aircraft internal fires p 326 A90-17593
- Fire science and aircraft safety p 326 A90-17596
- Forced and natural venting of aircraft cabin fires: A numerical simulation p 326 A90-17597
- Time development of convection flow patterns in aircraft cabins under post-crash fire exposure p 327 A90-17598
- Fire hardening of an aircraft passenger cabin p 328 A90-17606
- New materials for civil aircraft furnishing p 328 A90-17609
- Flammability testing of aircraft cabin materials p 328 A90-17611
- Preliminary fire extinguishing tests with handheld bottles: A comparison of extinguishing compounds [DOT/FAA/CT-TN89/60] p 370 A90-17930
- Floor pull test of a transport airframe section [DOT/FAA/CT-TN88/14] p 497 A90-20072
- Boeing 727-100 test project (high energy radiated field tests) [DOT/FAA/CT-88/33] p 542 A90-21247
- The Shock and Vibration Digest, volume 21, no. 6 p 614 A90-22363
- Noise transmission into propeller-driven airplanes p 614 A90-22364
- Fire hazards of aerosol cans in aircraft cargo compartments [DOT/FAA/CT-89/32] p 636 A90-23369
- Problems of internal acoustics in two and three dimensional cavities with deformable walls using the MSC/Nastran code [DLC/STR-INT-TN-004] p 699 A90-24876
- B-1B improved windshield development, Volume 2: Magna analysis: Baseline and parametric [AD-A221501] p 845 A90-26828
- Toxicity of thermolysis products from the materials of airplane cockpits [CEAT-PV-M6/5924/02] p 876 A90-27895
- Tests for aircraft interior materials in fire accident [LR-622] p 914 A90-29337
- AIRCRAFT CONFIGURATIONS**
- Study of advanced technology impact on cycle characteristics and aircraft sizing (using multivariable optimization techniques) p 29 A90-12612
- A full scale, VSTOL, ground environment test facility p 58 A90-12631
- Influence of joint fixity on the structural static and dynamic response of a joined-wing aircraft. I - Static response [SAE PAPER 891060] p 100 A90-14361
- Automated aircraft configuration design and analysis [SAE PAPER 891072] p 101 A90-14368
- NMG - A system of numerical representation of aircraft geometry p 103 A90-15877
- Supersonic/hypersonic Euler flowfield prediction method for aircraft configurations p 145 A90-16767
- Results from a numerical simulation of an F-16A configuration at a supersonic Mach number p 146 A90-16769
- Underexpanded jet-freestream interactions on an axisymmetric afterbody configuration p 154 A90-18141
- Incompressible potential flow about complete aircraft configurations p 156 A90-18443
- Applications of Lagrangian blending functions for grid generation around airplane geometries [AIAA PAPER 90-0009] p 216 A90-19630
- The fickle effect of nose microasymmetry on the high-alpha aerodynamics [AIAA PAPER 90-0067] p 161 A90-19663
- A study of sonic boom overpressure trends with respect to weight, altitude, Mach number, and vehicle shaping [AIAA PAPER 90-0367] p 164 A90-19816
- AIAA Lighter-Than-Air Systems Technology Conference, 8th, Jacksonville, FL, Oct. 5-7, 1989, Technical Papers p 221 A90-20576
- A new type of non-rigid airship system [AIAA PAPER 89-3175] p 244 A90-20583
- TW-68 tilt wing high speed commercial VTOL p 246 A90-21712
- An investigation of strake fence flaps on a canard-configured aircraft [AIAA PAPER 90-0762] p 230 A90-22259
- Aircraft of unconventional configuration (2nd revised and enlarged edition) --- Russian book p 247 A90-22734
- Incompressible viscous flow about aircraft configurations p 233 A90-23290
- The influence of selected geometrical and mass parameters on the structural dynamics of an aircraft with a variable-geometry airfoil p 346 A90-24284
- The role of computational fluid dynamics (CFD) in aircraft design [AIAA PAPER 90-1801] p 335 A90-25175
- Automatic mesh generation for complex three-dimensional regions using a constrained Delaunay triangulation p 375 A90-26022
- Techniques in multiblock domain decomposition and surface grid generation p 309 A90-26526
- Application of a multiblock grid generation approach to aircraft configurations p 310 A90-26527
- Generation of tetrahedral meshes around complete aircraft p 310 A90-26536
- Application of a three-dimensional finite element grid generation scheme for an F-16 aircraft configuration p 336 A90-26541
- Grid generation for an aft-fuselage-mounted nacelle/pylon configuration p 311 A90-26543
- Zonal grid generation for fighter aircraft p 311 A90-26544
- Interactive grid generation for fighter aircraft geometries p 311 A90-26546
- Multiple-block grid adaption for an airplane geometry p 311 A90-26547
- Using the method of symmetric singularities for calculating flow past subsonic flight vehicles p 386 A90-28979
- Whirl flutter stability of a pusher configuration subject to a nonuniform flow [AIAA PAPER 90-1162] p 393 A90-29397
- Practical design considerations for integrating the propulsion system with the aircraft for jetborne flight [ASME PAPER 89-GT-310] p 490 A90-32257
- Calculations of propeller/airframe interference effects using the potential/multienergy flow method p 490 A90-32452
- Starship - A model for future designs p 493 A90-33714
- Flow visualization in flight testing [AIAA PAPER 90-1273] p 496 A90-34148
- Capability of current supercomputers for the computational fluid dynamics p 546 A90-34382
- Yakovlev strikes back p 579 A90-35848
- Boundary-element shape optimization system for aircraft structural components p 680 A90-39786
- YF-23A previews design features of future fighters p 643 A90-40344
- A modeling technique for STOVL ejector and volume dynamics [AIAA PAPER 90-2417] p 663 A90-42168
- Application of the KTRAN transonic small disturbance code to the complete CF-18 aircraft with stores p 629 A90-42416
- Focusing propulsion and lift system development for an evolving special operations aircraft [AIAA PAPER 90-2277] p 730 A90-42768
- The McDonnell Douglas MD-11 ... or, how the DC-10 grew bigger p 730 A90-43766
- Mirage 2000 - A French success that is no illusion p 731 A90-43768
- Support backbone for the Soviet air forces ... The Ilyushin 'Candid' family p 731 A90-43769
- Aerodynamic design considerations for aircraft radomes [AIAA PAPER 90-2843] p 711 A90-45163
- Approach to side force alleviation through modification of the pointed forebody geometry [AIAA PAPER 90-2834] p 712 A90-45165
- Transonic analysis of complex configurations using TRANAIR program [SAE PAPER 892289] p 714 A90-45467
- Stability characteristics of a conical aerospace plane concept [SAE PAPER 892313] p 757 A90-45475
- AIRPLANE - Experiences, benchmarks and improvements [AIAA PAPER 90-2998] p 787 A90-45848
- Numerical simulation of the viscous flow around a simplified F/A-18 at high angles of attack [AIAA PAPER 90-2999] p 787 A90-45849
- Reduction of the side force on pointed forebodies through add-on tip devices [AIAA PAPER 90-3005] p 788 A90-45854
- On optimal supersonic/hypersonic bodies [AIAA PAPER 90-3072] p 796 A90-45918
- VTOL military research aircraft --- Book p 828 A90-46002
- Supersonic aerodynamic characteristics of a Mach 3 high-speed civil transport configuration [AIAA PAPER 90-3210] p 811 A90-48836
- The MH-60K - A special rotorcraft for special operations [AIAA PAPER 90-3266] p 835 A90-48860
- Comparison of equivalent plate and finite element analysis of a realistic aircraft structural configuration [AIAA PAPER 90-3293] p 837 A90-48877
- Configuring tactical aircraft [AIAA PAPER 90-3305] p 837 A90-48886
- Design synthesis and optimization of joined-wing transports [AIAA PAPER 90-3197] p 838 A90-49102
- Application of boundary layer control to HSCAT low speed configuration [AIAA PAPER 90-3199] p 812 A90-49103
- Obtaining precise LTR with Luenberger type observer with arbitrary observer poles and finite gain [AIAA PAPER 90-3228] p 868 A90-49113
- The North American Rockwell XTV-12A - Reflections and some lessons [AIAA PAPER 90-3240] p 839 A90-49118
- The design of a sport aircraft configured to emulate jet fighter characteristics [AIAA PAPER 90-3244] p 839 A90-49119
- ATF prototypes outstrip F-15 in size and thrust p 841 A90-49477
- Aerostructural considerations for the power plant of overlapping wing configuration p 841 A90-49488
- Starship sails through p 842 A90-49825
- Characterization of configuration effects on lightning simulation/qualification testing p 819 A90-49835
- A numerical method for solving transonic flow past aircraft in Cartesian coordinates [NAL-TR-1008] p 18 A90-10003
- Computation of transonic flow about stores [AD-A210402] p 18 A90-10009
- Supersonic flow computations over aerospace configurations using an Euler marching solver [NASA-CR-4085] p 19 A90-10012
- Static aeroelastic analysis for generic configuration aircraft [NASA-TM-89423] p 52 A90-10042
- Grid generation procedure using the integral equation method [NAL-TR-1009] p 77 A90-10630
- Robust control design for flight control [AD-A211957] p 119 A90-11756
- Installed tailplane lift-curve slope at subsonic speeds [ESDU-89029] p 236 A90-15081
- Dynamic derivatives of missiles and fighter-type configurations at high angles of attack p 337 A90-17554
- Fuselage design for a specified Mach-sliced area distribution [NASA-TP-2975] p 414 A90-18385
- Influence of forebody geometry on aerodynamic characteristics and a design guide for defining departure/spin resistant forebody configurations [AD-A216714] p 414 A90-18388
- A user's manual for the method of moments Aircraft Modeling Code (AMC) [NASA-CR-186371] p 415 A90-18390
- Subsonic flutter analysis using MSC/NASTRAN [PB90-166786] p 522 A90-21041
- Prediction of forces and moments for flight vehicle control effectors. Part 1: Validation of methods for predicting hypersonic vehicle controls forces and moments [NASA-CR-186571] p 571 A90-21734
- Grid patching approaches for complex three-dimensional configurations p 573 A90-21985
- Multiblock topology specification and grid generation for complete aircraft configurations p 582 A90-21986
- A discussion on issues relating to multiblock grid generation p 608 A90-21991
- Automatic grid generation in complex three-dimensional configurations using a frontal system p 608 A90-21992
- Unstructured finite element mesh generation and adaptive procedures for CFD p 608 A90-21993
- Dynamic ground-effect measurements on the F-15 STOL and Maneuver Technology Demonstrator (S/MTD) configuration [NASA-TP-3000] p 573 A90-22531
- A modeling technique for STOVL ejector and volume dynamics [NASA-TM-103167] p 589 A90-22566
- Supersonic flow computations for an ASTOVL aircraft configuration, phase 2, part 2 [NASA-CR-4284] p 610 A90-22746
- The influence of adjacent seating configurations on egress through a type 3 emergency exit [AD-A218393] p 636 A90-23371
- Actuated forebody strakes [NASA-CASE-LAR-13983-1] p 648 A90-23390
- Preliminary design of a supersonic Short Takeoff and Vertical Landing (STOVL) fighter aircraft [NASA-CR-186670] p 649 A90-23394
- Composite reduced Navier Stokes procedures for flow problems with strong pressure interactions [AD-A219621] p 689 A90-23687
- Activities report in aerospace and aerodynamics [ETN-90-96774] p 699 A90-24224

- NASA/USRA high altitude reconnaissance aircraft
[NASA-CR-186685] p 650 N90-24266
- Helicopter controllability
[AD-A220078] p 672 N90-24275
- Feasibility study for a microwave-powered ozone sniffer aircraft, volume 2
[NASA-CR-186676] p 735 N90-25967
- ARLSUPER version 1.0, program users guide
[AD-A222693] p 815 N90-26793
- Aircraft lightning protection handbook
[AD-A222716] p 820 N90-27668
- Aircraft evacuations: The effect of passenger motivation and cabin configuration adjacent to the exit
[CAA-PAPER-89019] p 913 N90-29336
- AIRCRAFT CONSTRUCTION MATERIALS**
- Material requirements for future aeroengines
p 62 A90-12534
- Materials and structures for hypersonic vehicles
p 31 A90-13015
- Composite-embedded optical fibers for communication links
p 139 A90-13847
- Scaling effects in the impact response of graphite-epoxy composite beams
[SAE PAPER 891014] p 128 A90-14326
- Composite driveshaft designs
[SAE PAPER 891031] p 128 A90-14339
- Propeller development for the Rutan Voyager
[SAE PAPER 891034] p 100 A90-14341
- Beech Starship interior noise experimental studies
[SAE PAPER 891082] p 101 A90-14374
- Thermoplastic composite fighter forward fuselage
p 81 A90-14659
- Durability characteristics of the LAK-12 Letuva glider made of composite materials at the stage of certification
p 102 A90-15560
- Advantage Airbus?
p 102 A90-15746
- IHPET epawns engines for 21st century
p 188 A90-16702
- Advanced materials to fly high in NASP
p 203 A90-17297
- Materials pace aerospace technology
p 203 A90-17298
- The strength and weakness of carbon composite structures --- for military and civil aircraft
p 180 A90-17679
- Stronger starlifter
p 143 A90-17919
- The case for titanium
p 204 A90-17922
- Developing aluminium
p 204 A90-17924
- In process failure investigations in aeronautics
p 181 A90-18489
- Material of the '90s?
p 265 A90-20259
- More composites in commercial transports?
p 265 A90-20263
- Resin transfer molding of composite structures
p 270 A90-20264
- An AEW metalclad airship
[AIAA PAPER 89-3158] p 244 A90-20579
- Design criteria, constructions, and materials for the Dornier 328 airframe
p 246 A90-21610
- The coming age of the tiltrotor. I
p 246 A90-21711
- Material progress
p 221 A90-21715
- The impact of composites on the aerospace industry
p 221 A90-22649
- Aerospace materials research opportunities
p 267 A90-23177
- Efficient structural material distribution in the main frame of a flight vehicle
p 363 A90-24092
- Composites for aeronautical structures
p 286 A90-24291
- beta CEZ, a high performance titanium alloy for aerospace engines
[ONERA, TP NO. 1990-8] p 356 A90-25356
- Metal matrix composites - Ready for take-off?
p 356 A90-26865
- Materials get smarter
p 356 A90-27598
- Improvement in structural integrity and long term durability of aerospace composite components
p 441 A90-28189
- The use of fibre reinforced thermoplastics for helicopter primary structures and their engineering substantiation
p 441 A90-28191
- Evaluation of 3-D reinforcements in commingled, thermoplastic structural elements
p 441 A90-28192
- Analysis and testing of fiber-reinforced thermoplastic composite vertical stabilizer skins for an advanced attack helicopter
p 441 A90-28193
- Design and analysis of composite structures with manufacturing flaws
p 445 A90-28234
- Effects of damage on post-buckled skin-stiffener composite skin panels
p 409 A90-28235
- AIAA/ASME/ASCE/AHS/ASC Structures, Structural Dynamics and Materials Conference, 31st, Long Beach, CA, Apr. 2-4, 1990, Technical Papers. Part 3 - Structural dynamics I
p 449 A90-29359
- Sealing the future --- sealants and adhesives for military aircraft
p 442 A90-29638
- The challenge of LHX --- composite materials in light military helicopters
p 382 A90-29641
- Aerospace materials - Trends and potential
p 529 A90-31902
- Fabrication of aircraft structures from thermoplastic drapeable preforms
p 468 A90-33125
- Airbus A320 CFRP-rudder structural requirements
p 493 A90-33707
- Core composites in Swissair aircraft
p 493 A90-33709
- Repairing the damage
p 530 A90-33712
- Al-Li alloys and ultrahigh-strength steels for U.S. Navy aircraft
p 599 A90-37441
- Aluminum alloy 6013 sheet for new U.S. Navy aircraft
p 599 A90-37442
- Ultrahigh-strength steels for aerospace applications
p 599 A90-37443
- Development of a simulated bird-strike test method --- of aircraft turbine engine fan blade materials
p 600 A90-37444
- The mechanisms and benefits of aeroelastic tailoring
p 641 A90-39286
- The influence of material quality on airframe structural durability
p 676 A90-41336
- Advanced materials for landing gear
p 677 A90-41900
- Advanced material applications for direct lift engines
[AIAA PAPER 90-2753] p 664 A90-42226
- Eight years of flight operations with composite rotorblades
p 635 A90-42481
- Application of advanced materials to aircraft gas turbine engines
[AIAA PAPER 90-2281] p 764 A90-42769
- Aluminum surface preparation for aircraft field repair
p 764 A90-43204
- A friendly alloy --- aircraft construction materials
p 764 A90-44173
- Lose weight with Al-Li
p 765 A90-44175
- Toxicology in aviation
p 722 A90-44662
- Dornier Composite Aircraft - Economical and faultless
p 732 A90-44751
- Certification of composites for commercial aircraft
[SAE PAPER 892212] p 772 A90-45430
- Titanium matrix composite landing gear development
[SAE PAPER 892337] p 733 A90-45491
- Certifying the Speed Canard
p 833 A90-48699
- Titanium aluminides for advanced aircraft engines
p 874 A90-49000
- Unique features and innovative application of advanced composites to the MD-11
[AIAA PAPER 90-3217] p 838 A90-49108
- Comparison of processing techniques for Filmix unidirectional commingled fabric
p 940 A90-50058
- Durability and damage tolerance of graphite/epoxy honeycomb structures
p 942 A90-50085
- Material development and second source qualification of carbon fiber/epoxy prepreps for primary and secondary Airbus structures
p 948 A90-50225
- Castings Airworthiness
[AGARD-R-762] p 64 N90-10231
- Castings factors imposed by the French regulation for foundry castings used in military aircraft
p 64 N90-10233
- The question of the casting factor
p 64 N90-10238
- Choice and characterization of new materials for aerospace applications
[ETN-89-95219] p 126 N90-11819
- A new test procedure for a wing made with carbon fiber composites
[ETN-89-95220] p 126 N90-11820
- The evolution of light alloys in the aerospace industry
[ETN-89-95216] p 126 N90-11872
- Aluminium alloy development for aero engines
[PNR90548] p 126 N90-11874
- A vision of the future: The new engine technology
[PNR90566] p 115 N90-12603
- Material requirements for future aeroengines
[PNR90595] p 116 N90-12610
- Composite materials for future aeroengines
[PNR90584] p 127 N90-12667
- The future of non ferrous metals in aerospace engines
[PNR90572] p 127 N90-12720
- Fatigue behavior of specimens under compression load spectra
[ETN-89-95207] p 137 N90-12954
- An investigation on combined extension and bending of thin sheets with a central crack
[LR-561] p 137 N90-12958
- Some new techniques for aircraft fuselage skin tests
[LR-547] p 184 N90-13379
- New Light Alloys
[AGARD-CP-444] p 267 N90-15185
- Properties of Al-Li alloys
p 267 N90-15191
- Putting alloy 2091 to work
p 268 N90-15197
- Bird impact tests on asymmetric sandwich structures made in Kevlar 49
[CEAT-NT-10/S/83-5] p 323 N90-16727
- Bird impact tests on curved structures of the type Sandwich-Kevlar-Nida for normal and angular shooting
[CEAT-NT-10/S/83-4] p 324 N90-16728
- New materials for civil aircraft furnishing
p 328 N90-17609
- Heat release rate measurement for evaluating the flammability of aircraft materials
p 328 N90-17610
- Flammability testing of aircraft cabin materials
p 328 N90-17611
- Investigation of the failure modes in a metal matrix composite under thermal cycling
[AD-A216195] p 357 N90-17825
- Simple shear tests of the FMI 23.5.06 adhesive cured at low pressure (12 PSI)
[INFORME-I-298/88] p 357 N90-17871
- Pressure air tightness tests of laminated panels for wing leading edge heat shields
[INFORME-I-377/89] p 357 N90-17873
- Compendium of abstracts and viewgraphs.
[AD-A217189] p 532 N90-20140
- Boeing/NASA composite components flight service evaluation
[NASA-CR-181898] p 601 N90-22609
- Investigation on sheet material of 8090 and 2091 aluminium-lithium alloy
[MBB-UT-122/89-PUB] p 766 N90-25090
- Damage tolerance demonstration for A310-300 CFRP components
[MBB-UT-012/89-PUB] p 766 N90-25091
- Towards 2000: The composite engine
[PNR90646] p 750 N90-26000
- The impact and requirements of new materials on aeroengines
[PNR90671] p 750 N90-26003
- Metal matrix composites and powder processing for aero-engine applications
[PNR90617] p 767 N90-26087
- Materials and structures for 2000 and beyond: An attempted forecast by the DLR Materials and Structures Department
[ESA-TT-1154-REV] p 775 N90-26173
- AGARD highlights 90/1
p 783 N90-26788
- Design of helicopter components in metal matrix composites
[REPT-100-20-55] p 874 N90-26894
- Toxicity of thermolysis products from the materials of airplane cockpits
[CEAT-PV-M6/5924/02] p 876 N90-27895
- Static and dynamic characterization of the ATR 72 rods made of Ti 10.2.3 titanium alloy
[REPT-49-238] p 953 N90-28722
- Tests for aircraft interior materials in fire accident
[LR-622] p 914 N90-29337
- Fatigue, static tensile strength and stress corrosion of aircraft materials and structures. Part 1: Text
[LR-630-PT-1-REV] p 961 N90-29682
- Fatigue, static tensile strength and stress corrosion of aircraft materials and structures. Part 2: Figures
[LR-630-PT-2] p 961 N90-29683
- AIRCRAFT CONTROL**
- A knowledge-based system design/information tool for aircraft flight control systems
[AIAA PAPER 89-2978] p 55 A90-10491
- Optic multiplex for aircraft sensors - Issues and options
p 38 A90-11660
- Direct frequency modulation in interferometric systems
p 68 A90-11662
- Toward fly-by-light aircraft
p 39 A90-11664
- The application of linear maximum likelihood estimation of aerodynamic derivatives for the Bell-205 and Bell-206
p 30 A90-12773
- Airplane design. Part 7 - Determination of stability, control and performance characteristics: Far and military requirements --- Book
p 57 A90-12872
- On a pitch control law for a constant glide slope through windshears
p 117 A90-13784
- Minimum-time turns using vectored thrust
p 118 A90-14728
- Theory for aircraft handling qualities based upon a structural pilot model
p 118 A90-14730
- An analysis of the possibility of using direct control of the lifting force for modifying the flying qualities of aircraft
p 118 A90-15423
- The analysis of entry into and recovery from a spin for the J16 aircraft
p 195 A90-16854
- A separated algorithm and applications to flight test
p 216 A90-16857
- Generation of motion control for direction finders in a goniometer system
p 187 A90-17137
- The fundamentals of vectored propulsion
p 180 A90-17461
- Applications of fuzzy sets to rule-based expert system development
p 216 A90-18050

- Design of direct lift control systems against vertical gust p 196 A90-18592
- Modal aggregation and its application in flight mechanics p 196 A90-18595
- Analysis and design of sidestick controller systems for general aviation aircraft p 196 A90-19554
- Experimental investigation of a new device to control the asymmetric flowfield on forebodies at large angles of attack p 161 A90-19665
- [AIAA PAPER 90-0069] p 161 A90-19665
- High angle of attack flying qualities criteria p 197 A90-19738
- [AIAA PAPER 90-0219] p 197 A90-19738
- Control configured airship design p 244 A90-20585
- [AIAA PAPER 89-3170] p 244 A90-20585
- The National Aero-Space Plane, the guidance and control engineer's dream or nightmare? p 264 A90-21546
- [AAS PAPER 89-040] p 264 A90-21546
- Precision navigation using an integrated GPS-IMU system p 242 A90-21720
- A variable structure system (VSS) to robust control of aircraft p 257 A90-21987
- Application of dynamical systems theory to the high angle of attack dynamics of the F-14 p 257 A90-22184
- [AIAA PAPER 90-0221] p 257 A90-22184
- The fast-response requirement of powerplant thrust in the set of engineering and economic criteria of an aircraft p 254 A90-23354
- Flight-mechanics tasks in solving problems of active control p 257 A90-23358
- An application of generalized predictive control to rotorcraft terrain-following flight p 257 A90-23478
- Concise design of aircraft longitudinal model reference adaptive command augmentation system p 345 A90-24002
- Mean-square approximation by an even nonnegative polynomial p 374 A90-24101
- The performance and longitudinal stability and control of large receiver aircraft during air to air refueling p 346 A90-24338
- Aerodynamic control of aircraft by forebody vortex manipulation p 301 A90-25167
- [AIAA PAPER 90-1827] p 301 A90-25167
- An analysis of feel system effects on lateral flying qualities p 346 A90-25168
- [AIAA PAPER 90-1824] p 346 A90-25168
- Identification of moderately nonlinear flight mechanics systems with additive process and measurement noise p 347 A90-25987
- Toward a human-centered aircraft automation philosophy p 347 A90-26177
- ADAM 2.0 - An ASE analysis code for aircraft with digital flight control systems p 431 A90-29385
- [AIAA PAPER 90-1077] p 431 A90-29385
- Aircraft flight control system identification p 431 A90-30105
- A flight-test methodology for identification of an aerodynamic model for a V/STOL aircraft p 413 A90-30107
- Toward the panoramic cockpit, and 3-D cockpit displays p 419 A90-30682
- Accurate ILS and MLS performance evaluation in presence of site errors p 404 A90-30693
- Modeling and analysis tools for aircraft control system evaluations p 431 A90-30703
- Integrated structure/control concepts for oblique wing roll control and trim p 433 A90-31282
- Sensitivity derivatives of flutter characteristics and stability margins for aeroservoelastic design p 433 A90-31287
- Studies of predicting departure characteristics of aircraft p 433 A90-31480
- Comparison of test signals for aircraft frequency domain identification p 490 A90-33057
- Aeroservoelastic tailoring for lateral control enhancement p 516 A90-33060
- Cooperative synthesis of control and display augmentation in approach and landing p 516 A90-33061
- Review of active structural control systems and flight test techniques for dynamic stability investigations p 516 A90-33352
- Interactions of active controls and structural loads p 517 A90-33404
- Use of ground-based and in-flight simulation for flight control system development p 519 A90-33907
- [AIAA PAPER 90-1286] p 519 A90-33907
- A flight test investigation of certification requirements for laminar-flow general aviation airplanes p 496 A90-33920
- [AIAA PAPER 90-1310] p 496 A90-33920
- DIGITAC - A unique digital flight control testbed aircraft p 519 A90-33931
- [AIAA PAPER 90-1288] p 519 A90-33931
- Analysis of perturbed longitudinal dynamics of an aircraft taking into consideration the stationary aeroelastic effects and the atmospheric perturbances p 520 A90-34822
- A design method for real-time computer control hydraulic force system p 590 A90-36434
- The method of random variable structure optimal control for aircraft p 590 A90-37220
- A study of the control technique for aircraft spin recovery p 590 A90-37226
- AV-8B shipboard ski jump evaluation p 574 A90-38535
- Proportional control of asymmetric forebody vortices with the unsteady bleed technique p 591 A90-38758
- [AIAA PAPER 90-1629] p 591 A90-38758
- Concept development of automatic guidance for rotorcraft obstacle avoidance p 669 A90-41632
- MLS - A total system approach p 640 A90-41710
- Large receiver aircraft - The performance and longitudinal stability and control during air to air refueling p 669 A90-41767
- Computation of vectoring nozzle performance p 627 A90-42225
- [AIAA PAPER 90-2752] p 627 A90-42225
- Development of the stall warning/stick pusher system for the Boeing/de Havilland Dash 8 Series 300 p 645 A90-42420
- Direct drive servovalves: Why and how - The Magnaghi Milano answer p 688 A90-42484
- Problems in the synthesis of advanced aircraft control systems p 751 A90-44723
- The integrated control of a propulsion-airframe system [ASME PAPER 89-WA/DSC-12] p 751 A90-44847
- The ascending trajectories performance and control to minimize the heat load for the transatmospheric aero-space planes p 763 A90-45135
- [AIAA PAPER 90-2828] p 763 A90-45135
- Unified flying qualities criteria for longitudinal tracking p 752 A90-45141
- [AIAA PAPER 90-2806] p 752 A90-45141
- Control of forebody flow asymmetry - A critical review p 711 A90-45164
- [AIAA PAPER 90-2833] p 711 A90-45164
- Optimal control system design for departure prevention p 754 A90-45167
- [AIAA PAPER 90-2837] p 754 A90-45167
- Control of an aircraft in downbursts p 755 A90-45331
- Forebody vortex manipulation for aerodynamic control of aircraft at high angles of attack p 756 A90-45437
- [SAE PAPER 892220] p 756 A90-45437
- Numerical study of asymmetric air injection to control high angle-of-attack forebody vortices on the X-29 aircraft p 788 A90-45853
- [AIAA PAPER 90-3004] p 788 A90-45853
- Exploratory wind tunnel investigation of the stability and control characteristics of a three-surface, forward-swept wing advanced turboprop model p 797 A90-45920
- [AIAA PAPER 90-3074] p 797 A90-45920
- Stiffness of an aircraft pneumatic rudder drive p 828 A90-46479
- Parametric synthesis of the decoupling filter in the manual control system of VTOL aircraft p 859 A90-46483
- AIAA Guidance, Navigation and Control Conference, Portland, OR, Aug. 20-22, 1990, Technical Papers, Parts 1 & 2 p 862 A90-47576
- Robust hover control for a short takeoff/vertical landing aircraft p 862 A90-47593
- [AIAA PAPER 90-3333] p 862 A90-47593
- Application of a design method for integrated control to a VTOL airplane in hover p 862 A90-47594
- [AIAA PAPER 90-3334] p 862 A90-47594
- H-infinity based integrated flight/p propulsion control design for a STOVL aircraft in transition flight p 862 A90-47595
- [AIAA PAPER 90-3335] p 862 A90-47595
- Stochastic performance robustness of aircraft control systems p 865 A90-47665
- [AIAA PAPER 90-3410] p 865 A90-47665
- Robust control design for relaxed static stability aircraft p 865 A90-47696
- [AIAA PAPER 90-3443] p 865 A90-47696
- Robustness evaluation of a flexible aircraft control system p 890 A90-47698
- [AIAA PAPER 90-3445] p 890 A90-47698
- Local adaptive maneuvering optimization for fighter aircraft p 890 A90-47706
- [AIAA PAPER 90-3453] p 890 A90-47706
- Flight investigation of variations in rotorcraft control and display dynamics for hover p 866 A90-47731
- [AIAA PAPER 90-3482] p 866 A90-47731
- Optimal rigid body reorientation problem p 867 A90-47734
- [AIAA PAPER 90-3485] p 867 A90-47734
- Optimal periodic cruise with singular control p 833 A90-47738
- [AIAA PAPER 90-3490] p 833 A90-47738
- Nonconvex polytope approximations of attracting basin boundaries for nonlinear systems p 891 A90-47758
- [AIAA PAPER 90-3512] p 891 A90-47758
- Design of a close-support aircraft p 835 A90-48849
- [AIAA PAPER 90-3241] p 835 A90-48849
- The Bell Helicopter XV-3 and XV-15 experimental aircraft - Lessons learned p 835 A90-48859
- [AIAA PAPER 90-3265] p 835 A90-48859
- A self-compensating aircraft recovery system (SCARS) [AIAA PAPER 90-3273] p 818 A90-48864
- CONDOR - high altitude long endurance (HALE) autonomously piloted vehicle (APV) p 836 A90-48866
- [AIAA PAPER 90-3279] p 836 A90-48866
- Reconfigurable aircraft flight control system via robust direct adaptive control p 868 A90-49111
- [AIAA PAPER 90-3226] p 868 A90-49111
- Propulsion system design specifications based on STOVL flight control requirements p 839 A90-49112
- [AIAA PAPER 90-3227] p 839 A90-49112
- The implementation of STOVL task-tailored control modes in a fighter cockpit p 839 A90-49114
- [AIAA PAPER 90-3229] p 839 A90-49114
- Analyzing manipulator and feel system effects in aircraft flight control p 934 A90-51154
- Classification and reduction of pilot error p 24 N90-10014
- [NASA-CR-181867] p 24 N90-10014
- Real-time support for high performance aircraft operation p 57 N90-10075
- [NASA-CR-185475] p 57 N90-10075
- The active flexible wing aeroservoelastic wind-tunnel test program p 33 N90-10119
- The active control of an unstable canard aircraft p 57 N90-10894
- Robust control design for flight control p 119 N90-11756
- [AD-A211957] p 119 N90-11756
- Evolution of flight commands in Aeritalia design p 120 N90-11759
- [ETN-89-95211] p 120 N90-11759
- Integration of a centralized multiplexed control unit into the cockpit of an aircraft p 120 N90-12622
- [F6150-DT410-1-88329] p 120 N90-12622
- Aircraft SAR simulation Sargen 1.0 p 135 N90-12823
- [FEL-1989-44] p 135 N90-12823
- Aerodynamics of thrust vectoring p 172 N90-13354
- [NASA-CR-185074] p 172 N90-13354
- A knowledge-based system design/information tool for aircraft flight control systems p 217 N90-13990
- [NASA-TM-101704] p 217 N90-13990
- Laboratory test methodology for evaluating the effects of electromagnetic disturbances on fault-tolerant control systems p 217 N90-14061
- [NASA-TM-101665] p 217 N90-14061
- Design of a spanloader cargo aircraft p 184 N90-14216
- [NASA-CR-186046] p 184 N90-14216
- Turbulence effects of aircraft flight dynamics and control p 258 N90-15055
- Aircraft performance enhancement with active compressor stabilization p 249 N90-15097
- [AD-A213652] p 249 N90-15097
- Relative merits of reactive and forward-look detection for wind-shear encounters during landing approach for various microburst escape strategies p 259 N90-15108
- [NASA-TM-4158] p 259 N90-15108
- Experimental evaluation of impedance control for robotic aircraft refueling p 337 N90-16755
- [AD-A215532] p 337 N90-16755
- Results of aircraft open-loop tests of an experimental magnetic leader cable system for guidance during roll-out and turnoff p 348 N90-16768
- [NASA-TM-4135] p 348 N90-16767
- Design of integrated pitch axis for autopilot/autothrottle and integrated lateral axis for autopilot/yaw damper for NASA TSRV airplane using integral LQG methodology p 348 N90-16768
- [NASA-CR-4268] p 348 N90-16768
- Stability characteristics of a combat aircraft with control surface failure p 350 N90-17646
- [AD-A216196] p 350 N90-17646
- Hypercube expert system shell-applying production parallelism p 377 N90-18173
- [AD-A215762] p 377 N90-18173
- Possible piloting techniques at hypersonic speeds p 415 N90-18392
- [ISL-CO-216/88] p 415 N90-18392
- Practical methods for robust multivariable control p 462 N90-18920
- [AD-A216937] p 462 N90-18920
- Unsteady aerodynamics of delta wings performing maneuvers to high angle of attack p 398 N90-19196
- Joint University Program for Air Transportation Research, 1988-1989 p 468 N90-20921
- [NASA-CP-3063] p 468 N90-20921
- Neural networks for aircraft control p 521 N90-20937
- Perspectives on the use of rule-based control p 521 N90-20940
- Optimization and guidance of flight trajectories in the presence of windshear p 574 N90-21747
- [NASA-CR-186163] p 574 N90-21747
- The insertion of human dynamics models in the flight control loops of V/STOL research aircraft. Appendix 2: The optimal control model of a pilot in V/STOL aircraft control loops p 598 N90-21776
- [NASA-CR-186598] p 598 N90-21776
- An adaptive human response mechanism controlling the V/STOL aircraft. Appendix 3: The adaptive control model of a pilot in V/STOL aircraft control loops p 598 N90-21777
- [NASA-CR-186599] p 598 N90-21777

- Application of numerical optimization techniques to control system design for nonlinear dynamic models of aircraft p 593 N90-23032
- Preliminary airworthiness evaluation of the RC-12K [AD-A219545] p 648 N90-23387
- Actuated forebody strakes [NASA-CASE-LAR-13983-1] p 648 N90-23390
- An investigation of the use of singular perturbation methods and modal control theory in the derivation of aircraft control schemes [MATHS-REPT-A-106] p 758 N90-26014
- Aerodynamic/dynamic interaction [AD-A222263] p 815 N90-26798
- Past, present and future: Aircraft integrated monitoring systems: An ever-developing technology p 848 N90-27618
- Performance assessment of MIL-STD-1553B on the avionics systems demonstrator rig of British Aerospace p 849 N90-27624
- Aerodynamics of Combat Aircraft Controls and of Ground Effects [AGARD-CP-465] p 920 N90-28513
- Combat aircraft control requirements p 934 N90-28515
- Control research in the NASA high-alpha technology program p 934 N90-28516
- Combat aircraft control requirements for agility p 935 N90-28517
- Effective optimal control of a fighter aircraft engine p 928 N90-28548
- A sensor stabilization/tracking system for unmanned air vehicles [AD-A224008] p 936 N90-28579
- An expert system to perform on-line controller restructuring for abrupt model changes [NASA-TM-103609] p 964 N90-29121
- Evaluation for DLC-Flap Monitoring System of the VSRA [NAL-TM-607] p 928 N90-29391
- Short period control using angular acceleration feedback: Compensation for first lag servo [NAL-TM-600] p 936 N90-29399
- AIRCRAFT DESIGN**
- An objective methodology for definition and evaluation of advanced avionics architectures [AIAA PAPER 89-3035] p 36 A90-10535
- The aerodynamic assistant [AIAA PAPER 89-3132] p 75 A90-10608
- Computer-aided design of flight vehicle instrument bays --- Russian book p 76 A90-10837
- Air Force smart structures/skins program overview p 38 A90-11205
- The birth of the airplane: The first designs and constructions --- Russian book p 79 A90-12478
- History of the airframe. IV p 30 A90-12791
- Development and application of a computer-based system for conceptual aircraft design --- Book p 30 A90-12860
- Airplane design. Part 1 - Preliminary sizing of airplanes --- Book p 30 A90-12866
- Airplane design. Part 2 - Preliminary configuration design and integration of the propulsion system --- Book p 30 A90-12867
- Airplane design. Part 3 - Layout design of cockpit, fuselage, wing and empennage: Cutaways and inboard profiles --- Book p 30 A90-12868
- Airplane design. Part 4 - Layout design of landing gear and systems --- Book p 31 A90-12869
- Airplane design. Part 5 - Component weight estimation --- Book p 31 A90-12870
- Airplane design. Part 6 - Preliminary calculation of aerodynamic, thrust and power characteristics --- Book p 31 A90-12871
- Airplane design. Part 7 - Determination of stability, control and performance characteristics: Far and military requirements --- Book p 57 A90-12872
- Materials and structures for hypersonic vehicles p 31 A90-13015
- Structural optimization of lifting surfaces with divergence and control reversal constraints p 127 A90-13770
- General Dynamics F-16 p 100 A90-13791
- Propeller development for the Rutan Voyager [SAE PAPER 891034] p 100 A90-14341
- Designing the next generation flying test bed [SAE PAPER 891049] p 100 A90-14353
- Automated aircraft configuration design and analysis [SAE PAPER 891072] p 101 A90-14368
- Designing the V-22 'Osprey' tiltrotor V/STOL aircraft for maintenance and serviceability [SAE PAPER 891075] p 101 A90-14369
- Enhanced combat damage tolerance/supportability for improved combat sustainability [SAE PAPER 891078] p 101 A90-14370
- Design for maintainability [SAE PAPER 891079] p 81 A90-14371
- Beech Starship interior noise experimental studies [SAE PAPER 891082] p 101 A90-14374
- Structural analysis of the horizontal tail surfaces of subsonic transport aircraft p 102 A90-14556
- Stress-strain analysis of structural elements of incompressible or nearly incompressible materials by the finite element method p 129 A90-14557
- Increasing the heat conductivity of elastic damping elements of MR material p 102 A90-14580
- Aeroelastic characteristics of wings in subsonic flow p 102 A90-14615
- The Soviets' French revelation. II - Aircraft p 81 A90-14800
- Innovation in general aviation p 81 A90-14997
- Wing boundary layer calculation and its application to aircraft design p 84 A90-15151
- Leading edge flap influence on aerodynamic efficiency p 85 A90-15240
- Advantage Airbus? p 102 A90-15746
- Airframe structural design: Practical design information and data on aircraft structures --- Book p 103 A90-16624
- A refined optimality criterion technique applied to aircraft wing structural design p 206 A90-16718
- Numerical simulation of separated and vortical flows on bodies at large angles of attack p 146 A90-16772
- The relevance of unsteady aerodynamics for highly maneuverable and agile aircraft p 146 A90-16775
- The computer aided weight engineering of aircraft - (CAWE) system p 179 A90-16860
- SPF/DB takes off p 208 A90-17293
- Aircraft design: A conceptual approach --- Book p 179 A90-17307
- Boeing 720B design modification challenges p 179 A90-17309
- HSCT research focuses on environmental issues p 143 A90-17780
- Direct search method to aeroelastic tailoring of a composite wing under multiple constraints p 208 A90-17865
- Fighter design from the Soviet perspective [AIAA PAPER 89-2074] p 181 A90-18135
- The critical role of aerodynamic heating effects in the design of hypersonic vehicles p 155 A90-18249
- The application and design of large integral panels for SH-5 aircraft p 211 A90-18632
- Preliminary results from a subsonic high-angle-of-attack flush airdata sensing (HI-FADS) system - Design, calibration, algorithm development, and flight test evaluation [AIAA PAPER 90-0232] p 187 A90-19746
- AIAA Lighter-Than-Air Systems Technology Conference, 8th, Jacksonville, FL, Oct. 5-7, 1989, Technical Papers p 221 A90-20576
- An AEW metalclad airship [AIAA PAPER 89-3158] p 244 A90-20579
- Preliminary feasibility study for a new hybrid airship (Heliship) [AIAA PAPER 89-3161] p 244 A90-20581
- A new hybrid LTA vehicle, 'Heliship' - Its philosophy, outline [AIAA PAPER 89-3162] p 244 A90-20582
- A new type of non-rigid airship system [AIAA PAPER 89-3175] p 244 A90-20583
- Modern technology in airship design [AIAA PAPER 89-3169] p 244 A90-20584
- Control configured airship design [AIAA PAPER 89-3170] p 244 A90-20585
- Parametric sizing of modern naval airships [AIAA PAPER 89-3171] p 244 A90-20586
- Design criteria, constructions, and materials for the Dornier 328 airframe p 246 A90-21610
- A calculation method for ducted propellers p 226 A90-21626
- Stowing the tilt-rotor p 246 A90-21703
- Cockpit evolution in Airbus Scenarion 2000 p 247 A90-22434
- [MBB-UD-560/89] p 222 A90-22698
- Aircraft of unconventional configuration (2nd revised and enlarged edition) --- Russian book p 247 A90-22734
- Dynamic properties of a system for the roll control of a model electromagnetically suspended in a wind tunnel p 262 A90-22762
- Sizing up the Stealth --- B-2 bomber aircraft p 247 A90-23200
- Minimizing life cycle cost for subsonic commercial aircraft p 283 A90-23282
- The application of the discrete vortex method in aircraft design p 257 A90-23357
- Selection of the blended wing configuration for light aircraft p 234 A90-23401
- Prediction of the strength-related reliability of structural elements at the design stage p 274 A90-23402
- Design for assembly of aerospace structures - A qualitative, interactive approach [SME PAPER MS89-158] p 222 A90-23683
- Aerodynamic design methods for transonic wings p 293 A90-23978
- Efficient structural material distribution in the main frame of a flight vehicle p 363 A90-24092
- Application of the MARS system in aircraft-structure design p 374 A90-24127
- Supersonic flight vehicles --- Russian book p 299 A90-24233
- Stealth - Deception, evasion, and concealment in the air --- Book p 285 A90-24265
- Aviation Week editor flies Soviet-based MiG-29 fighter p 334 A90-24964
- B-2 aerodynamic design [AIAA PAPER 90-1802] p 334 A90-25174
- The role of computational fluid dynamics (CFD) in aircraft design [AIAA PAPER 90-1801] p 335 A90-25175
- European research and testing facilities requested for participation to SST/HST projects [ONERA, TP NO. 1990-12] p 351 A90-25358
- The design of supersonic aircraft and space vehicles by using global optimization techniques p 353 A90-25781
- Unified optimal criterion method - Combination of direction of gradient and ejection line p 367 A90-26077
- Design of low Reynolds number airfoils. I p 307 A90-26129
- Efficient method for computing transonic and supersonic flows about aircraft p 307 A90-26132
- Design for hypersonic speed p 335 A90-26343
- Design priorities for an air-superiority fighter p 335 A90-26344
- Application of a three-dimensional finite element grid generation scheme for an F-16 aircraft configuration p 336 A90-26541
- Navier-Stokes computations useful in aircraft design [AIAA PAPER 90-1800] p 315 A90-27311
- Creditable commuter --- civil aircraft p 405 A90-27975
- A practical flight path for microwave-powered airplanes p 429 A90-28007
- A review of the V-22 dynamics validation program p 406 A90-28155
- Optimization of rotor performance in hover and axial flight using a free wake analysis p 407 A90-28175
- Designers as users - Design supports based on crew system design practices p 457 A90-28184
- Unique methodology used in the Bell-Boeing V-22 main landing gear landing loads analysis and drop tests p 409 A90-28236
- V-22 aerodynamic loads analysis and development of loads alleviation flight control system p 410 A90-28239
- Aerodynamic design of the V-22 Osprey propotor p 385 A90-28241
- Tiltrotor aeroservoelastic design methodology at BHTI p 410 A90-28244
- Aerodynamics of human-powered flight p 386 A90-28552
- A study of the strength characteristics of a twin-fuselage aircraft with a trapezoid wing system p 410 A90-28993
- The use of automated parametric analysis for selecting efficient structural schemes for wings p 410 A90-29191
- Exploratory design studies using an integrated multidisciplinary synthesis capability for actively controlled composite wings [AIAA PAPER 90-0953] p 411 A90-29238
- Evaluation of current multiobjective optimization methods for aerodynamic problems using CFD codes [AIAA PAPER 90-0955] p 411 A90-29240
- Static aeroelastic behavior of an adaptive laminated piezoelectric composite wing [AIAA PAPER 90-1078] p 412 A90-29386
- Pilot report - MiG-29 p 413 A90-29661
- The all-composite airframe - Design and certification p 413 A90-29890
- Composite certification for commercial aircraft p 382 A90-29892
- Massively parallel computing p 458 A90-29897
- Virtual principles in aircraft structures. Volume 1 - Analysis. Volume 2 - Design, plates, finite elements --- Book p 452 A90-29977
- A status review of non-helicopter V/STOL aircraft development. I p 413 A90-30117
- Fly-by-wire controls key to 'pure' stealth aircraft --- F-117A Aircraft p 413 A90-30222
- Fundamentals of the design and development of parts and mechanisms for flight vehicles --- Russian book p 414 A90-30275
- Digital simulation of flight control systems for post-stall aircraft p 431 A90-30704
- Flying qualities lessons learned - 1988 p 431 A90-30705

Sukhoi and Gulfstream go supersonic --- joint development of business aircraft p 383 A90-31247
 Static stability and control characteristics of scissor wing configurations p 433 A90-31277
 Integrated structure/control concepts for oblique wing roll control and trim p 433 A90-31282
 Subcomponent tests for composite fuselage technology readiness p 490 A90-33105
 Design flutter calculations on PC p 545 A90-33379
 An analytical sensitivity method for use in integrated aeroservoelastic aircraft design p 517 A90-33405
 Starship - A model for future designs p 493 A90-33714
 Onboard maintenance system testing - The Boeing 747-400 Central Maintenance Computer [AIAA PAPER 90-1303] p 505 A90-33917
 Flight testing for aircraft agility [AIAA PAPER 90-1308] p 519 A90-33918
 Half transport aircraft cryogenic model for T2 wind tunnel p 524 A90-34242
 The vortex flap F-106B, overcoming safety and data problems in flight testing [AIAA PAPER 90-1280] p 496 A90-34725
 Agility as a contribution to design balance --- in fighter aircraft [AIAA PAPER 90-1305] p 579 A90-35300
 Water borne again p 579 A90-35846
 Flight beyond normal limits p 589 A90-35847
 Yakovlev strikes back p 579 A90-35848
 Some aspects of the control system and power unit lead tests using in-flight simulator systems and flying test-beds [AIAA PAPER 90-1323] p 580 A90-36031
 A study on mechanical model of the helicopter 'ground resonance' p 580 A90-36423
 A status review of non-helicopter V/STOL aircraft development. II p 580 A90-38028
 V-22 developmental status p 581 A90-38529
 Low speed maneuverability and agility design considerations for V/STOL aircraft p 581 A90-38536
 Development of the XV-15 tiltrotor research aircraft - Lessons learned p 581 A90-38540
 Boundary-element shape optimization system for aircraft structural components p 680 A90-39786
 Fatigue methodology III; Proceedings of the AHS National Technical Specialists' Meeting on Advanced Rotorcraft Structures, Scottsdale, AZ, Oct. 3-5, 1989 p 641 A90-39976
 Considerations of reliability design for rotorcraft p 680 A90-39977
 Designing rotorcraft dynamic components to reliability requirements p 641 A90-39978
 YF-23A previews design features of future fighters p 643 A90-40344
 Strake camber and thickness design procedure for low alpha supersonic flow p 622 A90-40678
 Static aeroelastic tailoring for oblique wing lateral trim p 667 A90-40689
 Technological preparations of civil aircraft programs p 617 A90-41110
 Design and analysis aid for evaluating aircraft structures p 694 A90-41188
 Critical review of design philosophies for recent transport WIG effect vehicles --- Wing-in Ground p 684 A90-41753
 Requirements for business jet aircraft [AIAA PAPER 90-2038] p 644 A90-41991
 Airframe/propulsion integration of supersonic cruise vehicles [AIAA PAPER 90-2151] p 644 A90-42047
 Exploration of concepts for multi-role fighters [AIAA PAPER 90-2276] p 644 A90-42104
 Integrated air vehicle/propulsion technology for a multirole fighter - A MCAIR perspective [AIAA PAPER 90-2278] p 644 A90-42105
 Propulsion system-flight control integration-flight evaluation and technology transition [AIAA PAPER 90-2280] p 644 A90-42106
 A remote tip-driven fan powered supersonic fighter concept [AIAA PAPER 90-2415] p 663 A90-42167
 Preliminary design and analysis of propellers p 645 A90-42407
 Eurofar - Status of the European tilt-rotor project p 645 A90-42441
 Principles underlying the integration of an aircraft and its engine --- Russian book p 729 A90-42520
 The Dash 8 Series 400 regional airliner p 729 A90-42664
 Some considerations in ultra light aircraft design p 730 A90-42673
 Demonstrating technologies for enhanced fighter manoeuvrability - The Rockwell/MBB X-31 p 731 A90-43767
 Mirage 2000 - A French success that is no illusion p 731 A90-43768

Civil supersonics - A less distant thunder p 731 A90-44223
 Parametric aeroelastic stability analysis of a generic X-wing aircraft p 731 A90-44737
 Supersonic STOVL - The future is now p 732 A90-44781
 Aerodynamic design considerations for aircraft radomes [AIAA PAPER 90-2843] p 711 A90-45163
 Technology issues for high-speed civil transports [SAE PAPER 892201] p 778 A90-45422
 The effect of solidity on propeller normal force [SAE PAPER 892205] p 713 A90-45424
 Douglas aging aircraft programs [SAE PAPER 892206] p 732 A90-45425
 Maintenance and economic benefits of non-painted aircraft operations [SAE PAPER 892208] p 732 A90-45427
 Design and certification of the all-composite airframe [SAE PAPER 892210] p 732 A90-45429
 Flight deck modernization [SAE PAPER 892231] p 732 A90-45447
 Application considerations for integral gas turbine electric starter/generator revisited [SAE PAPER 892252] p 746 A90-45454
 Rotary servoing actuator [SAE PAPER 892261] p 733 A90-45458
 A VSAERO analysis of several canard configured aircraft. II [SAE PAPER 892287] p 714 A90-45465
 Application of divergent trailing-edge airfoil technology to the design of a derivative wing [SAE PAPER 892288] p 714 A90-45466
 Thick airfoil designs for a HALE vehicle --- High Altitude Long Endurance [AIAA PAPER 90-3036] p 791 A90-45875
 Design of supersonic wings using an optimization strategy coupled with a solution scheme for the Euler equations [AIAA PAPER 90-3060] p 794 A90-45895
 The role of CFD applied to high performance aircraft [AIAA PAPER 90-3071] p 796 A90-45917
 Design and experimental investigation of a laminar horizontal tail [AIAA PAPER 90-3042] p 798 A90-45934
 Old lamps for new - A photoelastic design tool for weight and cost saving on aircraft structures p 878 A90-46039
 The design of a low Reynolds number RPV p 828 A90-46385
 Sensitivity analysis in the design of composite structures p 880 A90-46478
 Identification of a stress-strain computation model and planning of tensometry points in strength and stability studies p 880 A90-46482
 Wing design optimization under stress-strain constraints using full-strength and minimum mass criteria p 804 A90-46554
 Optimum aircraft design: Multipurpose approach --- Russian book p 829 A90-46618
 The impact of total quality management (TQM) and concurrent engineering on the aircraft design process p 785 A90-46927
 The evolution of design/development requirements for avionics/mission equipment (MEP) insertion p 846 A90-46932
 Optimal camber distributions with multiple constraints p 810 A90-48078
 Vertical tail design for base-line configuration of military combat aircraft p 810 A90-48080
 Airbrake design for base-line configuration of advanced jet trainers/light attack airplanes and military combat airplanes p 810 A90-48081
 Flying the giant --- An-124 Ruslan aircraft p 833 A90-48522
 Certificating the Speed Canard p 833 A90-48699
 Integrated product development (IPD) at General Dynamics FORTH Worth [AIAA PAPER 90-3192] p 786 A90-48828
 Thick-wing spanloader all-freighter - A design concept for tomorrow's air cargo [AIAA PAPER 90-3198] p 834 A90-48831
 The Hiller X-18 experimental aircraft - Lessons learned [AIAA PAPER 90-3203] p 834 A90-48832
 The Canadair CL-84 experimental aircraft - Lessons learned [AIAA PAPER 90-3205] p 834 A90-48833
 Conceptual design and feasibility study of very large passenger aircraft [AIAA PAPER 90-3220] p 834 A90-48841
 Preliminary design of a supersonic short takeoff and vertical landing (STOVL) fighter aircraft [AIAA PAPER 90-3231] p 834 A90-48844

The AVRO VZ-9 experimental aircraft - Lessons learned [AIAA PAPER 90-3237] p 835 A90-48847
 The Hawker P1127 vectored thrust fighter program - Lessons learned [AIAA PAPER 90-3238] p 835 A90-48848
 Design of a close-support aircraft [AIAA PAPER 90-3241] p 835 A90-48849
 Ride quality criteria for the B-2 bomber [AIAA PAPER 90-3256] p 835 A90-48852
 Analytic models for technology integration in aircraft design [AIAA PAPER 90-3262] p 835 A90-48857
 Subsystem thermal integration - A new challenge to the aircraft designer [AIAA PAPER 90-3274] p 836 A90-48865
 Comparison of equivalent plate and finite element analysis of a realistic aircraft structural configuration [AIAA PAPER 90-3293] p 837 A90-48877
 The BAe (commercial aircraft) LTD transport aircraft synthesis and optimisation program (TASOP) [AIAA PAPER 90-3295] p 837 A90-48879
 Advanced rotorcraft V/STOL - Technology needs for high-speed rotorcraft [AIAA PAPER 90-3298] p 837 A90-48880
 Configuring tactical aircraft [AIAA PAPER 90-3305] p 837 A90-48886
 Upgrading the cockpit - A multidisciplinary approach p 848 A90-48995
 Parametric analysis of swept-wing geometry with sheared wing tips [AIAA PAPER 90-3196] p 812 A90-49101
 Design synthesis and optimization of joined-wing transports [AIAA PAPER 90-3197] p 838 A90-49102
 X-wing experimental aircraft - Lessons learned [AIAA PAPER 90-3208] p 838 A90-49105
 CFD needs in conceptual design [AIAA PAPER 90-3209] p 813 A90-49106
 Twin-engine transports - A look at the future [AIAA PAPER 90-3215] p 818 A90-49107
 Taguchi methods in conceptual design for life cycle cost [AIAA PAPER 90-3222] p 839 A90-49109
 A hypersonic research vehicle to develop scramjet engines [AIAA PAPER 90-3232] p 839 A90-49115
 The North American Rockwell XFV-12A - Reflections and some lessons [AIAA PAPER 90-3240] p 839 A90-49118
 The design of a sport aircraft configured to emulate jet fighter characteristics [AIAA PAPER 90-3244] p 839 A90-49119
 CFD support of NASP design [AIAA PAPER 90-3252] p 872 A90-49120
 The (airplane) design professor as shepherd - An industry role in enhancing engineering education [AIAA PAPER 90-3259] p 897 A90-49121
 A method for lifting surface design using nonlinear optimization [AIAA PAPER 90-3290] p 813 A90-49122
 A efficient technique for multiobjective design optimization [AIAA PAPER 90-3291] p 892 A90-49123
 STOVL option for the multi-role fighter [AIAA PAPER 90-3296] p 840 A90-49124
 Selected design issues of some high speed rotorcraft concepts [AIAA PAPER 90-3297] p 840 A90-49125
 Aircraft subsystem waste energy recovery and management [SAE PAPER 901218] p 840 A90-49293
 ATF prototypes outstrip F-15 in size and thrust p 841 A90-49477
 Gripen wins its wings --- Swedish JAS39 aircraft testing and development p 842 A90-49823
 Commuter from Khodinka --- IL-114 airliner p 842 A90-49824
 Starship sails through p 842 A90-49825
 Application of the 'K-gage' to aircraft structural testing p 926 A90-49891
 Design of aircraft wings subjected to gust loads - A system reliability approach p 958 A90-52044
 High temperature VSCF (Variable Speed Constant Frequency) generator system [AD-A210823] p 71 N90-10351
 Turbulence management: Application aspects p 72 N90-10378
 Low-speed, high-lift aerodynamic characteristics of slender, hypersonic accelerator-type configurations [NASA-TP-2945] p 20 N90-10830
 See and avoid/cockpit visibility [DOT/FAA/CT-TN89/18] p 24 N90-10843
 ATTAS flight testing experiences p 34 N90-10862
 P-180 AVANTI: Project and flight test program comprehensive overview p 34 N90-10863

- The Experimental Aircraft Flight Test Programme p 34 N90-10865
- Flight test techniques adopted by Avions Marcel Dassault-Breguet Aviation p 34 N90-10867
- Flight testing and flight research: From the age of the tower jumper to the age of the astronaut p 35 N90-10882
- Integrated multidisciplinary design optimization of rotorcraft
- [NASA-TM-101642] p 36 N90-10889
- Wind tunnel test of CAD USB-STOL semi-borne prototype
- [NAL-TM-566] p 88 N90-11696
- Computer simulation of aircraft aerodynamics
- [NASA-TM-102221] p 88 N90-11699
- Development of direct-inverse 3-D methods for applied transonic aerodynamic wing design and analysis
- [NASA-CR-186036] p 103 N90-11733
- A design procedure for the handling qualities optimization of the X-29A aircraft
- [NASA-TM-4142] p 119 N90-11753
- Evolution of flight commands in Aeritalia design
- [ETN-89-95211] p 120 N90-11759
- Stall/spin/flight simulation
- [DOT/FAA/CT-88/28] p 122 N90-11765
- The aerodynamic experimental center of Aeritalia: Combat aircraft group
- [ETN-89-95213] p 122 N90-11766
- Choice and characterization of new materials for aerospace applications
- [ETN-89-95219] p 126 N90-11819
- The evolution of light alloys in the aerospace industry
- [ETN-89-95216] p 126 N90-11872
- General data processing support from project planning to workshop control
- [MBB-UD-526/88-PUB] p 138 N90-12208
- On the occasion of the 100th birthday of Ernst Heinkel
- [MBB/LW/3015/S/PUB/321] p 141 N90-12494
- LFC: A maturing concept
- [DOUGLAS-PAPER-7878] p 90 N90-12505
- Lockheed laminar-flow control systems development and applications
- p 90 N90-12506
- Laminar flow: The Cessna perspective
- p 91 N90-12507
- Long-range LFC transport
- p 104 N90-12508
- Development flight tests of JetStar LFC leading-edge flight test experiment
- p 104 N90-12509
- The right wing of the LEFT airplane
- p 91 N90-12510
- Research in Natural Laminar Flow and Laminar-Flow Control, part 2
- [NASA-CP-2487-PT-2] p 91 N90-12519
- Research in Natural Laminar Flow and Laminar-Flow Control, part 3
- [NASA-CP-2487-PT-3] p 92 N90-12539
- The design of an airfoil for a high-altitude, long-endurance remotely piloted vehicle
- p 104 N90-12545
- The 757 NLF glove flight test results
- p 104 N90-12546
- Nacelle design
- p 105 N90-12551
- Project, implementation, and utilization of composite structures
- [ETN-89-95209] p 127 N90-12665
- Study of high-speed civil transports
- [NASA-CR-4235] p 183 N90-13370
- The S.D.G., P.S.D. and the nonlinear airplane
- [NLR-MP-88018-U] p 183 N90-13371
- Efficient methods for integrated structural-aerodynamic wing optimum design
- p 184 N90-13376
- California air transportation study: A transportation system for the California Corridor of the year 2010
- [NASA-CR-186219] p 176 N90-14212
- Design of a spanloader cargo aircraft
- [NASA-CR-186046] p 184 N90-14216
- Preliminary design of four aircraft to service the California Corridor in the year 2010: The California Condor, California Sky-Hopper, high capacity short range transport tilt rotor aircraft needed to simplify intercity transportation
- [NASA-CR-186232] p 186 N90-14226
- Canard versus aft-tail ride qualities performance and pilot command response
- p 258 N90-15053
- The interference of flightmechanical control laws with those of load alleviation and its influence on structural design
- p 258 N90-15054
- Turbulence effects of aircraft flight dynamics and control
- p 258 N90-15055
- Aircraft performance enhancement with active compressor stabilization
- [AD-A213652] p 249 N90-15097
- Aluminum-lithium: Application of plate and sheet to fighter aircraft
- p 268 N90-15202
- Application of Lagrangian blending functions for grid generation around airplane geometries
- [NASA-CR-186318] p 237 N90-15891
- Fuel Tank Technology
- [AGARD-R-771] p 250 N90-15904
- The repair of aircraft integral fuel tanks in the RAF: A user's view of fuel tank technology
- p 250 N90-15908
- Integral fuel tank certification and test methods
- p 251 N90-15916
- Semi-empirical transition criteria for the design of laminar profiles
- p 276 N90-16174
- The use of prototypes in selected foreign fighter aircraft development programs: Rafale, EAP, Lavi, and Gripen
- [AD-A214500] p 287 N90-16707
- NASA supercritical airfoils: A matrix of family-related airfoils
- [NASA-TP-2969] p 315 N90-16710
- Analysis of indirect effects of lightning on a metallic A 300 wing: Test report
- [REPT-E87/645800] p 323 N90-16726
- Preliminary design of a family of three close air support aircraft
- [NASA-CR-186070] p 336 N90-16751
- Preliminary results from a subsonic high angle-of-attack flush airdata sensing (HI-FADS) system: Design, calibration, and flight test evaluation
- [NASA-TM-101713] p 339 N90-16758
- The integration of stores on modern tactical aircraft: Where we have been, and what we should do for the future
- p 337 N90-17552
- Objectives and results of cabin fire research in Germany
- p 325 N90-17588
- Characteristics of transport, aircraft fires measured by full-scale tests
- p 325 N90-17591
- Aircraft internal fires
- p 326 N90-17593
- Hot surface ignition studies of aviation fluids
- p 327 N90-17600
- US Navy aircraft fire protection technology
- p 327 N90-17603
- Fire hardening of an aircraft passenger cabin
- p 328 N90-17606
- Advanced materials for interior and equipment related to fire safety in aviation
- p 328 N90-17608
- The technology challenge of the advanced tactical fighter: A study of the technology transition process
- [AD-A216109] p 338 N90-17630
- GTDT/UTD: Brief history of successive development of theory and recent advances. Applications to antennas on ships and aircraft
- p 370 N90-17939
- Research on a two-dimensional inlet for a supersonic V-STOL propulsion system. Appendix A
- [NASA-CR-174945] p 396 N90-18364
- Fuselage design for a specified Mach-sliced area distribution
- [NASA-TP-2975] p 414 N90-18385
- Influence of forebody geometry on aerodynamic characteristics and a design guide for defining departure/spin resistant forebody configurations
- [AD-A216714] p 414 N90-18388
- Analysis and design of symmetrical airfoils
- [PD-CF-8943] p 400 N90-19213
- Flow simulation for aircraft
- [NLR-MP-87082-U] p 455 N90-19543
- A note on an acoustic response during an engine nacelle flight experiment
- [NASA-TM-102585] p 464 N90-19821
- Implications of Advanced Technologies for Air and Spacecraft Escape
- [AGARD-CP-472] p 483 N90-20054
- Development of an ejection seat specification for a new fighter aircraft
- p 483 N90-20057
- Compression pylon
- [NASA-CASE-LAR-13777-1] p 498 N90-20078
- The NASA digital VGH program. Exploration of methods and final results. Volume 1: Development of methods
- [NASA-CR-181909-VOL-1] p 505 N90-20081
- The NASA digital VGH program. Exploration of methods and final results. Volume 3: B 727 data 1978-1980: 1765 hours
- [NASA-CR-181909-VOL-3] p 505 N90-20082
- The NASA digital VGH program. Exploration of methods and final results. Volume 4: B 747 data 1978-1980, 1689 hours
- [NASA-CR-181909-VOL-4] p 506 N90-20083
- The NASA digital VGH program. Exploration of methods and final results. Volume 5: DC 10 data 1981-1982, 129 hours
- [NASA-CR-181909-VOL-5] p 506 N90-20084
- Aerofoil design techniques
- p 500 N90-20978
- A system for transonic wing design with geometric constraints based on an inverse method
- p 501 N90-20983
- Numerical optimization of wings in transonic flow
- p 502 N90-20997
- Aerodynamic design via control theory
- p 546 N90-20998
- Conceptual design optimization study
- [NASA-CR-4298] p 582 N90-21755
- Design and testing of a multiblock grid-generation procedure for aircraft design and research
- p 582 N90-21984
- Multiblock topology specification and grid generation for complete aircraft configurations
- p 582 N90-21986
- Feature-associated mesh embedding for complex configurations
- p 608 N90-21988
- Aircraft crash survival design guide. Volume 1: Design criteria and checklists
- [AD-A218434] p 575 N90-22545
- Aircraft crash survival design guide. Volume 2: Aircraft design crash impact conditions and human tolerance
- [AD-A218435] p 575 N90-22546
- Aircraft technology management and the related significance of the supercomputer
- p 612 N90-22975
- The use of supercomputers for the design and analysis of constructions
- p 612 N90-22977
- The automation management to support research and development
- p 612 N90-22978
- Design trends for Army/Air Force airplanes in the United States
- [NASA-TM-4179] p 615 N90-23338
- Aircraft drawings index
- p 618 N90-23340
- Preliminary design of a supersonic Short Takeoff and Vertical Landing (STOVL) fighter aircraft
- [NASA-CR-186670] p 649 N90-23394
- AVION: A detailed report on the preliminary design of a 79-passenger, high-efficiency, commercial transport aircraft
- [NASA-CR-186663] p 649 N90-23395
- High speed civil transport
- [NASA-CR-186661] p 649 N90-23396
- Feasibility study for a microwave-powered ozone sniffer aircraft
- [NASA-CR-186660] p 650 N90-23397
- Nonflammable hydraulic power system for tactical aircraft. Volume 1: Aircraft system definition, design and analysis
- [AD-A218493] p 671 N90-23409
- Conceptual design for aerospace vehicles
- p 651 N90-25043
- Design of a low cost short takeoff-vertical landing export fighter/attack aircraft
- [NASA-CR-186658] p 734 N90-25132
- From 1959-1989: 30 years of service experience with ramjets
- [PNR90677] p 748 N90-25139
- Prediction methodologies for nonlinear aerodynamic characteristics of control surfaces
- [NIAR-90-17] p 718 N90-25937
- Technical evaluation report on the Fluid Dynamics Panel Symposium on Computational Methods for Aerodynamic Design (Inverse) and Optimization
- [AGARD-AR-267] p 720 N90-25947
- Formation of design envelope criterion in terms of deterministic spectral procedure
- [RAE-TM-SS-9] p 721 N90-25953
- Feasibility study for a microwave-powered ozone sniffer aircraft, volume 2
- [NASA-CR-186676] p 735 N90-25967
- Global Sentry: NASA/USRA high altitude reconnaissance aircraft design, volume 2
- [NASA-CR-186820-VOL-2] p 736 N90-25971
- A contribution to the economic, optimal dimensioning, and shaping of aircraft structures using a design model
- [ETN-90-96966] p 737 N90-25976
- Towards 2000: The composite engine
- [PNR90646] p 750 N90-26000
- Prediction of rotating disc flow and heat transfer in gas turbine engines
- [PNR90650] p 750 N90-26001
- A computer module used to calculate the horizontal control surface size of a conceptual aircraft design
- [NASA-CR-186872] p 780 N90-26515
- Lessons learned from the T-46A durability and damage tolerance program
- p 842 N90-26812
- Photoelasticity: A cost effective design tool
- p 883 N90-26819
- The SKY SHARK: An RPV designed to investigate the pressure distribution on a lifting surface
- [NASA-CR-186222] p 844 N90-26824
- Active control of aerothermoelastic effects for a conceptual hypersonic aircraft
- [NASA-TM-102713] p 869 N90-27725
- Impact of Emerging NDE-NDI Methods on Aircraft Design, Manufacture, and Maintenance
- [AGARD-CP-462] p 885 N90-28068
- Inspection reliability
- p 885 N90-28072
- Impact of NDE-NDI methods on aircraft design, manufacture, and maintenance, from the fundamental point of view
- p 887 N90-28093
- Hypersonic Arbitrary-Body Aerodynamics (HABA) for conceptual design
- [DE90-014750] p 910 N90-28495
- Combat aircraft control requirements for agility
- p 935 N90-28517

- Effects of canard position on the aerodynamic characteristics of a close-coupled canard configuration at low speed. p 920 A90-28519
- Innovative control concepts and component integration for a generic-supercruise fighter. p 935 A90-28521
- Control of vortex aerodynamics at high angles of attack. p 921 A90-28523
- Inflight thrust vectoring: A further degree of freedom in the aerodynamic/flight mechanical design of modern fighter aircraft. p 921 A90-28528
- Dynamic ground effects. p 922 A90-28531
- Determination of the ground effect on the characteristics of the A320 aircraft. p 922 A90-28534
- Life cycle cost in the conceptual design of subsonic commercial aircraft, volumes 1 and 2. p 923 A90-28535
- System reliability optimization of aircraft wings. p 923 A90-28536
- The aerodynamic design of the oblique flying wing supersonic transport [NASA-CR-177552]. p 923 A90-28540
- Energy efficient engine program technology benefit/cost study, volume 2. p 931 A90-28565
- [NASA-CR-174766-VOL-2]. p 931 A90-28565
- A knowledge-based system design/information tool [NASA-CR-4316]. p 965 A90-29143
- Some topics in computational transonic aerodynamics: Revision. p 912 A90-29332
- [NAL-TR-1018T]. p 912 A90-29332
- Aircraft evacuations: The effect of passenger motivation and cabin configuration adjacent to the exit [CAA-PAPER-89019]. p 913 A90-29336
- Aircraft design for mission performance using nonlinear multiobjective optimization methods [NASA-CR-4328]. p 925 A90-29384
- WingDesign: Program for the structural design of a wing cross-section [LR-627]. p 925 A90-29390
- AIRCRAFT DETECTION**
- Concept of an MTI search radar. p 487 A90-33613
- Passive location and tracking using DOA and TOA measurements of single nonmaneuvering observer. p 576 A90-35709
- EH101 Advance Technology Rotorcraft low detectability/good neighbor design. p 579 A90-35774
- Performance assessment for airborne surveillance systems incorporating sensor fusion. p 583 A90-37088
- Neural networks for adaptive shape tracking. p 638 A90-39959
- Use of pulse radars for helicopters detection - Design constraints. p 683 A90-41073
- A nonlinear aircraft tracking filter utilizing control variable estimation [AIAA PAPER 90-3402]. p 822 A90-47657
- Comparison of 1-D and 2-D aircraft images. p 927 A90-52884
- AIRCRAFT ENGINES**
- The study of the theoretical calculation method for power stall dynamic characteristics of multiple-engine propeller airplane. p 29 A90-10349
- Fundamentals of turbine design for aircraft engines --- Russian book. p 40 A90-10839
- 3D calculations of reacting flows within aircraft engine combustion chambers [ONERA, TP NO. 1989-153]. p 67 A90-11173
- Three-dimensional modeling of turbulent transonic flow at the exit of a twin engine [AAAF PAPER NT 88-16]. p 4 A90-11434
- Aircraft compressor flutter analysis. p 41 A90-11797
- Flutter of cascade blades composed of blades having arbitrarily different natural frequencies. p 42 A90-11798
- The flutter characteristic analysis and optimization design of mistuning blade. p 42 A90-11799
- The features of FJR 710 engine. p 42 A90-12011
- Mechanical rig test of FJR 710/600 engine components. p 43 A90-12016
- International Symposium on Air Breathing Engines, 9th, Athens, Greece, Sept. 3-8, 1989, Proceedings, Volumes 1 & 2. p 43 A90-12501
- Highly loaded axial flow compressors - History and current developments. p 44 A90-12503
- Swedish philosophy in aeroengine development. p 44 A90-12504
- The active control of engine instabilities. p 44 A90-12505
- Some issues in the growth of small gas turbine aircraft propulsion engines. p 44 A90-12508
- Hydrogen fueled subsonic-ram-combustor model tests for an air-turbo-ram engine. p 44 A90-12529
- Experimental study of static pressure and mean velocity profiles inside a two-dimensional dump-type combustor model. p 45 A90-12530
- A study of two-phase flow for a ramjet combustor. p 45 A90-12532

- Material requirements for future aeroengines. p 62 A90-12534
- Extending the overhaul interval for gas turbine engines through the use of alternative coatings on first stage blades. p 63 A90-12539
- Design and off-design performance predictions of axial turbines. p 45 A90-12540
- Controlled mixing and variable geometry combustor design effects on emissions and combustion characteristics. p 45 A90-12547
- The performance of a small combustor operated over a wide range of conditions. p 45 A90-12548
- Aircraft engine vibration analysis. p 46 A90-12568
- Three dimensional numerical simulation for an aircraft engine type combustion chamber [ONERA, TP NO. 1989-120]. p 49 A90-12591
- Study of advanced technology impact on cycle characteristics and aircraft sizing (using multivariable optimization techniques). p 29 A90-12612
- Gearless crisp - The logical step to economic engines for high thrust. p 50 A90-12616
- Engine diagnostics - An application for expert system concepts. p 50 A90-12632
- Airplane design, Part 6 - Preliminary calculation of aerodynamic, thrust and power characteristics --- Book. p 31 A90-12871
- Materials and structures for hypersonic vehicles. p 31 A90-13015
- Augmented heat transfer in rectangular channels of narrow aspect ratios with rib turbulators. p 70 A90-13091
- A discrete dynamic model of the crankshaft-aircrew assembly of an aircraft piston engine for the purpose of vibration analysis by the method of finite elements. p 51 A90-13220
- Numerical simulation of valveless pulsed combustors. p 127 A90-13767
- Endurance of aircraft gas turbine mainshaft ball bearings-analysis using improved fatigue life theory. II - Application to a bearing operating under difficult lubrication conditions. p 128 A90-13845
- History of aircraft piston engine oils - The last forty years [SAE PAPER 891037]. p 124 A90-14343
- Design and development of the Garrett F109 turbofan engine [SAE PAPER 891046]. p 109 A90-14350
- Garrett TPF351-20 turboprop fan engine development [SAE PAPER 891047]. p 109 A90-14351
- The variable cycle diesel as an aircraft engine [SAE PAPER 891065]. p 110 A90-14365
- Simulation of a turbocompound two-stroke diesel engine [SAE PAPER 891066]. p 110 A90-14366
- Validation of the accelerated equivalent testing of gas turbine engines for multivariant applications. p 110 A90-14568
- A minimal permissible radial clearance in a gas turbine. p 110 A90-14569
- Estimation of the technical risk criterion in selecting the operating parameters of aircraft gas turbine engines. p 110 A90-14570
- The principle of jet engine thrust generation. p 110 A90-14571
- Effect of pressure on the electrophysical properties of two-phase flows in nozzles. p 110 A90-14572
- Design of a language for the testing of aircraft engines. p 137 A90-14573
- Determination of the effective areas of the mixing exhaust ducts of a bypass engine from autonomous test results. p 102 A90-14584
- Effect of the radial clearance on the efficiency of a partial microturbine. p 111 A90-14586
- Calculation of vibrational combustion limits in Helmholtz resonator-type chambers. p 125 A90-14588
- Operation of a compressor with intermediate air bleed. p 111 A90-14589
- Effect of the angle of attack on the efficiency and thrust ratio of axial-flow microturbines with full admission. p 111 A90-14590
- Classification of methods for eliminating surging in gas turbine engines. p 111 A90-14591
- An investigation into the internal heat transfer characteristics of a thermally anti-cold aero-engine intake lipskin. p 111 A90-15390
- Applied technology in gas turbine aircraft engine development. p 112 A90-16001
- XXG40 - Rolls-Royce advanced fighter engine demonstrator. p 112 A90-16002
- Squeeze film damping for aircraft gas turbines. p 113 A90-16009
- Diffusion bonding aeroengine components. p 131 A90-16012
- Dynamics of aviation gas turbine engines --- Russian book. p 113 A90-16049

- The VSCF system has arrived - The way in which a new constant-frequency electrical generation system in aeronautics has been developed. p 187 A90-16696
- Sharing power and profit. p 188 A90-16701
- CHS-IHPTET spawns engines for 21st century. p 188 A90-16702
- Aeroengine condition monitoring and fault diagnosis system. p 188 A90-16851
- A component modal synthesis technique for the lateral vibration analysis of aircraft engine systems. p 179 A90-16983
- TBCs for better engine efficiency --- thermal barrier coatings. p 203 A90-17294
- Aircraft propulsion systems technology and design --- Book. p 188 A90-17308
- Cost effective technology --- CAD/CAM techniques for aircraft engines. p 188 A90-17447
- Application of computational systems to aircraft engine components development. p 188 A90-17448
- Atomization and spray research for gas turbine engines. p 189 A90-17688
- Jet futures. p 190 A90-18526
- A study of ground vortex. p 158 A90-18590
- Gas turbine engine condition monitoring and fault diagnostics. p 190 A90-18594
- Digital control experiment research on the engine JT15D-4. p 190 A90-18600
- The eigenvalue sensitivity analysis and design for integrated flight/propulsion control systems. p 196 A90-18601
- Three dimensional photoelastic analysis of aeroengine parts. p 270 A90-20077
- Gas turbine combustion - A personal perspective. p 283 A90-20604
- Thermodynamics and the future turbine engines [ONERA, TP NO. 1989-165]. p 253 A90-21031
- Parametric studies of advanced turboprops. p 253 A90-21225
- Oils for flight turbine engines - Research and development in the 90s. p 266 A90-21473
- Some aspects of the erosive wear of components of aircraft turbine engines. p 253 A90-21627
- Hydrogen propulsion and the next century - A challenge that raises questions and problems. p 266 A90-21774
- Infrared sources of jet propulsion system and their suppression. p 252 A90-22614
- A study of the working process and losses in annular turbine nozzle cascades with a low contraction ratio. p 254 A90-23407
- Optimal selection of the parameters to be measured during the identification of gas turbine engines. I - Problem statement. p 255 A90-23410
- Effect of the control of turbocompressor guide vanes on the throttle characteristics of a bypass engine. p 255 A90-23425
- A method for the computer-aided hydraulic analysis of the turbine cooling systems of aviation gas turbine engines. p 255 A90-23430
- Effect of reduced aft diameter and increased blade number of high-speed counterrotation propeller performance [AIAA PAPER 89-0438]. p 234 A90-23650
- The properties and characteristics of electroless nickel coatings applied to gas turbine engine components [ASME PAPER 89-GT-4]. p 354 A90-23751
- Overview on test cases for computation of internal flows in turbomachines [ASME PAPER 89-GT-46]. p 288 A90-23772
- Vibration analysis for immediate assessment of battle-damaged gas turbine engines [ASME PAPER 89-GT-96]. p 341 A90-23811
- An automatic system for the programmed control of the parameters of the vibrational and thermal testing of the blades of gas turbine engines. p 343 A90-24216
- Burner rig hot corrosion of silicon carbide and silicon nitride. p 355 A90-25267
- beta CEZ, a high performance titanium alloy for aerospace engines [ONERA, TP NO. 1990-8]. p 356 A90-25356
- Computational and experimental analysis of transonic fanjet engine flow field using 3-D Euler code. p 306 A90-25809
- Acoustic characteristics of counterrotating unducted fans from model scale tests. p 378 A90-26138
- Basic approach in the development of TURBISTAN, a loading standard for fighter aircraft engine disks. p 368 A90-26754
- Metal matrix composites - Ready for take-off? p 356 A90-26865
- Swirling flow in thrust nozzles. p 421 A90-27962
- Use of swirl for flow control in propulsion nozzles. p 421 A90-27963
- Adaptive elective fuel control test techniques. p 421 A90-28168

- Advanced technology's impact on compressor design and development - A perspective
[SAE SP-800] p 423 A90-28571
- Composites boost 21st-century aircraft engines
p 442 A90-29704
- Cleaner superalloys via improved melting practices
p 442 A90-29707
- Gear vibration control with viscoelastic damping material in aeroengine
p 451 A90-29911
- Digital electronic control for WJ6G4A engine
p 424 A90-29919
- Modelling and simulation of turboprop engine behaviour
p 424 A90-29946
- Coatings for high temperature corrosion in aero and industrial gas turbines
p 443 A90-30479
- A very high speed switched-reluctance starter-generator for aircraft engine applications
p 452 A90-30791
- Design of an aero-engine thrust reverser blocker door
p 467 A90-31651
- Propulsion systems for supersonic V/STOL aircraft
[ASME PAPER 89-GT-309] p 507 A90-32259
- Configuration E-7 supersonic fighter/attack technology program
[ASME PAPER 89-GT-308] p 490 A90-32260
- A method of sizing multi-cycle engines for hypersonic aircraft
[ASME PAPER 89-GT-281] p 507 A90-32261
- Evaluation of control techniques for aircraft propulsion systems
p 507 A90-32262
- Multivariable control of jet engines
p 507 A90-32421
- A model gas turbine combustor with wall jets and optical access for turbulent mixing, fuel effects, and spray studies
p 507 A90-32808
- Investigation of cowl vent slots for supercritical stability enhancement in dual-mode ramjet inlets
p 507 A90-32951
- Endurance of aircraft gas turbine mainshaft ball bearings-analysis using improved fatigue life theory. I - Application to a long-life bearing
p 537 A90-33557
- Surface roughness measurements on gas turbine blades
[ASME PAPER 89-GT-285] p 508 A90-33559
- Influence of fuel drop size and combustor operating conditions on pollutant emissions
p 508 A90-33591
- The next AIAA engine design competition - A commercial engine
[AIAA PAPER 89-2258] p 550 A90-33675
- F-15E/GE-129 Increased Performance Engine initial development flight test program
[AIAA PAPER 90-1266] p 509 A90-33894
- An expert system for real-time aircraft monitoring
[AIAA PAPER 90-1311] p 545 A90-33921
- Thermomechanical processing of superalloys
p 531 A90-34156
- Fiber reinforced superalloys
p 532 A90-34169
- Rotary damping in aircraft motion due to jet propulsion system
p 520 A90-34820
- Microstructures of rapidly-solidified binary TiAl alloys
p 532 A90-34990
- Aeroelastic instabilities in aircraft engines - Application to a SNECMA fan stage
p 584 A90-35174
- Gas turbine engines for combat aviation - Current realities and perspectives for the near future
p 584 A90-35513
- Wide chord fan club
p 584 A90-35600
- Simulation research on the afterburning dynamic characteristics of engine control system
p 585 A90-35708
- Study on process control of aeroengine using microcomputer
p 586 A90-37239
- Development of a simulated bird-strike test method --- of aircraft turbine engine fan blade materials
p 600 A90-37444
- A status review of non-helicopter V/STOL aircraft development. II
p 580 A90-38028
- Control of a switched-reluctance aircraft engine starter-generator over a very wide speed range
p 586 A90-38130
- Technology update of early gas turbine designs
p 586 A90-38531
- Progress in certifying F402-RR-408 - The improved Pegasus engine for AV-8B and Harrier II Plus
p 587 A90-38532
- Tilt rotor requirements on engine design and qualification
p 587 A90-38534
- V-22 engine installation and removal tool - Designing support equipment with the aircraft, not after
p 581 A90-38538
- Power transfer devices for V/STOL convertible engine systems
p 587 A90-38539
- Expert diagnosis system for FJR engine troubles
p 587 A90-38597
- Total temperature separation in jets
[AIAA PAPER 90-1621] p 607 A90-38750
- UV spectroradiometric output of an F404 turbojet aircraft engine
p 652 A90-40195
- Application of leaned blades to an aeroengine
p 654 A90-40503
- Acoustic characteristics of a research step combustor
[AIAA PAPER 90-1851] p 655 A90-40530
- Numerical simulation of the behaviour of internal combustion supercharged engines
[AIAA PAPER 90-1873] p 655 A90-40539
- Identification of multivariable models of jet engines
[AIAA PAPER 90-1874] p 655 A90-40540
- Design of digital self-selecting multivariable controllers for jet engines
[AIAA PAPER 90-1875] p 655 A90-40541
- Computational modeling of inlet hamshock wave generation
[AIAA PAPER 90-2005] p 621 A90-40592
- Glass-ceramic matrix composites for advanced gas turbines
[AIAA PAPER 90-2014] p 676 A90-40594
- Fiber-optic turbine inlet temperature measurement system (FOTITMS)
[AIAA PAPER 90-2033] p 657 A90-40603
- High-temperature electronics for aircraft engines
[AIAA PAPER 90-2035] p 657 A90-40604
- The application of an expert maintenance and diagnostic tool to aircraft engines
[AIAA PAPER 90-2036] p 657 A90-40605
- Full authority digital electronic engine control system provides needed reliability
[AIAA PAPER 90-2037] p 658 A90-40606
- Convertible engine system for high speed rotorcraft
[AIAA PAPER 90-2512] p 658 A90-40643
- Rationale for determining information associated with aircraft gas turbine engines that is of historical importance
[AIAA PAPER 90-2754] p 617 A90-40648
- Aircraft engine technology gets a second wind
p 659 A90-41166
- Applying qualitative knowledge to aircraft engine system design
p 694 A90-41189
- Developmental tests on the M 88 engine are on track
p 660 A90-41761
- Automated aircraft engine costing using artificial intelligence
[AIAA PAPER 90-1887] p 660 A90-41981
- Design and analysis of a large-plug inlet ADP nacelle and pylon --- Advanced Ducted Prop
[AIAA PAPER 90-2015] p 673 A90-41986
- Development of high temperature actuation systems for advanced aircraft engines
[AIAA PAPER 90-2031] p 660 A90-41990
- GE's CF34 engine for business and regional jets
[AIAA PAPER 90-2041] p 661 A90-41992
- Viscous flow analysis for advanced inlet particle separators
[AIAA PAPER 90-2136] p 661 A90-42038
- Inclement weather induced aircraft engine power loss
[AIAA PAPER 90-2169] p 662 A90-42055
- Direct lift STOVL engine integration
[AIAA PAPER 90-2274] p 644 A90-42103
- Initiation of spalling in aircraft gas turbine bearings
[AIAA PAPER 90-2291] p 686 A90-42110
- Trend analysis and diagnostics codes for training purposes
[AIAA PAPER 90-2394] p 617 A90-42156
- The promise of advanced materials for a 21st century UBE --- ultrahigh bypass ratio engine
[AIAA PAPER 90-2396] p 662 A90-42157
- Ultra high bypass turbofan technologies for the twenty-first century
[AIAA PAPER 90-2397] p 662 A90-42158
- Propulsion control system designs for advanced Navy multimission aircraft
[AIAA PAPER 90-2403] p 663 A90-42160
- JFS190 turbine engine performance optimized using Taguchi methods
[AIAA PAPER 90-2419] p 663 A90-42169
- Engineering design models for ramjet efficiency and lean blowoff
[AIAA PAPER 90-2453] p 663 A90-42176
- CFE738 - A case for joint engine development
[AIAA PAPER 90-2522] p 664 A90-42197
- Turbine configuration impact on advanced IHPTET engine system mission capabilities
[AIAA PAPER 90-2739] p 664 A90-42221
- Co-development of CT7-6 engines - A continued tradition in technology and reliability
p 665 A90-42485
- Principles underlying the integration of an aircraft and its engine --- Russian book
p 729 A90-42520
- Performance improvement of an eroded axial flow compressor using water injection
[AIAA PAPER 90-2016] p 741 A90-42718
- Aircraft propulsion control systems for the next century
[AIAA PAPER 90-2034] p 742 A90-42720
- Transient behavior of supersonic flow through inlets
[AIAA PAPER 90-2130] p 704 A90-42734
- Application of advanced materials to aircraft gas turbine engines
[AIAA PAPER 90-2281] p 764 A90-42769
- Optimization studies for the PW305 turbofan
[AIAA PAPER 90-2520] p 744 A90-42813
- The LF500 and the regional airline market
[AIAA PAPER 90-2521] p 744 A90-42814
- The GMA 2100 and GMA 3007 engines for regional aircraft
[AIAA PAPER 90-2523] p 744 A90-42815
- The history of aviation engine development in the USSR and the 60th anniversary of CIAM
[AIAA PAPER 90-2761] p 783 A90-42828
- The propan ... What future now?
p 744 A90-43763
- The standard-setting Hornet
p 730 A90-43764
- Wide-chord fan proved in nearly five years of service
p 744 A90-44594
- Advanced developments of the Turbo-Union RB199
p 745 A90-44595
- Future development of the 535E4 engine
p 745 A90-44596
- Propulsion systems for the '90s
p 745 A90-44605
- Aircraft engine inspection
p 771 A90-44606
- Mathematical simulation model of an aircraft gas turbine
p 745 A90-44721
- Digital servomechanism for the tachometer of the M 602 engine
p 737 A90-44722
- Catalytic conversion of oil in bleed air - A maintenance tool
[SAE PAPER 892214] p 732 A90-45431
- Considerations for successful application of integrated drive generators to aircraft
[SAE PAPER 892226] p 746 A90-45442
- Power system for 21st century fighter aircraft
[SAE PAPER 892253] p 746 A90-45455
- Designing and tuning the digital controller of an electronic fuel control unit for small gas turbine engines
[SAE PAPER 892255] p 747 A90-45457
- Considerations in using broad specification fuels for aircraft propulsion
[SAE PAPER 892330] p 765 A90-45487
- V2500 turbofan engine
[SAE PAPER 892363] p 747 A90-45512
- The PW2000 - A mature engine with an eye to the future
[SAE PAPER 892365] p 748 A90-45514
- Prediction and measurement of rotor blade/stator vane dynamic characteristics of a modern aero-engine axial compressor
p 878 A90-46036
- Design of computer-aided aircraft testing systems. II
p 785 A90-46498
- Interchangeability of Soviet-made and foreign mineral oils for aviation gas turbine engines
p 873 A90-46525
- Technical and economic efficiency of aviation gas turbine engines in service --- Russian book
p 851 A90-46624
- Power struggle --- Advanced Tactical Fighter engine proposals
p 851 A90-46650
- NASA's HITEMP program for UHBR engines
[AIAA PAPER 90-2395] p 852 A90-47218
- Combustor technology for future aircraft
[AIAA PAPER 90-2400] p 852 A90-47219
- Titanium aluminides for advanced aircraft engines
p 874 A90-49000
- Twin-engine transports - A look at the future
[AIAA PAPER 90-3215] p 818 A90-49107
- Aerostructural considerations for the power plant of overlapping wing configuration
p 841 A90-49488
- The survivability of centrifugal compressors in modern aircraft engines
p 928 A90-49883
- Structural and dynamic analysis of the A330/340 composite RAT blade --- ram air turbine
p 942 A90-50083
- Aspects of the design of a hypersonic engine system and the selection of the intake and tail
[DGLR PAPER 88-040] p 928 A90-50233
- Automotive gasoline - A fuel for modern aircraft piston engines
p 950 A90-51620
- Ethanol and methanol in intermittent combustion engines
p 950 A90-51622
- A proposal for fuel specification activities relating to general aviation intermittent combustion engines
p 951 A90-51625
- Airbus technologies - An evolutionary process
p 902 A90-52699
- A supersonic through-flow fan engine airframe integration study
[NASA-CR-185140] p 18 A90-10004
- Full scale technology demonstration of a modern counterrotating unducted fan engine concept: Component test
[NASA-CR-180868] p 53 A90-10047

- Full scale technology demonstration of a modern counterrotating unducted fan engine concept. Design report
[NASA-CR-180867] p 53 N90-10048
- Full scale technology demonstration of a modern counterrotating unducted fan engine concept. Engine test
[NASA-CR-180869] p 53 N90-10049
- Combustor influence on fighter engine operability -
p 64 N90-10193
- Dynamic instability characteristics of aircraft turbine engine combustors p 53 N90-10195
- Advanced technologies impact on compressor design and development: A perspective
[NASA-TM-102341] p 54 N90-10891
- Future military powerplants --- fighter aircraft engines
[PNR90554] p 114 N90-11749
- Aluminium alloy development for aero engines
[PNR90548] p 126 N90-11874
- Flanged joints of aeroengines
[PNR90594] p 116 N90-12609
- Aviation Engine Test Facilities (AETF) fire protection study
[AD-A211483] p 134 N90-12777
- Effect of reduced aft diameter and increased blade number on high-speed counterrotation propeller performance
[NASA-TM-102077] p 172 N90-13352
- Study of the engine bird ingestion experience of the Boeing 737 aircraft
[DOT/FAA/CT-89/16] p 176 N90-13360
- X.2 limited flight test plan
[AD-A214412] p 249 N90-15099
- An experimental investigation of thrust vectoring two-dimensional convergent-divergent nozzles installed in a twin-engine fighter model at high angles of attack
[NASA-TM-4155] p 237 N90-15884
- Using goal programming to determine the optimal engine mix for UH-1 helicopters
[AD-A214893] p 343 N90-16762
- Analysis of hydraulic fluids and lubricating oils for the formation of Trimethylolpropane Phosphate (TMP-P)
[AD-A215188] p 357 N90-16939
- AGARD/SMP Review: Damage Tolerance for Engine Structures. 2: Defects and Quantitative Materials Behaviour --- conference
[AGARD-R-769] p 425 N90-18396
- In-flight evaluations of turbine fuel extenders
[DOT/FAA/CT-89/33] p 444 N90-19387
- Structural tailoring of select fiber composite structures
[NASA-TM-102484] p 533 N90-21137
- Attachment of lead wires to thin film thermocouples mounted on high temperature materials using the parallel gap welding process
[NASA-TM-102442] p 543 N90-21361
- Aeropropulsion facilities configuration control: Procedures manual
[NASA-TM-102541] p 543 N90-21399
- Control of flow separation and mixing by aerodynamic excitation
[NASA-TM-103131] p 571 N90-21733
- Preliminary development of an intelligent computer assistant for engine monitoring
[NASA-TM-101702] p 612 N90-22322
- Preliminary airworthiness evaluation of the RC-12K
[AD-A219545] p 648 N90-23387
- Fatigue crack growth investigation of a Ti-6Al-4V forging under complex loading conditions: NATO/AGARD supplemental engine disk program
[AD-A220239] p 678 N90-23538
- Processing of advanced ceramics which have potential for use in gas turbine aero engines
[AD-A220988] p 766 N90-25226
- Stage 2 re-engining: The only way to achieve a real stage 3 aircraft
[PNR90636] p 737 N90-25977
- Towards 2000: The composite engine
[PNR90646] p 750 N90-26000
- Prediction of rotating disc flow and heat transfer in gas turbine engines
[PNR90650] p 750 N90-26001
- Prediction and measurement of rotor blade/stator vane dynamic characteristics of a modern aero-engine axial compressor
[PNR90667] p 750 N90-26002
- The impact and requirements of new materials on aeroengines
[PNR90671] p 750 N90-26003
- Aircraft exhaust emissions: An engine manufacturer's perspective
[PNR90675] p 750 N90-26004
- Handbook of uncertainty methodology for engine testing at Pyestock (England)
[RAE-TM-P-1179] p 751 N90-26007
- Metal matrix composites and powder processing for aero-engine applications
[PNR90617] p 767 N90-26087
- NDT in aerospace: The next decade (1990's)
[PNR90628] p 777 N90-26348
- Elevated temperature crack growth
[NASA-CR-182247] p 777 N90-26355
- Bringing aircraft noise testing down to Earth
[PNR90642] p 783 N90-26637
- Effective optimal control of a fighter aircraft engine
p 928 N90-28548
- Energy efficient engine program technology benefit/cost study. Volume 1: Executive summary
[NASA-CR-174766-VOL-1] p 931 N90-28564
- Energy efficient engine program technology benefit/cost study, volume 2
[NASA-CR-174766-VOL-2] p 931 N90-28565
- Energy Efficient Engine: Control system preliminary definition report
[NASA-CR-179578] p 932 N90-28569
- High Temperature Surface Interactions.
[AGARD-CP-461] p 951 N90-28698
- Fretting fatigue strength of Ti-6Al-4V at room and elevated temperatures and ways of improving it
p 952 N90-28709
- Audibility and annoyance of en route noise of unducted fan engines
[AD-A223687] p 966 N90-30035
- ### AIRCRAFT EQUIPMENT
- Radar systems of aircraft --- Russian book
p 26 A90-10841
- Electrostatic description of a positive leader ignition from an aircraft
[ONERA, TP NO. 1989-149] p 23 A90-11171
- A small inert gas generator
p 180 A90-17405
- An advanced pneumatic impulse ice protection system (PIIP) for aircraft
[AIAA PAPER 90-0492] p 182 A90-19875
- Design of computer-aided testing systems for aviation equipment. I
p 222 A90-23416
- Aviation equipment --- Russian book
p 338 A90-24200
- The selection of actuation devices for aircraft pneumatic valves in systems under computer control
[SAE PAPER 891456] p 368 A90-27425
- Mechanical considerations for reliable interfaces in next generation electronics packaging
p 453 A90-30813
- Characteristics of 5x5 and 6x6 inch taut shadow mask CRTs for cockpit displays
p 737 A90-45239
- Aircraft measurements of sea surface conditions and their relationship to marine boundary-layer dynamics
p 888 A90-47572
- Subsystem thermal integration - A new challenge to the aircraft designer
[AIAA PAPER 90-3274] p 836 A90-48865
- Aeronautical fatigue in the electronic era; Proceedings of the Fifteenth ICAF Symposium, Jerusalem, Israel, June 21-23, 1989
p 901 A90-49876
- Airborne digital computers and systems --- Russian book
p 927 A90-52410
- Electro-impulse de-icing testing analysis and design
[NASA-CR-4175] p 32 N90-10031
- Meeting Review: Workshop on Airborne Instrumentation
[PB89-174775] p 39 N90-10032
- Numerical simulation of aeroplane response to a lightning injection
[ETN-89-95271] p 96 N90-11716
- Acoustic recording systems for use in military aircraft
[RAE-TM-MM-11] p 140 N90-13207
- Results of aircraft open-loop tests of an experimental magnetic leader cable system for guidance during roll-out and turnoff
[NASA-TM-4135] p 348 N90-16767
- Failure analysis handbook
[AD-A219747] p 689 N90-23752
- Multichannel on-board load and fatigue monitoring
p 849 N90-27621
- AIMS test and simulation equipment
p 892 N90-27623
- Performance assessment of MIL-STD-1553B on the avionics systems demonstrator rig of British Aerospace
p 849 N90-27624
- Integrated Air Traffic Management
[DLR-MITT-89-23] p 825 N90-27676
- A reliable, maintenance-free oxygen sensor for aircraft using an oxygen-sensitive coating on potentiometric electrodes
[AD-A22696] p 927 N90-28545
- ### AIRCRAFT FUEL SYSTEMS
- Fire deaths in aircraft without the crashworthy fuel system
p 22 A90-10266
- Integral fuel tanks - design, production, aging, repair
p 250 N90-15906
- ### AIRCRAFT FUELS
- Atomization of synthetic jet fuel
p 63 A90-12602
- Straight alcohol fuels for general aviation aircraft
[SAE PAPER 891038] p 124 A90-14344
- Laboratory analysis of antiwear properties of turbine-engine fuels
p 131 A90-15878
- Effect of pressure and temperature on residue formation in aviation kerosenes
p 203 A90-17281
- Development of a heavy fuel engine for an unmanned air vehicle
[AIAA PAPER 90-2170] p 662 A90-42056
- Experimental turbofan using liquid hydrogen and liquid natural gas as fuel
[AIAA PAPER 90-2421] p 663 A90-42170
- Considerations in using broad specification fuels for aircraft propulsion
[SAE PAPER 892330] p 765 A90-45487
- Future fuels for general aviation; Proceedings of the Symposium on Future Fuels for General Aviation Intermittent Combustion, Baltimore, MD, June 29, 1988
[ASTM STP-1048] p 950 A90-51616
- Manufacturing aviation gasoline
p 950 A90-51617
- Aircraft field experience with automotive gasoline in the United States
p 912 A90-51618
- Field experience with type certificated civil aircraft operated on motor gasolines and worldwide survey of motor gasoline characteristics
p 912 A90-51619
- Automotive gasoline - A fuel for modern aircraft piston engines
p 950 A90-51620
- The performance of alternate fuels in general aviation aircraft
p 950 A90-51621
- Ethanol and methanol in intermittent combustion engines
p 950 A90-51622
- Investigations into gasoline/alcohol blends for use in general aviation aircraft
p 950 A90-51623
- Future use of automotive gasoline in light aircraft
p 951 A90-51624
- A proposal for fuel specification activities relating to general aviation intermittent combustion engines
p 951 A90-51625
- Aircraft fuel tank construction and testing experience
p 250 N90-15907
- The repair of aircraft integral fuel tanks in the RAF: A user's view of fuel tank technology
p 250 N90-15908
- Ignitability of jet-A fuel vapors in aircraft fuel tanks
p 326 N90-17594
- The stability of fuel fires
p 327 N90-17601
- Production of high density aviation fuels via novel zeolite catalyst routes
[AD-A216444] p 443 N90-18601
- Low-energy gamma ray attenuation characteristics of aviation fuels
[NASA-TP-2974] p 462 N90-18882
- Turbine fuel alternatives (near term)
[AD-A219405] p 601 N90-22695
- Micro separator and ball-on-cylinder lubricity evaluator tests or corrosion inhibitor/lubricity improver additives
[AD-A221339] p 766 N90-25228
- Advanced fuel properties, phase 1
[AD-A219788] p 766 N90-25236
- Study of high-speed civil transports. Summary
[NASA-CR-4236] p 735 N90-25966
- Development of a mathematical model for the thermal decomposition of aviation fuels
[AD-A221673] p 875 N90-26994
- ### AIRCRAFT GUIDANCE
- Acceleration, gamma, and theta guidance for abort landing in a windshear
p 98 A90-14733
- Digital map for helicopter navigation and guidance
p 252 A90-21609
- Aircraft program motion along a predetermined trajectory. I - Mathematical modelling
p 345 A90-23979
- Design considerations for achieving MLS Category III requirements
p 331 A90-25575
- Fully automatic guidance for rotorcraft nap-of-the-earth (NOE) flight following planned profiles
p 403 A90-28219
- Automatic landing with GPS - Design of the flight guidance and flight control system
[AIAA PAPER 90-1301] p 487 A90-33915
- Improved guidance and control of vehicles and personnel on the ground will benefit airport traffic capacity
p 760 A90-44549
- Simulator evaluation of 'basic' mode back azimuth issues in departure and missed approach usage
[SAE PAPER 892216] p 728 A90-45433
- AIAA Guidance, Navigation and Control Conference, Portland, OR, Aug. 20-22, 1990, Technical Papers. Parts 1 & 2
p 862 A90-47576
- Application of energy turn g-limiting for aircraft high performance turns
[AIAA PAPER 90-3328] p 862 A90-47590
- Real-time piloted simulation of fully automatic guidance and control for rotorcraft nap-of-the-earth (NOE) flight following planned profiles
[AIAA PAPER 90-3372] p 864 A90-47630

- Artificial intelligence (AI) based tactical guidance for fighter aircraft
[AIAA PAPER 90-3435] p 889 A90-47688
- Guidance simulation and test support for differential GPS flight experiment
[NASA-CR-177471] p 28 N90-10021
- Trajectory optimization and guidance for an aerospace plane
[NASA-CR-185884] p 183 N90-13369
- Relative merits of reactive and forward-look detection for wind-shear encounters during landing approach for various microburst escape strategies
[NASA-TM-4158] p 259 N90-15108
- Guidance analysis of the aeroglide plane change maneuver as a turning point problem
[NASA-TM-101639] p 259 N90-15110
- Integrated flight guidance system using differential-GPS for landing approach guidance p 332 N90-16735
- Results of aircraft open-loop tests of an experimental magnetic leader cable system for guidance during roll-out and turnoff
[NASA-TM-4135] p 348 N90-16767
- A head up display format for application to V/STOL aircraft approach and landing
[NASA-TM-102216] p 340 N90-17632
- The Fourteenth Biennial Guidance Test Symposium, volume 1
[AD-A216925] p 405 N90-18383
- Automation of the readout, transcription and evaluation of digital flight data at DLR p 893 N90-27645
- On-board planning and control of 4D-trajectories in the TMA p 826 N90-27680
- Four-dimensional navigation and Flight Management Systems p 826 N90-27681
- Four-dimensional planner: A ground based planning system for time accurate approach guidance p 826 N90-27683
- Description of the primary flight display and flight guidance system logic in the NASA B-737 transport systems research vehicle
[NASA-TM-102710] p 927 N90-28546
- AIRCRAFT HAZARDS**
- Intelligent situation assessment and response aiding in flight emergencies
[AIAA PAPER 89-2999] p 36 A90-10507
- Electromagnetic characterization of lightning on aircraft
[ONERA, TP NO. 1989-131] p 22 A90-11155
- Experimental-theoretical comparison for current injection on an aircraft model
[ONERA, TP NO. 1989-133] p 22 A90-11157
- Electrostatic field conditions on an aircraft stricken by lightning
[ONERA, TP NO. 1989-148] p 23 A90-11170
- Flight over the sea with twin or triple jet aircraft p 179 A90-17048
- A program to improve aircraft icing forecasts
[AIAA PAPER 90-0196] p 216 A90-19733
- Hydrogen propulsion and the next century - A challenge that raises questions and problems p 266 A90-21774
- The effect of experimental uncertainties on icing test results
[AIAA PAPER 90-0665] p 322 A90-26977
- Flight test safety and 'high risk' tests - The Aerialia approach
[AIAA PAPER 90-1315] p 483 A90-33924
- Aircraft Ground Deicing Conference, Denver, CO, Sept. 20-22, 1988, Proceedings
[SAE P-217] p 817 A90-46004
- Highlights of RAE lightning strike investigations p 818 A90-49827
- Comparison of four lightning simulation tests on a composite test bed aircraft p 818 A90-49831
- Comparison of the swept frequency continuous wave, current pulse, and shock-excitation lightning simulation techniques p 818 A90-49832
- An assessment of analytical methods and lightning simulation test techniques used in lightning qualification and surveillance testing p 818 A90-49833
- Final results of the NASA storm hazards program p 819 A90-49834
- Characterization of configuration effects on lightning simulation/qualification testing p 819 A90-49835
- Lightning testing and test analyses of the JAS39 aircraft p 842 A90-49836
- Visualization of corona discharges p 819 A90-49839
- Grumman/FAA lightning study - A potential countermeasure for lightning induced flashblindness of aircrew members p 819 A90-49843
- In-flight aircraft lightning surface current model p 819 A90-49844
- Validation of GEMACS for prediction of lightning induced electromagnetic fields --- General Electromagnetic Model for Analysis of Complex Systems p 819 A90-49845
- The behavior of electric currents in graphite/epoxy structures p 883 A90-49846
- Electric charge acquired by airplanes penetrating thunderstorms p 913 A90-52093
- Remote sensing techniques of the Wave Propagation Laboratory for the measurement of supercooled liquid water: Applications to aircraft icing
[PB89-208102] p 24 N90-10842
- Meeting review: The Second NCAR (National Center for Atmospheric Research) Research Aircraft Fleet Workshop
[PB89-20901] p 137 N90-12113
- The human factors relating to escape and survival from helicopters ditching in water
[AGARD-AG-305(E)] p 176 N90-13358
- Flight in adverse environmental conditions
[AGARD-AR-277] p 185 N90-14218
- Wind shear models for aircraft hazard investigation p 280 N90-15044
- NASA's program on icing research and technology p 239 N90-15062
- Principal characteristics of lightning on aircraft p 239 N90-15067
- International Aircraft Occupant Safety Conference and Workshop proceedings
[AD-A214452] p 239 N90-15085
- The collection of non-conus aircraft icing data along with an identification of the geographical areas of potential severe icing and a study of a method of remote determining atmospheric icing data
[AD-A215055] p 323 N90-16724
- RAAF Orion aircraft A9-300 oxygen fire
[AD-A215496] p 323 N90-16725
- Investigation of air transportation technology at the Massachusetts Institute of Technology, 1988-1989 p 484 N90-20922
- Cockpit display of hazardous wind shear information p 484 N90-20924
- Modeling of surface roughness effects on glaze ice accretion p 485 N90-20925
- Ultrasonic techniques for aircraft ice accretion measurement p 485 N90-20926
- Investigation of surface water behavior during glaze ice accretion p 485 N90-20927
- The influence of ice accretion physics on the forecasting of aircraft icing conditions p 485 N90-20928
- Cockpit display of hazardous weather information p 485 N90-20929
- Advanced instrumentation for aircraft icing research
[NASA-CR-185225] p 506 N90-21006
- Fire hazards of aerosol cans in aircraft cargo compartments
[DOT/FAA/CT-89/32] p 636 N90-23369
- A quantitative technique to estimate microburst wind shear hazard to aircraft p 692 N90-25040
- A NASA/university/industry consortium for research on aircraft ice protection
[IAR-89-18] p 736 N90-25969
- AIRCRAFT HYDRAULIC SYSTEMS**
- Dynamic stiffness of a hydraulic damper in the system of a front landing gear strut p 102 A90-14555
- Generalized relations for estimating the efficiency and basic dimensions of screw pumps and hydraulic turbines of pump units p 111 A90-14583
- A method for the computer-aided hydraulic analysis of the turbine cooling systems of aviation gas turbine engines p 255 A90-23430
- Automated aircraft hydraulics testing p 551 A90-37899
- AIRCRAFT INDUSTRY**
- Installation and implementation of an extrusion cell in aircraft industry utilizing group technology
[SAE PAPER 891025] p 81 A90-14336
- Development of fatigue loading spectra
[ASTM STP-1006] p 367 A90-26751
- The future of the U.S. aircraft industry p 467 A90-32275
- Toward total quality in industry p 684 A90-41768
- The propan... What future now? p 744 A90-43763
- The economics of the organization and the planning of civil aviation --- Russian book p 897 A90-46629
- Innovation and investment for survival and prosperity - The new Battle of Britain --- UK military aircraft industry
[AIAA PAPER 90-3189] p 786 A90-48826
- Implementation of integrated product development --- in aircraft industry
[AIAA PAPER 90-3194] p 786 A90-48829
- A review of Australian and New Zealand investigations on aeronautical fatigue during the period April 1987 to March 1989
[AD-A210373] p 32 N90-10026
- The use of prototypes in selected foreign fighter aircraft development programs: Rafale, EAP, Lavi, and Gripen
[AD-A214500] p 287 N90-16707
- FAA (Federal Aviation Administration) aviation forecasts, fiscal years 1990-2001 p 552 N90-22530
- [AD-A219165] p 552 N90-22530
- Aircraft modifications cost analysis. Volume 1: Overview of the study
[AD-A220764] p 702 N90-25074
- The Federal Aviation Administration plan for research, engineering and development. Volume 1: Program plan
[AD-A221263] p 783 N90-25930
- Radiation-curable prepreg composites
[DE90-629740] p 951 N90-28674
- AIRCRAFT INSTRUMENTS**
- Computer-aided design of flight vehicle instrument bays --- Russian book p 76 A90-10837
- Air Force smart structures/skins program overview p 38 A90-11205
- Fiber optic systems for mobile platforms II: Proceedings of the Meeting, Boston, MA, Sept. 6, 7, 1988
[SPIE-989] p 67 A90-11659
- A review of fiber optic flight experience - Past problems, future direction p 38 A90-11661
- Wavelength division multiplexed fiber optic sensors for aircraft applications p 38 A90-11663
- Toward fly-by-light aircraft p 39 A90-11664
- The performance of linear fiber optic data buses p 68 A90-11665
- Fiber optic sensors for aircraft p 68 A90-11704
- Magnetic recording on board aircraft p 39 A90-12195
- The VSCF system has arrived - The way in which a new constant-frequency electrical generation system in aeronautics has been developed p 187 A90-16696
- A GPS-based flight-control concept p 242 A90-21719
- Aviation equipment --- Russian book p 338 A90-24200
- A review of the V-22 health monitoring system p 417 A90-28209
- Design criteria for helicopter night pilotage sensors p 417 A90-28221
- The microphysical structure of severe downdrafts from radar and aircraft observations in CINDE --- Convection Initiation and Downburst Experiment p 455 A90-28582
- Airborne telemetry trends for the 1990's p 418 A90-28874
- Development of airborne data reduction system in IPTN flight test p 418 A90-28895
- Development of an acceptability window for a ground proximity avoidance system p 419 A90-30730
- Evaluation of sensor management systems p 461 A90-30789
- 3-D in pictorial formats for aircraft cockpits p 420 A90-31331
- Advanced integrated avionics test support concepts
[AIAA PAPER 90-1259] p 504 A90-33889
- Microminiature flight test instrumentation
[AIAA PAPER 90-1274] p 504 A90-33898
- Electronic cartography - A new need for commercial aircraft p 576 A90-35351
- Applications of fiber optic sensors in the aerospace and marine industries p 603 A90-36782
- Equipment and capability trends in Loran-C RNAV p 576 A90-36918
- Performance assessment for airborne surveillance systems incorporating sensor fusion p 583 A90-37088
- The EH101 electronic instrument system p 652 A90-40462
- Multiple model adaptive controller for the STOL F-15 with sensor/actuator failures p 668 A90-40878
- Dual cross-polarization planar arrays in the C and X bands p 638 A90-40979
- Demonstration of MLS advanced approach techniques p 640 A90-41711
- Spectral response of a UV flame sensor for a modern turbojet aircraft engine p 769 A90-43285
- Evaluation of the dynamic characteristics of a helicopter instrument panel p 829 A90-46499
- Eight years of experience with small computerized retrofit load monitoring systems p 926 A90-49882
- Operation of aviation radio and electronic equipment (Handbook) --- Russian book p 914 A90-50747
- Cockpit lighting compatibility with image intensification night imaging systems: Issues and answers
[AD-A210503] p 32 N90-10028
- Optimal integral controller with sensor failure accommodation p 61 N90-10123
- Flight simulator evaluation of a head-down display
[NAL-TM-573] p 59 N90-10898
- Devices and procedures for the calibration of sensors and measurement: Systems of the flight test support system ATTAS
[DFVLR-MITT-89-06] p 134 N90-12007
- Principal characteristics of lightning on aircraft p 239 N90-15067

Display interface concepts for automated fault diagnosis
[NASA-TM-101610] p 252 N90-15102

A simulation evaluation of the engine monitoring and control system display
[NASA-TP-2960] p 420 N90-18393

Three input concepts for flight crew interaction with information presented on a large-screen electronic cockpit display
[NASA-TM-4173] p 420 N90-18394

Simulator comparison of thumbball, thumb switch, and touch screen input concepts for interaction with a large screen cockpit display format
[NASA-TM-102587] p 506 N90-21005

Continued development and analysis of a new extended Kalman filter for the Completely Integrated Reference Instrumentation System (CIRIS)
[AD-A220106] p 654 N90-23400

Qualitative evaluation of a conformational velocity vector display for use at high angles-of-attack in fighter aircraft
[NASA-TM-102629] p 739 N90-25981

Aircraft Integrated Monitoring Systems
[DLR-MITT-90-04] p 786 N90-27617

Past, present and future: Aircraft integrated monitoring systems: An ever-developing technology
p 848 N90-27618

Harrier Information Management System (HIMS): The system and the approach
p 884 N90-27630

AIMS for helicopters
p 820 N90-27639

Airborne CO₂ Doppler lidar for wind shear detection
p 849 N90-27640

The new US flight recorder regulations
p 849 N90-27642

The Canadian Aviation Safety Board's flight recorder facility
p 849 N90-27643

Australian experience in flight recorder readout and analysis
p 820 N90-27644

Automation of the readout, transcription and evaluation of digital flight data at DLR
p 893 N90-27645

Position finding and ground target direction finding by an aircraft with a gimbaled video camera
[DLR-FB-89-62] p 825 N90-27673

AIRCRAFT LANDING

Optimization of helicopter takeoff and landing
p 29 A90-11006

Autoland with GPS
p 97 A90-13985

Beech Starship occupant protection evaluation in emergency landing scenario
[SAE PAPER 891015] p 100 A90-14327

Penetration landing guidance trajectories in the presence of windshear
p 98 A90-14732

Acceleration, gamma, and theta guidance for abort landing in a windshear
p 98 A90-14733

Landing gear integrity - The bottom line of aircraft safety
p 180 A90-17408

Simulation of helicopter landing on a ship deck
p 181 A90-17705

Effect of wind shear on flight safety
p 175 A90-17973

Numerical simulation of the actuation system for the ALDF's propulsion control valve --- Aircraft Landing Dynamics Facility
[AIAA PAPER 90-0079] p 211 A90-19674

A GPS-based flight-control concept
p 242 A90-21719

Differential GPS (DGPS) as an approach and landing aid
p 242 A90-21722

Wind shear and hyperbolic distributions
p 280 A90-23632

Friction measurements under winter runway conditions
p 321 A90-23924

Visual information for simulated landing approaches
p 347 A90-26189

Basic areas of research in the development of a future ATM system --- air traffic management
p 551 A90-35685

Influence of ground effect on helicopter takeoff and landing performance
p 645 A90-42278

Effect of wind shear on the airspeed during the airplane landing approach
[AIAA PAPER 90-2838] p 754 A90-45160

Simulation of MLS-ATC procedures in the New York and San Francisco Terminal Control Areas
[SAE PAPER 892217] p 728 A90-45434

The mythology of first-come-first-serve landing order
p 821 A90-46394

Advanced architecture for domestic and global aviation systems
p 822 A90-46398

A theoretical and experimental investigation into the prerotation of aircraft tires
[AIAA PAPER 90-3272] p 836 A90-48863

Requirements for meteorological equipment designed for the acquisition of meteorological data essential for the takeoff and landing of aircraft at civil airports
p 962 A90-50777

Backside landing control of a STOL aircraft using approximate perfect servo
p 934 A90-52801

A simulation study of landing time allocation procedures for use in computer-assisted air traffic management systems
[AD-A212159] p 99 N90-11722

Ice runways near the South Pole
[AD-A211606] p 133 N90-11908

Autonomous automatic landing through computer vision
p 332 N90-16734

Integrated flight guidance system using differential-GPS for landing approach guidance
p 332 N90-16735

A head up display format for application to V/STOL aircraft approach and landing
[NASA-TM-102216] p 340 N90-17632

Airplane takeoff and landing performance monitoring system
[NASA-CASE-LAR-13734-1-CU] p 526 N90-20096

Runway rubber removal
[AD-A218349] p 526 N90-20100

Optimization and guidance of flight trajectories in the presence of windshear
[NASA-CR-186163] p 574 N90-21747

Dynamic ground-effect measurements on the F-15 STOL and Maneuver Technology Demonstrator (S/MTD) configuration
[NASA-TP-3000] p 573 N90-22531

Preliminary airworthiness evaluation of the RC-12K
[AD-A219545] p 648 N90-23387

Electro-optics engineering support for the integrated launch and recovery television surveillance system
[AD-A223450] p 938 N90-29406

AIRCRAFT LAUNCHING DEVICES

Accelerators and decelerators for large, hypersonic aircraft
[AIAA PAPER 90-1986] p 674 A90-40582

AIRCRAFT LIGHTS

The automatic detection of anti-collision lights
[RSRE-MEMO-4272] p 240 N90-15896

AIRCRAFT MAINTENANCE

APG-70 radar test package development aid
[AIAA PAPER 89-3044] p 1 A90-10624

Aerospace structures supportability
[SAE PAPER 891058] p 129 A90-14360

Design for maintainability
[SAE PAPER 891079] p 81 A90-14371

Aeroengine condition monitoring and fault diagnosis system
p 188 A90-16851

Stronger startlifter
p 143 A90-17919

Safer primers from 3M
p 204 A90-17925

Repair of composite aircraft parts - An operator's viewpoint
p 221 A90-20606

The Robotic Canopy Polishing System
[SME PAPER MS89-134] p 222 A90-23680

Caring for the elderly jet
p 285 A90-24280

Standardization in aerospace plating and coating
[SAE PAPER 890913] p 365 A90-24681

Electromagnetic dent removal for aircraft repair
[SAE PAPER 890923] p 286 A90-24689

Robotic dry stripping of airframes - Phase II
[SAE PAPER 890926] p 365 A90-24691

Automated aircraft paint strip cell
[SAE PAPER 890936] p 286 A90-24699

Automating and controlling dry paint stripping
[SAE PAPER 890939] p 365 A90-24702

Materials get smarter
p 356 A90-27598

A comprehensive diagnostic system for the T800-APW-800 engine
p 422 A90-28181

A review of the V-22 health monitoring system
p 417 A90-28209

Auxiliary power unit maintenance aid - Flight line engine diagnostics
p 382 A90-28348

Emerging new technologies at Sikorsky aircraft
p 382 A90-30114

An adaptive-learning expert system for maintenance diagnostics
p 460 A90-30754

Robotics for flightline servicing
p 383 A90-30760

The IMIS F-16 interactive diagnostic demonstration
p 383 A90-30768

Rapid low-temperature cure patching system for field repair
p 467 A90-31529

An apparatus to prepare composites for repair
p 533 A90-31574

Repair adhesives - Development criteria for field level conditions
p 528 A90-31575

Adhesive-bonded composite-patching repair of cracked aircraft structure
p 467 A90-31576

Evaluation of various non-asbestos epoxy adhesives for aircraft repair
p 529 A90-33078

Expert systems for design of battle damage repairs
p 467 A90-33094

In the shadow of Aloha
p 468 A90-33174

Repairing the damage
p 530 A90-33712

Onboard maintenance system testing - The Boeing 747-400 Central Maintenance Computer
[AIAA PAPER 90-1303] p 505 A90-33917

Canadians develop composite techniques for CF-18 battle damage repair program
p 551 A90-36300

V-22 engine installation and removal tool - Designing support equipment with the aircraft, not after
p 581 A90-38538

AV-8B composite repair program
p 551 A90-38542

Transport aircraft corrosion control
p 617 A90-40345

The application of an expert maintenance and diagnostic tool to aircraft engines
[AIAA PAPER 90-2036] p 657 A90-40605

Concept demonstration of the use of interactive fault diagnosis and isolation for TF30 engines
p 617 A90-41177

Jet Engine Technical Advisor (JETA)
p 693 A90-41184

The modular HUM system --- Health and Usage Monitoring instruments for rotary wing aircraft failure detection
p 618 A90-42476

The LF500 and the regional airline market
[AIAA PAPER 90-2521] p 744 A90-42814

Aluminum surface preparation for aircraft field repair
p 764 A90-43204

More power for the Harrier
p 745 A90-44597

Aircraft engine inspection
p 771 A90-44606

Douglas aging aircraft programs
[SAE PAPER 892206] p 732 A90-45425

Boeing 737 fuselage structural integrity program
[SAE PAPER 892207] p 701 A90-45426

Maintenance and economic benefits of non-painted aircraft operations
[SAE PAPER 892208] p 732 A90-45427

Dealing with the aging fleet
[SAE PAPER 892209] p 701 A90-45428

The PW2000 - A mature engine with an eye to the future
[SAE PAPER 892365] p 748 A90-45514

The economics of the organization and the planning of civil aviation --- Russian book
p 897 A90-46629

Unique features and innovative application of advanced composites to the MD-11
[AIAA PAPER 90-3217] p 838 A90-49108

Tracking B-1B aircraft with a structural data recorder
p 926 A90-49880

Re-assessing the F-16 damage tolerance and durability life of the RNLA F-16 aircraft
p 901 A90-49881

Aging jet transport structural evaluation programs
p 901 A90-49889

Development of a double crack growth gage algorithm for application to fleet tracking of fatigue damage
p 901 A90-49890

A probabilistic approach for the establishment of an aircraft structure inspection program
p 902 A90-49892

Induction heating development for aircraft repair
p 955 A90-50164

Aircraft accident report: Aloha Airlines, Flight 243, Boeing 737-200, N73711, near Maui, Hawaii, April 28, 1988
[PB89-910404] p 24 N90-10013

An appraisal of a number of power assessment procedures being proposed for use in Chinook-Lycoming T55 engine
[AD-A210482] p 52 N90-10041

The RB199: An in-service success
[PNR90544] p 114 N90-11746

Repair of composites by means of wet-lay-up
[LR-551] p 205 N90-13617

Integral fuel tanks - design, production, aging, repair
p 250 N90-15906

The repair of aircraft integral fuel tanks in the RAF: A user's view of fuel tank technology
p 250 N90-15908

Fuel resistant coatings for metal and composite fuel tanks
p 269 N90-15911

Spray sealing: A breakthrough in integral fuel tank sealing technology
p 276 N90-15912

Design philosophy and construction techniques for integral fuselage fuel tanks
p 250 N90-15913

Integral fuel tank certification and test methods
p 251 N90-15916

Cost effectiveness of composite materials on the F-15 and F-16 aircrafts
[AD-A216353] p 338 N90-17631

Damage tolerance demonstration for A310-300 CFRP components
[MBB-UT-012/89-PUB] p 766 N90-25091

From 1959-1989: 30 years of service experience with ramjets
[PNR90677] p 748 N90-25139

CREW CHIEF: A computer graphics simulation of an aircraft maintenance technician
p 779 N90-25515

Modeling strength data for CREW CHIEF
p 780 N90-25516

Success in tutoring electronic troubleshooting
p 780 N90-25568

- Second Annual International Conference on Aging Aircraft
[AD-A222715] p 724 N90-25961
- Robotic-aided system for inspection of aging aircraft [NIAR-90-9] p 777 N90-26346
- Computerized corrosion forecasting model for C-5 aircraft p 843 N90-26815
- Individual Helicopter Tracking Program (IHTP) for the MH-53J helicopter p 843 N90-26818
- Peak identification techniques p 844 N90-26822
- B-1B improved windshield development. Volume 2: Magna analysis: Baseline and parametric [AD-A221501] p 845 N90-26828
- Impact of NDE-NDI methods on aircraft design, manufacture, and maintenance, from the fundamental point of view p 887 N90-28093
- AIRCRAFT MANEUVERS**
- Pre-escape and escape aircraft maneuvers and gyrations - A critical under-reported problem affecting escape system performance and aircrew safety p 21 A90-10264
- Reflexive navigation for autonomous aircraft [AIAA PAPER 89-2991] p 25 A90-10502
- Dynamic interaction of separate INS/GPS Kalman filters (Filter-driving - Filter dynamics) p 124 A90-13996
- Development of a stall improvement package for the Gulfstream IV [SAE PAPER 891021] p 83 A90-14333
- The relevance of unsteady aerodynamics for highly maneuverable and agile aircraft p 146 A90-16775
- Experimental and computational studies of dynamic stall p 147 A90-16780
- Investigation of a nonlinear Kalman filter for estimating aircraft state variables p 195 A90-16850
- The analysis of entry into and recovery from a spin for the J6 aircraft p 195 A90-16854
- The fundamentals of vectored propulsion p 180 A90-17461
- Decoupled ultimate boundedness control of systems and large aircraft maneuver p 196 A90-19461
- Analysis and design of sidestick controller systems for general aviation aircraft p 196 A90-19554
- Attitude projection method for analyzing large-amplitude airplane maneuvers p 197 A90-19555
- Simple analyses of paths through windshears and downdrafts [AIAA PAPER 90-0222] p 197 A90-19740
- Preliminary results from a subsonic high-angle-of-attack flush airdata sensing (HI-FADS) system - Design, calibration, algorithm development, and flight test evaluation [AIAA PAPER 90-0232] p 187 A90-19746
- Analysis of aircraft performance during lateral maneuvering for microburst avoidance [AIAA PAPER 90-0568] p 197 A90-19920
- Potential applications of satellite navigation p 264 A90-21716
- A GPS-based flight-control concept p 242 A90-21719
- Differential GPS (DGPS) as an approach and landing aid p 242 A90-21722
- Pneumatic vortical flow control at high angles of attack [AIAA PAPER 90-0098] p 227 A90-22164
- Evaluation and measurement of airplane flutter interference - in television reception p 272 A90-22529
- Aerodynamic characteristics of an aircraft model at large angles of attack and large sideslip angles p 233 A90-23361
- Pay-offs and pitfalls of fly-by-wire p 346 A90-24281
- Aircraft program motion along a predetermined trajectory. II - Numerical simulation with application of spline functions to trajectory definitions p 347 A90-25199
- Nonlinear aerodynamics of two-dimensional airfoils in severe maneuver p 301 A90-25276
- Avoiding a maneuvering aircraft with TCAS - Traffic Alert and Collision Avoidance System p 347 A90-26222
- Application of higher harmonic control (HHC) to rotors operating at high speed and maneuvering flight p 429 A90-28157
- Helicopter design optimization for maneuverability and agility p 408 A90-28212
- Real time estimation of aircraft angular attitude p 431 A90-30103
- The STOL maneuver technology demonstrator manned simulation test program p 439 A90-30716
- Aeroelastic analysis using finite element models p 492 A90-33388
- Maneuver performance comparison between the XV-15 and an advanced tiltrotor design p 518 A90-33622
- F-15 STOL and Maneuver Technology Demonstrator flight test progress report [AIAA PAPER 90-1269] p 494 A90-33896
- Agility as a contribution to design balance - in fighter aircraft p 579 A90-35300
- [AIAA PAPER 90-1305] p 589 A90-35888
- Air combat beyond the stall p 589 A90-35888
- Piloted simulator assessments of agility [AIAA PAPER 90-1306] p 589 A90-36030
- Hypervelocity, minimum-radii, coordinated turns p 667 A90-40691
- Flight control application of eigenstructure assignment with optimization of robustness to structured state space uncertainty p 693 A90-40885
- Ultimate boundedness control of uncertain systems with application to roll coupled aircraft maneuver p 668 A90-40886
- Active control of tiltrotor blade in-plane loads during maneuvers p 670 A90-42463
- Estimation of rotor blade incidence and blade deformation from the measurement of pressures and strains in flight p 647 A90-42497
- Demonstrating technologies for enhanced fighter maneuverability - The Rockwell/MBB X-31 p 731 A90-43767
- An experimental investigation of roll agility in air-to-air combat [AIAA PAPER 90-2809] p 752 A90-45144
- Two dimensional post stall maneuver of a NACA 0015 airfoil at high pitching rates [AIAA PAPER 90-2810] p 710 A90-45150
- Parameter identification of linear systems based on smoothing [AIAA PAPER 90-2800] p 753 A90-45156
- Dynamics and control of maneuverable towed flight vehicles [AIAA PAPER 90-2841] p 754 A90-45161
- Control of forebody flow asymmetry - A critical review [AIAA PAPER 90-2833] p 711 A90-45164
- Optimal control system design for departure prevention [AIAA PAPER 90-2837] p 754 A90-45167
- Unsteady aerodynamics of delta wings, undergoing ramp-maneuvering in pitch to post-stall angle of attack p 806 A90-46857
- Application of energy turn g-limiting for aircraft high performance turns [AIAA PAPER 90-3328] p 862 A90-47590
- STOL Maneuver Technology Demonstrator aeroservoelasticity [AIAA PAPER 90-3336] p 863 A90-47596
- Inversion of nonlinear I-O map, zero dynamics and flight control system design [AIAA PAPER 90-3370] p 863 A90-47628
- Multivariable control law for flat-turn strafing maneuver by a supermaneuverable aircraft [AIAA PAPER 90-3371] p 863 A90-47629
- Local adaptive maneuvering optimization for fighter aircraft [AIAA PAPER 90-3453] p 890 A90-47706
- A comparison of inverse control with optimal control [AIAA PAPER 90-3484] p 866 A90-47733
- Exceptions to the C(n beta, dyn) criterion for aircraft stability at high angles of attack p 867 A90-48515
- Analytic models for technology integration in aircraft design [AIAA PAPER 90-3262] p 835 A90-48857
- An investigation of aircraft maneuverability and agility [AIAA PAPER 90-3300] p 868 A90-48882
- Description and reconstitution of manoeuvre loadings p 919 A90-49878
- Nonlinear maneuver autopilot for the F-15 aircraft [NASA-CR-179442] p 77 N90-11487
- FPG2: A flight profile generator program [AD-A212408] p 107 N90-12595
- Flow visualization of the effect of pitch rate on the vortex development on the scale model of a F-18 fighter aircraft [AD-A214244] p 236 N90-15080
- Relative merits of reactive and forward-look detection for wind-shear encounters during landing approach for various microburst escape strategies [NASA-TM-4158] p 259 N90-15108
- Preliminary results from a subsonic high angle-of-attack flush airdata sensing (HI-FADS) system: Design, calibration, and flight test evaluation [NASA-TM-101713] p 339 N90-16758
- Estimation and control of nonlinear and hybrid systems with applications to air-to-air guidance [AD-A214542] p 348 N90-16770
- Unsteady aerodynamics of delta wings performing maneuvers to high angle of attack p 398 N90-19196
- A study of flows over highly-swept wings designed for maneuver at supersonic speeds [AD-A216837] p 399 N90-19202
- A study of supermaneuver aerodynamics [AD-A218378] p 631 N90-23349
- Fighter agility metrics, research, and test [NASA-CR-186118] p 648 N90-23386
- Aerodynamics of Combat Aircraft Controls and of Ground Effects [AGARD-CP-465] p 920 N90-28513
- Combat aircraft control requirements p 934 N90-28515
- Observability of relative navigation using range-only measurements p 917 N90-29360
- Analysis of dynamic transient response and postflutter behavior of super-maneuvering airplane [AD-A224126] p 925 N90-29386
- Fighter agility metrics [NASA-CR-187289] p 925 N90-29389
- AIRCRAFT MODELS**
- Experimental-theoretical comparison for current injection on an aircraft model [ONERA, TP NO. 1989-133] p 22 A90-11157
- Connection of structures by laboratory-generated electrical discharges [ONERA, TP NO. 1989-147] p 58 A90-11169
- Identification of a coupled flapping/inflow model for the PUMA helicopter from flight test data p 56 A90-12767
- System identification strategies for helicopter rotor models incorporating induced flow p 30 A90-12768
- Flight simulation model validation procedure, a systematic approach p 30 A90-12770
- A frequency-domain system identification approach to helicopter flight mechanics model validation p 56 A90-12772
- An iterative non-linear, lifting line model for wings with unsymmetrical stall [SAE PAPER 891020] p 83 A90-14332
- Comparison of the analytical and experimental modes of a model airplane using finite element analysis and multi-reference testing p 207 A90-16986
- Flutter analysis on a non-linear wing model p 207 A90-17009
- Transonic Navier-Stokes solutions about a complex high-speed accelerator configuration [AIAA PAPER 90-0430] p 166 A90-19844
- Computer-aided simulation of aircraft motion including nonlinearities in aerodynamic-coefficient relationships p 257 A90-23359
- Aerodynamic characteristics of an aircraft model at large angles of attack and large sideslip angles p 233 A90-23361
- Wind tunnel testing of a helicopter model at HAL p 335 A90-26350
- Effect of the leading edge bluntness of a moderately swept wing on the aerodynamic characteristics of an aircraft model at subsonic and transonic velocities p 388 A90-29005
- A flight-test methodology for identification of an aerodynamic model for a V/STOL aircraft p 413 A90-30107
- Application of time domain decomposition techniques to aircraft ground and flutter test data p 491 A90-33373
- A study of symbolic processing and computational aspects in helicopter dynamics p 545 A90-34103
- Surface flow visualization in the cryogenic wind tunnel p 539 A90-34234
- Half transport aircraft cryogenic model for T2 wind tunnel p 524 A90-34242
- Higher harmonic control of a helicopter model rotor to reduce blade/vortex interaction noise p 496 A90-34360
- A study on mechanical model of the helicopter 'ground resonance' p 580 A90-36423
- Simulation of the reduction characteristics of scattering from an aircraft coated with a thin-type absorber by the spatial network method p 638 A90-39855
- Parameter identification of linear systems based on smoothing [AIAA PAPER 90-2800] p 753 A90-45156
- Measurements of pressures on the wing of an aircraft model during steady rotation [AIAA PAPER 90-2842] p 754 A90-45162
- Nonlinear flight control design via sliding methods p 756 A90-45335
- Wind tunnel studies of support strut interference on a 3 percent YF-17 fighter aircraft model at high angles of attack [AIAA PAPER 90-3083] p 794 A90-45899
- Identification of a stress-strain computation model and planning of tensometry points in strength and stability studies p 880 A90-46482
- Modeling of the buffeting of flight vehicles p 803 A90-46500
- Lateral-directional control of an aircraft using mu synthesis [AIAA PAPER 90-3442] p 865 A90-47695
- Bifurcation analysis of a model fighter aircraft with control augmentation [AIAA PAPER 90-2836] p 934 A90-50640

- Measurements of pressures on the tail and aft fuselage of an airplane model during rotary motions at spin attitudes
[NASA-TP-2939] p 20 N90-10829
- The spinning of aircraft: A discussion of spin prediction techniques including a chronological bibliography
[ARL-AERO-R-177] p 36 N90-10888
- Stability and control derivatives of the De Havilland DHC-2 BEAVER aircraft
[PB89-217525] p 119 N90-11754
- Sequential design of experiments with physically based models 23
[AD-A211918] p 138 N90-12239
- The precise calculation of the inviscid leading edge flow on a laminar airfoil using simple methods and verification by measurements on the TLF pilot model
p 277 N90-16180
- Stability characteristics of a combat aircraft with control surface failure
[AD-A216196] p 350 N90-17646
- Automation of an RCS (Radar Cross Section) measurement system and its application to investigate the electromagnetic scattering from scale model aircraft canopies
[AD-A215741] p 371 N90-17970
- Aerofoil design techniques
p 500 N90-20978
- Prediction methodologies for nonlinear aerodynamic characteristics of control surfaces
[NIAR-90-17] p 718 N90-25937
- Wind tunnel study of wake downwash behind A 6 percent scale model B1-B aircraft
[DE90-011783] p 719 N90-25941
- The effects of foreplanes on the static and dynamic characteristics of a combat aircraft model
p 920 N90-28520
- Study of ground effects on flying scaled models
p 922 N90-28532

AIRCRAFT NOISE

- A statistical model of helicopter noise
p 77 A90-10229
- Twenty-five years of rotorcraft aeroacoustics - Historical prospective and important issues
p 78 A90-11878
- Interior noise control of the Saab 340 aircraft
[SAE PAPER 891080] p 101 A90-14372
- Finite element calculations of the interior noise of the Saab 340 aircraft
[SAE PAPER 891081] p 101 A90-14373
- Effect of an isolated shell on interior noise levels in a turboprop aircraft
[SAE PAPER 891083] p 102 A90-14375
- Free-field correction factor for spherical acoustic waves impinging on cylinders
p 218 A90-17984
- Technical-scientific possibilities for helicopter noise research in the German-Dutch wind tunnel
p 283 A90-21474
- EUROFAR - European project for a commercial vertical-takeoff aircraft
[MBB-UD-553/89] p 221 A90-22696
- Digital control of local sound fields in an aircraft passenger compartment
p 247 A90-23113
- Aircraft noise --- Book
p 373 A90-24253
- HARF model rotor test at the DNW --- Hughes Advanced Rotor Program
p 406 A90-28167
- Considerations of noise for the use of compressed speech in a cockpit environment
p 404 A90-31334
- Noise of a simulated installed model counterrotation propeller at angle-of-attack and takeoff/approach conditions
[AIAA PAPER 90-0283] p 547 A90-32505
- Installation effects on propeller wake/vortex-induced structure-borne noise transmissions
p 579 A90-35761
- EH101 Advance Technology Rotorcraft low detectability/good neighbor design
p 579 A90-35774
- Acoustics
p 614 A90-36541
- Fuselage boundary-layer effects on sound propagation and scattering
p 695 A90-39781
- Acoustics of ultralight airplanes
p 643 A90-40685
- Experiments on the active control of the transmission of sound through a clamped rectangular plate
p 695 A90-41109
- Wind-tunnel measurement of noise emitted by helicopter rotors at high speed
[ONERA, TP NO. 1990-28] p 695 A90-41207
- A new noise certification method for 'light propeller aircraft' in testing
p 635 A90-41728
- Twin jet screech suppression concepts tested for 4.7 percent axisymmetric and two-dimensional nozzle configurations
[AIAA PAPER 90-2150] p 696 A90-42046
- A new class of random processes with application to helicopter noise
p 781 A90-42874
- Interior noise in the untreated Gulfstream II Propfan Test Assessment aircraft
p 731 A90-44736
- Effects of stage 3 rules on the airliner market
[SAE PAPER 892292] p 723 A90-45468

- Stages are for theaters - Decibels are for airplane noise measurements
[SAE PAPER 892293] p 778 A90-45469
- The MDE method for aircraft cabin interior noise prediction --- matrix difference equation
[SAE PAPER 892372] p 782 A90-45519
- The ROTONET prediction system and initial comparisons with far-field acoustics measurements for the XV-15 tilt-rotor aircraft
p 894 A90-46947
- Active control of propeller-induced noise fields inside a flexible cylinder
p 833 A90-47306
- Improved noise rejection in automatic carrier landing systems
[AIAA PAPER 90-3374] p 864 A90-47632
- Twin-jet screech suppression
p 894 A90-48957
- Measurement resolution of noise directivity patterns from acoustic flight tests
[NASA-TM-4134] p 79 N90-10679
- Profan Test Assessment (PTA): Flight test report
[NASA-CR-182278] p 113 N90-11738
- The NASA experience in aeronautical R and D: Three case studies with analysis
[AD-A211486] p 82 N90-12496
- Near-field noise predictions of an aircraft in cruise
p 140 N90-12538
- Acoustic design considerations: Review of rotor acoustic sources
p 106 N90-12585
- UHB demonstrator interior noise control flight tests and analysis
[NASA-CR-181897] p 140 N90-13198
- Mobility power flow analysis of an L-shaped plate structure subjected to acoustic excitation
[NASA-CR-186130] p 214 N90-13817
- A two dimensional power spectral estimate for some nonstationary processes
[NASA-CR-186100] p 217 N90-14843
- Evaluation of analysis techniques for low frequency interior noise and vibration of commercial aircraft
[NASA-CR-181851] p 220 N90-14866
- Cumulative airport noise exposure metrics: An assessment of evidence for time-of-day weightings, revision
[AD-A214878] p 352 N90-16773
- Comparison between design and installed acoustic characteristics of NASA Lewis 9- by 15-foot low-speed wind tunnel acoustic treatment
[NASA-TP-2996] p 440 N90-19242
- Noise of a simulated installed model counterrotation propeller at angle-of-attack and takeoff/approach conditions
[NASA-TM-102440] p 548 N90-20794
- Lateral attenuation of military aircraft flight noise
[AD-A218041] p 548 N90-20799
- The Shock and Vibration Digest, volume 21, no. 6
p 614 N90-22363
- Noise transmission into propeller-driven airplanes
p 614 N90-22364
- Evaluation of speech recognizers for use in advanced combat helicopter crew station research and development
[NASA-CR-177547] p 650 N90-24265
- FAA/NASA En Route Noise Symposium
[NASA-CP-3067] p 696 N90-24853
- Proposed definition of the term en route in en route aircraft noise
p 696 N90-24854
- PTA en route noise measurements
p 696 N90-24855
- En route noise: NASA propfan test aircraft (calculated source noise)
[DOT-TSC-FA953-LR5] p 697 N90-24857
- En route noise of two turboprop aircraft
[DLR-MITT-89-18] p 697 N90-24859
- Sound propagation elements in evaluation of en route noise of advanced turbofan aircraft
p 697 N90-24861
- Preliminary thoughts on an acoustic metric for the wilderness aircraft overflight study
p 697 N90-24862
- When propfans cruise, will LDN 65 fly
p 697 N90-24864
- Additive evaluation criteria for aircraft noise
p 698 N90-24867
- Social survey findings on en route noise annoyance issues
p 698 N90-24868
- En route noise annoyance laboratory test: Preliminary results
p 698 N90-24870
- Problems related to aircraft noise in Switzerland
p 698 N90-24871
- An aircraft noise study in Norway
p 698 N90-24872
- Problems of internal acoustics in two and three dimensional cavities with deformable walls, using the MSC/Nastran code
[DLC/STR-INT-TN-004] p 699 N90-24876
- High speed turboprop aeroacoustic study (counterrotation). Volume 1: Model development
[NASA-CR-185241] p 782 N90-26633
- Bringing aircraft noise testing down to Earth
[PNR90642] p 783 N90-26637

- BASEOPS default profiles for civil aircraft
[AD-A223161] p 844 N90-26825
- Air Force procedure for predicting aircraft noise around airbases: Airbase operations program (BASEOPS) description
[AD-A223069] p 895 N90-27466
- Air Force procedure for predicting aircraft noise around airbases: Noise Exposure Model (NOISEMAP): User's manual
[AD-A223162] p 895 N90-27467
- Aviation acoustical noise measurement
[AD-A222014] p 896 N90-27469
- Public-sector aviation issues, 1987 to 1988 graduate research award papers
[PB90-191206] p 820 N90-27667
- Structure-borne noise estimates for the PTA aircraft
[NASA-CR-4315] p 896 N90-28396
- A process for analysis, evaluation, and development of aerial servicing noise reduction measures in civil aircraft
[ETN-90-97300] p 896 N90-28398
- Comparison of speech intelligibility in cockpit noise using SPH-4 flight helmet with and without active noise reduction
[NASA-CR-177564] p 915 N90-28510
- Audibility and annoyance of en route noise of unducted fan engines
[AD-A223687] p 966 N90-30035
- Assessment - System for Aircraft Noise (ASAN): Development of alpha-test prototype system software
[AD-A223770] p 966 N90-30036
- AIRCRAFT PARTS**
- Computer-aided design of flight vehicle instrument bays --- Russian book
p 76 A90-10837
- Airplane design. Part 5 - Component weight estimation --- Book
p 31 A90-12870
- Wildhaber-Novikov circular arc gears - Some properties of relevance to their design
p 70 A90-12999
- Installation and implementation of an extrusion cell in aircraft industry utilizing group technology
[SAE PAPER 891025] p 81 A90-14336
- Vibration analysis of aircraft panels
p 207 A90-17026
- Damage tolerance analysis of dynamic components of rotary wing aircraft
p 179 A90-17312
- Looking inside a structure
p 209 A90-17920
- Repair of composite aircraft parts: An operator's viewpoint
p 221 A90-20606
- An investigation of the behavior of the dynamic load distribution versus operating speed and torque on heavily loaded, high speed aircraft gearing
p 271 A90-21129
- Durability of equipment assemblies and elements of life-support systems for flight vehicles --- Russian book
p 246 A90-21275
- Tradeoffs in honeycomb cored designs
p 538 A90-33708
- Repairing the damage
p 530 A90-33712
- Determination of additive contents in aviation and turbine oils
p 532 A90-34681
- Redesign of an electro-optical shroud in graphite/epoxy
p 676 A90-40215
- Dornier Composite Aircraft - Economical and faultless
p 732 A90-44751
- Fabrication of complex composite structures using advanced fiber placement technology
p 954 A90-50111
- Castings Airworthiness
[AGARD-R-762] p 64 N90-10231
- Casting factors imposed by the French regulation for foundry castings used in military aircraft
p 64 N90-10233
- The question of the casting factor
p 64 N90-10238
- Expert system diagnostics and parts life tracking as applied to the AV-8B aircraft for the USMC
p 884 N90-27629
- Evaluation of composite components on the Bell 206L and Sikorsky S-76 helicopters
[NASA-TM-4195] p 876 N90-27787
- In-service inspection of composite components on aircraft at depot and field levels
p 885 N90-28078
- AIRCRAFT PERFORMANCE**
- Wing-section effects on the flight performance of a remotely piloted vehicle
p 29 A90-11007
- Airplane aerodynamics and performance --- Book
p 17 A90-12865
- The Soviets' French revelation. II - Aircraft
p 81 A90-14800
- Leading edge flap influence on aerodynamic efficiency
p 85 A90-15240
- Safety management in aircraft testing and certification
p 180 A90-17421
- Effect of wind shear on flight safety
p 175 A90-17973
- On the level 2 ratings of the Cooper-Harper scale --- for pilot assessment of aircraft flying qualities
p 197 A90-19577

Analysis of aircraft performance during lateral maneuvering for microburst avoidance [AIAA PAPER 90-0568] p 197 A90-19920

An AEW metalclad airship [AIAA PAPER 89-3158] p 244 A90-20579

Preliminary feasibility study for a new hybrid airship (Heliship) [AIAA PAPER 89-3161] p 244 A90-20581

Parametric sizing of modern naval airships [AIAA PAPER 89-3171] p 244 A90-20586

Low- and high-speed tests with the Dornier 328 wind-tunnel model p 246 A90-21611

East coast Osprey flies p 246 A90-21713

The performance and longitudinal stability and control of large receiver aircraft during air to air refueling p 346 A90-24338

A status review of non-helicopter V/STOL aircraft development. I p 413 A90-30117

The variable-diameter rotor - A key to high performance rotorcraft p 413 A90-30118

Modeling and analysis tools for aircraft control system evaluations p 431 A90-30703

The STOL maneuver technology demonstrator manned simulation test program p 439 A90-30716

Flight testing for aircraft agility [AIAA PAPER 90-1308] p 519 A90-33918

Piloted simulator assessments of agility [AIAA PAPER 90-1306] p 589 A90-36030

Configuration aerodynamics p 557 A90-36540

Large receiver aircraft - The performance and longitudinal stability and control during air to air refueling p 669 A90-41767

More power for the Harrier p 745 A90-44597

Large aircraft flying qualities revisited [AIAA PAPER 90-2847] p 754 A90-45175

The problem of aircraft test flight correction p 828 A90-46485

Jet engines performance deterioration p 852 A90-46871

The MH-60K - A special rotorcraft for special operations [AIAA PAPER 90-3266] p 835 A90-48860

Application of advanced air vehicle and mission equipment technologies to the Light Helicopter (LH) [AIAA PAPER 90-3268] p 836 A90-48861

Air Force use of civil airworthiness criteria for testing and acceptance of military derivative transport aircraft [AIAA PAPER 90-3289] p 818 A90-48875

Helicopter of tiltrotor - A Soviet view p 838 A90-48952

The LTV XC-142 experimental aircraft lessons learned [AIAA PAPER 90-3204] p 838 A90-49104

X-29 ECS high-alpha modifications [SAE PAPER 901221] p 840 A90-49295

Field experience with type certificated civil aircraft operated on motor gasolines and worldwide survey of motor gasoline characteristics p 912 A90-51619

On the interactive computer program IPIS for aircraft parameter identification [NAL-TR-1000] p 77 N90-10586

Introduction to data items on flight path optimization [ESDU-89015] p 185 N90-14221

Influence of windshear, downdraft and turbulence on flight safety p 238 N90-15048

Classification of windshear severity p 281 N90-15049

A pitch control law for compensation of the phugoid mode induced by windshears p 258 N90-15051

Aircraft response and pilot behaviour during a wake vortex encounter perpendicular to the vortex axis p 259 N90-15057

Ice induced aerodynamic performance degradation of rotorcraft: An overview p 248 N90-15063

Aircraft performance enhancement with active compressor stabilization [AD-A213652] p 249 N90-15097

A UK perspective on the uniform engine test programme [RAE-TM-P-1172] p 257 N90-15922

Application of multifunction inertial reference systems to fighter aircraft p 332 N90-16740

Longitudinal stability and control characteristics of the Quiet Short-Haul Research Aircraft (QSRA) [NASA-TP-2965] p 349 N90-17639

The effects of wind tunnel data uncertainty on aircraft point performance predictions [AD-A216091] p 414 N90-18387

Development of a preliminary high-angle-of-attack nose-down pitch control requirement for high-performance aircraft [NASA-TM-101684] p 399 N90-19206

Potential role of avionics in escape systems p 483 N90-20060

The implementation and operation of a variable-response electronic throttle control system for a TF-104G aircraft [NASA-TM-101696] p 509 N90-20086

Airplane takeoff and landing performance monitoring system [NASA-CASE-LAR-13734-1-CU] p 526 N90-20096

Flight test investigation of certification issues pertaining to general-aviation-type aircraft with natural laminar flow [NASA-CR-181967] p 480 N90-20952

Flight path reconstruction using extended Kalman filtering techniques [PD-FC-9001] p 489 N90-20970

Supersonic through-flow fan engine and aircraft mission performance [NASA-TM-102304] p 516 N90-21038

Preliminary airworthiness evaluation of the RC-12K [AD-A219545] p 648 N90-23387

Initial flight test of half-scale unmanned air vehicle [AD-A219584] p 648 N90-23388

Estimating short-period dynamics using an extended Kalman filter [NASA-TM-101722] p 648 N90-23392

Lateral-directional stability and control characteristics of the Quiet Short-Haul Research Aircraft (QSRA) [NASA-TM-102250] p 671 N90-23413

A quantitative technique to estimate microburst wind shear hazard to aircraft p 692 N90-25040

Effects of simplifying assumptions on optimal trajectory estimation for a high-performance aircraft [NASA-TM-101721] p 757 N90-25142

Handbook of uncertainty methodology for engine testing at Pyestock (England) [RAE-TM-P-1179] p 751 N90-26007

Model tilt-rotor hover performance and surface pressure measurement [AD-A222535] p 845 N90-26827

Aircraft Integrated Monitoring Systems [DLR-MITT-90-04] p 786 N90-27617

Past, present and future: Aircraft integrated monitoring systems: An ever-developing technology p 848 N90-27618

Comparative Engine Performance Measurements [AGARD-LS-169] p 856 N90-27711

Survivable penetration p 917 N90-29363

Multi-disciplinary optimization of aeroservoelastic systems [NASA-CR-185931] p 925 N90-29385

AIRCRAFT PILOTS

Pilot's Associate - A perspective on Demonstration 2 [AIAA PAPER 89-3023] p 36 A90-10524

Theory for aircraft handling qualities based upon a structural pilot model p 118 A90-14730

Avoiding a maneuvering aircraft with TCAS - Traffic Alert and Collision Avoidance System p 347 A90-26222

Research in a high-fidelity acceleration environment p 439 A90-30734

Reassessment and extensions of pilot ratings with new data - of aircraft handling qualities [AIAA PAPER 90-2823] p 753 A90-45158

Design and evaluation of the ATC interface - Planning system for approach flight p 937 A90-52617

Peacetime replacement and crash damage factors for army aircraft [AD-A218544] p 636 N90-23372

Cognitive requirements for aircraft navigation [NASA-CR-186933] p 824 N90-26804

Evaluation of existing aircraft operator data bases [DOT/FAA/CT-90/18] p 898 N90-28463

AIRCRAFT POWER SUPPLIES

Power supply of aircraft - Russian book p 43 A90-12474

The VSCF system has arrived - The way in which a new constant-frequency electrical generation system in aeronautics has been developed p 187 A90-16896

The fast-response requirement of powerplant thrust in the set of engineering and economic criteria of an aircraft p 254 A90-23354

A parametric optimization algorithm for the electrical distribution circuits of civil aircraft p 255 A90-23417

A practical flight path for microwave-powered airplanes p 429 A90-28007

The evolution of built-in test for an electrical power generating system (EPGS) p 424 A90-30699

Advanced power system for 21st century fighter aircraft p 508 A90-33347

New power system architecture for the 747-400 p 508 A90-33349

Electrical power systems for high Mach vehicles p 586 A90-38129

Applying AVIP to high voltage power supply designs - Avionic Integrity Program p 605 A90-38132

Extracting pulse power from batteries p 605 A90-38175

Preliminary design of a long-endurance Mars aircraft [AIAA PAPER 90-2000] p 674 A90-40587

Use of smart actuators for the tail rotor collective pitch control p 688 A90-42483

High-performance EHA controls using an interior permanent magnet motor - electrohydraulic actuator for aircraft power systems p 730 A90-43152

EHA loading on the 270-Vdc bus [SAE PAPER 892225] p 746 A90-45441

Design features of the 747-400 Electric Power System [SAE PAPER 892227] p 746 A90-45443

VSCF cycloconverter reliability review of the 30/40 KVA F/A-18 electrical generating system - variable speed, constant frequency [SAE PAPER 892228] p 746 A90-45444

Power system for 21st century fighter aircraft [SAE PAPER 892253] p 746 A90-45455

Battery configurations for multi-megawatt pulse power p 873 A90-49763

A modular 550 watt, 25 watts per cubic inch power supply for next generation aircraft p 958 A90-52954

Civil air transport: A fresh look at power-by-wire and fly-by-light [NASA-TM-102574] p 542 N90-21283

Preliminary design of a long-endurance Mars aircraft [NASA-CR-185243] p 588 N90-21763

AIRCRAFT PRODUCTION

The advantages of automation in aerospace production p 130 A90-15357

Monitoring of aircraft assembly: Optical and laser methods - Russian book p 285 A90-24229

Automatic testing in aircraft building - Russian book p 285 A90-24231

Manufacturing and handling techniques used in the assembly of polished commercial aircraft [SAE PAPER 890925] p 286 A90-24690

Laser machining developments at McDonnell Douglas p 453 A90-31028

Teamwork for excellence [AIAA PAPER 89-3195] p 549 A90-31686

Smart structures concept study p 504 A90-32876

Wide chord fan club p 584 A90-35600

Toxicology in aviation p 722 A90-44662

A leap forward in aircraft construction technology - High-speed cutting sets new production standards p 881 A90-46720

The impact of total quality management (TQM) and concurrent engineering on the aircraft design process p 785 A90-46927

Practical aspects of European collaboration - procurement in helicopter industry p 785 A90-46928

Automated prepreg tow placement for composite structures p 954 A90-50113

Scenario 2000 [MBB-UD-500/89-PUB] p 734 N90-25092

AIRCRAFT PRODUCTION COSTS

V-22 - The prospects now - production costs of Bell Boeing tilt-rotor aircraft p 497 A90-34900

Aircraft modifications cost analysis. Volume 1: Overview of the study [AD-A220764] p 702 N90-25074

AIRCRAFT RELIABILITY

Placards, warning labels and operation manuals - An aircraft manufacturer's duty to warn p 79 A90-11396

Endurance test of FJR 710/600S engine p 42 A90-12012

Mechanical rig rest of FJR 710/600 engine components p 43 A90-12016

Aerospace structures supportability [SAE PAPER 891058] p 129 A90-14360

The anti-shimmy and break-proof study of nose landing gear p 178 A90-16856

Damage tolerance analysis of dynamic components of rotary wing aircraft p 179 A90-17312

Stronger starliner p 143 A90-17919

Durability of equipment assemblies and elements of life-support systems for flight vehicles - Russian book p 246 A90-21275

Design criteria, constructions, and materials for the Dornier 328 airframe p 246 A90-21610

Modeling strategies for crashworthiness analysis of landing gears p 409 A90-28233

In the shadow of Aloha p 468 A90-33174

Advancements in rotor and airframe structural flight testing developed during the SH-60B G.W./C.G. expansion program [AIAA PAPER 90-1281] p 495 A90-33902

Onboard maintenance system testing - The Boeing 747-400 Central Maintenance Computer [AIAA PAPER 90-1303] p 505 A90-33917

Transport aircraft corrosion control p 617 A90-40345

The effect on fatigue crack growth under spectrum loading of an imposed placard 'G' limit p 643 A90-41339

- Fracture control via DRM-Algorithm p 694 A90-41343
- The LF500 and the regional airline market [AIAA PAPER 90-2521] p 744 A90-42814
- Certification of composites for commercial aircraft [SAE PAPER 892212] p 772 A90-45430
- Flight testing Navy low Reynolds Number (LRN) unmanned aircraft p 828 A90-46387
- MDHC technical assessment of advanced rotor and control concepts p 861 A90-46948
- Fighter design econometrics = ownership affordability? [AIAA PAPER 90-3223] p 897 A90-48842
- Re-assessing the F-16 damage tolerance and durability life of the RNLA F-16 aircraft p 901 A90-49881
- Damage tolerance for helicopters p 919 A90-49888
- Health monitoring aircraft p 902 A90-50544
- Aircraft accident report: Aloha Airlines, Flight 243, Boeing 737-200, N73711, near Maui, Hawaii, April 28, 1988 [PB89-910404] p 24 N90-10013
- Airworthiness and flight characteristics test of the UH-60A Black Hawk helicopter equipped with the XM-139 multiple mine dispensing system (VOLCANO) [AD-A210271] p 32 N90-10025
- Castings Airworthiness [AGARD-R-762] p 64 N90-10231
- Casting airworthiness joint European civil authorities view-point p 64 N90-10234
- Royal Aerospace Establishment: No place for a castings factor p 64 N90-10235
- Combined advanced foundry and quality control techniques to enhance reliability of castings for the aerospace industry p 64 N90-10240
- Preliminary airworthiness evaluation of the Woodward hydromechanical unit installed on T700-GE-700 engines in the UH-60A helicopter [AD-A216751] p 428 N90-18430
- Airworthiness and flight characteristics evaluation of the McDonnell Douglas Helicopter Corporation (MDHC) 530FF helicopter [AD-A218253] p 498 N90-20076
- The NASA digital VGH program. Exploration of methods and final results. Volume 1: Development of methods [NASA-CR-181909-VOL-1] p 505 N90-20081
- The NASA digital VGH program. Exploration of methods and final results. Volume 3: B 727 data 1978-1980: 1765 hours [NASA-CR-181909-VOL-3] p 505 N90-20082
- The NASA digital VGH program: Exploration of methods and final results. Volume 4: B 747 data 1978-1980, 1689 hours [NASA-CR-181909-VOL-4] p 506 N90-20083
- The NASA digital VGH program: Exploration of methods and final results. Volume 5: DC 10 data 1981-1982, 129 hours [NASA-CR-181909-VOL-5] p 506 N90-20084
- The role of structural analysis in airworthiness certification [BR112064] p 499 N90-20972
- Preliminary airworthiness evaluation of the RC-12K [AD-A219545] p 648 N90-23387
- From 1959-1989: 30 years of service experience with ramjets [PNR90677] p 748 N90-25139
- Ground-simulation investigations of VTOL airworthiness criteria for terminal-area operations [NASA-TM-102810] p 757 N90-25141
- Program plan: International aircraft operator data base [IAR-90-1] p 783 N90-25697
- Second Annual International Conference on Aging Aircraft [AD-A22715] p 724 N90-25961
- Estimation of defective rate of mechanic-hydraulic components [ETN-90-97275] p 884 N90-27120
- Aircraft Integrated Monitoring Systems [DLR-MITT-90-04] p 786 N90-27617
- Computer modeling and data processing methods: An essential part of jet engine condition monitoring and fault diagnosis p 855 N90-27626
- Impact of Emerging NDE-NDI Methods on Aircraft Design, Manufacture, and Maintenance [AGARD-CP-462] p 885 N90-28068
- Inspection reliability p 885 N90-28072
- System reliability optimization of aircraft wings p 923 N90-28536
- Tests for aircraft interior materials in fire accident [LR-622] p 914 N90-29337
- Application of multifunction inertial reference systems to fighter aircraft p 916 N90-29341
- AIRCRAFT SAFETY**
- Coping with bomb threats to civil aviation p 23 A90-12781
- Methods of safety analysis for Beech Model 2000 - Starship 1 [SAE PAPER 891064] p 101 A90-14364
- Aircraft and ground vehicle friction measurements obtained under winter runway conditions [SAE PAPER 891070] p 95 A90-14367
- Flight over the sea with twin or triple jet aircraft p 179 A90-17048
- Landing gear integrity - The bottom line of aircraft safety p 180 A90-17408
- Modeling of air-to-air visual acquisition p 282 A90-21385
- The U.S. airline industry - Coping with an aging fleet p 221 A90-21702
- Airborne Doppler radar detection of low-altitude wind shear p 252 A90-23284
- Development of an automated windshear detection system using Doppler weather radar p 373 A90-25567
- The role of expert systems in aircraft safety management p 375 A90-26225
- Modeling and analysis tools for aircraft control system evaluations p 431 A90-30703
- Automation of flight safety control - Russian book p 589 A90-36157
- The safety analysis approach for the EH101 p 635 A90-42456
- Eddy current detection of subsurface cracks p 882 A90-48629
- A theoretical and experimental investigation into the prerotation of aircraft tires [AIAA PAPER 90-3272] p 836 A90-48863
- Aeronautical fatigue in the electronic era; Proceedings of the Fifteenth ICAF Symposium, Jerusalem, Israel, June 21-23, 1989 p 901 A90-49876
- Requirements for meteorological equipment designed for the acquisition of meteorological data essential for the takeoff and landing of aircraft at civil airports p 962 A90-50777
- Aircraft accident report: Aloha Airlines, Flight 243, Boeing 737-200, N73711, near Maui, Hawaii, April 28, 1988 [PB89-910404] p 24 N90-10013
- Safer skies with TCAS: Traffic Alert and Collision Avoidance System [PB89-169221] p 27 N90-10016
- Electro-impulse de-icing testing analysis and design [NASA-CR-4175] p 32 N90-10031
- Design of a final approach spacing tool for TRACON air traffic control [NASA-TM-102229] p 24 N90-10841
- Test and evaluation: Reducing risks to military aircraft from bird collisions. Report to the Chairman, Legislation, and National Security Subcommittee, Committee on Government Operations, House of Representatives [AD-A210670] p 25 N90-10845
- Aircraft cabin fire suppression by means of an interior water spray system [CAA-PAPER-88014] p 96 N90-11719
- The 1987 survey of track keeping and altitudes on Heathrow and Gatwick standard instrument departure routes (DAY) [CAA-PAPER-88010] p 99 N90-11729
- The human factors relating to escape and survival from helicopters ditching in water [AGARD-AG-305(E)] p 176 N90-13358
- Adverse weather operations during the Canadian Atlantic storms program p 281 N90-15052
- See and avoid/cockpit visibility [AD-A214214] p 239 N90-15084
- International Aircraft Occupant Safety Conference and Workshop proceedings [AD-A214452] p 239 N90-15085
- Application of experimental techniques to store release problems p 316 N90-17545
- Aircraft fires: A study of transport accidents from 1975 to the present p 324 N90-17583
- Aircraft fire safety: Learning from past accidents p 324 N90-17584
- Objectives and results of cabin fire research in Germany p 325 N90-17588
- New aircraft cabin and cargo flammability standards for transport category aircraft p 325 N90-17589
- Fire prevention in transport airplane passenger cabins p 325 N90-17590
- Characteristics of transport, aircraft fires measured by full-scale tests p 325 N90-17591
- Aircraft internal fires p 326 N90-17593
- Fire science and aircraft safety p 326 N90-17596
- The stability of fuel fires p 327 N90-17601
- US Navy aircraft fire protection technology p 327 N90-17603
- Aircraft fire safety in the Canadian Forces p 327 N90-17604
- New materials for civil aircraft furnishing p 328 N90-17609
- Weather data dissemination to aircraft p 486 N90-20934
- Statistics on aircraft gas turbine engine rotor failures that occurred in US commercial aviation during 1986 [DOT/FAA/CT-89/30] p 511 N90-21008
- Aircraft accident report, United Airlines Flight 811, Boeing 747-122, N4713U, Honolulu, Hawaii, February 24, 1989 [PB90-910401] p 574 N90-21748
- Aviation security: Corrective actions underway, but better inspection guidance still needed. Report to the Chairwoman, Government Activities and Transportation Subcommittee, Committee on Government Operations, House of Representatives [GAO/RCED-88-160] p 635 N90-23367
- Aeronautical decisionmaking for air ambulance program administrators [DOT/FAA/DS-88/8] p 635 N90-23368
- Aviation safety: Conditions within the air traffic control work force. Fact sheet for congressional requesters [GAO/RCED-89-113FS] p 724 N90-25958
- Aviation safety: Serious problems continue to trouble the air traffic control work force. Report to congressional requesters [GAO/RCED-89-112] p 724 N90-25959
- Safety net functions p 826 N90-27685
- Modeling and analysis of airport and aircraft operations [PB90-222167] p 915 N90-28511
- AIRCRAFT SPECIFICATIONS**
- Aircraft/airport compatibility: Some strategic, tactical, and operational issues [TT-8902] p 202 N90-13409
- Analysis of indirect effects of lightning on a metallic A 300 wing: Test report [REPT-E87/645800] p 323 N90-16726
- Preliminary design of a family of three close air support aircraft [NASA-CR-186070] p 336 N90-16751
- AIRCRAFT SPIN**
- A low cost stall/spin simulator [SAE PAPER 891022] p 117 A90-14334
- The analysis of entry into and recovery from a spin for the J6 aircraft p 195 A90-16854
- A summary of spin-recovery parachute experience on light airplanes [AIAA PAPER 90-1317] p 519 A90-33926
- A study of the control technique for aircraft spin recovery p 590 A90-37226
- Measurements of pressures on the wing of an aircraft model during steady rotation [AIAA PAPER 90-2842] p 754 A90-45162
- Stall/spin aerodynamic data project [DOT/FAA/CT-88/29] p 185 N90-14222
- AM-X high incidence trials, development and results [ETN-90-97277] p 759 N90-26016
- A flight dynamic model of aircraft spinning [AR-005-600] p 935 N90-28576
- AIRCRAFT STABILITY**
- On the 'inverse phugoid problem' as an instance of non-linear stability in pitch p 55 A90-10221
- Airplane design. Part 7 - Determination of stability, control and performance characteristics: Far and military requirements - Book p 57 A90-12872
- Supersonic boundary layer stability analysis with and without suction on aircraft wings p 148 A90-16792
- A separated algorithm and applications to flight test p 216 A90-16857
- The induced velocity distribution and the flap-pitch-torsion coupling on the stability and control of the helicopter in flight condition with lateral velocity p 196 A90-18633
- Rapid prediction of slender-wing-aircraft stability characteristics [AIAA PAPER 90-0301] p 163 A90-19782
- Application of dynamical systems theory to the high angle of attack dynamics of the F-14 [AIAA PAPER 90-0221] p 257 A90-22184
- Flight-mechanics tasks in solving problems of active control p 257 A90-23358
- A unified approach to the overall body motion stability and flutter characteristics of elastic aircraft p 346 A90-25102
- Static and dynamic loss of stability of elements of a supersonic aeroplane covering - Numerical analysis p 346 A90-25186
- Dynamics of spatial motion of an aeroplane after drop of loads p 346 A90-25189
- Optimal reflex camber p 308 A90-26347
- The Modular Flighttest Instrumentation/MFI 90 - A helicopter measuring system p 418 A90-28850
- Algorithm for simultaneous stabilization of single-input systems via dynamic feedback p 462 A90-31108
- Studies of predicting departure characteristics of aircraft p 433 A90-31480

- Review of active structural control systems and flight test techniques for dynamic stability investigations p 516 A90-33352
- On the prediction of the aeroelastic behaviour of lifting systems due to flow separation p 491 A90-33369
- Whole helicopter aeroelasticity - Experience with a new approach p 492 A90-33380
- Equation decoupling - A new approach to the aerodynamic identification of unstable aircraft [AIAA PAPER 90-1276] p 518 A90-33900
- A flight test investigation of certification requirements for laminar-flow general aviation airplanes [AIAA PAPER 90-1310] p 496 A90-33920
- Control of asymmetric vortical flows over delta wings at high angles of attack p 553 A90-35759
- A novel synthetic method for studying nonlinear flight stability p 645 A90-42355
- A new simplification method for analysing the rapid rolling stability of aircraft p 669 A90-42367
- The influence of the inertia coupling on the stability and control of the helicopter and the response of helicopter gust p 671 A90-42472
- Aeroelastic effects on stability and control of hingeless rotor helicopters p 647 A90-42473
- Helicopter stability and control modeling improvements and verification on two helicopters p 671 A90-42474
- The effect of solidity on propeller normal force [SAE PAPER 892205] p 713 A90-45424
- Stability characteristics of a conical aerospace plane concept [SAE PAPER 892313] p 757 A90-45475
- Exploratory wind tunnel investigation of the stability and control characteristics of a three-surface, forward-swept wing advanced turboprop model [AIAA PAPER 90-3074] p 797 A90-45920
- Aircraft passing through a sinusoidal gust p 811 A90-48090
- Aerospace - Collected translations of selected papers --- Book p 786 A90-48510
- Longitudinal stability analysis for deformable aircraft p 867 A90-48514
- Exceptions to the $C(n, \beta, \gamma)$ criterion for aircraft stability at high angles of attack p 867 A90-48515
- The Bell X-22A V/STOL, Variable Stability Research Airplane - Lessons learned [AIAA PAPER 90-3207] p 834 A90-48835
- Design of a close-support aircraft [AIAA PAPER 90-3241] p 835 A90-48849
- A new method of aircraft motion error extraction from radar raw data for real-time motion compensation p 824 A90-49675
- Structural stability augmentation system design using BODEDIRECT: A quick and accurate approach p 33 A90-10116
- The active control of an unstable canard aircraft p 57 A90-10894
- Stability and control derivatives of the De Havilland DHC-2 BEAVER aircraft [PB89-217525] p 119 A90-11754
- Aerodynamics of thrust vectoring [NASA-CR-185074] p 172 A90-13354
- On the application of modified stepwise regression for the estimation of aircraft stability and control parameters [REPT-8905] p 198 A90-13400
- Design of a spanloader cargo aircraft [NASA-CR-186046] p 184 A90-14216
- An aerodynamic tradeoff study of the scissor wing configuration [NASA-CR-186576] p 481 A90-20965
- Helicopter controllability [AD-A220078] p 672 A90-24275
- The role of $C_{sub} n, \beta, \gamma$ in the aircraft stability at high angles of attack [AD-A221586] p 868 A90-26833
- The DELTA MONSTER: An RPV designed to investigate the aerodynamics of a delta wing platform [NASA-CR-186226] p 924 A90-29381
- AIRCRAFT STRUCTURES**
- Some unconventional cases of the dynamical testing of helicopters p 28 A90-10227
- Fiber optic sensor systems for smart aerospace structures p 38 A90-11208
- Optical fiber sensing considerations for a smart aerospace structure p 38 A90-11210
- Modern dynamic components for helicopters [MBB-UD-556-89-PUB] p 29 A90-12253
- Impact evaluation of composite floor sections [SAE PAPER 891018] p 100 A90-14330
- Electrochromic windows - Applications for aircraft [SAE PAPER 891063] p 129 A90-14363
- Nonlinear transverse oscillations of a composite dynamic system p 129 A90-14558
- Dynamic analysis of lifting surfaces of small relative thickness in the case of finite displacements p 129 A90-14560
- Highly damage tolerant carbon fiber epoxy composites for primary aircraft structural applications p 125 A90-14660
- Computers boost structural technology p 138 A90-14799
- DB/SPF cooler outlet duct for aircraft application p 132 A90-16620
- Airframe structural design: Practical design information and data on aircraft structures --- Book p 103 A90-16624
- The case for titanium p 204 A90-17922
- Postbuckling behavior of laminated plates using a direct energy-minimization technique p 209 A90-17993
- Numerical study of balanced patch repairs to cracked sheets p 210 A90-18442
- An application of SQP and Ada to the structural optimisation of aircraft wings p 216 A90-18444
- The application and design of large integral panels for SH-5 aircraft p 211 A90-18632
- Experimental determination of the short crack effect for metals p 265 A90-20084
- Significance of the short crack effect on aerospace structures p 269 A90-20065
- Application of the dynamic stiffness method to the free and forced vibrations of aircraft panels p 270 A90-20599
- A study on initial fatigue quality of typical aircraft structures (fastener holes) p 272 A90-22004
- Random response and noise transmission of discretely stiffened composite panels p 283 A90-23288
- Determination of the torsion rigidity of a multiple-rib torsion box of an aircraft lifting surface p 364 A90-24134
- A method for determining equivalents during the fatigue testing of structures in an acoustic field p 364 A90-24153
- Multicriterial optimization of lugs in hinge joints p 364 A90-24162
- Calculation of the vibrations of aircraft with elastic suspended loads p 345 A90-24171
- Composites for aeronautical structures p 286 A90-24291
- Buckling analysis of FRP faced cylindrical sandwich panel under combined loading p 365 A90-24376
- Postbuckling finite element analysis of composite panels p 365 A90-24377
- Automated procedure for creating flight-by-flight spectra p 376 A90-26755
- Simplified analysis of helicopter fatigue loading spectra p 336 A90-26758
- Compilation of procedures for fatigue crack propagation testing under complex load sequences p 368 A90-26759
- Development of a phase Doppler based probe for icing cloud droplet characterization [AIAA PAPER 90-0667] p 368 A90-26978
- Examination of dynamic characteristics of UH-60A and EH-60A airframe structures p 406 A90-28154
- The effects of aerial combat on helicopter structural integrity p 406 A90-28166
- UCAR 2040, A novel wear resistant coating for aircraft structural components p 441 A90-28231
- A method for recalculating the temperature fields of aircraft structures for different experimental conditions p 448 A90-28994
- Approximation of frequency characteristics using identification with a complex mass matrix p 448 A90-29001
- Efficiency of using a multiple-wall torsion box in the load-bearing structures of lifting surfaces p 410 A90-29188
- Generalized Transition Finite-Boundary Elements for high speed flight structures [AIAA PAPER 90-1105] p 449 A90-29286
- Thermal structures - Four decades of progress [AIAA PAPER 90-0971] p 411 A90-29305
- The prediction and measurement of thermoacoustic response of plate structures [AIAA PAPER 90-0988] p 451 A90-29400
- Electrochromic aircraft windows p 451 A90-29891
- Meteoropod, an airborne system for measurements of mean wind, turbulence, and other meteorological parameters p 418 A90-29943
- Virtual principles in aircraft structures. Volume 1 - Analysis. Volume 2 - Design, plates, finite elements --- Book p 452 A90-29977
- Honeycomb sandwich primary structure applications on the Boeing Model 360 helicopter p 490 A90-31558
- Adhesive-bonded composite-patching repair of cracked aircraft structure p 467 A90-31576
- Sandwich structures on Aerospace helicopters p 467 A90-31657
- Aerospace materials - Trends and potential p 529 A90-31902
- Some smart structures concepts p 503 A90-32858
- Fiber optics smart structures program at UTIAS p 535 A90-32864
- Development of a fibre optic damage detection system for an aircraft leading edge p 504 A90-32873
- Application of effective baselines to smart structures p 536 A90-32885
- Erosive wear of fibrous PEEK composites p 530 A90-33127
- Ground vibration testing of aeroplanes with a sequence of single-point excitations - Simple and effective p 522 A90-33371
- Flutter analysis from ambient random responses p 491 A90-33374
- Identification of time varying modal parameters p 536 A90-33375
- Design flutter calculations on PC p 545 A90-33379
- Gyroscopic matrices in computation of vibration p 547 A90-33381
- Structural-acoustic analysis of aircraft fuselage structures using general purpose finite element codes p 492 A90-33385
- The influence of mathematical optimization methods on the design of aircraft structures p 492 A90-33387
- Aeroelastic tailoring validation by windtunnel model testing p 492 A90-33389
- Structural optimization in view of aeroelastic constraints p 536 A90-33391
- A modal parameter identification technique and its application to large complex structures with multiple steady sinusoidal excitation p 602 A90-35670
- Exact solutions to the oscillations of composite aircraft wings with warping constraint and elastic coupling p 603 A90-36271
- An advanced X-ray technique for NDI p 604 A90-37901
- Automated helicopter structural analysis data processing p 611 A90-38533
- Multi-level models for diagnosis of complex electro-mechanical systems p 693 A90-38888
- Discrete Fourier transform with high resolution for low frequencies applied to the modal analysis of aircraft vibration p 679 A90-38975
- Multilevel optimization of large-scale structures in a parallel computing environment p 693 A90-39180
- Development and application of an optimization procedure for space and aircraft structures p 679 A90-39186
- Boundary-element shape optimization system for aircraft structural components p 680 A90-39786
- Stress concentration factors - Comparison of theory with fatigue test data p 680 A90-39979
- Certification testing methodology for fighter hybrid structure p 642 A90-40128
- Design and analysis aid for evaluating aircraft structures p 694 A90-41188
- Estimation of fatigue crack growth in patched cracked panels p 684 A90-41335
- NASA investigation of a claimed 'overlap' between two gust response analysis methods p 771 A90-44730
- Boeing 737 fuselage structural integrity program [SAE PAPER 892207] p 701 A90-45426
- Dealing with the aging fleet [SAE PAPER 892209] p 701 A90-45428
- Old lamps for new - A photoelastic design tool for weight and cost saving on aircraft structures p 878 A90-46039
- Multicriteria optimal layouts of aircraft and spacecraft structures p 889 A90-46046
- Wing design optimization under stress-strain constraints using full-strength and minimum mass criteria p 804 A90-46554
- A method for reducing a buckled skin under combined loading p 860 A90-46571
- Effect of shock waves and jets on structural elements: Mathematical modeling in nonstationary gas dynamics --- Russian book p 806 A90-46621
- A leap forward in aircraft construction technology - High-speed cutting sets new production standards p 881 A90-46720
- Developments in the acoustic fatigue design process for composite aircraft structures p 882 A90-48047
- Aging fleet Structures Working Group activities [AIAA PAPER 90-3219] p 786 A90-48840
- Comparison of equivalent plate and finite element analysis of a realistic aircraft structural configuration [AIAA PAPER 90-3293] p 837 A90-48877
- Upgrading the cockpit - A multidisciplinary approach p 848 A90-48995
- Metal laminates for aerospace applications p 874 A90-48997
- Analysis of failures in aircraft structures p 882 A90-48998
- Commuter from Khodinka --- Il-114 airliner p 842 A90-49824
- Assessment of service load experience p 901 A90-49877

- Tracking B-1B aircraft with a structural data recorder
p 926 A90-49880
- Fractographic techniques for the assessment of aircraft component cracking
p 954 A90-49885
- Application of the 'K-gage' to aircraft structural testing
p 926 A90-49891
- A probabilistic approach for the establishment of an aircraft structure inspection program
p 902 A90-49892
- Understanding composite fatigue - New trends
p 940 A90-49893
- Damage tolerance demonstration for A310-300 CFRP-components
p 919 A90-49894
- Safety and health trends in aerospace composite materials
p 947 A90-50188
- Material development and second source qualification of carbon fiber/epoxy prepreps for primary and secondary Airbus structures
p 948 A90-50225
- Analysis and interpretation of aircraft component defects using quantitative fractography
p 956 A90-50555
- The application of TSIM software to act design and analysis on flexible aircraft
p 60 N90-10086
- Modifying high-order aeroelastic math model of a jet transport using maximum likelihood estimation
p 61 N90-10106
- Flexible aircraft dynamic modeling for dynamic analysis and control synthesis
p 61 N90-10112
- Aircraft modal suppression system: Existing design approach and its shortcomings
p 33 N90-10115
- Structural stability augmentation system design using BODEDIRECT: A quick and accurate approach
p 33 N90-10116
- Thin walled cast high-strength structural parts
p 65 N90-10242
- Fatigue crack initiation mechanics of metal aircraft structures
[AD-A210567]
p 65 N90-10255
- Transport composite fuselage technology: Impact dynamics and acoustic transmission
[NASA-CR-4035]
p 126 N90-11821
- Investigation of difficult component effects on finite element model vibration prediction for the Bell AG-1G helicopter. Volume 2: Correlation results
[NASA-CR-181916-VOL-2]
p 213 N90-13814
- The microstructure and properties of aluminum-lithium alloys
p 267 N90-15187
- Fabrication of test-articles from Al-Li 2091 for Fokker 100
p 267 N90-15196
- Current status of the application of conventional aluminium-lithium alloys and the potential for future developments
p 268 N90-15203
- Integral fuel tanks - design, production, aging, repair
p 250 N90-15906
- A dynamicist's view of fuel tank skin durability
p 251 N90-15915
- Analysis of damaged components from DOE security helicopter N7EG
[DE90-004488]
p 324 N90-16729
- Optimum element density studies for finite-element thermal analysis of hypersonic aircraft structures
[NASA-TM-4163]
p 369 N90-17074
- Experimental investigation to suppress flow-induced pressure oscillations in open cavities
[AD-A216285]
p 320 N90-17578
- Flammability testing of aircraft cabin materials
p 328 N90-17611
- A study of the structural efficiency of fluted core graphite-epoxy panels
[NASA-TM-101681]
p 373 N90-18070
- X-29A aircraft structural loads flight testing
[NASA-TM-101715]
p 416 N90-19225
- A new method for measuring the transmissivity of aircraft transparencies
[AD-A216953]
p 464 N90-19842
- Computer-aided structural optimisation of aircraft structures
[BR112837]
p 499 N90-20973
- Robots for aircraft coatings removal: Parameters and requirements
[DE90-009429]
p 609 N90-22048
- Multilevel decomposition approach to the preliminary sizing of a transport aircraft wing
[NASA-CR-4296]
p 583 N90-22557
- NASA-UVA light aerospace alloy and structures technology program
[NASA-CR-182607]
p 601 N90-22651
- Some 1-(diorganoxyphosphonyl)methyl-2,4- and -2,6-dinitro-benzenes
[NASA-CASE-ARC-11425-3]
p 678 N90-23475
- Modeling growth of fatigue cracks which originate at rivet holes
p 691 N90-25060
- Flexural fatigue life prediction of closed hat-section using materially nonlinear axial fatigue characteristics
p 691 N90-25062
- Elevator tab assembly producibility study
[IAR-89-16]
p 734 N90-25133
- The effect of aircraft size on cabin floor dynamic pulses
[DOT/FAA/CT-88/15]
p 735 N90-25136
- Mechanical paint removal techniques for aircraft structures
[IAR-89-23]
p 773 N90-25254
- Behavior of composite/metal aircraft structural elements and components under crash type loads: What are they telling us
[NASA-TM-102681]
p 774 N90-25368
- Calculation of flight vibration levels of the AH-1G helicopter and correlation with existing flight vibration measurements
[NASA-CR-182031]
p 775 N90-25375
- Computational crash dynamics. Project 1.2: Computational crash dynamics analysis
[IAR-89-19]
p 724 N90-25956
- A contribution to the economic, optimal dimensioning, and shaping of aircraft structures using a design model
[ETN-90-96966]
p 737 N90-25976
- Mechanical paint removal techniques for aircraft structures
[NIAR-90-12]
p 775 N90-26166
- Materials and structures for 2000 and beyond: An attempted forecast by the DLR Materials and Structures Department
[ESA-TT-1154-REV]
p 775 N90-26173
- Neural networks for detecting defects in aircraft structures
[IAR-90-4]
p 777 N90-26345
- Proceedings of the 1987 Aircraft/Engine Structural Integrity Program (ASIP/ENSIP) Conference
[AD-A198037]
p 842 N90-26807
- Lessons learned for composite aircraft structures qualification
p 842 N90-26808
- An aluminum quality breakthrough for aircraft structural reliability
p 843 N90-26816
- Application of damage tolerance
p 843 N90-26817
- Photoelasticity: A cost effective design tool
p 883 N90-26819
- Finite element models of USAF aircraft structures
p 844 N90-26820
- Automated analysis of MXU-553 flight data
p 844 N90-26821
- A review of crashworthiness of composite aircraft structures
[AD-A221555]
p 846 N90-27697
- A Protection And Detection Surface (PADS) for damage tolerance
[NASA-TP-3011]
p 876 N90-27788
- Reinforcing fibers and technology development for resin composites. Consequences for aircraft structures
[FOA-C-20777-2.5]
p 876 N90-27883
- Characterization of the 7175 T7352. Dissection of a die casting standard spar
[CEAT-PV-M5/528900]
p 877 N90-27906
- NDI-concept for composites in future military aircraft
p 877 N90-28070
- An ultrasonic system for in-service non-destructive inspection of composite structures
p 885 N90-28076
- A technique for rapid inspection of composite aircraft structure for impact damage
p 846 N90-28077
- In-service inspection of composite components on aircraft at depot and field levels
p 885 N90-28078
- Neutron radiography: Applications and systems
p 886 N90-28080
- New aspects in aircraft inspection using eddy current methods
p 886 N90-28085
- Inspection system for in-situ inspection of aircraft composite structures
p 886 N90-28091
- Use of acoustic emission for continuous surveillance of aircraft structures
p 887 N90-28092
- Aircraft battle damage repair of transparencies
[AD-A224168]
p 925 N90-29387
- Evaluation of static and fatigue properties of thin sheets of 8090-T8 aluminum-lithium alloy and observation of its fracture surfaces
[NAL-TR-1039]
p 953 N90-29499
- Fatigue, static tensile strength and stress corrosion of aircraft materials and structures. Part 1: Text
[LR-630-PT-1-REV]
p 961 N90-29682
- Fatigue, static tensile strength and stress corrosion of aircraft materials and structures. Part 2: Figures
[LR-630-PT-2]
p 961 N90-29683
- AIRCRAFT SURVIVABILITY**
- Pilot's Associate - A perspective on Demonstration 2
[AIAA PAPER 89-3023]
p 36 A90-10524
- Enhanced combat damage tolerance/supportability for improved combat sustainability
[SAE PAPER 891078]
p 101 A90-14370
- V-22 ballistic vulnerability hardening program
p 408 A90-28223
- Strike tolerant main rotor blade tip
p 409 A90-28232
- Smart structures concept study
p 504 A90-32876
- Control of an aircraft in downbursts
p 755 A90-45331
- Composite flight control actuators
p 874 A90-48993
- In service life monitoring system using g-meter readings and mass configuration control
[ETN-89-95218]
p 134 N90-12035
- Multichannel on-board load and fatigue monitoring
p 849 N90-27621
- Advanced algorithms design and implementation in on-board microprocessor systems for engine life usage monitoring
p 892 N90-27628
- Survivable penetration
p 917 N90-29363
- AIRCRAFT TIRES**
- Elastic-viscoplastic finite-element program for modeling tire/soil interaction
p 401 A90-31285
- Analysis of aircraft tires via semianalytic finite elements
p 496 A90-34740
- Evaluation of critical speeds in high speed aircraft tires
[SAE PAPER 892349]
p 733 A90-45500
- Frictionless contact of aircraft tires
[SAE PAPER 892350]
p 733 A90-45501
- Aircraft tire/pavement pressure distributions
[SAE PAPER 892351]
p 734 A90-45502
- A theoretical and experimental investigation into the prerotation of aircraft tires
[AIAA PAPER 90-3272]
p 836 A90-48863
- Evaluation of two transport aircraft and several ground test vehicle friction measurements obtained for various runway surface types and conditions. A summary of test results from joint FAA/NASA Runway Friction Program
[NASA-TP-2917]
p 249 N90-15902
- Runaway rubber removal
[AD-A218349]
p 526 N90-20100
- Reliability and performance of friction measuring tires and friction equipment correlation
[AD-A223694]
p 939 N90-29408
- AIRCRAFT WAKES**
- Propeller wakes and their interaction with wings
p 14 A90-12614
- Wake behaviour of a large deflection turbine rotor linear cascade
p 157 A90-18481
- Effect of ground on wake roll-up behind a lifting surface
p 160 A90-19436
- Effects of splitter plates on the wake flow behind a bluff body
p 469 A90-32453
- Preliminary flight test investigation of an airborne wake vortex detection concept
[AIAA PAPER 90-1282]
p 495 A90-33903
- Installation effects on propeller wake/vortex-induced structure-borne noise transmissions
p 579 A90-35761
- The effect of Mach number on the stability of a plane supersonic wake
p 557 A90-36524
- Vorticity distribution of vortex street in the wake of a circular cylinder
p 623 A90-41751
- The low frequency oscillation in the flow over a NACA0012 airfoil with an 'iced' leading edge
p 801 A90-46377
- The wake vortex problem revisited
p 817 A90-46395
- Free wake analysis of rotor configurations for reduced vibratory airloads
p 833 A90-46975
- Measurements of simulated wake/rotor interaction phenomena in turbomachinery
p 814 A90-49475
- Development of a VSAERO (Vortex Separation Aerodynamics) model of the F/A-18
[AD-A212442]
p 95 N90-12566
- Effect of pylon wake with and without pylon blowing on propeller thrust
[NASA-TM-4162]
p 173 N90-14190
- Wind tunnel study of wake downwash behind A6 percent scale model B1-B aircraft
[DE90-011783]
p 719 N90-25941
- AIRDROPS**
- Modeling the effects of the use of GPS (Global Positioning System) derived altitude indication in the C-17A airdrop system
[AD-A215366]
p 333 N90-16748
- Advanced recovery systems wind tunnel test report
[NASA-CR-177563]
p 816 N90-27653
- AIRFIELD SURFACE MOVEMENTS**
- Fatigue damage of an aircraft due to movement on the airfield
p 247 A90-23352
- Elastic-viscoplastic finite-element program for modeling tire/soil interaction
p 401 A90-31285
- Current status of Joint FAA/NASA Runway Friction Program
[SAE PAPER 892340]
p 760 A90-45494
- Aircraft tire/pavement pressure distributions
[SAE PAPER 892351]
p 734 A90-45502
- Possibilities for improving traffic flows
p 823 A90-49272
- AIRFOIL FENCES**
- An investigation of strake fence flaps on a canard-configured aircraft
[AIAA PAPER 90-0762]
p 230 A90-22259

AIRFOIL OSCILLATIONS

Oscillating thin wings in inviscid incompressible flow
p 2 A90-10224

A numerical method solving 2-D unsteady flow field around cascade of oscillating airfoils with arbitrary camber and thickness
p 7 A90-11788

Self-excited oscillation of shock waves on an airfoil in two-dimensional transonic channel flow
p 8 A90-11808

Numerical calculation of unsteady aerodynamic forces for three-dimensional subsonic oscillating cascades by a finite element method
p 9 A90-12219

Hot wire measurements in the wake of an oscillating airfoil
p 15 A90-12635

Identification of rotor flapping equation of motion from flight measurements with the RSRA compound helicopter
p 56 A90-12769

Vortex interactions in fixed and oscillating delta wings (water tunnel visualizations)
p 16 A90-12784

Unified super/hypersonic similitude for steady and oscillating cones and ogives
p 82 A90-13786

A critique of the experimental aerodynamic data base for an oscillating straked wing at high angles
p 147 A90-16779

Hot-wire measurements of near wakes behind an oscillating airfoil
p 154 A90-18138

Numerical method for solving the Euler equation for unsteady transonic flows over oscillating airfoils
p 157 A90-18578

Unsteady surface pressure distributions on a delta wing undergoing large amplitude pitching motions
[AIAA PAPER 90-0311]
p 164 A90-19790

Amplitude effects on dynamic stall of an oscillating airfoil
[AIAA PAPER 90-0575]
p 167 A90-19925

Viscous oscillating cascade aerodynamics and flutter by a locally analytical method
[AIAA PAPER 90-0579]
p 168 A90-19929

Investigation of oscillating airfoil shock phenomena
[AIAA PAPER 90-0695]
p 169 A90-19981

Controlled three-dimensionality in unsteady separated flows about a sinusoidally oscillating flat plate
[AIAA PAPER 90-0689]
p 230 A90-22244

Unsteady transonic aerodynamics of oscillating airfoils in supersonic freestream
p 232 A90-23277

Self-excited oscillation of transonic flow around an airfoil in two-dimensional channel
[ASME PAPER 89-GT-58]
p 290 A90-23784

Vortex formation around an oscillating and translating airfoil at large incidences
p 303 A90-25588

Newtonian flow over oscillating two-dimensional airfoils at moderate or large incidence
p 383 A90-27976

The effect of an unsteady three-dimensional wake on elastic blade-flapping eigenvalues in hover
p 385 A90-28228

Periodic response of thin-walled composite blades
p 408 A90-28229

Relative aeromechanical stability characteristics for hingeless and bearingless rotors
p 409 A90-28230

Design and development of a facility for compressible dynamic stall studies of a rapidly pitching airfoil
p 436 A90-28255

Nonlinear aeroelasticity
[AIAA PAPER 90-1031]
p 391 A90-29375

Chaotic response of aerosurfaces with structural nonlinearities (Status report)
[AIAA PAPER 90-1034]
p 392 A90-29378

Computational prediction of stall flutter in cascaded airfoils
[AIAA PAPER 90-1116]
p 392 A90-29388

Simple marching-vortex model for two-dimensional unsteady aerodynamics
p 395 A90-31288

State-space representation of unsteady airfoil behavior
p 469 A90-32461

Oscillatory shock motion caused by transonic shock boundary-layer interaction
p 470 A90-32478

Unsteady airloads due to separated flow on airfoils and wings
p 471 A90-33311

Computation of unsteady transonic flows around oscillating airfoils using full potential and Euler equations
p 472 A90-33357

Two-dimensional compressible unsteady aerodynamics in the Laplace domain
p 472 A90-33360

Numerical analysis of unsteady forces on oscillating ring airfoils and jet engines
p 473 A90-33364

A modern course in aeroelasticity (2nd revised and enlarged edition) --- Book
p 497 A90-34968

Thrust generation by an airfoil in hover modes
[AD-A223602]
p 552 A90-35137

Dynamic stall experiments on the NACA 23012 airfoil
p 552 A90-35140

Euler flutter analysis of airfoils using unstructured dynamic meshes
p 602 A90-35760

Parameter effects on oscillatory airfoil in transonic flows
[AIAA PAPER 90-1473]
p 563 A90-38629

Flow visualization studies of the Mach number effects on dynamic stall of an oscillating airfoil
p 622 A90-40683

Flow induced forced response of an incompressible radial cascade including profile and incidence effects
[AIAA PAPER 90-2352]
p 626 A90-42136

Self-induced roll oscillations of low-aspect-ratio rectangular wings
[AIAA PAPER 90-2811]
p 753 A90-45151

An experimental study of the nonlinear dynamic phenomenon known as wing rock
[AIAA PAPER 90-2812]
p 753 A90-45152

Delta wing surface pressures for high angle of attack maneuvers
p 711 A90-45153

Numerical solutions for unsteady aerofoil by internal singularity method
p 716 A90-45536

Effect of leading edge roundness on a delta wing in wing-rock motion
[AIAA PAPER 90-3080]
p 795 A90-45911

Transient aeroelastic computations using multiple moving frames of reference
[AIAA PAPER 90-3053]
p 798 A90-45932

The low frequency oscillation in the flow over a NACA0012 airfoil with an 'iced' leading edge
p 801 A90-46377
p 806 A90-46850

Interactive grid adaption
p 806 A90-46850

Interactive boundary-layer method for unsteady airfoil flows - Quasisteady model
p 812 A90-48953

Effects of transition on wind tunnel simulation of vehicle dynamics
p 870 A90-49273

Numerical simulation of transonic flow through oscillating and multi-row two-dimensional airfoil cascades
p 814 A90-49460

A panel method computation for oscillating aerofoil in compressible flow
p 906 A90-51483

Dynamic testing techniques and applications for an aeroelastic rotor test facility
p 201 A90-13406

Nonlinear phenomena in computational transonic aeroelasticity
p 235 A90-15070

An interactive boundary-layer method for unsteady airfoil flows. Part 1: Quasi-steady-state model
[AD-A221220]
p 634 A90-24250

Flow visualization of dynamic stall on an oscillating airfoil
[AD-A222202]
p 815 A90-26797

AIRFOIL PROFILES

The effect of pitch location on dynamic stall
p 2 A90-10641

An experimental investigation of the effect of incidence on the two-dimensional performance of an axial turbine cascade
p 11 A90-12520

Turbulent separated flow over and downstream of a two-element airfoil
p 16 A90-12738

Investigation of flow separation on a supercritical airfoil
p 17 A90-13023

Transonic flow over a single wedge
p 85 A90-15237

Experimental study of 2D/3D interactions between a vortical flow and a lifting surface
p 86 A90-15849

Three-dimensional aerodynamics of an annular airfoil cascade including loading effects
p 87 A90-15889

Airfoil noise in a uniform flow
p 139 A90-16330

An interactive boundary layer method for subsonic airfoil flows
p 144 A90-16754

The flow around wing-body junctions
p 145 A90-16765

Calculation of flow over airfoil with slat and flap
p 149 A90-16797

Airfoils in supersonic source and sink flows
p 149 A90-16844

Aircraft design: A conceptual approach --- Book
p 179 A90-17307

Low Reynolds number airfoils evaluation program
p 151 A90-17692

Sound radiation from an airfoil encountering an oblique gust in its plane of motion
p 218 A90-17998

Experimental investigation of flowfield about a multielement airfoil
p 154 A90-18137

Simulation of high incidence unsteady flow past Joukowski airfoils
p 156 A90-18301

Comparison of NACA 65, CDA, and tandem bladed cascades
p 190 A90-18484

An investigation of unsteady leading edge separation of rapidly pitched airfoils
p 157 A90-18587

Wall interference correction of high-lift multi-component airfoils
p 158 A90-18604

Experimental investigation of trailing-edge and near wake flow of a symmetric airfoil
p 160 A90-19449

Alleviation of shock oscillations in transonic flow by passive controls
[AIAA PAPER 90-0046]
p 161 A90-19648

Calculation of low Reynolds number flows at high angles of attack
[AIAA PAPER 90-0569]
p 167 A90-19921

The influence of a rotating leading edge on accelerating starting flow over an airfoil
[AIAA PAPER 90-0583]
p 168 A90-19932

Application of an adaptive algorithm to single and two-element airfoils in turbulent flow
[AIAA PAPER 90-0698]
p 169 A90-19983

Fortified LEWICE with viscous effects --- Lewis Ice Accretion Prediction Code
[AIAA PAPER 90-0754]
p 176 A90-20009

A computer aided manufacturing procedure for experimental two-dimensional aerofils
p 270 A90-20609

Analysis of transonic integral equations. I - Artificial viscosity
p 232 A90-23124

Unconventional leading edges of airfoils
p 233 A90-23356

An approximate method for calculating flow past a wing profile with allowance for viscosity
p 234 A90-23422

Design of symmetric profiles with maximum critical flow Mach number under prescribed constraints
p 295 A90-24095

Application of Fedorenko's multigrid method for calculating transonic flow past a profile
p 295 A90-24103

Numerical solutions of the linearized Euler equations for unsteady vortical flows around lifting airfoils
[AIAA PAPER 90-0694]
p 300 A90-25041

Topological study of three-dimensional vortex interactions
p 367 A90-25885

A semi-analytical procedure for the conformal mapping of arbitrary airfoil contours
p 309 A90-26498

Measurements in a separation bubble on an airfoil using laser velocimetry
p 384 A90-27977

Droplet impaction on a supersonic wedge - Consideration of similitude
p 400 A90-27986

Fast adaptive grid method for compressible flows
p 445 A90-28006

Effect of a jet on transonic flow past an airfoil
p 388 A90-29181

Prediction of heat transfer coefficient on turbine blade profiles
p 423 A90-29904

Wind-tunnel investigation of wing-in-ground effects
p 395 A90-31276

Galerkin finite element method for transonic flow about airfoils and wings
p 396 A90-31486

Vortex method modelling the unsteady motion of a thick airfoil
p 396 A90-31489

Multi-element aerofils in viscous flow
p 469 A90-32451

Experimental investigation of the flow development of an airfoil at high angles of attack
p 473 A90-33366

An improved incidence losses prediction method for turbine airfoils
[ASME PAPER 89-GT-284]
p 475 A90-33563

Correlation of lift and thickness noise sources in vortex-airfoil interaction
p 547 A90-34090

An implicit scheme with flow correction for the numerical solution of the Euler equation
p 477 A90-34674

Dynamic stall of a constant-rate pitching airfoil
p 553 A90-35754

Freestream turbulence effects on airfoil boundary-layer behavior at low Reynolds numbers
p 554 A90-35768

Unsteady aerodynamic gust response including steady flow separation
p 556 A90-36262

Interaction between boundary layer and wakes of different bodies
p 602 A90-38263

Effect of surface grooves on base pressure for a blunt trailing-edge airfoil
p 556 A90-36280

Wall interference assessment/correction (WIA) for transonic airfoil data from porous and shaped wall test sections
[AIAA PAPER 90-1406]
p 595 A90-37945

A numerical study on the use of sulfur hexafluoride as a test gas for wind tunnels
[AIAA PAPER 90-1421]
p 605 A90-37958

The effect of an oscillatory freestream-flow on a NACA-4412 profile at large relative amplitudes and low Reynolds-numbers
p 560 A90-38495

Newton solution of coupled viscous/inviscid multielement airfoil flows
[AIAA PAPER 90-1470]
p 562 A90-38627

Numerical prediction of transonic viscous flows around airfoils through an Euler/boundary layer interaction method
[AIAA PAPER 90-1537]
p 564 A90-38681

Direct simulation of low-density flow over airfoils
[AIAA PAPER 90-1539]
p 564 A90-38683

A general decomposition algorithm applied to multi-element airfoil grids
[AIAA PAPER 90-1606]
p 567 A90-38737

The organized nature of a turbulent trailing vortex
[AIAA PAPER 90-1625]
p 568 A90-38754

Temporal-adaptive Euler/Navier-Stokes algorithm for unsteady aerodynamic analysis of airfoils using unstructured dynamic meshes
[AIAA PAPER 90-1650]
p 569 A90-38778

Algebraic turbulence modeling for unstructured and adaptive meshes
[AIAA PAPER 90-1653] p 608 A90-38781

Mathematical modeling of plane parallel separated flows past bodies --- Russian book p 619 A90-39475

An introduction to chaos theory in CFD
[AIAA PAPER 90-1440] p 680 A90-39725

Transonic flow around airfoils with relaxation and energy supply by homogeneous condensation p 620 A90-39782

A visualization study of the interaction of a free vortex with the wake behind an airfoil p 623 A90-41119

Application of 3-D Navier-Stokes computation to bowed stacking turbine vane design
[AIAA PAPER 90-2129] p 625 A90-42035

Bonded airfoil attachments - A path to rotor structural efficiency
[AIAA PAPER 90-2177] p 686 A90-42061

Wind tunnel results and numerical computations for the NAE deHavilland series of natural laminar flow airfoils p 628 A90-42403

A Volterra kernel identification scheme applied to aerodynamic reactions
[AIAA PAPER 90-2803] p 712 A90-45178

Application of divergent trailing-edge airfoil technology to the design of a derivative wing
[SAE PAPER 892288] p 714 A90-45466

Some remarks on the Kutta condition p 716 A90-45738

Trajectories of vortex lines beneath a free surface or above a plane p 716 A90-45740

Thick airfoil designs for a HALE vehicle --- High Altitude Long Endurance
[AIAA PAPER 90-3036] p 791 A90-45875

On the drag reduction of bluff bodies through momentum injection
[AIAA PAPER 90-3076] p 797 A90-45922

An unstructured-mesh Euler method for multielement airfoil geometries
[AIAA PAPER 90-3051] p 797 A90-45930

Wake effects on the prediction of transonic viscous flows around airfoils with an Euler/boundary layer interaction approach
[AIAA PAPER 90-3061] p 798 A90-45933

Low Reynolds number aerodynamics; Proceedings of the Conference, University of Notre Dame, IN, June 5-7, 1989 p 799 A90-46358

Low Reynolds number airfoil design and wind tunnel testing at Princeton University p 799 A90-46362

The low frequency oscillation in the flow over a NACA0012 airfoil with an 'iced' leading edge p 801 A90-46377

Low Reynolds number airfoil design for subsonic compressible flow p 802 A90-46380

Profiling of the supersonic components of three-dimensional corrugated nozzles p 804 A90-46563

Some possibilities of the vortex layer method for calculating the aerodynamic characteristics of an augmented airfoil interacting with the engine jet p 804 A90-46564

Determination of the laminar-turbulent transition point for a turbulent layer on a yawing wing p 805 A90-46566

Acoustic excitation of boundary layer oscillations on a yawing wing p 805 A90-46567

The servo flap - An advanced rotor control system p 860 A90-46934

Improvement to interactive two dimensional rotor section design p 808 A90-46943

Airfoil design and data --- Book p 809 A90-47608

Airfoil static-pressure thrust - Flight-test verification
[AIAA PAPER 90-3286] p 812 A90-48873

The inverse problem in the multielement airfoil theory p 906 A90-51531

Design of the low-speed NLF(1)-0414F and the high-speed HSNLF(1)-0213 airfoils with high-lift systems p 93 N90-12540

Wind tunnel results of the high-speed NLF(1)-0213 airfoil p 93 N90-12542

Design and test of a natural laminar flow/large Reynolds number airfoil with a high design cruise lift coefficient p 93 N90-12543

Residual interference assessment in adaptive wall wind tunnels
[NASA-CR-181896] p 123 N90-12625

Computation of unsteady transonic flow about airfoils in frequency domain using the full-potential equation p 174 N90-14198

Detection of flow instabilities at airfoil profiles using piezoelectric arrays p 276 N90-16175

Use of the film-of-oil technique for profile measurements in the Transonic Wind tunnel Brunswick (TWB) p 238 N90-16252

CAST-10-2/DOA 2 Airfoil Studies Workshop Results
[NASA-CP-3052] p 352 N90-17647

Investigation of CAST-10-2/DOA 2 airfoil in NAE high Reynolds number two-dimensional test facility p 321 N90-17654

Experimental and theoretical aerodynamic characteristics of a high-lift semispan wing model
[NASA-TP-2990] p 477 N90-20046

Optimum hypersonic airfoils with attached shocks p 481 N90-20960

The MANTA: An RPV design to investigate forces and moments on a lifting surface
[NASA-CR-186227] p 499 N90-20971

Inverse design of airfoil contours: Constraints, numerical method, and applications p 500 N90-20980

An efficient airfoil design method using the Navier-Stokes equations p 500 N90-20981

Numerical optimization of target pressure distributions for subsonic and transonic airfoil design p 502 N90-20993

Adaptive grid embedding for the two-dimensional flux-split Euler equations
[NASA-CR-186533] p 547 N90-21571

The SKY SHARK: An RPV designed to investigate the pressure distribution on a lifting surface
[NASA-CR-186222] p 844 N90-26824

A two dimensional study of rotor/airfoil interaction in hover
[NASA-CR-183272] p 845 N90-27694

WingDesign: Program for the structural design of a wing cross-section
[LR-627] p 925 N90-29390

AIRFOILS

Numerical analysis of flow of an ideal fluid past an airfoil p 2 A90-10228

USA - A system to represent airfoils throughout the product life cycle
[AIAA PAPER 89-2972] p 73 A90-10487

Color schlieren system using square color filter and its application to aerofoil test in transonics p 66 A90-10748

An improved method for the computation of unsteady transonic potential flow - Application for airfoil and blade performance prediction
[ONERA, TP NO. 1989-154] p 4 A90-11175

On unsteady surface forces, and sound produced by the normal chopping of a rectilinear vortex p 5 A90-11604

Evaluation of two numerical techniques for the prediction of flow around blades p 10 A90-12512

Comparative cascade studies of some high diffusion compressor bladings p 15 A90-12637

Numerical solution of transonic flows on a streamfunction co-ordinate system p 17 A90-13238

The effect of trailing edge extensions on the performance of the Goettingen 797 and the Wortmann FX 63-137 aerofoil section at Reynolds numbers between 3×10^5 to the 5th and 1×10^6 to the 6th p 82 A90-13783

Computation of flow over airfoils under high lift separated flow condition p 86 A90-15741

Predictions of airfoil aerodynamic performance degradation due to icing p 144 A90-16753

Computation of multi-element airfoil flows including confluence effects p 144 A90-16755

Prediction of post-stall flows on airfoils p 145 A90-16757

Further work on aerofoils at Reynolds numbers between 3×10^5 to the 5th and 1×10^6 to the 6th p 145 A90-16758

On the effects of wind tunnel turbulence on steady and unsteady airfoil characteristics p 147 A90-16777

Transition phenomena on airfoils operating at low chord Reynolds numbers in steady and unsteady flow p 148 A90-16786

Prediction of transition on airfoils with separation bubbles, swept wings and bodies of revolution at incidence p 148 A90-16790

Transition effects on airfoil dynamics and the implications for subscale tests p 152 A90-17862

Computation of viscous transonic flow over porous airfoils p 153 A90-17864

Essential ingredients of a method for low Reynolds-number airfoils p 153 A90-17979

Mechanism of sidewall effect studied with oil flow visualization p 154 A90-18002

Effect of moving surfaces on the airfoil boundary-layer control p 159 A90-19388

Unsteady incompressible aerodynamics and forced response of detuned blade rows
[AIAA PAPER 90-0340] p 191 A90-19805

An advanced pneumatic impulse ice protection system (PIIP) for aircraft
[AIAA PAPER 90-0492] p 182 A90-19875

A numerical study of general viscous flows around multi-element airfoils
[AIAA PAPER 90-0572] p 167 A90-19922

Development of an unstructured mesh/Navier-Stokes method for aerodynamics of aircraft with ice accretions
[AIAA PAPER 90-0758] p 169 A90-20011

Convective heat transfer measurements from a NACA 0012 airfoil in flight and in the NASA Lewis Icing Research Tunnel
[AIAA PAPER 90-0199] p 272 A90-22180

A zonal flow analysis method for two-dimensional airfoils
[AIAA PAPER 90-0571] p 230 A90-22230

Airfoil pressure measurements during a blade vortex interaction and a comparison with theory p 232 A90-23105

Integral solution of unsteady full-potential equation for a transonic pitching airfoil p 232 A90-23280

The influence of selected geometrical and mass parameters on the structural dynamics of an aircraft with a variable-geometry airfoil p 346 A90-24284

Nonlinear aerodynamics of two-dimensional airfoils in severe maneuver p 301 A90-25276

A high-order time-accurate scheme and its applications p 304 A90-25732

Numerical calculation of bubbly two phase flow around an airfoil p 304 A90-25783

Design of low Reynolds number airfoils. I p 307 A90-26129

Air/water two-phase flow test tunnel for airfoil studies p 352 A90-26842

Infrared imaging and tufts studies of boundary layer flow regimes on a NACA 0012 airfoil p 446 A90-28268

Instrumentation requirements for laminar flow research in the NLR high speed wind tunnel HST p 447 A90-28283

Development of a dual strain gage balance system for measuring light loads p 437 A90-28289

A strong viscous-inviscid interaction method for computing unsteady transonic airloads for use in aeroelastics p 471 A90-33355

Transition from order to chaos in the wake of an airfoil p 474 A90-33506

Fiber reinforced superalloys p 532 A90-34169

An abbreviated Reynolds stress turbulence model for airfoil flows
[AIAA PAPER 90-1468] p 562 A90-38625

Numerical prediction of turbulent flow over airfoil sections with a new nonequilibrium turbulence model
[AIAA PAPER 90-1469] p 562 A90-38626

Interactive airfoil calculations with higher-order viscous-flow equations
[AIAA PAPER 90-1533] p 564 A90-38678

A flow around airfoil with slat and flap
[AIAA PAPER 90-1535] p 564 A90-38679

Determination of aerodynamic sensitivity coefficients based on the transonic small perturbation formulation p 622 A90-40682

A transonic airfoil design method and examples p 627 A90-42351

Higher-order boundary-layer approximations in interactive airfoil calculations p 628 A90-42402

Application of the moving surface boundary layer control to a two dimensional airfoil p 628 A90-42405

Nonlinear unsteady airfoil response studies p 628 A90-42406

Automated generation of two-dimensional non-overlapping structured grids for multiple element airfoils with Euler solutions p 629 A90-42422

Computation of viscous aerodynamic characteristics of 2-D airfoils for helicopter applications p 631 A90-42440

An aerofoil testing technique for low supersonic speeds in an adaptive flexible-walled wind tunnel
[AIAA PAPER 90-3086] p 795 A90-45900

Angle-of-attack validation of a new zonal CFD method for airfoil simulations
[AIAA PAPER 90-3077] p 795 A90-45908

A characterization and search technique for unsteady flow control problems
[AIAA PAPER 90-3102] p 796 A90-45914

An experimental study of a closely coupled tandem wing configuration at low Reynolds numbers
[AIAA PAPER 90-3094] p 797 A90-45923

Adaptive grid embedding for the two-dimensional Euler equations
[AIAA PAPER 90-3049] p 797 A90-45929

Low Reynolds number aerodynamics; Proceedings of the Conference, University of Notre Dame, IN, June 5-7, 1989 p 799 A90-46358

Prediction of aerodynamic performance of airfoils in low Reynolds number flows p 799 A90-46360

A fast method for computation of airfoil characteristics p 799 A90-46361

Study of low-Reynolds number separated flow past the Wortmann FX 63-137 airfoil p 799 A90-46363

An interactive boundary-layer stability-transition approach for low Reynolds-number airfoils p 799 A90-46364

- A review of low Reynolds number aerodynamic research at the University of Glasgow p 800 A90-46367
- Experimental aerodynamic characteristics of the airfoils LA 5055 and DU 86-084/18 at low Reynolds numbers p 800 A90-46368
- Performance measurements of an airfoil at low Reynolds numbers p 800 A90-46369
- Correlation of theory to wind-tunnel data at Reynolds numbers below 500,000 p 800 A90-46370
- A method to determine the performance of low-Reynolds-number airfoils under off-design unsteady freestream conditions p 801 A90-46375
- Control of low-Reynolds-number airfoils - A review p 801 A90-46376
- Detachment of turbulent boundary layers with varying free-stream turbulence and lower Reynolds numbers p 802 A90-46378
- Compressible Navier-Stokes solutions over low Reynolds number airfoils p 802 A90-46382
- Summary of experimental testing of a transonic low Reynolds number airfoil p 802 A90-46384
- Unsteady Euler airfoil solutions using unstructured dynamic meshes p 809 A90-47307
- Control of wall-separated flow by internal acoustic excitation p 809 A90-47314
- Airfoil design and data --- Book p 809 A90-47608
- Subsonic and transonic low-Reynolds-number airfoils with reduced pitching moments p 812 A90-48838
- [AIAA PAPER 90-3212] p 812 A90-48838
- Experimental investigation of multielement airfoil ice accretion and resulting performance degradation p 812 A90-48954
- Control of low-speed airfoil aerodynamics p 814 A90-49776
- Basic studies of the unsteady flow past high angle of attack airfoils p 18 N90-10008
- [AD-A210252] p 18 N90-10008
- Goertler instability on an airfoil: Comparison of marching solution with experimental observations p 19 N90-10364
- Simultaneous detection of separation and transition in surface shear layers p 72 N90-10368
- The structure of separated flow regions occurring near the leading edge of airfoils - including transition [NASA-CR-185853] p 87 N90-11695
- Goertler instability on an airfoil p 91 N90-12517
- The design of an airfoil for a high-altitude, long-endurance remotely piloted vehicle p 104 N90-12545
- Studies of gas turbine heat transfer airfoil surfaces and end-wall cooling effects [AD-A212451] p 117 N90-12620
- Analysis of experimental data for CAST 10-2/DOA 2 supercritical airfoil at low Reynolds numbers and application to high Reynolds number flow [AD-A211654] p 170 N90-13326
- Convective heat transfer measurements from a NACA 0012 airfoil in flight and in the NASA Lewis Icing Research Tunnel [NASA-TM-102448] p 213 N90-13750
- Navier-Stokes solutions of 2-D transonic flow over unconventional airfoils p 173 N90-14195
- A one equation turbulence model for transonic airfoils p 174 N90-14199
- Computational investigation of incompressible airfoil flows at high angles of attack [AD-A205885] p 174 N90-14201
- Stall/spin aerodynamic data project [DOT/FAA/CT-88/29] p 185 N90-14222
- Unsteady aerodynamics of oscillating and rapidly pitched airfoils p 235 N90-15074
- Experimental measurements of the laminar separation bubble on an Eppler 387 airfoil at low Reynolds numbers [NASA-CR-186263] p 275 N90-15380
- Test techniques for cryogenic wind tunnels p 263 N90-15952
- Models for cryogenic wind tunnels p 263 N90-15956
- An interactive method for the flow calculation of airfoils with local separation regions p 278 N90-16190
- Convergence speeding up in the calculation of the viscous flow about an airfoil p 279 N90-16194
- Periodically unsteady effects on profiles, induced by separation p 279 N90-16196
- An improvement of convection fidelity in Euler calculations p 315 N90-16709
- Numerical solutions of the linearized Euler equations for unsteady vortical flows around lifting airfoils [NASA-TM-102466] p 318 N90-17562
- Effect of riblets on flow separation from a cylinder and an airfoil in subsonic flow [AD-A216197] p 319 N90-17574
- CAST-10-2/DOA 2 Airfoil Studies Workshop Results [NASA-CP-3052] p 352 N90-17647
- Nonlinear transonic Wall-Interference Assessment/Correction (WIAC) procedures - and application to cast-10 airfoil results from the NASA 0.3-m TCT 8- by 24-inch Slotted Wall Test Section (SWTS) p 352 N90-17648
- High Reynolds number tests of the CAST-10-2/DOA 2 transonic airfoil at ambient and cryogenic temperature conditions p 320 N90-17650
- Some Navier-Stokes calculations for the CAST-10 airfoil p 320 N90-17651
- Main results of CAST-10 airfoil tested in T2 cryogenic wind tunnel p 321 N90-17652
- An experimental AWTS process and comparisons of ONERA T2 and 0.3-m TCT AWTS data for the ONERA CAST-10 airfoil p 321 N90-17653
- Investigation of CAST-10-2/DOA 2 airfoil in NAE high Reynolds number two-dimensional test facility p 321 N90-17654
- Comparison of NAE porous wall and NASA adaptive wall test results using the NAE CAST-10 airfoil model p 353 N90-17656
- Comparison of two- and three-dimensional Navier-Stokes solutions with NASA experimental data for CAST-10 airfoil p 321 N90-17658
- Unsteady viscous calculation method for cascades with leading edge induced separation p 426 N90-18408
- Asymptotic analysis of transonic flow through oscillating cascades p 427 N90-18421
- Measurement of velocity profiles and Reynolds stresses on an oscillating airfoil p 397 N90-18427
- Calculation of excrescence drag magnification due to pressure gradient at high subsonic speeds [ESDU-87004] p 397 N90-19195
- Heat transfer measurements from a NACA 0012 airfoil in flight and in the NASA Lewis icing research tunnel [NASA-CR-4278] p 399 N90-19203
- Analysis and design of symmetrical airfoils [PD-CF-8943] p 400 N90-19213
- Numerical simulations of supersonic flow through oscillating cascade sections [NASA-TM-103100] p 478 N90-20051
- Ultrasonic techniques for aircraft ice accretion measurement p 485 N90-20926
- Comparison of C- and O-grid generation methods using a NACA 0012 airfoil [AD-A216375] p 479 N90-20948
- Progress in inverse design and optimization in aerodynamics p 482 N90-20977
- An efficient airfoil design method using the Navier-Stokes equations p 500 N90-20981
- A fast collocation method for transonic airfoil design p 501 N90-20984
- A computational design method for shock free transonic cascades and airfoils p 501 N90-20986
- A tool for automatic design of airfoils in different operating conditions p 502 N90-20994
- The use of numerical optimization for helicopter airfoil and blade design p 502 N90-20995
- Aerodynamic design by optimization p 502 N90-20996
- Optimization of aerodynamic designs using computational fluid dynamics p 541 N90-20999
- The effects of compressor endwall flow on airfoil incidence and deviation p 512 N90-21011
- Research on cascade secondary and tip-leakage flows: Periodicity and surface flow visualization p 514 N90-21026
- Control of flow separation and mixing by aerodynamic excitation [NASA-TM-103131] p 571 N90-21733
- A computer code for the prediction of aerodynamic characteristics of lifting airfoils at transonic speed [DLC-EST-TN-030] p 632 N90-23359
- Prediction of aerodynamic performance of airfoils in low Reynolds number flows [DLC-EST-TN-031] p 632 N90-23360
- Euler code predicted separation at the airfoil trailing edge [FFA-TN-1989-30] p 632 N90-23364
- The computation of turbulent thin shear flows associated with flow around multielement aeroflows p 633 N90-24240
- An analytic study of nonsteady two-phase laminar boundary layer around an airfoil p 691 N90-25051
- Computation of viscous aerodynamic characteristics of 2-D airfoils for helicopter applications [NLR-MP-88052-U] p 720 N90-25951
- On central-difference and upwind schemes [NASA-CR-182061] p 781 N90-26595
- Flow visualization of dynamic stall on an oscillating airfoil [AD-A222202] p 815 N90-26797
- A heat transfer analysis for rough turbine airfoils [AD-A221942] p 854 N90-26831
- A comparison of two central difference schemes for solving the Navier-Stokes equations [NASA-TM-102815] p 816 N90-27654
- Development of a linearized unsteady aerodynamic analysis for cascade gust response predictions [NASA-CR-4308] p 816 N90-27655
- Aerodynamics of a linear oscillating cascade [NASA-TM-103250] p 817 N90-27657
- The effect of rapid spoiler deployment on the transient forces on an aerofoil p 921 N90-28527
- A boundary-layer transition model for the Navier-Stokes computation for a natural-laminar-flow airfoil [NAL-TR-1038T] p 912 N90-29328
- The computation and analysis of acoustic waves in transonic airfoil-vortex interactions p 966 N90-30031
- ### AIRFRAME MATERIALS
- History of the airframe. IV p 30 A90-12791
- Advanced materials to fly high in NASP p 203 A90-17297
- Materials pace aerospace technology p 203 A90-17298
- Demonstration of probabilistic-based durability analysis method for metallic airframes p 273 A90-23287
- Testing of statistical hypotheses and derivation of confidence intervals from inspection data samples p 363 A90-24087
- Efficient structural material distribution in the main frame of a flight vehicle p 363 A90-24092
- Examination of dynamic characteristics of UH-60A and EH-60A airframe structures p 406 A90-28154
- Avionics and electromagnetic compatibility (EMC) considerations on a helicopter with an advanced composite airframe p 417 A90-28217
- The all-composite airframe - Design and certification p 413 A90-29890
- Strength substantiation of the all composite airframe (A materials data base approach) p 490 A90-31519
- Automated R.T.M. for an airframe component --- Resin Transfer Molding p 534 A90-31881
- Usage monitoring of military helicopters p 651 A90-39984
- SH-2F airframe fatigue test program p 642 A90-39989
- The analysis and testing of composite panels subject to muzzle blast effects p 675 A90-39991
- The influence of material quality on airframe structural durability p 676 A90-41336
- Maritime environment airframe material fatigue testing p 764 A90-42675
- Quench sensitivity of airframe aluminium alloys p 765 A90-44348
- Safety and health trends in aerospace composite materials p 947 A90-50188
- Aircraft crash survival design guide. Volume 5: Aircraft postcrash survival [AD-A218438] p 575 N90-22549
- The stress and temperature dependence of creep in an Al-2.0 wt percent Li alloy [AD-A223676] p 953 N90-29480
- ### AIRFRAMES
- A review of fiber optic flight experience - Past problems, future direction p 38 A90-11661
- Airframe structural design: Practical design information and data on aircraft structures --- Book p 103 A90-16624
- Analysis methods of tie-down loads and airframe stress for shipboard-helicopters p 199 A90-16855
- New progress in airframe durability requirements p 246 A90-22001
- Development of jet transport airframe fatigue test spectra p 351 A90-26753
- Prediction and measurement of the aerodynamic interactions between a rotor and airframe in forward flight p 384 A90-28176
- Stochastic crack growth analysis methodologies for metallic structures [AIAA PAPER 90-1015] p 449 A90-29340
- Time domain simulations of a flexible wing in subsonic, compressible flow [AIAA PAPER 90-1153] p 390 A90-29365
- Natural honeycomb --- use of balsa wood in sandwich panel cores for advanced composite airframes p 442 A90-29643
- Three approaches to reliability analysis p 452 A90-30706
- Air Force manufacturing technology NDE programs supporting manufacturing and maintenance p 452 A90-30779
- The cryogenic wind tunnel as a testing tool for airframe/propulsion systems p 672 A90-40400
- Recent advances in fatigue life analysis methods for aerospace applications p 677 A90-41338
- The standard-setting Hornet p 730 A90-43764
- Mi-14 - The Soviet Sea King p 730 A90-43765
- The McDonnell Douglas MD-11 ... or, how the DC-10 grew bigger p 730 A90-43766

Building the B-2 p 701 A90-43826
Design and certification of the all-composite airframe
[SAE PAPER 892210] p 732 A90-45429
A generalized relation for the aerodynamic efficiency of plane bodies p 804 A90-46559
Experiences in NASTRAN airframe vibration prediction at Bell Helicopter Textron p 832 A90-46964
V-22 MSC/NASTRAN airframe vibration analysis and correlation p 832 A90-46969
Developments in ground vibration test and data analysis techniques for airframe structures p 832 A90-46970
A supersonic through-flow fan engine airframe integration study p 18 N90-10004
[NASA-CR-185140]
A review of Australian and New Zealand investigations on aeronautical fatigue during the period April 1987 to March 1989 p 32 N90-10026
[AD-A210373]
Airframe structural dynamic considerations in rotor design optimization p 134 N90-12057
[NASA-TM-101646]
Investigation of difficult component effects on finite element model vibration prediction for the Bell AH-1G helicopter. Volume 1: Ground vibration test results p 134 N90-12058
[NASA-CR-181916-VOL-1]
Airframe design considerations: Overview --- rotor design optimization p 106 N90-12586
Investigation of difficult component effects on finite element model vibration prediction for the Bell AG-1G helicopter. Volume 2: Correlation results p 213 N90-13814
[NASA-CR-181916-VOL-2]
An experimental investigation of the interaction between a model rotor and airframe in forward flight p 185 N90-14219
An analytical method for the prediction of unsteady rotor/airframe interactions in forward flight p 186 N90-14223
Application of the joined wing to tiltrotor aircraft [NASA-CR-177543] p 248 N90-15093
The use of prototypes in selected foreign fighter aircraft development programs: Rafale, EAP, Lavi, and Gripen [AD-A214500] p 287 N90-16707
Hypersonic nozzle/afterbody performance at low Mach numbers p 319 N90-17575
[AD-A216223]
Calculation of flight vibration levels of the AH-1G helicopter and correlation with existing flight vibration measurements p 454 N90-18743
[NASA-CR-181923]
Fatigue crack initiation and small crack growth in several airframe alloys p 454 N90-18746
[NASA-TM-102598]
Static strength and damage tolerance tests on the Fokker 100 airframe p 416 N90-19228
[NLR-MP-88023-U]
Floor pull test of a transport airframe section p 497 N90-20072
[DOT/FAA/CT-TN88/14]
Compendium of abstracts and viewgraphs p 532 N90-20140
[AD-A217189]
Plan, formulate, and discuss a NASTRAN finite element model of the UH-60A helicopter airframe p 541 N90-20439
[NASA-CR-181975]
NASA airframe structural integrity program p 543 N90-21422
[NASA-TM-102637]
Aircraft crash survival design guide. Volume 3: Aircraft structural crash resistance p 575 N90-22547
[AD-A218436]
Flutter investigations on a Transavia PL12/T-400 aircraft p 593 N90-22570
[AD-A219108]
Characterisation of fatigue of aluminium alloys by acoustic emission. Part 2: Discrimination between primary and other emissions p 678 N90-23523
[AERE-R-13303-PT-2]
Ground shake test of the UH-60A helicopter airframe and comparison with NASTRAN finite element model predictions p 758 N90-25143
[NASA-CR-181993]
Velocity measurements on a lifting rotor/airframe configuration in low speed forward flight p 815 N90-26790
Aircraft lightning protection handbook [AD-A222716] p 820 N90-27668
Acoustic emission detection of crack presence and crack advance during flight p 886 N90-28082
NASA Langley Research Center National Aero-Space Plane Mission simulation profile sets p 924 N90-28541
[NASA-TM-102670]
Correlation of AH-1G airframe flight vibration data with a coupled rotor-fuselage analysis p 959 N90-28865
[NASA-CR-181974]
Plan, execute, and discuss vibration measurements and correlations to evaluate a NASTRAN finite element model of the AH-64 helicopter airframe p 960 N90-28866
[NASA-CR-181973]

Proceedings of damping '89. Volume 1: Pages AAB-1 through DCD-11 p 960 N90-29664
[AD-A223431]
Fractographic analysis of fatigue failures of airframe equipment parts: Examples of a rod end housing and a rod end cap p 961 N90-29686
[NAL-TR-1047]
AIRLINE OPERATIONS
In the shadow of Aloha p 468 A90-33174
Transport aircraft corrosion control p 617 A90-40345
The planning of air transportation on airlines --- Russian book p 721 A90-42648
Effects of stage 3 rules on the airliner market [SAE PAPER 892292] p 723 A90-45468
Air transportation in COMECON countries --- Russian book p 785 A90-46616
Aging fleet Structures Working Group activities [AIAA PAPER 90-3219] p 786 A90-48840
Commercial aircraft DOC methods [AIAA PAPER 90-3224] p 897 A90-48843
Organization of air traffic control --- Russian book p 915 A90-52415
Airport technology international 1989/1990 --- Book p 937 A90-52857
National Airspace System flight planning operational concept [DOT/FAA/DS-89/30] p 177 N90-13362
Indianapolis Downtown Heliport: Operations analysis and marketing history [REPT-90RR-13] p 527 N90-21049
FAA (Federal Aviation Administration) aviation forecasts, fiscal years 1990-2001 p 552 N90-22530
[AD-A219165]
The effect of noise-abatement profiles on noise immissions and human annoyance underneath a subsequent climbpath p 698 N90-24865
Stage 2 re-engineing: The only way to achieve a real stage 3 aircraft [PNR90636] p 737 N90-25977
Application of a company data link at Lufthansa German Airlines p 827 N90-27689
Evaluation of existing aircraft operator data bases [DOT/FAA/CT-90/18] p 898 N90-28463
Modeling and analysis of airport and aircraft operations [PB90-222167] p 915 N90-28511
Airline productivity relating on the fuel cost. (2): Fuel consumption values and fuel efficiency [NAL-TM-604-2] p 913 N90-29333
AIRPORT PLANNING
Organization of air traffic control --- Russian book p 915 A90-52415
Development and evaluation at ATCEU of executive and support operations, phase 4A/3D --- ATCEU (Air Traffic Control Evaluation Unit) [CAA-PAPER-88017] p 99 N90-12572
Aircraft/airport compatibility: Some strategic, tactical, and operational issues [TT-8902] p 202 N90-13409
The Federal Aviation Administration plan for research, engineering and development. Volume 1: Program plan [AD-A221263] p 783 N90-25930
The potential for an extra runway at Heathrow: A preliminary feasibility study [TT-9007] p 938 N90-29403
AIRPORT SECURITY
Aviation security: Corrective actions underway, but better inspection guidance still needed. Report to the Chairwoman, Government Activities and Transportation Subcommittee, Committee on Government Operations, House of Representatives [GAO/RCED-88-160] p 635 N90-23367
AIRPORT SURFACE DETECTION EQUIPMENT
Advances in primary-radar technology p 241 A90-21380
Propagation of Mode S beacon signals on the airport surface p 241 A90-21381
Wind shear detection with airport surveillance radars p 241 A90-21387
Approach towards a future integrated airport surface traffic management p 827 N90-27686
Experimental study towards a future airport ground movement simulator p 827 N90-27687
AIRPORT TOWERS
FAA air traffic activity: Fiscal year 1988 [AD-A211338] p 99 N90-12570
FAA air traffic control operations concepts. Volume 7: ATCT (Airport Traffic Control Towers) tower controllers [AD-A210455] p 332 N90-16730
Atlanta tower simulation, volume 1 [DOT/FAA/CT-TN89/27-VOL-1] p 870 N90-26835
Atlanta tower simulation. Volume 2: Appendixes [DOT/FAA/CT-TN89/27-VOL-2] p 870 N90-26836
AIRPORTS
Aviation Security (Avsec) p 23 A90-12782

The FAA technical classification of aircraft and airports p 96 A90-15876
ICAO airfield reference code p 261 A90-21628
Ground navigation in airport traffic p 242 A90-21725
The influence of weather on flight operations at the Atlanta Hartsfield International Airport p 279 A90-22688
National Airspace System demand and capacity modeling p 330 A90-25562
Fog formation at Perth Airport p 611 A90-37748
Wind shear at Pantelleria airport p 692 A90-39702
Improved guidance and control of vehicles and personnel on the ground will benefit airport traffic capacity p 760 A90-44549
Efforts continue to increase airport/airspace capacity p 722 A90-44550
An automated method for predicting the height of the lower cloud boundary p 888 A90-48359
Vertical wind shears in lower-level jet stream over some airfields in the Urals and Siberia p 888 A90-48362
Some characteristics of the meteorological conditions of low cloud formation around the Baku airport p 888 A90-48364
Application possibilities of expert systems in modern maintenance for increasing operational security p 892 A90-49271
Analysis and synthesis of meteorological support systems for airports p 914 A90-50778
Measurement of wind characteristics at airports p 962 A90-50780
Semiautomatic coding of weather phenomenon groups in the meteorological reports of automatic airport stations p 962 A90-50783
Inversions and associated wind-shear warnings must be related to airport characteristics p 962 A90-52051
Airport technology international 1989/1990 --- Book p 937 A90-52857
ILS (Instrument Landing System) mathematical modeling study on the effects of proposed hangar construction west of runway 18R on localizer performance at Dallas-Fort Worth International Airport p 27 N90-10019
[AD-A210631]
A simulation study of landing time allocation procedures for use in computer-assisted air traffic management systems p 99 N90-11722
[AD-A212159]
Development and evaluation at ATCEU of executive and support operations, phase 4A/3D --- ATCEU (Air Traffic Control Evaluation Unit) [CAA-PAPER-88017] p 99 N90-12572
California air transportation study: A transportation system for the California Corridor of the year 2010 [NASA-CR-186219] p 176 N90-14212
National airspace system: Airport movement area control operational concept [WP-89W00181] p 243 N90-15086
Cumulative airport noise exposure metrics: An assessment of evidence for time-of-day weightings, revision p 352 N90-16773
[AD-A214878]
Synthetic aperture radar imagery of airports and surrounding areas: Archived SAR data [NASA-CR-4275] p 401 N90-18371
Synthetic aperture radar imagery of airports and surrounding areas: Philadelphia Airport [NASA-CR-4280] p 401 N90-18372
Low-energy gamma ray attenuation characteristics of aviation fuels p 462 N90-18882
[NASA-TP-2974]
Airfields on antarctic glacier ice p 526 N90-20097
[AD-A217638]
Criteria for polymer concrete on airport pavements [DOT/FAA/DS-89/18] p 527 N90-21045
MLS mathematical model validation study using airborne MLS data from Midway Airport engineering flight tests, August 1988 p 640 N90-23378
[DOT/FAA/CT-TN90/2]
Synthetic aperture radar imagery of airports and surrounding areas: Denver Stapleton International Airport p 637 N90-24257
[NASA-CR-4305]
Criteria for coal tar seal coats on airport pavements. Volume 2: Laboratory and field studies [AD-A220167] p 674 N90-24277
FAA/NASA En Route Noise Symposium [NASA-CP-3067] p 696 N90-24853
The effect of noise-abatement profiles on noise immissions and human annoyance underneath a subsequent climbpath p 698 N90-24865
En route noise annoyance laboratory test: Preliminary results p 698 N90-24870
An aircraft noise study in Norway p 698 N90-24872
Replication of NASPAC Dallas/Fort Worth study [DOT/FAA/CT-TN90/26] p 729 N90-25123

Atlanta tower simulation, volume 1
[DOT/FAA/CT-TN89/27-VOL-1] p 870 N90-26835

Atlanta tower simulation, Volume 2: Appendixes
[DOT/FAA/CT-TN89/27-VOL-2] p 870 N90-26836

Air Force procedure for predicting aircraft noise around
airbases: Airbase operations program (BASEOPS)
description
[AD-A223069] p 895 N90-27466

Public-sector aviation issues, 1987 to 1988 graduate
research award papers
[PB90-191206] p 820 N90-27667

Real-time adaptive aircraft scheduling
[NASA-CR-177558] p 820 N90-27669

Approach towards a future integrated airport surface
traffic management p 827 N90-27686

Airport pavement drainage
[DOT/FAA/RD-90/24] p 872 N90-27728

Airport capacity enhancement plan 1989
[PB90-197997] p 913 N90-28507

Modeling and analysis of airport and aircraft
operations
[PB90-222167] p 915 N90-28511

Proceedings of a workshop on Future Airport Passenger
Terminals
[PB90-213620] p 937 N90-28580

Development of acceptance plans for airport pavement
materials. Volume 1: Development
[DOT/FAA/RD-90/15] p 937 N90-28581

Development of a thickness design procedure for
stabilized layers under rigid airfield pavements
[DOT/FAA/RD-90/22] p 937 N90-28582

The cost of air service fragmentation
[TT-9010] p 913 N90-29334

The potential for an extra runway at Heathrow: A
preliminary feasibility study
[TT-9007] p 938 N90-29403

AIRSHIPS

A new hybrid airship ('Heliship') for commuter
transport p 29 A90-11875

The airship - An economical answer to air cargo
[TABES PAPER 89-1203] p 238 A90-20390

AIAA Lighter-Than-Air Systems Technology Conference,
8th, Jacksonville, FL, Oct. 5-7, 1989, Technical Papers
p 221 A90-20576

An AEW metalclad airship
[AIAA PAPER 89-3158] p 244 A90-20579

Preliminary feasibility study for a new hybrid airship
(Heliship)
[AIAA PAPER 89-3161] p 244 A90-20581

A new hybrid LTA vehicle, 'Heliship' - Its philosophy,
outline
[AIAA PAPER 89-3162] p 244 A90-20582

A new type of non-rigid airship system
[AIAA PAPER 89-3175] p 244 A90-20583

Modern technology in airship design
[AIAA PAPER 89-3169] p 244 A90-20584

Control configured airship design
[AIAA PAPER 89-3170] p 244 A90-20585

Parametric sizing of modern naval airships
[AIAA PAPER 89-3171] p 244 A90-20586

Prediction of aerostat and airship mooring mast loads
by nonlinear dynamic simulation
[AIAA PAPER 89-3172] p 245 A90-20587

Airship survival - Damage avoidance and control for large
ocean-going airships
[AIAA PAPER 89-3166] p 238 A90-20588

An analytical technique for addressing airship ditching
behavior
[AIAA PAPER 89-3167] p 238 A90-20589

Estimation of the flight dynamic characteristics of the
YEZ-2A
[AIAA PAPER 89-3173] p 245 A90-20590

AIRSPACE

More cruising levels expected at higher altitudes
p 721 A90-44548

Efforts continue to increase airport/airspace capacity
p 722 A90-44550

National airspace system plan: Facilities, equipment,
associated development and other capital needs
[AD-A215882] p 402 N90-18373

An early overview of tiltrotor aircraft characteristics and
pilot procedures in civil transport applications
[DOT/FAA/DS-89/37] p 503 N90-21003

Proposed definition of the term en route in en route
aircraft noise p 696 N90-24854

Airport capacity enhancement plan 1989
[PB90-197997] p 913 N90-28507

An analysis of GPS as the sole means navigation system
in US Navy aircraft p 917 N90-29350

AIRSPEED

Investigation of a nonlinear Kalman filter for estimating
aircraft state variables p 195 A90-16850

Hypersonic propulsion p 253 A90-21949

Flight tests to explore tail rotor limitations in the low
speed envelope p 647 A90-42498

Effect of wind shear on the airspeed during the airplane
landing approach
[AIAA PAPER 90-2838] p 754 A90-45160

Winds aloft measurement and airspeed calibration using
Loran
[AIAA PAPER 90-3331] p 847 A90-47592

A new method of aircraft motion error extraction from
radar raw data for real-time motion compensation
p 824 A90-49675

Evaluation of the improved OV-ID anti-icing system,
phase 2
[AD-A213928] p 239 N90-15083

Low air speed computation for helicopters: A new
approach p 333 N90-16744

Reducing C130E Hercules operating costs in the Royal
Australian Air Force and the United States Air Force by
increasing cruise speeds
[AD-A215747] p 338 N90-17629

Optimal control of an aircraft flying through a
downburst p 591 N90-21765

ALCOHOLS

Analysis of the T63-A-700 engine used in alcohol turbine
fuel extender test
[DOT/FAA/CT-TN90/18] p 928 N90-28549

ALERTNESS

Collision alert p 847 A90-48521

ALGORITHMS

Application of an adaptive algorithm to single and
two-element airfoils in turbulent flow
[AIAA PAPER 90-0698] p 169 A90-19983

Multilevel method for calculating aerodynamic loads on
a flight vehicle p 296 A90-24122

Automatic vibration reduction at a four bladed hingeless
model rotor - A wind tunnel demonstration
p 335 A90-25424

Simulator motion-drive algorithms - A designer's
perspective p 375 A90-25997

Generation of tetrahedral meshes around complete
aircraft p 310 A90-26536

On the combination of structured-unstructured meshes
p 311 A90-26540

Grid generation and its application to separated flows
p 312 A90-26552

A method for recalculating the temperature fields of
aircraft structures for different experimental conditions
p 448 A90-28994

Unsteady aerodynamics methods for transonic
aeroelastic analysis p 471 A90-33353

Optimization of complex data processing algorithms in
multichannel radio direction finding p 576 A90-36115

A primitive variable, strongly implicit calculation
procedure for viscous flows at all speeds
[AIAA PAPER 90-1521] p 563 A90-38666

Fracture control via DRM-Algorithm
p 694 A90-41343

A unified pressure correction algorithm for computing
complex fluid flows p 772 A90-45528

Application of energy turn g-limiting for aircraft high
performance turns
[AIAA PAPER 90-3328] p 862 A90-47590

Local adaptive maneuvering optimization for fighter
aircraft p 890 A90-47706

[AIAA PAPER 90-3453] p 890 A90-47706

Model reduction with a finite-interval H(infinity)
criterion
[AIAA PAPER 90-3473] p 890 A90-47723

Genetic algorithms in control system optimization
[AIAA PAPER 90-3488] p 867 A90-47736

Some computational and experimental aspects of
optimal design process of composite structures
p 882 A90-48050

Computation of transonic flow about stores
[AD-A210402] p 18 N90-10009

On the generation of a variable structure airport surface
traffic control system
[AD-A211306] p 99 N90-11724

Sequential design of experiments with physically based
models 23
[AD-A211918] p 138 N90-12239

Chordwise loading and camber for two-dimensional thin
sections
[AD-A213318] p 95 N90-12568

Automatic processing of images from the GRATE flight
test tool
[DLR-FB-89-28] p 109 N90-12599

Navier-Stokes solutions of 2-D transonic flow over
unconventional airfoils p 173 N90-14195

Advanced detection, isolation, and accommodation of
sensor failures in turbofan engines: Real-time
microcomputer implementation
[NASA-TP-2925] p 259 N90-15112

Advances in techniques and technologies for air vehicle
navigation and guidance
[AGARD-AR-276] p 243 N90-15899

Experience with strain-gage balances for cryogenic wind
tunnels p 264 N90-15958

Estimation and control of nonlinear and hybrid systems
with applications to air-to-air guidance
[AD-A214542] p 348 N90-16770

Tracking a hypersonic aircraft from a space platform
[AD-A216399] p 371 N90-17984

Numerical algorithms for parallel computers
[AD-A216812] p 377 N90-18181

Visual servicing for autonomous aircraft refueling
[AD-A216042] p 414 N90-18386

Wind-tunnel investigation of a flush airdata system at
Mach numbers from 0.7 to 1.4
[NASA-TM-101697] p 421 N90-18395

A streamwise upwind algorithm applied to vortical flow
over a delta wing
[NASA-TM-102225] p 398 N90-19201

Heli/SITAN: A terrain referenced navigation algorithm
for helicopters
[DE90-005193] p 405 N90-19217

Lateral attenuation of military aircraft flight noise
[AD-A218041] p 548 N90-20799

Comparison of C- and O-grid generation methods using
a NACA 0012 airfoil
[AD-A216375] p 479 N90-20948

A two-dimensional unsteady analysis for transonic and
supersonic cascade flows p 480 N90-20955

Flight path reconstruction using extended Kalman
filtering techniques
[PD-FC-9001] p 489 N90-20970

Windshear case study: Denver, Colorado, July 11,
1988
[DOT/FAA/DS-89/19] p 544 N90-21509

Adaptive grid embedding for the two-dimensional
flux-split Euler equations
[NASA-CR-186533] p 547 N90-21571

Extension of a streamwise upwind algorithm to a moving
grid system
[NASA-TM-102800] p 572 N90-21739

First-order weight corrections for real-time flight path
management
[LR-580] p 578 N90-21751

Kalman filter based range estimation for autonomous
navigation using imaging sensors p 578 N90-22238

Algorithms for computing the multivariable stability
margin p 612 N90-22999

Application of optimal tracking methods to aircraft terrain
following
[AD-A221099] p 641 N90-24264

En route noise: NASA proplan test aircraft (calculated
source noise)
[DOT-TSC-FA953-LR5] p 697 N90-24857

Evaluation of nonlinear motion-drive algorithms for flight
simulators
[UTIAS-TN-272] p 761 N90-25148

Supersonic combustor modeling p 749 N90-25992

Fluid Dynamics Panel Working Group 12 on Adaptive
Wind Tunnel Walls: Technology and Applications
[AGARD-AR-269] p 870 N90-26838

Advanced algorithms design and implementation in
on-board microprocessor systems for engine life usage
monitoring p 892 N90-27628

Expert system diagnostics and parts life tracking as
applied to the AV-8B aircraft for the USMC
p 884 N90-27629

Sideslip-induced static pressure errors in flight-test
measurements
[NASA-TM-102846] p 849 N90-27702

Studies in automatic speech recognition and its
application in aerospace p 958 N90-28759

Real-time aerodynamic heating and surface temperature
calculations for hypersonic flight simulation
[NASA-TM-4222] p 959 N90-28815

Independent ground monitor coverage of Global
Positioning System (GPS) satellites for use by civil
aviation p 918 N90-29364

Optimal trajectories for hypervelocity flight
p 918 N90-29378

Windshear estimation along the trajectory of an
aircraft p 963 N90-29745

ALIGNMENT

A waveform alignment approach to positioning airborne
radar-sounding data p 332 A90-26651

ALKYL COMPOUNDS

Some 1-(diorganooxyphosphonyl)methyl-2,4- and
-2,6-dinitro-benzenes
[NASA-CASE-ARC-11425-3] p 678 N90-23475

ALL-WEATHER AIR NAVIGATION

Kalman Filter Integration of Modern Guidance and
Navigation Systems
[AGARD-LS-166] p 28 N90-10847

Flight in Adverse Environmental Conditions
[AGARD-CP-470] p 222 N90-15041

The human element: The key to safe, civil operations
in adverse weather p 248 N90-15042

Adverse weather operations during the Canadian
Atlantic storms program p 281 N90-15052

Position computation without elevation information for computed centerline operations
[DOT/FAA/CT-TN89/42] p 640 N90-23379
The integration of multiple avionics sensors and technologies for future military helicopters p 916 N90-29344

ALLOCATIONS

A simulation study of landing time allocation procedures for use in computer-assisted air traffic management systems
[AD-A212159] p 99 N90-11722
Profiles-aeronautical/astronautical engineering: Human resources and funding
[PB90-103988] p 369 N90-16969

ALLOYING

Influence of alloying elements on the oxidation behavior of NbAl₃ p 355 A90-24861
Mechanical alloying spreads its wings p 950 A90-51200

ALLOYS

Thermal mechanical fatigue of coated blade materials
[AD-A21258] p 256 N90-15107

ALLYL COMPOUNDS

Improved thermal performance using allylnadecimides p 946 A90-50175

ALTERNATING DIRECTION IMPLICIT METHODS

Numerical simulation of supersonic unsteady flow using Euler equations
[AIAA PAPER 90-0415] p 229 A90-22215

ALTIMETERS

The accuracy of barometric altimeters with respect to geometric altitude p 108 A90-14012
Temperature insensitive fiber coil sensor for altimeters p 339 A90-26374
Modeling the effects of the use of GPS (Global Positioning System) derived altitude indication in the C-17A air drop system
[AD-A215366] p 333 N90-16748

ALTIMETRY

An update to the system safety study of TCAS 2
[DOT/FAA/SA-89/3] p 177 N90-13363

ALTITUDE

Modeling the effects of the use of GPS (Global Positioning System) derived altitude indication in the C-17A air drop system
[AD-A215366] p 333 N90-16748

ALTITUDE CONTROL

On a pitch control law for a constant glide slope through windshears p 117 A90-13784
The benefits and costs of automation in advanced helicopters - An empirical study p 348 A90-26258
Analytical evaluation of helicopter true air speed and associated flight tests p 647 A90-42499
Stability characteristics of a combat aircraft with control surface failure
[AD-A216196] p 350 N90-17646

ALTITUDE TESTS

Altitude testing of the 2D V/STOL ADEN demonstrator on an F404 engine p 345 N90-17638
[NASA-CR-174824] p 856 N90-27712
Design of the UETP experiment p 856 N90-27712
Comparison of altitude test cell results p 856 N90-27715
Comparison of ground-level test cells and ground-level to altitude test cells p 857 N90-27716
Experience in developing an improved altitude test capability p 857 N90-27719

ALUMINIDES

Extending the overhaul interval for gas turbine engines through the use of alternative coatings on first stage blades p 63 A90-12539
Observations on the brittle to ductile transition temperatures of B2 nickel aluminides with and without zirconium p 205 A90-19153
Microstructures of rapidly-solidified binary TiAl alloys p 532 A90-34990

Titanium aluminides for advanced aircraft engines p 874 A90-49000

Thermal mechanical fatigue of coated blade materials
[AD-A21258] p 256 N90-15107
Improved toughness alloys based on titanium aluminides
[AD-A218149] p 533 N90-20208

ALUMINUM

Aluminum surface preparation for aircraft field repair p 764 A90-43204

Chrome free electrolytic deoxidizer for aluminum p 956 A90-50216

Rolling of ARALL laminates (an alternative method for post-stretching ARALL laminates)
[LR-560] p 135 N90-12778

Fatigue crack growth investigation of a Ti-6Al-4V forging under complex loading conditions: NATO/AGARD supplemental engine disk program
[AD-A220239] p 678 N90-23538

ALUMINUM ALLOYS

Tough(er) aluminum-lithium alloys p 62 A90-11575
Intermetallic compounds for strong high-temperature materials - Status and potential p 125 A90-15022
The creep behavior of the Ti3Al alloy Ti-24Al-11Nb p 125 A90-15214

The manufacture of SPF military aircraft doors in aluminium alloy --- superplastically formed p 132 A90-16616

Production of Ti6Al4V-components for a new turbo-fan-engine p 132 A90-16618

Developing aluminium p 204 A90-17924

In process failure investigations in aeronautics p 181 A90-18489

Experimental determination of the short crack effect for metals p 265 A90-20064

Influence of alloying elements on the oxidation behavior of NbAl₃ p 355 A90-24861

The effect of elevated temperature exposure on the tensile and creep properties of Ti-24Al-11Nb p 355 A90-24865

Sliding and abrasive wear behaviour of an aluminium (2014)-SiC particle reinforced composite p 530 A90-33344

Al-Li alloys and ultrahigh-strength steels for U.S. Navy aircraft p 599 A90-37441

Aluminum alloy 6013 sheet for new U.S. Navy aircraft p 599 A90-37442

Reconstitution of crack growth from fractographic observations after flight simulation loading p 682 A90-40650

The influence of material quality on airframe structural durability p 676 A90-41336

Aircraft applications of advanced composite fiber/metal pressure vessels p 686 A90-42133

[AIAA PAPER 90-2344] Maritime environment airframe material fatigue testing p 764 A90-42675

Loss weight with Al-Li p 765 A90-44175

Quench sensitivity of airframe aluminium alloys p 765 A90-44348

The surface pretreatment of aluminium-lithium alloys for structural bonding p 881 A90-47118

Aerospace Arall - The advancement in aircraft materials p 947 A90-50186

Mechanical alloying spreads its wings p 950 A90-51200

Fatigue crack initiation mechanics of metal aircraft structures
[AD-A210567] p 65 N90-10255

Effects of a heat cycle on material strength
[NAL-TM-562] p 113 N90-11737

Aluminum alloy development for aero engines
[PNR90548] p 126 N90-11874

New Light Alloys
[AGARD-CP-444] p 267 N90-15185

The microstructure and properties of aluminum-lithium alloys p 267 N90-15187

Properties of Al-Li alloys p 267 N90-15191

Investigation on sheet material of 8090 and 2091 aluminium-lithium alloy p 267 N90-15192

Aluminum lithium alloys for Navy aircraft p 267 N90-15193

Fabrication of test-articles from Al-Li 2091 for Fokker 100 p 267 N90-15196

Putting alloy 2091 to work p 268 N90-15197

Fabrication characteristics of 8090 alloy p 268 N90-15198

Point of view of a civil aircraft manufacturer on Al-Li alloy p 268 N90-15200

Uses and properties of Al-Li on the new EH101 helicopter p 268 N90-15201

Aluminum-lithium: Application of plate and sheet to fighter aircraft p 268 N90-15202

Current status of the application of conventional aluminium-lithium alloys and the potential for future developments p 268 N90-15203

Fatigue of aluminium alloy joints with various fastener systems. Low load transfer
[ESDU-89046] p 370 N90-17193

Crack stoppers and ARALL laminates
[PB90-166588] p 533 N90-21142

Characterisation of fatigue of aluminium alloys by acoustic emission. Part 2: Discrimination between primary and other emissions p 678 N90-23523

[AERE-R-13303-PT-2] Fractographic observations on fatigue crack growth in 2024-T3 sheet material under flight-simulation loading
[LR-592] p 689 N90-23760

Investigation on sheet material of 8090 and 2091 aluminium-lithium alloy
[MBB-UT-122/89-PUB] p 766 N90-25090

Mechanical paint removal techniques for aircraft structures
[IAR-89-23] p 773 N90-25254

Mechanical paint removal techniques for aircraft structures
[NIAR-90-12] p 775 N90-26166

Investigation of crack-closure prediction models for fatigue in aluminium alloy sheet under flight-simulation loading
[LR-619] p 777 N90-26369

An aluminum quality breakthrough for aircraft structural reliability p 843 N90-26816

Characterization of the CP 214 T851. Dissection of a cast flat bar for a standard spar
[CEAT-PV-M4/462200] p 876 N90-27905

Characterization of the 7175 T7352. Dissection of a die casting standard spar
[CEAT-PV-M5/528900] p 877 N90-27906

Characterization of the 7175 T7352 101. Dissection of a die casting standard spar
[CEAT-PV-M5/5288] p 877 N90-27907

Characterization of the 7010 T73651. Dissection of a sheet billet for a standard spar
[CEAT-PV-M5/521700] p 877 N90-27908

The stress and temperature dependence of creep in an Al-2.0 wt percent Li alloy
[AD-A223676] p 953 N90-29480

Evaluation of static and fatigue properties of thin sheets of 8090-T8 aluminum-lithium alloy and observation of its fracture surfaces
[NAL-TR-1039] p 953 N90-29499

ALUMINUM CARBIDES
The application of cast SiC/Al to rotary engine components
[NASA-CR-179610] p 192 N90-13385

ALUMINUM OXIDES
Processing and mechanical properties of Al₂O₃/Y₃Al₅O₁₂ (YAG) eutectic composite p 951 A90-51966

AMPHIBIOUS AIRCRAFT
Glassy waters for Seastar --- corrosion-resistant GFRP for turboprop amphibious aircraft airframes p 382 A90-29637

Water borne again p 579 A90-35846

Mi-14 - The Soviet Sea King p 730 A90-43765

AMPLITUDE MODULATION
Direct frequency modulation in interferometric systems p 68 A90-11662

A fiber optic headset compatible with power-by-light p 504 A90-32906

AMPLITUDES
Amplitude effects on dynamic stall of an oscillating airfoil
[AIAA PAPER 90-0575] p 167 A90-19925

ANALOG CIRCUITS
Design of control amplifier for FJR 710 engine p 43 A90-12017

Electrical analog circuit for heat transfer measurements on a flat plate simulating turbine vane heat transfer in turbulent flow
[AIAA PAPER 90-2412] p 687 A90-42164

ANALOG SIMULATION
LDA processor TSI model 1990 analog input module reconstruction p 451 A90-29654

ANALOG TO DIGITAL CONVERTERS
Database for LDV signal processor performance analysis p 447 A90-28278

A new type of calibration rig for wind tunnel balances p 438 A90-28305

Clutter rejection and transmitter-receiver requirements in an airborne radar p 738 A90-45354

ANALOGS
Introducing the VRT gas turbine combustor
[AIAA PAPER 90-2452] p 743 A90-42808

Introducing the VRT gas turbine combustor
[NASA-TM-103176] p 688 N90-23591

ANECHOIC CHAMBERS
Airfoil noise in a uniform flow p 139 A90-16330

Tests of an ultra-light tunnel in the anechoic wind tunnel facility CEPRA 19
[ONERA-RF-20/7294-PH] p 872 N90-27729

ANGLE OF ATTACK
The effect of pitch location on dynamic stall p 2 A90-10641

Numerical simulation of reversed flow over a supersonic delta wing at high angle of attack
[AIAA PAPER 89-1802] p 8 A90-11849

Navier-Stokes computations of a prolate spheroid at angle of attack p 17 A90-13018

Spanwise distribution of lift and drag at high angles of attack
[SAE PAPER 891019] p 83 A90-14331

Effect of the angle of attack on the efficiency and thrust ratio of axial-flow microturbines with full admission p 111 A90-14590

Results from a numerical simulation of an F-16A configuration at a supersonic Mach number p 146 A90-16769

- Numerical simulation of separated and vortical flows on bodies at large angles of attack p 146 A90-16772
- A critique of the experimental aerodynamic data base for an oscillating straked wing at high angles p 147 A90-16779
- Wing-body mutual influence coefficients at angles-of-attack to 24 deg p 151 A90-17693
- Unsteady aerodynamic forces on rolling delta wings at high angle of attack p 159 A90-19426
- Rotational aerodynamics of elliptic bodies at high angles of attack p 161 A90-19664
- [AIAA PAPER 90-0068]
- Experimental investigation of a new device to control the asymmetric flowfield on forebodies at large angles of attack p 161 A90-19665
- [AIAA PAPER 90-0069]
- Investigation of high angle of attack vortical flows over delta wings p 162 A90-19682
- [AIAA PAPER 90-0101]
- High angle of attack flying qualities criteria p 197 A90-19738
- [AIAA PAPER 90-0219]
- In-flight flow field analysis on the NASA F-18 high alpha research vehicle with comparisons to ground facility data p 163 A90-19745
- [AIAA PAPER 90-0231]
- Preliminary results from a subsonic high-angle-of-attack flush airdata sensing (HI-FADS) system: Design, calibration, algorithm development, and flight test evaluation p 187 A90-19746
- [AIAA PAPER 90-0232]
- Rapid prediction of slender-wing-aircraft stability characteristics p 163 A90-19782
- [AIAA PAPER 90-0301]
- Lift development of delta wings undergoing constant acceleration from rest p 164 A90-19789
- [AIAA PAPER 90-0310]
- Impact of nose-probe chines on the vortex flows about the F-16C p 165 A90-19828
- [AIAA PAPER 90-0386]
- Calculation of low Reynolds number flows at high angles of attack p 167 A90-19921
- [AIAA PAPER 90-0569]
- Pneumatic vortical flow control at high angles of attack p 227 A90-22164
- [AIAA PAPER 90-0098]
- An investigation of asymmetric vortical flows over delta wings with tangential leading-edge blowing at high angles of attack p 227 A90-22167
- [AIAA PAPER 90-0103]
- Application of dynamical systems theory to the high angle of attack dynamics of the F-14 p 257 A90-22184
- [AIAA PAPER 90-0221]
- Wind-tunnel investigation on the effect of a crescent planform on drag p 228 A90-22196
- [AIAA PAPER 90-0300]
- Aerodynamic characteristics of an aircraft model at large angles of attack and large sideslip angles p 233 A90-23361
- [AIAA PAPER 90-0339]
- Unsteady Euler analysis of the flowfield of a propan at an angle of attack p 300 A90-25028
- [AIAA PAPER 90-0339]
- Aerodynamic control of aircraft by forebody vortex manipulation p 301 A90-25167
- [AIAA PAPER 90-1827]
- Shock sensitivity in parabolized Navier-Stokes solution of high angle-of-attack supersonic flow p 302 A90-25280
- [AIAA PAPER 90-0309]
- Topology of computed incompressible three-dimensional separated flow field around high-angle-of-attack cone-cylinders p 366 A90-25764
- [AIAA PAPER 90-0050]
- The hemisphere-cylinder at an angle of attack p 313 A90-26907
- [AIAA PAPER 90-0100]
- Numerical simulation of an F-16A at angle of attack p 313 A90-26911
- [AIAA PAPER 90-0309]
- Unsteady aerodynamic characteristics of a fighter model undergoing large-amplitude pitching motions at high angles of attack p 313 A90-26933
- [AIAA PAPER 90-0309]
- Newtonian flow over oscillating two-dimensional airfoils at moderate or large incidence p 383 A90-27976
- [AIAA PAPER 90-0309]
- An optical angle of attack sensor p 446 A90-28263
- [AIAA PAPER 90-0309]
- Model incidence measurement using the SAAB Elopotos system --- IR instrumentation for measuring angle of attack in transonic wind tunnel models p 446 A90-28264
- [AIAA PAPER 90-0309]
- Comparison of calculated and experimental nonstationary aerodynamic characteristics of a delta wing pitching at large angles of attack p 387 A90-28988
- [AIAA PAPER 90-0309]
- Development of high angle of attack flying qualities criteria using ground-based manned simulators p 433 A90-30717
- [AIAA PAPER 90-0309]
- Studies of predicting departure characteristics of aircraft p 433 A90-31480
- [AIAA PAPER 90-0309]
- Multi-element aerofoils in viscous flow p 469 A90-32451
- [AIAA PAPER 90-0309]
- Vortex shedding over delta wings p 470 A90-32479
- Experimental investigation of the flow development of an airfoil at high angles of attack p 473 A90-33366
- [AIAA PAPER 90-1289]
- The use of simulation in support of the high AOA flight test program of the AM-X aircraft p 495 A90-33909
- [AIAA PAPER 90-1289]
- A summary of spin-recovery parachute experience on light airplanes p 519 A90-33926
- [AIAA PAPER 90-1317]
- A dynamic optical model attitude measurement system p 539 A90-34236
- [AIAA PAPER 90-1317]
- Blockage corrections at high angles of attack in a wind tunnel p 593 A90-35756
- [AIAA PAPER 90-1317]
- Control of asymmetric vortical flows over delta wings at high angles of attack p 553 A90-35759
- [AIAA PAPER 90-1317]
- Comment on 'Improved thin-airfoil theory' p 554 A90-35772
- [AIAA PAPER 90-1317]
- Solution of Euler equations for fighter forebody-inlet combination at high angle of attack p 556 A90-36419
- [AIAA PAPER 90-1317]
- A numerical method in aeroelasticity for wings with separation at large angle of attack p 557 A90-37209
- [AIAA PAPER 90-1317]
- Flow field measurements near a fighter model at high angles of attack p 559 A90-37968
- [AIAA PAPER 90-1431]
- Comparison of high-angle-of-attack slender-body theory and exact solutions for potential flow over an ellipsoid p 622 A90-40692
- [AIAA PAPER 90-1431]
- The influence of control-surface compensation parameters on the hinge moment characteristics p 643 A90-41737
- [AIAA PAPER 90-1431]
- Yaw damping of elliptic bodies at high angles of attack p 709 A90-44740
- [AIAA PAPER 90-1431]
- Design of wing profiles for application in nonstall conditions in a given angle-of-attack range p 710 A90-44936
- [AIAA PAPER 90-1431]
- Delta wing surface pressures for high angle of attack maneuvers p 711 A90-45153
- [AIAA PAPER 90-2813]
- Control of forebody flow asymmetry - A critical review p 711 A90-45164
- [AIAA PAPER 90-2833]
- Unsteady flow separation on slender bodies at high angles of attack p 712 A90-45166
- [AIAA PAPER 90-2835]
- Optimal control system design for departure prevention p 754 A90-45167
- [AIAA PAPER 90-2837]
- Numerical simulation of the viscous flow around a simplified F/A-18 at high angles of attack p 787 A90-45849
- [AIAA PAPER 90-2999]
- Numerical simulation of the effects of variation of angle of attack and sweep angle on vortex breakdown over delta wings p 788 A90-45850
- [AIAA PAPER 90-3000]
- Numerical study of asymmetric air injection to control high angle-of-attack forebody vortices on the X-29 aircraft p 788 A90-45853
- [AIAA PAPER 90-3004]
- The effect of turbulence models on the numerical prediction of the flowfield about a prolate spheroid at high angle of attack p 789 A90-45855
- [AIAA PAPER 90-3106]
- Rapid prediction of slender-wing aircraft dynamics p 791 A90-45876
- [AIAA PAPER 90-3037]
- F-18 high alpha research vehicle surface pressures - Initial in-flight results and correlation with flow visualization and wind-tunnel data p 792 A90-45885
- [AIAA PAPER 90-3018]
- A laser sheet flow visualization and aerodynamic force data evaluation of a 3 percent YF-17 fighter aircraft model at high angles of attack p 792 A90-45886
- [AIAA PAPER 90-3019]
- Static and dynamic water tunnel tests of slender wings and wing-body configurations at extreme angles of attack p 869 A90-45888
- [AIAA PAPER 90-3021]
- Wind tunnel studies of support strut interference on a 3 percent YF-17 fighter aircraft model at high angles of attack p 794 A90-45899
- [AIAA PAPER 90-3083]
- Angle-of-attack validation of a new zonal CFD method for airfoil simulations p 795 A90-45908
- [AIAA PAPER 90-3077]
- Finite wing lift prediction at high angles of attack p 795 A90-45910
- [AIAA PAPER 90-3079]
- Outflow boundary conditions using Duhamel's equation p 798 A90-45937
- [AIAA PAPER 90-3014]
- Interference between a vortex filament and shock waves in free flow and in nonisobaric jets p 804 A90-46550
- [AIAA PAPER 90-3014]
- Using the smoking-wire visualization method in the study of wing models at large angles of attack in subsonic wind tunnels p 881 A90-46561
- [AIAA PAPER 90-3014]
- Calculation of three-dimensional flow past a plane supersonic air intake at angles of attack and sideslip p 805 A90-46573
- [AIAA PAPER 90-3014]
- Unsteady aerodynamics of delta wings, undergoing ramp-maneuvering in pitch to post-stall angle of attack p 806 A90-46857
- [AIAA PAPER 90-3014]
- A dynamic inversion based control law with application to the high angle-of-attack research vehicle p 864 A90-47662
- [AIAA PAPER 90-3407]
- Exceptions to the C(n beta, dyn) criterion for aircraft stability at high angles of attack p 867 A90-48515
- [AIAA PAPER 90-3407]
- X-29 high angle-of-attack flight testing - Program status p 837 A90-48885
- [AIAA PAPER 90-3303]
- X-29 ECS high-alpha modifications p 840 A90-49295
- [SAE PAPER 901221]
- Effect of incoming flow turbulence on the aerodynamic characteristics of a smooth symmetric body at large angles of attack p 904 A90-50817
- [SAE PAPER 901221]
- Prediction of pressure distribution on optimum-optimum delta wing at higher angles of attack in supersonic flow and its agreement with experimental results p 907 A90-51538
- [SAE PAPER 901221]
- High alpha --- angles of attack of fighter aircraft p 902 A90-52575
- [SAE PAPER 901221]
- Basic studies of the unsteady flow past high angle of attack airfoils p 18 N90-10008
- [AD-A210252]
- Normal-force-curve and pitching-moment-curve slopes of forebody-cylinder combinations at zero angle of attack for Mach numbers up to 5 p 89 N90-11709
- [ESDU-89008]
- Flutter clearance of the F-18 high-angle-of-attack research vehicle with experimental wingtip instrumentation pods p 103 N90-11732
- [NASA-TM-4148]
- Prediction of unsteady blade surface pressures on an advanced propeller at an angle of attack p 94 N90-12560
- [NASA-TM-102374]
- Normal force, pitching moment, and side force of forebody-cylinder combinations for angles of attack up to 90 degrees and Mach numbers up to 5 p 173 N90-14192
- [ESDU-89014]
- Flow visualization of the effect of pitch rate on the vortex development on the scale model of a F-18 fighter aircraft p 236 N90-15080
- [AD-A214244]
- Body effect on wing angle of attack and pitching moment at zero lift at low speeds p 337 N90-16757
- [ESDU-89042]
- Preliminary results from a subsonic high angle-of-attack flush airdata sensing (HI-FADS) system: Design, calibration, and flight test evaluation p 339 N90-16758
- [NASA-TM-101713]
- Dynamic derivatives of missiles and fighter-type configurations at high angles of attack p 337 N90-17554
- [NASA-TM-101713]
- Unsteady Euler analysis of the flow field of a propan at an angle of attack p 380 N90-18229
- [NASA-TM-102426]
- Influence of forebody geometry on aerodynamic characteristics and a design guide for defining departure/spin resistant forebody configurations p 414 N90-18388
- [AD-A216714]
- Application of variable-gain output feedback for high-alpha control p 434 N90-18434
- [NASA-TM-102603]
- Unsteady aerodynamics of delta wings performing maneuvers to high angle of attack p 398 N90-19196
- [NASA-TM-102603]
- Development of a preliminary high-angle-of-attack nose-down pitch control requirement for high-performance aircraft p 399 N90-19206
- [NASA-TM-101684]
- F-15B high angle-of-attack phenomena and spin prediction using bifurcation analysis p 498 N90-20073
- [AD-A217366]
- Numerical simulation of hypersonic flow around a space plane. Part 2: Application to high angles of attack flow [NAL-TR-1011T] p 570 N90-21726
- [NAL-TR-1011T]
- An experimental investigation of support strut interference on a three-percent fighter model at high angles of attack p 631 N90-23353
- [AD-A219793]
- An experimental and theoretical investigation of the flow over plane delta wings with supersonic leading edges [LR-588] p 717 N90-25114
- [LR-588]
- Qualitative evaluation of a conformal velocity vector display for use at high angles-of-attack in fighter aircraft [NASA-TM-102629] p 739 N90-25981
- [NASA-TM-102629]
- AM-X high incidence trials, development and results [ETN-90-97277] p 759 N90-26516
- [ETN-90-97277]
- The role of C(sub n beta, dyn) in the aircraft stability at high angles of attack p 868 N90-26833
- [AD-A221586]
- Control research in the NASA high-alpha technology program p 934 N90-28516
- [AD-A221586]
- Development of non-conventional control methods for high angle of attack flight using vortex manipulation p 935 N90-28522
- [AD-A221586]

Control of vortex aerodynamics at high angles of attack p 921 N90-28523
Aerodynamic parameters of High-Angle-of attack Research Vehicle (HARV) estimated from flight data [NASA-TM-102692] p 936 N90-28578

ANGLES (GEOMETRY)

Measurement of angles and angle characteristics with accelerometers and gyroscopes p 653 A90-41730

ANGULAR ACCELERATION

Analysis of the effect of rotor-angular-acceleration on the features of gas flow in turbomachinery p 6 A90-11780

Short period control using angular acceleration feedback: Compensation for first lag servo [NAL-TM-600] p 936 N90-29399

ANGULAR VELOCITY

Tail rotor dynamics during the translational turn maneuver of a helicopter p 334 A90-24148

Synthesis of optimal multidimensional digital systems for the simulation of the angular motions of a flight vehicle under random loading p 669 A90-41957

Nonlinear inversion flight control for a supermaneuverable aircraft [AIAA PAPER 90-3406] p 864 A90-47661

Optimal rigid body reorientation problem [AIAA PAPER 90-3485] p 867 A90-47734

Construction of a hybrid angular velocity reference system for investigation of the dynamic characteristics of strapdown gyros [ESA-TT-1181] p 774 N90-25332

ANISOTROPIC MEDIA

Design, realization, and qualification of model composite rotor blades p 384 A90-24293

The anisotropy of the mechanical behaviour in nickel-based single crystal superalloys for turbine blades [ONERA, TP NO. 1989-205] p 355 A90-25339

ANISOTROPIC PLATES

Structural analysis and optimum design of geodesically stiffened composite panels [NASA-CR-186944] p 959 N90-28862

ANISOTROPIC SHELLS

Analysis of aircraft tires via semianalytic finite elements p 496 A90-34740

ANISOTROPY

Effect of structural anisotropy on the dynamic characteristics of the wing and critical flutter speed p 386 A90-28985

ANNULAR DUCTS

Effect of the cross-sectional shape of a straight duct on supersonic flow stagnation p 296 A90-24110

ANNULAR FLOW

Unsteady flow visualization in a vibrating annular turbine cascade operating in the transonic flow regime p 7 A90-11786

Experimental investigation of the time-dependent flow in a vibrating annular cascade operating in the transonic flow regime p 7 A90-11787

Selection of a suitable combustion system for a small gas turbine engine p 112 A90-16005

Experimental investigation of coannular jet flow with swirl along a centerbody [AIAA PAPER 90-1622] p 567 A90-38751

Experimental studies of combustor dilution zone aerodynamics. II - Jet development p 659 A90-40947

Numerical analysis of the flows in annular slinger combustors [AIAA PAPER 90-2164] p 685 A90-42052

Mean loading effects on flutter of subsonic rotating annular cascade p 853 A90-49453

ANNULAR NOZZLES

Experimental investigation on the performance of an annular nozzle cascade of a highly-loaded transonic turbine stage p 152 A90-17787

A study of the working process and losses in annular turbine nozzle cascades with a low contraction ratio p 254 A90-23407

An experimental study of the gasdynamic characteristics of annular nozzle cascades with small flow exit angles p 255 A90-23409

ANOMALIES

The basis for facility comparison p 856 N90-27713

ANTARCTIC REGIONS

Improving snow roads and airstrips in Antarctica [AD-A211588] p 133 N90-11907

Ice runways near the South Pole [AD-A211606] p 133 N90-11908

ANTENNA ARRAYS

Airborne array antennas for satellite communication p 265 A90-23202

An array-fed reflector antenna with built-in calibration facility p 402 A90-27781

Dual cross-polarization planar arrays in the C and X bands p 638 A90-40979

ANTENNA DESIGN

The role of adaptive antenna systems when used with GPS p 128 A90-13995

An array-fed reflector antenna with built-in calibration facility p 402 A90-27781

Measurement and computer simulation of antennas on ships and aircraft for results of operational reliability p 370 N90-17936

Antenna installation on aircraft: Theory and practice p 371 N90-17941

ANTENNA FEEDS

An array-fed reflector antenna with built-in calibration facility p 402 A90-27781

ANTENNA RADIATION PATTERNS

McDonnell Douglas Helicopter Company Apache telemetry antenna analysis p 403 A90-28839

Analytical evaluation of radiation patterns of a TACAN antenna p 404 A90-30695

Applications of slotted cable antennas in the instrument landing system p 639 A90-41708

The addition of Bendix MLS (Microwave Landing System) antenna patterns to MLS mathematical model [AD-A210633] p 27 N90-10020

Measurement and computer simulation of antennas on ships and aircraft for results of operational reliability p 370 N90-17936

Antenna installation on aircraft: Theory and practice p 371 N90-17941

The Helicopter Antenna Radiation Prediction Code (HARP) [NASA-CR-186925] p 884 N90-27946

ANTENNAS

The addition of Bendix MLS (Microwave Landing System) antenna patterns to MLS mathematical model [AD-A210633] p 27 N90-10020

ANTIFRICTION BEARINGS

Life of concentrated contacts in the mixed EHD and boundary film regimes [AD-A216673] p 454 N90-18738

ANTIICING ADDITIVES

Aircraft Ground Deicing Conference, Denver, CO, Sept. 20-22, 1988, Proceedings [SAE P-217] p 817 A90-46004

Flight and wind tunnel investigation of aerodynamic effects of aircraft ground deicing/antiicing fluids p 235 N90-15064

ANTIOXIDANTS

Aging and antioxidant surveillance studies on turbine fuel JP-5 and JP-10 p 442 A90-29492

ANTISUBMARINE WARFARE

EH101 design and development status p 407 A90-28211

The Franco-German helicopter programme HAP, PAH-2/HAC p 618 A90-42478

ANTONOV AIRCRAFT

Flying the giant --- An-124 Russian aircraft p 833 A90-48522

APERTURES

Effect of the radial clearance on the efficiency of a partial microturbine p 111 A90-14586

APPLICATION SPECIFIC INTEGRATED CIRCUITS

A test and maintenance architecture demonstrated on SEM-E modules for fiber optic networks p 458 A90-28342

APPLICATIONS PROGRAMS (COMPUTERS)

GTU/UTD: Brief history of successive development of theory and recent advances. Applications to antennas on ships and aircraft p 370 N90-17939

Software verification plan for GCS --- guidance and control software [NASA-TM-101668] p 372 N90-18057

Design and testing of a multiblock grid-generation procedure for aircraft design and research p 582 N90-21984

Extension of a three-dimensional viscous wing flow analysis user's manual: VISTA 3-D code [NASA-CR-182024] p 574 N90-22538

Development of a software package for automatic data acquisition, analysis, and controls in an axial flow compressor test rig [PD-PR-8910] p 965 N90-29926

APPROACH

Evaluation and measurement of airplane flutter interference --- in television reception p 272 A90-22529

Effect of wind shear on the airspeed during the airplane landing approach [AIAA PAPER 90-2838] p 754 A90-45160

A head up display format for application to V/STOL aircraft approach and landing [NASA-TM-102216] p 340 N90-17632

Helipoint visual approach surface high temperature and high altitude tests [DOT/FAA/CT-TN89/34] p 825 N90-27675

Vibration responses of two house structures during the Edwards Air Force Base phase of the national sonic boom program [NASA-CR-182089] p 966 N90-29169

APPROACH AND LANDING TESTS (STS)

Prediction of longitudinal pilot induced oscillations using the optimal control model [AD-A220593] p 671 N90-23412

APPROACH CONTROL

Differential GPS (DGPS) as an approach and landing aid p 242 A90-21722

Development of obstacle clearance criteria and standards for MLS and MLS/RNAV precision approaches and development of an MLS collision risk model [SAE PAPER 892215] p 728 A90-45432

Simulator evaluation of 'basic' mode back azimuth issues in departure and missed approach usage [SAE PAPER 892216] p 728 A90-45433

National airspace system approach and departure sequencing operational concept [NAS-SR-1322] p 27 N90-10017

Operational trial of effect of raising minimum stack level in Heathrow stacks [CAA-PAPER-89003] p 99 N90-12573

Parallel approach separation and controller performance: A study of the impact of two separation standards [DOT/FAA/CT-TN89/50] p 99 N90-12574

Analysis of sequencing and scheduling methods for arrival traffic [NASA-TM-102795] p 636 N90-23373

Replication of NASPAC Dallas/Fort Worth study [DOT/FAA/CT-TN90/26] p 729 N90-25123

Four-dimensional planner: A ground based planning system for time accurate approach guidance p 826 N90-27683

Approach towards a future integrated airport surface traffic management p 827 N90-27686

Independent ground monitor coverage of Global Positioning System (GPS) satellites for use by civil aviation p 918 N90-29364

APPROACH INDICATORS

Cooperative synthesis of control and display augmentation in approach and landing p 516 A90-33061

Helicopter Visual Segment Approach Lighting System (HALS) [ACD-330] p 28 N90-10856

APPROXIMATION

Mean-square approximation by an even nonnegative polynomial p 374 A90-24101

A reduced cost rational-function approximation for unsteady aerodynamics [AIAA PAPER 90-1155] p 390 A90-29367

An approximate model for the performance and acoustic predictions of counterrotating propeller configurations [NASA-CR-180667] p 379 N90-18228

An approximate viscous shock layer method for calculating the hypersonic flow over blunt-nosed bodies p 479 N90-20947

An experimental and theoretical investigation of the flow over plane delta wings with supersonic leading edges [LR-588] p 717 N90-25114

An approximate method for calculating three-dimensional inviscid hypersonic flow fields [NASA-TD-3018] p 883 N90-27066

Unsteady aerodynamics of controls p 935 N90-28525

An enhanced integrated aerodynamic load/dynamic optimization procedure for helicopter rotor blades [NASA-CR-4326] p 924 N90-29383

ARC HEATING

A model for the electrohydrodynamic flow in a constricted arc heater p 131 A90-15393

Development and calibration of a continuous-flow arc-heated hypersonic wind tunnel [AIAA PAPER 90-1381] p 594 A90-37930

ARCHITECTURE (COMPUTERS)

An objective methodology for definition and evaluation of advanced avionics architectures [AIAA PAPER 89-3035] p 36 A90-10535

Trends in telemetry front end architecture [AIAA PAPER 89-3085] p 25 A90-10571

Trends in real-time flight systems [AIAA PAPER 89-3086] p 25 A90-10572

A heterogeneous parallel processing architecture for avionic and aerospace applications [AIAA PAPER 89-3108] p 74 A90-10590

Embedded knowledge based avionics [AIAA PAPER 89-3141] p 75 A90-10615

Categorization and performance analysis of advanced avionics algorithms on parallel processing architectures p 461 A90-30786

Integrated Diagnostics (ID) for advanced avionics architectures [SAE PAPER 892359] p 738 A90-45509

Parallel processing implementation of a flight controller p 333 N90-16743

Numerical algorithms for parallel computers [AD-A216812] p 377 N90-18181

SUBJECT INDEX

- Integrated circuits for avionics
[AD-A217964] p 540 N90-20312
- Software Management Environment (SME) concepts and architecture
[NASA-TM-103306] p 547 N90-21543
- AIRNET: A real-time communications network for aircraft
[NASA-CR-186140] p 690 N90-24514
- Conceptual design for aerospace vehicles
p 651 N90-25043
- Technical evaluation report on the Guidance and Control Panel 49th Symposium on Fault Tolerant Design Concepts for Highly Integrated Flight Critical Guidance and Control Systems
[AGARD-AR-281] p 758 N90-26012
- Aircraft condition monitoring system for future Airbus aircraft: New concept for programming and data recording
p 848 N90-27619
- Multichannel on-board load and fatigue monitoring
p 849 N90-27621
- Distributed control architecture for CNI preprocessors
p 917 N90-29356
- High speed bus technology development
[AD-A224486] p 960 N90-29565
- Small multipurpose stored data acquisition system
[DE90-010823] p 967 N90-30134
- AREA NAVIGATION**
- MLS RNAV accuracy flight tests
[SAE PAPER 892218] p 728 A90-45435
- Analytical studies for computed center line operations
[SAE PAPER 892219] p 729 A90-45436
- A conflict analysis of 4D descent strategies in a metered, multiple-arrival route environment
[NASA-CR-182019] p 593 N90-21772
- An evaluation of the accuracy of a microwave landing system area navigation system at Miami/Tamiami Florida Airport
[DOT/FAA/CT-TN89/40] p 640 N90-23377
- ARGON**
- A Mach 6 external nozzle experiment with Argon-Freon exhaust simulation
[SAE PAPER 892315] p 714 A90-45477
- AROMATIC COMPOUNDS**
- Toughened cyanates for aerospace applications
p 942 A90-50088
- ARRAYS**
- Detection of flow instabilities at airfoil profiles using piezoelectric arrays
p 276 N90-16175
- Aerodynamic study on forced vibrations on stator rows of axial compressors
p 426 N90-18412
- ARRIVALS**
- National Airspace System demand and capacity modeling
p 330 A90-25562
- Computer-based tools for assisting air traffic controllers with arrivals flow management
[RSRE-88001] p 178 N90-13366
- ARROW WINGS**
- Accumulated span loadings of an arrow wing having vortex flow
p 17 A90-13025
- ARTIFICIAL INTELLIGENCE**
- Pilot's Associate - A perspective on Demonstration 2
[AIAA PAPER 89-3023] p 36 A90-10524
- Linking artificial intelligence (AI) and computer aided engineering (CAE) to analyze the testability of electronic designs
[AIAA PAPER 89-3070] p 74 A90-10559
- Adapting an AI-based application from its LISP environment into a real-time embedded system
[AIAA PAPER 89-3142] p 75 A90-10616
- Artificial intelligence techniques applied to the non-cooperative identification (NCID) problem
[AIAA PAPER 89-3005] p 75 A90-10619
- Incorporation of alarm states into a real time decision making process
[AIAA PAPER 89-3006] p 76 A90-10620
- An intelligent system for autonomous navigation of airborne vehicles
p 26 A90-11696
- Real-time decision making for autonomous flight control
[SAE PAPER 891053] p 118 A90-14355
- Applying artificial intelligence techniques to air traffic control automation
p 282 A90-21389
- Future ATC automation aids based upon AI technology
p 375 A90-25563
- Advances in weather technology for the aviation system
p 373 A90-25572
- Computers and the aerospace engineer
p 375 A90-25719
- The role of expert systems in aircraft safety management
p 375 A90-26225
- Smart structures with nerves of glass
p 444 A90-27951
- Reasoning from uncertain data - A BIT enhancement
p 457 A90-28330
- Auxiliary power unit maintenance aid - Flight line engine diagnostics
p 382 A90-28348

- AAIIC '88 - Aerospace Applications of Artificial Intelligence; Proceedings of the Fourth Annual Conference, Dayton, OH, Oct. 25-27, 1988. Volumes 1 & 2
p 458 A90-30226
- An adaptive-learning expert system for maintenance diagnostics
p 460 A90-30754
- A Distributed Artificial Intelligence approach to object identification and classification
p 545 A90-34185
- Artificial intelligence (AI) based tactical guidance for fighter aircraft
[AIAA PAPER 90-3435] p 889 A90-47688
- Probabilistic reasoning for intelligent wind shear avoidance
[AIAA PAPER 90-3437] p 890 A90-47690
- Application possibilities of expert systems in modern maintenance for increasing operational security
p 892 A90-49271
- Real-time support for high performance aircraft operation
[NASA-CR-185475] p 57 N90-10075
- A knowledge-based system design/information tool for aircraft flight control systems
[NASA-TM-101704] p 217 N90-13990
- A knowledge-based flight status monitor for real-time application in digital avionics systems
[NASA-TM-101710] p 217 N90-13995
- Perspectives on the use of rule-based control
p 521 N90-20940
- A study of supermaneuver aerodynamics
[AD-A218378] p 631 N90-23349
- NDI-concept for composites in future military aircraft
p 877 N90-28070
- Use of acoustic emission for continuous surveillance of aircraft structures
p 887 N90-28092
- Model authoring system for fail safe analysis
[NASA-CR-4317] p 964 N90-29142
- A knowledge-based system design/information tool
[NASA-CR-4316] p 965 N90-29143
- ASCENT**
- Helipod visual approach surface high temperature and high altitude tests
[DOT/FAA/CT-TN89/34] p 825 N90-27675
- ASCENT PROPULSION SYSTEMS**
- ETO (Earth-To-Orbit): A trajectory program for aerospace vehicles
[AD-A218157] p 528 N90-20103
- ASPECT RATIO**
- Influence of blade leaning on the flow field behind turbine rectangular cascades with different incidences and aspect ratios
p 11 A90-12519
- Lift development of delta wings undergoing constant acceleration from rest
[AIAA PAPER 90-0310] p 164 A90-19789
- Nonsymmetric vortex breakdown and aerodynamic hysteresis in flow past a low-aspect-ratio wing/fuselage configuration
p 294 A90-24076
- An experimental study of separated flow past a low-aspect-ratio delta wing
p 294 A90-24077
- An iterative solution to aeroelastic effects in potential flow
[AD-A216291] p 320 N90-17580
- ASPHALT**
- Design temperatures for flexible airfield pavement design
[AD-A214141] p 262 N90-15115
- Evaluation of two transport aircraft and several ground test vehicle friction measurements obtained for various runway surface types and conditions. A summary of test results from joint FAA/NASA Runway Friction Program
[NASA-TP-2917] p 249 N90-15902
- Criteria for coal tar seal coats on airport pavements. Volume 2: Laboratory and field studies
[AD-A220167] p 674 N90-24277
- ASSEMBLER ROUTINES**
- The function of the Interactive Model Assembly Program (IMAP) for a flight simulator
[NAL-TR-1034] p 939 N90-29412
- ASSEMBLING**
- Design for assembly of aerospace structures - A qualitative, interactive approach
[SME PAPER MS89-158] p 222 A90-23683
- Manufacturing and handling techniques used in the assembly of polished commercial aircraft
[SAE PAPER 890925] p 286 A90-24690
- Harnessing detailed assembly process knowledge with CASE
p 535 A90-32504
- ASSEMBLY LANGUAGE**
- Yaw rate control of an air bearing vehicle
p 435 N90-19420
- ASSESSMENTS**
- Assessment of voice coders for ATC/pilot voice communications via satellite digital communication channels
[CAA-PAPER-89004] p 135 N90-12807

ATMOSPHERIC ELECTRICITY

- Risk assessment and its application to flight safety analysis
[DE90-004985] p 323 N90-16722
- ASTROGUIDE NAVIGATION SYSTEM**
- Strapdown astro-inertial navigation (SAIN) utilizing the optical wide-angle lens startracker (OWLS)
p 824 A90-49503
- ASTRONAUT TRAINING**
- Activities report in German aerospace
[ISSN-0070-3968] p 465 N90-19189
- ASTRONAUTICS**
- Profiles-aeronautical/astronautical engineering: Human resources and funding
[PB90-103888] p 369 N90-16969
- ASYMMETRY**
- Study of forces and moments on wing-bodies at high incidence, volumes 1 and 2
p 171 N90-13350
- Analytical study of the origin and behavior of asymmetric vortices
[NASA-TM-102796] p 573 N90-21746
- Development of non-conventional control methods for high angle of attack flight using vortex manipulation
p 935 N90-28522
- ASYMPTOTIC METHODS**
- An asymptotic theory for the periodic turbulent boundary layer in zero mean-pressure gradient
[AD-A222832] p 66 A90-10222
- Asymptotic calculation of flow parameters in the problem of hypersonic flow past blunt axisymmetric bodies
p 10 A90-12268
- Asymptotic solution of the optimal-deflection problem for a wing leading edge at subsonic flow velocities
p 295 A90-24094
- On the instabilities of supersonic mixing layers - A high-Mach-number asymptotic theory
p 702 A90-42644
- Asymptotic analysis of transonic flow through oscillating cascades
p 427 N90-18421
- ASYMPTOTIC SERIES**
- Asymptotic modal analysis and statistical energy analysis
[NASA-CR-186732] p 782 N90-26634
- ATMOSPHERIC ATTENUATION**
- Concept of an MTI search radar
p 487 A90-33613
- En route noise: NASA propfan test aircraft (calculated source noise)
[DOT-TSC-FA853-LR5] p 697 N90-24857
- ATMOSPHERIC BOUNDARY LAYER**
- An automated method for predicting the height of the lower cloud boundary
p 888 A90-48359
- Glancing shock-boundary layer interactions
p 319 N90-17571
- Wind tunnel design of heat island turbulent boundary layer
[IHW-ET/50] p 455 N90-19542
- ATMOSPHERIC CHEMISTRY**
- New high-speed air transport system and stratospheric pollution
[ONERA, TP NO. 1989-202] p 279 A90-22445
- Mesoscale acid deposition modeling studies
[NASA-CR-4262] p 140 N90-13228
- Global stratospheric change: Requirements for a Very-High-Altitude Aircraft for Atmospheric Research
[NASA-CP-10041] p 185 N90-14220
- ATMOSPHERIC CIRCULATION**
- Airdata calibration of a high-performance aircraft for measuring atmospheric wind profiles
[NASA-TM-101714] p 186 N90-14228
- ATMOSPHERIC COMPOSITION**
- Meeting Review: Workshop on Airborne Instrumentation
[PB89-174775] p 39 N90-10032
- ATMOSPHERIC EFFECTS**
- Estimation of atmospheric and transponder survey errors with a navigation Kalman filter
p 459 A90-30689
- The STOL maneuver technology demonstrator manned simulation test program
p 439 A90-30716
- Flight in Adverse Environmental Conditions
[AGARD-CP-470] p 222 N90-15041
- Adverse weather operations during the Canadian Atlantic storms program
p 281 N90-15052
- ATMOSPHERIC ELECTRICITY**
- Transall 88 - Lightning characterization program
[ONERA, TP NO. 1989-142] p 22 A90-11164
- Electrostatic description of a positive leader ignition from an aircraft
[ONERA, TP NO. 1989-149] p 23 A90-11171
- Multistroke cloud-to-ground strike to the NASA F-106B airplane
p 482 A90-32304
- 1988 International Aerospace and Ground Conference on Lightning and Static Electricity, Oklahoma City, OK, Apr. 19-22, 1988, Addendum to the Proceedings
p 888 A90-49826
- Aircraft lightning protection handbook
[AD-A222716] p 820 N90-27668

ATMOSPHERIC LASERS

Extended communication path length scintillation measurements and model - A discussion of results --- of atmospheric laser experiments p 725 A90-43230

ATMOSPHERIC MODELS

Mesoscale acid deposition modeling studies [NASA-CR-4262] p 140 N90-13228

Description of atmospheric turbulence p 280 N90-15043

Windshear case study: Denver, Colorado, July 11, 1988 [DOT/FAA/DS-89/19] p 544 N90-21509

Effects of simplifying assumptions on optimal trajectory estimation for a high-performance aircraft [NASA-TM-101721] p 757 N90-25142

ATMOSPHERIC MOISTURE

Using cloud moisture calculations for estimating aircraft icing p 888 A90-48358

Moisture absorption in graphite/epoxy laminates p 951 A90-52799

ATMOSPHERIC OPTICS

Variability characteristics of the meteorological optical range field in an optically inhomogeneous atmosphere p 962 A90-50784

ATMOSPHERIC SOUNDING

Meteopod, an airborne system for measurements of mean wind, turbulence, and other meteorological parameters p 418 A90-29943

ATMOSPHERIC TURBULENCE

Rotor noise due to atmospheric turbulence ingestion. I - Fluid mechanics p 219 A90-19385

Rotor noise due to atmospheric turbulence ingestion. II - Aeroacoustic results p 219 A90-19386

A Monte Carlo simulation technique for low-altitude, wind-shear turbulence [AIAA PAPER 90-0564] p 216 A90-19917

Meteopod, an airborne system for measurements of mean wind, turbulence, and other meteorological parameters p 418 A90-29943

Concept of an MTI search radar p 487 A90-33613

Helicopter response to atmospheric turbulence in forward flight p 518 A90-33625

Digital generation of two-dimensional field of turbulence for flight simulation p 611 A90-36427

The response of helicopter to dispersed gust p 670 A90-42470

Extended communication path length scintillation measurements and model - A discussion of results --- of atmospheric laser experiments p 725 A90-43230

Cloud features suggesting low level wind shear and turbulence p 778 A90-44545

Simulating turbulence and gusts for handling qualities evaluation [AIAA PAPER 90-2845] p 754 A90-45174

Modeling of turbulence and downbursts for flight simulators p 870 A90-48956

Some implications of the isotropic momentarily frozen assumptions for the SPAN-MAT program [NASA-CR-181937] p 88 N90-11704

The S.D.G., P.S.D. and the nonlinear airplane [NLR-MP-88018-U] p 183 N90-13371

Description of atmospheric turbulence p 280 N90-15043

ATMOSPHERICS

An airborne instrument for characterizing the 10,000 electromagnetic signals generated by one lightning flash p 848 A90-49830

ATOMIC SPECTRA

Shock layer vacuum UV spectroscopy in an arc-jet wind tunnel [NASA-TM-102258] p 370 N90-17112

ATOMIZERS

Influence of the continuous and dispersed phases on the symmetry of a gas turbine air-blast atomizer [ASME PAPER 89-GT-303] p 273 A90-22651

Symmetry assessment of an air-blast atomizer spray p 682 A90-40930

Effect of vane twist on the performance of dome swirlers for gas turbine airblast atomizers [AIAA PAPER 90-1955] p 881 A90-47203

Effect of vane twist on the performance of dome swirlers for gas turbine airblast atomizers [NASA-TM-103195] p 773 N90-25289

ATOMIZING

Investigation and improvement of ground starting characteristics of a combustor with airblast nozzles p 45 A90-12546

A study on spray characteristics down stream from a gutter-atomizer p 368 A90-26893

Effect of vane twist on the performance of dome swirlers for gas turbine airblast atomizers p 881 A90-47203

Effect of vane twist on the performance of dome swirlers for gas turbine airblast atomizers [NASA-TM-103195] p 773 N90-25289

ATTACK AIRCRAFT

The Battle Captain Expert System - A mission management decision support system for attack helicopter operations [AIAA PAPER 89-3098] p 37 A90-10583

Damage tolerance analysis and testing of a welded cluster gear for the main transmission of the Advanced Attack Helicopter p 445 A90-28187

Fly-by-wire controls key to 'pure' stealth aircraft --- F-117A Aircraft p 413 A90-30222

Flight/propulsion control integration for V/STOL fighter/attack aircraft p 591 A90-38530

Computational analysis of an open-nosed fighter/attack inlet [AIAA PAPER 90-2145] p 704 A90-42737

Building the B-2 p 701 A90-43826

VTOL military research aircraft --- Book p 828 A90-46002

The servo flap - An advanced rotor control system p 860 A90-46934

Airbrake design for base-line configuration of advanced jet trainers/light attack airplanes and military combat airplanes p 810 A90-48081

Estimating the relationships between the state of the art of technology and production cost for the US aircraft [AD-A212127] p 82 N90-12495

Evaluation of a damaged F/A-18 horizontal stabilizer [AD-A212573] p 107 N90-12597

Development of a least squares time response lower-order equivalent systems technique [AD-A220527] p 648 N90-23389

AM-X high incidence trials, development and results [ETN-90-97277] p 759 N90-26016

Expert system for pilot assistance: The challenge of an intensive prototyping [ETN-90-97274] p 825 N90-27674

Combat aircraft control requirements p 934 N90-28515

Combat aircraft control requirements for agility p 935 N90-28517

The effects of foreplanes on the static and dynamic characteristics of a combat aircraft model p 920 N90-28520

The steady and time-dependent aerodynamic characteristics of a combat aircraft with a delta or swept canard p 921 N90-28526

The potential for digital databases in flight planning and flight aiding for combat aircraft p 918 N90-29371

ATTACKING (ASSAULTING)

Time-optimal aircraft pursuit-evasion with a weapon envelope constraint [NASA-CR-186640] p 734 N90-25126

ATTENUATORS

Operational effects on crashworthy seat attenuators [AD-A221148] p 637 N90-24259

ATTITUDE (INCLINATION)

Real time estimation of aircraft angular attitude p 431 A90-30103

Model attitude measurement system p 539 A90-34235

A dynamic optical model attitude measurement system p 539 A90-34236

Optimization of the effective GPS data rate p 489 N90-20932

Coupled rotor-body equations of motion hover flight [NASA-CR-186710] p 717 N90-25111

ATTITUDE CONTROL

Design of attitude and rate command systems for helicopters using eigenstructure assignment p 118 A90-14729

Attitude projection method for analyzing large-amplitude airplane maneuvers p 197 A90-19555

OPST1 - An optical yaw control system for high performance helicopters p 430 A90-28220

A study on the application of controllability and observability concepts in the design of flight control systems p 693 A90-39303

Nonlinear inversion flight control for a supermaneuverable aircraft [AIAA PAPER 90-3406] p 864 A90-47661

Analyzing the flared landing task with pitch-rate flight control systems [AIAA PAPER 90-3483] p 866 A90-47732

LOG/LTR controller design using a reduced order model p 964 A90-52877

Low-speed wind-tunnel study of reaction control-jet effectiveness for hover and transition of a STOVL fighter concept [NASA-TM-4147] p 119 N90-11751

Aircraft SAR simulation Sargen 1.0 [FEL-1989-44] p 135 N90-12823

Aerodynamics of thrust vectoring [NASA-CR-185074] p 172 N90-13354

Techniques for extreme attitude suspension of a wind tunnel model in a magnetic suspension and balance system [NASA-CR-181895] p 202 N90-14245

Possible piloting techniques at hypersonic speeds [ISL-CO-216/88] p 415 N90-18392

Short period control using angular acceleration feedback: Compensation for first lag servo [NAL-TM-600] p 936 N90-29399

ATTITUDE STABILITY

Techniques for extreme attitude suspension of a wind tunnel model in a magnetic suspension and balance system [NASA-CR-181895] p 202 N90-14245

AUDITORY TASKS

Security audit for embedded avionics systems p 957 A90-50649

AUSTRALIA

An examination of the fatigue meter records from the RAAF Orion P-3C fleet [AD-A214000] p 338 N90-17628

AUTOCALVES

Cooking an aeroplane p 209 A90-17918

AUTOCALVING

Integrally heated tooling for economical, nonautoclave production of thermoplastic parts p 956 A90-50200

AUTOCORRELATION

A new class of random processes with application to helicopter noise p 781 A90-42874

Spanwise measurements of vertical components of atmospheric turbulence [NASA-TP-2963] p 456 N90-19718

AUTOMATED PILOT ADVISORY SYSTEM

The influence of ice accretion physics on the forecasting of aircraft icing conditions p 485 N90-20928

AUTOMATED RADAR TERMINAL SYSTEM

Experimental examination of the benefits of improved terminal air traffic control planning p 241 A90-21388

The development result of SPEKTR automated air traffic control (ATC) system with extended grade of automation for terminal and hub areas p 639 A90-41058

AUTOMATIC CONTROL

Adaptive automatic control systems. Number 16 --- Russian book p 76 A90-10844

Inverse problems in controlled system dynamics: Nonlinear models --- Russian book p 77 A90-12471

Digital control experiment research on the engine JT15D-4 p 190 A90-18600

The fast-response requirement of powerplant thrust in the set of engineering and economic criteria of an aircraft p 254 A90-23354

Aircraft program motion along a predetermined trajectory. I - Mathematical modelling p 345 A90-23979

An automatic system for the programmed control of the parameters of the vibrational and thermal testing of the blades of gas turbine engines p 343 A90-24216

Automating and controlling dry paint stripping [SAE PAPER 890939] p 365 A90-24702

The trend in navais inspection is to automatic operation p 329 A90-25495

The US air traffic control system architecture p 330 A90-25561

Advanced Automation System design p 375 A90-25566

Toward a human-centered aircraft automation philosophy p 347 A90-26177

Microprocessor control of a vapor-cycle cooling system [SAE PAPER 891457] p 339 A90-27426

An automated vorticity surveying system using a rotating hot-wire probe p 447 A90-28284

Instrumentation and operation of NDA cryogenic wind tunnel p 437 A90-28293

Fully automatic calibration machine for internal 6-component wind tunnel balance including cryogenic balances p 437 A90-28294

Eshbach's handbook of engineering fundamentals /4th edition/ p 448 A90-28825

Flying qualities lessons learned - 1988 p 431 A90-30705

A microcomputer-based airspace control simulation and prototype human-machine interface p 461 A90-30800

Cryogenic wind tunnels in Japan p 523 A90-34228

Concept development of automatic guidance for rotorcraft obstacle avoidance p 669 A90-41632

Monitoring and maintenance of automatic control systems in aviation --- Russian book p 778 A90-42524

Dynamics and control of maneuverable towed flight vehicles [AIAA PAPER 90-2841] p 754 A90-45161

Expert system technology applied to the automatic control of multiple unmanned aerial vehicles [AIAA PAPER 90-3280] p 892 A90-48867

- Automatic environmental control system for electronic equipment platforms p 840 A90-49292
[SAE PAPER 901217]
- Backside landing control of a STOL aircraft using approximate perfect servo p 934 A90-52801
- Apparatus for cooling electronic components in aircraft
[AD-D014207] p 183 N90-13373
- Flight deck automation: Promises and realities
[NASA-CP-10036] p 187 N90-13384
- Automatic control of cryogenic wind tunnels p 263 N90-15957
- A sensor stabilization/tracking system for unmanned air vehicles
[AD-A224008] p 936 N90-28579
- AUTOMATIC FLIGHT CONTROL**
- The research of cubic spline optimal terrain following system p 196 A90-18584
- A GPS-based flight-control concept p 242 A90-21719
- An in-flight interaction of the X-29A canard and flight control system
[AIAA PAPER 90-1240] p 348 A90-26820
- Fully automatic guidance for rotorcraft nap-of-the-earth (NOE) flight following planned profiles p 403 A90-28219
- Testing of a highly integrated automatic flight system - The 747-400 Flight Management Computer System
[AIAA PAPER 90-1302] p 505 A90-33916
- Developments in automation of flight test analysis and report generation
[AIAA PAPER 90-1313] p 487 A90-33923
- Autopilot flight test experience with BK 117 hingeless rotor
[AIAA PAPER 90-1267] p 505 A90-33930
- Flight-testing of the self-repairing flight control system using the F-15 highly integrated digital electronic control flight research facility
[AIAA PAPER 90-1321] p 520 A90-34149
- Automation of flight safety control --- Russian book p 589 A90-36157
- Application of transformational ideas to automatic flight control design p 589 A90-36433
- Digital map reader for helicopters p 653 A90-42448
- The Super Puma MKII automatic flight control system p 669 A90-42449
- Determination of the extreme values of the efficiency criteria for a flight vehicle control system in the probable scatter range of its characteristics p 859 A90-46569
- Fault tolerant architecture for a fly-by-light flight control computer p 860 A90-46931
- Application of energy turn g-limiting for aircraft high performance turns
[AIAA PAPER 90-3328] p 862 A90-47590
- Real-time piloted simulation of fully automatic guidance and control for rotorcraft nap-of-the-earth (NOE) flight following planned profiles
[AIAA PAPER 90-3372] p 864 A90-47630
- Flight controller design with nonlinear aerodynamics, large parameter uncertainty, and pilot compensation
[AIAA PAPER 90-3478] p 866 A90-47728
- Simulation investigation of multiple axis flying qualities
[AIAA PAPER 90-3480] p 866 A90-47729
- Synthesis of a simulator-based automated helicopter hover trainer
[AIAA PAPER 90-3481] p 891 A90-47730
- Flight investigation of variations in rotorcraft control and display dynamics for hover
[AIAA PAPER 90-3482] p 866 A90-47731
- Application of multifunction inertial reference systems to fighter aircraft p 332 N90-16740
- Design of a helicopter automatic flight control system using adaptive control p 522 N90-21040
- First-order weight corrections for real-time flight path management
[LR-580] p 578 N90-21751
- Helicopter controllability
[AD-A220078] p 672 N90-24275
- Flight service automation system, model 1 full capacity, NAS operational test and evaluation integration test plan
[DOT/FAA/CT-TN90/4] p 825 N90-27672
- Flight test investigation of flight director and autopilot functions for helicopter decelerating instrument approaches
[DOT/FAA/CT-TN89/54] p 869 N90-27724
- AUTOMATIC GAIN CONTROL**
- An in-flight interaction of the X-29A canard and flight control system
[AIAA PAPER 90-1240] p 348 A90-26820
- Automated measurement of aircraft-level electromagnetic interference p 404 A90-30752
- AUTOMATIC LANDING CONTROL**
- Autoland with GPS p 97 A90-13985
- Integrated system of differential Global Positioning System and inertial measurement unit - A position determination system for automatic landing
[AIAA PAPER 90-1300] p 487 A90-33914
- Automatic landing with GPS - Design of the flight guidance and flight control system
[AIAA PAPER 90-1301] p 487 A90-33915
- Simulation of MLS-ATC procedures in the New York and San Francisco Terminal Control Areas
[SAE PAPER 892217] p 728 A90-45434
- Improved noise rejection in automatic carrier landing systems
[AIAA PAPER 90-3374] p 864 A90-47632
- AUTOMATIC PILOTS**
- Intelligent situation assessment and response aiding in flight emergencies
[AIAA PAPER 89-2999] p 36 A90-10507
- Adaptive autopilot design via model expansion method p 55 A90-11124
- Real-time decision making for autonomous flight control
[SAE PAPER 891053] p 118 A90-14355
- Evaluation of the dynamic properties of the auto-pilot servo of a single-rotor helicopter through laboratory testing p 118 A90-15424
- Aircraft program motion along a predetermined trajectory. I - Mathematical modelling p 345 A90-23979
- Aircraft program motion along a predetermined trajectory. II - Numerical simulation with application of spline functions to trajectory definitions p 347 A90-25199
- Toward a human-centered aircraft automation philosophy p 347 A90-26177
- Autopilot flight test experience with BK 117 hingeless rotor
[AIAA PAPER 90-1267] p 505 A90-33930
- Digital autopilot for light aircraft p 653 A90-41741
- The Super Puma MKII automatic flight control system p 669 A90-42449
- An explicit model-matching approach to lateral-axis autopilot design p 756 A90-45413
- A mixed H2 and H(infinity) approach to an autopilot design problem
[AIAA PAPER 90-3441] p 865 A90-47694
- Genetic algorithms in control system optimization
[AIAA PAPER 90-3488] p 867 A90-47736
- CONDOR - high altitude long endurance (HALE) autonomously piloted vehicle (APV)
[AIAA PAPER 90-3279] p 836 A90-48866
- Nonlinear maneuver autopilot for the F-15 aircraft
[NASA-CR-179442] p 77 N90-11487
- Pilotless airplanes
[AD-A211719] p 103 N90-11734
- An autopilot design methodology for bank-to-turn missiles
[AD-A213379] p 198 N90-13399
- Design of integrated pitch axis for autopilot/autothrottle and integrated lateral axis for autopilot/yaw damper for NASA TSRV airplane using integral LQG methodology
[NASA-CR-4268] p 348 N90-16768
- The NASA digital VGH program: Exploration of methods and final results. Volume 2: L 1011 data 1978-1979: 1619 hours
[NASA-CR-181909-VOL-2] p 505 N90-20080
- Robustness evaluation of H2 and H(infinity) control theory as applied to a transport aircraft
[AD-A222795] p 759 N90-26018
- Flight test investigation of flight director and autopilot functions for helicopter decelerating instrument approaches
[DOT/FAA/CT-TN89/54] p 869 N90-27724
- AUTOMATIC TEST EQUIPMENT**
- Automatic testing in aircraft building --- Russian book p 285 A90-24231
- A microprocessor-based system for monitoring gas turbines p 350 A90-24359
- AUTOTESTCON '89 - IEEE International Automatic Testing Conference, Philadelphia, PA, Sept. 25-28, 1989, Conference Record p 457 A90-28310
- The two level maintenance - I level dilemma p 381 A90-28319
- Reasoning from uncertain data - A BIT enhancement p 457 A90-28330
- From a sow's ear - Quantitative diagnostic design requirements from anecdotal references p 448 A90-28337
- Intelligent built-in test and stress management p 448 A90-28343
- Auxiliary power unit maintenance aid - Flight line engine diagnostics p 382 A90-28348
- Advanced technology ATE for fuel accessory testing p 439 A90-30770
- Automated aircraft hydraulics testing p 551 A90-37899
- Next-generation automatic test equipment for military support p 767 A90-42667
- Design of computer-aided aircraft testing systems. II p 785 A90-46498
- AUTOMATIC TRAFFIC ADVISORY AND RESOLUTION**
- TCAS - A system for preventing midair collisions p 252 A90-21383
- Applying artificial intelligence techniques to air traffic control automation p 282 A90-21389
- AUTOMATIC WEATHER STATIONS**
- Semiautomatic coding of weather phenomenon groups in the meteorological reports of automatic airport stations p 962 A90-50783
- AUTOMATION**
- Computer-aided design of flight vehicle instrument bays --- Russian book p 76 A90-10837
- The advantages of automation in aerospace production p 130 A90-15357
- Automated aircraft paint strip cell
[SAE PAPER 890936] p 286 A90-24699
- Future ATC automation aids based upon AI technology p 375 A90-25563
- The benefits and costs of automation in advanced helicopters - An empirical study p 348 A90-26258
- Automation of an RCS (Radar Cross Section) measurement system and its application to investigate the electromagnetic scattering from scale model aircraft canopies
[AD-A215741] p 371 N90-17970
- AUTOMOBILE ENGINES**
- Advanced Turbine Technology Applications Project (ATTAP)
[NASA-CR-185133] p 51 N90-10036
- AUTOMOBILE FUELS**
- Aircraft field experience with automotive gasoline in the United States p 912 A90-51618
- Field experience with type certificated civil aircraft operated on motor gasolines and worldwide survey of motor gasoline characteristics p 912 A90-51619
- Automotive gasoline - A fuel for modern aircraft piston engines p 950 A90-51620
- Future use of automotive gasoline in light aircraft p 951 A90-51624
- AUTONOMIC NERVOUS SYSTEM**
- Neurocontrol systems and wing-fluid interactions underlying dragonfly flight p 434 N90-19240
- AUTONOMOUS NAVIGATION**
- Reflexive navigation for autonomous aircraft
[AIAA PAPER 89-2991] p 25 A90-10502
- An intelligent system for autonomous navigation of airborne vehicles p 26 A90-11696
- A reconfigurable integrated navigation and flight management system for military transport aircraft p 433 A90-30794
- The case for both RAIM and GIC working together - The ultimate solution to the GPS integrity problem p 576 A90-36916
- Control system validation in the autonomous helicopter p 667 A90-38908
- Autonomous integrated GPS/INS navigation experiment for OMV, Phase 1: Feasibility study
[NASA-CR-4267] p 489 N90-20969
- Kalman filter based range estimation for autonomous navigation using imaging sensors p 578 N90-22238
- The potential for digital databases in flight planning and flight aiding for combat aircraft p 918 N90-29371
- AUTONOMY**
- Technology and evaluation of unmanned air vehicles p 252 N90-15934
- Autonomous automatic landing through computer vision p 332 N90-16734
- AUTOPSIES**
- The use of soot analysis as an investigative tool in aircraft fires p 22 A90-10269
- AUTOREGRESSIVE PROCESSES**
- High resolution spectrum analysis for airborne pulse Doppler radars p 339 A90-24329
- Adaptive clutter rejection filters for airborne Doppler weather radar applied to the detection of low altitude windshear
[NASA-CR-186211] p 214 N90-14453
- AUTOROTATION**
- Analytical study of dynamic response of helicopter in autorotative flight p 670 A90-42469
- Optimal autorotational descent of a helicopter with control and state inequality constraints p 756 A90-45344
- AUXILIARY POWER SOURCES**
- Starter systems and auxiliary power units p 660 A90-41760
- Fast start ceramic auxiliary power unit
[SAE PAPER 892254] p 747 A90-45456
- AVAILABILITY**
- MDHC technical assessment of advanced rotor and control concepts p 861 A90-46948

AVALANCHE DIODES

A semiconductor laser-Doppler-anemometer for applications in aerodynamic research

p 447 A90-28273

AVERAGE

Development of a mass averaging temperature probe

p 427 N90-18418

AVIATION METEOROLOGY

A program to improve aircraft icing forecasts

[AIAA PAPER 90-0196] p 216 A90-19733

Colorado mountain flying - Crashes and weather

[AIAA PAPER 90-0369] p 175 A90-19818

Litigation and the National Weather Service

[AIAA PAPER 90-0371] p 220 A90-19819

Aviation litigation - An ATC perspective

[AIAA PAPER 90-0372] p 175 A90-19820

Use of Computer-Aided Video Display technology in aviation weather litigation

[AIAA PAPER 90-0373] p 216 A90-19821

Real time winds data for flight management

[AIAA PAPER 90-0565] p 197 A90-19918

The influence of weather on flight operations at the Atlanta Hartsfield International Airport

p 279 A90-22688

Environmental conditions associated with the Dallas microburst storm determined from satellite soundings

p 280 A90-22689

Multiple vortex ring model of the DFW microburst

p 280 A90-23286

Wind shear and hyperbolic distributions

p 280 A90-23632

Advances in weather technology for the aviation system

p 373 A90-25572

The source region and evolution of a microburst downdraft

p 456 A90-28612

Aviation meteorology - Panel report

p 692 A90-39403

Cloud features suggesting low level wind shear and turbulence

p 778 A90-44545

Optimal paths through downbursts

p 755 A90-45330

Control of an aircraft in downbursts

p 755 A90-45331

Analysis and prediction of weather for aviation

p 888 A90-48351

Using cloud moisture calculations for estimating aircraft icing

p 888 A90-48358

An automated method for predicting the height of the lower cloud boundary

p 888 A90-48359

Vertical wind shears in lower-level jet stream over some airfields in the Urals and Siberia

p 888 A90-48362

Requirements for meteorological equipment designed for the acquisition of meteorological data essential for the takeoff and landing of aircraft at civil airports

p 962 A90-50777

Analysis and synthesis of meteorological support systems for airports

p 914 A90-50778

Coordination strategies in a hierarchical air traffic control system with allowance for meteorological conditions

p 914 A90-50779

Measurement of wind characteristics at airports

p 962 A90-50780

Inversions and associated wind-shear warnings must be related to airport characteristics

p 962 A90-52051

Maximum expected concentrations of hail in thunderstorm precipitation

p 962 A90-52052

A scalar/vector potential solution for aerodynamic coefficients in wind shear

p 21 N90-10838

Description of atmospheric turbulence

p 280 N90-15043

AVIONICS

RISC lifting off in avionics --- Reduced Instruction Set Computer

[AIAA PAPER 89-2967] p 73 A90-10483

An objective methodology for definition and evaluation of advanced avionics architectures

[AIAA PAPER 89-3035] p 36 A90-10535

Linking artificial intelligence (AI) and computer aided engineering (CAE) to analyze the testability of electronic designs

[AIAA PAPER 89-3070] p 74 A90-10559

A methodology for validating software reliability

[AIAA PAPER 89-3081] p 74 A90-10567

An experimental investigation of fault tolerant software structures in an avionics application

[AIAA PAPER 89-3082] p 74 A90-10568

Trends in real-time flight systems

[AIAA PAPER 89-3086] p 25 A90-10572

Benchmarking blackboards to support cockpit information management

[AIAA PAPER 89-3095] p 37 A90-10580

Problem focus mechanisms for cockpit automation

[AIAA PAPER 89-3096] p 37 A90-10581

Real-time fault monitoring for aircraft applications using quantitative simulation and expert systems

[AIAA PAPER 89-3103] p 37 A90-10586

High level language programming for avionic vector processors

[AIAA PAPER 89-3107] p 74 A90-10589

A heterogeneous parallel processing architecture for avionic and aerospace applications

[AIAA PAPER 89-3108] p 74 A90-10590

Graphical interface tools for an avionics system

[AIAA PAPER 89-3130] p 75 A90-10606

The NIMBLE Project - Real-time common LISP for embedded expert systems applications

[AIAA PAPER 89-3140] p 75 A90-10614

Embedded knowledge based avionics

[AIAA PAPER 89-3141] p 75 A90-10615

Adapting an AI-based application from its LISP environment into a real-time embedded system

[AIAA PAPER 89-3142] p 75 A90-10616

Artificial intelligence techniques applied to the non-cooperative identification (NCID) problem

[AIAA PAPER 89-3005] p 75 A90-10619

Incorporation of alarm states into a real time decision making process

[AIAA PAPER 89-3006] p 76 A90-10620

Applications of neural networks to avionics systems

[AIAA PAPER 89-3093] p 76 A90-10627

An analysis of reliability in fiber optic ring and star networks

p 78 A90-11666

Fiber optics for advanced aircraft

p 68 A90-11702

Acquisition and recording of AMX A/C Aerialia experience and present trends

p 26 A90-12194

Power supply of aircraft --- Russian book

p 43 A90-12474

Composite-embedded optical fibers for communication links

p 139 A90-13847

Avionic system based on global navigational satellite system

p 97 A90-13984

Mode S transponders - A new avionics product

[SAE PAPER 891055] p 98 A90-14357

The design and study of the information transfer mechanism for a distributed avionics system

p 207 A90-16858

Low-expansion MMCs boost avionics

p 203 A90-17291

The Model 360 - Advanced composite helicopter

p 180 A90-17678

Digital electronic control unit for the European-Fighter Aircraft (EFA)

p 253 A90-21607

An operational perspective of potential benefits of microwave landing systems

p 242 A90-23242

Trends in avionics - From analog black boxes to integrated digital avionics systems

p 252 A90-23245

Flight testing the F-15E terrain following system

p 334 A90-24272

Recovery concepts for propulsion and avionics components --- for booster stage in launch vehicles

[AIAA PAPER 90-1810] p 353 A90-25172

The trend in navais inspection is to automatic operation

p 329 A90-25495

Interstitial materials for low thermal resistance joints in avionic equipment

[SAE PAPER 891441] p 356 A90-27412

Avionics and electromagnetic compatibility (EMC) considerations on a helicopter with an advanced composite airframe

p 417 A90-28217

The two level maintenance - I level dilemma

p 381 A90-28319

Two-level maintenance concept for advanced avionics architectures

p 457 A90-28321

Reasoning from uncertain data - A BIT enhancement

p 457 A90-28330

From a sow's ear - Quantitative diagnostic design requirements from anecdotal references

p 448 A90-28337

A test and maintenance architecture demonstrated on SEM-E modules for fiber optic networks

p 458 A90-28342

Intelligent built-in test and stress management

p 448 A90-28343

Telemetry systems of the future

p 458 A90-28829

AAIC '88 - Aerospace Applications of Artificial Intelligence; Proceedings of the Fourth Annual Conference, Dayton, OH, Oct. 25-27, 1988. Volumes 1 & 2

p 458 A90-30226

Integration of intelligent avionics systems for crew decision aiding

p 459 A90-30236

Information display management in a pilot's associate

p 418 A90-30238

Challenges of tomorrow - The future of secure avionics

p 419 A90-30723

Embedded computer system integration support --- avionics

p 419 A90-30724

Strategic aircraft engineering design simulation

p 439 A90-30729

An adaptive-learning expert system for maintenance diagnostics

p 460 A90-30754

Real-time adaptive control of knowledge based avionics tasks

p 460 A90-30764

An integrated diagnostics approach to embedded and flight-line support systems

p 460 A90-30767

The automated software development project - at McDonnell Aircraft Company (The Software Factory)

p 460 A90-30782

Categorization and performance analysis of advanced avionics algorithms on parallel processing architectures

p 461 A90-30786

Evaluation of sensor management systems

p 461 A90-30789

Software architecture concepts for avionics

p 461 A90-30806

Logistics support planning for standardized avionics

p 383 A90-30809

Commonality of MASA modules --- Modular Avionics System Architecture

p 462 A90-30816

Modular avionic architectures

p 453 A90-30819

After Habsheim

p 401 A90-31388

The impact of fiber optics (photonics) on future aircraft

p 504 A90-32863

The airborne supercomputer

p 538 A90-33775

Advanced integrated avionics test support concepts

[AIAA PAPER 90-1259] p 504 A90-33889

The multi-function RLG system comes of age - A technical update

p 578 A90-36931

A ground simulation-inspection system for avionic devices

p 594 A90-37232

High Voltage Design Guide summary

p 605 A90-38097

Polysilicon active-matrix liquid crystal displays for cockpit applications

p 681 A90-40393

Holographic combiner design to obtain uniform symbol brightness at head-up display video camera

p 652 A90-40394

Application of fracture mechanics to microscale phenomena in electronic assemblies

p 684 A90-41334

USCG HH-65A/SRR GPS integration and test results

p 726 A90-43705

The standard-setting Hornet

p 730 A90-43764

An interfacing solution for real-time avionics development

[SAE PAPER 892357] p 738 A90-45508

Integrated Diagnostics (ID) for advanced avionics architectures

[SAE PAPER 892359] p 738 A90-45509

Development of common GPS and GLONASS avionics standards

p 821 A90-46391

The evolution of design/development requirements for avionics/mission equipment (MEP) insertion

p 846 A90-46932

Near-term applications of knowledge based systems to combat helicopters

[AIAA PAPER 90-3301] p 847 A90-48883

Multi-role advance technology rotorcraft - The EH101

[AIAA PAPER 90-3302] p 837 A90-48884

Evaluation and control of an Integrated Closed Environmental Control System (ICECS)

[SAE PAPER 901237] p 841 A90-49307

Enhanced environmental control for the Harrier II Plus

[SAE PAPER 901238] p 841 A90-49308

The behavior of electric currents in graphite/epoxy structures

p 883 A90-49846

Aeronautical fatigue in the electronic era; Proceedings of the Fifteenth ICAF Symposium, Jerusalem, Israel, June 21-23, 1989

p 901 A90-49876

Security audit for embedded avionics systems

p 957 A90-50649

The E-SAT 300A - A multichannel satellite communication system for aircraft

p 914 A90-51339

8 x 8-inch full color cockpit display

p 927 A90-52953

Kalman Filter Integration of Modern Guidance and Navigation Systems

[AGARD-LS-166] p 28 N90-10847

Flight Test Techniques

[AGARD-CP-452] p 33 N90-10860

Flight testing of the Tornado Terrain Following System

p 35 N90-10875

Air Combat Environment Test and Evaluation Facility (ACETEF)

p 58 N90-10883

Flight test instrumentation and data processing at British Aerospace, Warton, U.K.

p 59 N90-10887

- Mirach 100 flight control system p 260 N90-15926
 The use of prototypes in selected foreign fighter aircraft development programs: Rafale, EAP, Lavi, and Gripen [AD-A214500] p 287 N90-16707
 Analysis and test of a wide angle spectrometer [AD-A215819] p 372 N90-18030
 Marshall Avionics Testbed System (MAST) p 421 N90-19417
 Potential role of avionics in escape systems p 483 N90-20060
 Controllable propulsion for escape systems control p 484 N90-20064
 Integrated circuits for avionics [AD-A217964] p 540 N90-20312
 Joint University Program for Air Transportation Research, 1988-1989 [NASA-CP-3063] p 468 N90-20921
 Optimization of the effective GPS data rate p 489 N90-20932
 Correlation/validation of finite element code analyses for vibration assessment of avionic equipment [AD-A220393] p 654 N90-23398
 Success in tutoring electronic troubleshooting p 780 N90-25568
 Hardware and software reliability estimation using simulations [NASA-CR-186637] p 780 N90-25580
 Equipment feasibility study: Very high frequency communication equipment (136-137 megahertz) [DOT/FAA/CT-TN89/72] p 775 N90-26210
 Hover position sensing system p 848 N90-27448
 Performance assessment of MIL-STD-1553B on the avionic systems demonstrator rig of British Aerospace p 849 N90-27624
 Position finding and ground target direction finding by an aircraft with a gimbaled video camera [DLR-FB-89-62] p 825 N90-27673
 PHARE: Concept and programme p 827 N90-27690
 Economical graphics display system for flight simulation avionics [NASA-CR-186886] p 849 N90-27701
 Advanced transport operating system software upgrade: Flight management/flight controls software description [NASA-CR-181936] p 893 N90-28366
 Validation of the F-18 high alpha research vehicle flight control and avionics systems modifications [NASA-TM-101723] p 924 N90-28542
 Studies in automatic speech recognition and its application in aerospace p 958 N90-28759
 The integration of multiple avionic sensors and technologies for future military helicopters p 916 N90-29344
 Distributed control architecture for CNI preprocessors p 917 N90-29356
 Integrated navigation/flight control for future high performance aircraft p 917 N90-29362
 Survivable penetration p 917 N90-29363
 The potential for digital databases in flight planning and flight aiding for combat aircraft p 918 N90-29371
 High speed bus technology development [AD-A224486] p 960 N90-29565
- AXIAL FLOW**
 Highly loaded axial flow compressors - History and current developments p 44 A90-12503
 Calculation of unsteady boundary layer development on axial-flow turbomachinery blading p 48 A90-12588
 Stall inception in axial compressors [ASME PAPER 89-GT-63] p 290 A90-23786
 Application of recess vaned casing treatment to axial flow fans [ASME PAPER 89-GT-68] p 341 A90-23791
 Axial flow compressor design optimization. I - Pitchline analysis and multivariable objective function influence [ASME PAPER 89-GT-201] p 342 A90-23873
 Flow rate and thrust coefficients for biaxial flows in a convergent nozzle p 395 A90-30344
 Laser anemometer measurements in a transonic axial-flow fan rotor [NASA-TP-2879] p 73 N90-11245
 Stage effects on stalling and recovery of a high-speed 10-stage axial-flow compressor p 115 N90-12600
 Temporally and spatially resolved flow in a two-stage axial compressor. Part 2: Computational assessment [NASA-TM-102273] p 194 N90-14236
 Relating flow between counter-rotating propellers to aerodynamic interaction noise p 479 N90-20944
 Flow coupling between a rotor and a stator in turbomachinery [AD-A223882] p 932 N90-28572
- AXIAL FLOW PUMPS**
 The use of circumferentially varying stagger guide vanes in an axial flow pump or compressor p 537 A90-33566
 An investigation of end-wall vortex cavitation in a high Reynolds number axial-flow pump [AD-A211426] p 133 N90-11982
- AXIAL FLOW TURBINES**
 The solution of the unsteady transonic flow through a blade passage in an axial turbine p 5 A90-11777
 An experimental investigation of the effect of incidence on the two-dimensional performance of an axial turbine cascade p 11 A90-12520
 Design and off-design performance predictions of axial turbines p 45 A90-12540
 Turbomachinery tip gap aerodynamics - A review p 13 A90-12557
 A study on the performance of the turbo-ramjet engines at high speed flight p 49 A90-12608
 Effect of the angle of attack on the efficiency and thrust ratio of axial-flow microturbines with full admission p 111 A90-14590
 A method for aerodynamic design calculation of axial gas turbine stages with cooling air mixing p 152 A90-17781
 An experimental study of tip clearance effects on the performance of an axial transonic turbine p 189 A90-17788
 Study of calculating an approximately constant reaction turbine stage with a tension spline streamline curvature method p 157 A90-18537
 A kinematical/numerical analysis of rotor-stator interaction noise [AIAA PAPER 90-0281] p 219 A90-19770
 Inlet skew and the growth of secondary losses and vorticity in a turbine cascade [ASME PAPER 89-GT-65] p 290 A90-23788
 Computer controlled test bench for axial turbines and propellers p 437 A90-28288
 Optimal computer-aided design of the blading of axial-flow turbines - Russian book p 452 A90-30268
 Unsteady transition in an axial-flow turbine. I - Measurements on the turbine rotor. II - Cascade measurements and modeling [ASME PAPER 89-GT-289] p 474 A90-33562
 An improved incidence losses prediction method for turbine airfoils [ASME PAPER 89-GT-284] p 475 A90-33563
 Calculation of an axial-flow birotary turbine p 880 A90-46492
 Effect of the nozzle ring vane height on the efficiency of axial-flow full-admission microturbines p 851 A90-46509
 Numerical solution of 2-D transonic flow through an axial turbine stage p 814 A90-49464
 Calculation of the secondary flow in an axial turbine p 513 N90-21022
 Research on cascade secondary and tip-leakage flows: Periodicity and surface flow visualization p 514 N90-21026
 Computational prediction and measurement of the flow in axial turbine cascades and stages p 514 N90-21028
- AXIAL LOADS**
 Numerical study of balanced patch repairs to cracked sheets p 210 A90-18442
- AXIAL STRAIN**
 Finite element analysis of structural components using viscoplastic models with application to a cowl lip problem [NASA-CR-185189] p 690 N90-23769
- AXIAL STRESS**
 The investigation of stress at an enter-gas nozzle of main landing gears for fighter aeroplanes p 181 A90-18606
- AXISYMMETRIC BODIES**
 Asymptotic calculation of flow parameters in the problem of hypersonic flow past blunt axisymmetric bodies p 10 A90-12268
 Numerical solution of unsteady Navier-Stokes equations for laminar/turbulent flows past axisymmetric bodies at angle of attack p 85 A90-15235
 Design of axisymmetric bodies with minimum transonic drag p 154 A90-17997
 Supersonic nonuniform flow of a gas past oblong axisymmetric bodies p 159 A90-19237
 Active soot reduction in a spray-fired, axisymmetric model gas turbine combustor [AIAA PAPER 90-0039] p 191 A90-19644
 Design optimization of natural laminar flow fuselages in compressible flow [AIAA PAPER 90-0303] p 182 A90-19784
 Formation of shocks within axisymmetric nozzles [AIAA PAPER 90-1655] p 570 A90-38782
 Gasdynamic characteristics of a plane or axisymmetric nozzle with a rectilinear generatrix of the supersonic section p 805 A90-46575
 Effect of incoming flow turbulence on the aerodynamic characteristics of a smooth symmetric body at large angles of attack p 904 A90-50817
- Sting-support interference on afterbody drag at transonic speeds [NAL-TM-EA-8902] p 909 N90-28492
 Prediction of subsonic vortex shedding from forebodies with chines [NASA-CR-4323] p 909 N90-28494
- AXISYMMETRIC FLOW**
 Turbulent mixing in helicopter jet diluters - Navier-Stokes calculations and correlations [AAAF PAPER NT 88-13] p 40 A90-11432
 An investigation of artificial compressor surge p 11 A90-12526
 Calculation of axisymmetric flows in turbomachines, through an explicit time-splitting method p 14 A90-12622
 Calculation of transonic axisymmetric flow past an engine nacelle with allowance for viscosity p 296 A90-24107
 Simulation of sound propagation in axisymmetric jet p 378 A90-25872
 Non-axisymmetric viscous lower-branch modes in axisymmetric supersonic flows p 474 A90-33509
 Effectiveness of passive devices for axisymmetric base drag reduction at Mach 2 p 555 A90-36184
 An efficient finite-difference algorithm for computing axisymmetric transonic nacelle flow fields p 557 A90-37205
 Hypersonic flow calculations with a hybrid Navier-Stokes/Monte Carlo method [AIAA PAPER 90-1691] p 560 A90-38394
 Finite element simulation of turbulent propeller flowfields p 703 A90-42658
 Transonic flow computations in convergent propulsion nozzles using the time-dependent mode p 708 A90-44459
 Profiling of the supersonic components of three-dimensional corrugated nozzles p 804 A90-46563
 Geometrical factors influencing the flow field in a propulsive nozzle p 807 A90-46876
 The radiation of sound from a propeller at angle of attack [NASA-CR-4264] p 548 N90-21602
 Theory and numerical analysis of single and multi-element nozzle propellers [LR-579] p 572 N90-21741
 Prediction of two-dimensional time-dependent gasdynamic flows for hypersonic studies [UTIAS-335] p 718 N90-25935
 Design of an axisymmetric, contoured nozzle for the HEG [DLR-FB-90-04] p 959 N90-28812
- AZIMUTH**
 ILS/MLS comparison tests at Miami/Tamiami, Florida Airport [ACD-330] p 27 N90-10018

B

B-1 AIRCRAFT

- B-1B Doppler error compensation based on flight data analysis p 404 A90-30790
 Expanding the B-1B flight envelope p 644 A90-41899
 Tracking B-1B aircraft with a structural data recorder p 926 A90-49880
 Wind tunnel study of wake downwash behind A6 percent scale model B1-B aircraft [DE90-011783] p 719 N90-25941
 B-1B improved windshield development. Volume 2: Magna analysis: Baseline and parametric [AD-A221501] p 845 N90-26828

B-52 AIRCRAFT

- Application of fracture mechanics and half-cycle method to the prediction of fatigue life of B-52 aircraft pylon components [NASA-TM-88277] p 214 N90-13820

B-58 AIRCRAFT

- Sonic boom signature data from cruciform microphone array experiments during the 1966-1967 EAFB national sonic boom evaluation program [NASA-CR-182027] p 549 N90-21605

B-70 AIRCRAFT

- Sonic boom signature data from cruciform microphone array experiments during the 1966-1967 EAFB national sonic boom evaluation program. [NASA-CR-182027] p 549 N90-21605

BACKSCATTERING

- LDA processor TSI model 1990 analog input module reconstruction p 451 A90-29654
 Development of an X-ray backscatter densitometer for measurement of freestream density during hypersonic flight [AIAA PAPER 90-1384] p 604 A90-37933

BACKWARD FACING STEPS

- Supersonic combustion of hydrogen jets behind a backward-facing step p 266 A90-22183
- [AIAA PAPER 90-0204]
- Prediction of turbulent combustion flowfields behind a backward-facing step p 529 A90-32952
- Supersonic flow over an axisymmetric backward-facing step p 566 A90-38717
- [AIAA PAPER 90-1580]
- Some characteristics of interference between shock waves and the aerodynamic wake behind a body p 804 A90-46551

BAGGAGE

- Fire hazards of aerosol cans in aircraft cargo compartments [DOT/FAA/CT-89/32] p 636 N90-23369

BALANCE

- A new type of calibration rig for wind tunnel balances p 438 A90-28305
- Effect of control surface mass unbalance on the stability of a closed-loop active control system [NASA-TP-2952] p 134 N90-12042
- Cryogenic temperature effects on sting-balance deflections in the National Transonic Facility [NASA-TM-4157] p 202 N90-14244

BALANCING

- Fully automatic calibration machine for internal 6-component wind tunnel balance including cryogenic balances p 437 A90-28294
- Spray automated balancing of rotors - How process parameters influence performance p 879 A90-46228
- An application process for dynamic balancing of turbomachinery shafting [NASA-TM-102537] p 541 N90-20392
- Aerodynamic control design: Experience and results at Aermacchi p 935 N90-28518

BALL BEARINGS

- Endurance of aircraft gas turbine mainshaft ball bearings-analysis using improved fatigue life theory. II - Application to a bearing operating under difficult lubrication conditions p 128 A90-13845
- Endurance of aircraft gas turbine mainshaft ball bearings-analysis using improved fatigue life theory. I - Application to a long-life bearing p 537 A90-33557
- Retirement lives of rolling element bearings p 680 A90-39980

BALLAST (MASS)

- Schleicher ASK-21 glider (TG-9) stall and spin [AD-A213513] p 249 N90-15096

BALLISTICS

- External flow computations for a finned 60mm ramjet in steady supersonic flight [AD-A216998] p 428 N90-19233

BALLOON FLIGHT

- Recent results and major activities in the NASA Balloon Program [IAF PAPER 89-468] p 81 A90-13557

BALLOON SOUNDING

- Recent results and major activities in the NASA Balloon Program [IAF PAPER 89-468] p 81 A90-13557

BALLOON-BORNE INSTRUMENTS

- Recent results and major activities in the NASA Balloon Program [IAF PAPER 89-468] p 81 A90-13557

BAROMETERS

- The accuracy of barometric altimeters with respect to geometric altitude p 108 A90-14012

BARS

- Characterization of the CP 214 T851. Dissection of a cast flat bar for a standard spar [CEAT-PV-M4/462200] p 876 N90-27905

BATCH PROCESSING

- Effective use of Cray supercomputers p 546 A90-34436
- Adaptive control of helicopter vibrations via the impulse response method [AD-A213728] p 260 N90-15113

BAYES THEOREM

- Reasoning from uncertain data - A BIT enhancement p 457 A90-28330

BAYS (STRUCTURAL UNITS)

- Experimental investigation to suppress flow-induced pressure oscillations in open cavities [AD-A216285] p 320 N90-17578

BEAMS (SUPPORTS)

- Vibration analysis of composite turbopropellers using a nonlinear beam-type finite-element approach p 70 A90-12844
- Scaling effects in the impact response of graphite-epoxy composite beams [SAE PAPER 891014] p 128 A90-14326
- The effect of impact loading on residual strength of CFRP composite beams p 208 A90-17683
- Theoretical modelling of composite rotating beams p 208 A90-17684

- Homogenization of composite beams in dynamical flexure p 878 A90-46184

BEARING (DIRECTION)

- A bearing error in the VHF omnirange due to sea surface reflection p 402 A90-27875
- Analytical evaluation of radiation patterns of a TACAN antenna p 404 A90-30695
- Visualization of three dimensional data p 782 N90-25553

BEARINGLESS ROTORS

- Relative aeromechanical stability characteristics for hingeless and bearingless rotors p 409 A90-28230
- Perspectives in aeromechanical stability of helicopter rotors p 831 A90-46953
- Application of a general-purpose mechanical systems analysis code to rotorcraft dynamics problems p 831 A90-46955
- Theoretical and experimental investigation of the aeroelastic stability of an advanced bearingless rotor in hover and forward flight p 831 A90-46958

BEARINGS

- Rub interactions of flexible casing rotor systems p 41 A90-11554
- Development of new segment carbon seal for use at low sealing pressure region FJR710/600S turbo fan engine p 69 A90-11950
- Optimum weight design of a rotor bearing system with dynamic behavior constraints [ASME PAPER 89-GT-74] p 358 A90-23795
- Threshold performance optimization of a rotor-bearing system subjected to leakage excitation [ASME PAPER 89-GT-126] p 360 A90-23825
- A combined Riccati transfer matrix-direct integration method with its applications p 611 A90-37218
- Evaluation of solid lubricant powder delivery system for turbine bearing lubrication [AIAA PAPER 90-2046] p 684 A90-41997
- The nature and control of skidding in lightly loaded intershaft bearings [PNR90591] p 136 N90-12933

BEECHCRAFT AIRCRAFT

- Beech Starship occupant protection evaluation in emergency landing scenario [SAE PAPER 891015] p 100 A90-14327
- Methods of safety analysis for Beech Model 2000 - Starship 1 [SAE PAPER 891064] p 101 A90-14364
- Strength substantiation of the all composite airframe (A materials data base approach) p 490 A90-31519
- Starship - A model for future designs p 493 A90-33714
- Starship sails through p 842 A90-49825
- Elevator tab assembly producibility study [IAR-89-16] p 734 N90-25133

BELL AIRCRAFT

- The application of linear maximum likelihood estimation of aerodynamic derivatives for the Bell-205 and Bell-206 p 30 A90-12773
- The Bell Helicopter XV-3 and XV-15 experimental aircraft - Lessons learned [AIAA PAPER 90-3265] p 835 A90-48859

BEND TESTS

- Correlation of radial-to-axial vaneless turns for centrifugal compressors [AIAA PAPER 90-1917] p 656 A90-40556
- Characterization of the CP 214 T851. Dissection of a cast flat bar for a standard spar [CEAT-PV-M4/462200] p 876 N90-27905
- Characterization of the 7175 T7352. Dissection of a die casting standard spar [CEAT-PV-M5/528900] p 877 N90-27906
- Characterization of the 7175 T7352 101. Dissection of a die casting standard spar [CEAT-PV-M5/5288] p 877 N90-27907
- Characterization of the 7010 T73651. Dissection of a sheet billet for a standard spar [CEAT-PV-M5/521700] p 877 N90-27908

BENDING

- Aircraft modal suppression system: Existing design approach and its shortcomings p 33 N90-10115
- Structural stability augmentation system design using BODEDIRECT: A quick and accurate approach p 33 N90-10116
- Development of a finite element based delamination analysis for laminates subject to extension, bending, and torsion p 679 N90-25049

BENDING FATIGUE

- Rotating system load monitoring using minimum fixed system instrumentation p 651 A90-39982
- An investigation on combined extension and bending of thin sheets with a central crack [LR-561] p 137 N90-12958
- Flexural fatigue life prediction of closed hat-section using materially nonlinear axial fatigue characteristics p 691 N90-25062

BENDING MOMENTS

- Divergence of thin-walled composite rods of closed profile in gas flow p 388 A90-29012
- The response of helicopter rotors to vibratory airflow p 832 A90-46971
- An examination of helicopter rotor load calculations p 833 A90-46972
- The response of helicopter rotors to vibratory airflow [AD-A215678] p 337 N90-16756

BENDING THEORY

- Effects of aeroelastic tailoring on anisotropic composite material beam models of helicopter blades [AD-A213478] p 249 N90-15095

BENDING VIBRATION

- A discrete dynamic model of the crankshaft-aircrew assembly of an aircraft piston engine for the purpose of vibration analysis by the method of finite elements p 51 A90-13220
- Active control of gust- and interference-induced vibration of tilt-rotor aircraft p 429 A90-28201
- Exact solutions to the oscillations of composite aircraft wings with warping constraint and elastic coupling p 603 A90-36271
- Vibration equations for a helicopter rotor blade p 604 A90-37830

BENZENE

- The 1-((diorganoxyphosphonyl)-methyl)-2,4- and -2,6-diamido benzenes [NASA-CASE-ARC-11425-4] p 532 N90-20133
- Some 1-((diorganoxyphosphonyl)methyl)-2,4- and -2,6-dinitro-benzenes [NASA-CASE-ARC-11425-3] p 678 N90-23475

BIAS

- An accurate numerical technique for determining flight test rate gyroscopes biases prior to takeoff [AD-A220987] p 739 N90-25138
- Visualization of three dimensional data p 782 N90-25553
- The basis for facility comparison p 856 N90-27713

BIBLIOGRAPHIES

- Noise and sonic boom impact technology. Effects of aircraft noise and sonic booms on structures: An assessment of the current state-of-knowledge [AD-A213919] p 378 N90-17409
- The Shock and Vibration Digest, volume 21, no. 2 p 609 N90-22059
- The Shock and Vibration Digest, volume 21, no. 6 p 614 N90-22363
- Supersonic wind tunnel nozzles: A selected, annotated bibliography to aid in the development of quiet wind tunnel technology [NASA-CR-4294] p 762 N90-26019
- FAA Rotorcraft Research, Engineering, and Development Bibliography 1962-1989 [AD-A224256] p 902 N90-29299

BILLETS

- Characterization of the 7010 T73651. Dissection of a sheet billet for a standard spar [CEAT-PV-M5/521700] p 877 N90-27908

BINDERS (MATERIALS)

- Calculation of thick wall fiber binders for rotor components of modern helicopters [MBB-UD-554/84-PUB] p 735 N90-25137

BIOCHEMISTRY

- The use of soot analysis as an investigative tool in aircraft fires p 22 A90-10269

BIODEGRADATION

- Enhanced bioreclamation of jet fuels: A full-scale test at Eglin AFB, Florida [AD-A222348] p 875 N90-26992

BIODYNAMICS

- Escape systems research at RAE p 483 N90-20058

BIPLANES

- Aerostructural considerations for the power plant of overlapping wing configuration p 841 A90-49488
- The Stealth biplane: A proposal in response to a low Reynolds Number station keeping mission [NASA-CR-186680] p 734 N90-25127

BIRD-AIRCRAFT COLLISIONS

- Prospects are good for using ATC radar to detect birds p 329 A90-25496
- Why birds kill - Cross-sectional analysis of U.S. Air Force bird strike data p 400 A90-30587
- Test and evaluation: Reducing risks to military aircraft from bird collisions. Report to the Chairman, Legislation, and National Security Subcommittee, Committee on Government Operations, House of Representatives [AD-A210670] p 25 N90-10845
- Study of the engine bird ingestion experience of the Boeing 737 aircraft [DOT/FAA/CT-89/16] p 176 N90-13360
- Full-scale birdstrike testing of in-service aged F-111 ADBIRT windshield transparencies [AD-A218035] p 484 N90-20069

- Forward canopy feasibility and Thru-The-Canopy (TTC) ejection system study [AD-A220360] p 637 N90-24258
- Study of the engine bird ingestion experience of the Boeing 737 aircraft (October 1986 to September 1988) [DOT/FAA/CT-89/29] p 723 N90-25119
- BIRDS**
- Study of the engine bird ingestion experience of the Boeing 737 aircraft [DOT/FAA/CT-89/16] p 176 N90-13360
- Bird impact tests on asymmetric sandwich structures made in Kevlar 49 [CEAT-NT-10/S/83-5] p 323 N90-16727
- Bird impact tests on curved structures of the type Sandwich-Kevlar-Nida for normal and angular shooting [CEAT-NT-10/S/83-4] p 324 N90-16728
- Study of bird ingestions into small inlet area, aircraft turbine engines (May 1987 to April 1988) [DOT/FAA/CT-89/17] p 402 N90-18375
- Bird impact tests on a Kevlar 49 structure. Monolithic plates. Oblique-angled impact [REPT-S3-4273] p 402 N90-18376
- BISMALEIMIDE**
- A third-generation bismaleimide prepreg system p 943 A90-50131
- Injectable bismaleimide systems p 943 A90-50132
- Fracture morphology of toughened bismaleimide/carbon fiber composites p 948 A90-50205
- Freeze drying for morphological control of inter-penetrating polymer networks p 948 A90-50214
- BLADE SLAP NOISE**
- Some processes of sound generation in a vortex-airfoil system with parallel axes p 218 A90-18448
- Rotor blade-vortex interaction impulsive noise source localization p 463 A90-27978
- Higher harmonic control of a helicopter model rotor to reduce blade/vortex interaction noise p 496 A90-34360
- CFD and transonic helicopter sound. p 696 A90-42433
- BLADE TIPS**
- Influence of the control law on the performance of a helicopter model rotor [ONERA, TP NO. 1989-136] p 4 A90-11158
- Unsteady aerodynamic characteristics of oscillating cascade with tip clearance p 8 A90-11793
- The interaction between tip clearance flow and the passage flowfield in an axial compressor cascade p 11 A90-12525
- Turbomachinery tip gap aerodynamics - A review p 13 A90-12557
- Theoretical and experimental analysis of a model rotor blade incorporating a swept tip p 151 A90-17586
- An experimental study of tip clearance effects on the performance of an axial transonic turbine p 189 A90-17788
- Effect of downstream elements on the flow at the exit of centrifugal compressor rotor p 157 A90-18483
- Propeller tip vortex interactions [AIAA PAPER 90-0437] p 166 A90-19846
- Performance and aerodynamic development of the Super Puma Mk II main rotor with new SPP8 blade tip design [ONERA, TP NO. 1989-181] p 245 A90-21041
- Correlation of Puma airfoils - Evaluation of CFD prediction methods [ONERA, TP NO. 1989-185] p 224 A90-21045
- Tip leakage losses in a linear turbine cascade [ASME PAPER 89-GT-56] p 290 A90-23782
- Effect of blade tip configuration on tip clearance loss of a centrifugal impeller [ASME PAPER 89-GT-80] p 358 A90-23801
- Secondary flow due to the tip clearance at the exit of centrifugal impellers [ASME PAPER 89-GT-81] p 358 A90-23802
- Entrapment plating of abrasive particles for jet engine clearance control [SAE PAPER 890918] p 286 A90-24685
- Calculation of tip leakage flow with three-dimensional Euler code p 304 A90-25772
- Rotor blade-vortex interaction impulsive noise source localization p 463 A90-27978
- Strike tolerant main rotor blade tip p 409 A90-28232
- Structural optimization with aeroelastic constraints of rotor blades with straight and swept tips p 535 A90-32475
- Estimation of losses in semi-open centrifugal impellers p 537 A90-33597
- Measurement of the interaction between a rotor tip vortex and a cylinder p 555 A90-36255
- Computation of flow through a centrifugal impeller with tip leakage [AIAA PAPER 90-2021] p 684 A90-41987
- Improvement in turbine blade aerodynamic force in the tip region p 809 A90-47854
- Dynamic tip clearance measurements in axial flow compressors [PNR90597] p 116 N90-12612
- Rotor induced-inflow-ratio measurements and CAMRAD calculations [NASA-TP-2946] p 237 N90-15882
- An experimental investigation of viscous aspects of propeller blade flow p 315 N90-16711
- Losses in the tip-leakage flow of a planar cascade of turbine blades p 514 N90-21027
- Analysis of the rotor tip leakage flow with tip cooling air ejection p 515 N90-21029
- The validation and application of a rotor acoustic prediction computer program [NASA-TM-101794] p 895 N90-27465
- Noise from tip vortex and bubble cavitation [AD-A221962] p 896 N90-27468
- Structural testing and analytical research of turbine components [AD-A23516] p 933 N90-29396
- Noncontact measurement of rotating blade vibrations [NAL-TR-1033] p 961 N90-29687
- BLADE-VORTEX INTERACTION**
- Rotor-blades excitation due to differential interference of vane wakes between upstream stator-rows in an axial compressor p 6 A90-11784
- The influence of the wake structure on the dynamic blade load p 6 A90-11785
- Numerical analysis of rotating stall by a vortex model p 13 A90-12590
- Recent research on external helicopter noise at ONERA p 218 A90-16825
- An experiment study of rotor aerodynamic in ground effect at low speed p 149 A90-16826
- Some processes of sound generation in a vortex-airfoil system with parallel axes p 218 A90-18448
- Airfoil pressure measurements during a blade vortex interaction and a comparison with theory p 232 A90-23105
- Reduction of blade-vortex interaction noise through higher harmonic pitch control p 377 A90-23937
- Winglets on rotor blades in forward flight - A theoretical and experimental investigation p 303 A90-25422
- Blade-vortex interaction experiments - Velocity and vorticity fields [AIAA PAPER 90-0030] p 312 A90-26903
- Rotor blade-vortex interaction impulsive noise source localization p 463 A90-27978
- High resolution flow field prediction for tail rotor aeroacoustics p 463 A90-28158
- Aeroacoustic flowfield and acoustics of a model helicopter tail rotor at high advance ratio p 463 A90-28160
- HARP model rotor test at the DNW --- Hughes Advanced Rotor Program p 406 A90-28167
- The effect of an unsteady three-dimensional wake on elastic blade-flapping eigenvalues in hover p 385 A90-28228
- Noise of a simulated installed model counterrotation propeller at angle-of-attack and takeoff/approach conditions [AIAA PAPER 90-0283] p 547 A90-32505
- Correlation of lift and thickness noise sources in vortex-airfoil interaction p 547 A90-34090
- Higher harmonic control of a helicopter model rotor to reduce blade/vortex interaction noise p 496 A90-34360
- Measurement of the interaction between a rotor tip vortex and a cylinder p 555 A90-36255
- Aerodynamic loads and blade vortex interaction noise prediction p 614 A90-38520
- Euler solutions for self-generated rotor blade-vortex interactions [AIAA PAPER 90-1588] p 566 A90-38723
- CFD and transonic helicopter sound p 696 A90-42433
- A study of the influence of a helicopter rotor blade on the following blades using Euler equations p 630 A90-42435
- Estimation of rotor blade incidence and blade deformation from the measurement of pressures and strains in flight p 647 A90-42497
- Numerical simulations of three-dimensional rotor blade-vortex interactions p 807 A90-46879
- Rotor loads computation using singularity methods and application to the noise prediction p 807 A90-46880
- Numerical simulation of wakes with application to blade-vortex interaction p 807 A90-46881
- Two and three dimensional indicial methods for rotor dynamic airloads p 808 A90-46973
- Experimental observations of two-dimensional blade-vortex interaction p 809 A90-47303
- An investigation of counterrotating tip vortex interaction [NASA-CR-185135] p 79 N90-11549
- Review and analysis of the DNW/Model 360 rotor acoustic data base [NASA-TM-102253] p 81 N90-11692
- Rotor induced-inflow-ratio measurements and CAMRAD calculations [NASA-TP-2946] p 237 N90-15882
- Prediction of rotor blade-vortex interaction noise from 2-D aerodynamic calculations and measurements [ISL-CO-243/88] p 396 N90-18365
- Study of the blade/vortice interaction on a one-blade rotor during forward flight (incompressible, non viscous fluid) [ISL-R-115/88] p 415 N90-18391
- Development of a mass averaging temperature probe p 427 N90-18418
- Airloads, wakes, and aeroelasticity [NASA-CR-177551] p 572 N90-21738
- Extension of a three-dimensional viscous wing flow analysis [NASA-CR-182023] p 631 N90-23348
- Aerodynamic loads and blade vortex interaction noise prediction [ISL-PU-310/89] p 719 N90-25942
- Noise from tip vortex and bubble cavitation [AD-A221962] p 896 N90-27468
- The acoustic results of a United Technologies scale model helicopter rotor tested at DNW [NASA-TM-101879] p 896 N90-27471
- Numerical simulations of blade-vortex interactions and lifting hovering rotor flows [AD-A224238] p 911 N90-29302
- BLAST LOADS**
- Boeing Transonic Windblast Generator System (BTWGS) p 199 A90-17413
- Microstructural effects of plastic media blasting on graphite epoxy composites [SAE PAPER 890928] p 286 A90-24693
- The analysis and testing of composite panels subject to muzzle blast effects p 675 A90-39991
- BLIND LANDING**
- Flight evaluations of several hover control and display combinations for precise blind vertical landings [AIAA PAPER 90-3479] p 867 A90-47764
- BLOCKING**
- Application of panel methods to wind-tunnel wall interference corrections [AIAA PAPER 90-0007] p 200 A90-19629
- BLOWDOWN WIND TUNNELS**
- Wave cancellation properties of a splitter-plate porous wall configuration p 57 A90-11005
- Separation shock dynamics in Mach 5 turbulent interactions induced by cylinders p 153 A90-17981
- Applications of infra-red thermography in a hypersonic blowdown wind tunnel p 438 A90-28300
- Infrared thermography in blowdown and intermittent hypersonic facilities p 440 A90-31302
- The new high Reynolds number Mach 8 capability in the NSWC Hypervelocity Wind Tunnel 9 [AIAA PAPER 90-1379] p 594 A90-37928
- Wind tunnel studies of F/A-18 tail buffet [AIAA PAPER 90-1432] p 559 A90-37969
- New transonic test sections for the NAE 5ftx5ft trisonic wind tunnel p 630 A90-42431
- The University of Toronto-Ryerson Polytechnical Institute hypersonic gun tunnel p 673 A90-42432
- BLOWING**
- Research on film-cooling of turbine blade p 190 A90-17795
- Characteristics of turbulent separation flows on a porous surface under conditions of injection p 231 A90-22422
- Effects of endwall suction and blowing on compressor stability enhancement [ASME PAPER 89-GT-64] p 290 A90-23787
- Pneumatic vortex flow control on a 55-degree cropped delta wing with chined forebody [AIAA PAPER 90-1430] p 559 A90-37967
- Effect of pylon wake with and without pylon blowing on propeller thrust [NASA-TM-4162] p 173 N90-14190
- Controlled vortical flow on delta wings through unsteady leading edge blowing [NASA-CR-186267] p 316 N90-16712
- Control of vortex aerodynamics at high angles of attack p 921 N90-28523
- BLUFF BODIES**
- Development of bluff body wake in a longitudinally curved stream p 86 A90-15745
- Calculations of the flow past bluff bodies, including tilt-rotor wing sections at alpha = 90 deg [AIAA PAPER 90-0032] p 227 A90-22156
- Effects of splitter plates on the wake flow behind a bluff body p 469 A90-32453

- Interaction between boundary layer and wakes of different bodies p 602 A90-36263
- Time-resolved measurements of total temperature and pressure in the vortex street behind a cylinder p 557 A90-36522
- On the drag reduction of bluff bodies through momentum injection
- [AIAA PAPER 90-3076] p 797 A90-45922
- Acoustic wave excitation during the aerodynamic interaction between a fan blade and a bluff obstacle p 965 A90-52289
- Fluctuating wind forces measured on a bluff body extending from a cavity p 371 N90-18020
- BLUNT BODIES**
- Measurements of pressure fluctuations in the interaction regions of shock waves and turbulent boundary layers induced by blunt fins p 9 A90-12218
- Asymptotic calculation of flow parameters in the problem of hypersonic flow past blunt axisymmetric bodies p 10 A90-12268
- Hypersonic flow past blunt edges at low Reynolds numbers p 10 A90-12284
- Surface roughness effect on the aerodynamic characteristics of a blunt body p 16 A90-12740
- Direct simulation of three-dimensional hypersonic flow about intersecting blunt wedges p 16 A90-12835
- Application of the hypersonic analogy for validation of numerical simulations p 16 A90-12838
- Aerodynamic heating in shock wave/turbulent boundary layer interaction regions induced by blunt fins p 82 A90-13775
- Verification of a Navier-Stokes code for solving the hypersonic blunt body problem p 146 A90-16774
- Comparison of thin and full viscous shock layer models in the problem of supersonic flow of a viscous gas past blunt cones p 231 A90-22396
- A study of flow of a vibrationally nonequilibrium dissociated gas past a blunt body p 234 A90-23435
- Determination of pressure and heat flow on the front surface of smooth blunt bodies p 299 A90-24166
- Effect of a recess on the aerodynamic characteristics of very blunt bodies at supersonic velocities p 299 A90-24167
- Hyperbolic grid generation techniques for blunt body configurations p 376 A90-26490
- Hypersonic reactive flow computations p 315 A90-27131
- Applications of infra-red thermography in a hypersonic blowdown wind tunnel p 438 A90-28300
- Effect of the leading edge bluntness of a moderately swept wing on the aerodynamic characteristics of an aircraft model at subsonic and transonic velocities p 388 A90-29005
- Combined effect of viscosity and bluntness on the aerodynamic efficiency of a delta wing in flow with a high supersonic velocity p 388 A90-29184
- High-resolution shock-capturing schemes for inviscid and viscous hypersonic flows p 476 A90-34545
- Effect of surface grooves on base pressure for a blunt trailing-edge airfoil p 556 A90-36280
- Comments on 'Effect of nose bluntness and cone angle on slender-vehicle transition' p 620 A90-39814
- Numerical study of heat transfer for unsteady viscous supersonic blunt body flows p 707 A90-44432
- The effect of vibration-dissociation interaction on heat transfer and drag during the hypersonic flow past bodies p 710 A90-44934
- Viscous flow characteristics over a blunt cone at hypersonic Mach numbers by using a PNS code p 810 A90-48085
- Hypervelocity flow of dissociating nitrogen downstream of a blunt nose p 811 A90-48712
- The formation of vortex streets in supersonic flows p 907 A90-51539
- Blunt-nose inviscid airflows with coupled nonequilibrium processes p 171 N90-13336
- Optimum shape of a blunt forebody in hypersonic flow [NASA-CR-181955] p 171 N90-13351
- Fluctuating wind forces measured on a bluff body extending from a cavity p 371 N90-18020
- Interaction of an oblique shock wave with supersonic flow over a blunt body p 398 N90-19197
- An approximate viscous shock layer method for calculating the hypersonic flow over blunt-nosed bodies p 479 N90-20947
- Numerical analysis of three-dimensional particle-laden flow equations p 775 N90-26268
- BLUNT LEADING EDGES**
- Semi-implicit Navier-Stokes solver (SINSS) calculations of separated flows around blunt delta wings [AIAA PAPER 90-0590] p 168 A90-19936

- Effect of similarity parameters on the aerodynamic quality and moment characteristics of a supersonic wing with blunt edges p 298 A90-24150
- Effects of nose bluntness and shock-shock interactions on blunt bodies in viscous hypersonic flows [NASA-CR-186451] p 479 N90-20950
- BO-105 HELICOPTER**
- The rotor-signal-module of MF190 --- for digital data acquisition from BO-105 helicopter rotary wings p 418 A90-28849
- Usage monitoring of military helicopters p 651 A90-39984
- Influence of ground effect on helicopter takeoff and landing performance p 645 A90-42278
- BODIES OF REVOLUTION**
- On steady subsonic flow past slender bodies of revolution p 144 A90-16736
- Numerical simulation of separated and vortical flows on bodies at large angles of attack p 146 A90-16772
- Prediction of transition on airfoils with separation bubbles, swept wings and bodies of revolution at incidence p 148 A90-16790
- Design of axisymmetric bodies with minimum transonic drag p 154 A90-17997
- Optimal nose shapes of bodies of revolution in transonic flow p 299 A90-24165
- Low-speed pressure distribution on semi-infinite two-dimensional bodies with elliptical noses p 553 A90-35766
- Computational results for the effects of external disturbances on transition location of bodies of revolution from subsonic to supersonic speeds and comparisons with experimental data p 715 A90-45522
- [SAE PAPER 892381] p 715 A90-45522
- Incompressible flow about ellipsoids of revolution [REPT-88-02] p 90 N90-11713
- Effect of vortex generators on the aerodynamic wing characteristics and body of revolution [AD-A22813] p 721 N90-25955
- BODY KINEMATICS**
- Computer-aided analysis of three-dimensional multiloop mechanisms p 669 A90-42328
- BODY-WING AND TAIL CONFIGURATIONS**
- An application of the surface-singularity method to wing-body-tail configurations p 9 A90-12229
- Airplane design. Part 2 - Preliminary configuration design and integration of the propulsion system --- Book p 30 A90-12867
- Airplane design. Part 3 - Layout design of cockpit, fuselage, wing and empennage: Outaways and inboard profiles --- Book p 30 A90-12868
- Numerical investigation of airfoil/jet/fuselage-undersurface flowfields in ground effect [AIAA PAPER 90-0597] p 168 A90-19939
- Algebraic boundary-conforming grid generation around wing/tail-body configurations p 308 A90-26480
- CTR-1000 civil tiltrotor concept p 829 A90-46939
- Vertical tail design for base-line configuration of military combat aircraft p 810 A90-48080
- BODY-WING CONFIGURATIONS**
- Separated flow over slender wing, body and wing-body combination p 85 A90-15232
- The flow around wing-body junctions p 145 A90-16765
- Wing-body mutual influence coefficients at angles-of-attack to 24 deg p 151 A90-17693
- An Euler method for wing-body-winglet flows [AIAA PAPER 90-0436] p 229 A90-22218
- Time-dependent and time-averaged turbulence structure near the nose of a wing-body junction p 231 A90-23036
- Unsteady supersonic computations of arbitrary wing-body configurations including external stores p 232 A90-23278
- Selection of the blended wing configuration for light aircraft p 234 A90-23401
- Nonsymmetric vortex breakdown and aerodynamic hysteresis in flow past a low-aspect-ratio wing/fuselage configuration p 294 A90-24076
- Flow past a wing/fuselage combination with separation from the side edges of the wing p 295 A90-24088
- An investigation of fillets in wing-fuselage joints at subsonic velocities p 297 A90-24131
- Algebraic boundary-conforming grid generation around wing/tail-body configurations p 308 A90-26480
- Calculations of transonic flows over wing-body combinations p 395 A90-31479
- The TSP methods applied to the calculation of transonic flow about wing/body/nacelle/pylon-configurations --- Transonic Small Perturbation p 554 A90-35868
- An interactive scheme for transonic wing/body flows based on Euler and inverse boundary-layer equations [AIAA PAPER 90-1586] p 566 A90-38721
- Developing the Canadair Regional Jet airliner p 729 A90-42656

- On aerodynamic characteristics of canard in canard-forward-swept wing configuration p 709 A90-44833
- Some aerodynamic characteristics of the scissor wing configuration [SAE PAPER 892202] p 713 A90-45423
- Static and dynamic water tunnel tests of slender wings and wing-body configurations at extreme angles of attack [AIAA PAPER 90-3021] p 869 A90-45888
- An evaluation of Euler solvers for transonic flowfield computations on wing-fuselage geometries [AIAA PAPER 90-3015] p 798 A90-45935
- A study of the stability and thermal stability of complex reinforced structures p 880 A90-46541
- Incompressible potential flow about three-dimensional configurations p 810 A90-48082
- Aerostructural considerations for the power plant of overlapping wing configuration p 841 A90-49488
- A closer look at the induced drag of crescent-shaped wings [AIAA PAPER 90-3063] p 903 A90-50638
- Low-speed, high-lift aerodynamic characteristics of slender, hypersonic accelerator-type configurations [NASA-TP-2945] p 20 N90-10830
- Study of forces and moments on wing-bodies at high incidence, volumes 1 and 2 p 171 N90-13350
- Body effect on wing angle of attack and pitching moment at zero lift at low speeds p 337 N90-16757
- [ESDU-89042] p 337 N90-16757
- Initial flight test of half-scale unmanned air vehicle [AD-A219584] p 648 N90-23388
- Three-dimensional model testing in the transonic self-streamlining wind tunnel p 938 N90-28583
- BOEING AIRCRAFT**
- Boeing 720B design modification challenges p 179 A90-17309
- Boeing Transonic Windblast Generator System (BTWGS) p 199 A90-17413
- Friction measurements under winter runway conditions p 321 A90-23924
- The prediction of loads on the Boeing Helicopters Model 360 rotor p 410 A90-28240
- Honeycomb sandwich primary structure applications on the Boeing Model 360 helicopter p 490 A90-31558
- Boeing Condor raises UAV performance levels p 496 A90-34028
- Boeing 727-100 test project (high energy radiated field tests) [DOT/FAA/CT-88/33] p 542 N90-21247
- BOEING 727 AIRCRAFT**
- Current status of Joint FAA/NASA Runway Friction Program [SAE PAPER 892340] p 760 A90-45494
- The NASA digital VGH program. Exploration of methods and final results. Volume 3: B 727 data 1978-1980: 1765 hours [NASA-CR-181909-VOL-3] p 505 N90-20082
- BOEING 737 AIRCRAFT**
- Extending an airliner's life p 244 A90-20262
- Boeing 737 fuselage structural integrity program [SAE PAPER 892207] p 701 A90-45426
- Current status of Joint FAA/NASA Runway Friction Program [SAE PAPER 892340] p 760 A90-45494
- Aircraft accident report: Aloha Airlines, Flight 243, Boeing 737-200, N73711, near Maui, Hawaii, April 28, 1988 [PB89-910404] p 24 N90-10013
- Study of the engine bird ingestion experience of the Boeing 737 aircraft (October 1986 to September 1988) [DOT/FAA/CT-89/29] p 723 N90-25119
- BOEING 747 AIRCRAFT**
- New power system architecture for the 747-400 p 508 A90-33349
- Design features of the 747-400 Electric Power System [SAE PAPER 892227] p 746 A90-45443
- Foil gas bearings for turbomachinery [SAE PAPER 901236] p 841 A90-49306
- The NASA digital VGH program: Exploration of methods and final results. Volume 4: B 747 data 1978-1980, 1689 hours [NASA-CR-181909-VOL-4] p 506 N90-20083
- Aircraft accident report, United Airlines Flight 811, Boeing 747-122, N4713U, Honolulu, Hawaii, February 24, 1989 [PB90-910401] p 574 N90-21748
- An experimental study of fault propagation in a jet-engine controller [NASA-CR-181335] p 665 N90-23401
- BOEING 757 AIRCRAFT**
- Flight survey of the 757 wing noise field and its effects on laminar boundary layer transition. Volume 3: Extended data analysis [NASA-CR-178419] p 380 N90-18233

BOLTED JOINTS

- Carbon fibre composite bolted joints
p 130 A90-15354
- Recent studies on the behaviour of interference fit pins in composite plates
p 132 A90-16320
- Fatigue evaluation of C/MH-53E main rotor damper threaded joints
p 642 A90-39988
- Viscoelastic relaxation in bolted thermoplastic composite joints
p 945 A90-50158
- Flanged joints of aeroengines
[PNR90594]
p 116 N90-12609

BOLTS

- Experimental investigation into the effects of rotating and static bolts on both windage heating and local heat transfer coefficients in a rotor/stator cavity
[ASME PAPER 89-GT-196]
p 362 A90-23870
- Advanced NDE techniques for quantitative characterization of aircraft
p 886 N90-28088

BOMBER AIRCRAFT

- Automated aircraft configuration design and analysis
[SAE PAPER 891072]
p 101 A90-14368
- Sizing up the Stealth --- B-2 bomber aircraft
p 247 A90-23200

- B-2 aerodynamic design
[AIAA PAPER 90-1802]
p 334 A90-25174
- Strategic aircraft engineering design simulation
p 439 A90-30729

- Ride quality criteria for the B-2 bomber
[AIAA PAPER 90-3256]
p 835 A90-48852
- Encyclopedia of US Air Force aircraft and missile systems. Volume 2: Post-World War 2 bombers, 1945-1973
[AD-A209273]
p 1 N90-10001

BOMBS

- Coping with bomb threats to civil aviation
p 23 A90-12781

BONDING

- Advanced NDE techniques for quantitative characterization of aircraft
p 886 N90-28088

BOOMS (EQUIPMENT)

- Numerical analysis of vibrations of a helicopter tail boom
p 31 A90-13224
- Self-retracting helicopter rescue hoist
p 829 A90-46935

BOOSTER RECOVERY

- Recovery concepts for propulsion and avionics components --- for booster stage in launch vehicles
[AIAA PAPER 90-1810]
p 353 A90-25172

BOOSTER ROCKET ENGINES

- Review of the Aerospace Safety Advisory Panel report for NASA fiscal year 1990 authorization
[GPO-24-234]
p 177 N90-14213

BORON

- Combustion characteristics of a boron-fueled SFRJ with aft-burner
p 62 A90-12514
- An investigation on boron used as a component of solid propellant
p 765 A90-45708
- Regression and combustion characteristics of boron containing fuels for solid fuel ramjets
p 858 N90-27928

BORON COMPOUNDS

- Metallized fuel particle size study in a solid fuel ramjet
[AD-A220079]
p 679 N90-24451

BORON-EPOXY COMPOSITES

- Adhesive-bonded composite-patching repair of cracked aircraft structure
p 467 A90-31576

BOUNDARY CONDITIONS

- A method for the active control of the boundary layer condition
p 296 A90-24114
- Boundary conditions for Euler equations at internal block faces of multi-block domains using local grid refinement
[AIAA PAPER 90-1590]
p 607 A90-38725
- A two-dimensional unsteady potential solver in internal aerodynamics flow problems
p 707 A90-44430
- Outflow boundary conditions using Duhamel's equation
[AIAA PAPER 90-3014]
p 798 A90-45937
- Calculation of temperature distribution in various turbine blades using a boundary-fitted coordinate transformation method
p 929 N90-28550

BOUNDARY ELEMENT METHOD

- Complex variable boundary element method for external potential flows
[AIAA PAPER 90-0127]
p 162 A90-19694
- Analysis of transonic integral equations. II - Boundary element methods
p 302 A90-25301
- Boundary element solution of the transonic integro-differential equation
p 383 A90-27947
- Generalized Transition Finite-Boundary Elements for high speed flight structures
[AIAA PAPER 90-1105]
p 449 A90-29286
- Boundary element method for solving direct aerodynamic problem of aerofoil cascades on an arbitrary stream surface of revolution
p 554 A90-35830
- Boundary-element shape optimization system for aircraft structural components
p 680 A90-39786

- Calculation of stability derivatives for slender bodies using boundary element method
p 620 A90-40181
- Advanced applications of BEM to gas turbine engine structures
p 772 A90-45769
- Solution of potential flow past an elastic body using the boundary element technique
[AD-A213843]
p 275 N90-15390

BOUNDARY INTEGRAL METHOD

- Calculation of three-dimensional boundary layers including hypersonic flows
p 146 A90-16773
- Boundary integral equations method for compressible Navier-Stokes equations
p 209 A90-18262
- An approximate method for calculating flow past a wing profile with allowance for viscosity
p 234 A90-23422
- Numerical prediction of transonic viscous flows around airfoils through an Euler/boundary layer interaction method
[AIAA PAPER 90-1537]
p 564 A90-38681
- Boundary integral formulation for compressible nonlinear potential and Navier-Stokes equations
p 706 A90-44406

- Boundary-integral method for calculating aerodynamic sensitivities with illustration for lifting-surface theory
p 806 A90-46841

BOUNDARY LAYER COMBUSTION

- Effect of hydrogen combustion in a supersonic boundary layer on friction coefficient
p 355 A90-24116
- Regression and combustion characteristics of boron containing fuels for solid fuel ramjets
p 858 N90-27928

BOUNDARY LAYER CONTROL

- Prediction and control of transition in supersonic and hypersonic boundary layers
p 16 A90-12828
- Effect of moving surfaces on the airfoil boundary-layer control
p 159 A90-19388
- Further investigations of transonic shock-wave boundary-layer interaction with passive control
p 159 A90-19390

- Alleviation of shock oscillations in transonic flow by passive controls
[AIAA PAPER 90-0046]
p 161 A90-19648

- A method for the active control of the boundary layer condition
p 296 A90-24114
- Investigation of wall pressure pulsations during the passive control of shock/boundary layer interaction
p 378 A90-24132

- The boundary-layer fence - Barrier against the separation process
p 396 A90-31493
- Modification of large eddies in turbulent boundary layers
p 474 A90-33514
- Control of asymmetric vortical flows over delta wings at high angles of attack
p 553 A90-35759

- Laminar flow test installation in the Boeing Research Wind Tunnel
[AIAA PAPER 90-1425]
p 559 A90-37962

- Advanced Mach 3.5 Axisymmetric Quiet Nozzle
[AIAA PAPER 90-1592]
p 566 A90-38727

- Investigation of several passive and active methods for turbulent flow separation control
[AIAA PAPER 90-1598]
p 607 A90-38730

- Application of the moving surface boundary layer control to a two dimensional airfoil
p 628 A90-42405
- Control of forebody flow asymmetry - A critical review
[AIAA PAPER 90-2833]
p 711 A90-45164

- Design for a natural laminar flow glove for a transport aircraft
[AIAA PAPER 90-3043]
p 792 A90-45880

- Flight tests with a natural laminar flow glove on a transport aircraft
[AIAA PAPER 90-3044]
p 828 A90-45881

- A characterization and search technique for unsteady flow control problems
[AIAA PAPER 90-3102]
p 796 A90-45914

- On the drag reduction of bluff bodies through momentum injection
[AIAA PAPER 90-3076]
p 797 A90-45922

- Experimental aerodynamic characteristics of the airfoils LA 5055 and DU 86-084/18 at low Reynolds numbers
p 800 A90-46368

- Control of low-Reynolds-number airfoils - A review
p 801 A90-46376

- Application of localized surface heating to actively control the boundary layer separation
p 806 A90-46848

- Application of boundary layer control to HSCT low speed configuration
[AIAA PAPER 90-3199]
p 812 A90-49103

- Control of low-speed airfoil aerodynamics
p 814 A90-49776

- Laminar flow control perforated wing panel development
[NASA-CR-178166]
p 63 N90-10187

- Control and modification of turbulence
p 72 N90-10377

- Turbulence management: Application aspects
p 72 N90-10378

- Dynamics and control of turbulent shear flows
[AD-A210396]
p 72 N90-10402

- Active control of unsteady and separated flow structures
[AD-A212109]
p 89 N90-11707

- Research in Natural Laminar Flow and Laminar-Flow Control, part 1
[NASA-CP-2487-PT-1]
p 90 N90-12503

- Laminar flow: Challenge and potential
p 90 N90-12504

- LFC: A maturing concept
[DOUGLAS-PAPER-7878]
p 90 N90-12505

- Lockheed laminar-flow control systems development and applications
p 90 N90-12506

- Laminar flow: The Cessna perspective
p 91 N90-12507

- Long-range LFC transport
p 104 N90-12508

- Development flight tests of JetStar LFC leading-edge flight test experiment
p 104 N90-12509

- The right wing of the LEFT airplane
p 91 N90-12510

- Performance of laminar-flow leading-edge test articles in cloud encounters
p 104 N90-12511

- Simulated airline service experience with laminar-flow control leading-edge systems
p 104 N90-12512

- Goertler instability on an airfoil
p 91 N90-12517

- Research in Natural Laminar Flow and Laminar-Flow Control, part 2
[NASA-CP-2487-PT-2]
p 91 N90-12519

- Experimental studies on Goertler vortices
p 91 N90-12529

- An experimental evaluation of slots versus porous strips for laminar-flow applications
p 92 N90-12530

- Boundary-layer stability analysis of Langley Research Center 8-foot LFC experimental data
p 92 N90-12532

- Theoretical methods and design studies for NLF and HLFC swept wings at subsonic and supersonic speeds
p 92 N90-12535

- Application of sound and temperature to control boundary-layer transition
p 92 N90-12537

- Research in Natural Laminar Flow and Laminar-Flow Control, part 3
[NASA-CP-2487-PT-3]
p 92 N90-12539

- Design and test of an NLF wing glove for the variable-sweep transition flight experiment
p 104 N90-12544

- F-14 VSTFE and results of the cleanup flight test program
p 105 N90-12547

- Status report on a natural laminar-flow nacelle flight experiment
p 105 N90-12550

- Nacelle design
p 105 N90-12551

- Nacelle aerodynamic performance
p 105 N90-12552

- Supersonic laminar-flow control
p 93 N90-12554

- The effects of wall surface defects on boundary-layer transition in quiet and noisy supersonic flow
p 94 N90-12556

- Supersonic boundary-layer transition on the LaRC F-106 and the DFRF F-15 aircraft. Part 1: Transition measurements and stability analysis
p 94 N90-12558

- Simulated-airline-service flight tests of laminar-flow control with perforated-surface suction system
[NASA-TP-2966]
p 338 N90-17627

- Experimental and theoretical aerodynamic characteristics of a high-lift semispan wing model
[NASA-TP-2990]
p 477 N90-20046

- A study of supermaneuver aerodynamics
[AD-A218378]
p 631 N90-23349

- Application of laminar flow control to supersonic transport configurations
[NASA-CR-181917]
p 719 N90-25944

- Control of submersible vortex flows
[NASA-TM-102693]
p 909 N90-28493

BOUNDARY LAYER EQUATIONS

- Wing boundary layer calculation and its application to aircraft design
p 84 A90-15151

- Prediction of post-stall flows on airfoils
p 145 A90-16757

- Calculation of low Reynolds number flows at high angles of attack
[AIAA PAPER 90-0569]
p 167 A90-19921

- The prediction of boundary layers with rotation and variation of stream filament thickness
[ASME PAPER 89-GT-227]
p 362 A90-23882

- Newton solution of coupled viscous/inviscid multielement airfoil flows
[AIAA PAPER 90-1470]
p 562 A90-38627

- Interactive airfoil calculations with higher-order viscous-flow equations
[AIAA PAPER 90-1533]
p 564 A90-38678

- Higher-order boundary-layer approximations in interactive airfoil calculations
p 628 A90-42402

- Experimental study of the flow around an helicopter fuselage - Comparison with three-dimensional boundary layer calculations
p 630 A90-42438

- Wake effects on the prediction of transonic viscous flows around airfoils with an Euler/boundary layer interaction approach
[AIAA PAPER 90-3061] p 798 A90-45933
- A three-dimensional linear stability approach to transition on wings at incidence p 20 N90-10373
- Boundary-layer receptivity and laminar-flow airfoil design p 91 N90-12516
- Theoretical methods and design studies for NLF and HLFC swept wings at subsonic and supersonic speeds p 92 N90-12535
- Unsteady three-dimensional thin-layer Navier Stokes solutions on dynamic blocked grids
[AD-A212377] p 136 N90-12899
- An efficient solver of the Eigenvalue problem of the linear stability equations for three dimensional, compressible boundary-layer flows p 276 N90-16172
- Extension of a three-dimensional viscous wing flow analysis user's manual: VISTA 3-D code
[NASA-CR-182024] p 574 N90-22538
- The discretization of the three dimensional boundary layer equations
[ETN-90-97292] p 884 N90-27987
- ### BOUNDARY LAYER FLOW
- On the length scales of laminar shock/boundary-layer interaction p 5 A90-11610
- Flow in compressor interstage ducts p 11 A90-12521
- Boundary layer growth on low aspect ratio compressor blades p 12 A90-12553
- Axissymmetric afterbody flow separation at transonic speeds in presence of jet exhaust p 13 A90-12576
- Shock-wave/boundary-layer interaction at a swept compression corner p 16 A90-12850
- Experimental investigations of effects of the stagger angle on secondary flows in plane compressor cascades p 83 A90-13787
- Essential ingredients of a method for low Reynolds-number airfoils p 153 A90-17979
- Mach number effects on conical surface features of swept shock-wave/boundary-layer interactions p 154 A90-18147
- Large-scale motions in a supersonic turbulent boundary layer on a curved surface
[AIAA PAPER 90-0019] p 160 A90-19636
- Nonequilibrium recombination-dissociation boundary layer flows along arbitrarily-catalytic hypersonic vehicles
[AIAA PAPER 90-0055] p 161 A90-19652
- Numerical solution of the boundary-layer equations for a general aviation fuselage
[AIAA PAPER 90-0305] p 163 A90-19786
- Calculation of the side-wall boundary layer in axial turbomachines, accounting for the internal flow near the blades p 225 A90-21595
- Secondary loss generation in a linear cascade of high-turning turbine blades
[ASME PAPER 89-GT-47] p 289 A90-23773
- Compressor blade boundary layers. II - Measurements with incident wakes
[ASME PAPER 89-GT-51] p 289 A90-23777
- Infrared imaging and tufts studies of boundary layer flow regimes on a NACA 0012 airfoil p 446 A90-28268
- Oscillatory shock motion caused by transonic shock boundary-layer interaction p 470 A90-32478
- Higher-order effects in boundary-layer premixed combustion p 529 A90-32953
- The trailing edge loss of transonic turbine blades
[ASME PAPER 89-GT-278] p 475 A90-33564
- Interaction between boundary layer and wakes of different bodies p 602 A90-36263
- A numerical study of supersonic flow over a compression corner with different incoming boundary-layer profiles
[AIAA PAPER 90-1453] p 561 A90-38612
- Influence of bulk turbulence and entrance boundary layer thickness on the curved duct flow field
[AIAA PAPER 90-1502] p 606 A90-38651
- Correlation of separation shock motion in a compression ramp interaction with pressure fluctuations in the incoming boundary layer
[AIAA PAPER 90-1646] p 569 A90-38774
- Relationship between velocity circulation around a wing profile and vorticity dispersion in a boundary layer p 620 A90-39539
- The influence of the inlet Mach number on the boundary layer development on turbomachinery blade surfaces p 621 A90-40504
- Non-steady flow loss mechanisms associated with vaneless diffusers
[AIAA PAPER 90-2508] p 682 A90-40641
- Sidewall boundary-layer removal and wall adaptation studies p 672 A90-40680
- Investigations of the influence of slot blowing from the upper wing surface on the flow around the wing and its aerodynamic characteristics p 623 A90-41740
- Modelling of boundary layer and trailing edge thickness effects for the Euler equations using surface transpiration p 629 A90-42412
- A method to determine the performance of low-Reynolds-number airfoils under off-design unsteady freestream conditions p 801 A90-46375
- Wind-tunnel investigations of wings with serrated sharp trailing edges p 802 A90-46379
- Interactive boundary-layer method for unsteady airfoil flows - Quasisteady model p 812 A90-48953
- The receptivity of laminar boundary layer flow to leading edge vibrations p 815 A90-49800
- The aerodynamic design of the contraction for a subsonic wind tunnel p 907 A90-51545
- The three-dimensional vortex sheet structure on delta wings p 19 N90-10367
- Experimental and numerical analyses of laminar boundary-layer flow stability over an aircraft fuselage forebody p 93 N90-12549
- Reduction of turbulent drag: Boundary layer manipulators
[CERT-RSF-OA-74/2259-AYD] p 136 N90-12889
- Generalized similarity solutions for three dimensional, laminar, steady, compressible boundary layer flows on swept profile cylinders p 212 N90-13725
- Wake interaction effects on the transition process on turbine blades
[AD-A214492] p 343 N90-16759
- Experimental investigation of the mechanisms underlying vortex kinematics in unsteady separated flows
[AD-A217889] p 540 N90-20346
- Relating flow between counter-rotating propellers to aerodynamic interaction noise p 479 N90-20944
- Comparison of C- and O-grid generation methods using a NACA 0012 airfoil
[AD-A216375] p 479 N90-20948
- Low-density flow effects for hypervelocity vehicles, phase 2
[AD-A221034] p 634 N90-24249
- An interactive boundary-layer method for unsteady airfoil flows. Part 1: Quasi-steady-state model
[AD-A221220] p 634 N90-24250
- Numeric fluid mechanics p 960 N90-29161
- ### BOUNDARY LAYER SEPARATION
- Marginal separation of laminar axisymmetric boundary layers p 1 A90-10074
- Unsteady viscous calculation of cascade flows with leading-edge-induced separation
[ONERA, TP NO. 1989-116] p 3 A90-11148
- Numerical analysis of rotating stall by a vortex model p 13 A90-12590
- Investigation of flow separation on a supercritical airfoil p 17 A90-13023
- Transition effects on airfoil dynamics and the implications for subscale tests p 152 A90-17862
- Separation shock dynamics in Mach 5 turbulent interactions induced by cylinders p 153 A90-17981
- High Reynolds number wedge-induced separation lengths at Mach 6 p 154 A90-18001
- Video visualization of separation shock motion from measured wall pressure signals in a Mach 5 compression ramp interaction
[AIAA PAPER 90-0074] p 162 A90-19670
- Swept shock/boundary-layer interactions - Tutorial and update
[AIAA PAPER 90-0375] p 228 A90-22207
- Separation development and its effect on the aerodynamics of supercritical profiles at transonic velocities p 297 A90-24142
- Measurements in a separation bubble on an airfoil using laser velocimetry p 384 A90-27977
- Boundary layer turbulence structure in the presence of embedded streamwise vortex pairs p 552 A90-35193
- Vortex generator jets - Means for flow separation control p 555 A90-36257
- Boundary layer diagnostics by means of an infrared scanning radiometer p 605 A90-38493
- Mathematical modeling of plane parallel separated flows past bodies --- Russian book p 619 A90-39475
- Drag reduction by controlling flow separation using stepped afterbodies p 622 A90-40690
- Boundary-layer transition and separation on a turbine blade in a plane cascade
[AIAA PAPER 90-2263] p 625 A90-42102
- An airfoil theory of bifurcating laminar separation from thin obstacles p 702 A90-42639
- Design of wing profiles for application in nonstall conditions in a given angle-of-attack range p 710 A90-44936
- Unsteady flow separation on slender bodies at high angles of attack
[AIAA PAPER 90-2835] p 712 A90-45166
- Effect of riblets on flow separation in a subsonic diffuser p 712 A90-45261
- 2D vs. 3D - Selection of pressure distributions to delay separation on wings
[AIAA PAPER 90-3026] p 790 A90-45868
- The effect of separation on turbulent boundary layer characteristics over a smooth surface at Mach 6.0
[AIAA PAPER 90-3028] p 790 A90-45870
- A computational study of incipient leading-edge separation on a 65-deg delta wing at $M = 1.60$
[AIAA PAPER 90-3029] p 791 A90-45871
- Active flow control on low Reynolds number airfoils
[AIAA PAPER 90-3039] p 792 A90-45878
- Numerical investigation of laminar separated viscous trailing-edge flow using triple-deck theory
[AIAA PAPER 90-3046] p 792 A90-45883
- The instability of two-dimensional laminar separation p 800 A90-46365
- Bursting in separating flow and in transition p 800 A90-46366
- A computationally efficient modelling of laminar separation bubbles p 801 A90-46372
- Unsteady aerodynamics of Wortmann FX63-137 airfoil at low Reynolds numbers p 801 A90-46374
- Flow past bodies within a narrow class of cross-sectional shapes with stationary separation zones at large Reynolds numbers p 805 A90-46568
- Application of localized surface heating to actively control the boundary layer separation p 806 A90-46848
- Improvement in turbine blade aerodynamic force in the tip region p 809 A90-47854
- Effect of the Mach number and shape of the front part of the obstacle on the separation zone length in supersonic flow p 903 A90-50816
- Application of a vortex lattice numerical model in the calculation of inviscid incompressible flow around delta wings p 904 A90-51017
- The calculation of incompressible separated turbulent boundary layers p 905 A90-51025
- New methods of buffeting prediction on civil aircraft p 908 A90-52620
- Dynamics and control of turbulent shear flows
[AD-A210396] p 72 N90-10402
- Active control of unsteady and separated flow structures
[AD-A212109] p 89 N90-11707
- Simulation of glancing shock wave and boundary layer interaction
[NASA-TM-102233] p 133 N90-11970
- Some observations on transitory stall in conical diffusers
[NASA-TM-102387] p 94 N90-12561
- A computationally efficient modelling of laminar separation bubbles
[NASA-CR-185854] p 136 N90-12872
- Computation of Navier-Stokes equations for three-dimensional flow separation
[NASA-TM-102266] p 172 N90-13353
- Navier-Stokes solutions of 2-D transonic flow over unconventional airfoils p 173 N90-14195
- Navier-Stokes analysis of airfoils with leading edge ice accretions p 174 N90-14196
- Computational investigation of incompressible airfoil flows at high angles of attack
[AD-A205885] p 174 N90-14201
- Experimental measurements of the laminar separation bubble on an Eppler 387 airfoil at low Reynolds numbers
[NASA-CR-186263] p 275 N90-15380
- Flows with Separation
[DGLR-PAPERS-88-05] p 276 N90-16169
- An interactive method for the flow calculation of airfoils with local separation regions p 278 N90-16190
- Calculation of the flap profile flows with separation based on coupled potential and boundary layer solutions p 278 N90-16191
- Inverse solutions for boundary layers with separation or close to separation under locally infinite swept wing conditions p 279 N90-16192
- Periodically unsteady effects on profiles, induced by separation p 279 N90-16196
- Glancing shock-boundary layer interactions p 319 N90-17571
- Effect of riblets on flow separation from a cylinder and an airfoil in subsonic flow
[AD-A216197] p 319 N90-17574
- Experimental investigation of the influence of rotor wakes on the development of the profile boundary layer and the performance of an annular compressor cascade p 427 N90-18425
- Measurement of velocity profiles and Reynolds stresses on an oscillating airfoil p 397 N90-18427
- Contribution to the study of three-dimensional separation in turbulent incompressible flow
[ESA-TT-1169] p 454 N90-18697
- Influence of friction and separation phenomena on the dynamic blade loading of transonic turbine cascades
[MITT-88-04] p 428 N90-19235

- Control of flow separation and mixing by aerodynamic excitation
[NASA-TM-103131] p 571 N90-21733
- Numerical investigation of some control methods for 3-D turbulent interactions due to sharp fins
p 591 N90-21764
- A study of supermaneuver aerodynamics
[AD-A218378] p 631 N90-23349
- Euler code predicted separation at the airfoil trailing edge
[FFA-TN-1989-30] p 632 N90-23364
- An interactive boundary-layer method for unsteady airfoil flows. Part 1: Quasi-steady-state model
[AD-A221220] p 634 N90-24250
- A computational efficient modelling of laminar separation bubbles
[NASA-CR-186729] p 774 N90-25291
- Report of the Fluid Dynamics Panel Working Group 10 on calculation of 3D separate turbulent flows in boundary layer limit
[AGARD-AR-255] p 776 N90-26280
- In-flight flow visualization with pressure measurements at low speeds on the NASA F-18 high alpha research vehicle
[NASA-TM-101726] p 910 N90-28505
- Dynamic separation: Search for the cause of dynamic stall and search for its control
[AD-A223412] p 911 N90-29305
- BOUNDARY LAYER STABILITY**
- Curvature effects on the stability of laminar boundary layers on swept wings p 148 A90-16788
- Supersonic boundary layer stability analysis with and without suction on aircraft wings p 148 A90-16792
- Experimental transition and boundary-layer stability analysis for a slotted swept laminar flow control airfoil p 148 A90-16793
- On the Goertler vortex instability mechanism at hypersonic speeds p 158 A90-18886
- Numerical modeling of a flame in a confined, unstable shear layer
[AIAA PAPER 90-0647] p 205 A90-19966
- Instability and susceptibility of a boundary layer in the vicinity of two-dimensional surface inhomogeneities p 535 A90-32675
- The inviscid axisymmetric stability of the supersonic flow along a circular cylinder p 554 A90-35916
- A study of boundary layer stability in the case of an increased incoming stream turbulence in gradient flows p 555 A90-36065
- Effects of shock on the stability of hypersonic boundary layers
[AIAA PAPER 90-1448] p 561 A90-38608
- Stability limits for three-dimensional supersonic boundary layers p 564 A90-38673
- Advanced Mach 3.5 Axisymmetric Quiet Nozzle
[AIAA PAPER 90-1592] p 566 A90-38727
- Boundary layer stability in the case of transonic external flow p 619 A90-39514
- Comments on 'Effect of nose bluntness and cone angle on slender-vehicle transition' p 620 A90-39814
- Subharmonic instability of compressible boundary layers p 706 A90-44005
- Excitation and development of unstable perturbations in a supersonic boundary layer p 710 A90-44928
- An interactive boundary-layer stability-transition approach for low Reynolds-number airfoils p 799 A90-46364
- Determination of the laminar-turbulent transition point for a turbulent layer on a yawing wing p 805 A90-46566
- Response of a subsonic boundary layer to a pulsed oscillation of a localized region of the surface in the flow p 811 A90-48295
- Fluid Dynamics of Three-Dimensional Turbulent Shear Flows and Transition
[AGARD-CP-438] p 71 N90-10356
- Stability and transition of three-dimensional boundary layers p 71 N90-10357
- Direct numerical study of leading-edge contamination p 19 N90-10361
- Experimental study of transition and leading edge contamination on swept wings p 71 N90-10362
- Curvature effects on the stability of three-dimensional laminar boundary layers p 71 N90-10366
- The three-dimensional vortex sheet structure on delta wings p 19 N90-10367
- Simultaneous detection of separation and transition in surface shear layers p 72 N90-10368
- A three-dimensional linear stability approach to transition on wings at incidence p 20 N90-10373
- Boundary-layer receptivity and laminar-flow airfoil design p 91 N90-12516
- Predicted and hot-film measured Tollmien-Schlichting wave characteristics p 91 N90-12523
- Experimental studies on Goertler vortices p 91 N90-12529
- An experimental evaluation of slots versus porous strips for laminar-flow applications p 92 N90-12530
- Results of LFC experiment on slotted swept supercritical airfoil in Langley's 8-foot transonic pressure tunnel p 92 N90-12531
- Boundary-layer stability analysis of Langley Research Center 8-foot LFC experimental data p 92 N90-12532
- Theoretical methods and design studies for NLF and HLFC swept wings at subsonic and supersonic speeds p 92 N90-12535
- Research in Natural Laminar Flow and Laminar-Flow Control, part 3
[NASA-CP-2487-PT-3] p 92 N90-12539
- Design of the low-speed NLF(1)-0414F and the high-speed HSNLF(1)-0213 airfoils with high-lift systems p 93 N90-12540
- Design and test of an NLF wing glove for the variable-sweep transition flight experiment p 104 N90-12544
- Variable-Sweep Transition Flight Experiment (VSTFE): Stability code development and clean-up glove data analysis p 105 N90-12548
- Experimental and numerical analyses of laminar boundary-layer flow stability over an aircraft fuselage forebody p 93 N90-12549
- Experimental and theoretical investigation of boundary-layer instability mechanisms on a swept leading edge at Mach 3.5 p 94 N90-12557
- Supersonic boundary-layer transition on the LaRC F-106 and the DFRF F-15 aircraft. Part 1: Transition measurements and stability analysis p 94 N90-12558
- Experiments on the laminar-turbulent transition on swept wings p 276 N90-16170
- An efficient solver of the Eigenvalue problem of the linear stability equations for three dimensional, compressible boundary-layer flows p 276 N90-16172
- Detection of flow instabilities at airfoil profiles using piezoelectric arrays p 276 N90-16175
- Direct measurement of laminar instability amplification factors in flight p 277 N90-16178
- Numerical simulation of supersonic free shear layers [AD-A216289] p 320 N90-17579
- Effects of forebody geometry on subsonic boundary-layer stability
[NASA-CR-4314] p 718 N90-25939
- Application of laminar flow control to supersonic transport configurations
[NASA-CR-181917] p 719 N90-25944
- BOUNDARY LAYER TRANSITION**
- Adverse pressure gradient effects on boundary layer transition in a turbulent free stream p 15 A90-12639
- Prediction and control of transition in supersonic and hypersonic boundary layers p 16 A90-12828
- In-flight boundary-layer transition measurements on a swept wing p 17 A90-13017
- Disturbance growth in an unstable three-dimensional boundary layer p 148 A90-16787
- Leading edge contamination and relaminarisation on a swept wing at incidence p 148 A90-16789
- Experimental transition and boundary-layer stability analysis for a slotted swept laminar flow control airfoil p 148 A90-16793
- Perturbations of a three-dimensional boundary layer produced by body irregularities p 150 A90-17107
- The application of infrared thermography to the measurement of heat fluxes in a wind tunnel [ONERA, TP NO. 1989-192] p 261 A90-21051
- Flight and wind-tunnel investigations on boundary-layer transition p 233 A90-23283
- A study of the laminar-turbulent boundary layer transition on the windward side of a delta wing with a conical surface p 298 A90-24144
- In quest of the laminar-flow airliner - Flight experiments on a T-33 jet trainer p 300 A90-24825
- A transition detection study at Mach 1.5, 2.0, and 2.5 using a micro-thin hot-film system p 436 A90-28260
- Infrared imaging and tufts studies of boundary layer flow regimes on a NACA 0012 airfoil p 446 A90-28268
- The boundary-layer fence - Barrier against the separation process p 396 A90-31493
- The influence of boundary layer state on vortex shedding from flat plates and turbine cascades
[ASME PAPER 89-GT-296] p 474 A90-33560
- Unsteady transition in an axial-flow turbine. I - Measurements on the turbine rotor. II - Cascade measurements and modeling
[ASME PAPER 89-GT-289] p 474 A90-33562
- Flight-measured streamwise disturbance instabilities in laminar flow
[AIAA PAPER 90-1283] p 495 A90-33904
- An infrared camera system for detection of boundary layer transition in the ETW p 539 A90-34249
- Design and operational features of low-disturbance wind tunnels at NASA Langley for Mach numbers from 3.5 to 18
[AIAA PAPER 90-1391] p 594 A90-37936
- Boundary layer diagnostics by means of an infrared scanning radiometer p 605 A90-38493
- The effect of an oscillatory freestream-flow on a NACA-4412 profile at large relative amplitudes and low Reynolds-numbers p 560 A90-38495
- The influence of interaction aerodynamics of rotor-fuselage-interferences on the fuselage flow p 561 A90-38523
- Infrared cameras for detection of boundary layer transition in transonic and subsonic wind tunnels
[AIAA PAPER 90-1450] p 606 A90-38610
- Liquid crystal coatings for surface shear stress visualization in hypersonic flows
[AIAA PAPER 90-1513] p 563 A90-38660
- Comments on 'Effect of nose bluntness and cone angle on slender-vehicle transition' p 620 A90-39814
- Boundary-layer transition and separation on a turbine blade in a plane cascade
[AIAA PAPER 90-2263] p 625 A90-42102
- Flow over a leading edge with distributed roughness p 703 A90-42646
- In-flight flow visualization using infrared imaging p 731 A90-44731
- In-flight flow visualization characteristics of the NASA F-18 high alpha research vehicle at high angles of attack
[SAE PAPER 892222] p 713 A90-45439
- Design for a natural laminar flow glove for a transport aircraft
[AIAA PAPER 90-3043] p 792 A90-45880
- XFOIL - An analysis and design system for low Reynolds number airfoils p 799 A90-46359
- A fast method for computation of airfoil characteristics p 799 A90-46361
- An interactive boundary-layer stability-transition approach for low Reynolds-number airfoils p 799 A90-46364
- Bursting in separating flow and in transition p 800 A90-46366
- A computationally efficient modelling of laminar separation bubbles p 801 A90-46372
- Acoustic excitation of boundary layer oscillations on a yawing wing p 805 A90-46567
- Effects of transition on wind tunnel simulation of vehicle dynamics p 870 A90-49273
- Prediction of transition on a swept wing p 908 A90-52592
- Fluid Dynamics of Three-Dimensional Turbulent Shear Flows and Transition
[AGARD-CP-438] p 71 N90-10356
- Stability and transition of three-dimensional boundary layers p 71 N90-10357
- Experimental investigation of attachment-line transition in low-speed, high-lift wind-tunnel testing p 71 N90-10358
- Direct numerical study of leading-edge contamination p 19 N90-10361
- Experimental study of transition and leading edge contamination on swept wings p 71 N90-10362
- Simultaneous detection of separation and transition in surface shear layers p 72 N90-10368
- A three-dimensional linear stability approach to transition on wings at incidence p 20 N90-10373
- Control and modification of turbulence p 72 N90-10377
- The structure of separated flow regions occurring near the leading edge of airfoils - including transition
[NASA-CR-185853] p 87 N90-11695
- Normal-force-curve and pitching-moment-curve slopes of forebody-cylinder combinations at zero angle of attack for Mach numbers up to 5
[ESDU-89008] p 89 N90-11709
- Research in Natural Laminar Flow and Laminar-Flow Control, part 1
[NASA-CP-2487-PT-1] p 90 N90-12503
- Performance of laminar-flow leading-edge test articles in cloud encounters p 104 N90-12511
- Boundary-layer receptivity and laminar-flow airfoil design p 91 N90-12516
- Research in Natural Laminar Flow and Laminar-Flow Control, part 2
[NASA-CP-2487-PT-2] p 91 N90-12519
- Hot-film system for transition detection in cryogenic wind tunnels p 122 N90-12522
- Remote detection of boundary-layer transition by an optical system p 139 N90-12524
- Theoretical methods and design studies for NLF and HLFC swept wings at subsonic and supersonic speeds p 92 N90-12535
- Application of sound and temperature to control boundary-layer transition p 92 N90-12537

Research in Natural Laminar Flow and Laminar-Flow Control, part 3 [NASA-CP-2487-PT-3] p 92 N90-12539

Wind tunnel results of the low-speed NLF(1)-0414F airfoil p 93 N90-12541

Design and test of an NLF wing glove for the variable-sweep transition flight experiment p 104 N90-12544

The 757 NLF glove flight test results p 104 N90-12546

F-14 VSTFE and results of the cleanup flight test program p 105 N90-12547

Variable-Sweep Transition Flight Experiment (VSTFE): Stability code development and clean-up glove data analysis p 105 N90-12548

Experimental and numerical analyses of laminar boundary-layer flow stability over an aircraft fuselage forebody p 93 N90-12549

Status report on a natural laminar-flow nacelle flight experiment p 105 N90-12550

Nacelle design p 105 N90-12551

Nacelle aerodynamic performance p 105 N90-12552

Supersonic laminar-flow control p 93 N90-12554

Design and fabrication requirements for low noise supersonic/hypersonic wind tunnels p 122 N90-12555

The effects of wall surface defects on boundary-layer transition in quiet and noisy supersonic flow p 94 N90-12556

Supersonic boundary-layer transition on the LaRC F-106 and the DFRF F-15 aircraft. Part 1: Transition measurements and stability analysis p 94 N90-12558

Supersonic boundary-layer transition on the LaRC F-106 and the DFRF F-15 aircraft. Part 2: Aerodynamic predictions p 94 N90-12559

A computationally efficient modelling of laminar separation bubbles [NASA-CR-185854] p 136 N90-12872

Transition in surface boundary layers [CERT-RSF-OA-43/5018-AYD] p 136 N90-12897

Numerical simulation of transition in three-dimensional boundary layers [DLR-FB-89-12] p 212 N90-13728

Flows with Separation [DGLR-PAPERS-88-05] p 276 N90-16169

Semi-empirical transition criteria for the design of laminar profiles p 276 N90-16174

Determination of the N-factor in the Brunswick (Federal Rep. of Germany) transonic wind tunnel using measurements of pressure distributions and transition points, and the Sally method p 276 N90-16177

Development of transition criteria on the basis of e to the N power for three dimensional wing boundary layers p 277 N90-16179

Wake interaction effects on the transition process on turbine blades [AD-A214492] p 343 N90-16759

A review of high-speed, convective, heat-transfer computation methods p 316 N90-17548

Opportunities for improved understanding of supersonic and hypersonic flows p 318 N90-17566

Some Navier-Stokes calculations for the CAST-10 airfoil p 320 N90-17651

Main results of CAST-10 airfoil tested in T2 cryogenic wind tunnel p 321 N90-17652

An experimental AWTS process and comparisons of ONERA T2 and 0.3-m TCT AWTS data for the ONERA CAST-10 aerofoil p 321 N90-17653

Investigation of CAST-10-2/DOA 2 airfoil in NAE high Reynolds number two-dimensional test facility p 321 N90-17654

Flight survey of the 757 wing noise field and its effects on laminar boundary layer transition. Volume 3: Extended data analysis [NASA-CR-178419] p 380 N90-18233

Modelling unsteady transition and its effects on profile loss p 427 N90-18423

Experimental investigation of the influence of rotor wakes on the development of the profile boundary layer and the performance of an annular compressor cascade p 427 N90-18425

Flight test investigation of certification issues pertaining to general-aviation-type aircraft with natural laminar flow [NASA-CR-181967] p 480 N90-20952

Current Japanese supercomputers for computational fluid dynamics applications p 610 N90-23172

Flow unsteadiness effects on boundary layers [NASA-CR-186067] p 690 N90-24557

A brief review of some mechanisms causing boundary layer transition at high speeds [NASA-TM-102834] p 720 N90-25945

Use of liquid crystals for qualitative and quantitative 2-D studies of transition and skin friction [RAE-TM-AERO-2159] p 958 N90-28800

Numeric fluid mechanics p 960 N90-29161

A boundary-layer transition model for the Navier-Stokes computation for a natural-laminar-flow airfoil [NAL-TR-1038T] p 912 N90-29328

BOUNDARY LAYERS

Tangential mass addition for the control of shock wave/boundary layer interactions in scramjet inlets p 13 A90-12586

A CFD study of precombustion shock-trains from Mach 3-6 [AIAA PAPER 90-2220] p 705 A90-42751

General buckling tests with thin-walled shells [DLR-MITT-89-13] p 213 N90-13816

An experimental investigation of viscous aspects of propeller blade flow p 315 N90-16711

Predicted and measured boundary layer refraction for advanced turboprop propeller noise [NASA-TM-102365] p 379 N90-17413

Shock-shock boundary layer interactions p 318 N90-17569

Glancing shock-boundary layer interactions p 319 N90-17571

Some Navier-Stokes calculations for the CAST-10 airfoil p 320 N90-17651

Investigation of CAST-10-2/DOA 2 airfoil in NAE high Reynolds number two-dimensional test facility p 321 N90-17654

Experience with some repeat tests on the 9 inch chord CAST-10-2/DOA 2 airfoil model in the Langley 0.3-m TCT adaptive wall test section p 321 N90-17657

Aerodynamics of unsteady systems. Numerical study of potential flow/boundary layer coupling [ETN-90-96257] p 396 N90-18367

Flow unsteadiness effects on boundary layers [NASA-CR-186067] p 690 N90-24557

A computationally efficient modelling of laminar separation bubbles [NASA-CR-186729] p 774 N90-25291

A brief review of some mechanisms causing boundary layer transition at high speeds [NASA-TM-102834] p 720 N90-25945

Unsteady aerodynamics of controls p 935 N90-28525

BOUNDARY VALUE PROBLEMS

Construction of a straight single-row airfoil lattice by the method of quasi-solutions for inverse boundary value problems p 84 A90-14564

The method of matched integral representations in viscous fluid dynamics p 129 A90-14565

On the coupling of finite elements and boundary elements for transonic potential flows p 155 A90-18297

Boundary conditions for Euler equations at internal block faces of multi-block domains using local grid refinement [AIAA PAPER 90-1590] p 607 A90-38725

Design of wing profiles for application in nonstall conditions in a given angle-of-attack range p 710 A90-44936

Calculation of the heat flux at a three-dimensional critical point in supersonic flow past a body p 803 A90-46536

Construction of wing profiles in subsonic gas flow by the method of quasi-solutions for inverse boundary value problems p 803 A90-46542

Goertler instability on an airfoil p 91 N90-12517

Evaluation of the indirect effects of lightning on a system: Double transfer function method [RAE-TRANS-2172] p 176 N90-14211

A direct-inverse method for transonic and separated flows about airfoils [NASA-CR-4270] p 235 N90-15072

Guidance analysis of the aeroglide plane change maneuver as a turning point problem [NASA-TM-101639] p 259 N90-15110

A system for transonic wing design with geometric constraints based on an inverse method p 501 N90-20983

Subsonic and transonic blade design by means of analysis codes p 510 N90-20985

A computational design method for shock free transonic cascades and airfoils p 501 N90-20986

A study of supermaneuver aerodynamics [AD-A218378] p 631 N90-23349

Extension-torsion coupling behavior of advanced composite tilt-rotor blades p 651 N90-25057

Proceedings of damping '89. Volume 1: Pages AAB-1 through DCD-11 [AD-A223431] p 960 N90-29664

BOV WAVES

Airfoils in supersonic source and sink flows p 149 A90-16844

Modeling of liquid jets injected transversely into a supersonic crossflow p 153 A90-17985

A study of the limitations of linear theory methods as applied to sonic boom calculations [AIAA PAPER 90-0368] p 219 A90-19817

The effect of shock/shock interactions on the design of hypersonic inlets [AIAA PAPER 90-2217] p 705 A90-42748

Shock layer vacuum UV spectroscopy in an arc-jet wind tunnel [NASA-TM-102258] p 370 N90-17112

Glancing shock-boundary layer interactions p 319 N90-17571

BOX BEAMS

Determination of the torsion rigidity of a multiple-rib torsion box of an aircraft lifting surface p 364 A90-24134

BOXES (CONTAINERS)

Advanced gearbox technology [NASA-CR-179625] p 666 N90-24274

BRAKES (FOR ARRESTING MOTION)

Accelerators and decelerators for large, hypersonic aircraft [AIAA PAPER 90-1986] p 674 A90-40582

BRACING

Aircraft and ground vehicle friction measurements obtained under winter runway conditions [SAE PAPER 891070] p 95 A90-14367

BRANCHING (MATHEMATICS)

Unfolding of double-zero eigenvalue bifurcations for supersonic flow past a pitching wedge p 347 A90-25995

Bifurcation analysis of a model fighter aircraft with control augmentation [AIAA PAPER 90-2836] p 934 A90-50640

F-15B high angle-of-attack phenomena and spin prediction using bifurcation analysis [AD-A217366] p 498 N90-20073

BRAYTON CYCLE

Performance potential of an advanced technology Mach 3 turbojet engine installed on a conceptual high-speed civil transport [NASA-TM-4144] p 51 N90-10034

BRAZING

Braze repair of MA754 aero gas turbine engine nozzles [ASME PAPER 89-GT-235] p 342 A90-23886

Two special cost-effective applications for electrochemical metallizing for improved brazing and bonding [SAE PAPER 890927] p 365 A90-24692

BREATHING APPARATUS

Development of improved fire safety standards adopted by the Federal Aviation Administration p 324 N90-17585

BRIGHTNESS

A new method for measuring the transmissivity of aircraft transparencies [AD-A216953] p 464 N90-19842

BRISTOL-SIDDELEY BS 53 ENGINE

Progress in certifying F402-RR-408 - The improved Pegasus engine for AV-8B and Harrier II Plus p 587 A90-38532

More power for the Harrier p 745 A90-44597

Operation of the Rolls-Royce Pegasus Engine on low grade non-aviation fuels [SAE PAPER 892329] p 747 A90-45486

BRITTLENESS

Observations on the brittle to ductile transition temperatures of B2 nickel aluminides with and without zirconium p 205 A90-19153

Freeze drying for morphological control of inter-penetrating polymer networks p 948 A90-50214

BROADBAND

Audibility and annoyance of en route noise of unducted fan engines [AD-A223687] p 966 N90-30035

BROWNIAN MOVEMENTS

Brownian motion far from equilibrium - A hypersonic approach p 555 A90-35917

Stochastic propagation of an array of parallel cracks: Exploratory work on matrix fatigue damage in composite laminates [DE89-017837] p 126 N90-11813

BUBBLE MEMORY DEVICES

Bubble memory applications for aircraft systems p 418 A90-30681

BUBBLE TECHNIQUE

Application of the hydrogen bubble visualization method to the water tunnels of ONERA [ONERA, TP NO. 1989-107] p 58 A90-11140

BUBBLES

Numerical calculation of bubbly two phase flow around an airfoil p 304 A90-25783

Flow visualization via laser-induced reflection from bubble sheets p 680 A90-39784

A computationally efficient modelling of laminar separation bubbles p 801 A90-46372

A computationally efficient modelling of laminar separation bubbles [NASA-CR-185854] p 136 N90-12872

- Experimental measurements of the laminar separation bubble on an Eppler 387 airfoil at low Reynolds numbers [NASA-CR-186263] p 275 N90-15380
- A computational efficient modelling of laminar separation bubbles [NASA-CR-186729] p 774 N90-25291
- Noise from tip vortex and bubble cavitation [AD-A221962] p 896 N90-27468
- BUCKLING**
- Experimental study on the buckling and postbuckling of carbon fibre composite panels with and without interply disbonds p 130 A90-15355
- Postbuckling behavior of laminated plates using a direct energy-minimization technique p 209 A90-17993
- Postbuckling finite element analysis of composite panels p 365 A90-24377
- Damage tolerance of a postbuckling soft skin hat stiffened compression panel p 534 A90-31647
- Torsional buckling and post-buckling of composite geodetic cylinders with special reference to joint flexibility p 878 A90-45971
- General buckling tests with thin-walled shells [DLR-MITT-89-13] p 213 N90-13816
- Structural analysis and optimum design of geodesically stiffened composite panels [NASA-CR-186944] p 959 N90-28862
- BUDGETING**
- Studies of the European transonic wind tunnel [ONERA-RSF-12/0694-GY] p 141 N90-13278
- BUFFETING**
- An investigation of the buffet excitation parameter p 473 A90-33368
- On the prediction of the aeroelastic behaviour of lifting systems due to flow separation p 491 A90-33369
- Wind tunnel studies of F/A-18 tail buffet [AIAA PAPER 90-1432] p 559 A90-37969
- Wide angle diffusers with passive boundary-layer control [AIAA PAPER 90-1600] p 567 A90-38732
- An experimental and analytical investigation of the buffet excitation parameter p 645 A90-42417
- Modeling of the buffeting of flight vehicles p 803 A90-46500
- New methods of buffeting prediction on civil aircraft p 908 A90-52620
- Assessment of computational prediction of tail buffeting [NASA-TM-101613] p 237 N90-15886
- BULKHEADS**
- Study on SPF and SPF/DB of the bulk-head structure with nonsymmetric shape p 132 A90-16619
- BUOYANCY**
- Navier-Stokes computations of three-dimensional laminar flows with buoyancy in a channel with wing-type vortex generators p 772 A90-45728
- BURAN SPACE SHUTTLE**
- Landing tests for Buran shuttle with jet engine-equipped mock-up p 61 N90-10904
- BURNERS**
- Burner rig hot corrosion of silicon carbide and silicon nitride p 355 A90-25267
- Externally vaporizing system for turbine combustor [AD-D014284] p 256 N90-15918
- Modification and improvement of software for modeling multidimensional reacting fuel flows [AD-A217789] p 533 N90-20235
- BURNING RATE**
- Numerical modeling of the combustion kinetics of hydrocarbon fuels in an annular combustion chamber with allowance for the formation of harmful impurities p 124 A90-14582
- BURNS (INJURIES)**
- Fire deaths in aircraft without the crashworthy fuel system p 22 A90-10266
- BURSTS**
- Spray automated balancing of rotors - How process parameters influence performance p 879 A90-46228
- BUS CONDUCTORS**
- Laboratory implementation of the Continuously Reconfiguring Multi-Microprocessor Flight Control System (CRMFCFS) [AD-A217730] p 520 N90-20094
- BYPASS RATIO**
- Ultra High Bypass (UHB) engine critical component technology [ASME PAPER 89-GT-229] p 342 A90-23884
- Investigation of very high bypass ratio engines for subsonic transports p 659 A90-40945
- Turbofans turn to UHB propulsion p 659 A90-41165
- The promise of advanced materials for a 21st century UBE - ultrahigh bypass ratio engine [AIAA PAPER 90-2396] p 662 A90-42157
- Ultra high bypass turbofan technologies for the twenty-first century [AIAA PAPER 90-2397] p 662 A90-42158

- Analysis of installed wind tunnel test results on large bypass ratio engine/nacelle installations [AIAA PAPER 90-2146] p 705 A90-42738
- NASA's HITEMP program for UHBR engines [AIAA PAPER 90-2395] p 852 A90-47218
- Aerodynamic losses in conventional fan blades of high by pass turbo engine p 854 A90-49487

BYPASSES

- Holographic flow visualisation of turbofan by-pass and core nozzle streams [ASME PAPER 89-GT-260] p 363 A90-23891

C**C (PROGRAMMING LANGUAGE)**

- Development and testing of methodology for evaluating the performance of multi-input/multi-output digital control systems [AIAA PAPER 90-3501] p 867 A90-47747
- Yaw rate control of an air bearing vehicle p 435 N90-19420

C BAND

- Dual cross-polarization planar arrays in the C and X bands p 638 A90-40979

C-130 AIRCRAFT

- Improving snow roads and airstrips in Antarctica [AD-A215588] p 133 N90-11907
- Reducing C130E Hercules operating costs in the Royal Australian Air Force and the United States Air Force by increasing cruise speeds [AD-A215747] p 338 N90-17629

C-135 AIRCRAFT

- Parabolic flight experiments on fluid surfaces and wetting KC-135R low altitude air refueling flight test program [AIAA PAPER 90-1265] p 494 A90-33893
- The use of the CFM56 engine in the KC-135 tanker [SAE PAPER 892362] p 747 A90-45511
- Combustion Experiments During KC-135 Parabolic Flights [ESA-SP-1113] p 368 N90-16958

C-140 AIRCRAFT

- Ground vibration test results of a JetStar airplane using impulsive sine excitation p 179 A90-16963
- The right wing of the LEFT airplane p 91 N90-12510

- Simulated airline service experience with laminar-flow control leading-edge systems p 104 N90-12512

- Simulated-airline-service flight tests of laminar-flow control with perforated-surface suction system [NASA-TP-2966] p 338 N90-17627

C-141 AIRCRAFT

- Stronger stratiifier p 143 A90-17919

C-5 AIRCRAFT

- Computerized corrosion forecasting model for C-5 aircraft p 843 N90-26815

CABIN ATMOSPHERES

- The optimum control and adaptive control for airplane cabin pressure p 182 A90-18627

- Contamination of cabin air by synthetic oil and breakdown products [SAE PAPER 891455] p 323 A90-27424

- Microprocessor control of a vapor-cycle cooling system [SAE PAPER 891457] p 339 A90-27426

- Analysis and improvement of cabin temperature control system p 580 A90-37241

- Use of ECS-conditioned air for FLIR avionics thermal control - Fighter aircraft [SAE PAPER 901219] p 840 A90-49294

- F-15 Environment Control System improvements [SAE PAPER 901235] p 841 A90-49305

- Characteristics of transport, aircraft fires measured by full-scale tests p 325 N90-17591

CALCIUM FLUORIDES

- Self-lubricating surfaces by ion beam processing [AD-A22489] p 884 N90-27118

CALCULUS

- A fractional calculus model of aeroelasticity [AD-A216244] p 377 N90-18212

CALCULUS OF VARIATIONS

- Application of a self-adaptive grid method to complex flows [NASA-TM-102223] p 143 N90-13324

CALENDARS

- Calendar of selected aeronautical and space meetings [AGARD-CAL-90/1] p 464 N90-19060

CALIBRATING

- Liquid water content and droplet size calibration of the NASA Lewis Icing Research Tunnel [AIAA PAPER 90-0669] p 261 A90-22242

- An array-fed reflector antenna with built-in calibration facility p 402 A90-27781

- Automatic calibration machine for cryogenic and conventional internal strain gage balances [AIAA PAPER 90-1396] p 595 A90-37939

- Winds aloft measurement and airspeed calibration using Loran [AIAA PAPER 90-3331] p 847 A90-47592

- Devices and procedures for the calibration of sensors and measurement: Systems of the flight test support system ATTAS [DFVLR-MITT-89-06] p 134 N90-12007

- Dynamic testing techniques and applications for an aeroelastic rotor test facility p 201 N90-13406

- Liquid water content and droplet size calibration of the NASA Lewis Icing Research Tunnel [NASA-TM-102447] p 213 N90-13797

- Airdata calibration of a high-performance aircraft for measuring atmospheric wind profiles [NASA-TM-101714] p 186 N90-14228

- Design and calibration of an in-stack, low-pressure impactor [AD-A213531] p 255 N90-15105

- Cryogenic balances for the US NTF p 264 N90-15959

- Evaluation of various thrust calculation techniques on an F404 engine [NASA-TP-3001] p 735 N90-25134

- An accurate numerical technique for determining flight test rate gyroscope biases prior to takeoff [AD-A220987] p 739 N90-25138

- An automated calibration laboratory for flight research instrumentation: Requirements and a proposed design approach [NASA-TM-101719] p 781 N90-26564

- Three-dimensional model testing in the transonic self-streamlining wind tunnel p 938 N90-28583

- Procedure for calibrating fly-by-wire control chains of the flying testbed ATTAS [DLR-MITT-90-02] p 936 N90-29401

- Noncontact measurement of rotating blade vibrations [NAL-TR-1033] p 961 N90-29687

CALORIMETERS

- Improved Thermo-Oxidative-Deposition screening tests for turbine lubricants [AD-A217795] p 533 N90-21188

CAMBER

- Numerical simulation of unsteady flow about cambered plates p 159 A90-19389

- The maximum lift coefficient of plain wings at subsonic speeds [ESDU-89034] p 236 N90-15082

- A study of flows over highly-swept wings designed for maneuver at supersonic speeds [AD-A216837] p 399 N90-19202

CAMBERED WINGS

- An application of the surface-singularity method to wing-body-tail configurations p 9 A90-12229

- Leading- and trailing-edge flaps on supersonic delta wings p 233 A90-23285

- Optimal reflex camber p 308 A90-26347

- Strake camber and thickness design procedure for low alpha supersonic flow p 622 A90-40678

- Aerodynamic characteristics of forward sweep [AIAA PAPER 90-3041] p 792 A90-45879

CAMERAS

- The new light weight, high performance reconnaissance camera KRB 8/24 F p 847 A90-48607

- Video photographic considerations for measuring the proximity of a probe aircraft with a smoke seeded trailing vortex [NASA-TM-102691] p 724 N90-25120

CANADA

- Adverse weather operations during the Canadian Atlantic storms program p 281 N90-15052

- Aircraft fire safety: Learning from past accidents p 324 N90-17584

- Aircraft fire safety in the Canadian Forces p 327 N90-17604

- The Canadian Aviation Safety Board's flight recorder facility p 849 N90-27643

CANADAIR AIRCRAFT

- Canadians develop composite techniques for CF-18 battle damage repair program p 551 A90-36300

- Developing the Canadair Regional Jet airliner p 729 A90-42656

- CF 18 480 Gallon External Fuel Tank Stores Clearance Program p 35 N90-10877

CANARD CONFIGURATIONS

- Canard-wing interaction in unsteady supersonic flow p 3 A90-11010

- An investigation of strake fence flaps on a canard-configured aircraft [AIAA PAPER 90-0762] p 230 A90-22259

- Pay-offs and pitfalls of fly-by-wire p 346 A90-24281

- An in-flight interaction of the X-29A canard and flight control system [AIAA PAPER 90-1240] p 348 A90-26820

- The numerical simulation of the low speed aerodynamic characteristics of a set of close-coupled canard configurations p 396 A90-31485
- On aerodynamic characteristics of canard in canard-forward-swept wing configuration p 709 A90-44833
- Canard-wing vortex interactions at subsonic through supersonic speeds [AIAA PAPER 90-2814] p 711 A90-45154
- A VSAERO analysis of several canard configured aircraft II [SAE PAPER 892287] p 714 A90-45465
- Numerical simulation of vortical flows over a strake-delta wing and a close coupled delta-canard configuration [AIAA PAPER 90-3002] p 788 A90-45851
- Numerical simulation of vortical flows over close-coupled canard-wing configuration [AIAA PAPER 90-3003] p 788 A90-45852
- Self-induced roll oscillations of lifting systems with thin delta wings p 860 A90-46570
- Certifying the Speed Canard p 833 A90-48699
- The active control of an unstable canard aircraft p 57 N90-10894
- Validation of a computer code for analysis of subsonic aerodynamic performance of wings with flaps in combination with a canard or horizontal tail and an application to optimization [NASA-TP-2961] p 173 N90-14187
- Canard versus aft-tail ride qualities performance and pilot command response p 258 N90-15053
- Wind tunnel investigations on the configuration of the international vortex flow experiment p 277 N90-16181
- X-29A aircraft structural loads flight testing [NASA-TM-101715] p 416 N90-19225
- Constrained spanload optimization for minimum drag of multi-lifting-surface configurations p 501 N90-20992
- Feasibility study for a microwave-powered ozone sniffer aircraft [NASA-CR-186660] p 650 N90-23397
- Effect of tail size reductions on longitudinal aerodynamic characteristics of a three surface F-15 model with nonaxisymmetric nozzles [NASA-TP-3036] p 718 N90-25938
- An in-flight interaction of the X-29A canard and flight control system [NASA-TM-101718] p 736 N90-25973
- A computer module used to calculate the horizontal control surface size of a conceptual aircraft design [NASA-CR-186872] p 780 N90-26515
- Aerodynamic and propulsive control development of the STOL and maneuver technology demonstrator p 920 N90-28514
- Effects of canard position on the aerodynamic characteristics of a close-coupled canard configuration at low speed p 920 N90-28519
- The effects of foreplanes on the static and dynamic characteristics of a combat aircraft model p 920 N90-28520
- The steady and time-dependent aerodynamic characteristics of a combat aircraft with a delta or swept canard p 921 N90-28526
- An in-flight investigation of ground effect on a forward-swept wing airplane p 922 N90-28533
- CANOPIES**
- Canopy fragilization using embedded detonating cord p 180 A90-17417
- The Robotic Canopy Polishing System [SME PAPER MS89-134] p 222 A90-23680
- The shape assumed by a soft conical shell in fluid flow p 300 A90-24752
- Analytical solution of the problem of nonaxisymmetric potential flow past a spherical canopy - A summary of the principal asymptotic formulas and qualitative analysis p 300 A90-24753
- An improved canopy stiffness scaling law for determining opening time of flat circular parachutes [AIAA PAPER 90-3058] p 790 A90-45863
- Automation of an RCS (Radar Cross Section) measurement system and its application to investigate the electromagnetic scattering from scale model aircraft canopies [AD-A215741] p 371 N90-17970
- A new method for measuring the transmissivity of aircraft transparencies [AD-A216953] p 464 N90-19842
- Water-tunnel study results of a TFA-18 and F/A-18 canopy flow visualization [NASA-TM-101705] p 573 N90-22532
- Nondestructive measurement of residual stresses in aircraft transparencies [AD-A218680] p 689 N90-23762
- Forward canopy feasibility and Thru-The-Canopy (TTC) ejection system study [AD-A220360] p 637 N90-24258

CANS

- Fire hazards of aerosol cans in aircraft cargo compartments [DOT/FAA/CT-89/32] p 636 N90-23369

CANTILEVER BEAMS

- A new generation of innovative ultra-advanced intelligent composite materials featuring electro-rheological fluids - An experimental investigation p 204 A90-17962
- Sensitivity analysis using resonance and anti-resonance frequencies - A guide to structural modification p 536 A90-33396

CANTILEVER PLATES

- Dynamic structural correlation via nonlinear programming techniques p 208 A90-17372
- Nonlinear stall flutter and divergence analysis of cantilevered graphite/epoxy wings [AIAA PAPER 90-0983] p 450 A90-29373

CAPACITANCE

- Simulator comparison of thumbball, thumb switch, and touch screen input concepts for interaction with a large screen cockpit display format [NASA-TM-102587] p 506 N90-21005

CAPILLARY FLOW

- Some technological errors in the use of capillary inspection in gas turbine engine repair p 769 A90-43039

CAPTIVE TESTS

- Captive carry testing of remotely piloted vehicles p 828 A90-46386

CARBON DIOXIDE

- The changes of structures and properties in PAN-based carbon fibers during heat treatment in carbon dioxide p 945 A90-50145
- Aircraft exhaust emissions: An engine manufacturer's perspective [PNR90675] p 750 N90-26004

CARBON DIOXIDE LASERS

- A laser obstacle avoidance and display system p 419 A90-30694
- Laser machining developments at McDonnell Douglas p 453 A90-31028
- Airborne CO₂ Doppler lidar for wind shear detection p 849 N90-27640

CARBON FIBER REINFORCED PLASTICS

- Highly damage tolerant carbon fiber epoxy composites for primary aircraft structural applications p 125 A90-14660
- Carbon fibre composite bolted joints p 130 A90-15354
- Experimental study on the buckling and postbuckling of carbon fibre composite panels with and without interply disbands p 130 A90-15355
- The advantages of automation in aerospace production p 130 A90-15357
- The strength and weakness of carbon composite structures --- for military and civil aircraft p 180 A90-17679
- The effect of impact loading on residual strength of CFRP composite beams p 208 A90-17683
- Material of the '90s? p 265 A90-20259
- Design and fabrication of the carbon fiber/epoxy A-320 horizontal tailplane p 286 A90-25221
- A study on flaw detection method for CFRP composite laminates. I. The measurement of crack extension in CFRP composites by electrical potential method p 441 A90-28003
- Toughened thermosets for damage tolerant carbon fiber reinforced composites p 443 A90-29825
- Fibre reinforced thermoplastic integral constructions in modular build-up technology - The 'thermoplastic in-situ-technique' p 534 A90-31879
- Thermoplastic composites, past, present and future p 529 A90-31882
- Design, fabrication and experimental test of hi-temperature CFRP stiffened structures --- rotating cowling panels for unducted fan engines p 534 A90-31892

- Aerospace materials - Trends and potential p 529 A90-31902
- Airbus A320 CFRP-rudder structural requirements p 493 A90-33707
- Damage tolerance of carbon fibre reinforced plastic sandwich panels p 675 A90-40047
- Structural components of fiber-reinforced thermoplastics p 676 A90-41111
- EH-101 main rotor hub application of thick carbon fiber unidirectional tension bands p 618 A90-42489
- A comparison of honeycomb-core and foam-core carbon-fibre/epoxy sandwich panels p 764 A90-43855
- Damage tolerance demonstration for A310-300 CFRP-components p 819 A90-49894
- High temperature behavior of the innovation carbon/CSPI composite p 941 A90-50067

Chemical resistance of carbon fiber reinforced polyether ether ketone and polyphenylene sulfide composites p 944 A90-50142

Aerospace Arall - The advancement in aircraft materials p 947 A90-50186

A study of filament wound high modulus carbon fiber reinforced cylinders p 948 A90-50218

A new test procedure for a wing made with carbon fiber composites [ETN-89-95220] p 126 N90-11820

Simple shear tests of the FMI 23.5.06 adhesive cured at low pressure (12 PSI) p 357 N90-17871

[INFORME-I-298/88] p 357 N90-17871

Impact of composites in the aerospace industry [ETN-90-96231] p 443 N90-18527

Damage tolerance demonstration for A310-300 CFRP components [MBB-UT-012/89-PUB] p 766 N90-25091

CARBON FIBERS

High performance thermoplastic composites with poly(etherketoneketone) matrix p 529 A90-31846

Aircraft applications of advanced composite fiber/metal pressure vessels [AIAA PAPER 90-2344] p 686 A90-42133

Domestic precursor technology - A unique route to current and future generation carbon fibers p 940 A90-50057

Vapor grown carbon fiber for space thermal management systems p 943 A90-50128

Monolithic CFC-Main Landing Gear Door for Tornado p 955 A90-50136

The changes of structures and properties in PAN-based carbon fibers during heat treatment in carbon dioxide p 945 A90-50145

Fracture morphology of toughened bismaleimide/carbon fiber composites p 948 A90-50205

Electrostatic dry powder prepregging of carbon fiber p 948 A90-50215

Mechanical influences on crystallization in PEEK matrix/carbon fiber reinforced composites p 949 A90-50227

Project, implementation, and utilization of composite structures [ETN-89-95209] p 127 N90-12665

Reinforcing fibers and technology development for resin composites. Consequences for aircraft structures [FOA-C-20777-2.5] p 876 N90-27883

CARBON MONOXIDE

Predicting the CO, HC, and NO(x) emission and combustion efficiency of small turbine engines from the combustion chamber bench test results p 125 A90-15425

CARBON STEELS

Improved steel for landing gear design [SAE PAPER 892335] p 765 A90-45490

CARBON-CARBON COMPOSITES

Carbon-carbon for NASP p 599 A90-36672

Performance evaluations of oxidation-resistant carbon-carbon composites in simulated hypersonic vehicle environments p 874 A90-48131

Chemical vapor deposition of Hf/Si compounds as a high temperature coating for carbon/carbon composites p 955 A90-50159

Carbon-carbon composites: Emerging materials for hypersonic flight [NASA-TM-103472] p 767 N90-26080

NASA Langley Research Center National Aero-Space Plane Mission simulation profile sets [NASA-TM-102670] p 924 N90-28541

CARBONIZATION

The changes of structures and properties in PAN-based carbon fibers during heat treatment in carbon dioxide p 945 A90-50145

CARGO

New aircraft cabin and cargo flammability standards for transport category aircraft p 325 N90-17589

CARGO AIRCRAFT

Thick-wing spanloader all-freighter - A design concept for tomorrow's air cargo [AIAA PAPER 90-3198] p 834 A90-48831

Design of a spanloader cargo aircraft [NASA-CR-186046] p 184 N90-14216

CARRIAGES

The integration of stores on modern tactical aircraft: Where we have been, and what we should do for the future p 337 N90-17552

CARRIER FREQUENCIES

Processing of undifferenced GPS carrier beat phase measurements and adjustment computations [TR-5-1988] p 178 N90-13368

CARTESIAN COORDINATES

Full-potential calculations using Cartesian grids p 86 A90-15740

- A numerical method for solving transonic flow past aircraft in Cartesian coordinates
[NAL-TR-1008] p 18 A90-10003
- CASCADE FLOW**
- Calculation of three-dimensional turbulent flow in a linear turbine cascade
[ONERA, TP NO. 1989-115] p 3 A90-11147
- Unsteady viscous calculation of cascade flows with leading-edge-induced separation
[ONERA, TP NO. 1989-116] p 3 A90-11148
- Unsteady aerodynamics and aeroelasticity of turbomachines and propellers; Proceedings of the Fourth International Symposium, Aachen, Federal Republic of Germany, Sept. 6-10, 1987 p 5 A90-11776
- The solution of the unsteady transonic flow through a blade passage in an axial turbine p 5 A90-11777
- Calculation of unsteady Euler flows in turbomachinery using the linearized Euler equations p 5 A90-11778
- Analysis of nonuniform subsonic flows about a row of moving blades p 6 A90-11779
- The effect of the magnitude of the inlet-boundary disturbance on the unsteady forces on axial gas-turbine blades p 6 A90-11781
- Unsteady 2D flow calculation in turbomachinery cascades p 6 A90-11782
- The influence of the wake structure on the dynamic blade load p 6 A90-11785
- Experimental investigation of the time-dependent flow in a vibrating annular cascade operating in the transonic flow regime p 7 A90-11787
- A numerical method solving 2-D unsteady flow field around cascade of oscillating airfoils with arbitrary camber and thickness p 7 A90-11788
- The unsteady aerodynamics of an oscillating cascade in a compressible flow field p 7 A90-11789
- Numerical investigation of unsteady compressible flow through nozzles and cascades p 7 A90-11790
- Unsteady aerodynamic characteristics of oscillating cascade with tip clearance p 8 A90-11793
- Progress towards the development of an inviscid-viscous interaction method for unsteady flows in turbomachinery cascades p 8 A90-11806
- Computation of unsteady compressible turbulent boundary layers in cascade flow with controlled inlet perturbation p 8 A90-11807
- Finite element method for unsteady three-dimensional subsonic flows through a cascade oscillating with steady loading p 9 A90-11873
- Numerical calculation of unsteady aerodynamic forces for three-dimensional subsonic oscillating cascades by a finite element method p 9 A90-12219
- Numerical calculation of unsteady aerodynamic forces for two-dimensional supersonic oscillating cascades by finite element method p 9 A90-12238
- Evaluation of two numerical techniques for the prediction of flow around blades p 10 A90-12512
- Studies on the influence of Mach number on profile losses of a reaction turbine cascade p 10 A90-12517
- Influence of blade leaning on the flow field behind turbine rectangular cascades with different incidences and aspect ratios p 11 A90-12519
- An experimental investigation of the effect of incidence on the two-dimensional performance of an axial turbine cascade p 11 A90-12520
- The interaction between tip clearance flow and the passage flowfield in an axial compressor cascade p 11 A90-12525
- The development of an exact conservative scheme associated with the supersonic trailing edge separation modelling for the computation of the transonic 2D cascade p 12 A90-12551
- Computation of three dimensional turbulent boundary layers in internal flows, including turbomachinery rotor blades p 12 A90-12555
- Experimental investigation of the transonic centrifugal compressor inducer straight cascades p 13 A90-12592
- Computation of transonic turbine cascade flow using Navier-Stokes equations p 14 A90-12621
- A solution adaptive finite element method applied to two-dimensional unsteady viscous compressible cascade flow p 15 A90-12624
- PCISM method for two dimensional compressible viscous cascade flow calculation p 15 A90-12625
- Application of the double linearization theory to three-dimensional subsonic and supersonic cascade flutter p 50 A90-12638
- Experimental investigations of effects of the stagger angle on secondary flows in plane compressor cascades p 83 A90-13787
- Construction of a straight single-row airfoil lattice by the method of quasi-solutions for inverse boundary value problems p 84 A90-14564
- Three-dimensional aerodynamics of an annular airfoil cascade including loading effects p 87 A90-15889
- Theoretical prediction of high Reynolds number viscid/inviscid interaction phenomena in cascades p 145 A90-16759
- An approach for calculating steady subsonic and transonic blade to blade flows p 152 A90-17784
- Computation of transonic flow in a plane cascade with an unfactored flux splitting implicit method p 152 A90-17785
- A relaxation method for transonic potential flows through 2-D cascade with large camber angle p 152 A90-17786
- Experimental investigation on the performance of an annular nozzle cascade of a highly-loaded transonic turbine stage p 152 A90-17787
- Secondary flows in a transonic cascade - Comparison between experimental and numerical results p 157 A90-18501
- The experiments for gas turbine plane cascade in a shock tunnel p 160 A90-19441
- Unsteady incompressible aerodynamics and forced response of detuned blade rows p 191 A90-19805
- [AIAA PAPER 90-0340] p 191 A90-19805
- Calculation of the side-wall boundary layer in axial turbomachines, accounting for the internal flow near the blades p 225 A90-21595
- A finite element solution of unsteady two-dimensional flow in cascades p 226 A90-21946
- A study of the working process and losses in annular turbine nozzle cascades with a low contraction ratio p 254 A90-23407
- An experimental study of the gasdynamic characteristics of annular nozzle cascades with small flow exit angles p 255 A90-23409
- Inviscid cascade flow calculations using a multigrid method p 288 A90-23763
- [ASME PAPER 89-GT-22] p 288 A90-23763
- Overview on test cases for computation of internal flows in turbomachines p 288 A90-23772
- [ASME PAPER 89-GT-46] p 288 A90-23772
- Secondary loss generation in a linear cascade of high-turning turbine blades p 289 A90-23773
- [ASME PAPER 89-GT-47] p 289 A90-23773
- 3D Mean-Stream-Line Method - A new engineering approach to the inverse problem of 3D cascade p 289 A90-23774
- [ASME PAPER 89-GT-48] p 289 A90-23774
- Development of the tip-leakage flow downstream of a planar cascade of turbine blades - Vorticity field p 289 A90-23781
- [ASME PAPER 89-GT-55] p 289 A90-23781
- Tip leakage losses in a linear turbine cascade p 290 A90-23782
- [ASME PAPER 89-GT-56] p 290 A90-23782
- Inlet skew and the growth of secondary losses and vorticity in a turbine cascade p 290 A90-23788
- [ASME PAPER 89-GT-65] p 290 A90-23788
- Application of low-solidity cascade diffuser to transonic centrifugal compressor p 290 A90-23789
- [ASME PAPER 89-GT-66] p 290 A90-23789
- Mach number effects on secondary flow development downstream of a turbine cascade p 290 A90-23790
- [ASME PAPER 89-GT-67] p 290 A90-23790
- Three-dimensional separated flow field in the endwall region of an annular compressor cascade in the presence of rotor-stator interaction. II - Unsteady flow and pressure field p 291 A90-23798
- [ASME PAPER 89-GT-77] p 291 A90-23798
- Comparison of steady and unsteady secondary flows in a turbine stator cascade p 291 A90-23800
- [ASME PAPER 89-GT-79] p 291 A90-23800
- Viscous flow in a controlled diffusion compressor cascade with increasing incidence p 291 A90-23829
- [ASME PAPER 89-GT-131] p 291 A90-23829
- Aerodynamics of cooling jets introduced in the secondary flow of a low speed turbine cascade p 362 A90-23868
- [ASME PAPER 89-GT-192] p 362 A90-23868
- The effect of uniform spanwise vorticity on the two-dimensional flow through cascades p 293 A90-23996
- Investigation of the flow structure behind the rotating blades in the elbow of a wind tunnel in the case of acoustic excitation p 297 A90-24124
- Navier-Stokes study of rotating stall in compressor cascades p 302 A90-25292
- Numerical methods for transonic cascade flow problems p 305 A90-25796
- A numerical method for solving the unsteady compressible Navier-Stokes equations p 306 A90-25827
- C-grid generation for turbomachinery cascades p 312 A90-26554
- Time domain flutter analysis of cascades using a full-potential solver p 391 A90-29374
- [AIAA PAPER 90-0984] p 391 A90-29374
- Computational prediction of stall flutter in cascaded airfoils p 392 A90-29388
- [AIAA PAPER 90-1116] p 392 A90-29388
- Aeroelastic problems in turbomachines p 393 A90-29393
- [AIAA PAPER 90-1157] p 393 A90-29393
- A calculation of the aerodynamic lift acting on cascade blades in a steady, viscous flow at high Reynolds number p 469 A90-32425
- The influence of boundary layer state on vortex shedding from flat plates and turbine cascades p 474 A90-33560
- [ASME PAPER 89-GT-296] p 474 A90-33560
- The trailing edge loss of transonic turbine blades p 475 A90-33564
- [ASME PAPER 89-GT-278] p 475 A90-33564
- Estimation of losses in semi-open centrifugal impellers p 537 A90-33597
- An investigation of the flow characteristics of transonic nozzle blades p 475 A90-33700
- Boundary element method for solving direct aerodynamic problem of aerofoil cascades on an arbitrary stream surface of revolution p 554 A90-35830
- Unsteady transonic cascade flow with in-passage shock wave p 556 A90-36281
- Calculation of two- and three-dimensional flow in a transonic turbine cascade with particular regard to the losses p 565 A90-38686
- [AIAA PAPER 90-1542] p 565 A90-38686
- Calculation of unsteady rotor/stator interaction p 565 A90-38688
- [AIAA PAPER 90-1544] p 565 A90-38688
- Simulation of inviscid blade-row interaction using a linearized potential code p 621 A90-40555
- [AIAA PAPER 90-1916] p 621 A90-40555
- Three-component LDA measurements in an axial-flow compressor p 683 A90-40943
- Viscous-inviscid interaction method for calculating the flow in compressor cascade blade passages and wake with separation p 624 A90-42032
- [AIAA PAPER 90-2125] p 624 A90-42032
- Inviscid and viscous flows in transonic and supersonic cascades using an implicit upwind relaxation algorithm p 625 A90-42034
- [AIAA PAPER 90-2128] p 625 A90-42034
- Application of 3-D Navier-Stokes computation to bowed stacking turbine vane design p 625 A90-42035
- [AIAA PAPER 90-2129] p 625 A90-42035
- Boundary-layer transition and separation on a turbine blade in a plane cascade p 625 A90-42102
- [AIAA PAPER 90-2263] p 625 A90-42102
- Flow induced forced response of an incompressible radial cascade including profile and incidence effects p 626 A90-42136
- [AIAA PAPER 90-2352] p 626 A90-42136
- Linearized unsteady aerodynamics for turbomachinery aeroelastic applications p 626 A90-42137
- [AIAA PAPER 90-2355] p 626 A90-42137
- Investigation of unsteady flow through a transonic turbine stage. II - Data/prediction comparison for time-averaged and phase-resolved pressure data p 626 A90-42162
- [AIAA PAPER 90-2409] p 626 A90-42162
- Development of a robust calculation method for transonic viscous blade-to-blade flows p 703 A90-42671
- Computation of turbine flowfields with a Navier-Stokes code p 704 A90-42731
- [AIAA PAPER 90-2122] p 704 A90-42731
- Turbulent flow simulation of a three-dimensional turbine cascade p 704 A90-42732
- [AIAA PAPER 90-2124] p 704 A90-42732
- Analysis of transonic turbine rotor cascade flows using a finite-volume total variation diminishing (TVD) scheme p 704 A90-42733
- [AIAA PAPER 90-2127] p 704 A90-42733
- Effects of inlet turbulence scale on turbine blade surface heat transfer in a linear cascade p 768 A90-42761
- [AIAA PAPER 90-2264] p 768 A90-42761
- Compressor aerodynamics --- Book p 706 A90-44052
- Numerical solution of 2D transonic flows in a turbine cascade p 709 A90-44601
- Experimental investigation of turbulence in a supersonic flow p 710 A90-44931
- Calculation of nonstationary forces in a three-row compressor cascade p 803 A90-46502
- Mean loading effects on flutter of subsonic rotating annular cascade p 853 A90-49453
- Variational formulation of 2-D unsteady transonic aerodynamics of oscillating cascades p 813 A90-49458
- Flow field around an oscillating cascade p 814 A90-49459
- Numerical simulation of transonic flow through oscillating and multi-row two-dimensional airfoil cascades p 814 A90-49460
- Noise generation by swept cascade p 895 A90-49486
- Cascade aerodynamic gust response including steady loading effects p 904 A90-51006
- A comprehensive analysis of the viscous incompressible flow in quasi-three-dimensional aerofoil cascades p 905 A90-51028
- Unsteady lifting surface theory for a rotating cascade of swept blades p 906 A90-51259
- [ASME PAPER 89-GT-306] p 906 A90-51259

An application of topological analysis to studying the three-dimensional flow in cascades. I - Topological rules for skin-friction lines and section streamlines p 908 A90-52607

An investigation of characteristics of transonic and viscous flows for turbine cascades p 909 A90-52779

Unsteady Aerodynamic Phenomena in Turbomachines [AGARD-CP-468] p 425 N90-18405

Numerical investigation of unsteady flow in oscillating turbine and compressor cascades p 426 N90-18407

Unsteady viscous calculation method for cascades with leading edge induced separation p 426 N90-18408

Asymptotic analysis of transonic flow through oscillating cascades p 427 N90-18421

Experiments on the unsteady flow in a supersonic compressor stage p 427 N90-18422

Experimental investigation of the influence of rotor wakes on the development of the profile boundary layer and the performance of an annular compressor cascade p 427 N90-18425

Influence of friction and separation phenomena on the dynamic blade loading of transonic turbine cascades [MITT-88-04] p 428 N90-19235

A two-dimensional unsteady analysis for transonic and supersonic cascade flows p 480 N90-20955

A computational design method for shock free transonic cascades and airfoils p 501 N90-20986

An inverse method for the design of turbomachine blades p 511 N90-20988

Secondary flows and Reynolds stress distributions downstream of a turbine cascade at different expansion ratios p 512 N90-21015

An investigation of secondary flows in nozzle guide vanes p 512 N90-21016

Secondary flow in a turbine guide vane with low aspect ratio p 513 N90-21018

Measurement of the flow field in the blade passage and side-wall region of a plane turbine cascade p 513 N90-21019

Centrifugal impeller geometry and its influence on secondary flows p 513 N90-21020

Calculation of the three dimensional turbulent flow in a linear turbine blade p 513 N90-21021

Research on cascade secondary and tip-leakage flows: Periodicity and surface flow visualization p 514 N90-21026

Losses in the tip-leakage flow of a planar cascade of turbine blades p 514 N90-21027

Computational prediction and measurement of the flow in axial turbine cascades and stages p 514 N90-21028

The effect of secondary flow on the redistribution of the total temperature field downstream of a stationary turbine cascade p 515 N90-21033

Aerodynamics of a linear oscillating cascade [NASA-TM-103250] p 817 N90-27657

CASCADE WIND TUNNELS

Comparative cascade studies of some high diffusion compressor bladings p 15 A90-12637

Wake behaviour of a large deflection turbine rotor linear cascade p 157 A90-18481

Comparison of NACA 65, CDA, and tandem bladed cascades p 190 A90-18484

Experimental studies of 90 deg corner cascades in the National Full-Scale Aerodynamic Complex [AIAA PAPER 90-1622] p 307 A90-25935

CASE HISTORIES

The history of aviation engine development in the USSR and the 60th anniversary of CIAM p 783 A90-42828

The NASA experience in aeronautical R and D: Three case studies with analysis [AD-A211486] p 82 N90-12496

CASES (CONTAINERS)

Casing vibration and gas turbine operating conditions [ASME PAPER 89-GT-78] p 358 A90-23799

CASING

An analysis of cavity resonance in the aeroengine casing during rig testing p 894 A90-49481

CAST ALLOYS

Metallurgy of investment cast superalloy components p 531 A90-34154

Investment-cast superalloys a good investment p 949 A90-51198

Constitutive modeling for isotropic materials (HOST) [NASA-CR-179522] p 193 N90-13390

Constitutive modeling for isotropic materials (HOST) [NASA-CR-174718] p 193 N90-13391

CASTING

Characterization of the CP 214 T851. Dissection of a cast flat bar for a standard spar [CEAT-PV-M4/462200] p 876 N90-27905

Characterization of the 7175 T7352. Dissection of a die casting standard spar [CEAT-PV-M5/528900] p 877 N90-27906

Characterization of the 7175 T7352 101. Dissection of a die casting standard spar [CEAT-PV-M5/5288] p 877 N90-27907

Characterization of the 7010 T73651. Dissection of a sheet billet for a standard spar [CEAT-PV-M5/521700] p 877 N90-27908

CASTINGS

Castings Airworthiness [AGARD-R-762] p 64 N90-10231

Casting factors imposed by the French regulation for foundry castings used in military aircraft p 64 N90-10233

Casting airworthiness joint European civil authorities view-point p 64 N90-10234

Royal Aerospace Establishment: No place for a castings factor p 64 N90-10235

The question of the casting factor p 64 N90-10238

Combined advanced foundry and quality control techniques to enhance reliability of castings for the aerospace industry p 64 N90-10240

Thin walled cast high-strength structural parts p 65 N90-10242

Defects in monoblock cast turbine wheels p 443 N90-18400

CATALYSIS

Effects of thermochemistry, nonequilibrium, and surface catalysis on the design of hypersonic vehicles p 224 A90-21159

CATALYSTS

Catalytic conversion of oil in bleed air - A maintenance tool [SAE PAPER 892214] p 732 A90-45431

Production of high density aviation fuels via novel zeolite catalyst routes [AD-A216444] p 443 N90-18601

CATASTROPHE THEORY

A study of the control technique for aircraft spin recovery p 590 A90-37226

CATHODE RAY TUBES

New technology advances for brighter color CRT displays p 652 A90-40399

Characteristics of 5x5 and 6x6 inch flat shadow mask CRTs for cockpit displays p 737 A90-45239

The interaction of chromostereopsis and stereopsis in stereoscopic CRT (Cathode Ray Tubes) displays [AD-A217906] p 927 N90-28544

CAUCHY INTEGRAL FORMULA

Complex variable boundary element method for external potential flows [AIAA PAPER 90-0127] p 162 A90-19694

CAVITATION FLOW

Numerical calculation of bubbly two phase flow around an airfoil p 304 A90-25783

Measurements in a separation bubble on an airfoil using laser velocimetry p 384 A90-27977

An investigation of end-wall vortex cavitation in a high Reynolds number axial-flow pump [AD-A211426] p 133 N90-11982

Noise from tip vortex and bubble cavitation [AD-A221962] p 896 N90-27468

CAVITIES

Pressure pulsation in a cavity in the path of subsonic and supersonic gas flow p 10 A90-12279

Experimental investigation into the effects of rotating and static bolts on both windage heating and local heat transfer coefficients in a rotor/stator cavity [ASME PAPER 89-GT-196] p 362 A90-23870

Visualization studies in rotating disk cavity flows p 475 A90-33568

An experimental investigation of supersonic flow over two cavities in tandem [AIAA PAPER 90-3087] p 795 A90-45901

Experimental investigation to suppress flow-induced pressure oscillations in open cavities [AD-A216285] p 320 N90-17578

Fluctuating wind forces measured on a bluff body extending from a cavity [AD-A216414] p 371 N90-18020

Passive venting technique for shallow cavities [NASA-CASE-LAR-14031-1] p 499 N90-20079

Problems of internal acoustics in two and three dimensional cavities with deformable walls using the MSC/Nastran code [DLC/STR-INT-TN-004] p 699 N90-24876

Cavity aeroacoustics [AD-A223853] p 911 N90-29307

CAVITY RESONATORS

An analysis of cavity resonance in the aeroengine casing during rig testing p 894 A90-49481

CEMENTS

Criteria for polymer concrete on airport pavements [DOT/FAA/DS-89/18] p 527 N90-21045

Development and testing of rapid repair methods for war damaged runways [AD-A223970] p 938 N90-28586

CENSUS

Census of US civil aircraft [PB90-120296] p 468 N90-20920

CENTER OF GRAVITY

The computer aided weight engineering of aircraft - (CAWE) system p 179 A90-16860

CENTER OF MASS

A study of the errors of a gyroscopic instrument for measuring linear accelerations p 771 A90-45133

CENTERBODIES

Experimental investigation of coannular jet flow with swirl along a centerbody [AIAA PAPER 90-1622] p 567 A90-38751

CENTRAL PROCESSING UNITS

Concurrent processing adaptation of aeroplastic analysis of propfans [NASA-TM-102455] p 215 N90-14656

CENTRIFUGAL COMPRESSORS

Acoustic resonance in centrifugal compressors induced by interaction between rotor and stator p 78 A90-11803

Experimental investigation of the transonic centrifugal compressor inducer straight cascades p 13 A90-12592

Two-stage two-spool experimental centrifugal compressor investigation p 49 A90-12593

A secondary flow calculation method for one stage centrifugal compressor p 14 A90-12597

Unsteady flow in centrifugal compressors due to downstream circumferential distortions p 14 A90-12598

Effect of environmental particles on a radial compressor p 113 A90-16373

Effect of downstream elements on the flow at the exit of centrifugal compressor rotor p 157 A90-18483

Analysis of blade loadings in centrifugal compressors p 158 A90-18591

Experimental and theoretical study of the swirling flow in centrifugal compressor volutes [ASME PAPER 89-GT-183] p 273 A90-22663

Application of low-solidity cascade diffuser to transonic centrifugal compressor [ASME PAPER 89-GT-66] p 290 A90-23789

An approximate 3-D aerodynamic design method for centrifugal impeller blades [ASME PAPER 89-GT-73] p 291 A90-23794

Effect of blade tip configuration on tip clearance loss of a centrifugal impeller [ASME PAPER 89-GT-80] p 358 A90-23801

Secondary flow due to the tip clearance at the exit of centrifugal impellers [ASME PAPER 89-GT-81] p 358 A90-23802

Dual pressure ratio compressor [ASME PAPER 89-GT-121] p 341 A90-23820

Laser transit anemometry investigation of a high speed centrifugal compressor [ASME PAPER 89-GT-155] p 360 A90-23843

A new design method for centrifugal compressor vaned diffusers [ASME PAPER 89-GT-156] p 292 A90-23844

A method of predicting the energy losses in vaneless diffusers of centrifugal compressors [ASME PAPER 89-GT-158] p 292 A90-23846

Mathematical formulation of blade surfaces in turbomachinery. I - Theoretical surface formulations [ASME PAPER 89-GT-160] p 360 A90-23848

Mathematical formulation of blade surfaces in turbomachinery. II - Practical examples of determined surfaces [ASME PAPER 89-GT-161] p 361 A90-23849

The influence of diffuser vane leading edge geometry on the performance of a centrifugal compressor [ASME PAPER 89-GT-163] p 292 A90-23851

Estimation of losses in semi-open centrifugal impellers p 537 A90-33597

An experimental investigation of rotating stall in a centrifugal compressor with vaneless diffuser p 621 A90-40513

Correlation of radial-to-axial vaneless turns for centrifugal compressors [AIAA PAPER 90-1917] p 656 A90-40556

Characterization of helicopter turboshaft engine noise p 660 A90-41759

Computation of flow through a centrifugal impeller with tip leakage [AIAA PAPER 90-2021] p 684 A90-41987

Advanced analysis of multi-ring liquid seals p 880 A90-46236

The survivability of centrifugal compressors in modern aircraft engines p 928 A90-49883

Flow in a forward swept centrifugal fan, volumes 1 and 2 p 481 N90-20959

CENTRIFUGAL FORCE

Computation of three dimensional turbulent boundary layers in internal flows, including turbomachinery rotor blades p 12 A90-12555

- Theoretical modelling of composite rotating beams
p 208 A90-17684
- Optimum design of rotational wheels under transient thermal and centrifugal loading
p 270 A90-20770
- CENTRIFUGAL PUMPS**
- Numerical study of centrifugal impeller response to an outlet pressure distortion
p 68 A90-11804
- Experimental investigations on the spatial and time-dependent structure of part-load recirculations in centrifugal pumps
p 83 A90-13788
- CERAMIC COATINGS**
- Thermal barrier characteristics of partially stabilized zirconia coatings on Incoloy alloy 909 (A controlled expansion alloy)
[ASME PAPER 89-GT-146]
p 354 A90-23839
- Ceramic materials and coatings for future aerospace applications - Challenge of the 1990's
p 942 A90-50071
- Chemical vapor deposition of Hf/Si compounds as a high temperature coating for carbon/carbon composites
p 955 A90-50159
- CERAMIC FIBERS**
- Ceramic materials and coatings for future aerospace applications - Challenge of the 1990's
p 942 A90-50071
- High temperature deformation studies on CVD silicon carbide fibers
p 945 A90-50147
- CERAMIC MATRIX COMPOSITES**
- Analysis of whisker-toughened ceramic components - A design engineer's viewpoint
p 205 A90-19149
- Noninteractive macroscopic reliability model for ceramic matrix composites with orthotropic material symmetry
[ASME PAPER 89-GT-129]
p 360 A90-23827
- A review of failure models for ceramic matrix composite laminates under monotonic loads
[ASME PAPER 89-GT-153]
p 354 A90-23842
- Engineering design of tough ceramic matrix composites for turbine components
[ASME PAPER 89-GT-294]
p 343 A90-23892
- Industry turns to ceramic composites
p 356 A90-27597
- Analysis and practical design of ceramic-matrix composite components
p 445 A90-28135
- Development of monolithic and composite ceramics at Allied-Signal Aerospace Company
p 599 A90-35950
- Glass-ceramic matrix composites for advanced gas turbines
[AIAA PAPER 90-2014]
p 676 A90-40594
- Composites applications - The future is now
p 678 A90-42372
- The application of engineering ceramics in gas turbines
[PNR90676]
p 750 N90-26005
- CERAMICS**
- Ceramic heat exchangers in gas turbine
[ONERA, TP NO. 1989-109]
p 40 A90-11142
- Thermal/structural analyses of several hydrogen-cooled leading-edge concepts for hypersonic flight vehicles
[AIAA PAPER 90-0053]
p 274 A90-23702
- Current status of ceramic gas turbine R&D in Japan
[ASME PAPER 89-GT-114]
p 359 A90-23818
- Advanced turbine technology applications project (ATTAP) - Overview, status, and outlook
[ASME PAPER 89-GT-118]
p 360 A90-23819
- Injection molding development of ceramic turbine components
[ASME PAPER 89-GT-170]
p 361 A90-23855
- Reliability evaluation system for ceramic gas turbine components
p 444 A90-27678
- High-temperature corrosion and mechanical properties of some silicon nitride ceramics
p 531 A90-33985
- Probabilistic design technology for ceramic components
p 601 A90-35507
- The role of NDE in ceramic turbine engine component development
p 601 A90-35508
- MRS International Meeting on Advanced Materials, 1st, Tokyo, Japan, May 31-June 3, 1988, Proceedings. Volume 5 - Structural ceramics/Fracture mechanics
p 599 A90-35926
- Development of monolithic and composite ceramics at Allied-Signal Aerospace Company
p 599 A90-35950
- Development of ceramic components for high-temperature gas turbines
p 602 A90-35951
- Development of impact design methods for ceramic gas turbine components
[AIAA PAPER 90-2413]
p 687 A90-42165
- Slip-cast hot isostatically pressed silicon nitride gas turbine components
p 765 A90-44816
- Fast start ceramic auxiliary power unit
[SAE PAPER 89-2254]
p 747 A90-45456
- Advanced Turbine Technology Applications Project (ATTAP)
[NASA-CR-185133]
p 51 N90-10036
- Improved silicon carbide for advanced heat engines
[NASA-CR-180831]
p 65 N90-10293
- Development of an advanced fan blade containment system
[DOT/FAA/CT-89/20]
p 192 N90-13386
- Thermal barrier coatings for gas turbine and diesel engines
[NASA-TM-102408]
p 205 N90-13636
- Advanced Turbine Technology Applications Project (ATTAP)
[NASA-CR-185109]
p 220 N90-14153
- Thermal/structural analyses of several hydrogen-cooled leading-edge concepts for hypersonic flight vehicles
[NASA-TM-102391]
p 215 N90-14511
- Summary report of the Summer Conference of the DARPA-Materials Research Council
[AD-A217380]
p 532 N90-20143
- Processing of advanced ceramics which have potential for use in gas turbine aero engines
[AD-A220988]
p 766 N90-25226
- Towards 2000: The composite engine
[PNR90646]
p 750 N90-26000
- Energy efficient engine pin fin and ceramic composite segmented liner combustor sector rig test report
[NASA-CR-179534]
p 932 N90-28567
- CERMETS**
- Composite matrix cooling scheme for small gas turbine combustors
[AIAA PAPER 90-2158]
p 852 A90-47210
- CERTIFICATION**
- A flight test investigation of certification requirements for laminar-flow general aviation airplanes
[AIAA PAPER 90-1310]
p 496 A90-33920
- Certification testing methodology for fighter hybrid structure
p 642 A90-40128
- A new noise certification method for 'light propeller aircraft' in testing
p 635 A90-41728
- Certification of composites for commercial aircraft
[SAE PAPER 89-212]
p 772 A90-45430
- Royal Aerospace Establishment: No place for a castings factor
p 64 N90-10235
- CF 18 480 Gallon External Fuel Tank Stores Clearance Program
p 35 N90-10877
- Integral fuel tank certification and test methods
p 251 N90-15916
- Software verification plan for GCS --- guidance and control software
[NASA-TM-101668]
p 372 N90-18057
- Sole means navigation and integrity through hybrid Loran-C and NAVSTAR GPS
p 489 N90-20933
- Brake performance of the McDonnell Douglas DC-10-30/40 during high speed, high energy rejected takeoffs
[PB90-917004]
p 503 N90-21000
- The role of NDI in the certification of turbine engine components
[PNR90629]
p 777 N90-26349
- The role of NDI in the certification of turbine engine components
p 859 N90-28069
- An analysis of GPS as the sole means navigation system in US Navy aircraft
p 917 N90-29350
- CESSNA AIRCRAFT**
- Laminar flow: The Cessna perspective
p 91 N90-12507
- CH-47 HELICOPTER**
- A rule-based paradigm for intelligent adaptive flight control
p 434 N90-19238
- CHANNEL CAPACITY**
- Feasibility of using frequency offset on very high frequency air/ground voice channels
[DOT/FAA/CT-TN89/71]
p 542 N90-21248
- Throughput and delay characteristics for a slow-frequency hopped aircraft-to-aircraft packet radio network
[AD-A220525]
p 688 N90-23609
- CHANNEL FLOW**
- Computation of laminar mixed convection flow in a channel with wing type built-in obstacles
p 67 A90-11114
- Variable-velocity flow at the initial mixing section in a diffuser channel
p 84 A90-14563
- Determination of the effective areas of the mixing exhaust ducts of a bypass engine from autonomous test results
p 102 A90-14584
- Studies on supersonic radial flow behavior in disk channel
p 87 A90-16104
- Self-excited oscillation of transonic flow around an airfoil in two-dimensional channel
[ASME PAPER 89-GT-58]
p 290 A90-23784
- Pressure loss and heat transfer in channels roughened on two opposed walls
[ASME PAPER 89-GT-86]
p 358 A90-23805
- Effect of rib-angle orientation on local mass transfer distribution in a three-pass rib-roughened channel
[ASME PAPER 89-GT-98]
p 359 A90-23812
- Local convection heat transfer on a plane wall in the vicinity of strong streamwise accelerations
p 535 A90-32174
- A laser based computer aided non-intrusive technique for full field flow characterization in macroscopic curved channels
p 535 A90-32293
- Development of a new low-Reynolds-number type Reynolds stress model and its application to a lobe mixer flow --- to improve thrust efficiency and suppress jet noise in turbofan engines
p 584 A90-35229
- Experimental investigation of GDL diffusers
[AIAA PAPER 90-1512]
p 563 A90-38659
- Navier-Stokes computations of three-dimensional laminar flows with buoyancy in a channel with wing-type vortex generators
p 772 A90-45728
- Carrier wing profile in nonstationary current
[ETN-90-95368]
p 399 N90-19208
- CHANNELS (DATA TRANSMISSION)**
- Studies in automatic speech recognition and its application in aerospace
p 958 N90-28759
- CHAOS**
- Chaotic response of aerosurfaces with structural nonlinearities (Status report)
[AIAA PAPER 90-1034]
p 392 A90-29378
- Transition from order to chaos in the wake of an airfoil
p 474 A90-33506
- An introduction to chaos theory in CFD
[AIAA PAPER 90-1440]
p 680 A90-39725
- CHAPLYGIN EQUATION**
- Solution of sonic flow problems
p 470 A90-32712
- Calculation of nonseparated flow past a wing profile at large Reynolds numbers
p 706 A90-42995
- CHARACTERISTICS**
- Fabrication characteristics of 8090 alloy
p 268 N90-15198
- CHARACTERIZATION**
- Choice and characterization of new materials for aerospace applications
[ETN-89-95219]
p 126 N90-11819
- Characterization of chemicals on engine exhaust particles
[AD-A213566]
p 256 N90-15106
- Characterisation of fatigue of aluminium alloys by acoustic emission. Part 2: Discrimination between primary and other emissions
[AERE-R-13303-PT-2]
p 678 N90-23523
- Radiation-curable prepreg composites
[DE90-629740]
p 951 N90-28674
- CHARGE COUPLED DEVICES**
- A daylight stellar sensor using a charge-coupled device
p 637 A90-39002
- Optoelectronic guidance sensors (5th revised and enlarged edition) --- Russian book
p 881 A90-46620
- CHARGE FLOW DEVICES**
- Requirements in the 1990's for high enthalpy ground test facilities for CFD validation
[AIAA PAPER 90-1401]
p 597 A90-38489
- CHEBYSHEV APPROXIMATION**
- Spectral simulation of unsteady compressible flow past a circular cylinder
[NASA-CR-182030]
p 478 N90-20050
- CHECKOUT**
- A review of the V-22 health monitoring system
p 417 A90-28209
- The US National Transonic Facility, NTF
p 262 N90-15942
- CHEMICAL ANALYSIS**
- HPLC analysis of helicopter rotor blade materials
[AD-A221121]
p 650 N90-24270
- CHEMICAL BONDS**
- The 1-((diorganoxyphosphonyl)-methyl)-2,4- and -2,6-diamido benzenes
[NASA-CASE-ARC-11425-4]
p 532 N90-20133
- CHEMICAL COMPOSITION**
- Influence of fuel composition on flame radiation in gas turbine combustors
p 659 A90-40946
- Thermal stability of jet fuel
[DE90-002760]
p 269 N90-15288
- HPLC analysis of helicopter rotor blade materials
[AD-A221121]
p 650 N90-24270
- CHEMICAL ENERGY**
- Acoustic-vortex-chemical interactions in an idealized ramjet
p 54 N90-10206
- CHEMICAL LASERS**
- Experimental investigation of a chemical laser cavity flowfield
[AD-A216398]
p 372 N90-18038
- CHEMICAL PROPERTIES**
- Mechanical considerations for reliable interfaces in next generation electronics packaging
p 453 A90-30813
- Poly(arylene ether ketone)/poly(aryl imide) homo- and polydimethylsiloxane segmented copolymer blends - Influence of chemical structure on miscibility and physical property behavior
p 941 A90-50063
- Chemical resistance of carbon fiber reinforced polyether ether ketone and polyphenylene sulfide composites
p 944 A90-50142
- Spray sealing: A breakthrough in integral fuel tank sealing technology
p 276 A90-15912

CHEMICAL REACTIONS

- Balance model of the perfectly stirred reactor with the discontinuity surface p 125 A90-14652
- Numerical study of chemically reacting flows using a lower-upper symmetric successive overrelaxation scheme p 153 A90-17989
- A three-dimensional upwind parabolized Navier-Stokes code for chemically reacting flows [AIAA PAPER 90-0394] p 165 A90-19831
- Full scale study of a cabin fire in an A300 fuselage section p 326 A90-17592
- Modification and improvement of software for modeling multidimensional reacting fuel flows [AD-A217789] p 533 A90-20235
- Computation of nonequilibrium chemically reacting flows in hypersonic flow field p 480 A90-20954
- Supersonic combustor modeling p 749 A90-25992

CHEMICAL REACTORS

- Balance model of the perfectly stirred reactor with the discontinuity surface p 125 A90-14652

CHIPS (ELECTRONICS)

- Integrated circuits for avionics [AD-A217964] p 540 A90-20312
- An experimental study of fault propagation in a jet-engine controller [NASA-CR-181335] p 665 A90-23401
- Miniaturization of flight deflection measurement system [NASA-CASE-LAR-13628-1] p 689 A90-23707
- Comparative evaluation of Allison T56 engine chip detectors [AD-A221864] p 855 A90-26832

CHIRP

- Direct frequency modulation in interferometric systems p 68 A90-11662

CHLORINE COMPOUNDS

- Effects on aerospace alloys of residual chlorine in chlorinated-solvent primers p 956 A90-50187

CHLORINE FLUORIDES

- Nonflammable hydraulic power system for tactical aircraft. Volume 1: Aircraft system definition, design and analysis [AD-A218493] p 671 A90-23409

CHOLESKY FACTORIZATION

- A parallel-vector algorithm for rapid structural analysis on high-performance computers [AIAA PAPER 90-1149] p 458 A90-29293

CHROMIUM STEELS

- Gear steels for future helicopter transmissions p 265 A90-20607

CIRCUIT BOARDS

- Correlation/validation of finite element code analyses for vibration assessment of avionic equipment [AD-A220393] p 654 A90-23398

CIRCUIT RELIABILITY

- Smart microsensors for high temperature applications, phase 1 [AD-A224151] p 959 A90-28828

CIRCUITS

- A parametric optimization algorithm for the electrical distribution circuits of civil aircraft p 255 A90-23417

CIRCULAR CONES

- Suppression of vortex asymmetry behind circular cones p 556 A90-36282

CIRCULAR CYLINDERS

- Separation shock dynamics in Mach 5 turbulent interactions induced by cylinders p 153 A90-17981
- The inviscid axisymmetric stability of the supersonic flow along a circular cylinder p 554 A90-35916
- Vorticity distribution of vortex street in the wake of a circular cylinder p 623 A90-41751
- Numerical modeling of transverse flow past a cylinder using Euler equations p 709 A90-44922
- Computation of hypersonic unsteady viscous flow over a cylinder p 397 A90-19194
- An experimental study of the aeroelastic behaviour of two parallel interfering circular cylinders p 455 A90-19609

- Spectral simulation of unsteady compressible flow past a circular cylinder [NASA-CR-182030] p 478 A90-20050

CIRCULAR TUBES

- A multipurpose aerodynamic research facility utilizing the abandoned Cincinnati subway tubes [AIAA PAPER 90-1424] p 596 A90-37961

CIRCULATION CONTROL AIRFOILS

- Method for calculating the unsteady flow of an elliptical circulation-control airfoil p 3 A90-11003
- Dynamic stall of circulation control airfoils [AIAA PAPER 90-0573] p 167 A90-19923
- Navier-Stokes methods to predict circulation control airfoil performance [AIAA PAPER 90-0574] p 167 A90-19924
- A finite element method for solving lifting airfoil in transonic flow p 226 A90-21984

- Higher harmonic and trim control of the X-wing circulation control wind tunnel model rotor p 435 A90-28156

- Circulation control tail boom aerodynamic prediction and validation p 385 A90-28243

- Active flow control on low Reynolds number airfoils [AIAA PAPER 90-3039] p 792 A90-45878
- Aeroelastic characteristics of aircraft with circulation control wings p 497 A90-20070

CIRCULATION CONTROL ROTORS

- Perspectives in aeromechanical stability of helicopter rotors p 831 A90-46953

CIRCULATION DISTRIBUTION

- Relationship between velocity circulation around a wing profile and vorticity dispersion in a boundary layer p 620 A90-39539
- Minimum induced drag for wings with spanwise camber p 709 A90-44733
- Optimum spanwise camber for minimum induced drag [BU-403] p 397 A90-18369
- The application of the finite element method to an aerodynamic problem specific to propeller design [LR-614] p 718 A90-25116

CIVIL AVIATION

- Eurofix p 25 A90-10239
- Recent cases and developments in aviation law p 79 A90-11393
- Coping with bomb threats to civil aviation p 23 A90-12781
- Aviation Security (Avsec) p 23 A90-12782
- A study of the limitations of linear theory methods as applied to sonic boom calculations [AIAA PAPER 90-0368] p 219 A90-19817
- Advanced technology rotorcraft - Civil short haul transport of the future p 246 A90-21710
- Potential applications of satellite navigation p 264 A90-21716
- Status and potential of GPS-receiver development p 265 A90-21717
- A parametric optimization algorithm for the electrical distribution circuits of civil aircraft p 255 A90-23417
- From the DC-3 to hypersonic flight - ICAO in a changing environment p 222 A90-23662
- The disadvantages of GPS - Comparative study of solutions adapted to civil aviation p 329 A90-23994
- Institutional stepping stones for FANS - Future Air Navigation Systems p 403 A90-27923
- Creditable commuter --- civil aircraft p 405 A90-27975

- Sting design feasibility for E.T.W. cryogenic civil transport aircraft p 524 A90-34245
- Tests of automatic dependent surveillance (ADS) in Western Europe - Possible future developments p 574 A90-35353
- Technological preparations of civil aircraft programs p 617 A90-41110
- Euromat - The European aviation research and technology program p 617 A90-41112
- Monitoring and maintenance of automatic control systems in aviation --- Russian book p 778 A90-42524

- Civil supersonics - A less distant thunder p 731 A90-44223

- More cruising levels expected at higher altitudes p 721 A90-44548

- Technology issues for high-speed civil transports [SAE PAPER 892201] p 778 A90-45422

- The economics of the organization and the planning of civil aviation --- Russian book p 897 A90-46629

- Recent developments in EEC aviation law - 'The second phase' p 897 A90-46648

- Commercial aircraft DOC methods [AIAA PAPER 90-3224] p 897 A90-48843

- Application of boundary layer control to HSCT low speed configuration [AIAA PAPER 90-3199] p 812 A90-49103

- Financing of civil aircraft - Purchases and leasing p 898 A90-49616

- U.S. deregulation - Evidence from ten years of experience p 898 A90-49619

- Anatomy of airline regulation - Towards a pluriform, plurilateral, pluralistic, flexible world-wide regulatory framework for air transport p 898 A90-49620

- Assuring the future of civil aircraft industry in Germany [DGLR PAPER 88-004] p 902 A90-50232

- Pursuit of the high-speed civil transport [AIAA PAPER 90-1814] p 919 A90-51450

- New methods of buffeting prediction on civil aircraft p 908 A90-52620

- Airport technology international 1989/1990 --- Book p 937 A90-52857

- Casting airworthiness joint European civil authorities view-point p 64 A90-10234

- Flight testing in the Netherlands: An overview p 36 A90-10884

- Simulated airline service experience with laminar-flow control leading-edge systems p 104 A90-12512

- Fine resolution errors in secondary surveillance radar altitude reporting amongst aircraft transmitting the conspicuity codes 4321 and 4322 [RSRE-88004] p 135 A90-12816

- Study of high-speed civil transports [NASA-CR-4235] p 183 A90-13370

- Aircraft accident report: Delta Air Lines, Inc., Boeing 727-232, N473DA, Dallas-Fort Worth International Airport, Texas, August 31, 1988 [PB89-910406] p 240 A90-15895

- Investigation and characteristics of major fire-related accidents in civil air transports over the past ten years p 324 A90-17582

- Aircraft fire safety: Learning from past accidents p 324 A90-17584

- Fire safety in civil aviation p 325 A90-17586

- Fire hardening of an aircraft passenger cabin p 328 A90-17606

- New materials for civil aircraft furnishing p 328 A90-17609

- Interoperability issues in the use of satellite-based navigation systems for civil aviation purposes [AD-A217279] p 405 A90-19223

- Census of US civil aircraft [PB90-120296] p 468 A90-20920

- Civil air transport: A fresh look at power-by-wire and fly-by-light [NASA-TM-102574] p 542 A90-21283

- Aerodynamic development perspective for traffic aeroplanes [DGLR-89-141] p 637 A90-24260

- The 30th Airlines International Electronics Meeting Proceedings [ETN-90-96973] p 637 A90-24261

- The effect of noise-abatement profiles on noise immissions and human annoyance underneath a subsequent climbpath p 698 A90-24865

- Study of high-speed civil transports. Summary [NASA-CR-4236] p 735 A90-25966

- Mobile satellite communications for civil aviation [NLR-MP-88066-U] p 775 A90-26238

- BASEOPS default profiles for civil aircraft [AD-A223161] p 844 A90-26825

- New features of JAL's ground station p 872 A90-27633

- Application of a company data link at Lufthansa German Airlines p 827 A90-27689

- High-speed civil transport study: Special factors [NASA-CR-181881] p 923 A90-28537

- GPS integrity requirements for use by civil aviation p 916 A90-29339

- Independent ground monitor coverage of Global Positioning System (GPS) satellites for use by civil aviation p 918 A90-29364

- CL-84 AIRCRAFT The Canadair CL-84 experimental aircraft - Lessons learned [AIAA PAPER 90-3205] p 834 A90-48833

- CLASSIFICATIONS The FAA technical classification of aircraft and airports p 96 A90-15876

- ICAO airfield reference code p 261 A90-21628

- Classification and reduction of pilot error [NASA-CR-181867] p 24 A90-10014

- Gas identification system using graded temperature sensor and neural net interpretation [AD-A213359] p 205 A90-13627

- Classification of windshear severity p 281 A90-15049

- Design and calibration of an in-stack, low-pressure impactor [AD-A213531] p 255 A90-15105

- CLEAR AIR TURBULENCE Analysis of severe atmospheric disturbances from airline flight records p 280 A90-15045

- CLEARANCES An experimental study of tip clearance effects on the performance of an axial transonic turbine p 189 A90-17788

- Effect of blade tip configuration on tip clearance loss of a centrifugal impeller [ASME PAPER 89-GT-80] p 358 A90-23801

- CF 18 480 Gallon External Fuel Tank Stores Clearance Program p 35 A90-10877

- Helicopter surface maneuvering test results [ACD-330] p 59 A90-10897

- Flutter clearance of the F-18 high-angle-of-attack research vehicle with experimental wingtip instrumentation pods [NASA-TM-4148] p 103 A90-11732

- An investigation of end-wall vortex cavitation in a high Reynolds number axial-flow pump [AD-A211426] p 133 A90-11982

- Dynamic tip clearance measurements in axial flow compressors [PNR90597] p 116 A90-12612

SUBJECT INDEX

- Assessment of worm gearing for helicopter transmissions
[NASA-TM-102441] p 257 N90-15923
- NASA/GE Energy Efficient Engine low pressure turbine scaled test vehicle performance report
[NASA-CR-168290] p 931 N90-28563
- ### CLIMBING FLIGHT
- Airplane takeoff and landing performance monitoring system
[NASA-CASE-LAR-13734-1-CU] p 526 N90-20096
- The SKY SHARK: An RPV designed to investigate the pressure distribution on a lifting surface
[NASA-CR-186222] p 844 N90-26824
- ### CLOCKS
- Real-time simulation clock
[NASA-CASE-LAR-14056-1] p 689 N90-23713
- ### CLOUD COVER
- Concept of an MTI search radar p 487 A90-33613
- Cloud-to-ground strikes to the NASA F-106 airplane p 574 A90-35767
- An automated method for predicting the height of the lower cloud boundary p 888 A90-48359
- Some characteristics of the meteorological conditions of low cloud formation around the Baku airport p 888 A90-48364
- ### CLOUD GLACIATION
- Using cloud moisture calculations for estimating aircraft icing p 888 A90-48358
- ### CLOUD PHYSICS
- Remote sensing techniques of the Wave Propagation Laboratory for the measurement of supercooled liquid water: Applications to aircraft icing
[PB89-208102] p 24 N90-10842
- The signals of an ice warning device in dependence on total water content and normalized icing degree
[ESA-TT-1207] p 963 N90-29692
- ### CLOUDS (METEOROLOGY)
- Performance of laminar-flow leading-edge test articles in cloud encounters p 104 N90-12511
- Mesoscale acid deposition modeling studies
[NASA-CR-4262] p 140 N90-13228
- Adverse weather operations during the Canadian Atlantic storms program p 281 N90-15052
- The signals of an ice warning device in dependence on total water content and normalized icing degree
[ESA-TT-1207] p 963 N90-29692
- ### CLUTTER
- A powerful range-Doppler clutter rejection strategy for navigational radars p 403 A90-30688
- Airborne early warning radar --- Book p 727 A90-45200
- Clutter rejection and transmitter-receiver requirements in an airborne radar p 738 A90-45354
- ASR-9 weather channel test report
[AD-A211749] p 133 N90-11934
- Adaptive clutter rejection filters for airborne Doppler weather radar applied to the detection of low altitude windshear p 214 N90-14453
- Synthetic aperture radar imagery of airports and surrounding areas: Archived SAR data
[NASA-CR-4275] p 401 N90-18371
- Synthetic aperture radar imagery of airports and surrounding areas: Philadelphia Airport
[NASA-CR-4280] p 401 N90-18372
- Synthetic aperture radar imagery of airports and surrounding areas: Denver Stapleton International Airport
[NASA-CR-4305] p 637 N90-24257
- ### COAL
- Criteria for coal tar seal coats on airport pavements. Volume 2: Laboratory and field studies
[AD-A220167] p 674 N90-24277
- ### COAL DERIVED LIQUIDS
- Production of jet fuels from coal-derived liquids. Volume 11: Production of advanced endothermic fuel blends from Great Plains Gasification Plant naphtha by-product stream
[AD-A210251] p 65 N90-11184
- Production of jet fuels from coal derived liquids. Volume 10: Jet fuels production by-products, utility, and sulfur emissions control integration study
[AD-A213872] p 357 N90-16951
- ### COAL GASIFICATION
- Production of jet fuels from coal-derived liquids. Volume 13: Evaluation of storage and thermal stability of jet fuels derived from coal liquids
[AD-A224576] p 954 N90-29527
- ### COALESCING
- Investigation of surface water behavior during glaze ice accretion p 485 N90-20927
- ### COANDA EFFECT
- Control of flow separation and mixing by aerodynamic excitation
[NASA-TM-103131] p 571 N90-21733

COLLISION AVOIDANCE

- Automatic speech recognition in air-ground data link p 690 N90-25037
- Toxicity of thermolysis products from the materials of airplane cockpits
[CEAT-PV-M6/5924/02] p 876 N90-27895
- The function of the Interactive Model Assembly Program (IMAP) for a flight simulator
[NAL-TR-1034] p 939 N90-29412
- ### COEFFICIENT OF FRICTION
- Effect of hydrogen combustion in a supersonic boundary layer on friction coefficient p 355 A90-24116
- Internal rotor friction instability
[NASA-CR-183942] p 543 N90-21395
- ### COGNITION
- Cognitive requirements for aircraft navigation
[NASA-CR-186933] p 824 N90-26804
- ### COHERENT RADAR
- Shadow-tracking algorithm for moving target detection p 488 A90-34137
- Simulation of airborne target imagery - Dependence on frequency and bistatic angle p 488 A90-34146
- ### COLD FLOW TESTS
- Swirling flow in thrust nozzles p 421 A90-27962
- Large-eddy simulations of flows in a ramjet combustor p 772 A90-45534
- Aerodynamic and heat transfer measurements on blading for a high rim-speed transonic turbine
[RAE-TM-P-1151] p 256 N90-15920
- ### COLD WEATHER
- Definition of research needs to address airport pavement distress in cold regions
[DOT/FAA/DS-89/13] p 59 N90-10896
- ### COLLISION AVOIDANCE
- Design philosophy for a general aviation TCAS display --- Traffic Advisory and Collision Avoidance System
[SAE PAPER 891052] p 108 A90-14354
- Air traffic control development at Lincoln Laboratory p 240 A90-21378
- TCAS - A system for preventing midair collisions p 252 A90-21383
- Modeling of air-to-air visual acquisition p 282 A90-21385
- TCAS - A lengthy but beneficial development effort p 339 A90-25494
- Development and operation of the Traffic Alert and Collision Avoidance System (TCAS) p 331 A90-25573
- Avoiding a maneuvering aircraft with TCAS --- Traffic Alert and Collision Avoidance System p 347 A90-26222
- TCAS for commuter aircraft p 487 A90-33348
- A surveillance 360 deg television orientation and ranging system as an aid to collision avoidance p 577 A90-36922
- Development of obstacle clearance criteria and standards for MLS and MLS/RNAV precision approaches and development of an MLS collision risk model
[SAE PAPER 892215] p 728 A90-45432
- Collision alert p 847 A90-48521
- Safer skies with TCAS: Traffic Alert and Collision Avoidance System p 27 N90-10016
- See and avoid/cockpit visibility p 24 N90-10843
- Test and evaluation: Reducing risks to military aircraft from bird collisions. Report to the Chairman, Legislation, and National Security Subcommittee, Committee on Government Operations, House of Representatives
[AD-A210670] p 25 N90-10845
- Ground and Obstacle Avoidance (GOA) concept of operations
[DOT/FAA/DS-89/08] p 28 N90-10855
- UK airmisses involving commercial air transport, May-August 1988 p 96 N90-11717
- UK airmisses involving commercial air transport
[CAA-2/88] p 96 N90-11718
- An update to the system safety study of TCAS 2
[DOT/FAA/SA-89/3] p 177 N90-13363
- See and avoid/cockpit visibility p 239 N90-15084
- The automatic detection of anti-collision lights
[RSRE-MEMO-4272] p 240 N90-15896
- UK airmisses involving commercial air transport, September to December 1988 p 240 N90-15897
- Development of an automatic ground collision avoidance system using a digital terrain database
[AD-A216247] p 329 N90-17621
- UK airmisses involving commercial air transport, January - April 1989 p 575 N90-22544
- Results of TCAS-2 simulations in reconstructed dangerous encounters (Jul. 1986 to Jun. 1989)
[ETN-90-96474] p 636 N90-23375
- Safety net functions p 826 N90-27685

COLLISION PARAMETERS

UK airmisses involving commercial air transport: May - August 1989
[ISSN-0951-6301] p 913 N90-29335

COLLISION PARAMETERS

Charging of aircraft - High-velocity collisions
p 322 A90-26131

COLLOCATION

Collocation methods and lifting-surfaces
p 9 A90-12023
Optimal solutions to flight mechanics problems using a Nonlinear Programming and Collocation technique
[AIAA PAPER 90-3415] p 889 A90-47669
A panel process for the calculation of the flow around a wing with front angle damping
[ETN-90-95367] p 399 N90-19207
A fast collocation method for transonic airfoil design
p 501 N90-20984

COLOR

New technology advances for brighter color CRT displays
p 652 A90-40399

COLOR PHOTOGRAPHY

Color schlieren system using square color filter and its application to aerofoil test in transonics
p 66 A90-10748

COLOR VISION

A new method for measuring the transmissivity of aircraft transparencies
[AD-A216953] p 464 N90-19842

COLOR-COLOR DIAGRAM

Performance of full color active-matrix-LCD in the cockpit environment
p 681 A90-40392

COMBAT

The Battle Captain Expert System - A mission management decision support system for attack helicopter operations
[AIAA PAPER 89-3098] p 37 A90-10583
Enhanced combat damage tolerance/supportability for improved combat sustainability
[SAE PAPER 891078] p 101 A90-14370
The effects of aerial combat on helicopter structural integrity
p 406 A90-28166
Air-to-Air Combat Test IV (AACT IV) and the AACT data base
p 381 A90-28169
The challenge of LHX --- composite materials in light military helicopters
p 382 A90-29641
Air combat beyond the stall
p 589 A90-35888
Preliminary flight evaluation of the SA 365 Panther helicopter in air-to-air combat manoeuvres
p 647 A90-42494
An experimental investigation of roll agility in air-to-air combat
[AIAA PAPER 90-2809] p 752 A90-45144
Near-term applications of knowledge based systems to combat helicopters
[AIAA PAPER 90-3301] p 847 A90-48883
Air Combat Environment Test and Evaluation Facility (ACETEF)
p 58 N90-10883
Evaluation of speech recognizers for use in advanced combat helicopter crew station research and development
[NASA-CR-177547] p 650 N90-24265
Time-optimal aircraft pursuit-evasion with a weapon envelope constraint
[NASA-CR-186640] p 734 N90-25126
Combat aircraft control requirements for agility
p 935 N90-28517
Counterair situation awareness display for Army aviation
p 964 N90-28982
The potential for digital databases in flight planning and flight aiding for combat aircraft
p 918 N90-29371

COMBINED STRESS

Theoretical modelling of composite rotating beams
p 208 A90-17684
Buckling analysis of FRP faced cylindrical sandwich panel under combined loading
p 365 A90-24376
A method for reducing a buckled skin under combined loading
p 860 A90-46571

COMBUSTIBLE FLOW

3D calculations of reacting flows within aircraft engine combustion chambers
[ONERA, TP NO. 1989-153] p 67 A90-11173
An experimental investigation of isothermal swirling flow in a model of a dump combustor
p 47 A90-12572
Numerical study of chemically reacting flows using a lower-upper symmetric successive overrelaxation scheme
p 153 A90-17989
Upwind adaptive finite element investigations of the two-dimensional reactive interaction of supersonic gaseous jets
p 209 A90-18264
Velocity and scalar measurements in model and real gas turbine combustors
p 191 A90-19005
Simultaneous CARS measurements of temperature and H₂, H₂O concentrations in hydrogen-fueled supersonic combustion
[AIAA PAPER 90-0158] p 205 A90-19713

Large-eddy simulations of combustion instability in an axisymmetric ramjet combustor
[AIAA PAPER 90-0267] p 191 A90-19764
Hydraulic analogy application in the study of a two-phase mixture combustion flow
[AIAA PAPER 90-0451] p 211 A90-19850
Numerical calculation of gaseous reacting flows in a model of gas turbine combustors
p 271 A90-21979
A numerical study of mixing enhancement in a supersonic combustor
[AIAA PAPER 90-0203] p 272 A90-22182
Chemically reacting supersonic flow calculation using an assumed PDF model
[AIAA PAPER 90-0731] p 230 A90-22256
Numerical study of three methods for solving reacting flows
p 305 A90-25804
Application of Lomax-Bailey implicit scheme to reactive flows
p 367 A90-25861
Inlet swirl effects on dump combustor flows
[AIAA PAPER 90-0035] p 312 A90-26904
Hypersonic reactive flow computations
p 315 A90-27131
Prediction of turbulent combustion flowfields behind a backward-facing step
p 529 A90-32952
Laser Doppler velocimetry investigation of swirler flowfields
p 682 A90-40929
Numerical analysis of the flows in annular slinger combustors
[AIAA PAPER 90-2164] p 685 A90-42052
Direct measurements of skin friction in a scramjet combustor
[AIAA PAPER 90-2342] p 626 A90-42132
Suppression of 'Buzz' instability by geometrical design of the flameholder
[AIAA PAPER 90-1966] p 741 A90-42706
Operation of the ram accelerator in the transdetonative velocity regime
[AIAA PAPER 90-1985] p 741 A90-42712
A computational investigation of flow losses in a supersonic combustor
[AIAA PAPER 90-2093] p 742 A90-42728
Mixing and combustion enhancement in supersonic reacting flows
p 744 A90-44410
Numerical simulation of flow through the Langley parametric scramjet engine
[SAE PAPER 892314] p 747 A90-45476
A planar reacting shear layer system for the study of fluid dynamics-combustion interaction
[NASA-TM-102422] p 194 N90-13393
Modification and improvement of software for modeling multidimensional reacting fuel flows
[AD-A217789] p 533 N90-20235
Subsonic combustor flow modeling: State of the art of CFD techniques for reacting and combustor flow
p 749 N90-25991

COMBUSTION

On the use of external burning to reduce aerospace vehicle transonic drag
[AIAA PAPER 90-1935] p 656 A90-40562
Analytical studies of three-dimensional combustion processes
[AD-A211903] p 126 N90-11837
Thermochemical calculations with inert compounds
[FOA-C-20759-2.1] p 206 N90-13677
Acoustic-vortical-combustion interaction in a solid fuel ramjet simulator
p 194 N90-14234
Full scale study of a cabin fire in an A300 fuselage section
p 326 N90-17592
Full-scale air transport category fuselage burnthrough tests
[DOT/FAA/CT-TN89/65] p 486 N90-20967
On the use of external burning to reduce aerospace vehicle transonic drag
[NASA-TM-103107] p 588 N90-21762
Supersonic reacting internal flow fields
[NASA-TM-103480] p 767 N90-26094
Modeling of supersonic reacting flow fields
p 855 N90-26898
The reduction of smoke emissions from Allison T56 engines
[ARL-PROP-R-182] p 928 N90-28547
Energy Efficient Engine combustor test hardware detailed design report
[NASA-CR-168301] p 929 N90-28554

COMBUSTION CHAMBERS

3D calculations of reacting flows within aircraft engine combustion chambers
[ONERA, TP NO. 1989-153] p 67 A90-11173
Similarity and scale effects in solid fuel ramjet combustors
p 60 A90-12513
Full-scale liquid fuel ramjet combustor tests
p 44 A90-12528
Hydrogen fueled subsonic-ram-combustor model tests for an air-turbo-ram engine
p 44 A90-12529

SUBJECT INDEX

Experimental study of static pressure and mean velocity profiles inside a two-dimensional dump-type combustor model
p 45 A90-12530
A study of two-phase flow for a ramjet combustor
p 45 A90-12532
Investigation and improvement of ground starting characteristics of a combustor with airblast nozzles
p 45 A90-12548
Controlled mixing and variable geometry combustor design effects on emissions and combustion characteristics
p 45 A90-12547
The performance of a small combustor operated over a wide range of conditions
p 45 A90-12548
Experimental study on autoignition in a scramjet combustor
p 46 A90-12559
Hypersonic combustion of hydrogen in a shock tunnel
p 46 A90-12560
The use of pulse facilities for testing supersonic combustion ramjet (scramjet) combustors in simulated hypersonic flight conditions
p 46 A90-12562
An experimental investigation of isothermal swirling flow in a model of a dump combustor
p 47 A90-12572
Effect of primary air swirl on emissions formations in gas turbine combustors
p 47 A90-12573
On the weak extinction of gas turbine combustors
p 47 A90-12574
Three dimensional numerical simulation for an aircraft engine type combustion chamber
[ONERA, TP NO. 1989-120] p 49 A90-12591
Numerical simulation of valveless pulsed combustors
p 127 A90-13767
Numerical modeling of the combustion kinetics of hydrocarbon fuels in an annular combustion chamber with allowance for the formation of harmful impurities
p 124 A90-14582
Exhaust emission performance of a vaporizer tube combustor as compared with a single tube combustor
p 111 A90-14614
A circular combustor configuration with multiple injection ports for mixing enhancement
p 130 A90-15389
Predicting the CO, HC, and NO(x) emission and combustion efficiency of small turbine engines from the combustion chamber bench test results
p 125 A90-15425
Advanced combustor liner cooling technology for gas turbines
p 112 A90-16004
Selection of a suitable combustion system for a small gas turbine engine
p 112 A90-16005
Calculation of flowfields in side-inlet ramjet combustors with an algebraic Reynolds stress model
p 87 A90-16367
Velocity and scalar measurements in model and real gas turbine combustors
p 191 A90-19005
Future test rigs
p 200 A90-19012
Active soot reduction in a spray-fired, axisymmetric model gas turbine combustor
[AIAA PAPER 90-0039] p 191 A90-19644
Numerical modeling of a flame in a confined, unstable shear layer
[AIAA PAPER 90-0647] p 205 A90-19966
Gas turbine combustion - A personal perspective
p 283 A90-20604
Numerical calculation of gaseous reacting flows in a model of gas turbine combustors
p 271 A90-21979
A numerical study of mixing enhancement in a supersonic combustor
[AIAA PAPER 90-0203] p 272 A90-22182
Mathematical model of turboprop engine behaviour
p 254 A90-23351
On-line temperature profile display system
[ASME PAPER 89-GT-10] p 374 A90-23755
Development of a dual fuel injector for a gas turbine combustor
[ASME PAPER 89-GT-25] p 340 A90-23764
Inlet swirl effects on dump combustor flows
[AIAA PAPER 90-0035] p 312 A90-26904
Experimental and theoretical investigations of turbulent flow in a side-inlet rectangular combustor
p 421 A90-27959
Small gas turbine using a second-generation pulse combustor
p 421 A90-27972
The effect of swirler on short reversal-flow annular combustor
p 423 A90-29906
Aerothermomechanical design of turbine-engine combustion chambers
p 424 A90-29922
A test facility for high-pressure high-temperature combustion chambers
p 438 A90-29924
A model gas turbine combustor with wall jets and optical access for turbulent mixing, fuel effects, and spray studies
p 507 A90-32808
Experimental studies of combustor dilution zone aerodynamics. I - Mean flowfields
p 508 A90-32962
Turbine combustor preliminary design approach
p 508 A90-32966
Influence of fuel drop size and combustor operating conditions on pollutant emissions
p 508 A90-33591

Heat transfer in a solid fuel ramjet combustor
[AIAA PAPER 90-1783] p 586 A90-38472

Experimental investigation of a supersonic swept ramp injector using laser-induced iodine fluorescence
[AIAA PAPER 90-1518] p 606 A90-38663

Combustion characteristics of a model can-type combustor
p 676 A90-40479

Fuel effects on gas turbine combustor dynamics
[AIAA PAPER 90-1957] p 676 A90-40570

Hydrocarbon-fueled scramjet combustor investigation
[AIAA PAPER 90-2337] p 658 A90-40622

Development of the jet-swirl high loading combustor
[AIAA PAPER 90-2451] p 658 A90-40633

Multistep dump combustor design to reduce combustion instabilities
p 659 A90-40934

Influence of fuel composition on flame radiation in gas turbine combustors
p 659 A90-40946

Experimental studies of combustor dilution zone aerodynamics. II - Jet development
p 659 A90-40947

Military engines - Cradle of technology
p 660 A90-41758

Some governing parameters of plasma torch igniter/flameholder in a scramjet combustor
[AIAA PAPER 90-2098] p 661 A90-42017

Multiple swirl dome combustor for high temperature rise applications
[AIAA PAPER 90-2159] p 661 A90-42050

Modeling gas turbine combustor performance under transient conditions
[AIAA PAPER 90-2161] p 661 A90-42051

Numerical analysis of the flows in annular slinger combustors
[AIAA PAPER 90-2164] p 685 A90-42052

The performance of a combustor pre-diffuser incorporating compressor outlet guide vanes
[AIAA PAPER 90-2165] p 661 A90-42053

Influences on the uniformity of sprays produced by gas turbine high shear nozzle/swirler assemblies
[AIAA PAPER 90-2193] p 686 A90-42068

Numerical simulations of gas turbine combustor flows
[AIAA PAPER 90-2305] p 686 A90-42116

Direct measurements of skin friction in a scramjet combustor
[AIAA PAPER 90-2342] p 626 A90-42132

Structure analysis of burning liquid-fueled spray in a confined combustor
[AIAA PAPER 90-2444] p 677 A90-42174

Engineering design models for ramjet efficiency and lean blowoff
[AIAA PAPER 90-2453] p 663 A90-42176

Radio frequency (RF) heated supersonic flow laboratory
[AIAA PAPER 90-2469] p 673 A90-42186

Mixing characteristics of dilution jets in small gas turbine combustors
[AIAA PAPER 90-2728] p 664 A90-42217

An experimental investigation of the velocity field in a reverse-flow combustor
p 739 A90-42657

Numerical simulation of nonpremixed turbulent flow in a dump combustor
[AIAA PAPER 90-1858] p 768 A90-42685

A computational investigation of flow losses in a supersonic combustor
[AIAA PAPER 90-2093] p 742 A90-42728

Flow establishment in a generic scramjet combustor
[AIAA PAPER 90-2096] p 742 A90-42729

Measurements in an annular combustor-diffuser system
[AIAA PAPER 90-2162] p 768 A90-42740

Parametric evaluation of the aerodynamic performance of an annular combustor-diffuser system
[AIAA PAPER 90-2163] p 742 A90-42741

Measured operating characteristics of a rectangular combustor/inlet isolator
[AIAA PAPER 90-2221] p 742 A90-42752

A validation study of the Spark Navier Stokes code for nonreacting scramjet combustor flowfields
[AIAA PAPER 90-2360] p 706 A90-42784

Introducing the VRT gas turbine combustor
[AIAA PAPER 90-2452] p 743 A90-42808

A study of the electrophysical phenomena in the combustion chambers of jet engines
p 765 A90-45028

Operation of the Rolls-Royce Pegasus Engine on low grade non-aviation fuels
[SAE PAPER 892329] p 747 A90-45486

Computation of complex flows in gas turbine combustors with a multi-level additive correction technique
p 881 A90-46899

Effect of vane twist on the performance of dome swirlers for gas turbine airblast atomizers
[AIAA PAPER 90-1955] p 881 A90-47203

Composite matrix cooling scheme for small gas turbine combustors
[AIAA PAPER 90-2158] p 852 A90-47210

Combustor influence on fighter engine operability
p 64 N90-10193

Dynamic instability characteristics of aircraft turbine engine combustors
p 53 N90-10195

Recent developments in Ramjet pressure oscillation technology
p 53 N90-10199

Numerical simulation of pressure oscillations in a ramjet combustor
p 54 N90-10202

MATE (Materials for Advanced Turbine Engines) Program, Project 3. Volume 2: Design, fabrication and evaluation of an oxide dispersion strengthened sheet alloy combustor liner
[NASA-CR-180892] p 357 N90-17868

Introducing the VRT gas turbine combustor
[NASA-TM-103176] p 688 N90-23591

Metallized fuel particle size study in a solid fuel ramjet
[AD-A220079] p 679 N90-24451

Effect of vane twist on the performance of dome swirlers for gas turbine airblast atomizers
[NASA-TM-103195] p 773 N90-25289

Combustion in the gas turbine. Part 1: Combustor types and design
[CIT/SME/VKI/RS/1] p 748 N90-25986

Combustion in the gas turbine. Part 2: Preliminary design and performance
[CIT/SME/VKI/RS/3] p 748 N90-25987

Aircraft exhaust emissions: An engine manufacturer's perspective
[PNR90675] p 750 N90-26004

A heat transfer analysis for rough turbine airfoils
[AD-A221942] p 854 N90-26831

Modeling of supersonic reacting flow fields
p 855 N90-26898

Flame extinction in compressible flow
p 883 N90-26899

Concentration, temperature, and density in a hydrogen-air flame by excimer-induced Raman scattering
p 875 N90-26903

Energy Efficient Engine combustor test hardware detailed design report
[NASA-CR-168301] p 929 N90-28554

Energy Efficient Engine (E3) combustion system component technology performance report
[NASA-CR-168274] p 930 N90-28555

Energy efficient engine pin fin and ceramic composite segmented liner combustor sector rig test report
[NASA-CR-179534] p 932 N90-28567

Solid fuel combustion chamber
[LR-634] p 939 N90-29433

COMBUSTION CHEMISTRY

Controlled mixing and variable geometry combustor design effects on emissions and combustion characteristics
p 45 A90-12547

Fuel molecular structure and flame temperature effects on soot formation in gas turbine combustors
[ASME PAPER 89-GT-288] p 253 A90-22652

Higher-order effects in boundary-layer premixed combustion
p 529 A90-32953

The influence of swirl on velocity, temperature and species characteristics in a can combustor
[AIAA PAPER 90-2454] p 664 A90-42177

Critical evaluation of Jet-A spray combustion using propane chemical kinetics in gas turbine combustion simulated by KIVA-II
[AIAA PAPER 90-2439] p 949 A90-50645

Fire science and aircraft safety
p 326 N90-17596

Time development of convection flow patterns in aircraft cabins under post-crash fire exposure
p 327 N90-17598

Fire hardening of an aircraft passenger cabin
p 328 N90-17606

Gas Turbine Combustion, volume 1
[VKI-LS-1990-02-VOL-1] p 748 N90-25985

Turbulent combustion modeling for turbo-jet combustion chambers
p 749 N90-25993

Chemistry of combustion processes
p 749 N90-25994

COMBUSTION CONTROL

Active combustion control in a coaxial dump combustor
[AIAA PAPER 90-2447] p 743 A90-42806

COMBUSTION EFFICIENCY

Studies on the influence of Mach number on profile losses of a reaction turbine cascade
p 10 A90-12517

Full-scale liquid fuel ramjet combustor tests
p 44 A90-12528

Investigation and improvement of ground starting characteristics of a combustor with airblast nozzles
p 45 A90-12546

The performance of a small combustor operated over a wide range of conditions
p 45 A90-12548

Predicting the CO, HC, and NO(x) emission and combustion efficiency of small turbine engines from the combustion chamber bench test results
p 125 A90-15425

The experimental study on the coaxial dump combustor with inner swirl inlet under the combustion condition
p 585 A90-36786

Engineering design models for ramjet efficiency and lean blowoff
[AIAA PAPER 90-2453] p 663 A90-42176

An investigation on boron used as a component of solid propellant
p 765 A90-45708

Combustion process in a gas turbine combustor when using H₂, NH₃ and LPG fuels
p 873 A90-46882

Effect of vane twist on the performance of dome swirlers for gas turbine airblast atomizers
[AIAA PAPER 90-1955] p 881 A90-47203

Cycle analysis of scramjet engines
[NAL-TR-1002] p 51 N90-10035

Aircraft propulsion: Leading the way in aviation
[LR-532] p 194 N90-13395

Metallized fuel particle size study in a solid fuel ramjet
[AD-A220079] p 679 N90-24451

Effect of vane twist on the performance of dome swirlers for gas turbine airblast atomizers
[NASA-TM-103195] p 773 N90-25289

Gas Turbine Combustion, volume 1
[VKI-LS-1990-02-VOL-1] p 748 N90-25985

Pollutants: Production and methods of reduction
[CIT/SME/VKI/RS/6] p 749 N90-25990

Subsonic combustor flow modeling: State of the art of CFD techniques for reacting and combustor flow
p 749 N90-25991

Supersonic combustor modeling
p 749 N90-25992

Turbulent combustion modeling for turbo-jet combustion chambers
p 749 N90-25993

Subsonic combustor testing
p 749 N90-25997

Raman scattering measurements using UV excimer lasers
p 874 N90-26902

Calculation of the combustion distribution in a liquid-fuel ramjet
p 858 N90-27931

An investigation of solid-fuel, dual-mode combustion ramjets
p 859 N90-27933

Photo-sensitized ignition of hydrogen/oxygen mixtures for hypersonic flight vehicles
p 877 N90-27935

Energy Efficient Engine combustor test hardware detailed design report
[NASA-CR-168301] p 929 N90-28554

Energy Efficient Engine (E3) combustion system component technology performance report
[NASA-CR-168274] p 930 N90-28555

Energy efficient engine program technology benefit/cost study. Volume 1: Executive summary
[NASA-CR-174766-VOL-1] p 931 N90-28564

Energy efficient engine program technology benefit/cost study, volume 2
[NASA-CR-174766-VOL-2] p 931 N90-28565

Solid fuel combustion chamber
[LR-634] p 939 N90-29433

COMBUSTION PHYSICS

Instrumentation for combustion and flow in engines; Proceedings of the NATO Advanced Study Institute, Vimeiro, Portugal, Sept. 13-26, 1987
p 211 A90-19004

Gas turbine combustion - A personal perspective
p 283 A90-20604

Supersonic combustion of hydrogen jets behind a backward-facing step
[AIAA PAPER 90-0204] p 266 A90-22183

Structure analysis of burning liquid-fueled spray in a confined combustor
[AIAA PAPER 90-2444] p 677 A90-42174

The influence of swirl on velocity, temperature and species characteristics in a can combustor
[AIAA PAPER 90-2454] p 664 A90-42177

Combustion of PMMA, PE, and PS in a ramjet
p 764 A90-43670

Combustion Experiments During KC-135 Parabolic Flights
[ESA-SP-1113] p 368 N90-16958

COMBUSTION PRODUCTS

Controlled mixing and variable geometry combustor design effects on emissions and combustion characteristics
p 45 A90-12547

Effect of primary air swirl on emissions formations in gas turbine combustors
p 47 A90-12573

Effect of pressure on the electrophysical properties of two-phase flows in nozzles
p 110 A90-14572

Predicting the CO, HC, and NO(x) emission and combustion efficiency of small turbine engines from the combustion chamber bench test results
p 125 A90-15425

Study of the expansion of hydrocarbon-oxygen products through supersonic nozzle
p 852 A90-46907

Characterization of chemicals on engine exhaust particles
[AD-A213566] p 256 N90-15106

Device for quickly sensing the amount of O₂ in a combustion product gas
[NASA-CASE-LAR-13816-1] p 609 N90-22025

The reduction of smoke emissions from Allison T56 engines

[ARL-PROP-R-182] p 928 N90-28547

COMBUSTION STABILITY

Simulation and second law analysis of the unsteady combustion of a non-ideal pulsating ramjet

p 44 A90-12516

Numerical simulation of valveless pulsed combustors

p 127 A90-13767

Large-eddy simulations of pressure oscillations and combustion instability in a ramjet

p 111 A90-15388

Large-eddy simulations of combustion instability in an axisymmetric ramjet combustor

[AIAA PAPER 90-0267] p 191 A90-19764

A one-dimensional model of ramjet combustion instability

[AIAA PAPER 90-0271] p 266 A90-22192

The effect of swirler on short reversal-flow annular combustor

p 423 A90-29906

Acoustic characteristics of a research step combustor

[AIAA PAPER 90-1851] p 655 A90-40530

Fuel effects on gas turbine combustor dynamics

[AIAA PAPER 90-1957] p 676 A90-40570

Multistep dump combustor design to reduce combustion instabilities

p 659 A90-40934

Active combustion control in a coaxial dump combustor

[AIAA PAPER 90-2447] p 743 A90-42806

Large-eddy simulations of flows in a ramjet combustor

p 772 A90-45534

Combustion Instabilities in Liquid-Fuelled Propulsion Systems

[AGARD-CP-450] p 63 N90-10191

Combustion instabilities in liquid-fueled propulsion systems: An overview

p 63 N90-10192

Numerical simulation of unsteady combustion in a dump combustor

p 54 N90-10203

Very-low-frequency oscillations in liquid-fueled ramjets

p 54 N90-10204

Acoustic-vortex-chemical interactions in an idealized ramjet

p 54 N90-10206

Gas Turbine Combustion, volume 1

[VKI-LS-1990-02-VOL-1] p 748 N90-25985

Combustion in the gas turbine. Part 3: Fuel injection, ignition and stability

[CIT/SME/VKI/RS/4] p 748 N90-25988

Liquid fueled ramjet combustion instability: Acoustical and vortical interactions with burning sprays

[AD-A222752] p 767 N90-26104

Calculation of the combustion distribution in a liquid-fuel ramjet

p 858 N90-27931

Numerical simulations of flowfields in a central-dump ramjet combustor. 3: Effects of chemistry

[AD-A224145] p 933 N90-28573

COMBUSTION TEMPERATURE

Simultaneous CARS measurements of temperature and H₂, H₂O concentrations in hydrogen-fueled supersonic combustion

[AIAA PAPER 90-0158] p 205 A90-19713

Combustor technology for future aircraft

[AIAA PAPER 90-2400] p 852 A90-47219

COMBUSTION VIBRATION

Calculation of vibrational combustion limits in Helmholtz resonator-type chambers

p 125 A90-14588

Combustion oscillations in ducts

p 204 A90-19006

COMMAND AND CONTROL

Concise design of aircraft longitudinal model reference adaptive command augmentation system

p 345 A90-24002

Throughput and delay characteristics for a slow-frequency hopped aircraft-to-aircraft packet radio network

[AD-A220525] p 688 N90-23609

Replay and transmission of AIMS-data to mainframe computer using remote transmitters

p 892 N90-27634

COMMAND LANGUAGES

Advanced Automation System design

p 375 A90-25566

A user's manual for the method of moments Aircraft Modeling Code (AMC)

[NASA-CR-186371] p 415 N90-18390

COMMERCIAL AIRCRAFT

Coping with bomb threats to civil aviation

p 23 A90-12781

More composites in commercial transports?

p 265 A90-20263

The U.S. airline industry - Coping with an aging fleet

p 221 A90-21702

TW-68 tilt wing high speed commercial VTOL

p 246 A90-21712

EUROFAR - European project for a commercial vertical-takeoff aircraft

[MBB-UD-553/89] p 221 A90-22696

Minimizing life cycle cost for subsonic commercial aircraft

p 283 A90-23282

Composites for aeronautical structures

p 286 A90-24291

Manufacturing and handling techniques used in the assembly of polished commercial aircraft

[SAE PAPER 890925] p 286 A90-24690

Pattern representations and syntactic classification of radar measurements of commercial aircraft

p 417 A90-28407

Composite certification for commercial aircraft

p 382 A90-29892

Methodology for developing an assessment expert system using a planning paradigm

p 460 A90-30757

An optically interfaced propulsion management system applied to a commercial transport aircraft

p 424 A90-30811

The future of the U.S. aircraft industry

p 467 A90-32275

Configuration aerodynamics

p 557 A90-36540

Transport aircraft corrosion control

p 617 A90-40345

Requirements for business jet aircraft

[AIAA PAPER 90-2038] p 644 A90-41991

The Dash 8 Series 400 regional airliner

p 729 A90-42664

Design and certification of the all-composite airframe

[SAE PAPER 892210] p 732 A90-45429

Certification of composites for commercial aircraft

[SAE PAPER 892212] p 772 A90-45430

Design features of the 747-400 Electric Power System

[SAE PAPER 892227] p 746 A90-45443

Induced drag - Historical perspective

[SAE PAPER 892341] p 715 A90-45495

The RB211-535E4 - A commercially proven engine for the military of tomorrow

[SAE PAPER 892364] p 748 A90-45513

The economics of the organization and the planning of civil aviation - Russian book

p 897 A90-46629

NASA's HITEMP program for UHBR engines

[AIAA PAPER 90-2395] p 852 A90-47218

Commercial aircraft DOC methods

[AIAA PAPER 90-3224] p 897 A90-48843

The BAe (commercial aircraft) LTD transport aircraft synthesis and optimisation program (TASOP)

[AIAA PAPER 90-3295] p 837 A90-48879

Certification impact of introducing G.P.S. into commercial transport navigation systems

p 824 A90-49501

Health monitoring aircraft

p 902 A90-50544

Airport technology international 1989/1990 - Book

p 937 A90-52857

UK airmisses involving commercial air transport

[CAA-2/88] p 96 N90-11718

International Aircraft Occupant Safety Conference and Workshop proceedings

[AD-A214452] p 239 N90-15085

UK airmisses involving commercial air transport, September to December 1988

[ISSN-0951-6301] p 240 N90-15897

Aircraft accident report, United Airlines Flight 811, Boeing 747-122, N4713U, Honolulu, Hawaii, February 24, 1989

[PB90-910401] p 574 N90-21748

First-order weight corrections for real-time flight path management

[LR-580] p 578 N90-21751

Aircraft drawings index

p 618 N90-23340

AVION: A detailed report on the preliminary design of a 79-passenger, high-efficiency, commercial transport aircraft

[NASA-CR-186663] p 649 N90-23395

High speed civil transport

[NASA-CR-186661] p 649 N90-23396

The 30th Airlines International Electronics Meeting Proceedings

[ETN-90-96973] p 637 N90-24261

Study of high-speed civil transports. Summary

[NASA-CR-4236] p 735 N90-25966

Knowledge-based system for flight information management

[NASA-TM-102685] p 780 N90-26511

BASEOPS default profiles for civil aircraft

[AD-A223161] p 844 N90-26825

World jet airplane inventory at year-end 1989

[PB90-207218] p 902 N90-28489

Life cycle cost in the conceptual design of subsonic commercial aircraft, volumes 1 and 2

p 923 N90-28535

Airline productivity relating on the fuel cost. (2): Fuel consumption values and fuel efficiency

[NAL-TM-604-2] p 913 N90-29333

UK airmisses involving commercial air transport: May - August 1989

[ISSN-0951-6301] p 913 N90-29335

COMMONALITY

Commonality of MASA modules - Modular Avionics System Architecture

p 462 A90-30816

Modular avion architectures

p 453 A90-30819

Preliminary design of a family of three close air support aircraft

[NASA-CR-186070] p 336 N90-16751

General test plan

p 857 N90-27721

COMMUNICATION

Rotorcraft low altitude CNS benefit/cost analysis: Rotorcraft operations data

[DOT/FAA/DS-89/9] p 141 N90-12406

Communications Interface Driver (CID) test plan

[DOT/FAA/CT-TN89/35] p 958 N90-28762

COMMUNICATION EQUIPMENT

AIRNET: A real-time communications network for aircraft

[NASA-CR-186140] p 690 N90-24514

COMMUNICATION NETWORKS

Data Link Processor (DLP) operational test and evaluation/integration test plan

[DOT/FAA/CT-TN89/32] p 214 N90-14404

Throughput and delay characteristics for a slow-frequency hopped aircraft-to-aircraft packet radio network

[AD-A220525] p 688 N90-23609

COMMUNICATION SATELLITES

CRL's mobile satellite communication experiments using ETS-V

[AIAA PAPER 90-0775] p 366 A90-25602

A new hybrid airship ('Heliship') for commuter transport

p 29 A90-11875

Creditable commuter - civil aircraft

p 405 A90-27975

Sukhoi and Gulfstream go supersonic - joint development of business aircraft

p 383 A90-31247

TCAS for commuter aircraft

p 487 A90-33348

Aeroelastic analysis for a composite T-tailplane of a turboprop commuter aircraft

p 492 A90-33390

Preliminary design of four aircraft to service the California Corridor in the year 2010: The California Condor, California Sky-Hopper, high capacity short range transport tilt rotor aircraft needed to simplify intercity transportation

[NASA-CR-186232] p 186 N90-14226

Low-speed wind-tunnel investigation of the flight dynamic characteristics of an advanced turboprop business/commuter aircraft configuration

[NASA-TP-2982] p 434 N90-19239

COMPACTING

Improving snow roads and airstrips in Antarctica

[AD-A211588] p 133 N90-11907

COMPATIBILITY

The integration of stores on modern tactical aircraft: Where we have been, and what we should do for the future

p 337 N90-17552

COMPENSATORS

Approximate loop transfer recovery method for designing fixed-order compensators

p 375 A90-25989

Design of adaptive digital controllers incorporating dynamic pole-assignment compensators for high-performance aircraft

p 432 A90-30714

The development of an airborne synthetic aperture radar motion compensation system

p 333 N90-16745

COMPENSATORY TRACKING

Simulation investigation of multiple axis flying qualities

[AIAA PAPER 90-3480] p 866 A90-47729

Application of optimal tracking methods to aircraft terrain following

[AD-A221099] p 641 N90-24264

COMPLEX SYSTEMS

A numerical solution for instruction tracing problem

p 424 A90-29918

Perspectives on the use of rule-based control

p 521 N90-20940

COMPLEX VARIABLES

Complex variable boundary element method for external potential flows

[AIAA PAPER 90-0127] p 162 A90-19694

COMPONENT RELIABILITY

Mechanical considerations for reliable interfaces in next generation electronics packaging

p 453 A90-30813

The survivability of centrifugal compressors in modern aircraft engines

p 928 A90-49883

The role of component testing

[PNR90589] p 115 N90-12608

Advanced Turbine Technology Applications Project (ATTAP)

[NASA-CR-185109] p 220 N90-14153

A study of variable geometry in advanced gas turbines

p 255 N90-15104

Estimation of defective rate of mechanic-hydraulic components

[ETN-90-97275] p 884 N90-27120

Recommended practices for measurement of gas path pressures and temperatures for performance assessment of aircraft turbine engines and components

COMPOSITE MATERIALS

Durability characteristics of the LAK-12 Letuva glider made of composite materials at the stage of certification p 102 A90-15560

A new generation of innovative ultra-advanced intelligent composite materials featuring electro-rheological fluids - An experimental investigation p 204 A90-17962

Aeroelastic tailoring applied to composite wing p 211 A90-18580

Material progress p 221 A90-21715

High-performance composite materials in air and space travel - State of the art and future perspectives [MBB-Z-0279/89] p 266 A90-22595

The impact of composites on the aerospace industry p 221 A90-22649

Aerospace materials research opportunities p 267 A90-23177

The challenge of LHX --- composite materials in light military helicopters p 382 A90-29641

Composites boost 21st-century aircraft engines p 442 A90-29704

Lightning strike protection concepts for composite materials p 528 A90-31617

Design of an aero-engine thrust reverser blocker door p 467 A90-31651

Development of a fibre optic damage detection system for an aircraft leading edge p 504 A90-32873

Designing with advanced composites; Report on the European Core Conference, 1st, Zurich, Switzerland, Oct. 20, 21, 1988, Conference Papers p 530 A90-33701

Aeroelastic tailoring of composite wing structures p 580 A90-37217

Fatigue methodology III; Proceedings of the AHS National Technical Specialists' Meeting on Advanced Rotorcraft Structures, Scottsdale, AZ, Oct. 3-5, 1989 p 641 A90-39976

The analysis and testing of composite panels subject to muzzle blast effects p 675 A90-39991

Towards a damage tolerance philosophy for composite materials and structures p 675 A90-40127

Design and manufacturing of composite materials blade models p 618 A90-42492

Hydraulic accumulators and high pressure bottles in composite material p 688 A90-42493

Building the B-2 p 701 A90-43826

Dornier Composite Aircraft - Economical and faultless p 732 A90-44751

Certification of composites for commercial aircraft [SAE PAPER 892212] p 772 A90-45430

Fast start ceramic auxiliary power unit [SAE PAPER 892254] p 747 A90-45456

Composite matrix cooling scheme for small gas turbine combustors [AIAA PAPER 90-2158] p 852 A90-47210

Iterative preliminary design tools for composite structures p 882 A90-48045

Developments in the acoustic fatigue design process for composite aircraft structures p 882 A90-48047

Certifying the Speed Canard p 833 A90-48699

Comparison of processing techniques for Filmix unidirectional commingled fabric p 940 A90-50058

Process optimization of high temperature composite materials p 943 A90-50130

A third-generation bismaleimide prepreg system p 943 A90-50131

Damage tolerance evaluation of several elevated temperature graphite composite materials p 945 A90-50155

Variations in impact test methods for tough composites p 946 A90-50167

Safety and health trends in aerospace composite materials p 947 A90-50188

Flammability regulations affecting advanced composite materials p 947 A90-50190

Freeze drying for morphological control of inter-penetrating polymer networks p 948 A90-50214

The application of 'PT' resins to high temperature aerospace structures p 949 A90-50230

Choice and characterization of new materials for aerospace applications [ETN-89-952/19] p 126 A90-11819

Material requirements for future aeroengines [PNR90595] p 116 A90-12610

Nondestructive analysis of aileron fatigue and aging in a Mirage F1 [REPT-M6-594000] p 184 A90-13378

The application of cast SiC/Al to rotary engine components [NASA-CR-179610] p 192 A90-13385

Repair of composites by means of wet-lay-up [LR-551] p 205 A90-13617

Effects of lightning on operations of aerospace vehicles p 239 A90-15065

Cost effectiveness of composite materials on the F-15 and F-16 aircrafts [AD-A216353] p 338 A90-17631

Computational crash dynamics. Project 1.2: Computational crash dynamics analysis [IAR-89-19] p 724 A90-25956

The impact and requirements of new materials on aeroengines [PNR90671] p 750 A90-26003

Applications of digital image processing in testing and evaluation of composite materials [AD-A222839] p 874 A90-26887

Evaluation of composite components on the Bell 206L and Sikorsky S-76 helicopters [NASA-TM-4195] p 876 A90-27787

In-service inspection of composite components on aircraft at depot and field levels p 885 A90-28078

Radiation-curable prepreg composites [DE90-629740] p 951 A90-28674

COMPOSITE STRUCTURES

Design of an advanced pneumatic deicer for the composite rotor blade p 29 A90-11009

Fiber optic sensors for composite monitoring p 37 A90-11203

Vibration analysis of composite turbopropellers using a nonlinear beam-type finite-element approach p 70 A90-12844

Beech Starship occupant protection evaluation in emergency landing scenario [SAE PAPER 891015] p 100 A90-14327

Impact evaluation of composite floor sections [SAE PAPER 891018] p 100 A90-14330

Composite driveshaft designs [SAE PAPER 891031] p 128 A90-14339

The warping restraint effect in the critical and subcritical static aeroelastic behavior of swept forward composite wing structures [SAE PAPER 891056] p 129 A90-14358

Beech Starship interior noise experimental studies [SAE PAPER 891082] p 101 A90-14374

Carbon fibre composite bolted joints p 130 A90-15354

Experimental study on the buckling and postbuckling of carbon fibre composite panels with and without interply disbonds p 130 A90-15355

Durability characteristics of the LAK-12 Letuva glider made of composite materials at the stage of certification p 102 A90-15560

Recent studies on the behaviour of interference fit pins in composite plates p 132 A90-16320

Sensitivity and optimization of composite structures in MSC/NASTRAN p 208 A90-17370

The Model 360 - Advanced composite helicopter p 180 A90-17678

The strength and weakness of carbon composite structures --- for military and civil aircraft p 180 A90-17679

The effect of impact loading on residual strength of CFRP composite beams p 208 A90-17683

Theoretical modelling of composite rotating beams p 208 A90-17684

Design and calculation of composite air-cooled blades in a highly-loaded transonic turbine p 189 A90-17790

Calculation of coolant flow and heat transfer inside composite air-cooled turbine p 189 A90-17791

Experimental investigation on composite air-cooled blades of highly-loaded transonic turbine p 189 A90-17793

Direct search method to aeroelastic tailoring of a composite wing under multiple constraints p 208 A90-17865

The static aeroelastic behavior of sweptforward composite wing structures taking into account their warping restraint effect p 210 A90-18407

Crashworthiness of composite floor sections p 243 A90-20261

Resin transfer molding of composite structures p 270 A90-20264

Repair of composite aircraft parts - An operator's viewpoint p 221 A90-20606

Optimum design of composite structures p 272 A90-22135

Random response and noise transmission of discretely stiffened composite panels p 283 A90-23288

Design, realization, and qualification of model composite rotor blades p 364 A90-24293

Postbuckling finite element analysis of composite panels p 365 A90-24377

Aeroelastic tailoring of a wing with composite skin p 366 A90-25108

Review of composite rotor blade modeling p 366 A90-25303

Improvement in structural integrity and long term durability of aerospace composite components p 441 A90-28189

Avionics and electromagnetic compatibility (EMC) considerations on a helicopter with an advanced composite airframe p 417 A90-28217

Periodic response of thin-walled composite blades p 408 A90-28229

Design and analysis of composite structures with manufacturing flaws p 445 A90-28234

Effects of damage on post-buckled skin-stiffener composite skin panels p 409 A90-28235

Divergence of thin-walled composite rods of closed profile in gas flow p 388 A90-29012

Exploratory design studies using an integrated multidisciplinary synthesis capability for actively controlled composite wings [AIAA PAPER 90-0953] p 411 A90-29238

Design and fabrication of a prototype resin matrix composite interceptor structure [AIAA PAPER 90-1004] p 442 A90-29275

An approach for analysis and design of composite rotor blades [AIAA PAPER 90-1005] p 449 A90-29276

Flutter analysis of composite panels in supersonic flow [AIAA PAPER 90-1180] p 450 A90-29379

Static aeroelastic behavior of an adaptive laminated piezoelectric composite wing [AIAA PAPER 90-1078] p 412 A90-29386

Natural honeycomb --- use of balsa wood in sandwich panel cores for advanced composite airframes p 442 A90-29643

The all-composite airframe - Design and certification p 413 A90-29890

Composite certification for commercial aircraft p 382 A90-29892

Honeycomb sandwich primary structure applications on the Boeing Model 360 helicopter p 490 A90-31558

An apparatus to prepare composites for repair p 533 A90-31574

Repair adhesives - Development criteria for field level conditions p 528 A90-31575

Design and fabrication considerations for composite structures with embedded fiber optic sensors p 536 A90-32871

Subcomponent tests for composite fuselage technology readiness p 490 A90-33105

Aeroelastic tailoring validation by windtunnel model testing p 492 A90-33389

Aeroelastic analysis for a composite T-tailplane of a turboprop commuter aircraft p 492 A90-33390

Designing with advanced composites; Report on the European Core Conference, 1st, Zurich, Switzerland, Oct. 20, 21, 1988, Conference Papers p 530 A90-33701

The story of sandwich construction p 538 A90-33702

Manufacture of honeycomb p 538 A90-33704

Honeycomb quality requirements - A user's perspective p 538 A90-33705

Design with honeycomb, state of the art p 538 A90-33706

Airbus A320 CFRP-rudder structural requirements p 493 A90-33707

Tradeoffs in honeycomb cored designs p 538 A90-33708

Core composites in Swissair aircraft p 493 A90-33709

Aircraft cabin interior systems meeting new FAA regulations p 482 A90-33710

Repairing the damage p 530 A90-33712

Exact solutions to the oscillations of composite aircraft wings with warping constraint and elastic coupling p 603 A90-36271

Optimum design of composite wing structures subjected to displacement constraints p 680 A90-39276

Finite element analysis of composite panel flutter p 681 A90-40032

Towards a damage tolerance philosophy for composite materials and structures p 675 A90-40127

Certification testing methodology for fighter hybrid structure p 642 A90-40128

Advanced materials for landing gear p 677 A90-41900

Analysis of composite rotor blades via Saint Venant's solutions p 688 A90-42491

Design and certification of the all-composite airframe [SAE PAPER 892210] p 732 A90-45429

Torsional buckling and post-buckling of composite geodetic cylinders with special reference to joint flexibility p 878 A90-45971

Homogenization of composite beams in dynamical flexure p 878 A90-46184

Sensitivity analysis in the design of composite structures p 880 A90-46478

NASA's HITEMP program for UHBR engines [AIAA PAPER 90-2395] p 852 A90-47218

Iterative preliminary design tools for composite structures p 882 A90-48045

Developments in the acoustic fatigue design process for composite aircraft structures p 882 A90-48047

Some computational and experimental aspects of optimal design process of composite structures p 882 A90-48050

Composite flight control actuators p 874 A90-48993

Unique features and innovative application of advanced composites to the MD-11 [AIAA PAPER 90-3217] p 838 A90-49108

Understanding composite fatigue - New trends p 940 A90-49893

Damage tolerance demonstration for A310-300 CFRP-components p 919 A90-49894

Innovative design concepts for thermoplastic composite materials p 940 A90-50059

Repair of thermoplastic composite structures by fusion bonding p 941 A90-50060

Fabrication of complex composite structures using advanced fiber placement technology p 954 A90-50111

Automated prepreg tow placement for composite structures p 954 A90-50113

Viscoelastic relaxation in bolted thermoplastic composite joints p 945 A90-50158

High performance needled structures in composites p 955 A90-50173

Composites for aerospace application from Kevlar aramid reinforced PEKK thermoplastic p 946 A90-50176

Flammability regulations affecting advanced composite materials p 947 A90-50190

PMR graphite engine duct development [NASA-CR-182228] p 51 N90-10037

Development of pressure containment and damage tolerance technology for composite fuselage structures in large transport aircraft [NASA-CR-3996] p 63 N90-10186

Transport composite fuselage technology: Impact dynamics and acoustic transmission [NASA-CR-4035] p 126 N90-11821

Evaluation of a damaged F/A-18 horizontal stabilizer [AD-A212573] p 107 N90-12597

Project, implementation, and utilization of composite structures [ETN-89-95209] p 127 N90-12665

Aeroelastic control of composite lifting surfaces: Integrated aeroelastic control optimization p 198 N90-13396

New Light Alloys [AGARD-CP-444] p 267 N90-15185

Proceedings of the 1988 Structural Integrity Program Conference [AD-A213545] p 275 N90-15486

Advanced materials for interior and equipment related to fire safety in aviation p 328 N90-17608

New materials for civil aircraft furnishing p 328 N90-17609

COCOMAT: A Computer Aided Engineering (CAE) system for composite structures design [NLR-MP-87078-U] p 462 N90-19756

A review of the analytical simulation of aircraft crash dynamics [NASA-TM-102595] p 484 N90-20068

Structural tailoring of select fiber composite structures [NASA-TM-102484] p 533 N90-21137

Boeing/NASA composite components flight service evaluation [NASA-CR-181898] p 601 N90-22609

Unique failure behavior of metal/composite aircraft structural components under crash type loads [NASA-TM-102679] p 690 N90-24660

Extension-torsion coupling, behavior of advanced composite tilt-rotor blades p 651 N90-25057

Behavior of composite/metal aircraft structural elements and components under crash type loads: What are they telling us [NASA-TM-102681] p 774 N90-25368

Proceedings of the 1987 Aircraft/Engine Structural Integrity Program (ASIP/ENSIP) Conference [AD-A198037] p 842 N90-26807

Lessons learned for composite aircraft structures qualification p 842 N90-26808

A review of crashworthiness of composite aircraft structures [AD-A221555] p 846 N90-27697

A Protection And Detection Surface (PADS) for damage tolerance [NASA-TP-3011] p 876 N90-27788

NDI-concept for composites in future military aircraft p 877 N90-28070

An ultrasonic system for in-service non-destructive inspection of composite structures p 885 N90-28076

A technique for rapid inspection of composite aircraft structure for impact damage p 846 N90-28077

Development of an automated ultrasonic inspection system for composite structure on in-service aircraft p 885 N90-28079

The application of infrared thermography to the nondestructive testing of composite materials p 886 N90-28084

Inspection system for in-situ inspection of aircraft composite structures p 886 N90-28091

Energy efficient engine pin fin and ceramic composite segmented liner combustor sector rig test report [NASA-CR-179534] p 932 N90-28567

Structural analysis and optimum design of geodesically stiffened composite panels [NASA-CR-186944] p 959 N90-28862

A low cost shadow moire device for the nondestructive evaluation of impact damage in composite laminates [AD-A223451] p 953 N90-29442

Proceedings of damping '89. Volume 1: Pages AAB-1 through DCD-11 [AD-A223431] p 960 N90-29664

COMPOSITE WRAPPING

A study of filament wound high modulus carbon fiber reinforced cylinders p 948 A90-50218

COMPOUND HELICOPTERS

Modelling aspects for the synthesis and performance assessment of some future advanced helicopters p 829 A90-46937

COMPRESSED AIR

Thermodynamic calculation of the compressors of gas turbine engines and powerplants at high air pressures p 130 A90-14585

COMPRESSIBILITY

Compression pylon [NASA-CASE-LAR-13777-1] p 498 N90-20078

Summary report of the Summer Conference of the DARPA-Materials Research Council [AD-A217380] p 532 N90-20143

Study of the compressibility effects on the turbulence of supersonic drags [ETN-90-97448] p 817 N90-27661

COMPRESSIBILITY EFFECTS

Effects of compressibility on the characteristics of free shear layers p 302 A90-25285

Study of compressibility effects in mixing layer by numerical simulation [AIAA PAPER 90-1464] p 562 A90-38621

COMPRESSIBLE BOUNDARY LAYER

Computation of unsteady compressible turbulent boundary layers in cascade flow with controlled inlet perturbation p 8 A90-11807

Prediction and control of transition in supersonic and hypersonic boundary layers p 16 A90-12828

The detection of large scale structure in undisturbed and disturbed compressible turbulent free shear layers [AIAA PAPER 90-0711] p 230 A90-22251

Fourth-order accurate three-dimensional compressible boundary-layer calculations p 308 A90-26136

Study of compressibility effects in mixing layer by numerical simulation [AIAA PAPER 90-1464] p 562 A90-38621

Subharmonic instability of compressible boundary layers p 706 A90-44005

Wake effects on the prediction of transonic viscous flows around airfoils with an Euler/boundary layer interaction approach [AIAA PAPER 90-3061] p 798 A90-45933

Generalized similarity solutions for three-dimensional laminar compressible wing boundary layers p 907 A90-51543

A method of predicting 3-D compressible boundary layer on the rotating blade of turbomachinery p 908 A90-52777

Generalized similarity solutions for three dimensional, laminar, steady, compressible boundary layer flows on swept profile cylinders [DLR-FB-89-34] p 212 N90-13725

A computational model for thickening boundary layers with mass addition for hypersonic engine inlet testing [AD-A216246] p 319 N90-17576

COMPRESSIBLE FLOW

The unsteady aerodynamics of an oscillating cascade in a compressible flow field p 7 A90-11789

Numerical investigation of unsteady compressible flow through nozzles and cascades p 7 A90-11790

A multi-domain 3D Euler solver for flows in turbomachines [ONERA, TP NO. 1989-119] p 15 A90-12623

A solution adaptive finite element method applied to two-dimensional unsteady viscous compressible cascade flow p 15 A90-12624

PCISM method for two dimensional compressible viscous cascade flow calculation p 15 A90-12625

Computational and experimental studies of compressible dynamic stall p 146 A90-16776

Transonic flow in throat region of supersonic nozzles p 149 A90-16799

Modeling of liquid jets injected transversely into a supersonic crossflow p 153 A90-17985

Solving compressible flow problems using adaptive finite quadtree and octree grids p 155 A90-18243

Boundary integral equations method for compressible Navier-Stokes equations p 209 A90-18262

Finite element simulation of compressible turbulent flows - Validation and application to internal aerodynamic in gas-turbine engines p 210 A90-18343

Some processes of sound generation in a vortex-airfoil system with parallel axes p 218 A90-18448

Block multigrid implicit solution of the Euler equations of compressible fluid flow [AIAA PAPER 90-0106] p 162 A90-19684

Design optimization of natural laminar flow fuselages in compressible flow [AIAA PAPER 90-0303] p 182 A90-19784

Embedded function methods for supersonic turbulent boundary layers [AIAA PAPER 90-0306] p 163 A90-19787

Application of a rotary-wing viscous flow solver on a massively parallel computer [AIAA PAPER 90-0334] p 164 A90-19802

Development of finite element methods for compressible Navier-Stokes flow simulations in aerospace design [AIAA PAPER 90-0403] p 166 A90-19833

The sonic eddy - A model for compressible turbulence [AIAA PAPER 90-0495] p 167 A90-19876

Compressibility effects in free shear layers [AIAA PAPER 90-0705] p 212 A90-19984

Chemically reacting supersonic flow calculation using an assumed PDF model [AIAA PAPER 90-0731] p 230 A90-22256

Turbulence modeling for aerodynamic flows [AIAA PAPER 89-0606] p 234 A90-23647

Ideal propeller in compressible gas flow in a wind tunnel p 298 A90-24156

Free-wake analysis of compressible rotor flows p 302 A90-25283

Effects of compressibility on the characteristics of free shear layers p 302 A90-25285

A numerical method for solving the unsteady compressible Navier-Stokes equations p 306 A90-25827

Fast adaptive grid method for compressible flows p 445 A90-28006

Time domain simulations of a flexible wing in subsonic, compressible flow [AIAA PAPER 90-1153] p 390 A90-29365

State-space representation of unsteady airfoil behavior p 469 A90-32461

Two-dimensional compressible unsteady aerodynamics in the Laplace domain p 472 A90-33360

Direct numerical simulations of transition in a compressible wake p 553 A90-35212

Oscillation of circular shock wave p 557 A90-36465

The k-kl turbulence model and wall layer model for compressible flows [AIAA PAPER 90-1483] p 563 A90-38637

A primitive variable, strongly implicit calculation procedure for viscous flows at all speeds [AIAA PAPER 90-1521] p 563 A90-38666

A locally implicit scheme for 3-D compressible viscous flows [AIAA PAPER 90-1525] p 563 A90-38670

Calculation of three-dimensional jet interaction flowfields [AIAA PAPER 90-2099] p 624 A90-42018

A colocated finite volume method for solving the Navier-Stokes equations for incompressible and compressible flows in turbomachinery - Results and applications p 703 A90-42659

Pressure-based real-time measurements in compressible free shear layers [AIAA PAPER 90-1980] p 703 A90-42709

Boundary integral formulation for compressible nonlinear potential and Navier-Stokes equations p 706 A90-44406

Numerical simulation of the compressible flow in a valve-cylinder assembly p 770 A90-44431

Solution of the Euler equations using unstructured polygonal meshes p 708 A90-44435

Numerical study of compressible nozzle flow p 708 A90-44437

A formulation for the solution of Euler equations for compressible flow using finite elements p 708 A90-44447

Compressible flow algorithms applied to structured/unstructured grids p 779 A90-44855

Tooth thickness effects on the performance of gas labyrinth seals p 771 A90-45300

Non-unique solutions of the Euler equations p 716 A90-45727

Schlieren studies of compressibility effects on dynamic stall of airfoils in transient pitching motion [AIAA PAPER 90-3038] p 791 A90-45877

Low Reynolds number airfoil design for subsonic compressible flow p 802 A90-46380

- Compressible Navier-Stokes solutions over low Reynolds number airfoils p 802 A90-46382
- Application of the inverse method of three-dimensional boundary layer analysis to the problem of flow past a wing with allowance for the effect of viscosity p 804 A90-46548
- Self-excited oscillations in internal transonic flows p 813 A90-49274
- Analysis of a propeller in compressible, steady flow p 814 A90-49778
- Least-squares finite element methods for compressible Euler equations p 904 A90-51013
- A panel method computation for oscillating aerofoil in compressible flow p 906 A90-51483
- Multigrid methods in computational fluid dynamics p 906 A90-51526
- The formation of vortex streets in supersonic flows p 907 A90-51539
- Multigrid scheme for the compressible Euler-equations p 907 A90-51559
- Three-dimensional unsteady transonic viscous-inviscid interaction p 18 N90-10005
- Experimental research on swept shock Wave/ Boundary layer interactions [AD-A211744] p 134 N90-11988
- An efficient solver of the Eigenvalue problem of the linear stability equations for three dimensional, compressible boundary-layer flows p 276 N90-16172
- Skin friction measurements by laser interferometry in supersonic flows p 317 N90-17557
- Numerical simulation of compressible vortices [AD-A216221] p 371 N90-18017
- Direct numerical simulation of aerodynamic noise [AD-A214122] p 379 N90-18225
- Spectral simulation of unsteady compressible flow past a circular cylinder [NASA-CR-182030] p 478 N90-20050
- Analysis of flow-, thermal-, and structural-interaction of hypersonic structures subjected to severe aerodynamic heating [AD-A217882] p 478 N90-20053
- Comparison of C- and O-grid generation methods using a NACA 0012 airfoil [AD-A216375] p 479 N90-20948
- Numerical method for designing 3D turbomachinery blade rows p 511 N90-20990
- Flame extinction in compressible flow p 883 N90-26899
- Development of turbulence models for the analysis of compressible or incompressible unsteady flow [ETN-90-97486] p 958 N90-28810
- COMPRESSIBLE FLUIDS**
- The effect of energy input on the characteristics of profiles in compressible fluid media p 906 A90-51533
- COMPRESSION LOADS**
- Sensitivity and optimization of composite structures in MSC/NASTRAN p 208 A90-17370
- Effect of creep on the load-bearing capacity of compressed panels p 364 A90-24102
- Damage tolerance of a postbuckling soft skin hat stiffened compression panel p 534 A90-31647
- Variations in impact test methods for tough composites p 946 A90-50167
- COMPRESSION RATIO**
- An experimental study of a supersonic gas ejector p 851 A90-46546
- COMPRESSION TESTS**
- Two-stage two-spool experimental centrifugal compressor investigation p 49 A90-12593
- Investigation of some effects on the compressor characteristics of an advanced bleed air compressor design p 49 A90-12594
- COMPRESSIVE STRENGTH**
- High service temperature high compressive strength and tough prepreg system p 530 A90-33098
- Compressive viscoelastic effects (creep) of a unidirectional glass/epoxy composite material p 946 A90-50170
- COMPRESSOR BLADES**
- Computation of aerodynamic blade loads due to wake influence and aerodynamic damping of turbine and compressor cascades p 7 A90-11791
- Aircraft compressor flutter analysis p 41 A90-11797
- Acoustic resonance in centrifugal compressors induced by interaction between rotor and stator p 78 A90-11803
- The interaction between tip clearance flow and the passage flowfield in an axial compressor cascade p 11 A90-12525
- Unsteady loss in a low speed axial flow compressor during rotating stall p 12 A90-12527
- Boundary layer growth on low aspect ratio compressor blades p 12 A90-12553
- A quasi-3D design method of transonic compressor blade with the function of improving velocity distribution p 49 A90-12589
- Numerical analysis of rotating stall by a vortex model p 13 A90-12590
- Comparative cascade studies of some high diffusion compressor bladings p 15 A90-12637
- Experimental investigations of effects of the stagger angle on secondary flows in plane compressor cascades p 83 A90-13787
- Comparison of NACA 65, CDA, and tandem bladed cascades p 190 A90-18484
- Analysis of blade loadings in centrifugal compressors p 158 A90-18591
- Compressor blade boundary layers. II - Measurements with incident wakes [ASME PAPER 89-GT-51] p 289 A90-23777
- Effects of endwall suction and blowing on compressor stability enhancement [ASME PAPER 89-GT-64] p 290 A90-23787
- Secondary flow due to the tip clearance at the exit of centrifugal impellers [ASME PAPER 89-GT-81] p 358 A90-23802
- Viscous flow in a controlled diffusion compressor cascade with increasing incidence [ASME PAPER 89-GT-131] p 291 A90-23829
- Three-dimensional relief in turbomachinery blading [ASME PAPER 89-GT-151] p 292 A90-23840
- An ultrasonic fatigue facility for HCF/LCF interactive tests p 363 A90-23900
- Navier-Stokes study of rotating stall in compressor cascades p 302 A90-25292
- Development of erosion resistant coatings for compression airfoils p 443 A90-31120
- Boundary element method for solving direct aerodynamic problem of aerofoil cascades on an arbitrary stream surface of revolution p 554 A90-35830
- Application of leaned blades to an aeroengine p 654 A90-40503
- Stall margin improvement in axial-flow compressors by circumferential variation of stationary blade setting angles [AIAA PAPER 90-1912] p 656 A90-40554
- Viscous-inviscid interaction method for calculating the flow in compressor cascade blade passages and wake with separation [AIAA PAPER 90-2125] p 624 A90-42032
- Development of a robust calculation method for transonic viscous blade-to-blade flows p 703 A90-42671
- Comparison among modal analyses of axial compressor blade using experimental data of different measuring systems p 878 A90-46038
- Calculation of nonstationary forces in a three-row compressor cascade p 803 A90-46502
- Optimal blading density in axial-flow compressor stages with a developed three-dimensional flow p 851 A90-46505
- Blading design for multi-storage HP compressor [PNR90602] p 116 N90-12616
- Performance of a highly-loaded HP compressor [RAE-TM-P-1149] p 256 N90-15919
- A method for the prediction of supersonic compressor blade performance [CUED/A-TURBO/TR-126] p 344 N90-17634
- Inverse computation of transonic internal flows with application for multi-point-design of supercritical compressor blades p 501 N90-20987
- Forcing function effects on rotor row unsteady aerodynamic response in a multistage compressor p 573 N90-22536
- Application of neural networks to the F/A-18 engine condition monitoring system [AD-A219820] p 666 N90-24271
- Structural testing and analytical research of turbine components [AD-A223516] p 933 N90-29396
- COMPRESSOR EFFICIENCY**
- Highly loaded axial flow compressors - History and current developments p 44 A90-12503
- A study of flow structure in a contra-rotating axial compressor stage p 11 A90-12524
- Gas turbine compressor operating environment and material evaluation [ASME PAPER 89-GT-42] p 340 A90-23769
- Dual pressure ratio compressor [ASME PAPER 89-GT-121] p 341 A90-23820
- The influence of diffuser vane leading edge geometry on the performance of a centrifugal compressor [ASME PAPER 89-GT-163] p 292 A90-23851
- Advanced core technology - Key to subsonic propulsion benefits [ASME PAPER 89-GT-241] p 342 A90-23890
- An off-design loss and deviation prediction study for transonic axial compressors [ASME PAPER 89-GT-324] p 343 A90-23893
- Developmental tests on the M 88 engine are on track p 660 A90-41761
- Stall cell blockage in a high-speed multistage axial-flow compressor [AIAA PAPER 90-1913] p 740 A90-42693
- Performance improvement of an eroded axial flow compressor using water injection [AIAA PAPER 90-2016] p 741 A90-42718
- The interaction between distortion of inlet flow and blade stall flutter in axial-flow compressor p 854 A90-49466
- Dynamic tip clearance measurements in axial flow compressors [PNR90597] p 116 N90-12612
- Energy Efficient Engine acoustic supporting technology report [NASA-CR-174834] p 930 N90-28557
- COMPRESSOR ROTORS**
- The inclusion of a similarity representation of compressor rotation in the modeling of the interaction of cannon firing with air intakes at incidence [AAAF PAPER NT 88-18] p 4 A90-11435
- Experimental investigation of the transonic centrifugal compressor inducer straight cascades p 13 A90-12592
- Analyses of full 3D S1-S2 iterative solution in CAS transonic compressor rotor and comparison with quasi-3D S1-S2m iterative solution and L2F measurement p 157 A90-18532
- Computation and analysis of the shapes of S1 and S2 streamsurfaces in a transonic compressor rotor p 160 A90-19446
- Improvement of 3D full-potential method and computation of flowfield of CAS compressor rotor [ASME PAPER 89-GT-17] p 288 A90-23760
- Application of recess vaned casing treatment to axial flow fans [ASME PAPER 89-GT-68] p 341 A90-23791
- Three-dimensional separated flow field in the endwall region of an annular compressor cascade in the presence of rotor-stator interaction. II - Unsteady flow and pressure field [ASME PAPER 89-GT-77] p 291 A90-23798
- Analysis of fully stalled compressor p 383 A90-27966
- Advanced technology's impact on compressor design and development - A perspective [SAE SP-800] p 423 A90-28571
- Fracture mechanics assessment of EB-welded blisked rotors p 453 A90-31117
- Computer-aided design of compressor rotor blade rings p 851 A90-46497
- Noise generation by swept cascade p 895 A90-49486
- Advanced technologies impact on compressor design and development: A perspective [NASA-TM-102341] p 54 N90-10891
- Flow in a forward swept centrifugal fan, volumes 1 and 2 p 481 N90-20959
- Prediction and measurement of rotor blade/stator vane dynamic characteristics of a modern aero-engine axial compressor [PNR90667] p 750 N90-26002
- COMPRESSORS**
- Vortex-flow compressors --- Russian book p 69 A90-12479
- Flow in compressor interstage ducts p 11 A90-12521
- Simulation of compressor performance deterioration due to erosion [ASME PAPER 89-GT-182] p 254 A90-22665
- Estimation of the efficiency of a ramjet engine with a thermocompressor using fuel conversion products p 255 A90-23412
- Three-dimensional separated flow field in the endwall region of an annular compressor cascade in the presence of rotor-stator interaction. I - Quasi-steady flow field and comparison with steady-state data [ASME PAPER 89-GT-76] p 291 A90-23797
- Casing vibration and gas turbine operating conditions [ASME PAPER 89-GT-78] p 358 A90-23799
- Compressor aerodynamics --- Book p 706 A90-44052
- Stage effects on stalling and recovery of a high-speed 10-stage axial-flow compressor p 115 N90-12600
- Externally vaporizing system for turbine combustor [AD-D014284] p 256 N90-15918
- Numerical investigation of unsteady flow in oscillating turbine and compressor cascades p 426 N90-18407
- Experiments on the unsteady flow in a supersonic compressor stage p 427 N90-18422
- Experimental investigation of the influence of rotor wakes on the development of the profile boundary layer and the performance of an annular compressor cascade p 427 N90-18425
- Compressor performance tests in the compressor research facility p 427 N90-18428
- Secondary flows and radial mixing predictions in axial compressors p 512 N90-21010

- WINCOF-I code for prediction of fan compressor unit with water ingestion
[NASA-CR-185157] p 551 N90-21724
- The effects of a compressor rebuild on gas turbine engine performance: Final results p 552 N90-28701
- COMPUTATION**
- Thermochemical calculations with inert compounds [FOA-C-20759-2.1] p 206 N90-13677
- Example of procedure in calculation of control hinge moments
[ESDU-89010] p 199 N90-14240
- A review of high-speed, convective, heat-transfer computation methods p 316 N90-17548
- A computational model for thickening boundary layers with mass addition for hypersonic engine inlet testing [AD-A216246] p 319 N90-17576
- Hypercube expert system shell-applying production parallelism
[AD-A215762] p 377 N90-18173
- A matrix-free locally-implicit scheme for Navier-Stokes equations
[AD-A218298] p 541 N90-20349
- The Shock and Vibration Digest, volume 21, no. 2 p 609 N90-22059
- Effects of simplifying assumptions on optimal trajectory estimation for a high-performance aircraft
[NASA-TM-101721] p 757 N90-25142
- Computational crash dynamics. Project 1.2: Computational crash dynamics analysis
[IAR-89-19] p 724 N90-25956
- The Helicopter Antenna Radiation Prediction Code (HARP)
[NASA-CR-186925] p 884 N90-27946
- COMPUTATIONAL CHEMISTRY**
- Calculated chemical and vibrational nonequilibrium effects in hypersonic nozzles p 253 A90-21224
- COMPUTATIONAL FLUID DYNAMICS**
- Marginal separation of laminar axisymmetric boundary layers p 1 A90-10074
- Numerical analysis of flow of an ideal fluid past an airfoil p 2 A90-10228
- The numerical method for solving the high Reynolds hypersonic viscous shock layer p 2 A90-10340
- Calculation of confined swirling flows with a second moment closure p 66 A90-10640
- Method for calculating the unsteady flow of an elliptical circulation-control airfoil p 3 A90-11003
- Wing-section effects on the flight performance of a remotely piloted vehicle p 29 A90-11007
- Computation of laminar mixed convection flow in a channel with wing type built-in obstacles p 67 A90-11114
- Several problems posed by aerothermal calculations in machines
[ONERA, TP NO. 1989-102] p 67 A90-11136
- Calculation of three-dimensional turbulent flow in a linear turbine cascade
[ONERA, TP NO. 1989-115] p 3 A90-11147
- Unsteady viscous calculation of cascade flows with leading-edge-induced separation
[ONERA, TP NO. 1989-116] p 3 A90-11148
- Numerical simulation of three-dimensional unsteady flows in turbomachines
[ONERA, TP NO. 1989-118] p 4 A90-11149
- An improved method for the computation of unsteady transonic potential flow - Application for airfoil and blade performance prediction
[ONERA, TP NO. 1989-154] p 4 A90-11175
- Numerical calculation of unsteady aerodynamic forces for three-dimensional subsonic oscillating cascades by a finite element method p 9 A90-12219
- Advances in computational design and analysis of airbreathing propulsion systems p 43 A90-12502
- Numerical simulation of turbomachinery flows with a simple model of viscous effects - Comparison with experimental data
[ONERA, TP NO. 1989-122] p 10 A90-12510
- Evaluation of two numerical techniques for the prediction of flow around blades p 10 A90-12512
- Shock capturing and loss prediction for transonic turbine blades using a pressure correction method p 11 A90-12518
- Navier-Stokes methods applied to turbomachinery blade design p 12 A90-12549
- The development of an exact conservative scheme associated with the supersonic trailing edge separation modelling for the computation of the transonic 2D cascade p 12 A90-12551
- Computation of three dimensional turbulent boundary layers in internal flows, including turbomachinery rotor blades p 12 A90-12555
- Investigation of the mixing of parallel supersonic streams p 69 A90-12561
- A theoretical approach to particle separator design p 48 A90-12584

- Numerical simulation of three-dimensional hypersonic inlet flowfields p 13 A90-12587
- A quasi-3D design method of transonic compressor blade with the function of improving velocity distribution p 49 A90-12589
- Numerical analysis of rotating stall by a vortex model p 13 A90-12590
- Three dimensional numerical simulation for an aircraft engine type combustion chamber
[ONERA, TP NO. 1989-120] p 49 A90-12591
- Radial swirl flows between parallel disks at critical flow rate p 14 A90-12596
- A secondary flow calculation method for one stage centrifugal compressor p 14 A90-12597
- Unsteady flow in centrifugal compressors due to downstream circumferential distortions p 14 A90-12598
- Advanced computational techniques for hypersonic propulsion p 69 A90-12606
- Aerodynamic and propulsive performance of hypersonic detonation wave ramjets p 49 A90-12609
- Computation of transonic turbine cascade flow using Navier-Stokes equations p 14 A90-12621
- Calculation of axisymmetric flows in turbomachines, through an explicit time-splitting method p 14 A90-12622
- A multi-domain 3D Euler solver for flows in turbomachines
[ONERA, TP NO. 1989-119] p 15 A90-12623
- A solution adaptive finite element method applied to two-dimensional unsteady viscous compressible cascade flow p 15 A90-12624
- PCISIM method for two dimensional compressible viscous cascade flow calculation p 15 A90-12625
- CFD predictions of lobed mixer flowfields p 70 A90-12626
- New approach to small transonic perturbations finite element numerical solving method. I - Numerical developments. II - Numerical applications p 16 A90-12783
- Prediction and control of transition in supersonic and hypersonic boundary layers p 16 A90-12828
- Application of the hypersonic analogy for validation of numerical simulations p 16 A90-12838
- Closed-form solutions for nonlinear quasi-unsteady transonic aerodynamics p 16 A90-12839
- Critique of turbulence models for shock-induced flow separation p 17 A90-12851
- Numerical study of single impinging jets through a crossflow p 17 A90-13020
- Numerical solution of transonic flows on a streamfunction co-ordinate system p 17 A90-13238
- Unified super/hypersonic similitude for steady and oscillating cones and ogives p 82 A90-13786
- Experimental investigations of effects of the stagger angle on secondary flows in plane compressor cascades p 83 A90-13787
- Goertler vortices in supersonic and hypersonic boundary layers p 83 A90-14091
- The method of matched integral representations in viscous fluid dynamics p 129 A90-14565
- A numerical method for calculating supersonic nonisobaric jets p 84 A90-14566
- Wing boundary layer calculation and its application to aircraft design p 84 A90-15151
- Recent Navier/Stokes calculations in applications p 85 A90-15227
- Separated flow over slender wing, body and wing-body combination p 85 A90-15232
- Computation of transonic separated flow using the Euler equations p 85 A90-15233
- Numerical solution of unsteady Navier-Stokes equations for laminar/turbulent flows, past axisymmetric bodies at angle of attack p 85 A90-15235
- Transonic flow over a single wedge p 85 A90-15237
- Calculation of flow past delta wings in the thin shock layer approximation p 86 A90-15624
- Euler solutions with a multi-block structured code p 86 A90-15739
- Full-potential calculations using Cartesian grids p 86 A90-15740
- Computation of flow over airfoils under high lift separated flow condition p 86 A90-15741
- Wind tunnel testing of high blockage models p 121 A90-15743
- Convergence properties of high-Reynolds-number separated flow calculations p 86 A90-15820
- Gas turbine engine component development - An integrated approach p 112 A90-16006
- A study on surge and rotating stall in axial compressors - A summary of the measurement and fundamental analysis method p 87 A90-16105
- Computation of the thin-layer Navier-Stokes equations for a 2D flow p 87 A90-16332

- Calculation of flowfields in side-inlet ramjet combustors with an algebraic Reynolds stress model p 87 A90-16367
- Symposium on Numerical and Physical Aspects of Aerodynamic Flows, 4th, California State University, Long Beach, Jan. 16-19, 1989, Proceedings p 144 A90-16751
- Experiments are telling you something (Stewartson Memorial Lecture) --- about aerodynamic flows p 144 A90-16752
- An interactive boundary layer method for subsonic airfoil flows p 144 A90-16754
- Computation of multi-element airfoil flows including confluence effects p 144 A90-16755
- VISTRAFS - A simulation method for strongly-interacting viscous transonic flow p 144 A90-16756
- The flow around wing-body junctions p 145 A90-16765
- Supersonic/hypersonic Euler flowfield prediction method for aircraft configurations p 145 A90-16767
- Calculation of three-dimensional boundary layers including hypersonic flows p 146 A90-16773
- Verification of a Navier-Stokes code for solving the hypersonic blunt body problem p 146 A90-16774
- Computational and experimental studies of compressible dynamic stall p 146 A90-16776
- Experimental and computational studies of dynamic stall p 147 A90-16780
- Analysis of high-incidence separated flow past airfoils p 147 A90-16781
- The calculation of under-expanded impinging jets p 147 A90-16782
- Multigrid acceleration of transonic flow computations p 147 A90-16783
- Supersonic boundary layer stability analysis with and without suction on aircraft wings p 148 A90-16792
- Calculation of flow over airfoil with slat and flap p 149 A90-16797
- Multigrid solution method for the Euler equations --- Book p 149 A90-16841
- Numerical studies of incompressible flow around delta and double-delta wings p 150 A90-16845
- A numerical method for computing the aerodynamic loads on wings with sharp-edge separations at large angles of attack in subcritical transonic flows p 150 A90-16852
- Computation of the trailing edge flow downstream a flat plate with finite thickness p 151 A90-17464
- An approach for calculating steady subsonic and transonic blade to blade flows p 152 A90-17784
- Computation of transonic flow in a plane cascade with an unfactored flux splitting implicit method p 152 A90-17785
- A relaxation method for transonic potential flows through 2-D cascade with large camber angle p 152 A90-17786
- Computation of viscous transonic flow over porous airfoils p 153 A90-17864
- Rotor hover performance prediction using a free-wake, computational fluid dynamics method p 153 A90-17869
- High-resolution upwind scheme for vortical-flow simulations p 153 A90-17872
- Essential ingredients of a method for low Reynolds-number airfoils p 153 A90-17979
- Numerical study of chemically reacting flows using a lower-upper symmetric successive overrelaxation scheme p 153 A90-17989
- Hybrid finite volume approach to Euler solutions for supersonic flows p 154 A90-18144
- Solving compressible flow problems using adaptive finite quadtree and octree grids p 155 A90-18243
- Boundary integral equations method for compressible Navier-Stokes equations p 209 A90-18262
- Upwind adaptive finite element investigations of the two-dimensional reactive interaction of supersonic gaseous jets p 209 A90-18264
- Computation of hypersonic flows by a finite element least-squares method p 155 A90-18296
- On the coupling of finite elements and boundary elements for transonic potential flows: p 155 A90-18297
- A finite element solution for transonic flow around lifting fuselage with arbitrary cross sections from the minimum pressure integral p 156 A90-18298
- Simulation of high incidence unsteady flow past Joukowski airfoils p 156 A90-18301
- Numerical methods to solve the incompressible Euler and Navier-Stokes equations in 3D with applications p 209 A90-18302
- Optimization methods applied to aerodynamic design problems in computational fluid dynamics p 156 A90-18308
- Grid generation with the 1988 EAGLE code p 156 A90-18310

Finite element analysis of the flow of a propeller on a slender body with a two-equation turbulence model p 210 A90-18340

Finite element simulation of compressible turbulent flows - Validation and application to internal aerodynamic in gas-turbine engines p 210 A90-18343

Secondary flows in a transonic cascade - Comparison between experimental and numerical results p 157 A90-18501

Turbulent boundary layer development in the presence of small isolated two-dimensional surface discontinuities p 210 A90-18507

A new implicit hybrid schemes for the Euler equation of transonic flow p 158 A90-18608

Computations of unsteady transonic flows about thin airfoils by integral equation method p 158 A90-18609

On the Goertler vortex instability mechanism at hypersonic speeds p 158 A90-18886

Numerical modeling of a viscous separated flow in the near wake p 159 A90-19236

The computational method for the transonic wing design p 160 A90-19438

Block multigrid implicit solution of the Euler equations of compressible fluid flow [AIAA PAPER 90-0106] p 162 A90-19684

Fresh look at floating shock fitting [AIAA PAPER 90-0108] p 162 A90-19686

Complex variable boundary element method for external potential flows p 162 A90-19694

An efficient upwind relaxation-sweeping algorithm for three-dimensional Euler equations [AIAA PAPER 90-0129] p 162 A90-19695

Direct simulation of hypersonic rarefied flow about a delta wing [AIAA PAPER 90-0143] p 162 A90-19704

Numerical solution of the boundary-layer equations for a general aviation fuselage [AIAA PAPER 90-0305] p 163 A90-19786

Three-dimensional solution-adaptive grid generation on composite configurations [AIAA PAPER 90-0329] p 164 A90-19799

Application of a rotary-wing viscous flow solver on a massively parallel computer [AIAA PAPER 90-0334] p 164 A90-19802

Generalized fluxvectors for hypersonic shock-capturing [AIAA PAPER 90-0390] p 165 A90-19829

A three-dimensional upwind parabolized Navier-Stokes code for chemically reacting flows [AIAA PAPER 90-0394] p 165 A90-19831

Viscous supersonic flow computations over a delta-rectangular wing with slanting surfaces [AIAA PAPER 90-0419] p 166 A90-19841

Hypersonic rarefied flow and its solution over the stagnation region [AIAA PAPER 90-0420] p 166 A90-19842

Transonic Navier-Stokes solutions about a complex high-speed accelerator configuration [AIAA PAPER 90-0430] p 166 A90-19844

Hydraulic analogy application in the study of a two-phase mixture combustion flow [AIAA PAPER 90-0451] p 211 A90-19850

A numerical study of general viscous flows around multi-element airfoils [AIAA PAPER 90-0572] p 167 A90-19922

Navier-Stokes methods to predict circulation control airfoil performance [AIAA PAPER 90-0574] p 167 A90-19924

Semi-implicit Navier-Stokes solver (SINSS) calculations of separated flows around blunt delta wings [AIAA PAPER 90-0590] p 168 A90-19936

Prediction of steady and unsteady asymmetric vortical flows around cones [AIAA PAPER 90-0598] p 168 A90-19940

Counterrotating prop-fan simulations which feature a relative-motion multiblock grid decomposition enabling arbitrary time-steps [AIAA PAPER 90-0687] p 169 A90-19978

Application of an adaptive algorithm to single and two-element airfoils in turbulent flow [AIAA PAPER 90-0698] p 169 A90-19983

Development of an unstructured mesh/Navier-Stokes method for aerodynamics of aircraft with ice accretions [AIAA PAPER 90-0758] p 169 A90-20011

Parabolized Navier-Stokes predictions of three-dimensional hypersonic flows with strong crossflow effects p 223 A90-20508

Transonic integro-differential and integral equations with artificial viscosity p 223 A90-20988

Inviscid non equilibrium flow in ONERA F4 wind tunnel [ONERA, TP NO. 1989-161] p 223 A90-21029

Recent developments in calculation methods for internal flows by solution of Euler or Navier-Stokes equations [ONERA, TP NO. 1989-167] p 223 A90-21033

Hypersonics. Volume 2 - Computation and measurement of hypersonic flows; Proceedings of the First Joint Europe/U.S. Short Course on Hypersonics, Paris, France, Dec. 7-11, 1987 -- Book p 224 A90-21164

Computations of hypersonic flow by finite-volume methods p 224 A90-21168

Computation of hypersonic flow fields p 225 A90-21169

On the computations of hypersonic viscous flows p 225 A90-21170

The National Aero-Space Plane, the guidance and control engineer's dream or nightmare? [AAS PAPER 89-040] p 264 A90-21546

Calculation of the side-wall boundary layer in axial turbomachines, accounting for the internal flow near the blades p 225 A90-21595

Numerical simulation of transonic wing flows using a zonal Euler, boundary-layer, Navier-Stokes approach p 225 A90-21596

Prediction of vortical flows on wings using incompressible Navier-Stokes equations p 226 A90-21935

Numerical calculation of gaseous reacting flows in a model of gas turbine combustors p 271 A90-21979

Computation of subsonic shrouded propeller flows [AIAA PAPER 90-0029] p 226 A90-22154

Subsonic calculation of propeller/wing interference [AIAA PAPER 90-0031] p 226 A90-22155

Calculations of the flow past bluff bodies, including tilt-rotor wing sections at $\alpha = 90$ deg [AIAA PAPER 90-0032] p 227 A90-22156

Navier-Stokes predictions of the flowfield around the F-18 (HARV) wing and fuselage at large incidence [AIAA PAPER 90-0099] p 227 A90-22165

Vortical flows over delta wings and numerical prediction of vortex breakdown [AIAA PAPER 90-0102] p 227 A90-22166

A numerical study of mixing enhancement in a supersonic combustor [AIAA PAPER 90-0203] p 272 A90-22182

A numerical method for three-dimensional viscous flows [AIAA PAPER 90-0236] p 228 A90-22186

Simulation and analysis of a delta planform with triple jets in ground effect [AIAA PAPER 90-0299] p 228 A90-22195

Unsteady transonic Navier-Stokes computations for an oscillating wing using single and multiple zones [AIAA PAPER 90-0313] p 228 A90-22197

Multi-processing on supercomputers for computational aerodynamics [AIAA PAPER 90-0337] p 282 A90-22199

Applications of an adaptive unstructured solution algorithm to the analysis of high speed flows [AIAA PAPER 90-0395] p 229 A90-22213

An embedded grid formulation applied to a delta wing [AIAA PAPER 90-0429] p 229 A90-22216

A zonal flow analysis method for two-dimensional airfoils [AIAA PAPER 90-0571] p 230 A90-22230

Chemically reacting supersonic flow calculation using an assumed PDF model [AIAA PAPER 90-0731] p 230 A90-22256

Navier-Stokes computations of vortical flows over low-aspect-ratio wings p 232 A90-23103

Upwind differencing scheme for the time-accurate incompressible Navier-Stokes equations p 232 A90-23109

Analysis of transonic integral equations. I - Artificial viscosity p 232 A90-23124

Structure of velocity and temperature fields in laminar channel flows with longitudinal vortex generators p 273 A90-23207

Unsteady supersonic computations of arbitrary wing-body configurations including external stores p 232 A90-23278

Measurements and calculations of the aerodynamic characteristics of the propeller sections series V3 p 233 A90-23355

Turbulence modeling for aerodynamic flows [AIAA PAPER 89-0606] p 234 A90-23647

Viscous flow calculations in turbomachinery channels [ASME PAPER 89-GT-5] p 287 A90-23752

Measurement and calculation of the three-dimensional flow in axial compressor stators, with and without end-bends [ASME PAPER 89-GT-6] p 287 A90-23753

Improvement of 3D full-potential method and computation of flowfield of CAS compressor rotor [ASME PAPER 89-GT-17] p 288 A90-23760

Inviscid cascade flow calculations using a multigrid method [ASME PAPER 89-GT-22] p 288 A90-23763

Accelerated computation of viscous, steady incompressible flows [ASME PAPER 89-GT-45] p 288 A90-23771

Overview on test cases for computation of internal flows in turbomachines [ASME PAPER 89-GT-46] p 288 A90-23772

Self-excited oscillation of transonic flow around an airfoil in two-dimensional channel [ASME PAPER 89-GT-58] p 290 A90-23784

Three-dimensional solutions for inviscid incompressible flow in turbomachines [ASME PAPER 89-GT-140] p 291 A90-23837

Three-dimensional relief in turbomachinery blading [ASME PAPER 89-GT-151] p 292 A90-23840

Verification of an impeller design by laser measurements and 3D-viscous flow calculations [ASME PAPER 89-GT-159] p 292 A90-23847

An analysis methodology for internal swirling flow systems with a rotating wall [ASME PAPER 89-GT-185] p 361 A90-23863

The extension and application of three-dimensional time marching analyses to incompressible turbomachinery flows [ASME PAPER 89-GT-212] p 293 A90-23878

The prediction of boundary layers with rotation and variation of stream filament thickness [ASME PAPER 89-GT-227] p 362 A90-23882

A simplified model for unstable temperature field calculation of gas turbine rotor [ASME PAPER 89-GT-234] p 363 A90-23885

Calculation of nonseparated transonic flow past swept wings with allowance for viscosity p 294 A90-24079

Application of Fedorenko's multigrid method for calculating transonic flow past a profile p 295 A90-24103

A new quick method for integrating Euler equations for plane transonic flows p 295 A90-24105

Calculation of transonic axisymmetric flow past an engine nacelle with allowance for viscosity p 296 A90-24107

Calculation of flows of an ideal gas in nozzles and jets by the relaxation method p 296 A90-24109

Multilevel method for calculating aerodynamic loads on a flight vehicle p 296 A90-24122

Calculation of supersonic flow past a wing/fuselage combination with the resolution of a compression shock from the wing p 297 A90-24138

Using third-fourth order compact schemes for calculating gas flows in nozzles with high supersonic M numbers on the basis of simplified Navier-Stokes equations p 299 A90-24157

Numerical solutions of the linearized Euler equations for unsteady vortical flows around lifting airfoils [AIAA PAPER 90-0694] p 300 A90-25041

The role of computational fluid dynamics (CFD) in aircraft design [AIAA PAPER 90-1801] p 335 A90-25175

Comparison of inviscid and viscous separated flows p 302 A90-25277

Free-wake analysis of compressible rotor flows p 302 A90-25283

Three-dimensional adaptive grid generation on a composite-block grid p 374 A90-25289

Analysis of transonic integral equations. II - Boundary element methods p 302 A90-25301

Comparisons among grid generation using elliptic partial differential equations p 374 A90-25478

On efficiency and accuracy of numerical methods for solving aerodynamic equations p 304 A90-25730

A high-order time-accurate scheme and its applications p 304 A90-25732

Application of a digital control theory for generating adaptive grids p 366 A90-25734

The transonic nonisentropic potential calculation p 304 A90-25739

Topology of computed incompressible three-dimensional separated flow field around high-angle-of-attack cone-cylinders p 366 A90-25764

Problem areas in applied computational fluid dynamics p 366 A90-25770

Computation of steady three dimensional transonic internal flows p 304 A90-25771

Calculation of tip leakage flow with three-dimensional Euler code p 304 A90-25772

Flow-calculation over a delta-wing using the thin-layer Navier-Stokes equations p 304 A90-25773

Non-equilibrium hypersonic flows - Physics and numerics p 304 A90-25777

Numerical calculation of bubbly two phase flow around an airfoil p 304 A90-25783

Numerical simulations of unsteady shock reflections by ramps p 305 A90-25795

Numerical methods for transonic cascade flow problems p 305 A90-25796

Navier-Stokes simulations around a high-speed propeller p 305 A90-25797

Analysis of three-dimensional aerospace configurations using the Euler and Navier-Stokes equations p 305 A90-25798

- Numerical aerodynamics via formal integration - Laplace, Euler, Prandtl, Navier-Stokes and Reynolds equations p 305 A90-25800
- Computation of 2D Navier-Stokes equations p 367 A90-25801
- An automatic Euler solver using unstructured upwind method p 367 A90-25811
- Turbulence models for 3D transonic viscous flows. II p 306 A90-25820
- A numerical method for solving the unsteady compressible Navier-Stokes equations p 306 A90-25827
- Flow dependent grid for aerodynamic designers p 306 A90-25831
- Transonic aerodynamics analysis of unconventional wing configurations by 3D-Euler code p 306 A90-25835
- Navier-Stokes computations for the investigation of flowfields about a Space-Plane p 306 A90-25836
- Numerical simulation of separated flows around a wing section by a discrete vortex method p 307 A90-25846
- Numerical simulation of wing in ground effect p 307 A90-25863
- Simulation of sound propagation in axisymmetric jet p 378 A90-25872
- Automatic mesh generation for complex three-dimensional regions using a constrained Delaunay triangulation p 375 A90-26022
- Efficient method for computing transonic and supersonic flows about aircraft p 307 A90-26132
- Fourth-order accurate three-dimensional compressible boundary-layer calculations p 308 A90-26136
- Numerical prediction of wakes of different bodies p 308 A90-26341
- Adaptive wall wind tunnels - Marriage between experiments and computations p 351 A90-26351
- Numerical grid generation in computational fluid mechanics '88; Proceedings of the Second International Conference, Miami Beach, FL, Dec. 5-8, 1988 p 376 A90-26476
- Knowledge-based flow field zoning p 308 A90-26478
- Quasi-three-dimensional grid generation by an algebraic homotopy procedure p 376 A90-26481
- Effect of the grid system on the solution of Euler equations p 309 A90-26494
- Solution-adaptive grids for transonic flows p 309 A90-26508
- The construction of component-adaptive grids for aerodynamic geometries p 309 A90-26513
- Techniques in multiblock domain decomposition and surface grid generation p 309 A90-26526
- Application of a multiblock grid generation approach to aircraft configurations p 310 A90-26527
- Interactive multi-block grid generation p 310 A90-26528
- 2-D and 3-D unstructured mesh adaption relying on physical analogy p 310 A90-26534
- On the combination of structured-unstructured meshes p 311 A90-26540
- Application of I-DEAS grid generator for three-dimensional transonic flow analysis p 311 A90-26542
- Grid generation for an aft-fuselage-mounted nacelle/pylon configuration p 311 A90-26543
- Zonal grid generation for fighter aircraft p 311 A90-26544
- Geometric modelling of complex aerodynamic surfaces and three-dimensional grid generation p 311 A90-26545
- Interactive grid generation for fighter aircraft geometries p 311 A90-26546
- Multiple-block grid adaption for an airplane geometry p 311 A90-26547
- Grid generation and its application to separated flows p 312 A90-26552
- Numerical interactive grid generation for 3D-flow calculations p 312 A90-26556
- Inlet swirl effects on dump combustor flows [AIAA PAPER 90-0035] p 312 A90-26904
- Analysis of unsteady rotor-stator interactions using a viscous explicit method [AIAA PAPER 90-0342] p 313 A90-26937
- Unsteady hypersonic viscous flow in impulse facilities [AIAA PAPER 90-0421] p 313 A90-26947
- A flux-split solution procedure for unsteady inlet flows [AIAA PAPER 90-0585] p 314 A90-26967
- Comparison of 3-D viscous flow computations of Mach 5 inlet with experimental data [AIAA PAPER 90-0600] p 314 A90-26970
- Viscous computations using a direct solver p 315 A90-27133
- Navier-Stokes computations useful in aircraft design [AIAA PAPER 90-1800] p 315 A90-27311
- Boundary element solution of the transonic integro-differential equation p 383 A90-27947
- Effects of turbulence model constants on computation of confined swirling flows p 444 A90-27999
- Wave formation on a liquid layer for de-icing airplane wings p 445 A90-28137
- Efficient free wake calculations using Analytical/Numerical Matching and far-field linearization p 384 A90-28171
- A numerical analysis of the British Experimental Rotor Program blade p 384 A90-28194
- Advanced rotor computations with a corrected potential method p 385 A90-28197
- Investigation of aerodynamic interactions between a rotor and fuselage in forward flight p 385 A90-28198
- Rotor loads validation utilizing a coupled aeroelastic analysis with refined aerodynamic modeling p 408 A90-28226
- Measurements, visualization and interpretation of 3-D flows - Application within base flows p 386 A90-28252
- Development and extension of diagnostic techniques for advancing high speed aerodynamic research p 436 A90-28281
- Numerical solution of the problem of supersonic flow of an ideal gas past a trapezoidal wedge p 386 A90-28980
- Calculation of flow characteristics in the core of a vortex sheet p 386 A90-28981
- Impact of multigrid smoothing analysis on three-dimensional potential flow calculations p 449 A90-29147
- Effect of a jet on transonic flow past an airfoil p 388 A90-29181
- Evaluation of current multiobjective optimization methods for aerodynamic problems using CFD codes [AIAA PAPER 90-0955] p 411 A90-29240
- Computation of steady and unsteady control surface loads in transonic flow [AIAA PAPER 90-0935] p 389 A90-29361
- Implicit flux-split Euler schemes for unsteady aerodynamic analysis involving unstructured dynamic meshes [AIAA PAPER 90-0936] p 389 A90-29362
- Unsteady flow computation of oscillating flexible wings [AIAA PAPER 90-0937] p 389 A90-29363
- Computational requirements for hypersonic flight performance estimates p 440 A90-29686
- Unsteady transonic aerodynamics p 393 A90-29882
- Physical phenomena associated with unsteady transonic flows p 394 A90-29883
- Basic equations for unsteady transonic flow p 394 A90-29884
- Basic numerical methods --- of unsteady and transonic flow p 394 A90-29886
- Application of transonic flow analysis to helicopter rotor problems p 394 A90-29887
- Alternative methods for modeling unsteady transonic flows p 394 A90-29889
- Massively parallel computing p 458 A90-29897
- Numerical solutions of the linearized Euler equations for unsteady vortical flows around lifting airfoils p 394 A90-30264
- An integral method for transonic flows p 395 A90-31119
- Comparison between experimental and numerical results for a research hypersonic aircraft p 395 A90-31278
- Calculations of transonic flows over wing-body combinations p 395 A90-31479
- Numerical simulation of separated flow around two-dimensional wing section by a discrete vortex method p 469 A90-32067
- Calculation of internal flows using a single-pass, parabolized Navier-Stokes analysis p 469 A90-32458
- Unsteady aerodynamics methods for transonic aeroelastic analysis p 471 A90-33353
- Application of the CAP-TSD unsteady transonic small disturbance program to wing flutter --- Computational Aeroelasticity Program p 491 A90-33354
- Computation of unsteady transonic flows around oscillating airfoils using full potential and Euler equations p 472 A90-33357
- Aeroelastic analysis using finite element models p 492 A90-33388
- Calculation of flow on a flat plate at angle of attack by numerical solution of Navier-Stokes equations p 537 A90-33424
- Numerical simulation of separated flows around a wing section at pitching motion by a discrete vortex method p 475 A90-33753
- Numerical simulation of vortex breakdown by solving the Euler equations for an incompressible fluid p 476 A90-34323
- Benchmark calculations with an unstructured grid flow solver on a SIMD computer p 546 A90-34378
- Computational aerothermodynamics p 476 A90-34380
- Capability of current supercomputers for the computational fluid dynamics p 546 A90-34382
- Computational fluid dynamics - Current capabilities and directions for the future p 540 A90-34385
- High-resolution shock-capturing schemes for inviscid and viscous hypersonic flows p 476 A90-34545
- A numerical method for calculating supersonic flows of a viscous gas p 476 A90-34672
- On a lifting line theory for supersonic flow. II - A supersonic lifting line theory for wings p 477 A90-34817
- Direct numerical simulations of transition in a compressible wake p 553 A90-35212
- Numerical calculation of the jet-interaction induced separation with respect to thrust vector control p 584 A90-35228
- Unsteady inviscid and viscous computations for vortex-dominated flows p 553 A90-35752
- Boundary element method for solving direct aerodynamic problem of aerofoil cascades on an arbitrary stream surface of revolution p 554 A90-35830
- The TSP methods applied to the calculation of transonic flow about wing/body/nacelle/pylon-configurations --- Transonic Small Perturbation p 554 A90-35868
- The inviscid axisymmetric stability of the supersonic flow along a circular cylinder p 554 A90-35916
- Navier-Stokes computation of flow around a round-edged double-delta wing p 555 A90-36251
- Computational methods in design aerodynamics p 557 A90-36539
- An efficient finite-difference algorithm for computing axisymmetric transonic nacelle flow fields p 557 A90-37205
- An analytic solution on hypersonic flow over an arbitrary slender body with near power-law profile p 558 A90-37736
- A method for solving three-dimensional viscous incompressible flows over slender bodies p 558 A90-37890
- The challenging process of validating CFD codes [AIAA PAPER 90-1402] p 558 A90-37943
- A numerical study on the use of sulfur hexafluoride as a test gas for wind tunnels [AIAA PAPER 90-1421] p 605 A90-37958
- Hypersonic flow calculations with a hybrid Navier-Stokes/Monte Carlo method [AIAA PAPER 90-1691] p 560 A90-38394
- Evaluation of transonic wall interference assessment and correction for semi-span wing data [AIAA PAPER 90-1433] p 597 A90-38487
- The influence of interactional aerodynamics of rotor-fuselage-interferences on the fuselage flow p 561 A90-38523
- A numerical study of supersonic flow over a compression corner with different incoming boundary-layer profiles [AIAA PAPER 90-1453] p 561 A90-38612
- Numerical simulation of confined, spatially-developing mixing layers - Comparison to the temporal shear layer [AIAA PAPER 90-1462] p 562 A90-38619
- Flow over inclined finite length and width flat plates at low and high Reynolds numbers [AIAA PAPER 90-1467] p 562 A90-38624
- An abbreviated Reynolds stress turbulence model for airfoil flows [AIAA PAPER 90-1468] p 562 A90-38625
- Numerical prediction of turbulent flow over airfoil sections with a new nonequilibrium turbulence model [AIAA PAPER 90-1469] p 562 A90-38626
- Newton solution of coupled viscous/inviscid multielement airfoil flows [AIAA PAPER 90-1470] p 562 A90-38627
- Parameter effects on oscillatory aerofoil in transonic flows [AIAA PAPER 90-1473] p 563 A90-38629
- The k-k1 turbulence model and wall layer model for compressible flows [AIAA PAPER 90-1483] p 563 A90-38637
- Versatility of an algebraic backflow turbulence model [AIAA PAPER 90-1485] p 563 A90-38639
- A locally implicit scheme for 3-D compressible viscous flows [AIAA PAPER 90-1525] p 563 A90-38670
- Interactive airfoil calculations with higher-order viscous-flow equations [AIAA PAPER 90-1533] p 564 A90-38678
- A flow around airfoil with slat and flap [AIAA PAPER 90-1535] p 564 A90-38679
- Numerical prediction of transonic viscous flows around airfoils through an Euler/boundary layer interaction method [AIAA PAPER 90-1537] p 564 A90-38681
- Unsteady Navier-Stokes solutions for a low aspect ratio delta wing [AIAA PAPER 90-1538] p 564 A90-38682

- The free-wake computation of rotor-body flows
[AIAA PAPER 90-1540] p 565 A90-38684
- Calculation of two- and three-dimensional flow in a transonic turbine cascade with particular regard to the losses
[AIAA PAPER 90-1542] p 565 A90-38686
- Calculation of unsteady rotor/stator interaction
[AIAA PAPER 90-1544] p 565 A90-38688
- A grid generation method for an aft-fuselage mounted capped-nacelle/pylon configuration with an actuator disk
[AIAA PAPER 90-1564] p 565 A90-38703
- A comparison of adaptive-grid redistribution and embedding for steady transonic flows
[AIAA PAPER 90-1565] p 565 A90-38704
- A hybrid Reynolds averaged/PDF closure model for supersonic turbulent combustion
[AIAA PAPER 90-1573] p 600 A90-38711
- Computational study for passive control of supersonic asymmetric vortical flows around cones
[AIAA PAPER 90-1581] p 566 A90-38718
- An interactive scheme for transonic wing/body flows based on Euler and inverse boundary-layer equations
[AIAA PAPER 90-1586] p 566 A90-38721
- Boundary conditions for Euler equations at internal block faces of multi-block domains using local grid refinement
[AIAA PAPER 90-1590] p 607 A90-38725
- Two and three dimensional grid generation by an algebraic homotopy procedure
[AIAA PAPER 90-1603] p 567 A90-38734
- A computational study of the taxonomy of vortex breakdown
[AIAA PAPER 90-1624] p 568 A90-38753
- Application of vortex embedding to aircraft flows
[AIAA PAPER 90-1626] p 568 A90-38755
- Navier-Stokes computations of vortical flows
[AIAA PAPER 90-1628] p 568 A90-38757
- Numerical simulation of a turbulent flow through a shock wave
[AIAA PAPER 90-1641] p 608 A90-38769
- Three-dimensional flux-split Euler schemes involving unstructured dynamic meshes
[AIAA PAPER 90-1649] p 569 A90-38777
- Temporal-adaptive Euler/Navier-Stokes algorithm for unsteady aerodynamic analysis of airfoils using unstructured dynamic meshes
[AIAA PAPER 90-1650] p 569 A90-38778
- A three-dimensional finite element Navier-Stokes solver with k-epsilon turbulence model for unstructured grids
[AIAA PAPER 90-1652] p 570 A90-38780
- Algebraic turbulence modeling for unstructured and adaptive meshes
[AIAA PAPER 90-1653] p 608 A90-38781
- Formation of shocks within axisymmetric nozzles
[AIAA PAPER 90-1655] p 570 A90-38782
- A computational study of the impingement region of an unsteady subsonic jet
[AIAA PAPER 90-1657] p 570 A90-38784
- Calculation of hypersonic forebody/inlet flow fields
[AIAA PAPER 90-1493] p 619 A90-39049
- Boundary layer stability in the case of transonic external flow
[AIAA PAPER 90-1659] p 619 A90-39514
- Perturbations of higher modes in a supersonic jet
[AIAA PAPER 90-1661] p 619 A90-39516
- The problem of supersonic flow past a thin wing of finite span with fully subsonic leading edges
[AIAA PAPER 90-1663] p 620 A90-39519
- Relationship between velocity circulation around a wing profile and vorticity dispersion in a boundary layer
[AIAA PAPER 90-1665] p 620 A90-39539
- An introduction to chaos theory in CFD
[AIAA PAPER 90-1440] p 680 A90-39725
- Simulation of inviscid blade-row interaction using a linearised potential code
[AIAA PAPER 90-1916] p 621 A90-40555
- CFD applications in an aerospace engine test facility
[AIAA PAPER 90-2003] p 681 A90-40590
- Computational modeling of inlet hammer shock wave generation
[AIAA PAPER 90-2005] p 621 A90-40592
- Application of CFD to pitch/yaw thrust vectoring spherical convergent flap nozzles
[AIAA PAPER 90-2023] p 657 A90-40597
- A numerical investigation of supersonic inlet using implicit TVD scheme
[AIAA PAPER 90-2135] p 621 A90-40612
- Transverse fuel-injection model for a scramjet propulsion system
[AIAA PAPER 90-2027] p 659 A90-40927
- Numerical simulation of the growth of instabilities in supersonic free shear layers
[AIAA PAPER 90-2125] p 623 A90-40941
- CFD propels NASP propulsion progress
[AIAA PAPER 90-2125] p 624 A90-42032
- Quasi-3D viscous flow computations in subsonic and transonic turbomachinery bladings
[AIAA PAPER 90-2126] p 625 A90-42033
- Computation of multiple normal shock wave/turbulent boundary layer interactions
[AIAA PAPER 90-2133] p 685 A90-42037
- Numerical analysis of the flows in annular slinger combustors
[AIAA PAPER 90-2164] p 685 A90-42052
- Numerical modeling of an impinging jet in cross-flow
[AIAA PAPER 90-2246] p 686 A90-42093
- Turbulence model performance in V/STOL flow field simulation
[AIAA PAPER 90-2248] p 625 A90-42094
- Boundary-layer transition and separation on a turbine blade in a plane cascade
[AIAA PAPER 90-2263] p 625 A90-42102
- Numerical simulations of gas turbine combustor flows
[AIAA PAPER 90-2305] p 686 A90-42116
- Investigation of unsteady flow through transonic turbine stage. I - Analysis
[AIAA PAPER 90-2408] p 626 A90-42161
- A modeling technique for STOVL ejector and volume dynamics
[AIAA PAPER 90-2417] p 663 A90-42168
- Mixing characteristics of dilution jets in small gas turbine combustors
[AIAA PAPER 90-2728] p 664 A90-42217
- Navier-Stokes analysis of an ejector and mixer-ejector operating at pressure ratios in the range 2-4
[AIAA PAPER 90-2730] p 626 A90-42218
- Calculation of viscous-inviscid strong interaction for transonic flows over aerofoils
[AIAA PAPER 90-2730] p 627 A90-42364
- Wind tunnel results and numerical computations for the NAE deHavilland series of natural laminar flow airfoils
[AIAA PAPER 90-2730] p 628 A90-42403
- Application of the KTRAN transonic small disturbance code to the complete CF-18 aircraft with stores
[AIAA PAPER 90-2730] p 629 A90-42416
- CFD and transonic helicopter sound
[AIAA PAPER 90-2730] p 696 A90-42433
- Comparison with experiment of various computational methods of airflow on three helicopter fuselages
[AIAA PAPER 90-2730] p 630 A90-42436
- Rotorcraft computational fluid dynamics - Recent developments at McDonnell Douglas
[AIAA PAPER 90-2730] p 630 A90-42439
- A new Lagrangian method for steady supersonic flow computation. I - Godunov scheme
[AIAA PAPER 90-2730] p 631 A90-42506
- Finite element simulation of turbulent propeller flowfields
[AIAA PAPER 90-2730] p 703 A90-42658
- A collocated finite volume method for solving the Navier-Stokes equations for incompressible and compressible flows in turbomachinery - Results and applications
[AIAA PAPER 90-2730] p 703 A90-42659
- Film cooling of turbine blades - Two dimensional experiments and numerical simulations
[AIAA PAPER 90-2730] p 739 A90-42670
- Development of a robust calculation method for transonic viscous blade-to-blade flows
[AIAA PAPER 90-2730] p 703 A90-42671
- Computational analysis of the flowfield of a two-dimensional ejector nozzle
[AIAA PAPER 90-1901] p 740 A90-42690
- A computational investigation of flow losses in a supersonic combustor
[AIAA PAPER 90-2093] p 742 A90-42728
- Flow establishment in a generic scramjet combustor
[AIAA PAPER 90-2096] p 742 A90-42729
- Computation of turbine flowfields with a Navier-Stokes code
[AIAA PAPER 90-2122] p 704 A90-42731
- Turbulent flow simulation of a three-dimensional turbine cascade
[AIAA PAPER 90-2124] p 704 A90-42732
- Computational analysis of an open-nosed fighter/attack inlet
[AIAA PAPER 90-2145] p 704 A90-42737
- Computational investigation of two-dimensional ejector nozzle flow fields
[AIAA PAPER 90-2148] p 768 A90-42739
- A CFD study of precombustion shock-trains from Mach 3-6
[AIAA PAPER 90-2220] p 705 A90-42751
- Numerical simulation of droplet deformation in convective flows
[AIAA PAPER 90-2309] p 769 A90-42773
- Unsteady analysis of hot streak migration in a turbine stage
[AIAA PAPER 90-2354] p 769 A90-42782
- Using 3D Euler flow simulations to assess effects of periodic unsteady flow through turbines
[AIAA PAPER 90-2357] p 706 A90-42783
- A validation study of the Spark Navier Stokes code for nonreacting scramjet combustor flowfields
[AIAA PAPER 90-2360] p 706 A90-42784
- Numerical simulation of hypersonic viscous continuum flow
[AIAA PAPER 90-2360] p 707 A90-44407
- Numerical study of heat transfer for unsteady viscous supersonic blunt body flows
[AIAA PAPER 90-2360] p 707 A90-44432
- Numerical study of compressible nozzle flow
[AIAA PAPER 90-2360] p 708 A90-44437
- A formulation for the solution of Euler equations for compressible flow using finite elements
[AIAA PAPER 90-2360] p 708 A90-44447
- Transonic flow computations in convergent propulsion nozzles using the time-dependent mode
[AIAA PAPER 90-2360] p 708 A90-44459
- Development and application of a fractional-step method for the solution of transonic and supersonic flow problems
[AIAA PAPER 90-2360] p 709 A90-44461
- Numerical predictions for the flow and the heat transfer in gas turbine cooling systems
[AIAA PAPER 90-2360] p 770 A90-44464
- Numerical solution of 2D transonic flows in a turbine cascade
[AIAA PAPER 90-2360] p 709 A90-44601
- Zonal Navier-Stokes methodology for flow simulation about a complete aircraft
[AIAA PAPER 90-2360] p 709 A90-44727
- Compressible flow algorithms on structured/unstructured grids
[AIAA PAPER 90-2360] p 779 A90-44855
- Numerical modeling of transverse flow past a cylinder using Euler equations
[AIAA PAPER 90-2360] p 709 A90-44922
- Effects of turbulence models on the prediction of transonic wing flows
[AIAA PAPER 90-2360] p 713 A90-45440
- Application of divergent trailing-edge airfoil technology to the design of a derivative wing
[AIAA PAPER 90-2360] p 714 A90-45466
- Transonic analysis of complex configurations using TRANAIR program
[AIAA PAPER 90-2360] p 714 A90-45467
- Hypersonic CFD applications for the National Aero-Space Plane
[AIAA PAPER 90-2360] p 714 A90-45473
- Hypersonic forebody lift-induced drag
[AIAA PAPER 90-2360] p 715 A90-45497
- Computational results for the effects of external disturbances on transition location of bodies of revolution from subsonic to supersonic speeds and comparisons with experimental data
[AIAA PAPER 90-2360] p 715 A90-45522
- A unified pressure correction algorithm for computing complex fluid flows
[AIAA PAPER 90-2360] p 772 A90-45528
- Large-eddy simulations of flows in a ramjet combustor
[AIAA PAPER 90-2360] p 772 A90-45534
- Numerical solutions for unsteady aerofoil by internal singularity method
[AIAA PAPER 90-2360] p 716 A90-45536
- Non-unique solutions of the Euler equations
[AIAA PAPER 90-2360] p 716 A90-45727
- Navier-Stokes computations of three-dimensional laminar flows with buoyancy in a channel with wing-type vortex generators
[AIAA PAPER 90-2360] p 772 A90-45728
- Linear instability of the supersonic wake behind a flat plate aligned with a uniform stream
[AIAA PAPER 90-2360] p 716 A90-45783
- Simulation of leading-edge vortex flows
[AIAA PAPER 90-2360] p 716 A90-45785
- AIAA Applied Aerodynamics Conference, 8th, Portland, OR, Aug. 20-22, 1990, Technical Papers, Parts 1 & 2
[AIAA PAPER 90-2360] p 787 A90-45845
- CFD validation for aerodynamic flows - Challenge for the '90's
[AIAA PAPER 90-2360] p 787 A90-45846
- Supersonic flow computations for an ASTOVL aircraft configuration
[AIAA PAPER 90-2360] p 787 A90-45847
- AIRPLANE - Experiences, benchmarks and improvements
[AIAA PAPER 90-2360] p 787 A90-45848
- Numerical simulation of the viscous flow around a simplified F/A-18 at high angles of attack
[AIAA PAPER 90-2360] p 787 A90-45849
- Numerical simulation of the effects of variation of angle of attack and sweep angle on vortex breakdown over delta wings
[AIAA PAPER 90-3000] p 788 A90-45850
- Numerical simulation of vortical flows over a strake-delta wing and a close coupled delta-canard configuration
[AIAA PAPER 90-3002] p 788 A90-45851
- Numerical simulation of vortical flows over close-coupled canard-wing configuration
[AIAA PAPER 90-3003] p 788 A90-45852
- Numerical study of asymmetric air injection to control high angle-of-attack forebody vortices on the X-29 aircraft
[AIAA PAPER 90-3004] p 788 A90-45853
- The effect of turbulence models on the numerical prediction of the flowfield about a prolate spheroid at high angle of attack
[AIAA PAPER 90-3106] p 789 A90-45855
- Euler procedure for calculation of the steady rotor flow with emphasis on wake evolution
[AIAA PAPER 90-3007] p 789 A90-45857

- Experimental and numerical study of the British Experimental Rotor Programme blade
[AIAA PAPER 90-3008] p 789 A90-45858
- Navier-Stokes simulation of transonic afterbody flows with jet exhaust
[AIAA PAPER 90-3057] p 790 A90-45862
- 2D vs. 3D - Selection of pressure distributions to delay separation on wings
[AIAA PAPER 90-3026] p 790 A90-45868
- Numerical investigation of laminar separated viscous trailing-edge flow using triple-deck theory
[AIAA PAPER 90-3046] p 792 A90-45883
- Computational simulation of flows about hypersonic geometries with sharp leading edges
[AIAA PAPER 90-3065] p 793 A90-45891
- Experimental and computational surface and flow-field results for an all-body hypersonic aircraft
[AIAA PAPER 90-3067] p 793 A90-45893
- Calculation of three-dimensional viscous and inviscid hypersonic flows using split-matrix marching methods
[AIAA PAPER 90-3070] p 794 A90-45894
- Sideslip-induced static pressure errors in flight-test measurements
[AIAA PAPER 90-3082] p 794 A90-45898
- Angle-of-attack validation of a new zonal-CFD method for airfoil simulations
[AIAA PAPER 90-3077] p 795 A90-45908
- Relative efficiency and accuracy of two Navier-Stokes codes for simulating attached transonic flow over wings
[AIAA PAPER 90-3078] p 795 A90-45909
- An upwind approach to unsteady flowfield simulation
[AIAA PAPER 90-3100] p 796 A90-45912
- A characterization and search technique for unsteady flow control problems
[AIAA PAPER 90-3102] p 796 A90-45914
- Application of a streamwise upwind algorithm for unsteady transonic computations over oscillating wings
[AIAA PAPER 90-3103] p 796 A90-45915
- The role of CFD applied to high performance aircraft
[AIAA PAPER 90-3071] p 796 A90-45917
- On optimal supersonic/hypersonic bodies
[AIAA PAPER 90-3072] p 796 A90-45918
- Adaptive grid embedding for the two-dimensional Euler equations
[AIAA PAPER 90-3049] p 797 A90-45929
- An unstructured-mesh Euler method for multielement airfoil geometries
[AIAA PAPER 90-3051] p 797 A90-45930
- Transient aeroelastic computations using multiple moving frames of reference
[AIAA PAPER 90-3053] p 798 A90-45932
- Numerical study of vortical flow over a sideslipping delta wing
[AIAA PAPER 90-3001] p 798 A90-45936
- Outflow boundary conditions using Duhamel's equation
[AIAA PAPER 90-3014] p 798 A90-45937
- A fast method for computation of airfoil characteristics
p 799 A90-46361
- Study of low-Reynolds number separated flow past the Wortmann FX 63-137 airfoil
p 799 A90-46363
- Compressible Navier-Stokes solutions over low Reynolds number airfoils
p 802 A90-46382
- Boundary-integral method for calculating aerodynamic sensitivities with illustration for lifting-surface theory
p 806 A90-46841
- Unsteady aerodynamics - Physical issues and numerical predictions
p 806 A90-46843
- Interactive grid adaption
p 806 A90-46850
- Two-dimensional convergent-divergent nozzle flow with wall velocity slip and temperature jump
p 807 A90-46884
- Numerical calculations of flows with shock waves by flux vector splitting method
p 808 A90-47299
- Numerical study of interaction of a jet with a supersonic cross flow
p 808 A90-47300
- Speed-up of the strongly implicit procedure with application to subsonic/transonic potential flows
p 809 A90-47301
- Unsteady Euler airfoil solutions using unstructured dynamic meshes
p 809 A90-47307
- Winger - Computer code for aerodynamic analysis of wings
p 810 A90-48077
- Solutions of two-dimensional Euler equations with multigrid acceleration
p 810 A90-48086
- Aircraft passing through a sinusoidal gust
p 811 A90-48090
- Wave interactions in a three-dimensional attachment-line boundary layer
p 811 A90-48715
- A numerical method for relating two- and three-dimensional pressure distributions on transonic wings
[AIAA PAPER 90-3211] p 812 A90-48837
- TRANAIR applications to engine/airframe integration
p 838 A90-48958
- CFD needs in conceptual design
[AIAA PAPER 90-3209] p 813 A90-49106
- CFD support of NASP design
[AIAA PAPER 90-3252] p 872 A90-49120
- Numerical simulation of transonic flow through oscillating and multi-row two-dimensional airfoil cascades
p 814 A90-49460
- Numerical solution of 2-D transonic flow through an axial turbine stage
p 814 A90-49464
- A design method for turbomachinery blading in three-dimensional flow
p 904 A90-51003
- Cascade aerodynamic gust response including steady loading effects
p 904 A90-51006
- Least-squares finite element methods for compressible Euler equations
p 904 A90-51013
- An improved SIP scheme for numerical solutions of transonic streamfunction equations - strongly implicit procedure
p 904 A90-51014
- Numerical simulation of three-dimensional transonic flows
p 905 A90-51020
- The calculation of incompressible separated turbulent boundary layers
p 905 A90-51025
- A comprehensive analysis of the viscous incompressible flow in quasi-three-dimensional aerfoil cascades
p 905 A90-51028
- Multigrid methods in computational fluid dynamics
p 906 A90-51526
- Multigrid acceleration of TVD schemes in transonic Euler flow calculation
p 908 A90-52030
- Varying specific heat gasdynamic function formulae simplification and analytical solution of normal shock waves
p 908 A90-52776
- A method of predicting 3-D compressible boundary layer on the rotating blade of turbomachinery
p 908 A90-52777
- Analysis and calculation for interaction between shock wave and laminar boundary layer
p 909 A90-52778
- An investigation of characteristics of transonic and viscous flows for turbine cascades
p 909 A90-52779
- Three-dimensional unsteady transonic viscous-inviscid interaction
p 18 N90-10005
- An integrated CFD/experimental analysis of aerodynamic forces and moments
[NASA-TM-102195] p 18 N90-10006
- Fluid Dynamics of Three-Dimensional Turbulent Shear Flows and Transition
[AGARD-CP-438] p 71 N90-10356
- Stability and transition of three-dimensional boundary layers
p 71 N90-10357
- Direct numerical study of leading-edge contamination
p 19 N90-10361
- Control and modification of turbulence
p 72 N90-10377
- Linear instability of supersonic plane wakes
[NASA-CR-181911] p 20 N90-10833
- An experimental investigation of the aerodynamic characteristics of slanted base ogive cylinders using magnetic suspension technology
[NASA-CR-181708] p 21 N90-10834
- Computer simulation of aircraft aerodynamics
[NASA-TM-102221] p 88 N90-11699
- Analytical studies of three-dimensional combustion processes
[AD-A211903] p 126 N90-11837
- Simulation of glancing shock wave and boundary layer interaction
[NASA-TM-102233] p 133 N90-11970
- Research in Natural Laminar Flow and Laminar-Flow Control, part 2
[NASA-CP-2487-PT-2] p 91 N90-12519
- CFD methods for drag prediction and analysis currently in use in UK
[RAE-TM-AERO-2146] p 95 N90-12563
- Analysis of experimental data for CAST 10-2/DOA 2 supercritical airfoil at low Reynolds numbers and application to high Reynolds number flow
[AD-A211654] p 170 N90-13326
- Correlation of Puma airloads: Lifting-line and wake calculation
[NASA-TM-102212] p 170 N90-13327
- Block-structured solution of three-dimensional transonic flows using parallel processing
[AD-A212851] p 170 N90-13330
- Study of the integration of wind tunnel and computational methods for aerodynamic configurations
[NASA-TM-102196] p 170 N90-13332
- A CFD study of tilt rotor flowfields
[NASA-CR-186116] p 171 N90-13349
- Computation of Navier-Stokes equations for three-dimensional flow separation
[NASA-TM-102266] p 172 N90-13353
- Recent progress in research pertaining to estimates of gas-side heat transfer in an aircraft gas turbine
[NASA-TM-102460] p 194 N90-13394
- Multigrid and defect correction for the steady Navier-Stokes equations: Applications to aerodynamics
[ETN-90-96011] p 212 N90-13727
- Numerical simulation of transition in three-dimensional boundary layers
[DLR-FB-89-12] p 212 N90-13728
- Navier-Stokes simulation of the crossflow instability in swept-wing flows
[NASA-CR-186122] p 212 N90-13744
- Temporally and spatially resolved flow in a two-stage axial compressor. Part 2: Computational assessment
[NASA-TM-102273] p 194 N90-14236
- A dynamic multiblock approach to solving the unsteady Euler equations about complex configurations
p 214 N90-14497
- Unsteady aerodynamics of oscillating and rapidly pitched airfoils
p 235 N90-15074
- Finite difference techniques and rotor blade aeroelastic partial differential equations with quasisteady aerodynamics
p 236 N90-15075
- Assessment of computational prediction of tail buffeting
[NASA-TM-101613] p 237 N90-15886
- Calculation of the flow field of a multiblade helicopter rotor using a Euler method including the wake
p 278 N90-16189
- Calculation of the flap profile flows with separation based on coupled potential and boundary layer solutions
p 278 N90-16191
- NASA aerodynamics program
[NASA-TM-4175] p 373 N90-17235
- Prediction methods for store separation
p 317 N90-17549
- Numerical solutions of the linearized Euler equations for unsteady vortical flows around lifting airfoils
[NASA-TM-102466] p 318 N90-17562
- Analysis and numerical solution of flow over airfoil with control flap
p 318 N90-17564
- Opportunities for improved understanding of supersonic and hypersonic flows
p 318 N90-17566
- Shock-shock boundary layer interactions
p 318 N90-17569
- Viscous three-dimensional analyses for nozzles for hypersonic propulsion
[NASA-CR-185197] p 344 N90-17635
- Prediction of rotor blade-vortex interaction noise from 2-D aerodynamic calculations and measurements
[ISL-CO-243/88] p 396 N90-18365
- Aerodynamics of unsteady systems. Numerical study of potential flow/boundary layer coupling
[ETN-90-96257] p 396 N90-18367
- Study of the blade/vortice interaction on a one-blade rotor during forward flight (incompressible, non viscous fluid)
[ISL-R-115/88] p 415 N90-18391
- Unsteady Aerodynamic Phenomena in Turbomachines
[AGARD-CP-468] p 425 N90-18405
- Unsteady blade loads due to wake influence
p 426 N90-18413
- Numerical prediction of axial turbine stage aerodynamics
p 426 N90-18416
- Modelling unsteady transition and its effects on profile loss
p 427 N90-18423
- Measurement of velocity profiles and Reynolds stresses on an oscillating airfoil
p 397 N90-18427
- Stall and recovery in multistage axial flow compressors
p 428 N90-18429
- Computation of hypersonic unsteady viscous flow over a cylinder
p 397 N90-19194
- A streamwise upwind algorithm applied to vortical flow over a delta wing
[NASA-TM-102225] p 398 N90-19201
- External flow computations for a finned 60mm ramjet in steady supersonic flight
[AD-A216998] p 428 N90-19233
- Experimental and theoretical investigations of flowfields and heat transfer in modern gas turbines
[AD-A217663] p 429 N90-19237
- The influence of a wall function on turbine blade heat transfer prediction
p 429 N90-19421
- Flow simulation for aircraft
[NLR-MP-87082-U] p 455 N90-19543
- Numerical simulations of supersonic flow through oscillating cascade sections
[NASA-TM-103100] p 478 N90-20051
- Comparison of 3-D viscous flow computations of Mach 5 inlet with experimental data
[NASA-TM-102518] p 510 N90-20090
- On total variation diminishing schemes for transonic turbulent flow computation
p 479 N90-20945
- Comparison of C- and O-grid generation methods using a NACA 0012 airfoil
[AD-A216375] p 479 N90-20948
- Convergence acceleration of hypersonic flow calculations: A nonlinear relaxation factor
p 480 N90-20957

Computational Methods for Aerodynamic Design (Inverse) and Optimization [AGARD-CP-463] p 500 N90-20976

An efficient airfoil design method using the Navier-Stokes equations p 500 N90-20981

A computational design method for shock free transonic cascades and airfoils p 501 N90-20986

Inverse computation of transonic internal flows with application for multi-point-design of supersonic compressor blades p 501 N90-20987

An inverse method for the design of turbomachine blades p 511 N90-20988

Optimization of aerodynamic designs using computational fluid dynamics p 541 N90-20999

Secondary Flows in Turbomachines [AGARD-CP-469] p 511 N90-21009

Secondary flows and radial mixing predictions in axial compressors p 512 N90-21010

A study on secondary flow and spanwise mixing in axial flow compressors p 512 N90-21012

Parabolized calculations of turbulent three dimensional flows in a turbine duct p 482 N90-21013

Experimental and numerical study on basic phenomena of secondary flows in turbines p 512 N90-21014

An investigation of secondary flows in nozzle guide vanes p 512 N90-21016

Secondary flow predictions for a transonic nozzle guide vane p 513 N90-21017

Secondary flow in a turbine guide vane with low aspect ratio p 513 N90-21018

Centrifugal impeller geometry and its influence on secondary flows p 513 N90-21020

Calculation of the three dimensional turbulent flow in a linear turbine blade p 513 N90-21021

Calculation of the secondary flow in an axial turbine p 513 N90-21022

Secondary flow calculations for axial and radial compressors p 514 N90-21024

Computational prediction and measurement of the flow in axial turbine cascades and stages p 514 N90-21028

Analysis of the rotor tip leakage flow with tip cooling air ejection p 515 N90-21029

Numerical simulation of hypersonic flow around a space plane. Part 2: Application to high angles of attack flow [NAL-TR-10117] p 570 N90-21726

Swept wing ice accretion modeling [NASA-TM-103114] p 570 N90-21727

Extension of a streamwise upwind algorithm to a moving grid system [NASA-TM-102800] p 572 N90-21739

Analytical study of the origin and behavior of asymmetric vortices [NASA-TM-102796] p 573 N90-21746

Mesh generation for flow computation in turbomachine p 588 N90-21981

Design and testing of a multiblock grid-generation procedure for aircraft design and research p 582 N90-21984

Grid patching approaches for complex three-dimensional configurations p 573 N90-21985

Multiblock topology specification and grid generation for complete aircraft configurations p 582 N90-21986

Feature-associated mesh embedding for complex configurations p 608 N90-21988

A discussion on issues relating to multiblock grid generation p 608 N90-21991

Automatic grid generation in complex three-dimensional configurations using a frontal system p 608 N90-21992

Unstructured finite element mesh generation and adaptive procedures for CFD p 608 N90-21993

Development of a computational fluid dynamics and chemistry model for the fouling of jet fuels [DE90-005664] p 608 N90-22003

European research on viscous flow (EuroVisc) p 609 N90-22014

[NLR-TP-89077-U] p 609 N90-22014

Extension of a three-dimensional viscous wing flow analysis user's manual: VISTA 3-D code [NASA-CR-182024] p 574 N90-22538

A modeling technique for STOVL ejector and volume dynamics [NASA-TM-103167] p 589 N90-22566

Supersonic flow computations for an ASTOVL aircraft configuration, phase 2, part 2 [NASA-CR-4284] p 610 N90-22746

Numerical flow simulation and supercomputers: More than a digital wind tunnel p 612 N90-22976

Current Japanese supercomputers for computational fluid dynamics applications p 610 N90-23172

Extension of a three-dimensional viscous wing flow analysis [NASA-CR-182023] p 631 N90-23348

The computation of turbulent thin shear flows associated with flow around multielement aerofoils p 633 N90-24240

Experimental and analytical study of close-coupled ventral nozzles for ASTOVL aircraft [NASA-TM-103170] p 666 N90-24273

Technical evaluation report on the Fluid Dynamics Panel Symposium on Computational Methods for Aerodynamic Design (Inverse) and Optimization [AGARD-AR-267] p 720 N90-25947

Computation of viscous aerodynamic characteristics of 2-D airfoils for helicopter applications [NLR-MP-88052-U] p 720 N90-25951

Liquid fueled ramjet combustion instability: Acoustical and vortical interactions with burning sprays [AD-A222752] p 767 N90-26104

Report of the Fluid Dynamics Panel Working Group 10 on calculation of 3D separate turbulent flows in boundary layer limit [AGARD-AR-255] p 776 N90-26280

Development of a system for the numerical simulation of Euler flows, with results of preliminary 3-D propeller-slipstream/exhaust-jet calculations [NLR-TR-88008-U] p 776 N90-26285

Informatics aspects of large flow calculations on the SX-2 supercomputer [NLR-MP-88037-U] p 776 N90-26290

Fluid Dynamics Panel Working Group 12 on Adaptive Wind Tunnel Walls: Technology and Applications [AGARD-AR-269] p 870 N90-26838

Turbulent reacting flows and supersonic combustion [AD-A221793] p 875 N90-26933

Development of a mathematical model for the thermal decomposition of aviation fuels [AD-A221673] p 875 N90-26994

A comparison of two central difference schemes for solving the Navier-Stokes equations [NASA-TM-102815] p 816 N90-27654

Aerodynamics of a linear oscillating cascade [NASA-TM-103250] p 817 N90-27657

Efficient solution of the steady Euler equations with a centered implicit method p 884 N90-27999

The effect of rapid spoiler deployment on the transient forces on an aerofoil p 921 N90-28527

Study of the ground effects in the CEAT aerohydrodynamic tunnel: Using the results p 922 N90-28530

The aerodynamic design of the oblique flying wing supersonic transport [NASA-CR-177552] p 923 N90-28540

Measurement of the steady surface pressure distribution on a single rotation large scale advanced prop-fan blade at Mach numbers from 0.03 to 0.78 [NASA-CR-182124] p 929 N90-28552

Development of turbulence models for the analysis of compressible or incompressible unsteady flow [ETN-90-97486] p 958 N90-28810

Numeric fluid mechanics p 980 N90-29161

Some topics in computational transonic aerodynamics: Revision [NAL-TR-1018T] p 912 N90-29332

COMPUTATIONAL GEOMETRY

NMG - A system of numerical representation of aircraft geometry p 103 N90-15877

Surface grid generation for complex three-dimensional geometries p 376 N90-26484

The construction of component-adaptive grids for aerodynamic geometries p 309 N90-26513

Unstructured finite element mesh generation and adaptive procedures for CFD p 608 N90-21993

COMPUTATIONAL GRIDS

Grid generation and adaptation for the direct simulation Monte Carlo method p 67 N90-11102

A class of implicit upwind schemes for Euler simulations with unstructured meshes p 5 N90-11597

Multigrid acceleration of transonic flow computations p 147 N90-16783

Multigrid solution method for the Euler equations --- Book p 149 N90-16841

Three-dimensional solution-adaptive grid generation on composite configurations [AIAA PAPER 90-0329] p 164 N90-19799

Application of an adaptive algorithm to single and two-element airfoils in turbulent flow [AIAA PAPER 90-0698] p 169 N90-19983

Development of an unstructured mesh/Navier-Stokes method for aerodynamics of aircraft with ice accretions [AIAA PAPER 90-0758] p 169 N90-20011

Vortical flows over delta wings and numerical prediction of vortex breakdown [AIAA PAPER 90-0102] p 227 N90-22166

Finite element mesh refinement criteria for stress analysis p 273 N90-23013

A three-dimensional space marching algorithm for the solution of the Euler equations on unstructured grids [AIAA PAPER 90-0014] p 234 N90-23701

Automation of the development of a finite element model for shells of the wing type p 364 N90-24118

Three-dimensional adaptive grid generation on a composite-block grid p 374 N90-25289

Application of a digital control theory for generating adaptive grids p 366 N90-25734

Flow dependent grid for aerodynamic designers p 306 N90-25831

Application of multiple grids topology to supersonic internal/external flow interactions p 308 N90-26135

Numerical grid generation in computational fluid mechanics '88; Proceedings of the Second International Conference, Miami Beach, FL, Dec.-5-8, 1988 p 376 N90-26476

Knowledge-based flow field zoning p 308 N90-26478

Algebraic boundary-conforming grid generation around wing/tail-body configurations p 308 N90-26480

Hyperbolic grid generation techniques for blunt body configurations p 376 N90-26490

Effect of the grid system on the solution of Euler equations p 309 N90-26494

A comparison of two adaptive grid techniques p 309 N90-26507

Solution-adaptive grids for transonic flows p 309 N90-26508

Application of a multiblock grid generation approach to aircraft configurations p 310 N90-26527

Interactive multi-block grid generation p 310 N90-26528

The generation of unstructured triangular meshes using Delaunay triangulation --- applications to hypersonic inlets p 310 N90-26533

Generation of tetrahedral meshes around complete aircraft p 310 N90-26536

Interactive generation of unstructured grids for three dimensional problems p 310 N90-26537

On the combination of structured-unstructured meshes p 311 N90-26540

Application of I-DEAS grid generator for three-dimensional transonic flow analysis p 311 N90-26542

Multiple-block grid adaption for an airplane geometry p 311 N90-26547

Grid generation and its application to separated flows p 312 N90-26552

Interactive grid generation for turbomachinery flow field simulations p 312 N90-26553

C-grid generation for turbomachinery cascades p 312 N90-26554

Numerical interactive grid generation for 3D-flow calculations p 312 N90-26556

Calculation of transonic flows with separation past arbitrary inlets at incidence p 384 N90-27979

Fast adaptive grid method for compressible flows p 445 N90-28006

Implicit flux-split Euler schemes for unsteady aerodynamic analysis involving unstructured dynamic meshes p 389 N90-29362

[AIAA PAPER 90-0936] p 389 N90-29362

Aeroelastic analysis of wings using the Euler equations with a deforming mesh [AIAA PAPER 90-1032] p 391 N90-29376

Benchmark calculations with an unstructured grid flow solver on a SIMD computer p 546 N90-34378

Euler flutter analysis of airfoils using unstructured dynamic meshes p 602 N90-35760

Solution of Euler equations with unstructured meshes p 558 N90-37343

A comparison of adaptive-grid redistribution and embedding for steady transonic flows [AIAA PAPER 90-1565] p 565 N90-38704

Boundary conditions for Euler equations at internal block faces of multi-block domains using local grid refinement [AIAA PAPER 90-1590] p 607 N90-38725

A general decomposition algorithm applied to multi-element airfoil grids [AIAA PAPER 90-1606] p 567 N90-38737

Application of vortex embedding to aircraft flows [AIAA PAPER 90-1626] p 568 N90-38755

A three-dimensional finite element Navier-Stokes solver with k-epsilon turbulence model for unstructured grids [AIAA PAPER 90-1652] p 570 N90-38780

Algebraic turbulence modeling for unstructured and adaptive meshes [AIAA PAPER 90-1653] p 608 N90-38781

Application of a new adaptive grid for aerodynamic analysis of shock containing single jets [AIAA PAPER 90-2025] p 624 N90-41988

Numerical simulations of gas turbine combustor flows [AIAA PAPER 90-2305] p 686 N90-42116

Euler and Navier-Stokes computations for airfoil geometries using unstructured meshes p 630 N90-42425

A multistage method for the solution of the Euler equations on unstructured grids p 708 N90-44460

Compressible flow algorithms on structured/unstructured grids p 779 N90-44855

Hypersonic forebody lift-induced drag
[SAE PAPER 892345] p 715 A90-45497
Interactive grid adaption p 806 A90-46850
Unsteady Euler airfoil solutions using unstructured dynamic meshes p 809 A90-47307
Euler analysis comparison with LDV data for an advanced counter-rotation propfan at cruise
[AIAA PAPER 90-3033] p 903 A90-50637
Solution of the thin-layer Navier-Stokes equations for laminar transonic flow
[PB89-221600] p 136 N90-12879
Multigrid solution method for the Euler equations
[PB89-219463] p 138 N90-13116
Multigrid calculations of 3-D turbulent viscous flows
[NASA-CR-185154] p 143 N90-13323
Application of a self-adaptive grid method to complex flows
[NASA-TM-102223] p 143 N90-13324
Multigrid and defect correction for the steady Navier-Stokes equations: Applications to aerodynamics
[ETN-90-96011] p 212 N90-13727
Comparison of C- and O-grid generation methods using a NACA 0012 airfoil
[AD-A216375] p 479 N90-20948
Convergence acceleration of hypersonic flow calculations: A nonlinear relaxation factor p 480 N90-20957
A fast collocation method for transonic airfoil design p 501 N90-20984
A computational design method for shock free transonic cascades and airfoils p 501 N90-20986
Secondary flow predictions for a transonic nozzle guide vane p 513 N90-21017
Adaptive grid embedding for the two-dimensional flux-split Euler equations
[NASA-CR-186533] p 547 N90-21571
Extension of a streamwise upwind algorithm to a moving grid system
[NASA-TM-102800] p 572 N90-21739
Mesh generation for flow computation in turbomachine p 588 N90-21981
Design and testing of a multiblock grid-generation procedure for aircraft design and research p 582 N90-21984
Grid patching approaches for complex three-dimensional configurations p 573 N90-21985
Feature-associated mesh embedding for complex configurations p 608 N90-21988
A discussion on issues relating to multiblock grid generation p 608 N90-21991
Automatic grid generation in complex three-dimensional configurations using a frontal system p 608 N90-21992
Unstructured finite element mesh generation and adaptive procedures for CFD p 608 N90-21993
Current Japanese supercomputers for computational fluid dynamics applications p 610 N90-23172
Composite reduced Navier Stokes procedures for flow problems with strong pressure interactions p 689 N90-23687
[AD-A219621] p 689 N90-23687
Euler analysis comparison with LDV data for an advanced counter-rotation propfan at cruise
[NASA-TM-103249] p 720 N90-25946
Informatics aspects of large flow calculations on the SX-2 supercomputer
[NLR-MP-88037-U] p 776 N90-26290
Efficient solution of the steady Euler equations with a centered implicit method p 884 N90-27999
Calculation of temperature distribution in various turbine blades using a boundary-fitted coordinate transformation method p 929 N90-28550

COMPUTER AIDED DESIGN

USA - A system to represent airfoils throughout the product life cycle
[AIAA PAPER 89-2972] p 73 A90-10487
Linking artificial intelligence (AI) and computer aided engineering (CAE) to analyze the testability of electronic designs
[AIAA PAPER 89-3070] p 74 A90-10559
The aerodynamic assistant
[AIAA PAPER 89-3132] p 75 A90-10608
Computer-aided design of flight vehicle instrument bays --- Russian book p 76 A90-10837
Thermostructural behavior of electromagnetic windows - Elaboration of a code package
[ONERA, TP NO. 1989-145] p 76 A90-11167
Advances in computational design and analysis of airbreathing propulsion systems p 43 A90-12502
Design and off-design performance predictions of axial turbines p 45 A90-12540
A theoretical approach to particle separator design p 48 A90-12584
Operating aspects of counter-rotating propfan and planetary-differential gear coupling p 50 A90-12615

Development and application of a computer-based system for conceptual aircraft design --- Book p 30 A90-12860
Simulations of propeller/airframe interference effects using an Euler correction method p 31 A90-13019
Integrated navigation system design and performance with Phase III GPS user equipment p 98 A90-13997
Accuracy considerations for GPS TSPI system design p 98 A90-14001
Propeller development for the Rutan Voyager
[SAE PAPER 891034] p 100 A90-14341
Aerospace structures supportability
[SAE PAPER 891058] p 129 A90-14360
Automated aircraft configuration design and analysis
[SAE PAPER 891072] p 101 A90-14368
Computers boost structural technology p 138 A90-14799
NMG - A system of numerical representation of aircraft geometry p 103 A90-15877
Gas turbine engine component development - An integrated approach p 112 A90-16006
Integrated approach to design and manufacture of gas turbine components based on group theory p 113 A90-16010
The computer aided weight engineering of aircraft - (CAWE) system p 179 A90-16860
Minimum weight design of helicopter rotor blades with frequency constraints p 180 A90-17313
Cost effective technology --- CAD/CAM techniques for aircraft engines p 188 A90-17447
Application of computational systems to aircraft engine components development p 188 A90-17448
Direct search method to aeroelastic tailoring of a composite wing under multiple constraints p 208 A90-17865
Optimization methods applied to aerodynamic design problems in computational fluid dynamics p 156 A90-18308
Aerodynamic design of an HP compressor stage using advanced computation codes p 156 A90-18479
Computerized structural analysis for engine components p 190 A90-18486
Analysis of whisker-toughened ceramic components - A design engineer's viewpoint p 205 A90-19149
Beyond the limits - Flight enters the computer age --- Book p 282 A90-20380
Modern technology in airship design
[AIAA PAPER 89-3169] p 244 A90-20584
A calculation method for ducted propellers p 226 A90-21626
Optimum design of composite structures p 272 A90-22135
Multi-processing on supercomputers for computational aerodynamics
[AIAA PAPER 90-0337] p 282 A90-22199
Design of computer-aided testing systems for aviation equipment. I p 222 A90-23416
Air Force application of injection molding technology
[SME PAPER EM89-103] p 274 A90-23686
A new design method for centrifugal compressor vaned diffusers p 292 A90-23844
[ASME PAPER 89-GT-156] p 292 A90-23844
Automation of the development of a finite element model for shells of the wing type p 364 A90-24118
Application of the MARS system in aircraft-structure design p 374 A90-24127
Design and fabrication of the carbon fiber/epoxy A-320 horizontal tailplane p 286 A90-25221
Minimum weight design of rotorcraft blades with multiple frequency and stress constraints p 335 A90-25304
Advanced Traffic Management System automation p 330 A90-25565
Computers and the aerospace engineer p 375 A90-25719
Surface grid generation for complex three-dimensional geometries p 376 A90-26484
Navier-Stokes computations useful in aircraft design
[AIAA PAPER 90-1800] p 315 A90-27311
Designers as users - Design supports based on crew system design practices p 457 A90-28184
Airborne telemetry trends for the 1990's p 418 A90-28874
A method for recalculating the temperature fields of aircraft structures for different experimental conditions p 448 A90-28994
Influence of structural and aerodynamic modeling on flutter analysis
[AIAA PAPER 90-0954] p 411 A90-29239
Evaluation of current: multiojective optimization methods for aerodynamic problems using CFD codes
[AIAA PAPER 90-0955] p 411 A90-29240
An application of structural optimization in wind tunnel model design
[AIAA PAPER 90-0956] p 438 A90-29241
Optimal computer-aided design of the blading of axial-flow turbines --- Russian book p 452 A90-30268

A computer-aided control engineering environment for multi-disciplinary expert-aided analysis and design (MEAD) p 461 A90-30796
Algorithm for simultaneous stabilization of single-input systems via dynamic feedback p 462 A90-31108
Multi-level models for diagnosis of complex electro-mechanical systems p 693 A90-38888
Multilevel optimization of large-scale structures in a parallel computing environment p 693 A90-39180
Development and application of an optimization procedure for space and aircraft structures p 679 A90-39186
Design and analysis aid for evaluating aircraft structures p 694 A90-41188
Applying qualitative knowledge to aircraft engine system design p 694 A90-41189
SMAS - An expert system for configuring a research flight simulator p 694 A90-41191
Application of 3-D viscous code in the design of a high performance compressor p 740 A90-42694
[AIAA PAPER 90-1914] p 740 A90-42694
Ada real-time GPS/INS simulation approach to system development p 751 A90-43706
Preliminary design and load distributions of high performance mechanical systems p 771 A90-45281
Finite element analysis of the Twelve Foot Pressurized Wind Tunnel p 760 A90-45296
Flight deck modernization
[SAE PAPER 892231] p 732 A90-45447
3D transonic nacelle and winglet design
[AIAA PAPER 90-3064] p 794 A90-45897
Computer-aided design of compressor rotor blade rings p 851 A90-46497
Improvement to interactive two dimensional rotor section design p 808 A90-46943
Structural mode significance using INCA --- Interactive Controls Analysis computer program
[AIAA PAPER 90-3346] p 889 A90-47606
Integrated product development (IPD) at General Dynamics Forth Worth p 786 A90-48828
[AIAA PAPER 90-3192] p 786 A90-48828
Implementation of integrated product development --- in aircraft industry p 786 A90-48829
[AIAA PAPER 90-3194] p 786 A90-48829
Configuring tactical aircraft p 837 A90-48886
[AIAA PAPER 90-3305] p 837 A90-48886
Upgrading the cockpit - A multidisciplinary approach p 848 A90-48995
Wind tunnel test of CAD USB-STOL semi-borne prototype p 88 N90-11696
[NAL-TM-566] p 88 N90-11696
Development of direct-inverse 3-D methods for applied transonic aerodynamic wing design and analysis
[NASA-CR-186036] p 103 N90-11733
Advanced technology in military gas turbine design and manufacture p 114 N90-11747
[PNR90545] p 114 N90-11747
General data processing support from project planning to workshop control p 138 N90-12208
[MBB-UD-526/88-PUB] p 138 N90-12208
The design of an airfoil for a high-altitude, long-endurance remotely piloted vehicle p 104 N90-12545
Supersonic boundary-layer transition on the LaRC F-106 and the DFRF F-15 aircraft. Part 2: Aerodynamic predictions p 94 N90-12559
A vision of the future: The new engine technology
[PNR90566] p 115 N90-12603
A computer integrated approach to dimensional inspection p 116 N90-12611
[PNR90596] p 116 N90-12611
Efficient methods for integrated structural-aerodynamic wing optimum design p 184 N90-13376
Aircraft performance enhancement with active compressor stabilization p 249 N90-15097
[AD-A213652] p 249 N90-15097
COCOMAT: A Computer Aided Engineering (CAE) system for composite structures design p 462 N90-19756
[NLR-MP-87078-U] p 462 N90-19756
The role of structural analysis in airworthiness certification
[BR112064] p 499 N90-20972
Computer-aided structural optimisation of aircraft structures
[BR112837] p 499 N90-20973
Conceptual design optimization study
[NASA-CR-4298] p 582 N90-21755
Aircraft technology management and the related significance of the supercomputer p 612 N90-22975
Numerical flow simulation and supercomputers: More than a digital wind tunnel p 612 N90-22976
The use of supercomputers for the design and analysis of constructions p 612 N90-22977
The development of a system for the numerical simulation of Euler flows p 612 N90-22980

- Multidisciplinary Expert-aided Analysis and Design (MEAD) p 613 N90-23050
- Conceptual design for aerospace vehicles p 651 N90-25043
- Development and application of an optimization procedure for space and aircraft structures [MBB-FW-522/S/PUB-383] p 779 N90-25078
- Integral-equation methods in steady and unsteady subsonic, transonic and supersonic aerodynamics for interdisciplinary design [NASA-TM-102677] p 716 N90-25110
- CREW CHIEF: A computer graphics simulation of an aircraft maintenance technician p 779 N90-25515
- Modeling strength data for CREW CHIEF p 780 N90-25516
- Feasibility study for a microwave-powered ozone sniffer aircraft, volume 2 [NASA-CR-186676] p 735 N90-25967
- Supersonic combustor modeling p 749 N90-25992
- A computer module used to calculate the horizontal control surface size of a conceptual aircraft design [NASA-CR-186872] p 780 N90-26515
- Development of a method to design helicopter rotors [REPT-100-30-03] p 845 N90-26830
- Hypersonic Arbitrary-Body Aerodynamics (HABA) for conceptual design [DE90-014750] p 910 N90-28495
- Flow coupling between a rotor and a stator in turbomachinery [AD-A223882] p 932 N90-28572
- WingDesign: Program for the structural design of a wing cross-section [LR-627] p 925 N90-29390
- COMPUTER AIDED MANUFACTURING**
- USA - A system to represent airfoils throughout the product life cycle [AIAA PAPER 89-2972] p 73 A90-10487
- Integrated approach to design and manufacture of gas turbine components based on group theory p 113 A90-16010
- Cost effective technology --- CAD/CAM techniques for aircraft engines p 188 A90-17447
- Looking inside a structure p 209 A90-17920
- A computer aided manufacturing procedure for experimental two-dimensional aerofoils p 270 A90-20609
- Computer integrated quality assurance for robotic workcells in aerospace manufacturing [SME PAPER MS89-152] p 283 A90-23681
- Design for assembly of aerospace structures - A qualitative, interactive approach [SME PAPER MS89-158] p 222 A90-23683
- Air Force application of injection molding technology [SME PAPER EM89-103] p 274 A90-23686
- Design and fabrication of the carbon fiber/epoxy A-320 horizontal tailplane p 286 A90-25221
- Computers and the aerospace engineer p 375 A90-25719
- AHS, Annual Forum, 45th, Boston, MA, May 22-24, 1989, Proceedings p 381 A90-28151
- McDonnell Douglas Helicopter Company Factory of the Future Project p 381 A90-28163
- Carbon/epoxy tooling evaluation and usage p 445 A90-28165
- Design and fabrication of a prototype resin matrix composite interceptor structure [AIAA PAPER 90-1004] p 442 A90-29275
- Automated R.T.M. for an airframe component --- Resin Transfer Molding p 534 A90-31881
- Manufacture of honeycomb p 538 A90-33704
- Metallurgy of investment cast superalloy components p 531 A90-34154
- Thermomechanical processing of superalloys p 531 A90-34156
- A leap forward in aircraft construction technology - High-speed cutting sets new production standards p 881 A90-46720
- Integrated product development (IPD) at General Dynamics FORTH Worth [AIAA PAPER 90-3192] p 786 A90-48828
- The AVRO VZ-9 experimental aircraft - Lessons learned [AIAA PAPER 90-3237] p 835 A90-48847
- Advanced technology in military gas turbine design and manufacture [PNR90545] p 114 N90-11747
- General data processing support from project planning to workshop control [MBB-UD-526/88-PUB] p 138 N90-12208
- A vision of the future: The new engine technology [PNR90566] p 115 N90-12603
- COCOMAT: A Computer Aided Engineering (CAE) system for composite structures design [NLR-MP-87078-U] p 462 N90-19756
- COMPUTER AIDED MAPPING**
- Electronic cartography - A new need for commercial aircraft p 576 A90-35351
- COMPUTER ANIMATION**
- Visual information for simulated landing approaches p 347 A90-26189
- COMPUTER ASSISTED INSTRUCTION**
- Computer aided analysis of gas turbine cycles p 779 A90-45289
- Success in tutoring electronic troubleshooting p 780 N90-25568
- Aspects of data link applications for ATC purposes p 827 N90-27688
- COMPUTER DESIGN**
- The airborne supercomputer p 538 A90-33775
- Use of Onboard Data Loaders [SAE PAPER 892327] p 738 A90-45485
- A mixed H2 and H(infinity) approach to an autopilot design problem [AIAA PAPER 90-3441] p 865 A90-47694
- COMPUTER GRAPHICS**
- Graphical interface tools for an avionics system [AIAA PAPER 89-3130] p 75 A90-10606
- Advances in computational design and analysis of airbreathing propulsion systems p 43 A90-12502
- Computerised structural analysis for engine components p 190 A90-18486
- Use of Computer-Aided Video Display technology in aviation weather litigation [AIAA PAPER 90-0373] p 216 A90-19821
- Realtime graphic flight simulations using multiple minicomputers p 351 A90-26203
- Interactive generation of unstructured grids for three dimensional problems p 310 A90-26537
- Interactive grid generation for turbomachinery flow field simulations p 312 A90-26553
- C-grid generation for turbomachinery cascades p 312 A90-26554
- A new data acquisition, display and control system for the ARA transonic wind tunnel p 436 A90-28256
- Expert system - Conventional processing interface p 460 A90-30753
- Flight simulator evaluation of a dot-matrix display for presentation of approach map formats p 419 A90-30787
- 3-D in pictorial formats for aircraft cockpits p 420 A90-31331
- The Real Time Display Builder (RTDB) p 546 N90-20656
- Preliminary development of an intelligent computer assistant for engine monitoring [NASA-TM-101702] p 612 N90-22322
- Conceptual design for aerospace vehicles p 651 N90-25043
- CREW CHIEF: A computer graphics simulation of an aircraft maintenance technician p 779 N90-25515
- Feasibility study for a microwave-powered ozone sniffer aircraft, volume 2 [NASA-CR-186676] p 735 N90-25967
- Economical graphics display system for flight simulation avionics [NASA-CR-186886] p 849 N90-27701
- The Helicopter Antenna Radiation Prediction Code (HARP) [NASA-CR-186925] p 884 N90-27946
- The function of the Interactive Model Assembly Program (IMAP) for a flight simulator [NAL-TR-1034] p 939 N90-29412
- Realtime multi-plot graphics system [NASA-CR-4304] p 965 N90-29919
- COMPUTER INFORMATION SECURITY**
- Security audit for embedded avionics systems p 957 A90-50649
- COMPUTER NETWORKS**
- International aircraft operator data base master requirements and implementation plan [DOT/FAA/CT-90/17] p 967 N90-29247
- COMPUTER PROGRAM INTEGRITY**
- A methodology for validating software reliability [AIAA PAPER 89-3081] p 74 A90-10567
- An experimental investigation of fault tolerant software structures in an avionics application [AIAA PAPER 89-3082] p 74 A90-10568
- The automated software development project at McDonnell Aircraft Company (The Software Factory) p 460 A90-30782
- COMPUTER PROGRAMMING**
- Computer-based tools for assisting air traffic controllers with arrivals flow management [RSRE-88001] p 178 N90-13366
- Apparatus for cooling electronic components in aircraft [AD-DO14207] p 183 N90-13373
- Software verification plan for GCS --- guidance and control software [NASA-TM-101668] p 372 N90-18057
- A data acquisition parallel bus for wind tunnels at ARL (Aeronautical Research Laboratory) p 526 N90-20098
- [AD-A218052] p 526 N90-20098
- Human centrifuge controller [NAL-TM-SE-8901] p 527 N90-21043
- Evolution of Ada technology in the flight dynamics area: Implementation/testing phase analysis [NASA-TM-103310] p 546 N90-21539
- System testing of a production Ada (trademark) project: The GRODY study [NASA-TM-103308] p 546 N90-21541
- Evolution of Ada technology in the flight dynamics area: Design phase analysis [NASA-TM-103307] p 547 N90-21542
- Software Management Environment (SME) concepts and architecture [NASA-TM-103306] p 547 N90-21543
- Implementation of a production Ada project: The GRODY study [NASA-TM-103305] p 547 N90-21544
- Development of a microcomputer based software system for use in crewmember ejection analysis [AD-A220398] p 723 N90-25117
- National Airspace System (NAS) software life cycle management study [AD-A221180] p 729 N90-25122
- An object-oriented solution example: A flight simulator electrical system [AD-A219190] p 761 N90-25145
- Development of a method to design helicopter rotors [REPT-100-30-03] p 845 N90-26830
- Design of helicopter components in metal matrix composites [REPT-100-20-55] p 874 N90-26894
- Aircraft condition monitoring system for future Airbus aircraft: New concept for programming and data recording p 848 N90-27619
- Development of a software package for automatic data acquisition, analysis, and controls in an axial flow compressor test rig [PD-PR-8910] p 965 N90-29926
- Assessment System for Aircraft Noise (ASAN): Development of alpha-test prototype system software [AD-A223770] p 966 N90-30036
- COMPUTER PROGRAMS**
- The aerodynamic assistant [AIAA PAPER 89-3132] p 75 A90-10608
- Real-time decision making for autonomous flight control [SAE PAPER 891053] p 118 A90-14355
- A refined optimality criterion technique applied to aircraft wing structural design p 206 A90-16718
- Predictions of airfoil aerodynamic performance degradation due to icing p 144 A90-16753
- Practical suggestions for modifying math models to correlate with actual modal test results p 207 A90-16979
- Grid generation with the 1988 EAGLE code p 156 A90-18310
- Fortified LEWICE with viscous effects --- Lewis Ice Accretion Prediction Code [AIAA PAPER 90-0754] p 176 A90-20009
- A finite element solution of unsteady two-dimensional flow in cascades p 226 A90-21946
- The integrated support station (ISS) - A modular Ada-based test system to support AN/ALE-47 countermeasure dispenser system testing, evaluation, and reprogramming p 457 A90-28323
- Applications of XTRAN3S and CAP-TSD to fighter aircraft [AIAA PAPER 90-1035] p 389 A90-29360
- ADAM 2.0 - An ASE analysis code for aircraft with digital flight control systems [AIAA PAPER 90-1077] p 431 A90-29385
- Numerical simulation of an adaptive-wall wind-tunnel - A comparison of two different strategies p 439 A90-30251
- Design flutter calculations on PC p 545 A90-33379
- Whole helicopter aeroelasticity - Experience with a new approach p 492 A90-33380
- A ground simulation-inspection system for avionics devices p 594 A90-37232
- The challenging process of validating CFD codes [AIAA PAPER 90-1402] p 558 A90-37943
- Influence of bulk turbulence and entrance boundary layer thickness on the curved duct flow field [AIAA PAPER 90-1502] p 606 A90-38651
- Modeling gas turbine combustor performance under transient conditions [AIAA PAPER 90-2161] p 661 A90-42051
- Trend analysis and diagnostics codes for training purposes [AIAA PAPER 90-2394] p 617 A90-42156
- Development and verification of software for flight safety critical strapdown systems p 694 A90-42454

The place of knowledge based systems in helicopter dynamic system condition prognosis

p 618 A90-42475

Next-generation automatic test equipment for military support

p 767 A90-42667

Computational analysis of the flowfield of a two-dimensional ejector nozzle

[AIAA PAPER 90-1901] p 740 A90-42690

A test matrix sequencer for research test facility automation

[AIAA PAPER 90-2386] p 759 A90-42791

Rockwell International's miniature high performance GPS receiver

p 726 A90-43701

RAIM - An implementation study

p 726 A90-43714

Computer aided analysis of gas turbine cycles

p 779 A90-45289

Tooth thickness effects on the performance of gas labyrinth seals

p 771 A90-45300

Transonic analysis of complex configurations using TRANAIR program

[SAE PAPER 892289] p 714 A90-45467

Improving computer techniques for real-time digital flight simulation

[SAE PAPER 892354] p 760 A90-45505

The evolution of design/development requirements for avionics/mission equipment (MEP) insertion

p 846 A90-46932

Application of a general-purpose mechanical systems analysis code to rotorcraft dynamics problems

p 831 A90-46955

Recent developments in rotor dynamics methodology in the U.S. industry

p 889 A90-46960

Development of the Second Generation Comprehensive Helicopter Analysis System (2GCHAS)

p 889 A90-46963

Application of the Westland CRFD program to total helicopter dynamics

p 832 A90-46965

Application to a helicopter of a general method for modifying a finite-element model to correlate with modal test data

p 832 A90-46968

Optimal solutions to flight mechanics problems using a Nonlinear Programming and Collocation technique

[AIAA PAPER 90-3415] p 889 A90-47669

Design synthesis and optimization of joined-wing transports

[AIAA PAPER 90-3197] p 838 A90-49102

Initial flight qualification and operational maintenance of X-29A flight software

[NASA-TM-101703] p 32 N90-10023

The application of TSIM software to act design and analysis on flexible aircraft

p 60 N90-10086

Control law synthesis and optimization software for large order aeroservoelastic systems

p 61 N90-10111

The MHOST finite element program: 3-D inelastic analysis methods for hot section components. Volume 3: Systems' manual

[NASA-CR-182236] p 73 N90-10451

On the interactive computer program IPIS for aircraft parameter identification

[NAL-TR-1000] p 77 N90-10586

A preliminary sensitivity analysis of the Generalized Escape System Simulation (GESS) computer program

[DE89-016891] p 24 N90-10844

GRATE: A new flight test tool for flying qualities evaluation

p 34 N90-10868

Flight testing of the Tornado Terrain Following System

p 35 N90-10875

Some implications of the isotropic momentarily frozen assumptions for the SPAN-MAT program

[NASA-CR-181937] p 88 N90-11704

Development of direct-inverse 3-D methods for applied transonic aerodynamic wing design and analysis

[NASA-CR-186036] p 103 N90-11733

Additions and corrections to SUPER: A program for calculating steady and oscillatory supersonic flow over a thin wing, tail plane and fin

[AD-A211771] p 90 N90-12501

Development of a VSAERO (Vortex Separation Aerodynamics) model of the F/A-18

[AD-A212442] p 95 N90-12566

FPG2: A flight profile generator program

[AD-A212408] p 107 N90-12595

Aircraft SAR simulation Sargen 1.0

[FEL-1989-44] p 135 N90-12823

Application of a self-adaptive grid method to complex flows

[NASA-TM-102223] p 143 N90-13324

Geodetic network adjustment using GPS triple difference observations and a priori stochastic information

[TR-1-1987] p 178 N90-13367

Trajectory optimization and guidance for an aerospace plane

[NASA-CR-185884] p 183 N90-13369

Software and hardware description of the helicopter motion equations for VAX computers

[AD-A213248] p 184 N90-13375

Application of a two-dimensional unsteady viscous analysis code to a supersonic throughflow fan stage

[NASA-TM-14141] p 192 N90-13387

Validation of a computer code for analysis of subsonic aerodynamic performance of wings with flaps in combination with a canard or horizontal tail and an application to optimization

[NASA-TP-2961] p 173 N90-14187

RAMSCRAM: A flexible ramjet/scramjet engine simulation program

[NASA-TM-102451] p 194 N90-14235

Data Link Processor (DLP) operational test and evaluation/integration test plan

[DOT/FAA/CT-TN89/32] p 214 N90-14404

User's guide to PMESH: A grid-generation program for single-rotation and counterrotation advanced turboprops

[NASA-CR-185156] p 217 N90-14783

Systems for airborne wind and turbulence measurement

p 281 N90-15046

Nonlinear phenomena in computational transonic aerelasticity

p 235 N90-15070

A study of variable geometry in advanced gas turbines

p 255 N90-15104

Design and calibration of an in-stack, low-pressure impactor

[AD-A213531] p 255 N90-15105

Solution of potential flow past an elastic body using the boundary element technique

[AD-A213843] p 275 N90-15390

Inclusion of nonlinear aerodynamics in the FLAP code

[DE89-009507] p 281 N90-15519

Rotor induced-inflow-ratio measurements and CAMRAD calculations

[NASA-TP-2946] p 237 N90-15882

The application of Z to the specification of air traffic control systems. 1: An initial specification of the radar processing activity

[RSRE-MEMO-4280] p 243 N90-15900

Distribution of hardware and software elements in unmanned air vehicle systems

p 251 N90-15933

The development of an airborne synthetic aperture radar motion compensation system

p 333 N90-16745

Noise and sonic boom impact technology. Initial development of an Assessment System for Aircraft Noise (ASAN). Volume 1: Executive summary

[AD-A214164] p 379 N90-17410

Noise and sonic boom impact technology. Initial development of an Assessment System for Aircraft Noise (ASAN). Volume 3: Technical description

[AD-A214455] p 379 N90-17412

Ignitability of jet-A fuel vapors in aircraft fuel tanks

p 326 N90-17594

Forced and natural venting of aircraft cabin fires: A numerical simulation

p 326 N90-17597

Time development of convection flow patterns in aircraft cabins under post-crash fire exposure

p 327 N90-17598

Analysis of the National Transonic Facility mishap

[NASA-TM-101686] p 328 N90-17620

Viscous three-dimensional analyses for nozzles for hypersonic propulsion

[NASA-CR-185197] p 344 N90-17635

Measurement and computer simulation of antennas on ships and aircraft for results of operational reliability

p 370 N90-17936

GTD/UTD: Brief history of successive development of theory and recent advances. Applications to antennas on ships and aircraft

p 370 N90-17939

Hypercube expert system shell-applying production parallelism

[AD-A215762] p 377 N90-18173

A user's manual for the method of moments Aircraft Modeling Code (AMC)

[NASA-CR-186371] p 415 N90-18390

Unsteady Aerodynamic Phenomena in Turbomachines [AGARD-CP-468] p 425 N90-18405

Numerical prediction of axial turbine stage aerodynamics

p 426 N90-18416

Automation and extension of LDV (Laser-Doppler Velocimetry) measurements of off-design flow in a subsonic cascade wind tunnel

[AD-A216627] p 453 N90-18670

Heat transfer measurements from a NACA 0012 airfoil in flight and in the NASA Lewis icing research tunnel

[NASA-CR-4278] p 399 N90-19203

Marshall Avionics Testbed System (MAST)

p 421 N90-19417

Yaw rate control of an air bearing vehicle

p 435 N90-19420

The influence of a wall function on turbine blade heat transfer prediction

p 429 N90-19421

Experimental and theoretical aerodynamic characteristics of a high-lift semispan wing model

[NASA-TP-2990] p 477 N90-20046

The application of active controls technology to a generic hypersonic aircraft configuration

[NASA-TM-101689] p 497 N90-20071

Comparison of 3-D viscous flow computations of Mach 5 inlet with experimental data

[NASA-TM-102518] p 510 N90-20090

Laboratory implementation of the Continuously Reconfiguring Multi-Microprocessor Flight Control System (CRMFCFS)

[AD-A217730] p 520 N90-20094

A data acquisition parallel bus for wind tunnels at ARL (Aeronautical Research Laboratory)

[AD-A218052] p 526 N90-20098

ETO (Earth-To-Orbit): A trajectory program for aerospace vehicles

[AD-A218157] p 528 N90-20103

Modification and improvement of software for modeling multidimensional reacting fuel flows

[AD-A217789] p 533 N90-20235

Air Force Boom Event Analyzer Recorder (BEAR): System description

[AD-A218048] p 548 N90-20800

Convergence acceleration of hypersonic flow calculations: A nonlinear relaxation factor

p 480 N90-20957

Aerofoil design techniques

p 500 N90-20978

Constrained spanload optimization for minimum drag of multi-lifting-surface configurations

p 501 N90-20992

Aerodynamic design by optimization

p 502 N90-20996

Numerical optimization of wings in transonic flow

p 502 N90-20997

Experimental and numerical study on basic phenomena of secondary flows in turbines

p 512 N90-21014

Secondary flow in a turbine guide vane with low aspect ratio

p 513 N90-21018

Generation and decay of secondary flows and their impact on aerodynamic performance of modern turbomachinery components

p 514 N90-21023

Computational prediction and measurement of the flow in axial turbine cascades and stages

p 514 N90-21028

Supersonic nozzle design of arbitrary cross-section

p 515 N90-21035

Structural tailoring of select fiber composite structures

[NASA-TM-102484] p 533 N90-21137

Aeropropulsion facilities configuration control: Procedures manual

[NASA-TM-102541] p 543 N90-21399

Evolution of Ada technology in the flight dynamics area: Implementation/testing phase analysis

[NASA-TM-103310] p 546 N90-21539

Software Management Environment (SME) concepts and architecture

[NASA-TM-103306] p 547 N90-21543

Implementation of a production Ada project: The GRODY study

[NASA-TM-103305] p 547 N90-21544

WINCOF-I code for prediction of fan compressor unit with water ingestion

[NASA-CR-185157] p 551 N90-21724

Prediction of forces and moments for flight vehicle control effectors. Part 2: An analysis of delta wing aerodynamic control effectiveness in ground effect

[NASA-CR-186572] p 571 N90-21735

A computer program for the prediction of nozzle-propeller performance

[LR-578] p 572 N90-21740

Mesh generation for flow computation in turbomachine

p 588 N90-21981

The development of a system for the numerical simulation of Euler flows

p 612 N90-22980

Multidisciplinary Expert-aided Analysis and Design (MEAD)

p 613 N90-23050

Current Japanese supercomputers for computational fluid dynamics applications

p 610 N90-23172

Continued development and analysis of a new extended Kalman filter for the Completely Integrated Reference Instrumentation System (CIRIS)

[AD-A220106] p 654 N90-23400

STARS: An integrated general-purpose finite element structural, aeroelastic, and aeroservoelastic analysis computer program

[NASA-TM-101709] p 689 N90-23768

IAPSA 2 small-scale system specification

[NASA-CR-182006] p 695 N90-24103

Extension-torsion coupling behavior of advanced composite tilt-rotor blades

p 651 N90-25057

Flexural fatigue life prediction of closed hat-section using materially nonlinear axial fatigue characteristics

p 691 N90-25062

Coupled robot-body equations of motion hover flight

[NASA-CR-186710] p 717 N90-25111

The application of the finite element method to an aerodynamic problem specific to propeller design

[LR-614] p 718 N90-25116

- Replication of NASPAC Dallas/Fort Worth study
[DOT/FAA/CT-TN90/26] p 729 N90-25123
- Advanced fuel properties, phase 1
[AD-A219788] p 766 N90-25236
- A simulation code for turbocompound diesel engines
[IAR-89-26] p 774 N90-25348
- Hardware and software reliability estimation using simulations
[NASA-CR-186637] p 780 N90-25580
- Reliability model generator specification
[NASA-CR-182005] p 780 N90-25638
- Informatics aspects of large flow calculations on the SX-2 supercomputer
[NLR-MP-88037-U] p 776 N90-26290
- A computer module used to calculate the horizontal control surface size of a conceptual aircraft design
[NASA-CR-186872] p 780 N90-26515
- ARLSUPER version 1.0, program users guide
[AD-A22693] p 815 N90-26793
- Proceedings of the 1987 Aircraft/Engine Structural Integrity Program (ASIP/ENSIP) Conference
[AD-A198037] p 842 N90-26807
- Application of damage tolerance p 843 N90-26817
- Automated analysis of MXU-553 flight data p 844 N90-26821
- BASEOPS default profiles for civil aircraft
[AD-A223161] p 844 N90-26825
- B-1B improved windshield development. Volume 2: Magna analysis: Baseline and parametric
[AD-A221501] p 845 N90-26828
- The validation and application of a rotor acoustic prediction computer program
[NASA-TM-101794] p 895 N90-27465
- A review of crashworthiness of composite aircraft structures
[AD-A221555] p 846 N90-27697
- Computer code for predicting coolant flow and heat transfer in turbomachinery
[NASA-TP-2985] p 858 N90-27722
- Calculation of the combustion distribution in a liquid-fuel ramjet
[NASA-TP-2985] p 858 N90-27931
- The Helicopter Antenna Radiation Prediction Code (HARP)
[NASA-CR-186925] p 884 N90-27946
- In-service inspection of composite components on aircraft at depot and field levels p 885 N90-28078
- Prediction of subsonic vortex shedding from forebodies with chines
[NASA-CR-4323] p 909 N90-28494
- Model authoring system for fail safe analysis
[NASA-CR-4317] p 964 N90-29142
- WingDesign: Program for the structural design of a wing cross-section
[LR-627] p 925 N90-29390
- Generalized Advanced Propeller Analysis System (GAPAS). Volume 2: Computer program user manual
[NASA-CR-185277] p 933 N90-29394
- Structural testing and analytical research of turbine components
[AD-A223516] p 933 N90-29396
- The function of the Interactive Model Assembly Program (IMAP) for a flight simulator
[NAL-TR-1034] p 939 N90-29412
- Realtime multi-plot graphics system
[NASA-CR-4304] p 965 N90-29919
- COMPUTER SYSTEMS DESIGN**
- A knowledge-based system design/information tool for aircraft flight control systems
[AIAA PAPER 89-2978] p 55 A90-10491
- A methodology for validating software reliability
[AIAA PAPER 89-3081] p 74 A90-10567
- Very-high-performance data acquisition/analysis/display/control systems based on the APTC I/O computer p 458 A90-28852
- Development and verification of software for flight safety critical strapdown systems p 694 A90-42454
- Airborne digital computers and systems --- Russian book p 927 A90-52410
- A knowledge-based system design/information tool for aircraft flight control systems
[NASA-TM-101704] p 217 N90-13990
- System testing of a production Ada (trademark) project: The GRODY study
[NASA-TM-103308] p 546 N90-21541
- Evolution of Ada technology in the flight dynamics area: Design phase analysis
[NASA-TM-103307] p 547 N90-21542
- The EFA integrated monitoring and recording system: Requirements and concept for implementation p 848 N90-27620
- AIMS test and simulation equipment p 892 N90-27623
- Knowledge based diagnosis of jet engines under consideration of model based methods p 855 N90-27631
- New features of JAL's ground station p 872 N90-27633
- Flight data replay and analysis system p 893 N90-27635
- Daily flight operation monitoring in JAL p 820 N90-27636
- Realtime multi-plot graphics system
[NASA-CR-4304] p 965 N90-29919
- COMPUTER SYSTEMS PERFORMANCE**
- Categorization and performance analysis of advanced avionics algorithms on parallel processing architectures p 461 A90-30786
- Efficient methods for integrated structural-aerodynamic wing optimum design p 184 N90-13376
- Integrated approach fault tolerance-current state and future requirements p 275 N90-15465
- System testing of a production Ada (trademark) project: The GRODY study
[NASA-TM-103308] p 546 N90-21541
- Inertial navigation system simulator: Behavioral specification, revision p 578 N90-22554
- [AD-A219294] p 578 N90-22554
- IAPSA 2 small-scale system specification
[NASA-CR-182008] p 695 N90-24103
- COMPUTER SYSTEMS PROGRAMS**
- Advanced software for turbine blade processing
[SME PAPER MS89-330] p 274 A90-23694
- Flight Test Techniques
[AGARD-CP-452] p 33 N90-10860
- Start-up built-in test for the DISCUS fault tolerant, fly-by-wire computer system p 869 N90-27625
- Development of a COMPAS prototype for the ATC Centre at Frankfurt (Fed. Republic of Germany) p 826 N90-27684
- Development of acceptance plans for airport pavement materials. Volume 1: Development
[DOT/FAA/RD-90/15] p 937 N90-28581
- COMPUTER SYSTEMS SIMULATION**
- The comparison of the airbase simulation models airbase and sustained p 123 N90-12629
- COMPUTER TECHNIQUES**
- Jet engine fault detection with differential gas path analysis at discrete operating points p 50 A90-12633
- Beyond the limits - Flight enters the computer age --- Book p 282 A90-20380
- A new data acquisition, display and control system for the ARA transonic wind tunnel p 436 A90-28256
- A parallel-vector algorithm for rapid structural analysis on high-performance computers
[AIAA PAPER 90-1149] p 458 A90-29293
- The IMIS F-16 interactive diagnostic demonstration p 383 A90-30768
- A laser based computer aided non-intrusive technique for full field flow characterization in macroscopic curved channels p 535 A90-32293
- Measurement of angles and angle characteristics with accelerometers and gyroscopes p 653 A90-41730
- Computer-aided analysis of three-dimensional multiloop mechanisms p 669 A90-42328
- Analytical studies for computed center line operations
[SAE PAPER 892219] p 729 A90-45436
- Improving computer techniques for real-time digital flight simulation
[SAE PAPER 892354] p 760 A90-45505
- Recent developments in rotor dynamics methodology in the U.S. industry p 889 A90-46960
- Fundamental dynamics issues for comprehensive rotorcraft analyses p 831 A90-46961
- An improved rotor/airframe coupling method for NASTRAN airframe vibration analysis p 831 A90-46962
- CFD needs in conceptual design
[AIAA PAPER 90-3209] p 813 A90-49106
- A closer look at the induced drag of crescent-shaped wings
[AIAA PAPER 90-3063] p 903 A90-50638
- Recent progress in research pertaining to estimates of gas-side heat transfer in an aircraft gas turbine
[NASA-TM-102460] p 194 N90-13394
- RADC fault tolerant system reliability evaluation facility
[AD-A215298] p 377 N90-17348
- Noise and sonic boom impact technology. Initial development of an Assessment System for Aircraft Noise (ASAN). Volume 2: System design strategy
[AD-A214454] p 379 N90-17411
- Noise and sonic boom impact technology. Initial development of an Assessment System for Aircraft Noise (ASAN). Volume 3: Technical description
[AD-A214455] p 379 N90-17412
- Life of concentrated contacts in the mixed EHD and boundary film regimes
[AD-A216673] p 454 N90-18738
- A matrix-free locally-implicit scheme for Navier-Stokes equations
[AD-A218298] p 541 N90-20349
- The automation management to support research and development p 612 N90-22978
- Computer modeling and data processing methods: An essential part of jet engine condition monitoring and fault diagnosis p 855 N90-27626
- A knowledge-based system design/information tool
[NASA-CR-4316] p 965 N90-29143
- COMPUTER VISION**
- The Robotic Canopy Polishing System
[SME PAPER MS89-134] p 222 A90-23680
- Multiple sensor data association and fusion in aerospace applications p 778 A90-44644
- Possibilities for improving traffic flows p 823 A90-49272
- Autonomous automatic landing through computer vision p 332 N90-16734
- Feasibility study for a microwave-powered ozone sniffer aircraft, volume 2
[NASA-CR-186676] p 735 N90-25967
- COMPUTERIZED SIMULATION**
- Intelligent situation assessment and response aiding in flight emergencies
[AIAA PAPER 89-2999] p 36 A90-10507
- Real-time fault monitoring for aircraft applications using quantitative simulation and expert systems
[AIAA PAPER 89-3103] p 37 A90-10586
- Wing-section effects on the flight performance of a remotely piloted vehicle p 29 A90-11007
- Grid generation and adaptation for the direct simulation Monte Carlo method p 67 A90-11102
- Numerical simulation of three-dimensional unsteady flows in turbomachines
[ONERA, TP NO. 1989-118] p 4 A90-11149
- A class of implicit upwind schemes for Euler simulations with unstructured meshes p 5 A90-11597
- Advances in computational design and analysis of airbreathing propulsion systems p 43 A90-12502
- Advanced computational techniques for hypersonic propulsion p 69 A90-12606
- Direct simulation of three-dimensional hypersonic flow about intersecting blunt wedges p 16 A90-12835
- Critique of turbulence models for shock-induced flow separation p 17 A90-12851
- Influence of joint fixity on the structural static and dynamic response of a joined-wing aircraft. I. - Static response
[SAE PAPER 891060] p 100 A90-14361
- Simulation of a turbocompound two-stroke diesel engine
[SAE PAPER 891066] p 110 A90-14366
- Predictions of airfoil aerodynamic performance degradation due to icing p 144 A90-16753
- High-resolution upwind scheme for vortical-flow simulations p 153 A90-17872
- The research of cubic spline optimal terrain following system p 196 A90-18584
- Numerical simulation of the actuation system for the ALDF's propulsion control valve --- Aircraft Landing Dynamics Facility
[AIAA PAPER 90-0079] p 211 A90-19674
- Direct simulation of hypersonic rarefied flow about a delta wing
[AIAA PAPER 90-0143] p 162 A90-19704
- Large-eddy simulations of combustion instability in an axisymmetric ramjet combustor
[AIAA PAPER 90-0267] p 191 A90-19764
- Beyond the limits - Flight enters the computer age --- Book p 282 A90-20380
- Prediction of aerostat and airship mooring mast loads by nonlinear dynamic simulation
[AIAA PAPER 89-3172] p 245 A90-20587
- New approach for Doppler ambiguities resolution in medium pulse repetition frequency radars p 240 A90-20937
- An investigation of the behavior of the dynamic load distribution versus operating speed and torque on heavily loaded, high speed aircraft gearing p 271 A90-21129
- Multipath modeling for simulating the performance of the microwave landing system p 241 A90-21384
- Computer-aided simulation of aircraft motion including nonlinearities in aerodynamic-coefficient relationships p 257 A90-23359
- Application of a lower-upper implicit scheme and an interactive grid generation for turbomachinery flow field simulations
[ASME PAPER 89-GT-20] p 288 A90-23762
- Simulation of cooling film density ratios in a mass transfer technique
[ASME PAPER 89-GT-200] p 362 A90-23872
- High resolution spectrum analysis for airborne pulse Doppler radars p 339 A90-24329
- A practical co-axial twin rotor model p 335 A90-25423

- National Airspace System demand and capacity modeling p 330 A90-25562
 Future ATC automation aids based upon AI technology p 375 A90-25563
 Computers and the aerospace engineer p 375 A90-25719
 Flow-calculation over a δ -wing using the thin-layer Navier-Stokes equations p 304 A90-25773
 Three-dimensional simulations of hypersonic flows p 306 A90-25823
 Realtime graphic flight simulations using multiple minicomputers p 351 A90-26203
 General aviation pilot error in computer simulated adverse weather scenarios p 322 A90-26254
 Simulation of separated flows using panel method p 308 A90-26349
 Interactive grid generation for turbomachinery flow field simulations p 312 A90-26553
 Helicopter simulation development by correlation with frequency sweep flight test data p 407 A90-28203
 External 6-component wind tunnel balances for aerospace simulation facilities p 438 A90-28296
 The rotor-signal-module of MF190 --- for digital data acquisition from BO-105 helicopter rotary wings p 418 A90-28849
 An aircraft flight control reconfiguration algorithm p 432 A90-30708
 A study of a propulsion control system for a VATOL aircraft (A direct design synthesis application) p 424 A90-30712
 Multivariable control design for the control reconfigurable combat aircraft (CRCA) p 432 A90-30715
 A microcomputer-based airspace control simulation and prototype human-machine interface p 461 A90-30800
 Numerical simulations of an oblique detonation wave engine p 508 A90-32964
 Numerical simulation of vortex breakdown by solving the Euler equations for an incompressible fluid p 476 A90-34323
 Simulation research on the afterburning dynamic characteristics of engine control system p 585 A90-35708
 Passive location and tracking using DOA and TOA measurements of single nonmaneuvering observer p 576 A90-35709
 A ground simulation-inspection system for avionic devices p 594 A90-37232
 Development and verification of an algorithm for helicopter inverse simulations p 591 A90-38522
 Direct simulation of low-density flow over airfoils [AIAA PAPER 90-1539] p 564 A90-38683
 Dynamic FLIR simulation in flight training research p 681 A90-40109
 Supercomputer applications in gas turbine flowfield simulation p 620 A90-40495
 Numerical simulation of the behaviour of internal combustion supercharged engines p 655 A90-40539
 Simulation of inviscid blade-row interaction using a linearised potential code p 621 A90-40555
 Analyses of Arrow Air DC-8-63 accident of December 12, 1985 - Gander, Newfoundland p 635 A90-40687
 Concept development of automatic guidance for rotorcraft obstacle avoidance p 669 A90-41632
 Modeling gas turbine combustor performance under transient conditions p 661 A90-42051
 Turbulence model performance in V/STOL flow field simulation p 625 A90-42094
 Active control of tiltrotor blade in-plane loads during maneuvers p 670 A90-42463
 A computational model for thickening boundary layers with mass addition for hypersonic engine inlet testing [AIAA PAPER 90-2219] p 705 A90-42750
 Introducing the VRT gas turbine combustor [AIAA PAPER 90-2452] p 743 A90-42808
 Ada real-time GPS/INS simulation approach to system development p 751 A90-43706
 RAIM - An implementation study p 726 A90-43714
 Numerical simulation of hypersonic viscous continuum flow p 707 A90-44407
 Numerical simulation of the compressible flow in a valve-cylinder assembly p 770 A90-44431
 Numerical simulation of transonic porous airfoil flows p 707 A90-44433
 Mathematical simulation model of an aircraft gas turbine p 745 A90-44721
 Dynamics and control of maneuverable towed flight vehicles p 754 A90-45161
 Simulation of MLS-ATC procedures in the New York and San Francisco Terminal Control Areas [SAE PAPER 892217] p 728 A90-45434
 Power system for 21st century fighter aircraft [SAE PAPER 892253] p 746 A90-45455
 Real time data collection and control in a distributed simulator system using Ethernet TCP/IP [SAE PAPER 892356] p 761 A90-45507
 An interfacing solution for real-time avionics development [SAE PAPER 892357] p 738 A90-45508
 Large-eddy simulations of flows in a ramjet combustor p 772 A90-45534
 Simulation of leading-edge vortex flows p 716 A90-45785
 Navier Stokes simulation of waverider flowfields [AIAA PAPER 90-3066] p 793 A90-45892
 Angle-of-attack validation of a new zonal CFD method for airfoil simulations p 795 A90-45908
 Relative efficiency and accuracy of two Navier-Stokes codes for simulating attached transonic flow over wings [AIAA PAPER 90-3078] p 795 A90-45909
 An upwind approach to unsteady flowfield simulation [AIAA PAPER 90-3100] p 796 A90-45912
 Navier-Stokes simulation of unsteady supersonic cavity flowfield with passive control p 796 A90-45913
 One wing for two airliners - Computer screens are technical trailblazers for a unique wing p 785 A90-46719
 Probabilistic reasoning for intelligent wind shear avoidance [AIAA PAPER 90-3437] p 890 A90-47690
 Validation of GEMACS for prediction of lightning induced electromagnetic fields --- General Electromagnetic Model for Analysis of Complex Systems p 819 A90-49845
 Critical evaluation of Jet-A spray combustion using propane chemical kinetics in gas turbine combustion simulated by KIVA-II [AIAA PAPER 90-2439] p 949 A90-50645
 Numerical simulation of three-dimensional transonic flows p 905 A90-51020
 Acoustic wave excitation during the aerodynamic interaction between a fan blade and a bluff obstacle p 965 A90-52289
 The application of TSIM, software to act design and analysis on flexible aircraft p 60 N90-10086
 Numerical simulation of pressure oscillations in a ramjet combustor p 54 N90-10202
 Numerical simulation of unsteady combustion in a dump combustor p 54 N90-10203
 On the interactive computer program IPIS for aircraft parameter identification [NAL-TR-1000] p 77 N90-10586
 A preliminary sensitivity analysis of the Generalized Escape System Simulation (GESS) computer program [DE89-016891] p 24 N90-10844
 Computer simulation of aircraft aerodynamics [NASA-TM-102221] p 88 N90-11699
 Post crash flight analysis: Visualizing flight recorder data [AD-A212063] p 96 N90-11715
 Numerical simulation of aeroplane response to a lightning injection [ETN-89-95271] p 96 N90-11716
 A simulation study of landing time allocation procedures for use in computer-assisted air traffic management systems [AD-A212159] p 99 N90-11722
 STOVL propulsion system volume dynamics approximations [NASA-TM-102397] p 114 N90-11740
 Simulation of glancing shock wave and boundary layer interaction [NASA-TM-102233] p 133 N90-11970
 Development and evaluation at ATCEU of executive and support operations, phase 4A/3D --- ATCEU (Air Traffic Control Evaluation Unit) p 99 N90-12572
 [CAA-PAPER-88017] p 99 N90-12572
 Real-time simulation of an F110/STOVL turbofan engine [NASA-TM-102409] p 117 N90-12618
 Aircraft SAR simulation Sargen 1.0 [FEL-1989-44] p 135 N90-12823
 The S.D.G., P.S.D. and the nonlinear airplane [NLR-MP-88018-U] p 183 N90-13371
 STOVL aircraft simulation for integrated flight and propulsion control research [NASA-TM-102419] p 193 N90-13389
 Mathematical model identification for flight simulation, based on flight and taxi tests [LR-550] p 202 N90-13410
 Navier-Stokes simulation of the crossflow instability in swept-wing flows [NASA-CR-186122] p 212 N90-13744
 RAMSCRAM: A flexible ramjet/scramjet engine simulation program [NASA-TM-102451] p 194 N90-14235
 Temporally and spatially resolved flow in a two-stage axial compressor. Part 2: Computational assessment [NASA-TM-102273] p 194 N90-14236
 A study of variable geometry in advanced gas turbines p 255 N90-15104
 Piloted simulation of a ground-based time-control concept for air traffic control [NASA-TM-101085] p 240 N90-15898
 NASA aerodynamics program p 373 N90-17235
 Direct multivariable adaptive controller with application to wing flutter p 349 N90-17642
 Measurement and computer simulation of antennas on ships and aircraft for results of operational reliability p 370 N90-17936
 Numerical simulation of compressible vortices [AD-A216221] p 371 N90-18017
 Delivery performance of conventional aircraft by terminal-area, time-based air traffic control: A real-time simulation evaluation [NASA-TP-2978] p 404 N90-18378
 Aeroservoelasticity [NASA-TM-102620] p 416 N90-19227
 Spectral simulation of unsteady compressible flow past a circular cylinder [NASA-CR-182030] p 478 N90-20050
 Escape systems research at RAE p 483 N90-20058
 Autonomous integrated GPS/INS navigation experiment for OMV, Phase 1: Feasibility study [NASA-CR-4267] p 489 N90-20969
 Calculation of the three dimensional turbulent flow in a linear turbine blade p 513 N90-21021
 The numerical simulation of multistage turbomachinery flows p 514 N90-21025
 Airborne Doppler radar flight experiments for the detection of microbursts p 542 N90-21243
 Swept wing ice accretion modeling [NASA-TM-103114] p 570 N90-21727
 A comparison of time-optimal interception trajectories for the F-8 and F-15 [NASA-CR-186300] p 581 N90-21753
 Quiet mode for nonlinear rotor models [NASA-TM-102236] p 582 N90-21758
 Optimal control of an aircraft flying through a downburst p 591 N90-21765
 Design and testing of a multiblock grid-generation procedure for aircraft design and research p 582 N90-21984
 Numerical flow simulation and supercomputers: More than a digital wind tunnel p 612 N90-22976
 Application of numerical optimization techniques to control system design for nonlinear dynamic models of aircraft p 593 N90-23032
 Real-time closed-loop simulation and upset evaluation of control systems in harsh electromagnetic environments p 613 N90-23069
 Simulator evaluation of the final approach spacing tool [NASA-TM-102807] p 636 N90-23374
 Introducing the VRT gas turbine combustor [NASA-TM-103176] p 688 N90-23591
 Real-time simulation clock [NASA-CASE-LAR-14056-1] p 689 N90-23713
 Low-density flow effects for hypervelocity vehicles, phase 2 [AD-A221034] p 634 N90-24249
 A quantitative technique to estimate microburst wind shear hazard to aircraft p 692 N90-25040
 Convex models of malfunction diagnosis in high performance aircraft [AD-A218514] p 702 N90-25073
 Replication of NASPAC Dallas/Fort Worth study [DOT/FAA/CT-TN90/26] p 729 N90-25123
 Lecture notes on flight simulation techniques [LR-596] p 762 N90-25153
 A simulation code for turbocompound diesel engines [IAR-89-26] p 774 N90-25348
 CREW CHIEF: A computer graphics simulation of an aircraft maintenance technician p 779 N90-25515
 Modeling strength data for CREW CHIEF p 780 N90-25516
 Hardware and software reliability estimation using simulations [NASA-CR-186637] p 780 N90-25580
 Two-dimensional Euler and Navier-Stokes Time accurate simulations of fan rotor flows [NASA-TM-102402] p 720 N90-25948
 Performance of a supercharged direct-injection stratified-charge rotary combustion engine [NASA-TM-103105] p 748 N90-25982
 Model following control system design: Preliminary ATTAS in-flight simulation test results [PD-FC-9003] p 758 N90-26010

- An investigation of the use of singular perturbation methods and modal control theory in the derivation or aircraft control schemes
[MATHS-REPT-A-106] p 758 N90-26014
Dallas/Fort Worth simulation, volume 1
[DOT/FAA/CT-TN89/28-VOL-1] p 824 N90-26802
Cognitive requirements for aircraft navigation
[NASA-CR-186933] p 824 N90-26804
Atlanta tower simulation, volume 1
[DOT/FAA/CT-TN89/27-VOL-1] p 870 N90-26835
Atlanta tower simulation, Volume 2: Appendixes
[DOT/FAA/CT-TN89/27-VOL-2] p 870 N90-26836
The EFA integrated monitoring and recording system: Requirements and concept for implementation
p 848 N90-27620
AIMS test and simulation equipment
p 892 N90-27623
Experimental study towards a future airport ground movement simulator
p 827 N90-27687
Econometric graphics display system for flight simulation avionics
[NASA-CR-186886] p 849 N90-27701
Dallas/Fort Worth simulation. Phase 2: Triple simultaneous parallel Instrument Landing System (ILS) approaches (turbojets)
[DOT/FAA/CT-90/2] p 915 N90-28509
Investigation of ATP blades, part 2. Validation of two-dimensional viscous flow simulation codes around thin airfoils
[NAL-TR-1046] p 912 N90-29326
The function of the Interactive Model Assembly Program (IMAP) for a flight simulator
[NAL-TR-1034] p 939 N90-29412
Three-dimensional numerical study of thunderstorm downdrafts and associated outflow boundaries
p 963 N90-29746
- CONCENTRATION (COMPOSITION)**
Low NO(x) potential of gas turbine engines
[NASA-TM-102452] p 345 N90-17636
- CONCORDE AIRCRAFT**
The next generation supersonic transport engine: Critical issues
[PNR90576] p 115 N90-12605
- CONCRETES**
Evaluation of two transport aircraft and several ground test vehicle friction measurements obtained for various runway surface types and conditions. A summary of test results from joint FAA/NASA Runway Friction Program
[NASA-TP-2917] p 249 N90-15902
Criteria for polymer concrete on airport pavements
[DOT/FAA/DS-89/18] p 527 N90-21045
Development and testing of rapid repair methods for war damaged runways
[AD-A223970] p 938 N90-28586
- CONCURRENT PROCESSING**
Concurrent processing adaptation of aeroelastic analysis of propfans
[AIAA PAPER 90-1036] p 450 A90-29380
A multiprocessor implementation of real-time control for a turbojet engine
p 746 A90-45415
Concurrent processing adaptation of aeroplastic analysis of propfans
[NASA-TM-102455] p 215 N90-14656
- CONDENSATION**
Effect of condensation in a diffuser on the flow field
p 603 A90-36784
Condensation in hypersonic nitrogen wind tunnels
[AIAA PAPER 90-1392] p 558 A90-37937
- CONDENSING**
Transonic flow around airfoils with relaxation and energy supply by homogeneous condensation
p 620 A90-39782
- CONDITIONED REFLEXES**
Reflexive navigation for autonomous aircraft
[AIAA PAPER 89-2991] p 25 A90-10502
- CONDUCTIVE HEAT TRANSFER**
Finite element analysis of nonstationary temperature fields in gas turbine components
p 271 A90-21324
- CONES**
Comparison of thin and full viscous shock layer models in the problem of supersonic flow of a viscous gas past blunt cones
p 231 A90-22396
- CONFERENCES**
Infrared technology XIV: Proceedings of the Meeting, San Diego, CA, Aug. 15-17, 1988
[SPIE-972] p 66 A90-10138
Fiber optic smart structures and skins: Proceedings of the Meeting, Boston, MA, Sept. 8, 9, 1988
[SPIE-986] p 37 A90-11201
Fiber optic systems for mobile platforms II: Proceedings of the Meeting, Boston, MA, Sept. 6, 7, 1988
[SPIE-989] p 67 A90-11659
Unsteady aerodynamics and aeroelasticity of turbomachines and propellers; Proceedings of the Fourth International Symposium, Aachen, Federal Republic of Germany, Sept. 6-10, 1987
p 5 A90-11776

- NAVSTAR-GPS: An evolution or a revolution, Ecole Supérieure d'Electricité, Gif-sur-Yvette, France, Feb. 11, 1987, Workshop
p 27 A90-12250
International Symposium on Air Breathing Engines, 9th, Athens, Greece, Sept. 3-8, 1989, Proceedings. Volumes 1 & 2
p 43 A90-12501
ION, Satellite Division's International Technical Meeting, Colorado Springs, CO, Sept. 19-23, 1988, Proceedings
p 123 A90-13976
Heat Transfer and Fluid Mechanics Institute, 31st, California State University, Sacramento, June 1, 2, 1989, Proceedings
p 130 A90-15387
Symposium on Numerical and Physical Aspects of Aerodynamic Flows, 4th, California State University, Long Beach, Jan. 16-19, 1989, Proceedings
p 144 A90-16751
Instrumentation for combustion and flow in engines; Proceedings of the NATO Advanced Study Institute, Vimeiro, Portugal, Sept. 13-26, 1987
p 211 A90-19004
AIAA Lighter-Than-Air Systems Technology Conference, 8th, Jacksonville, FL, Oct. 5-7, 1989, Technical Papers
p 221 A90-20576
Superalloy 718: Metallurgy and applications; Proceedings of the International Symposium, Pittsburgh, PA, June 12-14, 1989
p 266 A90-20775
Numerical grid generation in computational fluid mechanics '88; Proceedings of the Second International Conference, Miami Beach, FL, Dec. 5-8, 1988
p 376 A90-26476
Development of fatigue loading spectra
[ASTM STP-1006] p 367 A90-26751
AHS, Annual Forum, 45th, Boston, MA, May 22-24, 1989, Proceedings
p 381 A90-28151
AUTOTESTCON '89 - IEEE International Automatic Testing Conference, Philadelphia, PA, Sept. 25-28, 1989, Conference Record
p 457 A90-28310
AIAA/ASME/ASCE/AHS/ASC Structures, Structural Dynamics and Materials Conference, 31st, Long Beach, CA, Apr. 2-4, 1990, Technical Papers. Part 1 - Materials, engineering optimization and design
p 449 A90-29226
AIAA/ASME/ASCE/AHS/ASC Structures, Structural Dynamics and Materials Conference, 31st, Long Beach, CA, Apr. 2-4, 1990, Technical Papers. Part 3 - Structural dynamics I
p 449 A90-29359
AAIC '88 - Aerospace Applications of Artificial Intelligence; Proceedings of the Fourth Annual Conference, Dayton, OH, Oct. 25-27, 1988, Volumes 1 & 2
p 458 A90-30226
Heat transfer in gas turbine engines; Proceedings of the Symposium, ASME Winter Annual Meeting, San Francisco, CA, Dec. 10-15, 1989
p 534 A90-32166
European Forum on Aeroelasticity and Structural Dynamics, Aachen, Federal Republic of Germany, Apr. 17-19, 1989, Proceedings
[DGLR BERICHT 89-01] p 468 A90-33351
Designing with advanced composites; Report on the European Core Conference, 1st, Zurich, Switzerland, Oct. 20, 21, 1988, Conference Papers
p 530 A90-33701
AIAA/SFTE/DGLR/SETP, Biannual Flight Test Conference, 5th, Ontario, CA, May 22-24, 1990, Technical Papers
p 493 A90-33886
MRS International Meeting on Advanced Materials, 1st, Tokyo, Japan, May 31-June 3, 1988, Proceedings. Volume 5 - Structural ceramics/Fracture mechanics
p 599 A90-35926
National Technical Specialists' Meeting on Tactical V/STOL, New Bern, NC, Sept. 19-21, 1989, Proceedings
p 551 A90-38526
Fatigue methodology III; Proceedings of the AHS National Technical Specialists' Meeting on Advanced Rotorcraft Structures, Scottsdale, AZ, Oct. 3-5, 1989
p 641 A90-39976
Annual General Meeting of the Canadian Aeronautics and Space Institute, 36th, Ottawa, Canada, May 15, 16, 1989, Proceedings
p 701 A90-42652
Developments in mechanics. Volume 15 - Midwestern Mechanics Conference, 21st, Michigan Technological University, Houghton, Aug. 13-16, 1989, Proceedings
p 769 A90-42870
The 21st century in space; Proceedings of the Thirty-fifth Annual AAS Conference, Saint Louis, MO, Oct. 24-26, 1988
p 762 A90-43460
AIAA Atmospheric Flight Mechanics Conference, Portland, OR, Aug. 20-22, 1990, Technical Papers
p 751 A90-45134
Institute of Navigation, Annual Meeting, 45th, Alexandria, VA, June 27-29, 1989, Proceedings
p 727 A90-45226
AIAA Applied Aerodynamics Conference, 8th, Portland, OR, Aug. 20-22, 1990, Technical Papers. Parts 1 & 2
p 787 A90-45845
Low Reynolds number aerodynamics; Proceedings of the Conference, University of Notre Dame, IN, June 5-7, 1989
p 799 A90-46358
Radio Technical Commission for Aeronautics, Annual Assembly and Technical Symposium, Washington, DC, Dec. 4-6, 1989, Proceedings
p 821 A90-46390
Vertical Lift Aircraft Design Conference, San Francisco, CA, Jan. 17-19, 1990, Proceedings
p 829 A90-46926
AHS National Specialists' Meeting on Rotorcraft Dynamics, Arlington, TX, Nov. 13, 14, 1989, Proceedings
p 830 A90-46952
AIAA Guidance, Navigation and Control Conference, Portland, OR, Aug. 20-22, 1990, Technical Papers. Parts 1 & 2
p 862 A90-47576
National Conference on Aerodynamics, 5th, Poona, India, May 24, 25, 1990, Proceedings
p 809 A90-48076
Aerospace - Collected translations of selected papers --- Book
p 786 A90-48510
Unsteady aerodynamics and aeroelasticity of turbomachines and propellers; Proceedings of the Fifth International Symposium, Beijing, People's Republic of China, Sept. 18-21, 1989
p 853 A90-49451
Latin American Conference on International Air Transport and Activities in Outer Space, Mexico City, Mexico, Aug. 14-18, 1988, Proceedings
p 897 A90-49613
1988 International Aerospace and Ground Conference on Lightning and Static Electricity, Oklahoma City, OK, Apr. 19-22, 1988, Addendum to the Proceedings
p 888 A90-49826
Aeronautical fatigue in the electronic era; Proceedings of the Fifteenth ICAF Symposium, Jerusalem, Israel, June 21-23, 1989
p 901 A90-49876
International SAMPE Symposium and Exhibition, 35th, Anaheim, CA, Apr. 2-5, 1990, Proceedings. Books 1 & 2
p 940 A90-50056
Quantitative methods in fractography; Proceedings of the Symposium on Evaluation and Techniques in Fractography, Atlanta, GA, Nov. 10, 1988
[ASTM STP-1085] p 949 A90-50551
Future fuels for general aviation; Proceedings of the Symposium on Future Fuels for General Aviation Intermittent Combustion, Baltimore, MD, June 29, 1988
[ASTM STP-1048] p 950 A90-51616
Combustion instabilities in liquid-fueled propulsion systems
[AGARD-CP-450] p 63 N90-10191
Castings Airworthiness
[AGARD-R-762] p 64 N90-10231
Fluid Dynamics of Three-Dimensional Turbulent Shear Flows and Transition
[AGARD-CP-438] p 71 N90-10356
Kalman Filter Integration of Modern Guidance and Navigation Systems
[AGARD-LS-166] p 28 N90-10847
Flight Test Techniques
[AGARD-CP-452] p 33 N90-10860
Meeting review: The Second NCAR (National Center for Atmospheric Research) Research Aircraft Fleet Workshop
[PB89-200901] p 137 N90-12113
Research in Natural Laminar Flow and Laminar-Flow Control, part 1
[NASA-CP-2487-PT-1] p 90 N90-12503
Research in Natural Laminar Flow and Laminar-Flow Control, part 2
[NASA-CP-2487-PT-2] p 91 N90-12519
Research in Natural Laminar Flow and Laminar-Flow Control, part 3
[NASA-CP-2487-PT-3] p 92 N90-12539
Flight deck automation: Promises and realities
[NASA-CP-10036] p 187 N90-13384
Flight in adverse environmental conditions
[AGARD-AR-277] p 185 N90-14218
Flight in Adverse Environmental Conditions
[AGARD-CP-470] p 222 N90-15041
International Aircraft Occupant Safety Conference and Workshop proceedings
[AD-A214452] p 239 N90-15085
New Light Alloys
[AGARD-CP-444] p 267 N90-15185
Proceedings of the 1988 Structural Integrity Program Conference
[AD-A213545] p 275 N90-15486
Advances in techniques and technologies for air vehicle navigation and guidance
[AGARD-AR-276] p 243 N90-15899
Fuel Tank Technology
[AGARD-R-771] p 250 N90-15904
Guidance and Control of Unmanned Air Vehicles
[AGARD-CP-436] p 260 N90-15924
Advances in Techniques and Technologies for Air Vehicle Navigation and Guidance
[AGARD-CP-455] p 332 N90-16731
Aircraft Fire Safety
[AGARD-CP-467] p 324 N90-17581
CAST-10-2/DOA 2 Airfoil Studies
[NASA-CP-3052] p 352 N90-17647

- AGARD/SMP Review: Damage Tolerance for Engine Structures. 2: Defects and Quantitative Materials Behaviour --- conference
[AGARD-R-769] p 425 N90-18396
- Unsteady Aerodynamic Phenomena in Turbomachines [AGARD-CP-468] p 425 N90-18405
- Calendar of selected aeronautical and space meetings [AGARD-CAL-90/1] p 464 N90-19060
- Implications of Advanced Technologies for Air and Spacecraft Escape
[AGARD-CP-472] p 483 N90-20054
- Summary report of the Summer Conference of the DARPA-Materials Research Council
[AD-A217380] p 532 N90-20143
- Joint University Program for Air Transportation Research, 1988-1989
[NASA-CP-3063] p 468 N90-20921
- Computational Methods for Aerodynamic Design (Inverse) and Optimization
[AGARD-CP-463] p 500 N90-20976
- Secondary Flows in Turbomachines
[AGARD-CP-469] p 511 N90-21009
- Proceedings of the 13th International Congress on Instrumentation in Aerospace Simulation Facilities
[EOARD-LR-89-069] p 527 N90-21046
- Peacetime replacement and crash damage factors for army aircraft
[AD-A218544] p 636 N90-23372
- The 30th Airlines International Electronics Meeting Proceedings
[ETN-90-96973] p 637 N90-24261
- FAA/NASA En Route Noise Symposium
[NASA-CP-3067] p 696 N90-24853
- Second Annual International Conference on Aging Aircraft
[AD-A222715] p 724 N90-25961
- Technical evaluation report on the Guidance and Control Panel 49th Symposium on Fault Tolerant Design Concepts for Highly Integrated Flight Critical Guidance and Control Systems
[AGARD-AR-281] p 758 N90-26012
- Rotorcraft aeromechanical stability-methodology assessment. Phase 2: Workshop
[NASA-TM-102272] p 816 N90-26800
- Proceedings of the 1987 Aircraft/Engine Structural Integrity Program (ASIP/ENSIP) Conference
[AD-A198037] p 842 N90-26807
- Application of damage tolerance
[DLR-MITT-89-23] p 825 N90-27676
- AGARD/SMP Review Damage Tolerance for Engine Structures. 3: Component Behaviour and Life Management
[AGARD-R-770] p 855 N90-27704
- Impact of Emerging NDE-NDI Methods on Aircraft Design, Manufacture, and Maintenance
[AGARD-CP-462] p 885 N90-28068
- Aerodynamics of Combat Aircraft Controls and of Ground Effects
[AGARD-CP-465] p 920 N90-28513
- Proceedings of a workshop on Future Airport Passenger Terminals
[PB90-213620] p 937 N90-28580
- High Temperature Surface Interactions
[AGARD-CP-461] p 951 N90-28698
- The Second ARO Workshop on Rotorcraft Interactional Aerodynamics
[AD-A223310] p 911 N90-29304
- Analysis, Design and Synthesis Methods for Guidance and Control Systems
[AGARD-AG-314] p 916 N90-29338
- Proceedings of damping '89. Volume 1: Pages AAB-1 through DCD-11
[AD-A223431] p 960 N90-29664
- CONFIGURATION MANAGEMENT**
- The automated software development project at McDonnell Aircraft Company (The Software Factory)
p 460 A90-30782
- Application of 3-D viscous code in the design of a high performance compressor
[AIAA PAPER 90-1914] p 740 A90-42694
- Recent developments in rotor dynamics methodology in the U.S. industry
p 889 A90-46960
- Distribution of hardware and software elements in unmanned air vehicle systems
p 251 N90-15933
- Aeropropulsion facilities configuration control: Procedures manual
[NASA-TM-102541] p 543 N90-21399
- CONFORMAL MAPPING**
- Analysis of high-incidence separated flow past airfoils.
p 147 A90-16781
- Applications of Lagrangian blending functions for grid generation around airplane geometries
[AIAA PAPER 90-0009] p 216 A90-19630
- An embedded grid formulation applied to a delta wing
[AIAA PAPER 90-0429] p 229 A90-22216

- Application of multiple grids topology to supersonic internal/external flow interactions p 308 A90-26135
- A semi-analytical procedure for the conformal mapping of arbitrary airfoil contours p 309 A90-26498
- Grid generation for an aft-fuselage-mounted nacelle/pylon configuration p 311 A90-26543
- Aerodynamic loads and blade vortex interaction noise prediction p 614 A90-38520
- A grid generation method for an aft-fuselage mounted capped-nacelle/pylon configuration with an actuator disk
[AIAA PAPER 90-1564] p 565 A90-38703
- Analysis and numerical solution of flow over airfoil with control flap p 318 N90-17564
- Prediction of subsonic vortex shedding from forebodies with chines
[NASA-CR-4323] p 909 N90-28494
- CONGRESSIONAL REPORTS**
- Safer skies with TCAS: Traffic Alert and Collision Avoidance System
[PB89-169221] p 27 N90-10016
- Aviation security: Corrective actions underway, but better inspection guidance still needed. Report to the Chairwoman, Government Activities and Transportation Subcommittee, Committee on Government Operations, House of Representatives
[GAO/RCED-88-160] p 635 N90-23367
- Aviation safety: Conditions within the air traffic control work force. Fact sheet for congressional requesters
[GAO/RCED-89-113FS] p 724 N90-25958
- Aviation safety: Serious problems continue to trouble the air traffic control work force. Report to congressional requesters
[GAO/RCED-89-112] p 724 N90-25959
- CONICAL BODIES**
- Unified super/hypersonic similitude for steady and oscillating cones and ogives p 82 A90-13786
- Effect of the inertial nature of injection and temperature on the damping of body vibrations p 150 A90-17112
- Mach number effects on conical surface features of swept shock-wave/boundary-layer interactions p 154 A90-18147
- Prediction of steady and unsteady asymmetric vortical flows around cones
[AIAA PAPER 90-0598] p 168 A90-19940
- A study of the laminar-turbulent boundary layer transition on the windward side of a delta wing with a conical surface p 298 A90-24144
- Laminar separated flow on a biconical body at high supersonic velocities p 387 A90-28992
- Stability characteristics of a conical aerospace plane concept
[SAE PAPER 892313] p 757 A90-45475
- External flow computations for a finned 60mm ramjet in steady supersonic flight
[AD-A216998] p 428 N90-19233
- CONICAL FLOW**
- Calculation of cone drag p 84 A90-14579
- Navier-Stokes computations of lee-side flows over delta wings p 153 A90-17978
- Asymmetric separated flows at supersonic speeds
[AIAA PAPER 90-0595] p 230 A90-22233
- A method for calculating the location and intensity of a conical head shock on the lower surface of a delta wing with supersonic edges p 297 A90-24139
- Computational study for passive control of supersonic asymmetric vortical flows around cones
[AIAA PAPER 90-1581] p 566 A90-38718
- Structure of swept shock wave/boundary-layer interactions using conical shadowgraphy
[AIAA PAPER 90-1644] p 569 A90-38772
- The potential approximation in the theory of conical flows p 710 A90-44930
- Some observations on transitory stall in conical diffusers
[NASA-TM-102387] p 94 N90-12561
- The experimental investigation of flow in the core of a vortex structure
[BR114893] p 960 N90-29597
- CONICAL NOZZLES**
- Gasdynamic characteristics of a plane or axisymmetric nozzle with a rectilinear generatrix of the supersonic section p 805 A90-46575
- CONICAL SHELLS**
- The shape assumed by a soft conical shell in fluid flow p 300 A90-24752
- CONSCIOUSNESS**
- Development of an ejection seat specification for a new fighter aircraft p 483 N90-20057
- CONSERVATION EQUATIONS**
- Numerical study of three methods for solving reacting flows p 305 A90-25804
- Computation of complex flows in gas turbine combustors with a multi-level additive correction technique p 881 A90-46899

CONSERVATION LAWS

- Multigrid scheme for the compressible Euler-equations p 907 A90-51559

CONSTITUTIVE EQUATIONS

- Constitutive modeling for isotropic materials (HOST)
[NASA-CR-179522] p 193 N90-13390
- Constitutive modeling for isotropic materials (HOST)
[NASA-CR-174718] p 193 N90-13391

CONSTRUCTION

- Aircraft fuel tank construction and testing experience
[AD-A222716] p 250 N90-15907
- The US National Transonic Facility, NTF p 262 N90-15942
- The European Transonic Windtunnel (ETW) p 262 N90-15945
- Models for cryogenic wind tunnels p 263 N90-15956
- Aircraft lightning protection handbook
[AD-A222716] p 820 N90-27668

CONSTRUCTION MATERIALS

- Creep-fatigue interactions of gas turbine materials p 131 A90-16011
- The promise of advanced materials for a 21st century UBE --- ultrahigh bypass ratio engine
[AIAA PAPER 90-2396] p 662 A90-42157

CONTACT LOADS

- A quadratic programming method for solving three dimensional elastic-plastic contact problems p 603 A90-36417
- Frictionless contact of aircraft tires
[SAE PAPER 892350] p 733 A90-45501
- Aircraft tire/pavement pressure distributions
[SAE PAPER 892351] p 734 A90-45502

CONTAINMENT

- Development of an advanced fan blade containment system
[DOT/FAA/CT-89/20] p 192 N90-13386

CONTAMINANTS

- An overview of the joint FAA/NASA aircraft/ground runway friction program
[NASA-TM-103486] p 724 N90-25957

CONTAMINATION

- Catalytic conversion of oil in bleed air - A maintenance tool
[SAE PAPER 892214] p 732 A90-45431
- Direct numerical study of leading-edge contamination p 19 N90-10361

CONTINUOUS RADIATION

- Comparison of the swept frequency continuous wave, current pulse, and shock-excitation lightning simulation techniques p 818 A90-49832

CONTINUUM FLOW

- Numerical simulation of hypersonic viscous continuum flow p 707 A90-44407

CONTOURS

- A semi-analytical procedure for the conformal mapping of arbitrary airfoil contours p 309 A90-26498
- A two-dimensional adaptive-wall test section with ventilated walls in the Ames 2- by 2-foot transonic wind tunnel
[NASA-TM-102207] p 201 N90-13407
- Inverse design of airfoil contours: Constraints, numerical method, and applications p 500 N90-20980
- Generation of circumferential velocity contours associated with pulsed point suction on a rotating disk p 691 N90-25065

CONTRACT MANAGEMENT

- Studies of the European transonic wind tunnel
[ONERA-RS-12/0694-GY] p 141 N90-13278

CONTRACTION

- A study of the working process and losses in annular turbine nozzle cascades with a low contraction ratio p 254 A90-23407

CONTRACTORS

- The technology challenge of the advanced tactical fighter: A study of the technology transition process
[AD-A216109] p 338 N90-17630

CONTRACTS

- Eurofighter fights back p 221 A90-21714

CONTRA-ROTATING PROPELLERS

- A study of flow structure in a contra-rotating axial compressor stage p 11 A90-12524
- Noise prediction of a counter-rotation propfan p 218 A90-17861
- Propeller tip vortex interactions
[AIAA PAPER 90-0437] p 166 A90-19846
- A methodology proposal to design and analyse counterrotating high speed propellers
[ASME PAPER 89-GT-38] p 340 A90-23767
- A practical co-axial twin rotor model p 335 A90-25423
- Noise of a simulated installed model counterrotation propeller at angle-of-attack and takeoff/approach conditions
[AIAA PAPER 90-0283] p 547 A90-32505

- Counter-rotating propellant analysis using a frequency domain panel method p 623 A90-40937
- On the unsteady loading noise of counter-rotating propeller p 895 A90-49484
- User's guide to PMESH: A grid-generation program for single-rotation and counterrotation advanced turboprops [NASA-CR-185156] p 217 N90-14783
- In-plane forces and moments on installed inclined propellers at low forward speeds p 316 N90-16720
- An approximate model for the performance and acoustic predictions of counterrotating propeller configurations [NASA-CR-180667] p 379 N90-18228
- Relating flow between counter-rotating propellers to aerodynamic interaction noise p 479 N90-20944
- Experimental performance and acoustic investigation of modern, counterrotating blade concepts [NASA-CR-185158] p 649 N90-23393
- CONTRAST**
- The assessment of visibility from automatic contrast Measurements p 242 N90-15061
- CONTROL BOARDS**
- Description of the primary flight display and flight guidance system logic in the NASA B-737 transport systems research vehicle [NASA-TM-102710] p 927 N90-28546
- CONTROL CONFIGURED VEHICLES**
- An adaptive flight control system design for non-minimum phase CCV by relative order reduction p 196 A90-19428
- Control configured airship design [AIAA PAPER 89-3170] p 244 A90-20585
- Flight-testing of the self-repairing flight control system using the F-15 highly integrated digital electronic control flight research facility [AIAA PAPER 90-1321] p 520 A90-34149
- Adaptive flight control of CCV aircraft with limiting zeros [AIAA PAPER 90-3409] p 864 A90-47664
- Backside landing control of a STOL aircraft using approximate perfect servo p 934 A90-52801
- Flight-testing of the self-repairing flight control system using the F-15 highly integrated digital electronic control flight research facility [NASA-TM-101725] p 758 N90-25144
- CONTROL EQUIPMENT**
- Applications of fiber optic sensors in advanced engine controls p 68 A90-11703
- Dynamic properties of a system for the roll control of a model electromagnetically suspended in a wind tunnel p 262 A90-22762
- Integration of a centralized multiplexed control unit into the cockpit of an aircraft [F6150-DT410-1-88329] p 120 N90-12622
- Prediction of forces and moments for flight vehicle control effectors. Part 1: Validation of methods for predicting hypersonic vehicle controls forces and moments [NASA-CR-186571] p 571 N90-21734
- Prediction of forces and moments for flight vehicle control effectors. Part 2: An analysis of delta wing aerodynamic control effectiveness in ground effect [NASA-CR-186572] p 571 N90-21735
- Analysis, Design and Synthesis Methods for Guidance and Control Systems [AGARD-AG-314] p 916 N90-29338
- CONTROL MOMENT GYROSCOPES**
- A study of the errors of a gyroscopic instrument for measuring linear accelerations p 771 A90-45133
- CONTROL SIMULATION**
- Simulation research on the afterburning dynamic characteristics of engine control system p 48 A90-12581
- Digital control experiment research on the engine JT15D-4 p 190 A90-18600
- Numerical simulation of the actuation system for the ALDF's propulsion control valve --- Aircraft Landing Dynamics Facility [AIAA PAPER 90-0079] p 211 A90-19674
- Control sensitivity, bandwidth and disturbance rejection concerns for advanced rotorcraft p 430 A90-28204
- A model for active control of helicopter air resonance in hover and forward flight p 670 A90-42462
- An assessment of robustness of flight control systems based on variable structure techniques p 57 N90-10895
- Computer-based tools for assisting air traffic controllers with arrivals flow management [RSRE-88001] p 178 N90-13366
- Simulator evaluation of the final approach spacing tool [NASA-TM-102807] p 636 N90-23374
- Robustness evaluation of H2 and H(infinity) control theory as applied to a transport aircraft [AD-A222795] p 759 N90-26018
- CONTROL STABILITY**
- Adaptive autopilot design via model expansion method p 55 A90-11124
- Design of attitude and rate command systems for helicopters using eigenstructure assignment p 118 A90-14729
- Robust controller design using normalized coprime factor plant descriptions --- Book p 457 A90-27645
- Results of an A109 simulation validation and handling qualities study p 591 A90-38524
- Guaranteed cost control via optimal parametric LQ design p 693 A90-40810
- Energy based stability analysis of a fuzzy roll controller design for a flexible aircraft wing p 668 A90-40833
- Stability and controllability in proportional navigation p 725 A90-42990
- A pilot rating scale for evaluating failure transients in electronic flight control systems [AIAA PAPER 90-2827] p 754 A90-45159
- Exploratory wind tunnel investigation of the stability and control characteristics of a three-surface, forward-swept wing advanced turboprop model [AIAA PAPER 90-3074] p 797 A90-45920
- Stiffness of an aircraft pneumatic rudder drive p 828 A90-46479
- Robustness evaluation of a flexible aircraft control system [AIAA PAPER 90-3445] p 890 A90-47698
- Wind tunnel results of the low-speed NLF(1)-0414F airfoil p 93 N90-12541
- On the application of modified stepwise regression for the estimation of aircraft stability and control parameters [REPT-8905] p 198 N90-13400
- STARS: An integrated general-purpose finite element structural, aeroelastic, and aeroservoelastic analysis computer program [NASA-TM-101709] p 689 N90-23768
- CONTROL STICKS**
- Development of the stall warning/stick pusher system for the Boeing/de Havilland Dash 8 Series 300 p 645 A90-42420
- Simulator comparison of thumbball, thumb switch, and touch screen input concepts for interaction with a large screen cockpit display format [NASA-TM-102587] p 506 N90-21005
- CONTROL SURFACES**
- Structural optimization of lifting surfaces with divergence and control reversal constraints p 127 A90-13770
- Experimental transition and boundary-layer stability analysis for a slotted swept laminar flow control airfoil p 148 A90-16793
- Time-domain aeroservoelastic modeling using weighted unsteady aerodynamic forces p 195 A90-17698
- Effect of moving surfaces on the airfoil boundary-layer control p 159 A90-19388
- Pneumatic vortical flow control at high angles of attack [AIAA PAPER 90-0098] p 227 A90-22164
- Pay-offs and pitfalls of fly-by-wire p 346 A90-24281
- Conditions of the generation of autooscillations in aerodynamic control surfaces in nonseparated subsonic flow of a gas p 315 A90-27303
- Tiltrotor aeroservoelastic design methodology at BHTI p 410 A90-28244
- Computation of steady and unsteady control surface loads in transonic flow [AIAA PAPER 90-0935] p 389 A90-29361
- Simulation of static and dynamic aeroelastic behavior of a flexible wing with multiple control surfaces [AIAA PAPER 90-1075] p 392 A90-29383
- An aircraft flight control reconfiguration algorithm p 432 A90-30708
- Flutter analysis from ambient random responses p 491 A90-33374
- Multi-surface control law synthesis and wind tunnel test verification of active flutter suppression for a transport-type wing p 517 A90-33401
- Practical techniques of modelling aeroelastic systems for active control applications p 545 A90-33402
- Implementation of comprehensive actuation system models in aeroservoelastic analysis p 517 A90-33406
- Further studies of harmonic gradient method for supersonic aeroelastic applications p 473 A90-33410
- Vortex generator jets - Means for flow separation control p 555 A90-36257
- Computational study for passive control of supersonic asymmetric vortical flows around cones [AIAA PAPER 90-1581] p 566 A90-38718
- Flutter of shaft-supported low aspect-ratio control surfaces p 667 A90-38912
- The influence of control-surface compensation parameters on the hinge moment characteristics p 643 A90-41737
- Influence of some geometrical and design parameters on the hinge moment characteristics of rudders p 643 A90-41739
- The active flexible wing aeroservoelastic wind-tunnel test program p 33 N90-10119
- Effect of control surface mass unbalance on the stability of a closed-loop active control system [NASA-TP-2952] p 134 N90-12042
- Stall/spin aerodynamic data project [DOT/FAA/CT-88/29] p 185 N90-14222
- Example of procedure in calculation of control hinge moments [ESDU-89010] p 199 N90-14240
- Discrete proportional Plus Integral (PI) multivariable control laws for the Control Reconfigurable Combat Aircraft (CRCA) [AD-A215664] p 433 N90-18431
- Prediction of forces and moments for flight vehicle control effectors. Part 1: Validation of methods for predicting hypersonic vehicle controls forces and moments [NASA-CR-186571] p 571 N90-21734
- Research at NASA's NFAC wind tunnels [NASA-TM-102827] p 702 N90-25933
- Prediction methodologies for nonlinear aerodynamic characteristics of control surfaces [NIAI-90-17] p 718 N90-25937
- A computer module used to calculate the horizontal control surface size of a conceptual aircraft design [NASA-CR-186872] p 780 N90-26515
- Aerodynamic/dynamic interaction [AD-A22263] p 815 N90-26798
- Development of an automated ultrasonic inspection system for composite structure on in-service aircraft p 885 N90-28079
- Control of submersible vortex flows [NASA-TM-102693] p 909 N90-28493
- Aerodynamic control design: Experience and results at Aermacchi p 935 N90-28518
- Development of non-conventional control methods for high angle of attack flight using vortex manipulation p 935 N90-28522
- Control of vortex aerodynamics at high angles of attack p 921 N90-28523
- Unsteady aerodynamics of controls p 935 N90-28525
- CONTROL SYSTEMS DESIGN**
- A methodology for modeling, control design and simulation of aerospace mechanical systems [AIAA PAPER 89-3049] p 73 A90-10543
- A hardware and software fault tolerant safety controller [AIAA PAPER 89-3123] p 74 A90-10599
- Adaptive automatic control systems. Number 16 --- Russian book p 76 A90-10844
- The discontinuity condition in the optimal control problem for a composite system p 76 A90-10848
- Formalization and solution of covering problems in the synthesis of control and monitoring systems p 76 A90-10963
- Fiber optics for advanced aircraft p 68 A90-11702
- Design of control amplifier for FJR 710 engine p 43 A90-12017
- Advances in computational design and analysis of airbreathing propulsion systems p 43 A90-12502
- VSTOL power plant control lessons from Harrier experience p 13 A90-12582
- Identification of mathematical derivative models for the design of a model following control system --- for fly-by-wire helicopter p 56 A90-12764
- Airplane design. Part 7 - Determination of stability, control and performance characteristics: Far and military requirements --- Book p 57 A90-12872
- Synthesis of locally optimal aircraft control in the presence of delay p 137 A90-14561
- Design of attitude and rate command systems for helicopters using eigenstructure assignment p 118 A90-14729
- Literal singular-value-based flight control system design techniques p 118 A90-14747
- A simple active controller to suppress helicopter air resonance in hover and forward flight p 119 A90-16521
- Design of direct lift control systems against vertical gust p 196 A90-18592
- The eigenvalue sensitivity analysis and design for integrated flight/propulsion control systems p 196 A90-18601
- The establishment of mathematical model of engine control system and simulation research of afterburning dynamic characteristics p 190 A90-18613
- The optimum control and adaptive control for airplane cabin pressure p 182 A90-18627
- An adaptive flight control system design for non-minimum phase CCV by relative order reduction p 196 A90-19428
- Decoupled ultimate boundedness control of systems and large aircraft maneuver p 196 A90-19461

Analysis and design of sidestick controller systems for general aviation aircraft p 196 A90-19554

Design of a helicopter output feedback control law using modal and structured-robustness techniques p 282 A90-20557

Digital electronic control unit for the European Fighter Aircraft (EFA) p 253 A90-21607

A variable structure system (VSS) to robust control of aircraft p 257 A90-21987

Reduction of blade-vortex interaction noise through higher harmonic pitch control p 377 A90-23937

Concise design of aircraft longitudinal model reference adaptive command augmentation system p 345 A90-24002

Automatic vibration reduction at a four bladed hingeless model rotor - A wind tunnel demonstration p 335 A90-25424

Helicopter rotor dynamics and aeroelasticity - Some key ideas and insights p 335 A90-25425

Advanced Automation System design p 375 A90-25566

Design considerations for achieving MLS Category III requirements p 331 A90-25575

Approximate loop transfer recovery method for designing fixed-order compensators p 375 A90-25989

Robust control system design synthesis with observers p 375 A90-25994

Embedded digital control for aircraft environmental control systems - A practical vehicle management system approach [SAE PAPER 891438] p 339 A90-27409

Microprocessor control of a vapor-cycle cooling system [SAE PAPER 891457] p 339 A90-27426

Robust controller design using normalized coprime factor plant descriptions --- Book p 457 A90-27645

Helicopter flight control system design and evaluation for NOE operations using controller inversion techniques p 429 A90-28202

RSRA/X-Wing flight control system development - Lessons learned p 430 A90-28216

Helicopter obstacle avoidance system - The use of manned simulation to evaluate the contribution of key design parameters p 417 A90-28218

Linear control issues in the higher harmonic control of helicopter vibrations p 430 A90-28225

Eshbach's handbook of engineering fundamentals / 4th edition/ p 448 A90-28825

Very-high-performance data acquisition/analysis/display/control systems based on the APTEC I/O computer p 458 A90-28852

Time domain simulations of a flexible wing in subsonic, compressible flow [AIAA PAPER 90-1153] p 390 A90-29365

Digital-flutter-suppression-system investigations for the active flexible wing wind-tunnel model [AIAA PAPER 90-1074] p 430 A90-29382

A design of a twin variable control system for aero-turbojet engine p 423 A90-29917

Digital electronic control for WJ6G4A engine p 424 A90-29919

Aircraft flight control system identification p 431 A90-30105

Modeling and analysis tools for aircraft control system evaluations p 431 A90-30703

Reconfigurable flight controller for the STOL F-15 with sensor/actuator failures p 432 A90-30707

A study of a propulsion control system for a VATOL aircraft (A direct design synthesis application) p 424 A90-30712

Lessons learned in the development of a multivariable control system p 432 A90-30713

Design of adaptive digital controllers incorporating dynamic pole-assignment compensators for high-performance aircraft p 432 A90-30714

Multivariable control design for the control reconfigurable combat aircraft (CRCA) p 432 A90-30715

A computer-aided control engineering environment for multi-disciplinary expert-aided analysis and design (MEAD) p 461 A90-30796

Algorithm for simultaneous stabilization of single-input systems via dynamic feedback p 462 A90-31108

Active flutter suppression for a wing model p 433 A90-31283

Sensitivity derivatives of flutter characteristics and stability margins for aeroservoelastic design p 433 A90-31287

Evaluation of control techniques for aircraft propulsion systems p 507 A90-32262

Comparison of test signals for aircraft frequency domain identification p 490 A90-33057

Reduced-order modeling and controller design for a high-performance helicopter p 516 A90-33058

Aeroservoelastic tailoring for lateral control enhancement p 516 A90-33060

Recent activities within the aeroservoelasticity branch at the NASA Langley Research Center p 492 A90-33400

Interactions of active controls and structural loads p 517 A90-33404

An analytical sensitivity method for use in integrated aeroservoelastic aircraft design p 517 A90-33405

Implementation of comprehensive actuation system models in aeroservoelastic analysis p 517 A90-33406

A review of aeroelasticity research at the flight dynamics laboratory p 493 A90-33409

Use of ground-based and in-flight simulation for flight control system development [AIAA PAPER 90-1286] p 519 A90-33907

Automatic landing with GPS - Design of the flight guidance and flight control system [AIAA PAPER 90-1301] p 487 A90-33915

Simulation research on the afterburning dynamic characteristics of engine control system p 585 A90-35708

Application of transformational ideas to automatic flight control design p 589 A90-36433

A design method for real-time computer control hydraulic force system p 590 A90-36434

The study of transient suppression techniques for multimode flight control system p 590 A90-37219

The method of random variable structure optimal control for aircraft p 590 A90-37220

Analysis and improvement of cabin temperature control system p 580 A90-37241

Control system validation in the autonomous helicopter p 667 A90-38908

Improvement of helicopter handling qualities using H(infinity)-optimisation p 667 A90-38965

Implementation of a transputer-based flight controller p 667 A90-38966

A study on the application of controllability and observability concepts in the design of flight control systems p 693 A90-39303

Identification of multivariable models of jet engines [AIAA PAPER 90-1874] p 655 A90-40540

Design of digital self-selecting multivariable controllers for jet engines [AIAA PAPER 90-1875] p 655 A90-40541

Analysis of airframe/engine interactions - An integrated control perspective [AIAA PAPER 90-1918] p 667 A90-40557

A preliminary evaluation of an F100 engine parameter estimation process using flight data [AIAA PAPER 90-1921] p 656 A90-40559

Full authority digital electronic engine control system provides needed reliability [AIAA PAPER 90-2037] p 658 A90-40606

Guaranteed cost control via optimal parametric LQ design p 693 A90-40810

Helicopter control design using feedback linearization techniques p 668 A90-40817

Energy based stability analysis of a fuzzy roll controller design for a flexible aircraft wing p 668 A90-40833

Flight control application of eigenstructure assignment with optimization of robustness to structured state space uncertainty p 693 A90-40885

Ultimate boundedness control of uncertain systems with application to roll coupled aircraft maneuver p 668 A90-40886

Digital controller design for the pitch axis of the F-14 using an H(infinity) method p 668 A90-40912

Synthesis of optimal multidimensional digital systems for the simulation of the angular motions of a flight vehicle under random loading p 669 A90-41957

Propulsion control system designs for advanced Navy multimission aircraft [AIAA PAPER 90-2403] p 663 A90-42160

Design methodology for multivariable helicopter control systems p 669 A90-42461

A highly maneuverable helicopter in-flight simulator - Aspects of realization [AIAA PAPER 88-4607] p 670 A90-42466

A technique for the tuning of helicopter flight control systems p 670 A90-42467

Full Authority Digital Engine Control for the AS 355 N TM 319 engines p 665 A90-42486

Aircraft propulsion control systems for the next century [AIAA PAPER 90-2034] p 742 A90-42720

Active combustion control in a coaxial dump combustor [AIAA PAPER 90-2447] p 743 A90-42806

High-performance EHA controls using an interior permanent magnet motor --- electrohydraulic actuator for aircraft power systems p 730 A90-43152

Problems in the synthesis of advanced aircraft control systems p 751 A90-44723

The integrated control of a propulsion-airframe system [ASME PAPER 89-WA/DSC-12] p 751 A90-44847

Design of flight control systems to meet rotorcraft handling qualities specifications p 752 A90-45140

[AIAA PAPER 90-2805] p 752 A90-45140

Unified flying qualities criteria for longitudinal tracking [AIAA PAPER 90-2806] p 752 A90-45141

Assessment of proposed fighter agility metrics [AIAA PAPER 90-2807] p 752 A90-45142

Toward a theory of aircraft agility [AIAA PAPER 90-2808] p 752 A90-45143

A pilot rating scale for evaluating failure transients in electronic flight control systems [AIAA PAPER 90-2827] p 754 A90-45159

Optimal control system design for departure prevention [AIAA PAPER 90-2837] p 754 A90-45167

Handling qualities research at the Flight Research Laboratory, NAE/NRC, 1980 - 1990 and beyond [AIAA PAPER 90-2848] p 755 A90-45176

System identification requirements for high-bandwidth rotorcraft flight control system design p 755 A90-45333

Nonlinear flight control design via sliding methods p 756 A90-45335

An explicit model-matching approach to lateral-axis autopilot design p 756 A90-45413

Design features of the 747-400 Electric Power System [SAE PAPER 892227] p 746 A90-45443

Designing and tuning the digital controller of an electronic fuel control unit for small gas turbine engines [SAE PAPER 892255] p 747 A90-45457

BHTI's technical assessment of advanced rotor and control concepts p 861 A90-46949

Mechanisms of active control in cylindrical fuselage structures p 862 A90-47309

Structure/control design synthesis of active flutter suppression system by goal programming [AIAA PAPER 90-3325] p 872 A90-47587

Application of a design method for integrated control to a VTOL airplane in hover [AIAA PAPER 90-3334] p 862 A90-47594

H-infinity based integrated flight/propulsion control design for a STOVL aircraft in transition flight [AIAA PAPER 90-3335] p 862 A90-47595

STOL Maneuver Technology Demonstrator aeroservoelasticity [AIAA PAPER 90-3336] p 863 A90-47596

Structural mode significance using INCA --- Interactive Controls Analysis computer program [AIAA PAPER 90-3346] p 889 A90-47606

Inversion of nonlinear I-O map, zero dynamics and flight control system design [AIAA PAPER 90-3370] p 863 A90-47628

Improved noise rejection in automatic carrier landing systems [AIAA PAPER 90-3374] p 864 A90-47632

Nonlinear inversion flight control for a supermaneuverable aircraft [AIAA PAPER 90-3406] p 864 A90-47661

Robust flight control system design with multiple model approach [AIAA PAPER 90-3411] p 865 A90-47666

Robust control design for relaxed static stability aircraft [AIAA PAPER 90-3443] p 865 A90-47696

Extended implicit model following as applied to integrated flight and propulsion control [AIAA PAPER 90-3444] p 890 A90-47697

Robustness evaluation of a flexible aircraft control system [AIAA PAPER 90-3445] p 890 A90-47698

Flight controller design with nonlinear aerodynamics, large parameter uncertainty, and pilot compensation [AIAA PAPER 90-3478] p 866 A90-47728

Genetic algorithms in control system optimization [AIAA PAPER 90-3488] p 867 A90-47736

Development and testing of methodology for evaluating the performance of multi-input/multi-output digital control systems [AIAA PAPER 90-3501] p 867 A90-47747

Robust low norm output feedback design for flight control systems [AIAA PAPER 90-3505] p 891 A90-47751

Flight control design considerations for STOVL powered-lift flight [AIAA PAPER 90-3225] p 868 A90-49110

Reconfigurable aircraft flight control system via robust direct adaptive control [AIAA PAPER 90-3226] p 868 A90-49111

Obtaining precise LTR with Luenberger type observer with arbitrary observer poles and finite gain [AIAA PAPER 90-3228] p 868 A90-49113

Automatic environmental control system for electronic equipment platforms [SAE PAPER 901217] p 840 A90-49292

- Proven dynamic modeling techniques for concurrent design and analysis of ECS controllers
[SAE PAPER 901234] p 841 A90-49304
- Evaluation and control of an Integrated Closed Environmental Control System (ICECS)
[SAE PAPER 901237] p 841 A90-49307
- Enhanced environmental control for the Harrier II Plus
[SAE PAPER 901238] p 841 A90-49308
- The Mast Mounted Sight 771 processor upgrade program --- for helicopter p 926 A90-51058
- LQG/LTR controller design using a reduced order model p 964 A90-52877
- Real-time support for high performance aircraft operation
[NASA-CR-185475] p 57 N90-10075
- Structural stability augmentation system design using BODEDIRECT: A quick and accurate approach p 33 N90-10116
- ATTAS flight testing experiences p 34 N90-10862
- The active control of an unstable canard aircraft p 57 N90-10894
- An assessment of robustness of flight control systems based on variable structure techniques p 57 N90-10895
- Applications of flight control system methods to an advanced combat rotorcraft
[NASA-TM-101054] p 119 N90-11752
- A design procedure for the handling qualities optimization of the X-29A aircraft
[NASA-TM-4142] p 119 N90-11753
- Robust control design for flight control
[AD-A21957] p 119 N90-11756
- Discretization and model reduction for a class of nonlinear systems p 198 N90-13397
- An autopilot design methodology for bank-to-turn missiles
[AD-A213379] p 198 N90-13399
- A knowledge-based system design/information tool for aircraft flight control systems
[NASA-TM-101704] p 217 N90-13990
- Laboratory test methodology for evaluating the effects of electromagnetic disturbances on fault-tolerant control systems
[NASA-TM-101665] p 217 N90-14061
- Fly-by-light flight control system technology development plan
[NASA-CR-181953] p 259 N90-15111
- The US National Transonic Facility, NTF p 262 N90-15942
- Applications of modern control theory synthesis to a super-augmented aircraft
[AD-A215431] p 336 N90-16753
- Design of integrated pitch axis for autopilot/autothrottle and integrated lateral axis for autopilot/yaw damper for NASA TSRV airplane using integral LQG methodology
[NASA-CR-4268] p 348 N90-16768
- Estimation and control of nonlinear and hybrid systems with applications to air-to-air guidance
[AD-A214542] p 348 N90-16770
- The implications of using integrated software support environment for design of guidance and control systems software
[AGARD-AR-229] p 434 N90-18432
- Application of variable-gain output feedback for high-alpha control
[NASA-TM-102603] p 434 N90-18434
- Practical methods for robust multivariable control
[AD-A216937] p 462 N90-18920
- Laboratory implementation of the Continuously Reconfiguring Multi-Microprocessor Flight Control System (CRMMFCS)
[AD-A217730] p 520 N90-20094
- Joint University Program for Air Transportation Research, 1988-1989
[NASA-CP-3063] p 468 N90-20921
- Rule-based mechanisms of learning for intelligent adaptive flight control p 521 N90-20939
- Perspectives on the use of rule-based control p 521 N90-20940
- Stochastic robustness of linear control systems p 521 N90-20941
- Design of a helicopter automatic flight control system using adaptive control p 522 N90-21040
- Human centrifuge controller
[NAL-TM-SE-8901] p 527 N90-21043
- Advances in optimal active control techniques for aerospace systems; application to aircraft active landing gear p 592 N90-21769
- A methodology for knowledge-based restructurable control to accommodate system failures p 609 N90-22058
- Elements of active vibration control for rotating machinery
[NASA-TM-102368] p 610 N90-22703
- Integrated control-system design via generalized LQG (GLOG) theory p 613 N90-23023
- Application of numerical optimization techniques to control system design for nonlinear dynamic models of aircraft p 593 N90-23032
- Multidisciplinary Expert-aided Analysis and Design (MEAD) p 613 N90-23050
- Multivariable frequency weighted model order reduction for control synthesis
[AIAA-89-3558] p 613 N90-23060
- Six-degree-of-freedom aircraft simulation with mixed-data structure using the applied dynamics simulation language, ADSIM p 613 N90-23067
- Modeling flexible aircraft for flight control design
[AD-A219123] p 757 N90-25140
- Synthesis of individual rotor blade control system for gust alleviation
[NASA-TM-101886] p 736 N90-25972
- Hot gas ingestion characteristics and flow visualization of a vectored thrust STOVL concept p 751 N90-26009
- Model following control system design: Preliminary ATLAS in-flight simulation test results
[PD-FC-9003] p 758 N90-26010
- H-infinity based integrated flight-propulsion control design for a STOVL aircraft in transition flight
[NASA-TM-103198] p 758 N90-26011
- An investigation of the use of singular perturbation methods and modal control theory in the derivation of aircraft control schemes
[MATHS-REPT-A-106] p 758 N90-26014
- Aircraft Integrated Monitoring Systems
[DLR-MITT-90-04] p 786 N90-27617
- AIMS test and simulation equipment p 892 N90-27623
- Performance assessment of MIL-STD-1553B on the avionic systems demonstrator rig of British Aerospace p 849 N90-27624
- New features of JAL's ground station p 872 N90-27633
- Experimental characterization of the effects of pneumatic tubing on unsteady pressure measurements
[NASA-TM-4171] p 850 N90-27703
- Aerodynamics of Combat Aircraft Controls and of Ground Effects
[AGARD-CP-465] p 920 N90-28513
- Aerodynamic and propulsive control development of the STOL and maneuver technology demonstrator p 920 N90-28514
- Combat aircraft control requirements p 934 N90-28515
- Aerodynamic control design: Experience and results at Aermacchi p 935 N90-28518
- Innovative control concepts and component integration for a generic supercruise fighter p 935 N90-28521
- Development of non-conventional control methods for high angle of attack flight using vortex manipulation p 935 N90-28522
- Unsteady aerodynamics of controls p 935 N90-28525
- Validation of the F-18 high alpha research vehicle flight control and avionics systems modifications
[NASA-TM-101723] p 924 N90-28542
- Propulsion system-flight control integration and optimization: Flight evaluation and technology transition
[NASA-TM-4207] p 929 N90-28551
- Energy Efficient Engine: Control system preliminary definition report
[NASA-CR-179578] p 932 N90-28569
- A conceptual framework for fighter flight control systems
[PD-CP-9009] p 936 N90-28577
- An expert system to perform on-line controller restructuring for abrupt model changes
[NASA-TM-103609] p 964 N90-29121
- Analysis, Design and Synthesis Methods for Guidance and Control Systems
[AGARD-AG-314] p 916 N90-29338
- Integrated navigation/flight control for future high performance aircraft p 917 N90-29362
- Multi-disciplinary optimization of aeroservoelastic systems
[NASA-CR-185931] p 925 N90-29385
- ### CONTROL THEORY
- Inverse problems in controlled system dynamics: Nonlinear models --- Russian book p 77 A90-12471
- Parametric synthesis of piecewise constant locally optimal aircraft control under conditions of indeterminacy p 137 A90-14576
- Acceleration, gamma, and theta guidance for abort landing in a windshear p 98 A90-14733
- Effect of the control of turbocompressor guide vanes on the throttle characteristics of a bypass engine p 255 A90-23425
- Low speed testing and simulation of the STOL and Maneuver Technology Demonstrator
[AIAA PAPER 90-1820] p 334 A90-25169
- Application of a digital control theory for generating adaptive grids p 366 A90-25734
- Identification of moderately nonlinear flight mechanics systems with additive process and measurement noise p 347 A90-25987
- Restructurable control using proportional-integral-implicit model following --- for fighter aircraft
[AD-A220997] p 347 A90-25990
- Theoretical and experimental correlation of helicopter aeromechanics in hover p 429 A90-28200
- Helicopter flight control system design and evaluation for NOE operations using controller inversion techniques p 429 A90-28202
- Linear control issues in the higher harmonic control of helicopter vibrations p 430 A90-28225
- Lessons learned in the development of a multivariable control system p 432 A90-30713
- Flutter suppression control law synthesis for the active flexible wing model p 517 A90-33403
- Flying qualities problems of aerospace craft
[AIAA PAPER 90-2804] p 752 A90-45139
- Robustness of dynamic inversion vs mu synthesis - Lateral-directional flight control example
[AIAA PAPER 90-3338] p 863 A90-47598
- Multivariable control law for flat-turn strafing maneuver by a supermaneuverable aircraft
[AIAA PAPER 90-3371] p 863 A90-47629
- A dynamic inversion based control law with application to the high angle-of-attack research vehicle
[AIAA PAPER 90-3407] p 864 A90-47662
- Modifying high-order aeroelastic math model of a jet transport using maximum likelihood estimation p 61 A90-10106
- Control law synthesis and optimization software for large order aeroservoelastic systems p 61 N90-10111
- Flexible aircraft dynamic modeling for dynamic analysis and control synthesis p 61 N90-10112
- Aircraft modal suppression system: Existing design approach and its shortcomings p 33 N90-10115
- Nonlinear maneuver autopilot for the F-15 aircraft
[NASA-CR-179442] p 77 N90-11487
- Adaptive control law design for model uncertainty compensation
[AD-A211712] p 120 N90-11758
- An autopilot design methodology for bank-to-turn missiles
[AD-A213379] p 198 N90-13399
- A pitch control law for compensation of the phugoid mode induced by windshears p 258 N90-15051
- The interference of flightmechanical control laws with those of load alleviation and its influence on structural design p 258 N90-15054
- Adaptive control of helicopter vibrations via the impulse response method p 260 N90-15113
- Guidance and Control of Unmanned Air Vehicles
[AGARD-CP-436] p 260 N90-15924
- Synthesis of control law, on a RPV, in order to minimize the number of sensors p 260 N90-15925
- Automatic control of cryogenic wind tunnels p 263 N90-15957
- Parallel processing implementation of a flight controller p 333 N90-16743
- Applications of modern control theory synthesis to a super-augmented aircraft
[AD-A215431] p 336 N90-16753
- A fractional calculus model of aeroelasticity
[AD-A216244] p 377 N90-18212
- Application of variable-gain output feedback for high-alpha control
[NASA-TM-102603] p 434 N90-18434
- Practical methods for robust multivariable control
[AD-A216937] p 462 N90-18920
- Aeroservoelasticity
[NASA-TM-102620] p 416 N90-19227
- Output model-following control synthesis for an oblique-wing aircraft
[NASA-TM-100454] p 435 N90-19241
- Digital-flutter-suppression-system investigations for the active flexible wing wind-tunnel model
[NASA-TM-102618] p 520 N90-20093
- Joint University Program for Air Transportation Research, 1988-1989
[NASA-CP-3063] p 468 N90-20921
- An expert system for wind shear avoidance p 486 N90-20938
- Experimental and theoretical investigation of optimal control methods with model reduction p 521 N90-21039
- Advances in optimal active control techniques for aerospace systems; application to aircraft active landing gear p 592 N90-21769
- Integrated control-system design via generalized LQG (GLOG) theory p 613 N90-23023

- Multivariable frequency weighted model order reduction for control synthesis
[AIAA-89-3558] p 613 N90-23060
- Prediction of longitudinal pilot induced oscillations using the optimal control model
[AD-A220593] p 671 N90-23412
- Adaptive control of a system with periodic dynamics: Application of an impulse response method to the helicopter vibration problem p 694 N90-23990
- An investigation of the use of singular perturbation methods and modal control theory in the derivation of aircraft control schemes
[MATHS-REPT-A-106] p 758 N90-26014
- Low-speed wind tunnel investigation of the static stability and control characteristics of an advanced turboprop configuration with the propellers placed over the tail
[NASA-CR-186900] p 759 N90-26017
- Robustness evaluation of H2 and H(infinity) control theory as applied to a transport aircraft
[AD-A222795] p 759 N90-26018
- Development and testing of methodology for evaluating the performance of multi-input/multi-output digital control systems
[NASA-TM-102704] p 846 N90-27699
- Active control of aerothermoelastic effects for a conceptual hypersonic aircraft
[NASA-TM-102713] p 869 N90-27725
- Aerodynamic and propulsive control development of the STOL and maneuver technology demonstrator
p 920 N90-28514
- Control research in the NASA high-alpha technology program p 934 N90-28516
- Innovative control concepts and component integration for a generic supercruise fighter p 935 N90-28521
- Control and estimation for aerospace applications with system time delays p 918 N90-29367
- Proceedings of damping '89. Volume 1: Pages AAB-1 through DCD-11
[AD-A223431] p 960 N90-29664
- CONTROL VALVES**
- Numerical simulation of the actuation system for the ALDF's propulsion control valve --- Aircraft Landing Dynamics Facility
[AIAA PAPER 90-0079] p 211 A90-19674
- Direct drive servovalves: Why and how - The Magnaghi Milano answer p 688 A90-42484
- CONTROLLABILITY**
- East coast Osprey flies p 246 A90-21713
- Control sensitivity, bandwidth and disturbance rejection concerns for advanced rotorcraft p 430 A90-28204
- Ten years of stall testing
[AIAA PAPER 90-1268] p 518 A90-33895
- Estimating short-period dynamics using an extended Kalman filter --- for aircraft controllability
[AIAA PAPER 90-1277] p 518 A90-33901
- Techniques for improving precision of flying qualities assessment
[AIAA PAPER 90-1285] p 519 A90-33906
- Results of an A109 simulation validation and handling qualities study p 591 A90-38524
- AIAA Atmospheric Flight Mechanics Conference, Portland, OR, Aug. 20-22, 1990, Technical Papers
p 751 A90-45134
- Flying qualities problems of aerospace craft
[AIAA PAPER 90-2804] p 752 A90-45139
- Design of flight control systems to meet rotorcraft handling qualities specifications
[AIAA PAPER 90-2805] p 752 A90-45140
- Unified flying qualities criteria for longitudinal tracking
[AIAA PAPER 90-2806] p 752 A90-45141
- Assessment of proposed fighter agility metrics
[AIAA PAPER 90-2807] p 752 A90-45142
- Toward a theory of aircraft agility
[AIAA PAPER 90-2808] p 752 A90-45143
- An experimental investigation of roll agility in air-to-air combat
[AIAA PAPER 90-2809] p 752 A90-45144
- Reassessment and extensions of pilot ratings with new data --- of aircraft handling qualities
[AIAA PAPER 90-2823] p 753 A90-45158
- A pilot rating scale for evaluating failure transients in electronic flight control systems
[AIAA PAPER 90-2827] p 754 A90-45159
- Simulating turbulence and gusts for handling qualities evaluation
[AIAA PAPER 90-2845] p 754 A90-45174
- Large aircraft flying qualities revisited
[AIAA PAPER 90-2847] p 754 A90-45175
- Handling qualities research at the Flight Research Laboratory, NAE/NRC, 1980 - 1990 and beyond
[AIAA PAPER 90-2848] p 755 A90-45176
- Lessons learned from the S/MTD program for the Flying Qualities Specification
[AIAA PAPER 90-2849] p 755 A90-45177
- An investigation of aircraft maneuverability and agility
[AIAA PAPER 90-3300] p 868 A90-46882

- A design procedure for the handling qualities optimization of the X-29A aircraft
[NASA-TM-4142] p 119 N90-11753
- Elements of active vibration control for rotating machinery
[NASA-TM-102368] p 610 N90-22703
- Prediction of longitudinal pilot induced oscillations using the optimal control model
[AD-A220593] p 671 N90-23412
- Static wind-tunnel and radio-controlled flight test investigation of a remotely piloted vehicle having a delta wing planform
[NASA-TM-4200] p 632 N90-24238
- Helicopter controllability
[AD-A220078] p 672 N90-24275
- Combat aircraft control requirements
p 934 N90-28515
- Combat aircraft control requirements for agility
p 935 N90-28517
- Aerodynamic control design: Experience and results at Aermacchi p 935 N90-28518
- Innovative control concepts and component integration for a generic supercruise fighter p 935 N90-28521
- Noncontact measurement of rotating blade vibrations
[NAL-TR-1033] p 961 N90-29687
- CONTROLLERS**
- A hardware and software fault tolerant safety controller
[AIAA PAPER 89-3123] p 74 A90-10599
- Design of digital self-selecting multivariable controllers for jet engines
[AIAA PAPER 90-1875] p 655 A90-40541
- Digital controller design for the pitch axis of the F-14 using an H(infinity) method p 668 A90-40912
- Handling qualities research at the Flight Research Laboratory, NAE/NRC, 1980 - 1990 and beyond
[AIAA PAPER 90-2848] p 755 A90-45176
- Designing and tuning the digital controller of an electronic fuel control unit for small gas turbine engines
[SAE PAPER 892255] p 747 A90-45457
- Lateral-directional control of an aircraft using mu synthesis
[AIAA PAPER 90-3442] p 865 A90-47695
- A new methodology for model order reduction with application to eigenstructure controllers
[AIAA PAPER 90-3475] p 891 A90-47725
- Input/output coupling in eigenstructure assignment
[AIAA PAPER 90-3476] p 865 A90-47726
- Effects of stick dynamics on helicopter flying qualities
[AIAA PAPER 90-3477] p 866 A90-47727
- Flight controller design with nonlinear aerodynamics, large parameter uncertainty, and pilot compensation
[AIAA PAPER 90-3478] p 866 A90-47728
- Genetic algorithms in control system optimization
[AIAA PAPER 90-3488] p 867 A90-47736
- A robust wind shear stochastic controller-estimator
[AIAA PAPER 90-3489] p 867 A90-47737
- Proven dynamic modeling techniques for concurrent design and analysis of ECS controllers
[SAE PAPER 901234] p 841 A90-49304
- Flexible aircraft dynamic modeling for dynamic analysis and control synthesis p 61 N90-10112
- Optimal integral controller with sensor failure accommodation p 61 N90-10123
- A helicopter flight path controller design via a nonlinear transformation technique p 199 N90-14242
- Parallel processing implementation of a flight controller p 333 N90-16743
- Design of integrated pitch axis for autopilot/autothrottle and integrated lateral axis for autopilot/yaw damper for NASA TSRV airplane using integral LQG methodology
[NASA-CR-4268] p 348 N90-16768
- A rule-based paradigm for intelligent adaptive flight control p 434 N90-19238
- Output model-following control synthesis for an oblique-wing aircraft
[NASA-TM-100454] p 435 N90-19241
- Potential role of avionics in escape systems
p 483 N90-20060
- The implementation and operation of a variable-response electronic throttle control system for a TF-104G aircraft
[NASA-TM-101696] p 509 N90-20086
- Interaction of switch actuation on tracking with a four-axis flight control (cross-coupling)
[AD-A217981] p 520 N90-20095
- Perspectives on the use of rule-based control p 521 N90-20940
- Experimental and theoretical investigation of optimal control methods with model reduction p 521 N90-21039
- Human centrifuge controller
[NAL-TM-SE-8901] p 527 N90-21043
- A comparison of time-optimal interception trajectories for the F-8 and F-15
[NASA-CR-186300] p 581 N90-21753

- Real-time closed-loop simulation and upset evaluation of control systems in harsh electromagnetic environments p 613 N90-23069
- An experimental study of fault propagation in a jet-engine controller
[NASA-CR-181335] p 665 N90-23401
- H-infinity based integrated flight-propulsion control design for a STOVL aircraft in transition flight
[NASA-TM-103198] p 758 N90-26011
- Development and testing of methodology for evaluating the performance of multi-input/multi-output digital control systems
[NASA-TM-102704] p 846 N90-27699
- A digital controller for active aeroelastic controls
[NAL-TR-1014] p 936 N90-29402
- CONVECTION**
- An improvement of convection fidelity in Euler calculations p 315 N90-16709
- Time development of convection flow patterns in aircraft cabins under post-crash fire exposure p 327 N90-17598
- Analytical study of the origin and behavior of asymmetric vortices
[NASA-TM-102796] p 573 N90-21746
- Numerical simulations of the structure of supersonic shear layers
[AD-A224164] p 960 N90-29587
- Three-dimensional numerical study of thunderstorm downdrafts and associated outflow boundaries p 963 N90-29746
- CONVECTION CLOUDS**
- Cloud features suggesting low level wind shear and turbulence p 778 A90-44545
- CONVECTIVE FLOW**
- Computation of laminar mixed convection flow in a channel with wing type built-in obstacles p 67 A90-11114
- Compressibility effects in free shear layers
[AIAA PAPER 90-0705] p 212 A90-19984
- Numerical simulation of droplet deformation in convective flows
[AIAA PAPER 90-2309] p 769 A90-42773
- CONVECTIVE HEAT TRANSFER**
- Experimental investigation on composite cooling of a turbine blade p 190 A90-17794
- Convective heat transfer measurements from a NACA 0012 airfoil in flight and in the NASA Lewis Icing Research Tunnel
[AIAA PAPER 90-0199] p 272 A90-22180
- Impingement/effusion cooling - The influence of the number of impingement holes and pressure loss on the heat transfer coefficient
[ASME PAPER 89-GT-188] p 361 A90-23866
- Determination of convective transfer coefficients on a wind-tunnel model by stimulated infrared thermography
[ONERA, TP NO. 1989-218] p 351 A90-25351
- Local convection heat transfer on a plane wall in the vicinity of strong streamwise accelerations p 535 A90-32174
- Heat transfer in a solid fuel ramjet combustor
[AIAA PAPER 90-1783] p 586 A90-38472
- An experimental convective heat transfer investigation around a film-cooled gas turbine blade p 957 A90-51261
- Convective heat transfer measurements from a NACA 0012 airfoil in flight and in the NASA Lewis Icing Research Tunnel
[NASA-TM-102448] p 213 N90-13750
- A review of high-speed, convective, heat-transfer computation methods p 316 N90-17548
- Flammability testing of aircraft cabin materials p 328 N90-17611
- Heat transfer near the entrance to a film cooling hole in a gas turbine blade
[AD-A217396] p 510 N90-20089
- Calculation of temperature distribution in various turbine blades using a boundary-fitted coordinate transformation method p 929 N90-28550
- CONVERGENCE**
- Convergence aloft as a precursor to microbursts p 456 A90-28620
- A multistage method for the solution of the Euler equations on unstructured grids p 708 A90-44460
- Solutions of two-dimensional Euler equations with multigrid acceleration p 810 A90-48086
- Convergence speeding up in the calculation of the viscous flow about an airfoil p 279 N90-16194
- Convergence acceleration of hypersonic flow calculations: A nonlinear relaxation factor p 480 N90-20957
- Multilevel decomposition approach to the preliminary sizing of a transport aircraft wing
[NASA-CR-4296] p 583 N90-22557
- Low-density flow effects for hypervelocity vehicles, phase 2
[AD-A221034] p 634 N90-24249

CONVERGENT NOZZLES

- Determination of the specific thrust in open regimes and design of a nonseparating convergent nozzle profile p 395 A90-30339
- Flow rate and thrust coefficients for biaxial flows in a convergent nozzle p 395 A90-30344
- Transonic flow computations in convergent propulsion nozzles using the time-dependent mode p 708 A90-44459

CONVERGENT-DIVERGENT NOZZLES

- Computation of transonic flow in a plane cascade with an unfactored flux splitting implicit method p 152 A90-17785
- The use of a Laval nozzle and wall suction for blockage-free transonic wind-tunnel operation p 225 A90-21592
- Advanced Mach 3.5 Axisymmetric Quiet Nozzle [AIAA PAPER 90-1592] p 566 A90-38727
- High Mach exhaust system concept scale model test results [AIAA PAPER 90-1905] p 655 A90-40552
- Supersonic rectangular isothermal shrouded jets [AIAA PAPER 90-2028] p 621 A90-40599
- The sensitivity of near-field acoustics to the orientation of twin two-dimensional supersonic nozzles [AIAA PAPER 90-2149] p 625 A90-42045
- Experimental evaluation of expendable supersonic nozzle concepts [AIAA PAPER 90-1904] p 740 A90-42691
- Numerical study of compressible nozzle flow p 708 A90-44437
- Study of the expansion of hydrocarbon-oxygen products through supersonic nozzle p 852 A90-46907
- An experimental investigation of thrust vectoring two-dimensional convergent-divergent nozzles installed in a twin-engine fighter model at high angles of attack [NASA-TM-4155] p 237 N90-15884
- Static investigation of a two-dimensional convergent-divergent exhaust nozzle with multi-axis thrust-vectoring capability [NASA-TP-2973] p 397 N90-19193
- Computation of hypersonic unsteady viscous flow over a cylinder p 397 N90-19194

CONVERTIBLE FAN-SHAFT ENGINES

- Precursor convertible engine study [AIAA PAPER 90-2486] p 658 A90-40636
- Convertible engine system for high speed rotorcraft [AIAA PAPER 90-2512] p 658 A90-40643
- A hydrodynamic turbo-fan/shaft convertible engine p 665 A90-42487
- The selection of convertible engines with current gas generator technology for high speed rotorcraft p 852 A90-46933

CONVEXITY

- Design of cryogenic tanks for launch vehicles p 609 N90-22662

CONVOLUTION INTEGRALS

- Development of a mathematical model of an adaptive antituffler system p 769 A90-42911

COOLING

- Optimum trailing edge ejection for cooled gas turbine blades p 41 A90-11562
- Thermal/structural analyses of several hydrogen-cooled leading-edge concepts for hypersonic flight vehicles [AIAA PAPER 90-0053] p 274 A90-23702
- Characteristics of partial length circular pin fins as heat transfer augmentors for airfoil internal cooling passages [ASME PAPER 89-GT-87] p 359 A90-23806
- A numerical three-dimensional thermal stress analysis for cooled blades [ASME PAPER 89-GT-168] p 341 A90-23853
- A comparison between engine test results and design predictions of turbine blade cooling performance [ASME PAPER 89-GT-169] p 341 A90-23854
- Impingement/effusion cooling - The influence of the number of impingement holes and pressure loss on the heat transfer coefficient [ASME PAPER 89-GT-188] p 361 A90-23866
- Aerodynamics of cooling jets introduced in the secondary flow of a low speed turbine cascade [ASME PAPER 89-GT-192] p 362 A90-23868
- Application of formal optimization techniques in thermal/structural design of a heat-pipe-cooled panel for a hypersonic vehicle [NASA-TM-89131] p 72 N90-10409
- Design and demonstration of heat pipe cooling for NASP and evaluation of heating methods at high heating rates [DE89-016995] p 186 N90-14227
- Thermal/structural analyses of several hydrogen-cooled leading-edge concepts for hypersonic flight vehicles [NASA-TM-102391] p 215 N90-14511
- Flexible heat pipe cold plate [AD-A216053] p 434 N90-18433
- Analysis of the rotor tip leakage flow with tip cooling air ejection p 515 N90-21029

- The application of engineering ceramics in gas turbines [PNR90676] p 750 N90-26005

COOLING FINNS

- Heat transfer and pressure drop for short pin-fin arrays with pin-end wall fillet [ASME PAPER 89-GT-99] p 359 A90-23813

COOLING SYSTEMS

- DB/SPF cooler outlet duct for aircraft application p 132 A90-16620
- A method for the computer-aided hydraulic analysis of the turbine cooling systems of aviation gas turbine engines p 255 A90-23430
- Microprocessor control of a vapor-cycle cooling system [SAE PAPER 891457] p 339 A90-27426
- The investigation of heat transfer in cooled blades of gas turbines [AIAA PAPER 90-2144] p 685 A90-42043
- Numerical predictions for the flow and the heat transfer in gas turbine cooling systems p 770 A90-44464
- The flow field and heat transfer near a turbulator p 771 A90-44755
- Composite matrix cooling scheme for small gas turbine combustors [AIAA PAPER 90-2158] p 852 A90-47210
- Automatic environmental control system for electronic equipment platforms [SAE PAPER 901217] p 840 A90-49292
- Combustor cooling aspects [CIT/SME/VKI/RS/5] p 749 N90-25989
- Analysis of scramjet engine characteristics [NAL-TR-1041] p 933 N90-29398

COORDINATE TRANSFORMATIONS

- Calculation of temperature distribution in various turbine blades using a boundary-fitted coordinate transformation method p 929 N90-28550

COORDINATES

- Aerospace coordinate systems and transformations --- Book p 282 A90-23372
- Analysis and design of symmetrical airfoils [PD-CF-8943] p 400 N90-19213

COORDINATION

- National airspace system monitoring operational concept [NAS-SR-1330] p 178 N90-14214

COPOLYMERS

- Effect of molecular weight and end group control on the adhesion behavior of thermoplastic polyimides and poly(imide siloxane) segmented copolymers p 947 A90-50199

CORE FLOW

- Holographic flow visualization of turbofan by-pass and core nozzle streams [ASME PAPER 89-GT-260] p 363 A90-23891
- Calculation of flow characteristics in the core of a vortex sheet p 386 A90-28981
- Turbulent plane jet excited mechanically by an oscillating thin plate in the potential core p 553 A90-35262
- Evolution of engine cycles for STOVL propulsion concepts [AIAA PAPER 90-2272] p 743 A90-42767
- Energy Efficient Engine core design and performance report [NASA-CR-168069] p 930 N90-28559
- CORILIS EFFECT**
- Shaft flexibility effects on aeroelastic stability of a rotating bladed disk p 132 A90-16371
- Effect of downstream elements on the flow at the exit of centrifugal compressor rotor p 157 A90-18483

CORNER FLOW

- Shock-wave/boundary-layer interaction at a swept compression corner p 16 A90-12850
- Numerical simulation of supersonic and hypersonic turbulent compression corner flows using PNS equations p 85 A90-15242
- A numerical study of supersonic flow over a compression corner with different incoming boundary-layer profiles [AIAA PAPER 90-1453] p 561 A90-38612
- Wall pressure pulsation spectra ahead of internal corners p 804 A90-46545

CORRECTION

- Viscous corrections on wings in incompressible flow p 301 A90-25200
- Residual interference and wind tunnel wall adaption p 353 N90-17655
- First-order weight corrections for real-time flight path management [LR-580] p 578 N90-21751

CORRELATION

- Reliability and performance of friction measuring tires and friction equipment correlation [AD-A223694] p 939 N90-29408

CORRIDORS

- En route noise annoyance laboratory test: Preliminary results p 698 N90-24870

CORROSION

- NDI (Nondestructive Inspection) oriented corrosion control for Army aircraft. Phase 1: Inspection methods [AD-A213368] p 176 N90-13359
- A corrosion fatigue/stress corrosion testing facility at Materials Research Laboratory [MRL-TN-568] p 527 N90-21044
- Computerized corrosion forecasting model for C-5 aircraft p 843 N90-26815
- Effect of protective coatings on mechanical properties of superalloys p 952 N90-28707
- CORROSION PREVENTION**
- Corrosion protection and EMP/EMI shielding p 600 A90-37902
- Development of a water-borne non-chromated primer and topcoat for aerospace applications p 956 A90-50213
- NDI (Nondestructive Inspection) oriented corrosion control for Army aircraft. Phase 1: Inspection methods [AD-A213368] p 176 N90-13359
- Nonflammable hydraulic power system for tactical aircraft. Volume 1: Aircraft system definition, design and analysis [AD-A218493] p 671 N90-23409
- Micro separator and ball-on-cylinder lubricity evaluator tests or corrosion inhibitor/lubricity improver additives [AD-A221339] p 766 N90-25228

CORROSION RESISTANCE

- Analysis of whisker-toughened ceramic components - A design engineer's viewpoint p 205 A90-19149
- Glassy waters for Seastar --- corrosion-resistant GFRP for turboprop amphibious aircraft airframes p 382 A90-29637
- A friendly alloy --- aircraft construction materials p 764 A90-44173
- Aerospace Arall - The advancement in aircraft materials p 947 A90-50186
- Aluminum lithium alloys for Navy aircraft p 267 N90-15193
- New aspects in aircraft inspection using eddy current methods p 886 N90-28085
- High Temperature Surface Interactions [AGARD-CP-461] p 951 N90-28698
- Molten salt induced high temperature degradation of thermal barrier coatings p 952 N90-28704
- Overview on hot gas tests and molten salt corrosion experiments at the DLR p 953 N90-28714

CORROSION TESTS

- Gas turbine compressor operating environment and material evaluation [ASME PAPER 89-GT-42] p 340 A90-23769
- Hot-gas corrosion test of Si3N4 and SiC p 531 A90-33987
- Coatings for gas turbine compressors [NLR-MP-88045-U] p 115 N90-11750
- NDI (Nondestructive Inspection) oriented corrosion control for Army aircraft. Phase 1: Inspection methods [AD-A213368] p 176 N90-13359
- A corrosion fatigue/stress corrosion testing facility at Materials Research Laboratory [MRL-TN-568] p 527 N90-21044

COST ANALYSIS

- The manufacture of SPF military aircraft doors in aluminium alloy --- superplastically formed p 132 A90-16616
- The integrated test vehicle, (I.T.V.) - A vehicle for cost-effective hypersonic testing [AIAA PAPER 90-0630] p 352 A90-26974
- Aerospace materials - Trends and potential p 529 A90-31902
- Design of aeroengines in a low-fuel price scenario p 739 A90-42653
- The LF500 and the regional airline market [AIAA PAPER 90-2521] p 744 A90-42814
- The economics of the organization and the planning of civil aviation --- Russian book p 897 A90-46629
- Conceptual design and feasibility study of very large passenger aircraft [AIAA PAPER 90-3220] p 834 A90-48841
- Lessons learned from the integration of flight systems p 35 N90-10874
- Rotorcraft low altitude CNS benefit/cost analysis: Rotorcraft operations data [DOT/FAA/DS-89/9] p 141 N90-12406
- HOTOL: A future launcher for Europe p 353 N90-16800
- Reducing C130E Hercules operating costs in the Royal Australian Air Force and the United States Air Force by increasing cruise speeds [AD-A215747] p 338 N90-17629
- Cost effectiveness of composite materials on the F-15 and F-16 aircraft [AD-A216353] p 338 N90-17631
- Criteria for polymer concrete on airport pavements [DOT/FAA/DS-89/18] p 527 N90-21045

Peacetime replacement and crash damage factors for army aircraft

[AD-A218544] p 636 N90-23372

Preliminary design of a supersonic Short Takeoff and Vertical Landing (STOVL) fighter aircraft

[NASA-CR-186670] p 649 N90-23394

Aircraft modifications cost analysis. Volume 1: Overview of the study

[AD-A220764] p 702 N90-25074

Airline productivity relating on the fuel cost. (2): Fuel consumption values and fuel efficiency

[NAL-TM-604-2] p 913 N90-29333

COST EFFECTIVENESS

Generalized relations for estimating the efficiency and basic dimensions of screw pumps and hydraulic turbines of pump units

p 111 A90-14583

SPF/DB takes off p 208 A90-17293

Cost effective technology --- CAD/CAM techniques for aircraft engines p 188 A90-17447

Two special cost-effective applications for electrochemical metallizing for improved brazing and bonding

[SAE PAPER 890927] p 365 A90-24692

The use of satellite technology for oceanic air traffic control p 330 A90-25570

Improvement in structural integrity and long term durability of aerospace composite components

p 441 A90-28189

Ground testing techniques in support of flight test

[AIAA PAPER 90-1309] p 523 A90-33919

A framework for the optimal design of instructor/operator stations in flight simulators p 779 A90-45373

Technical and economic efficiency of aviation gas turbine engines in service --- Russian book

p 851 A90-46624

Implementation of integrated product development --- in aircraft industry

[AIAA PAPER 90-3194] p 786 A90-48829

Fighter design econometrics = ownership affordability?

[AIAA PAPER 90-3223] p 897 A90-48842

Designing for reliable and low maintenance cost aero engines

[PNR90570] p 115 N90-12604

Aviation Engine Test Facilities (AETF) fire protection study

[AD-A211483] p 134 N90-12777

Repair of composites by means of wet-lay-up

[LR-551] p 205 N90-13617

Fly-by-light flight control system technology development plan

[NASA-CR-181953] p 259 N90-15111

The European Transonic Windtunnel (ETW)

p 262 N90-15945

Cost effectiveness of composite materials on the F-15 and F-16 aircrafts

[AD-A216353] p 338 N90-17631

Individual Helicopter Tracking Program (IHTP) for the MH-53J helicopter

p 843 N90-26818

Photoelasticity: A cost effective design tool

p 883 N90-26819

Finite element models of USAF aircraft structures

p 844 N90-26820

Cost effective technology

[PNR90664] p 883 N90-27002

Life cycle cost in the conceptual design of subsonic commercial aircraft, volumes 1 and 2

p 923 N90-28535

Energy efficient engine program technology benefit/cost study. Volume 1: Executive summary

[NASA-CR-174766-VOL-1] p 931 N90-28564

Energy Efficient Engine: High-pressure compressor test hardware detailed design report

[NASA-CR-180850] p 932 N90-28570

COST ESTIMATES

Automated aircraft engine costing using artificial intelligence

[AIAA PAPER 90-1887] p 660 A90-41981

Estimating the relationships between the state of the art of technology and production cost for the US aircraft

[AD-A212127] p 82 N90-12495

Aircraft modifications cost analysis. Volume 1: Overview of the study

[AD-A220764] p 702 N90-25074

COST REDUCTION

A computer aided manufacturing procedure for experimental two-dimensional aerofoils

p 270 A90-20609

Recovery concepts for propulsion and avionics components --- for booster stage in launch vehicles

[AIAA PAPER 90-1810] p 353 A90-25172

The promise of advanced materials for a 21st century VBE --- ultrahigh bypass ratio engine

[AIAA PAPER 90-2396] p 662 A90-42157

The Common/Same Type Rating - Human factors and other issues

[SAE PAPER 892229] p 723 A90-45445

Old lamps for new - A photoelastic design tool for weight and cost saving on aircraft structures

p 878 A90-46039

US Navy principal site testing concept and the F-18

p 33 N90-10861

Aluminum-lithium: Application of plate and sheet to fighter aircraft

p 268 N90-15202

Reducing C130E Hercules operating costs in the Royal Australian Air Force and the United States Air Force by increasing cruise speeds

[AD-A215747] p 338 N90-17629

Energy efficient engine program technology benefit/cost study, volume 2

[NASA-CR-174766-VOL-2] p 931 N90-28565

The cost of air service fragmentation

[TT-9010] p 913 N90-29334

COSTS

Using goal programming to determine the optimal engine mix for UH-1 helicopters

[AD-A214893] p 343 N90-16762

Individual Helicopter Tracking Program (IHTP) for the MH-53J helicopter

p 843 N90-26818

High productivity testing p 871 N90-26843

COUNTER ROTATION

Operating aspects of counter-rotating propfan and planetary-differential gear coupling

p 50 A90-12615

Counterrotating prop-fan simulations which feature a relative-motion multiblock grid decomposition enabling arbitrary time-steps

[AIAA PAPER 90-0687] p 169 A90-19978

Effect of reduced aft diameter and increased blade number of high-speed counterrotation propeller performance

[AIAA PAPER 89-0438] p 234 A90-23650

Acoustic characteristics of counterrotating unducted fans from model scale tests

p 378 A90-26138

An approximation model for the performance and acoustic predictions of counterrotating propeller configurations

[AIAA PAPER 90-0282] p 378 A90-26931

A nonlinear transient formulation of UHB aeroelastic response and stability. I - Theoretical formulation

[SAE PAPER 892322] p 715 A90-45481

Calculation of an axial-flow birotary turbine

p 880 A90-46492

On the unsteady loading noise of counter-rotating propeller

p 895 A90-49484

Euler analysis comparison with LDV data for an advanced counter-rotation propfan at cruise

[AIAA PAPER 90-3033] p 903 A90-50637

Full scale technology demonstration of a modern counterrotating unducted fan engine concept: Component test

[NASA-CR-180868] p 53 N90-10047

Full scale technology demonstration of a modern counterrotating unducted fan engine concept. Design report

[NASA-CR-180867] p 53 N90-10048

Full scale technology demonstration of a modern counterrotating unducted fan engine concept. Engine test

[NASA-CR-180869] p 53 N90-10049

Acoustic test and analysis of a counterrotating prop-fan model

[NASA-CR-179590] p 79 N90-10683

An investigation of counterrotating tip vortex interaction

[NASA-CR-185135] p 79 N90-11549

Effect of reduced aft diameter and increased blade number on high-speed counterrotation propeller performance

[NASA-TM-102077] p 172 N90-13352

Noise of a simulated installed model counterrotation propeller at angle-of-attack and takeoff/approach conditions

[NASA-TM-102440] p 548 N90-20794

Advanced gearbox technology

[NASA-CR-179625] p 666 N90-24274

Euler analysis comparison with LDV data for an advanced counter-rotation propfan at cruise

[NASA-TM-103249] p 720 N90-25946

High speed turboprop aeroacoustic study (counterrotation). Volume 1: Model development

[NASA-CR-185241] p 782 N90-26633

COUNTER-ROTATING WHEELS

Aerodynamic and torque characteristics of enclosed Co/counter rotating disks

[ASME PAPER 89-GT-177] p 361 A90-23858

COUNTERFLOW

Effect of tangential injection on flow in a laminar boundary layer

p 294 A90-24080

COUNTERMEASURES

Counterair situation awareness display for Army aviation p 964 N90-28982

COUPLED MODES

High performance single-mode coupler for harsh environments p 78 A90-11027

COUPLING

Input/output coupling in eigenstructure assignment [AIAA PAPER 90-3476] p 865 A90-47726

The effects of structural flap-lag and pitch-lag coupling on soft inplane hingeless rotor stability in hover

[NASA-TP-3002] p 910 N90-28503

Flow coupling between a rotor and a stator in turbomachinery

[AD-A223882] p 932 N90-28572

COVARIANCE

Passive location accuracy via a general covariance error model --- long-baseline interferometry from airborne platforms

p 914 A90-51060

COWLINGS

Design, fabrication and experimental test of hi-temperature CFRP stiffened structures --- rotating cowl panels for unducted fan engines

p 534 A90-31892

Finite element analysis of structural components using viscoplastic models with application to a cowl lip problem

[NASA-CR-185189] p 690 N90-23769

CRACK ARREST

Crack stoppers and ARALL laminates

[PB90-166588] p 533 N90-21142

CRACK CLOSURE

Numerical study of balanced patch repairs to cracked sheets

p 210 A90-18442

Elevated temperature crack growth

[NASA-CR-182247] p 777 N90-26355

Investigation of crack-closure prediction models for fatigue in aluminium alloy sheet under flight-simulation loading

[LR-619] p 777 N90-26369

Effects of blocks of overloads and underloads on fatigue crack growth in 2024-T351 sheet specimens: Fractographic analysis and crack closure predictions

[LR-629] p 961 N90-29681

CRACK GEOMETRY

Numerical study of balanced patch repairs to cracked sheets

p 210 A90-18442

Bulging cracks in pressurized fuselages - A procedure for computation

p 880 A90-46301

Modeling growth of fatigue cracks which originate at rivet holes

p 691 N90-25060

CRACK INITIATION

Fatigue life prediction method for gas turbine rotor disk alloy FV535

p 440 A90-27679

Designing rotorcraft dynamic components to reliability requirements

p 641 A90-39978

Fatigue crack initiation mechanics of metal aircraft structures

[AD-A210567] p 65 N90-10255

Thermal fatigue durability for advanced propulsion materials

[NASA-TM-102348] p 215 N90-14641

Fatigue crack initiation and small crack growth in several airframe alloys

[NASA-TM-102598] p 454 N90-18746

New aspects in aircraft inspection using eddy current methods

p 886 N90-28085

Fractographic analysis of fatigue crack growth under two-blocks loading on 2024-T351 sheet specimens

[LR-628] p 961 N90-29680

Effects of blocks of overloads and underloads on fatigue crack growth in 2024-T351 sheet specimens: Fractographic analysis and crack closure predictions

[LR-629] p 961 N90-29681

CRACK PROPAGATION

An oxidation fatigue interaction damage model for thermal fatigue crack growth

p 62 A90-11539

Predicting crack growth under thermo-mechanical cycling

p 209 A90-18169

Significance of the short crack effect on aerospace structures

p 269 A90-20065

Fatigue of thick-section cold-expanded holes with and without cracks

p 270 A90-20987

A study on initial fatigue quality of typical aircraft structures (fastener holes)

p 272 A90-22004

Compilation of procedures for fatigue crack propagation testing under complex load sequences

p 368 A90-26759

A study on flaw detection method for CFRP composite laminates. I - The measurement of crack extension in CFRP composites by electrical potential method

p 441 A90-28003

Stochastic crack growth analysis methodologies for metallic structures

[AIAA PAPER 90-1015] p 449 A90-29340

- Time dependent effects on high temperature low cycle fatigue and fatigue crack propagation on nickel base superalloys p 443 A90-29881
- Fracture mechanics assessment of EB-welded blisked rotors p 453 A90-31117
- Cyclic deformation, fatigue and fatigue crack propagation in Ni-base alloys p 531 A90-34162
- Designing rotorcraft dynamic components to reliability requirements p 641 A90-39978
- Reconstitution of crack growth from fractographic observations after flight simulation loading p 682 A90-40650
- Estimation of fatigue crack growth in patched cracked panels p 684 A90-41335
- Recent advances in fatigue life analysis methods for aerospace applications p 677 A90-41338
- The effect on fatigue crack growth under spectrum loading of an imposed placard 'G' limit p 643 A90-41339
- Probabilistic approach to fleet management p 701 A90-42674
- Acoustic emission and signal analysis p 781 A90-43782
- Development of process control procedure for ultrahigh-sensitivity fluorescent penetrant inspection systems p 771 A90-45225
- Cyclic fracture toughness of VT-3-1 and VT-25 titanium alloys p 873 A90-46514
- Fractographic techniques for the assessment of aircraft component cracking p 954 A90-49885
- Development of a double crack growth gage algorithm for application to fleet tracking of fatigue damage p 901 A90-49890
- Effects on aerospace alloys of residual chlorine in chlorinated-solvent primers p 956 A90-50187
- Analysis and interpretation of aircraft component defects using quantitative fractography p 956 A90-50555
- Effects of a heat cycle on material strength [NAL-TM-562] p 113 N90-11737
- Stochastic propagation of an array of parallel cracks: Exploratory work on matrix fatigue damage in composite laminates [DE89-017837] p 126 N90-11813
- An investigation on combined extension and bending of thin sheets with a central crack [LR-561] p 137 N90-12958
- Application of fracture mechanics and half-cycle method to the prediction of fatigue life of B-52 aircraft pylon components [NASA-TM-88277] p 214 N90-13820
- An evaluation of a fatigue crack growth prediction model for variable-amplitude loading (PREFFAS) [LR-537] p 214 N90-13822
- Thermal mechanical fatigue of coated blade materials [AD-A214258] p 256 N90-15107
- Fatigue crack initiation and small crack growth in several airframe alloys [NASA-TM-102598] p 454 N90-18746
- A corrosion fatigue/stress corrosion testing facility at Materials Research Laboratory [MRL-TN-568] p 527 N90-21044
- Crack stoppers and ARALL laminates [PB90-166588] p 533 N90-21142
- NASA airframe structural integrity program [NASA-TM-102637] p 543 N90-21422
- An evaluation of the pressure proof test concept for thin sheet 2024-T3 [NASA-TM-101675] p 543 N90-21424
- Characterisation of fatigue of aluminium alloys by acoustic emission. Part 2: Discrimination between primary and other emissions [AERE-R-13303-PT-2] p 678 N90-23523
- Fatigue crack growth investigation of a Ti-6Al-4V forging under complex loading conditions: NATO/AGARD supplemental engine disk program [AD-A220239] p 678 N90-23538
- Fractographic observations on fatigue crack growth in 2024-T3 sheet material under flight-simulation loading [LR-592] p 689 N90-23760
- Modeling growth of fatigue cracks which originate at rivet holes p 691 N90-25060
- Elevated temperature crack growth [NASA-CR-182247] p 777 N90-26355
- Computerized corrosion forecasting model for C-5 aircraft p 843 N90-26815
- Application of damage tolerance p 843 N90-26817
- Acoustic emission detection of crack presence and crack advance during flight p 886 N90-28082
- New aspects in aircraft inspection using eddy current methods p 886 N90-28085
- Damage tolerance of the fighter aircraft 37 Viggen. Part 1: Analytical assessment [FFA-TN-1990-12-PT-1] p 923 N90-28538
- Damage tolerance of the fighter aircraft 37 Viggen. Part 2: Experimental verification [FFA-TN-1990-13-PT-2] p 923 N90-28539
- Evaluation of static and fatigue properties of thin sheets of 8090-T8 aluminum-lithium alloy and observation of its fracture surfaces [NAL-TR-1039] p 953 N90-29499
- Fractographic observations on fatigue crack growth under miniTWIST flight-simulation loading (2024-T3 material) [LR-631] p 961 N90-29684
- CRACK TIPS**
- Non-conservative stability of a cracked thick rotating blade p 606 A90-38544
- CRACKING (FRACTURING)**
- Breakage of fan blades in the S1 wind tunnel at Mondane-Avrioux [ONERA, TP NO. 1989-104] p 57 A90-11138
- Fatigue evaluation of C/MH-53E main rotor damper threaded joints p 642 A90-39988
- Eddy current detection of subsurface cracks p 882 A90-48629
- Stress intensity factors for cracking metal structures under rapid thermal loading. Volume 2: Theoretical background [AD-A213297] p 213 N90-13812
- Thermal mechanical fatigue of coated blade materials [AD-A214258] p 256 N90-15107
- Defects in monoblock cast turbine wheels p 443 N90-18400
- CRACKS**
- Stochastic propagation of an array of parallel cracks: Exploratory work on matrix fatigue damage in composite laminates [DE89-017837] p 126 N90-11813
- Stress intensity factors for cracking metal structures under rapid thermal loading. Volume 2: Theoretical background [AD-A213297] p 213 N90-13812
- Design temperatures for flexible airfield pavement design [AD-A214141] p 262 N90-15115
- Inspection development for T-37 wing spar cap lug [AD-A214826] p 287 N90-16708
- An evaluation of the pressure proof test concept for thin sheet 2024-T3 [NASA-TM-101675] p 543 N90-21424
- Development of creep-fatigue damage detection method of rotor steel by ultrasonic wave measurement [DE90-503792] p 777 N90-26365
- Acoustic emission detection of crack presence and crack advance during flight p 886 N90-28082
- Fatigue, static tensile strength and stress corrosion of aircraft materials and structures. Part 1: Text [LR-630-PT-1-REV] p 961 N90-29682
- Fatigue, static tensile strength and stress corrosion of aircraft materials and structures. Part 2: Figures [LR-630-PT-2] p 961 N90-29683
- CRASH LANDING**
- Aft facing transport aircraft passenger seats under 16G dynamic crash simulation p 175 A90-17416
- Post crash flight analysis: Visualizing flight recorder data [AD-A21063] p 96 N90-11715
- Aircraft crash survival design guide. Volume 2: Aircraft design crash impact conditions and human tolerance [AD-A218435] p 575 N90-22546
- CRASHES**
- A description of the Naval Air Development Center's ejection tower and crash test facilities and their uses p 200 A90-17426
- International Aircraft Occupant Safety Conference and Workshop proceedings [AD-A214452] p 239 N90-15085
- Aircraft accident report: Delta Air Lines, Inc., Boeing 727-232, N473DA, Dallas-Fort Worth International Airport, Texas, August 31, 1988 [PB89-910406] p 240 N90-15895
- Analysis of the National Transonic Facility mishap [NASA-TM-101686] p 328 N90-17620
- A review of the analytical simulation of aircraft crash dynamics [NASA-TM-102595] p 484 N90-20068
- Peacetime replacement and crash damage factors for army aircraft [AD-A218544] p 636 N90-23372
- The effect of aircraft size on cabin floor dynamic pulses [DOT/FAA/CT-88/15] p 735 N90-25136
- Behavior of composite/metal aircraft structural elements and components under crash type loads: What are they telling us [NASA-TM-102681] p 774 N90-25368
- Computational crash dynamics. Project 1.2: Computational crash dynamics analysis [IAR-89-19] p 724 N90-25956
- CRASHWORTHINESS**
- Fire deaths in aircraft without the crashworthy fuel system p 22 A90-10266
- Criteria for general aviation fuel systems crashworthiness [SAE PAPER 891016] p 109 A90-14328
- Dynamic testing of crashworthy fuel valves [SAE PAPER 891017] p 128 A90-14329
- Impact evaluation of composite floor sections [SAE PAPER 891018] p 100 A90-14330
- Crashworthiness of composite floor sections p 243 A90-20261
- Modeling strategies for crashworthiness analysis of landing gears p 409 A90-28233
- International Aircraft Occupant Safety Conference and Workshop proceedings [AD-A214452] p 239 N90-15085
- Aircraft fires: A study of transport accidents from 1975 to the present p 324 A90-17583
- Floor pull test of a transport airframe section [DOT/FAA/CT-TN88/14] p 497 N90-20072
- Aircraft crash survival design guide. Volume 1: Design criteria and checklists [AD-A218434] p 575 N90-22545
- Aircraft crash survival design guide. Volume 2: Aircraft design crash impact conditions and human tolerance [AD-A218435] p 575 N90-22546
- Aircraft crash survival design guide. Volume 3: Aircraft structural crash resistance [AD-A218436] p 575 N90-22547
- Aircraft crash survival design guide. Volume 4: Aircraft seats, restraints, litters, and cockpit/cabin dealthalization [AD-A218437] p 575 N90-22548
- Aircraft crash survival design guide. Volume 5: Aircraft postcrash survival [AD-A218438] p 575 N90-22549
- Operational effects on crashworthy seat attenuators [AD-A221148] p 637 N90-24259
- Computational crash dynamics. Project 1.2: Computational crash dynamics analysis [IAR-89-19] p 724 N90-25956
- A review of crashworthiness of composite aircraft structures [AD-A221555] p 846 N90-27697
- A review of research and development in crashworthiness of general aviation aircraft: Seats, restraints and floor structures [AD-A221557] p 846 N90-27698
- CRAY COMPUTERS**
- Effective use of Cray supercomputers p 546 A90-34436
- CREEP PROPERTIES**
- Creep-fatigue interactions of gas turbine materials p 131 A90-16011
- The effect of elevated temperature exposure on the tensile and creep properties of Ti-24Al-11Nb p 355 A90-24865
- Life prediction and fatigue p 532 A90-34163
- Compressive viscoelastic effects (creep) of a unidirectional glass/epoxy composite material p 946 A90-50170
- Study on application of ultrasonic wave measurement to creep-fatigue damage detection [DE89-782317] p 774 N90-25361
- Development of creep-fatigue damage detection method of rotor steel by ultrasonic wave measurement [DE90-503792] p 777 N90-26365
- The stress and temperature dependence of creep in an Al-2.0 wt percent Li alloy [AD-A223676] p 953 N90-29480
- CREEP RUPTURE STRENGTH**
- Recrystallization behavior of nickel-base single crystal superalloys p 440 A90-27681
- A friendly alloy --- aircraft construction materials p 764 A90-44173
- CREEP STRENGTH**
- The creep behavior of the Ti3Al alloy Ti-24Al-11Nb p 125 A90-15214
- Designing turbine blades for fatigue and creep p 112 A90-16007
- Laser welding of an advanced rapidly-solidified titanium alloy p 881 A90-47021
- Application of high performance metals in gas turbine engines [PNR90640] p 750 N90-25999
- CREEP TESTS**
- Effect of creep on the load-bearing capacity of compressed panels p 364 A90-24102
- CREW WORKSTATIONS**
- Aircraft design: A conceptual approach --- Book p 179 A90-17307
- Development of an acceptability window for a ground proximity avoidance system p 419 A90-30730
- F-15E terrain following test results [AIAA PAPER 90-1299] p 504 A90-33913
- Evaluation of speech recognizers for use in advanced combat helicopter crew station research and development [NASA-CR-177547] p 650 N90-24265

CREWS

- Operational effects on crashworthy seat attenuators
[AD-A221148] p 637 N90-24259

CRITERIA

- Additive evaluation criteria for aircraft noise
p 698 N90-24867
- Statistical treatment of slow strain rate data for assessment of hydrogen embrittlement in low alloy high strength steel
[ARL-MAT-R-122] p 767 N90-26106

CRITICAL FLOW

- Radial swirl flows between parallel disks at critical flow rate
p 14 A90-12596
- Design of symmetric profiles with maximum critical flow Mach number under prescribed constraints
p 295 A90-24095

CRITICAL LOADING

- Optimization of the relative thicknesses of a high-aspect-ratio wing in a multicriterial formulation
p 334 A90-24133

CRITICAL POINT

- Calculation of the heat flux at a three-dimensional critical point in supersonic flow past a body
p 803 A90-46536

CRITICAL VELOCITY

- Calculation of the front or rear part of a flat body in subsonic flow with the extremum value of the critical Mach number
p 296 A90-24120
- A method for determining aileron efficiency and critical reversal and divergence rates at transonic velocities
p 345 A90-24147
- Flutter and aileron reversal safety factors
p 345 A90-24164
- Effect of structural anisotropy on the dynamic characteristics of the wing and critical flutter speed
p 386 A90-28985
- A combined Riccati transfer matrix-direct integration method with its applications
p 611 A90-37218
- Evaluation of critical speeds in high speed aircraft tires
[SAE PAPER 892349] p 733 A90-45500

CROSS CORRELATION

- Spanwise measurements of vertical components of atmospheric turbulence
[NASA-TP-2963] p 456 N90-19718

CROSS COUPLING

- Analysis of airframe/engine interactions - An integrated control perspective
[AIAA PAPER 90-1918] p 667 A90-40557

CROSS FLOW

- Numerical study of single impinging jets through a crossflow
p 17 A90-13020
- Experiments in swept-wing transition
p 149 A90-16794
- Modeling of liquid jets injected transversely into a supersonic crossflow
p 153 A90-17985
- Numerical solution of the boundary-layer equations for a general aviation fuselage
[AIAA PAPER 90-0305] p 163 A90-19786
- Parabolized Navier-Stokes predictions of three-dimensional hypersonic flows with strong crossflow effects
p 223 A90-20508
- Topology of computed incompressible three-dimensional separated flow field around high-angle-of-attack cone-cylinders
p 366 A90-25764
- Finite element simulation of complex jets in a crossflow for V/STOL applications
p 585 A90-35753
- Stability limits for three-dimensional supersonic boundary layers
[AIAA PAPER 90-1528] p 564 A90-38673
- The effect of constructive and destructive interference on the downstream development of twin jets in a crossflow. I - Destructive interference of laterally spaced jets
[AIAA PAPER 90-1623] p 607 A90-38752
- Measurement of crossflow vortices, attachment-line flow, and transition using microthin hot films
[AIAA PAPER 90-1636] p 607 A90-38765
- The effect of constructive and destructive interference on the downstream development of twin jets in a crossflow. II - Interference effects of angularly displaced jets
[AIAA PAPER 90-2107] p 684 A90-42020
- Numerical modeling of an impinging jet in cross-flow
[AIAA PAPER 90-2246] p 686 A90-42093
- Solid fuel ignition and combustion characteristics under high-speed crossflows
[AIAA PAPER 90-2075] p 764 A90-42725
- The development of crossflow vortices on a 45 degree swept wing
[SAE PAPER 892245] p 713 A90-45452
- Surface flow on a flat plate induced by a supersonic jet exhausting normally into a low speed crossflow
[AIAA PAPER 90-3011] p 789 A90-45860
- Numerical study of interaction of a jet with a supersonic cross flow
p 808 A90-47300

- Design and test of an NLF wing glove for the variable-sweep transition flight experiment
p 104 N90-12544

The 757 NLF glove flight test results

- p 104 N90-12546
- A streamwise upwind algorithm applied to vortical flow over a delta wing
[NASA-TM-102225] p 398 N90-19201
- Generation of circumferential velocity contours associated with pulsed point suction on a rotating disk
p 691 N90-25065

CROSS POLARIZATION

- Dual cross-polarization planar arrays in the C and X bands
p 638 A90-40979

CROSS SECTIONS

- Effect of the cross-sectional shape of a straight duct on supersonic flow stagnation
p 296 A90-24110
- Aircraft drawings index
p 618 N90-23340

CRUISING FLIGHT

- Minimum fuel cruise by periodic optimization
p 182 A90-19429
- European research and testing facilities requested for participation to SST/HST projects
[ONERA, TP NO. 1990-12] p 351 A90-25358
- A study of approximately optimal cruising flight regimes of variable-mass aircraft
p 430 A90-29187
- Thrust law effects on the longitudinal stability of hypersonic cruise
[AIAA PAPER 90-2820] p 763 A90-45149
- Singular, periodic solutions in aircraft cruise-dash optimization
[AIAA PAPER 90-3369] p 863 A90-47627
- Thermal management for a Mach 5 cruise aircraft using endothermic fuel
[AIAA PAPER 90-3284] p 853 A90-48871
- System optimization for maximizing reconnaissance mission range of a hypersonic cruise vehicle
[AIAA PAPER 90-3292] p 837 A90-48876
- Reducing C130E Hercules operating costs in the Royal Australian Air Force and the United States Air Force by increasing cruise speeds
[AD-A215747] p 338 N90-17629
- An approach to on-board optimization of cruise at constant altitude
[LR-581] p 578 N90-21752

CRUSHING

- The effect of aircraft size on cabin floor dynamic pulses
[DOT/FAA/CT-88/15] p 735 N90-25136

CRYOGENIC COOLING

- Reduced voltage and restart testing of the 1-watt integral cryogenic cooler (HD-1033B/C/D)
[AD-A215133] p 369 N90-16971

CRYOGENIC EQUIPMENT

- Fully automatic calibration machine for internal 6-component wind tunnel balance including cryogenic balances
p 437 A90-28294
- Development of cryogenic instrumentation for ETW models
p 525 A90-34251
- Vibration dampers for cryogenic turbomachinery
[AIAA PAPER 90-2740] p 882 A90-47228

CRYOGENIC FLUID STORAGE

- Design of cryogenic tanks for launch vehicles
p 609 N90-22662

CRYOGENIC FLUIDS

- Rotordynamics of the Vulcan LH2 Turbopump - Comparison between test results and non-linear dynamic analysis
p 528 A90-33382

CRYOGENIC ROCKET PROPELLANTS

- The cycle evaluation of the advanced LACE performance
[IAF PAPER 89-313] p 109 A90-13447

CRYOGENIC TEMPERATURE

- Hot wire anemometry in transonic flows and cryogenic conditions
p 539 A90-34229
- Investigation of model rigging limitations on a high speed wind tunnel model at cryogenic temperature
p 523 A90-34232
- Experimental evaluation of a tuned electromagnetic damper for vibration control of cryogenic turbopump rotors
[NASA-TP-3005] p 665 N90-23403

CRYOGENIC WIND TUNNELS

- Cryogenic wind tunnels
p 199 A90-17346
- Status of the development programme for instrumentation and test techniques of the European Transonic Windtunnel - ETW
p 437 A90-28292
- Instrumentation and operation of NDA cryogenic wind tunnel
p 437 A90-28293
- Turbulence measurements and noise generation in a transonic cryogenic wind tunnel
[AIAA PAPER 88-2026] p 522 A90-32463
- Cryogenic wind tunnels in Japan
p 523 A90-34228
- Hot wire anemometry in transonic flows and cryogenic conditions
p 539 A90-34229

- The Kryo-Kanal Koeln, KKK: Description of tunnel conversion - Results of calibration tests under ambient and cryogenic conditions
p 523 A90-34230
- Investigation of model rigging limitations on a high speed wind tunnel model at cryogenic temperature
p 523 A90-34232

A measurement window for a cryogenic windtunnel

- p 523 A90-34233
- Surface flow visualization in the cryogenic wind tunnel
p 539 A90-34234

Design and manufacture of a cryogenic wind tunnel model

- p 523 A90-34238
- Flow quality in the T2 cryogenic wind-tunnel - Problems and solutions
p 524 A90-34240

- T2 ability concerning model design and instrumentation in short run processing
p 524 A90-34241
- Half transport aircraft cryogenic model for T2 wind tunnel
p 524 A90-34242

- Sting design feasibility for E.T.W. cryogenic civil transport aircraft
p 524 A90-34245

- A proposed automatic calibration facility for cryogenic balances
p 524 A90-34246

- Automatic calibration machine for internal cryogenic balances
p 524 A90-34247

- Development of cryogenic instrumentation for ETW models
p 525 A90-34251

- Measurement of temperature gradients and assessment of balance performance using the RAE cryogenic test duct
p 525 A90-34252

- Aeronautical facility requirements into the 2,000's
[AIAA PAPER 90-1375] p 594 A90-37926

- National Transonic Facility model and model support vibration problems
[AIAA PAPER 90-1416] p 596 A90-37953

- The cryogenic wind tunnel as a testing tool for airframe/propulsion systems
p 672 A90-40400

- Sidewall boundary-layer removal and wall adaptation studies
p 672 A90-40680

- Cryogenic wind tunnels
p 673 A90-41726

- Wind tunnel wall interference investigations in NAE/NRC High Reynolds Number 2D Facility and NASA Langley 0.3m Transonic Cryogenic Tunnel
p 628 A90-42404

- Characteristics of temperature and pressure generation and retention in flow inside cryogenic wind tunnel T-04
p 869 A90-46576

- Hot-film system for transition detection in cryogenic wind tunnels
p 122 N90-12522

- Residual interference assessment in adaptive wall wind tunnels
[NASA-CR-181896] p 123 N90-12625

- The NASA Langley 0.3-meter transonic cryogenic tunnel
p 262 N90-15941

- The cryogenic Ludwig tube tunnel at Goettingen
p 263 N90-15947

- Other cryogenic wind tunnel projects
p 263 N90-15948

- Test techniques for cryogenic wind tunnels
p 263 N90-15952

- Models for cryogenic wind tunnels
p 263 N90-15956

- Automatic control of cryogenic wind tunnels
p 263 N90-15957

- Experience with strain-gage balances for cryogenic wind tunnels
p 264 N90-15958

- Safety and cryogenic wind tunnels
p 264 N90-15960

- An experimental AWTS process and comparisons of ONERA T2 and 0.3-m TCT AWTS data for the ONERA CAST-10 aerofoil
p 321 N90-17653

CRYOGENICS

- Cryogenic temperature effects on sting-balance deflections in the National Transonic Facility
[NASA-TM-4157] p 202 N90-14244

- The NASA Langley 0.3-meter transonic cryogenic tunnel
p 262 N90-15941

- The US National Transonic Facility, NTF
p 262 N90-15942

- Cryogenic balances for the US NTF
p 264 N90-15959

CRYSTAL STRUCTURE

- The creep behavior of the Ti3Al alloy Ti-24Al-11Nb
p 125 A90-15214

CRYSTALLINITY

- Chemical resistance of carbon fiber reinforced polyether ether ketone and polyphenylene sulfide composites
p 944 A90-50142

CRYSTALLIZATION

- Characterization of LaRC-TPI 1500 powders - A new version with controlled molecular weight
p 946 A90-50177

- Mechanical influences on crystallization in PEEK matrix/carbon fiber reinforced composites
p 949 A90-50227

CUES

- Stereopsis cueing effects on hover-in-turbulence performance in a simulated rotorcraft
[NASA-TP-2980] p 506 N90-21004
- Fighter agility metrics, research, and test
[NASA-CR-186118] p 648 N90-23386
- Evaluation of nonlinear motion-drive algorithms for flight simulators
[UTIAS-TN-272] p 761 N90-25148
- The need for platform motion in modern piloted flight training simulators
[AD-A221720] p 871 N90-26847

CUMULATIVE DAMAGE

- A method for determining equivalents during the fatigue testing of structures in an acoustic field
p 364 A90-24153
- Investigation of variation in fatigue life calculated using damage fraction
p 537 A90-33624
- Considerations of reliability design for rotorcraft
p 680 A90-39977
- The collection of usage data to improve structural integrity of operational helicopters
p 651 A90-39983
- Fatigue life estimates for helicopter loading spectra
p 772 A90-45324
- Evaluation of a damaged F/A-18 horizontal stabilizer
[AD-A212573] p 107 N90-12597
- Fatigue life estimates for helicopter loading spectra
[NASA-CR-181941] p 279 N90-16294

CURING

- Rapid low-temperature cure patching system for field repair
p 467 A90-31529
- New cyanate ester resin with low temperature (125-200 C) cure capability
p 944 A90-50135
- Simple shear tests of the FMI 23.5.06 adhesive cured at low pressure (12 PSI)
[INFORME-I-298/88] p 357 N90-17871
- Radiation-curable prepreg composites
[DE90-629740] p 951 N90-28674

CURRENT DISTRIBUTION

- In-flight aircraft lightning surface current model
p 819 A90-49844

CURTISS-WRIGHT AIRCRAFT

- The Curtiss-Wright X-19 experimental aircraft - Lessons learned
[AIAA PAPER 90-3206] p 834 A90-48834

CURVATURE

- Curvature effects on the stability of laminar boundary layers on swept wings
p 148 A90-16788
- Curvature effects on the stability of three-dimensional laminar boundary layers
p 71 N90-10366

CURVE FITTING

- Identification of XV-15 aeroelastic modes using frequency-domain methods
[NASA-TM-101021] p 582 N90-21756

CURVED BEAMS

- Vibration dampers for cryogenic turbomachinery
[AIAA PAPER 90-2740] p 882 A90-47228

CURVED PANELS

- Nonlinear response and fatigue of stiffened panels
p 363 A90-23953
- Buckling analysis of FRP faced cylindrical sandwich panel under combined loading
p 365 A90-24376
- Postbuckling finite element analysis of composite panels
p 365 A90-24377
- Experimental investigation of three-dimensional turbulent boundary layers on 'infinite' swept curved wings
p 303 A90-25589
- A generalized lifting-line theory for curved and swept wings
p 303 A90-25597
- Response of orthogonally stiffened cylindrical shell panels
p 603 A90-36285
- Effect of aerodynamic heating on deformation of composite cylindrical panels in a gas flow
p 773 A90-45788
- Analysis of self-excited vibrations of stiffened covering panels of an aeroplane wing
p 860 A90-46716

CUTTING

- A leap forward in aircraft construction technology - High-speed cutting sets new production standards
p 881 A90-46720

CYANATES

- High service temperature, damage tolerant prepreg systems based on cyanate chemistry
p 941 A90-50069
- Toughened cyanates for aerospace applications
p 942 A90-50088
- New cyanate ester resin with low temperature (125-200 C) cure capability
p 944 A90-50135

CYBERNETICS

- Formalization and solution of covering problems in the synthesis of control and monitoring systems
p 76 A90-10963
- AAAI '88 - Aerospace Applications of Artificial Intelligence; Proceedings of the Fourth Annual Conference, Dayton, OH, Oct. 25-27, 1988. Volumes 1 & 2
p 458 A90-30226

CYCLIC LOADS

- Simplified analysis of helicopter fatigue loading spectra
p 336 A90-26758
- Carbon/epoxy tooling evaluation and usage
p 445 A90-28165
- Cyclic stress-strain behavior and low cycle fatigue of Ti 6242
p 530 A90-33523
- Cyclic deformation, fatigue and fatigue crack propagation in Ni-base alloys
p 531 A90-34162
- Three dimensional turbine blade analysis in thermo-viscoplasticity
p 540 A90-34324
- A simple prediction method for low-cycle fatigue life of structures
p 604 A90-37240
- A rate theory investigation of cyclic loading and plastic deformation in the high stress and ambient temperature range
p 954 A90-49884

CYCLOTRON RESONANCE DEVICES

- History and status of beamed power technology and applications at 2.45 Gigahertz
p 61 N90-10150

CYLINDERS

- Effects of splitter plates on the wake flow behind a bluff body
p 469 A90-32453
- Flow past two cylinders and two spheres
p 903 A90-50815

CYLINDRICAL BODIES

- The effect of flow curvature on the aerodynamic characteristics of an ogive-cylinder body
p 82 A90-13785
- Experimental study of nonsteady asymmetric flow around an ogive-cylinder at incidence
p 384 A90-27985
- Numerical simulation of the compressible flow in a valve-cylinder assembly
p 770 A90-44431
- Aerodynamic effects of body roughness
[AIAA PAPER 90-2850] p 712 A90-45168
- Mechanisms of active control in cylindrical fuselage structures
p 862 A90-47309
- An experimental investigation of the aerodynamic characteristics of slanted base ogive cylinders using magnetic suspension technology
[NASA-CR-181708] p 21 N90-10834
- Normal-force-curve and pitching-moment-curve slopes of forebody-cylinder combinations at zero angle of attack for Mach numbers up to 5
[ESDU-89008] p 89 N90-11709
- Effect of riblets on flow separation from a cylinder and an airfoil in subsonic flow
[AD-A216197] p 319 N90-17574
- Subsonic sting interference on the aerodynamic characteristics of a family of slanted-base ogive-cylinders
[NASA-CR-4299] p 633 N90-24242

CYLINDRICAL SHELLS

- Structure-borne noise transmission in cylindrical enclosures due to random excitation
[AIAA PAPER 90-0990] p 463 A90-29402
- Response of orthogonally stiffened cylindrical shell panels
p 603 A90-36285
- Effect of aerodynamic heating on deformation of composite cylindrical panels in a gas flow
p 773 A90-45788
- Torsional buckling and post-buckling of composite geodetic cylinders with special reference to joint flexibility
p 878 A90-45971
- Active control of sound transmission through a cylindrical shell
p 893 A90-46192
- Bulging cracks in pressurized fuselages - A procedure for computation
p 880 A90-46301
- Theoretical studies of the active control of propeller-induced cabin noise
p 893 A90-46351

D

DAMAGE

- Damage tolerance of a postbuckling soft skin hat stiffened compression panel
p 534 A90-31647
- Expert systems for design of battle damage repairs
p 467 A90-33094
- Use of unbalanced laminates as a screening method for microcracking
p 948 A90-50217
- Design temperatures for flexible airfield pavement design
[AD-A214141] p 262 N90-15115
- Point of view of a civil aircraft manufacturer on Al-Li alloy
p 268 N90-15200
- Analysis of the National Transonic Facility mishap
[NASA-TM-101686] p 328 N90-17620
- Stability characteristics of a combat aircraft with control surface failure
[AD-A216196] p 350 N90-17646
- AGARD/SMP Review: Damage Tolerance for Engine Structures. 2: Defects and Quantitative Materials Behaviour --- conference
[AGARD-R-769] p 425 N90-18396

- The need for a common approach within AGARD --- engine component defects
p 425 N90-18404
- Advances in optimal active control techniques for aerospace systems; application to aircraft active landing gear
p 592 N90-21769
- Peacetime replacement and crash damage factors for army aircraft
[AD-A218544] p 636 N90-23372
- An experimental study of fault propagation in a jet-engine controller
[NASA-CR-181335] p 665 N90-23401
- Damage tolerance demonstration for A310-300 CFPR components
[MBB-UT-012/89-PUB] p 766 N90-25091
- Study of the engine bird ingestion experience of the Boeing 737 aircraft (October 1986 to September 1988)
[DOT/FAA/CT-89/29] p 723 N90-25119
- Study on application of ultrasonic wave measurement to creep-fatigue damage detection
[DE89-782317] p 774 N90-25361
- Mechanical paint removal techniques for aircraft structures
[NIAR-90-12] p 775 N90-26166
- Development of creep-fatigue damage detection method of rotor steel by ultrasonic wave measurement
[DE90-503792] p 777 N90-26365
- Lessons learned for composite aircraft structures qualification
p 842 N90-26808
- An expert system advisor for damage repair of composite wing skins (repairman)
p 842 N90-26810
- Lessons learned from the T-46A durability and damage tolerance program
p 842 N90-26812
- Computerized corrosion forecasting model for C-5 aircraft
p 843 N90-26815
- Application of damage tolerance
p 843 N90-26817
- Individual Helicopter Tracking Program (IHTP) for the MH-53J helicopter
p 843 N90-26818
- Peak identification techniques
p 844 N90-26822
- Annual review of aircraft accident data: US general aviation, calendar year 1987
[PB90-138066] p 820 N90-27666
- Damage tolerance of the fighter aircraft 37 Viggen. Part 1: Analytical assessment
[FFA-TN-1990-12-PT-1] p 923 N90-28538
- Damage tolerance of the fighter aircraft 37 Viggen. Part 2: Experimental verification
[FFA-TN-1990-13-PT-2] p 923 N90-28539
- Development and testing of rapid repair methods for war damaged runways
[AD-A223970] p 938 N90-28586
- Evaluation of high temperature protective coatings for gas turbine engines under simulated service conditions
p 952 N90-28712
- Aircraft battle damage repair of transparencies
[AD-A224168] p 925 N90-29387

DAMAGE ASSESSMENT

- Enhanced combat damage tolerance/supportability for improved combat sustainability
[SAE PAPER 891078] p 101 A90-14370
- The anti-shimmy and break-proof study of nose landing gear
p 178 A90-16856
- Damage tolerance analysis of dynamic components of rotary wing aircraft
p 179 A90-17312
- Predicting crack growth under thermo-mechanical cycling
p 209 A90-18169
- Airship survival - Damage avoidance and control for large ocean-going airships
[AIAA PAPER 89-3166] p 238 A90-20588
- Fatigue damage of an aircraft due to movement on the airfield
p 247 A90-23352
- Vibration analysis for immediate assessment of battle-damaged gas turbine engines
[ASME PAPER 89-GT-96] p 341 A90-23811
- Caring for the elderly jet
p 285 A90-24280
- Review of composite rotor blade modeling
p 366 A90-25303
- Damage tolerance analysis and testing of a welded cluster gear for the main transmission of the Advanced Attack Helicopter
p 445 A90-28187
- Effects of damage on post-buckled skin-stiffener composite skin panels
p 409 A90-28235
- An apparatus to prepare composites for repair
p 533 A90-31574
- Development of a fibre optic damage detection system for an aircraft leading edge
p 504 A90-32873
- Repairing the damage
p 530 A90-33712
- Towards a damage tolerance philosophy for composite materials and structures
p 675 A90-40127
- Metal laminates for aerospace applications
p 874 A90-48997
- Highlights of RAE lightning strike investigations
p 818 A90-49827
- Damage tolerance for helicopters
p 919 A90-49888
- Development of a double crack growth gage algorithm for application to fleet tracking of fatigue damage
p 901 A90-49890

Damage tolerance demonstration for A310-300 CFRP-components p 919 A90-49894
High service temperature, damage tolerant prepreg systems based on cyanate chemistry p 941 A90-50069

Hierarchical damage tolerant controllers for smart structures [AD-A209422] p 31 N90-10022

Development of pressure containment and damage tolerance technology for composite fuselage structures in large transport aircraft [NASA-CR-3996] p 63 N90-10186

Study of the engine bird ingestion experience of the Boeing 737 aircraft [DOT/FAA/CT-89/16] p 176 N90-13360

Analysis of damaged components from DOE security helicopter N7EG [DE90-004488] p 324 N90-16729

Noise and sonic boom impact technology. Effects of aircraft noise and sonic booms on structures: An assessment of the current state-of-knowledge [AD-A213919] p 378 N90-17409

AGARD/SMP Review: Damage Tolerance for Engine Structures. 2: Defects and Quantitative Materials Behaviour --- conference [AGARD-R-769] p 425 N90-18396

Damage tolerance analysis for manned hypervelocity vehicles. Volume 2: Software user's manual [AD-A222136] p 845 N90-26826

Aircraft lightning protection handbook [AD-A222716] p 820 N90-27668

AGARD/SMP Review Damage Tolerance for Engine Structures. 3: Component Behaviour and Life Management [AGARD-R-770] p 855 N90-27704

AGARD damage tolerance concepts for engine structures Workshop 3, Component Behaviour and Life Management p 855 N90-27705

Component behaviour and life management: The need for common AGARD approaches and actions p 856 N90-27710

Inspection system for in-situ inspection of aircraft composite structures p 886 N90-28091

Damage tolerance analysis for manned hypervelocity vehicles. Volume 1: Final technical report [AD-A221970] p 887 N90-28106

DAMPERS

Unbalance response studies on a model rotor supported on uncentrally squeezed film dampers and the development experience of a jet engine p 69 A90-12579

Probabilistic method to compute the optimal slip load for a mistuned bladed disk assembly with friction dampers p 507 A90-32269

Fatigue evaluation of C/MH-53E main rotor damper threaded joints p 642 A90-39988

High temperature powder lubricated dampers for gas turbine engines [AIAA PAPER 90-2048] p 684 A90-41999

DAMPING

A study of roll response required in a low altitude slalom task --- in helicopter control p 347 A90-25421

Aircraft modal suppression system: Existing design approach and its shortcomings p 33 N90-10115

Numerical simulation of unsteady combustion in a dump combustor p 54 N90-10203

Control and stabilization of linear and nonlinear distributed systems [AD-A216446] p 462 N90-18908

An experimental study of the aeroelastic behaviour of two parallel interfering circular cylinders p 455 N90-19609

An investigation of the generation and radiation of aerodynamic noise in real piping systems p 614 N90-22368

DAMPING TESTS

A model for active control of helicopter air resonance in hover and forward flight p 670 A90-42462

DARK ADAPTATION

The assessment of visibility from automatic contrast Measurements p 242 N90-15061

DATA ACQUISITION

System identification - Multibus acquisition and simulation equipment p 26 A90-12192

Acquisition and recording of AMX A/C Aeritalia experience and present trends p 26 A90-12194

Testing facility and procedure of the ATTAS on-board data acquisition system p 39 A90-12202

A comfortable and universal data-acquisition-system for flight research p 39 A90-12204

A new data acquisition, display and control system for the ARA transonic wind tunnel p 436 A90-28256

An optical angle of attack sensor p 446 A90-28263

Instrumentation and operation of NDA cryogenic wind tunnel p 437 A90-28293

The rotor-signal-module of MF190 --- for digital data acquisition from BO-105 helicopter rotary wings p 418 A90-28849

Very-high-performance data acquisition/analysis/display/control systems based on the APTEC I/O computer p 458 A90-28852

Flight test data processing, plotting and analysis at your finger tips - A flexible, automated, integrated approach [AIAA PAPER 90-1322] p 545 A90-34150

The Meteorological Measurement System on the NASA ER-2 aircraft p 926 A90-51658

Noise data of four small propeller-driven airplanes [PB89-216980] p 139 N90-12291

Preliminary experience with high response pressure measurements in a multistage, high speed compressor [RAE-TM-P-1141] p 117 N90-12619

A real-time wind model using digital data from aircraft [RSRE-MEMO-4309] p 137 N90-13005

Data acquisition in aerodynamic research p 171 N90-13340

A data acquisition parallel bus for wind tunnels at ARL (Aeronautical Research Laboratory) [AD-A218052] p 526 N90-20098

The MANTA: An RPV design to investigate forces and moments on a lifting surface [NASA-CR-186227] p 499 N90-20971

Enhanced Low Level Wind Shear (LLWAS) 6-sensor improvement user's manual for data processing of field data [DOT/FAA/CT-TN90/8] p 583 N90-21759

Modeling strength data for CREW CHIEF p 780 N90-25516

ARLSUPER version 1.0, program users guide [AD-A222693] p 815 N90-26793

The Langley 14- by 22-foot subsonic tunnel: Description, flow characteristics, and guide for users [NASA-TP-3008] p 816 N90-27649

General test plan p 857 N90-27721

Acoustic emission detection of crack presence and crack advance during flight p 886 N90-28082

Analysis of heliport environmental data, Intracoastal City [DOT/FAA/CT-TN89/43] p 938 N90-28584

The DELTA MONSTER: An RPV designed to investigate the aerodynamics of a delta wing platform [NASA-CR-186226] p 924 N90-29381

Development of a software package for automatic data acquisition, analysis, and controls in an axial flow compressor test rig [PD-PR-8910] p 965 N90-29926

Small multipurpose stored data acquisition system [DE90-010823] p 967 N90-30134

DATA BASE MANAGEMENT SYSTEMS

A computer-aided control engineering environment for multi-disciplinary expert-aided analysis and design (MEAD) p 461 A90-30796

Assessment System for Aircraft Noise (ASAN) citation database. Volume 2: Database update manual [AD-A219176] p 615 N90-23189

Assessment System for Aircraft Noise (ASAN) citation database. Volume 3: New citation review procedures [AD-A219177] p 615 N90-23190

TRENDS: The aeronautical post-test database management system [NASA-TM-101025] p 761 N90-25149

DATA BASES

Air-to-Air Combat Test IV (AACT IV) and the AACT data base p 381 A90-28169

Database for LDV signal processor performance analysis p 447 A90-28278

A flight-test methodology for identification of an aerodynamic model for a V/STOL aircraft p 413 A90-30107

Data base correlation issues p 459 A90-30740

The IMIS F-16 interactive diagnostic demonstration p 383 A90-30768

Developments in automation of flight test analysis and report generation [AIAA PAPER 90-1313] p 487 A90-33923

Database management considerations for IFR certified earth-referenced navigation systems p 577 A90-36921

Review and analysis of the DNW/Model 360 rotor acoustic data base [NASA-TM-102253] p 81 N90-11692

The role of component testing [PNR90589] p 115 N90-12608

Mesoscale acid deposition modeling studies [NASA-CR-4262] p 140 N90-13228

Stall/spin aerodynamic data project [DOT/FAA/CT-88/29] p 185 N90-14222

The collection of non-conus aircraft icing data along with an identification of the geographical areas of potential severe icing and a study of a method of remote determining atmospheric icing data [AD-A215055] p 323 N90-16724

Verification of aerothermodynamic codes by means of a winged experimental re-entry vehicle p 354 N90-16842

Noise and sonic boom impact technology. Effects of aircraft noise and sonic booms on structures: An assessment of the current state-of-knowledge [AD-A213919] p 378 N90-17409

Development of an automatic ground collision avoidance system using a digital terrain database [AD-A216247] p 329 N90-17621

The influence of ice accretion physics on the forecasting of aircraft icing conditions p 485 N90-20928

Assessment System for Aircraft Noise (ASAN) citation database. Volume 1: User's manual [AD-A219175] p 615 N90-23188

Assessment System for Aircraft Noise (ASAN) citation database. Volume 3: New citation review procedures [AD-A219177] p 615 N90-23190

A comparison of lightning network data with surface weather observations [AD-A220003] p 692 N90-23832

Flow unsteadiness effects on boundary layers [NASA-CR-186067] p 690 N90-24557

TRENDS: The aeronautical post-test database management system [NASA-TM-101025] p 761 N90-25149

Program plan: International aircraft operator data base [IAR-90-1] p 783 N90-25697

An automated calibration laboratory for flight research instrumentation: Requirements and a proposed design approach [NASA-TM-101719] p 781 N90-26564

BASEOPS default profiles for civil aircraft [AD-A223161] p 844 N90-26825

Development of a mathematical model for the thermal decomposition of aviation fuels [AD-A221673] p 875 N90-26994

Evaluation of existing aircraft operator data bases [DOT/FAA/CT-90/18] p 898 N90-28463

A flight dynamic model of aircraft spinning [AR-005-600] p 935 N90-28576

International aircraft operator data base master requirements and implementation plan [DOT/FAA/CT-90/17] p 967 N90-29247

The potential for digital databases in flight planning and flight aiding for combat aircraft p 918 N90-29371

DATA COLLECTION PLATFORMS

Passive location accuracy via a general covariance error model --- long-baseline interferometry from airborne platforms p 914 A90-51060

The MANTA: An RPV design to investigate forces and moments on a lifting surface [NASA-CR-186227] p 499 N90-20971

DATA COMPRESSION

Weather data dissemination to aircraft p 486 N90-20934

Automated analysis of MXU-553 flight data p 844 N90-26821

DATA CORRELATION

Wind tunnel testing of high blockage models p 121 A90-15743

Iterative algorithm for correlation of strain gauge data with aerodynamic load p 709 A90-44739

DATA FLOW ANALYSIS

RISC lifting off in avionics --- Reduced Instruction Set Computer [AIAA PAPER 89-2967] p 73 A90-10483

The performance of linear fiber optic data buses p 68 A90-11665

Testing of statistical hypotheses and derivation of confidence intervals from inspection data samples p 363 A90-24087

B-1B Doppler error compensation based on flight data analysis p 404 A90-30790

Testing of a highly integrated automatic flight system - The 747-400 Flight Management Computer System [AIAA PAPER 90-1302] p 505 A90-33916

Preparations of the real-time data analyst to insure flight test safety [AIAA PAPER 90-1316] p 488 A90-33925

The application of an expert maintenance and diagnostic tool to aircraft engines [AIAA PAPER 90-2036] p 657 A90-40605

The development of a low cost data logging system for flight trials based on an IBM compatible PC [RAE-TM-FM-16] p 251 N90-15917

Past, present and future: Aircraft integrated monitoring systems: An ever-developing technology p 848 N90-27618

DATA INTEGRATION

Multiple sensor data association and fusion in aerospace applications p 778 A90-44644

DATA LINKS

The US air traffic control system architecture p 330 A90-25561

- Mode S system design and architecture p 330 A90-25569
- The use of satellite technology for oceanic air traffic control p 330 A90-25570
- Mode S - A data link for future air traffic control p 576 A90-35684
- Applications of Mode S secondary surveillance radar to civil air traffic control - Studies, experiments, and policy of the French Direction de la Navigation Aérienne p 639 A90-41056
- Range Applications Joint Program Office GPS Range System data link p 725 A90-43686
- Data Link Processor (DLP) operational test and evaluation/integration test plan [DOT/FAA/CT-TN89/32] p 214 N90-14404
- Operational evaluation of initial data link air traffic control services, volume 1 [DOT/FAA/CT-90/1-VOL-1] p 455 N90-19472
- Weather data dissemination to aircraft p 486 N90-20934
- Automatic speech recognition in air-ground data link p 690 N90-25037
- The disturbance processes on the data links of the mode-S air traffic control system [ETN-90-96960] p 729 N90-25965
- Data link test and analysis system/ATCRBS transponder test system technical reference [DOT/FAA/CT-TN90/7] p 824 N90-26803
- Aspects of data link applications for ATC purposes p 827 N90-27688
- Application of a company data link at Lufthansa German Airlines p 827 N90-27689
- DATA MANAGEMENT**
- Study of advanced technology impact on cycle characteristics and aircraft sizing (using multivariable optimization techniques) p 29 A90-12612
- Harrier Information Management System (HIMS): The system and the approach p 884 N90-27630
- DATA PROCESSING**
- Real-time test data processing system --- for helicopter flight testing p 458 A90-28860
- Flight test data processing, plotting and analysis at your finger tips - A flexible, automated, integrated approach [AIAA PAPER 90-1322] p 545 A90-34150
- Automated helicopter structural analysis data processing p 611 A90-38533
- Developments in ground vibration test and data analysis techniques for airframe structures p 832 A90-46970
- Application possibilities of expert systems in modern maintenance for increasing operational security p 892 A90-49271
- Guidance simulation and test support for differential GPS flight experiment [NASA-CR-177471] p 28 N90-10021
- Flight Test Techniques [AGARD-CP-452] p 33 N90-10860
- The Experimental Aircraft Flight Test Programme p 34 N90-10865
- Flight test techniques adopted by Avions Marcel Dassault-Breguet Aviation p 34 N90-10867
- Flight test instrumentation and data processing at British Aerospace, Warton, U.K. p 59 N90-10887
- General data processing support from project planning to workshop control [MBB-UD-526/88-PUB] p 138 N90-12208
- Data acquisition in aerodynamic research p 171 N90-13340
- The development of a low cost data logging system for flight trials based on an IBM compatible PC [RAE-TM-FM-16] p 251 N90-15917
- Tracking a hypersonic aircraft from a space platform [AD-A216399] p 371 N90-17984
- Time and frequency-domain identification and verification of BO-105 dynamic models [AD-A216828] p 415 N90-18389
- Meteorologist Weather Processor (MWP) integration test plan [DOT/FAA/CT-TN89/62] p 544 N90-21500
- Enhanced Low Level Wind Shear (LLWAS) 6-sensor improvement user's manual for data processing of field data [DOT/FAA/CT-TN90/8] p 583 N90-21759
- Real-time simulation clock [NASA-CASE-LAR-14056-1] p 689 N90-23713
- Automated analysis of MXU-553 flight data p 844 N90-26821
- Computer modeling and data processing methods: An essential part of jet engine condition monitoring and fault diagnosis p 855 N90-27626
- Air traffic management in Europe: Structure, tasks, potential p 825 N90-27677
- Application of a company data link at Lufthansa German Airlines p 827 N90-27689
- Design of the UETP experiment p 856 N90-27712
- Experience in developing an improved design of experiment (lessons learned) p 857 N90-27718
- General test plan p 857 N90-27721
- Noncontact measurement of rotating blade vibrations [NAL-TR-1033] p 961 N90-29687
- DATA PROCESSING EQUIPMENT**
- Data Link Processor (DLP) operational test and evaluation/integration test plan [DOT/FAA/CT-TN89/32] p 214 N90-14404
- Throughput and delay characteristics for a slow-frequency hopped aircraft-to-aircraft packet radio network [AD-A220525] p 688 N90-23609
- DATA RECORDERS**
- Prospects of onboard magnetic tape recording during flight tests p 39 A90-12198
- Applications for a small format airborne recorder p 847 A90-48620
- The NASA digital VGH program: Exploration of methods and final results. Volume 2: L 1011 data 1978-1979: 1619 hours [NASA-CR-181909-VOL-2] p 505 N90-20080
- The NASA digital VGH program: Exploration of methods and final results. Volume 1: Development of methods [NASA-CR-181909-VOL-1] p 505 N90-20081
- The NASA digital VGH program: Exploration of methods and final results. Volume 3: B 727 data 1978-1980: 1765 hours [NASA-CR-181909-VOL-3] p 505 N90-20082
- The NASA digital VGH program: Exploration of methods and final results. Volume 4: B 747 data 1978-1980, 1689 hours [NASA-CR-181909-VOL-4] p 506 N90-20083
- The NASA digital VGH program: Exploration of methods and final results. Volume 5: DC 10 data 1981-1982, 129 hours [NASA-CR-181909-VOL-5] p 506 N90-20084
- DATA RECORDING**
- Acquisition and recording of AMX A/C Aeritalia experience and present trends p 26 A90-12194
- The importance of measured data as a contribution to reducing crew caused accidents [AIAA PAPER 89-3219] p 482 A90-31703
- The collection of usage data to improve structural integrity of operational helicopters p 651 A90-39983
- Acoustic recording systems for use in military aircraft [RAE-TM-MM-11] p 140 N90-13207
- Aircraft condition monitoring system for future Airbus aircraft: New concept for programming and data recording p 848 N90-27619
- The EFA integrated monitoring and recording system: Requirements and concept for implementation p 848 N90-27620
- DATA REDUCTION**
- Heat transfer and pressure drop for short pin-fin arrays with pin-endwall fillet [ASME PAPER 89-GT-99] p 359 A90-23813
- Development of airborne data reduction system in IPTN flight test p 418 A90-28895
- Testing of a highly integrated automatic flight system - The 747-400 Flight Management Computer System [AIAA PAPER 90-1302] p 505 A90-33916
- Developments in ground vibration test and data analysis techniques for airframe structures p 832 A90-46970
- New methods of buffering prediction on civil aircraft p 908 A90-52620
- The Experimental Aircraft Flight Test Programme p 34 N90-10865
- Prediction methodologies for nonlinear aerodynamic characteristics of control surfaces [NIAR-90-17] p 718 N90-25937
- Automated analysis of MXU-553 flight data p 844 N90-26821
- DATA SAMPLING**
- Conditional sampling --- technique for aerodynamic characteristics measurement from wind-tunnel experiments [ONERA, TP NO. 1989-187] p 261 A90-21047
- DATA SIMULATION**
- Aircraft SAR simulation Sargen 1.0 [FEL-1989-44] p 135 N90-12823
- DATA SMOOTHING**
- Parameter identification of linear systems based on smoothing [AIAA PAPER 90-2800] p 753 A90-45156
- DATA STORAGE**
- Developments in automation of flight test analysis and report generation [AIAA PAPER 90-1313] p 487 A90-33923
- The MHOST finite element program: 3-D inelastic analysis methods for hot section components. Volume 3: Systems' manual [NASA-CR-182236] p 73 N90-10451
- Noise and sonic boom impact technology. Initial development of an Assessment System for Aircraft Noise (ASAN). Volume 3: Technical description [AD-A214455] p 379 N90-17412
- Assessment System for Aircraft Noise (ASAN) citation database. Volume 2: Database update manual [AD-A219176] p 615 N90-23189
- DATA STRUCTURES**
- An international civil integrity complement to GPS and GLONASS p 821 A90-46392
- DATA SYSTEMS**
- A test matrix sequencer for research test facility automation [AIAA PAPER 90-2386] p 759 A90-42791
- The Real Time Display Builder (RTDB) p 546 N90-20656
- Cockpit display of hazardous wind shear information p 484 N90-20924
- Weather data dissemination to aircraft p 486 N90-20934
- DATA TRANSMISSION**
- Trends in telemetry front end architecture [AIAA PAPER 89-3085] p 25 A90-10571
- High performance single-mode coupler for harsh environments p 78 A90-11027
- The performance of linear fiber optic data buses p 68 A90-11665
- An analysis of reliability in fiber optic ring and star networks p 78 A90-11666
- Research on transmission quality of telemetry system in flight test p 26 A90-12189
- Decommunication techniques and their integration into post flight analysis system p 26 A90-12191
- The Modular Flighttest Instrumentation/MFI 90 - A helicopter measuring system p 418 A90-28850
- Range Applications Joint Program Office GPS Range System data link p 725 A90-43686
- Operational evaluation of initial data link air traffic control services, volume 1 [DOT/FAA/CT-90/1-VOL-1] p 455 N90-19472
- Optimization of the effective GPS data rate p 489 N90-20932
- Automatic speech recognition in air-ground data link p 690 N90-25037
- The disturbance processes on the data links of the mode-S air traffic control system [ETN-90-96960] p 729 N90-25965
- New features of JAL's ground station p 872 N90-27633
- Replay and transmission of AIMS-data to mainframe computer using remote transcribers p 892 N90-27634
- DAYTIME**
- Cumulative airport noise exposure metrics: An assessment of evidence for time-of-day weightings, revision [AD-A214878] p 352 N90-16773
- DC 10 AIRCRAFT**
- The McDonnell Douglas MD-11 ... or, how the DC-10 grew bigger p 730 A90-43766
- The NASA digital VGH program: Exploration of methods and final results. Volume 5: DC 10 data 1981-1982, 129 hours [NASA-CR-181909-VOL-5] p 506 N90-20084
- Brake performance of the McDonnell Douglas DC-10-30/40 during high speed, high energy rejected takeoffs [PB90-917004] p 503 N90-21000
- DEAD RECKONING**
- Observability of relative navigation using range-only measurements p 917 N90-29360
- DEATH**
- Fire deaths in aircraft without the crashworthy fuel system p 22 A90-10266
- DEBRIS**
- In-line wear monitor [AD-A217799] p 510 N90-20091
- DECCA NAVIGATION**
- Eurofix p 25 A90-10239
- DECELERATION**
- Airfoils in supersonic source and sink flows p 149 A90-16844
- An open-loop transient thermodynamic model of the Cougar turbojet [AD-A211774] p 114 N90-11745
- Flight test investigation of flight director and autopilot functions for helicopter decelerating instrument approaches [DOT/FAA/CT-TN89/54] p 869 N90-27724
- DECISION MAKING**
- The Battle Captain Expert System - A mission management decision support system for attack helicopter operations [AIAA PAPER 89-3098] p 37 A90-10583
- Artificial intelligence techniques applied to the non-cooperative identification (NCID) problem [AIAA PAPER 89-3005] p 75 A90-10619
- Incorporation of alarm states into a real time decision making process [AIAA PAPER 89-3006] p 76 A90-10620

- Multiobjective decision making in a fuzzy environment with applications to helicopter design p 405 A90-27993
- Integration of intelligent avionics systems for crew decision aiding p 459 A90-30236
- Real-time adaptive control of knowledge based avionics tasks p 460 A90-30764
- On the generation of a variable structure airport surface traffic control system p 99 N90-11724 [AD-A211306]
- Using goal programming to determine the optimal engine mix for UH-1 helicopters p 343 N90-16762 [AD-A214893]
- Aeronautical decisionmaking for air ambulance program administrators p 635 N90-23368 [DOT/FAA/DS-88/8]
- Replay and transmission of AIMS-data to mainframe computer using remote transcribers p 892 N90-27634
- DECISION THEORY**
- A decision-making aid for multi-layer radar absorbent coverings p 773 N90-25267 [ESA-TT-1173]
- DECODERS**
- Miniaturization of flight deflection measurement system p 689 N90-23707 [NASA-CASE-LAR-13628-1]
- DECOMMUTATORS**
- Decommutation techniques and their integration into post flight analysis system p 26 A90-12191
- DECOMPOSITION**
- Conceptual design optimization study p 582 N90-21755 [NASA-CR-4298]
- A discussion on issues relating to multiblock grid generation p 608 N90-21991
- Multilevel decomposition approach to the preliminary sizing of a transport aircraft wing p 583 N90-22557 [NASA-CR-4296]
- DECOUPLING**
- Decoupled ultimate boundedness control of systems and large aircraft maneuver p 196 A90-19461
- DEFECTS**
- Design and analysis of composite structures with manufacturing flaws p 445 A90-28234
- Analysis and interpretation of aircraft component defects using quantitative fractography p 956 A90-50555
- Reflection by defective diffusion bonds p 206 N90-13638 [AD-A212995]
- Fuel resistant coatings for metal and composite fuel tanks p 269 N90-15911
- Defects in monoblock cast turbine wheels p 443 N90-18400
- Review of modelling methods to take account of material structure and defects p 425 N90-18402
- The need for a common approach within AGARD --- engine component defects p 425 N90-18404
- Neural networks for detecting defects in aircraft structures p 777 N90-26345 [IAR-90-4]
- Estimation of defective rate of mechanic-hydraulic components p 884 N90-27120 [ETN-90-97275]
- Inspection system for in-situ inspection of aircraft composite structures p 886 N90-28091
- DEFENSE INDUSTRY**
- AGARD highlights 90/1 p 783 N90-26788
- DEFENSE PROGRAM**
- The technology challenge of the advanced tactical fighter: A study of the technology transition process p 338 N90-17630 [AD-A216109]
- Aircraft modifications cost analysis. Volume 1: Overview of the study p 702 N90-25074 [AD-A220764]
- An analysis of GPS as the sole means navigation system in US Navy aircraft p 917 N90-29350
- DEFINITION**
- A glossary of terms, definitions, acronyms, and abbreviations related to the National Airspace System [DOT/FAA/CT-TN89/53] p 967 N90-29249
- DEFLECTION**
- Vibrations of rectangular plates with moderately large initial deflections at elevated temperatures using finite element method p 451 A90-29429 [AIAA PAPER 90-1125]
- Cryogenic temperature effects on sting-balance deflections in the National Transonic Facility p 202 N90-14244 [NASA-TM-4157]
- Miniaturization of flight deflection measurement system p 689 N90-23707 [NASA-CASE-LAR-13628-1]
- Structural testing and analytical research of turbine components p 933 N90-29396 [AD-A223516]
- DEFORMATION**
- Cyclic deformation, fatigue and fatigue crack propagation in Ni-base alloys p 531 A90-34162

- A study of the influence of predeformations on the vibrations of blades p 585 A90-35673
- Design temperatures for flexible airfield pavement design p 262 N90-15115 [AD-A214141]
- Nonlinear static and dynamic modeling of composite rotor blades including warping effects p 924 N90-29382
- DEFROSTING**
- Grid and mesh patterned electrically conductive coatings in IR systems p 503 A90-32028
- DEGRADATION**
- Predictions of airfoil aerodynamic performance degradation due to icing p 144 A90-16753
- Experimental investigation of multielement airfoil ice accretion and resulting performance degradation p 812 A90-48954
- Ice induced aerodynamic performance degradation of rotorcraft: An overview p 248 N90-15063
- Computerized corrosion forecasting model for C-5 aircraft p 843 N90-26815
- B-1B improved windshield development. Volume 2: Magna analysis: Baseline and parametric [AD-A221501] p 845 N90-26828
- A technique for rapid inspection of composite aircraft structure for impact damage p 846 N90-28077
- Molten salt induced high temperature degradation of thermal barrier coatings p 952 N90-28704
- Effect of protective coatings on mechanical properties of superalloys p 952 N90-28707
- DEGREES OF FREEDOM**
- Whirl-flutter investigation on an advanced turboprop configuration p 40 A90-11008
- 5DOF dynamic loads on a jet vane p 675 A90-42147 [AIAA PAPER 90-2382]
- Helicopter stability and control modeling improvements and verification on two helicopters p 671 A90-42474
- Short time-dynamometer system for shock wave channels p 773 N90-25084 [MBB-UT-115/89-PUB]
- Coupled rotor-body equations of motion hover flight [NASA-CR-186710] p 717 N90-25111
- Inflight thrust vectoring: A further degree of freedom in the aerodynamic/flight mechanical design of modern fighter aircraft p 921 N90-28528
- DEICERS**
- Design of an advanced pneumatic deicer for the composite rotor blade p 29 A90-11009
- An advanced pneumatic impulse ice protection system (PIIP) for aircraft p 182 A90-19875 [AIAA PAPER 90-0492]
- Thin film eddy current impulse deicer p 183 A90-20012 [AIAA PAPER 90-0761]
- A comparison of a droplet impingement code to icing tunnel results p 352 A90-26979 [AIAA PAPER 90-0670]
- Evaluation of the improved OV-ID anti-icing system, phase 2 p 239 N90-15083 [AD-A213928]
- A NASA/university/industry consortium for research on aircraft ice protection p 736 N90-25969 [IAR-89-18]
- DEICING**
- Fatigue and electromagnetic interference test for Electro-Impulse De-Icing [SAE PAPER 891062] p 100 A90-14362
- Impact ice stresses in rotating airfoils p 175 A90-19735 [AIAA PAPER 90-0198]
- Wave formation on a liquid layer for de-icing airplane wings p 445 A90-28137
- Grid and mesh patterned electrically conductive coatings in IR systems p 503 A90-32028
- Deicing of solids using radiant heating p 769 A90-43309
- Aircraft Ground Deicing Conference, Denver, CO, Sept. 20-22, 1988, Proceedings p 817 A90-46004 [SAE P-217]
- Electro-impulse de-icing testing analysis and design [NASA-CR-4175] p 32 N90-10031
- NASA's program on icing research and technology p 239 N90-15062
- Flight and wind tunnel investigation of aerodynamic effects of aircraft ground deicing/antiflying fluids p 235 N90-15064
- Modeling of surface roughness effects on glaze ice accretion p 485 N90-20925
- DELAMINATING**
- Experimental study on the buckling and postbuckling of carbon fibre composite panels with and without interply disbonds p 130 A90-15355
- Evaluation of 3-D reinforcements in commingled, thermoplastic structural elements p 441 A90-28192
- Towards a damage tolerance philosophy for composite materials and structures p 675 A90-40127

- Investigation of the failure modes in a metal matrix composite under thermal cycling p 357 N90-17825 [AD-A216195]
- Development of a finite element based delamination analysis for laminates subject to extension, bending, and torsion p 679 N90-25049
- DELAY**
- The influence of weather on flight operations at the Atlanta Hartsfield International Airport p 279 A90-22688
- Replication of NASPAC Dallas/Fort Worth study [DOT/FAA/CT-TN90/26] p 729 N90-25123
- DELPHI METHOD (FORECASTING)**
- The future of aircraft paint removal methods [AD-A214946] p 356 N90-16936
- DELTA WINGS**
- The water tunnel test of delaying vortex breakdown over a delta wing using supplements p 2 A90-10346
- Application of the hydrogen bubble visualization method to the water tunnels of ONERA p 58 A90-11140 [ONERA, TP NO. 1989-107]
- Numerical simulation of reversed flow over a supersonic delta wing at high angle of attack p 8 A90-11849 [AIAA PAPER 89-1802]
- Lee-side heating of a delta wing in supersonic flow p 10 A90-12281
- Vortex interactions in fixed and oscillating delta wings (water tunnel visualizations) p 16 A90-12784
- Experimental and numerical investigation of vortex flow over a sideslipping delta wing p 17 A90-13016
- Computation of transonic separated flow using the Euler equations p 85 A90-15233
- Leading edge flap influence on aerodynamic efficiency p 85 A90-15240
- Calculation of flow past delta wings in the thin shock layer approximation p 86 A90-15624
- Numerical studies of incompressible flow around delta and double-delta wings p 150 A90-16845
- Navier-Stokes computations of lee-side flows over delta wings p 153 A90-17978
- Low-speed unsteady aerodynamics of a pitching straked wing at high incidence. I - Test program. II - Harmonic analysis p 159 A90-19387
- Unsteady aerodynamic forces on rolling delta wings at high angle of attack p 159 A90-19426
- Investigation of high angle of attack vortical flows over delta wings p 162 A90-19682 [AIAA PAPER 90-0101]
- Direct simulation of hypersonic rarefied flow about a delta wing p 162 A90-19704 [AIAA PAPER 90-0143]
- Large-amplitude high-rate roll experiments on a delta and double delta wing p 163 A90-19742 [AIAA PAPER 90-0224]
- Lift development of delta wings undergoing constant acceleration from rest p 164 A90-19789 [AIAA PAPER 90-0310]
- Unsteady surface pressure distributions on a delta wing undergoing large amplitude pitching motions p 164 A90-19790 [AIAA PAPER 90-0311]
- An investigation on the coiled-up of vortices on a double delta wing p 165 A90-19825 [AIAA PAPER 90-0382]
- Viscous supersonic flow computations over a delta-rectangular wing with slanting surfaces p 166 A90-19841 [AIAA PAPER 90-0419]
- Semi-implicit Navier-Stokes solver (SINSS) calculations of separated flows around blunt delta wings p 168 A90-19936 [AIAA PAPER 90-0590]
- Prediction of vortical flows on wings using incompressible Navier-Stokes equations p 226 A90-21935
- Vortical flows over delta wings and numerical prediction of vortex breakdown p 227 A90-22166 [AIAA PAPER 90-0102]
- An investigation of asymmetric vortical flows over delta wings with tangential leading-edge blowing at high angles of attack p 227 A90-22167 [AIAA PAPER 90-0103]
- Simulation and analysis of a delta platform with multiple jets in ground effect p 228 A90-22195 [AIAA PAPER 90-0299]
- An experimental investigation of sweep-angle influence on delta-wing flows p 228 A90-22210 [AIAA PAPER 90-0383]
- An embedded grid formulation applied to a delta wing p 229 A90-22216 [AIAA PAPER 90-0429]
- Vortex dynamics on a pitching delta wing p 233 A90-23281
- Leading- and trailing-edge flaps on supersonic delta wings p 233 A90-23285
- An experimental study of separated flow past a low-aspect-ratio delta wing p 294 A90-24077
- A method for calculating the location and intensity of a conical head shock on the lower surface of a delta wing with supersonic edges p 297 A90-24139

- A study of the laminar-turbulent boundary layer transition on the windward side of a delta wing with a conical surface p 298 A90-24144
- Flow-calculation over a delta-wing using the thin-layer Navier-Stokes equations p 304 A90-25773
- Vortex dynamics of delta wings p 307 A90-26067
- Measurements on an oscillating 70-deg delta wing in subsonic flow p 307 A90-26130
- Measured forces and moments on a delta wing during pitch-up p 308 A90-26137
- Effects of a contoured apex on vortex breakdown p 308 A90-26141
- Comparison between thin layer and full Navier-Stokes simulations over a supersonic delta wing [AIAA PAPER 90-0589] p 314 A90-26968
- The flowfields of bursting vortices over moderately swept delta wings [AIAA PAPER 90-0599] p 314 A90-26969
- Calculation of flow characteristics in the core of a vortex sheet p 386 A90-28981
- Comparison of calculated and experimental nonstationary aerodynamic characteristics of a delta wing pitching at large angles of attack p 387 A90-28988
- Aerodynamic quality of a plane delta wing with blunted edges at large supersonic flow velocities p 387 A90-28991
- Combined effect of viscosity and bluntness on the aerodynamic efficiency of a delta wing in flow with a high supersonic velocity p 388 A90-29184
- Vortex shedding over delta wings p 470 A90-32479
- Unsteady airloads due to separated flow on airfoils and wings p 471 A90-33311
- Further studies of harmonic gradient method for supersonic aeroelastic applications p 473 A90-33410
- A technique for calculating nonlinear normal-force and pitching-moment coefficients for slender delta wings, accounting for wing thickness p 476 A90-34356
- Unsteady inviscid and viscous computations for vortex-dominated flows p 553 A90-35752
- Effect of vertical-ejector jet on the aerodynamics of delta wings p 553 A90-35755
- Control of asymmetric vortical flows over delta wings at high angles of attack p 553 A90-35759
- Connection between leading-edge sweep, vortex lift, and vortex strength for delta wings p 554 A90-35770
- Navier-Stokes computation of flow around a round-edged double-delta wing p 555 A90-36251
- Leading-edge vortices due to low Reynolds number flow past a pitching delta wing p 555 A90-36258
- Transient response of leading-edge vortices to localized suction p 556 A90-36279
- Experimental study of incompressible flow on the upper surface of a delta wing p 558 A90-37346
- Large-amplitude high-rate roll oscillation system for the measurement of non-linear airloads [AIAA PAPER 90-1426] p 590 A90-37963
- Pneumatic vortex flow control on a 55-degree cropped delta wing with chined forebody [AIAA PAPER 90-1430] p 559 A90-37967
- Unsteady aerodynamic loading produced by a sinusoidally oscillating delta wing [AIAA PAPER 90-1536] p 564 A90-38680
- Unsteady Navier-Stokes solutions for a low aspect ratio delta wing [AIAA PAPER 90-1538] p 564 A90-38682
- Application of vortex embedding to aircraft flows [AIAA PAPER 90-1626] p 568 A90-38755
- Flow structure generated by oscillating delta-wing segments p 622 A90-40694
- An experimental study of the nonlinear dynamic phenomenon known as wing rock [AIAA PAPER 90-2812] p 753 A90-45152
- Delta wing surface pressures for high angle of attack maneuvers [AIAA PAPER 90-2813] p 711 A90-45153
- Numerical simulation of the effects of variation of angle of attack and sweep angle on vortex breakdown over delta wings [AIAA PAPER 90-3000] p 788 A90-45850
- Numerical simulation of vortical flows over a strake-delta wing and a close coupled delta-canard configuration [AIAA PAPER 90-3002] p 788 A90-45851
- Numerical simulation of vortical flows over close-coupled canard-wing configuration [AIAA PAPER 90-3003] p 788 A90-45852
- A computational study of incipient leading-edge separation on a 65-deg delta wing at $M = 1.60$ [AIAA PAPER 90-3029] p 791 A90-45871
- Rapid prediction of slender-wing aircraft dynamics [AIAA PAPER 90-3037] p 791 A90-45876
- Effect of leading edge roundness on a delta wing in wing-rock motion [AIAA PAPER 90-3080] p 795 A90-45911
- Numerical study of vortical flow over a sideslipping delta wing [AIAA PAPER 90-3001] p 798 A90-45936
- Self-induced roll oscillations of lifting systems with thin delta wings p 860 A90-46570
- Unsteady aerodynamics of delta wings, undergoing ramp-maneuvering in pitch to post-stall angle of attack p 806 A90-46857
- Numerical simulation of steady and unsteady vortical flows around wings and bodies p 806 A90-46869
- Computational and experimental studies on ground effect of a slender wing tailless delta aircraft p 810 A90-48083
- Application of a vortex lattice numerical model in the calculation of inviscid incompressible flow around delta wings p 904 A90-51017
- Theoretical prediction of pressure distribution on wedged delta wing at higher supersonic Mach numbers and its agreement with experimental results p 907 A90-51537
- Prediction of pressure distribution on optimum-optimum delta wing at higher angles of attack in supersonic flow and its agreement with experimental results p 907 A90-51538
- An integrated CFD/experimental analysis of aerodynamic forces and moments [NASA-TM-102195] p 18 N90-10006
- The three-dimensional vortex sheet structure on delta wings p 19 N90-10367
- Unsteady aerodynamics with applications to flight mechanics [AD-A211944] p 89 N90-11706
- Experimental transonic flutter characteristics of two 72 deg-sweep delta-wing models [NASA-TM-101659] p 175 N90-14205
- Flows with Separation [DGLR-PAPERS-88-05] p 276 N90-16169
- Flow field visualization study on a 65 deg delta wing at $M = 0.85$ p 277 N90-16182
- Research on three different Euler's schemes applied to a delta wing with vortical flows p 278 N90-16184
- Force and moment measurements on delta wings in unsteady flow p 278 N90-16185
- Numerical simulation of the laminar and turbulent three dimensional flow on a delta wing with sharp leading edge p 278 N90-16186
- Controlled vortical flow on delta wings through unsteady leading edge blowing [NASA-CR-186267] p 316 N90-16712
- An experimental study of the effect of streamwise vortices on unsteady turbulent boundary-layer separation p 369 N90-17045
- Surface pressure distributions on a delta wing undergoing large amplitude pitching oscillations [NASA-CR-186326] p 317 N90-17558
- Numerical simulation of compressible vortices [AD-A216221] p 371 N90-18017
- Unsteady aerodynamics of delta wings performing maneuvers to high angle of attack p 398 N90-19196
- Leading edge vortex dynamics on a pitching delta wing [NASA-CR-186327] p 398 N90-19198
- A streamwise upwind algorithm applied to vortical flow over a delta wing [NASA-TM-102225] p 398 N90-19201
- Conical Euler solution for a highly-swept delta wing undergoing wing-rock motion [NASA-TM-102609] p 400 N90-19211
- A video-based experimental investigation of wing rock [AD-A218244] p 498 N90-20075
- Experimental and numerical investigation of the vortex flow over a sharp edged delta wing; with and without sideslip [PB90-167131] p 481 N90-20964
- Prediction of forces and moments for flight vehicle control effectors. Part 2: An analysis of delta wing aerodynamic control effectiveness in ground effect [NASA-CR-186572] p 571 N90-21735
- A video-based experimental investigation of wing rock p 592 N90-21771
- An experimental and theoretical investigation of the flow over plane delta wings with supersonic leading edges [LR-588] p 717 N90-25114
- Investigation of the vortex flow over a sharp-edged delta wing in the transonic speed regime [LR-594] p 717 N90-25115
- Experimental study on vortex and shock wave development on a 65 deg delta wing [NLR-MP-88033-U] p 720 N90-25950
- Experiments with unsteady, free surface, three-dimensional vortices in a thermally stable, stratified fluid [AD-A222088] p 815 N90-26796
- Experimental investigations on the stability and vorticity of the vortex breakdown phenomenon above delta wings, measured by the ultrasonic laser method [ESA-TT-1079] p 910 N90-28498
- Control of vortex aerodynamics at high angles of attack p 921 N90-28523
- The steady and time-dependent aerodynamic characteristics of a combat aircraft with a delta or swept canard p 921 N90-28526
- The aerodynamic design of the oblique flying wing supersonic transport [NASA-CR-177552] p 923 N90-28540
- The DELTA MONSTER: An RPV designed to investigate the aerodynamics of a delta wing platform [NASA-CR-186226] p 924 N90-29381
- DEMODULATORS**
- Multiple channel frequency demodulator p 69 A90-12190
- DENSITOMETERS**
- Development of an X-ray backscatter densitometer for measurement of freestream density during hypersonic flight [AIAA PAPER 90-1384] p 604 A90-37933
- DENSITY DISTRIBUTION**
- Measurement of mean and fluctuating flow properties in hypersonic shear layers [AIAA PAPER 90-1409] p 560 A90-38488
- DEOXIDIZING**
- Chrome free electrolytic deoxidizer for aluminum p 956 A90-50216
- DEPENDENT VARIABLES**
- A nonlinear aircraft tracking filter utilizing control variable estimation [AIAA PAPER 90-3402] p 822 A90-47657
- DEPLOYMENT**
- Yaw fin deployment apparatus for ejection seat [AD-D014512] p 723 N90-25118
- The effect of rapid spoiler deployment on the transient forces on an aerofoil p 921 N90-28527
- DEPOSITION**
- Mesoscale acid deposition modeling studies [NASA-CR-4262] p 140 N90-13228
- Development of a computational fluid dynamics and chemistry model for the fouling of jet fuels [DE90-005664] p 608 N90-22003
- Development of a mathematical model for the thermal decomposition of aviation fuels [AD-A221673] p 875 N90-26994
- DEPOSITS**
- Development of a mathematical model for the thermal decomposition of aviation fuels [AD-A221673] p 875 N90-26994
- DERIVATION**
- Incompressible flow about ellipsoids of revolution [REPT-88-02] p 90 N90-11713
- DESCENT**
- Piloted simulation of a ground-based time-control concept for air traffic control [NASA-TM-101085] p 240 N90-15898
- Optimal control of an aircraft flying through a downburst p 591 N90-21765
- A conflict analysis of 4D descent strategies in a metered, multiple-arrival route environment [NASA-CR-182019] p 593 N90-21772
- Dynamic ground effects p 922 N90-28531
- DESCENT TRAJECTORIES**
- Optimal autorotational descent of a helicopter with control and state inequality constraints p 756 A90-45344
- DESCRIPTIVE GEOMETRY**
- Rotary-Jet thrust augmentor with jet-flapped blades p 633 N90-24243
- DESIGN ANALYSIS**
- Linking artificial intelligence (AI) and computer aided engineering (CAE) to analyze the testability of electronic designs [AIAA PAPER 89-3070] p 74 A90-10559
- Fundamentals of turbine design for aircraft engines --- Russian book p 40 A90-10839
- Advances in computational design and analysis of airbreathing propulsion systems p 43 A90-12502
- Design for maintainability [SAE PAPER 891079] p 81 A90-14371
- Smoothing the way to future designs - A new technique for wind-tunnel measurements p 121 A90-15873
- The design and study of the information transfer mechanism for a distributed avionics system p 207 A90-16858
- Sensitivity and optimization of composite structures in MSC/NASTRAN p 208 A90-17370
- New progress in airframe durability requirements p 246 A90-22001
- Cockpit evolution in Airbus p 247 A90-22434
- Numerical optimization of axial compressor designs [ASME PAPER 89-GT-14] p 340 A90-23758
- A proposal for optimized design of multistage compressors [ASME PAPER 89-GT-34] p 288 A90-23766
- A methodology proposal to design and analyse counterrotating high speed propellers [ASME PAPER 89-GT-38] p 340 A90-23767

Optimum weight design of a rotor bearing system with dynamic behavior constraints
[ASME PAPER 89-GT-74] p 358 A90-23795

A three dimensional inverse method in turbomachinery. II - Experimental verification
[ASME PAPER 89-GT-137] p 360 A90-23834

Verification of an impeller design by laser measurements and 3D-viscous flow calculations
[ASME PAPER 89-GT-159] p 292 A90-23847

A comparison between engine test results and design predictions of turbine blade cooling performance
[ASME PAPER 89-GT-169] p 341 A90-23854

Axial flow compressor design optimization. I - Pitchline analysis and multivariable objective function influence
[ASME PAPER 89-GT-201] p 342 A90-23873

An off-design loss and deviation prediction study for transonic axial compressors
[ASME PAPER 89-GT-324] p 343 A90-23893

Laminar flow control leading-edge systems in simulated airline service
p 335 A90-26134

Adaptive wall wind tunnels - Marriage between experiments and computations
p 351 A90-26351

AIAA/ASME/ASCE/AHS/ASC Structures, Structural Dynamics and Materials Conference, 31st, Long Beach, CA, Apr. 2-4, 1990, Technical Papers, Part 1 - Materials, engineering optimization and design p 449 A90-29226

Exploratory design studies using an integrated multidisciplinary synthesis capability for actively controlled composite wings
[AIAA PAPER 90-0953] p 411 A90-29238

Influence of structural and aerodynamic modeling on flutter analysis
[AIAA PAPER 90-0954] p 411 A90-29239

Turbine combustor preliminary design approach
p 508 A90-32966

An analytical sensitivity method for use in integrated aeroservoelastic aircraft design
p 517 A90-33405

T2 ability concerning model design and instrumentation in short run processing
p 524 A90-34241

Development of cryogenic instrumentation for ETW models
p 525 A90-34251

Design and operational features of low-disturbance wind tunnels at NASA Langley for Mach numbers from 3.5 to 18
[AIAA PAPER 90-1391] p 594 A90-37936

Development of the jet-swirl high loading combustor
[AIAA PAPER 90-2451] p 658 A90-40633

Cryogenic wind tunnels
p 673 A90-41726

Toward total quality in industry
p 684 A90-41768

Design and performance of a small, high speed axial compressor
[AIAA PAPER 90-1911] p 624 A90-41983

Multiple swirler dome combustor for high temperature rise applications
[AIAA PAPER 90-2159] p 661 A90-42050

On- and off-design performance analysis of hypersonic detonation wave ramjets
[AIAA PAPER 90-2473] p 664 A90-42188

A novel synthetic method for studying nonlinear flight stability
p 645 A90-42355

Application of 3-D flow analysis to the design of a high work transonic turbine
p 628 A90-42395

Preliminary design and analysis of propellers
p 645 A90-42407

Flight tests to explore tail rotor limitations in the low speed envelope
p 647 A90-42498

Application of sweep to improve the efficiency of a transonic fan. I - Design
[AIAA PAPER 90-1915] p 741 A90-42695

Suppression of 'Buzz' instability by geometrical design of the flameholder
[AIAA PAPER 90-1966] p 741 A90-42706

Task-oriented display design - Concept and example
[SAE PAPER 892230] p 738 A90-45446

Conceptual design and feasibility study of very large passenger aircraft
[AIAA PAPER 90-3220] p 834 A90-48841

Multi-role advance technology rotorcraft - The EH101
[AIAA PAPER 90-3302] p 837 A90-48884

Taguchi methods in conceptual design for life cycle cost
[AIAA PAPER 90-3222] p 839 A90-49109

Selected design issues of some high speed rotorcraft concepts
[AIAA PAPER 90-3297] p 840 A90-49125

ATF prototypes outstrip F-15 in size and thrust
p 841 A90-49477

A design method for turbomachinery blading in three-dimensional flow
p 904 A90-51003

At a depth of 500 meters - The TU Dresden supersonic wind tunnel
p 937 A90-52700

Large scale prop-fan structural design study. Volume 1: Initial concepts
[NASA-CR-174992] p 52 N90-10043

Large scale prop-fan structural design study. Volume 2: Preliminary design of SR-7
[NASA-CR-174993] p 52 N90-10044

Full scale technology demonstration of a modern counterrotating unducted fan engine concept. Design report
[NASA-CR-180867] p 53 N90-10048

Integrated multidisciplinary design optimization of rotorcraft
[NASA-TM-101642] p 36 N90-10889

An assessment of robustness of flight control systems based on variable structure techniques
p 57 N90-10895

Viscoelastic tuned dampers for control of structural dynamics
p 73 N90-10999

Performance and quality of a wing type parachute: Parametric analysis
[REPT-88-19] p 89 N90-11710

Development of direct-inverse 3-D methods for applied transonic aerodynamic wing design and analysis
[NASA-CR-186036] p 103 N90-11733

Blading design for multi-storage HP compressor
[PNR90602] p 116 N90-12616

Performance of a highly-loaded HP compressor
[RAE-TM-P-1149] p 256 N90-15919

Numerical solutions of the linearized Euler equations for unsteady vortical flows around lifting airfoils
[NASA-TM-102466] p 318 N90-17562

Research on a two-dimensional inlet for a supersonic V/STOL propulsion system. Appendix A
[NASA-CR-174945] p 396 N90-18364

Aerodynamic analysis of a US Navy and Marine Corps unmanned air vehicle
[AD-A218282] p 498 N90-20077

The NASA digital VGH program: Exploration of methods and final results. Volume 4: B 747 data 1978-1980, 1689 hours
[NASA-CR-181909-VOL-4] p 506 N90-20083

An application process for dynamic balancing of turbomachinery shafting
[NASA-TM-102537] p 541 N90-20392

Plan, formulate, and discuss a NASTRAN finite element model of the UH-60A helicopter airframe
[NASA-CR-181975] p 541 N90-20439

Design of a natural laminar flow airfoil for an unmanned aircraft
[PD-CF-9004] p 499 N90-20975

Aerodynamic design techniques at DLR Institute for Design Aerodynamics
p 500 N90-20979

Inverse design of airfoil contours: Constraints, numerical method, and applications
p 500 N90-20980

An efficient airfoil design method using the Navier-Stokes equations
p 500 N90-20981

A system for transonic wing design with geometric constraints based on an inverse method
p 501 N90-20983

A fast collocation method for transonic airfoil design
p 501 N90-20984

Subsonic and transonic blade design by means of analysis codes
p 510 N90-20985

A computational design method for shock free transonic cascades and airfoils
p 501 N90-20986

Inverse computation of transonic internal flows with application for multi-point-design of supercritical compressor blades
p 501 N90-20987

An inverse method for the design of turbomachine blades
p 511 N90-20988

Application of an inverse method to the design of a radial inflow turbine
p 511 N90-20989

Aerodynamic optimization by simultaneously updating flow variables and design parameters
p 501 N90-20991

Numerical optimization of target pressure distributions for subsonic and transonic airfoil design
p 502 N90-20993

A tool for automatic design of airfoils in different operating conditions
p 502 N90-20994

The use of numerical optimization for helicopter airfoil and blade design
p 502 N90-20995

Aerodynamic design by optimization
p 502 N90-20996

Numerical optimization of wings in transonic flow
p 502 N90-20997

Aerodynamic design via control theory
p 546 N90-20998

Optimization of aerodynamic designs using computational fluid dynamics
p 541 N90-20999

Conceptual design optimization study
[NASA-CR-4298] p 582 N90-21755

Aircraft crash survival design guide. Volume 1: Design criteria and checklists
[AD-A218434] p 575 N90-22545

Multilevel decomposition approach to the preliminary sizing of a transport aircraft wing
[NASA-CR-4296] p 583 N90-22557

Supersonic flow computations for an ASTOVL aircraft configuration, phase 2, part 2
[NASA-CR-4284] p 610 N90-22746

Integrated control-system design via generalized LQG (GLQG) theory
p 613 N90-23023

Application of numerical optimization techniques to control system design for nonlinear dynamic models of aircraft
p 593 N90-23032

Nonflammable hydraulic power system for tactical aircraft. Volume 1: Aircraft system definition, design and analysis
[AD-A218493] p 671 N90-23409

An approach for design and analysis of composite rotor blades
[AD-A219257] p 734 N90-25125

Ground shake test of the UH-60A helicopter airframe and comparison with NASTRAN finite element model predictions
[NASA-CR-181993] p 758 N90-25143

A computational efficient modelling of laminar separation bubbles
[NASA-CR-186729] p 774 N90-25291

Calculation of flight vibration levels of the AH-1G helicopter and correlation with existing flight vibration measurements
[NASA-CR-182031] p 775 N90-25375

Prediction methodologies for nonlinear aerodynamic characteristics of control surfaces
[NIAR-90-17] p 718 N90-25937

Background, current status, and prognosis of the ongoing slush hydrogen technology development program for the NASP
[NASA-TM-103220] p 763 N90-26055

A computer module used to calculate the horizontal control surface size of a conceptual aircraft design
[NASA-CR-186872] p 780 N90-26515

Lessons learned from the T-46A durability and damage tolerance program
p 842 N90-26812

Finite element models of USAF aircraft structures
p 844 N90-26820

Device for the dilution of hot exhaust jets
[ETN-90-97435] p 858 N90-27723

Energy Efficient Engine integrated core/low spool test hardware design report
[NASA-CR-168137] p 931 N90-28566

Energy Efficient Engine: High-pressure compressor test hardware detailed design report
[NASA-CR-180850] p 932 N90-28570

Development of a thickness design procedure for stabilized layers under rigid airfield pavements
[DOT/FAA/RD-90/22] p 937 N90-28582

A knowledge-based system design/information tool
[NASA-CR-4316] p 965 N90-29143

An enhanced integrated aerodynamic load/dynamic optimization procedure for helicopter rotor blades
[NASA-CR-4326] p 924 N90-29383

Aircraft design for mission performance using nonlinear multiobjective optimization methods
[NASA-CR-4328] p 925 N90-29384

DESIGN TO COST

Cost effective technology --- CAD/CAM techniques for aircraft engines
p 188 A90-17447

Potential application of automotive fatigue technology in rotorcraft design
p 681 A90-39987

Automated aircraft engine costing using artificial intelligence
[AIAA PAPER 90-1887] p 660 A90-41981

The Franco-German helicopter programme HAP, PAH-2/HAC
p 618 A90-42478

GTPDP - A rotary wing aircraft preliminary design and performance estimation program including optimization and cost
p 830 A90-46944

Fighter design econometrics = ownership affordability?
[AIAA PAPER 90-3223] p 897 A90-48842

DESTRUCTIVE TESTS

Towards a unified method of causing impact damage in thick laminated composites
p 946 A90-50168

Floor pull test of a transport airframe section
[DOT/FAA/CT-TN88/14] p 497 N90-20072

DETECTION

Relative merits of reactive and forward-look detection for wind-shear encounters during landing approach for various microburst escape strategies
[NASA-TM-4158] p 259 N90-15108

Inspection development for T-37 wing spar cap lug
[AD-A214826] p 287 N90-16708

Formulation and verification of a technique for compensation of pneumatic attenuation errors in airborne pressure sensing devices
p 369 N90-17084

Analysis and test of a wide angle spectrometer
[AD-A215819] p 372 N90-18030

Device for quickly sensing the amount of O₂ in a combustion product gas
[NASA-CASE-LAR-13816-1] p 609 N90-22025

- A comparison of lightning network data with surface weather observations
[AD-A220003] p 692 N90-23832
- Neural networks for detecting defects in aircraft structures
[IAR-90-4] p 777 N90-26345
- DETERIORATION**
- The analysis and solution of the performance deterioration problem of WP7 engine under the full reheating condition p 191 A90-18624
- Applications of digital image processing in testing and evaluation of composite materials
[AD-A222939] p 874 N90-26887
- DETONABLE GAS MIXTURES**
- Operation of the ram accelerator in the transdetonative velocity regime
[AIAA PAPER 90-1985] p 741 A90-42712
- A study of the electrophysical phenomena in the combustion chambers of jet engines p 765 A90-45028
- DETONATION**
- Canopy fragilization using embedded detonating cord p 180 A90-17417
- DETONATION WAVES**
- Aerodynamic and propulsive performance of hypersonic detonation wave ramjets p 49 A90-12609
- Numerical simulations of an oblique detonation wave engine p 508 A90-32964
- On- and off-design performance analysis of hypersonic detonation wave ramjets
[AIAA PAPER 90-2473] p 664 A90-42188
- DEVIATION**
- Radio deviation of airborne goniometers --- Russian book p 242 A90-22733
- The effects of compressor and wall flow on airfoil incidence and deviation p 512 N90-21011
- DHC 2 AIRCRAFT**
- Stability and control derivatives of the De Havilland DHC-2 BEAVER aircraft
[PB89-217525] p 119 N90-11754
- DIAGNOSIS**
- An adaptive-learning expert system for maintenance diagnostics p 460 A90-30754
- The IMIS F-16 interactive diagnostic demonstration p 383 A90-30768
- Advanced technology ATE for fuel accessory testing p 439 A90-30770
- Gear noise, vibration, and diagnostic studies at NASA Lewis Research Center
[NASA-TM-102435] p 372 N90-18041
- Convex models of malfunction diagnosis in high performance aircraft
[AD-A218514] p 702 N90-25073
- DIAMETERS**
- Effect of reduced aft diameter and increased blade number of high-speed counterrotation propeller performance
[AIAA PAPER 89-0438] p 234 A90-23650
- Effect of reduced aft diameter and increased blade number on high-speed counterrotation propeller performance
[NASA-TM-102077] p 172 N90-13352
- DICTIONARIES**
- A glossary of terms, definitions, acronyms, and abbreviations related to the National Airspace System
[DOT/FAA/CT-TN89/53] p 967 N90-29249
- DIES**
- Characterization of the 7175 T7352. Dissection of a die casting standard spar
[CEAT-PV-M5/528900] p 877 N90-27906
- Characterization of the 7175 T7352 101. Dissection of a die casting standard spar
[CEAT-PV-M5/5288] p 877 N90-27907
- DIESEL ENGINES**
- The variable cycle diesel as an aircraft engine
[SAE PAPER 891065] p 110 A90-14365
- Two-dimensional analysis of two-phase reacting flow in a firing direct-injection diesel engine
[NASA-TM-102069] p 194 N90-13392
- A simulation code for turbocompound diesel engines
[IAR-89-26] p 774 N90-25348
- DIFFERENCE EQUATIONS**
- Implicit flux-split schemes for the Euler equations p 602 A90-36254
- The MDE method for aircraft cabin interior noise prediction --- matrix difference equation
[SAE PAPER 892372] p 782 A90-45519
- Compressible Navier-Stokes solutions over low Reynolds number airfoils p 802 A90-46382
- DIFFERENTIAL EQUATIONS**
- Boundary element solution of the transonic integro-differential equation p 383 A90-27947
- Numerical solutions of the linearized Euler equations for unsteady vortical flows around lifting airfoils p 394 A90-30264
- Numerical solutions of the linearized Euler equations for unsteady vortical flows around lifting airfoils
[NASA-TM-102466] p 318 N90-17562
- Adaptive grid embedding for the two-dimensional flux-split Euler equations
[NASA-CR-186533] p 547 N90-21571
- Application of a dynamic stall model to rotor trim and aeroelastic response p 583 N90-22556
- Time-optimal aircraft pursuit-evasion with a weapon envelope constraint
[NASA-CR-186640] p 734 N90-25126
- The discretization of the three dimensional boundary layer equations p 884 N90-27987
- [ETN-90-97292]
- DIFFERENTIAL GEOMETRY**
- Differential-geometrical technique of signal transformation and estimation of position, rate and acceleration parameters using supplementary data sources p 638 A90-41004
- DIFFERENTIAL INTERFEROMETRY**
- Remote detection of boundary-layer transition by an optical system p 139 N90-12524
- DIFFERENTIAL PRESSURE**
- The Meteorological Measurement System on the NASA ER-2 aircraft p 926 A90-51658
- DIFFUSERS**
- Comparative cascade studies of some high diffusion compressor bladings p 15 A90-12637
- Variable-velocity flow at the initial mixing section in a diffuser channel p 84 A90-14563
- Application of low-solidity cascade diffuser to transonic centrifugal compressor
[ASME PAPER 89-GT-66] p 290 A90-23789
- A new design method for centrifugal compressor vaned diffusers
[ASME PAPER 89-GT-156] p 292 A90-23844
- Effect of the design of a diffuser with tangential injection on the starting and separation ratios of pressures p 295 A90-24099
- Aeroelastic deformation of a crescent-shaped rigid support in the diffuser chamber of a wind tunnel p 364 A90-24112
- Effect of condensation in a diffuser on the flow field p 603 A90-36784
- Wide angle diffusers with passive boundary-layer control
[AIAA PAPER 90-1600] p 567 A90-38732
- The normal shock generator - An inlet throat region research apparatus for high Mach applications
[AIAA PAPER 90-1930] p 759 A90-42698
- Measurements in an annular combustor-diffuser system
[AIAA PAPER 90-2162] p 768 A90-42740
- Parametric evaluation of the aerodynamic performance of an annular combustor-diffuser system
[AIAA PAPER 90-2163] p 742 A90-42741
- DIFFUSION**
- Viscous flow in a controlled diffusion compressor cascade with increasing incidence
[ASME PAPER 89-GT-131] p 291 A90-23829
- Some observations on transitory stall in conical diffusers
[NASA-TM-102387] p 94 N90-12561
- DIFFUSION COEFFICIENT**
- Moisture absorption in graphite/epoxy laminates p 951 A90-52799
- DIFFUSION FLAMES**
- Flame extinction in compressible flow p 883 N90-26899
- Raman scattering measurements using UV excimer lasers p 874 N90-26902
- DIFFUSION WELDING**
- Diffusion bonding aeroengine components p 131 A90-16012
- Study on SPF and SPF/DB of the bulk-head structure with nonsymmetric shape p 132 A90-16619
- SPF/DB takes off p 208 A90-17293
- Reflection by defective diffusion bonds
[AD-A212995] p 206 N90-13638
- Diffusion bonding of metals p 206 N90-14330
- DIGITAL COMMAND SYSTEMS**
- Recent activities within the aeroservoelasticity branch at the NASA Langley Research Center p 492 A90-33400
- DIGITAL COMPUTERS**
- Laboratory test methodology for evaluating the effects of electromagnetic disturbances on fault-tolerant control systems
[NASA-TM-101665] p 217 N90-14061
- Synthesis of control law, on a RPV, in order to minimize the number of sensors p 260 N90-15925
- Conceptual design for aerospace vehicles p 651 N90-25043
- Control and estimation for aerospace applications with system time delays p 918 N90-29367
- DIGITAL DATA**
- A real-time wind model using digital data from aircraft
[RSRE-MEMO-4309] p 137 N90-13005
- Survivable penetration p 917 N90-29363
- DIGITAL ELECTRONICS**
- Trends in avionics - From analog black boxes to integrated digital avionics systems p 252 A90-23245
- Adaptive elective fuel control test techniques p 421 A90-28168
- High-temperature electronics for aircraft engines
[AIAA PAPER 90-2035] p 657 A90-40604
- Digital servomechanism for the tachometer of the M 602 engine p 737 A90-44722
- A real time microcomputer implementation of sensor failure detection for turbofan engines p 745 A90-45414
- Advanced detection, isolation, and accommodation of sensor failures in turbofan engines: Real-time microcomputer implementation
[NASA-TP-2925] p 259 N90-15112
- Energy Efficient Engine: Control system preliminary definition report
[NASA-CR-179578] p 932 N90-28569
- DIGITAL FILTERS**
- Range determination in a multipath prone environment p 877 A90-45960
- In-flight experiments on the active control of propeller-induced cabin noise p 893 A90-46352
- DIGITAL NAVIGATION**
- F-16/GPS integration test results p 726 A90-43710
- Loran-C/GPS Interoperable Computerized Algorithms (LOGICAL) p 823 A90-49494
- Development of an automatic ground collision avoidance system using a digital terrain database
[AD-A216247] p 329 N90-17621
- DIGITAL RADAR SYSTEMS**
- Advances in primary-radar technology p 241 A90-21380
- Wind shear detection with pencil-beam radars p 279 A90-21386
- Data Link Processor (DLP) operational test and evaluation/integration test plan
[DOT/FAA/CT-TN89/32] p 214 N90-14404
- DIGITAL SIMULATION**
- Numerical simulation of reversed flow over a supersonic delta wing at high angle of attack
[AIAA PAPER 89-1802] p 8 A90-11849
- Numerical simulation of supersonic and hypersonic turbulent compression corner flows using PNS equations p 85 A90-15242
- Numerical simulation of an impinging jet on a flat plate p 86 A90-15821
- Results from a numerical simulation of an F-16A configuration at a supersonic Mach number p 146 A90-16769
- A numerical study of mixing and chemical heat release in supersonic mixing layers
[AIAA PAPER 90-0152] p 163 A90-19710
- Numerical simulation of transonic wing flows using a zonal Euler, boundary-layer, Navier-Stokes approach p 225 A90-21596
- Simulation and analysis of a delta planform with multiple jets in ground effect
[AIAA PAPER 90-0299] p 228 A90-22195
- Topology of computed incompressible three-dimensional separated flow field around high-angle-of-attack cone-cylinders p 366 A90-25764
- Numerical simulation of an F-16A at angle of attack
[AIAA PAPER 90-0100] p 313 A90-26911
- A numerical study of transverse jets into supersonic flows and influence of pressure waves
[AIAA PAPER 90-0733] p 314 A90-26985
- Digital simulation of flight control systems for post-stall aircraft p 431 A90-30704
- Numerical simulation of separated flow around two-dimensional wing section by a discrete vortex method p 469 A90-32067
- Capability of current supercomputers for the computational fluid dynamics p 546 A90-34382
- Alternate table look-up routine for real-time digital flight simulation p 611 A90-35769
- Digital generation of two-dimensional field of turbulence for flight simulation p 611 A90-36427
- Study of compressibility effects in mixing layer by numerical simulation
[AIAA PAPER 90-1464] p 562 A90-38621
- Numerical simulation of flow through the Langley parametric scramjet engine
[SAE PAPER 892314] p 747 A90-45476
- Numerical simulation of steady and unsteady vortical flows around wings and bodies p 806 A90-46869
- Numerical simulations of three-dimensional rotor blade-vortex interactions p 807 A90-46879
- Numerical simulation of wakes with application to blade-vortex interaction p 807 A90-46881

- Effects of transition on wind tunnel simulation of vehicle dynamics p 870 A90-49273
- Numerical simulation of nonreactive flows in turbomachines p 908 A90-52621
- Numerical simulation of leading-edge vortex rollup and bursting p 20 N90-10831
- A robust digital model following controller for helicopters [ESA-TT-1041] p 120 N90-12621
- Aircraft response and pilot behaviour during a wake vortex encounter perpendicular to the vortex axis p 259 N90-15057
- Flows with Separation [DGLR-PAPERS-88-05] p 276 N90-16169
- Numerical simulation of the laminar and turbulent three dimensional flow on a delta wing with sharp leading edge p 278 N90-16186
- Direct numerical simulation of aerodynamic noise [AD-A214122] p 379 N90-18225
- Flow simulation for aircraft [NLR-MP-87082-U] p 455 N90-19543
- Comparison of C- and O-grid generation methods using a NACA 0012 airfoil [AD-A216375] p 479 N90-20948
- Numerical flow simulation and supercomputers: More than a digital wind tunnel p 612 N90-22976
- The automation management to support research and development p 612 N90-22978
- The development of a system for the numerical simulation of Euler flows p 612 N90-22980
- Numerical simulations of the structure of supersonic shear layers [AD-A224164] p 960 N90-29587
- DIGITAL SYSTEMS**
- Signal processing in a digital GPS receiver p 128 A90-14006
- An adaptive flight control system design for non-minimum phase CCV by relative order reduction p 196 A90-19428
- Digital electronic control unit for the European Fighter Aircraft (EFA) p 253 A90-21607
- Embedded digital control for aircraft environmental control systems - A practical vehicle management system approach [SAE PAPER 891438] p 339 A90-27409
- A preliminary evaluation of an F100 engine parameter estimation process using flight data [AIAA PAPER 90-1921] p 656 A90-40559
- Full authority digital electronic engine control system provides needed reliability [AIAA PAPER 90-2037] p 658 A90-40606
- Digital autopilot for light aircraft p 653 A90-41741
- Synthesis of optimal multidimensional digital systems for the simulation of the angular motions of a flight vehicle under random loading p 669 A90-41957
- Digital map reader for helicopters p 653 A90-42448
- The Super Puma MKII automatic flight control system p 669 A90-42449
- Main characteristics of an integrated flight and display system for AS MKII Super-Puma p 653 A90-42450
- Flight test results of a complex precise digital flight control system p 35 N90-10870
- Applications of flight control system methods to an advanced combat rotorcraft [NASA-TM-101054] p 119 N90-11752
- Advanced actuation systems development, volume 1 [AD-A213334] p 121 N90-12624
- Advanced actuation systems development, volume 2 [AD-A213378] p 198 N90-13398
- A knowledge-based flight status monitor for real-time application in digital avionics systems [NASA-TM-101710] p 217 N90-13995
- Development of the triplex digital flight control system of the STOL research aircraft ASKA [NAL-TR-1013] p 349 N90-17640
- The Advanced Digital-Optical Control System (ADOCS) user demonstration program [AD-A215984] p 349 N90-17644
- Digital-flutter-suppression-system investigations for the active flexible wing wind-tunnel model [NASA-TM-102618] p 520 N90-20093
- Applications of digital image processing in testing and evaluation of composite materials [AD-A222939] p 874 N90-26887
- Development and testing of methodology for evaluating the performance of multi-input/multi-output digital control systems [NASA-TM-102704] p 846 N90-27699
- A conceptual framework for fighter flight control systems [PD-CF-9009] p 936 N90-28577
- A digital controller for active aeroelastic controls [NAL-TR-1014] p 936 N90-29402
- DIGITAL TECHNIQUES**
- Aircraft interface with the future ATC system p 331 A90-25574

- Digital X-ray inspection p 445 A90-28162
- Operating principles of a terrain-recognition air navigation system p 403 A90-29655
- An optically interfaced propulsion management system applied to a commercial transport aircraft p 424 A90-30811
- Design of digital self-selecting multivariable controllers for jet engines [AIAA PAPER 90-1875] p 655 A90-40541
- Digital control of magnetic bearings supporting a multimass flexible rotor p 682 A90-40712
- Onboard digital recording system for flight tests p 653 A90-41742
- Engine controls for the 1990's [PNR90546] p 114 N90-11748
- DIGITAL TRANSDUCERS**
- Fault tolerant architecture for a fly-by-light flight control computer p 860 A90-46931
- Data acquisition in aerodynamic research p 171 N90-13340
- DILUTION**
- Experimental studies of combustor dilution zone aerodynamics. I - Mean flowfields p 508 A90-32962
- Experimental studies of combustor dilution zone aerodynamics. II - Jet development p 659 A90-40947
- Mixing characteristics of dilution jets in small gas turbine combustors [AIAA PAPER 90-2728] p 664 A90-42217
- DIMENSIONAL ANALYSIS**
- Development and application of an optimization procedure for space and aircraft structures [MBB-FW-522/S/PUB-383] p 779 N90-25078
- A contribution to the economic, optimal dimensioning, and shaping of aircraft structures using a design model [ETN-90-96966] p 737 N90-25976
- DIRECT LIFT CONTROLS**
- Advanced material applications for direct lift engines [AIAA PAPER 90-2753] p 664 A90-42226
- Evaluation for DLC-Flap Monitoring System of the VSRA [NAL-TM-607] p 928 N90-29391
- DIRECTION FINDING**
- Generation of motion control for direction finders in a goniometer system p 187 A90-17137
- Optimization of complex data processing algorithms in multichannel radio direction finding p 576 A90-36115
- DIRECTIONAL CONTROL**
- Robustness of dynamic inversion vs mu synthesis - Lateral-directional flight control example [AIAA PAPER 90-3338] p 863 A90-47598
- DIRECTIONAL STABILITY**
- Yaw rate control of an air bearing vehicle p 435 N90-19420
- The effects of foreplanes on the static and dynamic characteristics of a combat aircraft model p 920 N90-28520
- DIRECTIVITY**
- Measurement resolution of noise directivity patterns from acoustic flight tests [NASA-TM-4134] p 79 N90-10679
- DIRICHLET PROBLEM**
- Inverse design of airfoil contours: Constraints, numerical method, and applications p 500 N90-20980
- DISCRETE ADDRESS BEACON SYSTEM**
- Aircraft Reply and Interference Environment Simulator (ARIES) hardware principles of operation, Volume 2: Appendixes [DOT/FAA/CT-TN88/4-2] p 135 N90-12781
- Aircraft Reply and Interference Environment Simulator (ARIES) hardware principles of operation, Volume 1 [DOT/FAA/CT-TN88/4-1] p 135 N90-12782
- DISCRETE FUNCTIONS**
- Convergence of the method of discrete vortices when applied to steady-state aerodynamics problems p 231 A90-22816
- Control point selection in the discrete vortex method p 470 A90-32567
- Discretization and model reduction for a class of nonlinear systems p 198 N90-13397
- The discretization of the three dimensional boundary layer equations [ETN-90-97292] p 884 N90-27987
- A digital controller for active aeroelastic controls [NAL-TR-1014] p 936 N90-29402
- DISCRIMINATION**
- Gas identification system using graded temperature sensor and neural net interpretation [AD-A213359] p 205 N90-13627
- DISKS (SHAPES)**
- Studies on supersonic radial flow behavior in disk channel p 87 A90-16104
- Probabilistic method to compute the optimal slip load for a mistuned bladed disk assembly with friction dampers p 507 A90-32269

- Slotted-wall research with disk and parachute models in a low-speed wind tunnel [AIAA PAPER 90-1407] p 595 A90-37946
- Coherent vortex structures in the wake of a sphere and a circular disk at rest and under forced vibrations p 623 A90-40749
- DISPERSION**
- MATE (Materials for Advanced Turbine Engines) Program, Project 3. Volume 2: Design, fabrication and evaluation of an oxide dispersion strengthened sheet alloy combustor liner [NASA-CR-180892] p 357 N90-17868
- DISPLACEMENT**
- Optimum design of composite wing structures subjected to displacement constraints p 680 A90-39276
- Self compensation of rigid displacements in holographic interferometry [ISL-CO-219/88] p 370 N90-17113
- DISPLACEMENT MEASUREMENT**
- Measurement of wind tunnel model deformation under airflow p 522 A90-33370
- Feasibility study of RADAC stereo optoelectronic model deformation measurement system for ETW p 539 A90-34239
- DISPLAY DEVICES**
- Design philosophy for a general aviation TCAS display --- Traffic Advisory and Collision Avoidance System [SAE PAPER 891052] p 108 A90-14354
- Two effective methods of approach and landing by visual display [SAE PAPER 891054] p 108 A90-14356
- Use of Computer-Aided Video Display technology in aviation weather litigation [AIAA PAPER 90-0373] p 216 A90-19821
- On-line temperature profile display system [ASME PAPER 89-GT-10] p 374 A90-23755
- Information display management in a pilot's associate p 418 A90-30238
- Toward the panoramic cockpit, and 3-D cockpit displays p 419 A90-30682
- A laser obstacle avoidance and display system p 419 A90-30694
- Data base correlation issues p 459 A90-30740
- Flight simulator evaluation of a dot-matrix display for presentation of approach map formats p 419 A90-30787
- Cognitive perspectives on map displays for helicopter flight p 419 A90-31329
- 3-D in pictorial formats for aircraft cockpits p 420 A90-31331
- Design and evaluation of a cockpit display for hovering flight p 490 A90-33059
- Cooperative synthesis of control and display augmentation in approach and landing p 516 A90-33061
- Three-dimensional measurement, display, and interpretation of fluid flow datasets p 679 A90-38854
- Flight testing and application of a Peripheral Vision Display p 652 A90-40381
- Taking a new look at cockpit vertical situation displays p 652 A90-40382
- Performance of full color active-matrix-LCD in the cockpit environment p 681 A90-40392
- Polysilicon active-matrix liquid crystal displays for cockpit applications p 681 A90-40393
- Multifunction displays optimized for viewability p 652 A90-40398
- New technology advances for brighter color CRT displays p 652 A90-40399
- The all glass helicopter cockpit p 653 A90-42447
- Main characteristics of an integrated flight and display system for AS MKII Super-Puma p 653 A90-42450
- Next-generation automatic test equipment for military support p 767 A90-42667
- Characteristics of 5x5 and 6x6 inch taut shadow mask CRTs for cockpit displays p 737 A90-45239
- Task-oriented display design - Concept and example [SAE PAPER 892230] p 738 A90-45446
- Dual servo optical projection system (SOPS) - A solution for two crewmember and night vision goggle display needs [SAE PAPER 892353] p 760 A90-45504
- Evaluation of the dynamic characteristics of a helicopter instrument panel p 829 A90-46499
- Flight-path display can improve safety, operational efficiency p 847 A90-48982
- 8 x 8-inch full color cockpit display p 927 A90-52953
- Classification and reduction of pilot error [NASA-CR-181867] p 24 N90-10014
- Flight simulator evaluation of a head-down display [NAL-TM-573] p 59 N90-10898
- Independent Orbiter Assessment (IOA): Analysis of the displays and controls subsystem [NASA-CR-185563] p 124 N90-11774

- Integration of a centralized multiplexed control unit into the cockpit of an aircraft
[F6150-DT410-1-88329] p 120 N90-12622
- A candidate concept for display of forward-looking wind shear information
[NASA-TM-101585] p 187 N90-14232
- Display interface concepts for automated fault diagnosis
[NASA-TM-101610] p 252 N90-15102
- Application of multifunction inertial reference systems to fighter aircraft
p 332 N90-16740
- A simulation evaluation of the engine monitoring and control system display
[NASA-TP-2960] p 420 N90-18393
- Three input concepts for flight crew interaction with information presented on a large-screen electronic cockpit display
[NASA-TM-4173] p 420 N90-18394
- The Real Time Display Builder (RTDB)
p 546 N90-20656
- Investigation of air transportation technology at the Massachusetts Institute of Technology, 1988-1989
p 484 N90-20922
- Cockpit display of hazardous wind shear information
p 484 N90-20924
- Cockpit display of hazardous weather information
p 485 N90-20929
- Stereopsis cueing effects on hover-in-turbulence performance in a simulated rotorcraft
[NASA-TP-2980] p 506 N90-21004
- Simulator comparison of thumbball, thumb switch, and touch screen input concepts for interaction with a large screen cockpit display format
[NASA-TM-102587] p 506 N90-21005
- Model-based method for terrain-following display design
[AD-A219302] p 583 N90-22563
- Simulator evaluation of the final approach spacing tool
[NASA-TM-102807] p 636 N90-23374
- Automatic speech recognition in air-ground data link
p 690 N90-25037
- Visualization of three dimensional data
p 782 N90-25553
- Qualitative evaluation of a conformal velocity vector display for use at high angles-of-attack in fighter aircraft
[NASA-TM-102629] p 739 N90-25981
- Knowledge-based system for flight information management
[NASA-TM-102685] p 780 N90-26511
- Cognitive requirements for aircraft navigation
[NASA-CR-186933] p 824 N90-26804
- The Canadian Aviation Safety Board's flight recorder facility
p 849 N90-27643
- Australian experience in flight recorder readout and analysis
p 820 N90-27644
- Economical graphics display system for flight simulation avionics
[NASA-CR-186886] p 849 N90-27701
- The interaction of chromostereopsis and stereopsis in stereoscopic CRT (Cathode Ray Tubes) displays
[AD-A217906] p 927 N90-28544
- Description of the primary flight display and flight guidance system logic in the NASA B-737 transport systems research vehicle
[NASA-TM-102710] p 927 N90-28546
- Counterair situation awareness display for Army aviation
p 964 N90-28982
- DISSIPATION**
Analysis and mitigation of numerical dissipation in inviscid and viscous computation of vortex-dominated flows
[NASA-CR-186887] p 776 N90-26281
- On central-difference and upwind schemes
[NASA-CR-182061] p 781 N90-26595
- DISTANCE**
Taxiway sign effectiveness under reduced visibility conditions
[DOT/FAA/CT-TN90/20] p 761 N90-25150
- DISTANCE MEASURING EQUIPMENT**
Image based range determination
[AIAA PAPER 90-3404] p 822 A90-47659
- DISTORTION**
Engine inlet distortion in a 9.2 percent scale vectored thrust STOVL model in ground effect
[NASA-TM-102358] p 318 N90-17561
- Free-field propagation of high intensity noise
[NASA-CR-186577] p 549 N90-21604
- DISTRIBUTED PARAMETER SYSTEMS**
Dynamic damping of vibrations in mechanical systems by means of elastic links with distributed parameters
p 139 A90-15568
- The design and study of the information transfer mechanism for a distributed avionics system
p 207 A90-16858
- Decentralized systems --- Book p 888 A90-46001
- Distributed control architecture for CNI preprocessors
p 917 N90-29356
- DISTRIBUTED PROCESSING**
Trends in telemetry front end architecture
[AIAA PAPER 89-3085] p 25 A90-10571
- Software fault tolerance analysis and testing for the Advanced Automation System
[AIAA PAPER 89-3124] p 75 A90-10600
- The design and study of the information transfer mechanism for a distributed avionics system
p 207 A90-16858
- Telemetry systems of the future
p 458 A90-28829
- A Distributed Artificial Intelligence approach to object identification and classification
p 545 A90-34185
- Real time data collection and control in a distributed simulator system using Ethernet TCP/IP
[SAE PAPER 892356] p 761 A90-45507
- Real-time simulation clock
[NASA-CASE-LAR-14056-1] p 689 N90-23713
- An automated calibration laboratory for flight research instrumentation: Requirements and a proposed design approach
[NASA-TM-101719] p 781 N90-26564
- Performance assessment of MIL-STD-1553B on the avionics systems demonstrator rig of British Aerospace
p 849 N90-27624
- DISTRIBUTION FUNCTIONS**
Analysis of distributions of Visual Meteorological Conditions (VMC) heliport data
[DOT/FAA/CT-TN89/67] p 544 N90-21508
- DITCHING (LANDING)**
An analytical technique for addressing airship ditching behavior
[AIAA PAPER 89-3167] p 238 A90-20589
- Escape and survival following helicopter ditching - Training aspects
p 722 A90-44658
- Escape and survival following helicopter ditching - Research aspects
p 722 A90-44659
- The human factors relating to escape and survival from helicopters ditching in water
[AGARD-AG-305(E)] p 176 N90-13358
- DIURNAL VARIATIONS**
Some characteristics of the meteorological conditions of low cloud formation around the Baku airport
p 888 A90-48364
- DIVERGENCE**
Aeroelastic analysis of a low aspect ratio wing
p 619 A90-38915
- DIVERGENT NOZZLES**
Numerical calculation of turbulent separated flows in an abruptly expanding channel
p 803 A90-46487
- Exhaust environment measurements of a turbofan engine equipped with an afterburner and 2D nozzle
[NASA-CR-4289] p 588 N90-21760
- DOORS**
The manufacture of SPF military aircraft doors in aluminium alloy --- superplastically formed
p 132 A90-16616
- Aircraft accident report, United Airlines Flight 811, Boeing 747-122, N4713U, Honolulu, Hawaii, February 24, 1989
[PB90-910401] p 574 N90-21748
- Aircraft evacuations: The effect of passenger motivation and cabin configuration adjacent to the exit
[CAA-PAPER-89019] p 913 N90-29336
- DOPED CRYSTALS**
The gas source molecular beam epitaxial growth of Al(x)Ga(1-x)P on (100) GaP
p 894 A90-48657
- DOPPLER EFFECT**
B-1B Doppler error compensation based on flight data analysis
p 404 A90-30790
- Integration and automation of navigation functions using Kalman filters
p 915 A90-52615
- DOPPLER NAVIGATION**
Prototype testing of an integrated Doppler/GPS navigation system
p 577 A90-36926
- Modern strapdown system for helicopter
p 653 A90-42451
- DOPPLER RADAR**
Terminal Doppler Weather Radar System - Wind shear detection will warn pilots of danger
p 25 A90-10462
- Advances in primary-radar technology
p 241 A90-21380
- Development of an automated windshear detection system using Doppler weather radar
p 373 A90-25567
- Advances in weather technology for the aviation system
p 373 A90-25572
- Microburst precursors observed with Doppler radar
p 456 A90-28613
- Range obscuration mitigation by adaptive PRF selection for the TDWR system --- Pulse Repetition Frequency for Terminal Doppler Weather Radar
p 456 A90-28617
- Convergence aloft as a precursor to microbursts
p 456 A90-28620
- Microburst divergence detection for terminal Doppler weather radar
p 456 A90-28625
- A powerful range-Doppler clutter rejection strategy for navigational radars
p 403 A90-30688
- Doppler-rate filtering for detecting moving targets with synthetic aperture radars
p 488 A90-34138
- Low-level windshear alert systems and Doppler radar in aircraft terminal operations
p 574 A90-35758
- Aviation meteorology - Panel report
p 692 A90-39403
- Range determination in a multipath prone environment
p 877 A90-45960
- Adaptive clutter rejection filters for airborne Doppler weather radar applied to the detection of low altitude windshear
[NASA-CR-186211] p 214 N90-14453
- Turbulence spectral widths view angle independence as observed by Doppler radar
[DOT/FAA/SA-89/2] p 281 N90-15566
- Advanced instrumentation for aircraft icing research
[NASA-CR-185225] p 506 N90-21006
- Airborne Doppler radar flight experiments for the detection of microbursts
p 542 N90-21243
- DORNIER AIRCRAFT**
Design criteria, constructions, and materials for the Dornier 328 airframe
p 246 A90-21610
- Low- and high-speed tests with the Dornier 328 wind-tunnel model
p 246 A90-21611
- Water borne again
p 579 A90-35846
- Dornier Composite Aircraft - Economical and faultless
p 732 A90-44751
- DOUGLAS AIRCRAFT**
Douglas aging aircraft programs
[SAE PAPER 892206] p 732 A90-45425
- Flight deck modernization
[SAE PAPER 892231] p 732 A90-45447
- DOWNWASH**
An experimental investigation of the downwash beneath a lifting rotor and low advance ratios
p 151 A90-17585
- Rotorwash flow fields - Flight test measurement, prediction methodologies, and operational issues
p 817 A90-46930
- Analysis of heliport environmental data: Indianapolis downtown heliport, Wall Street heliport. Volume 2: Wall Street heliport data plots
[DOT/FAA/CT-TN87/54-VOL-2] p 121 N90-11761
- Analysis of heliport environmental data: Indianapolis downtown heliport, Wall Street heliport. Volume 3: Indianapolis downtown heliport data plots
[AD-A217412] p 544 N90-20500
- Wind tunnel study of wake downwash behind A 6 percent scale model B1-B aircraft
[DE90-011783] p 719 N90-25941
- Analysis of heliport environmental data, Intracoastal City
[DOT/FAA/CT-TN89/43] p 938 N90-28584
- Three-dimensional numerical study of thunderstorm downdrafts and associated outflow boundaries
p 963 N90-29746
- DRAFT (GAS FLOW)**
Simple analyses of paths through windshears and downdrafts
[AIAA PAPER 90-0222] p 197 A90-19740
- DRAG**
Reduction of profile drag by modifying the structure next to the wake area
[IMFL-88/35] p 172 N90-13356
- Induced drag for non-planar wings
[LR-521] p 172 N90-13357
- Calculation of excrescence drag magnification due to pressure gradient at high subsonic speeds
[ESDU-87004] p 397 N90-19195
- An analytic study of nonsteady two-phase laminar boundary layer around an airfoil
p 691 N90-25051
- Study of the ground effects in the CEAT aerohydrodynamic tunnel: Using the results
p 922 N90-28530
- DRAG CHUTES**
An experimental investigation of wall-interference effects for parachutes in closed wind tunnels
[DE90-001802] p 236 N90-15076
- DRAG COEFFICIENTS**
Airplane design. Part 6 - Preliminary calculation of aerodynamic, thrust and power characteristics --- Book
p 31 A90-12871
- Calculation of cone drag
p 84 A90-14579
- Turbulent boundary layer development in the presence of small isolated two-dimensional surface discontinuities
p 210 A90-18507
- Optimal nose shapes of bodies of revolution in transonic flow
p 299 A90-24165
- Drag measurements on a modified prolate spheroid using a magnetic suspension and balance system
p 672 A90-40684

DRAG MEASUREMENT

- A proposed automatic calibration facility for cryogenic balances p 524 A90-34246
 Drag measurements on a modified prolate spheroid using a magnetic suspension and balance system p 672 A90-40684
 Recent aerodynamic measurements with Magnetic Suspension Systems p 759 A90-44399
 An experimental study of low-speed single-surface airfoils with faired leading edges p 801 A90-46371
 Study of the flow around the prototype of A300: Results of the third test campaign at F2 and comparison with calculations [CERT-33/5025-29-DERAT] p 817 N90-27663
- DRAG REDUCTION**
 Advantage Airbus? p 102 A90-15746
 Low Reynolds number airfoils evaluation program p 151 A90-17692
 Comment on 'Drag reduction factor due to ground effect' p 159 A90-19396
 The application of the discrete vortex method in aircraft design p 257 A90-23357
 The local surface variation method in profile shape optimization problems p 297 A90-24136
 Reductions in induced drag by the use of aft swept wing tips p 299 A90-24342
 Modification of large eddies in turbulent boundary layers p 474 A90-33514
 Takeoff characteristics of turbofan engines p 585 A90-35764
 Effectiveness of passive devices for axisymmetric base drag reduction at Mach 2 p 555 A90-36184
 Supersonic aircraft drag reduction [AIAA PAPER 90-1596] p 567 A90-38729
 On the use of external burning to reduce aerospace vehicle transonic drag [AIAA PAPER 90-1935] p 656 A90-40562
 Drag reduction by controlling flow separation using stepped afterbodies p 622 A90-40690
 Effect of detailed surface geometry on riblet drag reduction performance p 622 A90-40693
 Numerical simulation of transonic porous airfoil flows p 707 A90-44433
 Minimum induced drag for wings with spanwise camber p 709 A90-44733
 Induced drag - Historical perspective [SAE PAPER 892341] p 715 A90-45495
 An entropy method for induced drag minimization [SAE PAPER 892344] p 715 A90-45496
 On optimal supersonic/hypersonic bodies [AIAA PAPER 90-3072] p 796 A90-45918
 On the drag reduction of bluff bodies through momentum injection [AIAA PAPER 90-3076] p 797 A90-45922
 Control of low-Reynolds-number airfoils - A review p 801 A90-46376
 Wind-tunnel investigations of wings with serrated sharp trailing edges p 802 A90-46379
 The design of a low Reynolds number RPV p 828 A90-46385
 Control of low-speed airfoil aerodynamics p 814 A90-49776
 Control and modification of turbulence p 72 N90-10377
 Turbulence management: Application aspects p 72 N90-10378
 An experimental investigation of helicopter rotor hub fairing drag characteristics [NASA-TM-102182] p 88 N90-11701
 Application of sound and temperature to control boundary-layer transition p 92 N90-12537
 Design of the low-speed NLF(1)-0414F and the high-speed HSNLF(1)-0213 airfoils with high-lift systems p 93 N90-12540
 Experimental and numerical analyses of laminar boundary-layer flow stability over an aircraft fuselage forebody p 93 N90-12549
 Status report on a natural laminar-flow nacelle flight experiment p 105 N90-12550
 Nacelle design p 105 N90-12551
 Reduction of turbulent drag: Boundary layer manipulators [CERT-RSF-OA-74/2259-AYD] p 136 N90-12889
 NASA aerodynamics program [NASA-TM-4175] p 373 N90-17235
 Effect of riblets on flow separation from a cylinder and an airfoil in subsonic flow [AD-A216197] p 319 N90-17574
 Optimum spanwise camber for minimum induced drag [BU-403] p 397 N90-18369
 Aerodynamic analysis of a US Navy and Marine Corps unmanned air vehicle [AD-A218282] p 498 N90-20077
 Compression pylon [NASA-CASE-LAR-13777-1] p 498 N90-20078

- Passive venting technique for shallow cavities [NASA-CASE-LAR-14031-1] p 499 N90-20079
 A fast collocation method for transonic airfoil design p 501 N90-20984
 Constrained spanload optimization for minimum drag of multi-lifting-surface configurations p 501 N90-20992
 On the use of external burning to reduce aerospace vehicle transonic drag [NASA-TM-103107] p 588 N90-21762
- DRAINAGE**
 Analytical and experimental study of runway runoff with wind effects [PTI-8948] p 123 N90-12627
 Airport pavement drainage [DOT/FAA/RD-90/24] p 872 N90-27728
- DRAWINGS**
 Aircraft drawings index p 618 N90-23340
- DRONE AIRCRAFT**
 The new light weight, high performance reconnaissance camera KFB 8/24 F p 847 A90-48607
 LOG/LTR controller design using a reduced order model p 964 A90-52877
- DROP SIZE**
 Atomization of synthetic jet fuel p 63 A90-12602
 Atomization and spray research for gas turbine engines p 189 A90-17688
 Liquid water content and droplet size calibration of the NASA Lewis Icing Research Tunnel [AIAA PAPER 90-0669] p 261 A90-22242
 Comparison of two droplet sizing systems in an icing wind tunnel [AIAA PAPER 90-0668] p 274 A90-23711
 Development of a phase Doppler based probe for icing cloud droplet characterization [AIAA PAPER 90-0667] p 368 A90-26978
 Influence of fuel drop size and combustor operating conditions on pollutant emissions p 508 A90-33591
 Rain erosion testing --- on polymethyl methacrylate specimens p 525 A90-34578
 Liquid water content and droplet size calibration of the NASA Lewis Icing Research Tunnel [NASA-TM-102447] p 213 N90-13797
 Comparison of two droplet sizing systems in an icing wind tunnel [NASA-TM-102456] p 215 N90-14617
- DROP TESTS**
 Unique methodology used in the Bell-Boeing V-22 main landing gear landing loads analysis and drop tests p 409 A90-28236
 Preliminary characterization of parachute wake recontact p 622 A90-40681
- DROP TRANSFER**
 A comparison of a droplet impingement code to icing tunnel results [AIAA PAPER 90-0670] p 352 A90-26979
- DROPS (LIQUIDS)**
 A novel method of atomization with potential gas turbine applications p 131 A90-16003
 Droplet impaction on a supersonic wedge - Consideration of similitude p 400 A90-27986
 Aerodynamic breakup of liquid jets - A review [AIAA PAPER 90-1616] p 607 A90-38746
 The effects of toughening stresses on liquid impact induced fracture p 692 A90-41315
 Numerical simulation of droplet deformation in convective flows [AIAA PAPER 90-2309] p 769 A90-42773
 Liquid fueled ramjet combustion instability: Acoustical and vortical interactions with burning sprays [AD-A222752] p 767 N90-26104
- DRY FRICTION**
 Vibration of turbine blades damped by dry friction forces p 879 A90-46190
- DUCTED BODIES**
 Computational modeling of inlet hammer shock wave generation [AIAA PAPER 90-2005] p 621 A90-40592
- DUCTED FAN ENGINES**
 3D Euler analysis of ducted propfan flowfields [AIAA PAPER 90-3034] p 791 A90-45873
 The turbofan of tomorrow p 850 A90-46150
- DUCTED FANS**
 Recent propeller development and studies conducted at ONERA [ONERA, TP NO. 1990-16] p 683 A90-41201
- DUCTED FLOW**
 Computation of laminar mixed convection flow in a channel with wing type built-in obstacles p 67 A90-11114
 Flow in compressor interstage ducts p 11 A90-12521
 A study of flow structure in a contra-rotating axial compressor stage p 11 A90-12524
 The propagation of a normal shock in a varying area duct p 130 A90-15045

- Development of bluff body wake in a longitudinally curved stream p 86 A90-15745
 Pseudoshock and separated flow in rectangular ducts p 295 A90-24089
 An experimental investigation on control of flow dynamic distortions downstream under strong shock-boundary layer interaction in the two-dimensional flow field p 471 A90-33288
 Injectant mole fraction measurements of transverse injection in constant area supersonic ducts [AIAA PAPER 90-1632] p 587 A90-38761
 Directivity of the noise radiation emitted from the inlet duct of a turbofan helicopter engine [ONERA, TP NO. 1990-26] p 695 A90-41205
 Interaction between a high-level steady acoustic field and a ducted turbulent flow [ONERA, TP NO. 1990-27] p 695 A90-41206
 Analysis of internal flow in a ventral nozzle for STOVL aircraft [AIAA PAPER 90-1899] p 739 A90-42688
 Self-excited oscillations in internal transonic flows p 813 A90-49274
 Analysis of internal flow in a ventral nozzle for STOVL aircraft [NASA-TM-103123] p 666 N90-23404
- DUCTED ROCKET ENGINES**
 Analytical studies of three-dimensional combustion processes [AD-A211903] p 126 N90-11837
- DUCTILITY**
 Observations on the brittle to ductile transition temperatures of B2 nickel aluminides with and without zirconium p 205 A90-19153
- DUCTS**
 Combustion oscillations in ducts p 204 A90-19006
 PMR graphite engine duct development [NASA-CR-182228] p 51 N90-10037
 Numerical method for designing 3D turbomachinery blade rows p 511 N90-20990
 Inflatable fuel tank buffer [AD-D014446] p 503 N90-21002
 Parabolized calculations of turbulent three dimensional flows in a turbine duct p 482 N90-21013
 Experimental and analytical study of close-coupled ventral nozzles for ASTOVL aircraft [NASA-TM-103170] p 666 N90-24273
- DUMP COMBUSTORS**
 Experimental study of static pressure and mean velocity profiles inside a two-dimensional dump-type combustor model p 45 A90-12530
 Nonaxisymmetric instabilities in a dump combustor with a swirling inlet flow p 253 A90-21228
 Inlet swirl effects on dump combustor flows [AIAA PAPER 90-0035] p 312 A90-26904
 Experimental and theoretical investigations of turbulent flow in a side-inlet rectangular combustor p 421 A90-27959
 Swirling flow in thrust nozzles p 421 A90-27962
 An experimental study on flowfields in a dual inlet swirl-dump combustor p 471 A90-33283
 The experimental study on the coaxial dump combustor with inner swirl inlet under the combustion condition p 585 A90-36786
 Multistep dump combustor design to reduce combustion instabilities p 659 A90-40934
 Numerical simulation of nonpremixed turbulent flow in a dump combustor [AIAA PAPER 90-1858] p 768 A90-42685
 Active combustion control in a coaxial dump combustor [AIAA PAPER 90-2447] p 743 A90-42806
 Numerical simulation of unsteady combustion in a dump combustor p 54 N90-10203
 Very-low-frequency oscillations in liquid-fueled ramjets p 54 N90-10204
 Calculation of the combustion distribution in a liquid-fuel ramjet p 858 N90-27931
- DURABILITY**
 Durability characteristics of the LAK-12 Letuva glider made of composite materials at the stage of certification p 102 A90-15560
 Improvement in structural integrity and long term durability of aerospace composite components p 441 A90-28189
 The U.S. Army Helicopter Structural Integrity Program - 1989 European Rotorcraft Forum p 581 A90-38525
 Introducing the VRT gas turbine combustor [AIAA PAPER 90-2452] p 743 A90-42808
 Dealing with the aging fleet [SAE PAPER 892209] p 701 A90-45428
 Durability and damage tolerance of S-2 glass/PEEK composites p 944 A90-50140
 A dynamicist's view of fuel tank skin durability p 251 N90-15915
 Introducing the VRT gas turbine combustor [NASA-TM-103176] p 688 N90-23591

SUBJECT INDEX

Lessons learned from the T-46A durability and damage tolerance program p 842 A90-26812

DYNAMIC CHARACTERISTICS

Dynamics of aviation gas turbine engines --- Russian book p 113 A90-16049

The establishment of mathematical model of engine control system and simulation research of afterburning dynamic characteristics p 190 A90-18613

Compensating for pneumatic distortion in pressure sensing devices p 211 A90-19956

[AIAA PAPER 90-0631] p 211 A90-19956

Dynamic properties of a system for the roll control of a model electromagnetically suspended in a wind tunnel p 262 A90-22762

Dynamic characteristics of one-dimensional gas flow with friction p 296 A90-24115

Examination of dynamic characteristics of UH-60A and F-1-60A airframe structures p 406 A90-28154

Effect of structural anisotropy on the dynamic characteristics of the wing and critical flutter speed p 386 A90-28985

A study of symbolic processing and computational aspects in helicopter dynamics p 545 A90-34103

Prediction and measurement of rotor blade/stator vane dynamic characteristics of a modern aero-engine axial compressor p 878 A90-46036

Leading edge vortex dynamics on a pitching delta wing [NASA-CR-186327] p 398 A90-19198

Compensating for pneumatic distortion in pressure sensing devices [NASA-TM-101716] p 415 A90-19224

Performance of an optimized rotor blade at off-design flight conditions [NASA-CR-4288] p 416 A90-19226

Low-speed wind-tunnel investigation of the flight dynamic characteristics of an advanced turboprop business/commuter aircraft configuration [NASA-TP-2982] p 434 A90-19239

An applicational process for dynamic balancing of turbomachinery shafting [NASA-TM-102537] p 541 A90-20392

Plan, formulate, and discuss a NASTRAN finite element model of the UH-60A helicopter airframe [NASA-CR-181975] p 541 A90-20439

Application of numerical optimization techniques to control system design for nonlinear dynamic models of aircraft p 593 A90-23032

Behavior of composite/metal aircraft structural elements and components under crash type loads: What are they telling us [NASA-TM-102681] p 774 A90-25368

Flow visualization of dynamic stall on an oscillating airfoil [AD-A222202] p 815 A90-26797

The effects of foreplanes on the static and dynamic characteristics of a combat aircraft model p 920 A90-28520

Static and dynamic characterization of the ATR 72 rods made of Ti 10.2.3 titanium alloy [REPT-49-238] p 953 A90-28722

DYNAMIC CONTROL

Tail rotor dynamics during the translational turn maneuver of a helicopter p 334 A90-24148

Comparison of test signals for aircraft frequency domain identification p 490 A90-33057

A technique for the tuning of helicopter flight control systems p 670 A90-42467

The place of knowledge based systems in helicopter dynamic system condition prognosis p 618 A90-42475

3-D analysis of laser measurements of vortex bursting on a chined forebody fighter configuration [AIAA PAPER 90-3020] p 793 A90-45887

A dynamic inversion based control law with application to the high angle-of-attack research vehicle [AIAA PAPER 90-3407] p 864 A90-47662

Viscoelastic tuned dampers for control of structural dynamics p 73 A90-10999

Adaptive control law design for model uncertainty compensation [AD-A211712] p 120 A90-11758

Dallas/Fort Worth simulation, volume 1 [DOT/FAA/CT-TN89/28-VOL-1] p 824 A90-26802

Dynamic separation: Search for the cause of dynamic stall and search for its control [AD-A223412] p 911 A90-29305

DYNAMIC LOADS

The influence of the wake structure on the dynamic blade load p 6 A90-11785

Experimental and analytical evaluation of dynamic load vibration of a 2240-kW (3000-hp) rotorcraft transmission p 127 A90-13750

An investigation of the behavior of the dynamic load distribution versus operating speed and torque on heavily loaded, high speed aircraft gearing p 271 A90-21129

A dynamic optical model attitude measurement system p 539 A90-34236

Gearbox system design for ultra-high bypass engines [AIAA PAPER 90-2152] p 685 A90-42048

Prediction and alleviation of V-22 rotor dynamic loads p 833 A90-46974

Influence of friction and separation phenomena on the dynamic blade loading of transonic turbine cascades [MITT-88-04] p 428 A90-19235

DYNAMIC MODELS

Simulation research on the afterburning dynamic characteristics of engine control system p 48 A90-12581

A discrete dynamic model of the crankshaft-aircrew assembly of an aircraft piston engine for the purpose of vibration analysis by the method of finite elements p 51 A90-13220

Numerical analysis of vibrations of a helicopter tail boom p 31 A90-13224

Criteria for evaluating the flight dynamics model of flight simulators p 121 A90-15422

Dynamic simulation of cross-shafted propulsion system for tilt nacelle application [AIAA PAPER 90-0439] p 191 A90-19847

Modeling strategies for crashworthiness analysis of landing gears p 409 A90-28233

A dynamic optical model attitude measurement system p 539 A90-34236

Linear dynamics of supersonic ramjet p 655 A90-40519

A simple dynamic engine model for use in a real-time aircraft simulation with thrust vectoring [AIAA PAPER 90-2166] p 662 A90-42054

A comprehensive approach to coupled rotor-fuselage dynamics p 646 A90-42460

Helicopter stability and control modeling improvements and verification on two helicopters p 671 A90-42474

Dynamics and control of maneuverable towed flight vehicles [AIAA PAPER 90-2841] p 754 A90-45161

Proven dynamic modeling techniques for concurrent design and analysis of ECS controllers [SAE PAPER 901234] p 841 A90-49304

Adaptive control law design for model uncertainty compensation [AD-A211712] p 120 A90-11758

AcSim: Aircraft simulation program with application to flight profile generation [AD-A212466] p 185 A90-14217

Wind shear models for aircraft hazard investigation p 280 A90-15044

Adaptive control of helicopter vibrations via the impulse response method [AD-A213728] p 260 A90-15113

Formulation and verification of a technique for compensation of pneumatic attenuation errors in airborne pressure sensing devices p 369 A90-17084

Fire science and aircraft safety p 326 A90-17596

Time and frequency-domain identification and verification of BO-105 dynamic models [AD-A216828] p 415 A90-18389

Application of numerical optimization techniques to control system design for nonlinear dynamic models of aircraft p 593 A90-23032

Convex models of malfunction diagnosis in high performance aircraft [AD-A218514] p 702 A90-25073

Research at NASA's NFAC wind tunnels [NASA-TM-102827] p 702 A90-25933

Formation of design envelope criterion in terms of deterministic spectral procedure [RAE-TM-SS-9] p 721 A90-25953

A flight dynamic model of aircraft spinning [AR-005-600] p 935 A90-28576

Nonlinear static and dynamic modeling of composite rotor blades including warping effects p 924 A90-29382

DYNAMIC PRESSURE

Fuel effects on gas turbine combustor dynamics [AIAA PAPER 90-1957] p 676 A90-40570

An experimental investigation of turbine rotor wakes for the development of a fiber optic pressure sensor [AIAA PAPER 90-2411] p 687 A90-42163

External nozzle flap dynamic load measurements on F-15 S/MTD model [AIAA PAPER 90-1910] p 740 A90-42692

Analysis of scramjet engine characteristics [NAL-TR-1041] p 933 A90-29398

DYNAMIC PROGRAMMING

Optimal input design for aircraft parameter estimation using dynamic programming principles [AIAA PAPER 90-2801] p 753 A90-45157

DYNAMIC RESPONSE

Identification of an adequate model for collective response dynamics of a Sea King helicopter in hover p 56 A90-12766

DYNAMIC STRUCTURAL ANALYSIS

Random response and noise transmission of discretely stiffened composite panels p 283 A90-23288

The effect of structural variations on the dynamic characteristics of helicopter rotor blades [AIAA PAPER 90-1161] p 450 A90-29396

Response characteristics of a two-dimensional wing subjected to turbulence near the flutter boundary p 519 A90-34082

Aeroelastic response characteristics of a rotor executing arbitrary harmonic blade pitch variations p 646 A90-42464

The response of helicopter to dispersed gust p 670 A90-42470

Acoustic fatigue analysis by the finite element method p 954 A90-49886

Rotor blade dynamic design p 106 A90-12583

Experimental aeroelasticity history, status and future in brief [NASA-TM-102651] p 527 A90-21047

Development and application of a generalized dynamic wake theory for lifting rotors p 570 A90-21731

Application of a dynamic stall model to rotor trim and aeroelastic response p 583 A90-22556

Coupled rotor-body equations of motion hover flight [NASA-CR-186710] p 717 A90-25111

The effect of aircraft size on cabin floor dynamic pulses [DOT/FAA/CT-88/15] p 735 A90-25136

Construction of a hybrid angular velocity reference system for investigation of the dynamic characteristics of strapdown gyros [ESA-TT-1181] p 774 A90-25332

Computational crash dynamics. Project 1.2: Computational crash dynamics analysis [IAR-89-19] p 724 A90-25956

An in-flight interaction of the X-29A canard and flight control system [NASA-TM-101718] p 736 A90-25973

An investigation of the use of singular perturbation methods and modal control theory in the derivation of aircraft control schemes [MATHS-REPT-A-106] p 758 A90-26014

Structural dynamics branch research and accomplishments [NASA-TM-102488] p 778 A90-26373

Development of a linearized unsteady aerodynamic analysis for cascade gust response predictions [NASA-CR-4308] p 816 A90-27655

Effective optimal control of a fighter aircraft engine p 928 A90-28548

Analysis of dynamic transient response and postflutter behavior of super-maneuvering airplane [AD-A224126] p 925 A90-29386

DYNAMIC STABILITY

A study of the stability of a wing aileron in supersonic flow p 222 A90-20442

Static and dynamic loss of stability of elements of a supersonic aeroplane covering - Numerical analysis p 346 A90-25186

Eliminating the TF30 P-111 + engine rotor-instability problem p 508 A90-32961

On dynamic stability boundaries for binary systems p 538 A90-33698

A study on mechanical model of the helicopter 'ground resonance' p 580 A90-36423

The role of bearing support stiffness anisotropy in suppression of rotordynamic instability p 879 A90-46215

The response of helicopter rotors to vibratory airload p 832 A90-46971

Combustor influence on fighter engine operability p 64 A90-10193

Dynamic instability characteristics of aircraft turbine engine combustors p 53 A90-10195

Rotorcraft aeromechanical stability-methodology assessment. Phase 2: Workshop [NASA-TM-102272] p 816 A90-26800

DYNAMIC STRUCTURAL ANALYSIS

Some unconventional cases of the dynamical testing of helicopters p 28 A90-10227

Design and application of a finite element package for modelling turbomachinery vibrations p 70 A90-13011

Dynamic analysis of lifting surfaces of small relative thickness in the case of finite displacements p 129 A90-14560

Practical suggestions for modifying math models to correlate with actual modal test results p 207 A90-16979

A component modal synthesis technique for the lateral vibration analysis of aircraft engine systems p 179 A90-16983

Comparison of the analytical and experimental modes of a model airplane using finite element analysis and multi-reference testing p 207 A90-16986

Vibration analysis of aircraft panels p 207 A90-17026

Dynamic structural correlation via nonlinear programming techniques p 208 A90-17372

A new generation of innovative ultra-advanced intelligent composite materials featuring electro-rheological fluids - An experimental investigation p 204 A90-17962

The influence of selected geometrical and mass parameters on the structural dynamics of an aircraft with a variable-geometry airfoil p 346 A90-24284

Review of composite rotor blade modeling p 366 A90-25303

Unique methodology used in the Bell-Boeing V-22 main landing gear landing loads analysis and drop tests p 409 A90-28236

Approximation of frequency characteristics using identification with a complex mass matrix p 448 A90-29001

AIAA/ASME/ASCE/AHS/ASC Structures, Structural Dynamics and Materials Conference, 31st, Long Beach, CA, Apr. 2-4, 1990, Technical Papers. Part 1 - Materials, engineering optimization and design p 449 A90-29226

Influence of structural and aerodynamic modeling on flutter analysis [AIAA PAPER 90-0954] p 411 A90-29239

AIAA/ASME/ASCE/AHS/ASC Structures, Structural Dynamics and Materials Conference, 31st, Long Beach, CA, Apr. 2-4, 1990, Technical Papers. Part 3 - Structural dynamics I p 449 A90-29359

Rotary-wing aeroelasticity with application to VTOL vehicles [AIAA PAPER 90-1115] p 392 A90-29387

Dynamic analysis of rotor blades with rotor retention design variations [AIAA PAPER 90-1159] p 412 A90-29394

Aeroelastic tailoring analysis for preliminary design of advanced turbo propellers with composite blades p 412 A90-29395

Vibrations of rectangular plates with moderately large initial deflections at elevated temperatures using finite element method [AIAA PAPER 90-1125] p 451 A90-29429

Numerical model of unsteady subsonic aeroelastic behavior p 535 A90-32471

Structural optimization with aeroelastic constraints of rotor blades with straight and swept tips p 535 A90-32475

European Forum on Aeroelasticity and Structural Dynamics, Aachen, Federal Republic of Germany, Apr. 17-19, 1989, Proceedings [DGLR BERICHT 89-01] p 468 A90-33351

Review of active structural control systems and flight test techniques for dynamic stability investigations p 516 A90-33352

Ground vibration testing of aeroplanes with a sequence of single-point excitations - Simple and effective p 522 A90-33371

Identification of time varying modal parameters p 536 A90-33375

Rotordynamics of the Vulcain LH2 Turbopump - Comparison between test results and non-linear dynamic analysis p 528 A90-33382

Sensitivity analysis using resonance and anti-resonance frequencies - A guide to structural modification p 536 A90-33396

A review of aeroelasticity research at the flight dynamics laboratory p 493 A90-33409

Dynamics of multi-spool gas turbines using the matrix transfer method - Applications p 509 A90-33594

Dynamics of multi-spool gas turbines using the matrix transfer method - Theory p 509 A90-33595

On dynamic stability boundaries for binary systems p 538 A90-33698

Dynamic analysis of airport pavement p 593 A90-36418

Vibration equations for a helicopter rotor blade p 604 A90-37830

Numerical methods for the treatment of periodic systems with applications to structural dynamics and helicopter rotor dynamics p 604 A90-37881

Non-conservative stability of a cracked thick rotating blade p 606 A90-38544

Aeroelastic analysis of a low aspect ratio wing p 619 A90-38915

Annual General Meeting of the Canadian Aeronautics and Space Institute, 36th, Ottawa, Canada, May 15, 16, 1989, Proceedings p 701 A90-42652

Large-order modal analysis techniques in the Aeroelastic Design Optimization Program (ADOP) [SAE PAPER 892323] p 772 A90-45482

Frictionless contact of aircraft tires [SAE PAPER 892350] p 733 A90-45501

Homogenization of composite beams in dynamical flexure p 878 A90-46184

V-22 MSC/NASTRAN airframe vibration analysis and correlation p 832 A90-46969

STOL Maneuver Technology Demonstrator aeroservoelasticity [AIAA PAPER 90-3336] p 863 A90-47596

Structural and dynamic analysis of the A330/340 composite RAT blade --- ram air turbine p 942 A90-50083

Flexible aircraft dynamic modeling for dynamic analysis and control synthesis p 61 N90-10112

Viscoelastic tuned dampers for control of structural dynamics p 73 N90-10999

Airframe structural dynamic considerations in rotor design optimization [NASA-TM-101646] p 134 N90-12057

RAN (Royal Australian Navy) vibration analysis system operator's guide [AD-A212441] p 107 N90-12596

Investigation of difficult component effects on finite element model vibration prediction for the Bell AG-1G helicopter. Volume 2: Correlation results [NASA-CR-181916-VOL-2] p 213 N90-13814

Active control system for gust load alleviation and structural damping p 259 N90-15056

Analysis of the National Transonic Facility mishap [NASA-TM-101686] p 328 N90-17620

An experimental study of the aeroelastic behaviour of two parallel interfering circular cylinders p 455 N90-19609

A review of the analytical simulation of aircraft crash dynamics [NASA-TM-102595] p 484 N90-20068

Plan, formulate, and discuss a NASTRAN finite element model of the UH-60A helicopter airframe [NASA-CR-181975] p 541 N90-20439

Performance data from a wind-tunnel test of two main-rotor blade designs for a utility-class helicopter [NASA-TM-4183] p 499 N90-20974

Development and application of a generalized dynamic wake theory for lifting rotors p 570 N90-21731

Airloads, wakes, and aeroelasticity [NASA-CR-177551] p 572 N90-21738

Aircraft crash survival design guide. Volume 3: Aircraft structural crash resistance [AD-A218436] p 575 N90-22547

Unique failure behavior of metal/composite aircraft structural components under crash type loads [NASA-TM-102679] p 690 N90-24660

Ground shake test of the UH-60A helicopter airframe and comparison with NASTRAN finite element model predictions [NASA-CR-181993] p 758 N90-25143

Calculation of flight vibration levels of the AH-1G helicopter and correlation with existing flight vibration measurements [NASA-CR-182031] p 775 N90-25375

An in-flight interaction of the X-29A canard and flight control system [NASA-TM-101718] p 736 N90-25973

Structural dynamics branch research and accomplishments [NASA-TM-102488] p 778 N90-26373

Nonlinear static and dynamic modeling of composite rotor blades including warping effects p 924 N90-29382

DYNAMIC TESTS

A multifunctional system of helicopter dynamics simulations p 28 A90-10226

Some unconventional cases of the dynamical testing of helicopters p 28 A90-10227

Dynamic testing of crashworthy fuel valves [SAE PAPER 891017] p 128 A90-14329

Evaluation of the dynamic properties of the auto-pilot servo of a single-rotor helicopter through laboratory testing p 118 A90-15424

MAVIS flight load simulation --- Multi Axis Vibration System p 202 A90-17003

Aft facing transport aircraft passenger seats under 16G dynamic crash simulation p 175 A90-17416

A review of the V-22 dynamics validation program p 406 A90-28155

Full scale technology demonstration of a modern counterrotating unducted fan engine concept: Component test [NASA-CR-180868] p 53 N90-10047

Dynamic testing techniques and applications for an aeroelastic rotor test facility p 201 N90-13406

Results of aircraft open-loop tests of an experimental magnetic leader cable system for guidance during roll-out and turnoff [NASA-TM-4135] p 348 N90-16767

Dynamic derivatives of missiles and fighter-type configurations at high angles of attack p 337 N90-17554

The 59th Shock and Vibration Symposium, volume 2 [AD-A214579] p 372 N90-18065

Experimental identification of helicopter engine dynamics from closed loop data p 855 N90-27627

DYNAMICAL SYSTEMS

Inverse problems in controlled system dynamics: Nonlinear models --- Russian book p 77 A90-12471

Simulation model-building procedure for dynamic systems integration p 138 A90-14744

Dynamic damping of vibrations in mechanical systems by means of elastic links with distributed parameters p 139 A90-15568

Application of dynamical systems theory to the high angle of attack dynamics of the F-14 [AIAA PAPER 90-0221] p 257 A90-22184

Recent developments in rotor dynamics methodology in the U.S. industry p 889 A90-46960

A new methodology for model order reduction with application to eigenstructure controllers [AIAA PAPER 90-3475] p 891 A90-47725

Effects of stick dynamics on helicopter flying qualities [AIAA PAPER 90-3477] p 886 A90-47727

The application of TSIM software to act design and analysis on flexible aircraft p 60 N90-10086

A contribution to the improvement of the accuracy in the parameter identification of nonlinear processes, by example of the aircraft motion [ETN-90-96961] p 736 N90-25974

DYNAMOMETERS

Short time-dynamometer system for shock wave channels [MBB-UT-115/89-PUB] p 773 N90-25084

E

EARLY WARNING SYSTEMS

Incorporation of alarm states into a real time decision making process [AIAA PAPER 89-3006] p 76 A90-10620

Airborne early warning radar --- Book p 727 A90-45200

EARPHONES

A fiber optic headset compatible with power-by-light p 504 A90-32906

EARTH OBSERVATIONS (FROM SPACE)

Activities report in German aerospace [ISSN-0070-3966] p 465 N90-19189

EARTH ORBITS

ETO (Earth-To-Orbit): A trajectory program for aerospace vehicles [AD-A218157] p 528 N90-20103

EARTH TERMINALS

Harrier Information Management System (HIMS): The system and the approach p 884 N90-27630

ECHO SOUNDING

Ultrasonic regression rate measurement in solid fuel ramjets [AIAA PAPER 90-1963] p 656 A90-40573

ECONOMIC ANALYSIS

The fast-response requirement of powerplant thrust in the set of engineering and economic criteria of an aircraft p 254 A90-23354

California air transportation study: A transportation system for the California Corridor of the year 2010 [NASA-CR-186219] p 176 N90-14212

A contribution to the economic, optimal dimensioning, and shaping of aircraft structures using a design model [ETN-90-96966] p 737 N90-25976

Airline productivity relating on the fuel cost. (2): Fuel consumption values and fuel efficiency [NAL-TM-604-2] p 913 N90-29333

ECONOMIC DEVELOPMENT

Air transportation in COMECON countries --- Russian book p 785 A90-46616

ECONOMIC FACTORS

Effect of the angle of attack on the efficiency and thrust ratio of axial-flow microturbines with full admission p 111 A90-14590

Maintenance and economic benefits of non-painted aircraft operations [SAE PAPER 892208] p 732 A90-45427

ECONOMICS

FAA (Federal Aviation Administration) aviation forecasts, fiscal years 1990-2001 [AD-A219165] p 552 N90-22530

Study of high-speed civil transports. Summary [NASA-CR-4236] p 735 N90-25966

Proceedings of a workshop on Future Airport Passenger Terminals [PB90-213620] p 937 N90-28580

ECONOMY

The cost of air service fragmentation [TT-9010] p 913 N90-29334

EDDY CURRENTS

Thin film eddy current impulse deicer [AIAA PAPER 90-0761] p 183 A90-20012

Comparison among modal analyses of axial compressor blade using experimental data of different measuring systems p 878 A90-46038

- Eddy current detection of subsurface cracks
p 882 A90-48629
- Inspection development for T-37 wing spar cap lug
[AD-A214826] p 287 N90-16708
- Inspection reliability p 885 N90-28072
- New aspects in aircraft inspection using eddy current methods p 886 N90-28085
- EDDY VISCOSITY**
Problem areas in applied computational fluid dynamics p 366 A90-25770
- Numerical prediction of turbulent flow over airfoil sections with a new nonequilibrium turbulence model [AIAA PAPER 90-1469] p 562 A90-38626
- Navier-Stokes solutions of 2-D transonic flow over unconventional airfoils p 173 N90-14195
- The computation of turbulent thin shear flows associated with flow around multielement aerofoils p 633 N90-24240
- EDUCATION**
Computer aided analysis of gas turbine cycles p 779 A90-45289
- Calendar of selected aeronautical and space meetings [AGARD-CAL-90/1] p 464 N90-19060
- Success in tutoring electronic troubleshooting p 780 N90-25568
- EFFECTIVE PERCEIVED NOISE LEVELS**
Noise levels from a VSTOL aircraft measured at ground level and at 1.2 m above the ground [NPL-RSA(EXT)-009] p 464 N90-18999
- EGRESS**
The influence of adjacent seating configurations on egress through a type 3 emergency exit [AD-A218393] p 636 N90-23371
- EIGENVALUES**
Design of attitude and rate command systems for helicopters using eigenstructure assignment p 118 A90-14729
- The eigenvalue sensitivity analysis and design for integrated flight/propulsion control systems p 196 A90-18601
- Eigenvalue problem in the theory of flow past thin profiles at high supersonic velocity p 295 A90-24096
- Unfolding of double-zero eigenvalue bifurcations for supersonic flow past a pitching wedge p 347 A90-25995
- High-quality approximation of eigenvalues in structural optimization p 603 A90-36277
- Development of a mathematical model of an adaptive antilflutter system p 769 A90-42911
- Robust low norm output feedback design for flight control systems [AIAA PAPER 90-3505] p 891 A90-47751
- AcSim: Aircraft simulation program with application to flight profile generation [AD-A212466] p 185 N90-14217
- An efficient solver of the Eigenvalue problem of the linear stability equations for three dimensional, compressible boundary-layer flows p 276 N90-16172
- A fractional calculus model of aeroelasticity [AD-A216244] p 377 N90-18212
- A comparison of flutter calculations based on eigenvalue and energy method p 425 N90-18406
- EIGENVECTORS**
Input/output coupling in eigenstructure assignment [AIAA PAPER 90-3476] p 865 A90-47726
- AcSim: Aircraft simulation program with application to flight profile generation [AD-A212466] p 185 N90-14217
- A comparison of two central difference schemes for solving the Navier-Stokes equations [NASA-TM-102815] p 816 N90-27654
- EJECTION INJURIES**
Canopy fragilization using embedded detonating cord p 180 A90-17417
- Development of a microcomputer based software system for use in crewmember ejection analysis [AD-A220398] p 723 N90-25117
- EJECTION SEATS**
A description of the Naval Air Development Center's ejection tower and crash test facilities and their uses p 200 A90-17426
- Aerodynamic testing of a new semi-prone ejection seat design [AIAA PAPER 90-0234] p 182 A90-19748
- Escape system evolution p 722 A90-44656
- A preliminary sensitivity analysis of the Generalized Escape System Simulation (GESS) computer program [DE89-016891] p 24 N90-10844
- Parachute opening shocks during high speed ejections: Normalization p 497 N90-20056
- Development of an ejection seat specification for a new fighter aircraft p 483 N90-20057
- Escape systems research at RAE p 483 N90-20058
- Fighter escape system: The next step forward p 483 N90-20059
- Windblast protection for advanced ejection seats p 483 N90-20063
- Yaw fin deployment apparatus for ejection seat [AD-D014512] p 723 N90-25118
- EJECTORS**
Rotating primary flow induction using jet-flapped blades p 48 A90-12585
- Navier-Stokes analysis of an ejector and mixer-ejector operating at pressure ratios in the range 2-4 [AIAA PAPER 90-2730] p 626 A90-42218
- Computational analysis of the flowfield of a two-dimensional ejector nozzle [AIAA PAPER 90-1901] p 740 A90-42690
- An experimental study of a supersonic gas ejector p 851 A90-46546
- Characteristics of temperature and pressure generation and retention in flow inside cryogenic wind tunnel T-04 p 869 A90-46576
- Investigation of advanced mixer-ejector exhaust system [AD-A211943] p 89 N90-11705
- Rotary-Jet thrust augmentor with jet-flapped blades p 633 N90-24243
- ELASTIC BARS**
Calculation of the vibrations of aircraft with elastic suspended loads p 345 A90-24171
- ELASTIC BODIES**
Dynamic analysis of lifting surfaces of small relative thickness in the case of finite displacements p 129 A90-14560
- Nonstationary motion of an elastic profile in subsonic incompressible flow p 300 A90-24741
- Solution of potential flow past an elastic body using the boundary element technique [AD-A213843] p 275 N90-15390
- ELASTIC BUCKLING**
Buckling analysis of FRP faced cylindrical sandwich panel under combined loading p 365 A90-24376
- ELASTIC CYLINDERS**
Active control of propeller-induced noise fields inside a flexible cylinder p 833 A90-47306
- ELASTIC DAMPING**
Increasing the heat conductivity of elastic damping elements of MR material p 102 A90-14580
- Dynamic damping of vibrations in mechanical systems by means of elastic links with distributed parameters p 139 A90-15568
- ELASTIC DEFORMATION**
Development status of epicyclic gears p 271 A90-21141
- Aeroelastic deformation of a crescent-shaped rigid support in the diffuser chamber of a wind tunnel p 364 A90-24112
- High temperature deformation studies on CVD silicon carbide fibers p 945 A90-50147
- Static aeroelastic analysis of a three-dimensional generic wing [NASA-TM-102231] p 509 N90-20087
- Analysis of dynamic transient response and postflutter behavior of super-maneuvering airplane [AD-A224126] p 925 N90-29386
- ELASTIC PROPERTIES**
The story of sandwich construction p 538 A90-33702
- Advanced applications of BEM to gas turbine engine structures p 772 A90-45769
- Homogenization of composite beams in dynamical flexure p 878 A90-46184
- ELASTIC SHEETS**
Manufacture of honeycomb p 538 A90-33704
- ELASTIC SHELLS**
Equilibrium of an elastic porous shell in supersonic gas flow p 150 A90-17109
- ELASTIC WAVES**
A numerical study of transverse jets into supersonic flows and influence of pressure waves [AIAA PAPER 90-0733] p 314 A90-26985
- Acoustic emission and signal analysis p 781 A90-43782
- Unsteady blade surface pressures on a large-scale advanced propeller - Prediction and data [AIAA PAPER 90-2402] p 808 A90-47220
- ELASTODYNAMICS**
A unified approach to the overall body motion stability and flutter characteristics of elastic aircraft p 346 A90-25102
- ELASTOMERS**
Spray sealing: A breakthrough in integral fuel tank sealing technology p 276 N90-15912
- Equilibrium swelling of elastomeric materials in solvent environments [DE90-010164] p 678 N90-24430
- ELASTOPLASTICITY**
A quadratic programming method for solving three dimensional elastic-plastic contact problems p 603 A90-36417
- A simple prediction method for low-cycle fatigue life of structures p 604 A90-37240
- The MHOSE finite element program: 3-D inelastic analysis methods for hot section components. Volume 3: Systems' manual [NASA-CR-182236] p 73 N90-10451
- ELECTRIC BATTERIES**
Battery configurations for multi-megawatt pulse power p 873 A90-49763
- Flight termination system battery guidelines [AD-A217310] p 520 N90-20092
- ELECTRIC CHARGE**
Electric charge acquired by airplanes penetrating thunderstorms p 913 A90-52093
- ELECTRIC CONDUCTORS**
Flexible heat pipe cold plate [AD-A216053] p 434 N90-18433
- ELECTRIC CORONA**
Visualization of corona discharges p 819 A90-49839
- ELECTRIC CURRENT**
The behavior of electric currents in graphite/epoxy structures p 883 A90-49846
- ELECTRIC DISCHARGES**
Connection of structures by laboratory-generated electrical discharges [ONERA, TP NO. 1989-147] p 58 A90-11169
- A fatigue study of electrical discharge machine (EDM) strain-gage balance materials p 448 A90-28295
- ELECTRIC EQUIPMENT TESTS**
The evolution of built-in test for an electrical power generating system (EPGS) p 424 A90-30699
- A captive store flight vibration simulation project p 672 A90-40476
- Evaluation for DLC-Flap Monitoring System of the VSRA [NAL-TM-607] p 928 N90-29391
- ELECTRIC FIELD STRENGTH**
A new generation of innovative ultra-advanced intelligent composite materials featuring electro-rheological fluids - An experimental investigation p 204 A90-17962
- ELECTRIC FIELDS**
Grid generation procedure using the integral equation method [NAL-TR-1009] p 77 N90-10630
- ELECTRIC GENERATORS**
Considerations for successful application of integrated drive generators to aircraft [SAE PAPER 892226] p 746 A90-45442
- VSCF cycloconverter reliability review of the 30/40 KVA F/A-18 electrical generating system --- variable speed, constant frequency [SAE PAPER 892228] p 746 A90-45444
- Application considerations for integral gas turbine electric starter/generator revisited [SAE PAPER 892252] p 746 A90-45454
- Assessment of High Temperature Superconducting (HTS) electric motors for rotorcraft propulsion [NASA-CR-185222] p 588 N90-21761
- ELECTRIC MOTORS**
Control of a switched-reluctance aircraft engine starter-generator over a very wide speed range p 588 A90-38130
- High-performance EHA controls using an interior permanent magnet motor --- electrohydrostatic actuator for aircraft power systems p 730 A90-43152
- EHA loading on the 270-Vdc bus [SAE PAPER 892225] p 746 A90-45441
- Assessment of High Temperature Superconducting (HTS) electric motors for rotorcraft propulsion [NASA-CR-185222] p 588 N90-21761
- ELECTRIC POTENTIAL**
A study on flaw detection method for CFRP composite laminates. I - The measurement of crack extension in CFRP composites by electrical potential method p 441 A90-28003
- Device for quickly sensing the amount of O₂ in a combustion product gas [NASA-CASE-LAR-13816-1] p 609 N90-22025
- ELECTRIC POWER SUPPLIES**
Power supply of aircraft --- Russian book p 43 A90-12474
- Electrical power systems for high Mach vehicles p 586 A90-38129
- Applying AVIP to high voltage power supply designs --- Avionic Integrity Program p 605 A90-38132
- Design features of the 747-400 Electric Power System [SAE PAPER 892227] p 746 A90-45443
- Flight termination system battery guidelines [AD-A217310] p 520 N90-20092
- ELECTRIC PROPULSION**
EHA loading on the 270-Vdc bus [SAE PAPER 892225] p 746 A90-45441
- Application considerations for integral gas turbine electric starter/generator revisited [SAE PAPER 892252] p 746 A90-45454

ELECTRIC PULSES

- Fatigue and electromagnetic interference test for Electro-Impulse De-Icing
[SAE PAPER 891062] p 100 A90-14362
- Extracting pulse power from batteries p 605 A90-38175
- Battery configurations for multi-megawatt pulse power p 873 A90-49763

ELECTRIC WIRE

- Helicopter wire strike accident and high voltage electrocution - A case report p 22 A90-10265

ELECTRICAL ENGINEERING

- An object-oriented solution example: A flight simulator electrical system
[AD-A219190] p 761 N90-25145

ELECTRICAL FAULTS

- A parametric optimization algorithm for the electrical distribution circuits of civil aircraft p 255 A90-23417
- From a sow's ear - Quantitative diagnostic design requirements from anecdotal references p 448 A90-28337
- A test and maintenance architecture demonstrated on SEM-E modules for fiber optic networks p 458 A90-28342
- The evolution of built-in test for an electrical power generating system (EPGS) p 424 A90-30699
- Applying AVIP to high voltage power supply designs --- Avionic Integrity Program p 605 A90-38132
- An experimental study of fault propagation in a jet-engine controller
[NASA-CR-181335] p 665 N90-23401

ELECTRICAL INSULATION

- High Voltage Design Guide summary p 605 A90-38097

ELECTRICAL MEASUREMENT

- Electrostatic field conditions on an aircraft stricken by lightning
[ONERA, TP NO. 1989-148] p 23 A90-11170
- Evaluation and measurement of airplane flutter interference --- in television reception p 272 A90-22529
- Inspection development for T-37 wing spar cap lug
[AD-A214826] p 287 N90-16708

ELECTRICAL PROPERTIES

- High Voltage Design Guide summary p 605 A90-38097
- Aircraft lightning protection handbook
[AD-A222716] p 820 N90-27668

ELECTRICAL RESISTIVITY

- Connection of structures by laboratory-generated electrical discharges
[ONERA, TP NO. 1989-147] p 58 A90-11169
- Effect of pressure on the electrophysical properties of two-phase flows in nozzles p 110 A90-14572
- A study on flaw detection method for CFRP composite laminates. I - The measurement of crack extension in CFRP composites by electrical potential method p 441 A90-28003

ELECTRIFICATION

- Electric charge acquired by airplanes penetrating thunderstorms p 913 A90-52093

ELECTRO-OPTICS

- Design criteria for helicopter night pilotage sensors p 417 A90-28221
- Redesign of an electro-optical shroud in graphite/epoxy p 676 A90-40215
- Electro-optics engineering support for the integrated launch and recovery television surveillance system
[AD-A223450] p 938 N90-29406

ELECTROCHROMISM

- Electrochromic windows - Applications for aircraft
[SAE PAPER 891063] p 129 A90-14363
- Electrochromic aircraft windows p 451 A90-29891

ELECTRODEPOSITION

- Two special cost-effective applications for electrochemical metallizing for improved brazing and bonding
[SAE PAPER 890927] p 365 A90-24692

ELECTRODYNAMICS

- Electrodynamic properties of engine exhaust jets p 265 A90-23428

ELECTROHYDRODYNAMICS

- A model for the electrohydrodynamic flow in a constricted arc heater p 131 A90-15393

ELECTROLESS DEPOSITION

- The properties and characteristics of electroless nickel coatings applied to gas turbine engine components
[ASME PAPER 89-GT-4] p 354 A90-23751

ELECTROMAGNETIC ABSORPTION

- Electrochromic windows - Applications for aircraft
[SAE PAPER 891063] p 129 A90-14363

ELECTROMAGNETIC COMPATIBILITY

- Avionics and electromagnetic compatibility (EMC) considerations on a helicopter with an advanced composite airframe p 417 A90-28217

- Automated measurement of aircraft-level electromagnetic interference p 404 A90-30752

ELECTROMAGNETIC COUPLING

- Boeing 727-100 test project (high energy radiated field tests)
[DOT/FAA/CT-88/33] p 542 N90-21247

ELECTROMAGNETIC FIELDS

- Electromagnetic characterization of lightning on aircraft
[ONERA, TP NO. 1989-131] p 22 A90-11155
- Experimental-theoretical comparison for current injection on an aircraft model
[ONERA, TP NO. 1989-133] p 22 A90-11157
- An airborne instrument for characterizing the 10,000 electromagnetic signals generated by one lightning flash p 848 A90-49830
- An assessment of analytical methods and lightning simulation test techniques used in lightning qualification and surveillance testing p 818 A90-49833
- Validation of GEMACS for prediction of lightning induced electromagnetic fields --- General Electromagnetic Model for Analysis of Complex Systems p 819 A90-49845
- Electro-impulse de-icing testing analysis and design
[NASA-CR-4175] p 32 N90-10031
- Boeing 727-100 test project (high energy radiated field tests)
[DOT/FAA/CT-88/33] p 542 N90-21247

ELECTROMAGNETIC HAMMERS

- Electromagnetic dent removal for aircraft repair
[SAE PAPER 890923] p 286 A90-24689

ELECTROMAGNETIC INTERFERENCE

- Optic multiplex for aircraft sensors - Issues and options p 38 A90-11660
- The role of adaptive antenna systems when used with GPS p 128 A90-13995
- Fatigue and electromagnetic interference test for Electro-Impulse De-Icing
[SAE PAPER 891062] p 100 A90-14362
- Interference detection and suppression in Loran-C receivers p 240 A90-20504
- Evaluation and measurement of airplane flutter interference --- in television reception p 272 A90-22529

- Automated measurement of aircraft-level electromagnetic interference p 404 A90-30752
- Corrosion protection and EMP/EMI shielding p 600 A90-37902

- Laboratory test methodology for evaluating the effects of electromagnetic disturbances on fault-tolerant control systems
[NASA-TM-101665] p 217 N90-14061

- Aircraft testing in the electromagnetic environment p 248 N90-15066

- The disturbance processes on the data links of the mode-S air traffic control system
[ETN-90-96960] p 729 N90-25965

- Aircraft testing in the electromagnetic environment p 248 N90-15066

- The disturbance processes on the data links of the mode-S air traffic control system
[ETN-90-96960] p 729 N90-25965

- Aircraft testing in the electromagnetic environment p 248 N90-15066

- Aircraft testing in the electromagnetic environment p 248 N90-15066

- Aircraft testing in the electromagnetic environment p 248 N90-15066

- Aircraft testing in the electromagnetic environment p 248 N90-15066

- Aircraft testing in the electromagnetic environment p 248 N90-15066

- Aircraft testing in the electromagnetic environment p 248 N90-15066

- Aircraft testing in the electromagnetic environment p 248 N90-15066

- Aircraft testing in the electromagnetic environment p 248 N90-15066

- Aircraft testing in the electromagnetic environment p 248 N90-15066

- Aircraft testing in the electromagnetic environment p 248 N90-15066

- Aircraft testing in the electromagnetic environment p 248 N90-15066

- Aircraft testing in the electromagnetic environment p 248 N90-15066

- Aircraft testing in the electromagnetic environment p 248 N90-15066

- Aircraft testing in the electromagnetic environment p 248 N90-15066

- Aircraft testing in the electromagnetic environment p 248 N90-15066

- Aircraft testing in the electromagnetic environment p 248 N90-15066

- Aircraft testing in the electromagnetic environment p 248 N90-15066

- Aircraft testing in the electromagnetic environment p 248 N90-15066

- Aircraft testing in the electromagnetic environment p 248 N90-15066

- Aircraft testing in the electromagnetic environment p 248 N90-15066

ELECTROMECHANICAL DEVICES

- Multi-level models for diagnosis of complex electro-mechanical systems p 693 A90-38888

ELECTROMECHANICS

- Aerospace induction motor actuators driven from a 20-kHz power link
[NASA-TM-102482] p 509 N90-20085

ELECTRON BEAM WELDING

- Fracture mechanics assessment of EB-welded blisked rotors p 453 A90-31117

ELECTRON BEAMS

- Self-lubricating surfaces by ion beam processing
[AD-A222489] p 884 N90-27118
- Radiation-curable prepreg composites
[DE90-629740] p 951 N90-28674

ELECTRON MICROSCOPY

- Fractographic analysis of fatigue crack growth under two-blocks loading on 2024-T351 sheet specimens
[LR-628] p 961 N90-29680
- Effects of blocks of overloads and underloads on fatigue crack growth in 2024-T351 sheet specimens: Fractographic analysis and crack closure predictions
[LR-629] p 961 N90-29681

ELECTRON OPTICS

- Failure analysis handbook
[AD-A219747] p 689 N90-23752

ELECTRONIC CONTROL

- Design of control amplifier for FJR 710 engine p 43 A90-12017
- Digital electronic control unit for the European Fighter Aircraft (EFA) p 253 A90-21607
- Flight testing of the Chandler Evans adaptive fuel control on the S-76A helicopter p 422 A90-28178
- Mission effectiveness testing of an adaptive electronic fuel control on an S-76A p 422 A90-28199
- Computer controlled test bench for axial turbines and propellers p 437 A90-28288
- Digital electronic control for WJ6G4A engine p 424 A90-29919
- Electric controls for a high-performance EHA using an interior permanent magnet motor drive p 452 A90-30711

- Flight-testing of the self-repairing flight control system using the F-15 highly integrated digital electronic control flight research facility
[AIAA PAPER 90-1321] p 520 A90-34149

- Composite electronic enclosures for engine-mounted environments p 657 A90-40601

- High-temperature electronics for aircraft engines
[AIAA PAPER 90-2035] p 657 A90-40604

- Full authority digital electronic engine control system provides needed reliability
[AIAA PAPER 90-2037] p 658 A90-40606

- A pilot rating scale for evaluating failure transients in electronic flight control systems p 754 A90-45159

- Multivariable optimization scheme for tuning the controller of an electronic fuel control unit for small gas turbine engines p 745 A90-45301

- A real time microcomputer implementation of sensor failure detection for turbofan engines p 745 A90-45414

- Engine controls for the 1990's
[PNR90546] p 114 N90-11748

- Apparatus for cooling electronic components in aircraft
[AD-D014207] p 183 N90-13373

- Advanced detection, isolation, and accommodation of sensor failures in turbofan engines: Real-time microcomputer implementation
[NASA-TP-2925] p 259 N90-15112

- The implementation and operation of a variable-response electronic throttle control system for a TF-104G aircraft
[NASA-TM-101696] p 509 N90-20086

- Human centrifuge controller
[NAL-TM-SE-8901] p 527 N90-21043

- Propulsion system-flight control integration and optimization: Flight evaluation and technology transition
[NASA-TM-4207] p 929 N90-28551

- Propulsion system-flight control integration and optimization: Flight evaluation and technology transition
[NASA-TM-4207] p 929 N90-28551

- Propulsion system-flight control integration and optimization: Flight evaluation and technology transition
[NASA-TM-4207] p 929 N90-28551

- Propulsion system-flight control integration and optimization: Flight evaluation and technology transition
[NASA-TM-4207] p 929 N90-28551

- Propulsion system-flight control integration and optimization: Flight evaluation and technology transition
[NASA-TM-4207] p 929 N90-28551

- Propulsion system-flight control integration and optimization: Flight evaluation and technology transition
[NASA-TM-4207] p 929 N90-28551

- Propulsion system-flight control integration and optimization: Flight evaluation and technology transition
[NASA-TM-4207] p 929 N90-28551

- Propulsion system-flight control integration and optimization: Flight evaluation and technology transition
[NASA-TM-4207] p 929 N90-28551

- Propulsion system-flight control integration and optimization: Flight evaluation and technology transition
[NASA-TM-4207] p 929 N90-28551

- Propulsion system-flight control integration and optimization: Flight evaluation and technology transition
[NASA-TM-4207] p 929 N90-28551

- Propulsion system-flight control integration and optimization: Flight evaluation and technology transition
[NASA-TM-4207] p 929 N90-28551

- Propulsion system-flight control integration and optimization: Flight evaluation and technology transition
[NASA-TM-4207] p 929 N90-28551

- Propulsion system-flight control integration and optimization: Flight evaluation and technology transition
[NASA-TM-4207] p 929 N90-28551

- Propulsion system-flight control integration and optimization: Flight evaluation and technology transition
[NASA-TM-4207] p 929 N90-28551

SUBJECT INDEX

- Automatic environmental control system for electronic equipment platforms
[SAE PAPER 901217] p 840 A90-49292
- Spectra composite enhances portability and survivability of electronic equipment p 947 A90-50189
- Operation of aviation radio and electronic equipment (Handbook) — Russian book p 914 A90-50747
- Numerical simulation of aeroplane response to a lightning injection [ETN-89-95271] p 96 N90-11716

ELECTRONIC EQUIPMENT TESTS

- A test and maintenance architecture demonstrated on SEM-E modules for fiber optic networks p 458 A90-28342
- Intelligent built-in test and stress management p 448 A90-28343

ELECTRONIC MODULES

- Commonality of MASA modules — Modular Avionics System Architecture p 462 A90-30816
- Modular avionics architectures p 453 A90-30819

ELECTRONIC PACKAGING

- Low-expansion MMCs boost avionics p 203 A90-17291
- Mechanical considerations for reliable interfaces in next generation electronics packaging p 453 A90-30813

ELECTRONICS

- Eschbach's handbook of engineering fundamentals / 4th edition/ p 448 A90-28825

ELECTROPLATING

- Entrapment plating of abrasive particles for jet engine clearance control [SAE PAPER 890918] p 286 A90-24685
- Two special cost-effective applications for electrochemical metallizing for improved brazing and bonding [SAE PAPER 890927] p 365 A90-24692

ELECTROSTATIC BONDING

- Electrostatic dry powder prepegging of carbon fiber p 948 A90-50215

ELECTROSTATICS

- Electrostatic field conditions on an aircraft stricken by lightning [ONERA, TP NO. 1989-148] p 23 A90-11170

ELEVATION

- Position computation without elevation information for computed centerline operations [DOT/FAA/CT-TN89/42] p 640 N90-23379
- Noise measurements of turboprop airplanes at different overflight elevations p 697 N90-24860

ELEVATION ANGLE

- Analytical studies for computed center line operations [SAE PAPER 892219] p 729 A90-45436
- Lateral attenuation of military aircraft flight noise [AD-A218041] p 548 N90-20799

ELEVATORS (CONTROL SURFACES)

- Hinge moment coefficient derivatives for trailing-edge controls on wings at subsonic speeds [ESDU-89009] p 198 N90-14239
- Boeing/NASA composite components flight service evaluation [NASA-CR-181898] p 601 N90-22609
- Short period control using angular acceleration feedback: Compensation for first lag servo [NAL-TM-600] p 936 N90-29399

ELLIPSOIDS

- Low-speed pressure distribution on semi-infinite two-dimensional bodies with elliptical noses p 553 A90-35766
- Incompressible flow about ellipsoids of revolution [REPT-88-02] p 90 N90-11713
- Contribution to the study of three-dimensional separation in turbulent incompressible flow [ESA-TT-1169] p 454 N90-18697

ELLIPTIC DIFFERENTIAL EQUATIONS

- Comparisons among grid generation using elliptic partial differential equations p 374 A90-25478
- Surface grid generation through elliptic PDEs p 309 A90-26496
- The construction of component-adaptive grids for aerodynamic geometries p 309 A90-26513

ELLIPTICITY

- Rotational aerodynamics of elliptic bodies at high angles of attack [AIAA PAPER 90-0068] p 161 A90-19664
- Yaw damping of elliptic bodies at high angles of attack p 709 A90-44740

EMBEDDED COMPUTER SYSTEMS

- The NIMBLE Project - Real-time common LISP for embedded expert systems applications [AIAA PAPER 89-3140] p 75 A90-10614
- Embedded knowledge based avionics [AIAA PAPER 89-3141] p 75 A90-10615
- Adapting an AI-based application from its LISP environment into a real-time embedded system [AIAA PAPER 89-3142] p 75 A90-10616

- Embedded computer system integration support — avionics p 419 A90-30724
- An integrated diagnostics approach to embedded and flight-line support systems p 460 A90-30767
- The Super Puma MKII automatic flight control system p 669 A90-42449
- Main characteristics of an integrated flight and display system for AS MKII Super-Puma p 653 A90-42450
- The evolution of design/development requirements for avionics/mission equipment (MEP) insertion p 846 A90-46932
- Security audit for embedded avionics systems p 957 A90-50649

EMBEDDING

- Smart Skins - A development roadmap p 504 A90-32860
- Fiber optics smart structures program at UTIAS p 535 A90-32864
- Design and fabrication considerations for composite structures with embedded fiber optic sensors p 536 A90-32871
- Embedded GPS - The Canadian Marconi approach p 725 A90-43700
- Structural tailoring of select fiber composite structures [NASA-TM-102484] p 533 N90-21137
- Feature-associated mesh embedding for complex configurations p 608 N90-21988

EMERGENCIES

- Intelligent situation assessment and response aiding in flight emergencies [AIAA PAPER 89-2999] p 36 A90-10507
- Beech Starship occupant protection evaluation in emergency landing scenario [SAE PAPER 891015] p 100 A90-14327
- Aircraft accident report: Delta Air Lines, Inc., Boeing 727-232, N473DA, Dallas-Fort Worth International Airport, Texas, August 31, 1988 [PB89-910406] p 240 N90-15895
- Aircraft fire safety in the Canadian Forces p 327 N90-17604
- Perspectives on the use of rule-based control p 521 N90-20940
- The influence of adjacent seating configurations on egress through a type 3 emergency exit [AD-A218393] p 636 N90-23371

EMISSION SPECTRA

- Free-field propagation of high intensity noise [NASA-CR-186577] p 549 N90-21604

EMULSIONS

- Criteria for coal tar seal coats on airport pavements. Volume 2: Laboratory and field studies [AD-A220167] p 674 N90-24277

ENCLOSURES

- Composite electronic enclosures for engine-mounted environments [AIAA PAPER 90-2030] p 657 A90-40601

END PLATES

- A method for calculating axial turbomachine end wall turbulent boundary layers [ASME PAPER 89-GT-15] p 287 A90-23759

ENDOTHERMIC FUELS

- Thermal management for a Mach 5 cruise aircraft using endothermic fuel [AIAA PAPER 90-3284] p 853 A90-48871
- Production of jet fuels from coal-derived liquids. Volume 11: Production of advanced endothermic fuel blends from Great Plains Gasification Plant naphtha by-product stream [AD-A210251] p 65 N90-11184

ENERGY ABSORPTION

- Low-energy gamma ray attenuation characteristics of aviation fuels [NASA-TP-2974] p 462 N90-18882
- Aircraft crash survival design guide. Volume 4: Aircraft seats, restraints, litters, and cockpit/cabin dealthalization [AD-A218437] p 575 N90-22548
- Operational effects on crashworthy seat attenuators [AD-A221148] p 637 N90-24259
- A review of crashworthiness of composite aircraft structures [AD-A221555] p 846 N90-27697

ENERGY BUDGETS

- An experimental study of a turbulent jet impinging on a wedge p 553 A90-35274

ENERGY CONSERVATION

- Nonflammable hydraulic power system for tactical aircraft. Volume 1: Aircraft system definition, design and analysis [AD-A218493] p 671 N90-23409
- Energy Efficient Engine: Flight propulsion system final design and analysis [NASA-CR-168219] p 930 N90-28558
- Energy Efficient Engine core design and performance report [NASA-CR-168069] p 930 N90-28559

ENGINE AIRFRAME INTEGRATION

- Energy Efficient Engine integrated core/low spool design and performance report [NASA-CR-168211] p 931 N90-28561
- Energy efficient engine program technology benefit/cost study. Volume 1: Executive summary [NASA-CR-174766-VOL-1] p 931 N90-28564
- Energy Efficient Engine: Control system preliminary definition report [NASA-CR-179578] p 932 N90-28569

ENERGY CONVERSION

- Production of jet fuels from coal derived liquids. Volume 10: Jet fuels production by-products, utility, and sulfur emissions control integration study [AD-A213872] p 357 N90-16951

ENERGY CONVERSION EFFICIENCY

- Energy Efficient Engine high pressure turbine component test performance report [NASA-CR-168289] p 929 N90-28553
- Energy Efficient Engine acoustic supporting technology report [NASA-CR-174834] p 930 N90-28557
- Energy Efficient Engine: Flight propulsion system final design and analysis [NASA-CR-168219] p 930 N90-28558
- Energy Efficient Engine program advanced turbofan nacelle definition study [NASA-CR-174942] p 930 N90-28560

ENERGY DISSIPATION

- A method of predicting the energy losses in vaneless diffusers of centrifugal compressors [ASME PAPER 89-GT-158] p 292 A90-23846
- Power dissipation in smooth and honeycomb labyrinth seals [ASME PAPER 89-GT-220] p 362 A90-23881
- Estimation of losses in semi-open centrifugal impellers p 537 A90-33597
- Non-steady flow loss mechanisms associated with vaneless diffusers [AIAA PAPER 90-2508] p 682 A90-40641
- An investigation of secondary flows in nozzle guide vanes p 512 N90-21016
- Losses in the tip-leakage flow of a planar cascade of turbine blades p 514 N90-21027

ENERGY METHODS

- A study of the nonlinear deformation of a shell of revolution with a surface bend p 129 A90-14574
- A comparison of flutter calculations based on eigenvalue and energy method p 425 N90-18406
- An approximate viscous shock layer method for calculating the hypersonic flow over blunt-nosed bodies p 479 N90-20947

ENERGY TECHNOLOGY

- History and status of beamed power technology and applications at 2.45 Gigahertz p 61 N90-10150

ENERGY TRANSFER

- Transfer of the atomic ion energy of supersonic flow of a partially dissociated gas to a solid surface p 234 A90-23432
- The numerical simulation of multistage turbomachinery flows p 514 N90-21025

ENGINE AIRFRAME INTEGRATION

- Simulations of propeller/airframe interference effects using an Euler correction method p 31 A90-13019
- Calculation of transonic flows for novel engine-airframe installations p 145 A90-16768
- Mach 6 testing of two generic three-dimensional sidewall compression scramjet inlets in tetrafluoromethane [AIAA PAPER 90-0530] p 192 A90-19895
- Holographic flow visualisation of turbofan by-pass and core nozzle streams [ASME PAPER 89-GT-260] p 363 A90-23891
- Propulsion system integration in high-performance aircraft p 333 A90-23922
- Aerodynamic interference of prismatic engine nacelles with the wing at supersonic velocities p 294 A90-24078
- The LHTEC T800-LHT-800 engine integration into the Agusta A129 helicopter p 422 A90-28177
- Practical design considerations for integrating the propulsion system with the aircraft for jetborne flight [ASME PAPER 89-GT-310] p 490 A90-32257
- Evaluation of control techniques for aircraft propulsion systems p 507 A90-32262
- Calculations of propeller/airframe interference effects using the potential/multienergy flow method p 490 A90-32452
- Calculation of hypersonic forebody/inlet flow fields [AIAA PAPER 90-1493] p 619 A90-39049
- Analysis of airframe/engine interactions - An integrated control perspective [AIAA PAPER 90-1918] p 667 A90-40557
- The challenge of demonstrating the X-30 p 659 A90-41162
- 3-D Euler calculations for aft-propfan integration [AIAA PAPER 90-2147] p 625 A90-42044

- Airframe/propulsion integration of supersonic cruise vehicles
 [AIAA PAPER 90-2151] p 644 A90-42047
- Direct lift STOVL engine integration
 [AIAA PAPER 90-2274] p 644 A90-42103
- Integrated air vehicle/propulsion technology for a multirole fighter - A MCAIR perspective
 [AIAA PAPER 90-2278] p 644 A90-42105
- Principles underlying the integration of an aircraft and its engine --- Russian book p 729 A90-42520
- Optimization studies for the PW305 turbofan
 [AIAA PAPER 90-2520] p 744 A90-42813
- The integrated control of a propulsion-airframe system
 [ASME PAPER 89-WA/DSC-12] p 751 A90-44847
- VTOL military research aircraft --- Book p 828 A90-46002
- Extended implicit model following as applied to integrated flight and propulsion control
 [AIAA PAPER 90-3444] p 890 A90-47697
- TRANAIR applications to engine/airframe integration p 838 A90-48958
- The North American Rockwell XFV-12A - Reflections and some lessons
 [AIAA PAPER 90-3240] p 839 A90-49118
- STOVL option for the multi-role fighter
 [AIAA PAPER 90-3296] p 840 A90-49124
- A supersonic through-flow fan engine airframe integration study
 [NASA-CR-185140] p 18 N90-10004
- Re-engine with the Rolls-Royce Tay 670, the route to significant noise reduction
 [PNR90585] p 115 N90-12606
- Analysis of scramjet engine characteristics
 [NAL-TR-1041] p 933 N90-29398
- ENGINE ANALYZERS**
- Engine diagnostics - An application for expert system concepts p 50 A90-12632
- Gas turbine engine condition monitoring and fault diagnostics p 190 A90-18594
- Turbofan engine analysis and optimization using spreadsheets p 779 A90-45290
- ENGINE CONTROL**
- Applications of fiber optic sensors in advanced engine controls p 68 A90-11703
- The active control of engine instabilities p 44 A90-12505
- Simulation research on the afterburning dynamic characteristics of engine control system p 48 A90-12581
- VSTOL power plant control lessons from Harrier experience p 13 A90-12582
- Classification of methods for eliminating surging in gas turbine engines p 111 A90-14591
- The eigenvalue sensitivity analysis and design for integrated flight/propulsion control systems p 196 A90-18601
- The establishment of mathematical model of engine control system and simulation research of afterburning dynamic characteristics p 190 A90-18613
- Dynamic simulation of cross-shafted propulsion system for tilt nacelle application
 [AIAA PAPER 90-0439] p 191 A90-19847
- Digital electronic control unit for the European Fighter Aircraft (EFA) p 253 A90-21607
- Effect of the control of turbocompressor guide vanes on the throttle characteristics of a bypass engine p 255 A90-23425
- Electrodynamic properties of engine exhaust jets p 265 A90-23428
- Mission effectiveness testing of an adaptive electronic fuel control on an S-76A p 422 A90-28199
- A numerical solution for instruction tracing problem p 424 A90-29918
- Digital electronic control for WJ6G4A engine p 424 A90-29919
- Advanced technology ATE for fuel accessory testing p 439 A90-30770
- An optically interfaced propulsion management system applied to a commercial transport aircraft p 424 A90-30811
- Evaluation of control techniques for aircraft propulsion systems p 507 A90-32262
- Multivariable control of jet engines p 507 A90-32421
- Simulation research on the afterburning dynamic characteristics of engine control system p 585 A90-35708
- Study on process control of aeroengine using microcomputer p 586 A90-37239
- An application of expert system to jet engine diagnostic procedures p 587 A90-38596
- Expert diagnosis system for FJR engine troubles p 587 A90-38597
- Identification of multivariable models of jet engines
 [AIAA PAPER 90-1874] p 655 A90-40540
- Design of digital self-selecting multivariable controllers for jet engines
 [AIAA PAPER 90-1875] p 655 A90-40541
- A preliminary evaluation of an F100 engine parameter estimation process using flight data
 [AIAA PAPER 90-1921] p 656 A90-40559
- Composite electronic enclosures for engine-mounted environments
 [AIAA PAPER 90-2030] p 657 A90-40601
- Lightweight fuel pump and metering component for advanced gas turbine engine control
 [AIAA PAPER 90-2032] p 657 A90-40602
- Fiber-optic turbine inlet temperature measurement system (FOTITMS)
 [AIAA PAPER 90-2033] p 657 A90-40603
- High-temperature electronics for aircraft engines
 [AIAA PAPER 90-2035] p 657 A90-40604
- Full authority digital electronic engine control system provides needed reliability
 [AIAA PAPER 90-2037] p 658 A90-40606
- Development of high temperature actuation systems for advanced aircraft engines
 [AIAA PAPER 90-2031] p 660 A90-41990
- Propulsion control system designs for advanced Navy multimission aircraft
 [AIAA PAPER 90-2403] p 663 A90-42160
- UH-60A helicopter stability augmentation study p 670 A90-42471
- Full Authority Digital Engine Control for the AS 355 N TM 319 engines p 665 A90-42486
- Aircraft propulsion control systems for the next century p 742 A90-42720
- The integrated control of a propulsion-airframe system
 [ASME PAPER 89-WA/DSC-12] p 751 A90-44847
- H-infinity based integrated flight/propulsion control design for a STOVL aircraft in transition flight
 [AIAA PAPER 90-3335] p 862 A90-47595
- Fault-tolerant transputer-based controller configurations for gas-turbine engines p 852 A90-48529
- Full scale technology demonstration of a modern counterrotating unducted fan engine concept. Engine test
 [NASA-CR-180869] p 53 N90-10049
- An open-loop transient thermodynamic model of the Cougar turbojet
 [AD-A211774] p 114 N90-11745
- Engine controls for the 1990's p 114 N90-11748
- Software verification plan for GCS --- guidance and control software
 [NASA-TM-101668] p 372 N90-18057
- The implementation and operation of a variable-response electronic throttle control system for a TF-104G aircraft
 [NASA-TM-101696] p 509 N90-20086
- Propulsion system-flight control integration and optimization: Flight evaluation and technology transition
 [NASA-TM-4207] p 929 N90-28551
- Smart microsensors for high temperature applications, phase 1
 [AD-A224151] p 959 N90-28828
- ENGINE COOLANTS**
- Calculation of coolant flow and heat transfer inside composite air-cooled turbine p 189 A90-17791
- A method for the computer-aided hydraulic analysis of the turbine cooling systems of aviation gas turbine engines p 255 A90-23430
- Pressure loss and heat transfer in channels roughened on two opposed walls
 [ASME PAPER 89-GT-86] p 358 A90-23805
- Characteristics of partial length circular pin fins as heat transfer augmentors for airfoil internal cooling passages
 [ASME PAPER 89-GT-87] p 359 A90-23806
- Gas turbine engine brush seal applications
 [AIAA PAPER 90-2142] p 685 A90-42041
- Numerical predictions for the flow and the heat transfer in gas turbine cooling systems p 770 A90-44464
- Thermal management for a Mach 5 cruise aircraft using endothermic fuel
 [AIAA PAPER 90-3284] p 853 A90-48871
- Computer code for predicting coolant flow and heat transfer in turbomachinery
 [NASA-TP-2985] p 858 N90-27722
- ENGINE DESIGN**
- USA - A system to represent airfoils throughout the product life cycle
 [AIAA PAPER 89-2972] p 73 A90-10487
- Fundamentals of turbine design for aircraft engines --- Russian book p 40 A90-10839
- Ceramic heat exchangers in gas turbine
 [ONERA, TP NO. 1989-109] p 40 A90-11142
- The flutter characteristic analysis and optimization design of mistuning blade p 42 A90-11799
- The features of FJR 710 engine p 42 A90-12011
- International Symposium on Air Breathing Engines, 9th, Athens, Greece, Sept. 3-8, 1989, Proceedings, Volumes 1 & 2 p 43 A90-12501
- Swedish philosophy in aeroengine development p 44 A90-12504
- Some issues in the growth of small gas turbine aircraft propulsion engines p 44 A90-12508
- Hydrogen fueled subsonic-ram-combustor model tests for an air-turbo-ram engine p 44 A90-12529
- Design and off-design performance predictions of axial turbines p 45 A90-12540
- Application of three-dimensional methods for the calculation of gas dynamic and thermal processes at the design of gas turbines for air breathing engines p 46 A90-12552
- Unbalance response studies on a model rotor supported on uncentrally squeezed film dampers and the development experience of a jet engine p 69 A90-12579
- A study of particle trajectories in a gas turbine intake p 48 A90-12583
- Investigation of some effects on the compressor characteristics of an advanced bleed air compressor design p 49 A90-12594
- Advanced airbreathing powerplant for hypersonic vehicles p 49 A90-12607
- Study of advanced technology impact on cycle characteristics and aircraft sizing (using multivariable optimization techniques) p 29 A90-12612
- Operating aspects of counter-rotating propfan and planetary-differential gear coupling p 50 A90-12615
- Gearless crank - The logical step to economic engines for high thrust p 50 A90-12616
- Non-iterative analytical methods for off-design turbofan calculations with or without mixed-flows p 70 A90-12628
- Development study of air turbo-ramjet for future space plane
 [IAF PAPER 89-311] p 109 A90-13445
- The cycle evaluation of the advanced LACE performance
 [IAF PAPER 89-313] p 109 A90-13447
- Design and development of the Garrett F109 turbofan engine
 [SAE PAPER 891046] p 109 A90-14350
- Garrett TPF351-20 turboprop fan engine development
 [SAE PAPER 891047] p 109 A90-14351
- Successful performance development program for the T800-LHT-800 turboshaft engine
 [SAE PAPER 891048] p 110 A90-14352
- Simulation of a turbocompound two-stroke diesel engine
 [SAE PAPER 891066] p 110 A90-14366
- A minimal permissible radial clearance in a gas turbine p 110 A90-14569
- Increasing the heat conductivity of elastic damping elements of MR material p 102 A90-14580
- Thermodynamic calculation of the compressors of gas turbine engines and powerplants at high air pressures p 130 A90-14585
- XG40 - Rolls-Royce advanced fighter engine demonstrator p 112 A90-16002
- Gas turbine engine component development - An integrated approach p 112 A90-16006
- Sharing power and profit p 188 A90-16701
- IHPET spawns engines for 21st century p 188 A90-16702
- Turboshafts on tenterhooks p 188 A90-16703
- Payoffs in growth engines p 188 A90-16823
- Recent research on external helicopter noise at ONERA p 218 A90-16825
- TBCs for better engine efficiency --- thermal barrier coatings p 203 A90-17294
- Aircraft propulsion systems technology and design --- Book p 188 A90-17308
- Cost effective technology --- CAD/CAM techniques for aircraft engines p 188 A90-17447
- Application of computational systems to aircraft engine components development p 188 A90-17448
- A method for aerodynamic design calculation of axial gas turbine stages with cooling air mixing p 152 A90-17781
- An aerodynamic design and calculation method for gas turbine with cooling air mixing p 189 A90-17782
- Design and calculation of composite air-cooled blades in a highly-loaded transonic turbine p 189 A90-17790
- Jet futures p 190 A90-18526
- Study of calculating an approximately constant reaction turbine stage with a tension spline streamline curvature method p 157 A90-18537
- The analysis and solution of the performance deterioration problem of WP7 engine under the full reheating condition p 191 A90-18624
- Dynamic simulation of cross-shafted propulsion system for tilt nacelle application
 [AIAA PAPER 90-0439] p 191 A90-19847

- Numerical optimization of axial compressor designs
[ASME PAPER 89-GT-14] p 340 A90-23758
- A proposal for optimized design of multistage compressors
[ASME PAPER 89-GT-34] p 288 A90-23766
- Optimum weight design of a rotor bearing system with dynamic behavior constraints
[ASME PAPER 89-GT-74] p 358 A90-23795
- A review of failure models for ceramic matrix composite laminates under monotonic loads
[ASME PAPER 89-GT-153] p 354 A90-23842
- The design and test of a two stage transonic axial flow compressor
[ASME PAPER 89-GT-164] p 341 A90-23852
- Axial flow compressor design optimization. I - Pitchline analysis and multivariable objective function influence
[ASME PAPER 89-GT-201] p 342 A90-23873
- Axial flow compressor design optimization. II - Through-flow analysis
[ASME PAPER 89-GT-202] p 342 A90-23874
- An off-design loss and deviation prediction study for transonic axial compressors
[ASME PAPER 89-GT-324] p 343 A90-23893
- Effect of the design of a diffuser with tangential injection on the starting and separation ratios of pressures
p 295 A90-24099
- Acoustic characteristics of counterrotating unducted fans from model scale tests
p 378 A90-26138
- Use of swirl for flow control in propulsion nozzles
p 421 A90-27963
- A synergistic approach to logistics planning and engine design
p 422 A90-28207
- The revolution continuous --- performance of military helicopters
[MBB-UD-557-89-PUB] p 381 A90-28242
- Advanced technology's impact on compressor design and development - A perspective
[SAE SP-800] p 423 A90-28571
- Cleaner superalloys via improved melting practices
p 442 A90-29707
- Aerothermomechanical design of turbine-engine combustion chambers
p 424 A90-29922
- Modelling and simulation of turboprop engine behaviour
p 424 A90-29946
- Cycle analysis for helicopter gas turbine engines
[ASME PAPER 89-GT-328] p 506 A90-32258
- Propulsion systems for supersonic V/STOL aircraft
[ASME PAPER 89-GT-309] p 507 A90-32259
- A method of sizing multi-cycle engines for hypersonic aircraft
[ASME PAPER 89-GT-281] p 507 A90-32261
- Design of an air-cooled metallic high-temperature radial turbine
p 507 A90-32960
- Numerical simulations of an oblique detonation wave engine
p 508 A90-32964
- An improved incidence losses prediction method for turbine airfoils
[ASME PAPER 89-GT-284] p 475 A90-33563
- The next AIAA engine design competition - A commercial engine
[AIAA PAPER 89-2258] p 550 A90-33675
- F-15E/GE-129 Increased Performance Engine initial development flight test program
[AIAA PAPER 90-1266] p 509 A90-33894
- Gas turbine engines for combat aviation - Current realities and perspectives for the near future
p 584 A90-35513
- Wide chord fan club
p 584 A90-35600
- The T800-LHT-800 engine - Designed for supportability
p 585 A90-35773
- Technology update of early gas turbine designs
p 586 A90-38531
- Progress in certifying F402-RR-408 - The improved Pegasus engine for AV-8B and Harrier II Plus
p 587 A90-38532
- Tilt rotor requirements on engine design and qualification
p 587 A90-38534
- V-22 engine installation and removal tool - Designing support equipment with the aircraft, not after
p 581 A90-38538
- Power transfer devices for V/STOL convertible engine systems
p 587 A90-38539
- Linear dynamics of supersonic ramjet
p 655 A90-40519
- Acoustic characteristics of a research step combustor
[AIAA PAPER 90-1851] p 655 A90-40530
- Lightweight fuel pump and metering component for advanced gas turbine engine control
[AIAA PAPER 90-2032] p 657 A90-40602
- Convertible engine system for high speed rotorcraft
[AIAA PAPER 90-2512] p 658 A90-40643
- Rationale for determining information associated with aircraft gas turbine engines that is of historical importance
[AIAA PAPER 90-2754] p 617 A90-40648
- Transverse fuel-injection model for a scramjet propulsion system
p 659 A90-40927
- Multistep dump combustor design to reduce combustion instabilities
p 659 A90-40934
- Investigation of very high bypass ratio engines for subsonic transports
p 659 A90-40945
- Aircraft engine technology gets a second wind
p 659 A90-41166
- Applying qualitative knowledge to aircraft engine system design
p 694 A90-41189
- Starter systems and auxiliary power units
p 660 A90-41760
- Design and analysis of a large-plug inlet ADP nacelle and pylon --- Advanced Ducted Prop
[AIAA PAPER 90-2015] p 673 A90-41986
- Development of high temperature actuation systems for advanced aircraft engines
[AIAA PAPER 90-2031] p 660 A90-41990
- Evaluation of brush seals for limited-life engines
[AIAA PAPER 90-2140] p 685 A90-42040
- Gas turbine engine brush seal applications
[AIAA PAPER 90-2142] p 685 A90-42041
- Gearbox system design for ultra-high bypass engines
[AIAA PAPER 90-2152] p 685 A90-42048
- The development of a probabilistic turbine rotor design system
[AIAA PAPER 90-2176] p 662 A90-42060
- The promise of advanced materials for a 21st century UBE --- ultrahigh bypass ratio engine
[AIAA PAPER 90-2396] p 662 A90-42157
- Ultra high bypass turbofan technologies for the twenty-first century
[AIAA PAPER 90-2397] p 662 A90-42158
- Component arrangement studies for an 8000 shp turboshaft high technology core
[AIAA PAPER 90-2398] p 663 A90-42159
- Development of impact design methods for ceramic gas turbine components
[AIAA PAPER 90-2413] p 687 A90-42165
- Engineering design models for ramjet efficiency and lean blowoff
[AIAA PAPER 90-2453] p 663 A90-42176
- CFE738 - A case for joint engine development
[AIAA PAPER 90-2522] p 664 A90-42197
- Turbine configuration impact on advanced IHPET engine system mission capabilities
[AIAA PAPER 90-2739] p 664 A90-42221
- Advanced material applications for direct lift engines
[AIAA PAPER 90-2753] p 664 A90-42226
- Co-development of CT7-6 engines - A continued tradition in technology and reliability
p 665 A90-42485
- Contribution of engine improvement on next future rotorcraft
p 665 A90-42488
- Design of aeroengines in a low-fuel price scenario
p 739 A90-42653
- Methods for determining the internal thrust of scramjet engine modules from experimental data
[AIAA PAPER 90-2340] p 743 A90-42777
- IHPET technology mission payoffs at the component level - A look at Phase II technologies --- Integrated High Performance Turbine Engine Technology
[AIAA PAPER 90-2404] p 701 A90-42794
- Optimization studies for the PW305 turbofan
[AIAA PAPER 90-2520] p 744 A90-42813
- The GMA 2100 and GMA 3007 engines for regional aircraft
[AIAA PAPER 90-2523] p 744 A90-42815
- Advanced developments of the Turbo-Union RB199
p 745 A90-44595
- Propulsion systems for the '90s
p 745 A90-44605
- Turbofan engine analysis and optimization using spreadsheets
p 779 A90-45290
- V2500 turbofan engine
[SAE PAPER 892363] p 747 A90-45512
- The RB211-535E4 - A commercially proven engine for the military of tomorrow
[SAE PAPER 892364] p 748 A90-45513
- The PW2000 - A mature engine with an eye to the future
[SAE PAPER 892365] p 748 A90-45514
- The turbofan of tomorrow
p 850 A90-46150
- A method for the matching of structural and geometric parameters of the turbocompressors of small gas turbine engines in computer-aided design
p 850 A90-46491
- Calculation of an axial-flow birotary turbine
p 880 A90-46492
- Calculation of the efficiency of an active partial-admission gas turbine for counterpressures varying over a wide range
p 850 A90-46495
- Calculation of nonstationary forces in a three-row compressor cascade
p 803 A90-46502
- Power struggle --- Advanced Tactical Fighter engine proposals
p 851 A90-46650
- Benefits of advanced materials, structures, and aerodynamics in future high speed civil transport propulsion systems
[AIAA PAPER 90-3285] p 853 A90-48872
- Aspects of the design of a hypersonic engine system and the selection of the intake and tail
[DGLR PAPER 88-040] p 928 A90-50233
- A supersonic through-flow fan engine airframe integration study
[NASA-CR-185140] p 18 N90-10004
- Performance potential of an advanced technology Mach 3 turbojet engine installed on a conceptual high-speed civil transport
[NASA-TM-4144] p 51 N90-10034
- Advanced Turbine Technology Applications Project (ATTAP)
[NASA-CR-185133] p 51 N90-10036
- Large-scale Advanced Prop-fan (LAP) technology assessment report
[NASA-CR-182142] p 53 N90-10046
- Full scale technology demonstration of a modern counterrotating unducted fan engine concept. Design report
[NASA-CR-180867] p 53 N90-10048
- Revolutionary opportunities for materials and structures study
[NASA-CR-179642] p 63 N90-10184
- Combustor influence on fighter engine operability
p 64 N90-10193
- Advanced technologies impact on compressor design and development: A perspective
[NASA-TM-102341] p 54 N90-10891
- Advanced technology in military gas turbine design and manufacture
[PNR90545] p 114 N90-11747
- Engine controls for the 1990's
[PNR90546] p 114 N90-11748
- Future military powerplants --- fighter aircraft engines
[PNR90554] p 114 N90-11749
- A vision of the future: The new engine technology
[PNR90566] p 115 N90-12603
- Designing for reliable and low maintenance cost aero engines
[PNR90570] p 115 N90-12604
- The next generation supersonic transport engine: Critical issues
[PNR90576] p 115 N90-12605
- Material requirements for future aeroengines
[PNR90595] p 116 N90-12610
- A computer integrated approach to dimensional inspection
[PNR90596] p 116 N90-12611
- Gas turbine performance analysis
[PNR90599] p 116 N90-12614
- Blading design for multi-storage HP compressor
[PNR90602] p 116 N90-12616
- Composite materials for future aeroengines
[PNR90584] p 127 N90-12667
- The future of non ferrous metals in aerospace engines
[PNR90572] p 127 N90-12720
- The commercial aircraft noise problem
[PNR90577] p 140 N90-13203
- Advanced Turbine Technology Applications Project (ATTAP)
[NASA-CR-185109] p 220 N90-14153
- A study of variable geometry in advanced gas turbines
p 255 N90-15104
- AGARD/SMP Review: Damage Tolerance for Engine Structures. 2: Defects and Quantitative Materials Behaviour --- conference
[AGARD-R-769] p 425 N90-18396
- Compressor performance tests in the compressor research facility
p 427 N90-18428
- Stall and recovery in multistage axial flow compressors
p 428 N90-18429
- Development and fabrication of structural components for a scramjet engine
[NASA-CR-181945] p 510 N90-20088
- Supersonic through-flow fan engine and aircraft mission performance
[NASA-TM-102304] p 516 N90-21038
- Study of the engine bird ingestion experience of the Boeing 737 aircraft (October 1986 to September 1988)
[DOT/FAA/CT-89/29] p 723 N90-25119
- From 1959-1989: 30 years of service experience with ramjets
[PNR90677] p 748 N90-25139
- Combustion in the gas turbine. Part 1: Combustor types and design
[CIT/SME/VKI/RS/1] p 748 N90-25986
- Combustion in the gas turbine. Part 2: Preliminary design and performance
[CIT/SME/VKI/RS/3] p 748 N90-25987
- Combustion in the gas turbine. Part 3: Fuel injection, ignition and stability
[CIT/SME/VKI/RS/4] p 748 N90-25988

- Combustor cooling aspects
[CIT/SME/VKI/RS/5] p 749 N90-25989
- Prediction and measurement of rotor blade/stator vane dynamic characteristics of a modern aero-engine axial compressor
[PNR90667] p 750 N90-26002
- The impact and requirements of new materials on aeroengines
[PNR90671] p 750 N90-26003
- Research and development of advanced gas turbine
[DE90-503377] p 776 N90-26335
- Comparative Engine Performance Measurements
[AGARD-LS-169] p 856 N90-27711
- Design of the UETP experiment p 856 N90-27712
- The basis for facility comparison p 856 N90-27713
- Energy Efficient Engine combustor test hardware detailed design report
[NASA-CR-168301] p 929 N90-28554
- Energy Efficient Engine (E3) combustion system component technology performance report
[NASA-CR-168274] p 930 N90-28555
- Energy Efficient Engine exhaust mixer model technology report addendum; phase 3 test program
[NASA-CR-174799] p 930 N90-28556
- Energy Efficient Engine: Flight propulsion system final design and analysis
[NASA-CR-168219] p 930 N90-28558
- Energy Efficient Engine core design and performance report
[NASA-CR-168069] p 930 N90-28559
- Energy Efficient Engine program advanced turbofan nacelle definition study
[NASA-CR-174942] p 930 N90-28560
- Energy Efficient Engine: Control system component performance report
[NASA-CR-174651] p 931 N90-28562
- NASA/GE Energy Efficient Engine low pressure turbine scaled test vehicle performance report
[NASA-CR-168290] p 931 N90-28563
- Energy Efficient Engine integrated core/low spool test hardware design report
[NASA-CR-168137] p 931 N90-28566
- ENGINE FAILURE**
- Breakage of fan blades in the S1 wind tunnel at Mondane-Avriex
[ONERA, TP NO. 1989-104] p 57 A90-11138
- Jet engine fault detection with differential gas path analysis at discrete operating points p 50 A90-12633
- Aeroengine condition monitoring and fault diagnosis system p 188 A90-16851
- Flight over the sea with twin or triple jet aircraft p 179 A90-17048
- Effect of wind shear on flight safety p 175 A90-17973
- Gas turbine engine condition monitoring and fault diagnostics p 190 A90-18594
- Digital control experiment research on the engine JT15D-4 p 190 A90-18600
- A comparison between the design point and near-stall performance of an axial compressor
[ASME PAPER 89-GT-70] p 254 A90-22667
- Vibration analysis for immediate assessment of battle-damaged gas turbine engines
[ASME PAPER 89-GT-96] p 341 A90-23811
- A comprehensive diagnostic system for the T800-APW-800 engine p 422 A90-28181
- Concept demonstration of the use of interactive fault diagnosis and isolation for TF30 engines p 617 A90-41177
- Inclement weather induced aircraft engine power loss
[AIAA PAPER 90-2169] p 662 A90-42055
- Trend analysis and diagnostics codes for training purposes
[AIAA PAPER 90-2394] p 617 A90-42156
- Prompt identification of a troubled engine can help avoid catastrophe p 721 A90-44222
- The survivability of centrifugal compressors in modern aircraft engines p 928 A90-49883
- Report on an overseas visit, June 1988
[AD-A210374] p 52 N90-10040
- Statistics on aircraft gas turbine engine rotor failures that occurred in US commercial aviation during 1986
[DOT/FAA/CT-89/30] p 511 N90-21008
- Application of neural networks to the F/A-18 engine condition monitoring system
[AD-A219820] p 666 N90-24271
- ENGINE INLETS**
- Wind-tunnel test of the air intake of an unducted fan
[AAAF PAPER NT 88-19] p 4 A90-11436
- Theoretical analysis of an icing test apparatus for turbine engine air intakes
[AAAF PAPER NT 88-20] p 23 A90-11437
- A theoretical approach to particle separator design p 48 A90-12584

- Tangential mass addition for the control of shock wave/boundary layer interactions in scramjet inlets p 13 A90-12586
- An investigation into the internal heat transfer characteristics of a thermally anti-iced aero-engine intake lipskin p 111 A90-15390
- A numerical parametric study of a scramjet inlet in a Mach 6 arc heated test facility
[AIAA PAPER 90-0531] p 167 A90-19896
- Development of an anti-icing runback model
[AIAA PAPER 90-0759] p 238 A90-22258
- Effect of inlet flow angle on the erosion of radial turbine guide vanes
[ASME PAPER 89-GT-208] p 254 A90-22664
- Aerodynamic interference of prismatic engine nacelles with the wing at supersonic velocities p 294 A90-24078
- Calculation of transonic axisymmetric flow past an engine nacelle with allowance for viscosity p 296 A90-24107
- Engine inlet distortion in a 9.2 percent scaled vectored thrust STOVL model in ground effect
[AIAA PAPER 89-2910] p 301 A90-25043
- Damping of the inlet vortex in a turbojet engine p 301 A90-25185
- Three-dimensional shock-shock interactions on the scramjet inlet
[AIAA PAPER 90-0529] p 314 A90-26963
- Investigation of cowl vent slots for supercritical stability enhancement in dual-mode ramjet inlets p 507 A90-32951
- Effect of condensation in a diffuser on the flow field p 603 A90-36784
- Influence of bulk turbulence and entrance boundary layer thickness on the curved duct flow field
[AIAA PAPER 90-1502] p 606 A90-38651
- Inlet radial temperature redistribution in a transonic turbine stage
[AIAA PAPER 90-1543] p 565 A90-38687
- CFD applications in an aerospace engine test facility
[AIAA PAPER 90-2003] p 681 A90-40590
- Small-scale inlet testing for low cost screening applications
[AIAA PAPER 90-1926] p 741 A90-42696
- Analysis of shock interactions and flow structure in high speed inlets
[AIAA PAPER 90-2132] p 704 A90-42735
- Computational analysis of an open-nosed fighter/attack inlet
[AIAA PAPER 90-2145] p 704 A90-42737
- Analysis of installed wind tunnel test results on large bypass ratio engine/nacelle installations
[AIAA PAPER 90-2146] p 705 A90-42738
- A computational model for thickening boundary layers with mass addition for hypersonic engine inlet testing
[AIAA PAPER 90-2219] p 705 A90-42750
- Measured operating characteristics of a rectangular combustor/inlet isolator
[AIAA PAPER 90-2221] p 742 A90-42752
- Effect of riblets on flow separation in a subsonic diffuser p 712 A90-45261
- Combustor technology for future aircraft
[AIAA PAPER 90-2400] p 852 A90-47219
- Aspects of the design of a hypersonic engine system and the selection of the intake and tail
[DGLR PAPER 88-040] p 928 A90-50233
- Development of a VSAERO (Vortex Separation Aerodynamics) model of the F/A-18
[AD-A212442] p 95 N90-12566
- Engine inlet distortion in a 9.2 percent scale vectored thrust STOVL model in ground effect
[NASA-TM-102358] p 318 N90-17561
- Study of bird ingestions into small inlet area, aircraft turbine engines (May 1987 to April 1988)
[DOT/FAA/CT-89/17] p 402 N90-18375
- Control of flow separation and mixing by aerodynamic excitation
[NASA-TM-103131] p 571 N90-21733
- Finite element elastic-plastic-creep and cyclic life analysis of a cowl lip
[NASA-TM-102342] p 610 N90-22808
- Finite element analysis of structural components using viscoplastic models with application to a cowl lip problem
[NASA-CR-185189] p 690 N90-23769
- Research and development of advanced gas turbine
[DE90-503377] p 776 N90-26335
- Modeling of supersonic reacting flow fields p 855 N90-26898

ENGINE MONITORING INSTRUMENTS

- A multichannel wide FOV infrared radiometric system p 67 A90-11410
- Turbomachinery blade vibration and dynamic stress measurements utilizing nonintrusive techniques p 41 A90-11558

- Development of a remaining useful life of a lubricant evaluation technique. III - Cyclic voltammetric methods p 125 A90-15732
- Noninterference blade-vibration measurement system for gas turbine engines p 132 A90-16372
- Aeroengine condition monitoring and fault diagnosis system p 188 A90-16851
- Gas turbine engine condition monitoring and fault diagnostics p 190 A90-18594
- Instrumentation for combustion and flow in engines; Proceedings of the NATO Advanced Study Institute, Vimeiro, Portugal, Sept. 13-26, 1987 p 211 A90-19004
- On-line temperature profile display system
[ASME PAPER 89-GT-10] p 374 A90-23755
- Casing vibration and gas turbine operating conditions
[ASME PAPER 89-GT-78] p 358 A90-23799
- A microprocessor-based system for monitoring gas turbines p 350 A90-24359
- A comprehensive diagnostic system for the T800-APW-800 engine p 422 A90-28181
- F-111/TF30 engine monitoring system - A fusion of past, present, and future technology p 425 A90-30817
- Onboard maintenance system testing - The Boeing 747-400 Central Maintenance Computer
[AIAA PAPER 90-1303] p 505 A90-33917
- Study on process control of aeroengine using microcomputer p 586 A90-37239
- V-22 engine installation and removal tool - Designing support equipment with the aircraft, not after p 581 A90-38538
- Expert diagnosis system for FJR engine troubles p 587 A90-38597
- Prompt identification of a troubled engine can help avoid catastrophe p 721 A90-44222
- A simulation evaluation of the engine monitoring and control system display
[NASA-TP-2960] p 420 N90-18393
- Preliminary development of an intelligent computer assistant for engine monitoring
[NASA-TM-101702] p 612 N90-22322
- Application of neural networks to the F/A-18 engine condition monitoring system
[AD-A219820] p 666 N90-24271
- Computer modeling and data processing methods: An essential part of jet engine condition monitoring and fault diagnosis p 855 N90-27626
- Experimental identification of helicopter engine dynamics from closed loop data p 855 N90-27627
- Advanced algorithms design and implementation in on-board microprocessor systems for engine life usage monitoring p 892 N90-27628
- Harrier Information Management System (HIMS): The system and the approach p 884 N90-27630
- ENGINE NOISE**
- Recent research on external helicopter noise at ONERA p 218 A90-16825
- Directivity of the noise radiation emitted from the inlet duct of a turboshaft helicopter engine
[ONERA, TP NO. 1990-26] p 695 A90-41205
- Future development of the 535E4 engine p 745 A90-44596
- A source of discrete noise components in the flow path of gas turbines and fans p 894 A90-46506
- Near-field noise predictions of an aircraft in cruise p 140 N90-12538
- The 757 NLF glove flight test results p 104 N90-12546
- Re-engine with the Rolls-Royce Tay 670, the route to significant noise reduction
[PNR90585] p 115 N90-12606
- The commercial aircraft noise problem
[PNR90577] p 140 N90-13203
- Evaluation of analysis techniques for low frequency interior noise and vibration of commercial aircraft
[NASA-CR-181851] p 220 N90-14866
- A/F32T-9 large turbo fan engine enclosed noise suppressor system (T-9 NSS), exterior far-field and interior noise, McConnell AFB, Kansas
[AD-A220535] p 665 N90-23402
- Noise measurements of turboprop airplanes at different overflight elevations p 697 N90-24860
- Stage 2 re-engining: The only way to achieve a real stage 3 aircraft
[PNR90636] p 737 N90-25977
- Air Force procedure for predicting aircraft noise around airbases: Airbase operations program (BASEOPS) description
[AD-A223069] p 895 N90-27466
- Air Force procedure for predicting aircraft noise around airbases: Noise Exposure Model (NOISEMAP). User's manual
[AD-A223162] p 895 N90-27467

- Vibration responses of two house structures during the Edwards Air Force Base phase of the national sonic boom program
[NASA-CR-182089] p 966 N90-29169
- Audibility and annoyance of en route noise of unducted fan engines
[AD-A223687] p 966 N90-30035
- ### ENGINE PARTS
- Mechanical rig rest of FJR 710/600 engine components p 43 A90-12016
- Gas turbine engine component development - An integrated approach p 112 A90-16006
- Integrated approach to design and manufacture of gas turbine components based on group theory p 113 A90-16010
- Diffusion bonding aeroengine components p 131 A90-16012
- Production of Ti6Al4V-components for a new turbo-fan-engine p 132 A90-16618
- Application of computational systems to aircraft engine components development p 188 A90-17448
- Computerised structural analysis for engine components p 190 A90-18486
- Three dimensional photoelastic analysis of aeroengine parts p 270 A90-20077
- Finite element analysis of nonstationary temperature fields in gas turbine components p 271 A90-21324
- Some aspects of the erosive wear of components of aircraft turbine engines p 253 A90-21627
- Advanced turbine technology applications project (ATTAP) - Overview, status, and outlook
[ASME PAPER 89-GT-118] p 360 A90-23819
- Thermal barrier characteristics of partially stabilized zirconia coatings on Incoloy alloy 909 (A controlled expansion alloy)
[ASME PAPER 89-GT-146] p 354 A90-23839
- A review of failure models for ceramic matrix composite laminates under monotonic loads
[ASME PAPER 89-GT-153] p 354 A90-23842
- Injection molding development of ceramic turbine components
[ASME PAPER 89-GT-170] p 361 A90-23855
- Ultra High Bypass (UHB) engine critical component technology
[ASME PAPER 89-GT-229] p 342 A90-23884
- Engineering design of tough ceramic matrix composites for turbine components
[ASME PAPER 89-GT-294] p 343 A90-23892
- Basic approach in the development of TURBISTAN, a loading standard for fighter aircraft engine disks p 368 A90-26754
- Reliability evaluation system for ceramic gas turbine components p 444 A90-27678
- Desktop failure analysis on a microcomputer using Weibull, lognormal, and renewal data
[ASME PAPER 89-GT-275] p 535 A90-32263
- Metallurgy of investment cast superalloy components p 531 A90-34154
- Probabilistic design technology for ceramic components p 601 A90-35507
- The role of NDE in ceramic turbine engine component development p 601 A90-35508
- Wide chord fan club p 584 A90-35600
- Component arrangement studies for an 8000 shp turboshaft high technology core
[AIAA PAPER 90-2398] p 663 A90-42159
- Development of impact design methods for ceramic gas turbine components p 687 A90-42165
- CFE738 - A case for joint engine development
[AIAA PAPER 90-2522] p 664 A90-42197
- Aircraft engine inspection p 771 A90-44606
- Slip-cast hot isostatically pressed silicon nitride gas turbine components p 765 A90-44816
- Design of the optimal hardening treatment for the metal surfaces of gas turbine engine components p 873 A90-46496
- Full scale technology demonstration of a modern counterrotating unducted fan engine concept: Component test
[NASA-CR-180868] p 53 N90-10047
- Improved silicon carbide for advanced heat engines
[NASA-CR-180831] p 65 N90-10293
- Effects of a heat cycle on material strength
[NAL-TM-562] p 113 N90-11737
- Advanced technology in military gas turbine design and manufacture
[PNR90545] p 114 N90-11747
- Aluminium alloy development for aero engines
[PNR90548] p 126 N90-11874
- The role of component testing
[PNR90589] p 115 N90-12608
- Real-time simulation of an F110/STOVL turbofan engine
[NASA-TM-102409] p 117 N90-12618
- Constitutive modeling for isotropic materials (HOST)
[NASA-CR-179522] p 193 N90-13390
- Constitutive modeling for isotropic materials (HOST)
[NASA-CR-174718] p 193 N90-13391
- A study of variable geometry in advanced gas turbines p 255 N90-15104
- Proceedings of the 1988 Structural Integrity Program Conference
[AD-A213545] p 275 N90-15486
- AGARD/SMP Review: Damage Tolerance for Engine Structures. 2: Defects and Quantitative Materials Behaviour --- conference
[AGARD-R-769] p 425 N90-18396
- Defects in monoblock cast turbine wheels p 443 N90-18400
- Review of modelling methods to take account of material structure and defects p 425 N90-18402
- The need for a common approach within AGARD --- engine component defects p 425 N90-18404
- Compendium of abstracts and viewgraphs.
[AD-A217189] p 532 N90-20140
- Attachment of lead wires to thin film thermocouples mounted on high temperature materials using the parallel gap welding process
[NASA-TM-102442] p 543 N90-21361
- Combustion in the gas turbine. Part 2: Preliminary design and performance
[CIT/SME/VKI/RS/3] p 748 N90-25987
- The application of engineering ceramics in gas turbines
[PNR90676] p 750 N90-26005
- The role of NDI in the certification of turbine engine components
[PNR90629] p 777 N90-26349
- AGARD damage tolerance concepts for engine structures Workshop 3, Component Behaviour and Life Management p 855 N90-27705
- Life management planning p 856 N90-27709
- Component behaviour and life management: The need for common AGARD approaches and actions p 856 N90-27710
- The role of NDI in the certification of turbine engine components p 859 N90-28069
- Critical inspection of high performance turbine engine components: The RFC concept p 859 N90-28073
- Energy Efficient Engine: Control system component performance report
[NASA-CR-174651] p 931 N90-28562
- Evaluation of high temperature protective coatings for gas turbine engines under simulated service conditions p 952 N90-28712
- Surface property improvement in titanium alloy gas turbine components through ion implantation p 953 N90-28713
- ### ENGINE STARTERS
- Start characteristics of FJR 710/600S engine p 42 A90-12013
- Restart characteristics of turbofan engines p 50 A90-12627
- A very high speed switched-reluctance starter-generator for aircraft engine applications p 452 A90-30791
- Control of a switched-reluctance aircraft engine starter-generator over a very wide speed range p 586 A90-38130
- Starter systems and auxiliary power units p 660 A90-41760
- Application considerations for integral gas turbine electric starter/generator revisited
[SAE PAPER 892252] p 746 A90-45454
- Effect of the fluid level of a hydraulic shock absorber on the characteristics of the gas supply system p 851 A90-46504
- ### ENGINE TESTS
- Endurance test of FJR 710/600S engine p 42 A90-12012
- Start characteristics of FJR 710/600S engine p 42 A90-12013
- Oil migration of FJR 710/600S engine p 43 A90-12014
- Steady state performance of FJR 710/600S engine p 43 A90-12015
- Mechanical rig rest of FJR 710/600 engine components p 43 A90-12016
- The use of pulse facilities for testing supersonic combustion ramjet (scramjet) combustors in simulated hypersonic flight conditions p 46 A90-12562
- Aircraft engine vibration analysis p 46 A90-12568
- A study on the performance of the turbo-ramjet engines at high speed flight p 49 A90-12608
- Icing test techniques for air intake screens on helicopters functioning in temperatures around 0 C p 23 A90-12619
- Designing the next generation flying test bed
[SAE PAPER 891049] p 100 A90-14353
- Validation of the accelerated equivalent testing of gas turbine engines for multivariant applications p 110 A90-14568
- Design of a language for the testing of aircraft engines p 137 A90-14573
- Future test rigs p 200 A90-19012
- Efficiency testing of a helicopter transmission planetary reduction stage p 271 A90-21113
- Optimal selection of the parameters to be measured during the identification of gas turbine engines. I - Problem statement p 255 A90-23410
- Experimental examination of the aerothermal performance of a gas turbine engine test facility
[ASME PAPER 89-GT-94] p 341 A90-23810
- The design and test of a two stage transonic axial flow compressor
[ASME PAPER 89-GT-164] p 341 A90-23852
- A comparison between engine test results and design predictions of turbine blade cooling performance
[ASME PAPER 89-GT-169] p 341 A90-23854
- Experimental investigation of supersonic turbine performance
[ASME PAPER 89-GT-238] p 342 A90-23888
- The effect of experimental uncertainties on icing test results
[AIAA PAPER 90-0665] p 322 A90-26977
- A test facility for high-pressure high-temperature combustion chambers p 438 A90-29924
- Advanced technology ATE for fuel accessory testing p 439 A90-30770
- Eliminating the TF30 P-111 + engine rotor-instability problem p 508 A90-32961
- Some aspects of the control system and power unit lead tests using in-flight simulator systems and flying test-beds
[AIAA PAPER 90-1323] p 580 A90-36031
- Scramjet testing from Mach 4 to 20 - Present capability and needs for the nineties
[AIAA PAPER 90-1388] p 597 A90-38485
- An application of expert system to jet engine diagnostic procedures p 587 A90-38596
- CFD applications in an aerospace engine test facility
[AIAA PAPER 90-2003] p 681 A90-40590
- Adjusting turbine engine transient performance for the effects of environmental variances
[AIAA PAPER 90-2501] p 658 A90-40639
- Developmental tests on the M 88 engine are on track p 660 A90-41761
- Gas turbine engine brush seal applications
[AIAA PAPER 90-2142] p 685 A90-42041
- Multiple swirler dome combustor for high temperature rise applications
[AIAA PAPER 90-2159] p 661 A90-42050
- The GMA 2100 and GMA 3007 engines for regional aircraft
[AIAA PAPER 90-2523] p 744 A90-42815
- A real time microcomputer implementation of sensor failure detection for turbofan engines p 745 A90-45414
- Considerations in using broad specification fuels for aircraft propulsion
[SAE PAPER 892330] p 765 A90-45487
- Design of computer-aided aircraft testing systems. II p 785 A90-46498
- An analysis of cavity resonance in the aeroengine casing during rig testing p 894 A90-49481
- Performance potential of an advanced technology Mach 3 turbojet engine installed on a conceptual high-speed civil transport
[NASA-TM-4144] p 51 N90-10034
- Full scale technology demonstration of a modern counterrotating unducted fan engine concept: Component test
[NASA-CR-180868] p 53 N90-10047
- Full scale technology demonstration of a modern counterrotating unducted fan engine concept: Engine test
[NASA-CR-180869] p 53 N90-10049
- Test and evaluation: Reducing risks to military aircraft from bird collisions. Report to the Chairman, Legislation, and National Security Subcommittee, Committee on Government Operations, House of Representatives
[AD-A210670] p 25 N90-10845
- The role of component testing
[PNR90589] p 115 N90-12608
- Aviation Engine Test Facilities (AETF) fire protection study
[AD-A211483] p 134 N90-12777
- Advanced Turbine Technology Applications Project (ATTAP)
[NASA-CR-185109] p 220 N90-14153
- Advanced detection, isolation, and accommodation of sensor failures in turbofan engines: Real-time microcomputer implementation
[NASA-TP-2925] p 259 N90-15112

- The Uniform Engine Test Programme
[AGARD-AR-248] p 428 N90-19232
- Evaluation of various thrust calculation techniques on an F404 engine
[NASA-TP-3001] p 735 N90-25134
- Gas Turbine Combustion, volume 2
[VKI-LS-1990-02-VOL-2] p 749 N90-25995
- Subsonic combustor testing p 749 N90-25997
- Handbook of uncertainty methodology for engine testing at Pyestock (England)
[RAE-TM-P-1179] p 751 N90-26007
- Bringing aircraft noise testing down to Earth
[PNR90642] p 783 N90-26637
- Comparative evaluation of Allison T56 engine chip detectors
[AD-A221864] p 855 N90-26832
- AGARD/SMP Review Damage Tolerance for Engine Structures. 3: Component Behaviour and Life Management
[AGARD-R-770] p 855 N90-27704
- AGARD damage tolerance concepts for engine structures Workshop 3, Component Behaviour and Life Management p 855 N90-27705
- Component behaviour and life management: The need for common AGARD approaches and actions p 856 N90-27710
- Comparative Engine Performance Measurements
[AGARD-LS-169] p 856 N90-27711
- Design of the UETP experiment p 856 N90-27712
- The basis for facility comparison p 856 N90-27713
- Comparison of ground-level test cells and ground-level to altitude test cells p 857 N90-27716
- Experience in developing an improved design of experiment (lessons learned) p 857 N90-27718
- Experience in developing an improved altitude test capability p 857 N90-27719
- General test plan p 857 N90-27721
- Engine testing of thermographic phosphors
[DE90-013269] p 885 N90-28059
- The reduction of smoke emissions from Allison T56 engines
[ARL-PROP-R-182] p 928 N90-28547
- Energy Efficient Engine: Control system component performance report
[NASA-CR-174651] p 931 N90-28562
- Energy Efficient Engine integrated core/low spool test hardware design report
[NASA-CR-168137] p 931 N90-28566
- Source emission test of gas turbine engine test facility, Kelly AFB, TX
[AD-A223869] p 932 N90-28571
- The effects of a compressor rebuild on gas turbine engine performance: Final results p 952 N90-28701
- ENGINEERING**
Eshbach's handbook of engineering fundamentals / 4th edition/ p 448 A90-28825
- ENGINEERING MANAGEMENT**
The impact of total quality management (TQM) and concurrent engineering on the aircraft design process p 785 A90-46927
- ENTHALPY**
Embedded function methods for supersonic turbulent boundary layers
[AIAA PAPER 90-0306] p 163 A90-19787
- Enthalpy damping for high Mach number Euler solutions
[AIAA PAPER 90-1585] p 566 A90-38720
- Radio frequency (RF) heated supersonic flow laboratory
[AIAA PAPER 90-2469] p 673 A90-42186
- High enthalpy hypersonic wind tunnel F4: General description and associated instrumentation p 673 N90-24228
- Design of an axisymmetric, contoured nozzle for the HEG
[DLR-FB-90-04] p 959 N90-28812
- ENTRAINMENT**
The sonic eddy - A model for compressible turbulence
[AIAA PAPER 90-0495] p 167 A90-19876
- Leading edge vortex dynamics on a pitching delta wing
[NASA-CR-186327] p 398 N90-19198
- ENTRAPMENT**
Entrapment plating of abrasive particles for jet engine clearance control
[SAE PAPER 890918] p 286 A90-24685
- ENTROPY**
The transonic nonisentropic potential calculation p 304 A90-25739
- Entropy wave instability in compact ramjets p 858 N90-27932
- ENVIRONMENT EFFECTS**
Coatings for gas turbine compressors
[NLR-MP-88045-U] p 115 N90-11750

- The next generation supersonic transport engine: Critical issues
[PNR90576] p 115 N90-12605
- Noise and sonic boom impact technology. Initial development of an Assessment System for Aircraft Noise (ASAN). Volume 1: Executive summary
[AD-A214164] p 379 N90-17410
- Noise and sonic boom impact technology. Initial development of an Assessment System for Aircraft Noise (ASAN). Volume 2: System design strategy
[AD-A214454] p 379 N90-17411
- Evaluation of composite components on the Bell 206L and Sikorsky S-76 helicopters
[NASA-TM-4195] p 876 N90-27787
- Assessment System for Aircraft Noise (ASAN): Development of alpha-test prototype system software
[AD-A223770] p 966 N90-30036
- ENVIRONMENT POLLUTION**
Proposed definition of the term en route in en route aircraft noise p 696 N90-24854
- En route noise of two turboprop aircraft
[DLR-MITT-89-18] p 697 N90-24859
- The effect of noise-abatement profiles on noise immissions and human annoyance underneath a subsequent climbpath p 698 N90-24865
- Problems related to aircraft noise in Switzerland p 698 N90-24871
- ENVIRONMENT SIMULATION**
Results of aerodynamic testing of large-scale wing sections in a simulated natural rain environment
[AIAA PAPER 90-0486] p 167 A90-19874
- Adjusting turbine engine transient performance for the effects of environmental variances
[AIAA PAPER 90-2501] p 658 A90-40639
- Simulating turbulence and gusts for handling qualities evaluation
[AIAA PAPER 90-2845] p 754 A90-45174
- An assessment of analytical methods and lightning simulation test techniques used in lightning qualification and surveillance testing p 818 A90-49833
- Analysis of indirect effects of lightning on a metallic A 300 wing: Test report
[REPT-E87/645800] p 323 N90-16726
- Proceedings of the 13th International Congress on Instrumentation in Aerospace Simulation Facilities
[EOARD-LR-89-069] p 527 N90-21046
- ENVIRONMENT SIMULATORS**
Aircraft Reply and Interference Environment Simulator (ARIES) hardware principles of operation. Volume 2: Appendixes
[DOT/FAA/CT-TN88/4-2] p 135 N90-12781
- Aircraft Reply and Interference Environment Simulator (ARIES) hardware principles of operation, volume 1
[DOT/FAA/CT-TN88/4-1] p 135 N90-12782
- ENVIRONMENTAL CONTROL**
Embedded digital control for aircraft environmental control systems - A practical vehicle management system approach
[SAE PAPER 891438] p 339 A90-27409
- Microprocessor control of a vapor-cycle cooling system
[SAE PAPER 891457] p 339 A90-27426
- Automatic environmental control system for electronic equipment platforms
[SAE PAPER 901217] p 840 A90-49292
- Aircraft subsystem waste energy recovery and management
[SAE PAPER 901218] p 840 A90-49293
- Use of ECS-conditioned air for FLIR avionics thermal control - Fighter aircraft
[SAE PAPER 901219] p 840 A90-49294
- Proven dynamic modeling techniques for concurrent design and analysis of ECS controllers
[SAE PAPER 901234] p 841 A90-49304
- F-15 Environment Control System improvements
[SAE PAPER 901235] p 841 A90-49305
- Evaluation and control of an Integrated Closed Environmental Control System (ICECS)
[SAE PAPER 901237] p 841 A90-49307
- Enhanced environmental control for the Harrier II Plus
[SAE PAPER 901238] p 841 A90-49308
- ENVIRONMENTAL MONITORING**
Meeting Review: Workshop on Airborne Instrumentation
[PB89-174775] p 39 N90-10032
- ENVIRONMENTAL QUALITY**
The US National Transonic Facility, NTF p 262 N90-15942
- Synthetic aperture radar imagery of airports and surrounding areas: Philadelphia Airport
[NASA-CR-4280] p 401 N90-18372
- ENVIRONMENTAL SURVEYS**
Noise and sonic boom impact technology. Initial development of an Assessment System for Aircraft Noise (ASAN). Volume 1: Executive summary
[AD-A214164] p 379 N90-17410

- Noise and sonic boom impact technology. Initial development of an Assessment System for Aircraft Noise (ASAN). Volume 2: System design strategy
[AD-A214454] p 379 N90-17411
- Noise and sonic boom impact technology. Initial development of an Assessment System for Aircraft Noise (ASAN). Volume 3: Technical description
[AD-A214455] p 379 N90-17412
- Assessment System for Aircraft Noise (ASAN) citation database. Volume 3: New citation review procedures
[AD-A219177] p 615 N90-23190
- Air Force procedure for predicting aircraft noise around airbases: Airbase operations program (BASEOPS) description
[AD-A223069] p 895 N90-27466
- ENVIRONMENTAL TESTS**
High performance single-mode coupler for harsh environments p 78 A90-11027
- Water ingestion simulation - Test needs p 23 A90-12620
- A full scale, VSTOL, ground environment test facility p 58 A90-12631
- Scenario 2000
[MBB-UD-560/89] p 222 A90-22698
- New concept for improved nonmetallic erosion protection systems p 407 A90-28188
- Strength substantiation of the all composite airframe (A materials data base approach) p 490 A90-31519
- Rain erosion testing --- on polymethyl methacrylate specimens p 525 A90-34578
- Applying AVIP to high voltage power supply designs --- Avionic Integrity Program p 605 A90-38132
- Adjusting turbine engine transient performance for the effects of environmental variances
[AIAA PAPER 90-2501] p 658 A90-40639
- EPOXY COMPOUNDS**
Compressive viscoelastic effects (creep) of a unidirectional glass/epoxy composite material p 946 A90-50170
- EPOXY MATRIX COMPOSITES**
The advantages of automation in aerospace production p 130 A90-15357
- Design and fabrication of the carbon fiber/epoxy A-320 horizontal tailplane p 286 A90-25221
- Core composites in Swissair aircraft p 493 A90-33709
- A comparison of honeycomb-core and foam-core carbon-fibre/epoxy sandwich panels p 764 A90-43855
- 977 - Characterization of a family of new toughened epoxy resins p 943 A90-50089
- Development of a high toughness heat resistant 177 C (350 F) curing film adhesive for aerospace bonding applications - FM 377 adhesive p 955 A90-50126
- Rigidite 5255-3 - A highly damage tolerant prepreg resin system with a well balanced property profile p 944 A90-50139
- Impact of composites in the aerospace industry
[ETN-90-96231] p 443 N90-18527
- Development of an automated ultrasonic inspection system for composite structure on in-service aircraft p 885 N90-28079
- EPOXY RESINS**
Repair of composite aircraft parts - An operator's viewpoint p 221 A90-20606
- Repair adhesives - Development criteria for field level conditions p 528 A90-31575
- Evaluation of various non-asbestos epoxy adhesives for aircraft repair p 529 A90-33078
- High service temperature high compressive strength and tough prepreg system p 530 A90-33098
- 977 - Characterization of a family of new toughened epoxy resins p 943 A90-50089
- A high performance aerospace resin for Resin Transfer Molding p 945 A90-50163
- Criteria for polymer concrete on airport pavements
[DOT/FAA/DS-89/18] p 527 N90-21045
- EQUATIONS OF MOTION**
Whole helicopter aeroelasticity - Experience with a new approach p 492 A90-33380
- Rotary damping in aircraft motion due to jet propulsion system p 520 A90-34820
- Kane's methods in rotorblade dynamics p 646 A90-42458
- Stability and controllability in proportional navigation p 725 A90-42990
- The role of bearing support stiffness anisotropy in suppression of rotordynamic instability p 879 A90-46215
- Stall/spin/flight simulation
[DOT/FAA/CT-88/28] p 122 N90-11765
- Software and hardware description of the helicopter motion equations for VAX computers
[AD-A213248] p 184 N90-13375

AcSim: Aircraft simulation program with application to flight profile generation
[AD-A212466] p 185 N90-14217

Introduction to data items on flight path optimisation
[ESDU-89015] p 185 N90-14221

Calculation of the flow field of a multiblade helicopter rotor using a Euler method including the wake
p 278 N90-16189

Equations of motion of slung load systems with results for dual lift
[NASA-TM-102246] p 349 N90-17641

ETO (Earth-To-Orbit): A trajectory program for aerospace vehicles
[AD-A218157] p 528 N90-20103

Design of a helicopter automatic flight control system using adaptive control
p 522 N90-21040

Coupled rotor-body equations of motion hover flight
[NASA-CR-186710] p 717 N90-25111

Modeling flexible aircraft for flight control design
[AD-A219123] p 757 N90-25140

Identification of aerodynamic models for maneuvering aircraft
[NASA-CR-186630] p 719 N90-25943

Windshear estimation along the trajectory of an aircraft
p 963 N90-29745

Three-dimensional numerical study of thunderstorm downdrafts and associated outflow boundaries
p 963 N90-29746

EQUILIBRIUM EQUATIONS
Transient aeroelastic computations using multiple moving frames of reference
[AIAA PAPER 90-3053] p 798 A90-45932

EQUILIBRIUM FLOW
Equilibrium of an elastic porous shell in supersonic gas flow
p 150 A90-17109

EQUILIBRIUM METHODS
An examination of helicopter rotor load calculations
p 833 A90-46972

EQUIPMENT SPECIFICATIONS
Requirements for meteorological equipment designed for the acquisition of meteorological data essential for the takeoff and landing of aircraft at civil airports
p 962 A90-50777

EROSION
Effect of environmental particles on a radial compressor
p 113 A90-16373

Some aspects of the erosive wear of components of aircraft turbine engines
p 253 A90-21627

Performance improvement of an eroded axial flow compressor using water injection
[AIAA PAPER 90-2016] p 741 A90-42718

Jet engines performance deterioration
p 852 A90-46871

EROSIVE BURNING
Effect of inlet flow angle on the erosion of radial turbine guide vanes
[ASME PAPER 89-GT-208] p 254 A90-22664

Simulation of compressor performance deterioration due to erosion
[ASME PAPER 89-GT-182] p 254 A90-22665

Inverse heat transfer studies and the effects of propellant aluminum on TVC jet vane heating and erosion
[AIAA PAPER 90-1860] p 655 A90-40533

ERROR ANALYSIS
A methodology for validating software reliability
[AIAA PAPER 89-3081] p 74 A90-10567

Mean-square approximation by an even nonnegative polynomial
p 374 A90-24101

Design considerations for achieving MLS Category III requirements
p 331 A90-25575

Global Positioning System: Arrival in the fleet - A GPS AN/SRN-25(V) receiver assessment
p 331 A90-26338

A bearing error in the VHF omnirange due to sea surface reflection
p 402 A90-27875

Estimation of atmospheric and transponder survey errors with a navigation Kalman filter
p 459 A90-30689

A dynamic optical model attitude measurement system
p 539 A90-34236

Concept demonstration of the use of interactive fault diagnosis and isolation for TF30 engines
p 617 A90-41177

LDV measurements and the flow analysis in the vortex region of a radial inflow turbine
p 511 N90-21007

Handbook of uncertainty methodology for engine testing at Pyestock (England)
p 751 N90-26007

[RAE-TM-P-1179]

Obtaining consistent models of helicopter flight-data measurement errors using kinematic-compatibility and state-reconstruction methods
[AD-A222533] p 815 N90-26799

ERROR CORRECTING DEVICES
Optimal selection of GPS sets to minimize emitter location errors
p 97 A90-13992

ERROR DETECTION CODES

Real-time fault monitoring for aircraft applications using quantitative simulation and expert systems
[AIAA PAPER 89-3103] p 37 A90-10586

Fine resolution errors in secondary surveillance radar altitude reporting amongst aircraft transmitting the conspicuity codes 4321 and 4322
[RSRE-88004] p 135 N90-12816

Multigrid and defect correction for the steady Navier-Stokes equations: Applications to aerodynamics
[ETN-90-96011] p 212 N90-13727

Computer modeling and data processing methods: An essential part of jet engine condition monitoring and fault diagnosis
p 855 N90-27626

Knowledge based diagnosis of jet engines under consideration of model based methods
p 855 N90-27631

Fault Detection and Isolation (FDI) techniques for guidance and control systems
p 918 N90-29366

ERROR SIGNALS

Dynamic interaction of separate INS/GPS Kalman filters (Filter-driving - Filter dynamics)
p 124 A90-13996

MLS - A total system approach
p 640 A90-41710

Estimation of the efficiency of various operational modes of a navigation complex
p 725 A90-42924

ERRORS

Formulation and verification of a technique for compensation of pneumatic attenuation errors in airborne pressure sensing devices
p 369 N90-17084

Dallas/Fort Worth simulation, volume 1
[DOT/FAA/CT-TN89/28-VOL-1] p 824 N90-26802

Sideslip-induced static pressure errors in flight-test measurements
[NASA-TM-102846] p 849 N90-27702

Studies in automatic speech recognition and its application in aerospace
p 958 N90-28759

ESCAPE (ABANDONMENT)

An analysis of factors impeding passenger escape from aircraft fires
p 322 A90-26018

The human factors relating to escape and survival from helicopters ditching in water
[AGARD-AG-305(E)] p 176 N90-13358

ESCAPE SYSTEMS

Pre-escape and escape aircraft maneuvers and gyrations - A critical under-reported problem affecting escape system performance and aircrew safety
p 21 A90-10264

Boeing Transonic Windblast Generator System (BTWGS)
p 199 A90-17413

Canopy fragilization using embedded detonating cord
p 180 A90-17417

Escape system evolution
p 722 A90-44656

Escape and survival following helicopter ditching - Research aspects
p 722 A90-44659

A preliminary sensitivity analysis of the Generalized Escape System Simulation (GESS) computer program [DE89-016891] p 24 N90-10844

Supersonic aerodynamic characteristics of a proposed Assured Crew Return Capability (ACRC) lifting-body configuration
[NASA-TM-4136] p 317 N90-17560

Implications of Advanced Technologies for Air and Spacecraft Escape
[AGARD-CP-472] p 483 N90-20054

Development of an ejection seat specification for a new fighter aircraft
p 483 N90-20057

Escape systems research at RAE
p 483 N90-20058

Fighter escape system: The next step forward
p 483 N90-20059

Potential role of avionics in escape systems
p 483 N90-20060

Controllable propulsion for escape systems control
p 484 N90-20064

Forward canopy feasibility and Thru-The-Canopy (TTC) ejection system study
[AD-A220360] p 637 N90-24258

Development of a microcomputer based software system for use in crewmember ejection analysis
[AD-A220398] p 723 N90-25117

ESTIMATES

On the application of modified stepwise regression for the estimation of aircraft stability and control parameters [REPT-8905] p 198 N90-13400

A quantitative technique to estimate microburst wind shear hazard to aircraft
p 692 N90-25040

Structure-borne noise estimates for the PTA aircraft
[NASA-CR-4315] p 896 N90-28396

ESTIMATING

Methodology for estimating helicopter performance and weights using limited data
p 829 A90-46936

Normal force, pitching moment, and side force of forebody-cylinder combinations for angles of attack up to 90 degrees and Mach numbers up to 5
[ESDU-89014] p 173 N90-14192

Example of procedure in calculation of control hinge moments
[ESDU-89010] p 199 N90-14240

The effect of aircraft size on cabin floor dynamic pulses
[DOT/FAA/CT-88/15] p 735 N90-25136

An accurate numerical technique for determining flight test rate gyroscope biases prior to takeoff
[AD-A220987] p 739 N90-25138

Effects of simplifying assumptions on optimal trajectory estimation for a high-performance aircraft
[NASA-TM-101721] p 757 N90-25142

Structure-borne noise estimates for the PTA aircraft
[NASA-CR-4315] p 896 N90-28396

Windshear estimation along the trajectory of an aircraft
p 963 N90-29745

ESTIMATORS

Parameter sensitivity analysis of one kind of flight path reconstruction estimator
p 779 A90-44832

A robust wind shear stochastic controller-estimator [AIAA PAPER 90-3489] p 867 A90-47737

ETCHING

Chrome free electrolytic deoxidizer for aluminum
p 956 A90-50216

ETHYL ALCOHOL

Straight alcohol fuels for general aviation aircraft
[SAE PAPER 891038] p 124 A90-14344

Ethanol and methanol in intermittent combustion engines
p 950 A90-51622

Investigations into gasoline/alcohol blends for use in general aviation aircraft
p 950 A90-51623

A proposal for fuel specification activities relating to general aviation intermittent combustion engines
p 951 A90-51625

In-flight evaluations of turbine fuel extenders
[DOT/FAA/CT-89/33] p 444 N90-19387

Turbine fuel alternatives (near term)
[AD-A219405] p 601 N90-22695

ETHYLENE

Nonflammable hydraulic power system for tactical aircraft. Volume 1: Aircraft system definition, design and analysis
[AD-A218493] p 671 N90-23409

EULER EQUATIONS OF MOTION

A class of implicit upwind schemes for Euler simulations with unstructured meshes
p 5 A90-11597

Calculation of unsteady Euler flows in turbomachinery using the linearized Euler equations
p 5 A90-11778

Numerical Euler solution for the interaction between oscillating cascade and forced inlet unsteadiness
p 8 A90-11792

Computation of transonic separated flow using the Euler equations
p 85 A90-15233

Euler solutions with a multi-block structured code
p 86 A90-15739

Supersonic/hypersonic Euler flowfield prediction method for aircraft configurations
p 145 A90-16767

Calculation of two-dimensional transonic flow of Euler equations with multigrid method
p 149 A90-16835

Multigrid solution method for the Euler equations -- Book
p 149 A90-16841

Hybrid finite volume approach to Euler solutions for supersonic flows
p 154 A90-18144

Solving compressible flow problems using adaptive finite quadtree and octree grids
p 155 A90-18243

Euler and Navier-Stokes solutions for hypersonic flows
p 155 A90-18254

Numerical methods to solve the incompressible Euler and Navier-Stokes equations in 3D with applications
p 209 A90-18302

Aerodynamic design of an HP compressor stage using advanced computation codes
p 156 A90-18479

Numerical method for solving the Euler equation for unsteady transonic flows over oscillating airfoils
p 157 A90-18578

A new implicit hybrid schemes for the Euler equation of transonic flow
p 158 A90-18608

Block multigrid implicit solution of the Euler equations of compressible fluid flow
[AIAA PAPER 90-0106] p 162 A90-19684

Fresh look at floating shock fitting
[AIAA PAPER 90-0108] p 162 A90-19686

An efficient upwind relaxation-sweeping algorithm for three-dimensional Euler equations
[AIAA PAPER 90-0129] p 162 A90-19695

Recent developments in calculation methods for internal flows by solution of Euler or Navier-Stokes equations [ONERA, TP NO. 1989-167] p 223 A90-21033

Application of an efficient hybrid scheme for aeroelastic analysis of advanced propellers
[AIAA PAPER 90-0028] p 226 A90-22153

Numerical simulation of supersonic unsteady flow using Euler equations
[AIAA PAPER 90-0415] p 229 A90-22215

An Euler method for wing-body-winglet flows
[AIAA PAPER 90-0436] p 229 A90-22218

A three-dimensional space marching algorithm for the solution of the Euler equations on unstructured grids
[AIAA PAPER 90-0014] p 234 A90-23701

Design of symmetric profiles with maximum critical flow Mach number under prescribed constraints
p 295 A90-24095

A new quick method for integrating Euler equations for plane transonic flows
p 295 A90-24105

Unsteady Euler analysis of the flowfield of a propan at an angle of attack
[AIAA PAPER 90-0339] p 300 A90-25028

Numerical solutions of the linearized Euler equations for unsteady vortical flows around lifting airfoils
[AIAA PAPER 90-0694] p 300 A90-25041

Unsteady aerodynamic and aeroelastic calculations for wings using Euler equations
p 302 A90-25288

Numerical simulation of vortex breakdown via 3-D Euler equations
[ONERA, TP NO. 1989-211] p 303 A90-25344

Analysis of three-dimensional aerospace configurations using the Euler and Navier-Stokes equations
p 305 A90-25798

Numerical aerodynamics via formal integration - Laplace, Euler, Prandtl, Navier-Stokes and Reynolds equations
p 305 A90-25800

Computational and experimental analysis of transonic fanjet engine flow field using 3-D Euler code
p 306 A90-25809

An automatic Euler solver using unstructured upwind method
p 367 A90-25811

Transonic aerodynamics analysis of unconventional wing configurations by 3D-Euler code
p 306 A90-25835

Effect of the grid system on the solution of Euler equations
p 309 A90-26494

Implicit flux-split Euler schemes for unsteady aerodynamic analysis involving unstructured dynamic meshes
[AIAA PAPER 90-0936] p 389 A90-29362

Aeroelastic analysis of wings using the Euler equations with a deforming mesh
[AIAA PAPER 90-1032] p 391 A90-29376

Gyroscopic matrices in computation of vibration
p 547 A90-33381

Numerical simulation of vortex breakdown by solving the Euler equations for an incompressible fluid
p 476 A90-34323

An implicit scheme with flow correction for the numerical solution of the Euler equation
p 477 A90-34674

Implicit flux-split schemes for the Euler equations
p 602 A90-36254

Transonic Euler solutions on mutually interfering finned bodies
p 555 A90-36256

Solution of Euler equations for fighter forebody-inlet combination at high angle of attack
p 556 A90-36419

Computational methods in design aerodynamics
p 557 A90-36539

Solution of Euler equations with unstructured meshes
p 558 A90-37343

Enthalpy damping for high Mach number Euler solutions
[AIAA PAPER 90-1585] p 566 A90-38720

Euler solutions for self-generated rotor blade-vortex interactions
[AIAA PAPER 90-1588] p 566 A90-38723

Boundary conditions for Euler equations at internal block faces of multi-block domains using local grid refinement
[AIAA PAPER 90-1590] p 607 A90-38725

A general decomposition algorithm applied to multi-element airfoil grids
[AIAA PAPER 90-1606] p 567 A90-38737

Three-dimensional flux-split Euler schemes involving unstructured dynamic meshes
[AIAA PAPER 90-1649] p 569 A90-38777

Temporal-adaptive Euler/Navier-Stokes algorithm for unsteady aerodynamic analysis of airfoils using unstructured dynamic meshes
[AIAA PAPER 90-1650] p 569 A90-38778

3-D Euler calculations for aft-propan integration
[AIAA PAPER 90-2147] p 625 A90-42044

Modelling of boundary layer and trailing edge thickness effects for the Euler equations using surface transpiration
p 629 A90-42412

Finite volume solutions of two-dimensional Euler equations on adapted structured meshes
p 629 A90-42413

Automated generation of two-dimensional non-overlapping structured grids for multiple element airfoils with Euler solutions
p 629 A90-42422

Euler and Navier-Stokes computations for airfoil geometries using unstructured meshes
p 630 A90-42425

A study of the influence of a helicopter rotor blade on the following blades using Euler equations
p 630 A90-42435

Unsteady Euler analysis of the redistribution of an inlet temperature distortion in a turbine
[AIAA PAPER 90-2262] p 768 A90-42759

Using 3D Euler flow simulations to assess effects of periodic unsteady flow through turbines
[AIAA PAPER 90-2357] p 706 A90-42783

Development of supersonic and hypersonic Euler solvers using shock fitting in two and three dimensions
p 707 A90-44426

Shock-fitting in three space dimensions
p 707 A90-44434

Solution of the Euler equations using unstructured polygonal meshes
p 708 A90-44435

A formulation for the solution of Euler equations for compressible flow using finite elements
p 708 A90-44447

A weighted residual formulation for finite element solutions of the steady Euler equations
p 770 A90-44457

A multistage method for the solution of the Euler equations on unstructured grids
p 708 A90-44460

Off-design performance of hypersonic waveriders
p 763 A90-44735

Numerical modeling of transverse flow past a cylinder using Euler equations
p 709 A90-44922

Non-unique solutions of the Euler equations
p 716 A90-45727

AIRPLANE - Experiences, benchmarks and improvements
[AIAA PAPER 90-2998] p 787 A90-45848

Euler procedure for calculation of the steady rotor flow with emphasis on wake evolution
[AIAA PAPER 90-3007] p 789 A90-45857

3D Euler analysis of ducted propan flowfields
[AIAA PAPER 90-3034] p 791 A90-45873

Validation of propeller slipstream calculations using a multi-block Euler code
[AIAA PAPER 90-3035] p 791 A90-45874

Design of supersonic wings using an optimization strategy coupled with a solution scheme for the Euler equations
[AIAA PAPER 90-3060] p 794 A90-45895

Adaptive grid embedding for the two-dimensional Euler equations
[AIAA PAPER 90-3049] p 797 A90-45929

Wake effects on the prediction of transonic viscous flows around airfoils with an Euler/boundary layer interaction approach
[AIAA PAPER 90-3061] p 798 A90-45933

Analytical studies of the transonic flutter of aircraft
p 860 A90-46577

Unsteady Euler airfoil solutions using unstructured dynamic meshes
p 809 A90-47307

Solutions of two-dimensional Euler equations with multigrid acceleration
p 810 A90-48086

Least-squares finite element methods for compressible Euler equations
p 904 A90-51013

Analysis of three-dimensional turbomachinery flows on C-type grids using an implicit Euler solver
[ASME PAPER 89-GT-85] p 905 A90-51258

Multigrid scheme for the compressible Euler-equations
p 907 A90-51559

Multigrid acceleration of TVD schemes in transonic Euler flow calculation
p 908 A90-52030

Supersonic flow computations over aerospace configurations using an Euler marching solver
[NASA-CR-4085] p 19 N90-10012

Numerical simulation of leading-edge vortex rollup and bursting
p 20 N90-10831

Numerical simulation of unsteady rotational flow over propan configurations
[NASA-CR-186037] p 90 N90-12500

Improvements in the formulations and numerical solution of the Euler problem for swept wings
[RAE-TM-AERO-2139] p 95 N90-12562

Euler equation solutions applied to a helicopter rotor in forward moving flight
[ONERA-RSF-1/3731-AY-346A] p 107 N90-12592

Multigrid solution method for the Euler equations
[PB89-219463] p 138 N90-13116

Block-structured solution of three-dimensional transonic flows using parallel processing
[AD-A212851] p 170 N90-13330

Transonic Euler solutions on mutually interfering finned bodies
[AD-A213395] p 170 N90-13331

Computation of flow fields around propellers and hovering rotors based on the solution of the Euler equations
[DLR-FB-89-37] p 170 N90-13333

Application of an efficient hybrid scheme for aeroelastic analysis of advanced propellers
[NASA-TM-102428] p 172 N90-13355

Multigrid and defect correction for the steady Navier-Stokes equations: Applications to aerodynamics
[ETN-90-96011] p 212 N90-13727

A dynamic multiblock approach to solving the unsteady Euler equations about complex configurations
p 214 N90-14497

Research on three different Euler's schemes applied to a delta wing with vortical flows
p 278 N90-16184

Unsteady Euler analysis of the flow field of a propan at an angle of attack
[NASA-TM-102426] p 380 N90-18229

Numerical investigation of unsteady flow in oscillating turbine and compressor cascades
p 426 N90-18407

Numerical simulations of supersonic flow through oscillating cascade sections
[NASA-TM-103100] p 478 N90-20051

Computation of nonequilibrium chemically reacting flows in hypersonic flow field
p 480 N90-20954

An evaluation of the two-dimensional Euler and Navier-Stokes calculations based on a flux-vector splitting
[PB90-166778] p 481 N90-20963

Optimization of aerodynamic designs using computational fluid dynamics
p 541 N90-20999

Adaptive grid embedding for the two-dimensional flux-split Euler equations
[NASA-CR-186533] p 547 N90-21571

Grid patching approaches for complex three-dimensional configurations
p 573 N90-21985

Feature-associated mesh embedding for complex configurations
p 608 N90-21988

The development of a system for the numerical simulation of Euler flows
p 612 N90-22980

Euler code predicted separation at the airfoil trailing edge
[FFA-TN-1989-30] p 632 N90-23364

Analysis and mitigation of numerical dissipation in inviscid and viscous computation of vortex-dominated flows
[NASA-CR-186887] p 776 N90-26281

Development of a system for the numerical simulation of Euler flows, with results of preliminary 3-D propeller-slipstream/exhaust-jet calculations
[NLR-TR-88008-U] p 776 N90-26285

An approximate method for calculating three-dimensional inviscid hypersonic flow fields
[NASA-TP-3018] p 883 N90-27066

Efficient solution of the steady Euler equations with a centered implicit method
p 884 N90-27999

Solution of Euler equations applied to a rotor of a helicopter in steady flight
[ONERA-RSF-1/3731-AY-002A] p 910 N90-28500

Transonic 3-D Euler analysis of flows around fanjet engine and TPS (Turbine Powered Simulator). Comparison with wind tunnel experiment, evaluation of TPS testing method and 3-D flow
[NAL-TR-1045] p 912 N90-29327

EULER-LAGRANGE EQUATION

Application of vortex embedding to aircraft flows
[AIAA PAPER 90-1626] p 568 A90-38755

A new Lagrangian method for steady supersonic flow computation. I - Godunov scheme
p 631 A90-42506

Numerical simulation of droplet deformation in convective flows
[AIAA PAPER 90-2309] p 769 A90-42773

Application of Lagrangian blending functions for grid generation around airplane geometries
[NASA-CR-186318] p 237 N90-15891

EUROPEAN AIRBUS

Advantage Airbus?
p 102 A90-15746

Hydrogen propulsion and the next century - A challenge that raises questions and problems
p 266 A90-21774

Airbus A320 CFRP-rudder structural requirements
p 493 A90-33707

Results of wind tunnel ground effect measurements on Airbus A320 using turbine power simulation and moving tunnel floor techniques
[AIAA PAPER 90-1427] p 559 A90-37964

The Airbus ... a challenge launched twenty years ago
p 699 A90-41769

Software maintenance on the Airbus family
[SAE PAPER 892326] p 738 A90-45484

One wing for two airliners - Computer screens are technical trailblazers for a unique wing
p 785 A90-46719

Assuring the future of civil aircraft industry in Germany
[DGLR PAPER 88-004] p 902 A90-50232

Airbus technologies - An evolutionary process
p 902 A90-52699

Properties of Al-Li alloys
p 267 N90-15191

Fire hardening of aircraft through upgrades of materials and designs
p 327 N90-17605

Aerodynamic development perspective for traffic aeroplanes
[DGLR-89-141] p 637 N90-24260

Simulation of transport aeroplanes
[MBB-UT-007/89-PUB] p 723 N90-25089

EUTECTIC COMPOSITES

Processing and mechanical properties of Al2O3/Y3Al5O12 (YAG) eutectic composite p 951 A90-51966

EUTECTICS

Effect of protective coatings on mechanical properties of superalloys p 952 N90-28707

EVAUATING (TRANSPORTATION)

The influence of adjacent seating configurations on egress through a type 3 emergency exit [AD-A218393] p 636 N90-23371

Aircraft evacuations: The effect of passenger motivation and cabin configuration adjacent to the exit [CAA-PAPER-89019] p 913 N90-29336

EVALUATION

Experimental and analytical evaluation of dynamic load vibration of a 2240-kW (3000-hp) rotorcraft transmission p 127 A90-13750

Evaluation of various non-asbestos epoxy adhesives for aircraft repair p 529 A90-33078

The evaluation of flight recorders p 653 A90-41729

Numerical simulation of aeroplane response to a lightning injection [ETN-89-95271] p 96 N90-11716

EVAPORATION

Externally vaporizing system for turbine combustor [AD-D014284] p 256 N90-15918

EVASIVE ACTIONS

Avoiding a maneuvering aircraft with TCAS --- Traffic Alert and Collision Avoidance System p 347 A90-26222

EVOLUTION (DEVELOPMENT)

Evolution of flight commands in Aeritalia design [ETN-89-95211] p 120 N90-11759

EXCIMER LASERS

Raman scattering measurements using UV excimer lasers p 874 N90-26902

Concentration, temperature, and density in a hydrogen-air flame by excimer-induced Raman scattering p 875 N90-26903

EXCITATION

Ground vibration test results of a JetStar airplane using impulsive sine excitation p 179 A90-16963

The effectiveness of vane-aileron excitation in the experimental determination of flutter speed by parameter identification [NASA-TP-2971] p 249 N90-15100

EXHAUST DIFFUSERS

The performance of a combustor pre-diffuser incorporating compressor outlet guide vanes [AIAA PAPER 90-2165] p 661 A90-42053

Device for the dilution of hot exhaust jets [ETN-90-97435] p 858 N90-27723

EXHAUST EMISSION

Exhaust emission performance of a vaporizer tube combustor as compared with a single tube combustor p 111 A90-14614

Low NO(x) potential of gas turbine engines [AIAA PAPER 90-0550] p 343 A90-25036

Influence of fuel drop size and combustor operating conditions on pollutant emissions p 508 A90-33591

Characterization of helicopter turboshaft engine noise p 660 A90-41759

Technology issues for high-speed civil transports [SAE PAPER 892201] p 778 A90-45422

Pollutants: Production and methods of reduction [CIT/SME/VKI/RS/6] p 749 N90-25990

Aircraft exhaust emissions: An engine manufacturer's perspective [PNR90675] p 750 N90-26004

The reduction of smoke emissions from Allison T56 engines [ARL-PROP-R-182] p 928 N90-28547

Energy Efficient Engine exhaust mixer model technology report addendum: phase 3 test program [NASA-CR-174799] p 930 N90-28556

Source emission test of gas turbine engine test facility, Kelly AFB, TX [AD-A223869] p 932 N90-28571

EXHAUST FLOW SIMULATION

Analysis of internal flow in a ventral nozzle for STOVL aircraft p 739 A90-42688

A Mach 6 external nozzle experiment with Argon-Freon exhaust simulation [SAE PAPER 892315] p 714 A90-45477

Steady and unsteady potential flow around thin annular wings and engines with simulation of jet engine flow [DFVLR-FB-89-18] p 89 N90-11711

Analysis of a six-component, flow-through, strain-gage, force balance used for hypersonic wind tunnel models with scramjet exhaust flow simulation p 597 N90-21775

Analysis of internal flow in a ventral nozzle for STOVL aircraft [NASA-TM-103123] p 666 N90-23404

Device for the dilution of hot exhaust jets [ETN-90-97435] p 858 N90-27723

EXHAUST GASES

Aerosol effects on jet-engine IR radiation p 40 A90-10152

Infrared radiation model for aircraft and reentry vehicle p 77 A90-10169

Three-dimensional modeling of turbulent transonic flow at the exit of a twin engine [AAAF PAPER NT 88-16] p 4 A90-11434

Basic principles of measuring thrust through exhaust to inlet total pressure ratio - Engine Pressure Ratio (EPR) p 191 A90-18635

Infrared sources of jet propulsion system and their suppression p 252 A90-22614

Contamination of cabin air by synthetic oil and breakdown products [SAE PAPER 891455] p 323 A90-27424

Hot gas environment around STOVL aircraft in ground proximity. I - Experimental study [AIAA PAPER 90-2269] p 742 A90-42765

Hot gas environment around STOVL aircraft in ground proximity. II - Numerical study [AIAA PAPER 90-2270] p 743 A90-42766

Surface flow on a flat plate induced by a supersonic jet exhausting normally into a low speed crossflow [AIAA PAPER 90-3011] p 789 A90-45860

TRANAIR applications to engine/airframe integration p 838 A90-48958

Gas identification system using graded temperature sensor and neural net interpretation [AD-A213359] p 205 N90-13627

Exhaust environment measurements of a turbofan engine equipped with an afterburner and 2D nozzle [NASA-CR-4289] p 588 N90-21760

EXHAUST NOZZLES

Exhaust nozzle system design considerations for turbofanjet propulsion systems p 48 A90-12577

Braze repair of MA754 aero gas turbine engine nozzles [ASME PAPER 89-GT-235] p 342 A90-23886

Performance characteristics of a one-third-scale, vectorable ventral nozzle for SSTOVL aircraft [AIAA PAPER 90-2271] p 586 A90-37562

High Mach exhaust system concept scale model test results [AIAA PAPER 90-1905] p 655 A90-40552

Flight test results of the F-15 SMTD thrust vectoring/thrust reversing exhaust nozzle --- STOL/Maneuvering Technology Demonstrator [AIAA PAPER 90-1906] p 660 A90-41982

On and off-design performance prediction of single spool turbojets using gasdynamics [AIAA PAPER 90-2393] p 662 A90-42155

Experimental evaluation of expendable supersonic nozzle concepts [AIAA PAPER 90-1904] p 740 A90-42691

Nozzle design optimization by method-of-characteristics [AIAA PAPER 90-2024] p 741 A90-42719

Computational investigation of two-dimensional ejector nozzle flow fields [AIAA PAPER 90-2148] p 768 A90-42739

Investigation of advanced mixer-ejector exhaust system [AD-A211943] p 89 N90-11705

Altitude testing of the 2D V-STOL ADEN demonstrator on an F404 engine [NASA-CR-174824] p 345 N90-17638

Static investigation of a two-dimensional convergent-divergent exhaust nozzle with multi-axis thrust-vectoring capability [NASA-TP-2973] p 397 N90-19193

Exhaust nozzles for propulsion systems with emphasis on supersonic cruise aircraft [NASA-RP-1235] p 516 N90-21037

Performance characteristics of a one-third-scale, vectorable ventral nozzle for SSTOVL aircraft [NASA-TM-103120] p 552 N90-21725

Exhaust environment measurements of a turbofan engine equipped with an afterburner and 2D nozzle [NASA-CR-4289] p 588 N90-21760

Experimental and analytical study of close-coupled ventral nozzles for ASTOVL aircraft [NASA-TM-103170] p 666 N90-24273

Hot gas ingestion characteristics and flow visualization of a vectored thrust STOVL concept [NASA-TM-103212] p 751 N90-26009

Entropy wave instability in compact ramjets p 858 N90-27932

EXHAUST SYSTEMS

Propulsion system integration in high-performance aircraft p 333 A90-23922

High Mach exhaust system concept scale model test results [AIAA PAPER 90-1905] p 655 A90-40552

X.2 limited flight test plan [AD-A214412] p 249 N90-15099

EXHAUST VELOCITY

Mean and turbulent velocity measurements in a turbojet exhaust p 423 A90-28272

EXOTHERMIC REACTIONS

A numerical study of mixing and chemical heat release in supersonic mixing layers [AIAA PAPER 90-0152] p 163 A90-19710

EXPERIMENT DESIGN

Theoretical analysis of an icing test apparatus for turbine engine air intakes [AAAF PAPER NT 88-20] p 23 A90-11437

Experience with multi-step test inputs for helicopter parameter identification p 56 A90-12775

An aeroflot testing technique for low supersonic speeds in an adaptive flexible-walled wind tunnel [AIAA PAPER 90-3086] p 795 A90-45900

Design of the UETP experiment p 856 N90-27712

Experience in developing an improved design of experiment (lessons learned) p 857 N90-27718

EXPERIMENTATION

Experiments on the unsteady flow in a supersonic compressor stage p 427 N90-18422

EXPERT SYSTEMS

Benchmarking blackboards to support cockpit information management [AIAA PAPER 89-3095] p 37 A90-10580

Problem focus mechanisms for cockpit automation [AIAA PAPER 89-3096] p 37 A90-10581

The Battle Captain Expert System - A mission management decision support system for attack helicopter operations [AIAA PAPER 89-3098] p 37 A90-10583

Real-time fault monitoring for aircraft applications using quantitative simulation and expert systems [AIAA PAPER 89-3103] p 37 A90-10586

The aerodynamic assistant [AIAA PAPER 89-3132] p 75 A90-10608

The NIMBLE Project - Real-time common LISP for embedded expert systems applications [AIAA PAPER 89-3140] p 75 A90-10614

Embedded knowledge based avionics [AIAA PAPER 89-3141] p 75 A90-10615

APG-70 radar test package development aid [AIAA PAPER 89-3044] p 1 A90-10624

An intelligent system for autonomous navigation of airborne vehicles p 26 A90-11696

Engine diagnostics - An application for expert system concepts p 50 A90-12632

Applications of fuzzy sets to rule-based expert system development p 216 A90-18050

Future ATC automation aids based upon AI technology p 375 A90-25563

The role of expert systems in aircraft safety management p 375 A90-26225

Rotor smoothing expert system p 381 A90-28164

Auxiliary power unit maintenance aid - Flight line engine diagnostics p 382 A90-28348

AAAI '88 - Aerospace Applications of Artificial Intelligence; Proceedings of the Fourth Annual Conference, Dayton, OH, Oct. 25-27, 1988. Volumes 1 & 2 p 458 A90-30226

Automating acquisition of plans for an intelligent assistant by observing user behavior p 459 A90-30230

Information display management in a pilot's associate p 418 A90-30238

An American knowledge base in England - Alternate implementations of an expert system flight status monitor p 459 A90-30719

Expert system - Conventional processing interface p 460 A90-30753

An adaptive-learning expert system for maintenance diagnostics p 460 A90-30754

Methodology for developing an assessment expert system using a planning paradigm p 460 A90-30757

An integrated diagnostics approach to embedded and flight-line support systems p 460 A90-30767

A computer-aided control engineering environment for multi-disciplinary expert-aided analysis and design (MEAD) p 461 A90-30786

A microcomputer-based airspace control simulation and prototype human-machine interface p 461 A90-30800

Harnessing detailed assembly process knowledge with CASE p 535 A90-32504

Expert systems for design of battle damage repairs p 467 A90-33094

An expert system for real-time aircraft monitoring [AIAA PAPER 90-1311] p 545 A90-33921

A design method for real-time computer control hydraulic force system p 590 A90-36434

An application of expert system to jet engine diagnostic procedures p 587 A90-38596

Expert diagnosis system for FJR engine troubles p 587 A90-38597

- Multi-level models for diagnosis of complex electro-mechanical systems p 693 A90-38888
- The application of an expert maintenance and diagnostic tool to aircraft engines p 657 A90-40605
- Concept demonstration of the use of interactive fault diagnosis and isolation for TF30 engines p 617 A90-41177
- Jet Engine Technical Advisor (JETA) p 693 A90-41184
- Design and analysis aid for evaluating aircraft structures p 694 A90-41188
- Applying qualitative knowledge to aircraft engine system design p 694 A90-41189
- SMAS - An expert system for configuring a research flight simulator p 694 A90-41191
- The place of knowledge based systems in helicopter dynamic system condition prognosis p 618 A90-42475
- Next-generation automatic test equipment for military support p 767 A90-42667
- Probabilistic reasoning for intelligent wind shear avoidance p 890 A90-47690
- [AIAA PAPER 90-3437] p 890 A90-47690
- Expert system technology applied to the automatic control of multiple unmanned aerial vehicles p 892 A90-48867
- [AIAA PAPER 90-3280] p 892 A90-48867
- Near-term applications of knowledge based systems to combat helicopters p 847 A90-48883
- [AIAA PAPER 90-3301] p 847 A90-48883
- Application possibilities of expert systems in modern maintenance for increasing operational security p 892 A90-49271
- Hierarchical damage tolerant controllers for smart structures [AD-A209422] p 31 N90-10022
- Real-time support for high performance aircraft operation p 57 N90-10075
- [NASA-CR-185475] p 57 N90-10075
- Nonlinear maneuver autopilot for the F-15 aircraft p 77 N90-11487
- [NASA-CR-179442] p 77 N90-11487
- A knowledge-based system design/information tool for aircraft flight control systems p 217 N90-13990
- [NASA-TM-101704] p 217 N90-13990
- A knowledge-based flight status monitor for real-time application in digital avionics systems p 217 N90-13995
- [NASA-TM-101710] p 217 N90-13995
- Advances in Techniques and Technologies for Air Vehicle Navigation and Guidance p 332 N90-16731
- [AGARD-CP-455] p 332 N90-16731
- Hypercube expert system shell-applying production parallelism p 377 N90-18173
- [AD-A215762] p 377 N90-18173
- A rule-based paradigm for intelligent adaptive flight control p 434 N90-19238
- Investigation of air transportation technology at Princeton University, 1988-1989 p 486 N90-20935
- An expert system for wind shear avoidance p 486 N90-20938
- Rule-based mechanisms of learning for intelligent adaptive flight control p 521 N90-20939
- Progress in inverse design and optimization in aerodynamics p 482 N90-20977
- Preliminary development of an intelligent computer assistant for engine monitoring p 612 N90-22322
- [NASA-TM-101702] p 612 N90-22322
- Multidisciplinary Expert-aided Analysis and Design (MEAD) p 613 N90-23050
- Flight-testing of the self-repairing flight control system using the F-15 highly integrated digital electronic control flight research facility p 758 N90-25144
- [NASA-TM-101725] p 758 N90-25144
- Advanced fuel properties, phase 1 p 766 N90-25236
- [AD-A219788] p 766 N90-25236
- Neural networks for detecting defects in aircraft structures p 777 N90-26345
- [IAR-90-4] p 777 N90-26345
- Robotic-aided system for inspection of aging aircraft p 777 N90-26346
- [NIAR-90-9] p 777 N90-26346
- Knowledge-based system for flight information management p 780 N90-26511
- [NASA-TM-102685] p 780 N90-26511
- Proceedings of the 1987 Aircraft/Engine Structural Integrity Program (ASIP/ENSIP) Conference p 842 N90-26807
- [AD-A198037] p 842 N90-26807
- An expert system advisor for damage repair of composite wing skins (repairman) p 842 N90-26810
- Past, present and future: Aircraft integrated monitoring systems: An ever-developing technology p 848 N90-27618
- Expert system diagnostics and parts life tracking as applied to the AV-8B aircraft for the USMC p 884 N90-27629
- Knowledge based diagnosis of jet engines under consideration of model based methods p 855 N90-27631
- Public-sector aviation issues, 1987 to 1988 graduate research award papers p 820 N90-27667
- [PB90-191206] p 820 N90-27667
- Expert system for pilot assistance: The challenge of an intensive prototyping p 825 N90-27674
- [ETN-90-97274] p 825 N90-27674
- Use of acoustic emission for continuous surveillance of aircraft structures p 887 N90-28092
- An expert system to perform on-line controller restructuring for abrupt model changes p 964 N90-29121
- [NASA-TM-103609] p 964 N90-29121
- Model authoring system for fail safe analysis p 964 N90-29142
- [NASA-CR-4317] p 964 N90-29142
- A knowledge-based system design/information tool p 965 N90-29143
- [NASA-CR-4316] p 965 N90-29143
- EXPLOSION SUPPRESSION**
- Fuel tank explosion protection p 251 N90-15914
- Onboard fire- and explosion suppression for fighter aircraft p 327 N90-17602
- EXPLOSIVES**
- Application of the hypersonic analogy for validation of numerical simulations p 16 A90-12838
- EXPLOSIVES**
- Coping with bomb threats to civil aviation p 23 A90-12781
- EXPOSURE**
- Fuel resistant coatings for metal and composite fuel tanks p 269 N90-15911
- Integral fuel tank certification and test methods p 251 N90-15916
- EXTENSOMETERS**
- New inflight experiments to measure aerodynamics loads [ETN-90-97276] p 868 N90-26834
- EXTERNAL STORE SEPARATION**
- Aerodynamics of store separation p 629 A90-42418
- Helicopter store separation - Predictive techniques and flight testing p 647 A90-42495
- Application of experimental techniques to store release problems p 316 N90-17545
- Prediction methods for store separation p 317 N90-17549
- EXTERNAL STORES**
- Unsteady supersonic computations of arbitrary wing-body configurations including external stores p 232 A90-23278
- A captive store flight vibration simulation project p 672 A90-40476
- Application of the KTRAN transonic small disturbance code to the complete CF-18 aircraft with stores p 629 A90-42416
- Measurements of aerodynamic forces on aircraft external stores in the NAE trisonic blowdown wind-tunnel p 629 A90-42419
- Incompressible potential flow about three-dimensional configurations p 810 A90-48082
- Computation of transonic flow about stores p 18 N90-10009
- [AD-A210402] p 18 N90-10009
- CF 18 480 Gallon External Fuel Tank Stores Clearance Program p 35 N90-10877
- The integration of stores on modern tactical aircraft: Where we have been, and what we should do for the future p 337 N90-17552
- Water-tunnel investigation of concepts for alleviation of adverse inlet spillage interactions with external stores [NASA-TM-4181] p 398 N90-19199
- EXTRAPOLATION**
- Sequential design of experiments with physically based models 23 p 138 N90-12239
- [AD-A211918] p 138 N90-12239
- EXTRUDING**
- Installation and implementation of an extrusion cell in aircraft industry utilizing group technology p 81 A90-14336
- [SAE PAPER 891025] p 81 A90-14336
- EYE (ANATOMY)**
- The interaction of chromostereopsis and stereopsis in stereoscopic CRT (Cathode Ray Tubes) displays p 927 N90-28544
- [AD-A217906] p 927 N90-28544
- F**
- F-104 AIRCRAFT**
- Airdata calibration of a high-performance aircraft for measuring atmospheric wind profiles p 186 N90-14228
- [NASA-TM-101714] p 186 N90-14228
- Sonic boom signature data from cruciform microphone array experiments during the 1966-1967 EAFB national sonic boom evaluation program p 549 N90-21605
- [NASA-CR-182027] p 549 N90-21605
- F-106 AIRCRAFT**
- Study of vortex breakdown of F-106B by Euler code p 233 A90-23289
- The vortex flap F-106B, overcoming safety and data problems in flight testing p 496 A90-34725
- [AIAA PAPER 90-1280] p 496 A90-34725
- Cloud-to-ground strikes to the NASA F-106 airplane p 574 A90-35767
- F-111 AIRCRAFT**
- F-111/TF30 engine monitoring system - A fusion of past, present, and future technology p 425 A90-30817
- F-14 AIRCRAFT**
- Application of dynamical systems theory to the high angle of attack dynamics of the F-14 p 257 A90-22184
- [AIAA PAPER 90-0221] p 257 A90-22184
- Digital controller design for the pitch axis of the F-14 using an H(infinity) method p 668 A90-40912
- Considerations for successful application of integrated drive generators to aircraft p 746 A90-45442
- [SAE PAPER 892226] p 746 A90-45442
- The role of CFD applied to high performance aircraft p 796 A90-45917
- [AIAA PAPER 90-3071] p 796 A90-45917
- F-14 VSTFE and results of the cleanup flight test program p 105 N90-12547
- Flutter clearance of the F-14A variable-sweep transition flight experiment airplane, phase 2 p 735 N90-25135
- [NASA-TM-101717] p 735 N90-25135
- F-15 AIRCRAFT**
- Flight testing the F-15E terrain following system p 334 A90-24272
- High-temperature bootstrap compared with F-15 growth air cycle air conditioning system p 336 A90-27407
- [SAE PAPER 891436] p 336 A90-27407
- Reconfigurable flight controller for the STOL F-15 with sensor/actuator failures p 432 A90-30707
- Design of adaptive digital controllers incorporating dynamic pole-assignment compensators for high-performance aircraft p 432 A90-30714
- F-15 STOL and Maneuver Technology Demonstrator flight test progress report p 494 A90-33896
- [AIAA PAPER 90-1269] p 494 A90-33896
- F-15E terrain following test results p 504 A90-33913
- [AIAA PAPER 90-1299] p 504 A90-33913
- Flight-testing of the self-repairing flight control system using the F-15 highly integrated digital electronic control flight research facility p 520 A90-34149
- [AIAA PAPER 90-1321] p 520 A90-34149
- Flow field measurements near a fighter model at high angles of attack p 559 A90-37968
- [AIAA PAPER 90-1431] p 559 A90-37968
- Full authority digital electronic engine control system provides needed reliability p 658 A90-40606
- [AIAA PAPER 90-2037] p 658 A90-40606
- Multiple model adaptive controller for the STOL F-15 with sensor/actuator failures p 668 A90-40878
- Flight test results of the F-15 SMTD thrust vectoring/thrust reversing exhaust nozzle --- STOL/Maneuvering Technology Demonstrator p 660 A90-41982
- [AIAA PAPER 90-1906] p 660 A90-41982
- External nozzle flap dynamic load measurements on F-15 S/MTD model p 740 A90-42692
- [AIAA PAPER 90-1910] p 740 A90-42692
- Titanium matrix composite landing gear development p 733 A90-45491
- [SAE PAPER 892337] p 733 A90-45491
- Flight test of a trajectory controller using linearizing transformations with measurement feedback p 864 A90-47631
- [AIAA PAPER 90-3373] p 864 A90-47631
- F-15 Environment Control System improvements p 841 A90-49305
- [SAE PAPER 901235] p 841 A90-49305
- ATF prototypes outstrip F-15 in size and thrust p 841 A90-49477
- Bifurcation analysis of a model fighter aircraft with control augmentation p 934 A90-50640
- [AIAA PAPER 90-2836] p 934 A90-50640
- Nonlinear maneuver autopilot for the F-15 aircraft p 77 N90-11487
- [NASA-CR-179442] p 77 N90-11487
- Cost effectiveness of composite materials on the F-15 and F-16 aircraft p 338 N90-17631
- [AD-A216353] p 338 N90-17631
- A comparison of time-optimal interception trajectories for the F-8 and F-15 p 581 N90-21753
- [NASA-CR-186300] p 581 N90-21753
- Dynamic ground-effect measurements on the F-15 STOL and Maneuver Technology Demonstrator (S/MTD) configuration p 573 N90-22531
- [NASA-TP-3000] p 573 N90-22531
- Flight-testing of the self-repairing flight control system using the F-15 highly integrated digital electronic control flight research facility p 758 N90-25144
- [NASA-TM-101725] p 758 N90-25144
- Success in tutoring electronic troubleshooting p 780 N90-25568
- Effect of tail size reductions on longitudinal aerodynamic characteristics of a three surface F-15 model with nonaxisymmetric nozzles p 718 N90-25938
- [NASA-TP-3036] p 718 N90-25938
- Application of multifunction inertial reference systems to fighter aircraft p 916 N90-29341
- Integrated navigation/flight control for future high performance aircraft p 917 N90-29362
- F-16 AIRCRAFT**
- General Dynamics F-16 p 100 A90-13791

- Results from a numerical simulation of an F-16A configuration at a supersonic Mach number p 146 A90-16769
- Impact of nose-probe chines on the vortex flows about the F-16C [AIAA PAPER 90-0386] p 165 A90-19828
- Application of a three-dimensional finite element grid generation scheme for an F-16 aircraft configuration p 336 A90-26541
- Numerical simulation of an F-16A at angle of attack [AIAA PAPER 90-0100] p 313 A90-26911
- The IMIS F-16 interactive diagnostic demonstration p 383 A90-30768
- Flight control application of eigenstructure assignment with optimization of robustness to structured state space uncertainty p 693 A90-40885
- F-16/GPS integration test results p 726 A90-43710
- Zonal Navier-Stokes methodology for flow simulation about a complete aircraft p 709 A90-44727
- Integrated product development (IPD) at General Dynamics Fort Worth p 786 A90-48828
- Proven dynamic modeling techniques for concurrent design and analysis of ECS controllers [SAE PAPER 901234] p 841 A90-49304
- Re-assessing the F-16 damage tolerance and durability life of the RNLAF F-16 aircraft p 901 A90-49881
- Cost effectiveness of composite materials on the F-15 and F-16 aircrafts [AD-A216353] p 338 N90-17631
- Stability characteristics of a combat aircraft with control surface failure [AD-A216196] p 350 N90-17646
- F-17 AIRCRAFT**
- A laser sheet flow visualization and aerodynamic force data evaluation of a 3 percent YF-17 fighter aircraft model at high angles of attack [AIAA PAPER 90-3019] p 792 A90-45886
- Wind tunnel studies of support strut interference on a 3 percent YF-17 fighter aircraft model at high angles of attack [AIAA PAPER 90-3083] p 794 A90-45899
- An experimental investigation of support strut interference on a three-percent fighter model at high angles of attack [AD-A219793] p 631 N90-23353
- F-18 AIRCRAFT**
- Simulation model-building procedure for dynamic systems integration p 138 A90-14744
- In-flight flow field analysis on the NASA F-18 high alpha research vehicle with comparisons to ground facility data [AIAA PAPER 90-0231] p 163 A90-19745
- Navier-Stokes predictions of the flowfield around the F-18 (HARV) wing and fuselage at large incidence [AIAA PAPER 90-0099] p 227 A90-22165
- Wind tunnel studies of F/A-18 tail buffet [AIAA PAPER 90-1432] p 559 A90-37969
- A simple dynamic engine model for use in a real-time aircraft simulation with thrust vectoring [AIAA PAPER 90-2166] p 662 A90-42054
- The standard-setting Hornet p 730 A90-43764
- In-flight flow visualization characteristics of the NASA F-18 high alpha research vehicle at high angles of attack [SAE PAPER 892222] p 713 A90-45439
- VSCF cycloconverter reliability review of the 30/40 KVA F/A-18 electrical generating system --- variable speed, constant frequency [SAE PAPER 892228] p 746 A90-45444
- Numerical simulation of the viscous flow around a simplified F/A-18 at high angles of attack [AIAA PAPER 90-2999] p 787 A90-45849
- F-18 high alpha research vehicle surface pressures - Initial in-flight results and correlation with flow visualization and wind-tunnel data [AIAA PAPER 90-3018] p 792 A90-45885
- CF 18 480 Gallon External Fuel Tank Stores Clearance Program p 35 N90-10877
- Flutter clearance of the F-18 high-angle-of-attack research vehicle with experimental wingtip instrumentation pods [NASA-TM-4148] p 103 N90-11732
- Flow visualization of the effect of pitch rate on the vortex development on the scale model of a F-18 fighter aircraft [AD-A214244] p 236 N90-15080
- Water-tunnel study results of a TFA-18 and F/A-18 canopy flow visualization [NASA-TM-101705] p 573 N90-22532
- Fighter agility metrics, research, and test [NASA-CR-186118] p 648 N90-23386
- Application of neural networks to the F/A-18 engine condition monitoring system [AD-A219820] p 666 N90-24271
- A knowledge-based system design/information tool [NASA-CR-4316] p 965 N90-29143
- F-4 AIRCRAFT**
- Cost effectiveness of composite materials on the F-15 and F-16 aircrafts [AD-A216353] p 338 N90-17631
- F-8 AIRCRAFT**
- A comparison of time-optimal interception trajectories for the F-8 and F-15 [NASA-CR-186300] p 581 N90-21753
- F-86 AIRCRAFT**
- Scientific justification and development plan for a mid-sized jet research aircraft [PB89-208995] p 103 N90-11731
- FABRICATION**
- Material progress p 221 A90-21715
- Design, fabrication and experimental test of hi-temperature CFRP stiffened structures --- rotating cowl panels for unducted fan engines p 534 A90-31892
- Fabrication of aircraft structures from thermoplastic drapable preforms p 468 A90-33125
- Designing aerospace structures with Du Pont's LDF thermoplastic composites p 530 A90-33126
- Fabrication of complex composite structures using advanced fiber placement technology p 954 A90-50111
- Automated prepreg tow placement for composite structures p 954 A90-50113
- PMR graphite engine duct development [NASA-CR-182228] p 51 N90-10037
- Design and calibration of an in-stack, low-pressure impactor [AD-A213531] p 255 N90-15105
- Fabrication of test-articles from Al-Li 2091 for Fokker 100 p 267 N90-15196
- Fabrication characteristics of 8090 alloy p 268 N90-15198
- Aluminum-lithium: Application of plate and sheet to fighter aircraft p 268 N90-15202
- Models for cryogenic wind tunnels p 263 N90-15956
- Experience with strain-gage balances for cryogenic wind tunnels p 264 N90-15958
- Cryogenic balances for the US NTF p 264 N90-15959
- Heat pipes for wing leading edges of hypersonic vehicles [NASA-CR-181922] p 369 N90-17055
- Development and fabrication of structural components for a scramjet engine [NASA-CR-181945] p 510 N90-20088
- An applicational process for dynamic balancing of turbomachinery shafting [NASA-TM-102537] p 541 N90-20392
- The Stealth biplane: A proposal in response to a low Reynolds Number station keeping mission [NASA-CR-186680] p 734 N90-25127
- Carbon-carbon composites: Emerging materials for hypersonic flight [NASA-TM-103472] p 767 N90-26080
- FABRICS**
- Comparison of processing techniques for Filmix unidirectional commingled fabric p 940 A90-50058
- High performance needed structures in composites p 955 A90-50173
- FACTORIZATION**
- On efficiency and accuracy of numerical methods for solving aerodynamic equations p 304 A90-25730
- Implicit flux-split schemes for the Euler equations p 602 A90-36254
- A comparison of two central difference schemes for solving the Navier-Stokes equations [NASA-TM-102815] p 816 N90-27654
- FAIL-SAFE SYSTEMS**
- Towards a damage tolerance philosophy for composite materials and structures p 675 A90-40127
- Model authoring system for fail safe analysis [NASA-CR-4317] p 964 N90-29142
- FAILURE**
- Optimal integral controller with sensor failure accommodation p 61 N90-10123
- Display interface concepts for automated fault diagnosis [NASA-TM-101610] p 252 N90-15102
- Natural icing re-evaluation of the EH-60A Quick Fix helicopter [AD-A214728] p 323 N90-16723
- Effect of temperature on the storage life of polysulfide aircraft sealants [MRL-TR-89-31] p 444 N90-19364
- A Protection And Detection Surface (PADS) for damage tolerance [NASA-TP-3011] p 876 N90-27788
- FAILURE ANALYSIS**
- Breakage of fan blades in the S1 wind tunnel at Mondane-Avrieux [ONERA, TP NO. 1989-104] p 57 A90-11138
- Methods of safety analysis for Beech Model 2000 - Starship 1 [SAE PAPER 891064] p 101 A90-14364
- In process failure investigations in aeronautics p 181 A90-18489
- Gas turbine engine condition monitoring and fault diagnostics p 190 A90-18594
- Prediction of the strength-related reliability of structural elements at the design stage p 274 A90-23402
- Reasoning from uncertain data - A BIT enhancement p 457 A90-28330
- An aircraft flight control reconfiguration algorithm p 432 A90-30708
- F/A-18 aileron smart servoactuator p 432 A90-30710
- Desktop failure analysis on a microcomputer using Weibull, lognormal, and renewal data [ASME PAPER 89-GT-275] p 535 A90-32263
- A fracture analysis using eight-node-isoparametric singular elements and its application in fuselage panels p 603 A90-36431
- Application of fracture mechanics to microscale phenomena in electronic assemblies p 684 A90-41334
- Initiation of spalling in aircraft gas turbine bearings [AIAA PAPER 90-2291] p 686 A90-42110
- A 'new' philosophy of structural reliability, fail safe versus safe life p 688 A90-42490
- Probabilistic approach to fleet management p 701 A90-42674
- A real time microcomputer implementation of sensor failure detection for turbofan engines p 745 A90-45414
- Analysis of failures in aircraft structures p 882 A90-48998
- RAN (Royal Australian Navy) vibration analysis system operator's guide [AD-A212441] p 107 N90-12596
- The nature and control of skidding in lightly loaded intershaft bearings [PNR0591] p 136 N90-12933
- Thermal barrier coating life prediction model development, phase 1 [NASA-CR-182230] p 193 N90-13388
- Evaluation of the improved OV-ID anti-icing system, phase 2 [AD-A213928] p 239 N90-15083
- Analysis of damaged components from DOE security helicopter N7EG [DE90-004488] p 324 N90-16729
- Analysis of the National Transonic Facility mishap [NASA-TM-101686] p 328 N90-17620
- A study of the structural efficiency of fluted core graphite-epoxy panels [NASA-TM-101681] p 373 N90-18070
- Discrete proportional Plus Integral (PI) multivariable control laws for the Control Reconfigurable Combat Aircraft (CRCA) [AD-A215664] p 433 N90-18431
- A methodology for knowledge-based restructurable control to accommodate system failures p 609 N90-22058
- Computational and experimental investigations of rotating stall in compressor cascades p 588 N90-22565
- Thermal/structural analysis of the shaft-disk region of a fan drive system [NASA-TM-101687] p 610 N90-22807
- Failure analysis handbook [AD-A219747] p 689 N90-23752
- Development of a finite element based delamination analysis for laminates subject to extension, bending, and torsion p 679 N90-25049
- Behavior of composite/metal aircraft structural elements and components under crash type loads: What are they telling us [NASA-TM-102681] p 774 N90-25368
- Hardware and software reliability estimation using simulations [NASA-CR-186637] p 780 N90-25580
- Reliability model generator specification [NASA-CR-182005] p 780 N90-25638
- Molten salt induced high temperature degradation of thermal barrier coatings p 952 N90-28704
- Fractographic analysis of fatigue failures of airframe equipment parts: Examples of a rod end housing and a rod end cap [NAL-TR-1047] p 961 N90-29686
- FAILURE MODES**
- Carbon fibre composite bolted joints p 130 A90-15354
- A review of failure models for ceramic matrix composite laminates under monotonic loads [ASME PAPER 89-GT-153] p 354 A90-23842

From a sow's ear - Quantitative diagnostic design requirements from anecdotal references

p 448 A90-28337

Three approaches to reliability analysis

p 452 A90-30706

Subcomponent tests for composite fuselage technology readiness

p 490 A90-33105

The modular HUM system --- Health and Usage Monitoring instruments for rotary wing aircraft failure detection

p 618 A90-42476

A comparison of honeycomb-core and foam-core carbon-fibre/epoxy sandwich panels

p 764 A90-43855

Analysis of failures in aircraft structures

p 882 A90-48998

Independent Orbiter Assessment (IOA): Analysis of the displays and controls subsystem [NASA-CR-185563]

p 124 A90-11774

Failure analysis handbook

[AD-A219747]

p 689 A90-23752

Unique failure behavior of metal/composite aircraft structural components under crash type loads

[NASA-TM-102679]

p 690 A90-24660

Development of a finite element based delamination analysis for laminates subject to extension, bending, and torsion

p 679 A90-25049

Reliability model generator specification [NASA-CR-182005]

p 780 A90-25638

Use of acoustic emission for continuous surveillance of aircraft structures

p 887 A90-28092

System reliability optimization of aircraft wings

p 923 A90-28536

Model authoring system for fail safe analysis [NASA-CR-4317]

p 964 A90-29142

FAIRINGS

An experimental study of low-speed single-surface airfoils with faired leading edges

p 801 A90-46371

An experimental investigation of helicopter rotor hub fairing drag characteristics

[NASA-TM-102182]

p 88 A90-11701

FALSE ALARMS

Safety net functions

p 826 A90-27685

FAN BLADES

Breakage of fan blades in the S1 wind tunnel at Mondane-Avrieux

[ONERA, TP NO. 1989-104]

p 57 A90-11138

Blade mistuning coupled with shaft flexibility effects in rotor aeroelasticity

[ASME PAPER 89-GT-330]

p 343 A90-23896

Development of a simulated bird-strike test method --- of aircraft turbine engine fan blade materials

p 600 A90-37444

Nonlinear finite-element analysis to predict fan-blade damage due to soft-body impact

p 683 A90-40939

Metal matrix composite fan blade development [AIAA PAPER 90-2178]

p 677 A90-42062

Application of sweep to improve the efficiency of a transonic fan. I - Design

[AIAA PAPER 90-1915]

p 741 A90-42695

Wide-chord fan proved in nearly five years of service

p 744 A90-44594

Aerodynamic losses in conventional fan blades of high by pass turbo engine

p 854 A90-49487

Acoustic wave excitation during the aerodynamic interaction between a fan blade and a bluff obstacle

p 965 A90-52289

Laser anemometer measurements in a transonic axial-flow fan rotor

[NASA-TP-2879]

p 73 A90-11245

Development of an advanced fan blade containment system

[DOT/FAA/CT-89/20]

p 192 A90-13386

Thermal/structural analysis of the shaft-disk region of a fan drive system

[NASA-TM-101687]

p 610 A90-22807

FAN IN WING AIRCRAFT

Propulsion systems for vertical flight aircraft

[AIAA PAPER 90-3299]

p 853 A90-48881

FANS

WINCOF-I code for prediction of fan compressor unit with water ingestion

[NASA-CR-185157]

p 551 A90-21724

FAR FIELDS

Efficient free wake calculations using Analytical/Numerical Matching and far-field linearization

p 384 A90-28171

Simulation of the reduction characteristics of scattering from an aircraft coated with a thin-type absorber by the spatial network method

p 638 A90-39855

Estimation of subsonic far-field jet-mixing noise from single-stream circular nozzles

[ESDU-89041]

p 316 A90-16721

FAR ULTRAVIOLET RADIATION

Shock layer vacuum UV spectroscopy in an arc-jet wind tunnel

[NASA-TM-102258]

p 370 A90-17112

FAST FOURIER TRANSFORMATIONS

Discrete Fourier transform with high resolution for low frequencies applied to the modal analysis of aircraft vibration

p 679 A90-38975

FASTENERS

Fatigue of aluminium alloy joints with various fastener systems. Low load transfer

[ESDU-89046]

p 370 A90-17193

Neural networks for detecting defects in aircraft structures

[IAR-90-4]

p 777 A90-26345

B-1B improved windshield development. Volume 2: Magna analysis: Baseline and parametric

[AD-A221501]

p 845 A90-26828

New aspects in aircraft inspection using eddy current methods

p 886 A90-28085

FATIGUE (MATERIALS)

Breakage of fan blades in the S1 wind tunnel at Mondane-Avrieux

[ONERA, TP NO. 1989-104]

p 57 A90-11138

An ultrasonic fatigue facility for HCF/LCF interactive tests

p 363 A90-23900

Fatigue methodology III; Proceedings of the AHS National Technical Specialists' Meeting on Advanced Rotorcraft Structures, Scottsdale, AZ, Oct. 3-5, 1989

p 641 A90-39976

Estimation of fatigue crack growth in patched cracked panels

p 684 A90-41335

Dealing with the aging fleet [SAE PAPER 892209]

p 701 A90-45428

Aeronautical fatigue in the electronic era; Proceedings of the Fifteenth ICAF Symposium, Jerusalem, Israel, June 21-23, 1989

p 901 A90-49876

The Operational Loads Monitoring System (OLMS)

p 926 A90-49879

Acoustic fatigue analysis by the finite element method

p 954 A90-49886

Damage tolerance for helicopters

p 919 A90-49888

Development of a double crack growth gage algorithm for application to fleet tracking of fatigue damage

p 901 A90-49890

Understanding composite fatigue - New trends

p 940 A90-49893

Aerospace Arall - The advancement in aircraft materials

p 947 A90-50186

A review of Australian and New Zealand investigations on aeronautical fatigue during the period April 1987 to March 1989

[AD-A210373]

p 32 A90-10026

Effects of a heat cycle on material strength [NAL-TM-562]

p 113 A90-11737

Stochastic propagation of an array of parallel cracks: Exploratory work on matrix fatigue damage in composite laminates

[DE89-017837]

p 126 A90-11813

Nondestructive analysis of aileron fatigue and aging in a Mirage F1

[REPT-M6-594000]

p 184 A90-13378

Design temperatures for flexible airfield pavement design

[AD-A214141]

p 262 A90-15115

Inspection development for T-37 wing spar cap lug

[AD-A214826]

p 287 A90-16708

AGARD/SMP Review: Damage Tolerance for Engine Structures. 2: Defects and Quantitative Materials Behaviour --- conference

[AGARD-R-769]

p 425 A90-18396

Life of concentrated contacts in the mixed EHD and boundary film regimes

[AD-A216673]

p 454 A90-18738

Crack stoppers and ARALL laminates

[PB90-166588]

p 533 A90-21142

NASA airframe structural integrity program

[NASA-TM-102637]

p 543 A90-21422

NASA-UVA light aerospace alloy and structures technology program

[NASA-CR-182607]

p 601 A90-22651

Fatigue crack growth investigation of a Ti-6Al-4V forging under complex loading conditions: NATO/AGARD supplemental engine disk program

[AD-A220239]

p 678 A90-23538

Failure analysis handbook

[AD-A219747]

p 689 A90-23752

Modeling growth of fatigue cracks which originate at rivet holes

[MBB-UT-122/89-PUB]

p 766 A90-25090

Investigation on sheet material of 8090 and 2091

[DE89-782317]

p 774 A90-25361

Development of creep-fatigue damage detection method of rotor steel by ultrasonic wave measurement

[DE90-503792]

p 777 A90-26365

Energy efficient engine pin fin and ceramic composite segmented liner combustor sector rig test report

[NASA-CR-179534]

p 932 A90-28567

Fretting fatigue strength of Ti-6Al-4V at room and elevated temperatures and ways of improving it

p 952 A90-28709

Evaluation of static and fatigue properties of thin sheets of 8090-T8 aluminum-lithium alloy and observation of its fracture surfaces

[NAL-TR-1039]

p 953 A90-29499

Fractographic analysis of fatigue crack growth under two-blocks loading on 2024-T351 sheet specimens

[LR-628]

p 961 A90-29680

Effects of blocks of overloads and underloads on fatigue crack growth in 2024-T351 sheet specimens: Fractographic analysis and crack closure predictions

[LR-629]

p 961 A90-29681

Fatigue, static tensile strength and stress corrosion of aircraft materials and structures. Part 1: Text

[LR-630-PT-1-REV]

p 961 A90-29682

Fatigue, static tensile strength and stress corrosion of aircraft materials and structures. Part 2: Figures

[LR-630-PT-2]

p 961 A90-29683

Fractographic observations on fatigue crack growth under miniTWIST flight-simulation loading (2024-T3 material)

[LR-631]

p 961 A90-29684

Fractographic analysis of fatigue failures of airframe equipment parts: Examples of a rod end housing and a rod end cap

[NAL-TR-1047]

p 961 A90-29686

FATIGUE LIFE

Rub interactions of flexible casing rotor systems

p 41 A90-11554

Endurance of aircraft gas turbine mainshaft ball bearings-analysis using improved fatigue life theory. II - Application to a bearing operating under difficult lubrication conditions

p 128 A90-13845

Designing turbine blades for fatigue and creep

p 112 A90-16007

Experimental determination of the short crack effect for metals

p 265 A90-20064

A study on initial fatigue quality of typical aircraft structures (fastener holes)

p 272 A90-22004

Nonlinear response and fatigue of stiffened panels

p 363 A90-23953

Standardized stress-time histories - An overview

p 368 A90-26752

Development of jet transport airframe fatigue test spectra

p 351 A90-26753

Automated procedure for creating flight-by-flight spectra

p 376 A90-26755

Fatigue spectra development for airborne stores

p 336 A90-26757

Simplified analysis of helicopter fatigue loading spectra

p 336 A90-26758

Compilation of procedures for fatigue crack propagation testing under complex load sequences

p 368 A90-26759

Reliability evaluation system for ceramic gas turbine components

p 444 A90-27678

Fatigue life prediction method for gas turbine rotor disk alloy FV535

p 440 A90-27679

A fatigue study of electrical discharge machine (EDM) strain-gage balance materials

p 448 A90-28295

Methodology of variable amplitude fatigue tests

p 451 A90-29866

The in service multi-axial-stress situation in an uncooled gas turbine blade

p 423 A90-29880

Interactions of active controls and structural loads

p 517 A90-33404

Endurance of aircraft gas turbine mainshaft ball bearings-analysis using improved fatigue life theory. I - Application to a long-life bearing

p 537 A90-33557

Investigation of variation in fatigue life calculated using damage fraction

p 537 A90-33624

Life prediction and fatigue

p 532 A90-34163

A simple prediction method for low-cycle fatigue life of structures

- Recent advances in fatigue life analysis methods for aerospace applications p 677 A90-41338
- The effect on fatigue crack growth under spectrum loading of an imposed placard 'G' limit p 643 A90-41339
- Shaft flexibility effects on the forced response of a bladed-disk assembly p 744 A90-43218
- Fatigue life assessment of a leaded electronic component under a combined thermal and random vibration environment p 770 A90-43734
- Fatigue life estimates for helicopter loading spectra p 772 A90-45324
- The survivability of centrifugal compressors in modern aircraft engines p 928 A90-49883
- Damage tolerance for helicopters p 919 A90-49888
- A review of Australian and New Zealand investigations on aeronautical fatigue during the period April 1987 to March 1989 p 32 N90-10026
- In service life monitoring system using g-meter readings and mass configuration control p 134 N90-12035
- Application of fracture mechanics and half-cycle method to the prediction of fatigue life of B-52 aircraft pylon components p 214 N90-13820
- [NASA-TM-88277] p 214 N90-13820
- Fatigue analysis and reconstruction of helicopter load spectra p 206 N90-14304
- Thermal fatigue durability for advanced propulsion materials p 215 N90-14641
- [NASA-TM-102348] p 215 N90-14641
- Thermal mechanical fatigue of coated blade materials p 256 N90-15107
- [AD-A214258] p 256 N90-15107
- Fatigue life estimates for helicopter loading spectra [NASA-CR-181941] p 279 N90-16294
- An evaluation of the pressure proof test concept for thin sheet 2024-T3 p 543 N90-21424
- [NASA-TM-101675] p 543 N90-21424
- Flexural fatigue life prediction of closed hat-section using materially nonlinear axial fatigue characteristics p 691 N90-25062
- Retirement for cause of the F100 engine p 843 N90-26813
- Damage tolerance analysis for manned hypervelocity vehicles. Volume 2: Software user's manual p 845 N90-26826
- [AD-A222136] p 845 N90-26826
- Multichannel on-board load and fatigue monitoring p 849 N90-27621
- Life management planning p 856 N90-27709
- Use of acoustic emission for continuous surveillance of aircraft structures p 887 N90-28092
- FATIGUE TESTS**
- Effect of protective coatings on mechanical properties of superalloys p 62 A90-11126
- [ONERA, TP NO. 1989-88] p 62 A90-11126
- Fatigue and electromagnetic interference test for Electro-Impulse De-Icing p 100 A90-14362
- [SAE PAPER 891062] p 100 A90-14362
- Creep-fatigue interactions of gas turbine materials p 131 A90-16011
- Fatigue of thick-section cold-expanded holes with and without cracks p 270 A90-20987
- Development status of epicyclic gears p 271 A90-21141
- Fatigue damage of an aircraft due to movement on the airfield p 247 A90-23352
- Fatigue tests of samples of flanged joints of wings p 274 A90-23353
- A method for determining equivalents during the fatigue testing of structures in an acoustic field p 364 A90-24153
- Development of fatigue loading spectra p 367 A90-26751
- [ASTM STP-1006] p 367 A90-26751
- Standardized stress-time histories - An overview p 368 A90-26752
- Development of jet transport airframe fatigue test spectra p 351 A90-26753
- Basic approach in the development of TURBISTAN, a loading standard for fighter aircraft engine disks p 368 A90-26754
- Automated procedure for creating flight-by-flight spectra p 376 A90-26755
- Fatigue spectra development for airborne stores p 336 A90-26757
- Simplified analysis of helicopter fatigue loading spectra p 336 A90-26758
- Compilation of procedures for fatigue crack propagation testing under complex load sequences p 368 A90-26759
- UCAR 2040, A novel wear resistant coating for aircraft structural components p 441 A90-28231
- A fatigue study of electrical discharge machine (EDM) strain-gage balance materials p 448 A90-28295
- Methodology of variable amplitude fatigue tests p 451 A90-29866
- Stress concentration factors - Comparison of theory with fatigue test data p 680 A90-39979
- Improvements to the fatigue substantiation of the H-60 composite tail rotor blade p 642 A90-39985
- Potential application of automotive fatigue technology in rotorcraft design p 681 A90-39987
- SH-2F airframe fatigue test program p 642 A90-39989
- Certification plan for an all-composite main rotor flexbeam p 642 A90-39992
- Maritime environment airframe material fatigue testing p 764 A90-42675
- Douglas aging aircraft programs p 732 A90-45425
- [SAE PAPER 892206] p 732 A90-45425
- Metal laminates for aerospace applications p 874 A90-48997
- Understanding composite fatigue - New trends p 940 A90-49893
- Estimation of the safety factor of turbine blades under thermal cycling and vibration loading p 958 A90-52356
- Fatigue behavior of specimens under compression load spectra [ETN-89-95207] p 137 N90-12954
- Some new techniques for aircraft fuselage skin tests [LR-547] p 184 N90-13379
- An evaluation of a fatigue crack growth prediction model for variable-amplitude loading (PREFFAS) p 214 N90-13822
- [LR-537] p 214 N90-13822
- Design temperatures for flexible airfield pavement design p 262 N90-15115
- [AD-A214141] p 262 N90-15115
- Inspection development for T-37 wing spar cap lug [AD-A214826] p 287 N90-16708
- The need for a common approach within AGARD --- engine component defects p 425 N90-18404
- Static strength and damage tolerance tests on the Fokker 100 airframe p 416 N90-19228
- [NLR-MP-88023-U] p 416 N90-19228
- A corrosion fatigue/stress corrosion testing facility at Materials Research Laboratory p 527 N90-21044
- [MRL-TN-568] p 527 N90-21044
- Characterisation of fatigue of aluminium alloys by acoustic emission. Part 2: Discrimination between primary and other emissions p 678 N90-23523
- [AERE-R-13303-PT-2] p 678 N90-23523
- Fatigue crack growth investigation of a Ti-6Al-4V forging under complex loading conditions: NATO/AGARD supplemental engine disk program p 678 N90-23538
- [AD-A220239] p 678 N90-23538
- Investigation of crack-closure prediction models for fatigue in aluminium alloy sheet under flight-simulation loading p 777 N90-26369
- [LR-619] p 777 N90-26369
- An aluminum quality breakthrough for aircraft structural reliability p 843 N90-26816
- An ultrasonic system for in-service non-destructive inspection of composite structures p 885 N90-28076
- Static and dynamic characterization of the ATR 72 rods made of Ti 10.2.3 titanium alloy p 953 N90-28722
- [REPT-49-238] p 953 N90-28722
- Evaluation of static and fatigue properties of thin sheets of 8090-T8 aluminum-lithium alloy and observation of its fracture surfaces p 953 N90-29499
- [NAL-TR-1039] p 953 N90-29499
- Fractographic observations on fatigue crack growth under miniTWIST flight-simulation loading (2024-T3 material) p 961 N90-29684
- [LR-631] p 961 N90-29684
- FAULT TOLERANCE**
- A methodology for validating software reliability p 74 A90-10567
- [AIAA PAPER 89-3081] p 74 A90-10567
- An experimental investigation of fault tolerant software structures in an avionics application p 74 A90-10568
- [AIAA PAPER 89-3082] p 74 A90-10568
- A hardware and software fault tolerant safety controller p 74 A90-10599
- [AIAA PAPER 89-3123] p 74 A90-10599
- Software fault tolerance analysis and testing for the Advanced Automation System p 75 A90-10600
- [AIAA PAPER 89-3124] p 75 A90-10600
- Mode S system design and architecture p 330 A90-25569
- Restructurable control using proportional-integral implicit model following --- for fighter aircraft p 347 A90-25990
- [AD-A220997] p 347 A90-25990
- Advanced technology ATE for fuel accessory testing p 439 A90-30770
- The use of non-dedicated redundancy in the AMCAD fault tolerant control system p 461 A90-30793
- Modified fault tolerant inertial navigation system p 578 A90-37211
- Fault tolerant architecture for a fly-by-light flight control computer p 860 A90-46931
- Fault-tolerant transputer-based controller configurations for gas-turbine engines p 852 A90-48529
- Development of pressure containment and damage tolerance technology for composite fuselage structures in large transport aircraft p 63 N90-10186
- [NASA-CR-3996] p 63 N90-10186
- An open-loop transient thermodynamic model of the Couguar turbojet p 114 N90-11745
- [AD-A211774] p 114 N90-11745
- Software fault tolerance p 99 N90-12575
- [RSRE-MEMO-4237] p 99 N90-12575
- Laboratory test methodology for evaluating the effects of electromagnetic disturbances on fault-tolerant control systems p 217 N90-14061
- [NASA-TM-101665] p 217 N90-14061
- Integrated approach fault tolerance-current state and future requirements p 275 N90-15465
- [AD-A214402] p 275 N90-15465
- RADC fault tolerant system reliability evaluation facility [AD-A215298] p 377 N90-17348
- Neural networks for aircraft control p 521 N90-20937
- Real-time closed-loop simulation and upset evaluation of control systems in harsh electromagnetic environments p 613 N90-23069
- An experimental study of fault propagation in a jet-engine controller p 665 N90-23401
- [NASA-CR-181335] p 665 N90-23401
- Technical evaluation report on the Guidance and Control Panel 49th Symposium on Fault Tolerant Design Concepts for Highly Integrated Flight Critical Guidance and Control Systems p 758 N90-26012
- [AGARD-AR-281] p 758 N90-26012
- Aircraft Integrated Monitoring Systems p 786 N90-27617
- [DLR-MITT-90-04] p 786 N90-27617
- Formal design and verification of a reliable computing platform for real-time control. Phase 1: Results p 965 N90-29965
- [NASA-TM-102716] p 965 N90-29965
- FAULTS**
- Two-level maintenance concept for advanced avionics architectures p 457 A90-28321
- Main characteristic parameter model for jet engine fault diagnosis p 585 A90-37210
- Fault Detection and Isolation (FDI) techniques for guidance and control systems p 918 N90-29366
- FEASIBILITY**
- Conceptual design and feasibility study of very large passenger aircraft p 834 A90-48841
- [AIAA PAPER 90-3220] p 834 A90-48841
- FEASIBILITY ANALYSIS**
- A feasibility study for a combat aircraft model sting for the European transonic wind tunnel p 524 A90-34243
- Design of a close-support aircraft p 835 A90-48849
- [AIAA PAPER 90-3241] p 835 A90-48849
- A wind tunnel study of a sting-mounted circulation control wing p 319 N90-17577
- [AD-A216248] p 319 N90-17577
- Forward canopy feasibility and Thru-The-Canopy (TTC) ejection system study p 637 N90-24258
- [AD-A220360] p 637 N90-24258
- FEEDBACK**
- Formulation and verification of a technique for compensation of pneumatic attenuation errors in airborne pressure sensing devices p 369 N90-17084
- Passive navigation using image irradiance tracking p 578 N90-22232
- FEEDBACK CONTROL**
- Applications of fuzzy sets to rule-based expert system development p 216 A90-18050
- Design of direct lift control systems against vertical gust p 196 A90-18592
- Decoupled ultimate boundedness control of systems and large aircraft maneuver p 196 A90-19461
- Design of a helicopter output feedback control law using modal and structured-robustness techniques p 282 A90-20557
- Approximate loop transfer recovery method for designing fixed-order compensators p 375 A90-25989
- Very-high-performance data acquisition/analysis/display/control systems based on the APTEC I/O computer p 458 A90-28852
- A numerical solution for instruction tracing problem p 424 A90-29918
- F/A-18 aileron smart servoactuator p 432 A90-30710
- Multivariable control design for the control reconfigurable combat aircraft (CRCA) p 432 A90-30715
- Algorithm for simultaneous stabilization of single-input systems via dynamic feedback p 462 A90-31108
- Analysis and improvement of cabin temperature control system p 580 A90-37241
- Improvement of helicopter handling qualities using H(infinity)-optimisation p 667 A90-38965
- Analysis of airframe/engine interactions - An integrated control perspective p 667 A90-40557
- [AIAA PAPER 90-1918] p 667 A90-40557

Guaranteed cost control via optimal parametric LQ design p 693 A90-40810

Helicopter control design using feedback linearization techniques p 668 A90-40817

Ultimate boundedness control of uncertain systems with application to roll coupled aircraft maneuver p 668 A90-40886

Design of flight control systems to meet rotorcraft handling qualities specifications [AIAA PAPER 90-2805] p 752 A90-45140

Active vibration control for flexible rotor by optimal direct-output feedback control p 879 A90-46222

Helicopter individual blade control through optimal output feedback p 861 A90-46956

Structure/control design synthesis of active flutter suppression system by goal programming [AIAA PAPER 90-3325] p 872 A90-47587

Flight test of a trajectory controller using linearizing transformations with measurement feedback [AIAA PAPER 90-3373] p 864 A90-47631

Control of a twin lift helicopter system using nonlinear state feedback [AIAA PAPER 90-3408] p 817 A90-47663

A mixed H2 and H(infinity) approach to an autopilot design problem [AIAA PAPER 90-3441] p 865 A90-47694

Lateral-directional control of an aircraft using mu synthesis [AIAA PAPER 90-3442] p 865 A90-47695

Robustness evaluation of a flexible aircraft control system [AIAA PAPER 90-3445] p 890 A90-47698

Multivariable flight control synthesis and literal robustness analysis for an aeroelastic vehicle [AIAA PAPER 90-3446] p 890 A90-47699

Rotorcraft pursuit-evasion in nap-of-the-earth flight [AIAA PAPER 90-3455] p 786 A90-47707

A new methodology for model order reduction with application to eigenstructure controllers [AIAA PAPER 90-3475] p 891 A90-47725

Input/output coupling in eigenstructure assignment [AIAA PAPER 90-3476] p 865 A90-47726

Flight controller design with nonlinear aerodynamics, large parameter uncertainty, and pilot compensation [AIAA PAPER 90-3478] p 866 A90-47728

Simulation investigation of multiple axis flying qualities [AIAA PAPER 90-3480] p 866 A90-47729

Analyzing the flared landing task with pitch-rate flight control systems [AIAA PAPER 90-3483] p 866 A90-47732

A comparison of inverse control with optimal control [AIAA PAPER 90-3484] p 866 A90-47733

Robust low norm output feedback design for flight control systems [AIAA PAPER 90-3505] p 891 A90-47751

Obtaining precise LTR with Luenberger type observer with arbitrary observer poles and finite gain [AIAA PAPER 90-3228] p 868 A90-49113

Structural stability augmentation system design using BODEDIRECT: A quick and accurate approach p 33 N90-10116

Optimal integral controller with sensor failure accommodation p 61 N90-10123

Flight test results of a complex precise digital flight control system p 35 N90-10870

Adaptive control law design for model uncertainty compensation [AD-A211712] p 120 N90-11758

Effect of control surface mass unbalance on the stability of a closed-loop active control system [NASA-TP-2952] p 134 N90-12042

A robust digital model following controller for helicopters [ESA-TT-1041] p 120 N90-12621

Turbulence effects of aircraft flight dynamics and control p 258 N90-15055

Advanced detection, isolation, and accommodation of sensor failures in turbofan engines: Real-time microcomputer implementation [NASA-TP-2925] p 259 N90-15112

Discrete proportional Plus Integral (PI) multivariable control laws for the Control Reconfigurable Combat Aircraft (CRCA) [AD-A215664] p 433 N90-18431

Application of variable-gain output feedback for high-alpha control [NASA-TM-102603] p 434 N90-18434

Practical methods for robust multivariable control [AD-A216937] p 462 N90-18920

Output model-following control synthesis for an oblique-wing aircraft [NASA-TM-100454] p 435 N90-19241

Stochastic robustness of linear control systems p 521 N90-20941

Algorithms for computing the multivariable stability margin p 612 N90-22999

Integrated control-system design via generalized LQG (GLOG) theory p 613 N90-23023

Multivariable frequency weighted model order reduction for control synthesis [AIAA-89-3558] p 613 N90-23060

Real-time closed-loop simulation and upset evaluation of control systems in harsh electromagnetic environments p 613 N90-23069

Helicopter Airborne Laser Positioning System (HALPS) [NASA-TM-102814] p 654 N90-23399

Adaptive control of a system with periodic dynamics: Application of an impulse response method to the helicopter vibration problem p 694 N90-23990

Modeling flexible aircraft for flight control design [AD-A219123] p 757 N90-25140

Synthesis of individual rotor blade control system for gust alleviation [NASA-TM-101886] p 736 N90-25972

Robustness evaluation of H2 and H(infinity) control theory as applied to a transport aircraft [AD-A222795] p 759 N90-26018

An expert system to perform on-line controller restructuring for abrupt model changes [NASA-TM-103609] p 964 N90-29121

Control and estimation for aerospace applications with system time delays p 918 N90-29367

Short period control using angular acceleration feedback: Compensation for first lag servo [NAL-TM-600] p 936 N90-29399

FEEDFORWARD CONTROL

Applications of neural networks to avionics systems [AIAA PAPER 89-3093] p 76 A90-10627

FELTS

New metallic felts with improved resistance to high temperature oxidation [ONERA, TP NO. 1989-210] p 366 A90-25343

FIBER COMPOSITES

Resin transfer molding of composite aircraft structures [SAE PAPER 891042] p 128 A90-14347

High-performance composite materials in air and space travel - State of the art and future perspectives [MBB-Z-0279/89] p 266 A90-22595

Composites for aeronautical structures p 286 A90-24291

Buckling analysis of FRP faced cylindrical sandwich panel under combined loading p 365 A90-24376

Postbuckling finite element analysis of composite panels p 365 A90-24377

Metal matrix composites - Ready for take-off? p 356 A90-26865

The use of fibre reinforced thermoplastics for helicopter primary structures and their engineering substantiation p 441 A90-28191

Evaluation of 3-D reinforcements in commingled, thermoplastic structural elements p 441 A90-28192

Analysis and testing of fiber-reinforced thermoplastic composite vertical stabilizer skins for an advanced attack helicopter p 441 A90-28193

Aeroelastic tailoring analysis for preliminary design of advanced turbo propellers with composite blades p 412 A90-29395

Structure-borne noise transmission in cylindrical enclosures due to random excitation [AIAA PAPER 90-0990] p 463 A90-29402

Composites boost 21st-century aircraft engines p 442 A90-29704

The status of high temperature polymers for composites - Likely candidates p 528 A90-31516

Strength substantiation of the all composite airframe (A materials data base approach) p 490 A90-31519

Designing aerospace structures with Du Pont's LDF thermoplastic composites p 530 A90-33126

Erosive wear of fibrous PEEK composites p 530 A90-33127

Fiber reinforced superalloys p 532 A90-34169

Carbon-carbon for NASP p 599 A90-36672

A technique for rapid impact damage detection with implication for composite aircraft structures p 600 A90-37662

Glass-ceramic matrix composites for advanced gas turbines [AIAA PAPER 90-2014] p 676 A90-40594

Metal matrix composite fan blade development [AIAA PAPER 90-2178] p 677 A90-42062

Aircraft applications of advanced composite fiber/metal pressure vessels [AIAA PAPER 90-2344] p 686 A90-42133

Composites applications - The future is now p 678 A90-42372

Eight years of flight operations with composite rotorblades p 835 A90-42481

Analysis of composite rotor blades via Saint Venant's solutions p 688 A90-42491

Application of advanced materials to aircraft gas turbine engines [AIAA PAPER 90-2281] p 764 A90-42769

Lightweight, composite flight control actuators [SAE PAPER 892264] p 733 A90-45459

Understanding composite fatigue - New trends p 940 A90-49893

International SAMPE Symposium and Exhibition, 35th, Anaheim, CA, Apr. 2-5, 1990, Proceedings. Books 1 & 2 p 940 A90-50056

Domestic precursor technology - A unique route to current and future generation carbon fibers p 940 A90-50057

Interfaces properties of high temperature polymer composite systems p 941 A90-50062

Poly(arylene ether ketone)/poly(aryl imide) homo- and polydimethylsiloxane segmented copolymer blends - Influence of chemical structure on miscibility and physical property behavior p 941 A90-50063

Thermo-oxidative stability studies of PMR-15 polymer matrix composites reinforced with various continuous fibers p 941 A90-50068

Structural and dynamic analysis of the A330/340 composite RAT blade --- ram air turbine p 942 A90-50083

Fabrication of complex composite structures using advanced fiber placement technology p 954 A90-50111

Monolithic CFC-Main Landing Gear Door for Tornado p 955 A90-50136

Durability and damage tolerance of S-2 glass/PEEK composites p 944 A90-50140

High performance needed structures in composites p 955 A90-50173

Fracture morphology of toughened bismaleimide/carbon fiber composites p 948 A90-50205

Use of unbalanced laminates as a screening method for microcracking p 948 A90-50217

Material development and second source qualification of carbon fiber/epoxy prepreps for primary and secondary Airbus structures p 948 A90-50225

Mechanical influences on crystallization in PEEK matrix/carbon fiber reinforced composites p 949 A90-50227

The application of 'PT' resins to high temperature aerospace structures p 949 A90-50230

Structural tailoring of select fiber composite structures [NASA-TM-102484] p 533 N90-21137

Neutron radiography: Applications and systems p 886 N90-28080

FIBER OPTICS

High performance single-mode coupler for harsh environments p 78 A90-11027

Comparison of three concepts for a long stroke displacement transducer p 66 A90-11041

Review of fiber optic methods for strain monitoring and non-destructive testing p 67 A90-11042

Fiber optic smart structures and skins; Proceedings of the Meeting, Boston, MA, Sept. 8, 9, 1988 [SPIE-986] p 37 A90-11201

Overview of fiber optic smart structures for aerospace applications p 37 A90-11202

Fiber optic sensors for composite monitoring p 37 A90-11203

Air Force smart structures/skins program overview p 38 A90-11205

Fiber optic sensor systems for smart aerospace structures p 38 A90-11208

Optical fiber, sensing considerations for a smart aerospace structure p 38 A90-11210

Producibility and life cycle cost issues in applications of embedded fiber optic sensors in smart skins p 38 A90-11221

Fiber optic systems for mobile platforms II; Proceedings of the Meeting, Boston, MA, Sept. 6, 7, 1988 [SPIE-989] p 67 A90-11659

Optic multiplex for aircraft sensors - Issues and options p 38 A90-11660

A review of fiber optic flight experience - Past problems, future direction p 38 A90-11661

Wavelength division multiplexed fiber optic sensors for aircraft applications p 38 A90-11663

Toward fly-by-light aircraft p 39 A90-11664

The performance of linear fiber optic data buses p 68 A90-11665

An analysis of reliability in fiber optic ring and star networks p 78 A90-11666

Fiber optics for advanced aircraft p 68 A90-11702

Applications of fiber optic sensors in advanced engine controls p 68 A90-11703

Fiber optic sensors for aircraft p 68 A90-11704

A fiberoptic LAN for aircraft and other applications p 282 A90-23241

Temperature insensitive fiber coil sensor for altimeters p 339 A90-26374

Development of a phase Doppler based probe for icing cloud droplet characterization [AIAA PAPER 90-0667] p 368 A90-26978

- Smart structures with nerves of glass
p 444 A90-27951
- A test and maintenance architecture demonstrated on SEM-E modules for fiber optic networks
p 458 A90-28342
- Some smart structures concepts
p 503 A90-32858
- Smart Skins - A development roadmap
p 504 A90-32860
- The impact of fiber optics (photonics) on future aircraft
p 504 A90-32863
- Fiber optics smart structures program at UTIAS
p 535 A90-32864
- Design and fabrication considerations for composite structures with embedded fiber-optic sensors
p 536 A90-32871
- Development of a fibre optic damage detection system for an aircraft leading edge
p 504 A90-32873
- Smart structures concept study
p 504 A90-32876
- A fiber optic headset compatible with power-by-light
p 504 A90-32906
- Applications of fiber optic sensors in the aerospace and marine industries
p 603 A90-36782
- Reduced insertion loss of X-band RF fiber optic links
p 695 A90-41240
- An experimental investigation of turbine rotor wakes for the development of a fiber optic pressure sensor
[AIAA PAPER 90-2411] p 687 A90-42163
- Silicon-etalon fiber-optic temperature sensor
[NASA-TM-102389] p 187 A90-13381
- Fly-by-light flight control system technology development plan
[NASA-CR-181953] p 259 A90-15111
- The Advanced Digital-Optical Control System (ADOCS) user demonstration program
[AD-A215984] p 349 A90-17644
- Advanced instrumentation for aircraft icing research
[NASA-CR-185225] p 506 A90-21006
- Civil air transport: A fresh look at power-by-wire and fly-by-light
[NASA-TM-102574] p 542 A90-21283
- High speed bus technology development
[AD-A224486] p 960 A90-29565
- FIBER ORIENTATION**
EH-101 main rotor hub application of thick carbon fiber unidirectional tension bands
p 618 A90-42489
- FIBER STRENGTH**
High-performance composite materials in air and space travel - State of the art and future perspectives
[MBB-Z-0279/89] p 266 A90-22595
- FIBERS**
Investigation of the failure modes in a metal matrix composite under thermal cycling
[AD-A216195] p 357 A90-17825
- Calculation of thick wall fiber binders for rotor components of modern helicopters
[MBB-UD-554/84-PUB] p 735 A90-25137
- Towards 2000: The composite engine
[PNR90646] p 750 A90-26000
- FIELD OF VIEW**
An image analysis method for vehicle stabilization
p 668 A90-40914
- Dual servo optical projection system (SOPS) - A solution for two crewmember and night vision goggle display needs
[SAE PAPER 892353] p 760 A90-45504
- Flight-path display can improve safety, operational efficiency
p 847 A90-48982
- FIELD STRENGTH**
Comparative evaluation of Allison T56 engine chip detectors
[AD-A221864] p 855 A90-26832
- FIGHTER AIRCRAFT**
A knowledge-based system design/information tool for aircraft flight control systems
[AIAA PAPER 89-2978] p 55 A90-10491
- Pilot's Associate - A perspective on Demonstration 2
[AIAA PAPER 89-3023] p 36 A90-10524
- Artificial intelligence techniques applied to the non-cooperative identification (NCID) problem
[AIAA PAPER 89-3005] p 75 A90-10619
- APG-70 radar test package development aid
[AIAA PAPER 89-3044] p 1 A90-10624
- Study of advanced technology impact on cycle characteristics and aircraft sizing (using multivariable optimization techniques)
p 29 A90-12612
- Dynamic interaction of separate INS/GPS Kalman filters (Filter-driving - Filter dynamics)
p 124 A90-13996
- Literal singular-value-based flight control system design techniques
p 118 A90-14747
- The Soviets' French revelation. II - Aircraft
p 81 A90-14800
- XG40 - Rolls-Royce advanced fighter engine demonstrator
p 112 A90-16002
- Investigation on the determination of airplane tail loads by flight tests
p 178 A90-16853
- The fundamentals of vectored propulsion
p 180 A90-17461
- Further analysis of wing rock generated by forebody vortices
p 153 A90-17868
- Fighter design from the Soviet perspective
[AIAA PAPER 89-2074] p 181 A90-18135
- The investigation of stress at an enter-gas nozzle of main landing gears for fighter aeroplanes
p 181 A90-18606
- Static aeroelastic analysis of fighter aircraft using a three-dimensional Navier-Stokes algorithm
[AIAA PAPER 90-0435] p 166 A90-19845
- Eurofighter fights back
p 221 A90-21714
- Demonstration of probabilistic-based durability analysis method for metallic airframes
p 273 A90-23287
- Propulsion system integration in high-performance aircraft
p 333 A90-23922
- Aerodynamic control of aircraft by forebody vortex manipulation
[AIAA PAPER 90-1827] p 301 A90-25167
- Restructurable control using proportional-integral implicit model following --- for fighter aircraft
[AD-A220997] p 347 A90-25990
- Efficient method for computing transonic and supersonic flows about aircraft
p 307 A90-26132
- Design priorities for an air-superiority fighter
p 335 A90-26344
- Optimal reflex camber
p 308 A90-26347
- Zonal grid generation for fighter aircraft
p 311 A90-26544
- Interactive grid generation for fighter aircraft geometries
p 311 A90-26546
- Basic approach in the development of TURBISTAN, a loading standard for fighter aircraft engine disks
p 368 A90-26754
- Fatigue spectra development for airborne stores
p 336 A90-26757
- Unsteady aerodynamic characteristics of a fighter model undergoing large-amplitude pitching motions at high angles of attack
[AIAA PAPER 90-0309] p 313 A90-26933
- Stealth comes of age
p 336 A90-27596
- A test and maintenance architecture demonstrated on SEM-E modules for fiber optic networks
p 458 A90-28342
- Design and fabrication of a prototype resin matrix composite interceptor structure
[AIAA PAPER 90-1004] p 442 A90-29275
- Applications of XTRAN3S and CAP-TSD to fighter aircraft
[AIAA PAPER 90-1035] p 389 A90-29360
- Digital simulation of flight control systems for post-stall aircraft
p 431 A90-30704
- Multivariable control design for the control reconfigurable combat aircraft (CRCA)
p 432 A90-30715
- Development of high angle of attack flying qualities criteria using ground-based manned simulators
p 433 A90-30717
- Challenges of tomorrow - The future of secure avionics
p 419 A90-30723
- Research in a high-fidelity acceleration environment
p 439 A90-30734
- An adaptive-learning expert system for maintenance diagnostics
p 460 A90-30754
- Evaluation of sensor management systems
p 461 A90-30789
- The boundary-layer fence - Barrier against the separation process
p 396 A90-31493
- Configuration E-7 supersonic fighter/attack technology program
[ASME PAPER 89-GT-308] p 490 A90-32260
- The impact of fiber optics (photonics) on future aircraft
p 504 A90-32863
- Smart structures concept study
p 504 A90-32876
- Advanced power system for 21st century fighter aircraft
p 508 A90-33347
- Interactions of active controls and structural loads
p 517 A90-33404
- The use of simulation in support of the high AOA flight test program of the AM-X aircraft
[AIAA PAPER 90-1289] p 495 A90-33909
- Flight testing for aircraft agility
[AIAA PAPER 90-1308] p 519 A90-33918
- Ground testing techniques in support of flight test
[AIAA PAPER 90-1309] p 523 A90-33919
- A feasibility study for a combat aircraft model sting for the European transonic wind tunnel
p 524 A90-34243
- Computational fluid dynamics - Current capabilities and directions for the future
p 540 A90-34385
- Table top experimental simulation of hypersonic aero-optical effects --- encountered by cooled window on interceptor
p 525 A90-34586
- Agility as a contribution to design balance --- in fighter aircraft
[AIAA PAPER 90-1305] p 579 A90-35300
- Gas turbine engines for combat aviation - Current realities and perspectives for the near future
p 584 A90-35513
- Flight beyond normal limits
p 589 A90-35847
- Air combat beyond the stall
p 589 A90-35888
- Canadians develop composite techniques for CF-18 battle damage repair program
p 551 A90-36300
- Solution of Euler equations for fighter forebody-inlet combination at high angle of attack
p 556 A90-36419
- Analysis of serious mechanical trouble in a retractable main landing gear of a jet fighter
p 580 A90-36438
- Flight/propulsion control integration for V/STOL fighter/attack aircraft
p 591 A90-38530
- Certification testing methodology for fighter hybrid structure
p 642 A90-40128
- YF-23A previews design features of future fighters
p 643 A90-40344
- Multifunction displays optimized for viewability
p 652 A90-40398
- New technology advances for brighter color CRT displays
p 652 A90-40399
- Experimental windtunnel studies for EFA
p 672 A90-41113
- Exploration of concepts for multi-role fighters
[AIAA PAPER 90-2276] p 644 A90-42104
- Integrated air vehicle/propulsion technology for a multirole fighter - A MCAIR perspective
[AIAA PAPER 90-2278] p 644 A90-42105
- Propulsion control system designs for advanced Navy multimission aircraft
[AIAA PAPER 90-2403] p 663 A90-42160
- A remote tip-driven fan powered supersonic fighter concept
[AIAA PAPER 90-2415] p 663 A90-42167
- Computational analysis of an open-nozzle fighter/attack inlet
[AIAA PAPER 90-2145] p 704 A90-42737
- Demonstrating technologies for enhanced fighter manoeuvrability - The Rockwell/MBB X-31
p 731 A90-43767
- Supersonic STOVL - The future is now
p 732 A90-44781
- Assessment of proposed fighter agility metrics
[AIAA PAPER 90-2807] p 752 A90-45142
- Toward a theory of aircraft agility
[AIAA PAPER 90-2808] p 752 A90-45143
- An experimental investigation of roll agility in air-to-air combat
[AIAA PAPER 90-2809] p 752 A90-45144
- Steady and unsteady force testing of fighter aircraft models in a water tunnel
[AIAA PAPER 90-2815] p 711 A90-45155
- Lessons learned from the S/MTD program for the Flying Qualities Specification
[AIAA PAPER 90-2849] p 755 A90-45177
- Forebody vortex manipulation for aerodynamic control of aircraft at high angles of attack
[SAE PAPER 892220] p 756 A90-45437
- Vortex control for tail buffet alleviation on a twin-tail fighter configuration
[SAE PAPER 892221] p 756 A90-45438
- Power system for 21st century fighter aircraft
[SAE PAPER 892253] p 746 A90-45455
- 3-D analysis of laser measurements of vortex bursting on a chined forebody fighter configuration
[AIAA PAPER 90-3020] p 793 A90-45887
- Power struggle --- Advanced Tactical Fighter engine proposals
p 851 A90-46650
- Artificial intelligence (AI) based tactical guidance for fighter aircraft
[AIAA PAPER 90-3435] p 889 A90-47688
- A comparison of inverse control with optimal control
[AIAA PAPER 90-3484] p 866 A90-47733
- Vertical tail design for base-line configuration of military combat aircraft
p 810 A90-48080
- Computational and experimental studies on ground effect of a slender wing tailless delta aircraft
p 810 A90-48083
- Innovation and investment for survival and prosperity - The new Battle of Britain --- UK military aircraft industry
[AIAA PAPER 90-3189] p 786 A90-48826
- Fighter design econometrics = ownership affordability?
[AIAA PAPER 90-3223] p 897 A90-48842
- Preliminary design of a supersonic short takeoff and vertical landing (STOVL) fighter aircraft
[AIAA PAPER 90-3231] p 834 A90-48844
- The Hawker P1127 vectored thrust fighter program - Lessons learned
[AIAA PAPER 90-3238] p 835 A90-48848
- Analytic models for technology integration in aircraft design
[AIAA PAPER 90-3262] p 835 A90-48857
- Propulsion system flight test analysis using modeling techniques
[AIAA PAPER 90-3288] p 853 A90-48874

Configuring tactical aircraft
[AIAA PAPER 90-3305] p 837 A90-48886

Status of the STOL and Maneuver Technology Demonstrator flight test program
[AIAA PAPER 90-3306] p 838 A90-48887

The implementation of STOVL task-tailored control modes in a fighter cockpit
[AIAA PAPER 90-3229] p 839 A90-49114

The design of a sport aircraft configured to emulate jet fighter characteristics
[AIAA PAPER 90-3244] p 839 A90-49119

STOVL option for the multi-role fighter
[AIAA PAPER 90-3296] p 840 A90-49124

Use of ECS-conditioned air for FLIR avionics thermal control - Fighter aircraft
[SAE PAPER 901219] p 840 A90-49294

A blackboard approach for diagnosis in Pilot's Associate
p 892 A90-49741

Lightning testing and test analyses of the JAS39 aircraft
p 842 A90-49836

Monolithic CFC-Main Landing Gear Door for Tornado
p 955 A90-50136

Military navigation - The fourth generation
p 914 A90-50775

Aviation Week editor flies top Soviet interceptor
p 920 A90-52574

Wind tunnel support system effects on a fighter aircraft model at Mach numbers from 0.6 to 2.0
[AD-A210614] p 19 N90-10010

Problems related to the acquisition, processing and utilization of the modal parameters measured in flight tests in order to obtain the full envelope for flutter
[ETN-89-95210] p 103 N90-11735

Future military powerplants --- fighter aircraft engines
[PNR90554] p 114 A90-11749

Low-speed wind-tunnel study of reaction control-jet effectiveness for hover and transition of a STOVL fighter concept
[NASA-TM-4147] p 119 N90-11751

The aerodynamic experimental center of Aerialia: Combat aircraft group
[ETN-89-95213] p 122 N90-11766

Estimating the relationships between the state of the art of technology and production cost for the US aircraft
[AD-A212127] p 82 N90-12495

Development and applications of reliability and maintainability design criteria in military aircraft
[ETN-89-95208] p 107 N90-12591

An experimental investigation of thrust vectoring two-dimensional convergent-divergent nozzles installed in a twin-engine fighter model at high angles of attack
[NASA-TM-4155] p 237 N90-15884

The use of prototypes in selected foreign fighter aircraft development programs: Rafale, EAP, Lavi, and Gripen
[AD-A214500] p 287 N90-16707

Application of multifunction inertial reference systems to fighter aircraft
p 332 N90-16740

The integration of stores on modern tactical aircraft: Where we have been, and what we should do for the future
p 337 N90-17552

Dynamic derivatives of missiles and fighter-type configurations at high angles of attack
p 337 N90-17554

Onboard fire- and explosion suppression for fighter aircraft
p 327 N90-17602

The technology challenge of the advanced tactical fighter: A study of the technology transition process
[AD-A216109] p 338 N90-17630

The effects of wind tunnel data uncertainty on aircraft point performance predictions
[AD-A216091] p 414 N90-18387

Influence of forebody geometry on aerodynamic characteristics and a design guide for defining departure/spin resistant forebody configurations
[AD-A216714] p 414 N90-18388

Development of an ejection seat specification for a new fighter aircraft
p 483 N90-20057

F-15B high angle-of-attack phenomena and spin prediction using bifurcation analysis
[AD-A217366] p 498 N90-20073

The implementation and operation of a variable-response electronic throttle control system for a TF-104G aircraft
[NASA-TM-101696] p 509 N90-20086

Preliminary design of a supersonic Short Takeoff and Vertical Landing (STOVL) fighter aircraft
[NASA-CR-186670] p 649 N90-23394

Throughput and delay characteristics for a slow-frequency hopped aircraft-to-aircraft packet radio network
[AD-A220525] p 688 N90-23609

A study of the technology required for advanced vertical take-off aircraft
[ETN-90-96786] p 650 N90-24268

Convex models of malfunction diagnosis in high performance aircraft
[AD-A218514] p 702 N90-25073

Time-optimal aircraft pursuit-evasion with a weapon envelope constraint
[NASA-CR-186640] p 734 N90-25126

Design of a low cost short takeoff-vertical landing export fighter/attack aircraft
[NASA-CR-186658] p 734 N90-25132

Qualitative evaluation of a conformal velocity vector display for use at high angles-of-attack in fighter aircraft
[NASA-TM-102629] p 739 N90-25981

Special essays for the 40th anniversary of the revolution: The chief designer discusses the F-8 2 and future fighter planes
[AD-A221587] p 845 N90-26829

Innovative control concepts and component integration for a generic supercruise fighter
p 935 N90-28521

A look at tomorrow today
p 921 N90-28524

Inflight thrust vectoring: A further degree of freedom in the aerodynamic/light mechanical design of modern fighter aircraft
p 921 N90-28528

Aerodynamic interferences of in-flight thrust reversers in ground effect
p 921 N90-28529

Damage tolerance of the fighter aircraft 37 Viggen. Part 1: Analytical assessment
[FFA-TN-1990-12-PT-1] p 923 N90-28538

Damage tolerance of the fighter aircraft 37 Viggen. Part 2: Experimental verification
[FFA-TN-1990-13-PT-2] p 923 N90-28539

Effective optimal control of a fighter aircraft engine
p 928 N90-28548

A conceptual framework for fighter flight control systems
[PD-CF-9009] p 936 N90-28577

Fighter agility metrics
[NASA-CR-187289] p 925 N90-29389

FILAMENT WINDING

Aircraft applications of advanced composite fiber/metal pressure vessels
[AIAA PAPER 90-2344] p 686 A90-42133

Injectable bismaleimide systems
p 943 A90-50132

A study of filament wound high modulus carbon fiber reinforced cylinders
p 948 A90-50218

FILE MAINTENANCE (COMPUTERS)

Initial flight qualification and operational maintenance of X-29A flight software
[NASA-TM-101703] p 32 N90-10023

Assessment System for Aircraft Noise (ASAN) citation database. Volume 2: Database update manual
[AD-A219176] p 615 N90-23189

FILLETS

An investigation of fillets in wing-fuselage joints at subsonic velocities
p 297 A90-24131

Effective methods of controlling a junction vortex system in an incompressible, three-dimensional, turbulent flow
p 571 N90-21732

FILM COOLING

Pressure surface trailing edge slot cooling
[ONERA, TP NO. 1989-123] p 47 A90-12569

Cooling characteristics of a radial water blade
p 47 A90-12571

Advanced combustor liner cooling technology for gas turbines
p 112 A90-16004

Experimental investigation on composite air-cooled blades of highly-loaded transonic turbine
p 189 A90-17793

Experimental investigation on composite cooling of a turbine blade
p 190 A90-17794

Research on film-cooling of turbine blade
p 190 A90-17795

An experimental study of turbine vane heat transfer with leading edge and downstream film cooling
[ASME PAPER 89-GT-69] p 358 A90-23792

An experimental study of heat transfer and film cooling on low aspect ratio turbine nozzles
[ASME PAPER 89-GT-187] p 361 A90-23865

Effects of an embedded vortex on injectant from a single film-cooling hole in a turbulent boundary layer
[ASME PAPER 89-GT-189] p 362 A90-23867

Simulation of cooling film density ratios in a mass transfer technique
[ASME PAPER 89-GT-200] p 362 A90-23872

Prediction of heat transfer coefficient on turbine blade profiles
p 423 A90-29904

Experimental investigation of external heat transfer coefficients on film-cooled turbine blade leading edge
p 585 A90-36787

Film cooling of turbine blades - Two dimensional experiments and numerical simulations
p 739 A90-42670

An experimental investigation of film cooling effectiveness for slots of various exit geometries
[AIAA PAPER 90-2266] p 768 A90-42763

An experimental convective heat transfer investigation around a film-cooled gas turbine blade
p 957 A90-51261

Heat transfer near the entrance to a film cooling hole in a gas turbine blade
[AD-A217396] p 510 N90-20089

Further studies of turbulence structure resulting from interactions between embedded vortices and wall jets at high blowing ratios
[AD-A223296] p 960 N90-29593

FINANCIAL MANAGEMENT

Financing of civil aircraft - Purchases and leasing materials. Volume 1: Development
[DOT/FAA/RD-90/15] p 937 N90-28581

FINITE DIFFERENCE THEORY

Calculation of three-dimensional turbulent flow in a linear turbine cascade
[ONERA, TP NO. 1989-115] p 3 A90-11147

A model for the electrohydrodynamic flow in a constricted arc heater
p 131 A90-15393

Computation of multi-element airfoil flows including confluence effects
p 144 A90-16755

Prediction of post-stall flows on airfoils
p 145 A90-16757

Calculation of low Reynolds number flows at high angles of attack
[AIAA PAPER 90-0569] p 167 A90-19921

Recent developments in calculation methods for internal flows by solution of Euler or Navier-Stokes equations
[ONERA, TP NO. 1989-167] p 223 A90-21033

Prediction of vortical flows on wings using incompressible Navier-Stokes equations
p 226 A90-21935

Upwind differencing scheme for the time-accurate incompressible Navier-Stokes equations
p 232 A90-23109

Unsteady aerodynamic and aeroelastic calculations for wings using Euler equations
p 302 A90-25288

Numerical methods for transonic cascade flow problems
p 305 A90-25796

Alternative methods for modeling unsteady transonic flows
p 394 A90-29889

An efficient finite-difference algorithm for computing axisymmetric transonic nacelle flow fields
p 557 A90-37205

CFD and transonic helicopter sound
p 696 A90-42433

Structural and aerodynamic analysis of a large scale advanced propeller blade
[AIAA PAPER 90-2401] p 743 A90-42793

Tooth thickness effects on the performance of gas labyrinth seals
p 771 A90-45300

Simulation of time-dependent viscous flows using central and upwind-biased finite-difference techniques
[AIAA PAPER 90-3012] p 790 A90-45864

Computational simulation of flows about hypersonic geometries with sharp leading edges
[AIAA PAPER 90-3065] p 793 A90-45891

Computation of unsteady transonic flow about airfoils in frequency domain using the full-potential equation
p 174 A90-14198

Finite difference techniques and rotor blade aeroelastic partial differential equations with quasisteady aerodynamics
p 236 N90-15075

An examination of helicopter rotor load calculations
[AD-A214295] p 249 N90-15098

A review of high-speed, convective, heat-transfer computation methods
p 316 N90-17548

Shock-shock boundary layer interactions
p 318 N90-17569

Computation of hypersonic unsteady viscous flow over a cylinder
p 397 N90-19194

Three-dimensional viscous rotor flow calculations using a viscous-inviscid interaction approach
[NASA-TM-102235] p 399 N90-19204

A fast collocation method for transonic airfoil design
p 501 N90-20984

Application of an inverse method to the design of a radial inflow turbine
p 511 N90-20989

Numerical method for designing 3D turbomachinery blade rows
p 511 N90-20990

Optimization of aerodynamic designs using computational fluid dynamics
p 541 N90-20999

ARLSUPER version 1.0, program users guide
[AD-A222693] p 815 N90-26793

A comparison of two central difference schemes for solving the Navier-Stokes equations
[NASA-TM-102815] p 816 N90-27654

Calculation of temperature distribution in various turbine blades using a boundary-fitted coordinate transformation method
p 929 N90-28550

Numerical simulations of blade-vortex interactions and lifting hovering rotor flows
[AD-A224238] p 911 N90-29302

FINITE ELEMENT METHOD

Finite element method for unsteady three-dimensional subsonic flows through a cascade oscillating with steady loading p 9 A90-11873

Numerical calculation of unsteady aerodynamic forces for three-dimensional subsonic oscillating cascades by a finite element method p 9 A90-12219

Numerical calculation of unsteady aerodynamic forces for two-dimensional supersonic oscillating cascades by finite element method p 9 A90-12238

A solution adaptive finite element method applied to two-dimensional unsteady viscous compressible cascade flow p 15 A90-12624

New approach to small transonic perturbations finite element numerical solving method. I - Numerical developments. II - Numerical applications p 16 A90-12783

Vibration analysis of composite turbopropellers using a nonlinear beam-type finite-element approach p 70 A90-12844

Design and application of a finite element package for modelling turbomachinery vibrations p 70 A90-13011

Influence of joint fixity on the structural static and dynamic response of a joined-wing aircraft. I - Static response [SAE PAPER 891060] p 100 A90-14361

Stress-strain analysis of structural elements of incompressible or nearly incompressible materials by the finite element method p 129 A90-14557

The tape method for the automatic partitioning of an arbitrary region when calculating temperature stresses p 138 A90-14587

A refined optimality criterion technique applied to aircraft wing structural design p 206 A90-16718

Flutter analysis of composite panels using high-precision finite elements p 207 A90-16725

Modal characteristics of swept plate flutter models p 207 A90-16962

Practical suggestions for modifying math models to correlate with actual modal test results p 207 A90-16979

Comparison of the analytical and experimental modes of a model airplane using finite element analysis and multi-reference testing p 207 A90-16986

Sensitivity and optimization of composite structures in MSC/NASTRAN p 208 A90-17370

Dynamic structural correlation via nonlinear programming techniques p 208 A90-17372

Euler and Navier-Stokes solutions for hypersonic flows p 155 A90-18254

Upwind adaptive finite element investigations of the two-dimensional reactive interaction of supersonic gaseous jets p 209 A90-18264

Computation of hypersonic flows by a finite element least-squares method p 155 A90-18296

On the coupling of finite elements and boundary elements for transonic potential flows p 155 A90-18297

A finite element solution for transonic flow around lifting fuselage with arbitrary cross sections from the minimum pressure integral p 156 A90-18298

Application of the finite element method to the problem of rotational flow around wings p 156 A90-18305

Finite element analysis of the flow of a propeller on a slender body with a two-equation turbulence model p 210 A90-18340

Finite element simulation of compressible turbulent flows - Validation and application to internal aerodynamic in gas-turbine engines p 210 A90-18343

Variational principle with variable domain discontinuous finite element method for transonic flow and determining automatically the position and shape of the shock waves p 160 A90-19434

Impact ice stresses in rotating airfoils [AIAA PAPER 90-0198] p 175 A90-19735

Development of finite element methods for compressible Navier-Stokes flow simulations in aerospace design [AIAA PAPER 90-0403] p 166 A90-19833

Application of the dynamic stiffness method to the free and forced vibrations of aircraft panels p 270 A90-20599

Finite element analysis of nonstationary temperature fields in gas turbine components p 271 A90-21324

A finite element solution of unsteady two-dimensional flow in cascades p 226 A90-21946

A finite element method for solving lifting airfoil in transonic flow p 226 A90-21984

Finite element mesh refinement criteria for stress analysis p 273 A90-23013

Automation of the development of a finite element model for shells of the wing type p 364 A90-24118

Review of composite rotor blade modeling p 366 A90-25303

Application of a three-dimensional finite element grid generation scheme for an F-16 aircraft configuration p 336 A90-26541

Hypersonic reactive flow computations

p 315 A90-27131

Generalized Transition Finite-Boundary Elements for high speed flight structures [AIAA PAPER 90-1105] p 449 A90-29286

Finite element two-dimensional panel flutter at high supersonic speeds and elevated temperature [AIAA PAPER 90-0982] p 450 A90-29372

Vibrations of rectangular plates with moderately large initial deflections at elevated temperatures using finite element method [AIAA PAPER 90-1125] p 451 A90-29429

Virtual principles in aircraft structures. Volume 1 - Analysis. Volume 2 - Design, plates, finite elements --- Book p 452 A90-29977

Elastic-viscoplastic finite-element program for modeling tire/soil interaction p 401 A90-31285

Galerkin finite element method for transonic flow about airfoils and wings p 396 A90-31486

Subcomponent tests for composite fuselage technology readiness p 490 A90-33105

Structural-acoustic analysis of aircraft fuselage structures using general purpose finite element codes p 492 A90-33385

The influence of mathematical optimization methods on the design of aircraft structures p 492 A90-33387

Aeroelastic analysis using finite element models p 492 A90-33388

The story of sandwich construction p 538 A90-33702

Design with honeycomb, state of the art p 538 A90-33706

Force balance errors due to temperature changes in ETW p 539 A90-34231

Analysis of aircraft tires via semianalytic finite elements p 496 A90-34740

Finite element simulation of complex jets in a crossflow for V/STOL applications p 585 A90-35753

Finite element numerical analysis for transonic flows around lifting fuselages p 558 A90-37216

Aeroelastic tailoring of composite wing structures p 580 A90-37217

Solution of Euler equations with unstructured meshes p 558 A90-37343

Hierarchical finite element method for rotating beams p 605 A90-38353

Air resonance stability of hingeless rotors in forward flight p 590 A90-38519

A three-dimensional finite element Navier-Stokes solver with k-epsilon turbulence model for unstructured grids [AIAA PAPER 90-1652] p 570 A90-38780

Formation of shocks within axisymmetric nozzles [AIAA PAPER 90-1655] p 570 A90-38782

Finite element analysis of composite panel flutter p 681 A90-40032

Simulation of inviscid blade-row interaction using a linearised potential code [AIAA PAPER 90-1916] p 621 A90-40555

Planet gear sleeve spinning analysis [AIAA PAPER 90-2154] p 681 A90-40613

Nonlinear finite-element analysis to predict fan-blade damage due to soft-body impact p 683 A90-40939

Finite-element analysis of large spur and helical gear systems p 683 A90-40940

An improvement on upwinding technique used in the Galerkin finite element method for the computation of inviscid transonic flow with shock waves p 627 A90-42361

Finite element simulation of unsteady two-dimensional incompressible viscous flows p 629 A90-42423

Finite element simulation of turbulent propeller flowfields p 703 A90-42658

Fatigue life assessment of a leaded electronic component under a combined thermal and random vibration environment p 770 A90-43734

Fully vectorized implicit scheme for 2-D viscous hypersonic flow using adaptive finite element methods p 708 A90-44439

A formulation for the solution of Euler equations for compressible flow using finite elements p 708 A90-44447

A weighted residual formulation for finite element solutions of the steady Euler equations p 770 A90-44457

A multistage method for the solution of the Euler equations on unstructured grids p 708 A90-44460

Preliminary design and load distributions of high performance mechanical systems p 771 A90-45281

Finite element analysis of the Twelve Foot Pressurized Wind Tunnel p 760 A90-45296

Transonic analysis of complex configurations using TRANAIR program [SAE PAPER 892289] p 714 A90-45467

The MDE method for aircraft cabin interior noise prediction --- matrix difference equation [SAE PAPER 892372] p 782 A90-45519

Non-unique solutions of the Euler equations

p 716 A90-45727

Fundamental dynamics issues for comprehensive rotorcraft analyses p 831 A90-46961

Application to a helicopter of a general method for modifying a finite-element model to correlate with modal test data p 832 A90-46968

Some computational and experimental aspects of optimal design process of composite structures p 882 A90-48050

Comparison of equivalent plate and finite element analysis of a realistic aircraft structural configuration [AIAA PAPER 90-3293] p 837 A90-48877

Acoustic fatigue analysis by the finite element method p 954 A90-49886

Structural and dynamic analysis of the A330/340 composite RAT blade --- ram air turbine p 942 A90-50083

A design method for turbomachinery blading in three-dimensional flow p 904 A90-51003

Least-squares finite element methods for compressible Euler equations p 904 A90-51013

The MHOST finite element program: 3-D inelastic analysis methods for hot section components. Volume 3: Systems' manual [NASA-CR-182236] p 73 N90-10451

Investigation of difficult component effects on finite element modal vibration prediction for the Bell AH-1G helicopter. Volume 1: Ground vibration test results [NASA-CR-181916-VOL-1] p 134 N90-12058

Constitutive modeling for isotropic materials (HOST) [NASA-CR-174718] p 193 N90-13391

Investigation of difficult component effects on finite element modal vibration prediction for the Bell AG-1G helicopter. Volume 2: Correlation results [NASA-CR-181916-VOL-2] p 213 N90-13814

Effects of aeroelastic tailoring on anisotropic composite material beam models of helicopter blades [AD-A213478] p 249 N90-15095

Solution of potential flow past an elastic body using the boundary element technique [AD-A213843] p 275 N90-15390

Optimum element density studies for finite-element thermal analysis of hypersonic aircraft structures [NASA-TM-4163] p 369 N90-17074

Shock-shock boundary layer interactions p 318 N90-17569

Analysis of the National Transonic Facility mishap [NASA-TM-101686] p 328 N90-17620

A review of the analytical simulation of aircraft crash dynamics [NASA-TM-102595] p 484 N90-20068

Rotordynamic analysis with shell elements for the transfer matrix method [AD-A217455] p 541 N90-20434

Plan, formulate, and discuss a NASTRAN finite element model of the UH-60A helicopter airframe [NASA-CR-181975] p 541 N90-20439

Comparison of C- and O-grid generation methods using a NACA 0012 airfoil [AD-A216375] p 479 N90-20948

The role of structural analysis in airworthiness certification [BR112064] p 499 N90-20972

An inverse method for the design of turbomachine blades p 511 N90-20988

A study on secondary flow and spanwise mixing in axial flow compressors p 512 N90-21012

Analysis of the rotor tip leakage flow with tip cooling air ejection p 515 N90-21029

Automatic grid generation in complex three-dimensional configurations using a frontal system p 608 N90-21992

Unstructured finite element mesh generation and adaptive procedures for CFD p 608 N90-21993

Design of cryogenic tanks for launch vehicles p 609 N90-22662

Thermal/structural analysis of the shaft-disk region of a fan drive system [NASA-TM-101687] p 610 N90-22807

Finite element elastic-plastic-creep and cyclic life analysis of a cowl lip [NASA-TM-102342] p 610 N90-22808

Correlation/validation of finite element code analyses for vibration assessment of avionic equipment [AD-A220393] p 654 N90-23398

STARS: An integrated general-purpose finite element structural, aeroelastic, and aeroservoelastic analysis computer program [NASA-TM-101709] p 689 N90-23768

Finite element analysis of structural components using viscoplastic models with application to a cowl lip problem [NASA-CR-185189] p 690 N90-23769

- Short time Force and moment measurement System for shock tubes (SFS) for measuring times less than 10 ms p 674 N90-24233
- Rotary-Jet thrust augmentor with jet-flapped blades p 633 N90-24243
- Development of a finite element based delamination analysis for laminates subject to extension, bending, and torsion p 679 N90-25049
- Extension-torsion coupling behavior of advanced composite tilt-rotor blades p 651 N90-25057
- Development and application of an optimization procedure for space and aircraft structures [MBB-FW-522/S/PUB-383] p 779 N90-25078
- The application of the finite element method to an aerodynamic problem specific to propeller design [LR-614] p 718 N90-25116
- Calculation of thick wall fiber binders for rotor components of modern helicopters p 735 N90-25137
- Ground shake test of the UH-60A helicopter airframe and comparison with NASTRAN finite element model predictions [NASA-CR-181993] p 758 N90-25143
- Calculation of flight vibration levels of the AH-1G helicopter and correlation with existing flight vibration measurements [NASA-CR-182031] p 775 N90-25375
- Computational crash dynamics. Project 1.2: Computational crash dynamics analysis [IAR-89-19] p 724 N90-25956
- Photoelasticity: A cost effective design tool p 683 N90-26819
- Finite element models of USAF aircraft structures p 844 N90-26820
- B-1B improved windshield development. Volume 2: Magna analysis: Baseline and parametric [AD-A221501] p 845 N90-26828
- Correlation of AH-1G airframe flight vibration data with a coupled rotor-fuselage analysis [NASA-CR-181974] p 959 N90-28865
- Plan, execute, and discuss vibration measurements and correlations to evaluate a NASTRAN finite element model of the AH-64 helicopter airframe [NASA-CR-181973] p 960 N90-28866
- Nonlinear static and dynamic modeling of composite rotor blades including warping effects p 924 N90-29382
- Structural testing and analytical research of turbine components [AD-A223516] p 933 N90-29396
- FINITE VOLUME METHOD**
- 3D calculations of reacting flows within aircraft engine combustion chambers [ONERA, TP NO. 1989-153] p 67 A90-11173
- Turbulent mixing in helicopter jet diluters - Navier-Stokes calculations and correlations [AAAF PAPER NT 88-13] p 40 A90-11432
- Flow in compressor interstage ducts p 11 A90-12521
- CFD predictions of lobed mixer flowfields p 70 A90-12626
- Navier-Stokes computations of a prolate spheroid at angle of attack p 17 A90-13018
- Hybrid finite volume approach to Euler solutions for supersonic flows p 154 A90-18144
- Solving compressible flow problems using adaptive finite quadtree and octree grids p 155 A90-18243
- Solution of the parabolized Navier-Stokes equations using Osher's upwind scheme [AIAA PAPER 90-0392] p 165 A90-19830
- Chemical and vibrational non-equilibrium nozzle flow calculation by an implicit upwind method [ONERA, TP NO. 1989-175] p 223 A90-21037
- Computations of hypersonic flow by finite-volume methods p 224 A90-21168
- Asymmetric separated flows at supersonic speeds [AIAA PAPER 90-0595] p 230 A90-22233
- Navier-Stokes computations of vortical flows over low-aspect-ratio wings p 232 A90-23103
- Application of a lower-upper implicit scheme and an interactive grid generation for turbomachinery flow field simulations [ASME PAPER 89-GT-20] p 288 A90-23762
- Calculation of tip leakage flow with three-dimensional Euler code p 304 A90-25772
- Analysis of three-dimensional aerospace configurations using the Euler and Navier-Stokes equations p 305 A90-25798
- Quasi-three-dimensional grid generation by an algebraic homotopy procedure p 376 A90-26481
- The construction of component-adaptive grids for aerodynamic geometries p 309 A90-26513
- Hypersonic reactive flow computations p 315 A90-27131
- Calculation of transonic flows with separation past arbitrary inlets at incidence p 384 A90-27979
- Calculations of propeller/airframe interference effects using the potential/multienergy flow method p 490 A90-32452
- Development of a three-dimensional upwind parabolized Navier-Stokes code p 602 A90-36253
- An interactive scheme for transonic wing/body flows based on Euler and inverse boundary-layer equations [AIAA PAPER 90-1586] p 566 A90-38721
- Boundary conditions for Euler equations at internal block faces of multi-block domains using local grid refinement [AIAA PAPER 90-1590] p 607 A90-38725
- Three dimensional transonic and supersonic flow prediction in axi-vented nozzles using a finite volume method [AIAA PAPER 90-2026] p 624 A90-41989
- Modeling supersonic combustion using a fully-implicit numerical method [AIAA PAPER 90-2307] p 677 A90-42117
- Finite volume solutions of two-dimensional Euler equations on adapted structured meshes p 629 A90-42413
- A colocated finite volume method for solving the Navier-Stokes equations for incompressible and compressible flows in turbomachinery - Results and applications p 703 A90-42659
- Turbulent flow simulation of a three-dimensional turbine cascade [AIAA PAPER 90-2124] p 704 A90-42732
- Analysis of transonic turbine rotor cascade flows using a finite-volume total variation diminishing (TVD) scheme [AIAA PAPER 90-2127] p 704 A90-42733
- Development of supersonic and hypersonic Euler solvers using shock fitting in two and three dimensions p 707 A90-44426
- An upwind approach to unsteady flowfield simulation [AIAA PAPER 90-3100] p 796 A90-45912
- Computation of flow fields around propellers and hovering rotors based on the solution of the Euler equations [DLR-FB-89-37] p 170 N90-13333
- A computational design method for shock free transonic cascades and airfoils p 501 N90-20986
- Numerical simulation of hypersonic flow around a space plane. Part 2: Application to high angles of attack flow [NAL-TR-10117] p 570 N90-21726
- A computer code for the prediction of aerodynamic characteristics of lifting airfoils at transonic speed [DLC-EST-TN-030] p 632 N90-23359
- FINNED BODIES**
- Aerodynamic heating in shock wave/turbulent boundary layer interaction regions induced by blunt fins p 82 A90-13775
- Upstream-influence scaling of fin-generated shock wave boundary-layer interactions [AIAA PAPER 90-0376] p 164 A90-19822
- Transonic Euler solutions on mutually interfering finned bodies p 555 A90-36256
- Navier-Stokes predictions of pitch damping for finned projectiles using steady coning motion [AIAA PAPER 90-3088] p 795 A90-45902
- Transonic Euler solutions on mutually interfering finned bodies [AD-A213395] p 170 N90-13331
- External flow computations for a finned 60mm ramjet in steady supersonic flight [AD-A216998] p 428 N90-19233
- FINIS**
- Measurements of pressure fluctuations in the interaction regions of shock waves and turbulent boundary layers induced by blunt fins p 9 A90-12218
- Aerodynamic heating in the interaction regions of shock waves and turbulent boundary layers induced by sharp fins p 9 A90-12220
- Characteristics of partial length circular pin fins as heat transfer augmentors for airfoil internal cooling passages [ASME PAPER 89-GT-87] p 359 A90-23806
- The effect of longitudinal fins on turbulent friction drag p 297 A90-24123
- Structure of swept shock wave/boundary-layer interactions using conical shadowgraphy [AIAA PAPER 90-1644] p 569 A90-38772
- Simulation of glancing shock wave and boundary layer interaction [NASA-TM-102233] p 133 N90-11970
- Additions and corrections to SUPER: A program for calculating steady and oscillatory supersonic flow over a thin wing, tail plane and fin [AD-A211771] p 90 N90-12501
- Glancing shock-boundary layer interactions p 319 N90-17571
- Numerical investigation of some control methods for 3-D turbulent interactions due to sharp fins p 591 N90-21764
- Calculation of the aeroelastic blade stabilization with linearized process [MITT-87-01] p 666 N90-24272
- Yaw fin deployment apparatus for ejection seat [AD-D014512] p 723 N90-25118
- Damage tolerance of the fighter aircraft 37 Viggen. Part 1: Analytical assessment [FFA-TN-1990-12-PT-1] p 923 N90-28538
- Damage tolerance of the fighter aircraft 37 Viggen. Part 2: Experimental verification [FFA-TN-1990-13-PT-2] p 923 N90-28539
- FIR FILTERS**
- Adaptive clutter rejection filters for airborne Doppler weather radar applied to the detection of low altitude windshear [NASA-CR-186211] p 214 N90-14453
- FIRE CONTROL**
- F-16/GPS integration test results p 726 A90-43710
- China-built airborne synchronous laser ranger the new L-8 jet trainer aircraft [AD-A213835] p 275 N90-15422
- Application of multifunction inertial reference systems to fighter aircraft p 916 N90-29341
- FIRE EXTINGUISHERS**
- Aircraft cabin fire suppression by means of an interior water spray system [CAA-PAPER-88014] p 96 N90-11719
- Aviation Engine Test Facilities (AETF) fire protection study [AD-A211483] p 134 N90-12777
- US Navy aircraft fire protection technology p 327 N90-17603
- Preliminary fire extinguishing tests with handheld bottles: A comparison of extinguishing compounds [DOT/FAA/CT-TN89/60] p 370 N90-17930
- FIRE FIGHTING**
- Aircraft internal fires p 326 N90-17593
- FIRE PREVENTION**
- Aircraft cabin interior systems meeting new FAA regulations p 482 A90-33710
- Aircraft cabin fire suppression by means of an interior water spray system [CAA-PAPER-88014] p 96 N90-11719
- Aviation Engine Test Facilities (AETF) fire protection study [AD-A211483] p 134 N90-12777
- Investigation and characteristics of major fire-related accidents in civil air transports over the past ten years p 324 N90-17582
- Aircraft fires: A study of transport accidents from 1975 to the present p 324 N90-17583
- Development of improved fire safety standards adopted by the Federal Aviation Administration p 324 N90-17585
- Fire safety in civil aviation p 325 N90-17586
- A review of UK civil aviation fire and cabin safety research p 325 N90-17587
- Objectives and results of cabin fire research in Germany p 325 N90-17588
- New aircraft cabin and cargo flammability standards for transport category aircraft p 325 N90-17589
- Fire prevention in transport airplane passenger cabins p 325 N90-17590
- Fire science and aircraft safety p 326 N90-17596
- Hot surface ignition studies of aviation fluids p 327 N90-17600
- Onboard fire- and explosion suppression for fighter aircraft p 327 N90-17602
- US Navy aircraft fire protection technology p 327 N90-17603
- Aircraft fire safety in the Canadian Forces p 327 N90-17604
- Fire hardening of aircraft through upgrades of materials and designs p 327 N90-17605
- Fire hardening of an aircraft passenger cabin p 328 N90-17606
- Advanced materials for interior and equipment related to fire safety in aviation p 328 N90-17608
- Heat release rate measurement for evaluating the flammability of aircraft materials p 328 N90-17610
- FIREPROOFING**
- Aircraft cabin fire suppression by means of an interior water spray system [CAA-PAPER-88014] p 96 N90-11719
- Fire prevention in transport airplane passenger cabins p 325 N90-17590
- Onboard fire- and explosion suppression for fighter aircraft p 327 N90-17602
- FIRES**
- An analysis of factors impeding passenger escape from aircraft fires p 322 A90-26018
- Aviation Engine Test Facilities (AETF) fire protection study [AD-A211483] p 134 N90-12777
- RAAF Orion aircraft A9-300 oxygen fire [AD-A215496] p 323 N90-16725
- Aircraft Fire Safety [AGARD-CP-467] p 324 N90-17581

- Aircraft fires: A study of transport accidents from 1975 to the present p 324 N90-17583
- Aircraft fire safety: Learning from past accidents p 324 N90-17584
- Fire safety in civil aviation p 325 N90-17586
- A review of UK civil aviation fire and cabin safety research p 325 N90-17587
- Objectives and results of cabin fire research in Germany p 325 N90-17588
- Fire prevention in transport airplane passenger cabins p 325 N90-17590
- Characteristics of transport, aircraft fires measured by full-scale tests p 325 N90-17591
- Full scale study of a cabin fire in an A300 fuselage section p 326 N90-17592
- Aircraft internal fires p 326 N90-17593
- Fire science and aircraft safety p 326 N90-17596
- Forced and natural venting of aircraft cabin fires: A numerical simulation p 326 N90-17597
- Time development of convection flow patterns in aircraft cabins under post-crash fire exposure p 327 N90-17598
- Hot surface ignition studies of aviation fluids p 327 N90-17600
- The stability of fuel fires p 327 N90-17601
- Onboard fire- and explosion suppression for fighter aircraft p 327 N90-17602
- US Navy aircraft fire protection technology p 327 N90-17603
- Aircraft fire safety in the Canadian Forces p 327 N90-17604
- Fire hardening of aircraft through upgrades of materials and designs p 327 N90-17605
- Fire hardening of an aircraft passenger cabin p 328 N90-17606
- Advanced materials for interior and equipment related to fire safety in aviation p 328 N90-17608
- New materials for civil aircraft furnishing p 328 N90-17609
- Flammability testing of aircraft cabin materials p 328 N90-17611
- Preliminary fire extinguishing tests with handheld bottles: A comparison of extinguishing compounds [DOT/FAA/CT-TN89/60] p 370 N90-17930
- Full-scale air transport category fuselage burnthrough tests [DOT/FAA/CT-TN89/65] p 486 N90-20967
- Aircraft crash survival design guide, Volume 5: Aircraft postcrash survival [AD-A218438] p 575 N90-22549
- Fire hazards of aerosol cans in aircraft cargo compartments [DOT/FAA/CT-89/32] p 636 N90-23369
- Flammability of fire resistant, aircraft hydraulic fluid [DOT/FAA/CT-TN90/19] p 766 N90-25222
- FIXED WINGS**
- Response and hub loads sensitivity analysis of a helicopter rotor p 181 A90-18145
- BELLTECH - A multipurpose Navier-Stokes code for rotor blade and fixed wing configurations p 384 A90-28174
- Influence of joint fixity on the aeroelastic characteristics of a joined wing structure [AIAA PAPER 90-0980] p 390 A90-29370
- Propulsion systems for vertical flight aircraft [AIAA PAPER 90-3299] p 853 A90-48881
- X-wing experimental aircraft - Lessons learned [AIAA PAPER 90-3208] p 838 A90-49105
- Preliminary design of a family of three close air support aircraft [NASA-CR-186070] p 336 N90-16751
- Extension of a three-dimensional viscous wing flow analysis [NASA-CR-182023] p 631 N90-23348
- FLAME HOLDERS**
- Engineering design models for ramjet efficiency and lean blowoff [AIAA PAPER 90-2453] p 663 A90-42176
- Suppression of 'Buzz' instability by geometrical design of the flameholder [AIAA PAPER 90-1966] p 741 A90-42706
- FLAME IONIZATION**
- A study of the electrophysical phenomena in the combustion chambers of jet engines p 765 A90-45028
- FLAME PROPAGATION**
- Velocity and scalar measurements in model and real gas turbine combustors p 191 A90-19005
- Combustion oscillations in ducts p 204 A90-19006
- The effect of swirler on short reversal-flow annular combustor p 423 A90-29906
- Development of the jet-swirl high loading combustor [AIAA PAPER 90-2451] p 658 A90-40633
- Fuel tank explosion protection p 251 N90-15914
- Combustion Experiments During KC-135 Parabolic Flights [ESA-SP-1113] p 368 N90-16958
- Fire science and aircraft safety p 326 N90-17596
- Chemistry of combustion processes p 749 N90-25994
- FLAME RETARDANTS**
- Development of improved fire safety standards adopted by the Federal Aviation Administration p 324 N90-17585
- FLAME SPECTROSCOPY**
- Influence of fuel composition on flame radiation in gas turbine combustors p 659 A90-40946
- Spectral response of a UV flame sensor for a modern turbojet aircraft engine p 769 A90-43285
- FLAME STABILITY**
- On the use of external burning to reduce aerospace vehicle transonic drag [AIAA PAPER 90-1935] p 656 A90-40562
- Suppression of 'Buzz' instability by geometrical design of the flameholder [AIAA PAPER 90-1966] p 741 A90-42706
- Combustion process in a gas turbine combustor when using H₂,NH₃ and LPG fuels p 873 A90-46882
- On the use of external burning to reduce aerospace vehicle transonic drag [NASA-TM-103107] p 588 N90-21762
- Flame extinction in compressible flow p 883 N90-26899
- FLAME TEMPERATURE**
- Numerical modeling of a flame in a confined, unstable shear layer [AIAA PAPER 90-0647] p 205 A90-19966
- Fuel molecular structure and flame temperature effects on soot formation in gas turbine combustors [ASME PAPER 89-GT-288] p 253 A90-22652
- Experimental studies of combustor dilution zone aerodynamics. I - Mean flowfields p 508 A90-32962
- FLAMEOUT**
- In flight relight tests on AM-X single engine fly-by-wire aircraft p 34 N90-10869
- Application of neural networks to the F/A-18 engine condition monitoring system [AD-A219820] p 666 N90-24271
- FLAMES**
- Concentration, temperature, and density in a hydrogen-air flame by excimer-induced Raman scattering p 875 N90-26903
- FLAMMABILITY**
- Experimental and computational flammability limits in a solid fuel ramjet [AIAA PAPER 90-1964] p 676 A90-40574
- Flammability regulations affecting advanced composite materials p 947 A90-50190
- New aircraft cabin and cargo flammability standards for transport category aircraft p 325 N90-17589
- Ignitability of jet-A fuel vapors in aircraft fuel tanks p 326 N90-17594
- Hot surface ignition studies of aviation fluids p 327 N90-17600
- Heat release rate measurement for evaluating the flammability of aircraft materials p 328 N90-17610
- Flammability testing of aircraft cabin materials p 328 N90-17611
- Full-scale air transport category fuselage burnthrough tests [DOT/FAA/CT-TN89/65] p 486 N90-20967
- Flammability of fire resistant, aircraft hydraulic fluid [DOT/FAA/CT-TN90/19] p 766 N90-25222
- Toxicity of thermolysis products from the materials of airplane cockpits [CEAT-PV-M6/5924/02] p 876 N90-27895
- Tests for aircraft interior materials in fire accident [LR-622] p 914 N90-29337
- FLAMMABLE GASES**
- Fire hazards of aerosol cans in aircraft cargo compartments [DOT/FAA/CT-89/32] p 636 N90-23369
- FLANGES**
- Flanged joints of aeroplanes [PNR90594] p 116 N90-12609
- FLAPPING**
- An experimental and analytical investigation of isolated rotor flap-lag stability in forward flight p 518 A90-33623
- Synthesis of individual rotor blade control system for gust alleviation [NASA-TM-101886] p 736 N90-25972
- FLAPS (CONTROL SURFACES)**
- An analysis of the possibility of using direct control of the lifting force for modifying the flying qualities of aircraft p 118 A90-15423
- Calculation of flow over airfoil with slat and flap p 149 A90-16797
- An investigation of strake fence flaps on a canard-configured aircraft [AIAA PAPER 90-0762] p 230 A90-22259
- Unsteady, separated flow behind an oscillating, two-dimensional spoiler p 469 A90-32462
- A flow around airfoil with slat and flap [AIAA PAPER 90-1535] p 564 A90-38679
- Application of CFD to pitch/yaw thrust vectoring spherical convergent flap nozzles [AIAA PAPER 90-2023] p 657 A90-40597
- External nozzle flap dynamic load measurements on F-15 S/MTD model [AIAA PAPER 90-1910] p 740 A90-42692
- Vibration reduction on servo flap controlled rotor using HHC p 861 A90-46967
- An examination of helicopter rotor load calculations p 833 A90-46972
- Comparison of active control on a servo flap rotor using fixed system and rotating system parameters p 862 A90-46976
- Validation of a computer code for analysis of subsonic aerodynamic performance of wings with flaps in combination with a canard or horizontal tail and an application to optimization [NASA-TP-2961] p 173 N90-14187
- Calculation of the flap profile flows with separation based on coupled potential and boundary layer solutions p 278 N90-16191
- Analysis and numerical solution of flow over airfoil with control flap p 318 N90-17564
- The NASA digital VGH program: Exploration of methods and final results. Volume 2: L 1011 data 1978-1979: 1619 hours [NASA-CR-181909-VOL-2] p 505 N90-20080
- FLASH POINT**
- Considerations in using broad specification fuels for aircraft propulsion [SAE PAPER 892330] p 765 A90-45487
- FLAT PLATES**
- Application of the hydrogen bubble visualization method to the water tunnels of ONERA [ONERA, TP NO. 1989-107] p 58 A90-11140
- Adverse pressure gradient effects on boundary layer transition in a turbulent free stream p 15 A90-12639
- Numerical simulation of an impinging jet on a flat plate p 86 A90-15821
- The flow around wing-body junctions p 145 A90-16765
- Computation of the trailing edge flow downstream a flat plate with finite thickness p 151 A90-17464
- Effect of ground on wake roll-up behind a lifting surface p 160 A90-19436
- Solution of the parabolized Navier-Stokes equations using Osher's upwind scheme [AIAA PAPER 90-0392] p 165 A90-19830
- Viscous oscillating cascade aerodynamics and flutter by a locally analytical method [AIAA PAPER 90-0579] p 168 A90-19929
- The effect of longitudinal fins on turbulent friction drag p 297 A90-24123
- A transition detection study at Mach 1.5, 2.0, and 2.5 using a micro-thin hot-film system p 436 A90-28260
- Liquid crystal thermography for aerodynamic heating measurements in short duration hypersonic facilities p 446 A90-28262
- Calculation of flow on a flat plate at angle of attack by numerical solution of Navier-Stokes equations p 537 A90-33424
- The influence of boundary layer state on vortex shedding from flat plates and turbine cascades [ASME PAPER 89-GT-296] p 474 A90-33560
- Visualization studies in rotating disk cavity flows p 475 A90-33568
- Interaction of a plane shear layer with a downstream flat plate [AIAA PAPER 90-1460] p 561 A90-38617
- Flow over inclined finite length and width flat plates at low and high Reynolds numbers [AIAA PAPER 90-1467] p 562 A90-38624
- A numerical study of longitudinal vortex interaction with a boundary layer [AIAA PAPER 90-1630] p 568 A90-38759
- Wave structure of artificial perturbations in a supersonic boundary layer on a plate p 619 A90-39518
- Supersonic flutter of shear deformable laminated composite flat panels p 683 A90-41104
- Electrical analog circuit for heat transfer measurements on a flat plate simulating turbine vane heat transfer in turbulent flow [AIAA PAPER 90-2412] p 687 A90-42164
- Subharmonic instability of compressible boundary layers p 706 A90-44005
- Surface flow on a flat plate induced by a supersonic jet exhausting normally into a low speed crossflow [AIAA PAPER 90-3011] p 789 A90-45860

- A generalized relation for the aerodynamic efficiency of plane bodies p 804 A90-46559
- Empirical prediction of the blockage effect of a flat body on a rotor p 807 A90-46942
- The turbulent near wake of a flat plate at low Reynolds number p 811 A90-48711
- Linear instability of supersonic plane wakes [NASA-CR-181911] p 20 N90-10833
- Unsteady three-dimensional thin-layer Navier Stokes solutions on dynamic blocked grids [AD-A212377] p 136 N90-12899
- Computation of Navier-Stokes equations for three-dimensional flow separation [NASA-TM-102266] p 172 N90-13353
- Glancing shock-boundary layer interactions p 319 N90-17571
- Calculation of excrescence drag magnification due to pressure gradient at high subsonic speeds [ESDU-87004] p 397 N90-19195
- Leading edge vortex dynamics on a pitching delta wing [NASA-CR-186327] p 398 N90-19198
- Numerical simulations of supersonic flow through oscillating cascade sections [NASA-TM-103100] p 478 N90-20051
- The Helicopter Antenna Radiation Prediction Code (HARP) [NASA-CR-186925] p 884 N90-27946
- FLAT SURFACES**
- Wake-boundary layer interaction p 85 A90-15238
- Calculation of the front or rear part of a flat body in subsonic flow with the extremum value of the critical Mach number p 296 A90-24120
- Local heat transfer on a flat surface roughened with broken ribs p 534 A90-32169
- FLEXIBILITY**
- Blade mistuning coupled with shaft flexibility effects in rotor aeroelasticity [ASME PAPER 89-GT-330] p 343 A90-23896
- Numerical simulation of unsteady rotational flow over propfan configurations [NASA-CR-186037] p 90 N90-12500
- Structural testing and analytical research of turbine components [AD-A223516] p 933 N90-29396
- FLEXIBLE BODIES**
- Whirl-flutter investigation on an advanced turboprop configuration p 40 A90-11008
- Rub interactions of flexible casing rotor systems p 41 A90-11554
- A new type of non-rigid airship system [AIAA PAPER 89-3175] p 244 A90-20583
- Flight testing a highly flexible aircraft - Case study on the MIT Light Eagle p 414 A90-31284
- Certification plan for an all-composite main rotor flexbeam p 642 A90-39992
- Digital control of magnetic bearings supporting a multimass flexible rotor p 682 A90-40712
- Shaft flexibility effects on the forced response of a bladed-disk assembly p 744 A90-43218
- The application of TSIM software to act design and analysis on flexible aircraft p 60 N90-10086
- Flexible aircraft dynamic modeling for dynamic analysis and control synthesis p 61 N90-10112
- Aircraft modal suppression system: Existing design approach and its shortcomings p 33 N90-10115
- Structural stability augmentation system design using BODEDIRECT: A quick and accurate approach p 33 N90-10116
- Modeling flexible aircraft for flight control design [AD-A219123] p 757 N90-25140
- FLEXIBLE SPACECRAFT**
- Control law synthesis and optimization software for large order aeroservoelastic systems p 61 N90-10111
- FLEXIBLE WINGS**
- Unsteady flow computation of oscillating flexible wings [AIAA PAPER 90-0937] p 389 A90-29363
- Navier-Stokes computations on swept-tapered wings, including flexibility [AIAA PAPER 90-1152] p 389 A90-29364
- Time domain simulations of a flexible wing in subsonic, compressible flow [AIAA PAPER 90-1153] p 390 A90-29365
- Aeroservoelasticity [AIAA PAPER 90-1073] p 411 A90-29381
- Digital-flutter-suppression-system investigations for the active flexible wing wind-tunnel model [AIAA PAPER 90-1074] p 430 A90-29382
- Simulation of static and dynamic aeroelastic behavior of a flexible wing with multiple control surfaces [AIAA PAPER 90-1075] p 392 A90-29383
- Entry of a flexible airfoil into a vertical gust p 470 A90-32552
- Recent activities within the aeroservoelasticity branch at the NASA Langley Research Center p 492 A90-33400

- Flutter suppression control law synthesis for the active flexible wing model p 517 A90-33403
- Energy based stability analysis of a fuzzy roll controller design for a flexible aircraft wing p 668 A90-40833
- The active flexible wing aeroservoelastic wind-tunnel test program p 33 N90-10119
- Using transonic small disturbance theory for predicting the aeroelastic stability of a flexible wind-tunnel model [NASA-TM-102617] p 478 N90-20047
- Static aeroelastic analysis of a three-dimensional generic wing [NASA-TM-102231] p 509 N90-20087
- Digital-flutter-suppression-system investigations for the active flexible wing wind-tunnel model [NASA-TM-102618] p 520 N90-20093
- FLEXING**
- Homogenization of composite beams in dynamical flexure p 878 A90-46184
- Flexural fatigue life prediction of closed hat-section using materially nonlinear axial fatigue characteristics p 691 N90-25062
- FLIGHT ALTITUDE**
- The accuracy of barometric altimeters with respect to geometric altitude p 108 A90-14012
- A study of sonic boom overpressure trends with respect to weight, altitude, Mach number, and vehicle shaping [AIAA PAPER 90-0367] p 164 A90-19816
- More cruising levels expected at higher altitudes p 721 A90-44548
- Computation of hypersonic low density flows with thermochemical nonequilibrium p 477 N90-20044
- FLIGHT CHARACTERISTICS**
- Aerodynamic and dynamic principles of helicopter flight --- Russian book p 55 A90-12473
- An analysis of the possibility of using direct control of the lifting force for modifying the flying qualities of aircraft p 118 A90-15423
- High angle of attack flying qualities criteria [AIAA PAPER 90-0219] p 197 A90-19738
- Estimation of the flight dynamic characteristics of the YEZ-2A [AIAA PAPER 89-3173] p 245 A90-20590
- Flying qualities lessons learned - 1988 p 431 A90-30705
- Development of high angle of attack flying qualities criteria using ground-based manned simulators p 433 A90-30717
- The importance of measured data as a contribution to reducing crew caused accidents [AIAA PAPER 89-3219] p 482 A90-31703
- Flight testing for aircraft agility [AIAA PAPER 90-1308] p 519 A90-33918
- Flight test safety and 'high risk' tests - The Aeritalia approach [AIAA PAPER 90-1315] p 483 A90-33924
- The cryogenic wind tunnel as a testing tool for airframe/p propulsion systems p 672 A90-40400
- The response of helicopter to dispersed gust p 670 A90-42470
- Some considerations in ultra light aircraft design p 730 A90-42673
- Flying qualities problems of aerospace craft [AIAA PAPER 90-2804] p 752 A90-45139
- Large aircraft flying qualities revisited [AIAA PAPER 90-2847] p 754 A90-45175
- Singular, periodic solutions in aircraft cruise-dash optimization [AIAA PAPER 90-3369] p 863 A90-47627
- Airworthiness and flight characteristics test of the UH-60A Black Hawk helicopter equipped with the XM-139 multiple mine dispensing system (VOLCANO) [AD-A210271] p 32 N90-10025
- GRATE: A new flight test tool for flying qualities evaluation p 34 N90-10868
- Unsteady aerodynamics with applications to flight mechanics [AD-A211944] p 89 N90-11706
- Comparison of flying qualities derived from in-flight and ground-based simulators for a jet-transport airplane for the approach and landing pilot tasks [NASA-TP-2962] p 120 N90-11757
- Global stratospheric change: Requirements for a Very-High-Altitude Aircraft for Atmospheric Research [NASA-CP-10041] p 185 N90-14220
- Influence of windshear, downdraft and turbulence on flight safety p 238 N90-15048
- A pitch control law for compensation of the phugoid mode induced by windshears p 258 N90-15051
- Canard versus aft-tail ride qualities performance and pilot command response p 258 N90-15053
- The interference of flightmechanical control laws with those of load alleviation and its influence on structural design p 258 N90-15054
- Longitudinal stability and control characteristics of the Quiet Short-Haul Research Aircraft (QSRA) [NASA-TP-2965] p 349 N90-17639

- Low-speed wind-tunnel investigation of the flight dynamic characteristics of an advanced turboprop business/commuter aircraft configuration [NASA-TP-2982] p 434 N90-19239
- Airworthiness and flight characteristics evaluation of the McDonnell Douglas Helicopter Corporation (MDHC) 530FF helicopter [AD-A218253] p 498 N90-20076
- Flight path reconstruction using extended Kalman filtering techniques [PD-FC-9001] p 489 N90-20970
- Development of a least squares time response lower-order equivalent systems technique [AD-A220527] p 648 N90-23389
- Estimating short-period dynamics using an extended Kalman filter [NASA-TM-101722] p 648 N90-23392
- Static wind-tunnel and radio-controlled flight test investigation of a remotely piloted vehicle having a delta wing planform [NASA-TM-4200] p 632 N90-24238
- H-infinity based integrated flight-propulsion control design for a STOVL aircraft in transition flight [NASA-TM-103198] p 758 N90-26011
- The SKY SHARK: An RPV designed to investigate the pressure distribution on a lifting surface [NASA-CR-186222] p 844 N90-26824
- Monitoring and controlling flight in windshear p 820 N90-27641
- Comparison of altitude test cell results p 856 N90-27715
- Evaluation of composite components on the Bell 206L and Sikorsky S-76 helicopters [NASA-TM-4195] p 876 N90-27787
- Solution of Euler equations applied to a rotor of a helicopter in steady flight [ONERA-RSF-1/3731-AY-002A] p 910 N90-28500
- Aerodynamic parameters of High-Angle-of attack Research Vehicle (HARV) estimated from flight data [NASA-TM-102692] p 936 N90-28578
- Application of multifunction inertial reference systems to fighter aircraft p 916 N90-29341
- Fighter agility metrics [NASA-CR-187289] p 925 N90-29389
- FLIGHT CONDITIONS**
- The influence of weather on flight operations at the Atlanta Hartsfield International Airport p 279 A90-22688
- The application of the discrete vortex method in aircraft design p 257 A90-23357
- A survey of nonuniform inflow models for rotorcraft flight dynamics and control applications p 590 A90-38521
- Inclement weather induced aircraft engine power loss [AIAA PAPER 90-2169] p 662 A90-42055
- Analytical evaluation of helicopter true air speed and associated flight tests p 647 A90-42499
- Simulating turbulence and gusts for handling qualities evaluation [AIAA PAPER 90-2845] p 754 A90-45174
- The response of helicopter rotors to vibratory airload p 832 A90-46971
- A technique for the prediction of aerodynamics and aeroelasticity of rotor blades p 184 N90-13377
- Flight in adverse environmental conditions [AGARD-AR-277] p 185 N90-14218
- A survey of nonuniform inflow models for rotorcraft flight dynamics and control applications [NASA-TM-102219] p 260 N90-15938
- Measurement and prediction of propeller blade surface pressure distributions p 481 N90-20961
- The use of numerical optimization for helicopter airfoil and blade design p 502 N90-20995
- Comparison of altitude test cell results p 856 N90-27715
- Effects of canard position on the aerodynamic characteristics of a close-coupled canard configuration at low speed p 920 N90-28519
- FLIGHT CONTROL**
- On the 'inverse phugoid problem' as an instance of non-linear stability in pitch p 55 A90-10221
- A knowledge-based system design/information tool for aircraft flight control systems [AIAA PAPER 89-2978] p 55 A90-10491
- Comparison of three concepts for a long stroke displacement transducer p 66 A90-11041
- Toward fly-by-light aircraft p 39 A90-11664
- Optimization of the observations and control of aircraft --- Russian book p 60 A90-12468
- Airplane design, Part 4 - Layout design of landing gear and systems --- Book p 31 A90-12869
- Airplane design, Part 7 - Determination of stability, control and performance characteristics: Far and military requirements --- Book p 57 A90-12872
- On a pitch control law for a constant glide slope through windshears p 117 A90-13784

- Real-time decision making for autonomous flight control
[SAE PAPER 891053] p 118 A90-14355
- Synthesis of locally optimal aircraft control in the presence of delay p 137 A90-14561
- Parametric synthesis of piecewise constant locally optimal aircraft control under conditions of indeterminacy p 137 A90-14576
- Literal singular-value-based flight control system design techniques p 118 A90-14747
- The relevance of unsteady aerodynamics for highly maneuverable and agile aircraft p 146 A90-16775
- Recursive real-time identification of step-response matrices of helicopters for adaptive digital flight control p 195 A90-17703
- Modal aggregation and its application in flight mechanics p 196 A90-18595
- The eigenvalue sensitivity analysis and design for integrated flight/propulsion control systems p 196 A90-18601
- An adaptive flight control system design for non-minimum phase CCV by relative order reduction p 196 A90-19428
- Analysis and design of sidestick controller systems for general aviation aircraft p 196 A90-19554
- Compensating for pneumatic distortion in pressure sensing devices p 211 A90-19956
- [AIAA PAPER 90-0631] p 211 A90-19956
- Airship survival - Damage avoidance and control for large ocean-going airships p 238 A90-20588
- [AIAA PAPER 89-3166] p 238 A90-20588
- Flight-path measurement p 242 A90-21721
- A variable structure system (VSS) to robust control of aircraft p 257 A90-21987
- Trends in avionics - From analog black boxes to integrated digital avionics systems p 252 A90-23245
- An application of generalized predictive control to rotorcraft terrain-following flight p 257 A90-23478
- Pay-offs and pitfalls of fly-by-wire p 346 A90-24281
- Aviation Week editor flies Soviet-based MiG-29 fighter p 334 A90-24964
- Low speed testing and simulation of the STOL and Maneuver Technology Demonstrator [AIAA PAPER 90-1820] p 334 A90-25169
- Restructurable control using proportional-integral-implicit model following --- for fighter aircraft [AD-A220997] p 347 A90-25990
- Robust control system design synthesis with observers p 375 A90-25994
- Helicopter flight control system design and evaluation for NOE operations using controller inversion techniques p 429 A90-28202
- RSRA/X-Wing flight control system development - Lessons learned p 430 A90-28216
- OPST1 - An optical yaw control system for high performance helicopters p 430 A90-28220
- V-22 aerodynamic loads analysis and development of loads alleviation flight control system p 410 A90-28239
- A study of approximately optimal cruising flight regimes of variable-mass aircraft p 430 A90-29187
- ADAM 2.0 - An ASE analysis code for aircraft with digital flight control systems [AIAA PAPER 90-1077] p 431 A90-29385
- Aircraft flight control system identification p 431 A90-30105
- Modeling and analysis tools for aircraft control system evaluations p 431 A90-30703
- Digital simulation of flight control systems for post-stall aircraft p 431 A90-30704
- Flying qualities lessons learned - 1988 p 431 A90-30705
- Reconfigurable flight controller for the STOL F-15 with sensor/actuator failures p 432 A90-30707
- An aircraft flight control reconfiguration algorithm p 432 A90-30708
- F/A-18 aileron smart servoactuator p 432 A90-30710
- A study of a propulsion control system for a VATOL aircraft (A direct design synthesis application) p 424 A90-30712
- Lessons learned in the development of a multivariable control system p 432 A90-30713
- The STOL maneuver technology demonstrator manned simulation test program p 439 A90-30716
- An American knowledge base in England - Alternate implementations of an expert system flight status monitor p 459 A90-30719
- Reduced-order modeling and controller design for a high-performance helicopter p 516 A90-33058
- Design and evaluation of a cockpit display for hovering flight p 490 A90-33059
- Interactions of active controls and structural loads p 517 A90-33404
- Implementation of comprehensive actuation system models in aeroservoelastic analysis p 517 A90-33406
- Use of ground-based and in-flight simulation for flight control system development [AIAA PAPER 90-1286] p 519 A90-33907
- F-15E terrain following test results [AIAA PAPER 90-1299] p 504 A90-33913
- Automatic landing with GPS - Design of the flight guidance and flight control system [AIAA PAPER 90-1301] p 487 A90-33915
- DIGITAC - A unique digital flight control testbed aircraft [AIAA PAPER 90-1288] p 519 A90-33931
- Some aspects of the control system and power unit lead tests using in-flight simulator systems and flying test-beds [AIAA PAPER 90-1323] p 580 A90-36031
- The study of transient suppression techniques for multimode flight control system p 590 A90-37219
- A survey of nonuniform inflow models for rotorcraft flight dynamics and control applications p 590 A90-38521
- V-22 developmental status p 581 A90-38529
- Flight/propulsion control integration for V/STOL fighter/attack aircraft p 591 A90-38530
- Implementation of a transputer-based flight controller p 667 A90-38966
- A study on the application of controllability and observability concepts in the design of flight control systems p 693 A90-39303
- Flight control application of eigenstructure assignment with optimization of robustness to structured state space uncertainty p 693 A90-40885
- Ultimate boundedness control of uncertain systems with application to roll coupled aircraft maneuver p 668 A90-40886
- Digital controller design for the pitch axis of the F-14 using an H(infinity) method p 668 A90-40912
- MLS - A total system approach p 640 A90-41710
- Expanding the B-1B flight envelope p 644 A90-41899
- Propulsion system-flight control integration-flight evaluation and technology transition [AIAA PAPER 90-2280] p 644 A90-42106
- Main characteristics of an integrated flight and display system for AS MKII Super-Puma p 653 A90-42450
- Modern strapdown system for helicopter p 653 A90-42451
- A technique for the tuning of helicopter flight control systems p 670 A90-42467
- Use of smart actuators for the tail rotor collective pitch control p 688 A90-42483
- Direct drive servovalves: Why and how - The Magnaghi Milano answer p 688 A90-42484
- Developing the Canadair Regional Jet airliner p 729 A90-42656
- Improved guidance and control of vehicles and personnel on the ground will benefit airport traffic capacity p 760 A90-44549
- Optimization of glides for constant wind fields and course headings p 731 A90-44734
- Design of flight control systems to meet rotorcraft handling qualities specifications [AIAA PAPER 90-2805] p 752 A90-45140
- Dynamics and control of maneuverable towed flight vehicles [AIAA PAPER 90-2841] p 754 A90-45161
- Simulating turbulence and gusts for handling qualities evaluation [AIAA PAPER 90-2845] p 754 A90-45174
- Large aircraft flying qualities revisited [AIAA PAPER 90-2847] p 754 A90-45175
- Lessons learned from the S/MTD program for the Flying Qualities Specification [AIAA PAPER 90-2849] p 755 A90-45177
- Optimal paths through downbursts p 755 A90-45330
- System identification requirements for high-bandwidth rotorcraft flight control system design p 755 A90-45333
- Nonlinear flight control design via sliding methods p 756 A90-45335
- An explicit model-matching approach to lateral-axis autopilot design p 756 A90-45413
- Lightweight, composite flight control actuators [SAE PAPER 892264] p 733 A90-45459
- Simulation evaluation of transition and hover flying qualities of a mixed-flow, remote-lift STOVL aircraft [SAE PAPER 892284] p 757 A90-45464
- A multi-sensor approach to assuring GPS integrity p 821 A90-46396
- H-infinity based integrated flight/propulsion control design for a STOVL aircraft in transition flight [AIAA PAPER 90-3335] p 862 A90-47595
- Robustness of dynamic inversion vs mu synthesis - Lateral-directional flight control example [AIAA PAPER 90-3338] p 863 A90-47598
- Inversion of nonlinear I-O map, zero dynamics and flight control system design [AIAA PAPER 90-3370] p 863 A90-47628
- Nonlinear inversion flight control for a supermaneuverable aircraft [AIAA PAPER 90-3406] p 864 A90-47661
- Adaptive flight control of CCV aircraft with limiting zeros [AIAA PAPER 90-3409] p 864 A90-47664
- Robust flight control system design with multiple model approach [AIAA PAPER 90-3411] p 865 A90-47666
- Optimal solutions to flight mechanics problems using a Nonlinear Programming and Collocation technique [AIAA PAPER 90-3415] p 889 A90-47669
- A mixed H2 and H(infinity) approach to an autopilot design problem [AIAA PAPER 90-3441] p 865 A90-47694
- Robust control design for relaxed static stability aircraft [AIAA PAPER 90-3443] p 865 A90-47696
- Extended implicit model following as applied to integrated flight and propulsion control [AIAA PAPER 90-3444] p 890 A90-47697
- Robustness evaluation of a flexible aircraft control system [AIAA PAPER 90-3445] p 890 A90-47698
- Multivariable flight control synthesis and literal robustness analysis for an aeroelastic vehicle [AIAA PAPER 90-3446] p 890 A90-47699
- Model reduction with a finite-interval H(infinity) criterion [AIAA PAPER 90-3473] p 890 A90-47723
- Analyzing the flared landing task with pitch-rate flight control systems [AIAA PAPER 90-3483] p 866 A90-47732
- Robust low norm output feedback design for flight control systems [AIAA PAPER 90-3505] p 891 A90-47751
- Short take-off and landing maneuver technology demonstrator (STOL/MTD) lessons learned - Integrated flight/propulsion control (IFPC) [AIAA PAPER 90-3307] p 868 A90-48888
- Computerized MLS flight inspection system developed p 823 A90-48983
- Composite flight control actuators p 874 A90-48993
- The LTV XC-142 experimental aircraft lessons learned [AIAA PAPER 90-3204] p 838 A90-49104
- Flight control design considerations for STOVL powered-lift flight [AIAA PAPER 90-3225] p 868 A90-49110
- Reconfigurable aircraft flight control system via robust direct adaptive control [AIAA PAPER 90-3226] p 868 A90-49111
- Propulsion system design specifications based on STOVL flight control requirements [AIAA PAPER 90-3227] p 839 A90-49112
- Obtaining precise LTR with Luenberger type observer with arbitrary observer poles and finite gain [AIAA PAPER 90-3228] p 868 A90-49113
- Gripen wins its wings --- Swedish JAS39 aircraft testing and development p 842 A90-49823
- Analyzing manipulator and feel system effects in aircraft flight control p 934 A90-51154
- Hierarchical damage tolerant controllers for smart structures [AD-A209422] p 31 N90-10022
- Initial flight qualification and operational maintenance of X-29A flight software [NASA-TM-101703] p 32 N90-10023
- A320 flight tests: Particularities and innovations p 34 N90-10864
- Real-time flight test analysis and display techniques for the X-29A aircraft p 34 N90-10866
- Flight test results of a complex precise digital flight control system p 35 N90-10870
- An assessment of robustness of flight control systems based on variable structure techniques p 57 N90-10895
- Applications of flight control system methods to an advanced combat rotorcraft [NASA-TM-101054] p 119 N90-11752
- Robust control design for flight control [AD-A211957] p 119 N90-11756
- Comparison of flying qualities derived from in-flight and ground-based simulators for a jet-transport airplane for the approach and landing pilot tasks [NASA-TP-2962] p 120 N90-11757
- Adaptive control law design for model uncertainty compensation [AD-A211712] p 120 N90-11758
- Advanced actuation systems development, volume 1 [AD-A213334] p 121 N90-12624
- STOVL aircraft simulation for integrated flight and propulsion control research [NASA-TM-102419] p 193 N90-13389

A knowledge-based system design/information tool for aircraft flight control systems
 [NASA-TM-101704] p 217 N90-13990
 A helicopter flight path controller design via a nonlinear transformation technique p 199 N90-14242
 Wind shear models for aircraft hazard investigation p 280 N90-15044
 How to fly windshear using the fly-by-wire concept p 258 N90-15050
 Turbulence effects of aircraft flight dynamics and control p 258 N90-15055
 Fly-by-light flight control system technology development plan
 [NASA-CR-181953] p 259 N90-15111
 Integrated approach fault tolerance-current state and future requirements
 [AD-A214402] p 275 N90-15465
 Guidance and Control of Unmanned Air Vehicles
 [AGARD-CP-436] p 260 N90-15924
 Mirach 100 flight control system p 260 N90-15926
 A survey of nonuniform inflow models for rotorcraft flight dynamics and control applications
 [NASA-TM-102219] p 260 N90-15938
 Advances in Techniques and Technologies for Air Vehicle Navigation and Guidance
 [AGARD-CP-455] p 332 N90-16731
 Integrated flight guidance system using differential-GPS for landing approach guidance p 332 N90-16735
 Parallel processing implementation of a flight controller p 333 N90-16743
 Formulation and verification of a technique for compensation of pneumatic attenuation errors in airborne pressure sensing devices p 369 N90-17084
 Development of an automatic ground collision avoidance system using a digital terrain database
 [AD-A216247] p 329 N90-17621
 Development of the triplex digital flight control system of the STOL research aircraft ASKA
 [NAL-TR-1013] p 349 N90-17640
 The Advanced Digital-Optical Control System (ADOCS) user demonstration program
 [AD-A215984] p 349 N90-17644
 Software verification plan for GCS --- guidance and control software p 372 N90-18057
 [NASA-TM-101668] p 372 N90-18057
 Discrete proportional Plus Integral (PI) multivariable control laws for the Control Reconfigurable Combat Aircraft (CRCA)
 [AD-A215664] p 433 N90-18431
 The implications of using integrated software support environment for design of guidance and control systems software
 [AGARD-AR-229] p 434 N90-18432
 Flexible heat pipe cold plate p 434 N90-18433
 [AD-A216053] p 434 N90-18433
 Application of variable-gain output feedback for high-alpha control p 434 N90-18434
 [NASA-TM-102603] p 434 N90-18434
 Practical methods for robust multivariable control
 [AD-A216937] p 462 N90-18920
 Compensating for pneumatic distortion in pressure sensing devices p 415 N90-19224
 [NASA-TM-101716] p 415 N90-19224
 A rule-based paradigm for intelligent adaptive flight control p 434 N90-19238
 Neurocontrol systems and wing-fluid interactions underlying dragonfly flight p 434 N90-19240
 F-15B high angle-of-attack phenomena and spin prediction using bifurcation analysis
 [AD-A217366] p 498 N90-20073
 Flight termination system battery guidelines
 [AD-A217310] p 520 N90-20092
 Laboratory implementation of the Continuously Reconfiguring Multi-Microprocessor Flight Control System (CRMMFCS)
 [AD-A217730] p 520 N90-20094
 Interaction of switch actuation on tracking with a four-axis flight control (cross-coupling)
 [AD-A217981] p 520 N90-20095
 The Real Time Display Builder (RTDB) p 546 N90-20656
 Optimization of the effective GPS data rate p 489 N90-20932
 Investigation of air transportation technology at Princeton University, 1988-1989 p 486 N90-20935
 Application of stochastic robustness to aircraft control systems p 521 N90-20936
 An expert system for wind shear avoidance p 486 N90-20938
 Rule-based mechanisms of learning for intelligent adaptive flight control p 521 N90-20939
 Civil air transport: A fresh look at power-by-wire and fly-by-light
 [NASA-TM-102574] p 542 N90-21283

The insertion of human dynamics models in the flight control loops of V/STOL research aircraft. Appendix 2: The optimal control model of a pilot in V/STOL aircraft control loops
 [NASA-CR-186598] p 598 N90-21776
 Algorithms for computing the multivariable stability margin p 612 N90-22999
 Multidisciplinary Expert-aided Analysis and Design (MEAD) p 613 N90-23050
 Six-degree-of-freedom aircraft simulation with mixed-data structure using the applied dynamics simulation language, ADSIM p 613 N90-23067
 Prediction of longitudinal pilot induced oscillations using the optimal control model
 [AD-A220593] p 671 N90-23412
 Miniaturization of flight deflection measurement system
 [NASA-CASE-LAR-13628-1] p 689 N90-23707
 Development and test of software by safety critical aircraft systems
 [MBB-FE-363/S/PUB-384] p 723 N90-25103
 Modeling flexible aircraft for flight control design
 [AD-A219123] p 757 N90-25140
 Flight-testing of the self-repairing flight control system using the F-15 highly integrated digital electronic control flight research facility
 [NASA-TM-101725] p 758 N90-25144
 Reliability model generator specification
 [NASA-CR-182005] p 780 N90-25638
 Identification of aerodynamic models for maneuvering aircraft
 [NASA-CR-186630] p 719 N90-25943
 An in-flight interaction of the X-29A canard and flight control system
 [NASA-TM-101718] p 736 N90-25973
 Technical evaluation report on the Guidance and Control Panel 49th Symposium on Fault Tolerant Design Concepts for Highly Integrated Flight Critical Guidance and Control Systems
 [AGARD-AR-281] p 758 N90-26012
 Robustness evaluation of H2 and H(infinity) control theory as applied to a transport aircraft
 [AD-A222795] p 759 N90-26018
 Aerodynamic/dynamic interaction
 [AD-A222263] p 815 N90-26798
 New inflight experiments to measure aerodynamics loads
 [ETN-90-97276] p 868 N90-26834
 Daily flight operation monitoring in JAL p 820 N90-27636
 Monitoring and controlling flight in windshear p 820 N90-27641
 Advanced transport operating system software upgrade: Flight management/flight controls software description
 [NASA-CR-181936] p 893 N90-28366
 Aerodynamic and propulsive control development of the STOL and maneuver technology demonstrator p 920 N90-28514
 A look at tomorrow today p 921 N90-28524
 Validation of the F-18 high alpha research vehicle flight control and avionics systems modifications
 [NASA-TM-101723] p 924 N90-28542
 Description of the primary flight display and flight guidance system logic in the NASA B-737 transport systems research vehicle
 [NASA-TM-102710] p 927 N90-28546
 Propulsion system-flight control integration and optimization: Flight evaluation and technology transition
 [NASA-TM-4207] p 929 N90-28551
 A conceptual framework for fighter flight control systems
 [PD-CF-9009] p 936 N90-28577
 Model authoring system for fail safe analysis
 [NASA-CR-4317] p 964 N90-29142
 Flight test engineering with the ATTAS p 902 N90-29160
 Analysis, Design and Synthesis Methods for Guidance and Control Systems
 [AGARD-AG-314] p 916 N90-29338
 Application of multifunction inertial reference systems to fighter aircraft p 916 N90-29341
 Integrated navigation/flight control for future high performance aircraft p 917 N90-29362
 Fault Detection and Isolation (FDI) techniques for guidance and control systems p 918 N90-29366
 Fighter agility metrics
 [NASA-CR-187289] p 925 N90-29389
 Formal design and verification of a reliable computing platform for real-time control. Phase 1: Results
 [NASA-TM-102716] p 965 N90-29965

FLIGHT CREWS

Pre-escape and escape aircraft maneuvers and gyrations - A critical under-reported problem affecting escape system performance and aircrew safety p 21 N90-10264

Intelligent situation assessment and response aiding in flight emergencies
 [AIAA PAPER 89-2999] p 36 A90-10507
 Boeing Transonic Windblast Generator System (BTWGS) p 199 A90-17413
 Canopy fragilization using embedded detonating cord p 180 A90-17417
 Water test facilities for aviation life support equipment p 200 A90-17431
 Designers as users - Design supports based on crew system design practices p 457 A90-28184
 Integration of intelligent avionics systems for crew decision aiding p 459 A90-30236
 Considerations of noise for the use of compressed speech in a cockpit environment p 404 A90-31334
 The importance of measured data as a contribution to reducing crew caused accidents
 [AIAA PAPER 89-3219] p 482 A90-31703
 The Common/Same Type Rating - Human factors and other issues p 723 A90-45445
 Initial service experience with the Fokker 100 p 733 A90-45450
 [SAE PAPER 892238] p 733 A90-45450
 Upgrading the cockpit - A multidisciplinary approach p 848 A90-48995
 Display interface concepts for automated fault diagnosis p 252 N90-15102
 [NASA-TM-101610] p 252 N90-15102
 Delivery performance of conventional aircraft by terminal-area, time-based air traffic control: A real-time simulation evaluation p 404 N90-18378
 [NASA-TP-2978] p 404 N90-18378
 Three input concepts for flight crew interaction with information presented on a large-screen electronic cockpit display
 [NASA-TM-4173] p 420 N90-18394
 Windshear case study: Denver, Colorado, July 11, 1988 p 544 N90-21509
 [DOT/FAA/DS-89/19] p 544 N90-21509
 Development of a microcomputer based software system for use in crewmember ejection analysis
 [AD-A220398] p 723 N90-25117

FLIGHT ENVELOPES
 The effects of aerial combat on helicopter structural integrity p 406 A90-28166
 Expanding the B-1B flight envelope p 644 A90-41899
 Stability and control derivatives of the De Havilland DHC-2 BEAVER aircraft p 119 N90-11754
 [PB89-217525] p 119 N90-11754
 Identification of aerodynamic models for maneuvering aircraft p 719 N90-25943
 [NASA-CR-186630] p 719 N90-25943
 Combat aircraft control requirements p 934 N90-28515
 Application of multifunction inertial reference systems to fighter aircraft p 916 N90-29341

FLIGHT HAZARDS
 Terminal Doppler Weather Radar System - Wind shear detection will warn pilots of danger p 25 A90-10462
 Penetration landing guidance trajectories in the presence of windshear p 98 A90-14732
 A program to improve aircraft icing forecasts
 [AIAA PAPER 90-0196] p 216 A90-19733
 Colorado mountain flying - Crashes and weather
 [AIAA PAPER 90-0369] p 175 A90-19818
 Environmental conditions associated with the Dallas microburst storm determined from satellite soundings p 280 A90-22689
 Multiple vortex ring model of the DFW microburst p 280 A90-23286
 An analysis of factors impeding passenger escape from aircraft fires p 322 A90-26018
 Microburst precursors observed with Doppler radar p 456 A90-28613
 Underlying factors in air traffic control incidents p 401 A90-31335
 Multistroke cloud-to-ground strike to the NASA F-106B airplane p 482 A90-32304
 Low-level windshear alert systems and Doppler radar in aircraft terminal operations p 574 A90-35758
 Using cloud moisture calculations for estimating aircraft icing p 888 A90-48358
 Inversions and associated wind-shear warnings must be related to airport characteristics p 962 A90-52051
 Maximum expected concentrations of hail in thunderstorm precipitation p 962 A90-52052
 Effects of lightning on operations of aerospace vehicles p 239 N90-15065
 Relative merits of reactive and forward-look detection for wind-shear encounters during landing approach for various microburst escape strategies
 [NASA-TM-4158] p 259 N90-15108
 Bird impact tests on asymmetric sandwich structures made in Kevlar 49 p 323 N90-16727
 [CEAT-NT-10/S/83-5] p 323 N90-16727

- Bird impact tests on curved structures of the type Sandwich-Kevlar-Nida for normal and angular shooting [CEAT-NT-10/S/83-4] p 324 N90-16728
- A quantitative technique to estimate microburst wind shear hazard to aircraft p 692 N90-25040
- Development and test of software by safety critical aircraft systems [MBB-FE-363/S/PUB-384] p 723 N90-25103
- Aircraft lightning protection handbook [AD-A22716] p 820 N90-27668
- FLIGHT INSTRUMENTS**
- Flight simulator evaluation of a head-down display [NAL-TM-573] p 59 N90-10898
- Independent Orbiter Assessment (IOA): Analysis of the displays and controls subsystem [NASA-CR-185563] p 124 N90-11774
- Natural icing re-evaluation of the EH-60A Quick Fix helicopter [AD-A214728] p 323 N90-16723
- A simulation evaluation of the engine monitoring and control system display [NASA-TP-2960] p 420 N90-18393
- Flexible heat pipe cold plate [AD-A216053] p 434 N90-18433
- The interaction of chromostereopsis and stereopsis in stereoscopic CRT (Cathode Ray Tubes) displays [AD-A217906] p 927 N90-28544
- FLIGHT LOAD RECORDERS**
- Multichannel on-board load and fatigue monitoring p 849 N90-27621
- FLIGHT MANAGEMENT SYSTEMS**
- Real time winds data for flight management [AIAA PAPER 90-0565] p 197 A90-19918
- Aircraft interface with the future ATC system p 331 A90-25574
- A reconfigurable integrated navigation and flight management system for military transport aircraft p 433 A90-30794
- Testing of a highly integrated automatic flight system - The 747-400 Flight Management Computer System [AIAA PAPER 90-1302] p 505 A90-33916
- Basic areas of research in the development of a future ATM system --- air traffic management p 551 A90-35685
- An interfacing solution for real-time avionics development [SAE PAPER 892357] p 738 A90-45508
- Development of common GPS and GLONASS avionics standards p 821 A90-46391
- Advanced architecture for domestic and global aviation systems p 822 A90-46398
- Towards a quantitative assessment of benefits which INS/GPS integration can offer to civil aviation operating in a non-jamming environment p 823 A90-49496
- Development and evaluation at ATCEU of executive and support operations, phase 4A/3D --- ATCEU (Air Traffic Control Evaluation Unit) [CAA-PAPER-88017] p 99 N90-12572
- Operational trial of effect of raising minimum stack level in Heathrow stacks [CAA-PAPER-89003] p 99 N90-12573
- Computer-based tools for assisting air traffic controllers with arrivals flow management [RSRE-88001] p 178 N90-13366
- A knowledge-based system design/information tool for aircraft flight control systems [NASA-TM-101704] p 217 N90-13990
- A knowledge-based flight status monitor for real-time application in digital avionics systems [NASA-TM-101710] p 217 N90-13995
- The development of a low cost data logging system for flight trials based on an IBM compatible PC [RAE-TM-FM-16] p 251 N90-15917
- First-order weight corrections for real-time flight path management [LR-580] p 578 N90-21751
- A conflict analysis of 4D descent strategies in a metered, multiple-arrival route environment [NASA-CR-182019] p 593 N90-21772
- The 30th Airlines International Electronics Meeting Proceedings [ETN-90-96973] p 637 N90-24261
- Replay and transmission of AIMS-data to mainframe computer using remote transcribers p 892 N90-27634
- Flight data replay and analysis system p 893 N90-27635
- Daily flight operation monitoring in JAL p 820 N90-27636
- Expert system for pilot assistance: The challenge of an intensive prototyping [ETN-90-97274] p 825 N90-27674
- Integrated Air Traffic Management [DLR-MITT-89-23] p 825 N90-27676
- Air traffic management in Europe: Structure, tasks, potential p 825 N90-27677
- On-board planning and control of 4D-trajectories in the TMA p 826 N90-27680
- Four-dimensional navigation and Flight Management Systems p 826 N90-27681
- On the structure of a future flight operations system p 826 N90-27682
- Development of a COMPAS prototype for the ATC Centre at Frankfurt (Fed. Republic of Germany) p 826 N90-27684
- Safety net functions p 826 N90-27685
- Aspects of data link applications for ATC purposes p 827 N90-27688
- Application of a company data link at Lufthansa German Airlines p 827 N90-27689
- PHARE: Concept and programme p 827 N90-27690
- Integration of flight 'management and air traffic management systems [RAE-TM-FM-41] p 827 N90-27693
- Advanced transport operating system software upgrade: Flight management/flight controls software description [NASA-CR-181936] p 893 N90-28366
- FLIGHT MECHANICS**
- Helicopter dynamics: Limiting flight conditions --- Russian book p 55 A90-12481
- System identification collaboration - The role of AGARD p 1 A90-12763
- A frequency-domain system identification approach to helicopter flight mechanics model validation p 56 A90-12772
- Modal aggregation and its application in flight mechanics p 196 A90-18595
- Identification of moderately nonlinear flight mechanics systems with additive process and measurement noise p 347 A90-25987
- A study of symbolic processing and computational aspects in helicopter dynamics p 545 A90-34103
- Helicopter store separation - Predictive techniques and flight testing p 647 A90-42495
- AIAA Atmospheric Flight Mechanics Conference, Portland, OR, Aug. 20-22, 1990, Technical Papers p 751 A90-45134
- Rapid prediction of slender-wing aircraft dynamics [AIAA PAPER 90-3037] p 791 A90-45876
- Optimal solutions to flight mechanics problems using a Nonlinear Programming and Collocation technique [AIAA PAPER 90-3415] p 889 A90-47669
- Optimal periodic cruise with singular control [AIAA PAPER 90-3490] p 833 A90-47738
- Unsteady aerodynamics with applications to flight mechanics [AD-A211944] p 89 N90-11706
- Flight in adverse environmental conditions [AGARD-AR-277] p 185 N90-14218
- Flight in Adverse Environmental Conditions [AGARD-CP-470] p 222 N90-15041
- Description of atmospheric turbulence p 280 N90-15043
- A pitch control law for compensation of the phugoid mode induced by windshears p 258 N90-15051
- The interference of flightmechanical control laws with those of load alleviation and its influence on structural design p 258 N90-15054
- A study of the effects of Rotating Frame Turbulence (RFT) on helicopter flight mechanics p 248 N90-15058
- Optimization and guidance of flight trajectories in the presence of windshear [NASA-CR-186163] p 574 N90-21747
- A comparison of time-optimal interception trajectories for the F-8 and F-15 [NASA-CR-186300] p 581 N90-21753
- The applicability of simple helicopter models for flight mechanics studies [ETN-90-96962] p 736 N90-25975
- Inflight thrust vectoring: A further degree of freedom in the aerodynamic/flight mechanical design of modern fighter aircraft p 921 N90-28528
- Flight test engineering with the ATTAS p 902 N90-29160
- FLIGHT OPERATIONS**
- Independent Orbiter Assessment (IOA): Analysis of the displays and controls subsystem [NASA-CR-185563] p 124 N90-11774
- Fuel tank explosion protection p 251 N90-15914
- An overview of the joint FAA/NASA aircraft/ground runway friction program [NASA-TM-103486] p 724 N90-25957
- Modeling and analysis of airport and aircraft operations [PB90-222167] p 915 N90-28511
- FLIGHT OPTIMIZATION**
- Optimization of helicopter takeoff and landing p 29 A90-11006
- The research of cubic spline optimal terrain following system p 196 A90-18584
- Minimum fuel cruise by periodic optimization p 182 A90-19429
- The problem of aircraft test flight correction p 828 A90-46485
- Sequential design of experiments with physically based models 23 [AD-A211918] p 138 N90-12239
- Induced drag for non-planar wings [LR-521] p 172 N90-13357
- An approach to on-board optimization of cruise at constant altitude [LR-581] p 578 N90-21752
- Life cycle cost in the conceptual design of subsonic commercial aircraft, volumes 1 and 2 p 923 N90-28535
- FLIGHT PATHS**
- On the 'inverse phugoid problem' as an instance of non-linear stability in pitch p 55 A90-10221
- Operating aspects of counter-rotating propfan and planetary-differential gear coupling p 50 A90-12615
- Effect of wind shear on flight safety p 175 A90-17973
- The research of cubic spline optimal terrain following system p 196 A90-18584
- Attitude projection method for analyzing large-amplitude airplane maneuvers p 197 A90-19555
- Simple analyses of paths through windshears and downdrafts [AIAA PAPER 90-0222] p 197 A90-19740
- Real time winds data for flight management [AIAA PAPER 90-0565] p 197 A90-19918
- Flight-path measurement p 242 A90-21721
- Aircraft program motion along a predetermined trajectory. I - Mathematical modelling p 345 A90-23979
- Aircraft program motion along a predetermined trajectory. II - Numerical simulation with application of spline functions to trajectory definitions p 347 A90-25199
- A practical flight path for microwave-powered airplanes p 429 A90-28007
- Differential-geometrical technique of signal transformation and estimation of position, rate and acceleration parameters using supplementary data sources p 638 A90-41004
- MLS - A total system approach p 640 A90-41710
- Analytical evaluation of helicopter true air speed and associated flight tests p 647 A90-42499
- Parameter sensitivity analysis of one kind of flight path reconstruction estimator p 779 A90-44832
- Development of obstacle clearance criteria and standards for MLS and MLS/RNAV precision approaches and development of an MLS collision risk model [SAE PAPER 892215] p 728 A90-45432
- Optimal solutions to flight mechanics problems using a Nonlinear Programming and Collocation technique [AIAA PAPER 90-3415] p 889 A90-47669
- Flight-path display can improve safety, operational efficiency p 847 A90-48982
- The 1987 survey of track keeping and altitudes on Heathrow and Gatwick standard instrument departure routes (DAY) [CAA-PAPER-88010] p 99 N90-11729
- Operational trial of effect of raising minimum stack level in Heathrow stacks [CAA-PAPER-89003] p 99 N90-12573
- FGP2: A flight profile generator program [AD-A212408] p 107 N90-12595
- AcSim: Aircraft simulation program with application to flight profile generation [AD-A212466] p 185 N90-14217
- Introduction to data items on flight path optimisation [ESDU-89015] p 185 N90-14221
- A helicopter flight path controller design via a nonlinear transformation technique p 199 N90-14242
- Dallas/Fort Worth simulation. Volume 2: Appendixes D, E, and F [AD-A216613] p 405 N90-18380
- Flight path reconstruction using extended Kalman filtering techniques [PD-FC-9001] p 489 N90-20970
- A comparison of time-optimal interception trajectories for the F-8 and F-15 [NASA-CR-186300] p 581 N90-21753
- Optimal control of an aircraft flying through a downburst p 591 N90-21765
- Prediction of longitudinal pilot induced oscillations using the optimal control model [AD-A220593] p 671 N90-23412
- Application of optimal tracking methods to aircraft terrain following [AD-A221099] p 641 N90-24264
- When propfans cruise, will LDN 65 fly p 697 N90-24864
- An aircraft noise study in Norway p 698 N90-24872

R and D aspects of the future operational concept of the BFS p 826 N90-27679

On-board planning and control of 4D-trajectories in the TMA p 826 N90-27680

Four-dimensional navigation and Flight Management Systems p 826 N90-27681

A study of terrain following systems and the creation of flight paths for terrain following vehicles [FOA-C-20774-2.5] p 827 N90-27691

FLIGHT PLANS

Aircraft interface with the future ATC system p 331 A90-25574

Fully automatic guidance for rotorcraft nap-of-the-earth (NOE) flight following planned profiles p 403 A90-28219

Air traffic control --- Russian book p 638 A90-39581

Ground and Obstacle Avoidance (GOA) concept of operations [DOT/FAA/DS-89/08] p 28 N90-10855

National Airspace System flight planning operational concept [DOT/FAA/DS-89/30] p 177 N90-13362

Control outside of independent surveillance coverage operational concept [AD-A214163] p 243 N90-15090

The potential for digital databases in flight planning and flight aiding for combat aircraft p 918 N90-29371

FLIGHT RECORDERS

An electronic flight-recorder for a hang-glider p 39 A90-12234

The evaluation of flight recorders p 653 A90-41729

Onboard digital recording system for flight tests p 653 A90-41742

Post crash flight analysis: Visualizing flight recorder data [AD-A21063] p 96 N90-11715

The NASA digital VGH program: Exploration of methods and final results. Volume 2: L 1011 data 1978-1979: 1619 hours [NASA-CR-181909-VOL-2] p 505 N90-20080

The NASA digital VGH program: Exploration of methods and final results. Volume 1: Development of methods [NASA-CR-181909-VOL-1] p 505 N90-20081

The NASA digital VGH program: Exploration of methods and final results. Volume 3: B 727 data 1978-1980: 1765 hours [NASA-CR-181909-VOL-3] p 505 N90-20082

The NASA digital VGH program: Exploration of methods and final results. Volume 4: B 747 data 1978-1980: 1689 hours [NASA-CR-181909-VOL-4] p 506 N90-20083

The NASA digital VGH program: Exploration of methods and final results. Volume 5: DC 10 data 1981-1982: 129 hours [NASA-CR-181909-VOL-5] p 506 N90-20084

Windshear case study: Denver, Colorado, July 11, 1988 [DOT/FAA/DS-89/19] p 544 N90-21509

Aircraft Integrated Monitoring Systems [DLR-MITT-90-04] p 786 N90-27617

The EFA integrated monitoring and recording system: Requirements and concept for implementation p 848 N90-27620

Performance assessment of MIL-STD-1553B on the avionics systems demonstrator rig of British Aerospace p 849 N90-27624

Flight data replay and analysis system p 893 N90-27635

AIMS for helicopters p 820 N90-27639

Monitoring and controlling flight in windshear p 820 N90-27641

The new US flight recorder regulations p 849 N90-27642

The Canadian Aviation Safety Board's flight recorder facility p 849 N90-27643

Australian experience in flight recorder readout and analysis p 820 N90-27644

Automation of the readout, transcription and evaluation of digital flight data at DLR p 893 N90-27645

FLIGHT RULES

An analysis of GPS as the sole means navigation system in US Navy aircraft p 917 N90-29350

FLIGHT SAFETY

Pre-escape and escape aircraft maneuvers and gyrations - A critical under-reported problem affecting escape system performance and aircrew safety p 21 A90-10264

A hardware and software fault tolerant safety controller [AIAA PAPER 89-3123] p 74 A90-10599

Aviation Security (Avsec) p 23 A90-12782

Avionic system based on global navigational satellite system p 97 A90-13984

Effect of wind shear on flight safety p 175 A90-17973

UH-60 flight data replay and refly system state estimator analysis [AIAA PAPER 90-0181] p 197 A90-19723

Analysis of aircraft performance during lateral maneuvering for microburst avoidance [AIAA PAPER 90-0568] p 197 A90-19920

Development of an anti-icing runback model [AIAA PAPER 90-0759] p 238 A90-22258

Technical means and methods of flight safety assurance --- Russian book p 238 A90-22735

TCAS - A lengthy but beneficial development effort p 339 A90-25494

An analysis of factors impeding passenger escape from aircraft fires p 322 A90-26018

Probabilistic risk assessment and aviation system safety p 322 A90-26231

Peacekeeper IFSS - A TQM success story --- Instrumentation and Flight Safety System [AIAA PAPER 89-3218] p 549 A90-31702

The effect of winglets on aircraft wing flutter p 473 A90-33411

Flight test safety and 'high risk' tests - The Aeritalia approach [AIAA PAPER 90-1315] p 483 A90-33924

Preparations of the real-time data analyst to insure flight test safety [AIAA PAPER 90-1316] p 488 A90-33925

Electronic cartography - A new need for commercial aircraft p 576 A90-35351

The U.S. Army Helicopter Structural Integrity Program - 1989 European Rotorcraft Forum p 581 A90-38525

Flight safety performance of the microwave landing system p 639 A90-41705

ILS - A safe bet for your future landings p 639 A90-41707

Inclement weather induced aircraft engine power loss [AIAA PAPER 90-2169] p 662 A90-42055

Main characteristics of an integrated flight and display system for AS MKII Super-Puma p 653 A90-42450

System concept and performance criteria of modern helicopter navigation p 640 A90-42452

Development and verification of software for flight safety critical strapdown systems p 694 A90-42454

More cruising levels expected at higher altitudes p 721 A90-44548

Flight safety performance of the Microwave Landing System p 727 A90-45227

Aircraft Ground Deicing Conference, Denver, CO, Sept. 20-22, 1988, Proceedings [SAE P-217] p 817 A90-46004

Application possibilities of expert systems in modern maintenance for increasing operational security p 892 A90-49271

Experimental work station simulator at the test station of the Bundesanstalt fuer Flugsicherung p 937 A90-52616

Safer skies with TCAS: Traffic Alert and Collision Avoidance System [PB89-169221] p 27 N90-10016

See and avoid/cockpit visibility p 24 N90-10843

[DOT/FAA/CT-TN89/18] p 24 N90-10843

The Air Force Flight Test Center Flight Test Safety Program p 35 N90-10872

UK airmisses involving commercial air transport [CAA-2/88] p 96 N90-11718

National Airspace System airspace management operational concept [DOT/FAA/DS-89/29] p 177 N90-13361

National Airspace System flight planning operational concept [DOT/FAA/DS-89/30] p 177 N90-13362

An update to the system safety study of TCAS 2 [DOT/FAA/SA-89/3] p 177 N90-13363

Flight in adverse environmental conditions [AGARD-AR-277] p 185 N90-14218

Analysis of severe atmospheric disturbances from airline flight records p 280 N90-15045

Influence of windshear, downdraft and turbulence on flight safety p 238 N90-15048

Ice induced aerodynamic performance degradation of rotorcraft: An overview p 248 N90-15063

Effects of lightning on operations of aerospace vehicles p 239 N90-15065

Aircraft testing in the electromagnetic environment p 248 N90-15066

Turbulence spectral widths view angle independence as observed by Doppler radar [DOT/FAA/SA-89/2] p 281 N90-15566

Risk assessment and its application to flight safety analysis [DE90-004985] p 323 N90-16722

Aircraft fire safety in the Canadian Forces p 327 N90-17604

Dallas/Fort Worth simulation. Volume 2: Appendixes D, E, and F [AD-A216613] p 405 N90-18380

UK airmisses involving commercial air transport, January - April 1989 [ISSN-0951-6301] p 575 N90-22544

Aeronautical decisionmaking for air ambulance program administrators p 635 N90-23368

[DOT/FAA/DS-88/8] p 635 N90-23368

Results of TCAS-2 simulations in reconstructed dangerous encounters (Jul. 1986 to Jun. 1989) [ETN-90-96474] p 636 N90-23375

Development and test of software by safety critical aircraft systems [MBB-FE-363/S/PUB-384] p 723 N90-25103

An overview of the joint FAA/NASA aircraft/ground runway friction program [NASA-TM-103486] p 724 N90-25957

Aviation safety: Serious problems continue to trouble the air traffic control work force. Report to congressional requesters [GAO/RCED-89-112] p 724 N90-25959

Daily flight operation monitoring in JAL p 820 N90-27636

Monitoring and controlling flight in windshear p 820 N90-27641

The new US flight recorder regulations p 849 N90-27642

The Canadian Aviation Safety Board's flight recorder facility p 849 N90-27643

Air traffic management in Europe: Structure, tasks, potential p 825 N90-27677

Component behaviour and life management: The need for common AGARD approaches and actions p 856 N90-27710

Modeling and analysis of airport and aircraft operations [PB90-222167] p 915 N90-28511

FLIGHT SIMULATION

Rockwell's simulator emulates NASP flight characteristics p 60 A90-11650

Flight simulation model validation procedure, a systematic approach p 30 A90-12770

A low cost stall/spin simulator [SAE PAPER 891022] p 117 A90-14334

MAVIS flight load simulation --- Multi Axis Vibration System p 202 A90-17003

UH-60 flight data replay and refly system state estimator analysis [AIAA PAPER 90-0181] p 197 A90-19723

High angle of attack flying qualities criteria [AIAA PAPER 90-0219] p 197 A90-19738

Precision navigation using an integrated GPS-IMU system p 242 A90-21720

Low speed testing and simulation of the STOL and Maneuver Technology Demonstrator [AIAA PAPER 90-1820] p 334 A90-25169

Aircraft program motion along a predetermined trajectory. II - Numerical simulation with application of spline functions to trajectory definitions p 347 A90-25199

Visual information for simulated landing approaches p 347 A90-26189

Realtime graphic flight simulations using multiple minicomputers p 351 A90-26203

A review of flight simulation techniques p 435 A90-27953

Control sensitivity, bandwidth and disturbance rejection concerns for advanced rotorcraft p 430 A90-28204

Helicopter obstacle avoidance system - The use of manned simulation to evaluate the contribution of key design parameters p 417 A90-28218

Emerging new technologies at Sikorsky aircraft p 382 A90-30114

The STOL maneuver technology demonstrator manned simulation test program p 439 A90-30716

Development of high angle of attack flying qualities criteria using ground-based manned simulators p 433 A90-30717

Helmet mounted display systems for helicopter simulation p 420 A90-31344

Use of ground-based and in-flight simulation for flight control system development [AIAA PAPER 90-1286] p 519 A90-33907

The use of simulation in support of the high AOA flight test program of the AM-X aircraft [AIAA PAPER 90-1289] p 495 A90-33909

UH-60 helicopter simulator fidelity testing or how to make it fly like the real thing [AIAA PAPER 90-1290] p 522 A90-33910

Table top experimental simulation of hypersonic aero-optical effects --- encountered by cooled window on interceptor p 525 A90-34586

Alternate table look-up routine for real-time digital flight simulation p 611 A90-35769

Digital generation of two-dimensional field of turbulence for flight simulation p 611 A90-36427

A survey of nonuniform inflow models for rotorcraft flight dynamics and control applications p 590 A90-38521

SUBJECT INDEX

Results of an A109 simulation validation and handling qualities study p 591 A90-38524

Reconstitution of crack growth from fractographic observations after flight simulation loading p 682 A90-40650

The application of concentric vortex simulation to calculating the aerodynamic characteristics of bodies of revolution at high angles of attack p 627 A90-42357

Preliminary flight evaluation of the SA 365 Panther helicopter in air-to-air combat manoeuvres p 647 A90-42494

An experimental investigation of roll agility in air-to-air combat [AIAA PAPER 90-2809] p 752 A90-45144

Reassessment and extensions of pilot ratings with new data --- of aircraft handling qualities [AIAA PAPER 90-2823] p 753 A90-45158

Development of obstacle clearance criteria and standards for MLS and MLS/RNAV precision approaches and development of an MLS collision risk model [SAE PAPER 892215] p 728 A90-45432

Simulator evaluation of 'basic' mode back azimuth issues in departure and missed approach usage [SAE PAPER 892216] p 728 A90-45433

Simulation evaluation of transition and hover flying qualities of a mixed-flow, remote-lift STOVL aircraft [SAE PAPER 892284] p 757 A90-45464

Helmet-mounted display systems for flight simulation [SAE PAPER 892352] p 760 A90-45503

Managing man-in-the-loop simulations [SAE PAPER 892355] p 761 A90-45506

Effects of stick dynamics on helicopter flying qualities [AIAA PAPER 90-3477] p 866 A90-47727

Simulation investigation of multiple axis flying qualities [AIAA PAPER 90-3480] p 866 A90-47729

Flight investigation of variations in rotorcraft control and display dynamics for hover [AIAA PAPER 90-3482] p 866 A90-47731

Flight evaluations of several hover control and display combinations for precise blind vertical landings [AIAA PAPER 90-3479] p 867 A90-47764

Stereopsis as a visual cue in flight simulation p 870 A90-48960

Flight Test Techniques [AGARD-CP-452] p 33 N90-10860

ATTAS flight testing experiences p 34 N90-10862

GRATE: A new flight test tool for flying qualities evaluation p 34 N90-10868

Flight testing of the Tornado Terrain Following System p 35 N90-10875

Flight simulator evaluation of a head-down display [NAL-TM-573] p 59 N90-10898

Flight simulation test facility: Function and specification of the simulator cockpit system [NAL-TM-577] p 59 N90-10899

Stability and control derivatives of the De Havilland DHC-2 BEAVER aircraft [PB89-217525] p 119 N90-11754

Comparison of flying qualities derived from in-flight and ground-based simulators for a jet-transport airplane for the approach and landing pilot tasks [NASA-TP-2962] p 120 N90-11757

Stall/spin/flight simulation [DOT/FAA/CT-88/28] p 122 N90-11765

FPG2: A flight profile generator program [AD-A212408] p 107 N90-12595

The comparison of the airspace simulation models airspace and sustained [FEL-1988-66] p 123 N90-12629

Mathematical model identification for flight simulation, based on flight and taxi tests [LR-550] p 202 N90-13410

AcSim: Aircraft simulation program with application to flight profile generation [AD-A212468] p 185 N90-14217

Wind shear models for aircraft hazard investigation p 280 N90-15044

A survey of nonuniform inflow models for rotorcraft flight dynamics and control applications [NASA-TM-102219] p 260 N90-15938

The NASA Langley 0.3-meter transonic cryogenic tunnel p 262 N90-15941

Integrated flight guidance system using differential-GPS for landing approach guidance p 332 N90-16735

Hermes training aircraft p 354 N90-16827

Hypersonic nozzle/afterbody performance at low Mach numbers [AD-A216223] p 319 N90-17575

Time and frequency-domain identification and verification of BO-105 dynamic models [AD-A216828] p 415 N90-18389

Calculation and optimization of rotor start process [ETN-90-95894] p 416 N90-19229

Yaw rate control of an air bearing vehicle p 435 N90-19420

An early overview of tiltrotor aircraft characteristics and pilot procedures in civil transport applications [DOT/FAA/DS-89/37] p 503 N90-21003

Stereopsis cueing effects on hover-in-turbulence performance in a simulated rotorcraft [NASA-TP-2980] p 506 N90-21004

Aeroelastic simulation of higher harmonic control p 592 N90-21768

Six-degree-of-freedom aircraft simulation with mixed-data structure using the applied dynamics simulation language, ADSIM p 613 N90-23067

Results of TCAS-2 simulations in reconstructed dangerous encounters (Jul. 1986 to Jun. 1989) [ETN-90-96474] p 636 N90-23375

Fighter agility metrics, research, and test [NASA-CR-186118] p 648 N90-23386

Estimating short-period dynamics using an extended Kalman filter [NASA-TM-101722] p 648 N90-23392

Real-time simulation clock [NASA-CASE-LAR-14056-1] p 689 N90-23713

Fractographic observations on fatigue crack growth in 2024-T3 sheet material under flight-simulation loading [LR-592] p 689 N90-23760

IAPSA 2 small-scale system specification [NASA-CR-182006] p 695 N90-24103

Helicopter controllability [AD-A220078] p 672 N90-24275

Simulation of transport aeroplanes [MBB-UT-007/89-PUB] p 723 N90-25089

Lecture notes on flight simulation techniques [LR-596] p 762 N90-25153

Model following control system design: Preliminary ATTAS in-flight simulation test results [PD-FC-9003] p 758 N90-26010

Investigation of crack-closure prediction models for fatigue in aluminium alloy sheet under flight-simulation loading [LR-619] p 777 N90-26369

The need for platform motion in modern piloted flight training simulators [AD-A221720] p 871 N90-26847

Economical graphics display system for flight simulation avionics [NASA-CR-186886] p 849 N90-27701

Dallas/Forth Worth simulation. Phase 2: Triple simultaneous parallel Instrument Landing System (ILS) approaches (turbojets) [DOT/FAA/CT-90/2] p 915 N90-28509

Aerodynamic control design: Experience and results at Aermacchi p 935 N90-28518

An in-flight investigation of ground effect on a forward-swept wing airplane p 922 N90-28533

Real-time aerodynamic heating and surface temperature calculations for hypersonic flight simulation [NASA-TM-4222] p 959 N90-28815

Flight test engineering with the ATTAS p 902 N90-29160

Fighter agility metrics [NASA-CR-187289] p 925 N90-29389

Terrain visual cue analysis for simulating low-level flight: A multidimensional scaling approach [AD-A223564] p 938 N90-29407

Fractographic observations on fatigue crack growth under miniTWIST flight-simulation loading (2024-T3 material) [LR-631] p 961 N90-29684

FLIGHT SIMULATORS

Rockwell's simulator emulates NASP flight characteristics p 60 A90-11650

Identification of mathematical derivative models for the design of a model following control system --- for fly-by-wire helicopter p 56 A90-12764

Criteria for evaluating the flight dynamics model of flight simulators p 121 A90-15422

Simulator motion-drive algorithms - A designer's perspective p 375 A90-25997

Avoiding a maneuvering aircraft with TCAS --- Traffic Alert and Collision Avoidance System p 347 A90-26222

A review of flight simulation techniques p 435 A90-27953

Flying qualities lessons learned - 1988 p 431 A90-30705

Strategic aircraft engineering design simulation p 439 A90-30729

Development of an acceptability window for a ground proximity avoidance system p 419 A90-30730

Data base correlation issues p 459 A90-30740

Flight simulator evaluation of a dot-matrix display for presentation of approach map formats p 419 A90-30787

Augmenting flight simulator motion response to turbulence p 440 A90-31279

Helmet mounted display systems for helicopter simulation p 420 A90-31344

FLIGHT TEST INSTRUMENTS

SMAS - An expert system for configuring a research flight simulator p 694 A90-41191

ATHeS - A helicopter in-flight simulator for ACT testing p 643 A90-41727

A highly maneuverable helicopter in-flight simulator - Aspects of realization [AIAA PAPER 88-4607] p 670 A90-42466

Combining thermal and high level acoustics p 770 A90-43729

A framework for the optimal design of instructor/operator stations in flight simulators p 779 A90-45373

Improving computer techniques for real-time digital flight simulation [SAE PAPER 892354] p 760 A90-45505

Managing man-in-the-loop simulations [SAE PAPER 892355] p 761 A90-45506

Synthesis of a simulator-based automated helicopter hover trainer [AIAA PAPER 90-3481] p 891 A90-47730

The Bell X-22A V/STOL, Variable Stability Research Airplane - Lessons learned [AIAA PAPER 90-3207] p 834 A90-48835

Modeling of turbulence and downbursts for flight simulators p 870 A90-48956

Experimental work station simulator at the test station of the Bundesanstalt fuer Flugsicherung p 937 A90-52616

A robust digital model following controller for helicopters [ESA-TT-1041] p 120 N90-12621

Software and hardware description of the helicopter motion equations for VAX computers [AD-A213248] p 184 N90-13375

Hermes training aircraft p 354 N90-16827

Inertial navigation system simulator: Behavioral specification, revision [AD-A219294] p 578 N90-22554

Simulator evaluation of the final approach spacing tool [NASA-TM-102807] p 636 N90-23374

An object-oriented solution example: A flight simulator electrical system [AD-A219190] p 761 N90-25145

Evaluation of nonlinear motion-drive algorithms for flight simulators [UTIAS-TN-272] p 761 N90-25148

Lecture notes on flight simulation techniques [LR-596] p 762 N90-25153

The need for platform motion in modern piloted flight training simulators [AD-A221720] p 871 N90-26847

Economical graphics display system for flight simulation avionics [NASA-CR-186886] p 849 N90-27701

Real-time aerodynamic heating and surface temperature calculations for hypersonic flight simulation [NASA-TM-4222] p 959 N90-28815

The function of the Interactive Model Assembly Program (IMAP) for a flight simulator [NAL-TR-1034] p 939 N90-29412

FLIGHT STABILITY TESTS

Air resonance stability of hingeless rotors in forward flight p 590 A90-38519

A novel synthetic method for studying nonlinear flight stability p 645 A90-42355

UH-60A helicopter stability augmentation study p 670 A90-42471

Airworthiness and flight characteristics test of the UH-60A Black Hawk helicopter equipped with the XM-139 multiple mine dispensing system (VOLCANO) [AD-A210271] p 32 N90-10025

F-15B high angle-of-attack phenomena and spin prediction using bifurcation analysis [AD-A217366] p 498 N90-20073

The MANTA: An RPV design to investigate forces and moments on a lifting surface [NASA-CR-186227] p 499 N90-20971

FLIGHT TEST INSTRUMENTS

The rotor-signal-module of MF190 --- for digital data acquisition from BO-105 helicopter rotary wings p 418 A90-28849

The Modular Flighttest Instrumentation/MFI 90 - A helicopter measuring system p 418 A90-28850

Development of airborne data reduction system in IPTN flight test p 418 A90-28895

Devices and procedures for the calibration of sensors and measurement: Systems of the flight test support system ATTAS [DFVLR-MITT-89-06] p 134 N90-12007

Automatic processing of images from the GRATE flight test tool [DLR-FB-89-28] p 109 N90-12599

Continued development and analysis of a new extended Kalman filter for the Completely Integrated Reference Instrumentation System (CIRIS) [AD-A220106] p 654 N90-23400

FLIGHT TEST VEHICLES

Evaluation for DLC-Flap Monitoring System of the VSRA [NAL-TM-607] p 928 N90-29391

FLIGHT TEST VEHICLES

Maximum likelihood tuning of a vehicle motion filter p 755 A90-45334
The problem of aircraft test flight correction p 828 A90-46485
Initial flight test of half-scale unmanned air vehicle [AD-A219584] p 648 N90-23388
On-board planning and control of 4D-trajectories in the TMA p 826 N90-27680

FLIGHT TESTS

Trends in real-time flight systems [AIAA PAPER 89-3086] p 25 A90-10572
A review of fiber optic flight experience - Past problems, future direction p 38 A90-11661
Toward fly-by-light aircraft p 39 A90-11664
Endurance test of FJR 710/600S engine p 42 A90-12012
Oil migration of FJR 710/600S engine p 43 A90-12014
Research on transmission quality of telemetry system in flight test p 26 A90-12189
System identification - Multibus acquisition and simulation equipment p 26 A90-12192
Testing facility and procedure of the ATTAS on-board data acquisition system p 39 A90-12202
A comfortable and universal data-acquisition-system for flight research p 39 A90-12204
The small portable Global Positioning System tracking range of the future p 60 A90-12209
A study on the performance of the turbo-ramjet engines at high speed flight p 49 A90-12608
Gearless crisp - The logical step to economic engines for high trust p 50 A90-12616
Icing test techniques for air intake screens on helicopters functioning in temperatures around 0 C p 23 A90-12619
Water ingestion simulation - Test needs p 23 A90-12620
Restart characteristics of turbofan engines p 50 A90-12627
System identification collaboration - The role of AGARD p 1 A90-12763
Identification of a coupled flapping/inflow model for the PUMA helicopter from flight test data p 56 A90-12767
In-flight boundary-layer transition measurements on a swept wing p 17 A90-13017
Flight demonstration of two and three satellite navigation p 98 A90-13994
Development of a stall improvement package for the Gulfstream IV [SAE PAPER 891021] p 83 A90-14333
Designing the next generation flying test bed [SAE PAPER 891049] p 100 A90-14353
Investigation of a nonlinear Kalman filter for estimating aircraft state variables p 195 A90-16850
Investigation on the determination of airplane tail loads by flight tests p 178 A90-16853
A separated algorithm and applications to flight test p 216 A90-16857
Ground vibration test results of a JetStar airplane using impulsive sine excitation p 179 A90-16963
Boeing 720B design modification challenges p 179 A90-17309
Landing gear integrity - The bottom line of aircraft safety p 180 A90-17408
Safety management in aircraft testing and certification p 180 A90-17421
Preliminary results from a subsonic high-angle-of-attack flush airdata sensing (HI-FADS) system - Design, calibration, algorithm development, and flight test evaluation [AIAA PAPER 90-0232] p 187 A90-19746
Drag and propulsive efficiency of a light aircraft based on a new flight test technique [AIAA PAPER 90-0233] p 182 A90-19747
Hypersonic flight testing p 245 A90-21171
Technical-scientific possibilities for helicopter noise research in the German-Dutch wind tunnel p 283 A90-21474
East coast Osprey flies p 246 A90-21713
Precision navigation using an integrated GPS-IMU system p 242 A90-21720
Sizing up the Stealth --- B-2 bomber aircraft p 247 A90-23200
Flight and wind-tunnel investigations on boundary-layer transition p 233 A90-23283
Flight testing the F-15E terrain following system p 334 A90-24272
Aviation Week editor flies Soviet-based MiG-29 fighter p 334 A90-24964
A study of roll response required in a low altitude slalom task --- in helicopter control p 347 A90-25421

Laminar flow control leading-edge systems in simulated airline service p 335 A90-26134
A comparison of a droplet impingement code to icing tunnel results [AIAA PAPER 90-0670] p 352 A90-26979
Design, evaluation and proof-of-concept flights of a main rotor interblade viscoelastic damping system p 406 A90-28152
A review of the V-22 dynamics validation program p 406 A90-28155
Rotor smoothing expert system p 381 A90-28164
Air-to-Air Combat Test IV (AACT IV) and the AACT data base p 381 A90-28169
The Pointer - Test and evaluation of the tiltrotor UAV --- unmanned aerial vehicle p 406 A90-28170
Identification of retreating blade stall mechanisms using flight test pressure measurements p 384 A90-28172
Flight testing of the Chandler Evans adaptive fuel control on the S-76A helicopter p 422 A90-28178
Initial results from the joint NASA-Lewis/U.S. Army icing flight research tests p 400 A90-28180
Flight tests of Adaptive Fuel Control and decoupled rotor speed control systems p 422 A90-28183
Helicopter simulation development by correlation with frequency sweep flight test data p 407 A90-28203
McDonnell Douglas Helicopter Company Apache telemetry antenna analysis p 403 A90-28839
Real-time test data processing system --- for helicopter flight testing p 458 A90-28860
Pilot report - MiG-29 p 413 A90-29661
A flight-test methodology for identification of an aerodynamic model for a V/STOL aircraft p 413 A90-30107
A laser obstacle avoidance and display system p 419 A90-30694
Lessons learned in the development of a multivariable control system p 432 A90-30713
Development of high angle of attack flying qualities criteria using ground-based manned simulators p 433 A90-30717
B-1B Doppler error compensation based on flight data analysis p 404 A90-30790
Flight testing a highly flexible aircraft - Case study on the MIT Light Eagle p 414 A90-31284
Application of effective baselines to smart structures p 536 A90-32885
Review of active structural control systems and flight test techniques for dynamic stability investigations p 516 A90-33352
Maneuver performance comparison between the XV-15 and an advanced tiltrotor design p 518 A90-33622
AIAA/SFTE/DGLR/SETP, Biannual Flight Test Conference, 5th, Ontario, CA, May 22-24, 1990, Technical Papers p 493 A90-33886
Flight test and numerical analysis of a half-scale Unmanned Air Vehicle [AIAA PAPER 90-1260] p 494 A90-33890
Wind-tunnel and flight-test investigation of the exdrone remotely piloted vehicle configuration [AIAA PAPER 90-1261] p 494 A90-33891
A concept study on the use of remotely piloted, sub-scale aircraft for high Reynolds number testing [AIAA PAPER 90-1263] p 494 A90-33892
KC-135R low altitude air refueling flight test program [AIAA PAPER 90-1265] p 494 A90-33893
F-15E/GE-129 Increased Performance Engine initial development flight test program [AIAA PAPER 90-1266] p 509 A90-33894
Ten years of stall testing [AIAA PAPER 90-1268] p 518 A90-33895
F-15 STOL and Maneuver Technology Demonstrator flight test progress report [AIAA PAPER 90-1269] p 494 A90-33896
Fluorescence spectroscopy and thermometry for hypersonic flight research [AIAA PAPER 90-1272] p 538 A90-33897
Microminiature flight test instrumentation [AIAA PAPER 90-1274] p 504 A90-33898
Advanced parameter identification techniques for near real time flight flutter test analysis [AIAA PAPER 90-1275] p 494 A90-33899
Advancements in rotor and airframe structural flight testing developed during the SH-60B G.W./C.G. expansion program [AIAA PAPER 90-1281] p 495 A90-33902
Preliminary flight test investigation of an airborne wake vortex detection concept [AIAA PAPER 90-1282] p 495 A90-33903
Flight-measured streamwise disturbance instabilities in laminar flow [AIAA PAPER 90-1283] p 495 A90-33904
In flight flow angle measurements on the Ball-Bartoe Jetwing powered lift aircraft [AIAA PAPER 90-1284] p 495 A90-33905

SUBJECT INDEX

Techniques for improving precision of flying qualities assessment [AIAA PAPER 90-1285] p 519 A90-33906
The use of simulation in support of the high AOA flight test program of the AM-X aircraft [AIAA PAPER 90-1289] p 495 A90-33909
EH 101 Flight Test Program current status and future testing [AIAA PAPER 90-1296] p 495 A90-33912
F-15E terrain following test results [AIAA PAPER 90-1299] p 504 A90-33913
Testing of a highly integrated automatic flight system - The 747-400 Flight Management Computer System [AIAA PAPER 90-1302] p 505 A90-33916
Flight testing for aircraft agility [AIAA PAPER 90-1308] p 519 A90-33918
Ground testing techniques in support of flight test [AIAA PAPER 90-1309] p 523 A90-33919
A flight test investigation of certification requirements for laminar-flow general aviation airplanes [AIAA PAPER 90-1310] p 496 A90-33920
An expert system for real-time aircraft monitoring [AIAA PAPER 90-1311] p 545 A90-33921
Developments in automation of flight test analysis and report generation [AIAA PAPER 90-1313] p 487 A90-33923
Flight test safety and 'high risk' tests - The Aeritalia approach [AIAA PAPER 90-1315] p 483 A90-33924
Preparations of the real-time data analyst to insure flight test safety [AIAA PAPER 90-1316] p 488 A90-33925
A summary of spin-recovery parachute experience on light airplanes [AIAA PAPER 90-1317] p 519 A90-33926
Autopilot flight test experience with BK 117 hingeless rotor [AIAA PAPER 90-1267] p 505 A90-33930
Boeing Condor raises UAV performance levels p 496 A90-34028
Flow visualization in flight testing [AIAA PAPER 90-1273] p 496 A90-34148
Flight-testing of the self-repairing flight control system using the F-15 highly integrated digital electronic control flight research facility [AIAA PAPER 90-1321] p 520 A90-34149
Flight test data processing, plotting and analysis at your finger tips - A flexible, automated, integrated approach [AIAA PAPER 90-1322] p 545 A90-34150
The vortex flap F-106B, overcoming safety and data problems in flight testing [AIAA PAPER 90-1280] p 496 A90-34725
Flight testing of the Low Altitude/Airspeed Unmanned Research Aircraft (LAURA) [AIAA PAPER 90-1262] p 579 A90-36026
Flight tests of a helmet-mounted display synthetic visibility system [AIAA PAPER 90-1279] p 579 A90-36027
Some aspects of the control system and power unit lead tests using in-flight simulator systems and flying test-beds [AIAA PAPER 90-1323] p 580 A90-36031
Acoustics p 614 A90-36541
Results of an A109 simulation validation and handling qualities study p 591 A90-38524
Expert diagnosis system for FJR engine troubles p 587 A90-38597
Rotating system load monitoring using minimum fixed system instrumentation p 651 A90-39982
Improvements to the fatigue substantiation of the H-60 composite tail rotor blade p 642 A90-39985
SH-2F airframe fatigue test program p 642 A90-39989
Flight testing and application of a Peripheral Vision Display p 652 A90-40381
A captive store flight vibration simulation project p 672 A90-40476
Demonstration of MLS advanced approach techniques p 640 A90-41711
Onboard digital recording system for flight tests p 653 A90-41742
Developmental tests on the M 88 engine are on track p 660 A90-41761
Flight test results of the F-15 SMTD thrust vectoring/thrust reversing exhaust nozzle --- STOL/Maneuvering Technology Demonstrator [AIAA PAPER 90-1906] p 660 A90-41982
Influence of ground effect on helicopter takeoff and landing performance p 645 A90-42278
EH101 development progress p 646 A90-42442
The modular HUM system --- Health and Usage Monitoring instruments for rotary wing aircraft failure detection p 618 A90-42476
New systems for helicopter and aircraft vibration monitoring p 653 A90-42477

- The Franco-German helicopter programme HAP, PAH-2/HAC p 618 A90-42478
- Preliminary flight evaluation of the SA 365 Panther helicopter in air-to-air combat manoeuvres p 647 A90-42494
- Helicopter store separation - Predictive techniques and flight testing p 647 A90-42495
- Flight tests to explore tail rotor limitations in the low speed envelope p 647 A90-42498
- Analytical evaluation of helicopter true air speed and associated flight tests p 647 A90-42499
- UK reference station for Navstar GPS p 725 A90-43681
- USCG HH-65A/SRR GPS integration and test results p 726 A90-43705
- A flight test comparison of two GPS/INS integration approaches p 726 A90-43708
- In-flight flow visualization using infrared imaging p 731 A90-44731
- Development of a real-time aeroperformance analysis technique for the X-29A advanced technical demonstrator p 732 A90-44738
- Optimal input design for aircraft parameter estimation using dynamic programming principles [AIAA PAPER 90-2801] p 753 A90-45157
- MLS RNAV accuracy flight tests [SAE PAPER 892218] p 728 A90-45435
- Flight tests with a natural laminar flow glove on a transport aircraft [AIAA PAPER 90-3044] p 828 A90-45881
- Natural laminar flow - A wind tunnel test campaign and comparison with flight test data [AIAA PAPER 90-3045] p 792 A90-45882
- F-18 high alpha research vehicle surface pressures - Initial in-flight results and correlation with flow visualization and wind-tunnel data [AIAA PAPER 90-3018] p 792 A90-45885
- Sideslip-induced static pressure errors in flight-test measurements [AIAA PAPER 90-3082] p 794 A90-45898
- Flight testing Navy low Reynolds Number (LRN) unmanned aircraft p 828 A90-46387
- Rotorwash flow fields - Flight test measurement, prediction methodologies, and operational issues p 817 A90-46930
- The ROTONET prediction system and initial comparisons with far-field acoustics measurements for the XV-15 tilt-rotor aircraft p 894 A90-46947
- Flight test of a trajectory controller using linearizing transformations with measurement feedback [AIAA PAPER 90-3373] p 864 A90-47631
- Update 90 - A progress report on evaluation and flight testing of the small common RLG INS [AIAA PAPER 90-3375] p 847 A90-47763
- The Bell X-22A V/STOL, Variable Stability Research Airplane - Lessons learned [AIAA PAPER 90-3207] p 834 A90-48835
- The AVRO VZ-9 experimental aircraft - Lessons learned [AIAA PAPER 90-3237] p 835 A90-48847
- Airfoil static-pressure thrust - Flight-test verification [AIAA PAPER 90-3286] p 812 A90-48873
- Propulsion system flight test analysis using modeling techniques [AIAA PAPER 90-3288] p 853 A90-48874
- X-29 high angle-of-attack flight testing - Program status [AIAA PAPER 90-3303] p 837 A90-48885
- Status of the STOL and Maneuver Technology Demonstrator flight test program [AIAA PAPER 90-3306] p 838 A90-48887
- Unique features and innovative application of advanced composites to the MD-11 [AIAA PAPER 90-3217] p 838 A90-49108
- Gripen wins its wings --- Swedish JAS39 aircraft testing and development p 842 A90-49823
- Commuter from Khodinka --- Il-114 airliner p 842 A90-49824
- Analyzing manipulator and feel system effects in aircraft flight control p 934 A90-51154
- ILS/MLS comparison tests at Miami/Tamiami, Florida Airport [ACD-330] p 27 N90-10018
- Electro-impulse de-icing testing analysis and design [NASA-CR-4175] p 32 N90-10031
- On the interactive computer program IPIS for aircraft parameter identification [NAL-TR-1000] p 77 N90-10586
- Measurement resolution of noise directivity patterns from acoustic flight tests [NASA-TM-4134] p 79 N90-10679
- Flight Test Techniques [AGARD-CP-452] p 33 N90-10860
- US Navy principal site testing concept and the F-18 p 33 N90-10861
- ATTAS flight testing experiences p 34 N90-10862
- P-180 AVANTI: Project and flight test program comprehensive overview p 34 N90-10863
- A320 flight tests: Particularities and innovations p 34 N90-10864
- The Experimental Aircraft Flight Test Programme p 34 N90-10865
- Real-time flight test analysis and display techniques for the X-29A aircraft p 34 N90-10866
- Flight test techniques adopted by Avions Marcel Dassault-Breguet Aviation p 34 N90-10867
- GRATE: A new flight test tool for flying qualities evaluation p 34 N90-10868
- In flight reflight tests on AM-X single engine fly-by-wire aircraft p 34 N90-10869
- Flight test results of a complex precise digital flight control system p 35 N90-10870
- The Air Force Flight Test Center Flight Test Safety Program p 35 N90-10872
- Lessons learned from the integration of flight systems p 35 N90-10874
- Flight testing of the Tornado Terrain Following System p 35 N90-10875
- CF 18 480 Gallon External Fuel Tank Stores Clearance Program p 35 N90-10877
- Flight testing and flight research: From the age of the tower jumper to the age of the astronaut p 35 N90-10882
- Flight testing in the Netherlands: An overview p 36 N90-10884
- Flight test instrumentation and data processing at British Aerospace, Warton, U.K. p 59 N90-10887
- Heliport surface maneuvering test results [ACD-330] p 59 N90-10897
- Problems related to the acquisition, processing and utilization of the modal parameters measured in flight tests in order to obtain the full envelope for flutter [ETN-89-95210] p 103 N90-11735
- Proplan Test Assessment (PTA): Flight test report [NASA-CR-182278] p 113 N90-11738
- Proplan Test Assessment (PTA) [NASA-CR-185138] p 113 N90-11739
- Devices and procedures for the calibration of sensors and measurement: Systems of the flight test support system ATTAS [DFVLR-MITT-89-06] p 134 N90-12007
- Development flight tests of JetStar LFC leading-edge flight test experiment p 104 N90-12509
- The right wing of the LEFT airplane p 91 N90-12510
- Performance of laminar-flow leading-edge test articles in cloud encounters p 104 N90-12511
- Simulated airline service experience with laminar-flow control leading-edge systems p 104 N90-12512
- Design and test of an NLF wing glove for the variable-sweep transition flight experiment p 104 N90-12544
- F-14 VSTFE and results of the cleanup flight test program p 105 N90-12547
- Status report on a natural laminar-flow nacelle flight experiment p 105 N90-12550
- UHB demonstrator interior noise control flight tests and analysis [NASA-CR-181897] p 140 N90-13198
- Correlation of Puma airloads: Lifting-line and wake calculation [NASA-TM-102212] p 170 N90-13327
- LORAN C stability integrity assurance [AD-A12663] p 177 N90-13364
- An in-flight investigation of ground effect on a forward-swept wing airplane [NASA-TM-101708] p 175 N90-14202
- Flight evaluation of a pneumatic system for unsteady pressure measurements using conventional sensors [NASA-TM-4131] p 186 N90-14225
- Systems for airborne wind and turbulence measurement p 281 N90-15046
- NASA's program on icing research and technology p 239 N90-15062
- Flight and wind tunnel investigation of aerodynamic effects of aircraft ground deicing/antiicing fluids p 235 N90-15064
- Aircraft testing in the electromagnetic environment p 248 N90-15066
- Schleicher ASK-21 glider (TG-9) stall and spin [AD-A13513] p 249 N90-15096
- X-2 limited flight test plan [AD-A14412] p 249 N90-15099
- China-built airborne synchronous laser ranger the new L-8 jet trainer aircraft [AD-A13835] p 275 N90-15422
- Mirach 100 flight control system p 260 N90-15926
- Risk assessment and its application to flight safety analysis [DE90-004985] p 323 N90-16722
- Natural icing re-evaluation of the EH-60A Quick Fix helicopter [AD-A214728] p 323 N90-16723
- Integrated flight guidance system using differential-GPS for landing approach guidance p 332 N90-16735
- Preliminary results from a subsonic high angle-of-attack flush airdata sensing (HI-FADS) system: Design, calibration, and flight test evaluation [NASA-TM-101713] p 339 N90-16758
- Longitudinal stability and control characteristics of the Quiet Short-Haul Research Aircraft (OSRA) [NASA-TP-2965] p 349 N90-17639
- The Advanced Digital-Optical Control System (ADOCS) user demonstration program [AD-A215984] p 349 N90-17644
- Flight survey of the 757 wing noise field and its effects on laminar boundary layer transition. Volume 3: Extended data analysis [NASA-CR-178419] p 380 N90-18233
- Time and frequency-domain identification and verification of BO-105 dynamic models [AD-A216828] p 415 N90-18389
- Wind-tunnel investigation of a flush airdata system at Mach numbers from 0.7 to 1.4 [NASA-TM-101697] p 421 N90-18395
- Heat transfer measurements from a NACA 0012 airfoil in flight and in the NASA Lewis icing research tunnel [NASA-CR-4278] p 399 N90-19203
- Helicopter flight vibration of large transportation containers: A case for testing tailoring [DE90-007429] p 402 N90-19215
- X-29A aircraft structural loads flight testing [NASA-TM-101715] p 416 N90-19225
- Low-speed wind-tunnel investigation of the flight dynamic characteristics of an advanced turboprop business/commuter aircraft configuration [NASA-TP-2982] p 434 N90-19239
- In-flight evaluations of turbine fuel extenders [DOT/FAA/CT-89/33] p 444 N90-19387
- Sandia National Laboratories' new high level acoustic test facility [DE90-006810] p 464 N90-19820
- A note on an acoustic response during an engine nacelle flight experiment [NASA-TM-102585] p 464 N90-19821
- Airworthiness and flight characteristics evaluation of the McDonnell Douglas Helicopter Corporation (MDHC) 530FF helicopter [AD-A218253] p 498 N90-20076
- Aerodynamic analysis of a US Navy and Marine Corps unmanned air vehicle [AD-A218282] p 498 N90-20077
- Flight test investigation of certification issues pertaining to general-aviation-type aircraft with natural laminar flow [NASA-CR-181967] p 480 N90-20952
- Application of a dynamic stall model to rotor trim and aeroelastic response p 583 N90-22556
- Flutter investigations on a Transavia PL12/T-400 aircraft [AD-A219108] p 593 N90-22570
- Boeing/NASA composite components flight service evaluation [NASA-CR-181898] p 601 N90-22609
- Turbine fuel alternatives (near term) [AD-A219405] p 601 N90-22695
- An evaluation of the accuracy of a microwave landing system area navigation system at Miami/Tamiami Florida Airport [DOT/FAA/CT-TN89/40] p 640 N90-23377
- MLS mathematical model validation study using airborne MLS data from Midway Airport engineering flight tests, August 1988 [DOT/FAA/CT-TN90/2] p 640 N90-23378
- Fighter agility metrics, research, and test [NASA-CR-186118] p 648 N90-23386
- Preliminary airworthiness evaluation of the RC-12K [AD-A219545] p 648 N90-23387
- Initial flight test of half-scale unmanned air vehicle [AD-A219584] p 648 N90-23388
- Development of a least squares time response lower-order equivalent systems technique [AD-A220527] p 648 N90-23389
- Prediction of longitudinal pilot induced oscillations using the optimal control model [AD-A220593] p 671 N90-23412
- Static wind-tunnel and radio-controlled flight test investigation of a remotely piloted vehicle having a delta wing planform [NASA-TM-4200] p 632 N90-24238
- Helicopter controllability [AD-A220078] p 672 N90-24275
- En route noise of turboprop aircraft and their acceptability: Report of tests p 697 N90-24858

- Video photographic considerations for measuring the proximity of a probe aircraft with a smoke seeded trailing vortex
[NASA-TM-102691] p 724 N90-25120
- Evaluation of various thrust calculation techniques on an F404 engine
[NASA-TP-3001] p 735 N90-25134
- Flutter clearance of the F-14A variable-sweep transition flight experiment airplane, phase 2
[NASA-TM-101717] p 735 N90-25135
- An accurate numerical technique for determining flight test rate gyroscope biases prior to takeoff
[AD-A220987] p 739 N90-25138
- Flight-testing of the self-repairing flight control system using the F-15 highly integrated digital electronic control flight research facility
[NASA-TM-101725] p 758 N90-25144
- TRENDS: The aeronautical post-test database management system
[NASA-TM-101025] p 761 N90-25149
- Research at NASA's NFAC wind tunnels
[NASA-TM-102827] p 702 N90-25933
- Flight testing of a natural laminar flow airfoil using gliders
[PD-CF-9005] p 718 N90-25936
- Model following control system design: Preliminary ATTAS in-flight simulation test results
[PD-FC-9003] p 758 N90-26010
- Aeroacoustics of advanced propellers
[NASA-TM-103137] p 782 N90-26635
- Obtaining consistent models of helicopter flight-data measurement errors using kinematic-compatibility and state-reconstruction methods
[AD-A22533] p 815 N90-26799
- Automated analysis of MXU-553 flight data
p 844 N90-26821
- The SKY SHARK: An RPV designed to investigate the pressure distribution on a lifting surface
[NASA-CR-186222] p 844 N90-26824
- New inflight experiments to measure aerodynamics loads
[ETN-90-97276] p 868 N90-26834
- Heliprot visual approach surface high temperature and high altitude tests
[DOT/FAA/CT-TN89/34] p 825 N90-27675
- Sideslip-induced static pressure errors in flight-test measurements
[NASA-TM-102846] p 849 N90-27702
- Flight test investigation of flight director and autopilot functions for helicopter decelerating instrument approaches
[DOT/FAA/CT-TN89/54] p 869 N90-27724
- In-flight flow visualization with pressure measurements at low speeds on the NASA F-18 high alpha research vehicle
[NASA-TM-101726] p 910 N90-28505
- Aerodynamic and propulsive control development of the STOL and maneuver technology demonstrator
p 920 N90-28514
- Control research in the NASA high-alpha technology program
p 934 N90-28516
- Study of ground effects on flying scaled models
p 922 N90-28532
- Description of the primary flight display and flight guidance system logic in the NASA B-737 transport systems research vehicle
[NASA-TM-102710] p 927 N90-28546
- Flight test engineering with the ATTAS
p 902 N90-29160
- Vibration responses of two house structures during the Edwards Air Force Base phase of the national sonic boom program
[NASA-CR-182089] p 966 N90-29169
- Fighter agility metrics
[NASA-CR-187289] p 925 N90-29389
- Evaluation for DLC-Flap Monitoring System of the VSRA
[NAL-TM-607] p 928 N90-29391
- Procedure for calibrating fly-by-wire control chains of the flying testbed ATTAS
[DLR-MITT-90-02] p 936 N90-29401
- FLIGHT TIME**
Four-dimensional navigation and Flight Management Systems
p 826 N90-27681
- FLIGHT TRAINING**
Dynamic FLIR simulation in flight training research
p 681 A90-40109
- Escape and survival following helicopter ditching - Research aspects
p 722 A90-44659
- Synthesis of a simulator-based automated helicopter hover trainer
[AIAA PAPER 90-3481] p 891 A90-47730
- The need for platform motion in modern piloted flight training simulators
[AD-A221720] p 871 N90-26847

FLIGHT VEHICLES

- Adaptive automatic control systems. Number 16 --- Russian book
p 76 A90-10844
- An analysis of the possibility of expanding the information base of an adaptive control system for a flight vehicle surrounded by an ionized gas medium
p 60 A90-10845
- The discontinuity condition in the optimal control problem for a composite system
p 76 A90-10848
- A study of flow of a vibrationally nonequilibrium dissociated gas past a blunt body
p 234 A90-23435
- Some aspects of the numerical modeling of supersonic flow past flight vehicles
p 293 A90-24048
- Efficient structural material distribution in the main frame of a flight vehicle
p 363 A90-24092
- Multilevel method for calculating aerodynamic loads on a flight vehicle
p 296 A90-24122
- Calculation of flow past flight vehicles of complex configurations at high supersonic Mach numbers using the hypersonic theory of small perturbations
p 299 A90-24158
- Supersonic flight vehicles --- Russian book
p 299 A90-24233
- Experimental aeroelasticity - History, status and future in brief
[AIAA PAPER 90-0978] p 382 A90-29598
- Fundamentals of the design and development of parts and mechanisms for flight vehicles --- Russian book
p 414 A90-30275
- Hydroelastic problems in space flight vehicles
p 536 A90-33386
- Analysis of aeroelastic divergence for the slender flight vehicles
p 680 A90-39298
- An image analysis method for vehicle stabilization
p 668 A90-40914
- Synthesis of optimal multidimensional digital systems for the simulation of the angular motions of a flight vehicle under random loading
p 669 A90-41957
- Optoelectronic guidance sensors (5th revised and enlarged edition) --- Russian book
p 881 A90-46620
- Experimental aeroelasticity history, status and future in brief
[NASA-TM-102651] p 527 N90-21047
- FLIR DETECTORS**
F-15E terrain following test results
[AIAA PAPER 90-1299] p 504 A90-33913
- Dynamic FLIR simulation in flight training research
p 681 A90-40109
- Application of advanced air vehicle and mission equipment technologies to the Light Helicopter (LH)
[AIAA PAPER 90-3268] p 836 A90-48861
- Use of ECS-conditioned air for FLIR avionics thermal control - Fighter aircraft
[SAE PAPER 901219] p 840 A90-49294
- Reduced voltage and restart testing of the 1-watt integral cryogenic cooler (HD-1033B/C/D)
[AD-A215133] p 369 N90-16971
- FLOORS**
Impact evaluation of composite floor sections
[SAE PAPER 891018] p 100 A90-14330
- Crashworthiness of composite floor sections
p 243 A90-20261
- Development of improved fire safety standards adopted by the Federal Aviation Administration
p 324 N90-17585
- Floor pull test of a transport airframe section
[DOT/FAA/CT-TN88/14] p 497 N90-20072
- The effect of aircraft size on cabin floor dynamic pulses
[DOT/FAA/CT-88/15] p 735 N90-25136
- A review of research and development in crashworthiness of general aviation aircraft: Seats, restraints and floor structures
[AD-A221557] p 846 N90-27698
- FLOQUET THEOREM**
Rotor/fuselage vibration isolation studies by a Floquet-harmonic iteration technique
p 182 A90-19393
- Instabilities of supersonic shear flows
[AIAA PAPER 90-0712] p 314 A90-26983
- A study of symbolic processing and computational aspects in helicopter dynamics
p 545 A90-34103
- Subharmonic instability of compressible boundary layers
p 706 A90-44005
- FLOW CHARACTERISTICS**
Asymptotic calculation of flow parameters in the problem of hypersonic flow past blunt axisymmetric bodies
p 10 A90-12268
- An investigation of artificial compressor surge
p 11 A90-12526
- The effect of flow curvature on the aerodynamic characteristics of an ogive-cylinder body
p 82 A90-13785
- A study of ground vortex
p 158 A90-18590
- Experimental investigation of trailing-edge and near wake flow of a symmetric airfoil
p 160 A90-19449

- An investigation of asymmetric vortical flows over delta wings with tangential leading-edge blowing at high angles of attack
[AIAA PAPER 90-0103] p 227 A90-22167
- Characteristics of turbulent separation flows on a porous surface under conditions of injection
p 231 A90-22422
- Dual pressure ratio compressor
[ASME PAPER 89-GT-121] p 341 A90-23820
- Calculation of supersonic flow past a wing/fuselage combination with the resolution of a compression shock from the wing
p 297 A90-24138
- Interference between the pitot-static tube and the model in wind tunnel studies of flow parameters
p 350 A90-24169
- Comparison of model- and full-scale wind-tunnel performance
[AIAA PAPER 88-2536] p 351 A90-26133
- Calculation of flow characteristics in the core of a vortex sheet
p 386 A90-28981
- Effects of splitter plates on the wake flow behind a bluff body
p 469 A90-32453
- An investigation of the flow characteristics of transonic nozzle blades
p 475 A90-33700
- Flow quality in the T2 cryogenic wind-tunnel - Problems and solutions
p 524 A90-34240
- Boundary layer turbulence structure in the presence of embedded streamwise vortex pairs
p 552 A90-35193
- Structure of a reattaching supersonic shear layer
p 555 A90-36252
- Priorities for high-lift testing in the 1990s
[AIAA PAPER 90-1413] p 596 A90-37950
- The new FFA T1500 transonic wind tunnel initial operation, calibration, and test results
[AIAA PAPER 90-1420] p 596 A90-37957
- On the possibilities for improvement and modernization of subsonic wind tunnels
[AIAA PAPER 90-1423] p 596 A90-37960
- A multipurpose aerodynamic research facility utilizing the abandoned Cincinnati subway tubes
[AIAA PAPER 90-1424] p 596 A90-37961
- Flow and acoustic features of a supersonic tapered nozzle
[AIAA PAPER 90-1599] p 567 A90-38731
- Measurement of crossflow vortices, attachment-line flow, and transition using microthin hot films
[AIAA PAPER 90-1636] p 607 A90-38765
- The effect of constructive and destructive interference on the downstream development of twin jets in a crossflow. II - Interference effects of angularly displaced jets
[AIAA PAPER 90-2107] p 684 A90-42020
- Compressor aerodynamics --- Book
p 706 A90-44052
- CFD validation for aerodynamic flows - Challenge for the '90's
[AIAA PAPER 90-2995] p 787 A90-45846
- Relation between flow parameters of a gas turbine engine and rotor frequencies
p 851 A90-46539
- The determination of the aerodynamic characteristics of an ogive-cylinder body in subsonic, curved, incompressible flow, and an assessment of the effect of flow curvature
[REPT-87-13] p 89 N90-11712
- Navier-Stokes simulation of the crossflow instability in swept-wing flows
[NASA-CR-186122] p 212 N90-13744
- Automatic control of cryogenic wind tunnels
p 263 N90-15957
- Study of the blade/vortice interaction on a one-blade rotor during forward flight (incompressible, non viscous fluid)
[ISL-R-115/88] p 415 N90-18391
- Calculation of excrescence drag magnification due to pressure gradient at high subsonic speeds
[ESDU-87004] p 397 N90-19195
- Aerodynamic optimization by simultaneously updating flow variables and design parameters
p 501 N90-20991
- Computational and experimental investigations of rotating stall in compressor cascades
p 588 N90-22565
- A review of instability and noise propagation in supersonic flows
[NASA-CR-186800] p 717 N90-25112
- Raman scattering measurements using UV excimer lasers
p 874 N90-26902
- The Langley 14-by-22-foot subsonic tunnel: Description, flow characteristics, and guide for users
[NASA-TP-3008] p 816 N90-27649
- FLOW DEFLECTION**
Suppression of vortex asymmetry behind circular cones
p 556 A90-36282
- Experimental and analytical study of close-coupled ventral nozzles for ASTOVL aircraft
[NASA-TM-103170] p 666 N90-24273

FLOW DISTORTION

- Numerical study of centrifugal impeller response to an outlet pressure distortion p 68 A90-11804
- Unsteady flow in centrifugal compressors due to downstream circumferential distortions p 14 A90-12598
- Numerical simulation of three-dimensional flow around parachute canopies p 84 A90-14438
- The characteristic decay region of a class of three-dimensional wall jets p 85 A90-15241
- Large-scale motions in a supersonic turbulent boundary layer on a curved surface [AIAA PAPER 90-0019] p 160 A90-19636
- Compensating for pneumatic distortion in pressure sensing devices [AIAA PAPER 90-0631] p 211 A90-19956
- Investigation of the flow structure behind the rotating blades in the elbow of a wind tunnel in the case of acoustic excitation p 297 A90-24124
- Influence of wind tunnel circuit installations on test section flow quality p 436 A90-28287
- An experimental investigation on control of flow dynamic distortions downstream under strong shock-boundary layer interaction in the two-dimensional flow field p 471 A90-33288
- Inlet distortion generated periodic aerodynamic rotor response [ASME PAPER 89-GT-299] p 475 A90-33567
- Effect of condensation in a diffuser on the flow field p 603 A90-36784
- The effect of constructive and destructive interference on the downstream development of twin jets in a crossflow. I - Destructive interference of laterally spaced jets [AIAA PAPER 90-1623] p 607 A90-38752
- Perturbations of higher modes in a supersonic jet p 619 A90-39516
- Wave structure of artificial perturbations in a supersonic boundary layer on a plate p 619 A90-39518
- Calculation of stability derivatives for slender bodies using boundary element method p 620 A90-40181
- Excitation and development of unstable perturbations in a supersonic boundary layer p 710 A90-44928
- Experimental investigation of turbulence in a supersonic flow p 710 A90-44931
- Compensating for pneumatic distortion in pressure sensing devices [NASA-TM-101716] p 415 N90-19224
- Theoretical and experimental study of flow-control devices for inlets of indraft wind tunnels [NASA-TM-100050] p 598 N90-21778
- Experience in developing an improved design of experiment (lessons learned) p 857 N90-27718

FLOW DISTRIBUTION

- The unsteady aerodynamics of an oscillating cascade in a compressible flow field p 7 A90-11789
- Influence of blade leaning on the flow field behind turbine rectangular cascades with different incidences and aspect ratios p 11 A90-12519
- The interaction between tip clearance flow and the passage flowfield in an axial compressor cascade p 11 A90-12525
- Numerical simulation of three-dimensional hypersonic inlet flowfields p 13 A90-12587
- CFD predictions of lobed mixer flowfields p 70 A90-12626
- Heat Transfer and Fluid Mechanics Institute, 31st, California State University, Sacramento, June 1, 2, 1989, Proceedings p 130 A90-15387
- A model for the electrohydrodynamic flow in a constricted arc heater p 131 A90-15393
- Calculation of flowfields in side-inlet ramjet combustors with an algebraic Reynolds stress model p 87 A90-16367
- Supersonic/hypersonic Euler flowfield prediction method for aircraft configurations p 145 A90-16767
- Calculation of transonic flows for novel engine-airframe installations p 145 A90-16768
- Two-dimensional transonic flow field analysis with different turbulence models p 150 A90-16846
- Design and experimental verification of an equivalent forebody representation of flowing inlets p 152 A90-17863
- Numerical study of chemically reacting flows using a lower-upper symmetric successive overrelaxation scheme p 153 A90-17989
- Experimental investigation of flowfield about a multielement airfoil p 154 A90-18137
- An investigation of unsteady leading edge separation of rapidly pitched airfoils p 157 A90-18587
- Analysis of blade loadings in centrifugal compressors p 158 A90-18591
- Application of panel methods to wind-tunnel wall interference corrections [AIAA PAPER 90-0007] p 200 A90-19629

- In-flight flow field analysis on the NASA F-18 high alpha research vehicle with comparisons to ground facility data [AIAA PAPER 90-0231] p 163 A90-19745
- Experimental and numerical investigation of the flow in the core of a leading edge vortex [AIAA PAPER 90-0384] p 165 A90-19826
- Aerodynamic spike flowfields computed to select optimum configuration at Mach 2.5 with experimental validation [AIAA PAPER 90-0414] p 166 A90-19837
- The influence of a rotating leading edge on accelerating starting flow over an airfoil [AIAA PAPER 90-0583] p 168 A90-19932
- Numerical investigation of airfoil/jet/fuselage-undersurface flowfields in ground effect [AIAA PAPER 90-0597] p 168 A90-19939
- Hydrodynamic visualization of organized structures and turbulences in boundary layers, wakes, jets or propeller flows [ONERA, TP NO. 1989-158] p 223 A90-21026
- Correlation of Puma airfoils - Evaluation of CFD prediction methods [ONERA, TP NO. 1989-185] p 224 A90-21045
- Computation of hypersonic flow fields p 225 A90-21169
- Nonaxisymmetric instabilities in a dump combustor with a swirling inlet flow p 253 A90-21228
- Application of an efficient hybrid scheme for aeroelastic analysis of advanced propellers [AIAA PAPER 90-0028] p 226 A90-22153
- Pneumatic vortical flow control at high angles of attack [AIAA PAPER 90-0098] p 227 A90-22164
- Navier-Stokes predictions of the flowfield around the F-18 (HARV) wing and fuselage at large incidence [AIAA PAPER 90-0099] p 227 A90-22165
- Convective heat transfer measurements from a NACA 0012 airfoil in flight and in the NASA Lewis Icing Research Tunnel [AIAA PAPER 90-0199] p 272 A90-22180
- An experimental investigation of sweep-angle influence on delta-wing flows [AIAA PAPER 90-0383] p 228 A90-22210
- Experimental and theoretical study of the swirling flow in centrifugal compressor volutes [ASME PAPER 89-GT-183] p 273 A90-22663
- Turbulence modeling for aerodynamic flows [AIAA PAPER 89-0606] p 234 A90-23647
- Improvement of 3D full-potential method and computation of flowfield of CAS compressor rotor [ASME PAPER 89-GT-17] p 288 A90-23760
- Application of a lower-upper implicit scheme and an interactive grid generation for turbomachinery flow field simulations [ASME PAPER 89-GT-20] p 288 A90-23762
- Overview on test cases for computation of internal flows in turbomachines [ASME PAPER 89-GT-46] p 288 A90-23772
- Flow in a centrifugal fan of the squirrel cage type [ASME PAPER 89-GT-52] p 289 A90-23778
- Three-dimensional separated flow field in the endwall region of an annular compressor cascade in the presence of rotor-stator interaction. I - Quasi-steady flow field and comparison with steady-state data [ASME PAPER 89-GT-76] p 291 A90-23797
- Three-dimensional separated flow field in the endwall region of an annular compressor cascade in the presence of rotor-stator interaction. II - Unsteady flow and pressure field [ASME PAPER 89-GT-77] p 291 A90-23798
- LDV measurements and the flow analysis in the vaneless region of a radial inflow turbine [ASME PAPER 89-GT-157] p 292 A90-23845
- Axial flow compressor design optimization. II - Through-flow analysis [ASME PAPER 89-GT-202] p 342 A90-23874
- Unsteady Euler analysis of the flowfield of a propfan at an angle of attack [AIAA PAPER 90-0339] p 300 A90-25028
- Navier-Stokes computations for the investigation of flowfields about a Space-Plane p 306 A90-25836
- Efficient method for computing transonic and supersonic flows about aircraft p 307 A90-26132
- Knowledge-based flow field zoning p 308 A90-26478
- Interactive grid generation for turbomachinery flow field simulations p 312 A90-26553
- Numerical simulation of an F-16A at angle of attack [AIAA PAPER 90-0100] p 313 A90-26911
- The flowfields of bursting vortices over moderately swept delta wings [AIAA PAPER 90-0599] p 314 A90-26969
- High resolution flow field prediction for tail rotor aeroacoustics p 463 A90-28158

- Aeroacoustic flowfield and acoustics of a model helicopter tail rotor at high advance ratio p 463 A90-28160
- Measurements, visualization and interpretation of 3-D flows - Application within base flows p 386 A90-28252
- Observation and analysis of sidewall effect in a transonic airfoil test section p 436 A90-28257
- A laser fluorescence anemometer for water tunnel flowfield studies p 447 A90-28279
- Numerical simulation of an adaptive-wall wind-tunnel - A comparison of two different strategies p 439 A90-30251
- Galerkin finite element method for transonic flow about airfoils and wings p 396 A90-31486
- A laser based computer aided non-intrusive technique for full field flow characterization in macroscopic curved channels p 535 A90-32293
- Nonstationary hypersonic flow past a thin wing of variable shape p 470 A90-32559
- Numerical modeling of separated turbulent flows p 470 A90-32673
- Prediction of turbulent combustion flowfields behind a backward-facing step p 529 A90-32952
- An experimental study on flowfields in a dual inlet swirl-dump combustor p 471 A90-33283
- An experimental investigation on control of flow dynamic distortions downstream under strong shock-boundary layer interaction in the two-dimensional flow field p 471 A90-33288
- Experimental investigation of the flow development of an airfoil at high angles of attack p 473 A90-33366
- Calculation of flow on a flat plate at angle of attack by numerical solution of Navier-Stokes equations p 537 A90-33424
- Visualization studies in rotating disk cavity flows p 475 A90-33568
- Capability of current supercomputers for the computational fluid dynamics p 546 A90-34382
- Finite element simulation of complex jets in a crossflow for V/STOL applications p 585 A90-35753
- Navier-Stokes computation of flow around a round-edged double-delta wing p 555 A90-36251
- The effect of Mach number on the stability of a plane supersonic wake p 557 A90-36524
- Pneumatic vortex flow control on a 55-degree cropped delta wing with chined forebody [AIAA PAPER 90-1430] p 559 A90-37967
- Flow field measurements near a fighter model at high angles of attack p 559 A90-37968
- Measurement of mean and fluctuating flow properties in hypersonic shear layers [AIAA PAPER 90-1409] p 560 A90-38488
- Flow field studies behind a wing at low Reynolds numbers p 563 A90-38628
- Influence of bulk turbulence and entrance boundary layer thickness on the curved duct flow field [AIAA PAPER 90-1502] p 606 A90-38651
- A flow around airfoil with slat and flap [AIAA PAPER 90-1535] p 564 A90-38679
- Calculation of hypersonic forebody/inlet flow fields [AIAA PAPER 90-1493] p 619 A90-39049
- Confined jet thrust vector control nozzle studies [AIAA PAPER 90-2027] p 657 A90-40598
- A numerical investigation of supersonic inlet using implicit TVD scheme [AIAA PAPER 90-2135] p 621 A90-40612
- Flow structure generated by oscillating delta-wing segments p 622 A90-40694
- Symmetry assessment of an air-blast atomizer spray p 682 A90-40930
- Calculation of three-dimensional jet interaction flowfields [AIAA PAPER 90-2099] p 624 A90-42018
- The effect of constructive and destructive interference on the downstream development of twin jets in a crossflow. II - Interference effects of angularly displaced jets [AIAA PAPER 90-2107] p 684 A90-42020
- Model of a labyrinth seal with flow p 687 A90-42334
- The flow over a wing/nacelle combination in the presence of a propeller slipstream p 629 A90-42415
- Flow over a leading edge with distributed roughness p 703 A90-42646
- Finite element simulation of turbulent propeller flowfields p 703 A90-42658
- Computational analysis of the flowfield of a two-dimensional ejector nozzle [AIAA PAPER 90-1901] p 740 A90-42690
- Three-dimensional turbulent flow code calculations of hot gas ingestion p 745 A90-44726
- The flow field and heat transfer near a turbulator p 771 A90-44755

The effect of turbulence models on the numerical prediction of the flowfield about a prolate spheroid at high angle of attack
[AIAA PAPER 90-3106] p 789 A90-45855

Navier-Stokes simulation of unsteady supersonic cavity flowfield with passive control
[AIAA PAPER 90-3101] p 796 A90-45913

An evaluation of Euler solvers for transonic flowfield computations on wing-fuselage geometries
[AIAA PAPER 90-3015] p 798 A90-45935

The low frequency oscillation in the flow over a NACA0012 airfoil with an 'iced' leading edge
p 801 A90-46377

Flow past bodies within a narrow class of cross-sectional shapes with stationary separation zones at large Reynolds numbers
p 805 A90-46568

Geometrical factors influencing the flow field in a propulsive nozzle
p 807 A90-46876

Rotorwash flow fields - Flight test measurement, prediction methodologies, and operational issues
p 817 A90-46930

Flow field around an oscillating cascade
p 814 A90-49459

Euler analysis comparison with LDV data for an advanced counter-rotation propfan at cruise
[AIAA PAPER 90-3033] p 903 A90-50637

Flow past two cylinders and two spheres
p 903 A90-50815

A numerical method for solving transonic flow past aircraft in Cartesian coordinates
[NAL-TR-1008] p 18 N90-10003

Computation of transonic flow about stores
[AD-A210402] p 18 N90-10009

Experimental investigation of attachment-line transition in low-speed, high-lift wind-tunnel testing
p 71 N90-10358

Curvature effects on the stability of three-dimensional laminar boundary layers
p 71 N90-10366

Linear instability of supersonic plane wakes
[NASA-CR-181911] p 20 N90-10833

The structure of separated flow regions occurring near the leading edge of airfoils - including transition
[NASA-CR-185853] p 87 N90-11695

Investigation of advanced mixer-ejector exhaust system
[AD-A211943] p 89 N90-11705

Computation of ramjet internal flowfields
[AD-A212001] p 114 N90-11743

Analytical studies of three-dimensional combustion processes
[AD-A211903] p 126 N90-11837

Experimental research on swept shock wave/boundary layer interactions
[AD-A211744] p 134 N90-11988

Experimental and theoretical investigation of boundary-layer instability mechanisms on a swept leading edge at Mach 3.5
p 94 N90-12557

Reduction of turbulent drag: Boundary layer manipulators
[CERT-RSF-0A-74/2259-AYD] p 136 N90-12889

Multigrid solution method for the Euler equations
[PB89-219463] p 138 N90-13116

Application of a self-adaptive grid method to complex flows
[NASA-TM-102223] p 143 N90-13324

Analysis of experimental data for CAST 10-2/DOA 2 supercritical airfoil at low Reynolds numbers and application to high Reynolds number flow
[AD-A211654] p 170 N90-13326

Study of the integration of wind tunnel and computational methods for aerodynamic configurations
[NASA-TM-102196] p 170 N90-13332

Computation of flow fields around propellers and hovering rotors based on the solution of the Euler equations
[DLR-FB-89-37] p 170 N90-13333

Blunt-nose inviscid airflows with coupled nonequilibrium processes
p 171 N90-13336

A CFD study of tilt rotor flowfields
[NASA-CR-186116] p 171 N90-13349

Optimum shape of a blunt forebody in hypersonic flow
[NASA-CR-181955] p 171 N90-13351

Computation of Navier-Stokes equations for three-dimensional flow separation
[NASA-TM-102266] p 172 N90-13353

Application of an efficient hybrid scheme for aeroelastic analysis of advanced propellers
[NASA-TM-102428] p 172 N90-13355

A smoke generator system for aerodynamic flight research
[NASA-TM-4137] p 183 N90-13372

A planar reacting shear layer system for the study of fluid dynamics-combustion interaction
[NASA-TM-102422] p 194 N90-13393

A wall interference assessment/correction interface measurement system for the NASA/ARC 12-ft PWT
[NASA-CR-185474] p 200 N90-13401

Convective heat transfer measurements from a NACA 0012 airfoil in flight and in the NASA Lewis Icing Research Tunnel
[NASA-TM-102448] p 213 N90-13750

A computational analysis of the transonic flow field of two-dimensional minimum length nozzles
p 173 N90-14194

Navier-Stokes solutions of 2-D transonic flow over unconventional airfoils
p 173 N90-14195

Navier-Stokes analysis of airfoils with leading edge ice accretions
p 174 N90-14196

Computation of unsteady transonic flow about airfoils in frequency domain using the full-potential equation
p 174 N90-14198

Acoustic-vortical-combustion interaction in a solid fuel ramjet simulator
p 194 N90-14234

A dynamic multiblock approach to solving the unsteady Euler equations about complex configurations
p 214 N90-14497

Unsteady aerodynamics of oscillating and rapidly pitched airfoils
p 235 N90-15074

Performance of a highly-loaded HP compressor
[RAE-TM-P-1149] p 256 N90-15919

Use of the film-of-oil technique for profile measurements in the Transonic Wind tunnel Brunswick (TWB)
p 238 N90-16252

Controlled vortical flow on delta wings through unsteady leading edge blowing
[NASA-CR-186267] p 316 N90-16712

An experimental study of the effect of streamwise vortices on unsteady turbulent boundary-layer separation
p 369 N90-17045

Low speed flowfield characterization by infrared measurements of surface temperatures
p 317 N90-17556

Time development of convection flow patterns in aircraft cabins under post-crash fire exposure
p 327 N90-17598

Viscous three-dimensional analyses for nozzles for hypersonic propulsion
[NASA-CR-185197] p 344 N90-17635

CAST-10-2/DOA 2 Airfoil Studies. Workshop Results
[NASA-CP-3052] p 352 N90-17647

Nonlinear transonic Wall-Interference Assessment/Correction (WIAIC) procedures and application to cast-10 airfoil results from the NASA 0.3-m TCT 8- by 24-inch Slotted Wall Test Section (SWTS)
p 352 N90-17648

Residual interference and wind tunnel wall adaption
p 353 N90-17655

Comparison of two- and three-dimensional Navier-Stokes solutions with NASA experimental data for CAST-10 airfoil
p 321 N90-17658

Experimental investigation of a chemical laser cavity flowfield
[AD-A216398] p 372 N90-18038

Unsteady Euler analysis of the flow field of a propan at an angle of attack
[NASA-TM-102426] p 380 N90-18229

Automation and extension of LDV (Laser-Doppler Velocimetry) measurements of off-design flow in a subsonic cascade wind tunnel
[AD-A216627] p 453 N90-18670

Unsteady aerodynamics of delta wings performing maneuvers to high angle of attack
p 398 N90-19196

Interaction of an oblique shock wave with supersonic flow over a blunt body
p 398 N90-19197

A study of flows over highly-swept wings designed for maneuver at supersonic speeds
[AD-A216837] p 399 N90-19202

A panel process for the calculation of the flow around a wing with front angle damping
[ETN-90-95367] p 399 N90-19207

External flow computations for a finned 60mm ramjet in steady supersonic flight
[AD-A216998] p 428 N90-19233

Experimental and theoretical investigations of flowfields and heat transfer in modern gas turbines
[AD-A217663] p 429 N90-19237

Flow simulation for aircraft
[NLR-MP-87082-U] p 455 N90-19543

Spanwise measurements of vertical components of atmospheric turbulence
[NASA-TP-2963] p 456 N90-19718

Heat transfer near the entrance to a film cooling hole in a gas turbine blade
[AD-A217396] p 510 N90-20089

Experimental investigation of the mechanisms underlying vortex kinematics in unsteady separated flows
[AD-A217889] p 540 N90-20346

Laser-velocimeter-measured flow field around an advanced, swept, eight-blade propeller at Mach 0.8
[NASA-TP-2462] p 468 N90-20942

Users manual for the NASA Lewis Ice Accretion Prediction Code (LEWICE)
[NASA-CR-185129] p 468 N90-20943

On total variation diminishing schemes for transonic turbulent flow computation
p 479 N90-20945

An approximate viscous shock layer method for calculating the hypersonic flow over blunt-nosed bodies
p 479 N90-20947

Comparison of C- and O-grid generation methods using a NACA 0012 airfoil
[AD-A216375] p 479 N90-20948

Effects of nose bluntness and shock-shock interactions on blunt bodies in viscous hypersonic flows
[NASA-CR-186451] p 479 N90-20950

Computation of nonequilibrium chemically reacting flows in hypersonic flow field
p 480 N90-20954

Measurement of lift development on rapidly-accelerated wings
p 480 N90-20956

Convergence acceleration of hypersonic flow calculations: A nonlinear relaxation factor
p 480 N90-20957

Computation of viscous flow around a propeller-shaft configuration with infinite-pitch rectangular blades
p 481 N90-20958

Flow in a forward swept centrifugal fan, volumes 1 and 2
p 481 N90-20959

Optimum hypersonic airfoils with attached shocks
p 481 N90-20960

An evaluation of the two-dimensional Euler and Navier-Stokes calculations based on a flux-vector splitting
[PB90-166778] p 481 N90-20963

Experimental and numerical investigation of the vortex flow over a sharp edged delta wing: with and without sideslip
[PB90-167131] p 481 N90-20964

Aerodynamic design techniques at DLR Institute for Design Aerodynamics
p 500 N90-20979

Aerodynamic design via control theory
p 546 N90-20998

Secondary Flows in Turbomachines
[AGARD-CP-469] p 511 N90-21009

Measurement of the flow field in the blade passage and side-wall region of a plane turbine cascade
p 513 N90-21019

Centrifugal impeller geometry and its influence on secondary flows
p 513 N90-21020

The effect of secondary flow on the redistribution of the total temperature field downstream of a stationary turbine cascade
p 515 N90-21033

Supersonic nozzle design of arbitrary cross-section
p 515 N90-21035

Subsonic flutter analysis using MSC/NASTRAN
[PB90-166786] p 522 N90-21041

Adaptive grid embedding for the two-dimensional flux-split Euler equations
[NASA-CR-186533] p 547 N90-21571

Effective methods of controlling a junction vortex system in an incompressible, three-dimensional, turbulent flow
p 571 N90-21732

Extension of a streamwise upwind algorithm to a moving grid system
[NASA-TM-102800] p 572 N90-21739

Numerical investigation of some control methods for 3-D turbulent interactions due to sharp fins
p 591 N90-21764

An experimental investigation of the physical mechanisms controlling the asymmetric flow past slender bodies at large angles of attack
p 592 N90-21767

Theoretical and experimental study of flow-control devices for inlets of indraft wind tunnels
[NASA-TM-100050] p 598 N90-21778

A discussion on issues relating to multiblock grid generation
p 608 N90-21991

Water-tunnel study results of a TF/A-18 and F/A-18 canopy flow visualization
[NASA-TM-101705] p 573 N90-22532

Computational and experimental investigations of rotating stall in compressor cascades
p 588 N90-22565

Numerical flow simulation and supercomputers: More than a digital wind tunnel
p 612 N90-22976

The development of a system for the numerical simulation of Euler flows
p 612 N90-22980

Extension of a three-dimensional viscous wing flow analysis
[NASA-CR-182023] p 631 N90-23348

Three-dimensional analysis on flow and temperature distributions for aircraft fuel thermal stability
[AD-A219651] p 678 N90-23571

Composite reduced Navier Stokes procedures for flow problems with strong pressure interactions
[AD-A219621] p 689 N90-23687

- The interaction of a supersonic streamwise vortex and a normal shock wave p 633 N90-24241
- Unsteady potential flow past a propeller blade section [NASA-CR-4307] p 634 N90-24246
- Low-density flow effects for hypervelocity vehicles, phase 2 [AD-A221034] p 634 N90-24249
- Experimental and analytical study of close-coupled ventral nozzles for ASTOVL aircraft [NASA-TM-103170] p 666 N90-24273
- A review of instability and noise propagation in supersonic flows [NASA-CR-186800] p 717 N90-25112
- A lifting surface method for the calculation of steady and unsteady, incompressible propeller aerodynamics [ESA-TT-1151] p 717 N90-25113
- An experimental and theoretical investigation of the flow over plane delta wings with supersonic leading edges [LR-588] p 717 N90-25114
- Investigation of the vortex flow over a sharp-edged delta wing in the transonic speed regime [LR-594] p 717 N90-25115
- Identification of aerodynamic models for maneuvering aircraft [NASA-CR-186630] p 719 N90-25943
- Euler analysis comparison with LDV data for an advanced counter-rotation propfan at cruise [NASA-TM-103249] p 720 N90-25946
- Two-dimensional Euler and Navier-Stokes Time accurate simulations of fan rotor flows [NASA-TM-102402] p 720 N90-25948
- Effect of vortex generators on the aerodynamic wing characteristics and body of revolution [AD-A22813] p 721 N90-25955
- Hot gas ingestion characteristics and flow visualization of a vectored thrust STOVL concept [NASA-TM-103212] p 751 N90-26009
- Supersonic reacting internal flow fields [NASA-TM-103480] p 767 N90-26094
- Numerical analysis of three-dimensional particle-laden flow equations [IAR-90-2] p 775 N90-26268
- High speed turboprop aerodynamic study (counterrotation). Volume 1: Model development [NASA-CR-185241] p 782 N90-26633
- Velocity measurements on a lifting rotor/airframe configuration in low speed forward flight p 815 N90-26790
- Dallas/Fort Worth simulation, volume 1 [DOT/FAA/CT-TN89/28-VOL-1] p 824 N90-26802
- Modeling of supersonic reacting flow fields p 855 N90-26898
- An approximate method for calculating three-dimensional inviscid hypersonic flow fields [NASA-TP-3018] p 883 N90-27066
- Aerodynamics of a linear oscillating cascade [NASA-TM-103250] p 817 N90-27657
- Study of the compressibility effects on the turbulence of supersonic drags [ETN-90-97448] p 817 N90-27661
- Computer code for predicting coolant flow and heat transfer in turbomachinery [NASA-TP-2985] p 858 N90-27722
- Control of submersible vortex flows [NASA-TM-102693] p 909 N90-28493
- In-flight flow visualization with pressure measurements at low speeds on the NASA F-18 high alpha research vehicle [NASA-TM-101726] p 910 N90-28505
- Effects of canard position on the aerodynamic characteristics of a close-coupled canard configuration at low speed p 920 N90-28519
- Numerical simulations of flowfields in a central-dump ramjet combustor. 3: Effects of chemistry [AD-A224145] p 933 N90-28573
- Numerical simulations of blade-vortex interactions and lifting hovering rotor flows [AD-A224238] p 911 N90-29302
- Applications of LIF to high speed flows p 911 N90-29320
- Laser induced fluorescence: Practical applications. p 911 N90-29323
- FLOW EQUATIONS**
- A numerical method for calculating supersonic nonisobaric jets p 84 A90-14566
- Throughflow numerical calculations including influence of spanwise mixing in a multistage axial flow compressor p 157 A90-18534
- Inviscid drag prediction for transonic transport wings using a full-potential method [AIAA PAPER 90-0578] p 168 A90-19926
- Numerical method for the flow of an ideal fluid on a plane with subsonic and supersonic regions p 233 A90-23382
- Advantages of flow variables in thin viscous shock layer problems p 384 A90-24145
- Parallel computation of three-dimensional transonic flow problems with complex geometries [AIAA PAPER 90-0336] p 313 A90-26936
- Basic equations for unsteady transonic flow p 394 A90-29884
- Calculation of the complete transonic unsteady small disturbance equation by ADI method p 627 A90-42353
- Flow and heat transfer in rotating-disc systems. Volume I - Rotor-stator systems -- Book p 772 A90-45759
- Unsteady aerodynamics - Physical issues and numerical predictions p 806 A90-46843
- Analysis of a propeller in compressible, steady flow p 814 A90-49778
- CFD methods for drag prediction and analysis currently in use in UK [RAE-TM-AERO-2146] p 95 N90-12563
- Conical Euler solution for a highly-swept delta wing undergoing wing-rock motion [NASA-TM-102609] p 400 N90-19211
- Spectral simulation of unsteady compressible flow past a circular cylinder [NASA-CR-182030] p 478 N90-20050
- Multigrid accelerated relaxation solution of transonic full potential flow equation [PD-CF-8942] p 480 N90-20951
- Computation of nonequilibrium chemically reacting flows in hypersonic flow field p 480 N90-20954
- Aerodynamic design via control theory p 546 N90-20998
- Numerical analysis of three-dimensional particle-laden flow equations [IAR-90-2] p 775 N90-26268
- Efficient solution of the steady Euler equations with a centered implicit method p 884 N90-27999
- FLOW GEOMETRY**
- Computation of laminar mixed convection flow in a channel with wing type built-in obstacles p 67 A90-11114
- Test rig for the study of the flow in a rotor-stator system [ONERA, TP NO. 1989-124] p 58 A90-12634
- Augmented heat transfer in rectangular channels of narrow aspect ratios with rib turbulators p 70 A90-13091
- Determination of the effective areas of the mixing exhaust ducts of a bypass engine from autonomous test results p 102 A90-14584
- A circular combustor configuration with multiple injection ports for mixing enhancement p 130 A90-15389
- Curvature effects on the stability of laminar boundary layers on swept wings p 148 A90-16788
- Computation and analysis of the shapes of S1 and S2 streamsurfaces in a transonic compressor rotor p 160 A90-19446
- Large-scale motions in a supersonic turbulent boundary layer on a curved surface [AIAA PAPER 90-0019] p 160 A90-19636
- Development of the MZM numerical method for 3D boundary layer with interaction on complex configurations -- Multi-Zonal Marching [ONERA, TP NO. 1989-174] p 223 A90-21036
- The influence of diffuser vane leading edge geometry on the performance of a centrifugal compressor [ASME PAPER 89-GT-163] p 292 A90-23851
- Wing-fuselage interference regimes at supersonic flight velocities p 298 A90-24155
- Calculation of flow past flight vehicles of complex configurations at high supersonic Mach numbers using the hypersonic theory of small perturbations p 299 A90-24158
- A panel method for arbitrary moving boundaries problems p 302 A90-25284
- Numerical prediction of wakes of different bodies p 308 A90-26341
- Adaptive wall wind tunnels - Marriage between experiments and computations p 351 A90-26351
- Parallel computation of three-dimensional transonic flow problems with complex geometries [AIAA PAPER 90-0336] p 313 A90-26936
- Aerodynamic characteristics of wave riders based on flows behind axisymmetric shock waves p 395 A90-30342
- In flight flow angle measurements on the Ball-Bartoe Jetwing powered lift aircraft [AIAA PAPER 90-1284] p 495 A90-33905
- The free-wake computation of rotor-body flows [AIAA PAPER 90-1540] p 565 A90-38684
- Navier-Stokes solutions for vortical flows over a tangent-ogive cylinder p 620 A90-39780
- Solution of the Euler equations using unstructured polygonal meshes p 708 A90-44435
- Computational simulation of flows about hypersonic geometries with sharp leading edges [AIAA PAPER 90-3065] p 793 A90-45891
- Self-excited oscillations in internal transonic flows p 813 A90-49274
- Analytical studies of three-dimensional combustion processes [AD-A211903] p 126 N90-11837
- Block-structured solution of three-dimensional transonic flows using parallel processing [AD-A212851] p 170 N90-13330
- A computational analysis of the transonic flow field of two-dimensional minimum length nozzles p 173 N90-14194
- Analytical study of the origin and behavior of asymmetric vortices [NASA-TM-102796] p 573 N90-21746
- Generation of circumferential velocity contours associated with pulsed point suction on a rotating disk p 691 N90-25065
- Effects of forebody geometry on subsonic boundary-layer stability [NASA-CR-4314] p 718 N90-25939
- FLOW MEASUREMENT**
- Turbulence measurements in a flow generated by the collision of radially flowing wall jets p 2 A90-10699
- Influence of blade leaning on the flow field behind turbine rectangular cascades with different incidences and aspect ratios p 11 A90-12519
- In-flight boundary-layer transition measurements on a swept wing p 17 A90-13017
- Hot-wire measurements of near wakes behind an oscillating airfoil p 154 A90-18138
- Mean flow measurements of heated supersonic stream injection into a high Reynolds number supersonic stream [AIAA PAPER 90-0180] p 163 A90-19722
- Hypersonics. Volume 2 - Computation and measurement of hypersonic flows; Proceedings of the First Joint Europe/U.S. Short Course on Hypersonics, Paris, France, Dec. 7-11, 1987 -- Book p 224 A90-21164
- Measurement and calculation of the three-dimensional flow in axial compressor stators, with and without end-bends [ASME PAPER 89-GT-6] p 287 A90-23753
- Laser transit anemometry investigation of a high speed centrifugal compressor [ASME PAPER 89-GT-155] p 360 A90-23843
- Aerodynamic and heat transfer measurements on blading for a high rim-speed transonic turbine [ASME PAPER 89-GT-228] p 293 A90-23883
- Frontiers in experimental fluid mechanics p 367 A90-26059
- Turbulence measurements and noise generation in a transonic cryogenic wind tunnel [AIAA PAPER 88-2026] p 522 A90-32463
- In flight flow angle measurements on the Ball-Bartoe Jetwing powered lift aircraft [AIAA PAPER 90-1284] p 495 A90-33905
- Hot wire anemometry in transonic flows and cryogenic conditions p 539 A90-34229
- Review of vortical flow utilization [AIAA PAPER 90-1429] p 605 A90-37966
- Flow field measurements near a fighter model at high angles of attack [AIAA PAPER 90-1431] p 559 A90-37968
- The development of a 3-D laser velocimeter for the NASA Langley low turbulence pressure wind tunnel [AIAA PAPER 90-1385] p 597 A90-38484
- Measurement of mean and fluctuating flow properties in hypersonic shear layers [AIAA PAPER 90-1409] p 560 A90-38488
- The organized nature of a turbulent trailing vortex [AIAA PAPER 90-1625] p 568 A90-38754
- Measurement of crossflow vortices, attachment-line flow, and transition using microthin hot films [AIAA PAPER 90-1636] p 607 A90-38765
- Three-dimensional measurement, display, and interpretation of fluid flow datasets p 679 A90-38854
- Laser Doppler velocimetry investigation of swirler flowfields p 682 A90-40929
- The development of crossflow vortices on a 45 degree swept wing [SAE PAPER 892245] p 713 A90-45452
- A review of low Reynolds number aerodynamic research at the University of Glasgow p 800 A90-46367
- Wide-range fuel flowmeter, phase 2 [AD-A210547] p 72 N90-10424
- Hot-film system for transition detection in cryogenic wind tunnels p 122 N90-12522
- Predicted and hot-film measured Tollmien-Schlichting wave characteristics p 91 N90-12523
- Remote detection of boundary-layer transition by an optical system p 139 N90-12524
- Basic aerodynamic research facility for comparative studies of flow diagnostic techniques p 122 N90-12526
- Rotor induced-inflow-ratio measurements and CAMRAD calculations [NASA-TP-2946] p 237 N90-15882

Automation and extension of LDV (Laser-Doppler Velocimetry) measurements of off-design flow in a subsonic cascade wind tunnel
[AD-A216627] p 453 N90-18670

FLOW REGULATORS

Use of swirl for flow control in propulsion nozzles
p 421 A90-27963
A CFD study of precombustion shock-trains from Mach 3-6
[AIAA PAPER 90-2220] p 705 A90-42751

FLOW RESISTANCE

Calculation of cone drag p 84 A90-14579

FLOW STABILITY

Investigation of the mixing of parallel supersonic streams p 69 A90-12561
An experimental investigation of non-steady flow in vaneless diffusers p 14 A90-12595
Nonlinear stability of subsonic mixing layers with symmetric temperature variations p 223 A90-20501
Hydrodynamic visualization of organized structures and turbulences in boundary layers, wakes, jets or propeller flows

[ONERA, TP NO. 1989-158] p 223 A90-21026
Stability of flow through multistage axial compressors [ASME PAPER 89-GT-311] p 231 A90-22668
Stability analysis and numerical experiments for viscous-inviscid interaction in transonic flow p 293 A90-24009

Instabilities of supersonic shear flows
[AIAA PAPER 90-0712] p 314 A90-26983
The effect of walls on a spatially growing supersonic shear layer p 393 A90-29591
On the instability of hypersonic flow past a wedge p 554 A90-35902

The effect of Mach number on the stability of a plane supersonic wake p 557 A90-36524
Numerical simulation of confined, spatially-developing mixing layers - Comparison to the temporal shear layer [AIAA PAPER 90-1462] p 562 A90-38619

A device for introducing helical perturbations into a trailing line vortex
[AIAA PAPER 90-1627] p 568 A90-38756
Numerical simulation of the growth of instabilities in supersonic free shear layers p 623 A90-40941

On the instabilities of supersonic mixing layers - A high-Mach-number asymptotic theory p 702 A90-42644

Excitation and development of unstable perturbations in a supersonic boundary layer p 710 A90-44928
Computation of complex flows in gas turbine combustors with a multi-level additive correction technique p 881 A90-46899

Recent developments in Ramjet pressure oscillation technology p 53 N90-10199
Wide-range fuel flowmeter, phase 2 [AD-A210547] p 72 N90-10424

Research in Natural Laminar Flow and Laminar-Flow Control, part 1 [NASA-CP-2487-PT-1] p 90 N90-12503
Long-range LFC transport p 104 N90-12508

Detection of flow instabilities at airfoil profiles using piezoelectric arrays p 276 N90-16175
A method for the prediction of supersonic compressor blade performance [CUEP/A-TURBO/TR-126] p 344 N90-17634

Analytical study of the origin and behavior of asymmetric vortices [NASA-TM-102796] p 573 N90-21746
Generation of circumferential velocity contours associated with pulsed point suction on a rotating disk p 691 N90-25065

Entropy wave instability in compact ramjets p 858 N90-27932

Experimental investigations on the stability and vorticity of the vortex breakdown phenomenon above delta wings, measured by the ultrasonic laser method [ESA-TT-1079] p 910 N90-28498

FLOW THEORY

On a lifting line theory for supersonic flow. I - The velocity field due to a vortex line in supersonic flow p 143 A90-16735

Hypersonic rarefied flow and its solution over the stagnation region [AIAA PAPER 90-0420] p 166 A90-19842

Nonlinear stability of subsonic mixing layers with symmetric temperature variations p 223 A90-20501
Airfoil pressure measurements during a blade vortex interaction and a comparison with theory p 232 A90-23105

An approximate method for calculating flow past a wing profile with allowance for viscosity p 234 A90-23422
Eigenvalue problem in the theory of flow past thin profiles at high supersonic velocity p 295 A90-24096

Permeability of the porous walls of a wind tunnel at transonic velocities p 350 A90-24151

Calculation of flow past flight vehicles of complex configurations at high supersonic Mach numbers using the hypersonic theory of small perturbations p 299 A90-24158

A generalized lifting-line theory for curved and swept wings p 303 A90-25597
On a lifting line theory for supersonic flow. II - A supersonic lifting line theory for wings p 477 A90-34817

Research department fluid mechanics - Scientific report (1988) --- Book p 603 A90-36538
Mathematical modeling of plane parallel separated flows past bodies --- Russian book p 619 A90-39475

Perturbations of higher modes in a supersonic jet p 619 A90-39516
The potential approximation in the theory of conical flows p 710 A90-44930

A problem in the theory of optimal aerodynamic shapes p 803 A90-46503
Throughflow theory for nonaxisymmetric turbomachinery flow. I - Formulation. II - Assessment [ASME PAPER 89-GT-304] p 905 A90-51256

Applications of an adaptive unstructured solution algorithm to the analysis of high speed flows [AIAA PAPER 90-0395] p 229 A90-22213
Effect of surface riblets on the velocity profile of an incompressible boundary layer p 294 A90-24081

An experimental study of the effect of the Reynolds number on flow past a swept wing at transonic velocities p 294 A90-24082
Asymptotic solution of the optimal-deflection problem for a wing leading edge at subsonic flow velocities p 295 A90-24094

Calculation of the front or rear part of a flat body in subsonic flow with the extremum value of the critical Mach number p 296 A90-24120
Separation development and its effect on the aerodynamics of supercritical profiles at transonic velocities p 297 A90-24142

Determination of pressure and heat flow on the front surface of smooth blunt bodies p 299 A90-24166
Isothermal velocity and turbulence measurements downstream of a model multilobed turbofan mixer p 365 A90-24353

An automated vorticity surveying system using a rotating hot-wire probe p 447 A90-28284
Flow rate and thrust coefficients for biaxial flows in a convergent nozzle p 395 A90-30344

Turbulence statistics in a shock wave boundary layer interaction p 552 A90-35205
The development of a 3-D laser velocimeter for the NASA Langley low turbulence pressure wind tunnel [AIAA PAPER 90-1385] p 597 A90-38484

Study of compressibility effects in mixing layer by numerical simulation [AIAA PAPER 90-1464] p 562 A90-38621
The organized nature of a turbulent trailing vortex [AIAA PAPER 90-1625] p 568 A90-38754

Supersonic rectangular isothermal shrouded jets [AIAA PAPER 90-2028] p 621 A90-40599
Measurements of turbulent dual-jet interaction [AIAA PAPER 90-2105] p 624 A90-42019

An experimental investigation of the velocity field in a reverse-flow combustor p 739 A90-42657
Operation of the ram accelerator in the transdetonative velocity regime [AIAA PAPER 90-1985] p 741 A90-42712

Measurements in an annular combustor-diffuser system [AIAA PAPER 90-2162] p 768 A90-42740
Hypervelocity flow of dissociating nitrogen downstream of a blunt nose p 811 A90-48712

Wide-range fuel flowmeter, phase 2 [AD-A210547] p 72 N90-10424
Laser anemometer measurements in a transonic axial-flow fan rotor [NASA-TP-2879] p 73 N90-11245

Some implications of the isotropic momentarily frozen assumptions for the SPAN-MAT program [NASA-CR-181937] p 88 N90-11704
Experimental studies on Goertler vortices p 91 N90-12529

Stage effects on stalling and recovery of a high-speed 10-stage axial-flow compressor p 115 N90-12600
Practical systems for speckle velocimetry p 171 N90-13341

Laser two focus techniques p 212 N90-13348
Experimental measurements of the laminar separation bubble on an Eppler 387 airfoil at low Reynolds numbers [NASA-CR-186263] p 275 N90-15380

Numerical investigations of heat transfer and flow rates in rotating cavities. Simulation of the movement generated by wall temperature gradients, by source-sink mass flows or by the differential rotation of the walls, under the influence of Coriolis and centrifugal forces [ETN-90-96253] p 454 N90-18695

Relating flow between counter-rotating propellers to aerodynamic interaction noise p 479 N90-20944
LDV measurements and the flow analysis in the vortex region of a radial inflow turbine p 511 N90-21007
Laser induced fluorescence: Practical applications p 911 N90-29323

Analysis of scramjet engine characteristics [NAL-TR-1041] p 933 N90-29398

FLOW VISUALIZATION

Holographic interferometric study of shock wave propagation p 66 A90-10732
Application of the hydrogen bubble visualization method to the water tunnels of ONERA [ONERA, TP NO. 1989-107] p 58 A90-11140

Hydrodynamic visualization of the flow around a high-speed aircraft propeller [ONERA, TP NO. 1989-108] p 3 A90-11141
Flow around a jet and thrust measurement bias from static tests [AAAF PAPER NT 88-11] p 40 A90-11431

Unsteady flow visualization in a vibrating annular turbine cascade operating in the transonic flow regime p 7 A90-11786
Propeller wakes and their interaction with wings p 14 A90-12614

Complementary field method for interferometric tomographic reconstruction of high speed aerodynamic flows [AD-A219698] p 131 A90-15900
Experiments in swept-wing transition p 149 A90-16794

Transonic flow in throat region of supersonic nozzles p 149 A90-16799
An experiment study of rotor aerodynamic in ground effect at low speed p 149 A90-16826

Jets, vortices, and turbulence p 207 A90-17175
Design and experimental verification of an equivalent forebody representation of flowing inlets p 152 A90-17863

Mechanism of sidewall effect studied with oil flow visualization p 154 A90-18002
Effect of moving surfaces on the airfoil boundary-layer control p 159 A90-19388

Supersonic jet noise reduction by a porous single expansion ramp nozzle [AIAA PAPER 90-0366] p 219 A90-19815
Aerodynamic control of NASP-type vehicles through vortex manipulation [AIAA PAPER 90-0594] p 203 A90-19938

Hydrodynamic visualization of organized structures and turbulences in boundary layers, wakes, jets or propeller flows [ONERA, TP NO. 1989-158] p 223 A90-21026
Instrumentation being developed for the ONERA F4 wind tunnel [ONERA, TP NO. 1989-189] p 261 A90-21049

Controlled three-dimensionality in unsteady separated flows about a sinusoidally oscillating flat plate [AIAA PAPER 90-0689] p 230 A90-22244
Tip leakage losses in a linear turbine cascade [ASME PAPER 89-GT-56] p 290 A90-23782

Holographic flow visualization of turbofan by-pass and core nozzle streams [ASME PAPER 89-GT-260] p 363 A90-23891
In quest of the laminar-flow airliner - Flight experiments on a T-33 jet trainer p 300 A90-24825

Experimental study of nonsteady asymmetric flow around an ogive-cylinder at incidence p 384 A90-27985
Measurements, visualization and interpretation of 3-D flows - Application within base flows p 386 A90-28252

Observation and analysis of sidewall effect in a transonic airfoil test section p 436 A90-28257
Use of liquid crystals for qualitative and quantitative 2-D studies of transition and skin friction p 446 A90-28259

A laser fluorescence anemometer for water tunnel flowfield studies p 447 A90-28279
Development and extension of diagnostic techniques for advancing high speed aerodynamic research p 436 A90-28281

Status of the development programme for instrumentation and test techniques of the European Transonic Windtunnel - ETW p 437 A90-28292
New light on wind tunnel lasers p 439 A90-31248

Experimental investigation of the flow development of an airfoil at high angles of attack p 473 A90-33366

- An experimental investigation of the turbulent structure in a two-dimensional momentumless wake p 474 A90-33515
- Visualization studies in rotating disk cavity flows p 475 A90-33568
- Flow visualization in flight testing [AIAA PAPER 90-1273] p 496 A90-34148
- Surface flow visualization in the cryogenic wind tunnel p 539 A90-34234
- Suppression of vortex asymmetry behind circular cones p 556 A90-36282
- Flow field studies behind a wing at low Reynolds numbers [AIAA PAPER 90-1471] p 563 A90-38628
- A flow around airfoil with slat and flap [AIAA PAPER 90-1535] p 564 A90-38679
- Structure of swept shock wave/boundary-layer interactions using conical shadowgraphy [AIAA PAPER 90-1644] p 569 A90-38772
- Three-dimensional measurement, display, and interpretation of fluid flow datasets p 679 A90-38854
- Flow visualization via laser-induced reflection from bubble sheets p 680 A90-39784
- Flow visualization studies of the Mach number effects on dynamic stall of an oscillating airfoil p 622 A90-40683
- Flow structure generated by oscillating delta-wing segments p 622 A90-40694
- A visualization study of the interaction of a free vortex with the wake behind an airfoil p 623 A90-41119
- Aerodynamic applications of infrared thermography p 770 A90-44147
- In-flight flow visualization using infrared imaging p 731 A90-44731
- Visualization of the turbulent trailing vortex behind a finite wing in steady and unsteady flows p 712 A90-45260
- Vortex control for tail buffet alleviation on a twin-tail fighter configuration [SAE PAPER 892221] p 756 A90-45438
- In-flight flow visualization characteristics of the NASA F-18 high alpha research vehicle at high angles of attack [SAE PAPER 892222] p 713 A90-45439
- Application of a new visualization method to helicopter rotor flow [AIAA PAPER 90-3006] p 789 A90-45856
- F-18 high alpha research vehicle surface pressures - Initial in-flight results and correlation with flow visualization and wind-tunnel data [AIAA PAPER 90-3018] p 792 A90-45885
- A laser sheet flow visualization and aerodynamic force data evaluation of a 3 percent YF-17 fighter aircraft model at high angles of attack [AIAA PAPER 90-3019] p 792 A90-45886
- Experimental and computational surface and flow-field results for an all-body hypersonic aircraft [AIAA PAPER 90-3067] p 793 A90-45893
- An experimental study of a closely coupled tandem wing configuration at low Reynolds numbers [AIAA PAPER 90-3094] p 797 A90-45923
- Using the smoking-wire visualization method in the study of wing models at large angles of attack in subsonic wind tunnels p 861 A90-46561
- Application of the wide-field shadowgraph technique to rotor wake visualization [NASA-TM-102222] p 88 N90-11700
- Advanced technology in military gas turbine design and manufacture [PNR90545] p 114 N90-11747
- Experimental research on swept shock Wave/Boundary layer interactions [AD-A211744] p 134 N90-11988
- Recent flow visualization studies in the 0.3-m TCT p 122 N90-12528
- Experimental studies on Goertler vortices p 91 N90-12529
- Study of forces and moments on wing-bodies at high incidence, volumes 1 and 2 p 171 N90-13350
- A smoke generator system for aerodynamic flight research [NASA-TM-4137] p 183 N90-13372
- A vapor generator for transonic flow visualization [NASA-TM-101670] p 201 N90-13403
- Flow visualization of the effect of pitch rate on the vortex development on the scale model of a F-18 fighter aircraft [AD-A214244] p 236 N90-15080
- Flow field visualization study on a 65 deg delta wing at $M = 0.85$ p 277 N90-16182
- A wind tunnel study of a sting-mounted circulation control wing [AD-A216248] p 319 N90-17577
- Fluctuating wind forces measured on a bluff body extending from a cavity [AD-A216414] p 371 N90-18020
- Half model tests on an ONERA calibration model in the transonic wind tunnel Goettingen, Federal Republic of Germany [DLR-MITT-89-29] p 397 N90-18370
- Water-tunnel investigation of concepts for alleviation of adverse inlet spillage interactions with external stores [NASA-TM-4181] p 398 N90-19199
- Research on cascade secondary and tip-leakage flows: Periodicity and surface flow visualization p 514 N90-21026
- Water-tunnel study results of a TF/A-18 and F/A-18 canopy flow visualization [NASA-TM-101705] p 573 N90-22532
- Ground evaluation of seeding an in-flight wingtip vortex using infrared imaging flow visualization technique p 635 N90-25035
- Investigation of the vortex flow over a sharp-edged delta wing in the transonic speed regime [LR-594] p 717 N90-25115
- Space plane model for visual measurement of aerodynamic heating [DE90-505514] p 720 N90-25949
- Hot gas ingestion characteristics and flow visualization of a vectored thrust STOVL concept [NASA-TM-103212] p 751 N90-26009
- Informatics aspects of large flow calculations on the SX-2 supercomputer [NLR-MP-88037-U] p 776 N90-26290
- Experiments with unsteady, free surface, three-dimensional vortices in a thermally stable, stratified fluid [AD-A222088] p 815 N90-26796
- Flow visualization of dynamic stall on an oscillating airfoil [AD-A222202] p 815 N90-26797
- In-flight flow visualization with pressure measurements at low speeds on the NASA F-18 high alpha research vehicle [NASA-TM-101726] p 910 N90-28505
- Applications of LIF to high speed flows p 911 N90-29320
- Laser induced fluorescence: Practical applications p 911 N90-29323
- ### FLOWMETERS
- Lightweight fuel pump and metering component for advanced gas turbine engine control [AIAA PAPER 90-2032] p 657 A90-40602
- Wide-range fuel flowmeter, phase 2 [AD-A210547] p 72 N90-10424
- ### FLUID BOUNDARIES
- Solution of potential flow past an elastic body using the boundary element technique [AD-A213843] p 275 N90-15390
- ### FLUID DYNAMICS
- An experimental investigation of supersonic flow over two cavities in tandem [AIAA PAPER 90-3087] p 795 A90-45901
- Unsteady three-dimensional thin-layer Navier-Stokes solutions on dynamic blocked grids p 235 N90-15069
- An improvement of convection fidelity in Euler calculations p 315 N90-16709
- Modeling the wake as a continuous vortex sheet in a potential-flow solution using vortex panels [AD-A216220] p 371 N90-18016
- Aerodynamic analysis of a US Navy and Marine Corps unmanned air vehicle [AD-A218282] p 498 N90-20077
- Modification and improvement of software for modeling multidimensional reacting fuel flows [AD-A217789] p 533 N90-20235
- DURIP optical equipment for high-speed viscous-inviscid interaction research [AD-A217772] p 540 N90-20345
- WINCOF-I code for prediction of fan compressor unit with water ingestion [NASA-CR-185157] p 551 N90-21724
- Modeling of vortex-induced oscillations based on indicial response approach [NASA-CR-186560] p 572 N90-21736
- Fluid Dynamics Panel Working Group 12 on Adaptive Wind Tunnel Walls: Technology and Applications [AGARD-AR-269] p 870 N90-26838
- The reduction of smoke emissions from Allison T56 engines [ARL-PROP-R-182] p 928 N90-28547
- ### FLUID FILLED SHELLS
- Hydroelastic problems in space flight vehicles p 536 A90-33386
- ### FLUID FILMS
- Analysis of thermal gradient effects in oil ring seals p 682 A90-40716
- Use of the film-of-oil technique for profile measurements in the Transonic Wind tunnel Brunswick (TWB) p 238 N90-16252
- Life of concentrated contacts in the mixed EHD and boundary film regimes [AD-A216673] p 454 N90-18738
- ### FLUID FLOW
- Application of the finite element method to the problem of rotational flow around wings p 156 A90-18305
- The shape assumed by a soft conical shell in fluid flow p 300 A90-24752
- Analytical solution of the problem of nonaxisymmetric potential flow past a spherical canopy - A summary of the principal asymptotic formulas and qualitative analysis p 300 A90-24753
- Skin effect in flow of a disperse fluid past a wing profile p 395 A90-30334
- Application of splines to the calculation of flow past a wing profile p 805 A90-46615
- Numerical calculations of flows with shock waves by flux vector splitting method p 808 A90-47299
- Analytical studies of three-dimensional combustion processes [AD-A211903] p 126 N90-11837
- Application of a self-adaptive grid method to complex flows [NASA-TM-102223] p 143 N90-13324
- An experimental study of the aeroelastic behaviour of two parallel interfering circular cylinders p 455 N90-19609
- ### FLUID INJECTION
- Effects of an embedded vortex on injectant from a single film-cooling hole in a turbulent boundary layer [ASME PAPER 89-GT-189] p 362 A90-23867
- Effect of the design of a diffuser with tangential injection on the starting and separation ratios of pressures p 295 A90-24099
- Large-scale structure in a supersonic slot-injected flowfield p 602 A90-36265
- Effects of streamwise vorticity injection on turbulent mixing layer development [AIAA PAPER 90-1459] p 561 A90-38616
- Numerical study of asymmetric air injection to control high angle-of-attack forebody vortices on the X-29 aircraft [AIAA PAPER 90-3004] p 788 A90-45853
- ### FLUID JETS
- Aerodynamic breakup of liquid jets - A review [AIAA PAPER 90-1616] p 607 A90-38746
- ### FLUID MANAGEMENT
- Lightweight fuel pump and metering component for advanced gas turbine engine control [AIAA PAPER 90-2032] p 657 A90-40602
- ### FLUID MECHANICS
- Heat Transfer and Fluid Mechanics Institute, 31st, California State University, Sacramento, June 1, 2, 1989, Proceedings p 130 A90-15387
- Development process of turbulence in a round-nozzle air jet p 87 A90-16101
- Rotor noise due to atmospheric turbulence ingestion. I - Fluid mechanics p 219 A90-19385
- Frontiers in experimental fluid mechanics p 367 A90-26059
- Eshbach's handbook of engineering fundamentals / 4th edition/ p 448 A90-28825
- Research department fluid mechanics - Scientific report (1988) --- Book p 603 A90-36538
- Developments in mechanics, Volume 15 - Midwestern Mechanics Conference, 21st, Michigan Technological University, Houghton, Aug. 13-16, 1989, Proceedings p 769 A90-42870
- Test techniques for cryogenic wind tunnels p 263 N90-15952
- Development and application of a generalized dynamic wake theory for lifting rotors p 570 N90-21731
- An interactive boundary-layer method for unsteady airfoil flows. Part 1: Quasi-steady-state model [AD-A221220] p 634 N90-24250
- ARLSUPER version 1.0, program users guide [AD-A222693] p 815 N90-26793
- Study of ground effects on flying scaled models p 922 N90-28532
- ### FLUID PRESSURE
- Shock capturing and loss prediction for transonic turbine blades using a pressure correction method p 11 A90-12518
- ### FLUID-SOLID INTERACTIONS
- Investigation of adaptive-wall wind tunnels with two measured interfaces [AIAA PAPER 90-0186] p 200 A90-19728
- An experimental study of the effect of the Reynolds number on flow past a swept wing at transonic velocities p 294 A90-24082
- Application of Fedorenko's multigrad method for calculating transonic flow past a profile p 295 A90-24103
- A new quick method for integrating Euler equations for plane transonic flows p 295 A90-24105

Numerical simulation of separated flows around a wing section by a discrete vortex method p 307 A90-25846
Interaction between boundary layer and wakes of different bodies p 602 A90-36263
The design of the series of blade flutter rotor and the experimental investigation of flow-induced vibration p 586 A90-37230

Wind tunnel testing techniques on aerodynamic effects with small asymmetry [AIAA PAPER 90-1400] p 560 A90-38490

FLUORESCENCE

Development of process control procedure for ultrahigh-sensitivity fluorescent penetrant inspection systems p 771 A90-45225
Engine testing of thermographic phosphors [DE90-013269] p 885 N90-28059

FLUORINE COMPOUNDS

HF shock tunnel facility for studying supersonic combustion [AIAA PAPER 90-1551] p 600 A90-38693

FLUOROCARBONS

Mach 6 testing of two generic three-dimensional sidewall compression scramjet inlets in tetrafluoromethane [AIAA PAPER 90-0530] p 192 A90-19895

FLUOROSILICATES

Fluorosilicone sealants for aircraft fuel containment p 529 A90-31618

FLUSHING

Wind-tunnel investigation of a flush airdata system at Mach numbers from 0.7 to 1.4 [NASA-TM-101697] p 421 N90-18395

FLUTTER

Evaluation and measurement of airplane flutter interference --- in television reception p 272 A90-22529

Effect of structural anisotropy on the dynamic characteristics of the wing and critical flutter speed p 386 A90-28985

Flutter clearance of the F-18 high-angle-of-attack research vehicle with experimental wingtip instrumentation pods [NASA-TM-4148] p 103 N90-11732

Effect of control surface mass unbalance on the stability of a closed-loop active control system [NASA-TP-2952] p 134 N90-12042

The effectiveness of vane-aileron excitation in the experimental determination of flutter speed by parameter identification [NASA-TP-2971] p 249 N90-15100

Unsteady Aerodynamic Phenomena in Turbomachines [AGARD-CP-468] p 425 N90-18405

A comparison of flutter calculations based on eigenvalue and energy method p 425 N90-18406
Using transonic small disturbance theory for predicting the aeroelastic stability of a flexible wind-tunnel model [NASA-TM-102617] p 478 N90-20047

Digital-flutter-suppression-system investigations for the active flexible wing wind-tunnel model [NASA-TM-102618] p 520 N90-20093

An experimental study of tip shape effects on the flutter of aft-swept, flat-plate wings [NASA-TM-4180] p 582 N90-22555

Flutter clearance of the F-14A variable-sweep transition flight experiment airplane, phase 2 [NASA-TM-101717] p 735 N90-25135

A digital controller for active aeroelastic controls [NAL-TR-1014] p 936 N90-29402

FLUTTER ANALYSIS

Whirl-flutter investigation on an advanced turboprop configuration p 40 A90-11008
Flutter of turbine blades p 41 A90-11794
Systematic study of flutter characteristics of two-dimensional cascades in incompressible flow p 41 A90-11796

Aircraft compressor flutter analysis p 41 A90-11797
Flutter of cascade blades composed of blades having arbitrarily different natural frequencies p 42 A90-11798

The flutter characteristic analysis and optimization design of mistuning blade p 42 A90-11799

The effects of three centres of blade on flutter p 42 A90-11800

Flutter of mistuned cascades with structural coupling p 42 A90-11802

Mach number effects on transonic aeroelastic forces and flutter characteristics p 17 A90-13024

Blade surface pressure measurement on a pusher propeller in flight [SAE PAPER 891040] p 139 A90-14346

Aeroelastic characteristics of wings in subsonic flow p 102 A90-14615

A synthetic research for aircraft active flutter suppression p 195 A90-16827

Modal characteristics of swept plate flutter models p 207 A90-16962

Ground vibration test results of a JetStar airplane using impulsive sine excitation p 179 A90-16963

Flutter analysis on a non-linear wing model p 207 A90-17009

Boeing 720B design modification challenges p 179 A90-17309

Aeroelastic tailoring applied to composite wing p 211 A90-18580

Viscous oscillating cascade aerodynamics and flutter by a locally analytical method [AIAA PAPER 90-0579] p 168 A90-19929

A parametric study of the flutter stability of two-dimensional turbine and compressor cascades in incompressible flow p 225 A90-21593

Flutter and aileron reversal safety factors p 345 A90-24164

A unified approach to the overall body motion stability and flutter characteristics of elastic aircraft p 346 A90-25102

A semi-actuator disk theory for prediction of stall flutter in axial flow compressors p 301 A90-25105

Influence of structural and aerodynamic modeling on flutter analysis [AIAA PAPER 90-0954] p 411 A90-29239

Applications of XTRAN3S and CAP-TSD to fighter aircraft [AIAA PAPER 90-1035] p 389 A90-29360

A reduced cost rational-function approximation for unsteady aerodynamics [AIAA PAPER 90-1155] p 390 A90-29367

Influence of joint fixity on the aeroelastic characteristics of a joined wing structure [AIAA PAPER 90-0980] p 390 A90-29370

Nonlinear stall flutter and divergence analysis of cantilevered graphite/epoxy wings [AIAA PAPER 90-0983] p 450 A90-29373

Time domain flutter analysis of cascades using a full-potential solver [AIAA PAPER 90-0984] p 391 A90-29374

Aeroelastic analysis of wings using the Euler equations with a deforming mesh [AIAA PAPER 90-1032] p 391 A90-29376

Chaotic response of aerosurfaces with structural nonlinearities (Status report) [AIAA PAPER 90-1034] p 392 A90-29378

Flutter analysis of composite panels in supersonic flow [AIAA PAPER 90-1180] p 450 A90-29379

Digital-flutter-suppression-system investigations for the active flexible wing wind-tunnel model [AIAA PAPER 90-1074] p 430 A90-29382

Computational prediction of stall flutter in cascaded airfoils [AIAA PAPER 90-1116] p 392 A90-29388

Aeroelastic problems in turbomachines [AIAA PAPER 90-1157] p 393 A90-29393

Aeroelastic tailoring analysis for preliminary design of advanced turbo propellers with composite blades p 412 A90-29395

Whirl flutter stability of a pusher configuration subject to a nonuniform flow [AIAA PAPER 90-1162] p 393 A90-29397

Practical problems - Airplanes --- unsteady interactional aerodynamics, flutter characteristics, and active flight control p 394 A90-29885

Active flutter suppression for a wing model p 433 A90-31283

Sensitivity derivatives of flutter characteristics and stability margins for aeroservoelastic design p 433 A90-31287

Application of the CAP-TSD unsteady transonic small disturbance program to wing flutter --- Computational Aeroelasticity Program p 491 A90-33354

Comparison of two potential flow methods for transonic flutter analysis p 471 A90-33356

Applications of the unsteady full potential equation for wings p 472 A90-33358

Calculations of unsteady aerodynamics over oscillating wings p 472 A90-33362

Application of time domain decomposition techniques to aircraft ground and flutter test data p 491 A90-33373

Flutter analysis from ambient random responses p 491 A90-33374

Design flutter calculations on PC p 545 A90-33379

Structural optimization in view of aeroelastic constraints p 536 A90-33391

Flutter suppression control law synthesis for the active flexible wing model p 517 A90-33403

A review of aeroelasticity research at the flight dynamics laboratory p 493 A90-33409

Effects of tailplane aerodynamics and fuselage flexibility on the flutter of high aspect ratio, low speed aircraft p 493 A90-33414

Advanced parameter identification techniques for near real time flight flutter test analysis [AIAA PAPER 90-1275] p 494 A90-33899

Response characteristics of a two-dimensional wing subjected to turbulence near the flutter boundary p 519 A90-34082

Euler flutter analysis of airfoils using unstructured dynamic meshes p 602 A90-35760

The design of the series of blade flutter rotor and the experimental investigation of flow-induced vibration p 586 A90-37230

Flutter of shaft-supported low aspect-ratio control surfaces p 667 A90-38912

Aeroelastic analysis of a low aspect ratio wing p 619 A90-38915

Development of a mathematical model of an adaptive antiflutter system p 769 A90-42911

Full span analysis for flutter prediction of slender blade assemblies p 879 A90-46188

Effect of the drag on the critical flutter velocity p 828 A90-46480

Unsteady aerodynamics - Physical issues and numerical predictions p 806 A90-46843

Structure/control design synthesis of active flutter suppression system by goal programming [AIAA PAPER 90-3325] p 872 A90-47587

Aircraft passing through a sinusoidal gust p 811 A90-48090

A new method for high speed propeller flutter prediction p 854 A90-49454

A method for predicting stall flutter under variable interblade phase angle along rotating direction p 813 A90-49455

The interaction between distortion of inlet flow and blade stall flutter in axial-flow compressor p 854 A90-49466

A model of small-disturbance wave in large-scale separation zone associated with stall flutter p 883 A90-49469

Some explorations on the mechanism of blade flutter suppression by porous wall casing p 854 A90-49470

Recent results of numerical flutter studies in high performance gliders [DGLR PAPER 88-038] p 934 A90-50249

Problems related to the acquisition, processing and utilization of the modal parameters measured in flight tests in order to obtain the full envelope for flutter [ETN-89-95210] p 103 N90-11735

Experimental transonic flutter characteristics of two 72 deg-sweep delta-wing models [NASA-TM-101659] p 175 N90-14205

Nonlinear phenomena in computational transonic aeroelasticity p 235 N90-15070

Using transonic small disturbance theory for predicting the aeroelastic stability of a flexible wind-tunnel model [NASA-TM-102617] p 478 N90-20047

The application of active controls technology to a generic hypersonic aircraft configuration [NASA-TM-101689] p 497 N90-20071

Subsonic flutter analysis using MSC/NASTRAN [PB90-166786] p 522 N90-21041

An experimental study of tip shape effects on the flutter of aft-swept, flat-plate wings [NASA-TM-4180] p 582 N90-22555

Flutter investigations on a Transavia PL12/T-400 aircraft [AD-A219108] p 593 N90-22570

On simplified analytical flutter clearance procedures for light aircraft [DLR-FB-89-56] p 672 N90-24276

Effects of spoiler surfaces on the aeroelastic behavior of a low-aspect-ratio rectangular wing [NASA-TM-102622] p 846 N90-27700

Multi-disciplinary optimization of aeroservoelastic systems [NASA-CR-185931] p 925 N90-29385

FLUX DENSITY

Construction of a hybrid angular velocity reference system for investigation of the dynamic characteristics of strapdown gyros [ESA-TT-1181] p 774 N90-25332

FLUX VECTOR SPLITTING

Solving compressible flow problems using adaptive finite quadtree and octree grids p 155 A90-18243

An efficient upwind relaxation-sweeping algorithm for three-dimensional Euler equations [AIAA PAPER 90-0129] p 162 A90-19695

Generalized fluxvectors for hypersonic shock-capturing [AIAA PAPER 90-0390] p 165 A90-19829

Applications of an adaptive unstructured solution algorithm to the analysis of high speed flows [AIAA PAPER 90-0395] p 229 A90-22213

Comparison of inviscid and viscous separated flows p 302 A90-25277

A flux-split solution procedure for unsteady inlet flows [AIAA PAPER 90-0585] p 314 A90-26967

- Implicit flux-split Euler schemes for unsteady aerodynamic analysis involving unstructured dynamic meshes
[AIAA PAPER 90-0936] p 389 A90-29362
- Implicit flux-split schemes for the Euler equations
p 602 A90-36254
- Three-dimensional flux-split Euler schemes involving unstructured dynamic meshes
[AIAA PAPER 90-1649] p 569 A90-38777
- Transient behavior of supersonic flow through inlets
[AIAA PAPER 90-2130] p 704 A90-42734
- Adaptive grid embedding for the two-dimensional Euler equations
[AIAA PAPER 90-3049] p 797 A90-45929
- Numerical calculations of flows with shock waves by flux vector splitting method
p 808 A90-47299
- Solution of the thin-layer Navier-Stokes equations for laminar transonic flow
[PB89-221600] p 136 N90-12879
- Multigrid solution method for the Euler equations
[PB89-219463] p 138 A90-13116
- A dynamic multiblock approach to solving the unsteady Euler equations about complex configurations
p 214 N90-14497
- An evaluation of the two-dimensional Euler and Navier-Stokes calculations based on a flux-vector splitting
[PB90-166778] p 481 N90-20963
- FLY BY WIRE CONTROL**
- Identification of mathematical derivative models for the design of a model following control system --- for fly-by-wire helicopter
p 56 A90-12764
- The VSCF system has arrived - The way in which a new constant-frequency electrical generation system in aeronautics has been developed
p 187 A90-16696
- The coming age of the tiltrotor. I
p 246 A90-21711
- Pay-offs and pitfalls of fly-by-wire
p 346 A90-24281
- Fly-by-wire controls key to 'pure' stealth aircraft ---
F-117A Aircraft
p 413 A90-30222
- After Habsheim
p 401 A90-31388
- Problems in the synthesis of advanced aircraft control systems
p 751 A90-44723
- A pilot rating scale for evaluating failure transients in electronic flight control systems
[AIAA PAPER 90-2827] p 754 A90-45159
- Fault-tolerant transputer-based controller configurations for gas-turbine engines
p 852 A90-48529
- X-29 high angle-of-attack flight testing - Program status
[AIAA PAPER 90-3303] p 837 A90-48885
- Gripen wins its wings --- Swedish JAS39 aircraft testing and development
p 842 A90-49823
- Aviation Week editor files top Soviet interceptor
p 920 A90-52574
- ATTAS flight testing experiences
p 34 N90-10862
- In flight reflight tests on AM-X single engine fly-by-wire aircraft
p 34 N90-10869
- Engine controls for the 1990's
[PNR90546] p 114 N90-11748
- How to fly windshear using the fly-by-wire concept
p 258 N90-15050
- Applications of modern control theory synthesis to a super-augmented aircraft
[AD-A215431] p 336 N90-16753
- Model following control system design: Preliminary ATTAS in-flight simulation test results
[PD-FC-9003] p 758 N90-26010
- Start-up built-in test for the DISCUS fault tolerant, fly-by-wire computer system
p 869 N90-27625
- Procedure for calibrating fly-by-wire control chains of the flying testbed ATTAS
[DLR-MITT-90-02] p 936 N90-29401
- FOAMS**
- Aviation Engine Test Facilities (AETF) fire protection study
[AD-A211483] p 134 N90-12777
- FOG**
- Fog formation at Perth Airport
p 611 A90-37748
- FOIL BEARINGS**
- Foil gas bearings for turbomachinery
[SAE PAPER 901236] p 841 A90-49306
- FOKKER AIRCRAFT**
- Initial service experience with the Fokker 100
[SAE PAPER 892238] p 733 A90-45450
- Investigation of propeller slipstream effects on the Fokker 50 through in-flight pressure measurements
[AIAA PAPER 90-3084] p 806 A90-46645
- Static strength and damage tolerance tests on the Fokker 100 airframe
[NLR-MP-88023-U] p 416 N90-19228
- Activities report in aerospace and aerodynamics
[ETN-90-96774] p 699 N90-24224

FORCE DISTRIBUTION

- The warping restraint effect in the critical and subcritical static aeroelastic behavior of swept forward composite wing structures
[SAE PAPER 891056] p 129 A90-14358
- Minimum induced drag for wings with spanwise camber
p 709 A90-44733
- The effect of solidity on propeller normal force
[SAE PAPER 892205] p 713 A90-45424
- Wind tunnel tests of the influence of aerofoil thickness on the normal force and pitching moment of two slender wings at transonic and supersonic Mach numbers
[ESA-TT-1129] p 237 N90-15889
- Force and moment measurements on delta wings in unsteady flow
p 278 N90-16185
- Optimum spanwise camber for minimum induced drag
[BU-403] p 397 N90-18369
- The MANTA: An RPV design to investigate forces and moments on a lifting surface
[NASA-CR-186227] p 499 N90-20971
- Analysis of a six-component, flow-through, strain-gage, force balance used for hypersonic wind tunnel models with scramjet exhaust flow simulation
[NASA-CR-186585] p 597 N90-21775
- A flight dynamic model of aircraft spinning
[AR-005-600] p 935 N90-28576

FORCED CONVECTION

- Numerical simulation of droplet deformation in convective flows
[AIAA PAPER 90-2309] p 769 A90-42773

FORCED VIBRATION

- Application of the dynamic stiffness method to the free and forced vibrations of aircraft panels
p 270 A90-20599
- Study on travelling wave vibration of bladed disks in turbomachinery
p 423 A90-29908
- Large-amplitude high-rate roll oscillation system for the measurement of non-linear airloads
[AIAA PAPER 90-1426] p 590 A90-37963
- Coherent vortex structures in the wake of a sphere and a circular disk at rest and under forced vibrations
p 623 A90-40749
- Vibration of turbine blades damped by dry friction forces
p 879 A90-46190
- Aerodynamic study on forced vibrations on stator rows of axial compressors
p 426 N90-18412
- A video-based experimental investigation of wing rock
p 592 N90-21771

FOREBODIES

- Design and experimental verification of an equivalent forebody representation of flowing inlets
p 152 A90-17863
- Further analysis of wing rock generated by forebody vortices
p 153 A90-17868
- Aerodynamic control of aircraft by forebody vortex manipulation
[AIAA PAPER 90-1827] p 301 A90-25167
- The effect of windscreens bows and HUD pitch ladder on pilot performance during simulated flight
p 420 A90-31333
- Solution of Euler equations for fighter forebody-inlet combination at high angle of attack
p 556 A90-36419
- Pneumatic vortex flow control on a 55-degree cropped delta wing with chined forebody
[AIAA PAPER 90-1430] p 559 A90-37967
- Proportional control of asymmetric forebody vortices with the unsteady bleed technique
[AIAA PAPER 90-1629] p 591 A90-38758
- Strake camber and thickness design procedure for low alpha supersonic flow
p 622 A90-40678
- Approach to side force alleviation through modification of the pointed forebody geometry
[AIAA PAPER 90-2834] p 712 A90-45165
- Forebody vortex manipulation for aerodynamic control of aircraft at high angles of attack
[SAE PAPER 892220] p 756 A90-45437
- Hypersonic forebody lift-induced drag
[SAE PAPER 892345] p 715 A90-45497
- Numerical study of asymmetric air injection to control high angle-of-attack forebody vortices on the X-29 aircraft
[AIAA PAPER 90-3004] p 788 A90-45853
- Reduction of the side force on pointed forebodies through add-on tip devices
[AIAA PAPER 90-3005] p 788 A90-45854
- 3-D analysis of laser measurements of vortex bursting on a chined forebody fighter configuration
[AIAA PAPER 90-3020] p 793 A90-45887
- Normal-force-curve and pitching-moment-curve slopes of forebody-cylinder combinations at zero angle of attack for Mach numbers up to 5
[ESDU-89008] p 89 N90-11709
- Experimental and numerical analyses of laminar boundary-layer flow stability over an aircraft fuselage forebody
p 93 N90-12549

- Optimum shape of a blunt forebody in hypersonic flow
[NASA-CR-181955] p 171 N90-13351
- Normal force, pitching moment, and side force of forebody-cylinder combinations for angles of attack up to 90 degrees and Mach numbers up to 5
[ESDU-89014] p 173 N90-14192
- Influence of forebody geometry on aerodynamic characteristics and a design guide for defining departure/spin resistant forebody configurations
[AD-A216714] p 414 N90-18388
- Effects of nose bluntness and shock-shock interactions on blunt bodies in viscous hypersonic flows
[NASA-CR-186451] p 479 N90-20950
- Actuated forebody strakes
[NASA-CASE-LAR-13983-1] p 648 N90-23390
- Effects of forebody geometry on subsonic boundary-layer stability
[NASA-CR-4314] p 718 N90-25939
- Prediction of subsonic vortex shedding from forebodies with chines
[NASA-CR-4323] p 909 N90-28494
- The effects of foreplanes on the static and dynamic characteristics of a combat aircraft model
p 920 N90-28520
- Development of non-conventional control methods for high angle of attack flight using vortex manipulation
p 935 N90-28522

FORECASTING

- FAA (Federal Aviation Administration) aviation forecasts, fiscal years 1990-2001
[AD-A219165] p 552 N90-22530
- IFR aircraft handled forecast by air route traffic control center: Fiscal years 1990 to 2005
[AD-A220312] p 641 N90-24263
- Study of high-speed civil transports. Summary
[NASA-CR-4236] p 735 N90-25966
- Computerized corrosion forecasting model for C-5 aircraft
p 843 N90-26815

FORMAT

- A head up display format for application to V/STOL aircraft approach and landing
[NASA-TM-102216] p 340 N90-17632

FORMING TECHNIQUES

- The manufacture of SPF military aircraft doors in aluminium alloy --- superplastically formed
p 132 A90-16616
- Study on SPF and SPF/DB of the bulk-head structure with nonsymmetric shape
p 132 A90-16619
- DB/SPF cooler outlet duct for aircraft application
p 132 A90-16620
- Application investigation on superplastic forming/diffusion bonding combined technology of titanium alloy TC4
p 204 A90-18603
- Material of the '90s?
p 265 A90-20259
- Material progress
p 221 A90-21715
- Automated R.T.M. for an airframe component --- Resin Transfer Molding
p 534 A90-31881
- Designing aerospace structures with Du Pont's LDF thermoplastic composites
p 530 A90-33126

FORMULATIONS

- The acute, delayed neurotoxicity evaluation of two jet engine oil formulations
[AD-A222018] p 875 N90-26972
- An enhanced integrated aerodynamic load/dynamic optimization procedure for helicopter rotor blades
[NASA-CR-4326] p 924 N90-29383

FORTRAN

- A simulation code for turbocompound diesel engines
[IAR-89-26] p 774 N90-25348

FOULING

- Development of a computational fluid dynamics and chemistry model for the fouling of jet fuels
[DE90-005664] p 608 N90-22003
- Development of a mathematical model for the thermal decomposition of aviation fuels
[AD-A21673] p 875 N90-26994

FOURIER ANALYSIS

- Surface grid generation through elliptic PDEs
p 309 A90-26496

- Data acquisition in aerodynamic research
p 171 N90-13340
- Numerical simulations of the structure of supersonic shear layers
[AD-A224164] p 960 N90-29587

FOURIER SERIES

- Analysis of aircraft tires via semianalytic finite elements
p 496 A90-34740

FOURIER TRANSFORMATION

- Frequency domain aerodynamic analysis of interacting rotating systems
p 21 N90-10837
- Formation of design envelope criterion in terms of deterministic spectral procedure
[RAE-TM-SS-9] p 721 N90-25953

FRACTIONATION

- Thermal stability of jet fuel
[DE90-001160] p 206 N90-14385

FRACTOGRAPHY

- Reconstitution of crack growth from fractographic observations after flight simulation loading p 682 A90-40650
- Fractographic techniques for the assessment of aircraft component cracking p 954 A90-49885
- Fracture morphology of toughened bismaleimide/carbon fiber composites p 948 A90-50205
- Quantitative methods in fractography; Proceedings of the Symposium on Evaluation and Techniques in Fractography, Atlanta, GA, Nov. 10, 1988 [ASTM STP-1085] p 949 A90-50551
- Analysis and interpretation of aircraft component defects using quantitative fractography p 956 A90-50555
- Failure analysis handbook [AD-A219747] p 689 N90-23752
- Fractographic observations on fatigue crack growth in 2024-T3 sheet material under flight-simulation loading [LR-592] p 689 N90-23760
- Fractographic analysis of fatigue crack growth under two-blocks loading on 2024-T351 sheet specimens [LR-628] p 961 N90-29680
- Effects of blocks of overloads and underloads on fatigue crack growth in 2024-T351 sheet specimens: Fractographic analysis and crack closure predictions [LR-629] p 961 N90-29681
- Fractographic observations on fatigue crack growth under miniTWIST flight-simulation loading (2024-T3 material) [LR-631] p 961 N90-29684
- Fractographic analysis of fatigue failures of airframe equipment parts: Examples of a rod end housing and a rod end cap [NAL-TR-1047] p 961 N90-29686
- FRACTURE MECHANICS**
- Burner rig hot corrosion of silicon carbide and silicon nitride p 355 A90-25267
- Methodology of variable amplitude fatigue tests p 451 A90-29866
- Fracture mechanics assessment of EB-welded blisked rotors p 453 A90-31117
- MRS International Meeting on Advanced Materials, 1st, Tokyo, Japan, May 31-June 3, 1988, Proceedings. Volume 5 - Structural ceramics/Fracture mechanics p 599 A90-35926
- A fracture analysis using eight-node-isoparametric singular elements and its application in fuselage panels p 603 A90-36431
- Application of fracture mechanics to microscale phenomena in electronic assemblies p 684 A90-41334
- Estimation of fatigue crack growth in patched cracked panels p 684 A90-41335
- The influence of material quality on airframe structural durability p 676 A90-41336
- Recent advances in fatigue life analysis methods for aerospace applications p 677 A90-41338
- Fracture control via DRM-Algorithm p 694 A90-41343
- Fractographic techniques for the assessment of aircraft component cracking p 954 A90-49885
- Use of unbalanced laminates as a screening method for microcracking p 948 A90-50217
- Influence of microstructure and microdamage processes on fracture at high loading rates [AD-A210307] p 65 N90-10253
- Stress intensity factors for cracking metal structures under rapid thermal loading. Volume 2: Theoretical background [AD-A213297] p 213 N90-13812
- Application of fracture mechanics and half-cycle method to the prediction of fatigue life of B-52 aircraft pylon components [NASA-TM-88277] p 214 N90-13820
- AGARD/SMP Review: Damage Tolerance for Engine Structures. 2: Defects and Quantitative Materials Behaviour --- conference [AGARD-R-769] p 425 N90-18396
- Review of modelling methods to take account of material structure and defects p 425 N90-18402
- A corrosion fatigue/stress corrosion testing facility at Materials Research Laboratory [MRL-TN-568] p 527 N90-21044
- NASA airframe structural integrity program [NASA-TM-102637] p 543 N90-21422
- An evaluation of the pressure proof test concept for thin sheet 2024-T3 [NASA-TM-101675] p 543 N90-21424
- NASA-UVA light aerospace alloy and structures technology program [NASA-CR-182607] p 601 N90-22651
- Failure analysis handbook [AD-A219747] p 689 N90-23752
- Retirement for cause of the F100 engine p 843 N90-26813

- Damage tolerance analysis for manned hypervelocity vehicles. Volume 2: Software user's manual [AD-A222136] p 845 N90-26826
- Component behaviour and life management: The need for common AGARD approaches and actions p 856 N90-27710
- The role of NDI in the certification of turbine engine components p 859 N90-28069
- Damage tolerance analysis for manned hypervelocity vehicles. Volume 1: Final technical report [AD-A221970] p 887 N90-28106
- FRACTURE STRENGTH**
- Tough(er) aluminum-lithium alloys p 62 A90-11575
- Highly damage tolerant carbon fiber epoxy composites for primary aircraft structural applications p 125 A90-14660
- Analysis of whisker-toughened ceramic components - A design engineer's viewpoint p 205 A90-19149
- Strength of the guide vane components of gas turbines p 266 A90-21318
- Current status of ceramic gas turbine R&D in Japan [ASME PAPER 89-GT-114] p 359 A90-23818
- A method for calculating the stiffness characteristics of large-aspect-ratio wings with anisotropic panels in accordance with strength and aileron efficiency requirements p 334 A90-24161
- The effects of toughening stresses on liquid impact induced fracture p 692 A90-41315
- Cyclic fracture toughness of VT-3-1 and VT-25 titanium alloys p 873 A90-46514
- Improved damage tolerance by controlling thermoplastic solubility in thermoset composites p 944 A90-50138
- The effect of matrix toughness in the development of improved structural adhesives p 955 A90-50183
- Ways of providing for the strength and service life of aircraft structures made of polymer composites with allowance for damage p 957 A90-50843
- Influence of microstructure and microdamage processes on fracture at high loading rates [AD-A210307] p 65 N90-10253
- Investigation on sheet material of 8090 and 2091 aluminium-lithium alloy p 267 N90-15192
- Improved toughness alloys based on titanium aluminides [AD-A218149] p 533 N90-20208
- Study of the microstructure of a titanium alloy (6246) for turbomachine compressors [ETN-90-97450] p 876 N90-27900
- Fretting fatigue strength of Ti-6Al-4V at room and elevated temperatures and ways of improving it p 952 N90-28709
- FRACTURES (MATERIALS)**
- Summary report of the Summer Conference of the DARPA-Materials Research Council [AD-A217380] p 532 N90-20143
- FRACTURING**
- Evaluation of static and fatigue properties of thin sheets of 8090-T8 aluminium-lithium alloy and observation of its fracture surfaces [NAL-TR-1039] p 953 N90-29499
- FRAGMENTATION**
- Statistics on aircraft gas turbine engine rotor failures that occurred in US commercial aviation during 1986 [DOT/FAA/CT-89/30] p 511 N90-21008
- FREE BOUNDARIES**
- Deicing of solids using radiant heating p 769 A90-43309
- FREE FLIGHT**
- Application of piezoelectric foils in experimental aerodynamics p 446 A90-28258
- Development of two multi-sensor hot-film measuring techniques for free-flight experiments p 417 A90-28291
- Project Falke - Performance of free flight tests in the supersonic, transonic, and subsonic regimes from balloons [DGLR PAPER 88-018] p 903 A90-50235
- FREE FLOW**
- Adverse pressure gradient effects on boundary layer transition in a turbulent free stream p 15 A90-12639
- Airfoils in supersonic source and sink flows p 149 A90-16844
- Experimental investigation of flowfield about a multielement airfoil p 154 A90-18137
- Compressibility effects in free shear layers [AIAA PAPER 90-0705] p 212 A90-19984
- Unsteady transonic aerodynamics of oscillating airfoils in supersonic freestream p 232 A90-23277
- Prediction of heat transfer coefficient on turbine blade profiles p 423 A90-29904
- Freestream turbulence effects on airfoil boundary-layer behavior at low Reynolds numbers p 554 A90-35768
- The effect of an oscillatory freestream-flow on a NACA-4412 profile at large relative amplitudes and low Reynolds-numbers p 560 A90-38495

- Numerical simulation of the growth of instabilities in supersonic free shear layers p 623 A90-40941
- Measurements of turbulent dual-jet interaction [AIAA PAPER 90-2105] p 624 A90-42019
- The effect of constructive and destructive interference on the downstream development of twin jets in a crossflow. II - Interference effects of angularly displaced jets [AIAA PAPER 90-2107] p 684 A90-42020
- Pressure-based real-time measurements in compressible free shear layers [AIAA PAPER 90-1980] p 703 A90-42709
- Adaptive grid embedding for the two-dimensional Euler equations [AIAA PAPER 90-3049] p 797 A90-45929
- Detachment of turbulent boundary layers with varying free-stream turbulence and lower Reynolds numbers p 802 A90-46378
- Modelling free vortex flow on planar swept wing p 810 A90-48079
- A straight attached shock wave at the profile tip at freestream Mach number greater than about 1 p 907 A90-51534
- A study of flows over highly-swept wings designed for maneuver at supersonic speeds [AD-A216837] p 399 N90-19202
- Flame extinction in compressible flow p 883 N90-26899
- FREE JETS**
- Total temperature effects on centerline Mach number characteristics of freejets p 302 A90-25290
- Fast adaptive grid method for compressible flows p 445 A90-28006
- Supersonic rectangular isothermal shrouded jets [AIAA PAPER 90-2028] p 621 A90-40599
- FREE VIBRATION**
- Application of the dynamic stiffness method to the free and forced vibrations of aircraft panels p 270 A90-20599
- The influence of selected geometrical and mass parameters on the structural dynamics of an aircraft with a variable-geometry airfoil p 346 A90-24284
- Helicopter rotor dynamics and aeroelasticity - Some key ideas and insights p 335 A90-25425
- Exact solutions to the oscillations of composite aircraft wings with warping constraint and elastic coupling p 603 A90-36271
- On total variation diminishing schemes for transonic turbulent flow computation p 479 N90-20945
- FREE WING AIRCRAFT**
- An experimental study of tip shape effects on the flutter of aft-swept, flat-plate wings [NASA-TM-4180] p 582 N90-22555
- FREEZE DRYING**
- Freeze drying for morphological control of inter-penetrating polymer networks p 948 A90-50214
- FREIGHT COSTS**
- The airship - An economical answer to air cargo [TABES PAPER 89-1203] p 238 A90-20390
- FREON**
- A Mach 6 external nozzle experiment with Argon-Freon exhaust simulation [SAE PAPER 892315] p 714 A90-45477
- FREQUENCY CONVERTERS**
- VSCF cycloconverter reliability review of the 30/40 KVA F/A-18 electrical generating system --- variable speed, constant frequency [SAE PAPER 892228] p 746 A90-45444
- FREQUENCY DISTRIBUTION**
- Wind shear and hyperbolic distributions p 280 A90-23632
- A comparison of emergency medical helicopter accident rates in the United States and the Federal Republic of Germany p 722 A90-44640
- FREQUENCY HOPPING**
- New approach for Doppler ambiguities resolution in medium pulse repetition frequency radars p 240 A90-20937
- Throughput and delay characteristics for a slow-frequency hopped aircraft-to-aircraft packet radio network [AD-A220525] p 688 N90-23609
- FREQUENCY MODULATION**
- Direct frequency modulation in interferometric systems p 68 A90-11662
- Multiple channel frequency demodulator p 69 A90-12190
- FREQUENCY RANGES**
- Equipment feasibility study: Very high frequency communication equipment (136-137 megahertz) [DOT/FAA/CT-TN89/72] p 775 N90-26210
- FREQUENCY RESPONSE**
- Advancements in frequency-domain methods for rotorcraft system identification p 56 A90-12771
- Comparison of the analytical and experimental modes of a model airplane using finite element analysis and multi-reference testing p 207 A90-16986

An explicit model-matching approach to lateral-axis autopilot design p 756 A90-45413

FREQUENCY SHIFT KEYING
A powerful range-Doppler clutter rejection strategy for navigational radars p 403 A90-30688

FREQUENCY SYNCHRONIZATION
Omega - A low-cost precision synchronizer p 727 A90-45233

FRETTING
Fretting fatigue strength of Ti-6Al-4V at room and elevated temperatures and ways of improving it p 952 N90-28709
Surface property improvement in titanium alloy gas turbine components through ion implantation p 953 N90-28713

FRICTION
Dynamic characteristics of one-dimensional gas flow with friction p 296 A90-24115
Analytical study of mistuning/friction/aerodynamics interaction in a bladed disk assembly [AD-A211139] p 55 N90-10893
Life of concentrated contacts in the mixed EHD and boundary film regimes [AD-A216673] p 454 N90-18738
Runaway rubber removal [AD-A218349] p 526 N90-20100
An overview of the joint FAA/NASA aircraft/ground runway friction program [NASA-TM-103486] p 724 N90-25957
Reliability and performance of friction measuring tires and friction equipment correlation [AD-A223694] p 939 N90-29408

FRICTION DRAG
The effect of longitudinal fins on turbulent friction drag p 297 A90-24123
Airfoil static-pressure thrust - Flight-test verification [AIAA PAPER 90-3286] p 812 A90-48873
Control and modification of turbulence p 72 N90-10377
Turbulence management: Application aspects p 72 N90-10378
A brief review of some mechanisms causing boundary layer transition at high speeds [NASA-TM-102834] p 720 N90-25945

FRICTION FACTOR
An annular gas seal analysis using empirical entrance and exit region friction factors [ASME PAPER 89-TRIB-46] p 537 A90-33555
Test results for turbulent annular seals, using smooth rotors and helically grooved stators [ASME PAPER 89-TRIB-11] p 537 A90-33556

FRICTION MEASUREMENT
Aircraft and ground vehicle friction measurements obtained under winter runway conditions [SAE PAPER 891070] p 95 A90-14367
Friction measurements under winter runway conditions p 321 A90-23924
High temperature skin friction measurement p 448 A90-28306
Direct measurements of skin friction in a scramjet combustor [AIAA PAPER 90-2342] p 626 A90-42132
Current status of Joint FAA/NASA Runway Friction Program [SAE PAPER 892340] p 760 A90-45494
Evaluation of two transport aircraft and several ground test vehicle friction measurements obtained for various runway surface types and conditions. A summary of test results from joint FAA/NASA Runway Friction Program [NASA-TP-2917] p 249 N90-15902
Skin friction measurements by laser interferometry in supersonic flows p 317 N90-17557
Reliability and performance of friction measuring tires and friction equipment correlation [AD-A223694] p 939 N90-29408

FRICTION REDUCTION
An experimental study of the combined effect of longitudinal riblets and vortex breakers on turbulent friction p 805 A90-46565

FRICTIONLESS ENVIRONMENTS
Frictionless contact of aircraft tires [SAE PAPER 892350] p 733 A90-45501

FROST DAMAGE
Definition of research needs to address airport pavement distress in cold regions [DOT/FAA/DS-89/13] p 59 N90-10896

FROUDE NUMBER
The interaction between a counter-rotating vortex pair in vertical ascent and a free surface p 151 A90-17580

FUEL COMBUSTION
Numerical modeling of the combustion kinetics of hydrocarbon fuels in an annular combustion chamber with allowance for the formation of harmful impurities p 124 A90-14582

Ultrasonic regression rate measurement in solid fuel ramjets [AIAA PAPER 90-1963] p 656 A90-40573
Hydrocarbon-fueled scramjet combustor investigation [AIAA PAPER 90-2337] p 658 A90-40622
Influence of fuel composition on flame radiation in gas turbine combustors p 659 A90-40946
Combustion of PMMA, PE, and PS in a ramjet p 764 A90-43670
Combustion process in a gas turbine combustor when using H₂, NH₃ and LPG fuels p 873 A90-46882
Revolutionary opportunities for materials and structures study [NASA-CR-179642] p 63 N90-10184
Two-dimensional analysis of two-phase reacting flow in a firing direct-injection diesel engine [NASA-TM-102069] p 194 N90-13392
High speed commercial transport fuels considerations and research needs [NASA-TM-102535] p 600 N90-21869
Performance of a supercharged direct-injection stratified-charge rotary combustion engine [NASA-TM-103105] p 748 N90-25982
Liquid fueled ramjet combustion instability: Acoustical and vortical interactions with burning sprays [AD-A222752] p 767 N90-26104
Regression and combustion characteristics of boron containing fuels for solid fuel ramjets p 858 N90-27928
Calculation of the combustion distribution in a liquid-fuel ramjet p 858 N90-27931
An investigation of solid-fuel, dual-mode combustion ramjets p 859 N90-27933
Overview on hot gas tests and molten salt corrosion experiments at the DLR p 953 N90-28714

FUEL CONSUMPTION
Gearless crank - The logical step to economic engines for high thrust p 50 A90-12616
Propeller development for the Rutan Voyager [SAE PAPER 891034] p 100 A90-14341
A circular combustor configuration with multiple injection ports for mixing enhancement p 130 A90-15389
XG40 - Rolls-Royce advanced fighter engine demonstrator p 112 A90-16002
Payoffs in growth engines p 188 A90-16823
Minimum fuel cruise by periodic optimization p 182 A90-19429
Industry turns to ceramic composites p 356 A90-27597
Takeoff characteristics of turbofan engines p 585 A90-35764
Accelerating hypersonic airplanes with ground-power p 586 A90-38186
Gearbox system design for ultra-high bypass engines [AIAA PAPER 90-2152] p 685 A90-42048
Design of aeroengines in a low-fuel price scenario p 739 A90-42653
The PW2000 - A mature engine with an eye to the future [SAE PAPER 892365] p 748 A90-45514
The turbofan of tomorrow p 850 A90-46150
Singular, periodic solutions in aircraft cruise-dash optimization [AIAA PAPER 90-3369] p 863 A90-47627
Optimal periodic cruise with singular control [AIAA PAPER 90-3490] p 833 A90-47738
Supersonic boundary-layer transition on the LaRC F-106 and the DFR F-15 aircraft. Part 1: Transition measurements and stability analysis p 94 N90-12558
Trajectory optimization and guidance for an aerospace plane [NASA-CR-185884] p 183 N90-13369
Guidance analysis of the aeroglide plane change maneuver as a turning point problem [NASA-TM-101639] p 259 N90-15110
Reducing C130E Hercules operating costs in the Royal Australian Air Force and the United States Air Force by increasing cruise speeds [AD-A215747] p 338 N90-17629
In-flight evaluations of turbine fuel extenders [DOT/FAA/CT-89/33] p 444 N90-19387
Civil air transport: A fresh look at power-by-wire and fly-by-light [NASA-TM-102574] p 542 N90-21283
An approach to on-board optimization of cruise at constant altitude [LR-581] p 578 N90-21752
Comparison of altitude test cell results p 856 N90-27715
Comparison of ground-level test cells and ground-level to altitude test cells p 857 N90-27716
General test plan p 857 N90-27721
Energy Efficient Engine acoustic supporting technology report [NASA-CR-174834] p 930 N90-28557

Energy Efficient Engine core design and performance report [NASA-CR-168069] p 930 N90-28559
Energy Efficient Engine program advanced turbofan nacelle definition study [NASA-CR-174942] p 930 N90-28560
Energy Efficient Engine integrated core/low spool design and performance report [NASA-CR-168211] p 931 N90-28561
Energy efficient engine program technology benefit/cost study, volume 2 [NASA-CR-174766-VOL-2] p 931 N90-28565
Energy Efficient Engine: Control system preliminary definition report [NASA-CR-179578] p 932 N90-28569
Energy Efficient Engine: High-pressure compressor test hardware detailed design report [NASA-CR-180850] p 932 N90-28570
Airline productivity relating on the fuel cost. (2): Fuel consumption values and fuel efficiency [NAL-TM-604-2] p 913 N90-29333

FUEL CONTROL
Design of control amplifier for FJR 710 engine p 43 A90-12017
Adaptive elective fuel control test techniques p 421 A90-28168
Flight testing of the Chandler Evans adaptive fuel control on the S-76A helicopter p 422 A90-28178
Flight tests of Adaptive Fuel Control and decoupled rotor speed control systems p 422 A90-28183
Mission effectiveness testing of an adaptive electronic fuel control on an S-76A p 422 A90-28199
Multivariable optimization scheme for tuning the controller of an electronic fuel control unit for small gas turbine engines p 745 A90-45301
Designing and tuning the digital controller of an electronic fuel control unit for small gas turbine engines [SAE PAPER 892255] p 747 A90-45457
Guidance and Control strategies for aerospace vehicles [NASA-CR-186195] p 199 N90-14243

FUEL FLOW
Study on process control of aeroengine using microcomputer p 586 A90-37239
Comparison of altitude test cell results p 856 N90-27715
Analysis of scramjet engine characteristics [NAL-TR-1041] p 933 N90-29398

FUEL FLOW REGULATORS
Multivariable optimization scheme for tuning the controller of an electronic fuel control unit for small gas turbine engines p 745 A90-45301

FUEL INJECTION
Full-scale liquid fuel ramjet combustor tests p 44 A90-12528
Experimental study on autoignition in a scramjet combustor p 46 A90-12559
A circular combustor configuration with multiple injection ports for mixing enhancement p 130 A90-15389
Selection of a suitable combustion system for a small gas turbine engine p 112 A90-16005
Air and spray patterns produced by gas turbine high-shear nozzle/swirler assemblies [AIAA PAPER 90-0465] p 192 A90-19857
Effects of pressure mismatch on slot injection in supersonic flow [AIAA PAPER 90-0092] p 227 A90-22161
A numerical study of mixing enhancement in a supersonic combustor [AIAA PAPER 90-0203] p 272 A90-22182
Influence of the continuous and dispersed phases on the symmetry of a gas turbine air-blast atomizer [ASME PAPER 89-GT-303] p 273 A90-22651
Development of a dual fuel injector for a gas turbine combustor [ASME PAPER 89-GT-25] p 340 A90-23764
Influence of fuel drop size and combustor operating conditions on pollutant emissions p 508 A90-33591
Aerodynamic breakup of liquid jets - A review [AIAA PAPER 90-1616] p 607 A90-38746
Injectant mole fraction measurements of transverse injection in constant area supersonic ducts [AIAA PAPER 90-1632] p 587 A90-38761
Transverse fuel-injection model for a scramjet propulsion system p 659 A90-40927
Military engines - Cradle of technology p 660 A90-41758
Further validation of a semi-analytical approach for fuel injectors of different concepts [AIAA PAPER 90-2190] p 686 A90-42067
An experimental investigation of the velocity field in a reverse-flow combustor p 739 A90-42657
Effect of vane twist on the performance of dome swirlers for gas turbine airblast atomizers [AIAA PAPER 90-1955] p 881 A90-47203

- Numerical simulation of unsteady combustion in a dump combustor p 54 N90-10203
- Two-dimensional analysis of two-phase reacting flow in a firing direct-injection diesel engine [NASA-TM-102069] p 194 N90-13392
- Externally vaporizing system for turbine combustor [AD-D014284] p 256 N90-15918
- Effect of vane twist on the performance of dome swirlers for gas turbine airblast atomizers [NASA-TM-103195] p 773 N90-25289
- Combustion in the gas turbine. Part 3: Fuel injection, ignition and stability [CIT/SME/VKI/RS/4] p 748 N90-25988
- Calculation of the combustion distribution in a liquid-fuel ramjet p 558 N90-27931
- FUEL OILS**
- Development of new segment carbon seal for use at low sealing pressure region FJR710/600S turbo fan engine p 69 A90-11950
- FUEL PRODUCTION**
- Manufacturing aviation gasoline p 950 A90-51617
- Production of jet fuels from coal-derived liquids. Volume 11: Production of advanced endothermic fuel blends from Great Plains Gasification Plant naphtha by-product stream [AD-A210251] p 65 N90-11184
- FUEL PUMPS**
- Classification of methods for eliminating surging in gas turbine engines p 111 A90-14591
- Lightweight fuel pump and metering component for advanced gas turbine engine control [AIAA PAPER 90-2032] p 657 A90-40602
- Compatibility of fuel system components with high density fuel [AD-A210381] p 32 N90-10027
- FUEL SPRAYS**
- Investigation and improvement of ground starting characteristics of a combustor with airblast nozzles p 45 A90-12546
- Atomization of synthetic jet fuel p 63 A90-12602
- A novel method of atomization with potential gas turbine applications p 131 A90-16003
- Atomization and spray research for gas turbine engines p 189 A90-17688
- Active soot reduction in a spray-fired, axisymmetric model gas turbine combustor [AIAA PAPER 90-0039] p 191 A90-19644
- Air and spray patterns produced by gas turbine high-shear nozzle/swirler assemblies [AIAA PAPER 90-0465] p 192 A90-19857
- Influence of the continuous and dispersed phases on the symmetry of a gas turbine air-blast atomizer [ASME PAPER 89-GT-303] p 273 A90-22651
- A study on spray characteristics down stream from a gutter-atomizer p 368 A90-26893
- A model gas turbine combustor with wall jets and optical access for turbulent mixing, fuel effects, and spray studies p 507 A90-32808
- Influence of fuel drop size and combustor operating conditions on pollutant emissions p 508 A90-33591
- Further validation of a semi-analytical approach for fuel injectors of different concepts [AIAA PAPER 90-2190] p 686 A90-42067
- Structure analysis of burning liquid-fueled spray in a confined combustor [AIAA PAPER 90-2444] p 677 A90-42174
- Introducing the VRT gas turbine combustor [AIAA PAPER 90-2452] p 743 A90-42808
- Critical evaluation of Jet-A spray combustion using propane chemical kinetics in gas turbine combustion simulated by KIVA-II p 949 A90-50645
- The stability of fuel fires p 327 N90-17601
- Introducing the VRT gas turbine combustor [NASA-TM-103176] p 688 N90-23591
- FUEL SYSTEMS**
- Criteria for general aviation fuel systems crashworthiness [SAE PAPER 891016] p 109 A90-14328
- Compatibility of fuel system components with high density fuel [AD-A210381] p 32 N90-10027
- Fuel resistant coatings for metal and composite fuel tanks p 269 N90-15911
- Externally vaporizing system for turbine combustor [AD-D014284] p 256 N90-15918
- Low-energy gamma ray attenuation characteristics of aviation fuels [NASA-TP-2974] p 462 N90-18882
- Aircraft crash survival design guide. Volume 1: Design criteria and checklists [AD-A218434] p 575 N90-22545
- Aircraft crash survival design guide. Volume 5: Aircraft postcrash survival [AD-A218438] p 575 N90-22549

FUEL TANKS

- A small inert gas generator p 180 A90-17405
- Fluorosilicone sealants for aircraft fuel containment p 529 A90-31618
- Aircraft applications of advanced composite fiber/metal pressure vessels [AIAA PAPER 90-2344] p 686 A90-42133
- CF 18 480 Gallon External Fuel Tank Stores Clearance Program p 35 N90-10877
- Fuel Tank Technology [AGARD-R-771] p 250 N90-15904
- Integral fuel tank sealing practice at British Aerospace (Kingston) p 250 N90-15905
- Integral fuel tanks - design, production, aging, repair p 250 N90-15906
- Aircraft fuel tank construction and testing experience p 250 N90-15907
- The repair of aircraft integral fuel tanks in the RAF: A user's view of fuel tank technology p 250 N90-15908
- The effect of primer age on adhesion of polysulphide sealant p 269 N90-15909
- Fuel resistant coatings for metal and composite fuel tanks p 269 N90-15911
- Spray sealing: A breakthrough in integral fuel tank sealing technology p 276 N90-15912
- Design philosophy and construction techniques for integral fuselage fuel tanks p 250 N90-15913
- Fuel tank explosion protection p 251 N90-15914
- A dynamicist's view of fuel tank skin durability p 251 N90-15915
- Integral fuel tank certification and test methods p 251 N90-15916
- Application of experimental techniques to store release problems p 316 N90-17545
- Ignitability of jet-A fuel vapors in aircraft fuel tanks p 326 N90-17594
- Inflatable fuel tank buffer [AD-D014446] p 503 N90-21002
- FUEL TESTS**
- Laboratory analysis of antiwear properties of turbine-engine fuels p 131 A90-15878
- Effect of pressure and temperature on residue formation in aviation kerosenes p 203 A90-17281
- Fuel effects on gas turbine combustor dynamics [AIAA PAPER 90-1957] p 676 A90-40570
- Operation of the Rolls-Royce Pegasus Engine on low grade non-aviation fuels [SAE PAPER 892329] p 747 A90-45486
- Modelling of fuel effects on naval aircraft operations [SAE PAPER 892331] p 765 A90-45488
- Investigations into gasoline/alcohol blends for use in general aviation aircraft p 950 A90-51623
- In-flight evaluations of turbine fuel extenders [DOT/FAA/CT-89/33] p 444 N90-19387
- Turbine fuel alternatives (near term) [AD-A219405] p 601 N90-22695
- Subsonic combustor testing p 749 N90-25997
- Comparison of ground-level test cells and ground-level to altitude test cells p 857 N90-27716
- FUEL VALVES**
- Dynamic testing of crashworthy fuel valves [SAE PAPER 891017] p 128 A90-14329
- FUEL-AIR RATIO**
- Non-iterative analytical methods for off-design turbofan calculations with or without mixed-flows p 70 A90-12628
- Fuel effects on gas turbine combustor dynamics [AIAA PAPER 90-1957] p 676 A90-40570
- Very-low-frequency oscillations in liquid-fueled ramjets p 54 N90-10204
- A planar reacting shear layer system for the study of fluid dynamics-combustion interaction [NASA-TM-102422] p 194 N90-13393
- FUELS**
- Modification and improvement of software for modeling multidimensional reacting fuel flows [AD-A217789] p 533 N90-20235
- FULL SCALE TESTS**
- STOVL wind tunnel tests demonstrate ejector viability p 245 A90-21000
- Approximation of frequency characteristics using identification with a complex mass matrix p 448 A90-29001
- Application of the 'K-gage' to aircraft structural testing p 926 A90-49891
- Characteristics of transport, aircraft fires measured by full-scale tests p 325 N90-17591
- Full scale study of a cabin fire in an A300 fuselage section p 326 N90-17592
- Full-scale air transport category fuselage burnthrough tests [DOT/FAA/CT-TN89/65] p 486 N90-20867
- FUNCTIONAL DESIGN SPECIFICATIONS**
- Designing the V-22 'Osprey' tiltrotor V/Stol aircraft for maintenance and serviceability [SAE PAPER 891075] p 101 A90-14389

- Rotorcraft analytical improvement needed to reduce developmental risk - The 1989 Alexander A. Nikolsky Lecture p 285 A90-23934
- Design priorities for an air-superiority fighter p 335 A90-26344
- Optimum aircraft design: Multipurpose approach --- Russian book p 829 A90-46618
- CTR-1000 civil tiltrotor concept p 829 A90-46939
- GTPDP - A rotary wing aircraft preliminary design and performance estimation program including optimization and cost p 830 A90-46944
- Communications Interface Driver (CID) test plan [DOT/FAA/CT-TN89/35] p 958 N90-28762
- FUSELAGES**
- Application of localized active control to reduce propeller noise transmitted through fuselage surface p 78 A90-11884
- Impact evaluation of composite floor sections [SAE PAPER 891018] p 100 A90-14330
- Finite element calculations of the interior noise of the Saab 340 aircraft [SAE PAPER 891081] p 101 A90-14373
- Thermoplastic composite fighter forward fuselage p 81 A90-14659
- Numerical simulation of separated and vortical flows on bodies at large angles of attack p 146 A90-16772
- A finite element solution for transonic flow around lifting fuselage with arbitrary cross sections from the minimum pressure integral p 156 A90-18298
- Rotor/fuselage vibration isolation studies by a Floquet-harmonic iteration technique p 182 A90-19393
- Design optimization of natural laminar flow fuselages in compressible flow [AIAA PAPER 90-0303] p 182 A90-19784
- Numerical solution of the boundary-layer equations for a general aviation fuselage [AIAA PAPER 90-0305] p 163 A90-19786
- Extending an airliner's life p 244 A90-20262
- The application of the engineering approach for analyzing crack tolerance of fuselage panels to a transport airplane p 272 A90-22014
- Navier-Stokes predictions of the flowfield around the F-18 (HARV) wing and fuselage at large incidence [AIAA PAPER 90-0099] p 227 A90-22165
- 'Flow past a wing/fuselage combination with separation from the side edges of the wing' p 295 A90-24088
- An investigation of fillets in wing-fuselage joints at subsonic velocities p 297 A90-24131
- Calculation of supersonic flow past a wing/fuselage combination with the resolution of a compression shock from the wing p 297 A90-24138
- Wing-fuselage interference regimes at supersonic flight velocities p 298 A90-24155
- The influence of the helicopter fuselage on its rotor p 301 A90-25101
- Fourth-order accurate three-dimensional compressible boundary-layer calculations p 308 A90-26136
- Calculation of flow characteristics in the core of a vortex sheet p 386 A90-28981
- A study of the strength characteristics of a twin-fuselage aircraft with a trapezoid wing system p 410 A90-28993
- Rotor/airframe aeroelastic analyses using the transfer matrix approach [AIAA PAPER 90-1119] p 392 A90-29391
- Subcomponent tests for composite fuselage technology readiness p 490 A90-33105
- Structural-acoustic analysis of aircraft fuselage structures using general purpose finite element codes p 492 A90-33385
- A fracture analysis using eight-node-isoparametric singular elements and its application in fuselage panels p 603 A90-36431
- Finite element numerical analysis for transonic flows around lifting fuselages p 558 A90-37216
- The influence of interactional aerodynamics of rotor-fuselage-interferences on the fuselage flow p 561 A90-38523
- Fuselage boundary-layer effects on sound propagation and scattering p 695 A90-39781
- Comparison with experiment of various computational methods of airflow on three helicopter fuselages p 630 A90-42436
- Experimental study of the flow around an helicopter fuselage - Comparison with three-dimensional boundary layer calculations p 630 A90-42438
- Helicopter ground and air resonance dynamics p 646 A90-42457
- A comprehensive approach to coupled rotor-fuselage dynamics p 646 A90-42460
- An unsteady helicopter rotor-fuselage aerodynamic interaction analysis p 712 A90-45323
- Boeing 737 fuselage structural integrity program [SAE PAPER 892207] p 701 A90-45426

Maintenance and economic benefits of non-painted aircraft operations
[SAE PAPER 892208] p 732 A90-45427

Bulging cracks in pressurized fuselages - A procedure for computation p 880 A90-46301

Mechanisms of active control in cylindrical fuselage structures p 862 A90-47309

A method for calculating the rotor-fuselage interference in helicopters
[DGLR PAPER 88-060] p 919 A90-50246

Development of pressure containment and damage tolerance technology for composite fuselage structures in large transport aircraft
[NASA-CR-3996] p 63 N90-10186

Measurements of pressures on the tail and aft fuselage of an airplane model during rotary motions at spin attitudes
[NASA-TP-2939] p 20 N90-10829

Transport composite fuselage technology: Impact dynamics and acoustic transmission
[NASA-CR-4035] p 126 N90-11821

Experimental and numerical analyses of laminar boundary-layer flow stability over an aircraft fuselage forebody p 93 N90-12549

Some new techniques for aircraft fuselage skin tests
[LR-547] p 184 N90-13379

An analytical method for the prediction of unsteady rotor/airframe interactions in forward flight p 186 N90-14223

Investigation on sheet material of 8090 and 2091 aluminium-lithium alloy p 267 N90-15192

Design philosophy and construction techniques for integral fuselage fuel tanks p 250 N90-15913

Full scale study of a cabin fire in an A300 fuselage section p 326 N90-17592

Forced and natural venting of aircraft cabin fires: A numerical simulation p 326 N90-17597

Fuselage design for a specified Mach-sliced area distribution
[NASA-TP-2975] p 414 N90-18385

Floor pull test of a transport airframe section
[DOT/FAA/CT-TN88/14] p 497 N90-20072

Full-scale air transport category fuselage burnthrough tests
[DOT/FAA/CT-TN89/65] p 486 N90-20967

NASA airframe structural integrity program
[NASA-TM-102637] p 543 N90-21422

An evaluation of the pressure proof test concept for thin sheet 2024-T3
[NASA-TM-101675] p 543 N90-21424

Water-tunnel study results of a TF/A-18 and F/A-18 canopy flow visualization
[NASA-TM-101705] p 573 N90-22532

Aircraft crash survival design guide. Volume 3: Aircraft structural crash resistance
[AD-A218436] p 575 N90-22547

Feasibility study for a microwave-powered ozone sniffer aircraft
[NASA-CR-186660] p 650 N90-23397

Asymptotic modal analysis and statistical energy analysis
[NASA-CR-186732] p 782 N90-26634

Correlation of AH-1G airframe flight vibration data with a coupled rotor-fuselage analysis
[NASA-CR-181974] p 959 N90-28865

FUSION (MELTING)

Repair of thermoplastic composite structures by fusion bonding p 941 A90-50060

Aircraft battle damage repair of transparencies
[AD-A224168] p 925 N90-29387

FUZZY SETS

Applications of fuzzy sets to rule-based expert system development p 216 A90-18050

A decision-making aid for multi-layer radar absorbent coverings
[ESA-TT-1173] p 773 N90-25267

FUZZY SYSTEMS

Multiobjective decision making in a fuzzy environment with applications to helicopter design p 405 A90-27993

Energy based stability analysis of a fuzzy roll controller design for a flexible aircraft wing p 668 A90-40833

G

GALERKIN METHOD

Development of finite element methods for compressible Navier-Stokes flow simulations in aerospace design
[AIAA PAPER 90-0403] p 166 A90-19833

Non-unique solutions of the Euler equations p 718 A90-45727

Application of a dynamic stall model to rotor trim and aeroelastic response p 583 N90-22556

GALLIUM ARSENIDE LASERS

Direct frequency modulation in interferometric systems p 68 A90-11662

GALLIUM PHOSPHIDES

The gas source molecular beam epitaxial growth of Al(x)Ga(1-x)P on (100) GaP p 894 A90-48657

GAME THEORY

Time-optimal aircraft pursuit-evasion with a weapon envelope constraint
[NASA-CR-186640] p 734 N90-25126

GAMMA RAY ABSORPTION

Low-energy gamma ray attenuation characteristics of aviation fuels
[NASA-TP-2974] p 462 N90-18882

GAMMA RAYS

Low-energy gamma ray attenuation characteristics of aviation fuels
[NASA-TP-2974] p 462 N90-18882

GANGLIA

Neurocontrol systems and wing-fluid interactions underlying dragonfly flight p 434 N90-19240

GAPS

A minimal permissible radial clearance in a gas turbine p 110 A90-14569

GAS ANALYSIS

Jet engine fault detection with differential gas path analysis at discrete operating points p 50 A90-12633

Device for quickly sensing the amount of O₂ in a combustion product gas
[NASA-CASE-LAR-13816-1] p 609 N90-22025

GAS ATOMIZATION

A novel method of atomization with potential gas turbine applications p 131 A90-16003

Atomization and spray research for gas turbine engines p 189 A90-17688

Air and spray patterns produced by gas turbine high-shear nozzle/swirler assemblies
[AIAA PAPER 90-0465] p 192 A90-19857

GAS BEARINGS

Foil gas bearings for turbomachinery
[SAE PAPER 901236] p 841 A90-49306

Yaw rate control of an air bearing vehicle p 435 N90-19420

GAS COOLING

Experimental studies of combustor dilution zone aerodynamics. I - Mean flowfields p 508 A90-32962

Particulate trajectories and impact characteristics in hypersonic flight involving gas coolant shielding p 476 A90-34583

GAS DENSITY

Computation of hypersonic low density flows with thermochemical nonequilibrium p 477 N90-20044

GAS DETECTORS

Gas identification system using graded temperature sensor and neural net interpretation
[AD-A213359] p 205 N90-13627

GAS DISSOCIATION

Approximations for nonequilibrium hypervelocity aerodynamics p 154 A90-17990

Transfer of the atomic ion energy of supersonic flow of a partially dissociated gas to a solid surface p 234 A90-23432

A study of flow of a vibrationally nonequilibrium dissociated gas past a blunt body p 234 A90-23435

GAS DYNAMICS

A study of three-dimensional supersonic flow of a real gas past axisymmetric bodies p 3 A90-10938

Application of three-dimensional methods for the calculation of gas dynamic and thermal processes at the design of gas turbines for air breathing engines p 46 A90-12552

The principle of jet engine thrust generation p 110 A90-14571

Numerical calculation of gaseous reacting flows in a model of gas turbine combustors p 271 A90-21979

An experimental study of the gasdynamic characteristics of annular nozzle cascades with small flow exit angles p 255 A90-23409

A study of flow of a vibrationally nonequilibrium dissociated gas past a blunt body p 234 A90-23435

Aerodynamic characteristics of thin bodies moving in a gas with shock waves p 297 A90-24140

Using third-fourth order compact schemes for calculating gas flows in nozzles with high supersonic M numbers on the basis of simplified Navier-Stokes equations p 289 A90-24157

Conditions of the generation of autooscillations in aerodynamic control surfaces in nonseparated subsonic flow of a gas p 315 A90-27303

On and off-design performance prediction of single spool turbojets using gasdynamics
[AIAA PAPER 90-2393] p 682 A90-42155

A weighted residual formulation for finite element solutions of the steady Euler equations p 770 A90-44457

Gasdynamic characteristics of a plane or axisymmetric nozzle with a rectilinear generatrix of the supersonic section p 805 A90-46575

Effect of shock waves and jets on structural elements: Mathematical modeling in nonstationary gas dynamics - Russian book p 806 A90-46621

Least-squares finite element methods for compressible Euler equations p 904 A90-51013

Varying specific heat gasdynamic function formulae simplification and analytical solution of normal shock waves p 908 A90-52776

Hypersonic nozzle/afterbody performance at low Mach numbers
[AD-A216223] p 319 N90-17575

Experimental investigation of a chemical laser cavity flowfield
[AD-A216398] p 372 N90-18038

Spectral simulation of unsteady compressible flow past a circular cylinder
[NASA-CR-182030] p 478 N90-20050

Computation of nonequilibrium chemically reacting flows in hypersonic flow field p 480 N90-20954

Prediction of two-dimensional time-dependent gasdynamic flows for hypersonic studies
[UTIAS-335] p 718 N90-25935

GAS EXPANSION

Study of the expansion of hydrocarbon-oxygen products through supersonic nozzle p 852 A90-46907

GAS FLOW

Analysis of the effect of rotor-angular-acceleration on the features of gas flow in turbomachinery p 6 A90-11780

Pressure pulsation in a cavity in the path of subsonic and supersonic gas flow p 10 A90-12279

Equilibrium of an elastic porous shell in supersonic gas flow p 150 A90-17109

Supersonic nonuniform flow of a gas past oblong axisymmetric bodies p 159 A90-19237

Comparison of thin and full viscous shock layer models in the problem of supersonic flow of a viscous gas past blunt cones p 231 A90-22396

An experimental study of separated flow past a low-aspect-ratio delta wing p 294 A90-24077

Dynamic characteristics of one-dimensional gas flow with friction p 296 A90-24115

Acoustic noise emitted from vessels in an impulse-type wind tunnel p 378 A90-24125

Ideal propeller in compressible gas flow in a wind tunnel p 298 A90-24156

Calculation of the effect of the engine nacelle on transonic flow past a wing p 387 A90-28990

Laminar separated flow on a biconical body at high supersonic velocities p 387 A90-28992

Divergence of thin-walled composite rods of closed profile in gas flow p 388 A90-29012

Calculation of the drag of fuselage tail sections of different shapes in supersonic flow of a nonviscous gas p 388 A90-29182

Flow rate and thrust coefficients for biaxial flows in a convergent nozzle p 395 A90-30344

Local convection heat transfer on a plane wall in the vicinity of strong streamwise accelerations p 535 A90-32174

An investigation of the flow characteristics of transonic nozzle blades p 475 A90-33700

A numerical method for calculating supersonic flows of a viscous gas p 476 A90-34672

Condensation in hypersonic nitrogen wind tunnels
[AIAA PAPER 90-1392] p 558 A90-37937

Application of the LAURA code for slender-vehicle aerothermodynamics
[AIAA PAPER 90-1714] p 560 A90-38416

Requirements in the 1990's for high enthalpy ground test facilities for CFD validation
[AIAA PAPER 90-1401] p 597 A90-38489

Recent advances in H₂/O₂ high pressure coaxial injector performance analysis
[AIAA PAPER 90-1959] p 762 A90-42705

Numerical predictions for the flow and the heat transfer in gas turbine cooling systems p 770 A90-44464

Effect of aerodynamic heating on deformation of composite cylindrical panels in a gas flow p 773 A90-45788

A study of gas flow in hypersonic nozzles at large Reynolds numbers using simplified Navier-Stokes equations p 803 A90-46538

Construction of wing profiles in subsonic gas flow by the method of quasi-solutions for inverse boundary value problems p 803 A90-46542

An experimental study of a supersonic gas ejector p 851 A90-46546

Supersonic flow computations over aerospace configurations using an Euler marching solver
[NASA-CR-4085] p 19 N90-10012

- Recent progress in research pertaining to estimates of gas-side heat transfer in an aircraft gas turbine
[NASA-TM-102480] p 194 N90-13394
- Prediction of two-dimensional time-dependent gasdynamic flows for hypersonic studies
[UTIAS-335] p 718 N90-25935
- Combustion in the gas turbine. Part 2: Preliminary design and performance
[CIT/SME/VKI/RS/3] p 748 N90-25987
- Numerical analysis of three-dimensional particle-laden flow equations
[IAR-90-2] p 775 N90-26268

GAS GENERATORS

- A small inert gas generator p 180 A90-17405
- Performance potential and technology issues of MHD augmented hypersonic simulation facilities
[AIAA PAPER 90-1380] p 598 A90-37929

GAS INJECTION

- Effect of the inertial nature of injection and temperature on the damping of body vibrations p 150 A90-17112
- Mean flow measurements of heated supersonic slot injection into a high Reynolds number supersonic stream
[AIAA PAPER 90-0180] p 163 A90-19722
- Effect of tangential injection on flow in a laminar boundary layer p 294 A90-24080
- Numerical calculation of the jet-interaction induced separation with respect to thrust vector control
p 584 A90-35228
- The effect of constructive and destructive interference on the downstream development of twin jets in a crossflow. I - Destructive interference of laterally spaced jets
[AIAA PAPER 90-1623] p 607 A90-38752
- Recent advances in H₂/O₂ high pressure coaxial injector performance analysis
[AIAA PAPER 90-1959] p 762 A90-42705
- Operation of a gas ejector in the pulsed regime
p 850 A90-46488
- Effect of the fluid level of a hydraulic shock absorber on the characteristics of the gas supply system
p 851 A90-46504
- Analysis of the rotor tip leakage flow with tip cooling air ejection p 515 N90-21029
- Analysis of a six-component, flow-through, strain-gage, force balance used for hypersonic wind tunnel models with scramjet exhaust flow simulation
[NASA-CR-186585] p 597 N90-21775

GAS JETS

- Aerosol effects on jet-engine IR radiation
p 40 A90-10152
- Effect of shock waves and jets on structural elements: Mathematical modeling in nonstationary gas dynamics --- Russian book p 806 A90-46621
- A review of instability and noise propagation in supersonic flows
[NASA-CR-186800] p 717 N90-25112

GAS MIXTURES

- A study of the radiation of hydrogen-xenon mixtures near models flying at high supersonic velocities
p 470 A90-32509
- Study of the expansion of hydrocarbon-oxygen products through supersonic nozzle p 852 A90-46907
- Gas identification system using graded temperature sensor and neural net interpretation
[AD-A213359] p 205 N90-13627
- Externally vaporizing system for turbine combustor [AD-D014284] p 256 N90-15918
- Concentration, temperature, and density in a hydrogen-air flame by excimer-induced Raman scattering p 875 N90-26903

GAS PRESSURE

- An annular gas seal analysis using empirical entrance and exit region friction factors
[ASME PAPER 89-TRIB-46] p 537 A90-33555
- Tests for integrating measurement of gas pressures in flight propellers
[ETN-90-96498] p 634 N90-24253

GAS STREAMS

- Production of jet fuels from coal derived liquids. Volume 10: Jet fuels production by-products, utility, and sulfur emissions control integration study
[AD-A213872] p 357 N90-16951
- Modeling of supersonic reacting flow fields
p 855 N90-26898

GAS TEMPERATURE

- The Kryo-Kanal Koeln, KKK: Description of tunnel conversion - Results of calibration tests under ambient and cryogenic conditions p 523 A90-34230
- Gas identification system using graded temperature sensor and neural net interpretation
[AD-A213359] p 205 N90-13627
- Overview on hot gas tests and molten salt corrosion experiments at the DLR p 953 N90-28714

GAS TURBINE ENGINES

- Fundamentals of turbine design for aircraft engines --- Russian book p 40 A90-10839

- Effect of protective coatings on mechanical properties of superalloys
[ONERA, TP NO. 1989-88] p 62 A90-11126
- Applications of fiber optic sensors in advanced engine controls p 68 A90-11703
- Some issues in the growth of small gas turbine aircraft propulsion engines p 44 A90-12508
- IMI 834 - A new high temperature capability titanium alloy for engine use p 62 A90-12535
- Properties and characterisation of novel thermal barrier systems for gas turbines p 62 A90-12538
- Extending the overhaul interval for gas turbine engines through the use of alternative coatings on first stage blades p 63 A90-12539
- Application of three-dimensional methods for the calculation of gas dynamic and thermal processes at the design of gas turbines for air breathing engines
p 46 A90-12552
- Turbomachinery tip gap aerodynamics - A review
p 13 A90-12557
- Aircraft engine vibration analysis p 46 A90-12568
- Temperature scaling of turbine blade heat transfer with and without shock wave passing p 47 A90-12570
- Cooling characteristics of a radial water blade
p 47 A90-12571
- Effect of primary air swirl on emissions formations in gas turbine combustors p 47 A90-12573
- On the weak extinction of gas turbine combustors
p 47 A90-12574
- Unbalance response studies on a model rotor supported on decentralised squeeze film dampers and the development experience of a jet engine
p 69 A90-12579
- The remote sensing of temperature in gas turbine engine components using epithermal neutrons
p 70 A90-12630
- Engine diagnostics - An application for expert system concepts p 50 A90-12632
- Augmented heat transfer in rectangular channels of narrow aspect ratios with rib turbulators
p 70 A90-13091
- Validation of the accelerated equivalent testing of gas turbine engines for multivariant applications
p 110 A90-14568
- A minimal permissible radial clearance in a gas turbine
p 110 A90-14569
- Estimation of the technical risk criterion in selecting the operating parameters of aircraft gas turbine engines
p 110 A90-14570
- Effect of the roughness of deposits in a compressor cascade on the flow lag angle p 84 A90-14578
- Numerical modeling of the combustion kinetics of hydrocarbon fuels in an annular combustion chamber with allowance for the formation of harmful impurities
p 124 A90-14582
- Generalized relations for estimating the efficiency and basic dimensions of screw pumps and hydraulic turbines of pump units p 111 A90-14583
- Thermodynamic calculation of the compressors of gas turbine engines and powerplants at high air pressures
p 130 A90-14585
- The tape method for the automatic partitioning of an arbitrary region when calculating temperature stresses
p 138 A90-14587
- Classification of methods for eliminating surging in gas turbine engines p 111 A90-14591
- Exhaust emission performance of a vaporizer tube combustor as compared with a single tube combustor
p 111 A90-14614
- A circular combustor configuration with multiple injection ports for mixing enhancement p 130 A90-15389
- Development of a remaining useful life of a lubricant evaluation technique. III - Cyclic voltammetric methods
p 125 A90-15732
- Laboratory analysis of antiwear properties of turbine-engine fuels p 131 A90-15878
- Applied technology in gas turbine aircraft engine development p 112 A90-16001
- A novel method of atomization with potential gas turbine applications p 131 A90-16003
- Advanced combustor liner cooling technology for gas turbines p 112 A90-16004
- Selection of a suitable combustion system for a small gas turbine engine p 112 A90-16005
- Gas turbine engine component development - An integrated approach p 112 A90-16006
- Squeeze film damping for aircraft gas turbines
p 113 A90-16009
- Integrated approach to design and manufacture of gas turbine components based on group theory
p 113 A90-16010
- Creep-fatigue interactions of gas turbine materials
p 131 A90-16011
- Dynamics of aviation gas turbine engines --- Russian book p 113 A90-16049

- Noninterference blade-vibration measurement system for gas turbine engines p 132 A90-16372
- Atomization and spray research for gas turbine engines p 189 A90-17688
- Finite element simulation of compressible turbulent flows - Validation and application to internal aerodynamic in gas-turbine engines p 210 A90-18343
- Gas turbine engine condition monitoring and fault diagnostics p 190 A90-18594
- The analysis and solution of the performance deterioration problem of WP7 engine under the full reheating condition p 191 A90-18624
- Instrumentation for combustion and flow in engines; Proceedings of the NATO Advanced Study Institute, Vimeiro, Portugal, Sept. 13-26, 1987
p 211 A90-19004

- The experiments for gas turbine plane cascade in a shock tunnel p 160 A90-19441
- Active soot reduction in a spray-fired, axisymmetric model gas turbine combustor
[AIAA PAPER 90-0039] p 191 A90-19644
- Air and spray patterns produced by gas turbine high-shear nozzle/swirler assemblies
[AIAA PAPER 90-0465] p 192 A90-19857
- Effect of the nonuniform rotation of the gas turbine rotor on blade vibrations p 253 A90-20431
- Strength of the guide vane components of gas turbines p 266 A90-21318
- Finite element analysis of nonstationary temperature fields in gas turbine components p 271 A90-21324
- Numerical calculation of gaseous reacting flows in a model of gas turbine combustors p 271 A90-21979
- Influence of the continuous and dispersed phases on the symmetry of a gas turbine air-blast atomizer
[ASME PAPER 89-GT-303] p 273 A90-22651
- Fuel molecular structure and flame temperature effects on soot formation in gas turbine combustors
[ASME PAPER 89-GT-288] p 253 A90-22652
- Simulation of compressor performance deterioration due to erosion
[ASME PAPER 89-GT-182] p 254 A90-22665
- Mathematical model of turboprop engine behaviour
p 254 A90-23351
- Optimal selection of the parameters to be measured during the identification of gas turbine engines. I - Problem statement p 255 A90-23410
- A method for the computer-aided hydraulic analysis of the turbine cooling systems of aviation gas turbine engines p 255 A90-23430
- The properties and characteristics of electroless nickel coatings applied to gas turbine engine components
[ASME PAPER 89-GT-4] p 354 A90-23751
- Development of a dual fuel injector for a gas turbine combustor
[ASME PAPER 89-GT-25] p 340 A90-23764
- Mach number effects on secondary flow development downstream of a turbine cascade
[ASME PAPER 89-GT-67] p 290 A90-23790
- An experimental study of turbine vane heat transfer with leading edge and downstream film cooling
[ASME PAPER 89-GT-69] p 358 A90-23792
- Casing vibration and gas turbine operating conditions
[ASME PAPER 89-GT-78] p 358 A90-23799
- Pressure loss and heat transfer in channels roughened on two opposed walls
[ASME PAPER 89-GT-86] p 358 A90-23805
- Experimental examination of the aerothermal performance of a gas turbine engine test facility
[ASME PAPER 89-GT-94] p 341 A90-23810
- Vibration analysis for immediate assessment of battle-damaged gas turbine engines
[ASME PAPER 89-GT-96] p 341 A90-23811
- Effect of rib-angle orientation on local mass transfer distribution in a three-pass rib-roughened channel
[ASME PAPER 89-GT-98] p 359 A90-23812
- Current status of ceramic gas turbine R&D in Japan
[ASME PAPER 89-GT-114] p 359 A90-23818
- Advanced turbine technology applications project (ATTAP) - Overview, status, and outlook
[ASME PAPER 89-GT-118] p 360 A90-23819
- Three-dimensional relief in turbomachinery blading
[ASME PAPER 89-GT-151] p 292 A90-23840
- The design and test of a two stage transonic axial flow compressor
[ASME PAPER 89-GT-164] p 341 A90-23852
- A numerical three-dimensional thermal stress analysis for cooled blades
[ASME PAPER 89-GT-168] p 341 A90-23853
- Injection molding development of ceramic turbine components
[ASME PAPER 89-GT-170] p 361 A90-23855
- A theoretical study of ingress for shrouded rotating disc systems with radial outflow --- sealing rotor-stator cavities
[ASME PAPER 89-GT-178] p 361 A90-23859

- Axial flow compressor design optimization. II - Through-flow analysis
[ASME PAPER 89-GT-202] p 342 A90-23874
- A simplified model for unstable temperature field calculation of gas turbine rotor
[ASME PAPER 89-GT-234] p 363 A90-23885
- Braze repair of MA754 aero gas turbine engine nozzles
[ASME PAPER 89-GT-235] p 342 A90-23886
- The selection and performance of thermal sprayed abradable seal coatings for gas turbine engines
[SAE PAPER 890929] p 286 A90-24694
- Low NO(x) potential of gas turbine engines
[AIAA PAPER 90-0550] p 343 A90-25036
- Reliability evaluation system for ceramic gas turbine components
p 444 A90-27678
- Fatigue life prediction method for gas turbine rotor disk alloy FV535
p 440 A90-27679
- Small gas turbine using a second-generation pulse combustor
p 421 A90-27972
- A synergistic approach to logistics planning and engine design
p 422 A90-28207
- Advanced technology's impact on compressor design and development - A perspective
[SAE SP-800] p 423 A90-28571
- The in service multi-axial-stress situation in an uncooled gas turbine blade
p 423 A90-29880
- Aerothermomechanical design of turbine-engine combustion chambers
p 424 A90-29922
- Coatings for high temperature corrosion in aero and industrial gas turbines
p 443 A90-30479
- Air Force manufacturing technology NDE programs supporting manufacturing and maintenance
p 452 A90-30779
- A very high speed switched-reluctance starter-generator for aircraft engine applications
p 452 A90-30791
- Heat transfer in gas turbine engines; Proceedings of the Symposium, ASME Winter Annual Meeting, San Francisco, CA, Dec. 10-15, 1989
p 534 A90-32166
- Local convection heat transfer on a plane wall in the vicinity of strong streamwise accelerations
p 535 A90-32174
- Cycle analysis for helicopter gas turbine engines
[ASME PAPER 89-GT-328] p 506 A90-32258
- Desktop failure analysis on a microcomputer using Weibull, lognormal, and renewal data
[ASME PAPER 89-GT-275] p 535 A90-32263
- A model gas turbine combustor with wall jets and optical access for turbulent mixing, fuel effects, and spray studies
p 507 A90-32808
- Navier-Stokes analyses of the redistribution of inlet temperature distortions in a turbine
p 471 A90-32959
- Design of an air-cooled metallic high-temperature radial turbine
p 507 A90-32960
- Endurance of aircraft gas turbine mainshaft ball bearings-analysis using improved fatigue life theory. I - Application to a long-life bearing
p 537 A90-33557
- Surface roughness measurements on gas turbine blades
[ASME PAPER 89-GT-285] p 508 A90-33559
- Dynamics of multi-spool gas turbines using the matrix transfer method - Applications
p 509 A90-33594
- Dynamics of multi-spool gas turbines using the matrix transfer method - Theory
p 509 A90-33595
- Powder metallurgy and oxide dispersion processing of superalloys
p 531 A90-34158
- Fiber reinforced superalloys
p 532 A90-34169
- Development of ceramic components for high-temperature gas turbines
p 602 A90-35951
- Control of a switched-reluctance aircraft engine starter-generator over a very wide speed range
p 586 A90-38130
- Technology update of early gas turbine designs
p 586 A90-38531
- Inlet radial temperature redistribution in a transonic turbine stage
[AIAA PAPER 90-1543] p 565 A90-38687
- The effect of constructive and destructive interference on the downstream development of twin jets in a crossflow. I - Destructive interference of laterally spaced jets
[AIAA PAPER 90-1623] p 607 A90-38752
- Combustion characteristics of a model can-type combustor
p 676 A90-40479
- Application of leaned blades to an aeroengine
p 654 A90-40503
- Partial similarity and a real-time model of twin-spool gas turbine
p 654 A90-40512
- Acoustic characteristics of a research step combustor
[AIAA PAPER 90-1851] p 655 A90-40530
- Numerical simulation of the behaviour of internal combustion supercharged engines
[AIAA PAPER 90-1873] p 655 A90-40539
- Fuel effects on gas turbine combustor dynamics
[AIAA PAPER 90-1957] p 676 A90-40570
- Glass-ceramic matrix composites for advanced gas turbines
[AIAA PAPER 90-2014] p 676 A90-40594
- Lightweight fuel pump and metering component for advanced gas turbine engine control
[AIAA PAPER 90-2032] p 657 A90-40602
- Fiber-optic turbine inlet temperature measurement system (FOTITMS)
[AIAA PAPER 90-2033] p 657 A90-40603
- Development of the jet-swirl high loading combustor
[AIAA PAPER 90-2451] p 658 A90-40633
- Rationale for determining information associated with aircraft gas turbine engines that is of historical importance
[AIAA PAPER 90-2754] p 617 A90-40648
- Laser Doppler velocimetry investigation of swirler flowfields
p 682 A90-40929
- Design and performance of a small, high speed axial compressor
[AIAA PAPER 90-1911] p 624 A90-41983
- High temperature solid lubricant requirements for advanced high performance gas turbine engines
[AIAA PAPER 90-2042] p 661 A90-41993
- High temperature powder lubricated dampers for gas turbine engines
[AIAA PAPER 90-2048] p 684 A90-41999
- Viscous flow analysis for advanced inlet particle separators
[AIAA PAPER 90-2136] p 661 A90-42038
- Evaluation of brush seals for limited-life engines
[AIAA PAPER 90-2140] p 685 A90-42040
- Gas turbine engine brush seal applications
[AIAA PAPER 90-2142] p 685 A90-42041
- The investigation of heat transfer in cooled blades of gas turbines
[AIAA PAPER 90-2144] p 685 A90-42043
- Modeling gas turbine combustor performance under transient conditions
[AIAA PAPER 90-2161] p 661 A90-42051
- The development of a probabilistic turbine rotor design system
[AIAA PAPER 90-2176] p 662 A90-42060
- Influences on the uniformity of sprays produced by gas turbine high shear nozzle/swirler assemblies
[AIAA PAPER 90-2193] p 686 A90-42068
- Direct lift STOVL engine integration
[AIAA PAPER 90-2274] p 644 A90-42103
- Initiation of spalling in aircraft gas turbine bearings
[AIAA PAPER 90-2291] p 686 A90-42110
- Numerical simulations of gas turbine combustor flows
[AIAA PAPER 90-2305] p 686 A90-42116
- Component arrangement studies for an 8000 shp turboshaft high technology core
[AIAA PAPER 90-2398] p 663 A90-42159
- An experimental investigation of turbine rotor wakes for the development of a fiber optic pressure sensor
[AIAA PAPER 90-2411] p 687 A90-42163
- Electrical analog circuit for heat transfer measurements on a flat plate simulating turbine vane heat transfer in turbulent flow
[AIAA PAPER 90-2412] p 687 A90-42164
- Development of impact design methods for ceramic gas turbine components
[AIAA PAPER 90-2413] p 687 A90-42165
- Review of mixed flow and radial turbine options
[AIAA PAPER 90-2414] p 687 A90-42166
- JFS190 turbine engine performance optimized using Taguchi methods
[AIAA PAPER 90-2419] p 663 A90-42169
- The influence of swirl on velocity, temperature and species characteristics in a can combustor
[AIAA PAPER 90-2454] p 664 A90-42177
- Mixing characteristics of dilution jets in small gas turbine combustors
[AIAA PAPER 90-2728] p 664 A90-42217
- Stall cell blockage in a high-speed multistage axial-flow compressor
[AIAA PAPER 90-1913] p 740 A90-42693
- Measurements in an annular combustor-diffuser system
[AIAA PAPER 90-2162] p 768 A90-42740
- Parametric evaluation of the aerodynamic performance of an annular combustor-diffuser system
[AIAA PAPER 90-2163] p 742 A90-42741
- Application of advanced materials to aircraft gas turbine engines
[AIAA PAPER 90-2281] p 764 A90-42769
- Unsteady analysis of hot streak migration in a turbine stage
[AIAA PAPER 90-2354] p 769 A90-42782
- Using 3D Euler flow simulations to assess effects of periodic unsteady flow through turbines
[AIAA PAPER 90-2357] p 706 A90-42783
- Introducing the VRT gas turbine combustor
[AIAA PAPER 90-2452] p 743 A90-42808
- Some technological errors in the use of capillary inspection in gas turbine engine repair
p 769 A90-43039
- Advanced developments of the Turbo-Union RB199
p 745 A90-44595
- Mathematical simulation model of an aircraft gas turbine
p 745 A90-44721
- The flow field and heat transfer near a turbulator
p 771 A90-44755
- Slip-cast hot isostatically pressed silicon nitride gas turbine components
p 765 A90-44816
- Computer aided analysis of gas turbine cycles
p 779 A90-45289
- Tooth thickness effects on the performance of gas labyrinth seals
p 771 A90-45300
- Multivariable optimization scheme for tuning the controller of an electronic fuel control unit for small gas turbine engines
p 745 A90-45301
- Application considerations for integral gas turbine electric starter/generator revisited
[SAE PAPER 892252] p 746 A90-45454
- Fast start ceramic auxiliary power unit
[SAE PAPER 892254] p 747 A90-45456
- Designing and tuning the digital controller of an electronic fuel control unit for small gas turbine engines
[SAE PAPER 892255] p 747 A90-45457
- Advanced applications of BEM to gas turbine engine structures
p 772 A90-45769
- Theoretical and experimental determination of natural frequencies of laced blading
p 878 A90-46037
- Unbalance response of a Jeffcott rotor incorporating long squeeze film dampers
p 880 A90-46237
- A method for the matching of structural and geometric parameters of the turbocompressors of small gas turbine engines in computer-aided design
p 850 A90-46491
- Optimal choice of measured parameters during the identification of gas turbine engines. II - Combined confidence regions and intervals of the identification results
p 850 A90-46493
- Design of the optimal hardening treatment for the metal surfaces of gas turbine engine components
p 873 A90-46496
- Cyclic fracture toughness of VT3-1 and VT-25 titanium alloys
p 873 A90-46514
- Interchangeability of Soviet-made and foreign mineral oils for aviation gas turbine engines
p 873 A90-46525
- Relation between flow parameters of a gas turbine engine and rotor frequencies
p 851 A90-46539
- Technical and economic efficiency of aviation gas turbine engines in service --- Russian book
p 851 A90-46624
- Jet engines performance deterioration
p 852 A90-46871
- Combustion process in a gas turbine combustor when using H₂, NH₃ and LPG fuels
p 873 A90-46882
- Computation of complex flows in gas turbine combustors with a multi-level additive correction technique
p 881 A90-46899
- The selection of convertible engines with current gas generator technology for high speed rotorcraft
p 852 A90-46933
- Effect of vane twist on the performance of dome swirlers for gas turbine airblast atomizers
[AIAA PAPER 90-1955] p 881 A90-47203
- Composite matrix cooling scheme for small gas turbine combustors
[AIAA PAPER 90-2158] p 852 A90-47210
- Combustor technology for future aircraft
[AIAA PAPER 90-2400] p 852 A90-47219
- Fault-tolerant transputer-based controller configurations for gas-turbine engines
p 852 A90-48529
- Critical evaluation of Jet-A spray combustion using propane chemical kinetics in gas turbine combustion simulated by KIVA-II
[AIAA PAPER 90-2439] p 949 A90-50645
- Performance potential of an advanced technology Mach 3 turbojet engine installed on a conceptual high-speed civil transport
[NASA-TM-4144] p 51 N90-10034
- Advanced Turbine Technology Applications Project (ATTAP)
[NASA-CR-185133] p 51 N90-10036
- Report on an overseas visit, June 1988
[AD-A210374] p 52 N90-10040
- Combustor influence on fighter engine operability
p 64 N90-10193
- The MHOST finite element program: 3-D inelastic analysis methods for hot section components. Volume 3: Systems' manual
[NASA-CR-182236] p 73 N90-10451
- Advanced technologies impact on compressor design and development: A perspective
[NASA-TM-102341] p 54 N90-10891
- Advanced technology in military gas turbine design and manufacture
[PNR90545] p 114 N90-11747

- Gas turbine performance analysis
[PNR90599] p 116 N90-12614
- The nature and control of skidding in lightly loaded
intershaft bearings
[PNR90591] p 136 N90-12933
- Constitutive modeling for isotropic materials (HOST)
[NASA-CR-179522] p 193 N90-13390
- Constitutive modeling for isotropic materials (HOST)
[NASA-CR-174718] p 193 N90-13391
- Recent progress in research pertaining to estimates of
gas-side heat transfer in an aircraft gas turbine
[NASA-TM-102460] p 194 N90-13394
- A study of variable geometry in advanced gas turbines
p 255 N90-15104
- Cycle analysis for helicopter gas turbine engines
[RAE-TM-P-1154] p 256 N90-15921
- Low NO(x) potential of gas turbine engines
[NASA-TM-102452] p 345 N90-17636
- Study of bird ingestions into small inlet area, aircraft
turbine engines (May 1987 to April 1988)
[DOT/FAA/CT-89/17] p 402 N90-18375
- AGARD/SMP Review: Damage Tolerance for Engine
Structures. 2: Defects and Quantitative Materials
Behaviour — conference
[AGARD-R-769] p 425 N90-18396
- Review of modelling methods to take account of material
structure and defects p 425 N90-18402
- The need for a common approach within AGARD —
engine component defects p 425 N90-18404
- Experimental and theoretical investigations of flowfields
and heat transfer in modern gas turbines
[AD-A217663] p 429 N90-19237
- In-flight evaluations of turbine fuel extenders
[DOT/FAA/CT-89/33] p 444 N90-19387
- Heat transfer near the entrance to a film cooling hole
in a gas turbine blade
[AD-A217396] p 510 N90-20089
- Statistics on aircraft gas turbine engine rotor failures
that occurred in US commercial aviation during 1986
[DOT/FAA/CT-89/30] p 511 N90-21008
- Fatigue crack growth investigation of a Ti-6Al-4V forging
under complex loading conditions: NATO/AGARD
supplemental engine disk program
[AD-A220239] p 678 N90-23538
- Introducing the VRT gas turbine combustor
[NASA-TM-103176] p 688 N90-23591
- Processing of advanced ceramics which have potential
for use in gas turbine aero engines
[AD-A220988] p 766 N90-25226
- Effect of vane twist on the performance of dome swirlers
for gas turbine airblast atomizers
[NASA-TM-103195] p 773 N90-25289
- Gas Turbine Combustion, volume 1
[VKI-LS-1990-02-VOL-1] p 748 N90-25985
- Combustion in the gas turbine. Part 1: Combustor types
and design
[CIT/SME/VKI/RS/1] p 748 N90-25986
- Combustion in the gas turbine. Part 2: Preliminary design
and performance
[CIT/SME/VKI/RS/3] p 748 N90-25987
- Combustion in the gas turbine. Part 3: Fuel injection,
ignition and stability
[CIT/SME/VKI/RS/4] p 748 N90-25988
- Combustor cooling aspects
[CIT/SME/VKI/RS/5] p 749 N90-25989
- Pollutants: Production and methods of reduction
[CIT/SME/VKI/RS/6] p 749 N90-25990
- Subsonic combustor flow modeling: State of the art of
CFD techniques for reacting and combustor flow
p 749 N90-25991
- Chemistry of combustion processes
p 749 N90-25994
- Gas Turbine Combustion, volume 2
[VKI-LS-1990-02-VOL-2] p 749 N90-25995
- Towards 2000: The composite engine
[PNR90646] p 750 N90-26000
- Prediction of rotating disc flow and heat transfer in gas
turbine engines
[PNR90650] p 750 N90-26001
- Aircraft exhaust emissions: An engine manufacturer's
perspective
[PNR90675] p 750 N90-26004
- The application of engineering ceramics in gas
turbines
[PNR90676] p 750 N90-26005
- Elevated temperature crack growth
[NASA-CR-182247] p 777 N90-26355
- Retirement for cause of the F100 engine
p 843 N90-26813
- Comparative evaluation of Allison T56 engine chip
detectors
[AD-A221864] p 855 N90-26832
- Cost effective technology
[PNR90664] p 883 N90-27002
- Self-lubricating surfaces by ion beam processing
[AD-A222489] p 884 N90-27118
- Experimental identification of helicopter engine
dynamics from closed loop data p 855 N90-27627
- AGARD damage tolerance concepts for engine
structures Workshop 3, Component Behaviour and Life
Management p 855 N90-27705
- Life management planning p 856 N90-27709
- Experience in developing an improved altitude test
capability p 857 N90-27719
- The role of NDI in the certification of turbine engine
components p 859 N90-28069
- Critical inspection of high performance turbine engine
components: The RFC concept p 859 N90-28073
- Analysis of the T63-A-700 engine used in alcohol turbine
fuel extender test
[DOT/FAA/CT-TN90/18] p 928 N90-28549
- Calculation of temperature distribution in various turbine
blades using a boundary-fitted coordinate transformation
method p 929 N90-28550
- Energy Efficient Engine exhaust mixer model technology
report addendum; phase 3 test program
[NASA-CR-174799] p 930 N90-28556
- Energy Efficient Engine integrated core/low spool
design and performance report
[NASA-CR-168211] p 931 N90-28561
- Energy Efficient Engine integrated core/low spool test
hardware design report
[NASA-CR-168137] p 931 N90-28566
- Energy Efficient Engine: High-pressure compressor test
hardware detailed design report
[NASA-CR-180850] p 932 N90-28570
- Source emission test of gas turbine engine test facility,
Kelly AFB, TX
[AD-A223869] p 932 N90-28571
- The effects of a compressor rebuild on gas turbine
engine performance: Final results p 952 N90-28701
- Effect of protective coatings on mechanical properties
of superalloys p 952 N90-28707
- Evaluation of high temperature protective coatings for
gas turbine engines under simulated service conditions
p 952 N90-28712
- Surface property improvement in titanium alloy gas
turbine components through ion implantation
p 953 N90-28713
- Overview on hot gas tests and molten salt corrosion
experiments at the DLR p 953 N90-28714
- Recommended practices for measurement of gas path
pressures and temperatures for performance assessment
of aircraft turbine engines and components
[AGARD-AR-245] p 933 N90-29393
- ### GAS TURBINES
- Ceramic heat exchangers in gas turbine
[ONERA, TP NO. 1989-109] p 40 A90-11142
- Optimum trailing edge ejection for cooled gas turbine
blades p 41 A90-11562
- The effect of the magnitude of the inlet-boundary
disturbance on the unsteady forces on axial gas-turbine
blades p 6 A90-11781
- Unsteady flow visualization in a vibrating annular turbine
cascade operating in the transonic flow regime
p 7 A90-11786
- Stress analysis of gas turbine bladed disc for structural
integrity applying the concept of cyclic symmetry
p 46 A90-12564
- A study of particle trajectories in a gas turbine intake
p 48 A90-12583
- A method for aerodynamic design calculation of axial
gas turbine stages with cooling air mixing
p 152 A90-17781
- An aerodynamical design and calculation method for
gas turbine with cooling air mixing p 189 A90-17782
- Velocity and scalar measurements in model and real
gas turbine combustors p 191 A90-19005
- Future test rigs p 200 A90-19012
- Gas turbine combustion - A personal perspective
p 283 A90-20604
- Study of various factors affecting secondary loss vortices
downstream a straight turbine cascade
[ASME PAPER 89-GT-12] p 287 A90-23757
- Gas turbine compressor operating environment and
material evaluation
[ASME PAPER 89-GT-42] p 340 A90-23769
- Mathematical formulation of blade surfaces in
turbomachinery. I - Theoretical surface formulations
[ASME PAPER 89-GT-160] p 360 A90-23848
- A microprocessor-based system for monitoring gas
turbines p 350 A90-24359
- Turbine combustor preliminary design approach
p 508 A90-32966
- Supercomputer applications in gas turbine flowfield
simulation p 620 A90-40495
- Influence of fuel composition on flame radiation in gas
turbine combustors p 659 A90-40946
- Bonded airfoil attachments - A path to rotor structural
efficiency
[AIAA PAPER 90-2177] p 686 A90-42061
- Life estimation of a gas turbine afterburner spraybar
p 739 A90-42662
- Numerical predictions for the flow and the heat transfer
in gas turbine cooling systems p 770 A90-44464
- Vibration analysis of faced blades p 878 A90-46186
- Calculation of the efficiency of an active
partial-admission gas turbine for counterpressures varying
over a wide range p 850 A90-46495
- A source of discrete noise components in the flow path
of gas turbines and fans p 894 A90-46506
- Effect of vane twist on the performance of dome swirlers
for gas turbine airblast atomizers
[AIAA PAPER 90-1955] p 881 A90-47203
- An experimental convective heat transfer investigation
around a film-cooled gas turbine blade
p 957 A90-51261
- Improved silicon carbide for advanced heat engines
[NASA-CR-180831] p 65 N90-10293
- Studies of gas turbine heat transfer airfoil surfaces and
end-wall cooling effects
[AD-A212451] p 117 N90-12620
- Wake interaction effects on the transition process on
turbine blades
[AD-A214492] p 343 N90-16759
- Advanced gearbox technology
[NASA-CR-179625] p 666 N90-24274
- Effect of vane twist on the performance of dome swirlers
for gas turbine airblast atomizers
[NASA-TM-103195] p 773 N90-25289
- Research and development of advanced gas turbine
[DE90-503377] p 776 N90-26335
- Comparison of ground-level test cells and ground-level
altitude test cells p 857 N90-27716
- Further studies of turbulence structure resulting from
interactions between embedded vortices and wall jets at
high blowing ratios
[AD-A223296] p 960 N90-29593
- ### GAS VALVES
- The selection of actuation devices for aircraft pneumatic
valves in systems under computer control
[SAE PAPER 891456] p 368 A90-27425
- ### GAS-GAS INTERACTIONS
- Effect of tangential injection on flow in a laminar
boundary layer p 294 A90-24080
- ### GAS-LIQUID INTERACTIONS
- Recent advances in H₂/O₂ high pressure coaxial
injector performance analysis
[AIAA PAPER 90-1959] p 762 A90-42705
- ### GAS-SOLID INTERFACES
- Comparisons of one- and two- interface methods for
tunnel wall interference calculation p 870 A90-48961
- ### GASEOUS FUELS
- Prediction of turbulent combustion flowfields behind a
backward-facing step p 529 A90-32952
- Combustion process in a gas turbine combustor when
using H₂, NH₃ and LPG fuels p 873 A90-46882
- Gas identification system using graded temperature
sensor and neural net interpretation
[AD-A213359] p 205 N90-13627
- Externally vaporizing system for turbine combustor
[AD-D014284] p 256 N90-15918
- Production of jet fuels from coal derived liquids. Volume
10: Jet fuels production by-products, utility, and sulfur
emissions control integration study
[AD-A213872] p 357 N90-16951
- Advanced fuel properties, phase 1
[AD-A219788] p 766 N90-25236
- ### GASIFICATION
- Production of jet fuels from coal-derived liquids. Volume
11: Production of advanced endothermic fuel blends from
Great Plains Gasification Plant naphtha by-product
stream
[AD-A210251] p 65 N90-11184
- ### GASOLINE (FUEL)
- Investigations into gasoline/alcohol blends for use in
general aviation aircraft p 950 A90-51623
- ### GASOLINE
- Manufacturing aviation gasoline p 950 A90-51617
- Aircraft field experience with automotive gasoline in the
United States p 912 A90-51618
- Field experience with type certificated civil aircraft
operated on motor gasolines and worldwide survey of
motor gasoline characteristics p 912 A90-51619
- Automotive gasoline - A fuel for modern aircraft piston
engines p 950 A90-51620
- Future use of automotive gasoline in light aircraft
p 951 A90-51624
- ### GAUZE
- The production of uniformly sheared streams by means
of double gauzes in wind tunnels - A mathematical
analysis p 131 A90-15887
- ### GEAR TEETH
- Development status of epicyclic gears
p 271 A90-21141
- Preliminary design and load distributions of high
performance mechanical systems p 771 A90-45281

- Gear noise, vibration, and diagnostic studies at NASA Lewis Research Center [NASA-TM-102435] p 372 N90-18041
- GEARS**
- Operating aspects of counter-rotating propfan and planetary-differential gear coupling p 50 A90-12615
- Wildhaber-Novikov circular arc gears - Some properties of relevance to their design p 70 A90-12999
- Gear steels for future helicopter transmissions p 265 A90-20607
- Efficiency testing of a helicopter transmission planetary reduction stage p 271 A90-21113
- An investigation of the behavior of the dynamic load distribution versus operating speed and torque on heavily loaded, high speed aircraft gearing p 271 A90-21129
- Damage tolerance analysis and testing of a welded cluster gear for the main transmission of the Advanced Attack Helicopter p 445 A90-28187
- Gear vibration control with viscoelastic damping material in aeroengine p 451 A90-29911
- Multiple-power-path nonplanetary main gearbox of the Mi-26 heavy-lift transport helicopter p 452 A90-30115
- Finite-element analysis of large spur and helical gear systems p 683 A90-40940
- Gearbox system design for ultra-high bypass engines [AIAA PAPER 90-2152] p 685 A90-42048
- The modular HUM system --- Health and Usage Monitoring instruments for rotary wing aircraft failure detection p 618 A90-42476
- RAN (Royal Australian Navy) vibration analysis system operator's guide [AD-A212441] p 107 N90-12596
- Assessment of worm gearing for helicopter transmissions [NASA-TM-102441] p 257 N90-15923
- Gear noise, vibration, and diagnostic studies at NASA Lewis Research Center [NASA-TM-102435] p 372 N90-18041
- Life of concentrated contacts in the mixed EHD and boundary film regimes [AD-A216673] p 454 A90-18738
- Transmission research activities at NASA Lewis Research Center [NASA-TM-103132] p 543 N90-21394
- Advanced gearbox technology [NASA-CR-179625] p 666 N90-24274
- GENERAL AVIATION AIRCRAFT**
- Criteria for general aviation fuel systems crashworthiness [SAE PAPER 891016] p 109 A90-14328
- Straight alcohol fuels for general aviation aircraft [SAE PAPER 891038] p 124 A90-14344
- Innovation in general aviation p 81 A90-14997
- The coming age of the tiltrotor, II p 413 A90-30119
- A flight test investigation of certification requirements for laminar-flow general aviation airplanes [AIAA PAPER 90-1310] p 496 A90-33920
- GE's CF34 engine for business and regional jets [AIAA PAPER 90-2041] p 661 A90-41992
- Annual General Meeting of the Canadian Aeronautics and Space Institute, 36th, Ottawa, Canada, May 15, 16, 1989, Proceedings p 701 A90-42652
- BD-10J supersonic homebuilt aircraft p 730 A90-42672
- Design and experimental investigation of a laminar horizontal tail [AIAA PAPER 90-3042] p 798 A90-45934
- CTR-1000 civil tiltrotor concept p 829 A90-46939
- Starship sails through p 842 A90-48825
- Future fuels for general aviation; Proceedings of the Symposium on Future Fuels for General Aviation Intermittent Combustion, Baltimore, MD, June 29, 1988 [ASTM STP-1048] p 950 A90-51616
- Automotive gasoline - A fuel for modern aircraft piston engines p 950 A90-51620
- Investigations into gasoline/alcohol blends for use in general aviation aircraft p 950 A90-51623
- Future use of automotive gasoline in light aircraft p 951 A90-51624
- A proposal for fuel specification activities relating to general aviation intermittent combustion engines p 951 A90-51625
- The spinning of aircraft: A discussion of spin prediction techniques including a chronological bibliography [ARL-AERO-R-177] p 36 N90-10888
- Census of US civil aircraft [PB90-120296] p 468 N90-20920
- Annual review of aircraft accident data: US general aviation calendar year 1987 p 486 N90-20966
- The Federal Aviation Administration plan for research, engineering and development, Volume 1: Program plan [AD-A221263] p 783 N90-25930
- The Federal Aviation Administration plan for research, engineering and development, Volume 2: Project descriptions p 783 N90-25931
- [AD-A221264] p 783 N90-25931
- BASEOPS default profiles for civil aircraft [AD-A223161] p 844 N90-26825
- Annual review of aircraft accident data: US general aviation, calendar year 1987 p 820 N90-27666
- [PB90-138066] p 820 N90-27666
- Public-sector aviation issues, 1987 to 1988 graduate research award papers [PB90-191206] p 820 N90-27667
- A review of research and development in crashworthiness of general aviation aircraft: Seats, restraints and floor structures [AD-A221557] p 846 N90-27698
- GENERAL DYNAMICS AIRCRAFT**
- General Dynamics F-16 p 100 A90-13791
- What can we do after we've done it all? --- total quality management and leadership philosophy in practice [AIAA PAPER 89-3209] p 549 A90-31696
- GEOCENTRIC COORDINATES**
- Database management considerations for IFR certified earth-referenced navigation systems p 577 A90-36921
- GEODETTIC SURVEYS**
- A test of kinematic GPS combined with aerial photography - Organization, logistics and results p 97 A90-13983
- ASHTech XII - A new GPS technology p 576 A90-36917
- GEOMETRIC DILUTION OF PRECISION**
- Ridge regression processing p 489 N90-20931
- GEOMETRIC THEORY OF DIFFRACTION**
- GTD/UTD: Brief history of successive development of theory and recent advances. Applications to antennas on ships and aircraft p 370 N90-17939
- The Helicopter Antenna Radiation Prediction Code (HARP) [NASA-CR-186925] p 884 N90-27946
- GEOMETRY**
- Euler and Navier-Stokes computations for airfoil geometries using unstructured meshes p 630 A90-42425
- A study of variable geometry in advanced gas turbines p 255 N90-15104
- Application of Lagrangian blending functions for grid generation around airplane geometries [NASA-CR-186318] p 237 N90-15891
- Glancing shock-boundary layer interactions p 319 N90-17571
- A user's manual for the method of moments Aircraft Modeling Code (AMC) [NASA-CR-186371] p 415 N90-18390
- A system for transonic wing design with geometric constraints based on an inverse method p 501 N90-20983
- Subsonic and transonic blade design by means of analysis codes p 510 N90-20985
- GLACIERS**
- Airfields on antarctic glacier ice [AD-A217638] p 526 N90-20097
- GLASS**
- Glass-ceramic matrix composites for advanced gas turbines [AIAA PAPER 90-2014] p 676 A90-40594
- The all glass helicopter cockpit p 653 A90-42447
- Impact testing of glass/phenolic honeycomb panels with graphite/epoxy facesheets p 946 A90-50166
- Project, implementation, and utilization of composite structures [ETN-89-95209] p 127 N90-12665
- GLASS FIBER REINFORCED PLASTICS**
- Glassy waters for Seastar --- corrosion-resistant GFRP for turboprop amphibious aircraft airframes p 382 A90-29637
- Core composites in Swissair aircraft p 493 A90-33709
- Durability and damage tolerance of S-2 glass/PEEK composites p 944 A90-50140
- Compressive viscoelastic effects (creep) of a unidirectional glass/epoxy composite material p 946 A90-50170
- Improved fiber reinforced polyphenylene sulfide thermoplastic composites p 947 A90-50180
- Pressure air tightness tests of laminated panels for wing leading edge heat shields [INFORME-I-377/89] p 357 N90-17873
- GLIDE PATHS**
- On a pitch control law for a constant glide slope through windshears p 117 A90-13784
- Optimization of glides for constant wind fields and course headings p 731 A90-44734
- ILS mathematical modeling study of the effects of proposed hangar construction at the Orlando International Airport, Runway 17R, Orlando, Florida [DOT/FAA/CT-TN89/52] p 121 N90-11762
- GLIDERS**
- Durability characteristics of the LAK-12 Letuva glider made of composite materials at the stage of certification p 102 A90-15560
- Effects of tailplane aerodynamics and fuselage flexibility on the flutter of high aspect ratio, low speed aircraft p 493 A90-33414
- Recent results of numerical flutter studies in high performance gliders [DGLR PAPER 88-038] p 934 A90-50249
- Schleicher ASK-21 glider (TG-9) stall and spin [AD-A213513] p 249 A90-15096
- Flight testing of a natural laminar flow airfoil using gliders [PD-CF-9005] p 718 N90-25936
- GLIDING**
- Effects of random initial conditions and deterministic winds on simulated parachute motion p 22 A90-11002
- Drag and propulsive efficiency of a light aircraft based on a new flight test technique [AIAA PAPER 90-0233] p 182 A90-19747
- GLOBAL POSITIONING SYSTEM**
- Eurofix p 25 A90-10239
- The small portable Global Positioning System tracking range of the future p 60 A90-12209
- NAVSTAR-GPS: An evolution or a revolution, Ecole Supérieure d'Electricité, Gif-sur-Yvette, France, Feb. 11, 1987, Workshop p 27 A90-12250
- ION, Satellite Division's International Technical Meeting, Colorado Springs, CO, Sept. 19-23, 1988, Proceedings p 123 A90-13976
- International satellite radionavigation and radiolocation - Choosing among the options p 96 A90-13979
- Kinematic and pseudo-kinematic GPS p 96 A90-13980
- A test of airborne kinematic GPS positioning for aerial photography - Methodology p 97 A90-13982
- A test of kinematic GPS combined with aerial photography - Organization, logistics and results p 97 A90-13983
- Avionic system based on global navigational satellite system p 97 A90-13984
- Autoland with GPS p 97 A90-13985
- GPS Hover Position Sensing System p 108 A90-13986
- GPS: Arrival in the fleet - A GPS AN/SRN-25 receiver assessment p 97 A90-13989
- Integration of GPS with the Carrier Aircraft Inertial Navigation System (CAINS) p 97 A90-13990
- Optimal selection of GPS sets to minimize emitter location errors p 97 A90-13992
- Influence of satellite geometry, range, clock, and altimeter errors on two-satellite GPS navigation p 123 A90-13993
- Flight demonstration of two and three satellite navigation p 98 A90-13994
- The role of adaptive antenna systems when used with GPS p 128 A90-13995
- Dynamic interaction of separate INS/GPS Kalman filters (Filter-driving - Filter dynamics) p 124 A90-13996
- Integrated navigation system design and performance with Phase III GPS user equipment p 98 A90-13997
- Architecture options for GPS/Carousel IV integration p 108 A90-13999
- Accuracy considerations for GPS TSPI system design p 98 A90-14001
- Signal processing in a digital GPS receiver p 128 A90-14006
- The accuracy of barometric altimeters with respect to geometric altitude p 108 A90-14012
- Loran-aided GPS integrity p 98 A90-14013
- GPS monitor alarm limits for nonprecision approaches p 98 A90-15315
- Potential applications of satellite navigation p 264 A90-21716
- Status and potential of GPS-receiver development p 265 A90-21717
- A GPS-based flight-control concept p 242 A90-21719
- Precision navigation using an integrated GPS-IMU system p 242 A90-21720
- Flight-path measurement p 242 A90-21721
- Differential GPS (DGPS) as an approach and landing aid p 242 A90-21722
- The disadvantages of GPS - Comparative study of solutions adapted to civil aviation p 329 A90-23994

- Integrated navigation - Employing LIRU/GPS p 329 A90-23995
- Performance study of an integrated NAVSTAR GPS/SINS navigation system p 329 A90-24003
- The US air traffic control system architecture p 330 A90-25561
- The use of satellite technology for oceanic air traffic control p 330 A90-25570
- Applicability of an augmented GPS for navigation in the National Airspace System p 331 A90-25571
- Global Positioning System: Arrival in the fleet - A GPS AN/SRN-25(V) receiver assessment p 331 A90-26338
- Prospects are very good for using satellites for aeronautical navigation p 403 A90-27924
- Integrated system of differential Global Positioning System and inertial measurement unit - A position determination system for automatic landing [AIAA PAPER 90-1300] p 487 A90-33914
- Automatic landing with GPS - Design of the flight guidance and flight control system [AIAA PAPER 90-1301] p 487 A90-33915
- The case for both RAIM and GIC working together - The ultimate solution to the GPS integrity problem p 576 A90-36916
- ASHTech XII - A new GPS technology p 576 A90-36917
- Prototype testing of an integrated Doppler/GPS navigation system p 577 A90-36926
- Omega-GPS interoperability for the long haul p 577 A90-36927
- Low cost QUBIK IMU for integration with GPS, Omega, Loran-C, and SDI systems p 577 A90-36929
- UK reference station for Navstar GPS p 725 A90-43661
- Range Applications Joint Program Office GPS Range System data link p 725 A90-43686
- Embedded GPS - The Canadian Marconi approach p 725 A90-43700
- Rockwell International's miniature high performance GPS receiver p 726 A90-43701
- USCG HH-65A/SRR GPS integration and test results p 726 A90-43705
- Ada real-time GPS/INS simulation approach to system development p 751 A90-43706
- Reduced order INS/GPS guided unmanned air vehicle study p 726 A90-43707
- A flight test comparison of two GPS/INS integration approaches p 726 A90-43708
- F-16/GPS integration test results p 726 A90-43710
- A robust RAIM scheme using GPS/GLONASS systems p 726 A90-43713
- RAIM - An implementation study p 726 A90-43714
- Integration of the LTN-72 INS with the DOD GPS 3A set p 728 A90-45236
- GPSNOTAM - A demonstration system for GPS status notification p 728 A90-45238
- Radio Technical Commission for Aeronautics, Annual Assembly and Technical Symposium, Washington, DC, Dec. 4-6, 1989, Proceedings p 821 A90-46390
- Development of common GPS and GLONASS avionics standards p 821 A90-46391
- An international civil integrity complement to GPS and GLONASS p 821 A90-46392
- A multi-sensor approach to assuring GPS integrity p 821 A90-46396
- Advanced architecture for domestic and global aviation systems p 822 A90-46398
- The use of onboard sensor data in aerial triangulation - GPS, pressure sensors, laser telemetry p 822 A90-47901
- An integrated GPS/GLONASS receiver p 822 A90-47909
- 1990-1995, a period of international decision making for the navigation community - Is our planning as good as it should be? p 823 A90-49490
- An analysis of GPS receiver performance capabilities and trends p 823 A90-49491
- Loran-C/GPS Interoperable Computerized Algorithms (LOGICAL) p 823 A90-49494
- Towards a quantitative assessment of benefits which INS/GPS integration can offer to civil aviation operating in a non-jamming environment p 823 A90-49496
- Phase III GPS Manpack receiver operation and navigation performance p 823 A90-49497
- Certification impact of introducing G.P.S. into commercial transport navigation systems p 824 A90-49501
- Military navigation - The fourth generation p 914 A90-50775
- A supplement to GPS/Navstar for civil use p 915 A90-52613
- Inspection of instrument landing systems p 915 A90-52614
- Integration and automation of navigation functions using Kalman filters p 915 A90-52615
- Guidance simulation and test support for differential GPS flight experiment [NASA-CR-177471] p 28 N90-10021
- Test network Delta [ETN-90-96009] p 177 N90-13365
- Geodetic network adjustment using GPS triple difference observations and a priori stochastic information [TR-1-1987] p 178 N90-13367
- Processing of undifferenced GPS carrier beat phase measurements and adjustment computations [TR-5-1988] p 178 N90-13368
- Advances in techniques and technologies for air vehicle navigation and guidance [AGARD-AR-276] p 243 N90-15899
- Advances in Techniques and Technologies for Air Vehicle Navigation and Guidance [AGARD-CP-455] p 332 N90-16731
- Integrated flight guidance system using differential-GPS for landing approach guidance p 332 N90-16735
- Modeling the effects of the use of GPS (Global Positioning System) derived altitude indication in the C-17A airdrop system [AD-A215366] p 333 N90-16748
- The Fourteenth Biennial Guidance Test Symposium, volume 1 [AD-A216925] p 405 N90-18383
- Interoperability issues in the use of satellite-based navigation systems for civil aviation purposes [AD-A217279] p 405 N90-19223
- Ridge regression processing p 489 N90-20931
- Optimization of the effective GPS data rate p 489 N90-20932
- Sole means navigation and integrity through hybrid Loran-C and NAVSTAR GPS p 489 N90-20933
- Autonomous integrated GPS/INS navigation experiment for OMV. Phase 1: Feasibility study [NASA-CR-4267] p 489 N90-20969
- Continued development and analysis of a new extended Kalman filter for the Completely Integrated Reference Instrumentation System (CIRIS) [AD-A220106] p 654 N90-23400
- FAA Loran early implementation project [AD-A221866] p 824 N90-26805
- Analysis, Design and Synthesis Methods for Guidance and Control Systems [AGARD-AG-314] p 916 N90-29338
- GPS integrity requirements for use by civil aviation p 916 N90-29339
- An analysis of GPS as the sole means navigation system in US Navy aircraft p 917 N90-29350
- Independent ground monitor coverage of Global Positioning System (GPS) satellites for use by civil aviation p 918 N90-29364
- Fault Detection and Isolation (FDI) techniques for guidance and control systems p 918 N90-29366
- GOAL THEORY**
- Structure/control design synthesis of active flutter suppression system by goal programming [AIAA PAPER 90-3325] p 872 A90-47587
- GOALS**
- Langley aerospace test highlights, 1989 [NASA-TM-102631] p 699 N90-24221
- GOERTLER INSTABILITY**
- Goertler vortices in supersonic and hypersonic boundary layers p 83 A90-14091
- On the Goertler vortex instability mechanism at hypersonic speeds p 158 A90-18886
- Goertler instability on an airfoil: Comparison of marching solution with experimental observations p 19 N90-10364
- Goertler instability on an airfoil p 91 N90-12517
- Experimental studies on Goertler vortices p 91 N90-12529
- GOGGLES**
- Dual servo optical projection system (SOPS) - A solution for two crewmember and night vision goggle display needs [SAE PAPER 892353] p 760 A90-45504
- GONIOMETERS**
- Generation of motion control for direction finders in a goniometer system p 187 A90-17137
- GOVERNMENT PROCUREMENT**
- Eurofighter fights back p 221 A90-21714
- Practical aspects of European collaboration --- procurement in helicopter industry p 785 A90-46928
- Aircraft modifications cost analysis. Volume 1: Overview of the study [AD-A220764] p 702 N90-25074
- GOVERNMENT/INDUSTRY RELATIONS**
- Eurofighter fights back p 221 A90-21714
- V-22 - The prospects now --- production costs of Bell Boeing tilt-rotor aircraft p 497 A90-34900
- GOVERNMENTS**
- The influence of adjacent seating configurations on egress through a type 3 emergency exit [AD-A218393] p 636 N90-23371
- GRADIENTS**
- A decision-making aid for multi-layer radar absorbent coverings [ESA-TT-1173] p 773 N90-25267
- GRAIN BOUNDARIES**
- Recrystallization behavior of nickel-base single crystal superalloys p 440 A90-27681
- GRAIN SIZE**
- Fatigue crack initiation mechanics of metal aircraft structures [AD-A210567] p 65 N90-10255
- GRAPHIC ARTS**
- Post crash flight analysis: Visualizing flight recorder data [AD-A212063] p 96 N90-11715
- GRAPHITE**
- PMR graphite engine duct development [NASA-CR-182228] p 51 N90-10037
- GRAPHITE-EPOXY COMPOSITES**
- Scaling effects in the impact response of graphite-epoxy composite beams [SAE PAPER 891014] p 128 A90-14326
- Highly damage tolerant carbon fiber epoxy composites for primary aircraft structural applications p 125 A90-14660
- Design and evaluation of graphite/epoxy truss core sandwich panels p 210 A90-18406
- Crashworthiness of composite floor sections p 243 A90-20261
- Microstructural effects of plastic media blasting on graphite epoxy composites [SAE PAPER 890928] p 286 A90-24693
- Carbon/epoxy tooling evaluation and usage p 445 A90-28165
- Nonlinear stall flutter and divergence analysis of cantilevered graphite/epoxy wings [AIAA PAPER 90-0983] p 450 A90-29373
- Strength substantiation of the all composite airframe (A materials data base approach) p 490 A90-31519
- Adhesive-bonded composite-patching repair of cracked aircraft structure p 467 A90-31576
- Design and fabrication considerations for composite structures with embedded fiber optic sensors p 536 A90-32871
- The analysis and testing of composite panels subject to muzzle blast effects p 675 A90-35991
- Certification testing methodology for fighter hybrid structure p 642 A90-40128
- Impact damage and residual strength analysis of composite panels with bonded stiffeners --- for primary aircraft structures p 642 A90-40130
- Redesign of an electro-optical shroud in graphite/epoxy p 676 A90-40215
- Design and certification of the all-composite airframe [SAE PAPER 892210] p 732 A90-45429
- Comparison of four lightning simulation tests on a composite test bed aircraft p 818 A90-49831
- The behavior of electric currents in graphite/epoxy structures p 883 A90-49846
- Durability and damage tolerance of graphite/epoxy honeycomb structures p 942 A90-50085
- Vapor grown carbon fiber for space thermal management systems p 943 A90-50128
- Advanced joint of 3-D composite materials for space structure p 944 A90-50137
- Damage tolerance evaluation of several elevated temperature graphite composite materials p 945 A90-50155
- Plastic media blast (PMB) paint removal from composites p 945 A90-50162
- Impact testing of glass/phenolic honeycomb panels with graphite/epoxy facesheets p 946 A90-50166
- Evaluation of the thermoplastic film interleaf concept for improved damage tolerance p 946 A90-50179
- Moisture absorption in graphite/epoxy laminates p 951 A90-52799
- A study of the structural efficiency of fluted core graphite-epoxy panels [NASA-TM-101681] p 373 N90-18070
- Boeing/NASA composite components flight service evaluation [NASA-CR-181898] p 601 N90-22609
- GRAPHS (CHARTS)**
- Airfoil design and data --- Book p 809 A90-47608
- GRAVITY WAVES**
- The interaction between a counter-rotating vortex pair in vertical ascent and a free surface p 151 A90-17580
- GRAZING FLOW**
- Parametric studies of acoustic duct attenuation perforated-plate-on-honeycomb absorber [NAL-TM-603] p 966 N90-30030
- GRID GENERATION (MATHEMATICS)**
- Grid generation and adaptation for the direct simulation Monte Carlo method p 67 A90-11102

SUBJECT INDEX

A class of implicit upwind schemes for Euler simulations with unstructured meshes p 5 A90-11597

Euler solutions with a multi-block structured code p 86 A90-15739

Full-potential calculations using Cartesian grids p 86 A90-15740

Solving compressible flow problems using adaptive finite quadtree and octree grids p 155 A90-18243

Grid generation with the 1988 EAGLE code p 156 A90-18310

Applications of Lagrangian blending functions for grid generation around airplane geometries [AIAA PAPER 90-0009] p 216 A90-19630

Three-dimensional solution-adaptive grid generation on composite configurations [AIAA PAPER 90-0329] p 164 A90-19799

Static aeroelastic analysis of fighter aircraft using a three-dimensional Navier-Stokes algorithm [AIAA PAPER 90-0435] p 166 A90-19845

Applications of an adaptive unstructured solution algorithm to the analysis of high speed flows [AIAA PAPER 90-0395] p 229 A90-22213

An embedded grid formulation applied to a delta wing [AIAA PAPER 90-0429] p 229 A90-22216

Finite element mesh refinement criteria for stress analysis p 273 A90-23013

A three-dimensional space marching algorithm for the solution of the Euler equations on unstructured grids [AIAA PAPER 90-0014] p 234 A90-23701

Application of a lower-upper implicit scheme and an interactive grid generation for turbomachinery flow field simulations [ASME PAPER 89-GT-20] p 288 A90-23762

Three-dimensional adaptive grid generation on a composite-block grid p 374 A90-25289

Comparisons among grid generation using elliptic partial differential equations p 374 A90-25478

Application of a digital control theory for generating adaptive grids p 366 A90-25734

An automatic Euler solver using unstructured upwind method p 367 A90-25811

Numerical simulation of wing in ground effect p 307 A90-25863

Automatic mesh generation for complex three-dimensional regions using a constrained Delaunay triangulation p 375 A90-26022

Application of multiple grids topology to supersonic internal/external flow interactions p 308 A90-26135

Numerical grid generation in computational fluid mechanics '88; Proceedings of the Second International Conference, Miami Beach, FL, Dec. 5-8, 1988 p 376 A90-26476

Knowledge-based flow field zoning p 308 A90-26478

Algebraic boundary-conforming grid generation around wing/tail-body configurations p 308 A90-26480

Quasi-three-dimensional grid generation by an algebraic homotopy procedure p 376 A90-26481

Surface grid generation for complex three-dimensional geometries p 376 A90-26484

Hyperbolic grid generation techniques for blunt body configurations p 376 A90-26490

Effect of the grid system on the solution of Euler equations p 309 A90-26494

Surface grid generation through elliptic PDEs p 309 A90-26496

A semi-analytical procedure for the conformal mapping of arbitrary airfoil contours p 309 A90-26498

The construction of component-adaptive grids for aerodynamic geometries p 309 A90-26513

Techniques in multiblock domain decomposition and surface grid generation p 309 A90-26526

Application of a multiblock grid generation approach to aircraft configurations p 310 A90-26527

Interactive multi-block grid generation p 310 A90-26528

Adaptive mesh generation for viscous flows using Delaunay triangulation p 310 A90-26531

The generation of unstructured triangular meshes using Delaunay triangulation --- applications to hypersonic inlets p 310 A90-26533

2-D and 3-D unstructured mesh adaption relying on physical analogy p 310 A90-26534

Generation of tetrahedral meshes around complete aircraft p 310 A90-26536

Interactive generation of unstructured grids for three dimensional problems p 310 A90-26537

On the combination of structured-unstructured meshes p 311 A90-26540

Application of a three-dimensional finite element grid generation scheme for an F-16 aircraft configuration p 336 A90-26541

Application of I-DEAS grid generator for three-dimensional transonic flow analysis p 311 A90-26542

Grid generation for an aft-fuselage-mounted nacelle/pylon configuration p 311 A90-26543

Zonal grid generation for fighter aircraft p 311 A90-26544

Geometric modelling of complex aerodynamic surfaces and three-dimensional grid generation p 311 A90-26545

Interactive grid generation for fighter aircraft geometries p 311 A90-26546

Multiple-block grid adaption for an airplane geometry p 311 A90-26547

Grid generation and its application to separated flows p 312 A90-26552

Interactive grid generation for turbomachinery flow field simulations p 312 A90-26553

C-grid generation for turbomachinery cascades p 312 A90-26554

Numerical interactive grid generation for 3D-flow calculations p 312 A90-26556

Computational fluid dynamics - Current capabilities and directions for the future p 540 A90-34385

Solution of Euler equations for fighter forebody-inlet combination at high angle of attack p 556 A90-36419

Unsteady Navier-Stokes solutions for a low aspect ratio delta wing [AIAA PAPER 90-1538] p 564 A90-36862

A grid generation method for an aft-fuselage mounted capped-nacelle/pylon configuration with an actuator disk [AIAA PAPER 90-1564] p 565 A90-36703

Two and three dimensional grid generation by an algebraic homotopy procedure [AIAA PAPER 90-1603] p 567 A90-36734

An algebraic adaptive-grid technique for the solution of Navier-Stokes equations [AIAA PAPER 90-1605] p 567 A90-36736

VisualGrid - A software package for interactive grid generation [AIAA PAPER 90-1607] p 612 A90-36738

Three-dimensional flux-split Euler schemes involving unstructured dynamic meshes [AIAA PAPER 90-1649] p 569 A90-36777

Temporal-adaptive Euler/Navier-Stokes algorithm for unsteady aerodynamic analysis of airfoils using unstructured dynamic meshes [AIAA PAPER 90-1650] p 569 A90-36778

An introduction to chaos theory in CFD [AIAA PAPER 90-1440] p 680 A90-39725

Investigation of unsteady flow through transonic turbine stage. I - Analysis [AIAA PAPER 90-2408] p 626 A90-42161

A computational investigation of flow losses in a supersonic combustor [AIAA PAPER 90-2093] p 742 A90-42728

Flow establishment in a generic scramjet combustor [AIAA PAPER 90-2096] p 742 A90-42729

Computation of turbine flowfields with a Navier-Stokes code [AIAA PAPER 90-2122] p 704 A90-42731

Turbulent flow simulation of a three-dimensional turbine cascade [AIAA PAPER 90-2124] p 704 A90-42732

Solution of the Euler equations using unstructured polygonal meshes p 708 A90-44435

Compressible flow algorithms on structured/unstructured grids p 779 A90-44855

An unstructured-mesh Euler method for multielement airfoil geometries [AIAA PAPER 90-3051] p 797 A90-45930

Analysis of three-dimensional turbomachinery flows on C-type grids using an implicit Euler solver [ASME PAPER 89-GT-85] p 905 A90-51258

Computation of transonic flow about stores [AD-A210402] p 18 N90-10009

Grid generation procedure using the integral equation method [NAL-TR-1009] p 77 N90-10630

Transonic Euler solutions on mutually interfering finned bodies [AD-A213395] p 170 N90-13331

User's guide to PMESH: A grid-generation program for single-rotation and counterrotation advanced turboprops [NASA-CR-185156] p 217 N90-14783

Application of Lagrangian blending functions for grid generation around airplane geometries [NASA-CR-186318] p 237 N90-15891

Mesh generation for flow computation in turbomachine p 588 N90-21981

Grid patching approaches for complex three-dimensional configurations p 573 N90-21985

Multiblock topology specification and grid generation for complete aircraft configurations p 582 N90-21986

A discussion on issues relating to multiblock grid generation p 608 N90-21991

Automatic grid generation in complex three-dimensional configurations using a frontal system p 608 N90-21992

GROUND EFFECT (AERODYNAMICS)

Unstructured finite element mesh generation and adaptive procedures for CFD p 608 N90-21993

Supersonic flow computations for an ASTOVL aircraft configuration, phase 2, part 2. [NASA-CR-4284] p 610 N90-22746

GROUND BASED CONTROL

The trend in navids inspection is to automatic operation p 329 A90-25495

Aircraft interface with the future ATC system p 331 A90-25574

Expert system technology applied to the automatic control of multiple unmanned aerial vehicles [AIAA PAPER 90-3280] p 892 A90-48867

IFR aircraft handled forecast by air route traffic control center: Fiscal years 1990 to 2005 [AD-A220312] p 641 N90-24263

GROUND EFFECT (AERODYNAMICS)

An experiment study of rotor aerodynamic in ground effect at low speed p 149 A90-16826

Numerical simulation of wings in steady and unsteady ground effects p 153 A90-17866

Comment on 'Drag reduction factor due to ground effect' p 159 A90-19396

Effect of ground on wake roll-up behind a lifting surface p 160 A90-19436

Turbulence modeling for impinging jets [AIAA PAPER 90-0022] p 211 A90-19639

Numerical investigation of airfoil/jet/fuselage-undersurface flowfields in ground effect [AIAA PAPER 90-0597] p 168 A90-19939

Determination of the ground effect on the characteristics of the A320 aircraft [ONERA, TP NO. 1989-188] p 245 A90-21048

Simulation and analysis of a delta planform with multiple jets in ground effect [AIAA PAPER 90-0299] p 228 A90-22195

Engine inlet distortion in a 9.2 percent scaled vectored thrust STOVL model in ground effect [AIAA PAPER 89-2910] p 301 A90-25043

Numerical simulation of wing in ground effect p 307 A90-25863

Prediction and measurement of low-frequency harmonic noise of a hovering model helicopter rotor p 463 A90-28159

Tip vortex geometry of a hovering helicopter rotor in ground effect p 407 A90-28196

Wind-tunnel investigation of wing-in-ground effects p 395 A90-31276

Takeoff characteristics of turbofan engines p 585 A90-35764

Results of wind tunnel ground effect measurements on Airbus A320 using turbine power simulation and moving tunnel floor techniques [AIAA PAPER 90-1427] p 559 A90-37964

A computational study of the impingement region of an unsteady subsonic jet [AIAA PAPER 90-1657] p 570 A90-38784

Influence of ground effect on helicopter takeoff and landing performance p 645 A90-42278

Influence of ground effect on helicopter takeoff and landing performance p 646 A90-42468

Hot gas environment around STOVL aircraft in ground proximity. I - Experimental study [AIAA PAPER 90-2269] p 742 A90-42765

Hot gas environment around STOVL aircraft in ground proximity. II - Numerical study [AIAA PAPER 90-2270] p 743 A90-42766

Three-dimensional turbulent flow code calculations of hot gas ingestion p 745 A90-44726

Low-speed aerodynamic characteristics of a powered NASP-like configuration in ground effect [SAE PAPER 892312] p 714 A90-45474

Computational and experimental studies on ground effect of a slender wing tailless delta aircraft p 810 A90-48083

An in-flight investigation of ground effect on a forward-swept wing airplane [NASA-TM-101708] p 175 N90-14202

Engine inlet distortion in a 9.2 percent scale vectored thrust STOVL model in ground effect [NASA-TM-102358] p 318 N90-17561

Calculation and optimization of rotor start process [ETN-90-95894] p 416 N90-19229

Prediction of forces and moments for flight vehicle control effectors. Part 2: An analysis of delta wing aerodynamic control effectiveness in ground effect [NASA-CR-186572] p 571 N90-21735

Dynamic ground-effect measurements on the F-15 STOL and Maneuver Technology Demonstrator (S/MTD) configuration [NASA-TP-3000] p 573 N90-22531

Aerodynamic performance of a 0.27-scale model of an AH-64 helicopter with baseline and alternate rotor blade sets [NASA-TM-4201] p 632 N90-24237

The Langley 14- by 22-foot subsonic tunnel: Description, flow characteristics, and guide for users
[NASA-TP-3008] p 816 N90-27649

A two dimensional study of rotor/airfoil interaction in hover
[NASA-CR-183272] p 845 N90-27694

Aerodynamics of Combat Aircraft Controls and of Ground Effects
[AGARD-CP-465] p 920 N90-28513

Aerodynamic interferences of in-flight thrust reversers in ground effect
p 921 N90-28529

Study of the ground effects in the CEAT aerohydrodynamic tunnel: Using the results
p 922 N90-28530

Dynamic ground effects
p 922 N90-28531

Study of ground effects on flying scaled models
p 922 N90-28532

An in-flight investigation of ground effect on a forward-swept wing airplane
p 922 N90-28533

Determination of the ground effect on the characteristics of the A320 aircraft
p 922 N90-28534

GROUND EFFECT MACHINES

Numerical simulation of wing in ground effect
p 307 A90-25863

Simulation evaluation of transition and hover flying qualities of a mixed-flow, remote-lift STOVL aircraft
[SAE PAPER 892284] p 757 A90-45464

GROUND HANDLING

Aircraft and ground vehicle friction measurements obtained under winter runway conditions
[SAE PAPER 891070] p 95 A90-14367

An overview of the joint FAA/NASA aircraft/ground runway friction program
[NASA-TM-103486] p 724 N90-25957

GROUND OPERATIONAL SUPPORT SYSTEM

Harrier Information Management System (HIMS): The system and the approach
p 884 N90-27630

GROUND RESONANCE

Helicopter ground/air resonance including rotor shaft flexibility and control coupling
p 406 A90-28153

A study on mechanical model of the helicopter 'ground resonance'
p 580 A90-36423

Experimental study of the effects of nonlinearities on ground resonance
p 643 A90-40172

Helicopter ground and air resonance dynamics
p 646 A90-42457

GROUND SPEED

Evaluation of critical speeds in high speed aircraft tires
[SAE PAPER 892349] p 733 A90-45500

GROUND STATIONS

A bearing error in the VHF omnirange due to sea surface reflection
p 402 A90-27875

Telemetry systems of the future
p 458 A90-28829

Development of high angle of attack flying qualities criteria using ground-based manned simulators
p 433 A90-30717

Research in a high-fidelity acceleration environment
p 439 A90-30734

Test network Delft
[ETN-90-96009] p 177 N90-13365

Bringing aircraft noise testing down to Earth
[PNR90642] p 783 N90-26637

New features of JAL's ground station
p 872 N90-27633

Independent ground monitor coverage of Global Positioning System (GPS) satellites for use by civil aviation
p 918 N90-29364

GROUND SUPPORT EQUIPMENT

Ground aviation equipment: Handbook --- in Russian
p 593 A90-36153

Design of a final approach spacing tool for TRACON air traffic control
[NASA-TM-102229] p 24 N90-10841

Replay and transmission of AIMS-data to mainframe computer using remote transcribers
p 892 N90-27634

Four-dimensional planner: A ground based planning system for time accurate approach guidance
p 826 N90-27683

GROUND SUPPORT SYSTEMS

The small portable Global Positioning System tracking range of the future
p 60 A90-12209

Robotics for flightline servicing
p 383 A90-30760

The Canadian Airspace Systems Plan - Maintaining the safety and efficiency of the air navigation system
p 725 A90-42655

Efforts continue to increase airport/airspace capacity
p 722 A90-44550

GROUND TESTS

Water ingestion simulation - Test needs
p 23 A90-12620

A full scale, VSTOL, ground environment test facility
p 58 A90-12631

Ground vibration test results of a JetStar airplane using impulsive sine excitation
p 179 A90-16963

MAVIS flight load simulation --- Multi Axis Vibration System
p 202 A90-17003

Results of aerodynamic testing of large-scale wing sections in a simulated natural rain environment
[AIAA PAPER 90-0486] p 167 A90-19874

The effect of experimental uncertainties on icing test results
[AIAA PAPER 90-0665] p 322 A90-26977

The Pointer - Test and evaluation of the tiltrotor UAV --- unmanned aerial vehicle
p 406 A90-28170

Initial results from the joint NASA-Lewis/U.S. Army icing flight research tests
p 400 A90-28180

Application of time domain decomposition techniques to aircraft ground and flutter test data
p 491 A90-33373

Ground testing techniques in support of flight test.
[AIAA PAPER 90-1309] p 523 A90-33919

Requirements in the 1990's for high enthalpy ground test facilities for CFD validation
[AIAA PAPER 90-1401] p 597 A90-38489

CFD applications in an aerospace engine test facility
[AIAA PAPER 90-2003] p 681 A90-40590

Developmental tests on the M 88 engine are on track
p 660 A90-41761

EH101 development progress
p 646 A90-42442

Captive carry testing of remotely piloted vehicles
p 828 A90-46386

Developments in ground vibration test and data analysis techniques for airframe structures
p 832 A90-46970

The AVRO VZ-9 experimental aircraft - Lessons learned
[AIAA PAPER 90-3237] p 835 A90-48847

Full scale technology demonstration of a modern counterrotating unducted fan engine concept. Engine test
[NASA-CR-180869] p 53 N90-10049

Acoustic-thermal environment for USB flap structure. Report 1: Ground simulation test results
[NAL-TM-567] p 88 N90-11697

Helicopter rotor test rig (RoTeSt) in DNW: Application and results
[RAE-TRANS-2171] p 201 N90-13408

NASA's program on icing research and technology
p 239 N90-15062

Evaluation of two transport aircraft and several ground test vehicle friction measurements obtained for various runway surface types and conditions. A summary of test results from joint FAA/NASA Runway Friction Program
[NASA-TP-2917] p 249 N90-15902

Dynamic ground-effect measurements on the F-15 STOL and Maneuver Technology Demonstrator (S/MTD) configuration
[NASA-TP-3000] p 573 N90-22531

Helicopter Airborne Laser Positioning System (HALPS)
[NASA-TM-102814] p 654 N90-23399

En route noise: NASA proplan test aircraft (corrected data - simplified procedure)
[DOT-TSC-FA953-LR4] p 696 N90-24856

Ground shake test of the UH-60A helicopter airframe and comparison with NASTRAN finite element model predictions
[NASA-CR-181993] p 758 N90-25143

General test plan
p 857 N90-27721

Control research in the NASA high-alpha technology program
p 934 N90-28516

Evaluation for DLC-Flap Monitoring System of the VSRA
[NAL-TM-607] p 928 N90-29391

GROUND-AIR-GROUND COMMUNICATION

The Mode S beacon radar system
p 241 A90-21379

Propagation of Mode S beacon signals on the airport surface
p 241 A90-21381

ATC ground communications system optimization techniques
p 330 A90-25568

Air-ground information transfer in the National Airspace System
p 380 A90-26235

Tests of automatic dependent surveillance (ADS) in Western Europe - Possible future developments
p 574 A90-35353

The Canadian Airspace Systems Plan - Maintaining the safety and efficiency of the air navigation system
p 725 A90-42655

Aircraft Reply and Interference Environment Simulator (ARIES) hardware principles of operation. Volume 2: Appendixes
[DOT/FAA/CT-TN88/4-2] p 135 N90-12781

Aircraft Reply and Interference Environment Simulator (ARIES) hardware principles of operation, volume 1
[DOT/FAA/CT-TN88/4-1] p 135 N90-12782

National airspace system air-ground communications operational concept
[DOT/FAA/DS-90/2] p 542 N90-21249

New features of JAL's ground station
p 872 N90-27633

Integrated Air Traffic Management
[DLR-MITT-89-23] p 825 N90-27676

Airline requirements for a future air traffic management system
p 825 N90-27678

Aspects of data link applications for ATC purposes
p 827 N90-27688

GROUP THEORY

Integrated approach to design and manufacture of gas turbine components based on group theory
p 113 A90-16010

GUIDANCE (MOTION)

Guidance and Control strategies for aerospace vehicles
[NASA-CR-186195] p 199 N90-14243

Estimation and control of nonlinear and hybrid systems with applications to air-to-air guidance
[AD-A214542] p 348 N90-16770

Software verification plan for GCS --- guidance and control software
[NASA-TM-101668] p 372 N90-18057

The implications of using integrated software support environment for design of guidance and control systems software
[AGARD-AR-229] p 434 N90-18432

GUIDANCE SENSORS

System concept and performance criteria of modern helicopter navigation
p 640 A90-42452

Optoelectronic guidance sensors (5th revised and enlarged edition) --- Russian book
p 881 A90-46620

GUIDE VANES

Strength of the guide vane components of gas turbines
p 266 A90-21318

Effect of inlet flow angle on the erosion of radial turbine guide vanes
[ASME PAPER 89-GT-208] p 254 A90-22664

Effect of the control of turbocompressor guide vanes on the throttle characteristics of a bypass engine
p 255 A90-23425

The use of circumferentially varying stagger guide vanes in an axial flow pump or compressor
p 537 A90-33566

The performance of a combustor pre-diffuser incorporating compressor outlet guide vanes
[AIAA PAPER 90-2165] p 661 A90-42053

LDV measurements and the flow analysis in the vortex region of a radial inflow turbine
p 511 N90-21007

An investigation of secondary flows in nozzle guide vanes
p 512 N90-21016

Secondary flow predictions for a transonic nozzle guide vane
p 513 N90-21017

Secondary flow in a turbine guide vane with low aspect ratio
p 513 N90-21018

Theoretical and experimental study of flow-control devices for inlets of indraft wind tunnels
[NASA-TM-100050] p 598 N90-21778

GUNFIRE

The inclusion of a similarity representation of compressor rotation in the modeling of the interaction of cannon firing with air intakes at incidence
[AAAF PAPER NT 88-18] p 4 A90-11435

Air-to-Air Combat Test IV (AACT IV) and the AACT data base
p 381 A90-28169

GUST ALLEVIATORS

Design of direct lift control systems against vertical gust
p 196 A90-18592

Active control system for gust load alleviation and structural damping
p 259 N90-15056

Synthesis of individual rotor blade control system for gust alleviation
[NASA-TM-101886] p 736 N90-25972

GUST LOADS

Multistage compressor vane row aerodynamic gust response
p 6 A90-11783

Unsteady incompressible aerodynamics and forced response of detuned blade rows
[AIAA PAPER 90-0340] p 191 A90-19805

Active control of gust- and interference-induced vibration of tilt-rotor aircraft
p 429 A90-28201

Fast calculation of root loci of aeroelastic systems and of gust response in time domain
p 517 A90-33413

Helicopter response to atmospheric turbulence in forward flight
p 518 A90-33625

Correlation of lift and thickness noise sources in vortex-airfoil interaction
p 547 A90-34090

Unsteady aerodynamic gust response including steady flow separation
p 556 A90-36262

The response of helicopter to dispersed gust
p 870 A90-42470

The influence of the inertia coupling on the stability and control of the helicopter and the response of helicopter gust
p 871 A90-42472

NASA investigation of a claimed 'overlap' between two gust response analysis methods
p 771 A90-44730

Simulating turbulence and gusts for handling qualities evaluation
[AIAA PAPER 90-2845] p 754 A90-45174

- Lift and pitching moment measurements on a swept tapered wing in oscillatory vertical gusts p 811 A90-48089
- Aircraft passing through a sinusoidal gust p 811 A90-48090
- Cascade aerodynamic gust response including steady loading effects p 904 A90-51006
- Design of aircraft wings subjected to gust loads - A system reliability approach p 958 A90-52044
- Active control system for gust load alleviation and structural damping p 259 N90-15056
- GUSTS**
- Preliminary tests of a gust generator in the ONERA S3Ch transonic wind tunnel [ONERA, TP NO. 1989-171] p 261 A90-21035
- Turbulence effects of aircraft flight dynamics and control p 258 N90-15055
- Spanwise measurements of vertical components of atmospheric turbulence [NASA-TP-2963] p 456 N90-19718
- Development of a linearized unsteady aerodynamic analysis for cascade gust response predictions [NASA-CR-4308] p 816 N90-27655
- GYRATION**
- Pre-escape and escape aircraft maneuvers and gyrations - A critical under-reported problem affecting escape system performance and aircrew safety p 21 A90-10264
- Construction of a hybrid angular velocity reference system for investigation of the dynamic characteristics of strapdown gyros [ESA-TT-1181] p 774 N90-25332
- GYROSCOPES**
- The multi-function RLG system comes of age - A technical update p 578 A90-36931
- GYROSCOPIC STABILITY**
- Gyroscopic matrices in computation of vibration p 547 A90-33381
- A study of the errors of a gyroscopic instrument for measuring linear accelerations p 771 A90-45133
- An accurate numerical technique for determining flight test rate gyroscope biases prior to takeoff [AD-A220987] p 739 N90-25138

H

H-53 HELICOPTER

- Helicopter simulation development by correlation with frequency sweep flight test data p 407 A90-28203
- Fatigue evaluation of C/MH-53E main rotor damper threaded joints p 642 A90-39988
- Focusing propulsion and lift system development for an evolving special operations aircraft [AIAA PAPER 90-2277] p 730 A90-42768
- Application of damage tolerance p 843 N90-26817
- Individual Helicopter Tracking Program (IHTP) for the MH-53J helicopter p 843 N90-26818

H-60 HELICOPTER

- Improvements to the fatigue substantiation of the H-60 composite tail rotor blade p 642 A90-39985
- Helicopter surveillance - A look at current and proposed future programs p 642 A90-39986

HAFNIUM COMPOUNDS

- Chemical vapor deposition of Hf/Si compounds as a high temperature coating for carbon/carbon composites p 955 A90-50159

HAIL

- Maximum expected concentrations of hail in thunderstorm precipitation p 962 A90-52052

HALOGENATION

- Nonflammable hydraulic power system for tactical aircraft. Volume 1: Aircraft system definition, design and analysis [AD-A218493] p 671 N90-23409

HANDBOOKS

- Failure analysis handbook [AD-A219747] p 689 N90-23752
- Wright Research and Development Center test facilities handbook [AD-A222582] p 762 N90-26020

HANDLING EQUIPMENT

- Results of studies on a manipulator system for model handling in the ETW p 524 A90-34248

HANG GLIDERS

- An electronic flight-recorder for a hang-glider p 39 A90-12234

HANGARS

- ILS (Instrument Landing System) mathematical modeling study on the effects of proposed hangar construction west of runway 18R on localizer performance at Dallas-Fort Worth International Airport [AD-A210631] p 27 N90-10019

- ILS mathematical modeling study of the effects of proposed hangar construction at the Orlando International Airport, Runway 17R, Orlando, Florida [DOT/FAA/CT-TN89/52] p 121 N90-11762

HARDNESS

- Improving snow roads and airstrips in Antarctica [AD-A211588] p 133 N90-11907

HARDNESS TESTS

- Evaluation of static and fatigue properties of thin sheets of 8090-T8 aluminum-lithium alloy and observation of its fracture surfaces [NAL-TR-1039] p 953 N90-29499

HARDWARE

- A hardware and software fault tolerant safety controller [AIAA PAPER 89-3123] p 74 A90-10599
- A ground simulation-inspection system for avionic devices p 594 A90-37232
- IAPSA 2 small-scale system specification [NASA-CR-182006] p 695 N90-24103

HARMONIC ANALYSIS

- Low-speed unsteady aerodynamics of a pitching straked wing at high incidence. I - Test program. II - Harmonic analysis p 159 A90-19387

HARMONIC CONTROL

- Higher harmonic and trim control of the X-wing circulation control wind tunnel model rotor p 435 A90-28156
- Application of higher harmonic control (HHC) to rotors operating at high speed and maneuvering flight p 429 A90-28157
- Effects of higher harmonic control on rotor performance and control loads [AIAA PAPER 90-1158] p 412 A90-29467
- Vibration reduction on servo flap controlled rotor using HHC p 861 A90-46967
- Comparison of active control on a servo flap rotor using fixed system and rotating system parameters p 862 A90-46976
- Aeroelastic simulation of higher harmonic control p 592 N90-21768

HARMONIC EXCITATION

- A modal parameter identification technique and its application to large complex structures with multiple steady sinusoidal excitation p 602 A90-35670

HARMONIC FUNCTIONS

- A new class of random processes with application to helicopter noise p 781 A90-42874

HARMONIC MOTION

- Aeroelastic response characteristics of a rotor executing arbitrary harmonic blade pitch variations p 646 A90-42464

HARMONIC OSCILLATION

- Vortex formation around an oscillating and translating airfoil at large incidences p 303 A90-25588
- An interactive boundary-layer method for unsteady airfoil flows. Part 1: Quasi-steady-state model [AD-A221220] p 634 N90-24250

HARMONICS

- An experimental investigation of supersonic flow over two cavities in tandem [AIAA PAPER 90-3087] p 795 A90-45901
- An examination of helicopter rotor load calculations [AD-A14295] p 249 N90-15098
- Quiet mode for nonlinear rotor models [NASA-TM-102236] p 582 N90-21758

HARRIER AIRCRAFT

- VSTOL power plant control lessons from Harrier experience p 13 A90-12582
- Practical design considerations for integrating the propulsion system with the aircraft for jetborne flight [ASME PAPER 89-GT-310] p 490 A90-32257
- AV-8B shipboard ski jump evaluation p 574 A90-38535

- AV-8B composite repair program p 551 A90-38542
- Focusing propulsion and lift system development for an evolving special operations aircraft [AIAA PAPER 90-2277] p 730 A90-42768
- More power for the Harrier p 745 A90-44597
- Operation of the Rolls-Royce Pegasus Engine on low grade non-aviation fuels [SAE PAPER 892329] p 747 A90-45486

- Flight evaluations of several hover control and display combinations for precise blind vertical landings [AIAA PAPER 90-3479] p 867 A90-47764
- Enhanced environmental control for the Harrier II Plus [SAE PAPER 901238] p 841 A90-49308

HAZARDS

- Safety and cryogenic wind tunnels p 264 N90-15960
- Characteristics of transport, aircraft fires measured by full-scale tests p 325 N90-17591
- Ignitability of jet-A fuel vapors in aircraft fuel tanks p 326 N90-17594
- Fire science and aircraft safety p 326 N90-17596
- Advanced materials for interior and equipment related to fire safety in aviation p 328 N90-17608

- Flammability testing of aircraft cabin materials p 328 N90-17611

HEAD MOVEMENT

- Dual servo optical projection system (SOPS) - A solution for two crewmember and night vision goggle display needs [SAE PAPER 892353] p 760 A90-45504

HEAD-UP DISPLAYS

- Holographic head-up displays for air and ground applications p 108 A90-13885
- Synthetic holography applied to head-up displays p 218 A90-16692
- Toward the panoramic cockpit, and 3-D cockpit displays p 419 A90-30682
- The effect of windscreen bows and HUD pitch ladder on pilot performance during simulated flight p 420 A90-31333
- Cooperative synthesis of control and display augmentation in approach and landing p 516 A90-33061
- Dynamic FLIR simulation in flight training research p 681 A90-40109
- Holographic combiner design to obtain uniform symbol brightness at head-up display video camera p 652 A90-40394
- Flight-path display can improve safety, operational efficiency p 847 A90-48982
- Automatic processing of images from the GRATE flight test tool [DLR-FB-89-28] p 109 N90-12599
- A head up display format for application to V/STOL aircraft approach and landing [NASA-TM-102216] p 340 N90-17632
- Development of the triplex digital flight control system of the STOL research aircraft ASKA [NAL-TR-1013] p 349 N90-17640

HEALTH

- Safety and health trends in aerospace composite materials p 947 A90-50188
- Boeing 727-100 test project (high energy radiated field tests) [DOT/FAA/CT-88/33] p 542 N90-21247

HEAT EXCHANGERS

- Ceramic heat exchangers in gas turbine [ONERA, TP NO. 1989-109] p 40 A90-11142
- Handbook on heat exchangers --- Russian book p 273 A90-22743
- F-15 Environment Control System improvements [SAE PAPER 901235] p 841 A90-49305
- High temperature VSCF (Variable Speed Constant Frequency) generator system [AD-A210823] p 71 N90-10351
- Cycle analysis for helicopter gas turbine engines [RAE-TM-P-1154] p 256 N90-15921

HEAT FLUX

- Determination of pressure and heat flow on the front surface of smooth blunt bodies p 299 A90-24166
- A measurement window for a cryogenic windtunnel p 523 A90-34233
- Calculation of the heat flux at a three-dimensional critical point in supersonic flow past a body p 803 A90-46536

HEAT GENERATION

- A numerical study of mixing and chemical heat release in supersonic mixing layers [AIAA PAPER 90-0152] p 163 A90-19710

HEAT ISLANDS

- Wind tunnel design of heat island turbulent boundary layer [IHW-ET/50] p 455 N90-19542

HEAT MEASUREMENT

- Studies of gas turbine heat transfer airfoil surfaces and end-wall cooling effects [AD-A212451] p 117 N90-12620

HEAT OF COMBUSTION

- A study of the electrophysical phenomena in the combustion chambers of jet engines p 765 A90-45028
- Flammability testing of aircraft cabin materials p 328 N90-17611

HEAT PIPES

- Application of formal optimization techniques in thermal/structural design of a heat-pipe-cooled panel for a hypersonic vehicle [NASA-TM-89131] p 72 N90-10409
- Design and demonstration of heat pipe cooling for NASP and evaluation of heating methods at high heating rates [DE89-016995] p 186 N90-14227
- Heat pipes for wing leading edges of hypersonic vehicles [NASA-CR-181922] p 369 N90-17055
- Flexible heat pipe cold plate [AD-A216053] p 434 N90-18433

HEAT RESISTANT ALLOYS

- Effect of protective coatings on mechanical properties of superalloys
 [ONERA, TP NO. 1989-88] p 62 A90-11126
 An oxidation fatigue interaction damage model for thermal fatigue crack growth p 62 A90-11539
 IMI 834 - A new high temperature capability titanium alloy for engine use p 62 A90-12535
 Intermetallic compounds for strong high-temperature materials - Status and potential p 125 A90-15022
 Superalloy 718: Metallurgy and applications; Proceedings of the International Symposium, Pittsburgh, PA, June 12-14, 1989 p 266 A90-20775
 Aerospace materials research opportunities p 267 A90-23177
 Braze repair of MA754 aero gas turbine engine nozzles
 [ASME PAPER 89-GT-235] p 342 A90-23886
 Recent and prospective developments in single-crystal superalloys for the blades of advanced turbines p 355 A90-24288
 The anisotropy of the mechanical behaviour in nickel-based single crystal superalloys for turbine blades [ONERA, TP NO. 1989-205] p 355 A90-25339
 Development of a new nickel based single crystal turbine blade alloy for very high temperatures [ONERA, TP NO. 1989-206] p 356 A90-25340
 Recrystallization behavior of nickel-base single crystal superalloys p 440 A90-27681
 Cleaner superalloys via improved melting practices p 442 A90-29707
 Time dependent effects on high temperature low cycle fatigue and fatigue crack propagation on nickel base superalloys p 443 A90-29881
 Coatings for high temperature corrosion in aero and industrial gas turbines p 443 A90-30479
 Resources - Supply and availability --- of superalloys for United States aerospace industry p 531 A90-34152
 Metallurgy of investment cast superalloy components p 531 A90-34154
 Thermomechanical processing of superalloys p 531 A90-34156
 Powder metallurgy and oxide dispersion processing of superalloys p 531 A90-34158
 Cyclic deformation, fatigue and fatigue crack propagation in Ni-base alloys p 531 A90-34162
 Life prediction and fatigue p 532 A90-34163
 Fiber reinforced superalloys p 532 A90-34169
 A friendly alloy --- aircraft construction materials p 764 A90-44173
 Investment-cast superalloys a good investment p 949 A90-51198
 Mechanical alloying spreads its wings p 950 A90-51200
 Modeling of the oil quench for Ni-based superalloy turbine disks p 957 A90-51525
 Constitutive modeling for isotropic materials (HOST) [NASA-CR-179522] p 193 N90-13390
 Constitutive modeling for isotropic materials (HOST) [NASA-CR-174718] p 193 N90-13391
 Thermal fatigue durability for advanced propulsion materials [NASA-TM-102348] p 215 N90-14641
 Attachment of lead wires to thin film thermocouples mounted on high temperature materials using the parallel gap welding process [NASA-TM-102442] p 543 N90-21361
 Effect of protective coatings on mechanical properties of superalloys p 952 N90-28707
 The stress and temperature dependence of creep in an Al-2.0 wt percent U alloy [AD-A223676] p 953 N90-29480
- HEAT SHIELDING**
 Particulate trajectories and impact characteristics in hypersonic flight involving gas coolant shielding p 476 A90-34583
 Pressure air tightness tests of laminated panels for wing leading edge heat shields [INFORME-I-377/89] p 357 N90-17873
 Carbon-carbon composites: Emerging materials for hypersonic flight [NASA-TM-103472] p 767 N90-26080
- HEAT SINKS**
 Evaluation and control of an Integrated Closed Environmental Control System (ICECS) [SAE PAPER 901237] p 841 A90-49307
 Flexible heat pipe cold plate [AD-A216053] p 434 N90-18433
- HEAT TRANSFER**
 Lee-side heating of a delta wing in supersonic flow p 10 A90-12281
 Temperature scaling of turbine blade heat transfer with and without shock wave passing p 47 A90-12570

- Test rig for the study of the flow in a rotor-stator system [ONERA, TP NO. 1989-124] p 58 A90-12634
 Augmented heat transfer in rectangular channels of narrow aspect ratios with rib turbulators p 70 A90-13091
 Heat Transfer and Fluid Mechanics Institute, 31st, California State University, Sacramento, June 1, 2, 1989, Proceedings p 130 A90-15387
 Calculation of coolant flow and heat transfer inside composite air-cooled turbine p 189 A90-17791
 Research on film-cooling of turbine blade p 190 A90-17795
 Cooking an aeroplane p 209 A90-17918
 The critical role of aerodynamic heating effects in the design of hypersonic vehicles p 155 A90-18249
 Embedded function methods for supersonic turbulent boundary layers [AIAA PAPER 90-0306] p 163 A90-19787
 Handbook on heat exchangers --- Russian book p 273 A90-22743
 An experimental study of turbine vane heat transfer with leading edge and downstream film cooling [ASME PAPER 89-GT-69] p 358 A90-23792
 Pressure loss and heat transfer in channels roughened on two opposed walls p 358 A90-23805
 Prediction of the aerodynamic environment and heat transfer for rotor-stator configurations [ASME PAPER 89-GT-89] p 359 A90-23807
 Heat transfer and pressure drop for short pin-fin arrays with pin-end wall fillet [ASME PAPER 89-GT-99] p 359 A90-23813
 Aerodynamic and heat transfer measurements on blading for a high rim-speed transonic turbine [ASME PAPER 89-GT-228] p 293 A90-23883
 Determination of pressure and heat flow on the front surface of smooth blunt bodies p 299 A90-24166
 Aerodynamic heat transfer testing in hypersonic wind tunnels using an infrared imaging system [AIAA PAPER 90-0189] p 350 A90-25027
 Liquid crystal thermography for aerodynamic heating measurements in short duration hypersonic facilities p 446 A90-28262
 Development and extension of diagnostic techniques for advancing high speed aerodynamic research p 436 A90-28281
 Comparison between experimental and numerical results for a research hypersonic aircraft p 395 A90-31278
 Heat transfer in gas turbine engines; Proceedings of the Symposium, ASME Winter Annual Meeting, San Francisco, CA, Dec. 10-15, 1989 p 534 A90-32166
 Local heat transfer on a flat surface roughened with broken ribs p 534 A90-32169
 Heat transfer in supersonic coaxial reacting jets p 601 A90-35394
 Total temperature separation in jets [AIAA PAPER 90-1621] p 607 A90-38750
 Inverse heat transfer studies and the effects of propellant aluminum on TVC jet vane heating and erosion [AIAA PAPER 90-1860] p 655 A90-40533
 The investigation of heat transfer in cooled blades of gas turbines [AIAA PAPER 90-2144] p 685 A90-42043
 Radio frequency (RF) heated supersonic flow laboratory [AIAA PAPER 90-2469] p 673 A90-42186
 Effects of inlet turbulence scale on turbine blade surface heat transfer in a linear cascade [AIAA PAPER 90-2264] p 768 A90-42761
 Numerical predictions for the flow and the heat transfer in gas turbine cooling systems p 770 A90-44464
 The flow field and heat transfer near a turbulator p 771 A90-44755
 The effect of vibration-dissociation interaction on heat transfer and drag during the hypersonic flow past bodies p 710 A90-44934
 Flow and heat transfer in rotating-disc systems. Volume I - Rotor-stator systems --- Book p 772 A90-45759
 Flow separation in oblique shock wave turbulent boundary layer interactions p 807 A90-46872
 Recent progress in research pertaining to estimates of gas-side heat transfer in an aircraft gas turbine [NASA-TM-102460] p 194 N90-13394
 Design and demonstration of heat pipe cooling for NASP and evaluation of heating methods at high heating rates [DE89-016995] p 186 N90-14227
 Aerodynamic and heat transfer measurements on blading for a high rim-speed transonic turbine [RAE-TM-P-1151] p 256 N90-15920
 Wake interaction effects on the transition process on turbine blades [AD-A214492] p 343 N90-16759
 Shock-shock boundary layer interactions p 318 N90-17569

- Glancing shock-boundary layer interactions p 319 N90-17571
 Heat release rate measurement for evaluating the flammability of aircraft materials p 328 N90-17610
 Viscous three-dimensional analyses for nozzles for hypersonic propulsion [NASA-CR-185187] p 344 N90-17635
 Numerical investigations of heat transfer and flow rates in rotating cavities. Simulation of the movement generated by wall temperature gradients, by source-sink mass flows or by the differential rotation of the walls, under the influence of coriolis and centrifugal forces [ETN-90-96253] p 454 N90-18695
 Experimental and theoretical investigations of flowfields and heat transfer in modern gas turbines [AD-A217663] p 429 N90-19237
 The influence of a wall function on turbine blade heat transfer prediction p 429 N90-19421
 Ultrasonic techniques for aircraft ice accretion measurement p 485 N90-20926
 Users manual for the NASA Lewis Ice Accretion Prediction Code (LEWICE) [NASA-CR-185129] p 468 N90-20943
 Secondary Flows in Turbomachines [AGARD-CP-469] p 511 N90-21009
 Navier-Stokes analysis of turbine blade heat transfer [NASA-TM-102496] p 542 N90-21300
 WINCOF-I code for prediction of fan compressor unit with water ingestion [NASA-CR-185157] p 551 N90-21724
 Performance of a supercharged direct-injection stratified-charge rotary combustion engine [NASA-TM-103105] p 748 N90-25982
 Combustor cooling aspects [CIT/SME/VKI/RS/5] p 749 N90-25989
 Prediction of rotating disc flow and heat transfer in gas turbine engines [PNR90650] p 750 N90-26001
 A heat transfer analysis for rough turbine airfoils [AD-A221942] p 854 N90-26831
 Computer code for predicting coolant flow and heat transfer in turbomachinery [NASA-TP-2985] p 858 N90-27722
- HEAT TRANSFER COEFFICIENTS**
 Convective heat transfer measurements from a NACA 0012 airfoil in flight and in the NASA Lewis Icing Research Tunnel [AIAA PAPER 90-0199] p 272 A90-22180
 Effect of rib-angle orientation on local mass transfer distribution in a three-pass rib-roughened channel [ASME PAPER 89-GT-98] p 359 A90-23812
 An experimental study of heat transfer and film cooling on low aspect ratio turbine nozzles [ASME PAPER 89-GT-187] p 361 A90-23865
 Impingement/effusion cooling - The influence of the number of impingement holes and pressure loss on the heat transfer coefficient [ASME PAPER 89-GT-188] p 361 A90-23866
 Experimental investigation into the effects of rotating and static bolts on both windage heating and local heat transfer coefficients in a rotor/stator cavity [ASME PAPER 89-GT-196] p 362 A90-23870
 Determination of convective transfer coefficients on a wind-tunnel model by stimulated infrared thermography [ONERA, TP NO. 1989-218] p 351 A90-25351
 Prediction of heat transfer coefficient on turbine blade profiles p 423 A90-29904
 Experimental investigation of external heat transfer coefficients on film-cooled turbine blade leading edge p 585 A90-36787
 Heat transfer in a solid fuel ramjet combustor [AIAA PAPER 90-1783] p 586 A90-38472
 Electrical analog circuit for heat transfer measurements on a flat plate simulating turbine vane heat transfer in turbulent flow [AIAA PAPER 90-2412] p 687 A90-42164
 Convective heat transfer measurements from a NACA 0012 airfoil in flight and in the NASA Lewis Icing Research Tunnel [NASA-TM-102448] p 213 N90-13750
 Ultrasonic techniques for aircraft ice accretion measurement p 485 N90-20926
- HEAT TRANSMISSION**
 Studies of gas turbine heat transfer airfoil surfaces and end-wall cooling effects [AD-A212451] p 117 N90-12620
- HEAT TREATMENT**
 The changes of structures and properties in PAN-based carbon fibers during heat treatment in carbon dioxide p 945 A90-50145
- HEATING**
 The analysis and solution of the performance deterioration problem of WP7 engine under the full reheating condition p 191 A90-18624
 Application of sound and temperature to control boundary-layer transition p 92 N90-12537

HEAVY LIFT HELICOPTERS

- Helicopter simulation development by correlation with frequency sweep flight test data p 407 A90-28203
 Multiple-power-path nonplanetary main gearbox of the Mi-26 heavy-lift transport helicopter p 452 A90-30115
 USCG HH-65A/SRR GPS integration and test results p 726 A90-43705

- Control of a twin lift helicopter system using nonlinear state feedback
 [AIAA PAPER 90-3408] p 817 A90-47663

HEINKEL AIRCRAFT

- On the occasion of the 100th birthday of Ernst Heinkel
 [MBB/LW/3015/S/PUB/321] p 141 N90-12494

HELICAL WINDINGS

- Finite-element analysis of large spur and helical gear systems p 683 A90-40940

HELICOPTER CONTROL

- Influence of the control law on the performance of a helicopter model rotor
 [ONERA, TP NO. 1989-136] p 4 A90-11158
 New rotor test rig in the large Modane wind tunnel [ONERA, TP NO. 1989-137] p 58 A90-11159
 Identification of mathematical derivative models for the design of a model following control system — for fly-by-wire helicopter p 56 A90-12764
 System identification strategies for helicopter rotor models incorporating induced flow p 30 A90-12768
 Design of attitude and rate command systems for helicopters using eigenstructure assignment p 118 A90-14729
 Evaluation of the dynamic properties of the auto-pilot servo of a single-rotor helicopter through laboratory testing p 118 A90-15424
 A simple active controller to suppress helicopter air resonance in hover and forward flight p 119 A90-16521

- Recursive real-time identification of step-response matrices of helicopters for adaptive digital flight control p 195 A90-17703
 The induced velocity distribution and the flap-pitch-torsion coupling on the stability and control of the helicopter in flight condition with lateral velocity p 196 A90-18633

- Design of a helicopter output feedback control law using modal and structured-robustness techniques p 282 A90-20557
 Nonlinear effects in helicopter rotor forward flight forced response p 347 A90-25420
 A study of roll response required in a low altitude slalom task — in helicopter control p 347 A90-25421
 Automatic vibration reduction at a four bladed hingeless model rotor - A wind tunnel demonstration p 335 A90-25424

- The benefits and costs of automation in advanced helicopters - An empirical study p 348 A90-26258
 Application of higher harmonic control (HHC) to rotors operating at high speed and maneuvering flight p 429 A90-28157
 The effects of aerial combat on helicopter structural integrity p 406 A90-28166
 Theoretical and experimental correlation of helicopter aeromechanics in hover p 429 A90-28200
 Helicopter flight control system design and evaluation for NOE operations using controller inversion techniques p 429 A90-28202

- RSRA/X-Wing flight control system development - Lessons learned p 430 A90-28216
 Fully automatic guidance for rotorcraft nap-of-the-earth (NOE) flight following planned profiles p 403 A90-28219

- OPST1 - An optical yaw control system for high performance helicopters p 430 A90-28220
 Design criteria for helicopter night pilotage sensors p 417 A90-28221

- Linear control issues in the higher harmonic control of helicopter vibrations p 430 A90-28225
 The Modular Flighttest Instrumentation/MFI 90 - A helicopter measuring system p 418 A90-28850
 Piezoelectric actuators for helicopter rotor control [AIAA PAPER 90-1076] p 411 A90-29384
 Effects of higher harmonic control on rotor performance and control loads p 412 A90-29467

- Comparison of test signals for aircraft frequency domain identification p 490 A90-33057
 Whole helicopter aeroelasticity - Experience with a new approach p 492 A90-33380
 EH 101 Flight Test Program current status and future testing p 495 A90-33912

- Some aspects of the control system and power unit lead tests using in-flight simulator systems and flying test-beds [AIAA PAPER 90-1296] p 580 A90-36031

- Control system validation in the autonomous helicopter p 667 A90-38908
 Improvement of helicopter handling qualities using H(infinity)-optimisation p 667 A90-38965
 Helicopter control design using feedback linearization techniques p 668 A90-40817
 ATTHes - A helicopter in-flight simulator for ACT testing p 643 A90-41727

- Active control of helicopter cabin noise p 645 A90-42434
 Modern strapdown system for helicopter p 653 A90-42451
 Design methodology for multivariable helicopter control systems p 669 A90-42461

- A model for active control of helicopter air resonance in hover and forward flight p 670 A90-42462
 A technique for the tuning of helicopter flight control systems p 670 A90-42467
 The influence of the inertia coupling on the stability and control of the helicopter and the response of helicopter gust p 671 A90-42472

- Aeroelastic effects on stability and control of hingeless rotor helicopters p 647 A90-42473
 Helicopter stability and control modeling improvements and verification on two helicopters p 671 A90-42474
 Estimation of rotor blade incidence and blade deformation from the measurement of pressures and strains in flight p 647 A90-42497

- Analytical evaluation of helicopter true air speed and associated flight tests p 647 A90-42499
 Design of flight control systems to meet rotorcraft handling qualities specifications [AIAA PAPER 90-2805] p 752 A90-45140

- A pilot rating scale for evaluating failure transients in electronic flight control systems [AIAA PAPER 90-2827] p 754 A90-45159
 Helicopter trim with flap-lag-torsion and stall by an optimized controller p 755 A90-45332
 System identification requirements for high-bandwidth rotorcraft flight control system design p 755 A90-45333

- Optimal autorotational descent of a helicopter with control and state inequality constraints p 756 A90-45344
 Helicopter individual blade control through optimal output feedback p 861 A90-46956
 A study of fundamental issues in higher harmonic control using aeroelastic simulation p 861 A90-46966
 Vibration reduction on servo flap controlled rotor using HHC p 861 A90-46967

- Control of a twin lift helicopter system using nonlinear state feedback [AIAA PAPER 90-3408] p 817 A90-47663
 Rotorcraft pursuit-evasion in nap-of-the-earth flight [AIAA PAPER 90-3455] p 788 A90-47707
 Effects of stick dynamics on helicopter flying qualities [AIAA PAPER 90-3477] p 866 A90-47727
 A linear quadratic regulator approach to the stabilization of uncertain linear systems [AIAA PAPER 90-3509] p 891 A90-47755
 The Mast Mounted Sight 771 processor upgrade program — for helicopter p 926 A90-51058
 Helicopter flight path controller design via a nonlinear transformation technique p 199 N90-14242
 Airworthiness and flight characteristics evaluation of the McDonnell Douglas Helicopter Corporation (MDHC) 530FF helicopter [AD-A218253] p 498 N90-20076
 Interaction of switch actuation on tracking with a four-axis flight control (cross-coupling) [AD-A217981] p 520 N90-20095
 Design of a helicopter automatic flight control system using adaptive control p 522 N90-21040
 ROSAR (Helicopter-Rotor based Synthetic Aperture Radar) p 541 N90-21229
 Aeroelastic simulation of higher harmonic control p 592 N90-21768
 Adaptive control of a system with periodic dynamics: Application of an impulse response method to the helicopter vibration problem p 694 N90-23990
 Helicopter controllability [AD-A220078] p 672 N90-24275
 Coupled rotor-body equations of motion hover flight [NASA-CR-186710] p 717 N90-25111
 AIMS for helicopters p 820 N90-27639

HELICOPTER DESIGN

- A multifunctional system of helicopter dynamics simulations p 28 A90-10226
 Some unconventional cases of the dynamical testing of helicopters p 28 A90-10227
 Modern dynamic components for helicopters [MBB-UD-556-89-PUB] p 29 A90-12253

- Rotor concepts for the European Future Advanced Rotorcraft (Eurofar) [MBB-UD-0551-89-PUB] p 29 A90-12258

- Aerodynamic and dynamic principles of helicopter flight — Russian book p 55 A90-12473
 Wildhaber-Novikov circular arc gears - Some properties of relevance to their design p 70 A90-12999
 Aerospatiale's military helicopter programs p 143 A90-16824

- Damage tolerance analysis of dynamic components of rotary wing aircraft p 179 A90-17312
 Minimum weight design of helicopter rotor blades with frequency constraints p 180 A90-17313
 Theoretical and experimental analysis of a model rotor blade incorporating a swept tip p 151 A90-17586
 The Model 360 - Advanced composite helicopter p 180 A90-17678

- Response and hub loads sensitivity analysis of a helicopter rotor p 181 A90-18145
 Dynamic stall of circulation control airfoils [AIAA PAPER 90-0573] p 187 A90-19923
 Design of a helicopter output feedback control law using modal and structured-robustness techniques p 282 A90-20557

- Gear steels for future helicopter transmissions p 265 A90-20607
 Helicopter transmissions - Design for safety and reliability p 270 A90-20608
 Performance and aerodynamic development of the Super Puma Mk II main rotor with new SPP8 blade tip design [ONERA, TP NO. 1989-181] p 245 A90-21041
 Equipment procurement - EH101 helicopter p 282 A90-22435
 Optimal placement of tuning masses for vibration reduction in helicopter rotor blades p 247 A90-23117
 Rotorcraft analytical improvement needed to reduce developmental risk - The 1989 Alexander A. Nikolsky Lecture p 285 A90-23934
 Modeling of subsonic unsteady aerodynamics for rotary wing applications p 293 A90-23935
 Hub loads analysis of the SA349/2 helicopter p 333 A90-23936
 Nonlinear effects in helicopter rotor forward flight forced response p 347 A90-25420
 A practical co-axial twin rotor model p 335 A90-25423
 Wind tunnel testing of a helicopter model at HAL p 335 A90-26350
 Multiobjective decision making in a fuzzy environment with applications to helicopter design p 405 A90-27993
 AHS, Annual Forum, 45th, Boston, MA, May 22-24, 1989, Proceedings p 381 A90-28151
 Design, evaluation and proof-of-concept flights of a main rotor interblade viscoelastic damping system p 406 A90-28152
 McDonnell Douglas Helicopter Company Factory of the Future Project p 381 A90-28163
 Identification of retreating blade stall mechanisms using flight test pressure measurements p 384 A90-28172
 The LHTEC T800-LHT-800 engine integration into the Agusta A129 helicopter p 422 A90-28177
 The use of fibre reinforced thermoplastics for helicopter primary structures and their engineering substantiation p 441 A90-28191
 EH101 design and development status p 407 A90-28211
 Helicopter design optimization for maneuverability and agility p 408 A90-28212
 Avionics and electromagnetic compatibility (EMC) considerations on a helicopter with an advanced composite airframe p 417 A90-28217
 The prediction of loads on the Boeing Helicopters Model 360 rotor p 410 A90-28240
 Application of transonic flow analysis to helicopter rotor problems p 394 A90-29887
 The variable-diameter rotor - A key to high performance rotorcraft p 413 A90-30118
 Honeycomb sandwich primary structure applications on the Boeing Model 360 helicopter p 490 A90-31558
 Advancements in rotor and airframe structural flight testing developed during the SH-60B G.W./C.G. expansion program [AIAA PAPER 90-1281] p 495 A90-33902
 EH101 Advance Technology Rotorcraft low detectability/good neighbor design p 579 A90-35774
 Stability sensitivity analysis of a helicopter rotor p 580 A90-36273
 Application of optimization methods to helicopter rotor blade design p 604 A90-37337
 The influence of interactional aerodynamics of rotor-fuselage-interferences on the fuselage flow p 561 A90-38523
 The U.S. Army Helicopter Structural Integrity Program - 1989 European Rotorcraft Forum p 581 A90-38525
 National Technical Specialists' Meeting on Tactical V/STOL, New Bern, NC, Sept. 19-21, 1989, Proceedings p 551 A90-38526

Automated helicopter structural analysis data processing p 611 A90-38533
Improvement of helicopter handling qualities using H(infinity)-optimisation p 667 A90-38965
Potential application of automotive fatigue technology in rotorcraft design p 681 A90-39987
Characterization of helicopter turboshaft engine noise p 660 A90-41759
Comparison with experiment of various computational methods of airflow on three helicopter fuselages p 630 A90-42436
Improving tilt rotor aircraft performance with variable-diameter rotors p 646 A90-42445
The all glass helicopter cockpit p 653 A90-42447
A comprehensive approach to coupled rotor-fuselage dynamics p 646 A90-42460
The place of knowledge based systems in helicopter dynamic system condition prognosis p 618 A90-42475
The Franco-German helicopter programme HAP, PAH-2/HAC p 618 A90-42478
EH-101 main rotor hub application of thick carbon fiber unidirectional tension bands p 618 A90-42489
A 'new' philosophy of structural reliability, fail safe versus safe life p 688 A90-42490
Flight tests to explore tail rotor limitations in the low speed envelope p 647 A90-42498
Evaluation of the dynamic characteristics of a helicopter instrument panel p 829 A90-46499
An experimental study of instantaneous velocity perturbations over a rotor disk for low duty coefficients p 860 A90-46572
Aerodynamic design of the Cal Poly Da Vinci Human-Powered Helicopter p 830 A90-46950
An examination of helicopter rotor load calculations p 833 A90-46972
The MH-60K - A special rotorcraft for special operations p 835 A90-48860
[AIAA PAPER 90-3266] p 835 A90-48860
Application of advanced air vehicle and mission equipment technologies to the Light Helicopter (LH) [AIAA PAPER 90-3268] p 836 A90-48861
Multi-role advance technology rotorcraft - The EH101 [AIAA PAPER 90-3302] p 837 A90-48884
Coaxial helicopters - Current status and future developments p 838 A90-48951
Helicopter or tiltrotor - A Soviet view p 838 A90-48952
Controller design for active vibration suppression of a helicopter [DFVLR-FB-89-20] p 120 N90-11760
Integrated multidisciplinary optimization of rotorcraft: A plan for development [NASA-TM-101617] p 106 N90-12580
General approach and scope --- rotor blade design optimization p 106 N90-12581
Rotor blade aerodynamic design p 106 N90-12582
Airframe design considerations: Overview --- rotor design optimization p 106 N90-12586
Validation of the procedures --- integrated multidisciplinary optimization of rotorcraft p 107 N90-12587
Appendix: Results obtained to date --- integrated multidisciplinary optimization of rotorcraft p 107 N90-12588
Euler equation solutions applied to a helicopter rotor in forward moving flight [ONERA-RSF-32/1285-AY-346A] p 107 N90-12592
Calculation of flight vibration levels of the AH-1G helicopter and correlation with existing flight vibration measurements [NASA-CR-181923] p 454 N90-18743
Activities report in German aerospace [ISSN-0070-3966] p 465 N90-19189
Design of a helicopter automatic flight control system using adaptive control p 522 N90-21040
Scenario 2000 [MBB-UD-500/89-PUB] p 734 N90-25092
Research at NASA's NFAC wind tunnels [NASA-TM-102827] p 702 N90-25933
Development of a method to design helicopter rotors [REPT-100-30-03] p 845 N90-26830
Design of helicopter components in metal matrix composites [REPT-100-20-55] p 874 N90-26894
HELICOPTER ENGINES
Turbulent mixing in helicopter jet diluters - Navier-Stokes calculations and correlations [AAAF PAPER NT 88-13] p 40 A90-11432
Helicopter dynamics: Limiting flight conditions --- Russian book p 55 A90-12481
A study of particle trajectories in a gas turbine intake p 48 A90-12583
Icing test techniques for air intake screens on helicopters functioning in temperatures around 0 C p 23 A90-12619

Successful performance development program for the T800-LHT-800 turboshaft engine [SAE PAPER 891048] p 110 A90-14352
Turboshafts on tenterhooks p 188 A90-16703
Payoffs in growth engines p 188 A90-16823
Recent research on external helicopter noise at ONERA p 218 A90-16825
Efficiency testing of a helicopter transmission planetary reduction stage p 271 A90-21113
The LHTEC T800-LHT-800 engine integration into the Agusta A129 helicopter p 422 A90-28177
A comprehensive diagnostic system for the T800-APW-800 engine p 422 A90-28181
Flight tests of Adaptive Fuel Control and decoupled rotor speed control systems p 422 A90-28183
A synergistic approach to logistics planning and engine design p 422 A90-28207
The four-bladed main rotor system for the AH-1W helicopter p 408 A90-28214
Cycle analysis for helicopter gas turbine engines [ASME PAPER 89-GT-328] p 506 A90-32258
EH 101 Flight Test Program current status and future testing [AIAA PAPER 90-1296] p 495 A90-33912
The T800-LHT-800 engine - Designed for supportability p 585 A90-35773
Precursor convertible engine study [AIAA PAPER 90-2486] p 658 A90-40636
Directivity of the noise radiation emitted from the inlet duct of a turboshaft helicopter engine [ONERA, TP NO. 1990-26] p 695 A90-41205
Full Authority Digital Engine Control for the AS 355 N TM 319 engines p 665 A90-42486
Contribution of engine improvement on next future rotorcraft p 665 A90-42488
Application of advanced air vehicle and mission equipment technologies to the Light Helicopter (LH) [AIAA PAPER 90-3268] p 836 A90-48861
An appraisal of a number of power assessment procedures being proposed for use in Chinook-Lycoming T55 engine [AD-A210482] p 52 N90-10041
Coatings for gas turbine compressors [NLR-MP-88045-U] p 115 N90-11750
Cycle analysis for helicopter gas turbine engines [RAE-TM-P-1154] p 256 N90-15921
Preliminary airworthiness evaluation of the Woodward hydromechanical unit installed on T700-GE-700 engines in the UH-60A helicopter [AD-A216751] p 428 N90-18430
Experimental identification of helicopter engine dynamics from closed loop data p 855 N90-27627
HELICOPTER PERFORMANCE
Optimization of helicopter takeoff and landing p 29 A90-11006
Design of an advanced pneumatic deicer for the composite rotor blade p 29 A90-11009
System identification collaboration - The role of AGARD p 1 A90-12763
Identification of a coupled body/coning/inflow model of Puma vertical response in the hover p 56 A90-12765
Identification of an adequate model for collective response dynamics of a Sea King helicopter in hover p 56 A90-12766
Identification of a coupled flapping/inflow model for the PUMA helicopter from flight test data p 56 A90-12767
System identification strategies for helicopter rotor models incorporating induced flow p 30 A90-12768
Identification of rotor flapping equation of motion from flight measurements with the RSRA compound helicopter p 56 A90-12769
A frequency-domain system identification approach to helicopter flight mechanics model validation p 56 A90-12772
The application of linear maximum likelihood estimation of aerodynamic derivatives for the Bell-205 and Bell-206 p 30 A90-12773
Experience with multi-step test inputs for helicopter parameter identification p 56 A90-12775
New free-wake analysis of rotorcraft hover performance using influence coefficients p 181 A90-17867
Development of military helicopters p 181 A90-18488
Performance and aerodynamic development of the Super Puma Mk II main rotor with new SPP8 blade tip design [ONERA, TP NO. 1989-181] p 245 A90-21041
Correlation of Puma airfoils - Evaluation of CFD prediction methods [ONERA, TP NO. 1989-185] p 224 A90-21045
Mission effectiveness testing of an adaptive electronic fuel control on an S-76A p 422 A90-28199
The new Spheriflex tail rotor for the Super Puma Mark 2 p 408 A90-28213
A comparison of four versus five blades for the main rotor of a light helicopter p 408 A90-28215

Strike tolerant main rotor blade tip p 409 A90-28232
The revolution continuous --- performance of military helicopters [MBB-UD-557-89-PUB] p 381 A90-28242
Reduced-order modeling and controller design for a high-performance helicopter p 516 A90-33058
Development and verification of an algorithm for helicopter inverse simulations p 591 A90-38522
Results of an A109 simulation validation and handling qualities study p 591 A90-38524
Influence of ground effect on helicopter takeoff and landing performance p 645 A90-42278
EH101 development progress p 646 A90-42442
Improving tilt rotor aircraft performance with variable-diameter rotors p 646 A90-42445
Digital map reader for helicopters p 653 A90-42448
System concept and performance criteria of modern helicopter navigation p 640 A90-42452
A highly maneuverable helicopter in-flight simulator - Aspects of realization [AIAA PAPER 88-4607] p 670 A90-42466
Influence of ground effect on helicopter takeoff and landing performance p 646 A90-42468
Analytical study of dynamic response of helicopter in autorotative flight p 670 A90-42469
The response of helicopter to dispersed gust p 670 A90-42470
Eight years of flight operations with composite rotorblades p 635 A90-42481
Preliminary flight evaluation of the SA 365 Panther helicopter in air-to-air combat manoeuvres p 647 A90-42494
Fatigue life estimates for helicopter loading spectra p 772 A90-45324
Methodology for estimating helicopter performance and weights using limited data p 829 A90-46936
Modelling aspects for the synthesis and performance assessment of some future advanced helicopters p 829 A90-46937
MDHC technical assessment of advanced rotor and control concepts p 861 A90-46948
Application of the Westland CRFD program to total helicopter dynamics p 832 A90-46965
An investigation of aircraft maneuverability and agility [AIAA PAPER 90-3300] p 868 A90-48882
Multi-role advance technology rotorcraft - The EH101 [AIAA PAPER 90-3302] p 837 A90-48884
Coaxial helicopters - Current status and future developments p 838 A90-48951
Helicopter or tiltrotor - A Soviet view p 838 A90-48952
Damage tolerance for helicopters p 919 A90-49888
Airworthiness and flight characteristics test of the UH-60A Black Hawk helicopter equipped with the XM-139 multiple mine dispensing system (VOLCANO) [AD-A210271] p 32 N90-10025
Helicopter Visual Segment Approach Lighting System (HALS) [ACD-330] p 28 N90-10856
Heliprot surface maneuvering test results [ACD-330] p 59 N90-10897
Correlation of Puma airloads: Lifting-line and wake calculation [NASA-TM-102212] p 170 N90-13327
Software and hardware description of the helicopter motion equations for VAX computers [AD-A213248] p 184 N90-13375
Fatigue life estimates for helicopter loading spectra [NASA-CR-181941] p 279 N90-16294
Helicopter flight vibration of large transportation containers: A case for testing tailoring [DE90-007429] p 402 N90-19215
Airworthiness and flight characteristics evaluation of the McDonnell Douglas Helicopter Corporation (MDHC) 530FF helicopter [AD-A218253] p 498 N90-20076
Performance data from a wind-tunnel test of two main-rotor blade designs for a utility-class helicopter [NASA-TM-4183] p 499 N90-20974
An early overview of tiltrotor aircraft characteristics and pilot procedures in civil transport applications [DOT/FAA/DS-89/37] p 503 N90-21003
Indianapolis Downtown Heliprot: Operations analysis and marketing history [REPT-90RR-13] p 527 N90-21049
Aeronautical decisionmaking for air ambulance program administrators [DOT/FAA/DS-88/8] p 635 N90-23368
Aerodynamic performance of a 0.27-scale model of an AH-64 helicopter with baseline and alternate rotor blade sets [NASA-TM-4201] p 632 N90-24237
Helicopter controllability [AD-A220078] p 672 N90-24275

Agusta methodology for pitch link loads prediction in preliminary design phase
[ETN-90-97270] p 737 N90-25978

Obtaining consistent models of helicopter flight-data measurement errors using kinematic-compatibility and state-reconstruction methods
[AD-A22533] p 815 N90-26799

Heliport visual approach surface high temperature and high altitude tests
[DOT/FAA/CT-TN89/34] p 825 N90-27675

Flight test investigation of flight director and autopilot functions for helicopter decelerating instrument approaches
[DOT/FAA/CT-TN89/54] p 869 N90-27724

Evaluation of composite components on the Bell 206L and Sikorsky S-76 helicopters
[NASA-TM-4195] p 876 N90-27787

HELICOPTER PROPELLER DRIVE

Influence of the control law on the performance of a helicopter model rotor
[ONERA, TP NO. 1989-136] p 4 A90-11158

Tail rotor dynamics during the translational turn maneuver of a helicopter
p 334 A90-24148

Efficiency study comparing two helicopter planetary reduction stages
[AIAA PAPER 90-2156] p 956 A90-50644

Efficiency study comparing two helicopter planetary reduction stages
[NASA-TM-103106] p 776 N90-26334

HELICOPTER TAIL ROTORS

Numerical analysis of vibrations of a helicopter tail boom
p 31 A90-13224

Sound radiation from an airfoil encountering an oblique gust in its plane of motion
p 218 A90-17998

Prediction of the interaction noise emitted by helicopter fenestrans
p 218 A90-18449

Technical-scientific possibilities for helicopter noise research in the German-Dutch wind tunnel
p 283 A90-21474

High resolution flow field prediction for tail rotor aeracoustics
p 463 A90-28158

Aeracoustic flowfield and acoustics of a model helicopter tail rotor at high advance ratio
p 463 A90-28160

HARP model rotor test at the DNW — Hughes Advanced Rotor Program
p 406 A90-28167

Icing Research Tunnel test of a model helicopter rotor
p 400 A90-28179

New concept for improved nonmetallic erosion protection systems
p 407 A90-28188

The new Spheriflex tail rotor for the Super Puma Mark 2
p 408 A90-28213

Circulation control tail boom aerodynamic prediction and validation
p 385 A90-28243

Flight tests to explore tail rotor limitations in the low speed envelope
p 647 A90-42498

Mi-14 - The Soviet Sea King
p 730 A90-43765

A model suitable for predicting the noise associated with the ducted tail rotor of a helicopter
[ECL-88-09] p 220 N90-14074

The applicability of simple helicopter models for flight mechanics studies
[ETN-90-96962] p 736 N90-25975

HELICOPTER WAKES

New free-wake analysis of rotorcraft hover performance using influence coefficients
p 181 A90-17867

Rotor hover performance prediction using a free-wake, computational fluid dynamics method
p 153 A90-17869

Rotor blade-vortex interaction impulsive noise source localization
p 463 A90-27978

High resolution flow field prediction for tail rotor aeracoustics
p 463 A90-28158

The effect of an unsteady three-dimensional wake on elastic blade-flapping eigenvalues in hover
p 385 A90-28228

Recent advancement in helicopter rotor wake study
p 556 A90-36413

An unsteady helicopter rotor-fuselage aerodynamic interaction analysis
p 712 A90-45323

Application of the wide-field shadowgraph technique to rotor wake visualization
[NASA-TM-102222] p 88 N90-11700

Analysis of heliport environmental data: Indianapolis downtown heliport, Wall Street heliport. Volume 2: Wall Street heliport data plots
[DOT/FAA/CT-TN87/54-VOL-2] p 121 N90-11761

Rotor induced-inflow-ratio measurements and CAMRAD calculations
[NASA-TP-2946] p 237 N90-15882

Calculation of the flow field of a multiblade helicopter rotor using a Euler method including the wake
p 278 N90-16189

Analysis of heliport environmental data: Indianapolis downtown heliport, Wall Street heliport. Volume 3: Indianapolis downtown heliport data plots
[AD-A217412] p 544 N90-20500

The Second ARO Workshop on Rotorcraft Interactional Aerodynamics
[AD-A223310] p 911 N90-29304

HELICOPTERS

A statistical model of helicopter noise
p 77 A90-10229

Wind tunnel tests of models of helicopter rotors
p 29 A90-10230

Helicopter wire strike accident and high voltage electrocution - A case report
p 22 A90-10265

Prospects of onboard magnetic tape recording during flight tests
p 39 A90-12198

Simulation of helicopter landing on a ship deck
p 181 A90-17705

Preliminary feasibility study for a new hybrid airship (HeliShip)
[AIAA PAPER 89-3161] p 244 A90-20581

Effect of advanced component technology on helicopter transmissions
p 271 A90-21115

Digital map for helicopter navigation and guidance
p 252 A90-21609

Simplified analysis of helicopter fatigue loading spectra
p 336 A90-26758

Helmet mounted display systems for helicopter simulation
p 420 A90-31344

Sandwich structures on Aerospace helicopters
p 467 A90-31657

A study of symbolic processing and computational aspects in helicopter dynamics
p 545 A90-34103

The EH101 electronic instrument system
p 652 A90-40462

Obstacle warning system for helicopters
p 653 A90-41114

Wind-tunnel measurement of noise emitted by helicopter rotors at high speed
[ONERA, TP NO. 1990-28] p 695 A90-41207

Experimental study of the flow around an helicopter fuselage - Comparison with three-dimensional boundary layer calculations
p 630 A90-42438

Computation of viscous aerodynamic characteristics of 2-D airfoils for helicopter applications
p 631 A90-42440

Helicopter ground and air resonance dynamics
p 646 A90-42457

A new class of random processes with application to helicopter noise
p 781 A90-42874

Application of a new visualization method to helicopter rotor flow
[AIAA PAPER 90-3006] p 789 A90-45856

Torsional buckling and post-buckling of composite geodetic cylinders with special reference to joint flexibility
p 878 A90-45971

Synthesis of a simulator-based automated helicopter hover trainer
[AIAA PAPER 90-3481] p 891 A90-47730

An experimental investigation of helicopter rotor hub fairing drag characteristics
[NASA-TM-102182] p 88 N90-11701

Sequential design of experiments with physically based models 23
[AD-A211918] p 138 N90-12239

Rotorcraft low altitude CNS benefit/cost analysis: Rotorcraft operations data
[DOT/FAA/DS-89/9] p 141 N90-12406

RAN (Royal Australian Navy) vibration analysis system operator's guide
[AD-A212441] p 107 N90-12596

A robust digital model following controller for helicopters
[ESA-TT-1041] p 120 N90-12621

The human factors relating to escape and survival from helicopters ditching in water
[AGARD-AG-305(E)] p 176 N90-13358

Helicopter rotor test rig (RoTeSt) in DNW: Application and results
[RAE-TRANS-2171] p 201 N90-13408

Effect of blade planform variation on a small-scale hovering rotor
[NASA-TM-4146] p 173 N90-14186

An experimental investigation of the interaction between a model rotor and airframe in forward flight
p 185 N90-14219

An analytical method for the prediction of unsteady rotor/airframe interactions in forward flight
p 186 N90-14223

A helicopter flight path controller design via a nonlinear transformation technique
p 199 N90-14242

Fatigue analysis and reconstruction of helicopter load spectra
p 206 N90-14304

A two dimensional power spectral estimate for some nonstationary processes
[NASA-CR-186100] p 217 N90-14843

A study of the effects of Rotating Frame Turbulence (RFT) on helicopter flight mechanics
p 248 N90-15058

Effects of aeroelastic tailoring on anisotropic composite material beam models of helicopter blades
[AD-A213478] p 249 N90-15095

An examination of helicopter rotor load calculations
[AD-A214295] p 249 N90-15098

Adaptive control of helicopter vibrations via the impulse response method
[AD-A213728] p 260 N90-15113

Uses and properties of Al-Li on the new EH101 helicopter
p 268 N90-15201

Assessment of worm gearing for helicopter transmissions
[NASA-TM-102441] p 257 N90-15923

Natural icing re-evaluation of the EH-60A Quick Fix helicopter
[AD-A214728] p 323 N90-16723

Analysis of damaged components from DOE security helicopter N7EG
[DE90-004488] p 324 N90-16729

Low air speed computation for helicopters: A new approach
p 333 N90-16744

Preliminary design of a family of three close air support aircraft
[NASA-CR-186070] p 336 N90-16751

Equations of motion of slung load systems with results for dual lift
[NASA-TM-102246] p 349 N90-17641

Force determination sensitivities study for full-scale helicopter ground vibration testing
[AD-A215983] p 349 N90-17643

The Advanced Digital-Optical Control System (ADOCS) user demonstration program
[AD-A215984] p 349 N90-17644

Time and frequency-domain identification and verification of BO-105 dynamic models
[AD-A216828] p 415 N90-18389

Life of concentrated contacts in the mixed EHD and boundary film regimes
[AD-A216673] p 454 N90-18738

Heli/SITAN: A terrain referenced navigation algorithm for helicopters
[DE90-005193] p 405 N90-19217

The use of numerical optimization for helicopter airfoil and blade design
p 502 N90-20995

Helicopter Airborne Laser Positioning System (HALPS)
[NASA-TM-102814] p 654 N90-23399

Adaptive control of a system with periodic dynamics: Application of an impulse response method to the helicopter vibration problem
p 694 N90-23990

Operational effects on crashworthy seat attenuators
[AD-A221148] p 637 N90-24259

Evaluation of speech recognizers for use in advanced combat helicopter crew station research and development
[NASA-CR-177547] p 650 N90-24265

HPLC analysis of helicopter rotor blade materials
[AD-A221121] p 650 N90-24270

Helicopter controllability
[AD-A220078] p 672 N90-24275

Extension-torsion coupling behavior of advanced composite tilt-rotor blades
p 651 N90-25057

Coupled rotor-body equations of motion hover flight
[NASA-CR-186710] p 717 N90-25111

Computation of viscous aerodynamic characteristics of 2-D airfoils for helicopter applications
[NLR-MP-88052-U] p 720 N90-25951

Flow visualization of dynamic stall on an oscillating airfoil
[AD-A222202] p 815 N90-26797

Rotorcraft aeromechanical stability-methodology assessment. Phase 2: Workshop
[NASA-TM-102272] p 816 N90-26800

Device for the dilution of hot exhaust jets
[ETN-90-97435] p 858 N90-27723

The Helicopter Antenna Radiation Prediction Code (HARP)
[NASA-CR-186925] p 884 N90-27946

Solution of Euler equations applied to a rotor of a helicopter in steady flight
[ONERA-RSF-1/3731-AY-002A] p 910 N90-28500

Velocity filtering applied to optical flow calculations
[NASA-TM-102802] p 916 N90-28512

Analysis of heliport environmental data, Intracoastal City
[DOT/FAA/CT-TN89/43] p 938 N90-28584

FAA Rotorcraft Research, Engineering, and Development Bibliography 1962-1989
[AD-A224256] p 902 N90-29299

HELIPORTS

Heliport surface maneuvering test results
[ACD-330] p 59 N90-10897

- Analysis of heliport environmental data: Indianapolis downtown heliport, Wall Street heliport. Volume 2: Wall Street heliport data plots
[DOT/FAA/CT-TN87/54-VOL-2] p 121 N90-11761
- Analysis of heliport environmental data: Indianapolis downtown heliport, Wall Street heliport. Volume 3: Indianapolis downtown heliport data plots
[AD-A217412] p 544 N90-20500
- Indianapolis Downtown Heliport: Operations analysis and marketing history
[REPT-90RR-13] p 527 N90-21049
- Analysis of distributions of Visual Meteorological Conditions (VMC) heliport data
[DOT/FAA/CT-TN89/67] p 544 N90-21508
- Heliport visual approach surface high temperature and high altitude tests
[DOT/FAA/CT-TN89/34] p 825 N90-27675
- Analysis of heliport environmental data, Intracoastal City
[DOT/FAA/CT-TN89/43] p 938 N90-28584
- FAA Rotorcraft Research, Engineering, and Development Bibliography 1962-1989
[AD-A224256] p 902 N90-29299

HELMET MOUNTED DISPLAYS

- Helicopter obstacle avoidance system - The use of manned simulation to evaluate the contribution of key design parameters
p 417 A90-28218
- Design criteria for helicopter night pilotage sensors
p 417 A90-28221
- Toward the panoramic cockpit, and 3-D cockpit displays
p 419 A90-30682
- Helmet mounted display systems for helicopter simulation
p 420 A90-31344
- Flight tests of a helmet-mounted display synthetic visibility system
[AIAA PAPER 90-1279] p 579 A90-36027
- Helmet-mounted display systems for flight simulation
[SAE PAPER 892352] p 760 A90-45503

HELMHOLTZ RESONATORS

- Calculation of vibrational combustion limits in Helmholtz resonator-type chambers
p 125 A90-14588
- An analysis of cavity resonance in the aeroengine casing during rig testing
p 890 A90-49481

HEMISPHERE CYLINDER BODIES

- The hemisphere-cylinder at an angle of attack
[AIAA PAPER 90-0050] p 313 A90-26907

HERMES MANNED SPACEPLANE

- Aerodynamic work for Hermes spaceplane
p 675 A90-41115
- Flows with Separation
[DGLR-PAPERS-88-05] p 276 N90-16169
- Hermes training aircraft
p 354 N90-16827

HERMETIC SEALS

- Optimization of the shape of a sealed shell and of the size and location of its reinforcements
p 957 A90-50773

HETERODYNING

- Feasibility of using frequency offset on very high frequency air/ground voice channels
[DOT/FAA/CT-TN89/71] p 542 N90-21248

HEURISTIC METHODS

- Applications of fuzzy sets to rule-based expert system development
p 216 A90-18050
- A multiprocessor implementation of real-time control for a turbojet engine
p 746 A90-45415
- Real-time adaptive aircraft scheduling
[NASA-CR-177558] p 820 N90-27669

HF LASERS

- HF shock tunnel facility for studying supersonic combustion
[AIAA PAPER 90-1551] p 600 A90-38693

HIGH ALTITUDE

- Restart characteristics of turbofan engines
p 50 A90-12627
- Nonlinear mechanics of unstable plasmas as related to high altitude aerodynamics
[AD-A215126] p 464 N90-19852
- NASA/USRA high altitude reconnaissance aircraft
[NASA-CR-186685] p 650 N90-24266
- Global Sentry: NASA/USRA high altitude reconnaissance aircraft design, volume 2
[NASA-CR-186820-VOL-2] p 736 N90-25971

HIGH ASPECT RATIO

- Aeroelastic characteristics of aircraft with circulation control wings
p 497 N90-20070

HIGH FREQUENCIES

- Feasibility of using frequency offset on very high frequency air/ground voice channels
[DOT/FAA/CT-TN89/71] p 542 N90-21248
- Equipment feasibility study: Very high frequency communication equipment (136-137 megahertz)
[DOT/FAA/CT-TN89/72] p 775 N90-26210

HIGH LEVEL LANGUAGES

- High level language programming for avionic vector processors
[AIAA PAPER 89-3107] p 74 A90-10589

HIGH PRESSURE

- Cooking an aeroplane
p 209 A90-17918
- A test facility for high-pressure high-temperature combustion chambers
p 438 A90-29924
- Small-scale inlet testing for low cost screening applications
[AIAA PAPER 90-1926] p 741 A90-42696
- Advanced actuation systems development, volume 1
[AD-A213334] p 121 N90-12624
- Nonflammable hydraulic power system for tactical aircraft. Volume 1: Aircraft system definition, design and analysis
[AD-A218493] p 671 N90-23409

HIGH PRESSURE OXYGEN

- RAAF Orion aircraft A9-300 oxygen fire
[AD-A215496] p 323 N90-16725

HIGH REYNOLDS NUMBER

- The numerical method for solving the high Reynolds hypersonic viscous shock layer
p 2 A90-10340
- Convergence properties of high-Reynolds-number separated flow calculations
p 86 A90-15820
- Further work on aerofoils at Reynolds numbers between 3×10^6 to the 5th and 1×10^7 to the 6th
p 145 A90-16758
- Theoretical prediction of high Reynolds number viscid/inviscid interaction phenomena in cascades
p 145 A90-16759
- High Reynolds number wedge-induced separation lengths at Mach 6
p 154 A90-18001
- Unsteady streamlines near the trailing edge of NACA 0012 airfoil at a Reynolds number of 125,000
p 155 A90-18158

- Compressibility effects in free shear layers
[AIAA PAPER 90-0705] p 212 A90-19984
- Development of the MZM numerical method for 3D boundary layer with interaction on complex configurations --- Multi-Zonal Marching
[ONERA, TP NO. 1989-174] p 223 A90-21036

- The detection of large scale structure in undisturbed and disturbed compressible turbulent free shear layers
[AIAA PAPER 90-0711] p 230 A90-22251
- Flight and wind-tunnel investigations on boundary-layer transition
p 233 A90-23283

- Effects of compressibility on the characteristics of free shear layers
p 302 A90-25285
- A concept study on the use of remotely piloted, sub-scale aircraft for high Reynolds number testing
[AIAA PAPER 90-1263] p 494 A90-33892

- A proposed automatic calibration facility for cryogenic balances
p 524 A90-34246
- Dynamics of the outgoing turbulent boundary layer in a Mach 5 unswept compression ramp interaction
[AIAA PAPER 90-1645] p 569 A90-38773
- Coherent vortex structures in the wake of a sphere and a circular disk at rest and under forced vibrations
p 623 A90-40749

- Cryogenic wind tunnels
p 673 A90-41726
- Correlation of theory to wind-tunnel data at Reynolds numbers below 500,000
p 800 A90-46370
- Flow past bodies within a narrow class of cross-sectional shapes with stationary separation zones at large Reynolds numbers
p 805 A90-46568

- A study of high-lift airfoils at high Reynolds numbers in the Langley low-turbulence pressure tunnel
[NASA-TM-89125] p 1 N90-10002
- An investigation of end-wall vortex cavitation in a high Reynolds number axial-flow pump
[AD-A211426] p 133 N90-11982

- Design and test of a natural laminar flow/large Reynolds number airfoil with a high design cruise lift coefficient
p 93 N90-12543

- Low speed testing of a laminar flow airfoil in an adaptive wall wind tunnel
[FFA-TN-1989-08] p 632 N90-23363

HIGH SPEED

- Hydrodynamic visualization of the flow around a high-speed aircraft propeller
[ONERA, TP NO. 1989-108] p 3 A90-11141
- A study on the performance of the turbo-ranjet engines at high speed flight
p 49 A90-12608
- An investigation of the behavior of the dynamic load distribution versus operating speed and torque on heavily loaded, high speed aircraft gearing
p 271 A90-21129
- Generalized Transition Finite-Boundary Elements for high speed flight structures
[AIAA PAPER 90-1105] p 449 A90-29286
- Evaluation of critical speeds in high speed aircraft tires
[SAE PAPER 892349] p 733 A90-45500
- Large-scale Advanced Prop-fan (LAP) high speed wind tunnel test report
[NASA-CR-182125] p 52 N90-10045
- A review of high-speed, convective, heat-transfer computation methods
p 316 N90-17548
- Aerofoil design techniques
p 500 N90-20978

- High speed civil transport
[NASA-CR-186661] p 649 N90-23396
- Study of high-speed civil transports. Summary
[NASA-CR-4236] p 735 N90-25966

HIGH SPEED CAMERAS

- Regression and combustion characteristics of boron containing fuels for solid fuel ramjets
p 858 N90-27928

HIGH STRENGTH

- Current status of the application of conventional aluminium-lithium alloys and the potential for future developments
p 268 N90-15203

HIGH STRENGTH ALLOYS

- IMI 834 - A new high temperature capability titanium alloy for engine use
p 62 A90-12535
- Intermetallic compounds for strong high-temperature materials - Status and potential
p 125 A90-15022
- Effects on aerospace alloys of residual chlorine in chlorinated-solvent primers
p 956 A90-50187
- MATE (Materials for Advanced Turbine Engines) Program, Project 3. Volume 2: Design, fabrication and evaluation of an oxide dispersion strengthened sheet alloy combustor liner
[NASA-CR-180892] p 357 N90-17868

HIGH STRENGTH STEELS

- Al-Li alloys and ultrahigh-strength steels for U.S. Navy aircraft
p 599 A90-37441
- Ultrahigh-strength steels for aerospace applications
p 599 A90-37443
- Improved steel for landing gear design
[SAE PAPER 892335] p 765 A90-45490
- Statistical treatment of slow strain rate data for assessment of hydrogen embrittlement in low alloy high strength steel
[ARL-MAT-R-122] p 767 N90-26106

HIGH TEMPERATURE

- Cooking an aeroplane
p 209 A90-17918
- Total temperature effects on centerline Mach number characteristics of freejets
p 302 A90-25290
- New metallic felts with improved resistance to high temperature oxidation
[ONERA, TP NO. 1989-210] p 366 A90-25343
- High-temperature electronics for aircraft engines
[AIAA PAPER 90-2035] p 657 A90-40604
- High temperature powder lubricated dampers for gas turbine engines
[AIAA PAPER 90-2048] p 684 A90-41999
- Multiple swirler dome combustor for high temperature rise applications
[AIAA PAPER 90-2159] p 661 A90-42050
- Spray automated balancing of rotors - How process parameters influence performance
p 879 A90-46228
- Stress intensity factors for cracking metal structures under rapid thermal loading. Volume 2: Theoretical background
[AD-A213297] p 213 N90-13812
- Carbon-carbon composites: Emerging materials for hypersonic flight
[NASA-TM-103472] p 767 N90-26080
- Elevated temperature crack growth
[NASA-CR-182247] p 777 N90-26355
- Engine testing of thermographic phosphors
[DE90-013269] p 885 N90-28059
- Analysis of the T63-A-700 engine used in alcohol turbine fuel extender test
[DOT/FAA/CT-TN90/18] p 928 N90-28549
- High Temperature Surface Interactions
[AGARD-CP-461] p 951 N90-28698
- Molten salt induced high temperature degradation of thermal barrier coatings
p 952 N90-28704
- Evaluation of high temperature protective coatings for gas turbine engines under simulated service conditions
p 952 N90-28712
- Surface property improvement in titanium alloy gas turbine components through ion implantation
p 953 N90-28713

HIGH TEMPERATURE ENVIRONMENTS

- Inverse cycle engine for hypersonic air-breathing propulsion
[ONERA, TP NO. 1989-121] p 50 A90-12611
- Development of high temperature actuation systems for advanced aircraft engines
[AIAA PAPER 90-2031] p 660 A90-41990
- Damage tolerance evaluation of several elevated temperature graphite composite materials
p 945 A90-50155
- Thermal interaction between an impinging hot jet and a conducting solid surface
[AIAA PAPER 90-3010] p 956 A90-50636
- High temperature VSCF (Variable Speed Constant Frequency) generator system
[AD-A210823] p 71 N90-10351

HIGH TEMPERATURE GASES

- Advanced turbine technology applications project (ATTAP) - Overview, status, and outlook
[ASME PAPER 89-GT-118] p 360 A90-23819

- The in service multi-axial-stress situation in an uncooled gas turbine blade p 423 A90-29880
- Design of an air-cooled metallic high-temperature radial turbine p 507 A90-32960
- Hot-gas corrosion test of Si3N4 and SiC p 531 A90-33987
- Development of ceramic components for high-temperature gas turbines p 602 A90-35951
- Hot gas environment around STOVL aircraft in ground proximity. I - Experimental study [AIAA PAPER 90-2269] p 742 A90-42765
- Hot gas environment around STOVL aircraft in ground proximity. II - Numerical study [AIAA PAPER 90-2270] p 743 A90-42766
- Three-dimensional turbulent flow code calculations of hot gas ingestion p 745 A90-44726
- Hot gas ingestion characteristics and flow visualization of a vectored thrust STOVL concept [NASA-TM-103212] p 751 N90-26009
- Overview on hot gas tests and molten salt corrosion experiments at the DLR p 953 N90-28714
- HIGH TEMPERATURE LUBRICANTS**
- High temperature solid lubricant requirements for advanced high performance gas turbine engines [AIAA PAPER 90-2042] p 661 A90-41993
- HIGH TEMPERATURE SUPERCONDUCTORS**
- Assessment of High Temperature Superconducting (HTS) electric motors for rotorcraft propulsion [NASA-CR-185222] p 588 N90-21761
- HIGH TEMPERATURE TESTS**
- An automatic system for the programmed control of the parameters of the vibrational and thermal testing of the blades of gas turbine engines p 343 A90-24216
- The effect of elevated temperature exposure on the tensile and creep properties of Ti-24Al-11Nb p 355 A90-24865
- Carbon/epoxy tooling evaluation and usage p 445 A90-28165
- High temperature skin friction measurement p 448 A90-28306
- A test facility for high-pressure high-temperature combustion chambers p 438 A90-29924
- The status of high temperature polymers for composites - Likely candidates p 528 A90-31516
- High service temperature high compressive strength and tough prepreg system p 530 A90-33098
- High-temperature corrosion and mechanical properties of some silicon nitride ceramics p 531 A90-33985
- The experimental study on the coaxial dump combustor with inner swirl inlet under the combustion condition p 585 A90-36786
- High temperature deformation studies on CVD silicon carbide fibers p 945 A90-50147
- The application of 'PT' resins to high temperature aerospace structures p 949 A90-50230
- HIGH VOLTAGES**
- High Voltage Design Guide summary p 605 A90-38097
- Applying AVIP to high voltage power supply designs - Avionic Integrity Program p 605 A90-38132
- HIGHLY MANEUVERABLE AIRCRAFT**
- Flight beyond normal limits p 589 A90-35847
- Air combat beyond the stall p 589 A90-35888
- A highly maneuverable helicopter in-flight simulator - Aspects of realization [AIAA PAPER 88-4607] p 670 A90-42466
- Multivariable control law for flat-turn strafe maneuver by a supermaneuverable aircraft [AIAA PAPER 90-3371] p 863 A90-47629
- A nonlinear aircraft tracking filter utilizing control variable estimation [AIAA PAPER 90-3402] p 822 A90-47657
- Nonlinear inversion flight control for a supermaneuverable aircraft [AIAA PAPER 90-3406] p 864 A90-47661
- HILLER AIRCRAFT**
- The Hiller X-18 experimental aircraft - Lessons learned [AIAA PAPER 90-3203] p 834 A90-48832
- HINGES**
- Rotary servohinge actuator [SAE PAPER 89-2261] p 733 A90-45458
- Hinge moment coefficient derivatives for trailing-edge controls on wings at subsonic speeds [ESDU-89009] p 198 N90-14239
- Example of procedure in calculation of control hinge moments [ESDU-89010] p 199 N90-14240
- HISTORIES**
- The birth of the airplane: The first designs and constructions - Russian book p 79 A90-12478
- History of the airplane. IV p 30 A90-12791
- Encyclopedia of US Air Force aircraft and missile systems. Volume 2: Post-World War 2 bombers, 1945-1973 [AD-A209273] p 1 N90-10001
- Flight testing and flight research: From the age of the tower jumper to the age of the astronaut p 35 N90-10882
- LFC: A maturing concept [DOUGLAS-PAPER-7878] p 90 N90-12505
- The NASA Langley 0.3-meter transonic cryogenic tunnel p 262 N90-15941
- The aims and history of adaptive wall wind tunnels p 871 N90-26839
- A look at tomorrow today p 921 N90-28524
- HODOGRAPHS**
- Solution of sonic flow problems p 470 A90-32712
- HOLE DISTRIBUTION**
- Impingement/effusion cooling - The influence of the number of impingement holes and pressure loss on the heat transfer coefficient [ASME PAPER 89-GT-188] p 361 A90-23866
- HOLE GEOMETRY (MECHANICS)**
- Fatigue of thick-section cold-expanded holes with and without cracks p 270 A90-20987
- HOLES (MECHANICS)**
- Wave cancellation properties of a splitter-plate porous wall configuration p 57 A90-11005
- A study on initial fatigue quality of typical aircraft structures (fastener holes) p 272 A90-22004
- Heat transfer near the entrance to a film cooling hole in a gas turbine blade [AD-A217396] p 510 N90-20089
- Modeling growth of fatigue cracks which originate at rivet holes p 691 N90-25060
- A technique for rapid inspection of composite aircraft structure for impact damage p 846 N90-28077
- HOLOGRAPHIC INTERFEROMETRY**
- Holographic interferometric study of shock wave propagation p 66 A90-10732
- Complementary field method for interferometric tomographic reconstruction of high speed aerodynamic flows [AD-A219698] p 131 A90-15900
- Simulation of cooling film density ratios in a mass transfer technique [ASME PAPER 89-GT-200] p 362 A90-23872
- Self compensation of rigid displacements in holographic interferometry [ISL-CO-219/88] p 370 N90-17113
- HOLOGRAPHY**
- Holographic head-up displays for air and ground applications p 108 A90-13885
- Synthetic holography applied to head-up displays p 218 A90-16692
- Holographic combiner design to obtain uniform symbol brightness at head-up display video camera p 652 A90-40394
- HOMOTOPY THEORY**
- Quasi-three-dimensional grid generation by an algebraic homotopy procedure p 376 A90-26481
- HONEYCOMB CORES**
- Repair of composite aircraft parts - An operator's viewpoint p 221 A90-20606
- Natural honeycomb - use of balsa wood in sandwich panel cores for advanced composite airframes p 442 A90-29643
- Manufacture of honeycomb p 538 A90-33704
- Honeycomb quality requirements - A user's perspective p 538 A90-33705
- Design with honeycomb, state of the art p 538 A90-33706
- Tradeoffs in honeycomb cored designs p 538 A90-33708
- Core composites in Swissair aircraft p 493 A90-33709
- A comparison of honeycomb-core and foam-core carbon-fibre/epoxy sandwich panels p 764 A90-43855
- Parametric studies of acoustic duct attenuation perforated-plate-on-honeycomb absorber [NAL-TM-603] p 966 N90-30030
- HONEYCOMB STRUCTURES**
- Mean and pulse characteristics of supersonic flow in a wind tunnel with a honeycomb nozzle p 231 A90-22421
- Power dissipation in smooth and honeycomb labyrinth seals [ASME PAPER 89-GT-220] p 362 A90-23881
- Electromagnetic dent removal for aircraft repair [SAE PAPER 89-0923] p 286 A90-24689
- Honeycomb sandwich primary structure applications on the Boeing Model 360 helicopter p 490 A90-31558
- Manufacture of honeycomb p 538 A90-33704
- Honeycomb quality requirements - A user's perspective p 538 A90-33705
- Design with honeycomb, state of the art p 538 A90-33706
- Tradeoffs in honeycomb cored designs p 538 A90-33708
- Wide-chord fan proved in nearly five years of service p 744 A90-44594
- Durability and damage tolerance of graphite/epoxy honeycomb structures p 942 A90-50085
- Impact testing of glass/phenolic honeycomb panels with graphite/epoxy facesheets p 946 A90-50166
- Development of an automated ultrasonic inspection system for composite structure on in-service aircraft p 885 N90-28079
- A low cost shadow moire device for the nondestructive evaluation of impact damage in composite laminates [AD-A223451] p 953 N90-29442
- HORIZONTAL FLIGHT**
- Optimization of rotor performance in hover and axial flight using a free wake analysis p 407 A90-28175
- Prediction and measurement of the aerodynamic interactions between a rotor and airframe in forward flight p 384 A90-28176
- Three-dimensional viscous rotor flow calculations using a viscous-inviscid interaction approach [NASA-TM-102235] p 399 N90-19204
- Velocity measurements on a lifting rotor/airframe configuration in low speed forward flight p 815 N90-26790
- HORIZONTAL TAIL SURFACES**
- Aeroelastic analysis for a composite T-tailplane of a turboprop commuter aircraft p 492 A90-33390
- Effects of tailplane aerodynamics and fuselage flexibility on the flutter of high aspect ratio, low speed aircraft p 493 A90-33414
- Design and experimental investigation of a laminar horizontal tail [AIAA PAPER 90-3042] p 798 A90-45934
- Validation of a computer code for analysis of subsonic aerodynamic performance of wings with flaps in combination with a canard or horizontal tail and an application to optimization p 173 N90-14187
- Installed tailplane lift-curve slope at subsonic speeds [ESDU-89029] p 236 N90-15081
- HORSESHOE VORTICES**
- Effective methods of controlling a junction vortex system in an incompressible, three-dimensional, turbulent flow p 571 N90-21732
- HOT CORROSION**
- Burner rig hot corrosion of silicon carbide and silicon nitride p 355 A90-25267
- New metallic felts with improved resistance to high temperature oxidation [ONERA, TP NO. 1989-210] p 366 A90-25343
- Coatings for high temperature corrosion in aero and industrial gas turbines p 443 A90-30479
- High-temperature corrosion and mechanical properties of some silicon nitride ceramics p 531 A90-33985
- Molten salt induced high temperature degradation of thermal barrier coatings p 952 N90-28704
- Evaluation of high temperature protective coatings for gas turbine engines under simulated service conditions p 952 N90-28712
- Overview on hot gas tests and molten salt corrosion experiments at the DLR p 953 N90-28714
- HOT ISOSTATIC PRESSING**
- Slip-cast hot isostatically pressed silicon nitride gas turbine components p 765 A90-44816
- Processing of advanced ceramics which have potential for use in gas turbine aero engines [AD-A220988] p 766 N90-25226
- HOT SURFACES**
- Mean flow measurements of heated supersonic slot injection into a high Reynolds number supersonic stream [AIAA PAPER 90-0180] p 163 A90-19722
- Hot surface ignition studies of aviation fluids p 327 N90-17600
- The stability of fuel fires p 327 N90-17601
- HOT WORKING**
- Thermomechanical processing of superalloys p 531 A90-34156
- HOT-FILM ANEMOMETERS**
- In quest of the laminar-flow airliner - Flight experiments on a T-33 jet trainer p 300 A90-24825
- A transition detection study at Mach 1.5, 2.0, and 2.5 using a micro-thin hot-film system p 436 A90-28260
- Development of two multi-sensor hot-film measuring techniques for free-flight experiments p 417 A90-28291
- Status of the development programme for instrumentation and test techniques of the European Transonic Windtunnel - ETW p 437 A90-28292
- Measurement of crossflow vortices, attachment-line flow, and transition using microthin hot films [AIAA PAPER 90-1636] p 607 A90-38765
- Hot-film system for transition detection in cryogenic wind tunnels p 122 N90-12522
- Predicted and hot-film measured Tollmien-Schlichting wave characteristics p 91 N90-12523

Relating flow between counter-rotating propellers to aerodynamic interaction noise p 479 N90-20944

HOT-WIRE ANEMOMETERS

A theoretical and experimental investigation of the Reynolds and apparent stresses in axial compressors p 12 A90-12554

Hot wire measurements in the wake of an oscillating airfoil p 15 A90-12635

An experimental investigation of the downwash beneath a lifting rotor and low advance ratios p 151 A90-17585

Hot-wire measurements of near wakes behind an oscillating airfoil p 154 A90-18138

Measurements in a separation bubble on an airfoil using laser velocimetry p 384 A90-27977

An automated vorticity surveying system using a rotating hot-wire probe p 447 A90-28284

Hot wire anemometry in transonic flows and cryogenic conditions p 539 A90-34229

Basic aerodynamic research facility for comparative studies of flow diagnostic techniques p 122 N90-12526

HOT-WIRE FLOWMETERS

Experimental investigations on the spatial and time-dependent structure of part-load recirculations in centrifugal pumps p 83 A90-13788

Unsteady transition in an axial-flow turbine. I - Measurements on the turbine rotor. II - Cascade measurements and modeling p 474 A90-33562

Vorticity distribution of vortex street in the wake of a circular cylinder p 623 A90-41751

HOTOL LAUNCH VEHICLE

HOTOL: A future launcher for Europe p 353 N90-16800

Aerodynamic and structural design challenges of a reusable single stage to orbit air-breathing launch vehicle p 354 N90-16814

HOTSHOT WIND TUNNELS

High enthalpy hypersonic wind tunnel F4: General description and associated instrumentation p 673 N90-24228

HOUSINGS

The application of cast SiC/Al to rotary engine components p 192 N90-13385

Gear noise, vibration, and diagnostic studies at NASA Lewis Research Center p 372 N90-18041

Fractographic analysis of fatigue failures of airframe equipment parts: Examples of a rod end housing and a rod end cap p 961 N90-29686

[NAL-TR-1047] p 961 N90-29686

HOVERCRAFT GROUND EFFECT MACHINES

A two dimensional study of rotor/airfoil interaction in hover p 845 N90-27694

HOVERING

Identification of a coupled body/coning/inflow model of Puma vertical response in the hover p 56 A90-12765

Identification of an adequate model for collective response dynamics of a Sea King helicopter in hover p 56 A90-12766

GPS Hover Position Sensing System p 108 A90-13986

A simple active controller to suppress helicopter air resonance in hover and forward flight p 119 A90-16521

New free-wake analysis of rotorcraft hover performance using influence coefficients p 181 A90-17867

Optimization of rotor performance in hover and axial flight using a free wake analysis p 407 A90-28175

Tip vortex geometry of a hovering helicopter rotor in ground effect p 407 A90-28196

Theoretical and experimental correlation of helicopter aeromechanics in hover p 429 A90-28200

Stability of hingeless rotors in hover using three-dimensional unsteady aerodynamics p 430 A90-28227

The effect of an unsteady three-dimensional wake on elastic blade-flapping eigenvalues in hover p 385 A90-28228

Relative aeromechanical stability characteristics for hingeless and bearingless rotors p 409 A90-28230

An experimental and analytical investigation of isolated rotor flap-lag stability in forward flight p 518 A90-33623

Thrust generation by an airfoil in hover modes [AD-A23602] p 552 A90-35137

Aerodynamic loads and blade vortex interaction noise prediction p 614 A90-38520

The free-wake computation of rotor-body flows [AIAA PAPER 90-1540] p 565 A90-38684

Application of mathematical modeling to the study of rigid helicopter rotors p 643 A90-41738

A review of tilt rotor download research p 630 A90-42437

Influence of ground effect on helicopter takeoff and landing performance p 646 A90-42468

Robust hover control for a short takeoff/vertical landing aircraft [AIAA PAPER 90-3333] p 862 A90-47593

Application of a design method for integrated control to a VTOL airplane in hover [AIAA PAPER 90-3334] p 862 A90-47594

Synthesis of a simulator-based automated helicopter hover trainer [AIAA PAPER 90-3481] p 891 A90-47730

Flight investigation of variations in rotorcraft control and display dynamics for hover [AIAA PAPER 90-3482] p 866 A90-47731

Low-speed wind-tunnel study of reaction control-jet effectiveness for hover and transition of a STOVLT fighter concept [NASA-TM-4147] p 119 N90-11751

Effect of blade planform variation on a small-scale hovering rotor [NASA-TM-4146] p 173 N90-14186

X.2 limited flight test plan [AD-A214412] p 249 N90-15099

Three-dimensional viscous rotor flow calculations using a viscous-inviscid interaction approach [NASA-TM-102235] p 399 N90-19204

Analysis of small-scale rotor hover performance data [NASA-TM-102271] p 540 N90-20325

Stereopsis cueing effects on hover-in-turbulence performance in a simulated rotorcraft [NASA-TP-2980] p 506 N90-21004

Coupled rotor-body equations of motion hover flight [NASA-CR-186710] p 717 N90-25111

Model tilt-rotor hover performance and surface pressure measurement [AD-A22535] p 845 N90-26827

Hover position sensing system p 848 N90-27448

A two dimensional study of rotor/airfoil interaction in hover [NASA-CR-183272] p 845 N90-27694

The effects of structural flap-lag and pitch-lag coupling on soft inplane hingeless rotor stability in hover [NASA-TP-3002] p 910 N90-28503

Numerical simulations of blade-vortex interactions and lifting hovering rotor flows [AD-A224238] p 911 N90-29302

HOVERING STABILITY

Supplemented visual cues for helicopter hovering above a moving ship deck p 195 A90-17704

Rotor hover performance prediction using a free-wake, computational fluid dynamics method p 153 A90-17869

A comprehensive hover test of the airloads and airflow of an extensively instrumented model helicopter rotor p 407 A90-28173

UH-60A helicopter stability augmentation study p 670 A90-42471

AHS National Specialists' Meeting on Rotorcraft Dynamics, Arlington, TX, Nov. 13, 14, 1989, Proceedings p 830 A90-46952

Theoretical and experimental investigation of the aeroelastic stability of an advanced bearingless rotor in hover and forward flight p 831 A90-46958

Flight evaluations of several hover control and display combinations for precise blind vertical landings [AIAA PAPER 90-3479] p 867 A90-47764

Airworthiness and flight characteristics test of the UH-60A Black Hawk helicopter equipped with the XM-139 multiple mine dispensing system (VOLCANO) [AD-A210271] p 32 N90-10025

The effects of structural flap-lag and pitch-lag coupling on soft inplane hingeless rotor stability in hover [NASA-TP-3002] p 910 N90-28503

HTPB PROPELLANTS

Solid fuel ignition and combustion characteristics under high-speed crossflows [AIAA PAPER 90-2075] p 764 A90-42725

HUBS

Hub loads analysis of the SA349/2 helicopter p 333 A90-23936

Vortex theory for the screw propeller with a hub p 620 A90-39538

EH-101 main rotor hub application of thick carbon fiber unidirectional tension bands p 618 A90-42489

An experimental investigation of helicopter rotor hub fairing drag characteristics [NASA-TM-102182] p 88 N90-11701

HUMAN BEHAVIOR

The insertion of human dynamics models in the flight control loops of V/STOL research aircraft. Appendix 2: The optimal control model of a pilot in V/STOL aircraft control loops [NASA-CR-186598] p 598 N90-21776

HUMAN CENTRIFUGES

Human centrifuge controller [NAL-TM-SE-8901] p 527 N90-21043

HUMAN FACTORS ENGINEERING

A description of the Naval Air Development Center's ejection tower and crash test facilities and their uses p 200 A90-17426

Advanced Automation System design p 375 A90-25566

Toward a human-centered aircraft automation philosophy p 347 A90-26177

Designers as users - Design supports based on crew system design practices p 457 A90-28184

Strategic aircraft engineering design simulation p 439 A90-30729

Underlying factors in air traffic control incidents p 401 A90-31335

Techniques for improving precision of flying qualities assessment [AIAA PAPER 90-1285] p 519 A90-33906

The Common/Same Type Rating - Human factors and other issues [SAE PAPER 892229] p 723 A90-45445

Task-oriented display design - Concept and example [SAE PAPER 892230] p 738 A90-45446

Advanced architecture for domestic and global aviation systems p 822 A90-46398

Upgrading the cockpit - A multidisciplinary approach p 848 A90-48995

Classification and reduction of pilot error [NASA-CR-181867] p 24 N90-10014

See and avoid/cockpit visibility [DOT/FAA/CT-TN89/18] p 24 N90-10843

Integration of a centralized multiplexed control unit into the cockpit of an aircraft [F6150-DT410-1-88329] p 120 N90-12622

The human factors relating to escape and survival from helicopters ditching in water [AGARD-AG-305(E)] p 176 N90-13358

Software and hardware description of the helicopter motion equations for VAX computers [AD-A213248] p 184 N90-13375

The human element: The key to safe, civil operations in adverse weather p 484 N90-15042

See and avoid/cockpit visibility [AD-A214214] p 239 N90-15084

A review of UK civil aviation fire and cabin safety research p 325 N90-17587

New aircraft cabin and cargo flammability standards for transport category aircraft p 325 N90-17589

Full scale study of a cabin fire in an A300 fuselage section p 326 N90-17592

Forced and natural venting of aircraft cabin fires: A numerical simulation p 326 N90-17597

Controllable propulsion for escape systems control p 484 N90-20064

Investigation of air transportation technology at the Massachusetts Institute of Technology, 1988-1989 p 484 N90-20922

The insertion of human dynamics models in the flight control loops of V/STOL research aircraft. Appendix 2: The optimal control model of a pilot in V/STOL aircraft control loops [NASA-CR-186598] p 598 N90-21776

Evaluation of speech recognizers for use in advanced combat helicopter crew station research and development [NASA-CR-177547] p 650 N90-24265

CREW CHIEF: A computer graphics simulation of an aircraft maintenance technician p 779 N90-25515

Modeling strength data for CREW CHIEF p 780 N90-25516

The need for platform motion in modern piloted flight training simulators [AD-A221720] p 871 N90-26847

PHARE: Concept and programme p 827 N90-27690

A conceptual framework for fighter flight control systems [PD-CF-9009] p 936 N90-28577

HUMAN PATHOLOGY

The use of soot analysis as an investigative tool in aircraft fires p 22 A90-10269

HUMAN PERFORMANCE

Peacekeeper IFSS - A TQM success story - Instrumentation and Flight Safety System [AIAA PAPER 89-3218] p 549 A90-31702

Correlation between vibration and computer operator response onboard a UH-1H helicopter p 737 A90-43727

Aeronautical decisionmaking for air ambulance program administrators [DOT/FAA/DS-88/8] p 635 N90-23368

Neural networks for detecting defects in aircraft structures [IAR-90-4] p 777 N90-26345

Robotic-aided system for inspection of aging aircraft
[NIAR-90-9] p 777 N90-26346

HUMAN REACTIONS
An adaptive human response mechanism controlling the V/STOL aircraft. Appendix 3: The adaptive control model of a pilot in V/STOL aircraft control loops
[NASA-CR-186599] p 598 N90-21777
Human response research update
p 699 N90-24873

HUMAN RESOURCES
Profiles-aeronautical/astronautical engineering: Human resources and funding
[PB90-103888] p 369 N90-16969

HUMAN TOLERANCES
Annoyance caused by advanced turboprop aircraft flyover noise: Counter-rotating-propeller configuration
[NASA-TP-3027] p 965 N90-29166

HYBRID NAVIGATION SYSTEMS
Integrated navigation - Employing LIRU/GPS
p 329 A90-23995
Sole means navigation and integrity through hybrid Loran-C and NAVSTAR GPS
p 489 N90-20933

HYBRID STRUCTURES
Reinforcing fibers and technology development for resin composites. Consequences for aircraft structures
[FOA-C-20777-2.5] p 876 N90-27883

HYDRAULIC ANALOGIES
Hydraulic analogy application in the study of a two-phase mixture combustion flow
[AIAA PAPER 90-0451] p 211 A90-19850
Investigation of oscillating airfoil shock phenomena
[AIAA PAPER 90-0695] p 169 A90-19981

HYDRAULIC CONTROL
A design method for real-time computer control hydraulic force system
p 590 A90-36434
Hydraulic accumulators and high pressure bottles in composite material
p 688 A90-42493

HYDRAULIC EQUIPMENT
Design and development of a facility for compressible dynamic stall studies of a rapidly pitching airfoil
p 436 A90-28255
Automated aircraft hydraulics testing
p 551 A90-37899
Hydraulic accumulators and high pressure bottles in composite material
p 688 A90-42493
Flexible heat pipe cold plate
[AD-A216053] p 434 N90-18433
Nonflammable hydraulic power system for tactical aircraft. Volume 1: Aircraft system definition, design and analysis
[AD-A218493] p 671 N90-23409

HYDRAULIC FLUIDS
Test and evaluation: Reducing risks to military aircraft from bird collisions. Report to the Chairman, Legislation, and National Security Subcommittee, Committee on Government Operations, House of Representatives
[AD-A210670] p 25 N90-10845
Analysis of hydraulic fluids and lubricating oils for the formation of Trimethylolpropane Phosphate (TMP-P)
[AD-A215188] p 357 N90-16939

HYDRAULIC TEST TUNNELS
Liquid water content and droplet size calibration of the NASA Lewis Icing Research Tunnel
[AIAA PAPER 90-0669] p 261 A90-22242
Pneumatic vortex flow control on a 55-degree cropped delta wing with chined forebody
[AIAA PAPER 90-1430] p 559 A90-37967
Liquid water content and droplet size calibration of the NASA Lewis Icing Research Tunnel
[NASA-TM-102447] p 213 N90-13797
Prediction of rotor blade-vortex interaction noise from 2-D aerodynamic calculations and measurements
[ISL-CQ-243/88] p 396 N90-18365
Experiments with unsteady, free surface, three-dimensional vortices in a thermally stable, stratified fluid
[AD-A222088] p 815 N90-26796

HYDROCARBON COMBUSTION
Combustion characteristics of a model can-type combustor
p 676 A90-40479
Study of the expansion of hydrocarbon-oxygen products through supersonic nozzle
p 852 A90-46907
Computation of ramjet internal flowfields
[AD-A212001] p 114 N90-11743

HYDROCARBON FUELS
The performance of a small combustor operated over a wide range of conditions
p 45 A90-12548
Numerical modeling of the combustion kinetics of hydrocarbon fuels in an annular combustion chamber with allowance for the formation of harmful impurities
p 124 A90-14582
Fuel molecular structure and flame temperature effects on soot formation in gas turbine combustors
[ASME PAPER 89-GT-288] p 253 A90-22652

Experimental and computational flammability limits in a solid fuel ramjet
[AIAA PAPER 90-1964] p 676 A90-40574
Hydrocarbon-fueled scramjet combustor investigation
[AIAA PAPER 90-2337] p 658 A90-40622
Flame extinction in compressible flow
p 883 N90-26899

HYDROCARBONS
Production of high density aviation fuels via novel zeolite catalyst routes
[AD-A216444] p 443 N90-18601
Fire hazards of aerosol cans in aircraft cargo compartments
[DOT/FAA/CT-89/32] p 636 N90-23369
Some 1-(diorganooxyphosphonyl)methyl-2,4- and -2,6-dinitro-benzenes
[NASA-CASE-ARC-11425-3] p 678 N90-23475

HYDROCRACKING
Production of high density aviation fuels via novel zeolite catalyst routes
[AD-A216444] p 443 N90-18601

HYDRODYNAMIC EQUATIONS
Brownian motion far from equilibrium - A hypersonic approach
p 555 A90-35917

HYDRODYNAMIC RAM EFFECT
Operation of the ram accelerator in the transdetonative velocity regime
[AIAA PAPER 90-1985] p 741 A90-42712
Inflatable fuel tank buffer
[AD-D014446] p 503 N90-21002

HYDRODYNAMICS
Three-dimensional adaptive grid generation on a composite-block grid
p 374 A90-25289
Wave interactions in a three-dimensional attachment-line boundary layer
p 811 A90-48715

HYDROELASTICITY
Hydroelastic problems in space flight vehicles
p 536 A90-33386

HYDROGEN
Simulation and second law analysis of the unsteady combustion of a non-ideal pulsating ramjet
p 44 A90-12516
Supersonic combustion of hydrogen jets behind a backward-facing step
[AIAA PAPER 90-0204] p 266 A90-22183
A study of the radiation of hydrogen-xenon mixtures near models flying at high supersonic velocities
p 470 A90-32509
On the use of external burning to reduce aerospace vehicle transonic drag
[AIAA PAPER 90-1935] p 656 A90-40562
The role of hydrogen/air chemistry in nozzle performance for a hypersonic propulsion system
[AIAA PAPER 90-2492] p 658 A90-40637
On the use of external burning to reduce aerospace vehicle transonic drag
[NASA-TM-103107] p 588 N90-21762
Concentration, temperature, and density in a hydrogen-air flame by excimer-induced Raman scattering
p 875 N90-26903

HYDROGEN COMPOUNDS
HF shock tunnel facility for studying supersonic combustion
[AIAA PAPER 90-1551] p 600 A90-38693

HYDROGEN EMBRITTLEMENT
Statistical treatment of slow strain rate data for assessment of hydrogen embrittlement in low alloy high strength steel
[ARL-MAT-R-122] p 767 N90-26106

HYDROGEN ENGINES
Gas Turbine Combustion, volume 2
[VKI-LS-1990-02-VOL-2] p 749 N90-25995

HYDROGEN FUELS
Hydrogen fueled subsonic-ram-combustor model tests for an air-turbo-ram engine
p 44 A90-12529
Experimental study on autoignition in a scramjet combustor
p 46 A90-12559
Hypersonic combustion of hydrogen in a shock tunnel
p 46 A90-12560
Simultaneous CARS measurements of temperature and H₂, H₂O concentrations in hydrogen-fueled supersonic combustion
[AIAA PAPER 90-0158] p 205 A90-19713
Hydrogen propulsion and the next century - A challenge that raises questions and problems
p 266 A90-21774
Effect of hydrogen combustion in a supersonic boundary layer on friction coefficient
p 355 A90-24116
Hydrogen in future energy and propulsion technology
p 692 A90-41736
Some governing parameters of plasma torch igniter/flameholder in a scramjet combustor
[AIAA PAPER 90-2098] p 661 A90-42017
Slush Hydrogen (SLH₂) technology development for application to the National Aerospace Plane (NASP)
[NASA-TM-102315] p 203 N90-14268

HYDROGEN OXYGEN ENGINES
Modeling supersonic combustion using a fully-implicit numerical method
[AIAA PAPER 90-2307] p 677 A90-42117
Cycle analysis of scramjet engines
[NAL-TR-1002] p 51 N90-10035

HYDROGEN PEROXIDE
Recent advances in H₂/O₂ high pressure coaxial injector performance analysis
[AIAA PAPER 90-1959] p 762 A90-42705
Enhanced bioreclamation of jet fuels: A full-scale test at Eglin AFB, Florida
[AD-A22348] p 875 N90-26992

HYDROGEN-BASED ENERGY
Hydrogen in future energy and propulsion technology
p 692 A90-41736

HYDROMECHANICS
Preliminary airworthiness evaluation of the Woodward hydromechanical unit installed on T700-GE-700 engines in the UH-60A helicopter
[AD-A216751] p 428 N90-18430

HYDROSTATICS
Electric controls for a high-performance EHA using an interior permanent magnet motor drive
p 452 A90-30711
EHA loading on the 270-Vdc bus
[SAE PAPER 892225] p 746 A90-45441
Assessment of worm gearing for helicopter transmissions
[NASA-TM-102441] p 257 N90-15923

HYGRAL PROPERTIES
Moisture absorption in graphite/epoxy laminates
p 951 A90-52799

HYPERBOLIC DIFFERENTIAL EQUATIONS
Unsteady three-dimensional thin-layer Navier-Stokes solutions on dynamic blocked grids
p 235 N90-15069

HYPERBOLIC FUNCTIONS
Hyperbolic grid generation techniques for blunt body configurations
p 376 A90-26490

HYPERBOLIC NAVIGATION
1990-1995, a period of international decision making for the navigation community - Is our planning as good as it should be?
p 823 A90-49490

HYPERCUBE MULTIPROCESSORS
Hypercube expert system shell-applying production parallelism
[AD-A215762] p 377 N90-18173

HYPERSONIC AIRCRAFT
Materials and structures for hypersonic vehicles
p 31 A90-13015
Thermodynamics and the future turbine engines
[ONERA, TP NO. 1989-165] p 253 A90-21031
Hypersonic propulsion
p 253 A90-21949
Aerospace materials research opportunities
p 267 A90-23177
European research and testing facilities requested for participation to SST/HST projects
[ONERA, TP NO. 1990-12] p 351 A90-25358
Comparison between experimental and numerical results for a research hypersonic aircraft
p 395 A90-31278
A method of sizing multi-cycle engines for hypersonic aircraft
[ASME PAPER 89-GT-281] p 507 A90-32261
Extracting pulse power from batteries
p 605 A90-38175
Accelerating hypersonic airplanes with ground-power
p 586 A90-38186
Accelerators and decelerators for large, hypersonic aircraft
[AIAA PAPER 90-1986] p 674 A90-40582
Nozzle design optimization by method-of-characteristics
[AIAA PAPER 90-2024] p 741 A90-42719
Off-design performance of hypersonic waveriders
p 763 A90-44735
SST/HST air traffic - Challenge for the future
p 763 A90-44752
Experimental and computational surface and flow-field results for an all-body hypersonic aircraft
[AIAA PAPER 90-3067] p 793 A90-45893
On optimal supersonic/hypersonic bodies
[AIAA PAPER 90-3072] p 796 A90-45918
Active control of aerothermoelastic effects for a conceptual hypersonic aircraft
[AIAA PAPER 90-3337] p 863 A90-47597
Thermal management for a Mach 5 cruise aircraft using endothermic fuel
[AIAA PAPER 90-3284] p 853 A90-48871
Thermal protection systems for hypersonic transport vehicles
[SAE PAPER 901306] p 882 A90-49358
Battery configurations for multi-megawatt pulse power
p 873 A90-49763

Aspects of the design of a hypersonic engine system and the selection of the intake and tail
[DGLR PAPER 88-040] p 928 A90-50233

HOTOL: A future launcher for Europe
p 353 N90-16800

National aero-spaceplane status and plans
p 337 N90-16801

Optimum element density studies for finite-element thermal analysis of hypersonic aircraft structures
[NASA-TM-4163] p 369 N90-17074

A computational model for thickening boundary layers with mass addition for hypersonic engine inlet testing
[AD-A216246] p 319 N90-17576

Investigation of the failure modes in a metal matrix composite under thermal cycling
[AD-A216195] p 357 N90-17825

Tracking a hypersonic aircraft from a space platform
[AD-A216399] p 371 N90-17984

The application of active controls technology to a generic hypersonic aircraft configuration
[NASA-TM-101689] p 497 N90-20071

Prediction of forces and moments for flight vehicle control effectors. Part 1: Validation of methods for predicting hypersonic vehicle controls forces and moments
[NASA-CR-186571] p 571 N90-21734

Prediction of forces and moments for flight vehicle control effectors. Part 2: An analysis of delta wing aerodynamic control effectiveness in ground effect
[NASA-CR-186572] p 571 N90-21735

Experimental aerothermodynamic research of hypersonic aircraft
[NASA-CR-186903] p 721 N90-25954

Maneuvering by means of lateral jets
[ISL-CO-255/88] p 758 N90-26015

Active control of aerothermoelastic effects for a conceptual hypersonic aircraft
[NASA-TM-102713] p 869 N90-27725

HYPERSONIC BOUNDARY LAYER

Prediction and control of transition in supersonic and hypersonic boundary layers
p 16 A90-12828

Goertler vortices in supersonic and hypersonic boundary layers
p 83 A90-14091

On the Goertler vortex instability mechanism at hypersonic speeds
p 158 A90-18886

Evaluation of equilibrium turbulence for a naturally developing hypersonic boundary layer at nonadiabatic wall conditions
[AIAA PAPER 90-1410] p 559 A90-37948

Effects of shock on the stability of hypersonic boundary layers
[AIAA PAPER 90-1448] p 561 A90-38608

HYPERSONIC COMBUSTION

Hypersonic combustion of hydrogen in a shock tunnel
p 46 A90-12560

Advanced computational techniques for hypersonic propulsion
p 69 A90-12606

Transverse fuel-injection model for a scramjet propulsion system
p 659 A90-40927

HYPERSONIC FLIGHT

Hypersonics revisited (The First Leslie Bedford Lecture)
p 60 A90-11458

The use of pulse facilities for testing supersonic combustion ramjet (scramjet) combustors in simulated hypersonic flight conditions
p 46 A90-12562

Advanced computational techniques for hypersonic propulsion
p 69 A90-12606

Aerodynamic and propulsive performance of hypersonic detonation wave ramjets
p 49 A90-12609

Rapid prediction of slender-wing-aircraft stability characteristics
[AIAA PAPER 90-0301] p 163 A90-19782

Rarefied gas dynamics
p 224 A90-21163

Hypersonic flight testing
p 245 A90-21171

Oils for flight turbine engines - Research and development in the 90s
p 266 A90-21473

Thermal/structural analyses of several hydrogen-cooled leading-edge concepts for hypersonic flight vehicles
[AIAA PAPER 90-0053] p 274 A90-23702

High temperature skin friction measurement
p 448 A90-28306

Computational requirements for hypersonic flight performance estimates
p 440 A90-29686

Fluorescence spectroscopy and thermometry for hypersonic flight research
[AIAA PAPER 90-1272] p 538 A90-33897

Particulate trajectories and impact characteristics in hypersonic flight involving gas coolant shielding
p 476 A90-34583

Design considerations for a compact table top hypersonic simulator of aero-optic effects
p 525 A90-34585

Development of an X-ray backscatter densitometer for measurement of freestream density during hypersonic flight
[AIAA PAPER 90-1384] p 604 A90-37933

Three dimensional Discrete Particle Simulation about the AFE geometry
[AIAA PAPER 90-1778] p 560 A90-38468

Thrust law effects on the longitudinal stability of hypersonic cruise
[AIAA PAPER 90-2820] p 763 A90-45149

Hypersonic CFD applications for the National Aero-Space Plane
[SAE PAPER 892310] p 714 A90-45473

System optimization for maximizing reconnaissance mission range of a hypersonic cruise vehicle
[AIAA PAPER 90-3292] p 837 A90-48876

The NASA experience in aeronautical R and D: Three case studies with analysis
[AD-A211486] p 82 N90-12496

Thermal/structural analyses of several hydrogen-cooled leading-edge concepts for hypersonic flight vehicles
[NASA-TM-102391] p 215 N90-14511

HOTOL: A future launcher for Europe
p 353 N90-16800

National aero-spaceplane status and plans
p 337 N90-16801

A computational model for thickening boundary layers with mass addition for hypersonic engine inlet testing
[AD-A216246] p 319 N90-17576

Viscous three-dimensional analyses for nozzles for hypersonic propulsion
[NASA-CR-185197] p 344 N90-17635

Possible piloting techniques at hypersonic speeds
[ISL-CO-216/88] p 415 N90-18392

Transpiration cooling in hypersonic flight
[NASA-CR-186435] p 478 N90-20052

Analysis of flow-, thermal-, and structural-interaction of hypersonic structures subjected to severe aerodynamic heating
[AD-A217882] p 478 N90-20053

Carbon-carbon composites: Emerging materials for hypersonic flight
[NASA-TM-103472] p 767 N90-26080

Real-time aerodynamic heating and surface temperature calculations for hypersonic flight simulation
[NASA-TM-4222] p 959 N90-28815

Optimal trajectories for hypervelocity flight
p 918 N90-29378

HYPERSONIC FLOW

The numerical method for solving the high Reynolds hypersonic viscous shock layer
p 2 A90-10340

Asymptotic calculation of flow parameters in the problem of hypersonic flow past blunt axisymmetric bodies
p 10 A90-12268

Hypersonic flow past blunt edges at low Reynolds numbers
p 10 A90-12284

Direct simulation of three-dimensional hypersonic flow about intersecting blunt wedges
p 16 A90-12835

Application of the hypersonic analogy for validation of numerical simulations
p 16 A90-12838

Unified super/hypersonic similitude for steady and oscillating cones and ogives
p 82 A90-13786

Supersonic/hypersonic flow past wedge and plane ogive in oscillation
p 85 A90-15231

Numerical simulation of supersonic and hypersonic turbulent compression corner flows using PNS equations
p 85 A90-15242

Calculation of flow past delta wings in the thin shock layer approximation
p 86 A90-15624

Computation of the thin-layer Navier-Stokes equations for a 2D flow
p 87 A90-16332

Supersonic/hypersonic Euler flowfield prediction method for aircraft configurations
p 145 A90-16767

Calculation of three-dimensional boundary layers including hypersonic flows
p 146 A90-16773

Verification of a Navier-Stokes code for solving the hypersonic blunt body problem
p 146 A90-16774

Euler and Navier-Stokes solutions for hypersonic flows
p 155 A90-18254

Computation of hypersonic flows by a finite element least-squares method
p 155 A90-18296

Video visualization of separation shock motion from measured wall pressure signals in a Mach 5 compression ramp interaction
[AIAA PAPER 90-0074] p 162 A90-19670

Direct simulation of hypersonic rarefied flow about a delta wing
[AIAA PAPER 90-0143] p 162 A90-19704

Generalized fluxvectors for hypersonic shock-capturing
[AIAA PAPER 90-0390] p 165 A90-19829

Solution of the parabolized Navier-Stokes equations using Osher's upwind scheme
[AIAA PAPER 90-0392] p 165 A90-19830

Hypersonic rarefied flow and its solution over the stagnation region
[AIAA PAPER 90-0420] p 166 A90-19842

Mach 6 testing of two generic three-dimensional sidewall compression scramjet inlets in tetrafluoromethane
[AIAA PAPER 90-0530] p 192 A90-19895

Parabolized Navier-Stokes predictions of three-dimensional hypersonic flows with strong crossflow effects
p 223 A90-20508

Hypersonics. Volume 2 - Computation and measurement of hypersonic flows; Proceedings of the First Joint Europe/U.S. Short Course on Hypersonics, Paris, France, Dec. 7-11, 1987 --- Book
p 224 A90-21164

Leading edge transition in hypersonic flows
p 224 A90-21167

Computations of hypersonic flow by finite-volume methods
p 224 A90-21168

Computation of hypersonic flow fields
p 225 A90-21169

On the computations of hypersonic viscous flows
p 225 A90-21170

Hypersonic propulsion
p 253 A90-21948

Representation of two-dimensional hypersonic inlet flows for one-dimensional scramjet cycle analysis
[AIAA PAPER 90-0527] p 229 A90-22226

Experimental studies of shock wave/wall jet interaction in hypersonic flow
[AIAA PAPER 90-0607] p 231 A90-22449

Calculation of flow past flight vehicles of complex configurations at high supersonic Mach numbers using the hypersonic theory of small perturbations
p 299 A90-24158

Non-equilibrium hypersonic flows - Physics and numerics
p 304 A90-25777

Three-dimensional simulations of hypersonic flows
p 306 A90-25823

Unsteady hypersonic viscous flow in impulse facilities
[AIAA PAPER 90-0421] p 313 A90-26947

Hypersonic reactive flow computations
p 315 A90-27131

Accurate Navier-Stokes results for the hypersonic flow over a spherical nose tip
p 393 A90-29687

Hypersonic viscous shock-layer solutions over long slender bodies. II - Low Reynolds number flows
p 393 A90-29695

Nonstationary hypersonic flow past a thin wing of variable shape
p 470 A90-32559

Unsteady aerodynamic forces of oscillating supersonic/hypersonic wings with attached shock waves
p 473 A90-33363

High-resolution shock-capturing schemes for inviscid and viscous hypersonic flows
p 476 A90-34545

Optical window materials for hypersonic flow
p 496 A90-34581

On the instability of hypersonic flow past a wedge
p 554 A90-35902

Development of a three-dimensional upwind parabolized Navier-Stokes code
p 602 A90-36253

An analytic solution on hypersonic flow over an arbitrary slender body with near power-law profile
p 558 A90-37736

Performance potential and technology issues of MHD augmented hypersonic simulation facilities
[AIAA PAPER 90-1380] p 598 A90-37929

Condensation in hypersonic nitrogen wind tunnels
[AIAA PAPER 90-1392] p 558 A90-37937

Hypersonic flow calculations with a hybrid Navier-Stokes/Monte Carlo method
[AIAA PAPER 90-1691] p 560 A90-38394

Measurement of mean and fluctuating flow properties in hypersonic shear layers
[AIAA PAPER 90-1409] p 560 A90-38488

Liquid crystal coatings for surface shear stress visualization in hypersonic flows
[AIAA PAPER 90-1513] p 563 A90-38660

Calculation of hypersonic forebody/inlet flow fields
[AIAA PAPER 90-1493] p 619 A90-39049

Supersonic/hypersonic laminar/turbulent transition
p 706 A90-42872

Numerical simulation of hypersonic viscous continuum flow
p 707 A90-44407

Development of supersonic and hypersonic Euler solvers using shock fitting in two and three dimensions
p 707 A90-44426

Fully vectorized implicit scheme for 2-D viscous hypersonic flow using adaptive finite element methods
p 708 A90-44439

The effect of vibration-dissociation interaction on heat transfer and drag during the hypersonic flow past bodies
p 710 A90-44934

The effect of separation on turbulent boundary layer characteristics over a smooth surface at Mach 6.0
[AIAA PAPER 90-3028] p 790 A90-45870

Computational simulation of flows about hypersonic geometries with sharp leading edges
[AIAA PAPER 90-3065] p 793 A90-45891

Calculation of three-dimensional viscous and inviscid hypersonic flows using split-matrix marching methods
[AIAA PAPER 90-3070] p 794 A90-45894

A problem in the theory of optimal aerodynamic shapes
p 803 A90-46503

SUBJECT INDEX

- Viscous flow characteristics over a blunt cone at hypersonic Mach numbers by using a PNS code
p 810 A90-48085
- Low-speed, high-lift aerodynamic characteristics of slender, hypersonic accelerator-type configurations
[NASA-TP-2945] p 20 N90-10830
- Hypersonic aerodynamics
p 171 N90-13335
- Optimum shape of a blunt forebody in hypersonic flow
[NASA-CR-181955] p 171 N90-13351
- Opportunities for improved understanding of supersonic and hypersonic flows
p 318 N90-17566
- Hypersonic nozzle/afterbody performance at low Mach numbers
[AD-A216223] p 319 N90-17575
- Computation of hypersonic unsteady viscous flow over a cylinder
p 397 N90-19194
- Computation of hypersonic, low density flows with thermochemical nonequilibrium
p 477 N90-20044
- An approximate viscous shock layer method for calculating the hypersonic flow over blunt-nosed bodies
p 479 N90-20947
- Effects of nose bluntness and shock-shock interactions on blunt bodies in viscous hypersonic flows
[NASA-CR-186451] p 479 N90-20950
- Computation of nonequilibrium chemically reacting flows in hypersonic flow field
p 480 N90-20954
- Convergence acceleration of hypersonic flow calculations: A nonlinear relaxation factor
p 480 N90-20957
- Optimum hypersonic airfoils with attached shocks
p 481 N90-20960
- Numerical simulation of hypersonic flow around a space plane. Part 2: Application to high angles of attack flow [NAL-TR-1011T] p 570 N90-21726
- Prediction of two-dimensional time-dependent gasdynamic flows for hypersonic studies
[UTIAS-335] p 718 N90-25935
- An approximate method for calculating three-dimensional inviscid hypersonic flow fields
[NASA-TP-3018] p 883 N90-27066
- Hypersonic Arbitrary-Body Aerodynamics (HABA) for conceptual design
[DE90-014750] p 910 N90-28495
- Applications of LIF to high speed flows
p 911 N90-29320
- HYPERSONIC FORCES**
- Possible piloting techniques at hypersonic speeds
[ISL-CO-216/88] p 415 N90-18392
- HYPERSONIC HEAT TRANSFER**
- Pressure and heat-transfer investigation of a hypersonic configuration
p 598 A90-35757
- HYPERSONIC INLETS**
- Tangential mass addition for the control of shock wave/boundary layer interactions in scramjet inlets
p 13 A90-12586
- Numerical simulation of three-dimensional hypersonic inlet flowfields
p 13 A90-12587
- High speed inlet testing in the NAVSWC wind tunnels
[AIAA PAPER 90-1412] p 595 A90-37949
- Analysis of shock interactions and flow structure in high speed inlets
[AIAA PAPER 90-2132] p 704 A90-42735
- The effect of shock/shock interactions on the design of hypersonic inlets
[AIAA PAPER 90-2217] p 705 A90-42748
- A computational model for thickening boundary layers with mass addition for hypersonic engine inlet testing
[AIAA PAPER 90-2219] p 705 A90-42750
- Finite element analysis of structural components using viscoplastic models with application to a cowl lip problem
[NASA-CR-185189] p 690 N90-23769
- Prediction of two-dimensional time-dependent gasdynamic flows for hypersonic studies
[UTIAS-335] p 718 N90-25935
- HYPERSONIC NOZZLES**
- Calculated chemical and vibrational nonequilibrium effects in hypersonic nozzles
p 253 A90-21224
- The role of hydrogen/air chemistry in nozzle performance for a hypersonic propulsion system
[AIAA PAPER 90-2492] p 658 A90-40637
- A Mach 6 external nozzle experiment with Argon-Freon exhaust simulation
[SAE PAPER 892315] p 714 A90-45477
- A study of gas flow in hypersonic nozzles at large Reynolds numbers using simplified Navier-Stokes equations
p 803 A90-46538
- Experimental investigation of a chemical laser cavity flowfield
[AD-A216398] p 372 N90-18038
- HYPERSONIC REENTRY**
- Infrared radiation model for aircraft and reentry vehicle
p 77 A90-10169
- Approximations for nonequilibrium hypervelocity aerodynamics
p 154 A90-17990

HYPERSONIC SHOCK

- The numerical method for solving the high Reynolds hypersonic viscous shock layer
p 2 A90-10340
- Spanwise properties of the unsteady separation shock in a Mach 5 unswept compression ramp interaction
[AIAA PAPER 90-0377] p 228 A90-22208
- Hypersonic aerodynamics
p 171 N90-13335
- Optimum hypersonic airfoils with attached shocks
p 481 N90-20960

HYPERSONIC SPEED

- The detection of large scale structure in undisturbed and disturbed compressible turbulent free shear layers
[AIAA PAPER 90-0711] p 230 A90-22251
- Dynamics of the outgoing turbulent boundary layer in a Mach 5 unswept compression ramp interaction
[AIAA PAPER 90-1645] p 569 A90-38773
- Streamtube analysis of supersonic combustion in an in-tube-scramjet
[AIAA PAPER 90-2339] p 762 A90-42776
- CFD support of NASP design
[AIAA PAPER 90-3252] p 872 A90-49120
- Hypersonic nozzle/afterbody performance at low Mach numbers
[AD-A216223] p 319 N90-17575
- An investigation of solid-fuel, dual-mode combustion ramjets
p 859 N90-27933

HYPERSONIC TEST APPARATUS

- The integrated test vehicle, (I.T.V.) - A vehicle for cost-effective hypersonic testing
[AIAA PAPER 90-0630] p 352 A90-26974
- Test and Measurement Technique in Hypersonics
[ILR-MITT-225(1989)] p 618 N90-24225
- The gun tunnel of the Brunswick Institute for Fluid Mechanics: Current development status
p 673 N90-24227

HYPERSONIC VEHICLES

- Hypersonics revisited (The First Leslie Bedford Lecture)
p 60 A90-11458
- Advanced airbreathing powerplant for hypersonic vehicles
p 49 A90-12607
- Inverse cycle engine for hypersonic air-breathing propulsion
[ONERA, TP NO. 1989-121] p 50 A90-12611
- The critical role of aerodynamic heating effects in the design of hypersonic vehicles
p 155 A90-18249
- Nonequilibrium recombination-dissociation boundary layer flows along arbitrarily-catalytic hypersonic vehicles
[AIAA PAPER 90-0055] p 161 A90-19852
- A three-dimensional upwind parabolized Navier-Stokes code for chemically reacting flows
[AIAA PAPER 90-0394] p 165 A90-19831
- Hypersonic airbreathing vehicle design - Focus on aero-space plane
p 245 A90-21156
- Effects of thermochemistry, nonequilibrium, and surface catalysis on the design of hypersonic vehicles
p 224 A90-21159
- Hypersonic flight testing
p 245 A90-21171
- Hypersonic aerospace sizing analysis for the preliminary design of aerospace vehicles
p 247 A90-23276
- Thermal/structural analyses of several hydrogen-cooled leading-edge concepts for hypersonic flight vehicles
[AIAA PAPER 90-0053] p 274 A90-23702
- Many means to NASP
p 285 A90-23917
- Design for hypersonic speed
p 335 A90-26343
- High temperature skin friction measurement
p 448 A90-28306
- Table top experimental simulation of hypersonic aero-optical effects --- encountered by cooled window on interceptor
p 525 A90-34586
- Development of a three-dimensional upwind parabolized Navier-Stokes code
p 602 A90-36253
- Large-scale structure in a supersonic slot-injected flowfield
p 602 A90-36265
- Hypersonic test facility requirements for the 1990's
[AIAA PAPER 90-1389] p 594 A90-37934
- The challenging process of validating CFD codes
[AIAA PAPER 90-1402] p 558 A90-37943
- Application of the LAURA code for slender-vehicle aerothermodynamics
[AIAA PAPER 90-1714] p 560 A90-38416
- Scramjet testing from Mach 4 to 20 - Present capability and needs for the nineties
[AIAA PAPER 90-1388] p 597 A90-38485
- The role of hydrogen/air chemistry in nozzle performance for a hypersonic propulsion system
[AIAA PAPER 90-2492] p 658 A90-40637
- On- and off-design performance analysis of hypersonic detonation wave ramjets
[AIAA PAPER 90-2473] p 664 A90-42188
- Hypersonic (T-D) 'pinch' and aerospaceplane propulsion
[AIAA PAPER 90-2474] p 675 A90-42189
- The effect of shock/shock interactions on the design of hypersonic inlets
[AIAA PAPER 90-2217] p 705 A90-42748

HYPERSONIC WIND TUNNELS

- Optimal plane change by low aerodynamic forces
[AIAA PAPER 90-2831] p 763 A90-45137
- Hypersonic forebody lift-induced drag
[SAE PAPER 892345] p 715 A90-45497
- The role of CFD applied to high performance aircraft
[AIAA PAPER 90-3071] p 796 A90-45917
- Determination of the extreme values of the efficiency criteria for a flight vehicle control system in the probable scatter range of its characteristics
p 859 A90-46569
- Performance evaluations of oxidation-resistant carbon-carbon composites in simulated hypersonic vehicle environments
p 874 A90-48131
- A hypersonic research vehicle to develop scramjet engines
[AIAA PAPER 90-3232] p 839 A90-49115
- Application of formal optimization techniques in thermal/structural design of a heat-pipe-cooled panel for a hypersonic vehicle
[NASA-TM-89131] p 72 N90-10409
- Adaptive control law design for model uncertainty compensation
[AD-A211712] p 120 N90-11758
- Thermal/structural analyses of several hydrogen-cooled leading-edge concepts for hypersonic flight vehicles
[NASA-TM-102391] p 215 N90-14511
- Aerodynamic and structural design challenges of a reusable single stage to orbit air-breathing launch vehicle
p 354 N90-16814
- Saenger propulsion system options
p 344 N90-16818
- Verification of aerothermodynamic codes by means of a winged experimental re-entry vehicle
p 354 N90-16842
- Heat pipes for wing leading edges of hypersonic vehicles
[NASA-CR-181922] p 369 N90-17055
- Aeroservoelasticity
[NASA-TM-102620] p 416 N90-19227
- Hypersonic waverider configurations for trans-atmospheric vehicles
[AD-A217925] p 498 N90-20074
- Low-density flow effects for hypervelocity vehicles, phase 2
[AD-A221034] p 634 N90-24249
- Supersonic reacting internal flow fields
[NASA-TM-103480] p 767 N90-26094
- Photo-sensitized ignition of hydrogen/oxygen mixtures for hypersonic flight vehicles
p 877 N90-27935
- Damage tolerance analysis for manned hypervelocity vehicles. Volume 1: Final technical report
[AD-A217920] p 887 N90-28106
- Real-time aerodynamic heating and surface temperature calculations for hypersonic flight simulation
[NASA-TM-4222] p 959 N90-28815
- HYPERSONIC WIND TUNNELS**
- Development of the UTA hypersonic shock tunnel
[AIAA PAPER 90-0080] p 200 A90-19675
- Inviscid non equilibrium flow in ONERA F4 wind tunnel
[ONERA, TP NO. 1989-161] p 223 A90-21029
- Instrumentation being developed for the ONERA F4 wind tunnel
[ONERA, TP NO. 1989-189] p 261 A90-21049
- Aerodynamic heat transfer testing in hypersonic wind tunnels using an infrared imaging system
[AIAA PAPER 90-0189] p 350 A90-25027
- European research and testing facilities requested for participation to SST/HST projects
[ONERA, TP NO. 1990-12] p 351 A90-25358
- Non-isentropic effects on the WRDC 20 inch hypersonic wind tunnel calibration
p 435 A90-28254
- Liquid crystal thermography for aerodynamic heating measurements in short duration hypersonic facilities
p 446 A90-28262
- Development and extension of diagnostic techniques for advancing high speed aerodynamic research
p 436 A90-28281
- Applications of infra-red thermography in a hypersonic blowdown wind tunnel
p 438 A90-28300
- Aerothermodynamics and transition in high-speed wind tunnels at NASA Langley
p 386 A90-28555
- Infrared thermography in blowdown and intermittent hypersonic facilities
p 440 A90-31302
- Aeronautical facility requirements into the 2,000's
[AIAA PAPER 90-1375] p 594 A90-37926
- Development and calibration of a continuous-flow arc-heated hypersonic wind tunnel
[AIAA PAPER 90-1381] p 594 A90-37930
- Hypersonic test facility requirements for the 1990's
[AIAA PAPER 90-1389] p 594 A90-37934
- Hypervelocity real gas capabilities of GASL's expansion tube (HYPULSE) facility
[AIAA PAPER 90-1390] p 594 A90-37935
- Condensation in hypersonic nitrogen wind tunnels
[AIAA PAPER 90-1392] p 558 A90-37937

Langley hypersonic aerodynamic/aerothermodynamic testing capabilities - Present and future
[AIAA PAPER 90-1376] p 596 A90-38483
Wind tunnel testing techniques on aerodynamic effects with small asymmetry
[AIAA PAPER 90-1400] p 560 A90-38490
The University of Toronto-Ryerson Polytechnical Institute hypersonic gun tunnel p 673 A90-42432
Design and fabrication requirements for low noise supersonic/hypersonic wind tunnels

p 122 N90-12555
Infrared thermography at hypersonic channel H2K
p 674 N90-24235
Infrared thermography p 911 N90-29325

HYPERSONICS

Design for hypersonic speed p 335 A90-26343
Computational fluid dynamics - Current capabilities and directions for the future p 540 A90-34385
Brownian motion far from equilibrium - A hypersonic approach p 555 A90-35917
NASA aerodynamics program
[NASA-TM-4175] p 373 N90-17235
Hypersonic nozzle/afterbody performance at low Mach numbers
[AD-A216223] p 319 N90-17575
Computation of hypersonic unsteady viscous flow over a cylinder p 397 N90-19194
Prediction of forces and moments for flight vehicle control effectors. Part 1: Validation of methods for predicting hypersonic vehicle controls forces and moments
[NASA-CR-186571] p 571 N90-21734
Test and Measurement Technique in Hypersonics
[ILR-MITT-225(1989)] p 618 N90-24225
High enthalpy hypersonic wind tunnel F4: General description and associated instrumentation
p 673 N90-24228
Prediction of two-dimensional time-dependent gasdynamic flows for hypersonic studies
[UTIAS-335] p 718 N90-25935
Hypersonic Arbitrary-Body Aerodynamics (HABA) for conceptual design
[DE90-014750] p 910 N90-28495

HYPERVELOCITY

Hypervelocity, minimum-radii, coordinated turns
p 667 A90-40691

HYPERVELOCITY FLOW

Approximations for nonequilibrium hypervelocity aerodynamics p 154 A90-17990
Performance potential and technology issues of MHD augmented hypersonic simulation facilities
[AIAA PAPER 90-1380] p 598 A90-37929
Hypervelocity real gas capabilities of GASL's expansion tube (HYPULSE) facility
[AIAA PAPER 90-1390] p 594 A90-37935
Hypervelocity flow of dissociating nitrogen downstream of a blunt nose p 811 A90-48712

HYPERVELOCITY WIND TUNNELS

The new high Reynolds number Mach 8 capability in the NSWC Hypervelocity Wind Tunnel 9
[AIAA PAPER 90-1379] p 594 A90-37928
Hypervelocity real gas capabilities of GASL's expansion tube (HYPULSE) facility
[AIAA PAPER 90-1390] p 594 A90-37935
Design and operational features of low-disturbance wind tunnels at NASA Langley for Mach numbers from 3.5 to 18
[AIAA PAPER 90-1391] p 594 A90-37936
High speed inlet testing in the NAVSWC wind tunnels
[AIAA PAPER 90-1412] p 595 A90-37949
Design of an axisymmetric, contoured nozzle for the HEG
[DLR-FB-90-04] p 959 N90-28812
Applications of LIF to high speed flows
p 911 N90-29320

HYSTERESIS

Nonsymmetric vortex breakdown and aerodynamic hysteresis in flow past a low-aspect-ratio wing/fuselage configuration p 294 A90-24076
Stall and recovery in multistage axial flow compressors p 428 N90-18429

IBM COMPUTERS

The development of a low cost data logging system for flight trials based on an IBM compatible PC
[RAE-TM-FM-16] p 251 N90-15917

ICE

Charging of aircraft - High-velocity collisions
p 322 A90-26131
Ice runways near the South Pole
[AD-A211606] p 133 N90-11908
Airfields on antarctic glacier ice
[AD-A217638] p 526 N90-20097

Modeling of surface roughness effects on glaze ice accretion p 485 N90-20925
Ultrasonic techniques for aircraft ice accretion measurement p 485 N90-20926
Investigation of surface water behavior during glaze ice accretion p 485 N90-20927
The influence of ice accretion physics on the forecasting of aircraft icing conditions p 485 N90-20928

ICE CLOUDS

Atmospheric conditions producing aircraft icing on 24-25 January 1989 - A case study utilizing combinations of surface and remote sensors
[AIAA PAPER 90-0197] p 175 A90-19734
Development of a phase Doppler based probe for icing cloud droplet characterization
[AIAA PAPER 90-0667] p 368 A90-26978
Initial results from the joint NASA-Lewis/U.S. Army icing flight research tests p 400 A90-28180

ICE FORMATION

Theoretical analysis of an icing test apparatus for turbine engine air intakes
[AAAF PAPER NT 88-20] p 23 A90-11437
Icing test techniques for air intake screens on helicopters functioning in temperatures around 0 C p 23 A90-12619

Predictions of airfoil aerodynamic performance degradation due to icing p 144 A90-16753
A program to improve aircraft icing forecasts
[AIAA PAPER 90-0196] p 216 A90-19733

Atmospheric conditions producing aircraft icing on 24-25 January 1989 - A case study utilizing combinations of surface and remote sensors
[AIAA PAPER 90-0197] p 175 A90-19734
Fortified LEWICE with viscous effects --- Lewis Ice Accretion Prediction Code
[AIAA PAPER 90-0754] p 176 A90-20009

Numerical study of the effects of icing on finite wing aerodynamics
[AIAA PAPER 90-0757] p 169 A90-20010
Development of an unstructured mesh/Navier-Stokes method for aerodynamics of aircraft with ice accretions
[AIAA PAPER 90-0758] p 169 A90-20011
Convective heat transfer measurements from a NACA 0012 airfoil in flight and in the NASA Lewis Icing Research Tunnel

[AIAA PAPER 90-0199] p 272 A90-22180
Liquid water content and droplet size calibration of the NASA Lewis Icing Research Tunnel

[AIAA PAPER 90-0669] p 261 A90-22242
Development of an anti-icing runback model
[AIAA PAPER 90-0759] p 238 A90-22258

Comparison of two droplet sizing systems in an icing wind tunnel
[AIAA PAPER 90-0668] p 274 A90-23711

Spray nozzle investigation for the Improved Helicopter Icing Spray System (IHSS)
[AIAA PAPER 90-0666] p 350 A90-25040

Swept wing ice accretion modeling
[AIAA PAPER 90-0756] p 300 A90-25042
The effect of experimental uncertainties on icing test results

[AIAA PAPER 90-0665] p 322 A90-26977
Development of a phase Doppler based probe for icing cloud droplet characterization

[AIAA PAPER 90-0667] p 368 A90-26978
A comparison of a droplet impingement code to icing tunnel results

[AIAA PAPER 90-0670] p 352 A90-26979
A study of ice shape prediction methodologies and comparison with experimental data

[AIAA PAPER 90-0753] p 322 A90-26986
Icing Research Tunnel test of a model helicopter rotor

p 400 A90-28179
Initial results from the joint NASA-Lewis/U.S. Army icing flight research tests p 400 A90-28180

Development of the improved helicopter icing spray system (IHSS) p 400 A90-28182
Measured aerodynamic performance of a swept wing with a simulated ice accretion

[AIAA PAPER 90-0490] p 557 A90-37063
Aircraft Ground Deicing Conference, Denver, CO, Sept. 20-22, 1988, Proceedings p 817 A90-46004

The low frequency oscillation in the flow over a NACA0012 airfoil with an 'iced' leading edge p 801 A90-46377

Experimental investigation of multi-element airfoil ice accretion and resulting performance degradation p 812 A90-48954

Remote sensing techniques of the Wave Propagation Laboratory for the measurement of supercooled liquid water: Applications to aircraft icing
[PB89-208102] p 24 N90-10842

Convective heat transfer measurements from a NACA 0012 airfoil in flight and in the NASA Lewis Icing Research Tunnel
[NASA-TM-102448] p 213 N90-13750

Liquid water content and droplet size calibration of the NASA Lewis Icing Research Tunnel
[NASA-TM-102447] p 213 N90-13797

Navier-Stokes analysis of airfoils with leading edge ice accretions p 174 N90-14196
Comparison of two droplet sizing systems in an icing wind tunnel

[NASA-TM-102456] p 215 N90-14617
Flight in Adverse Environmental Conditions
[AGARD-CP-470] p 222 N90-15041

NASA's program on icing research and technology p 239 N90-15062
Ice induced aerodynamic performance degradation of rotorcraft: An overview p 248 N90-15063

Flight and wind tunnel investigation of aerodynamic effects of aircraft ground deicing/antiicing fluids p 235 N90-15064

Evaluation of the improved OV-ID anti-icing system, phase 2 p 239 N90-15083
Natural icing re-evaluation of the EH-60A Quick Fix helicopter

[AD-A213928] p 323 N90-16723
[AD-A214728] p 323 N90-16723
The collection of non-conus aircraft icing data along with an identification of the geographical areas of potential severe icing and a study of a method of remote determining atmospheric icing data

[AD-A215055] p 323 N90-16724
Heat transfer measurements from a NACA 0012 airfoil in flight and in the NASA Lewis icing research tunnel

[NASA-CR-4278] p 399 N90-19203
Investigation of air transportation technology at the Massachusetts Institute of Technology, 1988-1989 p 484 N90-20922

Modeling of surface roughness effects on glaze ice accretion p 485 N90-20925
Ultrasonic techniques for aircraft ice accretion measurement p 485 N90-20926

Investigation of surface water behavior during glaze ice accretion p 485 N90-20927
The influence of ice accretion physics on the forecasting of aircraft icing conditions p 485 N90-20928

Users manual for the NASA Lewis Ice Accretion Prediction Code (LEWICE) p 468 N90-20943
[NASA-CR-185129] p 506 N90-21006

Advanced instrumentation for aircraft icing research
[NASA-CR-185225] p 570 N90-21272
Swept wing ice accretion modeling

[NASA-TM-103114] p 736 N90-25969
[AR-89-18] p 736 N90-25969
The signals of an ice warning device in dependence on total water content and normalized icing degree

[ESA-TT-1207] p 963 N90-29692
ICE PREVENTION

Theoretical analysis of an icing test apparatus for turbine engine air intakes
[AAAF PAPER NT 88-20] p 23 A90-11437

An investigation into the internal heat transfer characteristics of a thermally anti-iced aero-engine intake lipskin p 111 A90-15390

Impact ice stresses in rotating airfoils
[AIAA PAPER 90-0198] p 175 A90-19735
Development of an anti-icing runback model

[AIAA PAPER 90-0759] p 238 A90-22258
The effect of experimental uncertainties on icing test results

[AIAA PAPER 90-0665] p 322 A90-26977
NASA's program on icing research and technology p 239 N90-15062

Flight and wind tunnel investigation of aerodynamic effects of aircraft ground deicing/antiicing fluids p 235 N90-15064

Evaluation of the improved OV-ID anti-icing system, phase 2 p 239 N90-15083
[AD-A213928] p 485 N90-20925

Modeling of surface roughness effects on glaze ice accretion p 485 N90-20925
ICE REPORTING

A program to improve aircraft icing forecasts
[AIAA PAPER 90-0196] p 216 A90-19733
Impact ice stresses in rotating airfoils

[AIAA PAPER 90-0198] p 175 A90-19735
IDEAL FLUIDS

Numerical analysis of flow of an ideal fluid past an airfoil p 2 A90-10228
Numerical method for the flow of an ideal fluid on a plane with subsonic and supersonic regions p 233 A90-23362

Calculation of the induced drag of a wing with arbitrary deformation p 388 A90-29183

IDEAL GAS

- Nonlinear stability of subsonic mixing layers with symmetric temperature variations p 223 A90-20501
- Calculation of flows of an ideal gas in nozzles and jets by the relaxation method p 296 A90-24109
- Numerical solution of the problem of supersonic flow of an ideal gas past a trapezoidal wedge p 386 A90-28980
- Induced drag of a wing of low aspect ratio p 387 A90-28987
- Application of the LAURA code for slender-vehicle aerothermodynamics [AIAA PAPER 90-1714] p 560 A90-38416
- Generalized similarity solutions for three-dimensional laminar compressible wing boundary layers p 907 A90-51543

IDENTIFYING

- Gas identification system using graded temperature sensor and neural net interpretation [AD-A213359] p 205 N90-13627

IGNITERS

- Some governing parameters of plasma torch igniter/flameholder in a scramjet combustor [AIAA PAPER 90-2098] p 661 A90-42017

IGNITION

- Electrostatic description of a positive leader ignition from an aircraft [ONERA, TP NO. 1989-149] p 23 A90-11171
- Systems tunnel linear shaped charge lightning strike [NASA-CR-183832] p 201 N90-13404
- RAAF Orion aircraft A9-300 oxygen fire [AD-A215496] p 323 N90-16725
- Ignitability of jet-A fuel vapors in aircraft fuel tanks p 326 N90-17594
- Hot surface ignition studies of aviation fluids p 327 N90-17600
- Flammability of fire resistant, aircraft hydraulic fluid [DOT/FAA/CT-TN90/19] p 766 N90-25222
- Photo-sensitized ignition of hydrogen/oxygen mixtures for hypersonic flight vehicles p 877 N90-27935

IGNITION SYSTEMS

- Combustion in the gas turbine. Part 3: Fuel injection, ignition and stability [CIT/SME/VKI/RS/4] p 748 N90-25988

IGNITION TEMPERATURE

- Experimental study on autoignition in a scramjet combustor p 46 A90-12559

ILLUMINATING

- Improved lighting of taxiway/taxiway intersections for Instrument Flight Rules (IFR) operations [DOT/FAA/CT-TN89/64] p 243 N90-15089
- Modified touchdown zone lighting [DOT/FAA/CT-TN89/70] p 526 N90-21042

ILLUMINATION

- Flow visualization via laser-induced reflection from bubble sheets p 680 A90-39784

ILYUSHIN AIRCRAFT

- Support backbone for the Soviet air forces . . . The Ilyushin 'Candid' family p 731 A90-43769
- Commuter from Khodinka --- Il-114 airliner p 842 A90-49824

IMAGE ANALYSIS

- Vision guidance update - Synthetic aperture radar (SAR) multiple image exploitation for position and velocity determination p 488 A90-34140
- An image analysis method for vehicle stabilization p 668 A90-40914
- Optoelectronic guidance sensors (5th revised and enlarged edition) --- Russian book p 881 A90-46620
- Video photographic considerations for measuring the proximity of a probe aircraft with a smoke seeded trailing vortex [NASA-TM-102691] p 724 N90-25120

IMAGE INTENSIFIERS

- Cockpit lighting compatibility with image intensification night imaging systems: Issues and answers [AD-A210503] p 32 N90-10028

IMAGE MOTION COMPENSATION

- A new method of aircraft motion error extraction from radar raw data for real-time motion compensation p 824 A90-49675
- Self compensation of rigid displacements in holographic interferometry [ISL-CO-219/88] p 370 N90-17113
- Passive navigation using image irradiance tracking p 578 N90-22232

IMAGE PROCESSING

- Synthetic holography applied to head-up displays p 218 A90-16692
- A laser based computer aided non-intrusive technique for full field flow characterization in macroscopic curved channels p 535 A90-32293
- Advances in Techniques and Technologies for Air Vehicle Navigation and Guidance [AGARD-CP-455] p 332 N90-16731

- Autonomous automatic landing through computer vision p 332 N90-16734
- Applications of digital image processing in testing and evaluation of composite materials [AD-A222939] p 874 N90-26887
- Engine testing of thermographic phosphors [DE90-013269] p 885 N90-28059
- Electro-optics engineering support for the integrated launch and recovery television surveillance system [AD-A223450] p 938 N90-29406

IMAGE RECONSTRUCTION

- LDA processor TSI model 1990 analog input module reconstruction p 451 A90-29654

IMAGE RESOLUTION

- Characteristics of 5x5 and 6x6 inch taut shadow mask CRTs for cockpit displays p 737 A90-45239
- The development of an airborne synthetic aperture radar motion compensation system p 333 N90-16745

IMAGE VELOCITY SENSORS

- The automatic detection of anti-collision lights [RSRE-MEMO-4272] p 240 N90-15896

IMAGERY

- The function of the Interactive Model Assembly Program (IMAP) for a flight simulator [NAL-TR-1034] p 939 N90-29412

IMAGES

- Passive navigation using image irradiance tracking p 578 N90-22232
- A sensor stabilization/tracking system for unmanned air vehicles [AD-A224008] p 936 N90-28579

IMAGING TECHNIQUES

- Angular feature mapping - An optical method p 377 A90-23974
- The airborne synthetic cartographic indicator p 822 A90-46671
- Image based range determination [AIAA PAPER 90-3404] p 822 A90-47659
- Low speed flowfield characterization by infrared measurements of surface temperatures p 317 N90-17556
- Kalman filter based range estimation for autonomous navigation using imaging sensors p 578 N90-22238
- Ground evaluation of seeding an in-flight wingtip vortex using infrared imaging flow visualization technique p 635 N90-25035
- In-service inspection of composite components on aircraft at depot and field levels p 885 N90-28078

IMPACT DAMAGE

- Effect of environmental particles on a radial compressor p 113 A90-16373
 - Effects of damage on post-buckled skin-stiffener composite skin panels p 409 A90-28235
 - A technique for rapid impact damage detection with implication for composite aircraft structures p 600 A90-37662
 - Impact damage and residual strength analysis of composite panels with bonded stiffeners --- for primary aircraft structures p 642 A90-40130
 - Nonlinear finite-element analysis to predict fan-blade damage due to soft-body impact p 683 A90-40939
 - Development of impact design methods for ceramic gas turbine components [AIAA PAPER 90-2413] p 687 A90-42165
 - Durability and damage tolerance of graphite/epoxy honeycomb structures p 942 A90-50085
 - Damage tolerance evaluation of several elevated temperature graphite composite materials p 945 A90-50155
 - Towards a unified method of causing impact damage in thick laminated composites p 946 A90-50168
 - Evaluation of the thermoplastic film interleaf concept for improved damage tolerance p 946 A90-50179
 - Spectra composite enhances portability and survivability of electronic equipment p 947 A90-50189
 - Noise and sonic boom impact technology. Effects of aircraft noise and sonic booms on structures: An assessment of the current state-of-knowledge [AD-A213919] p 378 N90-17409
 - Unique failure behavior of metal/composite aircraft structural components under crash type loads [NASA-TM-102679] p 690 N90-24660
 - A Protection And Detection Surface (PADS) for damage tolerance [NASA-TP-3011] p 876 N90-27788
 - A technique for rapid inspection of composite aircraft structure for impact damage p 846 N90-28077
 - A low cost shadow moire device for the nondestructive evaluation of impact damage in composite laminates [AD-A223451] p 953 N90-29442
- # IMPACT LOADS
- Impact evaluation of composite floor sections [SAE PAPER 891018] p 100 A90-14330
 - The effect of impact loading on residual strength of CFRP composite beams p 208 A90-17683

- An analytical technique for addressing airship ditching behavior [AIAA PAPER 89-3167] p 238 A90-20589
- Particulate trajectories and impact characteristics in hypersonic flight involving gas coolant shielding p 476 A90-34583
- Development of a simulated bird-strike test method --- of aircraft turbine engine fan blade materials p 600 A90-37444

- A review of the analytical simulation of aircraft crash dynamics [NASA-TM-102595] p 484 N90-20068
- Full-scale birdstrike testing of in-service aged F-111 ADBIRT windshield transparencies [AD-A218035] p 484 N90-20069
- Runaway rubber removal [AD-A218349] p 526 N90-20100
- Aircraft crash survival design guide. Volume 2: Aircraft design crash impact conditions and human tolerance [AD-A218435] p 575 N90-22546

IMPACT PREDICTION

- The analysis and testing of composite panels subject to muzzle blast effects p 675 A90-39991

IMPACT RESISTANCE

- Scaling effects in the impact response of graphite-epoxy composite beams [SAE PAPER 891014] p 128 A90-14326
- The strength and weakness of carbon composite structures --- for military and civil aircraft p 180 A90-17679
- Strike tolerant main rotor blade tip p 409 A90-28232

- Development of impact design methods for ceramic gas turbine components [AIAA PAPER 90-2413] p 687 A90-42165
- Durability and damage tolerance of S-2 glass/PEEK composites p 944 A90-50140
- Transport composite fuselage technology: Impact dynamics and acoustic transmission [NASA-CR-4035] p 126 N90-11821
- Bird impact tests on a Kevlar 49 structure. Monolithic plates. Oblique-angled impact [REPT-S3-4273] p 402 N90-18376

IMPACT STRENGTH

- Improved toughness alloys based on titanium aluminides [AD-A218149] p 533 N90-20208

IMPACT TESTING MACHINES

- Multiple impact jet apparatus (MIJA) - Application to rain erosion studies p 525 A90-34580

IMPACT TESTS

- Scaling effects in the impact response of graphite-epoxy composite beams [SAE PAPER 891014] p 128 A90-14326
- Aft facing transport aircraft passenger seats under 16G dynamic crash simulation p 175 A90-17416
- Effects of damage on post-buckled skin-stiffener composite skin panels p 409 A90-28235
- Erosive wear of fibrous PEEK composites p 530 A90-33127
- Rain erosion testing --- on polymethyl methacrylate specimens p 525 A90-34578
- The effects of toughening stresses on liquid impact induced fracture p 692 A90-41315
- A comparison of honeycomb-core and foam-core carbon-fibre/epoxy sandwich panels p 764 A90-43855

- Impact testing of glass/phenolic honeycomb panels with graphite/epoxy facesheets p 946 A90-50166
- Variations in impact test methods for tough composites p 946 A90-50167
- The 59th Shock and Vibration Symposium, volume 2 [AD-A214579] p 372 N90-18065
- Bird impact tests on a Kevlar 49 structure. Monolithic plates. Oblique-angled impact [REPT-S3-4273] p 402 N90-18376
- The effect of aircraft size on cabin floor dynamic pulses [DOT/FAA/CT-88/15] p 735 N90-25136

IMPACT TOLERANCES

- Aircraft crash survival design guide. Volume 2: Aircraft design crash impact conditions and human tolerance [AD-A218435] p 575 N90-22546

IMPACTORS

- Design and calibration of an in-stack, low-pressure impactor [AD-A213531] p 255 N90-15105

IMPEDANCE

- Advanced actuation systems development, volume 2 [AD-A213378] p 198 N90-13398
- Experimental evaluation of impedance control for robotic aircraft refueling [AD-A215532] p 337 N90-16755

IMPELLERS

- Analysis of blade loadings in centrifugal compressors p 158 A90-18591

- An approximate 3-D aerodynamic design method for centrifugal impeller blades
[ASME PAPER 89-GT-73] p 291 A90-23794
- Effect of blade tip configuration on tip clearance loss of a centrifugal impeller
[ASME PAPER 89-GT-80] p 358 A90-23801
- Secondary flow due to the tip clearance at the exit of centrifugal impellers
[ASME PAPER 89-GT-81] p 358 A90-23802
- Verification of an impeller design by laser measurements and 3D-viscous flow calculations
[ASME PAPER 89-GT-159] p 292 A90-23847
- Estimation of losses in semi-open centrifugal impellers
p 537 A90-33597
- Analyses of revising the inlet profile of a radial inflow turbine impeller
p 602 A90-35831
- Computation of flow through a centrifugal impeller with tip leakage
[AIAA PAPER 90-2021] p 684 A90-41987
- Flow in a forward swept centrifugal fan, volumes 1 and 2
p 481 A90-20959
- Application of an inverse method to the design of a radial inflow turbine
p 511 A90-20989
- Centrifugal impeller geometry and its influence on secondary flows
p 513 A90-21020
- IMPINGEMENT**
- A comparison of a droplet impingement code to icing tunnel results
[AIAA PAPER 90-0670] p 352 A90-26979
- Interaction of a plane shear layer with a downstream flat plate
[AIAA PAPER 90-1460] p 561 A90-38617
- An experimental investigation of the interaction between a model rotor and airframe in forward flight
p 185 A90-14219
- IMPROVEMENT**
- Aviation security: Corrective actions underway, but better inspection guidance still needed. Report to the Chairwoman, Government Activities and Transportation Subcommittee, Committee on Government Operations, House of Representatives
[GAO/RCED-88-160] p 635 A90-23367
- Transonic wing charge improvements by passive shock boundary layer interference control: Development status and prospects
[ETN-90-96463] p 650 A90-24267
- IMPULSES**
- Unsteady hypersonic viscous flow in impulse facilities
[AIAA PAPER 90-0421] p 313 A90-26947
- Adaptive control of helicopter vibrations via the impulse response method
[AD-A213728] p 260 A90-15113
- Adaptive control of a system with periodic dynamics: Application of an impulse response method to the helicopter vibration problem
p 694 A90-23990
- IN-FLIGHT MONITORING**
- In-flight boundary-layer transition measurements on a swept wing
p 17 A90-13017
- In-flight flow field analysis on the NASA F-18 high alpha research vehicle with comparisons to ground facility data
[AIAA PAPER 90-0231] p 163 A90-19745
- An in-flight interaction of the X-29A canard and flight control system
[AIAA PAPER 90-1240] p 348 A90-26820
- An expert system for real-time aircraft monitoring
[AIAA PAPER 90-1311] p 545 A90-33921
- Preparations of the real-time data analyst to insure flight test safety
[AIAA PAPER 90-1316] p 488 A90-33925
- Autopilot flight test experience with BK 117 hingeless rotor
[AIAA PAPER 90-1267] p 505 A90-33930
- The Super Puma MKII automatic flight control system
p 669 A90-42449
- A highly maneuverable helicopter in-flight simulator - Aspects of realization
[AIAA PAPER 88-4607] p 670 A90-42466
- The modular HUM system - Health and Usage Monitoring instruments for rotary wing aircraft failure detection
p 618 A90-42476
- New systems for helicopter and aircraft vibration monitoring
p 653 A90-42477
- Estimation of rotor blade incidence and blade deformation from the measurement of pressures and strains in flight
p 647 A90-42497
- Development of a real-time aeroperformance analysis technique for the X-29A advanced technical demonstrator
p 732 A90-44738
- In-flight experiments on the active control of propeller-induced cabin noise
p 893 A90-46352
- Investigation of propeller slipstream effects on the Fokker 50 through in-flight pressure measurements
[AIAA PAPER 90-3084] p 806 A90-46645
- Propulsion system flight test analysis using modeling techniques
[AIAA PAPER 90-3288] p 853 A90-48874

- The Operational Loads Monitoring System (OLMS)
p 926 A90-49879
- Eight years of experience with small computerized retrofit load monitoring systems
p 926 A90-49882
- Measurement effects on the calculation of in-flight thrust for an F404 turbofan engine
[NASA-TM-4140] p 114 A90-11741
- A knowledge-based flight status monitor for real-time application in digital avionics systems
[NASA-TM-101710] p 217 A90-13995
- An in-flight investigation of ground effect on a forward-swept wing airplane
[NASA-TM-101708] p 175 A90-14202
- Systems for airborne wind and turbulence measurement
p 281 A90-15046
- Direct measurement of laminar instability amplification factors in flight
p 277 A90-16178
- Optimization of the effective GPS data rate
p 489 A90-20932
- Preliminary development of an intelligent computer assistant for engine monitoring
[NASA-TM-101702] p 612 A90-22322
- Calculation of flight vibration levels of the AH-1G helicopter and correlation with existing flight vibration measurements
[NASA-CR-182031] p 775 A90-25375
- An automated calibration laboratory for flight research instrumentation: Requirements and a proposed design approach
[NASA-TM-101719] p 781 A90-26564
- New in-flight experiments to measure aerodynamics loads
[ETN-90-97276] p 868 A90-26834
- The EFA integrated monitoring and recording system: Requirements and concept for implementation
p 848 A90-27620
- Start-up built-in test for the DISCUS fault tolerant, fly-by-wire computer system
p 869 A90-27625
- Expert system diagnostics and parts life tracking as applied to the AV-8B aircraft for the USMC
p 884 A90-27629
- Harrier Information Management System (HIMS): The system and the approach
p 884 A90-27630
- New features of JAL's ground station
p 872 A90-27633
- Daily flight operation monitoring in JAL
p 820 A90-27636
- AIMS for helicopters
p 820 A90-27639
- Monitoring and controlling flight in windshear
p 820 A90-27641
- An in-flight investigation of ground effect on a forward-swept wing airplane
p 922 A90-28533
- Evaluation for DLC-Flap Monitoring System of the VSRA
[NAL-TM-607] p 928 A90-29391
- INCIDENCE**
- The effects of compressor endwall flow on airfoil incidence and deviation
p 512 A90-21011
- Mechanical paint removal techniques for aircraft structures
[IAR-89-23] p 773 A90-25254
- INCOMPRESSIBILITY**
- Stress-strain analysis of structural elements of incompressible or nearly incompressible materials by the finite element method
p 129 A90-14557
- INCOMPRESSIBLE BOUNDARY LAYER**
- Effect of surface riblets on the velocity profile of an incompressible boundary layer
p 294 A90-24081
- INCOMPRESSIBLE FLOW**
- Oscillating thin wings in inviscid incompressible flow
p 2 A90-10224
- Method for calculating the unsteady flow of an elliptical circulation-control airfoil
p 3 A90-11003
- Systematic study of flutter characteristics of two-dimensional cascades in incompressible flow
p 41 A90-11796
- An application of the surface-singularity method to wing-body-tail configurations
p 9 A90-12229
- Calculation of flow over airfoil with slat and flap
p 149 A90-16797
- Numerical studies of incompressible flow around delta and double-delta wings
p 150 A90-16845
- Perturbations of a three-dimensional boundary layer produced by body irregularities
p 150 A90-17107
- Numerical methods to solve the incompressible Euler and Navier-Stokes equations in 3D with applications
p 209 A90-18302
- Incompressible potential flow about complete aircraft configurations
p 156 A90-18443
- Unsteady incompressible aerodynamics and forced response of detuned blade rows
[AIAA PAPER 90-0340] p 191 A90-19805
- Viscous oscillating cascade aerodynamics and flutter by a locally analytical method
[AIAA PAPER 90-0579] p 168 A90-19929

- A parametric study of the flutter stability of two-dimensional turbine and compressor cascades in incompressible flow
p 225 A90-21593
- Prediction of vortical flows on wings using incompressible Navier-Stokes equations
p 226 A90-21935
- Upwind differencing scheme for the time-accurate incompressible Navier-Stokes equations
p 232 A90-23109
- Incompressible viscous flow about aircraft configurations
p 233 A90-23290
- Viscous flow calculations in turbomachinery channels
[ASME PAPER 89-GT-5] p 287 A90-23752
- Accelerated computation of viscous, steady incompressible flows
[ASME PAPER 89-GT-45] p 288 A90-23771
- Tip leakage losses in a linear turbine cascade
[ASME PAPER 89-GT-56] p 290 A90-23782
- Three-dimensional solutions for inviscid incompressible flow in turbomachines
[ASME PAPER 89-GT-140] p 291 A90-23837
- The extension and application of three-dimensional time marching analyses to incompressible turbomachinery flows
[ASME PAPER 89-GT-212] p 293 A90-23878
- Construction of a wing surface in a nonviscous transonic flow from a given pressure distribution
p 298 A90-24149
- Nonstationary motion of an elastic profile in subsonic incompressible flow
p 300 A90-24741
- Viscous corrections on wings in incompressible flow
p 301 A90-25200
- A generalized lifting-line theory for curved and swept wings
p 303 A90-25597
- Numerical simulation of vortex breakdown by solving the Euler equations for an incompressible fluid
p 476 A90-34323
- A technique for calculating nonlinear normal-force and pitching-moment coefficients for slender delta wings, accounting for wing thickness
p 476 A90-34356
- Experimental study of incompressible flow on the upper surface of a delta wing
p 558 A90-37346
- A method for solving three-dimensional viscous incompressible flows over slender bodies
p 558 A90-37890
- Flow over inclined finite length and width flat plates at low and high Reynolds numbers
[AIAA PAPER 90-1467] p 562 A90-38624
- Experimental investigation of coannular jet flow with swirl along a centerbody
[AIAA PAPER 90-1622] p 567 A90-38751
- A computational study of the taxonomy of vortex breakdown
[AIAA PAPER 90-1624] p 568 A90-38753
- Navier-Stokes computations of vortical flows
[AIAA PAPER 90-1628] p 568 A90-38757
- A numerical study of longitudinal vortex interaction with a boundary layer
[AIAA PAPER 90-1630] p 568 A90-38759
- Navier-Stokes solutions for vortical flows over a tangent-ogive cylinder
p 620 A90-39780
- Viscous flow around a propeller-shaft configuration with infinite-pitch rectangular blades
p 683 A90-40938
- Flow induced forced response of an incompressible radial cascade including profile and incidence effects
[AIAA PAPER 90-2352] p 626 A90-42136
- A collocated finite volume method for solving the Navier-Stokes equations for incompressible and compressible flows in turbomachinery - Results and applications
p 703 A90-42659
- Computation of turbine flowfields with a Navier-Stokes code
[AIAA PAPER 90-2122] p 704 A90-42731
- Finite wing lift prediction at high angles of attack
[AIAA PAPER 90-3079] p 795 A90-45910
- Incompressible potential flow about three-dimensional configurations
p 810 A90-48082
- Cascade aerodynamic gust response including steady loading effects
p 904 A90-51006
- Application of a vortex lattice numerical model in the calculation of inviscid incompressible flow around delta wings
p 904 A90-51017
- The calculation of incompressible separated turbulent boundary layers
p 905 A90-51025
- A comprehensive analysis of the viscous incompressible flow in quasi-three-dimensional aerofoil cascades
p 905 A90-51028
- Multigrid methods in computational fluid dynamics
p 906 A90-51526
- The inverse problem in the multielement airfoil theory
p 906 A90-51531
- Prediction of transition on a swept wing
p 908 A90-52592
- Steady and unsteady potential flow around thin annular wings and engines with simulation of jet engine flow
[DFVLR-FB-89-18] p 89 A90-11711

Incompressible flow about ellipsoids of revolution
[REPT-88-02] p 90 N90-11713

Computational investigation of incompressible airflow at high angles of attack
[AD-A205885] p 174 N90-14201

Effective methods of controlling a junction vortex system in an incompressible, three-dimensional, turbulent flow
p 571 N90-21732

Modeling of vortex-induced oscillations based on indicial response approach
[NASA-CR-186560] p 572 N90-21736

The discretization of the three dimensional boundary layer equations
[ETN-90-97292] p 884 N90-27987

Development of turbulence models for the analysis of compressible or incompressible unsteady flow
[ETN-90-97486] p 958 N90-28810

INCOMPRESSIBLE FLUIDS

An approximate method for calculating flow past a wing profile with allowance for viscosity p 234 A90-23422

Calculation of the induced drag of a wing with arbitrary deformation p 388 A90-29183

Hydroelastic problems in space flight vehicles p 536 A90-33386

Calculation of nonseparated flow past a wing profile at large Reynolds numbers p 706 A90-42895

Application of splines to the calculation of flow past a wing profile p 805 A90-46615

INDEPENDENT VARIABLES

Advantages of flow variables in thin viscous shock layer problems p 364 A90-24145

INDEXES (DOCUMENTATION)

Aircraft drawings index p 618 N90-23340

FAA Rotorcraft Research, Engineering, and Development Bibliography 1962-1989
[AD-A224256] p 902 N90-29299

INDUCTION HEATING

Cleaner superalloys via improved melting practices p 442 A90-29707

Induction heating development for aircraft repair p 955 A90-50164

Aircraft battle damage repair of transparencies
[AD-A224168] p 925 N90-29387

INDUCTION MOTORS

Aerospace induction motor actuators driven from a 20-kHz power link
[NASA-TM-102482] p 509 N90-20085

INDUSTRIAL MANAGEMENT

Total quality management and the transitioning company - The perfect fit
[AIAA PAPER 89-3211] p 549 A90-31698

The future of the U.S. aircraft industry p 467 A90-32275

INDUSTRIES

Langley aerospace test highlights, 1989
[NASA-TM-102631] p 699 N90-24221

INERT ATMOSPHERE

A small inert gas generator p 180 A90-17405

INERTIA

The influence of the inertia coupling on the stability and control of the helicopter and the response of helicopter gust p 671 A90-42472

Effect of control surface mass unbalance on the stability of a closed-loop active control system
[NASA-TP-2952] p 134 N90-12042

INERTIAL NAVIGATION

GPS Hover Position Sensing System p 108 A90-13986

Integration of GPS with the Carrier Aircraft Inertial Navigation System (CAINS) p 97 A90-13990

Dynamic interaction of separate INS/GPS Kalman filters (Filter-driving - Filter dynamics) p 124 A90-13996

Integrated navigation system design and performance with Phase III GPS user equipment p 98 A90-13997

Architecture options for GPS/Carousel IV integration p 108 A90-13999

Accuracy considerations for GPS TSPI system design p 98 A90-14001

Potential applications of satellite navigation p 264 A90-21716

Flight-path measurement p 242 A90-21721

The trend in nav aids inspection is to automatic operation p 329 A90-25495

Estimation of atmospheric and transponder survey errors with a navigation Kalman filter p 459 A90-30689

Multisensor Integrated Navigation System p 577 A90-36924

Low cost QUBIK IMU for integration with GPS, Omega, Loran-C, and SDI systems p 577 A90-36929

The multi-function RLG system comes of age - A technical update p 578 A90-36931

Modified fault tolerant inertial navigation system p 578 A90-37211

Measurement of angles and angle characteristics with accelerometers and gyroscopes p 653 A90-41730

Modern strapdown system for helicopter p 653 A90-42451

System concept and performance criteria of modern helicopter navigation p 640 A90-42452

Ada real-time GPS/INS simulation approach to system development p 751 A90-43706

Reduced order INS/GPS guided unmanned air vehicle study p 726 A90-43707

A flight test comparison of two GPS/INS integration approaches p 726 A90-43708

Integration of the LTN-72 INS with the DOD GPS 3A set p 728 A90-45236

Image based range determination
[AIAA PAPER 90-3404] p 822 A90-47659

Update 90 - A progress report on evaluation and flight testing of the small common RLG INS
[AIAA PAPER 90-3375] p 847 A90-47763

Towards a quantitative assessment of benefits which INS/GPS integration can offer to civil aviation operating in a non-jamming environment p 823 A90-49496

Military navigation - The fourth generation p 914 A90-50775

Inspection of instrument landing systems p 915 A90-52614

Integration and automation of navigation functions using Kalman filters p 915 A90-52615

FPG2: A flight profile generator program
[AD-A212408] p 107 N90-12595

Advances in techniques and technologies for air vehicle navigation and guidance
[AGARD-AR-276] p 243 N90-15899

Optimization of the effective GPS data rate p 489 N90-20932

Autonomous integrated GPS/INS navigation experiment for OMV. Phase 1: Feasibility study
[NASA-CR-4267] p 489 N90-20969

Passive navigation using image irradiance tracking p 578 N90-22232

Inertial navigation system simulator: Behavioral specification, revision
[AD-A219294] p 578 N90-22554

Continued development and analysis of a new extended Kalman filter for the Completely Integrated Reference Instrumentation System (CIRIS)
[AD-A220106] p 654 N90-23400

Construction of a hybrid angular velocity reference system for investigation of the dynamic characteristics of strapdown gyros
[ESA-TT-1181] p 774 N90-25332

Integrated navigation/flight control for future high performance aircraft p 917 N90-29362

INERTIAL PLATFORMS

Precision navigation using an integrated GPS-IMU system p 242 A90-21720

Integrated system of differential Global Positioning System and inertial measurement unit - A position determination system for automatic landing
[AIAA PAPER 90-1300] p 487 A90-33914

Modified fault tolerant inertial navigation system p 578 A90-37211

INERTIAL REFERENCE SYSTEMS

Aerospace coordinate systems and transformations --- Book p 282 A90-23372

Integrated navigation - Employing LIRU/GPS p 329 A90-23995

Application of multifunction inertial reference systems to fighter aircraft p 332 N90-16740

Application of multifunction inertial reference systems to fighter aircraft p 916 N90-29341

INFINITE SPAN WINGS

Vibration of a wing of nonzero thickness in supersonic flow p 222 A90-20432

A study of the stability of a wing aileron in supersonic flow p 222 A90-20442

Wind-tunnel investigations of wings with serrated sharp trailing edges p 802 A90-46379

Local convergence of the solution in the discrete vortex method p 803 A90-46534

Prediction of transition on a swept wing p 908 A90-52592

INFLATABLE STRUCTURES

Inflatable fuel tank buffer
[AD-D014446] p 503 N90-21002

INFLATING

Wind tunnel tests of a 20-gore disk-gap-band parachute
[AD-A221326] p 634 N90-24251

INFLUENCE COEFFICIENT

Wing-body mutual influence coefficients at angles-of-attack to 24 deg p 151 A90-17693

New free-wake analysis of rotorcraft hover performance using influence coefficients p 181 A90-17867

INFORMATION DISSEMINATION

Conceptual design for aerospace vehicles p 651 N90-25043

INFORMATION MANAGEMENT

Benchmarking blackboards to support cockpit information management
[AIAA PAPER 89-3095] p 37 A90-10580

Problem focus mechanisms for cockpit automation
[AIAA PAPER 89-3096] p 37 A90-10581

Thermal management of closed computer modules utilizing high density circuitry --- in Airborne Information Management System
[AIAA PAPER 90-1748] p 583 A90-38441

Automatic speech recognition in air-ground data link p 690 N90-25037

Knowledge-based system for flight information management
[NASA-TM-102685] p 780 N90-26511

Flight data replay and analysis system p 893 N90-27635

Aspects of data link applications for ATC purposes p 827 N90-27688

INFORMATION PROCESSING (BIOLOGY)

The application of queuing theory to the modelling of CP-140 aircraft communications
[AD-A213479] p 274 N90-15310

INFORMATION RETRIEVAL

Assessment System for Aircraft Noise (ASAN) citation database. Volume 1: User's manual
[AD-A219175] p 615 N90-23188

Assessment System for Aircraft Noise (ASAN) citation database. Volume 2: Database update manual
[AD-A219176] p 615 N90-23189

Assessment System for Aircraft Noise (ASAN) citation database. Volume 3: New citation review procedures
[AD-A219177] p 615 N90-23190

Computer modeling and data processing methods: An essential part of jet engine condition monitoring and fault diagnosis p 855 N90-27626

INFORMATION SYSTEMS

Adaptive automatic control systems. Number 16 --- Russian book p 76 A90-10844

An analysis of the possibility of expanding the information base of an adaptive control system for a flight vehicle surrounded by an ionized gas medium p 60 A90-10845

Identification and diagnostics in the data processing and control systems of aerospace powerplants --- Russian book p 611 A90-36151

Investigation of air transportation technology at the Massachusetts Institute of Technology, 1988-1989 p 484 N90-20922

Evaluation of existing aircraft operator data bases
[DOT/FAA/CT-90/18] p 898 N90-28463

International aircraft operator data base master requirements and implementation plan
[DOT/FAA/CT-90/17] p 967 N90-29247

INFORMATION THEORY

Geodetic network adjustment using GPS triple difference observations and a priori stochastic information
[TR-1-1987] p 178 N90-13367

INFORMATION TRANSFER

The design and study of the information transfer mechanism for a distributed avionics system p 207 A90-16858

Air-ground information transfer in the National Airspace System p 380 A90-26235

Weather data dissemination to aircraft p 486 N90-20934

INFRARED DETECTORS

Instrumentation being developed for the ONERA F4 wind tunnel
[ONERA, TP NO. 1989-189] p 261 A90-21049

Ground navigation in airport traffic p 242 A90-21725

Optical window materials for hypersonic flow p 496 A90-34581

Development and operating experience on a zinc sulfide window for the Infrared Instrumentation System (IRIS) --- for gathering data on reentry vehicles p 505 A90-34584

INFRARED IMAGERY

Aerodynamic heat transfer testing in hypersonic wind tunnels using an infrared imaging system
[AIAA PAPER 90-0189] p 350 A90-25027

Infrared imaging and tufts studies of boundary layer flow regimes on a NACA 0012 airfoil p 446 A90-28268

Applications of infra-red thermography in a hypersonic blowdown wind tunnel p 438 A90-28300

Boundary layer diagnostics by means of an infrared scanning radiometer p 605 A90-38493

Dynamic FLIR simulation in flight training research p 681 A90-40109

Aerodynamic applications of infrared thermography p 770 A90-44147

In-flight flow visualization using infrared imaging p 731 A90-44731

INFRARED INSTRUMENTS

- Low speed flowfield characterization by infrared measurements of surface temperatures p 317 N90-17556
- Proceedings of the 13th International Congress on Instrumentation in Aerospace Simulation Facilities [EARD-IR-89-069] p 527 N90-21046
- Infrared thermography at hypersonic channel H2K p 674 N90-24235
- Ground evaluation of seeding an in-flight wingtip vortex using infrared imaging flow visualization technique p 635 N90-25035

INFRARED INSTRUMENTS

- Infrared technology XIV; Proceedings of the Meeting, San Diego, CA, Aug. 15-17, 1988 [SPIE-972] p 66 A90-10138

INFRARED PHOTOGRAPHY

- Infrared cameras for detection of boundary layer transition in transonic and subsonic wind tunnels [AIAA PAPER 90-1450] p 606 A90-38610
- Investigation of air transportation technology at the Massachusetts Institute of Technology, 1988-1989 p 484 N90-20922

INFRARED RADIATION

- Aerosol effects on jet-engine IR radiation p 40 A90-10152
- Infrared-radiation model for aircraft and reentry vehicle p 77 A90-10169
- Infrared sources of jet propulsion system and their suppression p 252 A90-22614
- The application of infrared thermography to the nondestructive testing of composite materials p 886 N90-28084

INFRARED RADIOMETERS

- A multichannel wide FOV infrared radiometric system p 67 A90-11410
- Infrared thermography in blowdown and intermittent hypersonic facilities p 440 A90-31302
- An infrared camera system for detection of boundary layer transition in the ETW p 539 A90-34249
- Boundary layer diagnostics by means of an infrared scanning radiometer p 605 A90-38493
- Infrared thermography p 911 N90-29325

INFRARED WINDOWS

- Thermostructural behavior of electromagnetic windows - Elaboration of a code package [ONERA, TP NO. 1989-145] p 76 A90-11167
- Grid and mesh patterned electrically conductive coatings in IR systems p 503 A90-32028
- Optical window materials for hypersonic flow p 496 A90-34581
- Development and operating experience on a zinc-sulfide window for the Infrared Instrumentation System (IRIS) --- for gathering data on reentry vehicles p 505 A90-34584
- Design considerations for a compact table top hypersonic simulator of aero-optic effects p 525 A90-34585
- Table top experimental simulation of hypersonic aero-optical effects --- encountered by cooled window on interceptor p 525 A90-34586

INGESTION (ENGINES)

- Water ingestion simulation - Test needs p 23 A90-12620
- Rotor noise due to atmospheric turbulence ingestion. II - Aeroacoustic results p 219 A90-19386
- Engine inlet distortion in a 9.2 percent scaled vectored thrust STOVL model in ground effect [AIAA PAPER 89-2910] p 301 A90-25043
- Hot gas environment around STOVL aircraft in ground proximity. I - Experimental study p 742 A90-42765
- Hot gas environment around STOVL aircraft in ground proximity. II - Numerical study [AIAA PAPER 90-2270] p 743 A90-42766
- Study of the engine bird ingestion experience of the Boeing 737 aircraft [DOT/FAA/CT-89/16] p 176 N90-13360
- Study of bird ingestions into small inlet area; aircraft turbine engines (May 1987 to April 1988) [DOT/FAA/CT-89/17] p 402 N90-18375

INJECTION

- Low NO(x) potential of gas turbine engines [NASA-TM-102452] p 345 N90-17636

INJECTION MOLDING

- Resin transfer molding of composite structures p 270 A90-20264
- Air Force application of injection molding technology [SME PAPER EM89-103] p 274 A90-23688
- Injection molding development of ceramic turbine components [ASME PAPER 89-GT-170] p 381 A90-23855
- Injectable bismaleimide systems p 943 A90-50132
- Improved silicon carbide for advanced heat engines [NASA-CR-180831] p 85 N90-10293

INJECTORS

- Experimental investigation of a supersonic swept ramp injector using laser-induced iodine fluorescence [AIAA PAPER 90-1518] p 606 A90-38663
- Subsonic combustor testing p 749 N90-25997
- Modeling of supersonic reacting flow fields p 855 N90-26898

INJURIES

- Windblast protection for advanced ejection seats p 483 N90-20063

INLET AIRFRAME CONFIGURATIONS

- Solution of Euler equations for fighter forebody-inlet combination at high angle of attack p 556 A90-36419

INLET FLOW

- The effect of the magnitude of the inlet-boundary disturbance on the unsteady forces on axial gas-turbine blades p 6 A90-11781
- Numerical Euler solution for the interaction between oscillating cascade and forced inlet unsteadiness p 8 A90-11792
- Computation of unsteady compressible turbulent boundary layers in cascade flow with controlled inlet perturbation p 8 A90-11807
- Advanced computational techniques for hypersonic propulsion p 69 A90-12606
- Experimental investigations on the spatial and time-dependent structure of part-load recirculations in centrifugal pumps p 83 A90-13788
- Design and experimental verification of an equivalent forebody representation of flowing inlets p 152 A90-17863
- A study of ground vortex p 158 A90-18590
- A numerical parametric study of a scramjet inlet in a Mach 6 arc heated test facility [AIAA PAPER 90-0531] p 167 A90-19896
- Investigation of oscillating airfoil shock phenomena [AIAA PAPER 90-0695] p 169 A90-19981
- Nonaxisymmetric instabilities in a dump combustor with a swirling inlet flow p 253 A90-21228
- Representation of two-dimensional hypersonic inlet flows for one-dimensional scramjet cycle analysis [AIAA PAPER 90-0527] p 229 A90-22226
- Effect of inlet flow angle on the erosion of radial turbine guide vanes [ASME PAPER 89-GT-208] p 254 A90-22664
- Inlet skew and the growth of secondary losses and vorticity in a turbine cascade [ASME PAPER 89-GT-65] p 290 A90-23788
- Damping of the inlet vortex in a turbojet engine p 301 A90-25185
- Inlet swirl effects on dump combustor flows [AIAA PAPER 90-0035] p 312 A90-26904
- Three-dimensional shock-shock interactions on the scramjet inlet [AIAA PAPER 90-0529] p 314 A90-26963
- A flux-split solution procedure for unsteady inlet flows [AIAA PAPER 90-0585] p 314 A90-26967
- Comparison of 3-D viscous flow computations of Mach 5 inlet with experimental data [AIAA PAPER 90-0600] p 314 A90-26970
- Calculation of transonic flows with separation past arbitrary inlets at incidence p 384 A90-27979
- An experimental study on flowfields in a dual inlet swirl-dump combustor p 471 A90-33283
- Inlet distortion generated periodic aerodynamic rotor response [ASME PAPER 89-GT-299] p 475 A90-33567
- Analyses of revising the inlet profile of a radial inflow turbine impeller p 602 A90-35831
- Influence of bulk turbulence and entrance boundary layer thickness on the curved duct flow field [AIAA PAPER 90-1502] p 606 A90-38651
- Calculation of hypersonic forebody/inlet flow fields [AIAA PAPER 90-1493] p 619 A90-39049
- The influence of the inlet Mach number on the boundary layer development on turbomachinery blade surfaces p 621 A90-40504
- Computational modeling of inlet hammer shock wave generation [AIAA PAPER 90-2005] p 621 A90-40592
- A numerical investigation of supersonic inlet using implicit TVD scheme [AIAA PAPER 90-2135] p 621 A90-40612
- Directivity of the noise radiation emitted from the inlet duct of a turboshaft helicopter engine [ONERA, TP NO. 1990-26] p 695 A90-41205
- Mixing characteristics of dilution jets in small gas turbine combustors [AIAA PAPER 90-2728] p 664 A90-42217
- Transient behavior of supersonic flow through inlets [AIAA PAPER 90-2130] p 704 A90-42734
- Analysis of shock interactions and flow structure in high speed inlets [AIAA PAPER 90-2132] p 704 A90-42735

Computational analysis of an open-nosed fighter/attack inlet

- [AIAA PAPER 90-2145] p 704 A90-42737
- Measurements in an annular combustor-diffuser system [AIAA PAPER 90-2162] p 768 A90-42740
- A numerical study of the effects of reverse sweep on a scramjet inlet performance [AIAA PAPER 90-2218] p 705 A90-42749
- A computational model for thickening boundary layers with mass addition for hypersonic engine inlet testing [AIAA PAPER 90-2219] p 705 A90-42750
- Effects of inlet turbulence scale on turbine blade surface heat transfer in a linear cascade [AIAA PAPER 90-2264] p 768 A90-42761
- A computational analysis of the transonic flow field of two-dimensional minimum length nozzles p 173 N90-14194
- Rotor induced inflow ratio measurements and CAMRAD calculations [NASA-TP-2946] p 237 N90-15882
- A method for the prediction of supersonic compressor blade performance [CUED/A-TURBO/TR-126] p 344 N90-17634
- Research on a two-dimensional inlet for a supersonic V/STOL propulsion system. Appendix A [NASA-CR-174945] p 396 N90-18364
- Water-tunnel investigation of concepts for alleviation of adverse inlet spillage interactions with external stores [NASA-TM-4181] p 398 N90-19199
- Application of an inverse method to the design of a radial inflow turbine p 511 N90-20989
- LDV measurements and the flow analysis in the vortex region of a radial inflow turbine p 511 N90-21007
- Control of flow separation and mixing by aerodynamic excitation [NASA-TM-103131] p 571 N90-21733
- Theoretical and experimental study of flow-control devices for inlets of indraft wind tunnels [NASA-TM-100050] p 598 N90-21778
- Aerodynamics of a linear oscillating cascade [NASA-TM-103250] p 817 N90-27657
- Experience in developing an improved design of experiment (lessons learned) p 857 N90-27718
- Experience in developing an improved altitude test capability p 857 N90-27719

INLET NOZZLES

- The investigation of stress at an enter-gas nozzle of main landing gears for fighter aeroplanes p 181 A90-18606
- Air and spray patterns produced by gas turbine high-shear nozzle/swirler assemblies [AIAA PAPER 90-0465] p 192 A90-19857
- A numerical parametric study of a scramjet inlet in a Mach 6 arc heated test facility [AIAA PAPER 90-0531] p 167 A90-19896
- Radio frequency (RF) heated supersonic flow laboratory [AIAA PAPER 90-2469] p 673 A90-42186

INLET PRESSURE

- Basic principles of measuring thrust through exhaust to inlet total pressure ratio - Engine Pressure Ratio (EPR) p 191 A90-18635
- Experimental investigation of terminal shock sensors in mixed-compression inlets [AIAA PAPER 90-1931] p 681 A90-40560

INLET TEMPERATURE

- Current status of ceramic gas turbine R&D in Japan [ASME PAPER 89-GT-114] p 359 A90-23818
- Navier-Stokes analyses of the redistribution of inlet temperature distortions in a turbine p 471 A90-32959
- Inlet radial temperature redistribution in a transonic turbine stage [AIAA PAPER 90-1543] p 565 A90-38687
- Fiber-optic turbine inlet temperature measurement system (FOTITMS) [AIAA PAPER 90-2033] p 657 A90-40603
- Unsteady Euler analysis of the redistribution of an inlet temperature distortion in a turbine [AIAA PAPER 90-2262] p 768 A90-42759
- Optimization studies for the PW305 turbofan [AIAA PAPER 90-2520] p 744 A90-42813
- Research and development of advanced gas turbine [DE90-503377] p 776 N90-26335

INOCULATION

- Ground evaluation of seeding an in-flight wingtip vortex using infrared imaging flow visualization technique p 635 N90-25035

INORGANIC COATINGS

- Grid and mesh patterned electrically conductive coatings in IR systems p 503 A90-32028

INPUT

- Three input concepts for flight crew interaction with information presented on a large-screen electronic cockpit display [NASA-TM-4173] p 420 N90-18394

SUBJECT INDEX

INPUT/OUTPUT ROUTINES

A test matrix sequencer for research test facility automation
[AIAA PAPER 90-2386] p 759 A90-42791

INSERTION LOSS

Reduced insertion loss of X-band RF fiber optic links
p 695 A90-41240

INSPECTION

Computer integrated quality assurance for robotic workcells in aerospace manufacturing
[SME PAPER MS89-152] p 283 A90-23681
Aircraft engine inspection p 771 A90-44606
A probabilistic approach for the establishment of an aircraft structure inspection program p 902 A90-49892

Stochastic propagation of an array of parallel cracks: Exploratory work on matrix fatigue damage in composite laminates
[DE89-017837] p 126 N90-11813

A computer integrated approach to dimensional inspection
[PNR90596] p 116 N90-12611

NDI (Nondestructive Inspection) oriented corrosion control for Army aircraft. Phase 1: Inspection methods
[AD-A213368] p 176 N90-13359

Inspection development for T-37 wing spar cap lug
[AD-A214826] p 287 N90-16708

Aviation security: Corrective actions underway, but better inspection guidance still needed. Report to the Chairwoman, Government Activities and Transportation Subcommittee, Committee on Government Operations, House of Representatives
[GAO/RCED-88-160] p 635 N90-23367

Modeling growth of fatigue cracks which originate at rivet holes p 691 N90-25060

Neural networks for detecting defects in aircraft structures
[IAR-90-4] p 777 N90-26345

Robotic-aided system for inspection of aging aircraft
[NIAR-90-9] p 777 N90-26346

NDT in aerospace: The next decade (1990's)
[PNR90628] p 777 N90-26348

The role of NDI in the certification of turbine engine components p 777 N90-26349

Individual Helicopter Tracking Program (IHTP) for the MH-53J helicopter p 843 N90-26818

Impact of Emerging NDE-NDI Methods on Aircraft Design, Manufacture, and Maintenance
[AGARD-CP-462] p 885 N90-28068

The role of NDI in the certification of turbine engine components p 859 N90-28069

NDI-concept for composites in future military aircraft p 877 N90-28070

Inspection reliability p 885 N90-28072

Critical inspection of high performance turbine engine components: The RFC concept p 859 N90-28073

An ultrasonic system for in-service non-destructive inspection of composite structures p 885 N90-28076

A technique for rapid inspection of composite aircraft structure for impact damage p 846 N90-28077

In-service inspection of composite components on aircraft at depot and field levels p 885 N90-28078

Development of an automated ultrasonic inspection system for composite structure on in-service aircraft p 885 N90-28079

Neutron radiography: Applications and systems p 886 N90-28080

New aspects in aircraft inspection using eddy current methods p 886 N90-28085

Inspection system for in-situ inspection of aircraft composite structures p 886 N90-28091

Use of acoustic emission for continuous surveillance of aircraft structures p 887 N90-28092

Impact of NDE-NDI methods on aircraft design, manufacture, and maintenance, from the fundamental point of view p 887 N90-28093

A low cost shadow moire device for the nondestructive evaluation of impact damage in composite laminates
[AD-A223451] p 953 N90-28442

Fractographic analysis of fatigue failures of airframe equipment parts: Examples of a rod end housing and a rod end cap
[NAL-TR-1047] p 961 N90-29686

INSSTALLING

Antenna installation on aircraft: Theory and practice p 371 N90-17941

INSTRUCTION SETS (COMPUTERS)

RISC lifting off in avionics — Reduced Instruction Set Computer
[AIAA PAPER 89-2967] p 73 A90-10483

INSTRUCTORS

A framework for the optimal design of instructor/operator stations in flight simulators p 779 A90-45373

INSTRUMENT APPROACH

Two effective methods of approach and landing by visual display
[SAE PAPER 891054] p 108 A90-14356

Demonstration of MLS advanced approach techniques p 640 A90-41711

Microwave landing system - A pilot's point of view p 640 A90-41712

Flight test investigation of flight director and autopilot functions for helicopter decelerating instrument approaches
[DOT/FAA/CT-TN89/54] p 869 N90-27724

Dallas/Forth Worth simulation. Phase 2: Triple simultaneous parallel Instrument Landing System (ILS) approaches (turbojets)
[DOT/FAA/CT-90/2] p 915 N90-28509

INSTRUMENT COMPENSATION

B-1B Doppler error compensation based on flight data analysis p 404 A90-30790

A proposed automatic calibration facility for cryogenic balances p 524 A90-34246

INSTRUMENT ERRORS

Modified fault tolerant inertial navigation system p 578 A90-37211

MLS - A total system approach p 640 A90-41710

A study of the errors of a gyroscopic instrument for measuring linear accelerations p 771 A90-45133

INSTRUMENT FLIGHT RULES

TCAS for commuter aircraft p 487 A90-33348

Handling qualities research at the Flight Research Laboratory, NAE/NRC, 1980 - 1990 and beyond
[AIAA PAPER 90-2848] p 755 A90-45176

Improved lighting of taxiway/taxiway intersections for Instrument Flight Rules (IFR) operations
[DOT/FAA/CT-TN89/64] p 243 N90-15089

IFR aircraft handled forecast by air route traffic control center: Fiscal years 1990 to 2005
[AD-A220312] p 641 N90-24263

INSTRUMENT LANDING SYSTEMS

Autolanding with GPS p 97 A90-13985

Two effective methods of approach and landing by visual display
[SAE PAPER 891054] p 108 A90-14356

Flight-path measurement p 242 A90-21721

Differential GPS (DGPS) as an approach and landing aid p 242 A90-21722

Accurate ILS and MLS performance evaluation in presence of site errors p 404 A90-30693

Strategic aircraft engineering design simulation p 439 A90-30729

Flight tests of a helmet-mounted display synthetic visibility system
[AIAA PAPER 90-1279] p 579 A90-36027

ILS - Past and present p 639 A90-41706

ILS - A safe bet for your future landings p 639 A90-41707

Applications of slotted cable antennas in the instrument landing system p 639 A90-41708

MLS - Keeping pace with the future p 640 A90-41709

Microwave landing system - A pilot's point of view p 640 A90-41712

Simulation of MLS-ATC procedures in the New York and San Francisco Terminal Control Areas
[SAE PAPER 892217] p 728 A90-45434

MLS RNAV accuracy flight tests p 728 A90-45435

Inspection of instrument landing systems p 915 A90-52614

ILS/MLS comparison tests at Miami/Tamiami, Florida Airport
[ACD-330] p 27 N90-10018

ILS (Instrument Landing System) mathematical modeling study on the effects of proposed hangar construction west of runway 18R on localizer performance at Dallas-Fort Worth International Airport
[AD-A210631] p 27 N90-10019

ILS mathematical modeling study of the effects of proposed hangar construction at the Orlando International Airport, Runway 17R, Orlando, Florida
[DOT/FAA/CT-TN89/52] p 121 N90-11762

An evaluation of the accuracy of a microwave landing system area navigation system at Miami/Tamiami Florida Airport
[DOT/FAA/CT-TN89/40] p 640 N90-23377

Dallas/Forth Worth simulation. Phase 2: Triple simultaneous parallel Instrument Landing System (ILS) approaches (turbojets)
[DOT/FAA/CT-90/2] p 915 N90-28509

INSURANCE (CONTRACTS)

Insurance aspects of airline liability p 898 A90-49615

INTAKE SYSTEMS

An investigation into the internal heat transfer characteristics of a thermally anti-iced aero-engine intake lipskin p 111 A90-15390

INTERACTIONAL AERODYNAMICS

Recent developments in Ramjet pressure oscillation technology p 53 N90-10199

Inflatable fuel tank buffer
[AD-D014446] p 503 N90-21002

A heat transfer analysis for rough turbine airfoils
[AD-A221942] p 854 N90-26831

Flow coupling between a rotor and a stator in turbomachinery
[AD-A223882] p 932 N90-28572

Numerical simulations of flowfields in a central-dump ramjet combustor. 3: Effects of chemistry
[AD-A224145] p 933 N90-28573

INTEGRAL EQUATIONS

The method of matched integral representations in viscous fluid dynamics p 129 A90-14565

Computations of unsteady transonic flows about thin airfoils by integral equation method p 158 A90-18609

Analysis of transonic integral equations. I - Artificial viscosity p 232 A90-23124

A panel method for arbitrary moving boundaries problems p 302 A90-25284

Analysis of transonic integral equations: II - Boundary element methods p 302 A90-25301

Boundary element solution of the transonic integro-differential equation p 383 A90-27947

Grid generation procedure using the integral equation method
[NAL-TR-1009] p 77 N90-10630

An alternative derivation for an integral equation for linearized subsonic flow over a wing
[AD-A214140] p 236 N90-15079

Integral-equation methods in steady and unsteady subsonic, transonic and supersonic aerodynamics for interdisciplinary design
[NASA-TM-102677] p 716 N90-25110

INTEGRALS

Elevated temperature crack growth
[NASA-CR-182247] p 777 N90-26355

INTEGRATED CIRCUITS

Thermal management of closed computer modules utilizing high density circuitry — in Airborne Information Management System
[AIAA PAPER 90-1748] p 583 A90-38441

INTEGRATED ENERGY SYSTEMS

Aircraft engine technology gets a second wind p 659 A90-41166

INTEGRATED OPTICS

The impact of fiber optics (photonics) on future aircraft
[AGARD-R-771] p 504 A90-32863

Fiber optics smart structures program at UTIAS p 535 A90-32864

Providing an inexpensive gyro for the navigation market p 848 A90-49502

INTEGRITY

Loran-aided GPS integrity p 98 A90-14013

The case for both RAIM and GIC working together - The ultimate solution to the GPS integrity problem p 576 A90-36916

Fuel Tank Technology
[AGARD-R-771] p 250 N90-15904

GPS integrity requirements for use by civil aviation p 916 N90-29339

INTELLIGENCE

Some problems on 'intelligence' of wind tunnel testing p 436 A90-28282

INTELLIGIBILITY

Comparison of speech intelligibility in cockpit noise using SPH-4 flight helmet with and without active noise reduction
[NASA-CR-177564] p 915 N90-28510

INTERACTIONAL AERODYNAMICS

A study of three-dimensional supersonic flow of a real gas past axisymmetric bodies p 3 A90-10938

Canard-wing interaction in unsteady supersonic flow p 3 A90-11010

A study of unsteady rotor-stator interactions p 67 A90-11557

On the length scales of laminar shock/boundary-layer interaction p 5 A90-11610

Analysis of the effect of rotor-angular-acceleration on the features of gas flow in turbomachinery p 6 A90-11780

The interaction between tip clearance flow and the passage flowfield in an axial compressor cascade p 11 A90-12525

Propeller wakes and their interaction with wings p 14 A90-12614

Identification of a coupled body/coning/inflow model of Puma vertical response in the hover p 56 A90-12765

Vortex interactions in fixed and oscillating delta wings (water tunnel visualizations) p 16 A90-12784

Numerical study of single impinging jets through a crossflow p 17 A90-13020

Investigation of flow separation on a supercritical airfoil p 17 A90-13023

Numerical simulation of three-dimensional flow around parachute canopies p 84 A90-14438
 Wake-boundary layer interaction p 85 A90-15238
 Experimental study of 2D/3D interactions between a vortical flow and a lifting surface p 86 A90-15849
 An interactive boundary layer method for subsonic airfoil flows p 144 A90-16754
 Interaction between strong longitudinal vortices and turbulent boundary layers p 145 A90-16764
 A viscous package for attached and separated flows on swept and tapered wings p 146 A90-16771
 On the effects of wind tunnel turbulence on steady and unsteady airfoil characteristics p 147 A90-16777
 Experimental and computational studies of dynamic stall p 147 A90-16780
 Computation of viscous transonic flow over porous airfoils p 153 A90-17864
 Further analysis of wing rock generated by forebody vortices p 153 A90-17868
 Essential ingredients of a method for low Reynolds-number airfoils p 153 A90-17979
 Separation shock dynamics in Mach 5 turbulent interactions induced by cylinders p 153 A90-17981
 High Reynolds number wedge-induced separation lengths at Mach 6 p 154 A90-18001
 Pressure fluctuations in the tip region of a blunt-tipped airfoil p 154 A90-18136
 Underexpanded jet-freestream interactions on an axisymmetric afterbody configuration p 154 A90-18141
 Mach number effects on conical surface features of swept shock-wave/boundary-layer interactions p 154 A90-18147
 Further investigations of transonic shock-wave boundary-layer interaction with passive control p 159 A90-19390
 Estimate of loads during wing-vortex interactions by Munk's transverse-flow method p 159 A90-19391
 A kinematical/numerical analysis of rotor-stator interaction noise p 219 A90-19770
 Upstream-influence scaling of fin-generated shock wave boundary-layer interactions p 164 A90-19822
 Impact of nose-probe chines on the vortex flows about the F-16C p 165 A90-19828
 Propeller tip vortex interactions p 166 A90-19846
 Calculation of low Reynolds number flows at high angles of attack p 167 A90-19921
 Fortified LEWICE with viscous effects --- Lewis Ice Accretion Prediction Code p 176 A90-20009
 Development of the MZM numerical method for 3D boundary layer with interaction on complex configurations --- Multi-Zonal Marching [ONERA, TP NO. 1989-174] p 223 A90-21036
 Swept shock/boundary-layer interactions - Tutorial and update p 228 A90-22207
 Experimental studies of shock wave/wall jet interaction in hypersonic flow p 231 A90-22449
 Airfoil pressure measurements during a blade vortex interaction and a comparison with theory p 232 A90-23105
 Three-dimensional separated flow field in the endwall region of an annular compressor cascade in the presence of rotor-stator interaction. II - Unsteady flow and pressure field [ASME PAPER 89-GT-77] p 291 A90-23798
 Aerodynamic design methods for transonic wings p 293 A90-23978
 Stability analysis and numerical experiments for viscous-inviscid interaction in transonic flow p 293 A90-24009
 Investigation of wall pressure pulsations during the passive control of shock/boundary layer interaction p 378 A90-24132
 Interaction between a vibrating compression shock and a boundary layer p 298 A90-24143
 Wing-fuselage interference regimes at supersonic flight velocities p 298 A90-24155
 On efficiency and accuracy of numerical methods for solving aerodynamic equations p 304 A90-25730
 Problem areas in applied computational fluid dynamics p 366 A90-25770
 Topological study of three-dimensional vortex interactions p 367 A90-25885
 Application of multiple grids topology to supersonic internal/external flow interactions p 308 A90-26135
 Blade-vortex interaction experiments - Velocity and vorticity fields p 312 A90-26903

Analysis of unsteady rotor-stator interactions using a viscous explicit method [AIAA PAPER 90-0342] p 313 A90-26937
 Conditions of the generation of autooscillations in aerodynamic control surfaces in nonseparated subsonic flow of a gas p 315 A90-27303
 Prediction and measurement of the aerodynamic interactions between a rotor and airframe in forward flight p 384 A90-28176
 Investigation of aerodynamic interactions between a rotor and fuselage in forward flight p 385 A90-28198
 Auxiliary hypotheses of the wave drag theory p 387 A90-29003
 Aeroservoelasticity [AIAA PAPER 90-1073] p 411 A90-29381
 Practical problems - Airplanes --- unsteady interactional aerodynamics, flutter characteristics, and active flight control p 394 A90-29885
 Basic numerical methods --- of unsteady and transonic flow p 394 A90-29886
 Infrared thermography in blowdown and intermittent hypersonic facilities p 440 A90-31302
 Multi-element aeroflows in viscous flow p 469 A90-32451
 Oscillatory shock motion caused by transonic shock boundary-layer interaction p 470 A90-32478
 A strong viscous-inviscid interaction method for computing unsteady transonic airloads for use in aerelastics p 471 A90-33355
 Non-axisymmetric viscous lower-branch modes in axisymmetric supersonic flows p 474 A90-33509
 Shock-fitting method for two-dimensional inviscid, steady supersonic flows in ducts p 477 A90-34864
 Turbulence statistics in a shock wave boundary layer interaction p 552 A90-35205
 Numerical calculation of the jet-interaction induced separation with respect to thrust vector control p 584 A90-35228
 Measurement of the interaction between a rotor tip vortex and a cylinder p 555 A90-36255
 Mach number effects on upstream influence in swept shock wave/turbulent boundary layer interactions p 556 A90-36415
 Acoustics p 614 A90-36541
 The influence of interactional aerodynamics of rotor-fuselage-interferences on the fuselage flow p 561 A90-38523
 Interaction of a plane shear layer with a downstream flat plate p 561 A90-38617
 Numerical prediction of transonic viscous flows around airfoils through an Euler/boundary layer interaction method [AIAA PAPER 90-1537] p 564 A90-38681
 Calculation of unsteady rotor/stator interaction [AIAA PAPER 90-1544] p 565 A90-38688
 An algebraic adaptive-grid technique for the solution of Navier-Stokes equations [AIAA PAPER 90-1605] p 567 A90-38736
 A numerical study of longitudinal vortex interaction with a boundary layer p 568 A90-38759
 Numerical simulation of a turbulent flow through a shock wave p 608 A90-38769
 Dynamics of the outgoing turbulent boundary layer in a Mach 5 unswept compression ramp interaction [AIAA PAPER 90-1645] p 569 A90-38773
 Correlation of separation shock motion in a compression ramp interaction with pressure fluctuations in the incoming boundary layer p 569 A90-38774
 Boundary layer stability in the case of transonic external flow p 619 A90-39514
 A visualization study of the interaction of a free vortex with the wake behind an airfoil p 623 A90-41119
 Interaction between a high-level steady acoustic field and a ducted turbulent flow [ONERA, TP NO. 1990-27] p 695 A90-41206
 Measurements of turbulent dual-jet interaction [AIAA PAPER 90-2105] p 624 A90-42019
 Computation of multiple normal shock wave/turbulent boundary layer interactions p 685 A90-42037
 Numerical analysis of viscous-inviscid interaction in transonic flow p 627 A90-42363
 Calculation of viscous-inviscid strong interaction for transonic flows over aeroflows p 627 A90-42364
 Higher-order boundary-layer approximations in interactive airfoil calculations p 628 A90-42402
 An investigation of oblique shock/boundary layer bleed interaction [AIAA PAPER 90-1928] p 703 A90-42697
 The effect of vibration-dissociation interaction on heat transfer and drag during the hypersonic flow past bodies p 710 A90-44934

Self-induced roll oscillations of low-aspect-ratio rectangular wings [AIAA PAPER 90-2811] p 753 A90-45151
 An experimental study of the nonlinear dynamic phenomenon known as wing rock [AIAA PAPER 90-2812] p 753 A90-45152
 Canard-wing vortex interactions at subsonic through supersonic speeds p 711 A90-45154
 An unsteady helicopter rotor-fuselage aerodynamic interaction analysis p 712 A90-45323
 Validation of propeller slipstream calculations using a multi-block Euler code p 791 A90-45874
 Static and dynamic water tunnel tests of slender wings and wing-body configurations at extreme angles of attack [AIAA PAPER 90-3021] p 869 A90-45888
 Multiple vortex and shock interactions at subsonic, transonic, and supersonic speeds [AIAA PAPER 90-3023] p 793 A90-45890
 Effect of leading edge roundness on a delta wing in wing-rock motion p 795 A90-45911
 Wake effects on the prediction of transonic viscous flows around airfoils with an Euler/boundary layer interaction approach [AIAA PAPER 90-3061] p 798 A90-45933
 Some characteristics of interference between shock waves and the aerodynamic wake behind a body p 804 A90-46551
 Some possibilities of the vortex layer method for calculating the aerodynamic characteristics of an augmented airfoil interacting with the engine jet p 804 A90-46564
 An experimental study of the combined effect of longitudinal riblets and vortex breakers on turbulent friction p 805 A90-46565
 Effect of shock waves and jets on structural elements: Mathematical modeling in nonstationary gas dynamics --- Russian book p 806 A90-46621
 Experimental observations of two-dimensional blade-vortex interaction p 809 A90-47303
 Wave interactions in a three-dimensional attachment-line boundary layer p 811 A90-48715
 Airfoil static-pressure thrust - Flight-test verification [AIAA PAPER 90-3286] p 812 A90-48873
 Interactive boundary-layer method for unsteady airfoil flows - Quasisteady model p 812 A90-48953
 Two- and three-dimensional problems of unsteady aerodynamics of low loaded turbomachinery blade rows stages p 813 A90-49452
 Numerical simulation of transonic flow through oscillating and multi-row two-dimensional airfoil cascades p 814 A90-49460
 The interaction between distortion of inlet flow and blade stall flutter in axial-flow compressor p 854 A90-49466
 Measurements of simulated wake/rotor interaction phenomena in turbomachinery p 814 A90-49475
 A method for calculating the rotor-fuselage interference in helicopters p 919 A90-50246
 A numerical technique for computing the unsteady transonic flow around a wing profile in arbitrary oscillation p 906 A90-51530
 An LDA investigation of the normal shock wave boundary layer interaction p 908 A90-52618
 Analysis and calculation for interaction between shock wave and laminar boundary layer p 909 A90-52778
 Frequency domain aerodynamic analysis of interacting rotating systems p 21 N90-10837
 A model suitable for predicting the noise associated with the ducted tail rotor of a helicopter [ECL-88-09] p 220 N90-14074
 Body effect on wing angle of attack and pitching moment at zero lift at low speeds [ESDU-89042] p 337 N90-16757
 A two dimensional study of rotor/airfoil interaction in hover [NASA-CR-183272] p 845 N90-27694
 The Second ARO Workshop on Rotorcraft Interactional Aerodynamics [AD-A223310] p 911 N90-29304
INTERACTIONS
 Three-dimensional unsteady transonic viscous-inviscid interaction p 18 N90-10005
 Numerical investigation of some control methods for 3-D turbulent interactions due to sharp fins p 591 N90-21764
INTERACTIVE CONTROL
 Interactive multi-block grid generation p 310 A90-26528
 Interactive generation of unstructured grids for three dimensional problems p 310 A90-26537
 Numerical interactive grid generation for 3D-flow calculations p 312 A90-26556

SUBJECT INDEX

- Concept demonstration of the use of interactive fault diagnosis and isolation for TF30 engines p 617 A90-41177
- Interactive grid adaption p 806 A90-46850
- An interactive method for the flow calculation of airfoils with local separation regions p 278 N90-16190
- INTERCEPTION**
- A comparison of time-optimal interception trajectories for the F-8 and F-15 [NASA-CR-186300] p 581 N90-21753
- INTERFACES**
- Display interface concepts for automated fault diagnosis [NASA-TM-101610] p 252 N90-15102
- INTERFERENCE**
- Residual interference assessment in adaptive wall wind tunnels [NASA-CR-181896] p 123 N90-12625
- INTERFERENCE DRAG**
- Analysis of installed wind tunnel test results on large bypass ratio engine/nacelle installations [AIAA PAPER 90-2146] p 705 A90-42738
- Wind tunnel support system effects on a fighter aircraft model at Mach numbers from 0.6 to 2.0 [AD-A210614] p 19 N90-10010
- An experimental investigation of helicopter rotor hub fairing drag characteristics [NASA-TM-102182] p 88 N90-11701
- Slotted-wall research with disk and parachute models in a low-speed wind tunnel [DE90-00289] p 572 N90-21737
- Subsonic sting interference on the aerodynamic characteristics of a family of slanted-base ogive-cylinders [NASA-CR-4299] p 633 N90-24242
- Sting-support interference on afterbody drag at transonic speeds [NAL-TM-EA-8902] p 909 N90-28492
- INTERFERENCE FIT**
- Internal rotor friction instability [NASA-CR-183942] p 543 N90-21395
- INTERFERENCE IMMUNITY**
- Optic multiplex for aircraft sensors - Issues and options p 38 A90-11660
- Clutter rejection and transmitter-receiver requirements in an airborne radar p 738 A90-45354
- INTERLAYERS**
- Evaluation of the thermoplastic film interleaf concept for improved damage tolerance p 946 A90-50179
- INTERMETALLICS**
- Intermetallic compounds for strong high-temperature materials - Status and potential p 125 A90-15022
- Application of advanced materials to aircraft gas turbine engines [AIAA PAPER 90-2281] p 764 A90-42769
- INTERNAL COMBUSTION ENGINES**
- Instrumentation for combustion and flow in engines; Proceedings of the NATO Advanced Study Institute, Vimeiro, Portugal, Sept. 13-26, 1987 p 211 A90-19004
- Smart microsensors for high temperature applications, phase 1 [AD-A224151] p 959 N90-28828
- INTERNAL COMPRESSION INLETS**
- Mach 6 testing of two generic three-dimensional sidewall compression scramjet inlets in tetrafluoromethane [AIAA PAPER 90-0530] p 192 A90-19895
- A numerical study of the effects of reverse sweep on a scramjet inlet performance [AIAA PAPER 90-2218] p 705 A90-42749
- INTERNAL FRICTION**
- Internal rotor friction instability [NASA-CR-183942] p 543 N90-21395
- INTERNATIONAL COOPERATION**
- The Soviets' French revelation. II - Aircraft p 81 A90-14800
- From the DC-3 to hypersonic flight - ICAO in a changing environment p 222 A90-23662
- The use of satellite technology for oceanic air traffic control p 330 A90-25570
- EH101 design and development status p 407 A90-28211
- Status of the development programme for instrumentation and test techniques of the European Transonic Windtunnel - ETW p 437 A90-28292
- Practical aspects of European collaboration - procurement in helicopter industry p 785 A90-46928
- Advocating international cooperation: The Eurofar program - An example and a hope - European Future Advanced Rotorcraft program p 785 A90-46929
- Innovation and investment for survival and prosperity - The new Battle of Britain - UK military aircraft industry [AIAA PAPER 90-3189] p 786 A90-48826
- The integration of Latin American transport - Realities and perspectives p 898 A90-49618

- Anatomy of airline regulation - Towards a pluriform, plurilateral, pluralistic, flexible world-wide regulatory framework for air transport p 898 A90-49620
- Integrated Air Traffic Management [DLR-MITT-89-23] p 825 N90-27676
- Airline requirements for a future air traffic management system p 825 N90-27678
- PHARE: Concept and programme p 827 N90-27690
- INTERNATIONAL LAW**
- A review of regulations - The Chicago Convention and the bilateral network p 898 A90-49614
- INTERPOLATION**
- Surface grid generation for complex three-dimensional geometries p 376 A90-26484
- A grid generation method for an aft-fuselage mounted capped-nacelle/pylon configuration with an actuator disk [AIAA PAPER 90-1564] p 565 A90-38703
- Application of Lagrangian blending functions for grid generation around airplane geometries [NASA-CR-186318] p 237 N90-15891
- Analysis and design of symmetrical airfoils [PD-CF-8943] p 400 N90-19213
- Quiet mode for nonlinear rotor models [NASA-TM-102236] p 582 N90-21758
- INTERPROCESSOR COMMUNICATION**
- Array processor supercomputers p 376 A90-26626
- INTERSECTIONS**
- Improved lighting of taxiway/taxiway intersections for Instrument Flight Rules (IFR) operations [DOT/FAA/CT-TN89/64] p 243 N90-15089
- INTERSTITIALS**
- Interstitial materials for low thermal resistance joints in avionic equipment [SAE PAPER 891441] p 356 A90-27412
- INVENTORIES**
- World jet airplane inventory at year-end 1989 [PB90-207218] p 902 N90-28489
- INVESTMENT CASTING**
- Metallurgy of investment cast superalloy components p 531 A90-34154
- Investment-cast superalloys a good investment p 949 A90-51198
- INVESTMENTS**
- Using goal programming to determine the optimal engine mix for UH-1 helicopters [AD-A214893] p 343 N90-16762
- INVISID FLOW**
- Oscillating thin wings in inviscid incompressible flow p 2 A90-10224
- An improved version of LTRAN2 p 2 A90-10350
- Analysis of the effect of rotor-angular-acceleration on the features of gas flow in turbomachinery p 6 A90-11780
- Progress towards the development of an inviscid-viscous interaction method for unsteady flows in turbomachinery cascades p 8 A90-11806
- An application of the surface-singularity method to wing-body-tail configurations p 9 A90-12229
- Calculation of axisymmetric flows in turbomachines, through an explicit time-splitting method p 14 A90-12622
- A multi-domain 3D Euler solver for flows in turbomachines [ONERA, TP NO. 1989-119] p 15 A90-12623
- Computation of multi-element airfoil flows including confluence effects p 144 A90-16755
- VISTRAFS - A simulation method for strongly-interacting viscous transonic flow p 144 A90-16756
- Prediction of post-stall flows on airfoils p 145 A90-16757
- Theoretical prediction of high Reynolds number viscous/inviscid interaction phenomena in cascades p 145 A90-16759
- A viscous package for attached and separated flows on swept and tapered wings p 146 A90-16771
- Experimental and computational studies of dynamic stall p 147 A90-16780
- Full 3D iterative solution of transonic flow for a swept wing test channel p 160 A90-19431
- Solution of the parabolized Navier-Stokes equations using Osher's upwind scheme [AIAA PAPER 90-0392] p 165 A90-19830
- Inviscid drag prediction for transonic transport wings using a full-potential method [AIAA PAPER 90-0576] p 168 A90-19926
- Inviscid non equilibrium flow in ONERA F4 wind tunnel [ONERA, TP NO. 1989-161] p 223 A90-21029
- Application of a lower-upper implicit scheme and an interactive grid generation for turbomachinery flow field simulations [ASME PAPER 89-GT-20] p 288 A90-23762
- Inviscid cascade flow calculations using a multigrid method [ASME PAPER 89-GT-22] p 288 A90-23763

INVISID FLOW

- Three-dimensional solutions for inviscid incompressible flow in turbomachines [ASME PAPER 89-GT-140] p 291 A90-23837
- Stability analysis and numerical experiments for viscous-inviscid interaction in transonic flow p 293 A90-24009
- Comparison of inviscid and viscous separated flows p 302 A90-25277
- A generalized lifting-line theory for curved and swept wings p 303 A90-25597
- Computation of steady three dimensional transonic internal flows p 304 A90-25771
- Automatic mesh generation for complex three-dimensional regions using a constrained Delaunay triangulation p 375 A90-26022
- A comparison of two adaptive grid techniques p 309 A90-26507
- Solution-adaptive grids for transonic flows p 309 A90-26508
- Calculation of transonic flows with separation past arbitrary inlets at incidence p 384 A90-27879
- A technique for calculating nonlinear normal-force and pitching-moment coefficients for slender delta wings, accounting for wing thickness p 476 A90-34356
- High-resolution shock-capturing schemes for inviscid and viscous hypersonic flows p 476 A90-34545
- Shock-fitting method for two-dimensional inviscid, steady supersonic flows in ducts p 477 A90-34864
- Unsteady inviscid and viscous computations for vortex-dominated flows p 553 A90-35752
- On the instability of hypersonic flow past a wedge p 554 A90-35902
- The inviscid axisymmetric stability of the supersonic flow along a circular cylinder p 554 A90-35916
- Newton solution of coupled viscous/inviscid multielement airfoil flows [AIAA PAPER 90-1470] p 562 A90-38627
- Interactive airfoil calculations with higher-order viscous-flow equations [AIAA PAPER 90-1533] p 564 A90-38678
- Simulation of inviscid blade-row interaction using a linearised potential code [AIAA PAPER 90-1916] p 621 A90-40555
- Viscous-inviscid interaction method for calculating the flow in compressor cascade blade passages and wake with separation p 624 A90-42032
- Inviscid and viscous flows in transonic and supersonic cascades using an implicit upwind relaxation algorithm [AIAA PAPER 90-2128] p 625 A90-42034
- Calculation of viscous-inviscid strong interaction for transonic flows over aerofoils p 627 A90-42364
- Numerical modeling of transverse flow past a cylinder using Euler equations p 709 A90-44922
- Some remarks on the Kutta condition p 716 A90-45738
- Trajectories of vortex lines beneath a free surface or above a plane p 716 A90-45740
- An unstructured-mesh Euler method for multielement airfoil geometries [AIAA PAPER 90-3051] p 787 A90-45930
- XFOIL - An analysis and design system for low Reynolds number airfoils p 799 A90-46359
- A fast method for computation of airfoil characteristics p 799 A90-46361
- Geometrical factors influencing the flow field in a propulsive nozzle p 807 A90-46876
- Numerical simulation of wakes with application to blade-vortex interaction p 807 A90-46881
- Supersonic aerodynamic characteristics of a Mach 3 high-speed civil transport configuration [AIAA PAPER 90-3210] p 811 A90-48836
- Cascade aerodynamic gust response including steady loading effects p 904 A90-51006
- Application of a vortex lattice numerical model in the calculation of inviscid incompressible flow around delta wings p 904 A90-51017
- Multigrid methods in computational fluid dynamics p 906 A90-51526
- The inverse problem in the multielement airfoil theory p 906 A90-51531
- Multigrid scheme for the compressible Euler-equations p 907 A90-51559
- Numerical simulation of nonreactive flows in turbomachines p 908 A90-52621
- Three-dimensional unsteady transonic viscous-inviscid interaction p 18 N90-10005
- A three-dimensional linear stability approach to transition on wings at incidence p 20 N90-10373
- Supersonic boundary-layer transition on the LaRC F-106 and the DFRF F-15 aircraft. Part 2: Aerodynamic predictions p 94 N90-12559
- Computation of flow fields around propellers and hovering rotors based on the solution of the Euler equations [DLR-FB-89-37] p 170 N90-13333

- Hypersonic aerodynamics p 171 N90-13335
Blunt-nose inviscid airflows with coupled nonequilibrium processes p 171 N90-13336
The precise calculation of the inviscid leading edge flow on a laminar airfoil using simple methods and verification by measurements on the TLF pilot model p 277 N90-16180
An improvement of convection fidelity in Euler calculations p 315 N90-16709
DURIP optical equipment for high-speed viscous-inviscid interaction research [AD-A217772] p 540 N90-20345
Numerical method for designing 3D turbomachinery blade rows p 511 N90-20990
Integral-equation methods in steady and unsteady subsonic, transonic and supersonic aerodynamics for interdisciplinary design [NASA-TM-102677] p 716 N90-25110
Analysis and mitigation of numerical dissipation in inviscid and viscous computation of vortex-dominated flows [NASA-CR-186887] p 776 N90-26281
An approximate method for calculating three-dimensional inviscid hypersonic flow fields [NASA-TP-3018] p 883 N90-27066
Do inviscid vortex sheets roll-up [PD-CF-9010] p 909 N90-28491
- ION IMPLANTATION**
Self-lubricating surfaces by ion beam processing [AD-A22489] p 884 N90-27118
Surface property improvement in titanium alloy gas turbine components through ion implantation p 953 N90-28713
- ION TEMPERATURE**
Transfer of the atomic ion energy of supersonic flow of a partially dissociated gas to a solid surface p 234 A90-23432
- IONIZED GASES**
An analysis of the possibility of expanding the information base of an adaptive control system for a flight vehicle surrounded by an ionized gas medium p 60 A90-10845
- IRRADIANCE**
Passive navigation using image irradiance tracking p 578 N90-22232
- IRRADIATION**
Radiation-curable prepreg composites [DE90-629740] p 951 N90-28674
- ISOENERGETIC PROCESSES**
The interaction of a supersonic streamwise vortex and a normal shock wave p 633 N90-24241
- ISOLATORS**
Measured operating characteristics of a rectangular combustor/inlet isolator [AIAA PAPER 90-2221] p 742 A90-42752
- ISOPARAMETRIC FINITE ELEMENTS**
Postbuckling finite element analysis of composite panels p 365 A90-24377
A fracture analysis using eight-node-isoparametric singular elements and its application in fuselage panels p 603 A90-36431
- ISOTHERMAL FLOW**
Isothermal velocity and turbulence measurements downstream of a model multilobed turbofan mixer p 365 A90-24353
Velocity and turbulence characteristics of isothermal lobed mixer flows --- in turbofan jet engines p 584 A90-35230
- ISOTROPIC TURBULENCE**
A Monte Carlo simulation technique for low-altitude, wind-shear turbulence [AIAA PAPER 90-0564] p 216 A90-19917
- ISOTROPY**
Some implications of the isotropic momentarily frozen assumptions for the SPAN-MAT program [NASA-CR-181937] p 88 N90-11704
Turbulence spectral widths view angle independence as observed by Doppler radar [DOT/FAA/SA-89/2] p 281 N90-15566
- ITERATION**
On efficiency and accuracy of numerical methods for solving aerodynamic equations p 304 A90-25730
Numerical algorithms for parallel computers [AD-A216812] p 377 N90-18181
A two-dimensional unsteady analysis for transonic and supersonic cascade flows p 480 N90-20955
Convergence acceleration of hypersonic flow calculations: A nonlinear relaxation factor p 480 N90-20957
Application of an inverse method to the design of a radial inflow turbine p 511 N90-20989
Computational prediction and measurement of the flow in axial turbine cascades and stages p 514 N90-21028

Nonlinear static and dynamic modeling of composite rotor blades including warping effects p 924 N90-29382

ITERATIVE SOLUTION

- An interactive boundary layer method for subsonic airfoil flows p 144 A90-16754
Analyses of full 3D S1-S2 iterative solution in CAS transonic compressor rotor and comparison with quasi-3D S1-S2m iterative solution and L2F measurement p 157 A90-18532
Rotor/fuselage vibration isolation studies by a Floquet-harmonic iteration technique p 182 A90-19393
Full 3D iterative solution of transonic flow for a swept wing test channel p 160 A90-19431
A method for solving three-dimensional viscous incompressible flows over slender bodies p 558 A90-37890
Iterative algorithm for correlation of strain gauge data with aerodynamic load p 709 A90-44739
Computation of complex flows in gas turbine combustors with a multi-level additive correction technique p 881 A90-46899
Iterative preliminary design tools for composite structures p 882 A90-48045
The MHOST finite element program: 3-D inelastic analysis methods for hot section components. Volume 3: Systems' manual [NASA-CR-182236] p 73 N90-10451
Solution of the thin-layer Navier-Stokes equations for laminar transonic flow [PB89-221600] p 136 N90-12879
Multigrid solution method for the Euler equations [PB89-219463] p 138 N90-13116
An iterative solution to aeroelastic effects in potential flow [AD-A216291] p 320 N90-17580

J**JAMMERS**

- A modular 550 watt, 25 watts per cubic inch power supply for next generation aircraft p 958 A90-52954

JAMMING

- The role of adaptive antenna systems when used with GPS p 128 A90-13995

JAPAN

- Current Japanese supercomputers for computational fluid dynamics applications p 610 N90-23172
Some topics in computational transonic aerodynamics: Revision [NAL-TR-1018T] p 912 N90-29332

JAPANESE SPACECRAFT

- CRL's mobile satellite communication experiments using ETS-V [AIAA PAPER 90-0775] p 366 A90-25602

JET AIRCRAFT

- Caring for the elderly jet p 285 A90-24280
Development of jet transport airframe fatigue test spectra p 351 A90-26753
Stealth comes of age p 336 A90-27596
Rotary damping in aircraft motion due to jet propulsion system p 520 A90-34820
Yakovlev strikes back p 579 A90-35848
Analysis of serious mechanical trouble in a retractable main landing gear of a jet fighter p 580 A90-36438
Requirements for business jet aircraft [AIAA PAPER 90-2038] p 644 A90-41991
GE's CF34 engine for business and regional jets [AIAA PAPER 90-2041] p 661 A90-41992
Developing the Canadair Regional Jet airliner p 729 A90-42656
The history of aviation engine development in the USSR and the 60th anniversary of CIAM [AIAA PAPER 90-2761] p 783 A90-42828
The McDonnell Douglas MD-11 ... or, how the DC-10 grew bigger p 730 A90-43766
Airbrake design for base-line configuration of advanced jet trainers/light attack airplanes and military combat airplanes p 810 A90-48081
Aging fleet Structures Working Group activities [AIAA PAPER 90-3219] p 786 A90-48840
Aging jet transport structural evaluation programs p 901 A90-49889
Modifying high-order aeroelastic math model of a jet transport using maximum likelihood estimation p 61 N90-10106
Comparison of flying qualities derived from in-flight and ground-based simulators for a jet-transport airplane for the approach and landing pilot tasks [NASA-TP-2962] p 120 N90-11757
Inspection development for T-37 wing spar cap lug [AD-A214826] p 287 N90-16708

Throughput and delay characteristics for a slow-frequency hopped aircraft-to-aircraft packet radio network

- [AD-A205255] p 688 N90-23609
Forward canopy feasibility and Thru-The-Canopy (TTC) ejection system study [AD-A20360] p 637 N90-24258
Special essays for the 40th anniversary of the revolution: The chief designer discusses the F-8 2 and future fighter planes [AD-A221587] p 845 N90-26829
World jet airplane inventory at year-end 1989 [PB90-207218] p 902 N90-28489

JET AIRCRAFT NOISE

- Supersonic jet noise reduction by a porous single expansion ramp nozzle [AIAA PAPER 90-0366] p 219 A90-19815
Optimization of the sound-absorption lining parameters of an ejector jet muffler p 378 A90-24117
Mixer-ejector nozzle for jet noise suppression [AIAA PAPER 90-1909] p 894 A90-47202
Twin-jet screech suppression p 894 A90-48957
An analysis of cavity resonance in the aeroengine casing during rig testing p 894 A90-49481
What should be done with those noisy old aircraft [PNR90562] p 107 N90-12593
Re-engine with the Rolls-Royce Tay 670, the route to significant noise reduction [PNR90585] p 115 N90-12606
The commercial aircraft noise problem [PNR90577] p 140 N90-13203
Noise levels from a VSTOL aircraft measured at ground level and at 1.2 m above the ground [NPL-RSA(EXT)-009] p 464 N90-18999
Exhaust environment measurements of a turbofan engine equipped with an afterburner and 2D nozzle [NASA-CR-4289] p 588 N90-21760
En route noise annoyance laboratory test: Preliminary results p 698 N90-24870

JET CONTROL

- Maneuvering by means of lateral jets [ISL-CO-255/88] p 758 N90-26015

JET ENGINE FUELS

- The effect of jet fuel absorption on advanced aerospace thermoset and thermoplastic composites p 942 A90-50082
Compatibility of fuel system components with high density fuel [AD-A210381] p 32 N90-10027
Wide-range fuel flowmeter, phase 2 [AD-A210547] p 72 N90-10424
Production of jet fuels from coal-derived liquids. Volume 11: Production of advanced endothermic fuel blends from Great Plains Gasification Plant naphtha by-product stream [AD-A210251] p 65 N90-11184
The prediction of middle distillate fuel properties using liquid chromatography-proton nuclear magnetic resonance spectroscopy data [AD-A211879] p 126 N90-11899
Thermal stability of jet fuel [DE90-001160] p 206 N90-14385
Thermal stability of jet fuel [DE90-002760] p 269 N90-15288
Production of jet fuels from coal derived liquids. Volume 10: Jet fuels production by-products, utility, and sulfur emissions control integration study [AD-A213872] p 357 N90-16951
Development of a computational fluid dynamics and chemistry model for the fouling of jet fuels [DE90-005664] p 608 N90-22003
Turbine fuel alternatives (near term) [AD-A219405] p 601 N90-22695
Three-dimensional analysis on flow and temperature distributions for aircraft fuel thermal stability [AD-A219551] p 678 N90-23571
Enhanced bioreclamation of jet fuels: A full-scale test at Eglin AFB, Florida [AD-A222348] p 875 N90-26992
Production of jet fuels from coal-derived liquids. Volume 13: Evaluation of storage and thermal stability of jet fuels derived from coal liquids [AD-A224576] p 954 N90-29527
- JET ENGINES**
Aerosol effects on jet-engine IR radiation p 40 A90-10152
A multichannel wide FOV infrared radiometric system p 67 A90-11410
Turbulent mixing in helicopter jet diluters - Navier-Stokes calculations and correlations [AAAF PAPER NT 88-13] p 40 A90-11432
Analytical methods for subsonic propulsion system integration p 29 A90-12613
Water ingestion simulation - Test needs p 23 A90-12620

- Jet engine fault detection with differential gas path analysis at discrete operating points p 50 A90-12633
The principle of jet engine thrust generation p 110 A90-14571
Flight over the sea with twin or triple jet aircraft p 179 A90-17048
Jet futures p 190 A90-18526
Basic principles of measuring thrust through exhaust to inlet total pressure ratio - Engine Pressure Ratio (EPR) p 191 A90-18635
Electrodynamic properties of engine exhaust jets p 265 A90-23428
Advanced software for turbine blade processing [SME PAPER MS89-330] p 274 A90-23694
Experimental examination of the aerothermal performance of a gas turbine engine test facility [ASME PAPER 89-GT-94] p 341 A90-23810
Entrapment plating of abrasive particles for jet engine clearance control p 286 A90-24685
[SAE PAPER 890918] p 286 A90-24685
Computational and experimental analysis of transonic fanjet engine flow field using 3-D Euler code p 306 A90-25809
Multivariable control of jet engines p 507 A90-32421
Numerical analysis of unsteady forces on oscillating ring airfoils and jet engines p 473 A90-33364
Main characteristic parameter model for jet engine fault diagnosis p 585 A90-37210
An application of expert system to jet engine diagnostic procedures p 587 A90-38596
A preliminary evaluation of an F100 engine parameter estimation process using flight data [AIAA PAPER 90-1921] p 656 A90-40559
Nonlinear finite-element analysis to predict fan-blade damage due to soft-body impact p 683 A90-40939
Jet Engine Technical Advisor (JETA) p 693 A90-41184
JFS190 turbine engine performance optimized using Taguchi methods [AIAA PAPER 90-2419] p 663 A90-42169
An experimental investigation of film cooling effectiveness for slots of various exit geometries [AIAA PAPER 90-2266] p 768 A90-42763
A study of the electrophysical phenomena in the combustion chambers of jet engines p 765 A90-45028
Development of process control procedure for ultrahigh-sensitivity fluorescent penetrant inspection systems p 771 A90-45225
Test and theory for piezoelectric actuator-active vibration control of rotating machinery p 879 A90-46226
Jet engines performance deterioration p 852 A90-46871
Modeling of the oil quench for Ni-based superalloy turbine disks p 957 A90-51525
The absorption of sound by perforated linings p 965 A90-51994
The determination of third order linear models from a seventh order nonlinear jet engine model p 964 A90-52881
Effects of a heat cycle on material strength [NAL-TM-562] p 113 N90-11737
The RB199: An in-service success [PNR90544] p 114 N90-11746
Coatings for gas turbine compressors [NLR-MP-88045-U] p 115 N90-11750
Aluminium alloy development for aero engines [PNR90548] p 126 N90-11874
Dynamic tip clearance measurements in axial flow compressors [PNR90597] p 116 N90-12612
Characterization of chemicals on engine exhaust particles [AD-A213566] p 256 N90-15106
WINCOF-I code for prediction of fan compressor unit with water ingestion [NASA-CR-185157] p 551 N90-21724
A/F32T-9 large turbo fan engine enclosed noise suppressor system (T-9 NSS), exterior far-field and interior noise, McConnell AFB, Kansas [AD-A220535] p 665 N90-23402
The jet engine: 1932 [ISBN-3-922010-49-0] p 763 N90-25189
Knowledge based diagnosis of jet engines under consideration of model based methods p 855 N90-27631
- JET EXHAUST**
Axisymmetric afterbody flow separation at transonic speeds in presence of jet exhaust p 13 A90-12576
Electrodynamic properties of engine exhaust jets p 265 A90-23428
The effect of constructive and destructive interference on the downstream development of twin jets in a crossflow. I - Destructive interference of laterally spaced jets [AIAA PAPER 90-1623] p 607 A90-38752
- The cryogenic wind tunnel as a testing tool for airframe propulsion systems p 672 A90-40400
Navier-Stokes simulation of transonic afterbody flows with jet exhaust [AIAA PAPER 90-3057] p 790 A90-45862
- JET FLAPS**
Rotating primary flow induction using jet-flapped blades p 48 A90-12585
Jet flap theory p 298 A90-24154
Rotary-Jet thrust augmentor with jet-flapped blades p 633 N90-24243
- JET FLOW**
Jets, vortices, and turbulence p 207 A90-17175
Modeling of liquid jets injected transversely into a supersonic crossflow p 153 A90-17985
Underexpanded jet-freestream interactions on an axisymmetric afterbody configuration p 154 A90-18141
A study of ground vortex p 158 A90-18590
Thrust augmentation characteristics of jet reactions [AIAA PAPER 90-0033] p 161 A90-19641
Supersonic combustion of hydrogen jets behind a backward-facing step [AIAA PAPER 90-0204] p 266 A90-22183
Aerodynamics of cooling jets introduced in the secondary flow of a low speed turbine cascade [ASME PAPER 89-GT-192] p 362 A90-23868
Calculation of flows of an ideal gas in nozzles and jets by the relaxation method p 296 A90-24109
Computational and experimental analysis of transonic fanjet engine flow field using 3-D Euler code p 306 A90-25809
Simulation of sound propagation in axisymmetric jet and influence of pressure waves [AIAA PAPER 90-0733] p 314 A90-26985
Mean and turbulent velocity measurements in a turbojet exhaust p 423 A90-28272
Effect of a jet on transonic flow past an airfoil p 388 A90-29181
An experimental investigation of the turbulent structure in a two-dimensional momentumless wake p 474 A90-33515
Vortex generator jets - Means for flow separation control p 555 A90-36257
Experimental investigation of coannular jet flow with swirl along a centerbody [AIAA PAPER 90-1622] p 567 A90-38751
Confined jet thrust vector control nozzle studies [AIAA PAPER 90-2027] p 657 A90-40598
Development of the jet-swirl high loading combustor [AIAA PAPER 90-2451] p 658 A90-40633
Measurements of turbulent dual-jet interaction [AIAA PAPER 90-2105] p 624 A90-42019
A validation study of the Spark Navier Stokes code for nonreacting scramjet combustor flowfields [AIAA PAPER 90-2360] p 706 A90-42784
Some possibilities of the vortex layer method for calculating the aerodynamic characteristics of an augmented airfoil interacting with the engine jet p 804 A90-46564
Numerical study of interaction of a jet with a supersonic cross flow p 808 A90-47300
Thermal interaction between an impinging hot jet and a conducting solid surface [AIAA PAPER 90-3010] p 956 A90-50636
The absorption of sound by perforated linings p 965 A90-51994
Steady and unsteady potential flow around thin annular wings and engines with simulation of jet engine flow [DFVLR-FB-89-18] p 89 N90-11711
Low-speed wind-tunnel study of reaction control-jet effectiveness for hover and transition of a STOVL fighter concept [NASA-TM-4147] p 119 N90-11751
Experimental study of velocity fields and turbulence in a turbojet engine [ISL-CO-231/88] p 344 N90-16766
Applications of LIF to high speed flows p 911 N90-29320
- JET IMPINGEMENT**
Numerical study of single impinging jets through a crossflow p 17 A90-13020
Numerical simulation of an impinging jet on a flat plate p 86 A90-15821
The calculation of under-expanded impinging jets p 147 A90-16782
Turbulence modeling for impinging jets [AIAA PAPER 90-0022] p 211 A90-19639
Impingement/effusion cooling ~The influence of the number of impingement holes and pressure loss on the heat transfer coefficient [ASME PAPER 89-GT-188] p 361 A90-23866
Multiple impact jet apparatus (MIJA) - Application to rain erosion studies p 525 A90-34580
- An experimental study of a turbulent jet impinging on a wedge p 553 A90-35274
Total temperature separation in jets [AIAA PAPER 90-1621] p 607 A90-38750
A computational study of the impingement region of an unsteady subsonic jet [AIAA PAPER 90-1657] p 570 A90-38784
Inverse heat transfer studies and the effects of propellant aluminum on TVC jet vane heating and erosion [AIAA PAPER 90-1860] p 655 A90-40533
Numerical modeling of an impinging jet in cross-flow [AIAA PAPER 90-2246] p 686 A90-42093
Thermal interaction between an impinging hot jet and a conducting solid surface [AIAA PAPER 90-3010] p 956 A90-50636
A wind tunnel study of a sting-mounted circulation control wing [AD-A216248] p 319 N90-17577
- JET LIFT**
Effect of vertical-ejector jet on the aerodynamics of delta wings p 553 A90-35755
- JET MIXING FLOW**
Turbulence measurements in a flow generated by the collision of radially flowing wall jets p 2 A90-10699
Variable-velocity flow at the initial mixing section in a diffuser channel p 84 A90-14563
Upwind adaptive finite element investigations of the two-dimensional reactive interaction of supersonic gaseous jets p 209 A90-18264
A numerical study of mixing enhancement in a supersonic combustor [AIAA PAPER 90-0203] p 272 A90-22182
Total temperature effects on centerline Mach number characteristics of freejets p 302 A90-25290
Experimental studies of combustor dilution zone aerodynamics. I - Mean flowfields p 508 A90-32962
Finite element simulation of complex jets in a crossflow for V/STOL applications p 585 A90-35753
Injectant mole fraction measurements of transverse injection in constant area supersonic ducts [AIAA PAPER 90-1632] p 587 A90-38761
Experimental studies of combustor dilution zone aerodynamics. II - Jet development p 659 A90-40947
Calculation of three-dimensional jet interaction flowfields [AIAA PAPER 90-2099] p 624 A90-42018
Mixing characteristics of dilution jets in small gas turbine combustors [AIAA PAPER 90-2728] p 664 A90-42217
Mixing and combustion enhancement in supersonic reacting flows p 744 A90-44410
Estimation of subsonic far-field jet-mixing noise from single-stream circular nozzles [ESDU-89041] p 316 N90-16721
- JET NOZZLES**
Dissipation thrust losses due to distortions of the jet nozzle profile p 254 A90-23405
The sensitivity of near-field acoustics to the orientation of twin two-dimensional supersonic nozzles [AIAA PAPER 90-2149] p 625 A90-42045
- JET PROPULSION**
Flow around a jet and thrust measurement bias from static tests [AAAF PAPER NT 88-11] p 40 A90-11431
Hypersonic propulsion p 253 A90-21949
Infrared sources of jet propulsion system and their suppression p 252 A90-22614
Advanced core technology - Key to subsonic propulsion benefits [ASME PAPER 89-GT-241] p 342 A90-23890
STOVL aircraft simulation for integrated flight and propulsion control research [NASA-TM-102419] p 193 N90-13389
- JET STREAMS (METEOROLOGY)**
Analysis and prediction of weather for aviation p 888 A90-48351
Vertical wind shears in lower-level jet stream over some airfields in the Urals and Siberia p 888 A90-48362
- JET THRUST**
The principle of jet engine thrust generation p 110 A90-14571
Thrust augmentation characteristics of jet reactions [AIAA PAPER 90-0033] p 161 A90-19641
Simulation and analysis of a delta planform with multiple jets in ground effect [AIAA PAPER 90-0299] p 228 A90-22195
Confined jet thrust vector control nozzle studies [AIAA PAPER 90-2027] p 657 A90-40598
- JET VANES**
Inverse heat transfer studies and the effects of propellant aluminum on TVC jet vane heating and erosion [AIAA PAPER 90-1860] p 655 A90-40533
5DOF dynamic loads on a jet vane [AIAA PAPER 90-2382] p 675 A90-42147
- JETTISONING**
Aerodynamics of store separation p 629 A90-42418

JOINED WINGS

- Influence of joint fixity on the structural static and dynamic response of a joined-wing aircraft. I - Static response
[SAE PAPER 891060] p 100 A90-14361
- Design synthesis and optimization of joined-wing transports
[AIAA PAPER 90-3197] p 838 A90-49102
- Application of the joined wing to tiltrotor aircraft
[NASA-CR-177543] p 248 N90-15093
- JOINTS (JUNCTIONS)**
- Diffusion bonding aeroengine components
p 131 A90-16012
- Fatigue tests of samples of flanged joints of wings
p 274 A90-23353
- Multicriterial optimization of lugs in hinge joints
p 364 A90-24162
- Interstitial materials for low thermal resistance joints in avionic equipment
[SAE PAPER 891441] p 356 A90-27412
- The surface pretreatment of aluminium-lithium alloys for structural bonding
p 881 A90-47118
- Advanced joint of 3-D composite materials for space structure
p 944 A90-50137
- The effect of matrix toughness in the development of improved structural adhesives
p 955 A90-50183
- Advanced NDE techniques for quantitative characterization of aircraft
p 886 N90-28088
- JOUKOWSKI TRANSFORMATION**
- Simulation of high incidence unsteady flow past Joukowski airfoils
p 156 A90-18301
- JOURNAL BEARINGS**
- Planet gear sleeve spinning analysis
[AIAA PAPER 90-2154] p 681 A90-40613
- Analysis of thermal gradient effects in oil ring seals
p 682 A90-40716
- JP-4 JET FUEL**
- In-flight evaluations of turbine fuel extenders
[DOT/FAA/CT-89/33] p 444 N90-19387
- Equilibrium swelling of elastomeric materials in solvent environments
[DE90-010164] p 678 N90-24430
- JP-5 JET FUEL**
- Aging and antioxidant surveillance studies on turbine fuel JP-5 and JP-10
p 442 A90-29492

K

K-EPSILON TURBULENCE MODEL

- Calculation of confined swirling flows with a second moment closure
p 66 A90-10640
- A study of two-phase flow for a ramjet combustor
p 45 A90-12532
- Wake-boundary layer interaction
p 85 A90-15238
- Numerical simulation of an impinging jet on a flat plate
p 86 A90-15821
- Turbulence modeling for impinging jets
[AIAA PAPER 90-0022] p 211 A90-19639
- Numerical investigation of
airfoil/jet/fuselage-undersurface flowfields in ground effect
[AIAA PAPER 90-0597] p 168 A90-19939
- Critical evaluation of three-dimensional supersonic combustor calculations
[AIAA PAPER 90-0207] p 272 A90-22265
- A three-dimensional finite element Navier-Stokes solver with k-epsilon turbulence model for unstructured grids
[AIAA PAPER 90-1652] p 570 A90-38780
- Numerical modeling of an impinging jet in cross-flow
[AIAA PAPER 90-2246] p 686 A90-42093
- Turbulence model performance in V/STOL flow field simulation
[AIAA PAPER 90-2248] p 625 A90-42094
- Multigrad calculations of 3-D turbulent viscous flows
[NASA-CR-185154] p 143 N90-13323
- The computation of turbulent thin shear flows associated with flow around multielement aerofoils
p 633 N90-24240

KALMAN FILTERS

- Dynamic interaction of separate INS/GPS Kalman filters (Filter-driving - Filter dynamics)
p 124 A90-13996
- Investigation of a nonlinear Kalman filter for estimating aircraft state variables
p 195 A90-16850
- UH-60 flight data replay and refly system state estimator analysis
[AIAA PAPER 90-0181] p 197 A90-19723
- Real time estimation of aircraft angular attitude
p 431 A90-30103
- Aircraft flight control system identification
p 431 A90-30105
- Estimation of atmospheric and transponder survey errors with a navigation Kalman filter
p 459 A90-30689
- Reconfigurable flight controller for the STOL F-15 with sensor/actuator failures
p 432 A90-30707

- An aircraft flight control reconfiguration algorithm
p 432 A90-30708
- Estimating short-period dynamics using an extended Kalman filter --- for aircraft controllability
[AIAA PAPER 90-1277] p 518 A90-33901
- A proposed Kalman filter algorithm for estimation of unmeasured output variables for an F100 turbofan engine
[AIAA PAPER 90-1920] p 656 A90-40558
- Multiple model adaptive controller for the STOL F-15 with sensor/actuator failures
p 668 A90-40878
- A flight test comparison of two GPS/INS integration approaches
p 726 A90-43708
- F-16/GPS integration test results
p 726 A90-43710
- A robust RAIM scheme using GPS/GLONASS systems
p 726 A90-43713
- Parameter sensitivity analysis of one kind of flight path reconstruction estimator
p 779 A90-44832
- Maximum likelihood tuning of a vehicle motion filter
p 755 A90-45334
- Integration and automation of navigation functions using Kalman filters
p 915 A90-52615
- Guidance simulation and test support for differential GPS flight experiment
[NASA-CR-177471] p 28 N90-10021
- Kalman Filter Integration of Modern Guidance and Navigation Systems
[AGARD-LS-166] p 28 N90-10847
- Tracking a hypersonic aircraft from a space platform
[AD-A216399] p 371 N90-17984
- Autonomous integrated GPS/INS navigation experiment for OMV, Phase 1: Feasibility study
[NASA-CR-4267] p 489 N90-20969
- Flight path reconstruction using extended Kalman filtering techniques
[PD-FC-9001] p 489 N90-20970
- An adaptive human response mechanism controlling the V/STOL aircraft. Appendix 3: The adaptive control model of a pilot in V/STOL aircraft control loops
[NASA-CR-186599] p 598 N90-21777
- Kalman filter based range estimation for autonomous navigation using imaging sensors
p 578 N90-22238
- Estimating short-period dynamics using an extended Kalman filter
[NASA-TM-101722] p 648 N90-23392
- Obtaining consistent models of helicopter flight-data measurement errors using kinematic-compatibility and state-reconstruction methods
[AD-A22533] p 815 N90-26799
- Observability of relative navigation using range-only measurements
p 917 N90-29360
- KARHUNEN-LOEVE EXPANSION**
- A proper orthogonal decomposition of a simulated supersonic shear layer
p 904 A90-51009
- KARMAN-BODEWADT FLOW**
- Prediction of rotating disc flow and heat transfer in gas turbine engines
[PNR90650] p 750 N90-26001
- KERNEL FUNCTIONS**
- A Volterra kernel identification scheme applied to aerodynamic reactions
[AIAA PAPER 90-2803] p 712 A90-45178
- KEROSENE**
- Effect of pressure and temperature on residue formation in aviation kerosenes
p 203 A90-17281
- KEVLAR (TRADEMARK)**
- Composites for aerospace application from Kevlar aramid reinforced PEKK thermoplastic
p 946 A90-50176
- Project, implementation, and utilization of composite structures
[ETN-89-95209] p 127 N90-12665
- Bird impact tests on asymmetric sandwich structures made in Kevlar 49
[CEAT-NT-10/S/83-5] p 323 N90-16727
- Bird impact tests on curved structures of the type Sandwich-Kevlar-Nida for normal and angular shooting
[CEAT-NT-10/S/83-4] p 324 N90-16728
- Bird impact tests on a Kevlar 49 structure. Monolithic plates. Oblique-angled impact
[REPT-S3-4273] p 402 N90-18376
- KINEMATIC EQUATIONS**
- Kinematic and pseudo-kinematic GPS
p 96 A90-13980
- Flight path reconstruction using extended Kalman filtering techniques
[PD-FC-9001] p 489 N90-20970
- KINEMATICS**
- A test of airborne kinematic GPS positioning for aerial photography - Methodology
p 97 A90-13982
- A test of kinematic GPS combined with aerial photography - Organization, logistics and results
p 97 A90-13983

- Experimental investigation of the mechanisms underlying vortex kinematics in unsteady separated flows
[AD-A217889] p 540 N90-20346
- Windshear estimation along the trajectory of an aircraft
p 963 N90-29745
- KINETIC ENERGY**
- An experimental study of the effect of streamwise vortices on unsteady turbulent boundary-layer separation
p 369 N90-17045
- Secondary flow calculations for axial and radial compressors
p 514 N90-21024
- KINETICS**
- Development of a computational fluid dynamics and chemistry model for the fouling of jet fuels
[DE90-005664] p 608 N90-22003
- KITS**
- An expert system advisor for damage repair of composite wing skins (repairman)
p 842 N90-26810
- KNOWLEDGE BASES (ARTIFICIAL INTELLIGENCE)**
- A knowledge-based system design/information tool for aircraft flight control systems
[AIAA PAPER 89-2978] p 55 A90-10491
- Intelligent situation assessment and response aiding in flight emergencies
[AIAA PAPER 89-2999] p 36 A90-10507
- Embedded knowledge based avionics
[AIAA PAPER 89-3141] p 75 A90-10615
- An American knowledge base in England - Alternate implementations of an expert system flight status monitor
p 459 A90-30719
- Expert system - Conventional processing interface
p 460 A90-30753
- Real-time adaptive control of knowledge based avionics tasks
p 460 A90-30764
- Harnessing detailed assembly process knowledge with CASE
p 535 A90-32504
- Control system validation in the autonomous helicopter
p 667 A90-38908
- Applying qualitative knowledge to aircraft engine system design
p 694 A90-41189
- Automated aircraft engine costing using artificial intelligence
[AIAA PAPER 90-1887] p 660 A90-41981
- The place of knowledge based systems in helicopter dynamic system condition prognosis
p 618 A90-42475
- A knowledge-based system design/information tool for aircraft flight control systems
[NASA-TM-101704] p 217 N90-13990
- A knowledge-based flight status monitor for real-time application in digital avionics systems
[NASA-TM-101710] p 217 N90-13995
- A methodology for knowledge-based restructurable control to accommodate system failures
p 609 N90-22058
- Knowledge-based system for flight information management
[NASA-TM-102685] p 780 N90-26511
- Model authoring system for fail safe analysis
[NASA-CR-4317] p 964 N90-29142
- A knowledge-based system design/information tool
[NASA-CR-4316] p 965 N90-29143
- KNOWLEDGE REPRESENTATION**
- The role of expert systems in aircraft safety management
p 375 A90-26225
- Knowledge-based flow field zoning
p 308 A90-26478
- SMAS - An expert system for configuring a research flight simulator
p 694 A90-41191
- Probabilistic reasoning for intelligent wind shear avoidance
[AIAA PAPER 90-3437] p 890 A90-47690
- KNUDSEN FLOW**
- Grid generation and adaptation for the direct simulation Monte Carlo method
p 67 A90-11102
- KUTTA-JOUKOWSKI CONDITION**
- On an extension of the Kutta-Joukowski theorem to the supersonic regime
p 477 A90-34819
- Some remarks on the Kutta condition
p 716 A90-45738
- Euler code predicted separation at the airfoil trailing edge
[FFA-TN-1989-30] p 632 N90-23364

L

L-1011 AIRCRAFT

- The NASA digital VGH program: Exploration of methods and final results. Volume 2: L 1011 data 1978-1979: 1619 hours
[NASA-CR-181909-VOL-2] p 505 N90-20080
- The NASA digital VGH program: Exploration of methods and final results. Volume 1: Development of methods
[NASA-CR-181909-VOL-1] p 505 N90-20081

LABORATORIES

An automated calibration laboratory for flight research instrumentation: Requirements and a proposed design approach
[NASA-TM-101719] p 781 N90-26564

LABYRINTH SEALS

Threshold performance optimization of a rotor-bearing system subjected to leakage excitation
[ASME PAPER 89-GT-126] p 360 A90-23825

Power dissipation in smooth and honeycomb labyrinth seals
[ASME PAPER 89-GT-220] p 362 A90-23881

An annular gas seal analysis using empirical entrance and exit region friction factors
[ASME PAPER 89-TRIB-46] p 537 A90-33555

Evaluation of brush seals for limited-life engines
[AIAA PAPER 90-2140] p 685 A90-42040

Model of a labyrinth seal with flow
p 687 A90-42334

LAMINAR BOUNDARY LAYER

Marginal separation of laminar axisymmetric boundary layers
p 1 A90-10074

On the lengthscales of laminar shock/boundary-layer interaction
p 5 A90-11610

Calculation of unsteady boundary layer development on axial-flow turbomachinery blading
p 48 A90-12588

Curvature effects on the stability of laminar boundary layers on swept wings
p 148 A90-16788

The prediction of boundary layers with rotation and variation of stream filament thickness
[ASME PAPER 89-GT-227] p 362 A90-23882

Effect of tangential injection on flow in a laminar boundary layer
p 294 A90-24080

Interaction between a vibrating compression shock and a boundary layer
p 298 A90-24143

A study of the laminar-turbulent boundary layer transition on the windward side of a delta wing with a conical surface
p 298 A90-24144

Use of liquid crystals for qualitative and quantitative 2-D studies of transition and skin friction
p 446 A90-28259

Infrared imaging and tufts studies of boundary layer flow regimes on a NACA 0012 airfoil
p 446 A90-28268

The boundary-layer fence - Barrier against the separation process
p 396 A90-31493

Experimental study of incompressible flow on the upper surface of a delta wing
p 558 A90-37346

Laminar flow test installation in the Boeing Research Wind Tunnel
[AIAA PAPER 90-1425] p 559 A90-37962

Effects of streamwise vorticity injection on turbulent mixing layer development
[AIAA PAPER 90-1459] p 561 A90-38616

The lateral spreading of finite-span instability waves in a laminar mixing layer
[AIAA PAPER 90-1532] p 606 A90-38677

Advanced Mach 3.5 Axisymmetric Quiet Nozzle
[AIAA PAPER 90-1592] p 566 A90-38727

An airfoil theory of bifurcating laminar separation from thin obstacles
p 702 A90-42639

An investigation of oblique shock/boundary layer bleed interaction
[AIAA PAPER 90-1928] p 703 A90-42697

Design for a natural laminar flow glove for a transport aircraft
[AIAA PAPER 90-3043] p 792 A90-45880

Flight tests with a natural laminar flow glove on a transport aircraft
[AIAA PAPER 90-3044] p 828 A90-45881

The instability of two-dimensional laminar separation
p 800 A90-46365

Unsteady aerodynamics of Wortmann FX63-137 airfoil at low Reynolds numbers
p 801 A90-46374

Determination of the laminar-turbulent transition point for a turbulent layer on a yawing wing
p 805 A90-46566

Response of a subsonic boundary layer to a pulsed oscillation of a localized region of the surface in the flow
p 811 A90-48295

The receptivity of laminar boundary layer flow to leading edge vibrations
p 815 A90-49800

Generalized similarity solutions for three-dimensional laminar compressible wing boundary layers
p 907 A90-51543

Prediction of transition on a swept wing
p 908 A90-52592

Analysis and calculation for interaction between shock wave and laminar boundary layer
p 909 A90-52778

Curvature effects on the stability of three-dimensional laminar boundary layers
p 71 N90-10366

Control and modification of turbulence
p 72 N90-10377

Research in Natural Laminar Flow and Laminar-Flow Control, part 1
[NASA-CP-2487-PT-1] p 90 N90-12503

Laminar flow: Challenge and potential

p 90 N90-12504

LFC: A maturing concept
[DOUGLAS-PAPER-7878] p 90 N90-12505

Lockheed laminar-flow control systems development and applications
p 80 N90-12506

Laminar flow: The Cessna perspective
p 81 N90-12507

Long-range LFC transport
p 104 N90-12508

Development flight tests of JetStar LFC leading-edge flight test experiment
p 104 N90-12509

The right wing of the LEFT airplane
p 91 N90-12510

Performance of laminar-flow leading-edge test articles in cloud encounters
p 104 N90-12511

Simulated airline service experience with laminar-flow control leading-edge systems
p 104 N90-12512

Goertler instability on an airfoil
p 91 N90-12517

Research in Natural Laminar Flow and Laminar-Flow Control, part 2
[NASA-CP-2487-PT-2] p 91 N90-12519

Predicted and hot-film measured Tollmien-Schlichting wave characteristics
p 91 N90-12523

Experimental studies on Goertler vortices
p 91 N90-12529

An experimental evaluation of slots versus porous strips for laminar-flow applications
p 92 N90-12530

Results of LFC experiment on slotted swept supercritical airfoil in Langley's 8-foot transonic pressure tunnel
p 92 N90-12531

Boundary-layer stability analysis of Langley Research Center 8-foot LFC experimental data
p 92 N90-12532

Theoretical methods and design studies for NLF and HLFC swept wings at subsonic and supersonic speeds
p 92 N90-12535

Near-field noise predictions of an aircraft in cruise
p 140 N90-12538

Design and test of an NLF wing glove for the variable-sweep transition flight experiment
p 104 N90-12544

Experimental and numerical analyses of laminar boundary-layer flow stability over an aircraft fuselage forebody
p 93 N90-12549

Status report on a natural laminar-flow nacelle flight experiment
p 105 N90-12550

Nacelle aerodynamic performance
p 105 N90-12552

Supersonic laminar-flow control
p 93 N90-12554

Unsteady three-dimensional thin-layer Navier-Stokes solutions on dynamic blocked grids
p 235 N90-15069

A direct-inverse method for transonic and separated flows about airfoils
[NASA-CR-4270] p 235 N90-15072

Experimental measurements of the laminar separation bubble on an Eppler 387 airfoil at low Reynolds numbers
[NASA-CR-186263] p 275 N90-15380

Experiments on the laminar-turbulent transition on swept wings
p 276 N90-16170

Direct measurement of laminar instability amplification factors in flight
p 277 N90-16178

Flight survey of the 757 wing noise field and its effects on laminar boundary layer transition. Volume 3: Extended data analysis
[NASA-CR-178419] p 380 N90-18233

Experimental and theoretical aerodynamic characteristics of a high-lift semispan wing model
[NASA-TP-2990] p 477 N90-20046

An analytic study of nonsteady two-phase laminar boundary layer around an airfoil
p 691 N90-25051

Interactive calculation procedures for mixed compression inlets
[NASA-CR-186581] p 718 N90-25934

Effects of forebody geometry on subsonic boundary-layer stability
[NASA-CR-4314] p 718 N90-25939

Application of laminar flow control to supersonic transport configurations
[NASA-CR-181917] p 719 N90-25944

LAMINAR FLOW

Natural laminar flow research for subsonic transport aircraft in the FRG
p 2 A90-10137

Computation of laminar mixed convection flow in a channel with wing type built-in obstacles
p 67 A90-11114

Numerical solution of unsteady Navier-Stokes equations for laminar/turbulent flows past axis-symmetric bodies at angle of attack
p 85 A90-15235

Computation of the thin-layer Navier-Stokes equations for a 2D flow
p 87 A90-16332

Experimental transition and boundary-layer stability analysis for a slotted swept laminar flow control airfoil
p 148 A90-16793

Euler and Navier-Stokes solutions for hypersonic flows
p 155 A90-18254

An investigation of unsteady leading edge separation of rapidly pitched airfoils
p 157 A90-18587

Numerical modeling of a viscous separated flow in the near wake
p 159 A90-19236

Design optimization of natural laminar flow fuselages in compressible flow
[AIAA PAPER 90-0303] p 182 A90-19784

The influence of sweep on dynamic stall produced by a rapidly pitching wing
[AIAA PAPER 90-0581] p 230 A90-22231

Structure of velocity and temperature fields in laminar channel flows with longitudinal vortex generators
p 273 A90-23207

In quest of the laminar-flow airliner - Flight experiments on a T-33 jet trainer
p 300 A90-24825

A high-order time-accurate scheme and its applications
p 304 A90-25732

Computation of 2D Navier-Stokes equations
p 367 A90-25801

Laminar flow control leading-edge systems in simulated airline service
p 335 A90-26134

Fourth-order accurate three-dimensional compressible boundary-layer calculations
p 308 A90-26136

Viscous computations using a direct solver
p 315 A90-27133

Instrumentation requirements for laminar flow research in the NLR high speed wind tunnel HST
p 447 A90-28283

Laminar separated flow on a biconical body at high supersonic velocities
p 387 A90-28992

Unsteady transition in an axial-flow turbine. I - Measurements on the turbine rotor. II - Cascade measurements and modeling
[ASME PAPER 89-GT-289] p 474 A90-33562

Flight-measured streamwise disturbance instabilities in laminar flow
[AIAA PAPER 90-1283] p 495 A90-33904

A flight test investigation of certification requirements for laminar-flow general aviation airplanes
[AIAA PAPER 90-1310] p 496 A90-33920

Wind tunnel results and numerical computations for the NAE deHavilland series of natural laminar flow airfoils
p 628 A90-42403

Navier-Stokes computations of three-dimensional laminar flows with buoyancy in a channel with wing-type vortex generators
p 772 A90-45728

Linear instability of the supersonic wake behind a flat plate aligned with a uniform stream
p 716 A90-45783

Design for a natural laminar flow glove for a transport aircraft
[AIAA PAPER 90-3043] p 792 A90-45880

Natural laminar flow - A wind tunnel test campaign and comparison with flight test data
[AIAA PAPER 90-3045] p 792 A90-45882

Numerical investigation of laminar separated viscous trailing-edge flow using triple-deck theory
[AIAA PAPER 90-3046] p 792 A90-45883

Navier Stokes simulation of waverider flowfields
[AIAA PAPER 90-3066] p 793 A90-45892

Design and experimental investigation of a laminar horizontal tail
[AIAA PAPER 90-3042] p 798 A90-45934

Prediction of aerodynamic performance of airfoils in low Reynolds number flows
p 799 A90-46360

Low Reynolds number airfoil design and wind tunnel testing at Princeton University
p 799 A90-46362

A computationally efficient modelling of laminar separation bubbles
p 801 A90-46372

The design of a low Reynolds number RPV
p 828 A90-46385

Supersonic aerodynamic characteristics of a Mach 3 high-speed civil transport configuration
[AIAA PAPER 90-3210] p 811 A90-48836

Laminar flow control perforated wing panel development
[NASA-CR-178166] p 63 N90-10187

Research in Natural Laminar Flow and Laminar-Flow Control, part 1
[NASA-CP-2487-PT-1] p 90 N90-12503

Laminar flow: Challenge and potential
p 90 N90-12504

LFC: A maturing concept
[DOUGLAS-PAPER-7878] p 90 N90-12505

Research in Natural Laminar Flow and Laminar-Flow Control, part 2
[NASA-CP-2487-PT-2] p 91 N90-12519

Research in Natural Laminar Flow and Laminar-Flow Control, part 3
[NASA-CP-2487-PT-3] p 92 N90-12539

The design of an airfoil for a high-altitude, long-endurance remotely piloted vehicle
p 104 N90-12545

F-14 VSTFE and results of the cleanup flight test program
p 105 N90-12547

Variable-Sweep Transition Flight Experiment (VSTFE): Stability code development and clean-up glove data analysis
p 105 N90-12548

- Nacelle aerodynamic performance p 105 N90-12552
- Effects of acoustic sources p 140 N90-12553
- Supersonic laminar-flow control p 93 N90-12554
- Supersonic boundary-layer transition on the LaRC F-106 and the DFRF F-15 aircraft. Part 1: Transition measurements and stability analysis p 94 N90-12558
- Supersonic boundary-layer transition on the LaRC F-106 and the DFRF F-15 aircraft. Part 2: Aerodynamic predictions p 94 N90-12559
- A computationally efficient modelling of laminar separation bubbles [NASA-CR-185854] p 136 N90-12872
- Solution of the thin-layer Navier-Stokes equations for laminar transonic flow [PB89-221600] p 136 N90-12879
- Transition in surface boundary layers [CERT-RSF-OA-43/5018-AYD] p 136 N90-12897
- Generalized similarity solutions for three dimensional, laminar, steady, compressible boundary layer flows on swept profile cylinders p 212 N90-13725
- Numerical simulation of transition in three-dimensional boundary layers [DLR-FB-89-12] p 212 N90-13728
- Numerical simulation of the laminar and turbulent three dimensional-flow on a delta wing with sharp leading edge p 278 N90-16186
- An experimental investigation of viscous aspects of propeller blade flow p 315 N90-16711
- Simulated-airline-service flight tests of laminar-flow control with perforated-surface suction system [NASA-TP-2966] p 338 N90-17627
- Numerical investigations of heat transfer and flow rates in rotating cavities. Simulation of the movement generated by wall temperature gradients, by source-sink mass flows or by the differential rotation of the walls, under the influence or coriolis and centrifugal forces [ETN-90-96253] p 454 N90-18695
- Computation of hypersonic unsteady viscous flow over a cylinder p 397 N90-19194
- Method and apparatus for detecting laminar flow separation and reattachment [NASA-CASE-LAR-13952-1-SB] p 455 N90-19534
- A note on an acoustic response during an engine nacelle flight experiment [NASA-TM-102585] p 464 N90-19821
- Modification and improvement of software for modeling multidimensional reacting fuel flows [AD-A217789] p 533 N90-20235
- Flight test investigation of certification issues pertaining to general-aviation-type aircraft with natural laminar flow [NASA-CR-181967] p 480 N90-20952
- An experimental investigation of the physical mechanisms controlling the asymmetric flow past slender bodies at large angles of attack p 592 N90-21767
- European research on viscous flow (EuroVisc) [NLR-TP-89077-U] p 609 N90-22014
- Prediction of aerodynamic performance of airfoils in low Reynolds number flows [DLC-EST-TN-031] p 632 N90-23360
- Low speed testing of a laminar flow airfoil in an adaptive wall wind tunnel [FFA-TN-1989-08] p 632 N90-23363
- Flutter clearance of the F-14A variable-sweep transition flight experiment airplane, phase 2 [NASA-TM-101717] p 735 N90-25135
- Chemistry of combustion processes p 749 N90-25994
- A boundary-layer transition model for the Navier-Stokes computation for a natural-laminar-flow airfoil [NAL-TR-10387] p 912 N90-29328
- LAMINAR FLOW AIRFOILS**
- XFOIL - An analysis and design system for low Reynolds number airfoils p 799 A90-46359
- Application of the inverse method of three-dimensional boundary layer analysis to the problem of flow past a wing with allowance for the effect of viscosity p 804 A90-46548
- Dynamics and control of turbulent shear flows [AD-A210396] p 72 N90-10402
- Research in Natural Laminar Flow and Laminar-Flow Control, part 1 [NASA-CP-2487-PT-1] p 90 N90-12503
- Laminar flow: Challenge and potential p 90 N90-12504
- Laminar flow: The Cessna perspective p 91 N90-12507
- Long-range LFC transport p 104 N90-12508
- Development flight tests of JetStar LFC leading-edge flight test experiment p 104 N90-12509
- The right wing of the LEFT airplane p 91 N90-12510
- Performance of laminar-flow leading-edge test articles in cloud encounters p 104 N90-12511
- Simulated airline service experience with laminar-flow control leading-edge systems p 104 N90-12512
- Boundary-layer receptivity and laminar-flow airfoil design p 91 N90-12516
- Goertler instability on an airfoil p 91 N90-12517
- Research in Natural Laminar Flow and Laminar-Flow Control, part 2 [NASA-CP-2487-PT-2] p 91 N90-12519
- Predicted and hot-film measured Tollmien-Schlichting wave characteristics p 91 N90-12523
- Results of LFC experiment on slotted swept supercritical airfoil in Langley's 8-foot transonic pressure tunnel p 92 N90-12531
- Boundary-layer stability analysis of Langley Research Center 8-foot LFC experimental data p 92 N90-12532
- Theoretical methods and design studies for NLF and HLFC swept wings at subsonic and supersonic speeds p 92 N90-12535
- Research in Natural Laminar Flow and Laminar-Flow Control, part 3 [NASA-CP-2487-PT-3] p 92 N90-12539
- Design of the low-speed NLF(1)-0414F and the high-speed HSNLF(1)-0213 airfoils with high-lift systems p 93 N90-12540
- Wind tunnel results of the low-speed NLF(1)-0414F airfoil p 93 N90-12541
- Wind tunnel results of the high-speed NLF(1)-0213 airfoil p 93 N90-12542
- Design and test of a natural laminar flow/large Reynolds number airfoil with a high design cruise lift coefficient p 93 N90-12543
- The 757 NLF glove flight test results p 104 N90-12546
- Nacelle design p 105 N90-12551
- Transition in surface boundary layers [CERT-RSF-OA-43/5018-AYD] p 136 N90-12897
- Unsteady three-dimensional thin-layer Navier Stokes solutions on dynamic blocked grids [AD-A212377] p 136 N90-12899
- Semi-empirical transition criteria for the design of laminar profiles p 276 N90-16174
- The precise calculation of the inviscid leading edge flow on a laminar airfoil using simple methods and verification by measurements on the TLF pilot model p 277 N90-16180
- Design of a natural laminar flow airfoil for an unmanned aircraft [PD-CF-9004] p 499 N90-20975
- Aerofoil design techniques p 500 N90-20978
- Low speed testing of a laminar flow airfoil in an adaptive wall wind tunnel [FFA-TN-1989-08] p 632 N90-23363
- Composite reduced Navier Stokes procedures for flow problems with strong pressure interactions [AD-A219621] p 689 N90-23687
- Flight testing of a natural laminar flow airfoil using gliders [PD-CF-9005] p 718 N90-25936
- LAMINAR HEAT TRANSFER**
- Studies of gas turbine heat transfer airfoil surfaces and end-wall cooling effects [AD-A212451] p 117 N90-12620
- LAMINAR MIXING**
- The lateral spreading of finite-span instability waves in a laminar mixing layer [AIAA PAPER 90-1532] p 606 A90-38677
- Investigation of supersonic mixing layers p 623 A90-40926
- LAMINAR WAKES**
- Transition from order to chaos in the wake of an airfoil p 474 A90-33506
- LAMINATES**
- Flutter analysis of composite panels using high-precision finite elements p 207 A90-16725
- Postbuckling behavior of laminated plates using a direct energy-minimization technique p 209 A90-17993
- The static aeroelastic behavior of sweptforward composite wing structures taking into account their warping restraint effect p 210 A90-18407
- New concept for improved nonmetallic erosion protection systems p 407 A90-28188
- Toughened thermosets for damage tolerant carbon fiber reinforced composites p 443 A90-29825
- High performance thermoplastic composites with poly(etherketoneketone) matrix p 529 A90-31646
- Thermoplastic composites, past, present and future p 529 A90-31882
- Design and fabrication considerations for composite structures with embedded fiber optic sensors p 536 A90-32871
- A technique for rapid impact damage detection with implication for composite aircraft structures p 600 A90-37662
- Certification plan for an all-composite main rotor flexbeam p 642 A90-39992
- Impact damage and residual strength analysis of composite panels with bonded stiffeners --- for primary aircraft structures p 642 A90-40130
- Supersonic flutter of shear deformable laminated composite flat panels p 683 A90-41104
- Metal laminates for aerospace applications p 874 A90-48997
- Innovative design concepts for thermoplastic composite materials p 940 A90-50059
- High temperature adhesives commercially available to be used for extended time with PMR15 laminates p 943 A90-50125
- Process optimization of high temperature composite materials p 943 A90-50130
- Variations in impact test methods for tough composites p 946 A90-50167
- Towards a unified method of causing impact damage in thick laminated composites p 946 A90-50168
- Evaluation of the thermoplastic film interleaf concept for improved damage tolerance p 946 A90-50179
- Improved fiber reinforced polyphenylene sulfide thermoplastic composites p 947 A90-50180
- Integrally heated tooling for economical, nonautoclave production of thermoplastic parts p 956 A90-50200
- Use of unbalanced laminates as a screening method for microcracking p 948 A90-50217
- Measurement and characterization of prepreg permeability with a modified bagging technique p 949 A90-50226
- Moisture absorption in graphite/epoxy laminates p 951 A90-52799
- Stochastic propagation of an array of parallel cracks: Exploratory work on matrix fatigue damage in composite laminates [DE89-017837] p 126 N90-11813
- Rolling of ARALL laminates (an alternative method for post-stretching ARALL laminates) [LR-560] p 135 N90-12778
- Effects of aeroelastic tailoring on anisotropic composite material beam models of helicopter blades [AD-A213478] p 249 N90-15095
- Compendium of abstracts and viewgraphs. [AD-A217189] p 532 N90-20140
- Crack stoppers and ARALL laminates [PB90-166588] p 533 N90-21142
- Development of a finite element based delamination analysis for laminates subject to extension, bending, and torsion p 679 N90-25049
- An approach for design and analysis of composite rotor blades [AD-A219257] p 734 N90-25125
- Calculation of thick wall fiber binders for rotor components of modern helicopters [MBB-UD-554/84-PUB] p 735 N90-25137
- Aircraft battle damage repair of transparencies [AD-A224168] p 925 N90-29387
- A low cost shadow moire device for the nondestructive evaluation of impact damage in composite laminates [AD-A223451] p 953 N90-29442
- LAND MOBILE SATELLITE SERVICE**
- Tests of automatic dependent surveillance (ADS) in Western Europe - Possible future developments p 574 A90-35353
- LAND USE**
- Airborne MSS for land cover classification II p 737 A90-43376
- Aircraft/airport compatibility: Some strategic, tactical, and operational issues [TT-8902] p 202 N90-13409
- LANDING**
- Relative merits of reactive and forward-look detection for wind-shear encounters during landing approach for various microburst escape strategies [NASA-TM-4158] p 259 N90-15108
- Replication of NASPAC Dallas/Fort Worth study [DOT/FAA/CT-TN90/26] p 729 N90-25123
- BASEOPS default profiles for civil aircraft [AD-A223161] p 844 N90-26825
- LANDING AIDS**
- The mythology of first-come-first-serve landing order p 821 A90-46394
- Modified touchdown zone lighting [DOT/FAA/CT-TN89/70] p 526 N90-21042
- Four-dimensional navigation and Flight Management Systems p 826 N90-27681
- Approach towards a future integrated airport surface traffic management p 827 N90-27686
- LANDING GEAR**
- Airplane design. Part 4 - Layout design of landing gear and systems --- Book p 31 A90-12869
- Dynamic stiffness of a hydraulic damper in the system of a front landing gear strut p 102 A90-14555
- The anti-shimmy and break-proof study of nose landing gear p 178 A90-16856
- Landing gear integrity - The bottom line of aircraft safety p 180 A90-17408

- The investigation of stress at an enter-gas nozzle of main landing gears for fighter aeroplanes
p 181 A90-18606
- Fatigue damage of an aircraft due to movement on the airfield
p 247 A90-23352
- Modeling strategies for crashworthiness analysis of landing gears
p 409 A90-28233
- Unique methodology used in the Bell-Boeing V-22 main landing gear landing loads analysis and drop tests
p 409 A90-28236
- Analysis of serious mechanical trouble in a retractable main landing gear of a jet fighter
p 580 A90-36438
- Advanced materials for landing gear
p 677 A90-41900
- Improved steel for landing gear design
[SAE PAPER 892335] p 765 A90-45490
- Titanium matrix composite landing gear development
[SAE PAPER 892337] p 733 A90-45491
- Advances in optimal active control techniques for aerospace systems; application to aircraft active landing gear
p 592 N90-21769
- LANDING INSTRUMENTS**
Cooperative synthesis of control and display augmentation in approach and landing
p 516 A90-33061
- LANDING RADAR**
Independent operations on closely spaced runways
p 821 A90-46393
- LANDING SIMULATION**
Multipath modeling for simulating the performance of the microwave landing system
p 241 A90-21384
- Analyzing the flared landing task with pitch-rate flight control systems
[AIAA PAPER 90-3483] p 866 A90-47732
- Wind shear models for aircraft hazard investigation
p 280 N90-15044
- Hermes training aircraft
p 354 N90-16827
- Vibration responses of two house structures during the Edwards Air Force Base phase of the national sonic boom program
[NASA-CR-182089] p 966 N90-29169
- LANDING SITES**
Improving snow roads and airstrips in Antarctica
[AD-A211588] p 133 N90-11907
- Ice runways near the South Pole
[AD-A211606] p 133 N90-11908
- LANDING SPEED**
Accelerators and decelerators for large, hypersonic aircraft
[AIAA PAPER 90-1986] p 674 A90-40582
- LAP JOINTS**
An apparatus to prepare composites for repair
p 533 A90-31574
- LAPLACE EQUATION**
Numerical aerodynamics via formal integration - Laplace, Euler, Prandtl, Navier-Stokes and Reynolds equations
p 305 A90-25800
- Two-dimensional compressible unsteady aerodynamics in the Laplace domain
p 472 A90-33360
- LASER ANEMOMETERS**
Instrumentation being developed for the ONERA F4 wind tunnel
[ONERA, TP NO. 1989-189] p 261 A90-21049
- Laser transit anemometry investigation of a high speed centrifugal compressor
[ASME PAPER 89-GT-155] p 360 A90-23843
- Measurements in a separation bubble on an airfoil using laser velocimetry
p 384 A90-27977
- A laser fluorescence anemometer for water tunnel flowfield studies
p 447 A90-28279
- Laser anemometer measurements in a transonic axial-flow fan rotor
[NASA-TP-2879] p 73 N90-11245
- Laser two focus techniques
p 212 N90-13348
- Experimental study of velocity fields and turbulence in a turbojet engine
[ISL-CO-231/88] p 344 N90-16766
- LASER APPLICATIONS**
Verification of an impeller design by laser measurements and 3D-viscous flow calculations
[ASME PAPER 89-GT-159] p 292 A90-23847
- Integrated navigation - Employing LIRU/GPS
p 329 A90-23995
- Monitoring of aircraft assembly: Optical and laser methods - Russian book
p 285 A90-24229
- A study on spray characteristics down stream from a gutter-atomizer
p 368 A90-26893
- A laser based computer aided non-intrusive technique for full field flow characterization in macroscopic curved channels
p 535 A90-32293
- Flow visualization via laser-induced reflection from bubble sheets
p 680 A90-39784
- Optoelectronic guidance sensors (5th revised and enlarged edition) - Russian book
p 881 A90-46620
- Volumetric analysis by spontaneous Raman diffusion in a supersonic wind tunnel
[ISL-R-109/88] p 95 N90-12564
- Laser applications in supersonic unsteady flow
p 212 N90-13344
- Laser two focus techniques
p 212 N90-13348
- China-built airborne synchronous laser ranger the new L-8 jet trainer aircraft
[AD-A213835] p 275 N90-15422
- Analysis and test of a wide angle spectrometer
[AD-A215819] p 372 N90-18030
- LASER BEAMS**
Laser two focus techniques
p 212 N90-13348
- Control and estimation for aerospace applications with system time delays
p 918 N90-29367
- LASER CAVITIES**
Experimental investigation of a chemical laser cavity flowfield
[AD-A216398] p 372 N90-18038
- LASER CUTTING**
Laser machining developments at McDonnell Douglas
p 453 A90-31028
- LASER DOPPLER VELOCIMETERS**
Propeller wakes and their interaction with wings
p 14 A90-12614
- Time-dependent and time-averaged turbulence structure near the nose of a wing-body junction
p 231 A90-23036
- LDV measurements and the flow analysis in the vaneless region of a radial inflow turbine
[ASME PAPER 89-GT-157] p 292 A90-23845
- Isothermal velocity and turbulence measurements downstream of a model multilobed turbofan mixer
p 365 A90-24353
- Blade-vortex interaction experiments - Velocity and vorticity fields
[AIAA PAPER 90-0030] p 312 A90-26903
- Development of a phase Doppler based probe for icing cloud droplet characterization
[AIAA PAPER 90-0667] p 368 A90-26978
- Measurements, visualization and interpretation of 3-D flows - Application within base flows
p 386 A90-28252
- Design of a three dimensional Doppler anemometer for T2 transonic wind tunnel
p 447 A90-28271
- Mean and turbulent velocity measurements in a turbojet exhaust
p 423 A90-28272
- A semiconductor laser-Doppler-anemometer for applications in aerodynamic research
p 447 A90-28273
- Database for LDV signal processor performance analysis
p 447 A90-28278
- LDA processor TSI model 1990 analog input module reconstruction
p 451 A90-29654
- The development of a 3-D laser velocimeter for the NASA Langley low turbulence pressure wind tunnel
[AIAA PAPER 90-1385] p 597 A90-38484
- Laser Doppler velocimetry investigation of swirler flowfields
p 682 A90-40929
- Three-component LDA measurements in an axial-flow compressor
p 683 A90-40943
- Measurements in an annular combustor-diffuser system
[AIAA PAPER 90-2162] p 768 A90-42740
- Euler analysis comparison with LDV data for an advanced counter-rotation propfan at cruise
[AIAA PAPER 90-3033] p 903 A90-50637
- An LDA investigation of the normal shock wave boundary layer interaction
p 908 A90-52618
- Basic aerodynamic research facility for comparative studies of flow diagnostic techniques
p 122 N90-12526
- Experimental studies on Goertler vortices
p 91 N90-12529
- Practical systems for speckle velocimetry
p 171 N90-13341
- Laser applications in supersonic unsteady flow
p 212 N90-13344
- Automation and extension of LDV (Laser-Doppler Velocimetry) measurements of off-design flow in a subsonic cascade wind tunnel
[AD-A216627] p 453 N90-18670
- Laser-velocimeter-measured flow field around an advanced, swept, eight-blade propeller at Mach 0.8
[NASA-TP-2462] p 468 N90-20942
- LDV measurements and the flow analysis in the vortex region of a radial inflow turbine
p 511 N90-21007
- Euler analysis comparison with LDV data for an advanced counter-rotation propfan at cruise
[NASA-TM-103249] p 720 N90-25946
- LASER GYROSCOPES**
Providing an inexpensive gyro for the navigation mass market
p 848 A90-49502
- Construction of a hybrid angular velocity reference system for investigation of the dynamic characteristics of strapdown gyros
[ESA-TT-1181] p 774 N90-25332
- LASER INDUCED FLUORESCENCE**
A laser fluorescence anemometer for water tunnel flowfield studies
p 447 A90-28279
- Fluorescence spectroscopy and thermometry for hypersonic flight research
[AIAA PAPER 90-1272] p 538 A90-33897
- Experimental investigation of a supersonic swept ramp injector using laser-induced iodine fluorescence
[AIAA PAPER 90-1518] p 606 A90-38663
- Aircraft engine inspection
p 771 A90-44606
- Applications of LIF to high speed flows
p 911 N90-29320
- Laser induced fluorescence: Practical applications
p 911 N90-29323
- LASER INTERFEROMETRY**
Skin friction measurements by laser interferometry in swept shock/boundary-layer interactions
p 154 A90-18153
- The experiments for gas turbine plane cascade in a shock tunnel
p 160 A90-19441
- Simulation of cooling film density ratios in a mass transfer technique
[ASME PAPER 89-GT-200] p 362 A90-23872
- Remote detection of boundary-layer transition by an optical system
p 139 N90-12524
- Skin friction measurements by laser interferometry in supersonic flows
p 317 N90-17557
- LASER RANGE FINDERS**
China-built airborne synchronous laser ranger the new L-8 jet trainer aircraft
[AD-A213835] p 275 N90-15422
- LASER WELDING**
Laser machining developments at McDonnell Douglas
p 453 A90-31028
- Laser welding of an advanced rapidly-solidified titanium alloy
p 881 A90-47021
- LASERS**
New light on wind tunnel lasers
p 439 A90-31248
- Engine testing of thermographic phosphors
[DE90-013269] p 885 N90-28059
- Experimental investigations on the stability and vorticity of the vortex breakdown phenomenon above delta wings, measured by the ultrasonic laser method
[ESA-TT-1079] p 910 N90-28498
- LATERAL CONTROL**
Attitude projection method for analyzing large-amplitude airplane maneuvers
p 197 A90-19555
- Analysis of aircraft performance during lateral maneuvering for microburst avoidance
[AIAA PAPER 90-0568] p 197 A90-19920
- An investigation of asymmetric vortical flows over delta wings with tangential leading-edge blowing at high angles of attack
[AIAA PAPER 90-0103] p 227 A90-22167
- Dynamic properties of a system for the roll control of a model electromagnetically suspended in a wind tunnel
p 262 A90-22762
- An analysis of feel system effects on lateral flying qualities
[AIAA PAPER 90-1824] p 346 A90-25168
- A study of roll response required in a low altitude slalom task - in helicopter control
p 347 A90-25421
- Integrated structure/control concepts for oblique wing roll control and trim
p 433 A90-31282
- Aeroservoelastic tailoring for lateral control enhancement
p 516 A90-33060
- Energy based stability analysis of a fuzzy roll controller design for a flexible aircraft wing
p 668 A90-40833
- Ultimate boundedness control of uncertain systems with application to roll coupled aircraft maneuver
p 668 A90-40886
- An image analysis method for vehicle stabilization
p 668 A90-40914
- Robustness of dynamic inversion vs mu synthesis - Lateral-directional flight control example
[AIAA PAPER 90-3338] p 863 A90-47598
- Lateral-directional control of an aircraft using mu synthesis
[AIAA PAPER 90-3442] p 865 A90-47695
- A comparison of inverse control with optimal control
[AIAA PAPER 90-3484] p 866 A90-47733
- Synthesis of control law, on a RPV, in order to minimize the number of sensors
p 260 N90-15925
- Results of aircraft open-loop tests of an experimental magnetic leader cable system for guidance during roll-out and turnoff
[NASA-TM-4135] p 348 N90-16767
- Design of integrated pitch axis for autopilot/autothrottle and integrated lateral axis for autopilot/yaw damper for NASA TSRV airplane using integral LQG methodology
[NASA-CR-4268] p 348 N90-16768

- Fighter agility metrics, research, and test
[NASA-CR-186118] p 648 A90-23386
- Lateral-directional stability and control characteristics of the Quiet Short-Haul Research Aircraft (QSRA)
[NASA-TM-102250] p 671 A90-23413
- Maneuvering by means of lateral jets
[ISL-CO-255/88] p 758 A90-26015

LATERAL OSCILLATION

- Self-induced roll oscillations of lifting systems with thin delta wings p 860 A90-46570

LATERAL STABILITY

- The induced velocity distribution and the flap-pitch-torsion coupling on the stability and control of the helicopter in flight condition with lateral velocity p 196 A90-18633
- The lateral spreading of finite-span instability waves in a laminar mixing layer
[AIAA PAPER 90-1532] p 606 A90-38677
- Lateral-directional stability and control characteristics of the Quiet Short-Haul Research Aircraft (QSRA)
[NASA-TM-102250] p 671 A90-23413
- The effects of foreplanes on the static and dynamic characteristics of a combat aircraft model p 920 A90-28520

LATTICES (MATHEMATICS)

- A nonlinear vortex-lattice method for the calculation of interference effects between free vortex sheets and wings p 277 A90-16183

LAUNCH VEHICLE CONFIGURATIONS

- Parametric assessment of propulsion system mass for airbreathing launcher configurations p 344 A90-16819

LAUNCH VEHICLES

- Aerodynamic and structural design challenges of a reusable single stage to orbit air-breathing launch vehicle p 354 A90-16814
- Design of cryogenic tanks for launch vehicles p 609 A90-22662

LAUNCHING

- The SKY SHARK: An RPV designed to investigate the pressure distribution on a lifting surface
[NASA-CR-186222] p 844 A90-26824
- Electro-optics engineering support for the integrated launch and recovery television surveillance system
[AD-A223450] p 938 A90-29406

LAUNCHING SITES

- Accelerating hypersonic airplanes with ground-power p 586 A90-38186

LAYOUTS

- Airplane design. Part 3 - Layout design of cockpit, fuselage, wing and empennage: Cutaways and inboard profiles --- Book p 30 A90-12868

LEAD ACID BATTERIES

- Extracting pulse power from batteries p 605 A90-38175
- Battery configurations for multi-megawatt pulse power p 873 A90-49763

LEADING EDGE FLAPS

- Leading edge flap influence on aerodynamic efficiency p 85 A90-15240
- Leading- and trailing-edge flaps on supersonic delta wings p 233 A90-23285
- Navier-Stokes analysis of airfoils with leading edge ice accretions p 174 A90-14196

LEADING EDGE SLATS

- A flow around airfoil with slat and flap
[AIAA PAPER 90-1535] p 564 A90-38679

LEADING EDGE SWEEP

- Direct numerical study of leading-edge contamination p 19 A90-10361
- Computational design of low aspect ratio wing-winglet configurations for transonic wind-tunnel tests
[NASA-CR-181939] p 316 A90-17539

LEADING EDGES

- Unsteady viscous calculation of cascade flows with leading-edge-induced separation
[ONERA, TP NO. 1989-116] p 3 A90-11148
- Application of the hypersonic analogy for validation of numerical simulations p 16 A90-12838
- Development of a stall improvement package for the Gulfstream IV
[SAE PAPER 891021] p 83 A90-14333
- Investigations of modifications to improve the spin resistance of a high-wing, single-engine, light airplane
[SAE PAPER 891039] p 118 A90-14345
- Effect of the inlet diameter and neck edge radius on the flow coefficient of straight-generatrix nozzles p 84 A90-14577
- An investigation into the internal heat transfer characteristics of a thermally anti-iced aero-engine intake lipskin p 111 A90-15390
- Calculation of flow past delta wings in the thin shock layer approximation p 86 A90-15624
- Leading edge contamination and relaminarisation on a swept wing at incidence p 148 A90-16789
- The critical role of aerodynamic heating effects in the design of hypersonic vehicles p 155 A90-18249

- An investigation of unsteady leading edge separation of rapidly pitched airfoils p 157 A90-18587
- Experimental and numerical investigation of the flow in the core of a leading edge vortex
[AIAA PAPER 90-0384] p 165 A90-19826
- A numerical study of general viscous flows around multi-element airfoils p 167 A90-19922
- The influence of a rotating leading edge on accelerating starting flow over an airfoil
[AIAA PAPER 90-0583] p 168 A90-19932
- Development of an unstructured mesh/Navier-Stokes method for aerodynamics of aircraft with ice accretions
[AIAA PAPER 90-0758] p 169 A90-20011
- Leading edge transition in hypersonic flows p 224 A90-21167
- An investigation of asymmetric vortical flows over delta wings with tangential leading-edge blowing at high angles of attack
[AIAA PAPER 90-0103] p 227 A90-22167
- An experimental investigation of sweep-angle influence on delta-wing flows
[AIAA PAPER 90-0383] p 228 A90-22210
- Induced drag based on leading edge suction for a helicopter in forward flight p 232 A90-23102
- Vortex dynamics on a pitching delta wing p 233 A90-23281
- Unconventional leading edges of airfoils p 233 A90-23356
- Thermal/structural analyses of several hydrogen-cooled leading-edge concepts for hypersonic flight vehicles
[AIAA PAPER 90-0053] p 274 A90-23702
- An experimental study of turbine vane heat transfer with leading edge and downstream film cooling
[ASME PAPER 89-GT-69] p 358 A90-23792
- Three-dimensional relief in turbomachinery blading
[ASME PAPER 89-GT-151] p 292 A90-23840
- The influence of diffuser vane leading edge geometry on the performance of a centrifugal compressor
[ASME PAPER 89-GT-163] p 292 A90-23851
- Flow past a wing/fuselage combination with separation from the side edges of the wing p 295 A90-24088
- Asymptotic solution of the optimal-deflection problem for a wing leading edge at subsonic flow velocities p 295 A90-24094
- Eigenvalue problem in the theory of flow past thin profiles at high supersonic velocity p 295 A90-24096
- Flow-calculation over a delta-wing using the thin-layer Navier-Stokes equations p 304 A90-25773
- Vortex dynamics of delta wings p 307 A90-26067
- Laminar flow control leading-edge systems in simulated airline service p 335 A90-26134
- Blade-vortex interaction experiments - Velocity and vorticity fields
[AIAA PAPER 90-0030] p 312 A90-26903
- Observation and analysis of sidewall effect in a transonic airfoil test section p 436 A90-28257
- Effect of the leading edge bluntness of a moderately swept wing on the aerodynamic characteristics of an aircraft model at subsonic and transonic velocities p 388 A90-29005
- The numerical simulation of the low speed aerodynamic characteristics of a set of close-coupled canard configurations p 396 A90-31485
- Development of a fibre optic damage detection system for an aircraft leading edge p 504 A90-32873
- The development of leading-edge notches to improve the subsonic performance of wings of moderate sweep p 491 A90-33367
- Investigation of model rigging limitations on a high speed wind tunnel model at cryogenic temperature p 523 A90-34232
- Leading-edge vortices due to low Reynolds number flow past a pitching delta wing p 555 A90-36258
- Transient response of leading-edge vortices to localized suction p 556 A90-36279
- Experimental investigation of external heat transfer coefficients on film-cooled turbine blade leading edge p 585 A90-38787
- The problem of supersonic flow past a thin wing of finite span with fully subsonic leading edges p 620 A90-39519
- Flow over a leading edge with distributed roughness p 703 A90-42646
- Vortex control for tail buffet alleviation on a twin-tail fighter configuration
[SAE PAPER 892221] p 756 A90-45438
- Simulation of leading-edge vortex flows p 716 A90-45785
- A computational study of incipient leading-edge separation on a 65-deg delta wing at $M = 1.60$
[AIAA PAPER 90-3029] p 791 A90-45871
- Effect of leading edge roundness on a delta wing in wing-rock motion
[AIAA PAPER 90-3080] p 795 A90-45911

- An experimental study of low-speed single-surface airfoils with faired leading edges p 801 A90-46371
- The low frequency oscillation in the flow over a NACA0012 airfoil with an 'iced' leading edge p 801 A90-46377
- Local convergence of the solution in the discrete vortex method p 803 A90-46534
- Flow past bodies within a narrow class of cross-sectional shapes with stationary separation zones at large Reynolds numbers p 805 A90-46568
- The receptivity of laminar boundary layer flow to leading edge vibrations p 815 A90-49800
- Prediction of transition on a swept wing p 908 A90-52592
- Laminar flow control perforated wing panel development
[NASA-CR-178166] p 63 A90-10187
- Experimental study of transition and leading edge contamination on swept wings p 71 A90-10362
- Numerical simulation of leading-edge vortex rollup and bursting p 20 A90-10831
- The structure of separated flow regions occurring near the leading edge of airfoils - including transition
[NASA-CR-185853] p 87 A90-11695
- The right wing of the LEFT airplane p 91 A90-12510
- Performance of laminar-flow leading-edge test articles in cloud encounters p 104 A90-12511
- Simulated airline service experience with laminar-flow control leading-edge systems p 104 A90-12512
- Experimental and theoretical investigation of boundary-layer instability mechanisms on a swept leading edge at Mach 3.5 p 94 A90-12557
- Stall/spin aerodynamic data project
[DOT/FAA/CT-88/29] p 185 A90-14222
- Thermal/structural analyses of several hydrogen-cooled leading-edge concepts for hypersonic flight vehicles
[NASA-TM-102391] p 215 A90-14511
- The precise calculation of the inviscid leading edge flow on a laminar airfoil using simple methods and verification by measurements on the TLF pilot model p 277 A90-16180
- Controlled vortical flow on delta wings through unsteady leading edge blowing
[NASA-CR-186267] p 316 A90-16712
- Heat pipes for wing leading edges of hypersonic vehicles
[NASA-CR-181922] p 369 A90-17055
- Simulated-airline-service flight tests of laminar-flow control with perforated-surface suction system
[NASA-TP-2966] p 338 A90-17627
- Unsteady viscous calculation method for cascades with leading edge induced separation p 426 A90-18408
- Leading edge vortex dynamics on a pitching delta wing
[NASA-CR-186327] p 398 A90-19198
- Finite element elastic-plastic-creep and cyclic life analysis of a cowl lip p 610 A90-22808
- An experimental and theoretical investigation of the flow over plane delta wings with supersonic leading edges
[LR-588] p 717 A90-25114
- Experimental study on vortex and shock wave development on a 65 deg delta wing
[NLR-MP-88033-U] p 720 A90-25950

LEAKAGE

- Development of new segment carbon seal for use at low sealing pressure region FJR710/600S turbo fan engine p 69 A90-11950
- Development of the tip-leakage flow downstream of a planar cascade of turbine blades - Vorticity field
[ASME PAPER 89-GT-55] p 289 A90-23781
- Threshold performance optimization of a rotor-bearing system subjected to leakage excitation
[ASME PAPER 89-GT-126] p 360 A90-23825
- Test results for turbulent annular seals, using smooth rotors and helically grooved stators
[ASME PAPER 89-TRIB-11] p 537 A90-33556
- Computation of flow through a centrifugal impeller with tip leakage
[AIAA PAPER 90-2021] p 684 A90-41987
- Evaluation of brush seals for limited-life engines
[AIAA PAPER 90-2140] p 685 A90-42040
- Fuel Tank Technology
[AGARD-R-771] p 250 A90-15904
- Integral fuel tank sealing practice at British Aerospace (Kingston) p 250 A90-15905
- Integral fuel tanks - design, production, aging, repair p 250 A90-15906
- Aircraft fuel tank construction and testing experience p 250 A90-15907
- The repair of aircraft integral fuel tanks in the RAF: A user's view of fuel tank technology p 250 A90-15908
- Spray sealing: A breakthrough in integral fuel tank sealing technology p 276 A90-15912

- Design philosophy and construction techniques for integral fuselage fuel tanks p 250 N90-15913
- A dynamicist's view of fuel tank skin durability p 251 N90-15915
- Integral fuel tank certification and test methods p 251 N90-15916
- Research on cascade secondary and tip-leakage flows: Periodicity and surface flow visualization p 514 N90-21026
- Losses in the tip-leakage flow of a planar cascade of turbine blades p 514 N90-21027
- Analysis of the rotor tip leakage flow with tip cooling air ejection p 515 N90-21029
- LEAST SQUARES METHOD**
- Time domain parameter identification techniques applied to the UH-60A Black Hawk Helicopter p 77 A90-12774
- Computation of hypersonic flows by a finite element least-squares method p 155 A90-18296
- Surface grid generation through elliptic PDEs p 309 A90-26496
- Application of time domain decomposition techniques to aircraft ground and flutter test data p 491 A90-33373
- Identification of time varying modal parameters p 536 A90-33375
- Identification of multivariable models of jet engines [AIAA PAPER 90-1874] p 655 A90-40540
- A robust RAIM scheme using GPS/GLONASS systems p 726 A90-43713
- Least-squares finite element methods for compressible Euler equations p 904 A90-51013
- Development of a least squares time response lower-order equivalent systems technique [AD-A220527] p 648 N90-23389
- Adaptive control of a system with periodic dynamics: Application of an impulse response method to the helicopter vibration problem p 694 N90-23990
- Application of optimal tracking methods to aircraft terrain following [AD-A221099] p 641 N90-24264
- LEGAL LIABILITY**
- Litigation and the National Weather Service [AIAA PAPER 90-0371] p 220 A90-19819
- Use of Computer-Aided Video Display technology in aviation weather litigation [AIAA PAPER 90-0373] p 216 A90-19821
- Considerations on the legal regulation of air transport in the near future p 897 A90-46649
- Insurance aspects of airline liability p 898 A90-49615
- LIFE (DURABILITY)**
- Demonstration of probabilistic-based durability analysis method for metallic airframes p 273 A90-23287
- A 'new' philosophy of structural reliability, fail safe versus safe life p 688 A90-42490
- The PW2000 - A mature engine with an eye to the future [SAE PAPER 892365] p 748 A90-45514
- Advanced Turbine Technology Applications Project (ATTAP) [NASA-CR-185109] p 220 N90-14153
- Fuel Tank Technology [AGARD-R-771] p 250 N90-15904
- The effect of primer age on adhesion of polysulphide sealant p 269 N90-15909
- AGARD/SMP Review: Damage Tolerance for Engine Structures. 2: Defects and Quantitative Materials Behaviour --- conference [AGARD-R-769] p 425 N90-18396
- Review of modelling methods to take account of material structure and defects p 425 N90-18402
- Life of concentrated contacts in the mixed EHD and boundary film regimes [AD-A216873] p 454 N90-18738
- Effect of temperature on the storage life of polysulfide aircraft sealants [MRL-TR-89-31] p 444 N90-19364
- Finite element elastic-plastic-creep and cyclic life analysis of a cowl lip [NASA-TM-102342] p 610 N90-22808
- NDT in aerospace: The next decade (1990's) [PNR90628] p 777 N90-26348
- Lessons learned for composite aircraft structures qualification p 842 N90-26808
- An aluminum quality breakthrough for aircraft structural reliability p 843 N90-26816
- Peak identification techniques p 844 N90-26822
- Expert system diagnostics and parts life tracking as applied to the AV-8B aircraft for the USMC p 884 N90-27629
- Harrier Information Management System (HIMS): The system and the approach p 884 N90-27630
- Damage tolerance of the fighter aircraft 37 Viggen. Part 1: Analytical assessment [FFA-TN-1990-12-PT-1] p 923 N90-28538
- Damage tolerance of the fighter aircraft 37 Viggen. Part 2: Experimental verification [FFA-TN-1990-13-PT-2] p 923 N90-28539
- LIFE CYCLE COSTS**
- USA - A system to represent airfoils throughout the product life cycle [AIAA PAPER 89-2972] p 73 A90-10487
- Producibility and life cycle cost issues in applications of embedded fiber optic sensors in smart skins p 38 A90-11221
- Applied technology in gas turbine aircraft engine development p 112 A90-16001
- SPF/DB takes off p 208 A90-17293
- Minimizing life cycle cost for subsonic commercial aircraft p 283 A90-23282
- A comprehensive diagnostic system for the T800-APW-800 engine p 422 A90-28181
- What can we do after we've done it all? --- total quality management and leadership philosophy in practice [AIAA PAPER 89-3209] p 549 A90-31696
- Eight years of flight operations with composite rotorblades p 635 A90-42481
- Advanced developments of the Turbo-Union RB199 p 745 A90-44595
- Modelling of fuel effects on naval aircraft operations [SAE PAPER 892331] p 765 A90-45488
- Technical and economic efficiency of aviation gas turbine engines in service --- Russian book p 851 A90-46624
- Commercial aircraft DOC methods [AIAA PAPER 90-3224] p 897 A90-48843
- Subsystem thermal integration - A new challenge to the aircraft designer [AIAA PAPER 90-3274] p 836 A90-48865
- Taguchi methods in conceptual design for life cycle cost [AIAA PAPER 90-3222] p 839 A90-49109
- Compatibility of fuel system components with high density fuel [AD-A210381] p 32 N90-10027
- Cost effectiveness of composite materials on the F-15 and F-16 aircrafts [AD-A216353] p 338 N90-17631
- Preliminary design of a supersonic Short Takeoff and Vertical Landing (STOVL) fighter aircraft [NASA-CR-186670] p 649 N90-23394
- Retirement for cause of the F100 engine p 843 N90-26813
- Life cycle cost in the conceptual design of subsonic commercial aircraft, volumes 1 and 2 p 923 N90-28535
- LIFE SUPPORT SYSTEMS**
- Boeing Transonic Windblast Generator System (BTWGS) p 199 A90-17413
- Water test facilities for aviation life support equipment p 200 A90-17431
- Durability of equipment assemblies and elements of life-support systems for flight vehicles --- Russian book p 246 A90-21275
- The human factors relating to escape and survival from helicopters ditching in water [AGARD-AG-305(E)] p 176 N90-13358
- Implications of Advanced Technologies for Air and Spacecraft Escape [AGARD-CP-472] p 483 N90-20054
- LIFT**
- An analysis of the possibility of using direct control of the lifting force for modifying the flying qualities of aircraft p 118 A90-15423
- A finite element solution for transonic flow around lifting fuselage with arbitrary cross sections from the minimum pressure integral p 156 A90-18298
- The static aeroelastic behavior of sweptforward composite wing structures taking into account their warping restraint effect p 210 A90-18407
- Design of direct lift control systems against vertical gust p 196 A90-18592
- Wall interference correction of high-lift multi-component airfoils p 158 A90-18604
- Lift development of delta wings undergoing constant acceleration from rest [AIAA PAPER 90-0310] p 164 A90-19789
- Results of aerodynamic testing of large-scale wing sections in a simulated natural rain environment [AIAA PAPER 90-0486] p 167 A90-19874
- The influence of a rotating leading edge on accelerating starting flow over an airfoil [AIAA PAPER 90-0583] p 168 A90-19932
- Numerical solutions of the linearized Euler equations for unsteady vortical flows around lifting airfoils [AIAA PAPER 90-0694] p 300 A90-25041
- Vortex dynamics of delta wings p 307 A90-26067
- Induced drag of a wing of low aspect ratio p 387 A90-28987
- Studies of predicting departure characteristics of aircraft p 433 A90-31480
- A calculation of the aerodynamic lift acting on cascade blades in a steady, viscous flow at high Reynolds number p 469 A90-32425
- Unsteady lift and moment coefficients of an engine nacelle p 473 A90-33365
- On a lifting line theory for supersonic flow. II - A supersonic lifting line theory for wings p 477 A90-34817
- A verification of the supersonic lifting line theory for the case of infinite yawed wings p 477 A90-34821
- Comment on 'Improved thin-airfoil theory' p 554 A90-35772
- Wall interference correction for three-dimensional transonic flows [AIAA PAPER 90-1408] p 558 A90-37947
- Parameter effects on oscillatory aerofoil in transonic flows [AIAA PAPER 90-1473] p 563 A90-38629
- A flow around airfoil with slat and flap [AIAA PAPER 90-1535] p 564 A90-38679
- Unsteady aerodynamic loading produced by a sinusoidally oscillating delta wing [AIAA PAPER 90-1536] p 564 A90-38680
- Unsteady lift development on a constantly accelerated rectangular wing [AIAA PAPER 90-1633] p 569 A90-38762
- Lift response of a rectangular wing undergoing a step change in forward speed p 620 A90-39801
- Effects of unsteady blowing on the lift of a circulation controlled cylinder p 713 A90-45325
- An entropy method for induced drag minimization [SAE PAPER 892344] p 715 A90-45496
- Hypersonic forebody lift-induced drag [SAE PAPER 892345] p 715 A90-45497
- Aerodynamic characteristics of forward sweep [AIAA PAPER 90-3041] p 792 A90-45879
- Finite wing lift prediction at high angles of attack [AIAA PAPER 90-3079] p 795 A90-45910
- Correlation of theory to wind-tunnel data at Reynolds numbers below 500,000 p 800 A90-46370
- Wing theory --- Book p 809 A90-47700
- Lift and pitching moment measurements on a swept tapered wing in oscillatory vertical gusts p 811 A90-48089
- Experimental investigation of attachment-line transition in low-speed, high-lift wind-tunnel testing p 71 N90-10358
- Low-speed, high-lift aerodynamic characteristics of slender, hypersonic accelerator-type configurations [NASA-TP-2945] p 20 N90-10830
- Wind tunnel results of the low-speed NLF(1)-0414F airfoil p 93 N90-12541
- Powered-lift aircraft technology [NASA-SP-501] p 107 N90-12589
- Correlation of Puma airloads: Lifting-line and wake calculation [NASA-TM-102212] p 170 N90-13327
- Induced drag for non-planar wings [LR-521] p 172 N90-13357
- A direct-inverse method for transonic and separated flows about airfoils [NASA-CR-4270] p 235 N90-15072
- The maximum lift coefficient of plain wings at subsonic speeds [ESDU-89034] p 236 N90-15082
- Serrated trailing edges for improving lift and drag characteristics of lifting surfaces [NASA-CASE-LAR-13870-1] p 248 N90-15094
- Measurement of lift development on rapidly-accelerated wings p 480 N90-20956
- Application of a dynamic stall model to rotor trim and aeroelastic response p 583 N90-22556
- Unsteady potential flow past a propeller blade section [NASA-CR-4307] p 634 N90-24246
- Study of the ground effects in the CEAT aerohydrodynamic tunnel: Using the results p 922 N90-28530
- Numerical simulations of blade-vortex interactions and lifting hovering rotor flows [AD-A224238] p 911 N90-29302
- LIFT AUGMENTATION**
- Effect of vertical-ejector jet on the aerodynamics of delta wings p 553 A90-35755
- Priorities for high-lift testing in the 1990s [AIAA PAPER 90-1413] p 596 A90-37950
- Evolution of engine cycles for STOVL propulsion concepts [AIAA PAPER 90-2272] p 743 A90-42767
- Effects of unsteady blowing on the lift of a circulation controlled cylinder p 713 A90-45325
- Propulsive lift augmentation by side fences as applied to Japan's experimental STOL aircraft, ASKA [AIAA PAPER 90-3009] p 789 A90-45859
- On the drag reduction of bluff bodies through momentum injection [AIAA PAPER 90-3076] p 797 A90-45922

- Control of low-Reynolds-number airfoils - A review
p 801 A90-46376
- Modelling aspects for the synthesis and performance
assessment of some future advanced helicopters
p 829 A90-46937
- Control of low-speed airfoil aerodynamics
p 814 A90-49776
- ### LIFT DEVICES
- Effects of tailplane aerodynamics and fuselage flexibility
on the flutter of high aspect ratio, low speed aircraft
p 493 A90-33414
- Self-induced roll oscillations of lifting systems with thin
delta wings
p 860 A90-46570
- Wind tunnel results of the high-speed NLF(1)-0213
airfoil
p 93 A90-12542
- Aeroelastic control of composite lifting surfaces:
Integrated aeroelastic control optimization
p 198 A90-13396
- Installed tailplane lift-curve slope at subsonic speeds
[ESDU-89029]
p 236 A90-15081
- The maximum lift coefficient of plain wings at subsonic
speeds
[ESDU-89034]
p 236 A90-15082
- Serrated trailing edges for improving lift and drag
characteristics of lifting surfaces
[NASA-CASE-LAR-13870-1]
p 248 A90-15094
- The SKY SHARK: An RPV designed to investigate the
pressure distribution on a lifting surface
[NASA-CR-186222]
p 844 A90-26824
- ### LIFT DRAG RATIO
- Spanwise distribution of lift and drag at high angles of
attack
[SAE PAPER 891019]
p 83 A90-14331
- Propeller development for the Rutan Voyager
[SAE PAPER 891034]
p 100 A90-14341
- Further work on aerofoils at Reynolds numbers between
3 x 10 to the 5th and 1 x 10 to the 6th
p 145 A90-16758
- Wind-tunnel investigation on the effect of a crescent
planform on drag
[AIAA PAPER 90-0300]
p 228 A90-22196
- Supersonic aircraft drag reduction
[AIAA PAPER 90-1596]
p 567 A90-38729
- Some aerodynamic characteristics of the scissor wing
configuration
[SAE PAPER 892202]
p 713 A90-45423
- Design and test of a natural laminar flow/large Reynolds
number airfoil with a high design cruise lift coefficient
p 93 A90-12543
- Hypersonic waverider configurations for
trans-atmospheric vehicles
[AD-A217925]
p 498 A90-20074
- An aerodynamic tradeoff study of the scissor wing
configuration
[NASA-CR-186576]
p 481 A90-20965
- ### LIFT FANS
- A remote tip-driven fan powered supersonic fighter
concept
[AIAA PAPER 90-2415]
p 663 A90-42167
- ### LIFTING BODIES
- Collocation methods and lifting-surfaces
p 9 A90-12023
- On a lifting line theory for supersonic flow. I - The velocity
field due to a vortex line in supersonic flow
p 143 A90-16735
- Turbulent boundary layer development in the presence
of small isolated two-dimensional surface discontinuities
p 210 A90-18507
- Effect of ground on wake roll-up behind a lifting
surface
p 160 A90-19436
- A finite element method for solving lifting airfoil in
transonic flow
p 226 A90-21984
- Comment on 'Induced drag and the ideal wake of a
lifting wing'
p 233 A90-23291
- Determination of the torsion rigidity of a multiple-rib
torsion box of an aircraft lifting surface
p 364 A90-24134
- A generalized lifting-line theory for curved and swept
wings
p 303 A90-25597
- Using the lifting line theory for calculating straight wings
of arbitrary profile
p 387 A90-29004
- Wave rider volume distribution
p 388 A90-29006
- Efficiency of using a multiple-wall torsion box in the
load-bearing structures of lifting surfaces
p 410 A90-29188
- Numerical solutions of the linearized Euler equations
for unsteady vortical flows around lifting airfoils
p 394 A90-30264
- On the prediction of the aeroelastic behaviour of lifting
systems due to flow separation
p 491 A90-33369
- Correlation of lift and thickness noise sources in
vortex-airfoil interaction
p 547 A90-34090
- Finite element numerical analysis for transonic flows
around lifting fuselages
p 558 A90-37216

- Boundary-integral method for calculating aerodynamic
sensitivities with illustration for lifting-surface theory
p 806 A90-46841
- Parametric analysis of swept-wing geometry with
sheared wing tips
[AIAA PAPER 90-3196]
p 812 A90-49101
- A method for lifting surface design using nonlinear
optimization
[AIAA PAPER 90-3290]
p 813 A90-49122
- Unsteady lifting surface theory for a rotating cascade
of swept blades
[ASME PAPER 89-GT-306]
p 906 A90-51259
- Unsteady aerodynamics of oscillating and rapidly pitched
airfoils
p 235 A90-15074
- Supersonic aerodynamic characteristics of a proposed
Assured Crew Return Capability (ACRC) lifting-body
configuration
[NASA-TM-4136]
p 317 A90-17560
- Equations of motion of slung load systems with results
for dual lift
[NASA-TM-102246]
p 349 A90-17641
- A lifting surface method for the calculation of steady
and unsteady, incompressible propeller aerodynamics
[ESA-TT-1151]
p 717 A90-25113
- Aerodynamics of bodies in shear flow
p 910 A90-28496

LIFTING ROTORS

- An experimental investigation of the downwash beneath
a lifting rotor and low advance ratios
p 151 A90-17585
- An analytical method for the prediction of unsteady
rotor/airframe interactions in forward flight
p 186 A90-14223
- Performance of an optimized rotor blade at off-design
flight conditions
[NASA-CR-4288]
p 416 A90-19226
- Development and application of a generalized dynamic
wake theory for lifting rotors
p 570 A90-21731
- Numerical simulations of blade-vortex interactions and
lifting hovering rotor flows
[AD-A224238]
p 911 A90-29302
- ### LIGHT AIRCRAFT
- A low cost stall/spin simulator
[SAE PAPER 891022]
p 117 A90-14334
- Investigations of modifications to improve the spin
resistance of a high-wing, single-engine, light airplane
[SAE PAPER 891039]
p 118 A90-14345
- Innovation in general aviation
p 81 A90-14997
- Drag and propulsive efficiency of a light aircraft based
on a new flight test technique
[AIAA PAPER 90-0233]
p 182 A90-19747
- Selection of the blended wing configuration for light
aircraft
p 234 A90-23401
- A summary of spin-recovery parachute experience on
light airplanes
[AIAA PAPER 90-1317]
p 519 A90-33926
- A new noise certification method for 'light propeller
aircraft' in testing
p 635 A90-41728
- Digital autopilot for light aircraft
p 653 A90-41741
- The design of a sport aircraft configured to emulate jet
fighter characteristics
[AIAA PAPER 90-3244]
p 839 A90-49119
- On simplified analytical flutter clearance procedures for
light aircraft
[DLR-FB-89-56]
p 672 A90-24276

LIGHT ALLOYS

- The evolution of light alloys in the aerospace industry
[ETN-89-95216]
p 126 A90-11872
- NASA-UVA light aerospace alloy and structures
technology program
[NASA-CR-182607]
p 601 A90-22651

LIGHT HELICOPTERS

- Turboshafts on tenterhooks
p 188 A90-16703
- The LHTEC T800-LHT-800 engine integration into the
Agusta A129 helicopter
p 422 A90-28177
- Flight testing of the Chandler Evans adaptive fuel control
on the S-76A helicopter
p 422 A90-28178
- Development of the improved helicopter icing spray
system (IHSS)
p 400 A90-28182
- Helicopter design optimization for maneuverability and
agility
p 408 A90-28212
- A comparison of four versus five blades for the main
rotor of a light helicopter
p 408 A90-28215
- The challenge of LHX --- composite materials in light
military helicopters
p 382 A90-29641
- Application of advanced air vehicle and mission
equipment technologies to the Light Helicopter (LH)
[AIAA PAPER 90-3268]
p 836 A90-48861
- Hover position sensing system
p 848 A90-27448

LIGHT SCATTERING

- Nondestructive measurement of residual stresses in
aircraft transparencies
[AD-A218680]
p 689 A90-23762

LIGHT SOURCES

- Cockpit lighting compatibility with image intensification
night imaging systems: Issues and answers
[AD-A210503]
p 32 A90-10028

LIGHTING EQUIPMENT

- Cockpit lighting compatibility with image intensification
night imaging systems: Issues and answers
[AD-A210503]
p 32 A90-10028

LIGHTNING

- Electromagnetic characterization of lightning on
aircraft
[ONERA, TP NO. 1989-131]
p 22 A90-11155
- Experimental-theoretical comparison for current
injection on an aircraft model
[ONERA, TP NO. 1989-133]
p 22 A90-11157
- Transall 88 - Lightning characterization program
[ONERA, TP NO. 1989-142]
p 22 A90-11164
- Connection of structures by laboratory-generated
electrical discharges
[ONERA, TP NO. 1989-147]
p 58 A90-11169
- Electrostatic field conditions on an aircraft stricken by
lightning
[ONERA, TP NO. 1989-148]
p 23 A90-11170
- Electrostatic description of a positive leader ignition from
an aircraft
[ONERA, TP NO. 1989-149]
p 23 A90-11171
- Lightning strike protection concepts for composite
materials
p 528 A90-31617
- Multistroke cloud-to-ground strike to the NASA F-106B
airplane
p 482 A90-32304
- Cloud-to-ground strikes to the NASA F-106 airplane
p 574 A90-35767
- 1988 International Aerospace and Ground Conference
on Lightning and Static Electricity, Oklahoma City, OK,
Apr. 19-22, 1988, Addendum to the Proceedings
p 888 A90-49826
- Highlights of RAE lightning strike investigations
p 818 A90-49827
- An airborne instrument for characterizing the 10,000
electromagnetic signals generated by one lightning flash
p 848 A90-49830
- Comparison of four lightning simulation tests on a
composite test bed aircraft
p 818 A90-49831
- Comparison of the swept frequency continuous wave,
current pulse, and shock-excitation lightning simulation
techniques
p 818 A90-49832
- An assessment of analytical methods and lightning
simulation test techniques used in lightning qualification
and surveillance testing
p 818 A90-49833
- Final results of the NASA storm hazards program
p 819 A90-49834
- Characterization of configuration effects on lightning
simulation/qualification testing
p 819 A90-49835
- In-flight aircraft lightning surface current model
p 819 A90-49844
- Validation of GEMACS for prediction of lightning induced
electromagnetic fields --- General Electromagnetic Model
for Analysis of Complex Systems
p 819 A90-49845
- Numerical simulation of aeroplane response to a
lightning injection
[ETN-89-95271]
p 96 A90-11716
- Systems tunnel linear shaped charge lightning strike
[NASA-CR-183832]
p 201 A90-13404
- Evaluation of the indirect effects of lightning on a system:
Double transfer function method
[RAE-TRANS-2172]
p 176 A90-14211
- Effects of lightning on operations of aerospace
vehicles
p 239 A90-15065
- Principal characteristics of lightning on aircraft
p 239 A90-15067
- Analysis of indirect effects of lightning on a metallic A
300 wing: Test report
[REPT-E87/645800]
p 323 A90-16726
- The 1985 and 1986 direct strike lightning data, part 1
[NASA-TM-100533-PT-1]
p 374 A90-18125
- The 1985 and 1986 direct strike lightning data, part 2
[NASA-TM-100533-PT-2]
p 374 A90-18126
- A comparison of lightning network data with surface
weather observations
[AD-A220003]
p 692 A90-23832
- ### LIGHTNING SUPPRESSION
- Lightning testing and test analyses of the JAS39
aircraft
p 842 A90-49836
- Grumman/FAA lightning study - A potential
countermeasure for lightning induced flashblindness of
aircrew members
p 819 A90-49843
- The behavior of electric currents in graphite/epoxy
structures
p 883 A90-49846
- Aircraft lightning protection handbook
[AD-A222716]
p 820 A90-27668
- ### LINE OF SIGHT
- A new method of aircraft motion error extraction from
radar raw data for real-time motion compensation
p 824 A90-49675

LINEAR EQUATIONS

Efficient free wake calculations using
Analytical/Numerical Matching and far-field linearization
p 384 A90-28171

LINEAR EVOLUTION EQUATIONS

Control and stabilization of linear and nonlinear
distributed systems
[AD-A216446] p 462 N90-18908

LINEAR PREDICTION

A study of the limitations of linear theory methods as
applied to sonic boom calculations
[AIAA PAPER 90-0368] p 219 A90-19817

LINEAR PROGRAMMING

The research of cubic spline optimal terrain following
system p 196 A90-18584

Minimum induced drag for wings with spanwise
camber p 709 A90-44733

Using goal programming to determine the optimal engine
mix for UH-1 helicopters
[AD-A214893] p 343 N90-16762

Optimum spanwise camber for minimum induced drag
[BU-403] p 397 N90-18369

LINEAR QUADRATIC GAUSSIAN CONTROL

A simple active controller to suppress helicopter air
resonance in hover and forward flight
p 119 A90-16521

Multi-surface control law synthesis and wind tunnel test
verification of active flutter suppression for a transport-type
wing p 517 A90-33401

An analytical sensitivity method for use in integrated
aeroseuroelastic aircraft design p 517 A90-33405

Structure/control design synthesis of active flutter
suppression system by goal programming
[AIAA PAPER 90-3325] p 872 A90-47587

LQG/LTR controller design using a reduced order
model p 964 A90-52877

Design of integrated pitch axis for autopilot/autothrottle
and integrated lateral axis for autopilot/yaw damper for
NASA TSRV airplane using integral LQG methodology
[NASA-CR-4268] p 348 N90-16768

Integrated control-system design via generalized LQG
(GLQG) theory p 613 N90-23023

LINEAR QUADRATIC REGULATOR

Application of a digital control theory for generating
adaptive grids p 366 A90-25734

A design of a twin variable control system for
aero-turbojet engine p 423 A90-29917

Multivariable control of jet engines
p 507 A90-32421

Guaranteed cost control via optimal parametric LQ
design p 693 A90-40810

Robust flight control system design with multiple model
approach p 865 A90-47666

Extended implicit model following as applied to
integrated flight and propulsion control p 890 A90-47697

Multivariable flight control synthesis and lateral
robustness analysis for an aeroelastic vehicle p 890 A90-47699

A linear quadratic regulator approach to the stabilization
of uncertain linear systems p 891 A90-47755

[AIAA PAPER 90-3509]

LINEAR SYSTEMS

Approximate loop transfer recovery method for
designing fixed-order compensators p 375 A90-25989

Linear control issues in the higher harmonic control of
helicopter vibrations p 430 A90-28225

The method of random variable structure optimal control
for aircraft p 590 A90-37220

Parameter identification of linear systems based on
smoothing p 753 A90-45156

Decentralized systems --- Book p 888 A90-46001

Stochastic performance robustness of aircraft control
systems p 865 A90-47665

Robust low norm output feedback design for flight control
systems p 891 A90-47751

A linear quadratic regulator approach to the stabilization
of uncertain linear systems p 891 A90-47755

[AIAA PAPER 90-3509]

LQG/LTR controller design using a reduced order
model p 964 A90-52877

The determination of third order linear models from a
seventh order nonlinear jet engine model p 964 A90-52881

Advanced actuation systems development, volume 1
[AD-A213334] p 121 N90-12624

Advanced actuation systems development, volume 2
[AD-A213378] p 198 N90-13398

Numerical algorithms for parallel computers
[AD-A216812] p 377 N90-18181

Control and stabilization of linear and nonlinear
distributed systems [AD-A216446] p 462 N90-18908

Stochastic robustness of linear control systems
p 521 N90-20941

Control and estimation for aerospace applications with
system time delays p 918 N90-29367

LINEARIZATION

Helicopter control design using feedback linearization
techniques p 668 A90-40817

The discretization of the three dimensional boundary
layer equations [ETN-90-97292] p 884 N90-27987

LININGS

MATE (Materials for Advanced Turbine Engines)
Program, Project 3. Volume 2: Design, fabrication and
evaluation of an oxide dispersion strengthened sheet alloy
combustor liner [NASA-CR-180892] p 357 N90-17868

Energy efficient engine pin fin and ceramic composite
segmented liner combustor sector rig test report
[NASA-CR-179534] p 932 N90-28567

Parametric studies of acoustic duct attenuation
operforated-plate-on-honeycomb absorber [NAL-TM-603] p 966 N90-30030

LIQUEFIED GASES

High speed commercial transport fuels considerations
and research needs [NASA-TM-102535] p 600 N90-21869

LIQUEFIED NATURAL GAS

Experimental turbofan using liquid hydrogen and liquid
natural gas as fuel [AIAA PAPER 90-2421] p 663 A90-42170

LIQUID AIR CYCLE ENGINES
The cycle evaluation of the advanced LACE
performance [IAF PAPER 89-313] p 109 A90-13447

LIQUID ATOMIZATION

Atomization of synthetic jet fuel p 63 A90-12602

Further validation of a semi-analytical approach for fuel
injectors of different concepts [AIAA PAPER 90-2190] p 686 A90-42067

LIQUID CHROMATOGRAPHY

The prediction of middle distillate fuel properties using
liquid chromatography-proton nuclear magnetic resonance
spectroscopy data [AD-A211879] p 126 N90-11899

HPLC analysis of helicopter rotor blade materials
[AD-A221121] p 650 N90-24270

LIQUID CRYSTALS

Use of liquid crystals for qualitative and quantitative 2-D
studies of transition and skin friction p 446 A90-28259

Liquid crystal thermography for aerodynamic heating
measurements in short duration hypersonic facilities
p 446 A90-28262

Liquid crystal coatings for surface shear stress
visualization in hypersonic flows [AIAA PAPER 90-1513] p 563 A90-38660

Performance of full color active-matrix-LCD in the cockpit
environment p 681 A90-40392

Polysilicon active-matrix liquid crystal displays for cockpit
applications p 681 A90-40393

8 x 8-inch full color cockpit display p 927 A90-52953

Use of liquid crystals for qualitative and quantitative 2-D
studies of transition and skin friction [RAE-TM-AERO-2159] p 958 N90-28800

LIQUID FLOW
Nonstationary liquid flow of a fluid in the core of a conical
vortex sheet p 296 A90-24113

Wave formation on a liquid layer for de-icing airplane
wings p 445 A90-28137

Recent advances in H₂/O₂ high pressure coaxial
injector performance analysis [AIAA PAPER 90-1959] p 762 A90-42705

LIQUID FUELS
A one-dimensional model of ramjet combustion
instability [AIAA PAPER 90-0271] p 266 A90-22192

Influence of fuel composition on flame radiation in gas
turbine combustors p 659 A90-40946

Structure analysis of burning liquid-fueled spray in a
confined combustor [AIAA PAPER 90-2444] p 677 A90-42174

Very-low-frequency oscillations in liquid-fueled ramjets
p 54 N90-10204

The jet engine: 1932
[ISBN-3-922010-49-0] p 763 N90-25189

Liquid fueled ramjet combustion instability: Acoustical
and vortical interactions with burning sprays [AD-A222752] p 767 N90-26104

Calculation of the combustion distribution in a liquid-fuel
ramjet p 858 N90-27931

LIQUID HYDROGEN

Accelerating hypersonic airplanes with ground-power
p 586 A90-38186

Hydrogen in future energy and propulsion technology
p 692 A90-41736

Experimental turbofan using liquid hydrogen and liquid
natural gas as fuel [AIAA PAPER 90-2421] p 663 A90-42170

LIQUID INJECTION

Modeling of liquid jets injected transversely into a
supersonic crossflow p 153 A90-17985

LIQUID PROPELLANT ROCKET ENGINES

Full-scale liquid fuel ramjet combustor tests
p 44 A90-12528

The SEPR 844 reusable liquid rocket engine for Mirage
combat aircraft [AIAA PAPER 90-1835] p 655 A90-40526

Combustion instabilities in Liquid-Fuelled Propulsion
Systems [AGARD-CP-450] p 63 N90-10191

LIQUID ROCKET PROPELLANTS

Combustion instabilities in Liquid-Fuelled Propulsion
Systems [AGARD-CP-450] p 63 N90-10191

Combustion instabilities in liquid-fueled propulsion
systems: An overview p 63 N90-10192

LIQUID SURFACES

Inflatable fuel tank buffer
[AD-D014446] p 503 N90-21002

LIQUID-GAS MIXTURES

An experimental investigation of the physical
mechanisms controlling the asymmetric flow past slender
bodies at large angles of attack p 592 N90-21767

LISP (PROGRAMMING LANGUAGE)

The NIMBLE Project - Real-time common LISP for
embedded expert systems applications [AIAA PAPER 89-3140] p 75 A90-10614

Adapting an AI-based application from its LISP
environment into a real-time embedded system [AIAA PAPER 89-3142] p 75 A90-10616

Benchmark calculations with an unstructured grid flow
solver on a SIMD computer p 546 A90-34378

LITHIUM ALLOYS

Tough(er) aluminum-lithium alloys p 62 A90-11575

Al-Li alloys and ultrahigh-strength steels for U.S. Navy
aircraft p 599 A90-37441

Lose weight with Al-Li p 765 A90-44175

The surface pretreatment of aluminum-lithium alloys for
structural bonding p 881 A90-47118

New Light Alloys [AGARD-CP-444] p 267 N90-15185

The microstructure and properties of aluminum-lithium
alloys p 267 N90-15187

Properties of Al-Li alloys p 267 N90-15191

Investigation on sheet material of 8090 and 2091
aluminum-lithium alloy p 267 N90-15192

Aluminum lithium alloys for Navy aircraft
p 267 N90-15193

Fabrication of test-articles from Al-Li 2091 for Fokker
100 p 267 N90-15196

Putting alloy 2091 to work p 268 N90-15197

Fabrication characteristics of 8090 alloy
p 268 N90-15198

Point of view of a civil aircraft manufacturer on Al-Li
alloy p 268 N90-15200

Uses and properties of Al-Li on the new EH101
helicopter p 268 N90-15201

Aluminum-lithium: Application of plate and sheet to
fighter aircraft p 268 N90-15202

Current status of the application of conventional
aluminum-lithium alloys and the potential for future
developments p 268 N90-15203

Investigation on sheet material of 8090 and 2091
aluminum-lithium alloy [MBS-UT-122/89-PUB] p 766 N90-25090

The stress and temperature dependence of creep in
an Al-2.0 wt percent Li alloy [AD-A223676] p 953 N90-29480

Evaluation of static and fatigue properties of thin sheets
of 8090-T8 aluminum-lithium alloy and observation of its
fracture surfaces [NAL-TR-1039] p 953 N90-29499

LOAD DISTRIBUTION (FORCES)

Analysis of blade loadings in centrifugal compressors
p 158 A90-18591

Development status of epicyclic gears
p 271 A90-21141

Development of fatigue loading spectra
[ASTM STP-1006] p 367 A90-26751

Basic approach in the development of TURBISTAN, a
loading standard for fighter aircraft engine disks
p 368 A90-26754

Automated procedure for creating flight-by-flight
spectra p 376 A90-26755

Development of a dual strain gage balance system for
measuring light loads p 437 A90-28289

- Efficiency of using a multiple-wall torsion box in the load-bearing structures of lifting surfaces p 410 A90-29188
- Rotating system load monitoring using minimum fixed system instrumentation p 651 A90-39982
- Finite-element analysis of large spur and helical gear systems p 683 A90-40940
- The effect on fatigue crack growth under spectrum loading of an imposed placard 'G' limit p 643 A90-41339
- Approach to side force alleviation through modification of the pointed forebody geometry [AIAA PAPER 90-2834] p 712 A90-45165
- Preliminary design and load distributions of high performance mechanical systems p 771 A90-45281
- Fatigue life estimates for helicopter loading spectra p 772 A90-45324
- Assessment of service load experience p 901 A90-49877
- Description and reconstitution of manoeuvre loadings p 919 A90-49878
- The Operational Loads Monitoring System (OLMS) p 926 A90-49879
- Tracking B-1B aircraft with a structural data recorder p 926 A90-49880
- Eight years of experience with small computerized retrofit load monitoring systems p 926 A90-49882
- A rate theory investigation of cyclic loading and plastic deformation in the high stress and ambient temperature range p 954 A90-49884
- A new test procedure for a wing made with carbon fiber composites [ETN-89-95220] p 126 A90-11820
- Chordwise loading and camber for two-dimensional thin sections [AD-A213318] p 95 A90-12568
- Fatigue life estimates for helicopter loading spectra [NASA-CR-181941] p 279 A90-16294
- A lifting surface method for the calculation of steady and unsteady, incompressible propeller aerodynamics [ESA-TT-1151] p 717 A90-25113
- LOAD TESTS**
- Design and evaluation of graphite/epoxy truss core sandwich panels p 210 A90-18406
- Effect of creep on the load-bearing capacity of compressed panels p 364 A90-24102
- Composites boost 21st-century aircraft engines p 442 A90-29704
- Fatigue crack initiation mechanics of metal aircraft structures [AD-A210587] p 65 A90-10255
- A new test procedure for a wing made with carbon fiber composites [ETN-89-95220] p 126 A90-11820
- General buckling tests with thin-walled shells [DLR-MITT-89-13] p 213 A90-13816
- Floor pull test of a transport airframe section [DOT/FAA/CT-TN88/14] p 497 A90-20072
- Characterization of the CP 214 T851. Dissection of a cast flat bar for a standard spar [CEAT-PV-M4/462200] p 876 A90-27905
- Characterization of the 7175 T7352. Dissection of a die casting standard spar [CEAT-PV-M5/528900] p 877 A90-27906
- Characterization of the 7010 T73651. Dissection of a sheet billet for a standard spar [CEAT-PV-M5/521700] p 877 A90-27908
- LOADING MOMENTS**
- A method for reducing a buckled skin under combined loading p 860 A90-46571
- LOADING RATE**
- Fatigue of thick-section cold-expanded holes with and without cracks p 270 A90-20987
- Fatigue damage of an aircraft due to movement on the airfield p 247 A90-23352
- Reconstitution of crack growth from fractographic observations after flight simulation loading p 682 A90-40650
- Influence of microstructure and microdamage processes on fracture at high loading rates [AD-A210307] p 65 A90-10253
- An evaluation of a fatigue crack growth prediction model for variable-amplitude loading (PREFFAS) [LR-537] p 214 A90-13822
- LOADS (FORCES)**
- Hub loads analysis of the SA349/2 helicopter p 333 A90-23936
- Fatigue behavior of specimens under compression load spectra [ETN-89-95207] p 137 A90-12954
- Study of forces and moments on wing-bodies at high incidence, volumes 1 and 2 p 171 A90-13350
- Normal force, pitching moment, and side force of forebody-cylinder combinations for angles of attack up to 90 degrees and Mach numbers up to 5 [ESDU-89014] p 173 A90-14192

- Fatigue analysis and reconstruction of helicopter load spectra p 206 A90-14304
- An examination of the fatigue meter records from the RAAF Orion P-3C fleet [AD-A214000] p 338 A90-17628
- Equations of motion of slung load systems with results for dual lift [NASA-TM-102246] p 349 A90-17641
- A comparison of flutter calculations based on eigenvalue and energy method p 425 A90-18406
- Floor pull test of a transport airframe section [DOT/FAA/CT-TN88/14] p 497 A90-20072
- Unique failure behavior of metal/composite aircraft structural components under crash type loads [NASA-TM-102679] p 690 A90-24660
- Behavior of composite/metal aircraft structural elements and components under crash type loads: What are they telling us [NASA-TM-102681] p 774 A90-25368
- An unsteady lifting surface method for single rotation propellers [NASA-CR-4302] p 719 A90-25940
- Application of damage tolerance p 843 A90-26817
- The effect of rapid spoiler deployment on the transient forces on an aerofoil p 821 A90-28527
- Energy Efficient Engine high pressure turbine component test performance report [NASA-CR-168289] p 929 A90-28553
- An enhanced integrated aerodynamic load/dynamic optimization procedure for helicopter rotor blades [NASA-CR-4326] p 924 A90-29383
- Estimation of power spectral density of runway roughness [NAL-TR-1037] p 939 A90-29411
- Fatigue, static tensile strength and stress corrosion of aircraft materials and structures. Part 1: Text [LR-630-PT-1-REV] p 961 A90-29682
- Fatigue, static tensile strength and stress corrosion of aircraft materials and structures. Part 2: Figures [LR-630-PT-2] p 961 A90-29683

LOCAL AREA NETWORKS

- An analysis of reliability in fiber optic ring and star networks p 78 A90-11666
- A fiberoptic LAN for aircraft and other applications p 282 A90-23241
- Advanced Traffic Management System automation p 330 A90-25565
- Real time data collection and control in a distributed simulator system using Ethernet TCP/IP [SAE PAPER 892356] p 761 A90-45507
- AIRNET: A real-time communications network for aircraft [NASA-CR-186140] p 690 A90-24514
- An automated calibration laboratory for flight research instrumentation: Requirements and a proposed design approach [NASA-TM-101719] p 781 A90-26564
- Development of a COMPAS prototype for the ATC Centre at Frankfurt (Fed. Republic of Germany) p 826 A90-27684
- High speed bus technology development [AD-A224486] p 960 A90-29565

LOCI

- Fast calculation of root loci of aeroelastic systems and of gust response in time domain p 517 A90-33413

LOGISTICS

- Logistics support planning for standardized avionics p 383 A90-30809
- US Navy principal site testing concept and the F-18 p 33 A90-10861
- Experimental evaluation of impedance control for robotic aircraft refueling [AD-A215532] p 337 A90-16755
- RADC fault tolerant system reliability evaluation facility [AD-A215298] p 377 A90-17348
- Peace-time replacement and crash damage factors for army aircraft [AD-A218544] p 636 A90-23372
- Retirement for cause of the F100 engine p 843 A90-26813

LOGISTICS MANAGEMENT

- A synergistic approach to logistics planning and engine design p 422 A90-28207
- What can we do after we've done it all? — total quality management and leadership philosophy in practice [AIAA PAPER 89-3209] p 549 A90-31696

LONGITUDINAL CONTROL

- Digital controller design for the pitch axis of the F-14 using an H(infinity) method p 668 A90-40912
- Nonlinear flight control design via sliding methods p 756 A90-45335
- The active control of an unstable canard aircraft p 57 A90-10894

- An experimental investigation of thrust vectoring two-dimensional convergent-divergent nozzles installed in a twin-engine fighter model at high angles of attack [NASA-TM-41155] p 237 A90-15884
- Design of integrated pitch axis for autopilot/autothrottle and integrated lateral axis for autopilot/yaw damper for NASA TSRV airplane using integral LQG methodology [NASA-CR-4268] p 348 A90-16768
- Longitudinal stability and control characteristics of the Quiet Short-Haul Research Aircraft (QSRA) [NASA-TP-2965] p 349 A90-17639
- Development of a preliminary high-angle-of-attack nose-down pitch control requirement for high-performance aircraft [NASA-TM-101684] p 399 A90-19206
- Feasibility study for a microwave-powered ozone sniffer aircraft [NASA-CR-186660] p 650 A90-23397
- Short period control using angular acceleration feedback: Compensation for first lag servo [NAL-TM-600] p 936 A90-29399

LONGITUDINAL STABILITY

- On the 'inverse phugoid problem' as an instance of non-linear stability in pitch p 55 A90-10221
- The performance and longitudinal stability and control of large receiver aircraft during air to air refueling p 346 A90-24338
- Large receiver aircraft - The performance and longitudinal stability and control during air to air refuelling p 669 A90-41767
- Thrust law effects on the longitudinal stability of hypersonic cruise [AIAA PAPER 90-2820] p 763 A90-45149
- Longitudinal stability analysis for deformable aircraft p 867 A90-48514
- Dynamic derivatives of missiles and fighter-type configurations at high angles of attack p 337 A90-17554
- Longitudinal stability and control characteristics of the Quiet Short-Haul Research Aircraft (QSRA) [NASA-TP-2965] p 349 A90-17639

LONGITUDINAL WAVES

- Analysis of perturbed longitudinal dynamics of an aircraft taking into consideration the stationary aeroelastic effects and the atmospheric perturbances p 520 A90-34822

LORAN

- The US air traffic control system architecture p 330 A90-25561
- Database management considerations for IFR certified earth-referenced navigation systems p 577 A90-36921
- Winds aloft measurement and airspeed calibration using Loran [AIAA PAPER 90-3331] p 847 A90-47592
- The FAA gears up for Loran p 823 A90-49493
- FAA Loran early implementation project [AD-A21866] p 824 A90-26805

LORAN C

- Eurofix p 25 A90-10239
- Loran-aided GPS integrity p 98 A90-14013
- Interference detection and suppression in Loran-C receivers p 240 A90-20504
- Equipment and capability trends in Loran-C RNAV p 578 A90-36918
- Low cost QUBIK IMU for integration with GPS, Omega, Loran-C, and SDI systems p 577 A90-36929
- Loran-C/GPS Interoperable Computerized Algorithms (LOGICAL) p 823 A90-49494
- LORAN C stability integrity assurance [AD-A212663] p 177 A90-13364
- Sole means navigation and integrity through hybrid Loran-C and NAVSTAR GPS p 489 A90-20933

LOW ALTITUDE

- A Monte Carlo simulation technique for low-altitude, wind-shear turbulence [AIAA PAPER 90-0564] p 216 A90-19917
- Airborne Doppler radar detection of low-altitude wind shear p 252 A90-23284
- KC-135R low altitude air refueling flight test program [AIAA PAPER 90-1265] p 494 A90-33893
- Rotorcraft low altitude CNS benefit/cost analysis: Rotorcraft operations data [DOT/FAA/DS-89/9] p 141 A90-12406

LOW ASPECT RATIO

- Boundary layer growth on low aspect ratio compressor blades p 12 A90-12553
- Augmented heat transfer in rectangular channels of narrow aspect ratios with rib turbulators p 70 A90-13091
- An experimental study of heat transfer and film cooling on low aspect ratio turbine nozzles [ASME PAPER 89-GT-187] p 361 A90-23865
- Flutter of shaft-supported low aspect-ratio control surfaces p 667 A90-38912
- Secondary flow in a turbine guide vane with low aspect ratio p 513 A90-21018

LOW ASPECT RATIO WINGS

- Navier-Stokes computations of vortical flows over low-aspect-ratio wings p 232 A90-23103
- Wing-fuselage interference regimes at supersonic flight velocities p 298 A90-24155
- Induced drag of a wing of low aspect ratio p 387 A90-28987
- The use of automated parametric analysis for selecting efficient structural schemes for wings p 410 A90-29191
- Effects of spoiler surfaces on the aeroelastic behavior of a low-aspect-ratio rectangular wing [AIAA PAPER 90-0981] p 391 A90-29371
- Flow field studies behind a wing at low Reynolds numbers [AIAA PAPER 90-1471] p 563 A90-38628
- Unsteady Navier-Stokes solutions for a low aspect ratio delta wing [AIAA PAPER 90-1538] p 564 A90-38682
- Aeroelastic analysis of a low aspect ratio wing p 619 A90-38915
- On aerodynamic characteristics of canard in canard-forward-swept wing configuration p 709 A90-44833
- Self-induced roll oscillations of low-aspect-ratio rectangular wings [AIAA PAPER 90-2811] p 753 A90-45151
- Experimental transonic flutter characteristics of two 72 deg-sweep delta-wing models [NASA-TM-101659] p 175 A90-14205
- Computational design of low aspect ratio wing-winglet configurations for transonic wind-tunnel tests [NASA-CR-181939] p 316 A90-17539
- Effects of spoiler surfaces on the aeroelastic behavior of a low-aspect-ratio rectangular wing [NASA-TM-102622] p 846 A90-27700

LOW COST

- A low cost stall/spin simulator [SAE PAPER 891022] p 117 A90-14334
- Design of aeroengines in a low-fuel price scenario p 739 A90-42653
- Fighter escape system: The next step forward p 483 A90-20059

LOW DENSITY FLOW

- Supersonic low-density flow over airfoils p 153 A90-17871
- Direct simulation of low-density flow over airfoils [AIAA PAPER 90-1539] p 564 A90-38683
- Computation of hypersonic low density flows with thermochemical nonequilibrium p 477 A90-20044
- Low-density flow effects for hypervelocity vehicles, phase 2 [AD-A221034] p 634 A90-24249

LOW DENSITY MATERIALS

- Tough(er) aluminum-lithium alloys p 62 A90-11575
- Industry turns to ceramic composites p 356 A90-27597

LOW FREQUENCIES

- The low frequency oscillation in the flow over a NACA0012 airfoil with an 'iced' leading edge p 801 A90-46377

LOW LEVEL TURBULENCE

- Wind shear at Pantelleria airport p 692 A90-39702

LOW NOISE

- Design and fabrication requirements for low noise supersonic/hypersonic wind tunnels p 122 A90-12555

LOW PASS FILTERS

- Airborne MSS for land cover classification II p 737 A90-43376

LOW PRESSURE

- NASA/GE Energy Efficient Engine low pressure turbine scaled test vehicle performance report [NASA-CR-168290] p 931 A90-28563

LOW REYNOLDS NUMBER

- Hypersonic flow past blunt edges at low Reynolds numbers p 10 A90-12284
- The effect of trailing edge extensions on the performance of the Goettingen 797 and the Wortmann FX 63-137 aerofoil section at Reynolds numbers between 3 x 10 to the 5th and 1 x 10 to the 6th p 82 A90-13783
- Transition phenomena on airfoils operating at low chord Reynolds numbers in steady and unsteady flow p 148 A90-16786
- Low Reynolds number airfoils evaluation program p 151 A90-17692
- Essential ingredients of a method for low Reynolds-number airfoils p 153 A90-17979
- Calculation of low Reynolds number flows at high angles of attack [AIAA PAPER 90-0569] p 167 A90-19921
- Design of low Reynolds number airfoils. I p 307 A90-26129

Hypersonic viscous shock-layer solutions over long slender bodies. II - Low Reynolds number flows p 393 A90-29695

Development of a new low-Reynolds-number type Reynolds stress model and its application to a lobe mixer flow --- to improve thrust efficiency and suppress jet noise in turbofan engines p 584 A90-35229

Freestream turbulence effects on airfoil boundary-layer behavior at low Reynolds numbers p 554 A90-35768

Leading-edge vortices due to low Reynolds number flow past a pitching delta wing p 555 A90-36258

The effect of an oscillatory freestream-flow on a NACA-4412 profile at large relative amplitudes and low Reynolds-numbers p 560 A90-38495

Flow field studies behind a wing at low Reynolds numbers [AIAA PAPER 90-1471] p 563 A90-38628

Active flow control on low Reynolds number airfoils [AIAA PAPER 90-3039] p 792 A90-45878

An experimental study of a closely coupled tandem wing configuration at low Reynolds numbers [AIAA PAPER 90-3094] p 797 A90-45923

Low Reynolds number aerodynamics; Proceedings of the Conference, University of Notre Dame, IN, June 5-7, 1989 p 799 A90-46358

XFOIL - An analysis and design system for low Reynolds number airfoils p 799 A90-46359

Prediction of aerodynamic performance of airfoils in low Reynolds number flows p 799 A90-46360

A fast method for computation of airfoil characteristics p 799 A90-46361

Low Reynolds number airfoil design and wind tunnel testing at Princeton University p 799 A90-46362

Study of low-Reynolds number separated flow past the Wortmann FX 63-137 airfoil p 799 A90-46363

An interactive boundary-layer stability-transition approach for low Reynolds-number airfoils p 799 A90-46364

A review of low Reynolds number aerodynamic research at the University of Glasgow p 800 A90-46367

Experimental aerodynamic characteristics of the airfoils LA 5055 and DU 86-084/18 at low Reynolds numbers p 800 A90-46368

Performance measurements of an airfoil at low Reynolds numbers p 800 A90-46369

Correlation of theory to wind-tunnel data at Reynolds numbers below 500,000 p 800 A90-46370

An experimental study of low-speed single-surface airfoils with faired leading edges p 801 A90-46371

Unsteady aerodynamics of Wortmann FX63-137 airfoil at low Reynolds numbers p 801 A90-46374

A method to determine the performance of low-Reynolds-number airfoils under off-design unsteady freestream conditions p 801 A90-46375

Control of low-Reynolds-number airfoils - A review p 801 A90-46376

Detachment of turbulent boundary layers with varying free-stream turbulence and lower Reynolds numbers p 802 A90-46378

Low Reynolds number airfoil design for subsonic compressible flow p 802 A90-46380

Compressible Navier-Stokes solutions over low Reynolds number airfoils p 802 A90-46382

Shock/turbulent boundary layer interaction in low Reynolds number supercritical flows p 802 A90-46383

Summary of experimental testing of a transonic low Reynolds number airfoil p 802 A90-46384

The design of a low Reynolds number RPV p 828 A90-46385

Flight testing Navy low Reynolds Number (LRN) unmanned aircraft p 828 A90-46387

Wall pressure pulsation spectra ahead of internal corners p 804 A90-46545

The turbulent near wake of a flat plate at low Reynolds number p 811 A90-48711

Subsonic and transonic low-Reynolds-number airfoils with reduced pitching moments [AIAA PAPER 90-3212] p 812 A90-48838

Control of low-speed airfoil aerodynamics p 814 A90-49776

Prediction of aerodynamic performance of airfoils in low Reynolds number flows [DLC-EST-TN-031] p 632 A90-23360

The Stealth biplane: A proposal in response to a low Reynolds Number station keeping mission [NASA-CR-186680] p 734 A90-25127

LOW SPEED

- An experiment study of rotor aerodynamic in ground effect at low speed p 149 A90-16826
- Low air speed computation for helicopters: A new approach p 333 A90-16744
- Low speed flowfield characterization by infrared measurements of surface temperatures p 317 A90-17556

Velocity measurements on a lifting rotor/airframe configuration in low speed forward flight p 815 A90-26790

Effects of canard position on the aerodynamic characteristics of a close-coupled canard configuration at low speed p 920 A90-28519

LOW SPEED STABILITY

Low-speed wind tunnel investigation of the static stability and control characteristics of an advanced turboprop configuration with the propellers placed over the tail [NASA-CR-186900] p 759 A90-26017

LOW SPEED WIND TUNNELS

A critique of the experimental aerodynamic data base for an oscillating straked wing at high angles p 147 A90-16779

Engine inlet distortion in a 9.2 percent scaled vectored thrust STOVL model in ground effect [AIAA PAPER 89-2910] p 301 A90-25043

Experience with scale effects in non-airplane wind tunnel testing [AIAA PAPER 90-1822] p 350 A90-25165

Low speed testing and simulation of the STOL and Maneuver Technology Demonstrator [AIAA PAPER 90-1820] p 334 A90-25169

Low speed, indraft wind tunnels p 351 A90-26061

Unsteady aerodynamic characteristics of a fighter model undergoing large-amplitude pitching motions at high angles of attack [AIAA PAPER 90-0309] p 313 A90-26933

Influence of wind tunnel circuit installations on test section flow quality p 436 A90-28287

Development of two multi-sensor hot-film measuring techniques for free-flight experiments p 417 A90-28291

Cryogenic wind tunnels in Japan p 523 A90-34228

Slotted-wall research with disk and parachute models in a low-speed wind tunnel [AIAA PAPER 90-1407] p 595 A90-37946

Priorities for high-lift testing in the 1990s [AIAA PAPER 90-1413] p 596 A90-37950

On the possibilities for improvement and modernization of subsonic wind tunnels [AIAA PAPER 90-1423] p 596 A90-37960

A multipurpose aerodynamic research facility utilizing the abandoned Cincinnati subway tubes [AIAA PAPER 90-1424] p 596 A90-37961

Results of wind tunnel ground effect measurements on Airbus A320 using turbine power simulation and moving tunnel floor techniques [AIAA PAPER 90-1427] p 559 A90-37964

Vorticity distribution of vortex street in the wake of a circular cylinder p 623 A90-41751

Vortex control for tail buffet alleviation on a twin-tail fighter configuration [SAE PAPER 892221] p 756 A90-45438

At a depth of 500 meters - The TU Dresden supersonic wind tunnel p 937 A90-52700

Comparison of the results of tests on A300 aircraft in the RAE 5 metre and ONERA F1 wind tunnels [RAE-TM-AERO-2130] p 122 A90-11768

Comparison between design and installed acoustic characteristics of NASA Lewis 9- by 15-foot low-speed wind tunnel acoustic treatment [NASA-TP-2996] p 440 A90-19242

Design of a high angle of attack robotic sting mount for tests in a low speed wind tunnel [AD-A218105] p 526 A90-20099

Static wind-tunnel and radio-controlled flight test investigation of a remotely piloted vehicle having a delta wing planform [NASA-TM-4200] p 632 A90-24238

Innovative control concepts and component integration for a generic supercruise fighter p 935 A90-28521

LOW TEMPERATURE TESTS

Icing test techniques for air intake screens on helicopters functioning in temperatures around 0 C p 23 A90-12619

Interstitial materials for low thermal resistance joints in avionic equipment [SAE PAPER 891441] p 356 A90-27412

LOW TURBULENCE

SARL noise measurements [AIAA PAPER 90-0285] p 219 A90-19772

Development of a dual strain gage balance system for measuring light loads p 437 A90-28289

The development of a 3-D laser velocimeter for the NASA Langley low turbulence pressure wind tunnel [AIAA PAPER 90-1385] p 597 A90-38484

Acoustic excitation of boundary layer oscillations on a yawing wing p 805 A90-46567

LOW VISIBILITY

Flight in Adverse Environmental Conditions [AGARD-CP-470] p 222 A90-15041

Modified touchdown zone lighting [DOT/FAA/CT-TN89/70] p 526 A90-21042

LOW VOLTAGE

LOW VOLTAGE

Reduced voltage and restart testing of the 1-watt integral cryogenic cooler (HD-1033B/C/D)
[AD-A215133] p 369 N90-16971

LUBRICANT TESTS

Oil migration of FJR 710/600S engine

p 43 A90-12014

Development of a remaining useful life of a lubricant evaluation technique. III - Cyclic voltammetric methods
p 125 A90-15732

High temperature solid lubricant requirements for advanced high performance gas turbine engines
[AIAA PAPER 90-2042] p 661 A90-41993

Micro separator and ball-on-cylinder lubricity evaluator tests or corrosion inhibitor/lubricity improver additives
[AD-A221339] p 766 N90-25228

LUBRICANTS

Analysis of hydraulic fluids and lubricating oils for the formation of Trimethylolpropane Phosphate (TMP-P)
[AD-A215188] p 357 N90-16939

Life of concentrated contacts in the mixed EHD and boundary film regimes
[AD-A216673] p 454 N90-18738

Improved Thermo-Oxidative-Deposition screening tests for turbine lubricants
[AD-A217795] p 533 N90-21188

LUBRICATING OILS

Oil migration of FJR 710/600S engine

p 43 A90-12014

History of aircraft piston engine oils - The last forty years
[SAE PAPER 891037] p 124 A90-14343

Development of a remaining useful life of a lubricant evaluation technique. III - Cyclic voltammetric methods
p 125 A90-15732

Oils for flight turbine engines - Research and development in the 90s
p 266 A90-21473

Determination of additive contents in aviation and turbine oils
p 532 A90-34681

Catalytic conversion of oil in bleed air - A maintenance tool
[SAE PAPER 892214] p 732 A90-45431

Analysis of hydraulic fluids and lubricating oils for the formation of Trimethylolpropane Phosphate (TMP-P)
[AD-A215188] p 357 N90-16939

The acute, delayed neurotoxicity evaluation of two jet engine oil formulations
[AD-A222018] p 875 N90-26972

LUBRICATION

Endurance of aircraft gas turbine mainshaft ball bearings-analysis using improved fatigue life theory. II - Application to a bearing operating under difficult lubrication conditions
p 128 A90-13845

In-line wear monitor
[AD-A217799] p 510 N90-20091

LUBRICATION SYSTEMS

High temperature solid lubricant requirements for advanced high performance gas turbine engines
[AIAA PAPER 90-2042] p 661 A90-41993

Evaluation of solid lubricant powder delivery system for turbine bearing lubrication
[AIAA PAPER 90-2046] p 684 A90-41997

Life of concentrated contacts in the mixed EHD and boundary film regimes
[AD-A216673] p 454 N90-18738

LUGS

Multicriteria optimization of lugs in hinge joints
p 364 A90-24162

Inspection development for T-37 wing spar cap lug
[AD-A214826] p 287 N90-16708

LUMINAIRES

Improved lighting of taxiway/taxiway intersections for Instrument Flight Rules (IFR) operations
[DOT/FAA/CT-TN89/64] p 243 N90-15089

LUMINOUS INTENSITY

Electro-optics engineering support for the integrated launch and recovery television surveillance system
[AD-A223450] p 938 N90-29406

LUMPED PARAMETER SYSTEMS

Nonlinear mechanics of unstable plasmas as related to high altitude aerodynamics
[AD-A215126] p 464 N90-19852

M

MACH CONES

Irregular interaction of a strong shock wave with a thin profile
p 9 A90-12267

MACH NUMBER

Studies on the influence of Mach number on profile losses of a reaction turbine cascade
p 10 A90-12517

Mach number effects on transonic aeroelastic forces and flutter characteristics
p 17 A90-13024

High Reynolds number wedge-induced separation lengths at Mach 6
p 154 A90-18001

Mach number effects on conical surface features of swept shock-wave/boundary-layer interactions
p 154 A90-18147

A study of sonic boom overpressure trends with respect to weight, altitude, Mach number, and vehicle shaping
[AIAA PAPER 90-0367] p 164 A90-19816

Spanwise properties of the unsteady separation shock in a Mach 5 unswept compression ramp interaction
[AIAA PAPER 90-0377] p 228 A90-22208

The influence of sweep on dynamic stall produced by a rapidly pitching wing
[AIAA PAPER 90-0581] p 230 A90-22231

The detection of large scale structure in undisturbed and disturbed compressible turbulent free shear layers
[AIAA PAPER 90-0711] p 230 A90-22251

Unsteady supersonic computations of arbitrary wing-body configurations including external stores
p 232 A90-23278

Mach number effects on secondary flow development downstream of a turbine cascade
[ASME PAPER 89-GT-67] p 290 A90-23790

Pseudoshock and separated flow in rectangular ducts
p 295 A90-24089

Design of symmetric profiles with maximum critical flow Mach number under prescribed constraints
p 295 A90-24095

Effect of the cross-sectional shape of a straight duct on supersonic flow stagnation
p 296 A90-24110

Calculation of the front or rear part of a flat body in subsonic flow with the extremum value of the critical Mach number
p 296 A90-24120

Total temperature effects on centerline Mach number characteristics of freejets
p 302 A90-25290

Comparison of 3-D viscous flow computations of Mach 5 inlet with experimental data
[AIAA PAPER 90-0600] p 314 A90-26970

Effectiveness of passive devices for axisymmetric base drag reduction at Mach 2
p 555 A90-36184

Mach number effects on upstream influence in swept shock wave/turbulent boundary layer interactions
p 556 A90-36415

The effect of Mach number on the stability of a plane supersonic wake
p 557 A90-36524

An analytic solution on hypersonic flow over an arbitrary slender body with near power-law profile
p 558 A90-37736

Langley hypersonic aerodynamic/aerothermodynamic testing capabilities - Present and future
[AIAA PAPER 90-1376] p 596 A90-38483

Study of compressibility effects in mixing layer by numerical simulation
[AIAA PAPER 90-1464] p 562 A90-38621

Versatility of an algebraic backflow turbulence model
[AIAA PAPER 90-1485] p 563 A90-38639

Direct simulation of low-density flow over airfoils
[AIAA PAPER 90-1539] p 564 A90-38683

Numerical solution of the problem of supersonic flow of a viscous gas past a concave conical wing
p 619 A90-39465

The influence of the inlet Mach number on the boundary layer development on turbomachinery blade surfaces
p 621 A90-40504

High Mach exhaust system concept scale model test results
[AIAA PAPER 90-1905] p 655 A90-40552

Flow visualization studies of the Mach number effects on dynamic stall of an oscillating airfoil
p 622 A90-40683

On the instabilities of supersonic mixing layers - A high-Mach-number asymptotic theory
p 702 A90-42644

A CFD study of precombustion shock-trains from Mach 3-6
[AIAA PAPER 90-2220] p 705 A90-42751

A Mach 6 external nozzle experiment with Argon-Freon exhaust simulation
[SAE PAPER 892315] p 714 A90-45477

Linear instability of the supersonic wake behind a flat plate aligned with a uniform stream
p 716 A90-45783

A computational study of incipient leading-edge separation on a 65-deg delta wing at $M = 1.60$
[AIAA PAPER 90-3029] p 791 A90-45871

Effect of the Mach number and shape of the front part of the obstacle on the separation zone length in supersonic flow
p 903 A90-50816

A study of high-lift airfoils at high Reynolds numbers in the Langley low-turbulence pressure tunnel
[NASA-TM-89125] p 1 N90-10002

Wind tunnel support system effects on a fighter aircraft model at Mach numbers from 0.6 to 2.0
[AD-A210614] p 19 N90-10010

Normal-force-curve and pitching-moment-curve slopes of forebody-cylinder combinations at zero angle of attack for Mach numbers up to 5
[ESDU-89008] p 89 N90-11709

Experimental and theoretical investigation of boundary-layer instability mechanisms on a swept leading edge at Mach 3.5
p 94 N90-12557

Transition in surface boundary layers
[CERT-RSF-OA-43/5018-AYD] p 136 N90-12897

Normal force, pitching moment, and side force of forebody-cylinder combinations for angles of attack up to 90 degrees and Mach numbers up to 5
[ESDU-89014] p 173 N90-14192

Fuselage design for a specified Mach-sliced area distribution
[NASA-TP-2975] p 414 N90-18385

The gun tunnel of the Brunswick Institute for Fluid Mechanics: Current development status
p 673 N90-24227

Calculation of the aeroelastic blade stabilization with linearized process
[MITT-87-01] p 666 N90-24272

MACHINE LEARNING

Automating acquisition of plans for an intelligent assistant by observing user behavior
p 459 A90-30230

Rule-based mechanisms of learning for intelligent adaptive flight control
p 521 N90-20939

MACHINERY

Elements of active vibration control for rotating machinery
[NASA-TM-102368] p 610 N90-22703

MAGNESIUM ALLOYS

New Light Alloys
[AGARD-CP-444] p 267 N90-15185

MAGNETIC BEARINGS

Digital control of magnetic bearings supporting a multimass flexible rotor
p 682 A90-40712

MAGNETIC CONTROL

Results of aircraft open-loop tests of an experimental magnetic leader cable system for guidance during roll-out and turnoff
[NASA-TM-4135] p 348 N90-16767

MAGNETIC ENERGY STORAGE

Battery configurations for multi-megawatt pulse power
p 873 A90-49763

MAGNETIC LEVITATION VEHICLES

California air transportation study: A transportation system for the California Corridor of the year 2010
[NASA-CR-186219] p 176 N90-14212

MAGNETIC RECORDING

Magnetic recording on board aircraft
p 39 A90-12195

Prospects of onboard magnetic tape recording during flight tests
p 39 A90-12198

MAGNETIC SUSPENSION

Dynamic properties of a system for the roll control of a model electromagnetically suspended in a wind tunnel
p 262 A90-22762

Magnetic suspension - Today's marvel, tomorrow's tool
p 262 A90-23697

Drag measurements on a modified prolate spheroid using a magnetic suspension and balance system
p 672 A90-40684

The six component magnetic suspension system for wind tunnel testing
p 673 A90-41725

Recent aerodynamic measurements with Magnetic Suspension Systems
p 759 A90-44399

An experimental investigation of the aerodynamic characteristics of slanted base ogive cylinders using magnetic suspension technology
[NASA-CR-181708] p 21 N90-10834

Techniques for extreme attitude suspension of a wind tunnel model in a magnetic suspension and balance system
[NASA-CR-181895] p 202 N90-14245

MAGNETOHYDRODYNAMIC STABILITY

Nonlinear mechanics of unstable plasmas as related to high altitude aerodynamics
[AD-A215126] p 464 N90-19852

MAGNETOHYDRODYNAMICS

Performance potential and technology issues of MHD augmented hypersonic simulation facilities
[AIAA PAPER 90-1380] p 598 A90-37929

MAGNIFICATION

Calculation of excrescence drag magnification due to pressure gradient at high subsonic speeds
[ESDU-87004] p 397 N90-19195

MAINTAINABILITY

Designing the V-22 'Osprey' tiltrotor V/Stol aircraft for maintenance and serviceability
[SAE PAPER 891075] p 101 A90-14369

Design for maintainability
[SAE PAPER 891079] p 81 A90-14371

- What can we do after we've done it all? — total quality management and leadership philosophy in practice
[AIAA PAPER 89-3209] p 549 A90-31696
- MDHC technical assessment of advanced rotor and control concepts p 861 A90-46948
- Repair of thermoplastic composite structures by fusion bonding p 941 A90-50060
- The RB199: An in-service success
[PNR90544] p 114 N90-11746
- Development and applications of reliability and maintainability design criteria in military aircraft
[ETN-89-95208] p 107 N90-12591
- The repair of aircraft integral fuel tanks in the RAF: A user's view of fuel tank technology p 250 N90-15908
- Spray sealing: A breakthrough in integral fuel tank sealing technology p 276 N90-15912
- STOVL fighter propulsion reliability, maintainability, and supportability characterization
[AD-A224221] p 933 N90-28574
- Application of multifunction inertial reference systems to fighter aircraft p 916 N90-29341
- MAINTENANCE**
- Braze repair of MA754 aero gas turbine engine nozzles
[ASME PAPER 89-GT-235] p 342 A90-23886
- The two level maintenance - I level dilemma p 381 A90-28319
- Two-level maintenance concept for advanced avionics architectures p 457 A90-28321
- Some technological errors in the use of capillary inspection in gas turbine engine repair p 769 A90-43039
- Software maintenance on the Airbus family
[SAE PAPER 892326] p 738 A90-45484
- A review of Australian and New Zealand investigations on aeronautical fatigue during the period April 1987 to March 1989
[AD-A210373] p 32 N90-10026
- Improving snow roads and airstrips in Antarctica
[AD-A211588] p 133 N90-11907
- Evaluation of a damaged F/A-18 horizontal stabilizer
[AD-A212573] p 107 N90-12597
- Designing for reliable and low maintenance cost aero engines
[PNR90570] p 115 N90-12604
- Fuel Tank Technology
[AGARD-R-771] p 250 N90-15904
- Integral fuel tank sealing practice at British Aerospace (Kingston) p 250 N90-15905
- The effect of primer age on adhesion of polysulphide sealant p 269 N90-15909
- Fuel tank explosion protection p 251 N90-15914
- Brake performance of the McDonnell Douglas DC-10-30/40 during high speed, high energy rejected takeoffs
[PB90-917004] p 503 N90-21000
- Advances in optimal active control techniques for aerospace systems; application to aircraft active landing gear p 592 N90-21769
- An expert system advisor for damage repair of composite wing skins (repairman) p 842 N90-26810
- Impact of Emerging NDE-NDI Methods on Aircraft Design, Manufacture, and Maintenance
[AGARD-CP-462] p 885 N90-28068
- Neutron radiography: Applications and systems p 886 N90-28080
- Development and testing of rapid repair methods for war damaged runways
[AD-A223970] p 938 N90-28586
- Aircraft battle damage repair of transparencies
[AD-A224168] p 925 N90-29387
- Estimation of power spectral density of runway roughness
[NAL-TR-1037] p 939 N90-29411
- MAINTENANCE TRAINING**
- Trend analysis and diagnostics codes for training purposes
[AIAA PAPER 90-2394] p 617 A90-42156
- MALFUNCTIONS**
- Convex models of malfunction diagnosis in high performance aircraft
[AD-A218514] p 702 N90-25073
- MAN MACHINE SYSTEMS**
- Theory for aircraft handling qualities based upon a structural pilot model p 118 A90-14730
- Computer integrated quality assurance for robotic workcells in aerospace manufacturing
[SME PAPER MS89-152] p 283 A90-23681
- Air-ground information transfer in the National Airspace System p 380 A90-26235
- A microcomputer-based airspace control simulation and prototype human-machine interface p 461 A90-30800
- The T800-LHT-800 engine - Designed for supportability p 585 A90-35773
- The Common/Same Type Rating - Human factors and other issues
[SAE PAPER 892229] p 723 A90-45445
- Task-oriented display design - Concept and example
[SAE PAPER 892230] p 738 A90-45446
- Managing man-in-the-loop simulations
[SAE PAPER 892355] p 761 A90-45506
- A blackboard approach for diagnosis in Pilot's Associate p 892 A90-49741
- Design and evaluation of the ATC interface - Planning system for approach flight p 937 A90-52617
- Distribution of hardware and software elements in unmanned air vehicle systems p 251 N90-15933
- FAA air traffic control operations concepts. Volume 7: ATCT (Airport Traffic Control Towers) tower controllers
[AD-A210455] p 332 N90-16730
- Three input concepts for flight crew interaction with information presented on a large-screen electronic cockpit display
[NASA-TM-4173] p 420 N90-18394
- Simulator comparison of thumball, thumb switch, and touch screen input concepts for interaction with a large screen cockpit display format p 506 N90-21005
- [NASA-TM-102587] p 506 N90-21005
- An adaptive human response mechanism controlling the V/STOL aircraft. Appendix 3: The adaptive control model of a pilot in V/STOL aircraft control loops
[NASA-CR-186599] p 598 N90-21777
- Model-based method for terrain-following display design
[AD-A219302] p 583 N90-22563
- Qualitative evaluation of a conformal velocity vector display for use at high angles-of-attack in fighter aircraft
[NASA-TM-102629] p 739 N90-25981
- A conceptual framework for fighter flight control systems
[PD-CF-9009] p 936 N90-28577
- MAN POWERED AIRCRAFT**
- Aerodynamics of human-powered flight p 386 A90-28552
- Flight testing a highly flexible aircraft - Case study on the MIT Light Eagle p 414 A90-31284
- Aerodynamic design of the Cal Poly Da Vinci Human-Powered Helicopter p 830 A90-46950
- MAN-COMPUTER INTERFACE**
- Benchmarking blackboards to support cockpit information management
[AIAA PAPER 89-3095] p 37 A90-10580
- Problem focus mechanisms for cockpit automation
[AIAA PAPER 89-3096] p 37 A90-10581
- Graphical interface tools for an avionics system
[AIAA PAPER 89-3130] p 75 A90-10606
- Interactive grid generation for fighter aircraft geometries p 311 A90-26546
- Automating acquisition of plans for an intelligent assistant by observing user behavior p 459 A90-30230
- Information display management in a pilot's associate p 418 A90-30238
- A computer-aided control engineering environment for multi-disciplinary expert-aided analysis and design (MEAD) p 461 A90-30796
- SMAS - An expert system for configuring a research flight simulator p 694 A90-41191
- Managing man-in-the-loop simulations
[SAE PAPER 892355] p 761 A90-45506
- Flight deck automation: Promises and realities
[NASA-CP-10036] p 187 N90-13384
- Development and test of software by safety critical aircraft systems
[MBB-FE-363/S/PUB-384] p 723 N90-25103
- On the structure of a future flight operations system p 826 N90-27682
- Four-dimensional planner: A ground based planning system for time accurate approach guidance p 826 N90-27683
- Development of a COMPAS prototype for the ATC Centre at Frankfurt (Fed. Republic of Germany) p 826 N90-27684
- MANAGEMENT**
- Preliminary fire extinguishing tests with handheld bottles: A comparison of extinguishing compounds
[DOT/FAA/CT-TN89/60] p 370 N90-17930
- Airport capacity enhancement plan 1989
[PB90-197997] p 913 N90-28507
- MANAGEMENT METHODS**
- The Air Force Flight Test Center Flight Test Safety Program p 35 N90-10872
- MANAGEMENT PLANNING**
- The planning of air transportation on airlines --- Russian book p 721 A90-42648
- Development and evaluation at ATCEU of executive and support operations, phase 4A/3D --- ATCEU (Air Traffic Control Evaluation Unit)
[CAA-PAPER-88017] p 99 N90-12572
- National airspace system plan: Facilities, equipment, associated development and other capital needs
[AD-A215882] p 402 N90-18373
- Software Management Environment (SME) concepts and architecture
[NASA-TM-103306] p 547 N90-21543
- Flight service automation system, model 1 full capacity, NAS operational test and evaluation integration test plan
[DOT/FAA/CT-TN90/4] p 825 N90-27672
- International aircraft operator data base master requirements and implementation plan
[DOT/FAA/CT-90/17] p 967 N90-29247
- MANAGEMENT SYSTEMS**
- Advanced Traffic Management System automation p 330 A90-25565
- Auxiliary power unit maintenance aid - Flight line engine diagnostics p 382 A90-28348
- An optically interfaced propulsion management system applied to a commercial transport aircraft p 424 A90-30811
- Real-time adaptive aircraft scheduling
[NASA-CR-177558] p 820 N90-27669
- MANEUVERABILITY**
- Helicopter design optimization for maneuverability and agility p 408 A90-28212
- Low speed maneuverability and agility design considerations for V/STOL aircraft p 581 A90-38536
- Assessment of proposed fighter agility metrics
[AIAA PAPER 90-2807] p 752 A90-45142
- Toward a theory of aircraft agility
[AIAA PAPER 90-2808] p 752 A90-45143
- Approach to side force alleviation through modification of the pointed forebody geometry
[AIAA PAPER 90-2834] p 712 A90-45165
- Lessons learned from the S/MTD program for the Flying Qualities Specification
[AIAA PAPER 90-2849] p 755 A90-45177
- An investigation of aircraft maneuverability and agility
[AIAA PAPER 90-3300] p 868 A90-48882
- Possible piloting techniques at hypersonic speeds
[ISL-CO-216/88] p 415 N90-18392
- Discrete proportional Plus Integral (PI) multivariable control laws for the Control Reconfigurable Combat Aircraft (CRCA) p 433 N90-18431
- Identification of aerodynamic models for maneuvering aircraft
[NASA-CR-186630] p 719 N90-25943
- Combat aircraft control requirements for agility p 935 N90-28517
- Analysis of dynamic transient response and postflutter behavior of super-maneuvering airplane
[AD-A224126] p 925 N90-29386
- Fighter agility metrics
[NASA-CR-187289] p 925 N90-29389
- MANEUVERS**
- Potential role of avionics in escape systems p 483 N90-20060
- Identification of aerodynamic models for maneuvering aircraft
[NASA-CR-186630] p 719 N90-25943
- Maneuvering by means of lateral jets
[ISL-CO-255/88] p 758 N90-26015
- MANIFOLDS**
- The discontinuity condition in the optimal control problem for a composite system p 76 A90-10848
- MANIPULATORS**
- Results of studies on a manipulator system for model handling in the ETW p 524 A90-34248
- Analyzing manipulator and feel system effects in aircraft flight control p 934 A90-51154
- The Shock and Vibration Digest, volume 21, no. 3 p 609 N90-22064
- MANNED SPACECRAFT**
- Aerospace structures supportability
[SAE PAPER 891058] p 129 A90-14360
- MANUALS**
- User's manual for the ride motion simulator
[AD-A212855] p 201 N90-13402
- MANUFACTURING**
- Installation and implementation of an extrusion cell in aircraft industry utilizing group technology
[SAE PAPER 891025] p 81 A90-14336
- Manufacturing and handling techniques used in the assembly of polished commercial aircraft
[SAE PAPER 890925] p 286 A90-24690
- Design and analysis of composite structures with manufacturing flaws p 445 A90-28234
- Fibre reinforced thermoplastic integral constructions in modular build-up technology - The 'thermoplastic in-situ-technique' p 534 A90-31879
- Aircraft fuel tank construction and testing experience p 250 N90-15907
- Towards 2000: The composite engine
[PNR90646] p 750 N90-26000

- NDT in aerospace: The next decade (1990's)
[PNR90628] p 777 N90-26348
- Cost effective technology
[PNR90664] p 883 N90-27002
- Impact of Emerging NDE-NDI Methods on Aircraft Design, Manufacture, and Maintenance
[AGARD-CP-462] p 885 N90-28068
- Impact of NDE-NDI methods on aircraft design, manufacture, and maintenance, from the fundamental point of view p 887 N90-28093
- Life cycle cost in the conceptual design of subsonic commercial aircraft, volumes 1 and 2 p 923 N90-28535
- Radiation-curable prepreg composites
[DE90-629740] p 951 N90-28674
- MANY BODY PROBLEM**
- Fundamental dynamics issues for comprehensive rotorcraft analyses p 831 A90-46961
- MAP (PROGRAMMING LANGUAGE)**
- Application to a helicopter of a general method for modifying a finite-element model to correlate with modal test data p 832 A90-46968
- MAP MATCHING GUIDANCE**
- Dual mode radar fusion based on morphological processing p 459 A90-30249
- Position finding and ground target direction finding by an aircraft with a gimbaled video camera
[DLR-FB-89-62] p 825 N90-27673
- MAPPING**
- China-built airborne synchronous laser ranger the new L-8 jet trainer aircraft
[AD-A213835] p 275 N90-15422
- MAPS**
- Digital map for helicopter navigation and guidance p 252 A90-21609
- Cognitive perspectives on map displays for helicopter flight p 419 A90-31329
- MARINE ENVIRONMENTS**
- Maritime environment airframe material fatigue testing p 764 A90-42675
- MARINE METEOROLOGY**
- Aircraft measurements of sea surface conditions and their relationship to marine boundary-layer dynamics p 888 A90-47572
- Aerosol separator for use in aircraft
[PB90-142217] p 611 N90-22155
- MARINE PROPULSION**
- Computation of viscous flow around a propeller-shaft configuration with infinite-pitch rectangular blades p 481 N90-20958
- MARINE TECHNOLOGY**
- Materials pace aerospace technology p 203 A90-17298
- MARITIME SATELLITES**
- The E-SAT 300A - A multichannel satellite communication system for aircraft p 914 A90-51339
- MARKET RESEARCH**
- EUROFAR - European project for a commercial vertical-takeoff aircraft p 221 A90-22696
- The coming age of the tiltrotor. II p 413 A90-30119
- Euromart - The European aviation research and technology program p 617 A90-41112
- The Dash 8 Series 400 regional airliner p 729 A90-42664
- California air transportation study: A transportation system for the California Corridor of the year 2010
[NASA-CR-186219] p 176 N90-14212
- Indianapolis Downtown Heliport: Operations analysis and marketing history
[REPT-90RR-13] p 527 N90-21049
- MARKETING**
- Indianapolis Downtown Heliport: Operations analysis and marketing history
[REPT-90RR-13] p 527 N90-21049
- Scenario 2000
[MBB-UD-500/89-PUB] p 734 N90-25092
- MARKOV PROCESSES**
- Three approaches to reliability analysis p 452 A90-30706
- Optimization of complex data processing algorithms in multichannel radio direction finding p 576 A90-36115
- MARS ATMOSPHERE**
- Preliminary design of a long-endurance Mars aircraft
[AIAA PAPER 90-2000] p 674 A90-40587
- Preliminary design of a long-endurance Mars aircraft
[NASA-CR-185243] p 588 N90-21763
- MASS**
- Development of a mass averaging temperature probe p 427 N90-18418
- MASS DISTRIBUTION**
- Response and hub loads sensitivity analysis of a helicopter rotor p 181 A90-18145
- Effect of control surface mass unbalance on the stability of a closed-loop active control system
[NASA-TP-2952] p 134 N90-12042

MASS FLOW RATE

- Ultrasonic regression rate measurement in solid fuel ramjets
[AIAA PAPER 90-1963] p 656 A90-40573
- Film cooling of turbine blades - Two dimensional experiments and numerical simulations p 739 A90-42670

MASS TRANSFER

- Effect of rib-angle orientation on local mass transfer distribution in a three-pass rib-roughened channel
[ASME PAPER 89-GT-98] p 359 A90-23812
- Heat transfer and pressure drop for short pin-fin arrays with pin-endwall fillet
[ASME PAPER 89-GT-99] p 359 A90-23813
- Simulation of cooling film density ratios in a mass transfer technique
[ASME PAPER 89-GT-200] p 362 A90-23872
- Local heat transfer on a flat surface roughened with broken ribs p 534 A90-32169
- Studies of gas turbine heat transfer airfoil surfaces and end-wall cooling effects
[AD-A212451] p 117 N90-12620
- WINCOF-I code for prediction of fan compressor unit with water ingestion
[NASA-CR-185157] p 551 N90-21724

MASSIVELY PARALLEL PROCESSORS

- Application of a rotary-wing viscous flow solver on a massively parallel computer
[AIAA PAPER 90-0334] p 164 A90-19802
- Benchmark calculations with an unstructured grid flow solver on a SIMD computer p 546 A90-34378

MATCHING

- Development of a least squares time response lower-order equivalent systems technique
[AD-A220527] p 648 N90-23389

MATERIALS

- AIAA/ASME/ASCE/AHS/ASC Structures, Structural Dynamics and Materials Conference, 31st, Long Beach, CA, Apr. 2-4, 1990, Technical Papers. Part 1 - Materials, engineering optimization and design p 449 A90-29226

MATERIALS HANDLING

- Process optimization of high temperature composite materials p 943 A90-50130
- Modeling strength data for CREW CHIEF p 780 N90-25516

MATERIALS RECOVERY

- Enhanced bioreclamation of jet fuels: A full-scale test at Eglin AFB, Florida
[AD-A222348] p 875 N90-26992

MATERIALS SCIENCE

- Aerospace - Collected translations of selected papers --- Book p 786 A90-48510

MATERIALS TESTS

- Noninteractive macroscopic reliability model for ceramic matrix composites with orthotropic material symmetry
[ASME PAPER 89-GT-129] p 360 A90-23827
- Development of a simulated bird-strike test method --- of aircraft turbine engine fan blade materials p 600 A90-37444
- Tests for aircraft interior materials in fire accident
[LR-622] p 914 N90-29337

MATHEMATICAL MODELS

- Practical suggestions for modifying math models to correlate with actual modal test results p 207 A90-16979
- Aeroelastic detuning for stability enhancement of unstalled supersonic flutter p 189 A90-17462
- The establishment of mathematical model of engine control system and simulation research of afterburning dynamic characteristics p 190 A90-18613
- Numerical modeling of a flame in a confined, unstable shear layer
[AIAA PAPER 90-0647] p 205 A90-19966
- Advances in the efficient calculation of flows with friction p 225 A90-21475
- A one-dimensional model of ramjet combustion instability
[AIAA PAPER 90-0271] p 266 A90-22192
- Mathematical model of turboprop engine behaviour p 254 A90-23351
- Analysis of the mathematical modeling of an aircraft flight trajectory with consideration of engine thrust effect on the force ratio on the aircraft p 247 A90-23363
- Mathematical formulation of blade surfaces in turbomachinery. I - Theoretical surface formulations
[ASME PAPER 89-GT-160] p 360 A90-23848
- Mathematical formulation of blade surfaces in turbomachinery. II - Practical examples of determined surfaces
[ASME PAPER 89-GT-161] p 361 A90-23849
- Some aspects of the numerical modeling of supersonic flow past flight vehicles p 293 A90-24048
- Recent activities within the aeroservoelasticity branch at the NASA Langley Research Center p 492 A90-33400

- Reduced-order aeroelastic models via dynamic residualization p 579 A90-35762
- Main characteristic parameter model for jet engine fault diagnosis p 585 A90-37210
- Results of an A109 simulation validation and handling qualities study p 591 A90-38524
- Mathematical modeling of plane parallel separated flows past bodies --- Russian book p 619 A90-39475
- Application of mathematical modeling to the study of rigid helicopter rotors p 643 A90-41738
- A modeling technique for STOVL ejector and volume dynamics
[AIAA PAPER 90-2417] p 663 A90-42168
- Euler and Navier-Stokes computations for airfoil geometries using unstructured meshes p 630 A90-42425
- A model for active control of helicopter air resonance in hover and forward flight p 670 A90-42462
- Development of a mathematical model of an adaptive antilutter system p 769 A90-42911
- Extended communication path length scintillation measurements and model - A discussion of results --- of atmospheric laser experiments p 725 A90-43230
- Mathematical simulation model of an aircraft gas turbine p 745 A90-44721
- A computationally efficient modelling of laminar separation bubbles p 801 A90-46372
- Model reduction with a finite-interval H(infinity) criterion
[AIAA PAPER 90-3473] p 890 A90-47723
- A new methodology for model order reduction with application to eigenstructure controllers
[AIAA PAPER 90-3475] p 891 A90-47725
- In-flight aircraft lightning surface current model p 819 A90-49844
- Bifurcation analysis of a model fighter aircraft with control augmentation
[AIAA PAPER 90-2836] p 934 A90-50640
- ILS (Instrument Landing System) mathematical modelling study on the effects of proposed hangar construction west of runway 18R on localizer performance at Dallas-Fort Worth International Airport
[AD-A210631] p 27 N90-10019
- The addition of Bendix MLS (Microwave Landing System) antenna patterns to MLS mathematical model
[AD-A210633] p 27 N90-10020
- Compatibility of fuel system components with high density fuel
[AD-A210381] p 32 N90-10027
- Modifying high-order aeroelastic math model of a jet transport using maximum likelihood estimation p 61 N90-10106
- Flexible aircraft dynamic modeling for dynamic analysis and control synthesis p 61 N90-10112
- Aircraft modal suppression system: Existing design approach and its shortcomings p 33 N90-10115
- Dynamic instability characteristics of aircraft turbine engine combustors p 53 N90-10195
- Very-low-frequency oscillations in liquid-fueled ramjets p 54 N90-10204
- A preliminary sensitivity analysis of the Generalized Escape System Simulation (GESS) computer program
[DE89-016891] p 24 N90-10844
- Robust control design for flight control
[AD-A211957] p 119 N90-11756
- ILS mathematical modeling study of the effects of proposed hangar construction at the Orlando International Airport, Runway 17R, Orlando, Florida
[DOT/FAA/CT-TN89/52] p 121 N90-11762
- Sequential design of experiments with physically based models 23
[AD-A211918] p 138 N90-12239
- Euler equation solutions applied to a helicopter rotor in forward moving flight
[ONERA-RSF-32/1285-AY-346A] p 107 N90-12592
- Aircraft SAR simulation Sargen 1.0
[FEL-1989-44] p 135 N90-12823
- A computationally efficient modelling of laminar separation bubbles
[NASA-CR-185854] p 136 N90-12872
- Test network Delft
[ETN-90-96009] p 177 N90-13365
- Thermal barrier coating life prediction model development, phase 1
[NASA-CR-182230] p 193 N90-13388
- Constitutive modeling for isotropic materials (HOST)
[NASA-CR-179522] p 193 N90-13390
- Constitutive modeling for isotropic materials (HOST)
[NASA-CR-174718] p 193 N90-13391
- Discretization and model reduction for a class of nonlinear systems p 198 N90-13397
- Mathematical model identification for flight simulation, based on flight and taxi tests
[LR-550] p 202 N90-13410

- An evaluation of a fatigue crack growth prediction model for variable-amplitude loading (PREFFAS) [LR-537] p 214 N90-13822
- Slush Hydrogen (SLH2) technology development for application to the National Aerospace Plane (NASP) [NASA-TM-102315] p 203 N90-14268
- Thermal fatigue durability for advanced propulsion materials [NASA-TM-102348] p 215 N90-14641
- Analysis of severe atmospheric disturbances from airline flight records p 280 N90-15045
- Systems for airborne wind and turbulence measurement p 281 N90-15046
- A pitch control law for compensation of the phugoid mode induced by windshears p 258 N90-15051
- Aircraft response and pilot behaviour during a wake vortex encounter perpendicular to the vortex axis p 259 N90-15057
- The application of queueing theory to the modelling of CP-140 aircraft communications [AD-A213479] p 274 N90-15310
- Rotor induced-inflow-ratio measurements and CAMRAD calculations [NASA-TP-2946] p 237 N90-15882
- Assessment of computational prediction of tail buffeting [NASA-TM-101613] p 237 N90-15886
- Optimum element density studies for finite-element thermal analysis of hypersonic aircraft structures [NASA-TM-4163] p 369 N90-17074
- A computational model for thickening boundary layers with mass addition for hypersonic engine inlet testing [AD-A216246] p 319 N90-17576
- A review of UK civil aviation fire and cabin safety research p 325 N90-17587
- Forced and natural venting of aircraft cabin fires: A numerical simulation p 326 N90-17597
- Time development of convection flow patterns in aircraft cabins under post-crash fire exposure p 327 N90-17598
- Analysis of the National Transonic Facility mishap [NASA-TM-101686] p 328 N90-17620
- An examination of the fatigue meter records from the RAAF Orion P-3C fleet [AD-A214000] p 338 N90-17628
- A method for the prediction of supersonic compressor blade performance [CUEAD/TURBO/TR-126] p 344 N90-17634
- Measurement and computer simulation of antennas on ships and aircraft for results of operational reliability p 370 N90-17936
- Numerical simulation of compressible vortices [AD-A216221] p 371 N90-18017
- An approximate model for the performance and acoustic predictions of counterrotating propeller configurations [NASA-CR-180667] p 379 N90-18228
- Review of modelling methods to take account of material structure and defects p 425 N90-18402
- Unsteady viscous calculation method for cascades with leading edge induced separation p 426 N90-18408
- Aerodynamic study on forced vibrations on stator rows of axial compressors p 426 N90-18412
- Unsteady blade loads due to wake influence p 426 N90-18413
- Asymptotic analysis of transonic flow through oscillating cascades p 427 N90-18421
- Modelling unsteady transition and its effects on profile loss p 427 N90-18423
- Stall and recovery in multistage axial flow compressors p 428 N90-18429
- Calculation and optimization of rotor start process [ETN-90-95894] p 416 N90-19229
- Flow simulation for aircraft [NLR-MP-87082-U] p 455 N90-19543
- Using transonic small disturbance theory for predicting the aeroelastic stability of a flexible wind-tunnel model [NASA-TM-102617] p 478 N90-20047
- Aeroelastic characteristics of aircraft with circulation control wings p 497 N90-20070
- A video-based experimental investigation of wing rock [AD-A218244] p 498 N90-20075
- Summary report of the Summer Conference of the DARPA-Materials Research Council [AD-A217380] p 532 N90-20143
- Modification and improvement of software for modeling multidimensional reacting fuel flows [AD-A217789] p 533 N90-20235
- Plan, formulate, and discuss a NASTRAN finite element model of the UH-60A helicopter airframe [NASA-CR-181975] p 541 N90-20439
- A two-dimensional unsteady analysis for transonic and supersonic cascade flows p 480 N90-20955
- An efficient airfoil design method using the Navier-Stokes equations p 500 N90-20981
- An intensive procedure for the design of pressure-specified three-dimensional configurations at subsonic and supersonic speeds by means of a higher-order panel method p 500 N90-20982
- Subsonic and transonic blade design by means of analysis codes p 510 N90-20985
- Inverse computation of transonic internal flows with application for multi-point-design of supercritical compressor blades p 501 N90-20987
- Numerical method for designing 3D turbomachinery blade rows p 511 N90-20990
- Constrained spanload optimization for minimum drag of multi-lifting-surface configurations p 501 N90-20992
- Secondary flows and radial mixing predictions in axial compressors p 512 N90-21010
- A study on secondary flow and spanwise mixing in axial flow compressors p 512 N90-21012
- Parabolized calculations of turbulent three dimensional flows in a turbine duct p 482 N90-21013
- Experimental and numerical study on basic phenomena of secondary flows in turbines p 512 N90-21014
- Secondary flow calculations for axial and radial compressors p 514 N90-21024
- The numerical simulation of multistage turbomachinery flows p 514 N90-21025
- Research on cascade secondary and tip-leakage flows: Periodicity and surface flow visualization p 514 N90-21026
- Analysis of the rotor tip leakage flow with tip cooling air ejection p 515 N90-21029
- Experimental and theoretical investigation of optimal control methods with model reduction p 521 N90-21039
- Design of a helicopter automatic flight control system using adaptive control p 522 N90-21040
- Subsonic flutter analysis using MSC/NASTRAN [PB90-166786] p 522 N90-21041
- Development and application of a generalized dynamic wake theory for lifting rotors p 570 N90-21731
- Modeling of vortex-induced oscillations based on indicial response approach [NASA-CR-186560] p 572 N90-21736
- Analytical study of the origin and behavior of asymmetric vortices [NASA-TM-102796] p 573 N90-21746
- Conceptual design optimization study [NASA-CR-4298] p 582 N90-21755
- Quiet mode for nonlinear rotor models [NASA-TM-102236] p 582 N90-21758
- A conflict analysis of 4D descent strategies in a metered, multiple-arrival route environment [NASA-CR-182019] p 593 N90-21772
- The insertion of human dynamics models in the flight control loops of V/STOL research aircraft. Appendix 2: The optimal control model of a pilot in V/STOL aircraft control loops [NASA-CR-186598] p 598 N90-21776
- The Shock and Vibration Digest, volume 21, no. 2 p 609 N90-22059
- An investigation of the generation and radiation of aerodynamic noise in real piping systems p 614 N90-22368
- Application of a dynamic stall model to rotor trim and aeroelastic response p 583 N90-22556
- Model-based method for terrain-following display design [AD-A219302] p 583 N90-22563
- A modeling technique for STOVL ejector and volume dynamics [NASA-TM-103167] p 589 N90-22566
- Design of cryogenic tanks for launch vehicles p 609 N90-22662
- A study of supermaneuver aerodynamics [AD-A218378] p 631 N90-23349
- A computer code for the prediction of aerodynamic characteristics of lifting airfoils at transonic speed [DLC-EST-TN-030] p 632 N90-23359
- MLS mathematical model validation study using airborne MLS data from Midway Airport engineering flight tests, August 1988 [DOT/FAA/CT-TN90/2] p 640 N90-23378
- The computation of turbulent thin shear flows associated with flow around multielement airfoils p 633 N90-24240
- Sound propagation elements in evaluation of en route noise of advanced turbofan aircraft p 697 N90-24861
- A quantitative technique to estimate microburst wind shear hazard to aircraft p 692 N90-25040
- Development of a finite element based delamination analysis for laminates subject to extension, bending, and torsion p 679 N90-25049
- Extension-torsion coupling behavior of advanced composite tilt-rotor blades p 651 N90-25057
- A review of instability and noise propagation in supersonic flows [NASA-CR-186800] p 717 N90-25112
- Development of a microcomputer based software system for use in crewmember ejection analysis [AD-A220398] p 723 N90-25117
- The effect of aircraft size on cabin floor dynamic pulses [DOT/FAA/CT-88/15] p 735 N90-25136
- Ground shake test of the UH-60A helicopter airframe and comparison with NASTRAN finite element model predictions [NASA-CR-181993] p 758 N90-25143
- Lecture notes on flight simulation techniques [LR-596] p 762 N90-25153
- A computational efficient modelling of laminar separation bubbles [NASA-CR-186729] p 774 N90-25291
- Aerodynamic loads and blade vortex interaction noise prediction [ISL-PU-310/89] p 719 N90-25942
- The applicability of simple helicopter models for flight mechanics studies [ETN-90-96962] p 736 N90-25975
- Agusta methodology for pitch link loads prediction in preliminary design phase [ETN-90-97270] p 737 N90-25978
- Performance of a supercharged direct-injection stratified-charge rotary combustion engine [NASA-TM-103105] p 748 N90-25982
- Subsonic combustor flow modeling: State of the art of CFD techniques for reacting and combustor flow p 749 N90-25991
- Turbulent combustion modeling for turbo-jet combustion chambers p 749 N90-25993
- Background, current status, and prognosis of the ongoing slush hydrogen technology development program for the NASP [NASA-TM-103220] p 763 N90-26055
- Investigation of crack-closure prediction models for fatigue in aluminium alloy sheet under flight-simulation loading [LR-619] p 777 N90-26369
- A computer module used to calculate the horizontal control surface size of a conceptual aircraft design [NASA-CR-186872] p 780 N90-26515
- On central-difference and upwind schemes [NASA-CR-182061] p 781 N90-26595
- Velocity measurements on a lifting rotor/airframe configuration in low speed forward flight p 815 N90-26790
- Aerodynamic/dynamic interaction [AD-A222263] p 815 N90-26798
- Obtaining consistent models of helicopter flight-data measurement errors using kinematic-compatibility and state-reconstruction methods [AD-A222533] p 815 N90-26799
- Finite element models of USAF aircraft structures p 844 N90-26820
- Damage tolerance analysis for manned hypervelocity vehicles. Volume 2: Software user's manual [AD-A222136] p 845 N90-26826
- Air Force procedure for predicting aircraft noise around airbases: Noise Exposure Model (NOISEMAP). User's manual [AD-A223162] p 895 N90-27467
- Experimental identification of helicopter engine dynamics from closed loop data p 855 N90-27627
- Impact of NDE-NDI methods on aircraft design, manufacture, and maintenance, from the fundamental point of view p 887 N90-28093
- The effects of structural flap-lag and pitch-lag coupling on soft inplane hingeless rotor stability in hover [NASA-TP-30002] p 910 N90-28503
- Study of ground effects on flying scaled models p 922 N90-28532
- Structural analysis and optimum design of geodesically stiffened composite panels [NASA-CR-186944] p 959 N90-28862
- Correlation of AH-1G airframe flight vibration data with a coupled rotor-fuselage analysis [NASA-CR-181974] p 959 N90-28865
- Plan, execute, and discuss vibration measurements and correlations to evaluate a NASTRAN finite element model of the AH-64 helicopter airframe [NASA-CR-181973] p 960 N90-28866
- Multi-disciplinary optimization of aeroservoelastic systems [NASA-CR-185931] p 925 N90-29385
- Numerical simulations of the structure of supersonic shear layers [AD-A224164] p 960 N90-29587
- Proceedings of damping '89. Volume 1: Pages AAB-1 through DCD-11 [AD-A223431] p 960 N90-29664

MATHEMATICAL PROGRAMMING

- Modelling and simulation of turboprop engine behaviour p 424 A90-29946

MATRICES (MATHEMATICS)

- Rotor/airframe aeroelastic analyses using the transfer matrix approach
[AIAA PAPER 90-1119] p 392 A90-29391
A combined Riccati transfer matrix-direct integration method with its applications p 611 A90-37218
The application of the finite element method to an aerodynamic problem specific to propeller design
[LR-614] p 718 N90-25116

MATRIX MATERIALS

- Composites boost 21st-century aircraft engines
p 442 A90-29704
Investigation of the failure modes in a metal matrix composite under thermal cycling
[AD-A216195] p 357 N90-17825

MATRIX METHODS

- Dynamics of multi-spool gas turbines using the matrix transfer method - Applications p 509 A90-33594
Dynamics of multi-spool gas turbines using the matrix transfer method - Theory p 509 A90-33595
Calculation of three-dimensional viscous and inviscid hypersonic flows using split-matrix marching methods
[AIAA PAPER 90-3070] p 794 A90-45894
Passive location accuracy via a general covariance error model --- long-baseline interferometry from airborne platforms p 914 A90-51060
Rotordynamic analysis with shell elements for the transfer matrix method
[AD-A217455] p 541 N90-20434

MAXIMUM LIKELIHOOD ESTIMATES

- The application of linear maximum likelihood estimation of aerodynamic derivatives for the Bell-205 and Bell-206
p 30 A90-12773
Time domain parameter identification techniques applied to the UH-60A Black Hawk Helicopter
p 77 A90-12774
Pattern representations and syntactic classification of radar measurements of commercial aircraft
p 417 A90-28407
Identification of time varying modal parameters
p 536 A90-33375
Parameter identification of linear systems based on smoothing
[AIAA PAPER 90-2800] p 753 A90-45156
Maximum likelihood tuning of a vehicle motion filter
p 755 A90-45334
An orthogonal algorithm to the maximum likelihood estimation using an efficient method for computing sensitivities
[AIAA PAPER 90-3507] p 891 A90-47753
Modifying high-order aeroelastic math model of a jet transport using maximum likelihood estimation
p 61 N90-10106
Flight path reconstruction using extended Kalman filtering techniques
[PD-FC-9001] p 489 N90-20970
Experimental identification of helicopter engine dynamics from closed loop data p 855 N90-27627
Fault Detection and Isolation (FDI) techniques for guidance and control systems p 918 N90-29366

MCDONNELL DOUGLAS AIRCRAFT

- Rotocraft computational fluid dynamics - Recent developments at McDonnell Douglas
p 630 A90-42439
The McDonnell Douglas MD-11 ... or, how the DC-10 grew bigger
p 730 A90-43766
An interfacing solution for real-time avionics development
[SAE PAPER 892357] p 738 A90-45508

MEAN SQUARE VALUES

- Mean-square approximation by an even nonnegative polynomial p 374 A90-24101

MEASURING INSTRUMENTS

- External 6-component wind tunnel balances for aerospace simulation facilities p 438 A90-28296
A novel technique for aerodynamic force measurement in shock tubes p 438 A90-28302
Ultrasonic regression rate measurement in solid fuel ramjets
[AIAA PAPER 90-1963] p 656 A90-40573
Flight test instrumentation and data processing at British Aerospace, Warton, U.K. p 59 N90-10887
Devices and procedures for the calibration of sensors and measurement: Systems of the flight test support system ATTAS
[DFVLR-MITT-89-06] p 134 N90-12007
The assessment of visibility from automatic contrast Measurements p 242 N90-15061

MECHANICAL DEVICES

- Preliminary design and load distributions of high performance mechanical systems p 771 A90-45281

MECHANICAL DRIVES

- Composite driveshaft designs
[SAE PAPER 891031] p 128 A90-14339

- Assessment of worm gearing for helicopter transmissions
[NASA-TM-102441] p 257 N90-15923
The Shock and Vibration Digest, volume 21, no. 3
p 609 N90-22064

MECHANICAL ENGINEERING

- Stability and vibrations of mechanical systems --- Russian book p 270 A90-20426
Developments in mechanics. Volume 15 - Midwestern Mechanics Conference, 21st, Michigan Technological University, Houghton, Aug. 13-16, 1989, Proceedings p 769 A90-42870

MECHANICAL MEASUREMENT

- Experimental determination of the short crack effect for metals p 265 A90-20064

MECHANICAL PROPERTIES

- Effect of protective coatings on mechanical properties of superalloys
[ONERA, TP NO. 1989-88] p 62 A90-11126
Ceramic heat exchangers in gas turbine
[ONERA, TP NO. 1989-109] p 40 A90-11142
The case for titanium p 204 A90-17922
Developing aluminium p 204 A90-17924
Gear steels for future helicopter transmissions
p 265 A90-20607
The anisotropy of the mechanical behaviour in nickel-based single crystal superalloys for turbine blades
[ONERA, TP NO. 1989-205] p 355 A90-25339
Analysis and practical design of ceramic-matrix composite components p 445 A90-28135
Mechanical considerations for reliable interfaces in next generation electronics packaging p 453 A90-30813
The status of high temperature polymers for composites - Likely candidates p 528 A90-31516
Evaluation of various non-asbestos epoxy adhesives for aircraft repair p 529 A90-33078
High-temperature corrosion and mechanical properties of some silicon nitride ceramics p 531 A90-33985
Resources - Supply and availability --- of superalloys for United States aerospace industry
p 531 A90-34152

- Powder metallurgy and oxide dispersion processing of superalloys p 531 A90-34158
MRS International Meeting on Advanced Materials, 1st, Tokyo, Japan, May 31-June 3, 1988, Proceedings. Volume 5 - Structural ceramics/Fracture mechanics
p 599 A90-35926

Composites applications - The future is now

- p 678 A90-42372
Lose weight with Al-Li p 765 A90-44175
A method for reducing a buckled skin under combined loading p 860 A90-46571
Titanium aluminides for advanced aircraft engines
p 874 A90-49000
International SAMPE Symposium and Exhibition, 35th, Anaheim, CA, Apr. 2-5, 1990, Proceedings. Books 1 & 2
p 940 A90-50056
Thermo-oxidative stability studies of PMR-15 polymer matrix composites reinforced with various continuous fibers p 941 A90-50068
Effects of additives on the processing and properties of LARC-TPI polyimide p 942 A90-50070
Rigidite 5255-3 - A highly damage tolerant prepreg resin system with a well balanced property profile
p 944 A90-50139

- Chemical resistance of carbon fiber reinforced polyether ether ketone and polyphenylene sulfide composites
p 944 A90-50142
Improved fiber reinforced polyphenylene sulfide thermoplastic composites p 947 A90-50180
Mechanical influences on crystallization in PEEK matrix/carbon fiber reinforced composites
p 949 A90-50227

- Modeling of the oil quench for Ni-based superalloy turbine disks p 957 A90-51525
Processing and mechanical properties of Al2O3/Y3Al5O12 (YAG) eutectic composite
p 951 A90-51966
Combined advanced foundry and quality control techniques to enhance reliability of castings for the aerospace industry p 64 N90-10240
Thin walled cast high-strength structural parts
p 65 N90-10242

- Material requirements for future aeroengines
[PNR90595] p 116 N90-12610
Composite materials for future aeroengines
[PNR90584] p 127 N90-12667
Rolling of ARALL laminates (an alternative method for post-stretching ARALL laminates)
[LR-560] p 135 N90-12778

- The application of cast SiC/Al to rotary engine components
[NASA-CR-179610] p 192 N90-13385
New Light Alloys
[AGARD-CP-444] p 267 N90-15185

- The microstructure and properties of aluminum-lithium alloys p 267 N90-15187
Spray sealing: A breakthrough in integral fuel tank sealing technology p 276 N90-15912
Impact of composites in the aerospace industry
[ETN-90-96231] p 443 N90-18527
Lessons learned for composite aircraft structures qualification p 842 N90-26808
An aluminum quality breakthrough for aircraft structural reliability p 843 N90-26816
Applications of digital image processing in testing and evaluation of composite materials
[AD-A22939] p 874 N90-26887
Radiation-curable prepreg composites
[DE90-629740] p 951 N90-28674
Effect of protective coatings on mechanical properties of superalloys p 952 N90-28707
Structural testing and analytical research of turbine components
[AD-A23516] p 933 N90-29396
Evaluation of static and fatigue properties of thin sheets of 8090-T8 aluminum-lithium alloy and observation of its fracture surfaces
[NAL-TR-1039] p 953 N90-29499

MECHANICAL SHOCK

- The Shock and Vibration Digest, volume 21, no. 2
p 609 N90-22059
The Shock and Vibration Digest, volume 21, no. 3
p 609 N90-22064
The Shock and Vibration Digest, volume 21, no. 6
p 614 N90-22363

MECHANIZATION

- Technical evaluation report on the Guidance and Control Panel 49th Symposium on Fault Tolerant Design Concepts for Highly Integrated Flight Critical Guidance and Control Systems
[AGARD-AR-281] p 758 N90-26012

MEDICAL SERVICES

- A comparison of emergency medical helicopter accident rates in the United States and the Federal Republic of Germany p 722 A90-44640
Aeronautical decisionmaking for air ambulance program administrators
[DOT/FAA/DS-88/8] p 635 N90-23368

MELTING

- Improved melt flow and physical properties of Mitsui Toatsu's LARC-TPI 1500 series polyimide
p 943 A90-50134

MEMORY (COMPUTERS)

- Use of Onboard Data Loaders
[SAE PAPER 892327] p 738 A90-45485
The MHOST finite element program: 3-D inelastic analysis methods for hot section components. Volume 3: Systems' manual
[NASA-CR-182236] p 73 N90-10451
Concurrent processing adaptation of aeroplastic analysis of proflans
[NASA-TM-102455] p 215 N90-14656
The use of supercomputers for the design and analysis of constructions p 612 N90-22977

MERIDIONAL FLOW

- Secondary flow calculations for axial and radial compressors p 514 N90-21024

MESOSCALE PHENOMENA

- Fog formation at Perth Airport p 611 A90-37748
Mesoscale acid deposition modeling studies
[NASA-CR-4262] p 140 N90-13228
Three-dimensional numerical study of thunderstorm downdrafts and associated outflow boundaries
p 963 N90-29746

MESSAGE PROCESSING

- AIRNET: A real-time communications network for aircraft
[NASA-CR-186140] p 690 N90-24514
Communications Interface Driver (CID) test plan
[DOT/FAA/CT-TN89/35] p 958 N90-28762
Observability of relative navigation using range-only measurements p 917 N90-29360
High speed bus technology development
[AD-A224486] p 960 N90-29565

MESSAGES

- Taxiway sign effectiveness under reduced visibility conditions
[DOT/FAA/CT-TN90/20] p 761 N90-25150

METAL BONDING

- Diffusion bonding aeroengine components
p 131 A90-16012
Safer primers from 3M p 204 A90-17925
Application investigation on superplastic forming/diffusion bonding combined technology of titanium alloy TC4 p 204 A90-18603
Two special cost-effective applications for electrochemical metallizing for improved brazing and bonding
[SAE PAPER 890927] p 365 A90-24692

- Evaluation of various non-asbestos epoxy adhesives for aircraft repair p 529 A90-33078
- The surface pretreatment of aluminium-lithium alloys for structural bonding p 881 A90-47118
- Diffusion bonding of metals p 206 N90-14330
- METAL COATINGS**
- Extending the overhaul interval for gas turbine engines through the use of alternative coatings on first stage blades p 63 A90-12539
- Gas turbine compressor operating environment and material evaluation [ASME PAPER 89-GT-42] p 340 A90-23769
- Manufacturing and handling techniques used in the assembly of polished commercial aircraft [SAE PAPER 890925] p 286 A90-24690
- Fatigue life assessment of a leaded electronic component under a combined thermal and random vibration environment p 770 A90-43734
- Thermal mechanical fatigue of coated blade materials [AD-A214258] p 256 N90-15107
- METAL COMBUSTION**
- Combustion characteristics of a boron-fueled SFRJ with aft-burner p 62 A90-12514
- RAAF Orion aircraft A9-300 oxygen fire [AD-A21496] p 323 N90-16725
- Regression and combustion characteristics of boron containing fuels for solid fuel ramjets p 858 N90-27928
- METAL FATIGUE**
- IMI 834 - A new high temperature capability titanium alloy for engine use p 62 A90-12535
- Stochastic crack growth analysis methodologies for metallic structures [AIAA PAPER 90-1015] p 449 A90-29340
- Time dependent effects on high temperature low cycle fatigue and fatigue crack propagation on nickel base superalloys p 443 A90-29881
- Cyclic stress-strain behavior and low cycle fatigue of Ti 6242 p 530 A90-33523
- Reconstitution of crack growth from fractographic observations after flight simulation loading p 682 A90-40650
- Cyclic fracture toughness of VT3-1 and VT-25 titanium alloys p 873 A90-46514
- Analysis of failures in aircraft structures p 882 A90-48998
- Fatigue crack initiation mechanics of metal aircraft structures [AD-A210567] p 65 N90-10255
- Investigation on sheet material of 8090 and 2091 aluminium-lithium alloy p 267 N90-15192
- Aluminum lithium alloys for Navy aircraft p 267 N90-15193
- Uses and properties of Al-Li on the new EH101 helicopter p 268 N90-15201
- Proceedings of the 1988 Structural Integrity Program Conference [AD-A213545] p 275 N90-15486
- Fatigue of aluminium alloy joints with various fastener systems. Low load transfer [ESDU-89046] p 370 N90-17193
- Characterisation of fatigue of aluminium alloys by acoustic emission. Part 2: Discrimination between primary and other emissions [AERE-R-13303-PT-2] p 678 N90-23523
- AGARD/SMP Review Damage Tolerance for Engine Structures. 3: Component Behaviour and Life Management [AGARD-R-770] p 855 N90-27704
- Characterization of the CP 214 T851. Dissection of a cast flat bar for a standard spar [CEAT-PV-M4/462200] p 876 N90-27905
- Characterization of the 7175 T7352. Dissection of a die casting standard spar [CEAT-PV-M5/528900] p 877 N90-27906
- Characterization of the 7175 T7352 101. Dissection of a die casting standard spar [CEAT-PV-M5/5288] p 877 N90-27907
- Characterization of the 7010 T73651. Dissection of a sheet billet for a standard spar [CEAT-PV-M5/521700] p 877 N90-27908
- Damage tolerance analysis for manned hypervelocity vehicles. Volume 1: Final technical report [AD-A221970] p 887 N90-28106
- Fretting fatigue strength of Ti-6Al-4V at room and elevated temperatures and ways of improving it p 952 N90-28709
- METAL FIBERS**
- New metallic felts with improved resistance to high temperature oxidation [ONERA, TP NO. 1989-210] p 366 A90-25343
- METAL FUELS**
- Metallized fuel particle size study in a solid fuel ramjet [AD-A220079] p 679 N90-24451
- METAL JOINTS**
- Fatigue of aluminium alloy joints with various fastener systems. Low load transfer [ESDU-89046] p 370 N90-17193
- METAL MATRIX COMPOSITES**
- Composite-embedded optical fibers for communication links p 139 A90-13847
- Low-expansion MMCs boost avionics p 203 A90-17291
- The case for titanium p 204 A90-17922
- Metal matrix composites - Ready for take-off? p 356 A90-26865
- Sliding and abrasive wear behaviour of an aluminium (2014)-SiC particle reinforced composite p 530 A90-33344
- Advanced materials for landing gear p 677 A90-41900
- Metal matrix composites structural design experience [AIAA PAPER 90-2175] p 677 A90-42059
- Metal matrix composite fan blade development [AIAA PAPER 90-2178] p 677 A90-42062
- Composites applications - The future is now p 678 A90-42372
- Titanium matrix composite landing gear development [SAE PAPER 892337] p 733 A90-45491
- Investigation of the failure modes in a metal matrix composite under thermal cycling [AD-A216195] p 357 N90-17825
- Compendium of abstracts and viewgraphs. [AD-A217189] p 532 N90-20140
- Summary report of the Summer Conference of the DARPA-Materials Research Council [AD-A217380] p 532 N90-20143
- NASA-UVA light aerospace alloy and structures technology program [NASA-CR-182607] p 601 N90-22651
- Towards 2000: The composite engine [PNR90646] p 750 N90-26000
- Metal matrix composites and powder processing for aero-engine applications [PNR90617] p 767 N90-26087
- Design of helicopter components in metal matrix composites [REPT-100-20-55] p 874 N90-26894
- Proceedings of damping '89. Volume 1: Pages AAB-1 through DCD-11 [AD-A223431] p 960 N90-29664
- METAL OXIDES**
- Powder metallurgy and oxide dispersion processing of superalloys p 531 A90-34158
- METAL PLATES**
- The prediction and measurement of thermoacoustic response of plate structures [AIAA PAPER 90-0988] p 451 A90-29400
- Mobility power flow analysis of an L-shaped plate structure subjected to acoustic excitation [NASA-CR-186130] p 214 N90-13817
- METAL POLISHING**
- Manufacturing and handling techniques used in the assembly of polished commercial aircraft [SAE PAPER 890925] p 286 A90-24690
- METAL PROPELLANTS**
- Regression and combustion characteristics of boron containing fuels for solid fuel ramjets p 858 N90-27928
- METAL SHEETS**
- Numerical study of balanced patch repairs to cracked sheets p 210 A90-18442
- Aeroelastic tailoring applied to composite wing p 211 A90-18580
- Aluminum alloy 6013 sheet for new U.S. Navy aircraft p 599 A90-37442
- Metal laminates for aerospace applications p 874 A90-48997
- Investigation on sheet material of 8090 and 2091 aluminium-lithium alloy p 267 N90-15192
- Uses and properties of Al-Li on the new EH101 helicopter p 268 N90-15201
- Aluminum-lithium: Application of plate and sheet to fighter aircraft p 268 N90-15202
- An expert system advisor for damage repair of composite wing skins (repairman) p 842 N90-26810
- Evaluation of static and fatigue properties of thin sheets of 8090-T8 aluminium-lithium alloy and observation of its fracture surfaces [NAL-TR-1039] p 953 N90-29499
- Fractographic analysis of fatigue crack growth under two-blocks loading on 2024-T351 sheet specimens [LR-628] p 961 N90-29680
- Effects of blocks of overloads and underloads on fatigue crack growth in 2024-T351 sheet specimens: Fractographic analysis and crack closure predictions [LR-629] p 961 N90-29681
- METAL SHELLS**
- Demonstration of probabilistic-based durability analysis method for metallic airframes p 273 A90-23287
- METAL SURFACES**
- Application of localized active control to reduce propeller noise transmitted through fuselage surface p 78 A90-11884
- Thermal barrier characteristics of partially stabilized zirconia coatings on Incoloy alloy 909 (A controlled expansion alloy) [ASME PAPER 89-GT-146] p 354 A90-23839
- Electromagnetic dent removal for aircraft repair [SAE PAPER 890923] p 286 A90-24689
- Design of the optimal hardening treatment for the metal surfaces of gas turbine engine components p 873 A90-46496
- The effect of primer age on adhesion of polysulphide sealant p 269 N90-15909
- METAL WORKING**
- Rolling of ARALL laminates (an alternative method for post-stretching ARALL laminates) [LR-560] p 135 N90-12778
- Putting alloy 2091 to work p 268 N90-15197
- METAL-METAL BONDING**
- Reflection by defective diffusion bonds [AD-A212995] p 206 N90-13638
- METALLIZING**
- Two special cost-effective applications for electrochemical metallizing for improved brazing and bonding [SAE PAPER 890927] p 365 A90-24692
- METALLURGY**
- Superalloy 718: Metallurgy and applications; Proceedings of the International Symposium, Pittsburgh, PA, June 12-14, 1989 p 266 A90-20775
- METALS**
- New metallic felts with improved resistance to high temperature oxidation [ONERA, TP NO. 1989-210] p 366 A90-25343
- Stress intensity factors for cracking metal structures under rapid thermal loading. Volume 2: Theoretical background [AD-A213297] p 213 N90-13812
- Fuel resistant coatings for metal and composite fuel tanks p 269 N90-15911
- METEOROLOGICAL FLIGHT**
- Multistroke cloud-to-ground strike to the NASA F-106B airplane p 482 A90-32304
- Global stratospheric change: Requirements for a Very-High-Altitude Aircraft for Atmospheric Research [NASA-CP-10041] p 185 N90-14220
- METEOROLOGICAL INSTRUMENTS**
- Requirements for meteorological equipment designed for the acquisition of meteorological data essential for the takeoff and landing of aircraft at civil airports p 962 A90-50777
- Variability characteristics of the meteorological optical range field in an optically inhomogeneous atmosphere p 962 A90-50784
- The Meteorological Measurement System on the NASA ER-2 aircraft p 926 A90-51658
- Meeting Review: Workshop on Airborne Instrumentation [PB89-174775] p 39 N90-10032
- METEOROLOGICAL PARAMETERS**
- Meteopod, an airborne system for measurements of mean wind, turbulence, and other meteorological parameters p 418 A90-29943
- Microwave landing system - A pilot's point of view p 640 A90-41712
- Semiautomatic coding of weather phenomenon groups in the meteorological reports of automatic aircraft stations p 962 A90-50783
- The Meteorological Measurement System on the NASA ER-2 aircraft p 926 A90-51658
- ASR-9 weather channel test report [AD-A211749] p 133 N90-11934
- Weather data dissemination to aircraft p 486 N90-20934
- METEOROLOGICAL RADAR**
- Terminal Doppler Weather Radar System - Wind shear detection will warn pilots of danger p 25 A90-10462
- Air traffic control development at Lincoln Laboratory p 240 A90-21378
- Wind shear detection with pencil-beam radars p 279 A90-21386
- Development of an automated windshear detection system using Doppler weather radar p 373 A90-25567
- Advances in weather technology for the aviation system p 373 A90-25572
- The microphysical structure of severe downdrafts from radar and aircraft observations in CINDE --- Convection Initiation and Downburst Experiment p 455 A90-28582
- Microburst precursors observed with Doppler radar p 456 A90-28613

Range obscuration mitigation by adaptive PRF selection for the TDWR system --- Pulse Repetition Frequency for Terminal Doppler Weather Radar p 456 A90-28617
Convergence aloft as a precursor to microbursts p 456 A90-28620
Microburst divergence detection for terminal Doppler weather radar p 456 A90-28625
Design of new Polish primary radars AVIA DM/CM p 638 A90-41035
Maximum expected concentrations of hail in thunderstorm precipitation p 962 A90-52052
ASR-9 weather channel test report p 133 N90-11934
Adaptive clutter rejection filters for airborne Doppler weather radar applied to the detection of low altitude windshear p 214 N90-14453
Cockpit display of hazardous wind shear information p 484 N90-20924
Meteorologist Weather Processor (MWP) integration test plan [DOT/FAA/CT-TN89/62] p 544 N90-21500

METEOROLOGICAL RESEARCH AIRCRAFT
The Meteorological Measurement System on the NASA ER-2 aircraft p 926 A90-51658
Scientific justification and development plan for a mid-sized jet research aircraft p 103 N90-11731
Meeting review: The Second NCAR (National Center for Atmospheric Research) Research Aircraft Fleet Workshop [PB89-200901] p 137 N90-12113

METEOROLOGICAL SERVICES
Litigation and the National Weather Service [AIAA PAPER 90-0371] p 220 A90-19819
Wind shear at Pantelleria airport p 692 A90-39702
Analysis and synthesis of meteorological support systems for airports p 914 A90-50778
Coordination strategies in a hierarchical air traffic control system with allowance for meteorological conditions p 914 A90-50779
ASR-9 weather channel test report [AD-A211749] p 133 N90-11934
Plan for the FAA air traffic operational evaluation of the Automated Surface Observing System (ASOS) [DOT/FAA/CT-TN89/56] p 489 N90-20968
Meteorologist Weather Processor (MWP) integration test plan [DOT/FAA/CT-TN89/62] p 544 N90-21500
Flight service automation system, model 1 full capacity, NAS operational test and evaluation integration test plan [DOT/FAA/CT-TN90/4] p 825 N90-27672

METEOROLOGY
Scientific justification and development plan for a mid-sized jet research aircraft p 103 N90-11731
Meteorologist Weather Processor (MWP) integration test plan [DOT/FAA/CT-TN89/62] p 544 N90-21500
Windshear case study: Denver, Colorado, July 11, 1988 [DOT/FAA/DS-89/19] p 544 N90-21509

METHANE
High speed commercial transport fuels considerations and research needs [NASA-TM-102535] p 600 N90-21869

METHOD OF MOMENTS
A user's manual for the method of moments Aircraft Modeling Code (AMC) [NASA-CR-186371] p 415 N90-18390

METHODOLOGY
A review of failure models for ceramic matrix composite laminates under monotonic loads [ASME PAPER 89-GT-153] p 354 A90-23842
Tiltrotor aeroservoelastic design methodology at BHTI p 410 A90-28244
Methodology for developing an assessment expert system using a planning paradigm p 460 A90-30757

METHYL ALCOHOL
Straight alcohol fuels for general aviation aircraft [SAE PAPER 891038] p 124 A90-14344
Ethanol and methanol in intermittent combustion engines p 950 A90-51622
Investigations into gasoline/alcohol blends for use in general aviation aircraft p 950 A90-51623
A proposal for fuel specification activities relating to general aviation intermittent combustion engines p 951 A90-51625
Turbine fuel alternatives (near term) [AD-A219405] p 601 N90-22695

METHYL COMPOUNDS
Poly(arylene ether ketone)/poly(aryl imide) homo- and polydimethylsiloxane segmented copolymer blends - Influence of chemical structure on miscibility and physical property behavior p 941 A90-50063

The 1-((diorganoxyphosphonyl)-methyl)-2,4- and -2,6-diamido benzenes [NASA-CASE-ARC-11425-4] p 532 N90-20133
Some 1-((diorganoxyphosphonyl)methyl)-2,4- and -2,6-dinitro-benzenes [NASA-CASE-ARC-11425-3] p 678 N90-23475

METRIC SPACE
Visualization of three dimensional data p 782 N90-25553

MICROBURSTS (METEOROLOGY)
A Monte Carlo simulation technique for low-altitude, wind-shear turbulence [AIAA PAPER 90-0564] p 216 A90-19917
Analysis of aircraft performance during lateral maneuvering for microburst avoidance [AIAA PAPER 90-0568] p 197 A90-19920
Environmental conditions associated with the Dallas microburst storm determined from satellite soundings p 280 A90-22689
Airborne Doppler radar detection of low-altitude wind shear p 252 A90-23284
Multiple vortex ring model of the DFW microburst p 280 A90-23286
Development of an automated windshear detection system using Doppler weather radar p 373 A90-25567
The microphysical structure of severe downdrafts from radar and aircraft observations in CINDE --- Convection Initiation and Downburst Experiment p 455 A90-28582
The source region and evolution of a microburst downdraft p 456 A90-28612
Microburst precursors observed with Doppler radar p 456 A90-28613
Convergence aloft as a precursor to microbursts p 456 A90-28620
Microburst divergence detection for terminal Doppler weather radar p 456 A90-28625
Optimal paths through downbursts p 755 A90-45330
Control of an aircraft in downbursts p 755 A90-45331
A scalar/vector potential solution for aerodynamic coefficients in wind shear p 21 N90-10838
A candidate concept for display of forward-looking wind shear information [NASA-TM-101585] p 187 N90-14232
Analysis of severe atmospheric disturbances from airline flight records p 280 N90-15045
Influence of windshear, downdraft and turbulence on flight safety p 238 N90-15048
Relative merits of reactive and forward-look detection for wind-shear encounters during landing approach for various microburst escape strategies p 259 N90-15108
Synthetic aperture radar imagery of airports and surrounding areas: Archived SAR data [NASA-CR-4275] p 401 N90-18371
Synthetic aperture radar imagery of airports and surrounding areas: Philadelphia Airport [NASA-CR-4280] p 401 N90-18372
Cockpit display of hazardous weather information p 485 N90-20929
Airborne Doppler radar flight experiments for the detection of microbursts p 542 N90-21243
Windshear case study: Denver, Colorado, July 11, 1988 [DOT/FAA/DS-89/19] p 544 N90-21509
Synthetic aperture radar imagery of airports and surrounding areas: Denver Stapleton International Airport [NASA-CR-4305] p 637 N90-24257
A quantitative technique to estimate microburst wind shear hazard to aircraft p 692 N90-25040

MICROCOMPUTERS
A microcomputer-based airspace control simulation and prototype human-machine interface p 461 A90-30800
Desktop failure analysis on a microcomputer using Weibull, lognormal, and renewal data [ASME PAPER 89-GT-275] p 535 A90-32263
Study on process control of aeroengine using microcomputer p 586 A90-37239
A real time microcomputer implementation of sensor failure detection for turbofan engines p 745 A90-45414
Development of a microcomputer based software system for use in crewmember ejection analysis [AD-A220398] p 723 N90-25117

MICROCRACKS
Use of unbalanced laminates as a screening method for microcracking p 948 A90-50217
Mechanical paint removal techniques for aircraft structures [IAR-89-23] p 773 N90-25254

MICROELECTRONICS
Microminiature flight test instrumentation [AIAA PAPER 90-1274] p 504 A90-33898

MICROGRAVITY APPLICATIONS
Parabolic flight experiments on fluid surfaces and wetting p 363 A90-23904

MICROMECHANICS
Application of fracture mechanics to microscale phenomena in electronic assemblies p 684 A90-41334

MICROMINIATURIZATION
Smart microsensors for high temperature applications, phase 1 [AD-A224151] p 959 N90-28828

MICROMOTORS
Effect of the nozzle ring vane height on the efficiency of axial-flow full-admission microturbines p 851 A90-46509

MICROPROCESSORS
A microprocessor-based system for monitoring gas turbines p 350 A90-24359
The evolution of built-in test for an electrical power generating system (EPGS) p 424 A90-30699
The use of non-dedicated redundancy in the AMCAD fault tolerant control system p 461 A90-30793
Rockwell International's miniature high performance GPS receiver p 726 A90-43701
The Mast Mounted Sight 771 processor upgrade program --- for helicopter p 926 A90-51058
Autonomous automatic landing through computer vision p 332 N90-16734
Laboratory implementation of the Continuously Reconfiguring Multi-Microprocessor Flight Control System (CRMFCFS) [AD-A217730] p 520 N90-20094
An experimental study of fault propagation in a jet-engine controller [NASA-CR-181335] p 665 N90-23401
Advanced algorithms design and implementation in on-board microprocessor systems for engine life usage monitoring p 892 N90-27628
Small multipurpose stored data acquisition system [DE90-010823] p 967 N90-30134

MICROSTRIP ANTENNAS
Airborne array antennas for satellite communication p 265 A90-23202
Dual cross-polarization planar arrays in the C and X bands p 638 A90-40979

MICROSTRUCTURE
Safer primers from 3M p 204 A90-17925
Microstructural effects of plastic media blasting on graphite epoxy composites [SAE PAPER 890928] p 286 A90-24693
Microstructures of rapidly-solidified binary TiAl alloys p 532 A90-34990
Influence of microstructure and microdamage processes on fracture at high loading rates [AD-A210307] p 65 N90-10253
The microstructure and properties of aluminum-lithium alloys p 267 N90-15187
Application of high performance metals in gas turbine engines [PNR90640] p 750 N90-25999
Study of the microstructure of a titanium alloy (6246) for turbomachine compressors [ETN-90-97450] p 876 N90-27900
Characterization of the CP 214 T851. Dissection of a cast flat bar for a standard spar [CEAT-PV-M4/462200] p 876 N90-27905
Characterization of the 7175 T7352. Dissection of a die casting standard spar [CEAT-PV-M5/528900] p 877 N90-27906
Characterization of the 7175 T7352 101. Dissection of a die casting standard spar [CEAT-PV-M5/5288] p 877 N90-27907
Characterization of the 7010 T73651. Dissection of a sheet billet for a standard spar [CEAT-PV-M5/521700] p 877 N90-27908

MICROWAVE IMAGERY
Comparison of 1-D and 2-D aircraft images p 927 A90-52884

MICROWAVE LANDING SYSTEMS
Multipath modeling for simulating the performance of the microwave landing system p 241 A90-21384
EUROFAR - European project for a commercial vertical-takeoff aircraft [MBB-UD-553/89] p 221 A90-22696
An operational perspective of potential benefits of microwave landing systems p 242 A90-23242
Design considerations for achieving MLS Category III requirements p 331 A90-25575
Accurate ILS and MLS performance evaluation in presence of site errors p 404 A90-30693
Boeing Condor raises UAV performance levels p 496 A90-34028

Flight safety performance of the microwave landing system p 639 A90-41705

MLS - Keeping pace with the future p 640 A90-41709

MLS - A total system approach p 640 A90-41710

Demonstration of MLS advanced approach techniques p 640 A90-41711

Microwave landing system - A pilot's point of view p 640 A90-41712

Flight safety performance of the Microwave Landing System p 727 A90-45227

Development of obstacle clearance criteria and standards for MLS and MLS/RNAV precision approaches and development of an MLS collision risk model [SAE PAPER 892215] p 728 A90-45432

Simulator evaluation of 'basic' mode back azimuth issues in departure and missed approach usage [SAE PAPER 892216] p 728 A90-45433

Simulation of MLS-ATC procedures in the New York and San Francisco Terminal Control Areas [SAE PAPER 892217] p 728 A90-45434

MLS RNAV accuracy flight tests [SAE PAPER 892218] p 728 A90-45435

Analytical studies for computed center line operations [SAE PAPER 892219] p 729 A90-45436

Computerized MLS flight inspection system developed p 823 A90-48983

ILS/MLS comparison tests at Miami/Tamiami, Florida Airport [ACD-330] p 27 N90-10018

The addition of Bendix MLS (Microwave Landing System) antenna patterns to MLS mathematical model [AD-A210633] p 27 N90-10020

Helicopter Visual Segment Approach Lighting System (HALS) [ACD-330] p 28 N90-10856

An evaluation of the accuracy of a microwave landing system area navigation system at Miami/Tamiami Florida Airport [DOT/FAA/CT-TN89/40] p 640 N90-23377

MLS mathematical model validation study using airborne MLS data from Midway Airport engineering flight tests, August 1988 [DOT/FAA/CT-TN90/2] p 640 N90-23378

Position computation without elevation information for computed centerline operations [DOT/FAA/CT-TN89/42] p 640 N90-23379

MICROWAVE POWER BEAMING

A practical flight path for microwave-powered airplanes p 429 A90-28007

History and status of beamed power technology and applications at 2.45 Gigahertz p 61 N90-10150

MICROWAVE TRANSMISSION

ATC ground communications system optimization techniques p 330 A90-25568

Reduced insertion loss of X-band RF fiber optic links p 695 A90-41240

MIDAIR COLLISIONS

TCAS - A system for preventing midair collisions p 252 A90-21383

Modeling of air-to-air visual acquisition p 282 A90-21385

TCAS - A lengthy but beneficial development effort p 339 A90-25494

Development and operation of the Traffic Alert and Collision Avoidance System (TCAS) p 331 A90-25573

TCAS for commuter aircraft p 487 A90-33348

UK airmisses involving commercial air transport, May-August 1988 [ISSN-0951-6301] p 96 N90-11717

UK airmisses involving commercial air transport [CAA-2/88] p 96 N90-11718

UK airmisses involving commercial air transport, January - April 1989 [ISSN-0951-6301] p 575 N90-22544

UK airmisses involving commercial air transport: May - August 1989 [ISSN-0951-6301] p 913 N90-29335

MIG AIRCRAFT

The analysis of entry into and recovery from a spin for the Ju6 aircraft p 195 A90-16854

Aviation Week editor flies Soviet-based MiG-29 fighter p 334 A90-24964

Pilot report - MiG-29 p 413 A90-29661

Aviation Week editor flies top Soviet interceptor p 920 A90-52574

MILITARY AIR FACILITIES

A comparison of lightning network data with surface weather observations [AD-A220003] p 692 N90-23832

Source emission test of gas turbine engine test facility, Kelly AFB, TX [AD-A223869] p 932 N90-28571

MILITARY AIRCRAFT

Air Force smart structures/skins program overview p 38 A90-11205

Laser communication system design p 26 A90-11813

Acquisition and recording of AMX A/C Aeritalia experience and present trends p 26 A90-12194

Magnetic recording on board aircraft p 39 A90-12195

Airplane design. Part 7 - Determination of stability, control and performance characteristics: Far and military requirements --- Book p 57 A90-12872

The manufacture of SPF military aircraft doors in aluminium alloy --- superplastically formed p 132 A90-16616

Synthetic holography applied to head-up displays p 218 A90-16692

Sharing power and profit p 188 A90-16701

Materials pace aerospace technology p 203 A90-17298

Organic coatings - First line of defense p 204 A90-17300

Stronger starlifter p 143 A90-17919

Stealth - Deception, evasion, and concealment in the air --- Book p 285 A90-24265

Pay-offs and pitfalls of fly-by-wire p 346 A90-24281

Stealth comes of age p 336 A90-27596

Designers as users - Design supports based on crew system design practices p 457 A90-28184

Two-level maintenance concept for advanced avionics architectures p 457 A90-28321

The integrated support station (ISS) - A modular Ada-based test system to support AN/ALE-47 countermeasure dispenser system testing, evaluation, and reprogramming p 457 A90-28323

Sealing the future --- sealants and adhesives for military aircraft p 442 A90-29638

Massively parallel computing p 458 A90-29897

Why birds kill - Cross-sectional analysis of U.S. Air Force bird strike data p 400 A90-30587

A reconfigurable integrated navigation and flight management system for military transport aircraft p 433 A90-30794

Fluorosilicone sealants for aircraft fuel containment p 529 A90-31618

Impact of emerging technologies on future combat aircraft agility [AIAA PAPER 90-1304] p 580 A90-36029

Al-Li alloys and ultrahigh-strength steels for U.S. Navy aircraft p 599 A90-37441

Aluminum alloy 6013 sheet for new U.S. Navy aircraft p 599 A90-37442

Low speed maneuverability and agility design considerations for V/STOL aircraft p 581 A90-38536

Military engines - Cradle of technology p 660 A90-41758

Annual General Meeting of the Canadian Aeronautics and Space Institute, 36th, Ottawa, Canada, May 15, 16, 1989, Proceedings p 701 A90-42652

Supersonic STOVL - The future is now p 732 A90-44781

Overview of military technology at NASA Langley [SAE PAPER 892232] p 733 A90-45448

Propulsion integration for military aircraft [SAE PAPER 892234] p 733 A90-45449

Modelling of fuel effects on naval aircraft operations [SAE PAPER 892331] p 765 A90-45488

The RB211-535E4 - A commercially proven engine for the military of tomorrow [SAE PAPER 892364] p 748 A90-45513

VTOL military research aircraft --- Book p 828 A90-46002

Vertical tail design for base-line configuration of military combat aircraft p 810 A90-48080

Ride quality criteria for the B-2 bomber [AIAA PAPER 90-3256] p 835 A90-48852

The Bell Helicopter AH-1 Cobra - Past, present, and future [AIAA PAPER 90-3271] p 836 A90-48862

Air Force use of civil airworthiness criteria for testing and acceptance of military derivative transport aircraft [AIAA PAPER 90-3289] p 818 A90-48875

Composite flight control actuators p 874 A90-48993

X-29 ECS high-alpha modifications [SAE PAPER 901221] p 840 A90-49295

Evaluation and control of an Integrated Closed Environmental Control System (ICECS) [SAE PAPER 901237] p 841 A90-49307

Gripen wins its wings --- Swedish JAS39 aircraft testing and development p 842 A90-49823

NDI (Nondestructive Inspection) oriented corrosion control for Army aircraft. Phase 1: Inspection methods [AD-A213368] p 176 N90-13359

Design trends for Army/Air Force airplanes in the United States [NASA-TM-4179] p 615 N90-23338

Aircraft drawings index p 618 N90-23340

Model design of military aerospace vehicles [PB90-206301] p 787 N90-27646

MILITARY HELICOPTERS

Target classification by vibration sensing --- for helicopter detection p 1 A90-10170

Fire deaths in aircraft without the crashworthy fuel system p 22 A90-10266

The Battle Captain Expert System - A mission management decision support system for attack helicopter operations [AIAA PAPER 89-3098] p 37 A90-10583

Payoffs in growth engines p 188 A90-16823

Aerospatiale's military helicopter programs p 143 A90-16824

Analysis methods of tie-down loads and airframe stress for shipboard helicopters p 199 A90-16855

Supplemented visual cues for helicopter hovering above a moving ship deck p 195 A90-17704

Development of military helicopters p 181 A90-18488

Equipment procurement - EH101 helicopter p 282 A90-22435

Spray nozzle investigation for the Improved Helicopter Icing Spray System (HISS) [AIAA PAPER 90-0666] p 350 A90-25040

The prediction of the noise generating mechanisms of an Aerospatiale 365N-1 Dauphin helicopter p 463 A90-28161

The effects of aerial combat on helicopter structural integrity p 406 A90-28166

Air-to-Air Combat Test IV (AACT IV) and the AACT data base p 381 A90-28169

Initial results from the joint NASA-Lewis/U.S. Army icing flight research tests p 400 A90-28180

A comprehensive diagnostic system for the T800-APW-800 engine p 422 A90-28181

Damage tolerance analysis and testing of a welded cluster gear for the main transmission of the Advanced Attack Helicopter p 445 A90-28187

Analysis and testing of fiber-reinforced thermoplastic composite vertical stabilizer skins for an advanced attack helicopter p 441 A90-28193

Mission effectiveness testing of an adaptive electronic fuel control on an S-76A p 422 A90-28199

A synergistic approach to logistics planning and engine design p 422 A90-28207

EH101 design and development status p 407 A90-28211

Helicopter design optimization for maneuverability and agility p 408 A90-28212

The four-bladed main rotor system for the AH-1W helicopter p 408 A90-28214

The revolution continuous --- performance of military helicopters [MBB-UD-557-89-PUB] p 381 A90-28242

Real-time test data processing system --- for helicopter flight testing p 458 A90-28860

National Technical Specialists' Meeting on Tactical V/STOL, New Bern, NC, Sept. 19-21, 1989, Proceedings p 551 A90-38526

The Franco-German helicopter programme HAP, PAH-2/HAC p 618 A90-42478

Preliminary flight evaluation of the SA 365 Panther helicopter in air-to-air combat manoeuvres p 647 A90-42494

Helicopter store separation - Predictive techniques and flight testing p 647 A90-42495

EH101 vibration control p 647 A90-42496

Mi-14 - The Soviet Sea King p 730 A90-43765

Escape and survival following helicopter ditching - Training aspects p 722 A90-44658

Handling qualities research at the Flight Research Laboratory, NAE/NRC, 1980 - 1990 and beyond [AIAA PAPER 90-2848] p 755 A90-45176

An investigation of aircraft maneuverability and agility [AIAA PAPER 90-3300] p 868 A90-48882

Near-term applications of knowledge based systems to combat helicopters [AIAA PAPER 90-3301] p 847 A90-48883

Unmanned helicopters for battlefield and maritime surveillance p 920 A90-51899

Applications of flight control system methods to an advanced combat rotorcraft [NASA-TM-101054] p 119 N90-11752

Reduced voltage and restart testing of the 1-watt integral cryogenic cooler (HD-1033B/C/D) [AD-A215133] p 369 N90-16971

The integration of multiple avionic sensors and technologies for future military helicopters p 916 N90-29344

MILITARY OPERATIONS

Applications of neural networks to avionics systems [AIAA PAPER 89-3093] p 76 A90-10627

Flight testing in the Netherlands: An overview p 36 N90-10884

Hover position sensing system p 848 N90-27448

The potential for digital databases in flight planning and flight aiding for combat aircraft p 918 N90-29371

Electro-optics engineering support for the integrated launch and recovery television surveillance system [AD-A232450] p 938 N90-29406

MILITARY TECHNOLOGY

Interactive Videodisc training in aerospace applications [AIAA PAPER 89-3029] p 73 A90-10529

Integration of GPS with the Carrier Aircraft Inertial Navigation System (CAINS) p 97 A90-13990

The Soviets' French revelation. II - Aircraft p 81 A90-14800

Applied technology in gas turbine aircraft engine development p 112 A90-16001

XG40 - Rolls-Royce advanced fighter engine demonstrator p 112 A90-16002

Fighter design from the Soviet perspective [AIAA PAPER 89-2074] p 181 A90-18135

Total quality management and the transitioning company - The perfect fit [AIAA PAPER 89-3211] p 549 A90-31698

Impact of emerging technologies on future combat aircraft agility [AIAA PAPER 90-1304] p 580 A90-36029

Exploration of concepts for multi-role fighters [AIAA PAPER 90-2276] p 644 A90-42104

Next-generation automatic test equipment for military support p 767 A90-42667

Overview of military technology at NASA Langley [SAE PAPER 89-2232] p 733 A90-45448

Power struggle --- Advanced Tactical Fighter engine proposals p 851 A90-46650

Analytic models for technology integration in aircraft design [AIAA PAPER 90-3262] p 835 A90-48857

Encyclopedia of US Air Force aircraft and missile systems. Volume 2: Post-World War 2 bombers, 1945-1973 [AD-A209273] p 1 N90-10001

Post crash flight analysis: Visualizing flight recorder data [AD-A212063] p 96 A90-11715

Special essays for the 40th anniversary of the revolution: The chief designer discusses the F-8 2 and future fighter planes [AD-A221587] p 845 A90-26829

NDI-concept for composites in future military aircraft p 877 A90-28070

MILLIMETER WAVES

Advanced technology MMW seeker testbed, a multi-technology demonstration sensor p 488 A90-34143

MILLING

PMR graphite engine duct development [NASA-CR-182228] p 51 A90-10037

MINERAL OILS

Interchangeability of Soviet-made and foreign mineral oils for aviation gas turbine engines p 873 A90-46525

MINIATURIZATION

Experiments on the unsteady flow in a supersonic compressor stage p 427 A90-18422

Miniaturization of flight deflection measurement system [NASA-CASE-LAR-13628-1] p 689 A90-23707

MINICOMPUTERS

Realtime graphic flight simulations using multiple minicomputers p 351 A90-26203

MINIMA

A computational analysis of the transonic flow field of two-dimensional minimum length nozzles p 173 A90-14194

MINIMUM DRAG

Optimal camber distributions with multiple constraints p 810 A90-48078

Constrained spanload optimization for minimum drag of multi-lifting-surface configurations p 501 A90-20992

MINIMUM ENTROPY METHOD

An entropy method for induced drag minimization [SAE PAPER 89-2344] p 715 A90-45496

MINOR CIRCLE TURNING FLIGHT

Hypervelocity, minimum-radii, coordinated turns p 667 A90-40691

MIRAGE AIRCRAFT

Mirage 2000 - A French success that is no illusion p 731 A90-43768

MIRAGE 3 AIRCRAFT

The SEPR 844 reusable liquid rocket engine for Mirage combat aircraft [AIAA PAPER 90-1835] p 655 A90-40526

MISS DISTANCE

Dallas/Forth Worth simulation. Phase 2: Triple simultaneous parallel Instrument Landing System (ILS) approaches (turbojets) [DOT/FAA/CT-90/2] p 915 A90-28509

MISSILE CONFIGURATIONS

Aerodynamic spike flowfields computed to select optimum configuration at Mach 2.5 with experimental validation [AIAA PAPER 90-0414] p 166 A90-19837

Dynamic derivatives of missiles and fighter-type configurations at high angles of attack p 337 A90-17554

External flow computations for a finned 60mm ramjet in steady supersonic flight [AD-A216998] p 428 A90-19233

MISSILE CONTROL

Experimental investigation of a new device to control the asymmetric flowfield on forebodies at large angles of attack [AIAA PAPER 90-0069] p 161 A90-19665

The implications of using integrated software support environment for design of guidance and control systems software [AGARD-AR-229] p 434 A90-18432

MISSILE STRUCTURES

Resin transfer molding of composite structures p 270 A90-20264

Automated R.T.M. for an airframe component --- Resin Transfer Molding p 534 A90-31881

MISSILE SYSTEMS

Encyclopedia of US Air Force aircraft and missile systems. Volume 2: Post-World War 2 bombers, 1945-1973 [AD-A209273] p 1 N90-10001

MISSILE TESTS

Combining thermal and high level acoustics p 770 A90-43729

MISSILE TRACKING

The small portable Global Positioning System tracking range of the future p 60 A90-12209

MISSILES

Encyclopedia of US Air Force aircraft and missile systems. Volume 2: Post-World War 2 bombers, 1945-1973 [AD-A209273] p 1 N90-10001

Dynamic derivatives of missiles and fighter-type configurations at high angles of attack p 337 A90-17554

Model designation of military aerospace vehicles [PB90-206301] p 787 A90-27646

MISSION PLANNING

Reflexive navigation for autonomous aircraft [AIAA PAPER 89-2991] p 25 A90-10502

Data base correlation issues p 459 A90-30740

Mirach 100 flight control system p 260 A90-15926

Distribution of hardware and software elements in unmanned air vehicle systems p 251 A90-15933

Life cycle cost in the conceptual design of subsonic commercial aircraft, volumes 1 and 2 p 923 A90-28535

The DELTA MONSTER: An RPV designed to investigate the aerodynamics of a delta wing platform [NASA-CR-186226] p 924 A90-29381

Aircraft design for mission performance using nonlinear multiobjective optimization methods [NASA-CR-4328] p 925 A90-29384

MIXERS

Navier-Stokes analysis of a lobed mixer and nozzle [AIAA PAPER 90-0453] p 192 A90-19852

Isothermal velocity and turbulence measurements downstream of a model multilobed turbofan mixer p 365 A90-24353

Navier-Stokes analysis of an ejector and mixer-ejector operating at pressure ratios in the range 2-4 [AIAA PAPER 90-2730] p 626 A90-42218

Investigation of advanced mixer-ejector exhaust system [AD-A211943] p 89 A90-11705

Energy Efficient Engine exhaust mixer model technology report addendum; phase 3 test program [NASA-CR-174799] p 930 A90-28556

MIXING

A method for aerodynamic design calculation of axial gas turbine stages with cooling air mixing p 152 A90-17781

An aerodynamical design and calculation method for gas turbine with cooling air mixing p 189 A90-17782

Throughflow numerical calculations including influence of spanwise mixing in a multistage axial flow compressor p 157 A90-18534

Effect of vane twist on the performance of dome swirlers for gas turbine airblast atomizers [AIAA PAPER 90-1955] p 881 A90-47203

Secondary flows and radial mixing predictions in axial compressors p 512 A90-21010

A study on secondary flow and spanwise mixing in axial flow compressors p 512 A90-21012

Control of flow separation and mixing by aerodynamic excitation [NASA-TM-103131] p 571 A90-21733

Effect of vane twist on the performance of dome swirlers for gas turbine airblast atomizers [NASA-TM-103195] p 773 A90-25289

MIXING LAYERS (FLUIDS)

A numerical study of mixing and chemical heat release in supersonic mixing layers [AIAA PAPER 90-0152] p 163 A90-19710

Nonlinear stability of subsonic mixing layers with symmetric temperature variations p 223 A90-20501

Instabilities of supersonic shear flows [AIAA PAPER 90-0712] p 314 A90-26983

A numerical study of transverse jets into supersonic flows and influence of pressure waves [AIAA PAPER 90-0733] p 314 A90-26985

A laser fluorescence anemometer for water tunnel flowfield studies p 447 A90-28279

The effect of walls on a spatially growing supersonic shear layer p 393 A90-29591

Design considerations for a compact table top hypersonic simulator of aero-optic effects p 525 A90-34585

Table top experimental simulation of hypersonic aero-optic effects --- encountered by cooled window on interceptor p 525 A90-34586

Effects of streamwise vorticity injection on turbulent mixing layer development [AIAA PAPER 90-1459] p 561 A90-38616

Interaction of a plane shear layer with a downstream flat plate [AIAA PAPER 90-1460] p 561 A90-38617

Numerical simulation of confined, spatially-developing mixing layers - Comparison to the temporal shear layer [AIAA PAPER 90-1462] p 562 A90-38619

Study of compressibility effects in mixing layer by numerical simulation [AIAA PAPER 90-1464] p 562 A90-38621

The lateral spreading of finite-span instability waves in a laminar mixing layer [AIAA PAPER 90-1532] p 606 A90-38677

Investigation of supersonic mixing layers p 623 A90-40926

On the instabilities of supersonic mixing layers - A high-Mach-number asymptotic theory p 702 A90-42644

Two- and three-dimensional effects in the supersonic mixing layer [AIAA PAPER 90-1978] p 703 A90-42708

A planar reacting shear layer system for the study of fluid dynamics-combustion interaction [NASA-TM-102422] p 194 A90-13393

Supersonic combustor modeling p 749 A90-25992

Modeling of supersonic reacting flow fields p 855 A90-26898

MIXING LENGTH FLOW THEORY

CFD predictions of lobed mixer flowfields p 70 A90-12626

Non-iterative analytical methods for off-design turbofan calculations with or without mixed-flows p 70 A90-12628

A circular combustor configuration with multiple injection ports for mixing enhancement p 130 A90-15389

Navier-Stokes analysis of airfoils with leading edge ice accretions p 174 A90-14196

MIXTURES

WINCOF-I code for prediction of fan compressor unit with water ingestion [NASA-CR-185157] p 551 A90-21724

MOBILE COMMUNICATION SYSTEMS

CRL's mobile satellite communication experiments using ETS-V [AIAA PAPER 90-0775] p 366 A90-25802

Institutional stepping stones for FANS --- Future Air Navigation Systems p 403 A90-27923

Mobile satellite communications for civil aviation [NLR-MP-88066-U] p 775 A90-26238

MODAL RESPONSE

Interior noise control of the Saab 340 aircraft [SAE PAPER 891080] p 101 A90-14372

Modal characteristics of swept plate flutter models p 207 A90-16962

Practical suggestions for modifying math models to correlate with actual modal test results p 207 A90-16979

A component modal synthesis technique for the lateral vibration analysis of aircraft engine systems p 179 A90-16983

Comparison of the analytical and experimental modes of a model airplane using finite element analysis and multi-reference testing p 207 A90-16986

MAVIS flight load simulation --- Multi Axis Vibration System p 202 A90-17003

Flutter analysis on a non-linear wing model p 207 A90-17009

Modal aggregation and its application in flight mechanics p 196 A90-18595

- Design of a helicopter output feedback control law using modal and structured-robustness techniques p 282 A90-20557
- Linear control issues in the higher harmonic control of helicopter vibrations p 430 A90-28225
- Periodic response of thin-walled composite blades p 408 A90-28229
- A modal parameter identification technique and its application to large complex structures with multiple steady sinusoidal excitation p 602 A90-35670
- A study of the influence of predeformations on the vibrations of blades p 585 A90-35673
- A comprehensive approach to coupled rotor-fuselage dynamics p 646 A90-42460
- Comparison among modal analyses of axial compressor blade using experimental data of different measuring systems p 878 A90-46038
- Application to a helicopter of a general method for modifying a finite-element model to correlate with modal test data p 832 A90-46968
- Structural mode significance using INCA --- Interactive Controls Analysis computer program [AIAA PAPER 90-3346] p 889 A90-47606
- The receptivity of laminar boundary layer flow to leading edge vibrations p 815 A90-49800
- MODEL REFERENCE ADAPTIVE CONTROL**
- Adaptive autopilot design via model expansion method p 55 A90-11124
- Identification of mathematical derivative models for the design of a model following control system --- for fly-by-wire helicopter p 56 A90-12764
- Concise design of aircraft longitudinal model reference adaptive command augmentation system p 345 A90-24002
- Restructurable control using proportional-integral implicit model following --- for fighter aircraft [AD-A220997] p 347 A90-25990
- Reconfigurable flight controller for the STOL F-15 with sensor/actuator failures p 432 A90-30707
- Multiple model adaptive controller for the STOL F-15 with sensor/actuator failures p 668 A90-40878
- A self-compensating aircraft recovery system (SCARS) [AIAA PAPER 90-3273] p 818 A90-48864
- Direct multivariable adaptive controller with application to wing flutter p 349 A90-17642
- Rule-based mechanisms of learning for intelligent adaptive flight control p 521 A90-20939
- MODELS**
- Noninteractive macroscopic reliability model for ceramic matrix composites with orthotropic material symmetry [ASME PAPER 89-GT-129] p 360 A90-23827
- Acoustic test and analysis of a counterrotating prop-fan model [NASA-CR-179590] p 79 A90-10683
- An open-loop transient thermodynamic model of the Cougar turbojet p 114 A90-11745
- Development of a VSAERO (Vortex Separation Aerodynamics) model of the F/A-18 [AD-A212442] p 95 A90-12566
- Studies of gas turbine heat transfer airfoil surfaces and end-wall cooling effects [AD-A212451] p 117 A90-12620
- The comparison of the airbase simulation models airbase and sustained [FEL-1988-66] p 123 A90-12629
- Aeroelastic simulation of higher harmonic control p 592 A90-21768
- An experimental study of tip shape effects on the flutter of aft-swept, flat-plate wings [NASA-TM-4180] p 582 A90-22555
- An experimental investigation of support strut interference on a three-percent fighter model at high angles of attack [AD-A219793] p 631 A90-23353
- New transonic test sections for the NAE 5 ft x 5 ft trisonic wind tunnel [AD-A220933] p 674 A90-24278
- Unique failure behavior of metal/composite aircraft structural components under crash type loads [NASA-TM-102679] p 690 A90-24660
- Behavior of composite/metal aircraft structural elements and components under crash type loads: What are they telling us [NASA-TM-102681] p 774 A90-25368
- Space plane model for visual measurement of aerodynamic heating [DE90-505514] p 720 A90-25949
- H-infinity based integrated flight-propulsion control design for a STOVL aircraft in transition flight [NASA-TM-103198] p 758 A90-26011
- MODULES**
- Apparatus for cooling electronic components in aircraft [AD-D014207] p 183 A90-13373
- MODULUS OF ELASTICITY**
- Aerospace Arall - The advancement in aircraft materials p 947 A90-50186
- A study of filament wound high modulus carbon fiber reinforced cylinders p 948 A90-50218
- Calculation of thick wall fiber binders for rotor components of modern helicopters [MBS-UD-554/84-PUB] p 735 A90-25137
- MOIRE EFFECTS**
- Model attitude measurement system p 539 A90-34235
- MOISTURE CONTENT**
- Liquid water content and droplet size calibration of the NASA Lewis Icing Research Tunnel [AIAA PAPER 90-0669] p 261 A90-22242
- An automated method for predicting the height of the lower cloud boundary p 888 A90-48359
- Liquid water content and droplet size calibration of the NASA Lewis Icing Research Tunnel [NASA-TM-102447] p 213 A90-13797
- The signals of an ice warning device in dependence on total water content and normalized icing degree [ESA-TT-1207] p 963 A90-29692
- MOISTURE RESISTANCE**
- Moisture absorption in graphite/epoxy laminates p 951 A90-52799
- MOLDING MATERIALS**
- Resin transfer molding of composite aircraft structures [SAE PAPER 891042] p 128 A90-14347
- A high performance aerospace resin for Resin Transfer Molding p 945 A90-50163
- MOLDS**
- Automated R.T.M. for an airframe component --- Resin Transfer Molding p 534 A90-31881
- MOLECULAR BEAM EPITAXY**
- The gas source molecular beam epitaxial growth of Al(x)Ga(1-x)P on (100) GaP p 894 A90-48657
- MOLECULAR FLOW**
- Hypersonic rarefied flow and its solution over the stagnation region [AIAA PAPER 90-0420] p 166 A90-19842
- MOLECULAR OSCILLATIONS**
- Chemical and vibrational non-equilibrium nozzle flow calculation by an implicit upwind method [ONERA, TP NO. 1989-175] p 223 A90-21037
- A study of flow of a vibrationally nonequilibrium dissociated gas past a blunt body p 234 A90-23435
- MOLECULAR STRUCTURE**
- Fuel molecular structure and flame temperature effects on soot formation in gas turbine combustors [ASME PAPER 89-GT-288] p 253 A90-22652
- The prediction of middle distillate fuel properties using liquid chromatography-proton nuclear magnetic resonance spectroscopy data [AD-A211879] p 126 A90-11899
- Advanced fuel properties, phase 1 [AD-A219788] p 766 A90-25236
- MOLECULAR WEIGHT**
- Characterization of LaRC-TPI 1500 powders - A new version with controlled molecular weight p 946 A90-50177
- Effect of molecular weight and end group control on the adhesion behavior of thermoplastic polyimides and poly(imide siloxane) segmented copolymers p 947 A90-50199
- MOLTEN SALTS**
- Molten salt induced high temperature degradation of thermal barrier coatings p 952 A90-28704
- Overview on hot gas tests and molten salt corrosion experiments at the DLR p 953 A90-28714
- MOMENT DISTRIBUTION**
- The influence of control-surface compensation parameters on the hinge moment characteristics p 643 A90-41737
- Vortical sources of aerodynamic force and moment [SAE PAPER 892346] p 715 A90-45498
- Force and moment measurements on delta wings in unsteady flow p 278 A90-16185
- A flight dynamic model of aircraft spinning [AR-005-600] p 935 A90-28576
- MOMENTS**
- An integrated CFD/experimental analysis of aerodynamic forces and moments [NASA-TM-102195] p 18 A90-10006
- Study of forces and moments on wing-bodies at high incidence, volumes 1 and 2 p 171 A90-13350
- Hinge moment coefficient derivatives for trailing-edge controls on wings at subsonic speeds [ESDU-89009] p 198 A90-14239
- Example of procedure in calculation of control hinge moments [ESDU-89010] p 199 A90-14240
- In-plane forces and moments on installed inclined propellers at low forward speeds [ESDU-89047] p 316 A90-16720
- MOMENTUM TRANSFER**
- The numerical simulation of multistage turbomachinery flows p 514 A90-21025
- MONITORS**
- A microprocessor-based system for monitoring gas turbines p 350 A90-24359
- An appraisal of a number of power assessment procedures being proposed for use in Chinook-Lycoming T55 engine [AD-A210482] p 52 A90-10041
- Display interface concepts for automated fault diagnosis [NASA-TM-101610] p 252 A90-15102
- In-line wear monitor [AD-A217799] p 510 A90-20091
- Airplane takeoff and landing performance monitoring system [NASA-CASE-LAR-13734-1-CU] p 526 A90-20096
- Independent ground monitor coverage of Global Positioning System (GPS) satellites for use by civil aviation p 918 A90-29364
- MONOPULSE RADAR**
- Evaluating the feasibility of a radar separation minimum for a long-range SSR p 25 A90-10240
- MONTE CARLO METHOD**
- Grid generation and adaptation for the direct simulation Monte Carlo method p 67 A90-11102
- An analysis of reliability in fiber optic ring and star networks p 78 A90-11666
- Direct simulation of three-dimensional hypersonic flow about intersecting blunt wedges p 16 A90-12835
- A Monte Carlo simulation technique for low-altitude, wind-shear turbulence [AIAA PAPER 90-0564] p 216 A90-19917
- Testing of statistical hypotheses and derivation of confidence intervals from inspection data samples p 363 A90-24087
- Hypersonic flow calculations with a hybrid Navier-Stokes/Monte Carlo method [AIAA PAPER 90-1691] p 560 A90-38394
- Direct simulation of low-density flow over airfoils [AIAA PAPER 90-1539] p 564 A90-38683
- An autopilot design methodology for bank-to-turn missiles [AD-A213379] p 198 A90-13399
- A conflict analysis of 4D descent strategies in a metered, multiple-arrival route environment [NASA-CR-182019] p 593 A90-21772
- Low-density flow effects for hypervelocity vehicles, phase 2 [AD-A221034] p 634 A90-24249
- MOORING**
- Prediction of aerostat and airship mooring mast loads by nonlinear dynamic simulation [AIAA PAPER 89-3172] p 245 A90-20587
- MORALE**
- Aviation safety: Conditions within the air traffic control work force. Fact sheet for congressional requesters [GAO/RCED-89-113FS] p 724 A90-25958
- MORPHOLOGY**
- Fatigue crack initiation and small crack growth in several airframe alloys [NASA-TM-102598] p 454 A90-18746
- MOTION SIMULATION**
- Augmenting flight simulator motion response to turbulence p 440 A90-31279
- Development and verification of an algorithm for helicopter inverse simulations p 591 A90-38522
- MOTION SIMULATORS**
- Simulator motion-drive algorithms - A designer's perspective p 375 A90-25997
- User's manual for the ride motion simulator [AD-A212855] p 201 A90-13402
- MOTION STABILITY**
- A unified approach to the overall body motion stability and flutter characteristics of elastic aircraft p 346 A90-25102
- MOTOR VEHICLES**
- Flammability regulations affecting advanced composite materials p 947 A90-50190
- MOUNTAINS**
- Colorado mountain flying - Crashes and weather [AIAA PAPER 90-0369] p 175 A90-19818
- Ice runways near the South Pole [AD-A211606] p 133 A90-11908
- MOVING TARGET INDICATORS**
- Advances in primary-radar technology p 241 A90-21380
- Concept of an MTI search radar p 487 A90-33613
- Shadow-tracking algorithm for moving target detection p 488 A90-34137
- Doppler-rate filtering for detecting moving targets with synthetic aperture radars p 488 A90-34138
- The TVD 900 - A modern signal processing applied to primary civilian ATC radar p 638 A90-41034

MRCA AIRCRAFT

- Advanced developments of the Turbo-Union RB199 p 745 A90-44595
Fighter escape system: The next step forward p 483 N90-20059

MTBF

- The two level maintenance - I level dilemma p 381 A90-28319
Electrical power systems for high Mach vehicles p 586 A90-38129
Power system for 21st century fighter aircraft [SAE PAPER 892253] p 746 A90-45455

MUFFLERS

- Optimization of the sound-absorption lining parameters of an ejector jet muffler p 378 A90-24117

MULTIENGINE VEHICLES

- Flight over the sea with twin or triple jet aircraft p 179 A90-17048

MULTIGRID METHODS

- Calculation of transonic flows for novel engine-airframe installations p 145 A90-16768
Calculation of two-dimensional transonic flow of Euler equations with multigrid method p 149 A90-16835
Multigrid solution method for the Euler equations --- Book p 149 A90-16841
Block multigrid implicit solution of the Euler equations of compressible fluid flow [AIAA PAPER 90-0106] p 162 A90-19684
Viscous supersonic flow computations over a delta-rectangular wing with slanting surfaces [AIAA PAPER 90-0419] p 166 A90-19841
Inviscid cascade flow calculations using a multigrid method [ASME PAPER 89-GT-22] p 288 A90-23763
Application of Fedorenko's multigrid method for calculating transonic flow past a profile p 295 A90-24103

- Impact of multigrid smoothing analysis on three-dimensional potential flow calculations p 449 A90-29147

- Automated generation of two-dimensional non-overlapping structured grids for multiple element airfoils with Euler solutions p 629 A90-42422
Solution of the Euler equations using unstructured polygonal meshes p 708 A90-44435
Validation of propeller slipstream calculations using a multi-block Euler code [AIAA PAPER 90-3035] p 791 A90-45874

- Adaptive grid embedding for the two-dimensional Euler equations [AIAA PAPER 90-3049] p 797 A90-45929
Solutions of two-dimensional Euler equations with multigrid acceleration p 810 A90-48086
Numerical simulation of three-dimensional transonic flows p 905 A90-51020

- Multigrid methods in computational fluid dynamics p 906 A90-51526
Multigrid scheme for the compressible Euler-equations p 907 A90-51559
Multigrid acceleration of TVD schemes in transonic Euler flow calculation p 908 A90-52030

MULTIPATH TRANSMISSION

- Multipath modeling for simulating the performance of the microwave landing system p 241 A90-21384
Range determination in a multipath prone environment p 877 A90-45960

MULTIPHASE FLOW

- Review of mixed flow and radial turbine options [AIAA PAPER 90-2414] p 687 A90-42166

MULTIPLE ACCESS

- Multiple channel frequency demodulator p 69 A90-12190

MULTIPLEXING

- Automatic speech recognition in air-ground data link p 690 N90-25037

MULTIPROCESSING (COMPUTERS)

- Multi-processing on supercomputers for computational aerodynamics [AIAA PAPER 90-0337] p 282 A90-22199
A multiprocessor implementation of real-time control for a turbojet engine p 746 A90-45415
Laboratory implementation of the Continuously Reconfiguring Multi-Microprocessor Flight Control System (CRMFCFS) [AD-A217730] p 520 N90-20094

MULTISENSOR APPLICATIONS

- Development of two multi-sensor hot-film measuring techniques for free-flight experiments p 417 A90-28291
A Distributed Artificial Intelligence approach to object identification and classification p 545 A90-34185
Multisensor Integrated Navigation System p 577 A90-36924
Performance assessment for airborne surveillance systems incorporating sensor fusion p 583 A90-37088

- A multi-sensor approach to assuring GPS integrity p 821 A90-46396

MULTISPECTRAL BAND SCANNERS

- Airborne MSS for land cover classification II p 737 A90-43376
Description of the MARC measuring system [FEL-89-B170] p 963 N90-28887

MULTISPECTRAL RADAR

- Enhanced environmental control for the Harrier II Plus [SAE PAPER 901238] p 841 A90-49308

MULTISTAGE ROCKET VEHICLES

- Hypersonic (T-D) 'pinch' and aerospaceplane propulsion [AIAA PAPER 90-2474] p 675 A90-42189

MULTISTATIC RADAR

- Simulation of airborne target imagery - Dependence on frequency and bistatic angle p 488 A90-34146

MULTIVARIATE STATISTICAL ANALYSIS

- Multivariable control of jet engines p 507 A90-32421
Investigation of variation in fatigue life calculated using damage fraction p 537 A90-33624
Applications of modern control theory synthesis to a super-augmented aircraft [AD-A215431] p 336 N90-16753
Discrete proportional Plus Integral (PI) multivariable control laws for the Control Reconfigurable Combat Aircraft (CRCA) [AD-A215664] p 433 N90-18431
Practical methods for robust multivariable control [AD-A216937] p 462 N90-18920

MUSCULAR STRENGTH

- Modeling strength data for CREW CHIEF p 780 N90-25516

N

NACELLES

- Calculation of transonic flows for novel engine-airframe installations p 145 A90-16768
Aerodynamic interference of prismatic engine nacelles with the wing at supersonic velocities p 294 A90-24078
Calculation of transonic axisymmetric flow past an engine nacelle with allowance for viscosity p 296 A90-24107

- Calculation of the effect of the engine nacelle on transonic flow past a wing p 387 A90-28990
Calculation of the drag of fuselage tail sections of different shapes in supersonic flow of a nonviscous gas p 388 A90-29182

- Unsteady lift and moment coefficients of an engine nacelle p 473 A90-33365
An efficient finite-difference algorithm for computing axisymmetric transonic nacelle flow fields p 557 A90-37205

- A grid generation method for an aft-fuselage mounted capped-nacelle/pylon configuration with an actuator disk [AIAA PAPER 90-1564] p 565 A90-38703
Mi-14 - The Soviet Sea King p 730 A90-43765
3D transonic nacelle and winglet design [AIAA PAPER 90-3064] p 794 A90-45897

- Status report on a natural laminar-flow nacelle flight experiment p 105 N90-12550
Nacelle design p 105 N90-12551
Nacelle aerodynamic performance p 105 N90-12552

- Effects of acoustic sources p 140 N90-12553
A note on an acoustic response during an engine nacelle flight experiment [NASA-TM-102585] p 464 N90-19821

- Measurement and prediction of propeller blade surface pressure distributions p 481 N90-20961
Aerodynamic design techniques at DLR Institute for Design Aerodynamics p 500 N90-20979

- Interactive calculation procedures for mixed compression inlets [NASA-CR-186581] p 718 N90-25934
Energy Efficient Engine program advanced turbofan nacelle definition study [NASA-CR-174942] p 930 N90-28560

MAP-OF-THE-EARTH NAVIGATION

- Helicopter flight control system design and evaluation for NOE operations using controller inversion techniques p 429 A90-28202
Fully automatic guidance for rotorcraft nap-of-the-earth (NOE) flight following planned profiles p 403 A90-28219

- Development of an acceptability window for a ground proximity avoidance system p 419 A90-30730
Development and verification of an algorithm for helicopter inverse simulations p 591 A90-38522

- Concept development of automatic guidance for rotorcraft obstacle avoidance p 669 A90-41632

- Helmet-mounted display systems for flight simulation [SAE PAPER 892352] p 760 A90-45503
Real-time piloted simulation of fully automatic guidance and control for rotorcraft nap-of-the-earth (NOE) flight following planned profiles [AIAA PAPER 90-3372] p 864 A90-47630

- Rotorcraft pursuit-evasion in nap-of-the-earth flight [AIAA PAPER 90-3455] p 786 A90-47707
Survivable penetration p 917 N90-29363

NAPHTHALENE

- Production of jet fuels from coal-derived liquids. Volume 11: Production of advanced endothermic fuel blends from Great Plains Gasification Plant naphtha by-product stream [AD-A210251] p 65 N90-11184

NASA PROGRAMS

- A review and update of the NASA aircraft noise prediction program propeller analysis system [SAE PAPER 891032] p 139 A90-14340
In-flight flow field analysis on the NASA F-18 high alpha research vehicle with comparisons to ground facility data [AIAA PAPER 90-0231] p 163 A90-19745

- Comparison of model- and full-scale wind-tunnel performance [AIAA PAPER 88-2536] p 351 A90-26133
Development of pressure containment and damage tolerance technology for composite fuselage structures in large transport aircraft [NASA-CR-3996] p 63 N90-10186

- The NASA experience in aeronautical R and D: Three case studies with analysis [AD-A211486] p 82 N90-12496
Review of the Aerospace Safety Advisory Panel report for NASA fiscal year 1990 authorization [GPO-24-234] p 177 N90-14213

- FAA/NASA En Route Noise Symposium [NASA-CP-3087] p 696 N90-24853
En route noise: NASA propfan test aircraft (corrected data - simplified procedure) p 696 N90-24856

- En route noise: NASA propfan test aircraft (calculated source noise) [DOT-TSC-FA953-LR5] p 697 N90-24857

- Resources - Supply and availability --- of superalloys for United States aerospace industry p 531 A90-34152

NASA SPACE PROGRAMS

- Sensitivity and optimization of composite structures in MSC/NASTRAN p 208 A90-17370
Application of an efficient hybrid scheme for aeroelastic analysis of advanced propellers [AIAA PAPER 90-0028] p 226 A90-22153

- Structural and aerodynamic analysis of a large scale advanced propeller blade [AIAA PAPER 90-2401] p 743 A90-42793
Finite element analysis of the Twelve Foot Pressurized Wind Tunnel p 760 A90-45296

- An improved rotor/airframe coupling method for NASTRAN airframe vibration analysis p 831 A90-46962
Experiences in NASTRAN airframe vibration prediction at Bell Helicopter Textron p 832 A90-46964

- Application to a helicopter of a general method for modifying a finite-element model to correlate with modal test data p 832 A90-46968
V-22 MSC/NASTRAN airframe vibration analysis and correlation p 832 A90-46969

- Investigation of difficult component effects on finite element model vibration prediction for the Bell AH-1G helicopter. Volume 1: Ground vibration test results [NASA-CR-181916-VOL-1] p 134 N90-12058

- Application of an efficient hybrid scheme for aeroelastic analysis of advanced propellers [NASA-TM-102428] p 172 N90-13355
Investigation of difficult component effects on finite element model vibration prediction for the Bell AG-1G helicopter. Volume 2: Correlation results [NASA-CR-181916-VOL-2] p 213 N90-13814

- An iterative solution to aeroelastic effects in potential flow [AD-A216291] p 320 N90-17580
Static aeroelastic analysis of a three-dimensional generic wing [NASA-TM-102231] p 509 N90-20087

- Plan, formulate, and discuss a NASTRAN finite element model of the UH-60A helicopter airframe [NASA-CR-181975] p 541 N90-20439
Subsonic flutter analysis using MSC/NASTRAN [PB90-166786] p 522 N90-21041

- Ground shake test of the UH-60A helicopter airframe and comparison with NASTRAN finite element model predictions [NASA-CR-181993] p 758 N90-25143

Plan, execute, and discuss vibration measurements and correlations to evaluate a NASTRAN finite element model of the AH-64 helicopter airframe
[NASA-CR-181973] p 960 N90-28866

NATIONAL AEROSPACE PLANE PROGRAM

Rockwell's simulator emulates NASP flight characteristics p 60 A90-11650

Advanced materials to fly high in NASP p 203 A90-17297

Aerodynamic control of NASP-type vehicles through vortex manipulation
[AIAA PAPER 90-0594] p 203 A90-19938

Many means to NASP p 285 A90-23917

Pressure and heat-transfer investigation of a hypersonic configuration p 598 A90-35757

CFD propels NASP propulsion progress p 683 A90-41163

Hypersonic CFD applications for the National Aero-Space Plane
[SAE PAPER 892310] p 714 A90-45473

Low-speed aerodynamic characteristics of a powered NASP-like configuration in ground effect
[SAE PAPER 892312] p 714 A90-45474

Active control of aerothermoelastic effects for a conceptual hypersonic aircraft
[AIAA PAPER 90-3337] p 863 A90-47597

CFD support of NASP design
[AIAA PAPER 90-3252] p 872 A90-49120

Design and demonstration of heat pipe cooling for NASP and evaluation of heating methods at high heating rates
[DE89-016995] p 186 N90-14227

Slush Hydrogen (SLH2) technology development for application to the National Aerospace Plane (NASP)
[NASA-TM-102315] p 203 N90-14268

National aero-spaceplane status and plans p 337 N90-16801

Effects of nose bluntness and shock-shock interactions on blunt bodies in viscous hypersonic flows
[NASA-CR-186451] p 479 N90-20950

Background, current status, and prognosis of the ongoing slush hydrogen technology development program for the NASP
[NASA-TM-103220] p 763 N90-26055

Carbon-carbon composites: Emerging materials for hypersonic flight
[NASA-TM-103472] p 767 N90-26080

NASA Langley Research Center National Aero-Space Plane Mission simulation profile sets
[NASA-TM-102670] p 924 N90-28541

NATIONAL AIRSPACE SYSTEM

Air-ground information transfer in the National Airspace System p 380 A90-26235

Ground and Obstacle Avoidance (GOA) concept of operations
[DOT/FAA/DS-89/08] p 28 N90-10855

UK airmisses involving commercial air transport, May-August 1988
[ISSN-0951-6301] p 96 N90-11717

Rotorcraft low altitude CNS benefit/cost analysis: Rotorcraft operations data
[DOT/FAA/DS-89/9] p 141 N90-12406

National Airspace System airspace management operational concept
[DOT/FAA/DS-89/29] p 177 N90-13361

National Airspace System flight planning operational concept
[DOT/FAA/DS-89/30] p 177 N90-13362

National airspace system monitoring operational concept
[NAS-RR-1330] p 178 N90-14214

National airspace system: Airport movement area control operational concept
[WP-89W00181] p 243 N90-15086

Control outside of independent surveillance coverage operational concept
[AD-A214163] p 243 N90-15090

National airspace system plan: Facilities, equipment, associated development and other capital needs
[AD-A215882] p 402 N90-18373

Weather data dissemination to aircraft p 486 N90-20934

National airspace system air-ground communications operational concept
[DOT/FAA/DS-90/2] p 542 N90-21249

Meteorologist Weather Processor (MWP) integration test plan
[DOT/FAA/CT-TN89/62] p 544 N90-21500

National Airspace System (NAS) software life cycle management study
[AD-A221180] p 729 N90-25122

Replication of NASPAC Dallas/Fort Worth study
[DOT/FAA/CT-TN90/26] p 729 N90-25123

Flight service automation system, model 1 full capacity, NAS operational test and evaluation integration test plan
[DOT/FAA/CT-TN90/4] p 825 N90-27672

A glossary of terms, definitions, acronyms, and abbreviations related to the National Airspace System
[DOT/FAA/CT-TN89/53] p 967 N90-29249

NATIONAL AIRSPACE UTILIZATION SYSTEM

Operational trial of effect of raising minimum stack level in Heathrow stacks
[CAA-PAPER-89003] p 99 N90-12573

NATURAL GAS

Experimental turbofan using liquid hydrogen and liquid natural gas as fuel
[AIAA PAPER 90-2421] p 663 A90-42170

NAVIER-STOKES EQUATION

Grid generation and adaptation for the direct simulation Monte Carlo method p 67 A90-11102

Turbulent mixing in helicopter jet diluters - Navier-Stokes calculations and correlations
[AAAF PAPER NT 88-13] p 40 A90-11432

Navier-Stokes methods applied to turbomachinery blade design p 12 A90-12549

Computation of transonic turbine cascade flow using Navier-Stokes equations p 14 A90-12621

Navier-Stokes computations of a prolate spheroid at angle of attack p 17 A90-13018

Recent Navier/Stokes calculations in applications p 85 A90-15227

Numerical solution of unsteady Navier-Stokes equations for laminar/turbulent flows past axis-symmetric bodies at angle of attack p 85 A90-15235

Numerical simulation of supersonic and hypersonic turbulent compression corner flows using PNS equations p 85 A90-15242

Convergence properties of high-Reynolds-number separated flow calculations p 86 A90-15820

Computation of the thin-layer Navier-Stokes equations for a 2D flow p 87 A90-16332

Experiments are telling you something (Stewartson Memorial Lecture) --- about aerodynamic flows p 144 A90-16752

Interaction between strong longitudinal vortices and turbulent boundary layers p 145 A90-16764

Verification of a Navier-Stokes code for solving the hypersonic blunt body problem p 146 A90-16774

Analysis of high-incidence separated flow past airfoils p 147 A90-16781

Multigrid acceleration of transonic flow computations p 147 A90-16783

Navier-Stokes computations of lee-side flows over delta wings p 153 A90-17978

Euler and Navier-Stokes solutions for hypersonic flows p 155 A90-18254

Boundary integral equations method for compressible Navier-Stokes equations p 209 A90-18262

Numerical methods to solve the incompressible Euler and Navier-Stokes equations in 3D with applications p 209 A90-18302

A kinematical/numerical analysis of rotor-stator interaction noise
[AIAA PAPER 90-0281] p 219 A90-19770

Solution of the parabolized Navier-Stokes equations using Osher's upwind scheme
[AIAA PAPER 90-0392] p 165 A90-19830

A three-dimensional upwind parabolized Navier-Stokes code for chemically reacting flows
[AIAA PAPER 90-0394] p 165 A90-19831

Development of finite element methods for compressible Navier-Stokes flow simulations in aerospace design
[AIAA PAPER 90-0403] p 166 A90-19833

Transonic Navier-Stokes solutions about a complex high-speed accelerator configuration
[AIAA PAPER 90-0430] p 166 A90-19844

Navier-Stokes analysis of a lobed mixer and nozzle
[AIAA PAPER 90-0453] p 192 A90-19852

Dynamic stall of circulation control airfoils
[AIAA PAPER 90-0573] p 167 A90-19923

Navier-Stokes methods to predict circulation control airfoil performance
[AIAA PAPER 90-0574] p 167 A90-19924

Semi-implicit Navier-Stokes solver (SINSS) calculations of separated flows around blunt delta wings
[AIAA PAPER 90-0590] p 168 A90-19936

Development of an unstructured mesh/Navier-Stokes method for aerodynamics of aircraft with ice accretions
[AIAA PAPER 90-0758] p 169 A90-20011

Parabolized Navier-Stokes predictions of three-dimensional hypersonic flows with strong crossflow effects p 223 A90-20508

Recent developments in calculation methods for internal flows by solution of Euler or Navier-Stokes equations (ONERA, TP NO. 1989-167) p 223 A90-21033

Prediction of vortical flows on wings using incompressible Navier-Stokes equations p 226 A90-21935

Navier-Stokes predictions of the flowfield around the F-18 (HARV) wing and fuselage at large incidence
[AIAA PAPER 90-0099] p 227 A90-22165

Unsteady transonic Navier-Stokes computations for an oscillating wing using single and multiple zones
[AIAA PAPER 90-0313] p 228 A90-22197

Asymmetric separated flows at supersonic speeds
[AIAA PAPER 90-0595] p 230 A90-22233

Critical evaluation of three-dimensional supersonic combustor calculations
[AIAA PAPER 90-0207] p 272 A90-22265

Navier-Stokes computations of vortical flows over low-aspect-ratio wings p 232 A90-23103

Upwind differencing scheme for the time-accurate incompressible Navier-Stokes equations p 232 A90-23109

Using third-fourth order compact schemes for calculating gas flows in nozzles with high supersonic M numbers on the basis of simplified Navier-Stokes equations p 299 A90-24157

Shock sensitivity in parabolized Navier-Stokes solution of high angle-of-attack supersonic flow p 302 A90-25280

Navier-Stokes study of rotating stall in compressor cascades p 302 A90-25292

Flow-calculation over a delta-wing using the thin-layer Navier-Stokes equations p 304 A90-25773

Navier-Stokes simulations around a high-speed propeller p 305 A90-25797

Analysis of three-dimensional aerospace configurations using the Euler and Navier-Stokes equations p 305 A90-25798

Numerical aerodynamics via formal integration - Laplace, Euler, Prandtl, Navier-Stokes and Reynolds equations p 305 A90-25800

Computation of 2D Navier-Stokes equations p 367 A90-25801

Numerical study of three methods for solving reacting flows p 305 A90-25804

A numerical method for solving the unsteady compressible Navier-Stokes equations p 306 A90-25827

Flow dependent grid for aerodynamic designers p 306 A90-25831

Navier-Stokes computations for the investigation of flowfields about a Space-Plane p 306 A90-25836

A semi-analytical procedure for the conformal mapping of arbitrary airfoil contours p 309 A90-26498

Numerical simulation of an F-16A at angle of attack
[AIAA PAPER 90-0100] p 313 A90-26911

Comparison between thin layer and full Navier-Stokes simulations over a supersonic delta wing
[AIAA PAPER 90-0589] p 314 A90-26968

Navier-Stokes computations useful in aircraft design
[AIAA PAPER 90-1800] p 315 A90-27311

BELLTECH - A multipurpose Navier-Stokes code for rotor blade and fixed wing configurations p 384 A90-28174

Navier-Stokes computations on swept-tapered wings, including flexibility
[AIAA PAPER 90-1152] p 389 A90-29364

Accurate Navier-Stokes results for the hypersonic flow over a spherical nosetip p 393 A90-29687

Calculation of internal flows using a single-pass, parabolized Navier-Stokes analysis p 469 A90-32458

Navier-Stokes analyses of the redistribution of inlet temperature distortions in a turbine p 471 A90-32959

Calculations of unsteady aerodynamics over oscillating wings p 472 A90-33362

Calculation of flow on a flat plate at angle of attack by numerical solution of Navier-Stokes equations p 537 A90-33424

Navier-Stokes computation of flow around a round-edged double-delta wing p 555 A90-36251

Development of a three-dimensional upwind parabolized Navier-Stokes code p 602 A90-36253

Computational methods in design aerodynamics p 557 A90-36539

Hypersonic flow calculations with a hybrid Navier-Stokes/Monte Carlo method
[AIAA PAPER 90-1691] p 560 A90-38394

Application of the LAURA code for slender-vehicle aerothermodynamics
[AIAA PAPER 90-1714] p 560 A90-38416

Evaluation of transonic wall interference assessment and correction for semi-span wing data
[AIAA PAPER 90-1433] p 597 A90-38487

Numerical prediction of turbulent flow over airfoil sections with a new nonequilibrium turbulence model
[AIAA PAPER 90-1469] p 562 A90-38626

The k-kl turbulence model and wall layer model for compressible flows
[AIAA PAPER 90-1483] p 563 A90-38637

A primitive variable, strongly implicit calculation procedure for viscous flows at all speeds
[AIAA PAPER 90-1521] p 563 A90-38666

A locally implicit scheme for 3-D compressible viscous flows
[AIAA PAPER 90-1525] p 563 A90-38670

Interactive airfoil calculations with higher-order viscous-flow equations
[AIAA PAPER 90-1533] p 564 A90-38678

Unsteady Navier-Stokes solutions for a low aspect ratio delta wing
[AIAA PAPER 90-1538] p 564 A90-38682

An algebraic adaptive-grid technique for the solution of Navier-Stokes equations
[AIAA PAPER 90-1605] p 567 A90-38736

Navier-Stokes computations of vortical flows
[AIAA PAPER 90-1628] p 568 A90-38757

A numerical study of longitudinal vortex interaction with a boundary layer
[AIAA PAPER 90-1630] p 568 A90-38759

Temporal-adaptive Euler/Navier-Stokes algorithm for unsteady aerodynamic analysis of airfoils using unstructured dynamic meshes
[AIAA PAPER 90-1650] p 569 A90-38778

A three-dimensional finite element Navier-Stokes solver with k-epsilon turbulence model for unstructured grids
[AIAA PAPER 90-1652] p 570 A90-38780

Numerical solution of the problem of supersonic flow of a viscous gas past a concave conical wing
p 619 A90-39465

Navier-Stokes solutions for vortical flows over a tangent-ogive cylinder
p 620 A90-39780

A numerical investigation of supersonic inlet using implicit TVD scheme
[AIAA PAPER 90-2135] p 621 A90-40612

Calculation of three-dimensional jet interaction flowfields
[AIAA PAPER 90-2099] p 624 A90-42018

Application of 3-D Navier-Stokes computation to bowed stacking turbine vane design
[AIAA PAPER 90-2129] p 625 A90-42035

Navier-Stokes analysis of an ejector and mixer-ejector operating at pressure ratios in the range 2-4
[AIAA PAPER 90-2730] p 626 A90-42218

Euler and Navier-Stokes computations for airfoil geometries using unstructured meshes
p 630 A90-42425

Finite element simulation of turbulent propeller flowfields
p 703 A90-42658

A colocated finite volume method for solving the Navier-Stokes equations for incompressible and compressible flows in turbomachinery - Results and applications
p 703 A90-42659

Computational analysis of the flowfield of a two-dimensional ejector nozzle
[AIAA PAPER 90-1901] p 740 A90-42690

An investigation of oblique shock/boundary layer bleed interaction
[AIAA PAPER 90-1928] p 703 A90-42697

Computation of turbine flowfields with a Navier-Stokes code
[AIAA PAPER 90-2122] p 704 A90-42731

A CFD study of precombustion shock-trains from Mach 3-6
[AIAA PAPER 90-2220] p 705 A90-42751

Unsteady analysis of hot streak migration in a turbine stage
[AIAA PAPER 90-2354] p 769 A90-42782

A validation study of the Spark Navier Stokes code for nonreacting scramjet combustor flowfields
[AIAA PAPER 90-2360] p 706 A90-42784

Boundary integral formulation for compressible nonlinear potential and Navier-Stokes equations
p 706 A90-44406

Development and application of a fractional-step method for the solution of transonic and supersonic flow problems
p 709 A90-44461

Navier-Stokes computations of three-dimensional laminar flows with buoyancy in a channel with wing-type vortex generators
p 772 A90-45728

Simulation of leading-edge vortex flows
p 716 A90-45785

Navier-Stokes simulation of transonic afterbody flows with jet exhaust
[AIAA PAPER 90-3057] p 790 A90-45862

Navier Stokes simulation of waverider flowfields
[AIAA PAPER 90-3066] p 793 A90-45892

Navier-Stokes predictions of pitch damping for finned projectiles using steady coning motion
[AIAA PAPER 90-3088] p 795 A90-45902

Relative efficiency and accuracy of two Navier-Stokes codes for simulating attached transonic flow over wings
[AIAA PAPER 90-3078] p 795 A90-45909

Navier-Stokes simulation of unsteady supersonic cavity flowfield with passive control
[AIAA PAPER 90-3101] p 796 A90-45913

Numerical study of vortical flow over a sideslipping delta wing
[AIAA PAPER 90-3001] p 798 A90-45936

Study of low-Reynolds number separated flow past the Wortmann FX 63-137 airfoil
p 799 A90-46363

Compressible Navier-Stokes solutions over low Reynolds number airfoils
p 802 A90-46382

A study of gas flow in hypersonic nozzles at large Reynolds numbers using simplified Navier-Stokes equations
p 803 A90-46538

Numerical study of interaction of a jet with a supersonic cross flow
p 808 A90-47300

Prediction of separated transonic wing flows with nonequilibrium algebraic turbulence model
p 809 A90-47312

Viscous flow characteristics over a blunt cone at hypersonic Mach numbers by using a PNS code
p 810 A90-48085

Stability and transition of three-dimensional boundary layers
p 71 N90-10357

Direct numerical study of leading-edge contamination
p 19 N90-10361

Application of sound and temperature to control boundary-layer transition
p 92 N90-12537

Solution of the thin-layer Navier-Stokes equations for laminar transonic flow
[PB89-221600] p 136 N90-12879

Unsteady three-dimensional thin-layer Navier Stokes solutions on dynamic blocked grids
[AD-A212377] p 136 N90-12899

Multigrid calculations of 3-D turbulent viscous flows
[NASA-CR-185154] p 143 N90-13323

Multigrid and defect correction for the steady Navier-Stokes equations: Applications to aerodynamics
[ETN-90-96011] p 212 N90-13727

Numerical simulation of transition in three-dimensional boundary layers
[DLR-FB-89-12] p 212 N90-13728

Navier-Stokes simulation of the crossflow instability in swept-wing flows
[NASA-CR-186122] p 212 N90-13744

Navier-Stokes solutions of 2-D transonic flow over unconventional airfoils
p 173 N90-14195

Navier-Stokes analysis of airfoils with leading edge ice accretions
p 174 N90-14196

An improvement of convection fidelity in Euler calculations
p 315 N90-16709

Shock-shock boundary layer interactions
p 318 N90-17569

Numerical simulation of supersonic free shear layers
[AD-A216289] p 320 N90-17579

Viscous three-dimensional analyses for nozzles for hypersonic propulsion
[NASA-CR-185197] p 344 N90-17635

Some Navier-Stokes calculations for the CAST-10 airfoil
p 320 N90-17651

Comparison of two- and three-dimensional Navier-Stokes solutions with NASA experimental data for CAST-10 airfoil
p 321 N90-17658

Measurement of velocity profiles and Reynolds stresses on an oscillating airfoil
p 397 N90-18427

Comparison of 3-D viscous flow computations of Mach 5 inlet with experimental data
[NASA-TM-102518] p 510 N90-20090

A matrix-free locally-implicit scheme for Navier-Stokes equations
[AD-A218298] p 541 N90-20349

On total variation diminishing schemes for transonic turbulent flow computation
p 479 N90-20945

Comparison of C- and O-grid generation methods using a NACA 0012 airfoil
[AD-A216375] p 479 N90-20948

An evaluation of the two-dimensional Euler and Navier-Stokes calculations based on a flux-vector splitting
[PB90-166778] p 481 N90-20963

An efficient airfoil design method using the Navier-Stokes equations
p 500 N90-20981

Optimization of aerodynamic designs using computational fluid dynamics
p 541 N90-20999

Parabolized calculations of turbulent three dimensional flows in a turbine duct
p 482 N90-21013

Centrifugal impeller geometry and its influence on secondary flows
p 513 N90-21020

Calculation of the secondary flow in an axial turbine
p 513 N90-21022

Generation and decay of secondary flows and their impact on aerodynamic performance of modern turbomachinery components
p 514 N90-21023

Analysis of the rotor tip leakage flow with tip cooling air ejection
p 515 N90-21029

Navier-Stokes analysis of turbine blade heat transfer
[NASA-TM-102496] p 542 N90-21300

Numerical simulation of hypersonic flow around a space plane. Part 2: Application to high angles of attack flow
[NAL-TR-1011T] p 570 N90-21726

Modeling of vortex-induced oscillations based on indicial response approach
[NASA-CR-186560] p 572 N90-21736

Analytical study of the origin and behavior of asymmetric vortices
[NASA-TM-102796] p 573 N90-21746

Mesh generation for flow computation in turbomachine
p 588 N90-21981

Grid patching approaches for complex three-dimensional configurations
p 573 N90-21985

A study of supermaneuver aerodynamics
[AD-A218378] p 631 N90-23349

Composite reduced Navier Stokes procedures for flow problems with strong pressure interactions
[AD-A219621] p 689 N90-23687

The interaction of a supersonic streamwise vortex and a normal shock wave
p 633 N90-24241

Low-density flow effects for hypervelocity vehicles, phase 2
[AD-A221034] p 634 N90-24249

Experimental and analytical study of close-coupled ventral nozzles for ASTOVL aircraft
[NASA-TM-103170] p 666 N90-24273

Two-dimensional Euler and Navier-Stokes Time accurate simulations of fan rotor flows
[NASA-TM-102402] p 720 N90-25948

A comparison of two central difference schemes for solving the Navier-Stokes equations
[NASA-TM-102815] p 816 N90-27654

Numerical simulations of blade-vortex interactions and lifting hovering rotor flows
[AD-A224238] p 911 N90-29302

Investigation of ATP blades, part 2. Validation of two-dimensional viscous flow simulation codes around thin airfoils
[NAL-TR-1046] p 912 N90-29326

A boundary-layer transition model for the Navier-Stokes computation for a natural-laminar-flow airfoil
[NAL-TR-10387] p 912 N90-29328

Some topics in computational transonic aerodynamics: Revision
[NAL-TR-1018T] p 912 N90-29332

The computation and analysis of acoustic waves in transonic airfoil-vortex interactions
p 966 N90-30031

NAVIGATION

Institute of Navigation, Annual Meeting, 45th, Alexandria, VA, June 27-29, 1989, Proceedings
p 727 A90-45226

Mirach 100 flight control system
p 260 N90-15926

The development of an airborne synthetic aperture radar motion compensation system
p 333 N90-16745

Heli/SITAN: A terrain referenced navigation algorithm for helicopters
[DE90-005193] p 405 N90-19217

Sole means navigation and integrity through hybrid Loran-C and NAVSTAR GPS
p 489 N90-20933

Passive navigation using image irradiance tracking
p 578 N90-22232

An analysis of GPS as the sole means navigation system in US Navy aircraft
p 917 N90-29350

Distributed control architecture for CNI preprocessors
p 917 N90-29356

NAVIGATION AIDS

A precise flight reference system for evaluating airborne navigation aids
p 27 A90-12752

The role of adaptive antenna systems when used with GPS
p 128 A90-13995

Integrated navigation system design and performance with Phase III GPS user equipment
p 98 A90-13997

Architecture options for GPS/Carousel IV integration
p 108 A90-13999

Design philosophy for a general aviation TCAS display --- Traffic Advisory and Collision Avoidance System
[SAE PAPER 891052] p 108 A90-14354

Aerospace coordinate systems and transformations --- Book
p 282 A90-23372

The trend in nav aids inspection is to automatic operation
p 329 A90-25495

Estimation of atmospheric and transponder survey errors with a navigation Kalman filter
p 459 A90-30689

A reconfigurable integrated navigation and flight management system for military transport aircraft
p 433 A90-30794

Equipment and capability trends in Loran-C RNAV
p 576 A90-36918

Multisensor Integrated Navigation System
p 577 A90-36924

Differential Omega/VLF as a world-wide navigation aid in the 21st century
p 727 A90-45232

Omega - A low-cost precision synchronizer
p 727 A90-45233

Omega coverage - Analytical and empirical methods and solutions
p 728 A90-45234

The airborne synthetic cartographic indicator
p 822 A90-46671

Computerized MLS flight inspection system developed
p 823 A90-48983

1990-1995, a period of international decision making for the navigation community - Is our planning as good as it should be?
p 823 A90-49490

- The FAA gears up for Loran p 823 A90-49493
 Certification impact of introducing G.P.S. into commercial transport navigation systems p 824 A90-49501
 Operation of aviation radio and electronic equipment (Handbook) — Russian book p 914 A90-50747
 Guidance simulation and test support for differential GPS flight experiment [NASA-CR-177471] p 28 N90-10021
 Control outside of independent surveillance coverage operational concept [AD-A214163] p 243 N90-15090
 The automatic detection of anti-collision lights [RSRE-MEMO-4272] p 240 N90-15896
 Application of multifunction inertial reference systems to fighter aircraft p 332 N90-16740
 The Fourteenth Biennial Guidance Test Symposium, volume 1 [AD-A216925] p 405 N90-18383
 Sole means navigation and integrity through hybrid Loran-C and NAVSTAR GPS p 489 N90-20933
 Continued development and analysis of a new extended Kalman filter for the Completely Integrated Reference Instrumentation System (CIRIS) [AD-A220106] p 654 N90-23400
 Cognitive requirements for aircraft navigation [NASA-CR-186933] p 824 N90-26804
 Expert system for pilot assistance: The challenge of an intensive prototyping [ETN-90-97274] p 825 N90-27674
 Integrated Air Traffic Management [DLR-MITT-89-23] p 825 N90-27676
 R and D aspects of the future operational concept of the BFS p 826 N90-27679
 On-board planning and control of 4D-trajectories in the TMA p 826 N90-27680
 Four-dimensional navigation and Flight Management Systems p 826 N90-27681
 Advanced transport operating system software upgrade: Flight management/flight controls software description [NASA-CR-181936] p 893 N90-28366
 Observability of relative navigation using range-only measurements p 917 N90-29360
 The potential for digital databases in flight planning and flight aiding for combat aircraft p 918 N90-29371
- NAVIGATION INSTRUMENTS**
 Optimization of the observations and control of aircraft — Russian book p 60 A90-12468
 Architecture options for GPS/Carousel IV integration p 108 A90-13999
 Applications of fiber optic sensors in the aerospace and marine industries p 603 A90-36782
 A flight test comparison of two GPS/INS integration approaches p 726 A90-43708
 An analysis of GPS receiver performance capabilities and trends p 823 A90-49491
 Phase III GPS Manpack receiver operation and navigation performance p 823 A90-49497
 Providing an inexpensive gyro for the navigation mass market p 848 A90-49502
 Strapdown astro-inertial navigation (SAIN) utilizing the optical wide-angle lens startracker (OWLS) p 824 A90-49503
 Acquisition and recording an AMX A/C. Aeritalia experience and present trends [ETN-89-95217] p 109 N90-12598
- NAVIGATION SATELLITES**
 ION, Satellite Division's International Technical Meeting, Colorado Springs, CO, Sept. 19-23, 1988, Proceedings p 123 A90-13976
 International satellite radionavigation and radiolocation - Choosing among the options p 96 A90-13979
 Influence of satellite geometry, range, clock, and altimeter errors on two-satellite GPS navigation p 123 A90-13993
 Flight demonstration of two and three satellite navigation p 98 A90-13994
 Time synchronization/distribution applications of navigation signals repeated by geostationary satellites p 872 A90-46397
 An integrated GPS/GLONASS receiver p 822 A90-47909
 Interoperability issues in the use of satellite-based navigation systems for civil aviation purposes [AD-A217279] p 405 N90-19223
 Sole means navigation and integrity through hybrid Loran-C and NAVSTAR GPS p 489 N90-20933
 Independent ground monitor coverage of Global Positioning System (GPS) satellites for use by civil aviation p 918 N90-29364
- NAVSTAR SATELLITES**
 NAVSTAR-GPS: An evolution or a revolution, Ecole Supérieure d'Electricité, Gif-sur-Yvette, France, Feb. 11, 1987, Workshop p 27 A90-12250
 Differential GPS (DGPS) as an approach and landing aid p 242 A90-21722
- Performance study of an integrated NAVSTAR GPS/SINS navigation system p 329 A90-24003
 UK reference station for Navstar GPS p 725 A90-43681
 GPSNOTAM - A demonstration system for GPS status notification p 728 A90-45238
 Optimization of the effective GPS data rate p 489 N90-20932
 Sole means navigation and integrity through hybrid Loran-C and NAVSTAR GPS p 489 N90-20933
 Analysis, Design and Synthesis Methods for Guidance and Control Systems [AGARD-AG-314] p 916 N90-29338
- NAVY**
 US Navy principal site testing concept and the F-18 p 33 N90-10861
 US Navy aircraft fire protection technology p 327 N90-17603
- NEAR FIELDS**
 The sensitivity of near-field acoustics to the orientation of twin two-dimensional supersonic nozzles [AIAA PAPER 90-2149] p 625 A90-42045
 Near-field noise predictions of an aircraft in cruise p 140 N90-12538
- NEAR INFRARED RADIATION**
 Deicing of solids using radiant heating p 769 A90-43309
- NEAR WAKES**
 Hot-wire measurements of near wakes behind an oscillating airfoil p 154 A90-18138
 Numerical modeling of a viscous separated flow in the near wake p 159 A90-19236
 Experimental investigation of trailing-edge and near wake flow of a symmetric airfoil p 160 A90-19449
 Investigation of the near wake of a propan p 622 A90-40686
 The turbulent near wake of a flat plate at low Reynolds number p 811 A90-48711
 Linear instability of supersonic plane wakes [NASA-CR-181911] p 20 N90-10833
- NEODYMIUM LASERS**
 Laser communication system design p 26 A90-11813
- NERVOUS SYSTEM**
 The acute, delayed neurotoxicity evaluation of two jet engine oil formulations [AD-A222018] p 875 N90-26972
- NETHERLANDS**
 Flight testing in the Netherlands: An overview p 36 N90-10884
- NEURAL NETS**
 Applications of neural networks to avionics systems [AIAA PAPER 89-3093] p 76 A90-10627
 AAAC '88 - Aerospace Applications of Artificial Intelligence; Proceedings of the Fourth Annual Conference, Dayton, OH, Oct. 25-27, 1988, Volumes 1 & 2 p 458 A90-30226
 Neural networks for adaptive shape tracking p 638 A90-39959
 Real-time support for high performance aircraft operation [NASA-CR-185475] p 57 N90-10075
 Gas identification system using graded temperature sensor and neural net interpretation [AD-A213359] p 205 N90-13627
 Neural networks for aircraft control p 521 N90-20937
 Application of neural networks to the F/A-18 engine condition monitoring system [AD-A219820] p 666 N90-24271
 Neural networks for detecting defects in aircraft structures [IAR-90-4] p 777 N90-26345
- NEUROMUSCULAR TRANSMISSION**
 Analyzing manipulator and feel system effects in aircraft flight control p 934 A90-51154
- NEUROPHYSIOLOGY**
 Neurocontrol systems and wing-fluid interactions underlying dragonfly flight p 434 N90-19240
- NEUTRON BEAMS**
 The remote sensing of temperature in gas turbine engine components using epithermal neutrons p 70 A90-12630
- NEUTRON RADIOGRAPHY**
 Neutron radiography: Applications and systems p 886 N90-28080
- NEUTRON SOURCES**
 Neutron radiography: Applications and systems p 886 N90-28080
- NEWTON METHODS**
 Viscous computations using a direct solver p 315 A90-27133
 Newton solution of coupled viscous/inviscid multielement airfoil flows [AIAA PAPER 90-1470] p 562 A90-38627
- Computer-aided structural optimisation of aircraft structures [BR112837] p 499 N90-20973
- NEWTON THEORY**
 Optimum shape of a blunt forebody in hypersonic flow [NASA-CR-181955] p 171 N90-13351
- NEWTON-RAPHSON METHOD**
 A technique for the tuning of helicopter flight control systems p 670 A90-42467
- NEWTONIAN FLUIDS**
 Newtonian flow over oscillating two-dimensional airfoils at moderate or large incidence p 383 A90-27976
- NICKEL ALLOYS**
 Effect of protective coatings on mechanical properties of superalloys [ONERA, TP NO. 1989-88] p 62 A90-11126
 Intermetallic compounds for strong high-temperature materials - Status and potential p 125 A90-15022
 Recent and prospective developments in single-crystal superalloys for the blades of advanced turbines p 355 A90-24288
 The anisotropy of the mechanical behaviour in nickel-based single crystal superalloys for turbine blades [ONERA, TP NO. 1989-205] p 355 A90-25339
 Development of a new nickel based single crystal turbine blade alloy for very high temperatures [ONERA, TP NO. 1989-206] p 356 A90-25340
 Recrystallization behavior of nickel-base single crystal superalloys p 440 A90-27681
 Time dependent effects on high temperature low cycle fatigue and fatigue crack propagation on nickel base superalloys p 443 A90-29881
 Cyclic deformation, fatigue and fatigue crack propagation in Ni-base alloys p 531 A90-34162
 Investment-cast superalloys a good investment p 949 A90-51198
 Modeling of the oil quench for Ni-based superalloy turbine disks p 957 A90-51525
 Constitutive modeling for isotropic materials (HOST) [NASA-CR-179522] p 193 N90-13390
 Constitutive modeling for isotropic materials (HOST) [NASA-CR-174718] p 193 N90-13391
 Defects in monoblock cast turbine wheels p 443 N90-18400
- NICKEL COATINGS**
 The properties and characteristics of electroless nickel coatings applied to gas turbine engine components [ASME PAPER 89-GT-4] p 354 A90-23751
- NICKEL COMPOUNDS**
 Observations on the brittle to ductile transition temperatures of B2 nickel aluminides with and without zirconium p 205 A90-19153
- NICKEL STEELS**
 Gear steels for future helicopter transmissions p 265 A90-20607
- NIGHT**
 Cumulative airport noise exposure metrics: An assessment of evidence for time-of-day weightings, revision [AD-A214878] p 352 N90-16773
- NIGHT FLIGHTS (AIRCRAFT)**
 Helicopter obstacle avoidance system - The use of manned simulation to evaluate the contribution of key design parameters p 417 A90-28218
 Design criteria for helicopter night pilotage sensors p 417 A90-28221
- NIGHT VISION**
 Helicopter obstacle avoidance system - The use of manned simulation to evaluate the contribution of key design parameters p 417 A90-28218
 Design criteria for helicopter night pilotage sensors p 417 A90-28221
 Dual servo optical projection system (SOPS) - A solution for two crewmember and night vision goggle display needs [SAE PAPER 892353] p 760 A90-45504
 Cockpit lighting compatibility with image intensification night imaging systems: Issues and answers [AD-A210503] p 32 N90-10028
 The assessment of visibility from automatic contrast Measurements p 242 N90-15061
- NIOBIUM ALLOYS**
 The creep behavior of the Ti3Al alloy Ti-24Al-11Nb p 125 A90-15214
 Influence of alloying elements on the oxidation behavior of NbAl3 p 355 A90-24861
 The effect of elevated temperature exposure on the tensile and creep properties of Ti-24Al-11Nb p 355 A90-24865
- NITRATION**
 The 1-((diorganoxyphosphonyl)-methyl)-2,4- and -2,6-diamido benzenes [NASA-CASE-ARC-11425-4] p 532 N90-20133
 Some 1-((diorganoxyphosphonyl)methyl)-2,4- and -2,6-dinitro-benzenes [NASA-CASE-ARC-11425-3] p 678 N90-23475

NITRIC OXIDE

Computation of hypersonic low density flows with thermochemical nonequilibrium p 477 N90-20044

NITROGEN

A small inert gas generator p 180 A90-17405
 Condensation in hypersonic nitrogen wind tunnels [AIAA PAPER 90-1392] p 558 A90-37937
 Hypervelocity flow of dissociating nitrogen downstream of a blunt nose p 811 A90-48712

NITROGEN ATOMS

Computation of hypersonic low density flows with thermochemical nonequilibrium p 477 N90-20044

NITROGEN OXIDES

Predicting the CO, HC, and NO(x) emission and combustion efficiency of small turbine engines from the combustion chamber bench test results p 125 A90-15425

Low NO(x) potential of gas turbine engines [AIAA PAPER 90-0550] p 343 A90-25036
 Low NO(x) potential of gas turbine engines [NASA-TM-102452] p 345 N90-17636

Aircraft exhaust emissions: An engine manufacturer's perspective [PNR90675] p 750 N90-26004

NOISE (SOUND)

Acoustic noise emitted from vessels in an impulse-type wind tunnel p 378 A90-24125
 BASEOPS default profiles for civil aircraft [AD-A223161] p 844 N90-26825
 Noise from tip vortex and bubble cavitation [AD-A221962] p 896 N90-27468

NOISE GENERATORS

The prediction of the noise generating mechanisms of an Aerospatiale 365N-1 Dauphin helicopter p 463 A90-28161

Noise generation by swept cascade p 895 A90-49486
 Effects of acoustic sources p 140 N90-12553
 Influence of vane sweep on rotor-stator interaction noise p 169 N90-13325

NOISE INTENSITY

A statistical model of helicopter noise p 77 A90-10229

Acoustic noise emitted from vessels in an impulse-type wind tunnel p 378 A90-24125
 Prediction and measurement of low-frequency harmonic noise of a hovering model helicopter rotor p 463 A90-28159
 Aeroacoustic flowfield and acoustics of a model helicopter tail rotor at high advance ratio p 463 A90-28160

The prediction of the noise generating mechanisms of an Aerospatiale 365N-1 Dauphin helicopter p 463 A90-28161

Noise data of four small propeller-driven airplanes [PB89-216980] p 139 N90-12291

Cumulative airport noise exposure metrics: An assessment of evidence for time-of-day weightings, revision [AD-A214878] p 352 N90-16773

Noise levels from a VSTOL aircraft measured at ground level and at 1.2 m above the ground [NPL-RSA(EXT)-009] p 464 N90-18999

Lateral attenuation of military aircraft flight noise [AD-A218041] p 548 N90-20799

Free-field propagation of high intensity noise [NASA-CR-186577] p 549 N90-21604

Summary of sonic boom rise times observed during FAA community response studies over a 6-month period in the Oklahoma City area [NASA-CR-4277] p 696 N90-24852

Sound propagation elements in evaluation of en route noise of advanced turboprop aircraft p 697 N90-24861

Additive evaluation criteria for aircraft noise p 698 N90-24867

En route noise annoyance laboratory test: Preliminary results p 698 N90-24870

An aircraft noise study in Norway p 698 N90-24872

Aeroacoustics of advanced propellers [NASA-TM-103137] p 782 N90-26635

Structure-borne noise estimates for the PTA aircraft [NASA-CR-4315] p 896 N90-28396

Studies in automatic speech recognition and its application in aerospace p 958 N90-28759

Annoyance caused by advanced turboprop aircraft flyover noise: Counter-rotating-propeller configuration [NASA-TP-3027] p 965 N90-29166

Audibility and annoyance of en route noise of unducted fan engines [AD-A223687] p 966 N90-30035

NOISE MEASUREMENT

SARL noise measurements [AIAA PAPER 90-0285] p 219 A90-19772

Prediction and measurement of low-frequency harmonic noise of a hovering model helicopter rotor p 463 A90-28159

Pattern representations and syntactic classification of radar measurements of commercial aircraft p 417 A90-28407

Real time estimation of aircraft angular attitude p 431 A90-30103

The method of random variable structure optimal control for aircraft p 590 A90-37220

Broadband noise measurement in the transonic test section of the VTI T-38 wind tunnel [AIAA PAPER 90-1418] p 614 A90-37955

An experimental evaluation of test section noise in transonic wind tunnels [AIAA PAPER 90-1419] p 614 A90-37956

Wind-tunnel measurement of noise emitted by helicopter rotors at high speed [ONERA, TP NO. 1990-28] p 695 A90-41207

Noise-source measurements by thin-film pressure transducers in a subsonic turboprop model [ONERA, TP NO. 1990-36] p 659 A90-41212

Interior noise in the untreated Gulfstream II Propfan Test Assessment aircraft p 731 A90-44736

Stages are for theaters - Decibels are for airplane noise measurements [SAE PAPER 892293] p 778 A90-45469

Measurement resolution of noise directivity patterns from acoustic flight tests [NASA-TM-4134] p 79 N90-10679

The design and development of an acoustic test section for the ARA transonic wind tunnel [PNR90574] p 140 N90-13202

Acoustic recording systems for use in military aircraft [RAE-TM-MM-11] p 140 N90-13207

A model suitable for predicting the noise associated with the ducted tail rotor of a helicopter [ECL-88-09] p 220 N90-14074

Noise levels from a VSTOL aircraft measured at ground level and at 1.2 m above the ground [NPL-RSA(EXT)-009] p 464 N90-18999

Exhaust environment measurements of a turboprop engine equipped with an afterburner and 2D nozzle [NASA-CR-4289] p 588 N90-21760

PTA en route noise measurements p 696 N90-24855

En route noise: NASA propan test aircraft (corrected data - simplified procedure) [DOT-TSC-FA953-LR4] p 696 N90-24856

En route noise of two turboprop aircraft [DLR-MITT-89-18] p 697 N90-24859

Noise measurements of turboprop airplanes at different overflight elevations p 697 N90-24860

Preliminary thoughts on an acoustic metric for the wilderness aircraft overflight study p 697 N90-24862

En route noise annoyance laboratory test: Preliminary results p 698 N90-24870

Human response research update p 699 N90-24873

Bringing aircraft noise testing down to Earth [PNR90642] p 783 N90-26637

Aviation acoustical noise measurement [AD-A220214] p 896 N90-27469

Theoretical studies carried out in 1988 on helicopter rotor noise under subsonic conditions [ONERA-RS-82/5094-PY] p 896 N90-28402

NOISE POLLUTION
 Aircraft noise --- Book p 373 A90-24253

Fuselage boundary-layer effects on sound propagation and scattering p 695 A90-39781

Cumulative airport noise exposure metrics: An assessment of evidence for time-of-day weightings, revision [AD-A214878] p 352 N90-16773

A/F32T-9 large turbo fan engine enclosed noise suppressor system (T-9 NSS), exterior far-field and interior noise, McConnell AFB, Kansas [AD-A220535] p 665 N90-23402

Activities report in aerospace and aerodynamics [ETN-90-96774] p 699 N90-24224

FAA/NASA En Route Noise Symposium [NASA-CP-3067] p 696 N90-24853

Sound propagation elements in evaluation of en route noise of advanced turboprop aircraft p 697 N90-24861

Preliminary thoughts on an acoustic metric for the wilderness aircraft overflight study p 697 N90-24862

High-speed civil transport study: Special factors [NASA-CR-181881] p 923 N90-28537

NOISE PREDICTION
 A kinematical/numerical analysis of rotor-stator interaction noise [AIAA PAPER 90-0281] p 219 A90-19770

Aerodynamic loads and blade vortex interaction noise prediction p 614 A90-38520

The ROTONET prediction system and initial comparisons with far-field acoustics measurements for the XV-15 tilt-rotor aircraft p 894 A90-46947

Acoustic design considerations: Review of rotor acoustic sources p 106 N90-12585

Estimation of subsonic far-field jet-mixing noise from single-stream circular nozzles [ESDU-89041] p 316 N90-16721

En route noise annoyance laboratory test: Preliminary results p 698 N90-24870

High speed turboprop aeroacoustic study (counterrotation), Volume 1: Model development [NASA-CR-185241] p 782 N90-26633

NOISE PREDICTION (AIRCRAFT)

A statistical model of helicopter noise p 77 A90-10229

A review and update of the NASA aircraft noise prediction program propeller analysis system [SAE PAPER 891032] p 139 A90-14340

Airfoil noise in a uniform flow p 139 A90-16330

Recent research on external helicopter noise at ONERA p 218 A90-16825

Noise prediction of a counter-rotation propfan p 218 A90-17861

Prediction of the interaction noise emitted by helicopter fenestrons p 218 A90-18449

Prediction of transmission loss through an aircraft sidewall using statistical energy analysis --- study of cabin noise reduction p 219 A90-18599

Rotor noise due to atmospheric turbulence ingestion. I - Fluid mechanics p 219 A90-19385

Rotor noise due to atmospheric turbulence ingestion. II - Aeroacoustic results p 219 A90-19386

A study of the limitations of linear theory methods as applied to sonic boom calculations [AIAA PAPER 90-0368] p 219 A90-19817

High resolution flow field prediction for tail rotor aerodynamics p 463 A90-28158

Prediction and measurement of low-frequency harmonic noise of a hovering model helicopter rotor p 463 A90-28159

The prediction of the noise generating mechanisms of an Aerospatiale 365N-1 Dauphin helicopter p 463 A90-28161

Noise of a simulated installed model counterrotation propeller at angle-of-attack and takeoff/approach conditions [AIAA PAPER 90-0283] p 547 A90-32505

Structural-acoustic analysis of aircraft fuselage structures using general purpose finite element codes p 492 A90-33385

Acoustics of ultralight airplanes p 643 A90-40685

Characterization of helicopter turboshaft engine noise p 660 A90-41759

The MDE method for aircraft cabin interior noise prediction --- matrix difference equation [SAE PAPER 892372] p 782 A90-45519

Rotor loads computation using singularity methods and application to the noise prediction p 807 A90-46880

On numerical prediction of sound field generated by propeller p 895 A90-49485

Near-field noise predictions of an aircraft in cruise p 140 N90-12538

A model suitable for predicting the noise associated with the ducted tail rotor of a helicopter [ECL-88-09] p 220 N90-14074

Evaluation of analysis techniques for low frequency interior noise and vibration of commercial aircraft [NASA-CR-181851] p 220 N90-14866

Aerodynamic loads and blade vortex interaction noise prediction [ISL-PU-310/89] p 719 N90-25942

Aeroacoustics of advanced propellers [NASA-TM-103137] p 782 N90-26635

The validation and application of a rotor acoustic prediction computer program [NASA-TM-101794] p 895 N90-27465

Air Force procedure for predicting aircraft noise around airbases: Airbase operations program (BASEOPS) description [AD-A223069] p 895 N90-27466

Air Force procedure for predicting aircraft noise around airbases: Noise Exposure Model (NOISEMAP). User's manual [AD-A223162] p 895 N90-27467

Assessment System for Aircraft Noise (ASAN): Development of alpha-test prototype system software [AD-A223770] p 966 N90-30036

NOISE PROPAGATION
 Random response and noise transmission of discretely stiffened composite panels p 283 A90-23288

Installation effects on propeller wake/vortex-induced structure-borne noise transmissions p 579 A90-35761

Characterization of helicopter turboshaft engine noise p 660 A90-41759

Free-field propagation of high intensity noise [NASA-CR-186577] p 549 N90-21604

En route noise: NASA propan test aircraft (corrected data - simplified procedure) [DOT-TSC-FA953-LR4] p 696 N90-24856

En route noise: NASA propfan test aircraft (calculated source noise)
[DOT-TSC-FA953-LR5] p 697 N90-24857

A review of instability and noise propagation in supersonic flows
[NASA-CR-186800] p 717 N90-25112

The validation and application of a rotor acoustic prediction computer program
[NASA-TM-101794] p 895 N90-27465

Theoretical studies carried out in 1988 on helicopter rotor noise under subsonic conditions
[ONERA-RS-82/5094-PY] p 896 N90-28402

NOISE REDUCTION

Wave cancellation properties of a splitter-plate porous wall configuration
p 57 A90-11005

Application of localized active control to reduce propeller noise transmitted through fuselage surface
p 78 A90-11884

Interior noise control of the Saab 340 aircraft
[SAE PAPER 891080] p 101 A90-14372

Beech Starship interior noise experimental studies
[SAE PAPER 891082] p 101 A90-14374

Effect of an isolated shell on interior noise levels in a turboprop aircraft
[SAE PAPER 891083] p 102 A90-14375

Possibility of active propeller-noise suppression in piston-engine aircraft by changing the phase relation between the propeller and exhaust signals
p 218 A90-18450

Prediction of transmission loss through an aircraft sidewall using statistical energy analysis — study of cabin noise reduction
p 219 A90-18599

Supersonic jet noise reduction by a porous single expansion ramp nozzle
[AIAA PAPER 90-0366] p 219 A90-19815

Interference detection and suppression in Loran-C receivers
p 240 A90-20504

Effect of advanced component technology on helicopter transmissions
p 271 A90-21115

Digital control of local sound fields in an aircraft passenger compartment
p 247 A90-23113

Reduction of blade-vortex interaction noise through higher harmonic pitch control
p 377 A90-23937

Optimization of the sound-absorption lining parameters of an ejector jet muffler
p 378 A90-24117

Aircraft noise — Book
p 373 A90-24253

Application of active noise control to model propeller noise
p 548 A90-34091

Higher harmonic control of a helicopter model rotor to reduce blade/vortex interaction noise
p 496 A90-34360

Installation effects on propeller wake/vortex-induced structure-borne noise transmissions
p 579 A90-35761

EH101 Advance Technology Rotorcraft low detectability/good neighbor design
p 579 A90-35774

Experiments on the active control of the transmission of sound through a clamped rectangular plate
p 695 A90-41109

Wind-tunnel measurement of noise emitted by helicopter rotors at high speed
[ONERA, TP NO. 1990-28] p 695 A90-41207

Twin jet screech suppression concepts tested for 4.7 percent axisymmetric and two-dimensional nozzle configurations
[AIAA PAPER 90-2150] p 696 A90-42046

Active control of helicopter cabin noise
p 645 A90-42434

Technology issues for high-speed civil transports
[SAE PAPER 892201] p 778 A90-45422

Effects of stage 3 rules on the airliner market
[SAE PAPER 892292] p 723 A90-45468

The MDE method for aircraft cabin interior noise prediction — matrix difference equation
[SAE PAPER 892372] p 782 A90-45519

Theoretical studies of the active control of propeller-induced cabin noise
p 893 A90-46351

Mixer-ejector nozzle for jet noise suppression
[AIAA PAPER 90-1909] p 894 A90-47202

Active control of propeller-induced noise fields inside a flexible cylinder
p 833 A90-47306

Mechanisms of active control in cylindrical fuselage structures
p 862 A90-47309

Improved noise rejection in automatic carrier landing systems
[AIAA PAPER 90-3374] p 864 A90-47632

Twin-jet screech suppression
p 894 A90-48957

Noise generation by swept cascade
p 895 A90-49486

Review and analysis of the DNW/Model 360 rotor acoustic data base
[NASA-TM-102253] p 81 N90-11692

Noise data of four small propeller-driven airplanes
[PB89-216980] p 139 N90-12291

The NASA experience in aeronautical R and D: Three case studies with analysis
[AD-A211486] p 82 N90-12496

What should be done with those noisy old aircraft
[PNR90562] p 107 N90-12593

Re-engine with the Rolls-Royce Tay 670, the route to significant noise reduction
[PNR90585] p 115 N90-12606

UHB demonstrator interior noise control flight tests and analysis
[NASA-CR-181897] p 140 N90-13198

The commercial aircraft noise problem
[PNR90577] p 140 N90-13203

Fuselage design for a specified Mach-sliced area distribution
[NASA-TP-2975] p 414 N90-18385

Lateral attenuation of military aircraft flight noise
[AD-A218041] p 548 N90-20799

Transmission research activities at NASA Lewis Research Center
[NASA-TM-103132] p 543 N90-21394

The Shock and Vibration Digest, volume 21, no. 6
p 614 N90-22363

Noise transmission into propeller-driven airplanes
p 614 N90-22364

Integrated control-system design via generalized LQG (GLOG) theory
p 613 N90-23023

A/F32T-9 large turbo fan engine enclosed noise suppressor system (T-9 NSS), exterior far-field and interior noise, McConnell AFB, Kansas
[AD-A220535] p 665 N90-23402

The effect of noise-abatement profiles on noise immissions and human annoyance underneath a subsequent climbpath
p 698 N90-24865

Problems of internal acoustics in two and three dimensional cavities with deformable walls using the MSC/Nastran code
[DLC/STR-INT-TN-004] p 699 N90-24876

Stage 2 re-engineing: The only way to achieve a real stage 3 aircraft
[PNR90636] p 737 N90-25977

Low-speed wind tunnel investigation of the static stability and control characteristics of an advanced turboprop configuration with the propellers placed over the tail
[NASA-CR-186900] p 759 N90-26017

Aviation acoustical noise measurement
[AD-A222014] p 896 N90-27469

A process for analysis, evaluation, and development of aerial servicing noise reduction measures in civil aircraft
[ETN-90-97300] p 896 N90-28398

Comparison of speech intelligibility in cockpit noise using SPH-4 flight helmet with and without active noise reduction
[NASA-CR-177564] p 915 N90-28510

NOISE SPECTRA

The prediction of the noise generating mechanisms of an Aerospatiale 365N-1 Dauphin helicopter
p 463 A90-28161

Clutter rejection and transmitter-receiver requirements in an airborne radar
p 738 A90-45354

Effects of acoustic sources
p 140 N90-12553

Free-field propagation of high intensity noise
[NASA-CR-186577] p 549 N90-21604

NOISE TOLERANCE

FAA/NASA En Route Noise Symposium
[NASA-CP-3067] p 696 N90-24853

Proposed definition of the term en route in en route aircraft noise
p 696 N90-24854

The effect of noise-abatement profiles on noise immissions and human annoyance underneath a subsequent climbpath
p 698 N90-24865

Additive evaluation criteria for aircraft noise
p 698 N90-24867

Social survey findings on en route noise annoyance issues
p 698 N90-24868

Problems related to aircraft noise in Switzerland
p 698 N90-24871

Human response research update
p 699 N90-24873

Annoyance caused by advanced turboprop aircraft flyover noise: Counter-rotating-propeller configuration
[NASA-TP-3027] p 965 N90-29166

NONADIABATIC CONDITIONS

Evaluation of equilibrium turbulence for a naturally developing hypersonic boundary layer at nonadiabatic wall conditions
[AIAA PAPER 90-1410] p 559 A90-37948

NONDESTRUCTIVE TESTS

Review of fiber optic methods for strain monitoring and non-destructive testing
p 67 A90-11042

A study on flaw detection method for CFRP composite laminates. I - The measurement of crack extension in CFRP composites by electrical potential method
p 441 A90-28003

Air Force manufacturing technology NDE programs supporting manufacturing and maintenance
p 452 A90-30779

The role of NDE in ceramic turbine engine component development
p 601 A90-35508

A technique for rapid impact damage detection with implication for composite aircraft structures
p 600 A90-37662

An advanced X-ray technique for NDI
p 604 A90-37901

Some technological errors in the use of capillary inspection in gas turbine engine repair
p 769 A90-43039

Acoustic emission and signal analysis
p 781 A90-43782

Thermal nondestructive characterization of the integrity of protective coatings
p 770 A90-44325

Aircraft engine inspection
p 771 A90-44606

Development of process control procedure for ultrahigh-sensitivity fluorescent penetrant inspection systems
p 771 A90-45225

Eddy current detection of subsurface cracks
p 882 A90-48629

NDI (Nondestructive Inspection) oriented corrosion control for Army aircraft. Phase 1: Inspection methods
[AD-A213368] p 176 N90-13359

Nondestructive analysis of aileron fatigue and aging in a Mirage F1
[REPT-M6-594000] p 184 N90-13378

Diffusion bonding of metals
p 206 N90-14330

Nondestructive measurement of residual stresses in aircraft transparencies
[AD-A218680] p 689 N90-23762

Neural networks for detecting defects in aircraft structures
[IAR-90-4] p 777 N90-26345

NDT in aerospace: The next decade (1990's)
[PNR90628] p 777 N90-26348

The role of NDI in the certification of turbine engine components
[PNR90629] p 777 N90-26349

Development of creep-fatigue damage detection method of rotor steel by ultrasonic wave measurement
[DE90-503792] p 777 N90-26365

Retirement for cause of the F100 engine
p 843 N90-26813

Applications of digital image processing in testing and evaluation of composite materials
[AD-A222939] p 874 N90-26887

Impact of Emerging NDE-NDI Methods on Aircraft Design, Manufacture, and Maintenance
[AGARD-CP-462] p 885 N90-28068

The role of NDI in the certification of turbine engine components
p 859 N90-28069

NDI-concept for composites in future military aircraft
p 877 N90-28070

Inspection reliability
p 885 N90-28072

Critical inspection of high performance turbine engine components: The RFC concept
p 859 N90-28073

An ultrasonic system for in-service non-destructive inspection of composite structures
p 885 N90-28076

A technique for rapid inspection of composite aircraft structure for impact damage
p 846 N90-28077

In-service inspection of composite components on aircraft at depot and field levels
p 885 N90-28078

Development of an automated ultrasonic inspection system for composite structure on in-service aircraft
p 885 N90-28079

Neutron radiography: Applications and systems
p 886 N90-28080

Acoustic emission detection of crack presence and crack advance during flight
p 886 N90-28082

The application of infrared thermography to the nondestructive testing of composite materials
p 886 N90-28084

Advanced NDE techniques for quantitative characterization of aircraft
p 886 N90-28088

Use of acoustic emission for continuous surveillance of aircraft structures
p 887 N90-28092

Impact of NDE-NDI methods on aircraft design, manufacture, and maintenance, from the fundamental point of view
p 887 N90-28093

A low cost shadow moire device for the nondestructive evaluation of impact damage in composite laminates
[AD-A223451] p 953 N90-29442

NONEQUILIBRIUM FLOW

Approximations for nonequilibrium hypervelocity aerodynamics
p 154 A90-17990

Inviscid non equilibrium flow in ONERA F4 wind tunnel
[ONERA, TP NO. 1989-161] p 223 A90-21029

Chemical and vibrational non-equilibrium nozzle flow calculation by an implicit upwind method
[ONERA, TP NO. 1989-175] p 223 A90-21037

A study of flow of a vibrationally nonequilibrium dissociated gas past a blunt body
p 234 A90-23435

Non-equilibrium hypersonic flows - Physics and numerics
p 304 A90-25777

Numerical prediction of turbulent flow over airfoil sections with a new nonequilibrium turbulence model
[AIAA PAPER 90-1469] p 562 A90-38626

- Transonic flow around airfoils with relaxation and energy supply by homogeneous condensation p 620 A90-39782
- Streamtube analysis of supersonic combustion in an in-tube-scrumjet p 762 A90-42776
[AIAA PAPER 90-2339]
- NONEQUILIBRIUM THERMODYNAMICS**
- Nonequilibrium recombination-dissociation boundary layer flows along arbitrarily-catalytic hypersonic vehicles [AIAA PAPER 90-0055] p 161 A90-19652
- NONFERROUS METALS**
- The future of non ferrous metals in aerospace engines [PNR90572] p 127 N90-12720
- NONFLAMMABLE MATERIALS**
- Test and evaluation: Reducing risks to military aircraft from bird collisions. Report to the Chairman, Legislation, and National Security Subcommittee, Committee on Government Operations, House of Representatives [AD-A210670] p 25 N90-10845
- NONISENTROPICITY**
- The transonic nonisentropic potential calculation p 304 A90-25739
- Non-isentropic effects on the WRDC 20 inch hypersonic wind tunnel calibration p 435 A90-28254
- NONLINEAR EQUATIONS**
- Flutter analysis on a non-linear wing model p 207 A90-17009
- Nonlinear aeroelasticity p 391 A90-29375
[AIAA PAPER 90-1031]
- Boundary integral formulation for compressible nonlinear potential and Navier-Stokes equations p 706 A90-44406
- A dynamic inversion based control law with application to the high angle-of-attack research vehicle [AIAA PAPER 90-3407] p 864 A90-47662
- NONLINEAR FEEDBACK**
- Control of a twin lift helicopter system using nonlinear state feedback [AIAA PAPER 90-3408] p 817 A90-47663
- NONLINEAR FILTERS**
- Investigation of a nonlinear Kalman filter for estimating aircraft state variables p 195 A90-16850
- A nonlinear aircraft tracking filter utilizing control variable estimation [AIAA PAPER 90-3402] p 822 A90-47657
- Estimation and control of nonlinear and hybrid systems with applications to air-to-air guidance [AD-A214542] p 348 N90-16770
- NONLINEAR PROGRAMMING**
- Dynamic structural correlation via nonlinear programming techniques p 208 A90-17372
- The local surface variation method in profile shape optimization problems p 297 A90-24136
- Design methodology for multivariable helicopter control systems p 669 A90-42461
- Optimal solutions to flight mechanics problems using a Nonlinear Programming and Collocation technique [AIAA PAPER 90-3415] p 889 A90-47669
- Model reduction with a finite-interval $H(\infty)$ criterion [AIAA PAPER 90-3473] p 890 A90-47723
- Multilevel decomposition approach to the preliminary sizing of a transport aircraft wing [NASA-CR-4296] p 583 N90-22557
- NONLINEAR SYSTEMS**
- Inverse problems in controlled system dynamics: Nonlinear models — Russian book p 77 A90-12471
- Nonlinear transverse oscillations of a composite dynamic system p 129 A90-14558
- Decoupled ultimate boundedness control of systems and large aircraft maneuver p 196 A90-19461
- Application of dynamical systems theory to the high angle of attack dynamics of the F-14 [AIAA PAPER 90-0221] p 257 A90-22184
- Nonlinear response and fatigue of stiffened panels p 363 A90-23953
- Nonlinear effects in helicopter rotor forward flight forced response p 347 A90-25420
- Rotordynamics of the Vulcain LH2 Turbopump - Comparison between test results and non-linear dynamic analysis p 528 A90-33382
- Application of transformational ideas to automatic flight control design p 589 A90-36433
- An introduction to chaos theory in CFD [AIAA PAPER 90-1440] p 680 A90-39725
- Experimental study of the effects of nonlinearities on ground resonance p 643 A90-40172
- Helicopter control design using feedback linearization techniques p 668 A90-40817
- Nonlinear finite-element analysis to predict fan-blade damage due to soft-body impact p 683 A90-40939
- Nonlinear flight control design via sliding methods p 756 A90-45335
- Flight controller design with nonlinear aerodynamics, large parameter uncertainty, and pilot compensation [AIAA PAPER 90-3478] p 866 A90-47728

- Nonconvex polytope approximations of attracting basin boundaries for nonlinear systems p 891 A90-47758
[AIAA PAPER 90-3512]
- The determination of third order linear models from a seventh order nonlinear jet engine model p 964 A90-52881
- The application of TSIM software to act design and analysis on flexible aircraft p 60 N90-10086
- Correlation of Puma airloads: Lifting-line and wake calculation [NASA-TM-102212] p 170 N90-13327
- The S.D.G., P.S.D. and the nonlinear airplane [NLR-MP-88018-U] p 183 N90-13371
- Discretization and model reduction for a class of nonlinear systems p 198 N90-13397
- A helicopter flight path controller design via a nonlinear transformation technique p 199 N90-14242
- Estimation and control of nonlinear and hybrid systems with applications to air-to-air guidance [AD-A214542] p 348 N90-16770
- Control and stabilization of linear and nonlinear distributed systems p 462 N90-18908
- Nonlinear mechanics of unstable plasmas as related to high altitude aerodynamics p 464 N90-19852
- Quiet mode for nonlinear rotor models [NASA-TM-102236] p 582 N90-21758
- Estimating short-period dynamics using an extended Kalman filter [NASA-TM-101722] p 648 N90-23392
- A contribution to the improvement of the accuracy in the parameter identification of nonlinear processes, by example of the aircraft motion [ETN-90-96961] p 736 N90-25974
- Numeric fluid mechanics p 960 N90-29161
- NONLINEARITY**
- Nonlinear aerodynamics of two-dimensional airfoils in severe maneuver p 301 A90-25276
- Application of numerical optimization techniques to control system design for nonlinear dynamic models of aircraft p 593 N90-23032
- A time-marching method for calculating unsteady airloads on three-dimensional wings. Part 2: Full-potential formulation [DLR-FB-89-59] p 635 N90-24255
- Flexural fatigue life prediction of closed hat-section using materially nonlinear axial fatigue characteristics p 691 N90-25062
- Evaluation of nonlinear motion-drive algorithms for flight simulators [UTIAS-TN-272] p 761 N90-25148
- Prediction methodologies for nonlinear aerodynamic characteristics of control surfaces p 718 N90-25937
- Entropy wave instability in compact ramjets p 858 N90-27932
- Nonlinear static and dynamic modeling of composite rotor blades including warping effects p 924 N90-29382
- Aircraft design for mission performance using nonlinear multiobjective optimization methods [NASA-CR-4328] p 925 N90-29384
- Windshear estimation along the trajectory of an aircraft p 963 N90-29745
- The computation and analysis of acoustic waves in transonic airfoil-vortex interactions p 966 N90-30031
- NONUNIFORM FLOW**
- Analysis of nonuniform subsonic flows about a row of moving blades p 6 A90-11779
- Supersonic nonuniform flow of a gas past oblong axisymmetric bodies p 159 A90-19237
- Whirl flutter stability of a pusher configuration subject to a nonuniform flow [AIAA PAPER 90-1162] p 393 A90-29397
- A study of boundary layer stability in the case of an increased incoming stream turbulence in gradient flows p 555 A90-36065
- Effect of the nonuniformity of external supersonic flow and nozzle deflection angle on the base pressure behind an axisymmetric body with a single supersonic jet p 802 A90-46486
- NORMAL DENSITY FUNCTIONS**
- Determination of the extreme values of the efficiency criteria for a flight vehicle control system in the probable scatter range of its characteristics p 859 A90-46569
- Analysis of distributions of Visual Meteorological Conditions (VMC) heliport data [DOT/FAA/CT-TN89/67] p 544 N90-21508
- NORMAL SHOCK WAVES**
- The propagation of a normal shock in a varying area duct p 130 A90-15045
- Experimental investigation of terminal shock sensors in mixed-compression inlets [AIAA PAPER 90-1931] p 681 A90-40560

- Computation of multiple normal shock wave/turbulent boundary layer interactions [AIAA PAPER 90-2133] p 685 A90-42037
- The normal shock generator - An inlet throat region research apparatus for high Mach applications [AIAA PAPER 90-1930] p 759 A90-42698
- An LDA investigation of the normal shock wave boundary layer interaction p 908 A90-52618
- Varying specific heat gasdynamic function formulae simplification and analytical solution of normal shock waves p 908 A90-52776
- The interaction of a supersonic streamwise vortex and a normal shock wave p 633 N90-24241
- NORTH AMERICAN AIRCRAFT**
- Building the B-2 p 701 A90-43826
- NORTH ATLANTIC TREATY ORGANIZATION (NATO)**
- AGARD highlights 90/1 p 783 N90-26788
- NORWAY**
- An aircraft noise study in Norway p 698 N90-24872
- NOSE CONES**
- Low-speed pressure distribution on semi-infinite two-dimensional bodies with elliptical noses p 553 A90-35766
- Comments on 'Effect of nose bluntness and cone angle on slender-vehicle transition' p 620 A90-39814
- Viscous flow characteristics over a blunt cone at hypersonic Mach numbers by using a PNS code p 810 A90-48085
- Hypervelocity flow of dissociating nitrogen downstream of a blunt nose p 811 A90-48712
- Blunt-nose inviscid airflows with coupled nonequilibrium processes p 171 N90-13336
- NOSE TIPS**
- Optimal nose shapes of bodies of revolution in transonic flow p 299 A90-24165
- Accurate Navier-Stokes results for the hypersonic flow over a spherical nosetip p 393 A90-29687
- NOSE WHEELS**
- The anti-shimmy and break-proof study of nose landing gear p 178 A90-16856
- NOSES (FOREBODIES)**
- The fickle effect of nose microasymmetry on the high-alpha aerodynamics [AIAA PAPER 90-0067] p 161 A90-19663
- Rotational aerodynamics of elliptic bodies at high angles of attack [AIAA PAPER 90-0068] p 161 A90-19664
- Experimental investigation of a new device to control the asymmetric flowfield on forebodies at large angles of attack [AIAA PAPER 90-0069] p 161 A90-19665
- Impact of nose-probe chines on the vortex flows about the F-16C [AIAA PAPER 90-0386] p 165 A90-19828
- The hemisphere-cylinder at an angle of attack [AIAA PAPER 90-0050] p 313 A90-26907
- Accurate Navier-Stokes results for the hypersonic flow over a spherical nosetip p 393 A90-29687
- Forebody design for the aerospaceplane [AIAA PAPER 90-2472] p 762 A90-42810
- Yaw damping of elliptic bodies at high angles of attack p 709 A90-44740
- Control of forebody flow asymmetry - A critical review [AIAA PAPER 90-2833] p 711 A90-45164
- Development of a preliminary high-angle-of-attack nose-down pitch control requirement for high-performance aircraft [NASA-TM-101684] p 399 N90-19206
- Effects of nose bluntness and shock-shock interactions on blunt bodies in viscous hypersonic flows [NASA-CR-186451] p 479 N90-20950
- Effective methods of controlling a junction vortex system in an incompressible, three-dimensional, turbulent flow p 571 N90-21732
- NOTCH STRENGTH**
- A study on initial fatigue quality of typical aircraft structures (fastener holes) p 272 A90-22004
- NOTCHES**
- The development of leading-edge notches to improve the subsonic performance of wings of moderate sweep p 491 A90-33367
- NOWCASTING**
- Range obscuration mitigation by adaptive PRF selection for the TDWR system — Pulse Repetition Frequency for Terminal Doppler Weather Radar p 456 A90-28617
- Wind shear at Pantelleria airport p 692 A90-39702
- NOZZLE DESIGN**
- Investigation and improvement of ground starting characteristics of a combustor with airblast nozzles p 45 A90-12546
- Exhaust nozzle system design considerations for turboramjet propulsion systems p 48 A90-12577
- Advanced computational techniques for hypersonic propulsion p 69 A90-12606

- Supersonic jet noise reduction by a porous single expansion ramp nozzle
[AIAA PAPER 90-0366] p 219 A90-19815
- Calculated chemical and vibrational nonequilibrium effects in hypersonic nozzles p 253 A90-21224
- Propulsion system integration in high-performance aircraft p 333 A90-23922
- Development of the improved helicopter icing spray system (IHSS) p 400 A90-28182
- Computation of vectoring nozzle performance
[AIAA PAPER 90-2752] p 627 A90-42225
- Nozzle design optimization by method-of-characteristics
[AIAA PAPER 90-2024] p 741 A90-42719
- Effect of the nozzle ring vane height on the efficiency of axial-flow full-admission microturbines p 851 A90-46509
- Mixer-ejector nozzle for jet noise suppression
[AIAA PAPER 90-1909] p 894 A90-47202
- Parametric assessment of propulsion system mass for airbreathing launcher configurations p 344 A90-16819
- Static investigation of a two-dimensional convergent-divergent exhaust nozzle with multiaxis thrust-vectoring capability
[NASA-TP-2973] p 397 A90-19193
- An investigation of secondary flows in nozzle guide vanes p 512 A90-21016
- Secondary flow predictions for a transonic nozzle guide vane p 513 A90-21017
- Supersonic nozzle design of arbitrary cross-section p 515 A90-21035
- A computer program for the prediction of nozzle-propeller performance
[LR-578] p 572 A90-21740
- Theory and numerical analysis of single and multi-element nozzle propellers
[LR-579] p 572 A90-21741
- Recent improvements in the scope and accuracy of the performance prediction of nozzle propellers
[LR-598] p 572 A90-21742
- Design of an axisymmetric, contoured nozzle for the HEG
[DLR-FB-90-04] p 959 A90-28812
- NOZZLE EFFICIENCY**
- An experimental study of the gasdynamic characteristics of annular nozzle cascades with small flow exit angles p 255 A90-23409
- The role of hydrogen/air chemistry in nozzle performance for a hypersonic propulsion system
[AIAA PAPER 90-2492] p 658 A90-40637
- Static investigation of a two-dimensional convergent-divergent exhaust nozzle with multiaxis thrust-vectoring capability
[NASA-TP-2973] p 397 A90-19193
- Theory and numerical analysis of single and multi-element nozzle propellers
[LR-579] p 572 A90-21741
- Experimental and analytical study of close-coupled ventral nozzles for ASTOVL aircraft
[NASA-TM-103170] p 666 A90-24273
- NOZZLE FLOW**
- Numerical investigation of unsteady compressible flow through nozzles and cascades p 7 A90-11790
- An experimental investigation of non-steady flow in vaneless diffusers p 14 A90-12595
- Advanced computational techniques for hypersonic propulsion p 69 A90-12606
- CFD predictions of lobed mixer flowfields p 70 A90-12626
- Non-iterative analytical methods for off-design turbofan calculations with or without mixed-flows p 70 A90-12628
- Development process of turbulence in a round-nozzle air jet p 87 A90-16101
- Navier-Stokes analysis of a lobed mixer and nozzle
[AIAA PAPER 90-0453] p 192 A90-19852
- Chemical and vibrational non-equilibrium nozzle flow calculation by an implicit upwind method
[ONERA, TP NO. 1989-175] p 223 A90-21037
- Representation of two-dimensional hypersonic inlet flows for one-dimensional scramjet cycle analysis
[AIAA PAPER 90-0527] p 229 A90-22226
- Development of a dual fuel injector for a gas turbine combustor
[ASME PAPER 89-GT-25] p 340 A90-23764
- Holographic flow visualisation of turbofan by-pass and core nozzle streams
[ASME PAPER 89-GT-260] p 363 A90-23891
- Calculation of flows of an ideal gas in nozzles and jets by the relaxation method p 296 A90-24109
- Using third-fourth order compact schemes for calculating gas flows in nozzles with high supersonic M numbers on the basis of simplified Navier-Stokes equations p 299 A90-24157
- Use of swirl for flow control in propulsion nozzles p 421 A90-27963
- Mean and turbulent velocity measurements in a turbojet exhaust p 423 A90-28272
- Application of CFD to pitch/yaw thrust vectoring spherical convergent flap nozzles
[AIAA PAPER 90-2023] p 657 A90-40597
- The role of hydrogen/air chemistry in nozzle performance for a hypersonic propulsion system
[AIAA PAPER 90-2492] p 658 A90-40637
- Influences on the uniformity of sprays produced by gas turbine high shear nozzle/swirler assemblies
[AIAA PAPER 90-2193] p 688 A90-42068
- Analysis of internal flow in a ventral nozzle for STOVL aircraft
[AIAA PAPER 90-1899] p 739 A90-42688
- Computational analysis of the flowfield of a two-dimensional ejector nozzle
[AIAA PAPER 90-1901] p 740 A90-42690
- Computational investigation of two-dimensional ejector nozzle flow fields
[AIAA PAPER 90-2148] p 768 A90-42739
- Streamtube analysis of supersonic combustion in an in-tube-scrumjet
[AIAA PAPER 90-2339] p 762 A90-42776
- Numerical study of compressible nozzle flow p 708 A90-44437
- Non-unique solutions of the Euler equations p 716 A90-45727
- Effect of the nonuniformity of external supersonic flow and nozzle deflection angle on the base pressure behind an axisymmetric body with a single supersonic jet p 802 A90-46486
- Geometrical factors influencing the flow field in a propulsive nozzle p 807 A90-46876
- Two-dimensional convergent-divergent nozzle flow with wall velocity slip and temperature jump p 807 A90-46884
- Twin-jet screech suppression p 894 A90-48957
- Self-excited oscillations in internal transonic flows p 813 A90-49274
- Investigation of advanced mixer-ejector exhaust system
[AD-A211943] p 89 A90-11705
- A computational analysis of the transonic flow field of two-dimensional minimum length nozzles p 173 A90-14194
- Engine inlet distortion in a 9.2 percent scale vectored thrust STOVL model in ground effect
[NASA-TM-102358] p 318 A90-17561
- Viscous three-dimensional analyses for nozzles for hypersonic propulsion
[NASA-CR-185197] p 344 A90-17635
- Experimental investigation of a chemical laser cavity flowfield
[AD-A216398] p 372 A90-18038
- Computation of hypersonic unsteady viscous flow over a cylinder p 397 A90-19194
- Secondary flow predictions for a transonic nozzle guide vane p 513 A90-21017
- Secondary flow in a turbine guide vane with low aspect ratio p 513 A90-21018
- The effect of secondary flow on the redistribution of the total temperature field downstream of a stationary turbine cascade p 515 A90-21033
- Analysis of internal flow in a ventral nozzle for STOVL aircraft
[NASA-TM-103123] p 666 A90-23404
- Effect of tail size reductions on longitudinal aerodynamic characteristics of a three surface F-15 model with nonaxisymmetric nozzles
[NASA-TP-3036] p 718 A90-25938
- Hot gas ingestion characteristics and flow visualization of a vectored thrust STOVL concept
[NASA-TM-103212] p 751 A90-26009
- NOZZLE GEOMETRY**
- CFD predictions of lobed mixer flowfields p 70 A90-12626
- Effect of the inlet diameter and neck edge radius on the flow coefficient of straight-generatrix nozzles p 84 A90-14577
- Development process of turbulence in a round-nozzle air jet p 87 A90-16101
- Transonic flow in throat region of supersonic nozzles p 149 A90-16799
- The use of a Laval nozzle and wall suction for blockage-free transonic wind-tunnel operation p 225 A90-21592
- Mean and pulse characteristics of supersonic flow in a wind tunnel with a honeycomb nozzle p 231 A90-22421
- Dissipation thrust losses due to distortions of the jet nozzle profile p 254 A90-23405
- A study of the working process and losses in annular turbine nozzle cascades with a low contraction ratio p 254 A90-23407
- An experimental study of heat transfer and film cooling on low aspect ratio turbine nozzles
[ASME PAPER 89-GT-187] p 361 A90-23865
- Finite element simulation of complex jets in a crossflow for V/STOL applications p 585 A90-35753
- Flow and acoustic features of a supersonic tapered nozzle
[AIAA PAPER 90-1599] p 567 A90-38731
- Formation of shocks within axisymmetric nozzles
[AIAA PAPER 90-1655] p 570 A90-38782
- Confined jet thrust vector control nozzle studies
[AIAA PAPER 90-2027] p 657 A90-40598
- Three dimensional transonic and supersonic flow prediction in axi-vectored nozzles using a finite volume method p 624 A90-41989
- Twin jet screech suppression concepts tested for 4.7 percent axisymmetric and two-dimensional nozzle configurations
[AIAA PAPER 90-2150] p 696 A90-42046
- External nozzle flap dynamic load measurements on F-15 S/MTD model p 740 A90-42692
- Two-dimensional convergent-divergent nozzle flow with wall velocity slip and temperature jump p 807 A90-46884
- New experimental results on the origin and structure of Ferri and Dailey instabilities ('buzz') p 906 A90-51507
- A computational analysis of the transonic flow field of two-dimensional minimum length nozzles p 173 A90-14194
- Performance of an aero-space plane propulsion nozzle p 515 A90-21034
- Effect of tail size reductions on longitudinal aerodynamic characteristics of a three surface F-15 model with nonaxisymmetric nozzles p 718 A90-25938
- Design of an axisymmetric, contoured nozzle for the HEG
[DLR-FB-90-04] p 959 A90-28812
- NOZZLE THRUST COEFFICIENTS**
- Swirling flow in thrust nozzles p 421 A90-27962
- Aerodynamics of thrust vectoring
[NASA-CR-185074] p 172 A90-13354
- NOZZLE WALLS**
- Determination of the specific thrust in open regimes and design of a nonseparating convergent nozzle profile p 395 A90-30339
- Advanced Mach 3.5 Axisymmetric Quiet Nozzle
[AIAA PAPER 90-1592] p 566 A90-38727
- NUMERICAL ANALYSIS**
- Numerical analysis of flow of an ideal fluid past an airfoil p 2 A90-10228
- The production of uniformly sheared streams by means of double gauzes in wind tunnels - A mathematical analysis p 131 A90-15887
- Static and dynamic loss of stability of elements of a supersonic aeroplane covering - Numerical analysis p 346 A90-25186
- Finite element numerical analysis for transonic flows around lifting fuselages p 558 A90-37216
- Numerical analysis of viscous-inviscid interaction in transonic flow p 627 A90-42363
- Analysis of internal flow in a ventral nozzle for STOVL aircraft
[AIAA PAPER 90-1899] p 739 A90-42688
- On numerical prediction of sound field generated by propeller p 895 A90-49485
- Computation of ramjet internal flowfields
[AD-A212001] p 114 A90-11743
- Unsteady three-dimensional thin-layer Navier Stokes solutions on dynamic blocked grids
[AD-A212377] p 136 A90-12899
- Analysis and numerical solution of flow over airfoil with control flap p 318 A90-17584
- Numerical algorithms for parallel computers
[AD-A216812] p 377 A90-18181
- Modification and improvement of software for modeling multidimensional reacting fuel flows
[AD-A217789] p 533 A90-20235
- Theory and numerical analysis of single and multi-element nozzle propellers
[LR-579] p 572 A90-21741
- Analysis of internal flow in a ventral nozzle for STOVL aircraft
[NASA-TM-103123] p 666 A90-23404
- NUMERICAL CONTROL**
- Digital control experiment research on the engine JT15D-4 p 190 A90-18600
- Digital control of local sound fields in an aircraft passenger compartment p 247 A90-23113
- An automatic system for the programmed control of the parameters of the vibrational and thermal testing of the blades of gas turbine engines p 343 A90-24216

- The selection of actuation devices for aircraft pneumatic valves in systems under computer control
[SAE PAPER 891456] p 368 A90-27425
- Design and development of a facility for compressible dynamic stall studies of a rapidly pitching airfoil
p 436 A90-28255
- A new data acquisition, display and control system for the ARA transonic wind tunnel p 436 A90-28256
- Computer controlled test bench for axial turbines and propellers p 437 A90-28288
- A new type of calibration rig for wind tunnel balances p 438 A90-28305
- Digital-flutter-suppression-system investigations for the active flexible wing wind-tunnel model
[AIAA PAPER 90-1074] p 430 A90-29382
- Design of adaptive digital controllers incorporating dynamic pole-assignment compensators for high-performance aircraft p 432 A90-30714
- Multivariable control design for the control reconfigurable combat aircraft (CRCA)
p 432 A90-30715
- New power system architecture for the 747-400
p 508 A90-33349
- DIGITAC - A unique digital flight control testbed aircraft
[AIAA PAPER 90-1288] p 519 A90-33931
- A design method for real-time computer control hydraulic force system p 590 A90-36434
- Implementation of a transputer-based flight controller p 667 A90-38966
- Digital control of magnetic bearings supporting a multimass flexible rotor p 682 A90-40712
- Fracture control via DRM-Algorithm
p 694 A90-41343
- Digital autopilot for light aircraft p 653 A90-41741
- Use of smart actuators for the tail rotor collective pitch control p 688 A90-42483
- Full Authority Digital Engine Control for the AS 355 N TM 319 engines p 665 A90-42486
- A test matrix sequencer for research test facility automation
[AIAA PAPER 90-2386] p 759 A90-42791
- Designing and tuning the digital controller of an electronic fuel control unit for small gas turbine engines
[SAE PAPER 892255] p 747 A90-45457
- Development and testing of methodology for evaluating the performance of multi-input/multi-output digital control systems
[AIAA PAPER 90-3501] p 867 A90-47747
- Fabrication of complex composite structures using advanced fiber placement technology
p 954 A90-50111
- Automated prepreg tow placement for composite structures p 954 A90-50113
- Combined advanced foundry and quality control techniques to enhance reliability of castings for the aerospace industry p 64 A90-10240
- Application of numerical optimization techniques to control system design for nonlinear dynamic models of aircraft p 593 A90-23032
- NUMERICAL FLOW VISUALIZATION**
- Numerical simulation of reversed flow over a supersonic delta wing at high angle of attack
[AIAA PAPER 89-1802] p 8 A90-11849
- Numerical simulation of turbomachinery flows with a simple model of viscous effects - Comparison with experimental data
[ONERA, TP NO. 1989-122] p 10 A90-12510
- Three dimensional numerical simulation for an aircraft engine type combustion chamber
[ONERA, TP NO. 1989-120] p 49 A90-12591
- Application of the hypersonic analogy for validation of numerical simulations p 16 A90-12838
- Critique of turbulence models for shock-induced flow separation p 17 A90-12851
- Experimental and numerical investigation of vortex flow over a sideslipping delta wing p 17 A90-13016
- Numerical simulation of an impinging jet on a flat plate p 86 A90-15821
- Symposium on Numerical and Physical Aspects of Aerodynamic Flows, 4th, California State University, Long Beach, Jan. 16-19, 1989, Proceedings
p 144 A90-16751
- Numerical simulation of separated and vortical flows on bodies at large angles of attack p 146 A90-16772
- Computational and experimental studies of compressible dynamic stall p 146 A90-16776
- Numerical simulation of wings in steady and unsteady ground effects p 153 A90-17866
- High-resolution upwind scheme for vortical-flow simulations p 153 A90-17872
- Numerical modeling of a viscous separated flow in the near wake p 159 A90-19236
- Numerical simulation of unsteady flow about cambered plates p 159 A90-19389

- Video visualization of separation shock motion from measured wall pressure signals in a Mach 5 compression ramp interaction
[AIAA PAPER 90-0074] p 162 A90-19670
- Development of finite element methods for compressible Navier-Stokes flow simulations in aerospace design
[AIAA PAPER 90-0403] p 166 A90-19833
- Vortical flows over delta wings and numerical prediction of vortex breakdown
[AIAA PAPER 90-0102] p 227 A90-22166
- Numerical simulation of vortex breakdown via 3-D Euler equations
[ONERA, TP NO. 1989-211] p 303 A90-25344
- Comparison between thin layer and full Navier-Stokes simulations over a supersonic delta wing
[AIAA PAPER 90-0589] p 314 A90-26968
- A laser based computer aided non-intrusive technique for full field flow characterization in macroscopic curved channels p 535 A90-32293
- Numerical computations of transonic critical aerodynamic behavior p 469 A90-32457
- Numerical simulations of an oblique detonation wave engine p 508 A90-32964
- Solution of Euler equations with unstructured meshes p 558 A90-37343
- Supercomputer applications in gas turbine flowfield simulation p 620 A90-40495
- Numerical solution of 3-D hybrid problems in turbomachinery p 621 A90-40501
- Zonal Navier-Stokes methodology for flow simulation about a complete aircraft p 709 A90-44727
- A characterization and search technique for unsteady flow control problems
[AIAA PAPER 90-3102] p 796 A90-45914
- Prediction of aerodynamic performance of airfoils in low Reynolds number flows p 799 A90-46360
- Numerical simulation of three-dimensional nonstationary flows and variable aerodynamic forces in turbomachine stages p 814 A90-49465
- A proper orthogonal decomposition of a simulated supersonic shear layer p 904 A90-51009
- Numerical investigations of heat transfer and flow rates in rotating cavities. Simulation of the movement generated by wall temperature gradients, by source-sink mass flows or by the differential rotation of the walls, under the influence or conolis and centrifugal forces
[ETN-90-96253] p 454 A90-18695
- Prediction of aerodynamic performance of airfoils in low Reynolds number flows p 632 A90-23360
- [DLC-EST-TN-031] p 632 A90-23360
- Development of a system for the numerical simulation of Euler flows, with results of preliminary 3-D propeller-slipstream/exhaust-jet calculations
[NLR-TR-88008-U] p 776 A90-26285

NUMERICAL INTEGRATION

- A new quick method for integrating Euler equations for plane transonic flows p 295 A90-24105
- Numerical aerodynamics via formal integration - Laplace, Euler, Prandtl, Navier-Stokes and Reynolds equations p 305 A90-25800
- Supersonic nozzle design of arbitrary cross-section p 515 A90-21035

NUMERICAL STABILITY

- Development of a VSAERO (Vortex Separation Aerodynamics) model of the F/A-18
[AD-A212442] p 95 A90-12566

NUMERICAL WEATHER FORECASTING

- Fog formation at Perth Airport p 611 A90-37748

NUSSELT NUMBER

- Characteristics of partial length circular pin fins as heat transfer augmentors for airfoil internal cooling passages
[ASME PAPER 89-GT-87] p 359 A90-23806

**O RING SEALS**

- Analysis of thermal gradient effects in oil ring seals p 682 A90-40716

OBJECT PROGRAMS

- An object-oriented solution example: A flight simulator electrical system
[AD-A219190] p 761 A90-25145

OBLIQUE SHOCK WAVES

- On the lengthscales of laminar shock/boundary-layer interaction p 5 A90-11610
- Swept shock/boundary-layer interactions - Tutorial and update
[AIAA PAPER 90-0375] p 228 A90-22207
- Numerical simulations of an oblique detonation wave engine p 508 A90-32964
- Large-scale structure in a supersonic slot-injected flowfield p 602 A90-36265
- Glancing shock-boundary layer interactions p 319 A90-17571

- Interaction of an oblique shock wave with supersonic flow over a blunt body p 398 A90-19197
- Interactive calculation procedures for mixed compression inlets
[NASA-CR-186581] p 718 A90-25934
- OBLIQUE WINGS**
- Static stability and control characteristics of scissor wing configurations p 433 A90-31277
- Integrated structure/control concepts for oblique wing roll control and trim p 433 A90-31282
- Static aeroelastic tailoring for oblique wing lateral trim p 667 A90-40689
- Static aeroelastic analysis for generic configuration aircraft
[NASA-TM-89423] p 52 A90-10042
- Output model-following control synthesis for an oblique-wing aircraft
[NASA-TM-100454] p 435 A90-19241
- Static aeroelastic analysis of a three-dimensional generic wing
[NASA-TM-102231] p 509 A90-20087
- The aerodynamic design of the oblique flying wing supersonic transport
[NASA-CR-177552] p 923 A90-28540
- OBSERVABILITY (SYSTEMS)**
- Robust control system design synthesis with observers p 375 A90-25994
- A study on the application of controllability and observability concepts in the design of flight control systems p 693 A90-39303
- Elements of active vibration control for rotating machinery
[NASA-TM-102368] p 610 A90-22703
- Observability of relative navigation using range-only measurements p 917 A90-29360
- OBSERVATION AIRCRAFT**
- Pilotless airplanes p 103 A90-11734
- OBSTACLE AVOIDANCE**
- Helicopter obstacle avoidance system - The use of manned simulation to evaluate the contribution of key design parameters p 417 A90-28218
- A laser obstacle avoidance and display system p 419 A90-30694
- Obstacle warning system for helicopters p 653 A90-41114
- Concept development of automatic guidance for rotorcraft obstacle avoidance p 669 A90-41632
- Image based range determination
[AIAA PAPER 90-3404] p 822 A90-47659
- Kalman filter based range estimation for autonomous navigation using imaging sensors p 578 A90-22238
- Velocity filtering applied to optical flow calculations
[NASA-TM-102802] p 916 A90-28512
- OCCURRENCES**
- Additive evaluation criteria for aircraft noise p 698 A90-24867
- OCEAN DYNAMICS**
- Aircraft measurements of sea surface conditions and their relationship to marine boundary-layer dynamics p 888 A90-47572
- OCEAN SURFACE**
- A bearing error in the VHF omnirange due to sea surface reflection p 402 A90-27875
- OCEANOGRAPHIC PARAMETERS**
- Meeting Review: Workshop on Airborne Instrumentation
[PB89-174775] p 39 A90-10032
- OGIVES**
- The effect of flow curvature on the aerodynamic characteristics of an ogive-cylinder body p 82 A90-13785
- Unified super/hypersonic similitude for steady and oscillating cones and ogives p 82 A90-13786
- Supersonic/hypersonic flow past wedge and plane ogive in oscillation p 85 A90-15231
- Experimental study of nonsteady asymmetric flow around an ogive-cylinder at incidence p 384 A90-27985
- Aerodynamic effects of body roughness
[AIAA PAPER 90-2850] p 712 A90-45168
- An experimental investigation of the aerodynamic characteristics of slanted base ogive cylinders using magnetic suspension technology
[NASA-CR-181708] p 21 A90-10834
- The determination of the aerodynamic characteristics of an ogive-cylinder body in subsonic, curved, incompressible flow, and an assessment of the effect of flow curvature
[REPT-87-13] p 89 A90-11712
- Subsonic sting interference on the aerodynamic characteristics of a family of slanted-base ogive-cylinders
[NASA-CR-4299] p 633 A90-24242

OH-58 HELICOPTER

- The collection of usage data to improve structural integrity of operational helicopters p 651 A90-39983
 The Mast Mounted Sight 771 processor upgrade program -- for helicopter p 926 A90-51058

OIL ADDITIVES

- Determination of additive contents in aviation and turbine oils p 532 A90-34681

OILS

- High temperature VSCF (Variable Speed Constant Frequency) generator system [AD-A210823] p 71 N90-10351

OMEGA NAVIGATION SYSTEM

- Global Positioning System: Arrival in the fleet - A GPS AN/SRN-25(V) receiver assessment p 331 A90-26338
 Differential Omega/VLF as a world-wide navigation aid in the 21st century p 727 A90-45232
 Omega - A low-cost precision synchronizer p 727 A90-45233
 Omega coverage - Analytical and empirical methods and solutions p 728 A90-45234

ON-LINE SYSTEMS

- On-line temperature profile display system [ASME PAPER 89-GT-10] p 374 A90-23755
 Application possibilities of expert systems in modern maintenance for increasing operational security p 892 A90-49271
 Replay and transmission of AIMS-data to mainframe computer using remote transcribers p 892 N90-27634
 An expert system to perform on-line controller restructuring for abrupt model changes [NASA-TM-103609] p 964 N90-29121
 Noncontact measurement of rotating blade vibrations [NAL-TR-1033] p 961 N90-29687

ONBOARD DATA PROCESSING

- Magnetic recording on board aircraft p 39 A90-12195
 Testing facility and procedure of the ATTAS on-board data acquisition system p 39 A90-12202
 Rapsat - Application of onboard processing for communication and surveillance in air traffic control [AIAA PAPER 90-0883] p 331 A90-25702
 A review of the V-22 health monitoring system p 417 A90-28209
 Use of Onboard Data Loaders [SAE PAPER 89-2327] p 738 A90-45485
 The Operational Loads Monitoring System (OLMS) p 926 A90-49879
 An approach to on-board optimization of cruise at constant altitude [LR-581] p 578 N90-21752
 Past, present and future: Aircraft integrated monitoring systems: An ever-developing technology p 848 N90-27618
 Aircraft condition monitoring system for future Airbus aircraft: New concept for programming and data recording p 848 N90-27619
 The EFA integrated monitoring and recording system: Requirements and concept for implementation p 848 N90-27620
 Multichannel on-board load and fatigue monitoring p 849 N90-27621
 Advanced algorithms design and implementation in on-board microprocessor systems for engine life usage monitoring p 892 N90-27628
 Expert system diagnostics and parts life tracking as applied to the AV-8B aircraft for the USMC p 884 N90-27629
 AIMS for helicopters p 820 N90-27639
 The new US flight recorder regulations p 849 N90-27642
 Australian experience in flight recorder readout and analysis p 820 N90-27644
 On-board planning and control of 4D-trajectories in the TMA p 826 N90-27680
 On the structure of a future flight operations system p 826 N90-27682

ONBOARD EQUIPMENT

- Intelligent built-in test and stress management p 448 A90-28343
 Auxiliary power unit maintenance aid - Flight line engine diagnostics p 382 A90-28348
 An integrated diagnostics approach to embedded and flight-line support systems p 460 A90-30767
 Development of an automatic ground collision avoidance system using a digital terrain database [AD-A216247] p 329 N90-17621
 Passive navigation using image irradiance tracking p 578 N90-22232
 On-board planning and control of 4D-trajectories in the TMA p 826 N90-27680

ONE DIMENSIONAL FLOW

- Dynamic characteristics of one-dimensional gas flow with friction p 296 A90-24115

OPERATING COSTS

- Design of aeroengines in a low-fuel price scenario p 739 A90-42653
 Commercial aircraft DOC methods [AIAA PAPER 90-3224] p 897 A90-48843
 Revolutionary opportunities for materials and structures study [NASA-CR-179642] p 63 N90-10184
 Designing for reliable and low maintenance cost aero engines [PNR90570] p 115 N90-12604
 Reducing C130E Hercules operating costs in the Royal Australian Air Force and the United States Air Force by increasing cruise speeds [AD-A215747] p 338 N90-17629
 Energy Efficient Engine program advanced turbofan nacelle definition study [NASA-CR-174942] p 930 N90-28560
 Energy Efficient Engine: High-pressure compressor test hardware detailed design report p 932 N90-28570
 Airline productivity relating on the fuel cost. (2): Fuel consumption values and fuel efficiency [NAL-TM-604-2] p 913 N90-29333
 The cost of air service fragmentation [TT-9010] p 913 N90-29334

OPERATING SYSTEMS (COMPUTERS)

- Integrated approach fault tolerance-current state and future requirements [AD-A214402] p 275 N90-15465
 The implications of using integrated software support environment for design of guidance and control systems software [AGARD-AR-229] p 434 N90-18432
 TRENDS: The aeronautical post-test database management system [NASA-TM-101025] p 761 N90-25149
 Advanced transport operating system software upgrade: Flight management/flight controls software description [NASA-CR-181936] p 893 N90-28366

OPERATING TEMPERATURE

- High performance single-mode coupler for harsh environments p 78 A90-11027
 Gas turbine combustion - A personal perspective p 283 A90-20604
 Turbine fuel alternatives (near term) [AD-A21405] p 601 N90-22695

OPERATIONAL HAZARDS

- Independent operations on closely spaced runways p 821 A90-46393

OPERATIONS RESEARCH

- The comparison of the airbase simulation models airbase and sustained [FEL-1988-66] p 123 N90-12629
 Four-dimensional navigation and Flight Management Systems p 826 N90-27681

OPERATOR PERFORMANCE

- Parallel approach separation and controller performance: A study of the impact of two separation standards [DOT/FAA/CT-TN89/50] p 99 N90-12574
 The application of queueing theory to the modelling of CP-140 aircraft communications [AD-A213479] p 274 N90-15310
 Aviation safety: Serious problems continue to trouble the air traffic control work force. Report to congressional requesters [GAO/RCED-89-112] p 724 N90-25959

OPERATORS (PERSONNEL)

- A framework for the optimal design of instructor/operator stations in flight simulators p 779 A90-45373

OPTICAL COMMUNICATION

- An analysis of reliability in fiber optic ring and star networks p 78 A90-11666
 Fiber optics for advanced aircraft p 68 A90-11702
 Laser communication system design p 26 A90-11813
 Development of air-to-air laser communications p 487 A90-31938
 Extended communication path length scintillation measurements and model - A discussion of results -- of atmospheric laser experiments p 725 A90-43230

OPTICAL COMPUTERS

- Model attitude measurement system p 539 A90-34235

OPTICAL COUPLING

- High performance single-mode coupler for harsh environments p 78 A90-11027

OPTICAL EQUIPMENT

- Fiber optic systems for mobile platforms II; Proceedings of the Meeting, Boston, MA, Sept. 6, 7, 1988 [SPIE-989] p 67 A90-11659
 Applications of flight control system methods to an advanced combat rotorcraft [NASA-TM-101054] p 119 N90-11752

- The Advanced Digital-Optical Control System (ADOCS) user demonstration program [AD-A215984] p 349 N90-17644

OPTICAL FIBERS

- A review of fiber optic flight experience - Past problems, future direction p 38 A90-11661
 Composite-embedded optical fibers for communication links p 139 A90-13847
 Fiber-optic turbine inlet temperature measurement system (FOTITMS) [AIAA PAPER 90-2033] p 657 A90-40603
 Fault tolerant architecture for a fly-by-light flight control computer p 860 A90-46931
 Tests for integrating measurement of gas pressures in flight propellers [ETN-90-96498] p 634 N90-24253

OPTICAL FILTERS

- New technology advances for brighter color CRT displays p 652 A90-40399
 Velocity filtering applied to optical flow calculations [NASA-TM-102802] p 916 N90-28512

OPTICAL GYROSCOPES

- Measurement of angles and angle characteristics with accelerometers and gyroscopes p 653 A90-41730
 Providing an inexpensive gyro for the navigation mass market p 848 A90-49502

OPTICAL MATERIALS

- Optical window materials for hypersonic flow p 496 A90-34581

OPTICAL MEASUREMENT

- A dynamic optical model attitude measurement system p 539 A90-34236
 Design considerations for a compact table top hypersonic simulator of aero-optic effects p 525 A90-34585
 Remote detection of boundary-layer transition by an optical system p 139 N90-12524
 Analysis and test of a wide angle spectrometer [AD-A215819] p 372 N90-18030
 A video-based experimental investigation of wing rock p 592 N90-21771

OPTICAL MEASURING INSTRUMENTS

- Review of fiber optic methods for strain monitoring and non-destructive testing p 67 A90-11042
 Fiber optics for advanced aircraft p 68 A90-11702
 Applications of fiber optic sensors in advanced engine controls p 68 A90-11703
 Fiber optic sensors for aircraft p 68 A90-11704
 Monitoring of aircraft assembly: Optical and laser methods --- Russian book p 285 A90-24229
 Smart structures with nerves of glass p 444 A90-27951
 An optical angle of attack sensor p 448 A90-28263
 Model incidence measurement using the SAAB Elopotos system --- IR instrumentation for measuring angle of attack in transonic wind tunnel models p 446 A90-28264
 Fiber optics smart structures program at UTIAS p 535 A90-32864
 Design and fabrication considerations for composite structures with embedded fiber optic sensors p 536 A90-32871
 A measurement window for a cryogenic windtunnel p 523 A90-34233
 Applications of fiber optic sensors in the aerospace and marine industries p 603 A90-36782

OPTICAL PATHS

- Variability characteristics of the meteorological optical range field in an optically inhomogeneous atmosphere p 962 A90-50784

OPTICAL PROPERTIES

- Table top experimental simulation of hypersonic aero-optical effects --- encountered by cooled window on interceptor p 525 A90-34586

OPTICAL RADAR

- Target classification by vibration sensing --- for helicopter detection p 1 A90-10170
 Concept of an MTI search radar p 487 A90-33613
 Airborne CO2 Doppler lidar for wind shear detection p 849 N90-27640

OPTICAL REFLECTION

- A multichannel wide FOV infrared radiometric system p 67 A90-11410

OPTICAL SCANNERS

- Analysis and test of a wide angle spectrometer [AD-A215819] p 372 N90-18030

OPTICAL TRACKING

- Supplemented visual cues for helicopter hovering above a moving ship deck p 195 A90-17704

OPTIMAL CONTROL

- The discontinuity condition in the optimal control problem for a composite system p 76 A90-10848
 Optimization of the observations and control of aircraft --- Russian book p 60 A90-12468
 Synthesis of locally optimal aircraft control in the presence of delay p 137 A90-14561

Parametric synthesis of piecewise constant locally optimal aircraft control under conditions of indeterminacy p 137 A90-14576

A synthetic research for aircraft active flutter suppression p 195 A90-16827

The optimum control and adaptive control for airplane cabin pressure p 182 A90-18627

Minimum fuel cruise by periodic optimization p 182 A90-19429

Model problems of continuous control law optimization for a tensometric aerodynamic experiment p 295 A90-24086

A study of approximately optimal cruising flight regimes of variable-mass aircraft p 430 A90-29187

Flutter suppression control law synthesis for the active flexible wing model p 517 A90-33403

The method of random variable structure optimal control for aircraft p 590 A90-37220

Design methodology for multivariable helicopter control systems p 669 A90-42461

Analytical study of dynamic response of helicopter in autorotative flight p 670 A90-42469

Toward a theory of aircraft agility [AIAA PAPER 90-2808] p 752 A90-45143

Optimal input design for aircraft parameter estimation using dynamic programming principles [AIAA PAPER 90-2801] p 753 A90-45157

Optimal control system design for departure prevention [AIAA PAPER 90-2837] p 754 A90-45167

Optimal paths through downbursts p 755 A90-45330

Control of an aircraft in downbursts p 755 A90-45331

Helicopter trim with flap-lag-torsion and stall by an optimized controller p 755 A90-45332

Optimal autorotational descent of a helicopter with control and state inequality constraints p 756 A90-45344

Active vibration control for flexible rotor by optimal direct-output feedback control p 879 A90-46222

Helicopter individual blade control through optimal output feedback p 861 A90-46956

Singular, periodic solutions in aircraft cruise-dash optimization [AIAA PAPER 90-3369] p 863 A90-47627

Local adaptive maneuvering optimization for fighter aircraft [AIAA PAPER 90-3453] p 890 A90-47706

A comparison of inverse control with optimal control [AIAA PAPER 90-3484] p 866 A90-47733

Optimal rigid body reorientation problem [AIAA PAPER 90-3485] p 867 A90-47734

Optimal periodic cruise with singular control [AIAA PAPER 90-3490] p 833 A90-47738

System optimization for maximizing reconnaissance mission range of a hypersonic cruise vehicle [AIAA PAPER 90-3292] p 837 A90-48876

Integration of a centralized multiplexed control unit into the cockpit of an aircraft [F6150-DT410-1-88329] p 120 N90-12622

Aeroelastic control of composite lifting surfaces: Integrated aeroelastic control optimization p 198 N90-13396

Guidance and Control strategies for aerospace vehicles [NASA-CR-186195] p 199 N90-14243

Guidance analysis of the aeroglide plane change maneuver as a turning point problem [NASA-TM-101639] p 259 N90-15110

Output model-following control synthesis for an oblique-wing aircraft [NASA-TM-100454] p 435 N90-19241

Experimental and theoretical investigation of optimal control methods with model reduction p 521 N90-21039

Optimal control of an aircraft flying through a downburst p 591 N90-21765

Advances in optimal active control techniques for aerospace systems; application to aircraft active landing gear p 592 N90-21769

The insertion of human dynamics models in the flight control loops of V/STOL research aircraft. Appendix 2: The optimal control model of a pilot in V/STOL aircraft control loops [NASA-CR-186598] p 598 N90-21776

Prediction of longitudinal pilot induced oscillations using the optimal control model [AD-A220593] p 671 N90-23412

Model following control system design: Preliminary ATTAS in-flight simulation test results [PD-FC-9003] p 758 N90-26010

Effective optimal control of a fighter aircraft engine p 928 N90-28548

Control and estimation for aerospace applications with system time delays p 918 N90-29367

Optimal trajectories for hypervelocity flight p 918 N90-29378

Proceedings of damping '89. Volume 1: Pages AAB-1 through DCD-11 [AD-A223431] p 960 N90-29664

OPTIMIZATION

Structural optimization of lifting surfaces with divergence and control reversal constraints p 127 A90-13770

Optimization methods applied to aerodynamic design problems in computational fluid dynamics p 156 A90-18308

Optimum design of rotational wheels under transient thermal and centrifugal loading p 270 A90-20770

Optimum design of composite structures p 272 A90-22135

Optimal placement of tuning masses for vibration reduction in helicopter rotor blades p 247 A90-23117

Minimizing life cycle cost for subsonic commercial aircraft p 283 A90-23282

Selection of the blended wing configuration for light aircraft p 234 A90-23401

Optimal selection of the parameters to be measured during the identification of gas turbine engines. I - Problem statement p 255 A90-23410

A parametric optimization algorithm for the electrical distribution circuits of civil aircraft p 255 A90-23417

Numerical optimization of axial compressor designs [ASME PAPER 89-GT-14] p 340 A90-23758

A proposal for optimized design of multistage compressors [ASME PAPER 89-GT-34] p 288 A90-23766

Threshold performance optimization of a rotor-bearing system subjected to leakage excitation [ASME PAPER 89-GT-126] p 360 A90-23825

Axial flow compressor design optimization. I - Pitchline analysis and multivariable objective function influence [ASME PAPER 89-GT-201] p 342 A90-23873

Axial flow compressor design optimization. II - Through-flow analysis [ASME PAPER 89-GT-202] p 342 A90-23874

Efficient structural material distribution in the main frame of a flight vehicle p 363 A90-24092

Optimization of the sound-absorption lining parameters of an ejector jet muffler p 378 A90-24117

Application of the MARS system in aircraft-structure design p 374 A90-24127

Optimization of the relative thicknesses of a high-aspect-ratio wing in a multicriteria formulation p 334 A90-24133

The local surface variation method in profile shape optimization problems p 297 A90-24136

Multicriteria optimization of lugs in hinge joints p 364 A90-24162

ATC ground communications system optimization techniques p 330 A90-25568

The design of supersonic aircraft and space vehicles by using global optimization techniques p 353 A90-25781

Unified optimal criterion method - Combination of direction of gradient and ejection line p 367 A90-26077

Helicopter design optimization for maneuverability and agility p 408 A90-28212

AIAA/ASME/ASCE/AHS/ASC Structures, Structural Dynamics and Materials Conference, 31st, Long Beach, CA, Apr. 2-4, 1990, Technical Papers. Part 1 - Materials, engineering optimization and design p 449 A90-29226

Aeroelastic optimization of a helicopter rotor using an efficient sensitivity analysis [AIAA PAPER 90-0951] p 410 A90-29237

Exploratory design studies using an integrated multidisciplinary synthesis capability for actively controlled composite wings [AIAA PAPER 90-0953] p 411 A90-29238

Influence of structural and aerodynamic modeling on flutter analysis [AIAA PAPER 90-0954] p 411 A90-29239

Evaluation of current multiobjective optimization methods for aerodynamic problems using CFD codes [AIAA PAPER 90-0955] p 411 A90-29240

An application of structural optimization in wind tunnel model design [AIAA PAPER 90-0956] p 438 A90-29241

Optimal computer-aided design of the blading of axial-flow turbines --- Russian book p 452 A90-30268

Structural optimization with aeroelastic constraints of rotor blades with straight and swept tips p 535 A90-32475

The influence of mathematical optimization methods on the design of aircraft structures p 492 A90-33387

Stability sensitivity analysis of a helicopter rotor p 580 A90-36273

High-quality approximation of eigenvalues in structural optimization p 603 A90-36277

Application of optimization methods to helicopter rotor blade design p 604 A90-37337

Improvement of helicopter handling qualities using H(infinity)-optimization p 667 A90-38965

Multilevel optimization of large-scale structures in a parallel computing environment p 693 A90-39180

Development and application of an optimization procedure for space and aircraft structures p 679 A90-39186

Boundary-element shape optimization system for aircraft structural components p 680 A90-39786

Synthesis of optimal multidimensional digital systems for the simulation of the angular motions of a flight vehicle under random loading p 669 A90-41957

Propulsion system-flight control integration-flight evaluation and technology transition [AIAA PAPER 90-2280] p 644 A90-42106

Application of 3-D flow analysis to the design of a high work transonic turbine p 628 A90-42395

Nozzle design optimization by method-of-characteristics [AIAA PAPER 90-2024] p 741 A90-42719

Optimization of glides for constant wind fields and course headings p 731 A90-44734

Multivariable optimization scheme for tuning the controller of an electronic fuel control unit for small gas turbine engines p 745 A90-45301

Design of supersonic wings using an optimization strategy coupled with a solution scheme for the Euler equations [AIAA PAPER 90-3060] p 794 A90-45895

Decentralized systems --- Book p 888 A90-46001

Multicriteria optimal layouts of aircraft and spacecraft structures p 889 A90-46046

Wing design optimization under stress-strain constraints using full-strength and minimum mass criteria p 804 A90-46554

Optimum aircraft design: Multipurpose approach --- Russian book p 829 A90-46618

GTPDP - A rotary wing aircraft preliminary design and performance estimation program including optimization and cost p 830 A90-46944

Performance of an optimized rotor blade at off-design flight conditions p 830 A90-46946

Model reduction with a finite-interval H(infinity) criterion [AIAA PAPER 90-3473] p 890 A90-47723

Genetic algorithms in control system optimization [AIAA PAPER 90-3488] p 867 A90-47736

Iterative preliminary design tools for composite structures p 882 A90-48045

Some computational and experimental aspects of optimal design process of composite structures p 882 A90-48050

Optimal camber distributions with multiple constraints p 810 A90-48078

System optimization for maximizing reconnaissance mission range of a hypersonic cruise vehicle [AIAA PAPER 90-3292] p 837 A90-48876

The BAe (commercial aircraft) LTD transport aircraft synthesis and optimisation program (TASOP) [AIAA PAPER 90-3295] p 837 A90-48879

Design synthesis and optimization of joined-wing transports [AIAA PAPER 90-3197] p 838 A90-49102

A method for lifting surface design using nonlinear optimization [AIAA PAPER 90-3290] p 813 A90-49122

A efficient technique for multiobjective design optimization [AIAA PAPER 90-3291] p 892 A90-49123

Process optimization of high temperature composite materials p 943 A90-50130

Optimization of the shape of a sealed shell and of the size and location of its reinforcements p 957 A90-50773

Control law synthesis and optimization software for large order aeroservoelastic systems p 61 N90-10111

Integrated multidisciplinary design optimization of rotorcraft [NASA-TM-101642] p 36 N90-10889

A design procedure for the handling qualities optimization of the X-29A aircraft [NASA-TM-4142] p 119 N90-11753

Controller design for active vibration suppression of a helicopter [DFVLR-FB-89-20] p 120 N90-11760

Airframe structural dynamic considerations in rotor design optimization [NASA-TM-101646] p 134 N90-12057

Integrated multidisciplinary optimization of rotorcraft: A plan for development [NASA-TM-101617] p 106 N90-12580

General approach and scope --- rotor blade design optimization p 106 N90-12581

Validation of the procedures --- integrated multidisciplinary optimization of rotorcraft p 107 N90-12587

Appendix: Results obtained to date --- integrated multidisciplinary optimization of rotorcraft

- Reduction of turbulent drag: Boundary layer manipulators
[CERT-RSF-OA-74/2259-AYD] p 107 N90-12588
- Aeroelastic control of composite lifting surfaces: Integrated aeroelastic control optimization
p 198 N90-13396
- Discretization and model reduction for a class of nonlinear systems
p 198 N90-13397
- Introduction to data items on flight path optimization [ESDU-89015]
p 185 N90-14221
- Guidance analysis of the aeroglide plane change maneuver as a turning point problem
[NASA-TM-101639] p 259 N90-15110
- Synthesis of control law, on a RPV, in order to minimize the number of sensors
p 260 N90-15925
- Optimization of the effective GPS data rate
p 489 N90-20932
- Computer-aided structural optimisation of aircraft structures
[BR112837] p 499 N90-20973
- Computational Methods for Aerodynamic Design (Inverse) and Optimization
[AGARD-CP-463] p 500 N90-20976
- Progress in inverse design and optimization in aerodynamics
p 482 N90-20977
- Aerodynamic optimization by simultaneously updating flow variables and design parameters
p 501 N90-20991
- Constrained spanload optimization for minimum drag of multi-lifting-surface configurations
p 501 N90-20992
- Numerical optimization of target pressure distributions for subsonic and transonic airfoil design
p 502 N90-20993
- A tool for automatic design of airfoils in different operating conditions
p 502 N90-20994
- The use of numerical optimization for helicopter airfoil and blade design
p 502 N90-20995
- Aerodynamic design by optimization
p 502 N90-20996
- Numerical optimization of wings in transonic flow
p 502 N90-20997
- Aerodynamic design via control theory
p 546 N90-20998
- Optimization of aerodynamic designs using computational fluid dynamics
p 541 N90-20999
- Recent improvements in the scope and accuracy of the performance prediction of nozzle propellers
[LR-598] p 572 N90-21742
- Optimization and guidance of flight trajectories in the presence of windshear
[NASA-CR-186163] p 574 N90-21747
- A comparison of time-optimal interception trajectories for the F-8 and F-15
[NASA-CR-186300] p 581 N90-21753
- Conceptual design optimization study
[NASA-CR-4298] p 582 N90-21755
- Optimal control of an aircraft flying through a downburst
p 591 N90-21765
- Multilevel decomposition approach to the preliminary sizing of a transport aircraft wing
[NASA-CR-4296] p 583 N90-22557
- The use of supercomputers for the design and analysis of constructions
p 612 N90-22977
- Algorithms for computing the multivariable stability margin
p 612 N90-22999
- Application of numerical optimization techniques to control system design for nonlinear dynamic models of aircraft
p 593 N90-23032
- Development and application of an optimization procedure for space and aircraft structures
[MBB-FW-522/S/PUB-383] p 779 N90-25078
- An accurate numerical technique for determining flight test rate gyroscope biases prior to takeoff
[AD-A220987] p 739 N90-25138
- A decision-making aid for multi-layer radar absorbent coverings
[ESA-TT-1173] p 773 N90-25267
- A contribution to the economic, optimal dimensioning, and shaping of aircraft structures using a design model
[ETN-90-96966] p 737 N90-25976
- Development of a method to design helicopter rotors
[REPT-100-30-03] p 845 N90-26830
- Air traffic management in Europe: Structure, tasks, potential
p 825 N90-27677
- Four-dimensional navigation and Flight Management Systems
p 826 N90-27681
- Aerodynamic interferences of in-flight thrust reversers in ground effect
p 921 N90-28529
- System reliability optimization of aircraft wings
p 923 N90-28536
- An enhanced integrated aerodynamic load/dynamic optimization procedure for helicopter rotor blades
[NASA-CR-4326] p 924 N90-29383

- Aircraft design for mission performance using nonlinear multiobjective optimization methods
[NASA-CR-4328] p 925 N90-29384
- Multi-disciplinary optimization of aeroservoelastic systems
[NASA-CR-185931] p 925 N90-29385
- OPTOELECTRONIC DEVICES**
- Comparison of three concepts for a long stroke displacement transducer
p 66 A90-11041
- Optic multiplex for aircraft sensors - Issues and options
p 38 A90-11660
- OPST1 - An optical yaw control system for high performance helicopters
p 430 A90-28220
- Measurement of wind tunnel model deformation under airload
p 522 A90-33370
- Feasibility study of RADAC stereo optoelectronic model deformation measurement system for ETW
p 539 A90-34239
- Optoelectronic guidance sensors (5th revised and enlarged edition) --- Russian book
p 881 A90-46620
- ORBIT TRANSFER VEHICLES**
- Computational requirements for hypersonic flight performance estimates
p 440 A90-29686
- Guidance and Control strategies for aerospace vehicles
[NASA-CR-186195] p 199 N90-14243
- ORBITAL MANEUVERING VEHICLES**
- Autonomous integrated GPS/INS navigation experiment for OMV. Phase 1: Feasibility study
[NASA-CR-4267] p 489 N90-20969
- ORBITAL MANEUVERS**
- Optimal plane change by low aerodynamic forces
[AIAA PAPER 90-2831] p 763 A90-45137
- Guidance analysis of the aeroglide plane change maneuver as a turning point problem
[NASA-TM-101639] p 259 N90-15110
- ORGANIC COMPOUNDS**
- Development of a water-borne non-chromated primer and topcoat for aerospace applications
p 956 A90-50213
- ORGANIC MATERIALS**
- Organic coatings - First line of defense
p 204 A90-17300
- HPLC analysis of helicopter rotor blade materials
[AD-A221121] p 650 N90-24270
- ORGANIZATIONS**
- Calendar of selected aeronautical and space meetings
[AGARD-CAL-90/1] p 464 N90-19060
- ORIENTATION**
- Development of a preliminary high-angle-of-attack nose-down pitch control requirement for high-performance aircraft
[NASA-TM-101684] p 399 N90-19206
- ORIFICE FLOW**
- Large-scale structure in a supersonic slot-injected flowfield
p 602 A90-36265
- ORIFICES**
- Effect of the inlet diameter and neck edge radius on the flow coefficient of straight-generatrix nozzles
p 84 A90-14577
- ORTHOGONAL FUNCTIONS**
- An orthogonal algorithm to the maximum likelihood estimation using an efficient method for computing sensitivities
[AIAA PAPER 90-3507] p 891 A90-47753
- ORTHOGONALITY**
- Response of orthogonally stiffened cylindrical shell panels
p 603 A90-36285
- ORTHOTROPISM**
- Noninteractive macroscopic reliability model for ceramic matrix composites with orthotropic material symmetry
[ASME PAPER 89-GT-129] p 360 A90-23827
- OSCILLATING CYLINDERS**
- Response of orthogonally stiffened cylindrical shell panels
p 603 A90-36285
- OSCILLATING FLOW**
- An asymptotic theory for the periodic turbulent boundary layer in zero mean-pressure gradient
[AD-A22832] p 66 A90-10222
- The unsteady aerodynamics of an oscillating cascade in a compressible flow field
p 7 A90-11789
- Finite element method for unsteady three-dimensional subsonic flows through a cascade oscillating with steady loading
p 9 A90-11873
- Numerical calculation of unsteady aerodynamic forces for two-dimensional supersonic oscillating cascades by finite element method
p 9 A90-12238
- Unified super/hypersonic similitude for steady and oscillating cones and ogives
p 82 A90-13786
- Supersonic/hypersonic flow past wedge and plane ogive in oscillation
p 85 A90-15231
- Experimental study of 2D/3D interactions between a vortical flow and a lifting surface
p 86 A90-15849
- Potential flow calculation for three-dimensional wings and wing-body combination in oscillatory motion
p 153 A90-17976

- Alleviation of shock oscillations in transonic flow by passive controls
[AIAA PAPER 90-0046] p 161 A90-19648
- Nonaxisymmetric instabilities in a dump combustor with a swirling inlet flow
p 253 A90-21228
- Mean and pulse characteristics of supersonic flow in a wind tunnel with a honeycomb nozzle
p 231 A90-22421
- Self-excited oscillation of transonic flow around an airfoil in two-dimensional channel
[ASME PAPER 89-GT-58] p 290 A90-23784
- Interaction between a vibrating compression shock and a boundary layer
p 298 A90-24143
- Unsteady, separated flow behind an oscillating, two-dimensional spoiler
p 469 A90-32462
- Turbulent plane jet excited mechanically by an oscillating thin plate in the potential core
p 553 A90-35262
- Oscillation of circular shock wave
p 557 A90-36465
- The effect of an oscillatory freestream-flow on a NACA-4412 profile at large relative amplitudes and low Reynolds-numbers
p 560 A90-38495
- Model of a labyrinth seal with flow
p 687 A90-42334
- Large-eddy simulations of flows in a ramjet combustor
p 772 A90-45534
- Flow field around an oscillating cascade
p 814 A90-49459
- Numerical simulation of transonic flow through oscillating and multi-row two-dimensional airfoil cascades
p 814 A90-49460
- Experimental investigation to suppress flow-induced pressure oscillations in open cavities
[AD-A216285] p 320 N90-17578
- Extension of a streamwise upwind algorithm to a moving grid system
[NASA-TM-102800] p 572 N90-21739
- Numerical simulations of flowfields in a central-dump ramjet combustor. 3: Effects of chemistry
[AD-A224145] p 933 N90-28573
- OSCILLATIONS**
- Additions and corrections to SUPER: A program for calculating steady and oscillatory supersonic flow over a thin wing, tail plane and fin
[AD-A211771] p 90 N90-12501
- Unsteady aerodynamics of oscillating and rapidly pitched airfoils
p 235 N90-15074
- Surface pressure distributions on a delta wing undergoing large amplitude pitching oscillations
[NASA-CR-186326] p 317 N90-17558
- Unsteady Aerodynamic Phenomena in Turbomachines
[AGARD-CP-468] p 425 N90-18405
- Numerical investigation of unsteady flow in oscillating turbine and compressor cascades
p 426 N90-18407
- Asymptotic analysis of transonic flow through oscillating cascades
p 427 N90-18421
- Measurement of velocity profiles and Reynolds stresses on an oscillating airfoil
p 397 N90-18427
- An experimental study of the aeroelastic behaviour of two parallel interfering circular cylinders
p 455 N90-19609
- Numerical simulations of supersonic flow through oscillating cascade sections
[NASA-TM-103100] p 478 N90-20051
- A video-based experimental investigation of wing rock
[AD-A218244] p 498 N90-20075
- Modeling of vortex-induced oscillations based on indicial response approach
[NASA-CR-186560] p 572 N90-21736
- Evaluation of nonlinear motion-drive algorithms for flight simulators
[UTIAS-TN-272] p 761 N90-25148
- Entropy wave instability in compact ramjets
p 858 N90-27932
- OUTER SPACE TREATY**
- Latin American Conference on International Air Transport and Activities in Outer Space, Mexico City, Mexico, Aug. 14-18, 1988, Proceedings
p 897 A90-49613
- OUTLET FLOW**
- The performance of a combustor pre-diffuser incorporating compressor outlet guide vanes
[AIAA PAPER 90-2165] p 661 A90-42053
- Outflow boundary conditions using Duhamel's equation
[AIAA PAPER 90-3014] p 798 A90-45937
- OVERPRESSURE**
- A study of sonic boom overpressure trends with respect to weight, altitude, Mach number, and vehicle shaping
[AIAA PAPER 90-0367] p 164 A90-19816
- Summary of sonic boom rise times observed during FAA community response studies over a 6-month period in the Oklahoma City area
[NASA-CR-4277] p 696 N90-24852
- OXIDATION**
- An oxidation fatigue interaction damage model for thermal fatigue crack growth
p 62 A90-11539

- Thermo-oxidative stability studies of PMR-15 polymer matrix composites reinforced with various continuous fibers p 941 A90-50068
- Effect of temperature on the storage life of polysulfide aircraft sealants [MRL-TR-89-31] p 444 A90-19364
- Improved Thermo-Oxidative-Deposition screening tests for turbine lubricants [AD-A217795] p 533 A90-21188
- Carbon-carbon composites: Emerging materials for hypersonic flight [NASA-TM-103472] p 767 A90-26080
- Molten salt induced high temperature degradation of thermal barrier coatings p 952 A90-28704
- Evaluation of high temperature protective coatings for gas turbine engines under simulated service conditions p 952 A90-28712

OXIDATION RESISTANCE

- Influence of alloying elements on the oxidation behavior of NbAl₃ p 355 A90-24861
- New metallic felts with improved resistance to high temperature oxidation [ONERA, TP NO. 1989-210] p 366 A90-25343
- Performance evaluations of oxidation-resistant carbon-carbon composites in simulated hypersonic vehicle environments p 874 A90-48131
- NASA Langley Research Center National Aero-Space Plane Mission simulation profile sets [NASA-TM-102670] p 924 A90-28541

OXIDE FILMS

- In process failure investigations in aeronautics p 181 A90-18489

OXYGEN

- Device for quickly sensing the amount of O₂ in a combustion product gas [NASA-CASE-LAR-13816-1] p 609 A90-22025

OXYGEN ANALYZERS

- A reliable, maintenance-free oxygen sensor for aircraft using an oxygen-sensitive coating on potentiometric electrodes [AD-A222696] p 927 A90-28545

OXYGEN ATOMS

- Computation of hypersonic low density flows with thermochemical nonequilibrium p 477 A90-20044

OXYGEN SUPPLY EQUIPMENT

- RAAF Orion aircraft A9-300 oxygen fire [AD-A215496] p 323 A90-16725

OZONE

- Feasibility study for a microwave-powered ozone sniffer aircraft [NASA-CR-186660] p 650 A90-23397
- NASA/USRA high altitude reconnaissance aircraft [NASA-CR-186685] p 650 A90-24266

OZONOSPHERE

- NASA/USRA high altitude reconnaissance aircraft [NASA-CR-186685] p 650 A90-24266

P**P-I-N JUNCTIONS**

- Performance of full color active-matrix-LCD in the cockpit environment p 681 A90-40392
- 8 x 8-inch full color cockpit display p 927 A90-52953

P-1127 AIRCRAFT

- The Hawker P1127 vectored thrust fighter program - Lessons learned [AIAA PAPER 90-3238] p 835 A90-48848

P-3 AIRCRAFT

- RAAF Orion aircraft A9-300 oxygen fire [AD-A215496] p 323 A90-16725
- An examination of the fatigue meter records from the RAAF Orion P-3C fleet [AD-A214000] p 338 A90-17628
- The reduction of smoke emissions from Allison T56 engines [ARL-PROP-R-182] p 928 A90-28547

PAINTS

- Robotic dry stripping of airframes - Phase II [SAE PAPER 890926] p 365 A90-24691
- Microstructural effects of plastic media blasting on graphite epoxy composites [SAE PAPER 890928] p 286 A90-24693
- Automated aircraft paint strip cell [SAE PAPER 890936] p 286 A90-24699
- Automating and controlling dry paint stripping [SAE PAPER 890939] p 365 A90-24702
- Plastic media blast (PMB) paint removal from composites p 945 A90-50162
- The future of aircraft paint removal methods [AD-A214946] p 356 A90-16936
- Robots for aircraft coatings removal: Parameters and requirements [DE90-009429] p 609 A90-22048

- Mechanical paint removal techniques for aircraft structures [IAR-89-23] p 773 A90-25254
- Statistical treatment of slow strain rate data for assessment of hydrogen embrittlement in low alloy high strength steel [ARL-MAT-R-122] p 767 A90-26106
- Mechanical paint removal techniques for aircraft structures [NIAR-90-12] p 775 A90-26166

PALMGREN-MINER RULE

- Simplified analysis of helicopter fatigue loading spectra p 336 A90-26758

PANEL FLUTTER

- Flutter analysis of composite panels using high-precision finite elements p 207 A90-16725
- Vibration analysis of aircraft panels p 207 A90-17026
- Random response and noise transmission of discretely stiffened composite panels p 283 A90-23288
- Stochastic flutter of a panel subjected to random in-plane forces. I - Two mode interaction p 444 A90-27992
- Finite element two-dimensional panel flutter at high supersonic speeds and elevated temperature [AIAA PAPER 90-0982] p 450 A90-29372
- Stochastic flutter of a panel subjected to random in-plane forces. II - Two and three mode non-Gaussian solutions [AIAA PAPER 90-0986] p 451 A90-29399
- Finite element analysis of composite panel flutter p 681 A90-40032
- Effect of aerodynamic heating on deformation of composite cylindrical panels in a gas flow p 773 A90-45788

PANEL METHOD (FLUID DYNAMICS)

- Application of panel methods to wind-tunnel wall interference corrections [AIAA PAPER 90-0007] p 200 A90-19629
- A zonal flow analysis method for two-dimensional airfoils [AIAA PAPER 90-0571] p 230 A90-22230
- A panel method for arbitrary moving boundaries problems p 302 A90-25284
- Prediction of tip-clearance effects on a wing by the panel method p 307 A90-25871
- Propeller-wing interaction using a frequency domain panel method p 307 A90-26128
- Simulation of separated flows using panel method p 308 A90-26349
- Using the method of symmetric singularities for calculating flow past subsonic flight vehicles p 386 A90-28979
- An integral method for transonic flows p 395 A90-31119
- Numerical simulation of separated flow around two-dimensional wing section by a discrete vortex method p 469 A90-32067
- Calculation of unsteady subsonic and supersonic flow about oscillating wings and bodies by new panel methods p 472 A90-33359
- Computational methods in design aerodynamics p 557 A90-36539

- Counter-rotating propellant analysis using a frequency domain panel method p 623 A90-40937
- Forced response on turbomachinery blades due to passing wakes [AIAA PAPER 90-2353] p 705 A90-42781
- A VSAERO analysis of several canard configured aircraft. II [SAE PAPER 892287] p 714 A90-45465
- Induced drag of wings with highly swept and tapered wing tips [AIAA PAPER 90-3062] p 794 A90-45896
- An interactive boundary-layer stability-transition approach for low Reynolds-number airfoils p 799 A90-46364
- Winger - Computer code for aerodynamic analysis of wings p 810 A90-48077
- Application of a vortex lattice numerical model in the calculation of inviscid incompressible flow around delta wings p 904 A90-51017
- A panel method computation for oscillating aerofoil in compressible flow p 906 A90-51483
- Frequency domain aerodynamic analysis of interacting rotating systems p 21 A90-10837
- Study of the integration of wind tunnel and computational methods for aerodynamic configurations [NASA-TM-102196] p 170 A90-13332
- A technique for the prediction of aerodynamics and aeroelasticity of rotor blades p 184 A90-13377
- A panel process for the calculation of the flow around a wing with front angle damping [ETN-90-95367] p 399 A90-19207
- Experimental and theoretical aerodynamic characteristics of a high-lift semispan wing model [NASA-TP-2990] p 477 A90-20046

- Users manual for the NASA Lewis Ice Accretion Prediction Code (LEWICE) [NASA-CR-185129] p 468 A90-20943
- An intensive procedure for the design of pressure-specified three-dimensional configurations at subsonic and supersonic speeds by means of a higher-order panel method p 500 A90-20982
- A system for transonic wing design with geometric constraints based on an inverse method p 501 A90-20983

- A fast collocation method for transonic airfoil design p 501 A90-20984

- Probabilistic modeling for simulation of aerodynamic uncertainties in propulsion systems [NASA-TM-102472] p 515 A90-21036
- A time-marching method to calculate unsteady airloads on three-dimensional wings. Part 1: Linearized formulation [DLR-FB-89-58] p 634 A90-24254
- A time-marching method for calculating unsteady airloads on three-dimensional wings. Part 2: Full-potential formulation [DLR-FB-89-59] p 635 A90-24255
- A lifting surface method for the calculation of steady and unsteady, incompressible propeller aerodynamics [ESA-TT-1151] p 717 A90-25113
- An unsteady lifting surface method for single rotation propellers [NASA-CR-4302] p 719 A90-25940
- Aerodynamic/dynamic interaction [AD-A222263] p 815 A90-26798
- Study of the ground effects in the CEAT aerohydrodynamic tunnel: Using the results p 922 A90-28530

PANELS

- The application and design of large integral panels for SH-5 aircraft p 211 A90-18632
- The application of the engineering approach for analyzing crack tolerance of fuselage panels to a transport airplane p 272 A90-22014
- Design, fabrication and experimental test of hi-temperature CFRP stiffened structures --- rotating cowl panels for unducted fan engines p 534 A90-31892
- The analysis and testing of composite panels subject to muzzle blast effects p 675 A90-39991
- Damage tolerance of carbon fibre reinforced plastic sandwich panels p 675 A90-40047
- Supersonic flutter of shear deformable laminated composite flat panels p 683 A90-41104
- Estimation of fatigue crack growth in patched cracked panels p 684 A90-41335
- Impact testing of glass/phenolic honeycomb panels with graphite/epoxy facesheets p 946 A90-50166
- A study of the structural efficiency of fluted core graphite-epoxy panels [NASA-TM-101681] p 373 A90-18070
- Comparison between design and installed acoustic characteristics of NASA Lewis 9- by 15-foot low-speed wind tunnel acoustic treatment [NASA-TP-2996] p 440 A90-19242

PARABOLIC FLIGHT

- Parabolic flight experiments on fluid surfaces and wetting p 363 A90-23904
- Combustion Experiments During KC-135 Parabolic Flights [ESA-SP-1113] p 368 A90-16958
- External flow computations for a finned 60mm ramjet in steady supersonic flight [AD-A216998] p 428 A90-19233

PARACHUTE DESCENT

- Effects of random initial conditions and deterministic winds on simulated parachute motion p 22 A90-11002

- Performance and quality of a wing type parachute: Parametric analysis [REPT-88-19] p 89 A90-11710
- Wind tunnel study of wake downwash behind A 6 percent scale model B1-B aircraft [DE90-011783] p 719 A90-25941

PARACHUTE FABRICS

- Wind tunnel tests of a 20-gore disk-gap-band parachute [AD-A221326] p 634 A90-24251

PARACHUTES

- Numerical simulation of three-dimensional flow around parachute canopies p 84 A90-14438
- Numerical simulation of unsteady flow about cambered plates p 159 A90-19389
- The shape assumed by a soft conical shell in fluid flow p 300 A90-24752
- Analytical solution of the problem of nonaxisymmetric potential flow past a spherical canopy - A summary of the principal asymptotic formulas and qualitative analysis p 300 A90-24753
- High-performance parachutes p 400 A90-29803

Slotted-wall research with disk and parachute models in a low-speed wind tunnel p 595 A90-37946
 [AIAA PAPER 90-1407]
 Preliminary characterization of parachute wake recontact p 622 A90-40681
 An improved canopy stiffness scaling law for determining opening time of flat circular parachutes [AIAA PAPER 90-3058] p 790 A90-45863
 Wind tunnel tests of a 20-gore disk-gap-band parachute [AD-A221326] p 634 N90-24251

PARACHUTING INJURY
 Parachute opening shocks during high speed ejections: Normalization p 497 N90-20056

PARALLEL COMPUTERS
 Massively parallel computing p 458 A90-29897
 Multilevel optimization of large-scale structures in a parallel computing environment p 693 A90-39180
 Numerical algorithms for parallel computers [AD-A216812] p 377 N90-18181

PARALLEL FLOW
 Investigation of the mixing of parallel supersonic streams p 69 A90-12561
 Eigenvalue problem in the theory of flow past thin profiles at high supersonic velocity p 295 A90-24096
 Mathematical modeling of plane parallel separated flows past bodies --- Russian book p 619 A90-39475
 Measurements of turbulent dual-jet interaction [AIAA PAPER 90-2105] p 624 A90-42019
 The effect of constructive and destructive interference on the downstream development of twin jets in a crossflow. II - Interference effects of angularly displaced jets [AIAA PAPER 90-2107] p 684 A90-42020
 An experimental study of tip shape effects on the flutter of air-swept, flat-plate wings [NASA-TM-4180] p 582 N90-22555

PARALLEL PLATES
 Radial swirl flows between parallel disks at critical flow rate p 14 A90-12596

PARALLEL PROCESSING (COMPUTERS)
 A heterogeneous parallel processing architecture for avionic and aerospace applications [AIAA PAPER 89-3108] p 74 A90-10590
 Applications of neural networks to avionics systems [AIAA PAPER 89-3093] p 76 A90-10627
 Advances in computational design and analysis of airbreathing propulsion systems p 43 A90-12502
 Array processor supercomputers p 376 A90-26626
 Parallel computation of three-dimensional transonic flow problems with complex geometries [AIAA PAPER 90-0336] p 313 A90-26936
 A parallel-vector algorithm for rapid structural analysis on high-performance computers [AIAA PAPER 90-1149] p 458 A90-29293
 Categorization and performance analysis of advanced avionics algorithms on parallel processing architectures p 461 A90-30786
 Benchmark calculations with an unstructured grid flow solver on a SIMD computer p 546 A90-34378
 Implementation of a transputer-based flight controller p 667 A90-38966
 Fault-tolerant transputer-based controller configurations for gas-turbine engines p 852 A90-48529
 Block-structured solution of three-dimensional transonic flows using parallel processing [AD-A212851] p 170 N90-13330
 Parallel processing implementation of a flight controller p 333 N90-16743
 Visual servoing for autonomous aircraft refueling [AD-A216042] p 414 N90-18386

PARALLEL PROGRAMMING
 AIMS test and simulation equipment p 892 N90-27623

PARAMETER IDENTIFICATION
 Identification of an adequate model for collective response dynamics of a Sea King helicopter in hover p 56 A90-12766
 Identification of rotor flapping equation of motion from flight measurements with the RSRA compound helicopter p 56 A90-12769
 Time domain parameter identification techniques applied to the UH-60A Black Hawk Helicopter p 77 A90-12774
 Experience with multi-step test inputs for helicopter parameter identification p 56 A90-12775
 Optimal selection of the parameters to be measured during the identification of gas turbine engines. I - Problem statement p 255 A90-23410
 Identification of moderately nonlinear flight mechanics systems with additive process and measurement noise p 347 A90-25987
 Some problems on 'intelligence' of wind tunnel testing p 436 A90-28282
 A numerical solution for instruction tracing problem p 424 A90-29918

Aircraft flight control system identification p 431 A90-30105
 Application of time domain decomposition techniques to aircraft ground and flutter test data p 491 A90-33373
 Identification of time varying modal parameters p 536 A90-33375
 Advanced parameter identification techniques for near real time flight flutter test analysis [AIAA PAPER 90-1275] p 494 A90-33899
 Equation decoupling - A new approach to the aerodynamic identification of unstable aircraft [AIAA PAPER 90-1276] p 518 A90-33900
 A modal parameter identification technique and its application to large complex structures with multiple steady sinusoidal excitation p 602 A90-35670
 Identification and diagnostics in the data processing and control systems of aerospace powerplants --- Russian book p 611 A90-36151
 Main characteristic parameter model for jet engine fault diagnosis p 585 A90-37210
 Parameter identification of aeroelastic modes of rotary wings from transient time histories p 642 A90-40166
 Differential-geometrical technique of signal transformation and estimation of position, rate and acceleration parameters using supplementary data sources p 638 A90-41004
 Design methodology for multivariable helicopter control systems p 669 A90-42461
 Parametric evaluation of the aerodynamic performance of an annular combustor-diffuser system [AIAA PAPER 90-2163] p 742 A90-42741
 Parameter identification of linear systems based on smoothing [AIAA PAPER 90-2800] p 753 A90-45156
 Optimal input design for aircraft parameter estimation using dynamic programming principles [AIAA PAPER 90-2801] p 753 A90-45157
 Maximum likelihood tuning of a vehicle motion filter p 755 A90-45334
 Optimal choice of measured parameters during the identification of gas turbine engines. II - Combined confidence regions and intervals of the identification results p 850 A90-46493
 An orthogonal algorithm to the maximum likelihood estimation using an efficient method for computing sensitivities [AIAA PAPER 90-3507] p 891 A90-47753
 A parametric study of radial turbomachinery blade design in three-dimensional subsonic flow [ASME PAPER 89-GT-84] p 905 A90-51257
 The determination of third order linear models from a seventh order nonlinear jet engine model p 964 A90-52881
 On the interactive computer program IPIS for aircraft parameter identification [NAL-TR-1000] p 77 N90-10586
 The effectiveness of vane-aileron excitation in the experimental determination of flutter speed by parameter identification [NASA-TP-2971] p 249 N90-15100
 Estimating short-period dynamics using an extended Kalman filter [NASA-TM-101722] p 648 N90-23392
 A contribution to the improvement of the accuracy in the parameter identification of nonlinear processes, by example of the aircraft motion [ETN-90-96961] p 736 N90-25974

PARAMETERIZATION
 Parametric analysis of swept-wing geometry with sheared wing tips [AIAA PAPER 90-3196] p 812 A90-49101
 Performance and quality of a wing type parachute: Parametric analysis [REPT-88-19] p 89 N90-11710
 Parametric assessment of propulsion system mass for airbreathing launcher configurations p 344 N90-16819
 The Uniform Engine Test Programme [AGARD-AR-248] p 428 N90-19232

PARITY
 Fault Detection and Isolation (FDI) techniques for guidance and control systems p 918 N90-29366

PARTIAL DIFFERENTIAL EQUATIONS
 Three-dimensional adaptive grid generation on a composite-block grid p 374 A90-25289
 Comparisons among grid generation using elliptic partial differential equations p 374 A90-25478
 A comparison of two adaptive grid techniques p 309 A90-26507
 A weighted residual formulation for finite element solutions of the steady Euler equations p 770 A90-44457
 User's guide to PMESH: A grid-generation program for single-rotation and counterrotation advanced turboprops [NASA-CR-185156] p 217 N90-14783

Finite difference techniques and rotor blade aeroelastic partial differential equations with quasisteady aerodynamics p 236 N90-15075
 Application of an inverse method to the design of a radial inflow turbine p 511 N90-20989

PARTICLE DENSITY (CONCENTRATION)
 Performance of laminar-flow leading-edge test articles in cloud encounters p 104 N90-12511

PARTICLE EMISSION
 Characterization of chemicals on engine exhaust particles [AD-A213566] p 256 N90-15106

PARTICLE ENERGY
 The remote sensing of temperature in gas turbine engine components using epithermal neutrons p 70 A90-12630

PARTICLE LADEN JETS
 The future of aircraft paint removal methods [AD-A214946] p 356 N90-16936

PARTICLE SIZE DISTRIBUTION
 Comparison of two droplet sizing systems in an icing wind tunnel [AIAA PAPER 90-0668] p 274 A90-23711
 Comparison of two droplet sizing systems in an icing wind tunnel [NASA-TM-102456] p 215 N90-14617
 Metalized fuel particle size study in a solid fuel ramjet [AD-A220079] p 679 N90-24451

PARTICLE TRAJECTORIES
 A study of particle trajectories in a gas turbine intake p 48 A90-12583
 Particulate trajectories and impact characteristics in hypersonic flight involving gas coolant shielding p 476 A90-34583
 Viscous flow analysis for advanced inlet particle separators [AIAA PAPER 90-2136] p 661 A90-42038
 Swept wing ice accretion modeling [NASA-TM-103114] p 570 N90-21727

PARTICULATE SAMPLING
 Design and calibration of an in-stack, low-pressure impactor [AD-A213531] p 255 N90-15105

PARTICULATES
 Effect of environmental particles on a radial compressor p 113 A90-16373
 Sliding and abrasive wear behaviour of an aluminum (2014)-SiC particle reinforced composite p 530 A90-33344

PASSENGER AIRCRAFT
 Aft facing transport aircraft passenger seats under 16G dynamic crash simulation p 175 A90-17416
 Design criteria, constructions, and materials for the Dornier 328 airframe p 246 A90-21610
 Conceptual design and feasibility study of very large passenger aircraft [AIAA PAPER 90-3220] p 834 A90-48841
 International Aircraft Occupant Safety Conference and Workshop proceedings [AD-A214452] p 239 N90-15085
 Heat release rate measurement for evaluating the flammability of aircraft materials p 328 N90-17610
 AVION: A detailed report on the preliminary design of a 79-passenger, high-efficiency, commercial transport aircraft [NASA-CR-186663] p 649 N90-23395
 A process for analysis, evaluation, and development of aerial servicing noise reduction measures in civil aircraft [ETN-90-97300] p 896 N90-28398
 Aircraft evacuations: The effect of passenger motivation and cabin configuration adjacent to the exit [CAA-PAPER-89019] p 913 N90-29336

PASSENGERS
 An analysis of factors impeding passenger escape from aircraft fires p 322 A90-26018
 Fire safety in civil aviation p 325 N90-17586
 Fire hardening of an aircraft passenger cabin p 328 N90-17606
 The influence of adjacent seating configurations on egress through a type 3 emergency exit [AD-A218393] p 636 N90-23371
 High speed civil transport [NASA-CR-186661] p 649 N90-23396

PASTES
 Effect of temperature on the storage life of polysulfide aircraft sealants [MRL-TR-89-31] p 444 N90-19364

PATENTS
 Yaw fin deployment apparatus for ejection seat [AD-D014512] p 723 N90-25118

PATTERN RECOGNITION
 An intelligent system for autonomous navigation of airborne vehicles p 26 A90-11696
 Angular feature mapping - An optical method p 377 A90-23974

- Pattern representations and syntactic classification of radar measurements of commercial aircraft p 417 A90-28407
- Operating principles of a terrain-recognition air navigation system p 403 A90-29655
- Advanced technology MMW seeker testbed, a multi-technology demonstration sensor p 488 A90-34143
- A Distributed Artificial Intelligence approach to object identification and classification p 545 A90-34185
- Neural networks for adaptive shape tracking p 638 A90-39959
- Automatic processing of images from the GRATE flight test tool [DLR-FB-89-28] p 109 N90-12599
- Studies in automatic speech recognition and its application in aerospace p 958 N90-28759
- PAVEMENTS**
- Dynamic analysis of airport pavement p 593 A90-36418
- Aircraft tire/pavement pressure distributions [SAE PAPER 892351] p 734 A90-45502
- Definition of research needs to address airport pavement distress in cold regions [DOT/FAA/DS-89/13] p 59 N90-10896
- Design temperatures for flexible airfield pavement design [AD-A214141] p 262 N90-15115
- Criteria for polymer concrete on airport pavements [DOT/FAA/DS-89/18] p 527 N90-21045
- Criteria for coal tar seal coats on airport pavements. Volume 2: Laboratory and field studies [AD-A220167] p 674 N90-24277
- Airport pavement drainage [DOT/FAA/RD-90/24] p 872 N90-27728
- Development of acceptance plans for airport pavement materials. Volume 1: Development [DOT/FAA/RD-90/15] p 937 N90-28581
- Development of a thickness design procedure for stabilized layers under rigid airfield pavements [DOT/FAA/RD-90/22] p 937 N90-28582
- PAYLOADS**
- Unmanned air vehicles payloads and sensors p 251 N90-15930
- Feasibility study for a microwave-powered ozone sniffer aircraft [NASA-CR-186660] p 650 N90-23397
- PEACETIME**
- Peacetime replacement and crash damage factors for army aircraft [AD-A218544] p 636 N90-23372
- PEEK**
- Erosive wear of fibrous PEEK composites p 530 A90-33127
- Poly(arylene ether ketone)/poly(aryl imide) homo- and polydimethylsiloxane segmented copolymer blends - Influence of chemical structure on miscibility and physical property behavior p 941 A90-50063
- Durability and damage tolerance of S-2 glass/PEEK composites p 944 A90-50140
- Chemical resistance of carbon fiber reinforced polyether ether ketone and polyphenylene sulfide composites p 944 A90-50142
- Evaluation of the thermoplastic film interleaf concept for improved damage tolerance p 946 A90-50179
- Mechanical influences on crystallization in PEEK matrix/carbon fiber reinforced composites p 949 A90-50227
- PEELING**
- Robotic dry stripping of airframes - Phase II [SAE PAPER 890926] p 365 A90-24691
- Automated aircraft paint strip cell [SAE PAPER 890936] p 286 A90-24699
- Automating and controlling dry paint stripping [SAE PAPER 890939] p 365 A90-24702
- PENCIL BEAMS**
- Wind shear detection with pencil-beam radars p 279 A90-21386
- PENDULUMS**
- Measurement of angles and angle characteristics with accelerometers and gyroscopes p 653 A90-41730
- PENETRATION**
- Boeing 727-100 test project (high energy radiated field tests) [DOT/FAA/CT-88/33] p 542 N90-21247
- Survivable penetration p 917 N90-29363
- PERCEPTION**
- Cognitive requirements for aircraft navigation [NASA-CR-186933] p 824 N90-26804
- PERFORATED PLATES**
- Wave cancellation properties of a splitter-plate porous wall configuration p 57 A90-11005
- The absorption of sound by perforated linings p 965 A90-51994

- Laminar flow control perforated, wing panel development [NASA-CR-178166] p 63 N90-10187
- Comparison between design and installed acoustic characteristics of NASA Lewis 9- by 15-foot low-speed wind tunnel acoustic treatment [NASA-TP-2996] p 440 N90-19242
- Parametric studies of acoustic duct attenuation of perforated-plate-on-honeycomb absorber [NAL-TM-603] p 966 N90-30030
- PERFORATION**
- Simulated-airline-service flight tests of laminar-flow control with perforated-surface suction system [NASA-TP-2966] p 338 N90-17627
- PERFORMANCE PREDICTION**
- An iterative non-linear lifting line model for wings with unsymmetrical stall [SAE PAPER 891020] p 83 A90-14332
- Successful performance development program for the T800-LHT-800 turboshaft engine [SAE PAPER 891048] p 110 A90-14352
- Simulation of a turbocompound two-stroke diesel engine [SAE PAPER 891066] p 110 A90-14366
- Predictions of airfoil aerodynamic performance degradation due to icing p 144 A90-16753
- New free-wake analysis of rotorcraft hover performance using influence coefficients p 181 A90-17867
- The analysis and solution of the performance deterioration problem of WP7 engine under the full reheating condition p 191 A90-18624
- Hypersonic airbreathing vehicle design - Focus on aero-space plane p 245 A90-21156
- A hybrid method for prediction of propeller performance [AIAA PAPER 90-0440] p 229 A90-22219
- A method of predicting the energy losses in vaneless diffusers of centrifugal compressors [ASME PAPER 89-GT-158] p 292 A90-23846
- Reynolds number effects on the performance of a turbofan engine [ASME PAPER 89-GT-199] p 342 A90-23871
- Experimental investigation of supersonic turbine performance [ASME PAPER 89-GT-238] p 342 A90-23888
- Hub loads analysis of the SA349/2 helicopter p 333 A90-23936
- Performance study of an integrated NAVSTAR GPS/SINS navigation system p 329 A90-24003
- A semi-actuator disk theory for prediction of stall flutter in axial flow compressors p 301 A90-25105
- A study of ice shape prediction methodologies and comparison with experimental data [AIAA PAPER 90-0753] p 322 A90-26986
- High-temperature bootstrap compared with F-15 growth air cycle air conditioning system [SAE PAPER 891436] p 336 A90-27407
- High-performance parachutes p 400 A90-29803
- Helicopter surveillance - A look at current and proposed future programs p 642 A90-39986
- On and off-design performance prediction of single spool turbojets using gasdynamics [AIAA PAPER 90-2393] p 662 A90-42155
- A modeling technique for STOVL ejector and volume dynamics [AIAA PAPER 90-2417] p 663 A90-42168
- Helicopter store separation - Predictive techniques and flight testing p 647 A90-42495
- Off-design performance of hypersonic waveriders p 763 A90-44735
- Turbofan engine analysis and optimization using spreadsheets p 779 A90-45290
- Prediction of aerodynamic performance of airfoils in low Reynolds number flows p 799 A90-46360
- An interactive boundary-layer stability-transition approach for low Reynolds-number airfoils p 799 A90-46364
- A review of low Reynolds number aerodynamic research at the University of Glasgow p 800 A90-46367
- A method to determine the performance of low-Reynolds-number airfoils under off-design unsteady freestream conditions p 801 A90-46375
- GTPDP - A rotary wing aircraft preliminary design and performance estimation program including optimization and cost p 830 A90-46944
- BHT's technical assessment of advanced rotor and control concepts p 861 A90-46949
- Stochastic performance robustness of aircraft control systems [AIAA PAPER 90-3410] p 865 A90-47665
- ILS (Instrument Landing System) mathematical modeling study on the effects of proposed hangar construction west of runway 18R on localizer performance at Dallas-Fort Worth International Airport [AD-A210631] p 27 N90-10019

- Large-scale Advanced Prop-fan (LAP) high speed wind tunnel test report [NASA-CR-182125] p 52 N90-10045
- Review and analysis of the DNW/Model 360 rotor acoustic data base [NASA-TM-102253] p 81 N90-11692
- Some implications of the isotropic momentarily frozen assumptions for the SPAN-MAT program [NASA-CR-181937] p 88 N90-11704
- Numerical simulation of unsteady rotational flow over propfan configurations [NASA-CR-186037] p 90 N90-12500
- Normal force, pitching moment, and side force of forebody-cylinder combinations for angles of attack up to 90 degrees and Mach numbers up to 5 [ESDU-89014] p 173 N90-14192
- Hinge moment coefficient derivatives for trailing-edge controls on wings at subsonic speeds [ESDU-89009] p 198 N90-14239
- Computational design of low aspect ratio wing-winglet configurations for transonic wind-tunnel tests [NASA-CR-181939] p 316 N90-17539
- An examination of the fatigue meter records from the RAAF Orion P-3C fleet [AD-A214000] p 338 N90-17628
- A method for the prediction of supersonic compressor blade performance [CUE/A-TURBO/TR-126] p 344 N90-17634
- An approximate model for the performance and acoustic predictions of counterrotating propeller configurations [NASA-CR-180667] p 379 N90-18228
- The effects of wind tunnel data uncertainty on aircraft point performance predictions [AD-A216091] p 414 N90-18387
- Numerical prediction of axial turbine stage aerodynamics p 426 N90-18416
- Development of a mass averaging temperature probe p 427 N90-18418
- Application of variable-gain output feedback for high-alpha control [NASA-TM-102603] p 434 N90-18434
- Three-dimensional viscous rotor flow calculations using a viscous-inviscid interaction approach [NASA-TM-102235] p 399 N90-19204
- Aeroservoelasticity [NASA-TM-102620] p 416 N90-19227
- Using transonic small disturbance theory for predicting the aeroelastic stability of a flexible wind-tunnel model [NASA-TM-102617] p 478 N90-20047
- Airplane takeoff and landing performance monitoring system [NASA-CASE-LAR-13734-1-CU] p 526 N90-20096
- Secondary flow predictions for a transonic nozzle guide vane p 513 N90-21017
- Generation and decay of secondary flows and their impact on aerodynamic performance of modern turbomachinery components p 514 N90-21023
- Computational prediction and measurement of the flow in axial turbine cascades and stages p 514 N90-21028
- Recent improvements in the scope and accuracy of the performance prediction of nozzle propellers [LR-598] p 572 N90-21742
- A modeling technique for STOVL ejector and volume dynamics [NASA-TM-103167] p 589 N90-22566
- Integrated control-system design via generalized LOG (LOG) theory p 613 N90-23023
- Prediction of aerodynamic performance of airfoils in low Reynolds number flows [DLC-EST-TN-031] p 632 N90-23360
- Correlation/validation of finite element code analyses for vibration assessment of avionics equipment [AD-A220393] p 654 N90-23398
- Application of neural networks to the F/A-18 engine condition monitoring system [AD-A219820] p 666 N90-24271
- Evaluation of various thrust calculation techniques on an F404 engine [NASA-TP-3001] p 735 N90-25134
- Ground shake test of the UH-60A helicopter airframe and comparison with NASTRAN finite element model predictions [NASA-CR-181993] p 758 N90-25143
- Performance of a supercharged direct-injection stratified-charge rotary combustion engine [NASA-TM-103105] p 748 N90-25982
- Handbook of uncertainty methodology for engine testing at Pyestock (England) [RAE-TM-P-1179] p 751 N90-26007
- Retirement for cause of the F100 engine p 843 N90-26813
- Comparative Engine Performance Measurements [AGARD-LS-169] p 856 N90-27711
- Use of acoustic emission for continuous surveillance of aircraft structures p 887 N90-28092

PERFORMANCE TESTS

- Two-stage two-spool experimental centrifugal compressor investigation p 49 A90-12593
- Investigation of some effects on the compressor characteristics of an advanced bleed air compressor design p 49 A90-12594
- An experimental investigation of non-steady flow in vaneless diffusers p 14 A90-12595
- The development of a high response aerodynamic wedge probe and use on a high-speed research compressor p 69 A90-12618
- Non-iterative analytical methods for off-design turbofan calculations with or without mixed-flows p 70 A90-12628
- Effect of advanced component technology on helicopter transmissions p 271 A90-21115
- Design of computer-aided testing systems for aviation equipment I p 222 A90-23416
- A three dimensional inverse method in turbomachinery. II - Experimental verification [ASME PAPER 89-GT-137] p 360 A90-23834
- Automatic testing in aircraft building --- Russian book p 285 A90-24231
- The story of sandwich construction p 538 A90-33702
- Aircraft cabin interior systems meeting new FAA regulations p 482 A90-33710
- High Mach exhaust system concept scale model test results [AIAA PAPER 90-1905] p 655 A90-40552
- Reverse flow in multistage axial compressors p 623 A90-40942
- The BAe (commercial aircraft) LTD transport aircraft synthesis and optimisation program (TASOP) [AIAA PAPER 90-3295] p 837 A90-48879
- Experimental investigation of multielement airfoil ice accretion and resulting performance degradation p 812 A90-48954
- The performance of alternate fuels in general aviation aircraft p 950 A90-51621
- The role of component testing [PNR90589] p 115 A90-12608
- Effect of blade planform variation on a small-scale hovering rotor [NASA-TM-4146] p 173 A90-14186
- Fuel Tank Technology [AGARD-R-771] p 250 A90-15904
- Aircraft fuel tank construction and testing experience p 250 A90-15907
- Design philosophy and construction techniques for integral fuselage fuel tanks p 250 A90-15913
- Performance of a highly-loaded HP compressor [RAE-TM-P-1149] p 256 A90-15919
- A UK perspective on the uniform engine test programme [RAE-TM-P-1172] p 257 A90-15922
- Analysis of indirect effects of lightning on a metallic A 300 wing: Test report [REPT-E87/645800] p 323 A90-16726
- Experimental evaluation of impedance control for robotic aircraft refueling [AD-A215532] p 337 A90-16755
- Altitude testing of the 2D V-STOL ADEN demonstrator on an F404 engine [NASA-CR-174824] p 345 A90-17638
- Analysis and test of a wide angle spectrometer [AD-A215819] p 372 A90-18030
- Research on a two-dimensional inlet for a supersonic V-STOL propulsion system. Appendix A [NASA-CR-174945] p 396 A90-18364
- Compressor performance tests in the compressor research facility p 427 A90-18428
- Operational evaluation of initial data link air traffic control services, volume 1 [DOT/FAA/CT-90/1-VOL-1] p 455 A90-19472
- In-line wear monitor [AD-A217799] p 510 A90-20091
- Flight termination system battery guidelines [AD-A217310] p 520 A90-20092
- Performance data from a wind-tunnel test of two main-rotor blade designs for a utility-class helicopter [NASA-TM-4183] p 499 A90-20974
- Secondary flow predictions for a transonic nozzle guide vane p 513 A90-21017
- Operational effects on crashworthy seat attenuators [AD-A221148] p 637 A90-24259
- Human response research update p 699 A90-24873
- AIMS test and simulation equipment p 892 A90-27623
- Development and testing of methodology for evaluating the performance of multi-input/multi-output digital control systems [NASA-TM-102704] p 846 A90-27699
- The basis for facility comparison p 856 A90-27713

- Tests of an ultra-light tunnel in the anechoic wind tunnel facility CEPRA 19 [ONERA-RF-20/7294-PH] p 872 A90-27729
- A look at tomorrow today p 921 A90-28524
- Validation of the F-18 high alpha research vehicle flight control and avionics systems modifications [NASA-TM-101723] p 824 A90-28542
- Energy Efficient Engine exhaust mixer model technology report addendum; phase 3 test program [NASA-CR-174799] p 930 A90-28556
- Energy efficient engine pin fin and ceramic composite segmented liner combustor sector rig test report [NASA-CR-179534] p 932 A90-28567
- Source emission test of gas turbine engine test facility, Kelly AFB, TX [AD-A223869] p 932 A90-28571
- Communications Interface Driver (CID) test plan [DOT/FAA/CT-TN89/35] p 958 A90-28762
- Recommended practices for measurement of gas path pressures and temperatures for performance assessment of aircraft turbine engines and components [AGARD-AR-245] p 933 A90-29393
- Structural testing and analytical research of turbine components [AD-A223516] p 933 A90-29396
- PERIODIC FUNCTIONS**
- Numerical methods for the treatment of periodic systems with applications to structural dynamics and helicopter rotor dynamics p 604 A90-37881
- PERIODIC VARIATIONS**
- Periodically unsteady effects on profiles, induced by separation p 279 A90-16196
- Research on cascade secondary and tip-leakage flows: Periodicity and surface flow visualization p 514 A90-21026
- PERIPHERAL VISION**
- Flight testing and application of a Peripheral Vision Display p 652 A90-40381
- PERMANENT MAGNETS**
- Electric controls for a high-performance EHA using an interior permanent magnet motor drive p 452 A90-30711
- High-performance EHA controls using an interior permanent magnet motor --- electrohydraulic actuator for aircraft power systems p 730 A90-43152
- PERMEABILITY**
- Measurement and characterization of prepreg permeability with a modified bagging technique p 949 A90-50226
- Criteria for polymer concrete on airport pavements [DOT/FAA/DS-89/18] p 527 A90-21045
- PERSONAL COMPUTERS**
- Design flutter calculations on PC p 545 A90-33379
- Digital control of magnetic bearings supporting a multimass flexible rotor p 682 A90-40712
- Flight data replay and analysis system p 893 A90-27635
- PERSONNEL MANAGEMENT**
- Teamwork for excellence [AIAA PAPER 89-3195] p 549 A90-31686
- The (airplane) design professor as sheepherder - An industry role in enhancing engineering education [AIAA PAPER 90-3259] p 897 A90-49121
- PERTURBATION**
- A device for introducing helical perturbations into a trailing line vortex [AIAA PAPER 90-1627] p 568 A90-38756
- Algorithms for computing the multivariable stability margin p 612 A90-22999
- Aerodynamics of bodies in shear flow p 910 A90-28496
- PERTURBATION THEORY**
- A new methodology for model order reduction with application to eigenstructure controllers [AIAA PAPER 90-3475] p 891 A90-47725
- Using transonic small disturbance theory for predicting the aeroelastic stability of a flexible wind-tunnel model [NASA-TM-102617] p 478 A90-20047
- Numerical simulations of supersonic flow through oscillating cascade sections [NASA-TM-103100] p 478 A90-20051
- An experimental investigation of the physical mechanisms controlling the asymmetric flow past slender bodies at large angles of attack p 592 A90-21767
- An investigation of the use of singular perturbation methods and modal control theory in the derivation of aircraft control schemes [MATHS-REPT-A-106] p 758 A90-26014
- PETRI NETS**
- On the generation of a variable structure airport surface traffic control system [AD-A211306] p 99 A90-11724
- PETROLEUM PRODUCTS**
- Combustion process in a gas turbine combustor when using H₂, NH₃ and LPG fuels p 873 A90-46882

PHASE CONTROL

- Dynamics and control of turbulent shear flows [AD-A210396] p 72 A90-10402

PHASE DETECTORS

- Advanced instrumentation for aircraft icing research [NASA-CR-185225] p 506 A90-21006

PHASE LOCKED SYSTEMS

- Experimental investigation of the mechanisms underlying vortex kinematics in unsteady separated flows [AD-A217889] p 540 A90-20346

PHASE MODULATION

- Weather data dissemination to aircraft p 486 A90-20934

PHASE VELOCITY

- An experimental study of the effect of streamwise vortices on unsteady turbulent boundary-layer separation p 369 A90-17045

PHASED ARRAYS

- Airborne array antennas for satellite communication p 265 A90-23202

PHENOLIC RESINS

- Impact testing of glass/phenolic honeycomb panels with graphite/epoxy facesheets p 946 A90-50166
- The application of 'PT' resins to high temperature aerospace structures p 949 A90-50230

PHOSPHORIC ACIDS

- Chrome free electrolytic deoxidizer for aluminum p 956 A90-50216

PHOSPHORS

- Engine testing of thermographic phosphors [DE90-013269] p 885 A90-28059

PHOSPHORUS

- The 1-((diorganoxyphosphonyl)-methyl)-2,4- and -2,6-diamido benzenes p 946 A90-50166
- [NASA-CASE-ARC-11425-4] p 532 A90-20133
- Some 1-((diorganoxyphosphonyl)methyl)-2,4- and -2,6-dinitro-benzenes [NASA-CASE-ARC-11425-3] p 678 A90-23475

PHOTOCHEMICAL REACTIONS

- Characterization of chemicals on engine exhaust particles [AD-A213566] p 256 A90-15106
- Photo-sensitized ignition of hydrogen/oxygen mixtures for hypersonic flight vehicles p 877 A90-27935

PHOTOCHROMISM

- Grunman/FAA lightning study - A potential countermeasure for lightning induced flashblindness of aircrew members p 819 A90-49843

PHOTODIODES

- A semiconductor laser-Doppler-anemometer for applications in aerodynamic research p 447 A90-28273

PHOTODISSOCIATION

- Photo-sensitized ignition of hydrogen/oxygen mixtures for hypersonic flight vehicles p 877 A90-27935

PHOTOELASTIC ANALYSIS

- Three dimensional photoelastic analysis of aeroengine parts p 270 A90-20077
- Stress concentration factors - Comparison of theory with fatigue test data p 680 A90-39979
- Old lamps for new - A photoelastic design tool for weight and cost saving on aircraft structures p 878 A90-46039

PHOTOELASTICITY

- Photoelastic investigation of turbine rotor blade shrouds p 112 A90-16008
- Nondestructive measurement of residual stresses in aircraft transparencies [AD-A218680] p 689 A90-23762
- Photoelasticity: A cost effective design tool p 883 A90-26819

PHOTOGRAMMETRY

- A test of airborne kinematic GPS positioning for aerial photography - Methodology p 97 A90-13982

PHOTOGRAPHS

- Video photographic considerations for measuring the proximity of a probe aircraft with a smoke seeded trailing vortex [NASA-TM-102691] p 724 A90-25120

PHOTONICS

- The impact of fiber optics (photonics) on future aircraft p 504 A90-32863

PHOTOSTRESSES

- Liquid crystal coatings for surface shear stress visualization in hypersonic flows [AIAA PAPER 90-1513] p 563 A90-38660

PHYSICAL PROPERTIES

- Ceramic heat exchangers in gas turbine [ONERA, TP NO. 1889-109] p 40 A90-11142
- Improved melt flow and physical properties of Mitsui Toatsu's LARC-TPI 1500 series polyimide p 943 A90-50134

The prediction of middle distillate fuel properties using liquid chromatography-proton nuclear magnetic resonance spectroscopy data
[AD-A211879] p 126 N90-11899

PHYSIOLOGICAL EFFECTS

Windblast protection for advanced ejection seats
p 483 N90-20063
Assessment System for Aircraft Noise (ASAN) citation database. Volume 1: User's manual.
[AD-A219175] p 615 N90-23188
Assessment System for Aircraft Noise (ASAN) citation database. Volume 2: Database update manual
[AD-A219176] p 615 N90-23189
Assessment System for Aircraft Noise (ASAN) citation database. Volume 3: New citation review procedures
[AD-A219177] p 615 N90-23190

PIERCING

Bird impact tests on asymmetric sandwich structures made in Kevlar 49
[CEAT-NT-10/S/83-5] p 323 N90-16727
Bird impact tests on curved structures of the type Sandwich-Kevlar-Nida for normal and angular shooting
[CEAT-NT-10/S/83-4] p 324 N90-16728

PIEZOELECTRIC TRANSDUCERS

Application of piezoelectric foils in experimental aerodynamics
p 446 A90-28258
Piezoelectric actuators for helicopter rotor control
[AIAA PAPER 90-1076] p 411 A90-29384
Examples of force measurements in a wind tunnel using multicomponent piezoelectric transducers
p 540 A90-34352
Test and theory for piezoelectric actuator-active vibration control of rotating machinery
p 879 A90-46226
Detection of flow instabilities at airfoil profiles using piezoelectric arrays
p 276 N90-16175

PILOT ERROR

General aviation pilot error in computer simulated adverse weather scenarios
p 322 A90-26254
Reduced order INS/GPS guided unmanned air vehicle study
p 726 A90-43707
Classification and reduction of pilot error
[NASA-CR-181867] p 24 N90-10014

PILOT INDUCED OSCILLATION

Prediction of longitudinal pilot induced oscillations using the optimal control model
[AD-A220593] p 671 N90-23412

PILOT PERFORMANCE

Reflexive navigation for autonomous aircraft
[AIAA PAPER 89-2991] p 25 A90-10502
Applications of fuzzy sets to rule-based expert system development
p 216 A90-18050
On the level 2 ratings of the Cooper-Harper scale --- for pilot assessment of aircraft flying qualities
p 197 A90-19577
An analysis of feel system effects on lateral flying qualities
[AIAA PAPER 90-1824] p 346 A90-25168
General aviation pilot error in computer simulated adverse weather scenarios
p 322 A90-26254
Real-time adaptive control of knowledge based avionics tasks
p 460 A90-30764
Flight simulator evaluation of a dot-matrix display for presentation of approach map formats
p 419 A90-30787

Cognitive perspectives on map displays for helicopter flight
p 419 A90-31329
3-D in pictorial formats for aircraft cockpits
p 420 A90-31331

The effect of windscreen bows and HUD pitch ladder on pilot performance during simulated flight
p 420 A90-31333

After Habsheim
p 401 A90-31388
Multifunction displays optimized for viewability
p 652 A90-40398

ATTHes - A helicopter in-flight simulator for ACT testing
p 643 A90-41727

The airborne synthetic cartographic indicator
p 822 A90-46671

Simulation investigation of multiple axis flying qualities
[AIAA PAPER 90-3480] p 866 A90-47729
A blackboard approach for diagnosis in Pilot's Associate
p 892 A90-49741

Analyzing manipulator and feel system effects in aircraft flight control
p 934 A90-51154

Helicopter Visual Segment Approach Lighting System (HALS)
[ACD-330] p 28 N90-10856

Heliport surface maneuvering test results
[ACD-330] p 59 N90-10897

A candidate concept for display of forward-looking wind shear information
[NASA-TM-101585] p 187 N90-14232

The human element: The key to safe, civil operations in adverse weather
p 248 N90-15042

Classification of windshear severity
p 281 N90-15049

Canard versus aft-tail ride qualities performance and pilot command response
p 258 N90-15053

Aircraft response and pilot behaviour during a wake vortex encounter perpendicular to the vortex axis
p 259 N90-15057

Piloted simulation of a ground-based time-control concept for air traffic control
[NASA-TM-101085] p 240 N90-15898

Delivery performance of conventional aircraft by terminal-area, time-based air traffic control: A real-time simulation evaluation
[NASA-TP-2978] p 404 N90-18378

Three input concepts for flight crew interaction with information presented on a large-screen electronic cockpit display
[NASA-TM-4173] p 420 N90-18394

An early overview of tiltrotor aircraft characteristics and pilot procedures in civil transport applications
[DOT/FAA/DS-89/37] p 503 N90-21003

Stereopsis cueing effects on hover-in-turbulence performance in a simulated rotorcraft
[NASA-TP-2980] p 506 N90-21004

Model-based method for terrain-following display design
[AD-A219302] p 583 N90-22563

Fighter agility metrics, research, and test
[NASA-CR-186118] p 648 N90-23386

Helicopter controllability
[AD-A220078] p 672 N90-24275

Dallas/Fort Worth simulation, volume 1
[DOT/FAA/CT-TN89/28-VOL-1] p 824 N90-26802

Counterair situation awareness display for Army aviation
p 964 N90-28982

PILOT SELECTION

Aeronautical decisionmaking for air ambulance program administrators
[DOT/FAA/DS-88/8] p 635 N90-23368

PILOT TRAINING

Criteria for evaluating the flight dynamics model of flight simulators
p 121 A90-15422

UH-60 flight data replay and refly system state estimator analysis
[AIAA PAPER 90-0181] p 197 A90-19723

Visual information for simulated landing approaches
p 347 A90-26189

Aviation meteorology - Panel report
p 692 A90-39403

Escape and survival following helicopter ditching - Training aspects
p 722 A90-44658

The Common/Same Type Rating - Human factors and other issues
[SAE PAPER 892229] p 723 A90-45445

Initial service experience with the Fokker 100
[SAE PAPER 892238] p 733 A90-45450

Hermes training aircraft
p 354 N90-16827

Aeronautical decisionmaking for air ambulance program administrators
[DOT/FAA/DS-88/8] p 635 N90-23368

PILOTLESS AIRCRAFT

Captive carry testing of remotely piloted vehicles
p 828 A90-46386

Flight testing Navy low Reynolds Number (LRN) unmanned aircraft
p 828 A90-46387

CONDOR - high altitude long endurance (HALE) autonomously piloted vehicle (APV)
[AIAA PAPER 90-3279] p 836 A90-48866

All fabric N-wing unmanned powered flight systems
[AIAA PAPER 90-3282] p 836 A90-48869

Unmanned helicopters for battlefield and maritime surveillance
p 920 A90-51899

Guidance and Control of Unmanned Air Vehicles
[AGARD-CP-436] p 260 N90-15924

Unmanned air vehicles payloads and sensors
p 251 N90-15930

Distribution of hardware and software elements in unmanned air vehicle systems
p 251 N90-15933

Technology and evaluation of unmanned air vehicles
p 252 N90-15934

Design of a natural laminar flow airfoil for an unmanned aircraft
[PD-CF-9004] p 499 N90-20975

Initial flight test of half-scale unmanned air vehicle
[AD-A219584] p 648 N90-23388

PINS

Recent studies on the behaviour of interference fit pins in composite plates
p 132 A90-16320

PIPE FLOW

Effects of turbulence model constants on computation of confined swirling flows
p 444 A90-27999

PIPES (TUBES)

A study of filament wound high modulus carbon fiber reinforced cylinders
p 948 A90-50218

Estimation of subsonic far-field jet-mixing noise from single-stream circular nozzles
[ESDU-89041] p 316 N90-16721

An investigation of the generation and radiation of aerodynamic noise in real piping systems
p 614 N90-22368

Experimental characterization of the effects of pneumatic tubing on unsteady pressure measurements
[NASA-TM-4171] p 850 N90-27703

PISTON ENGINES

A discrete dynamic model of the crankshaft-aircrew assembly of an aircraft piston engine for the purpose of vibration analysis by the method of finite elements
p 51 A90-13220

History of aircraft piston engine oils - The last forty years
[SAE PAPER 891037] p 124 A90-14343

Possibility of active propeller-noise suppression in piston-engine aircraft by changing the phase relation between the propeller and exhaust signals
p 218 A90-18450

PITCH (INCLINATION)

On the 'inverse phugoid problem' as an instance of non-linear stability in pitch
p 55 A90-10221

The effect of pitch location on dynamic stall
p 2 A90-10641

On a pitch control law for a constant glide slope through windshears
p 117 A90-13784

Reduction of blade-vortex interaction noise through higher harmonic pitch control
p 377 A90-23937

Design and development of a facility for compressible dynamic stall studies of a rapidly pitching airfoil
p 436 A90-28255

The effect of windscreen bows and HUD pitch ladder on pilot performance during simulated flight
p 420 A90-31333

A comparison between theoretical and experimental results for a 3-D wing with damped pitching oscillations
p 472 A90-33361

Numerical simulation of separated flows around a wing section at pitching motion by a discrete vortex method
p 475 A90-33753

Dynamic stall of a constant-rate pitching airfoil
p 553 A90-35754

Leading-edge vortices due to low Reynolds number flow past a pitching delta wing
p 555 A90-36258

Digital controller design for the pitch axis of the F-14 using an H(infinity) method
p 668 A90-40912

The influence of control-surface compensation parameters on the hinge moment characteristics
p 643 A90-41737

Aeroelastic response characteristics of a rotor executing arbitrary harmonic blade pitch variations
p 646 A90-42464

Agusta methodology for pitch link loads prediction in preliminary design phase
p 646 A90-42465

Use of smart actuators for the tail rotor collective pitch control
p 688 A90-42483

The effect of solidity on propeller normal force
[SAE PAPER 892205] p 713 A90-45424

Unsteady aerodynamics of delta wings, undergoing ramp-maneuvering in pitch to post-stall angle of attack
p 806 A90-46857

Analyzing the flared landing task with pitch-rate flight control systems
[AIAA PAPER 90-3483] p 866 A90-47732

Unsteady aerodynamics with applications to flight mechanics
[AD-A211944] p 89 N90-11706

A pitch control law for compensation of the phugoid mode induced by windshears
p 258 N90-15051

Design of integrated pitch axis for autopilot/autothrottle and integrated lateral axis for autopilot/yaw damper for NASA TSRV airplane using integral LQG methodology
[NASA-CR-4268] p 348 N90-16768

PITCHING MOMENTS

The influence of sweep on dynamic stall produced by a rapidly pitching wing
[AIAA PAPER 90-0581] p 230 A90-22231

Integral solution of unsteady full-potential equation for a transonic pitching airfoil
p 232 A90-23280

Vortex dynamics on a pitching delta wing
p 233 A90-23281

Measured forces and moments on a delta wing during pitch-up
p 308 A90-26137

Comparison of calculated and experimental nonstationary aerodynamic characteristics of a delta wing pitching at large angles of attack
p 387 A90-28988

A technique for calculating nonlinear normal-force and pitching-moment coefficients for slender delta wings, accounting for wing thickness
p 476 A90-34356

Dynamic stall experiments on the NACA 23012 aerofoil
p 552 A90-35140

Wall interference correction for three-dimensional transonic flows
[AIAA PAPER 90-1408] p 558 A90-37947

Parameter effects on oscillatory aerofoil in transonic flows
[AIAA PAPER 90-1473] p 563 A90-38629

- Demonstrating technologies for enhanced fighter manoeuvrability - The Rockwell/MBB X-31 p 731 A90-43767
- Recent aerodynamic measurements with Magnetic Suspension Systems p 759 A90-44399
- Two dimensional post stall maneuver of a NACA 0015 airfoil at high pitching rates [AIAA PAPER 90-2610] p 710 A90-45150
- Schlieren studies of compressibility effects on dynamic stall of airfoils in transient pitching motion [AIAA PAPER 90-3038] p 791 A90-45877
- Navier-Stokes predictions of pitch damping for finned projectiles using steady coning motion [AIAA PAPER 90-3088] p 795 A90-45902
- Correlation of theory to wind-tunnel data at Reynolds numbers below 500,000 p 800 A90-46370
- Numerical simulation of wakes with application to blade-vortex interaction p 807 A90-46881
- Lift and pitching moment measurements on a swept tapered wing in oscillatory vertical gusts p 811 A90-48089
- Subsonic and transonic low-Reynolds-number airfoils with reduced pitching moments [AIAA PAPER 90-3212] p 812 A90-48838
- Normal-force-curve and pitching-moment-curve slopes of forebody-cylinder combinations at zero angle of attack for Mach numbers up to 5 [ESDU-89008] p 89 N90-11709
- Normal force, pitching moment, and side force of forebody-cylinder combinations for angles of attack up to 90 degrees and Mach numbers up to 5 [ESDU-89014] p 173 N90-14192
- Flow visualization of the effect of pitch rate on the vortex development on the scale model of a F-18 fighter aircraft [AD-A214244] p 236 N90-15080
- The response of helicopter rotors to vibratory airload [AD-A215678] p 337 N90-16756
- Body effect on wing angle of attack and pitching moment at zero lift at low speeds [ESDU-89042] p 337 N90-16757
- Study of the ground effects in the CEAT aerodynamic tunnel: Using the results p 922 N90-28530
- PITOT TUBES**
- Interference between the pitot-static tube and the model in wind tunnel studies of flow parameters p 350 A90-24169
- PITTING**
- Effects on aerospace alloys of residual chlorine in chlorinated-solvent primers p 956 A90-50187
- Coatings for gas turbine compressors [NLR-MP-88045-U] p 115 N90-11750
- PLANAR STRUCTURES**
- Optimal trajectories for hypervelocity flight p 918 N90-29378
- PLANE STRESS**
- Active control of tiltrotor blade in-plane loads during maneuvers p 670 A90-42463
- PLANE WAVES**
- Irregular interaction of a strong shock wave with a thin profile p 9 A90-12267
- Mobility power flow analysis of an L-shaped plate structure subjected to acoustic excitation [NASA-CR-186130] p 214 N90-13817
- PLANFORMS**
- Forebody design for the aerospaceplane [AIAA PAPER 90-2472] p 762 A90-42810
- Prediction of forces and moments for flight vehicle control effectors. Part 2: An analysis of delta wing aerodynamic control effectiveness in ground effect [NASA-CR-186572] p 571 N90-21735
- PLANNING**
- The Air Force Flight Test Center Flight Test Safety Program p 35 N90-10872
- PLASMA HEATING**
- Nonlinear mechanics of unstable plasmas as related to high altitude aerodynamics [AD-A215126] p 464 N90-19852
- PLASMA SPRAYING**
- Properties and characterisation of novel thermal barrier systems for gas turbines p 62 A90-12538
- PLASMA TORCHES**
- Some governing parameters of plasma torch igniter/flameholder in a scramjet combustor [AIAA PAPER 90-2098] p 661 A90-42017
- PLASMA TURBULENCE**
- Nonlinear mechanics of unstable plasmas as related to high altitude aerodynamics [AD-A215126] p 464 N90-19852
- PLASMAS (PHYSICS)**
- Nonlinear mechanics of unstable plasmas as related to high altitude aerodynamics [AD-A215126] p 464 N90-19852
- PLASTIC AIRCRAFT STRUCTURES**
- Resin transfer molding of composite aircraft structures [SAE PAPER 891042] p 128 A90-14347
- The strength and weakness of carbon composite structures --- for military and civil aircraft p 180 A90-17679
- Material of the '90s? p 265 A90-20259
- Crashworthiness of composite floor sections p 243 A90-20261
- More composites in commercial transports? p 265 A90-20263
- Material progress p 221 A90-21715
- The impact of composites on the aerospace industry p 221 A90-22649
- Air Force application of injection molding technology [SME PAPER EM89-103] p 274 A90-23686
- The use of fibre reinforced thermoplastics for helicopter primary structures and their engineering substantiation p 441 A90-28191
- Evaluation of 3-D reinforcements in commingled, thermoplastic structural elements p 441 A90-28192
- Analysis and testing of fiber-reinforced thermoplastic composite vertical stabilizer skins for an advanced attack helicopter p 441 A90-28193
- Toughened thermosets for damage tolerant carbon fiber reinforced composites p 443 A90-29825
- Fibre reinforced thermoplastic integral constructions in modular build-up technology - The 'thermoplastic in-situ-technique' p 534 A90-31879
- Design, fabrication and experimental test of hi-temperature CFRP stiffened structures --- rotating cowl panels for unducted fan engines p 534 A90-31892
- Fabrication of aircraft structures from thermoplastic drapable preforms p 468 A90-33125
- Designing aerospace structures with Du Pont's LDF thermoplastic composites p 530 A90-33126
- Canadians develop composite techniques for CF-18 battle damage repair program p 551 A90-36300
- A technique for rapid impact damage detection with implication for composite aircraft structures p 600 A90-37662
- Structural components of fiber-reinforced thermoplastics p 676 A90-41111
- Design and certification of the all-composite airframe [SAE PAPER 892210] p 732 A90-45429
- Innovative design concepts for thermoplastic composite materials p 940 A90-50059
- High temperature behavior of the innovation carbon/CSPI composite p 941 A90-50067
- Monolithic CFC-Main Landing Gear Door for Tornado p 955 A90-50136
- Ways of providing for the strength and service life of aircraft structures made of polymer composites with allowance for damage p 957 A90-50843
- PLASTIC DEFORMATION**
- A study of the nonlinear deformation of a shell of revolution with a surface bend p 129 A90-14574
- Wing design optimization under stress-strain constraints using full-strength and minimum mass criteria p 804 A90-46554
- A rate theory investigation of cyclic loading and plastic deformation in the high stress and ambient temperature range p 954 A90-49884
- Fatigue crack initiation mechanics of metal aircraft structures [AD-A210567] p 65 N90-10255
- PLASTICS**
- Aircraft battle damage repair of transparencies [AD-A224168] p 925 N90-29387
- PLATE THEORY**
- Supersonic flutter of shear deformable laminated composite flat panels p 683 A90-41104
- Comparison of equivalent plate and finite element analysis of a realistic aircraft structural configuration [AIAA PAPER 90-3293] p 837 A90-48877
- PLATES**
- Uses and properties of Al-Li on the new EH101 helicopter p 268 N90-15201
- Aluminum-lithium: Application of plate and sheet to fighter aircraft p 268 N90-15202
- PLATES (STRUCTURAL MEMBERS)**
- Effects of splitter plates on the wake flow behind a bluff body p 469 A90-32453
- PLATING**
- Standardization in aerospace plating and coating [SAE PAPER 890913] p 365 A90-24681
- PLOTTING**
- Realtime multi-plot graphics system [NASA-CR-4304] p 965 N90-29919
- PLUGS**
- Comparative evaluation of Allison T56 engine chip detectors [AD-A221864] p 855 N90-26832
- PLUMES**
- Investigation of advanced mixer-ejector exhaust system [AD-A211943] p 89 N90-11705
- PNEUMATIC CONTROL**
- Pneumatic vortical flow control at high angles of attack [AIAA PAPER 90-0098] p 227 A90-22164
- Prompt identification of a troubled engine can help avoid catastrophe p 721 A90-44222
- PNEUMATIC EQUIPMENT**
- Design of an advanced pneumatic deicer for the composite rotor blade p 29 A90-11009
- An advanced pneumatic impulse ice protection system (PIIP) for aircraft [AIAA PAPER 90-0492] p 182 A90-19875
- The selection of actuation devices for aircraft pneumatic valves in systems under computer control [SAE PAPER 891456] p 368 A90-27425
- Stiffness of an aircraft pneumatic rudder drive p 828 A90-46479
- Flight evaluation of a pneumatic system for unsteady pressure measurements using conventional sensors [NASA-TM-4131] p 186 N90-14225
- PNEUMATIC PROBES**
- Compensating for pneumatic distortion in pressure sensing devices [AIAA PAPER 90-0631] p 211 A90-19956
- Compensating for pneumatic distortion in pressure sensing devices [NASA-TM-101716] p 415 N90-19224
- Experimental characterization of the effects of pneumatic tubing on unsteady pressure measurements [NASA-TM-4171] p 850 N90-27703
- PNEUMATICS**
- Formulation and verification of a technique for compensation of pneumatic attenuation errors in airborne pressure sensing devices p 369 N90-17084
- POLAR CAPS**
- Airfields on antarctic glacier ice [AD-A217638] p 526 N90-20097
- POLARIZATION (CHARGE SEPARATION)**
- Charging of aircraft - High-velocity collisions p 322 A90-26131
- POLARIZATION CHARACTERISTICS**
- Electrostatic field conditions on an aircraft stricken by lightning [ONERA, TP NO. 1989-148] p 23 A90-11170
- POLICIES**
- Safety and cryogenic wind tunnels p 264 N90-15960
- Social survey findings on en route noise annoyance issues p 698 N90-24888
- AGARD highlights 90/1 p 783 N90-26788
- POLISHING**
- The Robotic Canopy Polishing System [SME PAPER MS89-134] p 222 A90-23680
- POLLUTION**
- Pollutants: Production and methods of reduction [CIT/SME/VKI/RS/6] p 749 N90-25990
- POLLUTION CONTROL**
- Active soot reduction in a spray-fired, axisymmetric model gas turbine combustor [AIAA PAPER 90-0039] p 191 A90-19644
- POLLUTION TRANSPORT**
- New high-speed air transport system and stratospheric pollution [ONERA, TP NO. 1989-202] p 279 A90-22445
- POLYACRYLONITRILE**
- Domestic precursor technology - A unique route to current and future generation carbon fibers p 940 A90-50057
- The changes of structures and properties in PAN-based carbon fibers during heat treatment in carbon dioxide p 945 A90-50145
- POLYESTER RESINS**
- New cyanate ester resin with low temperature (125-200 C) cure capability p 944 A90-50135
- POLYESTERS**
- Criteria for polymer concrete on airport pavements [DOT/FAA/DS-89/18] p 527 N90-21045
- POLYETHYLENES**
- Combustion of PMMA, PE, and PS in a ramjet p 764 A90-43670
- POLYHEDRONS**
- Formalization and solution of covering problems in the synthesis of control and monitoring systems p 76 A90-10963
- POLYIMIDE RESINS**
- Resin transfer molding of composite aircraft structures [SAE PAPER 891042] p 128 A90-14347
- In-situ measurement, modelling and control of the imidization reaction in PMR-15 --- polyimide resin for aerospace structures p 941 A90-50066
- High temperature behavior of the innovation carbon/CSPI composite p 941 A90-50067

Thermo-oxidative stability studies of PMR-15 polymer matrix composites reinforced with various continuous fibers p 941 A90-50068
Effects of additives on the processing and properties of LARC-TPI polyimide p 942 A90-50070
Characterization of LARC-TPI 1500 powders - A new version with controlled molecular weight p 946 A90-50177

Effect of molecular weight and end group control on the adhesion behavior of thermoplastic polyimides and poly(imide siloxane) segmented copolymers p 947 A90-50199

POLYIMIDES

Improved melt flow and physical properties of Mitsui Toatsu's LARC-TPI 1500 series polyimide p 943 A90-50134

Improved thermal performance using allylindiacid-imides p 946 A90-50175

Effect of molecular weight and end group control on the adhesion behavior of thermoplastic polyimides and poly(imide siloxane) segmented copolymers p 947 A90-50199

POLYMER BLENDS

Effects of additives on the processing and properties of LARC-TPI polyimide p 942 A90-50070

POLYMER MATRIX COMPOSITES

Composite-embedded optical fibers for communication links p 139 A90-13847

More composites in commercial transports? p 265 A90-20263

The status of high temperature polymers for composites - Likely candidates p 528 A90-31516

High performance thermoplastic composites with poly(etherketoneketone) matrix p 529 A90-31646
International SAMPE Symposium and Exhibition, 35th, Anaheim, CA, Apr. 2-5, 1990, Proceedings. Books 1 & 2 p 940 A90-50056

Interfaces properties of high temperature polymer composite systems p 941 A90-50062

Poly(arylene ether ketone)/poly(aryl imide) homo- and polydimethylsiloxane segmented copolymer blends - Influence of chemical structure on miscibility and physical property behavior p 941 A90-50063

Thermo-oxidative stability studies of PMR-15 polymer matrix composites reinforced with various continuous fibers p 941 A90-50068

Use of unbalanced laminates as a screening method for microcracking p 948 A90-50217

Ways of providing for the strength and service life of aircraft structures made of polymer composites with allowance for damage p 957 A90-50843

POLYMER PHYSICS

Freeze drying for morphological control of inter-penetrating polymer networks p 948 A90-50214

POLYMERIC FILMS

Application of piezoelectric foils in experimental aerodynamics p 446 A90-28258

Effects of additives on the processing and properties of LARC-TPI polyimide p 942 A90-50070

Development of a high toughness heat resistant 177 C (350 F) curing film adhesive for aerospace bonding applications - FM 377 adhesive p 955 A90-50126

Novel composite surfacing film p 948 A90-50212

A reliable, maintenance-free oxygen sensor for aircraft using an oxygen-sensitive coating on potentiometric electrodes [AD-A222696] p 927 N90-28545

POLYMERIZATION

In-situ measurement, modelling and control of the imidization reaction in PMR-15 ... polyimide resin for aerospace structures p 941 A90-50066

The 1-((diorganooxyphosphonyl)methyl)-2,4- and -2,6-diamido benzenes [NASA-CASE-ARC-11425-4] p 532 N90-20133

Some 1-((diorganooxyphosphonyl)methyl)-2,4- and -2,6-dinitro-benzenes [NASA-CASE-ARC-11425-3] p 678 N90-23475

POLYMETHYL METHACRYLATE

Rain erosion testing --- on polymethyl methacrylate specimens p 525 A90-34578

Combustion of PMMA, PE, and PS in a ramjet p 764 A90-43670

POLYNOMIALS

Mean-square approximation by an even nonnegative polynomial p 374 A90-24101

Determination of the extreme values of the efficiency criteria for a flight vehicle control system in the probable scatter range of its characteristics p 859 A90-46569

Sequential design of experiments with physically based models 23 [AD-A211918] p 138 N90-12239

Time-optimal aircraft pursuit-evasion with a weapon envelope constraint [NASA-CR-186640] p 734 N90-25126

Real-time adaptive aircraft scheduling [NASA-CR-177558] p 820 N90-27669

POLYSTYRENE

Combustion of PMMA, PE, and PS in a ramjet p 764 A90-43670

POLYSULFIDES

Integral fuel tank sealing practice at British Aerospace (Kingston) p 250 N90-15905

The effect of primer age on adhesion of polysulphide sealant p 269 N90-15909

Effect of temperature on the storage life of polysulfide aircraft sealants [MRL-TR-89-31] p 444 N90-19364

POLYTOPES

Nonconvex polytope approximations of attracting basin boundaries for nonlinear systems [AIAA PAPER 90-3512] p 891 A90-47758

PONTRYAGIN PRINCIPLE

A study of the control technique for aircraft spin recovery p 590 A90-37226

POROSITY

Supersonic jet noise reduction by a porous single expansion ramp nozzle [AIAA PAPER 90-0366] p 219 A90-19815

POROUS BOUNDARY LAYER CONTROL

Computation of viscous transonic flow over porous airfoils p 153 A90-17864

Permeability of the porous walls of a wind tunnel at transonic velocities p 350 A90-24151

Wide angle diffusers with passive boundary-layer control [AIAA PAPER 90-1600] p 567 A90-38732

An experimental evaluation of slots versus porous strips for laminar-flow applications p 92 N90-12530

Results of LFC experiment on slotted swept supercritical airfoil in Langley's 8-foot transonic pressure tunnel p 92 N90-12531

POROUS MATERIALS

Increasing the heat conductivity of elastic damping elements of MR material p 102 A90-14580

POROUS PLATES

Characteristics of turbulent separation flows on a porous surface under conditions of injection p 231 A90-22422

POROUS WALLS

Wave cancellation properties of a splitter-plate porous wall configuration p 57 A90-11005

Advanced combustor liner cooling technology for gas turbines p 112 A90-16004

Equilibrium of an elastic porous shell in supersonic gas flow p 150 A90-17109

An experimental investigation of pressure fluctuation mechanism for different transonic porous wall configurations [AIAA PAPER 90-1417] p 604 A90-37954

Broadband noise measurement in the transonic test section of the VTI T-38 wind tunnel [AIAA PAPER 90-1418] p 614 A90-37955

Some explorations on the mechanism of blade flutter suppression by porous wall casing p 854 A90-49470

Comparison of NAE porous wall and NASA adaptive wall test results using the NAE CAST-10 airfoil model p 353 N90-17656

PORTABLE EQUIPMENT

Spectra composite enhances portability and survivability of electronic equipment p 947 A90-50189

POSITION (LOCATION)

A waveform alignment approach to positioning airborne radar-sounding data p 332 A90-26651

Vision guidance update - Synthetic aperture radar (SAR) multiple image exploitation for position and velocity determination p 488 A90-34140

Differential-geometrical technique of signal transformation and estimation of position, rate and acceleration parameters using supplementary data sources p 638 A90-41004

Adaptive clutter rejection filters for airborne Doppler weather radar applied to the detection of low altitude windshear [NASA-CR-186211] p 214 N90-14453

National airspace system: Airport movement area control operational concept [WP-89W00181] p 243 N90-15086

Modeling the effects of the use of GPS (Global Positioning System) derived altitude indication in the C-17A airdrop system [AD-A215366] p 333 N90-16748

Position computation without elevation information for computed centerline operations [DOT/FAA/CT-TN89/42] p 640 N90-23379

Yaw fin deployment apparatus for ejection seat [AD-D014512] p 723 N90-25118

Visualization of three dimensional data p 782 N90-25553

Qualitative evaluation of a conformal velocity vector display for use at high angles-of-attack in fighter aircraft [NASA-TM-102629] p 739 N90-25981

Position finding and ground target direction finding by an aircraft with a gimbal video camera [DLR-FB-89-62] p 825 N90-27673

POSITION ERRORS

Optimal selection of GPS sets to minimize emitter location errors p 97 A90-13992

Influence of satellite geometry, range, clock, and altimeter errors on two-satellite GPS navigation p 123 A90-13993

Parameter sensitivity analysis of one kind of flight path reconstruction estimator p 779 A90-44832

Helicopter Airborne Laser Positioning System (HALPS) [NASA-TM-102814] p 654 N90-23399

POSITION INDICATORS

Dual mode radar fusion based on morphological processing p 459 A90-30249

Integrated system of differential Global Positioning System and inertial measurement unit - A position determination system for automatic landing [AIAA PAPER 90-1300] p 487 A90-33914

Analytical studies for computed center line operations [SAE PAPER 892219] p 729 A90-45436

Automatic processing of images from the GRATE flight test tool [DLR-FB-89-28] p 109 N90-12599

POSITION SENSING

Techniques for extreme attitude suspension of a wind tunnel model in a magnetic suspension and balance system [NASA-CR-181895] p 202 N90-14245

Heli/SITAN: A terrain referenced navigation algorithm for helicopters [DE90-005193] p 405 N90-19217

Hover position sensing system p 848 N90-27448

Position finding and ground target direction finding by an aircraft with a gimbal video camera [DLR-FB-89-62] p 825 N90-27673

POSITIONING

Helicopter Airborne Laser Positioning System (HALPS) [NASA-TM-102814] p 654 N90-23399

The potential for digital databases in flight planning and flight aiding for combat aircraft p 918 N90-29371

POSTFLIGHT ANALYSIS

Decommutation techniques and their integration into post flight analysis system p 26 A90-12191

Post crash flight analysis: Visualizing flight recorder data [AD-A212063] p 96 N90-11715

An automated calibration laboratory for flight research instrumentation: Requirements and a proposed design approach [NASA-TM-101719] p 781 N90-26564

POTENTIAL FLOW

An improved method for the computation of unsteady transonic potential flow - Application for airfoil and blade performance prediction [ONERA, TP NO. 1989-154] p 4 A90-11175

Analytical methods for subsonic propulsion system integration p 29 A90-12613

Full-potential calculations using Cartesian grids p 86 A90-15740

A relaxation method for transonic potential flows through 2-D cascade with large camber angle p 152 A90-17786

Potential flow calculation for three-dimensional wings and wing-body combination in oscillatory motion p 153 A90-17976

Experimental investigation of flowfield about a multielement airfoil p 154 A90-18137

On the coupling of finite elements and boundary elements for transonic potential flows p 155 A90-18297

Incompressible potential flow about complete aircraft configurations p 156 A90-18443

Complex variable boundary element method for external potential flows [AIAA PAPER 90-0127] p 162 A90-19694

Inviscid drag prediction for transonic transport wings using a full-potential method [AIAA PAPER 90-0576] p 168 A90-19926

A zonal flow analysis method for two-dimensional airfoils [AIAA PAPER 90-0571] p 230 A90-22230

Analytical solution of the problem of nonaxisymmetric potential flow past a spherical canopy - A summary of the principal asymptotic formulas and qualitative analysis p 300 A90-24753

Nonlinear aerodynamics of two-dimensional airfoils in severe maneuver p 301 A90-25276

Advanced rotor computations with a corrected potential method p 385 A90-28197

Impact of multigrid smoothing analysis on three-dimensional potential flow calculations p 449 A90-29147

SUBJECT INDEX

- Time domain flutter analysis of cascades using a full-potential solver
[AIAA PAPER 90-0984] p 391 A90-29374
- Three dimensional full potential method for the aeroelastic modeling of propfans
[AIAA PAPER 90-1120] p 393 A90-29392
- Calculations of transonic flows over wing-body combinations
p 395 A90-31479
- Multi-element aerofoils in viscous flow
p 469 A90-32451
- Calculations of propeller/airframe interference effects using the potential/multienergy flow method
p 490 A90-32452
- Comparison of two potential flow methods for transonic flutter analysis
p 471 A90-33356
- Applications of the unsteady full potential equation for wings
p 472 A90-33358
- Numerical analysis of unsteady forces on oscillating ring airfoils and jet engines
p 473 A90-33364
- Measurement of the interaction between a rotor tip vortex and a cylinder
p 555 A90-36255
- The free-wake computation of rotor-body flows
[AIAA PAPER 90-1540] p 565 A90-38684
- Simulation of inviscid blade-row interaction using a linearised potential code
[AIAA PAPER 90-1916] p 621 A90-40555
- Comparison of high-angle-of-attack slender-body theory and exact solutions for potential flow over an ellipsoid
p 622 A90-40692
- Boundary integral formulation for compressible nonlinear potential and Navier-Stokes equations
p 706 A90-44406
- A two-dimensional unsteady potential solver in internal aerodynamics flow problems
p 707 A90-44430
- Design of wing profiles for application in nonstall conditions in a given angle-of-attack range
p 710 A90-44936
- Speed-up of the strongly implicit procedure with application to subsonic/transonic potential flows
p 809 A90-47301
- Incompressible potential flow about three-dimensional configurations
p 810 A90-48082
- The aerodynamic design of the contraction for a subsonic wind tunnel
p 907 A90-51545
- Steady and unsteady potential flow around thin annular wings and engines with simulation of jet engine flow
[DFVLR-FB-89-18] p 89 A90-11711
- Solution of potential flow past an elastic body using the boundary element technique
[AD-A213843] p 275 A90-15390
- An iterative solution to aeroelastic effects in potential flow
[AD-A216291] p 320 A90-17580
- Modeling the wake as a continuous vortex sheet in a potential-flow solution using vortex panels
[AD-A216220] p 371 A90-18016
- Aerodynamics of unsteady systems. Numerical study of potential flow/boundary layer coupling
[ETN-90-96257] p 396 A90-18367
- Users manual for the NASA Lewis Ice Accretion Prediction Code (LEWICE)
[NASA-CR-185129] p 468 A90-20943
- Multigrid accelerated relaxation solution of transonic full potential flow equation
[PD-CF-8942] p 480 A90-20951
- Unsteady potential flow past a propeller blade section
[NASA-CR-4307] p 634 A90-24246
- Sideslip-induced static pressure errors in flight-test measurements
[NASA-TM-102846] p 849 A90-27702
- Flow coupling between a rotor and a stator in turbomachinery
[AD-A223882] p 932 A90-28572
- ### POTENTIAL THEORY
- Integral solution of unsteady full-potential equation for a transonic pitching airfoil
p 232 A90-23280
- Improvement of 3D full-potential method and computation of flowfield of CAS compressor rotor
[ASME PAPER 89-GT-17] p 288 A90-23760
- Basic equations for unsteady transonic flow
p 394 A90-29884
- Applications of the unsteady full potential equation for wings
p 472 A90-33358
- The potential approximation in the theory of conical flows
p 710 A90-44930
- An experimental investigation of viscous aspects of propeller blade flow
p 315 A90-16711
- ### POTENTIOMETRIC ANALYSIS
- A reliable, maintenance-free oxygen sensor for aircraft using an oxygen-sensitive coating on potentiometric electrodes
[AD-A222696] p 927 A90-28545
- ### POWDER (PARTICLES)
- Brownian motion far from equilibrium - A hypersonic approach
p 555 A90-35917

- Electrostatic dry powder prepping of carbon fiber
p 948 A90-50215
- ### POWDER METALLURGY
- Powder metallurgy and oxide dispersion processing of superalloys
p 531 A90-34158
- A friendly alloy --- aircraft construction materials
p 764 A90-44173
- New Light Alloys
[AGARD-CP-444] p 267 N90-15185
- Improved toughness alloys based on titanium aluminides
p 533 N90-20208
- Metal matrix composites and powder processing for aero-engine applications
[PNR90617] p 767 N90-26087
- ### POWER CONDITIONING
- Electrical power systems for high Mach vehicles
p 586 A90-38129
- ### POWER CONVERTERS
- Electric controls for a high-performance EHA using an interior permanent magnet motor drive
p 452 A90-30711
- Power transfer devices for V/STOL convertible engine systems
p 587 A90-38539
- ### POWER EFFICIENCY
- Effect of the radial clearance on the efficiency of a partial microturbine
p 111 A90-14586
- Effect of the angle of attack on the efficiency and thrust ratio of axial-flow microturbines with full admission
p 111 A90-14590
- Efficiency testing of a helicopter transmission planetary reduction stage
p 271 A90-21113
- Power dissipation in smooth and honeycomb labyrinth seals
[ASME PAPER 89-GT-220] p 362 A90-23881
- Review of mixed flow and radial turbine options
[AIAA PAPER 90-2414] p 687 A90-42166
- X.2 limited flight test plan
[AD-A214412] p 249 A90-15099
- Energy Efficient Engine exhaust mixer model technology report addendum; phase 3 test program
[NASA-CR-174799] p 930 A90-28556
- ### POWER LOSS
- Inclement weather induced aircraft engine power loss
[AIAA PAPER 90-2169] p 662 A90-42055
- ### POWER SPECTRA
- A new class of random processes with application to helicopter noise
p 781 A90-42874
- NASA investigation of a claimed 'overlap' between two gust response analysis methods
p 771 A90-44730
- The S.D.G., P.S.D. and the nonlinear airplane
[NLR-MP-88018-U] p 183 A90-13371
- A two dimensional power spectral estimate for some nonstationary processes
[NASA-CR-186100] p 217 A90-14843
- Construction of a hybrid angular velocity reference system for investigation of the dynamic characteristics of strapdown gyros
[ESA-TT-1181] p 774 A90-25332
- Formation of design envelope criterion in terms of deterministic spectral procedure
[RAE-TM-SS-9] p 721 A90-25953
- Estimation of power spectral density of runway roughness
[NAL-TR-1037] p 939 A90-29411
- ### POWER SUPPLIES
- Handbook on heat exchangers --- Russian book
p 273 A90-22743
- ### POWER SUPPLY CIRCUITS
- Power supply of aircraft --- Russian book
p 43 A90-12474
- ### POWERED LIFT AIRCRAFT
- In flight flow angle measurements on the Ball-Bartoe Jetwing powered lift aircraft
[AIAA PAPER 90-1284] p 495 A90-33905
- Focusing propulsion and lift system development for an evolving special operations aircraft
[AIAA PAPER 90-2277] p 730 A90-42768
- The NASA experience in aeronautical R and D: Three case studies with analysis
[AD-A211486] p 82 A90-12496
- Powered-lift aircraft technology
[NASA-SP-501] p 107 A90-12589
- FAA Rotorcraft Research, Engineering, and Development Bibliography 1962-1989
[AD-A224256] p 902 A90-29299
- ### PRECIPITATION (METEOROLOGY)
- The microphysical structure of severe downdrafts from radar and aircraft observations in CINDE --- Convection Initiation and Downburst Experiment
p 455 A90-28582
- Adverse weather operations during the Canadian Atlantic storms program
p 281 A90-15052

PREDICTION ANALYSIS TECHNIQUES

- The collection of non-conus aircraft icing data along with an identification of the geographical areas of potential severe icing and a study of a method of remote determining atmospheric icing data
[AD-A215055] p 323 N90-16724
- ### PRECIPITATION HARDENING
- Powder metallurgy and oxide dispersion processing of superalloys
p 531 A90-34158
- Quench sensitivity of airframe aluminium alloys
p 765 A90-44348
- ### PRECIPITATION PARTICLE MEASUREMENT
- Comparison of two droplet sizing systems in an icing wind tunnel
[AIAA PAPER 90-0668] p 274 A90-23711
- Comparison of two droplet sizing systems in an icing wind tunnel
[NASA-TM-102456] p 215 A90-14617
- ### PREDICTION ANALYSIS TECHNIQUES
- VISTRAFS - A simulation method for strongly-interacting viscous transonic flow
p 144 A90-16756
- Prediction of post-stall flows on airfoils
p 145 A90-16757
- Theoretical prediction of high Reynolds number viscid/inviscid interaction phenomena in cascades
p 145 A90-16759
- Supersonic/hypersonic Euler flowfield prediction method for aircraft configurations
p 145 A90-16767
- Predicting crack growth under thermo-mechanical cycling
p 209 A90-18169
- Prediction of the strength-related reliability of structural elements at the design stage
p 274 A90-23402
- Prediction of the aerodynamic environment and heat transfer for rotor-stator configurations
[ASME PAPER 89-GT-89] p 359 A90-23807
- A comparison between engine test results and design predictions of turbine blade cooling performance
[ASME PAPER 89-GT-169] p 341 A90-23854
- Prediction and measurement of the aerodynamic interactions between a rotor and airframe in forward flight
p 384 A90-28176
- The prediction of loads on the Boeing Helicopters Model 360 rotor
p 410 A90-28240
- Circulation control tail boom aerodynamic prediction and validation
p 385 A90-28243
- Prediction of turbulent combustion flowfields behind a backward-facing step
p 529 A90-32952
- On the prediction of the aeroelastic behaviour of lifting systems due to flow separation
p 491 A90-33369
- Flutter analysis from ambient random responses
p 491 A90-33374
- Life prediction and fatigue
p 532 A90-34163
- A simple prediction method for low-cycle fatigue life of structures
p 604 A90-37240
- Effects of turbulence models on the prediction of transonic wing flows
[SAE PAPER 892224] p 713 A90-45440
- Modelling of fuel effects on naval aircraft operations
[SAE PAPER 892331] p 765 A90-45488
- Full span analysis for flutter prediction of slender blade assemblies
p 879 A90-46188
- Unsteady aerodynamics - Physical issues and numerical predictions
p 806 A90-46843
- Unsteady blade surface pressures on a large-scale advanced propeller - Prediction and data
[AIAA PAPER 90-2402] p 808 A90-47220
- Method for simultaneous wing aerodynamic and structural load prediction
p 838 A90-48955
- Efficiency study comparing two helicopter planetary reduction stages
[AIAA PAPER 90-2156] p 956 A90-50644
- Theoretical prediction of pressure distribution on wedged delta wing at higher supersonic Mach numbers and its agreement with experimental results
p 907 A90-51537
- Goertler instability on an airfoil: Comparison of marching solution with experimental observations
p 19 A90-10364
- CFD methods for drag prediction and analysis currently in use in UK
[RAE-TM-AERO-2146] p 95 A90-12563
- A technique for the prediction of aerodynamics and aeroelasticity of rotor blades
p 184 A90-13377
- An evaluation of a fatigue crack growth prediction model for variable-amplitude loading (PREFFAS)
[LR-537] p 214 A90-13822
- Formulation and verification of a technique for compensation of pneumatic attenuation errors in airborne pressure sensing devices
p 369 A90-17084
- Predicted and measured boundary layer refraction for advanced turboprop propeller noise
[NASA-TM-102355] p 379 A90-17413
- Prediction methods for store separation
p 317 A90-17549
- Dynamic derivatives of missiles and fighter-type configurations at high angles of attack
p 337 A90-17554

- A study of the structural efficiency of fluted core graphite-epoxy panels
[NASA-TM-101681] p 373 N90-18070
- The effects of wind tunnel data uncertainty on aircraft point performance predictions
[AD-A216091] p 414 N90-18387
- Numerical investigation of unsteady flow in oscillating turbine and compressor cascades p 426 N90-18407
- The influence of a wall function on turbine blade heat transfer prediction p 429 N90-19421
- Escape systems research at RAE p 483 N90-20058
- Measurement and prediction of propeller blade surface pressure distributions p 481 N90-20961
- Aerodynamic design via control theory p 546 N90-20998
- Secondary Flows in Turbomachines
[AGARD-CP-469] p 511 N90-21009
- Secondary flows and radial mixing predictions in axial compressors p 512 N90-21010
- The effects of compressor endwall flow on airfoil incidence and deviation p 512 N90-21011
- Secondary flow in a turbine guide vane with low aspect ratio p 513 N90-21018
- Calculation of the secondary flow in an axial turbine p 513 N90-21022
- Losses in the tip-leakage flow of a planar cascade of turbine blades p 514 N90-21027
- NASA airframe structural integrity program
[NASA-TM-102637] p 543 N90-21422
- Recent improvements in the scope and accuracy of the performance prediction of nozzle propellers
[LR-598] p 572 N90-21742
- Multiblock topology specification and grid generation for complete aircraft configurations p 582 N90-21986
- The Shock and Vibration Digest, volume 21, no. 6 p 614 N90-22363
- Noise transmission into propeller-driven airplanes p 614 N90-22364
- A computer code for the prediction of aerodynamic characteristics of lifting airfoils at transonic speed
[DLC-EST-TN-030] p 632 N90-23359
- Low-density flow effects for hypervelocity vehicles, phase 2
[AD-A221034] p 634 N90-24249
- Flexural fatigue life prediction of closed hat-section using materially nonlinear axial fatigue characteristics p 691 N90-25062
- A computational efficient modelling of laminar separation bubbles
[NASA-CR-186729] p 774 N90-25291
- Efficiency study comparing two helicopter planetary reduction stages
[NASA-TM-103106] p 776 N90-26334
- Investigation of crack-closure prediction models for fatigue in aluminium alloy sheet under flight-simulation loading
[LR-619] p 777 N90-26369
- Aerocoustics of advanced propellers
[NASA-TM-103137] p 782 N90-26635
- Rotorcraft aeromechanical stability-methodology assessment. Phase 2: Workshop
[NASA-TM-102272] p 816 N90-26800
- Proceedings of the 1987 Aircraft/Engine Structural Integrity Program (ASIP/ENSIP) Conference
[AD-A198037] p 842 N90-26807
- Computerized corrosion forecasting model for C-5 aircraft p 843 N90-26815
- The validation and application of a rotor acoustic prediction computer program
[NASA-TM-101794] p 895 N90-27465
- Air Force procedure for predicting aircraft noise around airbases: Noise Exposure Model (NOISEMAP). User's manual
[AD-A223162] p 895 N90-27467
- Inspection reliability p 885 N90-28072
- Prediction of subsonic vortex shedding from forebodies with chines p 909 N90-28494
- [NASA-CR-4323] p 909 N90-28494
- Control research in the NASA high-alpha technology program p 934 N90-28516
- Unsteady aerodynamics of controls p 935 N90-28525
- Flow coupling between a rotor and a stator in turbomachinery
[AD-A223882] p 932 N90-28572
- Proceedings of damping '89. Volume 1: Pages AAB-1 through DCD-11
[AD-A223431] p 960 N90-29664
- PREDICTIONS**
- An investigation on combined extension and bending of thin sheets with a central crack
[LR-561] p 137 N90-12958
- Thermal barrier coating life prediction model development, phase 1
[NASA-CR-182230] p 193 N90-13388

- F-15B high angle-of-attack phenomena and spin prediction using bifurcation analysis
[AD-A217366] p 498 N90-20073
- Prediction of forces and moments for flight vehicle control effectors. Part 1: Validation of methods for predicting hypersonic vehicle controls forces and moments
[NASA-CR-186571] p 571 N90-21734
- The interaction of a supersonic streamwise vortex and a normal shock wave p 633 N90-24241
- A review of instability and noise propagation in supersonic flows
[NASA-CR-186800] p 717 N90-25112
- Elevated temperature crack growth
[NASA-CR-182247] p 777 N90-26355
- High productivity testing p 871 N90-26843
- Development of a linearized unsteady aerodynamic analysis for cascade gust response predictions
[NASA-CR-4308] p 816 N90-27655
- Effects of blocks of overloads and underloads on fatigue crack growth in 2024-T351 sheet specimens: Fractographic analysis and crack closure predictions
[LR-629] p 961 N90-29681
- PREDICTOR-CORRECTOR METHODS**
- Fracture control via DRM-Algorithm p 694 A90-41343
- 3D transonic nacelle and winglet design
[AIAA PAPER 90-3064] p 794 A90-45897
- Application of the inverse method of three-dimensional boundary layer analysis to the problem of flow past a wing with allowance for the effect of viscosity p 804 A90-46548
- Computation of hypersonic unsteady viscous flow over a cylinder p 397 N90-19194
- Numerical analysis of three-dimensional particle-laden flow equations
[IAIR-90-2] p 775 N90-26268
- PREFLIGHT ANALYSIS**
- The EFA integrated monitoring and recording system: Requirements and concept for implementation p 848 N90-27620
- Start-up built-in test for the DISCUS fault tolerant, fly-by-wire computer system p 869 N90-27625
- PREFLIGHT OPERATIONS**
- Analysis of extreme wind shear p 280 A90-23255
- PREFORMS**
- Fabrication of aircraft structures from thermoplastic drapeable preforms p 468 A90-33125
- PREMIXED FLAMES**
- Higher-order effects in boundary-layer premixed combustion p 529 A90-32953
- Combustion Experiments During KC-135 Parabolic Flights
[ESA-SP-1113] p 388 N90-16958
- PREMIXING**
- Low NO(x) potential of gas turbine engines
[NASA-TM-102452] p 345 N90-17636
- Turbulent combustion modeling for turbo-jet combustion chambers p 749 N90-25993
- PREPREGS**
- High service temperature high compressive strength and tough prepreg system p 530 A90-33098
- Fabrication of aircraft structures from thermoplastic drapeable preforms p 468 A90-33125
- High service temperature, damage tolerant prepreg systems based on cyanate chemistry p 941 A90-50069
- Automated prepreg tow placement for composite structures p 954 A90-50113
- A third-generation bismaleimide prepreg system p 943 A90-50131
- Rigidite 5255-3 - A highly damage tolerant prepreg resin system with a well balanced property profile p 944 A90-50139
- Improved fiber reinforced polyphenylene sulfide thermoplastic composites p 947 A90-50180
- Electrostatic dry powder preprepping of carbon fiber p 948 A90-50215
- Material development and second source qualification of carbon fiber/epoxy prepreps for primary and secondary Airbus structures p 948 A90-50225
- Measurement and characterization of prepreg permeability with a modified bagging technique p 949 A90-50226
- Radiation-curable prepreg composites
[DE90-629740] p 951 N90-28674
- PRESSURE DISTRIBUTION**
- Transonic flow over a single wedge p 85 A90-15237
- Noise prediction of a counter-rotation propfan p 218 A90-17861
- Design of axisymmetric bodies with minimum transonic drag p 154 A90-17997
- Mechanism of sidewall effect studied with oil flow visualization p 154 A90-18002

- Unsteady surface pressure distributions on a delta wing undergoing large amplitude pitching motions
[AIAA PAPER 90-0311] p 164 A90-19790
- An analytical technique for addressing airship ditching behavior
[AIAA PAPER 89-3167] p 238 A90-20589
- Effects of pressure mismatch on slot injection in supersonic flow
[AIAA PAPER 90-0092] p 227 A90-22161
- Construction of a wing surface in a nonviscous transonic flow from a given pressure distribution p 298 A90-24149
- Pressure and heat-transfer investigation of a hypersonic configuration p 598 A90-35757
- Low-speed pressure distribution on semi-infinite two-dimensional bodies with elliptical noses p 553 A90-35766
- Investigation of unsteady flow through a transonic turbine stage. II - Data/prediction comparison for time-averaged and phase-resolved pressure data
[AIAA PAPER 90-2409] p 626 A90-42162
- Delta wing surface pressures for high angle of attack maneuvers p 711 A90-45153
- Measurements of pressures on the wing of an aircraft model during steady rotation p 754 A90-45162
- Aircraft tire/pavement pressure distributions
[SAE PAPER 892351] p 734 A90-45502
- 2D vs. 3D - Selection of pressure distributions to delay separation on wings p 790 A90-45868
- Sideslip-induced static pressure errors in flight-test measurements p 794 A90-45898
- An evaluation of Euler solvers for transonic flowfield computations on wing-fuselage geometries
[AIAA PAPER 90-3015] p 798 A90-45935
- A computationally efficient modelling of laminar separation bubbles p 801 A90-46372
- Unsteady aerodynamics of Wortmann FX63-137 airfoil at low Reynolds numbers p 801 A90-46374
- A numerical method for relating two- and three-dimensional pressure distributions on transonic wings
[AIAA PAPER 90-3211] p 812 A90-48837
- The effect of energy input on the characteristics of profiles in compressible fluid media p 906 A90-51533
- Theoretical prediction of pressure distribution on wedged delta wing at higher supersonic Mach numbers and its agreement with experimental results p 907 A90-51537
- Prediction of pressure distribution on optimum-optimorum delta wing at higher angles of attack in supersonic flow and its agreement with experimental results p 907 A90-51538
- Status report on a natural laminar-flow nacelle flight experiment p 105 N90-12550
- Nacelle design p 105 N90-12551
- Nacelle aerodynamic performance p 105 N90-12552
- Effects of acoustic sources p 140 N90-12553
- Supersonic boundary-layer transition on the LaRC F-106 and the DFRF F-15 aircraft. Part 2: Aerodynamic predictions p 84 N90-12559
- Prediction of unsteady blade surface pressures on an advanced propeller at an angle of attack
[NASA-TM-102374] p 94 N90-12560
- Development of a VSAERO (Vortex Separation Aerodynamics) model of the F/A-18
[AD-A212442] p 95 N90-12566
- A computationally efficient modelling of laminar separation bubbles
[NASA-CR-185854] p 136 N90-12872
- Transonic Euler solutions on mutually interfering finned bodies p 170 N90-13331
- Pressure measurement technique in the wind tunnel division of DFVLR p 264 N90-15963
- Determination of the N-factor in the Brunswick (Federal Rep. of Germany) transonic wind tunnel using measurements of pressure distributions and transition points, and the SALLY method p 276 N90-16177
- Use of the film-of-oil technique for profile measurements in the Transonic Wind tunnel Brunswick (TWB) p 238 N90-16252
- Surface pressure distributions on a delta wing undergoing large amplitude pitching oscillations
[NASA-CR-186326] p 317 N90-17558
- Effect of riblets on flow separation from a cylinder and an airfoil in subsonic flow
[AD-A216197] p 319 N90-17574
- Experimental investigation to suppress flow-induced pressure oscillations in open cavities
[AD-A216285] p 320 N90-17578

Some Navier-Stokes calculations for the CAST-10 airfoil p 320 N90-17651

Calculation of excrescence drag magnification due to pressure gradient at high subsonic speeds [ESDU-87004] p 397 N90-19195

A panel process for the calculation of the flow around a wing with front angle damping [ETN-90-95367] p 399 N90-19207

Measurement and prediction of propeller blade surface pressure distributions p 481 N90-20961

An intensive procedure for the design of pressure-specified three-dimensional configurations at subsonic and supersonic speeds by means of a higher-order panel method p 500 N90-20982

A system for transonic wing design with geometric constraints based on an inverse method p 501 N90-20983

Numerical optimization of target pressure distributions for subsonic and transonic airfoil design p 502 N90-20993

Numerical optimization of wings in transonic flow p 502 N90-20997

Secondary Flows in Turbomachines [AGARD-CP-469] p 511 N90-21009

An experimental investigation of the physical mechanisms controlling the asymmetric flow past slender bodies at large angles of attack p 592 N90-21767

Unsteady potential flow past a propeller blade section [NASA-CR-4307] p 634 N90-24246

New transonic test sections for the NAE 5 ft x 5 ft trisonic wind tunnel [AD-A220933] p 674 N90-24278

Aerodynamic loads and blade vortex interaction noise prediction [ISL-PU-310/89] p 719 N90-25942

Application of laminar flow control to supersonic transport configurations [NASA-CR-181917] p 719 N90-25944

The SKY SHARK: An RPV designed to investigate the pressure distribution on a lifting surface [NASA-CR-186222] p 844 N90-26824

Model tilt-rotor hover performance and surface pressure measurement [AD-A225353] p 845 N90-26827

Study of the ground effects in the CEAT aerohydrodynamic tunnel: Using the results p 922 N90-28530

Measurement of the steady surface pressure distribution on a single rotation large scale advanced prop-fan blade at Mach numbers from 0.03 to 0.78 [NASA-CR-182124] p 929 N90-28552

PRESSURE DRAG

The effect of pitch location on dynamic stall p 2 A90-10641

Sting-support interference on afterbody drag at transonic speeds [NAL-TM-EA-8902] p 909 N90-28492

PRESSURE DROP

Secondary loss generation in a linear cascade of high-turning turbine blades [ASME PAPER 89-GT-47] p 289 A90-23773

Heat transfer and pressure drop for short pin-fin arrays with pin-endwall fillet [ASME PAPER 89-GT-99] p 359 A90-23813

Interaction between a high-level steady acoustic field and a ducted turbulent flow [ONERA, TP NO. 1990-27] p 695 A90-41206

PRESSURE EFFECTS

Effect of pressure on the electrophysical properties of two-phase flows in nozzles p 110 A90-14572

Characteristics of temperature and pressure generation and retention in flow inside cryogenic wind tunnel T-04 p 869 A90-46576

The performance of alternate fuels in general aviation aircraft p 950 A90-51621

A study of high-lift airfoils at high Reynolds numbers in the Langley low-turbulence pressure tunnel [NASA-TM-89125] p 1 N90-10002

Stage effects on stalling and recovery of a high-speed 10-stage axial-flow compressor p 115 N90-12600

Cavity aeroacoustics [AD-A223853] p 911 N90-29307

PRESSURE GAGES

The use of onboard sensor data in aerial triangulation - GPS, pressure sensors, laser telemetry p 822 A90-47901

PRESSURE GRADIENTS

An asymptotic theory for the periodic turbulent boundary layer in zero mean-pressure gradient [AD-A222832] p 66 A90-10222

Adverse pressure gradient effects on boundary layer transition in a turbulent free stream p 15 A90-12639

Influence of the radial component of total pressure gradient on tip clearance secondary flow in axial compressors [ASME PAPER 89-GT-19] p 288 A90-23761

A supersonic turbulent boundary layer in an adverse pressure gradient p 303 A90-25592

A study of boundary layer stability in the case of an increased incoming stream turbulence in gradient flows p 555 A90-36065

The instability of two-dimensional laminar separation p 800 A90-46365

Calculation of excrescence drag magnification due to pressure gradient at high subsonic speeds [ESDU-87004] p 397 N90-19195

PRESSURE MEASUREMENT

Unsteady pressure and structural response measurements on an elastic supercritical wing p 159 A90-19392

Investigation of adaptive-wall wind tunnels with two measured interfaces [AIAA PAPER 90-0186] p 200 A90-19728

Compensating for pneumatic distortion in pressure sensing devices [AIAA PAPER 90-0631] p 211 A90-19956

Conditional sampling --- technique for aerodynamic characteristics measurement from wind-tunnel experiments [ONERA, TP NO. 1989-187] p 261 A90-21047

Determination of the ground effect on the characteristics of the A320 aircraft [ONERA, TP NO. 1989-188] p 245 A90-21048

Airfoil pressure measurements during a blade vortex interaction and a comparison with theory p 232 A90-23105

Casing vibration and gas turbine operating conditions [ASME PAPER 89-GT-78] p 358 A90-23799

Determination of pressure and heat flow on the front surface of smooth blunt bodies p 299 A90-24166

Identification of retreating blade stall mechanisms using flight test pressure measurements p 384 A90-28172

Non-isentropic effects on the WRDC 20 inch hypersonic wind tunnel calibration p 435 A90-28254

Comparison between experimental, and numerical results for a research hypersonic aircraft p 395 A90-31278

Noise-source measurements by thin-film pressure transducers in a subsonic turbofan model [ONERA, TP NO. 1990-36] p 659 A90-41212

Estimation of rotor blade incidence and blade deformation from the measurement of pressures and strains in flight p 647 A90-42497

Pressure-based real-time measurements in compressible free shear layers [AIAA PAPER 90-1980] p 703 A90-42709

Recent aerodynamic measurements with Magnetic Suspension Systems p 759 A90-44399

Investigation of propeller slipstream effects on the Fokker 50 through in-flight pressure measurements [AIAA PAPER 90-3084] p 806 A90-46645

Measurements of pressures on the tail and aft fuselage of an airplane model during rotary motions at spin attitudes [NASA-TP-2939] p 20 N90-10829

Preliminary experience with high response pressure measurements in a multistage, high speed compressor. [RAE-TM-P-1141] p 117 N90-12619

A wall interference assessment/correction interface measurement system for the NASA/ARC 12-ft PWT [NASA-CR-185474] p 200 N90-13401

Flight evaluation of a pneumatic system for unsteady pressure measurements using conventional sensors [NASA-TM-4131] p 186 N90-14225

Pressure measurement technique in the wind tunnel division of DFVLR [ESA-TT-1145] p 264 N90-15963

Compensating for pneumatic distortion in pressure sensing devices [NASA-TM-101716] p 415 N90-19224

Exhaust environment measurements of a turbofan engine equipped with an afterburner and 2D nozzle [NASA-CR-4289] p 588 N90-21760

Investigation of the vortex flow over a sharp-edged delta wing in the transonic speed regime [LR-594] p 717 N90-25115

Experimental characterization of the effects of pneumatic tubing on unsteady pressure measurements [NASA-TM-4171] p 850 N90-27703

In-flight flow visualization with pressure measurements at low speeds on the NASA F-18 high alpha research vehicle [NASA-TM-101726] p 910 N90-28505

Determination of the ground effect on the characteristics of the A320 aircraft p 922 N90-28534

Recommended practices for measurement of gas path pressures and temperatures for performance assessment of aircraft turbine engines and components [AGARD-AR-245] p 933 N90-29393

PRESSURE OSCILLATIONS

Slipstream-induced pressure fluctuations on a wing panel p 77 A90-11004

Measurements of pressure fluctuations in the interaction regions of shock waves and turbulent boundary layers induced by blunt fins p 9 A90-12218

Large-eddy simulations of pressure oscillations and combustion instability in a ramjet p 111 A90-15388

Pressure fluctuations in the tip region of a blunt-tipped airfoil p 154 A90-18136

Wall pressure fluctuation spectra in supersonic flow past a forward facing step p 388 A90-29194

Oscillation of circular shock wave p 557 A90-36465

An experimental investigation of pressure fluctuation mechanism for different transonic porous wall configurations [AIAA PAPER 90-1417] p 604 A90-37954

A study of the unsteadiness of crossing shock wave turbulent boundary layer interactions [AIAA PAPER 90-1456] p 606 A90-38614

Wall pressure fluctuations in the reattachment region of a supersonic free shear layer [AIAA PAPER 90-1461] p 561 A90-38618

Computational modeling of inlet hammer shock wave generation [AIAA PAPER 90-2005] p 621 A90-40592

Multistep dump combustor design to reduce combustion instabilities p 659 A90-40934

An experimental investigation of turbine rotor wakes for the development of a fiber optic pressure sensor [AIAA PAPER 90-2411] p 687 A90-42163

Wall pressure pulsation spectra ahead of internal corners p 804 A90-46545

Unsteady blade surface pressures on a large-scale advanced propeller - Prediction and data [AIAA PAPER 90-2402] p 808 A90-47220

Combustion instabilities in liquid-fueled propulsion systems: An overview p 63 N90-10192

Characteristics of combustion driven pressure oscillations in advanced turbo-fan engines with afterburner p 64 N90-10194

Recent developments in Ramjet pressure oscillation technology p 53 N90-10199

Numerical simulation of pressure oscillations in a ramjet combustor p 54 N90-10202

Very-low-frequency oscillations in liquid-fueled ramjets p 54 N90-10204

Experimental investigation to suppress flow-induced pressure oscillations in open cavities [AD-A216285] p 320 N90-17578

PRESSURE PULSES

Pressure pulsation in a cavity in the path of subsonic and supersonic gas flow p 10 A90-12279

An experimental study of fluctuations in the front separation zone at supersonic flow velocities p 10 A90-12282

Investigation of wall pressure pulsations during the passive control of shock/boundary layer interaction p 378 A90-24132

PRESSURE RATIO

Basic principles of measuring thrust through exhaust to inlet total pressure ratio - Engine Pressure Ratio (EPR) p 191 A90-18635

Dual pressure ratio compressor [ASME PAPER 89-GT-121] p 341 A90-23820

Navier-Stokes analysis of an ejector and mixer-ejector operating at pressure ratios in the range 2-4 [AIAA PAPER 90-2730] p 626 A90-42218

Optimization studies for the PW305 turbofan [AIAA PAPER 90-2520] p 744 A90-42813

An experimental study of a supersonic gas ejector p 851 A90-46546

Experiments on the unsteady flow in a supersonic compressor stage p 427 N90-18422

PRESSURE RECOVERY

Some observations on transitory stall in conical diffusers [NASA-TM-102387] p 94 N90-12561

PRESSURE REDUCTION

Investigation of some effects on the compressor characteristics of an advanced bleed air compressor design p 49 A90-12594

Pressure loss and heat transfer in channels roughened on two opposed walls [ASME PAPER 89-GT-86] p 358 A90-23805

Impingement/effusion cooling - The influence of the number of impinging holes and pressure loss on the heat transfer coefficient [ASME PAPER 89-GT-188] p 361 A90-23866

Correlation of radial-to-axial vaneless turns for centrifugal compressors [AIAA PAPER 90-1917] p 656 A90-40556

An investigation of oblique shock/boundary layer bleed interaction [AIAA PAPER 90-1928] p 703 A90-42697

Secondary flow predictions for a transonic nozzle guide vane p 513 N90-21017

PRESSURE REGULATORS

Effect of the fluid level of a hydraulic shock absorber on the characteristics of the gas supply system
p 851 A90-46504

PRESSURE SENSORS

The development of a high response aerodynamic wedge probe and use on a high-speed research compressor
p 69 A90-12618

Compensating for pneumatic distortion in pressure sensing devices
[AIAA PAPER 90-0631] p 211 A90-19956

Experimental investigation of terminal shock sensors in mixed-compression inlets
[AIAA PAPER 90-1931] p 681 A90-40560

Noise-source measurements by thin-film pressure transducers in a subsonic turbofan model
[ONERA, TP NO. 1990-36] p 659 A90-41212

An experimental investigation of turbine rotor wakes for the development of a fiber optic pressure sensor
[AIAA PAPER 90-2411] p 687 A90-42163

Flight evaluation of a pneumatic system for unsteady pressure measurements using conventional sensors
[NASA-TM-4131] p 186 A90-14225

Pressure measurement technique in the wind tunnel division of DFVLR
[ESA-TT-1145] p 264 A90-15963

Formulation and verification of a technique for compensation of pneumatic attenuation errors in airborne pressure sensing devices
p 369 A90-17084

Compensating for pneumatic distortion in pressure sensing devices
[NASA-TM-101716] p 415 A90-19224

Tests for integrating measurement of gas pressures in flight propellers
[ETN-90-96498] p 634 A90-24253

A reliable, maintenance-free oxygen sensor for aircraft using an oxygen-sensitive coating on potentiometric electrodes
[AD-A22696] p 927 A90-28545

PRESSURE VESSEL DESIGN

Aircraft applications of advanced composite fiber/metal pressure vessels
[AIAA PAPER 90-2344] p 686 A90-42133

PRESSURE VESSELS

Cooking an aeroplane
p 209 A90-17918

Hydraulic accumulators and high pressure bottles in composite material
p 688 A90-42493

PRESSURIZED CABINS

The optimum control and adaptive control for airplane cabin pressure
p 182 A90-18627

Extending an airliner's life
p 244 A90-20262

Contamination of cabin air by synthetic oil and breakdown products
[SAE PAPER 891455] p 323 A90-27424

The MDE method for aircraft cabin interior noise prediction — matrix difference equation
[SAE PAPER 892372] p 782 A90-45519

Development of pressure containment and damage tolerance technology for composite fuselage structures in large transport aircraft
[NASA-CR-3996] p 63 A90-10186

PRESSURIZING

Starter systems and auxiliary power units
p 660 A90-41760

Bulging cracks in pressurized fuselages — A procedure for computation
p 880 A90-46301

PRESTRESSING

A study of the influence of predeformations on the vibrations of blades
p 585 A90-35673

PRIMERS

The effect of primer age on adhesion of polysulphide sealant
p 269 A90-15909

PRIMERS (COATINGS)

Safer primers from 3M
p 204 A90-17925

Effects on aerospace alloys of residual chlorine in chlorinated-solvent primers
p 956 A90-50187

Development of a water-borne non-chromated primer and topcoat for aerospace applications
p 956 A90-50213

PRINTED CIRCUITS

Correlation/validation of finite element code analyses for vibration assessment of avionic equipment
[AD-A220393] p 654 A90-23398

PRIORITIES

Social survey findings on en route noise annoyance issues
p 698 A90-24868

PROBABILITY DENSITY FUNCTIONS

Chemically reacting supersonic flow calculation using an assumed PDF model
[AIAA PAPER 90-0731] p 230 A90-22256

A hybrid Reynolds averaged/PDF closure model for supersonic turbulent combustion
[AIAA PAPER 90-1573] p 600 A90-38711

Probabilistic approach to fleet management
p 701 A90-42674

Numerical simulation of nonpremixed turbulent flow in a dump combustor
[AIAA PAPER 90-1858] p 768 A90-42685

Analytical study of mistuning/friction/aerodynamics interaction in a bladed disk assembly
[AD-A211139] p 55 A90-10893

PROBABILITY THEORY

Probabilistic method to compute the optimal slip load for a mistuned bladed disk assembly with friction dampers
p 507 A90-32269

Probabilistic design technology for ceramic components
p 601 A90-35507

The development of a probabilistic turbine rotor design system
[AIAA PAPER 90-2176] p 662 A90-42060

Estimation of the efficiency of various operational modes of a navigation complex
p 725 A90-42924

A probabilistic approach for the establishment of an aircraft structure inspection program
p 902 A90-49892

Stochastic robustness of linear control systems
p 521 A90-20941

Probabilistic modeling for simulation of aerodynamic uncertainties in propulsion systems
[NASA-TM-102472] p 515 A90-21036

Hardware and software reliability estimation using simulations
[NASA-CR-186637] p 780 A90-25580

Statistical treatment of slow strain rate data for assessment of hydrogen embrittlement in low alloy high strength steel
[ARL-MAT-R-122] p 767 A90-26106

Real-time adaptive aircraft scheduling
[NASA-CR-177558] p 820 A90-27669

Audibility and annoyance of en route noise of unducted fan engines
[AD-A223687] p 966 A90-30035

PROBLEM SOLVING

Formalization and solution of covering problems in the synthesis of control and monitoring systems
p 76 A90-10963

Introduction to data items on flight path optimisation
[ESDU-89015] p 185 A90-14221

A matrix-free locally-implicit scheme for Navier-Stokes equations
[AD-A218298] p 541 A90-20349

Subsonic and transonic blade design by means of analysis codes
p 510 A90-20985

Informatics aspects of large flow calculations on the SX-2 supercomputer
[NLR-MP-88037-U] p 776 A90-26290

PROCEDURES

En route noise: NASA proplan test aircraft (corrected data - simplified procedure)
[DOT-TSC-FA953-LR4] p 696 A90-24856

Experience in developing an improved altitude test capability
p 857 A90-27719

General test plan
p 857 A90-27721

Recommended practices for measurement of gas path pressures and temperatures for performance assessment of aircraft turbine engines and components
[AGARD-AR-245] p 933 A90-29393

PROCESS CONTROL (INDUSTRY)

Monitoring of aircraft assembly: Optical and laser methods — Russian book
p 285 A90-24229

Robotic dry stripping of airframes - Phase II
[SAE PAPER 890926] p 365 A90-24691

Development of process control procedure for ultrahigh-sensitivity fluorescent penetrant inspection systems
p 771 A90-45225

Integrated approach fault tolerance-current state and future requirements
[AD-A214402] p 275 A90-15465

PROCUREMENT

Equipment procurement - EH101 helicopter
p 282 A90-22435

PROCUREMENT MANAGEMENT

The use of the CFM56 engine in the KC-135 tanker
[SAE PAPER 892362] p 747 A90-45511

Practical aspects of European collaboration — procurement in helicopter industry
p 785 A90-46928

PRODUCT DEVELOPMENT

'Black Betsy' - The 6000C-4 rocket engine, 1945-1989.
[IAF PAPER 89-726] p 141 A90-13700

Design and development of the Garrett F109 turbofan engine
[SAE PAPER 891046] p 109 A90-14350

Developing aluminium
p 204 A90-17924

Development of the UTA hypersonic shock tunnel
[AIAA PAPER 90-0080] p 200 A90-19675

Eurofighter flights back
p 221 A90-21714

The role of NDE in ceramic turbine engine component development
p 601 A90-35508

Toward total quality in industry
p 684 A90-41768

The Airbus ... a challenge launched twenty years ago
p 699 A90-41769

Escape system evolution
p 722 A90-44656

Improving computer techniques for real-time digital flight simulation
[SAE PAPER 892354] p 760 A90-45505

An interfacing solution for real-time avionics development
[SAE PAPER 892357] p 738 A90-45508

The use of the CFM56 engine in the KC-135 tanker
[SAE PAPER 892362] p 747 A90-45511

The impact of total quality management (TQM) and concurrent engineering on the aircraft design process
p 785 A90-46927

Advocating international cooperation: The Eurofar program - An example and a hope — European Future Advanced Rotorcraft program
p 785 A90-46929

Integrated product development (IPD) at General Dynamics Forth Worth
[AIAA PAPER 90-3192] p 786 A90-48828

Implementation of integrated product development — in aircraft industry
[AIAA PAPER 90-3194] p 786 A90-48829

Lessons learned from the T-46A durability and damage tolerance program
p 842 A90-26812

Cost effective technology
[PNR90664] p 883 A90-27002

PRODUCTION COSTS

Production of Ti6Al4V-components for a new turbo-fan-engine
p 132 A90-16618

PRODUCTION ENGINEERING

Harnessing detailed assembly process knowledge with CASE
p 535 A90-32504

The impact of total quality management (TQM) and concurrent engineering on the aircraft design process
p 785 A90-46927

Estimating the relationships between the state of the art of technology and production cost for the US aircraft
[AD-A212127] p 82 A90-12495

PRODUCTION MANAGEMENT

Teamwork for excellence
[AIAA PAPER 89-3195] p 549 A90-31686

Total quality management and the transitioning company - The perfect fit
[AIAA PAPER 89-3211] p 549 A90-31698

Peacekeeper IFSS - A TQM success story — Instrumentation and Flight Safety System
[AIAA PAPER 89-3218] p 549 A90-31702

PRODUCTION PLANNING

Aircraft modifications cost analysis. Volume 1: Overview of the study
[AD-A220764] p 702 A90-25074

PRODUCTIVITY

National airspace system plan: Facilities, equipment, associated development and other capital needs
[AD-A215882] p 402 A90-18373

High productivity testing
p 871 A90-26843

PROFILOMETERS

Surface roughness measurements on gas turbine blades
[ASME PAPER 89-GT-285] p 508 A90-33559

PROGRAM VERIFICATION (COMPUTERS)

Verification of a Navier-Stokes code for solving the hypersonic blunt body problem
p 146 A90-16774

Initial flight qualification and operational maintenance of X-29A flight software
[NASA-TM-101703] p 32 A90-10023

ATTAS flight testing experiences
p 34 A90-10862

Validation of a computer code for analysis of subsonic aerodynamic performance of wings with flaps in combination with a canard or horizontal tail and an application to optimization
[NASA-TP-2961] p 173 A90-14187

Software verification plan for GCS — guidance and control software
[NASA-TM-101668] p 372 A90-18057

Formal design and verification of a reliable computing platform for real-time control. Phase 1: Results
[NASA-TM-102716] p 965 A90-29965

PROGRAMMING LANGUAGES

High level language programming for avionic vector processors
[AIAA PAPER 89-3107] p 74 A90-10589

Design of a language for the testing of aircraft engines
p 137 A90-14573

The application of Z to the specification of air traffic control systems. 1: An initial specification of the radar processing activity
[RSRE-MEMO-4280] p 243 A90-15900

Six-degree-of-freedom aircraft simulation with mixed-data structure using the applied dynamics simulation language, ADSIM
p 613 A90-23067

PROJECT MANAGEMENT

Peacekeeper IFSS - A TQM success story — Instrumentation and Flight Safety System
[AIAA PAPER 89-3218] p 549 A90-31702

- Activities report in German aerospace
[ISSN-0070-3966] p 465 N90-19189
- Operational evaluation of initial data link air traffic control services, volume 1
[DOT/FAA/CT-90/1-VOL-1] p 455 N90-19472
- The automation management to support research and development
p 612 N90-22978
- Program plan: International aircraft operator data base
[IAR-90-1] p 783 N90-25697
- R and D aspects of the future operational concept of the BFS
p 826 N90-27679
- GPS integrity requirements for use by civil aviation
p 916 N90-29339
- PROJECT PLANNING**
- Studies of the European transonic wind tunnel
[ONERA-RSF-12/0694-GY] p 141 N90-13278
- Program plan: International aircraft operator data base
[IAR-90-1] p 783 N90-25697
- The Federal Aviation Administration plan for research, engineering and development. Volume 1: Program plan
[AD-A221263] p 783 N90-25930
- The Federal Aviation Administration plan for research, engineering and development. Volume 2: Project descriptions
[AD-A221264] p 783 N90-25931
- Background, current status, and prognosis of the ongoing slush hydrogen technology development program for the NASP
[NASA-TM-103220] p 763 N90-26055
- Flight service automation system, model 1 full capacity, NAS operational test and evaluation integration test plan
[DOT/FAA/CT-TN90/4] p 825 N90-27672
- PROJECTILES**
- Numerical computations of transonic critical aerodynamic behavior
p 469 A90-32457
- Navier-Stokes predictions of pitch damping for finned projectiles using steady coning motion
[AIAA PAPER 90-3088] p 795 A90-45902
- External flow computations for a finned 60mm ramjet in steady supersonic flight
[AD-A216998] p 428 N90-19233
- PROLATE SPHEROIDS**
- Navier-Stokes computations of a prolate spheroid at angle of attack
p 17 A90-13018
- Drag measurements on a modified prolate spheroid using a magnetic suspension and balance system
p 672 A90-40684
- The effect of turbulence models on the numerical prediction of the flowfield about a prolate spheroid at high angle of attack
[AIAA PAPER 90-3106] p 789 A90-45855
- PRONE POSITION**
- Aerodynamic testing of a new semi-prone ejection seat design
[AIAA PAPER 90-0234] p 182 A90-19748
- PROP-FAN TECHNOLOGY**
- Hydrodynamic visualization of the flow around a high-speed aircraft propeller
[ONERA, TP NO. 1989-108] p 3 A90-11141
- Operating aspects of counter-rotating propfan and planetary-differential gear coupling
p 50 A90-12615
- Counterrotating prop-fan simulations which feature a relative-motion multiblock grid decomposition enabling arbitrary time-steps
[AIAA PAPER 90-0687] p 169 A90-19978
- Oils for flight turbine engines - Research and development in the 90s
p 266 A90-21473
- Ultra High Bypass (UHB) engine critical component technology
[ASME PAPER 89-GT-229] p 342 A90-23884
- Unsteady Euler analysis of the flowfield of a propfan at an angle of attack
[AIAA PAPER 90-0339] p 300 A90-25028
- Acoustic characteristics of counterrotating unducted fans from model scale tests
p 378 A90-26138
- Concurrent processing adaptation of aeroelastic analysis of propfans
[AIAA PAPER 90-1036] p 450 A90-29380
- Three dimensional full potential method for the aeroelastic modeling of propfans
[AIAA PAPER 90-1120] p 393 A90-29392
- Yakovlev strikes back
p 579 A90-35848
- Investigation of the near wake of a propfan
p 622 A90-40686
- The propfan ... What future now?
p 744 A90-43763
- Interior noise in the untreated Gulfstream II Propfan Test Assessment aircraft
p 731 A90-44736
- A nonlinear transient formulation of UHB aeroelastic response and stability. I - Theoretical formulation
[SAE PAPER 892322] p 715 A90-45481
- 3D Euler analysis of ducted propfan flowfields
[AIAA PAPER 90-3034] p 791 A90-45873
- The selection of convertible engines with current gas generator technology for high speed rotorcraft
p 852 A90-46933
- Euler analysis comparison with LDV data for an advanced counter-rotation propfan at cruise
[AIAA PAPER 90-3033] p 903 A90-50637
- Large scale prop-fan structural design study. Volume 1: Initial concepts
[NASA-CR-174992] p 52 N90-10043
- Large scale prop-fan structural design study. Volume 2: Preliminary design of SR-7
[NASA-CR-174993] p 52 N90-10044
- Large-scale Advanced Prop-fan (LAP) high speed wind tunnel test report
[NASA-CR-182125] p 52 N90-10045
- Large-scale Advanced Prop-fan (LAP) technology assessment report
[NASA-CR-182142] p 53 N90-10046
- Full scale technology demonstration of a modern counterrotating unducted fan engine concept: Component test
[NASA-CR-180868] p 53 N90-10047
- Full scale technology demonstration of a modern counterrotating unducted fan engine concept. Design report
[NASA-CR-180867] p 53 N90-10048
- Full scale technology demonstration of a modern counterrotating unducted fan engine concept. Engine test
[NASA-CR-180869] p 53 N90-10049
- Acoustic test and analysis of a counterrotating prop-fan model
[NASA-CR-179590] p 79 N90-10683
- Propfan Test Assessment (PTA): Flight test report
[NASA-CR-182278] p 113 N90-11738
- Propfan Test Assessment (PTA)
[NASA-CR-185138] p 113 N90-11739
- Numerical simulation of unsteady rotational flow over propfan configurations
[NASA-CR-186037] p 90 N90-12500
- Large-scale Advanced Prop-fan (LAP) static rotor test report
[NASA-CR-180848] p 117 N90-12617
- The design and development of an acoustic test section for the ARA transonic wind tunnel
[PNR90574] p 140 N90-13202
- Unsteady Euler analysis of the flow field of a propfan at an angle of attack
[NASA-TM-102426] p 380 N90-18229
- Structural tailoring of select fiber composite structures
[NASA-TM-102484] p 533 N90-21137
- Experimental performance and acoustic investigation of modern, counterrotating blade concepts
[NASA-CR-185158] p 649 N90-23393
- Advanced gearbox technology
[NASA-CR-179625] p 666 N90-24274
- En route noise: NASA propfan test aircraft (corrected data - simplified procedure)
[DOT-TSC-FA953-LR4] p 696 N90-24856
- En route noise: NASA propfan test aircraft (calculated source noise)
[DOT-TSC-FA953-LR5] p 697 N90-24857
- En route noise of turboprop aircraft and their acceptability: Report of tests
p 697 N90-24858
- En route noise of two turboprop aircraft
[DLR-MITT-89-18] p 697 N90-24859
- Noise measurements of turboprop airplanes at different overflight elevations
p 697 N90-24860
- When propfans cruise, will LDN 65 fly
p 697 N90-24864
- En route noise annoyance laboratory test: Preliminary results
p 698 N90-24870
- Euler analysis comparison with LDV data for a propfan advanced counter-rotation propfan at cruise
[NASA-TM-103249] p 720 N90-25946
- Aeroacoustics of advanced propellers
[NASA-TM-103137] p 782 N90-26635
- Measurement of the steady surface pressure distribution on a single rotation large scale advanced prop-fan blade at Mach numbers from 0.03 to 0.78
[NASA-CR-182124] p 929 N90-28552
- PROPAGATION VELOCITY**
- Significance of the short crack effect on aerospace structures
p 269 A90-20065
- PROPELLANT BINDERS**
- An investigation on boron used as a component of solid propellant
p 765 A90-45708
- PROPELLANT COMBUSTION**
- Combustion Instabilities in Liquid-Fuelled Propulsion Systems
[AGARD-CP-450] p 63 N90-10191
- Energy Efficient Engine (E3) combustion system component technology performance report
[NASA-CR-168274] p 930 N90-28555
- PROPELLANT GRAINS**
- Metallized fuel particle size study in a solid fuel ramjet
[AD-A220079] p 679 N90-24451
- PROPELLANT PROPERTIES**
- Aging and antioxidant surveillance studies on turbine fuel JP-5 and JP-10
p 442 A90-29492
- PROPELLANT STORAGE**
- Aging and antioxidant surveillance studies on turbine fuel JP-5 and JP-10
p 442 A90-29492
- PROPELLANTS**
- Thermochemical calculations with inert compounds
[FOA-C-20759-2.1] p 206 N90-13677
- Analysis of scramjet engine characteristics
[NAL-TR-1041] p 933 A90-29398
- PROPELLER BLADES**
- Analysis of nonuniform subsonic flows about a row of moving blades
p 6 A90-11779
- Propeller development for the Rutan Voyager
[SAE PAPER 891034] p 100 A90-14341
- Blade surface pressure measurement on a pusher propeller in flight
[SAE PAPER 891040] p 139 A90-14346
- Parametric studies of advanced turboprops
p 253 A90-21225
- Application of an efficient hybrid scheme for aeroelastic analysis of advanced propellers
[AIAA PAPER 90-0028] p 226 A90-22153
- A hybrid method for prediction of propeller performance
[AIAA PAPER 90-0440] p 229 A90-22219
- Measurements and calculations of the aerodynamic characteristics of the propeller sections series V3
p 233 A90-23355
- Effect of reduced aft diameter and increased blade number of high-speed counterrotation propeller performance
[AIAA PAPER 89-0438] p 234 A90-23650
- Tail rotor dynamics during the translational turn maneuver of a helicopter
p 334 A90-24148
- An approximation model for the performance and acoustic predictions of counterrotating propeller configurations
[AIAA PAPER 90-0282] p 378 A90-26931
- Aeroelastic tailoring analysis for preliminary design of advanced turbo propellers with composite blades
p 412 A90-29395
- Whirl flutter stability of a pusher configuration subject to a nonuniform flow
[AIAA PAPER 90-1162] p 393 A90-29397
- Calculations of propeller/airframe interference effects using the potential/multienergy flow method
p 490 A90-32452
- A study of the influence of predeformations on the vibrations of blades
p 585 A90-35673
- Viscous flow around a propeller-shaft configuration with infinite-pitch rectangular blades
p 683 A90-40938
- Nonlinear unsteady airfoil response studies
p 628 A90-42406
- Preliminary design and analysis of propellers
p 645 A90-42407
- Structural and aerodynamic analysis of a large scale advanced propeller blade
[AIAA PAPER 90-2401] p 743 A90-42793
- The effect of solidity on propeller normal force
[SAE PAPER 892205] p 713 A90-45424
- Unsteady blade surface pressures on a large-scale advanced propeller - Prediction and data
[AIAA PAPER 90-2402] p 808 A90-47220
- Prediction of unsteady blade surface pressures on an advanced propeller at an angle of attack
[NASA-TM-102374] p 94 N90-12560
- Large-scale Advanced Prop-fan (LAP) static rotor test report
[NASA-CR-180848] p 117 N90-12617
- Effect of reduced aft diameter and increased blade number on high-speed counterrotation propeller performance
[NASA-TM-102077] p 172 N90-13352
- Application of an efficient hybrid scheme for aeroelastic analysis of advanced propellers
[NASA-TM-102428] p 172 N90-13355
- An experimental investigation of viscous aspects of propeller blade flow
p 315 N90-18711
- Relating flow between counter-rotating propellers to aerodynamic interaction noise
p 479 N90-20944
- Measurement and prediction of propeller blade surface pressure distributions
p 481 N90-20961
- Aerofoil design techniques
p 500 N90-20978
- Unsteady potential flow past a propeller blade section
[NASA-CR-4307] p 634 N90-24246
- Agusta methodology for pitch link loads prediction in preliminary design phase
[ETN-90-97270] p 737 N90-25978
- Low-speed wind tunnel investigation of the static stability and control characteristics of an advanced turboprop configuration with the propellers placed over the tail
[NASA-CR-186900] p 759 N90-26017

Investigation of ATP blades, part 2. Validation of two-dimensional viscous flow simulation codes around thin airfoils

[NAL-TR-1046] p 912 N90-29326

PROPELLER DRIVE

Aerodynamic design of the Cal Poly Da Vinci Human-Powered Helicopter p 830 A90-46950

X.2 limited flight test plan

[AD-A214412] p 249 N90-15099

Computation of viscous flow around a propeller-shaft configuration with infinite-pitch rectangular blades

p 481 N90-20958

PROPELLER EFFICIENCY

The study of the theoretical calculation method for power stall dynamic characteristics of multiple-engine propeller airplane

p 29 A90-10349

Application of an efficient hybrid scheme for aeroelastic analysis of advanced propellers

[AIAA PAPER 90-0028] p 226 A90-22153

Measurement of propellers in the ARTI 3-meter wind tunnel

p 262 A90-23384

Ideal propeller in compressible gas flow in a wind tunnel

p 298 A90-24156

The design and development of an acoustic test section for the ARA transonic wind tunnel

[PNR90574] p 140 N90-13202

Application of an efficient hybrid scheme for aeroelastic analysis of advanced propellers

[NASA-TM-102428] p 172 N90-13355

Computation of viscous flow around a propeller-shaft configuration with infinite-pitch rectangular blades

p 481 N90-20958

A computer program for the prediction of nozzle-propeller performance

[LR-578] p 572 N90-21740

Theory and numerical analysis of single and multi-element nozzle propellers

[LR-579] p 572 N90-21741

Experimental performance and acoustic investigation of modern, counterrotating blade concepts

[NASA-CR-185158] p 649 N90-23393

PROPELLER FANS

Recent propeller development and studies conducted at ONERA

[ONERA, TP NO. 1990-16] p 683 A90-41201

A nonlinear transient formulation of UHB aeroelastic response and stability. I - Theoretical formulation

[SAE PAPER 892322] p 715 A90-45481

Calculation of the rotation noise of a single propeller with blades of arbitrary shape

p 894 A90-46552

Euler analysis comparison with LDV data for an advanced counter-rotation propfan at cruise

[AIAA PAPER 90-3033] p 903 A90-50637

Concurrent processing adaptation of aeroplastic analysis of propfans

[NASA-TM-102455] p 215 N90-14656

Unsteady Euler analysis of the flow field of a propfan at an angle of attack

[NASA-TM-102426] p 380 N90-18229

En route noise: NASA propfan test aircraft (corrected data - simplified procedure)

[DOT-TSC-FA953-LR4] p 696 N90-24856

En route noise: NASA propfan test aircraft (calculated source noise)

[DOT-TSC-FA953-LR5] p 697 N90-24857

En route noise of two turboprop aircraft

[DLR-MITT-89-18] p 697 N90-24859

Noise measurements of turboprop airplanes at different overflight elevations

p 697 N90-24860

When propfans cruise, will LDN 65 fly

p 697 N90-24864

Euler analysis comparison with LDV data for an advanced counter-rotation propfan at cruise

[NASA-TM-103249] p 720 N90-25946

Aeroacoustics of advanced propellers

[NASA-TM-103137] p 782 N90-26635

Structure-borne noise estimates for the PTA aircraft

[NASA-CR-4315] p 896 N90-28396

PROPELLER NOISE

Application of localized active control to reduce propeller noise transmitted through fuselage surface

p 78 A90-11884

A review and update of the NASA aircraft noise prediction program propeller analysis system

[SAE PAPER 891032] p 139 A90-14340

Interior noise control of the Saab 340 aircraft

[SAE PAPER 891080] p 101 A90-14372

Possibility of active propeller-noise suppression in piston-engine aircraft by changing the phase relation between the propeller and exhaust signals

p 218 A90-18450

Reduction of blade-vortex interaction noise through higher harmonic pitch control

p 377 A90-23937

Recent propeller development and studies conducted at ONERA

[ONERA, TP NO. 1990-16] p 683 A90-41201

Active control of sound transmission through a cylindrical shell

p 893 A90-46192

Theoretical studies of the active control of propeller-induced cabin noise

p 893 A90-46351

In-flight experiments on the active control of propeller-induced cabin noise

p 893 A90-46352

On the unsteady loading noise of counter-rotating propeller

p 895 A90-49484

On numerical prediction of sound field generated by propeller

p 895 A90-49485

An investigation of counterrotating tip vortex interaction

[NASA-CR-185135] p 79 N90-11549

Noise data of four small propeller-driven airplanes

[PB89-216980] p 139 N90-12291

Evaluation of analysis techniques for low frequency interior noise and vibration of commercial aircraft

[NASA-CR-181851] p 220 N90-14866

Predicted and measured boundary layer refraction for advanced turboprop propeller noise

[NASA-TM-102365] p 379 N90-17413

The radiation of sound from a propeller at angle of attack

[NASA-CR-4264] p 548 N90-21602

En route noise of turboprop aircraft and their acceptability: Report of tests

p 697 N90-24858

En route noise of two turboprop aircraft

[DLR-MITT-89-18] p 697 N90-24859

When propfans cruise, will LDN 65 fly

p 697 N90-24864

Annoyance caused by advanced turboprop aircraft flyover noise: Counter-rotating-propeller configuration

[NASA-TP-3027] p 965 N90-29166

PROPELLER SLIPSTREAMS

The study of the theoretical calculation method for power stall dynamic characteristics of multiple-engine propeller airplane

p 29 A90-10349

Slipstream-induced pressure fluctuations on a wing panel

p 77 A90-11004

Propeller wakes and their interaction with wings

p 14 A90-12614

Propeller tip vortex interactions

[AIAA PAPER 90-0437] p 166 A90-19846

Vortex theory for the screw propeller with a hub

p 620 A90-39538

The flow over a wing/nacelle combination in the presence of a propeller slipstream

p 629 A90-42415

Validation of propeller slipstream calculations using a multi-block Euler code

[AIAA PAPER 90-3035] p 791 A90-45874

Investigation of propeller slipstream effects on the Fokker 50 through in-flight pressure measurements

[AIAA PAPER 90-3084] p 806 A90-46645

Recent improvements in the scope and accuracy of the performance prediction of nozzle propellers

[LR-598] p 572 N90-21742

Development of a system for the numerical simulation of Euler flows, with results of preliminary 3-D propeller-slipstream/exhaust-jet calculations

[NLR-TR-88008-U] p 776 N90-26285

PROPELLERS

Hydrodynamic visualization of the flow around a high-speed aircraft propeller

[ONERA, TP NO. 1989-108] p 3 A90-11141

Unsteady aerodynamics and aeroelasticity of turbomachines and propellers; Proceedings of the Fourth International Symposium, Aachen, Federal Republic of Germany, Sept. 6-10, 1987

p 5 A90-11776

Simulations of propeller/airframe interference effects using an Euler correction method

p 31 A90-13019

Finite element analysis of the flow of a propeller on a slender body with a two-equation turbulence model

p 210 A90-18340

A calculation method for ducted propellers

p 226 A90-21626

Subsonic calculation of propeller/wing interference

[AIAA PAPER 90-0031] p 226 A90-22155

Navier-Stokes simulations around a high-speed propeller

p 305 A90-25797

Propeller-wing interaction using a frequency domain panel method

p 307 A90-26128

Computer controlled test bench for axial turbines and propellers

p 437 A90-28288

Installation effects on propeller wake/vortex-induced structure-borne noise transmissions

p 579 A90-35761

Finite element simulation of turbulent propeller flowfields

p 703 A90-42658

Active control of propeller-induced noise fields inside a flexible cylinder

p 833 A90-47306

Unsteady aerodynamics and aeroelasticity of turbomachines and propellers; Proceedings of the Fifth International Symposium, Beijing, People's Republic of China, Sept. 18-21, 1989

p 853 A90-49451

A new method for high speed propeller flutter prediction

p 854 A90-49454

Aeroelastic vibrations of turbomachine blades and propellers

p 854 A90-49482

Analysis of a propeller in compressible, steady flow

p 814 A90-49778

Large scale prop-fan structural design study. Volume 2: Preliminary design of SR-7

[NASA-CR-174993] p 52 N90-10044

Evaluation of the improved OV-ID anti-icing system, phase 2

[AD-A213928] p 239 N90-15083

An experimental investigation of viscous aspects of propeller blade flow

p 315 N90-16711

In-plane forces and moments on installed inclined propellers at low forward speeds

[ESDU-89047] p 316 N90-16720

Noise of a simulated installed model counterrotation propeller at angle-of-attack and takeoff/approach conditions

[NASA-TM-102440] p 548 N90-20794

Laser-velocimeter-measured flow field around an advanced, swept, eight-blade propeller at Mach 0.8

[NASA-TP-2462] p 468 N90-20942

Relating flow between counter-rotating propellers to aerodynamic interaction noise

p 479 N90-20944

Aerodynamic optimization by simultaneously updating flow variables and design parameters

p 501 N90-20991

Theory and numerical analysis of single and multi-element nozzle propellers

[LR-579] p 572 N90-21741

Tests for integrating measurement of gas pressures in flight propellers

[ETN-90-86498] p 634 N90-24253

FAA/NASA En Route Noise Symposium

[NASA-CP-3067] p 696 N90-24853

En route noise of turboprop aircraft and their acceptability: Report of tests

p 697 N90-24858

A lifting surface method for the calculation of steady and unsteady, incompressible propeller aerodynamics

[ESA-TT-1151] p 717 N90-25113

The application of the finite element method to an aerodynamic problem specific to propeller design

[LR-614] p 718 N90-25116

An unsteady lifting surface method for single rotation propellers

[NASA-CR-4302] p 719 N90-25940

Aeroacoustics of advanced propellers

[NASA-TM-103137] p 782 N90-26635

Noise from tip vortex and bubble cavitation

[AD-A221962] p 896 N90-27468

Structure-borne noise estimates for the PTA aircraft

[NASA-CR-4315] p 896 N90-28396

Investigation of ATP blades, part 2. Validation of two-dimensional viscous flow simulation codes around thin airfoils

[NAL-TR-1046] p 912 N90-29326

Generalized Advanced Propeller Analysis System (GAPAS). Volume 2: Computer program user manual

[NASA-CR-185277] p 933 N90-29394

PROPORTIONAL CONTROL

Restructurable control using proportional-integral implicit model following --- for fighter aircraft

[AD-A220997] p 347 A90-25990

Proportional control of asymmetric forebody vortices with the unsteady bleed technique

[AIAA PAPER 90-1629] p 591 A90-38758

Stability and controllability in proportional navigation

p 725 A90-42990

Robust flight control system design with multiple model approach

[AIAA PAPER 90-3411] p 865 A90-47666

Nonconvex polytope approximations of attracting basin boundaries for nonlinear systems

[AIAA PAPER 90-3512] p 891 A90-47758

Discrete proportional Plus Integral (PI) multivariable control laws for the Control Reconfigurable Combat Aircraft (CRCA)

[AD-A215664] p 433 N90-18431

PROPORTIONAL COUNTERS

In-line wear monitor

[AD-A217799] p 510 N90-20091

PULSION

Advanced computational techniques for hypersonic propulsion

p 69 A90-12606

H-infinity based integrated flight-propulsion control design for a STOVL aircraft in transition flight

[NASA-TM-103198] p 758 N90-26011

Supersonic reacting internal flow fields

[NASA-TM-103480] p 767 N90-26094

An investigation of solid-fuel, dual-mode combustion ramjets

p 859 N90-27933

STOVL fighter propulsion reliability, maintainability, and supportability characterization

[AD-A224221] p 933 N90-28574

Solid fuel combustion chamber

[LR-634] p 939 N90-29433

PROPULSION SYSTEM CONFIGURATIONS

- Advances in computational design and analysis of airbreathing propulsion systems p 43 A90-12502
- Advanced airbreathing powerplant for hypersonic vehicles p 49 A90-12607
- Analytical methods for subsonic propulsion system integration p 29 A90-12613
- Aircraft propulsion systems technology and design --- Book p 188 A90-17308
- The fundamentals of vectored propulsion p 180 A90-17461
- The eigenvalue sensitivity analysis and design for integrated flight/propulsion control systems p 196 A90-18601
- Dynamic simulation of cross-shafted propulsion system for tilt nacelle application [AIAA PAPER 90-0439] p 191 A90-19847
- An AEW metalclad airship [AIAA PAPER 89-3158] p 244 A90-20579
- The National Aero-Space Plane, the guidance and control engineer's dream or nightmare? [AAS PAPER 89-040] p 264 A90-21546
- Swirling flow in thrust nozzles p 421 A90-27962
- Practical design considerations for integrating the propulsion system with the aircraft for jetborne flight [ASME PAPER 89-GT-310] p 490 A90-32257
- Propulsion systems for supersonic V/STOL aircraft [ASME PAPER 89-GT-309] p 507 A90-32259
- Configuration E-7 supersonic fighter/attack technology program [ASME PAPER 89-GT-308] p 490 A90-32260
- A method of sizing multi-cycle engines for hypersonic aircraft [ASME PAPER 89-GT-281] p 507 A90-32261
- Precursor convertible engine study [AIAA PAPER 90-2486] p 658 A90-40636
- CFD propels NASP propulsion progress p 683 A90-41163
- Turbofans turn to UHB propulsion p 659 A90-41165
- Integrated air vehicle/propulsion technology for a multirole fighter - A MCAIR perspective [AIAA PAPER 90-2278] p 644 A90-42105
- Analysis of internal flow in a ventral nozzle for STOVL aircraft [AIAA PAPER 90-1899] p 739 A90-42688
- Experimental evaluation of expendable supersonic nozzle concepts [AIAA PAPER 90-1904] p 740 A90-42691
- Focusing propulsion and lift system development for an evolving special operations aircraft [AIAA PAPER 90-2277] p 730 A90-42768
- Propulsion systems for the '90s p 745 A90-44805
- High-speed rotorcraft V/STOL - An initial assessment p 829 A90-46938
- Thermal management for a Mach 5 cruise aircraft using endothermic fuel [AIAA PAPER 90-3284] p 853 A90-48871
- Benefits of advanced materials, structures, and aerodynamics in future high speed civil transport propulsion systems [AIAA PAPER 90-3285] p 853 A90-48872
- Propulsion systems for vertical flight aircraft [AIAA PAPER 90-3299] p 853 A90-48881
- Propulsion system design specifications based on STOVL flight control requirements [AIAA PAPER 90-3227] p 839 A90-49112
- Cycle analysis of scramjet engines [NAL-TR-1002] p 51 N90-10035
- History and status of beamed power technology and applications at 2.45 Gigahertz p 61 N90-10150
- Combustion Instabilities in Liquid-Fueled Propulsion Systems [AGARD-CP-450] p 63 N90-10191
- Combustion instabilities in liquid-fueled propulsion systems: An overview p 63 N90-10192
- STOVL propulsion system volume dynamics approximations [NASA-TM-102397] p 114 N90-11740
- Large-scale Advanced Prop-fan (LAP) static rotor test report [NASA-CR-180848] p 117 N90-12617
- Controllable propulsion for escape systems control p 484 N90-20064
- Performance of an aero-space plane propulsion nozzle p 515 N90-21034
- Probabilistic modeling for simulation of aerodynamic uncertainties in propulsion systems [NASA-TM-102472] p 515 N90-21036
- Exhaust nozzles for propulsion systems with emphasis on supersonic cruise aircraft [NASA-RP-1235] p 516 N90-21037
- AVION: A detailed report on the preliminary design of a 79-passenger, high-efficiency, commercial transport aircraft [NASA-CR-186663] p 649 N90-23395

- Analysis of internal flow in a ventral nozzle for STOVL aircraft [NASA-TM-103123] p 666 N90-23404
- Advanced gearbox technology [NASA-CR-179625] p 666 N90-24274
- PROPULSION SYSTEM PERFORMANCE**
- Steady state performance of FJR 710/600S engine p 43 A90-12015
- Studies on the influence of Mach number on profile losses of a reaction turbine cascade p 10 A90-12517
- The performance of a small combustor operated over a wide range of conditions p 45 A90-12548
- Aerodynamic and propulsive performance of hypersonic detonation wave ramjets p 49 A90-12609
- Preliminary analysis of methodology for assessment of propulsion system for aerospace plane [IAF PAPER 89-307] p 123 A90-13442
- Development study of air turbo-ramjet for future space plane [IAF PAPER 89-311] p 109 A90-13445
- Successful performance development program for the T800-LHT-800 turboshaft engine [SAE PAPER 891048] p 110 A90-14352
- The variable cycle diesel as an aircraft engine [SAE PAPER 891065] p 110 A90-14365
- Simulation of a turbocompound two-stroke diesel engine [SAE PAPER 891066] p 110 A90-14366
- Jet futures p 190 A90-18526
- Numerical simulation of the actuation system for the ALDF's propulsion control valve --- Aircraft Landing Dynamics Facility [AIAA PAPER 90-0079] p 211 A90-19674
- Simulation of compressor performance deterioration due to erosion [ASME PAPER 89-GT-182] p 254 A90-22665
- A comparison between the design point and near-stall performance of an axial compressor [ASME PAPER 89-GT-70] p 254 A90-22667
- Stability of flow through multistage axial compressors [ASME PAPER 89-GT-311] p 231 A90-22668
- Optimal selection of the parameters to be measured during the identification of gas turbine engines. I - Problem statement p 255 A90-23410
- Reynolds number effects on the performance of a turbofan engine [ASME PAPER 89-GT-199] p 342 A90-23871
- Propulsion system integration in high-performance aircraft p 333 A90-23922
- Small gas turbine using a second-generation pulse combustor p 421 A90-27972
- A test facility for high-pressure high-temperature combustion chambers p 438 A90-29924
- Three approaches to reliability analysis p 452 A90-30706
- A study of a propulsion control system for a VATOL aircraft (A direct design synthesis application) p 424 A90-30712
- An optically interfaced propulsion management system applied to a commercial transport aircraft p 424 A90-30811
- Cycle analysis for helicopter gas turbine engines [ASME PAPER 89-GT-328] p 506 A90-32258
- F-15E/GE-129 Increased Performance Engine initial development flight test program [AIAA PAPER 90-1266] p 509 A90-33894
- The cryogenic wind tunnel as a testing tool for airframe/propulsion systems p 672 A90-40400
- A preliminary evaluation of an F100 engine parameter estimation process using flight data [AIAA PAPER 90-1921] p 656 A90-40559
- Preliminary design of a long-endurance Mars aircraft [AIAA PAPER 90-2000] p 674 A90-40587
- Precursor convertible engine study [AIAA PAPER 90-2486] p 658 A90-40636
- Investigation of very high bypass ratio engines for subsonic transports p 659 A90-40945
- CFD propels NASP propulsion progress p 683 A90-41163
- Turbofans turn to UHB propulsion p 659 A90-41165
- Aircraft engine technology gets a second wind p 659 A90-41166
- Development of a heavy fuel engine for an unmanned air vehicle [AIAA PAPER 90-2170] p 662 A90-42056
- Propulsion system-flight control integration-flight evaluation and technology transition [AIAA PAPER 90-2280] p 644 A90-42106
- JFS190 turbine engine performance optimized using Taguchi methods [AIAA PAPER 90-2419] p 663 A90-42169
- On- and off-design performance analysis of hypersonic detonation wave ramjets [AIAA PAPER 90-2473] p 664 A90-42188
- A hydrodynamic turbo-fan/shaft convertible engine p 665 A90-42487

- A numerical study of the effects of reverse sweep on a scramjet inlet performance [AIAA PAPER 90-2218] p 705 A90-42749
- Measured operating characteristics of a rectangular combustor/inlet isolator [AIAA PAPER 90-2221] p 742 A90-42752
- Propulsion integration for military aircraft [SAE PAPER 892234] p 733 A90-45449
- Modelling of fuel effects on naval aircraft operations [SAE PAPER 892331] p 765 A90-45488
- Power struggle --- Advanced Tactical Fighter engine proposals p 851 A90-46650
- Extended implicit model following as applied to integrated flight and propulsion control [AIAA PAPER 90-3444] p 890 A90-47697
- Benefits of advanced materials, structures, and aerodynamics in future high speed civil transport propulsion systems [AIAA PAPER 90-3285] p 853 A90-48872
- Propulsion system flight test analysis using modeling techniques [AIAA PAPER 90-3288] p 853 A90-48874
- Performance potential of an advanced technology Mach 3 turbojet engine installed on a conceptual high-speed civil transport [NASA-TM-4144] p 51 N90-10034
- Report on an overseas visit, June 1988 [AD-A210374] p 52 N90-10040
- Gas turbine performance analysis [PNR90599] p 116 N90-12614
- Controllable propulsion for escape systems control p 484 N90-20064
- Performance of an aero-space plane propulsion nozzle p 515 N90-21034
- Probabilistic modeling for simulation of aerodynamic uncertainties in propulsion systems [NASA-TM-102472] p 515 N90-21036
- Exhaust nozzles for propulsion systems with emphasis on supersonic cruise aircraft [NASA-RP-1235] p 516 N90-21037
- Assessment of High Temperature Superconducting (HTS) electric motors for rotorcraft propulsion [NASA-CR-185222] p 588 N90-21761
- Preliminary design of a long-endurance Mars aircraft [NASA-CR-185243] p 588 N90-21763
- From 1959-1989: 30 years of service experience with ramjets [PNR90677] p 748 N90-25139
- Supersonic reacting internal flow fields [NASA-TM-103480] p 767 N90-26094
- Propulsion system-flight control integration and optimization: Flight evaluation and technology transition [NASA-TM-4207] p 929 N90-28551
- Solid fuel combustion chamber [LR-634] p 939 N90-29433
- PROPULSIVE EFFICIENCY**
- Drag and propulsive efficiency of a light aircraft based on a new flight test technique [AIAA PAPER 90-0233] p 182 A90-19747
- Parametric studies of advanced turboprops p 253 A90-21225
- Advanced core technology - Key to subsonic propulsion benefits [ASME PAPER 89-GT-241] p 342 A90-23890
- Small gas turbine using a second-generation pulse combustor p 421 A90-27972
- Aircraft propulsion: Leading the way in aviation [LR-532] p 194 N90-13395
- Parametric assessment of propulsion system mass for airbreathing launcher configurations p 344 N90-16819
- AVION: A detailed report on the preliminary design of a 79-passenger, high-efficiency, commercial transport aircraft [NASA-CR-186663] p 649 N90-23395
- Energy Efficient Engine (E3) combustion system component technology performance report [NASA-CR-168274] p 930 N90-28555
- Energy Efficient Engine core design and performance report [NASA-CR-168069] p 930 N90-28559
- Energy Efficient Engine integrated core/low spool test hardware design report [NASA-CR-168137] p 931 N90-28566
- Energy Efficient Engine: High-pressure compressor test hardware detailed design report [NASA-CR-180850] p 932 N90-28570
- PROTECTION**
- Effects of lightning on operations of aerospace vehicles p 239 N90-15065
- Fuel tank explosion protection p 251 N90-15914
- Aircraft Fire Safety [AGARD-CP-467] p 324 N90-17581
- A review of UK civil aviation fire and cabin safety research p 325 N90-17587
- Windblast protection for advanced ejection seats p 483 N90-20063

- Forward canopy feasibility and Thru-The-Canopy (TTC) ejection system study
[AD-A220360] p 637 N90-24258
- Carbon-carbon composites: Emerging materials for hypersonic flight
[NASA-TM-103472] p 767 N90-26080
- A Protection And Detection Surface (PADS) for damage tolerance
[NASA-TP-30111] p 876 N90-27788

PROTECTIVE COATINGS

- Effect of protective coatings on mechanical properties of superalloys
[ONERA, TP NO. 1989-88] p 62 A90-11126
- Properties and characterisation of novel thermal barrier systems for gas turbines
p 62 A90-12538
- Extending the overhaul interval for gas turbine engines through the use of alternative coatings on first stage blades
p 63 A90-12539
- TBCs for better engine efficiency --- thermal barrier coatings
p 203 A90-17294
- Organic coatings - First line of defense
p 204 A90-17300
- Gas turbine compressor operating environment and material evaluation
[ASME PAPER 89-GT-42] p 340 A90-23769
- Thermal barrier characteristics of partially stabilized zirconia coatings on Incoloy alloy 909 (A controlled expansion alloy)
[ASME PAPER 89-GT-146] p 354 A90-23839
- Standardization in aerospace plating and coating
[SAE PAPER 890913] p 365 A90-24681
- Entrapment plating of abrasive particles for jet engine clearance control
[SAE PAPER 890918] p 286 A90-24685
- The selection and performance of thermal sprayed abrasible seal coatings for gas turbine engines
[SAE PAPER 890929] p 286 A90-24694
- New concept for improved nonmetallic erosion protection systems
p 407 A90-28188
- UCAR 2040, A novel wear resistant coating for aircraft structural components
p 441 A90-28231
- Coating turbine engine components
p 451 A90-29893
- Coatings for high temperature corrosion in aero and industrial gas turbines
p 443 A90-30479
- Development of erosion resistant coatings for compression airfoils
p 443 A90-31120
- Lightning strike protection concepts for composite materials
p 528 A90-31617
- Corrosion protection and EMP/EMI shielding
p 600 A90-37902
- Thermal nondestructive characterization of the integrity of protective coatings
p 770 A90-44325
- Development of a water-borne non-chromated primer and topcoat for aerospace applications
p 956 A90-50213

- Fuel resistant coatings for metal and composite fuel tanks
p 269 N90-15911
- Criteria for coal tar seal coats on airport pavements. Volume 2: Laboratory and field studies
[AD-A220167] p 674 N90-24277
- Molten salt induced high temperature degradation of thermal barrier coatings
p 952 N90-28704
- Effect of protective coatings on mechanical properties of superalloys
p 952 N90-28707
- Evaluation of high temperature protective coatings for gas turbine engines under simulated service conditions
p 952 N90-28712
- Overview on hot gas tests and molten salt corrosion experiments at the DLR
p 953 N90-28714

PROTOCOL (COMPUTERS)

- High speed bus technology development
[AD-A224486] p 960 N90-29565

PROTON MAGNETIC RESONANCE

- The prediction of middle distillate fuel properties using liquid chromatography-proton nuclear magnetic resonance spectroscopy data
[AD-A211879] p 126 N90-11899

PROTOTYPES

- East coast Osprey flies
p 246 A90-21713
- Jet Engine Technical Advisor (JETA)
p 693 A90-41184
- The Experimental Aircraft Flight Test Programme
p 34 N90-10865
- The use of prototypes in selected foreign fighter aircraft development programs: Rafale, EAP, Lavi, and Gripen
[AD-A214500] p 287 N90-16707
- Noise and sonic boom impact technology. Initial development of an Assessment System for Aircraft Noise (ASAN). Volume 2: System design strategy
[AD-A214454] p 379 N90-17411
- An evaluation of the accuracy of a microwave landing system area navigation system at Miami/Tamiami Florida Airport
[DOT/FAA/CT-TN89/40] p 640 N90-23377

- Expert system for pilot assistance: The challenge of an intensive prototyping
[ETN-90-97274] p 825 N90-27674

PROVING

- Validation of the procedures --- integrated multidisciplinary optimization of rotorcraft
p 107 N90-12587

- Comparison of 3-D viscous flow computations of Mach 5 inlet with experimental data
[NASA-TM-102518] p 510 N90-20090

PSYCHOACOUSTICS

- Annoyance caused by advanced turboprop aircraft flyover noise: Counter-rotating-propeller configuration
[NASA-TP-3027] p 965 N90-29166

PSYCHOLOGY

- Joint University Program for Air Transportation Research, 1988-1989
[NASA-CP-3063] p 468 N90-20921

PULSE CODE MODULATION

- Real-time test data processing system --- for helicopter flight testing
p 458 A90-28860
- Acquisition and recording an AMX A/C. Aeritalia experience and present trends
[ETN-89-95217] p 109 N90-12598

PULSE COMMUNICATION

- The E-SAT 300A - A multichannel satellite communication system for aircraft
p 914 A90-51339
- Assessment of voice coders for ATC/pilot voice communications via satellite digital communication channels
[CAA-PAPER-89004] p 135 N90-12807

PULSE DOPPLER RADAR

- Antenna sidelobe requirements for the medium PRF mode of an airborne radar
p 37 A90-10985
- New approach for Doppler ambiguities resolution in medium pulse repetition frequency radars
p 240 A90-20937
- Wind shear detection with pencil-beam radars
p 279 A90-21386
- Airborne Doppler radar detection of low-altitude wind shear
p 252 A90-23284
- High resolution spectrum analysis for airborne pulse Doppler radars
p 339 A90-24329
- Use of pulse radars for helicopters detection - Design constraints
p 683 A90-41073

PULSE REPETITION RATE

- Antenna sidelobe requirements for the medium PRF mode of an airborne radar
p 37 A90-10985
- New approach for Doppler ambiguities resolution in medium pulse repetition frequency radars
p 240 A90-20937
- Doppler-rate filtering for detecting moving targets with synthetic aperture radars
p 488 A90-34138

PULSEJET ENGINES

- Simulation and second law analysis of the unsteady combustion of a non-ideal pulsating ramjet
p 44 A90-12516
- Small gas turbine using a second-generation pulse combustor
p 421 A90-27972
- Operation of a gas ejector in the pulsed regime
p 850 A90-46488

PUMP IMPELLERS

- Numerical study of centrifugal impeller response to an outlet pressure distortion
p 68 A90-11804
- Mathematical formulation of blade surfaces in turbomachinery. I - Theoretical surface formulations
[ASME PAPER 89-GT-160] p 360 A90-23848

PYLON MOUNTING

- Calculation of transonic flows for novel engine-airframe installations
p 145 A90-16768

PYLONS

- The TSP methods applied to the calculation of transonic flow about wing/body/nacelle/pylon-configurations --- Transonic Small Perturbation
p 554 A90-35868
- A grid generation method for an aft-fuselage mounted capped-nacelle/pylon configuration with an actuator disk
[AIAA PAPER 90-1564] p 565 A90-38703
- Application of fracture mechanics and half-cycle method to the prediction of fatigue life of B-52 aircraft pylon components
[NASA-TM-88277] p 214 N90-13820
- Effect of pylon wake with and without pylon blowing on propeller thrust
[NASA-TM-4162] p 173 N90-14190
- Compression pylon
[NASA-CASE-LAR-13777-1] p 498 N90-20078

PYROLYSIS

- Regression and combustion characteristics of boron containing fuels for solid fuel ramjets
p 858 N90-27928

Q

QUADRATIC PROGRAMMING

- An application of SQP and Ada to the structural optimisation of aircraft wings
p 216 A90-18444
- A quadratic programming method for solving three dimensional elastic-plastic contact problems
p 603 A90-36417

QUALIFICATIONS

- Sole means navigation and integrity through hybrid Loran-C and NAVSTAR GPS
p 489 N90-20933

QUALITY CONTROL

- Looking inside a structure
p 209 A90-17920
- Computer integrated quality assurance for robotic workcells in aerospace manufacturing
[SME PAPER MS89-152] p 283 A90-23681
- Advanced software for turbine blade processing
[SME PAPER MS89-330] p 274 A90-23694
- Air Force manufacturing technology NDE programs supporting manufacturing and maintenance
p 452 A90-30779
- Total quality management and the transitioning company - The perfect fit
[AIAA PAPER 89-3211] p 549 A90-31698
- Honeycomb quality requirements - A user's perspective
p 538 A90-33705
- Toward total quality in industry
p 684 A90-41768
- Development of process control procedure for ultrahigh-sensitivity fluorescent penetrant inspection systems
p 771 A90-45225
- The impact of total quality management (TQM) and concurrent engineering on the aircraft design process
p 785 A90-46927
- Implementation of integrated product development --- in aircraft industry
[AIAA PAPER 89-3194] p 786 A90-48829
- Ride quality criteria for the B-2 bomber
[AIAA PAPER 90-3256] p 835 A90-48852
- Castings Airworthiness
[AGARD-R-762] p 64 N90-10231
- Casting factors imposed by the French regulation for foundry castings used in military aircraft
p 64 N90-10233
- The question of the casting factor
p 64 N90-10238
- Combined advanced foundry and quality control techniques to enhance reliability of castings for the aerospace industry
p 64 N90-10240
- Thin walled cast high-strength structural parts
p 65 N90-10242

- The role of component testing
[PNR90589] p 115 N90-12608
- NDI (Nondestructive Inspection) oriented corrosion control for Army aircraft. Phase 1: Inspection methods
[AD-A213368] p 176 N90-13359
- Review of the Aerospace Safety Advisory Panel report for NASA fiscal year 1990 authorization
[GPO-24-234] p 177 N90-14213
- HPLC analysis of helicopter rotor blade materials
[AD-A221121] p 650 N90-24270
- Proceedings of the 1987 Aircraft/Engine Structural Integrity Program (ASIP/ENSIP) Conference
[AD-A198037] p 842 N90-26807
- An aluminum quality breakthrough for aircraft structural reliability
p 843 N90-26816
- Multichannel on-board load and fatigue monitoring
p 849 N90-27621
- Computer modeling and data processing methods: An essential part of jet engine condition monitoring and fault diagnosis
p 855 N90-27626
- Evaluation of composite components on the Bell 206L and Sikorsky S-76 helicopters
[NASA-TM-4195] p 876 N90-27787
- Neutron radiography: Applications and systems
p 886 N90-28080
- Development of acceptance plans for airport pavement materials. Volume 1: Development
[DOT/FAA/RD-90/15] p 937 N90-28581

QUARTZ LAMPS

- Deicing of solids using radiant heating
p 769 A90-43309

QUATERNARY ALLOYS

- Influence of alloying elements on the oxidation behavior of NbAl3
p 355 A90-24861

QUENCHING (COOLING)

- Quench sensitivity of airframe aluminum alloys
p 765 A90-44348
- Modeling of the oil quench for Ni-based superalloy turbine disks
p 957 A90-51525

QUEUEING THEORY

- Effective use of Cray supercomputers
p 546 A90-34436
- A simulation study of landing time allocation procedures for use in computer-assisted air traffic management systems
[AD-A212159] p 99 N90-11722

SUBJECT INDEX

- The application of queuing theory to the modelling of CP-140 aircraft communications
[AD-A213479] p 274 N90-15310
- QUIET ENGINE PROGRAM**
What should be done with those noisy old aircraft
[PNR90562] p 107 N90-12593
Re-engine with the Rolls-Royce Tay 670, the route to significant noise reduction
[PNR90585] p 115 N90-12606
The commercial aircraft noise problem
[PNR90577] p 140 N90-13203
- QUOTIENTS**
High-quality approximation of eigenvalues in structural optimization p 603 A90-36277

R

- RACKS (GEARS)**
Planet gear sleeve spinning analysis
[AIAA PAPER 90-2154] p 681 A90-40613
- RADAR ABSORBERS**
Simulation of the reduction characteristics of scattering from an aircraft coated with a thin-type absorber by the spatial network method p 638 A90-39855
Building the B-2 p 701 A90-43826
A decision-making aid for multi-layer radar absorbent coverings
[ESA-TT-1173] p 773 N90-25267
- RADAR ANTENNAS**
Antenna sidelobe requirements for the medium PRF mode of an airborne radar p 37 A90-10985
Antenna and radar signature technology at Dornier p 261 A90-21605
Radio deviation of airborne goniometers --- Russian book p 242 A90-22733
Software architecture concepts for avionics p 461 A90-30806
ROSAR (Helicopter-Rotor based Synthetic Aperture Radar) p 541 N90-21229
- RADAR APPROACH CONTROL**
Parallel runway monitor p 241 A90-21382
Aircraft Separation by Synchronized Transponder Interrogation (ASSTI) p 727 A90-43724
Design of a final approach spacing tool for TRACON air traffic control
[NASA-TM-102229] p 24 N90-10841
The application of Z to the specification of air traffic control systems. 1: An initial specification of the radar processing activity
[RSRE-MEMO-4280] p 243 N90-15900
Study improvement training facilities ground control air traffic controllers. Part 1: Alternative solutions and their consequences
[FEL-89-A257-PT-1] p 919 N90-29380
Study improvement training facilities ground control air traffic controllers. Part 2: Functional analysis approach control trainer
[FEL-89-A280-PT-2] p 939 N90-29409
- RADAR BEACONS**
Mode S transponders - A new avionics product
[SAE PAPER 891055] p 98 A90-14357
The Mode S beacon radar system p 241 A90-21379
Propagation of Mode S beacon signals on the airport surface p 241 A90-21381
Mode S system design and architecture p 330 A90-25569
Performances and new surveillance possibilities in SSR - Mode S p 639 A90-41036
Aircraft Separation by Synchronized Transponder Interrogation (ASSTI) p 727 A90-43724
Data link test and analysis system/ATCRBS transponder test system technical reference
[DOT/FAA/CT-TN90/7] p 824 N90-26803
- RADAR BEAMS**
Stealth comes of age p 336 A90-27596
ASR-4 long range radar will upgrade U.S. en-route surveillance p 403 A90-27925
- RADAR CROSS SECTIONS**
Antenna and radar signature technology at Dornier p 261 A90-21605
Stealth - Deception, evasion, and concealment in the air --- Book p 285 A90-24265
Fly-by-wire controls key to 'pure' stealth aircraft --- F-117A Aircraft p 413 A90-30222
Airborne early warning radar --- Book p 727 A90-45200
Automation of an RCS (Radar Cross Section) measurement system and its application to investigate the electromagnetic scattering from scale model aircraft canopies
[AD-A215741] p 371 N90-17970
- RADAR DATA**
Independent operations on closely spaced runways p 821 A90-46393

- Windshear case study: Denver, Colorado, July 11, 1988
[DOT/FAA/DS-89/19] p 544 N90-21509
- RADAR DETECTION**
Radio deviation of airborne goniometers --- Russian book p 242 A90-22733
Development of an automated windshear detection system using Doppler weather radar p 373 A90-25567
A powerful range-Doppler clutter rejection strategy for navigational radars p 403 A90-30688
Use of pulse radars for helicopters detection - Design constraints p 683 A90-41073
Adaptive clutter rejection filters for airborne Doppler weather radar applied to the detection of low altitude windshear
[NASA-CR-186211] p 214 N90-14453
Airborne Doppler radar flight experiments for the detection of microbursts p 542 N90-21243
- RADAR ECHOES**
Target classification by vibration sensing --- for helicopter detection p 1 A90-10170
- RADAR EQUIPMENT**
APG-70 radar test package development aid
[AIAA PAPER 89-3044] p 1 A90-10624
Radar systems of aircraft --- Russian book p 26 A90-10841
Radar systems --- Book p 208 A90-17305
Ground navigation in airport traffic p 242 A90-21725
The TVD 900 - A modern signal processing applied to primary civilian ATC radar p 638 A90-41034
Airborne early warning radar --- Book p 727 A90-45200
A modular 550 watt, 25 watts per cubic inch power supply for next generation aircraft p 958 A90-52954
Heli/SITAN: A terrain referenced navigation algorithm for helicopters
[DE90-005193] p 405 N90-19217
- RADAR IMAGERY**
Shadow-tracking algorithm for moving target detection p 488 A90-34137
Vision guidance update - Synthetic aperture radar (SAR) multiple image exploitation for position and velocity determination p 488 A90-34140
Simulation of airborne target imagery - Dependence on frequency and bistatic angle p 488 A90-34146
The development of an airborne synthetic aperture radar motion compensation system p 333 A90-16745
Synthetic aperture radar imagery of airports and surrounding areas: Archived SAR data p 401 N90-18371
Synthetic aperture radar imagery of airports and surrounding areas: Philadelphia Airport
[NASA-CR-4280] p 401 N90-18372
Synthetic aperture radar imagery of airports and surrounding areas: Denver Stapleton International Airport
[NASA-CR-4305] p 637 N90-24257
- RADAR MEASUREMENT**
Antenna and radar signature technology at Dornier p 261 A90-21605
A waveform alignment approach to positioning airborne radar-sounding data p 332 A90-26651
Pattern representations and syntactic classification of radar measurements of commercial aircraft p 417 A90-28407
The microphysical structure of severe downdrafts from radar and aircraft observations in CINDIE --- Convection Initiation and Downburst Experiment p 455 A90-28582
- RADAR NAVIGATION**
Dual mode radar fusion based on morphological processing p 459 A90-30249
Survivable penetration p 917 N90-29363
- RADAR RANGE**
Automation of an RCS (Radar Cross Section) measurement system and its application to investigate the electromagnetic scattering from scale model aircraft canopies
[AD-A215741] p 371 N90-17970
- RADAR RECEIVERS**
Rockwell International's miniature high performance GPS receiver p 726 A90-43701
RAIM - An implementation study p 726 A90-43714
- RADAR SCANNING**
The GE solid state air defence/ATC radar p 639 A90-41062
- RADAR SCATTERING**
Pattern representations and syntactic classification of radar measurements of commercial aircraft p 417 A90-28407
Simulation of the reduction characteristics of scattering from an aircraft coated with a thin-type absorber by the spatial network method p 638 A90-39855

RADIATION SHIELDING

- Airborne early warning radar --- Book p 727 A90-45200
Measurement and computer simulation of antennas on ships and aircraft for results of operational reliability p 370 N90-17936
Synthetic aperture radar imagery of airports and surrounding areas: Archived SAR data
[NASA-CR-4275] p 401 N90-18371
- RADAR SIGNATURES**
Antenna and radar signature technology at Dornier p 261 A90-21605
Prospects are good for using ATC radar to detect birds p 329 A90-25496
Stealth comes of age p 336 A90-27596
Simulation of airborne target imagery - Dependence on frequency and bistatic angle p 488 A90-34146
- RADAR TARGETS**
Target classification by vibration sensing --- for helicopter detection p 1 A90-10170
Antenna sidelobe requirements for the medium PRF mode of an airborne radar p 37 A90-10985
New approach for Doppler ambiguities resolution in medium pulse repetition frequency radars p 240 A90-20937
Shadow-tracking algorithm for moving target detection p 488 A90-34137
Advanced technology MMW seeker tested, a multi-technology demonstration sensor p 488 A90-34143
Simulation of airborne target imagery - Dependence on frequency and bistatic angle p 488 A90-34146
- RADAR TRACKING**
Using aircraft radar tracks to estimate wind aloft p 241 A90-21390
An array-fed reflector antenna with built-in calibration facility p 402 A90-27781
A powerful range-Doppler clutter rejection strategy for navigational radars p 403 A90-30688
Independent operations on closely spaced runways p 821 A90-46393
Turbulence spectral widths view angle independence as observed by Doppler radar
[DOT/FAA/SA-89/2] p 281 N90-15566
- RADARSAT**
The Radarsat system --- Canada/U.S. program for launching remote sensing satellite with SAR p 873 A90-49671
- RADIAL FLOW**
An experimental investigation of non-steady flow in vaneless diffusers p 14 A90-12595
Radial swirl flows between parallel disks at critical flow rate p 14 A90-12596
Studies on supersonic radial flow behavior in disk channel p 87 A90-16104
LDV measurements and the flow analysis in the vaneless region of a radial inflow turbine p 292 A90-23845
[ASME PAPER 89-GT-157] p 292 A90-23845
A theoretical study of ingress for shrouded rotating disc systems with radial outflow --- sealing rotor-stator cavities p 361 A90-23859
[ASME PAPER 89-GT-178] p 361 A90-23859
Design of an air-cooled metallic high-temperature radial turbine p 507 A90-32960
Analyses of revising the inlet profile of a radial inflow turbine impeller p 602 A90-35831
Oscillation of circular shock wave p 557 A90-36465
Flow induced forced response of an incompressible radial cascade including profile and incidence effects
[AIAA PAPER 90-2352] p 626 A90-42136
Review of mixed flow and radial turbine options
[AIAA PAPER 90-2414] p 687 A90-42166
An experimental investigation of viscous aspects of propeller blade flow p 315 N90-16711
- RADIAL VELOCITY**
Effect of the radial clearance on the efficiency of a partial microturbine p 111 A90-14586
- RADIANT HEATING**
Deicing of solids using radiant heating p 769 A90-43309
- RADIATION DETECTORS**
Coping with bomb threats to civil aviation p 23 A90-12781
- RADIATION EFFECTS**
Aircraft testing in the electromagnetic environment p 248 N90-15066
- RADIATION HAZARDS**
Boeing 727-100 test project (high energy radiated field tests)
[DOT/FAA/CT-88/33] p 542 N90-21247
- RADIATION MEASURING INSTRUMENTS**
UV spectroradiometric output of an F404 turbojet aircraft engine p 652 A90-40195
- RADIATION SHIELDING**
Corrosion protection and EMP/EMI shielding p 600 A90-37902

RADIATIVE HEAT TRANSFER

- A study of the radiation of hydrogen-xenon mixtures near models flying at high supersonic velocities p 470 A90-32509
- Deicing of solids using radiant heating p 769 A90-43309

RADIO ALTIMETERS

- Heli/SITAN: A terrain referenced navigation algorithm for helicopters [DE90-005193] p 405 N90-19217

RADIO COMMUNICATION

- ATC ground communications system optimization techniques p 330 A90-25568
- Automated measurement of aircraft-level electromagnetic interference p 404 A90-30752
- Automatic speech recognition in air-ground data link p 690 N90-25037

RADIO ECHOES

- A bearing error in the VHF omnirange due to sea surface reflection p 402 A90-27875

RADIO FREQUENCIES

- New approach for Doppler ambiguities resolution in medium pulse repetition frequency radars p 240 A90-20937
- Boeing 727-100 test project (high energy radiated field tests) [DOT/FAA/CT-88/33] p 542 N90-21247

RADIO FREQUENCY HEATING

- Radio frequency (RF) heated supersonic flow laboratory [AIAA PAPER 90-2469] p 673 A90-42186

RADIO NAVIGATION

- International satellite radionavigation and radiolocation - Choosing among the options p 96 A90-13979
- Omega-GPS interoperability for the long haul p 577 A90-36927
- Development of obstacle clearance criteria and standards for MLS and MLS/RNAV precision approaches and development of an MLS collision risk model [SAE PAPER 892215] p 728 A90-45432
- A multi-sensor approach to assuring GPS integrity p 821 A90-46396
- Computerized MLS flight inspection system developed p 823 A90-48983
- Operation of aviation radio and electronic equipment (Handbook) --- Russian book p 914 A90-50747
- Military navigation - The fourth generation p 914 A90-50775

RADIO RECEIVERS

- GPS: Arrival in the fleet - A GPS AN/SRN-25 receiver assessment p 97 A90-13989
- Interference detection and suppression in Loran-C receivers p 240 A90-20504
- Status and potential of GPS-receiver development p 265 A90-21717
- Global Positioning System: Arrival in the fleet - A GPS AN/SRN-25(V) receiver assessment p 331 A90-26338
- An integrated GPS/GLONASS receiver p 822 A90-47909
- An analysis of GPS receiver performance capabilities and trends p 823 A90-49491
- Phase III GPS Manpack receiver operation and navigation performance p 823 A90-49497

RADIO SIGNALS

- The role of adaptive antenna systems when used with GPS p 128 A90-13995
- Optimization of complex data processing algorithms in multichannel radio direction finding p 576 A90-36115

RADIOGONIOMETERS

- Radio deviation of airborne goniometers --- Russian book p 242 A90-22733

RADIOISOTOPE BATTERIES

- Preliminary design of a long-endurance Mars aircraft [AIAA PAPER 90-2000] p 674 A90-40587
- Preliminary design of a long-endurance Mars aircraft [NASA-CR-185243] p 588 N90-21763

RADIOMETERS

- Experiments with unsteady, free surface, three-dimensional vortices in a thermally stable, stratified fluid [AD-A222088] p 815 N90-26796

RADOMES

- Aerodynamic design considerations for aircraft radomes [AIAA PAPER 90-2843] p 711 A90-45163

RAIN

- Results of aerodynamic testing of large-scale wing sections in a simulated natural rain environment [AIAA PAPER 90-0486] p 167 A90-19874
- An analytic study of nonsteady two-phase laminar boundary layer around an airfoil p 691 N90-25051

RAIN EROSION

- New concept for improved nonmetallic erosion protection systems p 407 A90-28188

- Rain erosion testing --- on polymethyl methacrylate specimens p 525 A90-34578
- Multiple impact jet apparatus (MIJA) - Application to rain erosion studies p 525 A90-34580

RAINDROPS

- Operational considerations for aerodynamic testing of large-scale wing sections in a simulated natural rain environment [AIAA PAPER 90-0485] p 313 A90-26956

RAMAN LASERS

- Volumetric analysis by spontaneous Raman diffusion in a supersonic wind tunnel [ISL-R-109/88] p 95 N90-12564

RAMAN SPECTRA

- Raman scattering measurements using UV excimer lasers p 874 N90-26902
- Concentration, temperature, and density in a hydrogen-air flame by excimer-induced Raman scattering p 875 N90-26903

RAMAN SPECTROSCOPY

- Simultaneous CARS measurements of temperature and H₂, H₂O concentrations in hydrogen-fueled supersonic combustion [AIAA PAPER 90-0158] p 205 A90-19713
- Volumetric analysis by spontaneous Raman diffusion in a supersonic wind tunnel [ISL-R-109/88] p 95 N90-12564

RAMJET ENGINES

- Similarity and scale effects in solid fuel ramjet combustors p 60 A90-12513
- Combustion characteristics of a boron-fueled SFRJ with aft-burner p 62 A90-12514
- Simulation and second law analysis of the unsteady combustion of a non-ideal pulsating ramjet p 44 A90-12516
- Full-scale liquid fuel ramjet combustor tests p 44 A90-12528
- Hydrogen fueled subsonic-ram-combustor model tests for an air-turbo-ram engine p 44 A90-12529
- A study of two-phase flow for a ramjet combustor p 45 A90-12532
- Exhaust nozzle system design considerations for turbojet propulsion systems p 48 A90-12577
- Aerodynamic and propulsive performance of hypersonic detonation wave ramjets p 49 A90-12609
- Large-eddy simulations of pressure oscillations and combustion instability in a ramjet p 111 A90-15388
- Calculation of flowfields in side-inlet ramjet combustors with an algebraic Reynolds stress model p 87 A90-16367
- Large-eddy simulations of combustion instability in an axisymmetric ramjet combustor [AIAA PAPER 90-0267] p 191 A90-19764
- Numerical modeling of a flame in a confined, unstable shear layer [AIAA PAPER 90-0647] p 205 A90-19966
- A one-dimensional model of ramjet combustion instability [AIAA PAPER 90-0271] p 266 A90-22192
- Estimation of the efficiency of a ramjet engine with a thermocompressor using fuel conversion products p 255 A90-23412
- Heat transfer in a solid fuel ramjet combustor [AIAA PAPER 90-1783] p 586 A90-38472
- Linear dynamics of supersonic ramjet p 655 A90-40519
- Ultrasonic regression rate measurement in solid fuel ramjets [AIAA PAPER 90-1963] p 656 A90-40573
- Experimental and computational flammability limits in a solid fuel ramjet [AIAA PAPER 90-1964] p 676 A90-40574
- Engineering design models for ramjet efficiency and lean blowoff [AIAA PAPER 90-2453] p 663 A90-42176
- On- and off-design performance analysis of hypersonic detonation wave ramjets [AIAA PAPER 90-2473] p 664 A90-42188
- Hypersonic (T-D) 'pinch' and aerospaceplane propulsion [AIAA PAPER 90-2474] p 675 A90-42189
- Numerical simulation of nonpremixed turbulent flow in a dump combustor [AIAA PAPER 90-1858] p 768 A90-42685
- Operation of the ram accelerator in the transdetonative velocity regime [AIAA PAPER 90-1985] p 741 A90-42712
- Combustion of PMMA, PE, and PS in a ramjet p 764 A90-43670
- Large-eddy simulations of flows in a ramjet combustor p 772 A90-45534
- Recent developments in Ramjet pressure oscillation technology p 53 N90-10199
- Numerical simulation of pressure oscillations in a ramjet combustor p 54 N90-10202

- Very-low-frequency oscillations in liquid-fueled ramjets p 54 N90-10204
- Acoustic-vortex-chemical interactions in an idealized ramjet p 54 N90-10206
- Computation of ramjet internal flowfields [AD-A212001] p 114 N90-11743
- Analytical studies of three-dimensional combustion processes [AD-A211903] p 126 N90-11837
- Apparatus for cooling electronic components in aircraft [AD-D014207] p 183 N90-13373
- Acoustic-vortical-combustion interaction in a solid fuel ramjet simulator p 194 N90-14234
- External flow computations for a finned 60mm ramjet in steady supersonic flight [AD-A216998] p 428 N90-19233
- Modification and improvement of software for modeling multidimensional reacting fuel flows [AD-A217789] p 533 N90-20235
- Metallized fuel particle size study in a solid fuel ramjet [AD-A220079] p 679 N90-24451
- From 1959-1989: 30 years of service experience with ramjets [PNR90677] p 748 N90-25139
- Gas Turbine Combustion, volume 1 [VKI-LS-1990-02-VOL-1] p 748 N90-25985
- Liquid fueled ramjet combustion instability: Acoustical and vortical interactions with burning sprays [AD-A222752] p 767 N90-26104
- Regression and combustion characteristics of boron containing fuels for solid fuel ramjets p 858 N90-27928
- Calculation of the combustion distribution in a liquid-fuel ramjet p 858 N90-27931
- Entropy wave instability in compact ramjets p 858 N90-27932
- An investigation of solid-fuel, dual-mode combustion ramjets p 859 N90-27933
- Numerical simulations of flowfields in a central-dump ramjet combustor. 3: Effects of chemistry [AD-A224145] p 933 N90-28573
- Solid fuel combustion chamber [LR-634] p 939 N90-29433

RAMPS

- Numerical simulations of unsteady shock reflections by ramps p 305 A90-25795

RAMPS (STRUCTURES)

- Experimental investigation of a supersonic swept ramp injector using laser-induced iodine fluorescence [AIAA PAPER 90-1518] p 606 A90-38663
- Dynamics of the outgoing turbulent boundary layer in a Mach 5 unswep compression ramp interaction [AIAA PAPER 90-1645] p 569 A90-38773

RANDOM NOISE

- Structure-borne noise transmission in cylindrical enclosures due to random excitation [AIAA PAPER 90-0990] p 463 A90-29402

RANDOM PROCESSES

- Effects of random initial conditions and deterministic winds on simulated parachute motion p 22 A90-11002
- A new class of random processes with application to helicopter noise p 781 A90-42874

RANDOM VIBRATION

- Stochastic flutter of a panel subjected to random in-plane forces. I - Two mode interaction p 444 A90-27992
- Flutter analysis from ambient random responses p 491 A90-33374

RANGE AND RANGE RATE TRACKING

- The small portable Global Positioning System tracking range of the future p 60 A90-12209

RANGE FINDERS

- Observability of relative navigation using range-only measurements p 917 N90-29360

RANGEFINDING

- Analytical evaluation of radiation patterns of a TACAN antenna p 404 A90-30695
- Range determination in a multipath prone environment p 877 A90-45960

Image based range determination

- [AIAA PAPER 90-3404] p 822 A90-47659
- China-built airborne synchronous laser ranger the new L-8 jet trainer aircraft [AD-A213835] p 275 N90-15422
- Velocity filtering applied to optical flow calculations [NASA-TM-102802] p 916 N90-28512

RANKINE-HUGONIOT RELATION

- Effects of shock on the stability of hypersonic boundary layers [AIAA PAPER 90-1448] p 561 A90-38608

RAPID QUENCHING (METALLURGY)

- Microstructures of rapidly-solidified binary TiAl alloys p 532 A90-34990
- Laser welding of an advanced rapidly-solidified titanium alloy p 881 A90-47021

RAPID TRANSIT SYSTEMS

- A multipurpose aerodynamic research facility utilizing the abandoned Cincinnati subway tubes
[AIAA PAPER 90-1424] p 596 A90-37961
California air transportation study: A transportation system for the California Corridor of the year 2010
[NASA-CR-186219] p 176 N90-14212

RARE GASES

- A small inert gas generator p 180 A90-17405

RAREFIED GAS DYNAMICS

- Changes in supersonic flow past an obstacle due to the formation of a thin rarefaction channel ahead of the obstacle p 150 A90-17108
Supersonic low-density flow over airfoils p 153 A90-17871

- Direct simulation of hypersonic rarefied flow about a delta wing
[AIAA PAPER 90-0143] p 162 A90-19704
Hypersonic rarefied flow and its solution over the stagnation region
[AIAA PAPER 90-0420] p 166 A90-19842

- Rarefied gas dynamics p 224 A90-21163
Three dimensional Discrete Particle Simulation about the AFE geometry
[AIAA PAPER 90-1778] p 560 A90-38468

RASTER SCANNING

- The all glass helicopter cockpit p 653 A90-42447

RATES (PER TIME)

- Estimation of defective rate of mechanic-hydraulic components
[ETN-90-97275] p 884 N90-27120

RATINGS

- Proceedings of a workshop on Future Airport Passenger Terminals
[PB90-213620] p 937 N90-28580

RATIONAL FUNCTIONS

- A reduced cost rational-function approximation for unsteady aerodynamics
[AIAA PAPER 90-1155] p 390 A90-29367
Fast calculation of root loci for aeroelastic systems and of response in time domain
[AIAA PAPER 90-1156] p 390 A90-29368

RAY TRACING

- Accurate ILS and MLS performance evaluation in presence of site errors p 404 A90-30693
PTA en route noise measurements p 696 N90-24855

RAYLEIGH EQUATIONS

- Linear instability of the supersonic wake behind a flat plate aligned with a uniform stream p 716 A90-45783

RAYLEIGH SCATTERING

- Wall pressure fluctuations in the reattachment region of a supersonic free shear layer
[AIAA PAPER 90-1461] p 561 A90-38618

RAYLEIGH-RITZ METHOD

- Flutter of shaft-supported low aspect-ratio control surfaces p 667 A90-38912

REACTION BONDING

- Slip-cast hot isostatically pressed silicon nitride gas turbine components p 765 A90-44816

REACTION KINETICS

- Application of Lomax-Bailey implicit scheme to reactive flows p 367 A90-25861
Hypersonic reactive flow computations p 315 A90-27131

- HF shock tunnel facility for studying supersonic combustion
[AIAA PAPER 90-1551] p 600 A90-38693
On the use of external burning to reduce aerospace vehicle transonic drag
[AIAA PAPER 90-1935] p 656 A90-40562

- In-situ measurement, modelling and control of the imidization reaction in PMR-15 polyimide resin for aerospace structures p 941 A90-50066
Critical evaluation of Jet-A spray combustion using propane chemical kinetics in gas turbine combustion simulated by KIVA-II
[AIAA PAPER 90-2439] p 949 A90-50645

- Numerical modeling of supersonic turbulent reacting free shear layers p 174 A90-14197
Flammability testing of aircraft cabin materials p 328 N90-17611

- Low NO(x) potential of gas turbine engines
[NASA-TM-102452] p 345 N90-17636
Summary report of the Summer Conference of the DARPA-Materials Research Council
[AD-A217380] p 532 N90-20143

- On the use of external burning to reduce aerospace vehicle transonic drag
[NASA-TM-103107] p 588 N90-21762
Liquid fueled ramjet combustion instability: Acoustical and vortical interactions with burning sprays
[AD-A222752] p 767 N90-26104

- Flame extinction in compressible flow p 883 N90-26899

- Turbulent reacting flows and supersonic combustion
[AD-A221793] p 875 N90-26933
An investigation of solid-fuel, dual-mode combustion ramjets p 859 N90-27933

- Photo-sensitized ignition of hydrogen/oxygen mixtures for hypersonic flight vehicles p 877 N90-27935
Numerical simulations of flowfields in a central-dump ramjet combustor. 3: Effects of chemistry
[AD-A224145] p 933 N90-28573

REACTOR MATERIALS

- Study on application of ultrasonic wave measurement to creep-fatigue damage detection
[DE89-782317] p 774 N90-25361

READOUT

- Australian experience in flight recorder readout and analysis p 820 N90-27644
Automation of the readout, transcription and evaluation of digital flight data at DLR p 893 N90-27645

REAL GASES

- A study of three-dimensional supersonic flow of a real gas past axisymmetric bodies p 3 A90-10938
Hypervelocity real gas capabilities of GASL's expansion tube (HYPULSE) facility
[AIAA PAPER 90-1390] p 594 A90-37935

- Requirements in the 1990's for high enthalpy ground test facilities for CFD validation
[AIAA PAPER 90-1401] p 597 A90-38489
High enthalpy hypersonic wind tunnel F4: General description and associated instrumentation p 673 N90-24228

REAL TIME OPERATION

- Reflexive navigation for autonomous aircraft
[AIAA PAPER 89-2991] p 25 A90-10502
Trends in real-time flight systems p 25 A90-10572

- Real-time fault monitoring for aircraft applications using quantitative simulation and expert systems
[AIAA PAPER 89-3103] p 37 A90-10586
The NIMBLE Project - Real-time common LISP for embedded expert systems applications
[AIAA PAPER 89-3140] p 75 A90-10614

- Adapting an AI-based application from its LISP environment into a real-time embedded system
[AIAA PAPER 89-3142] p 75 A90-10616
Incorporation of alarm states into a real time decision making process p 76 A90-10620

- Real-time decision making for autonomous flight control
[SAE PAPER 891053] p 118 A90-14355
Recursive real-time identification of step-response matrices of helicopters for adaptive digital flight control p 195 A90-17703

- Real time winds data for flight management
[AIAA PAPER 90-0565] p 197 A90-19918
A GPS-based flight-control concept p 242 A90-21719

- Precision navigation using an integrated GPS-IMU system p 242 A90-21720
Advanced software for turbine blade processing
[SME PAPER MS89-330] p 274 A90-23694

- Realtime graphic flight simulations using multiple minicomputers p 351 A90-26203
McDonnell Douglas Helicopter Company Apache telemetry antenna analysis p 403 A90-28839

- Very-high-performance data acquisition/analysis/display/control systems based on the APTEC I/O computer p 458 A90-28852
Real-time test data processing system --- for helicopter flight testing p 458 A90-28860

- Real time estimation of aircraft angular attitude p 431 A90-30103
Real-time adaptive control of knowledge based avionics tasks p 460 A90-30764

- An integrated diagnostics approach to embedded and flight-line support systems p 460 A90-30767
The use of non-dedicated redundancy in the AMCAD fault tolerant control system p 461 A90-30793

- Advanced parameter identification techniques for near real time flight flutter test analysis
[AIAA PAPER 90-1275] p 494 A90-33899
An expert system for real-time aircraft monitoring
[AIAA PAPER 90-1311] p 545 A90-33921

- Preparations of the real-time data analyst to insure flight test safety p 488 A90-33925
Alternate table look-up routine for real-time digital flight simulation p 611 A90-35769

- Implementation of a transputer-based flight controller p 667 A90-38966
Partial similarity and a real-time model of twin-spool gas turbine p 654 A90-40512

- ATtHeS - A helicopter in-flight simulator for ACT testing p 643 A90-41727
Development and verification of software for flight safety critical strapdown systems p 694 A90-42454

- Development of a real-time aeroperformance analysis technique for the X-29A advanced technical demonstrator p 732 A90-44738

- A real time microcomputer implementation of sensor failure detection for turbofan engines p 745 A90-45414

- A multiprocessor implementation of real-time control for a turbojet engine p 746 A90-45415
Improving computer techniques for real-time digital flight simulation p 760 A90-45505

- An interfacing solution for real-time avionics development
[SAE PAPER 892354] p 738 A90-45508

- Real-time piloted simulation of fully automatic guidance and control for rotorcraft nap-of-the-earth (NOE) flight following planned profiles
[AIAA PAPER 90-3372] p 864 A90-47630

- Artificial intelligence (AI) based tactical guidance for fighter aircraft
[AIAA PAPER 90-3435] p 889 A90-47688
A new method of aircraft motion error extraction from radar raw data for real-time motion compensation p 824 A90-49675

- Security audit for embedded avionics systems p 857 A90-50649
Real-time support for high performance aircraft operation
[NASA-CR-185475] p 57 N90-10075

- Real-time flight test analysis and display techniques for the X-29A aircraft p 34 N90-10866
Flight test instrumentation and data processing at British Aerospace, Warton, U.K. p 59 N90-10887

- Real-time simulation of an F110/STOVL turbofan engine
[NASA-TM-102409] p 117 N90-12618
Preliminary experience with high response pressure measurements in a multistage, high speed compressor
[RAE-TM-P-1141] p 117 N90-12619

- A real-time wind model using digital data from aircraft
[RSRE-MEMO-4309] p 137 N90-13005
Computer-based tools for assisting air traffic controllers with arrivals flow management p 178 N90-13366

- A knowledge-based flight status monitor for real-time application in digital avionics systems
[NASA-TM-101710] p 217 N90-13995
Autonomous automatic landing through computer vision p 332 N90-16734

- Hypercube expert system shell-applying production parallelism
[AD-A215762] p 377 N90-16173
Delivery performance of conventional aircraft by terminal-area, time-based air traffic control: A real-time simulation evaluation p 404 N90-18378

- A rule-based paradigm for intelligent adaptive flight control p 434 N90-19238
Potential role of avionics in escape systems p 483 N90-20060

- Airplane takeoff and landing performance monitoring system
[NASA-CASE-LAR-13734-1-CU] p 526 N90-20096
A data acquisition parallel bus for wind tunnels at ARL (Aeronautical Research Laboratory)
[AD-A218052] p 526 N90-20098

- The Real Time Display Builder (RTDB) p 546 N90-20656
Rule-based mechanisms of learning for intelligent adaptive flight control p 521 N90-20939

- Perspectives on the use of rule-based control p 521 N90-20940
Inertial navigation system simulator: Behavioral specification, revision
[AD-A219294] p 578 N90-22554

- Model-based method for terrain-following display design
[AD-A219302] p 583 N90-22563
Six-degree-of-freedom aircraft simulation with mixed-data structure using the applied dynamics simulation language, ADSIM p 613 N90-23067

- Real-time closed-loop simulation and upset evaluation of control systems in harsh electromagnetic environments p 613 N90-23069
A comparison of lightning network data with surface weather observations p 692 N90-23832

- AIRNET: A real-time communications network for aircraft
[NASA-CR-186140] p 690 N90-24514
Evaluation of various thrust calculation techniques on an F404 engine p 735 N90-25134

- Real-time adaptive aircraft scheduling
[NASA-CR-177558] p 820 N90-27669

- Expert system for pilot assistance: The challenge of an intensive prototyping
[ETN-90-97274] p 825 N90-27674
- An ultrasonic system for in-service non-destructive inspection of composite structures p 885 N90-28076
- In-service inspection of composite components on aircraft at depot and field levels p 885 N90-28078
- Inspection system for in-situ inspection of aircraft composite structures p 886 N90-28091
- Real-time aerodynamic heating and surface temperature calculations for hypersonic flight simulation
[NASA-TM-4222] p 959 N90-28815
- An expert system to perform on-line controller restructuring for abrupt model changes
[NASA-TM-103609] p 964 N90-29121
- Distributed control architecture for CNI preprocessors p 917 N90-29356
- The function of the Interactive Model Assembly Program (IMAP) for a flight simulator
[NAL-TR-1034] p 939 N90-29412
- Real-time multi-plot graphics system
[NASA-CR-4304] p 965 N90-29919
- Formal design and verification of a reliable computing platform for real-time control. Phase 1: Results
[NASA-TM-102716] p 965 N90-29965
- REATTACHED FLOW**
- A viscous package for attached and separated flows on swept and tapered wings p 146 A90-16771
- Structure of a reattaching supersonic shear layer p 555 A90-36252
- Wall pressure fluctuations in the reattachment region of a supersonic free shear layer
[AIAA PAPER 90-1461] p 561 A90-38618
- Supersonic flow over an axisymmetric backward-facing step
[AIAA PAPER 90-1580] p 566 A90-38717
- Simultaneous detection of separation and transition in surface shear layers p 72 N90-10368
- Method and apparatus for detecting laminar flow separation and reattachment
[NASA-CASE-LAR-13952-1-SB] p 455 N90-19534
- RECEIVERS**
- Signal processing in a digital GPS receiver p 128 A90-14006
- Ridge regression processing p 489 N90-20931
- Feasibility of using frequency offset on very high frequency air/ground voice channels
[DOT/FAA/CT-TN89/71] p 542 N90-21248
- Miniaturization of flight deflection measurement system
[NASA-CASE-LAR-13628-1] p 689 N90-23707
- RECESSES**
- Effect of a recess on the aerodynamic characteristics of very blunt bodies at supersonic velocities p 299 A90-24167
- RECIRCULATIVE FLUID FLOW**
- A full scale, VSTOL, ground environment test facility p 58 A90-12631
- Experimental investigations on the spatial and time-dependent structure of part-load recirculations in centrifugal pumps p 83 A90-13788
- An experimental study on flowfields in a dual inlet swirl-dump combustor p 471 A90-33283
- Interference between a vortex filament and shock waves in free flow and in nonisobaric jets p 804 A90-46550
- Composite reduced Navier Stokes procedures for flow problems with strong pressure interactions
[AD-A19621] p 689 N90-23687
- RECOMBINATION REACTIONS**
- Nonequilibrium recombination-dissociation boundary layer flows along arbitrarily-catalytic hypersonic vehicles
[AIAA PAPER 90-0055] p 161 A90-19652
- RECOMMENDATIONS**
- Program plan: International aircraft operator data base
[IAR-90-1] p 783 N90-25697
- RECONNAISSANCE**
- Design of a natural laminar flow airfoil for an unmanned aircraft
[PD-CF-9004] p 499 N90-20975
- RECONNAISSANCE AIRCRAFT**
- System optimization for maximizing reconnaissance mission range of a hypersonic cruise vehicle
[AIAA PAPER 90-3292] p 837 A90-48876
- Unmanned helicopters for battlefield and maritime surveillance p 920 A90-51899
- Pilotless airplanes
[AD-A211719] p 103 N90-11734
- Global Sentry: NASA/USRA high altitude reconnaissance aircraft design, volume 2
[NASA-CR-186820-VOL-2] p 736 N90-25971
- RECONSTRUCTION**
- Fatigue analysis and reconstruction of helicopter load spectra p 206 N90-14304

RECORDS MANAGEMENT

- Past, present and future: Aircraft integrated monitoring systems: An ever-developing technology p 848 N90-27618

RECOVERY

- Stall and recovery in multistage axial flow compressors p 428 N90-18429

RECOVERY PARACHUTES

- A summary of spin-recovery parachute experience on light airplanes
[AIAA PAPER 90-1317] p 519 A90-33926

RECOVERY VEHICLES

- A self-compensating aircraft recovery system (SCARS)
[AIAA PAPER 90-3273] p 818 A90-48864

RECRYSTALLIZATION

- Recrystallization behavior of nickel-base single crystal superalloys p 440 A90-27681

RECTANGULAR PANELS

- Experimental study on the buckling and postbuckling of carbon fibre composite panels with and without interply disbonds p 130 A90-15355
- Application of the dynamic stiffness method to the free and forced vibrations of aircraft panels p 270 A90-20599

RECTANGULAR PLANFORMS

- An investigation of the buffet excitation parameter p 473 A90-33368
- Effect of blade planform variation on a small-scale hovering rotor
[NASA-TM-4146] p 173 N90-14186

RECTANGULAR PLATES

- Recent studies on the behaviour of interference fit pins in composite plates p 132 A90-16320
- Vibrations of rectangular plates with moderately large initial deflections at elevated temperatures using finite element method
[AIAA PAPER 90-1125] p 451 A90-29429
- Dynamic analysis of airport pavement p 593 A90-36418
- Experiments on the active control of the transmission of sound through a clamped rectangular plate p 695 A90-41109

RECTANGULAR WINGS

- Investigations of modifications to improve the spin resistance of a high-wing, single-engine, light airplane
[SAE PAPER 891039] p 118 A90-14345
- Aeroelastic characteristics of wings in subsonic flow p 102 A90-14615
- Estimate of loads during wing-vortex interactions by Munk's transverse-flow method p 159 A90-19391
- Viscous supersonic flow computations over a delta-rectangular wing with slanting surfaces
[AIAA PAPER 90-0419] p 166 A90-19841
- Prediction of tip-clearance effects on a wing by the panel method p 307 A90-25871
- Effect of structural anisotropy on the dynamic characteristics of the wing and critical flutter speed p 386 A90-26985
- Effects of spoiler surfaces on the aeroelastic behavior of a low-aspect-ratio rectangular wing
[AIAA PAPER 90-0981] p 391 A90-29371
- Nonlinear stall flutter and divergence analysis of cantilevered graphite/epoxy wings
[AIAA PAPER 90-0983] p 450 A90-29373
- A numerical method in aeroelasticity for wings with separation at large angle of attack p 557 A90-37209
- Unsteady lift development on a constantly accelerated rectangular wing
[AIAA PAPER 90-1633] p 569 A90-38762
- Lift response of a rectangular wing undergoing a step change in forward speed p 620 A90-39801
- Self-induced roll oscillations of low-aspect-ratio rectangular wings
[AIAA PAPER 90-2811] p 753 A90-45151
- Modeling the wake as a continuous vortex sheet in a potential-flow solution using vortex panels
[AD-A216220] p 371 N90-18016
- Effects of spoiler surfaces on the aeroelastic behavior of a low-aspect-ratio rectangular wing
[NASA-TM-102622] p 846 N90-27700

REDUCED GRAVITY

- Combustion Experiments During KC-135 Parabolic Flights
[ESA-SP-1113] p 368 N90-16958

REDUCED ORDER FILTERS

- Modal aggregation and its application in flight mechanics p 196 A90-18595
- Reduced size first-order subsonic and supersonic aeroelastic modeling
[AIAA PAPER 90-1154] p 390 A90-29366
- Reduced-order aeroelastic models via dynamic residualization p 493 A90-33412
- LQG/LTR controller design using a reduced order model p 964 A90-52877

- The determination of third order linear models from a seventh order nonlinear jet engine model p 964 A90-52881

REDUNDANCY

- Combat aircraft control requirements p 934 N90-28515

REDUNDANT COMPONENTS

- The use of non-dedicated redundancy in the AMCAD fault tolerant control system p 461 A90-30793

REENTRY GUIDANCE

- Multiple-step terminal control with parameter identification and prediction during flight vehicle descent p 872 A90-46484

REENTRY VEHICLES

- Infrared radiation model for aircraft and reentry vehicle p 77 A90-10169
- Geometric modelling of complex aerodynamic surfaces and three-dimensional grid generation p 311 A90-26545
- Development and operating experience on a zinc-sulfide window for the Infrared Instrumentation System (IRIS) --- for gathering data on reentry vehicles p 505 A90-34584
- Verification of aerothermodynamic codes by means of a winged experimental re-entry vehicle p 354 N90-16842

REFERENCE SYSTEMS

- A precise flight reference system for evaluating airborne navigation aids p 27 A90-12752
- Development of common GPS and GLONASS avionics standards p 821 A90-46391

REFLECTOR ANTENNAS

- An array-fed reflector antenna with built-in calibration facility p 402 A90-27781

REFRACTION

- Predicted and measured boundary layer refraction for advanced turboprop propeller noise
[NASA-TM-102365] p 379 N90-17413

REFRACTIVITY

- Recent flow visualization studies in the 0.3-m TCT p 122 N90-12528

REFRACTORY COATINGS

- TBCs for better engine efficiency --- thermal barrier coatings p 203 A90-17294

REFRACTORY MATERIALS

- High service temperature, damage tolerant prepreg systems based on cyanate chemistry p 941 A90-50069
- High temperature adhesives commercially available to be used for extended time with PMR15 laminates p 943 A90-50125
- Development of a high toughness heat resistant 177 C (350 F) curing film adhesive for aerospace bonding applications - FM 377 adhesive p 955 A90-50126
- Process optimization of high temperature composite materials p 943 A90-50130
- Chemical vapor deposition of Hf/Si compounds as a high temperature coating for carbon/carbon composites p 955 A90-50159
- The application of 'PT' resins to high temperature aerospace structures p 949 A90-50230
- Attachment of lead wires to thin film thermocouples mounted on high temperature materials using the parallel gap welding process
[NASA-TM-102442] p 543 N90-21361
- Metal matrix composites and powder processing for aero-engine applications
[PNR90617] p 767 N90-26087
- The stress and temperature dependence of creep in an Al-2.0 wt percent Li alloy
[AD-A223676] p 953 N90-29480

REFUELING

- Experimental evaluation of impedance control for robotic aircraft refueling
[AD-A215532] p 337 N90-16755

REGENERATIVE COOLING

- Development and fabrication of structural components for a scramjet engine
[NASA-CR-181945] p 510 N90-20088

REGRESSION ANALYSIS

- Estimating the relationships between the state of the art of technology and production cost for the US aircraft
[AD-A212127] p 82 N90-12495
- On the application of modified stepwise regression for the estimation of aircraft stability and control parameters
[REPT-8905] p 198 N90-13400

REGULATIONS

- Castings Airworthiness
[AGARD-R-762] p 64 N90-10231
- The question of the casting factor p 64 N90-10238
- Fire hardening of an aircraft passenger cabin p 328 N90-17606
- Advanced materials for interior and equipment related to fire safety in aviation p 328 N90-17608
- New materials for civil aircraft furnishing p 328 N90-17609

Flammability testing of aircraft cabin materials
p 328 N90-17611

Problems related to aircraft noise in Switzerland
p 698 N90-24871

The new US flight recorder regulations
p 849 N90-27642

System reliability optimization of aircraft wings
p 923 N90-28536

Tests for aircraft interior materials in fire accident
[LR-622] p 914 N90-29337

REGULATORY MECHANISMS (BIOLOGY)
Neurocontrol systems and wing-fluid interactions
underlying dragonfly flight p 434 N90-19240

REINFORCED PLATES
Postbuckling behavior of laminated plates using a direct
energy-minimization technique p 209 A90-17993
Flutter analysis of composite panels in supersonic
flow
[AIAA PAPER 90-1180] p 450 A90-29379
Manufacture of honeycomb p 538 A90-33704
A study of the stability and thermal stability of complex
reinforced structures p 880 A90-46541

REINFORCED SHELLS
Automation of the development of a finite element model
for shells of the wing type p 364 A90-24118
Response of orthogonally stiffened cylindrical shell
panels p 603 A90-36285
A study of the stability and thermal stability of complex
reinforced structures p 880 A90-46541
Optimization of the shape of a sealed shell and of the
size and location of its reinforcements p 957 A90-50773

REINFORCING FIBERS
Metal laminates for aerospace applications
p 874 A90-48997
Chemical resistance of carbon fiber reinforced polyether
ether ketone and polyphenylene sulfide composites
p 944 A90-50142
Composites for aerospace application from Kevlar
aramid reinforced PEKK thermoplastic
p 946 A90-50176
Spectra composite enhances portability and survivability
of electronic equipment p 947 A90-50189
Rolling of ARALL laminates (an alternative method for
post-stretching ARALL laminates)
[LR-560] p 135 N90-12778
Reinforcing fibers and technology development for resin
composites. Consequences for aircraft structures
[FOA-C-20777-2.5] p 876 N90-27883

REINFORCING MATERIALS
The application of cast SiC/Al to rotary engine
components
[NASA-CR-179610] p 192 N90-13385

RELAXATION (MECHANICS)
Viscoelastic relaxation in bolted thermoplastic
composite joints p 945 A90-50158

RELAXATION METHOD (MATHEMATICS)
Calculation of flows of an ideal gas in nozzles and jets
by the relaxation method p 296 A90-24109
Impact of multigrid smoothing analysis on
three-dimensional potential flow calculations
p 449 A90-29147
Inviscid and viscous flows in transonic and supersonic
cascades using an implicit upwind relaxation algorithm
[AIAA PAPER 90-2128] p 825 A90-42034
Multigrid accelerated relaxation solution of transonic full
potential flow equation
[PD-CF-8942] p 480 N90-20951

RELIABILITY
The RB199: An in-service success
[PNR90544] p 114 N90-11746
Software fault tolerance
[RSRE-MEMO-4237] p 99 N90-12575
LORAN C stability integrity assurance
[AD-A212663] p 177 N90-13364
Review of the Aerospace Safety Advisory Panel report for
NASA fiscal year 1990 authorization
[GPO-24-234] p 177 N90-14213
RADC fault tolerant system reliability evaluation facility
[AD-A215298] p 377 N90-17348
Measurement and computer simulation of antennas on
ships and aircraft for results of operational reliability
p 370 N90-17936
IAPSA 2 small-scale system specification
[NASA-CR-182006] p 695 N90-24103
Hardware and software reliability estimation using
simulations
[NASA-CR-186637] p 780 N90-25580
Inspection reliability
p 885 N90-28072
STOVL fighter propulsion reliability, maintainability, and
supportability characterization
[AD-A224221] p 933 N90-28574
Reliability and performance of friction measuring tires
and friction equipment correlation
[AD-A223694] p 939 N90-29408

RELIABILITY ANALYSIS

An experimental investigation of fault tolerant software
structures in an avionics application
[AIAA PAPER 89-3082] p 74 A90-10568
Aerospace structures supportability
[SAE PAPER 891058] p 129 A90-14360
Methods of safety analysis for Beech Model 2000 -
Starship 1
[SAE PAPER 891064] p 101 A90-14364
Estimation of the technical risk criterion in selecting the
operating parameters of aircraft gas turbine engines
p 110 A90-14570
Applied technology in gas turbine aircraft engine
development p 112 A90-16001
Helicopter transmissions - Design for safety and
reliability p 270 A90-20608
Aerospace materials research opportunities
p 267 A90-23177
Reliability evaluation system for ceramic gas turbine
components p 444 A90-27678
Three approaches to reliability analysis
p 452 A90-30706
What can we do after we've done it all? --- total quality
management and leadership philosophy in practice
[AIAA PAPER 89-3209] p 549 A90-31696
Onboard maintenance system testing - The Boeing
747-400 Central Maintenance Computer
[AIAA PAPER 90-1303] p 505 A90-33917
Electrical power systems for high Mach vehicles
p 586 A90-38129
Considerations of reliability design for rotorcraft
p 680 A90-39977
Designing rotorcraft dynamic components to reliability
requirements p 641 A90-39978
Application of fracture mechanics to microscale
phenomena in electronic assemblies
p 684 A90-41334
Power system for 21st century fighter aircraft
[SAE PAPER 892253] p 746 A90-45455
Subsystem thermal integration - A new challenge to the
aircraft designer
[AIAA PAPER 90-3274] p 836 A90-48865
Design of aircraft wings subjected to gust loads - A
system reliability approach p 958 A90-52044
Correlation/validation of finite element code analyses
for vibration assessment of avionic equipment
[AD-A220393] p 654 N90-23398
Reliability model generator specification
[NASA-CR-182005] p 780 N90-25638
Formal design and verification of a reliable computing
platform for real-time control. Phase 1: Results
[NASA-TM-102716] p 965 N90-29965

RELIABILITY ENGINEERING

New progress in airframe durability requirements
p 246 A90-22001
Mechanical considerations for reliable interfaces in next
generation electronics packaging p 453 A90-30813
Fatigue methodology III: Proceedings of the AHS
National Technical Specialists' Meeting on Advanced
Rotorcraft Structures, Scottsdale, AZ, Oct. 3-5, 1989
p 641 A90-39976
Full authority digital electronic engine control system
provides needed reliability
[AIAA PAPER 90-2037] p 658 A90-40606
Toward total quality in industry p 684 A90-41768
Co-development of CT7-6 engines - A continued tradition
in technology and reliability p 665 A90-42485
Combining thermal and high level acoustics
p 770 A90-43729
VSCF cycloconverter reliability review of the 30/40 KVA
F/A-18 electrical generating system --- variable speed,
constant frequency
[SAE PAPER 892228] p 746 A90-45444
Development and applications of reliability and
maintainability design criteria in military aircraft
[ETN-89-95208] p 107 N90-12591
Flanged joints of aeroengines
[PNR90594] p 116 N90-12609
Aviation Engine Test Facilities (AETF) fire protection
study
[AD-A211483] p 134 N90-12777
Laboratory test methodology for evaluating the effects
of electromagnetic disturbances on fault-tolerant control
systems
[NASA-TM-101665] p 217 N90-14061
NDT in aerospace: The next decade (1990's)
[PNR90628] p 777 N90-26348
Smart microsensors for high temperature applications,
phase 1
[AD-A224151] p 959 N90-28828

RELIEF MAPS
Digital map reader for helicopters p 653 A90-42448

RELUCTANCE
A very high speed switched-reluctance starter-generator
for aircraft engine applications p 452 A90-30791

REMOTE CONTROL

Priorities for high-lift testing in the 1990s
[AIAA PAPER 90-1413] p 596 A90-37950
Pilotless airplanes
[AD-A211719] p 103 N90-11734
X.2 limited flight test plan
[AD-A214412] p 249 N90-15099
Visualization of three dimensional data
p 782 N90-25553

REMOTE SENSING

The remote sensing of temperature in gas turbine engine
components using epithermal neutrons
p 70 A90-12630
Atmospheric conditions producing aircraft icing on 24-25
January 1989 - A case study utilizing combinations of
surface and remote sensors
[AIAA PAPER 90-0197] p 175 A90-19734
Airborne MSS for land cover classification II
p 737 A90-43376
The Radarsat system --- Canada/U.S. program for
launching remote sensing satellite with SAR
p 873 A90-49671
Remote sensing techniques of the Wave Propagation
Laboratory for the measurement of supercooled liquid
water: Applications to aircraft icing
[PB89-208102] p 24 N90-10842
Global stratospheric change: Requirements for a
Very-High-Altitude Aircraft for Atmospheric Research
[NASA-CP-10041] p 185 N90-14220
The collection of non-conus aircraft icing data along with
an identification of the geographical areas of potential
severe icing and a study of a method of remote determining
atmospheric icing data
[AD-A215055] p 323 N90-16724
Airborne CO2 Doppler lidar for wind shear detection
p 849 N90-27640

REMOTE SENSORS

The development of a high response aerodynamic
wedge probe and use on a high-speed research
compressor
[PNR90598] p 116 N90-12613

REMOTELY PILOTED VEHICLES

Wing-section effects on the flight performance of a
remotely piloted vehicle p 29 A90-11007
The Pointer - Test and evaluation of the tiltrotor UAV
--- unmanned aerial vehicle p 406 A90-28170
Comparison of test signals for aircraft frequency domain
identification p 490 A90-33057
Flight test and numerical analysis of a half-scale
Unmanned Air Vehicle
[AIAA PAPER 90-1260] p 494 A90-33890
Wind-tunnel and flight-test investigation of the exdrone
remotely piloted vehicle configuration
[AIAA PAPER 90-1261] p 494 A90-33891
A concept study on the use of remotely piloted, sub-scale
aircraft for high Reynolds number testing
[AIAA PAPER 90-1263] p 494 A90-33892
Boeing Condor raises UAV performance levels
p 496 A90-34028
Flight testing of the Low Altitude/Airspeed Unmanned
Research Aircraft (LAURA)
[AIAA PAPER 90-1262] p 579 A90-36026
Preliminary design of a long-endurance Mars aircraft
[AIAA PAPER 90-2000] p 674 A90-40587
Development of a heavy fuel engine for an unmanned
air vehicle
[AIAA PAPER 90-2170] p 662 A90-42056
Reduced order INS/GPS guided unmanned air vehicle
study p 726 A90-43707
Thick airfoil designs for a HALE vehicle --- High Altitude
Long Endurance
[AIAA PAPER 90-3036] p 791 A90-45875
The design of a low Reynolds number RPV
p 828 A90-46385
Captive carry testing of remotely piloted vehicles
p 828 A90-46386
Flight testing Navy low Reynolds Number (LRN)
unmanned aircraft p 828 A90-46387
An unmanned air vehicle concept with tipjet drive
p 830 A90-46951
CONDOR - high altitude long endurance (HALE)
autonomously piloted vehicle (APV)
[AIAA PAPER 90-3279] p 836 A90-48866
Expert system technology applied to the automatic
control of multiple unmanned aerial vehicles
[AIAA PAPER 90-3280] p 892 A90-48867
All fabric N-wing unmanned powered flight systems
[AIAA PAPER 90-3282] p 836 A90-48869
The design of an airfoil for a high-altitude,
long-endurance remotely piloted vehicle
p 104 N90-12545
Guidance and Control of Unmanned Air Vehicles
[AGARD-CP-436] p 260 N90-15924
Synthesis of control law, on a RPV, in order to minimize
the number of sensors p 260 N90-15925
Mirach 100 flight control system p 260 N90-15926

- Unmanned air vehicles payloads and sensors p 251 N90-15930
- Technology and evaluation of unmanned air vehicles p 252 N90-15934
- Aerodynamic analysis of a US Navy and Marine Corps unmanned air vehicle [AD-A218282] p 498 N90-20077
- The MANTA: An RPV design to investigate forces and moments on a lifting surface [NASA-CR-186227] p 499 N90-20971
- Preliminary design of a long-endurance Mars aircraft [NASA-CR-185243] p 588 N90-21763
- Initial flight test of half-scale unmanned air vehicle [AD-A219584] p 648 N90-23388
- Static wind-tunnel and radio-controlled flight test investigation of a remotely piloted vehicle having a delta wing planform [NASA-TM-4200] p 632 N90-24238
- The Stealth biplane: A proposal in response to a low Reynolds Number station keeping mission [NASA-CR-186680] p 734 N90-25127
- The SKY SHARK: An RPV designed to investigate the pressure distribution on a lifting surface [NASA-CR-186222] p 844 N90-26824
- The DELTA MONSTER: An RPV designed to investigate the aerodynamics of a delta wing platform [NASA-CR-186226] p 924 N90-29381
- REMOVAL**
- The future of aircraft paint removal methods [AD-A214946] p 356 N90-16936
- Robots for aircraft coatings removal: Parameters and requirements [DE90-009429] p 609 N90-22048
- Mechanical paint removal techniques for aircraft structures [NIAR-90-12] p 775 N90-26166
- REPLACING**
- Scientific justification and development plan for a mid-sized jet research aircraft [PB89-208995] p 103 N90-11731
- What should be done with those noisy old aircraft [PNR90562] p 107 N90-12593
- REQUIREMENTS**
- CASTING factors imposed by the French regulation for foundry castings used in military aircraft p 64 N90-10233
- Meeting review: The Second NCAR (National Center for Atmospheric Research) Research Aircraft Fleet Workshop [PB89-200901] p 137 N90-12113
- Fire hardening of aircraft through upgrades of materials and designs p 327 N90-17605
- Development of a mass averaging temperature probe p 427 N90-18418
- A study of the technology required for advanced vertical take-off aircraft [ETN-90-96786] p 650 N90-24268
- Program plan: International aircraft operator data base [IAR-90-1] p 783 N90-25697
- Cognitive requirements for aircraft navigation [NASA-CR-186933] p 824 N90-26804
- RESCUE OPERATIONS**
- Self-retracting helicopter rescue hoist p 829 A90-46935
- Aircraft internal fires p 326 N90-17593
- RESEARCH AIRCRAFT**
- A comfortable and universal data-acquisition-system for flight research p 39 A90-12204
- In-flight flow field analysis on the NASA F-18 high alpha research vehicle with comparisons to ground facility data [AIAA PAPER 90-0231] p 163 A90-19745
- HTTB - Industry's first STOL test bed --- High Technology Test Bed program for future tactical aircraft requirements p 414 A90-31246
- Comparison between experimental and numerical results for a research hypersonic aircraft p 395 A90-31278
- AIAA/SFTE/DGLR/SETP, Biannual Flight Test Conference, 5th, Ontario, CA, May 22-24, 1990, Technical Papers p 493 A90-33886
- Flight testing of the Low Altitude/Airspeed Unmanned Research Aircraft (LAURA) [AIAA PAPER 90-1262] p 579 A90-36026
- VTOL military research aircraft --- Book p 828 A90-46002
- The Hiller X-18 experimental aircraft - Lessons learned [AIAA PAPER 90-3203] p 834 A90-48832
- The Canadair CL-84 experimental aircraft - Lessons learned [AIAA PAPER 90-3205] p 834 A90-48833
- The Curtiss-Wright X-19 experimental aircraft - Lessons learned [AIAA PAPER 90-3206] p 834 A90-48834
- Ryan X-13 experimental aircraft - Lessons learned [AIAA PAPER 90-3236] p 834 A90-48846

- The AVRO VZ-9 experimental aircraft - Lessons learned [AIAA PAPER 90-3237] p 835 A90-48847
- CONDOR - high altitude long endurance (HALE) autonomously piloted vehicle (APV) [AIAA PAPER 90-3279] p 836 A90-48866
- Short take-off and landing maneuver technology demonstrator (STOL/MTD) lessons learned - Integrated flight/p propulsion control (IFPC) [AIAA PAPER 90-3307] p 868 A90-48888
- A hypersonic research vehicle to develop scramjet engines [AIAA PAPER 90-3232] p 839 A90-49115
- STOVL aircraft simulation for integrated flight and propulsion control research [NASA-TM-102419] p 193 N90-13389
- Longitudinal stability and control characteristics of the Quiet Short-Haul Research Aircraft (QSRA) [NASA-TP-2965] p 349 N90-17639
- Aerosol separator for use in aircraft [PB90-142217] p 611 N90-22155
- Lateral-directional stability and control characteristics of the Quiet Short-Haul Research Aircraft (QSRA) [NASA-TM-102250] p 671 N90-23413
- Experimental aerothermodynamic research of hypersonic aircraft [NASA-CR-186903] p 721 N90-25954
- An automated calibration laboratory for flight research instrumentation: Requirements and a proposed design approach [NASA-TM-101719] p 781 N90-26564
- Aerodynamic parameters of High-Angle-of attack Research Vehicle (HARV) estimated from flight data [NASA-TM-102692] p 936 N90-28578
- A knowledge-based system design/information tool [NASA-CR-4316] p 965 N90-29143
- Procedure for calibrating fly-by-wire control chains of the flying testbed ATTAS [DLR-MITT-90-02] p 936 N90-29401
- The signals of an ice warning device in dependence on total water content and normalized icing degree [ESA-TT-1207] p 963 N90-29692
- RESEARCH AND DEVELOPMENT**
- Natural laminar flow research for subsonic transport aircraft in the FRG p 2 A90-10137
- Highly loaded axial flow compressors - History and current developments p 44 A90-12503
- Swedish philosophy in aeroengine development p 44 A90-12504
- Keepers of the flame --- scramjet development programs p 141 A90-16300
- Oils for flight turbine engines - Research and development in the 90s p 266 A90-21473
- Advanced Traffic Management System automation p 330 A90-25565
- Development of monolithic and composite ceramics at Allied-Signal Aerospace Company p 599 A90-35950
- Development of ceramic components for high-temperature gas turbines p 602 A90-35951
- Research department fluid mechanics - Scientific report (1988) --- Book p 603 A90-36538
- Technological preparations of civil aircraft programs p 617 A90-41110
- Euromart - The European aviation research and technology program p 617 A90-41112
- The development of a probabilistic turbine rotor design system [AIAA PAPER 90-2176] p 662 A90-42060
- IHPDET technology mission payoffs at the component level - A look at Phase II technologies --- Integrated High Performance Turbine Engine Technology [AIAA PAPER 90-2404] p 701 A90-42794
- The propan ... What future now? p 744 A90-43763
- Airbus technologies - An evolutionary process p 902 A90-52699
- The NASA experience in aeronautical R and D: Three case studies with analysis [AD-A211486] p 82 N90-12496
- Acquisition and recording an AMX A/C. Aeritalia experience and present trends [ETN-89-95217] p 109 N90-12598
- Gas turbine performance analysis [PNR90599] p 116 N90-12614
- Other cryogenic wind tunnel projects p 263 N90-15948
- Development of a mass averaging temperature probe p 427 N90-18418
- Calendar of selected aeronautical and space meetings [AGARD-CAL-90/1] p 464 N90-19060
- The automation management to support research and development p 612 N90-22978
- Langley aerospace test highlights, 1989 [NASA-TM-102631] p 699 N90-24221
- Research at NASA's NFAC wind tunnels [NASA-TM-102827] p 702 N90-25933

- Wright Research and Development Center test facilities handbook [AD-A222582] p 762 N90-26020
- R and D aspects of the future operational concept of the BFS p 826 N90-27679
- PHARE: Concept and programme p 827 N90-27690
- Integration of flight management and air traffic management systems [RAE-TM-FM-41] p 827 N90-27693
- RESEARCH FACILITIES**
- A test matrix sequencer for research test facility automation [AIAA PAPER 90-2386] p 759 A90-42791
- Basic aerodynamic research facility for comparative studies of flow diagnostic techniques p 122 N90-12526
- RADC fault tolerant system reliability evaluation facility [AD-A215298] p 377 N90-17348
- Compressor performance tests in the compressor research facility p 427 N90-18428
- Proceedings of the 13th International Congress on Instrumentation in Aerospace Simulation Facilities [EOARD-LR-89-069] p 527 N90-21046
- Aeropropulsion facilities configuration control: Procedures manual [NASA-TM-102541] p 543 N90-21399
- Langley aerospace test highlights, 1989 [NASA-TM-102631] p 699 N90-24221
- Structural dynamics branch research and accomplishments [NASA-TM-102488] p 778 N90-26373
- Dynamic ground effects p 922 N90-28531
- Study of ground effects on flying scaled models p 922 N90-28532
- RESEARCH MANAGEMENT**
- The NASA experience in aeronautical R and D: Three case studies with analysis [AD-A211486] p 82 N90-12496
- Aircraft technology management and the related significance of the supercomputer p 612 N90-22975
- The Federal Aviation Administration plan for research, engineering and development. Volume 1: Program plan [AD-A221263] p 783 N90-25930
- The Federal Aviation Administration plan for research, engineering and development. Volume 2: Project descriptions [AD-A221264] p 783 N90-25931
- RESEARCH VEHICLES**
- A dynamic inversion based control law with application to the high angle-of-attack research vehicle [AIAA PAPER 90-3407] p 864 A90-47662
- Validation of the F-18 high alpha research vehicle flight control and avionics systems modifications [NASA-TM-101723] p 924 N90-28542
- Aerodynamic parameters of High-Angle-of attack Research Vehicle (HARV) estimated from flight data [NASA-TM-102692] p 936 N90-28578
- RESIDUAL STRENGTH**
- The effect of impact loading on residual strength of CFRP composite beams p 208 A90-17683
- Impact damage and residual strength analysis of composite panels with bonded stiffeners --- for primary aircraft structures p 642 A90-40130
- Durability and damage tolerance of graphite/epoxy honeycomb structures p 942 A90-50085
- Boeing/NASA composite components flight service evaluation [NASA-CR-181898] p 601 N90-22609
- RESIDUAL STRESS**
- Use of unbalanced laminates as a screening method for microcracking p 948 A90-50217
- Nondestructive measurement of residual stresses in aircraft transparencies [AD-A218680] p 689 N90-23762
- RESIDUES**
- Effect of pressure and temperature on residue formation in aviation kerosenes p 203 A90-17281
- RESIN MATRIX COMPOSITES**
- Thermoplastic composite fighter forward fuselage p 81 A90-14659
- Resin transfer molding of composite structures p 270 A90-20264
- The use of fibre reinforced thermoplastics for helicopter primary structures and their engineering substantiation p 441 A90-28191
- Design and fabrication of a prototype resin matrix composite interceptor structure [AIAA PAPER 90-1004] p 442 A90-29275
- Toughened thermosets for damage tolerant carbon fiber reinforced composites p 443 A90-29825
- Automated R.T.M. for an airframe component --- Resin Transfer Molding p 534 A90-31881
- Thermoplastic composites, past, present and future p 529 A90-31882

- Structural components of fiber-reinforced thermoplastics p 676 A90-41111
- Composites applications - The future is now p 678 A90-42372
- International SAMPE Symposium and Exhibition, 35th, Anaheim, CA, Apr. 2-5, 1990, Proceedings, Books 1 & 2 p 940 A90-50056
- Innovative design concepts for thermoplastic composite materials p 940 A90-50059
- Repair of thermoplastic composite structures by fusion bonding p 941 A90-50060
- High service temperature, damage tolerant prepreg systems based on cyanate chemistry p 941 A90-50069
- The effect of jet fuel absorption on advanced aerospace thermoset and thermoplastic composites p 942 A90-50082
- Toughened cyanates for aerospace applications p 942 A90-50088
- Automated prepreg tow placement for composite structures p 954 A90-50113
- Injectable bismaleimide systems p 943 A90-50132
- Improved melt flow and physical properties of Mitsui Toatsu's LARC-TPI 1500 series polyimide p 943 A90-50134
- Improved damage tolerance by controlling thermoplastic solubility in thermoset composites p 944 A90-50138
- Improved thermal performance using allylindole-imides p 946 A90-50175
- Novel composite surfacing film p 948 A90-50212
- RESINS**
- Design of an aero-engine thrust reverser blocker door p 467 A90-31651
- Elevator tab assembly producibility study (IAR-89-16) p 734 N90-25133
- RESISTANCE HEATING**
- Grid and mesh patterned electrically conductive coatings in IR systems p 503 A90-32028
- RESOLUTION**
- Measurement resolution of noise directivity patterns from acoustic flight tests (NASA-TM-4134) p 79 N90-10679
- RESONANCE TESTING**
- Air resonance stability of hingeless rotors in forward flight p 590 A90-38519
- RESONANT FREQUENCIES**
- Flutter of cascade blades composed of blades having arbitrarily different natural frequencies p 42 A90-11798
- Acoustic resonance in centrifugal compressors induced by interaction between rotor and stator p 78 A90-11803
- Minimum weight design of rotorcraft blades with multiple frequency and stress constraints p 335 A90-25304
- The effect of structural variations on the dynamic characteristics of helicopter rotor blades (AIAA PAPER 90-1161) p 450 A90-29396
- Sensitivity analysis using resonance and anti-resonance frequencies - A guide to structural modification p 536 A90-33396
- A study of the influence of predeformations on the vibrations of blades p 585 A90-35673
- High-quality approximation of eigenvalues in structural optimization p 603 A90-36277
- Application of mathematical modeling to the study of rigid helicopter rotors p 643 A90-41738
- A comprehensive approach to coupled rotor-fuselage dynamics p 646 A90-42460
- Theoretical and experimental determination of natural frequencies of laced blading p 878 A90-46037
- Vibration analysis of laced blades p 878 A90-46186
- Numerical analysis of natural vibrations of an airplane with symmetrically variable geometry wing p 860 A90-46715
- Forcing function effects on rotor row unsteady aerodynamic response in a multistage compressor p 573 N90-22536
- RESOURCES MANAGEMENT**
- Aircraft subsystem waste energy recovery and management (SAE PAPER 901218) p 840 A90-49293
- RETARDING**
- Infrared sources of jet propulsion system and their suppression p 252 A90-22614
- RETIREMENT FOR CAUSE**
- Air Force manufacturing technology NDE programs supporting manufacturing and maintenance p 452 A90-30779
- Retirement for cause of the F100 engine p 843 N90-26813
- Critical inspection of high performance turbine engine components: The RFC concept p 859 N90-28073
- RETRACTABLE EQUIPMENT**
- Analysis of serious mechanical trouble in a retractable main landing gear of a jet fighter p 580 A90-36438
- Self-retracting helicopter rescue hoist p 829 A90-46935
- RETROFITTING**
- Eight years of experience with small computerized retrofit load monitoring systems p 926 A90-49882
- What should be done with those noisy old aircraft (PNR90562) p 107 N90-12593
- Aircraft modifications cost analysis. Volume 1: Overview of the study (AD-A220764) p 702 N90-25074
- REUSABLE LAUNCH VEHICLES**
- Progress in airbreathing combined engines for future European launcher p 344 N90-16817
- Saenger propulsion system options p 344 N90-16818
- REUSABLE ROCKET ENGINES**
- The SEPR 844 reusable liquid rocket engine for Mirage combat aircraft (AIAA PAPER 90-1835) p 655 A90-40526
- Probabilistic modeling for simulation of aerodynamic uncertainties in propulsion systems (NASA-TM-102472) p 515 N90-21036
- REUSABLE SPACECRAFT**
- Carbon-carbon for NASP p 599 A90-36672
- Project Falke - Performance of free flight tests in the supersonic, transonic, and subsonic regimes from balloons (DGLR PAPER 88-018) p 903 A90-50235
- REVENUE**
- Proceedings of a workshop on Future Airport Passenger Terminals (PB90-213620) p 937 N90-28580
- REVERSED FLOW**
- Numerical simulation of reversed flow over a supersonic delta wing at high angle of attack (AIAA PAPER 89-1802) p 8 A90-11849
- Selection of a suitable combustion system for a small gas turbine engine p 112 A90-16005
- A method for determining aileron efficiency and critical reversal and divergence rates at transonic velocities p 345 A90-24147
- Measurements in a separation bubble on an airfoil using laser velocimetry p 384 A90-27977
- The effect of swirler on short reversal-flow annular combustor p 423 A90-29906
- Reverse flow in multistage axial compressors p 623 A90-40942
- An experimental investigation of the velocity field in a reverse-flow combustor p 739 A90-42657
- Bursting in separating flow and in transition p 800 A90-46366
- Interference between a vortex filament and shock waves in free flow and in nonisobaric jets p 804 A90-46550
- REVERSING**
- Aerodynamic and propulsive control development of the STOL and maneuver technology demonstrator p 920 N90-28514
- Inflight thrust vectoring: A further degree of freedom in the aerodynamic/flight mechanical design of modern fighter aircraft p 921 N90-28528
- REVISIONS**
- Aircraft modifications cost analysis. Volume 1: Overview of the study (AD-A220764) p 702 N90-25074
- REYNOLDS EQUATION**
- Numerical modeling of supersonic turbulent reacting free shear layers p 174 N90-14197
- REYNOLDS NUMBER**
- An experimental investigation of the effect of incidence on the two-dimensional performance of an axial turbine cascade p 11 A90-12520
- Wind-tunnel investigation on the effect of a crescent platform on drag (AIAA PAPER 90-0300) p 228 A90-22196
- Reynolds number effects on the performance of a turbofan engine (ASME PAPER 89-GT-199) p 342 A90-23871
- An experimental study of the effect of the Reynolds number on flow past a swept wing at transonic velocities p 294 A90-24082
- Langlely hypersonic aerodynamic/aerothermodynamic testing capabilities - Present and future (AIAA PAPER 90-1376) p 596 A90-38483
- Boundary layer diagnostics by means of an infrared scanning radiometer p 605 A90-38493
- Two-dimensional wall adaption in the transonic windtunnel of the AIA p 597 A90-38497
- Flow over inclined finite length and width flat plates at low and high Reynolds numbers (AIAA PAPER 90-1467) p 562 A90-38624
- A hybrid Reynolds averaged/PDF closure model for supersonic turbulent combustion (AIAA PAPER 90-1573) p 600 A90-38711
- Calculation of nonseparated flow past a wing profile at large Reynolds numbers p 706 A90-42995
- Linear instability of the supersonic wake behind a flat plate aligned with a uniform stream p 716 A90-45783
- A study of gas flow in hypersonic nozzles at large Reynolds numbers using simplified Navier-Stokes equations p 803 A90-46538
- Analysis of experimental data for CAST 10-2/DOA 2 supercritical airfoil at low Reynolds numbers and application to high Reynolds number flow (AD-A211654) p 170 N90-13326
- An experimental study of the effect of streamwise vortices on unsteady turbulent boundary-layer separation p 369 N90-17045
- CAST-10-2/DOA 2 Airfoil Studies Workshop Results (NASA-CP-3052) p 352 N90-17647
- Comparison of conventional and adaptive wall wind tunnel results with regard to Reynolds number effects p 352 N90-17649
- High Reynolds number tests of the CAST-10-2/DOA 2 transonic airfoil at ambient and cryogenic temperature conditions p 320 N90-17650
- Investigation of CAST-10-2/DOA 2 airfoil in NAE high Reynolds number two-dimensional test facility p 321 N90-17654
- Carrier wing profile in nonstationary current (ETN-90-95368) p 399 N90-19208
- Wind tunnel design of heat island turbulent boundary layer (IHW-ET/50) p 455 N90-19542
- Navier-Stokes analysis of turbine blade heat transfer (NASA-TM-102496) p 542 N90-21300
- The gun tunnel of the Brunswick Institute for Fluid Mechanics: Current development status p 673 N90-24227
- Hypersonic Arbitrary-Body Aerodynamics (HABA) for conceptual design (DE90-014750) p 910 N90-28495
- REYNOLDS STRESS**
- Calculation of confined swirling flows with a second moment closure p 66 A90-10640
- A theoretical and experimental investigation of the Reynolds and apparent stresses in axial compressors p 12 A90-12554
- Calculation of flowfields in side-inlet ramjet combustors with an algebraic Reynolds stress model p 87 A90-16367
- Interaction between strong longitudinal vortices and turbulent boundary layers p 145 A90-16764
- Time-dependent and time-averaged turbulence structure near the nose of a wing-body junction p 231 A90-23036
- Development of a new low-Reynolds-number type Reynolds stress model and its application to a lobe mixer flow - to improve thrust efficiency and suppress jet noise in turbofan engines p 584 A90-35229
- Effects of streamwise vorticity injection on turbulent mixing layer development (AIAA PAPER 90-1459) p 561 A90-38616
- An abbreviated Reynolds stress turbulence model for airfoil flows (AIAA PAPER 90-1468) p 562 A90-38625
- The k-kl turbulence model and wall layer model for compressible flows (AIAA PAPER 90-1483) p 563 A90-38637
- An experimental study of the effect of streamwise vortices on unsteady turbulent boundary-layer separation p 369 N90-17045
- Measurement of velocity profiles and Reynolds stresses on an oscillating airfoil p 397 N90-18427
- Secondary flows and Reynolds stress distributions downstream of a turbine cascade at different expansion ratios p 512 N90-21015

RHEOLOGY

A new generation of innovative ultra-advanced intelligent composite materials featuring electro-rheological fluids - An experimental investigation p 204 A90-17962
 Proceedings of damping '89. Volume 1: Pages AAB-1 through DCD-11 [AD-A223431] p 960 N90-29664

RIBBON PARACHUTES

Wall-interference corrections for parachutes in a closed wind tunnel p 440 A90-31281
 Performance and quality of a wing type parachute: Parametric analysis [REPT-88-19] p 89 N90-11710
 An experimental investigation of wall-interference effects for parachutes in closed wind tunnels [DE90-001802] p 236 N90-15076

RIBLETS

Effect of surface riblets on the velocity profile of an incompressible boundary layer p 294 A90-24081
 Effect of detailed surface geometry on riblet drag reduction performance p 622 A90-40693
 Effect of riblets on flow separation in a subsonic diffuser p 712 A90-45261
 Effect of riblets on flow separation from a cylinder and an airfoil in subsonic flow [AD-A216197] p 319 N90-17574

RIBS (SUPPORTS)

Determination of the torsion rigidity of a multiple-rib torsion box of an aircraft lifting surface p 364 A90-24134
 Local heat transfer on a flat surface roughened with broken ribs p 534 A90-32169

RICCATI EQUATION

A combined Riccati transfer matrix-direct integration method with its applications p 611 A90-37218
 Direct multivariable adaptive controller with application to wing flutter p 349 N90-17642

RIDING QUALITY

Canard versus aft-tail ride qualities performance and pilot command response p 258 N90-15053

RIEMANN MANIFOLD

Stability and controllability in proportional navigation p 725 A90-42990

RIGGING

Investigation of model rigging limitations on a high speed wind tunnel model at cryogenic temperature p 523 A90-34232

RIGID ROTOR HELICOPTERS

Hingeless rotor dynamics in coordinated turns [AIAA PAPER 90-1117] p 412 A90-29389
 Application of mathematical modeling to the study of rigid helicopter rotors p 643 A90-41738
 An unsteady helicopter rotor-fuselage aerodynamic interaction analysis p 712 A90-45323

RIGID ROTORS

Aerodynamic loads computation on coaxial hingeless helicopter rotors [AIAA PAPER 90-0070] p 161 A90-19666
 Automatic vibration reduction at a four bladed hingeless model rotor - A wind tunnel demonstration p 335 A90-25424
 Stability of hingeless rotors in hover using three-dimensional unsteady aerodynamics p 430 A90-28227
 Relative aeromechanical stability characteristics for hingeless and bearingless rotors p 409 A90-28230
 Aeroelastic optimization of a helicopter rotor using an efficient sensitivity analysis [AIAA PAPER 90-0951] p 410 A90-29237
 An experimental and analytical investigation of isolated rotor flap-lag stability in forward flight p 518 A90-33623

Helicopter response to atmospheric turbulence in forward flight p 518 A90-33625
 Autopilot flight test experience with BK 117 hingeless rotor [AIAA PAPER 90-1267] p 505 A90-33930

Air resonance stability of hingeless rotors in forward flight p 590 A90-38519
 A study of fundamental issues in higher harmonic control using aeroelastic simulation p 861 A90-46966
 A technique for the prediction of aerodynamics and aeroelasticity of rotor blades p 184 N90-13377
 The effects of structural flap-lag and pitch-lag coupling on soft inplane hingeless rotor stability in hover [NASA-TP-3002] p 910 N90-28503

RIGID STRUCTURES

Attitude projection method for analyzing large-amplitude airplane maneuvers p 197 A90-19555
 UH-60A helicopter stability augmentation study p 670 A90-42471
 Effect of a crescent-shaped rigid support on the aerodynamic characteristics of models in the presence of perforated boundaries p 869 A90-46537
 Optimal rigid body reorientation problem [AIAA PAPER 90-3485] p 867 A90-47734

Equations of motion of slung load systems with results for dual lift [NASA-TM-102246] p 349 N90-17641

Time and frequency-domain identification and verification of BO-105 dynamic models [AD-A216828] p 415 N90-18389

RIGID WINGS

COCOMAT: A Computer Aided Engineering (CAE) system for composite structures design [NLR-MP-87078-U] p 462 N90-19756

RIGIDITY

Dynamic stiffness of a hydraulic damper in the system of a front landing gear strut p 102 A90-14555
 Determination of the torsion rigidity of a multiple-rib torsion box of an aircraft lifting surface p 364 A90-24134

RING LASERS

The multi-function RLG system comes of age - A technical update p 578 A90-36931
 Update 90 - A progress report on evaluation and flight testing of the small common RLG INS [AIAA PAPER 90-3375] p 847 A90-47763

RING WINGS

Steady and unsteady potential flow around thin annular wings and engines with simulation of jet engine flow [DFVLR-FB-89-18] p 89 N90-11711

RISK

Estimation of the technical risk criterion in selecting the operating parameters of aircraft gas turbine engines p 110 A90-14570
 Rotorcraft analytical improvement needed to reduce developmental risk - The 1989 Alexander A. Nikolsky Lecture p 285 A90-23934
 Flight test safety and 'high risk' tests - The Aerialia approach [AIAA PAPER 90-1315] p 483 A90-33924
 Review of the Aerospace Safety Advisory Panel report for NASA fiscal year 1990 authorization [GPO-24-234] p 177 N90-14213
 Risk assessment and its application to flight safety analysis [DE90-004985] p 323 N90-16722
 Fire safety in civil aviation p 325 N90-17586
 Kalman filter based range estimation for autonomous navigation using imaging sensors p 578 N90-22238

RIVETS

Modeling growth of fatigue cracks which originate at rivet holes p 691 N90-25060
 Neural networks for detecting defects in aircraft structures [IAR-90-4] p 777 N90-26345

ROADS

Improving snow roads and airstrips in Antarctica [AD-A211588] p 133 N90-11907

ROBOT DYNAMICS

Nonconvex polytope approximations of attracting basin boundaries for nonlinear systems [AIAA PAPER 90-3512] p 891 A90-47758

ROBOTICS

The Robotic Canopy Polishing System [SME PAPER MS89-134] p 222 A90-23680
 Computer integrated quality assurance for robotic workcells in aerospace manufacturing [SME PAPER MS89-152] p 283 A90-23681
 Robotic dry stripping of airframes - Phase II [SAE PAPER 890926] p 365 A90-24691
 Robotics for flightline servicing p 383 A90-30760
 Experimental evaluation of impedance control for robotic aircraft refueling [AD-A215532] p 337 N90-16755
 Hypercube expert system shell-applying production parallelism [AD-A215762] p 377 N90-18173
 Visual servoing for autonomous aircraft refueling [AD-A216042] p 414 N90-18386
 Design of a high angle of attack robotic sting mount for tests in a low speed wind tunnel [AD-A218105] p 526 N90-20099
 Visualization of three dimensional data p 782 N90-25553
 Robotic-aided system for inspection of aging aircraft [NIAR-90-9] p 777 N90-26346

ROBOTS

Advanced software for turbine blade processing [SME PAPER MS89-330] p 274 A90-23694
 Robots for aircraft coatings removal: Parameters and requirements [DE90-009429] p 609 N90-22048
 The Shock and Vibration Digest, volume 21, no. 3 p 609 N90-22064
 Robotic-aided system for inspection of aging aircraft [NIAR-90-9] p 777 N90-26346

ROBUSTNESS (MATHEMATICS)

Design of a helicopter output feedback control law using modal and structured-robustness techniques p 282 A90-20557

A variable structure system (VSS) to robust control of aircraft p 257 A90-21987
 Robust control system design synthesis with observers p 375 A90-25994
 Viscous computations using a direct solver p 315 A90-27133

Robust controller design using normalized coprime factor plant descriptions --- Book p 457 A90-27645
 Practical techniques of modelling aeroelastic systems for active control applications p 545 A90-33402
 Guaranteed cost control via optimal parametric LQ design p 693 A90-40810
 Flight control application of eigenstructure assignment with optimization of robustness to structured state space uncertainty p 693 A90-40885
 Development of a robust calculation method for transonic viscous blade-to-blade flows p 703 A90-42671

Robust hover control for a short takeoff/vertical landing aircraft [AIAA PAPER 90-3333] p 862 A90-47593

Robustness of dynamic inversion vs mu synthesis - Lateral-directional flight control example [AIAA PAPER 90-3338] p 863 A90-47598

Stochastic performance robustness of aircraft control systems [AIAA PAPER 90-3410] p 865 A90-47665

Robust flight control system design with multiple model approach [AIAA PAPER 90-3411] p 865 A90-47666

A mixed H2 and H(infinity) approach to an autopilot design problem [AIAA PAPER 90-3441] p 865 A90-47694

Lateral-directional control of an aircraft using mu synthesis [AIAA PAPER 90-3442] p 865 A90-47695

Robust control design for relaxed static stability aircraft [AIAA PAPER 90-3443] p 865 A90-47696

Extended implicit model following as applied to integrated flight and propulsion control [AIAA PAPER 90-3444] p 890 A90-47697

Robustness evaluation of a flexible aircraft control system [AIAA PAPER 90-3445] p 890 A90-47698

Multivariable flight control synthesis and literal robustness analysis for an aeroelastic vehicle [AIAA PAPER 90-3446] p 890 A90-47699

A robust wind shear stochastic controller-estimator [AIAA PAPER 90-3489] p 867 A90-47737

Robust low norm output feedback design for flight control systems [AIAA PAPER 90-3505] p 891 A90-47751

Reconfigurable aircraft flight control system via robust direct adaptive control [AIAA PAPER 90-3226] p 868 A90-49111

Robust control design for flight control [AD-A211957] p 119 N90-11756

Application of stochastic robustness to aircraft control systems p 521 N90-20936

Stochastic robustness of linear control systems p 521 N90-20941

Algorithms for computing the multivariable stability margin p 612 N90-22999

Multivariable frequency weighted model order reduction for control synthesis [AIAA-89-3558] p 613 N90-23060

Robustness evaluation of H2 and H(infinity) control theory as applied to a transport aircraft [AD-A222795] p 759 N90-26018

ROCKET ENGINE CASES

Systems tunnel linear shaped charge lightning strike [NASA-CR-183832] p 201 N90-13404

ROCKET ENGINE DESIGN

'Black Betsy' - The 6000C-4 rocket engine, 1945-1989. I [IAF PAPER 89-726] p 141 A90-13700
 Turbofans turn to UHB propulsion p 659 A90-41165
 Progress in airbreathing combined engines for future European launcher p 344 N90-16817
 Saenger propulsion system options p 344 N90-16818

Parametric assessment of propulsion system mass for airbreathing launcher configurations p 344 N90-16819

ROCKET ENGINES

The cycle evaluation of the advanced LACE performance [IAF PAPER 89-313] p 109 A90-13447

Calculation of vibrational combustion limits in Helmholtz resonator-type chambers p 125 A90-14588

Experimental evaluation of a tuned electromagnetic damper for vibration control of cryogenic turbopump rotors [NASA-TP-3005] p 665 N90-23403

The jet engine: 1932 [ISBN-3-922010-49-0] p 763 N90-25189

ROCKET NOZZLES

- CFD applications in an aerospace engine test facility
[AIAA PAPER 90-2003] p 681 A90-40590
- Hypersonic nozzle/afterbody performance at low Mach numbers
[AD-A216223] p 319 N90-17575

ROCKET PROPELLANTS

- Aging and antioxidant surveillance studies on turbine fuel JP-5 and JP-10 p 442 A90-29492

ROCKET TEST FACILITIES

- CFD applications in an aerospace engine test facility
[AIAA PAPER 90-2003] p 681 A90-40590

RODS

- Divergence of thin-walled composite rods of closed profile in gas flow p 388 A90-29012
- Static and dynamic characterization of the ATR 72 rods made of Ti 10-2.3 titanium alloy
[REPT-49-238] p 953 N90-28722
- Fractographic analysis of fatigue failures of airframe equipment parts: Examples of a rod end housing and a rod end cap
[NAL-TR-1047] p 961 N90-29686

ROLL

- A study of roll response required in a low altitude slalom task --- in helicopter control p 347 A90-25421

ROLLER BEARINGS

- Development status of epicyclic gears p 271 A90-21141
- Retirement lives of rolling element bearings p 680 A90-39980

ROLLING

- Rolling of ARALL laminates (an alternative method for post-stretching ARALL laminates)
[LR-560] p 135 N90-12778

ROLLING MOMENTS

- Unsteady aerodynamic forces on rolling delta wings at high angle of attack p 159 A90-19426
- Large-amplitude high-rate roll experiments on a delta and double delta wing
[AIAA PAPER 90-0224] p 163 A90-19742
- Control sensitivity, bandwidth and disturbance rejection concerns for advanced rotorcraft p 430 A90-28204
- A new simplification method for analysing the rapid rolling stability of aircraft p 669 A90-42367
- An experimental investigation of roll agility in air-to-air combat
[AIAA PAPER 90-2809] p 752 A90-45144
- Self-induced roll oscillations of low-aspect-ratio rectangular wings
[AIAA PAPER 90-2811] p 753 A90-45151
- An experimental study of the nonlinear dynamic phenomenon known as wing rock
[AIAA PAPER 90-2812] p 753 A90-45152
- A video-based experimental investigation of wing rock
[AD-A218244] p 498 N90-20075
- A video-based experimental investigation of wing rock p 592 N90-21771

ROSS ICE SHELF

- Airfields on antarctic glacier ice
[AD-A217638] p 526 N90-20097

ROTARY ENGINES

- The application of cast SiC/Al to rotary engine components
[NASA-CR-179610] p 192 N90-13385
- Performance of a supercharged direct-injection stratified-charge rotary combustion engine
[NASA-TM-103105] p 748 N90-25982

ROTARY STABILITY

- Shaft flexibility effects on aeroelastic stability of a rotating bladed disk p 132 A90-16371
- Rotational aerodynamics of elliptic bodies at high angles of attack
[AIAA PAPER 90-0068] p 161 A90-19664
- An experimental and analytical investigation of isolated rotor flap-lag stability in forward flight p 518 A90-33623

- Yaw damping of elliptic bodies at high angles of attack p 709 A90-44740
- Active stabilization of aeromechanical systems
[AD-A216629] p 454 N90-18672

ROTARY WING AIRCRAFT

- Experimental and analytical evaluation of dynamic load vibration of a 2240-kW (3000-hp) rotorcraft transmission
p 127 A90-13750
- Advanced technology rotorcraft - Civil short haul transport of the future
Scenario 2000
[MBB-UD-560/89] p 222 A90-22698
- Minimum weight design of rotorcraft blades with multiple frequency and stress constraints p 335 A90-25304
- AHS, Annual Forum, 45th, Boston, MA, May 22-24, 1989, Proceedings p 381 A90-28151
- Rotor/airframe aeroelastic analyses using the transfer matrix approach
[AIAA PAPER 90-1119] p 392 A90-29391

- The variable-diameter rotor - A key to high performance rotorcraft p 413 A90-30118
- EH101 Advance Technology Rotorcraft low detectability/good neighbor design p 579 A90-35774
- A survey of nonuniform inflow models for rotorcraft flight dynamics and control applications p 590 A90-38521
- Experimental study of the effects of nonlinearities on ground resonance p 643 A90-40172
- Rotorcraft computational fluid dynamics - Recent developments at McDonnell Douglas p 630 A90-42439

- The modular HUM system --- Health and Usage Monitoring instruments for rotary wing aircraft failure detection p 618 A90-42476
- A hydrodynamic turbo-fan/shaft convertible engine p 665 A90-42487
- Vertical Lift Aircraft Design Conference, San Francisco, CA, Jan. 17-19, 1990, Proceedings p 829 A90-46926
- Rotorwash flow fields - Flight test measurement, prediction methodologies, and operational issues p 817 A90-46930

- The evolution of design/development requirements for avionics/mission equipment (MEP) insertion p 846 A90-46932
- High-speed rotorcraft V/STOL - An initial assessment p 829 A90-46938
- Mission performance comparison between tilt rotor, variable diameter tilt rotor and tilt wing aircraft p 830 A90-46940

- GTPDP - A rotary wing aircraft preliminary design and performance estimation program including optimization and cost p 830 A90-46944
- Development of the Second Generation Comprehensive Helicopter Analysis System (2GCHAS) p 889 A90-46963
- Rotorcraft pursuit-evasion in nap-of-the-earth flight
[AIAA PAPER 90-3455] p 786 A90-47707
- Propulsion systems for vertical flight aircraft
[AIAA PAPER 90-3299] p 853 A90-48881
- Integrated multidisciplinary optimization of rotorcraft: A plan for development
[NASA-TM-101617] p 106 N90-12580
- General approach and scope --- rotor blade design optimization p 106 N90-12581
- Validation of the procedures --- integrated multidisciplinary optimization of rotorcraft p 107 N90-12587
- Appendix: Results obtained to date --- integrated multidisciplinary optimization of rotorcraft p 107 N90-12588
- NASA's program on icing research and technology p 239 N90-15062

- A survey of nonuniform inflow models for rotorcraft flight dynamics and control applications
[NASA-TM-102219] p 260 N90-15938
- Compendium of abstracts and viewgraphs.
[AD-A217189] p 532 N90-20140
- Stereopsis cueing effects on hover-in-turbulence performance in a simulated rotorcraft
[NASA-TP-2980] p 506 N90-21004
- Transmission research activities at NASA Lewis Research Center
[NASA-TM-103132] p 543 N90-21394
- Development and application of a generalized dynamic wake theory for lifting rotors p 570 N90-21731
- Quiet mode for nonlinear rotor models
[NASA-TM-102236] p 582 N90-21758
- Assessment of High Temperature Superconducting (HTS) electric motors for rotorcraft propulsion
[NASA-CR-185222] p 588 N90-21761
- Passive navigation using image irradiance tracking p 578 N90-22232

- Kalman filter based range estimation for autonomous navigation using imaging sensors p 578 N90-22238
- Extension of a three-dimensional viscous wing flow analysis
[NASA-CR-182023] p 631 N90-23348
- TRENDS: The aeronautical post-test database management system
[NASA-TM-101025] p 761 N90-25149
- AGARD highlights 90/1 p 783 N90-26788
- The Second ARO Workshop on Rotorcraft Interactional Aerodynamics
[AD-A223310] p 911 N90-29304

ROTARY WINGS

- A multifunctional system of helicopter dynamics simulations p 28 A90-10226
- Wind tunnel tests of models of helicopter rotors p 29 A90-10230
- Design of an advanced pneumatic deicer for the composite rotor blade p 29 A90-11009
- Application of the hydrogen bubble visualization method to the water tunnels of ONERA
[ONERA, TP NO. 1989-107] p 58 A90-11140
- Influence of the control law on the performance of a helicopter model rotor
[ONERA, TP NO. 1989-136] p 4 A90-11158
- New rotor test rig in the large Modane wind tunnel
[ONERA, TP NO. 1989-137] p 58 A90-11159
- Rotor concepts for the European Future Advanced Rotorcraft (Eurofar)
[MBB-UD-0551-89-PUB] p 29 A90-12258
- Aerodynamic and dynamic principles of helicopter flight --- Russian book p 55 A90-12473
- Identification of a coupled flapping/inflow model for the PUMA helicopter from flight test data p 56 A90-12767
- Wildhaber-Novikov circular arc gears - Some properties of relevance to their design p 70 A90-12999
- Blade surface pressure measurement on a pusher propeller in flight
[SAE PAPER 891040] p 139 A90-14346
- Evaluation of the dynamic properties of the auto-pilot servo of a single-rotor helicopter through laboratory testing p 118 A90-15424
- Aerospatiale's military helicopter programs p 143 A90-16824
- Practical suggestions for modifying math models to correlate with actual modal test results p 207 A90-16979
- Effect of tip speed on rotor inflow p 151 A90-17311
- Minimum weight design of helicopter rotor blades with frequency constraints p 180 A90-17313
- Dynamic structural correlation via nonlinear programming techniques p 208 A90-17372
- An experimental investigation of the downwash beneath a lifting rotor and low advance ratios p 151 A90-17585
- Theoretical and experimental analysis of a model rotor blade incorporating a swept tip p 151 A90-17586
- Theoretical modelling of composite rotating beams p 208 A90-17684
- Response and hub loads sensitivity analysis of a helicopter rotor p 181 A90-18145
- Numerical approaches for solving parametric vibration problems in helicopter dynamics p 182 A90-18607
- Thrust augmentation characteristics of jet reactions
[AIAA PAPER 90-0033] p 161 A90-19641
- Aerodynamic loads computation on coaxial hingeless helicopter rotors
[AIAA PAPER 90-0070] p 161 A90-19666
- Impact ice stresses in rotating airfoils
[AIAA PAPER 90-0198] p 175 A90-19735
- Application of a rotary-wing viscous flow solver on a massively parallel computer
[AIAA PAPER 90-0334] p 164 A90-19802
- Performance and aerodynamic development of the Super Puma Mk II main rotor with new SPP8 blade tip design
[ONERA, TP NO. 1989-181] p 245 A90-21041
- Correlation of Puma airfoils - Evaluation of CFD prediction methods
[ONERA, TP NO. 1989-185] p 224 A90-21045
- Technical-scientific possibilities for helicopter noise research in the German-Dutch wind tunnel p 283 A90-21474
- Induced drag based on leading edge suction for a helicopter in forward flight p 232 A90-23102
- Optimal placement of tuning masses for vibration reduction in helicopter rotor blades p 247 A90-23117
- Modeling of subsonic unsteady aerodynamics for rotary wing applications p 293 A90-23935
- Analytical approach to the induced flow of a helicopter rotor in vertical descent p 293 A90-23938
- Design, realization, and qualification of model composite rotor blades p 364 A90-24293
- The influence of the helicopter fuselage on its rotor p 301 A90-25101
- Review of composite rotor blade modeling p 366 A90-25303
- Winglets on rotor blades in forward flight - A theoretical and experimental investigation p 303 A90-25422
- Helicopter rotor dynamics and aeroelasticity - Some key ideas and insights p 335 A90-25425
- Helicopter ground/air resonance including rotor shaft flexibility and control coupling p 406 A90-28153
- Prediction and measurement of low-frequency harmonic noise of a hovering model helicopter rotor p 463 A90-28159
- Rotor smoothing expert system p 381 A90-28164
- HARP model rotor test at the DNW --- Hughes Advanced Rotor Program p 406 A90-28167
- Efficient free wake calculations using Analytical/Numerical Matching and far-field linearization p 384 A90-28171
- Identification of retreating blade stall mechanisms using flight test pressure measurements p 384 A90-28172
- A comprehensive hover test of the airloads and airflow of an extensively instrumented model helicopter rotor p 407 A90-28173

BELLTECH - A multipurpose Navier-Stokes code for rotor blade and fixed wing configurations p 384 A90-28174

Icing Research Tunnel test of a model helicopter rotor p 400 A90-28179

A numerical analysis of the British Experimental Rotor Program blade p 384 A90-28194

Tip vortex geometry of a hovering helicopter rotor in ground effect p 407 A90-28196

Active control of gust- and interference-induced vibration of tilt-rotor aircraft p 429 A90-28201

The four-bladed main rotor system for the AH-1W helicopter p 408 A90-28214

A comparison of four versus five blades for the main rotor of a light helicopter p 408 A90-28215

RSRA/X-Wing flight control system development - Lessons learned p 430 A90-28216

Rotor loads validation utilizing a coupled aeroelastic analysis with refined aerodynamic modeling p 408 A90-28226

Periodic response of thin-walled composite blades p 408 A90-28229

Strike tolerant main rotor blade tip p 409 A90-28232

The prediction of loads on the Boeing Helicopters Model 360 rotor p 410 A90-28240

The revolution continuous --- performance of military helicopters [MBB-UD-557-89-PUB] p 381 A90-28242

The rotor-signal-module of MF190 --- for digital data acquisition from BO-105 helicopter rotary wings p 418 A90-28849

Aeroelastic optimization of a helicopter rotor using an efficient sensitivity analysis [AIAA PAPER 90-0951] p 410 A90-29237

Rotary-wing aeroelasticity with application to VTOL vehicles [AIAA PAPER 90-1115] p 392 A90-29387

Aeroelastic analysis of helicopter rotor blades with advanced tip shapes [AIAA PAPER 90-1118] p 392 A90-29390

The effect of structural variations on the dynamic characteristics of helicopter rotor blades [AIAA PAPER 90-1161] p 450 A90-29396

Effects of higher harmonic control on rotor performance and control loads [AIAA PAPER 90-1158] p 412 A90-29467

Application of transonic flow analysis to helicopter rotor problems p 394 A90-29887

EH 101 Flight Test Program current status and future testing [AIAA PAPER 90-1296] p 495 A90-33912

Correlation of lift and thickness noise sources in vortex-airfoil interaction p 547 A90-34090

Application of active noise control to model propeller noise p 548 A90-34091

Higher harmonic control of a helicopter model rotor to reduce blade/vortex interaction noise p 496 A90-34360

Stability sensitivity analysis of a helicopter rotor p 580 A90-36273

A study on mechanical model of the helicopter 'ground resonance' p 580 A90-36423

Acoustics p 614 A90-36541

Application of optimization methods to helicopter rotor blade design p 604 A90-37337

Vibration equations for a helicopter rotor blade p 604 A90-37830

Numerical methods for the treatment of periodic systems with applications to structural dynamics and helicopter rotor dynamics p 604 A90-37881

Euler solutions for self-generated rotor blade-vortex interactions [AIAA PAPER 90-1588] p 566 A90-38723

Certification plan for an all-composite main rotor flexbeam p 642 A90-39992

Parameter identification of aeroelastic modes of rotary wings from transient time histories p 642 A90-40166

Viscous flow around a propeller-shaft configuration with infinite-pitch rectangular blades p 683 A90-40938

Use of pulse radars for helicopters detection - Design constraints p 683 A90-41073

Recent propeller development and studies conducted at ONERA [ONERA, TP NO. 1990-16] p 683 A90-41201

Wind-tunnel measurement of noise emitted by helicopter rotors at high speed [ONERA, TP NO. 1990-28] p 695 A90-41207

Application of mathematical modeling to the study of rigid helicopter rotors p 643 A90-41738

Unsteady deformations of elastic rotor blades p 687 A90-42341

A study of the influence of a helicopter rotor blade on the following blades using Euler equations p 630 A90-42435

A review of tilt rotor download research p 630 A90-42437

Improving helicopter aerodynamics - A step ahead p 631 A90-42443

Kane's methods in rotorblade dynamics p 646 A90-42458

Eight years of flight operations with composite rotorblades p 635 A90-42481

EH-101 main rotor hub application of thick carbon fiber unidirectional tension bands p 618 A90-42489

Design and manufacturing of composite materials blade models p 618 A90-42492

EH101 vibration control p 647 A90-42496

Rotary servohinge actuator [SAE PAPER 892261] p 733 A90-45458

Application of a new visualization method to helicopter rotor flow [AIAA PAPER 90-3006] p 789 A90-45856

An experimental study of instantaneous velocity perturbations over a rotor disk for low duty coefficients p 860 A90-46572

Numerical simulations of three-dimensional rotor blade-vortex interactions p 807 A90-46879

A study of fundamental issues in higher harmonic control using aeroelastic simulation p 861 A90-46966

Experimental observations of two-dimensional blade-vortex interaction p 809 A90-47303

A method for calculating the rotor-fuselage interference in helicopters [DGLR PAPER 88-060] p 919 A90-50246

Integrated multidisciplinary design optimization of rotorcraft [NASA-TM-101642] p 36 N90-10889

Rotor blade aerodynamic design p 106 N90-12582

Rotor blade dynamic design p 106 N90-12583

Rotor blade structural design p 106 N90-12584

Acoustic design considerations: Review of rotor acoustic sources p 106 N90-12585

Airframe design considerations: Overview --- rotor design optimization p 106 N90-12586

Appendix: Results obtained to date --- integrated multidisciplinary optimization of rotorcraft p 107 N90-12588

Euler equation solutions applied to a helicopter rotor in forward moving flight [ONERA-RSF-32/1285-AY-346A] p 107 N90-12592

RAN (Royal Australian Navy) vibration analysis system operator's guide [AD-A212441] p 107 N90-12596

An experimental investigation of the interaction between a model rotor and airframe in forward flight p 185 N90-14219

Effects of aeroelastic tailoring on anisotropic composite material beam models of helicopter blades [AD-A213478] p 249 N90-15095

An examination of helicopter rotor load calculations [AD-A214295] p 249 N90-15098

Calculation of the flow field of a multiblade helicopter rotor using a Euler method including the wake p 278 N90-16189

The response of helicopter rotors to vibratory airload [AD-A215678] p 337 N90-16756

Prediction of rotor blade-vortex interaction noise from 2-D aerodynamic calculations and measurements [ISL-CO-243/88] p 396 N90-18365

Performance of an optimized rotor blade at off-design flight conditions [NASA-CR-4288] p 416 N90-19226

Unsteady free-wake viscous aerodynamic analysis of helicopter rotors [AD-A217166] p 478 N90-20048

Analysis of small-scale rotor hover performance data [NASA-TM-102271] p 540 N90-20325

Performance data from a wind-tunnel test of two main-rotor blade designs for a utility-class helicopter [NASA-TM-4183] p 499 N90-20974

ROSAR (Helicopter-Rotor based Synthetic Aperture Radar) p 541 N90-21229

Airloads, wakes, and aeroelasticity [NASA-CR-177551] p 572 N90-21738

Aerodynamic characteristics of two rotorcraft airfoils designed for application to the inboard region of a main rotor blade [NASA-TP-3009] p 633 N90-24239

HPLC analysis of helicopter rotor blade materials [AD-A221121] p 650 N90-24270

Scenario 2000 [MBB-UD-500/89-PUB] p 734 N90-25092

Rotorcraft aeromechanical assessment. Phase 2: Workshop [NASA-TM-102272] p 816 N90-26800

Development of a method to design helicopter rotors [REPT-100-30-03] p 845 N90-26830

Applications of digital image processing in testing and evaluation of composite materials [AD-A22939] p 874 N90-26887

The acoustic results of a United Technologies scale model helicopter rotor tested at DNW [NASA-TM-101879] p 896 N90-27471

Theoretical studies carried out in 1988 on helicopter rotor noise under subsonic conditions [ONERA-RS-82/5094-PY] p 896 N90-28402

Solution of Euler equations applied to a rotor of a helicopter in steady flight [ONERA-RSF-1/3731-AY-002A] p 910 N90-28500

The effects of structural flap-lag and pitch-lag coupling on soft inplane hingeless rotor stability in hover [NASA-TP-3002] p 910 N90-28503

An enhanced integrated aerodynamic load/dynamic optimization procedure for helicopter rotor blades [NASA-CR-4326] p 924 N90-29383

ROTATING BODIES

Theoretical modelling of composite rotating beams p 208 A90-17684

Optimum design of rotational wheels under transient thermal and centrifugal loading p 270 A90-20770

An analysis methodology for internal swirling flow systems with a rotating wall [ASME PAPER 89-GT-185] p 361 A90-23863

Experimental investigation into the effects of rotating and static bolts on both windage heating and local heat transfer coefficients in a rotor/stator cavity [ASME PAPER 89-GT-196] p 362 A90-23870

Hierarchical finite element method for rotating beams p 605 A90-38353

Rotating system load monitoring using minimum fixed system instrumentation p 651 A90-39982

A theoretical and experimental investigation into the prerotation of aircraft tires [AIAA PAPER 90-3272] p 836 A90-48863

The interaction of a supersonic streamwise vortex and a normal shock wave p 633 N90-24241

ROTATING CYLINDERS

Effect of moving surfaces on the airfoil boundary-layer control p 159 A90-19388

ROTATING DISKS

Stress analysis of gas turbine bladed disc for structural integrity applying the concept of cyclic symmetry p 46 A90-12564

Shaft flexibility effects on aeroelastic stability of a rotating bladed disk p 132 A90-16371

Aerodynamic and torque characteristics of enclosed Co/counter rotating disks [ASME PAPER 89-GT-177] p 361 A90-23858

A theoretical study of ingress for shrouded rotating disc systems with radial outflow --- sealing rotor-stator cavities [ASME PAPER 89-GT-178] p 361 A90-23859

Blade mistuning coupled with shaft flexibility effects in rotor aeroelasticity [ASME PAPER 89-GT-330] p 343 A90-23896

Fatigue life prediction method for gas turbine rotor disk alloy FV535 p 440 A90-27679

Visualization studies in rotating disk cavity flows p 475 A90-33568

Flow and heat transfer in rotating-disc systems. Volume I - Rotor-stator systems --- Book p 772 A90-45759

Spray automated balancing of rotors - How process parameters influence performance p 879 A90-46228

Numerical investigations of heat transfer and flow rates in rotating cavities. Simulation of the movement generated by wall temperature gradients, by source-sink mass flows or by the differential rotation of the walls, under the influence or coriolis and centrifugal forces [ETN-90-96253] p 454 N90-18695

Generation of circumferential velocity contours associated with pulsed point suction on a rotating disk p 691 N90-25065

ROTATING ENVIRONMENTS

Comparison of active control on a servo flap rotor using fixed system and rotating system parameters p 862 A90-46976

ROTATING FLUIDS

Rotating primary flow induction using jet-flapped blades p 48 A90-12585

The interaction between a counter-rotating vortex pair in vertical ascent and a free surface p 151 A90-17580

Application of the finite element method to the problem of rotational flow around wings p 156 A90-18305

ROTATING SHAFTS

Composite driveshaft designs [SAE PAPER 891031] p 128 A90-14339

Helicopter surveillance - A look at current and proposed future programs p 642 A90-39986

The Shock and Vibration Digest, volume 21, no. 3 p 609 N90-22064

ROTATING STALLS

Unsteady loss in a low speed axial flow compressor during rotating stall p 12 A90-12527

Numerical analysis of rotating stall by a vortex model p 13 A90-12590

- Radial swirl flows between parallel disks at critical flow rate p 14 A90-12596
- A study on surge and rotating stall in axial compressors - A summary of the measurement and fundamental analysis method p 87 A90-16105
- Navier-Stokes study of rotating stall in compressor cascades p 302 A90-25292
- An experimental investigation of rotating stall in a centrifugal compressor with vaneless diffuser p 621 A90-40513
- Reverse flow in multistage axial compressors p 623 A90-40942
- Stall cell blockage in a high-speed multistage axial-flow compressor [AIAA PAPER 90-1913] p 740 A90-42693
- Relation between flow parameters of a gas turbine engine and rotor frequencies p 851 A90-46539
- The interaction between distortion of inlet flow and blade stall flutter in axial-flow compressor p 854 A90-49466
- A model of small-disturbance wave in large-scale separation zone associated with stall flutter p 883 A90-49469
- Stage effects on stalling and recovery of a high-speed 10-stage axial-flow compressor p 115 N90-12600
- Computational and experimental investigations of rotating stall in compressor cascades p 588 N90-22565
- ROTATION**
- A study of the effects of Rotating Frame Turbulence (RFT) on helicopter flight mechanics p 248 N90-15058
- An unsteady lifting surface method for single rotation propellers [NASA-CR-4302] p 719 N90-25940
- ROTOR AERODYNAMICS**
- Hydrodynamic visualization of the flow around a high-speed aircraft propeller [ONERA, TP NO. 1989-108] p 3 A90-11141
- A study of unsteady rotor-stator interactions p 67 A90-11557
- Rotor concepts for the European Future Advanced Rotorcraft (Eurofar) [MBB-UD-0551-89-PUB] p 29 A90-12258
- Aerodynamic and dynamic principles of helicopter flight - Russian book p 55 A90-12473
- Identification of an adequate model for collective response dynamics of a Sea King helicopter in hover p 56 A90-12766
- Identification of a coupled flapping/inflow model for the PUMA helicopter from flight test data p 56 A90-12767
- System identification strategies for helicopter rotor models incorporating induced flow p 30 A90-12768
- Identification of rotor flapping equation of motion from flight measurements with the RSRA compound helicopter p 56 A90-12769
- Flight simulation model validation procedure, a systematic approach p 30 A90-12770
- Advancements in frequency-domain methods for rotorcraft system identification p 56 A90-12771
- A frequency-domain system identification approach to helicopter flight mechanics model validation p 56 A90-12772
- Blade surface pressure measurement on a pusher propeller in flight [SAE PAPER 891040] p 139 A90-14346
- An experiment study of rotor aerodynamic in ground effect at low speed p 149 A90-16826
- Effect of tip speed on rotor inflow p 151 A90-17311
- Rotor hover performance prediction using a free-wake, computational fluid dynamics method p 153 A90-17869
- Prediction of the interaction noise emitted by helicopter fenestrations p 218 A90-18449
- Numerical approaches for solving parametric vibration problems in helicopter dynamics p 182 A90-18607
- Rotor noise due to atmospheric turbulence ingestion. I - Fluid mechanics p 219 A90-19385
- Rotor noise due to atmospheric turbulence ingestion. II - Aeroacoustic results p 219 A90-19386
- Rotor/fuselage vibration isolation studies by a Floquet-harmonic iteration technique p 182 A90-19393
- Performance and aerodynamic development of the Super Puma Mk II main rotor with new SPP8 blade tip design [ONERA, TP NO. 1989-181] p 245 A90-21041
- Influence of the radial component of total pressure gradient on tip clearance secondary flow in axial compressors [ASME PAPER 89-GT-19] p 288 A90-23761
- Blade sweep for low-speed axial fans [ASME PAPER 89-GT-53] p 289 A90-23779
- Stall inception in axial compressors [ASME PAPER 89-GT-63] p 290 A90-23786
- Three-dimensional separated flow field in the endwall region of an annular compressor cascade in the presence of rotor-stator interaction. I - Quasi-steady flow field and comparison with steady-state data [ASME PAPER 89-GT-76] p 291 A90-23797
- Prediction of the aerodynamic environment and heat transfer for rotor-stator configurations [ASME PAPER 89-GT-89] p 359 A90-23807
- Aerodynamics of cooling jets introduced in the secondary flow of a low speed turbine cascade [ASME PAPER 89-GT-192] p 362 A90-23868
- Modeling of subsonic unsteady aerodynamics for rotary wing applications p 293 A90-23935
- Hub loads analysis of the SA349/2 helicopter p 333 A90-23936
- Analytical approach to the induced flow of a helicopter rotor in vertical descent p 293 A90-23938
- Investigation of the flow structure behind the rotating blades in the elbow of a wind tunnel in the case of acoustic excitation p 297 A90-24124
- The influence of the helicopter fuselage on its rotor p 301 A90-25101
- Free-wake analysis of compressible rotor flows p 302 A90-25283
- A panel method for arbitrary moving boundaries problems p 302 A90-25284
- Winglets on rotor blades in forward flight - A theoretical and experimental investigation p 303 A90-25422
- A practical co-axial twin rotor model p 335 A90-25423
- Acoustic characteristics of counterrotating unducted fans from model scale tests p 378 A90-26138
- AHS, Annual Forum, 45th, Boston, MA, May 22-24, 1989, Proceedings p 381 A90-28151
- HARP model rotor test at the DNW - Hughes Advanced Rotor Program p 406 A90-28167
- A numerical analysis of the British Experimental Rotor Program blade p 384 A90-28194
- Comparison of measured induced velocities with results from a closed-form finite state wake model in forward flight p 385 A90-28195
- Advanced rotor computations with a corrected potential method p 385 A90-28197
- Investigation of aerodynamic interactions between a rotor and fuselage in forward flight p 385 A90-28198
- Theoretical and experimental correlation of helicopter aeromechanics in hover p 429 A90-28200
- Rotor loads validation utilizing a coupled aeroelastic analysis with refined aerodynamic modeling p 408 A90-28226
- Stability of hingeless rotors in hover using three-dimensional unsteady aerodynamics p 430 A90-28227
- Tilt rotor aircraft aeroacoustics p 409 A90-28238
- Aerodynamic design of the V-22 Osprey proprotor p 385 A90-28241
- Multi-output implementation of a modified sparse time domain technique for rotor stability testing [AIAA PAPER 90-0946] p 412 A90-29405
- Navier-Stokes analyses of the redistribution of inlet temperature distortions in a turbine p 471 A90-32959
- Eliminating the TF30 P-111 + engine rotor-instability problem p 508 A90-32961
- Unsteady transition in an axial-flow turbine. I - Measurements on the turbine rotor. II - Cascade measurements and modeling [ASME PAPER 89-GT-289] p 474 A90-33562
- Inlet distortion generated periodic aerodynamic rotor response [ASME PAPER 89-GT-299] p 475 A90-33567
- Analyses of revising the inlet profile of a radial inflow turbine impeller p 602 A90-35831
- Recent advancement in helicopter rotor wake study p 556 A90-36413
- Acoustics of ultralight airplanes p 643 A90-40685
- Counter-rotating propellant analysis using a frequency domain panel method p 623 A90-40937
- Rotorcraft computational fluid dynamics - Recent developments at McDonnell Douglas p 630 A90-42439
- Computation of viscous aerodynamic characteristics of 2-D airfoils for helicopter applications p 631 A90-42440
- Improving helicopter aerodynamics - A step ahead p 631 A90-42443
- Helicopter ground and air resonance dynamics p 646 A90-42457
- Analytical study of dynamic response of helicopter in autorotative flight p 670 A90-42469
- The influence of the inertia coupling on the stability and control of the helicopter and the response of helicopter gust p 671 A90-42472
- Aeroelastic effects on stability and control of hingeless rotor helicopters p 647 A90-42473
- Application of sweep to improve the efficiency of a transonic fan. I - Design [AIAA PAPER 90-1915] p 741 A90-42695
- Unsteady Euler analysis of the redistribution of an inlet temperature distortion in a turbine p 768 A90-42759
- Forced response on turbomachinery blades due to passing wakes [AIAA PAPER 90-2353] p 705 A90-42781
- Helicopter trim with flap-lag-torsion and stall by an optimized controller p 755 A90-45332
- Application of a new visualization method to helicopter rotor flow [AIAA PAPER 90-3006] p 789 A90-45856
- Euler procedure for calculation of the steady rotor flow with emphasis on wake evolution [AIAA PAPER 90-3007] p 789 A90-45857
- Experimental and numerical study of the British Experimental Rotor Programme blade [AIAA PAPER 90-3008] p 789 A90-45858
- Relation between flow parameters of a gas turbine engine and rotor frequencies p 851 A90-46539
- An experimental study of instantaneous velocity perturbations over a rotor disk for low duty coefficients p 860 A90-46572
- Rotorwash flow fields - Flight test measurement, prediction methodologies, and operational issues p 817 A90-46930
- Mission performance comparison between tilt rotor, variable diameter tilt rotor and tilt wing aircraft p 830 A90-46940
- Empirical prediction of the blockage effect of a flat body on a rotor p 807 A90-46942
- Improvement to interactive two dimensional rotor section design p 808 A90-46943
- Performance of an optimized rotor blade at off-design flight conditions p 830 A90-46946
- BHT's technical assessment of advanced rotor and control concepts p 861 A90-46949
- Aerodynamic design of the Cal Poly Da Vinci Human-Powered Helicopter p 830 A90-46950
- AHS National Specialists' Meeting on Rotorcraft Dynamics, Arlington, TX, Nov. 13, 14, 1989, Proceedings p 830 A90-46952
- Perspectives in aeromechanical stability of helicopter rotors p 831 A90-46953
- Recent developments in rotor dynamics methodology in the U.S. industry p 889 A90-46960
- Fundamental dynamics issues for comprehensive rotorcraft analyses p 831 A90-46961
- An improved rotor/airframe coupling method for NASTRAN airframe vibration analysis p 831 A90-46962
- An examination of helicopter rotor load calculations p 833 A90-46972
- Two and three dimensional indicial methods for rotor dynamic airloads p 808 A90-46973
- Prediction and alleviation of V-22 rotor dynamic loads p 833 A90-46974
- Free wake analysis of rotor configurations for reduced vibratory airloads p 833 A90-46975
- Measurements of simulated wake/rotor interaction phenomena in turbomachinery p 814 A90-49475
- An investigation of counterrotating tip vortex interaction [NASA-CR-185135] p 79 N90-11549
- Prediction of unsteady blade surface pressures on an advanced propeller at an angle of attack [NASA-TM-102374] p 94 N90-12560
- Integrated multidisciplinary optimization of rotorcraft: A plan for development [NASA-TM-101617] p 106 N90-12580
- General approach and scope - rotor blade design optimization p 106 N90-12581
- Rotor blade aerodynamic design p 106 N90-12582
- Influence of vane sweep on rotor-stator interaction noise p 169 N90-13325
- Computation of flow fields around propellers and hovering rotors based on the solution of the Euler equations [DLR-FB-89-37] p 170 N90-13333
- Finite difference techniques and rotor blade aeroelastic partial differential equations with quasisteady aerodynamics p 236 N90-15075
- Measurement and prediction of propeller blade surface pressure distributions p 481 N90-20961
- The Shock and Vibration Digest, volume 21, no. 2 p 609 N90-22059
- Forcing function effects on rotor rotor unsteady aerodynamic response in a multistage compressor p 573 N90-22536
- Experimental performance and acoustic investigation of modern, counterrotating blade concepts [NASA-CR-185158] p 649 N90-23393

Aerodynamic performance of a 0.27-scale model of an AH-64 helicopter with baseline and alternate rotor blade sets
[NASA-TM-4201] p 632 N90-24237
The acoustic results of a United Technologies scale model helicopter rotor, tested at DNW
[NASA-TM-101879] p 896 N90-27471
Analysis of heliport environmental data, Intracoastal City
[DOT/FAA/CT-TN89/43] p 938 N90-28584

ROTOR BLADES
Wind tunnel tests of models of helicopter rotors
p 29 A90-10230
Design of an advanced pneumatic deicer for the composite rotor blade
p 29 A90-11009
An improved method for the computation of unsteady transonic potential flow - Application for airfoil and blade performance prediction
[ONERA, TP NO. 1989-154] p 4 A90-11175
The flutter characteristic analysis and optimization design of mistuning blade
p 42 A90-11799
The effects of three centres of blade on flutter
p 42 A90-11800
Flutter of mistuned cascades with structural coupling
p 42 A90-11802
Evaluation of two numerical techniques for the prediction of flow around blades
p 10 A90-12512
Cooling characteristics of a radial water blade
p 47 A90-12571
Photoelastic investigation of turbine rotor blade shrouds
p 112 A90-16008
Noninterference blade-vibration measurement system for gas turbine engines
p 132 A90-16372
Effect of environmental particles on a radial compressor
p 113 A90-16373
Aerospatiale's military helicopter programs
p 143 A90-16824
Theoretical and experimental analysis of a model rotor blade incorporating a swept tip
p 151 A90-17586
The Model 360 - Advanced composite helicopter
p 180 A90-17678
An experimental study of tip clearance effects on the performance of an axial transonic turbine
p 189 A90-17788
Aerodynamic design of an HP compressor stage using advanced computation codes
p 156 A90-18479
Comparison of NACA 65, CDA, and tandem bladed cascades
p 190 A90-18484
Development of military helicopters
p 181 A90-18488
Optimal placement of tuning masses for vibration reduction in helicopter rotor blades
p 247 A90-23117
Flow in a centrifugal fan of the squirrel cage type
[ASME PAPER 89-GT-52] p 289 A90-23778
Design, realization, and qualification of model composite rotor blades
p 364 A90-24293
Minimum weight design of rotorcraft blades with multiple frequency and stress constraints
p 335 A90-25304
Nonlinear effects in helicopter rotor forward flight forced response
p 347 A90-25420
Fatigue life prediction method for gas turbine rotor disk alloy FV535
p 440 A90-27679
Helicopter ground/air resonance including rotor shaft flexibility and control coupling
p 406 A90-28153
Identification of retreating blade stall mechanisms using flight test pressure measurements
p 384 A90-28172
BELLTECH - A multipurpose Navier-Stokes code for rotor blade and fixed wing configurations
p 384 A90-28174
New concept for improved nonmetallic erosion protection systems
p 407 A90-28188
The four-bladed main rotor system for the AH-1W helicopter
p 408 A90-28214
A comparison of four versus five blades for the main rotor of a light helicopter
p 408 A90-28215
Periodic response of thin-walled composite blades
p 408 A90-28229
Strike tolerant main rotor blade tip
p 409 A90-28232
The prediction of loads on the Boeing Helicopters Model 360 rotor
p 410 A90-28240
The revolution continuous performance of military helicopters
[MBB-UD-557-89-PUB] p 381 A90-28242
An approach for analysis and design of composite rotor blades
[AIAA PAPER 90-1005] p 449 A90-29276
Time domain flutter analysis of cascades using a full-potential solver
[AIAA PAPER 90-0984] p 391 A90-29374
Piezoelectric actuators for helicopter rotor control
[AIAA PAPER 90-1076] p 411 A90-29384
Aeroelastic analysis of helicopter rotor blades with advanced tip shapes
[AIAA PAPER 90-1118] p 392 A90-29390

Rotor/airframe aeroelastic analyses using the transfer matrix approach
[AIAA PAPER 90-1119] p 392 A90-29391
Dynamic analysis of rotor blades with rotor retention design variations
[AIAA PAPER 90-1159] p 412 A90-29394
The effect of structural variations on the dynamic characteristics of helicopter rotor blades
[AIAA PAPER 90-1161] p 450 A90-29396
Effects of higher harmonic control on rotor performance and control loads
[AIAA PAPER 90-1158] p 412 A90-29467
Structural optimization with aeroelastic constraints of rotor blades with straight and swept tips
p 535 A90-32475
Helicopter response to atmospheric turbulence in forward flight
p 518 A90-33625
The design of the series of blade flutter rotor and the experimental investigation of flow-induced vibration
p 586 A90-37230
Application of optimization methods to helicopter rotor blade design
p 604 A90-37337
Vibration equations for a helicopter rotor blade
p 604 A90-37830
Calculation of unsteady rotor/stator interaction
[AIAA PAPER 90-1544] p 565 A90-38688
Improvements to the fatigue substantiation of the H-60 composite tail rotor blade
p 642 A90-39985
Helicopter surveillance - A look at current and proposed future programs
p 642 A90-39986
Application of mathematical modeling to the study of rigid helicopter rotors
p 643 A90-41738
Unsteady deformations of elastic rotor blades
p 687 A90-42341
CFD and transonic helicopter sound
p 696 A90-42433
Improving tilt rotor aircraft performance with variable-diameter rotors
p 646 A90-42445
Kane's methods in rotorblade dynamics
p 646 A90-42458
Active control of tiltrotor blade in-plane loads during maneuvers
p 670 A90-42463
Aeroelastic response characteristics of a rotor executing arbitrary harmonic blade pitch variations
p 646 A90-42464
Agusta methodology for pitch link loads prediction in preliminary design phase
p 646 A90-42465
Design and manufacturing of composite materials blade models
p 618 A90-42492
Shaft flexibility effects on the forced response of a bladed-disk assembly
p 744 A90-43218
Prediction and measurement of rotor blade/stator vane dynamic characteristics of a modern aero-engine axial compressor
p 878 A90-46036
Full span analysis for flutter prediction of slender blade assemblies
p 879 A90-46188
Computer-aided design of compressor rotor blade rings
p 851 A90-46497
Rotor loads computation using singularity methods and application to the noise prediction
p 807 A90-46880
Mission performance comparison between tilt rotor, variable diameter tilt rotor and tilt wing aircraft
p 830 A90-46940
Empirical prediction of the blockage effect of a flat body on a rotor
p 807 A90-46942
Performance of an optimized rotor blade at off-design flight conditions
p 830 A90-46946
MDHC technical assessment of advanced rotor and control concepts
p 861 A90-46948
Perspectives in aeromechanical stability of helicopter rotors
p 831 A90-46953
Helicopter individual blade control through optimal output feedback
p 861 A90-46956
Theoretical and experimental investigation of the aeroelastic stability of an advanced bearingless rotor in hover and forward flight
p 831 A90-46958
Experiences in NASTRAN airframe vibration prediction at Bell Helicopter Textron
p 832 A90-46964
Application of the Westland CRFD program to total helicopter dynamics
p 832 A90-46965
A study of fundamental issues in higher harmonic control using aeroelastic simulation
p 861 A90-46966
Mean loading effects on flutter of subsonic rotating annular cascade
p 853 A90-49453
A method for predicting stall flutter under variable interblade phase angle along rotating direction
p 813 A90-49455
Some explorations on the mechanism of blade flutter suppression by porous wall casing
p 854 A90-49470
Application of a two-dimensional unsteady viscous analysis code to a supersonic throughflow fan stage
[NASA-TM-4141] p 192 N90-13387
Effect of blade planform variation on a small-scale hovering rotor
[NASA-TM-4146] p 173 N90-14186

Analysis of the rotor tip leakage flow with tip cooling air ejection
p 515 N90-21029
Extension-torsion coupling behavior of advanced composite tilt-rotor blades
p 651 N90-25057
Synthesis of individual rotor blade control system for gust alleviation
[NASA-TM-101886] p 736 N90-25972

ROTOR BLADES (TURBOMACHINERY)
The design of rotor blades taking into account the combined effects of vibratory and thermal loads
p 40 A90-11553
Rub interactions of flexible casing rotor systems
p 41 A90-11554
Rotor-blades excitation due to differential interference of vane wakes between upstream stator-rows in an axial compressor
p 6 A90-11784
Experimental investigation of the time-dependent flow in a vibrating annular cascade operating in the transonic flow regime
p 7 A90-11787
Improved double linearization method for prediction of mean loading effects on subsonic and supersonic cascade flutter
p 41 A90-11795
Systematic study of flutter characteristics of two-dimensional cascades in incompressible flow
p 41 A90-11796
Flutter of cascade blades composed of blades having arbitrarily different natural frequencies
p 42 A90-11798
Progress towards the development of an inviscid-viscous interaction method for unsteady flows in turbomachinery cascades
p 8 A90-11806
Navier-Stokes methods applied to turbomachinery blade design
p 12 A90-12549
A theoretical and experimental investigation of the Reynolds and apparent stresses in axial compressors
p 12 A90-12554
Computation of three dimensional turbulent boundary layers in internal flows, including turbomachinery rotor blades
p 12 A90-12555
Wake behaviour of a large deflection turbine rotor linear cascade
p 157 A90-18481
Effect of downstream elements on the flow at the exit of centrifugal compressor rotor
p 157 A90-18483
Effect of the nonuniform rotation of the gas turbine rotor on blade vibrations
p 253 A90-20431
A finite element solution of unsteady two-dimensional flow in cascades
p 226 A90-21946
An approximate 3-D aerodynamic design method for centrifugal impeller blades
p 291 A90-23794
Three-dimensional solutions for inviscid incompressible flow in turbomachines
[ASME PAPER 89-GT-140] p 291 A90-23837
A simplified model for unstable temperature field calculation of gas turbine rotor
[ASME PAPER 89-GT-234] p 363 A90-23885
Aeroelastic problems in turbomachines
[AIAA PAPER 90-1157] p 393 A90-29393
Unsteady aerodynamics for turbomachinery aeroelastic applications
p 394 A90-29888
Probabilistic method to compute the optimal slip load for a mistuned bladed disk assembly with friction dampers
p 507 A90-32269
Aeroelastic instabilities in aircraft engines - Application to a SNECMA fan stage
p 584 A90-35174
Non-conservative stability of a cracked thick rotating blade
p 606 A90-38544
Euler solutions for self-generated rotor blade-vortex interactions
[AIAA PAPER 90-1588] p 566 A90-38723
Analysis of composite rotor blades via Saint Venant's solutions
p 688 A90-42491
Experimental and numerical study of the British Experimental Rotor Programme blade
[AIAA PAPER 90-3008] p 789 A90-45858
Unsteady lifting surface theory for a rotating cascade of swept blades
[ASME PAPER 89-GT-306] p 906 A90-51259
An experimental convective heat transfer investigation around a film-cooled gas turbine blade
p 957 A90-51261
Laser anemometer measurements in a transonic axial-flow fan rotor
[NASA-TP-2879] p 73 N90-11245
Review and analysis of the DNW/Model 360 rotor acoustic data base
[NASA-TM-102253] p 81 N90-11692
An investigation of end-wall vortex cavitation in a high Reynolds number axial-flow pump
[AD-A211426] p 133 N90-11982
Airframe structural dynamic considerations in rotor design optimization
[NASA-TM-101646] p 134 N90-12057
Numerical simulation of unsteady rotational flow over propfan configurations
[NASA-CR-186037] p 90 N90-12500

- Dynamic tip clearance measurements in axial flow compressors
[PNR90597] p 116 N90-12612
- Blading design for multi-storage HP compressor
[PNR90602] p 116 N90-12616
- A study of the effects of Rotating Frame Turbulence (RFT) on helicopter flight mechanics p 248 N90-15058
- Wake interaction effects on the transition process on turbine blades
[AD-A214492] p 343 N90-16759
- Study of the blade/vortex interaction on a one-blade rotor during forward flight (incompressible, non viscous fluid)
[ISL-R-115/88] p 415 N90-18391
- Design guidance to minimize unsteady forces in turbomachines p 426 N90-18411
- Unsteady blade loads due to wake influence p 426 N90-18413
- Modelling unsteady transition and its effects on profile loss p 427 N90-18423
- Experimental investigation of the influence of rotor wakes on the development of the profile boundary layer and the performance of an annular compressor cascade p 427 N90-18425
- An inverse method for the design of turbomachine blades p 511 N90-20988
- Experimental and numerical study on basic phenomena of secondary flows in turbines p 512 N90-21014
- Measurement of the flow field in the blade passage and side-wall region of a plane turbine cascade p 513 N90-21019
- Forcing function effects on rotor row unsteady aerodynamic response in a multistage compressor p 573 N90-22536
- Theoretical studies carried out in 1988 on helicopter rotor noise under subsonic conditions
[ONERA-RS-82/5094-PY] p 896 N90-28402
- Measurement of the steady surface pressure distribution on a single rotation large scale advanced prop-fan blade at Mach numbers from 0.03 to 0.78
[NASA-CR-182124] p 929 N90-28552
- Flow coupling between a rotor and a stator in turbomachinery
[AD-A223882] p 932 N90-28572
- Analysis of heliport environmental data, Intracoastal City
[DOT/FAA/CT-TN89/43] p 938 N90-28584
- Nonlinear static and dynamic modeling of composite rotor blades including warping effects p 924 N90-29382
- ROTOR BODY INTERACTIONS**
- Rub interactions of flexible casing rotor systems p 41 A90-11554
- Numerical Euler solution for the interaction between oscillating cascade and forced inlet unsteadiness p 8 A90-11792
- Acoustic resonance in centrifugal compressors induced by interaction between rotor and stator p 78 A90-11803
- Propeller wakes and their interaction with wings p 14 A90-12614
- Three-dimensional separated flow field in the endwall region of an annular compressor cascade in the presence of rotor-stator interaction. I - Quasi-steady flow field and comparison with steady-state data
[ASME PAPER 89-GT-76] p 291 A90-23797
- Propeller-wing interaction using a frequency domain panel method p 307 A90-26128
- Prediction and measurement of the aerodynamic interactions between a rotor and airframe in forward flight p 384 A90-28176
- Investigation of aerodynamic interactions between a rotor and fuselage in forward flight p 385 A90-28198
- Multi-output implementation of a modified sparse time domain technique for rotor stability testing
[AIAA PAPER 90-0946] p 412 A90-29405
- Measurement of the interaction between a rotor tip vortex and a cylinder p 555 A90-38255
- Air resonance stability of hingeless rotors in forward flight p 590 A90-38519
- The influence of interactional aerodynamics of rotor-fuselage-interferences on the fuselage flow p 561 A90-38523
- The free-wake computation of rotor-body flows
[AIAA PAPER 90-1540] p 565 A90-38684
- Comparison with experiment of various computational methods of airflow on three helicopter fuselages p 630 A90-42436
- A comprehensive approach to coupled rotor-fuselage dynamics p 646 A90-42460
- A model for active control of helicopter air resonance in hover and forward flight p 670 A90-42462
- An unsteady helicopter rotor-fuselage aerodynamic interaction analysis p 712 A90-45323
- Empirical prediction of the blockage effect of a flat body on a rotor p 807 A90-46942
- AHS National Specialists' Meeting on Rotorcraft Dynamics, Arlington, TX, Nov. 13, 14, 1989, Proceedings p 830 A90-46952
- Fundamental dynamics issues for comprehensive rotorcraft analyses p 831 A90-46961
- An improved rotor/airframe coupling method for NASTRAN airframe vibration analysis p 831 A90-46962
- Experiences in NASTRAN airframe vibration prediction at Bell Helicopter Textron p 832 A90-46964
- Application of the Westland CRFD program to total helicopter dynamics p 832 A90-46965
- A method for calculating the rotor-fuselage interference in helicopters
[DGLR PAPER 88-060] p 919 A90-50246
- ROTOR DYNAMICS**
- Unbalance response studies on a model rotor supported on uncentralsed squeeze film dampers and the development experience of a jet engine p 69 A90-12579
- Automatic vibration reduction at a four bladed hingeless model rotor - A wind tunnel demonstration p 335 A90-25424
- Helicopter rotor dynamics and aeroelasticity - Some key ideas and insights p 335 A90-25425
- Hingeless rotor dynamics in coordinated turns
[AIAA PAPER 90-1117] p 412 A90-29389
- Rotor dynamics of the Vulcain LH2 Turbopump - Comparison between test results and non-linear dynamic analysis p 528 A90-33382
- Dynamics of multi-spool gas turbines using the matrix transfer method - Applications p 509 A90-33594
- Dynamics of multi-spool gas turbines using the matrix transfer method - Theory p 509 A90-33595
- Numerical methods for the treatment of periodic systems with applications to structural dynamics and helicopter rotor dynamics p 604 A90-37881
- The development of a probabilistic turbine rotor design system
[AIAA PAPER 90-2176] p 662 A90-42060
- Kane's methods in rotorblade dynamics p 646 A90-42458
- Unbalance response of a Jeffcott rotor incorporating long squeeze film dampers p 880 A90-46237
- Integrated multidisciplinary optimization of rotorcraft: A plan for development
[NASA-TM-101617] p 106 N90-12580
- General approach and scope --- rotor blade design optimization p 106 N90-12581
- Rotor blade aerodynamic design p 106 N90-12582
- Rotor blade dynamic design p 106 N90-12583
- Application of the joined wing to tiltrotor aircraft
[NASA-CR-177543] p 248 N90-15093
- Gear noise, vibration, and diagnostic studies at NASA Lewis Research Center
[NASA-TM-102435] p 372 N90-18041
- Rotor dynamic analysis with shell elements for the transfer matrix method
[AD-A217455] p 541 N90-20434
- Design of a helicopter automatic flight control system using adaptive control p 522 N90-21040
- Internal rotor friction instability
[NASA-CR-183942] p 543 N90-21395
- Quiet mode for nonlinear rotor models
[NASA-TM-102236] p 582 N90-21758
- Elements of active vibration control for rotating machinery
[NASA-TM-102368] p 610 N90-22703
- Experimental performance and acoustic investigation of modern, counterrotating blade concepts
[NASA-CR-185158] p 649 N90-23393
- The applicability of simple helicopter models for flight mechanics studies
[ETN-90-96962] p 736 N90-25975
- Correlation of AH-1G airframe flight vibration data with a coupled rotor-fuselage analysis
[NASA-CR-181974] p 959 N90-28865
- ROTOR LIFT**
- Free wake analysis of rotor configurations for reduced vibratory airloads p 833 A90-46957
- ROTOR SPEED**
- Comparison of NACA 65, CDA, and tandem bladed cascades p 190 A90-18484
- Optimal placement of tuning masses for vibration reduction in helicopter rotor blades p 247 A90-23117
- Resonant stress determination of a turbine blade with modal damping as a function of rotor speed and vibrational amplitude
[ASME PAPER 89-GT-27] p 340 A90-23765
- Application of higher harmonic control (HHC) to rotors operating at high speed and maneuvering flight p 429 A90-28157
- Flight tests of Adaptive Fuel Control and decoupled rotor speed control systems p 422 A90-28183
- Stability sensitivity analysis of a helicopter rotor p 580 A90-386273
- A simple prediction method for low-cycle fatigue life of structures p 604 A90-37240
- Non-conservative stability of a cracked thick rotating blade p 606 A90-38544
- An experimental investigation of turbine rotor wakes for the development of a fiber optic pressure sensor
[AIAA PAPER 90-2411] p 687 A90-42163
- Improving helicopter aerodynamics - A step ahead p 631 A90-42443
- An experimental study of instantaneous velocity perturbations over a rotor disk for low duty coefficients p 860 A90-46572
- Helicopter individual blade control through optimal output feedback p 861 A90-46956
- Experimental evaluation of a tuned electromagnetic damper for vibration control of cryogenic turbopump rotors
[NASA-TP-3005] p 665 N90-23403
- ROTORCRAFT AIRCRAFT**
- Twenty-five years of rotorcraft aeroacoustics - Historical perspective and important issues p 78 A90-11878
- Rotor concepts for the European Future Advanced Rotorcraft (Eurofar)
[MBB-UD-0551-89-PUB] p 29 A90-12258
- New free-wake analysis of rotorcraft hover performance using influence coefficients p 181 A90-17867
- An application of generalized predictive control to rotorcraft terrain-following flight p 257 A90-23478
- Rotorcraft analytical improvement needed to reduce developmental risk - The 1989 Alexander A. Nikolsky Lecture p 285 A90-23934
- Optimization of rotor performance in hover and axial flight using a free wake analysis p 407 A90-28175
- Control sensitivity, bandwidth and disturbance rejection concerns for advanced rotorcraft p 430 A90-28204
- Fatigue methodology III; Proceedings of the AHS National Technical Specialists' Meeting on Advanced Rotorcraft Structures, Scottsdale, AZ, Oct. 3-5, 1989 p 641 A90-39976
- Considerations of reliability design for rotorcraft p 680 A90-39977
- Designing rotorcraft dynamic components to reliability requirements p 641 A90-39978
- Convertible engine system for high speed rotorcraft
[AIAA PAPER 90-2512] p 658 A90-40643
- Concept development of automatic guidance for rotorcraft obstacle avoidance p 669 A90-41632
- The safety analysis approach for the EH101 p 635 A90-42456
- Contribution of engine improvement on next future rotorcraft p 665 A90-42488
- Vertical Lift Aircraft Design Conference, San Francisco, CA, Jan. 17-19, 1990, Proceedings p 829 A90-46926
- Advocating international cooperation: The Eurofar program - An example and a hope --- European Future Advanced Rotorcraft program p 785 A90-46929
- The servo flap - An advanced rotor control system p 860 A90-46934
- The ROTONET prediction system and initial comparisons with far-field acoustics measurements for the XV-15 tilt-rotor aircraft p 894 A90-46947
- AHS National Specialists' Meeting on Rotorcraft Dynamics, Arlington, TX, Nov. 13, 14, 1989, Proceedings p 830 A90-46952
- Application of a general-purpose mechanical systems analysis code to rotorcraft dynamics problems p 831 A90-46955
- Experimental observations of two-dimensional blade-vortex interaction p 809 A90-47303
- Real-time piloted simulation of fully automatic guidance and control for rotorcraft nap-of-the-earth (NOE) flight following planned profiles
[AIAA PAPER 90-3372] p 864 A90-47630
- Flight investigation of variations in rotorcraft control and display dynamics for hover p 866 A90-47731
- [AIAA PAPER 90-3482] p 866 A90-47731
- The MH-60K - A special rotorcraft for special operations
[AIAA PAPER 90-3266] p 835 A90-48860
- Multi-role advance technology rotorcraft - The EH101
[AIAA PAPER 90-3302] p 837 A90-48884
- Selected design issues of some high speed rotorcraft concepts
[AIAA PAPER 90-3297] p 840 A90-49125
- Integrated multidisciplinary design optimization of rotorcraft
[NASA-TM-101642] p 36 N90-10889
- Aerodynamic characteristics of two rotorcraft airfoils designed for application to the inboard region of a main rotor blade
[NASA-TP-3009] p 633 N90-24239

ROTORS

Optimum weight design of a rotor bearing system with dynamic behavior constraints
[ASME PAPER 89-GT-74] p 358 A90-23795

Threshold performance optimization of a rotor-bearing system subjected to leakage excitation
[ASME PAPER 89-GT-126] p 360 A90-23825

A three dimensional inverse method in turbomachinery. II - Experimental verification
[ASME PAPER 89-GT-137] p 360 A90-23834

Experimental investigation into the effects of rotating and static bolts on both windage heating and local heat transfer coefficients in a rotor/stator cavity
[ASME PAPER 89-GT-196] p 362 A90-23870

Test results for turbulent annular seals, using smooth rotors and helically grooved stators
[ASME PAPER 89-TRIB-11] p 537 A90-33556

A combined Riccati transfer matrix-direct integration method with its applications p 611 A90-37218

Digital control of magnetic bearings supporting a multibeam flexible rotor p 682 A90-40712

Flow and heat transfer in rotating-disc systems. Volume I - Rotor-stator systems --- Book p 772 A90-45759

The role of bearing support stiffness anisotropy in suppression of rotor dynamic instability p 879 A90-46215

Active vibration control for flexible rotor by optimal direct-output feedback control p 879 A90-46222

Spray automated balancing of rotors - How process parameters influence performance p 879 A90-46228

Improved silicon carbide for advanced heat engines [NASA-CR-180831] p 65 A90-10293

An experimental investigation of helicopter rotor hub fairing drag characteristics
[NASA-TM-102182] p 88 A90-11701

Large-scale Advanced Prop-fan (LAP) static rotor test report
[NASA-CR-180848] p 117 A90-12617

Influence of vane sweep on rotor-stator interaction noise p 169 A90-13325

The application of cast SiC/Al to rotary engine components
[NASA-CR-179610] p 192 A90-13385

Effect of blade planform variation on a small-scale hovering rotor
[NASA-TM-4146] p 173 A90-14186

Wake interaction effects on the transition process on turbine blades
[AD-A214492] p 343 A90-16759

Three-dimensional viscous rotor flow calculations using a viscous-inviscid interaction approach
[NASA-TM-102235] p 399 A90-19204

Calculation and optimization of rotor start process
[ETN-90-95894] p 416 A90-19229

Analysis of small-scale rotor hover performance data
[NASA-TM-102271] p 540 A90-20325

Noise of a simulated installed model counterrotation propeller at angle-of-attack and takeoff/approach conditions
[NASA-TM-102440] p 548 A90-20794

Statistics on aircraft gas turbine engine rotor failures that occurred in US commercial aviation during 1986
[DOT/FAA/CT-89/30] p 511 A90-21008

Internal rotor friction instability
[NASA-CR-183942] p 543 A90-21395

The Shock and Vibration Digest, volume 21, no. 2 p 609 A90-22059

The Shock and Vibration Digest, volume 21, no. 3 p 609 A90-22064

Application of a dynamic stall model to rotor trim and aeroelastic response p 583 A90-22556

Computational and experimental investigations of rotating stall in compressor cascades p 588 A90-22565

Experimental evaluation of a tuned electromagnetic damper for vibration control of cryogenic turbopump rotors
[NASA-TP-3005] p 665 A90-23403

Rotary-Jet thrust augmentor with jet-flapped blades p 633 A90-24243

Coupled rotor-body equations of motion hover flight
[NASA-CR-186710] p 717 A90-25111

An unsteady lifting surface method for single rotation propellers
[NASA-CR-4302] p 719 A90-25940

Two-dimensional Euler and Navier-Stokes Time accurate simulations of fan rotor flows
[NASA-TM-102402] p 720 A90-25948

Development of creep-fatigue damage detection method of rotor steel by ultrasonic wave measurement
[DE90-503792] p 777 A90-26365

Velocity measurements on a lifting rotor/airframe configuration in low speed forward flight p 815 A90-26790

Flow coupling between a rotor and a stator in turbomachinery
[AD-A223882] p 932 A90-28572

An enhanced integrated aerodynamic load/dynamic optimization procedure for helicopter rotor blades
[NASA-CR-4326] p 924 A90-29383

Noncontact measurement of rotating blade vibrations [NAL-TR-1033] p 961 A90-29687

ROUTES

Simulator evaluation of the final approach spacing tool
[NASA-TM-102807] p 636 A90-23374

IFR aircraft handled forecast by air route traffic control center: Fiscal years 1990 to 2005
[AD-A220312] p 641 A90-24263

FAA/NASA En Route Noise Symposium
[NASA-CP-3067] p 696 A90-24853

Proposed definition of the term en route in en route aircraft noise p 696 A90-24854

PTA en route noise measurements p 696 A90-24855

En route noise: NASA proplan test aircraft (corrected data - simplified procedure)
[DOT-TSC-FA953-LR4] p 696 A90-24856

En route noise: NASA proplan test aircraft (calculated source noise)
[DOT-TSC-FA953-LR5] p 697 A90-24857

En route noise of turboprop aircraft and their acceptability: Report of tests p 697 A90-24858

En route noise of two turboprop aircraft
[DLR-MITT-89-18] p 697 A90-24859

Sound propagation elements in evaluation of an en route noise of advanced turboprop aircraft p 697 A90-24861

When proplans cruise, will LDN 65 fly p 697 A90-24864

Social survey findings on en route noise annoyance issues p 698 A90-24868

En route noise annoyance laboratory test: Preliminary results p 698 A90-24870

Problems related to aircraft noise in Switzerland p 698 A90-24871

RUBBER

Runaway rubber removal
[AD-A218349] p 526 A90-20100

RUBBER COATINGS

Organic coatings - First line of defense p 204 A90-17300

RUDDERS

Examples of force measurements in a wind tunnel using multicomponent piezoelectric transducers p 540 A90-34352

Influence of some geometrical and design parameters on the hinge moment characteristics of rudders p 643 A90-41739

Stiffness of an aircraft pneumatic rudder drive p 628 A90-46479

Hinge moment coefficient derivatives for trailing-edge controls on wings at subsonic speeds
[ESDU-89009] p 198 A90-14239

Prediction of forces and moments for flight vehicle control effectors. Part 1: Validation of methods for predicting hypersonic vehicle controls forces and moments
[NASA-CR-186571] p 571 A90-21734

RUNGE-KUTTA METHOD

Trajectories of vortex lines beneath a free surface or above a plane p 716 A90-45740

A one equation turbulence model for transonic airfoils p 174 A90-14199

Conical Euler solution for a highly-swept delta wing undergoing wing-rock motion
[NASA-TM-102609] p 400 A90-19211

A video-based experimental investigation of wing rock
[AD-A218244] p 498 A90-20075

A computer code for the prediction of aerodynamic characteristics of lifting airfoils at transonic speed
[DLG-EST-TN-030] p 632 A90-23359

Two-dimensional Euler and Navier-Stokes Time accurate simulations of fan rotor flows
[NASA-TM-102402] p 720 A90-25948

RUNWAY ALIGNMENT

Parallel runway monitor p 241 A90-21382

Analytical studies for computed center line operations
[SAE PAPER 892219] p 729 A90-45436

RUNWAY CONDITIONS

Aircraft and ground vehicle friction measurements obtained under winter runway conditions
[SAE PAPER 891070] p 95 A90-14367

Friction measurements under winter runway conditions p 321 A90-23924

Dynamic analysis of airport pavement p 593 A90-36418

Analyses of Arrow Air DC-8-63 accident of December 12, 1985 - Gander, Newfoundland p 635 A90-40687

Current status of Joint FAA/NASA Runway Friction Program
[SAE PAPER 892340] p 760 A90-45494

Independent operations on closely spaced runways p 821 A90-46393

Evaluation of two transport aircraft and several ground test vehicle friction measurements obtained for various runway surface types and conditions. A summary of test results from joint FAA/NASA Runway Friction Program [NASA-TP-2917] p 249 A90-15902

RUNWAY LIGHTS

Helicopter Visual Segment Approach Lighting System (HALS)
[ACD-330] p 28 A90-10856

Modified touchdown zone lighting
[DOT/FAA/CT-TN89/70] p 526 A90-21042

RUNWAYS

Efforts continue to increase airport/airspace capacity p 722 A90-44550

Definition of research needs to address airport pavement distress in cold regions
[DOT/FAA/DS-89/13] p 59 A90-10896

Improving snow roads and airstrips in Antarctica
[AD-A211588] p 133 A90-11907

Ice runways near the South Pole
[AD-A211606] p 133 A90-11908

Analytical and experimental study of runway runoff with wind effects
[PTI-8948] p 123 A90-12627

Design temperatures for flexible airfield pavement design
[AD-A214141] p 262 A90-15115

Dallas/Fort Worth simulation. Volume 2: Appendixes D, E, and F
[AD-A216613] p 405 A90-18380

Airfields on antarctic glacier ice
[AD-A217638] p 526 A90-20097

Runaway rubber removal
[AD-A218349] p 526 A90-20100

Modified touchdown zone lighting
[DOT/FAA/CT-TN89/70] p 526 A90-21042

Criteria for coal tar seal coats on airport pavements. Volume 2: Laboratory and field studies
[AD-A220167] p 674 A90-24277

Taxiway sign effectiveness under reduced visibility conditions
[DOT/FAA/CT-TN90/20] p 761 A90-25150

An overview of the joint FAA/NASA aircraft/ground runway friction program
[NASA-TM-103486] p 724 A90-25957

Atlanta tower simulation, volume 1
[DOT/FAA/CT-TN89/27-VOL-1] p 870 A90-26835

Atlanta tower simulation. Volume 2: Appendixes
[DOT/FAA/CT-TN89/27-VOL-2] p 870 A90-26836

Development and testing of rapid repair methods for war damaged runways
[AD-A223970] p 938 A90-28586

The potential for an extra runway at Heathrow: A preliminary feasibility study
[TT-9007] p 938 A90-29403

Estimation of power spectral density of runway roughness
[NAL-TR-1037] p 939 A90-29411

RYAN AIRCRAFT

Ryan X-13 experimental aircraft - Lessons learned
[AIAA PAPER 90-3236] p 834 A90-48846

S

S-N DIAGRAMS

Designing rotorcraft dynamic components to reliability requirements p 641 A90-39978

SA-330 HELICOPTER

Theoretical and experimental correlation of helicopter aeromechanics in hover p 429 A90-28200

The new Spheriflex tail rotor for the Super Puma Mark 2 p 408 A90-28213

SAB AIRCRAFT

Swedish philosophy in aeroengine development p 44 A90-12504

Interior noise control of the Saab 340 aircraft
[SAE PAPER 891080] p 101 A90-14372

Finite element calculations of the interior noise of the Saab 340 aircraft
[SAE PAPER 891081] p 101 A90-14373

SAFETY

User's manual for the ride motion simulator
[AD-A212855] p 201 A90-13402

Aircraft/airport compatibility: Some strategic, tactical, and operational issues
[TT-8902] p 202 A90-13409

Evaluation of the improved OV-ID anti-icing system, phase 2
[AD-A213928] p 239 A90-15083

X.2 limited flight test plan
[AD-A214412] p 249 A90-15099

SUBJECT INDEX

Aircraft accident report: Delta Air Lines, Inc., Boeing 727-232, N473DA, Dallas-Fort Worth International Airport, Texas, August 31, 1988
[PB89-910406] p 240 N90-15895

Safety and cryogenic wind tunnels p 264 N90-15960

Analysis of hydraulic fluids and lubricating oils for the formation of Trimethylolpropane Phosphate (TMP-P) [AD-A215188] p 357 N90-16939

Investigation and characteristics of major fire-related accidents in civil air transports over the past ten years p 324 N90-17582

A review of UK civil aviation fire and cabin safety research p 325 N90-17587

Advanced materials for interior and equipment related to fire safety in aviation p 328 N90-17608

New aspects in aircraft inspection using eddy current methods p 886 N90-28085

SAFETY DEVICES

Aircraft cabin fire suppression by means of an interior water spray system [CAA-PAPER-88014] p 96 N90-11719

SAFETY FACTORS

Beech Starship occupant protection evaluation in emergency landing scenario [SAE PAPER 891015] p 100 A90-14327

Criteria for general aviation fuel systems crashworthiness [SAE PAPER 891016] p 109 A90-14328

Methods of safety analysis for Beech Model 2000 - Starship 1 [SAE PAPER 891064] p 101 A90-14364

Helicopter transmissions - Design for safety and reliability p 270 A90-20608

Flutter and aileron reversal safety factors p 345 A90-24164

Caring for the elderly jet p 285 A90-24280

Probabilistic risk assessment and aviation system safety p 322 A90-26231

Aircraft cabin interior systems meeting new FAA regulations p 482 A90-33710

Ground testing techniques in support of flight test [AIAA PAPER 90-1309] p 523 A90-33919

Aging fleet Structures Working Group activities [AIAA PAPER 90-3219] p 786 A90-48840

Twin-engine transports - A look at the future [AIAA PAPER 90-3215] p 818 A90-49107

Safety and health trends in aerospace composite materials p 947 A90-50188

Flammability regulations affecting advanced composite materials p 947 A90-50190

Risk assessment and its application to flight safety analysis [DE90-004985] p 323 N90-16722

Aircraft Fire Safety [AGARD-CP-467] p 324 N90-17581

Aviation safety: Conditions within the air traffic control work force. Fact sheet for congressional requesters [GAO/RCED-89-113FS] p 724 N90-25958

SAFETY MANAGEMENT

Safety management in aircraft testing and certification p 180 A90-17421

Technical means and methods of flight safety assurance --- Russian book p 238 A90-22735

The role of expert systems in aircraft safety management p 375 A90-26225

Probabilistic risk assessment and aviation system safety p 322 A90-26231

The safety analysis approach for the EH101 p 635 A90-42456

UK airmisses involving commercial air transport [CAA-2/88] p 96 N90-11718

Review of the Aerospace Safety Advisory Panel report for NASA fiscal year 1990 authorization [GPO-24-234] p 177 N90-14213

Aircraft fire safety: Learning from past accidents p 324 N90-17584

Development of improved fire safety standards adopted by the Federal Aviation Administration p 324 N90-17585

Fire safety in civil aviation p 325 N90-17586

Objectives and results of cabin fire research in Germany p 325 N90-17588

Forced and natural venting of aircraft cabin fires: A numerical simulation p 326 N90-17597

Hot surface ignition studies of aviation fluids p 327 N90-17600

The stability of fuel fires p 327 N90-17601

Fire hardening of aircraft through upgrades of materials and designs p 327 N90-17605

Heat release rate measurement for evaluating the flammability of aircraft materials p 328 N90-17610

Brake performance of the McDonnell Douglas DC-10-30/40 during high speed, high energy rejected takeoffs [PB90-917004] p 503 N90-21000

Aviation security: Corrective actions underway, but better inspection guidance still needed. Report to the Chairwoman, Government Activities and Transportation Subcommittee, Committee on Government Operations, House of Representatives [GAO/RCED-88-160] p 635 N90-23367

Life management planning p 856 N90-27709

SALT SPRAY TESTS

Maritime environment airframe material fatigue testing p 764 A90-42675

SAMPLING

Aerosol separator for use in aircraft [PB90-142217] p 611 N90-22155

SANDWICH STRUCTURES

Design and evaluation of graphite/epoxy truss core sandwich panels p 210 A90-18406

Buckling analysis of FRP faced cylindrical sandwich panel under combined loading p 365 A90-24376

Natural honeycomb --- use of balsa wood in sandwich panel cores for advanced composite airframes p 442 A90-29643

Honeycomb sandwich primary structure applications on the Boeing Model 360 helicopter p 490 A90-31558

Sandwich structures on Aerospatiale helicopters p 467 A90-31657

The story of sandwich construction p 538 A90-33702

Honeycomb quality requirements - A user's perspective p 538 A90-33705

Core composites in Swissair aircraft p 493 A90-33709

Damage tolerance of carbon fibre reinforced plastic sandwich panels p 675 A90-40047

BD-10J supersonic homebuilt aircraft p 730 A90-42672

A comparison of honeycomb-core and foam-core carbon-fibre/epoxy sandwich panels p 764 A90-43855

Bird impact tests on asymmetric sandwich structures made in Kevlar 49 [CEAT-NT-10/S/83-5] p 323 N90-16727

Bird impact tests on curved structures of the type Sandwich-Kevlar-Nida for normal and angular shooting [CEAT-NT-10/S/83-4] p 324 N90-16728

A study of the structural efficiency of fluted core graphite-epoxy panels [NASA-TM-101681] p 373 N90-18070

A low cost shadow moire device for the nondestructive evaluation of impact damage in composite laminates [AD-A223451] p 953 N90-29442

SATELLITE ALTIMETRY

Influence of satellite geometry, range, clock, and altimeter errors on two-satellite GPS navigation p 123 A90-13993

SATELLITE ANTENNAS

The role of adaptive antenna systems when used with GPS p 128 A90-13995

The E-SAT 300A - A multichannel satellite communication system for aircraft p 914 A90-51339

SATELLITE COMMUNICATION

NAVSTAR-GPS: An evolution or a revolution, Ecole Supérieure d'Electricité, Gif-sur-Yvette, France, Feb. 11, 1987, Workshop p 27 A90-12250

Airborne array antennas for satellite communication p 265 A90-23202

The use of satellite technology for oceanic air traffic control p 330 A90-25570

Rapsat - Application of onboard processing for communication and surveillance in air traffic control [AIAA PAPER 90-0883] p 331 A90-25702

Tests of automatic dependent surveillance (ADS) in Western Europe - Possible future developments p 574 A90-35353

The E-SAT 300A - A multichannel satellite communication system for aircraft p 914 A90-51339

Mobile satellite communications for civil aviation [NLR-MP-88066-U] p 775 N90-26238

SATELLITE IMAGERY

Airborne MSS for land cover classification II p 737 A90-43376

Cloud features suggesting low level wind shear and turbulence p 778 A90-44545

SATELLITE NAVIGATION SYSTEMS

Influence of satellite geometry, range, clock, and altimeter errors on two-satellite GPS navigation p 123 A90-13993

Flight demonstration of two and three satellite navigation p 98 A90-13994

Accuracy considerations for GPS TSPI system design p 98 A90-14001

Potential applications of satellite navigation p 264 A90-21716

Status and potential of GPS-receiver development p 265 A90-21717

Ground navigation in airport traffic p 242 A90-21725

Prospects are very good for using satellites for aeronautical navigation p 403 A90-27924

The case for both RAIM and GIC working together - The ultimate solution to the GPS integrity problem p 576 A90-36916

GPSNOTAM - A demonstration system for GPS status notification p 728 A90-45238

Radio Technical Commission for Aeronautics, Annual Assembly and Technical Symposium, Washington, DC, Dec. 4-6, 1989, Proceedings p 821 A90-46390

1990-1995, a period of international decision making for the navigation community - Is our planning as good as it should be? p 823 A90-49490

A supplement to GPS/Navstar for civil use p 915 A90-52613

SATELLITE NETWORKS

Optimal selection of GPS sets to minimize emitter location errors p 97 A90-13992

Flight demonstration of two and three satellite navigation p 98 A90-13994

Geodetic network adjustment using GPS triple difference observations and a priori stochastic information [TR-1-1987] p 178 N90-13367

SATELLITE OBSERVATION

The Radarsat system --- Canada/U.S. program for launching remote sensing satellite with SAR p 873 A90-49671

Test network Delft [ETN-90-96009] p 177 N90-13365

Geodetic network adjustment using GPS triple difference observations and a priori stochastic information [TR-1-1987] p 178 N90-13367

SATELLITE POWER TRANSMISSION

History and status of beamed power technology and applications at 2.45 Gigahertz p 61 N90-10150

SATELLITE SOUNDING

Environmental conditions associated with the Dallas microburst storm determined from satellite soundings p 280 A90-22689

SATELLITE TRACKING

ASHTech XII - A new GPS technology p 576 A90-36917

Embedded GPS - The Canadian Marconi approach p 725 A90-43700

A robust RAIM scheme using GPS/GLONASS systems p 726 A90-43713

SATELLITE-BORNE INSTRUMENTS

Airborne MSS for land cover classification II p 737 A90-43376

SCALE EFFECT

Similarity and scale effects in solid fuel ramjet combustors p 60 A90-12513

Scaling effects in the impact response of graphite-epoxy composite beams [SAE PAPER 891014] p 128 A90-14326

Experience with scale effects in non-airplane wind tunnel testing [AIAA PAPER 90-1822] p 350 A90-25165

Design considerations for a compact table top hypersonic simulator of aero-optic effects p 525 A90-34585

Priorities for high-lift testing in the 1990s [AIAA PAPER 90-1413] p 596 A90-37950

Terrain visual cue analysis for simulating low-level flight: A multidimensional scaling approach [AD-A23564] p 938 N90-29407

SCALE MODELS

Transition effects on airfoil dynamics and the implications for subscale tests p 152 A90-17862

Comparison of model- and full-scale wind-tunnel performance [AIAA PAPER 88-2536] p 351 A90-26133

Acoustic characteristics of counterrotating unducted fans from model scale tests p 378 A90-26138

An application of structural optimization in wind tunnel model design [AIAA PAPER 90-0956] p 438 A90-29241

Flight test and numerical analysis of a half-scale Unmanned Air Vehicle [AIAA PAPER 90-1260] p 494 A90-33890

A concept study on the use of remotely piloted, sub-scale aircraft for high Reynolds number testing [AIAA PAPER 90-1263] p 494 A90-33892

High Mach exhaust system concept scale model test results [AIAA PAPER 90-1905] p 655 A90-40552

A simple dynamic engine model for use in a real-time aircraft simulation with thrust vectoring [AIAA PAPER 90-2166] p 662 A90-42054

Experimental evaluation of expendable supersonic nozzle concepts [AIAA PAPER 90-1904] p 740 A90-42691

Small-scale inlet testing for low cost screening applications [AIAA PAPER 90-1926] p 741 A90-42696

- Effect of a crescent-shaped rigid support on the aerodynamic characteristics of models in the presence of perforated boundaries p 869 A90-46537
An unmanned air vehicle concept with tipjet drive p 830 A90-46951
Evolution and test history of the V-22 0.2-scale aeroelastic model p 831 A90-46954
Theoretical and experimental investigation of the aeroelastic stability of an advanced bearingless rotor in hover and forward flight p 831 A90-46958
Strain-gage applications in wind tunnel balances p 957 A90-52037
The spinning of aircraft: A discussion of spin prediction techniques including a chronological bibliography [ARL-AERO-R-177] p 36 N90-10888
Engine inlet distortion in a 9.2 percent scale vectored thrust STOVL model in ground effect [NASA-TM-102358] p 318 N90-17561
Measurement and computer simulation of antennas on ships and aircraft for results of operational reliability p 370 N90-17936
Automation of an RCS (Radar Cross Section) measurement system and its application to investigate the electromagnetic scattering from scale model aircraft canopies [AD-A215741] p 371 N90-17970
Wind tunnel study of wake downwash behind A 6 percent scale model B1-B aircraft [DE90-011783] p 719 N90-25941
- SCALING LAWS**
Upstream-influence scaling of fin-generated shock wave boundary-layer interactions [AIAA PAPER 90-0376] p 164 A90-19822
An improved canopy stiffness scaling law for determining opening time of flat circular parachutes [AIAA PAPER 90-3058] p 790 A90-45863
- SCARFING**
An apparatus to prepare composites for repair p 533 A90-31574
- SCATTEROMETERS**
Dual cross-polarization planar arrays in the C and X bands p 638 A90-40979
- SCENE ANALYSIS**
Terrain visual cue analysis for simulating low-level flight: A multidimensional scaling approach [AD-A223564] p 938 N90-29407
- SCHEDULES**
Calendar of selected aeronautical and space meetings [AGARD-CAL-90/1] p 464 N90-19060
Marshall Avionics Testbed System (MAST) p 421 N90-19417
- SCHEDULING**
Piloted simulation of a ground-based time-control concept for air traffic control [NASA-TM-101085] p 240 N90-15898
Investigation of air transportation technology at the Massachusetts Institute of Technology, 1988-1989 p 484 N90-20922
Analysis of sequencing and scheduling methods for arrival traffic [NASA-TM-102795] p 636 N90-23373
Real-time adaptive aircraft scheduling [NASA-CR-177558] p 820 N90-27669
- SCHLIEREN PHOTOGRAPHY**
Color schlieren system using square color filter and its application to aerofoil test in transonics p 66 A90-10748
The use of a Laval nozzle and wall suction for blockage-free transonic wind-tunnel operation p 225 A90-21592
Schlieren studies of compressibility effects on dynamic stall of airfoils in transient pitching motion [AIAA PAPER 90-3038] p 791 A90-45877
Investigation of the vortex flow over a sharp-edged delta wing in the transonic speed regime [LR-594] p 717 N90-25115
Flow visualization of dynamic stall on an oscillating airfoil [AD-A222202] p 815 N90-26797
Cavity aeroacoustics [AD-A223853] p 911 N90-29307
- SCHMIDT NUMBER**
Simulation of cooling film density ratios in a mass transfer technique [ASME PAPER 89-GT-200] p 362 A90-23872
- SCHWARTZ INEQUALITY**
Formation of design envelope criterion in terms of deterministic spectral procedure [RAE-TM-SS-9] p 721 N90-25953
- SCINTILLATION**
Extended communication path length scintillation measurements and model - A discussion of results --- of atmospheric laser experiments p 725 A90-43230

SCREEN EFFECT

- Optimal conditions of flow turbulence suppression in the working section of a wind tunnel using screens located in the prechamber p 438 A90-29185
The absorption of sound by perforated linings p 965 A90-51994

SEA SURFACE TEMPERATURE

- Aircraft measurements of sea surface conditions and their relationship to marine boundary-layer dynamics p 888 A90-47572

SEA WATER

- Glassy waters for Seastar --- corrosion-resistant GFRP for turboprop amphibious aircraft airframes p 382 A90-29637

SEALERS

- Sealing the future --- sealants and adhesives for military aircraft p 442 A90-29638
Fluorosilicone sealants for aircraft fuel containment p 529 A90-31618
Silicone sealants and adhesives for aerospace/defense applications p 529 A90-31619
The effect of primer age on adhesion of polysulphide sealant p 269 N90-15909
Fuel resistant coatings for metal and composite fuel tanks p 269 N90-15911
Effect of temperature on the storage life of polysulfide aircraft sealants [MRL-TR-89-31] p 444 N90-19364

SEALING

- A theoretical study of ingress for shrouded rotating disc systems with radial outflow --- sealing rotor-stator cavities [ASME PAPER 89-GT-178] p 361 A90-23859
Flanged joints of aeroengines [PNR90594] p 116 N90-12609
Advanced actuation systems development, volume 1 [AD-A213334] p 121 N90-12624
Integral fuel tank sealing practice at British Aerospace (Kingston) p 250 N90-15905
The repair of aircraft integral fuel tanks in the RAF: A user's view of fuel tank technology p 250 N90-15908
Fuel resistant coatings for metal and composite fuel tanks p 269 N90-15911
Spray sealing: A breakthrough in integral fuel tank sealing technology p 276 N90-15912
Design philosophy and construction techniques for integral fuselage fuel tanks p 250 N90-15913
Integral fuel tank certification and test methods p 251 N90-15916

SEALS (STOPPERS)

- Development of new segment carbon seal for use at low sealing pressure region FJR710/600S turbo fan engine p 69 A90-11950
The selection and performance of thermal sprayed abrasible seal coatings for gas turbine engines [SAE PAPER 890929] p 286 A90-24694
Test results for turbulent annular seals, using smooth rotors and helically grooved stators [ASME PAPER 89-TRIB-11] p 537 A90-33556
Gas turbine engine brush seal applications [AIAA PAPER 90-2142] p 685 A90-42041
Tooth thickness effects on the performance of gas labyrinth seals p 771 A90-45300
Advanced analysis of multi-ring liquid seals p 880 A90-46236

SEAPLANES

- Water borne again p 579 A90-35846

SEARCH RADAR

- ASR-9 weather channel test report [AD-A211749] p 133 N90-11934

SEATS

- Aft facing transport aircraft passenger seats under 16G dynamic crash simulation p 175 A90-17416
Preliminary fire extinguishing tests with handheld bottles: A comparison of extinguishing compounds [DOT/FAA/CT-TN89/60] p 370 N90-17930
Operational effects on crashworthy seat attenuators [AD-A221148] p 637 N90-24259
A review of research and development in crashworthiness of general aviation aircraft: Seats, restraints and floor structures [AD-A221557] p 846 N90-27698

SECONDARY FLOW

- A secondary flow calculation method for one stage centrifugal compressor p 14 A90-12597
Experimental investigations of effects of the stagger angle on secondary flows in plane compressor cascades p 83 A90-13787
Aerodynamic design of an HP compressor stage using advanced computation codes p 156 A90-18479
Secondary flows in a transonic cascade - Comparison between experimental and numerical results p 157 A90-18501
Calculation of the side-wall boundary layer in axial turbomachines, accounting for the internal flow near the blades p 225 A90-21595

- Influence of the radial component of total pressure gradient on tip clearance secondary flow in axial compressors [ASME PAPER 89-GT-19] p 288 A90-23761
Secondary loss generation in a linear cascade of high-turning turbine blades [ASME PAPER 89-GT-47] p 289 A90-23773
Inlet skew and the growth of secondary losses and vorticity in a turbine cascade [ASME PAPER 89-GT-65] p 290 A90-23788
Mach number effects on secondary flow development downstream of a turbine cascade [ASME PAPER 89-GT-67] p 290 A90-23790
Comparison of steady and unsteady secondary flows in a turbine stator cascade [ASME PAPER 89-GT-79] p 291 A90-23800
Secondary flow due to the tip clearance at the exit of centrifugal impellers [ASME PAPER 89-GT-81] p 358 A90-23802
Aerodynamics of cooling jets introduced in the secondary flow of a low speed turbine cascade [ASME PAPER 89-GT-192] p 362 A90-23868
Influence of bulk turbulence and entrance boundary layer thickness on the curved duct flow field [AIAA PAPER 90-1502] p 606 A90-38651
Turbulent flow simulation of a three-dimensional turbine cascade [AIAA PAPER 90-2124] p 704 A90-42732
Improvement in turbine blade aerodynamic force in the tip region p 809 A90-47854
Basic studies of the unsteady flow past high angle of attack airfoils [AD-A210252] p 18 N90-10008
Secondary Flows in Turbomachines [AGARD-CP-469] p 511 N90-21009
Secondary flows and radial mixing predictions in axial compressors p 512 N90-21010
The effects of compressor endwall flow on airfoil incidence and deviation p 512 N90-21011
A study on secondary flow and spanwise mixing in axial flow compressors p 512 N90-21012
Experimental and numerical study on basic phenomena of secondary flows in turbines p 512 N90-21014
Secondary flows and Reynolds stress distributions downstream of a turbine cascade at different expansion ratios p 512 N90-21015
An investigation of secondary flows in nozzle guide vanes p 512 N90-21016
Secondary flow predictions for a transonic nozzle guide vane p 513 N90-21017
Secondary flow in a turbine guide vane with low aspect ratio p 513 N90-21018
Measurement of the flow field in the blade passage and side-wall region of a plane turbine cascade p 513 N90-21019
Calculation of the three dimensional turbulent flow in a linear turbine blade p 513 N90-21021
Calculation of the secondary flow in an axial turbine p 513 N90-21022
Generation and decay of secondary flows and their impact on aerodynamic performance of modern turbomachinery components p 514 N90-21023
Secondary flow calculations for axial and radial compressors p 514 N90-21024
Research on cascade secondary and tip-leakage flows: Periodicity and surface flow visualization p 514 N90-21026
Losses in the tip-leakage flow of a planar cascade of turbine blades p 514 N90-21027
Computational prediction and measurement of the flow in axial turbine cascades and stages p 514 N90-21028
The effect of secondary flow on the redistribution of the total temperature field downstream of a stationary turbine cascade p 515 N90-21033
- SECONDARY RADAR**
Evaluating the feasibility of a radar separation minimum for a long-range SSR p 25 A90-10240
Applications of Mode S secondary surveillance radar to civil air traffic control - Studies, experiments, and policy of the French Direction de la Navigation Aérienne p 639 A90-41056
Experiments on Mode S secondary surveillance radar - The participation of the French Direction de la Navigation Aérienne in the European effort p 639 A90-41057
Aircraft Reply and Interference Environment Simulator (ARIES) hardware principles of operation. Volume 2: Appendixes [DOT/FAA/CT-TN88/4-2] p 135 N90-12781
Aircraft Reply and Interference Environment Simulator (ARIES) hardware principles of operation, volume 1 [DOT/FAA/CT-TN88/4-1] p 135 N90-12782
- SECURITY**
Analysis of damaged components from DOE security helicopter N7EG [DE90-004488] p 324 N90-16729

SEDIMENTS

Production of jet fuels from coal-derived liquids. Volume 13: Evaluation of storage and thermal stability of jet fuels derived from coal liquids
[AD-A224576] p 954 N90-29527

SELF EXCITATION

Self-excited oscillation of shock waves on an airfoil in two-dimensional transonic channel flow p 8 A90-11808

Study on travelling wave vibration of bladed disks in turbomachinery p 423 A90-29908

Analysis of self-excited vibrations of stiffened covering panels of an aeroplane wing p 860 A90-46716

SELF INDUCED VIBRATION

Analysis of self-excited vibrations of stiffened covering panels of an aeroplane wing p 860 A90-46716

SELF LUBRICATING MATERIALS

Self-lubricating surfaces by ion beam processing [AD-A222489] p 884 N90-27118

SELF OSCILLATION

Self-excited oscillation of transonic flow around an airfoil in two-dimensional channel [ASME PAPER 89-GT-58] p 290 A90-23784

Conditions of the generation of autooscillations in aerodynamic control surfaces in nonseparated subsonic flow of a gas p 315 A90-27303

Self-induced roll oscillations of lifting systems with thin delta wings p 860 A90-46570

Self-excited oscillations in internal transonic flows p 813 A90-49274

SELF REPAIRING DEVICES

Flight-testing of the self-repairing flight control system using the F-15 highly integrated digital electronic control flight research facility [AIAA PAPER 90-1321] p 520 A90-34149

Flight-testing of the self-repairing flight control system using the F-15 highly integrated digital electronic control flight research facility [NASA-TM-101725] p 758 N90-25144

SELF SEALING

Spray sealing: A breakthrough in integral fuel tank sealing technology p 276 N90-15912

SEMICONDUCTOR DEVICES

Summary report of the Summer Conference of the DARPA-Materials Research Council [AD-A217380] p 532 N90-20143

SEMICONDUCTOR DIODES

Direct frequency modulation in interferometric systems p 68 A90-11662

SEMICONDUCTOR LASERS

A semiconductor laser-Doppler-anemometer for applications in aerodynamic research p 447 A90-28273

SEMIEMPIRICAL EQUATIONS

Experimental investigation of trailing-edge and near wake flow of a symmetric airfoil p 160 A90-19449

SEMIWAKE MODELS

Measured aerodynamic performance of a swept wing with a simulated ice accretion [AIAA PAPER 90-0490] p 557 A90-37063

Experimental and theoretical aerodynamic characteristics of a high-lift semispan wing model [NASA-TP-2990] p 477 N90-20046

SENSITIVITY

Sensitivity analysis using resonance and anti-resonance frequencies - A guide to structural modification p 536 A90-33396

An analytical sensitivity method for use in integrated aeroservoelastic aircraft design p 517 A90-33405

SENSITOMETRY

Visualization of corona discharges p 819 A90-49839

SENSORS

Overview of fiber optic smart structures for aerospace applications p 37 A90-11202

Fiber optic sensors for composite monitoring p 37 A90-11203

Air Force smart structures/skins program overview p 38 A90-11205

Fiber optic sensor systems for smart aerospace structures p 38 A90-11208

Optical fiber sensing considerations for a smart aerospace structure p 38 A90-11210

Producibility and life cycle cost issues in applications of embedded fiber optic sensors in smart skins p 38 A90-11221

Temperature insensitive fiber coil sensor for altimeters p 339 A90-26374

Evaluation of sensor management systems p 461 A90-30789

Application of effective baselines to smart structures p 536 A90-32885

Multiple sensor data association and fusion in aerospace applications p 778 A90-44644

Devices and procedures for the calibration of sensors and measurement: Systems of the flight test support system ATTAS [DFVLR-MITT-89-06] p 134 N90-12007

SENSORY FEEDBACK

An analysis of feel system effects on lateral flying qualities [AIAA PAPER 90-1824] p 346 A90-25168

SEPARATED FLOW

An experimental study of fluctuations in the front separation zone at supersonic flow velocities p 10 A90-12282

Axisymmetric afterbody flow separation at transonic speeds in presence of jet exhaust p 13 A90-12576

Turbulent separated flow over and downstream of a two-element airfoil p 16 A90-12738

Shock-wave/boundary-layer interaction at a swept compression corner p 16 A90-12850

Critique of turbulence models for shock-induced flow separation p 17 A90-12851

Investigation of flow separation on a supercritical airfoil p 17 A90-13023

Accumulated span loadings of an arrow wing having vortex flow p 17 A90-13025

Recent Navier/Stokes calculations in applications p 85 A90-15227

Separated flow over slender wing, body and wing-body combination p 85 A90-15232

Computation of transonic separated flow using the Euler equations p 85 A90-15233

Computation of flow over airfoils under high lift separated flow condition p 86 A90-15741

Convergence properties of high-Reynolds-number separated flow calculations p 86 A90-15820

A viscous package for attached and separated flows on swept and tapered wings p 146 A90-16771

Numerical simulation of separated and vortical flows on bodies at large angles of attack p 146 A90-16772

Analysis of high-incidence separated flow past airfoils p 147 A90-16781

Prediction of transition on airfoils with separation bubbles, swept wings and bodies of revolution at incidence p 148 A90-16790

Transition effects on airfoil dynamics and the implications for subscale tests p 152 A90-17862

Navier-Stokes computations of lee-side flows over delta wings p 153 A90-17978

Experimental investigation of flowfield about a multielement airfoil p 154 A90-18137

Simulation of high incidence unsteady flow past Joukowski airfoils p 156 A90-18301

An investigation of unsteady leading edge separation of rapidly pitched airfoils p 157 A90-18587

Numerical modeling of a viscous separated flow in the near wake p 159 A90-19236

Unsteady aerodynamic forces on rolling delta wings at high angle of attack p 159 A90-19426

Semi-implicit Navier-Stokes solver (SINSS) calculations of separated flows around blunt delta wings [AIAA PAPER 90-0590] p 168 A90-19936

A computer aided manufacturing procedure for experimental two-dimensional aeroflows p 270 A90-20609

Swept shock/boundary-layer interactions - Tutorial and update [AIAA PAPER 90-0375] p 228 A90-22207

Spanwise properties of the unsteady separation shock in a Mach 5 unswept compression ramp interaction [AIAA PAPER 90-0377] p 228 A90-22208

Asymmetric separated flows at supersonic speeds [AIAA PAPER 90-0595] p 230 A90-22233

Controlled three-dimensionality in unsteady separated flows about a sinusoidally oscillating flat plate [AIAA PAPER 90-0689] p 230 A90-22244

Characteristics of turbulent separation flows on a porous surface under conditions of injection p 231 A90-22422

Three-dimensional separated flow field in the endwall region of an annular compressor cascade in the presence of rotor-stator interaction. I - Quasi-steady flow field and comparison with steady-state data [ASME PAPER 89-GT-76] p 291 A90-23797

Three-dimensional separated flow field in the endwall region of an annular compressor cascade in the presence of rotor-stator interaction. II - Unsteady flow and pressure field [ASME PAPER 89-GT-77] p 291 A90-23798

An experimental study of separated flow past a low-aspect-ratio delta wing p 294 A90-24077

Calculation of nonseparated transonic flow past swept wings with allowance for viscosity p 294 A90-24079

Flow past a wing/fuselage combination with separation from the side edges of the wing p 295 A90-24088

Pseudoshock and separated flow in rectangular ducts p 295 A90-24089

Comparison of inviscid and viscous separated flows p 302 A90-25277

Topology of computed incompressible three-dimensional separated flow field around high-angle-of-attack cone-cylinders p 366 A90-25764

Navier-Stokes computations for the investigation of flowfields about a Space-Plane p 306 A90-25836

Numerical simulation of separated flows around a wing section by a discrete vortex method p 307 A90-25846

Simulation of separated flows using panel method p 308 A90-26349

Grid generation and its application to separated flows p 312 A90-26552

The hemisphere-cylinder at an angle of attack [AIAA PAPER 90-0050] p 313 A90-26907

Calculation of transonic flows with separation past arbitrary inlets at incidence p 384 A90-27979

Laminar separated flow on a biconical body at high supersonic velocities p 387 A90-28992

Numerical simulation of separated flow around two-dimensional wing section by a discrete vortex method p 469 A90-32067

Multi-element aeroflows in viscous flow p 469 A90-32451

Unsteady, separated flow behind an oscillating, two-dimensional spoiler p 469 A90-32462

Numerical modeling of separated turbulent flows p 470 A90-32673

Unsteady airloads due to separated flow on airfoils and wings p 471 A90-33311

An investigation of the buffet excitation parameter p 473 A90-33368

On the prediction of the aeroelastic behaviour of lifting systems due to flow separation p 491 A90-33369

Numerical simulation of separated flows around a wing section at pitching motion by a discrete vortex method p 475 A90-33753

A numerical method for calculating supersonic flows of a viscous gas p 476 A90-34672

Unsteady aerodynamic gust response including steady flow separation p 556 A90-36262

Versatility of an algebraic backflow turbulence model [AIAA PAPER 90-1485] p 563 A90-38639

Investigation of several passive and active methods for turbulent flow separation control [AIAA PAPER 90-1598] p 607 A90-38730

Drag reduction by controlling flow separation using stepped afterbodies p 622 A90-40690

Investigations of the influence of slot blowing from the upper wing surface on the flow around the wing and its aerodynamic characteristics p 623 A90-41740

Viscous-inviscid interaction method for calculating the flow in compressor cascade blade passages and wake with separation [AIAA PAPER 90-2125] p 624 A90-42032

Flow separation on a supercritical airfoil p 627 A90-42394

Zonal Navier-Stokes methodology for flow simulation about a complete aircraft p 709 A90-44727

Numerical modeling of transverse flow past a cylinder using Euler equations p 709 A90-44922

In-flight flow visualization characteristics of the NASA F-18 high alpha research vehicle at high angles of attack [SAE PAPER 892222] p 713 A90-45439

Effects of turbulence models on the prediction of transonic wing flows [SAE PAPER 892224] p 713 A90-45440

Low Reynolds number airfoil design and wind tunnel testing at Princeton University p 799 A90-46362

Study of low-Reynolds number separated flow past the Wortmann FX 63-137 airfoil p 799 A90-46363

Numerical calculation of turbulent separated flows in an abruptly expanding channel p 803 A90-46487

Self-induced roll oscillations of lifting systems with thin delta wings p 860 A90-46570

Application of localized surface heating to actively control the boundary layer separation p 806 A90-46848

Flow separation in oblique shock wave turbulent boundary layer interactions p 807 A90-46872

Prediction of separated transonic wing flows with nonequilibrium algebraic turbulence model p 809 A90-47312

Control of wall-separated flow by internal acoustic excitation p 809 A90-47314

Basic studies of the unsteady flow past high angle of attack airfoils [AD-A210252] p 18 N90-10008

The three-dimensional vortex sheet structure on delta wings p 19 N90-10367

Simultaneous detection of separation and transition in surface shear layers p 72 N90-10368

The structure of separated flow regions occurring near the leading edge of airfoils - including transition [NASA-CR-185853] p 87 N90-11695

- A one equation turbulence model for transonic airfoils p 174 N90-14199
- A direct-inverse method for transonic and separated flows about airfoils [NASA-CR-4270] p 235 N90-15072
- Flows with Separation [DGLR-PAPERS-88-05] p 276 N90-16169
- An interactive method for the flow calculation of airfoils with local separation regions p 278 N90-16190
- Calculation of the flap profile flows with separation based on coupled potential and boundary layer solutions p 278 N90-16191
- Inverse solutions for boundary layers with separation or close to separation under locally infinite swept wing conditions p 279 N90-16192
- Periodically unsteady effects on profiles, induced by separation p 279 N90-16196
- Unsteady viscous calculation method for cascades with leading edge induced separation p 426 N90-18408
- Method and apparatus for detecting laminar flow separation and reattachment [NASA-CASE-LAR-13952-1-SB] p 455 N90-19534
- Experimental investigation of the mechanisms underlying vortex kinematics in unsteady separated flows [AD-A217889] p 540 N90-20346
- Measurement of the flow field in the blade passage and side-wall region of a plane turbine cascade p 513 N90-21019
- Navier-Stokes analysis of turbine blade heat transfer [NASA-TM-102496] p 542 N90-21300
- Control of flow separation and mixing by aerodynamic excitation [NASA-TM-103131] p 571 N90-21733
- Numerical investigation of some control methods for 3-D turbulent interactions due to sharp fins p 591 N90-21764
- A study of supermaneuver aerodynamics [AD-A218378] p 631 N90-23349
- Identification of aerodynamic models for maneuvering aircraft [NASA-CR-186630] p 719 N90-25943
- Report of the Fluid Dynamics Panel Working Group 10 on calculation of 3D separate turbulent flows in boundary layer limit [AGARD-AR-255] p 776 N90-26280
- Model tilt-rotor hover performance and surface pressure measurement [AD-A222535] p 845 N90-26827
- The effect of rapid spoiler deployment on the transient forces on an airfoil p 921 N90-28527
- ### SEPARATORS
- A theoretical approach to particle separator design p 48 A90-12584
- Viscous flow analysis for advanced inlet particle separators [AIAA PAPER 90-2138] p 661 A90-42038
- ### SEQUENCING
- National airspace system approach and departure sequencing operational concept [NAS-SR-1322] p 27 N90-10017
- Passive navigation using image irradiance tracking p 578 N90-22232
- Kalman filter based range estimation for autonomous navigation using imaging sensors p 578 N90-22238
- Analysis of sequencing and scheduling methods for arrival traffic [NASA-TM-102795] p 636 N90-23373
- ### SEQUENTIAL ANALYSIS
- An application of SQP and Ada to the structural optimisation of aircraft wings p 216 A90-18444
- ### SERVICE LIFE
- Endurance test of FJR 710/600S engine p 42 A90-12012
- Development of a remaining useful life of a lubricant evaluation technique. III - Cyclic voltammetric methods p 125 A90-15732
- Extending an airliner's life p 244 A90-20262
- Durability of equipment assemblies and elements of life-support systems for flight vehicles --- Russian book p 446 A90-21275
- The U.S. airline industry - Coping with an aging fleet p 221 A90-21702
- New progress in airframe durability requirements p 246 A90-22001
- The application of the engineering approach for analyzing crack tolerance of fuselage panels to a transport airplane p 282 A90-22014
- Caring for the elderly jet p 275 A90-24280
- Development of erosion resistant coatings for compression airfoils p 443 A90-31120
- Probabilistic design technology for ceramic components p 601 A90-35507
- Retirement lives of rolling element bearings p 680 A90-39980
- Development and verification of software for flight safety critical strapdown systems p 694 A90-42454
- Life estimation of a gas turbine afterburner spraybar p 739 A90-42662
- Probabilistic approach to fleet management p 701 A90-42674
- Douglas aging aircraft programs [SAE PAPER 892206] p 732 A90-45425
- Initial service experience with the Fokker 100 [SAE PAPER 892238] p 733 A90-45450
- Operation of the Rolls-Royce Pegasus Engine on low grade non-aviation fuels [SAE PAPER 892329] p 747 A90-45486
- The RB211-535E4 - A commercially proven engine for the military of tomorrow [SAE PAPER 892364] p 748 A90-45513
- Technical and economic efficiency of aviation gas turbine engines in service --- Russian book p 851 A90-46624
- Tracking B-1B aircraft with a structural data recorder p 926 A90-49880
- Re-assessing the F-16 damage tolerance and durability life of the RNLA F-16 aircraft p 901 A90-49881
- The survivability of centrifugal compressors in modern aircraft engines p 928 A90-49883
- Durability and damage tolerance of graphite/epoxy honeycomb structures p 942 A90-50085
- Ways of providing for the strength and service life of aircraft structures made of polymer composites with allowance for damage p 957 A90-50843
- The RB199: An in-service success [PNR90544] p 114 N90-11746
- In service life monitoring system using g-meter readings and mass configuration control [ETN-89-95218] p 134 N90-12035
- Thermal barrier coating life prediction model development, phase 1 [NASA-CR-182230] p 193 N90-13388
- Full-scale birdstrike testing of in-service aged F-111 ADBIRT windshield transparencies [AD-A218035] p 484 N90-20069
- Flow in a forward swept centrifugal fan, volumes 1 and 2 p 481 N90-20959
- Boeing/NASA composite components flight service evaluation [NASA-CR-181898] p 601 N90-22609
- National Airspace System (NAS) software life cycle management study [AD-A221180] p 729 N90-25122
- Study on application of ultrasonic wave measurement to creep-fatigue damage detection [DE89-782317] p 774 N90-25361
- Damage tolerance analysis for manned hypervelocity vehicles. Volume 2: Software user's manual [AD-A222136] p 845 N90-26826
- B-1B improved windshield development. Volume 2: Magna analysis: Baseline and parametric [AD-A221501] p 845 N90-26828
- Advanced algorithms design and implementation in on-board microprocessor systems for engine life usage monitoring p 892 N90-27628
- AGARD/SMP Review Damage Tolerance for Engine Structures. 3: Component Behaviour and Life Management [AGARD-R-770] p 855 N90-27704
- AGARD damage tolerance concepts for engine structures Workshop 3, Component Behaviour and Life Management p 855 N90-27705
- Life management planning p 856 N90-27709
- Evaluation of composite components on the Bell 206L and Sikorsky S-76 helicopters [NASA-TM-4195] p 876 N90-27787
- An ultrasonic system for in-service non-destructive inspection of composite structures p 885 N90-28076
- NASA Langley Research Center National Aero-Space Plane Mission simulation profile sets [NASA-TM-102670] p 924 N90-28541
- Energy Efficient Engine (E3) combustion system component technology performance report [NASA-CR-168274] p 930 N90-28555
- ### SERVOCONTROL
- Evaluation of the dynamic properties of the auto-pilot servo of a single-rotor helicopter through laboratory testing F/A-18 aileron smart servoactuator p 432 A90-30710
- A review of aeroelasticity research at the flight dynamics laboratory p 493 A90-33409
- A design method for real-time computer control hydraulic force system p 590 A90-36434
- Direct drive servovalves: Why and how - The Magnaghi Milano answer p 688 A90-42484
- High-performance EHA controls using an interior permanent magnet motor --- electrohydraulic actuator for aircraft power systems p 730 A90-43152
- Lightweight, composite flight control actuators [SAE PAPER 892264] p 733 A90-45459
- Vibration reduction on servo flap controlled rotor using HHC p 861 A90-46967
- Comparison of active control on a servo flap rotor using fixed system and rotating system parameters p 862 A90-46976
- STOL Maneuver Technology Demonstrator aeroservoelasticity [AIAA PAPER 90-3336] p 863 A90-47596
- Short period control using angular acceleration feedback: Compensation for first lag servo [NAL-TM-600] p 936 N90-29399
- ### SERVOMECHANISMS
- Recent activities within the aeroservoelasticity branch at the NASA Langley Research Center p 492 A90-33400
- Digital servomechanism for the tachometer of the M 602 engine p 737 A90-44722
- Rotary servohinge actuator [SAE PAPER 892261] p 733 A90-45458
- Advanced actuation systems development, volume 1 [AD-A213334] p 121 N90-12624
- Advanced actuation systems development, volume 2 [AD-A213378] p 198 N90-13398
- Modeling flexible aircraft for flight control design [AD-A219123] p 757 N90-25140
- ### SH-3 HELICOPTER
- Identification of an adequate model for collective response dynamics of a Sea King helicopter in hover p 56 A90-12766
- ### SHADOWGRAPH PHOTOGRAPHY
- Structure of swept shock wave/boundary-layer interactions using conical shadowgraphy [AIAA PAPER 90-1644] p 569 A90-38772
- Application of the wide-field shadowgraph technique to rotor wake visualization [NASA-TM-102222] p 88 N90-11700
- Recent flow visualization studies in the 0.3-m TCT p 122 N90-12528
- ### SHAFTS (MACHINE ELEMENTS)
- Composite driveshaft designs [SAE PAPER 891031] p 128 A90-14339
- Shaft flexibility effects on aeroelastic stability of a rotating bladed disk p 132 A90-16371
- Threshold performance optimization of a rotor-bearing system subjected to leakage excitation [ASME PAPER 89-GT-126] p 360 A90-23825
- Blade mistuning coupled with shaft flexibility effects in rotor aeroelasticity [ASME PAPER 89-GT-330] p 343 A90-23896
- Helicopter ground/air resonance including rotor shaft flexibility and control coupling p 406 A90-28153
- Endurance of aircraft gas turbine mainshaft ball bearings-analysis using improved fatigue life theory. I - Application to a long-life bearing p 537 A90-33557
- Flutter of shaft-supported low aspect-ratio control surfaces p 687 A90-38912
- Viscous flow around a propeller-shaft configuration with infinite-pitch rectangular blades p 683 A90-40938
- The nature and control of skidding in lightly loaded intershaft bearings [PNR90591] p 136 N90-12933
- An applicational process for dynamic balancing of turbomachinery shafting [NASA-TM-102537] p 541 N90-20392
- Assessment of High Temperature Superconducting (HTS) electric motors for rotorcraft propulsion [NASA-CR-185222] p 588 N90-21761
- Thermal/structural analysis of the shaft-disk region of a fan drive system [NASA-TM-101687] p 610 N90-22807
- Experimental evaluation of a tuned electromagnetic damper for vibration control of cryogenic turbopump rotors [NASA-TP-3005] p 665 N90-23403
- ### SHAKING
- Force determination sensitivities study for full-scale helicopter ground vibration testing [AD-A215983] p 349 N90-17643
- ### SHAPED CHARGES
- Systems tunnel linear shaped charge lightning strike [NASA-CR-183832] p 201 N90-13404
- ### SHAPES
- Development of a VSAERO (Vortex Separation Aerodynamics) model of the F/A-18 [AD-A212442] p 95 N90-12566
- A user's manual for the method of moments Aircraft Modeling Code (AMC) [NASA-CR-186371] p 415 N90-18390
- A tool for automatic design of airfoils in different operating conditions p 502 N90-20994
- Optimization of aerodynamic designs using computational fluid dynamics p 541 N90-20999
- Supersonic nozzle design of arbitrary cross-section p 515 N90-21035

- An experimental study of tip shape effects on the flutter of aft-swept, flat-plate wings
[NASA-TM-4180] p 582 N90-22555
- A contribution to the economic, optimal dimensioning, and shaping of aircraft structures using a design model [ETN-90-96966] p 737 N90-25976
- SHARP LEADING EDGES**
- The water tunnel test of delaying vortex breakdown over a delta wing using supplements p 2 A90-10346
- Connection between leading-edge sweep, vortex lift, and vortex strength for delta wings p 554 A90-35770
- Structure of swept shock wave/boundary-layer interactions using conical shadowgraphy [AIAA PAPER 90-1644] p 569 A90-38772
- Computational simulation of flows about hypersonic geometries with sharp leading edges [AIAA PAPER 90-3065] p 793 A90-45891
- Numerical simulation of the laminar and turbulent three dimensional flow on a delta wing with sharp leading edge p 278 N90-16186
- Glancing shock-boundary layer interactions p 319 N90-17571
- A video-based experimental investigation of wing rock [AD-A18244] p 498 N90-20075
- Experimental and numerical investigation of the vortex flow over a sharp edged delta wing; with and without sideslip [PB90-167131] p 481 N90-20964
- SHEAR FLOW**
- Development of bluff body wake in a longitudinally curved stream p 86 A90-15745
- The production of uniformly sheared streams by means of double gauzes in wind tunnels - A mathematical analysis p 131 A90-15887
- The flow around wing-body junctions p 145 A90-16765
- Supersonic viscous shear layers p 367 A90-25873
- Instabilities of supersonic shear flows [AIAA PAPER 90-0712] p 314 A90-26983
- Structure of a reattaching supersonic shear layer p 555 A90-36252
- Fluid Dynamics of Three-Dimensional Turbulent Shear Flows and Transition [AGARD-CP-438] p 71 N90-10356
- Dynamics and control of turbulent shear flows [AD-A210396] p 72 N90-10402
- A planar reacting shear layer system for the study of fluid dynamics-combustion interaction [NASA-TM-102422] p 194 N90-13393
- Control of flow separation and mixing by aerodynamic excitation [NASA-TM-103131] p 571 N90-21733
- The computation of turbulent thin shear flows associated with flow around multielement aerofoils p 633 N90-24240
- Aerodynamics of bodies in shear flow p 910 N90-28496
- Cavity aeroacoustics [AD-A223853] p 911 N90-29307
- SHEAR LAYERS**
- Numerical modeling of a flame in a confined, unstable shear layer [AIAA PAPER 90-0647] p 205 A90-19966
- Compressibility effects in free shear layers [AIAA PAPER 90-0705] p 212 A90-19984
- The detection of large scale structure in undisturbed and disturbed compressible turbulent free shear layers [AIAA PAPER 90-0711] p 230 A90-22251
- Effects of compressibility on the characteristics of free shear layers p 302 A90-25285
- Supersonic viscous shear layers p 367 A90-25873
- The effect of walls on a spatially growing supersonic shear layer p 393 A90-29591
- Table top experimental simulation of hypersonic aero-optical effects --- encountered by cooled window on interceptor p 525 A90-34586
- Review of vortical flow utilization [AIAA PAPER 90-1429] p 605 A90-37966
- Measurement of mean and fluctuating flow properties in hypersonic shear layers [AIAA PAPER 90-1409] p 560 A90-38488
- Interaction of a plane shear layer with a downstream flat plate [AIAA PAPER 90-1460] p 561 A90-38617
- Wall pressure fluctuations in the reattachment region of a supersonic free shear layer [AIAA PAPER 90-1461] p 561 A90-38618
- Numerical simulation of confined, spatially-developing mixing layers - Comparison to the temporal shear layer [AIAA PAPER 90-1462] p 562 A90-38619
- Investigation of supersonic mixing layers p 623 A90-40926
- Numerical simulation of the growth of instabilities in supersonic free shear layers p 623 A90-40941
- Pressure-based real-time measurements in compressible free shear layers [AIAA PAPER 90-1980] p 703 A90-42709
- A proper orthogonal decomposition of a simulated supersonic shear layer p 904 A90-51009
- New experimental results on the origin and structure of Ferri and Dailey instabilities ('buzz') p 906 A90-51507
- A planar reacting shear layer system for the study of fluid dynamics-combustion interaction [NASA-TM-102422] p 194 N90-13393
- Numerical modeling of supersonic turbulent reacting free shear layers p 174 N90-14197
- Opportunities for improved understanding of supersonic and hypersonic flows p 318 N90-17566
- Numerical simulation of supersonic free shear layers [AD-A216289] p 320 N90-17579
- Control of flow separation and mixing by aerodynamic excitation [NASA-TM-103131] p 571 N90-21733
- Cavity aeroacoustics [AD-A223853] p 911 N90-29307
- Numerical simulations of the structure of supersonic shear layers [AD-A224164] p 960 N90-29587
- SHEAR STRAIN**
- Flutter analysis of composite panels in supersonic flow [AIAA PAPER 90-1180] p 450 A90-29379
- SHEAR STRENGTH**
- Design and evaluation of graphite/epoxy truss core sandwich panels p 210 A90-18406
- SHEAR STRESS**
- An annular gas seal analysis using empirical entrance and exit region friction factors [ASME PAPER 89-TRIB-46] p 537 A90-33555
- Boundary layer turbulence structure in the presence of embedded streamwise vortex pairs p 552 A90-35193
- Liquid crystal coatings for surface shear stress visualization in hypersonic flows [AIAA PAPER 90-1513] p 563 A90-38660
- Improvements to the fatigue substantiation of the H-60 composite tail rotor blade p 642 A90-39985
- Simultaneous detection of separation and transition in surface shear layers p 72 N90-10368
- Simple shear tests of the FMI 23.5.06 adhesive cured at low pressure (12 PSI) [INFORME-I-298/88] p 357 N90-17871
- Method and apparatus for detecting laminar flow separation and reattachment [NASA-CASE-LAR-13952-1-SB] p 455 N90-19534
- SHELL STABILITY**
- A study of the nonlinear deformation of a shell of revolution with a surface bend p 129 A90-14574
- SHELL THEORY**
- Analysis of aircraft tires via semianalytic finite elements p 496 A90-34740
- SHELLS (STRUCTURAL FORMS)**
- Optimization of the shape of a sealed shell and of the size and location of its reinforcements p 957 A90-50773
- SHIELDING**
- Forward canopy feasibility and Thru-The-Canopy (TTC) ejection system study [AD-A220360] p 637 N90-24258
- SHIPS**
- GPS: Arrival in the fleet - A GPS AN/SRN-25 receiver assessment p 97 A90-13989
- Simulation of helicopter landing on a ship deck p 181 A90-17705
- AV-8B shipboard ski jump evaluation p 574 A90-38535
- GTD/UTD: Brief history of successive development of theory and recent advances. Applications to antennas on ships and aircraft p 370 N90-17939
- SHOCK (PHYSIOLOGY)**
- Parachute opening shocks during high speed ejections: Normalization p 497 N90-20056
- SHOCK ABSORBERS**
- Dynamic stiffness of a hydraulic damper in the system of a front landing gear strut p 102 A90-14555
- SHOCK FRONTS**
- Fresh look at floating shock fitting [AIAA PAPER 90-0108] p 162 A90-19686
- SHOCK HEATING**
- Aerodynamic heating in shock wave/turbulent boundary layer interaction regions induced by blunt fins p 82 A90-13775
- Thermal/structural analyses of several hydrogen-cooled leading-edge concepts for hypersonic flight vehicles [AIAA PAPER 90-0053] p 274 A90-23702
- Thermal/structural analyses of several hydrogen-cooled leading-edge concepts for hypersonic flight vehicles [NASA-TM-102391] p 215 N90-14511
- SHOCK LAYERS**
- The numerical method for solving the high Reynolds hypersonic viscous shock layer p 2 A90-10340
- Calculation of flow past delta wings in the thin shock layer approximation p 86 A90-15624
- Comparison of thin and full viscous shock layer models in the problem of supersonic flow of a viscous gas past blunt cones p 231 A90-22396
- Advantages of flow variables in thin viscous shock layer problems p 364 A90-24145
- Hypersonic viscous shock-layer solutions over long slender bodies. II - Low Reynolds number flows p 393 A90-29695
- The effect of vibration-dissociation interaction on heat transfer and drag during the hypersonic flow past bodies p 710 A90-44934
- Experimental research on swept shock wave/boundary layer interactions [AD-A211744] p 134 N90-11988
- Shock layer vacuum UV spectroscopy in an arc-jet wind tunnel [NASA-TM-102258] p 370 N90-17112
- An approximate viscous shock layer method for calculating the hypersonic flow over blunt-nosed bodies p 479 N90-20947
- Numerical investigation of some control methods for 3-D turbulent interactions due to sharp fins p 591 N90-21764
- SHOCK LOADS**
- Wind tunnel tests of a 20-gore disk-gap-band parachute [AD-A221326] p 634 N90-24251
- SHOCK TESTS**
- The 59th Shock and Vibration Symposium, volume 2 [AD-A214579] p 372 N90-18065
- SHOCK TUBES**
- A novel technique for aerodynamic force measurement in shock tubes p 438 A90-28302
- Short time Force and moment measurement System for shock tubes (SFS) for measuring times less than 10 ms p 674 N90-24233
- SHOCK TUNNELS**
- Hypersonic combustion of hydrogen in a shock tunnel p 46 A90-12560
- The use of pulse facilities for testing supersonic combustion ramjet (scramjet) combustors in simulated hypersonic flight conditions p 46 A90-12562
- The experiments for gas turbine plane cascade in a shock tunnel p 160 A90-19441
- Development of the UTA hypersonic shock tunnel [AIAA PAPER 90-0080] p 200 A90-19675
- A novel technique for aerodynamic force measurement in shock tubes p 438 A90-28302
- HF shock tunnel facility for studying supersonic combustion [AIAA PAPER 90-1551] p 600 A90-38693
- SHOCK WAVE ATTENUATION**
- The normal shock generator - An inlet throat region research apparatus for high Mach applications [AIAA PAPER 90-1930] p 759 A90-42698
- SHOCK WAVE CONTROL**
- Tangential mass addition for the control of shock wave/boundary layer interactions in scramjet inlets p 13 A90-12586
- SHOCK WAVE GENERATORS**
- Computational modeling of inlet hammershock wave generation [AIAA PAPER 90-2005] p 621 A90-40592
- The normal shock generator - An inlet throat region research apparatus for high Mach applications [AIAA PAPER 90-1930] p 759 A90-42698
- SHOCK WAVE INTERACTION**
- Holographic interferometric study of shock wave propagation p 66 A90-10732
- The inclusion of a similarity representation of compressor rotation in the modeling of the interaction of cannon firing with air intakes at incidence [AAAF PAPER NT 88-18] p 4 A90-11435
- On the lengthscales of laminar shock/boundary-layer interaction p 5 A90-11610
- Measurements of pressure fluctuations in the interaction regions of shock waves and turbulent boundary layers induced by blunt fins p 9 A90-12218
- Aerodynamic heating in the interaction regions of shock waves and turbulent boundary layers induced by sharp fins p 8 A90-12220
- Irregular interaction of a strong shock wave with a thin profile p 9 A90-12267
- Tangential mass addition for the control of shock wave/boundary layer interactions in scramjet inlets p 13 A90-12586
- Critique of turbulence models for shock-induced flow separation p 17 A90-12851
- Investigation of flow separation on a supercritical airfoil p 17 A90-13023

Mach number effects on conical surface features of swept shock-wave/boundary-layer interactions p 154 A90-18147

Skin friction measurements by laser interferometry in swept shock/boundary-layer interactions p 154 A90-18153

Alleviation of shock oscillations in transonic flow by passive controls [AIAA PAPER 90-0046] p 161 A90-19648

Video visualization of separation shock motion from measured wall pressure signals in a Mach 5 compression ramp interaction [AIAA PAPER 90-0074] p 162 A90-19670

Upstream-influence scaling of fin-generated shock wave boundary-layer interactions [AIAA PAPER 90-0376] p 164 A90-19822

Swept shock/boundary-layer interactions - Tutorial and update [AIAA PAPER 90-0375] p 228 A90-22207

Experimental studies of shock wave/wall jet interaction in hypersonic flow [AIAA PAPER 90-0607] p 231 A90-22449

Investigation of wall pressure pulsations during the passive control of shock/boundary layer interaction p 378 A90-24132

Calculation of supersonic flow past a wing/fuselage combination with the resolution of a compression shock from the wing p 297 A90-24138

A method for calculating the location and intensity of a conical head shock on the lower surface of a delta wing with supersonic edges p 297 A90-24139

Interaction between a vibrating compression shock and a boundary layer p 298 A90-24143

Shock sensitivity in parabolized Navier-Stokes solution of high angle-of-attack supersonic flow p 302 A90-25280

Problem areas in applied computational fluid dynamics p 366 A90-25770

Three-dimensional shock-shock interactions on the scramjet inlet [AIAA PAPER 90-0529] p 314 A90-26963

Conditions of the generation of autooscillations in aerodynamic control surfaces in nonseparated subsonic flow of a gas p 315 A90-27303

Basic numerical methods --- of unsteady and transonic flow p 394 A90-29886

Aerodynamic characteristics of wave riders based on flows behind axisymmetric shock waves p 395 A90-30342

Oscillatory shock motion caused by transonic shock boundary-layer interaction p 470 A90-32478

An experimental investigation on control of flow dynamic distortions downstream under strong shock-boundary layer interaction in the two-dimensional flow field p 471 A90-33288

High-resolution shock-capturing schemes for inviscid and viscous hypersonic flows p 476 A90-34545

Shock-fitting method for two-dimensional inviscid, steady supersonic flows in ducts p 477 A90-34864

Turbulence statistics in a shock wave boundary layer interaction p 552 A90-35205

Unsteady transonic cascade flow with in-passage shock wave p 556 A90-36281

Mach number effects on upstream influence in swept shock wave/turbulent boundary layer interactions p 556 A90-36415

Effects of shock on the stability of hypersonic boundary layers [AIAA PAPER 90-1448] p 561 A90-38608

A numerical study of supersonic flow over a compression corner with different incoming boundary-layer profiles [AIAA PAPER 90-1453] p 561 A90-38612

A study of the unsteadiness of crossing shock wave turbulent boundary layer interactions [AIAA PAPER 90-1456] p 606 A90-38614

A primitive variable, strongly implicit calculation procedure for viscous flows at all speeds [AIAA PAPER 90-1521] p 563 A90-38666

Numerical simulation of a turbulent flow through a shock wave [AIAA PAPER 90-1641] p 608 A90-38769

Structure of swept shock wave/boundary-layer interactions using conical shadowgraphy [AIAA PAPER 90-1644] p 569 A90-38772

Correlation of separation shock motion in a compression ramp interaction with pressure fluctuations in the incoming boundary layer [AIAA PAPER 90-1646] p 569 A90-38774

Formation of shocks within axisymmetric nozzles [AIAA PAPER 90-1655] p 570 A90-38782

Computation of multiple normal shock wave/turbulent boundary layer interactions [AIAA PAPER 90-2133] p 685 A90-42037

Flow separation on a supercritical airfoil p 627 A90-42394

An investigation of oblique shock/boundary layer bleed interaction [AIAA PAPER 90-1928] p 703 A90-42697

Analysis of shock interactions and flow structure in high speed inlets [AIAA PAPER 90-2132] p 704 A90-42735

The effect of shock/shock interactions on the design of hypersonic inlets [AIAA PAPER 90-2217] p 705 A90-42748

Canard-wing vortex interactions at subsonic through supersonic speeds [AIAA PAPER 90-2814] p 711 A90-45154

Multiple vortex and shock interactions at subsonic, transonic, and supersonic speeds [AIAA PAPER 90-3023] p 793 A90-45890

An upwind approach to unsteady flowfield simulation [AIAA PAPER 90-3100] p 796 A90-45912

Shock/turbulent boundary layer interaction in low Reynolds number supercritical flows p 802 A90-46383

Some characteristics of interference between shock waves and the aerodynamic wake behind a body p 804 A90-46551

Effect of shock waves and jets on structural elements: Mathematical modeling in nonstationary gas dynamics --- Russian book p 806 A90-46621

Flow separation in oblique shock wave turbulent boundary layer interactions p 807 A90-46872

Numerical calculations of flows with shock waves by flux vector splitting method p 808 A90-47299

An LDA investigation of the normal shock wave boundary layer interaction p 908 A90-52618

Analysis and calculation for interaction between shock wave and laminar boundary layer p 909 A90-52778

Experimental research on swept shock wave/Boundary layer interactions [AD-A211744] p 134 A90-11988

Automatic control of cryogenic wind tunnels p 263 A90-15957

Interaction of an oblique shock wave with supersonic flow over a blunt body p 398 A90-19197

Interactive calculation procedures for mixed compression inlets [NASA-CR-186581] p 718 A90-25934

SHOCK WAVE PROFILES

Variational principle with variable domain discontinuous finite element method for transonic flow and determining automatically the position and shape of the shock waves p 160 A90-19434

A straight attached shock wave at the profile tip at freestream Mach number greater than about 1 p 907 A90-51534

SHOCK WAVE PROPAGATION

Holographic interferometric study of shock wave propagation p 66 A90-10732

Shock-wave/boundary-layer interaction at a swept compression corner p 16 A90-12850

The propagation of a normal shock in a varying area duct p 130 A90-15045

Aerodynamic characteristics of thin bodies moving in a gas with shock waves p 297 A90-24140

Oscillation of circular shock wave p 557 A90-36465

SHOCK WAVES

Self-excited oscillation of shock waves on an airfoil in two-dimensional transonic channel flow p 8 A90-11808

Temperature scaling of turbine blade heat transfer with and without shock wave passing p 47 A90-12570

Changes in supersonic flow past an obstacle due to the formation of a thin rarefaction channel ahead of the obstacle p 150 A90-17108

Video visualization of separation shock motion from measured wall pressure signals in a Mach 5 compression ramp interaction [AIAA PAPER 90-0074] p 162 A90-19670

Generalized fluxvectors for hypersonic shock-capturing [AIAA PAPER 90-0390] p 165 A90-19829

Investigation of oscillating airfoil shock phenomena [AIAA PAPER 90-0695] p 169 A90-19981

Spanwise properties of the unsteady separation shock in a Mach 5 unswept compression ramp interaction [AIAA PAPER 90-0377] p 228 A90-22208

Shock sensitivity in parabolized Navier-Stokes solution of high angle-of-attack supersonic flow p 302 A90-25280

Numerical simulations of unsteady shock reflections by ramps p 305 A90-25795

Unsteady aerodynamic forces of oscillating supersonic/hypersonic wings with attached shock waves p 473 A90-33363

Application of a new adaptive grid for aerodynamic analysis of shock containing single jets [AIAA PAPER 90-2025] p 624 A90-41988

An improvement on upwinding technique used in the Galerkin finite element method for the computation of inviscid transonic flow with shock waves p 627 A90-42361

A CFD study of precombustion shock-trains from Mach 3-6 [AIAA PAPER 90-2220] p 705 A90-42751

Shock-fitting in three space dimensions p 707 A90-44434

Comparison of the swept frequency continuous wave, current pulse, and shock-excitation lightning simulation techniques p 818 A90-49832

A numerical method for solving transonic flow past aircraft in Cartesian coordinates [NAL-TR-1008] p 18 A90-10003

Simulation of glancing shock wave and boundary layer interaction [NASA-TM-102233] p 133 A90-11970

Shock layer vacuum UV spectroscopy in an arc-jet wind tunnel [NASA-TM-102258] p 370 A90-17112

Glancing shock-boundary layer interactions p 319 A90-17571

Calculation of excrescence drag magnification due to pressure gradient at high subsonic speeds [ESDU-87004] p 397 A90-19195

Short time-dynamometer system for shock wave channels [MBB-UT-115/89-PUB] p 773 A90-25084

Investigation of the vortex flow over a sharp-edged delta wing in the transonic speed regime [LR-594] p 717 A90-25115

Experimental study on vortex and shock wave development on a 65 deg delta wing [NLR-MP-88033-U] p 720 A90-25950

SHORT CRACKS

Experimental determination of the short crack effect for metals p 265 A90-20064

Significance of the short crack effect on aerospace structures p 269 A90-20065

SHORT HAUL AIRCRAFT

Advanced technology rotorcraft - Civil short haul transport of the future p 246 A90-21710

Longitudinal stability and control characteristics of the Quiet Short-Haul Research Aircraft (QSRA) [NASA-TP-2965] p 349 A90-17639

Lateral-directional stability and control characteristics of the Quiet Short-Haul Research Aircraft (QSRA) [NASA-TM-102250] p 671 A90-23413

SHORT TAKEOFF AIRCRAFT

Development of new segment carbon seal for use at low sealing pressure regime FJR710/600S turbo fan engine p 69 A90-11950

The features of FJR 710 engine p 42 A90-12011

Endurance test of FJR 710/600S engine p 42 A90-12012

Start characteristics of FJR 710/600S engine p 42 A90-12013

Steady state performance of FJR 710/600S engine p 43 A90-12015

VSTOL power plant control lessons from Harrier experience p 13 A90-12582

Restart characteristics of turbofan engines p 50 A90-12627

The effect of trailing edge extensions on the performance of the Goettingen 797 and the Wortmann FX 63-137 aerofoil section at Reynolds numbers between 3×10^6 to the 5th and 1×10^7 to the 6th p 82 A90-13783

The fundamentals of vectored propulsion p 180 A90-17461

STOVL wind tunnel tests demonstrate ejector viability p 245 A90-21000

Propulsion system integration in high-performance aircraft p 333 A90-23922

Engine inlet distortion in a 9.2 percent scaled vectored thrust STOVL model in ground effect [AIAA PAPER 89-2910] p 301 A90-25043

Low speed testing and simulation of the STOL and Maneuver Technology Demonstrator [AIAA PAPER 90-1820] p 334 A90-25169

A status review of non-helicopter V/STOL aircraft development. I p 413 A90-30117

Reconfigurable flight controller for the STOL F-15 with sensor/actuator failures p 432 A90-30707

Lessons learned in the development of a multivariable control system p 432 A90-30713

Design of adaptive digital controllers incorporating dynamic pole-assignment compensators for high-performance aircraft p 432 A90-30714

The STOL maneuver technology demonstrator manned simulation test program p 439 A90-30716

HTTB - Industry's first STOL test bed --- High Technology Test Bed program for future tactical aircraft requirements p 414 A90-31246

- Configuration E-7 supersonic fighter/attack technology program
[ASME PAPER 89-GT-308] p 490 A90-32260
- Cooperative synthesis of control and display augmentation in approach and landing
p 516 A90-33061
- F-15 STOL and Maneuver Technology Demonstrator flight test progress report
[AIAA PAPER 90-1269] p 494 A90-33896
- Performance characteristics of a one-third-scale, vectorable ventral nozzle for SSTOVL aircraft
[AIAA PAPER 90-2271] p 586 A90-37562
- Expert diagnosis system for FJR engine troubles
p 587 A90-38597
- Multiple model adaptive controller for the STOL F-15 with sensor/actuator failures
p 668 A90-40878
- Direct lift STOVOL engine integration
[AIAA PAPER 90-2274] p 644 A90-42103
- Hot gas environment around STOVOL aircraft in ground proximity. II - Numerical study
[AIAA PAPER 90-2270] p 743 A90-42766
- Evolution of engine cycles for STOVOL propulsion concepts
[AIAA PAPER 90-2272] p 743 A90-42767
- Focusing propulsion and lift system development for an evolving special operations aircraft
[AIAA PAPER 90-2277] p 730 A90-42768
- Three-dimensional turbulent flow code calculations of hot gas ingestion
p 745 A90-44726
- Lessons learned from the S/MTD program for the Flying Qualities Specification
[AIAA PAPER 90-2849] p 755 A90-45177
- Simulation evaluation of transition and hover flying qualities of a mixed-flow, remote-lift STOVOL aircraft
[SAE PAPER 89-2284] p 757 A90-45464
- Supersonic flow computations for an ASTOVL aircraft configuration
[AIAA PAPER 90-2997] p 787 A90-45847
- Propulsive lift augmentation by side fences as applied to Japan's experimental STOL aircraft, ASKA
[AIAA PAPER 90-3009] p 789 A90-45859
- Vertical Lift Aircraft Design Conference, San Francisco, CA, Jan. 17-19, 1990, Proceedings
p 829 A90-46926
- Robust hover control for a short takeoff/vertical landing aircraft
[AIAA PAPER 90-3333] p 862 A90-47593
- STOL Maneuver Technology Demonstrator aeroservoelasticity
[AIAA PAPER 90-3336] p 863 A90-47596
- Preliminary design of a supersonic short takeoff and vertical landing (STOVOL) fighter aircraft
[AIAA PAPER 90-3231] p 834 A90-48844
- Status of the STOL and Maneuver Technology Demonstrator flight test program
[AIAA PAPER 90-3306] p 838 A90-48887
- Short take-off and landing maneuver technology demonstrator (STOL/MTD) lessons learned - Integrated flight/propulsion control (IFPC)
[AIAA PAPER 90-3307] p 868 A90-48888
- Flight control design considerations for STOVOL powered-lift flight
[AIAA PAPER 90-3225] p 868 A90-49110
- Propulsion system design specifications based on STOVOL flight control requirements
[AIAA PAPER 90-3227] p 839 A90-49112
- The implementation of STOVOL task-tailored control modes in a fighter cockpit
[AIAA PAPER 90-3229] p 839 A90-49114
- STOVOL option for the multi-role fighter
[AIAA PAPER 90-3296] p 840 A90-49124
- Backside landing control of a STOL aircraft using approximate perfect servo
p 934 A90-52801
- Flight simulator evaluation of a head-down display
[NAL-TM-573] p 59 N90-10898
- Wind tunnel test of CAD USB-STOL semi-borne prototype
[NAL-TM-566] p 88 N90-11696
- Acoustic-thermal environment for USB flap structure. Report 1: Ground simulation test results
[NAL-TM-567] p 88 N90-11697
- STOVOL propulsion system volume dynamics approximations
[NASA-TM-102397] p 114 N90-11740
- Low-speed wind-tunnel study of reaction control-jet effectiveness for hover and transition of a STOVOL fighter concept
[NASA-TM-4147] p 119 N90-11751
- The NASA experience in aeronautical R and D: Three case studies with analysis
[AD-A211486] p 82 N90-12496
- Powered-lift aircraft technology
[NASA-SP-501] p 107 N90-12589
- Real-time simulation of an F110/STOVOL turbofan engine
[NASA-TM-102409] p 117 N90-12618
- STOVOL aircraft simulation for integrated flight and propulsion control research
[NASA-TM-102419] p 193 N90-13389
- Development of the triplex digital flight control system of the STOL research aircraft ASKA
[NAL-TR-1013] p 349 N90-17640
- Performance characteristics of a one-third-scale, vectorable ventral nozzle for SSTOVL aircraft
[NASA-TM-103120] p 552 N90-21725
- Dynamic ground-effect measurements on the F-15 STOL and Maneuver Technology Demonstrator (S/MTD) configuration
[NASA-TP-3000] p 573 N90-22531
- Aerodynamic and propulsive control development of the STOL and maneuver technology demonstrator
p 920 N90-28514
- SHOT PEENING**
Fretting fatigue strength of Ti-6Al-4V at room and elevated temperatures and ways of improving it
p 952 N90-28709
- SHROUDED NOZZLES**
Supersonic rectangular isothermal shrouded jets
[AIAA PAPER 90-2028] p 621 A90-40599
- SHROUDED PROPELLERS**
Computation of subsonic shrouded propeller flows
[AIAA PAPER 90-0029] p 226 A90-22154
- Design and analysis of a large-plug inlet ADP nacelle and pylon - Advanced Ducted Prop
[AIAA PAPER 90-2015] p 673 A90-41986
- A computer program for the prediction of nozzle-propeller performance
[LR-578] p 572 N90-21740
- Recent improvements in the scope and accuracy of the performance prediction of nozzle propellers
[LR-598] p 572 N90-21742
- SHROUDED TURBINES**
Photoelastic investigation of turbine rotor blade shrouds
p 112 A90-16008
- A theoretical study of ingress for shrouded rotating disc systems with radial outflow - sealing rotor-stator cavities
[ASME PAPER 89-GT-178] p 361 A90-23859
- Local convection heat transfer on a plane wall in the vicinity of strong streamwise accelerations
p 535 A90-32174
- Advanced Turbine Technology Applications Project (ATTAP)
[NASA-CR-185133] p 51 N90-10036
- SHROUDS**
Redesign of an electro-optical shroud in graphite/epoxy
p 676 A90-40215
- SIDE INLETS**
Experimental and theoretical investigations of turbulent flow in a side-inlet rectangular combustor
p 421 A90-27959
- SIDELOBES**
Antenna sidelobe requirements for the medium PRF mode of an airborne radar
p 37 A90-10985
- SIDESLIP**
Experimental and numerical investigation of vortex flow over a sideslipping delta wing
p 17 A90-13016
- Aerodynamic characteristics of an aircraft model at large angles of attack and large sideslip angles
p 233 A90-23361
- Sideslip-induced static pressure errors in flight-test measurements
[AIAA PAPER 90-3082] p 794 A90-45898
- Numerical study of vortical flow over a sideslipping delta wing
[AIAA PAPER 90-3001] p 798 A90-45936
- Calculation of three-dimensional flow past a plane supersonic air intake at angles of attack and sideslip
p 805 A90-46573
- Application of a vortex lattice numerical model in the calculation of inviscid incompressible flow around delta wings
p 904 A90-51017
- Experimental and numerical investigation of the vortex flow over a sharp edged delta wing: with and without sideslip
[PB90-167131] p 481 N90-20964
- Sideslip-induced static pressure errors in flight-test measurements
[NASA-TM-102846] p 849 N90-27702
- SIGNAL ANALYSIS**
Acoustic emission and signal analysis
p 781 A90-43782
- SIGNAL ANALYZERS**
Air Force Boom Event Analyzer Recorder (BEAR): System description
[AD-A218048] p 548 N90-20800
- Ridge regression processing
p 489 N90-20931
- SIGNAL DETECTION**
The validation and application of a rotor acoustic prediction computer program
[NASA-TM-101794] p 895 N90-27465
- A reliable, maintenance-free oxygen sensor for aircraft using an oxygen-sensitive coating on potentiometric electrodes
[AD-A222696] p 927 N90-28545
- SIGNAL DETECTORS**
Method and apparatus for detecting laminar flow separation and reattachment
[NASA-CASE-LAR-13952-1-SB] p 455 N90-19534
- SIGNAL DISTORTION**
Experimental characterization of the effects of pneumatic tubing on unsteady pressure measurements
[NASA-TM-4171] p 850 N90-27703
- SIGNAL ENCODING**
Semiautomatic coding of weather phenomenon groups in the meteorological reports of automatic airport stations
p 962 A90-50783
- SIGNAL PROCESSING**
Signal processing in a digital GPS receiver
p 128 A90-14006
- Radar systems - Book
p 208 A90-17305
- Status and potential of GPS-receiver development
p 265 A90-21717
- High resolution spectrum analysis for airborne pulse Doppler radars
p 339 A90-24329
- Mean and turbulent velocity measurements in a turbojet exhaust
p 423 A90-28272
- Database for LDV signal processor performance analysis
p 447 A90-28278
- Advanced technology MMW seeker testbed, a multi-technology demonstration sensor
p 488 A90-34143
- A Distributed Artificial Intelligence approach to object identification and classification
p 545 A90-34185
- Optimization of complex data processing algorithms in multichannel radio direction finding
p 576 A90-36115
- Differential-geometrical technique of signal transformation and estimation of position, rate and acceleration parameters using supplementary data sources
p 638 A90-41004
- The TVD 900 - A modern signal processing applied to primary civilian ATC radar
p 638 A90-41034
- Embedded GPS - The Canadian Marconi approach
p 725 A90-43700
- Rockwell International's miniature high performance GPS receiver
p 726 A90-43701
- A robust RAIM scheme using GPS/GLONASS systems
p 726 A90-43713
- Differential Omega/VLF as a world-wide navigation aid in the 21st century
p 727 A90-45232
- Range determination in a multipath prone environment
p 877 A90-45960
- Applications for a small format airborne recorder
p 847 A90-48620
- Fly-by-light flight control system technology development plan
[NASA-CR-181953] p 259 N90-15111
- Ridge regression processing
p 489 N90-20931
- MLS mathematical model validation study using airborne MLS data from Midway Airport engineering flight tests, August 1988
[DOT/FAA/CT-TN90/2] p 640 N90-23378
- The disturbance processes on the data links of the mode-S air traffic control system
[ETN-90-96960] p 729 N90-25965
- Development and testing of methodology for evaluating the performance of multi-input/multi-output digital control systems
[NASA-TM-102704] p 846 N90-27699
- Distributed control architecture for CNI preprocessors
p 917 N90-29356
- SIGNAL RECEPTION**
ILS/MLS comparison tests at Miami/Tamiami, Florida Airport
[ACD-330] p 27 N90-10018
- SIGNAL REFLECTION**
ILS mathematical modeling study of the effects of proposed hangar construction at the Orlando International Airport, Runway 17R, Orlando, Florida
[DOT/FAA/CT-TN89/52] p 121 N90-11762
- SIGNAL TO NOISE RATIOS**
Database for LDV signal processor performance analysis
p 447 A90-28278
- Obtaining consistent models of helicopter flight-data measurement errors using kinematic-compatibility and state-reconstruction methods
[AD-A225333] p 815 N90-26799
- Comparison of speech intelligibility in cockpit noise using SPH-4 flight helmet with and without active noise reduction
[NASA-CR-177564] p 915 N90-28510
- SIGNAL TRANSMISSION**
Airborne telemetry trends for the 1990's
p 418 A90-28874
- SIGNATURE ANALYSIS**
Target classification by vibration sensing - for helicopter detection
p 1 A90-10170

Simulation of airborne target imagery - Dependence on frequency and bistatic angle p 488 A90-34146
Sonic boom signature data from cruciform microphone array experiments during the 1966-1967 EAFB national sonic boom evaluation program [NASA-CR-182027] p 549 N90-21605

SIKORSKY AIRCRAFT

Emerging new technologies at Sikorsky aircraft p 382 A90-30114

SILICON

Silicon-etalon fiber-optic temperature sensor [NASA-TM-102389] p 187 N90-13381

SILICON CARBIDES

Burner rig hot corrosion of silicon carbide and silicon nitride p 355 A90-25267
Sliding and abrasive wear behaviour of an aluminum (2014)-SiC particle reinforced composite p 530 A90-33344

Hot-gas corrosion test of Si₃N₄ and SiC p 531 A90-33987

Metal matrix composite fan blade development [AIAA PAPER 90-2178] p 677 A90-42062

High temperature deformation studies on CVD silicon carbide fibers p 945 A90-50147
Improved silicon carbide for advanced heat engines [NASA-CR-180831] p 65 N90-10293

SILICON COMPOUNDS

Chemical vapor deposition of Hf/Si compounds as a high temperature coating for carbon/carbon composites p 955 A90-50159

SILICON NITRIDES

Burner rig hot corrosion of silicon carbide and silicon nitride p 355 A90-25267

High-temperature corrosion and mechanical properties of some silicon nitride ceramics p 531 A90-33985

Hot-gas corrosion test of Si₃N₄ and SiC p 531 A90-33987

Development of monolithic and composite ceramics at Allied-Signal Aerospace Company p 599 A90-35950

Development of ceramic components for high-temperature gas turbines p 602 A90-35951

Slip-cast hot isostatically pressed silicon nitride gas turbine components p 765 A90-44816

Self-lubricating surfaces by ion beam processing [AD-A222489] p 884 N90-27118

SILICON POLYMERS

Polysilicon active-matrix liquid crystal displays for cockpit applications p 681 A90-40393

SILICONES

Silicone sealants and adhesives for aerospace/defense applications p 529 A90-31619

Equilibrium swelling of elastomeric materials in solvent environments [DE90-010164] p 678 N90-24430

SILOXANES

Poly(arylene ether ketone)/poly(aryl imide) homo- and polydimethylsiloxane segmented copolymer blends - Influence of chemical structure on miscibility and physical property behavior p 941 A90-50063

SILVER

Self-lubricating surfaces by ion beam processing [AD-A222489] p 884 N90-27118

SIMD (COMPUTERS)

Array processor supercomputers p 376 A90-26626

Benchmark calculations with an unstructured grid flow solver on a SIMD computer p 546 A90-34378

SIMPLIFICATION

Multivariable frequency weighted model order reduction for control synthesis [AIAA-89-3558] p 613 N90-23060

On simplified analytical flutter clearance procedures for light aircraft [DLR-FB-89-58] p 672 N90-24276

Effects of simplifying assumptions on optimal trajectory estimation for a high-performance aircraft [NASA-TM-101721] p 757 N90-25142

SIMULATION

Simulation of three-dimensional viscous flow within a multistage turbine [ASME PAPER 89-GT-152] p 292 A90-23841

Basic studies of the unsteady flow past high angle of attack airfoils [AD-A210252] p 18 N90-10008

Computation of ramjet internal flowfields [AD-A212001] p 114 N90-11743

LORAN C stability integrity assurance [AD-A212663] p 177 N90-13364

Evaluation of the indirect effects of lightning on a system: Double transfer function method [RAE-TRANS-2172] p 176 N90-14211

Principal characteristics of lightning on aircraft [AD-A216613] p 239 N90-15067

Dallas/Fort Worth simulation. Volume 2: Appendixes D, E, and F [AD-A216613] p 405 N90-18380

Ground-simulation investigations of VTOL airworthiness criteria for terminal-area operations [NASA-TM-102810] p 757 N90-25141

Formation of design envelope criterion in terms of deterministic spectral procedure [RAE-TM-SS-9] p 721 N90-25953

Qualitative evaluation of a conformal velocity vector display for use at high angles-of-attack in fighter aircraft [NASA-TM-102629] p 739 N90-25981

A flight dynamic model of aircraft spinning [AR-005-600] p 935 N90-28576

Overview on hot gas tests and molten salt corrosion experiments at the DLR p 953 N90-28714

SIMULATORS

Acoustic-vortical-combustion interaction in a solid fuel ramjet simulator p 194 N90-14234

Simulator comparison of thumbball, thumb switch, and touch screen input concepts for interaction with a large screen cockpit display format [NASA-TM-102587] p 506 N90-21005

Transonic 3-D Euler analysis of flows around fanjet engine and TPS (Turbine Powered Simulator). Comparison with wind tunnel experiment, evaluation of TPS testing method and 3-D flow [NAL-TR-1045] p 912 N90-29327

SIMULTANEOUS EQUATIONS

The application of the finite element method to an aerodynamic problem specific to propeller design [LR-614] p 718 N90-25116

SINE WAVES

Ground vibration test results of a JetStar airplane using impulsive sine excitation p 179 A90-16963

SINGLE CRYSTALS

Recent and prospective developments in single-crystal superalloys for the blades of advanced turbines p 355 A90-24288

The anisotropy of the mechanical behaviour in nickel-based single crystal superalloys for turbine blades [ONERA, TP NO. 1989-205] p 355 A90-25339

Development of a new nickel based single crystal turbine blade alloy for very high temperatures [ONERA, TP NO. 1989-206] p 356 A90-25340

Recrystallization behavior of nickel-base single crystal superalloys p 440 A90-27681

SINGLE ENGINE AIRCRAFT

Investigations of modifications to improve the spin resistance of a high-wing, single-engine, light airplane [SAE PAPER 891039] p 118 A90-14345

Comparison of four lightning simulation tests on a composite test bed aircraft p 818 A90-49831

SINGLE EVENT UPSETS

Real-time closed-loop simulation and upset evaluation of control systems in harsh electromagnetic environments p 613 N90-23069

SINGLE STAGE TO ORBIT VEHICLES

Computational requirements for hypersonic flight performance estimates p 440 A90-29686

Scramjet testing from Mach 4 to 20 - Present capability and needs for the nineties [AIAA PAPER 90-1388] p 597 A90-38485

The challenge of demonstrating the X-30 [AIAA PAPER 90-2474] p 675 A90-42189

Hypersonic (T-D) 'pinch' and aerospaceplane propulsion [AIAA PAPER 90-3252] p 872 A90-49120

HOTOL structures and materials at British Aerospace, Warton, UK [EOARD-LR-90-001] p 503 N90-21001

SINGULAR INTEGRAL EQUATIONS

Convergence of the method of discrete vortices when applied to steady-state aerodynamics problems p 231 A90-22816

Local convergence of the solution in the discrete vortex method p 803 A90-46534

SINGULARITY (MATHEMATICS)

An application of the surface-singularity method to wing-body-tail configurations p 9 A90-12229

Computational methods in design aerodynamics p 557 A90-36539

Numerical solutions for unsteady aerofoil by internal singularity method p 716 A90-45536

Rotor loads computation using singularity methods and application to the noise prediction p 807 A90-46880

SISO (CONTROL SYSTEMS)

Algorithm for simultaneous stabilization of single-input systems via dynamic feedback p 462 A90-31108

SITE SELECTION

Ice runways near the South Pole [AD-A211606] p 133 N90-11908

The potential for an extra runway at Heathrow: A preliminary feasibility study [TT-9007] p 938 N90-29403

SIZE (DIMENSIONS)

Airplane design. Part 1 - Preliminary sizing of airplanes --- Book p 30 A90-12866

SIZE DETERMINATION

Atomization of synthetic jet fuel p 63 A90-12602

Airplane design. Part 1 - Preliminary sizing of airplanes --- Book p 30 A90-12866

Effect of the inlet diameter and neck edge radius on the flow coefficient of straight-generatrix nozzles ... p 84 A90-14577

SIZING

Hypersonic aerospace sizing analysis for the preliminary design of aerospace vehicles p 247 A90-23276

SKID LANDINGS

Simulation of helicopter landing on a ship deck p 181 A90-17705

SKIDDING

The nature and control of skidding in lightly loaded intershaft bearings [PNR90591] p 136 N90-12933

SKIN (STRUCTURAL MEMBER)

Fiber optic smart structures and skins; Proceedings of the Meeting, Boston, MA, Sept. 8, 9, 1988 [SPIE-986] p 37 A90-11201

Overview of fiber optic smart structures for aerospace applications p 37 A90-11202

Fiber optic sensors for composite monitoring p 37 A90-11203

Air Force smart structures/skins program overview p 38 A90-11205

Producibility and life cycle cost issues in applications of embedded fiber optic sensors in smart skins p 38 A90-11221

Aeroelastic tailoring of a wing with composite skin p 366 A90-25108

Analysis and testing of fiber-reinforced thermoplastic composite vertical stabilizer skins for an advanced attack helicopter p 441 A90-28193

Effects of damage on post-buckled skin-stiffener composite skin panels p 409 A90-28235

Damage tolerance of a postbuckling soft skin hat stiffened compression panel p 534 A90-31647

Smart Skins - A development roadmap p 504 A90-32860

The impact of fiber optics (photonics) on future aircraft p 504 A90-32863

Expert systems for design of battle damage repairs p 467 A90-33094

A method for reducing a buckled skin under combined loading p 860 A90-46571

Comparison of four lightning simulation tests on a composite test bed aircraft p 818 A90-49831

Some new techniques for aircraft fuselage skin tests [LR-547] p 184 N90-13379

A dynamicist's view of fuel tank skin durability p 251 N90-15915

SKIN FRICTION

Skin friction measurements by laser interferometry in swept shock/boundary-layer interactions p 154 A90-18153

Use of liquid crystals for qualitative and quantitative 2-D studies of transition and skin friction p 446 A90-28259

Development and extension of diagnostic techniques for advancing high speed aerodynamic research p 436 A90-28281

Instrumentation requirements for laminar flow research in the NLR high speed wind tunnel HST p 447 A90-28283

Development of two multi-sensor hot-film measuring techniques for free-flight experiments p 417 A90-28291

High temperature skin friction measurement p 448 A90-28306

Skin effect in flow of a disperse fluid past a wing profile p 395 A90-30334

Effect of detailed surface geometry on riblet drag reduction performance p 622 A90-40693

Direct measurements of skin friction in a scramjet combustor [AIAA PAPER 90-2342] p 626 A90-42132

Effect of riblets on flow separation in a subsonic diffuser p 712 A90-45281

Flow separation in oblique shock wave turbulent boundary layer interactions p 807 A90-46872

Airfoil static-pressure thrust - Flight-test verification [AIAA PAPER 90-3286] p 812 A90-48873

An application of topological analysis to studying the three-dimensional flow in cascades. I - Topological rules for skin-friction lines and section streamlines p 908 A90-52607

Simultaneous detection of separation and transition in surface shear layers p 72 N90-10368

Control and modification of turbulence p 72 N90-10377

- Lockheed laminar-flow control systems development and applications p 90 N90-12506
- A one equation turbulence model for transonic airfoils p 174 N90-14199
- Test techniques for cryogenic wind tunnels p 263 N90-15952
- Skin friction measurements by laser interferometry in supersonic flows p 317 N90-17557
- Viscous three-dimensional analyses for nozzles for hypersonic propulsion [NASA-CR-185197] p 344 N90-17635
- Hypersonic waverider configurations for trans-atmospheric vehicles [AD-A217925] p 498 N90-20074
- A brief review of some mechanisms causing boundary layer transition at high speeds [NASA-TM-102834] p 720 N90-25945
- Use of liquid crystals for qualitative and quantitative 2-D studies of transition and skin friction [RAE-TM-AERO-2159] p 958 N90-28800
- SKYDROL (TRADEMARK)**
- Flammability of fire resistant, aircraft hydraulic fluid [DOT/FAA/CT-TN90/19] p 766 N90-25222
- SLEEP**
- Cumulative airport noise exposure metrics: An assessment of evidence for time-of-day weightings, revision [AD-A214878] p 352 N90-16773
- SLENDER BODIES**
- Separated flow over slender wing, body and wing-body combination p 85 A90-15232
- On steady subsonic flow past slender bodies of revolution p 144 A90-16736
- Finite element analysis of the flow of a propeller on a slender body with a two-equation turbulence model p 210 A90-18340
- The fickle effect of nose microasymmetry on the high-alpha aerodynamics [AIAA PAPER 90-0067] p 161 A90-19663
- Experimental investigation of a new device to control the asymmetric flowfield on forebodies at large angles of attack [AIAA PAPER 90-0069] p 161 A90-19665
- Hypersonic viscous shock-layer solutions over long slender bodies. II - Low Reynolds number flows p 393 A90-29695
- An analytic solution on hypersonic flow over an arbitrary slender body with near power-law profile p 558 A90-37736
- A method for solving three-dimensional viscous incompressible flows over slender bodies p 558 A90-37890
- Analysis of aeroelastic divergence for the slender flight vehicles p 680 A90-39298
- Calculation of stability derivatives for slender bodies using boundary element method p 620 A90-40181
- Comparison of high-angle-of-attack slender-body theory and exact solutions for potential flow over an ellipsoid p 622 A90-40692
- Unsteady flow separation on slender bodies at high angles of attack [AIAA PAPER 90-2835] p 712 A90-45166
- Full span analysis for flutter prediction of slender blade assemblies p 879 A90-46188
- An experimental investigation of the physical mechanisms controlling the asymmetric flow past slender bodies at large angles of attack p 592 N90-21767
- SLENDER CONES**
- Application of the LAURA code for slender-vehicle aerothermodynamics [AIAA PAPER 90-1714] p 560 A90-38416
- Comments on 'Effect of nose bluntness and cone angle on slender-vehicle transition' p 620 A90-39814
- The application of concentric vortex simulation to calculating the aerodynamic characteristics of bodies of revolution at high angles of attack p 627 A90-42357
- SLENDER WINGS**
- Separated flow over slender wing, body and wing-body combination p 85 A90-15232
- The aerodynamic behaviours of vortices for slender-wing p 158 A90-18623
- Rapid prediction of slender-wing-aircraft stability characteristics [AIAA PAPER 90-0301] p 163 A90-19782
- Optimization of the relative thicknesses of a high-aspect-ratio wing in a multicriterial formulation p 334 A90-24133
- A method for calculating the stiffness characteristics of large-aspect-ratio wings with anisotropic panels in accordance with strength and aileron efficiency requirements p 334 A90-24161
- Using the lifting line theory for calculating straight wings of arbitrary profile p 387 A90-29004
- Divergence of thin-walled composite rods of closed profile in gas flow p 388 A90-29012
- Connection between leading-edge sweep, vortex lift, and vortex strength for delta wings p 554 A90-35770
- Review of vortical flow utilization [AIAA PAPER 90-1429] p 605 A90-37966
- Various sources of wing rock p 622 A90-40679
- Coupled aerodynamic forces due to unsteady stall on a high-aspect-ratio wing oscillating at high amplitude [ONERA, TP NO. 1990-24] p 623 A90-41203
- An experimental study of the nonlinear dynamic phenomenon known as wing rock [AIAA PAPER 90-2812] p 753 A90-45152
- Static and dynamic water tunnel tests of slender wings and wing-body configurations at extreme angles of attack [AIAA PAPER 90-3021] p 869 A90-45888
- Computational and experimental studies on ground effect of a slender wing tailless delta aircraft p 810 A90-48083
- SLIDING FRICTION**
- Sliding and abrasive wear behaviour of an aluminum (2014)-SiC particle reinforced composite p 530 A90-33344
- Current status of Joint FAA/NASA Runway Friction Program [SAE PAPER 892340] p 760 A90-45494
- SLIP FLOW**
- Supersonic low-density flow over airfoils p 153 A90-17871
- SLIPSTREAMS**
- Prediction of two-dimensional time-dependent gasdynamic flows for hypersonic studies [UTIAS-335] p 718 N90-25935
- SLOPES**
- Installed tailplane lift-curve slope at subsonic speeds [ESDU-89029] p 236 N90-15081
- SLOT ANTENNAS**
- Applications of slotted cable antennas in the instrument landing system p 639 A90-41708
- SLOTS**
- Pressure surface trailing edge slot cooling [ONERA, TP NO. 1989-123] p 47 A90-12569
- Mean flow measurements of heated supersonic slot injection into a high Reynolds number supersonic stream [AIAA PAPER 90-0180] p 163 A90-19722
- Investigation of cowl vent slots for supercritical stability enhancement in dual-mode ramjet inlets p 507 A90-32951
- An experimental investigation of film cooling effectiveness for slots of various exit geometries [AIAA PAPER 90-2266] p 768 A90-42763
- SLOTTED WIND TUNNELS**
- Slotted-wall research with disk and parachute models in a low-speed wind tunnel [AIAA PAPER 90-1407] p 595 A90-37946
- Slotted-wall research with disk and parachute models in a low-speed wind tunnel [DE90-002989] p 572 N90-21737
- SLURRIES**
- Subsonic combustor testing p 749 N90-25997
- SLUSH**
- Slush Hydrogen (SLH2) technology development for application to the National Aerospace Plane (NASP) [NASA-TM-102315] p 203 N90-14268
- SLUSH HYDROGEN**
- Background, current status, and prognosis of the ongoing slush hydrogen technology development program for the NASP [NASA-TM-103220] p 763 N90-26055
- SMALL PERTURBATION FLOW**
- New approach to small transonic perturbations finite element numerical solving method. I - Numerical developments. II - Numerical applications p 16 A90-12783
- Computations of unsteady transonic flows about thin airfoils by integral equation method p 158 A90-18609
- Transonic integro-differential and integral equations with artificial viscosity p 223 A90-20988
- Effects of pressure mismatch on slot injection in supersonic flow [AIAA PAPER 90-0092] p 227 A90-22161
- Unsteady transonic aerodynamics of oscillating airfoils in supersonic freestream p 232 A90-23277
- Construction of a wing surface in a nonviscous transonic flow from a given pressure distribution p 298 A90-24149
- Calculation of flow past flight vehicles of complex configurations at high supersonic Mach numbers using the hypersonic theory of small perturbations p 299 A90-24158
- Using transonic small disturbance theory for predicting the aerodynamic stability of a flexible wind-tunnel model [AIAA PAPER 90-1033] p 391 A90-29377
- Alternative methods for modeling unsteady transonic flows p 394 A90-29889
- On an extension of the Kutta-Joukowski theorem to the supersonic regime p 477 A90-34819
- A verification of the supersonic lifting line theory for the case of infinite yawed wings p 477 A90-34821
- Nonlinear effects in the two-dimensional adaptive-wall outer-flow problem p 554 A90-35771
- The TSP methods applied to the calculation of transonic flow about wing/body/nacelle/pylon-configurations --- Transonic Small Perturbation p 554 A90-35868
- A new method for high speed propeller flutter prediction p 854 A90-49454
- A model of small-disturbance wave in large-scale separation zone associated with stall flutter p 883 A90-49469
- SMART STRUCTURES**
- Fiber optic smart structures and skins; Proceedings of the Meeting, Boston, MA, Sept. 8, 9, 1988 [SPIE-986] p 37 A90-11201
- Overview of fiber optic smart structures for aerospace applications p 37 A90-11202
- Fiber optic sensors for composite monitoring p 37 A90-11203
- Air Force smart structures/skins program overview p 38 A90-11205
- Fiber optic sensor systems for smart aerospace structures p 38 A90-11208
- Optical fiber sensing considerations for a smart aerospace structure p 38 A90-11210
- Materials get smarter p 356 A90-27598
- Smart structures with nerves of glass p 444 A90-27951
- Some smart structures concepts p 503 A90-32858
- Smart Skins - A development roadmap p 504 A90-32860
- The impact of fiber optics (photonics) on future aircraft p 504 A90-32863
- Fiber optics smart structures program at UTIAS p 535 A90-32864
- Smart structures concept study p 504 A90-32876
- Application of effective baselines to smart structures p 536 A90-32885
- Smart microsensors for high temperature applications, phase 1 [AD-A224151] p 959 N90-28828
- SMOKE**
- A smoke generator system for aerodynamic flight research [NASA-TM-4137] p 183 N90-13372
- Aircraft Fire Safety [AGARD-CP-467] p 324 N90-17581
- Fire science and aircraft safety p 326 N90-17596
- Experimental investigation of the mechanisms underlying vortex kinematics in unsteady separated flows [AD-A217889] p 540 N90-20346
- Video photographic considerations for measuring the proximity of a probe aircraft with a smoke seeded trailing vortex [NASA-TM-102691] p 724 N90-25120
- The reduction of smoke emissions from Allison T56 engines [ARL-PROP-R-182] p 928 N90-28547
- SOFT LANDING**
- Recovery concepts for propulsion and avionics components --- for booster stage in launch vehicles [AIAA PAPER 90-1810] p 353 A90-25172
- SOFTWARE ENGINEERING**
- The aerodynamic assistant [AIAA PAPER 89-3132] p 75 A90-10608
- Design of a language for the testing of aircraft engines p 137 A90-14573
- Counterrotating prop-fan simulations which feature a relative-motion multiblock grid decomposition enabling arbitrary time-steps [AIAA PAPER 90-0687] p 169 A90-19978
- Simulator motion-drive algorithms - A designer's perspective p 375 A90-25997
- The use of automated parametric analysis for selecting efficient structural schemes for wings p 410 A90-29191
- Rotor/airframe aeroelastic analyses using the transfer matrix approach [AIAA PAPER 90-1119] p 392 A90-29391
- VisualGrid - A software package for interactive grid generation [AIAA PAPER 90-1607] p 612 A90-38738
- Automated aircraft engine costing using artificial intelligence [AIAA PAPER 90-1887] p 660 A90-41981
- Software maintenance on the Airbus family [SAE PAPER 892326] p 738 A90-45484
- Control law synthesis and optimization software for large order aeroservoelastic systems p 61 N90-10111
- Processing of undifferenced GPS carrier beat phase measurements and adjustment computations [TR-5-1988] p 178 N90-13368

The implications of using integrated software support environment for design of guidance and control systems software

[AGARD-AR-229] p 434 N90-18432
Marshall Avionics Testbed System (MAST) p 421 N90-19417

Human centrifuge controller p 527 N90-21043
Technical evaluation report on the Guidance and Control Panel 49th Symposium on Fault Tolerant Design Concepts for Highly Integrated Flight Critical Guidance and Control Systems

[AGARD-AR-281] p 758 N90-26012
Start-up built-in test for the DISCUS fault tolerant, fly-by-wire computer system p 869 N90-27625
Advanced algorithms design and implementation in on-board microprocessor systems for engine life usage monitoring p 892 N90-27628
Economical graphics display system for flight simulation avionics

[NASA-CR-186886] p 849 N90-27701
Advanced transport operating system software upgrade: Flight management/flight controls software description [NASA-CR-181936] p 893 N90-28366
A conceptual framework for fighter flight control systems [PD-CF-9009] p 936 N90-28577
A knowledge-based system design/information tool [NASA-CR-4316] p 965 N90-29143

SOFTWARE TOOLS

RISC lifting off in avionics --- Reduced Instruction Set Computer

[AIAA PAPER 89-2967] p 73 A90-10483
A methodology for validating software reliability

[AIAA PAPER 89-3081] p 74 A90-10567
An experimental investigation of fault tolerant software structures in an avionics application

[AIAA PAPER 89-3082] p 74 A90-10568
A hardware and software fault tolerant safety controller

[AIAA PAPER 89-3123] p 74 A90-10599
Software fault tolerance analysis and testing for the Advanced Automation System

[AIAA PAPER 89-3124] p 75 A90-10600
The aerodynamic assistant

[AIAA PAPER 89-3132] p 75 A90-10608
Automated aircraft configuration design and analysis

[SAE PAPER 891072] p 101 A90-14368
A microprocessor-based system for monitoring gas turbines

p 350 A90-24359
Advanced Automation System design

p 375 A90-25566
A new data acquisition, display and control system for the ARA transonic wind tunnel

p 436 A90-28256
Two-level maintenance concept for advanced avionics architectures

p 457 A90-28321
The integrated support station (ISS) - A modular Ada-based test system to support AN/ALE-47 countermeasure dispenser system testing, evaluation, and reprogramming

p 457 A90-28323
Development of an acceptability window for a ground proximity avoidance system

p 419 A90-30730
Methodology for developing an assessment expert system using a planning paradigm

p 460 A90-30757
Robotics for flightline servicing

p 383 A90-30760
The automated software development project at McDonnell Aircraft Company (The Software Factory)

p 460 A90-30782
A reconfigurable integrated navigation and flight management system for military transport aircraft

p 433 A90-30794
A computer-aided control engineering environment for multi-disciplinary expert-aided analysis and design (MEAD)

p 461 A90-30796
Software architecture concepts for avionics

p 461 A90-30806
Balance calibration and evaluation software --- in wind tunnel tests

p 523 A90-34237
Control of a switched-reluctance aircraft engine starter-generator over a very wide speed range

p 586 A90-38130
Digital map reader for helicopters

p 653 A90-42448
Software fault tolerance

[RSRE-MEMO-4237] p 99 N90-12575
Test network Delft

[ETN-90-96009] p 177 N90-13365
Computer-based tools for assisting air traffic controllers with arrivals flow management

[RSRE-88001] p 178 N90-13366
The application of Z to the specification of air traffic control systems. 1: An initial specification of the radar processing activity

[RSRE-MEMO-4280] p 243 N90-15900
Parallel processing implementation of a flight controller

p 333 N90-16743
Aerodynamics of unsteady systems. Numerical study of potential flow/boundary layer coupling

[ETN-90-96257] p 396 N90-18367
Multi-disciplinary optimization of aeroservoelastic systems

[NASA-CR-185931] p 925 N90-29385
Assessment System for Aircraft Noise (ASAN): Development of alpha-test prototype system software

[AD-A223770] p 966 N90-30036
SOILS
Enhanced bioreclamation of jet fuels: A full-scale test at Eglin AFB, Florida

[AD-A22348] p 875 N90-26992
Development and testing of rapid repair methods for war damaged runways

[AD-A223970] p 938 N90-28586
SOL-GEL PROCESSES
Properties and characterisation of novel thermal barrier systems for gas turbines

p 62 A90-12538
SOLAR ARRAYS
Preliminary design of a long-endurance Mars aircraft

[AIAA PAPER 90-2000] p 674 A90-40587
Preliminary design of a long-endurance Mars aircraft [NASA-CR-185243] p 588 N90-21763

SOLAR FLARES
Recent results and major activities in the NASA Balloon Program

[IAF PAPER 89-468] p 81 A90-13557
SOLAR POWER SATELLITES
History and status of beamed power technology and applications at 2.45 Gigahertz

p 61 N90-10150
SOLID LUBRICANTS
Evaluation of solid lubricant powder delivery system for turbine bearing lubrication

[AIAA PAPER 90-2046] p 684 A90-41997
High temperature powder lubricated dampers for gas turbine engines

[AIAA PAPER 90-2048] p 684 A90-41999
SOLID MECHANICS
NASA-UVA light aerospace alloy and structures technology program

[NASA-CR-182607] p 601 N90-22651
SOLID PROPELLANT COMBUSTION
Experimental and computational flammability limits in a solid fuel ramjet

[AIAA PAPER 90-1964] p 676 A90-40574
Solid fuel ignition and combustion characteristics under high-speed crossflows

[AIAA PAPER 90-2075] p 764 A90-42725
An investigation on boron used as a component of solid propellant

p 765 A90-45708
Solid fuel combustion chamber

[LR-634] p 939 N90-29433
SOLID PROPELLANT IGNITION
Solid fuel ignition and combustion characteristics under high-speed crossflows

[AIAA PAPER 90-2075] p 764 A90-42725
SOLID PROPELLANT ROCKET ENGINES
Flow around a jet and thrust measurement bias from static tests

[AAAF PAPER NT 88-11] p 40 A90-11431
5DOF dynamic loads on a jet vane

[AIAA PAPER 90-2382] p 675 A90-42147
An investigation on boron used as a component of solid propellant

p 765 A90-45708
Systems tunnel linear shaped charge lightning strike

[NASA-CR-183832] p 201 N90-13404
Review of the Aerospace Safety Advisory Panel report for NASA fiscal year 1990 authorization

[GPO-24-234] p 177 N90-14213
SOLID PROPELLANTS
Similarity and scale effects in solid fuel ramjet combustors

p 60 A90-12513
Combustion characteristics of a boron-fueled SFRJ with aft-burner

p 62 A90-12514
Heat transfer in a solid fuel ramjet combustor

[AIAA PAPER 90-1783] p 586 A90-38472
Inverse heat transfer studies and the effects of propellant aluminum on TVC jet vane heating and erosion

[AIAA PAPER 90-1860] p 655 A90-40533
The jet engine: 1932

[ISBN-3-922010-49-0] p 763 N90-25189
SOLID ROCKET PROPELLANTS
Metalized fuel particle size study in a solid fuel ramjet

[AD-A220079] p 679 N90-24451
SOLID SURFACES
A numerical method for three-dimensional viscous flows

[AIAA PAPER 90-0236] p 228 A90-22186
Infrared sources of jet propulsion system and their suppression

p 252 A90-22614
Effect of surface riblets on the velocity profile of an incompressible boundary layer

p 294 A90-24081
Automation of the development of a finite element model for shells of the wing type

p 364 A90-24118
Surface grid generation through elliptic PDEs

p 309 A90-26496
Experimental study of incompressible flow on the upper surface of a delta wing

p 558 A90-37346
Application of localized surface heating to actively control the boundary layer separation

p 806 A90-46848
Thermal interaction between an impinging hot jet and a conducting solid surface

[AIAA PAPER 90-3010] p 956 A90-50636
SOLIDIFICATION
Microstructures of rapidly-solidified binary TiAl alloys

p 532 A90-34990
SOLIDS FLOW
Effect of environmental particles on a radial compressor

p 113 A90-16373
SOLUBILITY
Improved damage tolerance by controlling thermoplastic solubility in thermoset composites

p 944 A90-50138
SOLVENTS
Equilibrium swelling of elastomeric materials in solvent environments

[DE90-010164] p 678 N90-24430
SONDES
The development of a high response aerodynamic wedge probe and use on a high-speed research compressor

[PNR90598] p 116 N90-12613
SONIC BOOMS
A study of sonic boom overpressure trends with respect to weight, altitude, Mach number, and vehicle shaping

[AIAA PAPER 90-0367] p 164 A90-19816
A study of the limitations of linear theory methods as applied to sonic boom calculations

[AIAA PAPER 90-0368] p 219 A90-19817
Civil supersonics - A less distant thunder

p 731 A90-44223
SST/HST air traffic - Challenge for the future

p 763 A90-44752
Technology issues for high-speed civil transports

[SAE PAPER 892201] p 778 A90-45422
Noise and sonic boom impact technology. Effects of aircraft noise and sonic booms on structures: An assessment of the current state-of-knowledge

[AD-A213919] p 378 N90-17409
Noise and sonic boom impact technology. Initial development of an Assessment System for Aircraft Noise (ASAN). Volume 1: Executive summary

[AD-A214164] p 379 N90-17410
Noise and sonic boom impact technology. Initial development of an Assessment System for Aircraft Noise (ASAN). Volume 2: System design strategy

[AD-A214454] p 379 N90-17411
Noise and sonic boom impact technology. Initial development of an Assessment System for Aircraft Noise (ASAN). Volume 3: Technical description

[AD-A214455] p 379 N90-17412
Air Force Boom Event Analyzer Recorder (BEAR): System description

[AD-A218048] p 548 N90-20800
Sonic boom signature data from cruciform microphone array experiments during the 1966-1967 EAFB national sonic boom evaluation program

[NASA-CR-182027] p 549 N90-21605
Assessment System for Aircraft Noise (ASAN) citation database. Volume 1: User's manual

[AD-A219175] p 615 N90-23188
Assessment System for Aircraft Noise (ASAN) citation database. Volume 2: Database update manual

[AD-A219176] p 615 N90-23189
Assessment System for Aircraft Noise (ASAN) citation database. Volume 3: New citation review procedures

[AD-A219177] p 615 N90-23190
Summary of sonic boom rise times observed during FAA community response studies over a 6-month period in the Oklahoma City area

[NASA-CR-4277] p 696 N90-24852
Vibration responses of two house structures during the Edwards Air Force Base phase of the national sonic boom program

[NASA-CR-182089] p 966 N90-29169
SOOT
The use of soot analysis as an investigative tool in aircraft fires

p 22 A90-10269
Active soot reduction in a spray-fired, axisymmetric model gas turbine combustor

[AIAA PAPER 90-0039] p 191 A90-19644
Fuel molecular structure and flame temperature effects on soot formation in gas turbine combustors

[ASME PAPER 89-GT-288] p 253 A90-22652
Combustor cooling aspects

[CIT/SME/VKI/RS/5] p 749 N90-25989
SORTIE SYSTEMS
Robotics for flightline servicing

p 383 A90-30760

SOUND FIELDS

Digital control of local sound fields in an aircraft passenger compartment p 247 A90-23113

On numerical prediction of sound field generated by propeller p 895 A90-49485

The radiation of sound from a propeller at angle of attack

[NASA-CR-4264] p 548 N90-21602

Asymptotic modal analysis and statistical energy analysis

[NASA-CR-186732] p 782 N90-26634

SOUND GENERATORS

Sound generation by a supersonic aerofoil cutting through a steady jet flow p 781 A90-42638

SOUND PRESSURE

Noise prediction of a counter-rotation propfan p 218 A90-17861

Calculation of the rotation noise of a single propeller with blades of arbitrary shape p 894 A90-46552

Estimation of subsonic far-field jet-mixing noise from single-stream circular nozzles

[ESDU-89041] p 316 N90-16721

Noise levels from a VSTOL aircraft measured at ground level and at 1.2 m above the ground

[NPL-RSA(EXT)-009] p 464 N90-18999

The radiation of sound from a propeller at angle of attack

[NASA-CR-4264] p 548 N90-21602

Free-field propagation of high intensity noise

[NASA-CR-186577] p 549 N90-21604

Annoyance caused by advanced turboprop aircraft flyover noise: Counter-rotating-propeller configuration

[NASA-TP-3027] p 965 N90-29166

SOUND PROPAGATION

Simulation of sound propagation in axisymmetric jet p 378 A90-25872

Fuselage boundary-layer effects on sound propagation and scattering p 695 A90-39781

Sound propagation elements in evaluation of en route noise of advanced turboprop aircraft p 697 N90-24861

SOUND TRANSMISSION

Prediction of transmission loss through an aircraft sidewall using statistical energy analysis --- study of cabin noise reduction p 219 A90-18599

Optimization of the sound-absorption lining parameters of an ejector jet muffler p 378 A90-24117

Structure-borne noise transmission in cylindrical enclosures due to random excitation

[AIAA PAPER 90-0990] p 463 A90-29402

Installation effects on propeller wake/vortex-induced structure-borne noise transmissions p 579 A90-35761

Experiments on the active control of the transmission of sound through a clamped rectangular plate

p 695 A90-41109

Active control of sound transmission through a cylindrical shell p 893 A90-46192

Mechanisms of active control in cylindrical fuselage structures p 862 A90-47309

The absorption of sound by perforated linings

p 965 A90-51994

UHB demonstrator interior noise control flight tests and analysis

[NASA-CR-181897] p 140 N90-13198

The Shock and Vibration Digest, volume 21, no. 6

p 614 N90-22363

Noise transmission into propeller-driven airplanes

p 614 N90-22364

Tests of an ultra-light tunnel in the anechoic wind tunnel facility CEPRA 19

[ONERA-RF-20/7294-PH] p 872 N90-27729

SOUND WAVES

Free-field correction factor for spherical acoustic waves impinging on cylinders p 218 A90-17984

Sound radiation from an airfoil encountering an oblique gust in its plane of motion p 218 A90-17998

Sound generation by a supersonic aerofoil cutting through a steady jet flow p 781 A90-42638

Combining thermal and high level acoustics

p 770 A90-43729

Acoustic-vortex-chemical interactions in an idealized ramjet p 54 N90-10206

Application of sound and temperature to control boundary-layer transition p 92 N90-12537

Gear noise, vibration, and diagnostic studies at NASA Lewis Research Center

[NASA-TM-102435] p 372 N90-18041

Sandia National Laboratories' new high level acoustic test facility

[DE90-006810] p 464 N90-19820

Free-field propagation of high intensity noise

[NASA-CR-186577] p 549 N90-21604

The computation and analysis of acoustic waves in transonic airfoil-vortex interactions p 966 N90-30031

SPACE CAPSULES

Verification of aerothermodynamic codes by means of a winged experimental re-entry vehicle

p 354 N90-16842

SPACE FLIGHT

Hydroelastic problems in space flight vehicles

p 536 A90-33386

Langley aerospace test highlights, 1989

[NASA-TM-102631] p 699 N90-24221

SPACE LAW

Latin American Conference on International Air Transport and Activities in Outer Space, Mexico City, Mexico, Aug. 14-18, 1988, Proceedings

p 897 A90-49613

SPACE NAVIGATION

Accuracy considerations for GPS TSP1 system design

p 98 A90-14001

Aerospace coordinate systems and transformations --- Book

p 282 A90-23372

AIAA Guidance, Navigation and Control Conference, Portland, OR, Aug. 20-22, 1990, Technical Papers, Parts 1 & 2

p 862 A90-47576

SPACE PERCEPTION

Cognitive perspectives on map displays for helicopter flight

p 419 A90-31329

Stereopsis as a visual cue in flight simulation

p 870 A90-48960

SPACE PLATFORMS

Fiber optic systems for mobile platforms II; Proceedings of the Meeting, Boston, MA, Sept. 6, 7, 1988

[SPIE-989] p 67 A90-11659

Tracking a hypersonic aircraft from a space platform

[AD-A216399] p 371 N90-17984

SPACE PROGRAMS

The 21st century in space; Proceedings of the Thirty-fifth Annual AAS Conference, Saint Louis, MO, Oct. 24-26, 1988

p 762 A90-43460

SPACE SHUTTLE MAIN ENGINE

Application of HOST technology to the SSME HPFTP blade

[ASME PAPER 89-GT-130] p 360 A90-23828

SPACE SHUTTLE ORBITERS

Independent Orbiter Assessment (IOA): Analysis of the displays and controls subsystem

p 124 N90-11774

[NASA-CR-185563] Prediction of forces and moments for flight vehicle control effectors. Part 1: Validation of methods for predicting hypersonic vehicle controls forces and moments

p 571 N90-21734

SPACE SHUTTLES

Hypersonics revisited (The First Leslie Bedford Lecture)

p 60 A90-11458

Analysis of extreme wind shear

p 280 A90-23255

Computational fluid dynamics - Current capabilities and directions for the future

p 540 A90-34385

Landing tests for Buran shuttle with jet engine-equipped mock-up

p 61 N90-10904

The Real Time Display Builder (RTDB)

p 546 N90-20656

Research at NASA's NFAC wind tunnels

[NASA-TM-102827] p 702 N90-25933

SPACE STATIONS

Review of the Aerospace Safety Advisory Panel report for NASA fiscal year 1990 authorization

[GPO-24-234] p 177 N90-14213

Aerospace induction motor actuators driven from a 20-kHz power link

[NASA-TM-102482] p 509 N90-20085

SPACE SURVEILLANCE (SPACEBORNE)

Development and operation of the Traffic Alert and Collision Avoidance System (TCAS)

p 331 A90-25573

Rapsat - Application of onboard processing for communication and surveillance in air traffic control

[AIAA PAPER 90-0883] p 331 A90-25702

Tests of automatic dependent surveillance (ADS) in Western Europe - Possible future developments

p 574 A90-35353

SPACE TRANSPORTATION

Keepers of the flame --- scramjet development programs

p 141 A90-16300

High-performance composite materials in air and space travel - State of the art and future perspectives

[MBB-Z-0279/89] p 266 A90-22595

Design for hypersonic speed

p 335 A90-26343

SST/HST air traffic - Challenge for the future

p 763 A90-44752

Aerodynamic and structural design challenges of a reusable single stage to orbit air-breathing launch vehicle

p 354 N90-16814

Progress in airbreathing combined engines for future European launcher

p 344 N90-16817

SPACE TRANSPORTATION SYSTEM

Review of the Aerospace Safety Advisory Panel report for NASA fiscal year 1990 authorization

[GPO-24-234] p 177 N90-14213

SPACEBORNE LASERS

Development of air-to-air laser communications

p 487 A90-31938

SPACECRAFT CONSTRUCTION MATERIALS

The National Aero-Space Plane, the guidance and control engineer's dream or nightmare?

[AAS PAPER 89-040] p 264 A90-21546

The impact of composites on the aerospace industry

p 221 A90-22649

Materials get smarter

p 356 A90-27598

AIAA/ASME/ASCE/AHS/ASC Structures, Structural Dynamics and Materials Conference, 31st, Long Beach, CA, Apr. 2-4, 1990, Technical Papers, Part 3 - Structural dynamics I

p 449 A90-29359

Carbon-carbon for NASP

p 599 A90-36672

Ceramic materials and coatings for future aerospace applications - Challenge of the 1990's

p 942 A90-50071

The effect of jet fuel absorption on advanced aerospace thermoset and thermoplastic composites

p 942 A90-50082

HOTOL structures and materials at British Aerospace, Warton, UK

[EOARD-LR-90-001] p 503 N90-21001

Materials and structures for 2000 and beyond: An attempted forecast by the DLR Materials and Structures Department

[ESA-TT-1154-REV] p 775 N90-26173

SPACECRAFT CONTROL

Optimization of the observations and control of aircraft --- Russian book

p 60 A90-12468

The National Aero-Space Plane, the guidance and control engineer's dream or nightmare?

[AAS PAPER 89-040] p 264 A90-21546

Flying qualities problems of aerospace craft

[AIAA PAPER 90-2804] p 752 A90-45139

AIAA Guidance, Navigation and Control Conference, Portland, OR, Aug. 20-22, 1990, Technical Papers, Parts 1 & 2

p 862 A90-47576

Independent Orbiter Assessment (IOA): Analysis of the displays and controls subsystem

[NASA-CR-185563] p 124 N90-11774

SPACECRAFT DESIGN

Rockwell's simulator emulates NASP flight characteristics

p 60 A90-11650

MAVIS flight load simulation --- Multi Axis Vibration System

p 202 A90-17003

Development of finite element methods for compressible Navier-Stokes flow simulations in aerospace design

[AIAA PAPER 90-0403] p 166 A90-19833

Hypersonic aerospace sizing analysis for the preliminary design of aerospace vehicles

p 247 A90-23276

The design of supersonic aircraft and space vehicles by using global optimization techniques

p 353 A90-25781

Aerodynamic work for Hermes spaceplane

p 675 A90-41115

Forebody design for the aerospaceplane

[AIAA PAPER 90-2472] p 762 A90-42810

Flight testing and flight research: From the age of the tower jumper to the age of the astronaut

p 35 N90-10882

National aero-spaceplane status and plans

p 337 N90-16801

Supersonic aerodynamic characteristics of a proposed Assured Crew Return Capability (ACRC) lifting-body configuration

[NASA-TM-4136] p 317 N90-17560

Implications of Advanced Technologies for Air and Spacecraft Escape

[AGARD-CP-472] p 483 N90-20054

Structural dynamics branch research and accomplishments

[NASA-TM-102488] p 778 N90-26373

SPACECRAFT DOCKING

Supersonic aerodynamic characteristics of a proposed Assured Crew Return Capability (ACRC) lifting-body configuration

[NASA-TM-4136] p 317 N90-17560

Yaw rate control of an air bearing vehicle

p 435 N90-19420

SPACECRAFT GUIDANCE

AIAA Guidance, Navigation and Control Conference, Portland, OR, Aug. 20-22, 1990, Technical Papers, Parts 1 & 2

p 862 A90-47576

Trajectory optimization and guidance for an aerospace plane

[NASA-CR-185884] p 183 N90-13369

SPACECRAFT INSTRUMENTS

Applications of fiber optic sensors in the aerospace and marine industries

p 603 A90-36782

Independent Orbiter Assessment (IOA): Analysis of the displays and controls subsystem

[NASA-CR-185563] p 124 N90-11774

SPACECRAFT LANDING

Landing tests for Buran shuttle with jet engine-equipped mock-up p 61 N90-10904

SPACECRAFT LAUNCHING

Analysis of extreme wind shear p 280 A90-23255

SPACECRAFT MODELS

Landing tests for Buran shuttle with jet engine-equipped mock-up p 61 N90-10904

SPACECRAFT PERFORMANCE

The ascending trajectories performance and control to minimize the heat load for the transatmospheric aero-space planes [AIAA PAPER 90-2828] p 763 A90-45135

SPACECRAFT POWER SUPPLIES

High Voltage Design Guide summary p 605 A90-38097

SPACECRAFT PROPULSION

Preliminary analysis of methodology for assessment of propulsion system for aerospace plane [IAF PAPER 89-307] p 123 A90-13442

Development study of air turbo-ramjet for future space plane [IAF PAPER 89-311] p 109 A90-13445

Hydrogen in future energy and propulsion technology p 692 A90-41736

SPACECRAFT RELIABILITY

Independent Orbiter Assessment (IOA): Analysis of the displays and controls subsystem [NASA-CR-185563] p 124 N90-11774

SPACECRAFT STABILITY

Hydroelastic problems in space flight vehicles p 536 A90-33386

Stability characteristics of a conical aerospace plane concept [SAE PAPER 892313] p 757 A90-45475

SPACECRAFT STRUCTURES

Fiber optic sensor systems for smart aerospace structures p 38 A90-11208

Optical fiber sensing considerations for a smart aerospace structure p 38 A90-11210

MAVIS flight load simulation --- Multi Axis Vibration System p 202 A90-17003

Generalized Transition Finite-Boundary Elements for high speed flight structures p 449 A90-29286

[AIAA PAPER 90-1105] p 449 A90-29286

Development and application of an optimization procedure for space and aircraft structures p 679 A90-39186

Multicriteria optimal layouts of aircraft and spacecraft structures p 889 A90-46046

Advanced joint of 3-D composite materials for space structure p 944 A90-50137

Safety and health trends in aerospace composite materials p 847 A90-50188

Hierarchical damage tolerant controllers for smart structures p 31 N90-10022

[AD-A209422] p 31 N90-10022

Materials and structures for 2000 and beyond: An attempted forecast by the DLR Materials and Structures Department p 775 N90-26173

[ESA-TT-1154-REV] p 775 N90-26173

SPACECRAFT TRACKING

Tracking a hypersonic aircraft from a space platform [AD-A216399] p 371 N90-17984

SPACERS

Critical inspection of high performance turbine engine components: The RFC concept p 859 N90-28073

SPACING

Simulator evaluation of the final approach spacing tool [NASA-TM-102807] p 636 N90-23374

SPALLING

Initiation of spalling in aircraft gas turbine bearings [AIAA PAPER 90-2291] p 686 A90-42110

Thermal barrier coating life prediction model development, phase 1 [NASA-CR-182230] p 193 N90-13388

SPAN

Full span analysis for flutter prediction of slender blade assemblies p 879 A90-46188

SPANLOADER AIRCRAFT

Design of a spanloader cargo aircraft [NASA-CR-186046] p 184 N90-14216

SPANWISE BLOWING

Spanwise distribution of lift and drag at high angles of attack [SAE PAPER 891019] p 83 A90-14331

Spanwise properties of the unsteady separation shock in a Mach 5 unswept compression ramp interaction [AIAA PAPER 90-0377] p 228 A90-22208

Control of asymmetric vortical flows over delta wings at high angles of attack p 553 A90-35759

SPATIAL DEPENDENCIES

Numerical simulation of confined, spatially-developing mixing layers - Comparison to the temporal shear layer [AIAA PAPER 90-1462] p 562 A90-38619

SPATIAL MARCHING

A three-dimensional space marching algorithm for the solution of the Euler equations on unstructured grids [AIAA PAPER 90-0014] p 234 A90-23701

Three-dimensional simulations of hypersonic flows p 306 A90-25823

Application of a new adaptive grid for aerodynamic analysis of shock containing single jets [AIAA PAPER 90-2025] p 624 A90-41988

Calculation of three-dimensional viscous and inviscid hypersonic flows using split-matrix marching methods [AIAA PAPER 90-3070] p 794 A90-45894

Supersonic flow computations over aerospace configurations using an Euler marching solver [NASA-CR-4085] p 19 N90-10012

SPATIAL RESOLUTION

Temporally and spatially resolved flow in a two-stage axial compressor. Part 2: Computational assessment [NASA-TM-102273] p 194 N90-14236

SPECIFIC HEAT

Varying specific heat gasdynamic function formulae simplification and analytical solution of normal shock waves p 908 A90-52776

SPECIFICATIONS

National airspace system: Airport movement area control operational concept [WP-89W00181] p 243 N90-15086

APSA 2 small-scale system specification [NASA-CR-182006] p 695 N90-24103

Reliability model generator specification [NASA-CR-182005] p 780 N90-25638

In-service inspection of composite components on aircraft at depot and field levels p 885 N90-28078

SPECIMEN GEOMETRY

Fatigue behavior of specimens under compression load spectra [ETN-89-95207] p 137 N90-12954

SPECKLE PATTERNS

Practical systems for speckle velocimetry p 171 N90-13341

SPECTRA

Fatigue analysis and reconstruction of helicopter load spectra p 206 N90-14304

SPECTRAL CORRELATION

A new class of random processes with application to helicopter noise p 781 A90-42874

SPECTRAL METHODS

High resolution spectrum analysis for airborne pulse Doppler radars p 339 A90-24329

Helicopter simulation development by correlation with frequency sweep flight test data p 407 A90-28203

A design method for turbomachinery blading in three-dimensional flow p 904 A90-51003

Spectral simulation of unsteady compressible flow past a circular cylinder [NASA-CR-182030] p 478 N90-20050

SPECTRORADIOMETERS

UV spectroradiometric output of an F404 turbojet aircraft engine p 652 A90-40195

SPECTROSCOPY

Visualization of corona discharges p 819 A90-49839

SPECTRUM ANALYSIS

Spectral simulation of unsteady compressible flow past a circular cylinder [NASA-CR-182030] p 478 N90-20050

SPEECH RECOGNITION

Considerations of noise for the use of compressed speech in a cockpit environment p 404 A90-31334

Investigation of air transportation technology at the Massachusetts Institute of Technology, 1988-1989 p 484 A90-20922

Automatic speech recognition in air traffic control p 488 N90-20923

Evaluation of speech recognizers for use in advanced combat helicopter crew station research and development [NASA-CR-177547] p 650 N90-24265

Automatic speech recognition in air-ground data link p 690 N90-25037

Studies in automatic speech recognition and its application in aerospace p 958 N90-28759

SPEED CONTROL

Computer controlled test bench for axial turbines and propellers p 437 A90-28288

Analytical evaluation of helicopter true air speed and associated flight tests p 647 A90-42499

SPHERES

Coherent vortex structures in the wake of a sphere and a circular disk at rest and under forced vibrations p 623 A90-40749

Flow past two cylinders and two spheres p 903 A90-50815

SPHERICAL SHELLS

Analytical solution of the problem of nonaxisymmetric potential flow past a spherical canopy - A summary of the principal asymptotic formulas and qualitative analysis p 300 A90-24753

SPHERICAL WAVES

Free-field correction factor for spherical acoustic waves impinging on cylinders p 218 A90-17984

SPIKES (AERODYNAMIC CONFIGURATIONS)

Aerodynamic spike flowfields computed to select optimum configuration at Mach 2.5 with experimental validation [AIAA PAPER 90-0414] p 166 A90-19837

SPILLING

Water-tunnel investigation of concepts for alleviation of adverse inlet spillage interactions with external stores [NASA-TM-4181] p 398 N90-19199

SPIN

The spinning of aircraft: A discussion of spin prediction techniques including a chronological bibliography [ARL-AERO-R-177] p 36 N90-10888

SPIN DYNAMICS

Investigations of modifications to improve the spin resistance of a high-wing, single-engine, light airplane [SAE PAPER 891039] p 118 A90-14345

The analysis of entry into and recovery from a spin for the J16 aircraft p 195 A90-16854

F-15B high angle-of-attack phenomena and spin prediction using bifurcation analysis [AD-A217366] p 498 N90-20073

Miniaturization of flight deflection measurement system [NASA-CASE-LAR-13628-1] p 689 N90-23707

SPIN STABILIZATION

Stall/spin/flight simulation [DOT/FAA/CT-88/28] p 122 N90-11765

SPIN TESTS

Measurements of pressures on the wing of an aircraft model during steady rotation [AIAA PAPER 90-2842] p 754 A90-45162

Measurements of pressures on the tail and aft fuselage of an airplane model during rotary motions at spin attitudes [NASA-TP-2939] p 20 N90-10829

The spinning of aircraft: A discussion of spin prediction techniques including a chronological bibliography [ARL-AERO-R-177] p 36 N90-10888

SPLINE FUNCTIONS

Study of calculating an approximately constant reaction turbine stage with a tension spline streamline curvature method p 157 A90-18537

Aircraft program motion along a predetermined trajectory. II - Numerical simulation with application of spline functions to trajectory definitions p 347 A90-25199

Application of splines to the calculation of flow past a wing profile p 805 A90-46615

A study of terrain following systems and the creation of flight paths for terrain following vehicles [FOA-C-20774-2.5] p 827 N90-27691

SPLINES

Application of Lagrangian blending functions for grid generation around airplane geometries [NASA-CR-186318] p 237 N90-15891

Internal rotor friction instability [NASA-CR-183942] p 543 N90-21395

SPOILERS

Effects of spoiler surfaces on the aeroelastic behavior of a low-aspect-ratio rectangular wing [AIAA PAPER 90-0981] p 391 A90-29371

Unsteady, separated flow behind an oscillating, two-dimensional spoiler p 469 A90-32462

Boeing/NASA composite components flight service evaluation [NASA-CR-181898] p 601 N90-22609

Effects of spoiler surfaces on the aeroelastic behavior of a low-aspect-ratio rectangular wing [NASA-TM-102622] p 846 N90-27700

The effect of rapid spoiler deployment on the transient forces on an aerofoil p 921 N90-28527

SPOOLS

Dynamics of multi-spool gas turbines using the matrix transfer method - Applications p 509 A90-33594

Dynamics of multi-spool gas turbines using the matrix transfer method - Theory p 509 A90-33595

SPRAY CHARACTERISTICS

Air and spray patterns produced by gas turbine high-shear nozzle/swirler assemblies [AIAA PAPER 90-0465] p 192 A90-19857

A study on spray characteristics down stream from a gutter-atomizer p 368 A90-26893

Further validation of a semi-analytical approach for fuel injectors of different concepts [AIAA PAPER 90-2190] p 686 A90-42067

SUBJECT INDEX

Influences on the uniformity of sprays produced by gas turbine high shear nozzle/swirler assemblies
[AIAA PAPER 90-2193] p 686 A90-42068

Subsonic combustor testing p 749 N90-25997

SPRAY NOZZLES

Spray nozzle investigation for the Improved Helicopter Icing Spray System (IHSS)
[AIAA PAPER 90-0666] p 350 A90-25040

Development of the improved helicopter icing spray system (IHSS) p 400 A90-28182

Life estimation of a gas turbine afterburner spraybar p 739 A90-42662

SPRAYED COATINGS

TBCs for better engine efficiency --- thermal barrier coatings p 203 A90-17294

Organic coatings - First line of defense p 204 A90-17300

The selection and performance of thermal sprayed abrasible seal coatings for gas turbine engines
[SAE PAPER 890929] p 286 A90-24694

Coating turbine engine components p 451 A90-29893

SPRAYERS

Symmetry assessment of an air-blast atomizer spray p 682 A90-40930

Spray sealing: A breakthrough in integral fuel tank sealing technology p 276 N90-15912

Aircraft internal fires p 326 N90-17593

Liquid fueled ramjet combustion instability: Acoustical and vortical interactions with burning sprays
[AD-A22752] p 767 N90-26104

SPREAD SPECTRUM TRANSMISSION

Throughput and delay characteristics for a slow-frequency hopped aircraft-to-aircraft packet radio network
[AD-A220525] p 688 N90-23609

SQUEEZE FILMS

Unbalance response studies on a model rotor supported on uncentralized squeeze film dampers and the development experience of a jet engine p 69 A90-12579

Squeeze film damping for aircraft gas turbines p 113 A90-16009

Unbalance response of a Jeffcott rotor incorporating long squeeze film dampers p 880 A90-46237

STABILITY

LORAN C stability integrity assurance
[AD-A212663] p 177 N90-13364

Supersonic aerodynamic characteristics of a proposed Assured Crew Return Capability (ACRC) lifting-body configuration
[NASA-TM-4136] p 317 N90-17560

The stability of fuel fires p 327 N90-17601

Low NO(x) potential of gas turbine engines
[NASA-TM-102452] p 345 N90-17636

Direct multivariable adaptive controller with application to wing flutter p 349 N90-17642

Development of an ejection seat specification for a new fighter aircraft p 483 N90-20057

Algorithms for computing the multivariable stability margin p 612 N90-22999

STABILITY AUGMENTATION

Results of an A109 simulation validation and handling qualities study p 591 A90-38524

System concept and performance criteria of modern helicopter navigation p 640 A90-42452

UH-60A helicopter stability augmentation study p 670 A90-42471

Bifurcation analysis of a model fighter aircraft with control augmentation p 934 A90-50640

Structural stability augmentation system design using BODEDIRECT: A quick and accurate approach p 33 N90-10116

Output model-following control synthesis for an oblique-wing aircraft
[NASA-TM-100454] p 435 N90-19241

Lateral-directional stability and control characteristics of the Quiet Short-Haul Research Aircraft (QSRA)
[NASA-TM-102250] p 671 N90-23413

Short period control using angular acceleration feedback: Compensation for first lag servo
[NAL-TM-600] p 936 N90-29399

STABILITY DERIVATIVES

The application of linear maximum likelihood estimation of aerodynamic derivatives for the Bell-205 and Bell-206 p 30 A90-12773

Sensitivity derivatives of flutter characteristics and stability margins for aeroservoelastic design p 433 A90-31287

Unsteady lift and moment coefficients of an engine nacelle p 473 A90-33365

Analysis of perturbed longitudinal dynamics of an aircraft taking into consideration the stationary aeroelastic effects and the atmospheric perturbances p 520 A90-34822

Calculation of stability derivatives for slender bodies using boundary element method p 620 A90-40181

Inversion of nonlinear I-O map, zero dynamics and flight control system design p 863 A90-47628

[AIAA PAPER 90-3370] p 867 A90-48515

Exceptions to the $C(n, \beta, \gamma)$ criterion for aircraft stability at high angles of attack p 867 A90-48515

The active flexible wing aeroservoelastic wind-tunnel test program p 33 N90-10119

Stability and control derivatives of the De Havilland DHC-2 BEAVER aircraft
[PB89-217525] p 119 N90-11754

Dynamic derivatives of missiles and fighter-type configurations at high angles of attack p 337 N90-17554

Aerodynamic interferences of in-flight thrust reversers in ground effect p 921 N90-28529

STABILITY TESTS

Multi-output implementation of a modified sparse time domain technique for rotor stability testing
[AIAA PAPER 90-0946] p 412 A90-29405

Performance and quality of a wing type parachute: Parametric analysis
[REPT-88-19] p 89 N90-11710

Computation of nonequilibrium chemically reacting flows in hypersonic flow field p 480 N90-20954

Aerodynamic control design: Experience and results at Aermacchi p 935 N90-28518

STABILIZATION

The stability of fuel fires p 327 N90-17601

Control and stabilization of linear and nonlinear distributed systems
[AD-A216446] p 462 N90-18908

Escape systems research at RAE p 483 N90-20058

Controllable propulsion for escape systems control p 484 N90-20064

Digital-flutter-suppression-system investigations for the active flexible wing wind-tunnel model
[NASA-TM-102618] p 520 N90-20093

Calculation of the aeroelastic blade stabilization with linearized process
[MITT-87-01] p 666 N90-24272

Experience in developing an improved design of experiment (lessons learned) p 857 N90-27718

Development and testing of rapid repair methods for war damaged runways
[AD-A223970] p 938 N90-28586

STABILIZERS (FLUID DYNAMICS)

Evaluation of a damaged F/A-18 horizontal stabilizer
[AD-A212573] p 107 N90-12597

Cost effectiveness of composite materials on the F-15 and F-16 aircrafts
[AD-A216353] p 338 N90-17631

The MANTA: An RPV design to investigate forces and moments on a lifting surface
[NASA-CR-186227] p 499 N90-20971

A sensor stabilization/tracking system for unmanned air vehicles
[AD-A224008] p 936 N90-28579

STAGNATION FLOW

Hypersonic rarefied flow and its solution over the stagnation region
[AIAA PAPER 90-0420] p 166 A90-19842

Secondary loss generation in a linear cascade of high-turning turbine blades
[ASME PAPER 89-GT-47] p 289 A90-23773

Effect of the cross-sectional shape of a straight duct on supersonic flow stagnation p 296 A90-24110

STAGNATION POINT

Brownian motion far from equilibrium - A hypersonic approach p 555 A90-35917

Flow over a leading edge with distributed roughness p 703 A90-42646

A formulation for the solution of Euler equations for compressible flow using finite elements p 708 A90-44447

Shock layer vacuum UV spectroscopy in an arc-jet wind tunnel
[NASA-TM-102258] p 370 N90-17112

An experimental and theoretical investigation of the flow over plane delta wings with supersonic leading edges
[LR-568] p 717 N90-25114

Real-time aerodynamic heating and surface temperature calculations for hypersonic flight simulation
[NASA-TM-4222] p 959 N90-28815

STAGNATION PRESSURE

The use of circumferentially varying stagger guide vanes in an axial flow pump or compressor p 537 A90-33566

Time-resolved measurements of total temperature and pressure in the vortex street behind a cylinder p 557 A90-36522

STATIC AERODYNAMIC CHARACTERISTICS

STAGNATION TEMPERATURE

Time-resolved measurements of total temperature and pressure in the vortex street behind a cylinder p 557 A90-36522

STAIRSTEPS

Wall pressure fluctuation spectra in supersonic flow past a forward facing step p 388 A90-29194

STALLING

Development of the stall warning/stick pusher system for the Boeing/de Havilland Dash 8 Series 300 p 645 A90-42420

Computation of viscous aerodynamic characteristics of 2-D airfoils for helicopter applications
[NLR-MP-88052-U] p 720 N90-25951

STANDARDIZATION

Aviation acoustical noise measurement
[AD-A222014] p 896 N90-27469

STANDARDS

Application of effective baselines to smart structures p 536 A90-32885

Castings Airworthiness
[AGARD-R-762] p 64 N90-10231

Aircraft Fire Safety
[AGARD-CP-467] p 324 N90-17581

Development of improved fire safety standards adopted by the Federal Aviation Administration p 324 N90-17585

New aircraft cabin and cargo flammability standards for transport category aircraft p 325 N90-17589

The Uniform Engine Test Programme
[AGARD-AR-248] p 428 N90-19232

The effect of noise-abatement profiles on noise immissions and human annoyance underneath a subsequent climbpath p 698 N90-24865

STANDING WAVES

Interaction between a high-level steady acoustic field and a ducted turbulent flow
[ONERA, TP NO. 1990-27] p 695 A90-41206

Evaluation of critical speeds in high speed aircraft tires
[SAE PAPER 892349] p 733 A90-45500

STAR TRACKERS

A daylight stellar sensor using a charge-coupled device p 637 A90-39002

Strapdown astro-inertial navigation (SAIN) utilizing the optical wide-angle lens startracker (OWLS) p 824 A90-49503

STARTING

Restart characteristics of turbofan engines p 50 A90-12627

Calculation and optimization of rotor start process
[ETN-90-95894] p 416 N90-19229

STATE ESTIMATION

UH-60 flight data replay and refly system state estimator analysis
[AIAA PAPER 90-0181] p 197 A90-19723

Identification of moderately nonlinear flight mechanics systems with additive process and measurement noise p 347 A90-25987

Real time estimation of aircraft angular attitude p 431 A90-30103

A flight-test methodology for identification of an aerodynamic model for a V/STOL aircraft p 413 A90-30107

Estimating short-period dynamics using an extended Kalman filter --- for aircraft controllability
[AIAA PAPER 90-1277] p 518 A90-33901

A proposed Kalman filter algorithm for estimation of unmeasured output variables for an F100 turbofan engine
[AIAA PAPER 90-1920] p 656 A90-40558

Maximum likelihood tuning of a vehicle motion filter p 755 A90-45334

Flight path reconstruction using extended Kalman filtering techniques
[PD-FC-9001] p 489 N90-20970

Experimental and theoretical investigation of optimal control methods with model reduction p 521 N90-21039

Estimating short-period dynamics using an extended Kalman filter
[NASA-TM-101722] p 648 N90-23392

STATE VECTORS

A proposed Kalman filter algorithm for estimation of unmeasured output variables for an F100 turbofan engine
[AIAA PAPER 90-1920] p 656 A90-40558

Parameter sensitivity analysis of one kind of flight path reconstruction estimator p 779 A90-44832

STATIC AERODYNAMIC CHARACTERISTICS

Interference between the pitot-static tube and the model in wind tunnel studies of flow parameters p 350 A90-24169

Simulation of static and dynamic aeroelastic behavior of a flexible wing with multiple control surfaces
[AIAA PAPER 90-1075] p 392 A90-29383

STATIC CHARACTERISTICS

- Static stability and control characteristics of scissor wing configurations p 433 A90-31277
A numerical method in aeroelasticity for wings with separation at large angle of attack p 557 A90-37209

STATIC CHARACTERISTICS

- Static aeroelastic tailoring for oblique wing lateral trim p 667 A90-40689
The effects of foreplanes on the static and dynamic characteristics of a combat aircraft model p 920 N90-28520
Static and dynamic characterization of the ATR 72 rods made of Ti 10.2.3 titanium alloy [REPT-49-238] p 953 N90-28722

STATIC DEFORMATION

- Effect of aerodynamic heating on deformation of composite cylindrical panels in a gas flow p 773 A90-45788

STATIC ELECTRICITY

- 1988 International Aerospace and Ground Conference on Lightning and Static Electricity, Oklahoma City, OK, Apr. 19-22, 1988, Addendum to the Proceedings p 888 A90-49826

STATIC LOADS

- Agusta methodology for pitch link loads prediction in preliminary design phase p 646 A90-42465
Aircraft tire/pavement pressure distributions [SAE PAPER 892351] p 734 A90-45502
Agusta methodology for pitch link loads prediction in preliminary design phase [ETN-90-97270] p 737 N90-25978

STATIC PRESSURE

- Numerical study of centrifugal impeller response to an outlet pressure distortion p 68 A90-11804
Experimental study of static pressure and mean velocity profiles inside a two-dimensional dump-type combustor model p 45 A90-12530
Studies on supersonic radial flow behavior in disk channel p 87 A90-16104
Investigation of adaptive-wall wind tunnels with two measured interfaces [AIAA PAPER 90-0186] p 200 A90-19728
An experimental investigation of pressure fluctuation mechanism for different transonic porous wall configurations [AIAA PAPER 90-1417] p 604 A90-37954
Correlation of radial-to-axial vaneless turns for centrifugal compressors [AIAA PAPER 90-1917] p 656 A90-40556
A unified pressure correction algorithm for computing complex fluid flows p 772 A90-45528
Sideslip-induced static pressure errors in flight-test measurements [AIAA PAPER 90-3082] p 794 A90-45898
Airfoil static-pressure thrust - Flight-test verification [AIAA PAPER 90-3286] p 812 A90-48873
The interaction of a supersonic streamwise vortex and a normal shock wave p 633 N90-24241
Sideslip-induced static pressure errors in flight-test measurements [NASA-TM-102846] p 849 N90-27702

STATIC STABILITY

- Structural analysis of the horizontal tail surfaces of subsonic transport aircraft p 102 A90-14556
Static and dynamic loss of stability of elements of a supersonic aeroplane covering - Numerical analysis p 346 A90-25186
Optimal reflex camber p 308 A90-26347
Static aeroelastic behavior of an adaptive laminated piezoelectric composite wing [AIAA PAPER 90-1078] p 412 A90-29386
Static stability and control characteristics of scissor wing configurations p 433 A90-31277
Robust control design for relaxed static stability aircraft [AIAA PAPER 90-3443] p 865 A90-47696
Airworthiness and flight characteristics test of the UH-60A Black Hawk helicopter equipped with the XM-139 multiple mine dispensing system (VOLCANO) [AD-A210271] p 32 N90-10025
Combustor influence on fighter engine operability p 64 N90-10193
Low-speed wind tunnel investigation of the static stability and control characteristics of an advanced turboprop configuration with the propellers placed over the tail [NASA-CR-186900] p 759 N90-26017

STATIC TESTS

- Flow around a jet and thrust measurement bias from static tests [AAAF PAPER NT 88-11] p 40 A90-11431
Static aeroelastic analysis for generic configuration aircraft [NASA-TM-89423] p 52 N90-10042
Large-scale Advanced Prop-fan (LAP) static rotor test report [NASA-CR-180848] p 117 N90-12617

- Results of aircraft open-loop tests of an experimental magnetic leader cable system for guidance during roll-out and turnoff [NASA-TM-4135] p 348 N90-16767

- Static investigation of a two-dimensional convergent-divergent exhaust nozzle with multiaxis thrust-vectoring capability [NASA-TP-2973] p 397 N90-19193

- Static strength and damage tolerance tests on the Fokker 100 airframe [NLR-MP-88023-U] p 416 N90-19228
Floor pull test of a transport airframe section [DOT/FAA/CT-TN88/14] p 497 N90-20072
Evaluation of static and fatigue properties of thin sheets of 8090-T8 aluminum-lithium alloy and observation of its fracture surfaces [NAL-TR-1039] p 953 N90-29499

STATICS

- ASR-9 weather channel test report [AD-A211749] p 133 N90-11934

STATISTICAL ANALYSIS

- A statistical model of helicopter noise p 77 A90-10229
Another look at aircraft accident statistics p 322 A90-26301
Desktop failure analysis on a microcomputer using Weibull, lognormal, and renewal data [ASME PAPER 89-GT-275] p 535 A90-32263
A comparison of emergency medical helicopter accident rates in the United States and the Federal Republic of Germany p 722 A90-44640
NASA investigation of a claimed 'overlap' between two gust response analysis methods p 771 A90-44730
Analytical study of mistuning/friction/aerodynamics interaction in a bladed disk assembly [AD-A211139] p 55 N90-10893
A real-time wind model using digital data from aircraft [RSRE-MEMO-4309] p 137 N90-13005
Study of the engine bird ingestion experience of the Boeing 737 aircraft [DOT/FAA/CT-89/16] p 176 N90-13360
Risk assessment and its application to flight safety analysis [DE90-004985] p 323 N90-16722
Aircraft fires: A study of transport accidents from 1975 to the present p 324 N90-17583
Objectives and results of cabin fire research in Germany p 325 N90-17588
The NASA digital VGH program. Exploration of methods and final results. Volume 3: B 727 data 1978-1980: 1765 hours [NASA-CR-181909-VOL-3] p 505 N90-20082
The NASA digital VGH program: Exploration of methods and final results. Volume 4: B 747 data 1978-1980, 1689 hours [NASA-CR-181909-VOL-4] p 506 N90-20083
The NASA digital VGH program: Exploration of methods and final results. Volume 5: DC 10 data 1981-1982, 129 hours [NASA-CR-181909-VOL-5] p 506 N90-20084
Ridge regression processing p 489 N90-20931
Annual review of aircraft accident data: US general aviation calendar year 1987 [PB90-138066] p 486 N90-20966
Statistics on aircraft gas turbine engine rotor failures that occurred in US commercial aviation during 1986 [DOT/FAA/CT-89/30] p 511 N90-21008
An investigation of the generation and radiation of aerodynamic noise in real piping systems p 614 N90-22368
A comparison of lightning network data with surface weather observations [AD-A220003] p 692 N90-23832
Adaptive control of a system with periodic dynamics: Application of an impulse response method to the helicopter vibration problem p 694 N90-23990
Study of the engine bird ingestion experience of the Boeing 737 aircraft (October 1986 to September 1988) [DOT/FAA/CT-89/29] p 723 N90-25119
Handbook of uncertainty methodology for engine testing at Pyestock (England) [RAE-TM-P-1179] p 751 N90-26007
Statistical treatment of slow strain rate data for assessment of hydrogen embrittlement in low alloy high strength steel [ARL-MAT-R-122] p 767 N90-26106
Asymptotic modal analysis and statistical energy analysis [NASA-CR-186732] p 782 N90-26634
Active control of aerothermoelastic effects for a conceptual hypersonic aircraft [NASA-TM-102713] p 869 N90-27725
Development of acceptance plans for airport pavement materials. Volume 1: Development [DOT/FAA/RD-90/15] p 937 N90-28581

SUBJECT INDEX

- UK airmisses involving commercial air transport: May - August 1989 [ISSN-0951-6301] p 913 N90-29335

STATISTICAL CORRELATION

- Additive evaluation criteria for aircraft noise p 698 N90-24867
System reliability optimization of aircraft wings p 923 N90-28536

STATISTICAL TESTS

- Testing of statistical hypotheses and derivation of confidence intervals from inspection data samples p 363 A90-24087

STATISTICAL WEATHER FORECASTING

- Some characteristics of the meteorological conditions of low cloud formation around the Baku airport p 888 A90-48364

STATOR BLADES

- Rotor-blades excitation due to differential interference of vane wakes between upstream stator-rows in an axial compressor p 6 A90-11784
Three-dimensional separated flow field in the endwall region of an annular compressor cascade in the presence of rotor-stator interaction. I - Quasi-steady flow field and comparison with steady-state data [ASME PAPER 89-GT-76] p 291 A90-23797
Comparison of steady and unsteady secondary flows in a turbine stator cascade [ASME PAPER 89-GT-79] p 291 A90-23800

STATORS

- A study of unsteady rotor-stator interactions p 67 A90-11557
Test rig for the study of the flow in a rotor-stator system [ONERA, TP NO. 1989-124] p 58 A90-12634
Measurement and calculation of the three-dimensional flow in axial compressor stators, with and without end-bends [ASME PAPER 89-GT-6] p 287 A90-23753
Experimental investigation into the effects of rotating and static bolts on both windage heating and local heat transfer coefficients in a rotor/stator cavity [ASME PAPER 89-GT-196] p 362 A90-23870
Test results for turbulent annular seals, using smooth rotors and helically grooved stators [ASME PAPER 89-TRIB-11] p 537 A90-33556
Calculation of unsteady rotor/stator interaction [AIAA PAPER 90-1544] p 565 A90-38688
Flow and heat transfer in rotating-disc systems. Volume I - Rotor-stator systems --- Book p 772 A90-45759
Prediction and measurement of rotor blade/stator vane dynamic characteristics of a modern aero-engine axial compressor p 878 A90-46036
Influence of vane sweep on rotor-stator interaction noise p 169 N90-13325
Aerodynamic study on forced vibrations on stator rows of axial compressors p 426 N90-18412
The numerical simulation of multistage turbomachinery flows p 514 N90-21025
The effect of secondary flow on the redistribution of the total temperature field downstream of a stationary turbine cascade p 515 N90-21033
Prediction and measurement of rotor blade/stator vane dynamic characteristics of a modern aero-engine axial compressor [PNR90667] p 750 N90-26002
Flow coupling between a rotor and a stator in turbomachinery [AD-A223882] p 932 N90-28572

STEADY FLOW

- Grid generation and adaptation for the direct simulation Monte Carlo method p 67 A90-11102
Collocation methods and lifting-surfaces p 9 A90-12023
An investigation of artificial compressor surge p 11 A90-12526
A multi-domain 3D Euler solver for flows in turbomachines [ONERA, TP NO. 1989-119] p 15 A90-12623
On steady subsonic flow past slender bodies of revolution p 144 A90-16736
Transition phenomena on airfoils operating at low chord Reynolds numbers in steady and unsteady flow p 148 A90-16786
An approach for calculating steady subsonic and transonic blade to blade flows p 152 A90-17784
Numerical simulation of wings in steady and unsteady ground effects p 153 A90-17866
Prediction of steady and unsteady asymmetric vortical flows around cones [AIAA PAPER 90-0598] p 168 A90-19940
Development of the MZM numerical method for 3D boundary layer with interaction on complex configurations --- Multi-Zonal Marching [ONERA, TP NO. 1989-174] p 223 A90-21036

Accelerated computation of viscous, steady incompressible flows
[ASME PAPER 89-GT-45] p 288 A90-23771

Comparison of steady and unsteady secondary flows in a turbine stator cascade
[ASME PAPER 89-GT-79] p 291 A90-23800

Computation of steady three dimensional transonic internal flows p 304 A90-25771

A comparison of two adaptive grid techniques p 309 A90-26507

Comparison between thin layer and full Navier-Stokes simulations over a supersonic delta wing
[AIAA PAPER 90-0589] p 314 A90-26968

Design of a three dimensional Doppler anemometer for T2 transonic wind tunnel p 447 A90-28271

An automated vorticity surveying system using a rotating hot-wire probe p 447 A90-28284

Computation of steady and unsteady control surface loads in transonic flow
[AIAA PAPER 90-0935] p 389 A90-28361

Three dimensional full potential method for the aeroelastic modeling of propfans
[AIAA PAPER 90-1120] p 393 A90-28392

A calculation of the aerodynamic lift acting on cascade blades in a steady, viscous flow at high Reynolds number p 469 A90-32425

Flow quality in the T2 cryogenic wind-tunnel - Problems and solutions p 524 A90-34240

Shock-fitting method for two-dimensional inviscid, steady supersonic flows in ducts p 477 A90-34864

Unsteady aerodynamic gust response including steady flow separation p 556 A90-36262

A comparison of adaptive-grid redistribution and embedding for steady transonic flows
[AIAA PAPER 90-1565] p 565 A90-38704

A new Lagrangian method for steady supersonic flow computation. I - Godunov scheme p 631 A90-42506

Sound generation by a supersonic aerofoil cutting through a steady jet flow p 781 A90-42638

An airfoil theory of bifurcating laminar separation from thin obstacles p 702 A90-42639

Shock-fitting in three space dimensions p 707 A90-44434

Visualization of the turbulent trailing vortex behind a finite wing in steady and unsteady flows p 712 A90-45260

Some remarks on the Kutta condition p 716 A90-45738

Euler procedure for calculation of the steady rotor flow with emphasis on wake evolution
[AIAA PAPER 90-3007] p 789 A90-45857

Numerical simulation of steady and unsteady vortical flows around wings and bodies p 806 A90-46869

Geometrical factors influencing the flow field in a propulsive nozzle p 807 A90-46876

Analysis of a propeller in compressible, steady flow p 814 A90-49778

The effect of energy input on the characteristics of profiles in compressible fluid media p 906 A90-51533

Steady and unsteady potential flow around thin annular wings and engines with simulation of jet engine flow
[DFVLR-FB-89-18] p 89 N90-11711

Additions and corrections to SUPER: A program for calculating steady and oscillatory supersonic flow over a thin wing, tail plane and fin
[AD-A211771] p 90 N90-12501

Unsteady three-dimensional thin-layer Navier Stokes solutions on dynamic blocked grids
[AD-A212377] p 136 N90-12899

Generalized similarity solutions for three dimensional, laminar, steady, compressible boundary layer flows on swept profile cylinders p 212 N90-13725

[DLR-FB-89-34]

Computational investigation of incompressible airfoil flows at high angles of attack
[AD-A205885] p 174 N90-14201

An improvement of convection fidelity in Euler calculations p 315 N90-16709

Carrier wing profile in nonstationary current
[ETN-90-95368] p 399 N90-19208

Convergence acceleration of hypersonic flow calculations: A nonlinear relaxation factor p 480 N90-20957

A lifting surface method for the calculation of steady and unsteady, incompressible propeller aerodynamics
[ESA-TT-1151] p 717 N90-25113

Analysis and mitigation of numerical dissipation in inviscid and viscous computation of vortex-dominated flows
[NASA-CR-186887] p 776 N90-26281

Adaptation for unsteady flow p 871 N90-26845

Efficient solution of the steady Euler equations with a centered implicit method p 884 N90-27999

Prediction of subsonic vortex shedding from forebodies with chines
[NASA-CR-4323] p 909 N90-28494

Solution of Euler equations applied to a rotor of a helicopter in steady flight
[ONERA-RSF-1/3731-AY-002A] p 910 N90-28500

STEADY STATE

Euler and Navier-Stokes computations for airfoil geometries using unstructured meshes p 630 A90-42425

A weighted residual formulation for finite element solutions of the steady Euler equations p 770 A90-44457

Compressor performance tests in the compressor research facility p 427 N90-18428

Comparison of altitude test cell results p 856 N90-27715

Calculation of the combustion distribution in a liquid-fuel ramjet p 858 N90-27931

Unsteady aerodynamics of controls p 935 N90-28525

STEAM TURBINES

Research and development of advanced gas turbine [DE90-503377] p 776 N90-26335

STEELS

Advanced materials for landing gear p 677 A90-41900

STEERING

A sensor stabilization/tracking system for unmanned air vehicles
[AD-A224008] p 936 N90-28579

STEREOSCOPIC VISION

The interaction of chromostereopsis and stereopsis in stereoscopic CRT (Cathode Ray Tubes) displays
[AD-A217906] p 927 N90-28544

STEREOSCOPY

Stereopsis as a visual cue in flight simulation p 870 A90-48960

STIFFENING

Damage tolerance of a postbuckling soft skin hat stiffened compression panel p 534 A90-31647

Structural analysis and optimum design of geodesically stiffened composite panels
[NASA-CR-186944] p 959 N90-28862

STIFFNESS

Nonlinear response and fatigue of stiffened panels p 363 A90-23953

An improved canopy stiffness scaling law for determining opening time of flat circular parachutes
[AIAA PAPER 90-3058] p 790 A90-45863

Current status of the application of conventional aluminum-lithium alloys and the potential for future developments p 268 N90-15203

STIFFNESS MATRIX

Whirl-flutter investigation on an advanced turboprop configuration p 40 A90-11008

STIRRING

Balance model of the perfectly stirred reactor with the discontinuity surface p 125 A90-14652

STOCHASTIC PROCESSES

Adaptive automatic control systems. Number 16 --- Russian book p 76 A90-10844

Stochastic crack growth analysis methodologies for metallic structures
[AIAA PAPER 90-1015] p 449 A90-29340

Stochastic flutter of a panel subjected to random in-plane forces. II - Two and three mode non-Gaussian solutions
[AIAA PAPER 90-0986] p 451 A90-29399

The method of random variable structure optimal control for aircraft p 590 A90-37220

Stochastic performance robustness of aircraft control systems
[AIAA PAPER 90-3410] p 865 A90-47665

A robust wind shear stochastic controller-estimator
[AIAA PAPER 90-3489] p 867 A90-47737

Test network Delft
[ETN-90-96009] p 177 N90-13365

An autopilot design methodology for bank-to-turn missiles
[AD-A213379] p 198 N90-13399

A two dimensional power spectral estimate for some nonstationary processes
[NASA-CR-186100] p 217 N90-14843

Application of stochastic robustness to aircraft control systems p 521 N90-20936

Stochastic robustness of linear control systems p 521 N90-20941

STOICHIOMETRY

An investigation of solid-fuel, dual-mode combustion ramjets p 859 N90-27933

STOPPING

Brake performance of the McDonnell Douglas DC-10-30/40 during high speed, high energy rejected takeoffs
[PB90-917004] p 503 N90-21000

STORAGE STABILITY

Repair adhesives - Development criteria for field level conditions p 528 A90-31575

Effect of temperature on the storage life of polysulfide aircraft sealants
[MRL-TR-89-31] p 444 N90-19364

STORAGE TANKS

Design of cryogenic tanks for launch vehicles p 609 N90-22662

STORM SUPPRESSION

ASR-9 weather channel test report
[AD-A211749] p 133 N90-11934

STOWAGE (ONBOARD EQUIPMENT)

Stowing the tilt-rotor p 246 A90-21703

STRAIN DISTRIBUTION

SH-2F airframe fatigue test program p 642 A90-39989

Finite element elastic-plastic-creep and cyclic life analysis of a cowl lip
[NASA-TM-102342] p 610 N90-22808

Finite element analysis of structural components using viscoplastic models with application to a cowl lip problem
[NASA-CR-185189] p 690 N90-23769

STRAIN GAGE BALANCES

Development of a multi-component internal strain-gauge balance for model tests in a cryogenic wind tunnel
[NLR-TR-88157-U] p 123 N90-12628

Experience with strain-gage balances for cryogenic wind tunnels p 264 N90-15958

Cryogenic balances for the US NTF p 264 N90-15959

Analysis of a six-component, flow-through, strain-gage, force balance used for hypersonic wind tunnel models with scramjet exhaust flow simulation
[NASA-CR-186585] p 597 N90-21775

STRAIN GAGES

Measurement of propellers in the ARTI 3-meter wind tunnel p 262 A90-23364

Smart structures with nerves of glass p 444 A90-27951

Development of a dual strain gage balance system for measuring light loads p 437 A90-28289

A fatigue study of electrical discharge machine (EDM) strain-gage balance materials p 448 A90-28295

External 6-component wind tunnel balances for aerospace simulation facilities p 438 A90-28296

Automatic calibration machine for cryogenic and conventional internal strain gage balances
[AIAA PAPER 90-1396] p 595 A90-37939

Iterative algorithm for correlation of strain gage data with aerodynamic load p 709 A90-44739

Development of a double crack growth gage algorithm for application to fleet tracking of fatigue damage p 901 A90-49890

Application of the 'K-gage' to aircraft structural testing p 926 A90-49891

Strain-gage applications in wind tunnel balances p 957 A90-52037

Development of a multi-component internal strain-gauge balance for model tests in a cryogenic wind tunnel
[NLR-TR-88157-U] p 123 N90-12628

STRAIN HARDENING

The effects of toughening stresses on liquid impact induced fracture p 692 A90-41315

STRAIN MEASUREMENT

Review of fiber optic methods for strain monitoring and non-destructive testing p 67 A90-11042

Smart structures concept study p 504 A90-32876

Feasibility study of RADAC stereo optoelectronic model deformation measurement system for ETW p 539 A90-34239

Estimation of rotor blade incidence and blade deformation from the measurement of pressures and strains in flight p 647 A90-42497

STRAIN RATE

Life prediction and fatigue p 532 A90-34163

Fatigue life estimates for helicopter loading spectra p 772 A90-45324

Fatigue life estimates for helicopter loading spectra
[NASA-CR-181941] p 279 N90-16294

Statistical treatment of slow strain rate data for assessment of hydrogen embrittlement in low alloy high strength steel
[ARL-MAT-R-122] p 767 N90-26106

STRAKES

A critique of the experimental aerodynamic data base for an oscillating straked wing at high angles p 147 A90-16779

Low-speed unsteady aerodynamics of a pitching straked wing at high incidence. I - Test program. II - Harmonic analysis p 159 A90-19387

An investigation of strake fence flaps on a canard-configured aircraft
[AIAA PAPER 90-0762] p 230 A90-22259

Strake camber and thickness design procedure for low alpha supersonic flow p 622 A90-40678

- Numerical simulation of vortical flows over a strake-delta wing and a close coupled delta-canard configuration [AIAA PAPER 90-3002] p 788 A90-45851
- Actuated forebody strakes [NASA-CASE-LAR-13983-1] p 648 N90-23390
- Development of non-conventional control methods for high angle of attack flight using vortex manipulation p 935 N90-28522
- STRANGE ATTRACTORS**
- Nonconvex polytope approximations of attracting basin boundaries for nonlinear systems [AIAA PAPER 90-3512] p 891 A90-47758
- STRAPDOWN INERTIAL GUIDANCE**
- Performance study of an integrated NAVSTAR GPS/SINS navigation system p 329 A90-24003
- Modified fault tolerant inertial navigation system p 578 A90-37211
- Modern strapdown system for helicopter p 653 A90-42451
- System concept and performance criteria of modern helicopter navigation p 640 A90-42452
- Development and verification of software for flight safety critical strapdown systems p 694 A90-42454
- Strapdown astro-inertial navigation (SAIN) utilizing the optical wide-angle lens startracker (OWLS) p 824 A90-49503
- The Fourteenth Biennial Guidance Test Symposium, volume 1 [AD-A216925] p 405 N90-18383
- Integrated navigation/flight control for future high performance aircraft p 917 N90-29362
- Fault Detection and Isolation (FDI) techniques for guidance and control systems p 918 N90-29366
- STRAPS**
- Aircraft crash survival design guide. Volume 4: Aircraft seats, restraints, litters, and cockpit/cabin dehalization [AD-A218437] p 575 N90-22548
- STRATEGIC MATERIALS**
- Resources - Supply and availability --- of superalloys for United States aerospace industry p 531 A90-34152
- STRATEGY**
- Fire hardening of aircraft through upgrades of materials and designs p 327 N90-17605
- Studies in automatic speech recognition and its application in aerospace p 958 N90-28759
- STRATIFICATION**
- Experiments with unsteady, free surface, three-dimensional vortices in a thermally stable, stratified fluid [AD-A222088] p 815 N90-26796
- STRATIFIED FLOW**
- Experiments with unsteady, free surface, three-dimensional vortices in a thermally stable, stratified fluid [AD-A222088] p 815 N90-26796
- STRATOSPHERE**
- New high-speed air transport system and stratospheric pollution [ONERA, TP NO. 1989-202] p 279 A90-22445
- Global stratospheric change: Requirements for a Very-High-Altitude Aircraft for Atmospheric Research [NASA-CP-10041] p 185 N90-14220
- STREAM FUNCTIONS (FLUIDS)**
- Numerical solution of transonic flows on a streamfunction co-ordinate system p 17 A90-13238
- Underexpanded jet-freestream interactions on an axisymmetric afterbody configuration p 154 A90-18141
- Unsteady streamlines near the trailing edge of NACA 0012 airfoil at a Reynolds number of 125,000 p 155 A90-18158
- Computation and analysis of the shapes of S1 and S2 streamsurfaces in a transonic compressor rotor p 160 A90-19446
- 3D Mean-Stream-Line Method - A new engineering approach to the inverse problem of 3D cascade [ASME PAPER 89-GT-48] p 289 A90-23774
- Stability analysis and numerical experiments for viscous-inviscid interaction in transonic flow p 293 A90-24009
- Flight-measured streamwise disturbance instabilities in laminar flow [AIAA PAPER 90-1283] p 495 A90-33904
- Calculation of viscous-inviscid strong interaction for transonic flows over aerofoils p 627 A90-42364
- An improved SIP scheme for numerical solutions of transonic streamfunction equations --- strongly implicit procedure p 904 A90-51014
- STREAMLINED BODIES**
- Boundary layer growth on low aspect ratio compressor blades p 12 A90-15233
- Interaction between boundary layer and wakes of different bodies p 602 A90-36263

- An application of topological analysis to studying the three-dimensional flow in cascades. I - Topological rules for skin-friction lines and section streamlines p 908 A90-52607
- STREAMLINING**
- Design and off-design performance predictions of axial turbines p 45 A90-12540
- Three-dimensional model testing in the transonic self-streamlining wind tunnel p 938 N90-28583
- STRESS (PHYSIOLOGY)**
- Windblast protection for advanced ejection seats p 483 N90-20063
- STRESS ANALYSIS**
- The design of rotor blades taking into account the combined effects of vibratory and thermal loads p 40 A90-11553
- Stress analysis of gas turbine bladed disc for structural integrity applying the concept of cyclic symmetry p 46 A90-12564
- Influence of joint fixity on the structural static and dynamic response of a joined-wing aircraft. I - Static response [SAE PAPER 891060] p 100 A90-14361
- Carbon fibre composite bolted joints p 130 A90-15354
- Photoelastic investigation of turbine rotor blade shrouds p 112 A90-16008
- Analysis methods of tie-down loads and airframe stress for shipboard-helicopters p 199 A90-16855
- The anti-shimmy and break-proof study of nose landing gear p 178 A90-16856
- Finite element mesh refinement criteria for stress analysis p 273 A90-23013
- Resonant stress determination of a turbine blade with modal damping as a function of rotor speed and vibrational amplitude [ASME PAPER 89-GT-27] p 340 A90-23765
- A numerical three-dimensional thermal stress analysis for cooled blades [ASME PAPER 89-GT-168] p 341 A90-23853
- Virtual principles in aircraft structures. Volume 1 - Analysis. Volume 2 - Design, plates, finite elements --- Book p 452 A90-29977
- Impact damage and residual strength analysis of composite panels with bonded stiffeners --- for primary aircraft structures p 642 A90-40130
- Advanced applications of BEM to gas turbine engine structures p 772 A90-45769
- Description and reconstitution of manoeuvre loadings p 919 A90-49878
- A rate theory investigation of cyclic loading and plastic deformation in the high stress and ambient temperature range p 954 A90-49884
- Casting airworthiness joint-European civil authorities view-point p 64 N90-10234
- Rotor blade structural design p 106 N90-12584
- Stress intensity factors for cracking metal structures under rapid thermal loading. Volume 2: Theoretical background [AD-A213297] p 213 N90-13812
- Application of fracture mechanics and half-cycle method to the prediction of fatigue life of B-52 aircraft pylon components [NASA-TM-88277] p 214 N90-13820
- The computation of turbulent thin shear flows associated with flow around multielement aerofoils p 633 N90-24240
- Application of damage tolerance p 843 N90-26817
- Photoelasticity: A cost effective design tool p 883 N90-26819
- Calculation of temperature distribution in various turbine blades using a boundary-fitted coordinate transformation method p 929 N90-28550
- Development of a thickness design procedure for stabilized layers under rigid airfield pavements [DOT/FAA/RD-90/22] p 937 N90-28582
- STRESS CONCENTRATION**
- Stress concentration factors - Comparison of theory with fatigue test data p 680 A90-39979
- STRESS CORROSION**
- Effects on aerospace alloys of residual chlorine in chlorinated-solvent primers p 956 A90-50187
- Fabrication of test-articles from Al-Li 2091 for Fokker 100 p 267 N90-15196
- STRESS CORROSION CRACKING**
- Tough(er) aluminum-lithium alloys p 62 A90-11575
- Adhesive-bonded composite-patching repair of cracked aircraft structure p 467 A90-31576
- Ultrahigh-strength steels for aerospace applications p 599 A90-37443
- Analysis of failures in aircraft structures p 882 A90-48998
- Fabrication of test-articles from Al-Li 2091 for Fokker 100 p 267 N90-15196

- A corrosion fatigue/stress corrosion testing facility at Materials Research Laboratory [MRL-TN-568] p 527 N90-21044
- STRESS CYCLES**
- Stress concentration factors - Comparison of theory with fatigue test data p 680 A90-39979
- Peak identification techniques p 844 N90-26822
- STRESS DISTRIBUTION**
- Flow in compressor interstage ducts p 11 A90-12521
- The strength and weakness of carbon composite structures --- for military and civil aircraft p 180 A90-17679
- The investigation of stress at an enter-gas nozzle of main landing gears for fighter aeroplanes p 181 A90-18606
- Generalized Transition Finite-Boundary Elements for high speed flight structures [AIAA PAPER 90-1105] p 449 A90-29286
- The in service multi-axial-stress situation in an uncooled gas turbine blade p 423 A90-29880
- Secondary flows and Reynolds stress distributions downstream of a turbine cascade at different expansion ratios p 512 N90-21015
- Finite element elastic-plastic-creep and cyclic life analysis of a cowl lip [NASA-TM-102342] p 610 N90-22808
- Finite element analysis of structural components using viscoplastic models with application to a cowl lip problem [NASA-CR-185189] p 690 N90-23769
- STRESS INTENSITY FACTORS**
- Numerical study of balanced patch repairs to cracked sheets p 210 A90-18442
- Three dimensional photoelastic analysis of aeroengine parts p 270 A90-20077
- The application of the engineering approach for analyzing crack tolerance of fuselage panels to a transport airplane p 272 A90-22014
- A fracture analysis using eight-node-isoparametric singular elements and its application in fuselage panels p 603 A90-36431
- The effects of toughening stresses on liquid impact induced fracture p 692 A90-41315
- Application of the 'K-gage' to aircraft structural testing p 926 A90-49891
- Fatigue behavior of specimens under compression load spectra [ETN-89-95207] p 137 N90-12954
- Stress intensity factors for cracking metal structures under rapid thermal loading. Volume 2: Theoretical background [AD-A213297] p 213 N90-13812
- Fatigue crack initiation and small crack growth in several airframe alloys [NASA-TM-102598] p 454 N90-18746
- Use of acoustic emission for continuous surveillance of aircraft structures p 887 N90-28092
- Damage tolerance of the fighter aircraft 37 Viggen. Part 1: Analytical assessment [FFA-TN-1990-12-PT-1] p 923 N90-28538
- Fatigue, static tensile strength and stress corrosion of aircraft materials and structures. Part 1: Text [LR-630-PT-1-REV] p 961 N90-29682
- Fatigue, static tensile strength and stress corrosion of aircraft materials and structures. Part 2: Figures [LR-630-PT-2] p 961 N90-29683
- STRESS MEASUREMENT**
- Turbomachinery blade vibration and dynamic stress measurements utilizing nonintrusive techniques p 41 A90-11558
- Intelligent built-in test and stress management p 448 A90-28343
- Methodology of variable amplitude fatigue tests p 451 A90-29866
- Eight years of experience with small computerized retrofit load monitoring systems p 926 A90-49882
- Nondestructive measurement of residual stresses in aircraft transparencies [AD-A218680] p 689 N90-23762
- STRESS WAVES**
- Fatigue life prediction method for gas turbine rotor disk alloy FV535 p 440 A90-27679
- STRESS-STRAIN RELATIONSHIPS**
- Stress-strain analysis of structural elements of incompressible or nearly incompressible materials by the finite element method p 129 A90-14557
- Cyclic stress-strain behavior and low cycle fatigue of Ti 6242 p 530 A90-33523
- Fatigue crack initiation mechanics of metal aircraft structures [AD-A210567] p 65 N90-10255
- Finite element analysis of structural components using viscoplastic models with application to a cowl lip problem [NASA-CR-185189] p 690 N90-23769

STRESS-STRAIN-TIME RELATIONS

- Standardized stress-time histories - An overview
p 368 A90-26752
- Considerations of reliability design for rotorcraft
p 680 A90-39977

STRESSES

- Development and application of an optimization procedure for space and aircraft structures
[MBB-FW-522/S/PUB-383] p 779 N90-25078
- The stress and temperature dependence of creep in an Al-2.0 wt percent U alloy
[AD-A223676] p 953 N90-29480

STRIPPING

- Microstructural effects of plastic media blasting on graphite epoxy composites
[SAE PAPER 890928] p 286 A90-24693
- Plastic media blast (PMB) paint removal from composites
p 945 A90-50162
- The future of aircraft paint removal methods
[AD-A214946] p 356 N90-16936

STRUCTURAL ANALYSIS

- Computerised structural analysis for engine components
p 190 A90-18486
- The application and design of large integral panels for SH-5 aircraft
p 211 A90-18632
- A new type of non-rigid airship system
[AIAA PAPER 89-3175] p 244 A90-20583
- Durability of equipment assemblies and elements of life-support systems for flight vehicles - Russian book
p 246 A90-21275
- Demonstration of probabilistic-based durability analysis method for metallic airframes
p 273 A90-23287
- Application of HOST technology to the SSME HPFTP blade
[ASME PAPER 89-GT-130] p 360 A90-23828
- Design and analysis of composite structures with manufacturing flaws
p 445 A90-28234
- Eshbach's handbook of engineering fundamentals / 4th edition/
p 448 A90-28825
- A parallel-vector algorithm for rapid structural analysis on high-performance computers
[AIAA PAPER 90-1149] p 458 A90-29293
- The all-composite airframe - Design and certification
p 413 A90-29890
- Virtual principles in aircraft structures. Volume 1 - Analysis. Volume 2 - Design, plates, finite elements - Book
p 452 A90-29977
- Structural-acoustic analysis of aircraft fuselage structures using general purpose finite element codes
p 492 A90-33385
- Automated helicopter structural analysis data processing
p 611 A90-38533
- Analysis of composite rotor blades via Saint Venant's solutions
p 688 A90-42491
- Structural and aerodynamic analysis of a large scale advanced propeller blade
[AIAA PAPER 90-2401] p 743 A90-42793
- Developments in mechanics. Volume 15 - Midwestern Mechanics Conference, 21st, Michigan Technological University, Houghton, Aug. 13-16, 1989, Proceedings
p 769 A90-42870
- Bulging cracks in pressurized fuselages - A procedure for computation
p 880 A90-46301
- Structural mode significance using INCA - Interactive Controls Analysis computer program
[AIAA PAPER 90-3346] p 889 A90-47606
- Some computational and experimental aspects of optimal design process of composite structures
p 882 A90-48050
- Aging jet transport structural evaluation programs
p 901 A90-49889
- Damage tolerance demonstration for A310-300 CFRP-components
p 919 A90-49894
- High performance needed structures in composites
p 955 A90-50173
- Static aeroelastic analysis for generic configuration aircraft
[NASA-TM-89423] p 52 N90-10042
- Integrated multidisciplinary optimization of rotorcraft: A plan for development
[NASA-TM-101617] p 106 N90-12580
- General approach and scope - rotor blade design optimization
p 106 N90-12581
- Rotor blade aerodynamic design
p 106 N90-12582
- Rotor blade structural design
p 106 N90-12584
- Validation of the procedures - integrated multidisciplinary optimization of rotorcraft
p 107 N90-12587
- Appendix: Results obtained to date - integrated multidisciplinary optimization of rotorcraft
p 107 N90-12588
- Evaluation of a damaged F/A-18 horizontal stabilator
[AD-A212573] p 107 N90-12597
- Constitutive modeling for isotropic materials (HOST)
[NASA-CR-179522] p 193 N90-13390

- Constitutive modeling for isotropic materials (HOST)
[NASA-CR-174718] p 193 N90-13391
- Mobility power flow analysis of an L-shaped plate structure subjected to acoustic excitation
[NASA-CR-186130] p 214 N90-13817
- An examination of helicopter rotor load calculations
[AD-A214295] p 249 N90-15098
- Solution of potential flow past an elastic body using the boundary element technique
[AD-A213843] p 275 N90-15390
- Proceedings of the 1988 Structural Integrity Program Conference
[AD-A213545] p 275 N90-15486
- Noise and sonic boom impact technology. Effects of aircraft noise and sonic booms on structures: An assessment of the current state-of-knowledge
[AD-A213919] p 378 N90-17409
- An experimental study of the aeroelastic behaviour of two parallel interfering circular cylinders
p 455 N90-19609
- COCOMAT: A Computer Aided Engineering (CAE) system for composite structures design
[NLR-MP-87078-U] p 462 N90-19756
- Analysis of flow, thermal, and structural-interaction of hypersonic structures subjected to severe aerodynamic heating
[AD-A217882] p 478 N90-20053
- The role of structural analysis in airworthiness certification
[BR112064] p 499 N90-20972
- Computer-aided structural optimisation of aircraft structures
[BR112837] p 499 N90-20973
- STARS: An integrated general-purpose finite element structural, aeroelastic, and aeroservoelastic analysis computer program
[NASA-TM-101709] p 689 N90-23768
- Finite element analysis of structural components using viscoplastic models with application to a cowl lip problem
[NASA-CR-185189] p 690 N90-23769
- Peak identification techniques
p 844 N90-26822
- Structural analysis and optimum design of geodesically stiffened composite panels
[NASA-CR-186944] p 959 N90-28862
- Generalized Advanced Propeller Analysis System (GAPAS). Volume 2: Computer program user manual
[NASA-CR-185277] p 933 N90-29394
- Structural testing and analytical research of turbine components
[AD-A223516] p 933 N90-29396

STRUCTURAL DESIGN

- The design of rotor blades taking into account the combined effects of vibratory and thermal loads
p 40 A90-11553
- Controlled mixing and variable geometry combustor design effects on emissions and combustion characteristics
p 45 A90-12547
- Computers boost structural technology
p 138 A90-14799
- Carbon fibre composite bolted joints
p 130 A90-15354
- Airframe structural design: Practical design information and data on aircraft structures - Book
p 103 A90-16624
- A refined optimality criterion technique applied to aircraft wing structural design
p 206 A90-16718
- Low Reynolds number airfoils evaluation program
p 151 A90-17692
- Design and evaluation of graphite/epoxy truss core sandwich panels
p 210 A90-18406
- Aerodynamic testing of a new semi-prone ejection seat design
[AIAA PAPER 90-0234] p 182 A90-19748
- Optimum design of rotational wheels under transient thermal and centrifugal loading
p 270 A90-20770
- Optimum design of composite structures
p 272 A90-22135
- Application of the MARS system in aircraft-structure design
p 374 A90-24127
- An application of structural optimization in wind tunnel model design
[AIAA PAPER 90-0956] p 438 A90-29241
- Design and fabrication of a prototype resin matrix composite interceptor structure
[AIAA PAPER 90-1004] p 442 A90-29275
- An approach for analysis and design of composite rotor blades
[AIAA PAPER 90-1005] p 449 A90-29276
- Composite certification for commercial aircraft
p 382 A90-29892
- Virtual principles in aircraft structures. Volume 1 - Analysis. Volume 2 - Design, plates, finite elements - Book
p 452 A90-29977
- High performance thermoplastic composites with poly(etherketoneketone) matrix
p 529 A90-31646

- The influence of mathematical optimization methods on the design of aircraft structures
p 492 A90-33387
- Aeroelastic tailoring validation by windtunnel model testing
p 492 A90-33389
- Structural optimization in view of aeroelastic constraints
p 536 A90-33391
- Recent activities within the aeroservoelasticity branch at the NASA Langley Research Center
p 492 A90-33400
- Designing with advanced composites; Report on the European Core Conference, 1st, Zurich, Switzerland, Oct. 20, 21, 1988, Conference Papers
p 530 A90-33701
- Design with honeycomb, state of the art
p 538 A90-33706
- Airbus A320 CFRP-rudder structural requirements
p 493 A90-33707
- Probabilistic design technology for ceramic components
p 601 A90-35507
- High-quality approximation of eigenvalues in structural optimization
p 603 A90-36277
- The design of the series of blade flutter rotor and the experimental investigation of flow-induced vibration
p 586 A90-37230
- Application of optimization methods to helicopter rotor blade design
p 604 A90-37337
- The U.S. Army Helicopter Structural Integrity Program - 1989 European Rotorcraft Forum
p 581 A90-38525
- Multilevel optimization of large-scale structures in a parallel computing environment
p 693 A90-39180
- Development and application of an optimization procedure for space and aircraft structures
p 679 A90-39186
- Redesign of an electro-optical shroud in graphite/epoxy
p 676 A90-40215
- Design of new Polish primary radars AVIA DM/CM
p 638 A90-41035
- Recent propeller development and studies conducted at ONERA
[ONERA, TP NO. 1990-16] p 683 A90-41201
- Influence of some geometrical and design parameters on the hinge moment characteristics of rudders
p 643 A90-41739
- Metal matrix composites structural design experience
[AIAA PAPER 90-2175] p 677 A90-42059
- Component arrangement studies for an 8000 shp turboshaft high technology core
[AIAA PAPER 90-2398] p 663 A90-42159
- Design and manufacturing of composite materials blade models
p 618 A90-42492
- Improved steel for landing gear design
[SAE PAPER 892335] p 765 A90-45490
- Design and experimental investigation of a laminar horizontal tail
[AIAA PAPER 90-3042] p 798 A90-45934
- Structure/control design synthesis of active flutter suppression system by goal programming
[AIAA PAPER 90-3325] p 872 A90-47587
- Iterative preliminary design tools for composite structures
p 882 A90-48045
- Developments in the acoustic fatigue design process for composite aircraft structures
p 882 A90-48047
- Some computational and experimental aspects of optimal design process of composite structures
p 882 A90-48050
- A method for lifting surface design using nonlinear optimization
[AIAA PAPER 90-3290] p 813 A90-49122
- Design of aircraft wings subjected to gust loads - A system reliability approach
p 958 A90-52044
- Large scale prop-fan structural design study. Volume 1: Initial concepts
[NASA-CR-174992] p 52 N90-10043
- Large scale prop-fan structural design study. Volume 2: Preliminary design of SR-7
[NASA-CR-174993] p 52 N90-10044
- Royal Aerospace Establishment: No place for a castings factor
p 64 N90-10235
- Application of formal optimization techniques in thermal/structural design of a heat-pipe-cooled panel for a hypersonic vehicle
[NASA-TM-89131] p 72 N90-10409
- Integrated multidisciplinary optimization of rotorcraft: A plan for development
[NASA-TM-101617] p 106 N90-12580
- General approach and scope - rotor blade design optimization
p 106 N90-12581
- Rotor blade aerodynamic design
p 106 N90-12582
- Rotor blade dynamic design
p 106 N90-12583
- Rotor blade structural design
p 106 N90-12584
- Acoustic design considerations: Review of rotor acoustic sources
p 106 N90-12585
- Airframe design considerations: Overview - rotor design optimization
p 106 N90-12586
- Appendix: Results obtained to date - integrated multidisciplinary optimization of rotorcraft
p 107 N90-12588

Efficient methods for integrated structural-aerodynamic wing optimum design p 184 N90-13376

Development of an advanced fan blade containment system [DOT/FAA/CT-89/20] p 192 N90-13386

Aeroelastic control of composite lifting surfaces: Integrated aeroelastic control optimization p 198 N90-13396

Design and demonstration of heat pipe cooling for NASP and evaluation of heating methods at high heating rates [DE89-016995] p 186 N90-14227

The interference of flightmechanical control laws with those of load alleviation and its influence on structural design p 258 N90-15054

Design and calibration of an in-stack, low-pressure impactor [AD-A213531] p 255 N90-15105

Design philosophy and construction techniques for integral fuselage fuel tanks p 250 N90-15913

Unmanned air vehicles payloads and sensors p 251 N90-15930

The European Transonic Windtunnel (ETW) p 262 N90-15945

The cryogenic Ludwig tube tunnel at Goettingen p 263 N90-15947

Aerodynamic and structural design challenges of a reusable single stage to orbit air-breathing launch vehicle p 354 N90-16814

Advanced materials for interior and equipment related to fire safety in aviation p 328 N90-17608

Design guidance to minimize unsteady forces in turbomachines p 426 N90-18411

X-29A aircraft structural loads flight testing [NASA-TM-101715] p 416 N90-19225

Aeroservoelasticity [NASA-TM-102620] p 416 N90-19227

Development and fabrication of structural components for a scramjet engine [NASA-CR-181945] p 510 N90-20088

Computational Methods for Aerodynamic Design (Inverse) and Optimization [AGARD-CP-463] p 500 N90-20976

Progress in inverse design and optimization in aerodynamics p 482 N90-20977

Inverse design of airfoil contours: Constraints, numerical method, and applications p 500 N90-20980

An intensive procedure for the design of pressure-specified three-dimensional configurations at subsonic and supersonic speeds by means of a higher-order panel method p 500 N90-20982

An inverse method for the design of turbomachine blades p 511 N90-20988

Application of an inverse method to the design of a radial inflow turbine p 511 N90-20989

Aerodynamic optimization by simultaneously updating flow variables and design parameters p 501 N90-20991

Calculation of the secondary flow in an axial turbine p 513 N90-21022

Generation and decay of secondary flows and their impact on aerodynamic performance of modern turbomachinery components p 514 N90-21023

Structural tailoring of select fiber composite structures [NASA-TM-102484] p 533 N90-21137

An experimental study of tip shape effects on the flutter of aft-swept, flat-plate wings [NASA-TM-4180] p 582 N90-22555

Design of cryogenic tanks for launch vehicles p 609 N90-22662

Aircraft drawings index p 618 N90-23340

Correlation/validation of finite element code analyses for vibration assessment of avionics equipment [AD-A220393] p 654 N90-23398

Modeling growth of fatigue cracks which originate at rivet holes p 691 N90-25060

Flexural fatigue life prediction of closed hat-section using materially nonlinear axial fatigue characteristics p 691 N90-25062

Behavior of composite/metal aircraft structural elements and components under crash type loads: What are they telling us [NASA-TM-102681] p 774 N90-25368

An expert system advisor for damage repair of composite wing skins (repairman) p 842 N90-26810

Airport pavement drainage [DOT/FAA/RD-90/24] p 872 N90-27728

Study of ground effects on flying scaled models p 922 N90-28532

Measurement of the steady surface pressure distribution on a single rotation large scale advanced prop-fan blade at Mach numbers from 0.03 to 0.78 [NASA-CR-182124] p 929 N90-28552

Multi-disciplinary optimization of aeroservoelastic systems [NASA-CR-185931] p 925 N90-29385

WingDesign: Program for the structural design of a wing cross-section [LR-627] p 925 N90-29390

Structural testing and analytical research of turbine components [AD-A223516] p 933 N90-29396

STRUCTURAL DESIGN CRITERIA

Stress-strain analysis of structural elements of incompressible or nearly incompressible materials by the finite element method p 129 A90-14557

An application of SQP and Ada to the structural optimisation of aircraft wings p 216 A90-18444

Optimization of the relative thicknesses of a high-aspect-ratio wing in a multicriterial formulation p 334 A90-24133

Multicriterial optimization of lugs in hinge joints p 364 A90-24162

Unified optimal criterion method - Combination of direction of gradient and ejection line p 367 A90-26077

Analysis of fully stalled compressor p 383 A90-27966

V-22 aerodynamic loads analysis and development of loads alleviation flight control system p 410 A90-28239

Aeroelastic optimization of a helicopter rotor using an efficient sensitivity analysis [AIAA PAPER 90-0951] p 410 A90-29237

Tradeoffs in honeycomb cored designs p 538 A90-33708

Optimum design of composite wing structures subjected to displacement constraints p 680 A90-39276

Design and analysis aid for evaluating aircraft structures p 694 A90-41188

Large-order modal analysis techniques in the Aeroelastic Design Optimization Program (ADOP) [SAE PAPER 892323] p 772 A90-45482

Multicriteria optimal layouts of aircraft and spacecraft structures p 889 A90-46046

Development and applications of reliability and maintainability design criteria in military aircraft [ETN-89-95208] p 107 N90-12591

Project, implementation, and utilization of composite structures [ETN-89-95209] p 127 N90-12665

Point of view of a civil aircraft manufacturer on Al-Li alloy p 268 N90-15200

Uses and properties of Al-Li on the new EH101 helicopter p 268 N90-15201

Semi-empirical transition criteria for the design of laminar profiles p 276 N90-16174

Development of transition criteria on the basis of ϵ to the N power for three dimensional wing boundary layers p 277 N90-16179

STRUCTURAL ENGINEERING

Fiber optic smart structures and skins; Proceedings of the Meeting, Boston, MA, Sept. 8, 9, 1988 [SPIE-986] p 37 A90-11201

Engineering design of tough ceramic matrix composites for turbine components [ASME PAPER 89-GT-294] p 343 A90-23892

The (airplane) design professor as shepherd - An industry role in enhancing engineering education [AIAA PAPER 90-3259] p 897 A90-49121

Aircraft fuel tank construction and testing experience p 250 N90-15907

Noise and sonic boom impact technology. Effects of aircraft noise and sonic booms on structures: An assessment of the current state-of-knowledge [AD-A213919] p 378 N90-17409

COCOMAT: A Computer Aided Engineering (CAE) system for composite structures design [NLR-MP-87078-U] p 462 N90-19756

Aircraft crash survival design guide. Volume 3: Aircraft structural crash resistance [AD-A218436] p 575 N90-22547

NASA-UVA light aerospace alloy and structures technology program [NASA-CR-182607] p 601 N90-22651

The application of engineering ceramics in gas turbines [PNR90676] p 750 N90-26005

STRUCTURAL FAILURE

Breakage of fan blades in the S1 wind tunnel at Mondane-Avrieux [ONERA, TP NO. 1989-104] p 57 A90-11138

Rub interactions of flexible casing rotor systems p 41 A90-11554

A method for reducing a buckled skin under combined loading p 860 A90-46571

Proceedings of the 1988 Structural Integrity Program Conference [AD-A213545] p 275 N90-15486

NASA airframe structural integrity program [NASA-TM-102637] p 543 N90-21422

An evaluation of the pressure proof test concept for thin sheet 2024-T3 [NASA-TM-101675] p 543 N90-21424

Advances in optimal active control techniques for aerospace systems; application to aircraft active landing gear p 592 N90-21769

Development of a finite element based delamination analysis for laminates subject to extension, bending, and torsion p 679 N90-25049

Proceedings of the 1987 Aircraft/Engine Structural Integrity Program (ASIP/ENSIP) Conference [AD-A198037] p 842 N90-26807

Lessons learned from the T-46A durability and damage tolerance program p 842 N90-26812

Automated analysis of MXU-553 flight data p 844 N90-26821

The role of NDI in the certification of turbine engine components p 859 N90-28069

Development of an automated ultrasonic inspection system for composite structure on in-service aircraft p 885 N90-28079

STRUCTURAL INFLUENCE COEFFICIENTS

Effect of structural anisotropy on the dynamic characteristics of the wing and critical flutter speed p 386 A90-28985

Influence of structural and aerodynamic modeling on flutter analysis [AIAA PAPER 90-0954] p 411 A90-29239

STRUCTURAL MEMBERS

Life of concentrated contacts in the mixed EHD and boundary film regimes [AD-A216673] p 454 N90-18738

STRUCTURAL RELIABILITY

New progress in airframe durability requirements p 246 A90-22001

Prediction of the strength-related reliability of structural elements at the design stage p 274 A90-23402

Noninteractive macroscopic reliability model for ceramic matrix composites with orthotropic material symmetry [ASME PAPER 89-GT-129] p 360 A90-23827

Improvement in structural integrity and long term durability of aerospace composite components p 441 A90-28189

V-22 ballistic vulnerability hardening program p 408 A90-28223

Stochastic crack growth analysis methodologies for metallic structures [AIAA PAPER 90-1015] p 449 A90-29340

Advancements in rotor and airframe structural flight testing developed during the SH-60B G.W./C.G. expansion program [AIAA PAPER 90-1281] p 495 A90-33902

The collection of usage data to improve structural integrity of operational helicopters p 651 A90-39983

Potential application of automotive fatigue technology in rotorcraft design p 681 A90-39987

Damage tolerance of carbon fibre reinforced plastic sandwich panels p 675 A90-40047

The influence of material quality on airframe structural durability p 676 A90-41336

A 'new' philosophy of structural reliability, fail safe versus safe life p 688 A90-42490

Probabilistic approach to fleet management p 701 A90-42674

Boeing 737 fuselage structural integrity program [SAE PAPER 892207] p 701 A90-45426

Dealing with the aging fleet [SAE PAPER 892209] p 701 A90-45428

Tracking B-1B aircraft with a structural data recorder p 926 A90-49880

Health monitoring aircraft p 902 A90-50544

Proceedings of the 1988 Structural Integrity Program Conference [AD-A213545] p 275 N90-15486

Boeing/NASA composite components flight service evaluation [NASA-CR-181898] p 601 N90-22609

Correlation/validation of finite element code analyses for vibration assessment of avionics equipment [AD-A220393] p 654 N90-23398

An aluminum quality breakthrough for aircraft structural reliability p 843 N90-26816

Multichannel on-board load and fatigue monitoring p 849 N90-27621

STRUCTURAL STABILITY

Postbuckling behavior of laminated plates using a direct energy-minimization technique p 209 A90-17993

Stability and vibrations of mechanical systems --- Russian book p 270 A90-20426

A method for calculating the stiffness characteristics of large-aspect-ratio wings with anisotropic panels in accordance with strength and aileron efficiency requirements p 334 A90-24161

Influence of joint fixity on the aeroelastic characteristics of a joined wing structure [AIAA PAPER 90-0980] p 390 A90-29370

Using transonic small disturbance theory for predicting the aeroelastic stability of a flexible wind-tunnel model [AIAA PAPER 90-1033] p 391 A90-29377

ADAM 2.0 - An ASE analysis code for aircraft with digital flight control systems p 431 A90-29385

Hingeless rotor dynamics in coordinated turns [AIAA PAPER 90-1117] p 412 A90-29389

Parametric aeroelastic stability analysis of a generic X-wing aircraft p 731 A90-44737

A study of the stability and thermal stability of complex reinforced structures p 880 A90-46541

Development of a VSAERO (Vortex Separation Aerodynamics) model of the F/A-18 [AD-A124442] p 95 N90-12566

Fatigue of aluminium alloy joints with various fastener systems. Low load transfer p 370 N90-17193

Active stabilization of aeromechanical systems [AD-A216629] p 454 N90-18672

Floor pull test of a transport airframe section [DOT/FAA/CT-TN88/14] p 497 N90-20072

Multivariable frequency weighted model order reduction for control synthesis p 613 N90-23060

Feasibility study for a microwave-powered ozone sniffer aircraft [NASA-CR-186660] p 650 N90-23397

STRUCTURAL STRAIN

Evaluation of a damaged F/A-18 horizontal stabilizer [AD-A212573] p 107 N90-12597

STRUCTURAL VIBRATION

Rotor-blades excitation due to differential interference of vane wakes between upstream stator-rows in an axial compressor p 6 A90-11784

Experimental investigation of the time-dependent flow in a vibrating annular cascade operating in the transonic flow regime p 7 A90-11787

Unsteady aerodynamic characteristics of oscillating cascade with tip clearance p 8 A90-11793

Improved double linearization method for prediction of mean loading effects on subsonic and supersonic cascade flutter p 41 A90-11795

Flutter of cascade blades composed of blades having arbitrarily different natural frequencies p 42 A90-11798

The effects of three centres of blade on flutter p 42 A90-11800

Flutter of mistuned cascades with structural coupling p 42 A90-11802

Vibration analysis of composite turbopropellers using a nonlinear beam-type finite-element approach p 70 A90-12844

Design and application of a finite element package for modelling turbomachinery vibrations p 70 A90-13011

Nonlinear transverse oscillations of a composite dynamic system p 129 A90-14558

Squeeze film damping for aircraft gas turbines p 113 A90-16009

A component modal synthesis technique for the lateral vibration analysis of aircraft engine systems p 179 A90-16983

Vibration analysis of aircraft panels p 207 A90-17026

Theoretical and experimental analysis of a model rotor blade incorporating a swept tip p 151 A90-17586

The Model 360 - Advanced composite helicopter p 180 A90-17678

Time-domain aeroservoelastic modeling using weighted unsteady aerodynamic forces p 195 A90-17698

Rotor/fuselage vibration isolation studies by a Floquet-harmonic iteration technique p 182 A90-19393

Stability and vibrations of mechanical systems --- Russian book p 270 A90-20426

Effect of the nonuniform rotation of the gas turbine rotor on blade vibrations p 253 A90-20431

Casing vibration and gas turbine operating conditions [ASME PAPER 89-GT-78] p 358 A90-23799

Vibration analysis for immediate assessment of battle-damaged gas turbine engines [ASME PAPER 89-GT-96] p 341 A90-23811

An ultrasonic fatigue facility for HCF/LCF interactive tests p 363 A90-23900

Automatic vibration reduction at a four bladed hingeless model rotor - A wind tunnel demonstration p 335 A90-25424

Examination of dynamic characteristics of UH-60A and EH-60A airframe structures p 406 A90-28154

Application of higher harmonic control (HHC) to rotors operating at high speed and maneuvering flight p 429 A90-28157

Rotor smoothing expert system p 381 A90-28164

Icing Research Tunnel test of a model helicopter rotor p 400 A90-28179

Vibrations of rectangular plates with moderately large initial deflections at elevated temperatures using finite element method [AIAA PAPER 90-1125] p 451 A90-29429

Effects of higher harmonic control on rotor performance and control loads p 412 A90-29467

Ground vibration testing of aeroplanes with a sequence of single-point excitations - Simple and effective p 522 A90-33371

Gyroscopic matrices in computation of vibration p 547 A90-33381

Sensitivity analysis using resonance and anti-resonance frequencies - A guide to structural modification p 536 A90-33396

Turbulent plane jet excited mechanically by an oscillating thin plate in the potential core p 553 A90-35262

Reduced-order aeroelastic models via dynamic residualization p 579 A90-35762

The design of the series of blade flutter rotor and the experimental investigation of flow-induced vibration p 586 A90-37230

National Transonic Facility model and model support vibration problems [AIAA PAPER 90-1416] p 596 A90-37953

Hierarchical finite element method for rotating beams p 605 A90-38353

Discrete Fourier transform with high resolution for low frequencies applied to the modal analysis of aircraft vibration p 679 A90-38975

Correlation between vibration and computer operator response onboard a UH-1H helicopter p 737 A90-43727

Fatigue life assessment of a leaded electronic component under a combined thermal and random vibration environment p 770 A90-43734

Large-order modal analysis techniques in the Aeroelastic Design Optimization Program (ADOP) [SAE PAPER 89-2323] p 772 A90-45482

Theoretical and experimental determination of natural frequencies of laced blading p 878 A90-46037

Vibration analysis of laced blades p 878 A90-46186

Full span analysis for flutter prediction of slender blade assemblies p 879 A90-46188

Vibration of turbine blades damped by dry friction forces p 879 A90-46190

Ride quality criteria for the B-2 bomber [AIAA PAPER 90-3256] p 835 A90-48852

The receptivity of laminar boundary layer flow to leading edge vibrations p 815 A90-49800

Modifying high-order aeroelastic math model of a jet transport using maximum likelihood estimation p 61 N90-10106

Aircraft modal suppression system: Existing design approach and its shortcomings p 33 N90-10115

Problems related to the acquisition, processing and utilization of the modal parameters measured in flight tests in order to obtain the full envelope for flutter [ETN-89-95210] p 103 N90-11735

Investigation of difficult component effects on finite element model vibration prediction for the Bell AH-1G helicopter. Volume 1: Ground vibration test results [NASA-CR-181916-VOL-1] p 134 N90-12058

Airframe design considerations: Overview --- rotor design optimization p 106 N90-12586

Investigation of difficult component effects on finite element model vibration prediction for the Bell AH-1G helicopter. Volume 2: Correlation results [NASA-CR-181916-VOL-2] p 213 N90-13814

Evaluation of analysis techniques for low frequency interior noise and vibration of commercial aircraft [NASA-CR-181851] p 220 N90-14866

Active control system for gust load alleviation and structural damping p 259 N90-15056

Force determination sensitivities study for full-scale helicopter ground vibration testing [AD-A215983] p 349 N90-17643

Helicopter flight vibration of large transportation containers: A case for testing tailoring [DE90-007429] p 402 N90-19215

Exhaust environment measurements of a turbofan engine equipped with an afterburner and 2D nozzle [NASA-CR-4289] p 588 N90-21760

The Shock and Vibration Digest, volume 21, no. 2 p 609 N90-22059

The Shock and Vibration Digest, volume 21, no. 6 p 614 N90-22363

Calculation of flight vibration levels of the AH-1G helicopter and correlation with existing flight vibration measurements [NASA-CR-182031] p 775 N90-25375

STRUCTURAL WEIGHT

Airplane design. Part 5 - Component weight estimation --- Book p 31 A90-12870

A study of sonic boom overpressure trends with respect to weight, altitude, Mach number, and vehicle shaping [AIAA PAPER 90-0367] p 164 A90-19816

Optimum weight design of a rotor bearing system with dynamic behavior constraints [ASME PAPER 89-GT-74] p 358 A90-23795

Efficient structural material distribution in the main frame of a flight vehicle p 363 A90-24092

Lightning strike protection concepts for composite materials p 528 A90-31617

AVION: A detailed report on the preliminary design of a 79-passenger, high-efficiency, commercial transport aircraft [NASA-CR-186663] p 649 N90-23395

STRUCTURES

AIAA/ASME/ASCE/AHS/ASC Structures, Structural Dynamics and Materials Conference, 31st, Long Beach, CA, Apr. 2-4, 1990, Technical Papers. Part 1 - Materials, engineering optimization and design p 449 A90-29226

STRUTS

Wind tunnel studies of support strut interference on a 3 percent YF-17 fighter aircraft model at high angles of attack [AIAA PAPER 90-3083] p 794 A90-45899

An experimental investigation of support strut interference on a three-percent fighter model at high angles of attack [AD-A219793] p 631 N90-23353

SUBCRITICAL FLOW

A numerical method for computing the aerodynamic loads on wings with sharp-edge separations at large angles of attack in subcritical transonic flows p 150 A90-16852

SUBMARINES

Control of submersible vortex flows [NASA-TM-102693] p 909 N90-28493

SUBSONIC AIRCRAFT

Natural laminar flow research for subsonic transport aircraft in the FRG p 2 A90-10137

On the 'inverse phugoid problem' as an instance of non-linear stability in pitch p 55 A90-10221

Hydrogen fueled subsonic-ram-combustor model tests for an air-turbo-ram engine p 44 A90-12529

Analytical methods for subsonic propulsion system integration p 29 A90-12613

Structural analysis of the horizontal tail surfaces of subsonic transport aircraft p 102 A90-14556

Preliminary results from a subsonic high-angle-of-attack flush airdata sensing (HI-FADS) system - Design, calibration, algorithm development, and flight test evaluation [AIAA PAPER 90-0232] p 187 A90-19746

Aerospace materials research opportunities p 267 A90-23177

Effects of nonplanar outboard wing forms on a wing p 232 A90-23279

Minimizing life cycle cost for subsonic commercial aircraft p 283 A90-23282

Analysis of the mathematical modeling of an aircraft flight trajectory with consideration of engine thrust effect on the force ratio on the aircraft p 247 A90-23363

Using the method of symmetric singularities for calculating flow past subsonic flight vehicles p 386 A90-28979

Investigation of very high bypass ratio engines for subsonic transports p 659 A90-40945

Noise-source measurements by thin-film pressure transducers in a subsonic turbofan model [ONERA, TP NO. 1990-36] p 659 A90-41212

Airbus technologies - An evolutionary process p 902 A90-52699

Lockheed laminar-flow control systems development and applications p 90 N90-12506

Preliminary results from a subsonic high angle-of-attack flush airdata sensing (HI-FADS) system: Design, calibration, and flight test evaluation [NASA-TM-101713] p 339 N90-16758

Life cycle cost in the conceptual design of subsonic commercial aircraft, volumes 1 and 2 p 923 N90-28535

High-speed civil transport study: Special factors [NASA-CR-181881] p 923 N90-28537

SUBSONIC FLOW

Analysis of nonuniform subsonic flows about a row of moving blades p 6 A90-11779

Finite element method for unsteady three-dimensional subsonic flows through a cascade oscillating with steady loading p 9 A90-11873

Numerical calculation of unsteady aerodynamic forces for three-dimensional subsonic oscillating cascades by a finite element method p 9 A90-12219

Pressure pulsation in a cavity in the path of subsonic and supersonic gas flow p 10 A90-12279

Aeroelastic characteristics of wings in subsonic flow p 102 A90-14615

On steady subsonic flow past slender bodies of revolution p 144 A90-16736

An interactive boundary layer method for subsonic airfoil flows p 144 A90-16754

Design optimization of natural laminar flow fuselages in compressible flow p 182 A90-19784

[AIAA PAPER 90-0303] p 182 A90-19784

Nonlinear stability of subsonic mixing layers with symmetric temperature variations p 223 A90-20501

Computation of subsonic shrouded propeller flows [AIAA PAPER 90-0029] p 226 A90-22154

Subsonic calculation of propeller/wing interference [AIAA PAPER 90-0031] p 226 A90-22155

An embedded grid formulation applied to a delta wing [AIAA PAPER 90-0429] p 229 A90-22216

Numerical method for the flow of an ideal fluid on a plane with subsonic and supersonic regions p 233 A90-23362

Modeling of subsonic unsteady aerodynamics for rotary wing applications p 293 A90-23935

An experimental study of separated flow past a low-aspect-ratio delta wing p 294 A90-24077

Asymptotic solution of the optimal-deflection problem for a wing leading edge at subsonic flow velocities p 295 A90-24094

Aeroelastic deformation of a crescent-shaped rigid support in the diffuser chamber of a wind tunnel p 364 A90-24112

Calculation of the front or rear part of a flat body in subsonic flow with the extremum value of the critical Mach number p 296 A90-24120

An investigation of fillets in wing-fuselage joints at subsonic velocities p 297 A90-24131

The local surface variation method in profile shape optimization problems p 297 A90-24136

Separation development and its effect on the aerodynamics of supercritical profiles at transonic velocities p 297 A90-24142

Construction of a wing surface in a nonviscous transonic flow from a given pressure distribution p 298 A90-24149

Permeability of the porous walls of a wind tunnel at transonic velocities p 350 A90-24151

Nonstationary motion of an elastic profile in subsonic incompressible flow p 300 A90-24741

Total temperature effects on centerline Mach number characteristics of freejets p 302 A90-25290

Measurements on an oscillating 70-deg delta wing in subsonic flow p 307 A90-26130

Conditions of the generation of autooscillations in aerodynamic control surfaces in nonseparated subsonic flow of a gas p 315 A90-27303

Effect of the leading edge bluntness of a moderately swept wing on the aerodynamic characteristics of an aircraft model at subsonic and transonic velocities p 388 A90-29005

Time domain simulations of a flexible wing in subsonic, compressible flow p 390 A90-29365

[AIAA PAPER 90-1153] p 390 A90-29365

Reduced size first-order subsonic and supersonic aeroelastic modeling [AIAA PAPER 90-1154] p 390 A90-29366

Numerical simulation of an adaptive-wall wind-tunnel - A comparison of two different strategies p 439 A90-30251

Calculation of unsteady subsonic and supersonic flow about oscillating wings and bodies by new panel methods p 472 A90-33359

The development of leading-edge notches to improve the subsonic performance of wings of moderate sweep p 491 A90-33367

An implicit scheme with flow correction for the numerical solution of the Euler equation p 477 A90-34674

A numerical method in aeroelasticity for wings with separation at large angle of attack p 557 A90-37209

A numerical study on the use of sulfur hexafluoride as a test gas for wind tunnels p 605 A90-37958

[AIAA PAPER 90-1421] p 605 A90-37958

A computational study of the impingement region of an unsteady subsonic jet p 570 A90-38784

[AIAA PAPER 90-1657] p 570 A90-38784

Experimental study of the turbulent boundary layer on a transport wing in subsonic flow p 709 A90-44728

Effect of riblets on flow separation in a subsonic diffuser p 712 A90-45261

Low-speed aerodynamic characteristics of a powered NASP-like configuration in ground effect [SAE PAPER 892312] p 714 A90-45474

Low Reynolds number airfoil design for subsonic compressible flow p 802 A90-46380

Construction of wing profiles in subsonic gas flow by the method of quasi-solutions for inverse boundary value problems p 803 A90-46542

Speed-up of the strongly implicit procedure with application to subsonic/transonic potential flows p 809 A90-47301

Response of a subsonic boundary layer to a pulsed oscillation of a localized region of the surface in the flow p 811 A90-48295

Subsonic and transonic low-Reynolds-number airfoils with reduced pitching moments [AIAA PAPER 90-3212] p 812 A90-48838

Flow past two cylinders and two spheres p 903 A90-50815

A parametric study of radial turbomachinery blade design in three-dimensional subsonic flow [ASME PAPER 89-GT-84] p 905 A90-51257

Computation of ramjet internal flowfields [AD-A212001] p 114 A90-11743

CFD methods for drag prediction and analysis currently in use in UK [RAE-TM-AERO-2146] p 95 A90-12563

Multigrid solution method for the Euler equations [PB89-219463] p 138 A90-13116

An alternative derivation for an integral equation for linearized subsonic flow over a wing [AD-A214140] p 236 A90-15079

Effect of riblets on flow separation from a cylinder and an airfoil in subsonic flow [AD-A216197] p 319 A90-17574

A matrix-free locally-implicit scheme for Navier-Stokes equations [AD-A218298] p 541 A90-20349

Subsonic and transonic blade design by means of analysis codes p 510 A90-20985

Numerical optimization of target pressure distributions for subsonic and transonic airfoil design p 502 A90-20993

Subsonic flutter analysis using MSC/NASTRAN [PB90-166786] p 522 A90-21041

STARS: An integrated general-purpose finite element structural, aeroelastic, and aeroservoelastic analysis computer program [NASA-TM-101709] p 689 A90-23768

Effects of forebody geometry on subsonic boundary-layer stability [NASA-CR-4314] p 718 A90-25939

Subsonic combustor flow modeling: State of the art of CFD techniques for reacting and combustor flow p 749 A90-25991

Flame extinction in compressible flow p 883 A90-26899

SUBSONIC FLUTTER

Improved double linearization method for prediction of mean loading effects on subsonic and supersonic cascade flutter p 41 A90-11795

Application of the double linearization theory to three-dimensional subsonic and supersonic cascade flutter p 50 A90-12638

Numerical model of unsteady subsonic aeroelastic behavior p 535 A90-32471

Mean loading effects on flutter of subsonic rotating annular cascade p 853 A90-49453

Subsonic flutter analysis using MSC/NASTRAN [PB90-166786] p 522 A90-21041

SUBSONIC SPEED

Advanced core technology - Key to subsonic propulsion benefits [ASME PAPER 89-GT-241] p 342 A90-23890

Project Falke - Performance of free flight tests in the supersonic, transonic, and subsonic regimes from balloons [DGLR PAPER 88-018] p 903 A90-50235

Hinge moment coefficient derivatives for trailing-edge controls on wings at subsonic speeds [ESDU-89009] p 198 A90-14239

Installed tailplane lift-curve slope at subsonic speeds [ESDU-89029] p 236 A90-15081

The maximum lift coefficient of plain wings at subsonic speeds [ESDU-89034] p 236 A90-15082

Body effect on wing angle of attack and pitching moment at zero lift at low speeds [ESDU-89042] p 337 A90-16757

An intensive procedure for the design of pressure-specified three-dimensional configurations at subsonic and supersonic speeds by means of a higher-order panel method p 500 A90-20982

AVION: A detailed report on the preliminary design of a 79-passenger, high-efficiency, commercial transport aircraft [NASA-CR-186663] p 649 A90-23395

Flow unsteadiness effects on boundary layers [NASA-CR-186067] p 690 A90-24557

Gas Turbine Combustion, volume 2 [VKI-LS-1990-02-VOL-2] p 749 A90-25995

Theoretical studies carried out in 1988 on helicopter rotor noise under subsonic conditions [ONERA-RS-82/5094-PY] p 896 A90-28402

SUBSONIC WIND TUNNELS

Wind-tunnel investigation on the effect of a crescent platform on drag [AIAA PAPER 90-0300] p 228 A90-22196

Effects of an embedded vortex on injectant from a single film-cooling hole in a turbulent boundary layer [ASME PAPER 89-GT-189] p 362 A90-23867

Investigation of the flow structure behind the rotating blades in the elbow of a wind tunnel in the case of acoustic excitation p 297 A90-24124

Database for LDV signal processor performance analysis p 447 A90-28278

Aerothermodynamics and transition in high-speed wind tunnels at NASA Langley p 386 A90-28555

Instability and susceptibility of a boundary layer in the vicinity of two-dimensional surface inhomogeneities p 535 A90-32675

A wall pressure correction method for half-model experiment in closed subsonic wind tunnel test section p 593 A90-36437

Measured aerodynamic performance of a swept wing with a simulated ice accretion [AIAA PAPER 90-0490] p 557 A90-37063

Aeronautical facility requirements into the 2,000's [AIAA PAPER 90-1375] p 594 A90-37926

On the possibilities for improvement and modernization of subsonic wind tunnels [AIAA PAPER 90-1423] p 596 A90-37960

Infrared cameras for detection of boundary layer transition in transonic and subsonic wind tunnels [AIAA PAPER 90-1450] p 606 A90-38610

Detachment of turbulent boundary layers with varying free-stream turbulence and lower Reynolds numbers p 802 A90-46378

Using the smoking-wire visualization method in the study of wing models at large angles of attack in subsonic wind tunnels p 881 A90-46561

Acoustic excitation of boundary layer oscillations on a yawing wing p 805 A90-46567

The aerodynamic design of the contraction for a subsonic wind tunnel p 907 A90-51545

The aerodynamic experimental center of Aeritalia: Combat aircraft group [ETN-89-95213] p 122 A90-11766

A data acquisition parallel bus for wind tunnels at ARL (Aeronautical Research Laboratory) [AD-A218052] p 526 A90-20098

The Langley 14- by 22-foot subsonic tunnel: Description, flow characteristics, and guide for users [NASA-TP-3008] p 816 A90-27649

Dynamic ground effects p 922 A90-28531

SUBSTITUTES

Re-engine with the Rolls-Royce Tay 670, the route to significant noise reduction [PNR90585] p 115 A90-12606

SUBSTRUCTURES

Design philosophy and construction techniques for integral fuselage fuel tanks p 250 A90-15913

Unique failure behavior of metal/composite aircraft structural components under crash type loads [NASA-TM-102679] p 690 A90-24660

SUCTION

Supersonic boundary layer stability analysis with and without suction on aircraft wings p 148 A90-16792

The use of a Laval nozzle and wall suction for blockage-free transonic wind-tunnel operation p 225 A90-21592

Induced drag based on leading edge suction for a helicopter in forward flight p 232 A90-23102

Effects of endwall suction and blowing on compressor stability enhancement [ASME PAPER 89-GT-64] p 290 A90-23787

Transient response of leading-edge vortices to localized suction p 556 A90-36279

Simulated-airline-service flight tests of laminar-flow control with perforated-surface suction system [NASA-TP-2966] p 338 A90-17627

Generation of circumferential velocity contours associated with pulsed point suction on a rotating disk p 691 A90-25065

SULFIDES

Improved fiber reinforced polyphenylene sulfide thermoplastic composites p 947 A90-50180

SULFUR FLUORIDES

A numerical study on the use of sulfur hexafluoride as a test gas for wind tunnels [AIAA PAPER 90-1421] p 605 A90-37958

SUPERCHARGERS

Numerical simulation of the behaviour of internal combustion supercharged engines [AIAA PAPER 90-1873] p 655 A90-40539

A simulation code for turbocompound diesel engines [IAR-89-26] p 774 A90-25348

SUPERCOMPUTERS

- Multi-processing on supercomputers for computational aerodynamics
[AIAA PAPER 90-0337] p 282 A90-22199
- Array processor supercomputers p 376 A90-26626
- The airborne supercomputer p 538 A90-33775
- Capability of current supercomputers for the computational fluid dynamics p 546 A90-34382
- Effective use of Cray supercomputers p 546 A90-34436
- Supercomputer applications in gas turbine flowfield simulation p 620 A90-40495
- Aircraft technology management and the related significance of the supercomputer p 612 N90-22975
- Numerical flow simulation and supercomputers: More than a digital wind tunnel p 612 N90-22976
- The use of supercomputers for the design and analysis of constructions p 612 N90-22977
- Current Japanese supercomputers for computational fluid dynamics applications p 610 N90-23172
- Informatics aspects of large flow calculations on the SX-2 supercomputer [NLR-MP-88037-U] p 776 N90-26290

SUPERCooling

- Condensation in hypersonic nitrogen wind tunnels [AIAA PAPER 90-1392] p 558 A90-37937
- Remote sensing techniques of the Wave Propagation Laboratory for the measurement of supercooled liquid water: Applications to aircraft icing [PB89-208102] p 24 N90-10842

SUPERCritical AIRFOILS

- Closed-form solutions for nonlinear quasi-unsteady transonic aerodynamics p 16 A90-12839
- Investigation of flow separation on a supercritical airfoil p 17 A90-13023
- Fresh look at floating shock fitting [AIAA PAPER 90-0108] p 162 A90-19686
- Separation development and its effect on the aerodynamics of supercritical profiles at transonic velocities p 297 A90-24142
- Two-dimensional wall adaption in the transonic windtunnel of the AIA p 597 A90-38497
- Sidewall boundary-layer removal and wall adaption studies p 672 A90-40680
- A transonic airfoil design method and examples p 627 A90-42351
- Flow separation on a supercritical airfoil p 627 A90-42394
- A study of high-lift airfoils at high Reynolds numbers in the Langley low-turbulence pressure tunnel [NASA-TM-89125] p 1 N90-10002
- A direct-inverse method for transonic and separated flows about airfoils [NASA-CR-4270] p 235 N90-15072
- NASA supercritical airfoils: A matrix of family-related airfoils [NASA-TP-2969] p 315 N90-16710
- Comparison of conventional and adaptive wall wind tunnel results with regard to Reynolds number effects p 352 N90-17649
- Experience with some repeat tests on the 9 inch chord CAST-10-2/DOA 2 airfoil model in the Langley 0.3-m TCT adaptive wall test section p 321 N90-17657
- Aerodynamic design techniques at DLR Institute for Design Aerodynamics p 500 N90-20979

SUPERCritical FLOW

- Shock/turbulent boundary layer interaction in low Reynolds number supercritical flows p 802 A90-46383
- Analysis of experimental data for CAST 10-2/DOA 2 supercritical airfoil at low Reynolds numbers and application to high Reynolds number flow [AD-A211654] p 170 N90-13326
- Aerofoil design techniques p 500 N90-20978
- Inverse design of airfoil contours: Constraints, numerical method, and applications p 500 N90-20980
- Inverse computation of transonic internal flows with application for multi-point-design of supercritical compressor blades p 501 N90-20987
- Limits of adaptation, residual interferences p 871 N90-26844

SUPERCritical WINGS

- Further investigations of transonic shock-wave boundary-layer interaction with passive control p 159 A90-19390
- Unsteady pressure and structural response measurements on an elastic supercritical wing p 159 A90-19392
- Results of LFC experiment on slotted swept supercritical airfoil in Langley's 8-foot transonic pressure tunnel p 92 N90-12531
- Boundary-layer stability analysis of Langley Research Center 8-foot LFC experimental data p 92 N90-12532

SUPERHIGH FREQUENCIES

- Reduced insertion loss of X-band RF fiber optic links p 695 A90-41240

SUPERPLASTICITY

- The manufacture of SPF military aircraft doors in aluminium alloy — superplastically formed p 132 A90-16616
- Study on SPF and SPF/DB of the bulk-head structure with nonsymmetric shape p 132 A90-16619
- DB/SPF cooler outlet duct for aircraft application p 132 A90-16620
- SPF/DB takes off p 208 A90-17293
- The case for titanium p 204 A90-17922
- Application investigation on superplastic forming/diffusion bonding combined technology of titanium alloy TC4 p 204 A90-18603
- Diffusion bonding of metals p 206 N90-14330
- Aluminum lithium alloys for Navy aircraft p 267 N90-15193
- Design of cryogenic tanks for launch vehicles p 609 N90-22662

SUPersonic AIRCRAFT

- HSCT research focuses on environmental issues p 143 A90-17780
- A study of sonic boom overpressure trends with respect to weight, altitude, Mach number, and vehicle shaping [AIAA PAPER 90-0367] p 164 A90-19816
- Thermodynamics and the future turbine engines [ONERA, TP NO. 1989-165] p 253 A90-21031
- New high-speed air transport system and stratospheric pollution [ONERA, TP NO. 1989-202] p 279 A90-22445
- Integral solution of unsteady full-potential equation for a transonic pitching airfoil p 232 A90-23280
- Analysis of the mathematical modeling of an aircraft flight trajectory with consideration of engine thrust effect on the force ratio on the aircraft p 247 A90-23363
- Effect of creep on the load-bearing capacity of compressed panels p 364 A90-24102
- Static and dynamic loss of stability of elements of a supersonic aeroplane covering - Numerical analysis p 346 A90-25186
- The design of supersonic aircraft and space vehicles by using global optimization techniques p 353 A90-25781
- Wave rider volume distribution p 388 A90-29006
- Experimental transonic flutter characteristics of supersonic cruise configurations [AIAA PAPER 90-0979] p 390 A90-29369
- Sukhoi and Gulfstream go supersonic — joint development of business aircraft p 383 A90-31247
- Propulsion systems for supersonic V/STOL aircraft [ASME PAPER 89-GT-309] p 507 A90-32259
- Configuration E-7 supersonic fighter/attack technology program [ASME PAPER 89-GT-308] p 490 A90-32260
- Supersonic aircraft drag reduction [AIAA PAPER 90-1596] p 567 A90-38729
- Hydrogen in future energy and propulsion technology p 692 A90-41736
- Airframe/propulsion integration of supersonic cruise vehicles [AIAA PAPER 90-2151] p 644 A90-42047
- A remote tip-driven fan powered supersonic fighter concept [AIAA PAPER 90-2415] p 663 A90-42167
- BD-10J supersonic homebuilt aircraft p 730 A90-42672
- Civil supersonics - A less distant thunder p 731 A90-44223
- Supersonic STOVL - The future is now p 732 A90-44781
- Propulsion integration for military aircraft [SAE PAPER 892234] p 733 A90-45449
- 3D transonic nacelle and winglet design [AIAA PAPER 90-3064] p 794 A90-45897
- On optimal supersonic/hypersonic bodies [AIAA PAPER 90-3072] p 796 A90-45918
- Analysis of self-excited vibrations of stiffened covering panels of an aeroplane wing p 860 A90-46716
- Multivariable flight control synthesis and literal robustness analysis for an aeroelastic vehicle [AIAA PAPER 90-3446] p 890 A90-47699
- Supersonic aerodynamic characteristics of a Mach 3 high-speed civil transport configuration [AIAA PAPER 90-3210] p 811 A90-48836
- Preliminary design of a supersonic short takeoff and vertical landing (STOVL) fighter aircraft [AIAA PAPER 90-3231] p 834 A90-48844
- Twin-jet screech suppression p 894 A90-48957
- A supersonic through-flow fan engine airframe integration study [NASA-CR-185140] p 18 N90-10004
- Passive venting technique for shallow cavities [NASA-CASE-LAR-14031-1] p 499 N90-20079
- Preliminary design of a supersonic Short Takeoff and Vertical Landing (STOVL) fighter aircraft [NASA-CR-186670] p 649 N90-23394

- Convex models of malfunction diagnosis in high performance aircraft [AD-A218514] p 702 N90-25073
- Interactive calculation procedures for mixed compression inlets [NASA-CR-186581] p 718 N90-25934
- High-speed civil transport study: Special factors [NASA-CR-181881] p 923 N90-28537

SUPersonic AIRFOILS

- Supersonic low-density flow over airfoils p 153 A90-17871
- Aerodynamic design methods for transonic wings p 293 A90-23978
- Comparison between thin layer and full Navier-Stokes simulations over a supersonic delta wing [AIAA PAPER 90-0589] p 314 A90-26968
- Observation and analysis of sidewall effect in a transonic airfoil test section p 436 A90-28257
- Instrumentation and operation of NDA cryogenic wind tunnel p 437 A90-28293
- A verification of the supersonic lifting line theory for the case of infinite yawed wings p 477 A90-34821
- Sound generation by a supersonic aerofoil cutting through a steady jet flow p 781 A90-42638
- Design of supersonic wings using an optimization strategy coupled with a solution scheme for the Euler equations [AIAA PAPER 90-3060] p 794 A90-45895

SUPersonic BOUNDARY LAYERS

- Marginal separation of laminar axisymmetric boundary layers p 1 A90-10074
- Prediction and control of transition in supersonic and hypersonic boundary layers p 16 A90-12828
- Goertler vortices in supersonic and hypersonic boundary layers p 83 A90-14091
- Supersonic boundary layer stability analysis with and without suction on aircraft wings p 148 A90-16792
- Large-scale motions in a supersonic turbulent boundary layer on a curved surface [AIAA PAPER 90-0019] p 160 A90-19636
- A numerical study of mixing and chemical heat release in supersonic mixing layers [AIAA PAPER 90-0152] p 163 A90-19710
- Embedded function methods for supersonic turbulent boundary layers [AIAA PAPER 90-0306] p 163 A90-19787
- Effect of hydrogen combustion in a supersonic boundary layer on friction coefficient p 355 A90-24116
- A supersonic turbulent boundary layer in an adverse pressure gradient p 303 A90-25592
- Turbulence statistics in a shock wave boundary layer interaction p 552 A90-35205
- A study of the unsteadiness of crossing shock wave turbulent boundary layer interactions [AIAA PAPER 90-1456] p 606 A90-38614
- Wall pressure fluctuations in the reattachment region of a supersonic free shear layer [AIAA PAPER 90-1461] p 561 A90-38618
- Wave structure of artificial perturbations in a supersonic boundary layer on a plate p 619 A90-39518
- Excitation and development of unstable perturbations in a supersonic boundary layer p 710 A90-44928
- Supersonic laminar-flow control p 93 N90-12554
- Supersonic boundary-layer transition on the LaRC F-106 and the DFRF F-15 aircraft. Part 1: Transition measurements and stability analysis p 94 N90-12558
- Supersonic boundary-layer transition on the LaRC F-106 and the DFRF F-15 aircraft. Part 2: Aerodynamic predictions p 94 N90-12559

SUPersonic COMBUSTION

- Simultaneous CARS measurements of temperature and H₂, H₂O concentrations in hydrogen-fueled supersonic combustion [AIAA PAPER 90-0158] p 205 A90-19713
- Hydraulic analogy application in the study of a two-phase mixture combustion flow [AIAA PAPER 90-0451] p 211 A90-19850
- A numerical study of mixing enhancement in a supersonic combustor [AIAA PAPER 90-0203] p 272 A90-22182
- Supersonic combustion of hydrogen jets behind a backward-facing step [AIAA PAPER 90-0204] p 266 A90-22183
- Chemically reacting supersonic flow calculation using an assumed PDF model [AIAA PAPER 90-0731] p 230 A90-22256
- Critical evaluation of three-dimensional supersonic combustor calculations [AIAA PAPER 90-0207] p 272 A90-22265
- Effect of hydrogen combustion in a supersonic boundary layer on friction coefficient p 355 A90-24116
- Application of Lomax-Bailey implicit scheme to reactive flows p 367 A90-25861
- Supersonic viscous shear layers p 367 A90-25873
- Numerical simulations of an oblique detonation wave engine p 508 A90-32964

- Heat transfer in supersonic coaxial reacting jets
p 601 A90-35394
- Experimental investigation of a supersonic swept ramp injector using laser-induced iodine fluorescence
[AIAA PAPER 90-1518] p 606 A90-38663
- HF shock tunnel facility for studying supersonic combustion
[AIAA PAPER 90-1551] p 600 A90-38693
- A hybrid Reynolds averaged/PDF closure model for supersonic turbulent combustion
[AIAA PAPER 90-1573] p 600 A90-38711
- Modeling supersonic combustion using a fully-implicit numerical method
[AIAA PAPER 90-2307] p 677 A90-42117
- A computational investigation of flow losses in a supersonic combustor
[AIAA PAPER 90-2093] p 742 A90-42728
- Streamtube analysis of supersonic combustion in an in-tube-scamjet
[AIAA PAPER 90-2339] p 762 A90-42776
- Computation of ramjet internal flowfields
[AD-A212001] p 114 N90-11743
- The next generation supersonic transport engine: Critical issues
[PNR90576] p 115 N90-12605
- Numerical modeling of supersonic turbulent reacting free shear layers
p 174 N90-14197
- Hypersonic nozzle/afterbody performance at low Mach numbers
[AD-A216223] p 319 N90-17575
- Supersonic combustor modeling
p 749 N90-25992
- Supersonic reacting internal flow fields
[NASA-TM-103480] p 767 N90-26094
- Flame extinction in compressible flow
p 883 N90-26899
- Raman scattering measurements using UV excimer lasers
p 874 N90-26902
- Concentration, temperature, and density in a hydrogen-air flame by excimer-induced Raman scattering
p 875 N90-26903
- Turbulent reacting flows and supersonic combustion
[AD-A221793] p 875 N90-26933
- Photo-sensitized ignition of hydrogen/oxygen mixtures for hypersonic flight vehicles
p 877 N90-27935
- SUPERSONIC COMBUSTION RAMJET ENGINES**
- Experimental study on autoignition in a scramjet combustor
p 46 A90-12559
- Hypersonic combustion of hydrogen in a shock tunnel
p 46 A90-12560
- The use of pulse facilities for testing supersonic combustion ramjet (scramjet) combustors in simulated hypersonic flight conditions
p 46 A90-12562
- Tangential mass addition for the control of shock wave/boundary layer interactions in scramjet inlets
p 13 A90-12586
- Keepers of the flame --- scramjet development programs
p 141 A90-16300
- Mach 6 testing of two generic three-dimensional sidewall compression scramjet inlets in tetrafluoromethane
[AIAA PAPER 90-0530] p 192 A90-19895
- A numerical parametric study of a scramjet inlet in a Mach 6 arc heated test facility
[AIAA PAPER 90-0531] p 167 A90-19896
- Calculated chemical and vibrational nonequilibrium effects in hypersonic nozzles
p 253 A90-21224
- Hypersonic propulsion
p 253 A90-21949
- Representation of two-dimensional hypersonic inlet flows for one-dimensional scramjet cycle analysis
[AIAA PAPER 90-0527] p 229 A90-22226
- Three-dimensional shock-shock interactions on the scramjet inlet
[AIAA PAPER 90-0529] p 314 A90-26963
- Investigation of cowl vent slots for supercritical stability enhancement in dual-mode ramjet inlets
p 507 A90-32951
- Scramjet testing from Mach 4 to 20 - Present capability and needs for the nineties
[AIAA PAPER 90-1388] p 597 A90-38485
- Injectant mole fraction measurements of transverse injection in constant area supersonic ducts
[AIAA PAPER 90-1632] p 587 A90-38761
- Linear dynamics of supersonic ramjet
p 655 A90-40519
- Hydrocarbon-fueled scramjet combustor investigation
[AIAA PAPER 90-2337] p 658 A90-40622
- Transverse fuel-injection model for a scramjet propulsion system
p 659 A90-40927
- Some governing parameters of plasma torch igniter/flameholder in a scramjet combustor
[AIAA PAPER 90-2098] p 661 A90-42017
- Direct measurements of skin friction in a scramjet combustor
[AIAA PAPER 90-2342] p 626 A90-42132
- Hypersonic (T-D) 'pinch' and aerospaceplane propulsion
[AIAA PAPER 90-2474] p 675 A90-42189
- Flow establishment in a generic scramjet combustor
[AIAA PAPER 90-2096] p 742 A90-42729
- A numerical study of the effects of reverse sweep on a scramjet inlet performance
[AIAA PAPER 90-2218] p 705 A90-42749
- Measured operating characteristics of a rectangular combustor/inlet isolator
[AIAA PAPER 90-2221] p 742 A90-42752
- Streamtube analysis of supersonic combustion in an in-tube-scamjet
[AIAA PAPER 90-2339] p 762 A90-42776
- Methods for determining the internal thrust of scramjet engine modules from experimental data
[AIAA PAPER 90-2340] p 743 A90-42777
- A validation study of the Spark Navier Stokes code for nonreacting scramjet combustor flowfields
[AIAA PAPER 90-2360] p 706 A90-42784
- Mixing and combustion enhancement in supersonic reacting flows
p 744 A90-44410
- Numerical simulation of flow through the Langley parametric scramjet engine
[SAE PAPER 892314] p 747 A90-45476
- A hypersonic research vehicle to develop scramjet engines
[AIAA PAPER 90-3232] p 839 A90-49115
- Cycle analysis of scramjet engines
[NAL-TR-1002] p 51 N90-10035
- Computation of ramjet internal flowfields
[AD-A212001] p 114 N90-11743
- Numerical modeling of supersonic turbulent reacting free shear layers
p 174 N90-14197
- RAMSCRAM: A flexible ramjet/scramjet engine simulation program
[NASA-TM-102451] p 194 N90-14235
- Hypersonic nozzle/afterbody performance at low Mach numbers
[AD-A216223] p 319 N90-17575
- Development and fabrication of structural components for a scramjet engine
[NASA-CR-181945] p 510 N90-20088
- Performance of an aero-space plane propulsion nozzle
p 515 N90-21034
- Supersonic combustor modeling
p 749 N90-25992
- Gas Turbine Combustion, volume 2
[VKI-LS-1990-02-VOL-2] p 749 N90-25995
- Supersonic reacting internal flow fields
[NASA-TM-103480] p 767 N90-26094
- Modeling of supersonic reacting flow fields
p 855 N90-26898
- Flame extinction in compressible flow
p 883 N90-26899
- Analysis of scramjet engine characteristics
[NAL-TR-1041] p 933 N90-29398
- SUPERSONIC COMMERCIAL AIR TRANSPORT**
- Technology issues for high-speed civil transports
[SAE PAPER 892201] p 778 A90-45422
- Benefits of advanced materials, structures, and aerodynamics in future high speed civil transport propulsion systems
[AIAA PAPER 90-3285] p 853 A90-48872
- The next generation supersonic transport engine: Critical issues
[PNR90576] p 115 N90-12605
- SUPERSONIC COMPRESSORS**
- Aircraft compressor flutter analysis
p 41 A90-11797
- The development of a high response aerodynamic wedge probe and use on a high-speed research compressor
p 69 A90-12618
- Laser transit anemometry investigation of a high speed centrifugal compressor
[ASME PAPER 89-GT-155] p 360 A90-23843
- Quasi-3D viscous flow computations in subsonic and transonic turbomachinery bladings
[AIAA PAPER 90-2126] p 625 A90-42033
- A method for the prediction of supersonic compressor blade performance
[CUED/A-TURBO/TR-126] p 344 N90-17634
- SUPERSONIC CRUISE AIRCRAFT RESEARCH**
- A supersonic through-flow fan engine airframe integration study
[NASA-CR-185140] p 18 N90-10004
- Study of high-speed civil transports
[NASA-CR-4235] p 183 N90-13370
- SUPERSONIC DIFFUSERS**
- Experimental investigation of GDL diffusers
[AIAA PAPER 90-1512] p 563 A90-38659
- A CFD study of precombustion shock-trains from Mach 3-6
[AIAA PAPER 90-2220] p 705 A90-42751
- Experimental investigation of a chemical laser cavity flowfield
[AD-A216398] p 372 N90-18038
- SUPERSONIC DRAG**
- Effectiveness of passive devices for axisymmetric base drag reduction at Mach 2
p 555 A90-36184
- Supersonic aircraft drag reduction
[AIAA PAPER 90-1596] p 567 A90-38729
- On optimal supersonic/hypersonic bodies
[AIAA PAPER 90-3072] p 796 A90-45918
- CFD methods for drag prediction and analysis currently in use in UK
[RAE-TM-AERO-2146] p 95 N90-12563
- Influence of friction and separation phenomena on the dynamic blade loading of transonic turbine cascades
[MITT-88-04] p 428 N90-19235
- SUPERSONIC FLIGHT**
- Thermostructural behavior of electromagnetic windows - Elaboration of a code package
[ONERA, TP NO. 1989-145] p 76 A90-11167
- Rapid prediction of slender-wing-aircraft stability characteristics
[AIAA PAPER 90-0301] p 163 A90-19782
- Supersonic flight vehicles --- Russian book
p 299 A90-24233
- Aerodynamic characteristics of wave riders based on flows behind axisymmetric shock waves
p 395 A90-30342
- A study of the radiation of hydrogen-xenon mixtures near models flying at high supersonic velocities
p 470 A90-32509
- Taking a new look at cockpit vertical situation displays
p 652 A90-40382
- RAMSCRAM: A flexible ramjet/scramjet engine simulation program
[NASA-TM-102451] p 194 N90-14235
- External flow computations for a finned 60mm ramjet in steady supersonic flight
[AD-A216998] p 428 N90-19233
- An aerodynamic tradeoff study of the scissor wing configuration
[NASA-CR-186576] p 481 N90-20965
- Thermal structures: Four decades of progress
[NASA-CR-186898] p 887 N90-28105
- SUPERSONIC FLOW**
- A study of three-dimensional supersonic flow of a real gas past axisymmetric bodies
p 3 A90-10938
- Canard-wing interaction in unsteady supersonic flow
p 3 A90-11010
- Numerical simulation of reversed flow over a supersonic delta wing at high angle of attack
p 8 A90-11849
- [AIAA PAPER 89-1802] p 8 A90-11849
- Numerical calculation of unsteady aerodynamic forces for two-dimensional supersonic oscillating cascades by finite element method
p 9 A90-12238
- Pressure pulsation in a cavity in the path of subsonic and supersonic gas flow
p 10 A90-12279
- Lee-side heating of a delta wing in supersonic flow
p 10 A90-12281
- An experimental study of fluctuations in the front separation zone at supersonic flow velocities
p 10 A90-12282
- Shock capturing and loss prediction for transonic turbine blades using a pressure correction method
p 11 A90-12518
- The development of an exact conservative scheme associated with the supersonic trailing edge separation modelling for the computation of the transonic 2D cascade
p 12 A90-12551
- Investigation of the mixing of parallel supersonic streams
p 69 A90-12561
- Shock-wave/boundary-layer interaction at a swept compression corner
p 16 A90-12850
- Unified super/hypersonic similitude for steady and oscillating cones and ogives
p 82 A90-13786
- Supersonic/hypersonic flow past wedge and plane ogive in oscillation
p 85 A90-15231
- Numerical simulation of supersonic and hypersonic turbulent compression corner flows using PNS equations
p 85 A90-15242
- Studies on supersonic radial flow behavior in disk channel
p 87 A90-16104
- On a lifting line theory for supersonic flow. I - The velocity field due to a vortex line in supersonic flow
p 143 A90-16735
- Supersonic/hypersonic Euler flowfield prediction method for aircraft configurations
p 145 A90-16767
- Results from a numerical simulation of an F-16A configuration at a supersonic Mach number
p 146 A90-16769
- Airfoils in supersonic source and sink flows
p 149 A90-16844
- Changes in supersonic flow past an obstacle due to the formation of a thin rarefaction channel ahead of the obstacle
p 150 A90-17108
- Equilibrium of an elastic porous shell in supersonic gas flow
p 150 A90-17109
- Design and experimental verification of an equivalent forebody representation of flowing inlets
p 152 A90-17863
- Supersonic low-density flow over airfoils
p 153 A90-17871

- High-resolution upwind scheme for vortical-flow simulations p 153 A90-17872
- Modeling of liquid jets injected transversely into a supersonic crossflow p 153 A90-17985
- Numerical study of chemically reacting flows using a lower-upper symmetric successive overrelaxation scheme p 153 A90-17989
- Hybrid finite volume approach to Euler solutions for supersonic flows p 154 A90-18144
- Mach number effects on conical surface features of swept shock-wave/boundary-layer interactions p 154 A90-18147
- Supersonic nonuniform flow of a gas past oblong axisymmetric bodies p 159 A90-19237
- Fresh look at floating shock fitting [AIAA PAPER 90-0108] p 162 A90-19686
- Mean flow measurements of heated supersonic slot injection into a high Reynolds number supersonic stream [AIAA PAPER 90-0180] p 163 A90-19722
- Solution of the parabolized Navier-Stokes equations using Osher's upwind scheme [AIAA PAPER 90-0392] p 165 A90-19830
- Aerodynamic spike flowfields computed to select optimum configuration at Mach 2.5 with experimental validation [AIAA PAPER 90-0414] p 166 A90-19837
- Viscous supersonic flow computations over a delta-rectangular wing with slanting surfaces [AIAA PAPER 90-0419] p 166 A90-19841
- Prediction of steady and unsteady asymmetric vortical flows around cones [AIAA PAPER 90-0598] p 168 A90-19940
- Investigation of oscillating airfoil shock phenomena [AIAA PAPER 90-0695] p 169 A90-19981
- Vibration of a wing of nonzero thickness in supersonic flow p 222 A90-20432
- A study of the stability of a wing aileron in supersonic flow p 222 A90-20442
- Effects of pressure mismatch on slot injection in supersonic flow [AIAA PAPER 90-0092] p 227 A90-22161
- Numerical simulation of supersonic unsteady flow using Euler equations [AIAA PAPER 90-0415] p 229 A90-22215
- Asymmetric separated flows at supersonic speeds [AIAA PAPER 90-0595] p 230 A90-22233
- Comparison of thin and full viscous shock layer models in the problem of supersonic flow of a viscous gas past blunt cones p 231 A90-22396
- Mean and pulse characteristics of supersonic flow in a wind tunnel with a honeycomb nozzle p 231 A90-22421
- Characteristics of turbulent separation flows on a porous surface under conditions of injection p 231 A90-22422
- Unsteady transonic aerodynamics of oscillating airfoils in supersonic freestream p 232 A90-23277
- Unsteady supersonic computations of arbitrary wing-body configurations including external stores p 232 A90-23278
- Leading- and trailing-edge flaps on supersonic delta wings p 233 A90-23285
- Numerical method for the flow of an ideal fluid on a plane with subsonic and supersonic regions p 233 A90-23362
- Transfer of the atomic ion energy of supersonic flow of a partially dissociated gas to a solid surface p 234 A90-23432
- Some aspects of the numerical modeling of supersonic flow past flight vehicles p 293 A90-24048
- Pseudoshock and separated flow in rectangular ducts p 295 A90-24089
- Eigenvalue problem in the theory of flow past thin profiles at high supersonic velocity p 295 A90-24096
- Effect of the cross-sectional shape of a straight duct on supersonic flow stagnation p 296 A90-24110
- Calculation of supersonic flow past a wing/fuselage combination with the resolution of a compression shock from the wing p 297 A90-24138
- A method for calculating the location and intensity of a conical head shock on the lower surface of a delta wing with supersonic edges p 297 A90-24139
- Aerodynamic characteristics of thin bodies moving in a gas with shock waves p 297 A90-24140
- Effect of similarity parameters on the aerodynamic quality and moment characteristics of a supersonic wing with blunt edges p 298 A90-24150
- Wing-fuselage interference regimes at supersonic flight velocities p 298 A90-24155
- Using third-fourth order compact schemes for calculating gas flows in nozzles with high supersonic M numbers on the basis of simplified Navier-Stokes equations p 299 A90-24157
- Calculation of flow past flight vehicles of complex configurations at high supersonic Mach numbers using the hypersonic theory of small perturbations p 299 A90-24158
- Determination of pressure and heat flow on the front surface of smooth blunt bodies p 299 A90-24166
- Effect of a recess on the aerodynamic characteristics of very blunt bodies at supersonic velocities p 299 A90-24167
- Shock sensitivity in parabolized Navier-Stokes solution of high angle-of-attack supersonic flow p 302 A90-25280
- Numerical study of three methods for solving reacting flows p 305 A90-25804
- Unfolding of double-zero eigenvalue bifurcations for supersonic flow past a pitching wedge p 347 A90-25995
- Efficient method for computing transonic and supersonic flows about aircraft p 307 A90-26132
- Application of multiple grids topology to supersonic internal/external flow interactions p 308 A90-26135
- Instabilities of supersonic shear flows [AIAA PAPER 90-0712] p 314 A90-26983
- A numerical study of transverse jets into supersonic flows and influence of pressure waves [AIAA PAPER 90-0733] p 314 A90-26985
- Newtonian flow over oscillating two-dimensional airfoils at moderate or large incidence p 383 A90-27976
- Droplet impaction on a supersonic wedge - Consideration of similitude p 400 A90-27986
- Numerical solution of the problem of supersonic flow of an ideal gas past a trapezoidal wedge p 386 A90-28980
- Aerodynamic quality of a plane delta wing with blunted edges at large supersonic flow velocities p 387 A90-28991
- Laminar separated flow on a biconical body at high supersonic velocities p 387 A90-28992
- Calculation of the drag of fuselage tail sections of different shapes in supersonic flow of a nonviscous gas p 388 A90-29182
- Combined effect of viscosity and bluntness on the aerodynamic efficiency of a delta wing in flow with a high supersonic velocity p 388 A90-29184
- Wall pressure fluctuation spectra in supersonic flow past a forward facing step p 388 A90-29194
- Reduced size first-order subsonic and supersonic aerodynamic modeling [AIAA PAPER 90-1154] p 390 A90-29366
- Flutter analysis of composite panels in supersonic flow [AIAA PAPER 90-1180] p 450 A90-29379
- Stochastic flutter of a panel subjected to random in-plane forces. II - Two and three mode non-Gaussian solutions [AIAA PAPER 90-0986] p 451 A90-29399
- The effect of walls on a spatially growing supersonic shear layer p 393 A90-29591
- Entry of a flexible airfoil into a vertical gust p 470 A90-32552
- Calculation of unsteady subsonic and supersonic flow about oscillating wings and bodies by new panel methods p 472 A90-33359
- Unsteady aerodynamic forces of oscillating supersonic/hypersonic wings with attached shock waves p 473 A90-33363
- Further studies of harmonic gradient method for supersonic aerodynamic applications p 473 A90-33410
- Non-axisymmetric viscous lower-branch modes in axisymmetric supersonic flows p 474 A90-33509
- A numerical method for calculating supersonic flows of a viscous gas p 476 A90-34672
- On a lifting line theory for supersonic flow. II - A supersonic lifting line theory for wings p 477 A90-34817
- On an extension of the Kutta-Joukowski theorem to the supersonic regime p 477 A90-34819
- Shock-fitting method for two-dimensional inviscid, steady supersonic flows in ducts p 477 A90-34864
- Dynamic stall of a constant-rate pitching airfoil p 553 A90-35754
- The inviscid axisymmetric stability of the supersonic flow along a circular cylinder p 554 A90-35916
- Effectiveness of passive devices for axisymmetric base drag reduction at Mach 2 p 555 A90-36184
- Structure of a reattaching supersonic shear layer p 555 A90-36252
- Implicit flux-split schemes for the Euler equations p 602 A90-36254
- Large-scale structure in a supersonic slot-injected flowfield p 602 A90-36265
- Oscillation of circular shock wave p 557 A90-36465
- A numerical study of supersonic flow over a compression corner with different incoming boundary-layer profiles [AIAA PAPER 90-1453] p 561 A90-38612
- Numerical simulation of confined, spatially-developing mixing layers - Comparison to the temporal shear layer [AIAA PAPER 90-1462] p 562 A90-38619
- Experimental investigation of GDL diffusers [AIAA PAPER 90-1512] p 563 A90-38659
- A locally implicit scheme for 3-D compressible viscous flows [AIAA PAPER 90-1525] p 563 A90-38670
- Stability limits for three-dimensional supersonic boundary layers [AIAA PAPER 90-1528] p 564 A90-38673
- Supersonic flow over an axisymmetric backward-facing step [AIAA PAPER 90-1580] p 566 A90-38717
- Enthalpy damping for high Mach number Euler solutions [AIAA PAPER 90-1585] p 566 A90-38720
- Injectant mole fraction measurements of transverse injection in constant area supersonic ducts [AIAA PAPER 90-1632] p 587 A90-38761
- Numerical solution of the problem of supersonic flow of a viscous gas past a concave conical wing p 619 A90-39465
- The problem of supersonic flow past a thin wing of finite span with fully subsonic leading edges p 620 A90-39519
- Aerodynamic detuning for control of supersonic rotor forced response [AIAA PAPER 90-2018] p 621 A90-40596
- Strake camber and thickness design procedure for low alpha supersonic flow p 622 A90-40678
- Determination of aerodynamic sensitivity coefficients based on the transonic small perturbation formulation p 622 A90-40682
- Numerical simulation of the growth of instabilities in supersonic free shear layers p 623 A90-40941
- Three dimensional transonic and supersonic flow prediction in axi-vented nozzles using a finite volume method [AIAA PAPER 90-2026] p 624 A90-41989
- Inviscid and viscous flows in transonic and supersonic cascades using an implicit upwind relaxation algorithm [AIAA PAPER 90-2128] p 625 A90-42034
- Radio frequency (RF) heated supersonic flow laboratory [AIAA PAPER 90-2469] p 673 A90-42186
- A new Lagrangian method for steady supersonic flow computation. I - Godunov scheme p 631 A90-42506
- On the instabilities of supersonic mixing layers - A high-Mach-number asymptotic theory p 702 A90-42644
- Two- and three-dimensional effects in the supersonic mixing layer [AIAA PAPER 90-1978] p 703 A90-42708
- A validation study of the Spark Navier Stokes code for nonreacting scramjet combustor flowfields [AIAA PAPER 90-2360] p 706 A90-42784
- Supersonic/hypersonic laminar/turbulent transition p 706 A90-42872
- Subharmonic instability of compressible boundary layers p 706 A90-44005
- Mixing and combustion enhancement in supersonic reacting flows p 744 A90-44410
- Development of supersonic and hypersonic Euler solvers using shock fitting in two and three dimensions p 707 A90-44426
- Numerical study of heat transfer for unsteady viscous supersonic blunt body flows p 707 A90-44432
- Shock-fitting in three space dimensions p 707 A90-44434
- Development and application of a fractional-step method for the solution of transonic and supersonic flow problems p 709 A90-44461
- The potential approximation in the theory of conical flows p 710 A90-44930
- Experimental investigation of turbulence in a supersonic flow p 710 A90-44931
- Aerodynamic drag of a pair of bodies in transonic and supersonic flow p 710 A90-44935
- Supersonic flow computations for an ASTOVL aircraft configuration [AIAA PAPER 90-2997] p 787 A90-45847
- Numerical investigation of laminar separated viscous trailing-edge flow using triple-deck theory [AIAA PAPER 90-3046] p 792 A90-45883
- An experimental investigation of supersonic flow over two cavities in tandem [AIAA PAPER 90-3087] p 795 A90-45901
- Navier-Stokes simulation of unsteady supersonic cavity flowfield with passive control [AIAA PAPER 90-3101] p 796 A90-45913
- Calculation of the heat flux at a three-dimensional critical point in supersonic flow past a body p 803 A90-46536
- An experimental study of a supersonic gas ejector p 851 A90-46546

Interference between a vortex filament and shock waves in free flow and in nonisobaric jets p 804 A90-46550
Calculation of three-dimensional flow past a plane supersonic air intake at angles of attack and sideslip p 805 A90-46573

Gasdynamic characteristics of a plane or axisymmetric nozzle with a rectilinear generatrix of the supersonic section p 805 A90-46575
Numerical study of interaction of a jet with a supersonic cross flow p 808 A90-47300

Effect of the Mach number and shape of the front part of the obstacle on the separation zone length in supersonic flow p 903 A90-50816

A proper orthogonal decomposition of a simulated supersonic shear layer p 904 A90-51009

Theoretical prediction of pressure distribution on wedged delta wing at higher supersonic Mach numbers and its agreement with experimental results p 907 A90-51537

Prediction of pressure distribution on optimum-optimum delta wing at higher angles of attack in supersonic flow and its agreement with experimental results p 907 A90-51538
The formation of vortex streets in supersonic flows p 907 A90-51539

Supersonic flow computations over aerospace configurations using an Euler marching solver [NASA-CR-4085] p 19 N90-10012
Additions and corrections to SUPER: A program for calculating steady and oscillatory supersonic flow over a thin wing, tail plane and fin [AD-A211771] p 90 N90-12501

The effects of wall surface defects on boundary-layer transition in quiet and noisy supersonic flow p 94 N90-12556
Multigrid solution method for the Euler equations [PB89-219463] p 138 N90-13116
Laser applications in supersonic unsteady flow p 212 N90-13344

Computation of Navier-Stokes equations for three-dimensional flow separation [NASA-TM-102266] p 172 N90-13353
Application of a two-dimensional unsteady viscous analysis code to a supersonic throughflow fan stage [NASA-TM-4141] p 192 N90-13387
A computational analysis of the transonic flow field of two-dimensional minimum length nozzles p 173 N90-14194

Skin friction measurements by laser interferometry in supersonic flows p 317 N90-17557
Opportunities for improved understanding of supersonic and hypersonic flows p 318 N90-17566
Numerical simulation of supersonic free shear layers [AD-A216289] p 320 N90-17579

Experimental investigation of a chemical laser cavity flowfield [AD-A216398] p 372 N90-18038
Experiments on the unsteady flow in a supersonic compressor stage p 427 N90-18422
Interaction of an oblique shock wave with supersonic flow over a blunt body p 398 N90-19197
Numerical simulations of supersonic flow through oscillating cascade sections [NASA-TM-103100] p 478 N90-20051

Compression pylon [NASA-CASE-LAR-13777-1] p 498 N90-20078
A two-dimensional unsteady analysis for transonic and supersonic cascade flows p 480 N90-20955
Exhaust nozzles for propulsion systems with emphasis on supersonic cruise aircraft [NASA-RP-1235] p 516 N90-21037
Supersonic flow computations for an ASTOVL aircraft configuration, phase 2, part 2 [NASA-CR-4284] p 610 N90-22746

STARS: An integrated general-purpose finite element structural, aeroelastic, and aeroservoelastic analysis computer program [NASA-TM-101709] p 689 N90-23768

A review of instability and noise propagation in supersonic flows [NASA-CR-186800] p 717 N90-25112

An experimental and theoretical investigation of the flow over plane delta wings with supersonic leading edges [LR-588] p 717 N90-25114

Supersonic reacting internal flow fields [NASA-TM-103480] p 767 N90-26094

Modeling of supersonic reacting flow fields p 855 N90-26898

Flame extinction in compressible flow p 883 N90-26899

Turbulent reacting flows and supersonic combustion [AD-A221793] p 875 N90-26933

Study of the compressibility effects on the turbulence of supersonic drags [ETN-90-97448] p 817 N90-27661

SUPERSONIC FLUTTER

Improved double linearization method for prediction of mean loading effects on subsonic and supersonic cascade flutter p 41 A90-11795

Application of the double linearization theory to three-dimensional subsonic and supersonic cascade flutter p 50 A90-12638

Flutter analysis of composite panels using high-precision finite elements p 207 A90-16725

Aeroelastic detuning for stability enhancement of unstalled supersonic flutter p 189 A90-17462

Stochastic flutter of a panel subjected to random in-plane forces. I - Two mode interaction p 444 A90-27992

Finite element two-dimensional panel flutter at high supersonic speeds and elevated temperature [AIAA PAPER 90-0982] p 450 A90-29372

Aeroelastic instabilities in aircraft engines - Application to a SNECMA fan stage p 584 A90-35174

Supersonic flutter of shear deformable laminated composite flat panels p 683 A90-41104

SUPERSONIC INLETS

High speed inlet testing in the NAVSWC wind tunnels [AIAA PAPER 90-1412] p 595 A90-37949

Experimental investigation of terminal shock sensors in mixed-compression inlets [AIAA PAPER 90-1931] p 681 A90-40560

Aerodynamic detuning for control of supersonic rotor forced response [AIAA PAPER 90-2018] p 621 A90-40596

A numerical investigation of supersonic inlet using implicit TVD scheme [AIAA PAPER 90-2135] p 621 A90-40612

The normal shock generator - An inlet throat region research apparatus for high Mach applications [AIAA PAPER 90-1930] p 759 A90-42698

Transient behavior of supersonic flow through inlets [AIAA PAPER 90-2130] p 704 A90-42734

Analysis of shock interactions and flow structure in high speed inlets [AIAA PAPER 90-2132] p 704 A90-42735

New experimental results on the origin and structure of Ferri and Dailey instabilities ('buzz') p 906 A90-51507

A method for the prediction of supersonic compressor blade performance [CUED/A-TURBO/TR-126] p 344 N90-17634

Comparison of 3-D viscous flow computations of Mach 5 inlet with experimental data [NASA-TM-102518] p 510 N90-20090

Numerical simulations of the structure of supersonic shear layers [AD-A224164] p 960 N90-29587

SUPERSONIC JET FLOW

A numerical method for calculating supersonic nonisobaric jets p 84 A90-14566

The calculation of under-expanded impinging jets p 147 A90-16782

Upwind adaptive finite element investigations of the two-dimensional reactive interaction of supersonic gaseous jets p 209 A90-18264

Supersonic jet noise reduction by a porous single expansion ramp nozzle [AIAA PAPER 90-0366] p 219 A90-19815

Heat transfer in supersonic coaxial reacting jets p 601 A90-35394

Perturbations of higher modes in a supersonic jet p 619 A90-39516

Supersonic rectangular isothermal shrouded jets [AIAA PAPER 90-2028] p 621 A90-40599

Application of a new adaptive grid for aerodynamic analysis of shock containing single jets [AIAA PAPER 90-2025] p 624 A90-41988

Sound generation by a supersonic aerofoil cutting through a steady jet flow p 781 A90-42638

Surface flow on a flat plate induced by a supersonic jet exhausting normally into a low speed crossflow [AIAA PAPER 90-3011] p 789 A90-45860

Effect of the nonuniformity of external supersonic flow and nozzle deflection angle on the base pressure behind an axisymmetric body with a single supersonic jet p 802 A90-46486

A review of instability and noise propagation in supersonic flows [NASA-CR-186800] p 717 N90-25112

SUPERSONIC NOZZLES

Transonic flow in throat region of supersonic nozzles p 149 A90-16799

Dissipation thrust losses due to distortions of the jet nozzle profile p 254 A90-23405

Numerical calculation of the jet-interaction induced separation with respect to thrust vector control p 584 A90-35228

Heat transfer in supersonic coaxial reacting jets p 601 A90-35394

Advanced Mach 3.5 Axisymmetric Quiet Nozzle [AIAA PAPER 90-1592] p 566 A90-38727

Flow and acoustic features of a supersonic tapered nozzle [AIAA PAPER 90-1599] p 567 A90-38731

Formation of shocks within axisymmetric nozzles [AIAA PAPER 90-1655] p 570 A90-38782

The sensitivity of near-field acoustics to the orientation of twin two-dimensional supersonic nozzles [AIAA PAPER 90-2149] p 625 A90-42045

Nozzle design optimization by method-of-characteristics [AIAA PAPER 90-2024] p 741 A90-42719

Profiling of the supersonic components of three-dimensional corrugated nozzles p 804 A90-46563

Geometrical factors influencing the flow field in a propulsive nozzle p 807 A90-46876

Study of the expansion of hydrocarbon-oxygen products through supersonic nozzle p 852 A90-46907

Supersonic nozzle design of arbitrary cross-section p 515 N90-21035

Exhaust nozzles for propulsion systems with emphasis on supersonic cruise aircraft [NASA-RP-1235] p 516 N90-21037

Supersonic wind tunnel nozzles: A selected, annotated bibliography to aid in the development of quiet wind tunnel technology [NASA-CR-4294] p 762 N90-26019

SUPERSONIC SPEED

Navier-Stokes computations of lee-side flows over delta wings p 153 A90-17978

Aerodynamic interference of prismatic engine nacelles with the wing at supersonic velocities p 294 A90-24078

Pseudoshock and separated flow in rectangular ducts p 295 A90-24089

Eigenvalue problem in the theory of flow past thin profiles at high supersonic velocity p 295 A90-24096

Project Falke - Performance of free flight tests in the supersonic, transonic, and subsonic regimes from balloons [DGLR PAPER 88-018] p 903 A90-50235

High temperature VSCF (Variable Speed Constant Frequency) generator system [AD-A210823] p 71 N90-10351

Supersonic aerodynamic characteristics of a proposed Assured Crew Return Capability (ACRC) lifting-body configuration [NASA-TM-4136] p 317 N90-17560

Hypersonic nozzle/afterbody performance at low Mach numbers [AD-A216223] p 319 N90-17575

A study of flows over highly-swept wings designed for maneuver at supersonic speeds [AD-A216837] p 399 N90-19202

An intensive procedure for the design of pressure-specified three-dimensional configurations at subsonic and supersonic speeds by means of a higher-order panel method p 500 N90-20982

High speed commercial transport fuels considerations and research needs [NASA-TM-102535] p 600 N90-21869

High speed civil transport [NASA-CR-186661] p 649 N90-23396

SUPERSONIC TEST APPARATUS

Laser induced fluorescence: Practical applications p 911 N90-29323

SUPERSONIC TRANSPORTS

Hypersonic aerospace sizing analysis for the preliminary design of aerospace vehicles p 247 A90-23276

European research and testing facilities requested for participation to SST/HST projects [ONERA, TP NO. 1990-12] p 351 A90-25358

SST/HST air traffic - Challenge for the future p 763 A90-44752

Pursuit of the high-speed civil transport [AIAA PAPER 90-1814] p 919 A90-51450

Revolutionary opportunities for materials and structures study [NASA-CR-179642] p 63 N90-10184

Study of high-speed civil transports [NASA-CR-4235] p 183 N90-13370

Supersonic through-flow fan engine and aircraft mission performance [NASA-TM-102304] p 516 N90-21038

Application of laminar flow control to supersonic transport configurations [NASA-CR-181917] p 719 N90-25944

The aerodynamic design of the oblique flying wing supersonic transport [NASA-CR-177552] p 923 N90-28540

SUPERSONIC TURBINES

An experimental study of tip clearance effects on the performance of an axial transonic turbine p 189 A90-17788

Effect of vane and blade numbers on performance of transonic turbine stage p 189 A90-17789

SUBJECT INDEX

Design and calculation of composite air-cooled blades in a highly-loaded transonic turbine p 189 A90-17790

Experimental investigation on composite air-cooled blades of highly-loaded transonic turbine p 189 A90-17793

Aerodynamic and heat transfer measurements on blading for a high rim-speed transonic turbine [ASME PAPER 89-GT-228] p 293 A90-23883

Experimental investigation of supersonic turbine performance [ASME PAPER 89-GT-238] p 342 A90-23888

Calculation of two- and three-dimensional flow in a transonic turbine cascade with particular regard to the losses [AIAA PAPER 90-1542] p 565 A90-38686

Investigation of unsteady flow through transonic turbine stage. I - Analysis [AIAA PAPER 90-2408] p 626 A90-42161

Application of 3-D flow analysis to the design of a high work transonic turbine p 628 A90-42395

Application of sweep to improve the efficiency of a transonic fan. I - Design [AIAA PAPER 90-1915] p 741 A90-42695

Analysis of transonic turbine rotor cascade flows using a finite-volume total variation diminishing (TVD) scheme [AIAA PAPER 90-2127] p 704 A90-42733

Revolutionary opportunities for materials and structures study [NASA-CR-179642] p 63 N90-10184

Aerodynamic and heat transfer measurements on blading for a high rim-speed transonic turbine [RAE-TM-P-1151] p 256 N90-15920

Influence of friction and separation phenomena on the dynamic blade loading of transonic turbine cascades [MITT-88-04] p 428 N90-19235

Supersonic through-flow fan engine and aircraft mission performance [NASA-TM-102304] p 516 N90-21038

SUPERSONIC WAKES

The effect of Mach number on the stability of a plane supersonic wake p 557 A90-36524

Linear instability of the supersonic wake behind a flat plate aligned with a uniform stream p 716 A90-45783

The formation of vortex streets in supersonic flows p 907 A90-51539

SUPERSONIC WIND TUNNELS

Mean and pulse characteristics of supersonic flow in a wind tunnel with a honeycomb nozzle p 231 A90-22421

An optical angle of attack sensor p 446 A90-28263

Aerothermodynamics and transition in high-speed wind tunnels at NASA Langley p 386 A90-28555

Aeronautical facility requirements into the 2,000's [AIAA PAPER 90-1375] p 594 A90-37926

Design and operational features of low-disturbance wind tunnels at NASA Langley for Mach numbers from 3.5 to 18 [AIAA PAPER 90-1391] p 594 A90-37936

High speed inlet testing in the NAVSWC wind tunnels [AIAA PAPER 90-1412] p 595 A90-37949

Wind tunnel testing techniques on aerodynamic effects with small asymmetry [AIAA PAPER 90-1400] p 560 A90-38490

Advanced Mach 3.5 Axisymmetric Quiet Nozzle [AIAA PAPER 90-1592] p 566 A90-38727

Investigation of supersonic mixing layers p 623 A90-40926

Experimental investigation of turbulence in a supersonic flow p 710 A90-44931

An aerofoil testing technique for low supersonic speeds in an adaptive flexible-walled wind tunnel [AIAA PAPER 90-3086] p 795 A90-45900

Euler analysis comparison with LDV data for an advanced counter-rotation propfan at cruise [AIAA PAPER 90-3033] p 903 A90-50637

An LDA investigation of the normal shock wave boundary layer interaction p 908 A90-52618

At a depth of 500 meters - The TU Dresden supersonic wind tunnel p 937 A90-52700

Design and fabrication requirements for low noise supersonic/hypersonic wind tunnels p 122 N90-12555

Volumetric analysis by spontaneous Raman diffusion in a supersonic wind tunnel [ISL-R-109/88] p 95 N90-12564

Comparison of 3-D viscous flow computations of Mach 5 inlet with experimental data [NASA-TM-102518] p 510 N90-20090

DURIP optical equipment for high-speed viscous-inviscid interaction research [AD-A217772] p 540 N90-20345

Euler analysis comparison with LDV data for an advanced counter-rotation propfan at cruise [NASA-TM-103249] p 720 N90-25946

Supersonic wind tunnel nozzles: A selected, annotated bibliography to aid in the development of quiet wind tunnel technology [NASA-CR-4294] p 762 N90-26019

SUPERSONICS

Aerodynamic development perspective for traffic aeroplanes [DGLR-89-141] p 637 N90-24260

Integral-equation methods in steady and unsteady subsonic, transonic and supersonic aerodynamics for interdisciplinary design [NASA-TM-102677] p 716 N90-25110

SUPPORT INTERFERENCE

Magnetic suspension - Today's marvel, tomorrow's tool p 262 A90-23697

An experimental investigation of support strut interference on a three-percent fighter model at high angles of attack [AD-A219793] p 631 N90-23353

Subsonic sting interference on the aerodynamic characteristics of a family of slanted-base ogive-cylinders [NASA-CR-4299] p 633 N90-24242

SUPPORT SYSTEMS

An integrated diagnostics approach to embedded and flight-line support systems p 460 A90-30767

Logistics support planning for standardized avionics p 383 A90-30809

Next-generation automatic test equipment for military support p 767 A90-42667

The role of bearing support stiffness anisotropy in suppression of rotordynamic instability p 879 A90-46215

SUPPORTS

Wind tunnel support system effects on a fighter aircraft model at Mach numbers from 0.6 to 2.0 [AD-A210614] p 19 N90-10010

Design of a high angle of attack robotic sting mount for tests in a low speed wind tunnel [AD-A218105] p 526 N90-20099

Sting-support interference on afterbody drag at transonic speeds [NAL-TM-EA-8902] p 909 N90-28492

SUPPRESSORS

Experimental investigation to suppress flow-induced pressure oscillations in open cavities [AD-A216285] p 320 N90-17578

SURFACE COOLING

Studies of gas turbine heat transfer airfoil surfaces and end-wall cooling effects [AD-A212451] p 117 N90-12620

SURFACE CRACKS

In process failure investigations in aeronautics p 181 A90-18489

Definition of research needs to address airport pavement distress in cold regions [DOT/FAA/DS-89/13] p 59 N90-10896

SURFACE DEFECTS

A study of the nonlinear deformation of a shell of revolution with a surface bend p 129 A90-14574

Electromagnetic dent removal for aircraft repair [SAE PAPER 890923] p 286 A90-24689

A study on flaw detection method for CFRP composite laminates. I - The measurement of crack extension in CFRP composites by electrical potential method p 441 A90-28003

The effects of wall surface defects on boundary-layer transition in quiet and noisy supersonic flow p 94 N90-12556

New aspects in aircraft inspection using eddy current methods p 886 N90-28085

SURFACE FINISHING

Safer primers from 3M p 204 A90-17925

Rapid low-temperature cure patching system for field repair p 467 A90-31529

Plastic media blast (PMB) paint removal from composites p 945 A90-50162

Design and fabrication requirements for low noise supersonic/hypersonic wind tunnels p 122 N90-12555

Fretting fatigue strength of Ti-6Al-4V at room and elevated temperatures and ways of improving it p 952 N90-28709

SURFACE GEOMETRY

Collocation methods and lifting-surfaces p 9 A90-12023

The warping restraint effect in the critical and subcritical static aeroelastic behavior of swept forward composite wing structures [SAE PAPER 891056] p 129 A90-14358

Effect of detailed surface geometry on riblet drag reduction performance p 622 A90-40693

SURFACE IONIZATION

Transfer of the atomic ion energy of supersonic flow of a partially dissociated gas to a solid surface p 234 A90-23432

SURFACE TEMPERATURE

SURFACE NAVIGATION

GPS: Arrival in the fleet - A GPS AN/SRN-25 receiver assessment p 97 A90-13989

Ground navigation in airport traffic p 242 A90-21725

A surveillance 360 deg television orientation and ranging system as an aid to collision avoidance p 577 A90-36922

SURFACE NOISE INTERACTIONS

Application of active noise control to model propeller noise p 548 A90-34091

The validation and application of a rotor acoustic prediction computer program [NASA-TM-101794] p 895 N90-27465

SURFACE PROPERTIES

Dynamic analysis of lifting surfaces of small relative thickness in the case of finite displacements p 129 A90-14560

Balance model of the perfectly stirred reactor with the discontinuity surface p 125 A90-14652

Effects of thermochemistry, nonequilibrium, and surface catalysis on the design of hypersonic vehicles p 224 A90-21159

Surface property improvement in titanium alloy gas turbine components through ion implantation p 953 N90-28713

SURFACE REACTIONS

Numerical study of three methods for solving reacting flows p 305 A90-25804

Regression and combustion characteristics of boron containing fuels for solid fuel ramjets p 858 N90-27928

High Temperature Surface Interactions [AGARD-CP-461] p 951 N90-28698

SURFACE ROUGHNESS

Surface roughness effect on the aerodynamic characteristics of a blunt body p 16 A90-12740

Convective heat transfer measurements from a NACA 0012 airfoil in flight and in the NASA Lewis Icing Research Tunnel [AIAA PAPER 90-0199] p 272 A90-22180

Fatigue damage of an aircraft due to movement on the airfield p 247 A90-23352

Pressure loss and heat transfer in channels roughened on two opposed walls [ASME PAPER 89-GT-86] p 358 A90-23805

A study of ice shape prediction methodologies and comparison with experimental data [AIAA PAPER 90-0753] p 322 A90-26986

Surface roughness measurements on gas turbine blades [ASME PAPER 89-GT-285] p 508 A90-33559

Flow over a leading edge with distributed roughness p 703 A90-42646

Convective heat transfer measurements from a NACA 0012 airfoil in flight and in the NASA Lewis Icing Research Tunnel [NASA-TM-102448] p 213 N90-13750

Heat transfer measurements from a NACA 0012 airfoil in flight and in the NASA Lewis icing research tunnel [NASA-CR-4278] p 399 N90-19203

Investigation of surface water behavior during glaze ice accretion p 485 N90-20927

Mechanical paint removal techniques for aircraft structures [IAR-89-23] p 773 N90-25254

Estimation of power spectral density of runway roughness [NAL-TR-1037] p 939 N90-29411

SURFACE ROUGHNESS EFFECTS

Effect of the roughness of deposits in a compressor cascade on the flow lag angle p 84 A90-14578

Local heat transfer on a flat surface roughened with broken ribs p 534 A90-32169

Instability and susceptibility of a boundary layer in the vicinity of two-dimensional surface inhomogeneities p 535 A90-32675

An annular gas seal analysis using empirical entrance and exit region friction factors [ASME PAPER 89-TRIB-46] p 537 A90-33555

Test results for turbulent annular seals, using smooth rotors and helically grooved stators [ASME PAPER 89-TRIB-11] p 537 A90-33556

Effect of surface grooves on base pressure for a blunt trailing-edge airfoil p 556 A90-36280

Aerodynamic effects of body roughness [AIAA PAPER 90-2850] p 712 A90-45168

The effects of wall surface defects on boundary-layer transition in quiet and noisy supersonic flow p 94 N90-12556

Modeling of surface roughness effects on glaze ice accretion p 485 N90-20925

SURFACE TEMPERATURE

Applications of infra-red thermography in a hypersonic blowdown wind tunnel p 438 A90-28300

Force balance errors due to temperature changes in ETW p 539 A90-34231
Thermal protection systems for hypersonic transport vehicles [SAE PAPER 901306] p 882 A90-49358
Low speed flowfield characterization by infrared measurements of surface temperatures p 317 N90-17556

Real-time aerodynamic heating and surface temperature calculations for hypersonic flight simulation [NASA-TM-4222] p 959 N90-28815

SURFACE TREATMENT

Aluminum surface preparation for aircraft field repair p 764 A90-43204
The surface pretreatment of aluminium-lithium alloys for structural bonding p 881 A90-47118
Chrome free electrolytic deoxidizer for aluminum p 956 A90-50216

SURFACE WATER

Investigation of surface water behavior during glaze ice accretion p 485 N90-20927

SURGES

An investigation of artificial compressor surge p 11 A90-12526
A study on surge and rotating stall in axial compressors - A summary of the measurement and fundamental analysis method p 87 A90-16105
An experimental study of fault propagation in a jet-engine controller [NASA-CR-181335] p 665 N90-23401

SURVEILLANCE

Rotorcraft low altitude CNS benefit/cost analysis: Rotorcraft operations data [DOT/FAA/DS-89/9] p 141 N90-12406
Control outside of independent surveillance coverage operational concept [AD-A214163] p 243 N90-15090
Aviation security: Corrective actions underway, but better inspection guidance still needed. Report to the Chairwoman, Government Activities and Transportation Subcommittee, Committee on Government Operations, House of Representatives [GAO/RCED-88-160] p 635 N90-23367

SURVEILLANCE RADAR

Evaluating the feasibility of a radar separation minimum for a long-range SSR p 25 A90-10240
Radar systems --- Book p 208 A90-17305
Air traffic control development at Lincoln Laboratory p 240 A90-21378

The Mode S beacon radar system p 241 A90-21379
Parallel runway monitor p 241 A90-21382
Wind shear detection with airport surveillance radars p 241 A90-21387
Mode S system design and architecture p 330 A90-25569

ARSR-4 long range radar will upgrade U.S. en-route surveillance p 403 A90-27925
The TVD 900 - A modern signal processing applied to primary civilian ATC radar p 638 A90-41034
Design of new Polish primary radars AVIA DM/CM p 638 A90-41035

Performances and new surveillance possibilities in SSR - Mode S p 639 A90-41036
Applications of Mode S secondary surveillance radar to civil air traffic control - Studies, experiments, and policy of the French Direction de la Navigation Aérienne p 639 A90-41056

Experiments on Mode S secondary surveillance radar - The participation of the French Direction de la Navigation Aérienne in the European effort p 639 A90-41057
Unmanned helicopters for battlefield and maritime surveillance p 920 A90-51899

ASR-9 weather channel test report [AD-A211749] p 133 N90-11934
Aircraft Reply and Interference Environment Simulator (ARIES) hardware principles of operation, Volume 2: Appendixes [DOT/FAA/CT-TN88/4-2] p 135 N90-12781

Aircraft Reply and Interference Environment Simulator (ARIES) hardware principles of operation, volume 1 [DOT/FAA/CT-TN88/4-1] p 135 N90-12782
Fine resolution errors in secondary surveillance radar altitude reporting amongst aircraft transmitting the conspicuity codes 4321 and 4322 [RSRE-88004] p 135 N90-12816

SURVEYS

A survey of nonuniform inflow models for rotorcraft flight dynamics and control applications p 590 A90-38521
Laser anemometer measurements in a transonic axial-flow fan rotor [NASA-TP-2879] p 73 N90-11245
Ice runways near the South Pole [AD-A211606] p 133 N90-11908

A survey of nonuniform inflow models for rotorcraft flight dynamics and control applications [NASA-TM-102219] p 260 N90-15938

Social survey findings on en route noise annoyance issues p 698 N90-24868

An aircraft noise study in Norway p 698 N90-24872
Aviation safety: Conditions within the air traffic control work force. Fact sheet for congressional requesters [GAO/RCED-89-113FS] p 724 N90-25958

Aviation safety: Serious problems continue to trouble the air traffic control work force. Report to congressional requesters [GAO/RCED-89-112] p 724 N90-25959

Facilities involved in adaptive wall research p 871 N90-26840

SURVIVAL

Escape and survival following helicopter ditching - Training aspects p 722 A90-44658

Escape and survival following helicopter ditching - Research aspects p 722 A90-44659

The human factors relating to escape and survival from helicopters ditching in water [AGARD-AG-305(E)] p 176 N90-13358

Aircraft fires: A study of transport accidents from 1975 to the present p 324 N90-17583
Implications of Advanced Technologies for Air and Spacecraft Escape [AGARD-CP-472] p 483 N90-20054

Aircraft crash survival design guide. Volume 1: Design criteria and checklists [AD-A218434] p 575 N90-22545

Aircraft crash survival design guide. Volume 4: Aircraft seats, restraints, litters, and cockpit/cabin dealthalization [AD-A218437] p 575 N90-22548

Aircraft crash survival design guide. Volume 5: Aircraft postcrash survival [AD-A218438] p 575 N90-22549

SUSPENDING (HANGING)

Calculation of the vibrations of aircraft with elastic suspended loads p 345 A90-24171
Equations of motion of slung load systems with results for dual lift [NASA-TM-102246] p 349 N90-17641

SWEPT ANGLE

Modal characteristics of swept plate flutter models p 207 A90-16962

An experimental investigation of sweep-angle influence on delta-wing flows [AIAA PAPER 90-0383] p 228 A90-22210

Numerical simulation of the effects of variation of angle of attack and sweep angle on vortex breakdown over delta wings [AIAA PAPER 90-3000] p 788 A90-45850

Induced drag of wings with highly swept and tapered wing tips [AIAA PAPER 90-3062] p 794 A90-45896

Experimental investigation of wingtip aerodynamic loading p 808 A90-46945
Computational design of low aspect ratio wing-winglet configurations for transonic wind-tunnel tests [NASA-CR-181939] p 316 N90-17539

SWEPT EFFECT

Parametric studies of advanced turboprops p 253 A90-21225

Connection between leading-edge sweep, vortex lift, and vortex strength for delta wings p 554 A90-35770

Application of sweep to improve the efficiency of a transonic fan. I - Design [AIAA PAPER 90-1915] p 741 A90-42695

Noise generation by swept cascade p 895 A90-49486

Design of the low-speed NLF(1)-0414F and the high-speed HSNLF(1)-0213 airfoils with high-lift systems p 93 N90-12540

Experimental and theoretical investigation of boundary-layer instability mechanisms on a swept leading edge at Mach 3.5 p 94 N90-12557

SWELLING

Equilibrium swelling of elastomeric materials in solvent environments [DE90-010164] p 678 N90-24430

SWEPT FORWARD WINGS

The warping restraint effect in the critical and subcritical static aeroelastic behavior of swept forward composite wing structures [SAE PAPER 891056] p 129 A90-14358

The static aeroelastic behavior of sweptforward composite wing structures taking into account their warping restraint effect p 210 A90-18407

Aerodynamic characteristics of forward sweep [AIAA PAPER 90-3041] p 792 A90-45879

Exploratory wind tunnel investigation of the stability and control characteristics of a three-surface, forward-swept wing advanced turboprop model [AIAA PAPER 90-3074] p 797 A90-45920

Analytical studies of the transonic flutter of aircraft p 860 A90-46577

High alpha --- angles of attack of fighter aircraft p 902 A90-52575

An in-flight investigation of ground effect on a forward-swept wing airplane [NASA-TM-101708] p 175 N90-14202

Applications of modern control theory synthesis to a super-augmented aircraft [AD-A215431] p 336 N90-16753

X-29A aircraft structural loads flight testing [NASA-TM-101715] p 416 N90-19225

A look at tomorrow today p 921 N90-28524

An in-flight investigation of ground effect on a forward-swept wing airplane p 922 N90-28533

SWEPT WINGS

The water tunnel test of delaying vortex breakdown over a delta wing using supplements p 2 A90-10346

In-flight boundary-layer transition measurements on a swept wing p 17 A90-13017

Structural optimization of lifting surfaces with divergence and control reversal constraints p 127 A90-13770

Recent Navier/Stokes calculations in applications p 85 A90-15227

A viscous package for attached and separated flows on swept and tapered wings p 146 A90-16771

Curvature effects on the stability of laminar boundary layers on swept wings p 148 A90-16788

Leading edge contamination and relaminarisation on a swept wing at incidence p 148 A90-16789

Prediction of transition on airfoils with separation bubbles, swept wings and bodies of revolution at incidence p 148 A90-16790

Experimental transition and boundary-layer stability analysis for a slotted swept laminar flow control airfoil p 148 A90-16793

Experiments in swept-wing transition p 149 A90-16794

Modal characteristics of swept plate flutter models p 207 A90-16962

Perturbations of a three-dimensional boundary layer produced by body irregularities p 150 A90-17107

Direct search method to aeroelastic tailoring of a composite wing under multiple constraints p 208 A90-17865

Full 3D iterative solution of transonic flow for a swept wing test channel p 160 A90-19431

Experimental and numerical investigation of the flow in the core of a leading edge vortex [AIAA PAPER 90-0384] p 165 A90-19826

The influence of sweep on dynamic stall produced by a rapidly pitching wing [AIAA PAPER 90-0581] p 230 A90-22231

Calculation of nonseparated transonic flow past swept wings with allowance for viscosity p 294 A90-24079

An experimental study of the effect of the Reynolds number on flow past a swept wing at transonic velocities p 294 A90-24082

A method for calculating the stiffness characteristics of large-aspect-ratio wings with anisotropic panels in accordance with strength and aileron efficiency requirements p 334 A90-24161

Reductions in induced drag by the use of aft swept wing tips p 299 A90-24342

Swept wing ice accretion modeling [AIAA PAPER 90-0756] p 300 A90-25042

Experimental investigation of three-dimensional turbulent boundary layers on 'infinite' swept curved wings p 303 A90-25589

A generalized lifting-line theory for curved and swept wings p 303 A90-25597

Fourth-order accurate three-dimensional compressible boundary-layer calculations p 308 A90-26136

The flowfields of bursting vortices over moderately swept delta wings [AIAA PAPER 90-0599] p 314 A90-26969

Use of liquid crystals for qualitative and quantitative 2-D studies of transition and skin friction p 446 A90-28259

Calculation of the effect of the engine nacelle on transonic flow past a wing p 387 A90-28990

Navier-Stokes computations on swept-tapered wings, including flexibility [AIAA PAPER 90-1152] p 389 A90-29364

Experimental transonic flutter characteristics of supersonic cruise configurations [AIAA PAPER 90-0979] p 390 A90-29369

Static aeroelastic behavior of an adaptive laminated piezoelectric composite wing [AIAA PAPER 90-1078] p 412 A90-29386

Aeroservoelastic tailoring for lateral control enhancement p 516 A90-33060

Further studies of harmonic gradient method for supersonic aeroelastic applications p 473 A90-33410

- Measured aerodynamic performance of a swept wing with a simulated ice accretion
[AIAA PAPER 90-0490] p 557 A90-37063
- Laminar flow test installation in the Boeing Research Wind Tunnel
[AIAA PAPER 90-1425] p 559 A90-37962
- Stability limits for three-dimensional supersonic boundary layers
[AIAA PAPER 90-1528] p 564 A90-38673
- Measurement of crossflow vortices, attachment-line flow, and transition using microthin hot films
[AIAA PAPER 90-1636] p 607 A90-38765
- Various sources of wing rock
p 622 A90-40679
- Experimental study of the turbulent boundary layer on a transport wing in subsonic flow
p 709 A90-44728
- On aerodynamic characteristics of canard in canard-forward-swept wing configuration
p 709 A90-44833
- The development of crossflow vortices on a 45 degree swept wing
[SAE PAPER 892245] p 713 A90-45452
- 2D vs. 3D - Selection of pressure distributions to delay separation on wings
[AIAA PAPER 90-3026] p 790 A90-45668
- Induced drag of wings with highly swept and tapered wing tips
[AIAA PAPER 90-3062] p 794 A90-45896
- Experimental investigation of wingtip aerodynamic loading
p 808 A90-46945
- Modelling free vortex flow on planar swept wing
p 810 A90-48079
- Lift and pitching moment measurements on a swept tapered wing in oscillatory vertical gusts
p 811 A90-48089
- Wave interactions in a three-dimensional attachment-line boundary layer
p 811 A90-48715
- X-29 high angle-of-attack flight testing - Program status
[AIAA PAPER 90-3303] p 837 A90-48885
- Parametric analysis of swept-wing geometry with sheared wing tips
[AIAA PAPER 90-3196] p 812 A90-49101
- X-29 ECS high-alpha modifications
[SAE PAPER 901221] p 840 A90-49295
- Prediction of transition on a swept wing
p 908 A90-52592
- Experimental study of transition and leading edge contamination on swept wings
p 71 N90-10362
- A three-dimensional linear stability approach to transition on wings at incidence
p 20 N90-10373
- A European collaborative investigation of the three-dimensional turbulent shear layers of a swept wing
p 20 N90-10380
- Boundary-layer stability analysis of Langley Research Center 8-foot LFC experimental data
p 92 N90-12532
- Theoretical methods and design studies for NLF and HLFC swept wings at subsonic and supersonic speeds
p 92 N90-12535
- Experimental and theoretical investigation of boundary-layer instability mechanisms on a swept leading edge at Mach 3.5
p 94 N90-12557
- Improvements in the formulations and numerical solution of the Euler problem for swept wings
[RAE-TM-AERO-2139] p 95 N90-12562
- Generalized similarity solutions for three dimensional, laminar, steady, compressible boundary layer flows on swept profile cylinders
[DLR-FB-89-34] p 212 N90-13725
- Navier-Stokes simulation of the crossflow instability in swept-wing flows
[NASA-CR-186122] p 212 N90-13744
- Experimental transonic flutter characteristics of two 72 deg-sweep delta-wing models
[NASA-TM-101659] p 175 N90-14205
- Experiments on the laminar-turbulent transition on swept wings
p 276 N90-16170
- The precise calculation of the inviscid leading edge flow on a laminar airfoil using simple methods and verification by measurements on the TLF pilot model
p 277 N90-16180
- A study of flows over highly-swept wings designed for maneuver at supersonic speeds
[AD-A216837] p 399 N90-19202
- Output model-following control synthesis for an oblique-wing aircraft
[NASA-TM-100454] p 435 N90-19241
- Swept wing ice accretion modeling
[NASA-TM-103114] p 570 N90-21727
- The steady and time-dependent aerodynamic characteristics of a combat aircraft with a delta or swept canard
p 921 N90-28526
- SWEPTBACK WINGS**
- Aeroelastic tailoring applied to composite wing
p 211 A90-18580
- Analytical studies of the transonic flutter of aircraft
p 860 A90-46577
- Aeroelastic characteristics of aircraft with circulation control wings
p 497 N90-20070
- An experimental study of tip shape effects on the flutter of aft-swept, flat-plate wings
[NASA-TM-4180] p 582 N90-22555
- SWIRLING**
- Calculation of confined swirling flows with a second moment closure
p 66 A90-10640
- An experimental investigation of isothermal swirling flow in a model of a dump combustor
p 47 A90-12572
- Effect of primary air swirl on emissions formations in gas turbine combustors
p 47 A90-12573
- Radial swirl flows between parallel disks at critical flow rate
p 14 A90-12596
- Atomization and spray research for gas turbine engines
p 189 A90-17688
- Air and spray patterns produced by gas turbine high-shear nozzle/swirler assemblies
[AIAA PAPER 90-0465] p 192 A90-19857
- Nonaxisymmetric instabilities in a dump combustor with a swirling inlet flow
p 253 A90-21228
- Experimental and theoretical study of the swirling flow in centrifugal compressor volutes
[ASME PAPER 89-GT-183] p 273 A90-22663
- An analysis methodology for internal swirling flow systems with a rotating wall
[ASME PAPER 89-GT-185] p 361 A90-23863
- Inlet swirl effects on dump combustor flows
[AIAA PAPER 90-0035] p 312 A90-26904
- Swirling flow in thrust nozzles
p 421 A90-27962
- Use of swirl for flow control in propulsion nozzles
p 421 A90-27963
- Effects of turbulence model constants on computation of confined swirling flows
p 444 A90-27999
- The effect of swirler on short reversal-flow annular combustor
p 423 A90-29906
- An experimental study on flowfields in a dual inlet swirl-dump combustor
p 471 A90-33283
- Experimental investigation of coannular jet flow with swirl along a centerbody
[AIAA PAPER 90-1622] p 567 A90-38751
- Development of the jet-swirl high loading combustor
[AIAA PAPER 90-2451] p 658 A90-40633
- Laser Doppler velocimetry investigation of swirler flowfields
p 682 A90-40929
- The influence of swirl on velocity, temperature and species characteristics in a can combustor
[AIAA PAPER 90-2454] p 664 A90-42177
- SWITCHES**
- Interaction of switch actuation on tracking with a four-axis flight control (cross-coupling)
[AD-A217981] p 520 N90-20095
- Simulator comparison of thumbball, thumb switch, and touch screen input concepts for interaction with a large screen cockpit display format
[NASA-TM-102587] p 506 N90-21005
- SWITCHING**
- Apparatus for cooling electronic components in aircraft
[AD-D014207] p 183 N90-13373
- SWITCHING CIRCUITS**
- A very high speed switched-reluctance starter-generator for aircraft engine applications
p 452 A90-30791
- 8 x 8-inch full color cockpit display
p 927 A90-52953
- SWITZERLAND**
- Problems related to aircraft noise in Switzerland
p 698 N90-24871
- SWIVELS**
- Performance characteristics of a one-third-scale, vectorable ventral nozzle for SSTOVL aircraft
[AIAA PAPER 90-2271] p 586 A90-37562
- Performance characteristics of a one-third-scale, vectorable ventral nozzle for SSTOVL aircraft
[NASA-TM-103120] p 552 N90-21725
- SYMBOLIC PROGRAMMING**
- Graphical interface tools for an avionics system
[AIAA PAPER 89-3130] p 75 A90-10606
- A study of symbolic processing and computational aspects in helicopter dynamics
p 545 A90-34103
- Hypercube expert system shell-applying production parallelism
[AD-A215762] p 377 N90-18173
- SYMBOLS**
- Taxiway sign effectiveness under reduced visibility conditions
[DOT/FAA/CT-TN90/20] p 761 N90-25150
- SYMMETRY**
- Symmetry assessment of an air-blast atomizer spray
p 682 A90-40930
- Liquid fueled ramjet combustion instability: Acoustical and vortical interactions with burning sprays
[AD-A222752] p 767 N90-26104
- Numerical simulations of flowfields in a central-dump ramjet combustor. 3: Effects of chemistry
[AD-A224145] p 933 N90-28573
- SYNCHRONOUS MOTORS**
- Electric controls for a high-performance EHA using an interior permanent magnet motor drive
p 452 A90-30711
- SYNCHRONOUS SATELLITES**
- An international civil integrity complement to GPS and GLONASS
p 821 A90-46392
- Time synchronization/distribution applications of navigation signals repeated by geostationary satellites
p 872 A90-46397
- Tracking a hypersonic aircraft from a space platform
[AD-A216399] p 371 N90-17984
- SYNOPTIC METEOROLOGY**
- Environmental conditions associated with the Dallas microburst storm determined from satellite soundings
p 280 A90-22689
- Analysis and prediction of weather for aviation
p 888 A90-48351
- SYNTHESIS (CHEMISTRY)**
- The 1-((diorganoxyphosphonyl)-methyl)-2,4- and -2,6-diamido benzenes
[NASA-CASE-ARC-11425-4] p 532 N90-20133
- SYNTHETIC APERTURE RADAR**
- Shadow-tracking algorithm for moving target detection
p 488 A90-34137
- Doppler-rate filtering for detecting moving targets with synthetic aperture radars
p 488 A90-34138
- Vision guidance update - Synthetic aperture radar (SAR) multiple image exploitation for position and velocity determination
p 488 A90-34140
- The Radarsat system --- Canada/U.S. program for launching remote sensing satellite with SAR
p 873 A90-49671
- A new method of aircraft motion error extraction from radar raw data for real-time motion compensation
p 824 A90-49675
- Aircraft SAR simulation Sargen 1.0
[FEL-1989-44] p 135 N90-12823
- The development of an airborne synthetic aperture radar motion compensation system
p 333 N90-16745
- Synthetic aperture radar imagery of airports and surrounding areas: Archived SAR data
[NASA-CR-4275] p 401 N90-18371
- Synthetic aperture radar imagery of airports and surrounding areas: Philadelphia Airport
[NASA-CR-4280] p 401 N90-18372
- Activities report in German aerospace
[ISSN-0070-3966] p 465 N90-19189
- ROSAR (Helicopter-Rotor based Synthetic Aperture Radar)
p 541 N90-21229
- Synthetic aperture radar imagery of airports and surrounding areas: Denver Stapleton International Airport
[NASA-CR-4305] p 637 N90-24257
- SYNTHETIC FUELS**
- Atomization of synthetic jet fuel
p 63 A90-12602
- Analysis of the T63-A-700 engine used in alcohol turbine fuel extender test
[DOT/FAA/CT-TN90/18] p 928 N90-28549
- Production of jet fuels from coal-derived liquids. Volume 13: Evaluation of storage and thermal stability of jet fuels derived from coal liquids
[AD-A224576] p 954 N90-29527
- SYSTEM EFFECTIVENESS**
- The disadvantages of GPS - Comparative study of solutions adapted to civil aviation
p 329 A90-23994
- Optimum aircraft design: Multipurpose approach --- Russian book
p 829 A90-46618
- Air Combat Environment Test and Evaluation Facility (ACETEF)
p 58 N90-10883
- Conceptual design for aerospace vehicles
p 651 N90-25043
- SYSTEM FAILURES**
- New power system architecture for the 747-400
p 508 A90-33349
- Multiple model adaptive controller for the STOL F-15 with sensor/actuator failures
p 668 A90-40878
- A methodology for knowledge-based restructurable control to accommodate system failures
p 609 N90-22058
- System reliability optimization of aircraft wings
p 923 N90-28536
- SYSTEM IDENTIFICATION**
- Artificial intelligence techniques applied to the non-cooperative identification (NCID) problem
[AIAA PAPER 89-3005] p 75 A90-10619
- System identification - Multibus acquisition and simulation equipment
p 26 A90-12192
- System identification collaboration - The role of AGARD
p 1 A90-12763
- Identification of mathematical derivative models for the design of a model following control system --- for fly-by-wire helicopter
p 56 A90-12764
- Identification of a coupled body/coning/inflow model of Puma vertical response in the hover
p 56 A90-12765

- Identification of a coupled flapping/inflow model for the PUMA helicopter from flight test data p 56 A90-12767
- System identification strategies for helicopter rotor models incorporating induced flow p 30 A90-12768
- Identification of rotor flapping equation of motion from flight measurements with the RSRA compound helicopter p 56 A90-12769
- Flight simulation model validation procedure, a systematic approach p 30 A90-12770
- Advancements in frequency-domain methods for rotorcraft system identification p 56 A90-12771
- A frequency-domain system identification approach to helicopter flight mechanics model validation p 56 A90-12772
- Identification of moderately nonlinear flight mechanics systems with additive process and measurement noise p 347 A90-25987
- Aircraft flight control system identification p 431 A90-30105
- System identification requirements for high-bandwidth rotorcraft flight control system design p 755 A90-45333
- AGARD highlights 90/1 p 783 A90-26788

SYSTEMS ANALYSIS

- Equipment procurement - EH101 helicopter p 282 A90-22435
- Modeling strategies for crashworthiness analysis of landing gears p 409 A90-28233
- Multi-level models for diagnosis of complex electro-mechanical systems p 693 A90-38888
- Decentralized systems --- Book p 888 A90-46001
- Review of the Aerospace Safety Advisory Panel report for NASA fiscal year 1990 authorization [GPO-24-234] p 177 A90-14213
- A UK perspective on the uniform engine test programme [RAE-TM-P-1172] p 257 A90-15922
- RADC fault tolerant system reliability evaluation facility [AD-A215298] p 377 A90-17348
- A fractional calculus model of aeroelasticity [AD-A216244] p 377 A90-18212
- Helicopter Airborne Laser Positioning System (HALPS) [NASA-TM-102814] p 654 A90-23399
- Nonflammable hydraulic power system for tactical aircraft. Volume 1: Aircraft system definition, design and analysis [AD-A218493] p 671 A90-23409
- The Federal Aviation Administration plan for research, engineering and development. Volume 2: Project descriptions [AD-A221264] p 783 A90-25931
- Knowledge based diagnosis of jet engines under consideration of model based methods p 855 A90-27631

SYSTEMS COMPATIBILITY

- Cockpit lighting compatibility with image intensification night imaging systems: Issues and answers [AD-A210503] p 32 A90-10028

SYSTEMS ENGINEERING

- Linking artificial intelligence (AI) and computer aided engineering (CAE) to analyze the testability of electronic designs [AIAA PAPER 89-3070] p 74 A90-10559
- Airplane design. Part 4 - Layout design of landing gear and systems --- Book p 31 A90-12869
- Thin film eddy current impulse deicer [AIAA PAPER 90-0761] p 183 A90-20012
- Handbook on heat exchangers --- Russian book p 273 A90-22743
- Numerical optimization of axial compressor designs [ASME PAPER 89-GT-14] p 340 A90-23758
- Advanced Traffic Management System automation p 330 A90-25565
- Mode S system design and architecture p 330 A90-25569
- High-temperature bootstrap compared with F-15 growth air cycle air conditioning system [SAE PAPER 891436] p 336 A90-27407
- Challenges of tomorrow - The future of secure avionics p 419 A90-30723
- Strategic aircraft engineering design simulation p 439 A90-30729
- Performance assessment for airborne surveillance systems incorporating sensor fusion p 583 A90-37088
- Integrated Diagnostics (ID) for advanced avionics architectures [SAE PAPER 892359] p 738 A90-45509
- Aircraft subsystem waste energy recovery and management [SAE PAPER 901218] p 840 A90-49293
- An appraisal of a number of power assessment procedures being proposed for use in Chinook-Lycoming T55 engine [AD-A210482] p 52 A90-10041

- Kalman Filter Integration of Modern Guidance and Navigation Systems [AGARD-LS-166] p 28 A90-10847
- Flight Test Techniques [AGARD-CP-452] p 33 A90-10860
- Flight test techniques adopted by Avions Marcel Dassault-Breguet Aviation p 34 A90-10867
- Advanced actuation systems development, volume 1 [AD-A213334] p 121 A90-12624
- Discretization and model reduction for a class of nonlinear systems p 198 A90-13397
- Advanced actuation systems development, volume 2 [AD-A213378] p 198 A90-13398
- Advances in techniques and technologies for air vehicle navigation and guidance [AGARD-AR-276] p 243 A90-15899
- Guidance and Control of Unmanned Air Vehicles [AGARD-CP-436] p 260 A90-15924
- Mirach 100 flight control system p 260 A90-15926
- Progress in airbreathing combined engines for future European launcher p 344 A90-16817
- National airspace system plan: Facilities, equipment, associated development and other capital needs [AD-A215882] p 402 A90-18373
- Potential role of avionics in escape systems p 483 A90-20060
- Evolution of Ada technology in the flight dynamics area: Implementation/testing phase analysis [NASA-TM-103310] p 546 A90-21539
- MLS mathematical model validation study using airborne MLS data from Midway Airport engineering flight tests, August 1988 [DOT/FAA/CT-TN90/2] p 640 A90-23378
- Cost effective technology [PNR90664] p 883 A90-27002
- Aircraft lightning protection handbook [AD-A222716] p 820 A90-27668
- Experimental study towards a future airport ground movement simulator p 827 A90-27687
- System reliability optimization of aircraft wings p 923 A90-28536
- A knowledge-based system design/information tool [NASA-CR-4316] p 965 A90-29143
- Flight test engineering with the ATTAS p 902 A90-29160
- Electro-optics engineering support for the integrated launch and recovery television surveillance system [AD-A223450] p 938 A90-29406

SYSTEMS INTEGRATION

- Software fault tolerance analysis and testing for the Advanced Automation System [AIAA PAPER 89-3124] p 75 A90-10600
- Airplane design. Part 2 - Preliminary configuration design and integration of the propulsion system --- Book p 30 A90-12867
- Integration of GPS with the Carrier Aircraft Inertial Navigation System (CAINS) p 97 A90-13990
- Simulation model-building procedure for dynamic systems integration p 138 A90-14744
- Trends in avionics - From analog black boxes to integrated digital avionics systems p 252 A90-23245
- Integrated navigation - Employing LIRU/GPS p 329 A90-23995
- Low speed, in draft wind tunnels p 351 A90-26061
- An analytical sensitivity method for use in integrated aeroservoelastic aircraft design p 517 A90-33405
- Advanced integrated avionics test support concepts [AIAA PAPER 90-1259] p 504 A90-33889
- Multisensor Integrated Navigation System p 577 A90-36924
- Prototype testing of an integrated Doppler/GPS navigation system p 577 A90-36926
- Omega-GPS interoperability for the long haul p 577 A90-36927
- Low cost QUBIK IMU for integration with GPS, Omega, Loran-C, and SDI systems p 577 A90-36929
- F-16/GPS integration test results p 726 A90-43710
- Integration of the LTN-72 INS with the DOD GPS 3A set p 728 A90-45236
- Considerations for successful application of integrated drive generators to aircraft [SAE PAPER 892226] p 746 A90-45442
- Design features of the 747-400 Electric Power System [SAE PAPER 892227] p 746 A90-45443
- Application considerations for integral gas turbine electric starter/generator revisited [SAE PAPER 892252] p 746 A90-45454
- H-infinity based integrated flight/propulsion control design for a STOVL aircraft in transition flight [AIAA PAPER 90-3335] p 862 A90-47595
- Analytic models for technology integration in aircraft design [AIAA PAPER 90-3262] p 835 A90-48857

- Short take-off and landing maneuver technology demonstrator (STOL/MTD) lessons learned - Integrated flight/propulsion control (IFPC) [AIAA PAPER 90-3307] p 868 A90-48888
- Evaluation and control of an integrated Closed Environmental Control System (ICECS) [SAE PAPER 901237] p 841 A90-49307
- Kalman Filter Integration of Modern Guidance and Navigation Systems [AGARD-LS-166] p 28 A90-10847
- Flight Test Techniques [AGARD-CP-452] p 33 A90-10860
- Real-time flight test analysis and display techniques for the X-29A aircraft p 34 A90-10866
- Flight test techniques adopted by Avions Marcel Dassault-Breguet Aviation p 34 A90-10867
- Lessons learned from the integration of flight systems p 35 A90-10874
- STOVL aircraft simulation for integrated flight and propulsion control research [NASA-TM-102419] p 193 A90-13389
- Integrated flight guidance system using differential-GPS for landing approach guidance p 332 A90-16735
- Antenna installation on aircraft: Theory and practice p 371 A90-17941
- The implications of using integrated software support environment for design of guidance and control systems software [AGARD-AR-229] p 434 A90-18432
- The Real Time Display Builder (RTDB) p 546 A90-20656
- Preliminary design of a supersonic Short Takeoff and Vertical Landing (STOVL) fighter aircraft [NASA-CR-186670] p 649 A90-23394
- Continued development and analysis of a new extended Kalman filter for the Completely Integrated Reference Instrumentation System (CIRIS) [AD-A220106] p 654 A90-23400
- Technical evaluation report on the Guidance and Control Panel 49th Symposium on Fault Tolerant Design Concepts for Highly Integrated Flight Critical Guidance and Control Systems [AGARD-AR-281] p 758 A90-26012
- Aircraft Integrated Monitoring Systems [DLR-MITT-90-04] p 786 A90-27617
- Performance assessment of MIL-STD-1553B on the avionic systems demonstrator rig of British Aerospace p 849 A90-27624
- Knowledge based diagnosis of jet engines under consideration of model based methods p 855 A90-27631
- New features of JAL's ground station p 872 A90-27633
- PHARE: Concept and programme p 827 A90-27690
- A look at tomorrow today p 921 A90-28524
- Description of the primary flight display, and flight guidance system logic in the NASA B-737 transport systems research vehicle [NASA-TM-102710] p 927 A90-28546
- Propulsion system-flight control integration and optimization: Flight evaluation and technology transition [NASA-TM-4207] p 929 A90-28551
- The integration of multiple avionic sensors and technologies for future military helicopters p 916 A90-29344
- Integrated navigation/flight control for future high performance aircraft p 917 A90-29362

SYSTEMS MANAGEMENT

- Effective use of Cray supercomputers p 546 A90-34436

SYSTEMS SIMULATION

- A methodology for modeling, control design and simulation of aerospace mechanical systems [AIAA PAPER 89-3049] p 73 A90-10543
- Simulation model-building procedure for dynamic systems integration p 138 A90-14744
- Noise of a simulated installed model counterrotation propeller at angle-of-attack and takeoff/approach conditions [AIAA PAPER 90-0283] p 547 A90-32505
- Probabilistic modeling for simulation of aerodynamic uncertainties in propulsion systems [NASA-TM-102472] p 515 A90-21036

SYSTEMS STABILITY

- Algorithm for simultaneous stabilization of single-input systems via dynamic feedback p 462 A90-31108
- Analysis of airframe/engine interactions - An integrated control perspective [AIAA PAPER 90-1918] p 667 A90-40557
- Decentralized systems --- Book p 888 A90-46001
- A linear quadratic regulator approach to the stabilization of uncertain linear systems [AIAA PAPER 90-3509] p 891 A90-47755

SYSTOLIC ARRAYS

- Array processor supercomputers p 376 A90-26626

T

T-2 AIRCRAFT

- Adaptive flight control of CCV aircraft with limiting zeros
[AIAA PAPER 90-3409] p 864 A90-47664

T-33 AIRCRAFT

- In quest of the laminar-flow airliner - Flight experiments on a T-33 jet trainer p 300 A90-24825

TABLES (DATA)

- Airfoil design and data --- Book p 809 A90-47608
Model designation of military aerospace vehicles
[PB90-206301] p 787 N90-27646
World jet airplane inventory at year-end 1989
[PB90-207218] p 902 N90-28489

TABS (CONTROL SURFACES)

- Elevator tab assembly producibility study
[IAR-89-16] p 734 N90-25133

TACAN

- Analytical evaluation of radiation patterns of a TACAN antenna p 404 A90-30695

TACHOMETERS

- Digital servomechanism for the tachometer of the M 602 engine p 737 A90-44722

TAIL ASSEMBLIES

- Investigation on the determination of airplane tail loads by flight tests p 178 A90-16853
Calculation of the drag of fuselage tail sections of different shapes in supersonic flow of a nonviscous gas p 388 A90-29182
Some considerations in ultra light aircraft design p 730 A90-42673

- Vortex control for tail buffet alleviation on a twin-tail fighter configuration
[SAE PAPER 892221] p 756 A90-45438

- Measurements of pressures on the tail and aft fuselage of an airplane model during rotary motions at spin attitudes
[NASA-TP-2939] p 20 N90-10829

- Additions and corrections to SUPER: A program for calculating steady and oscillatory supersonic flow over a thin wing, tail plane and fin
[AD-A211771] p 90 N90-12501

- Canard versus aft-tail ride qualities performance and pilot command response p 258 N90-15053
Assessment of computational prediction of tail buffeting
[NASA-TM-101613] p 237 N90-15886

- An experimental investigation of support strut interference on a three-percent fighter model at high angles of attack
[AD-A219793] p 631 N90-23353

- Effect of tail size reductions on longitudinal aerodynamic characteristics of a three surface F-15 model with nonaxisymmetric nozzles
[NASA-TP-3036] p 718 N90-25938

TAIL ROTORS

- Improvements to the fatigue substantiation of the H-60 composite tail rotor blade p 642 A90-39985
Helicopter surveillance - A look at current and proposed future programs p 642 A90-39986

- SH-2F airframe fatigue test program p 642 A90-39989

- Use of smart actuators for the tail rotor collective pitch control p 688 A90-42483

TAIL SURFACES

- Vertical tail design for base-line configuration of military combat aircraft p 810 A90-48080
Aspects of the design of a hypersonic engine system and the selection of the intake and tail
[DGLR PAPER 88-040] p 928 A90-50233

TAILLESS AIRCRAFT

- Optimal reflex camber p 308 A90-26347
Computational and experimental studies on ground effect of a slender wing tailless delta aircraft p 810 A90-48083

TAKEOFF

- Optimization of helicopter takeoff and landing p 29 A90-11006
Friction measurements under winter runway conditions p 321 A90-23924

- National Airspace System demand and capacity modeling p 330 A90-25562
Analyses of Arrow Air DC-8-63 accident of December 12, 1985 - Gander, Newfoundland p 635 A90-40687

- Influence of ground effect on helicopter takeoff and landing performance p 645 A90-42278
The 1987 survey of track keeping and altitudes on Heathrow and Gatwick standard instrument departure routes (DAY)
[CAA-PAPER-88010] p 99 N90-11729

- Airplane takeoff and landing performance monitoring system
[NASA-CASE-LAR-13734-1-CU] p 526 N90-20096

- Brake performance of the McDonnell Douglas DC-10-30/40 during high speed, high energy rejected takeoffs
[PB90-917004] p 503 N90-21000

- HOTOL structures and materials at British Aerospace, Warton, UK
[EOARD-LR-90-001] p 503 N90-21001

- Optimization and guidance of flight trajectories in the presence of windshear
[NASA-CR-186163] p 574 N90-21747

- En route noise annoyance laboratory test: Preliminary results p 698 N90-24870
A quantitative technique to estimate microburst wind shear hazard to aircraft p 692 N90-25040

- Replication of NASPAC Dallas/Fort Worth study
[DOT/FAA/CT-TN90/26] p 729 N90-25123

- An accurate numerical technique for determining flight test rate gyroscope biases prior to takeoff
[AD-A220987] p 739 N90-25138

- An overview of the joint FAA/NASA aircraft/ground runway friction program
[NASA-TM-103486] p 724 N90-25957

- BASEOPS default profiles for civil aircraft
[AD-A223161] p 844 N90-26825

- Vibration responses of two house structures during the Edwards Air Force Base phase of the national sonic boom program
[NASA-CR-182089] p 966 N90-29169

TAKEOFF RUNS

- Takeoff characteristics of turbofan engines p 585 A90-35764

TANDEM ROTOR HELICOPTERS

- A new hybrid LTA vehicle, 'Heliship' - Its philosophy, outline
[AIAA PAPER 89-3162] p 244 A90-20582

TANDEM WING AIRCRAFT

- An experimental study of a closely coupled tandem wing configuration at low Reynolds numbers
[AIAA PAPER 90-3094] p 797 A90-45923

- The Curtiss-Wright X-19 experimental aircraft - Lessons learned
[AIAA PAPER 90-3206] p 834 A90-48834

TAPERING

- Experimental investigation of wingtip aerodynamic loading p 808 A90-46945

TARGET ACQUISITION

- Modeling of air-to-air visual acquisition p 282 A90-21385

- Development and operation of the Traffic Alert and Collision Avoidance System (TCAS) p 331 A90-25573

- Neural networks for adaptive shape tracking p 638 A90-39959

- Unmanned helicopters for battlefield and maritime surveillance p 920 A90-51899

- Comparison of 1-D and 2-D aircraft images p 927 A90-52884

- Guidance and Control of Unmanned Air Vehicles
[AGARD-CP-436] p 260 N90-15924

- ROSAR (Helicopter-Rotor based Synthetic Aperture Radar) p 541 N90-21229

TARGET DRONE AIRCRAFT

- Pilotless airplanes
[AD-A211719] p 103 N90-11734

TARGET RECOGNITION

- Doppler-rate filtering for detecting moving targets with synthetic aperture radars p 488 A90-34138

- Optical window materials for hypersonic flow p 496 A90-34581

- Multiple sensor data association and fusion in aerospace applications p 778 A90-44644

- Mirach 100 flight control system p 260 N90-15926

TARGETS

- Qualitative evaluation of a conformal velocity vector display for use at high angles-of-attack in fighter aircraft
[NASA-TM-102629] p 739 N90-25981

TASKS

- Criteria for coal tar seal coats on airport pavements. Volume 2: Laboratory and field studies
[AD-A220167] p 674 N90-24277

TASKS

- Task-oriented display design - Concept and example
[SAE PAPER 892230] p 738 A90-45446

- FAA air traffic control operations concepts. Volume 7: ATCT (Airport Traffic Control Towers) tower controllers
[AD-A210455] p 332 N90-16730

TAXIING

- Results of aircraft open-loop tests of an experimental magnetic leader cable system for guidance during roll-out and turnoff
[NASA-TM-4135] p 348 N90-16767

TAXONOMY

- A computational study of the taxonomy of vortex breakdown
[AIAA PAPER 90-1624] p 568 A90-38753

TEAMS

- Teamwork for excellence
[AIAA PAPER 89-3195] p 549 A90-31688

TECHNOLOGICAL FORECASTING

- Material requirements for future aeroengines p 62 A90-12534

- IHPET spawns engines for 21st century p 188 A90-16702

- HSCT research focuses on environmental issues p 143 A90-17780

- Jet futures p 190 A90-18526
Advanced technology rotorcraft - Civil short haul transport of the future p 246 A90-21710

- Hydrogen propulsion and the next century - A challenge that raises questions and problems p 266 A90-21774

- McDonnell Douglas Helicopter Company Factory of the Future Project p 381 A90-28163

- Experimental aeroelasticity - History, status and future in brief
[AIAA PAPER 90-0978] p 382 A90-29598

- Sealing the future --- sealants and adhesives for military aircraft p 442 A90-29638

- Composites boost 21st-century aircraft engines p 442 A90-29704

- Advanced power system for 21st century fighter aircraft p 508 A90-33347

- Starship - A model for future designs p 493 A90-33714

- Mode S - A data link for future air traffic control p 576 A90-35684

- Basic areas of research in the development of a future ATM system --- air traffic management p 551 A90-35685

- Exploration of concepts for multi-role fighters
[AIAA PAPER 90-2276] p 644 A90-42104

- Contribution of engine improvement on next future rotorcraft p 665 A90-42488

- SST/HST air traffic - Challenge for the future p 763 A90-44752

- The turbofan of tomorrow p 850 A90-46150

- The Bell Helicopter AH-1 Cobra - Past, present, and future
[AIAA PAPER 90-3271] p 836 A90-48862

- Ceramic materials and coatings for future aerospace applications - Challenge of the 1990's p 942 A90-50071

- Airbus technologies - An evolutionary process p 902 A90-52699

- Future military powerplants --- fighter aircraft engines
[PNR90554] p 114 N90-11749

- A vision of the future: The new engine technology
[PNR90566] p 115 N90-12603

- The next generation supersonic transport engine: Critical issues
[PNR90576] p 115 N90-12605

- Material requirements for future aeroengines
[PNR90595] p 116 N90-12610

- Composite materials for future aeroengines
[PNR90584] p 127 N90-12667

- The future of non ferrous metals in aerospace engines
[PNR90572] p 127 N90-12720

- Experimental aeroelasticity history, status and future in brief
[NASA-TM-102651] p 527 N90-21047

- Materials and structures for 2000 and beyond: An attempted forecast by the DLR Materials and Structures Department
[ESA-TT-1154-REV] p 775 N90-26173

- The integration of multiple avionic sensors and technologies for future military helicopters p 916 N90-29344

TECHNOLOGY ASSESSMENT

- Innovation in general aviation p 81 A90-14997

- The coming age of the tiltrotor. I p 246 A90-21711

- A review of flight simulation techniques p 435 A90-27953

- Challenges of tomorrow - The future of secure avionics p 419 A90-30723

- Thermoplastic composites, past, present and future p 529 A90-31882

- ILS - Past and present p 639 A90-41706

- ILS - A safe bet for your future landings p 639 A90-41707

- Co-development of CT7-6 engines - A continued tradition in technology and reliability p 665 A90-42485

- IHPET technology mission payoffs at the component level - A look at Phase II technologies --- Integrated High Performance Turbine Engine Technology
[AIAA PAPER 90-2404] p 701 A90-42794

- Some technological errors in the use of capillary inspection in gas turbine engine repair p 769 A90-43039

- Technology issues for high-speed civil transports
[SAE PAPER 892201] p 778 A90-45422

- Overview of military technology at NASA Langley
[SAE PAPER 892232] p 733 A90-45448

- Methodology for estimating helicopter performance and weights using limited data p 829 A90-46936
- Modelling aspects for the synthesis and performance assessment of some future advanced helicopters p 829 A90-46937
- High-speed rotorcraft V/STOL - An initial assessment p 829 A90-46938
- The Bell Helicopter AH-1 Cobra - Past, present, and future [AIAA PAPER 90-3271] p 836 A90-48862
- Propulsion systems for vertical flight aircraft [AIAA PAPER 90-3299] p 853 A90-48881
- Coaxial helicopters - Current status and future developments p 838 A90-48951
- Large scale prop-fan structural design study. Volume 1: Initial concepts [NASA-CR-174992] p 52 N90-10043
- Large scale prop-fan structural design study. Volume 2: Preliminary design of SR-7 [NASA-CR-174993] p 52 N90-10044
- Estimating the relationships between the state of the art of technology and production cost for the US aircraft [AD-A212127] p 82 N90-12495
- LFC: A maturing concept [DOUGLAS-PAPER-7878] p 90 N90-12505
- LORAN C stability integrity assurance [AD-A212663] p 177 N90-13364
- Study of high-speed civil transports [NASA-CR-4235] p 183 N90-13370
- Technology and evaluation of unmanned air vehicles p 252 N90-15934
- Preliminary design of a supersonic Short Takeoff and Vertical Landing (STOVL) fighter aircraft [NASA-CR-186670] p 649 N90-23394
- A study of the technology required for advanced vertical take-off aircraft [ETN-90-96786] p 650 N90-24268
- Lecture notes on flight simulation techniques [LR-596] p 762 N90-25153
- Airport pavement drainage [DOT/FAA/RD-90/24] p 872 N90-27728
- Energy efficient engine program technology benefit/cost study. Volume 1: Executive summary [NASA-CR-174766-VOL-1] p 931 N90-28564
- TECHNOLOGY TRANSFER**
- Propulsion system-flight control integration-flight evaluation and technology transition [AIAA PAPER 90-2280] p 644 A90-42106
- Point of view of a civil aircraft manufacturer on Al-Li alloy p 268 N90-15200
- TECHNOLOGY UTILIZATION**
- Applications of fiber optic sensors in advanced engine controls p 68 A90-11703
- Holographic head-up displays for air and ground applications p 108 A90-13885
- Aircraft propulsion: Leading the way in aviation [LR-532] p 194 N90-13395
- Materials and structures for 2000 and beyond: An attempted forecast by the DLR Materials and Structures Department [ESA-TT-1154-REV] p 775 N90-26173
- Fluid Dynamics Panel Working Group 12 on Adaptive Wind Tunnel Walls: Technology and Applications [AGARD-AR-269] p 870 N90-26838
- TEETERING**
- Prediction and measurement of the aerodynamic interactions between a rotor and airframe in forward flight p 384 A90-28176
- TELEMETRY**
- Trends in telemetry front end architecture [AIAA PAPER 89-3085] p 25 A90-10571
- Trends in real-time flight systems [AIAA PAPER 89-3086] p 25 A90-10572
- Research on transmission quality of telemetry system in flight test p 26 A90-12189
- Prospects of onboard magnetic tape recording during flight tests p 39 A90-12198
- The small portable Global Positioning System tracking range of the future p 60 A90-12209
- Telemetry systems of the future p 458 A90-28829
- McDonnell Douglas Helicopter Company Apache telemetry antenna analysis p 403 A90-28839
- Airborne telemetry trends for the 1990's p 418 A90-28874
- Development of airborne data reduction system in IPTN flight test p 418 A90-28895
- Microminiature flight test instrumentation [AIAA PAPER 90-1274] p 504 A90-33898
- The use of onboard sensor data in aerial triangulation - GPS, pressure sensors, laser telemetry p 822 A90-47901
- Flight test instrumentation and data processing at British Aerospace, Warton, U.K. p 59 N90-10887
- X.2 limited flight test plan [AD-A214412] p 249 N90-15099

- The Real Time Display Builder (RTDB) p 546 N90-20656
- TELEOPERATORS**
- Visualization of three dimensional data p 782 N90-25553
- TELEVISION CAMERAS**
- Flight tests of a helmet-mounted display synthetic visibility system [AIAA PAPER 90-1279] p 579 A90-36027
- Holographic combiner design to obtain uniform symbol brightness at head-up display video camera p 652 A90-40394
- TELEVISION RECEIVERS**
- Evaluation and measurement of airplane flutter interference --- in television reception p 272 A90-22529
- TELEVISION SYSTEMS**
- A surveillance 360 deg television orientation and ranging system as an aid to collision avoidance p 577 A90-36922
- TEMPERATURE CONTROL**
- Analysis and improvement of cabin temperature control system p 580 A90-37241
- Thermal management of closed computer modules utilizing high density circuitry --- in Airborne Information Management System [AIAA PAPER 90-1748] p 583 A90-38441
- Subsystem thermal integration - A new challenge to the aircraft designer [AIAA PAPER 90-3274] p 836 A90-48865
- Use of ECS-conditioned air for FLIR avionics thermal control - Fighter aircraft [SAE PAPER 901219] p 840 A90-49294
- TEMPERATURE DEPENDENCE**
- Quench sensitivity of airframe aluminium alloys p 765 A90-44348
- Generalized similarity solutions for three-dimensional laminar compressible wing boundary layers p 907 A90-51543
- The stress and temperature dependence of creep in an Al-2.0 wt percent Li alloy [AD-A223676] p 953 N90-29480
- TEMPERATURE DISTRIBUTION**
- Finite element analysis of nonstationary temperature fields in gas turbine components p 271 A90-21324
- Structure of velocity and temperature fields in laminar channel flows with longitudinal vortex generators p 273 A90-23207
- On-line temperature profile display system [ASME PAPER 89-GT-10] p 374 A90-23755
- A simplified model for unstable temperature field calculation of gas turbine rotor [ASME PAPER 89-GT-234] p 363 A90-23885
- A method for recalculating the temperature fields of aircraft structures for different experimental conditions p 448 A90-28994
- Experimental studies of combustor dilution zone aerodynamics. I - Mean flowfields p 508 A90-32962
- Boundary layer diagnostics by means of an infrared scanning radiometer p 605 A90-38493
- Inlet radial temperature redistribution in a transonic turbine stage [AIAA PAPER 90-1543] p 565 A90-38687
- Total temperature separation in jets [AIAA PAPER 90-1621] p 607 A90-38750
- Unsteady Euler analysis of the redistribution of an inlet temperature distortion in a turbine [AIAA PAPER 90-2262] p 768 A90-42759
- A study of the electrophysical phenomena in the combustion chambers of jet engines p 765 A90-45028
- The effect of secondary flow on the redistribution of the total temperature field downstream of a stationary turbine cascade p 515 N90-21033
- Three-dimensional analysis on flow and temperature distributions for aircraft fuel thermal stability [AD-A219651] p 678 N90-23571
- Calculation of temperature distribution in various turbine blades using a boundary-fitted coordinate transformation method p 929 N90-28550
- TEMPERATURE EFFECTS**
- Total temperature effects on centerline Mach number characteristics of freejets p 302 A90-25290
- Characteristics of temperature and pressure generation and retention in flow inside cryogenic wind tunnel-T-04 p 869 A90-46576
- New cyanate ester resin with low temperature (125-200 C) cure capability p 944 A90-50135
- Effects of a heat cycle on material strength [NAL-TM-562] p 113 N90-11737
- Application of sound and temperature to control boundary-layer transition p 92 N90-12537
- Thermal barrier coatings for gas turbine and diesel engines [NASA-TM-102408] p 205 N90-13636

- Cryogenic temperature effects on sting-balance deflections in the National Transonic Facility [NASA-TM-4157] p 202 N90-14244
- Time development of convection flow patterns in aircraft cabins under post-crash fire exposure p 327 N90-17598
- Effect of temperature on the storage life of polysulfide aircraft sealants [MRL-TR-89-31] p 444 N90-19364
- Analysis of a six-component, flow-through, strain-gage, force balance used for hypersonic wind tunnel models with scramjet exhaust flow simulation [NASA-CR-186585] p 597 N90-21775
- High Temperature Surface Interactions [AGARD-CP-461] p 951 N90-28698
- Fretting fatigue strength of Ti-6Al-4V at room and elevated temperatures and ways of improving it p 952 N90-28709
- TEMPERATURE GRADIENTS**
- Measurement of temperature gradients and assessment of balance performance using the RAE cryogenic test duct p 525 A90-34252
- Analysis of thermal gradient effects in oil ring seals p 682 A90-40716
- TEMPERATURE INVERSIONS**
- Inversions and associated wind-shear warnings must be related to airport characteristics p 962 A90-52051
- TEMPERATURE MEASUREMENT**
- The remote sensing of temperature in gas turbine engine components using epithermal neutrons p 70 A90-12630
- Fluorescence spectroscopy and thermometry for hypersonic flight research [AIAA PAPER 90-1272] p 538 A90-33897
- Force balance errors due to temperature changes in ETW p 539 A90-34231
- Measurement of temperature gradients and assessment of balance performance using the RAE cryogenic test duct p 525 A90-34252
- Experimental investigation of a supersonic swept ramp injector using laser-induced iodine fluorescence [AIAA PAPER 90-1518] p 606 A90-38663
- Low speed flowfield characterization by infrared measurements of surface temperatures p 317 N90-17556
- Concentration, temperature, and density in a hydrogen-air flame by excimer-induced Raman scattering p 875 N90-26903
- Infrared thermography p 911 N90-29325
- Recommended practices for measurement of gas path pressures and temperatures for performance assessment of aircraft turbine engines and components [AGARD-AR-245] p 933 N90-29393
- TEMPERATURE MEASURING INSTRUMENTS**
- Silicon-etalon fiber-optic temperature sensor [NASA-TM-102389] p 187 N90-13381
- Development of a mass averaging temperature probe p 427 N90-18418
- TEMPERATURE PROBES**
- A reliable, maintenance-free oxygen sensor for aircraft using an oxygen-sensitive coating on potentiometric electrodes [AD-A222696] p 927 N90-28545
- TEMPERATURE SENSORS**
- Fiber-optic turbine inlet temperature measurement system (FOTITMS) [AIAA PAPER 90-2033] p 657 A90-40603
- Smart microsensors for high temperature applications, phase 1 [AD-A224151] p 959 N90-28828
- TEMPORAL RESOLUTION**
- Temporally and spatially resolved flow in a two-stage axial compressor. Part 2: Computational assessment [NASA-TM-102273] p 194 N90-14236
- TENSILE CREEP**
- Improved toughness alloys based on titanium aluminides [AD-A218149] p 533 N90-20208
- TENSILE PROPERTIES**
- The effect of elevated temperature exposure on the tensile and creep properties of Ti-24Al-11Nb p 355 A90-24865
- Study of the microstructure of a titanium alloy (6246) for turbomachine compressors [ETN-90-97450] p 876 N90-27900
- TENSILE STRENGTH**
- Effects of a heat cycle on material strength [NAL-TM-562] p 113 N90-11737
- Application of high performance metals in gas turbine engines [PNR90640] p 750 N90-25999
- Fatigue, static tensile strength and stress corrosion of aircraft materials and structures. Part 1: Text [LR-630-PT-1-REV] p 961 N90-29682

SUBJECT INDEX

- Fatigue, static tensile strength and stress corrosion of aircraft materials and structures. Part 2: Figures [LR-630-PT-2] p 961 N90-29683
- TENSILE STRESS**
Sensitivity and optimization of composite structures in MSC/NASTRAN p 208 A90-17370
Wing design optimization under stress-strain constraints using full-strength and minimum mass criteria p 804 A90-46554
- TENSILE TESTS**
EH-101 main rotor hub application of thick carbon fiber unidirectional tension bands p 618 A90-42489
Laser welding of an advanced rapidly-solidified titanium alloy p 881 A90-47021
Constitutive modeling for isotropic materials (HOST) [NASA-CR-179522] p 193 N90-13390
Static and dynamic characterization of the ATR 72 rods made of Ti 10.2.3 titanium alloy [REPT-49-238] p 953 N90-28722
- TENSOMETERS**
Measurement of propellers in the ARTI 3-meter wind tunnel p 262 A90-23364
Model problems of continuous control law optimization for a tensometric aerodynamic experiment p 295 A90-24086
Identification of a stress-strain computation model and planning of tensometry points in strength and stability studies p 880 A90-46482
- TERMINAL FACILITIES**
Advanced technology rotorcraft - Civil short haul transport of the future p 246 A90-21710
FAA air traffic activity: Fiscal year 1988 [AD-A211338] p 99 N90-12570
- TERMINAL GUIDANCE**
Multiple-step terminal control with parameter identification and prediction during flight vehicle descent p 872 A90-46484
- TERMS**
A glossary of terms, definitions, acronyms, and abbreviations related to the National Aerospace System [DOT/FAA/CT-TN89/53] p 967 N90-29249
- TERRAIN**
Development of an automatic ground collision avoidance system using a digital terrain database [AD-A216247] p 329 N90-17621
Heli/SITAN: A terrain referenced navigation algorithm for helicopters [DE90-005193] p 405 N90-19217
- TERRAIN ANALYSIS**
Operating principles of a terrain-recognition air navigation system p 403 A90-29655
Flight testing of the Tornado Terrain Following System p 35 N90-10875
Advances in techniques and technologies for air vehicle navigation and guidance [AGARD-AR-276] p 243 N90-15899
Technical evaluation report on the Guidance and Control Panel 49th Symposium on Fault Tolerant Design Concepts for Highly Integrated Flight Critical Guidance and Control Systems [AGARD-AR-281] p 758 N90-26012
Description of the MARC measuring system [FEL-89-B170] p 963 N90-28887
Survivable penetration p 917 N90-28363
Terrain visual cue analysis for simulating low-level flight: A multidimensional scaling approach [AD-A223564] p 938 N90-29407
- TERRAIN FOLLOWING AIRCRAFT**
The research of cubic spline optimal terrain following system p 196 A90-18584
An application of generalized predictive control to rotorcraft terrain-following flight p 257 A90-23478
Flight testing the F-15E terrain following system p 334 A90-24272
Accurate ILS and MLS performance evaluation in presence of site errors p 404 A90-30693
F-15E terrain following test results [AIAA PAPER 90-1299] p 504 A90-33913
The airborne synthetic cartographic indicator p 822 A90-46671
Image based range determination [AIAA PAPER 90-3404] p 822 A90-47659
Model-based method for terrain-following display design [AD-A219302] p 583 N90-22563
Application of optimal tracking methods to aircraft terrain following [AD-A221099] p 641 N90-24264
A study of terrain following systems and the creation of flight paths for terrain following vehicles [FOA-C-20774-2.5] p 827 N90-27691
- TEST CHAMBERS**
The NASA Langley 0.3-meter transonic cryogenic tunnel p 262 N90-15941
Research at NASA's NFAC wind tunnels [NASA-TM-102827] p 702 N90-25933

- The aims and history of adaptive wall wind tunnels p 871 N90-26839
- TEST EQUIPMENT**
New rotor test rig in the large Modane wind tunnel [ONERA, TP NO. 1989-137] p 58 A90-11159
Theoretical analysis of an icing test apparatus for turbine engine air intakes [AAAF PAPER NT 88-20] p 23 A90-11437
Test rig for the study of the flow in a rotor-stator system [ONERA, TP NO. 1989-124] p 58 A90-12634
Designing the next generation flying test bed [SAE PAPER 891049] p 100 A90-14353
Future test rigs p 200 A90-19012
Advanced technology ATE for fuel accessory testing p 439 A90-30770
- DIGITAC - A unique digital flight control testbed aircraft**
[AIAA PAPER 90-1288] p 519 A90-33931
Advanced technology MMW seeker testbed, a multi-technology demonstration sensor p 488 A90-34143
Automatic calibration machine for cryogenic and conventional internal strain gage balances [AIAA PAPER 90-1396] p 595 A90-37939
- TEST FACILITIES**
Testing facility and procedure of the ATTAS on-board data acquisition system p 39 A90-12202
A description of the Naval Air Development Center's ejection tower and crash test facilities and their uses p 200 A90-17426
Water test facilities for aviation life support equipment p 200 A90-17431
Separation shock dynamics in Mach 5 turbulent interactions induced by cylinders p 153 A90-17981
A numerical parametric study of a scramjet inlet in a Mach 6 arc heated test facility [AIAA PAPER 90-0531] p 167 A90-19896
European research and testing facilities requested for participation to SST/HST projects [ONERA, TP NO. 1990-12] p 351 A90-25358
The integrated test vehicle, (I.T.V.) - A vehicle for cost-effective hypersonic testing [AIAA PAPER 90-0630] p 352 A90-26974
Design and development of a facility for compressible dynamic stall studies of a rapidly pitching airfoil p 436 A90-28255
HTTB - Industry's first STOL test bed - High Technology Test Bed program for future tactical aircraft requirements p 414 A90-31246
Performance potential and technology issues of MHD augmented hypersonic simulation facilities [AIAA PAPER 90-1380] p 598 A90-37929
Hypersonic test facility requirements for the 1990's [AIAA PAPER 90-1389] p 594 A90-37934
Langley hypersonic aerodynamic/aerothermodynamic testing capabilities - Present and future [AIAA PAPER 90-1376] p 596 A90-38483
Requirements in the 1990's for high enthalpy ground test facilities for CFD validation [AIAA PAPER 90-1401] p 597 A90-38489
The normal shock generator - An inlet throat region research apparatus for high Mach applications [AIAA PAPER 90-1930] p 759 A90-42698
A test matrix sequencer for research test facility automation [AIAA PAPER 90-2386] p 759 A90-42791
Comparison of four lightning simulation tests on a composite test bed aircraft p 818 A90-49831
Characterization of configuration effects on lightning simulation/qualification testing p 819 A90-49835
Lightning testing and test analyses of the JAS39 aircraft p 842 A90-49836
US Navy principal site testing concept and the F-18 p 33 N90-10861
The Air Force Flight Test Center Flight Test Safety Program p 35 N90-10872
Air Combat Environment Test and Evaluation Facility (ACETEF) p 58 N90-10883
Flight simulation test facility: Function and specification of the simulator cockpit system [NAL-TM-577] p 59 N90-10899
Dynamic testing techniques and applications for an aeroelastic rotor test facility p 201 N90-13406
The Uniform Engine Test Programme [AGARD-AR-248] p 428 N90-19232
Marshall Avionics Testbed System (MAST) p 421 N90-19417
Sandia National Laboratories' new high level acoustic test facility [DE90-006810] p 464 N90-19820
A corrosion fatigue/stress corrosion testing facility at Materials Research Laboratory [MRL-TN-568] p 527 N90-21044

THERMAL CONTROL COATINGS

- Wright Research and Development Center test facilities handbook [AD-A22582] p 762 N90-26020
Bringing aircraft noise testing down to Earth [PNR90642] p 783 N90-26637
Design of the UETP experiment p 856 N90-27712
Comparison of altitude test cell results p 856 N90-27715
Comparison of ground-level test cells and ground-level to altitude test cells p 857 N90-27716
General test plan p 857 N90-27721
Source emission test of gas turbine engine test facility, Kelly AFB, TX [AD-A223869] p 932 N90-28571
Flight test engineering with the ATTAS p 902 N90-29160
- TEST PILOTS**
UH-60 helicopter simulator fidelity testing or how to make it fly like the real thing [AIAA PAPER 90-1290] p 522 A90-33910
Preparations of the real-time data analyst to insure flight test safety [AIAA PAPER 90-1316] p 488 A90-33925
DIGITAC - A unique digital flight control testbed aircraft [AIAA PAPER 90-1288] p 519 A90-33931
Flying the giant - An-124 Russian aircraft p 833 A90-48522
- TEST STANDS**
Analysis of small-scale rotor hover performance data [NASA-TM-102271] p 540 N90-20325
Experimental identification of helicopter engine dynamics from closed loop data p 855 N90-27627
Energy Efficient Engine acoustic supporting technology report [NASA-CR-174834] p 930 N90-28557
- TEST VEHICLES**
The integrated test vehicle, (I.T.V.) - A vehicle for cost-effective hypersonic testing [AIAA PAPER 90-0630] p 352 A90-26974
- TETRAHEDRONS**
Generation of tetrahedral meshes around complete aircraft p 310 A90-26536
- TF-30 ENGINE**
F-111/TF30 engine monitoring system - A fusion of past, present, and future technology p 425 A90-30817
Concept demonstration of the use of interactive fault diagnosis and isolation for TF30 engines p 617 A90-41177
- THERMAL ANALYSIS**
Finite element analysis of nonstationary temperature fields in gas turbine components p 271 A90-21324
Estimation of the efficiency of a ramjet engine with a thermocompressor using fuel conversion products p 255 A90-23412
A numerical three-dimensional thermal stress analysis for cooled blades [ASME PAPER 89-GT-168] p 341 A90-23853
Thermal structures - Four decades of progress [AIAA PAPER 90-0971] p 411 A90-29305
Dornier Composite Aircraft - Economical and faultless p 732 A90-44751
Subsystem thermal integration - A new challenge to the aircraft designer [AIAA PAPER 90-3274] p 836 A90-48865
Optimum element density studies for finite-element thermal analysis of hypersonic aircraft structures [NASA-TM-4163] p 369 N90-17074
Engine testing of thermographic phosphors [DE90-013269] p 885 N90-28059
- THERMAL BOUNDARY LAYER**
Thermal structures - Four decades of progress [AIAA PAPER 90-0971] p 411 A90-29305
- THERMAL BUCKLING**
The prediction and measurement of thermoacoustic response of plate structures [AIAA PAPER 90-0988] p 451 A90-29400
- THERMAL CONDUCTIVITY**
Increasing the heat conductivity of elastic damping elements of MR material p 102 A90-14580
Thermal/structural analyses of several hydrogen-cooled leading-edge concepts for hypersonic flight vehicles [AIAA PAPER 90-0053] p 274 A90-23702
Vapor grown carbon fiber for space thermal management systems p 943 A90-50128
Thermal interaction between an impinging hot jet and a conducting solid surface [AIAA PAPER 90-3010] p 956 A90-50636
Thermal/structural analyses of several hydrogen-cooled leading-edge concepts for hypersonic flight vehicles [NASA-TM-102391] p 215 N90-14511
- THERMAL CONTROL COATINGS**
Properties and characterisation of novel thermal barrier systems for gas turbines p 62 A90-12538
Carbon-carbon for NASP p 599 A90-36872

Thermal nondestructive characterization of the integrity of protective coatings p 770 A90-44325
 Thermal barrier coating life prediction model development, phase 1
 [NASA-CR-182230] p 193 N90-13388
 Thermal barrier coatings for gas turbine and diesel engines
 [NASA-TM-102408] p 205 N90-13636
 Molten salt induced high temperature degradation of thermal barrier coatings p 952 N90-28704
 Effect of protective coatings on mechanical properties of superalloys p 952 N90-28707

THERMAL CYCLING TESTS

Predicting crack growth under thermo-mechanical cycling p 209 A90-18169
 Strength of the guide vane components of gas turbines p 266 A90-21318
 A rate theory investigation of cyclic loading and plastic deformation in the high stress and ambient temperature range p 954 A90-49884
 Use of unbalanced laminates as a screening method for microcracking p 948 A90-50217
 Estimation of the safety factor of turbine blades under thermal cycling and vibration loading p 958 A90-52356

Investigation of the failure modes in a metal matrix composite under thermal cycling
 [AD-A216195] p 357 N90-17825
 The stress and temperature dependence of creep in an Al-2.0 wt percent Li alloy
 [AD-A223676] p 953 N90-29480

THERMAL DECOMPOSITION

Development of a mathematical model for the thermal decomposition of aviation fuels
 [AD-A221673] p 875 N90-26994
 Toxicity of thermolysis products from the materials of airplane cockpits
 [CEAT-PV-M6/5924/02] p 876 N90-27895

THERMAL DEGRADATION

Thermal stability of jet fuel
 [DE90-002760] p 269 N90-15288

THERMAL EMISSION

Aerosol effects on jet-engine IR radiation p 40 A90-10152
 Evaluation of a damaged F/A-18 horizontal stabilizer
 [AD-A212573] p 107 N90-12597

THERMAL ENVIRONMENTS

Prediction of the aerodynamic environment and heat transfer for rotor-stator configurations
 [ASME PAPER 89-GT-89] p 359 A90-23807
 Combining thermal and high level acoustics p 770 A90-43729
 Fatigue life assessment of a leaded electronic component under a combined thermal and random vibration environment p 770 A90-43734
 Acoustic-thermal environment for USB flap structure. Report 1: Ground simulation test results
 [NAL-TM-567] p 88 N90-11697
 Correlation/validation of finite element code analyses for vibration assessment of avionics equipment
 [AD-A220393] p 654 N90-23398

THERMAL EXPANSION

Low-expansion MMCs boost avionics p 203 A90-17291
 Thermal barrier characteristics of partially stabilized zirconia coatings on Incoloy alloy 909 (A controlled expansion alloy)
 [ASME PAPER 89-GT-146] p 354 A90-23839
 Composites boost 21st-century aircraft engines p 442 A90-29704
 A friendly alloy --- aircraft construction materials p 784 A90-44173
 Use of unbalanced laminates as a screening method for microcracking p 948 A90-50217

THERMAL FATIGUE

An oxidation fatigue interaction damage model for thermal fatigue crack growth p 62 A90-11539
 Designing turbine blades for fatigue and creep p 112 A90-18007
 Predicting crack growth under thermo-mechanical cycling p 209 A90-18169
 Time dependent effects on high temperature low cycle fatigue and fatigue crack propagation on nickel base superalloys p 443 A90-29881
 Coatings for high temperature corrosion in aero and industrial gas turbines p 443 A90-30479
 Cyclic deformation, fatigue and fatigue crack propagation in Ni-base alloys p 531 A90-34162
 Life prediction and fatigue p 532 A90-34163
 Recent advances in fatigue life analysis methods for aerospace applications p 677 A90-41338
 Acoustic-thermal environment for USB flap structure. Report 1: Ground simulation test results
 [NAL-TM-567] p 88 N90-11697

Thermal fatigue durability for advanced propulsion materials

[NASA-TM-102348] p 215 N90-14641
 Thermal mechanical fatigue of coated blade materials
 [AD-A214258] p 256 N90-15107
 Damage tolerance analysis for manned hypervelocity vehicles. Volume 1: Final technical report
 [AD-A221970] p 887 N90-28106
 Evaluation of high temperature protective coatings for gas turbine engines under simulated service conditions p 952 N90-28712

THERMAL INSULATION

Thermal/structural analysis of the shaft-disk region of a fan drive system
 [NASA-TM-101687] p 610 N90-22807
 Space plane model for visual measurement of aerodynamic heating
 [DE90-505514] p 720 N90-25949

THERMAL PROTECTION

TBCs for better engine efficiency --- thermal barrier coatings p 203 A90-17294
 The selection and performance of thermal sprayed abrasible seal coatings for gas turbine engines
 [SAE PAPER 890929] p 286 A90-24694
 Thermal protection systems for hypersonic transport vehicles
 [SAE PAPER 901306] p 882 A90-49358
 Ceramic materials and coatings for future aerospace applications - Challenge of the 1990's p 942 A90-50071

Development and fabrication of structural components for a scramjet engine
 [NASA-CR-181945] p 510 N90-20088

THERMAL RESISTANCE

Interstitial materials for low thermal resistance joints in avionic equipment
 [SAE PAPER 891441] p 356 A90-27412
 Interfaces properties of high temperature polymer composite systems p 941 A90-50062
 Finite element analysis of structural components using viscoplastic models with application to a cowl lip problem
 [NASA-CR-185189] p 690 N90-23769
 NASA Langley Research Center National Aero-Space Plane Mission simulation profile sets
 [NASA-TM-102670] p 924 N90-28541

THERMAL SIMULATION

Performance evaluations of oxidation-resistant carbon-carbon composites in simulated hypersonic vehicle environments p 874 A90-48131
 Acoustic-thermal environment for USB flap structure. Report 1: Ground simulation test results
 [NAL-TM-567] p 88 N90-11697

THERMAL STABILITY

Intermetallic compounds for strong high-temperature materials - Status and potential p 125 A90-15022
 Temperature insensitive fiber coil sensor for altimeters p 339 A90-26374
 Analysis and practical design of ceramic-matrix composite components p 445 A90-28135
 The status of high temperature polymers for composites - Likely candidates p 528 A90-31516
 Development of ceramic components for high-temperature gas turbines p 602 A90-35951
 A study of the stability and thermal stability of complex reinforced structures p 880 A90-48541
 High temperature behavior of the innovation carbon/CSPI composite p 941 A90-50067
 Thermo-oxidative stability studies of PMR-15 polymer matrix composites reinforced with various continuous fibers p 941 A90-50068
 Improved thermal performance using allylindac-imides p 946 A90-50175

Thermal stability of jet fuel
 [DE90-001180] p 206 N90-14385
 Thermal stability of jet fuel
 [DE90-002760] p 269 N90-15288
 High speed commercial transport fuels considerations and research needs
 [NASA-TM-102535] p 800 N90-21869
 Three-dimensional analysis on flow and temperature distributions for aircraft fuel thermal stability
 [AD-A219651] p 678 N90-23571

THERMAL STRESSES

Thermostructural behavior of electromagnetic windows - Elaboration of a code package
 [ONERA, TP NO. 1989-145] p 76 A90-11167
 The design of rotor blades taking into account the combined effects of vibratory and thermal loads p 40 A90-11553
 The tape method for the automatic partitioning of an arbitrary region when calculating temperature stresses p 138 A90-14587
 Optimum design of rotational wheels under transient thermal and centrifugal loading p 270 A90-20770

Thermal/structural analyses of several hydrogen-cooled leading-edge concepts for hypersonic flight vehicles

[AIAA PAPER 90-0053] p 274 A90-23702
 Redesign of an electro-optical shroud in graphite/epoxy p 676 A90-40215
 Life estimation of a gas turbine afterburner spraybar p 739 A90-42662
 Effects of a heat cycle on material strength
 [NAL-TM-562] p 113 N90-11737
 Stress intensity factors for cracking metal structures under rapid thermal loading. Volume 2: Theoretical background
 [AD-A213297] p 213 N90-13812
 Thermal/structural analyses of several hydrogen-cooled leading-edge concepts for hypersonic flight vehicles
 [NASA-TM-102391] p 215 N90-14511
 Optimum element density studies for finite-element thermal analysis of hypersonic aircraft structures
 [NASA-TM-4163] p 369 N90-17074
 Shock-shock boundary layer interactions p 318 N90-17569

Investigation of the failure modes in a metal matrix composite under thermal cycling
 [AD-A216195] p 357 N90-17825
 Calculation of temperature distribution in various turbine blades using a boundary-fitted coordinate transformation method p 929 N90-28550

THERMOCHEMISTRY

Thermochemical calculations with inert compounds [FOA-C-20759-2.1] p 206 N90-13677

THERMOCOUPLES

Attachment of lead wires to thin film thermocouples mounted on high temperature materials using the parallel gap welding process
 [NASA-TM-102442] p 543 N90-21361

THERMODYNAMIC CYCLES

Inverse cycle engine for hypersonic air-breathing propulsion
 [ONERA, TP NO. 1989-121] p 50 A90-12611
 Mathematical simulation model of an aircraft gas turbine p 745 A90-44721
 Computer aided analysis of gas turbine cycles p 779 A90-45289

Cycle analysis of scramjet engines
 [NAL-TR-1002] p 51 N90-10035

Cycle analysis for helicopter gas turbine engines
 [RAE-TM-P-1154] p 256 N90-15921
 Preliminary design of a supersonic Short Takeoff and Vertical Landing (STOVL) fighter aircraft
 [NASA-CR-186670] p 649 N90-23394

THERMODYNAMIC EFFICIENCY

Effect of vane and blade numbers on performance of transonic turbine stage p 189 A90-17789
 Estimation of the efficiency of a ramjet engine with a thermocompressor using fuel conversion products p 255 A90-23412
 Current status of ceramic gas turbine R&D in Japan
 [ASME PAPER 89-GT-114] p 359 A90-23818
 Research and development of advanced gas turbine [DE90-503377] p 776 N90-26335
 Overview on hot gas tests and molten salt corrosion experiments at the DLR p 953 N90-28714

THERMODYNAMIC EQUILIBRIUM

RAMSCRAM: A flexible ramjet/scramjet engine simulation program
 [NASA-TM-102451] p 194 N90-14235

THERMODYNAMIC PROPERTIES

Application of three-dimensional methods for the calculation of gas dynamic and thermal processes at the design of gas turbines for air breathing engines p 46 A90-12552

Thermodynamic calculation of the compressors of gas turbine engines and powerplants at high air pressures p 130 A90-14585

Mathematical model of turboprop engine behaviour p 254 A90-23351

Advanced core technology - Key to subsonic propulsion benefits
 [ASME PAPER 89-GT-241] p 342 A90-23890

The application of cast SiC/Al to rotary engine components
 [NASA-CR-179610] p 192 N90-13385

Investigation of surface water behavior during glaze ice accretion p 485 N90-20927

The stress and temperature dependence of creep in an Al-2.0 wt percent Li alloy
 [AD-A223876] p 953 N90-29480

THERMODYNAMICS

Thermodynamics and the future turbine engines
 [ONERA, TP NO. 1989-165] p 253 A90-21031
 An open-loop transient thermodynamic model of the Cougar turbojet
 [AD-A211774] p 114 N90-11745
 Thermal fatigue durability for advanced propulsion materials
 [NASA-TM-102348] p 215 N90-14641

- A study of variable geometry in advanced gas turbines p 255 N90-15104
- Performance of a supercharged direct-injection stratified-charge rotary combustion engine [NASA-TM-103105] p 748 N90-25982
- Concentration, temperature, and density in a hydrogen-air flame by excimer-induced Raman scattering p 875 N90-26903
- Molten salt induced high temperature degradation of thermal barrier coatings p 952 N90-28704
- Three-dimensional numerical study of thunderstorm downdrafts and associated outflow boundaries p 963 N90-29746
- THERMOELASTICITY**
 - Active control of aerothermoelastic effects for a conceptual hypersonic aircraft [AIAA PAPER 90-3337] p 863 A90-47597
 - Structural and dynamic analysis of the A330/340 composite RAT blade — ram air turbine p 942 A90-50083
- THERMOGRAPHY**
 - The application of infrared thermography to the measurement of heat fluxes in a wind tunnel [ONERA, TP NO. 1989-192] p 261 A90-21051
 - Determination of convective transfer coefficients on a wind-tunnel model by stimulated infrared thermography [ONERA, TP NO. 1989-218] p 351 A90-25351
 - Liquid crystal thermography for aerodynamic heating measurements in short duration hypersonic facilities p 446 A90-28262
 - Applications of infra-red thermography in a hypersonic blowdown wind tunnel p 438 A90-28300
 - Infrared thermography in blowdown and intermittent hypersonic facilities p 440 A90-31302
 - An infrared camera system for detection of boundary layer transition in the ETW p 539 A90-34249
 - Aerodynamic applications of infrared thermography p 770 A90-44147
 - Engine testing of thermographic phosphors [DE90-013269] p 885 N90-28059
 - The application of infrared thermography to the nondestructive testing of composite materials p 886 N90-28084
 - Infrared thermography p 911 N90-29325
- THERMOGRAVIMETRY**
 - Improved Thermo-Oxidative-Deposition screening tests for turbine lubricants [AD-A217795] p 533 N90-21188
- THERMOMECHANICAL TREATMENT**
 - Predicting crack growth under thermo-mechanical cycling p 209 A90-18169
 - Thermomechanical processing of superalloys p 531 A90-34156
 - Aluminum lithium alloys for Navy aircraft p 267 N90-15193
- THERMOPLASTIC FILMS**
 - Evaluation of the thermoplastic film interleaf concept for improved damage tolerance p 946 A90-50179
- THERMOPLASTIC RESINS**
 - Thermoplastic composite fighter forward fuselage p 81 A90-14659
 - Material of the '90s? p 265 A90-20259
 - Air Force application of injection molding technology [SME PAPER EM89-103] p 274 A90-23686
 - The use of fibre reinforced thermoplastics for helicopter primary structures and their engineering substantiation p 441 A90-28191
 - Evaluation of 3-D reinforcements in commingled, thermoplastic structural elements p 441 A90-28192
 - Analysis and testing of fiber-reinforced thermoplastic composite vertical stabilizer skins for an advanced attack helicopter p 441 A90-28193
 - Fibre reinforced thermoplastic integral constructions in modular build-up technology - The 'thermoplastic in-situ-technique' p 534 A90-31879
 - Thermoplastic composites, past, present and future p 529 A90-31882
 - Fabrication of aircraft structures from thermoplastic drapable preforms p 468 A90-33125
 - Designing aerospace structures with Du Pont's LDF thermoplastic composites p 530 A90-33126
 - Structural components of fiber-reinforced thermoplastics p 676 A90-41111
 - Comparison of processing techniques for Filmix unidirectional commingled fabric p 940 A90-50058
 - Innovative design concepts for thermoplastic composite materials p 940 A90-50059
 - Repair of thermoplastic composite structures by fusion bonding p 941 A90-50060
 - The effect of jet fuel absorption on advanced aerospace thermoset and thermoplastic composites p 942 A90-50082
 - Toughened cyanates for aerospace applications [AIAA PAPER 90-0761] p 942 A90-50088
 - 977 - Characterization of a family of new toughened epoxy resins p 943 A90-50089
- Improved melt flow and physical properties of Mitsui Toatsu's LARC-TPI 1500 series polyimide p 943 A90-50134
- Improved damage tolerance by controlling thermoplastic solubility in thermoset composites p 944 A90-50138
- Rigidite 5255-3 - A highly damage tolerant prepreg resin system with a well balanced property profile p 944 A90-50139
- Viscoelastic relaxation in bolted thermoplastic composite joints p 945 A90-50158
- Composites for aerospace application from Kevlar aramid reinforced PEKK thermoplastic p 946 A90-50176
- Characterization of LaRC-TPI 1500 powders - A new version with controlled molecular weight p 946 A90-50177
- Improved fiber reinforced polyphenylene sulfide thermoplastic composites p 947 A90-50180
- Effect of molecular weight and end group control on the adhesion behavior of thermoplastic polyimides and poly(imide siloxane) segmented copolymers p 947 A90-50199
- Integrally heated tooling for economical, nonautoclave production of thermoplastic parts p 956 A90-50200
- Electrostatic dry powder prepping of carbon fiber p 948 A90-50215
- THERMOPLASTICITY**
 - High performance thermoplastic composites with poly(etherketoneketone) matrix p 529 A90-31646
 - Three dimensional turbine blade analysis in thermo-viscoplasticity p 540 A90-34324
- THERMOSETTING RESINS**
 - Toughened thermosets for damage tolerant carbon fiber reinforced composites p 443 A90-29825
 - Strength substantiation of the all composite airframe (A materials data base approach) p 490 A90-31519
 - The effect of jet fuel absorption on advanced aerospace thermoset and thermoplastic composites p 942 A90-50082
 - Automated prepreg tow placement for composite structures p 954 A90-50113
 - New cyanate ester resin with low temperature (125-200 C) cure capability p 944 A90-50135
 - Improved damage tolerance by controlling thermoplastic solubility in thermoset composites p 944 A90-50138
- THICK WALLS**
 - Calculation of thick wall fiber binders for rotor components of modern helicopters [MBB-UD-554/84-PUB] p 735 N90-25137
- THICKNESS**
 - Optimization of the relative thicknesses of a high-aspect-ratio wing in a multicenteral formulation p 334 A90-24133
 - Ultrasonic techniques for aircraft ice accretion measurement p 485 N90-20926
- THIN AIRFOILS**
 - Irregular interaction of a strong shock wave with a thin profile p 9 A90-12267
 - Analysis of high-incidence separated flow past airfoils p 147 A90-16781
 - Pressure fluctuations in the tip region of a blunt-tipped airfoil p 154 A90-18136
 - Unsteady streamlines near the trailing edge of NACA 0012 airfoil at a Reynolds number of 125,000 p 155 A90-18158
 - Computations of unsteady transonic flows about thin airfoils by integral equation method p 158 A90-18609
 - An experimental investigation of the turbulent structure in a two-dimensional momentumless wake p 474 A90-33515
 - Comment on 'Improved thin-airfoil theory' p 554 A90-35772
 - A visualization study of the interaction of a free vortex with the wake behind an airfoil p 623 A90-41119
 - An airfoil theory of bifurcating laminar separation from thin obstacles p 702 A90-42639
 - Numerical simulation of transonic porous airfoil flows p 707 A90-44433
 - Two dimensional post stall maneuver of a NACA 0015 airfoil at high pitching rates [AIAA PAPER 90-2810] p 710 A90-45150
 - Effects of onset free-stream turbulence on the performance characteristics of an airfoil [AIAA PAPER 90-3025] p 790 A90-45867
- THIN BODIES**
 - Dynamic analysis of lifting surfaces of small relative thickness in the case of finite displacements p 129 A90-14560
 - Aerodynamic characteristics of thin bodies moving in a gas with shock waves p 297 A90-24140
- THIN FILMS**
 - Thin film eddy current impulse deicer [AIAA PAPER 90-0761] p 183 A90-20012
 - Application of piezoelectric foils in experimental aerodynamics p 446 A90-28258
- A transition detection study at Mach 1.5, 2.0, and 2.5 using a micro-thin hot-film system p 436 A90-28260
- Skin effect in flow of a disperse fluid past a wing profile p 395 A90-30334
- Attachment of lead wires to thin film thermocouples mounted on high temperature materials using the parallel gap welding process [NASA-TM-102442] p 543 N90-21361
- Self-lubricating surfaces by ion beam processing [AD-A222489] p 884 A90-27118
- A reliable, maintenance-free oxygen sensor for aircraft using an oxygen-sensitive coating on potentiometric electrodes [AD-A222696] p 927 N90-28545
- THIN LAYER CHROMATOGRAPHY**
 - Determination of additive contents in aviation and turbine oils p 532 A90-34681
- THIN PLATES**
 - Flutter analysis of composite panels using high-precision finite elements p 207 A90-16725
 - Eigenvalue problem in the theory of flow past thin profiles at high supersonic velocity p 295 A90-24096
 - Turbulent plane jet excited mechanically by an oscillating thin plate in the potential core p 553 A90-35262
 - An investigation on combined extension and bending of thin sheets with a central crack [LR-561] p 137 N90-12958
- THIN WALLED SHELLS**
 - Theoretical studies of the active control of propeller-induced cabin noise p 893 A90-46351
 - A study of the stability and thermal stability of complex reinforced structures p 880 A90-46541
 - General buckling tests with thin-walled shells [DLR-MITT-89-13] p 213 N90-13816
- THIN WALLS**
 - Periodic response of thin-walled composite blades p 408 A90-28229
 - Divergence of thin-walled composite rods of closed profile in gas flow p 388 A90-29012
 - Thin walled cast high-strength structural parts p 65 N90-10242
- THIN WINGS**
 - Oscillating thin wings in inviscid incompressible flow p 2 A90-10224
 - Effect of similarity parameters on the aerodynamic quality and moment characteristics of a supersonic wing with blunt edges p 298 A90-24150
 - Nonstationary motion of an elastic profile in subsonic incompressible flow p 300 A90-24741
 - Calculation of the induced drag of a wing with arbitrary deformation p 388 A90-29183
 - Nonstationary hypersonic flow past a thin wing of variable shape p 470 A90-32559
 - Control point selection in the discrete vortex method p 470 A90-32567
 - The problem of supersonic flow past a thin wing of finite span with fully subsonic leading edges p 620 A90-39519
 - Additions and corrections to SUPER: A program for calculating steady and oscillatory supersonic flow over a thin wing, tail plane and fin [AD-A211771] p 90 N90-12501
 - Chordwise loading and camber for two-dimensional thin sections [AD-A213318] p 95 N90-12568
 - Wind tunnel tests of the influence of aerofoil thickness on the normal force and pitching moment of two slender wings at transonic and supersonic Mach numbers [ESA-TT-1129] p 237 N90-15889
- THREAT EVALUATION**
 - UK airmasses involving commercial air transport, May-August 1988 [ISSN-0951-6301] p 96 N90-11717
- THREE AXIS STABILIZATION**
 - An image analysis method for vehicle stabilization p 668 A90-40914
- THREE DIMENSIONAL BODIES**
 - An application of the surface-singularity method to wing-body-tail configurations p 9 A90-12229
 - Flow past a wing/fuselage combination with separation from the side edges of the wing p 295 A90-24088
 - Analysis of three-dimensional aerospace configurations using the Euler and Navier-Stokes equations p 305 A90-25798
 - Surface grid generation for complex three-dimensional geometries p 376 A90-26484
 - A comparison between theoretical and experimental results for a 3-D wing with damped pitching oscillations p 472 A90-33361
 - Flow over inclined finite length and width flat plates at low and high Reynolds numbers [AIAA PAPER 90-1467] p 562 A90-38624
 - A grid generation method for an aft-fuselage mounted capped-nacelle/pylon configuration with an actuator disk [AIAA PAPER 90-1564] p 565 A90-38703

- Computer-aided analysis of three-dimensional multiloop mechanisms p 669 A90-42328
- Advanced applications of BEM to gas turbine engine structures p 772 A90-45769
- Incompressible potential flow about three-dimensional configurations p 810 A90-48082
- Effect of the Mach number and shape of the front part of the obstacle on the separation zone length in supersonic flow p 903 A90-50816
- A time-marching method to calculate unsteady airloads on three-dimensional wings. Part 1: Linearized formulation [DLR-FB-89-58] p 634 A90-24254
- A time-marching method for calculating unsteady airloads on three-dimensional wings. Part 2: Full-potential formulation [DLR-FB-89-59] p 635 A90-24255
- THREE DIMENSIONAL BOUNDARY LAYER**
- Computation of three dimensional turbulent boundary layers in internal flows, including turbomachinery rotor blades p 12 A90-12555
- Calculation of three-dimensional boundary layers including hypersonic flows p 146 A90-16773
- Disturbance growth in an unstable three-dimensional boundary layer p 148 A90-16787
- Perturbations of a three-dimensional boundary layer produced by body irregularities p 150 A90-17107
- Numerical solution of the boundary-layer equations for a general aviation fuselage [AIAA PAPER 90-0305] p 163 A90-19786
- Development of the MZM numerical method for 3D boundary layer with interaction on complex configurations -- Multi-Zonal Marching [ONERA, TP NO. 1989-174] p 223 A90-21036
- Viscous corrections on wings in incompressible flow p 301 A90-25200
- Experimental investigation of three-dimensional turbulent boundary layers on 'infinite' swept curved wings p 303 A90-25589
- Fourth-order accurate three-dimensional compressible boundary-layer calculations p 308 A90-26136
- Stability limits for three-dimensional supersonic boundary layers [AIAA PAPER 90-1528] p 564 A90-38673
- Direct measurements of skin friction in a scramjet combustor [AIAA PAPER 90-2342] p 626 A90-42132
- Experimental study of the flow around an helicopter fuselage - Comparison with three-dimensional boundary layer calculations p 630 A90-42438
- The development of crossflow vortices on a 45 degree swept wing [SAE PAPER 892245] p 713 A90-45452
- Application of the inverse method of three-dimensional boundary layer analysis to the problem of flow past a wing with allowance for the effect of viscosity p 804 A90-46548
- Acoustic excitation of boundary layer oscillations on a yawing wing p 805 A90-46567
- Wave interactions in a three-dimensional attachment-line boundary layer p 811 A90-48715
- Application of boundary layer control to HST low speed configuration [AIAA PAPER 90-3199] p 812 A90-49103
- Generalized similarity solutions for three-dimensional laminar compressible wing boundary layers p 907 A90-51543
- A method of predicting 3-D compressible boundary layer on the rotating blade of turbomachinery p 908 A90-52777
- Stability and transition of three-dimensional boundary layers p 71 N90-10357
- Curvature effects on the stability of three-dimensional laminar boundary layers p 71 N90-10366
- A three-dimensional linear stability approach to transition on wings at incidence p 20 N90-10373
- A European collaborative investigation of the three-dimensional turbulent shear layers of a swept wing p 20 N90-10380
- Numerical simulation of transition in three-dimensional boundary layers [DLR-FB-89-12] p 212 N90-13728
- An efficient solver of the Eigenvalue problem of the linear stability equations for three dimensional, compressible boundary-layer flows p 276 N90-16172
- Development of transition criteria on the basis of ϵ to the N power for three dimensional wing boundary layers p 277 N90-16179
- Numerical investigation of some control methods for 3-D turbulent interactions due to sharp fins p 591 N90-21764
- Generation of circumferential velocity contours associated with pulsed point suction on a rotating disk p 691 N90-25065

- Report of the Fluid Dynamics Panel Working Group 10 on calculation of 3D separate turbulent flows in boundary layer limit [AGARD-AR-255] p 776 N90-26280
- Study of the flow around the prototype of A300: Results of the third test campaign at F2 and comparison with calculations [CERT-33/5025-29-DERAT] p 817 N90-27663
- Numerical simulations of blade-vortex interactions and lifting hovering rotor flows [ADA-224238] p 911 N90-29302
- THREE DIMENSIONAL COMPOSITES**
- Engineering design of tough ceramic matrix composites for turbine components [ASME PAPER 89-GT-294] p 343 A90-23892
- Evaluation of 3-D reinforcements in commingled, thermoplastic structural elements p 441 A90-28192
- Advanced joint of 3-D composite materials for space structure p 944 A90-50137
- Reinforcing fibers and technology development for resin composites. Consequences for aircraft structures [FOA-C-20777-2.5] p 876 N90-27883
- THREE DIMENSIONAL FLOW**
- A study of three-dimensional supersonic flow of a real gas past axisymmetric bodies p 3 A90-10938
- Calculation of three-dimensional turbulent flow in a linear turbine cascade [ONERA, TP NO. 1989-115] p 3 A90-11147
- Numerical simulation of three-dimensional unsteady flows in turbomachines [ONERA, TP NO. 1989-118] p 4 A90-11149
- 3D calculations of reacting flows within aircraft engine combustion chambers [ONERA, TP NO. 1989-153] p 67 A90-11173
- Three-dimensional modeling of turbulent transonic flow at the exit of a twin engine [AAAF PAPER NT 88-16] p 4 A90-11434
- Analysis of nonuniform subsonic flows about a row of moving blades p 6 A90-11779
- Finite element method for unsteady three-dimensional subsonic flows through a cascade oscillating with steady loading p 9 A90-11873
- Numerical calculation of unsteady aerodynamic forces for three-dimensional subsonic oscillating cascades by a finite element method p 9 A90-12219
- Shock capturing and loss prediction for transonic turbine blades using a pressure correction method p 11 A90-12518
- Navier-Stokes methods applied to turbomachinery blade design p 12 A90-12549
- Application of three-dimensional methods for the calculation of gas dynamic and thermal processes at the design of gas turbines for air breathing engines p 46 A90-12552
- A theoretical and experimental investigation of the Reynolds and apparent stresses in axial compressors p 12 A90-12554
- Numerical simulation of three-dimensional hypersonic inlet flowfields p 13 A90-12587
- A quasi-3D design method of transonic compressor blade with the function of improving velocity distribution p 49 A90-12589
- Three dimensional numerical simulation for an aircraft engine type combustion chamber [ONERA, TP NO. 1989-120] p 49 A90-12591
- Computation of transonic turbine cascade flow using Navier-Stokes equations p 14 A90-12621
- Calculation of axisymmetric flows in turbomachines, through an explicit time-splitting method p 14 A90-12622
- A multi-domain 3D Euler solver for flows in turbomachines [ONERA, TP NO. 1989-119] p 15 A90-12623
- Application of the double linearization theory to three-dimensional subsonic and supersonic cascade flutter p 50 A90-12638
- Direct simulation of three-dimensional hypersonic flow about intersecting blunt wedges p 16 A90-12835
- Numerical simulation of three-dimensional flow around parachute canopies p 84 A90-14438
- Wing boundary layer calculation and its application to aircraft design p 84 A90-15151
- The characteristic decay region of a class of three-dimensional wall jets p 85 A90-15241
- Experimental study of 2D/3D interactions between a vortical flow and a lifting surface p 86 A90-15849
- Three-dimensional aerodynamics of an annular airfoil cascade including loading effects p 87 A90-15889
- Numerical studies of incompressible flow around delta and double-delta wings p 150 A90-16845
- The interaction between a counter-rotating vortex pair in vertical ascent and a free surface p 151 A90-17580
- Potential flow calculation for three-dimensional wings and wing-body combination in oscillatory motion p 153 A90-17976

- Analyses of full 3D S1-S2 iterative solution in CAS transonic compressor rotor and comparison with quasi-3D S1-S2m iterative solution and L2F measurement p 157 A90-18532
- Full 3D iterative solution of transonic flow for a swept wing test channel p 160 A90-19431
- The computational method for the transonic wing design p 160 A90-19438
- An efficient upwind relaxation-sweeping algorithm for three-dimensional Euler equations [AIAA PAPER 90-0129] p 162 A90-19695
- Three-dimensional solution-adaptive grid generation on composite configurations [AIAA PAPER 90-0329] p 164 A90-19799
- A three-dimensional upwind parabolized Navier-Stokes code for chemically reacting flows [AIAA PAPER 90-0394] p 165 A90-19831
- Navier-Stokes analysis of a lobed mixer and nozzle [AIAA PAPER 90-0453] p 192 A90-19852
- Parabolized Navier-Stokes predictions of three-dimensional hypersonic flows with strong crossflow effects p 223 A90-20508
- Numerical simulation of transonic wing flows using a zonal Euler, boundary-layer, Navier-Stokes approach p 225 A90-21596
- A numerical method for three-dimensional viscous flows [AIAA PAPER 90-0236] p 228 A90-22186
- Simulation and analysis of a delta planform with multiple jets in ground effect [AIAA PAPER 90-0299] p 228 A90-22195
- Controlled three-dimensionality in unsteady separated flows about a sinusoidally oscillating flat plate [AIAA PAPER 90-0689] p 230 A90-22244
- Critical evaluation of three-dimensional supersonic combustor calculations [AIAA PAPER 90-0207] p 272 A90-22265
- Experimental and theoretical study of the swirling flow in centrifugal compressor volutes [ASME PAPER 89-GT-183] p 273 A90-22663
- Time-dependent and time-averaged turbulence structure near the nose of a wing-body junction p 231 A90-23036
- Leading- and trailing-edge flaps on supersonic delta wings p 233 A90-23285
- A three-dimensional space marching algorithm for the solution of the Euler equations on unstructured grids [AIAA PAPER 90-0014] p 234 A90-23701
- Measurement and calculation of the three-dimensional flow in axial compressor stators, with and without end-bends [ASME PAPER 89-GT-6] p 287 A90-23753
- Improvement of 3D full-potential method and computation of flowfield of CAS compressor rotor [ASME PAPER 89-GT-17] p 288 A90-23760
- 3D Mean-Stream-Line Method - A new engineering approach to the inverse problem of 3D cascade [ASME PAPER 89-GT-48] p 289 A90-23774
- Mach number effects on secondary flow development downstream of a turbine cascade [ASME PAPER 89-GT-67] p 290 A90-23790
- An approximate 3-D aerodynamic design method for centrifugal impeller blades [ASME PAPER 89-GT-73] p 291 A90-23794
- Three-dimensional separated flow field in the endwall region of an annular compressor cascade in the presence of rotor-stator interaction. I - Quasi-steady flow field and comparison with steady-state data [ASME PAPER 89-GT-76] p 291 A90-23797
- Three-dimensional separated flow field in the endwall region of an annular compressor cascade in the presence of rotor-stator interaction. II - Unsteady flow and pressure field [ASME PAPER 89-GT-77] p 291 A90-23798
- Three-dimensional solutions for inviscid incompressible flow in turbomachines [ASME PAPER 89-GT-140] p 291 A90-23837
- Three-dimensional relief in turbomachinery blading [ASME PAPER 89-GT-151] p 292 A90-23840
- Simulation of three-dimensional viscous flow within a multistage turbine [ASME PAPER 89-GT-152] p 292 A90-23841
- Verification of an impeller design by laser measurements and 3D-viscous flow calculations [ASME PAPER 89-GT-159] p 292 A90-23847
- An experimental study of heat transfer and film cooling on low aspect ratio turbine nozzles [ASME PAPER 89-GT-187] p 361 A90-23865
- The extension and application of three-dimensional time marching analyses to incompressible turbomachinery flows [ASME PAPER 89-GT-212] p 293 A90-23878
- Topology of computed incompressible three-dimensional separated flow field around high-angle-of-attack cone-cylinders p 366 A90-25764

Computation of steady three dimensional transonic internal flows p 304 A90-25771

Calculation of tip leakage flow with three-dimensional Euler code p 304 A90-25772

Turbulence models for 3D transonic viscous flows. II p 306 A90-25820

Transonic aerodynamics analysis of unconventional wing configurations by 3D-Euler code p 306 A90-25835

Topological study of three-dimensional vortex interactions p 367 A90-25885

Experimental studies of 90 deg corner cascades in the National Full-Scale Aerodynamic Complex [AIAA PAPER 90-1826] p 307 A90-25935

Application of I-DEAS grid generator for three-dimensional transonic flow analysis p 311 A90-26542

Numerical interactive grid generation for 3D-flow calculations p 312 A90-26556

Parallel computation of three-dimensional transonic flow problems with complex geometries [AIAA PAPER 90-0336] p 313 A90-26936

Three-dimensional shock-shock interactions on the scramjet inlet [AIAA PAPER 90-0529] p 314 A90-26963

Comparison of 3-D viscous flow computations of Mach 5 inlet with experimental data [AIAA PAPER 90-0600] p 314 A90-26970

Measurements, visualization and interpretation of 3-D flows - Application within base flows p 386 A90-28252

Impact of multigrid smoothing analysis on three-dimensional potential flow calculations p 449 A90-29147

Unsteady aerodynamics for turbomachinery aeroelastic applications p 394 A90-29888

Calculation of internal flows using a single-pass, parabolized Navier-Stokes analysis p 469 A90-32458

Comparison of two potential flow methods for transonic flutter analysis p 471 A90-33356

On an extension of the Kutta-Joukowski theorem to the supersonic regime p 477 A90-34819

Development of a new low-Reynolds-number type Reynolds stress model and its application to a lobe mixer flow --- to improve thrust efficiency and suppress jet noise in turbofan engines p 584 A90-35229

Velocity and turbulence characteristics of isothermal lobed mixer flows --- in turbofan jet engines p 584 A90-35230

Navier-Stokes computation of flow around a round-edged double-delta wing p 555 A90-36251

An analytic solution on hypersonic flow over an arbitrary slender body with near power-law profile p 558 A90-37736

A method for solving three-dimensional viscous incompressible flows over slender bodies p 558 A90-37890

Wall interference correction for three-dimensional transonic flows [AIAA PAPER 90-1408] p 558 A90-37947

The development of a 3-D laser velocimeter for the NASA Langley low turbulence pressure wind tunnel [AIAA PAPER 90-1385] p 597 A90-38484

Evaluation of transonic wall interference assessment and correction for semi-span wing data [AIAA PAPER 90-1433] p 597 A90-38487

A locally implicit scheme for 3-D compressible viscous flows [AIAA PAPER 90-1525] p 563 A90-38670

Calculation of two- and three-dimensional flow in a transonic turbine cascade with particular regard to the losses [AIAA PAPER 90-1542] p 565 A90-38686

Navier-Stokes computations of vortical flows [AIAA PAPER 90-1628] p 568 A90-38757

Three-dimensional measurement, display, and interpretation of fluid flow datasets p 679 A90-38854

Navier-Stokes solutions for vortical flows over a tangent-ogive cylinder p 620 A90-39780

Numerical solution of 3-D hybrid problems in turbomachinery p 621 A90-40501

Application of CFD to pitch/yaw thrust vectoring spherical convergent flap nozzles [AIAA PAPER 90-2023] p 657 A90-40597

Three-component LDA measurements in an axial-flow compressor p 683 A90-40943

Three dimensional transonic and supersonic flow prediction in axi-vectorized nozzles using a finite volume method [AIAA PAPER 90-2026] p 624 A90-41989

Calculation of three-dimensional jet interaction flowfields [AIAA PAPER 90-2099] p 624 A90-42018

Application of 3-D Navier-Stokes computation to bowed stacking turbine vane design [AIAA PAPER 90-2129] p 625 A90-42035

Application of 3-D flow analysis to the design of a high work transonic turbine p 628 A90-42395

Two- and three-dimensional effects in the supersonic mixing layer [AIAA PAPER 90-1978] p 703 A90-42708

Turbulent flow simulation of a three-dimensional turbine cascade [AIAA PAPER 90-2124] p 704 A90-42732

Using 3D Euler flow simulations to assess effects of periodic unsteady flow through turbines [AIAA PAPER 90-2357] p 706 A90-42783

Supersonic/hypersonic laminar/turbulent transition p 706 A90-42872

Shock-fitting in three space dimensions p 707 A90-44434

In-flight flow visualization characteristics of the NASA F-18 high alpha research vehicle at high angles of attack [SAE PAPER 892222] p 713 A90-45439

Transonic analysis of complex configurations using TRANAIR program [SAE PAPER 892289] p 714 A90-45467

Hypersonic CFD applications for the National Aero-Space Plane [SAE PAPER 892310] p 714 A90-45473

Numerical simulation of flow through the Langley parametric scramjet engine [SAE PAPER 892314] p 747 A90-45476

A unified pressure correction algorithm for computing complex fluid flows p 772 A90-45528

Navier-Stokes computations of three-dimensional laminar flows with buoyancy in a channel with wing-type vortex generators p 772 A90-45728

3D Euler analysis of ducted propfan flowfields [AIAA PAPER 90-3034] p 791 A90-45873

3-D analysis of laser measurements of vortex bursting on a chined forebody fighter configuration [AIAA PAPER 90-3020] p 793 A90-45887

Navier Stokes simulation of waverider flowfields [AIAA PAPER 90-3066] p 793 A90-45892

Calculation of three-dimensional viscous and inviscid hypersonic flows using split-matrix marching methods [AIAA PAPER 90-3070] p 794 A90-45894

Relative efficiency and accuracy of two Navier-Stokes codes for simulating attached transonic flow over wings [AIAA PAPER 90-3078] p 795 A90-45909

Numerical study of vortical flow over a sideslipping delta wing [AIAA PAPER 90-3001] p 798 A90-45936

Optimal blading density in axial-flow compressor stages with a developed three-dimensional flow p 851 A90-46505

Calculation of the heat flux at a three-dimensional critical point in supersonic flow past a body p 803 A90-46536

Calculation of three-dimensional flow past a plane supersonic air intake at angles of attack and sideslip p 805 A90-46573

Numerical simulations of three-dimensional rotor blade-vortex interactions p 807 A90-46879

Two- and three-dimensional problems of unsteady aerodynamics of low loaded turbomachinery blade rows stages p 813 A90-49452

Numerical simulation of three-dimensional nonstationary flows and variable aerodynamic forces in turbomachine stages p 814 A90-49465

A design method for turbomachinery blading in three-dimensional flow p 904 A90-51003

Numerical simulation of three-dimensional transonic flows p 905 A90-51020

A parametric study of radial turbomachinery blade design in three-dimensional subsonic flow [ASME PAPER 89-GT-84] p 905 A90-51257

Analysis of three-dimensional turbomachinery flows on C-type grids using an implicit Euler solver [ASME PAPER 89-GT-85] p 905 A90-51258

Unsteady lifting surface theory for a rotating cascade of swept blades [ASME PAPER 89-GT-306] p 906 A90-51259

The aerodynamic design of the contraction for a subsonic wind tunnel p 907 A90-51545

An application of topological analysis to studying the three-dimensional flow in cascades. I - Topological rules for skin-friction lines and section streamlines p 908 A90-52607

Fluid Dynamics of Three-Dimensional Turbulent Shear Flows and Transition [AGARD-CP-438] p 71 A90-10356

Simulation of glancing shock wave and boundary layer interaction [NASA-TM-102233] p 133 A90-11970

Multigrid calculations of 3-D turbulent viscous flows [NASA-CR-185154] p 143 A90-13323

Block-structured solution of three-dimensional transonic flows using parallel processing [AD-A212851] p 170 A90-13330

Practical systems for speckle velocimetry p 171 N90-13341

Recent progress in research pertaining to estimates of gas-side heat transfer in an aircraft gas turbine [NASA-TM-102460] p 194 N90-13394

A dynamic multiblock approach to solving the unsteady Euler equations about complex configurations p 214 N90-14497

Numerical simulation of the laminar and turbulent three dimensional flow on a delta wing with sharp leading edge p 278 N90-16186

Numerical simulation of supersonic free shear layers [AD-A216289] p 320 N90-17579

Comparison of two- and three-dimensional Navier-Stokes solutions with NASA experimental data for CAST-10 airfoil p 321 N90-17658

Contribution to the study of three-dimensional separation in turbulent incompressible flow [ESA-TT-1169] p 454 N90-18697

Three-dimensional viscous rotor flow calculations using a viscous-inviscid interaction approach [NASA-TM-102235] p 399 N90-19204

On total variation diminishing schemes for transonic turbulent flow computation p 479 N90-20945

Secondary Flows in Turbomachines [AGARD-CP-469] p 511 N90-21009

Parabolized calculations of turbulent three dimensional flows in a turbine duct p 482 N90-21013

Experimental and numerical study on basic phenomena of secondary flows in turbines p 512 N90-21014

An investigation of secondary flows in nozzle guide vanes p 512 N90-21016

Measurement of the flow field in the blade passage and side-wall region of a plane turbine cascade p 513 N90-21019

Centrifugal impeller geometry and its influence on secondary flows p 513 N90-21020

Calculation of the three dimensional turbulent flow in a linear turbine blade p 513 N90-21021

Generation and decay of secondary flows and their impact on aerodynamic performance of modern turbomachinery components p 514 N90-21023

Swept wing ice accretion modeling [NASA-TM-103114] p 570 N90-21727

Effective methods of controlling a junction vortex system in an incompressible, three-dimensional, turbulent flow p 571 N90-21732

Extension of a three-dimensional viscous wing flow analysis user's manual: VISTA 3-D code [NASA-CR-182024] p 574 N90-22538

Extension of a three-dimensional viscous wing flow analysis [NASA-CR-182023] p 631 N90-23348

Three-dimensional analysis on flow and temperature distributions for aircraft fuel thermal stability [AD-A219651] p 678 N90-23571

Composite reduced Navier Stokes procedures for flow problems with strong pressure interactions [AD-A219621] p 689 N90-23687

Numerical analysis of three-dimensional particle-laden flow equations [IAR-90-2] p 775 N90-26268

Informatics aspects of large flow calculations on the SX-2 supercomputer [NLR-MP-88037-U] p 776 N90-26290

Experiments with unsteady, free surface, three-dimensional vortices in a thermally stable, stratified fluid [AD-A222088] p 815 N90-26796

An approximate method for calculating three-dimensional inviscid hypersonic flow fields [NASA-TP-3018] p 883 N90-27066

The discretization of the three dimensional boundary layer equations [ETN-90-97292] p 884 N90-27987

Transonic 3-D Euler analysis of flows around fanjet engine and TPS (Turbine Powered Simulator). Comparison with wind tunnel experiment, evaluation of TPS testing method and 3-D flow [NAL-TR-1045] p 912 N90-29327

THREE DIMENSIONAL MODELS

Numerical study of single impinging jets through a crossflow p 17 A90-13020

Static aeroelastic analysis of fighter aircraft using a three-dimensional Navier-Stokes algorithm [AIAA PAPER 90-0435] p 166 A90-19845

Numerical study of the effects of icing on finite wing aerodynamics [AIAA PAPER 90-0757] p 169 A90-20010

Three dimensional photoelastic analysis of aeroengine parts p 270 A90-20077

Multi-processing on supercomputers for computational aerodynamics [AIAA PAPER 90-0337] p 282 A90-22199

A three dimensional inverse method in turbomachinery.
II - Experimental verification
[ASME PAPER 89-GT-137] p 360 A90-23834

A numerical three-dimensional thermal stress analysis for cooled blades
[ASME PAPER 89-GT-168] p 341 A90-23853

Swept wing ice accretion modeling
[AIAA PAPER 90-0756] p 300 A90-25042

Numerical simulation of vortex breakdown via 3-D Euler equations
[ONERA, TP NO. 1989-211] p 303 A90-25344

Computational and experimental analysis of transonic fanjet engine flow field using 3-D Euler code
p 306 A90-25809

Three-dimensional simulations of hypersonic flows
p 306 A90-25823

Quasi-three-dimensional grid generation by an algebraic homotopy procedure
p 376 A90-26481

2-D and 3-D unstructured mesh adaption relying on physical analogy
p 310 A90-26534

Interactive generation of unstructured grids for three dimensional problems
p 310 A90-26537

Geometric modelling of complex aerodynamic surfaces and three-dimensional grid generation
p 311 A90-26545

Stability of hingeless rotors in hover using three-dimensional unsteady aerodynamics
p 430 A90-28227

Aeroelastic analysis of wings using the Euler equations with a deforming mesh
[AIAA PAPER 90-1032] p 391 A90-29376

Three dimensional full potential method for the aeroelastic modeling of propfans
[AIAA PAPER 90-1120] p 393 A90-29392

Three dimensional turbine blade analysis in thermo-viscoplasticity
p 540 A90-34324

Development of a new low-Reynolds-number type Reynolds stress model and its application to a lobe mixer flow --- to improve thrust efficiency and suppress jet noise in turbofan engines
p 584 A90-35229

Development of a three-dimensional upwind parabolized Navier-Stokes code
p 602 A90-36253

A quadratic programming method for solving three dimensional elastic-plastic contact problems
p 603 A90-36417

Three dimensional Discrete Particle Simulation about the AFE geometry
[AIAA PAPER 90-1778] p 560 A90-38468

Two and three dimensional grid generation by an algebraic homotopy procedure
p 567 A90-38734

A computational study of the taxonomy of vortex breakdown
[AIAA PAPER 90-1624] p 568 A90-38753

Three-dimensional flux-split Euler schemes involving unstructured dynamic meshes
[AIAA PAPER 90-1649] p 569 A90-38777

3-D Euler calculations for aft-propfan integration
[AIAA PAPER 90-2147] p 625 A90-42044

Application of 3-D viscous code in the design of a high performance compressor
[AIAA PAPER 90-1914] p 740 A90-42694

Introducing the VRT gas turbine combustor
[AIAA PAPER 90-2452] p 743 A90-42808

Flight deck modernization
[SAE PAPER 892231] p 732 A90-45447

2D vs. 3D - Selection of pressure distributions to delay separation on wings
[AIAA PAPER 90-3026] p 790 A90-45868

3D transonic nacelle and winglet design
[AIAA PAPER 90-3064] p 794 A90-45897

A numerical method for relating two- and three-dimensional pressure distributions on transonic wings
[AIAA PAPER 90-3211] p 812 A90-48837

Analytical studies of three-dimensional combustion processes
[AD-A211903] p 126 N90-11837

Navier-Stokes simulation of the crossflow instability in swept-wing flows
[NASA-CR-186122] p 212 N90-13744

Forced and natural venting of aircraft cabin fires: A numerical simulation
p 326 N90-17597

A fast collocation method for transonic airfoil design
p 501 N90-20984

Numerical method for designing 3D turbomachinery blade rows
p 511 N90-20990

Supersonic nozzle design of arbitrary cross-section
p 515 N90-21035

Swept wing ice accretion modeling
[NASA-TM-103114] p 570 N90-21727

Grid patching approaches for complex three-dimensional configurations
p 573 N90-21985

Introducing the VRT gas turbine combustor
[NASA-TM-103176] p 688 N90-23591

Rotary-Jet thrust augmentor with jet-flapped blades
p 633 N90-24243

Development of a finite element based delamination analysis for laminates subject to extension, bending, and torsion
p 679 N90-25049

Fluid Dynamics Panel Working Group 12 on Adaptive Wind Tunnel Walls: Technology and Applications
[AGARD-AR-269] p 870 N90-26838

Limits of adaptation, residual interferences
p 871 N90-26844

Three-dimensional model testing in the transonic self-streamlining wind tunnel
p 938 N90-28583

Three-dimensional numerical study of thunderstorm downdrafts and associated outflow boundaries
p 963 N90-29746

THREE DIMENSIONAL MOTION

A comparison of a droplet impingement code to icing tunnel results
[AIAA PAPER 90-0670] p 352 A90-26979

THROATS

Supersonic nozzle design of arbitrary cross-section
p 515 N90-21035

THROTTLING

Effect of the control of turbocompressor guide vanes on the throttle characteristics of a bypass engine
p 255 A90-23425

THRUST

Basic principles of measuring thrust through exhaust to inlet total pressure ratio - Engine Pressure Ratio (EPR)
p 191 A90-18635

Design of an aero-engine thrust reverser blocker door
p 467 A90-31651

A modeling technique for STOVL ejector and volume dynamics
[AIAA PAPER 90-2417] p 663 A90-42168

Methods for determining the internal thrust of scramjet engine modules from experimental data
[AIAA PAPER 90-2340] p 743 A90-42777

Thrust law effects on the longitudinal stability of hypersonic cruise
[AIAA PAPER 90-2820] p 763 A90-45149

Effect of pylon wake with and without pylon blowing on propeller thrust
[NASA-TM-4162] p 173 N90-14190

Engine inlet distortion in a 9.2 percent scale vectored thrust STOVL model in ground effect
[NASA-TM-102358] p 318 N90-17561

Optimal control of an aircraft flying through a downburst
p 591 N90-21765

A modeling technique for STOVL ejector and volume dynamics
[NASA-TM-103167] p 589 N90-22566

Evaluation of various thrust calculation techniques on an F404 engine
[NASA-TP-3001] p 735 N90-25134

THRUST AUGMENTATION

Gearless crisp - The logical step to economic engines for high thrust
p 50 A90-12616

Thrust augmentation characteristics of jet reactions
[AIAA PAPER 90-0033] p 161 A90-19641

Advanced material applications for direct lift engines
[AIAA PAPER 90-2753] p 664 A90-42226

The North American Rockwell XFV-12A - Reflections and some lessons
[AIAA PAPER 90-3240] p 839 A90-49118

Characteristics of combustion driven pressure oscillations in advanced turbo-fan engines with afterburner
p 64 N90-10194

Rotary-Jet thrust augmentor with jet-flapped blades
p 633 N90-24243

THRUST BEARINGS

Retirement lives of rolling element bearings
p 680 A90-39980

Initiation of spalling in aircraft gas turbine bearings
[AIAA PAPER 90-2291] p 686 A90-42110

THRUST CONTROL

The fast-response requirement of powerplant thrust in the set of engineering and economic criteria of an aircraft
p 254 A90-23354

Performance of an optimized rotor blade at off-design flight conditions
[NASA-CR-4288] p 416 N90-19226

A comparison of time-optimal interception trajectories for the F-8 and F-15
[NASA-CR-186300] p 581 N90-21753

THRUST DISTRIBUTION

Dissipation thrust losses due to distortions of the jet nozzle profile
p 254 A90-23405

Flow rate and thrust coefficients for biaxial flows in a convergent nozzle
p 395 A90-30344

A simple dynamic engine model for use in a real-time aircraft simulation with thrust vectoring
[AIAA PAPER 90-2166] p 662 A90-42054

Some aerodynamic characteristics of the scissor wing configuration
[SAE PAPER 892202] p 713 A90-45423

THRUST MEASUREMENT

Flow around a jet and thrust measurement bias from static tests
[AAAF PAPER NT 88-11] p 40 A90-11431

Determination of the specific thrust in open regimes and design of a nonseparating convergent nozzle profile
p 395 A90-30339

Measurement effects on the calculation of in-flight thrust for an F404 turbofan engine
[NASA-TM-4140] p 114 N90-11741

THRUST REVERSAL

Flight test results of the F-15 SMTD thrust vectoring/thrust reversing exhaust nozzle --- STOL/Maneuvering Technology Demonstrator
[AIAA PAPER 90-1906] p 660 A90-41982

Aerodynamic interferences of in-flight thrust reversers in ground effect
p 921 N90-28529

Dynamic ground effects
p 922 N90-28531

THRUST VECTOR CONTROL

Minimum-time turns using vectored thrust
p 118 A90-14728

The fundamentals of vectored propulsion
p 180 A90-17461

STOVL wind tunnel tests demonstrate ejector viability
p 245 A90-21000

Analysis of the mathematical modeling of an aircraft flight trajectory with consideration of engine thrust effect on the force ratio on the aircraft
p 247 A90-23363

Engine inlet distortion in a 9.2 percent scaled vectored thrust STOVL model in ground effect
[AIAA PAPER 89-2910] p 301 A90-25043

Lessons learned in the development of a multivariable control system
p 432 A90-30713

Numerical calculation of the jet-interaction induced separation with respect to thrust vector control
p 584 A90-35228

Inverse heat transfer studies and the effects of propellant aluminum on TVC jet vane heating and erosion
[AIAA PAPER 90-1860] p 655 A90-40533

Application of CFD to pitch/yaw thrust vectoring spherical convergent flap nozzles
[AIAA PAPER 90-2023] p 657 A90-40597

Confined jet thrust vector control nozzle studies
[AIAA PAPER 90-2027] p 657 A90-40598

Flight test results of the F-15 SMTD thrust vectoring/thrust reversing exhaust nozzle --- STOL/Maneuvering Technology Demonstrator
[AIAA PAPER 90-1906] p 660 A90-41982

A simple dynamic engine model for use in a real-time aircraft simulation with thrust vectoring
[AIAA PAPER 90-2166] p 662 A90-42054

SDOF dynamic loads on a jet vane
[AIAA PAPER 90-2382] p 675 A90-42147

Computation of vectored nozzle performance
[AIAA PAPER 90-2752] p 627 A90-42225

Demonstrating technologies for enhanced fighter maneuverability - The Rockwell/MBB X-31
p 731 A90-43767

The Hawker P1127 vectored thrust fighter program - Lessons learned
[AIAA PAPER 90-3238] p 835 A90-48848

Status of the STOL and Maneuver Technology Demonstrator flight test program
[AIAA PAPER 90-3306] p 838 A90-48887

Flight control design considerations for STOVL powered-lift flight
[AIAA PAPER 90-3225] p 868 A90-49110

High alpha --- angles of attack of fighter aircraft
p 902 A90-52575

Aerodynamics of thrust vectoring
[NASA-CR-185074] p 172 N90-13354

An experimental investigation of thrust vectoring two-dimensional convergent-divergent nozzles installed in a twin-engine fighter model at high angles of attack
[NASA-TM-4155] p 237 N90-15884

Static investigation of a two-dimensional convergent-divergent exhaust nozzle with multi-axis thrust-vectoring capability
[NASA-TP-2973] p 397 N90-19193

Aerodynamics of Combat Aircraft Controls and of Ground Effects
[AGARD-CP-465] p 920 N90-28513

Aerodynamic and propulsive control development of the STOL and maneuver technology demonstrator
p 920 N90-28514

Inflight thrust vectoring: A further degree of freedom in the aerodynamic/flight mechanical design of modern fighter aircraft
p 921 N90-28528

THRUST-WEIGHT RATIO

Material requirements for future aeroengines
p 62 A90-12534

XG40 - Rolls-Royce advanced fighter engine demonstrator
p 112 A90-16002

Creep-fatigue interactions of gas turbine materials
p 131 A90-16011

- Aircraft design: A conceptual approach --- Book p 179 A90-17307
- Computerised structural analysis for engine components p 190 A90-18486
- Bonded airfoil attachments - A path to rotor structural efficiency [AIAA PAPER 90-2177] p 686 A90-42061
- More power for the Harrier p 745 A90-44597
- The turbofan of tomorrow p 850 A90-46150
- Methodology for estimating helicopter performance and weights using limited data p 829 A90-46936
- ### THUNDERSTORMS
- Modeling of turbulence and downbursts for flight simulators p 870 A90-48956
- Final results of the NASA storm hazards program p 819 A90-49834
- Maximum expected concentrations of hail in thunderstorm precipitation p 962 A90-52052
- Electric charge acquired by airplanes penetrating thunderstorms p 913 A90-52093
- The 1985 and 1986 direct strike lightning data, part 1 [NASA-TM-100533-PT-1] p 374 A90-18125
- The 1985 and 1986 direct strike lightning data, part 2 [NASA-TM-100533-PT-2] p 374 A90-18126
- A comparison of lightning network data with surface weather observations p 692 A90-23832 [AD-A220003]
- Three-dimensional numerical study of thunderstorm downdrafts and associated outflow boundaries p 963 A90-29746
- ### TIGHTNESS
- Pressure air tightness tests of laminated panels for wing leading edge heat shields [INFORME-I-377/89] p 357 A90-17873
- ### TILT ROTOR AIRCRAFT
- Damage tolerance analysis of dynamic components of rotary wing aircraft p 179 A90-17312
- Helicopter transmissions - Design for safety and reliability p 270 A90-20608
- Stowing the tilt-rotor p 246 A90-21703
- Advanced technology rotorcraft - Civil short haul transport of the future p 246 A90-21710
- The coming age of the tiltrotor. I p 246 A90-21711
- East coast Osprey flies p 246 A90-21713
- Calculations of the flow past bluff bodies, including tilt-rotor wing sections at $\alpha = 90$ deg [AIAA PAPER 90-0032] p 227 A90-22156
- The Pointer - Test and evaluation of the tiltrotor UAV --- unmanned aerial vehicle p 406 A90-28170
- BELLTECH - A multipurpose Navier-Stokes code for rotor blade and fixed wing configurations p 384 A90-28174
- Active control of gust- and interference-induced vibration of tilt-rotor aircraft p 429 A90-28201
- Tilt rotor aircraft aeroacoustics p 409 A90-28238
- An approach for analysis and design of composite rotor blades [AIAA PAPER 90-1005] p 449 A90-29276
- The coming age of the tiltrotor. II p 413 A90-30119
- What's best to tilt - The rotor or the wing? p 580 A90-36850
- Tilt rotor requirements on engine design and qualification p 587 A90-38534
- Development of the XV-15 tiltrotor research aircraft - Lessons learned p 581 A90-38540
- A review of tilt rotor download research p 630 A90-42437
- Eurofar - Status of the European tilt-rotor project p 645 A90-42441
- Improving tilt rotor aircraft performance with variable-diameter rotors p 646 A90-42445
- Active control of tiltrotor blade in-plane loads during maneuvers p 670 A90-42463
- Advocating international cooperation: The Eurofar program - An example and a hope --- European Future Advanced Rotorcraft program p 785 A90-46929
- The selection of convertible engines with current gas generator technology for high speed rotorcraft p 852 A90-46933
- CTR-1000 civil tiltrotor concept p 829 A90-46939
- Advanced rotorcraft V/STOL - Technology needs for high-speed rotorcraft [AIAA PAPER 90-3298] p 837 A90-48880
- Helicopter or tiltrotor - A Soviet view p 838 A90-48952
- Application of the wide-field shadowgraph technique to rotor wake visualization [NASA-TM-102222] p 88 A90-11700
- A CFD study of tilt rotor flowfields [NASA-CR-186116] p 171 A90-13349
- Preliminary design of four aircraft to service the California Corridor in the year 2010: The California Condor, California Sky-Hopper, high capacity short range transport tilt rotor aircraft needed to simplify intercity transportation [NASA-CR-186232] p 186 A90-14226
- An early overview of tiltrotor aircraft characteristics and pilot procedures in civil transport applications [DOT/FAA/DS-89/37] p 503 A90-21003
- Extension-torsion coupling behavior of advanced composite tilt-rotor blades p 651 A90-25057
- Ground-simulation investigations of VTOL airworthiness criteria for terminal-area operations [NASA-TM-102810] p 757 A90-25141
- Model tilt-rotor hover performance and surface pressure measurement [AD-A222535] p 845 A90-26827
- FAA Rotorcraft Research, Engineering, and Development Bibliography 1962-1989 [AD-A224256] p 902 A90-29299
- ### TILT ROTOR RESEARCH AIRCRAFT PROGRAM
- Tiltrotor aeroservoelastic design methodology at BHTI p 410 A90-28244
- Development of the XV-15 tiltrotor research aircraft - Lessons learned p 581 A90-38540
- The Bell Helicopter XV-3 and XV-15 experimental aircraft - Lessons learned [AIAA PAPER 90-3265] p 835 A90-48859
- ### TILT WING AIRCRAFT
- TW-68 tilt wing high speed commercial VTOL p 246 A90-21712
- What's best to tilt - The rotor or the wing? p 580 A90-36850
- A status review of non-helicopter V/STOL aircraft development. II p 580 A90-38028
- The Canadair CL-84 experimental aircraft - Lessons learned [AIAA PAPER 90-3205] p 834 A90-48833
- Advanced rotorcraft V/STOL - Technology needs for high-speed rotorcraft [AIAA PAPER 90-3298] p 837 A90-48880
- The LTV XC-142 experimental aircraft lessons learned [AIAA PAPER 90-3204] p 838 A90-49104
- ### TILTED PROPELLERS
- The Curtiss-Wright X-19 experimental aircraft - Lessons learned [AIAA PAPER 90-3206] p 834 A90-48834
- ### TILTING ROTORS
- The selection of convertible engines with current gas generator technology for high speed rotorcraft p 852 A90-46933
- High-speed rotorcraft V/STOL - An initial assessment p 829 A90-46938
- Mission performance comparison between tilt rotor, variable diameter tilt rotor and tilt wing aircraft p 830 A90-46940
- Application of a general-purpose mechanical systems analysis code to rotorcraft dynamics problems p 831 A90-46955
- Experiences in NASTRAN airframe vibration prediction at Bell Helicopter Textron p 832 A90-46964
- Application of the wide-field shadowgraph technique to rotor wake visualization [NASA-TM-102222] p 88 A90-11700
- A CFD study of tilt rotor flowfields [NASA-CR-186116] p 171 A90-13349
- Identification of XV-15 aeroelastic modes using frequency-domain methods [NASA-TM-101021] p 582 A90-21756
- An approach for design and analysis of composite rotor blades [AD-A219257] p 734 A90-25125
- ### TIME DEPENDENCE
- Numerical simulation of confined, spatially-developing mixing layers - Comparison to the temporal shear layer [AIAA PAPER 90-1462] p 562 A90-38619
- Transonic flow computations in convergent propulsion nozzles using the time-dependent mode p 708 A90-44459
- A multistage method for the solution of the Euler equations on unstructured grids p 708 A90-44460
- Effects of unsteady blowing on the lift of a circulation controlled cylinder p 713 A90-45325
- An assessment of robustness of flight control systems based on variable structure techniques p 57 A90-10895
- Prediction of two-dimensional time-dependent gasdynamic flows for hypersonic studies [UTIAS-335] p 718 A90-25935
- The steady and time-dependent aerodynamic characteristics of a combat aircraft with a delta or swept canard p 921 A90-28526
- ### TIME DIVISION MULTIPLE ACCESS
- Rapsat - Application of onboard processing for communication and surveillance in air traffic control [AIAA PAPER 90-0883] p 331 A90-25702
- Range Applications Joint Program Office GPS Range System data link p 725 A90-43686
- ### TIME LAG
- An analysis of feel system effects on lateral flying qualities [AIAA PAPER 90-1824] p 346 A90-25168
- An experimental and analytical investigation of isolated rotor flap-lag stability in forward flight p 518 A90-33623
- Helicopter stability and control modeling improvements and verification on two helicopters p 671 A90-42474
- Model following control system design: Preliminary ATTS in-flight simulation test results [PD-FC-9003] p 758 A90-26010
- Control and estimation for aerospace applications with system time delays p 918 A90-29367
- ### TIME MARCHING
- The extension and application of three-dimensional time marching analyses to incompressible turbomachinery flows [ASME PAPER 89-GT-212] p 293 A90-23878
- Numerical methods for transonic cascade flow problems p 305 A90-25796
- Three-dimensional simulations of hypersonic flows p 306 A90-25823
- A numerical method for solving the unsteady compressible Navier-Stokes equations p 306 A90-25827
- Viscous computations using a direct solver p 315 A90-27133
- Temporal-adaptive Euler/Navier-Stokes algorithm for unsteady aerodynamic analysis of airfoils using unstructured dynamic meshes [AIAA PAPER 90-1650] p 569 A90-38778
- Modeling gas turbine combustor performance under transient conditions [AIAA PAPER 90-2161] p 661 A90-42051
- Simulation of time-dependent viscous flows using central and upwind-biased finite-difference techniques [AIAA PAPER 90-3012] p 790 A90-45864
- Calculation of three-dimensional viscous and inviscid hypersonic flows using split-matrix marching methods [AIAA PAPER 90-3070] p 794 A90-45894
- Extension of a streamwise upwind algorithm to a moving grid system [NASA-TM-102800] p 572 A90-21739
- Application of a dynamic stall model to rotor trim and aeroelastic response p 583 A90-22556
- A time-marching method to calculate unsteady airloads on three-dimensional wings. Part 1: Linearized formulation [DLR-FB-89-58] p 634 A90-24254
- A time-marching method for calculating unsteady airloads on three-dimensional wings. Part 2: Full-potential formulation [DLR-FB-89-59] p 635 A90-24255
- ### TIME MEASUREMENT
- Short time Force and moment measurement System for shock tubes (SFS) for measuring times less than 10 ms p 674 A90-24233
- ### TIME OPTIMAL CONTROL
- Sequential design of experiments with physically based models 23 [AD-A211918] p 138 A90-12239
- Control and stabilization of linear and nonlinear distributed systems [AD-A216448] p 462 A90-18908
- ### TIME RESPONSE
- Fast calculation of root loci for aeroelastic systems and of response in time domain [AIAA PAPER 90-1156] p 390 A90-29368
- ### TIME SHARING
- A Distributed Artificial Intelligence approach to object identification and classification p 545 A90-34185
- A data acquisition parallel bus for wind tunnels at ARL (Aeronautical Research Laboratory) [AD-A218052] p 526 A90-20098
- ### TIME TEMPERATURE PARAMETER
- Time dependent effects on high temperature low cycle fatigue and fatigue crack propagation on nickel base superalloys p 443 A90-29881
- In-situ measurement, modelling and control of the imidization reaction in PMR-15 --- polyimide resin for aerospace structures p 941 A90-50066
- ### TIP DRIVEN ROTORS
- A remote tip-driven fan powered supersonic fighter concept [AIAA PAPER 90-2415] p 663 A90-42167
- An unmanned air vehicle concept with tipjet drive p 830 A90-46951
- ### TIP SPEED
- Effect of tip speed on rotor inflow p 151 A90-17311
- An experimental investigation of the downwash beneath a lifting rotor and low advance ratios p 151 A90-17585
- En route noise of turboprop aircraft and their acceptability: Report of tests p 697 A90-24858
- ### TIRES
- An overview of the joint FAA/NASA aircraft/ground runway friction program [NASA-TM-103486] p 724 A90-25957

TITANIUM

- Metal matrix composite fan blade development
[AIAA PAPER 90-2178] p 677 A90-42062
- TITANIUM ALLOYS**
- IMI 834 - A new high temperature capability titanium alloy for engine use p 62 A90-12535
- The creep behavior of the Ti3Al alloy Ti-24Al-11Nb p 125 A90-15214
- Diffusion bonding aeroengine components p 131 A90-16012
- Production of Ti6Al4V-components for a new turbo-fan-engine p 132 A90-16618
- Study on SPF and SPF/DB of the bulk-head structure with nonsymmetric shape p 132 A90-16619
- DB/SPF cooler outlet duct for aircraft application p 132 A90-16620
- The case for titanium p 204 A90-17922
- Application investigation on superplastic forming/diffusion bonding combined technology of titanium alloy TC4 p 204 A90-18603
- The effect of elevated temperature exposure on the tensile and creep properties of Ti-24Al-11Nb p 355 A90-24865
- beta CEZ, a high performance titanium alloy for aerospace engines p 356 A90-25356
- Cyclic stress-strain behavior and low cycle fatigue of Ti 6242 p 530 A90-33523
- Microstructures of rapidly-solidified binary TiAl alloys p 532 A90-34990
- Titanium matrix composite landing gear development [SAE PAPER 892337] p 733 A90-45491
- Cyclic fracture toughness of VT3-1 and VT-25 titanium alloys p 873 A90-46514
- Laser welding of an advanced rapidly-solidified titanium alloy p 881 A90-47021
- Titanium aluminides for advanced aircraft engines p 874 A90-49000
- Influence of microstructure and microdamage processes on fracture at high loading rates [AD-A210307] p 65 N90-10253
- Improved toughness alloys based on titanium aluminides p 533 N90-20208
- Fatigue crack growth investigation of a Ti-6Al-4V forging under complex loading conditions: NATO/AGARD supplemental engine disk program [AD-A220239] p 678 N90-23538
- Application of high performance metals in gas turbine engines p 750 N90-25999
- Study of the microstructure of a titanium alloy (6246) for turbomachine compressors p 876 N90-27900
- Fretting fatigue strength of Ti-6Al-4V at room and elevated temperatures and ways of improving it p 952 N90-28709
- Surface property improvement in titanium alloy gas turbine components through ion implantation p 953 N90-28713
- Static and dynamic characterization of the ATR 72 rods made of Ti 10.2.3 titanium alloy [REPT-49-238] p 953 N90-28722
- TOLERANCES (MECHANICS)**
- Casting airworthiness joint European civil authorities view-point p 64 N90-10234
- Dynamic tip clearance measurements in axial flow compressors p 116 N90-12612
- Point of view of a civil aircraft manufacturer on Al-Li alloy p 268 N90-15200
- AGARD/SMP Review: Damage Tolerance for Engine Structures. 2: Defects and Quantitative Materials Behaviour - conference p 425 N90-18396
- Static strength and damage tolerance tests on the Fokker 100 airframe [NLR-MP-88023-U] p 416 N90-19228
- Damage tolerance demonstration for A310-300 CFPR components [MBB-UT-012/89-PUB] p 766 N90-25091
- Lessons learned for composite aircraft structures qualification p 842 N90-26808
- Lessons learned from the T-46A durability and damage tolerance program p 842 N90-26812
- Application of damage tolerance p 843 N90-26817
- Individual Helicopter Tracking Program (IHTP) for the MH-53J helicopter p 843 N90-26818
- Damage tolerance analysis for manned hypervelocity vehicles. Volume 2: Software user's manual [AD-A221136] p 845 N90-26826
- AGARD/SMP Review Damage Tolerance for Engine Structures. 3: Component Behaviour and Life Management [AGARD-R-770] p 855 N90-27704

AGARD damage tolerance concepts for engine structures Workshop 3, Component Behaviour and Life Management p 855 N90-27705

A Protection And Detection Surface (PADS) for damage tolerance [NASA-TP-3011] p 876 N90-27788

Damage tolerance analysis for manned hypervelocity vehicles. Volume 1: Final technical report [AD-A221970] p 887 N90-28106

TOLERANCES (PHYSIOLOGY)

Aircraft crash survival design guide. Volume 2: Aircraft design crash impact conditions and human tolerance [AD-A218435] p 575 N90-22546

TOLLMIE-SCHLICHTING WAVES

A method for the active control of the boundary layer condition p 296 A90-24114

Non-axisymmetric viscous lower-branch modes in axisymmetric supersonic flows p 474 A90-33509

On the instability of hypersonic flow past a wedge p 554 A90-35902

Long-range LFC transport p 104 N90-12508

Boundary-layer receptivity and laminar-flow airfoil design p 91 N90-12516

Predicted and hot-film measured Tollmien-Schlichting wave characteristics p 91 N90-12523

Design and test of an NLF wing glove for the variable-sweep transition flight experiment p 104 N90-12544

TOMAHAWK MISSILES

Developments in automation of flight test analysis and report generation [AIAA PAPER 90-1313] p 487 A90-33923

TOMOGRAPHY

Complementary field method for interferometric tomographic reconstruction of high speed aerodynamic flows [AD-A219698] p 131 A90-15900

Digital X-ray inspection p 445 A90-28162

TOOLING

Integrally heated tooling for economical, nonautoclave production of thermoplastic parts p 956 A90-50200

Development and fabrication of structural components for a scramjet engine [NASA-CR-181945] p 510 N90-20088

TOOLS

Carbon/epoxy tooling evaluation and usage p 445 A90-28165

Modeling strength data for CREW CHIEF p 780 N90-25516

TOPOLOGY

Topological study of three-dimensional vortex interactions p 367 A90-25885

Application of multiple grids topology to supersonic internal/external flow interactions p 308 A90-26135

An application of topological analysis to studying the three-dimensional flow in cascades. I - Topological rules for skin-friction lines and section streamlines p 908 A90-52607

Multiblock topology specification and grid generation for complete aircraft configurations p 582 N90-21986

TORQUE

An investigation of the behavior of the dynamic load distribution versus operating speed and torque on heavily loaded, high speed aircraft gearing p 271 A90-21129

Aerodynamic and torque characteristics of enclosed Co/counter rotating disks [ASME PAPER 89-GT-177] p 361 A90-23858

The influence of control-surface compensation parameters on the hinge moment characteristics p 643 A90-41737

Influence of some geometrical and design parameters on the hinge moment characteristics of rudders p 643 A90-41739

TORSION

Determination of the torsion rigidity of a multiple-rib torsion box of an aircraft lifting surface p 364 A90-24134

Helicopter trim with flap-lag-torsion and stall by an optimized controller p 755 A90-45332

Torsional buckling and post-buckling of composite geodetic cylinders with special reference to joint flexibility p 878 A90-45971

Development of a finite element based delamination analysis for laminates subject to extension, bending, and torsion p 679 N90-25049

TORSIONAL STRESS

Efficiency of using a multiple-wall torsion box in the load-bearing structures of lifting surfaces p 410 A90-29188

Agusta methodology for pitch link loads prediction in preliminary design phase p 646 A90-42465

Agusta methodology for pitch link loads prediction in preliminary design phase [ETN-90-97270] p 737 N90-25978

TORSIONAL VIBRATION

The effects of three centres of blade on flutter p 42 A90-11800

Agusta methodology for pitch link loads prediction in preliminary design phase p 646 A90-42465

The response of helicopter rotors to vibratory airflow [AD-A215678] p 337 N90-16756

TOUCHDOWN

Modified touchdown zone lighting [DOT/FAA/CT-TN89/70] p 526 N90-21042

TOUGHNESS

High service temperature high compressive strength and tough prepreg system p 530 A90-33098

The effect of matrix toughness in the development of improved structural adhesives p 955 A90-50183

Aerospace Arall - The advancement in aircraft materials p 947 A90-50186

Fracture morphology of toughened bismaleimide/carbon fiber composites p 948 A90-50205

Static and dynamic characterization of the ATR 72 rods made of Ti 10.2.3 titanium alloy [REPT-49-238] p 953 N90-28722

TOWED BODIES

Dynamics and control of maneuverable towed flight vehicles [AIAA PAPER 90-2841] p 754 A90-45161

TOXIC HAZARDS

Toxicology in aviation p 722 A90-44662

Aircraft cabin fire suppression by means of an interior water spray system [CAA-PAPER-88014] p 96 N90-11719

Analysis of hydraulic fluids and lubricating oils for the formation of Trimethylolpropane Phosphate (TMP-P) [AD-A215188] p 357 N90-16939

Aircraft Fire Safety [AGARD-CP-467] p 324 N90-17581

The acute, delayed neurotoxicity evaluation of two jet engine oil formulations [AD-A222018] p 875 N90-26972

TOXICITY

The acute, delayed neurotoxicity evaluation of two jet engine oil formulations [AD-A222018] p 875 N90-26972

Toxicity of thermolysis products from the materials of airplane cockpits [CEAT-PV-M6/5924/02] p 876 N90-27895

TOXICITY AND SAFETY HAZARD

An analysis of factors impeding passenger escape from aircraft fires p 322 A90-26018

TOXICOLOGY

Toxicology in aviation p 722 A90-44662

TRACKING (POSITION)

Passive location and tracking using DOA and TOA measurements of single nonmaneuvering observer p 576 A90-35709

Neural networks for adaptive shape tracking p 638 A90-39959

Unified flying qualities criteria for longitudinal tracking [AIAA PAPER 90-2806] p 752 A90-45141

Kalman Filter Integration of Modern Guidance and Navigation Systems [AGARD-LS-166] p 28 N90-10847

The 1987 survey of track keeping and altitudes on Heathrow and Gatwick standard instrument departure routes (DAY) [CAA-PAPER-88010] p 99 N90-11729

Estimation and control of nonlinear and hybrid systems with applications to air-to-air guidance [AD-A214542] p 348 N90-16770

Interaction of switch actuation on tracking with a four-axis flight control (cross-coupling) [AD-A217981] p 520 N90-20095

Passive navigation using image irradiance tracking p 578 N90-22232

Position finding and ground target direction finding by an aircraft with a gimbaled video camera [DLR-FB-89-62] p 825 N90-27673

A sensor stabilization/tracking system for unmanned air vehicles [AD-A224008] p 936 N90-28579

Control and estimation for aerospace applications with system time delays p 918 N90-29367

TRACKING FILTERS

Parametric synthesis of the decoupling filter in the manual control system of VTOL aircraft p 859 A90-46483

A nonlinear aircraft tracking filter utilizing control variable estimation [AIAA PAPER 90-3402] p 822 A90-47657

TRACKING NETWORKS

Multiple sensor data association and fusion in aerospace applications p 778 A90-44644

SUBJECT INDEX

TRACKING PROBLEM

Multivariable control design for the control reconfigurable combat aircraft (CRCA) p 432 A90-30715

TRACKING RADAR

The application of Z to the specification of air traffic control systems. 1: An initial specification of the radar processing activity [RSRE-MEMO-4280] p 243 N90-15900

TRACKING STATIONS

Passive location and tracking using DOA and TOA measurements of single nonmaneuvering observer p 576 A90-35709

TRAILING EDGE FLAPS

Experiments are telling you something (Stewartson Memorial Lecture) — about aerodynamic flows p 144 A90-16752
Leading- and trailing-edge flaps on supersonic delta wings p 233 A90-23285

TRAILING EDGES

Optimum trailing edge ejection for cooled gas turbine blades p 41 A90-11562
The development of an exact conservative scheme associated with the supersonic trailing edge separation modelling for the computation of the transonic 2D cascade p 12 A90-12551

Pressure surface trailing edge slot cooling [ONERA, TP NO. 1989-123] p 47 A90-12569

The effect of trailing edge extensions on the performance of the Goettingen 797 and the Wortmann FX 63-137 aerofoil section at Reynolds numbers between 3×10 to the 5th and 1×10 to the 6th p 82 A90-13783

Further work on aerofoils at Reynolds numbers between 3×10 to the 5th and 1×10 to the 6th p 145 A90-16758

Computation of the trailing edge flow downstream a flat plate with finite thickness p 151 A90-17464

Unsteady streamlines near the trailing edge of NACA 0012 airfoil at a Reynolds number of 125,000 p 155 A90-18158

Experimental investigation of trailing-edge and near wake flow of a symmetric airfoil p 160 A90-19449

The trailing edge loss of transonic turbine blades [ASME PAPER 89-GT-278] p 475 A90-33564

Investigation of model rigging limitations on a high speed wind tunnel model at cryogenic temperature p 523 A90-34232

Effect of surface grooves on base pressure for a blunt trailing-edge airfoil p 556 A90-36280

Modelling of boundary layer and trailing edge thickness effects for the Euler equations using surface transpiration p 629 A90-42412

Application of divergent trailing-edge airfoil technology to the design of a derivative wing p 714 A90-45466

Some remarks on the Kutta condition p 716 A90-45738

Numerical investigation of laminar separated viscous trailing-edge flow using triple-deck theory [AIAA PAPER 90-3046] p 792 A90-45883

An experimental study of low-speed single-surface airfoils with faired leading edges p 801 A90-46371

Wind-tunnel investigations of wings with serrated sharp trailing edges p 802 A90-46379

Local convergence of the solution in the discrete vortex method p 803 A90-46534

Flow past bodies within a narrow class of cross-sectional shapes with stationary separation zones at large Reynolds numbers p 805 A90-46568

Hinge moment coefficient derivatives for trailing-edge controls on wings at subsonic speeds p 198 N90-14239

Serrated trailing edges for improving lift and drag characteristics of lifting surfaces [NASA-CASE-LAR-13870-1] p 248 N90-15094

A wind tunnel study of a sting-mounted circulation control wing [AD-A216248] p 319 N90-17577

Calculation of excrescence drag magnification due to pressure gradient at high subsonic speeds p 397 N90-19195

[ESDU-87004] Euler code predicted separation at the airfoil trailing edge [FFA-TN-1989-30] p 632 N90-23364

TRAINING AIRCRAFT

Computer-aided simulation of aircraft motion including nonlinearities in aerodynamic-coefficient relationships p 257 A90-23359

TRAINING DEVICES

Interactive Videodisc training in aerospace applications [AIAA PAPER 89-3029] p 73 A90-10529

A review of flight simulation techniques p 435 A90-27953

A framework for the optimal design of instructor/operator stations in flight simulators p 779 A90-45373

TRAINING EVALUATION

The Common/Same Type Rating - Human factors and other issues [SAE PAPER 892229] p 723 A90-45445

The (airplane) design professor as shepherd - An industry role in enhancing engineering education [AIAA PAPER 90-3259] p 897 A90-49121

TRAINING SIMULATORS

Future ATC automation aids based upon AI technology p 375 A90-25563

Experimental study towards a future airport ground movement simulator p 827 N90-27687

Study improvement training facilities ground control air traffic controllers. Part 1: Alternative solutions and their consequences [FEL-89-A257-PT-1] p 919 N90-29380

Study improvement training facilities ground control air traffic controllers. Part 2: Functional analysis approach control trainer [FEL-89-A280-PT-2] p 939 N90-29409

TRAJECTORIES

Application of experimental techniques to store release problems p 316 N90-17545

Escape systems research at RAE p 483 N90-20058

Optimization and guidance of flight trajectories in the presence of windshear [NASA-CR-186163] p 574 N90-21747

First-order weight corrections for real-time flight path management [LR-580] p 578 N90-21751

A comparison of time-optimal interception trajectories for the F-8 and F-15 [NASA-CR-186300] p 581 N90-21753

Effects of simplifying assumptions on optimal trajectory estimation for a high-performance aircraft [NASA-TM-101721] p 757 N90-25142

Windshear estimation along the trajectory of an aircraft p 963 N90-29745

TRAJECTORY ANALYSIS

Analysis of the mathematical modeling of an aircraft flight trajectory with consideration of engine thrust effect on the force ratio on the aircraft p 247 A90-23363

Aircraft program motion along a predetermined trajectory. II - Numerical simulation with application of spline functions to trajectory definitions p 347 A90-25199

Rotorcraft pursuit-evasion in nap-of-the-earth flight [AIAA PAPER 90-3455] p 786 A90-47707

TRAJECTORY CONTROL

Inverse problems in controlled system dynamics: Nonlinear models — Russian book p 77 A90-12471

Generation of motion control for direction finders in a goniometer system p 187 A90-17137

Decoupled ultimate boundedness control of systems and large aircraft maneuver p 196 A90-19461

Ultimate boundedness control of uncertain systems with application to roll coupled aircraft maneuver p 668 A90-40886

The ascending trajectories performance and control to minimize the heat load for the transatmospheric aero-space planes [AIAA PAPER 90-2828] p 763 A90-45135

Optimal plane change by low aerodynamic forces [AIAA PAPER 90-2831] p 763 A90-45137

Inversion of nonlinear I-O map, zero dynamics and flight control system design [AIAA PAPER 90-3370] p 863 A90-47628

Flight test of a trajectory controller using linearizing transformations with measurement feedback [AIAA PAPER 90-3373] p 864 A90-47631

TRAJECTORY MEASUREMENT

Continued development and analysis of a new extended Kalman filter for the Completely Integrated Reference Instrumentation System (CIRIS) [AD-A220106] p 654 N90-23400

TRAJECTORY OPTIMIZATION

Minimum-time turns using vectored thrust p 118 A90-14728

Penetration landing guidance trajectories in the presence of windshear p 98 A90-14732

Acceleration, gamma, and theta guidance for abort landing in a windshear p 98 A90-14733

Minimum fuel cruise by periodic optimization p 182 A90-19429

The ascending trajectories performance and control to minimize the heat load for the transatmospheric aero-space planes [AIAA PAPER 90-2828] p 763 A90-45135

Optimal plane change by low aerodynamic forces [AIAA PAPER 90-2831] p 763 A90-45137

Thrust law effects on the longitudinal stability of hypersonic cruise [AIAA PAPER 90-2820] p 763 A90-45149

TRANSIENT OSCILLATIONS

Optimal paths through downbursts p 755 A90-45330

Control of an aircraft in downbursts p 755 A90-45331

Multiple-step terminal control with parameter identification and prediction during flight vehicle descent p 872 A90-46484

Singular, periodic solutions in aircraft cruise-dash optimization [AIAA PAPER 90-3369] p 863 A90-47627

Optimal periodic cruise with singular control [AIAA PAPER 90-3490] p 833 A90-47738

Nonlinear maneuver autopilot for the F-15 aircraft [NASA-CR-179442] p 77 N90-11487

Trajectory optimization and guidance for an aerospace plane [NASA-CR-185884] p 183 N90-13369

Guidance and Control strategies for aerospace vehicles [NASA-CR-186195] p 199 N90-14243

Guidance analysis of the aeroglide plane change maneuver as a turning point problem [NASA-TM-101639] p 259 N90-15110

ETO (Earth-To-Orbit): A trajectory program for aerospace vehicles [AD-A218157] p 528 N90-20103

An approach to on-board optimization of cruise at constant altitude [LR-581] p 578 N90-21752

Effects of simplifying assumptions on optimal trajectory estimation for a high-performance aircraft [NASA-TM-101721] p 757 N90-25142

Optimal trajectories for hypervelocity flight p 918 N90-29378

TRANSATMOSPHERIC VEHICLES

Computational requirements for hypersonic flight performance estimates p 440 A90-29686

The effect of Mach number on the stability of a plane supersonic wake p 557 A90-36524

Supersonic/hypersonic laminar/turbulent transition p 706 A90-42872

The ascending trajectories performance and control to minimize the heat load for the transatmospheric aero-space planes [AIAA PAPER 90-2828] p 763 A90-45135

Hypersonic waverider configurations for trans-atmospheric vehicles [AD-A217925] p 498 N90-20074

Comparison of three concepts for a long stroke displacement transducer p 66 A90-11041

New inflight experiments to measure aerodynamics loads [ETN-90-97276] p 868 N90-26834

An ultrasonic system for in-service non-destructive inspection of composite structures p 885 N90-28076

Dynamic characteristics of one-dimensional gas flow with friction p 296 A90-24115

A reduced cost rational-function approximation for unsteady aerodynamics [AIAA PAPER 90-1155] p 390 A90-29367

A combined Riccati transfer matrix-direct integration method with its applications p 611 A90-37218

Obtaining precise LTR with Luenberger type observer with arbitrary observer poles and finite gain [AIAA PAPER 90-3228] p 868 A90-49113

Comparison of the swept frequency continuous wave, current pulse, and shock-excitation lightning simulation techniques p 818 A90-49832

Backside landing control of a STOL aircraft using approximate perfect servo p 934 A90-52801

Evaluation of the indirect effects of lightning on a system: Double transfer function method [RAE-TRANS-2172] p 176 N90-14211

AcSim: Aircraft simulation program with application to flight profile generation [AD-A212466] p 185 N90-14217

Infrared thermography p 911 N90-29325

A digital controller for active aeroelastic controls [NAL-TR-1014] p 936 N90-29402

TRANSFER ORBITS

Optimal plane change by low aerodynamic forces [AIAA PAPER 90-2831] p 763 A90-45137

TRANSFORMATIONS (MATHEMATICS) Angular feature mapping - An optical method p 377 A90-23974

A helicopter flight path controller design via a nonlinear transformation technique p 199 N90-14242

TRANSIENT HEATING Force balance errors due to temperature changes in ETW p 539 A90-34231

TRANSIENT OSCILLATIONS Parameter identification of aeroelastic modes of rotary wings from transient time histories p 642 A90-40166

TRANSIENT PRESSURES

Composite reduced Navier Stokes procedures for flow problems with strong pressure interactions
[AD-A219621] p 689 N90-23687

TRANSIENT RESPONSE

Transient response of leading-edge vortices to localized suction p 556 A90-36279
Adjusting turbine engine transient performance for the effects of environmental variances p 658 A90-40639
[AIAA PAPER 90-2501]
Modeling gas turbine combustor performance under transient conditions p 661 A90-42051
[AIAA PAPER 90-2161]
Improved noise rejection in automatic carrier landing systems p 864 A90-47632
[AIAA PAPER 90-3374]
Estimating short-period dynamics using an extended Kalman filter p 648 N90-23392
[NASA-TM-101722]
An experimental study of fault propagation in a jet-engine controller p 665 N90-23401
[NASA-CR-181335]
Analysis of dynamic transient response and postflutter behavior of super-maneuvering airplane p 925 N90-29386
[AD-A224126]

TRANSITION FLIGHT

H-infinity based integrated flight/propulsion control design for a STOVL aircraft in transition flight
[AIAA PAPER 90-3335] p 862 A90-47595
H-infinity based integrated flight/propulsion control design for a STOVL aircraft in transition flight
[NASA-TM-103198] p 758 N90-26011

TRANSITION FLOW

Transition phenomena on airfoils operating at low chord Reynolds numbers in steady and unsteady flow p 148 A90-16786
Prediction of transition on airfoils with separation bubbles, swept wings and bodies of revolution at incidence p 148 A90-16790
Leading edge transition in hypersonic flows p 224 A90-21167
Instrumentation requirements for laminar flow research in the NLR high speed wind tunnel HST p 447 A90-28283
Development of two multi-sensor hot-film measuring techniques for free-flight experiments p 417 A90-28291
Aerothermodynamics and transition in high-speed wind tunnels at NASA Langley p 386 A90-28555
Optimal conditions of flow turbulence suppression in the working section of a wind tunnel using screens located in the prechamber p 438 A90-29185
Transition from order to chaos in the wake of an airfoil p 474 A90-33506
Direct numerical simulations of transition in a compressible wake p 553 A90-35212
Measurement of crossflow vortices, attachment-line flow, and transition using microthin hot films
[AIAA PAPER 90-1636] p 607 A90-38765
Wave structure of artificial perturbations in a supersonic boundary layer on a plate p 619 A90-39518
Supersonic/hypersonic laminar/turbulent transition p 706 A90-42872
Computational results for the effects of external disturbances on transition location of bodies of revolution from subsonic to supersonic speeds and comparisons with experimental data p 715 A90-45522
[SAE PAPER 892381]
Interactive boundary-layer method for unsteady airfoil flows - Quasisteady model p 812 A90-48953
Experiments on the laminar-turbulent transition on swept wings p 277 N90-16170
Development of transition criteria on the basis of ϵ to the N power for three dimensional wing boundary layers p 277 N90-16179
European research on viscous flow (EuroVisc) [NLR-TP-89077-U] p 609 N90-22014

TRANSITION POINTS
Determination of the laminar-turbulent transition point for a turbulent layer on a yawing wing p 805 A90-46566
Design and fabrication requirements for low noise supersonic/hypersonic wind tunnels p 122 N90-12555
Determination of the N-factor in the Brunswick (Federal Rep. of Germany) transonic wind tunnel using measurements of pressure distributions and transition points, and the SALLY method p 276 N90-16177

TRANSITION PRESSURE
Stall cell blockage in a high-speed multistage axial-flow compressor [AIAA PAPER 90-1913] p 740 A90-42693

TRANSITION TEMPERATURE
Observations on the brittle to ductile transition temperatures of B2 nickel aluminides with and without zirconium p 205 A90-19153

TRANSLATIONAL MOTION

Evaluation of nonlinear motion-drive algorithms for flight simulators [UTIAS-TN-272] p 761 N90-25148

TRANSMISSION EFFICIENCY

Research on transmission quality of telemetry system in flight test p 26 A90-12189

TRANSMISSION LINES

Helicopter wire strike accident and high voltage electrocution - A case report p 22 A90-10265

TRANSMISSION LOSS

An investigation of the generation and radiation of aerodynamic noise in real piping systems p 614 N90-22368

TRANSMISSIONS (MACHINE ELEMENTS)

Experimental and analytical evaluation of dynamic load vibration of a 2240-kW (3000-hp) rotorcraft transmission p 127 A90-13750
Gear steels for future helicopter transmissions p 265 A90-20607
Helicopter transmissions - Design for safety and reliability p 270 A90-20608
Efficiency testing of a helicopter transmission planetary reduction stage p 271 A90-21113
Effect of advanced component technology on helicopter transmissions p 271 A90-21115
Damage tolerance analysis and testing of a welded cluster gear for the main transmission of the Advanced Attack Helicopter p 445 A90-28187
Efficiency study comparing two helicopter planetary reduction stages [AIAA PAPER 90-2156] p 956 A90-50644
Assessment of worm gearing for helicopter transmissions [NASA-TM-102441] p 257 N90-15923
Life of concentrated contacts in the mixed EHD and boundary film regimes [AD-A216673] p 454 N90-18738
Transmission research activities at NASA Lewis Research Center p 543 N90-21394
[NASA-TM-103132]
Efficiency study comparing two helicopter planetary reduction stages [NASA-TM-103106] p 776 N90-26334

TRANSMISSIVITY

A new method for measuring the transmissivity of aircraft transparencies [AD-A216953] p 464 N90-19842

TRANSMITTER RECEIVERS

The performance of linear fiber optic data buses p 68 A90-11665
Clutter rejection and transmitter-receiver requirements in an airborne radar p 738 A90-45354
Equipment feasibility study: Very high frequency communication equipment (136-137 megahertz) [DOT/FAA/CT-TN89/72] p 775 N90-26210

TRANSMITTERS

Feasibility of using frequency offset on very high frequency air/ground voice channels [DOT/FAA/CT-TN89/71] p 542 N90-21248

TRANSCOENIC FLIGHT

Flight over the sea with twin or triple jet aircraft p 179 A90-17048

TRANSONIC COMPRESSORS

Shock capturing and loss prediction for transonic turbine blades using a pressure correction method p 11 A90-12518
A quasi-3D design method of transonic compressor blade with the function of improving velocity distribution p 49 A90-12589
Experimental investigation of the transonic centrifugal compressor inducer straight cascades p 13 A90-12592
Analyses of full 3D S1-S2 iterative solution in CAS transonic compressor rotor and comparison with quasi-3D S1-S2m iterative solution and L2F measurement p 157 A90-18532
Computation and analysis of the shapes of S1 and S2 streamsurfaces in a transonic compressor rotor p 160 A90-19446
Application of low-solidity cascade diffuser to transonic centrifugal compressor [ASME PAPER 89-GT-66] p 290 A90-23789
Aerodynamic and heat transfer measurements on blading for a high rim-speed transonic turbine [ASME PAPER 89-GT-228] p 293 A90-23883
An off-design loss and deviation prediction study for transonic axial compressors [ASME PAPER 89-GT-324] p 343 A90-23893
Calculation of tip leakage flow with three-dimensional Euler code p 304 A90-25772

TRANSONIC FLIGHT

The vortex flap F-106B, overcoming safety and data problems in flight testing [AIAA PAPER 90-1280] p 496 A90-34725

Flight tests with a natural laminar flow glove on a transport aircraft [AIAA PAPER 90-3044] p 828 A90-45881
A tool for automatic design of airfoils in different operating conditions p 502 N90-20994

TRANSONIC FLOW

An improved version of LTRAN2 p 2 A90-10350
Color schlieren system using square color filter and its application to aerofoil test in transonics p 66 A90-10748
An improved method for the computation of unsteady transonic potential flow - Application for airfoil and blade performance prediction [ONERA, TP NO. 1989-154] p 4 A90-11175
Three-dimensional modeling of turbulent transonic flow at the exit of a twin engine [AAAF PAPER NT 88-16] p 4 A90-11434
The solution of the unsteady transonic flow through a blade passage in an axial turbine p 5 A90-11777
Unsteady flow visualization in a vibrating annular turbine cascade operating in the transonic flow regime p 7 A90-11786
Self-excited oscillation of shock waves on an airfoil in two-dimensional transonic channel flow p 8 A90-11808
The development of an exact conservative scheme associated with the supersonic trailing edge separation modelling for the computation of the transonic 2D cascade p 12 A90-12551
Analytical methods for subsonic propulsion system integration p 29 A90-12613
Computation of transonic turbine cascade flow using Navier-Stokes equations p 14 A90-12621
PCISM method for two dimensional compressible viscous cascade flow calculation p 15 A90-12625
New approach to small transonic perturbations finite element numerical solving method. I - Numerical developments. II - Numerical applications p 16 A90-12783
Closed-form solutions for nonlinear quasi-unsteady transonic aerodynamics p 16 A90-12839
Numerical solution of transonic flows on a streamfunction co-ordinate system p 17 A90-13238
Recent Navier/Stokes calculations in applications p 85 A90-15227
Computation of transonic separated flow using the Euler equations p 85 A90-15233
Transonic flow over a single wedge p 85 A90-15237
VISTRAFS - A simulation method for strongly-interacting viscous transonic flow p 144 A90-16756
Calculation of transonic flows for novel engine-airframe installations p 145 A90-16768
The calculation of under-expanded impinging jets p 147 A90-16782
Multigrid acceleration of transonic flow computations p 147 A90-16783
Transonic flow in throat region of supersonic nozzles p 149 A90-16799
Calculation of two-dimensional transonic flow of Euler equations with multigrid method p 149 A90-16835
Airfoils in supersonic source and sink flows p 149 A90-16844
Two-dimensional transonic flow field analysis with different turbulence models p 150 A90-16846
A numerical method for computing the aerodynamic loads on wings with sharp-edge separations at large angles of attack in subcritical transonic flows p 150 A90-16852
An approach for calculating steady subsonic and transonic blade to blade flows p 152 A90-17784
Computation of transonic flow in a plane cascade with an unfactored flux splitting implicit method p 152 A90-17785
A relaxation method for transonic potential flows through 2-D cascade with large camber angle p 152 A90-17786
Experimental investigation on the performance of an annular nozzle cascade of a highly-loaded transonic turbine stage p 152 A90-17787
An experimental study of tip clearance effects on the performance of an axial transonic turbine p 189 A90-17788
Design and calculation of composite air-cooled blades in a highly-loaded transonic turbine p 189 A90-17790
Experimental investigation on composite air-cooled blades of highly-loaded transonic turbine p 189 A90-17793
Computation of viscous transonic flow over porous airfoils p 153 A90-17864
Rotor hover performance prediction using a free-wake, computational fluid dynamics method p 153 A90-17869
Design of axisymmetric bodies with minimum transonic drag p 154 A90-17997

- On the coupling of finite elements and boundary elements for transonic potential flows p 155 A90-18297
- A finite element solution for transonic flow around lifting fuselage with arbitrary cross sections from the minimum pressure integral p 156 A90-18298
- Secondary flows in a transonic cascade - Comparison between experimental and numerical results p 157 A90-18501
- Numerical method for solving the Euler equation for unsteady transonic flows over oscillating airfoils p 157 A90-18578
- A new implicit hybrid schemes for the Euler equation of transonic flow p 158 A90-18608
- Computations of unsteady transonic flows about thin airfoils by integral equation method p 158 A90-18609
- Further investigations of transonic shock-wave boundary-layer interaction with passive control p 159 A90-19390
- Full 3D iterative solution of transonic flow for a swept wing test channel p 160 A90-19431
- Variational principle with variable domain discontinuous finite element method for transonic flow and determining automatically the position and shape of the shock waves p 160 A90-19434
- The computational method for the transonic wing design p 160 A90-19438
- Alleviation of shock oscillations in transonic flow by passive controls p 161 A90-19648
- [AIAA PAPER 90-0046] p 161 A90-19648
- An efficient upwind relaxation-sweeping algorithm for three-dimensional Euler equations p 162 A90-19695
- [AIAA PAPER 90-0129] p 162 A90-19695
- Transonic Navier-Stokes solutions about a complex high-speed accelerator configuration p 166 A90-19844
- [AIAA PAPER 90-0430] p 166 A90-19844
- The sonic eddy - A model for compressible turbulence p 167 A90-19876
- [AIAA PAPER 90-0495] p 167 A90-19876
- Amplitude effects on dynamic stall of an oscillating airfoil p 167 A90-19925
- [AIAA PAPER 90-0575] p 167 A90-19925
- Inviscid drag prediction for transonic transport wings using a full-potential method p 168 A90-19926
- [AIAA PAPER 90-0576] p 168 A90-19926
- Investigation of oscillating airfoil shock phenomena p 169 A90-19981
- [AIAA PAPER 90-0695] p 169 A90-19981
- Transonic integro-differential and integral equations with artificial viscosity p 223 A90-20988
- Advances in the efficient calculation of flows with friction p 225 A90-21475
- Numerical simulation of transonic wing flows using a zonal Euler, boundary-layer, Navier-Stokes approach p 225 A90-21596
- A finite element solution of unsteady two-dimensional flow in cascades p 226 A90-21946
- A finite element method for solving lifting airfoil in transonic flow p 226 A90-21984
- Unsteady transonic Navier-Stokes computations for an oscillating wing using single and multiple zones p 228 A90-22197
- [AIAA PAPER 90-0313] p 228 A90-22197
- An Euler method for wing-body-winglet flows p 229 A90-22218
- [AIAA PAPER 90-0436] p 229 A90-22218
- Analysis of transonic integral equations. I - Artificial viscosity p 232 A90-23124
- Unsteady transonic aerodynamics of oscillating airfoils in supersonic freestream p 232 A90-23277
- Integral solution of unsteady full-potential equation for a transonic pitching airfoil p 232 A90-23280
- Self-excited oscillation of transonic flow around an airfoil in two-dimensional channel p 290 A90-23784
- [ASME PAPER 89-GT-58] p 290 A90-23784
- Mach number effects on secondary flow development downstream of a turbine cascade p 290 A90-23790
- [ASME PAPER 89-GT-67] p 290 A90-23790
- The design and test of a two stage transonic axial flow compressor p 341 A90-23852
- [ASME PAPER 89-GT-164] p 341 A90-23852
- The prediction of boundary layers with rotation and variation of stream filament thickness p 362 A90-23882
- [ASME PAPER 89-GT-227] p 362 A90-23882
- Aerodynamic design methods for transonic wings p 293 A90-23978
- Stability analysis and numerical experiments for viscous-inviscid interaction in transonic flow p 293 A90-24009
- Calculation of nonseparated transonic flow past swept wings with allowance for viscosity p 294 A90-24079
- Application of Fedorenko's multigrid method for calculating transonic flow past a profile p 295 A90-24103
- A new quick method for integrating Euler equations for plane transonic flows p 295 A90-24105
- Calculation of transonic axisymmetric flow past an engine nacelle with allowance for viscosity p 296 A90-24107
- A method for determining aileron efficiency and critical reversal and divergence rates at transonic velocities p 345 A90-24147
- Optimal nose shapes of bodies of revolution in transonic flow p 299 A90-24185
- Unsteady transonic flow around double-wedge profiles p 299 A90-24354
- Comparison of inviscid and viscous separated flows p 302 A90-25277
- Analysis of transonic integral equations. II - Boundary element methods p 302 A90-25301
- The transonic nonisentropic potential calculation p 304 A90-25739
- Problem areas in applied computational fluid dynamics p 366 A90-25770
- Computation of steady three dimensional transonic internal flows p 304 A90-25771
- Numerical methods for transonic cascade flow problems p 305 A90-25796
- Turbulence models for 3D transonic viscous flows. II p 306 A90-25820
- Transonic aerodynamics analysis of unconventional wing configurations by 3D-Euler code p 306 A90-25835
- Automatic mesh generation for complex three-dimensional regions using a constrained Delaunay triangulation p 375 A90-26022
- Efficient method for computing transonic and supersonic flows about aircraft p 307 A90-26132
- Solution-adaptive grids for transonic flows p 309 A90-26508
- Application of I-DEAS grid generator for three-dimensional transonic flow analysis p 311 A90-26542
- Numerical simulation of an F-16A at angle of attack p 313 A90-26911
- [AIAA PAPER 90-0100] p 313 A90-26911
- Parallel computation of three-dimensional transonic flow problems with complex geometries p 313 A90-26936
- [AIAA PAPER 90-0336] p 313 A90-26936
- Boundary element solution of the transonic integro-differential equation p 383 A90-27947
- Calculation of transonic flows with separation past arbitrary inlets at incidence p 384 A90-27979
- Fast adaptive grid method for compressible flows p 445 A90-28006
- Observation and analysis of sidewall effect in a transonic airfoil test section p 436 A90-28257
- Design of a three dimensional Doppler anemometer for T2 transonic wind tunnel p 447 A90-28271
- Some characteristics of changes in the nonstationary aerodynamic characteristics of a wing profile with an aileron in transonic flow p 387 A90-28989
- Calculation of the effect of the engine nacelle on transonic flow past a wing p 387 A90-28990
- Auxiliary hypotheses of the wave drag theory p 387 A90-29003
- Effect of the leading edge bluntness of a moderately swept wing on the aerodynamic characteristics of an aircraft model at subsonic and transonic velocities p 388 A90-29005
- Effect of a jet on transonic flow past an airfoil p 388 A90-29181
- Computation of steady and unsteady control surface loads in transonic flow p 389 A90-29361
- [AIAA PAPER 90-0935] p 389 A90-29361
- Using transonic small disturbance theory for predicting the aerodynamic stability of a flexible wind-tunnel model p 391 A90-29377
- [AIAA PAPER 90-1033] p 391 A90-29377
- Unsteady transonic aerodynamics p 393 A90-29882
- Physical phenomena associated with unsteady transonic flows p 394 A90-29883
- Basic equations for unsteady transonic flow p 394 A90-29884
- Practical problems - Airplanes --- unsteady interactional aerodynamics, flutter characteristics, and active flight control p 394 A90-29885
- Basic numerical methods --- of unsteady and transonic flow p 394 A90-29886
- Application of transonic flow analysis to helicopter rotor problems p 394 A90-29887
- Alternative methods for modeling unsteady transonic flows p 394 A90-29889
- An integral method for transonic flows p 395 A90-31119
- Calculations of transonic flows over wing-body combinations p 395 A90-31479
- Galerkin finite element method for transonic flow about airfoils and wings p 396 A90-31486
- Numerical computations of transonic critical aerodynamic behavior p 469 A90-32457
- Oscillatory shock motion caused by transonic shock boundary-layer interaction p 470 A90-32478
- Solution of sonic flow problems p 470 A90-32712
- A strong viscous-inviscid interaction method for computing unsteady transonic airloads for use in aeroelastics p 471 A90-33355
- Computation of unsteady transonic flows around oscillating airfoils using full potential and Euler equations p 472 A90-33357
- The trailing edge loss of transonic turbine blades [ASME PAPER 89-GT-278] p 475 A90-33564
- Hot wire anemometry in transonic flows and cryogenic conditions p 539 A90-34229
- Dynamic stall of a constant-rate pitching airfoil p 553 A90-35754
- The TSP methods applied to the calculation of transonic flow about wing/body/nacelle/pylon-configurations --- Transonic Small Perturbation p 554 A90-35868
- Implicit flux-split schemes for the Euler equations p 602 A90-36254
- Transonic Euler solutions on mutually interfering finned bodies p 555 A90-36256
- Unsteady transonic cascade flow with in-passage shock wave p 556 A90-36281
- An efficient finite-difference algorithm for computing axisymmetric transonic nacelle flow fields p 557 A90-37205
- Finite element numerical analysis for transonic flows around lifting fuselages p 558 A90-37216
- Solution of Euler equations with unstructured meshes p 558 A90-37343
- Adaptive wind tunnel walls: Compendium of final report - AGARD FDP working group 12 p 595 A90-37944
- [AIAA PAPER 90-1405] p 595 A90-37944
- Wall interference assessment/correction (WIAC) for transonic airfoil data from porous and shaped wall test sections p 595 A90-37945
- [AIAA PAPER 90-1406] p 595 A90-37945
- Wall interference correction for three-dimensional transonic flows p 558 A90-37947
- [AIAA PAPER 90-1408] p 558 A90-37947
- A numerical study on the use of sulfur hexafluoride as a test gas for wind tunnels p 605 A90-37958
- [AIAA PAPER 90-1421] p 605 A90-37958
- Evaluation of transonic wall interference assessment and correction for semi-span wing data p 597 A90-38487
- [AIAA PAPER 90-1433] p 597 A90-38487
- Parameter effects on oscillatory aerofoil in transonic flows p 563 A90-38629
- [AIAA PAPER 90-1473] p 563 A90-38629
- Numerical prediction of transonic viscous flows around airfoils through an Euler/boundary layer interaction method p 564 A90-38681
- [AIAA PAPER 90-1537] p 564 A90-38681
- Calculation of two- and three-dimensional flow in a transonic turbine cascade with particular regard to the losses p 565 A90-38686
- [AIAA PAPER 90-1542] p 565 A90-38686
- Inlet radial temperature redistribution in a transonic turbine stage p 565 A90-38687
- [AIAA PAPER 90-1543] p 565 A90-38687
- A comparison of adaptive-grid redistribution and embedding for steady transonic flows p 565 A90-38704
- [AIAA PAPER 90-1565] p 565 A90-38704
- An interactive scheme for transonic wing/body flows based on Euler and inverse boundary-layer equations p 566 A90-38721
- [AIAA PAPER 90-1586] p 566 A90-38721
- An algebraic adaptive-grid technique for the solution of Navier-Stokes equations p 567 A90-38736
- [AIAA PAPER 90-1605] p 567 A90-38736
- Boundary layer stability in the case of transonic external flow p 619 A90-39514
- Transonic flow around airfoils with relaxation and energy supply by homogeneous condensation p 620 A90-39782
- Determination of aerodynamic sensitivity coefficients based on the transonic small perturbation formulation p 622 A90-40682
- Three dimensional transonic and supersonic flow prediction in axi-vented nozzles using a finite volume method p 624 A90-41989
- [AIAA PAPER 90-2026] p 624 A90-41989
- Investigation of unsteady flow through a transonic turbine stage. II - Data/prediction comparison for time-averaged and phase-resolved pressure data p 626 A90-42162
- [AIAA PAPER 90-2409] p 626 A90-42162
- A transonic airfoil design method and examples p 627 A90-42351
- Calculation of the complete transonic unsteady small disturbance equation by ADI method p 627 A90-42353
- An improvement on upwinding technique used in the Galerkin finite element method for the computation of inviscid transonic flow with shock waves p 627 A90-42361
- Numerical analysis of viscous-inviscid interaction in transonic flow p 627 A90-42363
- Calculation of viscous-inviscid strong interaction for transonic flows over aerofoils p 627 A90-42364

- Application of the KTRAN transonic small disturbance code to the complete CF-18 aircraft with stores p 629 A90-42416
- CFD and transonic helicopter sound p 696 A90-42433
- Development of a robust calculation method for transonic viscous blade-to-blade flows p 703 A90-42671
- Analysis of transonic turbine rotor cascade flows using a finite-volume total variation diminishing (TVD) scheme [AIAA PAPER 90-2127] p 704 A90-42733
- Numerical simulation of transonic porous airfoil flows p 707 A90-44433
- Transonic flow computations in convergent propulsion nozzles using the time-dependent mode p 708 A90-44459
- A multistage method for the solution of the Euler equations on unstructured grids p 708 A90-44460
- Development and application of a fractional-step method for the solution of transonic and supersonic flow problems p 709 A90-44461
- Numerical solution of 2D transonic flows in a turbine cascade p 709 A90-44601
- Zonal Navier-Stokes methodology for flow simulation about a complete aircraft p 709 A90-44727
- Aerodynamic drag of a pair of bodies in transonic and supersonic flow p 710 A90-44935
- Effects of turbulence models on the prediction of transonic wing flows [SAE PAPER 892224] p 713 A90-45440
- Transonic analysis of complex configurations using TRANAIR program p 714 A90-45467
- Computational results for the effects of external disturbances on transition location of bodies of revolution from subsonic to supersonic speeds and comparisons with experimental data p 715 A90-45522
- Unsteady transonic flow --- Book p 716 A90-45760
- Navier-Stokes simulation of transonic afterbody flows with jet exhaust [AIAA PAPER 90-3057] p 790 A90-45862
- Relative efficiency and accuracy of two Navier-Stokes codes for simulating attached transonic flow over wings [AIAA PAPER 90-3078] p 795 A90-45909
- Application of a streamwise upwind algorithm for unsteady transonic computations over oscillating wings [AIAA PAPER 90-3103] p 796 A90-45915
- An unstructured-mesh Euler method for multielement airfoil geometries [AIAA PAPER 90-3051] p 797 A90-45930
- An evaluation of Euler solvers for transonic flowfield computations on wing-fuselage geometries [AIAA PAPER 90-3015] p 798 A90-45935
- Shock/turbulent boundary layer interaction in low Reynolds number supercritical flows p 802 A90-46383
- Summary of experimental testing of a transonic low Reynolds number airfoil p 802 A90-46384
- Speed-up of the strongly implicit procedure with application to subsonic/transonic potential flows p 809 A90-47301
- Prediction of separated transonic wing flows with nonequilibrium algebraic turbulence model p 809 A90-47312
- A numerical method for relating two- and three-dimensional pressure distributions on transonic wings [AIAA PAPER 90-3211] p 812 A90-48837
- Subsonic and transonic low-Reynolds-number airfoils with reduced pitching moments [AIAA PAPER 90-3212] p 812 A90-48838
- TRANAIR applications to engine/airframe integration p 838 A90-48958
- Self-excited oscillations in internal transonic flows p 813 A90-49274
- Numerical simulation of transonic flow through oscillating and multi-row two-dimensional airfoil cascades p 814 A90-49460
- Numerical solution of 2-D transonic flow through an axial turbine stage p 814 A90-49464
- Flow past two cylinders and two spheres p 903 A90-50815
- An improved SIP scheme for numerical solutions of transonic streamfunction equations --- strongly implicit procedure p 904 A90-51014
- Numerical simulation of three-dimensional transonic flows p 905 A90-51020
- Multigrid methods in computational fluid dynamics p 906 A90-51526
- A numerical technique for computing the unsteady transonic flow around a wing profile in arbitrary oscillation p 906 A90-51530
- The effect of energy input on the characteristics of profiles in compressible fluid media p 906 A90-51533
- Multigrid scheme for the compressible Euler-equations p 907 A90-51559
- Multigrid acceleration of TVD schemes in transonic Euler flow calculation p 908 A90-52030
- An investigation of characteristics of transonic and viscous flows for turbine cascades p 909 A90-52779
- A numerical method for solving transonic flow past aircraft in Cartesian coordinates [NAL-TR-1008] p 18 N90-10003
- Computation of transonic flow about stores [AD-A210402] p 18 N90-10009
- Laser anemometer measurements in a transonic axial-flow fan rotor [NASA-TP-2879] p 73 N90-11245
- Development of direct-inverse 3-D methods for applied transonic aerodynamic wing design and analysis [NASA-CR-186036] p 103 N90-11733
- Theoretical methods and design studies for NLF and HLF swept wings at subsonic and supersonic speeds p 92 N90-12535
- Improvements in the formulations and numerical solution of the Euler problem for swept wings [RAE-TM-AERO-2139] p 95 N90-12562
- Solution of the thin-layer Navier-Stokes equations for laminar transonic flow [PB89-221600] p 136 N90-12879
- Multigrid solution method for the Euler equations [PB89-219463] p 138 N90-13116
- Block-structured solution of three-dimensional transonic flows using parallel processing [AD-A212851] p 170 N90-13330
- Transonic Euler solutions on mutually interfering finned bodies [AD-A213395] p 170 N90-13331
- A vapor generator for transonic flow visualization [NASA-TM-101670] p 201 N90-13403
- A two-dimensional adaptive-wall test section with ventilated walls in the Ames 2- by 2-foot transonic wind tunnel [NASA-TM-102207] p 201 N90-13407
- A computational analysis of the transonic flow field of two-dimensional minimum length nozzles p 173 N90-14194
- Navier-Stokes solutions of 2-D transonic flow over unconventional airfoils p 173 N90-14195
- Computation of unsteady transonic flow about airfoils in frequency domain using the full-potential equation p 174 N90-14198
- Nonlinear phenomena in computational transonic aerelasticity p 235 N90-15070
- A direct-inverse method for transonic and separated flows about airfoils [NASA-CR-4270] p 235 N90-15072
- An improvement of convection fidelity in Euler calculations p 315 N90-16709
- Nonlinear transonic Wall-Interference Assessment/Correction (WIAC) procedures and application to cast-10 airfoil results from the NASA 0.3-m TCT 8- by 24-inch Slotted Wall Test Section (SWTS) p 352 N90-17648
- High Reynolds number tests of the CAST-10-2/DOA 2 transonic airfoil at ambient and cryogenic temperature conditions p 320 N90-17650
- Asymptotic analysis of transonic flow through oscillating cascades p 427 N90-18421
- A matrix-free locally-implicit scheme for Navier-Stokes equations [AD-A218298] p 541 N90-20349
- On total variation diminishing schemes for transonic turbulent flow computation p 479 N90-20945
- Multigrid accelerated relaxation solution of transonic full potential flow equation [PD-CF-8942] p 480 N90-20951
- A two-dimensional unsteady analysis for transonic and supersonic cascade flows p 480 N90-20955
- Subsonic and transonic blade design by means of analysis codes p 510 N90-20985
- Inverse computation of transonic internal flows with application for multi-point-design of supercritical compressor blades p 501 N90-20987
- Numerical optimization of target pressure distributions for subsonic and transonic airfoil design p 502 N90-20993
- Numerical optimization of wings in transonic flow p 502 N90-20997
- Secondary flow in a turbine guide vane with low aspect ratio p 513 N90-21018
- A discussion on issues relating to multiblock grid generation p 608 N90-21991
- Transonic wing charge improvements by passive shock boundary layer interference control: Development status and prospects [ETN-90-96463] p 650 N90-24267
- Integral-equation methods in steady and unsteady subsonic, transonic and supersonic aerodynamics for interdisciplinary design [NASA-TM-102677] p 716 N90-25110
- Study of the compressibility effects on the turbulence of supersonic drags [ETN-90-97448] p 817 N90-27661
- Solution of Euler equations applied to a rotor of a helicopter in steady flight [ONERA-RSF-1/3731-AY-002A] p 910 N90-28500
- Unsteady aerodynamics of controls p 935 N90-28525
- Some topics in computational transonic aerodynamics: Revision [NAL-TR-1018T] p 912 N90-29332
- The computation and analysis of acoustic waves in transonic airfoil-vortex interactions p 966 N90-30031
- TRANSONIC FLUTTER**
- Experimental investigation on the interference effect of FL-23 wind tunnel wall on transonic flutter p 57 A90-10347
- The acoustic phenomena of the stalling flutter p 78 A90-11801
- Mach number effects on transonic aeroelastic forces and flutter characteristics p 17 A90-13024
- Applications of XTRAN3S and CAP-TSD to fighter aircraft [AIAA PAPER 90-1035] p 389 A90-29360
- Experimental transonic flutter characteristics of supersonic cruise configurations [AIAA PAPER 90-0979] p 390 A90-29369
- Effects of spoiler surfaces on the aeroelastic behavior of a low-aspect-ratio rectangular wing [AIAA PAPER 90-0981] p 391 A90-29371
- Unsteady aerodynamics methods for transonic aeroelastic analysis p 471 A90-33353
- Application of the CAP-TSD unsteady transonic small disturbance program to wing flutter --- Computational Aeroelasticity Program p 491 A90-33354
- Comparison of two potential flow methods for transonic flutter analysis p 471 A90-33356
- Analytical studies of the transonic flutter of aircraft p 860 A90-46577
- A new method for high speed propeller flutter prediction p 854 A90-49454
- Variational formulation of 2-D unsteady transonic aerodynamics of oscillating cascades p 813 A90-49458
- Experimental transonic flutter characteristics of two 72 deg-sweep delta-wing models [NASA-TM-101659] p 175 N90-14205
- Effects of spoiler surfaces on the aeroelastic behavior of a low-aspect-ratio rectangular wing [NASA-TM-102622] p 846 N90-27700
- TRANSONIC NOZZLES**
- An investigation of the flow characteristics of transonic nozzle blades p 475 A90-33700
- TRANSONIC SPEED**
- Axisymmetric afterbody flow separation at transonic speeds in presence of jet exhaust p 13 A90-12576
- An experimental study of the effect of the Reynolds number on flow past a swept wing at transonic velocities p 294 A90-24082
- Project Falke - Performance of free flight tests in the supersonic, transonic, and subsonic regimes from balloons [DGLR PAPER 88-018] p 903 A90-50235
- Wind tunnel tests of the influence of airfoil thickness on the normal force and pitching moment of two slender wings at transonic and supersonic Mach numbers [ESA-TT-1129] p 237 N90-15889
- Flow unsteadiness effects on boundary layers [NASA-CR-186067] p 690 N90-24557
- Sting-support interference on afterbody drag at transonic speeds [NAL-TM-EA-8902] p 909 N90-28492
- TRANSONIC WIND TUNNELS**
- Cryogenic wind tunnels p 199 A90-17346
- Mechanism of sidewall effect studied with oil flow visualization p 154 A90-18002
- Preliminary tests of a gust generator in the ONERA S3Ch transonic wind tunnel [ONERA, TP NO. 1989-171] p 261 A90-21035
- The use of a Laval nozzle and wall suction for blockage-free transonic wind-tunnel operation p 225 A90-21592
- Computational and experimental analysis of transonic fanjet engine flow field using 3-D Euler code p 306 A90-25809
- A new data acquisition, display and control system for the ARA transonic wind tunnel p 436 A90-28256
- Model incidence measurement using the SAAB Elopotos system --- IR instrumentation for measuring angle of attack in transonic wind tunnel models p 446 A90-28264

Design of a three dimensional Doppler anemometer for T2 transonic wind tunnel p 447 A90-28271

Status of the development programme for instrumentation and test techniques of the European Transonic Windtunnel - ETW p 437 A90-28292

A new type of calibration rig for wind tunnel balances p 438 A90-28305

New light on wind tunnel lasers p 439 A90-31248

Turbulence measurements and noise generation in a transonic cryogenic wind tunnel [AIAA PAPER 88-2026] p 522 A90-32463

Reduced-order aeroelastic models via dynamic residualization p 493 A90-33412

PETW testing results --- Pilot European Transonic Windtunnel p 523 A90-34226

Cryogenic wind tunnels in Japan p 523 A90-34228

Force balance errors due to temperature changes in ETW p 539 A90-34231

Model attitude measurement system p 539 A90-34235

A dynamic optical model attitude measurement system p 539 A90-34236

Feasibility study of RADAC stereo optoelectronic model deformation measurement system for ETW p 539 A90-34239

Flow quality in the T2 cryogenic wind-tunnel - Problems and solutions p 524 A90-34240

T2 ability concerning model design and instrumentation in short run processing p 524 A90-34241

A feasibility study for a combat aircraft model sting for the European transonic wind tunnel p 524 A90-34243

Results of studies on a manipulator system for model handling in the ETW p 524 A90-34248

An infrared camera system for detection of boundary layer transition in the ETW p 539 A90-34249

Development of cryogenic instrumentation for ETW models p 525 A90-34251

Examples of force measurements in a wind tunnel using multicomponent piezoelectric transducers p 540 A90-34352

Aeronautical facility requirements into the 2,000's [AIAA PAPER 90-1375] p 594 A90-37926

Experience in the use of a viscous simulation methodology for tests in transonic tunnels [AIAA PAPER 90-1414] p 559 A90-37951

An experimental investigation of pressure fluctuation mechanism for different transonic porous wall configurations [AIAA PAPER 90-1417] p 604 A90-37954

Broadband noise measurement in the transonic test section of the VTI T-38 wind tunnel [AIAA PAPER 90-1418] p 614 A90-37955

An experimental evaluation of test section noise in transonic wind tunnels [AIAA PAPER 90-1419] p 614 A90-37956

The new FFA T1500 transonic wind tunnel initial operation, calibration, and test results [AIAA PAPER 90-1420] p 596 A90-37957

Two-dimensional wall adaption in the transonic windtunnel of the AIA p 597 A90-38497

Infrared cameras for detection of boundary layer transition in transonic and subsonic wind tunnels [AIAA PAPER 90-1450] p 606 A90-38610

Sidewall boundary-layer removal and wall adaptation studies p 672 A90-40680

New transonic test sections for the NAE 5ftx5ft trisonic wind tunnel p 630 A90-42431

Propulsion integration for military aircraft [SAE PAPER 892234] p 733 A90-45449

Basic aerodynamic research facility for comparative studies of flow diagnostic techniques p 122 N90-12526

Residual interference assessment in adaptive wall wind tunnels [NASA-CR-181896] p 123 N90-12625

The design and development of an acoustic test section for the ARA transonic wind tunnel [PNR90574] p 140 N90-13202

Studies of the European transonic wind tunnel [ONERA-RSF-12/0694-GY] p 141 N90-13278

A two-dimensional adaptive-wall test section with ventilated walls in the Ames 2- by 2-foot transonic wind tunnel [NASA-TM-102207] p 201 N90-13407

Cryogenic temperature effects on sting-balance deflections in the National Transonic Facility [NASA-TM-4157] p 202 N90-14244

The NASA Langley 0.3-meter transonic cryogenic tunnel p 262 N90-15941

The US National Transonic Facility, NTF p 262 N90-15942

The European Transonic Windtunnel (ETW) p 262 N90-15945

The cryogenic Ludwig tube tunnel at Goettingen p 263 N90-15947

Other cryogenic wind tunnel projects p 263 N90-15948

Test techniques for cryogenic wind tunnels p 263 N90-15952

Automatic control of cryogenic wind tunnels p 263 N90-15957

Cryogenic balances for the US NTF p 264 N90-15959

Safety and cryogenic wind tunnels p 264 N90-15960

Determination of the N-factor in the Brunswick (Federal Rep. of Germany) transonic wind tunnel using measurements of pressure distributions and transition points, and the Sally method p 276 N90-16177

Use of the film-of-oil technique for profile measurements in the Transonic Wind tunnel Brunswick (TWB) p 238 N90-16252

An experimental AWTs process and comparisons of ONERA T2 and 0.3-m TCT AWTs data for the ONERA CAST-10 aerofoil p 321 N90-17653

Half model tests on an ONERA calibration model in the transonic wind tunnel Goettingen, Federal Republic of Germany [DLR-MITT-89-20] p 397 N90-18370

New transonic test sections for the NAE 5 ft x 5 ft trisonic wind tunnel [AD-A220933] p 674 N90-24278

Investigation of the vortex flow over a sharp-edged delta wing in the transonic speed regime [LR-594] p 717 N90-25115

Effect of tail size reductions on longitudinal aerodynamic characteristics of a three surface F-15 model with nonaxisymmetric nozzles [NASA-TP-3036] p 718 N90-25938

Three-dimensional model testing in the transonic self-streamlining wind tunnel p 938 N90-28583

Transonic 3-D Euler analysis of flows around fanjet engine and TPS (Turbine Powered Simulator). Comparison with wind tunnel experiment, evaluation of TPS testing method and 3-D flow [NAL-TR-1045] p 912 N90-29327

TRANSPARENCY

A new method for measuring the transmissivity of aircraft transparencies [AD-A216953] p 464 N90-19842

TRANSPARATION

Modelling of boundary layer and trailing edge thickness effects for the Euler equations using surface transpiration p 629 A90-42412

Transpiration cooling in hypersonic flight [NASA-CR-186435] p 478 N90-20052

TRANSPONDERS

Mode S transponders - A new avionics product [SAE PAPER 891055] p 98 A90-14357

Estimation of atmospheric and transponder survey errors with a navigation Kalman filter p 459 A90-30689

Aircraft Separation by Synchronized Transponder Interrogation (ASSTI) p 727 A90-43724

Collision alert p 847 A90-48521

Data link test and analysis system/ATCRBS transponder test system technical reference [DOT/FAA/CT-TN90/7] p 824 N90-26803

TRANSPORT AIRCRAFT

Natural laminar flow research for subsonic transport aircraft in the FRG p 2 A90-10137

Analytical methods for subsonic propulsion system integration p 29 A90-12613

Structural analysis of the horizontal tail surfaces of subsonic transport aircraft p 102 A90-14556

The Soviets' French revelation. II - Aircraft p 81 A90-14800

Aft facing transport aircraft passenger seats under 16G dynamic crash simulation p 175 A90-17416

HSC research focuses on environmental issues p 143 A90-17780

Conditional sampling --- technique for aerodynamic characteristics measurement from wind-tunnel experiments [ONERA, TP NO. 1989-187] p 261 A90-21047

Numerical simulation of transonic wing flows using a zonal Euler, boundary-layer, Navier-Stokes approach p 225 A90-21596

The application of the engineering approach for analyzing crack tolerance of fuselage panels to a transport airplane p 272 A90-22014

Subsonic calculation of propeller/wing interference [AIAA PAPER 90-0031] p 226 A90-22155

Laminar flow control leading-edge systems in simulated airline service p 335 A90-26134

Development of jet transport airframe fatigue test spectra p 351 A90-26753

Multiple-power-path nonplanetary main gearbox of the Mi-26 heavy-lift transport helicopter p 452 A90-30115

A reconfigurable integrated navigation and flight management system for military transport aircraft p 433 A90-30794

An optically interfaced propulsion management system applied to a commercial transport aircraft p 424 A90-30811

Subcomponent tests for composite fuselage technology readiness p 490 A90-33105

Multi-surface control law synthesis and wind tunnel test verification of active flutter suppression for a transport-type wing p 517 A90-33401

Half transport aircraft cryogenic model for T2 wind tunnel p 524 A90-34242

Sting design feasibility for E.T.W. cryogenic civil transport aircraft p 524 A90-34245

Yakovlev strikes back p 579 A90-35848

Critical review of design philosophies for recent transport WIG effect vehicles --- Wing-in Ground p 684 A90-41753

Support backbone for the Soviet air forces . . . The Ilyushin 'Candid' family p 731 A90-43769

Experimental study of the turbulent boundary layer on a transport wing in subsonic flow p 709 A90-44728

Design for a natural laminar flow glove for a transport aircraft [AIAA PAPER 90-3043] p 792 A90-45880

Flight tests with a natural laminar flow glove on a transport aircraft [AIAA PAPER 90-3044] p 828 A90-45881

Flying the giant --- An-124 Ruslan aircraft p 833 A90-48522

Aging fleet Structures Working Group activities [AIAA PAPER 90-3219] p 786 A90-48840

Air Force use of civil airworthiness criteria for testing and acceptance of military derivative transport aircraft [AIAA PAPER 90-3289] p 818 A90-48875

The BAe (commercial aircraft) LTD transport aircraft synthesis and optimisation program (TASOP) [AIAA PAPER 90-3295] p 837 A90-48879

Advanced rotorcraft V/STOL - Technology needs for high-speed rotorcraft [AIAA PAPER 90-3298] p 837 A90-48880

Design synthesis and optimization of joined-wing transports [AIAA PAPER 90-3197] p 838 A90-49102

Twin-engine transports - A look at the future [AIAA PAPER 90-3215] p 818 A90-49107

Certification impact of introducing G.P.S. into commercial transport navigation systems p 824 A90-49501

Aging jet transport structural evaluation programs p 901 A90-49889

Modifying high-order aeroelastic math model of a jet transport using maximum likelihood estimation p 61 N90-10106

Development of pressure containment and damage tolerance technology for composite fuselage structures in large transport aircraft [NASA-CR-3996] p 63 N90-10186

Comparison of flying qualities derived from in-flight and ground-based simulators for a jet-transport airplane for the approach and landing pilot tasks [NASA-TP-2962] p 120 N90-11757

The aerodynamic experimental center of Aeritalia: Combat aircraft group [ETN-89-95213] p 122 N90-11766

Transport composite fuselage technology: Impact dynamics and acoustic transmission [NASA-CR-4035] p 126 N90-11821

Laminar flow: Challenge and potential p 90 N90-12504

Lockheed laminar-flow control systems development and applications p 90 N90-12506

Long-range LFC transport p 104 N90-12508

Preliminary design of four aircraft to service the California Corridor in the year 2010: The California Condor, California Sky-Hopper, high capacity short range transport tilt rotor aircraft needed to simplify intercity transportation [NASA-CR-186232] p 186 N90-14226

Relative merits of reactive and forward-look detection for wind-shear encounters during landing approach for various microburst escape strategies [NASA-TM-4158] p 259 N90-15108

Evaluation of two transport aircraft and several ground test vehicle friction measurements obtained for various runway surface types and conditions. A summary of test results from joint FAA/NASA Runway Friction Program [NASA-TP-2917] p 249 N90-15902

Investigation and characteristics of major fire-related accidents in civil air transports over the past ten years p 324 N90-17582

Development of improved fire safety standards adopted by the Federal Aviation Administration p 324 N90-17585

New aircraft cabin and cargo flammability standards for transport category aircraft p 325 N90-17589

Fire prevention in transport airplane passenger cabins p 325 N90-17590

- Characteristics of transport, aircraft fires measured by full-scale tests p 325 N90-17591
- Full-scale air transport category fuselage burnthrough tests [DOT/FAA/CT-TN89/65] p 486 N90-20967
- Simulator comparison of thumbball, thumb switch, and touch screen input concepts for interaction with a large screen cockpit display format [NASA-TM-102587] p 506 N90-21005
- Civil air transport: A fresh look at power-by-wire and fly-by-light [NASA-TM-102574] p 542 N90-21283
- An evaluation of the pressure proof test concept for thin sheet 2024-T3 [NASA-TM-101675] p 543 N90-21424
- High speed commercial transport fuels considerations and research needs [NASA-TM-102535] p 600 N90-21869
- UK airmisses involving commercial air transport, January - April 1989 [ISSN-0951-6301] p 575 N90-22544
- Multilevel decomposition approach to the preliminary sizing of a transport aircraft wing [NASA-CR-4296] p 583 N90-22557
- Fire hazards of aerosol cans in aircraft cargo compartments [DOT/FAA/CT-89/32] p 636 N90-23369
- AVION: A detailed report on the preliminary design of a 79-passenger, high-efficiency, commercial transport aircraft [NASA-CR-186663] p 649 N90-23395
- High speed civil transport [NASA-CR-186661] p 649 N90-23396
- Study of high-speed civil transports. Summary [NASA-CR-4236] p 735 N90-25966
- Robustness evaluation of H2 and H(infinity) control theory as applied to a transport aircraft [AD-A22795] p 759 N90-26018
- High-speed civil transport study: Special factors [NASA-CR-181881] p 923 N90-28537
- Energy Efficient Engine: Flight propulsion system final design and analysis [NASA-CR-168219] p 930 N90-28558
- TRANSPORT PROPERTIES**
- Calculation of confined swirling flows with a second moment closure p 66 A90-10640
- Development of a mathematical model for the thermal decomposition of aviation fuels [AD-A221673] p 875 N90-26994
- TRANSPORT THEORY**
- The numerical simulation of multistage turbomachinery flows p 514 N90-21025
- TRANSPORT VEHICLES**
- Thermal protection systems for hypersonic transport vehicles [SAE PAPER 901306] p 882 A90-49358
- TRANSPUTERS**
- Implementation of a transputer-based flight controller p 667 A90-38966
- Fault-tolerant transputer-based controller configurations for gas-turbine engines p 852 A90-48529
- TRANSVERSE OSCILLATION**
- Nonlinear transverse oscillations of a composite dynamic system p 129 A90-14558
- TRAPEZOIDAL WINGS**
- Effect of similarity parameters on the aerodynamic quality and moment characteristics of a supersonic wing with blunt edges p 298 A90-24150
- A study of the strength characteristics of a twin-fuselage aircraft with a trapezoid wing system p 410 A90-28993
- Wave rider volume distribution p 388 A90-29006
- TRAPPED VORTICES**
- On efficiency and accuracy of numerical methods for solving aerodynamic equations p 304 A90-25730
- TRAVELING WAVES**
- Study on travelling wave vibration of bladed disks in turbomachinery p 423 A90-29908
- Active stabilization of aeromechanical systems [AD-A216629] p 454 N90-18672
- TREND ANALYSIS**
- Trend analysis and diagnostics codes for training purposes [AIAA PAPER 90-2394] p 617 A90-42156
- TRENDS**
- The evolution of light alloys in the aerospace industry [ETN-89-95216] p 126 N90-11872
- Diffusion bonding of metals p 206 N90-14330
- Fighter escape system: The next step forward p 483 N90-20059
- Unique failure behavior of metal/composite aircraft structural components under crash type loads [NASA-TM-102679] p 690 N90-24660
- The effect of aircraft size on cabin floor dynamic pulses [DOT/FAA/CT-88/15] p 735 N90-25136

- Technical evaluation report on the Guidance and Control Panel 49th Symposium on Fault Tolerant Design Concepts for Highly Integrated Flight Critical Guidance and Control Systems [AGARD-AR-281] p 758 N90-26012
- Active control of aerothermoelastic effects for a conceptual hypersonic aircraft [NASA-TM-102713] p 869 N90-27725
- Impact of NDE-NDI methods on aircraft design, manufacture, and maintenance, from the fundamental point of view p 887 N90-28093
- TRIANGULATION**
- Automatic mesh generation for complex three-dimensional regions using a constrained Delaunay triangulation p 375 A90-26022
- Adaptive mesh generation for viscous flows using Delaunay triangulation p 310 A90-26531
- The generation of unstructured triangular meshes using Delaunay triangulation --- applications to hypersonic inlets p 310 A90-26533
- TRIAXIAL STRESSES**
- The in service multi-axial-stress situation in an uncooled gas turbine blade p 423 A90-29880
- TRIBOLOGY**
- Electrostatic field conditions on an aircraft stricken by lightning [ONERA, TP NO. 1989-148] p 23 A90-11170
- TRISONIC WIND TUNNELS**
- Broadband noise measurement in the transonic test section of the VTI T-38 wind tunnel [AIAA PAPER 90-1418] p 614 A90-37955
- Wind tunnel studies of F/A-18 tail buffet [AIAA PAPER 90-1432] p 559 A90-37969
- Small-scale inlet testing for low cost screening applications [AIAA PAPER 90-1926] p 741 A90-42696
- New transonic test sections for the NAE 5 ft x 5 ft trisonic wind tunnel [AD-A220933] p 674 N90-24278
- TRUSSES**
- Design and evaluation of graphite/epoxy truss core sandwich panels p 210 A90-18406
- TUNGSTEN**
- Fiber reinforced superalloys p 532 A90-34169
- TUNGSTEN OXIDES**
- Electrochromic windows - Applications for aircraft [SAE PAPER 891063] p 129 A90-14363
- Electrochromic aircraft windows p 451 A90-29891
- TUNING**
- Analytical study of mistuning/friction/aerodynamics interaction in a bladed disk assembly [AD-A211139] p 55 N90-10893
- TURBINE BLADES**
- Fundamentals of turbine design for aircraft engines --- Russian book p 40 A90-10839
- Calculation of three-dimensional turbulent flow in a linear turbine cascade [ONERA, TP NO. 1989-115] p 3 A90-11147
- Optimum trailing edge ejection for cooled gas turbine blades p 41 A90-11562
- The solution of the unsteady transonic flow through a blade passage in an axial turbine p 5 A90-11777
- The effect of the magnitude of the inlet-boundary disturbance on the unsteady forces on axial gas-turbine blades p 6 A90-11781
- A numerical method solving 2-D unsteady flow field around cascade of oscillating airfoils with arbitrary camber and thickness p 7 A90-11788
- Computation of aerodynamic blade loads due to wake influence and aerodynamic damping of turbine and compressor cascades p 7 A90-11791
- Flutter of turbine blades p 41 A90-11794
- Studies on the influence of Mach number on profile losses of a reaction turbine cascade p 10 A90-12517
- Shock capturing and loss prediction for transonic turbine blades using a pressure correction method p 11 A90-12518
- Influence of blade leaning on the flow field behind turbine rectangular cascades with different incidences and aspect ratios p 11 A90-12519
- An experimental investigation of the effect of incidence on the two-dimensional performance of an axial turbine cascade p 11 A90-12520
- Extending the overhaul interval for gas turbine engines through the use of alternative coatings on first stage blades p 63 A90-12539
- Stress analysis of gas turbine bladed disc for structural integrity applying the concept of cyclic symmetry p 46 A90-12564
- Pressure surface trailing edge slot cooling [ONERA, TP NO. 1989-123] p 47 A90-12569
- Temperature scaling of turbine blade heat transfer with and without shock wave passing p 47 A90-12570
- Computation of transonic turbine cascade flow using Navier-Stokes equations p 14 A90-12621

- Effect of the roughness of deposits in a compressor cascade on the flow lag angle p 84 A90-14578
- The tape method for the automatic partitioning of an arbitrary region when calculating temperature stresses p 138 A90-14587
- Designing turbine blades for fatigue and creep p 112 A90-16007
- Photoelastic investigation of turbine rotor blade shrouds p 112 A90-16008
- Shaft flexibility effects on aeroelastic stability of a rotating bladed disk p 132 A90-16371
- Dynamic structural correlation via nonlinear programming techniques p 208 A90-17372
- An approach for calculating steady subsonic and transonic blade to blade flows p 152 A90-17784
- Experimental investigation on the performance of an annular nozzle cascade of a highly-loaded transonic turbine stage p 152 A90-17787
- Effect of vane and blade numbers on performance of transonic turbine stage p 189 A90-17789
- Design and calculation of composite air-cooled blades in a highly-loaded transonic turbine p 189 A90-17790
- Calculation of coolant flow and heat transfer inside composite air-cooled turbine p 189 A90-17791
- Experimental investigation on composite air-cooled blades of highly-loaded transonic turbine p 189 A90-17793
- Experimental investigation on composite cooling of a turbine blade p 190 A90-17794
- Research on film-cooling of turbine blade p 190 A90-17795
- Wake behaviour of a large deflection turbine rotor linear cascade p 157 A90-18481
- Gas turbine combustion - A personal perspective p 283 A90-20604
- A parametric study of the flutter stability of two-dimensional turbine and compressor cascades in incompressible flow p 225 A90-21593
- Advanced software for turbine blade processing [SME PAPER MS89-330] p 274 A90-23694
- Study of various factors affecting secondary loss vortices downstream a straight turbine cascade [ASME PAPER 89-GT-12] p 287 A90-23757
- Resonant stress determination of a turbine blade with modal damping as a function of rotor speed and vibrational amplitude p 340 A90-23765
- Secondary loss generation in a linear cascade of high-turning turbine blades [ASME PAPER 89-GT-47] p 289 A90-23773
- Development of the tip-leakage flow downstream of a planar cascade of turbine blades - Vorticity field [ASME PAPER 89-GT-55] p 289 A90-23781
- Tip leakage losses in a linear turbine cascade [ASME PAPER 89-GT-56] p 290 A90-23782
- Comparison of steady and unsteady secondary flows in a turbine stator cascade [ASME PAPER 89-GT-79] p 291 A90-23800
- Characteristics of partial length circular pin fins as heat transfer augmentors for airfoil internal cooling passages [ASME PAPER 89-GT-87] p 359 A90-23806
- Mathematical formulation of blade surfaces in turbomachinery. I - Theoretical surface formulations [ASME PAPER 89-GT-160] p 360 A90-23848
- A numerical three-dimensional thermal stress analysis for cooled blades [ASME PAPER 89-GT-168] p 341 A90-23853
- A comparison between engine test results and design predictions of turbine blade cooling performance [ASME PAPER 89-GT-169] p 341 A90-23854
- Aerodynamic and heat transfer measurements on blading for a high rim-speed transonic turbine [ASME PAPER 89-GT-226] p 293 A90-23883
- Engineering design of tough ceramic matrix composites for turbine components [ASME PAPER 89-GT-294] p 343 A90-23892
- An automatic system for the programmed control of the parameters of the vibrational and thermal testing of the blades of gas turbine engines p 343 A90-24216
- Recent and prospective developments in single-crystal superalloys for the blades of advanced turbines p 355 A90-24288
- The anisotropy of the mechanical behaviour in nickel-based single crystal superalloys for turbine blades [ONERA, TP NO. 1989-205] p 355 A90-25339
- Development of a new nickel based single crystal turbine blade alloy for very high temperatures [ONERA, TP NO. 1989-206] p 356 A90-25340
- Digital X-ray inspection p 445 A90-28162
- The in service multi-axial-stress situation in an uncooled gas turbine blade p 423 A90-29880
- Prediction of heat transfer coefficient on turbine blade profiles p 423 A90-29904
- Optimal computer-aided design of the blading of axial-flow turbines --- Russian book p 452 A90-30268

A calculation of the aerodynamic lift acting on cascade blades in a steady, viscous flow at high Reynolds number p 469 A90-32425

Surface roughness measurements on gas turbine blades
[ASME PAPER 89-GT-285] p 508 A90-33559

The influence of boundary layer state on vortex shedding from flat plates and turbine cascades
[ASME PAPER 89-GT-296] p 474 A90-33560

An improved incidence losses prediction method for turbine airfoils
[ASME PAPER 89-GT-284] p 475 A90-33563

The trailing edge loss of transonic turbine blades
[ASME PAPER 89-GT-278] p 475 A90-33564

Three dimensional turbine blade analysis in thermo-viscoplasticity p 540 A90-34324

Wide chord fan club p 584 A90-35600

A study of the influence of predeformations on the vibrations of blades p 585 A90-35673

Boundary element method for solving direct aerodynamic problem of aerofoil cascades on an arbitrary stream surface of revolution p 554 A90-35830

Experimental investigation of external heat transfer coefficients on film-cooled turbine blade leading edge p 585 A90-35787

Development of a simulated bird-strike test method --- of aircraft turbine engine fan blade materials p 600 A90-37444

The influence of the inlet Mach number on the boundary layer development on turbomachinery blade surfaces p 621 A90-40504

Simulation of inviscid blade-row interaction using a linearised potential code
[AIAA PAPER 90-1916] p 621 A90-40555

Reverse flow in multistage axial compressors p 623 A90-40942

Application of 3-D Navier-Stokes computation to bowed stacking turbine vane design
[AIAA PAPER 90-2129] p 625 A90-42035

The investigation of heat transfer in cooled blades of gas turbines
[AIAA PAPER 90-2144] p 685 A90-42043

Boundary-layer transition and separation on a turbine blade in a plane cascade
[AIAA PAPER 90-2263] p 625 A90-42102

Investigation of unsteady flow through transonic turbine stage. I - Analysis
[AIAA PAPER 90-2408] p 626 A90-42161

Investigation of unsteady flow through a transonic turbine stage. II - Data/prediction comparison for time-averaged and phase-resolved pressure data
[AIAA PAPER 90-2409] p 626 A90-42162

Application of 3-D flow analysis to the design of a high work transonic turbine p 628 A90-42395

Film cooling of turbine blades - Two dimensional experiments and numerical simulations p 739 A90-42670

Effects of inlet turbulence scale on turbine blade surface heat transfer in a linear cascade
[AIAA PAPER 90-2264] p 768 A90-42761

Numerical solution of 2D transonic flows in a turbine cascade p 709 A90-44601

The flow field and heat transfer near a turbulator p 771 A90-44755

Theoretical and experimental determination of natural frequencies of laced blading p 878 A90-46037

Vibration of turbine blades damped by dry friction forces p 879 A90-46190

Improvement in turbine blade aerodynamic force in the tip region p 809 A90-47854

Two- and three-dimensional problems of unsteady aerodynamics of low loaded turbomachinery blade rows stages p 813 A90-49452

Structural and dynamic analysis of the A330/340 composite RAT blade --- ram air turbine p 942 A90-50083

An experimental convective heat transfer investigation around a film-cooled gas turbine blade p 957 A90-51261

Estimation of the safety factor of turbine blades under thermal cycling and vibration loading p 958 A90-52356

Large scale prop-fan structural design study. Volume 1: Initial concepts
[NASA-CR-174992] p 52 N90-10043

Large scale prop-fan structural design study. Volume 2: Preliminary design of SR-7
[NASA-CR-174993] p 52 N90-10044

Analytical study of mistuning/friction/aerodynamics interaction in a bladed disk assembly
[AD-A211139] p 55 N90-10893

A computer integrated approach to dimensional inspection
[PNR90596] p 116 N90-12611

Inclusion of nonlinear aerodynamics in the FLAP code
[DE89-009507] p 281 N90-15519

Aerodynamic and heat transfer measurements on blading for a high rim-speed transonic turbine
[RAE-TM-P-1151] p 256 N90-15920

Wake interaction effects on the transition process on turbine blades
[AD-A214492] p 343 N90-16759

A comparison of flutter calculations based on eigenvalue and energy method p 425 N90-18406

Influence of friction and separation phenomena on the dynamic blade loading of transonic turbine cascades
[MITT-88-04] p 428 N90-19235

The influence of a wall function on turbine blade heat transfer prediction p 429 N90-19421

Heat transfer near the entrance to a film cooling hole in a gas turbine blade
[AD-A217396] p 510 N90-20089

Subsonic and transonic blade design by means of analysis codes p 510 N90-20985

Calculation of the three dimensional turbulent flow in a linear turbine blade p 513 N90-21021

Calculation of the secondary flow in an axial turbine p 513 N90-21022

Losses in the tip-leakage flow of a planar cascade of turbine blades p 514 N90-21027

Navier-Stokes analysis of turbine blade heat transfer
[NASA-TM-102496] p 542 N90-21300

Calculation of the aeroelastic blade stabilization with linearized process
[MITT-87-01] p 666 N90-24272

Calculation of temperature distribution in various turbine blades using a boundary-fitted coordinate transformation method p 929 N90-28550

Flow coupling between a rotor and a stator in turbomachinery
[AD-A223882] p 932 N90-28572

The effects of a compressor rebuild on gas turbine engine performance: Final results p 952 N90-28701

Further studies of turbulence structure resulting from interactions between embedded vortices and wall jets at high blowing ratios p 960 N90-29593

TURBINE ENGINES

USA - A system to represent airfoils throughout the product life cycle
[AIAA PAPER 89-2972] p 73 A90-10487

Theoretical analysis of an icing test apparatus for turbine engine air intakes
[AAAF PAPER NT 88-20] p 23 A90-11437

Study of advanced technology impact on cycle characteristics and aircraft sizing (using multivariable optimization techniques) p 29 A90-12612

Simulation of a turbocompound two-stroke diesel engine
[SAE PAPER 891066] p 110 A90-14366

Predicting the CO, HC, and NO(x) emission and combustion efficiency of small turbine engines from the combustion chamber bench test results p 125 A90-15425

Thermodynamics and the future turbine engines
[ONERA, TP NO. 1989-165] p 253 A90-21031

Oils for flight turbine engines - Research and development in the 90s p 266 A90-21473

Some aspects of the erosive wear of components of aircraft turbine engines p 253 A90-21627

Effect of inlet flow angle on the erosion of radial turbine guide vanes
[ASME PAPER 89-GT-208] p 254 A90-22664

Heat transfer and pressure drop for short pin-fin arrays with pin-endwall fillet
[ASME PAPER 89-GT-99] p 359 A90-23813

A review of failure models for ceramic matrix composite laminates under monotonic loads
[ASME PAPER 89-GT-153] p 354 A90-23842

An experimental study of heat transfer and film cooling on low aspect ratio turbine nozzles
[ASME PAPER 89-GT-187] p 361 A90-23865

The LHTEC T800-LHT-800 engine integration into the Augusta A129 helicopter p 422 A90-28177

Coating turbine engine components p 451 A90-29893

Eliminating the TF30 P-111 + engine rotor-instability problem p 508 A90-32961

Composite electronic enclosures for engine-mounted environments
[AIAA PAPER 90-2030] p 657 A90-40601

Adjusting turbine engine transient performance for the effects of environmental variances
[AIAA PAPER 90-2501] p 658 A90-40639

Military engines - Cradle of technology p 660 A90-41758

Evaluation of solid lubricant powder delivery system for turbine bearing lubrication
[AIAA PAPER 90-2046] p 684 A90-41997

Metal matrix composites structural design experience
[AIAA PAPER 90-2175] p 677 A90-42059

Metal matrix composite fan blade development
[AIAA PAPER 90-2178] p 677 A90-42062

Turbine configuration impact on advanced IHPDET engine system mission capabilities
[AIAA PAPER 90-2739] p 664 A90-42221

Co-development of CT7-6 engines - A continued tradition in technology and reliability p 665 A90-42485

Unsteady Euler analysis of the redistribution of an inlet temperature distortion in a turbine
[AIAA PAPER 90-2262] p 768 A90-42759

An experimental investigation of film cooling effectiveness for slots of various exit geometries
[AIAA PAPER 90-2266] p 768 A90-42763

IHPDET technology mission payoffs at the component level - A look at Phase II technologies --- Integrated High Performance Turbine Engine Technology
[AIAA PAPER 90-2404] p 701 A90-42794

Vibration analysis of laced blades p 878 A90-46186

Calculation of the efficiency of an active partial-admission gas turbine for counterpressures varying over a wide range p 850 A90-46495

Effect of vane twist on the performance of dome swirlers for gas turbine airblast atomizers
[AIAA PAPER 90-1955] p 881 A90-47203

Vibration dampers for cryogenic turbomachinery
[AIAA PAPER 90-2740] p 882 A90-47228

Titanium aluminides for advanced aircraft engines p 874 A90-49000

An investigation of characteristics of transonic and viscous flows for turbine cascades p 909 A90-52779

Dynamic instability characteristics of aircraft turbine engine combustors p 53 N90-10195

A computer integrated approach to dimensional inspection
[PNR90596] p 116 N90-12611

Advanced Turbine Technology Applications Project (ATTAP)
[NASA-CR-185109] p 220 N90-14153

Aircraft performance enhancement with active compressor stabilization
[AD-A213652] p 249 N90-15097

Characterization of chemicals on engine exhaust particles
[AD-A213566] p 256 N90-15106

Improved Thermo-Oxidative-Deposition screening tests for turbine lubricants
[AD-A217795] p 533 N90-21188

Effect of vane twist on the performance of dome swirlers for gas turbine airblast atomizers
[NASA-TM-103195] p 773 N90-25289

The role of NDI in the certification of turbine engine components
[PNR90629] p 777 N90-26349

Engine testing of thermographic phosphors
[DE90-013269] p 885 N90-28059

Energy Efficient Engine: Flight propulsion system final design and analysis
[NASA-CR-168219] p 930 N90-28558

Energy Efficient Engine core design and performance report
[NASA-CR-168069] p 930 N90-28559

NASA/GE Energy Efficient Engine low pressure turbine scaled test vehicle performance report
[NASA-CR-168290] p 931 N90-28563

TURBINE EXHAUST NOZZLES

Device for the dilution of hot exhaust jets
[ETN-90-97435] p 858 N90-27723

TURBINE INSTRUMENTS

The remote sensing of temperature in gas turbine engine components using epithermal neutrons p 70 A90-12630

Instrumentation for combustion and flow in engines; Proceedings of the NATO Advanced Study Institute, Vimeiro, Portugal, Sept. 13-26, 1987 p 211 A90-19004

A microprocessor-based system for monitoring gas turbines p 350 A90-24359

Partial similarity and a real-time model of twin-spool gas turbine p 654 A90-40512

Optimal choice of measured parameters during the identification of gas turbine engines. II - Combined confidence regions and intervals of the identification results p 850 A90-46493

TURBINE PUMPS

Generalized relations for estimating the efficiency and basic dimensions of screw pumps and hydraulic turbines of pump units p 111 A90-14583

Application of HOST technology to the SSME HPFTP blade
[ASME PAPER 89-GT-130] p 360 A90-23828

Rotordynamics of the Vulcain LH2 Turbopump - Comparison between test results and non-linear dynamic analysis p 528 A90-33382

Probabilistic modeling for simulation of aerodynamic uncertainties in propulsion systems
[NASA-TM-102472] p 515 N90-21036

Experimental evaluation of a tuned electromagnetic damper for vibration control of cryogenic turbopump rotors
[NASA-TP-3005] p 665 A90-23403

TURBINE WHEELS

Test rig for the study of the flow in a rotor-stator system
[ONERA, TP NO. 1989-124] p 58 A90-12634

Experimental investigations on the spatial and time-dependent structure of part-load recirculations in centrifugal pumps
p 83 A90-13788

Effect of the radial clearance on the efficiency of a partial microturbine
p 111 A90-14586

Optimum design of rotational wheels under transient thermal and centrifugal loading
p 270 A90-20770

Analysis and practical design of ceramic-matrix composite components
p 445 A90-28135

Advanced technology's impact on compressor design and development - A perspective.
[SAE SP-800] p 423 A90-28571

Study on travelling wave vibration of bladed disks in turbomachinery
p 423 A90-29908

Visualization studies in rotating disk cavity flows
p 475 A90-33568

Non-steady flow loss mechanisms associated with vaneless diffusers
[AIAA PAPER 90-2508] p 682 A90-40641

A review of tilt rotor download research
p 630 A90-42437

Modeling of the oil quench for Ni-based superalloy turbine disks
p 957 A90-51525

Advanced technologies impact on compressor design and development: A perspective
[NASA-TM-102341] p 54 A90-10891

Defects in monoblock cast turbine wheels
p 443 A90-18400

TURBINES

An experimental study of the gasdynamic characteristics of annular nozzle cascades with small flow exit angles
p 255 A90-23409

LDF measurements and the flow analysis in the vaneless region of a radial inflow turbine
[ASME PAPER 89-GT-157] p 292 A90-23845

Aerodynamics of cooling jets introduced in the secondary flow of a low speed turbine cascade
[ASME PAPER 89-GT-192] p 362 A90-23868

A simulation code for turbocompound diesel engines
[IAR-89-26] p 774 A90-25348

A heat transfer analysis for rough turbine airfoils
[AD-A221942] p 854 A90-26831

Flow coupling between a rotor and a stator in turbomachinery
[AD-A223882] p 932 A90-28572

Transonic 3-D Euler analysis of flows around fanjet engine and TPS (Turbine Powered Simulator). Comparison with wind tunnel experiment, evaluation of TPS testing method and 3-D flow
[NAL-TR-1045] p 912 A90-29327

TURBOCOMPRESSORS

Multistage compressor vane row aerodynamic gust response
p 6 A90-11783

Highly loaded axial flow compressors - History and current developments
p 44 A90-12503

A study of flow structure in a contra-rotating axial compressor stage
p 11 A90-12524

The interaction between tip clearance flow and the passage flowfield in an axial compressor cascade
p 11 A90-12525

An investigation of artificial compressor surge
p 11 A90-12526

Unsteady loss in a low speed axial flow compressor during rotating stall
p 12 A90-12527

Design and off-design performance predictions of axial turbines
p 45 A90-12540

A theoretical and experimental investigation of the Reynolds and apparent stresses in axial compressors
p 12 A90-12554

Calculation of unsteady boundary layer development on axial-flow turbomachinery blading
p 48 A90-12588

The development of a high response aerodynamic wedge probe and use on a high-speed research compressor
p 69 A90-12618

Adverse pressure gradient effects on boundary layer transition in a turbulent free stream
p 15 A90-12639

Effect of the roughness of deposits in a compressor cascade on the flow lag angle
p 84 A90-14578

Thermodynamic calculation of the compressors of gas turbine engines and powerplants at high air pressures
p 130 A90-14585

Operation of a compressor with intermediate air bleed
p 111 A90-14589

A study on surge and rotating stall in axial compressors - A summary of the measurement and fundamental analysis method
p 87 A90-16105

Aerodynamic design of an HP compressor stage using advanced computation codes
p 156 A90-18479

Throughflow numerical calculations including influence of spanwise mixing in a multistage axial flow compressor
p 157 A90-18534

A parametric study of the flutter stability of two-dimensional turbine and compressor cascades in incompressible flow
p 225 A90-21593

Calculation of the side-wall boundary layer in axial turbomachines, accounting for the internal flow near the blades
p 225 A90-21595

A comparison between the design point and near-stall performance of an axial compressor
[ASME PAPER 89-GT-70] p 254 A90-22667

Stability of flow through multistage axial compressors
[ASME PAPER 89-GT-311] p 231 A90-22668

Effect of the control of turbocompressor guide vanes on the throttle characteristics of a bypass engine
p 255 A90-23425

Measurement and calculation of the three-dimensional flow in axial compressor stators, with and without end-bends
[ASME PAPER 89-GT-6] p 287 A90-23753

Numerical optimization of axial compressor designs
[ASME PAPER 89-GT-14] p 340 A90-23758

Influence of the radial component of total pressure gradient on tip clearance secondary flow in axial compressors
[ASME PAPER 89-GT-19] p 288 A90-23761

A proposal for optimized design of multistage compressors
[ASME PAPER 89-GT-34] p 288 A90-23766

Stall inception in axial compressors
[ASME PAPER 89-GT-63] p 290 A90-23786

Effects of endwall suction and blowing on compressor stability enhancement
[ASME PAPER 89-GT-64] p 290 A90-23787

Application of recess vane casing treatment to axial flow fans
[ASME PAPER 89-GT-68] p 341 A90-23791

Three-dimensional relief in turbomachinery blading
[ASME PAPER 89-GT-151] p 292 A90-23840

Simulation of three-dimensional viscous flow within a multistage turbine
[ASME PAPER 89-GT-152] p 292 A90-23841

The influence of diffuser vane leading edge geometry on the performance of a centrifugal compressor
[ASME PAPER 89-GT-163] p 292 A90-23851

The design and test of a two stage transonic axial flow compressor
[ASME PAPER 89-GT-164] p 341 A90-23852

Axial flow compressor design optimization. I - Pitchline analysis and multivariable objective function influence
[ASME PAPER 89-GT-201] p 342 A90-23873

Axial flow compressor design optimization. II - Through-flow analysis
[ASME PAPER 89-GT-202] p 342 A90-23874

The prediction of boundary layers with rotation and variation of stream filament thickness
[ASME PAPER 89-GT-227] p 362 A90-23882

An off-design loss and deviation prediction study for transonic axial compressors
[ASME PAPER 89-GT-324] p 343 A90-23893

An ultrasonic fatigue facility for HCF/LCF interactive tests
p 363 A90-23900

A semi-actuator disk theory for prediction of stall flutter in axial flow compressors
p 301 A90-25105

beta CEZ, a high performance titanium alloy for aerospace engines
[ONERA, TP NO. 1990-8] p 356 A90-25356

Calculation of tip leakage flow with three-dimensional Euler code
p 304 A90-25772

Analysis of unsteady rotor-stator interactions using a viscous explicit method
[AIAA PAPER 90-0342] p 313 A90-26937

Fracture mechanics assessment of EB-welded blisk rotors
p 453 A90-31117

Development of erosion resistant coatings for compressor airfoils
p 443 A90-31120

The use of circumferentially varying stagger guide vanes in an axial flow pump or compressor
p 537 A90-33566

Inlet distortion generated periodic aerodynamic rotor response
[ASME PAPER 89-GT-299] p 475 A90-33567

Aeroelastic instabilities in aircraft engines - Application to a SNECMA fan stage
p 584 A90-35174

Analyses of revising the inlet profile of a radial inflow turbine impeller
p 602 A90-35831

Numerical simulation of the behaviour of internal combustion supercharged engines
[AIAA PAPER 90-1873] p 655 A90-40539

Stall margin improvement in axial-flow compressors by circumferential variation of stationary blade setting angles
[AIAA PAPER 90-1912] p 656 A90-40554

Reverse flow in multistage axial compressors
p 623 A90-40942

Three-component LDA measurements in an axial-flow compressor
p 683 A90-40943

Military engines - Cradle of technology
p 660 A90-41758

Design and performance of a small, high speed axial compressor
[AIAA PAPER 90-1911] p 624 A90-41983

The performance of a combustor pre-diffuser incorporating compressor outlet guide vanes
[AIAA PAPER 90-2165] p 661 A90-42053

Linearized unsteady aerodynamics for turbomachinery aeroelastic applications
[AIAA PAPER 90-2355] p 626 A90-42137

Stall cell blockage in a high-speed multistage axial-flow compressor
[AIAA PAPER 90-1913] p 740 A90-42693

Application of 3-D viscous code in the design of a high performance compressor
[AIAA PAPER 90-1914] p 740 A90-42694

Performance improvement of an eroded axial flow compressor using water injection
[AIAA PAPER 90-2016] p 741 A90-42718

Prediction and measurement of rotor blade/stator vane dynamic characteristics of a modern aero-engine axial compressor
p 878 A90-46036

Theoretical and experimental determination of natural frequencies of laced blading
p 878 A90-46037

Comparison among modal analyses of axial compressor blade using experimental data of different measuring systems
p 878 A90-46038

A method for the matching of structural and geometric parameters of the turbocompressors of small gas turbine engines in computer-aided design
p 850 A90-46491

Optimal blading density in axial-flow compressor stages with a developed three-dimensional flow
p 851 A90-46505

Jet engines performance deterioration
p 852 A90-46871

Numerical simulation of nonreactive flows in turbomachines
p 908 A90-52621

Improved silicon carbide for advanced heat engines
[NASA-CR-180831] p 65 A90-10293

Coatings for gas turbine compressors
[NLR-MP-88045-U] p 115 A90-11750

The development of a high response aerodynamic wedge probe and use on a high-speed research compressor
[PNR90598] p 116 A90-12613

Blading design for multi-storage HP compressor
[PNR90602] p 116 A90-12616

Preliminary experience with high response pressure measurements in a multistage, high speed compressor
[RAE-TM-P-1141] p 117 A90-12619

Temporally and spatially resolved flow in a two-stage axial compressor. Part 2: Computational assessment
[NASA-TM-102273] p 194 A90-14236

Performance of a highly-loaded HP compressor
[RAE-TM-P-1149] p 256 A90-15919

Aerodynamic study on forced vibrations on stator rows of axial compressors
p 426 A90-18412

Numerical prediction of axial turbine stage aerodynamics
p 426 A90-18416

Stall and recovery in multistage axial flow compressors
p 428 A90-18429

The effects of compressor endwall flow on airfoil incidence and deviation
p 512 A90-21011

A study on secondary flow and spanwise mixing in axial flow compressors
p 512 A90-21012

Secondary flow calculations for axial and radial compressors
p 514 A90-21024

Forcing function effects on rotor row unsteady aerodynamic response in a multistage compressor
p 573 A90-22536

Computational and experimental investigations of rotating stall in compressor cascades
p 588 A90-22565

A simulation code for turbocompound diesel engines
[IAR-89-26] p 774 A90-25348

Application of high performance metals in gas turbine engines
[PNR90640] p 750 A90-25999

Prediction and measurement of rotor blade/stator vane dynamic characteristics of a modern aero-engine axial compressor
[PNR90667] p 750 A90-26002

Development of a software package for automatic data acquisition, analysis, and controls in an axial flow compressor test rig
[PD-PR-8910] p 965 A90-29926

TURBOFAN AIRCRAFT

Flight over the sea with twin or triple jet aircraft
p 179 A90-17048

Propulsion control system designs for advanced Navy multimission aircraft
[AIAA PAPER 90-2403] p 663 A90-42160

Sound propagation elements in evaluation of en route noise of advanced turbofan aircraft p 697 N90-24861

Energy efficient engine program technology benefit/cost study. Volume 1: Executive summary [NASA-CR-174766-VOL-1] p 931 N90-28564

Energy efficient engine program technology benefit/cost study, volume 2 [NASA-CR-174766-VOL-2] p 931 N90-28565

TURBOFAN ENGINES

Wind-tunnel test of the air intake of an unducted fan [AAAF PAPER NT 88-19] p 4 A90-11436

Development of new segment carbon seal for use at low sealing pressure region FJR710/600S turbo fan engine p 69 A90-11950

The features of FJR 710 engine p 42 A90-12011

Endurance test of FJR 710/600S engine p 42 A90-12012

Start characteristics of FJR 710/600S engine p 42 A90-12013

Oil migration of FJR 710/600S engine p 43 A90-12014

Steady state performance of FJR 710/600S engine p 43 A90-12015

Mechanical rig test of FJR 710/600 engine components p 43 A90-12016

Design of control amplifier for FJR 710 engine p 43 A90-12017

Exhaust nozzle system design considerations for turbofanjet propulsion systems p 48 A90-12577

Restart characteristics of turbofan engines p 50 A90-12627

Non-iterative analytical methods for off-design turbofan calculations with or without mixed-flows p 70 A90-12628

Jet engine fault detection with differential gas path analysis at discrete operating points p 50 A90-12633

Design and development of the Garrett F109 turbofan engine [SAE PAPER 891046] p 109 A90-14350

Garrett TPF351-20 turboprop fan engine development [SAE PAPER 891047] p 109 A90-14351

Production of Ti6Al4V-components for a new turbo-fan-engine p 132 A90-16618

Navier-Stokes analysis of a lobed mixer and nozzle [AIAA PAPER 90-0453] p 192 A90-19852

Reynolds number effects on the performance of a turbofan engine [ASME PAPER 89-GT-199] p 342 A90-23871

Ultra High Bypass (UHB) engine critical component technology [ASME PAPER 89-GT-229] p 342 A90-23884

Braze repair of MA754 aero gas turbine engine nozzles [ASME PAPER 89-GT-235] p 342 A90-23886

Advanced core technology - Key to subsonic propulsion benefits [ASME PAPER 89-GT-241] p 342 A90-23890

Holographic flow visualisation of turbofan by-pass and core nozzle streams [ASME PAPER 89-GT-260] p 363 A90-23891

Isothermal velocity and turbulence measurements downstream of a model multilobed turbofan mixer p 365 A90-24353

Use of swirl for flow control in propulsion nozzles p 421 A90-27963

Advanced technology's impact on compressor design and development - A perspective [SAE SP-800] p 423 A90-28571

Gas turbine engines for combat aviation - Current realities and perspectives for the near future p 584 A90-35513

Wide chord fan club p 584 A90-35600

Takeoff characteristics of turbofan engines p 585 A90-35764

Identification of multivariable models of jet engines [AIAA PAPER 90-1874] p 655 A90-40540

Design of digital self-selecting multivariable controllers for jet engines [AIAA PAPER 90-1875] p 655 A90-40541

A proposed Kalman filter algorithm for estimation of unmeasured output variables for an F100 turbofan engine p 656 A90-40558

Investigation of very high bypass ratio engines for subsonic transports p 659 A90-40945

Turbofans turn to UHB propulsion p 659 A90-41165

Noise-source measurements by thin-film pressure transducers in a subsonic turbofan model [ONERA, TP NO. 1990-36] p 659 A90-41212

Gearbox system design for ultra-high bypass engines [AIAA PAPER 90-2152] p 685 A90-42048

A simple dynamic engine model for use in a real-time aircraft simulation with thrust vectoring [AIAA PAPER 90-2166] p 662 A90-42054

Ultra high bypass turbofan technologies for the twenty-first century [AIAA PAPER 90-2397] p 662 A90-42158

Experimental turbofan using liquid hydrogen and liquid natural gas as fuel [AIAA PAPER 90-2421] p 663 A90-42170

CFE738 - A case for joint engine development [AIAA PAPER 90-2522] p 664 A90-42197

A hydrodynamic turbo-fan/shaft convertible engine p 665 A90-42487

Analysis of installed wind tunnel test results on large bypass ratio engine/nacelle installations [AIAA PAPER 90-2146] p 705 A90-42738

Optimization studies for the PW305 turbofan [AIAA PAPER 90-2520] p 744 A90-42813

The LF500 and the regional airline market [AIAA PAPER 90-2521] p 744 A90-42814

The GMA 2100 and GMA 3007 engines for regional aircraft [AIAA PAPER 90-2523] p 744 A90-42815

Wide-chord fan proved in nearly five years of service p 744 A90-44594

Future development of the 535E4 engine p 745 A90-44596

Propulsion systems for the '90s p 745 A90-44605

Turbofan engine analysis and optimization: using spreadsheets p 779 A90-45290

A real time microcomputer implementation of sensor failure detection for turbofan engines p 745 A90-45414

Considerations in using broad specification fuels for aircraft propulsion [SAE PAPER 892330] p 765 A90-45487

The use of the CFM56 engine in the KC-135 tanker [SAE PAPER 892362] p 747 A90-45511

V2500 turbofan engine [SAE PAPER 892363] p 747 A90-45512

The RB211-535E4 - A commercially proven engine for the military of tomorrow [SAE PAPER 892364] p 748 A90-45513

The turbofan of tomorrow p 850 A90-46150

Flying the giant --- An-124 Ruslan aircraft p 833 A90-48522

TRANAIR applications to engine/airframe integration p 838 A90-48958

Twin-engine transports - A look at the future [AIAA PAPER 90-3215] p 818 A90-49107

Aerodynamic losses in conventional fan blades of high bypass turbo engine p 854 A90-49487

PMR graphite engine duct development [NASA-CR-182228] p 51 N90-10037

Full scale technology demonstration of a modern counterrotating unducted fan engine concept: Component test [NASA-CR-180868] p 53 N90-10047

Full scale technology demonstration of a modern counterrotating unducted fan engine concept: Design report [NASA-CR-180867] p 53 N90-10048

Full scale technology demonstration of a modern counterrotating unducted fan engine concept: Engine test [NASA-CR-180869] p 53 N90-10049

Characteristics of combustion driven pressure oscillations in advanced turbo-fan engines with afterburner p 64 N90-10194

Advanced technologies impact on compressor design and development: A perspective [NASA-TM-102341] p 54 N90-10891

STOVL propulsion system volume dynamics approximations [NASA-TM-102397] p 114 N90-11740

Measurement effects on the calculation of in-flight thrust for an F404 turbofan engine [NASA-TM-4140] p 114 N90-11741

Near-field noise predictions of an aircraft in cruise p 140 N90-12538

The 757 NLF glove flight test results p 104 N90-12546

What should be done with those noisy old aircraft [PNR90562] p 107 N90-12593

Designing for reliable and low maintenance cost aero engines [PNR90570] p 115 N90-12604

Blading design for multi-storage HP compressor [PNR90602] p 116 N90-12616

Real-time simulation of an F110/STOVL turbofan engine [NASA-TM-102409] p 117 N90-12618

The commercial aircraft noise problem [PNR90577] p 140 N90-13203

Advanced detection, isolation, and accommodation of sensor failures in turbofan engines: Real-time microcomputer implementation [NASA-TP-2925] p 259 N90-15112

Altitude testing of the 2D V/STOL ADEN demonstrator on an F404 engine [NASA-CR-174824] p 345 N90-17638

In-line wear monitor [AD-A217799] p 510 N90-20091

Supersonic through-flow fan engine and aircraft mission performance [NASA-TM-102304] p 516 N90-21038

Exhaust environment measurements of a turbofan engine equipped with an afterburner and 2D nozzle [NASA-CR-4289] p 588 N90-21760

A/F32T-9 large turbo fan engine enclosed noise suppressor system (T-9 NSS), exterior far-field and interior noise, McConnell AFB, Kansas [AD-A220535] p 665 N90-23402

Design of a low cost short takeoff-vertical landing export fighter/attack aircraft [NASA-CR-186658] p 734 N90-25132

Effective optimal control of a fighter aircraft engine p 928 N90-28548

Energy Efficient Engine combustor test hardware detailed design report [NASA-CR-168301] p 929 N90-28554

Energy Efficient Engine (E3) combustion system component technology performance report [NASA-CR-168274] p 930 N90-28555

Energy Efficient Engine acoustic supporting technology report [NASA-CR-174834] p 930 N90-28557

Energy Efficient Engine program advanced turbofan nacelle definition study [NASA-CR-174942] p 930 N90-28560

Energy Efficient Engine: Control system component performance report [NASA-CR-174651] p 931 N90-28562

Energy efficient engine program technology benefit/cost study. Volume 1: Executive summary [NASA-CR-174766-VOL-1] p 931 N90-28564

Energy efficient engine program technology benefit/cost study, volume 2 [NASA-CR-174766-VOL-2] p 931 N90-28565

TURBOFANS

A study of the working process and losses in annular turbine nozzle cascades with a low contraction ratio p 254 A90-23407

Blade sweep for low-speed axial fans [ASME PAPER 89-GT-53] p 289 A90-23779

Application of sweep to improve the efficiency of a transonic fan. I - Design [AIAA PAPER 90-1915] p 741 A90-42695

Evolution of engine cycles for STOVL propulsion concepts [AIAA PAPER 90-2272] p 743 A90-42767

TURBOJET ENGINE CONTROL

A design of a twin variable control system for aero-turbojet engine p 423 A90-29917

A real time microcomputer implementation of sensor failure detection for turbofan engines p 745 A90-45414

A multiprocessor implementation of real-time control for a turbojet engine p 746 A90-45415

An experimental study of fault propagation in a jet-engine controller [NASA-CR-181335] p 665 N90-23401

TURBOJET ENGINES

Determination of the effective areas of the mixing exhaust ducts of a bypass engine from autonomous test results [NASA-CR-181335] p 102 A90-14584

Designing turbine blades for fatigue and creep p 112 A90-16007

Damping of the inlet vortex in a turbojet engine p 301 A90-25185

Mean and turbulent velocity measurements in a turbojet exhaust p 423 A90-28272

Simulation research on the afterburning dynamic characteristics of engine control system p 585 A90-35708

UV spectroradiometric output of an F404 turbojet aircraft engine p 652 A90-40195

On the use of external burning to reduce aerospace vehicle transonic drag [AIAA PAPER 90-1935] p 656 A90-40562

GE's CF34 engine for business and regional jets [AIAA PAPER 90-2041] p 661 A90-41992

Airframe/propulsion integration of supersonic cruise vehicles [AIAA PAPER 90-2151] p 644 A90-42047

On and off-design performance prediction of single spool turbojets using gasdynamics [AIAA PAPER 90-2393] p 662 A90-42155

The history of aviation engine development in the USSR and the 60th anniversary of CIAM [AIAA PAPER 90-2761] p 783 A90-42828

Spectral response of a UV flame sensor for a modern turbojet aircraft engine p 769 A90-43285

Propulsion systems for the '90s p 745 A90-44605

- An analysis of cavity resonance in the aeroengine casing during rig testing p 894 A90-49481
- An open-loop transient thermodynamic model of the Cougar turbojet [AD-A211774] p 114 N90-11745
- Experimental study of velocity fields and turbulence in a turbojet engine [ISL-CO-231/88] p 344 N90-16766
- The implementation and operation of a variable-response electronic throttle control system for a TF-104G aircraft [NASA-TM-101696] p 509 N90-20086
- On the use of external burning to reduce aerospace vehicle transonic drag [NASA-TM-103107] p 588 N90-21762
- Turbulent combustion modeling for turbo-jet combustion chambers p 749 N90-25993
- Comparative Engine Performance Measurements [AGARD-LS-169] p 856 N90-27711
- Comparison of ground-level test cells and ground-level to altitude test cells p 857 N90-27716

TURBOMACHINE BLADES

- Turbomachinery blade vibration and dynamic stress measurements utilizing noninvasive techniques p 41 A90-11558
- Calculation of unsteady boundary layer development on axial-flow turbomachinery blading p 48 A90-12588
- Construction of a straight single-row airfoil lattice by the method of quasi-solutions for inverse boundary value problems p 84 A90-14564
- Blade sweep for low-speed axial fans [ASME PAPER 89-GT-53] p 289 A90-23779
- Mathematical formulation of blade surfaces in turbomachinery. II - Practical examples of determined surfaces [ASME PAPER 89-GT-161] p 361 A90-23849
- C-grid generation for turbomachinery cascades p 312 A90-26554
- Study on travelling wave vibration of bladed disks in turbomachinery p 423 A90-29908
- Quasi-3D viscous flow computations in subsonic and transonic turbomachinery bladings [AIAA PAPER 90-2126] p 625 A90-42033
- Forced response on turbomachinery blades due to passing wakes [AIAA PAPER 90-2353] p 705 A90-42781
- Aeroelastic vibrations of turbomachine blades and propellers p 854 A90-49482
- A design method for turbomachinery blading in three-dimensional flow p 904 A90-51003
- A parametric study of radial turbomachinery blade design in three-dimensional subsonic flow [ASME PAPER 89-GT-84] p 905 A90-51257
- A method of predicting 3-D compressible boundary layer on the rotating blade of turbomachinery p 908 A90-52777
- Automation and extension of LDV (Laser-Doppler Velocimetry) measurements of off-design flow in a subsonic cascade wind tunnel [AD-A216627] p 453 N90-18670

TURBOMACHINERY

- Numerical simulation of three-dimensional unsteady flows in turbomachines [ONERA, TP NO. 1989-118] p 4 A90-11149
- Unsteady aerodynamics and aeroelasticity of turbomachines and propellers; Proceedings of the Fourth International Symposium, Aachen, Federal Republic of Germany, Sept. 6-10, 1987 p 5 A90-11776
- Calculation of unsteady Euler flows in turbomachinery using the linearized Euler equations p 5 A90-11778
- Analysis of the effect of rotor-angular-acceleration on the features of gas flow in turbomachinery p 6 A90-11780
- Unsteady 2D flow calculation in turbomachinery cascades p 6 A90-11782
- Numerical simulation of turbomachinery flows with a simple model of viscous effects - Comparison with experimental data [ONERA, TP NO. 1989-122] p 10 A90-12510
- Turbomachinery tip gap aerodynamics - A review p 13 A90-12557
- Calculation of axisymmetric flows in turbomachines, through an explicit time-splitting method p 14 A90-12622
- A multi-domain 3D Euler solver for flows in turbomachines [ONERA, TP NO. 1989-119] p 15 A90-12623
- Test rig for the study of the flow in a rotor-stator system [ONERA, TP NO. 1989-124] p 58 A90-12634
- Design and application of a finite element package for modelling turbomachinery vibrations p 70 A90-13011
- Aeroelastic detuning for stability enhancement of unstalled supersonic flutter p 189 A90-17462
- Computation of the trailing edge flow downstream a flat plate with finite thickness p 151 A90-17464

- Recent developments in calculation methods for internal flows by solution of Euler or Navier-Stokes equations [ONERA, TP NO. 1989-167] p 223 A90-21033
- Viscous flow calculations in turbomachinery channels [ASME PAPER 89-GT-5] p 287 A90-23752
- A method for calculating axial turbomachine end wall turbulent boundary layers [ASME PAPER 89-GT-15] p 287 A90-23759
- Improvement of 3D full-potential method and computation of flowfield of CAS compressor rotor [ASME PAPER 89-GT-17] p 288 A90-23760
- Application of a lower-upper implicit scheme and an interactive grid generation for turbomachinery flow field simulations [ASME PAPER 89-GT-20] p 288 A90-23762
- Overview on test cases for computation of internal flows in turbomachines [ASME PAPER 89-GT-46] p 288 A90-23772
- 3D Mean-Stream-Line Method - A new engineering approach to the inverse problem of 3D cascade [ASME PAPER 89-GT-48] p 289 A90-23774
- Threshold performance optimization of a rotor-bearing system subjected to leakage excitation [ASME PAPER 89-GT-126] p 360 A90-23825
- A three dimensional inverse method in turbomachinery. II - Experimental verification [ASME PAPER 89-GT-137] p 360 A90-23834
- Simulation of three-dimensional viscous flow within a multistage turbine [ASME PAPER 89-GT-152] p 292 A90-23841
- The extension and application of three-dimensional time marching analyses to incompressible turbomachinery flows [ASME PAPER 89-GT-212] p 293 A90-23878
- Interactive grid generation for turbomachinery flow field simulations p 312 A90-26553
- An annular gas seal analysis using empirical entrance and exit region friction factors [ASME PAPER 89-TRIB-46] p 537 A90-33555
- Numerical solution of 3-D hybrid problems in turbomachinery p 621 A90-40501
- Non-steady flow loss mechanisms associated with vaneless diffusers [AIAA PAPER 90-2508] p 682 A90-40641
- A colocated finite volume method for solving the Navier-Stokes equations for incompressible and compressible flows in turbomachinery - Results and applications p 703 A90-42659
- Test and theory for piezoelectric actuator-active vibration control of rotating machinery p 879 A90-46226
- Foil gas bearings for turbomachinery [SAE PAPER 901236] p 841 A90-49306
- Unsteady aerodynamics and aeroelasticity of turbomachines and propellers; Proceedings of the Fifth International Symposium, Beijing, People's Republic of China, Sept. 18-21, 1989 p 853 A90-49451
- Numerical simulation of three-dimensional nonstationary flows and variable aerodynamic forces in turbomachine stages p 814 A90-49465
- Throughflow theory for nonaxisymmetric turbomachinery flow. I - Formulation. II - Assessment [ASME PAPER 89-GT-304] p 905 A90-51256
- Analysis of three-dimensional turbomachinery flows on C-type grids using an implicit Euler solver [ASME PAPER 89-GT-85] p 905 A90-51258
- Data acquisition in aerodynamic research p 171 N90-13340
- Application of a two-dimensional unsteady viscous analysis code to a supersonic throughflow fan stage [NASA-TM-4141] p 192 N90-13387
- Unsteady Aerodynamic Phenomena in Turbomachines [AGARD-CP-468] p 425 N90-18405
- Numerical investigation of unsteady flow in oscillating turbine and compressor cascades p 426 N90-18407
- Numerical investigations of heat transfer and flow rates in rotating cavities. Simulation of the movement generated by wall temperature gradients, by source-sink mass flows or by the differential rotation of the walls, under the influence or coriolis and centrifugal forces [ETN-90-96253] p 454 N90-18695
- An applicational process for dynamic balancing of turbomachinery shafting [NASA-TM-102537] p 541 N90-20392
- Rotordynamic analysis with shell elements for the transfer matrix method [AD-A217455] p 541 N90-20434
- Computational Methods for Aerodynamic Design (Inverse) and Optimization [AGARD-CP-463] p 500 N90-20976
- Numerical method for designing 3D turbomachinery blade rows p 511 N90-20990
- Secondary Flows in Turbomachines [AGARD-CP-469] p 511 N90-21009
- Generation and decay of secondary flows and their impact on aerodynamic performance of modern turbomachinery components p 514 N90-21023

- The numerical simulation of multistage turbomachinery flows p 514 N90-21025
- Mesh generation for flow computation in turbomachine p 588 N90-21981
- The Shock and Vibration Digest, volume 21, no. 2 p 609 N90-22059
- Computer code for predicting coolant flow and heat transfer in turbomachinery [NASA-TP-2985] p 858 N90-27722
- TURBOPROP AIRCRAFT**
- Effect of an isolated shell on interior noise levels in a turboprop aircraft [SAE PAPER 891083] p 102 A90-14375
- The coming age of the tiltrotor. I p 246 A90-21711
- Digital control of local sound fields in an aircraft passenger compartment p 247 A90-23113
- Aeroelastic tailoring analysis for preliminary design of advanced turbo propellers with composite blades p 412 A90-29395
- Glassy waters for Seastar --- corrosion-resistant GFRP for turboprop amphibious aircraft airframes p 382 A90-29637
- Aeroelastic analysis for a composite T-tailplane of a turboprop commuter aircraft p 492 A90-33390
- Starship - A model for future designs p 493 A90-33714
- Application of active noise control to model propeller noise p 548 A90-34091
- 3-D Euler calculations for aft-propfan integration [AIAA PAPER 90-2147] p 625 A90-42044
- Exploratory wind tunnel investigation of the stability and control characteristics of a three-surface, forward-swept wing advanced turboprop model [AIAA PAPER 90-3074] p 797 A90-45920
- Commuter from Khodinka --- Il-114 airliner p 842 A90-49824
- Starship sails through p 842 A90-49825
- P-180 AVANTI: Project and flight test program comprehensive overview p 34 N90-10863
- Low-speed wind-tunnel investigation of the flight dynamic characteristics of an advanced turboprop business/commuter aircraft configuration [NASA-TP-2982] p 434 N90-19239
- Noise of a simulated installed model counterrotation propeller at angle-of-attack and takeoff/approach conditions [NASA-TM-102440] p 548 N90-20794
- En route noise of turboprop aircraft and their acceptability: Report of tests p 697 N90-24858
- En route noise of two turboprop aircraft [DLR-MITT-89-18] p 697 N90-24859
- High speed turboprop aeroacoustic study (counterrotation). Volume 1: Model development [NASA-CR-185241] p 782 N90-26633
- TURBOPROP ENGINES**
- Whirl-flutter investigation on an advanced turboprop configuration p 40 A90-11008
- Vibration analysis of composite turbopropellers using a nonlinear beam-type finite-element approach p 70 A90-12844
- Garrett TPF351-20 turboprop fan engine development [SAE PAPER 891047] p 109 A90-14351
- Parametric studies of advanced turboprops p 253 A90-21225
- A hybrid method for prediction of propeller performance [AIAA PAPER 90-0440] p 229 A90-22219
- Mathematical model of turboprop engine behaviour p 254 A90-23351
- Modelling and simulation of turboprop engine behaviour p 424 A90-29946
- Planet gear sleeve spinning analysis [AIAA PAPER 90-2154] p 681 A90-40613
- Investigation of the near wake of a propfan p 622 A90-40686
- Finite-element analysis of large spur and helical gear systems p 683 A90-40940
- Bonded airfoil attachments - A path to rotor structural efficiency [AIAA PAPER 90-2177] p 686 A90-42061
- The Dash 8 Series 400 regional airliner p 729 A90-42664
- The GMA 2100 and GMA 3007 engines for regional aircraft [AIAA PAPER 90-2523] p 744 A90-42815
- Large-scale Advanced Prop-fan (LAP) high speed wind tunnel test report [NASA-CR-182125] p 52 N90-10045
- Full scale technology demonstration of a modern counterrotating unducted fan engine concept. Design report [NASA-CR-180867] p 53 N90-10048
- Propfan Test Assessment (PTA) [NASA-CR-185138] p 113 N90-11739

- UHB demonstrator interior noise control flight tests and analysis
[NASA-CR-181897] p 140 N90-13198
- User's guide to PMESH: A grid-generation program for single-rotation and counterrotation advanced turboprops
[NASA-CR-185156] p 217 N90-14783
- The Shock and Vibration Digest, volume 21, no. 6
p 614 N90-22363
- Noise transmission into propeller-driven airplanes
p 614 N90-22364
- Advanced gearbox technology
[NASA-CR-179625] p 666 N90-24274
- TURBORAMJET ENGINES**
- A study on the performance of the turbo-ramjet engines at high speed flight p 49 A90-12608
- Development study of air turbo-ramjet for future space plane
[IAF PAPER 89-311] p 109 A90-13445
- Progress in airbreathing combined engines for future European launcher p 344 N90-16817
- Saenger propulsion system options p 344 N90-16818
- Parametric assessment of propulsion system mass for airbreathing launcher configurations p 344 N90-16819
- TURBOSHAPTS**
- Endurance of aircraft gas turbine mainshaft ball bearings-analysis using improved fatigue life theory. II - Application to a bearing operating under difficult lubrication conditions p 128 A90-13845
- Successful performance development program for the T800-LHT-800 turboshaft engine
[SAE PAPER 891048] p 110 A90-14352
- Turboshafts on tenterhooks p 188 A90-16703
- Digital electronic control for WJ6G4A engine p 424 A90-29919
- Directivity of the noise radiation emitted from the inlet duct of a turboshaft helicopter engine
[ONERA, TP NO. 1990-26] p 695 A90-41205
- Characterization of helicopter turboshaft engine noise p 660 A90-41759
- Component arrangement studies for an 8000 shp turboshaft high technology core
[AIAA PAPER 90-2398] p 663 A90-42159
- Co-development of CT7-6 engines - A continued tradition in technology and reliability p 665 A90-42485
- TURBULENCE**
- An experimental study of a turbulent jet impinging on a wedge p 553 A90-35274
- Control and modification of turbulence p 72 N90-10377
- Turbulence management: Application aspects p 72 N90-10378
- Two-dimensional analysis of two-phase reacting flow in a firing direct-injection diesel engine
[NASA-TM-102069] p 194 N90-13392
- Numerical modeling of supersonic turbulent reacting free shear layers p 174 N90-14197
- A one equation turbulence model for transonic airfoils p 174 N90-14199
- Systems for airborne wind and turbulence measurement p 281 N90-15046
- Influence of windshear, downdraft and turbulence on flight safety p 238 N90-15048
- Inclusion of nonlinear aerodynamics in the FLAP code [DE89-009507] p 281 N90-15519
- Turbulence spectral widths view angle independence as observed by Doppler radar
[DOT/FAA-SA-89/2] p 281 N90-15566
- Some Navier-Stokes calculations for the CAST-10 airfoil p 320 N90-17651
- Carrier wing profile in nonstationary current [ETN-90-95368] p 399 N90-19208
- Stereopsis cueing effects on hover-in-turbulence performance in a simulated rotorcraft
[NASA-TP-2980] p 506 N90-21004
- LDV measurements and the flow analysis in the vortex region of a radial inflow turbine p 511 N90-21007
- Secondary flows and Reynolds stress distributions downstream of a turbine cascade at different expansion ratios p 512 N90-21015
- Numerical investigation of some control methods for 3-D turbulent interactions due to sharp fins p 591 N90-21764
- The interaction of a supersonic streamwise vortex and a normal shock wave p 633 N90-24241
- New transonic test sections for the NAE 5 ft x 5 ft trisomic wind tunnel [AD-A220933] p 674 N90-24278
- A computational efficient modelling of laminar separation bubbles
[NASA-CR-186729] p 774 N90-25291
- Formation of design envelope criterion in terms of deterministic spectral procedure [RAE-TM-SS-9] p 721 N90-25953

TURBULENCE EFFECTS

- Rotor noise due to atmospheric turbulence ingestion. II - Aeroacoustic results p 219 A90-19386
- Prediction of aerostat and airship mooring mast loads by nonlinear dynamic simulation
[AIAA PAPER 89-3172] p 245 A90-20587
- A study of boundary layer stability in the case of an increased incoming stream turbulence in gradient flows p 555 A90-36065
- Interaction of a plane shear layer with a downstream flat plate
[AIAA PAPER 90-1460] p 561 A90-38617
- An experimental investigation of the velocity field in a reverse-flow combustor p 739 A90-42657
- Detachment of turbulent boundary layers with varying free-stream turbulence and lower Reynolds numbers p 802 A90-46378
- A study of high-lift airfoils at high Reynolds numbers in the Langley low-turbulence pressure tunnel
[NASA-TM-89125] p 1 N90-10002
- Turbulence effects of aircraft flight dynamics and control p 258 N90-15055
- A study of the effects of Rotating Frame Turbulence (RFT) on helicopter flight mechanics p 248 N90-15058
- Control of flow separation and mixing by aerodynamic excitation
[NASA-TM-103131] p 571 N90-21733
- TURBULENCE METERS**
- Isothermal velocity and turbulence measurements downstream of a model multilobed turbofan mixer p 365 A90-24353
- TURBULENCE MODELS**
- Critique of turbulence models for shock-induced flow separation p 17 A90-12851
- An interactive boundary layer method for subsonic airfoil flows p 144 A90-16754
- Interaction between strong longitudinal vortices and turbulent boundary layers p 145 A90-16764
- Two-dimensional transonic flow field analysis with different turbulence models p 150 A90-16846
- Finite element analysis of the flow of a propeller on a slender body with a two-equation turbulence model p 210 A90-18340
- Turbulence modeling for impinging jets
[AIAA PAPER 90-0022] p 211 A90-19639
- Navier-Stokes methods to predict circulation control airfoil performance
[AIAA PAPER 90-0574] p 167 A90-19924
- Effects of pressure mismatch on slot injection in supersonic flow
[AIAA PAPER 90-0092] p 227 A90-22161
- Turbulence modeling for aerodynamic flows
[AIAA PAPER 89-0606] p 234 A90-23647
- Problem areas in applied computational fluid dynamics p 366 A90-25770
- Turbulence models for 3D transonic viscous flows. II p 306 A90-25820
- Supersonic viscous shear layers p 367 A90-25873
- Effects of turbulence model constants on computation of confined swirling flows p 444 A90-27999
- Augmenting flight simulator motion response to turbulence p 440 A90-31279
- Numerical modeling of separated turbulent flows p 470 A90-32673
- Numerical calculation of the jet-interaction induced separation with respect to thrust vector control p 584 A90-35228
- Heat transfer in supersonic coaxial reacting jets p 601 A90-35394
- Freestream turbulence effects on airfoil boundary-layer behavior at low Reynolds numbers p 554 A90-35768
- Digital generation of two-dimensional field of turbulence for flight simulation p 611 A90-36427
- A numerical study of supersonic flow over a compression corner with different incoming boundary-layer profiles
[AIAA PAPER 90-1453] p 561 A90-38612
- An abbreviated Reynolds stress turbulence model for airfoil flows
[AIAA PAPER 90-1468] p 562 A90-38625
- Numerical prediction of turbulent flow over airfoil sections with a new nonequilibrium turbulence model
[AIAA PAPER 90-1469] p 562 A90-38626
- The k-kl turbulence model and wall layer model for compressible flows
[AIAA PAPER 90-1483] p 563 A90-38637
- Versatility of an algebraic backflow turbulence model
[AIAA PAPER 90-1485] p 563 A90-38639
- A hybrid Reynolds averaged/PDF closure model for supersonic turbulent combustion
[AIAA PAPER 90-1573] p 600 A90-38711
- Algebraic turbulence modeling for unstructured and adaptive meshes
[AIAA PAPER 90-1653] p 608 A90-38781

- Turbulence model performance in V/STOL flow field simulation
[AIAA PAPER 90-2248] p 625 A90-42094
- Euler and Navier-Stokes computations for airfoil geometries using unstructured meshes p 630 A90-42425
- Film cooling of turbine blades - Two dimensional experiments and numerical simulations p 739 A90-42670
- Computational investigation of two-dimensional ejector nozzle flow fields
[AIAA PAPER 90-2148] p 768 A90-42739
- Numerical simulation of the compressible flow in a valve-cylinder assembly p 770 A90-44431
- Effects of turbulence models on the prediction of transonic wing flows
[SAE PAPER 892224] p 713 A90-45440
- The effect of turbulence models on the numerical prediction of the flowfield about a prolate spheroid at high angle of attack
[AIAA PAPER 90-3106] p 789 A90-45855
- Prediction of separated transonic wing flows with nonequilibrium algebraic turbulence model p 809 A90-47312
- Modeling of turbulence and downbursts for flight simulators p 870 A90-48956
- Fluid Dynamics of Three-Dimensional Turbulent Shear Flows and Transition
[AGARD-CP-438] p 71 N90-10356
- A European collaborative investigation of the three-dimensional turbulent shear layers of a swept wing p 20 N90-10380
- A one equation turbulence model for transonic airfoils p 174 N90-14199
- Turbulence effects of aircraft flight dynamics and control p 258 N90-15055
- A study of the effects of Rotating Frame Turbulence (RFT) on helicopter flight mechanics p 248 N90-15058
- Some Navier-Stokes calculations for the CAST-10 airfoil p 320 N90-17651
- The influence of a wall function on turbine blade heat transfer prediction p 429 N90-19421
- Comparison of 3-D viscous flow computations of Mach 5 inlet with experimental data
[NASA-TM-102518] p 510 N90-20090
- An approximate viscous shock layer method for calculating the hypersonic flow over blunt-nosed bodies p 479 N90-20947
- An efficient airfoil design method using the Navier-Stokes equations p 500 N90-20981
- Centrifugal impeller geometry and its influence on secondary flows p 513 N90-21020
- Extension of a three-dimensional viscous wing flow analysis
[NASA-CR-182023] p 631 N90-23348
- Report of the Fluid Dynamics Panel Working Group 10 on calculation of 3D separate turbulent flows in boundary layer limit p 776 N90-26280
- [AGARD-AR-255] p 776 N90-26280
- A comparison of two central difference schemes for solving the Navier-Stokes equations
[NASA-TM-102815] p 816 N90-27654
- Development of turbulence models for the analysis of compressible or incompressible unsteady flow
[ETN-90-97486] p 958 N90-28810
- A boundary-layer transition model for the Navier-Stokes computation for a natural-laminar-flow airfoil
[NAL-TR-1038T] p 912 N90-29328
- TURBULENT BOUNDARY LAYER**
- An asymptotic theory for the periodic turbulent boundary layer in zero mean-pressure gradient
[AD-A222832] p 66 A90-10222
- Computation of unsteady compressible turbulent boundary layers in cascade flow with controlled inlet perturbation p 8 A90-11807
- Measurements of pressure fluctuations in the interaction regions of shock waves and turbulent boundary layers induced by blunt fins p 9 A90-12218
- Aerodynamic heating in the interaction regions of shock waves and turbulent boundary layers induced by sharp fins p 9 A90-12220
- Computation of three dimensional turbulent boundary layers in internal flows, including turbomachinery rotor blades p 12 A90-12555
- Calculation of unsteady boundary layer development on axial-flow turbomachinery blading p 48 A90-12588
- Aerodynamic heating in shock wave/turbulent boundary layer interaction regions induced by blunt fins p 82 A90-13775
- Wake-boundary layer interaction p 85 A90-15238
- Airfoil noise in a uniform flow p 139 A90-16330
- Interaction between strong longitudinal vortices and turbulent boundary layers p 145 A90-16764
- Leading edge contamination and relaminarisation on a swept wing at incidence p 148 A90-16789

Separation shock dynamics in Mach 5 turbulent interactions induced by cylinders p 153 A90-17981
 High Reynolds number wedge-induced separation lengths at Mach 6 p 154 A90-18001
 Skin friction measurements by laser interferometry in swept shock/boundary-layer interactions p 154 A90-18153
 Turbulent boundary layer development in the presence of small isolated two-dimensional surface discontinuities p 210 A90-18507
 Large-scale motions in a supersonic turbulent boundary layer on a curved surface [AIAA PAPER 90-0019] p 160 A90-19636
 Embedded function methods for supersonic turbulent boundary layers [AIAA PAPER 90-0306] p 163 A90-19787
 Upstream-influence scaling of fin-generated shock wave boundary-layer interactions [AIAA PAPER 90-0376] p 164 A90-19822
 Swept shock/boundary-layer interactions - Tutorial and update [AIAA PAPER 90-0375] p 228 A90-22207
 The detection of large scale structure in undisturbed and disturbed compressible turbulent free shear layers [AIAA PAPER 90-0711] p 230 A90-22251
 Experimental studies of shock wave/wall jet interaction in hypersonic flow [AIAA PAPER 90-0607] p 231 A90-22449
 Time-dependent and time-averaged turbulence structure near the nose of a wing-body junction p 231 A90-23036
 A method for calculating axial turbomachine end wall turbulent boundary layers [ASME PAPER 89-GT-15] p 287 A90-23759
 Effects of an embedded vortex on injectant from a single film-cooling hole in a turbulent boundary layer [ASME PAPER 89-GT-189] p 362 A90-23867
 The prediction of boundary layers with rotation and variation of stream filament thickness [ASME PAPER 89-GT-227] p 362 A90-23882
 Investigation of wall pressure pulsations during the passive control of shock/boundary layer interaction p 378 A90-24132
 Separation development and its effect on the aerodynamics of supercritical profiles at transonic velocities p 297 A90-24142
 A study of the laminar-turbulent boundary layer transition on the windward side of a delta wing with a conical surface p 298 A90-24144
 Experimental investigation of three-dimensional turbulent boundary layers on 'infinite' swept curved wings p 303 A90-25589
 A supersonic turbulent boundary layer in an adverse pressure gradient p 303 A90-25592
 Infrared imaging and tufts studies of boundary layer flow regimes on a NACA 0012 airfoil p 446 A90-28268
 A semiconductor laser-Doppler-anemometer for applications in aerodynamic research p 447 A90-28273
 Development and extension of diagnostic techniques for advancing high speed aerodynamic research p 436 A90-28281
 Wall pressure fluctuation spectra in supersonic flow past a forward facing step p 388 A90-29194
 The boundary-layer fence - Barrier against the separation process p 396 A90-31493
 Instability and susceptibility of a boundary layer in the vicinity of two-dimensional surface inhomogeneities p 535 A90-32675
 An experimental investigation on control of flow dynamic distortions downstream under strong shock-boundary layer interaction in the two-dimensional flow field p 471 A90-33288
 Modification of large eddies in turbulent boundary layers p 474 A90-33514
 Boundary layer turbulence structure in the presence of embedded streamwise vortex pairs p 552 A90-35193
 Turbulence statistics in a shock wave boundary layer interaction p 552 A90-35205
 Freestream turbulence effects on airfoil boundary-layer behavior at low Reynolds numbers p 554 A90-35768
 Structure of a reattaching supersonic shear layer p 555 A90-36252
 Mach number effects on upstream influence in swept shock wave/turbulent boundary layer interactions p 556 A90-36415
 Experimental study of incompressible flow on the upper surface of a delta wing p 558 A90-37346
 Evaluation of equilibrium turbulence for a naturally developing hypersonic boundary layer at nonadiabatic wall conditions [AIAA PAPER 90-1410] p 559 A90-37948
 A study of the unsteadiness of crossing shock wave turbulent boundary layer interactions [AIAA PAPER 90-1456] p 606 A90-38614

Wall pressure fluctuations in the reattachment region of a supersonic free shear layer [AIAA PAPER 90-1461] p 561 A90-38618
 The k-k1 turbulence model and wall layer model for compressible flows [AIAA PAPER 90-1483] p 563 A90-38637
 A numerical study of longitudinal vortex interaction with a boundary layer [AIAA PAPER 90-1630] p 568 A90-38759
 Structure of swept shock wave/boundary-layer interactions using conical shadowgraphy [AIAA PAPER 90-1644] p 569 A90-38772
 Dynamics of the outgoing turbulent boundary layer in a Mach 5 unswept compression ramp interaction [AIAA PAPER 90-1645] p 569 A90-38773
 Correlation of separation shock motion in a compression ramp interaction with pressure fluctuations in the incoming boundary layer [AIAA PAPER 90-1646] p 569 A90-38774
 Effect of detailed surface geometry on riblet drag reduction performance p 622 A90-40693
 Computation of multiple normal shock wave/turbulent boundary layer interactions [AIAA PAPER 90-2133] p 685 A90-42037
 Direct measurements of skin friction in a scramjet combustor [AIAA PAPER 90-2342] p 626 A90-42132
 Experimental study of the turbulent boundary layer on a transport wing in subsonic flow p 709 A90-44728
 Effect of riblets on flow separation in a subsonic diffuser p 712 A90-45261
 Effects of onset free-stream turbulence on the performance characteristics of an airfoil [AIAA PAPER 90-3025] p 790 A90-45867
 The effect of separation on turbulent boundary layer characteristics over a smooth surface at Mach 6.0 [AIAA PAPER 90-3028] p 790 A90-45870
 Detachment of turbulent boundary layers with varying free-stream turbulence and lower Reynolds numbers p 802 A90-46378
 Shock/turbulent boundary layer interaction in low Reynolds number supercritical flows p 802 A90-46383
 Application of the inverse method of three-dimensional boundary layer analysis to the problem of flow past a wing with allowance for the effect of viscosity p 804 A90-46548
 Flow separation in oblique shock wave turbulent boundary layer interactions p 807 A90-46872
 The calculation of incompressible separated turbulent boundary layers p 905 A90-51025
 An LDA investigation of the normal shock wave boundary layer interaction p 908 A90-52618
 Experimental research on swept shock Wave/Boundary layer interactions [AD-A211744] p 134 A90-11988
 Reduction of turbulent drag: Boundary layer manipulators [CERT-RSF-OA-74/2259-AYD] p 136 A90-12889
 Experiments on the laminar-turbulent transition on swept wings p 276 A90-16170
 An interactive method for the flow calculation of airfoils with local separation regions p 278 A90-16190
 Inverse solutions for boundary layers with separation or close to separation under locally infinite swept wing conditions p 279 A90-16192
 An experimental study of the effect of streamwise vortices on unsteady turbulent boundary-layer separation p 369 A90-17045
 A review of high-speed, convective, heat-transfer computation methods p 316 A90-17548
 Glancing shock-boundary layer interactions p 319 A90-17571
 Wind tunnel design of heat island turbulent boundary layer [IHV-ET/50] p 455 A90-19542
 European research on viscous flow (EuroVisc) [NLR-TP-89077-U] p 609 A90-22014
 Interactive calculation procedures for mixed compression inlets [NASA-CR-186581] p 718 A90-25934
 Report of the Fluid Dynamics Panel Working Group 10 on calculation of 3D separate turbulent flows in boundary layer limit [AGARD-AR-255] p 776 A90-26280
 Further studies of turbulence structure resulting from interactions between embedded vortices and wall jets at high blowing ratios [AD-A223296] p 960 A90-29593

TURBULENT DIFFUSION

Parabolized calculations of turbulent three dimensional flows in a turbine duct p 482 A90-21013
 The numerical simulation of multistage turbomachinery flows p 514 A90-21025

TURBULENT FLOW

Turbulence measurements in a flow generated by the collision of radially flowing wall jets p 2 A90-10699
 Calculation of three-dimensional turbulent flow in a linear turbine cascade [ONERA, TP NO. 1989-115] p 3 A90-11147
 3D calculations of reacting flows within aircraft engine combustion chambers [ONERA, TP NO. 1989-153] p 67 A90-11173
 A study of unsteady rotor-stator interactions p 67 A90-11557
 Adverse pressure gradient effects on boundary layer transition in a turbulent free stream p 15 A90-12639
 Turbulent separated flow over and downstream of a two-element airfoil p 16 A90-12738
 Shock-wave/boundary-layer interaction at a swept compression corner p 16 A90-12850
 Variable-velocity flow at the initial mixing section in a diffuser channel p 84 A90-14563
 Numerical solution of unsteady Navier-Stokes equations for laminar/turbulent flows past axis-symmetric bodies at angle of attack p 85 A90-15235
 Numerical simulation of supersonic and hypersonic turbulent compression corner flows using PNS equations p 85 A90-15242
 Calculation of flowfields in side-inlet ramjet combustors with an algebraic Reynolds stress model p 87 A90-16367
 The flow around wing-body junctions p 145 A90-16765
 On the effects of wind tunnel turbulence on steady and unsteady airfoil characteristics p 147 A90-16777
 Two-dimensional transonic flow field analysis with different turbulence models p 150 A90-16846
 Jets, vortices, and turbulence p 207 A90-17175
 Computation of the trailing edge flow downstream a flat plate with finite thickness p 151 A90-17464
 Finite element simulation of compressible turbulent flows - Validation and application to internal aerodynamic in gas-turbine engines p 210 A90-18343
 Large-eddy simulations of combustion instability in an axisymmetric ramjet combustor [AIAA PAPER 90-0267] p 191 A90-19764
 The sonic eddy - A model for compressible turbulence [AIAA PAPER 90-0495] p 167 A90-19876
 Application of an adaptive algorithm to single and two-element airfoils in turbulent flow [AIAA PAPER 90-0698] p 169 A90-19983
 Compressibility effects in free shear layers [AIAA PAPER 90-0705] p 212 A90-19984
 Hydrodynamic visualization of organized structures and turbulences in boundary layers, wakes, jets or propeller flows [ONERA, TP NO. 1989-158] p 223 A90-21026
 Chemically reacting supersonic flow calculation using an assumed PDF model [AIAA PAPER 90-0731] p 230 A90-22256
 Characteristics of turbulent separation flows on a porous surface under conditions of injection p 231 A90-22422
 Turbulence modeling for aerodynamic flows [AIAA PAPER 89-0606] p 234 A90-23647
 Effect of rib-angle orientation on local mass transfer distribution in a three-pass rib-roughened channel [ASME PAPER 89-GT-98] p 359 A90-23812
 The effect of longitudinal fins on turbulent friction drag p 297 A90-24123
 In quest of the laminar-flow airliner - Flight experiments on a T-33 jet trainer p 300 A90-24825
 A high-order time-accurate scheme, and its applications p 304 A90-25732
 Experimental and theoretical investigations of turbulent flow in a side-inlet rectangular combustor p 421 A90-27959
 Effects of turbulence model constants on computation of confined swirling flows p 444 A90-27999
 Influence of wind tunnel circuit installations on test section flow quality p 436 A90-28287
 Optimal conditions of flow turbulence suppression in the working section of a wind tunnel using screens located in the prechamber p 438 A90-29185
 Turbulence measurements and noise generation in a transonic cryogenic wind tunnel [AIAA PAPER 88-2026] p 522 A90-32463
 Prediction of turbulent combustion flowfields behind a backward-facing step p 529 A90-32952
 Response characteristics of a two-dimensional wing subjected to turbulence near the flutter boundary p 519 A90-34082
 Computational fluid dynamics - Current capabilities and directions for the future p 540 A90-34385
 Development of a new low-Reynolds-number type Reynolds stress model and its application to a lobe mixer flow --- to improve thrust efficiency and suppress jet noise in turbofan engines p 584 A90-35229

Velocity and turbulence characteristics of isothermal lobed mixer flows --- in turbfan jet engines p 584 A90-35230

A numerical study on the use of sulfur hexafluoride as a test gas for wind tunnels [AIAA PAPER 90-1421] p 605 A90-37958

An abbreviated Reynolds stress turbulence model for airfoil flows [AIAA PAPER 90-1468] p 562 A90-38625

Numerical prediction of turbulent flow over airfoil sections with a new nonequilibrium turbulence model [AIAA PAPER 90-1469] p 562 A90-38626

Versatility of an algebraic backflow turbulence model [AIAA PAPER 90-1485] p 563 A90-38639

Investigation of several passive and active methods for turbulent flow separation control [AIAA PAPER 90-1598] p 607 A90-38730

The organized nature of a turbulent trailing vortex [AIAA PAPER 90-1625] p 568 A90-38754

Numerical simulation of a turbulent flow through a shock wave [AIAA PAPER 90-1641] p 608 A90-38769

Interaction between a high-level steady acoustic field and a ducted turbulent flow [ONERA, TP NO. 1990-27] p 695 A90-41206

Computation of flow through a centrifugal impeller with tip leakage [AIAA PAPER 90-2021] p 684 A90-41987

Measurements of turbulent dual-jet interaction [AIAA PAPER 90-2105] p 624 A90-42019

Numerical analysis of the flows in annular slinger combustors [AIAA PAPER 90-2164] p 685 A90-42052

Electrical analog circuit for heat transfer measurements on a flat plate simulating turbine vane heat transfer in turbulent flow [AIAA PAPER 90-2412] p 687 A90-42164

Finite element simulation of turbulent propeller flowfields p 703 A90-42658

Numerical simulation of nonpremixed turbulent flow in a dump combustor [AIAA PAPER 90-1858] p 768 A90-42685

Recent advances in H₂/O₂ high pressure coaxial injector performance analysis [AIAA PAPER 90-1959] p 762 A90-42705

Computation of turbine flowfields with a Navier-Stokes code [AIAA PAPER 90-2122] p 704 A90-42731

Turbulent flow simulation of a three-dimensional turbine cascade [AIAA PAPER 90-2124] p 704 A90-42732

Three-dimensional turbulent flow code calculations of hot gas ingestion p 745 A90-44726

The flow field and heat transfer near a turbulator p 771 A90-44755

Experimental investigation of turbulence in a supersonic flow p 710 A90-44931

Numerical simulation of flow through the Langley parametric scramjet engine [SAE PAPER 892314] p 747 A90-45476

Large-eddy simulations of flows in a ramjet combustor p 772 A90-45534

Simulation of leading-edge vortex flows p 716 A90-45785

Effects of onset free-stream turbulence on the performance characteristics of an airfoil [AIAA PAPER 90-3025] p 790 A90-45867

XFOIL - An analysis and design system for low Reynolds number airfoils p 799 A90-46359

A fast method for computation of airfoil characteristics p 799 A90-46361

Bursting in separating flow and in transition p 800 A90-46366

Numerical calculation of turbulent separated flows in an abruptly expanding channel p 803 A90-46487

A study of gas flow in hypersonic nozzles at large Reynolds numbers using simplified Navier-Stokes equations p 803 A90-46538

An experimental study of the combined effect of longitudinal riblets and vortex breakers on turbulent friction p 805 A90-46565

Effect of incoming flow turbulence on the aerodynamic characteristics of a smooth symmetric body at large angles of attack p 904 A90-46817

Three-dimensional unsteady transonic viscous-inviscid interaction p 18 N90-10005

Fluid Dynamics of Three-Dimensional Turbulent Shear Flows and Transition [AGARD-CP-438] p 71 N90-10356

A European collaborative investigation of the three-dimensional turbulent shear layers of a swept wing p 20 N90-10380

Dynamics and control of turbulent shear flows [AD-A210396] p 72 N90-10402

Some implications of the isotropic momentarily frozen assumptions for the SPAN-MAT program [NASA-CR-181937] p 88 N90-11704

Transition in surface boundary layers [CERT-RSP-OA-43/5018-AYD] p 136 N90-12897

Multigrid calculations of 3-D turbulent viscous flows [NASA-CR-185154] p 143 N90-13323

Reduction of profile drag by modifying the structure next to the wake area [IMFL-88/35] p 172 N90-13356

A planar reacting shear layer system for the study of fluid dynamics-combustion interaction [NASA-TM-102422] p 194 N90-13393

Numerical simulation of transition in three-dimensional boundary layers [DLR-FB-89-12] p 212 N90-13728

A one equation turbulence model for transonic airfoils p 174 N90-14199

Acoustic-vortical-combustion interaction in a solid fuel ramjet simulator p 194 N90-14234

Assessment of computational prediction of tail buffeting [NASA-TM-101613] p 237 N90-15886

Numerical simulation of the laminar and turbulent three dimensional flow on a delta wing with sharp leading edge p 278 N90-16186

Experimental study of velocity fields and turbulence in a turbojet engine [ISL-CO-231/88] p 344 N90-16766

Direct numerical simulation of aerodynamic noise [AD-A214122] p 379 N90-18225

Contribution to the study of three-dimensional separation in turbulent incompressible flow [ESA-TT-1169] p 454 N90-18697

On total variation diminishing schemes for transonic turbulent flow computation p 479 N90-20945

Parabolized calculations of turbulent three dimensional flows in a turbine duct p 482 N90-21013

Calculation of the three dimensional turbulent flow in a linear turbine blade p 513 N90-21021

The computation of turbulent thin shear flows associated with flow around multielement aerofoils p 633 N90-24240

Turbulent combustion modeling for turbo-jet combustion chambers p 749 N90-25993

Chemistry of combustion processes p 749 N90-25994

Report of the Fluid Dynamics Panel Working Group 10 on calculation of 3D separate turbulent flows in boundary layer limit [AGARD-AR-255] p 776 N90-26280

Turbulent reacting flows and supersonic combustion [AD-A221793] p 875 N90-26933

Study of the compressibility effects on the turbulence of supersonic drags [ETN-90-97448] p 817 N90-27661

Numeric fluid mechanics p 960 N90-29161

TURBULENT HEAT TRANSFER

Structure of velocity and temperature fields in laminar channel flows with longitudinal vortex generators p 273 A90-23207

Further studies of turbulence structure resulting from interactions between embedded vortices and wall jets at high blowing ratios [AD-A223296] p 960 N90-29593

TURBULENT JETS

The characteristic decay region of a class of three-dimensional wall jets p 85 A90-15241

Development process of turbulence in a round-nozzle air jet p 87 A90-16101

Jet flap theory p 298 A90-24154

Turbulent plane jet excited mechanically by an oscillating thin plate in the potential core p 553 A90-35262

An experimental study of a turbulent jet impinging on a wedge p 553 A90-35274

Heat transfer in supersonic coaxial reacting jets p 601 A90-35394

Numerical modeling of supersonic turbulent reacting free shear layers p 174 N90-14197

Further studies of turbulence structure resulting from interactions between embedded vortices and wall jets at high blowing ratios [AD-A223296] p 960 N90-29593

TURBULENT MIXING

Turbulent mixing in helicopter jet diluters - Navier-Stokes calculations and correlations [AAAF PAPER NT 88-13] p 40 A90-11432

Three-dimensional modeling of turbulent transonic flow at the exit of a twin engine [AAAF PAPER NT 88-16] p 4 A90-11434

Investigation of the mixing of parallel supersonic streams p 69 A90-12561

A model gas turbine combustor with wall jets and optical access for turbulent mixing, fuel effects, and spray studies p 507 A90-32808

Development of a new low-Reynolds-number type Reynolds stress model and its application to a lobe mixer flow --- to improve thrust efficiency and suppress jet noise in turbfan engines p 584 A90-35229

Velocity and turbulence characteristics of isothermal lobed mixer flows --- in turbfan jet engines p 584 A90-35230

Effects of streamwise vorticity injection on turbulent mixing layer development [AIAA PAPER 90-1459] p 561 A90-38616

Two- and three-dimensional effects in the supersonic mixing layer [AIAA PAPER 90-1978] p 703 A90-42708

Numerical modeling of supersonic turbulent reacting free shear layers p 174 N90-14197

DURIP optical equipment for high-speed viscous-inviscid interaction research [AD-A217772] p 540 N90-20345

TURBULENT WAKES

Hot wire measurements in the wake of an oscillating airfoil p 15 A90-12635

Wake-boundary layer interaction p 85 A90-15238

Development of bluff body wake in a longitudinally curved stream p 86 A90-15745

Transition from order to chaos in the wake of an airfoil p 474 A90-33506

An experimental investigation of the turbulent structure in a two-dimensional momentumless wake p 474 A90-33515

Interaction between boundary layer and wakes of different bodies p 602 A90-36263

Visualization of the turbulent trailing vortex behind a finite wing in steady and unsteady flows p 712 A90-45260

Wake effects on the prediction of transonic viscous flows around airfoils with an Euler/boundary layer interaction approach [AIAA PAPER 90-3061] p 798 A90-45933

The wake vortex problem revisited p 817 A90-46395

The turbulent near wake of a flat plate at low Reynolds number p 811 A90-48711

Linear instability of supersonic plane wakes [NASA-CR-181911] p 20 N90-10833

Effect of pylon wake with and without pylon blowing on propeller thrust [NASA-TM-4162] p 173 N90-14190

An experimental investigation of viscous aspects of propeller blade flow p 315 N90-16711

TURNING FLIGHT

Minimum-time turns using vectored thrust p 118 A90-14728

Hingeless rotor dynamics in coordinated turns [AIAA PAPER 90-1117] p 412 A90-29389

Application of energy turn g-limiting for aircraft high performance turns [AIAA PAPER 90-3328] p 862 A90-47590

Multivariable control law for flat-turn strafe maneuver by a supermaneuverable aircraft [AIAA PAPER 90-3371] p 863 A90-47629

Guidance analysis of the aeroglide plane change maneuver as a turning point problem [NASA-TM-101639] p 259 N90-15110

The SKY SHARK: An RPV designed to investigate the pressure distribution on a lifting surface [NASA-CR-186222] p 844 N90-26824

TVD SCHEMES

A new implicit hybrid schemes for the Euler equation of transonic flow p 158 A90-18608

Numerical simulation of supersonic unsteady flow using Euler equations [AIAA PAPER 90-0415] p 229 A90-22215

Turbulence models for 3D transonic viscous flows. II p 306 A90-25820

A numerical investigation of supersonic inlet using implicit TVD scheme [AIAA PAPER 90-2135] p 621 A90-40612

Analysis of transonic turbine rotor cascade flows using a finite-volume total variation diminishing (TVD) scheme [AIAA PAPER 90-2127] p 704 A90-42733

Simulation of time-dependent viscous flows using central and upwind-biased finite-difference techniques [AIAA PAPER 90-3012] p 790 A90-45864

Multigrid acceleration of TVD schemes in transonic Euler flow calculation p 908 A90-52030

On total variation diminishing schemes for transonic turbulent flow computation p 479 N90-20945

Numerical simulation of hypersonic flow around a space plane. Part 2: Application to high angles of attack flow [NAL-TR-10117] p 570 N90-21726

Prediction of two-dimensional time-dependent gasdynamic flows for hypersonic studies [UTIAS-335] p 718 N90-25935

On central-difference and upwind schemes [NASA-CR-182061] p 781 N90-26595

TWISTING

- Parametric studies of advanced turboprops
p 253 A90-21225
- An approach for design and analysis of composite rotor blades
[AD-A219257] p 734 N90-25125
- ### TWO DIMENSIONAL BODIES
- Systematic study of flutter characteristics of two-dimensional cascades in incompressible flow
p 41 A90-11796
- Recent studies on the behaviour of interference fit pins in composite plates
p 132 A90-16320
- Turbulent boundary layer development in the presence of small isolated two-dimensional surface discontinuities
p 210 A90-18507
- Numerical simulation of unsteady flow about cambered plates
p 159 A90-19389
- A computer aided manufacturing procedure for experimental two-dimensional aerofoils
p 270 A90-20609
- Finite element two-dimensional panel flutter at high supersonic speeds and elevated temperature
[AIAA PAPER 90-0982] p 450 A90-29372
- Effects of splitter plates on the wake flow behind a bluff body
p 469 A90-32453
- Low-speed pressure distribution on semi-infinite two-dimensional bodies with elliptical noses
p 553 A90-35766
- Nonlinear effects in the two-dimensional adaptive-wall outer-flow problem
p 554 A90-35771
- The sensitivity of near-field acoustics to the orientation of twin two-dimensional supersonic nozzles
[AIAA PAPER 90-2149] p 625 A90-42045
- Computational investigation of two-dimensional ejector nozzle flow fields
[AIAA PAPER 90-2148] p 768 A90-42739
- A formulation for the solution of Euler equations for compressible flow using finite elements
p 708 A90-44447
- Flow past bodies within a narrow class of cross-sectional shapes with stationary separation zones at large Reynolds numbers
p 805 A90-46568
- A scalar/vector potential solution for aerodynamic coefficients in wind shear
p 21 N90-10838
- Aerodynamics of bodies in shear flow
p 910 N90-28496
- ### TWO DIMENSIONAL BOUNDARY LAYER
- Effect of surface riblets on the velocity profile of an incompressible boundary layer
p 294 A90-24081
- Viscous corrections on wings in incompressible flow
p 301 A90-25200
- Instability and susceptibility of a boundary layer in the vicinity of two-dimensional surface inhomogeneities
p 535 A90-32675
- The lateral spreading of finite-span instability waves in a laminar mixing layer
[AIAA PAPER 90-1532] p 606 A90-38677
- A computational model for thickening boundary layers with mass addition for hypersonic engine inlet testing
[AIAA PAPER 90-2219] p 705 A90-42750
- Subharmonic instability of compressible boundary layers
p 706 A90-44005
- The instability of two-dimensional laminar separation
p 800 A90-46365
- Heat transfer near the entrance to a film cooling hole in a gas turbine blade
[AD-A217396] p 510 N90-20089
- ### TWO DIMENSIONAL FLOW
- Method for calculating the unsteady flow of an elliptical circulation-control airfoil
p 3 A90-11003
- Unsteady 2D flow calculation in turbomachinery cascades
p 6 A90-11782
- A numerical method solving 2-D unsteady flow field around cascade of oscillating airfoils with arbitrary camber and thickness
p 7 A90-11788
- An experimental investigation of the effect of incidence on the two-dimensional performance of an axial turbine cascade
p 11 A90-12520
- The development of an exact conservative scheme associated with the supersonic trailing edge separation modelling for the computation of the transonic 2D cascade
p 12 A90-12551
- A solution adaptive finite element method applied to two-dimensional unsteady viscous compressible cascade flow
p 15 A90-12624
- PCISM method for two dimensional compressible viscous cascade flow calculation
p 15 A90-12625
- Convergence properties of high-Reynolds-number separated flow calculations
p 86 A90-15820
- Experimental study of 2D/3D interactions between a vortical flow and a lifting surface
p 86 A90-15849
- Computation of the thin-layer Navier-Stokes equations for a 2D flow
p 87 A90-16332
- Experiments are telling you something (Stewartson Memorial Lecture) --- about aerodynamic flows
p 144 A90-16752

- VISTRAFS - A simulation method for strongly-interacting viscous transonic flow
p 144 A90-16756
- Theoretical prediction of high Reynolds number viscid/inviscid interaction phenomena in cascades
p 145 A90-16759
- Calculation of two-dimensional transonic flow of Euler equations with multigrid method
p 149 A90-16835
- Two-dimensional transonic flow field analysis with different turbulence models
p 150 A90-16846
- A relaxation method for transonic potential flows through 2-D cascade with large camber angle
p 152 A90-17786
- Upwind adaptive finite element investigations of the two-dimensional reactive interaction of supersonic gaseous jets
p 209 A90-18264
- Fresh look at floating shock fitting
[AIAA PAPER 90-0108] p 162 A90-19686
- A kinematical/numerical analysis of rotor-stator interaction noise
[AIAA PAPER 90-0281] p 219 A90-19770
- Dynamic stall of circulation control airfoils
[AIAA PAPER 90-0573] p 167 A90-19923
- Numerical investigation of airfoil/jet/fuselage-undersurface flowfields in ground effect
[AIAA PAPER 90-0597] p 168 A90-19939
- Transonic integro-differential and integral equations with artificial viscosity
p 223 A90-20988
- A parametric study of the flutter stability of two-dimensional turbine and compressor cascades in incompressible flow
p 225 A90-21593
- A finite element solution of unsteady two-dimensional flow in cascades
p 226 A90-21946
- Representation of two-dimensional hypersonic inlet flows for one-dimensional scramjet cycle analysis
[AIAA PAPER 90-0527] p 229 A90-22226
- A zonal flow analysis method for two-dimensional airfoils
[AIAA PAPER 90-0571] p 230 A90-22230
- Viscous flow calculations in turbomachinery channels
[ASME PAPER 89-GT-5] p 287 A90-23752
- Overview on test cases for computation of internal flows in turbomachines
[ASME PAPER 89-GT-46] p 288 A90-23772
- The effect of uniform spanwise vorticity on the two-dimensional flow through cascades
p 293 A90-23996
- Effect of the design of a diffuser with tangential injection on the starting and separation ratios of pressures
p 295 A90-24099
- Nonlinear aerodynamics of two-dimensional airfoils in severe maneuver
p 301 A90-25276
- Computation of 2D Navier-Stokes equations
p 367 A90-25801
- An automatic Euler solver using unstructured upwind method
p 367 A90-25811
- A comparison of two adaptive grid techniques
p 309 A90-26507
- The hemisphere-cylinder at an angle of attack
[AIAA PAPER 90-0050] p 313 A90-26907
- A numerical study of transverse jets into supersonic flows and influence of pressure waves
[AIAA PAPER 90-0733] p 314 A90-26985
- Boundary element solution of the transonic integro-differential equation
p 383 A90-27947
- Newtonian flow over oscillating two-dimensional airfoils at moderate or large incidence
p 383 A90-27976
- Droplet impaction on a supersonic wedge - Consideration of similitude
p 400 A90-27986
- Numerical simulation of separated flow around two-dimensional wing section by a discrete vortex method
p 469 A90-32067
- An experimental investigation on control of flow dynamic distortions downstream under strong shock-boundary layer interaction in the two-dimensional flow field
p 471 A90-33288
- Two-dimensional compressible unsteady aerodynamics in the Laplace domain
p 472 A90-33360
- An experimental investigation of the turbulent structure in a two-dimensional momentumless wake
p 474 A90-33515
- Differential equation modeling of dynamic stall
p 476 A90-34325
- On a lifting line theory for supersonic flow. II - A supersonic lifting line theory for wings
p 477 A90-34817
- Shock-fitting method for two-dimensional inviscid, steady supersonic flows in ducts
p 477 A90-34864
- Nonlinear effects in the two-dimensional adaptive-wall outer-flow problem
p 554 A90-35771
- Digital generation of two-dimensional field of turbulence for flight simulation
p 611 A90-36427
- A numerical study of supersonic flow over a compression corner with different incoming boundary-layer profiles
[AIAA PAPER 90-1453] p 561 A90-38612

- Parameter effects on oscillatory aerofoil in transonic flows
[AIAA PAPER 90-1473] p 563 A90-38629
- A primitive variable, strongly implicit calculation procedure for viscous flows at all speeds
[AIAA PAPER 90-1521] p 563 A90-38666
- Calculation of two- and three-dimensional flow in a transonic turbine cascade with particular regard to the losses
[AIAA PAPER 90-1542] p 565 A90-38686
- A comparison of adaptive-grid redistribution and embedding for steady transonic flows
[AIAA PAPER 90-1565] p 565 A90-38704
- Investigation of several passive and active methods for turbulent flow separation control
[AIAA PAPER 90-1598] p 607 A90-38730
- Transonic flow around airfoils with relaxation and energy supply by homogeneous condensation
p 620 A90-39782
- Investigation of supersonic mixing layers
p 623 A90-40926
- Modeling supersonic combustion using a fully-implicit numerical method
[AIAA PAPER 90-2307] p 677 A90-42117
- Application of the moving surface boundary layer control to a two dimensional airfoil
p 628 A90-42405
- Finite volume solutions of two-dimensional Euler equations on adapted structured meshes
p 629 A90-42413
- Finite element simulation of unsteady two-dimensional incompressible viscous flows
p 629 A90-42423
- Two- and three-dimensional effects in the supersonic mixing layer
[AIAA PAPER 90-1978] p 703 A90-42708
- Pressure-based real-time measurements in compressible free shear layers
[AIAA PAPER 90-1980] p 703 A90-42709
- A two-dimensional unsteady potential solver in internal aerodynamics flow problems
p 707 A90-44430
- Numerical simulation of the compressible flow in a valve-cylinder assembly
p 770 A90-44431
- Solution of the Euler equations using unstructured polygonal meshes
p 708 A90-44435
- Development and application of a fractional-step method for the solution of transonic and supersonic flow problems
p 709 A90-44461
- Numerical solution of 2D transonic flows in a turbine cascade
p 709 A90-44601
- A Volterra kernel identification scheme applied to aerodynamic reactions
[AIAA PAPER 90-2803] p 712 A90-45178
- A unified pressure correction algorithm for computing complex fluid flows
p 772 A90-45528
- Some remarks on the Kutta condition
p 716 A90-45738
- Adaptive grid embedding for the two-dimensional Euler equations
[AIAA PAPER 90-3049] p 797 A90-45929
- Transient aeroelastic computations using multiple moving frames of reference
[AIAA PAPER 90-3053] p 798 A90-45932
- Numerical simulation of wakes with application to blade-vortex interaction
p 807 A90-46881
- Two-dimensional convergent-divergent nozzle flow with wall velocity slip and temperature jump
p 807 A90-46884
- Numerical study of interaction of a jet with a supersonic cross flow
p 808 A90-47300
- Solutions of two-dimensional Euler equations with multigrid acceleration
p 810 A90-48086
- Two- and three-dimensional problems of unsteady aerodynamics of low loaded turbomachinery blade rows stages
p 813 A90-49452
- Numerical solution of 2-D transonic flow through an axial turbine stage
p 814 A90-49464
- The calculation of incompressible separated turbulent boundary layers
p 905 A90-51025
- Throughflow theory for nonaxisymmetric turbomachinery flow. I - Formulation. II - Assessment
[ASME PAPER 89-GT-304] p 905 A90-51256
- Design of the low-speed NLF(1)-0414F and the high-speed HSNLF(1)-0213 airfoils with high-lift systems
p 93 N90-12540
- Wind tunnel results of the low-speed NLF(1)-0414F airfoil
p 93 N90-12541
- Wind tunnel results of the high-speed NLF(1)-0213 airfoil
p 93 N90-12542
- Navier-Stokes solutions of 2-D transonic flow over unconventional airfoils
p 173 N90-14195
- Computational investigation of incompressible airfoil flows at high angles of attack
[AD-A205885] p 174 N90-14201
- Wake interaction effects on the transition process on turbine blades
[AD-A214492] p 343 N90-16759

SUBJECT INDEX

- Comparison of two- and three-dimensional Navier-Stokes solutions with NASA experimental data for CAST-10 airfoil p 321 N90-17658
- An evaluation of the two-dimensional Euler and Navier-Stokes calculations based on a flux-vector splitting [PB90-166778] p 481 N90-20963
- The effect of rapid spoiler deployment on the transient forces on an aerofoil p 921 N90-28527
- Use of liquid crystals for qualitative and quantitative 2-D studies of transition and skin friction [RAE-TM-AERO-2159] p 958 N90-28800
- Investigation of ATP blades, part 2. Validation of two-dimensional viscous flow simulation codes around thin airfoils [NAL-TR-1046] p 912 N90-29326
- ### TWO DIMENSIONAL JETS
- Numerical simulation of an impinging jet on a flat plate p 86 A90-15821
- Turbulent plane jet excited mechanically by an oscillating thin plate in the potential core p 553 A90-35262
- ### TWO DIMENSIONAL MODELS
- Experimental study of static pressure and mean velocity profiles inside a two-dimensional dump-type combustor model p 45 A90-12530
- Numerical study of balanced patch repairs to cracked sheets p 210 A90-18442
- The generation of unstructured triangular meshes using Delaunay triangulation --- applications to hypersonic inlets p 310 A90-26533
- 2-D and 3-D unstructured mesh adaptation relying on physical analogy p 310 A90-26534
- Simple marching-vortex model for two-dimensional unsteady aerodynamics p 395 A90-31288
- Vortex method modelling the unsteady motion of a thick airfoil p 396 A90-31489
- State-space representation of unsteady airfoil behavior p 469 A90-32461
- Euler flutter analysis of airfoils using unstructured dynamic meshes p 602 A90-35760
- Numerical modeling of an impinging jet in cross-flow [AIAA PAPER 90-2246] p 686 A90-42093
- Numerical simulations of gas turbine combustor flows [AIAA PAPER 90-2305] p 686 A90-42116
- Two dimensional post stall maneuver of a NACA 0015 airfoil at high pitching rates p 710 A90-45150
- 2D vs. 3D - Selection of pressure distributions to delay separation on wings p 790 A90-45868
- Two and three dimensional indicial methods for rotor dynamic airloads p 808 A90-46973
- A numerical method for relating two- and three-dimensional pressure distributions on transonic wings [AIAA PAPER 90-3211] p 812 A90-48837
- Two-dimensional analysis of two-phase reacting flow in a firing direct-injection diesel engine [NASA-TM-102069] p 194 N90-13392
- A two dimensional power spectral estimate for some nonstationary processes [NASA-CR-186100] p 217 N90-14843
- PTA en route noise measurements p 696 N90-24855
- A two dimensional study of rotor/airfoil interaction in hover [NASA-CR-183272] p 845 N90-27694
- ### TWO PHASE FLOW
- A study of two-phase flow for a ramjet combustor p 45 A90-12532
- A theoretical approach to particle separator design p 48 A90-12584
- Effect of pressure on the electrophysical properties of two-phase flows in nozzles p 110 A90-14572
- Heat, Transfer and Fluid Mechanics Institute, 31st, California State University, Sacramento, June 1, 2, 1989, Proceedings p 130 A90-15387
- Hydraulic analogy application in the study of a two-phase mixture combustion flow [AIAA PAPER 90-0451] p 211 A90-19850
- Numerical calculation of bubbly two phase flow around an airfoil p 304 A90-25783
- Air/water two-phase flow test tunnel for airfoil studies p 352 A90-26842
- Brownian motion far from equilibrium - A hypersonic approach p 555 A90-35917
- Two-dimensional analysis of two-phase reacting flow in a firing direct-injection diesel engine [NASA-TM-102069] p 194 N90-13392
- An experimental investigation of the physical mechanisms controlling the asymmetric flow past slender bodies at large angles of attack p 592 N90-21767
- An analytic study of nonsteady two-phase laminar boundary layer around an airfoil p 691 N90-25051

- Numerical analysis of three-dimensional particle-laden flow equations [IAR-90-2] p 775 N90-26268
- ### TWO STAGE TURBINES
- A proposal for optimized design of multistage compressors [ASME PAPER 89-GT-34] p 288 A90-23766
- Partial similarity and a real-time model of twin-spool gas turbine p 654 A90-40512
- Turbine configuration impact on advanced IHPET engine system mission capabilities [AIAA PAPER 90-2739] p 664 A90-42221
- Energy Efficient Engine high pressure turbine component test performance report [NASA-CR-168289] p 929 N90-28553

U

- ### U.S.S.R.
- The history of aviation engine development in the USSR and the 60th anniversary of CIAM [AIAA PAPER 90-2761] p 783 A90-42828
- Aviation Week editor files top Soviet interceptor p 920 A90-52574
- ### U-2 AIRCRAFT
- Global stratospheric change: Requirements for a Very-High-Altitude Aircraft for Atmospheric Research [NASA-CP-10041] p 185 N90-14220
- NASA/USRA high altitude reconnaissance aircraft [NASA-CR-186685] p 650 N90-24266
- ### UDIMET ALLOYS
- Application of high performance metals in gas turbine engines [PNR90640] p 750 N90-25999
- ### UH-1 HELICOPTER
- Correlation between vibration and computer operator response onboard a UH-1H helicopter p 737 A90-43727
- Using goal programming to determine the optimal engine mix for UH-1 helicopters [AD-A214893] p 343 N90-16762
- ### UH-2 HELICOPTER
- Self-retracting helicopter rescue hoist p 829 A90-46935
- ### UH-60A HELICOPTER
- Time domain parameter identification techniques applied to the UH-60A Black Hawk Helicopter p 77 A90-12774
- UH-60 flight data replay and refly system state estimator analysis [AIAA PAPER 90-0181] p 197 A90-19723
- Examination of dynamic characteristics of UH-60A and EH-60A airframe structures p 406 A90-28154
- A comprehensive hover test of the airloads and airflow of an extensively instrumented model helicopter rotor p 407 A90-28173
- UH-60 helicopter simulator fidelity testing or how to make it fly like the real thing [AIAA PAPER 90-1290] p 522 A90-33910
- UH-60A helicopter stability augmentation study p 670 A90-42471
- Airworthiness and flight characteristics test of the UH-60A Black Hawk helicopter equipped with the XM-139 multiple mine dispensing system (VOLCANO) [AD-A210271] p 32 N90-10025
- Preliminary airworthiness evaluation of the Woodward hydromechanical unit installed on T700-GE-700 engines in the UH-60A helicopter [AD-A216751] p 428 N90-18430
- Plan, formulate, and discuss a NASTRAN finite element model of the UH-60A helicopter airframe [NASA-CR-181975] p 541 N90-20439
- Ground shake test of the UH-60A helicopter airframe and comparison with NASTRAN finite element model predictions [NASA-CR-181993] p 758 N90-25143
- ### ULLAGE
- Ignitability of jet-A fuel vapors in aircraft fuel tanks p 326 N90-17594
- ### ULTRAHIGH FREQUENCIES
- Rapsal - Application of onboard processing for communication and surveillance in air traffic control [AIAA PAPER 90-0883] p 331 A90-25702
- ### ULTRALIGHT AIRCRAFT
- Flight testing a highly flexible aircraft - Case study on the MIT Light Eagle p 414 A90-31284
- Acoustics of ultralight airplanes p 643 A90-40685
- Some considerations in ultra light aircraft design p 730 A90-42673
- ### ULTRASONIC AGITATION
- An ultrasonic fatigue facility for HCF/LCF interactive tests p 363 A90-23900
- ### ULTRASONIC FLAW DETECTION
- In process failure investigations in aeronautics p 181 A90-18489

UNIX (OPERATING SYSTEM)

- Development of creep-fatigue damage detection method of rotor steel by ultrasonic wave measurement [DE90-503792] p 777 N90-26365
- Development of an automated ultrasonic inspection system for composite structure on in-service aircraft p 885 N90-28079
- The application of infrared thermography to the nondestructive testing of composite materials p 886 N90-28084
- Advanced NDE techniques for quantitative characterization of aircraft p 886 N90-28088
- Inspection system for in-situ inspection of aircraft composite structures p 886 N90-28091
- ### ULTRASONIC SCANNERS
- Looking inside a structure p 209 A90-17920
- ### ULTRASONIC TESTS
- Ultrasonic regression rate measurement in solid fuel ramjets [AIAA PAPER 90-1963] p 656 A90-40573
- Nondestructive measurement of residual stresses in aircraft transparencies [AD-A218680] p 689 N90-23762
- ### ULTRASONIC WAVE TRANSDUCERS
- Ultrasonic techniques for aircraft ice accretion measurement p 485 N90-20926
- ### ULTRASONICS
- Experimental investigations on the stability and vorticity of the vortex breakdown phenomenon above delta wings, measured by the ultrasonic laser method [ESA-TT-1079] p 910 N90-28498
- ### ULTRAVIOLET DETECTORS
- Spectral response of a UV flame sensor for a modern turbojet aircraft engine p 769 A90-43285
- ### ULTRAVIOLET LASERS
- Raman scattering measurements using UV excimer lasers p 874 N90-26902
- ### ULTRAVIOLET RADIATION
- UV spectroradiometric output of an F404 turbojet aircraft engine p 652 A90-40195
- Grumman/FAA lightning study - A potential countermeasure for lightning induced flashblindness of aircrew members p 819 A90-49843
- ### ULTRAVIOLET SPECTRA
- Spectral response of a UV flame sensor for a modern turbojet aircraft engine p 769 A90-43285
- ### ULTRAVIOLET SPECTROSCOPY
- Shock layer vacuum UV spectroscopy in an arc-jet wind tunnel [NASA-TM-102258] p 370 N90-17112
- ### UNDAMPED OSCILLATIONS
- The response of helicopter rotors to vibratory airload p 832 A90-46971
- Prediction and alleviation of V-22 rotor dynamic loads p 833 A90-46974
- ### UNDERGROUND STRUCTURES
- At a depth of 500 meters - The TU Dresden supersonic wind tunnel p 937 A90-52700
- ### UNIFORM FLOW
- Airfoil noise in a uniform flow p 139 A90-16330
- The effect of uniform spanwise vorticity on the two-dimensional flow through cascades p 293 A90-23996
- Film cooling of turbine blades - Two dimensional experiments and numerical simulations p 739 A90-42670
- Outflow boundary conditions using Duhamel's equation [AIAA PAPER 90-3014] p 798 A90-45937
- Profiling of the supersonic components of three-dimensional corrugated nozzles p 804 A90-46563
- The inverse problem in the multielement airfoil theory p 906 A90-51531
- ### UNITED KINGDOM
- UK airmasses involving commercial air transport, September to December 1988 [ISSN-0951-6301] p 240 N90-15897
- A UK perspective on the uniform engine test programme [RAE-TM-P-1172] p 257 N90-15922
- A review of UK civil aviation fire and cabin safety research p 325 N90-17587
- ### UNIVERSAL TIME
- Time synchronization/distribution applications of navigation signals repeated by geostationary satellites p 872 A90-46397
- ### UNIVERSITIES
- Joint University Program for Air Transportation Research, 1988-1989 [NASA-CP-3063] p 468 N90-20921
- ### UNIVERSITY PROGRAM
- Investigation of air transportation technology at Princeton University, 1988-1989 p 486 N90-20935
- ### UNIX (OPERATING SYSTEM)
- Effective use of Cray supercomputers p 546 A90-34436

UNSTEADY AERODYNAMICS

- Oscillating thin wings in inviscid incompressible flow
p 2 A90-10224
- An improved version of LTRAN2 p 2 A90-10350
- Method for calculating the unsteady flow of an elliptical circulation-control airfoil p 3 A90-11003
- Canard-wing interaction in unsteady supersonic flow p 3 A90-11010
- On unsteady surface forces, and sound produced by the normal chopping of a rectilinear vortex p 5 A90-11604
- Unsteady aerodynamics and aeroelasticity of turbomachines and propellers; Proceedings of the Fourth International Symposium, Aachen, Federal Republic of Germany, Sept. 6-10, 1987 p 5 A90-11776
- The effect of the magnitude of the inlet-boundary disturbance on the unsteady forces on axial gas-turbine blades p 6 A90-11781
- Unsteady 2D flow calculation in turbomachinery cascades p 6 A90-11782
- Multistage compressor vane row aerodynamic gust response p 6 A90-11783
- The unsteady aerodynamics of an oscillating cascade in a compressible flow field p 7 A90-11789
- Numerical investigation of unsteady compressible flow through nozzles and cascades p 7 A90-11790
- Numerical Euler solution for the interaction between oscillating cascade and forced inlet unsteadiness p 8 A90-11792
- Unsteady aerodynamic characteristics of oscillating cascade with tip clearance p 8 A90-11793
- Progress towards the development of an inviscid-viscous interaction method for unsteady flows in turbomachinery cascades p 8 A90-11806
- Finite element method for unsteady three-dimensional subsonic flows through a cascade oscillating with steady loading p 9 A90-11873
- Numerical calculation of unsteady aerodynamic forces for three-dimensional subsonic oscillating cascades by a finite element method p 9 A90-12219
- Numerical calculation of unsteady aerodynamic forces for two-dimensional supersonic oscillating cascades by finite element method p 9 A90-12238
- An experimental study of fluctuations in the front separation zone at supersonic flow velocities p 10 A90-12282
- Unsteady loss in a low speed axial flow compressor during rotating stall p 12 A90-12527
- Identification of a coupled body/coning/inflow model of Puma vertical response in the hover p 56 A90-12765
- New approach to small transonic perturbations finite element numerical solving method. I - Numerical developments. II - Numerical applications p 16 A90-12783
- Closed-form solutions for nonlinear quasi-unsteady transonic aerodynamics p 16 A90-12839
- Mach number effects on transonic aeroelastic forces and flutter characteristics p 17 A90-13024
- Blade surface pressure measurement on a pusher propeller in flight [SAE PAPER 891040] p 139 A90-14346
- Variable-velocity flow at the initial mixing section in a diffuser channel p 84 A90-14563
- Supersonic/hypersonic flow past wedge and plane ogive in oscillation p 85 A90-15231
- A study on surge and rotating stall in axial compressors - A summary of the measurement and fundamental analysis method p 87 A90-16105
- A simple active controller to suppress helicopter air resonance in hover and forward flight p 119 A90-16521
- The relevance of unsteady aerodynamics for highly maneuverable and agile aircraft p 146 A90-16775
- On the effects of wind tunnel turbulence on steady and unsteady airfoil characteristics p 147 A90-16777
- A critique of the experimental aerodynamic data base for an oscillating straked wing at high angles p 147 A90-16779
- Analysis of high-incidence separated flow past airfoils p 147 A90-16781
- Aeroelastic detuning for stability enhancement of unstalled supersonic flutter p 189 A90-17462
- Time-domain aeroservoelastic modeling using weighted unsteady aerodynamic forces p 195 A90-17698
- Numerical simulation of wings in steady and unsteady ground effects p 153 A90-17866
- Sound radiation from an airfoil encountering an oblique gust in its plane of motion p 218 A90-17998
- Pressure fluctuations in the tip region of a blunt-tipped airfoil p 154 A90-18136
- An investigation of unsteady leading edge separation of rapidly pitched airfoils p 157 A90-18587
- Numerical approaches for solving parametric vibration problems in helicopter dynamics p 182 A90-18607

- Low-speed unsteady aerodynamics of a pitching straked wing at high incidence. I - Test program. II - Harmonic analysis p 159 A90-19387
- Unsteady pressure and structural response measurements on an elastic supercritical wing p 159 A90-19392
- Unsteady aerodynamic forces on rolling delta wings at high angle of attack p 159 A90-19426
- Unsteady surface pressure distributions on a delta wing undergoing large amplitude pitching motions [AIAA PAPER 90-0311] p 164 A90-19790
- Unsteady incompressible aerodynamics and forced response of detuned blade rows [AIAA PAPER 90-0340] p 191 A90-19805
- A numerical study of general viscous flows around multi-element airfoils [AIAA PAPER 90-0572] p 167 A90-19922
- Viscous oscillating cascade aerodynamics and flutter by a locally analytical method [AIAA PAPER 90-0579] p 168 A90-19929
- Parabolized Navier-Stokes predictions of three-dimensional hypersonic flows with strong crossflow effects p 223 A90-20508
- Inviscid non equilibrium flow in ONERA F4 wind tunnel [ONERA, TP NO. 1989-161] p 223 A90-21029
- Advances in the efficient calculation of flows with friction p 225 A90-21475
- Prediction of vortical flows on wings using incompressible Navier-Stokes equations p 226 A90-21935
- Unsteady transonic Navier-Stokes computations for an oscillating wing using single and multiple zones [AIAA PAPER 90-0313] p 228 A90-22197
- Spanwise properties of the unsteady separation shock in a Mach 5 unswept compression ramp interaction [AIAA PAPER 90-0377] p 228 A90-22208
- Numerical simulation of supersonic unsteady flow using Euler equations [AIAA PAPER 90-0415] p 229 A90-22215
- Asymmetric separated flows at supersonic speeds [AIAA PAPER 90-0595] p 230 A90-22233
- Controlled three-dimensionality in unsteady separated flows about a sinusoidally oscillating flat plate [AIAA PAPER 90-0689] p 230 A90-22244
- Induced drag based on leading edge suction for a helicopter in forward flight p 232 A90-23102
- Unsteady transonic aerodynamics of oscillating airfoils in supersonic freestream p 232 A90-23277
- Integral solution of unsteady full-potential equation for a transonic pitching airfoil p 232 A90-23280
- Prediction of the aerodynamic environment and heat transfer for rotor-stator configurations [ASME PAPER 89-GT-89] p 359 A90-23807
- Modeling of subsonic unsteady aerodynamics for rotary wing applications p 293 A90-23935
- Aerodynamic characteristics of thin bodies moving in a gas with shock waves p 297 A90-24140
- Nonstationary motion of an elastic profile in subsonic incompressible flow p 300 A90-24741
- Numerical solutions of the linearized Euler equations for unsteady vortical flows around lifting airfoils [AIAA PAPER 90-0694] p 300 A90-25041
- A unified approach to the overall body motion stability and flutter characteristics of elastic aircraft p 346 A90-25102
- Nonlinear aerodynamics of two-dimensional airfoils in severe maneuver p 301 A90-25276
- Unsteady aerodynamic and aeroelastic calculations for wings using Euler equations p 302 A90-25288
- A high-order time-accurate scheme and its applications p 304 A90-25732
- Vortex dynamics of delta wings p 307 A90-26067
- Propeller-wing interaction using a frequency domain panel method p 307 A90-26128
- Unsteady aerodynamic characteristics of a fighter model undergoing large-amplitude pitching motions at high angles of attack [AIAA PAPER 90-0309] p 313 A90-26933
- Analysis of unsteady rotor-stator interactions using a viscous explicit method [AIAA PAPER 90-0342] p 313 A90-26937
- Newtonian flow over oscillating two-dimensional airfoils at moderate or large incidence p 383 A90-27976
- Experimental study of nonsteady asymmetric flow around an ogive-cylinder at incidence p 384 A90-27985
- Comparison of measured induced velocities with results from a closed-form finite state wake model in forward flight p 385 A90-28195
- Advanced rotor computations with a corrected potential method p 385 A90-28197
- Rotor loads validation utilizing a coupled aeroelastic analysis with refined aerodynamic modeling p 408 A90-28226

- Stability of hingeless rotors in hover using three-dimensional unsteady aerodynamics p 430 A90-28227
- The effect of an unsteady three-dimensional wake on elastic blade-flapping eigenvalues in hover p 385 A90-28228
- Applications of XTRAN3S and CAP-TSD to fighter aircraft [AIAA PAPER 90-1035] p 389 A90-29360
- Computation of steady and unsteady control surface loads in transonic flow [AIAA PAPER 90-0935] p 389 A90-29361
- Implicit flux-split Euler schemes for unsteady aerodynamic analysis involving unstructured dynamic meshes [AIAA PAPER 90-0936] p 389 A90-29362
- Reduced size first-order subsonic and supersonic aeroelastic modeling [AIAA PAPER 90-1154] p 390 A90-29366
- A reduced cost rational-function approximation for unsteady aerodynamics [AIAA PAPER 90-1155] p 390 A90-29367
- Fast calculation of root loci for aeroelastic systems and of response in time domain [AIAA PAPER 90-1156] p 390 A90-29368
- Time domain flutter analysis of cascades using a full-potential solver [AIAA PAPER 90-0984] p 391 A90-29374
- Chaotic response of aerosurfaces with structural nonlinearities (Status report) [AIAA PAPER 90-1034] p 392 A90-29378
- Concurrent processing adaptation of aeroelastic analysis of propfans [AIAA PAPER 90-1036] p 450 A90-29380
- Aeroservoelasticity [AIAA PAPER 90-1073] p 411 A90-29381
- Rotary-wing aeroelasticity with application to VTOL vehicles [AIAA PAPER 90-1115] p 392 A90-29387
- Three dimensional full potential method for the aeroelastic modeling of propfans [AIAA PAPER 90-1120] p 393 A90-29392
- Accurate Navier-Stokes results for the hypersonic flow over a spherical nosetip p 393 A90-29687
- Unsteady transonic aerodynamics p 393 A90-29882
- Physical phenomena associated with unsteady transonic flows p 394 A90-29883
- Basic equations for unsteady transonic flow p 394 A90-29884
- Practical problems - Airplanes --- unsteady interactive aerodynamics, flutter characteristics, and active flight control p 394 A90-29885
- Application of transonic flow analysis to helicopter rotor problems p 394 A90-29887
- Unsteady aerodynamics for turbomachinery aeroelastic applications p 394 A90-29888
- Alternative methods for modeling unsteady transonic flows p 394 A90-29889
- Numerical solutions of the linearized Euler equations for unsteady vortical flows around lifting airfoils p 394 A90-30264
- Simple marching-vortex model for two-dimensional unsteady aerodynamics p 395 A90-31288
- Vortex method modelling the unsteady motion of a thick airfoil p 396 A90-31489
- State-space representation of unsteady airfoil behavior p 469 A90-32461
- Unsteady, separated flow behind an oscillating, two-dimensional spoiler p 469 A90-32462
- Entry of a flexible airfoil into a vertical gust p 470 A90-32552
- Unsteady airloads due to separated flow on airfoils and wings p 471 A90-33311
- Unsteady aerodynamics methods for transonic aeroelastic analysis p 471 A90-33353
- Application of the CAP-TSD unsteady transonic small disturbance program to wing flutter --- Computational Aeroelasticity Program p 491 A90-33354
- A strong viscous-inviscid interaction method for computing unsteady transonic airloads for use in aeroelastics p 471 A90-33355
- Comparison of two potential flow methods for transonic flutter analysis p 471 A90-33356
- Computation of unsteady transonic flows around oscillating airfoils using full potential and Euler equations p 472 A90-33357
- Applications of the unsteady full potential equation for wings p 472 A90-33358
- Calculation of unsteady subsonic and supersonic flow about oscillating wings and bodies by new panel methods p 472 A90-33359
- Two-dimensional compressible unsteady aerodynamics in the Laplace domain p 472 A90-33360

- A comparison between theoretical and experimental results for a 3-D wing with damped pitching oscillations
[AIAA PAPER 90-33361] p 472 A90-33361
- Calculations of unsteady aerodynamics over oscillating wings
[AIAA PAPER 90-33362] p 472 A90-33362
- Unsteady aerodynamic forces of oscillating supersonic/hypersonic wings with attached shock waves
[AIAA PAPER 90-33363] p 473 A90-33363
- Numerical analysis of unsteady forces on oscillating ring airfoils and jet engines
[AIAA PAPER 90-33364] p 473 A90-33364
- Unsteady lift and moment coefficients of an engine nacelle
[AIAA PAPER 90-33365] p 473 A90-33365
- Recent activities within the aeroservoelasticity branch at the NASA Langley Research Center
[AIAA PAPER 90-33400] p 492 A90-33400
- A review of aeroelasticity research at the flight dynamics laboratory
[AIAA PAPER 90-33409] p 493 A90-33409
- The effect of winglets on aircraft wing flutter
[AIAA PAPER 90-33411] p 473 A90-33411
- Fast calculation of root loci of aeroelastic systems and of gust response in time domain
[AIAA PAPER 90-33413] p 517 A90-33413
- Inlet distortion generated periodic aerodynamic rotor response
[ASME PAPER 89-GT-299] p 475 A90-33567
- Helicopter response to atmospheric turbulence in forward flight
[AIAA PAPER 90-33625] p 518 A90-33625
- Correlation of lift and thickness noise sources in vortex-airfoil interaction
[AIAA PAPER 90-34090] p 547 A90-34090
- Flow quality in the T2 cryogenic wind-tunnel - Problems and solutions
[AIAA PAPER 90-34240] p 524 A90-34240
- Unsteady inviscid and viscous computations for vortex-dominated flows
[AIAA PAPER 90-35752] p 553 A90-35752
- Reduced-order aeroelastic models via dynamic residualization
[AIAA PAPER 90-35762] p 579 A90-35762
- Leading-edge vortices due to low Reynolds number flow past a pitching delta wing
[AIAA PAPER 90-36258] p 555 A90-36258
- Unsteady aerodynamic gust response including steady flow separation
[AIAA PAPER 90-36262] p 556 A90-36262
- Unsteady transonic cascade flow with in-passage shock wave
[AIAA PAPER 90-36281] p 556 A90-36281
- Solution of Euler equations with unstructured meshes
[AIAA PAPER 90-37343] p 558 A90-37343
- Air resonance stability of hingeless rotors in forward flight
[AIAA PAPER 90-38519] p 590 A90-38519
- The lateral spreading of finite-span instability waves in a laminar mixing layer
[AIAA PAPER 90-1532] p 606 A90-38677
- Unsteady aerodynamic loading produced by a sinusoidally oscillating delta wing
[AIAA PAPER 90-1536] p 564 A90-38680
- Unsteady Navier-Stokes solutions for a low aspect ratio delta wing
[AIAA PAPER 90-1538] p 564 A90-38682
- Calculation of unsteady rotor/stator interaction
[AIAA PAPER 90-1544] p 565 A90-38688
- Unsteady lift development on a constantly accelerated rectangular wing
[AIAA PAPER 90-1633] p 569 A90-38762
- Temporal-adaptive Euler/Navier-Stokes algorithm for unsteady aerodynamic analysis of airfoils using unstructured dynamic meshes
[AIAA PAPER 90-1650] p 569 A90-38778
- Flow visualization via laser-induced reflection from bubble sheets
[AIAA PAPER 90-39784] p 680 A90-39784
- Lift response of a rectangular wing undergoing a step change in forward speed
[AIAA PAPER 90-39801] p 620 A90-39801
- Aerodynamic detuning for control of supersonic rotor forced response
[AIAA PAPER 90-2018] p 621 A90-40596
- Various sources of wing rock
[AIAA PAPER 90-40679] p 622 A90-40679
- Flow structure generated by oscillating delta-wing segments
[AIAA PAPER 90-40694] p 622 A90-40694
- Counter-rotating propellant analysis using a frequency domain panel method
[AIAA PAPER 90-40937] p 623 A90-40937
- Coupled aerodynamic forces due to unsteady stall on a high-aspect-ratio wing oscillating at high amplitude
[ONERA, TP NO. 1990-24] p 623 A90-41203
- Flow induced forced response of an incompressible radial cascade including profile and incidence effects
[AIAA PAPER 90-2352] p 626 A90-42136
- Linearized unsteady aerodynamics for turbomachinery aeroelastic applications
[AIAA PAPER 90-2355] p 626 A90-42137
- Calculation of the complete transonic unsteady small disturbance equation by ADI method
[AIAA PAPER 90-42353] p 627 A90-42353
- Flow separation on a supercritical airfoil
[AIAA PAPER 90-42394] p 627 A90-42394
- Nonlinear unsteady airfoil response studies
[AIAA PAPER 90-42406] p 628 A90-42406
- Computation of viscous aerodynamic characteristics of 2-D airfoils for helicopter applications
[AIAA PAPER 90-42440] p 631 A90-42440
- The effect of shock/shock interactions on the design of hypersonic inlets
[AIAA PAPER 90-2217] p 705 A90-42748
- Unsteady analysis of hot streak migration in a turbine stage
[AIAA PAPER 90-2354] p 769 A90-42782
- A two-dimensional unsteady potential solver in internal aerodynamics flow problems
[AIAA PAPER 90-44430] p 707 A90-44430
- Numerical modeling of transverse flow past a cylinder using Euler equations
[AIAA PAPER 90-44922] p 709 A90-44922
- Delta wing surface pressures for high angle of attack maneuvers
[AIAA PAPER 90-2813] p 711 A90-45153
- Unsteady flow separation on slender bodies at high angles of attack
[AIAA PAPER 90-2835] p 712 A90-45166
- A Volterra kernel identification scheme applied to aerodynamic reactions
[AIAA PAPER 90-2803] p 712 A90-45178
- An unsteady helicopter rotor-fuselage aerodynamic interaction analysis
[AIAA PAPER 90-45323] p 712 A90-45323
- Effects of unsteady blowing on the lift of a circulation controlled cylinder
[AIAA PAPER 90-45325] p 713 A90-45325
- The development of crossflow vortices on a 45 degree swept wing
[SAE PAPER 892245] p 713 A90-45452
- Unsteady transonic flow --- Book
[AIAA PAPER 90-45760] p 716 A90-45760
- Simulation of time-dependent viscous flows using central and upwind-biased finite-difference techniques
[AIAA PAPER 90-3012] p 790 A90-45864
- Effects of onset free-stream turbulence on the performance characteristics of an airfoil
[AIAA PAPER 90-3025] p 790 A90-45867
- Rapid prediction of slender-wing aircraft dynamics
[AIAA PAPER 90-3037] p 791 A90-45876
- Unsteady aerodynamics of Wortmann FX63-137 airfoil at low Reynolds numbers
[AIAA PAPER 90-46374] p 801 A90-46374
- A method to determine the performance of low-Reynolds-number airfoils under off-design unsteady freestream conditions
[AIAA PAPER 90-46375] p 801 A90-46375
- Boundary-integral method for calculating aerodynamic sensitivities with illustration for lifting-surface theory
[AIAA PAPER 90-46841] p 806 A90-46841
- Unsteady aerodynamics - Physical issues and numerical predictions
[AIAA PAPER 90-46843] p 806 A90-46843
- Unsteady aerodynamics of delta wings, undergoing ramp-maneuvering in pitch to post-stall angle of attack
[AIAA PAPER 90-46857] p 806 A90-46857
- Numerical simulation of wakes with application to blade-vortex interaction
[AIAA PAPER 90-46881] p 807 A90-46881
- Unsteady blade surface pressures on a large-scale advanced propeller - Prediction and data
[AIAA PAPER 90-2402] p 808 A90-47220
- Unsteady Euler airfoil solutions using unstructured dynamic meshes
[AIAA PAPER 90-47307] p 809 A90-47307
- Aircraft passing through a sinusoidal gust
[AIAA PAPER 90-48090] p 811 A90-48090
- Interactive boundary-layer method for unsteady airfoil flows - Quasisteady model
[AIAA PAPER 90-48953] p 812 A90-48953
- Unsteady aerodynamics and aeroelasticity of turbomachines and propellers; Proceedings of the Fifth International Symposium, Beijing, People's Republic of China, Sept. 18-21, 1989
[AIAA PAPER 90-49451] p 853 A90-49451
- Two- and three-dimensional problems of unsteady aerodynamics of low loaded turbomachinery blade rows stages
[AIAA PAPER 90-49452] p 813 A90-49452
- Variational formulation of 2-D unsteady transonic aerodynamics of oscillating cascades
[AIAA PAPER 90-49458] p 813 A90-49458
- Numerical simulation of three-dimensional nonstationary flows and variable aerodynamic forces in turbomachine stages
[AIAA PAPER 90-49465] p 814 A90-49465
- On the unsteady loading noise of counter-rotating propeller
[AIAA PAPER 90-49484] p 895 A90-49484
- Cascade aerodynamic gust response including steady loading effects
[AIAA PAPER 90-51006] p 904 A90-51006
- Unsteady lifting surface theory for a rotating cascade of swept blades
[ASME PAPER 89-GT-306] p 906 A90-51259
- A panel method computation for oscillating airfoil in compressible flow
[AIAA PAPER 90-51483] p 906 A90-51483
- New methods of buffeting prediction on civil aircraft
[AIAA PAPER 90-52620] p 908 A90-52620
- Numerical simulation of nonreactive flows in turbomachines
[AIAA PAPER 90-52621] p 908 A90-52621
- An investigation of counterrotating tip vortex interaction
[NASA-CR-185135] p 79 N90-11549
- Prediction of unsteady blade surface pressures on an advanced propeller at an angle of attack
[NASA-TM-102374] p 94 N90-12560
- Computation of unsteady transonic flow about airfoils in frequency domain using the full-potential equation
[AIAA PAPER 90-14198] p 174 N90-14198
- An analytical method for the prediction of unsteady rotor/airframe interactions in forward flight
[AIAA PAPER 90-14223] p 186 N90-14223
- Flight evaluation of a pneumatic system for unsteady pressure measurements using conventional sensors
[NASA-TM-4131] p 186 N90-14225
- Temporally and spatially resolved flow in a two-stage axial compressor. Part 2: Computational assessment
[NASA-TM-102273] p 194 N90-14236
- Concurrent processing adaptation of aeroplastic analysis of propfans
[NASA-TM-102455] p 215 N90-14656
- Canard versus aft-tail ride qualities performance and pilot command response
[NASA-TM-102503] p 258 N90-15053
- Unsteady aerodynamics of oscillating and rapidly pitched airfoils
[NASA-TM-105074] p 235 N90-15074
- Test techniques for cryogenic wind tunnels
[NASA-TM-105952] p 263 N90-15952
- Numerical solutions of the linearized Euler equations for unsteady vortical flows around lifting airfoils
[NASA-TM-102466] p 318 N90-17562
- Aerodynamics of unsteady systems. Numerical study of potential flow/boundary layer coupling
[ETN-90-96257] p 396 N90-18367
- Unsteady Aerodynamic Phenomena in Turbomachines
[AGARD-CP-468] p 425 N90-18405
- A comparison of flutter calculations based on eigenvalue and energy method
[AIAA PAPER 90-18406] p 425 N90-18406
- Design guidance to minimize unsteady forces in turbomachines
[AIAA PAPER 90-18411] p 426 N90-18411
- Unsteady blade loads due to wake influence
[AIAA PAPER 90-18413] p 426 N90-18413
- Numerical prediction of axial turbine stage aerodynamics
[AIAA PAPER 90-18416] p 426 N90-18416
- Unsteady aerodynamics of delta wings performing maneuvers to high angle of attack
[AIAA PAPER 90-19196] p 398 N90-19196
- Conical Euler solution for a highly-swept delta wing undergoing wing-rock motion
[NASA-TM-102609] p 400 N90-19211
- Aeroservoelasticity
[NASA-TM-102620] p 416 N90-19227
- Unsteady free-wake viscous aerodynamic analysis of helicopter rotors
[AD-A217166] p 478 N90-20048
- Aeroelastic characteristics of aircraft with circulation control wings
[AIAA PAPER 90-20070] p 497 N90-20070
- Development and application of a generalized dynamic wake theory for lifting rotors
[AIAA PAPER 90-21731] p 570 N90-21731
- Control of flow separation and mixing by aerodynamic excitation
[NASA-TM-103131] p 571 N90-21733
- Airloads, wakes, and aeroelasticity
[NASA-CR-177551] p 572 N90-21738
- Aeroelastic simulation of higher harmonic control
[AIAA PAPER 90-21768] p 592 N90-21768
- Forcing function effects on rotor row unsteady aerodynamic response in a multistage compressor
[AIAA PAPER 90-22536] p 573 N90-22536
- STARS: An integrated general-purpose finite element structural, aeroelastic, and aeroservoelastic analysis computer program
[NASA-TM-101709] p 689 N90-23768
- A time-marching method to calculate unsteady airloads on three-dimensional wings. Part 1: Linearized formulation
[DLR-FB-89-58] p 634 N90-24254
- A time-marching method for calculating unsteady airloads on three-dimensional wings. Part 2: Full-potential formulation
[DLR-FB-89-59] p 635 N90-24255
- Calculation of the aeroelastic blade stabilization with linearized process
[MITT-87-01] p 666 N90-24272
- Integral-equation methods in steady and unsteady subsonic, transonic and supersonic aerodynamics for interdisciplinary design
[NASA-TM-102677] p 716 N90-25110
- Identification of aerodynamic models for maneuvering aircraft
[NASA-CR-186630] p 719 N90-25943
- Two-dimensional Euler and Navier-Stokes Time accurate simulations of fan rotor flows
[NASA-TM-102402] p 720 N90-25948
- Aerodynamic/dynamic interaction
[AD-A222263] p 815 N90-26798
- Adaptation for unsteady flow
[AIAA PAPER 90-26845] p 871 N90-26845
- Development of a linearized unsteady aerodynamic analysis for cascade gust response predictions
[NASA-CR-4308] p 816 N90-27655
- Aerodynamics of a linear oscillating cascade
[NASA-TM-103250] p 817 N90-27657
- Unsteady aerodynamics of controls
[AIAA PAPER 90-28525] p 935 N90-28525

UNSTEADY FLOW

- Unsteady viscous calculation of cascade flows with leading-edge-induced separation
[ONERA, TP NO. 1989-116] p 3 A90-11148

Numerical simulation of three-dimensional unsteady flows in turbomachines
[ONERA, TP NO. 1989-118] p 4 A90-11149

An improved method for the computation of unsteady transonic potential flow - Application for airfoil and blade performance prediction
[ONERA, TP NO. 1989-154] p 4 A90-11175

A study of unsteady rotor-stator interactions
p 67 A90-11557

Unsteady aerodynamics and aeroelasticity of turbomachines and propellers; Proceedings of the Fourth International Symposium, Aachen, Federal Republic of Germany, Sept. 6-10, 1987 p 5 A90-11776

The solution of the unsteady transonic flow through a blade passage in an axial turbine p 5 A90-11777

Calculation of unsteady Euler flows in turbomachinery using the linearized Euler equations p 5 A90-11778

Unsteady flow visualization in a vibrating annular turbine cascade operating in the transonic flow regime p 7 A90-11786

A numerical method solving 2-D unsteady flow field around cascade of oscillating airfoils with arbitrary camber and thickness p 7 A90-11788

The unsteady aerodynamics of an oscillating cascade in a compressible flow field p 7 A90-11789

Computation of unsteady compressible turbulent boundary layers in cascade flow with controlled inlet perturbation p 8 A90-11807

Calculation of unsteady boundary layer development on axial-flow turbomachinery blading p 48 A90-12588

Unsteady flow in centrifugal compressors due to downstream circumferential distortions p 14 A90-12598

A solution adaptive finite element method applied to two-dimensional unsteady viscous compressible cascade flow p 15 A90-12624

Closed-form solutions for nonlinear quasi-unsteady transonic aerodynamics p 16 A90-12839

Numerical simulation of valveless pulsed combustors p 127 A90-13767

Numerical solution of unsteady Navier-Stokes equations for laminar/turbulent flows past axis-symmetric bodies at angle of attack p 85 A90-15235

Large-eddy simulations of pressure oscillations and combustion instability in a ramjet p 111 A90-15388

The relevance of unsteady aerodynamics for highly maneuverable and agile aircraft p 146 A90-16775

Transition phenomena on airfoils operating at low chord Reynolds numbers in steady and unsteady flow p 148 A90-16786

Experiments in swept-wing transition p 149 A90-16794

Transition effects on airfoil dynamics and the implications for subscale tests p 152 A90-17862

Unsteady streamlines near the trailing edge of NACA 0012 airfoil at a Reynolds number of 125,000 p 155 A90-18158

Simulation of high incidence unsteady flow past Joukowski airfoils p 156 A90-18301

Numerical method for solving the Euler equation for unsteady transonic flows over oscillating airfoils p 157 A90-18578

Computations of unsteady transonic flows about thin airfoils by integral equation method p 158 A90-18609

Numerical simulation of unsteady flow about cambered plates p 159 A90-19389

Application of a rotary-wing viscous flow solver on a massively parallel computer p 164 A90-19802

Prediction of steady and unsteady asymmetric vortical flows around cones p 168 A90-19940

Investigation of oscillating airfoil shock phenomena [AIAA PAPER 90-0695] p 169 A90-19981

A finite element solution of unsteady two-dimensional flow in cascades p 226 A90-21946

Numerical simulation of supersonic unsteady flow using Euler equations [AIAA PAPER 90-0415] p 229 A90-22215

Unsteady transonic aerodynamics of oscillating airfoils in supersonic freestream p 232 A90-23277

Unsteady supersonic computations of arbitrary wing-body configurations including external stores p 232 A90-23278

Three-dimensional separated flow field in the endwall region of an annular compressor cascade in the presence of rotor-stator interaction. II - Unsteady flow and pressure field [ASME PAPER 89-GT-77] p 291 A90-23798

Comparison of steady and unsteady secondary flows in a turbine stator cascade [ASME PAPER 89-GT-79] p 291 A90-23800

Unsteady transonic flow around double-wedge profiles p 299 A90-24354

Unsteady Euler analysis of the flowfield of a propan at an angle of attack [AIAA PAPER 90-0339] p 300 A90-25028

A numerical method for solving the unsteady compressible Navier-Stokes equations p 306 A90-25827

Simulation of sound propagation in axisymmetric jet p 378 A90-25872

A semi-analytical procedure for the conformal mapping of arbitrary airfoil contours p 309 A90-26498

Unsteady hypersonic viscous flow in impulse facilities [AIAA PAPER 90-0421] p 313 A90-26947

A flux-split solution procedure for unsteady inlet flows [AIAA PAPER 90-0585] p 314 A90-26967

Experimental study of nonsteady asymmetric flow around an ogive-cylinder at incidence p 384 A90-27985

Unsteady flow computation of oscillating flexible wings [AIAA PAPER 90-0937] p 389 A90-29363

Aeroelastic problems in turbomachines [AIAA PAPER 90-1157] p 393 A90-29393

Unsteady transonic aerodynamics p 393 A90-29882

Physical phenomena associated with unsteady transonic flows p 394 A90-29883

Basic equations for unsteady transonic flow p 394 A90-29884

Basic numerical methods --- of unsteady and transonic flow p 394 A90-29886

Unsteady aerodynamics for turbomachinery aeroelastic applications p 394 A90-29888

Numerical solutions of the linearized Euler equations for unsteady vortical flows around lifting airfoils p 394 A90-30264

Nonstationary hypersonic flow past a thin wing of variable shape p 470 A90-32559

Computation of unsteady transonic flows around oscillating airfoils using full potential and Euler equations p 472 A90-33357

Unsteady transition in an axial-flow turbine. I - Measurements on the turbine rotor. II - Cascade measurements and modeling [ASME PAPER 89-GT-289] p 474 A90-33562

Unsteady transonic cascade flow with in-passage shock wave p 556 A90-36281

Review of vortical flow utilization p 605 A90-37966

A study of the unsteadiness of crossing shock wave turbulent boundary layer interactions [AIAA PAPER 90-1456] p 606 A90-38614

A computational study of the taxonomy of vortex breakdown [AIAA PAPER 90-1624] p 568 A90-38753

Unsteady lift development on a constantly accelerated rectangular wing [AIAA PAPER 90-1633] p 569 A90-38762

A computational study of the impingement region of an unsteady subsonic jet [AIAA PAPER 90-1657] p 570 A90-38784

Non-steady flow loss mechanisms associated with vaneless diffusers [AIAA PAPER 90-2508] p 682 A90-40641

Investigation of unsteady flow through transonic turbine stage. I - Analysis [AIAA PAPER 90-2408] p 626 A90-42161

Investigation of unsteady flow through a transonic turbine stage. II - Data/prediction comparison for time-averaged and phase-resolved pressure data [AIAA PAPER 90-2409] p 626 A90-42162

Finite element simulation of unsteady two-dimensional incompressible viscous flows p 629 A90-42423

Flow establishment in a generic scramjet combustor [AIAA PAPER 90-2096] p 742 A90-42729

Transient behavior of supersonic flow through inlets [AIAA PAPER 90-2130] p 704 A90-42734

Unsteady Euler analysis of the redistribution of an inlet temperature distortion in a turbine [AIAA PAPER 90-2262] p 768 A90-42759

Using 3D Euler flow simulations to assess effects of periodic unsteady flow through turbines [AIAA PAPER 90-2357] p 706 A90-42783

Numerical study of heat transfer for unsteady viscous supersonic blunt body flows p 707 A90-44432

Unsteady flow separation on slender bodies at high angles of attack [AIAA PAPER 90-2835] p 712 A90-45166

Visualization of the turbulent trailing vortex behind a finite wing in steady and unsteady flows p 712 A90-45260

Numerical solutions for unsteady aerofoil by internal singularity method p 716 A90-45536

Unsteady transonic flow --- Book p 716 A90-45760

An upwind approach to unsteady flowfield simulation [AIAA PAPER 90-3100] p 796 A90-45912

Navier-Stokes simulation of unsteady supersonic cavity flowfield with passive control [AIAA PAPER 90-3101] p 796 A90-45913

A characterization and search technique for unsteady flow control problems [AIAA PAPER 90-3102] p 796 A90-45914

Application of a streamwise upwind algorithm for unsteady transonic computations over oscillating wings [AIAA PAPER 90-3103] p 796 A90-45915

An unstructured-mesh Euler method for multielement airfoil geometries [AIAA PAPER 90-3051] p 797 A90-45930

Transient aeroelastic computations using multiple moving frames of reference [AIAA PAPER 90-3053] p 798 A90-45932

Compressible Navier-Stokes solutions over low Reynolds number airfoils p 802 A90-46382

Interactive grid adaption p 806 A90-46850

Numerical simulation of steady and unsteady vortical flows around wings and bodies p 806 A90-46869

Effects of transition on wind tunnel simulation of vehicle dynamics p 870 A90-49273

A numerical technique for computing the unsteady transonic flow around a wing profile in arbitrary oscillation p 906 A90-51530

Numerical simulation of nonreactive flows in turbomachines p 908 A90-52621

Basic studies of the unsteady flow past high angle of attack airfoils [AD-A210252] p 18 A90-10008

Numerical simulation of unsteady combustion in a dump combustor p 54 A90-10203

Unsteady aerodynamics with applications to flight mechanics [AD-A211944] p 89 A90-11706

Active control of unsteady and separated flow structures [AD-A212109] p 89 A90-11707

Steady and unsteady potential flow around thin annular wings and engines with simulation of jet engine flow [DFVLR-FB-89-18] p 89 A90-11711

Numerical simulation of unsteady rotational flow over propfan configurations [NASA-CR-186037] p 90 A90-12500

Unsteady three-dimensional thin-layer Navier Stokes solutions on dynamic blocked grids [AD-A212377] p 136 A90-12899

Blunt-nose inviscid airflows with coupled nonequilibrium processes p 171 A90-13336

Laser applications in supersonic unsteady flow p 212 A90-13344

Application of a two-dimensional unsteady viscous analysis code to a supersonic throughflow fan stage [NASA-TM-4141] p 192 A90-13387

An alternative derivation for an integral equation for linearized subsonic flow over a wing [AD-A214140] p 236 A90-15079

Force and moment measurements on delta wings in unsteady flow p 278 A90-16185

Periodically unsteady effects on profiles, induced by separation p 279 A90-16196

Wake interaction effects on the transition process on turbine blades [AD-A214492] p 343 A90-16759

Numerical solutions of the linearized Euler equations for unsteady vortical flows around lifting airfoils [NASA-TM-102466] p 318 A90-17562

Unsteady Euler analysis of the flow field of a propan at an angle of attack [NASA-TM-102426] p 380 A90-18229

Numerical investigation of unsteady flow in oscillating turbine and compressor cascades p 426 A90-18407

Unsteady viscous calculation method for cascades with leading edge induced separation p 426 A90-18408

Aerodynamic study on forced vibrations on stator rows of axial compressors p 426 A90-18412

Experiments on the unsteady flow in a supersonic compressor stage p 427 A90-18422

Modelling unsteady transition and its effects on profile loss p 427 A90-18423

Experimental investigation of the influence of rotor wakes on the development of the profile boundary layer and the performance of an annular compressor cascade p 427 A90-18425

Active stabilization of aeromechanical systems [AD-A216629] p 454 A90-18672

Computation of hypersonic unsteady viscous flow over a cylinder p 397 A90-19194

Spectral simulation of unsteady compressible flow past a circular cylinder [NASA-CR-182030] p 478 A90-20050

Experimental investigation of the mechanisms underlying vortex kinematics in unsteady separated flows [AD-A217889] p 540 A90-20346

A two-dimensional unsteady analysis for transonic and supersonic cascade flows p 480 A90-20955

Measurement of lift development on rapidly-accelerated wings p 480 A90-20956

- Extension of a streamwise upwind algorithm to a moving grid system
[NASA-TM-102800] p 572 N90-21739
- Extension of a three-dimensional viscous wing flow analysis user's manual: VISTA 3-D code
[NASA-CR-182024] p 574 N90-22538
- Extension of a three-dimensional viscous wing flow analysis
[NASA-CR-182023] p 631 N90-23348
- Unsteady potential flow past a propeller blade section
[NASA-CR-4307] p 634 N90-24246
- An interactive boundary-layer method for unsteady airfoil flows. Part 1: Quasi-steady-state model
[AD-A221220] p 634 N90-24250
- A lifting surface method for the calculation of steady and unsteady, incompressible propeller aerodynamics [ESA-TT-1151] p 717 N90-25113
- An unsteady lifting surface method for single rotation propellers
[NASA-CR-4302] p 719 N90-25940
- Two-dimensional Euler and Navier-Stokes Time accurate simulations of fan rotor flows
[NASA-TM-102402] p 720 N90-25948
- Analysis and mitigation of numerical dissipation in inviscid and viscous computation of vortex-dominated flows
[NASA-CR-186887] p 776 N90-26281
- Aerodynamic/dynamic interaction
[AD-A22263] p 815 N90-26798
- Fluid Dynamics Panel Working Group 12 on Adaptive Wind Tunnel Walls: Technology and Applications
[AGARD-AR-269] p 870 N90-26838
- Adaptation for unsteady flow
[AGARD-AR-269] p 871 N90-26845
- Experimental characterization of the effects of pneumatic tubing on unsteady pressure measurements
[NASA-TM-4171] p 850 N90-27703
- Development of turbulence models for the analysis of compressible or incompressible unsteady flow
[ETN-90-97486] p 958 N90-28810
- UPGRADING**
- Aviation security: Corrective actions underway, but better inspection guidance still needed. Report to the Chairwoman, Government Activities and Transportation Subcommittee, Committee on Government Operations, House of Representatives
[GAO/RCED-88-160] p 635 N90-23367
- UPLINKING**
- Weather data dissemination to aircraft
p 486 N90-20934
- UPPER SURFACE BLOWING**
- Investigations of the influence of slot blowing from the upper wing surface on the flow around the wing and its aerodynamic characteristics
p 623 A90-41740
- UPPER SURFACE BLOWN FLAPS**
- Propulsive lift augmentation by side fences as applied to Japan's experimental STOL aircraft, ASKA
[AIAA PAPER 90-3009] p 789 A90-45859
- Acoustic-thermal environment for USB flap structure. Report 1: Ground simulation test results
[NAL-TM-567] p 88 N90-11697
- UPSTREAM**
- Mach number effects on upstream influence in swept shock wave/turbulent boundary layer interactions
p 556 A90-36415
- An upwind approach to unsteady flowfield simulation
[AIAA PAPER 90-3100] p 796 A90-45912
- UPWASH**
- Aircraft response and pilot behaviour during a wake vortex encounter perpendicular to the vortex axis
p 259 N90-15057
- URBAN TRANSPORTATION**
- Hydrogen in future energy and propulsion technology
p 692 A90-41736
- Possibilities for improving traffic flows
p 823 A90-49272
- USER MANUALS (COMPUTER PROGRAMS)**
- RAN (Royal Australian Navy) vibration analysis system operator's guide
[AD-A212441] p 107 N90-12596
- User's guide to PMESH: A grid-generation program for single-rotation and counterrotation advanced turboprops
[NASA-CR-185156] p 217 N90-14783
- A user's manual for the method of moments Aircraft Modeling Code (AMC)
[NASA-CR-186371] p 415 N90-18390
- ETO (Earth-To-Orbit): A trajectory program for aerospace vehicles
[AD-A218157] p 528 N90-20103
- Users manual for the NASA Lewis Ice Accretion Prediction Code (LEWICE)
[NASA-CR-185129] p 468 N90-20943
- Enhanced Low Level Wind Shear (LLWS) 6-sensor improvement user's manual for data processing of field data
[DOT/FAA/CT-TN90/8] p 583 N90-21759

- Extension of a three-dimensional viscous wing flow analysis user's manual: VISTA 3-D code
[NASA-CR-182024] p 574 N90-22538
- ARLSUPER version 1.0, program users guide
[AD-A222693] p 815 N90-26793
- Damage tolerance analysis for manned hypervelocity vehicles. Volume 2: Software user's manual
[AD-A22136] p 845 N90-26826
- Air Force procedure for predicting aircraft noise around airbases: Airbase operations program (BASEOPS) description
[AD-A223069] p 895 N90-27466
- Air Force procedure for predicting aircraft noise around airbases: Noise Exposure Model (NOISEMAP). User's manual
[AD-A223162] p 895 N90-27467
- Generalized Advanced Propeller Analysis System (GAPAS). Volume 2: Computer program user manual
[NASA-CR-185277] p 933 N90-29394
- USER REQUIREMENTS**
- Honeycomb quality requirements - A user's perspective
p 538 A90-33705
- Initial service experience with the Fokker 100
[SAE PAPER 892238] p 733 A90-45450
- Noise and sonic boom impact technology. Initial development of an Assessment System for Aircraft Noise (ASAN). Volume 3: Technical description
[AD-A214455] p 379 N90-17412
- The Langley 14- by 22-foot subsonic tunnel: Description, flow characteristics, and guide for users
[NASA-TP-3008] p 816 N90-27649
- R and D aspects of the future operational concept of the BFS
p 826 N90-27679
- Impact of Emerging NDE-NDI Methods on Aircraft Design, Manufacture, and Maintenance
[AGARD-CP-462] p 885 N90-28068
- GPS integrity requirements for use by civil aviation
p 916 N90-29339

V

V-22 AIRCRAFT

- Designing the V-22 'Osprey' tiltrotor V/Stol aircraft for maintenance and serviceability
[SAE PAPER 891075] p 101 A90-14369
- A review of the V-22 dynamics validation program
p 406 A90-28155
- A review of the V-22 health monitoring system
p 417 A90-28209
- V-22 ballistic vulnerability hardening program
p 408 A90-28223
- Unique methodology used in the Bell-Boeing V-22 main landing gear landing loads analysis and drop tests
p 409 A90-28236
- V-22 aerodynamic loads analysis and development of loads alleviation flight control system
p 410 A90-28239
- Aerodynamic design of the V-22 Osprey propeller
p 385 A90-28241
- V-22 - The prospects now --- production costs of Bell Boeing tilt-rotor aircraft
p 497 A90-34900
- V-22 developmental status
p 581 A90-38529
- V-22 engine installation and removal tool - Designing support equipment with the aircraft, not after
p 581 A90-38538
- Evolution and test history of the V-22 0.2-scale aeroelastic model
p 831 A90-46954
- Advanced rotorcraft V/STOL - Technology needs for high-speed rotorcraft
[AIAA PAPER 90-3298] p 837 A90-48880
- V/STOL AIRCRAFT**
- Turbulence measurements in a flow generated by the collision of radially flowing wall jets
p 2 A90-10699
- VSTOL power plant control lessons from Harrier experience
p 13 A90-12582
- A full scale, VSTOL, ground environment test facility
p 58 A90-12631
- Turbulence modeling for impinging jets
[AIAA PAPER 90-0022] p 211 A90-19639
- A flight-test methodology for identification of an aerodynamic model for a V/STOL aircraft
p 413 A90-30107
- Practical design considerations for integrating the propulsion system with the aircraft for jetborne flight
[ASME PAPER 89-GT-310] p 490 A90-32257
- Propulsion systems for supersonic V/STOL aircraft
[ASME PAPER 89-GT-309] p 507 A90-32259
- Finite element simulation of complex jets in a crossflow for V/STOL applications
p 585 A90-35753
- Effect of vertical-ejector jet on the aerodynamics of delta wings
p 553 A90-35755
- A status review of non-helicopter V/STOL aircraft development. II
p 580 A90-38028

- National Technical Specialists' Meeting on Tactical V/STOL, New Bern, NC, Sept. 19-21, 1989. Proceedings
p 551 A90-38526
- Flight/propulsion control integration for V/STOL fighter/attack aircraft
p 591 A90-38530
- Low speed maneuverability and agility design considerations for V/STOL aircraft
p 581 A90-38536
- Power transfer devices for V/STOL convertible engine systems
p 587 A90-38539
- A computational study of the impingement region of an unsteady subsonic jet
[AIAA PAPER 90-1657] p 570 A90-38784
- Turbulence model performance in V/STOL flow field simulation
[AIAA PAPER 90-2248] p 625 A90-42094
- Direct lift STOVL engine integration
[AIAA PAPER 90-2274] p 644 A90-42103
- A modeling technique for STOVL ejector and volume dynamics
[AIAA PAPER 90-2417] p 663 A90-42168
- Advanced material applications for direct lift engines
[AIAA PAPER 90-2753] p 664 A90-42226
- Analysis of internal flow in a ventral nozzle for STOVL aircraft
[AIAA PAPER 90-1899] p 739 A90-42688
- Hot gas environment around STOVL aircraft in ground proximity. I - Experimental study
[AIAA PAPER 90-2269] p 742 A90-42765
- More power for the Harrier
p 745 A90-44597
- Three-dimensional turbulent flow code calculations of hot gas ingestion
p 745 A90-44726
- Supersonic STOVL - The future is now
p 732 A90-44781
- Supersonic flow computations for an ASTOVL aircraft configuration
[AIAA PAPER 90-2997] p 787 A90-45847
- Reduction of the side force on pointed forebodies through add-on tip devices
[AIAA PAPER 90-3005] p 788 A90-45854
- Sideslip-induced static pressure errors in flight-test measurements
[AIAA PAPER 90-3082] p 794 A90-45898
- Parametric synthesis of the decoupling filter in the manual control system of VTOL aircraft
p 859 A90-46483
- Vertical Lift Aircraft Design Conference, San Francisco, CA, Jan. 17-19, 1990. Proceedings
p 829 A90-46926
- High-speed rotorcraft V/STOL - An initial assessment
p 829 A90-46938
- H-infinity based integrated flight/propulsion control design for a STOVL aircraft in transition flight
[AIAA PAPER 90-3335] p 862 A90-47595
- The Canadair CL-64 experimental aircraft - Lessons learned
[AIAA PAPER 90-3205] p 834 A90-48833
- Preliminary design of a supersonic short takeoff and vertical landing (STOVL) fighter aircraft
[AIAA PAPER 90-3231] p 834 A90-48844
- The Hawker P1127 vectored thrust fighter program - Lessons learned
[AIAA PAPER 90-3238] p 835 A90-48848
- Advanced rotorcraft V/STOL - Technology needs for high-speed rotorcraft
[AIAA PAPER 90-3298] p 837 A90-48880
- An investigation of aircraft maneuverability and agility
[AIAA PAPER 90-3300] p 868 A90-48882
- Configuring tactical aircraft
[AIAA PAPER 90-3305] p 837 A90-48886
- X-wing experimental aircraft - Lessons learned
[AIAA PAPER 90-3208] p 838 A90-49105
- The implementation of STOVL task-tailored control modes in a fighter cockpit
[AIAA PAPER 90-3229] p 839 A90-49114
- The North American Rockwell XFV-12A - Reflections and some lessons
[AIAA PAPER 90-3240] p 839 A90-49118
- STOVL option for the multi-role fighter
[AIAA PAPER 90-3296] p 840 A90-49124
- Engine inlet distortion in a 9.2 percent scale vectored thrust STOVL model in ground effect
[NASA-TM-102358] p 318 N90-17561
- A head up display format for application to V/STOL aircraft approach and landing
[NASA-TM-102216] p 340 N90-17632
- Research on a two-dimensional inlet for a supersonic V/STOL propulsion system. Appendix A
[NASA-CR-174945] p 396 N90-18364
- The insertion of human dynamics models in the flight control loops of V/STOL research aircraft. Appendix 2: The optimal control model of a pilot in V/STOL aircraft control loops
[NASA-CR-186598] p 598 N90-21776
- An adaptive human response mechanism controlling the V/STOL aircraft. Appendix 3: The adaptive control model of a pilot in V/STOL aircraft control loops
[NASA-CR-186599] p 598 N90-21777

- A modeling technique for STOVL ejector and volume dynamics
[NASA-TM-103167] p 589 N90-22566
- Supersonic flow computations for an ASTOVL aircraft configuration, phase 2, part 2
[NASA-CR-4284] p 610 N90-22746
- Preliminary design of a supersonic Short Takeoff and Vertical Landing (STOVL) fighter aircraft
[NASA-CR-186670] p 649 N90-23394
- Analysis of internal flow in a ventral nozzle for STOVL aircraft
[NASA-TM-103123] p 666 N90-23404
- Rotary-Jet thrust augmentor with jet-flapped blades
p 633 N90-24243
- Experimental and analytical study of close-coupled ventral nozzles for ASTOVL aircraft
[NASA-TM-103170] p 666 N90-24273
- Design of a low cost short takeoff-vertical landing export fighter/attack aircraft
[NASA-CR-186658] p 734 N90-25132
- Hot gas ingestion characteristics and flow visualization of a vectored thrust STOVL concept
[NASA-TM-103212] p 751 N90-26009
- H-infinity based integrated flight-propulsion control design for a STOVL aircraft in transition flight
[NASA-TM-103198] p 758 N90-26011
- Sideslip-induced static pressure errors in flight-test measurements
[NASA-TM-102846] p 849 N90-27702
- STOVL fighter propulsion reliability, maintainability, and supportability characterization
[AD-A224221] p 933 N90-28574
- VACUUM MELTING**
Cleaner superalloys via improved melting practices
p 442 A90-29707
- VALUE ENGINEERING**
Designing for reliable and low maintenance cost aero engines
[PNR90570] p 115 N90-12604
- VALVES**
Advanced actuation systems development, volume 1
[AD-A213334] p 121 N90-12624
- VANADIUM**
Fatigue crack growth investigation of a Ti-6Al-4V forging under complex loading conditions: NATO/AGARD supplemental engine disk program
[AD-A220239] p 678 N90-23538
- VANADIUM ALLOYS**
Production of Ti6Al4V-components for a new turbo-fan-engine
p 132 A90-16618
- VANELESS DIFFUSERS**
An experimental investigation of non-steady flow in vaneless diffusers
p 14 A90-12595
- Effect of downstream elements on the flow at the exit of centrifugal compressor rotor
p 157 A90-18483
- LDV measurements and the flow analysis in the vaneless region of a radial inflow turbine
p 292 A90-23845
- A method of predicting the energy losses in vaneless diffusers of centrifugal compressors
[ASME PAPER 89-GT-157] p 292 A90-23846
- An experimental investigation of rotating stall in a centrifugal compressor with vaneless diffuser
p 621 A90-40513
- Correlation of radial-to-axial vaneless turns for centrifugal compressors
[AIAA PAPER 90-1917] p 656 A90-40556
- Non-steady flow loss mechanisms associated with vaneless diffusers
[AIAA PAPER 90-2508] p 682 A90-40641
- VANES**
Multistage compressor vane row aerodynamic gust response
p 6 A90-11783
- Rotor-blades excitation due to differential interference of vane wakes between upstream stator-rows in an axial compressor
p 6 A90-11784
- Effect of vane and blade numbers on performance of transonic turbine stage
p 189 A90-17789
- Application of recess vane casing treatment to axial flow fans
[ASME PAPER 89-GT-68] p 341 A90-23791
- An experimental study of turbine vane heat transfer with leading edge and downstream film cooling
[ASME PAPER 89-GT-69] p 358 A90-23792
- A new design method for centrifugal compressor vane diffusers
[ASME PAPER 89-GT-156] p 292 A90-23844
- Investigation of unsteady flow through transonic turbine stage. I - Analysis
[AIAA PAPER 90-2408] p 626 A90-42161
- Turbine configuration impact on advanced IHPTET engine system mission capabilities
[AIAA PAPER 90-2739] p 664 A90-42221
- Application of 3-D flow analysis to the design of a high work transonic turbine
p 628 A90-42395

- Prediction and measurement of rotor blade/stator vane dynamic characteristics of a modern aero-engine axial compressor
p 878 A90-46036
- Effect of vane twist on the performance of dome swirlers for gas turbine airblast atomizers
[AIAA PAPER 90-1955] p 881 A90-47203
- Influence of vane sweep on rotor-stator interaction noise
p 169 N90-13325
- The effectiveness of vane-aileron excitation in the experimental determination of flutter speed by parameter identification
[NASA-TP-2971] p 249 N90-15100
- Navier-Stokes analysis of turbine blade heat transfer
[NASA-TM-102496] p 542 N90-21300
- Effect of vane twist on the performance of dome swirlers for gas turbine airblast atomizers
[NASA-TM-103195] p 773 N90-25289
- Prediction and measurement of rotor blade/stator vane dynamic characteristics of a modern aero-engine axial compressor
[PNR90667] p 750 N90-26002
- Validation of the F-18 high alpha research vehicle flight control and avionics systems modifications
[NASA-TM-101723] p 924 N90-28542
- Analysis of the T63-A-700 engine used in alcohol turbine fuel extender test
[DOT/FAA/CT-TN90/18] p 928 N90-28549
- The effects of a compressor rebuild on gas turbine engine performance: Final results
p 952 N90-28701
- VAPOR DEPOSITION**
Vapor grown carbon fiber for space thermal management systems
p 943 A90-50128
- High temperature deformation studies on CVD silicon carbide fibers
p 945 A90-50147
- Chemical vapor deposition of Hf/Si compounds as a high temperature coating for carbon/carbon composites
p 955 A90-50159
- Self-lubricating surfaces by ion beam processing
[AD-A222489] p 884 N90-27118
- VAPOR PHASES**
Microprocessor control of a vapor-cycle cooling system
[SAE PAPER 891457] p 339 A90-27426
- VAPORIZERS**
Exhaust emission performance of a vaporizer tube combustor as compared with a single tube combustor
p 111 A90-14614
- A vapor generator for transonic flow visualization
[NASA-TM-101670] p 201 N90-13403
- VAPORIZING**
Externally vaporizing system for turbine combustor
[AD-D014284] p 256 N90-15918
- VAPORS**
Gas identification system using graded temperature sensor and neural net interpretation
[AD-A213359] p 205 N90-13627
- Ignitability of jet-A fuel vapors in aircraft fuel tanks
p 326 N90-17594
- VARIABLE CYCLE ENGINES**
The variable cycle diesel as an aircraft engine
[SAE PAPER 891065] p 110 A90-14365
- Thermodynamics and the future turbine engines
[ONERA, TP NO. 1989-165] p 253 A90-21031
- A method of sizing multi-cycle engines for hypersonic aircraft
[ASME PAPER 89-GT-281] p 507 A90-32261
- Evolution of engine cycles for STOVL propulsion concepts
[AIAA PAPER 90-2272] p 743 A90-42767
- Power struggle --- Advanced Tactical Fighter engine proposals
p 851 A90-46650
- VARIABLE GEOMETRY STRUCTURES**
Controlled mixing and variable geometry combustor design effects on emissions and combustion characteristics
p 45 A90-12547
- The propagation of a normal shock in a varying area duct
p 130 A90-15045
- The influence of selected geometrical and mass parameters on the structural dynamics of an aircraft with a variable-geometry airfoil
p 346 A90-24284
- The variable-diameter rotor - A key to high performance rotorcraft
p 413 A90-30118
- Improving tilt rotor aircraft performance with variable-diameter rotors
p 646 A90-42445
- Numerical analysis of natural vibrations of an aeroplane with symmetrically variable geometry wing
p 860 A90-46715
- An assessment of robustness of flight control systems based on variable structure techniques
p 57 N90-10895
- VARIABLE MASS SYSTEMS**
A study of approximately optimal cruising flight regimes of variable-mass aircraft
p 430 A90-29187
- Rotary damping in aircraft motion due to jet propulsion system
p 520 A90-34820

VARIABLE PITCH PROPELLERS

- An approximate model for the performance and acoustic predictions of counterrotating propeller configurations
[NASA-CR-180667] p 379 N90-18228
- A computer program for the prediction of nozzle-propeller performance
[LR-578] p 572 N90-21740

VARIABLE STREAM CONTROL ENGINES

- Benefits of advanced materials, structures, and aerodynamics in future high speed civil transport propulsion systems
[AIAA PAPER 90-3285] p 853 A90-48872

VARIABLE SWEEP WINGS

- Static stability and control characteristics of scissor wing configurations
p 433 A90-31277
- Design and test of an NLF wing glove for the variable-sweep transition flight experiment
p 104 N90-12544

- F-14 VSTFE and results of the cleanup flight test program
p 105 N90-12547

- Variable-Sweep Transition Flight Experiment (VSTFE): Stability code development and clean-up glove data analysis
p 105 N90-12548

- An aerodynamic tradeoff study of the scissor wing configuration
[NASA-CR-186576] p 481 N90-20965

- Flutter clearance of the F-14A variable-sweep transition flight experiment airplane, phase 2
[NASA-TM-101717] p 735 N90-25135

VARIATIONAL PRINCIPLES

- Variational principle with variable domain discontinuous finite element method for transonic flow and determining automatically the position and shape of the shock waves
p 160 A90-19434

- Variational formulation of 2-D unsteady transonic aerodynamics of oscillating cascades
p 813 A90-49458

VATOL AIRCRAFT

- A study of a propulsion control system for a VATOL aircraft (A direct design synthesis application)
p 424 A90-30712

VAX COMPUTERS

- Artificial intelligence (AI) based tactical guidance for fighter aircraft
[AIAA PAPER 90-3435] p 889 A90-47688

- Software and hardware description of the helicopter motion equations for VAX computers
[AD-A213248] p 184 N90-13375

VECTOR ANALYSIS

- AcSim: Aircraft simulation program with application to flight profile generation
[AD-A212466] p 185 N90-14217

- Analysis of heliport environmental data: Indianapolis downtown heliport, Wall Street heliport. Volume 3: Indianapolis downtown heliport data plots
[AD-A217412] p 544 N90-20500

VECTOR PROCESSING (COMPUTERS)

- High level language programming for avionic vector processors
[AIAA PAPER 89-3107] p 74 A90-10589

- A parallel-vector algorithm for rapid structural analysis on high-performance computers
[AIAA PAPER 90-1149] p 458 A90-29293

VEHICLE WHEELS

- Dynamic stiffness of a hydraulic damper in the system of a front landing gear strut
p 102 A90-14555

VELOCITY

- Application of the joined wing to tiltrotor aircraft
[NASA-CR-177543] p 248 N90-15093

- Velocity filtering applied to optical flow calculations
[NASA-TM-102802] p 916 N90-28512

VELOCITY DISTRIBUTION

- Experimental study of static pressure and mean velocity profiles inside a two-dimensional dump-type combustor model
p 45 A90-12530

- A quasi-3D design method of transonic compressor blade with the function of improving velocity distribution
p 49 A90-12589

- Hot wire measurements in the wake of an oscillating airfoil
p 15 A90-12635

- On a lifting line theory for supersonic flow. I - The velocity field due to a vortex line in supersonic flow
p 143 A90-16735

- Wake behaviour of a large deflection turbine rotor linear cascade
p 157 A90-18481

- The induced velocity distribution and the flap-pitch-torsion coupling on the stability and control of the helicopter in flight condition with lateral velocity
p 196 A90-18633

- Structure of velocity and temperature fields in laminar channel flows with longitudinal vortex generators
p 273 A90-23207

- Wind shear and hyperbolic distributions
p 280 A90-23632

- Tip leakage losses in a linear turbine cascade
[ASME PAPER 89-GT-56] p 290 A90-23782

- Instrumentation and operation of NDA cryogenic wind tunnel p 437 A90-28293
- Relationship between velocity circulation around a wing profile and vorticity dispersion in a boundary layer p 620 A90-39539
- The performance of a combustor pre-diffuser incorporating compressor outlet guide vanes [AIAA PAPER 90-2165] p 661 A90-42053
- An experimental investigation of the velocity field in a reverse-flow combustor p 739 A90-42657
- Frequency domain aerodynamic analysis of interacting rotating systems p 21 N90-10837
- Laser anemometer measurements in a transonic axial-flow fan rotor [NASA-TP-2879] p 73 N90-11245
- Supersonic boundary-layer transition on the LaRC F-106 and the DFRF F-15 aircraft. Part 2: Aerodynamic predictions p 94 N90-12559
- Practical systems for speckle velocimetry p 171 N90-13341
- A wall interference assessment/correction interface measurement system for the NASA/ARC 12-ft PWT [NASA-CR-185474] p 200 N90-13401
- Experimental study of velocity fields and turbulence in a turbojet engine [ISL-CO-231/88] p 344 N90-16766
- Low speed flowfield characterization by infrared measurements of surface temperatures p 317 N90-17556
- Viscous three-dimensional analyses for nozzles for hypersonic propulsion [NASA-CR-185197] p 344 N90-17635
- Measurement of velocity profiles and Reynolds stresses on an oscillating airfoil p 397 N90-18427
- Theoretical and experimental study of flow-control devices for inlets of indraft wind tunnels [NASA-TM-100050] p 598 N90-21778
- An experimental and theoretical investigation of the flow over plane delta wings with supersonic leading edges [LR-588] p 717 N90-25114
- VELOCITY MEASUREMENT**
- Velocity and scalar measurements in model and real gas turbine combustors p 191 A90-19005
- Determination of the ground effect on the characteristics of the A320 aircraft [ONERA, TP NO. 1989-188] p 245 A90-21048
- Comparison of measured induced velocities with results from a closed-form finite state wake model in forward flight p 385 A90-28195
- Vision guidance update - Synthetic aperture radar (SAR) multiple image exploitation for position and velocity determination p 488 A90-34140
- Three-component LDA measurements in an axial-flow compressor p 683 A90-40943
- Measurements in an annular combustor-diffuser system [AIAA PAPER 90-2162] p 768 A90-42740
- Practical systems for speckle velocimetry p 171 N90-13341
- Laser two focus techniques p 212 N90-13348
- Low air speed computation for helicopters: A new approach p 333 N90-16744
- An experimental study of the effect of streamwise vortices on unsteady turbulent boundary-layer separation p 369 N90-17045
- Automation and extension of LDV (Laser-Doppler Velocimetry) measurements of off-design flow in a subsonic cascade wind tunnel [AD-A216627] p 453 N90-18670
- Velocity measurements on a lifting rotor/airframe configuration in low speed forward flight p 815 N90-26790
- Determination of the ground effect on the characteristics of the A320 aircraft p 922 N90-28534
- VENTILATION**
- Ignitability of jet-A fuel vapors in aircraft fuel tanks p 326 N90-17594
- Hot surface ignition studies of aviation fluids p 327 N90-17600
- Transonic wing charge improvements by passive shock boundary layer interference control: Development status and prospects [ETN-90-96463] p 650 N90-24267
- VENTILATION FANS**
- Flow in a centrifugal fan of the squirrel cage type [ASME PAPER 89-GT-52] p 289 A90-23778
- VENTING**
- Measurement and characterization of prepreg permeability with a modified bagging technique p 949 A90-50226
- The repair of aircraft integral fuel tanks in the RAF: A user's view of fuel tank technology p 250 N90-15908
- Forced and natural venting of aircraft cabin fires: A numerical simulation p 326 N90-17597
- Passive venting technique for shallow cavities [NASA-CASE-LAR-14031-1] p 499 N90-20079
- VERTICAL AIR CURRENTS**
- Multiple vortex ring model of the DFW microburst p 280 A90-23286
- The source region and evolution of a microburst downdraft p 456 A90-28612
- Entry of a flexible airfoil into a vertical gust p 470 A90-32552
- Modeling of turbulence and downbursts for flight simulators p 870 A90-48956
- Spanwise measurements of vertical components of atmospheric turbulence [NASA-TP-2963] p 456 N90-19718
- VERTICAL FLIGHT**
- Analytical approach to the induced flow of a helicopter rotor in vertical descent p 293 A90-23938
- VERTICAL LANDING**
- Supplemented visual cues for helicopter hovering above a moving ship deck p 195 A90-17704
- STOVL wind tunnel tests demonstrate ejector viability p 245 A90-21000
- The coming age of the tiltrotor. I p 246 A90-21711
- TW-68 tilt wing high speed commercial VTOL p 246 A90-21712
- Potential applications of satellite navigation p 264 A90-21716
- EUROFAR - European project for a commercial vertical-takeoff aircraft [MBB-UD-553/89] p 221 A90-22696
- Scenario 2000 [MBB-UD-560/89] p 222 A90-22698
- Performance characteristics of a one-third-scale, vectorable ventral nozzle for SSTOVL aircraft [AIAA PAPER 90-2271] p 586 A90-37562
- Influence of ground effect on helicopter takeoff and landing performance p 646 A90-42468
- A hydrodynamic turbo-fan/shaft convertible engine p 665 A90-42487
- Hot gas environment around STOVL aircraft in ground proximity. II - Numerical study [AIAA PAPER 90-2270] p 743 A90-42766
- Evolution of engine cycles for STOVL propulsion concepts [AIAA PAPER 90-2272] p 743 A90-42767
- Simulation evaluation of transition and hover flying qualities of a mixed-flow, remote-lift STOVL aircraft [SAE PAPER 892284] p 757 A90-45464
- Robust hover control for a short takeoff/vertical landing aircraft [AIAA PAPER 90-3333] p 862 A90-47593
- Application of a design method for integrated control to a VTOL airplane in hover [AIAA PAPER 90-3334] p 862 A90-47594
- Flight evaluations of several hover control and display combinations for precise blind vertical landings [AIAA PAPER 90-3479] p 867 A90-47764
- Ryan X-13 experimental aircraft - Lessons learned [AIAA PAPER 90-3236] p 834 A90-48846
- Flight control design considerations for STOVL powered-lift flight [AIAA PAPER 90-3225] p 868 A90-49110
- Propulsion system design specifications based on STOVL flight control requirements [AIAA PAPER 90-3227] p 839 A90-49112
- The implementation of STOVL task-tailored control modes in a fighter cockpit [AIAA PAPER 90-3229] p 839 A90-49114
- STOVL option for the multi-role fighter [AIAA PAPER 90-3296] p 840 A90-49124
- STOVL propulsion system volume dynamics approximations [NASA-TM-102397] p 114 N90-11740
- A head up display format for application to V/STOL aircraft approach and landing [NASA-TM-102216] p 340 N90-17632
- Performance characteristics of a one-third-scale, vectorable ventral nozzle for SSTOVL aircraft [NASA-TM-103120] p 552 N90-21725
- Ground-simulation investigations of VTOL airworthiness criteria for terminal-area operations [NASA-TM-102810] p 757 N90-25141
- VERTICAL MOTION**
- Identification of an adequate model for collective response dynamics of a Sea King helicopter in hover p 56 A90-12786
- VERTICAL MOTION SIMULATORS**
- Ground-simulation investigations of VTOL airworthiness criteria for terminal-area operations [NASA-TM-102810] p 757 N90-25141
- VERTICAL PERCEPTION**
- Taking a new look at cockpit vertical situation displays p 652 A90-40382
- VERTICAL TAKEOFF**
- TW-68 tilt wing high speed commercial VTOL p 246 A90-21712
- Simulation and analysis of a delta planform with multiple jets in ground effect [AIAA PAPER 90-0299] p 228 A90-22195
- EUROFAR - European project for a commercial vertical-takeoff aircraft [MBB-UD-553/89] p 221 A90-22696
- Scenario 2000 [MBB-UD-560/89] p 222 A90-22698
- Influence of ground effect on helicopter takeoff and landing performance p 646 A90-42468
- Full Authority Digital Engine Control for the AS 355 N TM 319 engines p 665 A90-42486
- The Curtiss-Wright X-19 experimental aircraft - Lessons learned [AIAA PAPER 90-3206] p 834 A90-48834
- A head up display format for application to V/STOL aircraft approach and landing [NASA-TM-102216] p 340 N90-17632
- Ground-simulation investigations of VTOL airworthiness criteria for terminal-area operations [NASA-TM-102810] p 757 N90-25141
- VERTICAL TAKEOFF AIRCRAFT**
- A full scale, VSTOL, ground environment test facility p 58 A90-12631
- Development of military helicopters p 181 A90-18488
- Thrust augmentation characteristics of jet reactions [AIAA PAPER 90-0033] p 161 A90-19641
- Dynamic simulation of cross-shafted propulsion system for tilt nacelle application [AIAA PAPER 90-0439] p 191 A90-19847
- Numerical investigation of airfoil/jet/fuselage-undersurface flowfields in ground effect [AIAA PAPER 90-0597] p 168 A90-19939
- Rotary-wing aeroelasticity with application to VTOL vehicles [AIAA PAPER 90-1115] p 392 A90-29387
- A status review of non-helicopter V/STOL aircraft development. I p 413 A90-30117
- What's best to tilt - The rotor or the wing? p 580 A90-36850
- Guaranteed cost control via optimal parametric LQ design p 693 A90-40810
- VTOL military research aircraft --- Book p 828 A90-46002
- Parametric synthesis of the decoupling filter in the manual control system of VTOL aircraft p 859 A90-46483
- Vertical Lift Aircraft Design Conference, San Francisco, CA, Jan. 17-19, 1990, Proceedings p 829 A90-46926
- An unmanned air vehicle concept with tipjet drive p 830 A90-46951
- Application of a design method for integrated control to a VTOL airplane in hover [AIAA PAPER 90-3334] p 862 A90-47594
- The Hiller X-18 experimental aircraft - Lessons learned [AIAA PAPER 90-3203] p 834 A90-48832
- The Bell X-22A V/STOL, Variable Stability Research Airplane - Lessons learned [AIAA PAPER 90-3207] p 834 A90-48835
- Ryan X-13 experimental aircraft - Lessons learned [AIAA PAPER 90-3236] p 834 A90-48846
- Propulsion systems for vertical flight aircraft [AIAA PAPER 90-3299] p 853 A90-48881
- The LTV XC-142 experimental aircraft lessons learned [AIAA PAPER 90-3204] p 838 A90-49104
- Powered-lift aircraft technology [NASA-SP-501] p 107 N90-12589
- Aircraft/airport compatibility: Some strategic, tactical, and operational issues [TT-8902] p 202 N90-13409
- A wind tunnel study of a sting-mounted circulation control wing [AD-A216248] p 319 N90-17577
- A study of the technology required for advanced vertical take-off aircraft [ETN-90-96786] p 650 N90-24268
- VERY HIGH FREQUENCIES**
- Equipment feasibility study: Very high frequency communication equipment (136-137 megahertz) [DOT/FAA/CT-TN89/72] p 775 N90-26210
- VERY LARGE SCALE INTEGRATION**
- Integrated circuits for avionics [AD-A217964] p 540 N90-20312
- VERY LOW BASE INTERFEROMETRY**
- Passive location accuracy via a general covariance error model --- long-baseline interferometry from airborne platforms p 914 A90-51060
- VERY LOW FREQUENCIES**
- Differential Omega/VLF as a world-wide navigation aid in the 21st century p 727 A90-45232
- VHF OMNIRANGE NAVIGATION**
- A bearing error in the VHF omnirange due to sea surface reflection p 402 A90-27875

- A surveillance 360 deg television orientation and ranging system as an aid to collision avoidance p 577 A90-36922
- VHSIC (CIRCUITS)**
- Two-level maintenance concept for advanced avionics architectures p 457 A90-28321
- VIBRATION**
- Analytical study of mistuning/friction/aerodynamics interaction in a bladed disk assembly [AD-A211139] p 55 N90-10893
- RAN (Royal Australian Navy) vibration analysis system operator's guide [AD-A212441] p 107 N90-12596
- Direct multivariable adaptive controller with application to wing flutter p 349 N90-17642
- Gear noise, vibration, and diagnostic studies at NASA Lewis Research Center [NASA-TM-102435] p 372 N90-18041
- Calculation of flight vibration levels of the AH-1G helicopter and correlation with existing flight vibration measurements [NASA-CR-181923] p 454 N90-18743
- Aeroelastic simulation of higher harmonic control p 592 N90-21768
- The Shock and Vibration Digest, volume 21, no. 3 p 609 N90-22064
- Computational and experimental investigations of rotating stall in compressor cascades p 588 N90-22565
- Adaptive control of a system with periodic dynamics: Application of an impulse response method to the helicopter vibration problem p 694 N90-23990
- An unsteady lifting surface method for single rotation propellers [NASA-CR-4302] p 719 N90-25940
- Asymptotic modal analysis and statistical energy analysis [NASA-CR-186732] p 782 N90-26634
- Studies in automatic speech recognition and its application in aerospace p 958 N90-28759
- Correlation of AH-1G airframe flight vibration data with a coupled rotor-fuselage analysis [NASA-CR-181974] p 959 N90-28865
- Vibration responses of two house structures during the Edwards Air Force Base phase of the national sonic boom program [NASA-CR-182089] p 966 N90-29169
- An enhanced integrated aerodynamic load/dynamic optimization procedure for helicopter rotor blades [NASA-CR-4326] p 924 N90-29383
- VIBRATION DAMPING**
- Computation of aerodynamic blade loads due to wake influence and aerodynamic damping of turbine and compressor cascades p 7 A90-11791
- Numerical Euler solution for the interaction between oscillating cascade and forced inlet unsteadiness p 8 A90-11792
- Unsteady aerodynamic characteristics of oscillating cascade with tip clearance p 8 A90-11793
- Flutter of turbine blades p 41 A90-11794
- Flutter of mistuned cascades with structural coupling p 42 A90-11802
- Design and application of a finite element package for modelling turbomachinery vibrations p 70 A90-13011
- Dynamic damping of vibrations in mechanical systems by means of elastic links with distributed parameters p 139 A90-15568
- Squeeze film damping for aircraft gas turbines p 113 A90-16009
- A synthetic research for aircraft active flutter suppression p 195 A90-16827
- Effect of the inertial nature of injection and temperature on the damping of body vibrations p 150 A90-17112
- Numerical approaches for solving parametric vibration problems in helicopter dynamics p 182 A90-18607
- Optimal placement of tuning masses for vibration reduction in helicopter rotor blades p 247 A90-23117
- Resonant stress determination of a turbine blade with modal damping as a function of rotor speed and vibrational amplitude [ASME PAPER 89-GT-27] p 340 A90-23765
- Minimum weight design of rotorcraft blades with multiple frequency and stress constraints p 335 A90-25304
- Active control of gust- and interference-induced vibration of tilt-rotor aircraft p 429 A90-28201
- Linear control issues in the higher harmonic control of helicopter vibrations p 430 A90-28225
- Approximation of frequency characteristics using identification with a complex mass matrix p 448 A90-29001
- Effects of spoiler surfaces on the aeroelastic behavior of a low-aspect-ratio rectangular wing [AIAA PAPER 90-0981] p 391 A90-29371
- Aeroservoelasticity [AIAA PAPER 90-1073] p 411 A90-29381

- Digital-flutter-suppression-system investigations for the active flexible wing wind-tunnel model [AIAA PAPER 90-1074] p 430 A90-29382
- Simulation of static and dynamic aeroelastic behavior of a flexible wing with multiple control surfaces [AIAA PAPER 90-1075] p 392 A90-29383
- Aeroelastic problems in turbomachines [AIAA PAPER 90-1157] p 393 A90-29393
- Multi-output implementation of a modified sparse time domain technique for rotor stability testing [AIAA PAPER 90-0946] p 412 A90-29405
- Practical problems - Airplanes - unsteady interaction aerodynamics, flutter characteristics, and active flight control p 394 A90-29885
- Gear vibration control with viscoelastic damping material in aeroengine p 451 A90-29911
- Active flutter suppression for a wing model p 433 A90-31283
- A comparison between theoretical and experimental results for a 3-D wing with damped pitching oscillations p 472 A90-33361
- Identification of time varying modal parameters p 536 A90-33375
- Structural optimization in view of aeroelastic constraints p 536 A90-33391
- Multi-surface control law synthesis and wind tunnel test verification of active flutter suppression for a transport-type wing p 517 A90-33401
- Practical techniques of modelling aeroelastic systems for active control applications p 545 A90-33402
- Flutter suppression control law synthesis for the active flexible wing model p 517 A90-33403
- Response characteristics of a two-dimensional wing subjected to turbulence near the flutter boundary p 519 A90-34082
- Rotary damping in aircraft motion due to jet propulsion system p 520 A90-34820
- National Transonic Facility model and model support vibration problems [AIAA PAPER 90-1416] p 596 A90-37953
- Parameter identification of aeroelastic modes of rotary wings from transient time histories p 642 A90-40166
- EH101 vibration control p 647 A90-42496
- Navier-Stokes predictions of pitch damping for finned projectiles using steady coning motion [AIAA PAPER 90-3088] p 795 A90-45902
- Vibration analysis of laced blades p 878 A90-46186
- Vibration of turbine blades damped by dry friction forces p 879 A90-46190
- Active vibration control for flexible rotor by optimal direct-output feedback control p 879 A90-46222
- Unbalance response of a Jeffcott rotor incorporating long squeeze film dampers p 880 A90-46237
- Vibration reduction on servo flap controlled rotor using HHC p 861 A90-46967
- Structure/control design synthesis of active flutter suppression system by goal programming [AIAA PAPER 90-3325] p 872 A90-47587
- STOL Maneuver Technology Demonstrator aeroservoelasticity [AIAA PAPER 90-3336] p 863 A90-47596
- Controller design for active vibration suppression of a helicopter [DFVLR-FB-89-20] p 120 N90-11760
- Active control system for gust load alleviation and structural damping p 259 N90-15056
- An experimental study of the aeroelastic behaviour of two parallel interfering circular cylinders p 455 N90-19609
- Digital-flutter-suppression-system investigations for the active flexible wing wind-tunnel model [NASA-TM-102618] p 520 N90-20093
- Internal rotor friction instability [NASA-CR-183942] p 543 N90-21395
- Development and application of a generalized dynamic wake theory for lifting rotors p 570 N90-21731
- Identification of XV-15 aeroelastic modes using frequency-domain methods [NASA-TM-101021] p 582 N90-21756
- Elements of active vibration control for rotating machinery [NASA-TM-102368] p 610 N90-22703
- Experimental evaluation of a tuned electromagnetic damper for vibration control of cryogenic turbopump rotors [NASA-TP-3005] p 665 N90-23403
- Adaptive control of a system with periodic dynamics: Application of an impulse response method to the helicopter vibration problem p 694 N90-23990
- Calculation of flight vibration levels of the AH-1G helicopter and correlation with existing flight vibration measurements [NASA-CR-182031] p 775 N90-25375
- Structural dynamics branch research and accomplishments [NASA-TM-102488] p 778 N90-26373

- Effects of spoiler surfaces on the aeroelastic behavior of a low-aspect-ratio rectangular wing [NASA-TM-102622] p 846 N90-27700
- Proceedings of damping '89. Volume 1: Pages AAB-1 through DCD-11 [AD-A223431] p 960 N90-29664
- VIBRATION EFFECTS**
- Correlation between vibration and computer operator response onboard a UH-1H helicopter p 737 A90-43727
- Response of a subsonic boundary layer to a pulsed oscillation of a localized region of the surface in the flow p 811 A90-48295
- The response of helicopter rotors to vibratory airflow [AD-A215678] p 337 N90-16756
- The Shock and Vibration Digest, volume 21, no. 3 p 609 N90-22064
- Correlation/validation of finite element code analyses for vibration assessment of avionics equipment [AD-A220393] p 654 N90-23398
- VIBRATION ISOLATORS**
- Unbalance response of a Jeffcott rotor incorporating long squeeze film dampers p 880 A90-46237
- Vibration dampers for cryogenic turbomachinery [AIAA PAPER 90-2740] p 882 A90-47228
- Viscoelastic tuned dampers for control of structural dynamics p 73 N90-10999
- Controller design for active vibration suppression of a helicopter [DFVLR-FB-89-20] p 120 N90-11760
- VIBRATION MEASUREMENT**
- Target classification by vibration sensing --- for helicopter detection p 1 A90-10170
- Turbomachinery blade vibration and dynamic stress measurements utilizing nonintrusive techniques p 41 A90-11558
- Aircraft engine vibration analysis p 46 A90-12568
- Experimental and analytical evaluation of dynamic load vibration of a 2240-KW (3000-hp) rotorcraft transmission p 127 A90-13750
- Noninterference blade-vibration measurement system for gas turbine engines p 132 A90-16372
- New systems for helicopter and aircraft vibration monitoring p 653 A90-42477
- Comparison among modal analyses of axial compressor blade using experimental data of different measuring systems p 878 A90-46038
- Calculation of flight vibration levels of the AH-1G helicopter and correlation with existing flight vibration measurements [NASA-CR-181923] p 454 N90-18743
- Calculation of flight vibration levels of the AH-1G helicopter and correlation with existing flight vibration measurements [NASA-CR-182031] p 775 N90-25375
- Plan, execute, and discuss vibration measurements and correlations to evaluate a NASTRAN finite element model of the AH-64 helicopter airframe [NASA-CR-181973] p 960 N90-28866
- Structural testing and analytical research of turbine components [AD-A223516] p 933 N90-29396
- Noncontact measurement of rotating blade vibrations [NAL-TR-1033] p 961 N90-29687
- VIBRATION MODE**
- Flutter of mistuned cascades with structural coupling p 42 A90-11802
- A synthetic research for aircraft active flutter suppression p 195 A90-16827
- Comparison of the analytical and experimental modes of a model airplane using finite element analysis and multi-reference testing p 207 A90-16986
- Flutter and aileron reversal safety factors p 345 A90-24164
- Stochastic flutter of a panel subjected to random in-plane forces. I - Two mode interaction p 444 A90-27992
- The effect of structural variations on the dynamic characteristics of helicopter rotor blades [AIAA PAPER 90-1161] p 450 A90-29396
- Stochastic flutter of a panel subjected to random in-plane forces. II - Two and three mode non-Gaussian solutions [AIAA PAPER 90-0986] p 451 A90-29399
- The prediction and measurement of thermoacoustic response of plate structures [AIAA PAPER 90-0988] p 451 A90-29400
- Ground vibration testing of aeroplanes with a sequence of single-point excitations - Simple and effective p 522 A90-33371
- Design flutter calculations on PC p 545 A90-33379
- Analysis of perturbed longitudinal dynamics of an aircraft taking into consideration the stationary aeroelastic effects and the atmospheric perturbances p 520 A90-34822
- Reduced-order aeroelastic models via dynamic residualization p 579 A90-35762
- Response of orthogonally stiffened cylindrical shell panels p 603 A90-36285

- Aeroelastic response characteristics of a rotor executing arbitrary harmonic blade pitch variations p 646 A90-42464
- Large-order modal analysis techniques in the Aeroelastic Design Optimization Program (ADOP) [SAE PAPER 892323] p 772 A90-45482
- An improved rotor/airframe coupling method for NASTRAN airframe vibration analysis p 831 A90-46962
- Experiences in NASTRAN airframe vibration prediction at Bell Helicopter Textron p 832 A90-46964
- Longitudinal stability analysis for deformable aircraft p 867 A90-48514
- Aeroelastic vibrations of turbomachine blades and propellers p 854 A90-49482
- Problems related to the acquisition, processing and utilization of the modal parameters measured in flight tests in order to obtain the full envelope for flutter [ETN-89-95210] p 103 N90-11735
- Experimental and theoretical investigation of optimal control methods with model reduction p 521 N90-21039
- An experimental study of tip shape effects on the flutter of aft-swept, flat-plate wings [NASA-TM-4180] p 582 N90-22555
- VIBRATION TESTS**
- Ground vibration test results of a JetStar airplane using impulsive sine excitation p 179 A90-16963
- A component modal synthesis technique for the lateral vibration analysis of aircraft engine systems p 179 A90-16983
- An automatic system for the programmed control of the parameters of the vibrational and thermal testing of the blades of gas turbine engines p 343 A90-24216
- Experimental transonic flutter characteristics of supersonic cruise configurations [AIAA PAPER 90-0979] p 390 A90-29369
- Ground vibration testing of aeroplanes with a sequence of single-point excitations - Simple and effective p 522 A90-33371
- A modal parameter identification technique and its application to large complex structures with multiple steady sinusoidal excitation p 602 A90-35670
- A captive store flight vibration simulation project p 672 A90-40476
- New systems for helicopter and aircraft vibration monitoring p 653 A90-42477
- EH101 vibration control p 647 A90-42496
- Vibration analysis of laced blades p 878 A90-46186
- Developments in ground vibration test and data analysis techniques for airframe structures p 832 A90-46970
- Investigation of difficult component effects on finite element model vibration prediction for the Bell AH-1G helicopter. Volume 1: Ground vibration test results [NASA-CR-181916-VOL-1] p 134 N90-12058
- Force determination sensitivities study for full-scale helicopter ground vibration testing [AD-A215983] p 349 N90-17643
- The 59th Shock and Vibration Symposium, volume 2 [AD-A214579] p 372 N90-18065
- Helicopter flight vibration of large transportation containers: A case for testing tailoring [DE90-007429] p 402 N90-19215
- Flutter investigations on a Transavia PL12/T-400 aircraft [AD-A219108] p 593 N90-22570
- On simplified analytical flutter clearance procedures for light aircraft [DLR-FB-89-56] p 672 N90-24276
- Plan, execute, and discuss vibration measurements and correlations to evaluate a NASTRAN finite element model of the AH-64 helicopter airframe [NASA-CR-181973] p 960 N90-28866
- VIBRATIONAL STRESS**
- Helicopter surveillance - A look at current and proposed future programs p 642 A90-39986
- VIBRATORY LOADS**
- The design of rotor blades taking into account the combined effects of vibratory and thermal loads p 40 A90-11553
- Response and hub loads sensitivity analysis of a helicopter rotor p 181 A90-18145
- Non-conservative stability of a cracked thick rotating blade p 606 A90-38544
- Rotating system load monitoring using minimum fixed system instrumentation p 651 A90-39982
- Performance of an optimized rotor blade at off-design flight conditions p 830 A90-46946
- V-22 MSC/NASTRAN airframe vibration analysis and correlation p 832 A90-46969
- The response of helicopter rotors to vibratory airload p 832 A90-46971
- Prediction and alleviation of V-22 rotor dynamic loads p 833 A90-46974
- Free wake analysis of rotor configurations for reduced vibratory airloads p 833 A90-46975
- Estimation of the safety factor of turbine blades under thermal cycling and vibration loading p 958 A90-52356
- Calculation of flight vibration levels of the AH-1G helicopter and correlation with existing flight vibration measurements [NASA-CR-181923] p 454 N90-18743
- VIDEO DISKS**
- Interactive Videodisc training in aerospace applications [AIAA PAPER 89-3029] p 73 A90-10529
- VIDEO EQUIPMENT**
- Applications for a small format airborne recorder p 847 A90-48620
- VIDEO LANDMARK ACQUISITION AND TRACKING**
- An image analysis method for vehicle stabilization p 668 A90-40914
- Position finding and ground target direction finding by an aircraft with a gimbaled video camera [DLR-FB-89-62] p 825 N90-27673
- VISCOELASTIC DAMPING**
- Design, evaluation and proof-of-concept flights of a main rotor interblade viscoelastic damping system p 406 A90-28152
- Gear vibration control with viscoelastic damping material in aeroengine p 451 A90-29911
- Dynamic analysis of airport pavement p 593 A90-36418
- Viscoelastic tuned dampers for control of structural dynamics p 73 N90-10999
- VISCOELASTICITY**
- Viscoelastic relaxation in bolted thermoplastic composite joints p 945 A90-50158
- Compressive viscoelastic effects (creep) of a unidirectional glass/epoxy composite material p 946 A90-50170
- VISCOPLASTICITY**
- Elastic-viscoplastic finite-element program for modeling tire/soil interaction p 401 A90-31285
- Three dimensional turbine blade analysis in thermo-viscoplasticity p 540 A90-34324
- NASA-UVA light aerospace alloy and structures technology program [NASA-CR-182607] p 601 N90-22651
- Finite element analysis of structural components using viscoplastic models with application to a cowl lip problem [NASA-CR-185189] p 690 N90-23769
- VISCOSITY**
- Numerical simulation of turbomachinery flows with a simple model of viscous effects - Comparison with experimental data [ONERA, TP NO. 1989-122] p 10 A90-12510
- Calculation of nonseparated transonic flow past swept wings with allowance for viscosity p 294 A90-24079
- Numerical simulation of leading-edge vortex rollup and bursting p 20 N90-10831
- An improvement of convection fidelity in Euler calculations p 315 N90-16709
- Measurement of lift development on rapidly-accelerated wings p 480 N90-20956
- VISCOUS DAMPING**
- Using transonic small disturbance theory for predicting the aeroelastic stability of a flexible wind-tunnel model [AIAA PAPER 90-1033] p 391 A90-29377
- VISCOUS DRAG**
- Supersonic aircraft drag reduction [AIAA PAPER 90-1596] p 567 A90-38729
- Some aerodynamic characteristics of the scissor wing configuration [SAE PAPER 892202] p 713 A90-45423
- Hypersonic waverider configurations for trans-atmospheric vehicles [AD-A217925] p 498 N90-20074
- VISCOUS FLOW**
- Unsteady viscous calculation of cascade flows with leading-edge-induced separation [ONERA, TP NO. 1989-116] p 3 A90-11148
- Progress towards the development of an inviscid-viscous interaction method for unsteady flows in turbomachinery cascades p 8 A90-11806
- Calculation of axisymmetric flows in turbomachines, through an explicit time-splitting method p 14 A90-12622
- A solution adaptive finite element method applied to two-dimensional unsteady viscous compressible cascade flow p 15 A90-12624
- PCISM method for two dimensional compressible viscous cascade flow calculation p 15 A90-12625
- Computation of the thin-layer Navier-Stokes equations for a 2D flow p 87 A90-16332
- VISTRAFS - A simulation method for strongly-interacting viscous transonic flow p 144 A90-16756
- Theoretical prediction of high Reynolds number viscid/inviscid interaction phenomena in cascades p 145 A90-16759
- A viscous package for attached and separated flows on swept and tapered wings p 146 A90-16771
- Experimental and computational studies of dynamic stall p 147 A90-16780
- Calculation of flow over airfoil with slat and flap p 149 A90-16797
- Numerical studies of incompressible flow around delta and double-delta wings p 150 A90-16845
- Two-dimensional transonic flow field analysis with different turbulence models p 150 A90-16846
- Perturbations of a three-dimensional boundary layer produced by body irregularities p 150 A90-17107
- Computation of viscous transonic flow over porous airfoils p 153 A90-17864
- Boundary integral equations method for compressible Navier-Stokes equations p 209 A90-18262
- Numerical modeling of a viscous separated flow in the near wake p 159 A90-19236
- Application of a rotary-wing viscous flow solver on a massively parallel computer [AIAA PAPER 90-0334] p 164 A90-19802
- Viscous supersonic flow computations over a delta-rectangular wing with slanting surfaces [AIAA PAPER 90-0419] p 166 A90-19841
- A numerical study of general viscous flows around multi-element airfoils [AIAA PAPER 90-0572] p 167 A90-19922
- Viscous oscillating cascade aerodynamics and flutter by a locally analytical method [AIAA PAPER 90-0579] p 168 A90-19929
- Fortified LEWICE with viscous effects --- Lewis Ice Accretion Prediction Code [AIAA PAPER 90-0754] p 176 A90-20009
- Transonic integro-differential and integral equations with artificial viscosity p 223 A90-20988
- Development of the MZM numerical method for 3D boundary layer with interaction on complex configurations --- Multi-Zonal Marching [ONERA, TP NO. 1989-174] p 223 A90-21036
- On the computations of hypersonic viscous flows p 225 A90-21170
- A numerical method for three-dimensional viscous flows [AIAA PAPER 90-0236] p 228 A90-22186
- Applications of an adaptive unstructured solution algorithm to the analysis of high speed flows [AIAA PAPER 90-0395] p 229 A90-22213
- Comparison of thin and full viscous shock layer models in the problem of supersonic flow of a viscous gas past blunt cones p 231 A90-22396
- Analysis of transonic integral equations. I - Artificial viscosity p 232 A90-23124
- Incompressible viscous flow about aircraft configurations p 233 A90-23290
- Viscous flow calculations in turbomachinery channels [ASME PAPER 89-GT-5] p 287 A90-23752
- Accelerated computation of viscous, steady incompressible flows [ASME PAPER 89-GT-45] p 288 A90-23771
- Viscous flow in a controlled diffusion compressor cascade with increasing incidence [ASME PAPER 89-GT-131] p 291 A90-23829
- Simulation of three-dimensional viscous flow within a multistage turbine [ASME PAPER 89-GT-152] p 292 A90-23841
- Verification of an impeller design by laser measurements and 3D-viscous flow calculations [ASME PAPER 89-GT-159] p 292 A90-23847
- Stability analysis and numerical experiments for viscous-inviscid interaction in transonic flow p 293 A90-24009
- Interaction between a vibrating compression shock and a boundary layer p 298 A90-24143
- Advantages of flow variables in thin viscous shock layer problems p 364 A90-24145
- Viscous corrections on wings in incompressible flow p 301 A90-25200
- Comparison of inviscid and viscous separated flows p 302 A90-25277
- Navier-Stokes simulations around a high-speed propeller p 305 A90-25797
- Computation of 2D Navier-Stokes equations p 367 A90-25801
- Turbulence models for 3D transonic viscous flows. II p 306 A90-25820
- Supersonic viscous shear layers p 367 A90-25873
- Solution-adaptive grids for transonic flows p 309 A90-26508
- Adaptive mesh generation for viscous flows using Delaunay triangulation p 310 A90-26531
- Analysis of unsteady rotor-stator interactions using a viscous explicit method [AIAA PAPER 90-0342] p 313 A90-26937
- Unsteady hypersonic viscous flow in impulse facilities [AIAA PAPER 90-0421] p 313 A90-26947

Comparison of 3-D viscous flow computations of Mach 5 inlet with experimental data [AIAA PAPER 90-0600] p 314 A90-26970

Viscous computations using a direct solver p 315 A90-27133

Combined effect of viscosity and bluntness on the aerodynamic efficiency of a delta wing in flow with a high supersonic velocity p 388 A90-29184

A calculation of the aerodynamic lift acting on cascade blades in a steady, viscous flow at high Reynolds number p 469 A90-32425

Multi-element airfoils in viscous flow p 469 A90-32451

Calculation of internal flows using a single-pass, parabolized Navier-Stokes analysis p 469 A90-32458

High-resolution shock-capturing schemes for inviscid and viscous hypersonic flows p 476 A90-34545

A numerical method for calculating supersonic flows of a viscous gas p 476 A90-34672

Velocity and turbulence characteristics of isothermal lobed mixer flows --- in turbofan jet engines p 584 A90-35230

Unsteady inviscid and viscous computations for vortex-dominated flows p 553 A90-35752

A method for solving three-dimensional viscous incompressible flows over slender bodies p 558 A90-37890

Wall interference correction for three-dimensional transonic flows [AIAA PAPER 90-1408] p 558 A90-37947

Experience in the use of a viscous simulation methodology for tests in transonic tunnels [AIAA PAPER 90-1414] p 559 A90-37951

Newton solution of coupled viscous/inviscid multielement airfoil flows [AIAA PAPER 90-1470] p 562 A90-38627

A primitive variable, strongly implicit calculation procedure for viscous flows at all speeds [AIAA PAPER 90-1521] p 563 A90-38666

A locally implicit scheme for 3-D compressible viscous flows [AIAA PAPER 90-1525] p 563 A90-38670

Interactive airfoil calculations with higher-order viscous-flow equations [AIAA PAPER 90-1533] p 564 A90-38678

Numerical prediction of transonic viscous flows around airfoils through an Euler/boundary layer interaction method [AIAA PAPER 90-1537] p 564 A90-38681

Navier-Stokes computations of vortical flows [AIAA PAPER 90-1628] p 568 A90-38757

Numerical solution of the problem of supersonic flow of a viscous gas past a concave conical wing p 619 A90-39465

Viscous flow around a propeller-shaft configuration with infinite-pitch rectangular blades p 683 A90-40938

Viscous-inviscid interaction method for calculating the flow in compressor cascade blade passages and wake with separation [AIAA PAPER 90-2125] p 624 A90-42032

Quasi-3D viscous flow computations in subsonic and transonic turbomachinery bladings [AIAA PAPER 90-2126] p 625 A90-42033

Inviscid and viscous flows in transonic and supersonic cascades using an implicit upwind relaxation algorithm [AIAA PAPER 90-2128] p 625 A90-42034

Viscous flow analysis for advanced inlet particle separators [AIAA PAPER 90-2136] p 661 A90-42038

Calculation of viscous-inviscid strong interaction for transonic flows over airfoils p 627 A90-42364

Computation of viscous aerodynamic characteristics of 2-D airfoils for helicopter applications p 631 A90-42440

Development of a robust calculation method for transonic viscous blade-to-blade flows p 703 A90-42671

Application of 3-D viscous code in the design of a high performance compressor [AIAA PAPER 90-1914] p 740 A90-42694

Numerical simulation of hypersonic viscous continuum flow p 707 A90-44407

Numerical study of heat transfer for unsteady viscous supersonic blunt body flows p 707 A90-44432

Fully vectorized implicit scheme for 2-D viscous hypersonic flow using adaptive finite element methods p 708 A90-44439

Zonal Navier-Stokes methodology for flow simulation about a complete aircraft p 709 A90-44727

Numerical simulation of the viscous flow around a simplified F/A-18 at high angles of attack [AIAA PAPER 90-2999] p 787 A90-45849

Simulation of time-dependent viscous flows using central and upwind-biased finite-difference techniques [AIAA PAPER 90-3012] p 790 A90-45864

Numerical investigation of laminar separated viscous trailing-edge flow using triple-deck theory [AIAA PAPER 90-3046] p 792 A90-45883

XFOIL - An analysis and design system for low Reynolds number airfoils p 799 A90-46359

Application of the inverse method of three-dimensional boundary layer analysis to the problem of flow past a wing with allowance for the effect of viscosity p 804 A90-46548

Viscous flow characteristics over a blunt cone at hypersonic Mach numbers by using a PNS code p 810 A90-48085

A comprehensive analysis of the viscous incompressible flow in quasi-three-dimensional airfoil cascades p 905 A90-51028

Numerical simulation of nonreactive flows in turbomachines p 908 A90-52621

An investigation of characteristics of transonic and viscous flows for turbine cascades p 909 A90-52779

Multigrid calculations of 3-D turbulent viscous flows [NASA-CR-185154] p 143 N90-13323

Hypersonic aerodynamics p 171 N90-13335

Application of a two-dimensional unsteady viscous analysis code to a supersonic throughflow fan stage [NASA-TM-4141] p 192 N90-13387

Convergence speeding up in the calculation of the viscous flow about an airfoil p 279 N90-16194

An experimental investigation of viscous aspects of propeller blade flow p 315 N90-16711

Viscous three-dimensional analyses for nozzles for hypersonic propulsion [NASA-CR-185197] p 344 N90-17635

Some Navier-Stokes calculations for the CAST-10 airfoil p 320 N90-17651

Unsteady viscous calculation method for cascades with leading edge induced separation p 426 N90-18408

Computation of hypersonic unsteady viscous flow over a cylinder p 397 N90-19194

Three-dimensional viscous rotor flow calculations using a viscous-inviscid interaction approach [NASA-TM-102235] p 399 N90-19204

Analysis of flow-, thermal-, and structural-interaction of hypersonic structures subjected to severe aerodynamic heating [AD-A217882] p 478 N90-20053

Comparison of 3-D viscous flow computations of Mach 5 inlet with experimental data [NASA-TM-102518] p 510 N90-20090

DURIP optical equipment for high-speed viscous-inviscid interaction research [AD-A217772] p 540 N90-20345

Relating flow between counter-rotating propellers to aerodynamic interaction noise p 479 N90-20944

Comparison of C- and O-grid generation methods using a NACA 0012 airfoil [AD-A216375] p 479 N90-20948

Effects of nose bluntness and shock-shock interactions on blunt bodies in viscous hypersonic flows [NASA-CR-186451] p 479 N90-20950

Computation of viscous flow around a propeller-shaft configuration with infinite-pitch rectangular blades p 481 N90-20958

Centrifugal impeller geometry and its influence on secondary flows p 513 N90-21020

Generation and decay of secondary flows and their impact on aerodynamic performance of modern turbomachinery components p 514 N90-21023

European research on viscous flow (EuroVisc) [NLR-TP-89077-U] p 609 N90-22014

Extension of a three-dimensional viscous wing flow analysis user's manual: VISTA 3-D code [NASA-CR-182024] p 574 N90-22538

Extension of a three-dimensional viscous wing flow analysis [NASA-CR-182023] p 631 N90-23348

An interactive boundary-layer method for unsteady airfoil flows. Part 1: Quasi-steady-state model [AD-A221220] p 634 N90-24250

Integral-equation methods in steady and unsteady subsonic, transonic and supersonic aerodynamics for interdisciplinary design [NASA-TM-102677] p 716 N90-25110

Computation of viscous aerodynamic characteristics of 2-D airfoils for helicopter applications [NLR-MP-88052-U] p 720 N90-25951

Numerical analysis of three-dimensional particle-laden flow equations [IAR-90-2] p 775 N90-26268

Do inviscid vortex sheets roll-up [PD-CF-9010] p 909 N90-28491

Investigation of ATP blades, part 2. Validation of two-dimensional viscous flow simulation codes around thin airfoils [NAL-TR-1046] p 912 N90-29326

VISCOUS FLUIDS

The method of matched integral representations in viscous fluid dynamics p 129 A90-14565

An approximate method for calculating flow past a wing profile with allowance for viscosity p 234 A90-23422

VISIBILITY

Variability characteristics of the meteorological optical range field in an optically inhomogeneous atmosphere p 962 A90-50784

The assessment of visibility from automatic contrast measurements p 242 N90-15061

Modified touchdown zone lighting [DOT/FAA/CT-TN89/70] p 526 N90-21042

Analysis of distributions of Visual Meteorological Conditions (VMC) heliport data [DOT/FAA/CT-TN89/67] p 544 N90-21508

Taxiway sign effectiveness under reduced visibility conditions [DOT/FAA/CT-TN90/20] p 761 N90-25150

VISION

Visualization of three dimensional data p 782 N90-25553

VISUAL ACUITY

A new method for measuring the transmissivity of aircraft transparencies [AD-A216953] p 464 N90-19842

VISUAL AIDS

Improved lighting of taxiway/taxiway intersections for Instrument Flight Rules (IFR) operations [DOT/FAA/CT-TN89/64] p 243 N90-15089

VISUAL FLIGHT

Modeling of air-to-air visual acquisition p 282 A90-21385

Heliport visual approach surface high temperature and high altitude tests [DOT/FAA/CT-TN89/34] p 825 N90-27675

VISUAL FLIGHT RULES

Visual information for simulated landing approaches p 347 A90-26189

VISUAL PERCEPTION

Visual servoing for autonomous aircraft refueling [AD-A216042] p 414 N90-18386

VISUAL PHOTOMETRY

Visualization of corona discharges p 819 A90-49839

VISUAL STIMULI

Terrain visual cue analysis for simulating low-level flight: A multidimensional scaling approach [AD-A223564] p 938 N90-29407

VISUAL TASKS

Stereopsis as a visual cue in flight simulation p 870 A90-48960

VOCODERS

Assessment of voice coders for ATC/pilot voice communications via satellite digital communication channels [CAA-PAPER-89004] p 135 N90-12807

VOICE COMMUNICATION

The US air traffic control system architecture p 330 A90-25561

ATC ground communications system optimization techniques p 330 A90-25568

Automatic speech recognition in air-ground data link p 690 N90-25037

Equipment feasibility study: Very high frequency communication equipment (136-137 megahertz) [DOT/FAA/CT-TN89/72] p 775 N90-26210

Comparison of speech intelligibility in cockpit noise using SPH-4 flight helmet with and without active noise reduction [NASA-CR-177564] p 915 N90-28510

VOICE CONTROL

The benefits and costs of automation in advanced helicopters - An empirical study p 348 A90-26258

Toward the panoramic cockpit, and 3-D cockpit displays p 419 A90-30682

VOLATILITY

Improved Thermo-Oxidative-Deposition screening tests for turbine lubricants [AD-A217795] p 533 N90-21188

VOLTERRA EQUATIONS

A Volterra kernel identification scheme applied to aerodynamic reactions [AIAA PAPER 90-2803] p 712 A90-45178

VOLUMETRIC ANALYSIS

Volumetric analysis by spontaneous Raman diffusion in a supersonic wind tunnel [ISL-R-109/88] p 95 N90-12564

VORTEX ADVISORY SYSTEM

The wake vortex problem revisited p 817 A90-46395

VORTEX ALLEVATION

Winglets on rotor blades in forward flight - A theoretical and experimental investigation p 303 A90-25422

SUBJECT INDEX

- Vortex control for tail buffet alleviation on a twin-tail fighter configuration
[SAE PAPER 892221] p 756 A90-45438
- The wake vortex problem revisited p 817 A90-46395
- Effective methods of controlling a junction vortex system in an incompressible, three-dimensional, turbulent flow p 571 N90-21732

VORTEX AVOIDANCE

- Preliminary flight test investigation of an airborne wake vortex detection concept
[AIAA PAPER 90-1282] p 495 A90-33903

VORTEX BREAKDOWN

- The water tunnel test of delaying vortex breakdown over a delta wing using supplements p 2 A90-10346
- A study of ground vortex p 158 A90-18590
- An investigation on the coiled-up of vortices on a double delta wing
[AIAA PAPER 90-0382] p 165 A90-19825
- Aerodynamic control of NASP-type vehicles through vortex manipulation
[AIAA PAPER 90-0594] p 203 A90-19938
- Vortical flows over delta wings and numerical prediction of vortex breakdown
[AIAA PAPER 90-0102] p 227 A90-22166
- An investigation of asymmetric vortical flows over delta wings with tangential leading-edge blowing at high angles of attack
[AIAA PAPER 90-0103] p 227 A90-22167
- Study of vortex breakdown of F-106B by Euler code p 233 A90-23289
- Nonsymmetric vortex breakdown and aerodynamic hysteresis in flow past a low-aspect-ratio wing/fuselage configuration p 294 A90-24076
- Numerical simulation of vortex breakdown via 3-D Euler equations
[ONERA, TP NO. 1989-211] p 303 A90-25344
- Effects of a contoured apex on vortex breakdown p 308 A90-26141
- Numerical simulation of vortex breakdown by solving the Euler equations for an incompressible fluid p 476 A90-34323
- Connection between leading-edge sweep, vortex lift, and vortex strength for delta wings p 554 A90-35770
- Leading-edge vortices due to low Reynolds number flow past a pitching delta wing p 555 A90-36258
- Transient response of leading-edge vortices to localized suction p 556 A90-36279
- A computational study of the taxonomy of vortex breakdown
[AIAA PAPER 90-1624] p 568 A90-38753
- Numerical simulation of the effects of variation of angle of attack and sweep angle on vortex breakdown over delta wings
[AIAA PAPER 90-3000] p 788 A90-45850
- 3-D analysis of laser measurements of vortex bursting on a chined forebody fighter configuration
[AIAA PAPER 90-3020] p 793 A90-45887
- Bursting in separating flow and in transition p 800 A90-46366
- Interference between a vortex filament and shock waves in free flow and in nonisobaric jets p 804 A90-46550
- An experimental study of the combined effect of longitudinal riblets and vortex breakers on turbulent friction p 805 A90-46565
- Numerical simulation of leading-edge vortex rollup and bursting p 20 N90-10831
- A smoke generator system for aerodynamic flight research
[NASA-TM-4137] p 183 N90-13372
- Surface pressure distributions on a delta wing undergoing large amplitude pitching oscillations
[NASA-CR-186326] p 317 N90-17558
- Leading edge vortex dynamics on a pitching delta wing
[NASA-CR-186327] p 398 N90-19198
- The interaction of a supersonic streamwise vortex and a normal shock wave p 633 N90-24241
- Investigation of the vortex flow over a sharp-edged delta wing in the transonic speed regime
[LR-594] p 717 N90-25115
- Control of submersible vortex flows
[NASA-TM-102693] p 909 N90-28493
- Experimental investigations on the stability and vorticity of the vortex breakdown phenomenon above delta wings, measured by the ultrasonic laser method
[ESA-TT-1079] p 910 N90-28498
- In-flight flow visualization with pressure measurements at low speeds on the NASA F-18 high alpha research vehicle
[NASA-TM-101726] p 910 N90-28505
- VORTEX FILAMENTS**
- A numerical method for three-dimensional viscous flows
[AIAA PAPER 90-0236] p 228 A90-22186

- Efficient free wake calculations using Analytical/Numerical Matching and far-field linearization p 384 A90-28171
- Measurement of the interaction between a rotor tip vortex and a cylinder p 555 A90-36255
- Trajectories of vortex lines beneath a free surface or above a plane p 716 A90-45740

VORTEX FLAPS

- The vortex flap F-106B, overcoming safety and data problems in flight testing
[AIAA PAPER 90-1280] p 496 A90-34725

VORTEX GENERATORS

- Structure of velocity and temperature fields in laminar channel flows with longitudinal vortex generators p 273 A90-23207
- Nonstationary liquid flow of a fluid in the core of a conical vortex sheet p 296 A90-24113
- Aerodynamic control of aircraft by forebody vortex manipulation
[AIAA PAPER 90-1827] p 301 A90-25167
- Damping of the inlet vortex in a turbojet engine p 301 A90-25185
- Boundary layer turbulence structure in the presence of embedded streamwise vortex pairs p 552 A90-35193
- Vortex generator jets - Means for flow separation control p 555 A90-36257
- Investigation of several passive and active methods for turbulent flow separation control
[AIAA PAPER 90-1598] p 607 A90-38730
- A device for introducing helical perturbations into a trailing line vortex
[AIAA PAPER 90-1627] p 568 A90-38756
- A numerical study of longitudinal vortex interaction with a boundary layer
[AIAA PAPER 90-1630] p 568 A90-38759
- Navier-Stokes computations of three-dimensional laminar flows with buoyancy in a channel with wing-type vortex generators p 772 A90-45728
- Trajectories of vortex lines beneath a free surface or above a plane p 716 A90-45740
- Improvements in the formulations and numerical solution of the Euler problem for swept wings
[RAE-TM-AERO-2139] p 95 N90-12562
- An experimental study of the effect of streamwise vortices on unsteady turbulent boundary-layer separation p 369 N90-17045
- Ground evaluation of seeding an in-flight wingtip vortex using infrared imaging flow visualization technique p 635 N90-25035
- Effect of vortex generators on the aerodynamic wing characteristics and body of revolution
[AD-A222813] p 721 N90-25955
- Further studies of turbulence structure resulting from interactions between embedded vortices and wall jets at high blowing ratios
[AD-A223296] p 960 N90-29593
- VORTEX RINGS**
- Multiple vortex ring model of the DFW microburst p 280 A90-23286
- Total temperature separation in jets
[AIAA PAPER 90-1621] p 607 A90-38750
- Analysis of severe atmospheric disturbances from airline flight records p 280 N90-15045
- VORTEX SHEDDING**
- Nonstationary liquid flow of a fluid in the core of a conical vortex sheet p 296 A90-24113
- Topological study of three-dimensional vortex interactions p 367 A90-25885
- Basic numerical methods --- of unsteady and transonic flow p 394 A90-29886
- The numerical simulation of the low speed aerodynamic characteristics of a set of close-coupled canard configurations p 396 A90-31485
- Vortex shedding over delta wings p 470 A90-32479
- The influence of boundary layer state on vortex shedding from flat plates and turbine cascades
[ASME PAPER 89-GT-296] p 474 A90-33560
- Flow field measurements near a fighter model at high angles of attack
[AIAA PAPER 90-1431] p 559 A90-37968
- Experimental investigation of coaxial jet flow with swirl along a centerbody
[AIAA PAPER 90-1622] p 567 A90-38751
- The instability of two-dimensional laminar separation p 800 A90-46365
- Flow visualization of the effect of pitch rate on the vortex development on the scale model of a F-18 fighter aircraft
[AD-A214244] p 236 N90-15080
- Modeling the wake as a continuous vortex sheet in a potential-flow solution using vortex panels
[AD-A216220] p 371 N90-18016
- Secondary flows and Reynolds stress distributions downstream of a turbine cascade at different expansion ratios p 512 N90-21015

VORTICES

- Flow visualization of dynamic stall on an oscillating airfoil
[AD-A222202] p 815 N90-26797
- Prediction of subsonic vortex shedding from forebodies with chines
[NASA-CR-4323] p 909 N90-28494
- Numerical simulations of flowfields in a central-dump ramjet combustor. 3: Effects of chemistry
[AD-A224145] p 933 N90-28573
- VORTEX SHEETS**
- Nonstationary liquid flow of a fluid in the core of a conical vortex sheet p 296 A90-24113
- Numerical simulation of separated flows around a wing section by a discrete vortex method p 307 A90-25846
- Calculation of flow characteristics in the core of a vortex sheet p 386 A90-28981
- Vortex method modelling the unsteady motion of a thick airfoil p 396 A90-31489
- Calculations of propeller/airframe interference effects using the potential/multienergy vortex method p 490 A90-32452
- Application of vortex embedding to aircraft flows
[AIAA PAPER 90-1626] p 568 A90-38755
- The three-dimensional vortex sheet structure on delta wings p 19 N90-10367
- Numerical simulation of leading-edge vortex rollup and bursting p 20 N90-10831
- An experimental investigation of the interaction between a model rotor and airframe in forward flight p 185 N90-14219
- A nonlinear vortex-lattice method for the calculation of interference effects between free vortex sheets and wings p 277 N90-16183
- An experimental investigation of viscous aspects of propeller blade flow p 315 N90-16711
- Modeling the wake as a continuous vortex sheet in a potential-flow solution using vortex panels
[AD-A216220] p 371 N90-18016
- Experiments with unsteady, free surface, three-dimensional vortices in a thermally stable, stratified fluid
[AD-A222088] p 815 N90-26796
- Do inviscid vortex sheets roll-up
[PD-CF-9010] p 909 N90-28491
- VORTEX STREETS**
- The influence of the wake structure on the dynamic blade load p 6 A90-11785
- The interaction between a counter-rotating vortex pair in vertical ascent and a free surface p 151 A90-17580
- Time-resolved measurements of total temperature and pressure in the vortex street behind a cylinder p 557 A90-36522
- The organized nature of a turbulent trailing vortex
[AIAA PAPER 90-1625] p 568 A90-38754
- Vorticity distribution of vortex street in the wake of a circular cylinder p 623 A90-41751
- The formation of vortex streets in supersonic flows p 907 A90-51539
- VORTICES**
- Vortex-flow compressors --- Russian book p 69 A90-12479
- Hot wire measurements in the wake of an oscillating airfoil p 15 A90-12635
- Experimental and numerical investigation of vortex flow over a sideslipping delta wing p 17 A90-13016
- Accumulated span loadings of an arrow wing having vortex flow p 17 A90-13025
- Goertler vortices in supersonic and hypersonic boundary layers p 83 A90-14091
- Experimental study of 2D/3D interactions between a vortical flow and a lifting surface p 86 A90-15849
- Numerical simulation of separated and vortical flows on bodies at large angles of attack p 146 A90-16772
- Experiments in swept-wing transition p 149 A90-16794
- Jets, vortices, and turbulence p 207 A90-17175
- Further analysis of wing rock generated by forebody vortices p 153 A90-17868
- Rotor hover performance prediction using a free-wake, computational fluid dynamics method p 153 A90-17869
- High-resolution upwind scheme for vortical-flow simulations p 153 A90-17872
- Navier-Stokes computations of lee-side flows over delta wings p 153 A90-17978
- Application of the finite element method to the problem of rotational flow around wings p 156 A90-18305
- Wake behaviour of a large deflection turbine rotor linear cascade p 157 A90-18481
- The aerodynamic behaviours of vortices for slender-wing p 158 A90-18623
- On the Goertler vortex instability mechanism at hypersonic speeds p 158 A90-18886
- Estimate of loads during wing-vortex interactions by Munk's transverse-flow method p 159 A90-18391

Unsteady aerodynamic forces on rolling delta wings at high angle of attack p 159 A90-19426
 Effect of ground on wake roll-up behind a lifting surface p 160 A90-19436
 Experimental investigation of a new device to control the asymmetric flowfield on forebodies at large angles of attack
 [AIAA PAPER 90-0069] p 161 A90-19665
 Investigation of high angle of attack vortical flows over delta wings
 [AIAA PAPER 90-0101] p 162 A90-19682
 Experimental and numerical investigation of the flow in the core of a leading edge vortex
 [AIAA PAPER 90-0384] p 165 A90-19826
 Propeller tip vortex interactions
 [AIAA PAPER 90-0437] p 166 A90-19846
 The sonic eddy - A model for compressible turbulence
 [AIAA PAPER 90-0495] p 167 A90-19876
 An experimental investigation of sweep-angle influence on delta-wing flows
 [AIAA PAPER 90-0383] p 228 A90-22210
 Convergence of the method of discrete vortices when applied to steady-state aerodynamics problems
 p 231 A90-22816
 Navier-Stokes computations of vortical flows over low-aspect-ratio wings p 232 A90-23103
 Vortex dynamics on a pitching delta wing
 p 233 A90-23281
 Study of various factors affecting secondary loss vortices downstream a straight turbine cascade
 [ASME PAPER 89-GT-12] p 287 A90-23757
 Inlet skew and the growth of secondary losses and vorticity in a turbine cascade
 [ASME PAPER 89-GT-65] p 290 A90-23788
 Effects of an embedded vortex on injectant from a single film-cooling hole in a turbulent boundary layer
 [ASME PAPER 89-GT-189] p 362 A90-23867
 The effect of uniform spanwise vorticity on the two-dimensional flow through cascades
 p 293 A90-23996
 Unsteady transonic flow around double-wedge profiles
 p 299 A90-24354
 Vortex formation around an oscillating and translating airfoil at large incidences p 303 A90-25588
 Flow-calculation over a delta-wing using the thin-layer Navier-Stokes equations p 304 A90-25773
 Vortex dynamics of delta wings p 307 A90-26067
 The flowfields of bursting vortices over moderately swept delta wings
 [AIAA PAPER 90-0599] p 314 A90-26969
 Numerical solutions of the linearized Euler equations for unsteady vortical flows around lifting airfoils
 p 394 A90-30264
 Simple marching-vortex model for two-dimensional unsteady aerodynamics p 395 A90-31288
 Control point selection in the discrete vortex method
 p 470 A90-32567
 Modification of large eddies in turbulent boundary layers p 474 A90-33514
 Numerical simulation of separated flows around a wing section at pitching motion by a discrete vortex method
 p 475 A90-33753
 Preliminary flight test investigation of an airborne wake vortex detection concept
 [AIAA PAPER 90-1282] p 495 A90-33903
 Flow quality in the T2 cryogenic wind-tunnel - Problems and solutions p 524 A90-34240
 Capability of current supercomputers for the computational fluid dynamics p 546 A90-34382
 On an extension of the Kutta-Joukowski theorem to the supersonic regime p 477 A90-34819
 Effect of vertical-ejector jet on the aerodynamics of delta wings p 553 A90-35755
 Recent advancement in helicopter rotor wake study
 p 556 A90-36413
 Review of vortical flow utilization
 [AIAA PAPER 90-1429] p 605 A90-37966
 Pneumatic vortex flow control on a 55-degree cropped delta wing with chined forebody
 [AIAA PAPER 90-1430] p 559 A90-37967
 Effects of streamwise vorticity injection on turbulent mixing layer development
 [AIAA PAPER 90-1459] p 561 A90-38616
 A device for introducing helical perturbations into a trailing line vortex
 [AIAA PAPER 90-1627] p 568 A90-38756
 Proportional control of asymmetric forebody vortices with the unsteady bleed technique
 [AIAA PAPER 90-1629] p 591 A90-38758
 Measurement of crossflow vortices, attachment-line flow, and transition using microthin hot films
 [AIAA PAPER 90-1636] p 607 A90-38765
 A computational study of the impingement region of an unsteady subsonic jet
 [AIAA PAPER 90-1657] p 570 A90-38784

Vortex theory for the screw propeller with a hub p 620 A90-39538
 Coherent vortex structures in the wake of a sphere and a circular disk at rest and under forced vibrations
 p 623 A90-40749
 A visualization study of the interaction of a free vortex with the wake behind an airfoil p 623 A90-41119
 The application of concentric vortex simulation to calculating the aerodynamic characteristics of bodies of revolution at high angles of attack p 627 A90-42357
 Visualization of the turbulent trailing vortex behind a finite wing in steady and unsteady flows p 712 A90-45260
 Forebody vortex manipulation for aerodynamic control of aircraft at high angles of attack
 [SAE PAPER 892220] p 756 A90-45437
 The development of crossflow vortices on a 45 degree swept wing
 [SAE PAPER 892245] p 713 A90-45452
 Simulation of leading-edge vortex flows
 p 716 A90-45785
 Numerical simulation of vortical flows over a strake-delta wing and a close coupled delta-canard configuration
 [AIAA PAPER 90-3002] p 788 A90-45851
 Numerical simulation of vortical flows over close-coupled canard-wing configuration
 [AIAA PAPER 90-3003] p 788 A90-45852
 Numerical study of asymmetric air injection to control high angle-of-attack forebody vortices on the X-29 aircraft
 [AIAA PAPER 90-3004] p 788 A90-45853
 Some characteristics of interference between shock waves and the aerodynamic wake behind a body
 p 804 A90-46551
 Some possibilities of the vortex layer method for calculating the aerodynamic characteristics of an augmented airfoil interacting with the engine jet
 p 804 A90-46564
 Numerical simulation of steady and unsteady vortical flows around wings and bodies p 806 A90-46869
 Improvement in turbine blade aerodynamic force in the tip region p 809 A90-47854
 Euler analysis comparison with LDV data for an advanced counter-rotation propfan at cruise
 [AIAA PAPER 90-3033] p 903 A90-50637
 Application of a vortex lattice numerical model in the calculation of inviscid incompressible flow around delta wings p 904 A90-51017
 Basic studies of the unsteady flow past high angle of attack airfoils
 [AD-A210252] p 18 N90-10008
 Acoustic-vortex-chemical interactions in an idealized ramjet p 54 N90-10206
 Goertler instability on an airfoil: Comparison of marching solution with experimental observations
 p 19 N90-10364
 A European collaborative investigation of the three-dimensional turbulent shear layers of a swept wing
 p 20 N90-10380
 An investigation of counterrotating tip vortex interaction
 [NASA-CR-185135] p 79 N90-11549
 An investigation of end-wall vortex cavitation in a high Reynolds number axial-flow pump
 [AD-A211426] p 133 N90-11982
 Goertler instability on an airfoil p 91 N90-12517
 Experimental studies on Goertler vortices
 p 91 N90-12529
 Development of a VSAERO (Vortex Separation Aerodynamics) model of the F/A-18
 [AD-A212442] p 95 N90-12566
 A smoke generator system for aerodynamic flight research
 [NASA-TM-4137] p 183 N90-13372
 An experimental investigation of the interaction between a model rotor and airframe in forward flight
 p 185 N90-14219
 Acoustic-vortical-combustion interaction in a solid fuel ramjet simulator p 194 N90-14234
 Aircraft response and pilot behaviour during a wake vortex encounter perpendicular to the vortex axis
 p 259 N90-15057
 Wind tunnel investigations on the configuration of the international vortex flow experiment p 277 N90-16181
 Flow field visualization study on a 65 deg delta wing at $M = 0.85$ p 277 N90-16182
 A nonlinear vortex-lattice method for the calculation of interference effects between free vortex sheets and wings p 277 N90-16183
 Research on three different Euler's schemes applied to a delta wing with vortical flows p 278 N90-16184
 An experimental investigation of viscous aspects of propeller blade flow p 315 N90-16711
 Controlled vortical flow on delta wings through unsteady leading edge blowing
 [NASA-CR-186267] p 316 N90-16712

An experimental study of the effect of streamwise vortices on unsteady turbulent boundary-layer separation
 p 369 N90-17045
 Numerical solutions of the linearized Euler equations for unsteady vortical flows around lifting airfoils
 [NASA-TM-102466] p 318 N90-17562
 Modeling the wake as a continuous vortex sheet in a potential-flow solution using vortex panels
 [AD-A216220] p 371 N90-18016
 Numerical simulation of compressible vortices
 [AD-A216221] p 371 N90-18017
 Study of the blade/vortex interaction on a one-blade rotor during forward flight (incompressible, non viscous fluid)
 [ISL-R-115/88] p 415 N90-18391
 Unsteady Aerodynamic Phenomena in Turbomachines
 [AGARD-CP-468] p 425 N90-18405
 Leading edge vortex dynamics on a pitching delta wing
 [NASA-CR-186327] p 398 N90-19198
 Water-tunnel investigation of concepts for alleviation of adverse inlet spillage interactions with external stores
 [NASA-TM-4181] p 398 N90-19199
 A streamwise upwind algorithm applied to vortical flow over a delta wing
 [NASA-TM-102225] p 398 N90-19201
 A video-based experimental investigation of wing rock
 [AD-A218244] p 498 N90-20075
 Experimental investigation of the mechanisms underlying vortex kinematics in unsteady separated flows
 [AD-A217889] p 540 N90-20346
 Measurement of lift development on rapidly-accelerated wings p 480 N90-20956
 Experimental and numerical investigation of the vortex flow over a sharp edged delta wing; with and without sideslip
 [PB90-167131] p 481 N90-20964
 LDV measurements and the flow analysis in the vortex region of a radial inflow turbine p 511 N90-21007
 Experimental and numerical study on basic phenomena of secondary flows in turbines p 512 N90-21014
 Secondary flows and Reynolds stress distributions downstream of a turbine cascade at different expansion ratios p 512 N90-21015
 Effective methods of controlling a junction vortex system in an incompressible, three-dimensional, turbulent flow
 p 571 N90-21732
 Modeling of vortex-induced oscillations based on indicial response approach
 [NASA-CR-186560] p 572 N90-21736
 Analytical study of the origin and behavior of asymmetric vortices
 [NASA-TM-102796] p 573 N90-21746
 The interaction of a supersonic streamwise vortex and a normal shock wave p 633 N90-24241
 Ground evaluation of seeding an in-flight wingtip vortex using infrared imaging flow visualization technique
 p 635 N90-25035
 Generation of circumferential velocity contours associated with pulsed point suction on a rotating disk
 p 691 N90-25065
 Video photographic considerations for measuring the proximity of a probe aircraft with a smoke seeded trailing vortex
 [NASA-TM-102691] p 724 N90-25120
 Identification of aerodynamic models for maneuvering aircraft
 [NASA-CR-186630] p 719 N90-25943
 Euler analysis comparison with LDV data for an advanced counter-rotation propfan at cruise
 [NASA-TM-103249] p 720 N90-25946
 Experimental study on vortex and shock wave development on a 65 deg delta wing
 [NLR-MP-88033-U] p 720 N90-25950
 Velocity measurements on a lifting rotor/airframe configuration in low speed forward flight
 p 815 N90-26790
 Experiments with unsteady, free surface, three-dimensional vortices in a thermally stable, stratified fluid
 [AD-A222088] p 815 N90-26796
 Flow visualization of dynamic stall on an oscillating airfoil
 [AD-A222202] p 815 N90-26797
 Noise from tip vortex and bubble cavitation
 [AD-A221962] p 896 N90-27468
 Control of submersible vortex flows
 [NASA-TM-102693] p 909 N90-28493
 Prediction of subsonic vortex shedding from forebodies with chines
 [NASA-CR-4323] p 909 N90-28494
 Aerodynamics of bodies in shear flow
 p 910 N90-28496

- In-flight flow visualization with pressure measurements at low speeds on the NASA F-18 high alpha research vehicle
[NASA-TM-101726] p 910 N90-28505
- Development of non-conventional control methods for high angle of attack flight using vortex manipulation
p 935 N90-28522
- Control of vortex aerodynamics at high angles of attack
p 921 N90-28523
- Dynamic ground effects
p 922 N90-28531
- A flight dynamic model of aircraft spinning
[AR-005-600] p 835 N90-28576
- Dynamic separation: Search for the cause of dynamic stall and search for its control
[AD-A223412] p 911 N90-29305
- Further studies of turbulence structure resulting from interactions between embedded vortices and wall jets at high blowing ratios
[AD-A23296] p 960 N90-29593
- The experimental investigation of flow in the core of a vortex structure
[BR114893] p 960 N90-29597
- The computation and analysis of acoustic waves in transonic airfoil-vortex interactions
p 966 N90-30031
- VORTICITY**
- On unsteady surface forces, and sound produced by the normal chopping of a rectilinear vortex
p 5 A90-11604
- Vortex interactions in fixed and oscillating delta wings (water tunnel visualizations)
p 16 A90-12784
- Large-eddy simulations of pressure oscillations and combustion instability in a ramjet
p 111 A90-15388
- On a lifting line theory for supersonic flow. I - The velocity field due to a vortex line in supersonic flow
p 143 A90-16735
- Interaction between strong longitudinal vortices and turbulent boundary layers
p 145 A90-16764
- Incompressible potential flow about complete aircraft configurations
p 156 A90-18443
- Large-eddy simulations of combustion instability in an axisymmetric ramjet combustor
[AIAA PAPER 90-0267] p 191 A90-19764
- Lift development of delta wings undergoing constant acceleration from rest
[AIAA PAPER 90-0310] p 164 A90-19789
- An investigation on the coiled-up of vortices on a double delta wing
[AIAA PAPER 90-0382] p 165 A90-19825
- Impact of nose-probe chines on the vortex flows about the F-16C
[AIAA PAPER 90-0386] p 165 A90-19828
- The influence of a rotating leading edge on accelerating starting flow over an airfoil
[AIAA PAPER 90-0583] p 168 A90-19932
- Prediction of steady and unsteady asymmetric vortical flows around cones
[AIAA PAPER 90-0598] p 168 A90-19940
- Prediction of vortical flows on wings using incompressible Navier-Stokes equations
p 226 A90-21935
- Vortical flows over delta wings and numerical prediction of vortex breakdown
[AIAA PAPER 90-0102] p 227 A90-22166
- Development of the tip-leakage flow downstream of a planar cascade of turbine blades - Vorticity field
[ASME PAPER 89-GT-55] p 289 A90-23781
- Numerical solutions of the linearized Euler equations for unsteady vortical flows around lifting airfoils
[AIAA PAPER 90-0694] p 300 A90-25041
- The transonic nonisentropic potential calculation
p 304 A90-25739
- An automated vorticity surveying system using a rotating hot-wire probe
p 447 A90-28284
- Numerical model of unsteady subsonic aeroelastic behavior
p 535 A90-32471
- On a lifting line theory for supersonic flow. II - A supersonic lifting line theory for wings
p 477 A90-34817
- Dynamic stall experiments on the NACA 23012 airfoil
p 552 A90-35140
- Control of asymmetric vortical flows over delta wings at high angles of attack
p 553 A90-35759
- Suppression of vortex asymmetry behind circular cones
p 556 A90-36282
- Relationship between velocity circulation around a wing profile and vorticity dispersion in a boundary layer
p 620 A90-39539
- Navier-Stokes solutions for vortical flows over a tangent-ogive cylinder
p 620 A90-39780
- Vorticity distribution of vortex street in the wake of a circular cylinder
p 623 A90-41751
- Computation of flow through a centrifugal impeller with tip leakage
[AIAA PAPER 90-2021] p 684 A90-41987
- An airfoil theory of bifurcating laminar separation from thin obstacles
p 702 A90-42639
- Flow over a leading edge with distributed roughness
p 703 A90-42646
- Canard-wing vortex interactions at subsonic through supersonic speeds
[AIAA PAPER 90-2814] p 711 A90-45154
- Vortical sources of aerodynamic force and moment
[SAE PAPER 892346] p 715 A90-45498
- Multiple vortex and shock interactions at subsonic, transonic, and supersonic speeds
[AIAA PAPER 90-3023] p 793 A90-45890
- The role of CFD applied to high performance aircraft
[AIAA PAPER 90-3071] p 796 A90-45917
- Numerical study of vortical flow over a sideslipping delta wing
[AIAA PAPER 90-3001] p 798 A90-45936
- A method to determine the performance of low-Reynolds-number airfoils under off-design unsteady freestream conditions
p 801 A90-46375
- Assessment of computational prediction of tail buffeting
[NASA-TM-101613] p 237 N90-15886
- Secondary flow calculations for axial and radial compressors
p 514 N90-21024
- VORTICITY EQUATIONS**
- The application of the discrete vortex method in aircraft design
p 257 A90-23357
- Optimization of rotor performance in hover and axial flight using a free wake analysis
p 407 A90-28175
- Unsteady inviscid and viscous computations for vortex-dominated flows
p 553 A90-35752
- The free-wake computation of rotor-body flows
[AIAA PAPER 90-1540] p 565 A90-38684
- Navier-Stokes computations of vortical flows
[AIAA PAPER 90-1628] p 568 A90-38757
- Modelling free vortex flow on planar swept wing
p 810 A90-48079
- VULCAN AIRCRAFT**
- Rotor dynamics of the Vulcain LH2 Turbopump - Comparison between test results and non-linear dynamic analysis
p 528 A90-33382
- VULNERABILITY**
- Fuel tank explosion protection
p 251 N90-15914
- Aviation security: Corrective actions underway, but better inspection guidance still needed. Report to the Chairwoman, Government Activities and Transportation Subcommittee, Committee on Government Operations, House of Representatives
[GAO/RCED-88-160] p 635 N90-23367
- W**
- WAFERS**
- Cooling characteristics of a radial water blade
p 47 A90-12571
- WAKES**
- The influence of the wake structure on the dynamic blade load
p 6 A90-11785
- Computation of aerodynamic blade loads due to wake influence and aerodynamic damping of turbine and compressor cascades
p 7 A90-11791
- Computation of the trailing edge flow downstream a flat plate with finite thickness
p 151 A90-17464
- The interaction between a counter-rotating vortex pair in vertical ascent and a free surface
p 151 A90-17580
- Comment on 'Induced drag and the ideal wake of a lifting wing'
p 233 A90-23291
- Compressor blade boundary layers. II - Measurements with incident wakes
[ASME PAPER 89-GT-51] p 289 A90-23777
- Free-wake analysis of compressible rotor flows
p 302 A90-25283
- Numerical prediction of wakes of different bodies
p 308 A90-26341
- Comparison of measured induced velocities with results from a closed-form finite state wake model in forward flight
p 385 A90-28195
- Direct numerical simulations of transition in a compressible wake
p 553 A90-35212
- Time-resolved measurements of total temperature and pressure in the vortex street behind a cylinder
p 557 A90-36522
- Preliminary characterization of parachute wake recontact
p 622 A90-40681
- Coherent vortex structures in the wake of a sphere and a circular disk at rest and under forced vibrations
p 623 A90-40749
- A visualization study of the interaction of a free vortex with the wake behind an airfoil
p 623 A90-41119
- Viscous-inviscid interaction method for calculating the flow in compressor cascade blade passages and wake with separation
[AIAA PAPER 90-2125] p 624 A90-42032
- Forced response on turbomachinery blades due to passing wakes
[AIAA PAPER 90-2353] p 705 A90-42781
- Euler procedure for calculation of the steady rotor flow with emphasis on wake evolution
[AIAA PAPER 90-3007] p 789 A90-45857
- Performance measurements of an airfoil at low Reynolds numbers
p 800 A90-46369
- An experimental investigation of the interaction between a model rotor and airframe in forward flight
p 185 N90-14219
- An analytical method for the prediction of unsteady rotor/airframe interactions in forward flight
p 186 N90-14223
- An experimental investigation of viscous aspects of propeller blade flow
p 315 N90-16711
- Wake interaction effects on the transition process on turbine blades
[AD-A214492] p 343 N90-16759
- Modeling the wake as a continuous vortex sheet in a potential-flow solution using vortex panels
[AD-A216220] p 371 N90-18016
- Design guidance to minimize unsteady forces in turbomachines
p 426 N90-18411
- Aerodynamic study on forced vibrations on stator rows of axial compressors
p 426 N90-18412
- Unsteady blade loads due to wake influence
p 426 N90-18413
- Modelling unsteady transition and its effects on profile loss
p 427 N90-18423
- Experimental investigation of the influence of rotor wakes on the development of the profile boundary layer and the performance of an annular compressor cascade
p 427 N90-18425
- Unsteady free-wake viscous aerodynamic analysis of helicopter rotors
[AD-A217166] p 478 N90-20048
- Spectral simulation of unsteady compressible flow past a circular cylinder
[NASA-CR-182030] p 478 N90-20050
- Comparison of C- and O-grid generation methods using a NACA 0012 airfoil
[AD-A216375] p 479 N90-20948
- Development and application of a generalized dynamic wake theory for lifting rotors
p 570 N90-21731
- Effective methods of controlling a junction vortex system in an incompressible, three-dimensional, turbulent flow
p 571 N90-21732
- Airloads, wakes, and aeroelasticity
[NASA-CR-177551] p 572 N90-21738
- Experiments with unsteady, free surface, three-dimensional vortices in a thermally stable, stratified fluid
[AD-A222088] p 815 N90-26796
- Do inviscid vortex sheets roll-up
[PD-CF-9010] p 909 N90-28491
- WALL FLOW**
- Wave cancellation properties of a splitter-plate porous wall configuration
p 57 A90-11005
- Experimental investigations of effects of the stagger angle on secondary flows in plane compressor cascades
p 83 A90-13787
- Wall interference correction of high-lift multi-component airfoils
p 158 A90-18604
- Video visualization of separation shock motion from measured wall pressure signals in a Mach 5 compression ramp interaction
[AIAA PAPER 90-0074] p 162 A90-19670
- Embedded function methods for supersonic turbulent boundary layers
[AIAA PAPER 90-0306] p 163 A90-19787
- The use of a Laval nozzle and wall suction for blockage-free transonic wind-tunnel operation
p 225 A90-21592
- A method for calculating axial turbomachine end wall turbulent boundary layers
[ASME PAPER 89-GT-15] p 287 A90-23759
- Observation and analysis of sidewall effect in a transonic airfoil test section
p 436 A90-28257
- The effect of walls on a spatially growing supersonic shear layer
p 393 A90-29591
- Wall-interference corrections for parachutes in a closed wind tunnel
p 440 A90-31281
- The k-k1 turbulence model and wall layer model for compressible flows
[AIAA PAPER 90-1483] p 563 A90-38637
- Two-dimensional convergent-divergent nozzle flow with wall velocity slip and temperature jump
p 807 A90-46884
- Control of wall-separated flow by internal acoustic excitation
p 809 A90-47314
- Study of the integration of wind tunnel and computational methods for aerodynamic configurations
[NASA-TM-102196] p 170 N90-13332

A two-dimensional adaptive-wall test section with ventilated walls in the Ames 2- by 2-foot transonic wind tunnel

[NASA-TM-102207] p 201 N90-13407

An experimental investigation of wall-interference effects for parachutes in closed wind tunnels

[DE90-001802] p 236 N90-15076

Nonlinear transonic Wall-Interference Assessment/Correction (WIA) procedures and application to cast-10 airfoil results from the NASA 0.3-m TCT 8- by 24-inch Slotted Wall Test Section (SWTS)

p 352 N90-17648

Comparison of conventional and adaptive wall wind tunnel results with regard to Reynolds number effects

p 352 N90-17649

Residual interference and wind tunnel wall adaptation

p 353 N90-17655

Aerodynamic optimization by simultaneously updating flow variables and design parameters

p 501 N90-20991

The effects of compressor endwall flow on airfoil incidence and deviation

p 512 N90-21011

New transonic test sections for the NAE 5 ft x 5 ft trisonic wind tunnel

[AD-A220933] p 674 N90-24278

Limits of adaptation, residual interferences

p 871 N90-26844

Adaptation for unsteady flow

p 871 N90-26845

Three-dimensional model testing in the transonic self-streamlining wind tunnel

p 938 N90-28583

WALL JETS

Turbulence measurements in a flow generated by the collision of radially flowing wall jets

p 2 A90-10699

The characteristic decay region of a class of three-dimensional wall jets

p 85 A90-15241

Experimental studies of shock wave/wall jet interaction in hypersonic flow

[AIAA PAPER 90-0607] p 231 A90-22449

Effect of tangential injection on flow in a laminar boundary layer

p 294 A90-24080

A model gas turbine combustor with wall jets and optical access for turbulent mixing, fuel effects, and spray studies

p 507 A90-32808

Further studies of turbulence structure resulting from interactions between embedded vortices and wall jets at high blowing ratios

[AD-A223296] p 960 N90-29593

WALL PRESSURE

Measurements of pressure fluctuations in the interaction regions of shock waves and turbulent boundary layers induced by blunt fins

p 9 A90-12218

Investigation of wall pressure pulsations during the passive control of shock/boundary layer interaction

p 378 A90-24132

Wall pressure fluctuation spectra in supersonic flow past a forward facing step

p 388 A90-29194

Effect of surface grooves on base pressure for a blunt trailing-edge airfoil

p 556 A90-36280

Unsteady transonic cascade flow with in-passage shock wave

p 556 A90-36281

A wall pressure correction method for half-model experiment in closed subsonic wind tunnel test section

p 593 A90-36437

A study of the unsteadiness of crossing shock wave turbulent boundary layer interactions

[AIAA PAPER 90-1456] p 606 A90-38614

Wall pressure fluctuations in the reattachment region of a supersonic free shear layer

[AIAA PAPER 90-1461] p 561 A90-38618

Dynamics of the outgoing turbulent boundary layer in a Mach 5 unswept compression ramp interaction

[AIAA PAPER 90-1645] p 569 A90-38773

Correlation of separation shock motion in a compression ramp interaction with pressure fluctuations in the incoming boundary layer

[AIAA PAPER 90-1646] p 569 A90-38774

Experimental investigation of terminal shock sensors in mixed-compression inlets

[AIAA PAPER 90-1931] p 681 A90-40560

Wall pressure pulsation spectra ahead of internal corners

p 804 A90-46545

A wall interference assessment/correction interface measurement system for the NASA/ARC 12-ft PWT

[NASA-CR-185474] p 200 N90-13401

WALL TEMPERATURE

Two-dimensional convergent-divergent nozzle flow with wall velocity slip and temperature jump

p 807 A90-46884

WALLS

The influence of a wall function on turbine blade heat transfer prediction

p 429 N90-19421

Further studies of turbulence structure resulting from interactions between embedded vortices and wall jets at high blowing ratios

[AD-A223296] p 960 N90-29593

WARNING SYSTEMS

GPS monitor alarm limits for nonprecision approaches

p 98 A90-15315

Wind shear detection with pencil-beam radars

p 279 A90-21386

A laser obstacle avoidance and display system

p 419 A90-30694

Development of an acceptability window for a ground proximity avoidance system

p 419 A90-30730

Low-level windshear alert systems and Doppler radar in aircraft terminal operations

p 574 A90-35758

Obstacle warning system for helicopters

p 653 A90-41114

Development of the stall warning/stick pusher system for the Boeing/de Havilland Dash 8 Series 300

p 645 A90-42420

Prompt identification of a troubled engine can help avoid catastrophe

p 721 A90-44222

Safer skies with TCAS: Traffic Alert and Collision Avoidance System

[PB89-169221] p 27 N90-10016

See and avoid/cockpit visibility

[DOT/FAA/CT-TN89/18] p 24 N90-10843

An update to the system safety study of TCAS 2

[DOT/FAA/SA-89/3] p 177 N90-13363

How to fly windshear using the fly-by-wire concept

p 258 N90-15050

Improved lighting of taxiway/taxiway intersections for Instrument Flight Rules (IFR) operations

[DOT/FAA/CT-TN89/64] p 243 N90-15089

Relative merits of reactive and forward-look detection for wind-shear encounters during landing approach for various microburst escape strategies

[NASA-TM-4158] p 259 N90-15108

The automatic detection of anti-collision lights

[RSRE-MEMO-4272] p 240 N90-15896

Onboard fire- and explosion suppression for fighter aircraft

p 327 N90-17602

US Navy aircraft fire protection technology

p 327 N90-17603

Joint University Program for Air Transportation Research, 1988-1989

[NASA-CP-3063] p 468 N90-20921

Cockpit display of hazardous weather information

p 485 N90-20929

WARPAGE

The static aeroelastic behavior of sweptforward composite wing structures taking into account their warping restraint effect

p 210 A90-18407

WASTE ENERGY UTILIZATION

Aircraft subsystem waste energy recovery and management

[SAE PAPER 901218] p 840 A90-49293

WASTE HEAT

Aircraft subsystem waste energy recovery and management

[SAE PAPER 901218] p 840 A90-49293

WASTE UTILIZATION

Production of jet fuels from coal-derived liquids. Volume 13: Evaluation of storage and thermal stability of jet fuels derived from coal liquids

[AD-A224576] p 954 N90-29527

WATER

Water ingestion simulation - Test needs

p 23 A90-12620

Aircraft internal fires

p 326 N90-17593

WINCOF-I code for prediction of fan compressor unit with water ingestion

[NASA-CR-185157] p 551 N90-21724

WATER FLOW

Air/water two-phase flow test tunnel for airfoil studies

p 352 A90-26842

WATER INJECTION

Performance improvement of an eroded axial flow compressor using water injection

[AIAA PAPER 90-2016] p 741 A90-42718

WATER LANDING

Water test facilities for aviation life support equipment

p 200 A90-17431

WATER POLLUTION

Enhanced bioreclamation of jet fuels: A full-scale test at Eglin AFB, Florida

[AD-A22348] p 875 N90-26992

WATER TUNNEL TESTS

The water tunnel test of delaying vortex breakdown over a delta wing using supplements

p 2 A90-10346

Application of the hydrogen bubble visualization method to the water tunnels of ONERA

[ONERA, TP NO. 1989-107] p 58 A90-11140

Vortex interactions in fixed and oscillating delta wings (water tunnel visualizations)

p 16 A90-12784

Aerodynamic control of NASP-type vehicles through vortex manipulation

[AIAA PAPER 90-0594] p 203 A90-19938

Hydrodynamic visualization of organized structures and turbulences in boundary layers, wakes, jets or propeller flows

[ONERA, TP NO. 1989-158] p 223 A90-21026

Air/water two-phase flow test tunnel for airfoil studies

p 352 A90-26842

Blade-vortex interaction experiments - Velocity and vorticity fields

[AIAA PAPER 90-0030] p 312 A90-26903

A laser fluorescence anemometer for water tunnel flowfield studies

p 447 A90-28279

Steady and unsteady force testing of fighter aircraft models in a water tunnel

[AIAA PAPER 90-2815] p 711 A90-45155

Static and dynamic water tunnel tests of slender wings and wing-body configurations at extreme angles of attack

[AIAA PAPER 90-3021] p 869 A90-45888

Effect of leading edge roundness on a delta wing in wing-rock motion

[AIAA PAPER 90-3080] p 795 A90-45911

Water-tunnel investigation of concepts for alleviation of adverse inlet spillage interactions with external stores

[NASA-TM-4181] p 398 N90-19199

A video-based experimental investigation of wing rock

p 592 N90-21771

The experimental investigation of flow in the core of a vortex structure

[BR114893] p 960 N90-29597

WATER VAPOR

Transonic flow around airfoils with relaxation and energy supply by homogeneous condensation

p 620 A90-39782

The effect of energy input on the characteristics of profiles in compressible fluid media

p 906 A90-51533

WAVE DIFFRACTION

Free-field correction factor for spherical acoustic waves impinging on cylinders

p 218 A90-17984

WAVE DRAG

Optimal nose shapes of bodies of revolution in transonic flow

p 299 A90-24165

Auxiliary hypotheses of the wave drag theory

p 387 A90-29003

Calculation of the drag of fuselage tail sections of different shapes in supersonic flow of a nonviscous gas

p 388 A90-29182

Supersonic aircraft drag reduction

[AIAA PAPER 90-1596] p 567 A90-38729

Some aerodynamic characteristics of the scissor wing configuration

[SAE PAPER 892202] p 713 A90-45423

Optimum shape of a blunt forebody in hypersonic flow

[NASA-CR-181955] p 171 N90-13351

WAVE EQUATIONS

The validation and application of a rotor acoustic prediction computer program

[NASA-TM-101794] p 895 N90-27465

WAVE EXCITATION

Wave structure of artificial perturbations in a supersonic boundary layer on a plate

p 619 A90-39518

Acoustic wave excitation during the aerodynamic interaction between a fan blade and a bluff obstacle

p 965 A90-52289

WAVE INTERACTION

Instabilities of supersonic shear flows

[AIAA PAPER 90-0712] p 314 A90-26983

Non-axisymmetric viscous lower-branch modes in axisymmetric supersonic flows

p 474 A90-33509

Wave interactions in a three-dimensional attachment-line boundary layer

p 811 A90-48715

Acoustic-vortex-chemical interactions in an idealized ramjet

p 54 N90-10206

Transonic 3-D Euler analysis of flows around fanjet engine and TPS (Turbine Powered Simulator). Comparison with wind tunnel experiment, evaluation of TPS testing method and 3-D flow

[NAL-TR-1045] p 912 N90-29327

WAVE PROPAGATION

The computation and analysis of acoustic waves in transonic airfoil-vortex interactions

p 966 N90-30031

WAVE REFLECTION

Numerical simulations of unsteady shock reflections by ramps

p 305 A90-25795

Reflection by defective diffusion bonds

[AD-A212995] p 206 N90-13638

WAVEFORMS

A waveform alignment approach to positioning airborne radar-sounding data

p 332 A90-26651

Air Force Boom Event Analyzer Recorder (BEAR): System description

[AD-A218048] p 548 N90-20800

Studies in automatic speech recognition and its application in aerospace

p 958 N90-28759

WAVEGUIDE ANTENNAS

Applications of slotted cable antennas in the instrument landing system

p 639 A90-41708

WAVELENGTH DIVISION MULTIPLEXING

- Optic multiplex for aircraft sensors - Issues and options p 38 A90-11660
- Wavelength division multiplexed fiber optic sensors for aircraft applications p 38 A90-11663
- A fiber optic headset compatible with power-by-light p 504 A90-32906

WAVERIDERS

- Wave rider volume distribution p 388 A90-29006
- Aerodynamic characteristics of wave riders based on flows behind axisymmetric shock waves p 395 A90-30342
- Off-design performance of hypersonic waveriders p 763 A90-44735
- Computational simulation of flows about hypersonic geometries with sharp leading edges [AIAA PAPER 90-3065] p 793 A90-45891
- Navier Stokes simulation of waverider flowfields [AIAA PAPER 90-3066] p 793 A90-45892
- Hypersonic waverider configurations for trans-atmospheric vehicles [AD-A217925] p 498 A90-20074

WEAPON SYSTEMS

- McDonnell Douglas Helicopter Company Factory of the Future Project p 381 A90-28163
- The two level maintenance - I level dilemma p 381 A90-28319
- Telemetry systems of the future p 458 A90-28829
- AIAA/SFTE/DGLR/SETP, Biannual Flight Test Conference, 5th, Ontario, CA, May 22-24, 1990, Technical Papers p 493 A90-33886
- Air Combat Environment Test and Evaluation Facility (ACEF) p 58 A90-10883
- China-built airborne synchronous laser ranger the new L-8 jet trainer aircraft [AD-A213835] p 275 A90-15422
- The integration of stores on modern tactical aircraft: Where we have been, and what we should do for the future p 337 A90-17552

WEAPONS

- The technology challenge of the advanced tactical fighter: A study of the technology transition process [AD-A216109] p 338 A90-17630

WEAR

- Some aspects of the erosive wear of components of aircraft turbine engines p 253 A90-21627
- Erosive wear of fibrous PEEK composites p 530 A90-33127
- Evaluation of brush seals for limited-life engines [AIAA PAPER 90-2140] p 685 A90-42040
- A theoretical and experimental investigation into the percolation of aircraft tires [AIAA PAPER 90-3272] p 836 A90-48863
- In-line wear monitor [AD-A217799] p 510 A90-20091
- Surface property improvement in titanium alloy gas turbine components through ion implantation p 953 A90-28713

WEAR INHIBITORS

- UCAR 2040, A novel wear resistant coating for aircraft structural components p 441 A90-28231

WEAR RESISTANCE

- Laboratory analysis of antiwear properties of turbine-engine fuels p 131 A90-15878
- UCAR 2040, A novel wear resistant coating for aircraft structural components p 441 A90-28231
- Development of erosion resistant coatings for compression airfoils p 443 A90-31120

WEAR TESTS

- Compatibility of fuel system components with high density fuel [AD-A210381] p 32 A90-10027

WEATHER

- General aviation pilot error in computer simulated adverse weather scenarios p 322 A90-26254
- Inclement weather induced aircraft engine power loss [AIAA PAPER 90-2169] p 662 A90-42055
- Flight in adverse environmental conditions [AGARD-AR-277] p 185 A90-14218
- Effects of lightning on operations of aerospace vehicles p 239 A90-15065
- Investigation of air transportation technology at the Massachusetts Institute of Technology, 1988-1989 p 484 A90-20922
- Cockpit display of hazardous wind shear information p 484 A90-20924
- Cockpit display of hazardous weather information p 485 A90-20929
- Weather data dissemination to aircraft p 486 A90-20934
- Plan for the FAA air traffic operational evaluation of the Automated Surface Observing System (ASOS) [DOT/FAA/CT-TN89/56] p 489 A90-20968
- Meteorologist Weather Processor (MWP) integration test plan [DOT/FAA/CT-TN89/62] p 544 A90-21500

- Analysis of distributions of Visual Meteorological Conditions (VMC) helipad data [DOT/FAA/CT-TN89/67] p 544 A90-21508

WEATHER FORECASTING

- A program to improve aircraft icing forecasts [AIAA PAPER 90-0196] p 216 A90-19733
- Atmospheric conditions producing aircraft icing on 24-25 January 1989 - A case study utilizing combinations of surface and remote sensors [AIAA PAPER 90-0197] p 175 A90-19734
- Real time winds data for flight management [AIAA PAPER 90-0565] p 197 A90-19918
- The influence of weather on flight operations at the Atlanta Hartsfield International Airport p 279 A90-22688

- Advances in weather technology for the aviation system p 373 A90-25572
- The Canadian Airspace Systems Plan - Maintaining the safety and efficiency of the air navigation system p 725 A90-42655

- Analysis and prediction of weather for aviation p 888 A90-48351

- The influence of ice accretion physics on the forecasting of aircraft icing conditions p 485 A90-20928
- A comparison of lightning network data with surface weather observations [AD-A220003] p 692 A90-23832

WEATHERING

- The performance of alternate fuels in general aviation aircraft p 950 A90-51621

WEDGE FLOW

- Direct simulation of three-dimensional hypersonic flow about intersecting blunt wedges p 16 A90-12835
- Supersonic/hypersonic flow past wedge and plane ogive in oscillation p 85 A90-15231
- Transonic flow over a single wedge p 85 A90-15237

- Droplet impaction on a supersonic wedge - Consideration of similitude p 400 A90-27986
- An experimental study of a turbulent jet impinging on a wedge p 553 A90-35274
- On the instability of hypersonic flow past a wedge p 554 A90-35902
- Theoretical prediction of pressure distribution on wedged delta wing at higher supersonic Mach numbers and its agreement with experimental results p 907 A90-51537

- Unsteady transonic flow around double-wedge profiles p 299 A90-24354

- Unfolding of double-zero eigenvalue bifurcations for supersonic flow past a pitching wedge p 347 A90-25995

- Numerical solution of the problem of supersonic flow of an ideal gas past a trapezoidal wedge p 386 A90-28980

- Desktop failure analysis on a microcomputer using Weibull, lognormal, and renewal data [ASME PAPER 89-GT-275] p 535 A90-32263

- The computer aided weight engineering of aircraft - (CAWE) system p 179 A90-16860

- Examples of force measurements in a wind tunnel using multicomponent piezoelectric transducers p 540 A90-34352

- Automatic calibration machine for cryogenic and conventional internal strain gage balances [AIAA PAPER 90-1396] p 595 A90-37939

- Minimum weight design of helicopter rotor blades with frequency constraints p 180 A90-17313

- Effect of advanced component technology on helicopter transmissions p 271 A90-21115

- Minimum weight design of rotorcraft blades with multiple frequency and stress constraints p 335 A90-25304

- Unified optimal criterion method - Combination of direction of gradient and ejection line p 367 A90-26077

- Electronic cartography - A new need for commercial aircraft p 576 A90-35351

- Optimum design of composite wing structures subjected to displacement constraints p 680 A90-39276

- Loss weight with Al-Li p 765 A90-44175

- Fast start ceramic auxiliary power unit [SAE PAPER 89-2254] p 747 A90-45456

- Lightweight, composite flight control actuators [SAE PAPER 89-2264] p 733 A90-45459

- Old lamps for new - A photoelastic design tool for weight and cost saving on aircraft structures p 878 A90-46039

- Design of a close-support aircraft [AIAA PAPER 90-3241] p 835 A90-48849
- Composite flight control actuators p 874 A90-48993

- Unique features and innovative application of advanced composites to the MD-11 [AIAA PAPER 90-3217] p 838 A90-49108

- Development of an advanced fan blade containment system [DOT/FAA/CT-89/20] p 192 A90-13386

- Aluminum-lithium: Application of plate and sheet to fighter aircraft p 268 A90-15202

- Transmission research activities at NASA Lewis Research Center [NASA-TM-103132] p 543 A90-21394

- The application of engineering ceramics in gas turbines [PNR90676] p 750 A90-26005

- Design of helicopter components in metal matrix composites [REPT-100-20-55] p 874 A90-26894

WEIGHTING FUNCTIONS

- A weighted residual formulation for finite element solutions of the steady Euler equations p 770 A90-44457

WELD STRENGTH

- Reflection by defective diffusion bonds [AD-A212995] p 206 A90-13638

WELD TESTS

- Damage tolerance analysis and testing of a welded cluster gear for the main transmission of the Advanced Attack Helicopter p 445 A90-28187

WELDING

- Attachment of lead wires to thin film thermocouples mounted on high temperature materials using the parallel gap welding process [NASA-TM-102442] p 543 A90-21361

WESTLAND AIRCRAFT

- Usage monitoring of military helicopters p 651 A90-39984

WETTING

- Parabolic flight experiments on fluid surfaces and wetting p 363 A90-23904

WHIRL TOWERS

- Empirical prediction of the blockage effect of a flat body on a rotor p 807 A90-46942

WHISKER COMPOSITES

- Analysis of whisker-toughened ceramic components - A design engineer's viewpoint p 205 A90-19149

WHITE LIGHT HOLOGRAPHY

- Holographic flow visualization of turbofan by-pass and core nozzle streams [ASME PAPER 89-GT-260] p 363 A90-23891

WIDE ANGLE LENSES

- Analysis and test of a wide angle spectrometer [AD-A215819] p 372 A90-18030

WILDERNESS

- Preliminary thoughts on an acoustic metric for the wilderness aircraft overflight study p 697 A90-24862

WIND (METEOROLOGY)

- Effects of random initial conditions and deterministic winds on simulated parachute motion p 22 A90-11002

- Airdata calibration of a high-performance aircraft for measuring atmospheric wind profiles [NASA-TM-101714] p 186 A90-14228

WIND DIRECTION

- Analytical and experimental study of runway runoff with wind effects [PTI-8948] p 123 A90-12627

WIND EFFECTS

- Boeing Transonic Windblast Generator System (BTWGS) p 199 A90-17413

- A study of the laminar-turbulent boundary layer transition on the windward side of a delta wing with a conical surface p 298 A90-24144

- Analytical and experimental study of runway runoff with wind effects [PTI-8948] p 123 A90-12627

- The effects of wind tunnel data uncertainty on aircraft point performance predictions [AD-A216091] p 414 A90-18387

- Aerodynamic analysis of a US Navy and Marine Corps unmanned air vehicle [AD-A218282] p 498 A90-20077

- Analysis of small-scale rotor hover performance data [NASA-TM-102271] p 540 A90-20325

WIND EROSION

- Erosive wear of fibrous PEEK composites p 530 A90-33127

WIND MEASUREMENT

- Meteopod, an airborne system for measurements of mean wind, turbulence, and other meteorological parameters p 418 A90-29943

- Winds aloft measurement and airspeed calibration using Loran [AIAA PAPER 90-3331] p 847 A90-47592
- Measurement of wind characteristics at airports p 962 A90-50780

Airdata calibration of a high-performance aircraft for measuring atmospheric wind profiles
[NASA-TM-101714] p 186 N90-14228

Systems for airborne wind and turbulence measurement p 281 N90-15046

Fluctuating wind forces measured on a bluff body extending from a cavity
[AD-A216414] p 371 N90-18020

WIND PRESSURE

Inclusion of nonlinear aerodynamics in the FLAP code [DE89-009507] p 281 N90-15519

WIND PROFILES

Advances in weather technology for the aviation system p 373 A90-25572

Aviation meteorology - Panel report p 692 A90-39403

Optimization of glides for constant wind fields and course headings p 731 A90-44734

Vertical wind shears in lower-level jet stream over some airfields in the Urals and Siberia p 888 A90-48362

A scalar/vector potential solution for aerodynamic coefficients in wind shear p 21 N90-10838

A real-time wind model using digital data from aircraft [RSRE-MEMO-4309] p 137 N90-13005

Airdata calibration of a high-performance aircraft for measuring atmospheric wind profiles [NASA-TM-101714] p 186 N90-14228

WIND SHEAR

Terminal Doppler Weather Radar System - Wind shear detection will warn pilots of danger p 25 A90-10462

On a pitch control law for a constant glide slope through windshears p 117 A90-13784

Penetration landing guidance trajectories in the presence of windshear p 98 A90-14732

Acceleration, gamma, and theta guidance for abort landing in a windshear p 98 A90-14733

Effect of wind shear on flight safety p 175 A90-17973

Simple analyses of paths through windshears and downdrafts p 197 A90-19740

[AIAA PAPER 90-0222] p 197 A90-19740

A Monte Carlo simulation technique for low-altitude, wind-shear turbulence p 216 A90-19917

[AIAA PAPER 90-0564] p 216 A90-19917

Wind shear detection with pencil-beam radars p 279 A90-21386

Wind shear detection with airport surveillance radars p 241 A90-21387

Analysis of extreme wind shear p 280 A90-23255

Airborne Doppler radar detection of low-altitude wind shear p 252 A90-23284

Wind shear and hyperbolic distributions p 280 A90-23632

Development of an automated windshear detection system using Doppler weather radar p 373 A90-25567

The source region and evolution of a microburst downdraft p 456 A90-28612

Range obscuration mitigation by adaptive PRF selection for the TDWR system - Pulse Repetition Frequency for Terminal Doppler Weather Radar p 456 A90-28617

Low-level windshear alert systems and Doppler radar in aircraft terminal operations p 574 A90-35758

Wind shear at Pantelleria airport p 692 A90-39702

The response of helicopter to dispersed gust p 670 A90-42470

Cloud features suggesting low level wind shear and turbulence p 778 A90-44545

Effect of wind shear on the airspeed during the airplane landing approach p 754 A90-45160

[AIAA PAPER 90-2838] p 754 A90-45160

Probabilistic reasoning for intelligent wind shear avoidance p 890 A90-47690

[AIAA PAPER 90-3437] p 890 A90-47690

Genetic algorithms in control system optimization p 867 A90-47736

[AIAA PAPER 90-3488] p 867 A90-47736

A robust wind shear stochastic controller-estimator [AIAA PAPER 90-3489] p 867 A90-47737

Inversions and associated wind-shear warnings must be related to airport characteristics p 962 A90-52051

A scalar/vector potential solution for aerodynamic coefficients in wind shear p 21 N90-10838

Mesoscale acid deposition modeling studies [NASA-CR-4262] p 140 N90-13228

A candidate concept for display of forward-looking wind shear information p 187 N90-14232

[NASA-TM-101585] p 187 N90-14232

Adaptive clutter rejection filters for airborne Doppler weather radar applied to the detection of low altitude windshear p 214 N90-14453

[NASA-CR-186211] p 214 N90-14453

Flight in Adverse Environmental Conditions [AGARD-CP-470] p 222 N90-15041

Wind shear models for aircraft hazard investigation p 280 N90-15044

Analysis of severe atmospheric disturbances from airline flight records p 280 N90-15045

Influence of windshear, downdraft and turbulence on flight safety p 238 N90-15048

Classification of windshear severity p 281 N90-15049

How to fly windshear using the fly-by-wire concept p 258 N90-15050

A pitch control law for compensation of the phugoid mode induced by windshears p 258 N90-15051

Relative merits of reactive and forward-look detection for wind-shear encounters during landing approach for various microburst escape strategies [NASA-TM-4156] p 259 N90-15108

Joint University Program for Air Transportation Research, 1988-1989 p 468 N90-20921

[NASA-CP-3063] p 468 N90-20921

Investigation of air transportation technology at the Massachusetts Institute of Technology, 1988-1989 p 484 N90-20922

Cockpit display of hazardous wind shear information p 484 N90-20924

Cockpit display of hazardous weather information p 485 N90-20929

Investigation of air transportation technology at Princeton University, 1988-1989 p 486 N90-20935

An expert system for wind shear avoidance p 486 N90-20938

Airborne Doppler radar flight experiments for the detection of microbursts p 542 N90-21243

Windshear case study: Denver, Colorado, July 11, 1988 p 544 N90-21509

[DOT/FAA/DS-89/19] p 544 N90-21509

Optimization and guidance of flight trajectories in the presence of windshear p 574 N90-21747

[NASA-CR-186163] p 574 N90-21747

Enhanced Low Level Wind Shear (LLWS) 6-sensor improvement user's manual for data processing of field data p 583 N90-21759

[DOT/FAA/CT-TN90/8] p 583 N90-21759

A quantitative technique to estimate microburst wind shear hazard to aircraft p 692 N90-25040

Airborne CO2 Doppler lidar for wind shear detection p 849 N90-27640

Monitoring and controlling flight in windshear p 820 N90-27641

Windshear estimation along the trajectory of an aircraft p 963 N90-29745

WIND TUNNEL APPARATUS

Cryogenic wind tunnels p 199 A90-17346

Instrumentation being developed for the ONERA F4 wind tunnel p 261 A90-21049

[ONERA, TP NO. 1989-189] p 261 A90-21049

Magnetic suspension - Today's marvel, tomorrow's tool p 262 A90-23697

Low speed, indraft wind tunnels p 351 A90-26061

Non-isentropic effects on the WRDC 20 inch hypersonic wind tunnel calibration p 435 A90-28254

Influence of wind tunnel circuit installations on test section flow quality p 436 A90-28287

Status of the development programme for instrumentation and test techniques of the European Transonic Windtunnel - ETW p 437 A90-28292

Instrumentation and operation of NDA cryogenic wind tunnel p 437 A90-28293

Fully automatic calibration machine for internal 6-component wind tunnel balance including cryogenic balances p 437 A90-28294

External 6-component wind tunnel balances for aerospace simulation facilities p 438 A90-28296

A new type of calibration rig for wind tunnel balances p 438 A90-28305

Optimal conditions of flow turbulence suppression in the working section of a wind tunnel using screens located in the prechamber p 438 A90-29185

PETW testing results - Pilot European Transonic Windtunnel p 523 A90-34226

Examples of force measurements in a wind tunnel using multicomponent piezoelectric transducers p 540 A90-34352

The new high Reynolds number Mach 8 capability in the NSWC Hypervelocity Wind Tunnel 9 p 594 A90-37928

[AIAA PAPER 90-1379] p 594 A90-37928

Development and calibration of a continuous-flow arc-heated hypersonic wind tunnel p 594 A90-37930

[AIAA PAPER 90-1381] p 594 A90-37930

Automatic calibration machine for cryogenic and conventional internal strain gage balances p 595 A90-37939

[AIAA PAPER 90-1396] p 595 A90-37939

Design of a three-component wall-mounted balance p 595 A90-37940

[AIAA PAPER 90-1397] p 595 A90-37940

The six component magnetic suspension system for wind tunnel testing p 673 A90-41725

New transonic test sections for the NAE 5ftx5ft trisonic wind tunnel p 630 A90-42431

The University of Toronto-Ryerson Polytechnical Institute hypersonic gun tunnel p 673 A90-42432

Wind tunnel support system effects on a fighter aircraft model at Mach numbers from 0.6 to 2.0 p 19 N90-10010

[AD-A210614] p 19 N90-10010

Hot-film system for transition detection in cryogenic wind tunnels p 122 N90-12522

Basic aerodynamic research facility for comparative studies of flow diagnostic techniques p 122 N90-12526

Development of a multi-component internal strain-gauge balance for model tests in a cryogenic wind tunnel [NLR-TR-88157-U] p 123 N90-12628

The design and development of an acoustic test section for the ARA transonic wind tunnel p 140 N90-13202

[PNR90574] p 140 N90-13202

A vapor generator for transonic flow visualization [NASA-TM-101670] p 201 N90-13403

Design of a high angle of attack robotic sting mount for tests in a low speed wind tunnel p 526 N90-20099

[AD-A218105] p 526 N90-20099

Test and Measurement Technique in Hypersonics [ILR-MITT-225(1989)] p 618 N90-24225

The Langley 14-by-22-foot subsonic tunnel: Description, flow characteristics, and guide for users [NASA-TP-3008] p 816 N90-27649

WIND TUNNEL CALIBRATION

Non-isentropic effects on the WRDC 20 inch hypersonic wind tunnel calibration p 435 A90-28254

An optical angle of attack sensor p 446 A90-28263

Fully automatic calibration machine for internal 6-component wind tunnel balance including cryogenic balances p 437 A90-28294

A new type of calibration rig for wind tunnel balances p 438 A90-28305

The Kryo-Kanal Koeln, KKK: Description of tunnel conversion - Results of calibration tests under ambient and cryogenic conditions p 523 A90-34230

Balance calibration and evaluation software - in wind tunnel tests p 523 A90-34237

Automatic calibration machine for internal cryogenic balances p 524 A90-34247

The new high Reynolds number Mach 8 capability in the NSWC Hypervelocity Wind Tunnel 9 p 594 A90-37928

[AIAA PAPER 90-1379] p 594 A90-37928

Development and calibration of a continuous-flow arc-heated hypersonic wind tunnel p 594 A90-37930

[AIAA PAPER 90-1381] p 594 A90-37930

The new FFA T1500 transonic wind tunnel initial operation, calibration, and test results p 596 A90-37957

[AIAA PAPER 90-1420] p 596 A90-37957

The design and development of an acoustic test section for the ARA transonic wind tunnel p 140 N90-13202

[PNR90574] p 140 N90-13202

Cryogenic temperature effects on sting-balance deflections in the National Transonic Facility [NASA-TM-4157] p 202 N90-14244

The US National Transonic Facility, NTF p 262 N90-15942

The cryogenic Ludwig tube tunnel at Goettingen p 263 N90-15947

Half model tests on an ONERA calibration model in the transonic wind tunnel Goettingen, Federal Republic of Germany p 397 N90-18370

[DLR-MITT-89-20] p 397 N90-18370

Flow unsteadiness effects on boundary layers [NASA-CR-186067] p 690 N90-24557

WIND TUNNEL DRIVES

Preliminary tests of a gust generator in the ONERA S3ch transonic wind tunnel p 261 A90-21035

[ONERA, TP NO. 1989-171] p 261 A90-21035

WIND TUNNEL MODELS

Smoothing the way to future designs - A new technique for wind-tunnel measurements p 121 A90-15873

Effect of tip speed on rotor inflow p 151 A90-17311

Design and experimental verification of an equivalent forebody representation of flowing inlets p 152 A90-17863

Experimental and numerical investigation of the flow in the core of a leading edge vortex p 165 A90-19826

[AIAA PAPER 90-0384] p 165 A90-19826

Low- and high-speed tests with the Dornier 328 wind-tunnel model p 246 A90-21611

Interference between the pitot-static tube and the model in wind tunnel studies of flow parameters p 350 A90-24169

Design, realization, and qualification of model composite rotor blades p 364 A90-24293

Experience with scale effects in non-airplane wind tunnel testing p 350 A90-25165

[AIAA PAPER 90-1822] p 350 A90-25165

Determination of convective transfer coefficients on a wind-tunnel model by stimulated infrared thermography [ONERA, TP NO. 1989-218] p 351 A90-25351

Wind tunnel testing of a helicopter cab at HAL p 335 A90-26350

- Model incidence measurement using the SAAB Elio-topos system --- IR instrumentation for measuring angle of attack in transonic wind tunnel models p 446 A90-28264
- An application of structural optimization in wind tunnel model design [AIAA PAPER 90-0956] p 438 A90-29241
- Reduced size first-order subsonic and supersonic aeroelastic modeling [AIAA PAPER 90-1154] p 390 A90-29366
- Using transonic small disturbance theory for predicting the aeroelastic stability of a flexible wind-tunnel model [AIAA PAPER 90-1033] p 391 A90-29377
- Digital-flutter-suppression-system investigations for the active flexible wing wind-tunnel model [AIAA PAPER 90-1074] p 430 A90-29382
- Simulation of static and dynamic aeroelastic behavior of a flexible wing with multiple control surfaces [AIAA PAPER 90-1075] p 392 A90-29383
- Piezoelectric actuators for helicopter rotor control [AIAA PAPER 90-1076] p 411 A90-29384
- Numerical simulation of an adaptive-wall wind-tunnel - A comparison of two different strategies p 439 A90-30251
- Measurement of wind tunnel model deformation under airflow p 522 A90-33370
- Reduced-order aeroelastic models via dynamic residualization p 493 A90-33412
- An experimental investigation of the turbulent structure in a two-dimensional momentumless wake p 474 A90-33515
- PETW testing results --- Pilot European Transonic Windtunnel p 523 A90-34226
- Investigation of model rigging limitations on a high speed wind tunnel model at cryogenic temperature p 523 A90-34232
- Surface flow visualization in the cryogenic wind tunnel p 539 A90-34234
- Design and manufacture of a cryogenic wind tunnel model p 523 A90-34238
- A feasibility study for a combat aircraft model sting for the European transonic wind tunnel p 524 A90-34243
- An infrared camera system for detection of boundary layer transition in the ETW p 539 A90-34249
- A wall pressure correction method for half-model experiment in closed subsonic wind tunnel test section p 593 A90-36437
- Slotted-wall research with disk and parachute models in a low-speed wind tunnel [AIAA PAPER 90-1407] p 595 A90-37946
- Experience in the use of a viscous simulation methodology for tests in transonic tunnels [AIAA PAPER 90-1414] p 559 A90-37951
- National Transonic Facility model and model support vibration problems [AIAA PAPER 90-1416] p 596 A90-37953
- Laminar flow test installation in the Boeing Research Wind Tunnel [AIAA PAPER 90-1425] p 559 A90-37962
- Large-amplitude high-rate roll oscillation system for the measurement of non-linear airloads [AIAA PAPER 90-1426] p 590 A90-37963
- Wind tunnel studies of F/A-18 tail buffet [AIAA PAPER 90-1432] p 559 A90-37969
- Aerodynamic drag of a pair of bodies in transonic and supersonic flow p 710 A90-44935
- Evolution and test history of the V-22 0.2-scale aeroelastic model p 831 A90-46954
- Development and testing of methodology for evaluating the performance of multi-input/multi-output digital control systems [AIAA PAPER 90-3501] p 867 A90-47747
- Effect of the Mach number and shape of the front part of the obstacle on the separation zone length in supersonic flow p 903 A90-50816
- Effect of incoming flow turbulence on the aerodynamic characteristics of a smooth symmetric body at large angles of attack p 904 A90-50817
- An integrated CFD/experimental analysis of aerodynamic forces and moments [NASA-TM-102195] p 18 A90-10006
- Wind tunnel support system effects on a fighter aircraft model at Mach numbers from 0.6 to 2.0 [AD-A210614] p 19 N90-10010
- Experimental investigation of attachment-line transition in low-speed, high-lift wind-tunnel testing p 71 N90-10358
- An experimental investigation of the aerodynamic characteristics of slanted base ogive cylinders using magnetic suspension technology [NASA-CR-181708] p 21 N90-10834
- Wind tunnel test of CAD USB-STOL semi-borne prototype [NAL-TM-566] p 88 N90-11696
- On the application of modified stepwise regression for the estimation of aircraft stability and control parameters [REPT-8905] p 198 N90-13400
- Techniques for extreme attitude suspension of a wind tunnel model in a magnetic suspension and balance system [NASA-CR-181895] p 202 N90-14245
- Test techniques for cryogenic wind tunnels p 263 N90-15952
- Models for cryogenic wind tunnels p 263 N90-15956
- Experience with strain-gage balances for cryogenic wind tunnels p 264 N90-15958
- High Reynolds number tests of the CAST-10-2/DOA 2 transonic airfoil at ambient and cryogenic temperature conditions p 320 N90-17650
- Main results of CAST-10 airfoil tested in T2 cryogenic wind tunnel p 321 N90-17652
- Comparison of NAE porous wall and NASA adaptive wall test results using the NAE CAST-10 airfoil model p 353 N90-17656
- Experience with some repeat tests on the 9 inch chord CAST-10-2/DOA 2 airfoil model in the Langley 0.3-m TCT adaptive wall test section p 321 N90-17657
- Comparison of two- and three-dimensional Navier-Stokes solutions with NASA experimental data for CAST-10 airfoil p 321 N90-17658
- Contribution to the study of three-dimensional separation in turbulent incompressible flow [ESA-TT-1169] p 454 N90-18697
- Using transonic small disturbance theory for predicting the aerodynamic stability of a flexible wind-tunnel model [NASA-TM-102617] p 478 N90-20047
- Digital-flutter-suppression-system investigations for the active flexible wing wind-tunnel model [NASA-TM-102618] p 520 N90-20093
- Design of a high angle of attack robotic sting mount for tests in a low speed wind tunnel [AD-A218105] p 526 N90-20099
- Slotted-wall research with disk and parachute models in a low-speed wind tunnel [DE90-002989] p 572 N90-21737
- Aerodynamic performance of a 0.27-scale model of an AH-64 helicopter with baseline and alternate rotor blade sets [NASA-TM-4201] p 632 N90-24237
- Wind tunnel study of wake downwash behind A6 percent scale model B1-B aircraft [DE90-011783] p 719 N90-25941
- Adaptation for unsteady flow p 871 N90-26845
- Development and testing of methodology for evaluating the performance of multi-input/multi-output digital control systems [NASA-TM-102704] p 846 N90-27699
- WIND TUNNEL NOZZLES**
- Design and fabrication requirements for low noise supersonic/hypersonic wind tunnels p 122 N90-12555
- WIND TUNNEL STABILITY TESTS**
- Wind tunnel tests of a 20-gore disk-gap-band parachute [AD-A221326] p 634 N90-24251
- WIND TUNNEL TESTS**
- Wind tunnel tests of models of helicopter rotors p 29 A90-10230
- Experimental investigation on the interference effect of FL-23 wind tunnel wall on transonic flutter p 57 A90-10347
- The effect of pitch location on dynamic stall p 2 A90-10641
- Slipstream-induced pressure fluctuations on a wing panel p 77 A90-11004
- Wing-section effects on the flight performance of a remotely piloted vehicle p 29 A90-11007
- Influence of the control law on the performance of a helicopter model rotor [ONERA, TP NO. 1989-136] p 4 A90-11158
- New rotor test rig in the large Modane wind tunnel [ONERA, TP NO. 1989-137] p 58 A90-11159
- The inclusion of a similarity representation of compressor rotation in the modeling of the interaction of cannon firing with air intakes at incidence [AAAF PAPER NT 88-18] p 4 A90-11435
- Wind-tunnel test of the air intake of an unducted fan [AAAF PAPER NT 88-19] p 4 A90-11436
- Pressure pulsation in a cavity in the path of subsonic and supersonic gas flow p 10 A90-12279
- Boundary layer growth on low aspect ratio compressor blades p 12 A90-12553
- Hot wire measurements in the wake of an oscillating airfoil p 15 A90-12635
- Comparative cascade studies of some high diffusion compressor bladings p 15 A90-12637
- Turbulent separated flow over and downstream of a two-element airfoil p 16 A90-12738
- Surface roughness effect on the aerodynamic characteristics of a blunt body p 16 A90-12740
- Fatigue and electromagnetic interference test for Electro-Impulse De-Icing [SAE PAPER 891062] p 100 A90-14362
- Wind tunnel testing of high blockage models p 121 A90-15743
- Smoothing the way to future designs - A new technique for wind-tunnel measurements p 121 A90-15873
- On the effects of wind tunnel turbulence on steady and unsteady airfoil characteristics p 147 A90-16777
- A critique of the experimental aerodynamic data base for an oscillating straked wing at high angles p 147 A90-16779
- Experiments in swept-wing transition p 149 A90-16794
- Effect of tip speed on rotor inflow p 151 A90-17311
- Cryogenic wind tunnels p 199 A90-17346
- Theoretical and experimental analysis of a model rotor blade incorporating a swept tip p 151 A90-17586
- Experimental investigation of flowfield about a multielement airfoil p 154 A90-18137
- Underexpanded jet-freestream interactions on an axisymmetric afterbody configuration p 154 A90-18141
- Wall interference correction of high-lift multi-component airfoils p 158 A90-18604
- Low-speed unsteady aerodynamics of a pitching straked wing at high incidence. I - Test program. II - Harmonic analysis p 159 A90-19387
- Effect of moving surfaces on the airfoil boundary-layer control p 159 A90-19388
- Large-scale motions in a supersonic turbulent boundary layer on a curved surface [AIAA PAPER 90-0018] p 160 A90-19636
- Large-amplitude high-rate roll experiments on a delta and double delta wing [AIAA PAPER 90-0224] p 163 A90-19742
- SARL noise measurements [AIAA PAPER 90-0285] p 219 A90-19772
- Unsteady surface pressure distributions on a delta wing undergoing large amplitude pitching motions [AIAA PAPER 90-0311] p 164 A90-19790
- Experimental and numerical investigation of the flow in the core of a leading edge vortex [AIAA PAPER 90-0384] p 165 A90-19826
- Impact of nose-probe chines on the vortex flows about the F-16C [AIAA PAPER 90-0386] p 165 A90-19828
- Thin film eddy current impulse deicer [AIAA PAPER 90-0761] p 183 A90-20012
- Estimation of the flight dynamic characteristics of the YEZ-2A [AIAA PAPER 89-3173] p 245 A90-20590
- STOVL wind tunnel tests demonstrate ejector viability p 245 A90-21000
- Inviscid non equilibrium flow in ONERA F4 wind tunnel [ONERA, TP NO. 1989-161] p 223 A90-21029
- Preliminary tests of a gust generator in the ONERA S3Ch transonic wind tunnel [ONERA, TP NO. 1989-171] p 261 A90-21035
- Conditional sampling --- technique for aerodynamic characteristics measurement from wind-tunnel experiments [ONERA, TP NO. 1989-187] p 261 A90-21047
- Determination of the ground effect on the characteristics of the A320 aircraft [ONERA, TP NO. 1989-188] p 245 A90-21048
- Technical-scientific possibilities for helicopter noise research in the German-Dutch wind tunnel p 283 A90-21474
- Low- and high-speed tests with the Dornier 328 wind-tunnel model p 246 A90-21611
- Wind-tunnel investigation on the effect of a crescent planform on drag [AIAA PAPER 90-0300] p 228 A90-22196
- A hybrid method for prediction of propeller performance [AIAA PAPER 90-0440] p 229 A90-22219
- Mean and pulse characteristics of supersonic flow in a wind tunnel with a honeycomb nozzle p 231 A90-22421
- Experimental studies of shock wave/wall jet interaction in hypersonic flow [AIAA PAPER 90-0607] p 231 A90-22449
- Dynamic properties of a system for the roll control of a model electromagnetically suspended in a wind tunnel p 262 A90-22762
- Flight and wind-tunnel investigations on boundary-layer transition p 233 A90-23283
- Measurement of propellers in the ARTI 3-meter wind tunnel p 262 A90-23364
- Magnetic suspension - Today's marvel, tomorrow's tool p 262 A90-23697

- Effects of an embedded vortex on injectant from a single film-cooling hole in a turbulent boundary layer
[ASME PAPER 89-GT-189] p 362 A90-23867
- Effect of the design of a diffuser with tangential injection on the starting and separation ratios of pressures
p 295 A90-24099
- Aeroelastic deformation of a crescent-shaped rigid support in the diffuser chamber of a wind tunnel
p 364 A90-24112
- Investigation of the flow structure behind the rotating blades in the elbow of a wind tunnel in the case of acoustic excitation
p 297 A90-24124
- Ideal propeller in compressible gas flow in a wind tunnel
p 298 A90-24156
- Design, realization, and qualification of model composite rotor blades
p 364 A90-24293
- Aerodynamic heat transfer testing in hypersonic wind tunnels using an infrared imaging system
[AIAA PAPER 90-0189] p 350 A90-25027
- Experience with scale effects in non-airplane wind tunnel testing
[AIAA PAPER 90-1822] p 350 A90-25165
- Low speed testing and simulation of the STOL and Maneuver Technology Demonstrator
[AIAA PAPER 90-1820] p 334 A90-25169
- The role of computational fluid dynamics (CFD) in aircraft design
[AIAA PAPER 90-1801] p 335 A90-25175
- Experimental studies of 90 deg corner cascades in the National Full-Scale Aerodynamic Complex
[AIAA PAPER 90-1826] p 307 A90-25935
- Measurements on an oscillating 70-deg delta wing in subsonic flow
p 307 A90-26130
- Comparison of model- and full-scale wind-tunnel performance
[AIAA PAPER 88-2536] p 351 A90-26133
- Measured forces and moments on a delta wing during pitch-up
p 308 A90-26137
- Wind tunnel testing of a helicopter model at HAL
p 335 A90-26350
- Operational considerations for aerodynamic testing of large-scale wing sections in a simulated natural rain environment
[AIAA PAPER 90-0485] p 313 A90-26956
- A comparison of a droplet impingement code to icing tunnel results
[AIAA PAPER 90-0670] p 352 A90-26979
- Higher harmonic and trim control of the X-wing circulation control wind tunnel model rotor
p 435 A90-28156
- HARP model rotor test at the DNW — Hughes Advanced Rotor Program
p 406 A90-28167
- The Pointer - Test and evaluation of the tiltrotor UAV — unmanned aerial vehicle
p 406 A90-28170
- Icing Research Tunnel test of a model helicopter rotor
p 400 A90-28179
- Initial results from the joint NASA-Lewis/U.S. Army icing flight research tests
p 400 A90-28180
- Investigation of aerodynamic interactions between a rotor and fuselage in forward flight
p 385 A90-28198
- Non-isentropic effects on the WRDC 20 inch hypersonic wind tunnel calibration
p 435 A90-28254
- Application of piezoelectric foils in experimental aerodynamics
p 446 A90-28258
- Use of liquid crystals for qualitative and quantitative 2-D studies of transition and skin friction
p 446 A90-28259
- A transition detection study at Mach 1.5, 2.0, and 2.5 using a micro-thin hot-film system
p 436 A90-28260
- An optical angle of attack sensor
p 446 A90-28263
- Model incidence measurement using the SAAB Elopotos system — IR instrumentation for measuring angle of attack in transonic wind tunnel models
p 446 A90-28264
- Design of a three dimensional Doppler anemometer for T2 transonic wind tunnel
p 447 A90-28271
- Some problems on 'intelligence' of wind tunnel testing
p 436 A90-28282
- Instrumentation requirements for laminar flow research in the NLR high speed wind tunnel HST
p 447 A90-28283
- Influence of wind tunnel circuit installations on test section flow quality
p 436 A90-28287
- Computer controlled test bench for axial turbines and propellers
p 437 A90-28288
- Development of a dual strain gage balance system for measuring light loads
p 437 A90-28289
- Aerothermodynamics and transition in high-speed wind tunnels at NASA Langley
p 386 A90-28555
- Experimental aeroelasticity - History, status and future in brief
[AIAA PAPER 90-0978] p 382 A90-29598
- Aerodynamic, thermal and mechanical problems in the aerospace field
p 382 A90-29921
- Wind-tunnel investigation of wing-in-ground effects
p 395 A90-31276
- Comparison between experimental and numerical results for a research hypersonic aircraft
p 395 A90-31278
- Turbulence measurements and noise generation in a transonic cryogenic wind tunnel
[AIAA PAPER 88-2026] p 522 A90-32463
- Noise of a simulated installed model counterrotation propeller at angle-of-attack and takeoff/approach conditions
[AIAA PAPER 90-0283] p 547 A90-32505
- Aeroelastic tailoring validation by windtunnel model testing
p 492 A90-33389
- Multi-surface control law synthesis and wind tunnel test verification of active flutter suppression for a transport-type wing
p 517 A90-33401
- The effect of winglets on aircraft wing flutter
p 473 A90-33411
- Wind-tunnel and flight-test investigation of the exdrone remotely piloted vehicle configuration
[AIAA PAPER 90-1261] p 494 A90-33891
- PETW testing results --- Pilot European Transonic Windtunnel
p 523 A90-34226
- The Krylo-Kanal Koeln, KKK: Description of tunnel conversion - Results of calibration tests under ambient and cryogenic conditions
p 523 A90-34230
- A dynamic optical model attitude measurement system
p 539 A90-34236
- Balance calibration and evaluation software --- in wind tunnel tests
p 523 A90-34237
- Differential equation modeling of dynamic stall
p 476 A90-34325
- Higher harmonic control of a helicopter model rotor to reduce blade/vortex interaction noise
p 496 A90-34360
- Blockage corrections at high angles of attack in a wind tunnel
p 593 A90-35756
- Pressure and heat-transfer investigation of a hypersonic configuration
p 598 A90-35757
- A study of boundary layer stability in the case of an increased incoming stream turbulence in gradient flows
p 555 A90-36065
- Structure of a reattaching supersonic shear layer
p 555 A90-36252
- A wall pressure correction method for half-model experiment in closed subsonic wind tunnel test section
p 593 A90-36437
- Acoustics
p 614 A90-36541
- Experimental study of incompressible flow on the upper surface of a delta wing
p 558 A90-37346
- The new high Reynolds number Mach 8 capability in the NSWCH Hypervelocity Wind Tunnel 9
[AIAA PAPER 90-1379] p 594 A90-37928
- Wall interference assessment/correction (WIAC) for transonic airfoil data from porous and shaped wall test sections
[AIAA PAPER 90-1406] p 595 A90-37945
- High speed inlet testing in the NAVSWC wind tunnels
[AIAA PAPER 90-1412] p 595 A90-37949
- Priorities for high-lift testing in the 1990s
[AIAA PAPER 90-1413] p 596 A90-37950
- Experience in the use of a viscous simulation methodology for tests in transonic tunnels
[AIAA PAPER 90-1414] p 559 A90-37951
- National Transonic Facility model and model support vibration problems
[AIAA PAPER 90-1416] p 596 A90-37953
- An experimental investigation of pressure fluctuation mechanism for different transonic porous wall configurations
[AIAA PAPER 90-1417] p 604 A90-37954
- Broadband noise measurement in the transonic test section of the VTI T-38 wind tunnel
[AIAA PAPER 90-1418] p 614 A90-37955
- An experimental evaluation of test section noise in transonic wind tunnels
[AIAA PAPER 90-1419] p 614 A90-37956
- The new FFA T1500 transonic wind tunnel initial operation, calibration, and test results
[AIAA PAPER 90-1420] p 596 A90-37957
- A numerical study on the use of sulfur hexafluoride as a test gas for wind tunnels
[AIAA PAPER 90-1421] p 605 A90-37958
- On the possibilities for improvement and modernization of subsonic wind tunnels
[AIAA PAPER 90-1423] p 596 A90-37960
- A multipurpose aerodynamic research facility utilizing the abandoned Cincinnati subway tubes
[AIAA PAPER 90-1424] p 596 A90-37961
- Laminar flow test installation in the Boeing Research Wind Tunnel
[AIAA PAPER 90-1425] p 559 A90-37962
- Large-amplitude high-rate roll oscillation system for the measurement of non-linear airloads
[AIAA PAPER 90-1426] p 590 A90-37963
- Results of wind tunnel ground effect measurements on Airbus A320 using turbine power simulation and moving tunnel floor techniques
[AIAA PAPER 90-1427] p 559 A90-37964
- Flow field measurements near a fighter model at high angles of attack
[AIAA PAPER 90-1431] p 559 A90-37968
- Wind tunnel studies of F/A-18 tail buffet
[AIAA PAPER 90-1432] p 559 A90-37969
- The development of a 3-D laser velocimeter for the NASA Langley low turbulence pressure wind tunnel
[AIAA PAPER 90-1385] p 597 A90-38484
- Measurement of mean and fluctuating flow properties in hypersonic shear layers
[AIAA PAPER 90-1409] p 560 A90-38488
- Wind tunnel testing techniques on aerodynamic effects with small asymmetry
[AIAA PAPER 90-1400] p 560 A90-38490
- Correlation of separation shock motion in a compression ramp interaction with pressure fluctuations in the incoming boundary layer
[AIAA PAPER 90-1646] p 569 A90-38774
- Wave structure of artificial perturbations in a supersonic boundary layer on a plate
p 619 A90-39518
- The cryogenic wind tunnel as a testing tool for airframe/propulsion systems
p 672 A90-40400
- Investigation of the near wake of a propfan
p 622 A90-40686
- Experimental windtunnel studies for EFA
p 672 A90-41113
- Wind-tunnel measurement of noise emitted by helicopter rotors at high speed
[ONERA, TP NO. 1990-28] p 695 A90-41207
- The six component magnetic suspension system for wind tunnel testing
p 673 A90-41725
- Cryogenic wind tunnels
p 673 A90-41726
- A new noise certification method for 'light propeller aircraft' in testing
p 635 A90-41728
- The influence of control-surface compensation parameters on the hinge moment characteristics
p 643 A90-41737
- Design and analysis of a large-plug inlet ADP nacelle and pylon --- Advanced Ducted Prop
[AIAA PAPER 90-2015] p 673 A90-41986
- Investigation of unsteady flow through a transonic turbine stage. II - Data/prediction comparison for time-averaged and phase-resolved pressure data
[AIAA PAPER 90-2409] p 626 A90-42162
- Wind tunnel results and numerical computations for the NAE deHavilland series of natural laminar flow airfoils
p 628 A90-42403
- Measurements of aerodynamic forces on aircraft external stores in the NAE trisonic blowdown wind-tunnel
p 629 A90-42419
- Improving tilt rotor aircraft performance with variable-diameter rotors
p 646 A90-42445
- Experimental evaluation of expendable supersonic nozzle concepts
[AIAA PAPER 90-1904] p 740 A90-42691
- Small-scale inlet testing for low cost screening applications
[AIAA PAPER 90-1926] p 741 A90-42696
- Two- and three-dimensional effects in the supersonic mixing layer
[AIAA PAPER 90-1978] p 703 A90-42708
- Analysis of installed wind tunnel test results on large bypass ratio engine/nacelle installations
[AIAA PAPER 90-2146] p 705 A90-42738
- Propulsion integration for military aircraft
[SAE PAPER 892234] p 733 A90-45449
- A computational study of incipient leading-edge separation on a 65-deg delta wing at M = 1.60
[AIAA PAPER 90-3029] p 791 A90-45871
- Thick airfoil designs for a HALE vehicle --- High Altitude Long Endurance
[AIAA PAPER 90-3036] p 791 A90-45875
- Natural laminar flow - A wind tunnel test campaign and comparison with flight test data
[AIAA PAPER 90-3045] p 792 A90-45882
- F-18 high alpha research vehicle surface pressures - Initial in-flight results and correlation with flow visualization and wind-tunnel data
[AIAA PAPER 90-3018] p 792 A90-45885
- Multiple vortex and shock interactions at subsonic, transonic, and supersonic speeds
[AIAA PAPER 90-3023] p 793 A90-45890
- Experimental and computational surface and flow-field results for an all-body hypersonic aircraft
[AIAA PAPER 90-3067] p 793 A90-45893
- Wind tunnel studies of support strut interference on a 3 percent YF-17 fighter aircraft model at high angles of attack
[AIAA PAPER 90-3083] p 794 A90-45899
- An aerolot testing technique for low supersonic speeds in an adaptive flexible-walled wind tunnel
[AIAA PAPER 90-3086] p 795 A90-45900

- An experimental investigation of supersonic flow over two cavities in tandem
[AIAA PAPER 90-3087] p 795 A90-45901
- Exploratory wind tunnel investigation of the stability and control characteristics of a three-surface, forward-swept wing advanced turboprop model
[AIAA PAPER 90-3074] p 797 A90-45920
- On the drag reduction of bluff bodies through momentum injection
[AIAA PAPER 90-3076] p 797 A90-45922
- An experimental study of a closely coupled tandem wing configuration at low Reynolds numbers
[AIAA PAPER 90-3094] p 797 A90-45923
- Low Reynolds number airfoil design and wind tunnel testing at Princeton University p 799 A90-46362
- Experimental aerodynamic characteristics of the airfoils LA 5055 and DU 86-084/18 at low Reynolds numbers p 800 A90-46368
- Performance measurements of an airfoil at low Reynolds numbers p 800 A90-46369
- Wind-tunnel investigations of wings with serrated sharp trailing edges p 802 A90-46379
- Summary of experimental testing of a transonic low Reynolds number airfoil p 802 A90-46384
- The design of a low Reynolds number RPV p 828 A90-46385
- An experimental study of the combined effect of longitudinal riblets and vortex breakers on turbulent friction p 805 A90-46565
- Investigation of propeller slipstream effects on the Fokker 50 through in-flight pressure measurements
[AIAA PAPER 90-3084] p 806 A90-46645
- Evolution and test history of the V-22 0.2-scale aeroelastic model p 831 A90-49554
- Mixer-ejector nozzle for jet noise suppression
[AIAA PAPER 90-1909] p 894 A90-47202
- Supersonic aerodynamic characteristics of a Mach 3 high-speed civil transport configuration
[AIAA PAPER 90-3210] p 811 A90-48836
- Experimental investigation of multielement airfoil ice accretion and resulting performance degradation p 812 A90-48954
- Effects of transition on wind tunnel simulation of vehicle dynamics p 870 A90-49273
- Flow past two cylinders and two spheres p 903 A90-50815
- Strain-gage applications in wind tunnel balances p 957 A90-52037
- New methods of buffeting prediction on civil aircraft p 908 A90-52620
- A study of high-lift airfoils at high Reynolds numbers in the Langley low-turbulence pressure tunnel
[NASA-TM-89125] p 1 N90-10002
- An integrated CFD/experimental analysis of aerodynamic forces and moments
[NASA-TM-102195] p 18 N90-10006
- Wind tunnel support system effects on a fighter aircraft model at Mach numbers from 0.6 to 2.0
[AD-A210614] p 19 N90-10010
- Large-scale Advanced Prop-fan (LAP) high speed wind tunnel test report
[NASA-CR-182125] p 52 N90-10045
- The active flexible wing aeroservoelastic wind-tunnel test program p 33 N90-10119
- Experimental investigation of attachment-line transition in low-speed, high-lift wind-tunnel testing p 71 N90-10358
- Wind tunnel test of CAD USB-STOL semi-borne prototype
[NAL-TM-566] p 88 N90-11696
- The determination of the aerodynamic characteristics of an ogive-cylinder body in subsonic, curved, incompressible flow, and an assessment of the effect of flow curvature
[REPT-87-13] p 89 N90-11712
- Low-speed wind-tunnel study of reaction control-jet effectiveness for hover and transition of a STOVL fighter concept
[NASA-TM-4147] p 119 N90-11751
- The aerodynamic experimental center of Aeritalia: Combat aircraft group
[ETN-89-95213] p 122 N90-11766
- Comparison of the results of tests on A300 aircraft in the RAE 5 metre and ONERA F1 wind tunnels
[RAE-TM-AERO-2130] p 122 N90-11768
- Research in Natural Laminar Flow and Laminar-Flow Control, part 2
[NASA-CP-2487-PT-2] p 91 N90-12519
- Results of LFC experiment on slotted swept supercritical airfoil in Langley's 8-foot transonic pressure tunnel p 92 N90-12531
- Boundary-layer stability analysis of Langley Research Center 8-foot LFC experimental data p 92 N90-12532
- Wind tunnel results of the low-speed NLF(1)-0414F airfoil p 93 N90-12541
- Wind tunnel results of the high-speed NLF(1)-0213 airfoil p 93 N90-12542
- Design and test of a natural laminar flow/large Reynolds number airfoil with a high design cruise lift coefficient p 93 N90-12543
- Residual interference assessment in adaptive wall wind tunnels
[NASA-CR-181896] p 123 N90-12625
- Development of a multi-component internal strain-gauge balance for model tests in a cryogenic wind tunnel
[NLR-TR-88157-U] p 123 N90-12628
- Analysis of experimental data for CAST 10-2/DOA 2 supercritical airfoil at low Reynolds numbers and application to high Reynolds number flow
[AD-A211654] p 170 N90-13326
- Study of the integration of wind tunnel and computational methods for aerodynamic configurations
[NASA-TM-102196] p 170 N90-13332
- Reduction of profile drag by modifying the structure next to the wake area
[IMFL-88/35] p 172 N90-13356
- A wall interference assessment/correction interface measurement system for the NASA/ARC 12-ft PWT
[NASA-CR-185474] p 200 N90-13401
- A two-dimensional adaptive-wall test section with ventilated walls in the Ames 2- by 2-foot transonic wind tunnel
[NASA-TM-102207] p 201 N90-13407
- Helicopter rotor test rig (RoTeSt) in DNW: Application and results
[RAE-TRANS-2171] p 201 N90-13408
- Cryogenic temperature effects on sting-balance deflections in the National Transonic Facility
[NASA-TM-4157] p 202 N90-14244
- Techniques for extreme attitude suspension of a wind tunnel model in a magnetic suspension and balance system
[NASA-CR-181895] p 202 N90-14245
- NASA's program on icing research and technology p 239 N90-15062
- Flight and wind tunnel investigation of aerodynamic effects of aircraft ground deicing/antiicing fluids p 235 N90-15064
- An experimental investigation of wall-interference effects for parachutes in closed wind tunnels
[DE90-001802] p 236 N90-15076
- Wind tunnel tests of the influence of airfoil thickness on the normal force and pitching moment of two slender wings at transonic and supersonic Mach numbers
[ESA-TT-1129] p 237 N90-15889
- Test techniques for cryogenic wind tunnels p 263 N90-15952
- Wind tunnel investigations on the configuration of the international vortex flow experiment p 277 N90-16181
- The response of helicopter rotors to vibratory airflow
[AD-A215678] p 337 N90-16756
- Computational design of low aspect ratio wing-winglet configurations for transonic wind-tunnel tests
[NASA-CR-181939] p 316 N90-17539
- Application of experimental techniques to store release problems p 316 N90-17545
- Dynamic derivatives of missiles and fighter-type configurations at high angles of attack p 337 N90-17554
- Surface pressure distributions on a delta wing undergoing large amplitude pitching oscillations
[NASA-CR-186326] p 317 N90-17558
- Supersonic aerodynamic characteristics of a proposed Assured Crew Return Capability (ACRC) lifting-body configuration
[NASA-TM-4136] p 317 N90-17560
- A wind tunnel study of a sting-mounted circulation control wing
[AD-A216248] p 319 N90-17577
- Stability characteristics of a combat aircraft with control surface failure
[AD-A216196] p 350 N90-17646
- CAST-10-2/DOA 2 Airfoil Studies Workshop Results
[NASA-CP-3052] p 352 N90-17647
- Nonlinear transonic Wall-Interference Assessment/Correction (WIA) procedures and application to cast-10 airfoil results from the NASA 0.3-m TCT 8- by 24-inch Slotted Wall Test Section (SWTS) p 352 N90-17648
- Comparison of conventional and adaptive wall wind tunnel results with regard to Reynolds number effects p 352 N90-17649
- High Reynolds number tests of the CAST-10-2/DOA 2 transonic airfoil at ambient and cryogenic temperature conditions p 320 N90-17650
- Main results of CAST-10 airfoil tested in T2 cryogenic wind tunnel p 321 N90-17652
- An experimental AWTS process and comparisons of ONERA T2 and 0.3-m TCT AWTS data for the ONERA CAST-10 aerofoil p 321 N90-17653
- Investigation of CAST-10-2/DOA 2 airfoil in NAE high Reynolds number two-dimensional test facility p 321 N90-17654
- Residual interference and wind tunnel wall adaption p 353 N90-17655
- Comparison of NAE porous wall and NASA adaptive wall test results using the NAE CAST-10 airfoil model p 353 N90-17656
- Experience with some repeat tests on the 9 inch chord CAST-10-2/DOA 2 airfoil model in the Langley 0.3-m TCT adaptive wall test section p 321 N90-17657
- Comparison of two- and three-dimensional Navier-Stokes solutions with NASA experimental data for CAST-10 airfoil p 321 N90-17658
- Half model tests on an ONERA calibration model in the transonic wind tunnel Goettingen, Federal Republic of Germany p 397 N90-18370
- [DLR-MITT-89-20] p 397 N90-18370
- The effects of wind tunnel data uncertainty on aircraft point performance predictions
[AD-A216091] p 414 N90-18387
- Wind-tunnel investigation of a flush airdata system at Mach numbers from 0.7 to 1.4
[NASA-TM-101697] p 421 N90-18395
- Automation and extension of LDV (Laser-Doppler Velocimetry) measurements of off-design flow in a subsonic cascade wind tunnel
[AD-A216627] p 453 N90-18670
- Heat transfer measurements from a NACA 0012 airfoil in flight and in the NASA Lewis icing research tunnel
[NASA-CR-4278] p 399 N90-19203
- Conical Euler solution for a highly-swept delta wing undergoing wing-rock motion
[NASA-TM-102609] p 400 N90-19211
- Aeroservoelasticity
[NASA-TM-102620] p 416 N90-19227
- Low-speed wind-tunnel investigation of the flight dynamic characteristics of an advanced turboprop business/commuter aircraft configuration
[NASA-TP-2982] p 434 N90-19239
- Windblast protection for advanced ejection seats p 483 N90-20063
- Aerodynamic analysis of a US Navy and Marine Corps unmanned air vehicle
[AD-A218282] p 498 N90-20077
- Digital-flutter-suppression-system investigations for the active flexible wing wind-tunnel model
[NASA-TM-102618] p 520 N90-20093
- A data acquisition parallel bus for wind tunnels at ARL (Aeronautical Research Laboratory)
[AD-A218052] p 526 N90-20098
- Noise of a simulated installed model counterrotation propeller at angle-of-attack and takeoff/approach conditions
[NASA-TM-102440] p 548 N90-20794
- Investigation of air transportation technology at the Massachusetts Institute of Technology, 1988-1989 p 484 N90-20922
- Laser-velocimeter-measured flow field around an advanced, swept, eight-blade propeller at Mach 0.8
[NASA-TP-2462] p 468 N90-20942
- An approximate viscous shock layer method for calculating the hypersonic flow over blunt-nosed bodies p 479 N90-20947
- Performance data from a wind-tunnel test of two main-rotor blade designs for a utility-class helicopter
[NASA-TM-4183] p 499 N90-20974
- Advanced instrumentation for aircraft icing research
[NASA-CR-185225] p 506 N90-21006
- Measurement of the flow field in the blade passage and side-wall region of a plane turbine cascade p 513 N90-21019
- Experimental aeroelasticity history, status and future in brief
[NASA-TM-102651] p 527 N90-21047
- Numerical simulation of hypersonic flow around a space plane. Part 2: Application to high angles of attack flow
[NAL-TR-10117] p 570 N90-21726
- Slotted-wall research with disk and parachute models in a low-speed wind tunnel
[DE90-002989] p 572 N90-21737
- A video-based experimental investigation of wing rock p 592 N90-21771
- Analysis of a six-component, flow-through, strain-gage, force balance used for hypersonic wind tunnel models with scramjet exhaust flow simulation
[NASA-CR-186585] p 597 N90-21775
- Low speed testing of a laminar flow airfoil in an adaptive wall wind tunnel
[FFA-TN-1989-08] p 632 N90-23363
- Experimental performance and acoustic investigation of modern, counterrotating blade concepts
[NASA-CR-185158] p 649 N90-23393

- Aerodynamic performance of a 0.27-scale model of an AH-64 helicopter with baseline and alternate rotor blade sets
[NASA-TM-4201] p 632 N90-24237
- Static wind-tunnel and radio-controlled flight test investigation of a remotely piloted vehicle having a delta wing planform
[NASA-TM-4200] p 632 N90-24238
- Subsonic sting interference on the aerodynamic characteristics of a family of slanted-base ogive-cylinders
[NASA-CR-4299] p 633 N90-24242
- Flow unsteadiness effects on boundary layers
[NASA-CR-186067] p 690 N90-24557
- Wind tunnel study of wake downwash behind A 6 percent scale model B1-B aircraft
[DE90-011783] p 719 N90-25941
- Experimental aerothermodynamic research of hypersonic aircraft
[NASA-CR-186903] p 721 N90-25954
- Adaptation for unsteady flow
p 871 N90-26845
- Advanced recovery systems wind tunnel test report
[NASA-CR-177563] p 816 N90-27653
- Study of the flow around the prototype of A300: Results of the third test campaign at F2 and comparison with calculations
[CERT-33/5025-29-DERAT] p 817 N90-27663
- Tests of an ultra-light tunnel in the anechoic wind tunnel facility CEPRA 19
[ONERA-RF-20/7294-PH] p 872 N90-27729
- Aerodynamic and propulsive control development of the STOL and maneuver technology demonstrator
p 920 N90-28514
- Control research in the NASA high-alpha technology program
p 934 N90-28516
- Aerodynamic control design: Experience and results at Aermacchi
p 935 N90-28518
- Effects of canard position on the aerodynamic characteristics of a close-coupled canard configuration at low speed
p 920 N90-28519
- Innovative control concepts and component integration for a generic supercruise fighter
p 935 N90-28521
- The steady and time-dependent aerodynamic characteristics of a combat aircraft with a delta or swept canard
p 921 N90-28526
- Determination of the ground effect on the characteristics of the A320 aircraft
p 922 N90-28534
- Aerodynamic parameters of High-Angle-of attack Research Vehicle (HARV) estimated from flight data
[NASA-TM-102692] p 936 N90-28578
- Transonic 3-D Euler analysis of flows around fanjet engine and TPS (Turbine Powered Simulator). Comparison with wind tunnel experiment, evaluation of TPS testing method and 3-D flow
[NAL-TR-1045] p 912 N90-29327
- WIND TUNNEL WALLS**
- Experimental investigation on the interference effect of FL-23 wind tunnel wall on transonic flutter
p 57 A90-10347
- Application of panel methods to wind-tunnel wall interference corrections
[AIAA PAPER 90-0007] p 200 A90-19629
- Investigation of adaptive-wall wind tunnels with two measured interfaces
[AIAA PAPER 90-0186] p 200 A90-19728
- Permeability of the porous walls of a wind tunnel at transonic velocities
p 350 A90-24151
- Adaptive wall wind tunnels - Marriage between experiments and computations
p 351 A90-26351
- Numerical simulation of an adaptive-wall wind-tunnel - A comparison of two different strategies
p 439 A90-30251
- Wall-interference corrections for parachutes in a closed wind tunnel
p 440 A90-31281
- Nonlinear effects in the two-dimensional adaptive-wall outer-flow problem
p 554 A90-35771
- Adaptive wind tunnel walls: Compendium of final report - AGARD FDP working group 12
[AIAA PAPER 90-1405] p 595 A90-37944
- Wall interference assessment/correction (WIAC) for transonic airfoil data from porous and shaped wall test sections
[AIAA PAPER 90-1406] p 595 A90-37945
- Slotted-wall research with disk and parachute models in a low-speed wind tunnel
[AIAA PAPER 90-1407] p 595 A90-37946
- Wall interference correction for three-dimensional transonic flows
[AIAA PAPER 90-1408] p 558 A90-37947
- Evaluation of equilibrium turbulence for a naturally developing hypersonic boundary layer at nonadiabatic wall conditions
[AIAA PAPER 90-1410] p 559 A90-37948
- An experimental investigation of pressure fluctuation mechanism for different transonic porous wall configurations
[AIAA PAPER 90-1417] p 604 A90-37954
- Two-dimensional wall adaption in the transonic wind-tunnel of the AIA
p 597 A90-38497
- Sidewall boundary-layer removal and wall adaptation studies
p 672 A90-40680
- Wind tunnel wall interference investigations in NAE/NRC High Reynolds Number 2D Facility and NASA Langley 0.3m Transonic Cryogenic Tunnel
p 628 A90-42404
- An aerofoil testing technique for low supersonic speeds in an adaptive flexible-walled wind tunnel
[AIAA PAPER 90-3086] p 795 A90-45900
- Comparisons of one- and two- interface methods for tunnel wall interference calculation
p 870 A90-48961
- The effects of wall surface defects on boundary-layer transition in quiet and noisy supersonic flow
p 94 N90-12556
- Residual interference assessment in adaptive wall wind tunnels
[NASA-CR-181896] p 123 N90-12625
- Study of the integration of wind tunnel and computational methods for aerodynamic configurations
[NASA-TM-102196] p 170 N90-13332
- A wall interference assessment/correction interface measurement system for the NASA/ARC 12-ft PWT
[NASA-CR-185474] p 200 N90-13401
- A two-dimensional adaptive-wall test section with ventilated walls in the Ames 2- by 2-foot transonic wind tunnel
[NASA-TM-102207] p 201 N90-13407
- An experimental investigation of wall-interference effects for parachutes in closed wind tunnels
[DE90-001802] p 236 N90-15076
- Nonlinear transonic Wall-Interference Assessment/Correction (WIAC) procedures and application to cast-10 airfoil results from the NASA 0.3-m TCT 8- by 24-inch Slotted Wall Test Section (SWTS)
p 352 N90-17648
- Comparison of conventional and adaptive wall wind tunnel results with regard to Reynolds number effects
p 352 N90-17649
- An experimental AWTs process and comparisons of ONERA T2 and 0.3-m TCT AWTs data for the ONERA CAST-10 airfoil
p 321 N90-17653
- Residual interference and wind tunnel wall adaption
p 353 N90-17655
- Comparison of NAE porous wall and NASA adaptive wall test results using the NAE CAST-10 airfoil model
p 353 N90-17656
- Experience with some repeat tests on the 9 inch chord CAST-10-2/DOA 2 airfoil model in the Langley 0.3-m TCT adaptive wall test section
p 321 N90-17657
- Slotted-wall research with disk and parachute models in a low-speed wind tunnel
[DE90-002889] p 572 N90-21737
- Low speed testing of a laminar flow airfoil in an adaptive wall wind tunnel
[FFA-TN-1989-08] p 632 N90-23363
- Fluid Dynamics Panel Working Group 12 on Adaptive Wind Tunnel Walls: Technology and Applications
[AGARD-AR-269] p 870 N90-26838
- The aims and history of adaptive wall wind tunnels
p 871 N90-26839
- Facilities involved in adaptive wall research
p 871 N90-26840
- High productivity testing
p 871 N90-26843
- Limits of adaptation, residual interferences
p 871 N90-26844
- Adaptation for unsteady flow
p 871 N90-26845
- Aerodynamics of a linear oscillating cascade
[NASA-TM-103250] p 817 N90-27657
- WIND TUNNELS**
- The production of uniformly sheared streams by means of double gauzes in wind tunnels - A mathematical analysis
p 131 A90-15887
- The application of infrared thermography to the measurement of heat fluxes in a wind tunnel
[ONERA, TP NO. 1989-192] p 261 A90-21051
- Comparison of two droplet sizing systems in an icing wind tunnel
[AIAA PAPER 90-0668] p 274 A90-23711
- Acoustic noise emitted from vessels in an impulse-type wind tunnel
p 378 A90-24125
- Finite element analysis of the Twelve Foot Pressurized Wind Tunnel
p 760 A90-45296
- Wind tunnel support system effects on a fighter aircraft model at Mach numbers from 0.6 to 2.0
[AD-A210614] p 19 N90-10010
- Comparison of two droplet sizing systems in an icing wind tunnel
[NASA-TM-102456] p 215 N90-14617
- Pressure measurement technique in the wind tunnel division of DFVLR
[ESA-TT-1145] p 264 N90-15963
- Shock layer vacuum UV spectroscopy in an arc-jet wind tunnel
[NASA-TM-102258] p 370 N90-17112
- Analysis of the National Transonic Facility mishap
[NASA-TM-101886] p 328 N90-17620
- Residual interference and wind tunnel wall adaption
p 353 N90-17655
- Fluctuating wind forces measured on a bluff body extending from a cavity
[AD-A216414] p 371 N90-18020
- Wind-tunnel investigation of a flush airdata system at Mach numbers from 0.7 to 1.4
[NASA-TM-101697] p 421 N90-18395
- Wind tunnel design of heat island turbulent boundary layer
[IHW-ET/50] p 455 N90-19542
- Modeling of surface roughness effects on glaze ice accretion
p 485 N90-20925
- Theoretical and experimental study of flow-control devices for inlets of indraft wind tunnels
[NASA-TM-100050] p 598 N90-21778
- Thermal/structural analysis of the shaft-disk region of a fan drive system
[NASA-TM-101687] p 610 N90-22807
- Langley aerospace test highlights, 1989
[NASA-TM-102631] p 699 N90-24221
- The gun tunnel of the Brunswick Institute for Fluid Mechanics: Current development status
p 673 N90-24227
- Research at NASA's NFAC wind tunnels
[NASA-TM-102827] p 702 N90-25933
- Low-speed wind tunnel investigation of the static stability and control characteristics of an advanced turboprop configuration with the propellers placed over the tail
[NASA-CR-186900] p 759 N90-26017
- Fluid Dynamics Panel Working Group 12 on Adaptive Wind Tunnel Walls: Technology and Applications
[AGARD-AR-269] p 870 N90-26838
- Facilities involved in adaptive wall research
p 871 N90-26840
- High productivity testing
p 871 N90-26843
- WIND TURBINES**
- Inclusion of nonlinear aerodynamics in the FLAP code
[DE89-009507] p 281 N90-15519
- WIND VARIATIONS**
- Vertical wind shears in lower-level jet stream over some airfields in the Urals and Siberia
p 888 A90-48362
- Measurement of wind characteristics at airports
p 962 A90-50780
- WIND VELOCITY**
- Wind shear and hyperbolic distributions
p 280 A90-23632
- Analysis of heliport environmental data: Indianapolis downtown heliport, Wall Street heliport. Volume 2: Wall Street heliport data plots
[DOT/FAA/CT-TN87/54-VOL-2] p 121 N90-11761
- Analytical and experimental study of runway runoff with wind effects
[PTI-8948] p 123 N90-12627
- Spanwise measurements of vertical components of atmospheric turbulence
[NASA-TP-2963] p 456 N90-19718
- Analysis of heliport environmental data: Indianapolis downtown heliport, Wall Street heliport. Volume 3: Indianapolis downtown heliport data plots
[AD-A217412] p 544 N90-20500
- WIND VELOCITY MEASUREMENT**
- Improved noise rejection in automatic carrier landing systems
[AIAA PAPER 90-3374] p 864 A90-47632
- WINDOWS (APERTURES)**
- Thermostructural behavior of electromagnetic windows - Elaboration of a code package
[ONERA, TP NO. 1989-145] p 76 A90-11167
- Electrochromic windows - Applications for aircraft
[SAE PAPER 891063] p 129 A90-14363
- Electrochromic aircraft windows
p 451 A90-29891
- A measurement window for a cryogenic windtunnel
p 523 A90-34233
- WINDS ALOFT**
- Real time winds data for flight management
[AIAA PAPER 90-0565] p 197 A90-19918
- Using aircraft radar tracks to estimate wind aloft
p 241 A90-21390
- Convergence aloft as a precursor to microbursts
p 456 A90-28620
- Winds aloft measurement and airspeed calibration using Loran
[AIAA PAPER 90-3331] p 847 A90-47592
- Airdata calibration of a high-performance aircraft for measuring atmospheric wind profiles
[NASA-TM-101714] p 186 N90-14228
- WINDSHIELDS**
- The effect of windscreen bows and HUD pitch ladder on pilot performance during simulated flight
p 420 A90-31333

- Grumman/FAA lightning study - A potential countermeasure for lightning induced flashblindness of aircrew members p 819 A90-49843
- Evaluation of the improved OV-ID anti-icing system, phase 2 [AD-A213928] p 239 N90-15083
- A new method for measuring the transmissivity of aircraft transparencies [AD-A216953] p 464 N90-19842
- Full-scale birdstrike testing of in-service aged F-111 ADBIRT windshield transparencies [AD-A218035] p 484 N90-20069
- Nondestructive measurement of residual stresses in aircraft transparencies [AD-A218680] p 689 N90-23762
- B-1B improved windshield development. Volume 2: Magna analysis: Baseline and parametric [AD-A221501] p 845 N90-26828
- WING CAMBER**
- Optimal reflex camber p 308 A90-26347
- Minimum induced drag for wings with spanwise camber p 709 A90-44733
- Optimal camber distributions with multiple constraints p 810 A90-48078
- Chordwise loading and camber for two-dimensional thin sections [AD-A213318] p 95 N90-12568
- Optimum spanwise camber for minimum induced drag [BU-403] p 397 N90-18369
- Aerodynamic development perspective for traffic aeroplanes [DGLR-89-141] p 637 N90-24260
- WING FLAPS**
- Viscous corrections on wings in incompressible flow p 301 A90-25200
- Applications of the unsteady full potential equation for wings p 472 A90-33358
- Modelling aspects for the synthesis and performance assessment of some future advanced helicopters p 829 A90-46937
- WING FLOW METHOD TESTS**
- An approximate method for calculating flow past a wing profile with allowance for viscosity p 234 A90-23422
- Aerodynamics of unsteady systems. Numerical study of potential flow/boundary layer coupling [ETN-90-96257] p 396 N90-18367
- WING LOADING**
- Accumulated span loadings of an arrow wing having vortex flow p 17 A90-13025
- A numerical method for computing the aerodynamic loads on wings with sharp-edge separations at large angles of attack in subcritical transonic flows p 150 A90-16852
- Aircraft design: A conceptual approach --- Book p 179 A90-17307
- Comment on 'Drag reduction factor due to ground effect' p 159 A90-19396
- The distribution of normal-wash for minimum induced drag of non-planar wings p 226 A90-21983
- Effect of creep on the load-bearing capacity of compressed panels p 364 A90-24102
- Operational considerations for aerodynamic testing of large-scale wing sections in a simulated natural rain environment [AIAA PAPER 90-0485] p 313 A90-26956
- A study of the strength characteristics of a twin-fuselage aircraft with a trapezoid wing system p 410 A90-28993
- The use of automated parametric analysis for selecting efficient structural schemes for wings p 410 A90-29191
- A verification of the supersonic lifting line theory for the case of infinite yawed wings p 477 A90-34821
- An experimental and analytical investigation of the buffet excitation parameter p 645 A90-42417
- Wing design optimization under stress-strain constraints using full-strength and minimum mass criteria p 804 A90-46554
- Method for simultaneous wing aerodynamic and structural load prediction p 838 A90-48955
- Design of aircraft wings subjected to gust loads - A system reliability approach p 958 A90-52044
- Advanced actuation systems development, volume 1 [AD-A213334] p 121 N90-12624
- A CFD study of tilt rotor flowfields [NASA-CR-186116] p 171 N90-13349
- Advanced actuation systems development, volume 2 [AD-A213378] p 198 N90-13398
- Transonic wing charge improvements by passive shock boundary layer interference control: Development status and prospects [ETN-90-96463] p 650 N90-24267
- Model tilt-rotor hover performance and surface pressure measurement [AD-A222535] p 845 N90-26827
- WING NACELLE CONFIGURATIONS**
- Aerodynamic interference of prismatic engine nacelles with the wing at supersonic velocities p 294 A90-24078
- Calculation of the effect of the engine nacelle on transonic flow past a wing p 387 A90-28990
- The TSP methods applied to the calculation of transonic flow about wing/body/nacelle/pylon-configurations --- Transonic Small Perturbation p 554 A90-35868
- Critical review of design philosophies for recent transport WIG effect vehicles --- Wing-in Ground p 684 A90-41753
- The flow over a wing/nacelle combination in the presence of a propeller slipstream p 629 A90-42415
- Analysis of installed wind tunnel test results on large bypass ratio engine/nacelle installations [AIAA PAPER 90-2146] p 705 A90-42738
- Aerostructural considerations for the power plant of overlapping wing configuration p 841 A90-49488
- WING OSCILLATIONS**
- Further analysis of wing rock generated by forebody vortices p 153 A90-17868
- Potential flow calculation for three-dimensional wings and wing-body combination in oscillatory motion p 153 A90-17976
- Vibration of a wing of nonzero thickness in supersonic flow p 222 A90-20432
- A numerical method for three-dimensional viscous flows [AIAA PAPER 90-0236] p 228 A90-22186
- Unsteady transonic Navier-Stokes computations for an oscillating wing using single and multiple zones [AIAA PAPER 90-0313] p 228 A90-22197
- Aeroelastic tailoring of a wing with composite skin p 366 A90-25108
- Unsteady aerodynamic and aeroelastic calculations for wings using Euler equations p 302 A90-25288
- Measurements on an oscillating 70-deg delta wing in subsonic flow p 307 A90-26130
- Unsteady flow computation of oscillating flexible wings [AIAA PAPER 90-0937] p 389 A90-29363
- Navier-Stokes computations on swept-tapered wings, including flexibility [AIAA PAPER 90-1152] p 389 A90-29364
- Aeroelastic analysis of wings using the Euler equations with a deforming mesh [AIAA PAPER 90-1032] p 391 A90-29376
- Active flutter suppression for a wing model p 433 A90-31283
- Calculation of unsteady subsonic and supersonic flow about oscillating wings and bodies by new panel methods p 472 A90-33359
- A comparison between theoretical and experimental results for a 3-D wing with damped pitching oscillations p 472 A90-33361
- Calculations of unsteady aerodynamics over oscillating wings p 472 A90-33362
- Unsteady aerodynamic forces of oscillating supersonic/hypersonic wings with attached shock waves p 473 A90-33363
- Multi-surface control law synthesis and wind tunnel test verification of active flutter suppression for a transport-type wing p 517 A90-33401
- Further studies of harmonic gradient method for supersonic aeroelastic applications p 473 A90-33410
- The effect of winglets on aircraft wing flutter p 473 A90-33411
- Response characteristics of a two-dimensional wing subjected to turbulence near the flutter boundary p 519 A90-34082
- Exact solutions to the oscillations of composite aircraft wings with warping constraint and elastic coupling p 603 A90-36271
- Aeroelastic tailoring of composite wing structures p 580 A90-37217
- Unsteady aerodynamic loading produced by a sinusoidally oscillating delta wing [AIAA PAPER 90-1536] p 564 A90-38680
- Various sources of wing rock p 622 A90-40679
- Flow structure generated by oscillating delta-wing segments p 622 A90-40694
- Coupled aerodynamic forces due to unsteady stall on a high-aspect-ratio wing oscillating at high amplitude [ONERA, TP NO. 1990-24] p 623 A90-41203
- Unsteady transonic flow --- Book p 716 A90-45760
- Application of a streamwise upwind algorithm for unsteady transonic computations over oscillating wings [AIAA PAPER 90-3103] p 796 A90-45915
- Numerical analysis of natural vibrations of an aeroplane with symmetrically variable geometry wing p 860 A90-46715
- Analysis of self-excited vibrations of stiffened covering panels of an aeroplane wing p 860 A90-46716
- Lift and pitching moment measurements on a swept tapered wing in oscillatory vertical gusts p 811 A90-48089
- A numerical technique for computing the unsteady transonic flow around a wing profile in arbitrary oscillation p 906 A90-51530
- Direct multivariable adaptive controller with application to wing flutter p 349 N90-17642
- A video-based experimental investigation of wing rock p 592 N90-21771
- An experimental study of tip shape effects on the flutter of aft-swept, flat-plate wings [NASA-TM-4180] p 582 N90-22555
- ARLSUPER version 1.0, program users guide [AD-A222693] p 815 N90-26793
- The steady and time-dependent aerodynamic characteristics of a combat aircraft with a delta or swept canard p 921 N90-28526
- Multi-disciplinary optimization of aeroservoelastic systems [NASA-CR-185931] p 925 N90-29385
- WING PANELS**
- Slipstream-induced pressure fluctuations on a wing panel p 77 A90-11004
- Fatigue tests of samples of flanged joints of wings p 274 A90-23353
- Effect of creep on the load-bearing capacity of compressed panels p 364 A90-24102
- A method for calculating the stiffness characteristics of large-aspect-ratio wings with anisotropic panels in accordance with strength and aileron efficiency requirements p 334 A90-24161
- Impact damage and residual strength analysis of composite panels with bonded stiffeners --- for primary aircraft structures p 642 A90-40130
- Laminar flow control perforated wing panel development [NASA-CR-178166] p 63 N90-10187
- Pressure air tightness tests of laminated panels for wing leading edge heat shields [INFORME-I-377/89] p 357 N90-17873
- WING PLANFORMS**
- Effects of nonplanar outboard wing forms on a wing p 232 A90-23279
- Selection of the blended wing configuration for light aircraft p 234 A90-23401
- A method for calculating the location and intensity of a conical head shock on the lower surface of a delta wing with supersonic edges p 297 A90-24139
- Induced drag of a wing of low aspect ratio p 387 A90-28887
- Application of the CAP-TSD unsteady transonic small disturbance program to wing flutter --- Computational Aeroelasticity Program p 491 A90-33354
- The development of leading-edge notches to improve the subsonic performance of wings of moderate sweep p 491 A90-33367
- An investigation of the buffet excitation parameter p 473 A90-33368
- Study of forces and moments on wing-bodies at high incidence, volumes 1 and 2 p 171 N90-13350
- Application of laminar flow control to supersonic transport configurations [NASA-CR-181917] p 719 N90-25944
- The experimental investigation of flow in the core of a vortex structure p 960 N90-29597
- [BR114893]
- WING PROFILES**
- Wing-section effects on the flight performance of a remotely piloted vehicle p 29 A90-11007
- Canard-wing interaction in unsteady supersonic flow p 3 A90-11010
- An iterative non-linear lifting line model for wings with unsymmetrical stall [SAE PAPER 891020] p 83 A90-14332
- Structural analysis of the horizontal tail surfaces of subsonic transport aircraft p 102 A90-14556
- A refined optimality criterion technique applied to aircraft wing structural design p 206 A90-16718
- Flutter analysis on a non-linear wing model p 207 A90-17009
- An application of SQP and Ada to the structural optimisation of aircraft wings p 216 A90-18444
- The computational method for the transonic wing design p 160 A90-19438
- Static aeroelastic analysis of fighter aircraft using a three-dimensional Navier-Stokes algorithm [AIAA PAPER 90-0435] p 166 A90-19845
- Results of aerodynamic testing of large-scale wing sections in a simulated natural rain environment [AIAA PAPER 90-0486] p 167 A90-19874
- Inviscid drag prediction for transonic transport wings using a full-potential method [AIAA PAPER 90-0576] p 168 A90-19926
- Numerical study of the effects of icing on finite wing aerodynamics [AIAA PAPER 90-0757] p 169 A90-20010
- Advances in the efficient calculation of flows with friction p 225 A90-21475

Numerical simulation of transonic wing flows using a zonal Euler, boundary-layer, Navier-Stokes approach p 225 A90-21596

The distribution of normal-wash for minimum induced drag of non-planar wings p 226 A90-21983

Convergence of the method of discrete vortices when applied to steady-state aerodynamics problems p 231 A90-22816

Aerodynamic design methods for transonic wings p 293 A90-23978

Asymptotic solution of the optimal-deflection problem for a wing leading edge at subsonic flow velocities p 295 A90-24094

Nonstationary liquid flow of a fluid in the core of a conical vortex sheet p 296 A90-24113

Automation of the development of a finite element model for shells of the wing type p 364 A90-24118

Optimization of the relative thicknesses of a high-aspect-ratio wing in a multicriterial formulation p 334 A90-24133

Calculation of supersonic flow past a wing/fuselage combination with the resolution of a compression shock from the wing p 297 A90-24138

Construction of a wing surface in a nonviscous transonic flow from a given pressure distribution p 298 A90-24149

Wing-fuselage interference regimes at supersonic flight velocities p 298 A90-24155

Nonstationary motion of an elastic profile in subsonic incompressible flow p 300 A90-24741

Numerical simulation of separated flows around a wing section by a discrete vortex method p 307 A90-25846

Numerical simulation of wing in ground effect p 307 A90-25863

Aerodynamics of human-powered flight p 386 A90-28552

Some characteristics of changes in the nonstationary aerodynamic characteristics of a wing profile with an aileron in transonic flow p 387 A90-28989

Using the lifting line theory for calculating straight wings of arbitrary profile p 387 A90-29004

Influence of joint fixity on the aeroelastic characteristics of a joined wing structure [AIAA PAPER 90-0980] p 390 A90-29370

Skin effect in flow of a disperse fluid past a wing profile p 395 A90-30334

Static stability and control characteristics of scissor wing configurations p 433 A90-31277

Galerkin finite element method for transonic flow about airfoils and wings p 396 A90-31486

The boundary-layer fence - Barrier against the separation process p 396 A90-31493

Numerical simulation of separated flow around two-dimensional wing section by a discrete vortex method p 469 A90-32067

Nonstationary hypersonic flow past a thin wing of variable shape p 470 A90-32559

Control point selection in the discrete vortex method p 470 A90-32567

Examples of force measurements in a wind tunnel using multicomponent piezoelectric transducers p 540 A90-34352

A technique for calculating nonlinear normal-force and pitching-moment coefficients for slender delta wings, accounting for wing thickness p 476 A90-34356

Aeroelastic tailoring of composite wing structures p 580 A90-37217

Numerical solution of the problem of supersonic flow of a viscous gas past a concave conical wing p 619 A90-39465

Relationship between velocity circulation around a wing profile and vorticity dispersion in a boundary layer p 620 A90-39539

Investigations of the influence of slot blowing from the upper wing surface on the flow around the wing and its aerodynamic characteristics p 623 A90-41740

Developing the Canadair Regional Jet airliner p 729 A90-42656

Calculation of nonseparated flow past a wing profile at large Reynolds numbers p 706 A90-42995

Design of wing profiles for application in nonstall conditions in a given angle-of-attack range p 710 A90-44936

Effects of turbulence models on the prediction of transonic wing flows [SAE PAPER 892224] p 713 A90-45440

Application of divergent trailing-edge airfoil technology to the design of a derivative wing [SAE PAPER 892288] p 714 A90-45466

An entropy method for induced drag minimization [SAE PAPER 892344] p 715 A90-45496

Unsteady transonic flow --- Book p 716 A90-45760

Application of a streamwise upwind algorithm for unsteady transonic computations over oscillating wings [AIAA PAPER 90-3103] p 796 A90-45915

An experimental study of a closely coupled tandem wing configuration at low Reynolds numbers [AIAA PAPER 90-3094] p 797 A90-45923

Construction of wing profiles in subsonic gas flow by the method of quasi-solutions for inverse boundary value problems p 803 A90-46542

Application of splines to the calculation of flow past a wing profile p 805 A90-46615

Numerical analysis of natural vibrations of an aeroplane with symmetrically variable geometry wing p 860 A90-46715

Wing theory --- Book p 809 A90-47700

Winger - Computer code for aerodynamic analysis of wings p 810 A90-48077

Integrated product development (IPD) at General Dynamics Forth Worth [AIAA PAPER 90-3192] p 786 A90-48828

Parametric analysis of swept-wing geometry with sheared wing tips [AIAA PAPER 90-3196] p 812 A90-49101

A numerical technique for computing the unsteady transonic flow around a wing profile in arbitrary oscillation p 906 A90-51530

The inverse problem in the multielement airfoil theory p 906 A90-51531

The effect of energy input on the characteristics of profiles in compressible fluid media p 906 A90-51533

A straight attached shock wave at the profile tip at freestream Mach number greater than about 1 p 907 A90-51534

Wind tunnel test of CAD USB-STOL semi-borne prototype [NAL-TM-566] p 88 A90-11696

Unsteady three-dimensional thin-layer Navier Stokes solutions on dynamic blocked grids [AD-A212377] p 136 A90-12899

Efficient methods for integrated structural-aerodynamic wing optimum design p 184 A90-13376

A panel process for the calculation of the flow around a wing with front angle damping [ETN-90-95367] p 399 A90-19207

Static aeroelastic analysis of a three-dimensional generic wing [NASA-TM-102231] p 509 A90-20087

Measurement of lift development on rapidly-accelerated wings p 480 A90-20956

Study of the ground effects in the CEAT aerohydrodynamic tunnel: Using the results p 922 A90-28530

The aerodynamic design of the oblique flying wing supersonic transport [NASA-CR-177552] p 923 A90-28540

WING ROOTS

Dynamic analysis of rotor blades with rotor retention design variations [AIAA PAPER 90-1159] p 412 A90-29394

Agusta methodology for pitch link loads prediction in preliminary design phase p 646 A90-42465

On aerodynamic characteristics of canard in canard-forward-swept wing configuration p 709 A90-44833

WING SLOTS

Experimental transition and boundary-layer stability analysis for a slotted swept laminar flow control airfoil p 148 A90-16793

An experimental evaluation of slots versus porous strips for laminar-flow applications p 92 A90-12530

WING SPAN

Spanwise distribution of lift and drag at high angles of attack [SAE PAPER 891019] p 83 A90-14331

Application of the finite element method to the problem of rotational flow around wings p 156 A90-18305

Fatigue tests of samples of flanged joints of wings p 274 A90-23353

Large-amplitude high-rate roll oscillation system for the measurement of non-linear airloads [AIAA PAPER 90-1426] p 590 A90-37963

Evaluation of transonic wall interference assessment and correction for semi-span wing data [AIAA PAPER 90-1433] p 597 A90-38487

A closer look at the induced drag of crescent-shaped wings [AIAA PAPER 90-3063] p 903 A90-50638

WING TIP VORTICES

Pressure fluctuations in the tip region of a blunt-tipped airfoil p 154 A90-18136

Aerodynamic control of NASP-type vehicles through vortex manipulation [AIAA PAPER 90-0594] p 203 A90-19938

Pneumatic vortical flow control at high angles of attack [AIAA PAPER 90-0098] p 227 A90-22164

Tip vortex geometry of a hovering helicopter rotor in ground effect p 407 A90-28196

Coupled aerodynamic forces due to unsteady stall on a high-aspect-ratio wing oscillating at high amplitude [ONERA, TP NO. 1990-24] p 623 A90-41203

Local convergence of the solution in the discrete vortex method p 803 A90-46534

Experimental investigations on the stability and vorticity of the vortex breakdown phenomenon above delta wings, measured by the ultrasonic laser method [ESA-TT-1079] p 910 A90-28498

WING TIPS

Flow past a wing/fuselage combination with separation from the side edges of the wing p 295 A90-24088

Reductions in induced drag by the use of aft swept wing tips p 299 A90-24342

Prediction of tip-clearance effects on a wing by the panel method p 307 A90-25871

An automated vorticity surveying system using a rotating hot-wire probe p 447 A90-28284

Aeroelastic analysis of helicopter rotor blades with advanced tip shapes [AIAA PAPER 90-1118] p 392 A90-29390

The effect of winglets on aircraft wing flutter p 473 A90-33411

Review of vortical flow utilization [AIAA PAPER 90-1429] p 605 A90-37966

Induced drag of wings with highly swept and tapered wing tips [AIAA PAPER 90-3062] p 794 A90-45896

Experimental investigation of wingtip aerodynamic loading p 808 A90-46945

Parametric analysis of swept-wing geometry with sheared wing tips [AIAA PAPER 90-3196] p 812 A90-49101

A straight attached shock wave at the profile tip at freestream Mach number greater than about 1 p 907 A90-51534

Flutter clearance of the F-18 high-angle-of-attack research vehicle with experimental wingtip instrumentation pods [NASA-TM-4148] p 103 A90-11732

Ground evaluation of seeding an in-flight wingtip vortex using infrared imaging flow visualization technique p 635 A90-25035

Video photographic considerations for measuring the proximity of a probe aircraft with a smoke seeded trailing vortex [NASA-TM-102691] p 724 A90-25120

WING-FUSELAGE STORES

Unsteady supersonic computations of arbitrary wing-body configurations including external stores p 232 A90-23278

WINGLETS

An Euler method for wing-body-winglet flows [AIAA PAPER 90-0436] p 229 A90-22218

Winglets on rotor blades in forward flight - A theoretical and experimental investigation p 303 A90-25422

The effect of winglets on aircraft wing flutter p 473 A90-33411

An entropy method for induced drag minimization [SAE PAPER 892344] p 715 A90-45496

3D transonic nacelle and winglet design [AIAA PAPER 90-3064] p 794 A90-45897

Computational design of low aspect ratio wing-winglet configurations for transonic wind-tunnel tests [NASA-CR-181939] p 316 A90-17539

WINGS

Wing boundary layer calculation and its application to aircraft design p 84 A90-15151

Supersonic boundary layer stability analysis with and without suction on aircraft wings p 148 A90-16792

Numerical simulation of wings in steady and unsteady ground effects p 153 A90-17866

Subsonic calculation of propeller/wing interference [AIAA PAPER 90-0031] p 226 A90-22155

Calculations of the flow past bluff bodies, including tilt-rotor wing sections at $\alpha = 90^\circ$ deg [AIAA PAPER 90-0032] p 227 A90-22156

Navier-Stokes predictions of the flowfield around the F-18 (HARV) wing and fuselage at large incidence [AIAA PAPER 90-0099] p 227 A90-22165

Flight and wind-tunnel investigations on boundary-layer transition p 233 A90-23283

Comment on 'Induced drag and the ideal wake of a lifting wing' p 233 A90-23291

Propeller-wing interaction using a frequency domain panel method p 307 A90-26128

Wave formation on a liquid layer for de-icing airplane wings p 445 A90-28137

Exploratory design studies using an integrated multidisciplinary synthesis capability for actively controlled composite wings [AIAA PAPER 90-0953] p 411 A90-29238

Evaluation of current multiobjective optimization methods for aerodynamic problems using CFD codes [AIAA PAPER 90-0955] p 411 A90-29240

- An integral method for transonic flows p 395 A90-31119
- Numerical simulation of separated flows around a wing section at pitching motion by a discrete vortex method p 475 A90-33753
- Boundary layer diagnostics by means of an infrared scanning radiometer p 605 A90-38493
- Optimum design of composite wing structures subjected to displacement constraints p 680 A90-39276
- Measurements of pressures on the wing of an aircraft model during steady rotation [AIAA PAPER 90-2842] p 754 A90-45162
- Finite wing lift prediction at high angles of attack [AIAA PAPER 90-3079] p 795 A90-45910
- One wing for two airliners - Computer screens are technical trailblazers for a unique wing p 785 A90-46719
- Wing theory — Book p 809 A90-47700
- A numerical method for relating two- and three-dimensional pressure distributions on transonic wings [AIAA PAPER 90-3211] p 812 A90-48837
- All fabric N-wing unmanned powered flight systems [AIAA PAPER 90-3282] p 836 A90-48869
- Development of direct-inverse 3-D methods for applied transonic aerodynamic wing design and analysis [NASA-CR-186036] p 103 A90-11733
- A new test procedure for a wing made with carbon fiber composites [ETN-89-95220] p 126 A90-11820
- Laminar flow: The Cessna perspective p 91 A90-12507
- Induced drag for non-planar wings [LR-521] p 172 A90-13357
- Unsteady three-dimensional thin-layer Navier-Stokes solutions on dynamic blocked grids p 235 A90-15069
- An alternative derivation for an integral equation for linearized subsonic flow over a wing [AD-A214140] p 236 A90-15079
- The maximum lift coefficient of plain wings at subsonic speeds [ESDU-89034] p 236 A90-15082
- Evaluation of the improved OV-ID anti-icing system, phase 2 [AD-A213928] p 239 A90-15083
- Test techniques for cryogenic wind tunnels p 263 A90-15952
- Inspection development for T-37 wing spar cap lug [AD-A214826] p 287 A90-16708
- Analysis of indirect effects of lightning on a metallic A 300 wing: Test report [REPT-E87/645800] p 323 A90-16726
- Body effect on wing angle of attack and pitching moment at zero lift at low speeds [ESDU-89042] p 337 A90-16757
- Heat pipes for wing leading edges of hypersonic vehicles [NASA-CR-181922] p 369 A90-17055
- Opportunities for improved understanding of supersonic and hypersonic flows p 318 A90-17566
- A wind tunnel study of a sting-mounted circulation control wing [AD-A216248] p 319 A90-17577
- Direct multivariable adaptive controller with application to wing flutter p 349 A90-17642
- Half model tests on an ONERA calibration model in the transonic wind tunnel Goettingen, Federal Republic of Germany [DLR-MITT-89-20] p 397 A90-18370
- Canier wing profile in nonstationary current [ETN-90-95368] p 399 A90-19208
- Progress in inverse design and optimization in aerodynamics p 482 A90-20977
- Aerofoil design techniques p 500 A90-20978
- A system for transonic wing design with geometric constraints based on an inverse method p 501 A90-20983
- Constrained spanload optimization for minimum drag of multi-lifting-surface configurations p 501 A90-20982
- Numerical optimization of wings in transonic flow p 502 A90-20997
- Extension of a streamwise upwind algorithm to a moving grid system [NASA-TM-102800] p 572 A90-21739
- Conceptual design optimization study [NASA-CR-4298] p 582 A90-21755
- Extension of a three-dimensional viscous wing flow analysis user's manual: VISTA 3-D code [NASA-CR-182024] p 574 A90-22538
- Multilevel decomposition approach to the preliminary sizing of a transport aircraft wing [NASA-CR-4296] p 583 A90-22557
- Application of laminar flow control to supersonic transport configurations [NASA-CR-181917] p 719 A90-25944
- Effect of vortex generators on the aerodynamic wing characteristics and body of revolution [AD-A222813] p 721 A90-25955
- Report of the Fluid Dynamics Panel Working Group 10 on calculation of 3D separate turbulent flows in boundary layer limit [AGARD-AR-255] p 776 A90-26280
- An expert system advisor for damage repair of composite wing skins (repairman) p 842 A90-26810
- Advanced recovery systems wind tunnel test report [NASA-CR-177563] p 816 A90-27653
- Do inviscid vortex sheets roll-up [PD-CF-9010] p 909 A90-28491
- Study of the ground effects in the CEAT aerohydrodynamic tunnel: Using the results p 922 A90-28530
- System reliability optimization of aircraft wings p 923 A90-28536
- Damage tolerance of the fighter aircraft 37 Viggen. Part 1: Analytical assessment [FFA-TN-1990-12-PT-1] p 923 A90-28538
- Damage tolerance of the fighter aircraft 37 Viggen. Part 2: Experimental verification [FFA-TN-1990-13-PT-2] p 923 A90-28539
- WingDesign: Program for the structural design of a wing cross-section [LR-627] p 925 A90-29390
- WINTER**
Friction measurements under winter runway conditions p 321 A90-23924
- WIRE**
Attachment of lead wires to thin film thermocouples mounted on high temperature materials using the parallel gap welding process [NASA-TM-102442] p 543 A90-21361
- WIRE CLOTH**
Grid and mesh patterned electrically conductive coatings in IR systems p 503 A90-32028
- WIRING**
Boeing 727-100 test project (high energy radiated field tests) [DOT/FAA/CT-88/33] p 542 A90-21247
- WORK SOFTENING**
A rate theory investigation of cyclic loading and plastic deformation in the high stress and ambient temperature range p 954 A90-49884
- WORKLOADS (PSYCHOPHYSIOLOGY)**
On the level 2 ratings of the Cooper-Harper scale --- for pilot assessment of aircraft flying qualities p 197 A90-19577
- Research in a high-fidelity acceleration environment p 439 A90-30734
- Flight simulator evaluation of a dot-matrix display for presentation of approach map formats p 419 A90-30787
- A candidate concept for display of forward-looking wind shear information [NASA-TM-101585] p 187 A90-14232
- The application of queueing theory to the modelling of CP-140 aircraft communications [AD-A213479] p 274 A90-15310
- Aviation safety: Conditions within the air traffic control work force. Fact sheet for congressional requesters [GAO/RCED-89-113FS] p 724 A90-25958
- Flight test investigation of flight director and autopilot functions for helicopter decelerating instrument approaches [DOT/FAA/CT-TN89/54] p 869 A90-27724
- WORKSTATIONS**
Expert system - Conventional processing interface p 460 A90-30753
- Experimental work station simulator at the test station of the Bundesanstalt fuer Flugsicherung p 937 A90-52616
- Simulator evaluation of the final approach spacing tool [NASA-TM-102807] p 636 A90-23374
- WRINKLING**
The story of sandwich construction p 538 A90-33702
- WROUGHT ALLOYS**
MATE (Materials for Advanced Turbine Engines) Program, Project 3. Volume 2: Design, fabrication and evaluation of an oxide dispersion strengthened sheet alloy combustor liner [NASA-CR-180892] p 357 A90-17868
- X**
- X RAY ANALYSIS**
The application of infrared thermography to the nondestructive testing of composite materials p 886 A90-28084
- X RAY FLUORESCENCE**
In-line wear monitor [AD-A217799] p 510 A90-20091
- X RAY INSPECTION**
Aviation Security (Avsec) p 23 A90-12782
- Digital X-ray inspection p 445 A90-28162
- An advanced X-ray technique for NDI p 604 A90-37901
- X RAY SCATTERING**
Development of an X-ray backscatter densitometer for measurement of freestream density during hypersonic flight [AIAA PAPER 90-1384] p 604 A90-37933
- X WING ROTORS:**
Higher harmonic and trim control of the X-wing circulation control wind tunnel model rotor p 435 A90-28156
- RSRA/X-Wing flight control system development - Lessons learned p 430 A90-28216
- Parametric aeroelastic stability analysis of a generic X-wing aircraft p 731 A90-44737
- X-wing experimental aircraft - Lessons learned [AIAA PAPER 90-3208] p 838 A90-49105
- X-1 AIRCRAFT**
'Black Betsy' - The 6000C-4 rocket engine, 1945-1989. [IAF PAPER 89-726] p 141 A90-13700
- X-13 AIRCRAFT**
Ryan X-13 experimental aircraft - Lessons learned [AIAA PAPER 90-3236] p 834 A90-48846
- X-15 AIRCRAFT**
Prediction of forces and moments for flight vehicle control effectors. Part 1: Validation of methods for predicting hypersonic vehicle controls forces and moments [NASA-CR-186571] p 571 A90-21734
- X-19 AIRCRAFT**
The Curtiss-Wright X-19 experimental aircraft - Lessons learned [AIAA PAPER 90-3206] p 834 A90-48834
- X-22A AIRCRAFT**
The Bell X-22A V/STOL, Variable Stability Research Airplane - Lessons learned [AIAA PAPER 90-3207] p 834 A90-48835
- X-29 AIRCRAFT**
A knowledge-based system design/information tool for aircraft flight control systems [AIAA PAPER 89-2978] p 55 A90-10491
- Development of a real-time aeroperformance analysis technique for the X-29A advanced technical demonstrator p 732 A90-44738
- Numerical study of asymmetric air injection to control high angle-of-attack forebody vortices on the X-29 aircraft [AIAA PAPER 90-3004] p 788 A90-45853
- The role of CFD applied to high performance aircraft [AIAA PAPER 90-3071] p 796 A90-45917
- X-29 high angle-of-attack flight testing - Program status [AIAA PAPER 90-3303] p 837 A90-48885
- X-29 ECS high-alpha modifications [SAE PAPER 901221] p 840 A90-49295
- High alpha --- angles of attack of fighter aircraft p 902 A90-52575
- Initial flight qualification and operational maintenance of X-29A flight software [NASA-TM-101703] p 32 A90-10023
- Real-time flight test analysis and display techniques for the X-29A aircraft p 34 A90-10866
- A design procedure for the handling qualities optimization of the X-29A aircraft [NASA-TM-4142] p 119 A90-11753
- X-29A aircraft structural loads flight testing [NASA-TM-101715] p 416 A90-19225
- An in-flight interaction of the X-29A canard and flight control system [NASA-TM-101718] p 736 A90-25973
- A look at tomorrow today p 921 A90-28524
- An in-flight investigation of ground effect on a forward-swept wing airplane p 922 A90-28533
- X-30 VEHICLE**
Carbon-carbon for NASP p 599 A90-36672
- The challenge of demonstrating the X-30 p 659 A90-41162
- CFD support of NASP design [AIAA PAPER 90-3252] p 872 A90-49120
- XC-142 AIRCRAFT**
The LTV XC-142 experimental aircraft lessons learned [AIAA PAPER 90-3204] p 838 A90-49104
- XENON**
A study of the radiation of hydrogen-xenon mixtures near models flying at high supersonic velocities p 470 A90-32509
- XV-15 AIRCRAFT**
Advancements in frequency-domain methods for rotorcraft system identification p 56 A90-12771
- Damage tolerance analysis of dynamic components of rotary wing aircraft p 179 A90-17312
- Maneuver performance comparison between the XV-15 and an advanced tiltrotor design p 518 A90-33622

XV-3 AIRCRAFT

- The Bell Helicopter XV-3 and XV-15 experimental aircraft
 - Lessons learned
 [AIAA PAPER 90-3265] p 835 A90-48859
 Ice induced aerodynamic performance degradation of
 rotorcraft: An overview p 248 N90-15063
 Application of the joined wing to tiltrotor aircraft
 [NASA-CR-177543] p 248 N90-15093
 Identification of XV-15 aeroelastic modes using
 frequency-domain methods
 [NASA-TM-101021] p 582 N90-21756

XV-3 AIRCRAFT

- The Bell Helicopter XV-3 and XV-15 experimental aircraft
 - Lessons learned
 [AIAA PAPER 90-3265] p 835 A90-48859

Y**YAG LASERS**

- Laser communication system design
 p 26 A90-11813

YAK 40 AIRCRAFT

- Practical aerodynamics of the Yak-42 aircraft --- Russian
 book p 334 A90-24218

YAW

- Experimental and numerical investigation of vortex flow
 over a sideslipping delta wing p 17 A90-13016
 Aircraft modal suppression system: Existing design
 approach and its shortcomings p 33 N90-10115
 Yaw rate control of an air bearing vehicle
 p 435 N90-19420
 Actuated forebody strakes
 [NASA-CASE-LAR-13983-1] p 648 N90-23390
 Yaw fin deployment apparatus for ejection seat
 [AD-D014512] p 723 N90-25118

YAWING MOMENTS

- OPST1 - An optical yaw control system for high
 performance helicopters p 430 A90-28220
 National Transonic Facility model and model support
 vibration problems
 [AIAA PAPER 90-1416] p 596 A90-37953
 The effect of solidity on propeller normal force
 [SAE PAPER 892205] p 713 A90-45424
 Method for simultaneous wing aerodynamic and
 structural load prediction p 838 A90-48955
 Development of non-conventional control methods for
 high angle of attack flight using vortex manipulation
 p 935 N90-28522

YIELD POINT

- Investigation on sheet material of 8090 and 2091
 aluminium-lithium alloy p 267 N90-15192
 Damage tolerance of the fighter aircraft 37 Viggen. Part
 1: Analytical assessment
 [FFA-TN-1990-12-PT-1] p 923 N90-28538
 Damage tolerance of the fighter aircraft 37 Viggen. Part
 2: Experimental verification
 [FFA-TN-1990-13-PT-2] p 923 N90-28539

YTTRIUM COMPOUNDS

- Thermal barrier coatings for gas turbine and diesel
 engines
 [NASA-TM-102408] p 205 N90-13636

YTTRIUM OXIDES

- MATE (Materials for Advanced Turbine Engines)
 Program, Project 3. Volume 2: Design, fabrication and
 evaluation of an oxide dispersion strengthened sheet alloy
 combustor liner
 [NASA-CR-180892] p 357 N90-17868

YTTRIUM-ALUMINUM GARNET

- Processing and mechanical properties of
 Al₂O₃/Y₃Al₅O₁₂ (YAG) eutectic composite
 p 951 A90-51966

Z**ZEOLITES**

- Production of high density aviation fuels via novel zeolite
 catalyst routes
 [AD-A216444] p 443 N90-18601

ZERO ANGLE OF ATTACK

- The radiation of sound from a propeller at angle of
 attack
 [NASA-CR-4264] p 548 N90-21602

ZERO LIFT

- Body effect on wing angle of attack and pitching moment
 at zero lift at low speeds
 [ESDU-89042] p 337 N90-16757

ZINC SULFIDES

- Development and operating experience on a zinc-sulfide
 window for the Infrared Instrumentation System (IRIS) ---
 for gathering data on reentry vehicles
 p 505 A90-34584

ZIRCONIUM

- Observations on the brittle to ductile transition
 temperatures of B2 nickel aluminides with and without
 zirconium p 205 A90-19153

ZIRCONIUM COMPOUNDS

- Thermal barrier coatings for gas turbine and diesel
 engines
 [NASA-TM-102408] p 205 N90-13636

ZIRCONIUM OXIDES

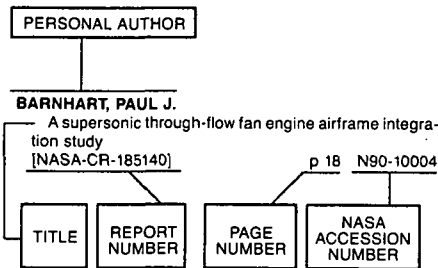
- Thermal barrier characteristics of partially stabilized
 zirconia coatings on Incoloy alloy 909 (A controlled
 expansion alloy)
 [ASME PAPER 89-GT-146] p 354 A90-23839

PERSONAL AUTHOR INDEX

AERONAUTICAL ENGINEERING / A Continuing Bibliography
1990 Cumulative Index

February 1991

Typical Personal Author Index Listing



Listings in this index are arranged alphabetically by personal author. The title of the document provides the user with a brief description of the subject matter. The report number helps to indicate the type of document listed (e.g., NASA report, translation, NASA contractor report). The page and accession numbers are located beneath and to the right of the title. Under any one author's name the accession numbers are arranged in sequence with the AIAA accession numbers appearing first.

A

- AAL, M. ABDEL**
Study of the expansion of hydrocarbon-oxygen products through supersonic nozzle p 852 A90-46907
- AAMODT, LEONARD C.**
Thermal nondestructive characterization of the integrity of protective coatings p 770 A90-44325
- AARINO, MICHAEL J.**
HF shock tunnel facility for studying supersonic combustion [AIAA PAPER 90-1551] p 600 A90-38693
- ABALAKOV, G. V.**
Effect of the inlet diameter and neck edge radius on the flow coefficient of straight-generatrix nozzles p 84 A90-14577
- ABBOTT, JOHN M.**
Control of flow separation and mixing by aerodynamic excitation [NASA-TM-103131] p 571 N90-21733
- ABBOTT, RIC**
Strength substantiation of the all composite airframe (A materials data base approach) p 490 A90-31519
Design and certification of the all-composite airframe [SAE PAPER 892210] p 732 A90-45429
Durability and damage tolerance of graphite/epoxy honeycomb structures p 942 A90-50085
- ABBOTT, TERENCE S.**
Task-oriented display design - Concept and example [SAE PAPER 892230] p 738 A90-45446
A simulation evaluation of the engine monitoring and control system display [NASA-TP-2960] p 420 N90-18393
- ABBOTT, WILLIAM Y.**
Airworthiness and flight characteristics evaluation of the McDonnell Douglas Helicopter Corporation (MDHC) 530FF helicopter [AD-A218253] p 498 N90-20076

- ABDALLA, H. A.**
Flow in compressor interstage ducts p 11 A90-12521
- ABDALLAH, S.**
Three-dimensional solutions for inviscid incompressible flow in turbomachines [ASME PAPER 89-GT-140] p 291 A90-23837
- ABDEL-MESSEH, W.**
Characteristics of partial length circular pin fins as heat transfer augmentors for airfoil internal cooling passages [ASME PAPER 89-GT-87] p 359 A90-23806
- ABDEL-RAHIM, A.**
Computational prediction of stall flutter in cascaded airfoils [AIAA PAPER 90-1116] p 392 A90-29388
- ABDELAZIK, MOHAMED A.**
The E-SAT 300A - A multichannel satellite communication system for aircraft p 914 A90-51339
- ABDOL-HAMID, KHALED S.**
Application of a new adaptive grid for aerodynamic analysis of shock containing single jets [AIAA PAPER 90-2025] p 624 A90-41988
Navier-Stokes simulation of transonic afterbody flows with jet exhaust [AIAA PAPER 90-3057] p 790 A90-45862
- ABDUL HUSAIN, R. A. A.**
Impingement/effusion cooling - The influence of the number of impingement holes and pressure loss on the heat transfer coefficient [ASME PAPER 89-GT-188] p 361 A90-23866
- ABELOFF, P. A.**
Thermal interaction between an impinging hot jet and a conducting solid surface [AIAA PAPER 90-3010] p 956 A90-50636
- ABID, RIDHA**
Effects of turbulence models on the prediction of transonic wing flows [SAE PAPER 892224] p 713 A90-45440
Prediction of separated transonic wing flows with nonequilibrium algebraic turbulence model p 809 A90-47312
- ABILEAH, ADI**
Performance of full color active-matrix-LCD in the cockpit environment p 681 A90-40392
- ABOLHASSANI, JAMSHID S.**
Applications of Lagrangian blending functions for grid generation around airplane geometries [AIAA PAPER 90-0009] p 216 A90-19630
Interactive grid adaption p 806 A90-46850
Application of Lagrangian blending functions for grid generation around airplane geometries [NASA-CR-186318] p 237 N90-15891
- ABOLHASSANI, JAMSHID SAMAREH**
Multiple-block grid adaption for an airplane geometry p 311 A90-26547
- ABOUDI, D.**
Low Reynolds number airfoils evaluation program p 151 A90-17692
- ABRAHAMSON, K.**
Application of a self-adaptive grid method to complex flows [NASA-TM-102223] p 143 N90-13324
- ABRAHAMSON, S.**
Visualization studies in rotating disk cavity flows p 475 A90-33568
- ABRAMOVICH, K. G.**
Analysis and prediction of weather for aviation p 888 A90-48351
- ABRATE, SERGE**
Composite driveshaft designs [SAE PAPER 891031] p 128 A90-14339
- ABU-HAKIMA, SUHAYYA**
Jet Engine Technical Advisor (JETA) p 693 A90-41184
- ABU-HIJLEH, B. A. K.**
Structure of a reattaching supersonic shear layer p 555 A90-36252
- ACAMPORA, G.**
EH-101 main rotor hub application of thick carbon fiber unidirectional tension bands p 618 A90-42489
- ACEVEDO, TERESA**
Challenges of tomorrow - The future of secure avionics p 419 A90-30723
- ACHENBACH, JAN D.**
Reflection by defective diffusion bonds [AD-A212995] p 206 N90-13638
- ACOSTA, WALDO A.**
Composite matrix cooling scheme for small gas turbine combustors [AIAA PAPER 90-2158] p 852 A90-47210
- ACREE, CECIL W., JR.**
Identification of XV-15 aeroelastic modes using frequency-domain methods [NASA-TM-101021] p 582 N90-21756
- ADACHI, TSUTOMU**
Improvement in turbine blade aerodynamic force in the tip region p 809 A90-47854
- ADAIR, D.**
Turbulent separated flow over and downstream of a two-element airfoil p 16 A90-12738
- ADAM, VOLKMAR**
On-board planning and control of 4D-trajectories in the TMA p 826 N90-27680
- ADAMCZYK, J. J.**
The numerical simulation of multistage turbomachinery flows p 514 N90-21025
- ADAMCZYK, JOHN J.**
Simulation of three-dimensional viscous flow within a multistage turbine [ASME PAPER 89-GT-152] p 292 A90-23841
- ADAMS, JOE H.**
Probabilistic design technology for ceramic components p 601 A90-35507
- ADAMS, KELLY J.**
The Air Force Flight Test Center Flight Test Safety Program p 35 N90-10872
- ADAMS, LOYCE M.**
Numerical algorithms for parallel computers [AD-A216812] p 377 N90-18181
- ADAMS, M. L.**
Turbomachinery blade vibration and dynamic stress measurements utilizing nonintrusive techniques p 41 A90-11558
- ADAMS, MARY S.**
Fuselage design for a specified Mach-sliced area distribution [NASA-TP-2975] p 414 N90-18385
- ADAMS, R. E.**
Parametric sizing of modern naval airships [AIAA PAPER 89-3171] p 244 A90-20586
Airship survival - Damage avoidance and control for large ocean-going airships [AIAA PAPER 89-3166] p 238 A90-20588
- ADAMS, R. J.**
Aeronautical decisionmaking for air ambulance program administrators [DOT/FAA/DS-88/8] p 635 N90-23368
- ADAMS, WENDELL G.**
The development of a 3-D laser velocimeter for the NASA Langley low turbulence pressure wind tunnel [AIAA PAPER 90-1385] p 597 A90-38484
- ADAMSON, J. D.**
The development of a probabilistic turbine rotor design system [AIAA PAPER 90-2176] p 662 A90-42060
- ADCOCK, JERRY B.**
Cryogenic temperature effects on sting-balance deflections in the National Transonic Facility [NASA-TM-4157] p 202 N90-14244
- ADDINGTON, GREGORY A.**
Controlled three-dimensionality in unsteady separated flows about a sinusoidally oscillating flat plate [AIAA PAPER 90-0689] p 230 A90-22244
- ADDISON, J. S.**
Unsteady transition in an axial-flow turbine. I - Measurements on the turbine rotor. II - Cascade measurements and modeling [ASME PAPER 89-GT-289] p 474 A90-33562
- ADELFGANG, STANLEY I.**
Analysis of extreme wind shear p 280 A90-23255

ADELMAN, HENRY

Numerical simulations of an oblique detonation wave engine p 508 A90-32964

ADELMAN, HOWARD M.

Optimal placement of tuning masses for vibration reduction in helicopter rotor blades p 247 A90-23117
Integrated multidisciplinary design optimization of rotorcraft

[NASA-TM-101642] p 36 N90-10889

Integrated multidisciplinary optimization of rotorcraft: A plan for development

[NASA-TM-101617] p 106 N90-12580

General approach and scope p 106 N90-12581

Rotor blade dynamic design p 106 N90-12583

ADGAMOV, RAVIL I.

Automatic testing in aircraft building p 285 A90-24231

ADLER, R. M.

Benefits of advanced materials, structures, and aerodynamics in future high speed civil transport propulsion systems

[AIAA PAPER 90-3285] p 853 A90-48872

ADLER, WILLIAM F.

Rain erosion testing p 525 A90-34578

ADRIAN, RONALD J.

Interaction of a plane shear layer with a downstream flat plate

[AIAA PAPER 90-1460] p 561 A90-38617

AESCHLIMAN, D. P.

Liquid crystal coatings for surface shear stress visualization in hypersonic flows

[AIAA PAPER 90-1513] p 563 A90-38660

AFANAS'EV, A. A.

Semiautomatic coding of weather phenomenon groups in the meteorological reports of automatic airport stations p 962 A90-50783

AFANAS'EV, I. V.

A study of the working process and losses in annular turbine nozzle cascades with a low contraction ratio p 254 A90-23407

AFTOSMIS, M. J.

Numerical simulation of an F-16A at angle of attack [AIAA PAPER 90-0100] p 313 A90-26911

AFZALI, HOSSEIN

Development and verification of software for flight safety critical strapdown systems p 694 A90-42454

AGARWAL, ARUN

High performance single-mode coupler for harsh environments p 78 A90-11027

AGARWAL, N. K.

Measurement of crossflow vortices, attachment-line flow, and transition using microthin hot films [AIAA PAPER 90-1636] p 607 A90-38765

AGARWAL, R.

Rotorcraft computational fluid dynamics - Recent developments at McDonnell Douglas p 630 A90-42439

AGARWAL, R. K.

Numerical simulation of three-dimensional hypersonic inlet flowfields p 13 A90-12587

Solution of the parabolized Navier-Stokes equations using Osher's upwind scheme [AIAA PAPER 90-0392] p 165 A90-19830

Numerical simulation of supersonic unsteady flow using Euler equations [AIAA PAPER 90-0415] p 229 A90-22215

A three-dimensional finite element Navier-Stokes solver with k-epsilon turbulence model for unstructured grids [AIAA PAPER 90-1652] p 570 A90-38780

AGARWAL, RAMESH K.

An algebraic adaptive-grid technique for the solution of Navier-Stokes equations [AIAA PAPER 90-1605] p 567 A90-38736

AGARWAL, TARUN K.

A parallel-vector algorithm for rapid structural analysis on high-performance computers [AIAA PAPER 90-1149] p 458 A90-29293

AGGARWAL, H. R.

Prediction and measurement of low-frequency harmonic noise of a hovering model helicopter rotor p 463 A90-28159

AGNELLO, MARK

Aircraft propulsion control systems for the next century [AIAA PAPER 90-2034] p 742 A90-42720

AGNIHOTRI, ASHOK

V-22 aerodynamic loads analysis and development of loads alleviation flight control system p 410 A90-28239

Prediction and alleviation of V-22 rotor dynamic loads p 833 A90-46974

AGRAWAL, D. P.

Effect of downstream elements on the flow at the exit of centrifugal compressor rotor p 157 A90-18483

AGRAWAL, G. L.

Foil gas bearings for turbomachinery [SAE PAPER 901236] p 841 A90-49306

AGRAWAL, S.

An evaluation of Euler solvers for transonic flowfield computations on wing-fuselage geometries [AIAA PAPER 90-3015] p 798 A90-45935

AGRAWAL, SHREEKANT

Supersonic boundary layer stability analysis with and without suction on aircraft wings p 148 A90-16792

AGRAWALA, A.

Categorization and performance analysis of advanced avionics algorithms on parallel processing architectures p 461 A90-30786

AGRICOLA, G. A.

The use of the CFM56 engine in the KC-135 tanker [SAE PAPER 892362] p 747 A90-45511

AGUERO, A.

Development of erosion resistant coatings for compression airfoils p 443 A90-31120

AGUIAR, A. J. N. M.

On the 'inverse phugoid problem' as an instance of non-linear stability in pitch p 55 A90-10221

AGULAR, A. J. N. M.

A pitch control law for compensation of the phugoid mode induced by windshears p 258 N90-15051

AHMED, ANWAR

In-flight boundary-layer transition measurements on a swept wing p 17 A90-13017

AHMED, S.

Numerical prediction of turbulent flow over airfoil sections with a new nonequilibrium turbulence model [AIAA PAPER 90-1469] p 562 A90-38626

Schlieren studies of compressibility effects on dynamic stall of airfoils in transient pitching motion [AIAA PAPER 90-3038] p 791 A90-45877

The Radarsat system p 873 A90-49671

AHMED, S. A.

An experimental investigation of isothermal swirling flow in a model of a dump combustor p 47 A90-12572

Inlet swirl effects on dump combustor flows [AIAA PAPER 90-0035] p 312 A90-26904

AHMED, S. R.

Comparison with experiment of various computational methods of airflow on three helicopter fuselages p 630 A90-42436

AHN, K. J.

Measurement and characterization of prepreg permeability with a modified bagging technique p 949 A90-50226

AHRENS, STEPHEN P.

Hover position sensing system p 848 N90-27448

AHUJA, K. K.

Application of localized active control to reduce propeller noise transmitted through fuselage surface p 78 A90-11884

AIELLO, R. A.

Parametric studies of advanced turboprops p 253 A90-21225

AIKAT, S.

Oscillating thin wings in inviscid incompressible flow p 2 A90-10224

Separated flow over slender wing, body and wing-body combination p 85 A90-15232

Potential flow calculation for three-dimensional wings and wing-body combination in oscillatory motion p 153 A90-17976

Incompressible potential flow about complete aircraft configurations p 156 A90-18443

AINSWORTH, R. W.

Data acquisition in aerodynamic research p 171 N90-13340

Wake interaction effects on the transition process on turbine blades [AD-A214492] p 343 N90-16759

AITKEN, G. S.

The Canadian Airspace Systems Plan - Maintaining the safety and efficiency of the air navigation system p 725 A90-42655

AKAMA, SHIN-YA

Endurance test of FJR 710/600S engine p 42 A90-12012

AKAY, M.

A comparison of honeycomb-core and foam-core carbon-fibre/epoxy sandwich panels p 764 A90-43855

AKIN, J. T.

Eliminating the TF30 P-111 + engine rotor-instability problem p 508 A90-32961

AKINYANJU, TED

Ground evaluation of seeding an in-flight wingtip vortex using infrared imaging flow visualization technique p 635 N90-25035

AKMANDOR, I. S.

A computational design method for shock free transonic cascades and airfoils p 501 N90-20986

AKMANDOR, I. SINAN

Simulation and second law analysis of the unsteady combustion of a non-ideal pulsating ramjet p 44 A90-12516

AL DABAGH, A. M.

Impingement/effusion cooling - The influence of the number of impingement holes and pressure loss on the heat transfer coefficient [ASME PAPER 89-GT-188] p 361 A90-23866

AL-GARNI, A.

The ascending trajectories performance and control to minimize the heat load for the transatmospheric aero-space planes [AIAA PAPER 90-2828] p 763 A90-45135

AL-KAYIEM, H. H.

A computer aided manufacturing procedure for experimental two-dimensional aerofoils p 270 A90-20609

AL-KHALIL, KAMEL M.

Development of an anti-icing runback model [AIAA PAPER 90-0759] p 238 A90-22258

AL'ES, M. IU.

Stress-strain analysis of structural elements of incompressible or nearly incompressible materials by the finite element method p 129 A90-14557

ALA, D.

Development and applications of reliability and maintainability design criteria in military aircraft [ETN-89-95208] p 107 N90-12591

ALAG, GURBUX S.

A proposed Kalman filter algorithm for estimation of unmeasured output variables for an F100 turbofan engine [AIAA PAPER 90-1920] p 656 A90-40558

ALBANIS, N.

Hot wire measurements in the wake of an oscillating airfoil p 15 A90-12635

ALBANO, G.

New approach for Doppler ambiguities resolution in medium pulse repetition frequency radars p 240 A90-20937

ALBERS, MARTIN

Saenger propulsion system options p 344 N90-16818

ALBERTS, T.

Optimal integral controller with sensor failure accommodation p 61 N90-10123

ALBERTSON, CINDY W.

Evaluation of equilibrium turbulence for a naturally developing hypersonic boundary layer at nonadiabatic wall conditions [AIAA PAPER 90-1410] p 559 A90-37948

ALBIN, A.

A probabilistic approach for the establishment of an aircraft structure inspection program p 902 A90-49892

ALBONE, C. M.

Feature-associated mesh embedding for complex configurations p 608 N90-21988

ALBRATEN, PER J.

A solution adaptive finite element method applied to two-dimensional unsteady viscous compressible cascade flow p 15 A90-12624

ALBRIGHT, C. A.

Laser welding of an advanced rapidly-solidified titanium alloy p 881 A90-47021

ALCORN, CHARLES W.

An experimental investigation of the aerodynamic characteristics of slanted base ogive cylinders using magnetic suspension technology [NASA-CR-181708] p 21 N90-10834

Subsonic sting interference on the aerodynamic characteristics of a family of slanted-base ogive-cylinders [NASA-CR-4299] p 633 N90-24242

ALDERETE, T. S.

Ground-simulation investigations of VTOL airworthiness criteria for terminal-area operations [NASA-TM-102810] p 757 N90-25141

ALDERFER, DAVID W.

Aerodynamic applications of infrared thermography p 770 A90-44147

ALEKSANDROV, A. IU.

The problem of aircraft test flight correction p 828 A90-46485

ALEKSEENKO, V. A.

Gasdynamic characteristics of a plane or axisymmetric nozzle with a rectilinear generatrix of the supersonic section p 805 A90-46575

ALEKSEVA, NATAL'IA A.

Fundamentals of the design and development of parts and mechanisms for flight vehicles p 414 A90-30275

- ALEKSEEVA, T. IA.**
Numerical modeling of the combustion kinetics of hydrocarbon fuels in an annular combustion chamber with allowance for the formation of harmful impurities p 124 A90-14582
- ALEMAN, M. A.**
Aviation Security (Avsec) p 23 A90-12782
- ALEMDAROGLU, N.**
Fortified LEWICE with viscous effects [AIAA PAPER 90-0754] p 176 A90-20009
- ALESHIN, VLADIMIR I.**
Organization of air traffic control p 915 A90-52415
- ALEXANDER, J. R.**
FAA air traffic control operations concepts. Volume 7: ATCT (Airport Traffic Control Towers) tower controllers [AD-A210455] p 332 A90-16730
- ALEXANDER, R. M.**
Test and theory for piezoelectric actuator-active vibration control of rotating machinery p 879 A90-46226
- ALEXANDER, RUSS I.**
Development of a real-time aeroperformance analysis technique for the X-29A advanced technical demonstrator p 732 A90-44738
- ALEXANDRU, MONA-LISA**
Global Sentry: NASA/USRA high altitude reconnaissance aircraft design, volume 2 [NASA-CR-186820-VOL-2] p 736 A90-25971
- ALEXE, CARMEN**
Analysis of perturbed longitudinal dynamics of an aircraft taking into consideration the stationary aeroleastic effects and the atmospheric perturbances p 520 A90-34822
- ALGEO, RICHARD D.**
Dallas/Fort Worth simulation. Volume 2: Appendixes D, E, and F [AD-A216613] p 405 A90-18380
Dallas/Fort Worth simulation, volume 1 [DOT/FAA/CT-TN89/28-VOL-1] p 824 A90-26802
Atlanta tower simulation, volume 1 [DOT/FAA/CT-TN89/27-VOL-1] p 870 A90-26835
Atlanta tower simulation: Volume 2: Appendixes [DOT/FAA/CT-TN89/27-VOL-2] p 870 A90-26836
- ALHERITIERE, E.**
beta CEZ, a high performance titanium alloy for aerospace engines [ONERA, TP NO. 1990-8] p 356 A90-25356
- ALHUSEIN, M. A.**
Turbulent boundary layer development in the presence of small isolated two-dimensional surface discontinuities p 210 A90-18507
- ALI, ALI Y.**
A/F32T-9 large turbo fan engine enclosed noise suppressor system (T-9 NSS), exterior far-field and interior noise, McConnell AFB, Kansas [AD-A220535] p 665 A90-23402
- ALISHAH, M. M.**
Algebraic boundary-conforming grid generation around wing/tail-body configurations p 308 A90-26480
- ALKALAI, K.**
Calculation of axisymmetric flows in turbomachines, through an explicit time-splitting method p 14 A90-12622
Development and application of a fractional-step method for the solution of transonic and supersonic flow problems p 709 A90-44461
- ALLAIRE, A. J. S.**
The effect of pitch location on dynamic stall p 2 A90-10641
- ALLAIRE, P. E.**
Digital control of magnetic bearings supporting a multimass flexible rotor p 682 A90-40712
- ALLAN, J. RICHARD**
Escape and survival following helicopter ditching. - Research aspects p 722 A90-44659
- ALLBRIGHT, CARL A.**
Advanced actuation systems development, volume 1 [AD-A213334] p 121 A90-12624
Advanced actuation systems development, volume 2 [AD-A213378] p 198 A90-13398
- ALLEN, DANIEL M.**
Real time data collection and control in a distributed simulator system using Ethernet TCP/IP [SAE PAPER 892356] p 761 A90-45507
- ALLEN, G. E.**
Benefits of advanced materials, structures, and aerodynamics in future high speed civil transport propulsion systems [AIAA PAPER 90-3285] p 853 A90-48872
- ALLEN, HOWARD G.**
The story of sandwich construction p 538 A90-33702
- ALLEN, JAMES G.**
A knowledge-based system design/information tool for aircraft flight control systems [AIAA PAPER 89-2978] p 55 A90-10491
- A knowledge-based system design/information tool for aircraft flight control systems [NASA-TM-101704] p 217 A90-13990
A knowledge-based system design/information tool [NASA-CR-4316] p 965 A90-29143
- ALLEN, M. G.**
Laser induced fluorescence: Practical applications p 911 A90-29323
- ALLEN, M. J.**
The remote sensing of temperature in gas turbine engine components using epithermal neutrons p 70 A90-12630
- ALLEN, S. M.**
Hierarchical damage tolerant controllers for smart structures [AD-A209422] p 31 A90-10022
- ALLEY, V. L.**
FAA air traffic control operations concepts. Volume 7: ATCT (Airport Traffic Control Towers) tower controllers [AD-A210455] p 332 A90-16730
- ALLIOT, J. C.**
Experimental-theoretical comparison for current injection on an aircraft model [ONERA, TP NO. 1989-133] p 22 A90-11157
Connection of structures by laboratory-generated electrical discharges [ONERA, TP NO. 1989-147] p 58 A90-11169
Electrostatic description of a positive leader ignition from an aircraft [ONERA, TP NO. 1989-149] p 23 A90-11171
- ALLONGUE, M.**
New rotor test rig in the large Modane wind tunnel [ONERA, TP NO. 1989-137] p 58 A90-11159
Performance and aerodynamic development of the Super Puma Mk II main rotor with new SPP8 blade tip design [ONERA, TP NO. 1989-181] p 245 A90-21041
The use of numerical optimization for helicopter airfoil and blade design p 502 A90-20995
- ALLSPACH, T.**
Highly damage tolerant carbon fiber epoxy composites for primary aircraft structural applications p 125 A90-14660
- ALLWRIGHT, S. E.**
Techniques in multiblock domain decomposition and surface grid generation p 309 A90-26526
- ALLWRIGHT, STEVE**
Multiblock topology specification and grid generation for complete aircraft configurations p 582 A90-21986
- ALMEN, G.**
Toughened cyanates for aerospace applications p 942 A90-50088
977 - Characterization of a family of new toughened epoxy resins p 943 A90-50089
- ALPAS, A. T.**
Sliding and abrasive wear behaviour of an aluminum (2014)-SiC particle reinforced composite p 530 A90-33344
- ALPERINE, SERGE**
Molten salt induced high temperature degradation of thermal barrier coatings p 952 A90-28704
- ALSALIH, ZUHEYR**
Compressible Navier-Stokes solutions over low Reynolds number airfoils p 802 A90-46382
- ALTHOFF, SUSAN L.**
Effect of tip speed on rotor inflow p 151 A90-17311
Effect of blade planform variation on a small-scale hovering rotor [NASA-TM-4146] p 173 A90-14186
- ALTOZ, F. E.**
Apparatus for cooling electronic components in aircraft [AD-D014207] p 183 A90-13373
- ALTSTADT, V.**
Highly damage tolerant carbon fiber epoxy composites for primary aircraft structural applications p 125 A90-14660
- ALTSTADT, V.**
Toughened thermosets for damage tolerant carbon fiber reinforced composites p 443 A90-29825
The effect of matrix toughness in the development of improved structural adhesives p 955 A90-50183
- ALTSTADT, VOLKER**
A third-generation bismaleimide prepreg system p 943 A90-50131
Rigidite 5255-3 - A highly damage tolerant prepreg resin system with a well balanced property profile p 944 A90-50139
- ALVERMANN, KLAUS**
Automatic processing of images from the GRATE flight test tool [DLR-FB-89-28] p 109 A90-12599
- ALVI, F. S.**
Structure of swept shock wave/boundary-layer interactions using conical shadowgraphy [AIAA PAPER 90-1644] p 569 A90-38772
- ALZIARY DE ROQUEFORT, T.**
Leading edge transition in hypersonic flows p 224 A90-21167
- AMAI, OSAMU**
Evaluating the feasibility of a radar separation minimum for a long-range SSR p 25 A90-10240
- AMALFITANO, MARGARET ERIAS**
X-29 ECS high-alpha modifications [SAE PAPER 901221] p 840 A90-49295
- AMANO, R. S.**
Grid generation and its application to separated flows p 312 A90-26552
- AMARANTOVA, I. I.**
Effect of a recess on the aerodynamic characteristics of very blunt bodies at supersonic velocities p 299 A90-24167
- AMATO, M.**
Numerical prediction of transonic viscous flows around airfoils through an Euler/boundary layer interaction method [AIAA PAPER 90-1537] p 564 A90-38681
Wake effects on the prediction of transonic viscous flows around airfoils with an Euler/boundary layer interaction approach [AIAA PAPER 90-3061] p 798 A90-45933
A computer code for the prediction of aerodynamic characteristics of lifting airfoils at transonic speed [DLC-EST-TN-030] p 632 A90-23359
- AMBUR, T. A.**
A dynamic optical model attitude measurement system p 539 A90-34236
- AMDAHL, DAVID J.**
Interactive multi-block grid generation p 310 A90-26528
- AMENDOLA, A.**
Design and testing of a multiblock grid-generation procedure for aircraft design and research p 582 A90-21984
- AMER, KENNETH B.**
A comparison of four versus five blades for the main rotor of a light helicopter p 408 A90-28215
A 'new' philosophy of structural reliability, fail safe versus safe life p 688 A90-42490
- AMICK, GROVER S.**
Unmanned air vehicles payloads and sensors p 251 A90-15930
- AMIELH, M.**
Device for the dilution of hot exhaust jets [ETN-90-97435] p 858 A90-27723
- AMJET, R. K.**
Rotor noise due to atmospheric turbulence ingestion. I - Fluid mechanics p 219 A90-19385
Rotor noise due to atmospheric turbulence ingestion. II - Aeroacoustic results p 219 A90-19386
- AMMANN, H.**
Initial service experience with the Fokker 100 [SAE PAPER 892238] p 733 A90-45450
- AMMARI, H. O.**
Simulation of cooling film density ratios in a mass transfer technique [ASME PAPER 89-GT-200] p 362 A90-23872
- AMMERMAN, H. L.**
FAA air traffic control operations concepts. Volume 7: ATCT (Airport Traffic Control Towers) tower controllers [AD-A210455] p 332 A90-16730
- AMOS, ANTHONY K.**
Chaotic response of aerosurfaces with structural nonlinearities (Status report) [AIAA PAPER 90-1034] p 392 A90-29378
- AMRANI, AHMED OMAR**
Parameter identification of aeroelastic modes of rotary wings from transient time histories p 642 A90-40166
- AMRO, J. P.**
Mechanical paint removal techniques for aircraft structures [IAR-89-23] p 773 A90-25254
- AMRO, JOE P.**
Mechanical paint removal techniques for aircraft structures [NIAR-90-12] p 775 A90-26166
- AMTSBERG, J.**
Comparison with experiment of various computational methods of airflow on three helicopter fuselages p 630 A90-42436
- AMUEDO, K. C.**
Engine inlet distortion in a 9.2 percent scaled vectored thrust STOVL model in ground effect [AIAA PAPER 89-2910] p 301 A90-25043
Engine inlet distortion in a 9.2 percent scale vectored thrust STOVL model in ground effect [NASA-TM-102358] p 318 A90-17561
- AMUEDO, KURT C.**
Hot gas ingestion characteristics and flow visualization of a vectored thrust STOVL concept [NASA-TM-103212] p 751 A90-26009

AN, JUNPING

- A fracture analysis using eight-node-isoparametric singular elements and its application in fuselage panels p 603 A90-36431

ANDEMARK, ROLF

- A study of terrain following systems and the creation of flight paths for terrain following vehicles [FOA-C-20774-2.5] p 827 N90-27691

ANDERSON, J. D., JR.

- Unsteady hypersonic viscous flow in impulse facilities [AIAA PAPER 90-0421] p 313 A90-26947

ANDERSON, J. R.

- Advances in primary-radar technology p 241 A90-21380

ANDERSON, J. THOMAS

- Airframe/propulsion integration of supersonic cruise vehicles [AIAA PAPER 90-2151] p 644 A90-42047

ANDERSON, JOHN A.

- Advanced actuation systems development, volume 1 [AD-A213334] p 121 N90-12624

- Advanced actuation systems development, volume 2 [AD-A213378] p 188 N90-13398

ANDERSON, JOHN D., JR.

- Hypersonic aerodynamics p 171 N90-13335

ANDERSON, JOHN M.

- From a sow's ear - Quantitative diagnostic design requirements from anecdotal references p 448 A90-28337

ANDERSON, MARK R.

- Modeling and analysis tools for aircraft control system evaluations p 431 A90-30703

- Robustness evaluation of a flexible aircraft control system [AIAA PAPER 90-3445] p 890 A90-47698

ANDERSON, N. E.

- Advanced gearbox technology [NASA-CR-179625] p 666 N90-24274

ANDERSON, R. P.

- Production of jet fuels from coal-derived liquids. Volume 13: Evaluation of storage and thermal stability of jet fuels derived from coal liquids [AD-A224576] p 954 N90-29527

ANDERSON, TORGER J.

- Simultaneous CARS measurements of temperature and H₂, H₂O concentrations in hydrogen-fueled supersonic combustion [AIAA PAPER 90-0158] p 205 A90-19713

ANDERSON, W. KYLE

- Navier-Stokes computations of vortical flows over low-aspect-ratio wings p 232 A90-23103

- A numerical study on the use of sulfur hexafluoride as a test gas for wind tunnels [AIAA PAPER 90-1421] p 605 A90-37958

ANDO, SHIGENORI

- A new hybrid airship ('Heliship') for commuter transport p 29 A90-11875

- Preliminary feasibility study for a new hybrid airship (Heliship) [AIAA PAPER 89-3161] p 244 A90-20581

- Critical review of design philosophies for recent transport WIG effect vehicles p 684 A90-41753

ANDRE, PIERRE

- Toward total quality in industry p 684 A90-41768

ANDRES, J.

- Eurofar - Status of the European tilt-rotor project p 645 A90-42441

ANDREW, D. N.

- The effect of uniform spanwise vorticity on the two-dimensional flow through cascades p 293 A90-23996

ANDREW, P.

- Unsteady loss in a low speed axial flow compressor during rotating stall p 12 A90-12527

ANDREWS, ALISON E.

- Knowledge-based flow field zoning p 308 A90-26478

ANDREWS, G. E.

- Impingement/effusion cooling - The influence of the number of impingement holes and pressure loss on the heat transfer coefficient [ASME PAPER 89-GT-188] p 361 A90-23866

ANDREWS, HAROLD

- The North American Rockwell XFV-12A - Reflections and some lessons [AIAA PAPER 90-3240] p 839 A90-49118

- An early overview of tiltrotor aircraft characteristics and pilot procedures in civil transport applications [DOT/FAA/DS-89/37] p 503 N90-21003

ANDREWS, J. W.

- Modeling of air-to-air visual acquisition p 282 A90-21385

- Experimental examination of the benefits of improved terminal air traffic control planning p 241 A90-21388

ANDRISANI, DOMINICK

- Estimating short-period dynamics using an extended Kalman filter [AIAA PAPER 90-1277] p 518 A90-33901

- Estimating short-period dynamics using an extended Kalman filter [NASA-TM-101722] p 648 N90-23392

ANEX, ROB

- Flight control design considerations for STOVL powered-lift flight [AIAA PAPER 90-3225] p 868 A90-49110

ANGELINI, J. J.

- New approach to small transonic perturbations finite element numerical solving method. I - Numerical developments. II - Numerical applications p 16 A90-12783

ANGRAND, FRANCOISE

- Fully vectorized implicit scheme for 2-D viscous hypersonic flow using adaptive finite element methods p 708 A90-44439

ANISHCHENKO, P. M.

- The development result of SPEKTR automated air traffic control (ATC) system with extended grade of automation for terminal and hub areas p 639 A90-41058

ANISKIN, L. V.

- Measurement of wind characteristics at airports p 962 A90-50780

ANISSIPOUR, AMIR A.

- Modifying high-order aeroelastic math model of a jet transport using maximum likelihood estimation p 61 N90-10106

ANJUM, M. I.

- Non-steady flow loss mechanisms associated with vaneless diffusers [AIAA PAPER 90-2508] p 682 A90-40641

ANJUM, MOHAMMAD I.

- An experimental investigation of non-steady flow in vaneless diffusers p 14 A90-12595

ANKUDINOV, A. L.

- Advantages of flow variables in thin viscous shock layer problems p 364 A90-24145

- Calculation of the heat flux at a three-dimensional critical point in supersonic flow past a body p 803 A90-46536

ANODINA, T. G.

- Prospects are very good for using satellites for aeronautical navigation p 403 A90-27924

- Basic areas of research in the development of a future ATM system p 551 A90-35685

ANSTEY, C. R.

- Large-amplitude high-rate roll oscillation system for the measurement of non-linear airloads [AIAA PAPER 90-1426] p 590 A90-37963

ANTOLOVICH, STEPHEN D.

- Cyclic deformation, fatigue and fatigue crack propagation in Ni-base alloys p 531 A90-34162

ANTON, D. J.

- Development of an ejection seat specification for a new fighter aircraft p 483 N90-20057

ANTONIEWICZ, ROBERT F.

- Flight test of a trajectory controller using linearizing transformations with measurement feedback [AIAA PAPER 90-3373] p 864 A90-47631

ANTONITIS, J. D.

- GPS Hover Position Sensing System p 108 A90-13986

ANTONOV, A. N.

- Pressure pulsation in a cavity in the path of subsonic and supersonic gas flow p 10 A90-12279

ANTUF'EV, B. A.

- Nonlinear transverse oscillations of a composite dynamic system p 129 A90-14558

ANURADHAKUMAAR, SMT.

- Stress analysis of gas turbine bladed disc for structural integrity applying the concept of cyclic symmetry p 46 A90-12564

AOKI, S.

- An experimental study of heat transfer and film cooling on low aspect ratio turbine nozzles [ASME PAPER 89-GT-187] p 361 A90-23865

AONO, H.

- Three dimensional photoelastic analysis of aeroengine parts p 270 A90-20077

AONO, HIRAO

- Mechanical rig rest of FJR 710/600 engine components p 43 A90-12016

APARICIO, J. P.

- Electrostatic description of a positive leader ignition from an aircraft [ONERA, TP NO. 1989-149] p 23 A90-11171

APKARIAN, P.

- Design of a helicopter output feedback control law using modal and structured-robustness techniques p 282 A90-20557

APOLONSKII, O. IU.

- A study of flow of a vibrationally nonequilibrium dissociated gas past a blunt body p 234 A90-23435

APONSO, BIMAL L.

- Reassessment and extensions of pilot ratings with new data [AIAA PAPER 90-2823] p 753 A90-45158

- Simulation investigation of multiple axis flying qualities [AIAA PAPER 90-3480] p 866 A90-47729

APPLIN, ZACHARY T.

- Experimental and theoretical aerodynamic characteristics of a high-lift semispan wing model [NASA-TP-2990] p 477 N90-20046

- The Langley 14-by 22-foot subsonic tunnel: Description, flow characteristics, and guide for users [NASA-TP-3008] p 816 N90-27649

ARABSHAHI, ABDOLLAH

- A dynamic multiblock approach to solving the unsteady Euler equations about complex configurations p 214 N90-14497

ARAKAWA, CHUICHI

- Navier-Stokes simulations around a high-speed propeller p 305 A90-25797

- Development of a new low-Reynolds-number type Reynolds stress model and its application to a lobe mixer flow p 584 A90-35229

ARALOV, A. P.

- Application of Fedorenko's multigrid method for calculating transonic flow past a profile p 295 A90-24103

ARBUCKLE, P. DOUGLAS

- Simulation model-building procedure for dynamic systems integration p 138 A90-14744

ARCHAMBAUD, J. P.

- T2 ability concerning model design and instrumentation in short run processing p 524 A90-34241

ARENA, A. S., JR.

- An experimental study of the nonlinear dynamic phenomenon known as wing rock [AIAA PAPER 90-2812] p 753 A90-45152

ARETZ, ANTHONY J.

- Cognitive requirements for aircraft navigation [NASA-CR-186933] p 824 N90-26804

ARGROW, BRIAN MAURICE

- A computational analysis of the transonic flow field of two-dimensional minimum length nozzles p 173 N90-14194

ARGYROPOULOS, ALEXANDRA

- National Airspace System flight planning operational concept [DOT/FAA/DS-89/30] p 177 N90-13362

ARIELI, RIMON

- Speed-up of the strongly implicit procedure with application to subsonic/transonic potential flows p 809 A90-47301

ARKAD'EV, A. B.

- Numerical simulation of transonic flow through oscillating and multi-row two-dimensional airfoil cascades p 814 A90-49460

ARKHAROVA, L. P.

- Interchangeability of Soviet-made and foreign mineral oils for aviation gas turbine engines p 873 A90-46525

ARMAND, C.

- Conditional sampling [ONERA, TP NO. 1989-187] p 261 A90-21047

ARMANDO, IA.

- Nondestructive analysis of aileron fatigue and aging in a Mirage F1 [REPT-M6-594000] p 184 N90-13378

ARMOUR, MICHAEL F.

- Flight test instrumentation and data processing at British Aerospace, Watton, U.K. p 59 N90-10887

ARMSTRONG, HERBERT B.

- Automatic speech recognition in air-ground data link p 690 N90-25037

ARMSTRONG, K. B.

- Repair of composite aircraft parts - An operator's viewpoint p 221 A90-20606

ARMSTRONG, KEITH B.

- Repairing the damage p 530 A90-33712

ARNAL, D.

- Leading edge contamination and relaminarisation on a swept wing at incidence p 148 A90-18789

- Prediction of transition on a swept wing p 908 A90-52592

- Experimental study of transition and leading edge contamination on swept wings p 71 N90-10362

- A three-dimensional linear stability approach to transition on wings at incidence p 20 N90-10373

- Control and modification of turbulence p 72 N90-10377

- Transition in surface boundary layers [CERT-RSF-OA-43/5018-AYD] p 136 N90-12897

- ARNETT, ERIC M.**
Propulsion control system designs for advanced Navy multimission aircraft
[AIAA PAPER 90-2403] p 663 A90-42160
- ARNETT, MICHAEL S.**
The effect of jet fuel absorption on advanced aerospace thermoset and thermoplastic composites
p 942 A90-50082
- ARNOLD, C. A.**
Poly(arylene ether ketone)/poly(aryl imide) homo- and polydimethylsiloxane segmented copolymer blends - Influence of chemical structure on miscibility and physical property behavior
p 941 A90-50063
Effect of molecular weight and end group control on the adhesion behavior of thermoplastic polyimides and poly(imide siloxane) segmented copolymers
p 947 A90-50199
- ARNOLD, F.**
Computation of multi-element airfoil flows including confluence effects
p 144 A90-16755
An interactive method for the flow calculation of airfoils with local separation regions
p 278 N90-16190
- ARNOLD, RICHARD**
MLS - Keeping pace with the future
p 640 A90-41709
- ARNONE, A. A.**
Inviscid cascade flow calculations using a multigrid method
[ASME PAPER 89-GT-22] p 288 A90-23763
- ARNTZ, NEIL J.**
CONDOR - high altitude long endurance (HALE) autonomously piloted vehicle (APV)
[AIAA PAPER 90-3279] p 836 A90-48866
- ARONOV, B. M.**
Computer-aided design of compressor rotor blade rings
p 851 A90-46497
- ARONSON, MOSES**
Taking a new look at cockpit vertical situation displays
p 652 A90-40382
- ARORA, R. P.**
A microprocessor-based system for monitoring gas turbines
p 350 A90-24359
- ARORA, S. C.**
Characteristics of partial length circular pin fins as heat transfer augmentors for airfoil internal cooling passages
[ASME PAPER 89-GT-87] p 359 A90-23806
- ARRIETA, VICTOR**
Chemical vapor deposition of Hf/Si compounds as a high temperature coating for carbon/carbon composites
p 955 A90-50159
- ARSENAUX, PETER J.**
Large-scale Advanced Prop-fan (LAP) high speed wind tunnel test report
[NASA-CR-182125] p 52 N90-10045
- ARSTENTO, G.**
The evolution of light alloys in the aerospace industry
[ETN-89-95216] p 126 N90-11872
- ARTEM'EV, V. I.**
Changes in supersonic flow past an obstacle due to the formation of a thin rarefaction channel ahead of the obstacle
p 150 A90-17108
- ARTILES, A.**
Internal rotor friction instability
[NASA-CR-183942] p 543 N90-21395
- ARTLEY, M. E.**
The influence of material quality on airframe structural durability
p 676 A90-41336
- ARTONI, E.**
Hydraulic accumulators and high pressure bottles in composite material
p 688 A90-42493
- ARTS, T.**
An experimental convective heat transfer investigation around a film-cooled gas turbine blade
p 957 A90-51261
- ARTT, D. W.**
The influence of diffuser vane leading edge geometry on the performance of a centrifugal compressor
[ASME PAPER 89-GT-163] p 292 A90-23851
- ARUNACHALAM, P.**
Selection of a suitable combustion system for a small gas turbine engine
p 112 A90-16005
- ARYANITIS, S.**
Planet gear sleeve spinning analysis
[AIAA PAPER 90-2154] p 681 A90-40613
- ARYA, V. K.**
Finite element analysis of structural components using viscoplastic models with application to a cowl lip problem
[NASA-CR-185189] p 690 N90-23769
- ARYA, VINOD K.**
Finite element elastic-plastic-creep and cyclic life analysis of a cowl lip
[NASA-TM-102342] p 610 N90-22808
- ASAHI, HIROAKI**
Flow dependent grid for aerodynamic designers
p 306 A90-25831
- ASAI, KEISUKE**
Computational and experimental analysis of transonic fanjet engine flow field using 3-D Euler code
p 306 A90-25809
The cryogenic wind tunnel as a testing tool for airframe/propulsion systems
p 672 A90-40400
Transonic 3-D Euler analysis of flows around fanjet engine and TPS (Turbine Powered Simulator). Comparison with wind tunnel experiment, evaluation of TPS testing method and 3-D flow
[NAL-TR-1045] p 912 N90-29327
- ASBURY, M. J. A.**
Towards a quantitative assessment of benefits which INS/GPS integration can offer to civil aviation operating in a non-jamming environment
p 823 A90-49496
- ASCOUGH, J. C.**
A UK perspective on the uniform engine test programme
[RAE-TM-P-1172] p 257 N90-15922
Handbook of uncertainty methodology for engine testing at Pyestock (England)
[RAE-TM-P-1179] p 751 N90-26007
- ASH, ROBERT L.**
Evaluation of equilibrium turbulence for a naturally developing hypersonic boundary layer at nonadiabatic wall conditions
[AIAA PAPER 90-1410] p 559 A90-37948
The organized nature of a turbulent trailing vortex
[AIAA PAPER 90-1625] p 568 A90-38754
A device for introducing helical perturbations into a trailing line vortex
[AIAA PAPER 90-1627] p 568 A90-38756
- ASHBY, DALE L.**
Study of the integration of wind tunnel and computational methods for aerodynamic configurations
[NASA-TM-102196] p 170 N90-13332
- ASHFORD, N.**
Modeling and analysis of airport and aircraft operations
[PB90-222167] p 915 N90-28511
- ASHFORD, N. J.**
The cost of air service fragmentation
[TT-9010] p 913 N90-29334
- ASHILL, P. R.**
CFD methods for drag prediction and analysis currently in use in UK
[RAE-TM-AERO-2146] p 95 N90-12563
A study of flows over highly-swept wings designed for maneuver at supersonic speeds
[AD-A216837] p 399 N90-19202
- ASHIZAWA, M.**
Unique features and innovative application of advanced composites to the MD-11
[AIAA PAPER 90-3217] p 838 A90-49108
- ASHJAE, JAVAD**
ASHTech XII - A new GPS technology
p 576 A90-36917
- ASHLEY, HOLT**
Unsteady aerodynamics with applications to flight mechanics
[AD-A211944] p 89 N90-11706
- ASHWOOD, PETER F.**
The Uniform Engine Test Programme
[AGARD-AR-248] p 428 N90-19232
- ASLANOV, S. K.**
Solution of sonic flow problems
p 470 A90-32712
- ASO, SHIGERU**
Measurements of pressure fluctuations in the interaction regions of shock waves and turbulent boundary layers induced by blunt fins
p 9 A90-12218
Aerodynamic heating in the interaction regions of shock waves and turbulent boundary layers induced by sharp fins
p 9 A90-12220
Aerodynamic heating in shock wave/turbulent boundary layer interaction regions induced by blunt fins
p 82 A90-13775
Numerical simulations of unsteady shock reflections by ramps
p 305 A90-25795
Numerical simulation of separated flows around a wing section by a discrete vortex method
p 307 A90-25846
Numerical simulation of separated flow around two-dimensional wing section by a discrete vortex method
p 469 A90-32067
Numerical simulation of separated flows around a wing section at pitching motion by a discrete vortex method
p 475 A90-33753
Numerical calculations of flows with shock waves by flux vector splitting method
p 808 A90-47299
- ASQUITH, G.**
The role of component testing
[PNR90589] p 115 N90-12608
- ASTAFEV, V. A.**
Effect of pressure and temperature on residue formation in aviation kerosenes
p 203 A90-17281
- ASTRIDGE, D. G.**
Helicopter transmissions - Design for safety and reliability
p 270 A90-20608
- ASWATH, C.**
Human centrifuge controller
[NAL-TM-SE-8901] p 527 N90-21043
- ATAMANCHUK, T. M.**
Aerodynamic and propulsive performance of hypersonic detonation wave ramjets
p 49 A90-12609
On- and off-design performance analysis of hypersonic detonation wave ramjets
[AIAA PAPER 90-2473] p 664 A90-42188
- ATASSI, H. M.**
Analysis of nonuniform subsonic flows about a row of moving blades
p 6 A90-11779
- ATASSI, HAFIZ M.**
Numerical solutions of the linearized Euler equations for unsteady vortical flows around lifting airfoils
[AIAA PAPER 90-0694] p 300 A90-25041
Numerical solutions of the linearized Euler equations for unsteady vortical flows around lifting airfoils
p 394 A90-30264
Numerical solutions of the linearized Euler equations for unsteady vortical flows around lifting airfoils
[NASA-TM-102466] p 318 N90-17562
- ATKIN, KEITH N.**
The EH101 electronic instrument system
p 652 A90-40462
- ATKINSON, A. STUART**
Rationale for determining information associated with aircraft gas turbine engines that is of historical importance
[AIAA PAPER 90-2754] p 617 A90-40648
- ATTA, ESSAM**
Static aeroelastic analysis of fighter aircraft using a three-dimensional Navier-Stokes algorithm
[AIAA PAPER 90-0435] p 166 A90-19845
- ATTA, ESSAM H.**
Zonal grid generation for fighter aircraft
p 311 A90-26544
- ATTA, RASHEED**
Leading-edge vortices due to low Reynolds number flow past a pitching delta wing
p 555 A90-36258
- ATWOOD, CHRISTOPHER A.**
An upwind approach to unsteady flowfield simulation
[AIAA PAPER 90-3100] p 796 A90-45912
- AU, ROBERT H.**
Optical window materials for hypersonic flow
p 496 A90-34581
- AUGUST, R.**
Structural and aerodynamic analysis of a large scale advanced propeller blade
[AIAA PAPER 90-2401] p 743 A90-42793
- AUGUSTIN, MICHAEL J.**
A review of the V-22 health monitoring system
p 417 A90-28209
- AUGUSTYN, THOMAS W.**
Applications for a small format airborne recorder
p 847 A90-48620
- AUL'CHENKO, S. M.**
Design of symmetric profiles with maximum critical flow Mach number under prescribed constraints
p 295 A90-24095
- AULEHLA, F.**
Aspects of the design of a hypersonic engine system and the selection of the intake and tail
[DGLR PAPER 88-040] p 928 A90-50233
- AULT, B. A.**
Active soot reduction in a spray-fired, axisymmetric model gas turbine combustor
[AIAA PAPER 90-0039] p 191 A90-19644
- AUME, NILSS M.**
CREW CHIEF: A computer graphics simulation of an aircraft maintenance technician
p 779 N90-25515
- AUPOIX, B.**
Calculation of three-dimensional boundary layers including hypersonic flows
p 146 A90-16773
- AVAGNINA, GIAN MARIO**
Evolution of flight commands in Aeritalia design
[ETN-89-95211] p 120 N90-11759
- EVERBACH, B. L.**
Initiation of spalling in aircraft gas turbine bearings
[AIAA PAPER 90-2291] p 686 A90-42110
- EVERY, JACK**
Enhanced combat damage tolerance/supportability for improved combat sustainability
[SAE PAPER 891078] p 101 A90-14370
- AVILA DE MELO, DENISE**
Analysis of aircraft performance during lateral maneuvering for microburst avoidance
[AIAA PAPER 90-0568] p 197 A90-19920
- AVILES, JAMES**
Equipment feasibility study: Very high frequency communication equipment (136-137 megahertz)
[DOT/FAA/CT-TN89/72] p 775 N90-26210

- AVRAN, P.**
Ceramic heat exchangers in gas turbine
[ONERA, TP NO. 1989-109] p 40 A90-11142
- AYLER, S. E.**
Recent developments in Ramjet pressure oscillation technology p 53 N90-10199
- AZAR, MASSOOD TABIB**
Silicon-etalon fiber-optic temperature sensor
[NASA-TM-102389] p 187 N90-13381
- AZIMIAN, A. R.**
Application of recess vane casing treatment to axial flow fans
[ASME PAPER 89-GT-68] p 341 A90-23791
- AZINHEIRA, J. R. C.**
A pitch control law for compensation of the phugoid mode induced by windshears p 258 N90-15051
- AZUMA, AKIRA**
Analytical study of dynamic response of helicopter in autorotative flight p 670 A90-42469
- AZZAZY, MEDHAT**
Remote detection of boundary-layer transition by an optical system p 139 N90-12524

B

- BAARSPUL, M.**
Mathematical model identification for flight simulation, based on flight and taxi tests
[LR-550] p 202 N90-13410
Lecture notes on flight simulation techniques
[LR-596] p 762 N90-25153
- BAARSPUL, MAX**
A review of flight simulation techniques p 435 A90-27953
- BAART, DOUGLAS**
Replication of NASPAC Dallas/Fort Worth study
[DOT/FAA/CT-TN90/26] p 729 N90-25123
- BABCHENKO, I. V.**
Effect of the design of a diffuser with tangential injection on the starting and separation ratios of pressures p 295 A90-24099
- BABIKOV, P. E.**
A study of flow of a vibrationally nonequilibrium dissociated gas past a blunt body p 234 A90-23435
- BACH, R. E., JR.**
A flight-test methodology for identification of an aerodynamic model for a V/STOL aircraft p 413 A90-30107
Analysis of severe atmospheric disturbances from airline flight records p 280 N90-15045
- BACH, RALPH E., JR.**
Sideslip-induced static pressure errors in flight-test measurements
[AIAA PAPER 90-3082] p 794 A90-45898
Sideslip-induced static pressure errors in flight-test measurements
[NASA-TM-102846] p 849 N90-27702
- BACHALO, W.**
Advanced instrumentation for aircraft icing research
[NASA-CR-185225] p 506 N90-21006
- BACHALO, W. D.**
Development of a phase Doppler based probe for icing cloud droplet characterization
[AIAA PAPER 90-0667] p 368 A90-26978
- BACHE, G.**
An analysis methodology for internal swirling flow systems with a rotating wall
[ASME PAPER 89-GT-185] p 361 A90-23863
- BADER, ANTON**
AIMS test and simulation equipment p 892 N90-27623
- BADGETT, M. E.**
Nonlinear maneuver autopilot for the F-15 aircraft
[NASA-CR-179442] p 77 N90-11487
- BADGLEY, ROBERT H.**
Vibration analysis for immediate assessment of battle-damaged gas turbine engines
[ASME PAPER 89-GT-96] p 341 A90-23811
- BADIAGIN, A. A.**
Selection of the blended wing configuration for light aircraft p 234 A90-23401
- BADINELLI, MARTIN**
Feasibility of using frequency offset on very high frequency air/ground voice channels
[DOT/FAA/CT-TN89/71] p 542 N90-21248
- BAE, YOON-YEONG**
Performance of an aero-space plane propulsion nozzle p 515 N90-21034
- BAEDER, J. D.**
Calculations of the flow past bluff bodies, including tilt-rotor wing sections at $\alpha = 90^\circ$ deg
[AIAA PAPER 90-0032] p 227 A90-22156
- BAEDER, JAMES DOUGLAS**
The computation and analysis of acoustic waves in transonic airfoil-vortex interactions p 966 N90-30031

- BAEHMANN, PEGGY L.**
Solving compressible flow problems using adaptive finite quadtree and octree grids p 155 A90-18243
- BAESLACK, W. A., III**
Laser welding of an advanced rapidly-solidified titanium alloy p 881 A90-47021
- BAEUMKER, MANFRED**
Analytical evaluation of helicopter true air speed and associated flight tests p 647 A90-42499
- BAGINOV, A. V.**
Parametric synthesis of piecewise constant locally optimal aircraft control under conditions of indeterminacy p 137 A90-14576
- BAHR, BEHNAM**
Neural networks for detecting defects in aircraft structures
[IAF-90-4] p 777 N90-26345
Robotic-aided system for inspection of aging aircraft
[NIAR-90-9] p 777 N90-26346
- BAHR, D. W.**
Fuel effects on gas turbine combustor dynamics
[AIAA PAPER 90-1957] p 676 A90-40570
Dynamic instability characteristics of aircraft turbine engine combustors p 53 N90-10195
- BAHREE, R.**
The design of rotor blades taking into account the combined effects of vibratory and thermal loads p 40 A90-11553
- BAI, J. M.**
Characterization of LaRC-TPI 1500 powders - A new version with controlled molecular weight p 946 A90-50177
- BAI, XUE-SONG**
The transonic nonisentropic potential calculation p 304 A90-25739
- BAIKOV, A. V.**
A source of discrete noise components in the flow path of gas turbines and fans p 894 A90-46506
- BAILE, MADHU**
Sealing the future p 442 A90-29638
Fluorosilicone sealants for aircraft fuel containment p 529 A90-31618
Silicone sealants and adhesives for aerospace/defense applications p 529 A90-31619
- BAILEY, J. D.**
Design and fabrication of a prototype resin matrix composite interceptor structure
[AIAA PAPER 90-1004] p 442 A90-29275
- BAILEY, J. E.**
Synthesis of a simulator-based automated helicopter hover trainer
[AIAA PAPER 90-3481] p 891 A90-47730
A robust wind shear stochastic controller-estimator
[AIAA PAPER 90-3489] p 867 A90-47737
- BAILEY, JOHN**
Flight beyond normal limits p 589 A90-35847
- BAILEY, M. MURRAY**
Thermal barrier coatings for gas turbine and diesel engines
[NASA-TM-102408] p 205 N90-13636
- BAILEY, M. W.**
Automated aircraft engine costing using artificial intelligence
[AIAA PAPER 90-1887] p 660 A90-41981
- BAILEY, SAMUEL A., JR.**
The Real Time Display Builder (RTDB) p 546 N90-20656
- BAILEY, T. A.**
Aircraft fire safety in the Canadian Forces p 327 N90-17604
- BAILEY, VINCE**
International SAMPE Symposium and Exhibition, 35th, Anaheim, CA, Apr. 2-5, 1990, Proceedings. Books 1 & 2 p 940 A90-50056
- BAILLARGEON, J. N.**
The gas source molecular beam epitaxial growth of $\text{Al}(\text{x})\text{Ga}(1-\text{x})\text{P}$ on (100) GaP p 894 A90-48657
- BAILLIE, STEWART**
Flight test investigation of flight director and autopilot functions for helicopter decelerating instrument approaches
[DOT/FAA/CT-TN89/54] p 869 N90-27724
- BAILLIE, STEWART W.**
Control sensitivity, bandwidth and disturbance rejection concerns for advanced rotorcraft p 430 A90-28204
Handling qualities research at the Flight Research Laboratory, NAE/NRC, 1980 - 1990 and beyond
[AIAA PAPER 90-2848] p 755 A90-45176
- BAIRAMOV, F. O.**
Dynamic damping of vibrations in mechanical systems by means of elastic links with distributed parameters p 139 A90-15568
- BAKER, DONALD J.**
Evaluation of composite components on the Bell 206L and Sikorsky S-76 helicopters
[NASA-TM-4195] p 876 N90-27787

- BAKER, GLENN D.**
Database for LDV signal processor performance analysis p 447 A90-28278
- BAKER, HENRY G.**
The NIMBLE Project - Real-time common LISP for embedded expert systems applications
[AIAA PAPER 89-3140] p 75 A90-10614
- BAKER, JOHN L.**
Mode S system design and architecture p 330 A90-25569
- BAKER, SUSAN P.**
Colorado mountain flying - Crashes and weather
[AIAA PAPER 90-0369] p 175 A90-19818
- BAKER, TIMOTHY J.**
Automatic mesh generation for complex three-dimensional regions using a constrained Delaunay triangulation p 375 A90-26022
Generation of tetrahedral meshes around complete aircraft p 310 A90-26536
- BAKER, V.**
Experimental evaluation of expendable supersonic nozzle concepts
[AIAA PAPER 90-1904] p 740 A90-42691
- BAKHLE, MILIND A.**
Time domain flutter analysis of cascades using a full-potential solver
[AIAA PAPER 90-0984] p 391 A90-29374
- BAKOS, ROBERT**
Hypervelocity real gas capabilities of GASL's expansion tube (HYPULSE) facility
[AIAA PAPER 90-1390] p 594 A90-37935
- BAKOW, L.**
Aluminum alloy 6013 sheet for new U.S. Navy aircraft p 599 A90-37442
- BAKSH, M. F.**
Fuel molecular structure and flame temperature effects on soot formation in gas turbine combustors
[ASME PAPER 89-GT-288] p 253 A90-22652
- BAKSHI, S.**
Holographic flow visualisation of turbofan by-pass and core nozzle streams
[ASME PAPER 89-GT-260] p 363 A90-23891
- BAKULIN, V. L.**
The experimental investigation of flow in the core of a vortex structure
[BR114893] p 960 N90-29597
- BAKUNIN, V. N.**
Determination of additive contents in aviation and turbine oils p 532 A90-34681
- BALABANOV, O. V.**
A study of approximately optimal cruising flight regimes of variable-mass aircraft p 430 A90-29187
- BALAGEAS, D.**
The application of infrared thermography to the measurement of heat fluxes in a wind tunnel
[ONERA, TP NO. 1989-192] p 261 A90-21051
Determination of convective transfer coefficients on a wind-tunnel model by stimulated infrared thermography
[ONERA, TP NO. 1989-218] p 351 A90-25351
- BALAKIMAR, PONNAMPALAM**
Supersonic/hypersonic laminar/turbulent transition p 706 A90-42872
- BALAKRISHNA, S.**
Automatic control of cryogenic wind tunnels p 263 N90-15957
- BALAKUMAR, PONNAMPALAM**
Stability limits for three-dimensional supersonic boundary layers
[AIAA PAPER 90-1528] p 564 A90-38673
- BALASANKARAN, A. V.**
Unbalance response studies on a model rotor supported on uncentrally squeezed film dampers and the development experience of a jet engine p 69 A90-12579
- BALD, W. B.**
Force balance errors due to temperature changes in ETW p 539 A90-34231
- BALDASARE, PAUL**
Evaluation of two transport aircraft and several ground test vehicle friction measurements obtained for various runway surface types and conditions. A summary of test results from joint FAA/NASA Runway Friction Program
[NASA-TP-2917] p 249 N90-15902
- BALDEN, T.**
Balance calibration and evaluation software p 523 A90-34237
Automatic calibration machine for internal cryogenic balances p 524 A90-34247
- BALDWIN, R. M.**
Spray automated balancing of rotors - How process parameters influence performance p 879 A90-46228
- BALDWIN, S. F.**
Flight tests to explore tail rotor limitations in the low speed envelope p 647 A90-42498

- BALENA, F. J.**
Transport composite fuselage technology: Impact dynamics and acoustic transmission
[NASA-CR-4035] p 126 N90-11821
- BALJEU, J. F.**
Development of a multi-component internal strain-gauge balance for model tests in a cryogenic wind tunnel
[NLR-TR-88157-U] p 123 N90-12628
- BALL, CALVIN L.**
Advanced technology's impact on compressor design and development - A perspective
[SAE SP-800] p 423 A90-28571
Advanced technologies impact on compressor design and development: A perspective
[NASA-TM-102341] p 54 N90-10891
- BALLAL, D. R.**
Acoustic characteristics of a research step combustor
[AIAA PAPER 90-1851] p 655 A90-40530
- BALLEY, E.**
Parallel processing implementation of a flight controller
p 333 N90-16743
- BALSA, THOMAS F.**
On the instabilities of supersonic mixing layers - A high-Mach-number asymptotic theory
p 702 A90-42644
- BALSONE, STEPHEN J.**
The effect of elevated temperature exposure on the tensile and creep properties of Ti-24Al-11Nb
p 355 A90-24865
- BAN, XIANLIN**
The application of concentric vortex simulation to calculating the aerodynamic characteristics of bodies of revolution at high angles of attack
p 627 A90-42357
- BANAS, RONALD P.**
Ceramic materials and coatings for future aerospace applications - Challenge of the 1990's
p 942 A90-50071
- BANDA, SIVA**
A mixed H2 and H(infinity) approach to an autopilot design problem
[AIAA PAPER 90-3441] p 865 A90-47694
- BANDO, TOSHIO**
Flight simulation test facility: Function and specification of the simulator cockpit system
[NAL-TM-577] p 59 N90-10899
- BANDYOPADHYAY, G.**
Application of a vortex lattice numerical model in the calculation of inviscid incompressible flow around delta wings
p 904 A90-51017
- BANDYOPADHYAY, PROMODE R.**
The organized nature of a turbulent trailing vortex
[AIAA PAPER 90-1625] p 568 A90-38754
- BANERJEE, J. R.**
Effects of tailplane aerodynamics and fuselage flexibility on the flutter of high aspect ratio, low speed aircraft
p 493 A90-33414
- BANERJEE, P. K.**
Advanced applications of BEM to gas turbine engine structures
p 772 A90-45769
- BANGLE, DONALD R.**
Development of a water-borne non-chromated primer and topcoat for aerospace applications
p 956 A90-50213
- BANKS, DANIEL W.**
F-18 high alpha research vehicle surface pressures - Initial in-flight results and correlation with flow visualization and wind-tunnel data
[AIAA PAPER 90-3018] p 792 A90-45885
- BANKS, P.**
Fine resolution errors in secondary surveillance radar altitude reporting amongst aircraft transmitting the conspicuity codes 4321 and 4322
[RSRE-88004] p 135 N90-12816
- BANKS, W. M.**
Experimental study on the buckling and postbuckling of carbon fibre composite panels with and without interply disbonds
p 130 A90-15355
- BANNINK, W. J.**
Investigation of the vortex flow over a sharp-edged delta wing in the transonic speed regime
[LR-594] p 717 N90-25115
- BANSOD, PRAKASH**
Computation of flow through a centrifugal impeller with tip leakage
[AIAA PAPER 90-2021] p 684 A90-41987
- BAO, HANLING**
Wing boundary layer calculation and its application to aircraft design
p 84 A90-15151
- BAO, YUN**
Calculation of two-dimensional transonic flow of Euler equations with multigrid method
p 149 A90-16835
- BAR-NIR, I. M.**
Coping with bomb threats to civil aviation
p 23 A90-12781
- BARAI, AMALESH**
Flutter of shaft-supported low aspect-ratio control surfaces
p 667 A90-38912
- BARANKIEWICZ, W. S.**
A modeling technique for STOVL ejector and volume dynamics
[AIAA PAPER 90-2417] p 663 A90-42168
A modeling technique for STOVL ejector and volume dynamics
[NASA-TM-103167] p 589 N90-22566
- BARANOV, P. A.**
Numerical simulation of three-dimensional flow around parachute canopies
p 84 A90-14438
- BARANOV, SERGEI K.**
Optimum aircraft design: Multipurpose approach
p 829 A90-46618
- BARANOVSKII, B. V.**
A method for the computer-aided hydraulic analysis of the turbine cooling systems of aviation gas turbine engines
p 255 A90-23430
- BARANOVSKY, S. I.**
Heat transfer in supersonic coaxial reacting jets
p 601 A90-35394
- BARATA, J. M. M.**
Numerical study of single impinging jets through a crossflow
p 17 A90-13020
- BARBANTINI, E.**
Blockage corrections at high angles of attack in a wind tunnel
p 593 A90-35756
The aerodynamic experimental center of Aeritalia: Combat aircraft group
[ETN-89-95213] p 122 N90-11766
- BARBAROSSA, S.**
Doppler-rate filtering for detecting moving targets with synthetic aperture radars
p 488 A90-34138
- BARBAUX, Y.**
Properties of Al-Li alloys
p 267 N90-15191
- BARBER, D. J.**
Preliminary design and analysis of propellers
p 645 A90-42407
- BARBER, JOHN W.**
Effect of temperature on the storage life of polysulfide aircraft sealants
[MRL-TR-89-31] p 444 N90-19364
- BARBER, S. A.**
Evaluation of solid lubricant powder delivery system for turbine bearing lubrication
[AIAA PAPER 90-2046] p 684 A90-41997
- BARBER, T. J.**
The role of hydrogen/air chemistry in nozzle performance for a hypersonic propulsion system
[AIAA PAPER 90-2492] p 658 A90-40637
- BARBIERI, SERGIO**
Results of an A109 simulation validation and handling qualities study
p 591 A90-38524
- BARBOT, ANDRE**
Developmental tests on the M 88 engine are on track
p 660 A90-41761
- BARCKLEY, K.**
Integrated navigation system design and performance with Phase III GPS user equipment
p 98 A90-13997
- BARDAKHANOV, S. P.**
Investigation of the flow structure behind the rotating blades in the elbow of a wind tunnel in the case of acoustic excitation
p 297 A90-24124
- BARISHIS, I. P.**
Durability characteristics of the LAK-12 Letuva glider made of composite materials at the stage of certification
p 102 A90-15560
- BARFIELD, F.**
Flight controller design with nonlinear aerodynamics, large parameter uncertainty, and pilot compensation
[AIAA PAPER 90-3478] p 866 A90-47728
- BARGER, RAYMOND L.**
Fuselage design for a specified Mach-sliced area distribution
[NASA-TP-2975] p 414 N90-18385
- BARINOV, V. A.**
An investigation of fillets in wing-fuselage joints at subsonic velocities
p 297 A90-24131
- BARIO, F.**
Aerodynamics of cooling jets introduced in the secondary flow of a low speed turbine cascade
[ASME PAPER 89-GT-192] p 362 A90-23868
- BARLOW, J.**
The ascending trajectories performance and control to minimize the heat load for the transatmospheric aero-space planes
[AIAA PAPER 90-2828] p 763 A90-45135
- BARLOW, J. B.**
Obtaining precise LTR with Luenberger type observer with arbitrary observer poles and finite gain
[AIAA PAPER 90-3228] p 868 A90-49113
- BARNDORFF-NIELSEN, O. E.**
Wind shear and hyperbolic distributions
p 280 A90-23632
- BARNES, MICHAEL**
The effect of windscreen bows and HUD pitch ladder on pilot performance during simulated flight
p 420 A90-31333
- BARNETT, MARK**
Theoretical prediction of high Reynolds number viscous/inviscid interaction phenomena in cascades
p 145 A90-16759
Simulation of three-dimensional viscous flow within a multistage turbine
[ASME PAPER 89-GT-152] p 292 A90-23841
- BARNETT, R. JOEL**
Detachment of turbulent boundary layers with varying free-stream turbulence and lower Reynolds numbers
p 802 A90-46378
- BARNETT, R. M.**
Investigation of high angle of attack vortical flows over delta wings
[AIAA PAPER 90-0101] p 162 A90-19682
- BARNHART, B.**
Influence of forebody geometry on aerodynamic characteristics and a design guide for defining departure/spin resistant forebody configurations
[AD-A216714] p 414 N90-18388
- BARNHART, BILLY P.**
Rotational aerodynamics of elliptic bodies at high angles of attack
[AIAA PAPER 90-0068] p 161 A90-19664
Yaw damping of elliptic bodies at high angles of attack
p 709 A90-44740
- BARNHART, PAUL J.**
A supersonic through-flow fan engine airframe integration study
[NASA-CR-185140] p 18 N90-10004
- BARNIV, YAIR**
Velocity filtering applied to optical flow calculations
[NASA-TM-102802] p 916 N90-28512
- BAROL, D.**
Modeling and analysis of airport and aircraft operations
[PB90-222167] p 915 N90-28511
- BARON, A.**
A tool for automatic design of airfoils in different operating conditions
p 502 N90-20994
- BARON, ADI ABILEAH YAIR**
8 x 8-inch full color cockpit display
p 927 A90-52953
- BARON, JUDSON R.**
Application of an adaptive algorithm to single and two-element airfoils in turbulent flow
[AIAA PAPER 90-0698] p 169 A90-19983
- BARON, SHELDON**
Intelligent situation assessment and response aiding in flight emergencies
[AIAA PAPER 89-2999] p 36 A90-10507
- BARON, TIMOTHY**
Local adaptive maneuvering optimization for fighter aircraft
[AIAA PAPER 90-3453] p 890 A90-47706
- BARR, D. W.**
AIMS for helicopters
p 820 N90-27639
- BARR, DALE C.**
The normal shock generator - An inlet throat region research apparatus for high Mach applications
[AIAA PAPER 90-1930] p 759 A90-42698
- BARRER, JOHN N.**
An operational perspective of potential benefits of microwave landing systems
p 242 A90-23242
- BARRERE, M.**
Thermodynamics and the future turbine engines
[ONERA, TP NO. 1989-165] p 253 A90-21031
- BARRETT, C. A.**
Influence of alloying elements on the oxidation behavior of NbAl3
p 355 A90-24861
- BARRETT, D. M.**
Performance evaluations of oxidation-resistant carbon-carbon composites in simulated hypersonic vehicle environments
p 874 A90-48131
- BARRETT, K. A.**
Injectable bismaleimide systems
p 943 A90-50132
- BARRETT, RODNEY V.**
An automated vorticity surveying system using a rotating hot-wire probe
p 447 A90-28284
- BARRETTE, ANNE K.**
Artificial intelligence techniques applied to the non-cooperative identification (NCID) problem
[AIAA PAPER 89-3005] p 75 A90-10619
- BARRICK, MICHAEL**
Application of effective baselines to smart structures
p 536 A90-32885
- BARRICK, MICHAEL D.**
Productibility and life cycle cost issues in applications of embedded fiber optic sensors in smart skins
p 38 A90-11221

- BARRIO CARDABA, A.**
Design and fabrication of the carbon fiber/epoxy A-320 horizontal tailplane p 286 A90-25221
- BARRON, RONALD M.**
Numerical solution of transonic flows on a streamfunction co-ordinate system p 17 A90-13238
- BARSKOV, V. V.**
Strength of the guide vane components of gas turbines p 266 A90-21318
- BARSONY-NAGY, A.**
Simulation of helicopter landing on a ship deck p 181 A90-17705
- BARTEL, H. W.**
Propfan Test Assessment (PTA): Flight test report [NASA-CR-182278] p 113 A90-11738
Propfan Test Assessment (PTA) [NASA-CR-185138] p 113 A90-11739
- BARTER, S. A.**
RAAF Orion aircraft A9-300 oxygen fire [AD-A215496] p 323 A90-16725
- BARTH, JAMES R.**
Fabrication of complex composite structures using advanced fiber placement technology p 954 A90-50111
- BARTHOLOMEW-BIGGS, M. C.**
An application of SQP and Ada to the structural optimisation of aircraft wings p 216 A90-18444
- BARTHOLOMEW, P.**
The role of structural analysis in airworthiness certification [BR112064] p 499 A90-20972
Computer-aided structural optimisation of aircraft structures [BR112837] p 499 A90-20973
- BARTLETT, C. SCOTT**
The effect of experimental uncertainties on icing test results [AIAA PAPER 90-0665] p 322 A90-26977
- BARTLETT, D. W.**
Curvature effects on the stability of laminar boundary layers on swept wings p 148 A90-16788
- BARTLETT, DENNIS W.**
F-14 VSTFE and results of the cleanup flight test program p 105 A90-12547
- BARTON, GEORGE G.**
A surveillance 360 deg television orientation and ranging system as an aid to collision avoidance p 577 A90-36922
- BARTON, H. A.**
Prediction and measurement of rotor blade/stator vane dynamic characteristics of a modern aero-engine axial compressor p 878 A90-46036
Prediction and measurement of rotor blade/stator vane dynamic characteristics of a modern aero-engine axial compressor [PNR90667] p 750 A90-26002
- BARTON, WILLIAM R.**
Risk assessment and its application to flight safety analysis [DE90-004985] p 323 A90-16722
- BARTRAND, TIMOTHY A.**
Performance of a supercharged direct-injection stratified-charge rotary combustion engine [NASA-TM-103105] p 748 A90-25982
- BARUZZI, G.**
Non-unique solutions of the Euler equations p 716 A90-45727
- BASERGA, CLAUDIO**
Methodology for estimating helicopter performance and weights using limited data p 829 A90-46936
- BASILE, JOHN P.**
Vibration reduction on servo flap controlled rotor using HHC p 861 A90-46967
- BASKARAN, V.**
Experimental investigation of three-dimensional turbulent boundary layers on 'infinite' swept curved wings p 303 A90-25589
- BASKHARONE, E. A.**
A comprehensive analysis of the viscous incompressible flow in quasi-three-dimensional aerofoil cascades p 905 A90-51028
- BASKIN, V. E.**
An experimental study of instantaneous velocity perturbations over a rotor disk for low duty coefficients p 860 A90-46572
- BASS, J.**
Integration of the LTN-72 INS with the DOD GPS 3A set p 728 A90-45236
- BASSI, F.**
Secondary flows in a transonic cascade - Comparison between experimental and numerical results p 157 A90-18501
- BASSIM, M. NABIL**
Use of acoustic emission for continuous surveillance of aircraft structures p 887 A90-28092
- BASTART, J.**
Test rig for the study of the flow in a rotor-stator system [ONERA, TP NO. 1989-124] p 58 A90-12634
- BASTIERE, ANNIE**
A decision-making aid for multi-layer radar absorbent coverings [ESA-TT-1173] p 773 A90-25267
- BASU, B. C.**
Oscillating thin wings in inviscid incompressible flow p 2 A90-10224
Potential flow calculation for three-dimensional wings and wing-body combination in oscillatory motion p 153 A90-17976
Incompressible potential flow about complete aircraft configurations p 156 A90-18443
Incompressible viscous flow about aircraft configurations p 233 A90-23290
Viscous corrections on wings in incompressible flow p 301 A90-25200
Multi-element aerofoils in viscous flow p 469 A90-32451
Lift and pitching moment measurements on a swept tapered wing in oscillatory vertical gusts p 811 A90-48089
- BATES, BRENT L.**
Transonic Navier-Stokes solutions about a complex high-speed accelerator configuration [AIAA PAPER 90-0430] p 166 A90-19844
- BATES, JACK R.**
Inflatable fuel tank buffer [AD-DO14446] p 503 A90-21002
- BATILL, S. M.**
Unsteady surface pressure distributions on a delta wing undergoing large amplitude pitching motions [AIAA PAPER 90-0311] p 164 A90-19790
Vortex dynamics on a pitching delta wing p 233 A90-23281
A concept study on the use of remotely piloted, sub-scale aircraft for high Reynolds number testing [AIAA PAPER 90-1263] p 494 A90-33892
Delta wing surface pressures for high angle of attack maneuvers [AIAA PAPER 90-2813] p 711 A90-45153
- BATILL, STEPHEN M.**
Low speed, in-draft wind tunnels p 351 A90-26061
- BATINA, JOHN T.**
Mach number effects on transonic aeroelastic forces and flutter characteristics p 17 A90-13024
Implicit flux-split Euler schemes for unsteady aerodynamic analysis involving unstructured dynamic meshes [AIAA PAPER 90-0936] p 389 A90-29362
Aeroelastic analysis of wings using the Euler equations with a deforming mesh [AIAA PAPER 90-1032] p 391 A90-29376
Unsteady aerodynamics methods for transonic aeroelastic analysis p 471 A90-33353
Application of the CAP-TSD unsteady transonic small disturbance program to wing flutter p 491 A90-33354
Euler flutter analysis of airfoils using unstructured dynamic meshes p 602 A90-35760
Three-dimensional flux-split Euler schemes involving unstructured dynamic meshes [AIAA PAPER 90-1649] p 569 A90-38777
Temporal-adaptive Euler/Navier-Stokes algorithm for unsteady aerodynamic analysis of airfoils using unstructured dynamic meshes [AIAA PAPER 90-1650] p 569 A90-38778
Unsteady Euler airfoil solutions using unstructured dynamic meshes p 809 A90-47307
Conical Euler solution for a highly-swept delta wing undergoing wing-rock motion [NASA-TM-102609] p 400 A90-19211
- BATSON, JAY D.**
Design and development of the Garrett F109 turbofan engine [SAE PAPER 891046] p 109 A90-14350
- BATTARBEE, D. I.**
EH101 vibration control p 647 A90-42496
- BATTEY, DAVID E.**
Holographic combiner design to obtain uniform symbol brightness at head-up display video camera p 652 A90-40394
- BATUR, C.**
Rub interactions of flexible casing rotor systems p 41 A90-11554
- BATY, G.**
The design and test of a two stage transonic axial flow compressor [ASME PAPER 89-GT-184] p 341 A90-23852
- BAUER, ANDREW B.**
Drag and propulsive efficiency of a light aircraft based on a new flight test technique [AIAA PAPER 90-0233] p 182 A90-19747
- BAUER, FRANK H.**
Structural mode significance using INCA [AIAA PAPER 90-3346] p 889 A90-47606
- BAUER, H. F.**
Hydroelastic problems in space flight vehicles p 536 A90-33386
- BAUER, JEFFREY E.**
Estimating short-period dynamics using an extended Kalman filter [AIAA PAPER 90-1277] p 518 A90-33901
Estimating short-period dynamics using an extended Kalman filter [NASA-TM-101722] p 648 A90-23392
- BAUM, JAMES P.**
Design for assembly of aerospace structures - A qualitative, interactive approach [SME PAPER MS89-158] p 222 A90-23683
- BAUM, JOSEPH D.**
Formation of shocks within axisymmetric nozzles [AIAA PAPER 90-1655] p 570 A90-38782
- BAUM, LARRY S.**
Benchmarking blackboards to support cockpit information management [AIAA PAPER 89-3095] p 37 A90-10580
- BAUM, LAWRENCE**
Problem focus mechanisms for cockpit automation [AIAA PAPER 89-3096] p 37 A90-10581
- BAUMANN, DANIEL D.**
Bifurcation analysis of a model fighter aircraft with control augmentation [AIAA PAPER 90-2836] p 934 A90-50640
F-15B high angle-of-attack phenomena and spin prediction using bifurcation analysis [AD-A217366] p 498 A90-20073
- BAUMBICK, ROBERT J.**
Fiber optics for advanced aircraft p 68 A90-11702
- BAUMGARDNER, DARREL**
Meeting Review: Workshop on Airborne Instrumentation [PB89-174775] p 39 A90-10032
- BAUSCH, WERNER**
Digital map for helicopter navigation and guidance p 252 A90-21609
- BAUST, HENRY D.**
Development and extension of diagnostic techniques for advancing high speed aerodynamic research p 436 A90-28281
- BAUWENS, LUC**
Numerical modeling of a flame in a confined, unstable shear layer [AIAA PAPER 90-0647] p 205 A90-19966
Entropy wave instability in compact ramjets p 858 A90-27932
- BAVARIAN, BEHZAD**
Chemical vapor deposition of Hf/Si compounds as a high temperature coating for carbon/carbon composites p 955 A90-50159
- BAVEJA, PREM**
In process failure investigations in aeronautics p 181 A90-18489
- BAVENDIEK, K.**
A comfortable and universal data-acquisition-system for flight research p 39 A90-12204
- BAXTER, B. J.**
A corrosion fatigue/stress corrosion testing facility at Materials Research Laboratory [MRL-TN-568] p 527 A90-21044
- BAXTER, D. R. J.**
Liquid crystal thermography for aerodynamic heating measurements in short duration hypersonic facilities p 446 A90-28262
- SAYBROOK, ROY**
Demonstrating technologies for enhanced fighter manoeuvrability - The Rockwell/MBB X-31 p 731 A90-43767
- BAYLE-LABOURE, G.**
Aerothermomechanical design of turbine-engine combustion chambers p 424 A90-29922
- BAYLISS, A.**
Application of sound and temperature to control boundary-layer transition p 92 A90-12537
- BAYLISS, EDWARD T.**
Development of common GPS and GLONASS avionics standards p 821 A90-46391
- BAZHAN, PAVEL I.**
Handbook on heat exchangers p 273 A90-22743
- BAZIN, MAURICE**
Breakage of fan blades in the S1 wind tunnel at Mondane-Avivieux [ONERA, TP NO. 1989-104] p 57 A90-11138
- BEACH, H. L. JR.**
Aeronautical facility requirements into the 2,000's [AIAA PAPER 90-1375] p 594 A90-37926
- BEACH, T. A.**
The numerical simulation of multistage turbomachinery flows p 514 A90-21025

- BEACH, TIM A.**
Simulation of three-dimensional viscous flow within a multistage turbine
[ASME PAPER 89-GT-152] p 292 A90-23841
- BEACHER, B. F.**
Three-dimensional relief in turbomachinery blading
[ASME PAPER 89-GT-151] p 292 A90-23840
- BEALE, J.**
High temperature deformation studies on CVD silicon carbide fibers p 945 A90-50147
- BEARMAN, P. W.**
The effect of rapid spoiler deployment on the transient forces on an aerofoil p 921 A90-28527
- BEAUCHAMP, G. M.**
An accurate numerical technique for determining flight test rate gyroscope biases prior to takeoff
[AD-A220987] p 739 N90-25138
- BEAUDOIN, JOSEPH A.**
Aviation litigation - An ATC perspective
[AIAA PAPER 90-0372] p 175 A90-19820
- BEAUDOIN, P.**
Parachute opening shocks during high speed ejections: Normalization p 497 N90-20056
- BEAVER, P. W.**
Fatigue of thick-section cold-expanded holes with and without cracks p 270 A90-20987
- BECHTEL, G. S.**
Application of HOST technology to the SSME HPFTP blade
[ASME PAPER 89-GT-130] p 360 A90-23828
- BECK, JEFFREY A.**
Bifurcation analysis of a model fighter aircraft with control augmentation
[AIAA PAPER 90-2836] p 934 A90-50640
- BECK, W.**
DB/SPF cooler outlet duct for aircraft application p 132 A90-15620
- BECKER, BRYAN R.**
The flow field and heat transfer near a turbulator p 771 A90-44755
- BECKER, CAROL S.**
The flow field and heat transfer near a turbulator p 771 A90-44755
- BECKER, K.**
The precise calculation of the inviscid leading edge flow on a laminar airfoil using simple methods and verification by measurements on the TLF pilot model p 277 N90-16180
- BECKER, WAYNE**
Elevator tab assembly producibility study
[JAR-89-16] p 734 N90-25133
- BECKMANN, M.**
Interference detection and suppression in Loran-C receivers p 240 A90-20504
- BECKWITH, I. E.**
Aerothermodynamics and transition in high-speed wind tunnels at NASA Langley p 386 A90-28555
Design and operational features of low-disturbance wind tunnels at NASA Langley for Mach numbers from 3.5 to 18
[AIAA PAPER 90-1391] p 594 A90-37936
- BECKWITH, IVAN E.**
Advanced Mach 3.5 Axisymmetric Quiet Nozzle
[AIAA PAPER 90-1592] p 566 A90-38727
Design and fabrication requirements for low noise supersonic/hypersonic wind tunnels p 122 N90-12555
Experimental and theoretical investigation of boundary-layer instability mechanisms on a swept leading edge at Mach 3.5 p 94 N90-12557
- BECKLE, J. P.**
Determination of the ground effect on the characteristics of the A320 aircraft
[ONERA, TP NO. 1989-188] p 245 A90-21048
Determination of the ground effect on the characteristics of the A320 aircraft p 922 N90-28534
- BEDARD, A. J., JR.**
Atmospheric conditions producing aircraft icing on 24-25 January 1989 - A case study utilizing combinations of surface and remote sensors
[AIAA PAPER 90-0197] p 175 A90-19734
- BEDDOES, T. S.**
Two and three dimensional indicial methods for rotor dynamic airloads p 808 A90-46973
- BEDE, JAMES R.**
BD-10J supersonic homebuilt aircraft p 730 A90-42672
- BEDOYA, CARLOS A.**
Application of multifunction inertial reference systems to fighter aircraft p 332 N90-16740
Application of multifunction inertial reference systems to fighter aircraft p 916 N90-29341
Survivable penetration p 917 N90-29363
- BEECH, ERIC**
Gripen wins its wings p 842 A90-49823
- BEEMAN, E. R., II**
Conceptual design optimization study
[NASA-CR-4298] p 582 N90-21755
- BEGG, LESTER L.**
Vapor grown carbon fiber for space thermal management systems p 943 A90-50128
- BEGUIER, C.**
Aerodynamics of unsteady systems. Numerical study of potential flow/boundary layer coupling
[ETN-90-96257] p 396 N90-18367
- BEGUIN, DANIEL**
Dual cross-polarization planar arrays in the C and X bands p 638 A90-40979
- BEHBEHANI, R. A.**
The 757 NLF glove flight test results p 104 N90-12546
- BEHEIM, GLENN**
Silicon-etalon fiber-optic temperature sensor
[NASA-TM-102389] p 187 N90-13381
- BEHME, ARTHUR K., JR.**
Plastic media blast (PMB) paint removal from composites p 945 A90-50162
- BEHNKE, BERND**
Model of a labyrinth seal with flow p 687 A90-42334
- BEHR, R.**
A nonlinear vortex-lattice method for the calculation of interference effects between free vortex sheets and wings p 277 N90-16183
- BEIER, K.**
Infrared radiation model for aircraft and reentry vehicle p 77 A90-10169
- BEIGHTOL, D. B.**
Helicopter flight vibration of large transportation containers: A case for testing tailoring
[DE90-007429] p 402 N90-19215
- BEILMAN, JOHN L.**
The Bell X-22A V/STOL, Variable Stability Research Airplane - Lessons learned
[AIAA PAPER 90-3207] p 834 A90-48835
- BEIN, THOMAS W.**
Flow coupling between a rotor and a stator in turbomachinery
[AD-A223882] p 932 N90-28572
- BEITLER, R. S.**
Energy Efficient Engine: Control system component performance report
[NASA-CR-174651] p 931 N90-28562
- BEKHTR, VLADIMIR P.**
Practical aerodynamics of the Yak-42 aircraft p 334 A90-24218
- BEKIR, E. C.**
Modeling flexible aircraft for flight control design
[AD-A219123] p 757 N90-25140
- BEKIR, ESMAT**
A new methodology for model order reduction with application to eigenstructure controllers
[AIAA PAPER 90-3475] p 891 A90-47725
- BELAICHUK, A. A.**
Testing of statistical hypotheses and derivation of confidence intervals from inspection data samples p 363 A90-24087
- BELAN, V. V.**
Synthesis of optimal multidimensional digital systems for the simulation of the angular motions of a flight vehicle under random loading p 669 A90-41957
- BELCASTRO, CELESTE M.**
Laboratory test methodology for evaluating the effects of electromagnetic disturbances on fault-tolerant control systems
[NASA-TM-101665] p 217 N90-14061
Real-time closed-loop simulation and upset evaluation of control systems in harsh electromagnetic environments p 613 N90-23069
- BELCHER, ANNE**
Design of a low cost short takeoff-vertical landing export fighter/attack aircraft
[NASA-CR-186658] p 734 N90-25132
- BELCHER, P. J.**
System optimization for maximizing reconnaissance mission range of a hypersonic cruise vehicle
[AIAA PAPER 90-3292] p 837 A90-48876
- BELETSKII, IU. M.**
Numerical modeling of transverse flow past a cylinder using Euler equations p 709 A90-44922
- BELIAEV, N. M.**
Numerical solution of the problem of supersonic flow of a viscous gas past a concave conical wing p 619 A90-39465
- BELIAKOV, A. R.**
Strength of the guide vane components of gas turbines p 266 A90-21318
- BELIANIN, N. M.**
Flow rate and thrust coefficients for biaxial flows in a convergent nozzle p 395 A90-30344
- BELIYANNIS, ANGELOS**
The potential for an extra runway at Heathrow: A preliminary feasibility study
[TT-9007] p 938 N90-29403
- BELL, I. C.**
Designing the next generation flying test bed
[SAE PAPER 891049] p 100 A90-14353
- BELL, JAMES H.**
Effects of streamwise vorticity injection on turbulent mixing layer development
[AIAA PAPER 90-1459] p 561 A90-38616
- BELLATI, B.**
New inflight experiments to measure aerodynamics loads
[ETN-90-97276] p 868 N90-26834
- BELLE, STEVE D.**
Effects of simplifying assumptions on optimal trajectory estimation for a high-performance aircraft
[NASA-TM-101721] p 757 N90-25142
- BELLER, R. C.**
Aviation Engine Test Facilities (AETF) fire protection study
[AD-A211483] p 134 N90-12777
- BELLINGER, N. C.**
Life estimation of a gas turbine afterburner spraybar p 739 A90-42662
Surface property improvement in titanium alloy gas turbine components through ion implantation p 953 N90-28713
- BELLMARD, LARRY**
Preliminary design of a supersonic Short Takeoff and Vertical Landing (STOVL) fighter aircraft
[NASA-CR-186670] p 649 N90-23394
- BELOTSEKOVETS, I. S.**
Effect of the nonuniformity of external supersonic flow and nozzle deflection angle on the base pressure behind an axisymmetric body with a single supersonic jet p 802 A90-46486
- BELOTSEKOVSKII, SERGEI M.**
Mathematical modeling of plane parallel separated flows past bodies p 619 A90-39475
- BELOUSOV, A. I.**
Increasing the heat conductivity of elastic damping elements of MR material p 102 A90-14580
- BELOUSOV, IURII A.**
Airborne digital computers and systems p 927 A90-52410
- BELTE, DAUMANTS**
Initial results from the joint NASA-Lewis/U.S. Army icing flight research tests p 400 A90-28180
- BEMENT, DAVID A.**
Measured operating characteristics of a rectangular combustor/inlet isolator
[AIAA PAPER 90-2221] p 742 A90-42752
- BEN BUEMI, S.**
Redesign of an electro-optical shroud in graphite/epoxy p 676 A90-40215
- BEN-AROSH, RACHEL**
Similarity and scale effects in solid fuel ramjet combustors p 60 A90-12513
- BEN-HAIM, YAKOV**
Convex models of malfunction diagnosis in high performance aircraft
[AD-A218514] p 702 N90-25073
- BEN-HARUSH, YITZHAK**
Application of the joined wing to tiltrotor aircraft
[NASA-CR-177543] p 248 N90-15093
- BENALLAL, A.**
Modeling of the oil quench for Ni-based superalloy turbine disks p 957 A90-51525
- BENCIC, TIMOTHY J.**
Hot gas ingestion characteristics and flow visualization of a vectored thrust STOVL concept
[NASA-TM-103212] p 751 N90-26009
- BENDER, KLAUS**
Unmanned helicopters for battlefield and maritime surveillance p 920 A90-51899
- BENDIKSEN, ODDVAR O.**
Aeroelastic problems in turbomachines
[AIAA PAPER 90-1157] p 393 A90-29393
- BENEK, J. A.**
A locally implicit scheme for 3-D compressible viscous flows
[AIAA PAPER 90-1525] p 563 A90-38670
- BENEL, RUSSELL A.**
Advanced Automation System design p 375 A90-25566
- BENETKA, JIRI**
Measurements and calculations of the aerodynamic characteristics of the propeller sections series V3 p 233 A90-23355
- BENETSCHIK, HANNES**
Inviscid and viscous flows in transonic and supersonic cascades using an implicit upwind relaxation algorithm
[AIAA PAPER 90-2128] p 625 A90-42034

BENNETT, BRADFORD C.

Calculation of hypersonic forebody/inlet flow fields
[AIAA PAPER 90-1493] p 619 A90-39049

BENNETT, CLIVE G.

Tough(er) aluminum-lithium alloys p 62 A90-11575

BENNETT, G. W.

Energy Efficient Engine: Control system component performance report
[NASA-CR-174651] p 931 N90-28562

BENNETT, JIM

Fighter design econometrics = ownership affordability?
[AIAA PAPER 90-3223] p 897 A90-48842

BENNETT, JOE

Lightweight fuel pump and metering component for advanced gas turbine engine control
[AIAA PAPER 90-2032] p 657 A90-40602

BENNETT, RICHARD L.

Design methodology for multivariable helicopter control systems p 669 A90-42461

BENNETT, ROBERT M.

Using transonic small disturbance theory for predicting the aerodynamic stability of a flexible wind-tunnel model
[AIAA PAPER 90-1033] p 391 A90-29377

Application of the CAP-TSD unsteady transonic small disturbance program to wing flutter p 491 A90-33354

Using transonic small disturbance theory for predicting the aerodynamic stability of a flexible wind-tunnel model
[NASA-TM-102617] p 478 N90-20047

BENNETT, W. A.

Investigation of unsteady flow through a transonic turbine stage. II - Data/prediction comparison for time-averaged and phase-resolved pressure data
[AIAA PAPER 90-2409] p 626 A90-42162

BENNETT, WILLIAM H.

Robust control design for relaxed static stability aircraft
[AIAA PAPER 90-3443] p 865 A90-47696

Robust control design for flight control
[AD-A211957] p 119 N90-11756

BENNINGTON, DONALD R.

Real-time simulation clock
[NASA-CASE-LAR-14056-1] p 689 N90-23713

BENSON, JOHN L.

Supersonic STOVL - The future is now p 732 A90-44781

BENSON, PATRICK

Rotor smoothing expert system p 381 A90-28164

BENSON, ROBERT L.

Peacetime replacement and crash damage factors for army aircraft
[AD-A218544] p 636 N90-23372

BENSON, RUSSELL A.

Modifying high-order aeroelastic math model of a jet transport using maximum likelihood estimation p 61 N90-10106

Design of integrated pitch axis for autopilot/autothrottle and integrated lateral axis for autopilot/yaw damper for NASA TSRV airplane using integral LQG methodology
[NASA-CR-4268] p 348 N90-16768

BENSON, T. J.

Comparison of 3-D viscous flow computations of Mach 5 inlet with experimental data
[AIAA PAPER 90-0600] p 314 A90-26970

Comparison of 3-D viscous flow computations of Mach 5 inlet with experimental data
[NASA-TM-102518] p 510 N90-20090

BENTSON, JAMES

Exact solutions to the oscillations of composite aircraft wings with warping constraint and elastic coupling p 603 A90-36271

BERA, RAJENDRA K.

Design priorities for an air-superiority fighter p 335 A90-26344

Do inviscid vortex sheets roll-up
[PD-CF-9010] p 909 N90-28491

A conceptual framework for fighter flight control systems
[PD-CF-9009] p 936 N90-28577

BERAK, PETR

Unconventional leading edges of airfoils p 233 A90-23356

BERAN, PHILIP S.

Analysis of transonic turbine rotor cascade flows using a finite-volume total variation diminishing (TVD) scheme
[AIAA PAPER 90-2127] p 704 A90-42733

BERANGER-BOURSIER, A. S.

Study of the microstructure of a titanium alloy (6246) for turbomachine compressors
[ETN-90-97450] p 876 N90-27900

BERENS, A. P.

Fatigue life estimates for helicopter loading spectra p 772 A90-45324

Fatigue life estimates for helicopter loading spectra
[NASA-CR-181941] p 279 N90-16294

BERG, A. J.

Measurement and characterization of prepreg permeability with a modified bagging technique p 949 A90-50226

BERG, DONALD F.

Propulsion system design specifications based on STOVL flight control requirements
[AIAA PAPER 90-3227] p 839 A90-49112

BERG, HANS-DIETER

Advanced materials for interior and equipment related to fire safety in aviation p 328 N90-17608

BERG, R. L.

Definition of research needs to address airport pavement distress in cold regions
[DOT/FAA/DS-89/13] p 59 N90-10896

BERGEL'SON, V. I.

Changes in supersonic flow past an obstacle due to the formation of a thin rarefaction channel ahead of the obstacle p 150 A90-17108

BERGER, E.

Coherent vortex structures in the wake of a sphere and a circular disk at rest and under forced vibrations p 623 A90-40749

BERGER, H.

On the coupling of finite elements and boundary elements for transonic potential flows p 155 A90-18297

BERGER, STANLEY A.

The interaction between a counter-rotating vortex pair in vertical ascent and a free surface p 151 A90-17580

BERGERON, HUGH

Design of a final approach spacing tool for TRACON air traffic control
[NASA-TM-102229] p 24 N90-10841

BERGMAN, C. M.

Development of supersonic and hypersonic Euler solvers using shock fitting in two and three dimensions p 707 A90-44426

BERGMANN, HEINRICH

Materials and structures for 2000 and beyond: An attempted forecast by the DLR Materials and Structures Department
[ESA-TT-1154-REV] p 775 N90-26173

BERHARDT, J. E.

Proportional control of asymmetric forebody vortices with the unsteady bleed technique
[AIAA PAPER 90-1629] p 591 A90-38758

BERIOS, G.

Jet engine fault detection with differential gas path analysis at discrete operating points p 50 A90-12633

BERK, J. V.

Software architecture concepts for avionics p 461 A90-30806

BERKHEEV, MANSUR M.

Automatic testing in aircraft building p 285 A90-24231

BERKOVITS, A.

Aeronautical fatigue in the electronic era; Proceedings of the Fifteenth ICAF Symposium, Jerusalem, Israel, June 21-23, 1989 p 901 A90-49876

BERKOWITZ, B. M.

Experimental investigation of multielement airfoil ice accretion and resulting performance degradation p 812 A90-48954

BERKOWITZ, BRIAN M.

Hypersonic aerospace sizing analysis for the preliminary design of aerospace vehicles p 247 A90-23276

Modeling of surface roughness effects on glaze ice accretion p 485 N90-20925

Users manual for the NASA Lewis Ice Accretion Prediction Code (LEWICE)
[NASA-CR-185129] p 468 N90-20943

BERNARD, J.

Calculation of the secondary flow in an axial turbine p 513 N90-21022

BERNER, C.

Measurements, visualization and interpretation of 3-D flows - Application within base flows p 386 A90-28252

BERNHARD, R. J.

Digital control of local sound fields in an aircraft passenger compartment p 247 A90-23113

BERNHART, W. D.

Electro-impulse de-icing testing analysis and design
[NASA-CR-4175] p 32 N90-10031

BERNINGER, DANIEL J.

Flight safety performance of the microwave landing system p 639 A90-41705

Flight safety performance of the Microwave Landing System p 727 A90-45227

BERNSTEIN, DENNIS S.

Integrated control-system design via generalized LQG (GLOG) theory p 613 N90-23023

BERRIER, B.

Experimental evaluation of expendable supersonic nozzle concepts
[AIAA PAPER 90-1904] p 740 A90-42691

BERRY, F. CLIFTON, JR.

High alpha p 902 A90-52575

BERRY, SCOTT

Boundary-layer stability analysis of Langley Research Center 8-foot LFC experimental data p 82 N90-12532

BERT, CHARLES W.

Effect of aerodynamic heating on deformation of composite cylindrical panels in a gas flow p 773 A90-45788

BETELRUD, ARILD

A fast method for computation of airfoil characteristics p 799 A90-46361

BERTIN, JOHN J.

Hypersonics. Volume 2 - Computation and measurement of hypersonic flows; Proceedings of the First Joint Europe/U.S. Short Course on Hypersonics, Paris, France, Dec. 7-11, 1987 p 224 A90-21164

Effect of the grid system on the solution of Euler equations p 309 A90-26494

BERWICK, J. W.

Fly-by-light flight control system technology development plan
[NASA-CR-181953] p 259 N90-15111

BESANT, C. B.

A computer integrated approach to dimensional inspection
[PNR90596] p 116 N90-12611

BESAW, HALIEN R.

Combining thermal and high level acoustics p 770 A90-43729

BESELER, JAN W.

An explicit model-matching approach to lateral-axis autopilot design p 756 A90-45413

BESHEARS, D. L.

Engine testing of thermographic phosphors
[DE90-013269] p 885 N90-28059

BESPALOV, V. A.

Dynamic stiffness of a hydraulic damper in the system of a front landing gear strut p 102 A90-14555

BESSONOV, D. A.

Interference between the pitot-static tube and the model in wind tunnel studies of flow parameters p 350 A90-24169

BETIAEV, S. K.

Skin effect in flow of a disperse fluid past a wing profile p 395 A90-30334

BETTNER, J. L.

Precursor convertible engine study
[AIAA PAPER 90-2486] p 658 A90-40636

BETTNER, JAMES L.

Component arrangement studies for an 8000 shp turboshaft high technology core
[AIAA PAPER 90-2398] p 663 A90-42159

BEVALOT, J.

Putting alloy 2091 to work p 268 N90-15197

BEWLEY, A. D.

Cycle analysis for helicopter gas turbine engines
[ASME PAPER 89-GT-328] p 506 A90-32258

Cycle analysis for helicopter gas turbine engines
[RAE-TM-P-1154] p 256 N90-15921

BEYER, R.

Experimental study towards a future airport ground movement simulator p 827 N90-27687

BEZARD, H.

An improved method for the computation of unsteady transonic potential flow - Application for airfoil and blade performance prediction
[ONERA, TP NO. 1989-154] p 4 A90-11175

BEZDEK, JAMES C.

An intelligent system for autonomous navigation of airborne vehicles p 26 A90-11696

BEZMENOV, V. IA.

Acoustic noise emitted from vessels in an impulse-type wind tunnel p 378 A90-24125

A study of gas flow in hypersonic nozzles at large Reynolds numbers using simplified Navier-Stokes equations p 803 A90-46538

BEZOS, GAUDY M.

Results of aerodynamic testing of large-scale wing sections in a simulated natural rain environment
[AIAA PAPER 90-0486] p 167 A90-19874

Operational considerations for aerodynamic testing of large-scale wing sections in a simulated natural rain environment
[AIAA PAPER 90-0485] p 313 A90-26956

BEZVESIL'NAIA, E. N.

A study of the errors of a gyroscopic instrument for measuring linear accelerations p 771 A90-45133

BHARADVAJ, BALA K.

Computation of steady and unsteady control surface loads in transonic flow
[AIAA PAPER 90-0935] p 389 A90-29361

- BHATTIA, R.**
A one-dimensional model of ramjet combustion instability
[AIAA PAPER 90-0271] p 266 A90-22192
Liquid fueled ramjet combustion instability: Acoustical and vortical interactions with burning sprays
[AD-A222752] p 767 N90-26104
- BHATT, VINAY**
Multilevel optimization of large-scale structures in a parallel computing environment p 693 A90-39180
- BHATTACHARYA, RABI S.**
Self-lubricating surfaces by ion beam processing
[AD-A222489] p 884 N90-27118
- BHATTACHARYA, S.**
Aircraft passing through a sinusoidal gust p 811 A90-48090
- BHATTACHARYA, T. K.**
A powerful range-Doppler clutter rejection strategy for navigational radars p 403 A90-30688
- BHUNGALLA, AMAR**
Correlation/validation of finite element code analyses for vibration assessment of avionic equipment
[AD-A220393] p 654 N90-23398
- BHUTTA, BILAL A.**
Parabolized Navier-Stokes predictions of three-dimensional hypersonic flows with strong crossflow effects p 223 A90-20508
- BI, N.**
Investigation of aerodynamic interactions between a rotor and fuselage in forward flight p 385 A90-28198
- BIANCO, CORRADO**
Aircraft fuel tank construction and testing experience p 250 N90-15907
- BIASIOL, ANDREA**
Development of a method to design helicopter rotors [REPT-100-30-03] p 845 N90-26830
- BIBKO, V. N.**
Wall pressure pulsation spectra ahead of internal corners p 804 A90-46545
- BICE, GREGORY W.**
Development of an automatic ground collision avoidance system using a digital terrain database
[AD-A216247] p 329 N90-17621
- BICEN, A. F.**
Combustion characteristics of a model can-type combustor p 676 A90-40479
- BIDWELL, C. S.**
Swept wing ice accretion modeling
[AIAA PAPER 90-0756] p 300 A90-25042
- BIDWELL, COLIN S.**
Predictions of airfoil aerodynamic performance degradation due to icing p 144 A90-16753
Swept wing ice accretion modeling
[NASA-TM-103114] p 570 N90-21727
- BIELAK, G. W.**
The 757 NLF glove flight test results p 104 N90-12546
- BIELER, H.**
Flight tests with a natural laminar flow glove on a transport aircraft
[AIAA PAPER 90-3044] p 828 A90-45881
Development of transition criteria on the basis of e to the N power for three dimensional wing boundary layers p 277 N90-16179
- BIEN, JOSEPH**
Dual servo optical projection system (SOPS) - A solution for two crewmember and night vision goggle display needs
[SAE PAPER 892353] p 760 A90-45504
- BIER, STEPHEN G.**
Evaluation of sensor management systems p 461 A90-30789
- BIESCHKE, BOB**
A modular 550 watt, 25 watts per cubic inch power supply for next generation aircraft p 958 A90-52954
- BIEZAD, D. J.**
GRATE: A new flight test tool for flying qualities evaluation p 34 N90-10868
- BIGGERS, SHERRILL B.**
A Protection And Detection Surface (PADS) for damage tolerance
[NASA-TP-3011] p 876 N90-27788
- BIHARI, B. L.**
Supersonic flow computations for an ASTOVL aircraft configuration
[AIAA PAPER 90-2997] p 787 A90-45847
- BIHRLE, W. JR.**
Influence of forebody geometry on aerodynamic characteristics and a design guide for defining departure/spin resistant forebody configurations
[AD-A216714] p 414 N90-18388
- BIL, CORNELIS**
Development and application of a computer-based system for conceptual aircraft design p 30 A90-12860
- BILEZIKJIAN, VAHE**
Aft facing transport aircraft passenger seats under 16G dynamic crash simulation p 175 A90-17416
- BILLIG, F. S.**
Effects of pressure mismatch on slot injection in supersonic flow
[AIAA PAPER 90-0092] p 227 A90-22161
- BILLIG, FREDERICK S.**
International Symposium on Air Breathing Engines, 9th, Athens, Greece, Sept. 3-8, 1989, Proceedings. Volumes 1 & 2 p 43 A90-12501
- BILLINGS, CHARLES E.**
Toward a human-centered aircraft automation philosophy p 347 A90-26177
- BILLMAN, BARRY**
Analytical studies for computed center line operations
[SAE PAPER 892219] p 729 A90-45436
- BILLMAN, BARRY R.**
Position computation without elevation information for computed centerline operations
[DOT/FAA/CT-TN89/42] p 640 N90-23379
- BILLMAN, L. C.**
Large scale prop-fan structural design study. Volume 1: Initial concepts
[NASA-CR-174992] p 52 N90-10043
Large scale prop-fan structural design study. Volume 2: Preliminary design of SR-7
[NASA-CR-174993] p 52 N90-10044
- BILLMANN, BARRY R.**
Helicopter Visual Segment Approach Lighting System (HALS)
[ACD-330] p 28 N90-10856
- BILLONNET, GILLES**
Numerical simulation of three-dimensional unsteady flows in turbomachines
[ONERA, TP NO. 1989-118] p 4 A90-11149
- BILODEAU, ANDREW R.**
A comprehensive diagnostic system for the T800-APW-800 engine p 422 A90-28181
- BIPPE, H.**
Disturbance growth in an unstable three-dimensional boundary layer p 148 A90-16787
Experiments on the laminar-turbulent transition on swept wings p 276 N90-16170
- BIRD, GRAEME A.**
Direct simulation of three-dimensional hypersonic flow about intersecting blunt wedges p 16 A90-12835
- BIRD, VICTOR J.**
Fiber-optic turbine inlet temperature measurement system (FOTITMS)
[AIAA PAPER 90-2033] p 657 A90-40603
- BIRKY, MERRITT M.**
The use of soot analysis as an investigative tool in aircraft fires p 22 A90-10269
- BIRMAN, V.**
Supersonic flutter of shear deformable laminated composite flat panels p 683 A90-41104
- BIRMAN, VICTOR**
Effect of aerodynamic heating on deformation of composite cylindrical panels in a gas flow p 773 A90-45788
- BIRNBAUM, MELVIN**
Range Applications Joint Program Office GPS Range System data link p 725 A90-43686
- BIRON, ANDRE**
Cyclic stress-strain behavior and low cycle fatigue of Ti 6242 p 530 A90-33523
- BISHOPP, J. A.**
The surface pretreatment of aluminium-lithium alloys for structural bonding p 881 A90-47118
- BISSET, JOHN W.**
Energy Efficient Engine integrated core/low spool test hardware design report
[NASA-CR-168137] p 931 N90-28566
- BISSINGER, NORBERT C.**
Generalized fluxvectors for hypersonic shock-capturing
[AIAA PAPER 90-0390] p 165 A90-19829
- BISWAS, DEWASHISH**
Studies on supersonic radial flow behavior in disk channel p 87 A90-16104
- BISWAS, G.**
Computation of laminar mixed convection flow in a channel with wing type built-in obstacles p 67 A90-11114
- BISWAS, GAUTAM**
Multi-level models for diagnosis of complex electro-mechanical systems p 693 A90-38888
Navier-Stokes computations of three-dimensional laminar flows with buoyancy in a channel with wing-type vortex generators p 772 A90-45728
- BITTNER, R. D.**
Flow establishment in a generic scramjet combustor
[AIAA PAPER 90-2096] p 742 A90-42729
- BITTNER, ROBERT D.**
Hypersonic CFD applications for the National Aero-Space Plane
[SAE PAPER 892310] p 714 A90-45473
- BJARKE, LISA J.**
An in-flight interaction of the X-29A canard and flight control system
[AIAA PAPER 90-1240] p 348 A90-26820
An in-flight interaction of the X-29A canard and flight control system
[NASA-TM-101718] p 736 N90-25973
- BJORKMAN, W. S.**
TRENDS: The aeronautical post-test database management system
[NASA-TM-101025] p 761 N90-25149
- BLACK, C. G.**
System identification strategies for helicopter rotor models incorporating induced flow p 30 A90-12768
A frequency-domain system identification approach to helicopter flight mechanics model validation p 56 A90-12772
- BLACK, G. THOMAS**
Flying qualities lessons learned - 1988 p 431 A90-30705
- BLACK, MARC**
Induction heating development for aircraft repair p 955 A90-50164
- BLACKBURN, MARTIN J.**
Improved toughness alloys based on titanium aluminides
[AD-A218149] p 533 N90-20208
- BLACKMAN, S. S.**
Multiple sensor data association and fusion in aerospace applications p 778 A90-44644
- BLACKWELDER, RON F.**
Modification of large eddies in turbulent boundary layers p 474 A90-33514
- BLACKWELL, R. H., JR.**
Higher harmonic and trim control of the X-wing circulation control wind tunnel model rotor p 435 A90-28156
- BLAIR, M.**
Time domain simulations of a flexible wing in subsonic, compressible flow
[AIAA PAPER 90-1153] p 390 A90-29365
- BLAIR, MAX**
A review of aeroelasticity research at the flight dynamics laboratory p 493 A90-33409
- BLAJER, W.**
Aircraft program motion along a predetermined trajectory. I - Mathematical modelling p 345 A90-23979
Aircraft program motion along a predetermined trajectory. II - Numerical simulation with application of spline functions to trajectory definitions p 347 A90-25199
- BLAKE, DAVID**
Flammability of fire resistant, aircraft hydraulic fluid
[DOT/FAA/CT-TN90/19] p 766 N90-25222
- BLAKE, DAVID R.**
Fire hazards of aerosol cans in aircraft cargo compartments
[DOT/FAA/CT-89/32] p 636 N90-23369
- BLAKE, WILLIAM B.**
Rotational aerodynamics of elliptic bodies at high angles of attack
[AIAA PAPER 90-0068] p 161 A90-19664
Low speed testing and simulation of the STOL and Maneuver Technology Demonstrator
[AIAA PAPER 90-1820] p 334 A90-25169
Yaw damping of elliptic bodies at high angles of attack p 709 A90-44740
- BLAKELEY, ANTHONY**
Structural and dynamic analysis of the A330/340 composite RAT blade p 942 A90-50083
- BLANCHARD, A.**
Flow quality in the T2 cryogenic wind-tunnel - Problems and solutions p 524 A90-34240
Main results of CAST-10 airfoil tested in T2 cryogenic wind tunnel p 321 N90-17652
- BLANCHARD, K. V.**
The nature and control of skidding in lightly loaded intershaft bearings
[PNR90591] p 136 N90-12933
- BLANDA, JOSEPH J.**
Range Applications Joint Program Office GPS Range System data link p 725 A90-43686
- BLANKSON, ISIAIAH**
NASA aerodynamics program
[NASA-TM-4175] p 373 N90-17235
- BLASZCZYK, J.**
Numerical analysis of natural vibrations of an aeroplane with symmetrically variable geometry wing p 860 A90-46715

BLASZCZYK, JAN

The influence of selected geometrical and mass parameters on the structural dynamics of an aircraft with a variable-geometry airfoil p 346 A90-24284

BLATT, J. R.

Energy Efficient Engine exhaust mixer model technology report addendum; phase 3 test program [NASA-CR-174799] p 930 N90-28556

BLAUVELT, H.

Reduced insertion loss of X-band RF fiber optic links p 695 A90-41240

BLEEKS, THOMAS W.

The properties and characteristics of electroless nickel coatings applied to gas turbine engine components [ASME PAPER 89-GT-4] p 354 A90-23751

BLEVINS, DAVID M.

Benchmarking blackboards to support cockpit information management [AIAA PAPER 89-3095] p 37 A90-10580

BLISS, D. B.

Optimization of rotor performance in hover and axial flight using a free wake analysis p 407 A90-28175
Free wake analysis of rotor configurations for reduced vibratory airloads p 833 A90-46975

BLISS, DONALD B.

New free-wake analysis of rotorcraft hover performance using influence coefficients p 181 A90-17867
High resolution flow field prediction for tail rotor aerodynamics p 463 A90-28158
Efficient free wake calculations using Analytical/Numerical Matching and far-field linearization p 384 A90-28171

BLOECHL, BERNHARD

Wind tunnel design of heat island turbulent boundary layer [IHW-ET/50] p 455 N90-19542

BLOEMHOF, HINNE

Flutter of mistuned cascades with structural coupling p 42 A90-11802

BLOM, ANDERS F.

Damage tolerance of the fighter aircraft 37 Viggen. Part 1: Analytical assessment [FFA-TN-1990-12-PT-1] p 923 N90-28538
Damage tolerance of the fighter aircraft 37 Viggen. Part 2: Experimental verification [FFA-TN-1990-13-PT-2] p 923 N90-28539

BLONDET, P.

Inspection system for in-situ inspection of aircraft composite structures p 886 N90-28091

BLOTTNER, FREDERICK G.

Verification of a Navier-Stokes code for solving the hypersonic blunt body problem p 146 A90-16774
Accurate Navier-Stokes results for the hypersonic flow over a spherical nosetip p 393 A90-29687

BLOY, A. W.

The performance and longitudinal stability and control of large receiver aircraft during air to air refueling p 346 A90-24338

BLOY, ALBERT W.

Large receiver aircraft - The performance and longitudinal stability and control during air to air refueling p 669 A90-41767

BLOZY, J. T.

Altitude testing of the 2D V-STOL ADEN demonstrator on an F404 engine [NASA-CR-174824] p 345 N90-17638

BLUME, HANS-J. C.

Airborne Doppler radar flight experiments for the detection of microbursts p 542 N90-21243

BLYSTONE, J. R.

The aerodynamic assistant [AIAA PAPER 89-3132] p 75 A90-10608

BOADEN, BRUCE

Future development of the 535E4 engine p 745 A90-44596

BOATMAN, JOE F.

Aerosol separator for use in aircraft [PB90-142217] p 611 N90-22155

BOBBITT, P. J.

Computational results for the effects of external disturbances on transition location of bodies of revolution from subsonic to supersonic speeds and comparisons with experimental data [SAE PAPER 89-2381] p 715 A90-45522

BOBIN, L.

Volumetric analysis by spontaneous Raman diffusion in a supersonic wind tunnel [ISL-R-109/88] p 95 N90-12564

BOBROW, J. E.

Active soot reduction in a spray-fired, axisymmetric model gas turbine combustor [AIAA PAPER 90-0039] p 191 A90-19644

BOCCI, A. J.

Aerofoil design techniques p 500 N90-20978

BOCIEK, STANISLAW

An analysis of the possibility of using direct control of the lifting force for modifying the flying qualities of aircraft p 118 A90-15423

Digital autopilot for light aircraft p 653 A90-41741

BOCK, DIANA M.

Cost effectiveness of composite materials on the F-15 and F-16 aircraft [AD-A216353] p 338 N90-17631

BOCK, K.-W.

Aerodynamic design by optimization p 502 N90-20996

BODDEN, D. S.

Configuration E-7 supersonic fighter/attack technology program [ASME PAPER 89-GT-308] p 490 A90-32260

BODDEN, DAVID S.

The implementation of STOVL task-tailored control modes in a fighter cockpit [AIAA PAPER 90-3229] p 839 A90-49114

BODDY, C. L.

Design of adaptive digital controllers incorporating dynamic pole-assignment compensators for high-performance aircraft p 432 A90-30714

BODEKER, DAN, III

Design of a low cost short takeoff-vertical landing export fighter/attack aircraft [NASA-CR-186658] p 734 N90-25132

BODNER, S. R.

Constitutive modeling for isotropic materials (HOST) [NASA-CR-179522] p 193 N90-13390
Constitutive modeling for isotropic materials (HOST) [NASA-CR-174718] p 193 N90-13391

BOEBEL, R.

Integration of the LTN-72 INS with the DOD GPS 3A set p 728 A90-45236

BOEHM, M.

Trends in avionics - From analog black boxes to integrated digital avionics systems p 252 A90-23245

BOEHRET, HARTMUT

Active control system for gust load alleviation and structural damping p 259 N90-15056

BOELCS, A.

Unsteady flow visualization in a vibrating annular turbine cascade operating in the transonic flow regime p 7 A90-11786

Experimental investigation of the time-dependent flow in a vibrating annular cascade operating in the transonic flow regime p 7 A90-11787

Numerical investigation of unsteady compressible flow through nozzles and cascades p 7 A90-11790

BOERMANS, L. M. M.

Experimental aerodynamic characteristics of the airfoils LA 5055 and DU 86-084/18 at low Reynolds numbers p 800 A90-46368

BOERSTOEL, J. W.

Numerical interactive grid generation for 3D-flow calculations p 312 A90-26556
Design and testing of a multiblock grid-generation procedure for aircraft design and research p 582 N90-21984

The development of a system for the numerical simulation of Euler flows p 612 N90-22980

Development of a system for the numerical simulation of Euler flows, with results of preliminary 3-D propeller-slipstream/exhaust-jet calculations [NLR-TR-88008-U] p 776 N90-26285

BOEV, BORIS V.

Identification and diagnostics in the data processing and control systems of aerospace powerplants p 611 A90-36151

BOFFADOSI, MAURIZIO

A fast collocation method for transonic airfoil design p 501 N90-20984

BOFILIOS, DIMITRI A.

Structure-borne noise transmission in cylindrical enclosures due to random excitation [AIAA PAPER 90-0990] p 463 A90-29402

BOGACHEV, A. S.

Optimization of complex data processing algorithms in multichannel radio direction finding p 576 A90-36115

BOGARDUS, SCOTT

High speed civil transport [NASA-CR-186661] p 649 N90-23396

BOGATKO, V. I.

Irregular interaction of a strong shock wave with a thin profile p 9 A90-12267

BOGDONOFF, S. M.

A study of the unsteadiness of crossing shock wave turbulent boundary layer interactions [AIAA PAPER 90-1456] p 606 A90-38614

BOGER, DAN C.

Aircraft modifications cost analysis. Volume 1: Overview of the study [AD-A220764] p 702 N90-25074

BOGOLEPOV, V. V.

Effect of tangential injection on flow in a laminar boundary layer p 294 A90-24080

BOGOMAZOV, V. I.

Using the smoking-wire visualization method in the study of wing models at large angles of attack in subsonic wind tunnels p 881 A90-46561

BOGOMOLOV, A. I.

Parametric synthesis of the decoupling filter in the manual control system of VTOL aircraft p 859 A90-46483

BOHLMANN, JONATHAN D.

Static aeroelastic tailoring for oblique wing lateral trim p 667 A90-40689

BOHN, HANS EINAR

An aircraft noise study in Norway p 698 N90-24872

BOIFFIER, JEAN-LUC

Synthesis of control law, on a RPV, in order to minimize the number of sensors p 260 N90-15925

BOIKO, A. V.

Instability and susceptibility of a boundary layer in the vicinity of two-dimensional surface inhomogeneities p 535 A90-32675

BOIKO, VLADIMIR I.

The planning of air transportation on airlines p 721 A90-42648

BOISSIERE, SERGE

Turbulent mixing in helicopter jet diluters - Navier-Stokes calculations and correlations [AAAF PAPER NT 88-13] p 40 A90-11432

BOISSON, H. C.

Development of turbulence models for the analysis of compressible or incompressible unsteady flow [ETN-90-97486] p 958 N90-28810

BOITNOTT, RICHARD L.

Impact evaluation of composite floor sections [SAE PAPER 891018] p 100 A90-14330

A review of the analytical simulation of aircraft crash dynamics [NASA-TM-102595] p 484 N90-20068

Behavior of composite/metal aircraft structural elements and components under crash type loads: What are they telling us [NASA-TM-102681] p 774 N90-25368

BOITNOTT, TAUNYA

Video visualization of separation shock motion from measured wall pressure signals in a Mach 5 compression ramp interaction [AIAA PAPER 90-0074] p 162 A90-19670

BOKSER, V. D.

Separation development and its effect on the aerodynamics of supercritical profiles at transonic velocities p 297 A90-24142

BOLDMAN, DONALD R.

The unsteady aerodynamics of an oscillating cascade in a compressible flow field p 7 A90-11789

BOLEY, G. D.

Classification and reduction of pilot error [NASA-CR-181867] p 24 N90-10014

BOLUKBASI, A.

Modeling strategies for crashworthiness analysis of landing gears p 409 A90-28233

BOLUKBASI, AKIF O.

Aircraft crash survival design guide. Volume 3: Aircraft structural crash resistance [AD-A218436] p 575 N90-22547

Aircraft crash survival design guide. Volume 4: Aircraft seats, restraints, litters, and cockpit/cabin dealthalization [AD-A218437] p 575 N90-22548

BOMAN, B. L.

Heat pipes for wing leading edges of hypersonic vehicles [NASA-CR-181922] p 369 N90-17055

BOMAN, PER-OLOF

Damage tolerance of the fighter aircraft 37 Viggen. Part 1: Analytical assessment [FFA-TN-1990-12-PT-1] p 923 N90-28538

Damage tolerance of the fighter aircraft 37 Viggen. Part 2: Experimental verification [FFA-TN-1990-13-PT-2] p 923 N90-28539

BOMMELAER, GUY

Icing test techniques for air intake screens on helicopters functioning in temperatures around 0 C p 23 A90-12619

BONAFE, J. L.

How to fly windshear using the fly-by-wire concept p 258 N90-15050

BONAITA, GIOVANNI

Results of an A109 simulation validation and handling qualities study p 591 A90-38524

BONCH-OSMOLOVSKII, LEV A.

Fundamentals of the design and development of parts and mechanisms for flight vehicles p 414 A90-30275

BOND, ALAN

Flight data replay and analysis system p 893 N90-27635

- BOND, LEONARD J.**
Impact of NDE-NDI methods on aircraft design, manufacture, and maintenance, from the fundamental point of view p 887 N90-28093
- BOND, THOMAS H.**
Icing Research Tunnel test of a model helicopter rotor p 400 A90-28179
- BONDI, M. J.**
TRENDS: The aeronautical post-test database management system [NASA-TM-101025] p 761 N90-25149
- BONHAUS, DARYL L.**
Strike camber and thickness design procedure for low alpha supersonic flow p 622 A90-40678
Relative efficiency and accuracy of two Navier-Stokes codes for simulating attached transonic flow over wings [AIAA PAPER 90-3078] p 795 A90-45909
- BONIFACIO, R.**
Co-development of CT7-6 engines - A continued tradition in technology and reliability p 665 A90-42485
- BONNET, J. P.**
Study of the compressibility effects on the turbulence of supersonic drags [ETN-90-97448] p 817 N90-27661
- BONNET, S.**
Calculation of three-dimensional boundary layers including hypersonic flows p 146 A90-16773
- BONTAUX, P.**
Numerical predictions for the flow and the heat transfer in gas turbine cooling systems p 770 A90-44464
Numerical investigations of heat transfer and flow rates in rotating cavities. Simulation of the movement generated by wall temperature gradients, by source-sink mass flows or by the differential rotation of the walls, under the influence or coriolis and centrifugal forces [ETN-90-96253] p 454 N90-18695
- BOOCOCK, RUSS**
Stress concentration factors - Comparison of theory with fatigue test data p 680 A90-39979
- BOORLA, RAGHUPATI**
Damage tolerance analysis of dynamic components of rotary wing aircraft p 179 A90-17312
- BOOTH, EARL R., JR.**
Reduction of blade-vortex interaction noise through higher harmonic pitch control p 377 A90-23937
Experimental observations of two-dimensional blade-vortex interaction p 809 A90-47303
Effect of pylon wake with and without pylon blowing on propeller thrust [NASA-TM-4162] p 173 N90-14190
- BOPPE, C. W.**
Hypersonic forebody lift-induced drag [SAE PAPER 892345] p 715 A90-45497
- BORAY, R. S.**
An experimental investigation of isothermal swirling flow in a model of a dump combustor p 47 A90-12572
Inlet swirl effects on dump combustor flows [AIAA PAPER 90-0035] p 312 A90-26904
- BORCHERS, I. U.**
Structural-acoustic analysis of aircraft fuselage structures using general purpose finite element codes p 492 A90-33385
- BORCHERS, PAUL**
Preliminary design of a supersonic Short Takeoff and Vertical Landing (STOVL) fighter aircraft [NASA-CR-186670] p 649 N90-23394
- BORDEN, ANDREW**
Incorporation of alarm states into a real time decision making process [AIAA PAPER 89-3006] p 76 A90-10620
- BORDER, JOHN**
Induction heating development for aircraft repair p 955 A90-50164
- BORDERS, M. E.**
Fuel tank explosion protection p 251 N90-15914
- BORELLA, H. M.**
Engine testing of thermographic phosphors [DE90-013269] p 885 N90-28059
- BORETTI, A. A.**
Two-dimensional Euler and Navier-Stokes Time accurate simulations of fan rotor flows [NASA-TM-102402] p 720 N90-25948
- BORGES, JOAO EDUARDO**
A three dimensional inverse method in turbomachinery. II - Experimental verification [ASME PAPER 89-GT-137] p 360 A90-23834
Application of an inverse method to the design of a radial inflow turbine p 511 N90-20989
- BORGHI, R.**
Turbulent combustion modeling for turbo-jet combustion chambers p 745 N90-25993
- BORGNOLO, F.**
EH-101 main rotor hub application of thick carbon fiber unidirectional tension bands p 618 A90-42489
- BORICIK, Z.**
Generalized similarity solutions for three-dimensional laminar compressible wing boundary layers p 907 A90-51543
- BORIS, J. P.**
A proper orthogonal decomposition of a simulated supersonic shear layer p 904 A90-51009
Acoustic-vortex-chemical interactions in an idealized ramjet p 54 N90-10206
- BORIS, JAY P.**
Numerical simulations of flowfields in a central-dump ramjet combustor. 3: Effects of chemistry [AD-A224145] p 933 N90-28573
- BORISOV, A. V.**
Numerical modeling of separated turbulent flows p 470 A90-32673
- BORISOV, S. IU.**
Characteristics of temperature and pressure generation and retention in flow inside cryogenic wind tunnel T-04 p 869 A90-46576
- BORNEMISZA, TIBOR**
Fast start ceramic auxiliary power unit [SAE PAPER 892254] p 747 A90-45456
- BOROFKA, JANINE C.**
Powder metallurgy and oxide dispersion processing of superalloys p 531 A90-34158
- BOROVSKII, B. I.**
Generalized relations for estimating the efficiency and basic dimensions of screw pumps and hydraulic turbines of pump units p 111 A90-14583
- BOROVSKII, S. M.**
Design of the optimal hardening treatment for the metal surfaces of gas turbine engine components p 873 A90-46496
- BORSHCH, A. M.**
Automation of flight safety control. p 589 A90-36157
- BORSHCH, V. L.**
Numerical solution of the problem of supersonic flow of a viscous gas past a concave conical wing p 619 A90-39465
- BORST, HENRY V.**
The Curtiss-Wright X-19 experimental aircraft - Lessons learned [AIAA PAPER 90-3206] p 834 A90-48834
- BORTNER, RAY**
Laboratory implementation of the Continuously Reconfiguring Multi-Microprocessor Flight Control System (CRMFCFS) [AD-A217730] p 520 N90-20094
- BORTOLUSSI, MICHAEL R.**
The benefits and costs of automation in advanced helicopters - An empirical study p 348 A90-26258
- BORTZ, G.**
Range determination in a multipath prone environment p 877 A90-45960
- BOS, H. J.**
Induced drag for non-planar wings [LR-521] p 172 N90-13357
- BOSCHER, D.**
The application of infrared thermography to the measurement of heat fluxes in a wind tunnel [ONERA, TP NO. 1989-192] p 261 A90-21051
Determination of convective transfer coefficients on a wind-tunnel model by stimulated infrared thermography [ONERA, TP NO. 1989-218] p 351 A90-25351
- BOSCHETTI, F.**
The evolution of light alloys in the aerospace industry [ETN-89-95216] p 126 N90-11872
An ultrasonic system for in-service non-destructive inspection of composite structures p 885 N90-28076
- BOSE, S.**
MATE (Materials for Advanced Turbine Engines) Program, Project 3. Volume 2: Design, fabrication and evaluation of an oxide dispersion strengthened sheet alloy combustor liner [NASA-CR-180892] p 357 N90-17868
- BOSNIAKOV, S. M.**
Calculation of supersonic flow past a wing/fuselage combination with the resolution of a compression shock from the wing p 297 A90-24138
Numerical solution of the problem of supersonic flow of an ideal gas past a trapezoidal wedge p 386 A90-28980
Calculation of three-dimensional flow past a plane supersonic air intake at angles of attack and sideslip p 805 A90-46573
- BOSSART, T. R.**
Practical design considerations for integrating the propulsion system with the aircraft for jetborne flight [ASME PAPER 89-GT-310] p 490 A90-32257
- BOSWORTH, JOHN T.**
A design procedure for the handling qualities optimization of the X-29A aircraft [NASA-TM-4142] p 119 N90-11753
- BOTIN, A. V.**
Hypersonic flow past blunt edges at low Reynolds numbers p 10 A90-12284
- BOTMAN, JEAN-PIERRE**
High service temperature, damage tolerant prepreg systems based on cyanate chemistry p 941 A90-50069
- BOTROS, DAVID F.**
Feasibility study for a microwave-powered ozone sniffer aircraft [NASA-CR-186660] p 650 N90-23397
- BOUCHARD, MICHAEL P.**
B-1B improved windshield development. Volume 2: Magna analysis: Baseline and parametric [AD-A21501] p 845 N90-26828
- BOUCHER, C. C.**
In-flight experiments on the active control of propeller-induced cabin noise p 893 A90-46352
- BOUCHERIT, A.**
Modeling of the oil quench for Ni-based superalloy turbine disks p 957 A90-51525
- BOUDIGUES, S.**
Ceramic heat exchangers in gas turbine [ONERA, TP NO. 1989-109] p 40 A90-11142
- BOUIS, X.**
Studies of the European transonic wind tunnel [ONERA-RSF-12/0694-GY] p 141 N90-13278
- BOUIS, XAVIER**
The European Transonic Windtunnel (ETW) p 262 N90-15945
- BOUKAMP, JOACHIM**
Antenna and radar signature technology at Dornier p 261 A90-21605
- BOULAY, J. L.**
Principal characteristics of lightning on aircraft p 239 N90-15067
- BOUNAJEM, ELIAS**
Flight test data processing, plotting and analysis at your finger tips - A flexible, automated, integrated approach [AIAA PAPER 90-1322] p 545 A90-34150
- BOUNIE, J. L.**
Composites for aeronautical structures p 286 A90-24291
- BOURGUIGNON, A. E.**
Pressure surface trailing edge slot cooling [ONERA, TP NO. 1989-123] p 47 A90-12569
Test rig for the study of the flow in a rotor-stator system [ONERA, TP NO. 1989-124] p 58 A90-12634
- BOUSE, G. K.**
Metallurgy of investment cast superalloy components p 531: A90-34154
- BOUSMAN, WILLIAM G.**
The response of helicopter rotors to vibratory airflow p 832 A90-46971
Correlation of Puma airloads: Lifting-line and wake calculation [NASA-TM-102212] p 170 N90-13327
The response of helicopter rotors to vibratory airflow [AD-A215678] p 337 N90-16756
Rotorcraft aeromechanical stability-methodology assessment. Phase 2: Workshop [NASA-TM-102272] p 816 N90-26800
The effects of structural flap-lag and pitch-lag coupling on soft inplane hingeless rotor stability in hover [NASA-TP-3002] p 910 N90-28503
- BOUSQUET, M. D.**
Mesoscale acid deposition modeling studies [NASA-CR-4262] p 140 N90-13228
- BOUTIER, A.**
Instrumentation being developed for the ONERA F4 wind tunnel [ONERA, TP NO. 1989-189] p 261 A90-21049
- BOUWER, G.**
A highly maneuverable helicopter in-flight simulator - Aspects of realization [AIAA PAPER 88-4607] p 670 A90-42466
- BOUWER, GERHARD**
ATThS - A helicopter in-flight simulator for ACT testing p 643 A90-41727
A robust digital model following controller for helicopters [ESA-TT-1041] p 120 N90-12621
- BOWEN, STUART W.**
The Meteorological Measurement System on the NASA ER-2 aircraft p 926 A90-51658
- BOWES, MICHAEL A.**
SH-2F airframe fatigue test program p 642 A90-39989
- BOWLES, KENNETH J.**
Thermo-oxidative stability studies of PMR-15 polymer matrix composites reinforced with various continuous fibers p 941 A90-50068
Use of unbalanced laminates as a screening method for microcracking p 948 A90-50217

BOWLES, R. L.

Acceleration, gamma, and theta guidance for abort landing in a windshear p 98 A90-14733

BOWLES, ROLAND L.

A Monte Carlo simulation technique for low-altitude, wind-shear turbulence [AIAA PAPER 90-0564] p 216 A90-19917

BOWLING, JOHN M.

Raman scattering measurements using UV excimer lasers p 874 A90-26902
Concentration, temperature, and density in a hydrogen-air flame by excimer-induced Raman scattering p 875 A90-26903

BOWMAN, C. T.

Turbulent reacting flows and supersonic combustion [AD-A221793] p 875 A90-26933

BOWMAN, DANIEL R.

Full-scale birdstrike testing of in-service aged F-111 ADBIT windshield transparencies [AD-A218035] p 484 A90-20069

BOWMAN, H. L.

Flow and acoustic features of a supersonic tapered nozzle [AIAA PAPER 90-1599] p 567 A90-38731
Supersonic rectangular isothermal shrouded jets [AIAA PAPER 90-2028] p 621 A90-40599

BOWMAN, JAMES S., JR.

Measurements of pressures on the wing of an aircraft model during steady rotation [AIAA PAPER 90-2842] p 754 A90-45162
Measurements of pressures on the tail and aft fuselage of an airplane model during rotary motions at spin attitudes [NASA-TP-2939] p 20 A90-10829

BOWMAN, K. B.

Structural optimization of lifting surfaces with divergence and control reversal constraints p 127 A90-13770

BOWMAN, P. S.

Acoustic emission detection of crack presence and crack advance during flight p 886 A90-28082

BOWMAN, R.

Observations on the brittle to ductile transition temperatures of B2 nickel aluminides with and without zirconium p 205 A90-19153

BOXWELL, D. A.

Prediction and measurement of low-frequency harmonic noise of a hovering model helicopter rotor p 463 A90-28159
Review and analysis of the DNW/Model 360 rotor acoustic data base [NASA-TM-102253] p 81 A90-11692

BOYD, JACK D.

A third-generation bismaleimide prepreg system p 943 A90-50131

BOYER, KEITH M.

Stall and recovery in multistage axial flow compressors p 428 A90-18429

BOYLE, M. A.

Variations in impact test methods for tough composites p 946 A90-50167

BOYLE, MAUREEN

High service temperature high compressive strength and tough prepreg system p 530 A90-33098

BOYLE, MAUREEN A.

High service temperature, damage tolerant prepreg systems based on cyanate chemistry p 941 A90-50069

BOYLE, R. J.

Navier-Stokes analysis of turbine blade heat transfer [NASA-TM-102496] p 542 A90-21300

BOZZOLA, P.

Use of smart actuators for the tail rotor collective pitch control p 688 A90-42483

BRACALENTE, E. M.

Airborne Doppler radar detection of low-altitude wind shear p 252 A90-23284
Airborne Doppler radar flight experiments for the detection of microbursts p 542 A90-21243

BRADFORD, E. R.

Using aircraft radar tracks to estimate wind aloft p 241 A90-21390

BRADLEY, R.

System identification strategies for helicopter rotor models incorporating induced flow p 30 A90-12768
Development and verification of an algorithm for helicopter inverse simulations p 591 A90-38522
Helicopter control design using feedback linearization techniques p 668 A90-40817

BRADSHAW, P.

Interaction between strong longitudinal vortices and turbulent boundary layers p 145 A90-16764
Experimental investigation of three-dimensional turbulent boundary layers on 'infinite' swept curved wings p 303 A90-25589

BRAFF, R.

Rapsat - Application of onboard processing for communication and surveillance in air traffic control [AIAA PAPER 90-0883] p 331 A90-25702

BRAGG, M.

A comparison of a droplet impingement code to icing tunnel results [AIAA PAPER 90-0670] p 352 A90-26979

BRAGG, M. B.

Measurements on an oscillating 70-deg delta wing in subsonic flow p 307 A90-26130
Measured forces and moments on a delta wing during pitch-up p 308 A90-26137
Measured aerodynamic performance of a swept wing with a simulated ice accretion [AIAA PAPER 90-0490] p 557 A90-37063

BRAHNEY, JAMES H.

Stowing the tilt-rotor p 246 A90-21703
An advanced X-ray technique for NDI p 604 A90-37901
Corrosion protection and EMP/EMI shielding p 600 A90-37902
Propulsion systems for the '90s p 745 A90-44605

BRAISTED, WILLIAM

B-1B improved windshield development. Volume 2: Magna analysis: Baseline and parametric [AD-A221501] p 845 A90-26828

BRANCH, GREG

The SKY SHARK: An RPV designed to investigate the pressure distribution on a lifting surface [NASA-CR-186222] p 844 A90-26824

BRAND, ALBERT

Prediction and measurement of the aerodynamic interactions between a rotor and airframe in forward flight p 384 A90-28176

BRAND, ALBERT GERARD

An experimental investigation of the interaction between a model rotor and airframe in forward flight p 185 A90-14219

BRANDER, J. R. G.

Modeling and analysis of airport and aircraft operations [PB90-222167] p 915 A90-28511

BRANDON, J. M.

Measurements on an oscillating 70-deg delta wing in subsonic flow p 307 A90-26130
In-flight flow visualization using infrared imaging p 731 A90-44731

BRANDON, JAY M.

Unsteady aerodynamic characteristics of a fighter model undergoing large-amplitude pitching motions at high angles of attack [AIAA PAPER 90-0309] p 313 A90-26933

BRANDSMA, F. J.

A system for transonic wing design with geometric constraints based on an inverse method p 501 A90-20983

BRANDT, J.

High-performance composite materials in air and space travel - State of the art and future perspectives [MBB-Z-0279/89] p 266 A90-22595

BRANDT, MADS H.

Flight data replay and analysis system p 893 A90-27635

BRANDT, STEVEN ALLAN

Numerical simulation of leading-edge vortex rollup and bursting p 20 A90-10831

BRANGIER, F.

Applications of Mode S secondary surveillance radar to civil air traffic control - Studies, experiments, and policy of the French Direction de la Navigation Aérienne p 639 A90-41056

BRANS, PATRICK

Design philosophy for a general aviation TCAS display [SAE PAPER 891052] p 108 A90-14354

BRANUM, LONNIE

Model tilt-rotor hover performance and surface pressure measurement [AD-A222535] p 845 A90-26827

BRASE, L. O.

Exhaust environment measurements of a turbofan engine equipped with an afterburner and 2D nozzle [NASA-CR-4289] p 588 A90-21760

BRASLOW, ALBERT L.

Simulated-airline-service flight tests of laminar-flow control with perforated-surface suction system [NASA-TP-2966] p 338 A90-17627

BRATTON, THOMAS

Communications Interface Driver (CID) test plan [DOT/FAA/CT-N89/35] p 958 A90-28762

BRAUN, G.

Helicopter rotor test rig (RoTeSt) in DNW: Application and results [RAE-TRANS-2171] p 201 A90-13408

BRAUN, M. J.

A laser based computer aided non-intrusive technique for full field flow characterization in macroscopic curved channels p 535 A90-32293

BRAUNE, ROLF

The Common/Same Type Rating - Human factors and other issues [SAE PAPER 892229] p 723 A90-45445

BRAVERMAN, ALEKSANDR S.

Helicopter dynamics: Limiting flight conditions p 55 A90-12481

BRAY, D.

Numerical modeling of an impinging jet in cross-flow [AIAA PAPER 90-2246] p 686 A90-42093

BRAYBROOK, ROY

General Dynamics F-16 p 100 A90-13791
The standard-setting Hornet p 730 A90-43764

BRAZA, M.

Development of turbulence models for the analysis of compressible or incompressible unsteady flow [ETN-90-97486] p 958 A90-28810

BRAZA, RUDY M.

Comparison of the swept frequency continuous wave, current pulse, and shock-excitation lightning simulation techniques p 818 A90-49832

BRAZSHKO, V. N.

Lee-side heating of a delta wing in supersonic flow p 10 A90-12281

BREEMAN, J. H.

Mathematical model identification for flight simulation, based on flight and taxi tests [LR-550] p 202 A90-13410

BREIDENTHAL, ROBERT E.

The sonic eddy - A model for compressible turbulence [AIAA PAPER 90-0495] p 167 A90-19876

BREIL, J. F.

Flow quality in the T2 cryogenic wind-tunnel - Problems and solutions p 524 A90-34240
Main results of CAST-10 airfoil tested in T2 cryogenic wind tunnel p 321 A90-17652

BREITKOPF, GUENTER E.

Basic approach in the development of TURBISTAN, a loading standard for fighter aircraft engine disks p 368 A90-26754

BRENDEL, M.

Transition phenomena on airfoils operating at low chord Reynolds numbers in steady and unsteady flow p 148 A90-16786

BRENNER, G.

Numerical simulation of hypersonic viscous continuum flow p 707 A90-44407

BRENNER, LOTHAR

Design criteria, constructions, and materials for the Dornier 328 airframe p 246 A90-21610

BRESCIA, JOSEPH A.

Evaluation of various non-asbestos epoxy adhesives for aircraft repair p 529 A90-33078

BRESINA, JOHN J.

NASA Langley Research Center National Aero-Space Plane Mission simulation profile sets [NASA-TM-102670] p 924 A90-28541

BRESLAU, RAY W.

Multisensor Integrated Navigation System p 577 A90-36924

BREUGELMANS, F. A. E.

Unsteady loss in a low speed axial flow compressor during rotating stall p 12 A90-12527

BRIDGEMAN, JOHN O.

Advanced rotor computations with a corrected potential method p 385 A90-28197

Three-dimensional viscous rotor flow calculations using a viscous-inviscid interaction approach [NASA-TM-102235] p 399 A90-19204

BRIDGEMAN, M. J.

NASA/GE Energy Efficient Engine low pressure turbine scaled test vehicle performance report [NASA-CR-168290] p 931 A90-28563

BRIDGES, ALAN L.

Integrated Diagnostics (ID) for advanced avionics architectures [SAE PAPER 892359] p 738 A90-45509

BRIDGES, PHILIP D.

Influence of satellite geometry, range, clock, and altimeter errors on two-satellite GPS navigation p 123 A90-13993

BRIEGER, JOHN T.

Tilt rotor aircraft aeroacoustics p 409 A90-28238

BRIGHT, CLARK I.

Grid and mesh patterned electrically conductive coatings in IR systems p 503 A90-32028

BRIGHT, MICHELLE

H-infinity based integrated flight/propulsion control design for a STOVL aircraft in transition flight [AIAA PAPER 90-3335] p 862 A90-47595

- BRIGHT, MICHELLE M.**
H-infinity based integrated flight-propulsion control design for a STOVL aircraft in transition flight
[NASA-TM-103198] p 758 N90-26011
- BRIGHT, PAUL**
Expert system diagnostics and parts life tracking as applied to the AV-8B aircraft for the USMC
p 884 N90-27629
- BRINDISI, FRANK, JR.**
The properties and characteristics of electroless nickel coatings applied to gas turbine engine components
[ASME PAPER 89-GT-4] p 354 A90-23751
- BRINDLEY, WILLIAM J.**
TBCs for better engine efficiency p 203 A90-17294
Thermal barrier coatings for gas turbine and diesel engines
[NASA-TM-102408] p 205 N90-13636
- BRINES, GERALD L.**
The turbofan of tomorrow p 850 A90-46150
- BRINK-SPALINK, J.**
Fast calculation of root loci for aeroelastic systems and of response in time domain
[AIAA PAPER 90-1156] p 390 A90-29368
Fast calculation of root loci of aeroelastic systems and of gust response in time domain p 517 A90-33413
- BRINKLEY, JAMES W.**
Windblast protection for advanced ejection seats
p 483 N90-20063
- BRISSART, J.**
Flow around a jet and thrust measurement bias from static tests
[AAAF PAPER NT 88-11] p 40 A90-11431
- BRISTEAU, M. O.**
Development of finite element methods for compressible Navier-Stokes flow simulations in aerospace design
[AIAA PAPER 90-0403] p 166 A90-19833
- BRITCHER, COLIN**
An experimental investigation of the aerodynamic characteristics of slanted base ogive cylinders using magnetic suspension technology
[NASA-CR-181708] p 21 N90-10834
- BRITCHER, COLIN P.**
Recent aerodynamic measurements with Magnetic Suspension Systems p 759 A90-44399
Subsonic sting interference on the aerodynamic characteristics of a family of slanted-base ogive-cylinders
[NASA-CR-4299] p 633 N90-24242
- BRITO, KARREN K.**
Vapor grown carbon fiber for space thermal management systems p 943 A90-50128
- BRITT, C. L.**
Airborne Doppler radar detection of low-altitude wind shear p 252 A90-23284
Airborne Doppler radar flight experiments for the detection of microbursts p 542 N90-21243
- BRITTON, R. K.**
A study of ice shape prediction methodologies and comparison with experimental data
[AIAA PAPER 90-0753] p 322 A90-26986
Ice induced aerodynamic performance degradation of rotorcraft: An overview p 248 N90-15063
- BROADBENT, E. G.**
Hypersonic (T-D) 'pinch' and aerospaceplane propulsion
[AIAA PAPER 90-2474] p 675 A90-42189
- BROCHET, J.**
A methodology proposal to design and analyse counterrotating high speed propellers
[ASME PAPER 89-GT-38] p 340 A90-23767
- BROCK, M. P.**
UHB demonstrator interior noise control flight tests and analysis
[NASA-CR-181897] p 140 N90-13198
- BROCKHAUS, R.**
Investigation of a nonlinear Kalman filter for estimating aircraft state variables p 195 A90-16850
- BROCKLEHURST, ALAN**
Experimental and numerical study of the British Experimental Rotor Programme blade
[AIAA PAPER 90-3008] p 789 A90-45858
- BROCKMAN, BOB**
Evaluation of critical speeds in high speed aircraft tires
[SAE PAPER 892349] p 733 A90-45500
- BROCKMEIER, U.**
Structure of velocity and temperature fields in laminar channel flows with longitudinal vortex generators
p 273 A90-23207
- BRODERSEN, ROLF**
A self-compensating aircraft recovery system (SCARS)
[AIAA PAPER 90-3273] p 818 A90-48864
- BRODETSKII, M. D.**
Aerodynamic interference of prismatic engine nacelles with the wing at supersonic velocities
p 294 A90-24078
- BROEDE, J.**
Advanced algorithms design and implementation in on-board microprocessor systems for engine life usage monitoring p 892 N90-27628
- BROGAN, F. A.**
Bulging cracks in pressurized fuselages - A procedure for computation p 880 A90-46301
- BROICHHAUSEN, K. O.**
Experiments on the unsteady flow in a supersonic compressor stage p 427 N90-18422
- BROIDA, T. J.**
Multiple sensor data association and fusion in aerospace applications p 778 A90-44644
- BROM, G.**
Volumetric analysis by spontaneous Raman diffusion in a supersonic wind tunnel
[ISL-R-109/88] p 95 N90-12564
- BROMMER, KARL**
High level language programming for avionic vector processors
[AIAA PAPER 89-3107] p 74 A90-10589
- BROOKS, A.**
Propulsion systems for vertical flight aircraft
[AIAA PAPER 90-3299] p 853 A90-48881
- BROOKS, C. J.**
The human factors relating to escape and survival from helicopters ditching in water
[AGARD-AG-305(E)] p 176 N90-13358
- BROOKS, CUYLER W., JR.**
Experimental transition and boundary-layer stability analysis for a slotted swept laminar flow control airfoil
p 148 A90-16793
Results of LFC experiment on slotted swept supercritical airfoil in Langley's 8-foot transonic pressure tunnel
p 92 N90-12531
Boundary-layer stability analysis of Langley Research Center 8-foot LFC experimental data p 92 N90-12532
- BROOKS, JEFFREY L.**
Logistics support planning for standardized avionics
p 383 A90-30809
- BROOKS, THOMAS F.**
Reduction of blade-vortex interaction noise through higher harmonic pitch control p 377 A90-23937
- BROPHY, CAROLYN ELIZABETH**
Implementation of a production Ada project: The GRODY study
[NASA-TM-103305] p 547 N90-21544
- BROQUERE, B.**
Analysis and practical design of ceramic-matrix composite components p 445 A90-28135
- BROSS, P. A.**
The EFA integrated monitoring and recording system: Requirements and concept for implementation
p 848 N90-27620
- BROUGHTON, T.**
Diffusion bonding aeroengine components
p 131 A90-16012
- BROUWER, J.**
Active soot reduction in a spray-fired, axisymmetric model gas turbine combustor
[AIAA PAPER 90-0039] p 191 A90-19644
A model gas turbine combustor with wall jets and optical access for turbulent mixing, fuel effects, and spray studies p 507 A90-32808
- BROWN, ALAN S.**
Material of the '90s? p 265 A90-20259
Stealth comes of age p 336 A90-27596
Materials get smarter p 356 A90-27598
- BROWN, ALISON**
A multi-sensor approach to assuring GPS integrity
p 821 A90-46396
- BROWN, ALISON K.**
GPS integrity requirements for use by civil aviation
p 916 N90-29339
- BROWN, CHRISTOPHER K.**
Computational design of low aspect ratio wing-winglet configurations for transonic wind-tunnel tests
[NASA-CR-181939] p 316 N90-17539
- BROWN, D.**
Wind tunnel studies of F/A-18 tail buffet
[AIAA PAPER 90-1432] p 559 A90-37969
Measurements of aerodynamic forces on aircraft external stores in the NAE trisonic blowdown wind-tunnel p 629 A90-42419
New transonic test sections for the NAE 5ftx5ft trisonic wind tunnel p 630 A90-42431
New transonic test sections for the NAE 5 ft x 5 ft trisonic wind tunnel
[AD-A220933] p 674 N90-24278
- BROWN, GERALD V.**
Experimental evaluation of a tuned electromagnetic damper for vibration control of cryogenic turbopump rotors
[NASA-TP-3005] p 665 N90-23403
- BROWN, H. A.**
A comparison of lightning network data with surface weather observations
[AD-A220003] p 692 N90-23832
- BROWN, J. M.**
RAIM - An implementation study p 726 A90-43714
- BROWN, JAMES M.**
Embedded GPS - The Canadian Marconi approach
p 725 A90-43700
- BROWN, JOHN E.**
Mode S transponders - A new avionics product
[SAE PAPER 891055] p 98 A90-14357
- BROWN, LEE MERRY**
ATC ground communications system optimization techniques p 330 A90-25568
- BROWN, P. C.**
Propan Test Assessment (PTA): Flight test report
[NASA-CR-182278] p 113 N90-11738
Propan Test Assessment (PTA)
[NASA-CR-185138] p 113 N90-11739
- BROWN, P. W.**
Investigations of modifications to improve the spin resistance of a high-wing, single-engine, light airplane
[SAE PAPER 891039] p 118 A90-14345
- BROWN, PAUL**
Acoustic test and analysis of a counterrotating prop-fan model
[NASA-CR-179590] p 79 N90-10683
- BROWN, PHILIP W.**
Multistroke cloud-to-ground strike to the NASA F-106B airplane p 482 A90-32304
The vortex flap F-106B, overcoming safety and data problems in flight testing
[AIAA PAPER 90-1280] p 496 A90-34725
Final results of the NASA storm hazards program p 819 A90-49834
- BROWN, R. GROVER**
Loran-aided GPS integrity p 98 A90-14013
The case for both RAIM and GIC working together - The ultimate solution to the GPS integrity problem
p 576 A90-36916
- BROWN, ROBERT L.**
Improving snow roads and airstrips in Antarctica
[AD-A211588] p 133 N90-11907
- BROWN, SQUIRE L.**
Exploration of concepts for multi-role fighters
[AIAA PAPER 90-2276] p 644 A90-42104
- BROWN, WILLIAM**
Atomization and spray research for gas turbine engines p 189 A90-17688
- BROWN, WILLIAM C.**
History and status of beamed power technology and applications at 2.45 Gigahertz p 61 N90-10150
- BROWNE, LINDSEY**
Application of panel methods to wind-tunnel wall interference corrections
[AIAA PAPER 90-0007] p 200 A90-19629
- BROWNE, LINDSEY E.**
Study of the integration of wind tunnel and computational methods for aerodynamic configurations
[NASA-TM-102196] p 170 N90-13332
- BRUCE, DAVID A.**
Inspection reliability p 885 N90-28072
- BRUCE, ROBERT A.**
A vapor generator for transonic flow visualization
[NASA-TM-101670] p 201 N90-13403
- BRUCE, WALTER E., JR.**
The US National Transonic Facility, NTF
p 262 N90-15942
- BRUCKNER, A. P.**
Operation of the ram accelerator in the transdetonative velocity regime
[AIAA PAPER 90-1985] p 741 A90-42712
- BRUDNYI, EDUARD O.**
Radio deviation of airborne goniometers
p 242 A90-22733
- BRUHIS, O.**
Flight simulation model validation procedure, a systematic approach p 30 A90-12770
- BRUHIS, OFER**
Identification of a coupled flapping/inflow model for the PUMA helicopter from flight test data p 56 A90-12767
- BRUINSMA, STAAS J. A.**
Review of fiber optic methods for strain monitoring and non-destructive testing p 67 A90-11042
- BRUN, G.**
Finite element simulation of compressible turbulent flows - Validation and application to internal aerodynamic in gas-turbine engines p 210 A90-18343
- BRUNE, C.**
Rotordynamics of the Vulcain LH2 Turbopump - Comparison between test results and non-linear dynamic analysis p 528 A90-33382
- BRUNEAU, CHARLES-HENRI**
Computation of hypersonic flows by a finite element least-squares method p 155 A90-18296

- BRUNEL, ERIC**
Preliminary tests of a gust generator in the ONERA S3Ch transonic wind tunnel
[ONERA, TP NO. 1989-171] p 261 A90-21035
- BRUNER, HUGH S.**
Development of a stall improvement package for the Gulfstream IV
[SAE PAPER 891021] p 83 A90-14333
- BRUNKEN, JOHN E.**
A review of the V-22 dynamics validation program
p 406 A90-28155
- BRUNKEN, JOHN E., JR.**
V-22 MSC/NASTRAN airframe vibration analysis and correlation
p 832 A90-46969
- BRUNNER, B.**
Eight years of experience with small computerized retrofit load monitoring systems
p 926 A90-49882
- BRUNNER, O.**
MAVIS flight load simulation
p 202 A90-17003
- BRUNNER, R.**
Improved thermal performance using allylnadac-imides
p 946 A90-50175
- BRUSKIN, DAVID E.**
Power supply of aircraft
p 43 A90-12474
- BRUSOV, VLADIMIR S.**
Optimum aircraft design: Multipurpose approach
p 829 A90-46618
- BRUTIAN, M. A.**
Jet flap theory
p 298 A90-24154
- BRUUN, H. H.**
A computer aided manufacturing procedure for experimental two-dimensional aerofoils
p 270 A90-20609
- BRYAN, KEVIN**
The MANTA: An RPV design to investigate forces and moments on a lifting surface
[NASA-CR-186227] p 499 N90-20971
- BRYAN, W. BARRY**
Flow induced forced response of an incompressible radial cascade including profile and incidence effects
[AIAA PAPER 90-2352] p 626 A90-42136
- BRYANSTON-CROSS, P. J.**
Holographic flow visualisation of turbofan by-pass and core nozzle streams
[ASME PAPER 89-GT-260] p 363 A90-23691
- BRYANT, T. D.**
Application of sound and temperature to control boundary-layer transition
p 92 N90-12537
- BRYCE, J. D.**
Preliminary experience with high response pressure measurements in a multistage, high speed compressor
[RAE-TM-P-1141] p 117 N90-12619
- BRYDGES, B. E.**
Amplitude effects on dynamic stall of an oscillating airfoil
[AIAA PAPER 90-0575] p 167 A90-19925
- BRYDGES, BRUCE E.**
Flow visualization of dynamic stall on an oscillating airfoil
[AD-A222202] p 815 N90-26797
- BRYSON, A. E.**
Simple analyses of paths through windshears and downdrafts
[AIAA PAPER 90-0222] p 197 A90-19740
Parameter identification of linear systems based on smoothing
[AIAA PAPER 90-2800] p 753 A90-45156
- BRYSON, A. E., JR.**
Optimal paths through downbursts
p 755 A90-45330
Control of an aircraft in downbursts
p 755 A90-45331
- BRYSON, ARTHUR E., JR.**
A comparison of inverse control with optimal control
[AIAA PAPER 90-3484] p 866 A90-47733
- BRYSON, ROBERT J.**
A review of the V-22 dynamics validation program
p 406 A90-28155
- BRYZGALIN, G. I.**
Multicriterial optimization of lugs in hinge joints
p 364 A90-24162
- BUCCI, R. J.**
The influence of material quality on airframe structural durability
p 676 A90-41336
An aluminum quality breakthrough for aircraft structural reliability
p 843 N90-26816
- BUCCIANTINI, G.**
The aerodynamic experimental center of Aeritalia: Combat aircraft group
[ETN-89-95213] p 122 N90-11766
- BUCHACKER, E.**
GRATE: A new flight test tool for flying qualities evaluation
p 34 N90-10868
- BUCHARLES, A.**
Advanced parameter identification techniques for near real time flight flutter test analysis
[AIAA PAPER 90-1275] p 494 A90-33899
- BUCHER, NANCY**
Helmet mounted display systems for helicopter simulation
p 420 A90-31344
- BUCHER, NANCY M.**
Helmet-mounted display systems for flight simulation
[SAE PAPER 892352] p 760 A90-45503
- BUCHMANN, O. A.**
Development and fabrication of structural components for a scramjet engine
[NASA-CR-181945] p 510 N90-20088
- BUCK, MELVIN L.**
Non-isentropic effects on the WRDC 20 inch hypersonic wind tunnel calibration
p 435 A90-28254
- BUCK, ROBERT N.**
Prompt identification of a troubled engine can help avoid catastrophe
p 721 A90-44222
- BUCKLEY, J. E.**
Unified flying qualities criteria for longitudinal tracking
[AIAA PAPER 90-2806] p 752 A90-45141
- BUCKLEY, P. L.**
Inlet swirl effects on dump combustor flows
[AIAA PAPER 90-0035] p 312 A90-26904
- BUCKNELL, R. L.**
Evolution of engine cycles for STOVL propulsion concepts
[AIAA PAPER 90-2272] p 743 A90-42767
- BUCKNER, RANDY L.**
The collection of usage data to improve structural integrity of operational helicopters
p 651 A90-39983
- BUDD, A. J.**
A simulation study of landing time allocation procedures for use in computer-assisted air traffic management systems
[AD-A212159] p 99 N90-11722
- BUELOW, PHILIP E.**
A three-dimensional upwind parabolized Navier-Stokes code for chemically reacting flows
[AIAA PAPER 90-0394] p 165 A90-19831
- BUENDIA, A.**
Pressure air tightness tests of laminated panels for wing leading edge heat shields
[INFORME-I-377/89] p 357 N90-17873
- BUERS, HARTMUT**
Low- and high-speed tests with the Dornier 328 wind-tunnel model
p 246 A90-21611
- BUETEFISCH, K. A.**
Experimental study on vortex and shock wave development on a 65 deg delta wing
[NLR-MP-88033-U] p 720 N90-25950
- BUETEFISCH, K.-A.**
Applications of LIF to high speed flows
p 911 N90-29320
- BUETEFISCH, KARL-ALOYS**
Flow field visualization study on a 65 deg delta wing at $M = 0.85$
p 277 N90-16182
- BUFACCHI, B.**
Aerodynamic control design: Experience and results at Aermacchi
p 935 N90-28518
- BUFFARDI, R.**
Development and applications of reliability and maintainability design criteria in military aircraft
[ETN-89-95208] p 107 N90-12591
Estimation of defective rate of mechanic-hydraulic components
[ETN-90-97275] p 884 N90-27120
- BUFFAT, M.**
Finite element simulation of compressible turbulent flows - Validation and application to internal aerodynamic in gas-turbine engines
p 210 A90-18343
- BUFFINGTON, R. J.**
Slotted-wall research with disk and parachute models in a low-speed wind tunnel
[AIAA PAPER 90-1407] p 595 A90-37946
Slotted-wall research with disk and parachute models in a low-speed wind tunnel
[DE90-002989] p 572 N90-21737
- BUFFINGTON, ROBERT J.**
Wall-interference corrections for parachutes in a closed wind tunnel
p 440 A90-31281
An experimental investigation of wall-interference effects for parachutes in closed wind tunnels
[DE90-001802] p 236 N90-15076
- BUFFUM, DANIEL H.**
The unsteady aerodynamics of an oscillating cascade in a compressible flow field
p 7 A90-11789
Aerodynamics of a linear oscillating cascade
[NASA-TM-103250] p 817 N90-27657
- BUGAJSKI, DANIEL J.**
A dynamic inversion based control law with application to the high angle-of-attack research vehicle
[AIAA PAPER 90-3407] p 864 A90-47662
- BUGGELN, RICHARD C.**
Hypersonic flow calculations with a hybrid Navier-Stokes/Monte Carlo method
[AIAA PAPER 90-1691] p 560 A90-38394
- BUGROVSKII, VIKTOR V.**
Identification and diagnostics in the data processing and control systems of aerospace powerplants
p 611 A90-36151
- BUI, M. N.**
An interactive scheme for transonic wing/body flows based on Euler and inverse boundary-layer equations
[AIAA PAPER 90-1586] p 566 A90-38721
- BUI, T. PAUL**
The Meteorological Measurement System on the NASA ER-2 aircraft
p 926 A90-51658
- BUJSEN, F.**
Numerical interactive grid generation for 3D-flow calculations
p 312 A90-26556
- BUIL, CHRISTIAN**
Visualization of corona discharges
p 819 A90-49839
- BUKOVSHIN, V. G.**
Effect of a recess on the aerodynamic characteristics of very blunt bodies at supersonic velocities
p 299 A90-24167
- BULBUL, E.**
Application of a three-dimensional finite element grid generation scheme for an F-16 aircraft configuration
p 336 A90-26541
- BULEKOV, V. P.**
Dynamic properties of a system for the roll control of a model electromagnetically suspended in a wind tunnel
p 262 A90-22762
- BULGAKOV, V. K.**
Stress-strain analysis of structural elements of incompressible or nearly incompressible materials by the finite element method
p 129 A90-14557
Numerical calculation of turbulent separated flows in an abruptly expanding channel
p 803 A90-46487
- BULLMORE, A. J.**
Theoretical studies of the active control of propeller-induced cabin noise
p 893 A90-46351
- BULLOCK, F.**
Automated prepreg tow placement for composite structures
p 954 A90-50113
- BULT, KENNETH R.**
The T800-LHT-800 engine - Designed for supportability
p 585 A90-35773
- BUNDICK, W. THOMAS**
Results of aircraft open-loop tests of an experimental magnetic leader cable system for guidance during roll-out and turnoff
[NASA-TM-4135] p 348 N90-16767
- BUNGER, S. R.**
The acute, delayed neurotoxicity evaluation of two jet engine oil formulations
[AD-A222018] p 875 N90-26972
- BUNK, W.**
Aerospace materials - Trends and potential
p 529 A90-31902
- BUNK, WOLFGANG**
Materials and structures for 2000 and beyond: An attempted forecast by the DLR Materials and Structures Department
[ESA-TT-1154-REV] p 775 N90-26173
- BURCH, I. A.**
A corrosion fatigue/stress corrosion testing facility at Materials Research Laboratory
[MRL-TN-568] p 527 N90-21044
- BURCHAM, FRANK W., JR.**
Propulsion system-flight control integration-flight evaluation and technology transition
[AIAA PAPER 90-2280] p 644 A90-42106
Propulsion system-flight control integration and optimization: Flight evaluation and technology transition
[NASA-TM-4207] p 929 N90-28551
- BURDGES, KENNETH P.**
Evaluation of transonic wall interference assessment and correction for semi-span wing data
[AIAA PAPER 90-1433] p 597 A90-38487
- BUREAU, J. L.**
Measurements of aerodynamic forces on aircraft external stores in the NAE trisonic blowdown wind-tunnel
p 629 A90-42419
- BURESTI, G.**
Boundary layer diagnostics by means of an infrared scanning radiometer
p 605 A90-38493
- BURGE, P. L.**
UHB demonstrator interior noise control flight tests and analysis
[NASA-CR-181897] p 140 N90-13198
- BURGER, BERND**
Application possibilities of expert systems in modern maintenance for increasing operational security
p 892 A90-49271

BURGGRAF, ODUS R.

Numerical investigation of laminar separated viscous trailing-edge flow using triple-deck theory
[AIAA PAPER 90-3046] p 792 A90-45883

BURGREEN, GREG W.

Particulate trajectories and impact characteristics in hypersonic flight involving gas coolant shielding
p 476 A90-34583

BURKHARDT, LEO A.

RAMSCRAM: A flexible ramjet/scramjet engine simulation program
[NASA-TM-102451] p 194 N90-14235

BURKE, MARY V.

Profiles-aeronautical/astronautical engineering: Human resources and funding
[PB90-103888] p 369 N90-16969

BURKEL, RICHARD H.

Aircraft engine inspection p 771 A90-44606

BURKETT, C. W.

Reductions in induced drag by the use of aft swept wing tips p 299 A90-24342

BURKHARD, ALAN H.

Application of fracture mechanics to microscale phenomena in electronic assemblies p 684 A90-41334

BURKHARDT, GARY L.

Inspection development for T-37 wing spar cap lug [AD-A214826] p 287 N90-16708

BURKHARDT, JAMES E.

Automatic environmental control system for electronic equipment platforms
[SAE PAPER 901217] p 840 A90-49292

BURLEY, JAMES R., II

Qualitative evaluation of a conformal velocity vector display for use at high angles-of-attack in fighter aircraft
[NASA-TM-102629] p 739 N90-25981

BURNER, ALPHEUS W.

Recent flow visualization studies in the 0.3-m TCT p 122 N90-12528

BURNET, L. A.

Carbon fibre composite bolted joints p 130 A90-15354

BURNETT, EDWARD J.

High performance needled structures in composites p 955 A90-50173

BURNHAM, E. A.

Operation of the ram accelerator in the transdetonative velocity regime
[AIAA PAPER 90-1985] p 741 A90-42712

BURNS, B. R. A.

Pay-offs and pitfalls of fly-by-wire p 346 A90-24281

BURNS, BRIAN R. A.

Aerodynamic and structural design challenges of a reusable single stage to orbit air-breathing launch vehicle p 354 N90-16814

BURNS, R. E.

Aviation Engine Test Facilities (AETF) fire protection study
[AD-A211483] p 134 N90-12777

BURRIN, R. H.

Application of active noise control to model propeller noise p 548 A90-34091

BURROWS, LEROY T.

Strike tolerant main rotor blade tip p 409 A90-28232

BURROWS, S. P.

Robust low norm output feedback design for flight control systems
[AIAA PAPER 90-3505] p 891 A90-47751

BURRUS, D. L.

Dynamic instability characteristics of aircraft turbine engine combustors p 53 N90-10195
Energy Efficient Engine combustor test hardware detailed design report
[NASA-CR-168301] p 929 N90-28554
Energy Efficient Engine (E3) combustion system component technology performance report
[NASA-CR-168274] p 930 N90-28555

BURSEY, R.

Flight test results of the F-15 SMTD thrust vectoring/thrust reversing exhaust nozzle
[AIAA PAPER 90-1906] p 660 A90-41982

BURT, E. G. C.

Hypersonic (T-D) 'pinch' and aerospaceplane propulsion
[AIAA PAPER 90-2474] p 675 A90-42189

BUSBRIDGE, M. L.

A laser obstacle avoidance and display system p 419 A90-30694

BUSH, ROBERT H.

Computational modeling of inlet hammer shock wave generation
[AIAA PAPER 90-2005] p 621 A90-40592

BUSHNELL, K. W.

Design of aeroengines in a low-fuel price scenario p 739 A90-42653

BUSHLOW, TODD

Steady and unsteady force testing of fighter aircraft models in a water tunnel
[AIAA PAPER 90-2815] p 711 A90-45155

BUSHNELL, D. M.

Aeronautical facility requirements into the 2,000's
[AIAA PAPER 90-1375] p 594 A90-37926

Supersonic aircraft drag reduction

[AIAA PAPER 90-1596] p 567 A90-38729
Investigation of several passive and active methods for turbulent flow separation control
[AIAA PAPER 90-1598] p 607 A90-38730

Control of submersible vortex flows

[NASA-TM-102693] p 909 N90-28493

BUSHNELL, DENNIS M.

Supersonic laminar-flow control p 93 N90-12554
Serrated trailing edges for improving lift and drag characteristics of lifting surfaces
[NASA-CASE-LAR-13870-1] p 248 N90-15094

BUSHNELL, PETER

Measurement of the steady surface pressure distribution on a single rotation large scale advanced prop-fan blade at Mach numbers from 0.03 to 0.78
[NASA-CR-182124] p 929 N90-28552

BUSSING, THOMAS R. A.

Transverse fuel-injection model for a scramjet propulsion system p 659 A90-40927

BUTENKO, K. K.

Two- and three-dimensional problems of unsteady aerodynamics of low loaded turbomachinery blade rows stages p 813 A90-49452

BUTKUS, LAWRENCE M.

Plastic media blast (PMB) paint removal from composites p 945 A90-50162

BUTLER, CARROLL

Cavity aeroacoustics
[AD-A223853] p 911 N90-29307

BUTLER, G. F.

An American knowledge base in England - Alternate implementations of an expert system flight status monitor p 459 A90-30719

A knowledge-based flight status monitor for real-time application in digital avionics systems
[NASA-TM-101710] p 217 N90-13995

BUTLER, GEORGE V.

The 21st century in space; Proceedings of the Thirty-fifth Annual AAS Conference, Saint Louis, MO, Oct. 24-26, 1988 p 762 A90-43460

BUTLER, RICKY W.

Formal design and verification of a reliable computing platform for real-time control. Phase 1: Results
[NASA-TM-102716] p 965 N90-29965

BUTOV, V. P.

An experimental study of instantaneous velocity perturbations over a rotor disk for low duty coefficients p 860 A90-46572

BUTT, G.

The effect of winglets on aircraft wing flutter p 473 A90-33411

BUTTLE, D. J.

Characterisation of fatigue of aluminium alloys by acoustic emission. Part 2: Discrimination between primary and other emissions
[AERE-R-13303-PT-2] p 678 N90-23523

BUTTRILL, CAREY S.

Simulation model-building procedure for dynamic systems integration p 138 A90-14744

Digital-flutter-suppression-system investigations for the active flexible wing wind-tunnel model
[AIAA PAPER 90-1074] p 430 A90-29382

Digital-flutter-suppression-system investigations for the active flexible wing wind-tunnel model
[NASA-TM-102618] p 520 N90-20093

BUTTS, STUART L.

Flight testing for aircraft agility
[AIAA PAPER 90-1308] p 519 A90-33918

BUXBAUM, O.

Description and reconstitution of manoeuvre loadings p 919 A90-49878

BUYUKATAMAN, K.

An investigation of the behavior of the dynamic load distribution versus operating speed and torque on heavily loaded, high speed aircraft gearing p 271 A90-21129

BUYUKATAMAN, KAYAALP

Gearbox system design for ultra-high bypass engines
[AIAA PAPER 90-2152] p 685 A90-42048

BUZOVERIA, N. P.

The local surface variation method in profile shape optimization problems p 297 A90-24136

BYERLEY, AARON R.

Heat transfer near the entrance to a film cooling hole in a gas turbine blade
[AD-A217396] p 510 N90-20089

BYERS, J. L.

Desktop failure analysis on a microcomputer using Weibull, lognormal, and renewal data
[ASME PAPER 89-GT-275] p 535 A90-32263

BYERS, THOMAS EDWARD

Automated aircraft paint strip cell
[SAE PAPER 890936] p 286 A90-24699

BYKOV, I. U. G.

Cyclic fracture toughness of VT-3-1 and VT-25 titanium alloys p 873 A90-46514

BYRAM, KENNETH V.

Independent operations on closely spaced runways p 821 A90-46393

BYRD, GREGORY P.

A quantitative technique to estimate microburst wind shear hazard to aircraft p 692 N90-25040

BYRKIN, A. P.

Using third-fourth order compact schemes for calculating gas flows in nozzles with high supersonic M numbers on the basis of simplified Navier-Stokes equations p 299 A90-24157

A study of gas flow in hypersonic nozzles at large Reynolds numbers using simplified Navier-Stokes equations p 803 A90-46538

BYRNE, KEVIN

The potential for an extra runway at Heathrow: A preliminary feasibility study
[TT-9007] p 938 N90-29403

BYUN, Y.

Unsteady hypersonic viscous flow in impulse facilities
[AIAA PAPER 90-0421] p 313 A90-26947

BYUN, YUNGHWAN

Computation of hypersonic unsteady viscous flow over a cylinder p 397 N90-19194

BYWORTH, S. P. Q.

Designing for reliable and low maintenance cost aero engines
[PNR90570] p 115 N90-12604

C**CABAK, A.**

Guidance simulation and test support for differential GPS flight experiment
[NASA-CR-177471] p 28 N90-10021

CABAK, ALGYTE

Reduced order INS/GPS guided unmanned air vehicle study p 726 A90-43707

CACOPARDI, S.

New approach for Doppler ambiguities resolution in medium pulse repetition frequency radars p 240 A90-20937

CADIOU, A.

Future test rigs p 200 A90-19012

A test facility for high-pressure high-temperature combustion chambers p 438 A90-29924

CAGLAYAN, A. K.

Hierarchical damage tolerant controllers for smart structures
[AD-A209422] p 31 N90-10022

CAGLAYAN, ALPER K.

An experimental investigation of fault tolerant software structures in an avionics application
[AIAA PAPER 89-3082] p 74 A90-10568

CAI, DAYING

Influence of blade leaning on the flow field behind turbine rectangular cascades with different incidences and aspect ratios p 11 A90-12519

CAI, H. J.

Wind tunnel testing techniques on aerodynamic effects with small asymmetry
[AIAA PAPER 90-1400] p 560 A90-38490

CAI, RUIXIAN

3D Mean-Stream-Line Method - A new engineering approach to the inverse problem of 3D cascade
[ASME PAPER 89-GT-48] p 289 A90-23774

CAI, XIAOBIN

A design method for real-time computer control hydraulic force system p 590 A90-36434

CAIN, BRENDAN G.

AIRNET: A real-time communications network for aircraft
[NASA-CR-186140] p 690 N90-24514

CAIRO, R. R.

Bonded airfoil attachments - A path to rotor structural efficiency
[AIAA PAPER 90-2177] p 686 A90-42061

CAL, A. A.

Effects of tailplane aerodynamics and fuselage flexibility on the flutter of high aspect ratio, low speed aircraft p 493 A90-33414

CALAPODAS, NICK

Force determination sensitivities study for full-scale helicopter ground vibration testing
[AD-A215983] p 349 N90-17643

CALDWELL, DARREL

Application of advanced air vehicle and mission equipment technologies to the Light Helicopter (LH)
[AIAA PAPER 90-3268] p 836 A90-48861

CALDWELL, JAMES L.

Formal design and verification of a reliable computing platform for real-time control. Phase 1: Results
[NASA-TM-102716] p 965 N90-29965

CALISE, ANTHONY J.

Approximate loop transfer recovery method for designing fixed-order compensators p 375 A90-25989
Helicopter individual blade control through optimal output feedback p 861 A90-46956
A comparison of time-optimal interception trajectories for the F-8 and F-15
[NASA-CR-186300] p 581 N90-21753

CALLAHAN, A. B.

Analysis of hydraulic fluids and lubricating oils for the formation of Trimethylolpropane Phosphate (TMP-P).
[AD-A215188] p 357 N90-16939

CALMON, JEAN

Military engines - Cradle of technology
p 660 A90-41758

CALVERT, W. J.

Performance of a highly-loaded HP compressor
[RAE-TM-P-1149] p 256 N90-15919

CAMARDA, CHARLES J.

Application of formal optimization techniques in thermal/structural design of a heat-pipe-cooled panel for a hypersonic vehicle
[NASA-TM-89131] p 72 N90-10409

CAMBIER, JEAN-LUC

Numerical simulations of an oblique detonation wave engine
p 508 A90-32964

CAMBIER, L.

Calculation of three-dimensional turbulent flow in a linear turbine cascade
[ONERA, TP NO. 1989-115] p 3 A90-11147
Recent developments in calculation methods for internal flows by solution of Euler or Navier-Stokes equations
[ONERA, TP NO. 1989-167] p 223 A90-21033
Calculation of the three dimensional turbulent flow in a linear turbine blade
p 513 N90-21021

CAMCI, C.

An experimental convective heat transfer investigation around a film-cooled gas turbine blade
p 957 A90-51261

CAMERON, C. D.

A model gas turbine combustor with wall jets and optical access for turbulent mixing, fuel effects, and spray studies
p 507 A90-32808
Symmetry assessment of an air-blast atomizer spray
p 682 A90-40930

CAMERON, WILLIAM L.

An intelligent system for autonomous navigation of airborne vehicles
p 26 A90-11696

CAMMAROTA, GIAN PAOLO

Design of helicopter components in metal matrix composites
[REPT-100-20-55] p 874 N90-26894

CAMMAROTA, JOSEPH P.

Research in a high-fidelity acceleration environment
p 439 A90-30734

CAMMAS, J. P.

Maximum expected concentrations of hail in thunderstorm precipitation
p 962 A90-52052

CAMPAGNAC, M. H.

Static and dynamic characterization of the ATR 72 rods made of Ti 10.2.3 titanium alloy
[REPT-49-238] p 953 N90-28722

CAMPBELL, BRIAN

Evaluation and control of an Integrated Closed Environmental Control System (ICECS)
[SAE PAPER 901237] p 841 A90-49307

CAMPBELL, BRYAN A.

Results of aerodynamic testing of large-scale wing sections in a simulated natural rain environment
[AIAA PAPER 90-0486] p 167 A90-19874
Operational considerations for aerodynamic testing of large-scale wing sections in a simulated natural rain environment
[AIAA PAPER 90-0485] p 313 A90-26956

CAMPBELL, E. L.

The application of queuing theory to the modelling of CP-140 aircraft communications
[AD-A213479] p 274 N90-15310

CAMPBELL, RICHARD L.

Design of the low-speed NLF(1)-0414F and the high-speed HSNLF(1)-0213 airfoils with high-lift systems
p 93 N90-12540
Design and test of an NLF wing glove for the variable-sweep transition flight experiment
p 104 N90-12544

CAMPBELL, S. D.

Wind shear detection with pencil-beam radars
p 279 A90-21386

CAMPBELL, WILLIAM A.

Large-scale Advanced Prop-fan (LAP) high speed wind tunnel test report
[NASA-CR-182125] p 52 N90-10045

CAMPOS, I. M. B. C.

A pitch control law for compensation of the phugoid mode induced by windshears
p 258 N90-15051

CAMPOS, L. M. B. C.

On the 'inverse phugoid problem' as an instance of non-linear stability in pitch
p 55 A90-10221
On a pitch control law for a constant glide slope through windshears
p 117 A90-13784

CANACCI, V. A.

A laser based computer aided non-intrusive technique for full field flow characterization in macroscopic curved channels
p 535 A90-32293

CANFIELD, R. A.

High-quality approximation of eigenvalues in structural optimization
p 603 A90-36277

CANNELLA, VINCENT

Performance of full color active-matrix-LCD in the cockpit environment
p 681 A90-40392
8 x 8-inch full color cockpit display
p 927 A90-52953

CANNON, M. R.

UHB demonstrator interior noise control flight tests and analysis
[NASA-CR-181897] p 140 N90-13198

CANTILLON, MARIELLE

Turbulent mixing in helicopter jet diluters - Navier-Stokes calculations and correlations
[AAAF PAPER NT 88-13] p 40 A90-11432

CANTWELL, BRIAN J.

Direct numerical simulations of transition in a compressible wake
p 553 A90-35212
The effect of Mach number on the stability of a plane supersonic wake
p 557 A90-36524

CAO, HOA V.

Numerical analysis of three-dimensional particle-laden flow equations
[IAR-90-2] p 775 N90-26268

CAO, QI

Analysis of blade loadings in centrifugal compressors
p 158 A90-18591

CAO, YIHUA

The induced velocity distribution and the flap-pitch-torsion coupling on the stability and control of the helicopter in flight condition with lateral velocity
p 196 A90-18633

CAPDEVILLE, G.

Multigrid acceleration of transonic flow computations
p 147 A90-16783

CAPECE, VINCENT R.

Multistage compressor vane row aerodynamic gust response
p 6 A90-11783
Unsteady aerodynamic gust response including steady flow separation
p 556 A90-36262

CAPELLO, G. P.

Combined advanced foundry and quality control techniques to enhance reliability of castings for the aerospace industry
p 64 N90-10240

CAPLOT, M.

Prediction of rotor blade-vortex interaction noise from 2-D aerodynamic calculations and measurements
[ISL-CO-243/88] p 396 N90-18365

Theoretical studies carried out in 1988 on helicopter rotor noise under subsonic conditions
[ONERA-RS-82/5094-PY] p 896 N90-28402

CAPON, J.

Multipath modeling for simulating the performance of the microwave landing system
p 241 A90-21384

CAPONE, FRANCIS J.

An experimental investigation of thrust vectoring two-dimensional convergent-divergent nozzles installed in a twin-engine fighter model at high angles of attack
[NASA-TM-4155] p 237 N90-15884

CAPPS, G. J.

Engine testing of thermographic phosphors
[DE90-013269] p 885 N90-28059

CAPRILE, C.

Understanding composite fatigue - New trends
p 940 A90-49893

CAPRIOTTI, D.

Infrared thermography in blowdown and intermittent hypersonic facilities
p 440 A90-31302

CAPRON, WILLIAM R.

Delivery performance of conventional aircraft by terminal-area, time-based air traffic control: A real-time simulation evaluation
[NASA-TP-2978] p 404 N90-18378

CARABINEANU, A.

On steady subsonic flow past slender bodies of revolution
p 144 A90-16736

CARADONNA, F. X.

Rotor hover performance prediction using a free-wake, computational fluid dynamics method
p 153 A90-17869

Application of transonic flow analysis to helicopter rotor problems
p 394 A90-29887
The free-wake computation of rotor-body flows
[AIAA PAPER 90-1540] p 565 A90-38684

CARADONNA, FRANCIS X.

Advanced rotor computations with a corrected potential method
p 385 A90-28197

CARADONNA, FRANK

The prediction of loads on the Boeing Helicopters Model 360 rotor
p 410 A90-28240

CARCHEDI, F.

The design and test of a two stage transonic axial flow compressor
[ASME PAPER 89-GT-164] p 341 A90-23852

CARDEN, HUEY D.

A review of the analytical simulation of aircraft crash dynamics
[NASA-TM-102595] p 484 N90-20068

Unique failure behavior of metal/composite aircraft structural components under crash type loads
[NASA-TM-102679] p 690 N90-24660

Behavior of composite/metal aircraft structural elements and components under crash type loads: What are they telling us
[NASA-TM-102681] p 774 N90-25368

CARDRICK, A. W.

Royal Aerospace Establishment: No place for a castings factor
p 64 N90-10235

CAREL, B.

Pressure surface trailing edge slot cooling
[ONERA, TP NO. 1989-123] p 47 A90-12569

CAREY, DAVE

The SKY SHARK: An RPV designed to investigate the pressure distribution on a lifting surface
[NASA-CR-186222] p 844 N90-26824

CAREY, G. F.

Shock sensitivity in parabolized Navier-Stokes solution of high angle-of-attack supersonic flow
p 302 A90-25280

Least-squares finite element methods for compressible Euler equations
p 904 A90-51013

CARICO, DEAN

Helicopter controllability
[AD-A220078] p 672 N90-24275

CARLISLE, D.

New high-speed air transport system and stratospheric pollution
[ONERA, TP NO. 1989-202] p 279 A90-22445

CARLIN, DIANA M.

The effect of jet fuel absorption on advanced aerospace thermoset and thermoplastic composites
p 942 A90-50082

CARLOMAGNO, G. M.

Boundary layer diagnostics by means of an infrared scanning radiometer
p 605 A90-38493

Infrared thermography
p 911 N90-29325

CARLSON, HAROLD

EHA loading on the 270-Vdc bus
[SAE PAPER 892225] p 746 A90-45441

CARLSON, HARRY W.

Validation of a computer code for analysis of subsonic aerodynamic performance of wings with flaps in combination with a canard or horizontal tail and an application to optimization
[NASA-TP-2961] p 173 N90-14187

CARLSON, LELAND A.

Determination of aerodynamic sensitivity coefficients based on the transonic small perturbation formulation
p 622 A90-40682

Development of direct-inverse 3-D methods for applied transonic aerodynamic wing design and analysis
[NASA-CR-186036] p 103 N90-11733

A direct-inverse method for transonic and separated flows about airfoils
[NASA-CR-4270] p 235 N90-15072

CARLSON, R. B.

TRANAIR applications to engine/airframe integration
p 838 A90-48958

CARLUCCIO, J. R.

The application of cast SiC/Al to rotary engine components
[NASA-CR-179610] p 192 N90-13385

CARMICHAEL, ALISTAIR A.

Radiation-curable prepreg composites
[DE90-629740] p 951 N90-28674

CARNEY, CURTIS S.

Stress intensity factors for cracking metal structures under rapid thermal loading. Volume 2: Theoretical background
[AD-A213297] p 213 N90-13812

- CARNEY, HAROLD K.**
The 1985 and 1986 direct strike lightning data, part 1 [NASA-TM-100533-PT-1] p 374 N90-18125
The 1985 and 1986 direct strike lightning data, part 2 [NASA-TM-100533-PT-2] p 374 N90-18126
- CAROLI, JOSEPH**
RADC fault tolerant system reliability evaluation facility [AD-A215298] p 377 N90-17348
- CARON, P.**
The anisotropy of the mechanical behaviour in nickel-based single crystal superalloys for turbine blades [ONERA, TP NO. 1989-205] p 355 A90-25339
Development of a new nickel based single crystal turbine blade alloy for very high temperatures [ONERA, TP NO. 1989-206] p 356 A90-25340
- CARONI, L.**
EH-101 main rotor hub application of thick carbon fiber unidirectional tension bands p 618 A90-42489
- CAROSSO, M.**
Combined advanced foundry and quality control techniques to enhance reliability of castings for the aerospace industry p 64 N90-10240
- CARPENTER, A.**
Tangential mass addition for the control of shock wave/boundary layer interactions in scramjet inlets p 13 A90-12586
- CARPENTER, MARK H.**
Mixing and combustion enhancement in supersonic reacting flows p 744 A90-44410
Supersonic combustor modeling p 749 N90-25992
- CARPENTER, P. W.**
Use of swirl for flow control in propulsion nozzles p 421 A90-27963
- CARPENTER, WILLIAM F.**
The evolution of built-in test for an electrical power generating system (EPGS) p 424 A90-30699
- CARPENTIER, J.**
Aerodynamic, thermal and mechanical problems in the aerospace field p 382 A90-29921
- CARPETIS, A.**
Hot wire measurements in the wake of an oscillating airfoil p 15 A90-12635
- CARR, L. W.**
Experimental and computational studies of dynamic stall p 147 A90-16780
Design and development of a facility for compressible dynamic stall studies of a rapidly pitching airfoil p 436 A90-28255
Flow visualization studies of the Mach number effects on dynamic stall of an oscillating airfoil p 622 A90-40683
Schlieren studies of compressibility effects on dynamic stall of airfoils in transient pitching motion [AIAA PAPER 90-3038] p 791 A90-45877
- CARRARA, W.**
Shadow-tracking algorithm for moving target detection p 488 A90-34137
- CARRAWAY, DEBRA L.**
A transition detection study at Mach 1.5, 2.0, and 2.5 using a micro-thin hot-film system p 436 A90-28260
Hot-film system for transition detection in cryogenic wind tunnels p 122 N90-12522
- CARREIRO, LOUIS R.**
ETO (Earth-To-Orbit): A trajectory program for aerospace vehicles [AD-A218157] p 528 N90-20103
- CARRESE, G.**
Multivariable optimization scheme for tuning the controller of an electronic fuel control unit for small gas turbine engines p 745 A90-45301
- CARRESE, GINO**
Designing and tuning the digital controller of an electronic fuel control unit for small gas turbine engines [SAE PAPER 892255] p 747 A90-45457
- CARRIER, M.**
Homogenization of composite beams in dynamical flexure p 878 A90-46184
- CARROLL, B. F.**
Computation of multiple normal shock wave/turbulent boundary layer interactions [AIAA PAPER 90-2133] p 685 A90-42037
- CARROTTE, J.**
The performance of a combustor pre-diffuser incorporating compressor outlet guide vanes [AIAA PAPER 90-2165] p 661 A90-42053
- CARROTTE, J. F.**
Experimental studies of combustor dilution zone aerodynamics. I - Mean flowfields p 508 A90-32962
Experimental studies of combustor dilution zone aerodynamics. II - Jet development p 659 A90-40947
- CARSCALLEN, W. E.**
The effect of secondary flow on the redistribution of the total temperature field downstream of a stationary turbine cascade p 515 N90-21033
- CARSON, GEORGE T., JR.**
Effect of tail size reductions on longitudinal aerodynamic characteristics of a three surface F-15 model with nonaxisymmetric nozzles [NASA-TP-3036] p 718 N90-25938
- CARSTENS, V.**
Computation of unsteady transonic flows around oscillating airfoils using full potential and Euler equations p 472 A90-33357
- CARTER, A. L.**
Application of fracture mechanics and half-cycle method to the prediction of fatigue life of B-52 aircraft pylon components [NASA-TM-88277] p 214 N90-13820
- CARTWRIGHT, D. J.**
Numerical study of balanced patch repairs to cracked sheets p 210 A90-18442
- CARUSO, STEVEN C.**
Development of an unstructured mesh/Navier-Stokes method for aerodynamics of aircraft with ice accretions [AIAA PAPER 90-0758] p 169 A90-20011
- CASALEGNO, L.**
Project, implementation, and utilization of composite structures [ETN-89-95209] p 127 N90-12665
- CASALIS, G.**
Prediction of transition on a swept wing p 908 A90-52592
- CASE, RICHARD I.**
EH101 design and development status p 407 A90-28211
- CASEY, JOHN A.**
Effects of stage 3 rules on the airliner market [SAE PAPER 892282] p 723 A90-45468
- CASEY, W. L.**
Laser communication system design p 26 A90-11813
- CASON, RANDALL W.**
Airworthiness and flight characteristics test of the UH-60A Black Hawk helicopter equipped with the XM-139 multiple mine dispensing system (VOLCANO) [AD-A210271] p 32 N90-10025
- CASSAING, J. J.**
Thermostructural behavior of electromagnetic windows - Elaboration of a code package [ONERA, TP NO. 1989-145] p 76 A90-11167
- CASSAN, H.**
Advanced parameter identification techniques for near real time flight flutter test analysis [AIAA PAPER 90-1275] p 494 A90-33899
- CASSENTI, B. N.**
Constitutive modeling for isotropic materials (HOST) [NASA-CR-174718] p 193 N90-13391
- CASTEX, A.**
Experimental study of 2D/3D interactions between a vortical flow and a lifting surface p 86 A90-15849
- CASTO, CHRIS**
Dual servo optical projection system (SOPS) - A solution for two crewmember and night vision goggle display needs [SAE PAPER 892353] p 760 A90-45504
- CASTONIA, JOHN C.**
Loran-C/GPS Interoperable Computerized Algorithms (LOGICAL) p 823 A90-49494
- CASTRO-LINARES, R.**
Helicopter control design using feedback linearization techniques p 688 A90-40817
- CATCHPOLE, C. E.**
Modelling aspects for the synthesis and performance assessment of some future advanced helicopters p 829 A90-46937
- CATES, M. R.**
Engine testing of thermographic phosphors [DE90-013269] p 885 N90-28059
- CATHERALL, D.**
Solution-adaptive grids for transonic flows p 309 A90-26508
- CATHERS, R. T.**
Pursuit of the high-speed civil transport [AIAA PAPER 90-1814] p 919 A90-51450
- CATTUNAR, S.**
Acquisition and recording of AMX A/C Aeritalia experience and present trends p 26 A90-12194
Acquisition and recording an AMX A/C Aeritalia experience and present trends [ETN-89-95217] p 109 N90-12538
- CAUGHEY, DAVID A.**
Block multigrid implicit solution of the Euler equations of compressible fluid flow [AIAA PAPER 90-0106] p 162 A90-19684
- CAULFIELD, THOMAS**
Fiber reinforced superalloys p 532 A90-34169
- CAVALIERE, M.**
Problems of internal acoustics in two and three dimensional cavities with deformable walls using the MSC/Nastran code [DLC/STR-INT-TN-004] p 699 N90-24876
- CAVES, R. E.**
The cost of air service fragmentation [TT-9010] p 813 N90-28334
- CAVES, ROBERT**
Aircraft/airport compatibility: Some strategic, tactical, and operational issues [TT-8902] p 202 N90-13409
- CAZALBOU, J. B.**
Numerical study of heat transfer for unsteady viscous supersonic blunt body flows p 707 A90-44432
- CAZIER, F. W., JR.**
Experimental transonic flutter characteristics of supersonic cruise configurations [AIAA PAPER 90-0979] p 390 A90-29369
- CEBECI, T.**
Progress towards the development of an inviscid-viscous interaction method for unsteady flows in turbomachinery cascades p 8 A90-11806
Calculation of low Reynolds number flows at high angles of attack [AIAA PAPER 90-0569] p 167 A90-19921
- CEBECI, TUNCER**
Prediction of post-stall flows on airfoils p 145 A90-16757
Prediction of transition on airfoils with separation bubbles, swept wings and bodies of revolution at incidence p 148 A90-16790
Essential ingredients of a method for low Reynolds-number airfoils p 153 A90-17979
Fortified LEWICE with viscous effects [AIAA PAPER 90-0754] p 176 A90-20009
An interactive boundary-layer stability-transition approach for low Reynolds-number airfoils p 799 A90-46364
Interactive boundary-layer method for unsteady airfoil flows - Quasisteady model p 812 A90-48953
A three-dimensional linear stability approach to transition on wings at incidence p 20 N90-10373
An interactive boundary-layer method for unsteady airfoil flows. Part 1: Quasi-steady-state model [AD-A221220] p 634 N90-24250
- CEDARLEAF, CALVIN**
Novel composite surfacing film p 948 A90-50212
- CEDOZ, R. W.**
Advanced gearbox technology [NASA-CR-179625] p 666 N90-24274
- CELENLIGIL, M. CEVDET**
Direct simulation of three-dimensional hypersonic flow about intersecting blunt wedges p 16 A90-12835
Direct simulation of hypersonic rarefied flow about a delta wing [AIAA PAPER 90-0143] p 162 A90-19704
- CELESTINA, M. L.**
The numerical simulation of multistage turbomachinery flows p 514 N90-21025
- CELESTINA, MARK L.**
Simulation of three-dimensional viscous flow within a multistage turbine [ASME PAPER 89-GT-152] p 292 A90-23841
- CELI, R.**
Structural optimization with aeroelastic constraints of rotor blades with straight and swept tips p 535 A90-32475
- CELI, ROBERTO**
Hingeless rotor dynamics in coordinated turns [AIAA PAPER 90-1117] p 412 A90-29389
Aeroelastic effects on stability and control of hingeless rotor helicopters p 647 A90-42473
- CELIK, Z.**
Control of asymmetric vortical flows over delta wings at high angles of attack p 553 A90-35759
- CELIK, ZEKI Z.**
An investigation of asymmetric vortical flows over delta wings with tangential leading-edge blowing at high angles of attack [AIAA PAPER 90-0103] p 227 A90-22167
- CELIKOVSKY, K.**
Experimental investigation of the transonic centrifugal compressor inducer straight cascades p 13 A90-12592
- CERBE, T.**
Optimization of helicopter takeoff and landing p 29 A90-11006
Influence of ground effect on helicopter takeoff and landing performance p 645 A90-42278
Influence of ground effect on helicopter takeoff and landing performance p 648 A90-42468
- CERBE, THOMAS**
Calculation and optimization of rotor start process [ETN-90-95894] p 416 N90-19229

CERBUS, CLIFFORD A.

The collection of non-conus aircraft icing data along with an identification of the geographical areas of potential severe icing and a study of a method of remote determining atmospheric icing data
[AD-A215055] p 323 N90-16724

CERCHIE, P. H.

Helicopter obstacle avoidance system - The use of manned simulation to evaluate the contribution of key design parameters p 417 A90-28218

CERNOSEK, JAN

Photoelasticity: A cost effective design tool p 883 N90-26819

CERONI, P.

Influence of the control law on the performance of a helicopter model rotor
[ONERA, TP NO. 1989-136] p 4 A90-11158

CERTAIN, BERNARD

Full Authority Digital Engine Control for the AS 355 N TM 319 engines p 665 A90-42486

CERUZZI, PAUL E.

Beyond the limits - Flight enters the computer age p 282 A90-20380

CETIN, M.

An off-design loss and deviation prediction study for transonic axial compressors
[ASME PAPER 89-GT-324] p 343 A90-23893

CETINKAYA, T. A.

A computational design method for shock free transonic cascades and airfoils p 501 N90-20986

CHA, C.

Simulation of airborne target imagery - Dependence on frequency and bistatic angle p 488 A90-34146

CHA, SOYOUNG S.

Complementary field method for interferometric tomographic reconstruction of high speed aerodynamic flows
[AD-A219698] p 131 A90-15900

CHACON, VINCE

Validation of the F-18 high alpha research vehicle flight control and avionics systems modifications
[NASA-TM-101723] p 924 N90-28542

CHADERJIAN, NEAL M.

Navier-Stokes predictions of the flowfield around the F-18 (HARV) wing and fuselage at large incidence
[AIAA PAPER 90-0099] p 227 A90-22165
Unsteady transonic Navier-Stokes computations for an oscillating wing using single and multiple zones
[AIAA PAPER 90-0313] p 228 A90-22197
Zonal Navier-Stokes methodology for flow simulation about a complete aircraft p 709 A90-44727

CHAHINE, G. L.

New concept for improved nonmetallic erosion protection systems p 407 A90-28188

CHAHROUR, C. A.

Energy Efficient Engine combustor test hardware detailed design report
[NASA-CR-168301] p 929 N90-28554
Energy Efficient Engine (E3) combustion system component technology performance report
[NASA-CR-168274] p 930 N90-28555

CHAI, G. B.

Experimental study on the buckling and postbuckling of carbon fibre composite panels with and without interply disbands p 130 A90-15355

CHAIKO, LEV

Assessment of worm gearing for helicopter transmissions
[NASA-TM-102441] p 257 N90-15923

CHAILLLOT, BERNARD

Technical evaluation report on the Guidance and Control Panel 49th Symposium on Fault Tolerant Design Concepts for Highly Integrated Flight Critical Guidance and Control Systems
[AGARD-AR-281] p 758 N90-26012

CHAKRABARTY, SUNIL KUMAR

Computation of 2D Navier-Stokes equations p 367 A90-25801

CHAKRAVARTHY, S. R.

Calculation of unsteady rotor/stator interaction
[AIAA PAPER 90-1544] p 565 A90-38688
Supersonic flow computations for an ASTOVL aircraft configuration
[AIAA PAPER 90-2997] p 787 A90-45847

CHAKRAVARTHY, SUKUMAR

Supersonic flow computations over aerospace configurations using an Euler marching solver
[NASA-CR-4085] p 19 N90-10012

CHAKRAVARTHY, SUKUMAR R.

Supersonic flow computations for an ASTOVL aircraft configuration, phase 2, part 2
[NASA-CR-4284] p 610 N90-22746

CHAKRAVARTY, A.

Fly-by-light flight control system technology development plan
[NASA-CR-181953] p 259 N90-15111

CHAKROUN, W. M.

Time-resolved measurements of total temperature and pressure in the vortex street behind a cylinder p 557 A90-36522

CHAMBERLAIN, R. R.

Calculation of three-dimensional jet interaction flowfields
[AIAA PAPER 90-2099] p 624 A90-42018

CHAMBERT, G.

Evaluation of the indirect effects of lightning on a system: Double transfer function method
[RAE-TRANS-2172] p 176 N90-14211

CHAMIS, C. C.

Parametric studies of advanced turboprops p 253 A90-21225

CHAMIS, CHRISTOS C.

Structural tailoring of select fiber composite structures
[NASA-TM-102484] p 533 N90-21137

CHAMPAGNE, G.

Benefits of advanced materials, structures, and aerodynamics in future high speed civil transport propulsion systems
[AIAA PAPER 90-3285] p 853 A90-48872

CHAMPETIER, C.

Design of a helicopter output feedback control law using modal and structured-robustness techniques p 282 A90-20557

CHAN, D. C.

Turbulent flow simulation of a three-dimensional turbine cascade
[AIAA PAPER 90-2124] p 704 A90-42732

CHAN, JEFFREY W.

Comparison of speech intelligibility in cockpit noise using SPH-4 flight helmet with and without active noise reduction
[NASA-CR-177564] p 915 N90-28510

CHAN, JOHN S.

Viscous supersonic flow computations over a delta-rectangular wing with slanting surfaces
[AIAA PAPER 90-0419] p 166 A90-19841

CHAN, K. ROLAND

The Meteorological Measurement System on the NASA ER-2 aircraft p 926 A90-51658

CHAN, KWAI S.

Constitutive modeling for isotropic materials (HOST)
[NASA-CR-179522] p 193 N90-13390
Constitutive modeling for isotropic materials (HOST)
[NASA-CR-174718] p 193 N90-13391

CHAN, S. C.

Design considerations for a compact table top hypersonic simulator of aero-optic effects p 525 A90-34585

CHAN, Y. Y.

Wind tunnel wall interference investigations in NAE/NRC High Reynolds Number 2D Facility and NASA Langley 0.3m Transonic Cryogenic Tunnel p 628 A90-42404
New transonic test sections for the NAE 5ftx5ft trisonic wind tunnel p 630 A90-42431

Analysis of experimental data for CAST 10-2/DOA 2 supercritical airfoil at low Reynolds numbers and application to high Reynolds number flow p 170 N90-13326

Investigation of CAST-10-2/DOA 2 airfoil in NAE high Reynolds number two-dimensional test facility p 321 N90-17654

New transonic test sections for the NAE 5 ft x 5 ft trisonic wind tunnel
[AD-A220933] p 674 N90-24278

CHAND, SUJEET

Energy based stability analysis of a fuzzy roll controller design for a flexible aircraft wing p 668 A90-40833

CHANDRA MOULY, M. C.

Analytical evaluation of radiation patterns of a TACAN antenna p 404 A90-30695

CHANDRA, RAMESH

Estimation of fatigue crack growth in patched cracked panels p 684 A90-41335

CHANDRASEKHARAN, M.

Computerised structural analysis for engine components p 190 A90-18486

CHANDRASEKHAR, U.

Photoelastic investigation of turbine rotor blade shrouds p 112 A90-16008

CHANDRASEKHARA, M. S.

Experimental and computational studies of dynamic stall p 147 A90-16780
Amplitude effects on dynamic stall of an oscillating airfoil
[AIAA PAPER 90-0575] p 167 A90-19925

Design and development of a facility for compressible dynamic stall studies of a rapidly pitching airfoil p 436 A90-28255

Flow visualization studies of the Mach number effects on dynamic stall of an oscillating airfoil p 622 A90-40683

Schlieren studies of compressibility effects on dynamic stall of airfoils in transient pitching motion
[AIAA PAPER 90-3038] p 791 A90-45877

CHANETZ, BRUNO

Contribution to the study of three-dimensional separation in turbulent incompressible flow
[ESA-TT-1169] p 454 N90-18697

CHANG, C. T.

A planar reacting shear layer system for the study of fluid dynamics-combustion interaction
[NASA-TM-102422] p 194 N90-13393

CHANG, CHAU-LYAN

Effects of shock on the stability of hypersonic boundary layers
[AIAA PAPER 90-1448] p 561 A90-38608

CHANG, GLENN E. C.

A third-generation bismaleimide prepreg system p 943 A90-50131

CHANG, I. Y.

Composites for aerospace application from Kevlar aramid reinforced PEKK thermoplastic p 946 A90-50176

CHANG, IKE Y.

High performance thermoplastic composites with poly(etheretherketone) matrix p 529 A90-31646

CHANG, K. C.

Prediction of post-stall flows on airfoils p 145 A90-16757

An Euler method for wing-body-winglet flows
[AIAA PAPER 90-0436] p 229 A90-22218

Performance assessment for airborne surveillance systems incorporating sensor fusion p 583 A90-37088

CHANG, KEUN-SHIK

An application of the surface-singularity method to wing-body-tail configurations p 9 A90-12229

CHANG, R. C.

An investigation on the coiled-up of vortices on a double delta wing
[AIAA PAPER 90-0382] p 165 A90-19825

CHANG, S. M.

Parallel computation of three-dimensional transonic flow problems with complex geometries
[AIAA PAPER 90-0336] p 313 A90-26936

CHANG, SHI-ING

Modification of large eddies in turbulent boundary layers p 474 A90-33514

CHAO, DERCHANG

Tiltrotor aeroservoelastic design methodology at BHTI p 410 A90-28244

CHAOUCHE, A.

Numerical predictions for the flow and the heat transfer in gas turbine cooling systems p 770 A90-44464

Numerical investigations of heat transfer and flow rates in rotating cavities. Simulation of the movement generated by wall temperature gradients, by source-sink mass flows or by the differential rotation of the walls, under the influence of coriolis and centrifugal forces
[ETN-90-96253] p 454 N90-18695

CHAPMAN, DOUGLAS M.

Air Force use of civil airworthiness criteria for testing and acceptance of military derivative transport aircraft
[AIAA PAPER 90-3289] p 818 A90-48875

CHAPMAN, G. M.

Theoretical and experimental determination of natural frequencies of laced blading p 878 A90-46037
Vibration analysis of laced blades p 878 A90-46186

CHAPMAN, GARY T.

Streamtube analysis of supersonic combustion in an in-tube-scamjet
[AIAA PAPER 90-2339] p 762 A90-42776

CHAPMAN, J. N.

Performance potential and technology issues of MHD augmented hypersonic simulation facilities
[AIAA PAPER 90-1380] p 598 A90-37929

CHAPOTON, CHARLES W.

Survivable penetration p 917 N90-29363

CHAPPELL, M. A.

Adjusting turbine engine transient performance for the effects of environmental variances
[AIAA PAPER 90-2501] p 658 A90-40639

CHAPPELL, SHERYL L.

Avoiding a maneuvering aircraft with TCAS p 347 A90-26222

CHARALAMBOUS, C. D.

Guidance and Control strategies for aerospace vehicles
[NASA-CR-186195] p 199 N90-14243

CHARGIN, MLADEN K.

Static aeroelastic analysis for generic configuration aircraft
[NASA-TM-89423] p 52 N90-10042

CHARGY, D.

Upwind adaptive finite element investigations of the two-dimensional reactive interaction of supersonic gaseous jets p 209 A90-18264

- CHARLES, B. D.**
Numerical simulations of three-dimensional rotor blade-vortex interactions p 807 A90-46879
- CHARLES, D.**
Metal matrix composites - Ready for take-off? p 356 A90-26865
- CHASHCHIN, V. A.**
Stiffness of an aircraft pneumatic rudder drive p 828 A90-46479
- CHASOVNIKOV, E. A.**
Comparison of calculated and experimental nonstationary aerodynamic characteristics of a delta wing pitching at large angles of attack p 387 A90-28988
- CHASSAING, P.**
Development of turbulence models for the analysis of compressible or incompressible unsteady flow [ETN-90-97486] p 958 A90-28810
- CHATSWORTH, TOM**
Global Sentry: NASA/USRA high altitude reconnaissance aircraft design, volume 2 [NASA-CR-186820-VOL-2] p 736 N90-25971
- CHATTOPADHYAY, A.**
Application of optimization methods to helicopter rotor blade design p 604 A90-37337
- CHATTOPADHYAY, ADITI**
Minimum weight design of helicopter rotor blades with frequency constraints p 180 A90-17313
Minimum weight design of rotorcraft blades with multiple frequency and stress constraints p 335 A90-25304
Performance of an optimized rotor blade at off-design flight conditions p 830 A90-46946
Appendix: Results obtained to date p 107 N90-12588
Performance of an optimized rotor blade at off-design flight conditions [NASA-CR-4288] p 416 N90-19226
An enhanced integrated aerodynamic load/dynamic optimization procedure for helicopter rotor blades [NASA-CR-4326] p 924 A90-29383
- CHAUSSÉE, DENNY S.**
Development of a three-dimensional upwind parabolized Navier-Stokes code p 602 A90-36253
- CHAUVE, M. P.**
Device for the dilution of hot exhaust jets [ETN-90-97435] p 858 N90-27723
- CHAVANON, PATRICK**
Performance and quality of a wing type parachute: Parametric analysis [REPT-88-19] p 89 N90-11710
- CHAVIARPOULOS, P.**
A two-dimensional unsteady potential solver in internal aerodynamics flow problems p 707 A90-44430
- CHAWLA, K.**
Simulation and analysis of a delta planform with multiple jets in ground effect [AIAA PAPER 90-0299] p 228 A90-22195
- CHAWLA, M. D.**
Wind-tunnel investigation of wing-in-ground effects p 395 A90-31276
- CHAWLA, MANGAL D.**
Robotics for flightline servicing p 383 A90-30760
- CHEATHAM, P. L.**
Computation of vectoring nozzle performance [AIAA PAPER 90-2752] p 627 A90-42225
- CHEESEMAN, I. C.**
An experimental investigation of the downwash beneath a lifting rotor and low advance ratios p 151 A90-17585
- CHEESEMAN, IAN C.**
The place of knowledge based systems in helicopter dynamic system condition prognosis p 618 A90-42475
- CHEFANOV, V. M.**
Effect of the inlet diameter and neck edge radius on the flow coefficient of straight-generatrix nozzles p 84 A90-14577
- CHEN, A. W.**
3D transonic nacelle and winglet design [AIAA PAPER 90-3064] p 794 A90-45897
TRANAIR applications to engine/airframe integration p 838 A90-48958
Application of boundary layer control to HSCT low speed configuration [AIAA PAPER 90-3199] p 812 A90-49103
The 757 NLF glove flight test results p 104 N90-12546
- CHEN, C. L.**
Calculation of unsteady rotor/stator interaction [AIAA PAPER 90-1544] p 565 A90-38688
- CHEN, C. P.**
Parameter effects on oscillatory aerofoil in transonic flows [AIAA PAPER 90-1473] p 563 A90-38629
- CHEN, CHING S.**
Advanced rotor computations with a corrected potential method p 385 A90-28197
- Three-dimensional viscous rotor flow calculations using a viscous-inviscid interaction approach [NASA-TM-102235] p 399 N90-19204
- CHEN, CHUANYAO**
A study on initial fatigue quality of typical aircraft structures (fastener holes) p 272 A90-22004
- CHEN, CHUNG-LUNG**
Computation of viscous transonic flow over porous airfoils p 153 A90-17864
- CHEN, D.**
Rolling of ARALL laminates (an alternative method for post-stretching ARALL laminates) [LR-560] p 135 N90-12778
An investigation on combined extension and bending of thin sheets with a central crack [LR-561] p 137 N90-12958
Some new techniques for aircraft fuselage skin tests [LR-547] p 184 N90-13379
- CHEN, D. R.**
Numerical solutions for unsteady aerofoil by internal singularity method p 716 A90-45536
- CHEN, DAGUANG**
Gas turbine engine condition monitoring and fault diagnostics p 190 A90-18594
- CHEN, F.-J.**
Design and operational features of low-disturbance wind tunnels at NASA Langley for Mach numbers from 3.5 to 18 [AIAA PAPER 90-1391] p 594 A90-37936
- CHEN, FANG-JENG**
Design and fabrication requirements for low noise supersonic/hypersonic wind tunnels p 122 N90-12555
- CHEN, FANG-JENG**
Advanced Mach 3.5 Axisymmetric Quiet Nozzle [AIAA PAPER 90-1592] p 566 A90-38727
- CHEN, H. C.**
The flow around wing-body junctions p 145 A90-16765
- CHEN, H. H.**
Prediction of transition on airfoils with separation bubbles, swept wings and bodies of revolution at incidence p 148 A90-16790
Calculation of low Reynolds number flows at high angles of attack [AIAA PAPER 90-0569] p 167 A90-19921
Fortified LEWICE with viscous effects [AIAA PAPER 90-0754] p 176 A90-20009
A three-dimensional linear stability approach to transition on wings at incidence p 20 N90-10373
- CHEN, HONGJI**
A quasi-3D design method of transonic compressor blade with the function of improving velocity distribution p 49 A90-12589
- CHEN, J. C.**
High temperature behavior of the innovation carbon/CSPI composite p 941 A90-50067
- CHEN, J.-L.**
Non-conservative stability of a cracked thick rotating blade p 606 A90-38544
- CHEN, JACQUELINE H.**
Direct numerical simulations of transition in a compressible wake p 553 A90-35212
The effect of Mach number on the stability of a plane supersonic wake p 557 A90-36524
- CHEN, JING-SONG**
Unsteady aerodynamic forces of oscillating supersonic/hypersonic wings with attached shock waves p 473 A90-33363
- CHEN, K.-H.**
A primitive variable, strongly implicit calculation procedure for viscous flows at all speeds [AIAA PAPER 90-1521] p 563 A90-38666
- CHEN, KANGMIN**
Variational principle with variable domain discontinuous finite element method for transonic flow and determining automatically the position and shape of the shock waves p 160 A90-19434
- CHEN, KENNY**
NASA/USRA high altitude reconnaissance aircraft [NASA-CR-186685] p 650 N90-24266
- CHEN, L. T.**
An interactive scheme for transonic wing/body flows based on Euler and inverse boundary-layer equations [AIAA PAPER 90-1586] p 566 A90-38721
- CHEN, L.-W.**
Non-conservative stability of a cracked thick rotating blade p 606 A90-38544
- CHEN, LEE T.**
A grid generation method for an aft-fuselage mounted capped-nacelle/pylon configuration with an actuator disk [AIAA PAPER 90-1564] p 565 A90-38703
- CHEN, MIAN**
Algorithm for simultaneous stabilization of single-input systems via dynamic feedback p 462 A90-31108
- CHEN, MING-HSIUNG**
On total variation diminishing schemes for transonic turbulent flow computation p 479 N90-20945
- CHEN, NAI-XING**
An improved SIP scheme for numerical solutions of transonic streamfunction equations p 904 A90-51014
- CHEN, NAI-XING**
Numerical solution of 3-D hybrid problems in turbomachinery p 621 A90-40501
- CHEN, P. C.**
Unsteady supersonic computations of arbitrary wing-body configurations including external stores p 232 A90-23278
Further studies of harmonic gradient method for supersonic aeroelastic applications p 473 A90-33410
- CHEN, QING**
A synthetic research for aircraft active flutter suppression p 195 A90-16827
- CHEN, REN LIANG**
The response of helicopter to dispersed gust p 670 A90-42470
- CHEN, REN-LIANG**
The influence of the inertia coupling on the stability and control of the helicopter and the response of helicopter gust p 671 A90-42472
- CHEN, ROBERT T. N.**
A survey of nonuniform inflow models for rotorcraft flight dynamics and control applications p 590 A90-38521
A survey of nonuniform inflow models for rotorcraft flight dynamics and control applications [NASA-TM-102219] p 260 N90-15938
- CHEN, RONG-GUO**
Some explorations on the mechanism of blade flutter suppression by porous wall casing p 854 A90-49470
- CHEN, RUILIN**
A ground simulation-inspection system for avionic devices p 594 A90-37232
- CHEN, RUIYI**
Color schlieren system using square color filter and its application to aerofoil test in transonics p 66 A90-10748
- CHEN, RUXIAN**
Calculation of viscous-inviscid strong interaction for transonic flows over aerofoils p 627 A90-42384
- CHEN, S.**
Probabilistic method to compute the optimal slip load for a mistuned bladed disk assembly with friction dampers p 507 A90-32269
- CHEN, S. H.**
Forced response on turbomachinery blades due to passing wakes [AIAA PAPER 90-2353] p 705 A90-42781
- CHEN, SHING**
Analytical study of mistuning/friction/aerodynamics interaction in a bladed disk assembly [AD-A211139] p 55 N90-10893
- CHEN, SHYI-YAUNG**
Extension of a three-dimensional viscous wing flow analysis user's manual: VISTA 3-D code [NASA-CR-182024] p 574 N90-22538
Extension of a three-dimensional viscous wing flow analysis [NASA-CR-182023] p 631 N90-23348
- CHEN, T. L. C.**
Application to a helicopter of a general method for modifying a finite-element model to correlate with modal test data p 832 A90-46968
- CHEN, W. C.**
An analysis methodology for internal swirling flow systems with a rotating wall [ASME PAPER 89-GT-185] p 361 A90-23863
- CHEN, WENJUN**
Analysis of aeroelastic divergence for the slender flight vehicles p 680 A90-39298
- CHEN, YAO-SONG**
An analytic solution on hypersonic flow over an arbitrary slender body with near power-law profile p 558 A90-37736
- CHEN, YONG-ZE**
An analytic solution on hypersonic flow over an arbitrary slender body with near power-law profile p 558 A90-37736
- CHEN, YOUNBIN**
Digital electronic control for WJ6G4A engine p 424 A90-29919
- CHEN, YUELIN**
Variational principle with variable domain discontinuous finite element method for transonic flow and determining automatically the position and shape of the shock waves p 160 A90-19434
- CHEN, YUH-WEN**
Hydraulic analogy application in the study of a two-phase mixture combustion flow [AIAA PAPER 90-0451] p 211 A90-19850

CHEN, ZONGJI

The eigenvalue sensitivity analysis and design for integrated flight/propulsion control systems p 196 A90-18601

CHEN, ZUOBIN

The computational method for the transonic wing design p 160 A90-19438
Calculations of transonic flows over wing-body combinations p 395 A90-31479

CHENG, C. W.

Reduction of the side force on pointed forebodies through add-on tip devices [AIAA PAPER 90-3005] p 788 A90-45854

CHENG, H. K.

An airfoil theory of bifurcating laminar separation from thin obstacles p 702 A90-42639

CHENG, K. Y.

The gas source molecular beam epitaxial growth of Al(x)Ga(1-x)P on (100) GaP p 894 A90-48657

CHENG, PETER Y.

STOL Maneuver Technology Demonstrator aeroservoelasticity [AIAA PAPER 90-3336] p 863 A90-47596

CHENG, SIN-I

Hypersonic rarefied flow and its solution over the stagnation region [AIAA PAPER 90-0420] p 166 A90-19842

CHENG, SIN-I

Hypersonic propulsion p 253 A90-21949

CHENG, V. H. L.

Rotorcraft pursuit-evasion in nap-of-the-earth flight [AIAA PAPER 90-3455] p 786 A90-47707

CHENG, VICTOR H. L.

Concept development of automatic guidance for rotorcraft obstacle avoidance p 669 A90-41632

CHENG, XINHUA

Effect of vane and blade numbers on performance of transonic turbine stage p 189 A90-17789

CHEREMUKHIN, G. A.

Aerodynamic interference of prismatic engine nacelles with the wing at supersonic velocities p 294 A90-24078

CHERENKOV, A. S.

Effect of pressure on the electrophysical properties of two-phase flows in nozzles p 110 A90-14572

CHEREPNIN, S. N.

A study of the electrophysical phenomena in the combustion chambers of jet engines p 765 A90-45028

CHERKASOVA, S. A.

Cyclic fracture toughness of VT-3-1 and VT-25 titanium alloys p 873 A90-46514

CHERNIAEVA, L. F.

The tape method for the automatic partitioning of an arbitrary region when calculating temperature stresses p 138 A90-14587

CHERRETT, M. A.

Preliminary experience with high response pressure measurements in a multistage, high speed compressor [RAE-TM-P-1141] p 117 N90-12619

CHERRY, D. G.

NASA/GE Energy Efficient Engine low pressure turbine scaled test vehicle performance report [NASA-CR-168290] p 931 N90-28563

CHESNAKAS, CHRISTOPHER J.

Three-component LDA measurements in an axial-flow compressor p 683 A90-40943

CHESNUTT, J. C.

Titanium aluminides for advanced aircraft engines p 874 A90-49000

CHETTY, SHYAM

Model following control system design: Preliminary ATTAS in-flight simulation test results [PD-FC-9003] p 758 N90-26010

CHEUNG, ANNY

Replication of NASPAC Dallas/Fort Worth study [DOT/FAA/CT-TN90/26] p 729 N90-25123

CHEUNG, SAMSON HOK-CHI

Convergence acceleration of hypersonic flow calculations: A nonlinear relaxation factor p 480 N90-20957

CHEVALLIER, J. P.

Instrumentation being developed for the ONERA F4 wind tunnel [ONERA, TP NO. 1989-189] p 261 A90-21049

High enthalpy hypersonic wind tunnel F4: General description and associated instrumentation p 673 N90-24228

The aims and history of adaptive wall wind tunnels p 871 N90-26839

CHEVERTON, K. J.

Design and fabrication of a prototype resin matrix composite interceptor structure [AIAA PAPER 90-1004] p 442 A90-29275

CHEW, JOHN W.

A theoretical study of ingress for shrouded rotating disc systems with radial outflow [ASME PAPER 89-GT-178] p 361 A90-23859

Prediction of rotating disc flow and heat transfer in gas turbine engines [PNR90650] p 750 N90-26001

CHI, RAY M.

Noninterference blade-vibration measurement system for gas turbine engines p 132 A90-16372

CHIA, K. N.

Analysis of high-incidence separated flow past airfoils p 147 A90-16781

CHIA, U.

Analysis of high-incidence separated flow past airfoils p 147 A90-16781

CHIANG, HSIAO-WEI D.

Unsteady incompressible aerodynamics and forced response of detuned blade rows [AIAA PAPER 90-0340] p 191 A90-19805

Unsteady aerodynamic gust response including steady flow separation p 556 A90-36262

Cascade aerodynamic gust response including steady loading effects p 904 A90-51006

CHIANG, RICHARD Y.

Algorithms for computing the multivariable stability margin p 612 N90-22999

CHIANG, S.

Laser welding of an advanced rapidly-solidified titanium alloy p 881 A90-47021

CHIANG, TING-LUNG

Effect of the grid system on the solution of Euler equations p 309 A90-26494

Computation of nonequilibrium chemically reacting flows in hypersonic flow field p 480 N90-20954

CHICHEROV, N. A.

Using the lifting line theory for calculating straight wings of arbitrary profile p 387 A90-29004

CHIESA, S.

Estimation of defective rate of mechanic-hydraulic components [ETN-90-97275] p 884 N90-27120

CHIGIER, NORMAN

Atomization and spray research for gas turbine engines p 189 A90-17688

Laser Doppler velocimetry investigation of swirler flowfields p 682 A90-40929

CHIGRINET, A. D.

Ground aviation equipment: Handbook p 593 A90-36153

CHIKARAISHI, M.

Development of ceramic components for high-temperature gas turbines p 602 A90-35951

CHIKATA, TETSUO

Mechanical rig rest of FJR 710/600 engine components p 43 A90-12016

CHILDERS, BROOKS A.

Video photographic considerations for measuring the proximity of a probe aircraft with a smoke seeded trailing vortex [NASA-TM-102691] p 724 N90-25120

CHILDS, D. W.

An annular gas seal analysis using empirical entrance and exit region friction factors [ASME PAPER 89-TRIB-46] p 537 A90-33555

Test results for turbulent annular seals, using smooth rotors and helically grooved stators [ASME PAPER 89-TRIB-11] p 537 A90-33556

CHILDS, E. P.

Turbulence model performance in V/STOL flow field simulation [AIAA PAPER 90-2248] p 625 A90-42094

CHILDS, ROBERT E.

Turbulence modeling for impinging jets [AIAA PAPER 90-0022] p 211 A90-19639

CHIMETTO, P.

The use of simulation in support of the high AOA flight test program of the AM-X aircraft [AIAA PAPER 90-1289] p 495 A90-33909

CHIN, JU SHAN

Influence of fuel composition on flame radiation in gas turbine combustors p 659 A90-40946

CHIN, SUEI

Identification of aerodynamic models for maneuvering aircraft [NASA-CR-186630] p 719 N90-25943

CHIN, Y. T.

Supersonic STOVL - The future is now [AIAA PAPER 90-3296] p 840 A90-49124

CHING, FRED

Lightweight, composite flight control actuators [SAE PAPER 89-2264] p 733 A90-45459

CHINITZ, WALLACE

Calculated chemical and vibrational nonequilibrium effects in hypersonic nozzles p 253 A90-21224

CHINZEI, NOBUO

Analysis of scramjet engine characteristics [NAL-TR-1041] p 933 N90-29398

CHIRANAIKADUL, PHAICHIT

The changes of structures and properties in PAN-based carbon fibers during heat treatment in carbon dioxide p 945 A90-50145

CHITTICK, WILLIAM A.

Integration of GPS with the Carrier Aircraft Inertial Navigation System (CAINS) p 97 A90-13990

CHITTUM, CHARLES B.

The influence of adjacent seating configurations on egress through a type 3 emergency exit [AD-A218393] p 636 N90-23371

CHIU, DI

Adaptive autopilot design via model expansion method p 55 A90-11124

CHIU, W. K.

The receptivity of laminar boundary layer flow to leading edge vibrations p 815 A90-49800

CHIU, Y. DANNY

An enhanced integrated aerodynamic load/dynamic optimization procedure for helicopter rotor blades [NASA-CR-4326] p 924 N90-29383

CHIVUKULA, VENU G.

Winds aloft measurement and airspeed calibration using Loran [AIAA PAPER 90-3331] p 847 A90-47592

CHIZHOV, V. V.

Calculation of an axial-flow birotary turbine p 880 A90-46492

CHMIELNIAK, T.

The solution of the unsteady transonic flow through a blade passage in an axial turbine p 5 A90-11777

CHMIELNIAK, TADEUSZ

Numerical solution of 2-D transonic flow through an axial turbine stage p 814 A90-49464

CHO, JINSOO

Propeller-wing interaction using a frequency domain panel method p 307 A90-26128

Counter-rotating propellant analysis using a frequency domain panel method p 623 A90-40937

Frequency domain aerodynamic analysis of interacting rotating systems p 21 N90-10837

CHO, MAENG-HYO

Flutter analysis of composite panels in supersonic flow [AIAA PAPER 90-1180] p 450 A90-29379

CHODY, JOSEPH R.

Combat aircraft control requirements for agility p 935 N90-28517

CHOI, GWAN SEUNG

An experimental study of fault propagation in a jet-engine controller [NASA-CR-181335] p 665 N90-23401

CHOI, JANG-SOO

An application of the surface-singularity method to wing-body-tail configurations p 9 A90-12229

Prediction of tip-clearance effects on a wing by the panel method p 307 A90-25871

CHOI, S. B.

A new generation of innovative ultra-advanced intelligent composite materials featuring electro-rheological fluids - An experimental investigation p 204 A90-17962

CHOI, SIU-TONG

Nonlinear response and fatigue of stiffened panels p 363 A90-23953

CHOI, Y. H.

Computational analysis of the flowfield of a two-dimensional ejector nozzle [AIAA PAPER 90-1901] p 740 A90-42690

CHOKANI, N.

Navier-Stokes simulation of unsteady supersonic cavity flowfield with passive control [AIAA PAPER 90-3101] p 796 A90-45913

CHOMIAK, J.

Controlled mixing and variable geometry combustor design effects on emissions and combustion characteristics p 45 A90-12547

CHONG, C. Y.

Performance assessment for airborne surveillance systems incorporating sensor fusion p 583 A90-37088

CHOO, YUNG K.

Application of a lower-upper implicit scheme and an interactive grid generation for turbomachinery flow field simulations [ASME PAPER 89-GT-20] p 288 A90-23762

Interactive grid generation for turbomachinery flow field simulations p 312 A90-26553

CHOPRA, INDERJIT

Response and hub loads sensitivity analysis of a helicopter rotor p 181 A90-18145

- Application of higher harmonic control (HHC) to rotors operating at high speed and maneuvering flight
p 429 A90-28157
- Rotor loads validation utilizing a coupled aeroelastic analysis with refined aerodynamic modeling
p 408 A90-28226
- Aeroelastic optimization of a helicopter rotor using an efficient sensitivity analysis
[AIAA PAPER 90-0951] p 410 A90-29237
- Aeroelastic analysis of helicopter rotor blades with advanced tip shapes
[AIAA PAPER 90-1118] p 392 A90-29390
- Multi-output implementation of a modified sparse time domain technique for rotor stability testing
[AIAA PAPER 90-0946] p 412 A90-29405
- Effects of higher harmonic control on rotor performance and control loads
[AIAA PAPER 90-1158] p 412 A90-29467
- Helicopter response to atmospheric turbulence in forward flight
p 518 A90-33625
- Stability sensitivity analysis of a helicopter rotor
p 580 A90-36273
- Air resonance stability of hingeless rotors in forward flight
p 590 A90-38519
- Perspectives in aeromechanical stability of helicopter rotors
p 831 A90-46953
- Theoretical and experimental investigation of the aeroelastic stability of an advanced bearingless rotor in hover and forward flight
p 831 A90-46958
- CHOUGHANE, MNAOUAR**
Helicopter trim with flap-lag-torsion and stall by an optimized controller
p 755 A90-45332
- Application of a dynamic stall model to rotor trim and aeroelastic response
p 583 N90-22556
- CHOW, CHUEN-YEN**
Computation of viscous transonic flow over porous airfoils
p 153 A90-17864
- CHOW, JOE H.**
An explicit model-matching approach to lateral-axis autopilot design
p 756 A90-45413
- CHOWDHRY, RAJIV S.**
Optimal rigid body reorientation problem
[AIAA PAPER 90-3485] p 867 A90-47734
- CHOY, F. K.**
Rub interactions of flexible casing rotor systems
p 41 A90-11554
- CHOY, FRED K.**
Experimental and analytical evaluation of dynamic load vibration of a 2240-kW (3000-hp) rotorcraft transmission
p 127 A90-13750
- CHRISS, R. M.**
An LDA investigation of the normal shock wave boundary layer interaction
p 908 A90-52618
- CHRISTIAN, MARK JAY**
Post crash flight analysis: Visualizing flight recorder data
[AD-A21063] p 96 N90-11715
- CHRISTIAN, T. F., JR.**
Fuel tank explosion protection
p 251 N90-15914
- CHRISTIAN, TOM**
An expert system advisor for damage repair of composite wing skins (repairman)
p 842 N90-26810
- CHRISTIANSEN, HOWARD**
Helicopter Airborne Laser Positioning System (HALPS)
[NASA-TM-102814] p 654 N90-23399
- CHRISTMORE, DAN L.**
Computational crash dynamics. Project 1.2: Computational crash dynamics analysis
[IAR-89-19] p 724 N90-25956
- CHRISTOPHE, J.**
High enthalpy hypersonic wind tunnel F4: General description and associated instrumentation
p 673 N90-24228
- CHRISTOPHER, P. A. T.**
Incompressible flow about ellipsoids of revolution
[REPT-88-02] p 90 N90-11713
- CHRYSAINTHO, A.**
Identification of multivariable models of jet engines
[AIAA PAPER 90-1874] p 655 A90-40540
- Design of digital self-selecting multivariable controllers for jet engines
[AIAA PAPER 90-1875] p 655 A90-40541
- CHU, ALPHONSE Y.**
Synthesis of individual rotor blade control system for gust alleviation
[NASA-TM-101886] p 736 N90-25972
- CHU, M. L.**
Impact ice stresses in rotating airfoils
[AIAA PAPER 90-0198] p 175 A90-19735
- CHU, SHIAW SHINN**
An improvement of convection fidelity in Euler calculations
p 315 N90-16709
- CHU, WULI**
An experimental investigation of rotating stall in a centrifugal compressor with vaneless diffuser
p 621 A90-40513
- CHUANG, H. ANDREW**
Unsteady flow computation of oscillating flexible wings
[AIAA PAPER 90-0937] p 389 A90-29363
- Unsteady inviscid and viscous computations for vortex-dominated flows
p 553 A90-35752
- CHUANG, J. C.**
Characterization of chemicals on engine exhaust particles
[AD-A213566] p 256 N90-15106
- CHUANG, SHU-HAO**
Numerical simulation of an impinging jet on a flat plate
p 86 A90-15821
- CHUBACHI, TATSUO**
Backside landing control of a STOL aircraft using approximate perfect servo
p 934 A90-52801
- CHUKHLANTSEV, S. G.**
Acoustic wave excitation during the aerodynamic interaction between a fan blade and a bluff obstacle
p 965 A90-52289
- CHUN, K.**
A circular combustor configuration with multiple injection ports for mixing enhancement
p 130 A90-15389
- CHUN, P. A.**
Recent developments in Ramjet pressure oscillation technology
p 53 N90-10199
- CHUNG, W. W.**
Ground-simulation investigations of VTOL airworthiness criteria for terminal-area operations
[NASA-TM-102810] p 757 N90-25141
- CHUNG, Y. L.**
Numerical simulations of gas turbine combustor flows
[AIAA PAPER 90-2305] p 686 A90-42116
- CHUPP, RAYMOND E.**
Evaluation of brush seals for limited-life engines
[AIAA PAPER 90-2140] p 685 A90-42040
- CHVYKOVA, E. M.**
Interchangeability of Soviet-made and foreign mineral oils for aviation gas turbine engines
p 873 A90-46525
- CHYLA, ANDRZEJ**
A statistical model of helicopter noise
p 77 A90-10229
- CHYU, M. K.**
Heat transfer and pressure drop for short pin-fin arrays with pin-endwall fillet
[ASME PAPER 89-GT-99] p 359 A90-23813
- Local heat transfer on a flat surface roughened with broken ribs
p 534 A90-32169
- CICHON, MICHAEL J.**
Repair adhesives - Development criteria for field level conditions
p 528 A90-31575
- CICOLANI, LUIGI S.**
Equations of motion of slung load systems with results for dual lift
[NASA-TM-102246] p 349 N90-17641
- CIEAUX, J. M.**
Homogenization of composite beams in dynamical flexure
p 878 A90-46184
- CIFONE, ANTHONY J.**
Combustor influence on fighter engine operability
p 64 N90-10193
- Dynamic instability characteristics of aircraft turbine engine combustors
p 53 N90-10195
- CIMBALA, J. M.**
An experimental investigation of the turbulent structure in a two-dimensional momentumless wake
p 474 A90-33515
- CIMBALISTA, M.**
Carbon/epoxy tooling evaluation and usage
p 445 A90-28165
- CIOFFI, L. V.**
Canard versus aft-tail ride qualities performance and pilot command response
p 258 N90-15053
- CIPRI, F.**
Choice and characterization of new materials for aerospace applications
[ETN-89-95219] p 126 N90-11819
- An ultrasonic system for in-service non-destructive inspection of composite structures
p 885 N90-28076
- CITRIN, K. M.**
Heat pipes for wing leading edges of hypersonic vehicles
[NASA-CR-181922] p 369 N90-17055
- CLARK, G.**
Fractographic techniques for the assessment of aircraft component cracking
p 954 A90-49885
- Analysis and interpretation of aircraft component defects using quantitative fractography
p 956 A90-50555
- Moisture absorption in graphite/epoxy laminates
p 951 A90-52799
- CLARK, JIM A.**
Modeling gas turbine combustor performance under transient conditions
[AIAA PAPER 90-2161] p 661 A90-42051
- CLARK, KENNETH**
Microstructural effects of plastic media blasting on graphite epoxy composites
[SAE PAPER 890928] p 286 A90-24693
- CLARK, MARIJO**
Process optimization of high temperature composite materials
p 943 A90-50130
- CLARK, R.**
In-situ measurement, modelling and control of the imidization reaction in PMR-15
p 941 A90-50066
- CLARK, R. L.**
Table top experimental simulation of hypersonic aero-optical effects
p 525 A90-34586
- CLARK, R. L., JR.**
Large-scale structure in a supersonic slot-injected flowfield
p 602 A90-36265
- CLARK, RODNEY L.**
Design considerations for a compact table top hypersonic simulator of aero-optic effects
p 525 A90-34585
- CLARK, ROGER W.**
Subsonic calculation of propeller/wing interference
[AIAA PAPER 90-0031] p 226 A90-22155
- CLARKE, GARRY K. C.**
A waveform alignment approach to positioning airborne radar-sounding data
p 332 A90-26265
- CLARY, JEFF S.**
Benchmark calculations with an unstructured grid flow solver on a SIMD computer
p 546 A90-34378
- CLAUS, R. O.**
Fiber optic sensor systems for smart aerospace structures
p 38 A90-11208
- CLAUSEN, ROBERT D.**
A computational model for thickening boundary layers with mass addition for hypersonic engine inlet testing
[AIAA PAPER 90-2219] p 705 A90-42750
- CLAUSEN, ROBERT DOUGLAS**
A computational model for thickening boundary layers with mass addition for hypersonic engine inlet testing
[AD-A216246] p 319 N90-17576
- CLAVEL, M.**
Study of the microstructure of a titanium alloy (6246) for turbomachine compressors
[ETN-90-97450] p 876 N90-27900
- CLEARY, JOSEPH W.**
Experimental and computational surface and flow-field results for an all-body hypersonic aircraft
[AIAA PAPER 90-3067] p 793 A90-45893
- Experimental aerothermodynamic research of hypersonic aircraft
[NASA-CR-186903] p 721 N90-25954
- CLEMENS, N. T.**
Two- and three-dimensional effects in the supersonic mixing layer
[AIAA PAPER 90-1978] p 703 A90-42708
- CLEMENT, WARREN F.**
Fully automatic guidance for rotorcraft nap-of-the-earth (NOE) flight following planned profiles
p 403 A90-28219
- Real-time piloted simulation of fully automatic guidance and control for rotorcraft nap-of-the-earth (NOE) flight following planned profiles
[AIAA PAPER 90-3372] p 864 A90-47630
- CLEMENTS, W. W.**
The influence of diffuser vane leading edge geometry on the performance of a centrifugal compressor
[ASME PAPER 89-GT-163] p 292 A90-23851
- CLEMONS, A.**
Evaluation of the thermoplastic film interleaf concept for improved damage tolerance
p 946 A90-50179
- CLER, A.**
Comparison with experiment of various computational methods of airflow on three helicopter fuselages
p 630 A90-42436
- Experimental study of the flow around an helicopter fuselage - Comparison with three-dimensional boundary layer calculations
p 630 A90-42438
- Improving helicopter aerodynamics - A step ahead
p 631 A90-42443
- CLER, STEPHANE**
High temperature adhesives commercially available to be used for extended time with PMR15 laminates
p 943 A90-50125
- CLIFF, E. M.**
Singular, periodic solutions in aircraft cruise-dash optimization
[AIAA PAPER 90-3369] p 863 A90-47627
- CLIFF, EUGENE M.**
Toward a theory of aircraft agility
[AIAA PAPER 90-2808] p 752 A90-45143
- Optimal rigid body reorientation problem
[AIAA PAPER 90-3485] p 867 A90-47734
- CLIFFORD, RICHARD J.**
Calculation of the combustion distribution in a liquid-fuel ramjet
p 858 N90-27931

CLINE, D. D.

Shock sensitivity in parabolized Navier-Stokes solution of high angle-of-attack supersonic flow p 302 A90-25280

CLINEDINST, WINSTON C.

Advanced transport operating system software upgrade: Flight management/flight controls software description [NASA-CR-181936] p 893 N90-28366

CLODFELTER, R. G.

Hot surface ignition studies of aviation fluids p 327 N90-17600

CLOFT, THOMAS G.

Ultra High Bypass (UHB) engine critical component technology [ASME PAPER 89-GT-229] p 342 A90-23884

CLOUGH, BRUCE T.

Short take-off and landing maneuver technology demonstrator (STOL/MTD) lessons learned - Integrated flight/propulsion control (IFPC) [AIAA PAPER 90-3307] p 868 A90-48888

CLOUSER, S.

Fuel effects on gas turbine combustor dynamics [AIAA PAPER 90-1957] p 676 A90-40570

CLOYD, J. D.

The effects of wind tunnel data uncertainty on aircraft point performance predictions [AD-A216091] p 414 N90-18387

COATS, G. D.

Mesoscale acid deposition modeling studies [NASA-CR-4262] p 140 N90-13228

COBLEIGH, BRENT R.

Aerodynamic parameters of High-Angle-of attack Research Vehicle (HARV) estimated from flight data [NASA-TM-102692] p 936 N90-28578

COCHRAN, J. E., JR.

Dynamics and control of maneuverable towed flight vehicles [AIAA PAPER 90-2841] p 754 A90-45161

COCHRAN, R. BRUCE

Hypersonic nozzle/afterbody performance at low Mach numbers [AD-A216223] p 319 N90-17575

COCKING, J. L.

Extending the overhaul interval for gas turbine engines through the use of alternative coatings on first stage blades p 63 A90-12539

COCKRELL, D. J.

Turbulent boundary layer development in the presence of small isolated two-dimensional surface discontinuities p 210 A90-18507

COCQUEREZ, J. L.

Study of ground effects on flying scaled models p 922 N90-28532

CODY, CHARLOTTE K.

Feasibility study for a microwave-powered ozone sniffer aircraft [NASA-CR-186660] p 650 N90-23397

CODY, WILLIAM J.

Designers as users - Design supports based on crew system design practices p 457 A90-28184

COE, PAUL L., JR.

Exploratory wind tunnel investigation of the stability and control characteristics of a three-surface, forward-swept wing advanced turboprop model [AIAA PAPER 90-3074] p 797 A90-45920

Low-speed wind-tunnel investigation of the flight dynamic characteristics of an advanced turboprop business/commuter aircraft configuration [NASA-TP-2982] p 434 N90-19239

COELHO, S. L. V.

The production of uniformly sheared streams by means of double gauzes in wind tunnels - A mathematical analysis p 131 A90-15887

COEN, PETER G.

Performance potential of an advanced technology Mach 3 turbojet engine installed on a conceptual high-speed civil transport [NASA-TM-4144] p 51 N90-10034

COFFMAN, STEVEN C.

Automated measurement of aircraft-level electromagnetic interference p 404 A90-30752

COGGESHALL, RANDY L.

Boeing/NASA composite components flight service evaluation [NASA-CR-181898] p 601 N90-22609

COHEN, GERALD C.

IAPSA 2 small-scale system specification [NASA-CR-182006] p 695 N90-24103
Reliability model generator specification [NASA-CR-182005] p 780 N90-25638

COHEN, J. D.

Considerations in using broad specification fuels for aircraft propulsion [SAE PAPER 892330] p 765 A90-45487

COHEN, J. M.

Air and spray patterns produced by gas turbine high-shear nozzle/swirler assemblies [AIAA PAPER 90-0465] p 192 A90-19857

Influences on the uniformity of sprays produced by gas turbine high shear nozzle/swirler assemblies [AIAA PAPER 90-2193] p 686 A90-42068

COHEN, S. B.

Experiments with unsteady, free surface, three-dimensional vortices in a thermally stable, stratified fluid [AD-A222088] p 815 N90-26796

COIRO, D.

Numerical prediction of transonic viscous flows around airfoils through an Euler/boundary layer interaction method [AIAA PAPER 90-1537] p 564 A90-38681

COIRO, D. P.

Wake effects on the prediction of transonic viscous flows around airfoils with an Euler/boundary layer interaction approach [AIAA PAPER 90-3061] p 798 A90-45933

COIRO, DOMENICO P.

Prediction of aerodynamic performance of airfoils in low Reynolds number flows p 799 A90-46360

A computer code for the prediction of aerodynamic characteristics of lifting airfoils at transonic speed [DLC-EST-TN-030] p 632 N90-23359

Prediction of aerodynamic performance of airfoils in low Reynolds number flows [DLC-EST-TN-031] p 632 N90-23360

COLE, GREGORY M.

Experimental measurements of the laminar separation bubble on an Eppler 387 airfoil at low Reynolds numbers [NASA-CR-186263] p 275 N90-15380

COLE, R. L.

Coping with bomb threats to civil aviation p 23 A90-12781

COLE, STANLEY R.

Experimental transonic flutter characteristics of supersonic cruise configurations [AIAA PAPER 90-0979] p 390 A90-29369

Effects of spoiler surfaces on the aeroelastic behavior of a low-aspect-ratio rectangular wing [AIAA PAPER 90-0981] p 391 A90-29371

Digital-flutter-suppression-system investigations for the active flexible wing wind-tunnel model [AIAA PAPER 90-1074] p 430 A90-29382

Digital-flutter-suppression-system investigations for the active flexible wing wind-tunnel model [NASA-TM-102618] p 520 N90-20093

Effects of spoiler surfaces on the aeroelastic behavior of a low-aspect-ratio rectangular wing [NASA-TM-102622] p 846 N90-27700

COLEHOUS, J. L.

Analytical methods for subsonic propulsion system integration p 29 A90-12613

Investigation of very high bypass ratio engines for subsonic transports p 659 A90-40945

COLEMAN, E. B.

Parametric evaluation of the aerodynamic performance of an annular combustor-diffuser system [AIAA PAPER 90-2163] p 742 A90-42741

COLEMAN, EDWARD E.

Design of integrated pitch axis for autopilot/autothrottle and integrated lateral axis for autopilot/yaw damper for NASA TSRV airplane using integral LQG methodology [NASA-CR-4268] p 348 N90-16768

COLLIER, ARNOLD S.

Aerodynamic heat transfer testing in hypersonic wind tunnels using an infrared imaging system [AIAA PAPER 90-0189] p 350 A90-25027

COLLIER, F. S., JR.

Curvature effects on the stability of laminar boundary layers on swept wings p 148 A90-16788

Curvature effects on the stability of three-dimensional laminar boundary layers p 71 N90-10366

COLLIER, FAYETTE S., JR.

Supersonic boundary-layer transition on the LaRC F-106 and the DFRF F-15 aircraft. Part 1: Transition measurements and stability analysis p 94 N90-12558

COLLINGE, KENNETH S.

A comprehensive diagnostic system for the T800-APW-800 engine p 422 A90-28181

COLLINS, J. F.

Materials pace aerospace technology p 203 A90-17298

COLLINS, JAMES

ASHTech XII - A new GPS technology p 576 A90-36917

COLLINS, JAMES A.

Intelligent built-in test and stress management p 448 A90-28343

COLLINS, JOHN

Full-scale air transport category fuselage burnthrough tests [DOT/FAA/CT-TN89/65] p 486 N90-20967

COLLINS, PATRICK K.

Aircraft subsystem waste energy recovery and management [SAE PAPER 901218] p 840 A90-49293

COLLINS, ROBERT E.

Leading- and trailing-edge flaps on supersonic delta wings p 233 A90-23285

COLLINS, WILLIAM G.

Mode S system design and architecture p 330 A90-25569

COLONIUS, TIM

Direct numerical simulation of aerodynamic noise [AD-A214122] p 379 N90-18225

COLOZZA, ANTHONY J.

Preliminary design of a long-endurance Mars aircraft [AIAA PAPER 90-2000] p 674 A90-40587

Preliminary design of a long-endurance Mars aircraft [NASA-CR-185243] p 588 N90-21763

COLTMAN, J. W.

Aircraft crash survival design guide. Volume 2: Aircraft design crash impact conditions and human tolerance [AD-A218435] p 575 N90-22546

COLUCCI, FRANK

Stronger starlifter p 143 A90-17919

The challenge of LHX p 382 A90-29641

Natural honeycomb p 442 A90-29643

Carbon-carbon for NASP p 599 A90-36672

COLVIN, G. N.

Development of a simulated bird-strike test method p 600 A90-37444

COLVIN, M. ALEXANDER

AIRNET: A real-time communications network for aircraft [NASA-CR-186140] p 690 N90-24514

COMBS, DAN

The MANTA: An RPV design to investigate forces and moments on a lifting surface [NASA-CR-186227] p 499 N90-20971

COMERFORD, T. J.

Aging fleet Structures Working Group activities [AIAA PAPER 90-3219] p 786 A90-48840

COMLY, KAREN

The SKY SHARK: An RPV designed to investigate the pressure distribution on a lifting surface [NASA-CR-186222] p 844 N90-26824

COMMON, CHRISTIAN J.

Propulsion control system designs for advanced Navy multimission aircraft [AIAA PAPER 90-2403] p 663 A90-42160

COMPTON, WILLIAM B., III

Navier-Stokes simulation of transonic afterbody flows with jet exhaust [AIAA PAPER 90-3057] p 790 A90-45862

CONCHIE, PETER J.

HOTOL: A future launcher for Europe p 353 N90-16800

CONDAMINAS, A.

Determination of the ground effect on the characteristics of the A320 aircraft [ONERA, TP NO. 1989-188] p 245 A90-21048

Determination of the ground effect on the characteristics of the A320 aircraft p 922 N90-28534

CONDON, DAVID

The MANTA: An RPV design to investigate forces and moments on a lifting surface [NASA-CR-186227] p 499 N90-20971

CONLIFFE, CALVIN H.

Turbofans turn to UHB propulsion p 659 A90-41165

CONNELLY, J. MICHAEL

Terminal Doppler Weather Radar System - Wind shear detection will warn pilots of danger p 25 A90-10462

CONNER, DAVID A.

Measurement resolution of noise directivity patterns from acoustic flight tests [NASA-TM-4134] p 79 N90-10679

CONNERS, TIMOTHY R.

Measurement effects on the calculation of in-flight thrust for an F404 turbofan engine [NASA-TM-4140] p 114 N90-11741

CONNETT, WILLIAM C.

An algebraic adaptive-grid technique for the solution of Navier-Stokes equations [AIAA PAPER 90-1605] p 567 A90-38736

CONNOLLY, KRISTEN

The DELTA MONSTER: An RPV designed to investigate the aerodynamics of a delta wing platform [NASA-CR-186226] p 924 N90-29381

CONRADY, NEAL

Local adaptive maneuvering optimization for fighter aircraft [AIAA PAPER 90-3453] p 890 A90-47706

- CONSIGNY, HERVE**
Preliminary tests of a gust generator in the ONERA S3Ch transonic wind tunnel
[ONERA, TP NO. 1989-171] p 261 A90-21035
- CONSTANCE, JOSEPH**
Industry turns to ceramic composites p 356 A90-27597
- CONSTANTINESCU, V. N.**
On a lifting line theory for supersonic flow. I - The velocity field due to a vortex line in supersonic flow p 143 A90-16735
On a lifting line theory for supersonic flow. II - A supersonic lifting line theory for wings p 477 A90-34817
- CONWAY, CHERYL VENTURA**
Auxiliary power unit maintenance aid - Flight line engine diagnostics p 382 A90-28348
- CONWAY, JOHN T.**
Modelling of boundary layer and trailing edge thickness effects for the Euler equations using surface transpiration p 629 A90-42412
- CONWAY, TIMOTHY J.**
Auxiliary power unit maintenance aid - Flight line engine diagnostics p 382 A90-28348
- COOK, JANET H.**
Incorporation of alarm states into a real time decision making process
[AIAA PAPER 89-3006] p 76 A90-10620
- COOK, M.**
Systems tunnel linear shaped charge lightning strike
[NASA-CR-183832] p 201 A90-13404
- COOK, M. V.**
On the application of modified stepwise regression for the estimation of aircraft stability and control parameters
[REPT-8905] p 198 A90-13400
- COOK, S. C.**
The development of a high response aerodynamic wedge probe and use on a high-speed research compressor
[PNR90598] p 116 A90-12613
Development of a mass averaging temperature probe p 427 A90-18418
- COOK, S. C. P.**
The development of a high response aerodynamic wedge probe and use on a high-speed research compressor p 69 A90-12618
- COOK, T. S.**
Application of HOST technology to the SSME HPFTP blade
[ASME PAPER 89-GT-130] p 360 A90-23828
- COOKE, G. A.**
Tests of automatic dependent surveillance (ADS) in Western Europe - Possible future developments p 574 A90-35353
- COOLEY, WILLIAM W.**
Comparison of four lightning simulation tests on a composite test bed aircraft p 818 A90-49831
- COONS, LEE**
IHPTET technology mission payoffs at the component level - A look at Phase II technologies
[AIAA PAPER 90-2404] p 701 A90-42794
- COOPER, E. E.**
Experimental examination of the aerothermal performance of a gas turbine engine test facility
[ASME PAPER 89-GT-94] p 341 A90-23810
- COOPER, G. K.**
CFD applications in an aerospace engine test facility
[AIAA PAPER 90-2003] p 681 A90-40590
- COOPER, J. E.**
Application of time domain decomposition techniques to aircraft ground and flutter test data p 491 A90-33373
Identification of time varying modal parameters p 536 A90-33375
- COOPER, JAY S.**
Architecture options for GPS/Carousel IV integration p 108 A90-13999
- COOPER, LAURENCE J.**
Reasoning from uncertain data - A BIT enhancement p 457 A90-28330
- COOPER, THOMAS D.**
Proceedings of the 1988 Structural Integrity Program Conference
[AD-A213545] p 275 A90-15486
The role of NDI in the certification of turbine engine components p 777 A90-26349
Proceedings of the 1987 Aircraft/Engine Structural Integrity Program (ASIP/ENSIP) Conference
[AD-A198037] p 842 A90-26807
The role of NDI in the certification of turbine engine components p 859 A90-28069
- COOPER, WILLIAM A.**
Meeting Review: Workshop on Airborne Instrumentation
[PB89-174775] p 39 A90-10032
- Scientific justification and development plan for a mid-sized jet research aircraft
[PB89-208995] p 103 A90-11731
Meeting review: The Second NCAR (National Center for Atmospheric Research) Research Aircraft Fleet Workshop
[PB89-200901] p 137 A90-12113
- COPENHAVER, R. M.**
Thermal stability of jet fuel
[DE90-001160] p 206 A90-14385
- COPENHAVER, RONALD M.**
Thermal stability of jet fuel
[DE90-002760] p 269 A90-15288
- COPENHAVER, W. W.**
Compressor performance tests in the compressor research facility p 427 A90-18428
- COPENHAVER, WILLIAM W.**
Stall cell blockage in a high-speed multistage axial-flow compressor
[AIAA PAPER 90-1913] p 740 A90-42693
- COPENHAVER, WILLIAM WARD**
Stage effects on stalling and recovery of a high-speed 10-stage axial-flow compressor p 115 A90-12600
- COPPENBARGER, RICHARD**
Real-time piloted simulation of fully automatic guidance and control for rotorcraft nap-of-the-earth (NOE) flight following planned profiles
[AIAA PAPER 90-3372] p 864 A90-47630
- COPPER, CHARLES**
Design of cryogenic tanks for launch vehicles p 609 A90-22662
- CORDEN, JOHN L.**
Manufacture of honeycomb p 538 A90-33704
- CORDIER, STEPHANE J.**
Rotating primary flow induction using jet-flapped blades p 48 A90-12585
- CORDIER, STEPHANE JEAN**
Rotary-Jet thrust augmentor with jet-flapped blades p 633 A90-24243
- CORDOVA, J. Q.**
VisualGrid - A software package for interactive grid generation
[AIAA PAPER 90-1607] p 612 A90-38738
- CORKER, KEVIN**
Intelligent situation assessment and response aiding in flight emergencies
[AIAA PAPER 89-2999] p 36 A90-10507
- CORLEY, JACK H.**
A test and maintenance architecture demonstrated on SEM-E modules for fiber optic networks p 458 A90-28342
- CORLISS, LLOYD D.**
RSRA/X-Wing flight control system development - Lessons learned p 430 A90-28216
- CORNELIUS, KENNETH C.**
3-D analysis of laser measurements of vortex bursting on a chined forebody fighter configuration
[AIAA PAPER 90-3020] p 793 A90-45887
An experimental evaluation of slots versus porous strips for laminar-flow applications p 92 A90-12530
- CORREA, S. M.**
Supersonic combustion of hydrogen jets behind a backward-facing step
[AIAA PAPER 90-0204] p 266 A90-22183
Flame extinction in compressible flow p 883 A90-26899
- CORTELLINI, FRANCESCO**
The safety analysis approach for the EH101 p 635 A90-42456
- COSNER, ANDREW A.**
Successful performance development program for the T800-LHT-800 turboshaft engine
[SAE PAPER 891048] p 110 A90-14352
- COSNER, RAYMOND R.**
Computational modeling of inlet hammer shock wave generation
[AIAA PAPER 90-2005] p 621 A90-40592
- COSTA OLIVEIRA, F.**
High-temperature corrosion and mechanical properties of some silicon nitride ceramics p 531 A90-33985
- COSTARD, JEAN**
Magnetic recording on board aircraft p 39 A90-12195
Flight test techniques adopted by Avions Marcel Dassault-Breguet Aviation p 34 A90-10867
- COSTES, J.-J.**
Coupled aerodynamic forces due to unsteady stall on a high-aspect-ratio wing oscillating at high amplitude
[ONERA, TP NO. 1990-24] p 623 A90-41203
- COSTES, M.**
An improved method for the computation of unsteady transonic potential flow - Application for airfoil and blade performance prediction
[ONERA, TP NO. 1989-154] p 4 A90-11175
- COSTILLA, MARCOS**
Interoperability issues in the use of satellite-based navigation systems for civil aviation purposes
[AD-A217279] p 405 A90-19223
- COTON, F. N.**
A review of low Reynolds number aerodynamic research at the University of Glasgow p 800 A90-46367
- COTON, P.**
Study of ground effects on flying scaled models p 922 A90-28532
- COTTON, JOHN C.**
Certification impact of introducing G.P.S. into commercial transport navigation systems p 824 A90-49501
- COTTRELL, CHARLES J.**
Drag reduction by controlling flow separation using stepped afterbodies p 622 A90-40690
- COUCH, B. D.**
A CFD study of precombustion shock-trains from Mach 3-6
[AIAA PAPER 90-2220] p 705 A90-42751
- COUCH, BRIAN P.**
The application of 'PT' resins to high temperature aerospace structures p 949 A90-50230
- COULTON, DAVID G.**
A new data acquisition, display and control system for the ARA transonic wind tunnel p 436 A90-28256
- COUSIN, J. M.**
The BAe (commercial aircraft) LTD transport aircraft synthesis and optimisation program (TASOP)
[AIAA PAPER 90-3295] p 837 A90-48879
- COUSTALAT, R.**
Software maintenance on the Airbus family
[SAE PAPER 892326] p 738 A90-45484
- COUSTEIX, J.**
Computation of the thin-layer Navier-Stokes equations for a 2D flow p 87 A90-16332
Calculation of three-dimensional boundary layers including hypersonic flows p 146 A90-16773
Control and modification of turbulence p 72 A90-10377
European research on viscous flow (EuroVisc)
[NLR-TP-89077-U] p 609 A90-22014
- COUSTOLS, E.**
Control and modification of turbulence p 72 A90-10377
Reduction of turbulent drag: Boundary layer manipulators
[CERT-RSF-OA-74/2259-AYD] p 136 A90-12889
- COUTANCEAU, MADELEINE**
Vortex formation around an oscillating and translating airfoil at large incidences p 303 A90-25588
- COUTS, WILFORD H., JR.**
Thermomechanical processing of superalloys p 531 A90-34156
- COVELL, PETER F.**
Stability characteristics of a conical aerospace plane concept
[SAE PAPER 892313] p 757 A90-45475
Supersonic aerodynamic characteristics of a Mach 3 high-speed civil transport configuration
[AIAA PAPER 90-3210] p 811 A90-48836
- COVERT, EUGENE E.**
On the effects of wind tunnel turbulence on steady and unsteady airfoil characteristics p 147 A90-16777
Unsteady streamlines near the trailing edge of NACA 0012 airfoil at a Reynolds number of 125,000 p 155 A90-18158
Unsteady aerodynamics of Wortmann FX63-137 airfoil at low Reynolds numbers p 801 A90-46374
- COWIN, RICHARD**
Real-time adaptive control of knowledge based avionics tasks p 460 A90-30764
- COWLES, B. A.**
Thermal mechanical fatigue of coated blade materials
[AD-A214258] p 256 A90-15107
- COWLEY, STEPHEN**
On the instability of hypersonic flow past a wedge p 554 A90-35902
- COWLING, D. A.**
Implementation of comprehensive actuation system models in aeroservoelastic analysis p 517 A90-33406
- COWLING, DAVID A.**
The active control of an unstable canard aircraft p 57 A90-10894
- COX, B. N.**
Fatigue crack initiation mechanics of metal aircraft structures
[AD-A210567] p 65 A90-10255
- COX, BRIAN**
Preliminary design of a supersonic short takeoff and vertical landing (STOVL) fighter aircraft
[AIAA PAPER 90-3231] p 834 A90-48844
Preliminary design of a family of three close air support aircraft
[NASA-CR-186070] p 336 A90-16751

- Preliminary design of a supersonic Short Takeoff and Vertical Landing (STOVL) fighter aircraft [NASA-CR-186670] p 649 N90-23394
- COX, G.**
Fire science and aircraft safety p 326 N90-17596
- COX, M. E.**
Tests of automatic dependent surveillance (ADS) in Western Europe - Possible future developments p 574 A90-35353
- COX, R. A.**
Navier-Stokes solutions of 2-D transonic flow over unconventional airfoils p 173 N90-14195
- COX, R. P.**
The Radarsat system p 873 A90-49671
- COX, RICHARD E.**
Managing man-in-the-loop simulations [SAE PAPER 892355] p 761 A90-45506
- COX, TIMOTHY H.**
A design procedure for the handling qualities optimization of the X-29A aircraft [NASA-TM-4142] p 119 N90-11753
- COY, JOHN J.**
Gear noise, vibration, and diagnostic studies at NASA Lewis Research Center [NASA-TM-102435] p 372 N90-18041
- COYNE, FRANCIS J.**
FAA Loran early implementation project [AD-A221866] p 824 N90-26805
- CRABILL, MONTY**
Air Force Boom Event Analyzer Recorder (BEAR): System description [AD-A218048] p 548 N90-20800
- CRABILL, NORMAN L.**
The NASA digital VGH program: Exploration of methods and final results. Volume 2: L 1011 data 1978-1979: 1619 hours [NASA-CR-181909-VOL-2] p 505 N90-20080
The NASA digital VGH program: Exploration of methods and final results. Volume 1: Development of methods [NASA-CR-181909-VOL-1] p 505 N90-20081
The NASA digital VGH program: Exploration of methods and final results. Volume 3: B 727 data 1978-1980: 1765 hours [NASA-CR-181909-VOL-3] p 505 N90-20082
The NASA digital VGH program: Exploration of methods and final results. Volume 4: B 747 data 1978-1980, 1689 hours [NASA-CR-181909-VOL-4] p 506 N90-20083
The NASA digital VGH program: Exploration of methods and final results. Volume 5: DC 10 data 1981-1982, 129 hours [NASA-CR-181909-VOL-5] p 506 N90-20084
- CRAMER, MICHAEL**
Intelligent situation assessment and response aiding in flight emergencies [AIAA PAPER 89-2999] p 36 A90-10507
- CRANE, PETER M.**
Dynamic FLIR simulation in flight training research p 681 A90-40109
- CRAUBNER, S.**
An infrared camera system for detection of boundary layer transition in the ETW p 539 A90-34249
- CRAW, JAMES M.**
Effective use of Cray supercomputers p 546 A90-34436
- CRAWFORD, CHARLES C., JR.**
Rotorcraft analytical improvement needed to reduce developmental risk - The 1989 Alexander A. Nikolsky Lecture p 285 A90-23934
- CRAWFORD, D. R.**
Generalized Advanced Propeller Analysis System (GAPAS). Volume 2: Computer program user manual [NASA-CR-185277] p 933 N90-29394
- CRAWFORD, DANIEL J.**
Real-time simulation clock [NASA-CASE-LAR-14056-1] p 689 N90-23713
- CRAWFORD, MARK R.**
The Air Force Flight Test Center Flight Test Safety Program p 35 N90-10872
- CRAWFORD, R. A.**
Performance potential and technology issues of MHD augmented hypersonic simulation facilities [AIAA PAPER 90-1380] p 598 A90-37929
- CRAWFORD, ROGER A.**
Influence of bulk turbulence and entrance boundary layer thickness on the curved duct flow field [AIAA PAPER 90-1502] p 806 A90-38651
- CRAWLEY, EDWARD F.**
Calculation of unsteady Euler flows in turbomachinery using the linearized Euler equations p 5 A90-11778
- CREAMER, PAUL M.**
GPSNOTAM - A demonstration system for GPS status notification p 728 A90-45238
- CREASMAN, S. F.**
An evaluation of Euler solvers for transonic flowfield computations on wing-fuselage geometries [AIAA PAPER 90-3015] p 798 A90-45935
- CREDEUR, LEONARD**
Delivery performance of conventional aircraft by terminal-area, time-based air traffic control: A real-time simulation evaluation [NASA-TP-2978] p 404 N90-18378
- CREEDON, JOHN F.**
Ceramic materials and coatings for future aerospace applications - Challenge of the 1990's p 942 A90-50071
- CREEK, ROBERT J.**
Manufacturing aviation gasoline p 950 A90-51617
- CREEK, ROGER S.**
The RB211-535E4 - A commercially proven engine for the military of tomorrow [SAE PAPER 892364] p 748 A90-45513
- CREEL, THEODORE R., JR.**
The effects of wall surface defects on boundary-layer transition in quiet and noisy supersonic flow p 94 N90-12556
Experimental and theoretical investigation of boundary-layer instability mechanisms on a swept leading edge at Mach 3.5 p 94 N90-12557
- CREISMEAS, PAUL**
Icing test techniques for air intake screens on helicopters functioning in temperatures around 0 C p 23 A90-12619
- CRISPI, PIERRE H.**
The development of a 3-D laser velocimeter for the NASA Langley low turbulence pressure wind tunnel [AIAA PAPER 90-1385] p 597 A90-38484
- CRITTENDEN, LORRI J.**
Considerations of noise for the use of compressed speech in a cockpit environment p 404 A90-31334
- CROCKER, SANDRA C.**
Range obscuration mitigation by adaptive PRF selection for the TDWR system p 456 A90-28617
- CRONKHITE, JAMES D.**
Experiences in NASTRAN airframe vibration prediction at Bell Helicopter Textron p 832 A90-46964
- CROOKS, R. S.**
Development of an X-ray backscatter densitometer for measurement of freestream density during hypersonic flight [AIAA PAPER 90-1384] p 604 A90-37933
- CROSS, ALVIN**
Captive carry testing of remotely piloted vehicles p 828 A90-46386
- CROSS, C. J.**
Metal matrix composites structural design experience [AIAA PAPER 90-2175] p 677 A90-42059
- CROSS, GUY M.**
A waveform alignment approach to positioning airborne radar-sounding data p 332 A90-26651
- CROSS, JEFFREY**
Helicopter Airborne Laser Positioning System (HALPS) [NASA-TM-102814] p 654 N90-23399
- CROWDER, JAMES P.**
Flow visualization in flight testing [AIAA PAPER 90-1273] p 496 A90-34148
Infrared cameras for detection of boundary layer transition in transonic and subsonic wind tunnels [AIAA PAPER 90-1450] p 606 A90-38610
- CROWTHER, T.**
Boeing 727-100 test project (high energy radiated field tests) [DOT/FAA/CT-88/33] p 542 N90-21247
- CUCCIO, J.**
Development of impact design methods for ceramic gas turbine components [AIAA PAPER 90-2413] p 687 A90-42165
- CUCCIO, JOHN S.**
Probabilistic design technology for ceramic components p 601 A90-35507
- CUESTA ALVAREZ, MARTIN**
Gas turbine engines for combat aviation - Current realities and perspectives for the near future p 584 A90-35513
- CUI, JINHUI**
Mach number effects on upstream influence in swept shock wave/turbulent boundary layer interactions p 556 A90-38415
- CUI, JIYA**
Basic principles of measuring thrust through exhaust to inlet total pressure ratio - Engine Pressure Ratio (EPR) p 191 A90-18635
- CUI, PINGYUAN**
An orthogonal algorithm to the maximum likelihood estimation using an efficient method for computing sensitivities [AIAA PAPER 90-3507] p 891 A90-47753
- CUI, ZHENYUAN**
The investigation of stress at an enter-gas nozzle of main landing gears for fighter aeroplanes p 181 A90-18606
- CULICK, F. E. C.**
Combustion instabilities in liquid-fueled propulsion systems: An overview p 63 N90-10192
- CULICK, FRED E. C.**
Application of dynamical systems theory to the high angle of attack dynamics of the F-14 [AIAA PAPER 90-0221] p 257 A90-22184
- CULLEN, DAVID C.**
The trend in navais inspection is to automatic operation p 329 A90-25495
- CULSHAW, BRIAN**
Applications of fiber optic sensors in the aerospace and marine industries p 603 A90-36782
- CUMMINGS, RUSSELL M.**
Numerical simulation of separated and vortical flows on bodies at large angles of attack p 146 A90-16772
Pneumatic vortical flow control at high angles of attack [AIAA PAPER 90-0098] p 227 A90-22164
Navier-Stokes predictions of the flowfield around the F-18 (HARV) wing and fuselage at large incidence [AIAA PAPER 90-0099] p 227 A90-22165
The effect of turbulence models on the numerical prediction of the flowfield about a prolate spheroid at high angle of attack [AIAA PAPER 90-3106] p 789 A90-45855
- CUMSTY, N. A.**
Compressor blade boundary layers. II - Measurements with incident wakes [ASME PAPER 89-GT-51] p 289 A90-23777
Stall inception in axial compressors [ASME PAPER 89-GT-63] p 290 A90-23786
Compressor aerodynamics p 706 A90-44052
A method for the prediction of supersonic compressor blade performance [CUD/A-TURBO/TR-126] p 344 N90-17634
- CUNAT, D.**
Pressure surface trailing edge slot cooling [ONERA, TP NO. 1989-123] p 47 A90-12569
- CUNLIFFE, F. R., III**
Automating and controlling dry paint stripping [SAE PAPER 890939] p 365 A90-24702
- CUNNINGHAM, A. M., JR.**
Low-speed unsteady aerodynamics of a pitching straked wing at high incidence. I - Test program. II - Harmonic analysis p 159 A90-19387
- CUNNINGHAM, ATLEE M., JR.**
A critique of the experimental aerodynamic data base for an oscillating straked wing at high angles p 147 A90-16779
Practical problems - Airplanes p 394 A90-29885
Steady and unsteady force testing of fighter aircraft models in a water tunnel [AIAA PAPER 90-2815] p 711 A90-45155
- CUNNINGHAM, JOSEPH R.**
Dynamic interaction of separate INS/GPS Kalman filters (Filter-driving - Filter dynamics) p 124 A90-13996
- CURA, FRANCESCA M.**
Flutter analysis on a non-linear wing model p 207 A90-17009
- CURLISS, DAVID B.**
The effect of jet fuel absorption on advanced aerospace thermoset and thermoplastic composites p 942 A90-50082
- CURRAN, PAUL J.**
Airborne MSS for land cover classification II p 737 A90-43376
- CURRY, ROBERT E.**
A smoke generator system for aerodynamic flight research [NASA-TM-4137] p 183 N90-13372
An in-flight investigation of ground effect on a forward-swept wing airplane [NASA-TM-101708] p 175 N90-14202
Flight evaluation of a pneumatic system for unsteady pressure measurements using conventional sensors [NASA-TM-4131] p 186 N90-14225
Experimental characterization of the effects of pneumatic tubing on unsteady pressure measurements [NASA-TM-4171] p 850 N90-27703
An in-flight investigation of ground effect on a forward-swept wing airplane p 822 N90-28533
- CURTIN, M. M.**
TRANAIR applications to engine/airframe integration p 838 A90-48958
- CURTISS, H. C.**
An experiment study of rotor aerodynamic in ground effect at low speed p 149 A90-16826
- CURTISS, H. C., JR.**
Influence of ground effect on helicopter takeoff and landing performance p 645 A90-42278

- Influence of ground effect on helicopter takeoff and landing performance p 646 A90-42468
Coupled rotor-body equations of motion hover flight [NASA-CR-186130] p 717 N90-25111
- CURTIS, HOWARD C., JR.**
A modern course in aeroelasticity (2nd revised and enlarged edition) p 497 A90-34968
- CURZIO, E. LARA**
High temperature deformation studies on CVD silicon carbide fibers p 945 A90-50147
- CUSCHIERI, J. M.**
Mobility power flow analysis of an L-shaped plate structure subjected to acoustic excitation [NASA-CR-186130] p 214 N90-13817
- CUSHMAN, ARTHUR**
Feasibility of using frequency offset on very high frequency air/ground voice channels [DOT/FAA/CT-TN89/71] p 542 N90-21248
- CUSWORTH, R. A.**
An experimental investigation of the velocity field in a reverse-flow combustor p 739 A90-42657
- CUTLER, A. D.**
Interaction between strong longitudinal vortices and turbulent boundary layers p 145 A90-16764
- CZAJKOWSKI, G.**
Production of jet fuels from coal-derived liquids. Volume 11: Production of advanced endothermic fuel blends from Great Plains Gasification Plant naphtha by-product stream [AD-A210251] p 65 N90-11184
- CZERWINSKI, ZBIGNIEW**
A statistical model of helicopter noise p 77 A90-10229
- D**
- D'AZZO, JOHN J.**
Multivariable control design for the control reconfigurable combat aircraft (CRCA) p 432 A90-30715
- D'EMILIA, G.**
Comparison among modal analyses of axial compressor blade using experimental data of different measuring systems p 878 A90-46038
- D'URSO, STEVEN J.**
Configuring tactical aircraft [AIAA PAPER 90-3305] p 837 A90-48886
- D'VARI, RON**
A nonlinear transient formulation of UHB aeroelastic response and stability. I - Theoretical formulation [SAE PAPER 892322] p 715 A90-45481
- DABBENE, DANILO**
Expert system for pilot assistance - The challenge of an intensive prototyping p 693 A90-38909
Expert system for pilot assistance: The challenge of an intensive prototyping [ETN-90-97274] p 825 N90-27674
- DADONE, ANDREA**
Computation of steady three dimensional transonic internal flows p 304 A90-25771
- DADONE, LEO**
The prediction of loads on the Boeing Helicopters Model 360 rotor p 410 A90-28240
- DAFNIS, A.**
The effect of winglets on aircraft wing flutter p 473 A90-33411
- DAGENHART, J. RAY**
Experiments in swept-wing transition p 149 A90-16794
The development of crossflow vortices on a 45 degree swept wing [SAE PAPER 892245] p 713 A90-45452
Goertler instability on an airfoil: Comparison of marching solution with experimental observations p 19 N90-10364
Goertler instability on an airfoil p 91 N90-12517
Predicted and hot-film measured Tollmien-Schlichting wave characteristics p 91 N90-12523
Experimental studies on Goertler vortices p 91 N90-12529
Boundary-layer stability analysis of Langley Research Center 8-foot LFC experimental data p 92 N90-12532
- DAHL, M. D.**
Some observations on transitory stall in conical diffusers [NASA-TM-102387] p 94 N90-12561
- DAHL, MILO D.**
Comparison between design and installed acoustic characteristics of NASA Lewis 9- by 15-foot low-speed wind tunnel acoustic treatment [NASA-TP-2996] p 440 N90-18242
- DAHLEN, HELMUT**
Acoustics of ultralight airplanes p 643 A90-40685
A new noise certification method for 'light propeller aircraft' in testing p 635 A90-41728
- DAI, DEPEI**
Vibration analysis of aircraft panels p 207 A90-17026
- DAI, GUANZHONG**
A design method for real-time computer control hydraulic force system p 590 A90-36434
- DAIGUJI, H.**
Numerical methods for transonic cascade flow problems p 305 A90-25796
A numerical method for solving the unsteady compressible Navier-Stokes equations p 306 A90-25827
- DAILEY, KATHLEEN B.**
AIRPLANE - Experiences, benchmarks and improvements [AIAA PAPER 90-2998] p 787 A90-45848
- DAILEY, SANDRA J.**
The evolution of built-in test for an electrical power generating system (EPGS) p 424 A90-30699
- DAILY, JOHN W.**
Numerical modeling of a flame in a confined, unstable shear layer [AIAA PAPER 90-0647] p 205 A90-19966
Entropy wave instability in compact ramjets p 858 N90-27932
- DALEY, DOUG E.**
Strike tolerant main rotor blade tip p 409 A90-28232
- DALLMANN, U.**
Flow over a leading edge with distributed roughness p 703 A90-42646
- DALLMANN, UWE**
Generalized similarity solutions for three dimensional, laminar, steady, compressible boundary layer flows on swept profile cylinders [DLR-FB-89-34] p 212 N90-13725
- DAMBRINE, BRUNO**
Designing turbine blades for fatigue and creep p 112 A90-16007
- DANBY, CLIVE M.**
Microprocessor control of a vapor-cycle cooling system [SAE PAPER 891457] p 339 A90-27426
- DANCEY, CLINTON L.**
Three-component LDA measurements in an axial-flow compressor p 683 A90-40943
- DANCEY, R. D.**
Software fault tolerance analysis and testing for the Advanced Automation System [AIAA PAPER 89-3124] p 75 A90-10600
- DANCEY, ROBERT D.**
Advanced Automation System design p 375 A90-25566
- DANEK, VLADIMIR**
The application of the discrete vortex method in aircraft design p 257 A90-23357
- DANG, T. Q.**
Simulations of propeller/airframe interference effects using an Euler correction method p 31 A90-13019
Calculations of propeller/airframe interference effects using the potential/multienergy flow method p 490 A90-32452
- DANIEL, JOHN G. B.**
Individual Helicopter Tracking Program (IHTP) for the MH-53J helicopter p 843 N90-26818
- DANIELS, W. A.**
Aerodynamic and torque characteristics of enclosed Co/counter rotating disks [ASME PAPER 89-GT-177] p 361 A90-23858
- DANIELSON, ARNOLD O.**
Inverse heat transfer studies and the effects of propellant aluminum on TVC jet vane heating and erosion [AIAA PAPER 90-1860] p 655 A90-40533
- DANILOVA, Z. K.**
A method for calculating the stiffness characteristics of large-aspect-ratio wings with anisotropic panels in accordance with strength and aileron efficiency requirements p 334 A90-24161
Effect of structural anisotropy on the dynamic characteristics of the wing and critical flutter speed p 386 A90-28985
- DANNENHOFFER, JOHN F., III**
A comparison of two adaptive grid techniques p 309 A90-26507
A comparison of adaptive-grid redistribution and embedding for steady transonic flows [AIAA PAPER 90-1565] p 565 A90-38704
- DANSBERRY, BRYAN E.**
An experimental study of tip shape effects on the flutter of aft-swept, flat-plate wings [NASA-TM-4180] p 582 N90-22555
- DANZEY, GERALD A.**
Attachment of lead wires to thin film thermocouples mounted on high temperature materials using the parallel gap welding process [NASA-TM-102442] p 543 N90-21361
- DARDEN, CHRISTINE M.**
A study of the limitations of linear theory methods as applied to sonic boom calculations [AIAA PAPER 90-0368] p 219 A90-19817
Validation of a computer code for analysis of subsonic aerodynamic performance of wings with flaps in combination with a canard or horizontal tail and an application to optimization [NASA-TP-2961] p 173 N90-14187
- DARGEL, G.**
Calculation of the flap profile flows with separation based on coupled potential and boundary layer solutions p 278 N90-16191
- DARGI, MICHAEL M.**
The behavior of electric currents in graphite/epoxy structures p 883 A90-49846
- DARGUE, JIM**
Simulation of MLS-ATC procedures in the New York and San Francisco Terminal Control Areas [SAE PAPER 892217] p 728 A90-45434
- DARIAN, ARMEN**
Analysis of shock interactions and flow structure in high speed inlets [AIAA PAPER 90-2132] p 704 A90-42735
- DARLINGTON, RALPH**
Unique methodology used in the Bell-Boeing V-22 main landing gear landing loads analysis and drop tests p 409 A90-28236
- DARRAH, PAUL**
Preliminary design of a family of three close air support aircraft [NASA-CR-186070] p 336 N90-16751
- DARYABEIGI, KAMRAN**
Aerodynamic applications of infrared thermography p 770 A90-44147
- DARYMOV, IURII P.**
Air traffic control p 638 A90-39581
Organization of air traffic control p 915 A90-52415
- DAS, A.**
Numerical simulation of vortical flows over close-coupled canard-wing configuration [AIAA PAPER 90-3003] p 788 A90-45852
- DAS, A. K.**
In process failure investigations in aeronautics p 181 A90-18489
- DASGUPTA, A.**
Studies on the influence of Mach number on profile losses of a reaction turbine cascade p 10 A90-12517
- DASO, ENDWELL O.**
Analysis of shock interactions and flow structure in high speed inlets [AIAA PAPER 90-2132] p 704 A90-42735
- DASS, THEODORE C., III**
Phase III GPS Manpack receiver operation and navigation performance p 823 A90-49497
- DAU, K.**
A strong viscous-inviscid interaction method for computing unsteady transonic airloads for use in aeroelasticity p 471 A90-33355
- DAUDPOTA, Q. ISA**
A review of instability and noise propagation in supersonic flows [NASA-CR-186800] p 717 N90-25112
- DAUMIT, G. P.**
Domestic precursor technology - A unique route to current and future generation carbon fibers p 940 A90-50057
- DAUSMAN, GEORGE E.**
The LTV XC-142 experimental aircraft lessons learned [AIAA PAPER 90-3204] p 838 A90-49104
- DAVADANT, JACQUES PAUL**
Computerized MLS flight inspection system developed p 823 A90-48983
- DAVIDOVICH, T. V.**
Vertical wind shears in lower-level jet stream over some airfields in the Urals and Siberia p 888 A90-48362
- DAVIDSON, C. J.**
Further work on aerofoils at Reynolds numbers between 3 x 10 to the 5th and 1 x 10 to the 6th p 145 A90-16758
- DAVIDSON, PHILIPPE**
Jet Engine Technical Advisor (JETA) p 693 A90-41184
- DAVIDSON, R.**
Aerosol effects on jet-engine IR radiation p 40 A90-10152
A multichannel wide FOV infrared radiometric system p 67 A90-11410
- DAVIES, C.**
Application of a self-adaptive grid method to complex flows [NASA-TM-102223] p 143 N90-13324
- DAVIES, CURTIS R.**
Certification of composites for commercial aircraft [SAE PAPER 892212] p 772 A90-45430

DAVIES, D. P.

DAVIES, D. P.

Gear steels for future helicopter transmissions
p 265 A90-20607

DAVIES, G. A. O.

The strength and weakness of carbon composite structures p 180 A90-17679
Torsional buckling and post-buckling of composite geodetic cylinders with special reference to joint flexibility p 878 A90-45971

DAVIES, P. N. H.

Multiple impact jet apparatus (MIJA) - Application to rain erosion studies p 525 A90-34580

DAVIS, BYRON A.

Aluminum-lithium: Application of plate and sheet to fighter aircraft p 268 N90-15202

DAVIS, DONALD Y.

Energy Efficient Engine: Flight propulsion system final design and analysis
[NASA-CR-168219] p 930 N90-28558

DAVIS, JAMES

Communications Interface Driver (CID) test plan
[DOT/FAA/CT-TN89/35] p 958 N90-28762

DAVIS, JAMES ARTHUR

Acoustic-vortical-combustion interaction in a solid fuel ramjet simulator p 194 N90-14234

DAVIS, M. H. A.

An image analysis method for vehicle stabilization p 668 A90-40914

DAVIS, PATRICK J.

Wind tunnel results of the low-speed NLF(1)-0414F airfoil p 93 N90-12541

DAVIS, R. A.

A practical co-axial twin rotor model p 335 A90-25423

DAVIS, RICHARD E.

Performance of laminar-flow leading-edge test articles in cloud encounters p 104 N90-12511

DAVIS, ROGER L.

Unsteady analysis of hot streak migration in a turbine stage
[AIAA PAPER 90-2354] p 769 A90-42782

DAVIS, S. J.

Laser induced fluorescence: Practical applications p 911 N90-29323

DAVIS, THOMAS J.

Design of a final approach spacing tool for TRACON air traffic control
[NASA-TM-102229] p 24 N90-10841
Piloted simulation of a ground-based time-control concept for air traffic control
[NASA-TM-101085] p 240 N90-15898
Simulator evaluation of the final approach spacing tool
[NASA-TM-102807] p 636 N90-23374

DAVIS, W. H.

Hypersonic forebody lift-induced drag
[SAE PAPER 892345] p 715 A90-45497
Numerical study of asymmetric air injection to control high angle-of-attack forebody vortices on the X-29 aircraft
[AIAA PAPER 90-3004] p 788 A90-45853
The role of CFD applied to high performance aircraft
[AIAA PAPER 90-3071] p 796 A90-45917

DAVIS, W. J.

Modeling flexible aircraft for flight control design
[AD-A219123] p 757 N90-25140

DAVIS, WILLIAM T.

Device for quickly sensing the amount of O₂ in a combustion product gas
[NASA-CASE-LAR-13816-1] p 609 N90-22025

DAVOUDZADEH, F.

Navier-Stokes study of rotating stall in compressor cascades p 302 A90-25292

DAVYDOV, PAVEL S.

Radar systems of aircraft p 26 A90-10841
Operation of aviation radio and electronic equipment (Handbook) p 914 A90-50747

DAWES, W. N.

The extension and application of three-dimensional time marching analyses to incompressible turbomachinery flows
[ASME PAPER 89-GT-212] p 283 A90-23878

DAWES, WILLIAM N.

A solution adaptive finite element method applied to two-dimensional unsteady viscous compressible cascade flow p 15 A90-12624

DAWHITFIELD, Q.

Aircraft cabin fire suppression by means of an interior water spray system
[CAA-PAPER-88014] p 96 N90-11719

DAWICK, D. S.

An evaluation of the pressure proof test concept for thin sheet 2024-T3
[NASA-TM-101675] p 543 N90-21424

DAWSON, G.

The repair of aircraft integral fuel tanks in the RAF: A user's view of fuel tank technology p 250 N90-15908

DAWSON, SETH

HARP model rotor test at the DNW p 406 A90-28167

DAY, A. J.

A computer aided manufacturing procedure for experimental two-dimensional aerofoils p 270 A90-20609

DAY, J.

The effect of primer age on adhesion of polysulphide sealant p 269 N90-15909

DAY, RICHARD W.

Passive location accuracy via a general covariance error model p 914 A90-51060

DAYTON, RONALD B.

Flight demonstration of two and three satellite navigation p 98 A90-13994
A flight test comparison of two GPS/INS integration approaches p 726 A90-43708

DE ABREU-GARCIA, J. ALEX

The determination of third order linear models from a seventh order nonlinear jet engine model p 964 A90-52881

DE BOER, E.

VISTRAFS - A simulation method for strongly-interacting viscous transonic flow p 144 A90-16756

DE BRUIN, A. C.

Comparison with experiment of various computational methods of airflow on three helicopter fuselages p 630 A90-42436

DE HOFF, RONALD L.

The application of an expert maintenance and diagnostic tool to aircraft engines
[AIAA PAPER 90-2036] p 657 A90-40605

DE JONG, FREDERIK J.

Hypersonic flow calculations with a hybrid Navier-Stokes/Monte Carlo method
[AIAA PAPER 90-1691] p 560 A90-38394

DE JONGE, J. B.

Assessment of service load experience p 901 A90-49877

DE LEEUW, J. H.

The application of linear maximum likelihood estimation of aerodynamic derivatives for the Bell-205 and Bell-206 p 30 A90-12773

DE LUCA, L.

Boundary layer diagnostics by means of an infrared scanning radiometer p 605 A90-38493

DE LUCCIA, J. J.

Materials pace aerospace technology p 203 A90-17298

DE MATTEIS, GUIDO

Effects of random initial conditions and deterministic winds on simulated parachute motion p 22 A90-11002

DE MATTEIS, P.

Numerical prediction of transonic viscous flows around airfoils through an Euler/boundary layer interaction method
[AIAA PAPER 90-1537] p 564 A90-38681

Wake effects on the prediction of transonic viscous flows around airfoils with an Euler/boundary layer interaction approach
[AIAA PAPER 90-3061] p 798 A90-45933

DE NICOLA, CARLO

Prediction of aerodynamic performance of airfoils in low Reynolds number flows p 799 A90-46360

DE OLIVEIRA, M. C. F.

Implementation of a transputer-based flight controller p 667 A90-38966

DE SAINT-VICTOR, X.

Experimental study of the flow around an helicopter fuselage - Comparison with three-dimensional boundary layer calculations p 630 A90-42438

DE SOCIO, LUCIANO M.

Effects of random initial conditions and deterministic winds on simulated parachute motion p 22 A90-11002

DE WILDE, J. P.

Heat transfer in a solid fuel ramjet combustor
[AIAA PAPER 90-1783] p 586 A90-38472

DE WITT, KENNETH J.

Development of an anti-icing runback model
[AIAA PAPER 90-0759] p 238 A90-22258

DEAN, P. D.

Fiber optic sensor systems for smart aerospace structures p 38 A90-11208

DEAN, RICHARD K.

Real-time test data processing system p 458 A90-28860

DEAN, S. J.

An array-fed reflector antenna with built-in calibration facility p 402 A90-27781

DEAN, WALTER N.

Equipment and capability trends in Loran-C RNAV p 576 A90-36918

DEATON, JOHN E.

The effect of windscreen bows and HUD pitch ladder on pilot performance during simulated flight p 420 A90-31333

DEBELLIS, WILLIAM B.

Interaction of switch actuation on tracking with a four-axis flight control (cross-coupling)
[AD-A217981] p 520 N90-20095
Counterair situation awareness display for Army aviation p 964 N90-28982

DEBURE, KELLY R.

Advanced transport operating system software upgrade: Flight management/flight controls software description
[NASA-CR-181936] p 893 N90-28366

DECASTRO, EMORY S.

A reliable, maintenance-free oxygen sensor for aircraft using an oxygen-sensitive coating on potentiometric electrodes
[AD-A222696] p 927 N90-28545

DECKER, FRIEDHELM

Application of vortex embedding to aircraft flows
[AIAA PAPER 90-1626] p 568 A90-38755

DECKER, W. A.

Ground-simulation investigations of VTOL airworthiness criteria for terminal-area operations
[NASA-TM-102810] p 757 N90-25141

DECKER, WILLIAM

Software Management Environment (SME) concepts and architecture
[NASA-TM-103306] p 547 N90-21543

DECKERT, W. H.

Powered-lift aircraft technology
[NASA-SP-501] p 107 N90-12589

DECONINCK, H.

Solution of the Euler equations using unstructured polygonal meshes p 708 A90-44435

DECRUYENAEDE, JEAN-PAUL

A sensor stabilization/tracking system for unmanned air vehicles
[AD-A224008] p 936 N90-28579

DEDEK, JINDRICH

Flight-mechanics tasks in solving problems of active control p 257 A90-23358

DEDOES, D.

Integrated navigation system design and performance with Phase III GPS user equipment p 98 A90-13997

DEGANI, D.

Experimental study of nonsteady asymmetric flow around an ogive-cylinder at incidence p 384 A90-27985

DEGANI, DAVID

Numerical simulation of separated and vortical flows on bodies at large angles of attack p 146 A90-16772
Analytical study of the origin and behavior of asymmetric vortices
[NASA-TM-102796] p 573 N90-21746

DEGEORGE, C. L.

Large-scale Advanced Prop-fan (LAP) technology assessment report
[NASA-CR-182142] p 53 N90-10046

DEGEORGE, CHARLES L.

Large-scale Advanced Prop-fan (LAP) static rotor test report
[NASA-CR-180848] p 117 N90-12617

DEGTIAREV, G. L.

Synthesis of locally optimal aircraft control in the presence of delay p 137 A90-14561

DEHAAN, MARK A.

Induced drag of wings with highly swept and tapered wing tips
[AIAA PAPER 90-3062] p 794 A90-45896

DEHN, JON D.

Advanced Automation System design p 375 A90-25566

DEHOFF, RONALD

Expert system diagnostics and parts life tracking as applied to the AV-8B aircraft for the USMC p 884 N90-27629

DEHONDT, D.

Numerical simulation of turbomachinery flows with a simple model of viscous effects - Comparison with experimental data
[ONERA, TP NO. 1989-122] p 10 A90-12510

DEIWERT, G. S.

Application of a self-adaptive grid method to complex flows
[NASA-TM-102223] p 143 N90-13324

DEIWERT, GEORGE S.

Computational aerothermodynamics p 476 A90-34380

DEJARNETTE, F. R.

Experimental investigation of a new device to control the asymmetric flowfield on forebodies at large angles of attack
[AIAA PAPER 90-0069] p 161 A90-19665

- DEJARNETTE, FRED R.**
An approximate method for calculating three-dimensional inviscid hypersonic flow fields [NASA-TP-3018] p 883 N90-27066
- DEJONG, A. N.**
Description of the MARC measuring system [FEL-89-B170] p 863 N90-28887
- DEJONG, W. G.**
Study improvement training facilities ground control air traffic controllers. Part 1: Alternative solutions and their consequences [FEL-89-A257-PT-1] p 919 N90-29380
Study improvement training facilities ground control air traffic controllers. Part 2: Functional analysis approach control trainer [FEL-89-A280-PT-2] p 939 N90-29409
- DEL FRATE, JOHN H.**
In-flight flow field analysis on the NASA F-18 high alpha research vehicle with comparisons to ground facility data [AIAA PAPER 90-0231] p 163 A90-19745
In-flight flow visualization characteristics of the NASA F-18 high alpha research vehicle at high angles of attack [SAE PAPER 892222] p 713 A90-45439
- DEL GUIDICE, P.**
Hybrid finite volume approach to Euler solutions for supersonic flows p 154 A90-18144
- DELAAT, JOHN C.**
A real time microcomputer implementation of sensor failure detection for turbofan engines p 745 A90-45414
Advanced detection, isolation, and accommodation of sensor failures in turbofan engines: Real-time microcomputer implementation. [NASA-TP-2925] p 259 N90-15112
- DELAMASANTIERE, CLAUDE**
Starter systems and auxiliary power units p 660 A90-41760
- DELANEUVILLE, R. E.**
The development of a probabilistic turbine rotor design system [AIAA PAPER 90-2176] p 662 A90-42060
- DELANEY, R. A.**
Investigation of unsteady flow through transonic turbine stage. I - Analysis [AIAA PAPER 90-2408] p 626 A90-42161
Investigation of unsteady flow through a transonic turbine stage. II - Data/prediction comparison for time-averaged and phase-resolved pressure data [AIAA PAPER 90-2409] p 626 A90-42162
Simulation of time-dependent viscous flows using central and upwind-biased finite-difference techniques [AIAA PAPER 90-3012] p 790 A90-45864
Analysis of three-dimensional turbomachinery flows on C-type grids using an implicit Euler solver [ASME PAPER 89-GT-85] p 905 A90-51258
- DELANEY, ROBERT A.**
3D Euler analysis of ducted propfan flowfields [AIAA PAPER 90-3034] p 791 A90-45873
- DELANNOY, A.**
Electrostatic field conditions on an aircraft stricken by lightning [ONERA, TP NO. 1989-148] p 23 A90-11170
Electrostatic description of a positive leader ignition from an aircraft [ONERA, TP NO. 1989-149] p 23 A90-11171
- DELAUNAY, C.**
New metallic felts with improved resistance to high temperature oxidation [ONERA, TP NO. 1989-210] p 366 A90-25343
- DELAURIER, JAMES**
Simple marching-vortex model for two-dimensional unsteady aerodynamics p 395 A90-31288
- DELAURIER, JAMES D.**
An experimental study of low-speed single-surface airfoils with faired leading edges p 801 A90-46371
- DELCLOPEZ, MARIA**
Software and hardware description of the helicopter motion equations for VAX computers [AD-A213248] p 184 N90-13375
- DELCOCO, R.**
Categorization and performance analysis of advanced avionics algorithms on parallel processing architectures p 461 A90-30786
- DELFRATE, JOHN H.**
In-flight flow visualization with pressure measurements at low speeds on the NASA F-18 high alpha research vehicle [NASA-TM-101726] p 910 N90-28505
- DELISI, J. W.**
F-15E/GE-129 Increased Performance Engine initial development flight test program [AIAA PAPER 90-1266] p 509 A90-33894
- DELLICKER, SCOTT H.**
F-16/GPS integration test results p 726 A90-43710
- DELPASSAND, MAJID**
A heat transfer analysis for rough turbine airfoils [AD-A221842] p 854 N90-26831
- DELPECH, P.**
The application of infrared thermography to the measurement of heat fluxes in a wind tunnel [ONERA, TP NO. 1989-192] p 261 A90-21051
Determination of convective transfer coefficients on a wind-tunnel model by stimulated infrared thermography [ONERA, TP NO. 1989-218] p 351 A90-25351
- DELUCIA, R. A.**
Statistics on aircraft gas turbine engine rotor failures that occurred in US commercial aviation during 1986 [DOT/FAA/CT-89/30] p 511 N90-21008
- DEMAEL, JACQUES J.**
On the generation of a variable structure airport surface traffic control system [AD-A211306] p 99 N90-11724
- DEMASI, JEANINE T.**
Thermal barrier coating life prediction model development, phase 1 [NASA-CR-182230] p 193 N90-13388
- DEMATTEIS, P. P.**
A computer code for the prediction of aerodynamic characteristics of lifting airfoils at transonic speed [DLC-EST-TN-030] p 632 N90-23359
- DEMEIS, RICHARD**
The Soviets' French revelation. II - Aircraft p 81 A90-14800
Innovation in general aviation p 81 A90-14997
Many means to NASP p 285 A90-23917
Sukhoi and Gulfstream go supersonic p 383 A90-31247
New light on wind tunnel lasers p 439 A90-31248
- DEMENT'EV, P. P.**
Fundamentals of the design and development of parts and mechanisms for flight vehicles p 414 A90-30275
- DEMMELE, JOHANN**
The signals of an ice warning device in dependence on total water content and normalized icing degree [ESA-TT-1207] p 963 N90-29692
- DEMOL, RENE**
The application of infrared thermography to the nondestructive testing of composite materials p 886 N90-28084
- DEMOTT, LARRY R.**
The T800-LHT-800 engine - Designed for supportability p 585 A90-35773
- DEMPSEY, BARRY J.**
Airport pavement drainage [DOT/FAA/RD-90/24] p 872 N90-27728
- DEMPSEY, RAY L.**
Damage tolerance evaluation of several elevated temperature graphite composite materials p 945 A90-50155
- DEMURIE, F.**
High Reynolds number tests of the CAST-10-2/DOA 2 transonic airfoil at ambient and cryogenic temperature conditions p 320 N90-17650
- DEN BOER, R. G.**
Low-speed unsteady aerodynamics of a pitching straked wing at high incidence. I - Test program. II - Harmonic analysis p 159 A90-19387
- DENG, G. B.**
Navier-Stokes computations of vortical flows [AIAA PAPER 90-1628] p 568 A90-38757
- DENG, HUAYU**
Design and calculation of composite air-cooled blades in a highly-loaded transonic turbine p 189 A90-17790
Calculation of coolant flow and heat transfer inside composite air-cooled turbine p 189 A90-17791
Experimental investigation on composite air-cooled blades of highly-loaded transonic turbine p 189 A90-17793
- DENG, SUGING**
The experiments for gas turbine plane cascade in a shock tunnel p 160 A90-19441
- DENG, SUGING**
Research on film-cooling of turbine blade p 190 A90-17795
- DENG, XUEYING**
The aerodynamic behaviours of vortices for slender-wing p 158 A90-18623
Mach number effects on upstream influence in swept shock wave/turbulent boundary layer interactions p 556 A90-36415
- DENG, ZHENG-TAO**
Numerical simulation of droplet deformation in convective flows [AIAA PAPER 90-2309] p 769 A90-42773
- DENICOLA, CARLO**
Prediction of aerodynamic performance of airfoils in low Reynolds number flows [DLC-EST-TN-031] p 632 N90-23360
- DENKE, P. H.**
The MDE method for aircraft cabin interior noise prediction [SAE PAPER 892372] p 782 A90-45519
- DENNER, BRETT W.**
An approximation model for the performance and acoustic predictions of counterrotating propeller configurations [AIAA PAPER 90-0282] p 378 A90-26931
- DENNER, BRETT WILLIAM**
An approximate model for the performance and acoustic predictions of counterrotating propeller configurations [NASA-CR-180667] p 379 N90-18228
- DENNING, R. M.**
The next generation supersonic transport engine: Critical issues [PNR90576] p 115 N90-12605
- DENT, LESLIE A.**
Software verification plan for GCS [NASA-TM-101668] p 372 N90-18057
- DENTON, J. D.**
The trailing edge loss of transonic turbine blades [ASME PAPER 89-GT-278] p 475 A90-33564
- DENYER, A. G.**
Tracking B-1B aircraft with a structural data recorder p 926 A90-49880
- DENYER, ANTHONY G.**
Automated procedure for creating flight-by-flight spectra p 376 A90-26755
- DEOM, A.**
The application of infrared thermography to the measurement of heat fluxes in a wind tunnel [ONERA, TP NO. 1989-192] p 261 A90-21051
Determination of convective transfer coefficients on a wind-tunnel model by stimulated infrared thermography [ONERA, TP NO. 1989-218] p 351 A90-25351
- DEPOMPEIS, R.**
P-180 AVANTI: Project and flight test program comprehensive overview p 34 N90-10863
- DEPONTE, SERGIO**
A fast collocation method for transonic airfoil design p 501 N90-20984
- DERBUNOVICH, G. I.**
Optimal conditions of flow turbulence suppression in the working section of a wind tunnel using screens located in the prechamber p 438 A90-29185
- DEREVIANKO, ALEKSANDR V.**
Fundamentals of turbine design for aircraft engines p 40 A90-10839
- DEROSA, S.**
Problems of internal acoustics in two and three dimensional cavities with deformable walls using the MSC/Nastran code [DLC/STR-INT-TN-004] p 699 N90-24876
- DERUYCK, J.**
Measurement of velocity profiles and Reynolds stresses on an oscillating airfoil p 397 N90-18427
Secondary flows and radial mixing predictions in axial compressors p 512 N90-21010
- DERVIEUX, A.**
Upwind adaptive finite element investigations of the two-dimensional reactive interaction of supersonic gaseous jets p 209 A90-18264
2-D and 3-D unstructured mesh adaption relying on physical analogy p 310 A90-26534
- DESAI, S. S.**
Full-potential calculations using Cartesian grids p 86 A90-15740
- DESAULTY, M.**
Finite element simulation of compressible turbulent flows - Validation and application to internal aerodynamic in gas-turbine engines p 210 A90-18343
- DESCH, DAVID A.**
Ada real-time GPS/INS simulation approach to system development p 751 A90-43706
- DESCHAMBAULT, R. L.**
The University of Toronto-Ryerson Polytechnical Institute hypersonic gun tunnel p 673 A90-42432
- DESCHAMPS, JACQUES**
Study of the ground effects in the CEAT aerohydrodynamic tunnel: Using the results p 922 N90-28530
- DESIDERI, J.-A.**
Hypersonic reactive flow computations p 315 A90-27131
- DESJARDINS, S. P.**
Aircraft crash survival design guide. Volume 4: Aircraft seats, restraints, litters, and cockpit/cabin dealthalization [AD-A218437] p 575 N90-22548
- DESMARIS, ROBERT N.**
Boundary-integral method for calculating aerodynamic sensitivities with illustration for lifting-surface theory p 806 A90-46841
- DESMOND, ANTHONY T.**
Evaluation of various non-asbestos epoxy adhesives for aircraft repair p 529 A90-33078

DESMOND, JOHN P.

Flight-path display can improve safety, operational efficiency p 847 A90-46882

DESOKY, A. A.

Effect of primary air swirl on emissions formations in gas turbine combustors p 47 A90-12573
Combustion process in a gas turbine combustor when using H₂, NH₃ and LPG fuels p 873 A90-46882

DESOPPER, A.

Influence of the control law on the performance of a helicopter model rotor
[ONERA, TP NO. 1989-136] p 4 A90-11158
Performance and aerodynamic development of the Super Puma Mk II main rotor with new SPP8 blade tip design
[ONERA, TP NO. 1989-181] p 245 A90-21041

DESOPPER, ANDRE

Correlation of Puma airfoils - Evaluation of CFD prediction methods
[ONERA, TP NO. 1989-185] p 224 A90-21045

DESROSIERS, MICHAEL J.

Developments in automation of flight test analysis and report generation
[AIAA PAPER 90-1313] p 487 A90-33923

DESSE, J. M.

The inclusion of a similarity representation of compressor rotation in the modeling of the interaction of cannon firing with air intakes at incidence
[AAAF PAPER NT 88-18] p 4 A90-11435

DESTARAC, D.

Numerical optimization of wings in transonic flow
p 502 N90-20997

DESTUYNDER, R.

New methods of buffeting prediction on civil aircraft
p 908 A90-52620

DETEMPLE-LAAKE, E.

Measurement of the flow field in the blade passage and side-wall region of a plane turbine cascade
p 513 N90-21019

DETROIT, MARK J.

Simulation investigation of multiple axis flying qualities
[AIAA PAPER 90-3480] p 866 A90-47729

DETURRIS, D. J.

Direct measurements of skin friction in a scramjet combustor
[AIAA PAPER 90-2342] p 626 A90-42132

DEVASENAPATHY, C.

Improved guidance and control of vehicles and personnel on the ground will benefit airport traffic capacity
p 760 A90-44549

DEVENPORT, WILLIAM J.

Time-dependent and time-averaged turbulence structure near the nose of a wing-body junction
p 231 A90-23036

DEVINE, KIRK

Inclement weather induced aircraft engine power loss
[AIAA PAPER 90-2169] p 662 A90-42055

DEVY, F.

Modeling of the oil quench for Ni-based superalloy turbine disks
p 957 A90-51525

DEWILDE, J. P.

Solid fuel combustion chamber
[LR-634] p 939 N90-29433

DEWITT, KENNETH J.

Convective heat transfer measurements from a NACA 0012 airfoil in flight and in the NASA Lewis Icing Research Tunnel
[AIAA PAPER 90-0199] p 272 A90-22180

Convective heat transfer measurements from a NACA 0012 airfoil in flight and in the NASA Lewis Icing Research Tunnel
[NASA-TM-102448] p 213 N90-13750

DEWITT, R. L.

Background, current status, and prognosis of the ongoing slush hydrogen technology development program for the NASP
[NASA-TM-103220] p 763 N90-26055

DEWITT, RICHARD L.

Slush Hydrogen (SLH₂) technology development for application to the National Aerospace Plane (NASP)
[NASA-TM-102315] p 203 N90-14268

DEXTER, ROBERT J.

Inspection development for T-37 wing spar cap lug
[AD-A214826] p 287 N90-16708

DHILLON, JASKIRAN

Global Sentry: NASA/USRA high altitude reconnaissance aircraft design, volume 2
[NASA-CR-186820-VOL-2] p 736 N90-25971

DHINGRA, A. K.

Multiobjective decision making in a fuzzy environment with applications to helicopter design
p 405 A90-27993

DI MARTINO, P.

Numerical simulation of the behaviour of internal combustion supercharged engines
[AIAA PAPER 90-1873] p 655 A90-40539

DIBROVA, GEORGII S.

The economics of the organization and the planning of civil aviation p 897 A90-46629

DICARLO, D. J.

Investigations of modifications to improve the spin resistance of a high-wing, single-engine, light airplane
[SAE PAPER 891039] p 118 A90-14345

DICKERSON, WALTER E.

Helicopter surface maneuvering test results
[ACD-330] p 59 N90-10897

DICKERSON, WILLIAM

When propfans cruise, will LDN 65 fly.
p 697 N90-24864

DICKES, E.

Influence of forebody geometry on aerodynamic characteristics and a design guide for defining departure/spin resistant forebody configurations
[AD-A216714] p 414 N90-18388

DICKEY, THOMAS A.

Contamination of cabin air by synthetic oil and breakdown products
[SAE PAPER 891455] p 323 A90-27424

Catalytic conversion of oil in bleed air - A maintenance tool
[SAE PAPER 892214] p 732 A90-45431

DICKINSON, JOSEPH D.

The Advanced Digital-Optical Control System (ADOCS) user demonstration program
[AD-A215984] p 349 N90-17644

DICKINSON, R.

Flight test results of the F-15 SMTD thrust vectoring/thrust reversing exhaust nozzle
[AIAA PAPER 90-1906] p 660 A90-41982

DICKMANN, E. D.

Autonomous automatic landing through computer vision
p 332 N90-16734

DICKSON, LAWRENCE W.

Radiation-curable prepreg composites
[DE90-629740] p 951 N90-28674

DICKSON, RICHARD W.

Advanced transport operating system software upgrade: Flight management/flight controls software description
[NASA-CR-181936] p 893 N90-28366

DIEDERICH, PIERRE

An international civil integrity complement to GPS and GLONASS
p 821 A90-46392

DIEFENDORF, R. J.

Compendium of abstracts and viewgraphs.
[AD-A217189] p 532 N90-20140

DIEMAN, CHARLES A., JR.

Canopy fragmentation using embedded detonating cord
p 180 A90-17417

DIEQIAN, WANG

The TSP methods applied to the calculation of transonic flow about wing/body/nacelle/pylon-configurations
p 554 A90-35868

DIEROFF, M.

A GPS-based flight-control concept
p 242 A90-21719

DIEROFF, MANFRED

Automatic landing with GPS - Design of the flight guidance and flight control system
[AIAA PAPER 90-1301] p 487 A90-33915

DIETENBERGER, MARK A.

Analyses of Arrow Air DC-8-63 accident of December 12, 1985 - Gander, Newfoundland
p 635 A90-40687

DIFILIPPO, D. J.

A precise flight reference system for evaluating airborne navigation aids
p 27 A90-12752

The development of an airborne synthetic aperture radar motion compensation system
p 333 N90-16745

DIFTLER, M. A.

UH-60A helicopter stability augmentation study
p 670 A90-42471

DIFTLER, MYRON A.

Helicopter simulation development by correlation with frequency sweep flight test data
p 407 A90-28203

DIJKSTRA, F.

Ultrasonic regression rate measurement in solid fuel ramjets
[AIAA PAPER 90-1963] p 656 A90-40573

Experimental and computational flammability limits in a solid fuel ramjet
[AIAA PAPER 90-1964] p 676 A90-40574

DILL, H. D.

Solid fuel combustion chamber
[LR-634] p 939 N90-29433

DILL, J.

Certification testing methodology for fighter hybrid structure
p 642 A90-40128

DILL, J.

Internal rotor friction instability
[NASA-CR-183942] p 543 N90-21395

DILLENUS, MARNIX F. E.

Prediction methods for store separation
p 317 N90-17549

DILLEY, A. DOUGLAS

Comparison between experimental and numerical results for a research hypersonic aircraft
p 395 A90-31278

DILLINGER, R.

Hypersonic CFD applications for the National Aero-Space Plane
[SAE PAPER 892310] p 714 A90-45473

DILLINGER, R.

Slip-cast hot isostatically pressed silicon nitride gas turbine components
p 765 A90-44816

DILLON, L. R.

Aerodynamic testing of a new semi-prone ejection seat design
[AIAA PAPER 90-0234] p 182 A90-19748

DIMEO, MARK

Analysis of heliport environmental data: Indianapolis downtown heliport, Wall Street heliport. Volume 2: Wall Street heliport data plots
[DOT/FAA/CT-TN87/54-VOL-2] p 121 N90-11761

Analysis of heliport environmental data: Indianapolis downtown heliport, Wall Street heliport. Volume 3: Indianapolis downtown heliport data plots
[AD-A217412] p 544 N90-20500

DIMICCO, R. G.

The effect of constructive and destructive interference on the downstream development of twin jets in a crossflow. I - Destructive interference of laterally spaced jets
[AIAA PAPER 90-1623] p 607 A90-38752

The effect of constructive and destructive interference on the downstream development of twin jets in a crossflow. II - Interference effects of angularly displaced jets
[AIAA PAPER 90-2107] p 684 A90-42020

DIMIDUK, D. M.

Intermetallic compounds for strong high-temperature materials - Status and potential
p 125 A90-15022

DIMMICK, R. L.

The effect of pitch location on dynamic stall
p 2 A90-10641

DIMOTAKIS, PAUL E.

The effect of walls on a spatially growing supersonic shear layer
p 393 A90-29591

DING, CHUAN-CH'U

Adaptive autopilot design via model expansion method
p 55 A90-11124

DING, CHUANXIN

The research of cubic spline optimal terrain following system
p 196 A90-18584

DINI, DINO

Contribution of engine improvement on next future rotorcraft
p 665 A90-42488

DINI, PAOLO

A computationally efficient modelling of laminar separation bubbles
p 801 A90-46372

A computationally efficient modelling of laminar separation bubbles
[NASA-CR-185854] p 136 N90-12872

A computational efficient modelling of laminar separation bubbles
[NASA-CR-186729] p 774 N90-25291

DINYOVSKY, P.

Plan, formulate, and discuss a NASTRAN finite element model of the UH-60A helicopter airframe
[NASA-CR-181975] p 541 N90-20439

DIPPE, D.

Four-dimensional planner: A ground based planning system for time accurate approach guidance
p 826 N90-27683

DIRUSSO, E.

Active vibration control for flexible rotor by optimal direct-output feedback control
p 879 A90-46222

DIRUSSO, ELISEO

Experimental evaluation of a tuned electromagnetic damper for vibration control of cryogenic turbopump rotors
[NASA-TP-3005] p 665 N90-23403

DISBROW, J. D.

An American knowledge base in England - Alternate implementations of an expert system flight status monitor
p 459 A90-30719

A knowledge-based flight status monitor for real-time application in digital avionics systems
[NASA-TM-101710] p 217 N90-13995

DISBROW, JAMES D.

Preliminary development of an intelligent computer assistant for engine monitoring
[NASA-TM-101702] p 612 N90-22322

DISDERO, M. C.

The airborne synthetic cartographic indicator
p 822 A90-46671

DISHART, PETER T.

Tip leakage losses in a linear turbine cascade
[ASME PAPER 89-GT-56] p 290 A90-23782

DISMILE, P. J.

A multipurpose aerodynamic research facility utilizing the abandoned Cincinnati subway tubes
[AIAA PAPER 90-1424] p 596 A90-37961

- The effect of constructive and destructive interference on the downstream development of twin jets in a crossflow.
I - Destructive interference of laterally spaced jets
[AIAA PAPER 90-1623] p 607 A90-38752
- The effect of constructive and destructive interference on the downstream development of twin jets in a crossflow.
II - Interference effects of angularly displaced jets
[AIAA PAPER 90-2107] p 684 A90-42020
- The effect of separation on turbulent boundary layer characteristics over a smooth surface at Mach 6.0
[AIAA PAPER 90-3028] p 790 A90-45870
- DISIMILE, PETER J.**
High Reynolds number wedge-induced separation lengths at Mach 6 p 154 A90-18001
- DITARANTO, R. A.**
Calculation of flight vibration levels of the AH-1G helicopter and correlation with existing flight vibration measurements
[NASA-CR-181923] p 454 N90-18743
- DITTMANN, GERALD L.**
Preparations of the real-time data analyst to insure flight test safety
[AIAA PAPER 90-1316] p 488 A90-33925
- DITTMAR, JAMES H.**
Predicted and measured boundary layer refraction for advanced turbo-prop propeller noise
[NASA-TM-102365] p 379 N90-17413
- DITTRICH, U.**
The effect of matrix toughness in the development of improved structural adhesives p 955 A90-50183
- DIVITO, BEN L.**
Formal design and verification of a reliable computing platform for real-time control. Phase 1: Results
[NASA-TM-102716] p 965 N90-29965
- DIWAKAR, PHILIP M.**
Numerical prediction of wakes of different bodies p 308 A90-26341
- DIX, DONALD M.**
Aircraft engine technology gets a second wind p 659 A90-41166
- DIX, RICHARD E.**
Cavity aeroacoustics
[AD-A223853] p 911 N90-29307
- DIXON, SIDNEY C.**
Materials and structures for hypersonic vehicles p 31 A90-13015
- DJILALI, N.**
Film cooling of turbine blades - Two dimensional experiments and numerical simulations p 739 A90-42670
- DJOMEHRI, J.**
Application of a self-adaptive grid method to complex flows
[NASA-TM-102223] p 143 N90-13324
- DJORDJEVIC, V. D.**
Nonlinear stability of subsonic mixing layers with symmetric temperature variations p 223 A90-20501
- DO, DUNG**
Full-scale air transport category fuselage burnthrough tests
[DOT/FAA/CT-TN89/65] p 486 N90-20967
- DO, HENRY**
Global Sentry: NASA/USRA high altitude reconnaissance aircraft design, volume 2
[NASA-CR-186820-VOL-2] p 736 N90-25971
- DOANE, PAUL**
Integrated air vehicle/propulsion technology for a multirole fighter - A MCAIR perspective
[AIAA PAPER 90-2278] p 644 A90-42105
- DOBBS, BILL**
High Voltage Design Guide summary p 605 A90-38097
- DOBRIANSKII, GEORGII V.**
Dynamics of aviation gas turbine engines p 113 A90-16049
- DOBRODEEV, V. P.**
Thermodynamic calculation of the compressors of gas turbine engines and powerplants at high air pressures p 130 A90-14585
- DOBROLENSKII, IURII P.**
Aviation equipment p 338 A90-24200
- DOBROVOL'SKII, V. A.**
Some problems on 'intelligence' of wind tunnel testing p 436 A90-28282
- DOBRYNSKI, WERNER**
Acoustics of ultralight airplanes p 643 A90-40685
A new noise certification method for 'light propeller aircraft' in testing p 635 A90-41728
En route noise of two turbo-prop aircraft
[DLR-MITT-89-18] p 697 N90-24859
- DOBYNE, JOHN**
The accuracy of barometric altimeters with respect to geometric altitude p 108 A90-14012
- DOBYNS, A. L.**
The analysis and testing of composite panels subject to muzzle blast effects p 675 A90-39991
- DODBELE, S. S.**
Status report on a natural laminar-flow nacelle flight experiment p 105 N90-12550
Nacelle aerodynamic performance p 105 N90-12552
- DODBELE, SIMHA S.**
Design optimization of natural laminar flow fuselages in compressible flow p 182 A90-19784
Effects of forebody geometry on subsonic boundary-layer stability
[NASA-CR-4314] p 718 N90-25939
- DODD, L. P.**
STOVL option for the multi-role fighter
[AIAA PAPER 90-3296] p 840 A90-49124
- DODD, STEVEN M.**
Expert systems for design of battle damage repairs p 467 A90-33094
- DODDS, W. J.**
Fuel effects on gas turbine combustor dynamics
[AIAA PAPER 90-1957] p 676 A90-40570
Multiple swirler dome combustor for high temperature rise applications
[AIAA PAPER 90-2159] p 661 A90-42050
- DOERFLER, T.**
Application of piezoelectric foils in experimental aerodynamics p 446 A90-28258
Detection of flow instabilities at airfoil profiles using piezoelectric arrays p 276 N90-16175
- DOERNBACH, JAY**
Assessment of High Temperature Superconducting (HTS) electric motors for rotorcraft propulsion
[NASA-CR-185222] p 588 N90-21761
- DOGGETT, J. W.**
Helicopter flight vibration of large transportation containers: A case for testing tailoring
[DE90-007429] p 402 N90-19215
- DOGGETT, ROBERT V., JR.**
Experimental transonic flutter characteristics of two 72 deg-sweep delta-wing models p 175 N90-14205
- DOGHA, ANJU S.**
Effect of vane twist on the performance of dome swirlers for gas turbine airblast atomizers
[AIAA PAPER 90-1955] p 881 A90-47203
Effect of vane twist on the performance of dome swirlers for gas turbine airblast atomizers
[NASA-TM-103195] p 773 N90-25289
- DOHME, J.**
Synthesis of a simulator-based automated helicopter hover trainer
[AIAA PAPER 90-3481] p 891 A90-47730
- DOHRMANN, ULRICH**
Transonic flow around airfoils with relaxation and energy supply by homogeneous condensation p 620 A90-39782
The effect of energy input on the characteristics of profiles in compressible fluid media p 906 A90-51533
- DOI, S.**
Daily flight operation monitoring in JAL p 820 N90-27636
- DOLEGA, BOGUSLAW**
Digital autopilot for light aircraft p 653 A90-41741
- DOLEZAL, JAROSLAV**
Mathematical model of turbo-prop engine behaviour p 254 A90-23351
Modelling and simulation of turbo-prop engine behaviour p 424 A90-29946
Mathematical simulation model of an aircraft gas turbine p 745 A90-44721
- DOLLING, D. S.**
Separation shock dynamics in Mach 5 turbulent interactions induced by cylinders p 153 A90-17981
Swept shock/boundary-layer interactions - Tutorial and update
[AIAA PAPER 90-0375] p 228 A90-22207
Spanwise properties of the unsteady separation shock in a Mach 5 unswept compression ramp interaction
[AIAA PAPER 90-0377] p 228 A90-22208
The detection of large scale structure in undisturbed and disturbed compressible turbulent free shear layers
[AIAA PAPER 90-0711] p 230 A90-22251
Correlation of separation shock motion in a compression ramp interaction with pressure fluctuations in the incoming boundary layer
[AIAA PAPER 90-1646] p 569 A90-38774
- DOLLING, DAVID S.**
Dynamics of the outgoing turbulent boundary layer in a Mach 5 unswept compression ramp interaction
[AIAA PAPER 90-1645] p 569 A90-38773
- DOLLYHIGH, SAMUEL M.**
Technology issues for high-speed civil transports
[SAE PAPER 892201] p 778 A90-45422
- DOLOU, P.**
Parachute opening shocks during high speed ejections: Normalization p 497 N90-20056
- DOMINY, R. G.**
An investigation of secondary flows in nozzle guide vanes p 512 N90-21016
- DOMPKA, R. V.**
Investigation of difficult component effects on finite element model vibration prediction for the Bell AH-1G helicopter. Volume 1: Ground vibration test results
[NASA-CR-181916-VOL-1] p 134 N90-12058
Investigation of difficult component effects on finite element model vibration prediction for the Bell AG-1G helicopter. Volume 2: Correlation results
[NASA-CR-181916-VOL-2] p 213 N90-13814
- DON, WAI-SUN**
Spectral simulation of unsteady compressible flow past a circular cylinder
[NASA-CR-182030] p 478 N90-20050
- DONALDSON, C. D.**
Control of submersible vortex flows
[NASA-TM-102693] p 909 N90-28493
- DONALDSON, JOHN O.**
Ceramic materials and coatings for future aerospace applications - Challenge of the 1990's p 942 A90-50071
- DONALDSON, PETER**
Cooking an aeroplane p 209 A90-17918
- DONALDSON, WAYNE A.**
ETO (Earth-To-Orbit): A trajectory program for aerospace vehicles
[AD-A218157] p 528 N90-20103
- DONE, G. T. S.**
Whole helicopter aeroelasticity - Experience with a new approach p 492 A90-33380
- DONELSON, M. J.**
Supersonic jet noise reduction by a porous single expansion ramp nozzle
[AIAA PAPER 90-0366] p 219 A90-19815
- DONER, WILLIAM D.**
Further studies of turbulence structure resulting from interactions between embedded vortices and wall jets at high blowing ratios
[AD-A223296] p 960 N90-29593
- DONG, BONIAN**
Numerical simulation of wakes with application to blade-vortex interaction p 807 A90-46881
- DONG, MING**
Numerical solution of 3-D hybrid problems in turbomachinery p 621 A90-40501
- DONG, Y.**
Compressor blade boundary layers. II - Measurements with incident wakes
[ASME PAPER 89-GT-51] p 289 A90-23777
- DONLAN, BRIAN**
Advanced integrated avionics test support concepts
[AIAA PAPER 90-1259] p 504 A90-33889
- DONNER, J. T.**
Advanced fuel properties, phase 1
[AD-A219788] p 766 N90-25236
- DONOVAN, J. F.**
Large-scale motions in a supersonic turbulent boundary layer on a curved surface
[AIAA PAPER 90-0019] p 160 A90-19636
Low Reynolds number airfoil design and wind tunnel testing at Princeton University p 799 A90-46362
- DONOVAN, JOHN F.**
Experimental investigation of terminal shock sensors in mixed-compression inlets
[AIAA PAPER 90-1931] p 681 A90-40560
- DONOVAN, STEVEN**
The Stealth biplane: A proposal in response to a low Reynolds Number station keeping mission
[NASA-CR-186680] p 734 N90-25127
- DONZELLI, GIANCARLO**
Design of helicopter components in metal matrix composites
[REPT-100-20-55] p 874 N90-26894
- DOOGOOD, P. N.**
The reduction of smoke emissions from Allison T56 engines
[ARL-PROP-R-182] p 928 N90-28547
- DOR, J. B.**
Flow quality in the T2 cryogenic wind-tunnel - Problems and solutions p 524 A90-34240
- DOREY, G.**
European research and testing facilities requested for participation to SST/HST projects
[ONERA, TP NO. 1990-12] p 351 A90-25358
- DORNEY, DANIEL J.**
Unsteady analysis of hot streak migration in a turbine stage
[AIAA PAPER 90-2354] p 769 A90-42782
- DORNHEIM, MICHAEL A.**
Fly-by-wire controls key to 'pure' stealth aircraft p 413 A90-30222
ATF prototypes outstrip F-15 in size and thrust p 841 A90-49477

DOSTAL, JAN

Measurements and calculations of the aerodynamic characteristics of the propeller sections series V3. p 233 A90-23355

DOTY, WAYNE A.

A flight test investigation of certification requirements for laminar-flow general aviation airplanes [AIAA PAPER 90-1310] p 496 A90-33920
Flight test investigation of certification issues pertaining to general-aviation-type aircraft with natural laminar flow [NASA-CR-181967] p 480 N90-20952

DOU, HUASHU

A method of predicting the energy losses in vaneless diffusers of centrifugal compressors [ASME PAPER 89-GT-158] p 292 A90-23846

DOUBLIER, MICHEL

Progress in airbreathing combined engines for future European launcher p 344 N90-16817

DOUCETT, NOEL A.

Data Link Processor (DLP) operational test and evaluation/integration test plan [DOT/FAA/CT-TN89/32] p 214 N90-14404

DOUGHERTY, F. C.

Thermal interaction between an impinging hot jet and a conducting solid surface [AIAA PAPER 90-3010] p 956 A90-50636

DOUGHERTY, F. CARROLL

Computational simulation of flows about hypersonic geometries with sharp leading edges [AIAA PAPER 90-3065] p 793 A90-45891

DOUGHTY, G. R.

Laser communication system design p 26 A90-11813

DOUGLAS, RANDAL K.

Robust hover control for a short takeoff/vertical landing aircraft [AIAA PAPER 90-3333] p 862 A90-47593

DOUVIKAS, D.

A secondary flow calculation method for one stage centrifugal compressor p 14 A90-12597
Secondary flow calculations for axial and radial compressors p 514 N90-21024

DOVGAL, A. V.

Instability and susceptibility of a boundary layer in the vicinity of two-dimensional surface inhomogeneities p 535 A90-32675

Acoustic excitation of boundary layer oscillations on a yawing wing p 805 A90-46567

DOVI, AUGUSTINE R.

Multilevel decomposition approach to the preliminary sizing of a transport aircraft wing [NASA-CR-4296] p 583 N90-22557

Aircraft design for mission performance using nonlinear multiobjective optimization methods [NASA-CR-4328] p 925 N90-29384

DOWELL, EARL H.

Nonlinear aeroelasticity [AIAA PAPER 90-1031] p 391 A90-29375
A modern course in aeroelasticity (2nd revised and enlarged edition) p 497 A90-34968
Asymptotic modal analysis and statistical energy analysis [NASA-CR-186732] p 782 N90-26634

DOWLING, A. P.

The absorption of sound by perforated linings p 965 A90-51994

DOWLING, N. E.

Simplified analysis of helicopter fatigue loading spectra p 336 A90-26758
Fatigue life estimates for helicopter loading spectra p 772 A90-45324
Fatigue life estimates for helicopter loading spectra [NASA-CR-181941] p 279 N90-16294

DOWNEY, D. C.

Enhanced bioreclamation of jet fuels: A full-scale test at Eglin AFB, Florida [AD-A22348] p 875 N90-26992

DOWNEY, DAVID A.

UH-60 helicopter simulator fidelity testing or how to make it fly like the real thing [AIAA PAPER 90-1290] p 522 A90-33910
Natural icing re-evaluation of the EH-60A Quick Fix helicopter [AD-A214728] p 323 N90-16723

DOWNEY, MARK

Unsteady free-wake viscous aerodynamic analysis of helicopter rotors [AD-A217166] p 478 N90-20048

DOWNING, DAVID R.

Analysis and design of sidestick controller systems for general aviation aircraft p 196 A90-19554
Assessment of proposed fighter agility metrics [AIAA PAPER 90-2807] p 752 A90-45142

DOWNING, JOHN P.

Structural mode significance using INCA [AIAA PAPER 90-3346] p 889 A90-47606

DOWSETT, M. J.

Development and evaluation at ATCEU of executive and support operations, phase 4A/3D [CAA-PAPER-88017] p 99 N90-12572

DRACOPOULOS, THEODORE NICOLAS

Aeroelastic control of composite lifting surfaces: Integrated aeroelastic control optimization p 198 N90-13396

DRAGOS, L.

On steady subsonic flow past slender bodies of revolution p 144 A90-16736

DRAJESKE, MARK H.

An experimental investigation of roll agility in air-to-air combat [AIAA PAPER 90-2809] p 752 A90-45144

DRAPER, ALFRED C.

Non-isentropic effects on the WRDC 20 inch hypersonic wind tunnel calibration p 435 A90-28254

DRELA, MARK

Aerodynamics of human-powered flight p 386 A90-28552
Newton solution of coupled viscous/inviscid multielement airfoil flows [AIAA PAPER 90-1470] p 562 A90-38627
XFoil - An analysis and design system for low Reynolds number airfoils p 799 A90-46359
Method for simultaneous wing aerodynamic and structural load prediction p 838 A90-48955

DRENGWITZ, MAGNUS

Position finding and ground target direction finding by an aircraft with a gimbaled video camera [DLR-FB-89-62] p 825 N90-27673

DRESS, DAVID A.

Drag measurements on a modified prolate spheroid using a magnetic suspension and balance system p 672 A90-40684

DRESSLER, U.

Flight tests with a natural laminar flow glove on a transport aircraft [AIAA PAPER 90-3044] p 828 A90-45881

DREVET, J.-P.

New rotor test rig in the large Modane wind tunnel [ONERA, TP NO. 1989-137] p 58 A90-11159

DRIGGERS, GERALD W.

Development and operating experience on a zinc-sulfide window for the Infrared Instrumentation System (IRIS) p 505 A90-34584

DRIKAKIS, D.

Multigrid scheme for the compressible Euler-equations p 907 A90-51559

DRING, R. P.

Throughflow theory for nonaxisymmetric turbomachinery flow. I - Formulation. II - Assessment [ASME PAPER 89-GT-304] p 905 A90-51256

DRING, ROBERT P.

Navier-Stokes analyses of the redistribution of inlet temperature distortions in a turbine p 471 A90-32959
Temporally and spatially resolved flow in a two-stage axial compressor. Part 2: Computational assessment [NASA-TM-102273] p 194 N90-14236
The effects of compressor endwall flow on airfoil incidence and deviation p 512 N90-21011

DRISCOLL, JOSEPH T.

Helicopter simulation development by correlation with frequency sweep flight test data p 407 A90-28203

DRIVER, D.

Towards 2000: The composite engine [PNR90646] p 750 N90-26000
Metal matrix composites and powder processing for aero-engine applications [PNR90617] p 767 N90-26087

DRIVER, DAVID

Aluminium alloy development for aero engines [PNR90548] p 126 N90-11874

DRIVER, MARK A.

Analysis of transonic turbine rotor cascade flows using a finite-volume total variation diminishing (TVD) scheme [AIAA PAPER 90-2127] p 704 A90-42733

DROSSIS, J.

An ultrasonic fatigue facility for HCF/LCF interactive tests p 363 A90-23900

DROUILHET, PAUL R., JR.

Air traffic control development at Lincoln Laboratory p 240 A90-21378

DROUIN, D. V.

Applications of XTRAN3S and CAP-TSD to fighter aircraft [AIAA PAPER 90-1035] p 389 A90-29360

DROZDA, THOMAS J.

Composites applications - The future is now p 678 A90-42372

DROZDOV, V. V.

A parametric optimization algorithm for the electrical distribution circuits of civil aircraft p 255 A90-23417

DRUEZ, P. M.

UHB demonstrator interior noise control flight tests and analysis [NASA-CR-181897] p 140 N90-13198

DRUILHET, AIME

Aircraft measurements of sea surface conditions and their relationship to marine boundary-layer dynamics p 888 A90-47572

DRUMMOND, C. K.

A modeling technique for STOVL ejector and volume dynamics [AIAA PAPER 90-2417] p 663 A90-42168
A modeling technique for STOVL ejector and volume dynamics [NASA-TM-103167] p 589 N90-22566

DRUMMOND, COLIN K.

STOVL propulsion system volume dynamics approximations [NASA-TM-102397] p 114 N90-11740
Real-time simulation of an F110/STOVL turbofan engine [NASA-TM-102409] p 117 N90-12618
STOVL aircraft simulation for integrated flight and propulsion control research [NASA-TM-102419] p 193 N90-13389

DRUMMOND, J. P.

Modeling of supersonic reacting flow fields p 855 N90-26898

DRUMMOND, J. PHILIP

A numerical study of mixing enhancement in a supersonic combustor [AIAA PAPER 90-0203] p 272 A90-22182
A hybrid Reynolds averaged/PDF closure model for supersonic turbulent combustion [AIAA PAPER 90-1573] p 600 A90-38711
Mixing and combustion enhancement in supersonic reacting flows p 744 A90-44410
Supersonic combustor modeling p 749 A90-25992
Supersonic reacting internal flow fields [NASA-TM-103480] p 767 N90-26094

DU VAL, R. W.

Flight simulation model validation procedure, a systematic approach p 30 A90-12770

DU VAL, RONALD

Identification of a coupled flapping/inflow model for the PUMA helicopter from flight test data p 56 A90-12767
Parameter identification of aeroelastic modes of rotary wings from transient time histories p 642 A90-40166

DUAN, S. Z.

Analysis of the effect of rotor-angular-acceleration on the features of gas flow in turbomachinery p 6 A90-11780

A numerical method solving 2-D unsteady flow field around cascade of oscillating airfoils with arbitrary camber and thickness p 7 A90-11788

DUAN, SHIZHONG

A model of small-disturbance wave in large-scale separation zone associated with stall flutter p 883 A90-49469

DUBELL, THOMAS L.

Combustor influence on fighter engine operability p 64 N90-10193

DUBIEL, D. J.

Energy efficient engine pin fin and ceramic composite segmented liner combustor sector rig test report [NASA-CR-179534] p 932 N90-28567

DUBOIS, S.

Development of a fibre optic damage detection system for an aircraft leading edge p 504 A90-32873

DUBOST, GERARD

Dual cross-polarization planar arrays in the C and X bands p 638 A90-40979

DUCK, PETER W.

Non-axisymmetric viscous lower-branch modes in axisymmetric supersonic flows p 474 A90-33509
The inviscid axisymmetric stability of the supersonic flow along a circular cylinder p 554 A90-35916

DUDAS, CHARLES

Communications Interface Driver (CID) test plan [DOT/FAA/CT-TN89/35] p 958 N90-28762

DUDLEY, SHARON E.

Expert system technology applied to the automatic control of multiple unmanned aerial vehicles [AIAA PAPER 90-3280] p 892 A90-48867

DUFFY, STEPHEN F.

Analysis of whisker-toughened ceramic components - A design engineer's viewpoint p 205 A90-19149
Noninteractive macroscopic reliability model for ceramic matrix composites with orthotropic material symmetry. [ASME PAPER 89-GT-129] p 360 A90-23827

DUGUNDJI, J.

Active stabilization of aeromechanical systems [AD-A216629] p 454 N90-18672

DUGUNDJI, JOHN

Postbuckling behavior of laminated plates using a direct energy-minimization technique p 209 A90-17993

- Nonlinear stall flutter and divergence analysis of cantilevered graphite/epoxy wings
[AIAA PAPER 90-0983] p 450 A90-29373
- DUKE, E. L.**
An American knowledge base in England - Alternate implementations of an expert system flight status monitor p 459 A90-30719
A knowledge-based flight status monitor for real-time application in digital avionics systems
[NASA-TM-101710] p 217 N90-13995
- DUKE, EUGENE L.**
Flight test of a trajectory controller using linearizing transformations with measurement feedback
[AIAA PAPER 90-3373] p 864 A90-47631
Preliminary development of an intelligent computer assistant for engine monitoring
[NASA-TM-101702] p 612 N90-22322
Effects of simplifying assumptions on optimal trajectory estimation for a high-performance aircraft
[NASA-TM-101721] p 757 N90-25142
- DUKE, P. A.**
Performance assessment of MIL-STD-1553B on the avionics systems demonstrator rig of British Aerospace p 849 N90-27624
- DULIEU, ANNIE**
Vortex formation around an oscillating and translating airfoil at large incidences p 303 A90-25588
- DULIKRAVICH, GEORGE S.**
Accelerated computation of viscous, steady incompressible flows
[ASME PAPER 89-GT-45] p 288 A90-23771
- DULY, K. R.**
The LF500 and the regional airline market
[AIAA PAPER 90-2521] p 744 A90-42814
- DUMANIS, A.**
Development of a double crack growth gage algorithm for application to fleet tracking of fatigue damage p 901 A90-49890
- DUMAS, R.**
Device for the dilution of hot exhaust jets
[ETN-90-97435] p 858 N90-27723
- DUNBAR, L. W.**
Turbine configuration impact on advanced IHPTET engine system mission capabilities
[AIAA PAPER 90-2739] p 664 A90-42221
- DUNBAR, W. G.**
High Voltage Design Guide summary p 605 A90-38097
- DUNBAR, WILLIAM**
Applying AVIP to high voltage power supply designs p 605 A90-38132
- DUNCAN, LARRY B.**
Application of fracture mechanics to microscale phenomena in electronic assemblies p 684 A90-41334
- DUNCAN, T. M.**
A daylight stellar sensor using a charge-coupled device p 637 A90-39002
- DUNFORD, P. G.**
EH101 development progress p 646 A90-42442
- DUNHAM, D. M.**
A hybrid method for prediction of propeller performance
[AIAA PAPER 90-0440] p 229 A90-22219
- DUNHAM, DANA MORRIS**
The effect of solidity on propeller normal force
[SAE PAPER 892205] p 713 A90-45424
- DUNHAM, R. EARL, JR.**
Results of aerodynamic testing of large-scale wing sections in a simulated natural rain environment
[AIAA PAPER 90-0486] p 167 A90-19874
Operational considerations for aerodynamic testing of large-scale wing sections in a simulated natural rain environment
[AIAA PAPER 90-0485] p 313 A90-26956
- DUNMIRE, H.**
Reduced voltage and restart testing of the 1-watt integral cryogenic cooler (HD-1033B/C/D)
[AD-A215133] p 369 N90-16971
- DUNN, DAVID A.**
HPLC analysis of helicopter rotor blade materials
[AD-A221121] p 650 N90-24270
- DUNN, H. J.**
The application of active controls technology to a generic hypersonic aircraft configuration
[NASA-TM-101689] p 497 N90-20071
- DUNN, JOE L.**
US Navy principal site testing concept and the F-18 p 33 N90-10861
- DUNN, M. G.**
Investigation of unsteady flow through a transonic turbine stage. II - Data/prediction comparison for time-averaged and phase-resolved pressure data
[AIAA PAPER 90-2409] p 626 A90-42162
- DUNN, PETER**
Nonlinear stall flutter and divergence analysis of cantilevered graphite/epoxy wings
[AIAA PAPER 90-0983] p 450 A90-29373
- DUNN, STEVEN C.**
Ground testing techniques in support of flight test
[AIAA PAPER 90-1309] p 523 A90-33919
- DUNN, WILLIAM R.**
RSRA/X-Wing flight control system development - Lessons learned p 430 A90-28216
- DUONG, L.**
Planet gear sleeve spinning analysis
[AIAA PAPER 90-2154] p 681 A90-40613
- DUPLIAKIN, V. M.**
Prediction of the strength-related reliability of structural elements at the design stage p 274 A90-23402
- DUPOIRIEUX, F.**
3D calculations of reacting flows within aircraft engine combustion chambers
[ONERA, TP NO. 1989-153] p 67 A90-11173
- DUPOIRIEUX, FRANCIS**
Three dimensional numerical simulation for an aircraft engine type combustion chamber
[ONERA, TP NO. 1989-120] p 49 A90-12591
- DUPONT, LEON**
Dual cross-polarization planar arrays in the C and X bands p 638 A90-40979
- DUPRIEZ, F.**
Half transport aircraft cryogenic model for T2 wind tunnel p 524 A90-34242
Sting design feasibility for E.T.W. cryogenic civil transport aircraft p 524 A90-34245
Design and manufacturing of composite materials blade models p 618 A90-42492
- DUPRIEZ, P.**
Design, realization, and qualification of model composite rotor blades p 364 A90-24293
- DUQUE, EARL P. N.**
A numerical analysis of the British Experimental Rotor Program blade p 384 A90-28194
Experimental and numerical study of the British Experimental Rotor Programme blade
[AIAA PAPER 90-3008] p 789 A90-45858
- DURAND, J.-M.**
The disadvantages of GPS - Comparative study of solutions adapted to civil aviation p 329 A90-23994
- DURAND, PIERRE**
Aircraft measurements of sea surface conditions and their relationship to marine boundary-layer dynamics p 888 A90-47572
- DURANTI, P.**
Flight test safety and 'high risk' tests - The Aeritalia approach
[AIAA PAPER 90-1315] p 483 A90-33924
New inflight experiments to measure aerodynamics loads
[ETN-90-97276] p 868 N90-26834
- DURAO, D. F. G.**
Numerical study of single impinging jets through a crossflow p 17 A90-13020
Instrumentation for combustion and flow in engines; Proceedings of the NATO Advanced Study Institute, Vimeiro, Portugal, Sept. 13-26, 1987 p 211 A90-19004
- DURHAM, MICHAEL H.**
Experimental transonic flutter characteristics of supersonic cruise configurations
[AIAA PAPER 90-0979] p 390 A90-29369
- DURNO, J. A.**
Ground shake test of the UH-60A helicopter airframe and comparison with NASTRAN finite element model predictions
[NASA-CR-181993] p 758 N90-25143
- DURNO, JASON A.**
Examination of dynamic characteristics of UH-60A and EH-60A airframe structures p 406 A90-28154
- DURRIE, J. E.**
STOVL option for the multi-role fighter
[AIAA PAPER 90-3296] p 840 A90-49124
- DURST, F.**
A semiconductor laser-Doppler-anemometer for applications in aerodynamic research p 447 A90-28273
- DURVASULA, S.**
Flutter of shaft-supported low aspect-ratio control surfaces p 667 A90-38912
- DUSA, D. J.**
Exhaust nozzle system design considerations for turbojet propulsion systems p 48 A90-12577
- DUSHIN, V. R.**
A study of three-dimensional supersonic flow of a real gas past axisymmetric bodies p 3 A90-10938
- DUSSA, R.**
Full scale study of a cabin fire in an A300 fuselage section p 326 N90-17592
- DUTHIE, A. C.**
The use of fibre reinforced thermoplastics for helicopter primary structures and their engineering substantiation p 441 A90-28191
- DUTOYA, D.**
Test rig for the study of the flow in a rotor-stator system
[ONERA, TP NO. 1989-124] p 58 A90-12634
- DUTOYA, DENIS**
Several problems posed by aerothermal calculations in machines
[ONERA, TP NO. 1989-102] p 67 A90-11136
- DUTTON, J. C.**
Investigation of supersonic mixing layers p 623 A90-40926
Computation of multiple normal shock wave/turbulent boundary layer interactions
[AIAA PAPER 90-2133] p 685 A90-42037
- DUTTON, PATRICIA L.**
Methodology for developing an assessment expert system using a planning paradigm p 460 A90-30757
- DUYVIS, F. J. DONKER**
Experimental aerodynamic characteristics of the airfoils LA 5055 and DU 86-084/18 at low Reynolds numbers p 800 A90-46368
- DWOYER, DOUGLAS L.**
CFD propels NASP propulsion progress p 683 A90-41163
- DYER, D. J.**
Wing-section effects on the flight performance of a remotely piloted vehicle p 29 A90-11007
- DYSON, A.**
Wildhaber-Novikov circular arc gears - Some properties of relevance to their design p 70 A90-12999
- DZHAMAI, V. V.**
Fundamentals of the design and development of parts and mechanisms for flight vehicles p 414 A90-30275
- DZIUBA, KATARZYNA**
A statistical model of helicopter noise p 77 A90-10229
- DZYGADLO, Z.**
Numerical analysis of vibrations of a helicopter tail boom p 31 A90-13224
Dynamics of spatial motion of an aeroplane after drop of loads p 346 A90-25189

E

- EARLS, MICHAEL R.**
Initial flight qualification and operational maintenance of X-29A flight software
[NASA-TM-101703] p 32 N90-10023
- EARNshaw, P. B.**
Comparison of the results of tests on A300 aircraft in the RAE 5 metre and ONERA F1 wind tunnels
[RAE-TM-AERO-2130] p 122 N90-11768
- EASON, MYRON O.**
Enhanced environmental control for the Harrier II Plus
[SAE PAPER 901238] p 841 A90-49308
- EASTEP, F. E.**
Structural optimization of lifting surfaces with divergence and control reversal constraints p 127 A90-13770
- EASTLAND, A.**
An analysis methodology for internal swirling flow systems with a rotating wall
[ASME PAPER 89-GT-185] p 361 A90-23863
- EASTLAND, A. H.**
Forced response on turbomachinery blades due to passing wakes
[AIAA PAPER 90-2353] p 705 A90-42781
- EASTWOOD, RAYMOND A.**
An integrated GPS/GLONASS receiver p 822 A90-47909
- EATON, J.**
Visualization studies in rotating disk cavity flows p 475 A90-33568
- EATON, JOHN K.**
Unsteady, separated flow behind an oscillating, two-dimensional spoiler p 469 A90-32462
Boundary layer turbulence structure in the presence of embedded streamwise vortex pairs p 552 A90-35193
Active control of unsteady and separated flow structures
[AD-A212109] p 89 N90-11707
- EATWELL, G. P.**
Active control of helicopter cabin noise p 645 A90-42434
- EBERHARDT, ARNT**
Dornier Composite Aircraft - Economical and faultless p 732 A90-44751
- EBERHARDT, D. SCOTT**
Numerical simulation of confined, spatially-developing mixing layers - Comparison to the temporal shear layer
[AIAA PAPER 90-1462] p 562 A90-38619

- EBERLE, ALBRECHT**
Generalized fluxvectors for hypersonic shock-capturing
[AIAA PAPER 90-0390] p 165 A90-19829
- EBERLE, W.**
Toughened thermosets for damage tolerant carbon fiber reinforced composites p 443 A90-29825
- EBERT, HANS J.**
On the occasion of the 100th birthday of Ernst Heinkel
[MBB/LW/3015/S/PUB/321] p 141 N90-12494
- EBNER, ROBERT E.**
Integrated navigation/flight control for future high performance aircraft p 917 N90-29362
- EBRAHIMI, YAGHOOB S.**
Design of integrated pitch axis for autopilot/autothrottle and integrated lateral axis for autopilot/yaw damper for NASA TSRV airplane using integral LQG methodology
[NASA-CR-4268] p 348 N90-16768
- ECER, A.**
Application of a three-dimensional finite element grid generation scheme for an F-16 aircraft configuration
p 336 A90-26541
Parallel computation of three-dimensional transonic flow problems with complex geometries
[AIAA PAPER 90-0336] p 313 A90-26936
- ECER, AKIN**
Block-structured solution of three-dimensional transonic flows using parallel processing
[AD-A212851] p 170 N90-13330
- ECHIN, A. I.**
Determination of additive contents in aviation and turbine oils p 532 A90-34681
- ECHIZENYA, YOSHIHIRO**
Current status of ceramic gas turbine R&D in Japan
[ASME PAPER 89-GT-114] p 359 A90-23818
- ECKARDT, D.**
Gearless crank - The logical step to economic engines for high thrust p 50 A90-12616
- ECKBRETH, ALAN C.**
Simultaneous CARS measurements of temperature and H₂, H₂O concentrations in hydrogen-fueled supersonic combustion
[AIAA PAPER 90-0158] p 205 A90-19713
- ECKERT, E. R.**
Studies of gas turbine heat transfer airfoil surfaces and end-wall cooling effects
[AD-A212451] p 117 N90-12620
- ECKHARD, K.**
MAVIS flight load simulation p 202 A90-17003
- ECKHARDT, DAVE E., JR.**
An experimental investigation of fault tolerant software structures in an avionics application
[AIAA PAPER 89-3082] p 74 A90-10568
- ECKSTROM, CLINTON V.**
Unsteady pressure and structural response measurements on an elastic supercritical wing p 159 A90-19392
Static aeroelastic tailoring for oblique wing lateral trim p 667 A90-40689
- EDENBOROUGH, H. KIPLING**
Research at NASA's NFAC wind tunnels
[NASA-TM-102827] p 702 N90-25933
- EDGAR, JON M.**
Evaluation and control of an integrated Closed Environmental Control System (ICECS)
[SAE PAPER 901237] p 841 A90-49307
- EDWARDS, D. K.**
Active soot reduction in a spray-fired, axisymmetric model gas turbine combustor
[AIAA PAPER 90-0039] p 191 A90-19844
- EDWARDS, DAVID E.**
Unsteady analysis of hot streak migration in a turbine stage
[AIAA PAPER 90-2354] p 769 A90-42782
- EDWARDS, JOHN A.**
An experimental investigation of supersonic flow over two cavities in tandem
[AIAA PAPER 90-3087] p 795 A90-45901
- EDWARDS, JOHN W.**
Unsteady airloads due to separated flow on airfoils and wings p 471 A90-33311
Unsteady aerodynamics - Physical issues and numerical predictions p 806 A90-46843
Assessment of computational prediction of tail buffeting
[NASA-TM-101613] p 237 N90-15886
- EDWARDS, KELVIN W.**
Hypersonic CFD applications for the National Aero-Space Plane
[SAE PAPER 892310] p 714 A90-45473
- EDWARDS, L. C.**
Wind-tunnel investigation of wing-in-ground effects p 395 A90-31276

- EDWARDS, S. J.**
Hierarchical damage tolerant controllers for smart structures
[AD-A209422] p 31 N90-10022
- EDWARDS, THOMAS A.**
Calculation of hypersonic forebody/inlet flow fields
[AIAA PAPER 90-1493] p 619 A90-39049
- EFIMOV, I. A.**
Effect of the control of turbocompressor guide vanes on the throttle characteristics of a bypass engine p 255 A90-23425
- EFIMTSOV, B. M.**
Wall pressure fluctuation spectra in supersonic flow past a forward facing step p 388 A90-29194
Wall pressure pulsation spectra ahead of internal corners p 804 A90-46545
- EGAMI, KOUICHI**
An automatic Euler solver using unstructured upwind method p 367 A90-25811
- EGAWA, KOUICHI**
Acoustic-thermal environment for USB flap structure. Report 1: Ground simulation test results
[NAL-TM-567] p 88 N90-11697
- EGGLESTON, B.**
Wind tunnel results and numerical computations for the NAE deHavilland series of natural laminar flow airfoils p 628 A90-42403
- EGGOLD, DAVID P.**
Assessment of proposed fighter agility metrics
[AIAA PAPER 90-2807] p 752 A90-45142
Fighter agility metrics, research, and test
[NASA-CR-186118] p 648 N90-23386
- EGOLF, T. ALAN**
Application of a rotary-wing viscous flow solver on a massively parallel computer
[AIAA PAPER 90-0334] p 164 A90-19802
An unsteady helicopter rotor-fuselage aerodynamic interaction analysis p 712 A90-45323
- EGOROV, I. N.**
Effect of the control of turbocompressor guide vanes on the throttle characteristics of a bypass engine p 255 A90-23425
- EHLERS, S. M.**
Static aeroelastic behavior of an adaptive laminated piezoelectric composite wing
[AIAA PAPER 90-1078] p 412 A90-29386
- EHRESMAN, C. M.**
Water ingestion simulation - Test needs p 23 A90-12620
- EHRLICH, F.**
The role of bearing support stiffness anisotropy in suppression of rotordynamic instability p 879 A90-46215
- EICHINGER, D.**
In-situ measurement, modelling and control of the imidization reaction in PMR-15 p 942 A90-50066
- EIDELMAN, SHMUEL**
Application of the hypersonic analogy for validation of numerical simulations p 16 A90-12838
- EIDSAUNE, DAVE**
Flight testing the F-15E terrain following system p 334 A90-24272
- EILTS, MICHAEL D.**
Convergence aloft as a precursor to microbursts p 456 A90-28620
- EISEMAN, PETER R.**
Numerical grid generation in computational fluid mechanics '88; Proceedings of the Second International Conference, Miami Beach, FL, Dec. 5-8, 1988 p 376 A90-26476
Interactive grid generation for turbomachinery flow field simulations p 312 A90-26553
- EISENBERG, JOSEPH D.**
The selection of convertible engines with current gas generator technology for high speed rotorcraft p 852 A90-46933
- EISENLOHR, GERNOT**
Investigation of some effects on the compressor characteristics of an advanced bleed air compressor design p 49 A90-12594
- EKATERINARIS, J.**
Experimental and computational studies of dynamic stall p 147 A90-16780
- EKATERINARIS, J. A.**
Vortical flows over delta wings and numerical prediction of vortex breakdown
[AIAA PAPER 90-0102] p 227 A90-22166
Numerical simulation of the effects of variation of angle of attack and sweep angle on vortex breakdown over delta wings
[AIAA PAPER 90-3000] p 788 A90-45850
- EKBLAD, MARK**
Reduced-order modeling and controller design for a high-performance helicopter p 516 A90-33058

- EKINS, JAMES**
HARP model rotor test at the DNW p 406 A90-28167
- EKLUND, DEAN R.**
A validation study of the Spark Navier Stokes code for nonreacting scramjet combustor flowfields
[AIAA PAPER 90-2360] p 706 A90-42784
- EKLUND, DEAN ROBERT**
Numerical modeling of supersonic turbulent reacting free shear layers p 174 A90-14197
- EKSTEDT, EDWARD E.**
Externally vaporizing system for turbine combustor
[AD-D014284] p 256 A90-15918
- EL-EMAM, S. H.**
Effect of primary air swirl on emissions formations in gas turbine combustors p 47 A90-12573
- EL-FOULY, M.**
Application of 3-D flow analysis to the design of a high work transonic turbine p 628 A90-42395
- EL-HADY, NABIT M.**
Application of localized surface heating to actively control the boundary layer separation p 806 A90-46848
- EL-KADY, M. A.**
Two-dimensional convergent-divergent nozzle flow with wall velocity slip and temperature jump p 807 A90-46884
- EL-MAHALLAWY, F. M.**
Combustion process in a gas turbine combustor when using H₂, NH₃ and LPG fuels p 873 A90-46882
- EL-SHAFFI, A.**
Unbalance response of a Jeffcott rotor incorporating long squeeze film dampers p 880 A90-46237
- ELANDJIAN, L.**
Effects of additives on the processing and properties of LARC-TPI polyimide p 842 A90-50070
- ELANDS, P. J. M.**
Experimental and computational flammability limits in a solid fuel ramjet
[AIAA PAPER 90-1964] p 676 A90-40574
Solid fuel combustion chamber
[LR-634] p 939 N90-29433
- ELAZAR, Y.**
Viscous flow in a controlled diffusion compressor cascade with increasing incidence
[ASME PAPER 89-GT-131] p 291 A90-23829
- ELBAHAR, OSAMA M. F.**
Computation of complex flows in gas turbine combustors with a multi-level additive correction technique p 881 A90-46899
- ELBANNA, HESHAM M.**
Determination of aerodynamic sensitivity coefficients based on the transonic small perturbation formulation p 622 A90-40682
- ELBIALY, E. I.**
Computation of the trailing edge flow downstream a flat plate with finite thickness p 151 A90-17464
- ELDER, J. E.**
Braze repair of MA754 aero gas turbine engine nozzles
[ASME PAPER 89-GT-235] p 342 A90-23886
Surface property improvement in titanium alloy gas turbine components through ion implantation p 953 N90-28713
- ELDER, R. L.**
A study of particle trajectories in a gas turbine intake p 48 A90-12583
Application of recess vane casing treatment to axial flow fans
[ASME PAPER 89-GT-68] p 341 A90-23791
Development of a mass averaging temperature probe p 427 N90-18418
- ELENA, M.**
Turbulence statistics in a shock wave boundary layer interaction p 552 A90-35205
Laser applications in supersonic unsteady flow p 212 N90-13344
- ELFSTROM, G. M.**
Wave cancellation properties of a splitter-plate porous wall configuration p 57 A90-11005
Broadband noise measurement in the transonic test section of the VTI T-38 wind tunnel
[AIAA PAPER 90-1418] p 614 A90-37955
- ELGERSMA, MICHAEL R.**
A dynamic inversion based control law with application to the high angle-of-attack research vehicle
[AIAA PAPER 90-3407] p 884 A90-47662
- ELIAS DE LOS REYES, DAVO**
Use of pulse radars for helicopters detection - Design constraints p 683 A90-41073
- ELIAS FUSTE, ANTONI**
Use of pulse radars for helicopters detection - Design constraints p 683 A90-41073

- ELIASSEN, PETER**
Numerical methods to solve the incompressible Euler and Navier-Stokes equations in 3D with applications p 209 A90-18302
- ELISHAKOFF, ISAAC**
Effect of aerodynamic heating on deformation of composite cylindrical panels in a gas flow p 773 A90-45788
- ELIZAROV, A. M.**
Design of wing profiles for application in nonstall conditions in a given angle-of-attack range p 710 A90-44936
- ELKADY, M. A.**
Study of the expansion of hydrocarbon-oxygen products through supersonic nozzle p 852 A90-46907
- ELLIOTT, ANDREW S.**
Helicopter response to atmospheric turbulence in forward flight p 518 A90-33625
Application of a general-purpose mechanical systems analysis code to rotorcraft dynamics problems p 831 A90-46955
- ELLIOTT, D. W.**
A remote tip-driven fan powered supersonic fighter concept [AIAA PAPER 90-2415] p 663 A90-42167
- ELLIOTT, G. S.**
Compressibility effects in free shear layers [AIAA PAPER 90-0705] p 212 A90-19984
Effects of compressibility on the characteristics of free shear layers p 302 A90-25285
Pressure-based real-time measurements in compressible free shear layers [AIAA PAPER 90-1980] p 703 A90-42709
- ELLIOTT, K.**
Correlation of radial-to-axial vaneless turns for centrifugal compressors [AIAA PAPER 90-1917] p 656 A90-40556
- ELLIOTT, S. J.**
Experiments on the active control of the transmission of sound through a clamped rectangular plate p 695 A90-41109
Active control of sound transmission through a cylindrical shell p 893 A90-46192
Theoretical studies of the active control of propeller-induced cabin noise p 893 A90-46351
In-flight experiments on the active control of propeller-induced cabin noise p 893 A90-46352
- ELLIS, F. A.**
Measurements of aerodynamic forces on aircraft external stores in the NAE trisonic blowdown wind-tunnel p 629 A90-42419
- ELLIS, JOHN**
International aircraft operator data base master requirements and implementation plan [DOT/FAA/CT-90/17] p 967 N90-29247
- ELLIS, KENNETH K.**
Electro-optics engineering support for the integrated launch and recovery television surveillance system [AD-A223450] p 938 N90-29406
- ELLIS, NEWTON C.**
Considerations of noise for the use of compressed speech in a cockpit environment p 404 A90-31334
- ELLIS, R. F.**
Nonlinear mechanics of unstable plasmas as related to high altitude aerodynamics [AD-A215126] p 464 N90-19852
- ELLIS, STEPHEN R.**
Visualization of three dimensional data p 782 N90-25553
- ELLROD, GARY**
Environmental conditions associated with the Dallas microburst storm determined from satellite soundings p 280 A90-22689
- ELMENDORF, W.**
Experiments on the unsteady flow in a supersonic compressor stage p 427 N90-18422
- ELMORE, KIMBERLY L.**
The source region and evolution of a microburst downdraft p 456 A90-28612
- ELROD, BRYANT D.**
Applicability of an augmented GPS for navigation in the National Airspace System p 331 A90-25571
- ELROD, D. A.**
An annular gas seal analysis using empirical entrance and exit region friction factors [ASME PAPER 89-TRIB-46] p 537 A90-33555
- ELROD, W. C.**
Electrical analog circuit for heat transfer measurements on a flat plate simulating turbine vane heat transfer in turbulent flow [AIAA PAPER 90-2412] p 687 A90-42164
- ELROD, WILLIAM C.**
Effects of inlet turbulence scale on turbine blade surface heat transfer in a linear cascade [AIAA PAPER 90-2264] p 768 A90-42761
- ELSENAAR, A.**
Instrumentation requirements for laminar flow research in the NLR high speed wind tunnel HST p 447 A90-28283
Experimental study on vortex and shock wave development on a 65 deg delta wing [NLR-MP-88033-U] p 720 N90-25950
- ELSHOLZ, E.**
Inverse solutions for boundary layers with separation or close to separation under locally infinite swept wing conditions p 279 N90-16192
- ELSTON, S. T.**
Prediction and measurement of rotor blade/stator vane dynamic characteristics of a modern aero-engine axial compressor p 878 A90-46036
Prediction and measurement of rotor blade/stator vane dynamic characteristics of a modern aero-engine axial compressor [PNR90667] p 750 N90-26002
- EMALETDINOV, R. I.**
Variable-velocity flow at the initial mixing section in a diffuser channel p 84 A90-14563
- EMBORG, URBAN**
Interior noise control of the Saab 340 aircraft [SAE PAPER 891080] p 101 A90-14372
- EMBURY, J. D.**
Sliding and abrasive wear behaviour of an aluminum (2014)-SiC particle reinforced composite p 530 A90-33344
- EMERY, EDWARD F.**
A test matrix sequencer for research test facility automation [AIAA PAPER 90-2386] p 759 A90-42791
- EMIN, O. N.**
A study of the working process and losses in annular turbine nozzle cascades with a low contraction ratio p 254 A90-23407
- ENAND, S.**
Integration of intelligent avionics systems for crew decision aiding p 459 A90-30236
- ENDE, H.**
A novel technique for aerodynamic force measurement in shock tubes p 438 A90-28302
- ENDERS, JOHN H.**
The human element: The key to safe, civil operations in adverse weather p 248 N90-15042
- ENDO, T.**
Application of the 'K-gage' to aircraft structural testing p 926 A90-49891
- ENDO, TAKASHI**
A study on flaw detection method for CFRP composite laminates. I - The measurement of crack extension in CFRP composites by electrical potential method p 441 A90-28003
- ENDOH, MASANORI**
Noncontact measurement of rotating blade vibrations [NAL-TR-1033] p 961 N90-29687
- ENDOH, SYUNJI**
Acoustic-thermal environment for USB flap structure. Report 1: Ground simulation test results [NAL-TM-567] p 88 N90-11697
- ENG, A. T.**
Organic coatings - First line of defense p 204 A90-17300
- ENGEDA, A.**
Mathematical formulation of blade surfaces in turbomachinery. I - Theoretical surface formulations [ASME PAPER 89-GT-160] p 360 A90-23848
Mathematical formulation of blade surfaces in turbomachinery. II - Practical examples of determined surfaces [ASME PAPER 89-GT-161] p 361 A90-23849
Estimation of losses in semi-open centrifugal impellers p 537 A90-33597
- ENGELGART, V. N.**
Asymptotic calculation of flow parameters in the problem of hypersonic flow past blunt axisymmetric bodies p 10 A90-12268
- ENGELAND, SHAWN A.**
Simulation evaluation of transition and hover flying qualities of a mixed-flow, remote-lift STOVL aircraft [SAE PAPER 892284] p 757 A90-45464
- ENGLER, NICHOLAS A.**
The collection of non-conus aircraft icing data along with an identification of the geographical areas of potential severe icing and a study of a method of remote determining atmospheric icing data [AD-A215055] p 323 N90-16724
- ENGLER, P.**
Injection molding development of ceramic turbine components [ASME PAPER 89-GT-170] p 361 A90-23855
- ENGLER, ROLF H.**
Experimental investigations on the stability and vorticity of the vortex breakdown phenomenon above delta wings, measured by the ultrasonic laser method [ESA-TT-1079] p 910 N90-28498
- ENIUTIN, G. V.**
The effect of longitudinal fins on turbulent friction drag p 297 A90-24123
An experimental study of the combined effect of longitudinal riblets and vortex breakers on turbulent friction p 805 A90-46565
- ENNS, DALE**
Robustness of dynamic inversion vs mu synthesis - Lateral-directional flight control example [AIAA PAPER 90-3338] p 863 A90-47598
Lateral-directional control of an aircraft using mu synthesis [AIAA PAPER 90-3442] p 865 A90-47695
- ENNS, DALE F.**
Nonlinear inversion flight control for a supermaneuverable aircraft [AIAA PAPER 90-3406] p 864 A90-47661
A dynamic inversion based control law with application to the high angle-of-attack research vehicle [AIAA PAPER 90-3407] p 864 A90-47662
- ENVIA, EDMANE**
Influence of vane sweep on rotor-stator interaction noise p 169 N90-13325
- EPIFANOV, S. V.**
Optimal selection of the parameters to be measured during the identification of gas turbine engines. I - Problem statement p 255 A90-23410
Optimal choice of measured parameters during the identification of gas turbine engines. II - Combined confidence regions and intervals of the identification results p 850 A90-46493
- EPIFANOV, V. M.**
Characteristics of turbulent separation flows on a porous surface under conditions of injection p 231 A90-22422
- EPEL, JOSEPH C.**
Helicopter Airborne Laser Positioning System (HALPS) [NASA-TM-102814] p 654 N90-23399
- EPLER, RICHARD**
Airfoil design and data p 809 A90-47608
- EPPS, J. A.**
Criteria for coal tar seal coats on airport pavements. Volume 2: Laboratory and field studies [AD-A220167] p 674 N90-24277
- EPSTEIN, A. H.**
Active stabilization of aeromechanical systems [AD-A216629] p 454 N90-18672
Experimental and theoretical investigations of flowfields and heat transfer in modern gas turbines [AD-A217663] p 429 N90-19237
- EPSTEIN, CHARLES S.**
The integration of stores on modern tactical aircraft: Where we have been, and what we should do for the future p 337 N90-17552
- ERDOS, J. I.**
The use of pulse facilities for testing supersonic combustion ramjet (scramjet) combustors in simulated hypersonic flight conditions p 46 A90-12562
- ERDOS, JOHN**
Hypervelocity real gas capabilities of GASL's expansion tube (HYPULSE) facility [AIAA PAPER 90-1390] p 594 A90-37935
- ERDOS, JOHN I.**
Calculated chemical and vibrational nonequilibrium effects in hypersonic nozzles p 253 A90-21224
- EREN, K.**
Geodetic network adjustment using GPS triple difference observations and a priori stochastic information [TR-1-1987] p 178 N90-13367
- ERENGIL, M. E.**
Correlation of separation shock motion in a compression ramp interaction with pressure fluctuations in the incoming boundary layer [AIAA PAPER 90-1646] p 569 A90-38774
- ERHARD, W.**
Experimental identification of helicopter engine dynamics from closed loop data p 855 N90-27627
- ERHART, J. J.**
Application of CFD to pitch/yaw thrust vectoring spherical convergent flap nozzles [AIAA PAPER 90-2023] p 657 A90-40597
- ERHEL, JOCELYNE**
Fully vectorized implicit scheme for 2-D viscous hypersonic flow using adaptive finite element methods p 708 A90-44439
- ERICKSON, G. E.**
Impact of nose-probe chines on the vortex flows about the F-16C [AIAA PAPER 90-0386] p 165 A90-19828

ERICKSON, GARY E.

- Canard-wing vortex interactions at subsonic through supersonic speeds
[AIAA PAPER 90-2814] p 711 A90-45154
Multiple vortex and shock interactions at subsonic, transonic, and supersonic speeds
[AIAA PAPER 90-3023] p 793 A90-45890

ERICKSON, J. C., JR.

- Adaptive wind tunnel walls: Compendium of final report - AGARD FDP working group 12
[AIAA PAPER 90-1405] p 595 A90-37944
Wall interference correction for three-dimensional transonic flows
[AIAA PAPER 90-1408] p 558 A90-37947
The aims and history of adaptive wall wind tunnels p 871 N90-26839
Limits of adaptation, residual interferences p 871 N90-26844

ERICKSON, KENNETH R.

- Embedded digital control for aircraft environmental control systems - A practical vehicle management system approach
[SAE PAPER 891438] p 339 A90-27409

ERICSSON, L. E.

- Critique of turbulence models for shock-induced flow separation p 17 A90-12851
Transition effects on airfoil dynamics and the implications for subscale tests p 152 A90-17862
Further analysis of wing rock generated by forebody vortices p 153 A90-17868
Rapid prediction of slender-wing-aircraft stability characteristics
[AIAA PAPER 90-0301] p 163 A90-19782
Various sources of wing rock p 622 A90-40679
Control of forebody flow asymmetry - A critical review
[AIAA PAPER 90-2833] p 711 A90-45164
Unsteady flow separation on slender bodies at high angles of attack
[AIAA PAPER 90-2835] p 712 A90-45166
Rapid prediction of slender-wing aircraft dynamics
[AIAA PAPER 90-3037] p 791 A90-45876
Effects of transition on wind tunnel simulation of vehicle dynamics p 870 A90-49273

ERICSSON, LARS E.

- The fickle effect of nose microasymmetry on the high-alpha aerodynamics
[AIAA PAPER 90-0067] p 161 A90-19663

ERKILET, MURAT

- A study on secondary flow and spanwise mixing in axial flow compressors p 512 N90-21012

ERLICHMAN, SCOTT

- Analysis of heliport environmental data: Indianapolis downtown heliport, Wall Street heliport. Volume 2: Wall Street heliport data plots
[DOT/FAA/CT-TN87/54-VOL-2] p 121 N90-11761
Analysis of heliport environmental data: Indianapolis downtown heliport, Wall Street heliport. Volume 3: Indianapolis downtown heliport data plots
[AD-A217412] p 544 N90-20500

ERLICHMAN, SCOTT L.

- Heliport surface maneuvering test results
[ACD-330] p 59 N90-10897

ERMER, PAUL G.

- Investigation of the failure modes in a metal matrix composite under thermal cycling
[AD-A216195] p 357 N90-17825

EROGU, H.

- Effect of inlet flow angle on the erosion of radial turbine guide vanes
[ASME PAPER 89-GT-208] p 254 A90-22664

ERSHOV, B. A.

- Vibration of a wing of nonzero thickness in supersonic flow p 222 A90-20432
Nonstationary motion of an elastic profile in subsonic incompressible flow p 300 A90-24741
Entry of a flexible airfoil into a vertical gust p 470 A90-32552

ERSHOV, S. V.

- Numerical simulation of transonic flow through oscillating and multi-row two-dimensional airfoil cascades p 814 A90-49460

ERZBERGER, HEINZ

- Design of a final approach spacing tool for TRACON air traffic control
[NASA-TM-102229] p 24 N90-10841
Analysis of sequencing and scheduling methods for arrival traffic
[NASA-TM-102795] p 636 N90-23373
Simulator evaluation of the final approach spacing tool
[NASA-TM-102807] p 636 N90-23374

ESCANDE, B.

- Calculation of three-dimensional turbulent flow in a linear turbine cascade
[ONERA, TP NO. 1989-115] p 3 A90-11147
Calculation of the three dimensional turbulent flow in a linear turbine blade p 513 N90-21021

ESCANES, J. C.

- Use of pulse radars for helicopters detection - Design constraints p 683 A90-41073

ESCH, HELMUT

- Wind tunnel tests of the influence of aerofoil thickness on the normal force and pitching moment of two slender wings at transonic and supersonic Mach numbers
[ESA-TT-1129] p 237 N90-15889

ESCH, PETER

- Low- and high-speed tests with the Dornier 328 wind-tunnel model p 246 A90-21611
Aerodynamic work for Hermes spaceplane p 675 A90-41115

ESCHENROEDER, ALAN Q.

- Blunt-nose inviscid airflows with coupled nonequilibrium processes p 171 N90-13336

ESER, S.

- Thermal stability of jet fuel
[DE90-001160] p 206 N90-14385

ESER, SEMIN

- Thermal stability of jet fuel
[DE90-002760] p 269 N90-15288

ESHOW, MICHELLE M.

- Results of an A109 simulation validation and handling qualities study p 591 A90-38524
A pilot rating scale for evaluating failure transients in electronic flight control systems
[AIAA PAPER 90-2827] p 754 A90-45159
Flight investigation of variations in rotorcraft control and display dynamics for hover
[AIAA PAPER 90-3482] p 866 A90-47731

ESKER, BARBARA S.

- Performance characteristics of a one-third-scale, vectorable ventral nozzle for SSTOVL aircraft
[AIAA PAPER 90-2271] p 586 A90-37562
Performance characteristics of a one-third-scale, vectorable ventral nozzle for SSTOVL aircraft
[NASA-TM-103120] p 552 N90-21725

ESKER, LINDA

- Evolution of Ada technology in the flight dynamics area: Implementation/testing phase analysis
[NASA-TM-103310] p 546 N90-21539
System testing of a production Ada (trademark) project: The GRODY study
[NASA-TM-103308] p 546 N90-21541
Evolution of Ada technology in the flight dynamics area: Design phase analysis
[NASA-TM-103307] p 547 N90-21542

ESPES, J. L.

- Aerospatiale's military helicopter programs p 143 A90-16824

ESSLINGER, P.

- Aerospace materials - Trends and potential p 529 A90-31902

ESTEBAN, E.

- Tests of automatic dependent surveillance (ADS) in Western Europe - Possible future developments p 574 A90-35353

ETCHETO, M.

- Bird impact tests on curved structures of the type Sandwich-Kevlar-Nida for normal and angular shooting
[CEAT-NT-10/S/83-4] p 324 N90-16728

EVANGELISTA, R.

- The design of a low Reynolds number RPV p 828 A90-46385

EVANGELISTA, RAQUEL

- Correlation of theory to wind-tunnel data at Reynolds numbers below 500,000 p 800 A90-46370

EVANS, ALYSON

- Aircraft evacuations: The effect of passenger motivation and cabin configuration adjacent to the exit
[CAA-PAPER-89019] p 913 N90-29336

EVANS, BRIAN

- More power for the Harrier p 745 A90-44597

EVANS, D. L.

- Eliminating the TF30 P-111 + engine rotor-instability problem p 508 A90-32961

EVANS, H. P.

- Wildhaber-Novikov circular arc gears - Some properties of relevance to their design p 70 A90-12999

EVANS, J. E.

- Multipath modeling for simulating the performance of the microwave landing system p 241 A90-21384

EVANS, JAMES

- Development of an automated windshear detection system using Doppler weather radar p 373 A90-25567

EVANS, R. L.

- Calculation of unsteady boundary layer development on axial-flow turbomachinery blading p 48 A90-12588

EVANS, RONALD J.

- Dynamic FLIR simulation in flight training research p 681 A90-40109

EVELETH, EDMUND L.

- Ethanol and methanol in intermittent combustion engines p 950 A90-51622

EVERDING, STEVEN

- Integrally heated tooling for economical, nonautoclave production of thermoplastic parts p 956 A90-50200

EVERETT, R. A., JR.

- Fatigue crack initiation and small crack growth in several airframe alloys
[NASA-TM-102598] p 454 N90-18746

EVERETT, SEYMOUR

- Design considerations for achieving MLS Category III requirements p 331 A90-25575

EVERMAN, WALTER

- Chaotic response of aerosurfaces with structural nonlinearities (Status report)
[AIAA PAPER 90-1034] p 392 A90-29378

EVERSMAN, W.

- A reduced cost rational-function approximation for unsteady aerodynamics
[AIAA PAPER 90-1155] p 390 A90-29367

EVERTON, ERIC L.

- Interactive grid generation for fighter aircraft geometries p 311 A90-26546
Interactive grid adaption p 806 A90-46850

EWALD, B.

- A measurement window for a cryogenic windtunnel p 523 A90-34233
Balance calibration and evaluation software p 523 A90-34237

- Automatic calibration machine for internal cryogenic balances p 524 A90-34247

- Automatic calibration machine for cryogenic and conventional internal strain gage balances
[AIAA PAPER 90-1396] p 595 A90-37939

EWALD, BERND

- Fully automatic calibration machine for internal 6-component wind tunnel balance including cryogenic balances p 437 A90-28294

EWALD, J.

- Helicopter ground and air resonance dynamics p 646 A90-42457

EWINS, D. J.

- Sensitivity analysis using resonance and anti-resonance frequencies - A guide to structural modification p 536 A90-33396

EXLEY, T.

- Correlation of radial-to-axial vaneless turns for centrifugal compressors
[AIAA PAPER 90-1917] p 656 A90-40556

- Numerical analysis of the flows in annular slinger combustors
[AIAA PAPER 90-2164] p 685 A90-42052

EXTREMET, G. P.

- Numerical investigations of heat transfer and flow rates in rotating cavities. Simulation of the movement generated by wall temperature gradients, by source-sink mass flows or by the differential rotation of the walls, under the influence or coriolis and centrifugal forces
[ETN-90-96253] p 454 N90-18695

F**FABRIS, D.**

- The effect of constructive and destructive interference on the downstream development of twin jets in a crossflow. I - Destructive interference of laterally spaced jets
[AIAA PAPER 90-1623] p 607 A90-38752

- The effect of constructive and destructive interference on the downstream development of twin jets in a crossflow. II - Interference effects of angularly displaced jets
[AIAA PAPER 90-2107] p 684 A90-42020

FABRY, JOHN M.

- A glossary of terms, definitions, acronyms, and abbreviations related to the National Airspace System
[DOT/FAA/CT-TN89/53] p 967 N90-29249

FADEN, DELMAR M.

- Aircraft interface with the future ATC system p 331 A90-25574

FADEEV, I. V.

- The effect of longitudinal fins on turbulent friction drag p 297 A90-24123

FADEEV, V. T.

- Identification of a stress-strain computation model and planning of tensometry points in strength and stability studies p 880 A90-46482

FAHERTY, M. F.

- Propulsion system flight test analysis using modeling techniques
[AIAA PAPER 90-3288] p 853 A90-48874

FAIN, HOWARD

- An intelligent system for autonomous navigation of airborne vehicles p 26 A90-11696

FAIRHURST, W. S.

- FAA air traffic control operations concepts. Volume 7: ATCT (Airport Traffic Control Towers) tower controllers
[AD-A210455] p 332 N90-16730

- FALABELLA, R.**
Variations in impact test methods for tough composites p 946 A90-50167
- FALCHETTI, F.**
Aerodynamic design of an HP compressor stage using advanced computation codes p 156 A90-18479
Calculation of the secondary flow in an axial turbine p 513 N90-21022
- FALEMPIN, G.**
Comparison with experiment of various computational methods of airflow on three helicopter fuselages p 630 A90-42436
- FALLAVOLLITA, MICHAEL A.**
Three dimensional Discrete Particle Simulation about the AFE geometry [AIAA PAPER 90-1778] p 560 A90-38468
- FALLS, J. R.**
Development of a simulated bird-strike test method p 600 A90-37444
- FALTUS, MILAN**
Problems in the synthesis of advanced aircraft control systems p 751 A90-44723
- FAN, DING**
Study on process control of aeroengine using microcomputer p 586 A90-37239
- FAN, RENZHOU**
A ground simulation-inspection system for avionic devices p 594 A90-37232
- FAN, ZUOMIN**
Main characteristic parameter model for jet engine fault diagnosis p 585 A90-37210
- FANCHER, M. F.**
Hot-film system for transition detection in cryogenic wind tunnels p 122 N90-12522
- FANG, JISHENG**
Analysis and calculation for interaction between shock wave and laminar boundary layer p 909 A90-52778
- FANG, Z.**
A weighted residual formulation for finite element solutions of the steady Euler equations p 770 A90-44457
- FANG, ZHENGPING**
The analysis of entry into and recovery from a spin for the J16 aircraft p 195 A90-16854
- FANN, F.**
Preliminary fire extinguishing tests with handheld bottles: A comparison of extinguishing compounds [DOT/FAA/CT-TN89/60] p 370 N90-17930
- FARAG, K.**
A comparison of a droplet impingement code to icing tunnel results [AIAA PAPER 90-0670] p 352 A90-26979
- FARHAT, C.**
Transient aeroelastic computations using multiple moving frames of reference [AIAA PAPER 90-3053] p 798 A90-45932
- FARID, M.**
Algebraic boundary-conforming grid generation around wing/tail-body configurations p 308 A90-26480
- FARJOLI, M.**
EH-101 main rotor hub application of thick carbon fiber unidirectional tension bands p 618 A90-42489
- FARMER, DOMINIC**
Signal processing in a digital GPS receiver p 128 A90-14006
- FARMER, ED**
Entrapment plating of abrasive particles for jet engine clearance control [SAE PAPER 890918] p 286 A90-24685
- FARMER, MOSES G.**
An experimental study of tip shape effects on the flutter of aft-swept, flat-plate wings [NASA-TM-4180] p 582 N90-22555
- FAROKHI, S.**
Blade surface pressure measurement on a pusher propeller in flight [SAE PAPER 891040] p 139 A90-14346
- FAROUK, B.**
Numerical simulations of the structure of supersonic shear layers [AD-A224164] p 960 N90-29587
- FARQUHAR, B. W.**
Analytical methods for subsonic propulsion system integration p 29 A90-12613
- FARRANDO, ALAIN**
Characterization of helicopter turboshaft engine noise p 660 A90-41759
- FARRELL, KEVIN J.**
An investigation of end-wall vortex cavitation in a high Reynolds number axial-flow pump [AD-A211426] p 133 N90-11982
- FARRELL, MICHAEL K.**
Aerodynamic design of the V-22 Osprey proprotor p 385 A90-28241
- FARRIS, GLENN G.**
A head up display format for application to V/STOL aircraft approach and landing [NASA-TM-102216] p 340 N90-17632
- FARSHCHI, M.**
Chemically reacting supersonic flow calculation using an assumed PDF model [AIAA PAPER 90-0731] p 230 A90-22256
Numerical simulation of a turbulent flow through a shock wave [AIAA PAPER 90-1641] p 608 A90-38769
- FASANELLA, EDWIN L.**
Scaling effects in the impact response of graphite-epoxy composite beams [SAE PAPER 891014] p 128 A90-14326
Impact evaluation of composite floor sections [SAE PAPER 891018] p 100 A90-14330
Analysis of the National Transonic Facility mishap [NASA-TM-101686] p 328 N90-17620
A review of the analytical simulation of aircraft crash dynamics [NASA-TM-102595] p 484 N90-20068
Behavior of composite/metal aircraft structural elements and components under crash type loads: What are they telling us [NASA-TM-102681] p 774 N90-25368
- FAUGHNAN, BRIAN W.**
Polysilicon active-matrix liquid crystal displays for cockpit applications p 681 A90-40393
- FAUST, G. K.**
Status report on a natural laminar-flow nacelle flight experiment p 105 N90-12550
Nacelle design p 105 N90-12551
- FAVALORO, S. C.**
Nonaxisymmetric instabilities in a dump combustor with a swirling inlet flow p 253 A90-21228
- FAVIER, D.**
Experimental study of 2D/3D interactions between a vortical flow and a lifting surface p 86 A90-15849
- FAVIN, S.**
Effects of pressure mismatch on slot injection in supersonic flow [AIAA PAPER 90-0092] p 227 A90-22161
- FECHER, FRANK J.**
In-service inspection of composite components on aircraft at depot and field levels p 885 A90-28078
- FEDCHENKO, VIKTOR S.**
Radio deviation of airborne goniometers p 242 A90-22733
- FEDELE, G.**
New approach for Doppler ambiguities resolution in medium pulse repetition frequency radars p 240 A90-20937
- FEDERSPIEL, JOHN**
Three dimensional transonic and supersonic flow prediction in axi-vectorized nozzles using a finite volume method [AIAA PAPER 90-2026] p 624 A90-41989
- FEDOROV, A. V.**
Excitation and development of unstable perturbations in a supersonic boundary layer p 710 A90-44928
- FEDOROV, ROMAN M.**
Mathematical modeling of plane parallel separated flows past bodies p 619 A90-39475
- FEDOSEEV, EFIM P.**
Airborne digital computers and systems p 927 A90-52410
- FEESER, KENNETH A.**
The STOL maneuver technology demonstrator manned simulation test program p 439 A90-30716
- FEHR, V. S.**
Eliminating the TF30 P-111 + engine rotor-instability problem p 508 A90-32961
- FEHRENBACHER, LARRY**
Improved Thermo-Oxidative-Deposition screening tests for turbine lubricants [AD-A217785] p 533 N90-21188
- FEHRING, NANCY P.**
The new high Reynolds number Mach 8 capability in the NSWV Hypervelocity Wind Tunnel 9 [AIAA PAPER 90-1379] p 594 A90-37928
- FEIEREISEN, WILLIAM J.**
Three dimensional Discrete Particle Simulation about the AFE geometry [AIAA PAPER 90-1778] p 560 A90-38468
- FEIG, PAUL D.**
The next AIAA engine design competition - A commercial engine [AIAA PAPER 89-2258] p 550 A90-33675
- FEIK, R. A.**
Identification of an adequate model for collective response dynamics of a Sea King helicopter in hover p 56 A90-12766
- FEJTEK, IAN**
A CFD study of tilt rotor flowfields [NASA-CR-186116] p 171 N90-13349
- FELDMAN, SIDNEY**
A surveillance 360 deg television orientation and ranging system as an aid to collision avoidance p 577 A90-36922
- FELDMANN, ROBERT J.**
Development of air-to-air laser communications p 487 A90-31938
Extended communication path length scintillation measurements and model - A discussion of results p 725 A90-43230
- FELKER, FORT F.**
A review of tilt rotor download research p 630 A90-42437
- FENG, GANG**
Design of direct lift control systems against vertical gust p 196 A90-18592
- FENG, Y. C.**
The acoustic phenomena of the stalling flutter p 78 A90-11801
- FENG, Y.-S.**
Unified optimal criterion method - Combination of direction of gradient and ejection line p 367 A90-26077
- FENG, YU CHENG**
The interaction between distortion of inlet flow and blade stall flutter in axial-flow compressor p 854 A90-49466
- FENG, ZHENGPING**
Analyses of revising the inlet profile of a radial inflow turbine impeller p 602 A90-35831
- FENTON, B. C.**
Statistics on aircraft gas turbine engine rotor failures that occurred in US commercial aviation during 1988 [DOT/FAA/CT-89/30] p 511 N90-21008
- FERG, D.**
Plan, execute, and discuss vibration measurements and correlations to evaluate a NASTRAN finite element model of the AH-64 helicopter airframe [NASA-CR-181973] p 960 N90-28866
- FERGUSON, DENNIS**
Microminiature flight test instrumentation [AIAA PAPER 90-1274] p 504 A90-33898
- FERGUSON, SAMUAL W.**
Rotorwash flow fields - Flight test measurement, prediction methodologies, and operational issues p 817 A90-46930
- FERMAN, M. A.**
A dynamicist's view of fuel tank skin durability p 251 N90-15915
- FERNANDEZ DE LA MORA, J.**
Brownian motion far from equilibrium - A hypersonic approach p 555 A90-35917
- FERNANDEZ, S. M.**
Fluorescence spectroscopy and thermometry for hypersonic flight research [AIAA PAPER 90-1272] p 538 A90-33897
- FERNANDO, E. M.**
A numerical study of mixing and chemical heat release in supersonic mixing layers [AIAA PAPER 90-0152] p 163 A90-19710
- FERNANDO, EMERICK M.**
A supersonic turbulent boundary layer in an adverse pressure gradient p 303 A90-25592
- FERNANDO, M. S. U. K.**
Application of the moving surface boundary layer control to a two dimensional airfoil p 628 A90-42405
- FERRAND, P.**
Parabolized calculations of turbulent three dimensional flows in a turbine duct p 482 N90-21013
- FERRARA, AUGUSTO M.**
Straight alcohol fuels for general aviation aircraft [SAE PAPER 891038] p 124 A90-14344
The performance of alternate fuels in general aviation aircraft p 950 A90-51621
Investigations into gasoline/alcohol blends for use in general aviation aircraft p 950 A90-51623
In-flight evaluations of turbine fuel extenders [DOT/FAA/CT-89/33] p 444 N90-19387
Turbine fuel alternatives (near term) [AD-A218405] p 601 N90-22695
- FERRARIS, PIER LUIGI**
Evolution of flight commands in Aeritalia design [ETN-89-95211] p 120 N90-11759
- FERRIS, ALICE T.**
Cryogenic balances for the US NTF p 264 N90-15959
- FERRIS, JAMES C.**
A study of high-lift airfoils at high Reynolds numbers in the Langley low-turbulence pressure tunnel [NASA-TM-89125] p 1 N90-10002
- FERTIG, TIM M.**
Redesign of an electro-optical shroud in graphite/epoxy p 676 A90-40215
- FERTIS, D. G.**
Parametric studies of advanced turboprops p 253 A90-21225

FESHCHENKO, S. A.

Effect of incoming flow turbulence on the aerodynamic characteristics of a smooth symmetric body at large angles of attack p 904 A90-50817

FESSLER, H.

Flanged joints of aeroengines [PNR90594] p 116 N90-12609

FESSOU, P.

Wind-tunnel test of the air intake of an unducted fan [AAAF PAPER NT 88-19] p 4 A90-11436

FEUERBACHER, BERNDT

Materials and structures for 2000 and beyond: An attempted forecast by the DLR Materials and Structures Department [ESA-TT-1154-REV] p 775 N90-26173

FEYZI, F.

Development of two multi-sensor hot-film measuring techniques for free-flight experiments p 417 A90-28291

FEZOU, L.

A class of implicit upwind schemes for Euler simulations with unstructured meshes p 5 A90-11597

FFOWCS WILLIAMS, J. E.

The active control of engine instabilities p 44 A90-12505

FIALA, R.

Full scale study of a cabin fire in an A300 fuselage section p 326 N90-17592

FICKE, J. M.

Application of fracture mechanics and half-cycle method to the prediction of fatigue life of B-52 aircraft pylon components [NASA-TM-88277] p 214 N90-13820

FIDELL, S. A.

Audibility and annoyance of en route noise of unducted fan engines [AD-A223687] p 966 N90-30035

FIDELL, SANFORD

Noise and sonic boom impact technology. Initial development of an Assessment System for Aircraft Noise (ASAN). Volume 1: Executive summary [AD-A214164] p 379 N90-17410

Noise and sonic boom impact technology. Initial development of an Assessment System for Aircraft Noise (ASAN). Volume 2: System design strategy [AD-A214454] p 379 N90-17411

Noise and sonic boom impact technology. Initial development of an Assessment System for Aircraft Noise (ASAN). Volume 3: Technical description [AD-A214455] p 379 N90-17412

FIDLER, JIFI

Mathematical model of turboprop engine behaviour p 254 A90-23351

Modelling and simulation of turboprop engine behaviour [AD-A214454] p 424 A90-29946

Mathematical simulation model of an aircraft gas turbine p 745 A90-44721

FIEBIG, DAVID A.

Full authority digital electronic engine control system provides needed reliability [AIAA PAPER 90-2037] p 658 A90-40606

FIEBIG, M.

Computation of laminar mixed convection flow in a channel with wing type built-in obstacles p 67 A90-11114

FIEBIG, MARTIN

Navier-Stokes computations of three-dimensional laminar flows with buoyancy in a channel with wing-type vortex generators p 772 A90-45728

FIEGIB, M.

Structure of velocity and temperature fields in laminar channel flows with longitudinal vortex generators p 273 A90-23207

FIELD, J. E.

Multiple impact jet apparatus (MIJA) - Application to rain erosion studies p 525 A90-34580

The effects of toughening stresses on liquid impact induced fracture p 692 A90-41315

FIELDS, JAMES M.

Cumulative airport noise exposure metrics: An assessment of evidence for time-of-day weightings, revision [AD-A214878] p 352 N90-16773

Social survey findings on en route noise annoyance issues p 698 N90-24868

FIELDSON, FRANK

RADC fault tolerant system reliability evaluation facility [AD-A215298] p 377 N90-17348

FILIPPOV, K. N.

Pressure pulsation in a cavity in the path of subsonic and supersonic gas flow p 10 A90-12279

FILIPPOVSKAIA, L. M.

Effect of the nonuniformity of external supersonic flow and nozzle deflection angle on the base pressure behind an axisymmetric body with a single supersonic jet p 802 A90-46486

FINAISH, F.

The influence of a rotating leading edge on accelerating starting flow over an airfoil [AIAA PAPER 90-0583] p 168 A90-19932

FINCH, W.

Computer-based tools for assisting air traffic controllers with arrivals flow management [RSRE-88001] p 178 N90-13366

FIROOZIAN, R.

Design and application of a finite element package for modelling turbomachinery vibrations p 70 A90-13011

FISCHER, ALBERTE

Aircraft measurements of sea surface conditions and their relationship to marine boundary-layer dynamics p 888 A90-47572

FISCHER, JOHN J.

Mechanical alloying spreads its wings p 950 A90-51200

FISCHER, MICHAEL C.

Development flight tests of JetStar LFC leading-edge flight test experiment p 104 N90-12509

Simulated airline service experience with laminar-flow control leading-edge systems p 104 N90-12512

FISCHERSWORTHING, A.

The in service multi-axial-stress situation in an uncooled gas turbine blade p 423 A90-29880

FISCHLER, J. E.

Laminar flow control perforated wing panel development [NASA-CR-178166] p 63 N90-10187

FISHER, BRUCE D.

Multistroke cloud-to-ground strike to the NASA F-106B airplane p 482 A90-32304

Cloud-to-ground strikes to the NASA F-106 airplane p 574 A90-35767

Final results of the NASA storm hazards program p 819 A90-49834

Effects of lightning on operations of aerospace vehicles p 239 N90-15065

FISHER, CARL E.

Detachment of turbulent boundary layers with varying free-stream turbulence and lower Reynolds numbers p 802 A90-46378

FISHER, D. F.

Laminar flow control leading-edge systems in simulated airline service p 335 A90-26134

FISHER, DAVID F.

In-flight flow visualization characteristics of the NASA F-18 high alpha research vehicle at high angles of attack [SAE PAPER 892222] p 713 A90-45439

F-18 high alpha research vehicle surface pressures - Initial in-flight results and correlation with flow visualization and wind-tunnel data [AIAA PAPER 90-3018] p 792 A90-45885

Development flight tests of JetStar LFC leading-edge flight test experiment p 104 N90-12509

Simulated airline service experience with laminar-flow control leading-edge systems p 104 N90-12512

Water-tunnel study results of a TF/A-18 and F/A-18 canopy flow visualization [NASA-TM-101705] p 573 N90-22532

In-flight flow visualization with pressure measurements at low speeds on the NASA F-18 high alpha research vehicle [NASA-TM-101726] p 910 N90-28505

FISHER, DIANA C.

Design and analysis aid for evaluating aircraft structures p 694 A90-41188

FISHER, F. A.

Aircraft lightning protection handbook [AD-A222716] p 820 N90-27668

FISHER, JAY L.

Inspection development for T-37 wing spar cap lug [AD-A214826] p 287 N90-16708

FISHER, V. A.

Engine controls for the 1990's [PNR90546] p 114 N90-11748

FITZGERALD, EDWARD J.

Measurements in a separation bubble on an airfoil using laser velocimetry p 384 A90-27977

FITZGERALD, JOHN H.

Inspection development for T-37 wing spar cap lug [AD-A214826] p 287 N90-16708

FITZGIBBON, K. T.

Autoland with GPS p 97 A90-13985

FITZPATRICK, G. A.

Diffusion bonding aeroengine components p 131 A90-16012

FITZSIMONS, P. M.

Time domain parameter identification techniques applied to the UH-60A Black Hawk Helicopter p 77 A90-12774

FITZSIMONS, PHILIP MATTHEW

Design of a helicopter automatic flight control system using adaptive control p 522 N90-21040

FLACKBERT, A. CLYDE

Helicopter obstacle avoidance system - The use of manned simulation to evaluate the contribution of key design parameters p 417 A90-28218

FLACKE, JOACHIM

Antenna and radar signature technology at Dornier p 261 A90-21605

FLAHERTY, JOSEPH E.

Solving compressible flow problems using adaptive finite quadtree and octree grids p 155 A90-18243

FLAIG, A.

Results of wind tunnel ground effect measurements on Airbus A320 using turbine power simulation and moving tunnel floor techniques [AIAA PAPER 90-1427] p 559 A90-37964

FLAMENT, C.

Chemical and vibrational non-equilibrium nozzle flow calculation by an implicit upwind method [ONERA, TP NO. 1989-175] p 223 A90-21037

FLAMENT, CYRIL

Inviscid non equilibrium flow in ONERA F4 wind tunnel [ONERA, TP NO. 1989-161] p 223 A90-21029

FLAMM, JEFFREY D.

Supersonic aerodynamic characteristics of a Mach 3 high-speed civil transport configuration [AIAA PAPER 90-3210] p 811 A90-48836

FLANDERS, JOEY B.

An expert system for real-time aircraft monitoring [AIAA PAPER 90-1311] p 545 A90-33921

FLANDERS, K.

The RB199: An in-service success [PNR90544] p 114 N90-11746

FLANNELLY, WILLIAM G.

Investigation of variation in fatigue life calculated using damage fraction p 537 A90-33624

FLATICO, JOSEPH M.

Silicon-etalon fiber-optic temperature sensor [NASA-TM-102389] p 187 N90-13381

FLECK, THOMAS

Flight testing of the Tornado Terrain Following System p 35 N90-10875

FLEETER, S.

Three-dimensional aerodynamics of an annular airfoil cascade including loading effects p 87 A90-15889

Inlet distortion generated periodic aerodynamic rotor response [ASME PAPER 89-GT-299] p 475 A90-33567

FLEETER, SANFORD

Multistage compressor vane row aerodynamic gust response p 6 A90-11783

The unsteady aerodynamics of an oscillating cascade in a compressible flow field p 7 A90-11789

Aeroelastic detuning for stability enhancement of unstalled supersonic flutter p 189 A90-17462

Unsteady incompressible aerodynamics and forced response of detuned blade rows [AIAA PAPER 90-0340] p 191 A90-19805

Viscous oscillating cascade aerodynamics and flutter by a locally analytical method [AIAA PAPER 90-0579] p 168 A90-19929

Investigation of oscillating airfoil shock phenomena [AIAA PAPER 90-0695] p 169 A90-19981

Unsteady aerodynamic gust response including steady flow separation p 556 A90-36262

Aerodynamic detuning for control of supersonic rotor forced response [AIAA PAPER 90-2018] p 621 A90-40596

Flow induced forced response of an incompressible radial cascade including profile and incidence effects [AIAA PAPER 90-2352] p 626 A90-42136

Cascade aerodynamic gust response including steady loading effects p 904 A90-51006

Aerodynamics of a linear oscillating cascade [NASA-TM-103250] p 817 N90-27657

FLEISCHER, R. L.

Intermetallic compounds for strong high-temperature materials - Status and potential p 125 A90-15022

FLEISCHMANN, DOMINIQUE

An analytical technique for addressing airship ditching behavior [AIAA PAPER 89-3167] p 238 A90-20589

FLEMING, O. P.

Active vibration control for flexible rotor by optimal direct-output feedback control p 879 A90-46222

Spray automated balancing of rotors - How process parameters influence performance p 879 A90-46228

FLEMING, P. J.

Implementation of a transputer-based flight controller p 667 A90-38966

Fault-tolerant transputer-based controller configurations for gas-turbine engines p 852 A90-48529

Parallel processing implementation of a flight controller p 333 N90-16743

- FLETCHER, DOUGLAS G.**
A validation study of the Spark Navier Stokes code for nonreacting scramjet combustor flowfields
[AIAA PAPER 90-2360] p 706 A90-42784
- FLETCHER, JAY W.**
Applications of flight control system methods to an advanced combat rotorcraft
[NASA-TM-101054] p 119 N90-11752
Time and frequency-domain identification and verification of BO-105 dynamic models
[AD-A216828] p 415 N90-18389
Obtaining consistent models of helicopter flight-data measurement errors using kinematic-compatibility and state-reconstruction methods
[AD-A22533] p 815 N90-26799
- FLEURY, CLAUDE**
Sensitivity and optimization of composite structures in MSC/NASTRAN p 208 A90-17370
- FLICK, JOHN**
New power system architecture for the 747-400 p 508 A90-33349
Design features of the 747-400 Electric Power System [SAE PAPER 892227] p 746 A90-45443
- FLOOD, J. D.**
Engine inlet distortion in a 9.2 percent scaled vectored thrust STOVL model in ground effect
[AIAA PAPER 89-2910] p 301 A90-25043
Engine inlet distortion in a 9.2 percent scale vectored thrust STOVL model in ground effect
[NASA-TM-102358] p 318 N90-17561
- FLOOD, JOSEPH D.**
Hot gas ingestion characteristics and flow visualization of a vectored thrust STOVL concept
[NASA-TM-103212] p 751 N90-26009
- FLORES, JOLEN**
Zonal Navier-Stokes methodology for flow simulation about a complete aircraft p 709 A90-44727
- FLORYAN, J. M.**
Flow over a leading edge with distributed roughness p 703 A90-42646
- FLOWERS, GEORGE T.**
Experimental study of the effects of nonlinearities on ground resonance p 643 A90-40172
- FLUGSTAD, T. H.**
High Mach exhaust system concept scale model test results
[AIAA PAPER 90-1905] p 655 A90-40552
- FLYNN, KEVIN T.**
The Stealth biplane: A proposal in response to a low Reynolds Number station keeping mission
[NASA-CR-186680] p 734 N90-25127
- FLYNN, MIKE**
The DELTA MONSTER: An RPV designed to investigate the aerodynamics of a delta wing platform
[NASA-CR-186226] p 924 N90-29381
- FOCH, RICHARD J.**
Flight testing of the Low Altitude/Airspeed Unmanned Research Aircraft (LAURA)
[AIAA PAPER 90-1262] p 579 A90-36026
Flight testing Navy low Reynolds Number (LRN) unmanned aircraft p 828 A90-46387
- FODALE, ROBERT**
Miniaturization of flight deflection measurement system
[NASA-CASE-LAR-13628-1] p 689 N90-23707
- FOELKER, JAMIE L.**
Discrete proportional Plus Integral (PI) multivariable control laws for the Control Reconfigurable Combat Aircraft (CRCA)
[AD-A215664] p 433 N90-18431
- FOERSCHING, H.**
A parametric study of the flutter stability of two-dimensional turbine and compressor cascades in incompressible flow p 225 A90-21593
- FOERSCHING, HANS**
Materials and structures for 2000 and beyond: An attempted forecast by the DLR Materials and Structures Department
[ESA-TT-1154-REV] p 775 N90-26173
- FOERSCHING, HANS W.**
Adaptation for unsteady flow p 871 N90-26845
- FOKIN, D. A.**
Design of wing profiles for application in nonstall conditions in a given angle-of-attack range p 710 A90-44936
Construction of wing profiles in subsonic gas flow by the method of quasi-solutions for inverse boundary value problems p 803 A90-46542
- FOLDA, T.**
Highly damage tolerant carbon fiber epoxy composites for primary aircraft structural applications p 125 A90-14660
Toughened thermosets for damage tolerant carbon fiber reinforced composites p 443 A90-29825
- FOLTZ, H. L.**
Energy Efficient Engine combustor test hardware detailed design report
[NASA-CR-168301] p 929 N90-28554
Energy Efficient Engine (E3) combustion system component technology performance report
[NASA-CR-168274] p 930 N90-28555
- FOMIN, V. M.**
Investigation of wall pressure pulsations during the passive control of shock/boundary layer interaction p 378 A90-24132
- FOMIN, V. N.**
Effect of the control of turbocompressor guide vanes on the throttle characteristics of a bypass engine p 255 A90-23425
- FONTAINE, J. P.**
Numerical investigations of heat transfer and flow rates in rotating cavities. Simulation of the movement generated by wall temperature gradients, by source-sink mass flows or by the differential rotation of the walls, under the influence of coriolis and centrifugal forces
[ETN-90-96253] p 454 N90-18695
- FOOTE, L.**
Plan, execute, and discuss vibration measurements and correlations to evaluate a NASTRAN finite element model of the AH-64 helicopter airframe
[NASA-CR-181973] p 960 N90-28866
- FORD, S. D.**
The (airplane) design professor as sheepherder - An industry role in enhancing engineering education
[AIAA PAPER 90-3259] p 897 A90-49121
- FORDEN, NOAH P.**
Feasibility study for a microwave-powered ozone sniffer aircraft
[NASA-CR-186660] p 650 N90-23397
- FORM, P.**
Safety net functions p 826 N90-27685
- FORNASIER, L.**
An intensive procedure for the design of pressure-specified three-dimensional configurations at subsonic and supersonic speeds by means of a higher-order panel method p 500 N90-20982
- FORNELL, PETER**
Honeycomb quality requirements - A user's perspective p 538 A90-33705
- FORNEY, L. J.**
Droplet impaction on a supersonic wedge - Consideration of similitude p 400 A90-27986
- FORRESTER, B. D.**
RAN (Royal Australian Navy) vibration analysis system operator's guide
[AD-A212441] p 107 N90-12596
- FORRESTER, PATRICK GRAHAM**
Effects of aeroelastic tailoring on anisotropic composite material beam models of helicopter blades
[AD-A213478] p 249 N90-15095
- FORSETH, DANIEL C.**
Rockwell International's miniature high performance GPS receiver p 726 A90-43701
- FORSYTH, GRAHAM F.**
Concept demonstration of the use of interactive fault diagnosis and isolation for TF30 engines p 617 A90-41177
- FORTUNATO, BERNARDO**
Computation of steady three dimensional transonic internal flows p 304 A90-25771
- FOSTER, JOHN E.**
Development of acceptance plans for airport pavement materials. Volume 1: Development
[DOT/FAA/RD-90/15] p 937 N90-28581
- FOSTER, JOHN V.**
Development of a preliminary high-angle-of-attack nose-down pitch control requirement for high-performance aircraft
[NASA-TM-101684] p 399 N90-19206
- FOSTER, ROBERT G.**
The effect of experimental uncertainties on icing test results
[AIAA PAPER 90-0665] p 322 A90-26977
- FOTTNER, LEONHARD**
Overview on test cases for computation of internal flows in turbomachines
[ASME PAPER 89-GT-46] p 288 A90-23772
- FOUQUES, B.**
Preliminary flight evaluation of the SA 365 Panther helicopter in air-to-air combat manoeuvres p 647 A90-42494
- FOURMAUX, ANTOINE**
Numerical simulation of three-dimensional unsteady flows in turbomachines
[ONERA, TP NO. 1989-118] p 4 A90-11149
- FOURNIER, D.**
Defects in monoblock cast turbine wheels p 443 N90-18400
- FOURNIER, FRANCETTE**
Prediction of the interaction noise emitted by helicopter fenestrons p 218 A90-18449
A model suitable for predicting the noise associated with the ducted tail rotor of a helicopter
[ECL-88-09] p 220 N90-14074
- FOURNIER, J.**
The application of infrared thermography to the measurement of heat fluxes in a wind tunnel
[ONERA, TP NO. 1989-192] p 261 A90-21051
- FOUSSEKIS, D.**
Aerodynamics of unsteady systems. Numerical study of potential flow/boundary layer coupling
[ETN-90-96257] p 396 N90-18367
- FOUTS, RANDALL S.**
Air Force use of civil airworthiness criteria for testing and acceptance of military derivative transport aircraft
[AIAA PAPER 90-3289] p 818 A90-48875
- FOWLER, D. K.**
Engineering design models for ramjet efficiency and lean blowoff
[AIAA PAPER 90-2453] p 663 A90-42176
- FOWLER, KEVIN R.**
Development of jet transport airframe fatigue test spectra p 351 A90-28753
- FOWLER, P. H.**
The remote sensing of temperature in gas turbine engine components using epithermal neutrons p 70 A90-12630
- FOX, D. S.**
Influence of alloying elements on the oxidation behavior of NbAl₃ p 355 A90-24861
- FOX, DENNIS S.**
Burner rig hot corrosion of silicon carbide and silicon nitride p 355 A90-25267
- FOX, MICHAEL**
Total temperature separation in jets
[AIAA PAPER 90-1621] p 607 A90-38750
- FOX, T. G.**
Development of a dual fuel injector for a gas turbine combustor
[ASME PAPER 89-GT-25] p 340 A90-23764
- FOZARD, JOHN W.**
The Hawker P1127 vectored thrust fighter program - Lessons learned
[AIAA PAPER 90-3238] p 835 A90-48848
- FRADENBURGH, EVAN A.**
The variable-diameter rotor - A key to high performance rotorcraft p 413 A90-30118
Improving tilt rotor aircraft performance with variable-diameter rotors p 646 A90-42445
- FRANCIS, DENISE M.**
Direct frequency modulation in interferometric systems p 68 A90-11662
- FRANCISCO, SHERMAN G.**
Aircraft Separation by Synchronized Transponder Interrogation (ASSTI) p 727 A90-43724
- FRANCISCUS, LEO C.**
RAMSCRAM: A flexible ramjet/scramjet engine simulation program
[NASA-TM-102451] p 194 N90-14235
Supersonic through-flow fan engine and aircraft mission performance
[NASA-TM-102304] p 516 N90-21038
- FRANCOIS, G.**
Instrumentation being developed for the ONERA F4 wind tunnel
[ONERA, TP NO. 1989-189] p 261 A90-21049
- FRANCOZ RIGALT, ANTONIO**
A review of regulations - The Chicago Convention and the bilateral network p 898 A90-49614
- FRANK, CHRISTOPHER L.**
Air Force application of injection molding technology
[SME PAPER EM89-103] p 274 A90-23686
- FRANKE, M. E.**
Navier-Stokes methods to predict circulation control airfoil performance
[AIAA PAPER 90-0574] p 167 A90-19924
Wind-tunnel investigation of wing-in-ground effects p 395 A90-31276
Confined jet thrust vector control nozzle studies
[AIAA PAPER 90-2027] p 657 A90-40598
Effect of riblets on flow separation in a subsonic diffuser p 712 A90-45261
- FRANKE, TH.**
Unsteady transonic flow around double-wedge profiles p 299 A90-24354
- FRANKEL, STEVEN H.**
A hybrid Reynolds averaged/PDF closure model for supersonic turbulent combustion
[AIAA PAPER 90-1573] p 600 A90-38711
- FRANKHAUSER, J. C.**
The microphysical structure of severe downdrafts from radar and aircraft observations in CINDE p 455 A90-28582

- FRANKLIN, J. A.**
Powered-lift aircraft technology
[NASA-SP-501] p 107 N90-12589
- FRANKLIN, JAMES A.**
Flight/propulsion control integration for V/STOL fighter/attack aircraft p 591 A90-38530
Simulation evaluation of transition and hover flying qualities of a mixed-flow, remote-lift STOVL aircraft [SAE PAPER 892284] p 757 A90-45464
- FRANSSON, T. H.**
Numerical investigation of unsteady compressible flow through nozzles and cascades p 7 A90-11790
- FRASER, STEPHANIE B.**
National Airspace System airspace management operational concept [DOT/FAA/DS-89/29] p 177 N90-13361
- FRASSINELLI, MARK C.**
Effect of tail size reductions on longitudinal aerodynamic characteristics of a three surface F-15 model with nonaxisymmetric nozzles [NASA-TP-3036] p 718 N90-25938
- FRATELLO, DAVID J.**
Wind-tunnel and flight-test investigation of the exordone remotely piloted vehicle configuration [AIAA PAPER 90-1261] p 494 A90-33891
Static wind-tunnel and radio-controlled flight test investigation of a remotely piloted vehicle having a delta wing planform [NASA-TM-4200] p 632 N90-24238
- FRÄUMIE, P.**
Aerodynamics of unsteady systems. Numerical study of potential flow/boundary layer coupling [ETN-90-96257] p 396 N90-18367
- FRAY, J. M. J.**
A system for transonic wing design with geometric constraints based on an inverse method p 501 N90-20983
- FRAZIER, J. L.**
Evaluation of the thermoplastic film interleaf concept for improved damage tolerance p 946 A90-50179
- FRAZIER, R. H.**
Evolution of engine cycles for STOVL propulsion concepts [AIAA PAPER 90-2272] p 743 A90-42767
- FREEMAN, C.**
A method for the prediction of supersonic compressor blade performance [CUED/A-TURBO/TR-126] p 344 N90-17634
- FREEMAN, W. G.**
Measurements in an annular combustor-diffuser system [AIAA PAPER 90-2162] p 768 A90-42740
Parametric evaluation of the aerodynamic performance of an annular combustor-diffuser system [AIAA PAPER 90-2163] p 742 A90-42741
- FREIMUTH, P.**
Comparison of conventional and adaptive wall wind tunnel results with regard to Reynolds number effects p 352 N90-17649
- FREMAUX, C. M.**
Parametric analysis of swept-wing geometry with sheared wing tips [AIAA PAPER 90-3196] p 812 A90-49101
- FRENCH, MARK**
An application of structural optimization in wind tunnel model design [AIAA PAPER 90-0956] p 438 A90-29241
- FRENCH, R. M.**
Modal characteristics of swept plate flutter models p 207 A90-16962
- FRENGLEY, MICHAEL C.**
Retirement lives of rolling element bearings p 680 A90-39980
- FRENNBERG, HANS M.**
Lightning testing and test analyses of the JAS39 aircraft p 842 A90-49836
- FRENSTER, JEFF**
The application of an expert maintenance and diagnostic tool to aircraft engines [AIAA PAPER 90-2036] p 657 A90-40605
Expert system diagnostics and parts life tracking as applied to the AV-8B aircraft for the USMC p 684 N90-27629
- FREUDINGER, LAWRENCE C.**
Flutter clearance of the F-18 high-angle-of-attack research vehicle with experimental wingtip instrumentation pods [NASA-TM-4148] p 103 N90-11732
Flutter clearance of the F-14A variable-sweep transition flight experiment airplane, phase 2 [NASA-TM-101717] p 735 N90-25135
- FREVERT, D. A.**
Software fault tolerance analysis and testing for the Advanced Automation System [AIAA PAPER 89-3124] p 75 A90-10600
- FREY, M. O.**
Experimental investigation of coannular jet flow with swirl along a centerbody [AIAA PAPER 90-1622] p 567 A90-38751
- FREYMUTH, P.**
Thrust generation by an airfoil in hover modes [AD-A223602] p 552 A90-35137
- FREYMUTH, PETER**
Dynamic separation: Search for the cause of dynamic stall and search for its control [AD-A223412] p 911 N90-29305
- FRIDDELL, J. H.**
Confined jet thrust vector control nozzle studies [AIAA PAPER 90-2027] p 657 A90-40598
- FRIDLAND, V. YA.**
Effect of vortex generators on the aerodynamic wing characteristics and body of revolution [AD-A22813] p 721 N90-25955
- FRIEDBERG, R. A.**
Electro-impulse de-icing testing analysis and design [NASA-CR-4175] p 32 N90-10031
- FRIEDEL, THOMAS**
Control system validation in the autonomous helicopter p 667 A90-38908
- FRIEDMAN, ART**
Challenges of tomorrow - The future of secure avionics p 419 A90-30723
- FRIEDMAN, W. D.**
Injection molding development of ceramic turbine components [ASME PAPER 89-GT-170] p 361 A90-23855
- FRIEDMANN, P. P.**
Vibration analysis of composite turbopropellers using a nonlinear beam-type finite-element approach p 70 A90-12844
A simple active controller to suppress helicopter air resonance in hover and forward flight p 119 A90-16521
Exploratory design studies using an integrated multidisciplinary synthesis capability for actively controlled composite wings [AIAA PAPER 90-0953] p 411 A90-29238
Structural optimization with aeroelastic constraints of rotor blades with straight and swept tips p 535 A90-32475
Numerical methods for the treatment of periodic systems with applications to structural dynamics and helicopter rotor dynamics p 604 A90-37881
A model for active control of helicopter air resonance in hover and forward flight p 670 A90-42462
- FRIEDMANN, PERETZ P.**
Helicopter rotor dynamics and aeroelasticity - Some key ideas and insights p 335 A90-25425
Rotary-wing aeroelasticity with application to VTOL vehicles [AIAA PAPER 90-1115] p 392 A90-29387
Aeroelastic tailoring analysis for preliminary design of advanced turbo propellers with composite blades p 412 A90-29395
A study of fundamental issues in higher harmonic control using aeroelastic simulation p 861 A90-46966
- FRIES, J. C.**
The effect of structural variations on the dynamic characteristics of helicopter rotor blades [AIAA PAPER 90-1161] p 450 A90-29396
- FRIN, ROGER**
Dual cross-polarization planar arrays in the C and X bands p 638 A90-40979
- FRITH, D. A.**
Engine diagnostics - An application for expert system concepts p 50 A90-12632
- FRITH, P. C.**
An open-loop transient thermodynamic model of the Cougar turbojet [AD-A211774] p 114 N90-11745
- FRITSCH, KLAUS**
Silicon-etalon fiber-optic temperature sensor [NASA-TM-102389] p 187 N90-13381
- FRITSKY, K. J.**
Turbine combustor preliminary design approach p 508 A90-32966
- FROLOV, V. M.**
Optimization of the relative thicknesses of a high-aspect-ratio wing in a multicriterial formulation p 334 A90-24133
Efficiency of using a multiple-wall torsion box in the load-bearing structures of lifting surfaces p 410 A90-29188
- FROLOVA, I. E.**
A method for the active control of the boundary layer condition p 296 A90-24114
- FROLOW, IGOR**
National Airspace System demand and capacity modeling p 330 A90-25562
- FRUSTIE, M. J.**
New materials for civil aircraft furnishing p 328 N90-17609
- FU, B.**
Injectable bismaleimide systems p 943 A90-50132
- FU, DEXUN**
On efficiency and accuracy of numerical methods for solving aerodynamic equations p 304 A90-25730
- FU, S. JOHNNY**
Local adaptive maneuvering optimization for fighter aircraft [AIAA PAPER 90-3453] p 890 A90-47706
- FU, YIBIN**
On the Goertler vortex instability mechanism at hypersonic speeds p 158 A90-18886
- FUCHS, HEINZ**
Dynamic derivatives of missiles and fighter-type configurations at high angles of attack p 337 N90-17554
- FUCHS, HENRY O.**
Fatigue spectra development for airborne stores p 336 A90-26757
- FUGEDY, JOHN**
Control system validation in the autonomous helicopter p 667 A90-38908
- FUGLSANG, D. F.**
Applications of XTRAN3S and CAP-TSD to fighter aircraft [AIAA PAPER 90-1035] p 389 A90-29360
- FUJIKSCHOT, P. H.**
Model incidence measurement using the SAAB Eloptopos system p 446 A90-28264
- FUJIEDA, KAKUTOSHI**
Wind tunnel test of CAD USB-STOL semi-borne prototype [NAL-TM-566] p 88 N90-11696
- FUJII, HIROSHI**
Application of Lomax-Bailey implicit scheme to reactive flows p 367 A90-25861
- FUJII, KOZO**
High-resolution upwind scheme for vortical-flow simulations p 153 A90-17872
Navier-Stokes computations for the investigation of flowfields about a Space-Plane p 306 A90-25836
Capability of current supercomputers for the computational fluid dynamics p 546 A90-34382
- FUJIMOTO, ATSUSHI**
Numerical simulation of separated flows around a wing section by a discrete vortex method p 307 A90-25846
Numerical simulation of separated flows around a wing section at pitching motion by a discrete vortex method p 475 A90-33753
- FUJIMOTO, ICHIRO**
Flutter of cascade blades composed of blades having arbitrarily different natural frequencies p 42 A90-11798
- FUJITA, TOSHIMI**
Wind tunnel test of CAD USB-STOL semi-borne prototype [NAL-TM-566] p 88 N90-11696
- FUJIWARA, TOSHI**
Supersonic viscous shear layers p 367 A90-25873
- FUJIYAMA, HIROSHI**
Expert diagnosis system for FJR engine troubles p 587 A90-38597
- FUKAI, I.**
Simulation of the reduction characteristics of scattering from an aircraft coated with a thin-type absorber by the spatial network method p 638 A90-39855
- FUKAMACHI, YASUO**
An electronic flight-recorder for a hang-glider p 39 A90-12234
- FUKUDA, KIZUKI**
Calculation of stability derivatives for slender bodies using boundary element method p 620 A90-40181
- FUKUDA, MASAHIRO**
Investigation of ATP blades, part 2. Validation of two-dimensional viscous flow simulation codes around thin airfoils [NAL-TR-1046] p 912 N90-29326
- FULKER, J. L.**
A study of flows over highly-swept wings designed for maneuver at supersonic speeds [AD-A216837] p 399 N90-19202
- FULLER, C. R.**
Free-field correction factor for spherical acoustic waves impinging on cylinders p 218 A90-17984
- FULLER, CHRIS R.**
Active control of propeller-induced noise fields inside a flexible cylinder p 833 A90-47306
Mechanisms of active control in cylindrical fuselage structures p 862 A90-47309
- FULTON, KEN**
The propan... What future now? p 744 A90-43763

- FULTON, MARK**
Helicopter trim with flap-lag-torsion and stall by an optimized controller p 755 A90-45332
- FUNAZAKI, K.**
Measurements of simulated wake/rotor interaction phenomena in turbomachinery p 814 A90-49475
- FUNG, K. Y.**
Unsteady transonic aerodynamics of oscillating airfoils in supersonic freestream p 232 A90-23277
- FURLAN, R.**
Production of Ti6Al4V-components for a new turbo-fan-engine p 132 A90-16618
- FURMAN, PETER J.**
Potential application of automotive fatigue technology in rotorcraft design p 681 A90-39987
- FURUKAWA, YASUMITSU**
Development process of turbulence in a round-nozzle air jet p 87 A90-16101
- FUSON, SCOTT E.**
Sealing the future p 442 A90-29638
Fluorosilicone sealants for aircraft fuel containment p 529 A90-31618
Silicone sealants and adhesives for aerospace/defense applications p 529 A90-31619
- FUTAMURA, HISAO**
A study on the performance of the turbo-ramjet engines at high speed flight p 49 A90-12608
- FUTATSUDERA, NAOKI**
Numerical simulation of separated flows around a wing section by a discrete vortex method p 307 A90-25846
Numerical simulation of separated flow around two-dimensional wing section by a discrete vortex method p 469 A90-32067
Numerical simulation of separated flows around a wing section at pitching motion by a discrete vortex method p 475 A90-33753
- ## G
- GABRIEL, CH. M.**
A technique for calculating nonlinear normal-force and pitching-moment coefficients for slender delta wings, accounting for wing thickness p 476 A90-34356
- GABRIELE, GARY A.**
Design for assembly of aerospace structures - A qualitative, interactive approach [SME PAPER MS89-158] p 222 A90-23683
- GABRIELLI, F.**
Time dependent effects on high temperature low cycle fatigue and fatigue crack propagation on nickel base superalloys p 443 A90-29881
- GAD-EL-HAK, MOHAMED**
Frontiers in experimental fluid mechanics p 367 A90-26059
Control of low-Reynolds-number airfoils - A review p 801 A90-46376
Control of low-speed airfoil aerodynamics p 814 A90-49776
- GADETSKII, V. M.**
An experimental study of the effect of the Reynolds number on flow past a swept wing at transonic velocities p 294 A90-24082
- GAFFNEY, R. L., JR.**
An abbreviated Reynolds stress turbulence model for airfoil flows [AIAA PAPER 90-1468] p 562 A90-38625
- GAGE, P. J.**
Comparative evaluation of Allison T56 engine chip detectors [AD-A221864] p 855 A90-26832
- GAGE, PETER J.**
Measurements of pressures on the wing of an aircraft model during steady rotation [AIAA PAPER 90-2842] p 754 A90-45162
- GAIFULLIN, A. M.**
Nonstationary liquid flow of a fluid in the core of a conical vortex sheet p 296 A90-24113
Calculation of flow characteristics in the core of a vortex sheet p 386 A90-28981
The experimental investigation of flow in the core of a vortex structure [BR114893] p 960 A90-29597
- GAINUTDINOV, V. G.**
Dynamic analysis of lifting surfaces of small relative thickness in the case of finite displacements p 129 A90-14560
Effect of the drag on the critical flutter velocity p 828 A90-46480
- GAITONDE, DATTA V.**
Numerical investigation of some control methods for 3-D turbulent interactions due to sharp fins p 591 A90-21764
- GAITSKILL, WILLIAM H.**
Development of the improved helicopter icing spray system (IHSS) p 400 A90-28182
- GAJEWSKI, T.**
Damping of the inlet vortex in a turbojet engine p 301 A90-25185
- GAL-OR, BENJAMIN**
The fundamentals of vectored propulsion p 180 A90-17461
- GALASSI, LELLO**
Effects of inlet turbulence scale on turbine blade surface heat transfer in a linear cascade [AIAA PAPER 90-2264] p 768 A90-42761
- GALBRAITH, R. A. MCD.**
A review of low Reynolds number aerodynamic research at the University of Glasgow p 800 A90-46367
- GALEA, E. R.**
Forced and natural venting of aircraft cabin fires: A numerical simulation p 326 A90-17597
- GALECKI, GREZEGORZ**
Chaotic response of aerosurfaces with structural nonlinearities (Status report) [AIAA PAPER 90-1034] p 392 A90-29378
- GALKIN, I. A.**
An analysis of the possibility of expanding the information base of an adaptive control system for a flight vehicle surrounded by an ionized gas medium p 60 A90-10845
- GALKIN, M. S.**
Approximation of frequency characteristics using identification with a complex mass matrix p 448 A90-29001
- GALLAGHER, DONALD**
Analysis of heliport environmental data: Indianapolis downtown heliport, Wall Street heliport. Volume 2: Wall Street heliport data plots [DOT/FAA/CT-TN87/54-VOL-2] p 121 A90-11761
Analysis of heliport environmental data: Indianapolis downtown heliport, Wall Street heliport. Volume 3: Indianapolis downtown heliport data plots [AD-A217412] p 544 A90-20500
- GALLAGHER, J. P.**
Fatigue life estimates for helicopter loading spectra p 772 A90-45324
Fatigue life estimates for helicopter loading spectra [NASA-CR-181941] p 279 A90-16294
- GALLAGHER, RANDY**
The DELTA MONSTER: An RPV designed to investigate the aerodynamics of a delta wing platform [NASA-CR-186226] p 924 A90-29381
- GALLAGHER, VIRGINIA M.**
Fatigue spectra development for airborne stores p 336 A90-26757
- GALLIMORE, P. L.**
The importance of measured data as a contribution to reducing crew caused accidents [AIAA PAPER 89-3219] p 482 A90-31703
- GALLMAN, JOHN W.**
Design synthesis and optimization of joined-wing transports [AIAA PAPER 90-3197] p 838 A90-49102
- GALLMAN, JUDITH M.**
The validation and application of a rotor acoustic prediction computer program [NASA-TM-101794] p 895 A90-27465
- GALLO, PAOLO**
Expert system for pilot assistance - The challenge of an intensive prototyping p 693 A90-38909
Expert system for pilot assistance: The challenge of an intensive prototyping [ETN-90-97274] p 825 A90-27674
- GALLON, M.**
Application of the hydrogen bubble visualization method to the water tunnels of ONERA [ONERA, TP NO. 1989-107] p 58 A90-11140
- GALLOWAY, JAMES N.**
Aerosol separator for use in aircraft [PB90-142217] p 611 A90-22155
- GALLUS, H. E.**
Unsteady aerodynamics and aeroelasticity of turbomachines and propellers; Proceedings of the Fourth International Symposium, Aachen, Federal Republic of Germany, Sept. 6-10, 1987 p 5 A90-11776
Computation of aerodynamic blade loads due to wake influence and aerodynamic damping of turbine and compressor cascades p 7 A90-11791
Three-dimensional separated flow field in the endwall region of an annular compressor cascade in the presence of rotor-stator interaction. I - Quasi-steady flow field and comparison with steady-state data [ASME PAPER 89-GT-76] p 291 A90-23797
Three-dimensional separated flow field in the endwall region of an annular compressor cascade in the presence of rotor-stator interaction. II - Unsteady flow and pressure field [ASME PAPER 89-GT-77] p 291 A90-23798
Numerical investigation of unsteady flow in oscillating turbine and compressor cascades p 426 A90-18407
- Unsteady blade loads due to wake influence p 426 A90-18413
- Experimental investigation of the influence of rotor wakes on the development of the profile boundary layer and the performance of an annular compressor cascade p 427 A90-18425
- Influence of friction and separation phenomena on the dynamic blade loading of transonic turbine cascades [MITT-88-04] p 428 A90-19235
- Computational prediction and measurement of the flow in axial turbine cascades and stages p 514 A90-21028
- GALLUS, HEINZ E.**
Inviscid and viscous flows in transonic and supersonic cascades using an implicit upwind relaxation algorithm [AIAA PAPER 90-2128] p 625 A90-42034
- GALPERIN, E. A.**
Fracture control via DRM-Algorithm p 694 A90-41343
- GALPIN, P. F.**
A colocated finite volume method for solving the Navier-Stokes equations for incompressible and compressible flows in turbomachinery - Results and applications p 703 A90-42659
- GALWAY, R. D.**
New transonic test sections for the NAE 5ftx5ft trisonic wind tunnel p 630 A90-42431
New transonic test sections for the NAE 5 ft x 5 ft trisonic wind tunnel [AD-A220933] p 674 A90-24278
- GAMACHE, R. N.**
Reverse flow in multistage axial compressors p 623 A90-40942
- GAMALERO, G.**
Flight test safety and 'high risk' tests - The Aeritalia approach [AIAA PAPER 90-1315] p 483 A90-33924
In flight reflight tests on AM-X single engine fly-by-wire aircraft p 34 A90-10869
- GAMMILL, TROY**
McDonnell Douglas Helicopter Company Apache telemetry antenna analysis p 403 A90-28839
- GAMULIN, A. G.**
Automation of flight safety control p 589 A90-36157
- GANABOV, V. I.**
Calculation of the rotation noise of a single propeller with blades of arbitrary shape p 894 A90-46552
- GANDHI, M. V.**
A new generation of innovative ultra-advanced intelligent composite materials featuring electro-rheological fluids - An experimental investigation p 204 A90-17962
- GANGAL, D. B.**
Comparative cascade studies of some high diffusion compressor bladings p 15 A90-12637
Comparison of NACA 65, CDA, and tandem bladed cascades p 190 A90-18484
- GANGLOFF, RICHARD P.**
NASA-UVA light aerospace alloy and structures technology program [NASA-CR-182607] p 601 A90-22651
- GANIEV, F. I.**
Calculation of the induced drag of a wing with arbitrary deformation p 388 A90-29183
- GANY, A.**
Combustion characteristics of a boron-fueled SFRJ with aft-burner p 62 A90-12514
Regression and combustion characteristics of boron containing fuels for solid fuel ramjets p 858 A90-27928
An investigation of solid-fuel, dual-mode combustion ramjets p 859 A90-27933
- GANY, ALON**
Similarity and scale effects in solid fuel ramjet combustors p 60 A90-12513
- GANZER, U.**
Assuring the future of civil aircraft industry in Germany [DGLR PAPER 88-004] p 902 A90-50232
- GAO, DEPING**
A simple prediction method for low-cycle fatigue life of structures p 604 A90-37240
- GAO, HAO**
A new simplification method for analysing the rapid rolling stability of aircraft p 669 A90-42367
- GAO, JINGMAN**
Application of leaned blades to an aeroengine p 654 A90-40503
- GAO, WEI-BING**
Algorithm for simultaneous stabilization of single-input systems via dynamic feedback p 462 A90-31108
- GAONKAR, G.**
A study of symbolic processing and computational aspects in helicopter dynamics p 545 A90-34103

- GAONKAR, G. H.**
A study of the effects of Rotating Frame Turbulence (RFT) on helicopter flight mechanics p 248 N90-15058
- GAONKAR, GOPAL H.**
An experimental and analytical investigation of isolated rotor flap-lag stability in forward flight p 518 A90-33623
- GARAEV, K. G.**
A problem in the theory of optimal aerodynamic shapes p 803 A90-46503
- GARBELL, MAURICE A.**
Proposed definition of the term en route in en route aircraft noise p 696 N90-24854
The effect of noise-abatement profiles on noise immissions and human annoyance underneath a subsequent climbpath p 698 N90-24865
- GARBER, DONALD P.**
PTA en route noise measurements p 696 N90-24855
- GARBER, F. D.**
Pattern representations and syntactic classification of radar measurements of commercial aircraft p 417 A90-28407
- GARCIA-FOGEDA, P.**
Two-dimensional compressible unsteady aerodynamics in the Laplace domain p 472 A90-33360
- GARCIA-NOCEITI, F.**
Implementation of a transputer-based flight controller p 667 A90-38966
- GARCIA, P.**
Airfoil noise in a uniform flow p 139 A90-16330
- GARCON, F.**
Wind-tunnel test of the air intake of an unducted fan [AAAF PAPER NT 88-19] p 4 A90-11436
- GARDINER, M. STROUP**
Criteria for coal tar seal coats on airport pavements. Volume 2: Laboratory and field studies [AD-A220167] p 674 N90-24277
- GARDNER, J. H.**
Acoustic-vortex-chemical interactions in an idealized ramjet p 54 N90-10206
- GARDNER, JOHN H.**
Numerical simulations of flowfields in a central-dump ramjet combustor. 3: Effects of chemistry [AD-A224145] p 933 N90-28573
- GARDNER, WILLIAM B.**
Energy efficient engine program technology benefit/cost study. Volume 1: Executive summary [NASA-CR-174766-VOL-1] p 931 N90-28564
Energy efficient engine program technology benefit/cost study, volume 2 [NASA-CR-174766-VOL-2] p 931 N90-28565
- GARG, SANJAY**
Cooperative synthesis of control and display augmentation in approach and landing p 516 A90-33061
Analysis of airframe/engine interactions - An integrated control perspective [AIAA PAPER 90-1918] p 667 A90-40557
H-infinity based integrated flight/propulsion control design for a STOVL aircraft in transition flight [AIAA PAPER 90-3335] p 862 A90-47595
H-infinity based integrated flight/propulsion control design for a STOVL aircraft in transition flight [NASA-TM-103198] p 758 N90-26011
- GARGIR, GENENE**
Hermes training aircraft p 354 N90-16827
- GARIBALDI, LUIGI**
Flutter analysis on a non-linear wing model p 207 A90-17009
- GARINO, ED**
The MANTA: An RPV design to investigate forces and moments on a lifting surface [NASA-CR-186227] p 499 N90-20971
- GARMIRE, E. M.**
A fiber optic headset compatible with power-by-light p 504 A90-32906
- GARNER, E. C.**
Heat pipes for wing leading edges of hypersonic vehicles [NASA-CR-181922] p 369 N90-17055
- GARNER, J. E.**
Proven dynamic modeling techniques for concurrent design and analysis of ECS controllers [SAE PAPER 901234] p 841 A90-49304
- GARNIER, F.**
Numerical simulation of unsteady combustion in a dump combustor p 54 N90-10203
- GARON, ANDRE**
Finite element simulation of turbulent propeller flowfields p 703 A90-42658
- GARRARD, WILLIAM L.**
Design of attitude and rate command systems for helicopters using eigenstructure assignment p 118 A90-14729
- Design of flight control systems to meet rotorcraft handling qualities specifications [AIAA PAPER 90-2805] p 752 A90-45140
- GARRARD, WILLIAM L., JR.**
Nonlinear inversion flight control for a supermaneuverable aircraft [AIAA PAPER 90-3406] p 864 A90-47661
- GARRETS, WELDON E.**
History of aircraft piston engine oils - The last forty years [SAE PAPER 891037] p 124 A90-14343
- GARRETT, AMY**
Smart structures concept study p 504 A90-32876
- GARRIS, C. A.**
Non-steady flow loss mechanisms associated with vaneless diffusers [AIAA PAPER 90-2508] p 682 A90-40641
- GARRIS, CHARLES A.**
An experimental investigation of non-steady flow in vaneless diffusers p 14 A90-12595
- GARRISON, W. M., JR.**
Ultrahigh-strength steels for aerospace applications p 599 A90-37443
- GARRIZ, JAVIER A.**
Evaluation of transonic wall interference assessment and correction for semi-span wing data [AIAA PAPER 90-1433] p 597 A90-38487
- GARTENBERG, EHUD**
Infrared imaging and tufts studies of boundary layer flow regimes on a NACA 0012 airfoil p 446 A90-28268
Low speed flowfield characterization by infrared measurements of surface temperatures p 317 N90-17556
- GARTRELL, LUTHER R.**
Basic aerodynamic research facility for comparative studies of flow diagnostic techniques p 122 N90-12526
- GARTSHORE, I.**
Film cooling of turbine blades - Two dimensional experiments and numerical simulations p 739 A90-42670
- GAT, URI**
Robots for aircraft coatings removal: Parameters and requirements [DE90-009429] p 609 N90-22048
- GATEWOOD, B. E.**
Virtual principles in aircraft structures. Volume 1 - Analysis. Volume 2 - Design, plates, finite elements p 452 A90-29977
- GATLIN, GREGORY M.**
Low-speed aerodynamic characteristics of a powered NASP-like configuration in ground effect [SAE PAPER 892312] p 714 A90-45474
Stability characteristics of a conical aerospace plane concept [SAE PAPER 892313] p 757 A90-45475
Low-speed, high-lift aerodynamic characteristics of slender, hypersonic accelerator-type configurations [NASA-TP-2945] p 20 N90-10830
The Langley 14-by-22-foot subsonic tunnel: Description, flow characteristics, and guide for users [NASA-TP-3008] p 816 N90-27649
- GATSKI, THOMAS B.**
A computational study of the taxonomy of vortex breakdown [AIAA PAPER 90-1624] p 568 A90-38753
- GAUBERT, MICHEL**
Hub loads analysis of the SA349/2 helicopter p 333 A90-23936
- GAUDET, L.**
Use of liquid crystals for qualitative and quantitative 2-D studies of transition and skin friction p 446 A90-28259
Use of liquid crystals for qualitative and quantitative 2-D studies of transition and skin friction [RAE-TM-AERO-2159] p 958 N90-28800
- GAUS, NORBERT**
Controller design for active vibration suppression of a helicopter [DFVLR-FB-89-20] p 120 N90-11760
- GAUTRONNEAU, E.**
Analysis and practical design of ceramic-matrix composite components p 445 A90-28135
- GAVALI, SHARAD**
Supercomputer applications in gas turbine flowfield simulation p 620 A90-40495
- GAVRILIDIS, JOSEPH**
The potential for an extra runway at Heathrow: A preliminary feasibility study [TT-9007] p 938 N90-29403
- GAVRILOV, VALERII N.**
Computer-aided design of flight vehicle instrument bays p 76 A90-10837
- GAY, A. M.**
The remote sensing of temperature in gas turbine engine components using epithermal neutrons p 70 A90-12630
- GAY, D.**
Homogenization of composite beams in dynamical flexure p 878 A90-46184
- GAYLE, E. ROSE**
Effect of reduced aft diameter and increased blade number of high-speed counterrotation propeller performance [AIAA PAPER 89-0438] p 234 A90-23650
- GAZAIX, M.**
Unsteady viscous calculation of cascade flows with leading-edge-induced separation [ONERA, TP NO. 1989-116] p 3 A90-11148
Unsteady viscous calculation method for cascades with leading edge induced separation p 426 N90-18408
- GE, FUYING**
Optimal control system design for departure prevention [AIAA PAPER 90-2837] p 754 A90-45167
Application of numerical optimization techniques to control system design for nonlinear dynamic models of aircraft p 593 N90-23032
- GE, SHAOYAN**
Research on film-cooling of turbine blade p 190 A90-17795
- GE, ZHOUFANG**
Color schlieren system using square color filter and its application to aerofoil test in transonics p 66 A90-10748
- GEDDES, NORMAN D.**
Information display management in a pilot's associate p 418 A90-30238
- GEE, KEN**
Numerical simulation of the viscous flow around a simplified F/A-18 at high angles of attack [AIAA PAPER 90-2999] p 787 A90-45849
The effect of turbulence models on the numerical prediction of the flowfield about a prolate spheroid at high angle of attack [AIAA PAPER 90-3106] p 789 A90-45855
- GEIDEL, H. A.**
Gearless crisp - The logical step to economic engines for high trust p 50 A90-12616
- GEIER, G. J.**
Guidance simulation and test support for differential GPS flight experiment [NASA-CR-177471] p 28 N90-10021
- GEIGER, ALAN L.**
Low-expansion MMCs boost avionics p 203 A90-17291
- GEIGER, R. H.**
Advanced recovery systems wind tunnel test report [NASA-CR-177563] p 816 N90-27653
- GEISELHART, KARL A.**
Performance potential of an advanced technology Mach 3 turbojet engine installed on a conceptual high-speed civil transport [NASA-CR-4144] p 51 N90-10034
- GEISSLER, W.**
A comparison between theoretical and experimental results for a 3-D wing with damped pitching oscillations p 472 A90-33361
- GELETUKHA, GEORGII N.**
Ground aviation equipment: Handbook p 593 A90-36153
- GELL, T. G.**
Use of liquid crystals for qualitative and quantitative 2-D studies of transition and skin friction p 446 A90-28259
Use of liquid crystals for qualitative and quantitative 2-D studies of transition and skin friction [RAE-TM-AERO-2159] p 958 N90-28800
- GEMAYEL, CHAOUKI A.**
Development of a thickness design procedure for stabilized layers under rigid airfield pavements [DOT/FAA/RD-90/22] p 937 N90-28582
- GENDRE, PASCAL**
Calculation of flow on a flat plate at angle of attack by numerical solution of Navier-Stokes equations p 537 A90-33424
- GENGO, JOSEPH T.**
Application of neural networks to the F/A-18 engine condition monitoring system [AD-A219820] p 666 N90-24271
- GENTRY, GARL L., JR.**
The effect of solidity on propeller normal force [SAE PAPER 892205] p 713 A90-45424
Effect of pylon wake with and without pylon blowing on propeller thrust [NASA-TM-4162] p 173 N90-14190
Experimental and theoretical aerodynamic characteristics of a high-lift semispan wing model [NASA-TP-2990] p 477 N90-20046

- The Langley 14- by 22-foot subsonic tunnel: Description, flow characteristics, and guide for users [NASA-TP-3008] p 816 N90-27649
- GEOFFROY, P.**
Design, realization, and qualification of model composite rotor blades p 364 A90-24293
Half transport aircraft cryogenic model for T2 wind tunnel p 524 A90-34242
Design and manufacturing of composite materials blade models p 618 A90-42492
- GEORGALA, J. M.**
The construction of component-adaptive grids for aerodynamic geometries p 309 A90-26513
A discussion on issues relating to multiblock grid generation p 608 N90-21991
- GEORGANTAS, A. I.**
Multivariable optimization scheme for tuning the controller of an electronic fuel control unit for small gas turbine engines p 745 A90-45301
- GEORGANTAS, ANTONIOS I.**
Designing and tuning the digital controller of an electronic fuel control unit for small gas turbine engines [SAE PAPER 892255] p 747 A90-45457
- GEORGE-FALVY, DEZSO**
In quest of the laminar-flow airliner - Flight experiments on a T-33 jet trainer p 300 A90-24825
Laminar flow test installation in the Boeing Research Wind Tunnel [AIAA PAPER 90-1425] p 559 A90-37962
- GEORGE, ALBERT R.**
Tilt rotor aircraft aeroacoustics p 409 A90-28238
- GEORGE, SAMUEL K.**
Architecture options for GPS/Carousel IV integration p 108 A90-13999
- GERA, JOSEPH**
Control research in the NASA high-alpha technology program p 934 N90-28516
- GERADIN, M.**
Three dimensional turbine blade analysis in thermo-viscoplasticity p 540 A90-34324
- GERARDI, TONY G.**
Health monitoring aircraft p 902 A90-50544
- GERASIMOV, A. P.**
Effect of the inlet diameter and neck edge radius on the flow coefficient of straight-generatrix nozzles p 84 A90-14577
- GERBE, J. P.**
Synthetic holography applied to head-up displays p 218 A90-16692
- GERBSCH, R. A.**
Solution of the parabolized Navier-Stokes equations using Osher's upwind scheme [AIAA PAPER 90-0392] p 165 A90-19830
- GERLING, W.**
Aspects of data link applications for ATC purposes p 827 N90-27688
- GERMANA, GUY T.**
The use of satellite technology for oceanic air traffic control p 330 A90-25570
- GERNERT, NELSON J.**
Flexible heat pipe cold plate [AD-A216053] p 434 N90-18433
- GEROLYMOS, G. A.**
Aircraft compressor flutter analysis p 41 A90-11797
- GERSTENFELD, ARTHUR**
Future ATC automation aids based upon AI technology p 375 A90-25563
- GERTEISEN, EDGAR A.**
Periodically unsteady effects on profiles, induced by separation p 279 N90-16196
- GERTH, D.**
Toughened thermosets for damage tolerant carbon fiber reinforced composites p 443 A90-29825
- GERTH, DALE**
A third-generation bismaleimide prepreg system p 943 A90-50131
- GESNER, JIM**
Bubble memory applications for aircraft systems p 418 A90-30681
- GESSNER, F. B.**
Experimental investigation of coannular jet flow with swirl along a centerbody [AIAA PAPER 90-1622] p 567 A90-38751
- GETSOV, L. B.**
Strength of the guide vane components of gas turbines p 266 A90-21318
- GEYER, GEORGE**
Full-scale air transport category fuselage burnthrough tests [DOT/FAA/CT-TN89/65] p 488 N90-20967
- GHAFFARI, FARHAD**
Transonic Navier-Stokes solutions about a complex high-speed accelerator configuration [AIAA PAPER 90-0430] p 166 A90-19844
- GHALLY, W. S.**
A design method for turbomachinery blading in three-dimensional flow p 904 A90-51003
A parametric study of radial turbomachinery blade design in three-dimensional subsonic flow [ASME PAPER 89-GT-84] p 905 A90-51257
- GHARIB, M.**
Transition from order to chaos in the wake of an airfoil p 474 A90-33506
- GHEE, TERENCE A.**
Effects of unsteady blowing on the lift of a circulation controlled cylinder p 713 A90-45325
- GHIA, K. N.**
Simulation of high incidence unsteady flow past Joukowski airfoils p 156 A90-18301
Study of low-Reynolds number separated flow past the Wortmann FX 63-137 airfoil p 799 A90-46363
- GHIA, U.**
Simulation of high incidence unsteady flow past Joukowski airfoils p 156 A90-18301
Study of low-Reynolds number separated flow past the Wortmann FX 63-137 airfoil p 799 A90-46363
- GHIEMI, L.**
A tool for automatic design of airfoils in different operating conditions p 502 N90-20994
- GHIRINGHELLI, G. L.**
Active flutter suppression for a wing model p 433 A90-31283
- GHORASHI, B.**
A circular combustor configuration with multiple injection ports for mixing enhancement p 130 A90-15389
A planar reacting shear layer system for the study of fluid dynamics-combustion interaction [NASA-TM-102422] p 194 N90-13393
- GHOSH, KUNAL**
Unified super/hypersonic similitude for steady and oscillating cones and ogives p 82 A90-13786
Supersonic/hypersonic flow past wedge and plane ogive in oscillation p 85 A90-15231
- GHURAYEB, JOSEPH**
Toward the panoramic cockpit, and 3-D cockpit displays p 419 A90-30682
- GIACOBBE, T.**
In service life monitoring system using g-meter readings and mass configuration control [ETN-89-95218] p 134 N90-12035
- GIANCHECCHI, U.**
The use of simulation in support of the high AOA flight test program of the AM-X aircraft [AIAA PAPER 90-1289] p 495 A90-33909
- GIANNAKOGLU, K.**
Calculation of axisymmetric flows in turbomachines, through an explicit time-splitting method p 14 A90-12622
Development and application of a fractional-step method for the solution of transonic and supersonic flow problems p 709 A90-44461
- GIAVOTTO, V.**
Understanding composite fatigue - New trends p 940 A90-49893
- GIBBENS, ROY P.**
The airship - An economical answer to air cargo [TABES PAPER 89-1203] p 238 A90-20390
- GIBSON, IVAN S.**
A computer program for the prediction of nozzle-propeller performance [LR-578] p 572 N90-21740
Theory and numerical analysis of single and multi-element nozzle propellers [LR-579] p 572 N90-21741
Recent improvements in the scope and accuracy of the performance prediction of nozzle propellers [LR-598] p 572 N90-21742
- GIBSON, J. C.**
Pay-offs and pitfalls of fly-by-wire p 346 A90-24281
- GIBSON, M. M.**
An interactive boundary layer method for subsonic airfoil flows p 144 A90-16754
- GIELDA, T. P.**
Numerical simulation of three-dimensional hypersonic inlet flowfields p 13 A90-12587
- GIELDA, THOMAS P.**
Computation of ramjet internal flowfields [AD-A212001] p 114 N90-11743
- GIESECKE, P.**
Automatic calibration machine for internal cryogenic balances p 524 A90-34247
Automatic calibration machine for cryogenic and conventional internal strain gage balances [AIAA PAPER 90-1396] p 595 A90-37939
- GIESECKE, PETER**
Fully automatic calibration machine for internal 6-component wind tunnel balance including cryogenic balances p 437 A90-28294
- GILBERT, B.**
Turbulence measurements in a flow generated by the collision of radially flowing wall jets p 2 A90-10699
- GILBERT, M. G.**
The application of active controls technology to a generic hypersonic aircraft configuration [NASA-TM-101689] p 497 N90-20071
- GILBERT, MICHAEL**
Recent activities within the aeroservoelasticity branch at the NASA Langley Research Center p 492 A90-33400
- GILBERT, MICHAEL G.**
An analytical sensitivity method for use in integrated aeroservoelastic aircraft design p 517 A90-33405
Parametric aeroelastic stability analysis of a generic X-wing aircraft p 731 A90-44737
Active control of aerothermoelastic effects for a conceptual hypersonic aircraft [AIAA PAPER 90-3337] p 863 A90-47597
Active control of aerothermoelastic effects for a conceptual hypersonic aircraft [NASA-TM-102713] p 869 N90-27725
- GILBERT, NEIL**
Correlation of Puma airloads: Lifting-line and wake calculation [NASA-TM-102212] p 170 N90-13327
- GILBERT, WILLIAM P.**
Control research in the NASA high-alpha technology program p 934 N90-28516
Dynamic ground effects p 922 N90-28531
- GILBRETH, CYNTHIA C.**
Development of a water-borne non-chromated primer and topcoat for aerospace applications p 956 A90-50213
- GILERT, WILLIAM P.**
Impact of emerging technologies on future combat aircraft agility [AIAA PAPER 90-1304] p 580 A90-36029
- GILES, GARY L.**
Comparison of equivalent plate and finite element analysis of a realistic aircraft structural configuration [AIAA PAPER 90-3293] p 837 A90-48877
- GILES, M. B.**
Experimental and theoretical investigations of flowfields and heat transfer in modern gas turbines [AD-A217663] p 429 N90-19237
- GILES, MICHAEL B.**
Inlet radial temperature redistribution in a transonic turbine stage [AIAA PAPER 90-1543] p 565 A90-38687
- GILHOUSEN, KLEIN S.**
Range Applications Joint Program Office GPS Range System data link p 725 A90-43686
- GILL, P. A.**
Blockage corrections at high angles of attack in a wind tunnel p 593 A90-35756
- GILKEY, R. D.**
Transonic analysis of complex configurations using TRANAIR program [SAE PAPER 892289] p 714 A90-45467
- GILLARD, W. J.**
X-29 high angle-of-attack flight testing - Program status [AIAA PAPER 90-3303] p 837 A90-48885
- GILLIAM, FRED T.**
Proceedings of the 13th International Congress on Instrumentation in Aerospace Simulation Facilities [EOARD-LR-89-069] p 527 N90-21046
- GILMORE, D.**
Dynamic simulation of cross-shafted propulsion system for tilt nacelle application [AIAA PAPER 90-0439] p 191 A90-19847
- GILMORE, JOHN F.**
Control system validation in the autonomous helicopter p 667 A90-38908
- GILPIN, TREVOR J.**
A review of UK civil aviation fire and cabin safety research p 325 N90-17587
- GILREATH, H. E.**
Investigation of the mixing of parallel supersonic streams p 69 A90-12561
Effects of pressure mismatch on slot injection in supersonic flow [AIAA PAPER 90-0092] p 227 A90-22161
- GILSON, CHARLES**
Turboshafts on tenterhooks p 188 A90-16703
- GILSON, D. J.**
Escape systems research at RAE p 483 N90-20058
- GILYARD, GLENN B.**
A proposed Kalman filter algorithm for estimation of unmeasured output variables for an F100 turbofan engine [AIAA PAPER 90-1920] p 656 A90-40558

- A preliminary evaluation of an F100 engine parameter estimation process using flight data
[AIAA PAPER 90-1921] p 656 A90-40559
- Propulsion system-flight control integration-flight evaluation and technology transition
[AIAA PAPER 90-2280] p 644 A90-42106
- Flight evaluation of a pneumatic system for unsteady pressure measurements using conventional sensors
[NASA-TM-4131] p 186 N90-14225
- Experimental characterization of the effects of pneumatic tubing on unsteady pressure measurements
[NASA-TM-4171] p 850 N90-27703
- Propulsion system-flight control integration and optimization: Flight evaluation and technology transition
[NASA-TM-4207] p 929 N90-28551
- GINDER, R. B.**
Performance of a highly-loaded HP compressor
[RAE-TM-P-1149] p 256 N90-15919
- GINERIS, DENISE J.**
Synthetic aperture radar imagery of airports and surrounding areas: Archived SAR data
[NASA-CR-4275] p 401 N90-18371
- Synthetic aperture radar imagery of airports and surrounding areas: Philadelphia Airport
[NASA-CR-4280] p 401 N90-18372
- Synthetic aperture radar imagery of airports and surrounding areas: Denver Stapleton International Airport
[NASA-CR-4305] p 637 N90-24257
- GINTY, B.**
The manufacture of SPF military aircraft doors in aluminium alloy
p 132 A90-16616
- GINZBURG, A. E.**
Strength of the guide vane components of gas turbines
p 266 A90-21318
- GIORDANENGO, PATRIZIA**
Expert system for pilot assistance - The challenge of an intensive prototyping
p 693 A90-38909
- Expert system for pilot assistance: The challenge of an intensive prototyping
[ETN-90-97274] p 825 N90-27674
- GIORDANO, DANIEL D.**
Investigation of oscillating airfoil shock phenomena
[AIAA PAPER 90-0695] p 169 A90-19981
- GIOVANOLA, J. H.**
Influence of microstructure and microdamage processes on fracture at high loading rates
[AD-A210307] p 65 N90-10253
- GIRAGOSIAN, PAKRAD A.**
Aerodynamic design considerations for aircraft radomes
[AIAA PAPER 90-2843] p 711 A90-45163
- GIRARD, A.**
Instrumentation being developed for the ONERA F4 wind tunnel
[ONERA, TP NO. 1989-189] p 261 A90-21049
- New high-speed air transport system and stratospheric pollution
[ONERA, TP NO. 1989-202] p 279 A90-22445
- High enthalpy hypersonic wind tunnel F4: General description and associated instrumentation
p 673 N90-24228
- GIRI, JAGANNATH**
Beech Starship occupant protection evaluation in emergency landing scenario
[SAE PAPER 891015] p 100 A90-14327
- Beech Starship interior noise experimental studies
[SAE PAPER 891082] p 101 A90-14374
- GIRODROUX-LAVIGNE, P.**
Unsteady viscous calculation of cascade flows with leading-edge-induced separation
[ONERA, TP NO. 1989-116] p 3 A90-11148
- Unsteady viscous calculation method for cascades with leading edge induced separation
p 426 N90-18408
- GISHVAROV, A. S.**
Validation of the accelerated equivalent testing of gas turbine engines for multivariant applications
p 110 A90-14568
- GISQUET, D.**
Numerical optimization of wings in transonic flow
p 502 N90-20997
- GITTOS, B. C.**
Gear steels for future helicopter transmissions
p 265 A90-20607
- GIULIANETTI, D. J.**
Evolution of engine cycles for STOVL propulsion concepts
[AIAA PAPER 90-2272] p 743 A90-42767
- GJESTLAND, TRULS T.**
An aircraft noise study in Norway
p 698 N90-24872
- GLADDEN, HERBERT J.**
Thermal/structural analyses of several hydrogen-cooled leading-edge concepts for hypersonic flight vehicles
[AIAA PAPER 90-0053] p 274 A90-23702
- Thermal/structural analyses of several hydrogen-cooled leading-edge concepts for hypersonic flight vehicles
[NASA-TM-102391] p 215 N90-14511
- GLADKIKH, V. A.**
Effect of pressure and temperature on residue formation in aviation kerosenes
p 203 A90-17281
- GLAESER, JOHN S.**
Analysis of the T63-A-700 engine used in alcohol turbine fuel extender test
[DOT/FAA/CT-TN90/18] p 928 N90-28549
- GLASS, ROBERT G.**
Microprocessor control of a vapor-cycle cooling system
[SAE PAPER 891457] p 339 A90-27426
- GLASSMAN, ARTHUR J.**
Advanced core technology - Key to subsonic propulsion benefits
[ASME PAPER 89-GT-241] p 342 A90-23890
- GLATT, L.**
Generalized Advanced Propeller Analysis System (GAPAS). Volume 2: Computer program user manual
[NASA-CR-185277] p 933 N90-29394
- GLATZ, J. D.**
A description of the Naval Air Development Center's ejection tower and crash test facilities and their uses
p 200 A90-17426
- GLAVINCEVSKI, B.**
Fuel molecular structure and flame temperature effects on soot formation in gas turbine combustors
[ASME PAPER 89-GT-288] p 253 A90-22652
- GLAZKOV, IU. A.**
Some technological errors in the use of capillary inspection in gas turbine engine repair
p 769 A90-43039
- GLAZUNOV, V. G.**
Vertical wind shears in lower-level jet stream over some airfields in the Urals and Siberia
p 888 A90-48362
- GLEASON, ALETA M.**
The Battle Captain Expert System - A mission management decision support system for attack helicopter operations
[AIAA PAPER 89-3098] p 37 A90-10583
- GLEASON, CLIFFORD C.**
Externally vaporizing system for turbine combustor
[AD-D014284] p 256 N90-15918
- GLEASON, DANIEL**
Digital simulation of flight control systems for post-stall aircraft
p 431 A90-30704
- GLEGG, STEWART A. L.**
Sound radiation from an airfoil encountering an oblique gust in its plane of motion
p 218 A90-17998
- GLENNY, D. E.**
Report on an overseas visit, June 1988
[AD-A210374] p 52 N90-10040
- An appraisal of a number of power assessment procedures being proposed for use in Chinook-Lycoming T55 engine
[AD-A210482] p 52 N90-10041
- GLEYZES, C.**
Calculation of three-dimensional boundary layers including hypersonic flows
p 146 A90-16773
- Experimental study of the flow around an helicopter fuselage - Comparison with three-dimensional boundary layer calculations
p 630 A90-42438
- Study of the flow around the prototype of A300: Results of the third test campaign at F2 and comparison with calculations
[CERT-33/5025-29-DERAT] p 817 N90-27663
- GLIEBE, P. R.**
Acoustic characteristics of counterrotating unducted fans from model scale tests
p 378 A90-26138
- An investigation of counterrotating tip vortex interaction
[NASA-CR-185135] p 79 N90-11549
- High speed turboprop aeroacoustic study (counterrotation). Volume 1: Model development
[NASA-CR-185241] p 782 N90-26633
- GLINSKY, N.**
Hypersonic reactive flow computations
p 315 A90-27131
- GLOMB, WALTER L., JR.**
Optic multiplex for aircraft sensors - Issues and options
p 38 A90-11660
- Direct frequency modulation in interferometric systems
p 68 A90-11662
- GLOSS, BLAIR B.**
National Transonic Facility model and model support vibration problems
[AIAA PAPER 90-1416] p 596 A90-37953
- The US National Transonic Facility, NTF
p 262 N90-15942
- GLOTOV, G. F.**
Interference between a vortex filament and shock waves in free flow and in nonisobaric jets
p 804 A90-46550
- GLOVER, KEITH**
Robust controller design using normalized coprime factor plant descriptions
p 457 A90-27645
- Robust control design for relaxed static stability aircraft
[AIAA PAPER 90-3443] p 865 A90-47696
- Robust control design for flight control
[AD-A211957] p 119 N90-11756
- GLOVER, RICHARD D.**
An automated calibration laboratory for flight research instrumentation: Requirements and a proposed design approach
[NASA-TM-101719] p 781 N90-26564
- GLOWINSKI, ROLAND**
Hypersonics. Volume 2 - Computation and measurement of hypersonic flows; Proceedings of the First Joint Europe/U.S. Short Course on Hypersonics, Paris, France, Dec. 7-11, 1987
p 224 A90-21164
- GLUSHKOV, N. N.**
Using the method of symmetric singularities for calculating flow past subsonic flight vehicles
p 386 A90-28879
- GNEMMI, P.**
Aerodynamic loads and blade vortex interaction noise prediction
p 614 A90-38520
- Aerodynamic loads and blade vortex interaction noise prediction
[ISL-PU-310/89] p 719 N90-25942
- GNESIN, V. I.**
Numerical simulation of three-dimensional nonstationary flows and variable aerodynamic forces in turbomachine stages
p 814 A90-49465
- GNOFFO, PETER A.**
Application of the LAURA code for slender-vehicle aerothermodynamics
[AIAA PAPER 90-1714] p 560 A90-38416
- GOAD, WILLIAM K.**
Recent flow visualization studies in the 0.3-m TCT
p 122 N90-12528
- GODDARD, K.**
Stage 2 re-engining: The only way to achieve a real stage 3 aircraft
[PNR90636] p 737 N90-25977
- GODENKO, A. E.**
Multicriterial optimization of lugs in hinge joints
p 364 A90-24162
- GODFREY, SARA**
Implementation of a production Ada project: The GRODY study
[NASA-TM-103305] p 547 N90-21544
- GODIO, GIANFRANCO**
The LHTEC T800-LHT-800 engine integration into the Agusta A129 helicopter
p 422 A90-28177
- GOEBEL, S. G.**
Investigation of supersonic mixing layers
p 623 A90-40926
- GOEING, M.**
Nozzle design optimization by method-of-characteristics
[AIAA PAPER 90-2024] p 741 A90-42719
- Aspects of the design of a hypersonic engine system and the selection of the intake and tail
[DGLR PAPER 88-040] p 928 A90-50233
- GOECKEN, TAHIR**
Computation of hypersonic low density flows with thermochemical nonequilibrium
p 477 N90-20044
- GOEKGOEL, OGUZ**
Damage tolerance demonstration for A310-300 CFPR components
[MBB-UT-012/89-PUB] p 766 N90-25091
- GOETZINGER, J. W.**
Production of jet fuels from coal-derived liquids. Volume 13: Evaluation of storage and thermal stability of jet fuels derived from coal liquids
[AD-A224576] p 954 N90-29527
- GOFORTH, A.**
Modeling flexible aircraft for flight control design
[AD-A219123] p 757 N90-25140
- GOGOLIN, V. P.**
Structural analysis of the horizontal tail surfaces of subsonic transport aircraft
p 102 A90-14556
- GOGUS, A. YALCIN**
Simulation and second law analysis of the unsteady combustion of a non-ideal pulsating ramjet
p 44 A90-12516
- GOIKHENBERG, M. M.**
The investigation of heat transfer in cooled blades of gas turbines
[AIAA PAPER 90-2144] p 685 A90-42043
- GOKA, TSUYOSHI**
Simulator evaluation of 'basic' mode back azimuth issues in departure and missed approach usage
[SAE PAPER 892216] p 728 A90-45433
- Simulation of MLS-ATC procedures in the New York and San Francisco Terminal Control Areas
[SAE PAPER 892217] p 728 A90-45434

- GOKGOL, O.**
Damage tolerance demonstration for A310-300 CFRP-components p 919 A90-49894
- GOLDIN, D. A.**
Identification and diagnostics in the data processing and control systems of aerospace powerplants p 611 A90-36151
- GOLAS, KATHARINE**
Interactive Videodisc training in aerospace applications [AIAA PAPER 89-3029] p 73 A90-10529
- GOLDBERG, DAVID E.**
Genetic algorithms in control system optimization [AIAA PAPER 90-3488] p 867 A90-47736
- GOLDBERG, LES**
Comparison of the analytical and experimental modes of a model airplane using finite element analysis and multi-reference testing p 207 A90-16986
- GOLDBERG, U. C.**
Versatility of an algebraic backflow turbulence model [AIAA PAPER 90-1485] p 563 A90-38639
- GOLDMAN, A.**
Flutter investigations on a Transavia PL12/T-400 aircraft [AD-A219108] p 593 N90-22570
- GOLDSCHMIED, FABIO R.**
Thick-wing spanloader all-freighter - A design concept for tomorrow's air cargo [AIAA PAPER 90-3198] p 834 A90-48831
Airfoil static-pressure thrust - Flight-test verification [AIAA PAPER 90-3286] p 812 A90-48873
- GOLDSMITH, N. T.**
Fractographic techniques for the assessment of aircraft component cracking p 954 A90-49885
Analysis and interpretation of aircraft component defects using quantitative fractography p 956 A90-50555
- GOLDSTEIN, M. E.**
On the instabilities of supersonic mixing layers - A high-Mach-number asymptotic theory p 702 A90-42644
- GOLDSTEIN, R. J.**
Studies of gas turbine heat transfer airfoil surfaces and end-wall cooling effects [AD-A212451] p 117 N90-12620
- GOLINVAL, J. C.**
Three dimensional turbine blade analysis in thermo-viscoplasticity p 540 A90-34324
- GOLLOMP, BERNARD P.**
Spectra composite enhances portability and survivability of electronic equipment p 947 A90-50189
- GOLOVACHEV, I. U. P.**
Determination of pressure and heat flow on the front surface of smooth blunt bodies p 299 A90-24166
Numerical modeling of transverse flow past a cylinder using Euler equations p 709 A90-44922
- GOLUB, ROBERT A.**
A review and update of the NASA aircraft noise prediction program propeller analysis system [SAE PAPER 891032] p 139 A90-14340
The prediction of the noise generating mechanisms of an Aerospatiale 365N-1 Dauphin helicopter p 463 A90-28161
The ROTONET prediction system and initial comparisons with far-field acoustics measurements for the XV-15 tilt-rotor aircraft p 894 A90-46947
- GOLUBKIN, V. N.**
Calculation of flow past delta wings in the thin shock layer approximation p 86 A90-15624
Aerodynamic characteristics of thin bodies moving in a gas with shock waves p 297 A90-24140
- GOMAN, M. G.**
Nonsymmetric vortex breakdown and aerodynamic hysteresis in flow past a low-aspect-ratio wing/fuselage configuration p 294 A90-24076
- GOMER, CHARLIE**
Preliminary design of a supersonic Short Takeoff and Vertical Landing (STOVL) fighter aircraft [NASA-CR-186670] p 649 N90-23394
- GOMES, S. B. V.**
Estimation of the flight dynamic characteristics of the YEZ-2A [AIAA PAPER 89-3173] p 245 A90-20590
- GOMUC, REHA**
Cyclic stress-strain behavior and low cycle fatigue of Ti 6242 p 530 A90-33523
- GOONCHAR, A. E.**
Effect of the leading edge bluntness of a moderately swept wing on the aerodynamic characteristics of an aircraft model at subsonic and transonic velocities p 388 A90-29005
- GONG, LESLIE**
Real-time aerodynamic heating and surface temperature calculations for hypersonic flight simulation [NASA-TM-4222] p 959 N90-28815
- GONG, YIFANG**
3D Mean-Stream-Line Method - A new engineering approach to the inverse problem of 3D cascade [ASME PAPER 89-GT-48] p 289 A90-23774
- GONSALVES, PAUL G.**
Model-based method for terrain-following display design [AD-A219302] p 583 N90-22563
- GONZALES, CESAR**
A proposal for fuel specification activities relating to general aviation intermittent combustion engines p 951 A90-51625
- GONZALEZ, CESAR**
Future fuels for general aviation; Proceedings of the Symposium on Future Fuels for General Aviation Intermittent Combustion, Baltimore, MD, June 29, 1988 [ASTM STP-1048] p 950 A90-51616
- GONZALEZ, HUGO A.**
Design of a three-component wall-mounted balance [AIAA PAPER 90-1397] p 595 A90-37940
- GOOBIE, S. M.**
An experimental investigation of the effect of incidence on the two-dimensional performance of an axial turbine cascade p 11 A90-12520
- GOODCHILD, PETER J.**
The modular HUM system p 618 A90-42476
- GOODMAN, R. K.**
Developments in ground vibration test and data analysis techniques for airframe structures p 832 A90-46970
- GOODMAN, ROBERT K.**
Examination of dynamic characteristics of UH-60A and EH-60A airframe structures p 406 A90-28154
- GOODNER, CLYDE E.**
An aircraft flight control reconfiguration algorithm p 432 A90-30708
- GOODRICH, KENNETH H.**
Artificial intelligence (AI) based tactical guidance for fighter aircraft [AIAA PAPER 90-3435] p 889 A90-47688
- GOODSON, EARL F., SR.**
The stress and temperature dependence of creep in an Al-2.0 wt percent Li alloy [AD-A223676] p 953 N90-29480
- GOODYER, M. J.**
Surface flow visualization in the cryogenic wind tunnel p 539 A90-34234
The six component magnetic suspension system for wind tunnel testing p 673 A90-41725
An airfoil testing technique for low supersonic speeds in an adaptive flexible-walled wind tunnel [AIAA PAPER 90-3086] p 795 A90-45900
- GOODYER, MICHAEL J.**
The aims and history of adaptive wall wind tunnels p 871 N90-26839
Limits of adaptation, residual interferences p 871 N90-26844
- GOOLD, IAN**
In the shadow of Aloha p 468 A90-33174
- GOORJIAN, PETER M.**
Application of a streamwise upwind algorithm for unsteady transonic computations over oscillating wings [AIAA PAPER 90-3103] p 796 A90-45915
A streamwise upwind algorithm applied to vortical flow over a delta wing [NASA-TM-102225] p 398 N90-19201
Extension of a streamwise upwind algorithm to a moving grid system [NASA-TM-102800] p 572 N90-21739
- GOPALAKRISHNA, H. S.**
Fatigue life assessment of a leaded electronic component under a combined thermal and random vibration environment p 770 A90-43734
- GOPALSWAMY, SWAMINATHAN**
Nonlinear flight control design via sliding methods p 756 A90-45335
- GORADIA, S. H.**
Computational results for the effects of external disturbances on transition location of bodies of revolution from subsonic to supersonic speeds and comparisons with experimental data [SAE PAPER 892381] p 715 A90-45522
- GORADIA, SURESH H.**
Theoretical methods and design studies for NLF and HLFC swept wings at subsonic and supersonic speeds p 92 N90-12535
- GORANSON, U. G.**
Aging jet transport structural evaluation programs p 901 A90-49889
- GORANSON, ULF G.**
Dealing with the aging fleet [SAE PAPER 892209] p 701 A90-45428
- GORANSSON, PETER**
Finite element calculations of the interior noise of the Saab 340 aircraft [SAE PAPER 891081] p 101 A90-14373
- GORDER, PATER J.**
Real-time piloted simulation of fully automatic guidance and control for rotorcraft nap-of-the-earth (NOE) flight following planned profiles [AIAA PAPER 90-3372] p 864 A90-47630
- GORDER, PETER J.**
Fully automatic guidance for rotorcraft nap-of-the-earth (NOE) flight following planned profiles p 403 A90-28219
Design and evaluation of a cockpit display for hovering flight p 490 A90-33059
- GORDNER, RAYMOND E.**
Unsteady Navier-Stokes solutions for a low aspect ratio delta wing [AIAA PAPER 90-1538] p 564 A90-38682
- GORDON, RACHEL**
Numerical simulation of vortical flows over a strake-delta wing and a close coupled delta-canard configuration [AIAA PAPER 90-3002] p 788 A90-45851
Speed-up of the strongly implicit procedure with application to subsonic/transonic potential flows p 809 A90-47301
- GORELOV, D. N.**
Control point selection in the discrete vortex method p 470 A90-32567
- GORELOV, V. A.**
The investigation of heat transfer in cooled blades of gas turbines [AIAA PAPER 90-2144] p 685 A90-42043
- GORENBUXH, P. I.**
Aerodynamic quality of a plane delta wing with blunted edges at large supersonic flow velocities p 387 A90-28991
Combined effect of viscosity and bluntness on the aerodynamic efficiency of a delta wing in flow with a high supersonic velocity p 388 A90-29184
A study of gas flow in hypersonic nozzles at large Reynolds numbers using simplified Navier-Stokes equations p 803 A90-46538
- GORIACHEV, V. V.**
Interchangeability of Soviet-made and foreign mineral oils for aviation gas turbine engines p 873 A90-46525
- GORLACH, I. A.**
Using cloud moisture calculations for estimating aircraft icing p 888 A90-48358
- GORODETSKII, V. G.**
Effect of pressure and temperature on residue formation in aviation kerosenes p 203 A90-17281
- GORRELL, STEVEN E.**
Stall cell blockage in a high-speed multistage axial-flow compressor [AIAA PAPER 90-1913] p 740 A90-42693
- GOSLIN, T. J.**
Aircraft modal suppression system: Existing design approach and its shortcomings p 33 N90-10115
Structural stability augmentation system design using BODEDIRECT: A quick and accurate approach p 33 N90-10116
- GOSTELOW, C. R.**
Component behaviour and life management: The need for common AGARD approaches and actions p 856 N90-27710
- GOSTELOW, J. P.**
Adverse pressure gradient effects on boundary layer transition in a turbulent free stream p 15 A90-12639
- GOSWAMI, TARUN**
Creep-fatigue interactions of gas turbine materials p 131 A90-16011
- GOTO, S.**
Development of the jet-swirl high loading combustor [AIAA PAPER 90-2451] p 658 A90-40633
- GOTOH, HARUO**
Oil migration of FJR 710/600S engine p 43 A90-12014
- GOTTLIEB, DAVID**
Spectral simulation of unsteady compressible flow past a circular cylinder [NASA-CR-182030] p 478 N90-20050
- GOTTLIEB, J. J.**
Prediction of two-dimensional time-dependent gasdynamic flows for hypersonic studies [UTIAS-335] p 718 N90-25935
- GOULAS, A.**
Evaluation of two numerical techniques for the prediction of flow around blades p 10 A90-12512
Hot wire measurements in the wake of an oscillating airfoil p 15 A90-12635
- GOULD, R. W.**
A technique for rapid impact damage detection with implication for composite aircraft structures p 600 A90-37662
- GOULD, RONALD W.**
A technique for rapid inspection of composite aircraft structure for impact damage p 846 N90-28077

GOULD, WARREN

Airworthiness and flight characteristics evaluation of the McDonnell Douglas Helicopter Corporation (MDHC) 530FF helicopter
[AD-A218253] p 498 N90-20076

GOULD, WARREN P.

Preliminary airworthiness evaluation of the RC-12K [AD-A219545] p 648 N90-23387

GOUNET, H.

Directivity of the noise radiation emitted from the inlet duct of a turboshaft helicopter engine
[ONERA, TP NO. 1990-26] p 695 A90-41205

GOUTINES, M.

Aerodynamic design of an HP compressor stage using advanced computation codes p 156 A90-18479
A methodology proposal to design and analyse counterrotating high speed propellers
[ASME PAPER 89-GT-38] p 340 A90-23767
Mesh generation for flow computation in turbomachine p 588 N90-21981

GOVARDHAN, M.

Wake behaviour of a large deflection turbine rotor linear cascade p 157 A90-18481

GOWDA, B. H. L.

Experimental study of static pressure and mean velocity profiles inside a two-dimensional dump-type combustor model p 45 A90-12530

GOWDA, R. M. S.

A numerical three-dimensional thermal stress analysis for cooled blades
[ASME PAPER 89-GT-168] p 341 A90-23853

GRABER, D. J.

Aerodynamic and torque characteristics of enclosed Co/counter rotating disks
[ASME PAPER 89-GT-177] p 361 A90-23858

GRACEY, CHRISTOPHER

Guidance analysis of the aeroglide plane change maneuver as a turning point problem
[NASA-TM-101639] p 259 N90-15110

GRAEWE, E.

Automatic calibration machine for internal cryogenic balances p 524 A90-34247
Automatic calibration machine for cryogenic and conventional internal strain gage balances
[AIAA PAPER 90-1396] p 595 A90-37939

GRAHAM, GARY M.

Two dimensional post stall maneuver of a NACA 0015 airfoil at high pitching rates
[AIAA PAPER 90-2810] p 710 A90-45150

GRAHAM, J. M. R.

The effect of rapid spoiler deployment on the transient forces on an aerofoil p 921 N90-28527

GRAHAM, ROBERT W.

Recent progress in research pertaining to estimates of gas-side heat transfer in an aircraft gas turbine
[NASA-TM-102460] p 194 N90-13394

GRAHAM, TODD

Theoretical and experimental investigation of the aeroelastic stability of an advanced bearingless rotor in hover and forward flight p 831 A90-46958

GRAHAM, WALTON

See and avoid/cockpit visibility
[DOT/FAA/CT-TN89/18] p 24 N90-10843
See and avoid/cockpit visibility
[AD-A214214] p 239 N90-15084

GRAHL, K. G.

Calculation of the side-wall boundary layer in axial turbomachines, accounting for the internal flow near the blades p 225 A90-21595

GRAHMANN, J. W.

Measurements in an annular combustor-diffuser system
[AIAA PAPER 90-2162] p 768 A90-42740
Parametric evaluation of the aerodynamic performance of an annular combustor-diffuser system
[AIAA PAPER 90-2163] p 742 A90-42741

GRALLERT, H.

Verification of aerothermodynamic codes by means of a winged experimental re-entry vehicle p 354 N90-16842

GRAMANN, RICHARD A.

Dynamics of the outgoing turbulent boundary layer in a Mach 5 unswep compression ramp interaction
[AIAA PAPER 90-1645] p 569 A90-38773

GRAMENOPOULOS, NICHOLAS

Concept of an MTI search radar p 487 A90-33613

GRANDHI, R. V.

Structural optimization of lifting surfaces with divergence and control reversal constraints p 127 A90-13770
System optimization for maximizing reconnaissance mission range of a hypersonic cruise vehicle
[AIAA PAPER 90-3292] p 837 A90-48876

GRANDO, J.

Experimental-theoretical comparison for current injection on an aircraft model
[ONERA, TP NO. 1989-133] p 22 A90-11157

GRANDPIERRE, L.

A probabilistic approach for the establishment of an aircraft structure inspection program p 902 A90-49892

GRANDT, A. F., JR.

The effect on fatigue crack growth under spectrum loading of an imposed placard 'G' limit p 643 A90-41339

Development of a double crack growth gage algorithm for application to fleet tracking of fatigue damage p 901 A90-49890

GRANOT, Z. H.

Acoustic fatigue analysis by the finite element method p 954 A90-49886

GRANOVSKII, A. V.

An investigation of the flow characteristics of transonic nozzle blades p 475 A90-33700

GRANTHAM, WILLIAM D.

Comparison of flying qualities derived from in-flight and ground-based simulators for a jet-transport airplane for the approach and landing pilot tasks
[NASA-TP-2962] p 120 N90-11757

GRANTZ, ARTHUR CHRISTIAN

An approximate viscous shock layer method for calculating the hypersonic flow over blunt-nosed bodies p 479 N90-20947

GRATZER, LOUIS B.

Conceptual design for aerospace vehicles p 651 N90-25043

GRAVELLE, A.

Measurement of wind tunnel model deformation under airflow p 522 A90-33370

GRAVES, A. T.

An American knowledge base in England - Alternate implementations of an expert system flight status monitor p 459 A90-30719

GRAY, C. C.

Vibrations of rectangular plates with moderately large initial deflections at elevated temperatures using finite element method
[AIAA PAPER 90-1125] p 451 A90-29429

GRAY, D. E.

Energy efficient engine program technology benefit/cost study. Volume 1: Executive summary
[NASA-CR-174766-VOL-1] p 931 N90-28564
Energy efficient engine program technology benefit/cost study, volume 2
[NASA-CR-174766-VOL-2] p 931 N90-28565

GRAY, DAVID E.

Turbofans turn to UHB propulsion p 659 A90-41165
Rockwell International's miniature high performance GPS receiver p 726 A90-43701

GREEK, CHRIS

The DELTA MONSTER: An RPV designed to investigate the aerodynamics of a delta wing platform
[NASA-CR-186226] p 924 N90-29381

GREEN, ANTHONY L.

Improved damage tolerance by controlling thermoplastic solubility in thermoset composites p 944 A90-50138

GREEN, DAVID L.

An early overview of tiltrotor aircraft characteristics and pilot procedures in civil transport applications
[DOT/FAA/DS-89/37] p 503 N90-21003

GREEN, DENNIS G.

Reducing C130E Hercules operating costs in the Royal Australian Air Force and the United States Air Force by increasing cruise speeds
[AD-A215747] p 338 N90-17629

GREEN, J.

GPS Hover Position Sensing System p 108 A90-13986

GREEN, J. B.

Production of jet fuels from coal-derived liquids. Volume 13: Evaluation of storage and thermal stability of jet fuels derived from coal liquids
[AD-A224576] p 954 N90-29527

GREEN, JOHN

Identification of a coupled flapping/inflow model for the PUMA helicopter from flight test data p 56 A90-12767

GREEN, JOHN A.

Static aeroelastic analysis of a three-dimensional generic wing
[NASA-TM-102231] p 509 N90-20087

GREEN, JOHN W.

Modelling gas turbine combustor performance under transient conditions
[AIAA PAPER 90-2161] p 661 A90-42051

GREEN, LAWRENCE L.

Wall interference assessment/correction (WIAC) for transonic airfoil data from porous and shaped wall test sections
[AIAA PAPER 90-1406] p 595 A90-37945

Nonlinear transonic Wall-Interference
Assessment/Correction (WIAC) procedures and application to cast-10 airfoil results from the NASA O.3-m TCT 8- by 24-inch Slotted Wall Test Section (SWTS) p 352 N90-17648

GREEN, M.

Investigation of aerodynamic interactions between a rotor and fuselage in forward flight p 385 A90-28198

GREEN, MICHAEL

Theoretical and experimental investigation of the aeroelastic stability of an advanced bearingless rotor in hover and forward flight p 831 A90-46958

GREEN, MICHAEL J.

CFD propels NASP propulsion progress p 683 A90-41163

GREEN, PETER F.

Equilibrium swelling of elastomeric materials in solvent environments
[DE90-010164] p 678 N90-24430

GREEN, STANLEY J.

Stages are for theaters - Decibels are for airplane noise measurements
[SAE PAPER 892293] p 778 A90-45469

GREEN, STEVEN M.

Piloted simulation of a ground-based time-control concept for air traffic control
[NASA-TM-101085] p 240 N90-15898
Simulator evaluation of the final approach spacing tool
[NASA-TM-102807] p 636 N90-23374

GREEN, THOMAS B.

Strategic aircraft engineering design simulation p 439 A90-30729

GREENBERG, CHARLES B.

Electrochromic windows - Applications for aircraft
[SAE PAPER 891063] p 129 A90-14363

GREENBERG, CHARLES E.

Adaptive selective fuel control test techniques p 421 A90-28168

GREENE, GEORGE C.

An entropy method for induced drag minimization
[SAE PAPER 892344] p 715 A90-45496

GREENE, J. B.

Nonflammable hydraulic power system for tactical aircraft. Volume 1: Aircraft system definition, design and analysis
[AD-A218493] p 671 N90-23409

GREENE, JANETTA ROSE

The effect of windscreen bows and HUD pitch ladder on pilot performance during simulated flight p 420 A90-31333

GREENOUGH, JEFFREY A.

Numerical simulation of confined, spatially-developing mixing layers - Comparison to the temporal shear layer
[AIAA PAPER 90-1462] p 562 A90-38619

GREGG, R. D.

Application of divergent trailing-edge airfoil technology to the design of a derivative wing
[SAE PAPER 892288] p 714 A90-45466

GREGOREK, G. M.

A hypersonic research vehicle to develop scramjet engines
[AIAA PAPER 90-3232] p 839 A90-49115

GREGORY-SMITH, D. G.

Inlet skew and the growth of secondary losses and vorticity in a turbine cascade
[ASME PAPER 89-GT-65] p 290 A90-23788

GREGORY, PEYTON B.

Thermal/structural analysis of the shaft-disk region of a fan drive system
[NASA-TM-101687] p 610 N90-22807

GREGORY, TOM J.

National aero-spaceplane status and plans p 337 N90-16801

GREITZER, E. M.

Rotor noise due to atmospheric turbulence ingestion. I - Fluid mechanics p 219 A90-19385
Effects of endwall suction and blowing on compressor stability enhancement
[ASME PAPER 89-GT-64] p 290 A90-23787

Reverse flow in multistage axial compressors p 623 A90-40942

Active stabilization of aeromechanical systems
[AD-A216629] p 454 N90-18672

GREK, G. R.

A study of boundary layer stability in the case of an increased incoming stream turbulence in gradient flows p 555 A90-38065

GRELLMANN, HANS W.

B-2 aerodynamic design
[AIAA PAPER 90-1802] p 334 A90-25174

GRENICH, A. F.

Compatibility of fuel system components with high density fuel
[AD-A210381] p 32 N90-10027

- GRIDLEY, M. C.**
Computation of vectoring nozzle performance
[AIAA PAPER 90-2752] p 627 A90-42225
- GRIEBLING, PHYLLIS C.**
A high performance aerospace resin for Resin Transfer Molding p 945 A90-50163
- GRIFFIN, L. W.**
Prediction of the aerodynamic environment and heat transfer for rotor-stator configurations
[ASME PAPER 89-GT-89] p 359 A90-23807
Numerical prediction of axial turbine stage aerodynamics p 426 N90-18416
- GRIFFITH, D. M.**
Fly-by-light flight control system technology development plan
[NASA-CR-181953] p 259 N90-15111
- GRIFFITH, D. O., II**
Turbulence measurements and noise generation in a transonic cryogenic wind tunnel
[AIAA PAPER 88-2026] p 522 A90-32463
- GRIFFITH, WAYLAND C.**
Condensation in hypersonic nitrogen wind tunnels
[AIAA PAPER 90-1392] p 558 A90-37937
- GRIFFITHS, BARRY E.**
Architecture options for GPS/Carousel IV integration p 108 A90-13999
- GRIFFITHS, G. R.**
Thermoplastic composites, past, present and future p 529 A90-31882
- GRIFFITHS, RICHARD W.**
Optical fiber sensing considerations for a smart aerospace structure p 38 A90-11210
- GRIGA, A. D.**
Optimal blading density in axial-flow compressor stages with a developed three-dimensional flow p 851 A90-46505
- GRIGOR'EV, B. V.**
Approximation of frequency characteristics using identification with a complex mass matrix p 448 A90-29001
- GRIGSBY, R. D.**
Production of jet fuels from coal-derived liquids. Volume 13: Evaluation of storage and thermal stability of jet fuels derived from coal liquids
[AD-A224576] p 954 N90-29527
- GRINA, KEN**
The Model 360 - Advanced composite helicopter p 180 A90-17678
- GRINKRUG, L. S.**
An experimental study of the gasdynamic characteristics of annular nozzle cascades with small flow exit angles p 255 A90-23409
- GROEGER, MONICA E.**
Flight simulator evaluation of a dot-matrix display for presentation of approach map formats p 419 A90-30787
- GROENEWEG, J. F.**
Unsteady Euler analysis of the flowfield of a propfan at an angle of attack
[AIAA PAPER 90-0339] p 300 A90-25028
Unsteady blade surface pressures on a large-scale advanced propeller - Prediction and data
[AIAA PAPER 90-2402] p 808 A90-47220
Prediction of unsteady blade surface pressures on an advanced propeller at an angle of attack
[NASA-TM-102374] p 94 N90-12560
Unsteady Euler analysis of the flow field of a propfan at an angle of attack
[NASA-TM-102426] p 380 N90-18229
- GROENEWEG, JOHN F.**
Aeroacoustics of advanced propellers
[NASA-TM-103137] p 782 N90-26635
- GROENIG, H.**
Experimental investigation of the flow development of an airfoil at high angles of attack p 473 A90-33366
- GROLL, D. B.**
Practical design considerations for integrating the propulsion system with the aircraft for jetborne flight
[ASME PAPER 89-GT-310] p 490 A90-32257
- GROMOV, G. V.**
Automation of flight safety control p 589 A90-36157
- GROMOV, GENNADI N.**
Differential-geometrical technique of signal transformation and estimation of position, rate and acceleration parameters using supplementary data sources p 638 A90-41004
- GROSCH, GERHARD**
Comparison of three concepts for a long stroke displacement transducer p 66 A90-11041
- GROSDEMANGE, HERVE**
The SEPR 844 reusable liquid rocket engine for Mirage combat aircraft
[AIAA PAPER 90-1835] p 655 A90-40526
- GROSS, R. L.**
Safety management in aircraft testing and certification p 180 A90-17421
- GROSS, UWE**
Design and manufacture of a cryogenic wind tunnel model p 523 A90-34238
- GROSSBACH, R.**
Parabolic flight experiments on fluid surfaces and wetting p 363 A90-23904
- GROSSI, D. R.**
The new US flight recorder regulations p 849 N90-27642
- GROSSIN, J.**
Software maintenance on the Airbus family
[SAE PAPER 892326] p 738 A90-45484
- GROTH, MARY**
Attachment of lead wires to thin film thermocouples mounted on high temperature materials using the parallel gap welding process
[NASA-TM-102442] p 543 N90-21361
- GRUBBS, JOHN H.**
Applications of digital image processing in testing and evaluation of composite materials
[AD-A222933] p 874 N90-26887
- GRUENHAGEN, WOLFGANG V.**
Time and frequency-domain identification and verification of BO-105 dynamic models
[AD-A216828] p 415 N90-18389
- GRUENINGER, GERHARD**
Materials and structures for 2000 and beyond: An attempted forecast by the DLR Materials and Structures Department
[ESA-TT-1154-REV] p 775 N90-26173
- GRUNDY, I. H.**
Additions and corrections to SUPER: A program for calculating steady and oscillatory supersonic flow over a thin wing, tail plane and fin
[AD-A211771] p 90 N90-12501
ARLSUPER version 1.0, program users guide
[AD-A222693] p 815 N90-26793
- GRUNNET, JAMES L.**
The new FFA T1500 transonic wind tunnel initial operation, calibration, and test results
[AIAA PAPER 90-1420] p 596 A90-37957
- GRUNWALD, A.**
Supplemented visual cues for helicopter hovering above a moving ship deck p 195 A90-17704
- GRUSKA, C. J.**
Large scale prop-fan structural design study. Volume 1: Initial concepts
[NASA-CR-174992] p 52 N90-10043
Large scale prop-fan structural design study. Volume 2: Preliminary design of SR-7
[NASA-CR-174993] p 52 N90-10044
- GRUZDEV, B. G.**
Radar systems of aircraft p 26 A90-10841
- GRUZDEV, V. N.**
Variable-velocity flow at the initial mixing section in a diffuser channel p 84 A90-14563
- GRZYBOWSKI, JOZEF**
Digital autopilot for light aircraft p 653 A90-41741
Onboard digital recording system for flight tests p 653 A90-41742
- GU, JIALIU**
Gear vibration control with viscoelastic damping material in aeroengine p 451 A90-29911
A combined Riccati transfer matrix-direct integration method with its applications p 611 A90-37218
- GU, S.-N.**
A modal parameter identification technique and its application to large complex structures with multiple steady sinusoidal excitation p 602 A90-35670
- GU, SONGSHI**
A simple prediction method for low-cycle fatigue life of structures p 604 A90-37240
- GU, ZHONGQUAN**
A study on mechanical model of the helicopter 'ground resonance' p 580 A90-36423
- GUADAGNO, M.**
Problems related to the acquisition, processing and utilization of the modal parameters measured in flight tests in order to obtain the full envelope for flutter
[ETN-89-95210] p 103 N90-11735
- GUAN, DE**
Aeroelastic tailoring applied to composite wing p 211 A90-18580
Aeroelastic tailoring of a wing with composite skin p 366 A90-25108
- GUASTAVINO, T. M.**
Preliminary fire extinguishing tests with handheld bottles: A comparison of extinguishing compounds
[DOT/FAA/CT-TN89/60] p 370 N90-17930
- GUDERLEY, KARL G.**
An alternative derivation for an integral equation for linearized subsonic flow over a wing
[AD-A214140] p 236 N90-15079
- GUDILIN, I. V.**
An experimental study of the combined effect of longitudinal riblets and vortex breakers on turbulent friction p 805 A90-46565
- GUDINO, JUAN**
NASA/USRA high altitude reconnaissance aircraft
[NASA-CR-186685] p 650 N90-24266
- GUDKOV, V. A.**
Jets, vortices, and turbulence p 207 A90-17175
- GUENETTE, G. R.**
Active stabilization of aeromechanical systems
[AD-A216629] p 454 N90-18672
Experimental and theoretical investigations of flowfields and heat transfer in modern gas turbines
[AD-A217663] p 429 N90-19237
- GUENTERMANN, T.**
Structure of velocity and temperature fields in laminar channel flows with longitudinal vortex generators p 273 A90-23207
- GUENZEL, UDO**
Cockpit evolution in Airbus p 247 A90-22434
- GUERDAL, ZAFER**
Structural analysis and optimum design of geodesically stiffened composite panels
[NASA-CR-186944] p 959 N90-28862
- GUERIN, G.**
Digital map reader for helicopters p 653 A90-42448
- GUERINONI, FABIO**
Solving compressible flow problems using adaptive finite quadtree and octree grids p 155 A90-18243
- GUERMOND, J.-L.**
Collocation methods and lifting-surfaces p 9 A90-12023
- GUERMOND, JEAN-LUC**
A generalized lifting-line theory for curved and swept wings p 303 A90-25597
- GUETTIER, MICHEL**
Experiments on Mode S secondary surveillance radar - The participation of the French Direction de la Navigation Aérienne in the European effort p 639 A90-41057
- GUIDOS, BERNARD J.**
External flow computations for a finned 60mm ramjet in steady supersonic flight
[AD-A216998] p 428 N90-19233
- GUIFFRE, G.**
Problems related to the acquisition, processing and utilization of the modal parameters measured in flight tests in order to obtain the full envelope for flutter
[ETN-89-95210] p 103 N90-11735
- GUIGNON, E. F.**
Fluorescence spectroscopy and thermometry for hypersonic flight research
[AIAA PAPER 90-1272] p 538 A90-33897
- GUILE, R. N.**
Hydrocarbon-fueled scramjet combustor investigation
[AIAA PAPER 90-2337] p 658 A90-40622
- GUILL, FREDERICK C.**
Pre-escape and escape aircraft maneuvers and gyrations - A critical under-reported problem affecting escape system performance and aircrew safety p 21 A90-10264
- GUILLEMOT, Y.**
Evaluation of the indirect effects of lightning on a system: Double transfer function method
[RAE-TRANS-2172] p 176 N90-14211
- GUIMBAL, BRUNO**
Design, evaluation and proof-of-concept flights of a main rotor interblade viscoelastic damping system p 406 A90-28152
The new Spheriflex tail rotor for the Super Puma Mark 2 p 408 A90-28213
- GULDER, O. L.**
Fuel molecular structure and flame temperature effects on soot formation in gas turbine combustors
[ASME PAPER 89-GT-288] p 253 A90-22652
- GULDNER, W.**
Aeroelastic tailoring validation by windtunnel model testing p 492 A90-33389
- GUMBERT, CLYDE**
Interactive generation of unstructured grids for three dimensional problems p 310 A90-26537
- GUMBERT, CLYDE R.**
Nonlinear transonic Wall-Interference Assessment/Correction (WIAC) procedures and application to cast-10 airfoil results from the NASA 0.3-m TCT 8- by 24-inch Slotted Wall Test Section (SWTS) p 352 N90-17648
- GUMMERE, ROBERT J.**
The technology challenge of the advanced tactical fighter: A study of the technology transition process
[AD-A216109] p 338 N90-17630
- GUNDAPPA, M.**
Turbulence measurements and noise generation in a transonic cryogenic wind tunnel
[AIAA PAPER 88-2026] p 522 A90-32463

GUNDY-BURLET, KAREN L.

Temporally and spatially resolved flow in a two-stage axial compressor. Part 2: Computational assessment [NASA-TM-102273] p 194 A90-14236

GUNN, J. A.

Hypersonic test facility requirements for the 1990's [AIAA PAPER 90-1389] p 594 A90-37934

GUNNINK, JAN WILLEM

Aerospace Arall - The advancement in aircraft materials p 947 A90-50186

GUNSALLUS, C. T.

Rotating system load monitoring using minimum fixed system instrumentation p 651 A90-39982

GUNSALLUS, CLIFFORD T.

Investigation of variation in fatigue life calculated using damage fraction p 537 A90-33624

GUNTER, E. J.

Dynamics of multi-spool gas turbines using the matrix transfer method - Applications p 509 A90-33594
Dynamics of multi-spool gas turbines using the matrix transfer method - Theory p 509 A90-33595

GUO, WEN

A novel synthetic method for studying nonlinear flight stability p 645 A90-42355

GUO, Y. P.

Sound generation by a supersonic aerofoil cutting through a steady jet flow p 781 A90-42638

GUO, YINGQING

A design of a twin variable control system for aero-turbojet engine p 423 A90-29917

GUPTA, A. K.

Controlled mixing and variable geometry combustor design effects on emissions and combustion characteristics p 45 A90-12547
Evaluation of high temperature protective coatings for gas turbine engines under simulated service conditions p 952 A90-28712

GUPTA, K. K.

STARS: An integrated general-purpose finite element structural, aeroelastic, and aeroservoelastic analysis computer program [NASA-TM-101709] p 689 A90-23768

GUPTA, P. C.

The next generation supersonic transport engine: Critical issues [PNR90576] p 115 A90-12605

GUPTA, R. N.

Hypersonic viscous shock-layer solutions over long slender bodies. II - Low Reynolds number flows p 393 A90-29695

GUPTA, ROOP M.

Low-density flow effects for hypervelocity vehicles, phase 2 [AD-A221034] p 634 A90-24249

GUPTA, S. C.

Leading edge flap influence on aerodynamic efficiency p 85 A90-15240
Optimal reflex camber p 308 A90-26347
Aerodynamic characteristics of forward sweep [AIAA PAPER 90-3041] p 792 A90-45879
Winger - Computer code for aerodynamic analysis of wings p 810 A90-48077
Optimal camber distributions with multiple constraints p 810 A90-48078
Modelling free vortex flow on planar swept wing p 810 A90-48079

GURA, G. V.

Interference between the pitot-static tube and the model in wind tunnel studies of flow parameters p 350 A90-24169

GURURAJ, D.

Photoelastic investigation of turbine rotor blade shrouds p 112 A90-16008

GURUSWAMY, GURU P.

Unsteady transonic Navier-Stokes computations for an oscillating wing using single and multiple zones [AIAA PAPER 90-0313] p 228 A90-22197
Unsteady aerodynamic and aeroelastic calculations for wings using Euler equations p 302 A90-25288
Navier-Stokes computations on swept-tapered wings, including flexibility [AIAA PAPER 90-1152] p 389 A90-29364
Application of a streamwise upwind algorithm for unsteady transonic computations over oscillating wings [AIAA PAPER 90-3103] p 796 A90-45915
Extension of a streamwise upwind algorithm to a moving grid system [NASA-TM-102800] p 572 A90-21739

GUSAROV, S. A.

Effect of the radial clearance on the efficiency of a partial microturbine p 111 A90-14586

GUSEINOV, N. SH.

Some characteristics of the meteorological conditions of low cloud formation around the Baku airport p 888 A90-48364

GUSEV, V. N.

Hypersonic flow past blunt edges at low Reynolds numbers p 10 A90-12284

GUSEVA, N. N.

An automated method for predicting the height of the lower cloud boundary p 888 A90-48359

GUSHCHIN, V. R.

Excitation and development of unstable perturbations in a supersonic boundary layer p 710 A90-44928

GUSHCHIN, V. V.

Identification and diagnostics in the data processing and control systems of aerospace powerplants p 611 A90-36151

GUTMANN, JAMES C.

Advanced Automation System design p 375 A90-25566

GUTMARK, E.

Flow and acoustic features of a supersonic tapered nozzle [AIAA PAPER 90-1599] p 567 A90-38731

Supersonic rectangular isothermal shrouded jets [AIAA PAPER 90-2028] p 621 A90-40599

Multistep dump combustor design to reduce combustion instabilities p 659 A90-40934

Suppression of 'Buzz' instability by geometrical design of the flameholder [AIAA PAPER 90-1966] p 741 A90-42706

Active combustion control in a coaxial dump combustor [AIAA PAPER 90-2447] p 743 A90-42806

GUVENEN, HALDUN

Aerodynamics of bodies in shear flow p 910 A90-28496

GUVERNIUK, S. V.

Equilibrium of an elastic porous shell in supersonic gas flow p 150 A90-17109

GUY, R. WAYNE

Scramjet testing from Mach 4 to 20 - Present capability and needs for the nineties [AIAA PAPER 90-1388] p 597 A90-38485

GUYOT, GERARD

A320 flight tests: Particularities and innovations p 34 A90-10864

GYEKENYESI, JOHN P.

A review of failure models for ceramic matrix composite laminates under monotonic loads [ASME PAPER 89-GT-153] p 354 A90-23842

H

HA MINH, H.

Numerical simulation of the compressible flow in a valve-cylinder assembly p 770 A90-44431

Numerical study of heat transfer for unsteady viscous supersonic blunt body flows p 707 A90-44432

HA, C. M.

Reconfigurable aircraft flight control system via robust direct adaptive control [AIAA PAPER 90-3226] p 868 A90-49111

HAAG, JOHN E.

VSCF cycloconverter reliability review of the 30/40 KVA F/A-18 electrical generating system [SAE PAPER 892228] p 746 A90-45444

HAAG, KARLHEINZ

A panel process for the calculation of the flow around a wing with front angle damping [ETN-90-95367] p 399 A90-19207

HAAS, DAVID JOSEPH

Aeroelastic characteristics of aircraft with circulation control wings p 497 A90-20070

HAAS, W.

Definition of research needs to address airport pavement distress in cold regions [DOT/FAA/DS-89/13] p 59 A90-10896

HAAS, WILBUR M.

Improving snow roads and airstrips in Antarctica [AD-A211588] p 133 A90-11907

HABASHI, W. G.

Non-unique solutions of the Euler equations p 716 A90-45727

HABER, JERALD M.

Noise and sonic boom impact technology. Effects of aircraft noise and sonic booms on structures: An assessment of the current state-of-knowledge [AD-A213919] p 378 A90-17409

HACISALIHZADE, SELIM

Visualization of three dimensional data p 782 A90-25553

HACK, K. H.

Inversions and associated wind-shear warnings must be related to airport characteristics p 962 A90-52051

HACKETT, STEVEN C.

A high performance aerospace resin for Resin Transfer Molding p 945 A90-50163

HADDAD, A.

Supersonic nozzle design of arbitrary cross-section p 515 A90-21035

HADDAD, A. H.

Estimation and control of nonlinear and hybrid systems with applications to air-to-air guidance [AD-A214542] p 348 A90-16770

HADDAD, WASSIM M.

Integrated control-system design via generalized LQG (GLQG) theory p 613 A90-23023

HADDOW, C.

An experimental investigation of the downwash beneath a lifting rotor and low advance ratios p 151 A90-17585

HADFIELD, MICHAEL

The multi-function RLG system comes of age - A technical update p 578 A90-36931

HADFIELD, MICHAEL J.

Update 90 - A progress report on evaluation and flight testing of the small common RLG INS [AIAA PAPER 90-3375] p 847 A90-47763

HADJISOPHOCLEOUS, G. V.

Time development of convection flow patterns in aircraft cabins under post-crash fire exposure p 327 A90-17598

HADZIDAKIS, M.

A two-dimensional unsteady potential solver in internal aerodynamics flow problems p 707 A90-44430

HAENDE, B. M.

Experimental and theoretical study of the swirling flow in centrifugal compressor volutes [ASME PAPER 89-GT-183] p 273 A90-22663

HAENEL, D.

On the computations of hypersonic viscous flows p 225 A90-21170

HAERING, EDWARD A., JR.

Airdata calibration of a high-performance aircraft for measuring atmospheric wind profiles [NASA-TM-101714] p 186 A90-14228

HAERTIG, J.

Aerodynamic loads and blade vortex interaction noise prediction p 614 A90-38520

Prediction of rotor blade-vortex interaction noise from 2-D aerodynamic calculations and measurements [ISL-CO-243/88] p 396 A90-18365

Study of the blade/vortex interaction on a one-blade rotor during forward flight (incompressible, non viscous fluid) [ISL-R-115/88] p 415 A90-18391

Aerodynamic loads and blade vortex interaction noise prediction [ISL-PU-310/89] p 719 A90-25942

HAERTIG, JACQUES

Rotor loads computation using singularity methods and application to the noise prediction p 807 A90-46880

HAEUSER, J.

Numerical grid generation in computational fluid mechanics '88; Proceedings of the Second International Conference, Miami Beach, FL, Dec. 5-8, 1988 p 376 A90-26476

HAEUSLER, S.

Structural-acoustic analysis of aircraft fuselage structures using general purpose finite element codes p 492 A90-33385

HAFEEZ, ARSHAD

Standardization in aerospace plating and coating [SAE PAPER 890913] p 365 A90-24681

HAFEZ, M. M.

Non-unique solutions of the Euler equations p 716 A90-45727

HAFTKA, R. T.

Design of aircraft wings subjected to gust loads - A system reliability approach p 958 A90-52044

HAGA, JANE

Teamwork for excellence [AIAA PAPER 89-3195] p 549 A90-31686

HAGEMAIER, DONALD J.

Eddy current detection of subsurface cracks p 882 A90-48629

HAGENBERG, T. H. M.

Mobile satellite communications for civil aviation [NLR-MP-88066-U] p 775 A90-26238

HAGENSON, R. L.

Improved fiber reinforced polyphenylene sulfide thermoplastic composites p 947 A90-50180

HAGG, D.

Production of Ti6Al4V-components for a new turbo-fan-engine p 132 A90-16618

HAGGE, JOHN K.

Mechanical considerations for reliable interfaces in next generation electronics packaging p 453 A90-30813

HAGHIGHAT, R.

Effects of additives on the processing and properties of LARC-TPI polyimide p 942 A90-50070

HAGINS, SAMUEL E.

Robotics for flightline servicing p 383 A90-30760

- HAGNAUER, GARY L.**
HPLC analysis of helicopter rotor blade materials
[AD-A221121] p 650 N90-24270
Applications of digital image processing in testing and evaluation of composite materials
[AD-A222939] p 874 N90-26887
- HAH, C.**
Generation and decay of secondary flows and their impact on aerodynamic performance of modern turbomachinery components p 514 N90-21023
Mesh generation for flow computation in turbomachine p 588 N90-21981
- HAHN, K.-U.**
Effect of wind shear on flight safety p 175 A90-17973
- HAHNE, DAVID E.**
Stability characteristics of a conical aerospace plane concept
[SAE PAPER 892313] p 757 A90-45475
Wind tunnel results of the high-speed NLF(1)-0213 airfoil p 93 N90-12542
Innovative control concepts and component integration for a generic supercruise fighter p 935 N90-28521
- HAIDER, O.**
Calculation of thick wall fiber binders for rotor components of modern helicopters
[MBB-UD-554/84-PUB] p 735 N90-25137
- HAIGLER, KARA J.**
Evaluation of transonic wall interference assessment and correction for semi-span wing data
[AIAA PAPER 90-1433] p 597 A90-38487
- HAINES, A. B.**
Experience in the use of a viscous simulation methodology for tests in transonic tunnels
[AIAA PAPER 90-1414] p 559 A90-37951
- HAINES, PATRICK A.**
The collection of non-conus aircraft icing data along with an identification of the geographical areas of potential severe icing and a study of a method of remote determining atmospheric icing data
[AD-A215055] p 323 N90-16724
- HAJIC, KENNETH J.**
Supersonic STOVL - The future is now p 732 A90-44781
- HALASZ, MIKE**
Jet Engine Technical Advisor (JETA) p 693 A90-41184
- HALEY, PHILIP J.**
Advanced turbine technology applications project (ATTAP) - Overview, status, and outlook
[ASME PAPER 89-GT-118] p 360 A90-23819
- HALFMANN, GUENTHER**
Low- and high-speed tests with the Dornier 328 wind-tunnel model p 246 A90-21611
- HALFORD, GARY R.**
Thermal fatigue durability for advanced propulsion materials
[NASA-TM-102348] p 215 N90-14641
Finite element elastic-plastic-creep and cyclic life analysis of a cowl lip
[NASA-TM-102342] p 610 N90-22808
- HALIM, AHMAD A. M.**
Numerical study of three methods for solving reacting flows p 305 A90-25804
- HALL, D. E.**
Alleviation of shock oscillations in transonic flow by passive controls
[AIAA PAPER 90-0046] p 161 A90-19648
- HALL, D. S.**
Aircraft crash survival design guide, Volume 5: Aircraft postcrash survival
[AD-A218438] p 575 N90-22549
- HALL, DOUGLAS R.**
Thick airfoil designs for a HALE vehicle
[AIAA PAPER 90-3036] p 791 A90-45875
- HALL, E. J.**
Simulation of time-dependent viscous flows using central and upwind-biased finite-difference techniques
[AIAA PAPER 90-3012] p 790 A90-45864
- HALL, E. L.**
Microstructures of rapidly-solidified binary TiAl alloys p 532 A90-34990
- HALL, EDWARD J.**
3D Euler analysis of ducted propfan flowfields
[AIAA PAPER 90-3034] p 791 A90-45873
- HALL, J. GORDON**
Blunt-nose inviscid airflows with coupled nonequilibrium processes p 171 N90-13336
- HALL, J. R.**
The need for platform motion in modern piloted flight training simulators
[AD-A221720] p 871 N90-26847
- HALL, KENNETH C.**
Calculation of unsteady Euler flows in turbomachinery using the linearized Euler equations p 5 A90-11778
- Development of a linearized unsteady aerodynamic analysis for cascade gust response predictions
[NASA-CR-4308] p 816 N90-27655
- HALL, M. G.**
Improvements in the formulations and numerical solution of the Euler problem for swept wings
[RAE-TM-AERO-2139] p 95 N90-12562
- HALL, MARK**
A synergistic approach to logistics planning and engine design p 422 A90-28207
- HALL, PATRICK G.**
The Pointer - Test and evaluation of the tiltrotor UAV p 406 A90-28170
- HALL, PHILIP**
On the Goertler vortex instability mechanism at hypersonic speeds p 158 A90-18886
Non-axisymmetric viscous lower-branch modes in axisymmetric supersonic flows p 474 A90-33509
On the instability of hypersonic flow past a wedge p 554 A90-35902
Wave interactions in a three-dimensional attachment-line boundary layer p 811 A90-48715
- HALL, R. M.**
Impact of nose-probe chines on the vortex flows about the F-16C
[AIAA PAPER 90-0386] p 165 A90-19828
Navier-Stokes solutions for vortical flows over a tangent-ogive cylinder p 620 A90-39780
- HALL, ROBERT M.**
Experimental investigation of a new device to control the asymmetric flowfield on forebodies at large angles of attack
[AIAA PAPER 90-0069] p 161 A90-19665
Remote detection of boundary-layer transition by an optical system p 139 N90-12524
- HALL, STEPHEN R.**
Iterative preliminary design tools for composite structures p 882 A90-48045
- HALL, STEVEN R.**
Linear control issues in the higher harmonic control of helicopter vibrations p 430 A90-28225
Piezoelectric actuators for helicopter rotor control
[AIAA PAPER 90-1076] p 411 A90-29384
- HALLER, F. F.**
Supersonic combustion of hydrogen-jets behind a backward-facing step
[AIAA PAPER 90-0204] p 266 A90-22183
- HALLIDAY, REGINALD D.**
Aircraft internal fires p 326 N90-17593
- HALLION, RICHARD P.**
Flight testing and flight research: From the age of the tower jumper to the age of the astronaut p 35 N90-10882
- HALLISSY, JAMES B.**
Design and test of an NLF wing glove for the variable-sweep transition flight experiment p 104 N90-12544
- HALLS, G. A.**
The nature and control of skidding in lightly loaded intershaft bearings
[PNR90591] p 136 N90-12933
- HALPERN, M. E.**
Application of optimal tracking methods to aircraft terrain following
[AD-A221099] p 641 N90-24264
- HALSEY, N. D.**
Grid generation for an aft-fuselage-mounted nacelle/pylon configuration p 311 A90-26543
- HALSEY, N. DOUGLAS**
Calculation of transonic flows for novel engine-airframe installations p 145 A90-16768
- HALSTEAD, D. E.**
Boundary-layer transition and separation on a turbine blade in a plane cascade
[AIAA PAPER 90-2263] p 625 A90-42102
- HALVERSTADT, D. E.**
Flight test data processing, plotting and analysis at your finger tips - A flexible, automated, integrated approach
[AIAA PAPER 90-1322] p 545 A90-34150
- HALVORSEN, WILLIAM G.**
Interior noise control of the Saab 340 aircraft
[SAE PAPER 891080] p 101 A90-14372
Viscoelastic tuned dampers for control of structural dynamics p 73 N90-10999
- HAM, NORMAN D.**
Active control of gust- and interference-induced vibration of tilt-rotor aircraft p 429 A90-28201
Active control of tiltrotor blade in-plane loads during maneuvers p 670 A90-42463
- HAMADA, SEIICHI**
Reliability evaluation system for ceramic gas turbine components p 444 A90-27678
- HAMAGUCHI, YASUMASA**
Evaluation of static and fatigue properties of thin sheets of 8090-T8 aluminum-lithium alloy and observation of its fracture surfaces
[NAL-TR-1039] p 953 N90-29499
- HAMANO, Y.**
Development of ceramic components for high-temperature gas turbines p 602 A90-35951
- HAMANO, YOSHITERU**
MRS International Meeting on Advanced Materials, 1st, Tokyo, Japan, May 31-June 3, 1988, Proceedings. Volume 5 - Structural ceramics/Fracture mechanics p 599 A90-35926
- HAMED, A.**
Effect of environmental particles on a radial compressor p 113 A90-16373
An investigation of oblique shock/boundary layer bleed interaction
[AIAA PAPER 90-1928] p 703 A90-42697
Jet engines performance deterioration p 852 A90-46871
Flow separation in oblique shock wave turbulent boundary layer interactions p 807 A90-46872
- HAMED, AWATEF**
Probabilistic modeling for simulation of aerodynamic uncertainties in propulsion systems
[NASA-TM-102472] p 515 N90-21036
- HAMED, M. A.**
Two-dimensional convergent-divergent nozzle flow with wall velocity slip and temperature jump p 807 A90-46884
- HAMEL, PETER**
System identification collaboration - The role of AGARD p 1 A90-12763
Flight test engineering with the ATTAS p 902 N90-29160
- HAMELUCK, DONALD**
Underlying factors in air traffic control incidents p 401 A90-31335
- HAMINH, H.**
Development of turbulence models for the analysis of compressible or incompressible unsteady flow
[ETN-90-97486] p 958 N90-28810
- HAMMER, JERRY**
Design and analysis of composite structures with manufacturing flaws p 445 A90-28234
- HAMMER, JOHN M.**
Information display management in a pilot's associate p 418 A90-30238
- HAMMESFAHR, J.**
A supplement to GPS/Navstar for civil use p 915 A90-52613
- HAMMOND, DARYL**
Multivariable control design for the control reconfigurable combat aircraft (CRCA) p 432 A90-30715
- HAMPTON, HERBERT R.**
Miniaturization of flight deflection measurement system
[NASA-CASE-LAR-13628-1] p 689 N90-23707
- HAMPTON, LAWRENCE**
Full-scale air transport category fuselage burnthrough tests
[DOT/FAA/CT-TN89/65] p 486 N90-20967
- HAMRICK, DAVID G.**
ATC ground communications system optimization techniques p 330 A90-25568
- HAN, CHAO**
Modal aggregation and its application in flight mechanics p 196 A90-18595
- HAN, J. C.**
Augmented heat transfer in rectangular channels of narrow aspect ratios with rib turbulators p 70 A90-13091
Effect of rib-angle orientation on local mass transfer distribution in a three-pass rib-roughened channel
[ASME PAPER 89-GT-98] p 359 A90-23812
Heat transfer in gas turbine engines; Proceedings of the Symposium, ASME Winter Annual Meeting, San Francisco, CA, Dec. 10-15, 1989 p 534 A90-32166
- HAN, JIANYUAN**
Effect of vane and blade numbers on performance of transonic turbine stage p 189 A90-17789
- HAN, LIT S.**
A heat transfer analysis for rough turbine airfoils
[AD-A221942] p 854 N90-26831
- HAN, WANJIN**
Influence of blade leaning on the flow field behind turbine rectangular cascades with different incidences and aspect ratios p 11 A90-12519
- HAN, ZHAOXUAN**
The design and study of the information transfer mechanism for a distributed avionics system p 207 A90-16858

- HANAGUD, S.**
Kane's methods in rotorblade dynamics p 646 A90-42458
- HANCOCK, G. J.**
Unsteady aerodynamics of controls p 935 N90-28525
- HANCOCK, JOHN P.**
An adaptive-learning expert system for maintenance diagnostics p 460 A90-30754
- HANCY, JEAN PIERRE**
PETW testing results p 523 A90-34226
- HAND, R. J.**
The effects of toughening stresses on liquid impact induced fracture p 692 A90-41315
- HANDELMAN, DAVID A.**
Rule-based mechanisms of learning for intelligent adaptive flight control p 521 N90-20939
Perspectives on the use of rule-based control p 521 N90-20940
- HANDELMAN, DAVID ANDREW**
A rule-based paradigm for intelligent adaptive flight control p 434 N90-19238
- HANDLEY, C. S.**
Flight tests to explore tail rotor limitations in the low speed envelope p 647 A90-42498
- HANDLEY, ROBERT M.**
TCAS - A lengthy but beneficial development effort p 339 A90-25494
- HANDSCHUH, R. F.**
Efficiency testing of a helicopter transmission planetary reduction stage p 271 A90-21113
- HANDSCHUH, ROBERT F.**
Efficiency study comparing two helicopter planetary reduction stages [AIAA PAPER 90-2156] p 956 A90-50644
Efficiency study comparing two helicopter planetary reduction stages [NASA-TM-103106] p 776 N90-26334
- HANFF, E. S.**
Large-amplitude high-rate roll experiments on a delta and double delta wing [AIAA PAPER 90-0224] p 163 A90-19742
Large-amplitude high-rate roll oscillation system for the measurement of non-linear airloads [AIAA PAPER 90-1426] p 590 A90-37963
- HANHELA, PETER J.**
Effect of temperature on the storage life of polysulfide aircraft sealants [MRL-TR-89-31] p 444 N90-19364
- HANKE, DIETRICH**
Hermes training aircraft p 354 N90-16827
- HANKEY, W. L.**
System optimization for maximizing reconnaissance mission range of a hypersonic cruise vehicle [AIAA PAPER 90-3292] p 837 A90-48876
- HANKEY, WILBUR L.**
Computation of ramjet internal flowfields [AD-A212001] p 114 N90-11743
- HANNA, R.**
A comparison of honeycomb-core and foam-core carbon-fibre/epoxy sandwich panels p 764 A90-43855
- HANNEMANN, KLAUS**
Design of an axisymmetric, contoured nozzle for the HEG [DLR-FB-90-04] p 959 N90-28812
- HANNIS, J. M.**
A comparison between engine test results and design predictions of turbine blade cooling performance [ASME PAPER 89-GT-169] p 341 A90-23854
- HANSEN, IRVING G.**
Aerospace induction motor actuators driven from a 20-kHz power link [NASA-TM-102482] p 509 N90-20085
- HANSEN, JAMES G. R.**
HOTOL structures and materials at British Aerospace, Warton, UK [EOARD-LR-90-001] p 503 N90-21001
- HANSEN, MARION G.**
Freeze drying for morphological control of inter-penetrating polymer networks p 948 A90-50214
- HANSEN, RICHARD C.**
Flight-path display can improve safety, operational efficiency p 847 A90-48982
- HANSEN, STEVE**
Energy based stability analysis of a fuzzy roll controller design for a flexible aircraft wing p 668 A90-40833
- HANSMAN, R. JOHN, JR.**
Analysis of aircraft performance during lateral maneuvering for microburst avoidance [AIAA PAPER 90-0568] p 197 A90-19920
Cockpit display of hazardous wind shear information p 484 N90-20924
Modeling of surface roughness effects on glaze ice accretion p 485 N90-20925
- Ultrasonic techniques for aircraft ice accretion measurement p 485 N90-20926
Investigation of surface water behavior during glaze ice accretion p 485 N90-20927
The influence of ice accretion physics on the forecasting of aircraft icing conditions p 485 N90-20928
Cockpit display of hazardous weather information p 485 N90-20929
- HANSON, D. B.**
Investigation of the near wake of a propfan p 622 A90-40686
- HANSON, FRANCIS V.**
Production of high density aviation fuels via novel zeolite catalyst routes [AD-A216444] p 443 N90-18601
- HANSON, RONALD K.**
Turbulent reacting flows and supersonic combustion [AD-A221793] p 875 N90-26933
- HAO, JIANG**
The study of transient suppression techniques for multimode flight control system p 590 A90-37219
- HARALSON, DAVID G.**
Toward the panoramic cockpit, and 3-D cockpit displays p 419 A90-30682
- HARASGAMA, S. P.**
Aerodynamic and heat transfer measurements on blading for a high rim-speed transonic turbine [ASME PAPER 89-GT-228] p 293 A90-23883
Aerodynamic and heat transfer measurements on blading for a high rim-speed transonic turbine [RAE-TM-P-1151] p 256 N90-15920
- HARDEGEN, H.**
Past, present and future: Aircraft integrated monitoring systems: An ever-developing technology p 848 N90-27618
- HARDERSEN, CHARLES P.**
SH-2F airframe fatigue test program p 642 A90-39989
- HARDIN, JAY C.**
A new class of random processes with application to helicopter noise p 781 A90-42874
- HARDING, J. W.**
Flight simulation model validation procedure, a systematic approach p 30 A90-12770
- HARDING, S. C.**
An investigation of secondary flows in nozzle guide vanes p 512 N90-21016
- HARDING, WILLIAM A.**
Hypercube expert system shell-applying production parallelism [AD-A215762] p 377 N90-18173
- HARDY, B. C.**
Experimental investigation of attachment-line transition in low-speed, high-lift wind-tunnel testing p 71 N90-10358
- HARDY, GORDON H.**
Simulation evaluation of transition and hover flying qualities of a mixed-flow, remote-lift STOVL aircraft [SAE PAPER 892284] p 757 A90-45464
Longitudinal stability and control characteristics of the Quiet Short-Haul Research Aircraft (QSRA) [NASA-TP-2965] p 349 N90-17639
Lateral-directional stability and control characteristics of the Quiet Short-Haul Research Aircraft (QSRA) [NASA-TM-102250] p 671 N90-23413
- HARDY, GROVER L.**
In-service inspection of composite components on aircraft at depot and field levels p 885 N90-28078
- HARDY, T. L.**
Background, current status, and prognosis of the ongoing slush hydrogen technology development program for the NASP [NASA-TM-103220] p 763 N90-26055
- HARDY, TERRY L.**
Slush Hydrogen (SLH2) technology development for application to the National Aerospace Plane (NASP) [NASA-TM-102315] p 203 N90-14268
- HARE, JEANETTE A.**
Airport pavement drainage [DOT/FAA/RD-90/24] p 872 N90-27728
- HARITOS, GEORGE K.**
Predicting crack growth under thermo-mechanical cycling p 209 A90-18169
- HARLOFF, G. J.**
Viscous three-dimensional analyses for nozzles for hypersonic propulsion [NASA-CR-185197] p 344 N90-17635
- HARLOFF, GARY J.**
Hypersonic aerospace sizing analysis for the preliminary design of aerospace vehicles p 247 A90-23276
- HARMAN, W. H.**
TCAS - A system for preventing midair collisions p 252 A90-21383
- HARMON, A. O.**
Nonflammable hydraulic power system for tactical aircraft. Volume 1: Aircraft system definition, design and analysis [AD-A218493] p 671 N90-23409
- HARMON, D. B.**
Aerodynamic breakup of liquid jets - A review [AIAA PAPER 90-1616] p 607 A90-38746
- HARMON, D. M.**
Damage tolerance analysis for manned hypervelocity vehicles. Volume 2: Software user's manual [AD-A222136] p 845 N90-26826
Damage tolerance analysis for manned hypervelocity vehicles. Volume 1: Final technical report [AD-A221970] p 887 N90-28106
- HARPER, P. J. G.**
Ground-simulation investigations of VTOL airworthiness criteria for terminal-area operations [NASA-TM-102810] p 757 N90-25141
- HARPUR, K.**
Acoustic recording systems for use in military aircraft [RAE-TM-MM-11] p 140 N90-13207
- HARRELL, TERRY L.**
The design of a sport aircraft configured to emulate jet fighter characteristics [AIAA PAPER 90-3244] p 839 A90-49119
- HARRIS, A. E.**
Holographic flow visualisation of turbofan by-pass and core nozzle streams [ASME PAPER 89-GT-260] p 363 A90-23891
- HARRIS, C. S.**
A conflict analysis of 4D descent strategies in a metered, multiple-arrival route environment [NASA-CR-182019] p 593 N90-21772
- HARRIS, CAROLINE S.**
Electrochromic windows - Applications for aircraft [SAE PAPER 891063] p 129 A90-14363
- HARRIS, CHARLES D.**
Experimental transition and boundary-layer stability analysis for a slotted swept laminar flow control airfoil p 148 A90-16793
Results of LFC experiment on slotted swept supercritical airfoil in Langley's 8-foot transonic pressure tunnel p 92 N90-12531
Boundary-layer stability analysis of Langley Research Center 8-foot LFC experimental data p 92 N90-12532
NASA supercritical airfoils: A matrix of family-related airfoils [NASA-TP-2969] p 315 N90-16710
- HARRIS, CHARLES E.**
NASA airframe structural integrity program [NASA-TM-102637] p 543 N90-21422
An evaluation of the pressure proof test concept for thin sheet 2024-T3 [NASA-TM-101675] p 543 N90-21424
- HARRIS, DAVID O.**
Application of fracture mechanics to microscale phenomena in electronic assemblies p 684 A90-41334
- HARRIS, J. A.**
Simulation of a turbocompound two-stroke diesel engine [SAE PAPER 891066] p 110 A90-14366
- HARRIS, J. L.**
Slotted-wall research with disk and parachute models in a low-speed wind tunnel [AIAA PAPER 90-1407] p 595 A90-37946
Slotted-wall research with disk and parachute models in a low-speed wind tunnel [DE90-002989] p 572 N90-21737
- HARRIS, JAMES A.**
A simulation code for turbocompound diesel engines [IAR-89-26] p 774 N90-25348
- HARRIS, JANE A.**
High performance needled structures in composites p 955 A90-50173
- HARRIS, JOHN A., JR.**
Retirement for cause of the F100 engine p 843 N90-26813
- HARRIS, JULIUS E.**
Numerical solution of the boundary-layer equations for a general aviation fuselage [AIAA PAPER 90-0305] p 163 A90-19786
Fourth-order accurate three-dimensional compressible boundary-layer calculations p 308 A90-26136
- HARRIS, MICHAEL**
Noise and sonic boom impact technology. Initial development of an Assessment System for Aircraft Noise (ASAN). Volume 1: Executive summary [AD-A214184] p 379 N90-17410
Noise and sonic boom impact technology. Initial development of an Assessment System for Aircraft Noise (ASAN). Volume 2: System design strategy [AD-A214454] p 379 N90-17411

- Noise and sonic boom impact technology. Initial development of an Assessment System for Aircraft Noise (ASAN). Volume 3: Technical description
[AD-A214455] p 379 N90-17412
- HARRIS, S. D.**
Air Combat Environment Test and Evaluation Facility (ACEF) p 58 N90-10883
- HARRIS, T.**
Endurance of aircraft gas turbine mainshaft ball bearings-analysis using improved fatigue life theory. II - Application to a bearing operating under difficult lubrication conditions p 128 A90-13845
- HARRIS, T. A.**
Endurance of aircraft gas turbine mainshaft ball bearings-analysis using improved fatigue life theory. I - Application to a long-life bearing p 537 A90-33557
- HARRIS, T. B.**
Measurement of mean and fluctuating flow properties in hypersonic shear layers
[AIAA PAPER 90-1409] p 560 A90-38488
- HARRIS, W. D.**
Damage tolerance analysis and testing of a welded cluster gear for the main transmission of the Advanced Attack Helicopter p 445 A90-28187
- HARRISON, J. M.**
Flight simulation model validation procedure, a systematic approach p 30 A90-12770
- HARRISON, R. J.**
Identification of retreating blade stall mechanisms using flight test pressure measurements p 384 A90-28172
- HARRISON, ROBIN T.**
Preliminary thoughts on an acoustic metric for the wilderness aircraft overflight study p 697 N90-24862
- HARRISON, S.**
Secondary loss generation in a linear cascade of high-turning turbine blades
[ASME PAPER 89-GT-47] p 289 A90-23773
- HARRISON, SCOTT RUSSELL**
Throughput and delay characteristics for a slow-frequency hopped aircraft-to-aircraft packet radio network
[AD-A220525] p 688 N90-23609
- HARSE, JAMES H.**
The four-bladed main rotor system for the AH-1W helicopter
The Bell Helicopter AH-1 Cobra - Past, present, and future
[AIAA PAPER 90-3271] p 836 A90-48862
- HARTER, JAMES A.**
Significance of the short crack effect on aerospace structures p 269 A90-20065
- HARTFIELD, ROY J.**
Experimental investigation of a supersonic swept ramp injector using laser-induced iodine fluorescence
[AIAA PAPER 90-1518] p 606 A90-38663
- HARTFIELD, ROY J., JR.**
Injectant mole fraction measurements of transverse injection in constant area supersonic ducts
[AIAA PAPER 90-1632] p 587 A90-38761
- HARTLEY, R. A.**
The Experimental Aircraft Flight Test Programme p 34 N90-10865
- HARTLEY, TOM T.**
The determination of third order linear models from a seventh order nonlinear jet engine model p 964 A90-52881
- HARTMAN, D. R.**
Durability and damage tolerance of S-2 glass/PEEK composites p 944 A90-50140
- HARTMAN, P.**
Viscous flow analysis for advanced inlet particle separators
[AIAA PAPER 90-2136] p 661 A90-42038
- HARTMAN, RANDOLPH**
Integrated navigation - Employing LIRU/GPS p 329 A90-23995
- HARTMANN, G.**
Three-dimensional simulations of hypersonic flows p 306 A90-25823
- Grid patching approaches for complex three-dimensional configurations p 573 N90-21985
- HARTMANN, K.**
Flow field visualization study on a 65 deg delta wing at $M = 0.85$ p 277 N90-16182
- HARTMANN, LAWRENCE**
Preliminary thoughts on an acoustic metric for the wilderness aircraft overflight study p 697 N90-24862
- HARTMANN, W.**
Monolithic CFC-Main Landing Gear Door for Tornado p 955 A90-50138
- HARTROPP, S. J.**
Design of aeroengines in a low-fuel price scenario p 739 A90-42653
- HARTWICH, PETER-M.**
Fresh look at floating shock fitting
[AIAA PAPER 90-0108] p 162 A90-19686
- Navier-Stokes solutions for vortical flows over a tangent-ogive cylinder p 620 A90-39760
- HARTZHEIM, WOLFGANG**
Development and application of an optimization procedure for space and aircraft structures p 679 A90-39186
- Development and application of an optimization procedure for space and aircraft structures
[MBB-FW-522/S/PUB-383] p 779 N90-25078
- HARVEY, J. F.**
A data acquisition parallel bus for wind tunnels at ARL (Aeronautical Research Laboratory)
[AD-A218052] p 526 N90-20098
- HARVEY, R. A.**
Optimization studies for the PW305 turbofan
[AIAA PAPER 90-2520] p 744 A90-42813
- HARVEY, W. D.**
Computational results for the effects of external disturbances on transition location of bodies of revolution from subsonic to supersonic speeds and comparisons with experimental data
[SAE PAPER 892381] p 715 A90-45522
- HARVEY, WILLIAM D.**
Experimental transition and boundary-layer stability analysis for a slotted swept laminar flow control airfoil p 148 A90-16793
- HARWOOD, KELLY**
Cognitive perspectives on map displays for helicopter flight p 419 A90-31329
- HASAN, S. A.**
Aerostructural considerations for the power plant of overlapping wing configuration p 841 A90-49488
- HASEGAWA, GIZO**
Aeroelastic response characteristics of a rotor executing arbitrary harmonic blade pitch variations p 646 A90-42464
- HASEGAWA, S.**
Hypersonic test facility requirements for the 1990's
[AIAA PAPER 90-1389] p 594 A90-37934
- HASEL, K. L.**
Ultra high bypass turbofan technologies for the twenty-first century
[AIAA PAPER 90-2397] p 662 A90-42158
- HASHEMI-KIA, MOSTAFA**
Dynamic testing techniques and applications for an aeroelastic rotor test facility p 201 N90-13406
- HASHIM, S. M.**
New transonic test sections for the NAE 5ftx5ft trisonic wind tunnel p 630 A90-42431
- New transonic test sections for the NAE 5 ft x 5 ft trisonic wind tunnel
[AD-A220933] p 674 N90-24278
- HASHIMOTO, MASAKATA**
Transonic aerodynamics analysis of unconventional wing configurations by 3D-Euler code p 306 A90-25835
- HASHIMOTO, TADAO**
Flow dependent grid for aerodynamic designers p 306 A90-25831
- HASHIMOTO, Y.**
CRL's mobile satellite communication experiments using ETS-V
[AIAA PAPER 90-0775] p 366 A90-25602
- HASHINO, R.**
Application of 3-D Navier-Stokes computation to bowed stacking turbine vane design
[AIAA PAPER 90-2129] p 625 A90-42035
- HASHISH, EMAM**
An improved rotor/airframe coupling method for NASTRAN airframe vibration analysis p 831 A90-46962
- HASKELL, R. W.**
Gas turbine compressor operating environment and material evaluation
[ASME PAPER 89-GT-42] p 340 A90-23769
- HASSAN, A. A.**
Euler solutions for self-generated rotor blade-vortex interactions
[AIAA PAPER 90-1588] p 566 A90-38723
- Rotorcraft computational fluid dynamics - Recent developments at McDonnell Douglas p 630 A90-42439
- Numerical simulations of three-dimensional rotor blade-vortex interactions p 807 A90-46879
- HASSAN, AHMED A.**
Improvement to interactive two dimensional rotor section design p 808 A90-46943
- HASSAN, H. A.**
Grid generation and adaptation for the direct simulation Monte Carlo method p 67 A90-11102
- An abbreviated Reynolds stress turbulence model for airfoil flows p 562 A90-38625
- A hybrid Reynolds averaged/PDF closure model for supersonic turbulent combustion
[AIAA PAPER 90-1573] p 600 A90-38711
- HASSAN, MAGGIE**
The SKY SHARK: An RPV designed to investigate the pressure distribution on a lifting surface
[NASA-CR-186222] p 844 N90-26824
- HASSELBRING, ALAN J.**
Update 90 - A progress report on evaluation and flight testing of the small common RLG INS
[AIAA PAPER 90-3375] p 847 A90-47763
- HASSENPLUG, WOLFGANG**
System concept and performance criteria of modern helicopter navigation p 640 A90-42452
- Development and verification of software for flight safety critical strapdown systems p 694 A90-42454
- Analytical evaluation of helicopter true air speed and associated flight tests p 647 A90-42499
- HASSIG, H.**
Modeling flexible aircraft for flight control design
[AD-A219123] p 757 N90-25140
- HASSOUN, JOHN A.**
Development of an acceptability window for a ground proximity avoidance system p 419 A90-30730
- HASTINGS, EARL C., JR.**
Status report on a natural laminar-flow nacelle flight experiment p 105 N90-12550
- HATAUE, ITARU**
Study of compressibility effects in mixing layer by numerical simulation
[AIAA PAPER 90-1464] p 562 A90-38621
- HATFIELD, DONALD W.**
High speed bus technology development
[AD-A22486] p 960 N90-29565
- HATHAWAY, MICHAEL D.**
Laser anemometer measurements in a transonic axial-flow fan rotor
[NASA-TP-2879] p 73 N90-11245
- HATTINGH, H. V.**
Atomization of synthetic jet fuel p 63 A90-12602
- HATTORI, TOSHIO**
Optimum design of rotational wheels under transient thermal and centrifugal loading p 270 A90-20770
- HAUENSTEIN, ANTHONY J.**
Chaotic response of aerosurfaces with structural nonlinearities (Status report)
[AIAA PAPER 90-1034] p 392 A90-29378
- HAUSER, G. C.**
Small multipurpose stored data acquisition system
[DE90-010823] p 967 N90-30134
- HAVEL, ROBERT F.**
Flight service automation system, model 1 full capacity, NAS operational test and evaluation integration test plan (DOT/FAA/CT-TN90/4) p 825 N90-27672
- HAVERLAND, MANFRED**
Flight-path measurement p 242 A90-21721
- Inspection of instrument landing systems p 915 A90-52614
- HAVEY, GARY**
Microminiature flight test instrumentation
[AIAA PAPER 90-1274] p 504 A90-33898
- HAVILAND, J. K.**
Adaptive control of helicopter vibrations via the impulse response method
[AD-A213728] p 260 N90-15113
- HAVILAND, JOHN K.**
NASA-UVA light aerospace alloy and structures technology program
[NASA-CR-182607] p 601 N90-22651
- Design of cryogenic tanks for launch vehicles p 609 N90-22662
- HAVRILLA, G. J.**
Injection molding development of ceramic turbine components
[ASME PAPER 89-GT-170] p 361 A90-23855
- HAWBOLDT, R. J.**
The University of Toronto-Ryerson Polytechnical Institute hypersonic gun tunnel p 673 A90-42432
- HAWK, J. D.**
Investigation of high angle of attack vortical flows over delta wings
[AIAA PAPER 90-0101] p 162 A90-19682
- HAWKEN, D. F.**
Prediction of two-dimensional time-dependent gasdynamic flows for hypersonic studies
[UTIAS-335] p 718 N90-25935
- HAWLEY, A. V.**
Subcomponent tests for composite fuselage technology readiness p 490 A90-33105
- HAWORTH, LORAN A.**
Helmet mounted display systems for helicopter simulation p 420 A90-31344
- HAWORTH, LOREN A.**
Helmet-mounted display systems for flight simulation
[SAE PAPER 892352] p 760 A90-45503
- HAY, N.**
Simulation of cooling film density ratios in a mass transfer technique
[ASME PAPER 89-GT-200] p 362 A90-23872

HAYAMI, H.

- Application of low-solidity cascade diffuser to transonic centrifugal compressor
[ASME PAPER 89-GT-66] p 290 A90-23789

HAYASHI, MASANORI

- Measurements of pressure fluctuations in the interaction regions of shock waves and turbulent boundary layers induced by blunt fins p 9 A90-12218
Aerodynamic heating in the interaction regions of shock waves and turbulent boundary layers induced by sharp fins p 9 A90-12220
Aerodynamic heating in shock wave/turbulent boundary layer interaction regions induced by blunt fins p 82 A90-13775
Numerical simulations of unsteady shock reflections by ramps p 305 A90-25795
Numerical simulation of separated flows around a wing section by a discrete vortex method p 307 A90-25846
Numerical simulation of separated flow around two-dimensional wing section by a discrete vortex method p 469 A90-32067
Numerical simulation of separated flows around a wing section at pitching motion by a discrete vortex method p 475 A90-33753

HAYDUK, ROBERT J.

- A review of the analytical simulation of aircraft crash dynamics
[NASA-TM-102595] p 484 A90-20068

HAYES, R. W.

- The creep behavior of the Ti3Al alloy Ti-24Al-11Nb p 125 A90-15214

HAYHURST, KELLY J.

- Software verification plan for GCS
[NASA-TM-101668] p 372 A90-18057

HAYNES, DAVY A.

- Design and experimental verification of an equivalent forebody representation of flowing inlets p 152 A90-17863

HAYNES, TIMOTHY S.

- Stability limits for three-dimensional supersonic boundary layers
[AIAA PAPER 90-1528] p 564 A90-38673

HAYNIE, D. A.

- New concept for improved nonmetallic erosion protection systems p 407 A90-28188

HAZARIKA, B.

- Measurement of velocity profiles and Reynolds stresses on an oscillating airfoil p 397 A90-18427

HE, CHENG JIAN

- Comparison of measured induced velocities with results from a closed-form finite state wake model in forward flight p 385 A90-28195

HE, CHENGJIAN

- Helicopter stability and control modeling improvements and verification on two helicopters p 671 A90-42474
Development and application of a generalized dynamic wake theory for lifting rotors p 570 A90-21731

HE, GUANGXIN

- A simplified model for unstable temperature field calculation of gas turbine rotor
[ASME PAPER 89-GT-234] p 363 A90-23885

HE, J.

- Embedded function methods for supersonic turbulent boundary layers
[AIAA PAPER 90-0306] p 163 A90-19787

HE, KAIFENG

- The study of the theoretical calculation method for power stall dynamic characteristics of multiple-engine propeller airplane p 29 A90-10349

HE, KEMIN

- Experimental investigation of trailing-edge and near wake flow of a symmetric airfoil p 160 A90-19449

HE, LI

- Numerical Euler solution for the interaction between oscillating cascade and forced inlet unsteadiness p 8 A90-11792
Computation of unsteady compressible turbulent boundary layers in cascade flow with controlled inlet perturbation p 8 A90-11807

HE, XIONG

- A new simplification method for analysing the rapid rolling stability of aircraft p 669 A90-42367

HE, YAQUN

- The method of random variable structure optimal control for aircraft p 590 A90-37220

HE, ZHIDAI

- A novel synthetic method for studying nonlinear flight stability p 645 A90-42355
Exceptions to the $C(n, \beta, \gamma)$ criterion for aircraft stability at high angles of attack p 867 A90-48515
The role of $C(\text{sub } n, \beta, \gamma)$ in the aircraft stability at high angles of attack
[AD-A221586] p 868 A90-26833

HE, ZHONGWEI

- An experimental investigation on control of flow dynamic distortions downstream under strong shock-boundary layer interaction in the two-dimensional flow field p 471 A90-33288

HEAD, V. L.

- Mixer-ejector nozzle for jet noise suppression
[AIAA PAPER 90-1909] p 894 A90-47202

HEALEY, M. D.

- A dynamicist's view of fuel tank skin durability p 251 A90-15915

HEAPHY, WILLIAM J.

- Advanced transport operating system software upgrade: Flight management/flight controls software description
[NASA-CR-181936] p 893 A90-28366

HEARSEY, RICHARD M.

- Numerical optimization of axial compressor designs
[ASME PAPER 89-GT-14] p 340 A90-23758

HEATHCO, CRAIG

- Tilt rotor requirements on engine design and qualification p 587 A90-38534

HEBBAR, SHESHAGIRI K.

- A laser sheet flow visualization and aerodynamic force data evaluation of a 3 percent YF-17 fighter aircraft model at high angles of attack
[AIAA PAPER 90-3019] p 792 A90-45886

- Wind tunnel studies of support strut interference on a 3 percent YF-17 fighter aircraft model at high angles of attack
[AIAA PAPER 90-3083] p 794 A90-45899

HEBERT, GREGORY J.

- Comparison of steady and unsteady secondary flows in a turbine stator cascade
[ASME PAPER 89-GT-79] p 291 A90-23800

HEBERT, JAMES L.

- Comparison of the swept frequency continuous wave, current pulse, and shock-excitation lightning simulation techniques p 818 A90-49832
An assessment of analytical methods and lightning simulation test techniques used in lightning qualification and surveillance testing p 818 A90-49833

- Characterization of configuration effects on lightning simulation/qualification testing p 819 A90-49835
Validation of GEMACS for prediction of lightning induced electromagnetic fields p 819 A90-49845

HEBERT, MARY P.

- An assessment of analytical methods and lightning simulation test techniques used in lightning qualification and surveillance testing p 818 A90-49833
Validation of GEMACS for prediction of lightning induced electromagnetic fields p 819 A90-49845

HEBSUR, M. G.

- Influence of alloying elements on the oxidation behavior of NbAl₃ p 355 A90-24861

HECHT, HERBERT

- A hardware and software fault tolerant safety controller
[AIAA PAPER 89-3123] p 74 A90-10599

HECHT, MYRON

- A hardware and software fault tolerant safety controller
[AIAA PAPER 89-3123] p 74 A90-10599

HECIAK, B.

- A probabilistic approach for the establishment of an aircraft structure inspection program p 902 A90-49892

HECKMANN, W.

- Highly damage tolerant carbon fiber epoxy composites for primary aircraft structural applications p 125 A90-14660

HECKMANN, WALTER

- A third-generation bismaleimide prepreg system p 943 A90-50131
Rigidite 5255-3 - A highly damage tolerant prepreg resin system with a well balanced property profile p 944 A90-50139

HEDAYATPOUR, ALI

- Influence of bulk turbulence and entrance boundary layer thickness on the curved duct flow field
[AIAA PAPER 90-1502] p 606 A90-38651

HEDLUND, ERIC R.

- The new high Reynolds number Mach 8 capability in the NSWC Hypervelocity Wind Tunnel 9
[AIAA PAPER 90-1378] p 594 A90-37928

HEDMAN, SVEN G.

- The TSP methods applied to the calculation of transonic flow about wing/body/nacelle/pylon-configurations p 554 A90-35868

HEDRICK, J. C.

- Poly(arylene ether ketone)/poly(aryl imide) homo- and polydimethylsiloxane segmented copolymer blends - Influence of chemical structure on miscibility and physical property behavior p 941 A90-50063

HEDRICK, J. KARL

- Nonlinear flight control design via sliding methods p 756 A90-45335

HEEG, J.

- The application of active controls technology to a generic hypersonic aircraft configuration
[NASA-TM-101689] p 497 A90-20071

HEEG, JENNIFER

- Active control of aerothermoelastic effects for a conceptual hypersonic aircraft
[AIAA PAPER 90-3337] p 863 A90-47597

- Active control of aerothermoelastic effects for a conceptual hypersonic aircraft
[NASA-TM-102713] p 869 A90-27725

HEFER, G.

- The cryogenic Ludwig tube tunnel at Goettingen p 263 A90-15947

HEFFERNAN, RUTH M.

- Hub loads analysis of the SA349/2 helicopter p 333 A90-23936

HEFFLEY, ROBERT K.

- Techniques for improving precision of flying qualities assessment
[AIAA PAPER 90-1285] p 519 A90-33906

HEFNER, JERRY N.

- Research in Natural Laminar Flow and Laminar-Flow Control, part 1
[NASA-CP-2487-PT-1] p 90 A90-12503

- Research in Natural Laminar Flow and Laminar-Flow Control, part 2
[NASA-CP-2487-PT-2] p 91 A90-12519

- Research in Natural Laminar Flow and Laminar-Flow Control, part 3
[NASA-CP-2487-PT-3] p 92 A90-12539

HEFTI, L. D.

- SPF/DB takes off p 208 A90-17293

HEGEDUS, C. R.

- Organic coatings - First line of defense p 204 A90-17300

HEIDE, W.

- Parabolic flight experiments on fluid surfaces and wetting p 363 A90-23904

HEIGES, MICHAEL WILLIAM

- A helicopter flight path controller design via a nonlinear transformation technique p 199 A90-14242

HEIJL, MARINUS C. F.

- More cruising levels expected at higher altitudes p 721 A90-44548

HEIKAL, H. A.

- Study of various factors affecting secondary loss vortices downstream a straight turbine cascade
[ASME PAPER 89-GT-12] p 287 A90-23757

HEIL, MICHAEL L.

- Predicting crack growth under thermo-mechanical cycling p 209 A90-18169

HEINE, J. E.

- Thermal mechanical fatigue of coated blade materials
[AD-A214258] p 256 A90-15107

HEINEMANN, H.

- The influence of boundary layer state on vortex shedding from flat plates and turbine cascades
[ASME PAPER 89-GT-296] p 474 A90-33560

HEINIG, K.

- A comparison of flutter calculations based on eigenvalue and energy method p 425 A90-18406

HEINRICH, J.

- Slip-cast hot isostatically pressed silicon nitride gas turbine components p 765 A90-44816

HEINZE, PETER

- Structural optimization in view of aeroelastic constraints p 538 A90-33391

HEIST, T. J.

- A multipurpose aerodynamic research facility utilizing the abandoned Cincinnati subway tubes
[AIAA PAPER 90-1424] p 596 A90-37961

HEISTER, S. D.

- Modeling of liquid jets injected transversely into a supersonic crossflow p 153 A90-17985

HEITOR, M. V.

- Velocity and scalar measurements in model and real gas turbine combustors p 191 A90-18005

HELD, WOLF

- En route noise of turboprop aircraft and their acceptability: Report of tests p 697 A90-24858

HELIN, HANK E.

- The relevance of unsteady aerodynamics for highly maneuverable and agile aircraft p 148 A90-16775

HELLBAUM, R. F.

- Direct measurements of skin friction in a scramjet combustor
[AIAA PAPER 90-2342] p 626 A90-42132

HELLENTHAL, G.

- The in service multi-axial-stress situation in an uncooled gas turbine blade p 423 A90-29880

HELLER, HANNO

- Technical-scientific possibilities for helicopter noise research in the German-Dutch wind tunnel p 283 A90-21474

- Acoustics of ultralight airplanes p 643 A90-40685

- A new noise certification method for 'light propeller aircraft' in testing p 635 A90-41728
- HELSING, MARTIN A.**
Feasibility study for a microwave-powered ozone sniffer aircraft
[NASA-CR-186660] p 650 N90-23397
- HELWEG-LARSEN, M.**
Audibility and annoyance of en route noise of unducted fan engines
[AD-A223687] p 966 N90-30035
- HEMANN, JOHN H.**
A review of failure models for ceramic matrix composite laminates under monotonic loads
[ASME PAPER 89-GT-153] p 354 A90-23842
- HEMDAN, HANDI T.**
Newtonian flow over oscillating two-dimensional airfoils at moderate or large incidence p 383 A90-27976
- HEMSCH, MICHAEL J.**
Connection between leading-edge sweep, vortex lift, and vortex strength for delta wings p 554 A90-35770
Comparison of high-angle-of-attack slender-body theory and exact solutions for potential flow over an ellipsoid p 622 A90-40692
- HENCKELS, A.**
Applications of infra-red thermography in a hypersonic blowdown wind tunnel p 438 A90-28300
Infrared thermography at hypersonic channel H2K p 674 N90-24235
- HENDERSON, B. E.**
Characteristics of combustion driven pressure oscillations in advanced turbo-fan engines with afterburner p 64 N90-10194
- HENDERSON, BRECK W.**
Boeing Condor raises UAV performance levels p 496 A90-34028
- HENDERSON, DEAN**
Preliminary design of a supersonic Short Takeoff and Vertical Landing (STOVL) fighter aircraft
[NASA-CR-186670] p 649 N90-23394
- HENDERSON, R. E.**
Design guidance to minimize unsteady forces in turbomachines p 426 N90-18411
- HENDERSON, WILLIAM P.**
Propulsion integration for military aircraft
[SAE PAPER 892234] p 733 A90-45449
Induced drag - Historical perspective
[SAE PAPER 892341] p 715 A90-45495
- HENDRICK, DAVID M.**
Sandia National Laboratories' new high level acoustic test facility
[DE90-006810] p 464 N90-19820
- HENDRICKS, R. C.**
A laser based computer aided non-intrusive technique for full field flow characterization in macroscopic curved channels p 535 A90-32293
- HENEGHAN, S. P.**
Acoustic characteristics of a research step combustor
[AIAA PAPER 90-1851] p 655 A90-40530
- HENFLING, J. F.**
Slotted-wall research with disk and parachute models in a low-speed wind tunnel
[AIAA PAPER 90-1407] p 595 A90-37946
Slotted-wall research with disk and parachute models in a low-speed wind tunnel
[DE90-002989] p 572 N90-21737
- HENKE, H.**
A strong viscous-inviscid interaction method for computing unsteady transonic airflows for use in aerelastics p 471 A90-33355
- HENKE, R.**
Natural laminar flow - A wind tunnel test campaign and comparison with flight test data
[AIAA PAPER 90-3045] p 792 A90-45882
The precise calculation of the inviscid leading edge flow on a laminar airfoil using simple methods and verification by measurements on the TLF pilot model p 277 N90-16180
- HENKEL, DAVID**
F-16/GPS integration test results p 726 A90-43710
- HENNE, J.**
Influence of friction and separation phenomena on the dynamic blade loading of transonic turbine cascades
[MITT-88-04] p 428 N90-19235
- HENNE, P. A.**
Application of divergent trailing-edge airfoil technology to the design of a derivative wing
[SAE PAPER 892288] p 714 A90-45466
- HENNE, PRESTON A.**
Technical evaluation report on the Fluid Dynamics Panel Symposium on Computational Methods for Aerodynamic Design (Inverse) and Optimization
[AGARD-AR-267] p 720 N90-25947
- HENRY, R.**
Aeroelastic instabilities in aircraft engines - Application to a SNECMA fan stage p 584 A90-35174
- Full span analysis for flutter prediction of slender blade assemblies p 879 A90-46188
- HENSCH, F.**
Model following control system design: Preliminary ATAS in-flight simulation test results
[PD-FC-9003] p 758 N90-26010
- HEPPENHEIMER, T. A.**
Keepers of the flame p 141 A90-16300
- HERAI, T.**
A study of filament wound high modulus carbon fiber reinforced cylinders p 948 A90-50218
- HERAKOVICH, CARL T.**
NASA-UVA light aerospace alloy and structures technology program
[NASA-CR-182607] p 601 N90-22651
- HERBER, ANDREAS**
Results of TCAS-2 simulations in reconstructed dangerous encounters (Jul. 1986 to Jun. 1989)
[ETN-90-96474] p 636 N90-23375
- HERNANDEZ, GLORIA**
Leading- and trailing-edge flaps on supersonic delta wings p 233 A90-23285
Supersonic aerodynamic characteristics of a Mach 3 high-speed civil transport configuration
[AIAA PAPER 90-3210] p 811 A90-48836
- HERRING, RALPH L.**
Subsystem thermal integration - A new challenge to the aircraft designer
[AIAA PAPER 90-3274] p 836 A90-48865
Aircraft subsystem waste energy recovery and management
[SAE PAPER 901218] p 840 A90-49293
- HERRMANN, G.**
Material development and second source qualification of carbon fiber/epoxy prepregs for primary and secondary Airbus structures p 948 A90-50225
- HERRMANN, J. W.**
A multipurpose aerodynamic research facility utilizing the abandoned Cincinnati subway tubes
[AIAA PAPER 90-1424] p 596 A90-37961
- HERRMANN, U.**
Analysis of three-dimensional aerospace configurations using the Euler and Navier-Stokes equations p 305 A90-25798
- HERSHEY, W.**
Rapsat - Application of onboard processing for communication and surveillance in air traffic control
[AIAA PAPER 90-0883] p 331 A90-25702
- HERTEL, J.**
Euler procedure for calculation of the steady rotor flow with emphasis on wake evolution
[AIAA PAPER 90-3007] p 789 A90-45857
Calculation of the flow field of a multiblade helicopter rotor using a Euler method including the wake p 278 N90-16189
- HERTEL, JOHANN**
A study of the influence of a helicopter rotor blade on the following blades using Euler equations p 630 A90-42435
- HERTZBERG, A.**
Operation of the ram accelerator in the transdetonative velocity regime
[AIAA PAPER 90-1985] p 741 A90-42712
- HESHMAT, H.**
High temperature powder lubricated dampers for gas turbine engines
[AIAA PAPER 90-2048] p 684 A90-41999
- HESS, LARRY L.**
Advanced technology ATE for fuel accessory testing p 439 A90-30770
- HESS, ROBERT W.**
A vapor generator for transonic flow visualization
[NASA-TM-101670] p 201 N90-13403
- HESS, RONALD A.**
Theory for aircraft handling qualities based upon a structural pilot model p 118 A90-14730
An application of generalized predictive control to rotorcraft terrain-following flight p 257 A90-23478
Design and evaluation of a cockpit display for hovering flight p 490 A90-33059
Analyzing the flared landing task with pitch-rate flight control systems
[AIAA PAPER 90-3483] p 866 A90-47732
Analyzing manipulator and feel system effects in aircraft flight control p 934 A90-51154
- HESELINK, LAMBERTUS**
Three-dimensional measurement, display, and interpretation of fluid flow datasets p 679 A90-38854
- HETTENA, E.**
Hypersonic reactive flow computations p 315 A90-27131
- HETU, JEAN-FRANCOIS**
Finite element simulation of turbulent propeller flowfields p 703 A90-42658
- HEWEDY, N. I. I.**
Two-dimensional convergent-divergent nozzle flow with wall velocity slip and temperature jump p 807 A90-46884
- HEWITT, F. A.**
Advanced airbreathing powerplant for hypersonic vehicles p 49 A90-12607
Parametric assessment of propulsion system mass for airbreathing launcher configurations p 344 A90-16819
- HEWITT, JACK**
RADIC fault tolerant system reliability evaluation facility
[AD-A215298] p 377 N90-17348
- HEYDER, E.**
Analysis of hydraulic fluids and lubricating oils for the formation of Trimethylolpropane Phosphate (TMP-P)
[AD-A215188] p 357 N90-16939
- HEYES, JAMES R.**
The integrated test vehicle, (I.T.V.) - A vehicle for cost-effective hypersonic testing
[AIAA PAPER 90-0630] p 352 A90-26974
- HEYMAN, JOSEPH S.**
Advanced NDE techniques for quantitative characterization of aircraft p 886 N90-28088
- HGUYEN, TU D.**
Design and analysis aid for evaluating aircraft structures p 694 A90-41188
- HIBBS, R. I.**
Tooth thickness effects on the performance of gas labyrinth seals p 771 A90-45300
- HIBEY, J. L.**
Guidance and Control strategies for aerospace vehicles
[NASA-CR-186195] p 199 N90-14243
- HICKOK, J. KYLE**
Vapor grown carbon fiber for space thermal management systems p 943 A90-50128
- HICKS, GARY**
NASA aerodynamics program
[NASA-TM-4175] p 373 N90-17235
- HICKS, JOHN W.**
Development of a real-time aeroperformance analysis technique for the X-29A advanced technical demonstrator p 732 A90-44738
Real-time flight test analysis and display techniques for the X-29A aircraft p 34 N90-10866
- HICKS, R.**
Subsonic and transonic low-Reynolds-number airfoils with reduced pitching moments
[AIAA PAPER 90-3212] p 812 A90-48838
- HIERGEIST, KARL**
Eight years of flight operations with composite rotorblades p 635 A90-42481
- HIGASHINO, KAZUYUKI**
Development study of air turbo-ramjet for future space plane
[IAF PAPER 89-311] p 109 A90-13445
- HIGGINS, CHRISTOPHER**
The potential for an extra runway at Heathrow: A preliminary feasibility study
[TT-9007] p 938 N90-29403
- HIGGINS, CRAIG W.**
The new high Reynolds number Mach 8 capability in the NSW Hypervelocity Wind Tunnel 9
[AIAA PAPER 90-1379] p 594 A90-37928
- HILBERS, G. RICHARD**
An airborne instrument for characterizing the 10,000 electromagnetic signals generated by one lightning flash p 848 A90-49930
- HILBIG, R.**
Aerodynamic development perspective for traffic aeroplanes
[DGLR-89-141] p 637 N90-24260
- HILDEBRAND, PETER H.**
Use of Computer-Aided Video Display technology in aviation weather litigation
[AIAA PAPER 90-0373] p 216 A90-19821
- HILGENSTOCK, A.**
Numerical simulation of the laminar and turbulent three dimensional flow on a delta wing with sharp leading edge p 278 N90-16186
- HILL, ACQUILLA S.**
CAST-10-2/DOA 2 Airfoil Studies Workshop Results
[NASA-CP-3052] p 352 N90-17647
- HILL, EUGENE G.**
Flight and wind tunnel investigation of aerodynamic effects of aircraft ground deicing/anticing fluids p 235 N90-15064
- HILL, I. R.**
An analysis of factors impeding passenger escape from aircraft fires p 322 A90-26018
- HILL, JEFF T.**
Constitutive modeling for isotropic materials (HOST)
[NASA-CR-179522] p 193 N90-13390

HILL, RICHARD G.

Investigation and characteristics of major fire-related accidents in civil air transports over the past ten years

p 324 N90-17582

Characteristics of transport, aircraft fires measured by full-scale tests

p 325 N90-17591

HILL, S. D.

A flight dynamic model of aircraft spinning

[AR-005-600] p 935 N90-28576

HILLEN, L. W.

RAAF Orion aircraft A9-300 oxygen fire

[AD-A215496] p 323 N90-16725

HILLER, M.

Computer-aided analysis of three-dimensional multiloop mechanisms

p 669 A90-42328

HILTON, W. F.

The aims and history of adaptive wall wind tunnels

p 871 N90-26839

HIMANSU, A.

Convergence properties of high-Reynolds-number separated flow calculations

p 86 A90-15820

HINCHEE, R. E.

Enhanced bioreclamation of jet fuels: A full-scale test at Eglin AFB, Florida

[AD-A222348] p 875 N90-26992

HINDASH, ISMAIL O.

Computational modeling of inlet hammer shock wave generation

[AIAA PAPER 90-2005] p 621 A90-40592

HINDS, H. A.

On the application of modified stepwise regression for the estimation of aircraft stability and control parameters

[REPT-8905] p 198 N90-13400

HINDSON, WILLIAM S.

A pilot rating scale for evaluating failure transients in electronic flight control systems

[AIAA PAPER 90-2827] p 754 A90-45159

HINGER, J.

Thermal protection systems for hypersonic transport vehicles

[SAE PAPER 901306] p 882 A90-49358

HINGST, W. R.

An LDA investigation of the normal shock wave boundary layer interaction

p 908 A90-52618

HINKLE, A. J.

The influence of material quality on airframe structural durability

p 676 A90-41336

HINTER, L. G.

A CFD study of precombustion shock-trains from Mach 3-6

[AIAA PAPER 90-2220] p 705 A90-42751

HINTON, DAVID A.

A candidate concept for display of forward-looking wind shear information

[NASA-TM-101585] p 187 N90-14232

Relative merits of reactive and forward-look detection for wind-shear encounters during landing approach for various microburst escape strategies

[NASA-TM-4158] p 259 N90-15108

HINTZE, M.

Boeing 727-100 test project (high energy radiated field tests)

[DOT/FAA/CT-88/33] p 542 N90-21247

HIRANO, K.

Total temperature separation in jets

[AIAA PAPER 90-1621] p 607 A90-38750

HIROKAWA, T.

Advanced joint of 3-D composite materials for space structure

p 944 A90-50137

HIROSE, NAOIKI

Computational and experimental analysis of transonic fanjet engine flow field using 3-D Euler code

p 306 A90-25809

Transonic aerodynamics analysis of unconventional wing configurations by 3D-Euler code

p 306 A90-25835

Investigation of ATP blades, part 2. Validation of two-dimensional viscous flow simulation codes around thin airfoils

[NAL-TR-1046] p 912 N90-29326

Transonic 3-D Euler analysis of flows around fanjet engine and TPS (Turbine Powered Simulator). Comparison with wind tunnel experiment, evaluation of TPS testing method and 3-D flow

[NAL-TR-1045] p 912 N90-29327

Some topics in computational transonic aerodynamics; Revision

[NAL-TR-1018T] p 912 N90-29332

HIROSE, TAKECHIRYO

Aeroelastic response characteristics of a rotor executing arbitrary harmonic blade pitch variations

p 646 A90-42464

HIROSE, Y.

Design and evaluation of graphite/epoxy truss core sandwich panels

p 210 A90-18406

HIRSCH, C.

Measurement of velocity profiles and Reynolds stresses on an oscillating airfoil

p 397 N90-18427

HIRSCH, CH.

An off-design loss and deviation prediction study for transonic axial compressors

[ASME PAPER 89-GT-324] p 343 A90-23893

Secondary flows and radial mixing predictions in axial compressors

p 512 N90-21010

HIRSCHEL, E. H.

Design for hypersonic speed

p 335 A90-26343

Turbulence management: Application aspects

p 72 N90-10378

HIRSCHEL, ERNEST HENRICH

Verification of aerothermodynamic codes by means of a winged experimental re-entry vehicle

p 354 N90-16842

HIRSCHKRON, R.

Convertible engine system for high speed rotorcraft

[AIAA PAPER 90-2512] p 658 A90-40643

HIRST, D. J.

Organic coatings - First line of defense

p 204 A90-17300

HITCHCOCK, LLOYD

Dallas/Fort Worth simulation. Volume 2: Appendixes D, E, and F

[AD-A216613] p 405 N90-18380

HITCHCOCK, LLOYD

Dallas/Fort Worth simulation, volume 1

[DOT/FAA/CT-TN89/28-VOL-1] p 824 N90-26802

Atlanta tower simulation, volume 1

[DOT/FAA/CT-TN89/27-VOL-1] p 870 N90-26835

Atlanta tower simulation. Volume 2: Appendixes

[DOT/FAA/CT-TN89/27-VOL-2] p 870 N90-26836

HIXSON, R. L.

Composite-embedded optical fibers for communication links

p 139 A90-13847

HIYAMA, R. M.

Conceptual design optimization study

[NASA-CR-4298] p 582 N90-21755

HO, CHIH-MING

Vortex dynamics of delta wings

p 307 A90-26067

HO, J. K.

Aircraft modal suppression system: Existing design approach and its shortcomings

p 33 N90-10115

Structural stability augmentation system design using BODEDIRECT: A quick and accurate approach

p 33 N90-10116

HO, P. Y.

Energy Efficient Engine acoustic supporting technology report

[NASA-CR-174834] p 930 N90-28557

HO, P.-Y.

An interactive boundary layer method for subsonic airfoil flows

p 144 A90-16754

HOA, S. V.

Repair of thermoplastic composite structures by fusion bonding

p 941 A90-50060

HOAD, DANNY R.

Rotor induced-inflow-ratio measurements and CAMRAD calculations

[NASA-TP-2946] p 237 N90-15882

HOADLEY, A. W.

Thermal management of closed computer modules utilizing high density circuitry

[AIAA PAPER 90-1748] p 583 A90-38441

HOADLEY, SHERWOOD T.

Digital-flutter-suppression-system investigations for the active flexible wing wind-tunnel model

[NASA-TM-102618] p 520 N90-20093

HOADLEY, SHERWOOD TIFFANY

Digital-flutter-suppression-system investigations for the active flexible wing wind-tunnel model

[AIAA PAPER 90-1074] p 430 A90-29382

Development and testing of methodology for evaluating the performance of multi-input/multi-output digital control systems

[AIAA PAPER 90-3501] p 867 A90-47747

Development and testing of methodology for evaluating the performance of multi-input/multi-output digital control systems

[NASA-TM-102704] p 846 N90-27699

HOANG, N.

The hemisphere-cylinder at an angle of attack

[AIAA PAPER 90-0050] p 313 A90-26907

HOBBS, D. E.

Application of sweep to improve the efficiency of a transonic fan. I - Design

[AIAA PAPER 90-1915] p 741 A90-42695

HOBSON, G. V.

Computation of turbine flowfields with a Navier-Stokes code

[AIAA PAPER 90-2122] p 704 A90-42731

HOCH, R. W.

Application of divergent trailing-edge airfoil technology to the design of a derivative wing

[SAE PAPER 892288] p 714 A90-45466

HOCKENBROCK, RICHARD

Multifunction displays optimized for viewability

p 652 A90-40398

New technology advances for brighter color CRT displays

p 652 A90-40399

Characteristics of 5x5 and 6x6 inch taut shadow mask CRTs for cockpit displays

p 737 A90-45239

HODAPP, JOHN F.

The E-SAT 300A - A multichannel satellite communication system for aircraft

p 914 A90-51339

HODGE, ANDREW J.

Impact testing of glass/phenolic honeycomb panels with graphite/epoxy facesheets

p 946 A90-50166

HODGES, DEWEY H.

Review of composite rotor blade modeling

p 366 A90-25303

Stability of hingeless rotors in hover using three-dimensional unsteady aerodynamics

p 430 A90-28227

HODGKINSON, JOHN

An analysis of feel system effects on lateral flying qualities

[AIAA PAPER 90-1824] p 346 A90-25168

Combat aircraft control requirements for agility

p 935 N90-28517

HODSON, H. P.

Unsteady transition in an axial-flow turbine. I - Measurements on the turbine rotor. II - Cascade measurements and modeling

[ASME PAPER 89-GT-289] p 474 A90-33562

Modelling unsteady transition and its effects on profile loss

p 427 N90-18423

HOEFENER, CARL

Accuracy considerations for GPS TSPI system design

p 98 A90-14001

HOEFENER, CARL E.

The small portable Global Positioning System tracking range of the future

p 60 A90-12209

HOEFFEL, JAMES D.

Critical inspection of high performance turbine engine components: The RFC concept

p 859 N90-28073

HOENLINGER, H.

Measurement of wind tunnel model deformation under airflow

p 522 A90-33370

Aeroelastic tailoring validation by windtunnel model testing

p 492 A90-33389

HOFF, G. E.

Experimental performance and acoustic investigation of modern, counterrotating blade concepts

[NASA-CR-185158] p 649 N90-23393

HOFF, KEITH

Force determination sensitivities study for full-scale helicopter ground vibration testing

[AD-A215983] p 349 N90-17643

HOFFMAN, DONNA KIM

The use of prototypes in selected foreign fighter aircraft development programs: Rafale, EAP, Lavi, and Gripen

[AD-A214500] p 287 N90-16707

HOFFMAN, J. D.

C-grid generation for turbomachinery cascades

p 312 A90-26554

HOFFMAN, KRISHNA

A nonlinear transient formulation of UHB aeroelastic response and stability. I - Theoretical formulation

[SAE PAPER 892322] p 715 A90-45481

HOFFMAN, PETER L. R.

Laser machining developments at McDonnell Douglas

p 453 A90-31028

HOFFMAN, W.

Verification of an impeller design by laser measurements and 3D-viscous flow calculations

[ASME PAPER 89-GT-159] p 292 A90-23847

HOFFMANN, ALEX

The potential for an extra runway at Heathrow: A preliminary feasibility study

[TT-9007] p 938 N90-29403

HOFFMANN, HANS-EBERHARD

The signals of an ice warning device in dependence on total water content and normalized icing degree

[ESA-TT-1207] p 963 N90-29692

HOFFMANN, JOE D.

Swirling flow in thrust nozzles

p 421 A90-27962

HOFFMANN, JON A.

Effects of onset free-stream turbulence on the performance characteristics of an airfoil

[AIAA PAPER 90-3025] p 790 A90-45867

HOFFMANN, KLAUS A.

Hyperbolic grid generation techniques for blunt body configurations

p 376 A90-26490

Effect of the grid system on the solution of Euler equations

p 309 A90-26494

- HOFFMANN, W.**
Secondary flow in a turbine guide vane with low aspect ratio p 513 N90-21018
Centrifugal impeller geometry and its influence on secondary flows p 513 N90-21020
- HOFFREN, JAAKKO**
Multigrid solution method for the Euler equations p 149 A90-16841
Solution of the thin-layer Navier-Stokes equations for laminar transonic flow [PB89-221600] p 136 N90-12879
Multigrid solution method for the Euler equations [PB89-219463] p 138 N90-13116
An evaluation of the two-dimensional Euler and Navier-Stokes calculations based on a flux-vector splitting [PB90-166778] p 481 N90-20963
- HOGABOOM, R.**
GPS Hover Position Sensing System p 108 A90-13986
- HOGG, D.**
Development of a fibre optic damage detection system for an aircraft leading edge p 504 A90-32873
- HOGGARD, AMOS W.**
Douglas aging aircraft programs [SAE PAPER 892206] p 732 A90-45425
- HOH, ROGER H.**
Flight test investigation of flight director and autopilot functions for helicopter decelerating instrument approaches [DOT/FAA/CT-TN89/54] p 869 N90-27724
- HOLANDA, RAYMOND**
Attachment of lead wires to thin film thermocouples mounted on high temperature materials using the parallel gap welding process [NASA-TM-102442] p 543 N90-21361
- HOLDEMAN, JAMES D.**
Three-dimensional turbulent flow code calculations of hot gas ingestion p 745 A90-44726
- HOLDEMAN, JONAS T.**
A preliminary sensitivity analysis of the Generalized Escape System Simulation (GESS) computer program [DE89-016891] p 24 N90-10844
- HOLDEN, MICHAEL S.**
Experimental studies of shock wave/wall jet interaction in hypersonic flow [AIAA PAPER 90-0607] p 231 A90-22449
Shock-shock boundary layer interactions p 318 N90-17569
- HOLLAND, ANNE D.**
Thermal/structural analysis of the shaft-disk region of a fan drive system [NASA-TM-101687] p 610 N90-22807
- HOLLAND, RAINER**
The rotor-signal-module of MF190 p 418 A90-28849
- HOLLAND, SCOTT D.**
Mach 6 testing of two generic three-dimensional sidewall compression scramjet inlets in tetrafluoromethane [AIAA PAPER 90-0530] p 192 A90-19895
- HOLLE, G. F.**
Gas turbine engine brush seal applications [AIAA PAPER 90-2142] p 685 A90-42041
- HOLLEY, O. M.**
A modular 550 watt, 25 watts per cubic inch power supply for next generation aircraft p 958 A90-52954
- HOLLIDAY, S.**
Development of erosion resistant coatings for compression airfoils p 443 A90-31120
- HOLLISTER, W. M.**
Using aircraft radar tracks to estimate wind aloft p 241 A90-21390
- HOLLISTER, WALTER M.**
Winds aloft measurement and airspeed calibration using Loran [AIAA PAPER 90-3331] p 847 A90-47592
Advances in techniques and technologies for air vehicle navigation and guidance [AGARD-AR-276] p 243 N90-15899
- HOLLMANN, MARTIN**
Design with honeycomb, state of the art p 538 A90-33706
- HOLLO, STEVEN D.**
Experimental investigation of a supersonic swept ramp injector using laser-induced iodine fluorescence [AIAA PAPER 90-1518] p 606 A90-38663
Injectant mole fraction measurements of transverse injection in constant area supersonic ducts [AIAA PAPER 90-1632] p 587 A90-38761
- HOLLOWELL, JEFF**
Heli/SITAN: A terrain referenced navigation algorithm for helicopters [DE90-005193] p 405 N90-19217
- HOLLOWELL, S. J.**
Conceptual design optimization study [NASA-CR-4298] p 582 N90-21755
- HOLLOWELL, WILLIAM**
Very-high-performance data acquisition/analysis/display/control systems based on the APTEC I/O computer p 458 A90-28852
- HOLLROCK, R. H.**
Self-retracting helicopter rescue hoist p 829 A90-46935
- HOLMBERG, ANDERS**
Euler code predicted separation at the airfoil trailing edge [FFA-TN-1989-30] p 632 N90-23364
- HOLMES, B. J.**
Wind-tunnel investigation on the effect of a crescent planform on drag [AIAA PAPER 90-0300] p 228 A90-22196
In-flight flow visualization using infrared imaging p 731 A90-44731
Wind-tunnel investigations of wings with serrated sharp trailing edges p 802 A90-46379
- HOLMES, BRUCE J.**
Induced drag - Historical perspective [SAE PAPER 892341] p 715 A90-45495
Experimental and numerical analyses of laminar boundary-layer flow stability over an aircraft fuselage forebody p 93 N90-12549
Serrated trailing edges for improving lift and drag characteristics of lifting surfaces [NASA-CASE-LAR-13870-1] p 248 N90-15094
NASA aerodynamics program [NASA-TM-4175] p 373 N90-17235
- HOLMES, D. GRAHAM**
The generation of unstructured triangular meshes using Delaunay triangulation p 310 A90-26533
- HOLMES, EDWARD M., III**
A comparison of emergency medical helicopter accident rates in the United States and the Federal Republic of Germany p 722 A90-44640
- HOLMES, HARLAN K.**
High temperature skin friction measurement p 448 A90-28306
- HOLMES, M.**
A UK perspective on the uniform engine test programme [RAE-TM-P-1172] p 257 N90-15922
- HOLMES, S. C.**
A numerical study of supersonic flow over a compression corner with different incoming boundary-layer profiles [AIAA PAPER 90-1453] p 561 A90-38612
- HOLMQUIST, HOWARD H.**
Chrome free electrolytic deoxidizer for aluminum p 956 A90-50216
- HOLST, TERRY L.**
Computation of viscous transonic flow over porous airfoils p 153 A90-17864
Navier-Stokes computations useful in aircraft design [AIAA PAPER 90-1800] p 315 A90-27311
CFD validation for aerodynamic flows - Challenge for the '90's [AIAA PAPER 90-2995] p 787 A90-45846
- HOLTROP, JOHN**
V-22 ballistic vulnerability hardening program p 408 A90-28223
- HONDA, TAKEKAZU**
Development study of air turbo-ramjet for future space plane [IAF PAPER 89-311] p 109 A90-13445
- HONG, STEVEN W.**
Helicopter simulation development by correlation with frequency sweep flight test data p 407 A90-28203
- HONG, TSAN-ZONG**
Aging and antioxidant surveillance studies on turbine fuel JP-5 and JP-10 p 442 A90-29492
- HONG, YAN**
The effect of swirler on short reversal-flow annular combustor p 423 A90-29906
- HONGOH, M.**
Fracture mechanics assessment of EB-welded blisk rotors p 453 A90-31117
- HOOGSTEDEN, W. P.**
Durability and damage tolerance of S-2 glass/PEEK composites p 944 A90-50140
- HOOPER, ED**
Beech Starship occupant protection evaluation in emergency landing scenario [SAE PAPER 891015] p 100 A90-14327
- HOOPER, EDWIN H.**
Starship - A model for future designs p 493 A90-33714
- HOOPER, STEVEN J.**
Development of a finite element based delamination analysis for laminates subject to extension, bending, and torsion p 679 N90-25049
- HOOS, JON A.**
The development of crossflow vortices on a 45 degree swept wing [SAE PAPER 892245] p 713 A90-45452
- HOOVER, ERIC J.**
Enhanced Low Level Wind Shear (LLWAS) 6-sensor improvement user's manual for data processing of field data [DOT/FAA/CT-TN90/8] p 583 N90-21759
- HOOVER, I. H.**
Boeing 737 fuselage structural integrity program [SAE PAPER 892207] p 701 A90-45426
- HOPPE, JOERG**
Airbus A320 CFRP-rudder structural requirements p 493 A90-33707
- HOPPING, B. M.**
Supersonic/hypersonic Euler flowfield prediction method for aircraft configurations p 145 A90-16767
- HORI, N.**
Adaptive flight control of CCV aircraft with limiting zeros [AIAA PAPER 90-3409] p 864 A90-47664
- HORIHAN, GREG**
Structural and dynamic analysis of the A330/340 composite RAT blade p 942 A90-50083
- HORIKAWA, TAKESHI**
Fatigue life prediction method for gas turbine rotor disk alloy FV535 p 440 A90-27679
- HORIUCHI, S.**
Hydrogen fueled subsonic-ram-combustor model tests for an air-turbo-ram engine p 44 A90-12529
- HORLEBEIN, A.**
The Franco-German helicopter programme HAP, PAH-2/HAC p 618 A90-42478
- HORLOCK, J. H.**
The use of circumferentially varying stagger guide vanes in an axial flow pump or compressor p 537 A90-33566
Design guidance to minimize unsteady forces in turbomachines p 426 N90-18411
- HORN, WALTER J.**
Viscoelastic relaxation in bolted thermoplastic composite joints p 945 A90-50158
Computational crash dynamics. Project 1.2: Computational crash dynamics analysis [IAR-89-19] p 724 N90-25956
- HORNAK, MICHELLE**
Very-high-performance data acquisition/analysis/display/control systems based on the APTEC I/O computer p 458 A90-28852
- HORNE, W. C.**
Turbulent separated flow over and downstream of a two-element airfoil p 16 A90-12738
- HORNER, MICHAEL B.**
Controlled three-dimensionality in unsteady separated flows about a sinusoidally oscillating flat plate [AIAA PAPER 90-0689] p 230 A90-22244
- HOROWITZ, E. J.**
Modeling flexible aircraft for flight control design [AD-A219123] p 757 N90-25140
- HOROWITZ, I. M.**
Flight controller design with nonlinear aerodynamics, large parameter uncertainty, and pilot compensation [AIAA PAPER 90-3478] p 866 A90-47728
- HORSTMAN, C. C.**
Mach number effects on conical surface features of swept shock-wave/boundary-layer interactions p 154 A90-18147
- HORSTMANN, K. H.**
Flight and wind-tunnel investigations on boundary-layer transition p 233 A90-23283
Design for a natural laminar flow glove for a transport aircraft [AIAA PAPER 90-3043] p 792 A90-45880
Flight tests with a natural laminar flow glove on a transport aircraft [AIAA PAPER 90-3044] p 828 A90-45881
- HORSTMANN, K.-H.**
Direct measurement of laminar instability amplification factors in flight p 277 N90-16178
Aerodynamic design techniques at DLR Institute for Design Aerodynamics p 500 N90-20979
- HORTON, G. C.**
Secondary flow predictions for a transonic nozzle guide vane p 513 N90-21017
- HORTON, RAY E.**
Damage tolerance evaluation of several elevated temperature graphite composite materials p 945 A90-50155
- HOSKINS, P. D.**
A remote tip-driven fan powered supersonic fighter concept [AIAA PAPER 90-2415] p 663 A90-42167
- HOSTETLER, C. M.**
FAA air traffic control operations concepts. Volume 7: ATCT (Airport Traffic Control Towers) tower controllers [AD-A210455] p 332 N90-16730

HOU, T. H.

Characterization of LaRC-TPI 1500 powders - A new version with controlled molecular weight p 946 A90-50177

HOUCK, JACOB A.

Delivery performance of conventional aircraft by terminal-area, time-based air traffic control: A real-time simulation evaluation [NASA-TP-2978] p 404 N90-18378

Digital-flutter-suppression-system investigations for the active flexible wing wind-tunnel model [NASA-TM-102618] p 520 N90-20093

HOUGHTON, P. D.

SMAS - An expert system for configuring a research flight simulator p 694 A90-41191

HOULIHAN, T.

Optimal integral controller with sensor failure accommodation p 61 N90-10123

HOUNJET, M. H. L.

Calculation of unsteady subsonic and supersonic flow about oscillating wings and bodies by new panel methods p 472 A90-33359

HOUPIS, C. H.

Flight controller design with nonlinear aerodynamics, large parameter uncertainty, and pilot compensation [AIAA PAPER 90-3478] p 866 A90-47728

HOURLING, LIH-WU

Comparisons among grid generation using elliptic partial differential equations p 374 A90-25478

HOUSER, MICHAEL J.

The development of a 3-D laser velocimeter for the NASA Langley low turbulence pressure wind tunnel [AIAA PAPER 90-1385] p 597 A90-38484

HOUSH, CLINTON S.

Some aerodynamic characteristics of the scissor wing configuration [SAE PAPER 892202] p 713 A90-45423

An aerodynamic tradeoff study of the scissor wing configuration [NASA-CR-186576] p 481 N90-20965

HOUSTON, J. G.

Laser communication system design p 26 A90-11813

HOUSTON, S. S.

Identification of a coupled body/coning/inflow model of Puma vertical response in the hover p 56 A90-12765
Theoretical and experimental correlation of helicopter aeromechanics in hover p 429 A90-28200

HOUTMAN, E. M.

Investigation of the vortex flow over a sharp-edged delta wing in the transonic speed regime [LR-594] p 717 N90-25115

HOUIWINK, R.

Computation of viscous aerodynamic characteristics of 2-D airfoils for helicopter applications p 631 A90-42440

Computation of viscous aerodynamic characteristics of 2-D airfoils for helicopter applications [NLR-MP-88052-U] p 720 N90-25951

HOVEY, PETER

Study of the engine bird ingestion experience of the Boeing 737 aircraft (October 1986 to September 1988) [DOT/FAA/CT-89/29] p 723 N90-25119

HOVEY, PETER W.

Study of the engine bird ingestion experience of the Boeing 737 aircraft [DOT/FAA/CT-89/16] p 176 N90-13360

HOWARD, BRIAN T.

Laser-velocimeter-measured flow field around an advanced, swept, eight-blade propeller at Mach 0.8 [NASA-TP-2462] p 468 N90-20942

HOWARD, CHARLES W.

Information display management in a pilot's associate p 418 A90-30238

HOWARD, F. G.

Investigation of several passive and active methods for turbulent flow separation control [AIAA PAPER 90-1598] p 607 A90-38730

Wind-tunnel investigations of wings with serrated sharp trailing edges p 802 A90-46379

HOWARD, FLOYD G.

Serrated trailing edges for improving lift and drag characteristics of lifting surfaces [NASA-CASE-LAR-13870-1] p 248 N90-15094

HOWARD, R. M.

Flight test and numerical analysis of a half-scale Unmanned Air Vehicle [AIAA PAPER 90-1260] p 494 A90-33890

HOWARD, RICHARD M.

Freestream turbulence effects on airfoil boundary-layer behavior at low Reynolds numbers p 554 A90-35768

HOWARD, WALTER H., JR.

A concept study on the use of remotely piloted, sub-scale aircraft for high Reynolds number testing [AIAA PAPER 90-1263] p 494 A90-33892

HOWE, DAVID C.

Energy Efficient Engine program advanced turbofan nacelle definition study [NASA-CR-174942] p 930 N90-28560

Energy Efficient Engine integrated core/low spool test hardware design report [NASA-CR-168137] p 931 N90-28566

Energy Efficient Engine: Control system preliminary definition report [NASA-CR-19578] p 932 N90-28569

Energy Efficient Engine: High-pressure compressor test hardware detailed design report [NASA-CR-180850] p 932 N90-28570

HOWE, M. S.

On unsteady surface forces, and sound produced by the normal chopping of a rectilinear vortex p 5 A90-11604

Correlation of lift and thickness noise sources in vortex-airfoil interaction p 547 A90-34090

HOWELL, GEORGE A.

Benchmark calculations with an unstructured grid flow solver on a SIMD computer p 546 A90-34378

HOWES, ROBERT L.

Effect of an isolated shell on interior noise levels in a turboprop aircraft [SAE PAPER 891083] p 102 A90-14375

HOWLAND, G. R.

Ground shake test of the UH-60A helicopter airframe and comparison with NASTRAN finite element model predictions [NASA-CR-181993] p 758 N90-25143

HOWSON, TIMOTHY E.

Thermomechanical processing of superalloys p 531 A90-34156

HOYNIK, DANIEL

Aeroelastic detuning for stability enhancement of unstalled supersonic flutter p 189 A90-17462

HRABAR, MAUREEN

Data base correlation issues p 459 A90-30740

HREHOV, DANIEL W.

Testing of a highly integrated automatic flight system - The 747-400 Flight Management Computer System [AIAA PAPER 90-1302] p 505 A90-33916

HSIAO, FEI-BIN

Control of wall-separated flow by internal acoustic excitation p 809 A90-47314

HSIAO, T.

Rapsat - Application of onboard processing for communication and surveillance in air traffic control [AIAA PAPER 90-0883] p 331 A90-25702

HSIEH, K. C.

The gas source molecular beam epitaxial growth of Al(x)Ga(1-x)P on (100) GaP p 894 A90-48657

HSIEH, SHENG-JUI

Numerical simulation of transonic porous airfoil flows p 707 A90-44433

HSU, C.-H.

Prediction of vortical flows on wings using incompressible Navier-Stokes equations p 226 A90-21935

Navier-Stokes computation of flow around a round-edged double-delta wing p 555 A90-36251

Simulation of leading-edge vortex flows p 716 A90-45785

Numerical study of vortical flow over a sideslipping delta wing [AIAA PAPER 90-3001] p 798 A90-45936

HSU, K. C.

The influence of swirl on velocity, temperature and species characteristics in a can combustor [AIAA PAPER 90-2454] p 664 A90-42177

HSU, S. E.

High temperature behavior of the innovation carbon/CSPI composite p 941 A90-50067

HSU, YU-KAO

An analytic study of nonsteady two-phase laminar boundary layer around an airfoil p 691 N90-25051

HU, H. X.

Guaranteed cost control via optimal parametric LQ design p 693 A90-40810

HU, HONG

Integral solution of unsteady full-potential equation for a transonic pitching airfoil p 232 A90-23280

HU, J. T. C.

An experimental investigation of the velocity field in a reverse-flow combustor p 739 A90-42657

HU, JINMING

The experiments for gas turbine plane cascade in a shock tunnel p 160 A90-19441

HU, MENGJUE

The experimental study on the coaxial dump combustor with inner swirl inlet under the combustion condition p 585 A90-36786

HU, SHOUSONG

The method of random variable structure optimal control for aircraft p 590 A90-37220

HU, XUANLI

Vibration analysis of aircraft panels p 207 A90-17026

HU, Z. A.

The acoustic phenomena of the stalling flutter p 78 A90-11801

HU, ZHAOFENG

A synthetic research for aircraft active flutter suppression p 195 A90-16827

HU, ZONG-AN

On the unsteady loading noise of counter-rotating propeller p 895 A90-49484

HU, ZONGAN

Noise generation by swept cascade p 895 A90-49486

HUA, JUN

A transonic airfoil design method and examples p 627 A90-42351

HUA, KAI

A design of a twin variable control system for aero-turbojet engine p 423 A90-29917

HUA, YAONAN

The prediction of boundary layers with rotation and variation of stream filament thickness [ASME PAPER 89-GT-227] p 362 A90-23882

A method of predicting 3-D compressible boundary layer on the rotating blade of turbomachinery p 908 A90-52777

HUANG, CHANGYOU

The computational method for the transonic wing design p 160 A90-19438

HUANG, CHIEN Y.

Restructurable control using proportional-integral implicit model following [AD-A220997] p 347 A90-25990

Multivariable control law for flat-turn straining maneuver by a supermaneuverable aircraft [AIAA PAPER 90-3371] p 863 A90-47629

HUANG, CHIEN YU

A methodology for knowledge-based restructurable control to accommodate system failures p 609 N90-22058

HUANG, CHUANQI

Aeroelastic tailoring of composite wing structures p 580 A90-37217

Optimum design of composite wing structures subjected to displacement constraints p 680 A90-39276

HUANG, DONGTAO

Computation of transonic flow in a plane cascade with an unfactored flux splitting implicit method p 152 A90-17785

HUANG, H. T.

Application of HOST technology to the SSME HPFTP blade [ASME PAPER 89-GT-130] p 360 A90-23828

HUANG, L.

Unsteady loss in a low speed axial flow compressor during rotating stall p 12 A90-12527

HUANG, L. S.

Application of sound and temperature to control boundary-layer transition p 92 N90-12537

HUANG, L. X.

Analysis of the effect of rotor-angular-acceleration on the features of gas flow in turbomachinery p 6 A90-11780

HUANG, LAN

Analysis methods of tie-down loads and airframe stress for shipboard-helicopters p 199 A90-16855

HUANG, LI-XI

On numerical prediction of sound field generated by propeller p 895 A90-49485

HUANG, MINGKE

An efficient finite-difference algorithm for computing axisymmetric transonic nacelle flow fields p 557 A90-37205

HUANG, ROBERT H. E.

Effect of temperature on the storage life of polysulfide aircraft sealants [MRL-TR-89-31] p 444 N90-19364

HUANG, SHYH-CHIN

Microstructures of rapidly-solidified binary TiAl alloys p 532 A90-34990

HUANG, WEIGUANG

Numerical study of interaction of a jet with a supersonic cross flow p 808 A90-47300

HUANG, X. Z.

Wind tunnel testing techniques on aerodynamic effects with small asymmetry [AIAA PAPER 90-1400] p 560 A90-38490

HUANG, XIAOYAN

A new design method for centrifugal compressor vaned diffusers [ASME PAPER 89-GT-156] p 292 A90-23844

HUANG, XINMEI

Fog formation at Perth Airport p 611 A90-37748

HUANG, ZHENWEI

Analysis of serious mechanical trouble in a retractable main landing gear of a jet fighter p 580 A90-36438

HUANG, ZHONGHU

A method for aerodynamic design calculation of axial gas turbine stages with cooling air mixing p 152 A90-17781

Experimental investigation on the performance of an annular nozzle cascade of a highly-loaded transonic turbine stage p 152 A90-17787

An experimental study of tip clearance effects on the performance of an axial transonic turbine p 189 A90-17788

HUBAND, G. W.

Results from a numerical simulation of an F-16A configuration at a supersonic Mach number p 146 A90-16769

Numerical simulation of an F-16A at angle of attack [AIAA PAPER 90-0100] p 313 A90-26911

X-29 high angle-of-attack flight testing - Program status [AIAA PAPER 90-3303] p 837 A90-48885

HUBBARD, H. H.

Sonic boom signature data from cruciform microphone array experiments during the 1966-1967 EAFB national sonic boom evaluation program [NASA-CR-182027] p 549 N90-21605

HUBBARD, HARVEY H.

Vibration responses of two house structures during the Edwards Air Force Base phase of the national sonic boom program [NASA-CR-182089] p 966 N90-29169

HUBBARD, ROBERT

Application of advanced air vehicle and mission equipment technologies to the Light Helicopter (LH) [AIAA PAPER 90-3268] p 836 A90-48861

HUBER, D. A.

Production of jet fuels from coal derived liquids. Volume 10: Jet fuels production by-products, utility, and sulfur emissions control integration study [AD-A213872] p 357 N90-16951

HUBER, FREDERICK E.

Near-term applications of knowledge based systems to combat helicopters [AIAA PAPER 90-3301] p 847 A90-48883

HUBER, HELMUT

EUROFAR - European project for a commercial vertical-takeoff aircraft [MBB-UD-553/89] p 221 A90-22696

HUBER, J.

Slip-cast hot isostatically pressed silicon nitride gas turbine components p 765 A90-44816

HUBER, WILFRED

Meteorologist Weather Processor (MWP) integration test plan [DOT/FAA/CT-TN89/62] p 544 N90-21500

HUCHLER, M.

Thermal protection systems for hypersonic transport vehicles [SAE PAPER 901306] p 882 A90-49358

HUCULAK, P.

A review of research and development in crashworthiness of general aviation aircraft: Seats, restraints and floor structures [AD-A221557] p 846 N90-27698

HUDDLESTON, D. H.

Optimization methods applied to aerodynamic design problems in computational fluid dynamics p 156 A90-18308

Optimization of aerodynamic designs using computational fluid dynamics p 541 N90-20999

HUDLICKA, EVA

Intelligent situation assessment and response aiding in flight emergencies [AIAA PAPER 89-2999] p 38 A90-10507

HUDSON, MAURICE G.

Airport technology international 1989/1990 p 937 A90-52857

HUDSON, SUSAN T.

Condensation in hypersonic nitrogen wind tunnels [AIAA PAPER 90-1392] p 558 A90-37837

HUEBERT, B. J.

Airborne aerosol inlet passing efficiency measurement p 927 A90-52077

HUEBNER, S.

Numerical analysis of the flows in annular slinger combustors [AIAA PAPER 90-2184] p 685 A90-42052

HUET, F.

Automatic grid generation in complex three-dimensional configurations using a frontal system p 608 N90-21992

HUFF, D. B.

Reduced insertion loss of X-band RF fiber optic links p 695 A90-41240

HUFF, D. L.

Application of an efficient hybrid scheme for aeroelastic analysis of advanced propellers [AIAA PAPER 90-0028] p 226 A90-22153

Application of an efficient hybrid scheme for aeroelastic analysis of advanced propellers [NASA-TM-102428] p 172 N90-13355

HUFF, DENNIS L.

Numerical simulations of supersonic flow through oscillating cascade sections [NASA-TM-103100] p 478 N90-20051

HUGHEN, JAMES H.

Advanced technology MMW seeker testbed, a multi-technology demonstration sensor p 488 A90-34143

HUGHES, A. J.

A real-time wind model using digital data from aircraft [RSRE-MEMO-4309] p 137 N90-13005

HUGHES, DAVID

Canadians develop composite techniques for CF-18 battle damage repair program p 551 A90-36300

HUGHES, G. W.

The advantages of automation in aerospace production p 130 A90-15357
The manufacture of SPF military aircraft doors in aluminium alloy p 132 A90-16616

HUGHES, I. J.

Active control of helicopter cabin noise p 645 A90-42434
The absorption of sound by perforated linings p 965 A90-51994

HUGUES, E. C.

Thermostructural behavior of electromagnetic windows - Elaboration of a code package [ONERA, TP NO. 1989-145] p 76 A90-11167

HUI, K.

The application of linear maximum likelihood estimation of aerodynamic derivatives for the Bell-205 and Bell-206 p 30 A90-12773

HUI, PATRICK J.

Embedded GPS - The Canadian Marconi approach p 725 A90-43700

HUI, W. H.

A new Lagrangian method for steady supersonic flow computation. I - Godunov scheme p 631 A90-42506

HULL, P. R.

Convertible engine system for high speed rotorcraft [AIAA PAPER 90-2512] p 658 A90-40643

HULTBERG, RANDY S.

Measurements of pressures on the wing of an aircraft model during steady rotation [AIAA PAPER 90-2842] p 754 A90-45162

Measurements of pressures on the tail and aft fuselage of an airplane model during rotary motions at spin attitudes [NASA-TP-2939] p 20 N90-10829

HUMMEL, D.

The gun tunnel of the Brunswick Institute for Fluid Mechanics: Current development status p 673 N90-24227

Effects of canard position on the aerodynamic characteristics of a close-coupled canard configuration at low speed p 920 N90-28519

HUMMEL, THOMAS C.

Multidisciplinary Expert-aided Analysis and Design (MEAD) p 613 N90-23050

HUMPHREY, R. B.

An interfacing solution for real-time avionics development [SAE PAPER 892357] p 738 A90-45508

HUMPHREYS, D. A.

European research on viscous flow (EuroVisc) [NLR-TP-89077-U] p 609 N90-22014

HUMPHREYS, WILLIAM WARREN

An experimental study of the effect of streamwise vortices on unsteady turbulent boundary-layer separation p 369 N90-17045

HUND, RON

Beech Starship interior noise experimental studies [SAE PAPER 891082] p 101 A90-14374

HUNG, CHING-MAO

Simulation of glancing shock wave and boundary layer interaction [NASA-TM-102233] p 133 N90-11970

Computation of Navier-Stokes equations for three-dimensional flow separation [NASA-TM-102266] p 172 N90-13353

HUNT, D. R.

The reduction of smoke emissions from Allison T56 engines [ARL-PROP-R-182] p 928 N90-28547

HUNT, JAMES L.

Hypersonic airbreathing vehicle design - Focus on aero-space plane p 245 A90-21156

HUNTER, JOHN A.

ARSR-4 long range radar will upgrade U.S. en-route surveillance p 403 A90-27925

HUO, PEI-FENG

Research on transmission quality of telemetry system in flight test p 26 A90-12189

HURST, DAVID W.

Surface flow on a flat plate induced by a supersonic jet exhausting normally into a low speed crossflow [AIAA PAPER 90-3011] p 789 A90-45860

HURST, LORI E.

SH-2F airframe fatigue test program p 642 A90-39989

HUSAIN, C. I.

Impingement/effusion cooling - The influence of the number of impingement holes and pressure loss on the heat transfer coefficient [ASME PAPER 89-GT-188] p 361 A90-23866

HUSBAND, E. G.

Large aircraft flying qualities revisited [AIAA PAPER 90-2847] p 754 A90-45175

HUSSAINI, M. YOUSUFF

Effects of shock on the stability of hypersonic boundary layers [AIAA PAPER 90-1448] p 561 A90-38608

HUSSON, D.

Maximum expected concentrations of hail in thunderstorm precipitation p 962 A90-52052

HUSTON, RONALD L.

Finite element mesh refinement criteria for stress analysis p 273 A90-23013

HUTCHINGS, L. A.

Audibility and annoyance of en route noise of unducted fan engines [AD-A223687] p 966 N90-30035

HUTCHINSON, B. R.

A collocated finite volume method for solving the Navier-Stokes equations for incompressible and compressible flows in turbomachinery - Results and applications p 703 A90-42659

HUTCHINSON, JOHN

Evaluation of existing aircraft operator data bases [DOT/FAA/CT-90/18] p 898 N90-28463

HUTCHINSON, JOHN J.

Program plan: International aircraft operator data base [IAR-90-1] p 783 N90-25697

International aircraft operator data base master requirements and implementation plan [DOT/FAA/CT-90/17] p 967 N90-29247

HUTIN, PIERRE-MARIE

Description of atmospheric turbulence p 280 N90-15043

HUTTSSELL, LAWRENCE

A review of aeroelasticity research at the flight dynamics laboratory p 493 A90-33409

HUYER, STEPHEN A.

Unsteady aerodynamic loading produced by a sinusoidally oscillating delta wing [AIAA PAPER 90-1536] p 564 A90-38680

HVIZD, JAMES J.

Ada real-time GPS/INS simulation approach to system development p 751 A90-43706

HWANG, C. J.

Numerical investigation of airfoil/jet/fuselage-undersurface flowfields in ground effect [AIAA PAPER 90-0597] p 168 A90-19939

HWANG, CHIN-KUAN

Comparisons among grid generation using elliptic partial differential equations p 374 A90-25478

HWANG, D. Q.

High temperature behavior of the innovation carbon/CSPI composite p 841 A90-50067

HWANG, DAU-GWEI

Aging and antioxidant surveillance studies on turbine fuel JP-5 and JP-10 p 442 A90-29492

HWANG, HORNG-REN

Computation of unsteady transonic flow about airfoils in frequency domain using the full-potential equation p 174 N90-14198

HWANG, JON LI

Optimum weight design of a rotor bearing system with dynamic behavior constraints [ASME PAPER 89-GT-74] p 358 A90-23795

HWANG, Y.-H.

Calculation of flowfields in side-inlet ramjet combustors with an algebraic Reynolds stress model p 87 A90-16367

Experimental and theoretical investigations of turbulent flow in a side-inlet rectangular combustor p 421 A90-27959

HYDE, T. H.

Flanged joints of aeroengines [PNR90594] p 116 N90-12609

HYLAND, DAVID C.

Integrated control-system design via generalized LQG (GLOG) theory p 613 N90-23023

HYLTON, L. D.

An experimental study of turbine vane heat transfer with leading edge and downstream film cooling [ASME PAPER 89-GT-69] p 358 A90-23792

HYNES, T. P.

Stability of flow through multistage axial compressors [ASME PAPER 89-GT-311] p 231 A90-22668
Stall inception in axial compressors [ASME PAPER 89-GT-63] p 290 A90-23786

HYTOPOULOS, E.

Flow over inclined finite length and width flat plates at low and high Reynolds numbers [AIAA PAPER 90-1467] p 562 A90-38624

IADELUCIA, JOSEPH P.

National airspace system approach and departure sequencing operational concept [NAS-SR-1322] p 27 N90-10017

IAGODKIN, V. N.

Evaluation of the dynamic characteristics of a helicopter instrument panel p 829 A90-46499

IAGUDIN, S. V.

Calculation of the drag of fuselage tail sections of different shapes in supersonic flow of a nonviscous gas p 388 A90-29182

IAKOVLEV, S. V.

Formalization and solution of covering problems in the synthesis of control and monitoring systems p 76 A90-10963

IAKUSHEV, S. A.

Effect of the Mach number and shape of the front part of the obstacle on the separation zone length in supersonic flow p 903 A90-50816

IANKOV, V. P.

Using the smoking-wire visualization method in the study of wing models at large angles of attack in subsonic wind tunnels p 881 A90-46561

IAROV, V. N.

A source of discrete noise components in the flow path of gas turbines and fans p 894 A90-46506

IATSENKO, I. N.

Optimal blading density in axial-flow compressor stages with a developed three-dimensional flow p 851 A90-46505

IATSEVICH, N. S.

Calculation of three-dimensional flow past a plane supersonic air intake at angles of attack and sideslip p 805 A90-46573

IBRAHIM, AZMAN SYED

Vibration dampers for cryogenic turbomachinery [AIAA PAPER 90-2740] p 882 A90-47228

IBRAHIM, K.

Vertical tail design for base-line configuration of military combat aircraft p 810 A90-48080
Airbrake design for base-line configuration of advanced jet trainers/light attack airplanes and military combat airplanes p 810 A90-48081

IBRAHIM, R. A.

Stochastic flutter of a panel subjected to random in-plane forces. I - Two mode interaction p 444 A90-27992
Stochastic flutter of a panel subjected to random in-plane forces. II - Two and three mode non-Gaussian solutions [AIAA PAPER 90-0986] p 451 A90-29399

ICHIKAWA, Y.

Air/water two-phase flow test tunnel for airfoil studies p 352 A90-26842

IDAN, M.

Parameter identification of linear systems based on smoothing [AIAA PAPER 90-2800] p 753 A90-45156

IDDINGS, F. A.

NDI (Nondestructive Inspection) oriented corrosion control for Army aircraft. Phase 1: Inspection methods [AD-A213368] p 176 N90-13359

IDE, H.

Evaluation of current multiobjective optimization methods for aerodynamic problems using CFD codes [AIAA PAPER 90-0955] p 411 A90-29240
Simulation of static and dynamic aeroelastic behavior of a flexible wing with multiple control surfaces [AIAA PAPER 90-1075] p 392 A90-29383

IDE, R. F.

Comparison of two droplet sizing systems in an icing wind tunnel [NASA-TM-102456] p 215 N90-14617

IDE, ROBERT F.

Liquid water content and droplet size calibration of the NASA Lewis Icing Research Tunnel [AIAA PAPER 90-0669] p 261 A90-22242

Comparison of two droplet sizing systems in an icing wind tunnel [AIAA PAPER 90-0668] p 274 A90-23711

Liquid water content and droplet size calibration of the NASA Lewis Icing Research Tunnel [NASA-TM-102447] p 213 N90-13797

IDE, T.

CRL's mobile satellite communication experiments using ETS-V [AIAA PAPER 90-0775] p 366 A90-25602

IERUSALIMSKII, K. M.

A study of the stability and thermal stability of complex reinforced structures p 880 A90-46541
A method for reducing a buckled skin under combined loading p 860 A90-46571

IEVALTS, JOHN O.

A three-dimensional upwind parabolized Navier-Stokes code for chemically reacting flows [AIAA PAPER 90-0394] p 165 A90-19831

IGNATEV, V. N.

Numerical modeling of the combustion kinetics of hydrocarbon fuels in an annular combustion chamber with allowance for the formation of harmful impurities p 124 A90-14582

IINUMA, KAZU

A new hybrid LTA vehicle, 'Heliship' - Its philosophy, outline [AIAA PAPER 89-3162] p 244 A90-20582

IIZUKA, KELGO

Temperature insensitive fiber coil sensor for altimeters p 339 A90-26374

IKAWA, KATSUYA

Transonic 3-D Euler analysis of flows around fanjet engine and TPS (Turbine Powered Simulator). Comparison with wind tunnel experiment, evaluation of TPS testing method and 3-D flow [NAL-TR-1045] p 912 N90-29327

IKAWA, KATUYA

Computational and experimental analysis of transonic fanjet engine flow field using 3-D Euler code p 306 A90-25809

IKEDA, MASAKAZU

Robust control system design synthesis with observers p 375 A90-25994

IKEDA, TAMEHARU

Effects of a heat cycle on material strength [NAL-TM-562] p 113 N90-11737

IKELS, KENNETH G.

A small inert gas generator p 180 A90-17405

IL'ICHEV, V. D.

Multilevel method for calculating aerodynamic loads on a flight vehicle p 296 A90-24122

IL'INSKII, N. B.

Construction of a straight single-row airfoil lattice by the method of quasi-solutions for inverse boundary value problems p 84 A90-14564

Construction of wing profiles in subsonic gas flow by the method of quasi-solutions for inverse boundary value problems p 803 A90-46542

ILK, B.

Development of two multi-sensor hot-film measuring techniques for free-flight experiments p 417 A90-28291

IMAI, Y.

Temperature insensitive fiber coil sensor for altimeters p 339 A90-26374

IMAIZUMI, TAKAO

Cloud features suggesting low level wind shear and turbulence p 778 A90-44545

IMMARIGEON, J.-P.

Evaluation of high temperature protective coatings for gas turbine engines under simulated service conditions p 952 N90-28712

IMMEN, FREDERICK H.

The U.S. Army Helicopter Structural Integrity Program - 1989 European Rotorcraft Forum p 581 A90-38525

IMMENSCHUH, WILLIAM T.

Ryan X-13 experimental aircraft - Lessons learned [AIAA PAPER 90-3236] p 834 A90-48846

INENAGA, ANDREW S.

The development of a 3-D laser velocimeter for the NASA Langley low turbulence pressure wind tunnel [AIAA PAPER 90-1385] p 597 A90-38484

INESHIN, IU. L.

An investigation of fillets in wing-fuselage joints at subsonic velocities p 297 A90-24131
Using the method of symmetric singularities for calculating flow past subsonic flight vehicles p 386 A90-28979

INGALLS, CHARLES

Methodology for estimating helicopter performance and weights using limited data p 829 A90-46936

INGALLS, S. A.

Taguchi methods in conceptual design for life cycle cost [AIAA PAPER 90-3222] p 839 A90-49109

INGEN, C. V.

Aircraft crash survival design guide. Volume 2: Aircraft design crash impact conditions and human tolerance [AD-A218435] p 575 N90-22546

INGER, G. R.

Nonequilibrium recombination-dissociation boundary layer flows along arbitrarily-catalytic hypersonic vehicles [AIAA PAPER 90-0055] p 161 A90-19652
Shock/turbulent boundary layer interaction in low Reynolds number supercritical flows p 802 A90-46383

INGLE, G.

Parallel processing implementation of a flight controller p 333 N90-16743

INGLESE, B.

Development and applications of reliability and maintainability design criteria in military aircraft [ETN-89-95208] p 107 N90-12591

INNOCENTI, M.

Dynamics and control of maneuverable towed flight vehicles [AIAA PAPER 90-2841] p 754 A90-45161

INOKUCHI, HAMAKI

Propulsive lift augmentation by side fences as applied to Japan's experimental STOL aircraft, ASKA [AIAA PAPER 90-3009] p 789 A90-45859

INOUE, TAKASHI

Propulsive lift augmentation by side fences as applied to Japan's experimental STOL aircraft, ASKA [AIAA PAPER 90-3009] p 789 A90-45859

INOUE, MAMORU

Computer simulation of aircraft aerodynamics [NASA-TM-102221] p 88 N90-11699

INSHAKOV, S. I.

Using the smoking-wire visualization method in the study of wing models at large angles of attack in subsonic wind tunnels p 881 A90-46561

IOANNIDES, E.

Endurance of aircraft gas turbine mainshaft ball bearings-analysis using improved fatigue life theory. II - Application to a bearing operating under difficult lubrication conditions p 128 A90-13845
Endurance of aircraft gas turbine mainshaft ball bearings-analysis using improved fatigue life theory. I - Application to a long-life bearing p 537 A90-33557

IPRI, ALFRED C.

Polysilicon active-matrix liquid crystal displays for cockpit applications p 681 A90-40393

IRVING, RUSSELL

A blackboard approach for diagnosis in Pilot's Associate p 892 A90-49741

ISAAC, G. A.

Adverse weather operations during the Canadian Atlantic storms program p 281 N90-15052

ISAAC, K. M.

Navier Stokes simulation of waverider flowfields [AIAA PAPER 90-3066] p 793 A90-45892

ISAACS, N. C. G.

Identification of retreating blade stall mechanisms using flight test pressure measurements p 384 A90-28172

ISHAI, ORI

The effect of impact loading on residual strength of CFRP composite beams p 208 A90-17683

ISHIDA, MASAHIRO

Effect of blade tip configuration on tip clearance loss of a centrifugal impeller [ASME PAPER 89-GT-80] p 358 A90-23801

Secondary flow due to the tip clearance at the exit of centrifugal impellers [ASME PAPER 89-GT-81] p 358 A90-23802

ISHIDA, TAIICHI

TW-68 tilt wing high speed commercial VTOL p 246 A90-21712

ISHIGURO, TOMIKO

Turbulence models for 3D transonic viscous flows. II p 306 A90-25820

ISHII, HIROSHI

A study on surge and rotating stall in axial compressors - A summary of the measurement and fundamental analysis method p 87 A90-16105

ISHII, MASAHIRO

An electronic flight-recorder for a hang-glider p 39 A90-12234

ISHIKAWA, KAZUTOSHI

Evaluation for DLC-Flap Monitoring System of the VSRA [NAL-TM-607] p 928 N90-29391

ISHIWATA, SHOJI

Current status of ceramic gas turbine R&D in Japan [ASME PAPER 89-GT-114] p 359 A90-23818

ISHIZAWA, HIROSHI

An application of expert system to jet engine diagnostic procedures p 587 A90-38596

ISING, S. J.

New cyanate ester resin with low temperature (125-200 C) cure capability p 944 A90-50135

- ISKRA, A. L.**
Characteristics of temperature and pressure generation and retention in flow inside cryogenic wind tunnel T-04
p 869 A90-46576
- ISOGAI, KOJI**
Direct search method to aeroelastic tailoring of a composite wing under multiple constraints
p 208 A90-17865
- ISPOLOV, I. U. G.**
Finite element analysis of nonstationary temperature fields in gas turbine components
p 271 A90-21324
- ISRAELI, MOSHE**
A method for solving three-dimensional viscous incompressible flows over slender bodies
p 558 A90-37890
- ISSAC, F.**
Electromagnetic characterization of lightning on aircraft
[ONERA, TP NO. 1989-131] p 22 A90-11155
Experimental-theoretical comparison for current injection on an aircraft model
[ONERA, TP NO. 1989-133] p 22 A90-11157
Transall 88 - Lightning characterization program
[ONERA, TP NO. 1989-142] p 22 A90-11164
Connection of structures by laboratory-generated electrical discharges
[ONERA, TP NO. 1989-147] p 58 A90-11169
Electrostatic description of a positive leader ignition from an aircraft
[ONERA, TP NO. 1989-149] p 23 A90-11171
- ITAHARA, HIROHARU**
Oil migration of FJR 710/600S engine
p 43 A90-12014
- ITO, A.**
The effect of trailing edge extensions on the performance of the Goettingen 797 and the Wortmann FX 63-137 aerofoil section at Reynolds numbers between 3×10^6 to the 5th and 1×10^7 to the 6th
p 82 A90-13783
Further work on aerofoils at Reynolds numbers between 3×10^6 to the 5th and 1×10^7 to the 6th
p 145 A90-16758
- ITO, TAKESHI**
A practical flight path for microwave-powered airplanes
p 429 A90-28007
- ITOH, HIDEKI**
Cloud features suggesting low level wind shear and turbulence
p 778 A90-44545
- ITOH, K.**
Holographic interferometric study of shock wave propagation
p 66 A90-10732
- ITOH, SHUICHI**
An electronic flight-recorder for a hang-glider
p 39 A90-12234
- IUDIN, G. A.**
An investigation of fillets in wing-fuselage joints at subsonic velocities
p 297 A90-24131
- IUGOV, OLEG K.**
Principles underlying the integration of an aircraft and its engine
p 729 A90-42520
- IUSHIN, A. I.**
A study of the laminar-turbulent boundary layer transition on the windward side of a delta wing with a conical surface
p 298 A90-24144
- IVANUSHKIN, A. K.**
Some characteristics of interference between shock waves and the aerodynamic wake behind a body
p 804 A90-46551
- IVANOV, A. M.**
Effect of the control of turbocompressor guide vanes on the throttle characteristics of a bypass engine
p 255 A90-23425
- IVANOV, M. I.**
Application of three-dimensional methods for the calculation of gas dynamic and thermal processes at the design of gas turbines for air breathing engines
p 46 A90-12552
- IVANOV, O. N.**
Flow past two cylinders and two spheres
p 903 A90-50815
- IVANOV, O. V.**
Validation of the accelerated equivalent testing of gas turbine engines for multivariate applications
p 110 A90-14568
- IVANOV, PETR A.**
Operation of aviation radio and electronic equipment (Handbook)
p 914 A90-50747
- IVANOV, S. A.**
Asymptotic calculation of flow parameters in the problem of hypersonic flow past blunt axisymmetric bodies
p 10 A90-12268
- IVERSON, D. E.**
Performance assessment for airborne surveillance systems incorporating sensor fusion
p 583 A90-37088
- IWASAKI, AKIHITO**
Wind tunnel test of CAD USB-STOL semi-borne prototype
[NAL-TM-566] p 88 N90-11696
- IVER, VENKIT**
Fourth-order accurate three-dimensional compressible boundary-layer calculations
p 308 A90-26136
- IZARD, M.**
Test rig for the study of the flow in a rotor-stator system
[ONERA, TP NO. 1989-124] p 58 A90-12634
- IZMAILOV, R. A.**
Acoustic resonance in centrifugal compressors induced by interaction between rotor and stator
p 78 A90-11803
- IZUMI, K. H.**
A conflict analysis of 4D descent strategies in a metered, multiple-arrival route environment
[NASA-CR-182019] p 593 N90-21772
- IZUTSU, N.**
Topological study of three-dimensional vortex interactions
p 367 A90-25885
- J**
- JACAZIO, G.**
Use of smart actuators for the tail rotor collective pitch control
p 688 A90-42483
- JACKSON, A. C.**
Transport composite fuselage technology: Impact dynamics and acoustic transmission
[NASA-CR-4035] p 126 N90-11821
- JACKSON, A. J. B.**
Gas turbine performance analysis
[PNR90599] p 116 N90-12614
- JACKSON, CHARLIE M., JR.**
Overview of military technology at NASA Langley
[SAE PAPER 892232] p 733 A90-45448
- JACKSON, KAREN E.**
Scaling effects in the impact response of graphite-epoxy composite beams
[SAE PAPER 891014] p 128 A90-14326
- JACKSON, MICHAEL**
Low-expansion MMCs boost avionics
p 203 A90-17291
- JACKSON, MIKE**
Lateral-directional control of an aircraft using mu synthesis
[AIAA PAPER 90-3442] p 865 A90-47695
- JACKSON, PAUL**
Mirage 2000 - A French success that is no illusion
p 731 A90-43768
- JACOB, TH.**
Precision navigation using an integrated GPS-IMU system
p 242 A90-21720
- JACOB, THOMAS**
Integrated system of differential Global Positioning System and inertial measurement unit - A position determination system for automatic landing
[AIAA PAPER 90-1300] p 487 A90-33914
Integrated flight guidance system using differential-GPS for landing approach guidance
p 332 N90-16735
- JACOBS, J. M. J. W.**
Numerical interactive grid generation for 3D-flow calculations
p 312 A90-26556
Design and testing of a multiblock grid-generation procedure for aircraft design and research
p 582 N90-21984
- JACOBS, P. A.**
Flow establishment in a generic scramjet combustor
[AIAA PAPER 90-2096] p 742 A90-42729
- JACOBS, TAVIS**
Preliminary design of a supersonic Short Takeoff and Vertical Landing (STOVL) fighter aircraft
[NASA-CR-188670] p 649 N90-23394
- JACOBSON, S.**
Aerosol effects on jet-engine IR radiation
p 40 A90-10152
A multichannel wide FOV infrared radiometric system
p 67 A90-11410
- JACOBSON, STEVEN B.**
Ride quality criteria for the B-2 bomber
[AIAA PAPER 90-3256] p 835 A90-48852
- JACQUES, CLAUDE**
The VSCF system has arrived - The way in which a new constant-frequency electrical generation system in aeronautes has been developed
p 187 A90-16696
- JACQUOTTE, OLIVIER-PIERRE**
An inverse method for the design of turbomachine blades
p 511 N90-20988
- JADAYEL, O. C.**
A theoretical and experimental investigation of the Reynolds and apparent stresses in axial compressors
p 12 A90-12554
- JADIC, I.**
On a lifting line theory for supersonic flow. I - The velocity field due to a vortex line in supersonic flow
p 143 A90-16735
On a lifting line theory for supersonic flow. II - A supersonic lifting line theory for wings
p 477 A90-34817
On an extension of the Kutta-Joukowski theorem to the supersonic regime
p 477 A90-34819
A verification of the supersonic lifting line theory for the case of infinite yawed wings
p 477 A90-34821
- JAGO, JOANN C.**
Radio Technical Commission for Aeronautics, Annual Assembly and Technical Symposium, Washington, DC, Dec. 4-6, 1989, Proceedings
p 821 A90-46390
- JAHN, THOMAS P.**
Flight deck modernization
[SAE PAPER 892231] p 732 A90-45447
- JAHNKE, CRAIG C.**
Application of dynamical systems theory to the high angle of attack dynamics of the F-14
[AIAA PAPER 90-0221] p 257 A90-22184
- JAHS, T. M.**
Electric controls for a high-performance EHA using an interior permanent magnet motor drive
p 452 A90-30711
- JAHS, THOMAS M.**
High-performance EHA controls using an interior permanent magnet motor
p 730 A90-43152
- JAKOB, H.**
The precise calculation of the inviscid leading edge flow on a laminar airfoil using simple methods and verification by measurements on the TLF pilot model
p 277 N90-16180
Calculation of the flap profile flows with separation based on coupled potential and boundary layer solutions
p 278 N90-16191
- JALAMANI, ZAKARIA A.**
A computational study of the impingement region of an unsteady subsonic jet
[AIAA PAPER 90-1657] p 570 A90-38784
- JALOTE, PANKAJ**
Integrated approach fault tolerance-current state and future requirements
[AD-A214402] p 275 N90-15465
- JAMERSON, LAWRENCE C.**
Artificial intelligence techniques applied to the non-cooperative identification (NCID) problem
[AIAA PAPER 89-3005] p 75 A90-10619
- JAMES, D. K.**
Unsteady transonic aerodynamics of oscillating airfoils in supersonic freestream
p 232 A90-23277
Further studies of harmonic gradient method for supersonic aeroelastic applications
p 473 A90-33410
- JAMES, E. H.**
An investigation into the internal heat transfer characteristics of a thermally anti-iced aero-engine intake lipskin
p 111 A90-15390
- JAMES, M. R.**
Fatigue crack initiation mechanics of metal aircraft structures
[AD-A210567] p 65 N90-10255
- JAMESON, A.**
Efficient method for computing transonic and supersonic flows about aircraft
p 307 A90-26132
- JAMESON, ANTONY**
Aerodynamic design via control theory
p 546 N90-20998
- JANAKIRAM, R. D.**
Rotorcraft computational fluid dynamics - Recent developments at McDonnell Douglas
p 630 A90-42439
- JANARDAN, B. A.**
Acoustic characteristics of counterrotating unducted fans from model scale tests
p 378 A90-26138
- JANETZKE, DAVID C.**
Concurrent processing adaptation of aeroelastic analysis of propfans
[AIAA PAPER 90-1036] p 450 A90-29380
Concurrent processing adaptation of aeroplastic analysis of propfans
[NASA-TM-102455] p 215 N90-14656
- JANG, HONG-MING**
Interactive boundary-layer method for unsteady airfoil flows - Quasisteady model
p 812 A90-48953
An interactive boundary-layer method for unsteady airfoil flows. Part 1: Quasi-steady-state model
[AD-A221220] p 634 N90-24250
- JANG, JINSEOK**
Air resonance stability of hingeless rotors in forward flight
p 590 A90-38519
- JANICKI, GERRY**
International SAMPE Symposium and Exhibition, 35th, Anaheim, CA, Apr. 2-5, 1990, Proceedings. Books 1 & 2
p 940 A90-50056

JANKOVITZ, JACK

Application of multifunction inertial reference systems to fighter aircraft p 332 N90-16740

JANSEN, WILLEM

Gas turbine engine component development - An integrated approach p 112 A90-16006

JANTZEN, EILHARD

Oils for flight turbine engines - Research and development in the 90s p 266 A90-21473

JANUS, J. MARK

Counterrotating prop-fan simulations which feature a relative-motion multiblock grid decomposition enabling arbitrary time-steps [AIAA PAPER 90-0687] p 169 A90-19978

JANZEN, DOYLE B.

Schleicher ASK-21 glider (TG-9) stall and spin [AD-A213513] p 249 N90-15096

JAPIKSE, DAVID

Laser transit anemometry investigation of a high speed centrifugal compressor [ASME PAPER 89-GT-155] p 360 A90-23843

JARCHOW, F.

Development status of epicyclic gears p 271 A90-21141

JARRAH, MOHAMMAD-AMEEN M.

Unsteady aerodynamics of delta wings, undergoing ramp-maneuvering in pitch to post-stall angle of attack p 806 A90-46857

JARRAH, MOHAMMAD-AMEEN MAHMOUD

Unsteady aerodynamics of delta wings performing maneuvers to high angle of attack p 398 N90-19196

JARYMOWYCZ, T. A.

Solid fuel ignition and combustion characteristics under high-speed crossflows [AIAA PAPER 90-2075] p 764 A90-42725

JATEGAONKAR, RAVINDRA V.

Identification of moderately nonlinear flight mechanics systems with additive process and measurement noise p 347 A90-25987

JAU, JULAN

Prediction of post-stall flows on airfoils p 145 A90-16757

JAWAHARLAL, M.

Integrated approach to design and manufacture of gas turbine components based on group theory p 113 A90-16010

JAYASIMHA, P.

Computational and experimental studies on ground effect of a slender wing tailless delta aircraft p 810 A90-48083

JEAL, R. H.

The future of non ferrous metals in aerospace engines [PNR90572] p 127 N90-12720
AGARD damage tolerance concepts for engine structures Workshop 3, Component Behaviour and Life Management p 855 N90-27705

JEANDEL, D.

Finite element simulation of compressible turbulent flows - Validation and application to internal aerodynamic in gas-turbine engines p 210 A90-18343

JECKO, B.

Numerical simulation of aeroplane response to a lightning injection [ETN-89-95271] p 96 N90-11716

JEFFERIES, R. W.

The influence of a rotating leading edge on accelerating starting flow over an airfoil [AIAA PAPER 90-0583] p 168 A90-19932

JEFFREY, J. R.

Nonflammable hydraulic power system for tactical aircraft. Volume 1: Aircraft system definition, design and analysis [AD-A218493] p 671 N90-23409

JEGLEY, DAWN C.

A study of the structural efficiency of fluted core graphite-epoxy panels [NASA-TM-101681] p 373 N90-18070

JENG, SAN-MOU

Numerical simulation of droplet deformation in convective flows [AIAA PAPER 90-2309] p 769 A90-42773

JENISTA, J. E.

Configuration E-7 supersonic fighter/attack technology program [ASME PAPER 89-GT-308] p 490 A90-32260

JENKEL, S. D.

Bonded airfoil attachments - A path to rotor structural efficiency [AIAA PAPER 90-2177] p 686 A90-42061

JENKINS, D. B.

Fine resolution errors in secondary surveillance radar altitude reporting amongst aircraft transmitting the conspicuity codes 4321 and 4322 [RSRE-88004] p 135 N90-12816

JENKINS, JERRY E.

A Volterra kernel identification scheme applied to aerodynamic reactions [AIAA PAPER 90-2803] p 712 A90-45178

JENKINS, RENALDO

An experimental AWTS process and comparisons of ONERA T2 and 0.3-m TCT AWTS data for the ONERA CAST-10 aerofoil p 321 N90-17653

JENKINS, S. B.

Large-amplitude high-rate roll experiments on a delta and double delta wing [AIAA PAPER 90-0224] p 163 A90-19742

JENKINS, S. W.

Criteria for coal tar seal coats on airport pavements. Volume 2: Laboratory and field studies [AD-A220167] p 674 N90-24277

JENKINS, SCOTT A.

Optimization of glides for constant wind fields and course headings p 731 A90-44734

JENKS, MARK D.

Development of the improved helicopter icing spray system (IHSS) p 400 A90-28182

JENNETT, LISA A.

Simulated airline service experience with laminar-flow control leading-edge systems p 104 N90-12512

JENNEY, GAVIN D.

Advanced actuation systems development, volume 1 [AD-A213334] p 121 N90-12624

Advanced actuation systems development, volume 2 [AD-A213378] p 198 N90-13398

JENNINGS, CRAIG H.

VSCF cycloconverter reliability review of the 30/40 KVA F/A-18 electrical generating system [SAE PAPER 892228] p 746 A90-45444

JENNINGS, T. M.

Fuel tank explosion protection p 251 N90-15914

JENSEN, CURTIS A.

A test and maintenance architecture demonstrated on SEM-E modules for fiber optic networks p 458 A90-28342

JENSEN, DAVID W.

Optical fiber sensing considerations for a smart aerospace structure p 38 A90-11210

JENSEN, J. L.

Wind shear and hyperbolic distributions p 280 A90-23632

JERACKI, ROBERT J.

Effect of reduced aft diameter and increased blade number of high-speed counterrotation propeller performance [AIAA PAPER 89-0438] p 234 A90-23650

Effect of reduced aft diameter and increased blade number on high-speed counterrotation propeller performance [NASA-TM-102077] p 172 N90-13352

JERAULD, GARY D.

The Advanced Digital-Optical Control System (ADOCS) user demonstration program [AD-A215984] p 349 N90-17644

JESKE, JAMES A.

Lateral-directional stability and control characteristics of the Quiet Short-Haul Research Aircraft (QSRA) [NASA-TM-102250] p 671 N90-23413

JESSE, D.

AIMS for helicopters p 820 N90-27639

JESSUP, STUART DODGE

An experimental investigation of viscous aspects of propeller blade flow p 315 N90-16711

JEUSETTE, JEAN-PIERRE

Postbuckling finite element analysis of composite panels p 365 A90-24377

JEWELL, WAYNE F.

Fully automatic guidance for rotorcraft nap-of-the-earth (NOE) flight following planned profiles p 403 A90-28219

Real-time piloted simulation of fully automatic guidance and control for rotorcraft nap-of-the-earth (NOE) flight following planned profiles [AIAA PAPER 90-3372] p 864 A90-47630

JHOU, JITAI

Influence of joint fixity on the structural static and dynamic response of a joined-wing aircraft. I - Static response [SAE PAPER 891060] p 100 A90-14361

Influence of joint fixity on the aeroelastic characteristics of a joined wing structure [AIAA PAPER 90-0980] p 390 A90-29370

JHONG, HONGHU

Experimental investigation on composite cooling of a turbine blade p 190 A90-17794

JH, WENHAI

Application investigation on superplastic forming/diffusion bonding combined technology of titanium alloy TC4 p 204 A90-18603

JIA, CHAOSHENG

The anti-shimmy and break-proof study of nose landing gear p 178 A90-16858

JIA, WEI

Calculation of flow over airfoil with slat and flap p 149 A90-16797

A flow around airfoil with slat and flap [AIAA PAPER 90-1535] p 564 A90-38679

JIANG, BO-NAN

Least-squares finite element methods for compressible Euler equations p 904 A90-51013

JIANG, DAZHONG

Digital control experiment research on the engine JT15D-4 p 190 A90-18600

JIANG, GUOAN

The computer aided weight engineering of aircraft - (CAWE) system p 179 A90-16860

JIANG, IVAN CHEN WEN

Flow coupling between a rotor and a stator in turbomachinery [AD-A223882] p 932 N90-28572

JIANG, J.-S.

A modal parameter identification technique and its application to large complex structures with multiple steady sinusoidal excitation p 602 A90-35670

JIANG, MING

A study of the control technique for aircraft spin recovery p 590 A90-37226

JIANG, TONG

An experimental investigation of rotating stall in a centrifugal compressor with vaneless diffuser p 621 A90-40513

JIANG, W. T.

Numerical simulations of gas turbine combustor flows [AIAA PAPER 90-2305] p 686 A90-42116

JIANG, ZIKANG

An investigation of characteristics of transonic and viscous flows for turbine cascades p 909 A90-52779

JIN, SHI

An aerodynamical design and calculation method for gas turbine with cooling air mixing p 189 A90-17782

JOBLING, D.

The surface pretreatment of aluminium-lithium alloys for structural bonding p 881 A90-47118

JOHAL, K. L.

Prediction and measurement of rotor blade/stator vane dynamic characteristics of a modern aero-engine axial compressor p 878 A90-46036

Prediction and measurement of rotor blade/stator vane dynamic characteristics of a modern aero-engine axial compressor [PNR90667] p 750 N90-26002

JOHANNESSEN, R.

1990-1995, a period of international decision making for the navigation community - Is our planning as good as it should be? p 823 A90-49490

Towards a quantitative assessment of benefits which INS/GPS integration can offer to civil aviation operating in a non-jamming environment p 823 A90-49496

JOHANNESSEN, ROLF

The role of adaptive antenna systems when used with GPS p 128 A90-13995

JOHN, REJI

Stress intensity factors for cracking metal structures under rapid thermal loading. Volume 2: Theoretical background [AD-A213297] p 213 N90-13812

JOHNS, ALBERT L.

Engine inlet distortion in a 9.2 percent scaled vectored thrust STOVL model in ground effect [AIAA PAPER 89-2910] p 301 A90-25043

Engine inlet distortion in a 9.2 percent scale vectored thrust STOVL model in ground effect [NASA-TM-102358] p 318 N90-17561

Hot gas ingestion characteristics and flow visualization of a vectored thrust STOVL concept [NASA-TM-103212] p 751 N90-26009

JOHNSON, A. A.

Safety management in aircraft testing and certification p 180 A90-17421

JOHNSON, A. B.

Temperature scaling of turbine blade heat transfer with and without shock wave passing p 47 A90-12570

JOHNSON, A. E.

Development and evaluation at ATCEU of executive and support operations, phase 4A/3D [CAA-PAPER-88017] p 99 N90-12572

Operational trial of effect of raising minimum stack level in Heathrow stacks [CAA-PAPER-89003] p 99 N90-12573

JOHNSON, A. M.

Application of advanced materials to aircraft gas turbine engines [AIAA PAPER 90-2281] p 764 A90-42769

- Compatibility of fuel system components with high density fuel
[AD-A210381] p 32 N90-10027
- JOHNSON, ALLAN H.**
Enhanced combat damage tolerance/supportability for improved combat sustainability
[SAE PAPER 891078] p 101 A90-14370
- JOHNSON, B. V.**
Aerodynamic and torque characteristics of enclosed Co/counter rotating disks
[ASME PAPER 89-GT-177] p 361 A90-23858
- JOHNSON, C. B.**
High Reynolds number tests of the CAST-10-2/DOA 2 transonic airfoil at ambient and cryogenic temperature conditions
p 320 N90-17650
- JOHNSON, CHARLES B.**
A transition detection study at Mach 1.5, 2.0, and 2.5 using a micro-thin hot-film system p 436 A90-28260
Hot-film system for transition detection in cryogenic wind tunnels p 122 N90-12522
- JOHNSON, DALE E.**
Database management considerations for IFR certified earth-referenced navigation systems p 577 A90-36921
- JOHNSON, DENNIS A.**
Effects of turbulence models on the prediction of transonic wing flows
[SAE PAPER 892224] p 713 A90-45440
Prediction of separated transonic wing flows with nonequilibrium algebraic turbulence model p 809 A90-47312
- JOHNSON, DICK**
Floor pull test of a transport airframe section
[DOT/FAA/CT-TN88/14] p 497 N90-20072
- JOHNSON, G. A.**
Study of forces and moments on wing-bodies at high incidence, volumes 1 and 2 p 171 N90-13350
- JOHNSON, G. I.**
A new type of calibration rig for wind tunnel balances p 438 A90-28305
- JOHNSON, JACK R.**
V-22 ballistic vulnerability hardening program p 408 A90-28223
- JOHNSON, JAMES R.**
AAAI '88 - Aerospace Applications of Artificial Intelligence; Proceedings of the Fourth Annual Conference, Dayton, OH, Oct. 25-27, 1988. Volumes 1 & 2 p 458 A90-30226
- JOHNSON, JOSEPH B.**
Supersonic boundary-layer transition on the LaRC F-106 and the DFRF F-15 aircraft. Part 1: Transition measurements and stability analysis p 94 N90-12558
- JOHNSON, M. RICHARD**
Dealing with the aging fleet
[SAE PAPER 892209] p 701 A90-45428
- JOHNSON, N. B.**
Aircraft crash survival design guide. Volume 2: Aircraft design crash impact conditions and human tolerance [AD-A218435] p 575 N90-22546
Aircraft crash survival design guide. Volume 5: Aircraft postcrash survival [AD-A218438] p 575 N90-22549
- JOHNSON, R. C.**
A practical co-axial twin rotor model p 335 A90-25423
- JOHNSON, RUSSELL W.**
Production of jet fuels from coal-derived liquids. Volume 11: Production of advanced endothermic fuel blends from Great Plains Gasification Plant naphtha by-product stream [AD-A210251] p 65 N90-11184
- JOHNSON, STEVEN A.**
A simple dynamic engine model for use in a real-time aircraft simulation with thrust vectoring
[AIAA PAPER 90-2166] p 662 A90-42054
Water-tunnel study results of a TF/A-18 and F/A-18 canopy flow visualization [NASA-TM-101705] p 573 N90-22532
- JOHNSON, VICKI S.**
Minimizing life cycle cost for subsonic commercial aircraft p 283 A90-23282
Life cycle cost in the conceptual design of subsonic commercial aircraft, volumes 1 and 2 p 923 N90-28535
- JOHNSON, WARREN B.**
Scientific justification and development plan for a mid-sized jet research aircraft
[PB89-208995] p 103 N90-11731
Meeting review: The Second NCAR (National Center for Atmospheric Research) Research Aircraft Fleet Workshop [PB89-200901] p 137 N90-12113
- JOHNSON, WAYNE**
Hub loads analysis of the SA349/2 helicopter p 333 A90-23936
- Correlation of Puma airloads: Lifting-line and wake calculation
[NASA-TM-102212] p 170 N90-13327
Application of the joined wing to tiltrotor aircraft [NASA-CR-177543] p 248 N90-15093
Airloads, wakes, and aeroelasticity [NASA-CR-177551] p 572 N90-21738
- JOHNSTON, G. R.**
Extending the overhaul interval for gas turbine engines through the use of alternative coatings on first stage blades p 63 A90-12539
- JOHNSTON, G. W.**
Interactive airfoil calculations with higher-order viscous-flow equations
[AIAA PAPER 90-1533] p 564 A90-38678
Higher-order boundary-layer approximations in interactive airfoil calculations p 628 A90-42402
Nonlinear unsteady airfoil response studies p 628 A90-42406
- JOHNSTON, JAMES P.**
Vortex generator jets - Means for flow separation control p 555 A90-36257
- JOHNSTON, N. J.**
Improved melt flow and physical properties of Mitsui Toatsu's LARC-TPI 1500 series polyimide p 943 A90-50134
- JOHNSTON, R. T.**
Propeller wakes and their interaction with wings p 14 A90-12614
- JOHNSTON, RICHARD P.**
The variable cycle diesel as an aircraft engine
[SAE PAPER 891065] p 110 A90-14365
- JOHNSTON, ROBERT T.**
Propeller tip vortex interactions
[AIAA PAPER 90-0437] p 166 A90-19846
- JOHNSTON, S. H.**
The manufacture of SPF military aircraft doors in aluminum alloy p 132 A90-16616
- JOHNSTONE, ROBERT**
CONDOR - high altitude long endurance (HALE) autonomously piloted vehicle (APV)
[AIAA PAPER 90-3279] p 836 A90-48866
- JOHST, EBERHARD**
Design criteria, constructions, and materials for the Dornier 328 airframe p 246 A90-21610
- JOLLES, F.**
Unsteady flow visualization in a vibrating annular turbine cascade operating in the transonic flow regime p 7 A90-11786
- JOLLY, J. RALPH, JR.**
Reduction of blade-vortex interaction noise through higher harmonic pitch control p 377 A90-23937
- JONCKHEERE, EDMOND A.**
Practical methods for robust multivariable control
[AD-A216937] p 462 N90-18920
- JONES, A.**
Analysis of failures in aircraft structures p 882 A90-48998
- JONES, A. H.**
Identification of multivariable models of jet engines
[AIAA PAPER 90-1874] p 655 A90-40540
Design of digital self-selecting multivariable controllers for jet engines
[AIAA PAPER 90-1875] p 655 A90-40541
- JONES, ALAN**
Correlation of Puma airfoils - Evaluation of CFD prediction methods
[ONERA, TP NO. 1989-185] p 224 A90-21045
- JONES, ALAN B.**
Development of obstacle clearance criteria and standards for MLS and MLS/RNAV precision approaches and development of an MLS collision risk model
[SAE PAPER 892215] p 728 A90-45432
- JONES, C. M.**
Implementation of a transputer-based flight controller p 667 A90-38966
Parallel processing implementation of a flight controller p 333 N90-16743
- JONES, C. W.**
Mixer-ejector nozzle for jet noise suppression
[AIAA PAPER 90-1909] p 894 A90-47202
- JONES, CHARLES H.**
An expert system for real-time aircraft monitoring
[AIAA PAPER 90-1311] p 545 A90-33921
- JONES, D. J.**
Wind tunnel results and numerical computations for the NAE deHavilland series of natural laminar flow airfoils p 628 A90-42403
- JONES, DENISE R.**
Three input concepts for flight crew interaction with information presented on a large-screen electronic cockpit display
[NASA-TM-4173] p 420 N90-18394
- Simulator comparison of thumbball, thumb switch, and touch screen input concepts for interaction with a large screen cockpit display format
[NASA-TM-102587] p 506 N90-21005
- JONES, GREGORY S.**
Qualitative evaluation of a conformal velocity vector display for use at high angles-of-attack in fighter aircraft [NASA-TM-102629] p 739 N90-25981
- JONES, G. S.**
The hemisphere-cylinder at an angle of attack
[AIAA PAPER 90-0050] p 313 A90-26907
- JONES, GREGORY S.**
The development of a 3-D laser velocimeter for the NASA Langley low turbulence pressure wind tunnel
[AIAA PAPER 90-1385] p 597 A90-38484
Basic aerodynamic research facility for comparative studies of flow diagnostic techniques p 122 N90-12526
- JONES, H.**
A test of airborne kinematic GPS positioning for aerial photography - Methodology p 97 A90-13982
- JONES, HENRY**
Performance of an optimized rotor blade at off-design flight conditions p 830 A90-46946
- JONES, J. G.**
Formation of design envelope criterion in terms of deterministic spectral procedure
[RAE-TM-SS-9] p 721 N90-25953
- JONES, J. J.**
Electric charge acquired by airplanes penetrating thunderstorms p 913 A90-52093
- JONES, JESSE D.**
The addition of Bendix MLS (Microwave Landing System) antenna patterns to MLS mathematical model [AD-A210633] p 27 N90-10020
MLS mathematical model validation study using airborne MLS data from Midway Airport engineering flight tests, August 1988
[DOT/FAA/CT-TN90/2] p 640 N90-23378
- JONES, JOHN H.**
Effects on aerospace alloys of residual chlorine in chlorinated-solvent primers p 956 A90-50187
- JONES, K. J.**
Composite-embedded optical fibers for communication links p 139 A90-13847
- JONES, KEVIN D.**
Computational simulation of flows about hypersonic geometries with sharp leading edges
[AIAA PAPER 90-3065] p 793 A90-45891
- JONES, MICHAEL G.**
Status report on a natural laminar-flow nacelle flight experiment p 105 N90-12550
Effects of acoustic sources p 140 N90-12553
- JONES, PAUL H.**
Modified touchdown zone lighting
[DOT/FAA/CT-TN89/70] p 526 N90-21042
Taxiway sign effectiveness under reduced visibility conditions
[DOT/FAA/CT-TN90/20] p 761 N90-25150
- JONES, ROBERT**
The servo flap - An advanced rotor control system p 860 A90-46934
Vibration reduction on servo flap controlled rotor using HHC p 861 A90-46967
Comparison of active control on a servo flap rotor using fixed system and rotating system parameters p 862 A90-46976
- JONES, ROBERT A.**
Opportunities for improved understanding of supersonic and hypersonic flows p 318 N90-17566
- JONES, ROBERT C.**
STOL Maneuver Technology Demonstrator aeroservoelasticity
[AIAA PAPER 90-3336] p 863 A90-47596
- JONES, ROBERT T.**
Wing theory p 809 A90-47700
- JONES, S. P.**
Prediction of aerostat and airship mooring mast loads by nonlinear dynamic simulation
[AIAA PAPER 89-3172] p 245 A90-20587
- JONES, STUART C.**
Thermal management for a Mach 5 cruise aircraft using endothermic fuel
[AIAA PAPER 90-3284] p 853 A90-48871
- JONES, T.**
Development of high temperature actuation systems for advanced aircraft engines
[AIAA PAPER 90-2031] p 660 A90-41990
- JONES, T. V.**
Temperature scaling of turbine blade heat transfer with and without shock wave passing p 47 A90-12570
- JONES, W. P.**
Calculation of confined swirling flows with a second moment closure p 66 A90-10640
Numerical simulation of nonpremixed turbulent flow in a dump combustor
[AIAA PAPER 90-1858] p 768 A90-42685

JONES, W. R.

- Airborne Doppler radar detection of low-altitude wind shear p 252 A90-23284
Airborne Doppler radar flight experiments for the detection of microbursts p 542 N90-21243

JONES, W. VERNON

- Recent results and major activities in the NASA Balloon Program [IAF PAPER 89-468] p 81 A90-13557

JONES, WILLIAM D.

- A very high speed switched-reluctance starter-generator for aircraft engine applications p 452 A90-30791

JONNAVITHULA, SREENADH S.

- Computational and experimental investigations of rotating stall in compressor cascades p 588 N90-22565

JORDAN, DAVID

- HARP model rotor test at the DNW p 406 A90-28167

JORDAN, FRANK L., JR.

- Wind tunnel results of the low-speed NLF(1)-0414F airfoil p 93 N90-12541
Wind tunnel results of the high-speed NLF(1)-0213 airfoil p 93 N90-12542

JOSLYN, H. DAVID

- The effects of compressor endwall flow on airfoil incidence and deviation p 512 N90-21011

JOST, G. S.

- A review of Australian and New Zealand investigations on aeronautical fatigue during the period April 1987 to March 1989 [AD-A210373] p 32 N90-10026

JOST, RANDY J.

- Comparison of the swept frequency continuous wave, current pulse, and shock-excitation lightning simulation techniques p 818 A90-49832
An assessment of analytical methods and lightning simulation test techniques used in lightning qualification and surveillance testing p 818 A90-49833
Characterization of configuration effects on lightning simulation/qualification testing p 819 A90-49835
Validation of GEMACS for prediction of lightning induced electromagnetic fields p 819 A90-49845

JOU, WEN-HUEI

- Large-eddy simulations of pressure oscillations and combustion instability in a ramjet p 111 A90-15388
Large-eddy simulations of combustion instability in an axisymmetric ramjet combustor [AIAA PAPER 90-0267] p 191 A90-19764
Large-eddy simulations of flows in a ramjet combustor p 772 A90-45534
Numerical simulation of pressure oscillations in a ramjet combustor p 54 N90-10202

JOUAILLEC, F.

- Recent propeller development and studies conducted at ONERA [ONERA, TP NO. 1990-16] p 683 A90-41201

JOUAN, J. Y.

- Electromagnetic characterization of lightning on aircraft [ONERA, TP NO. 1989-131] p 22 A90-11155
Transall 88 - Lightning characterization program [ONERA, TP NO. 1989-142] p 22 A90-11164

JOUBERT, H.

- Wind-tunnel test of the air intake of an unducted fan [AAAF PAPER NT 88-19] p 4 A90-11436
Aircraft compressor flutter analysis p 41 A90-11797
Aerodynamic study on forced vibrations on stator rows of axial compressors p 426 N90-18412

JOYCE, GAYNOR

- Feature-associated mesh embedding for complex configurations p 608 N90-21988

JOZWIAK, ROBERT

- The influence of control-surface compensation parameters on the hinge moment characteristics p 643 A90-41737
Influence of some geometrical and design parameters on the hinge moment characteristics of rudders p 643 A90-41739
Investigations of the influence of slot blowing from the upper wing surface on the flow around the wing and its aerodynamic characteristics p 623 A90-41740

JUBIS, REBECCA

- Underlying factors in air traffic control incidents p 401 A90-31335

JUDGE, KEVIN C.

- Two-level maintenance concept for advanced avionics architectures p 457 A90-28321

JUGGINS, P. T. W.

- A comprehensive approach to coupled rotor-fuselage dynamics p 646 A90-42460
Application of the Westland CRFD program to total helicopter dynamics p 832 A90-46965

JUILLEN, J. C.

- Leading edge contamination and relaminarisation on a swept wing at incidence p 148 A90-16789

- Experimental study of transition and leading edge contamination on swept wings p 71 N90-10362
Transition in surface boundary layers [CERT-RSF-OA-43/5018-AYD] p 136 N90-12897

JULIAN, STEVE

- The SKY SHARK: An RPV designed to investigate the pressure distribution on a lifting surface [NASA-CR-186222] p 844 N90-26824

JUMPER, E. J.

- The effect of pitch location on dynamic stall p 2 A90-10641

JUNG, YOON C.

- An application of generalized predictive control to rotorcraft terrain-following flight p 257 A90-23478

JUNGLAUS, G.

- New experimental results on the origin and structure of Ferri and Dailey instabilities ('buzz') p 906 A90-51507

JUNKER, B.

- Helicopter rotor test rig (RoTeSt) in DNW: Application and results [RAE-TRANS-2171] p 201 N90-13408

JURIK, MARIAN

- Numerical solution of 2D transonic flows in a turbine cascade p 709 A90-44601

JUTRAS, THOMAS H.

- Feasibility study for a microwave-powered ozone sniffer aircraft [NASA-CR-186660] p 650 N90-23397

K

KABA, HIDEKEI

- Instrumentation and operation of NDA cryogenic wind tunnel p 437 A90-28293

KACHANOV, B. O.

- Development of a mathematical model of an adaptive antiflutter system p 769 A90-42911

KACKER, S. C.

- An improved incidence losses prediction method for turbine airfoils [ASME PAPER 89-GT-284] p 475 A90-33563

KADAMBI, J. R.

- Turbomachinery blade vibration and dynamic stress measurements utilizing nonintrusive techniques p 41 A90-11558

KADAR, IVAN

- Neural networks for adaptive shape tracking p 638 A90-39959

KAERCHER, RAINER

- Digital electronic control unit for the European Fighter Aircraft (EFA) p 253 A90-21607

KAESER, R.

- Eight years of experience with small computerized retrofit load monitoring systems p 926 A90-49882

KAFYEKE, F.

- Application of the KTRAN transonic small disturbance code to the complete CF-18 aircraft with stores p 629 A90-42416

KAGERBAUER, G.

- Design philosophy and construction techniques for integral fuselage fuel tanks p 250 N90-15913

KAHANE, R. H.

- Mode S - A data link for future air traffic control p 576 A90-35684

KAHANEK, VACLAV

- Fatigue tests of samples of flanged joints of wings p 274 A90-23353

KAILASANATH, K.

- A numerical study of transverse jets into supersonic flows and influence of pressure waves [AIAA PAPER 90-0733] p 314 A90-26985
Supersonic flow over an axisymmetric backward-facing step [AIAA PAPER 90-1580] p 566 A90-38717

- Acoustic-vortex-chemical interactions in an idealized ramjet p 54 N90-10206

- Numerical simulations of the structure of supersonic shear layers [AD-A224164] p 960 N90-29587

KAILASANATH, KAZHIKATHRA

- Numerical simulations of flowfields in a central-dump ramjet combustor. 3: Effects of chemistry [AD-A224145] p 933 N90-28573

KAISER, K. J.

- Integration of intelligent avionics systems for crew decision aiding p 459 A90-30236

KAISER, KIMBERLY

- Problem focus mechanisms for cockpit automation [AIAA PAPER 89-3096] p 37 A90-10581

KAISER, ROBERT D.

- Analysis and test of a wide angle spectrometer [AD-A215819] p 372 N90-18030

KAISER, W. O.

- Supersonic combustion of hydrogen jets behind a backward-facing step [AIAA PAPER 90-0204] p 266 A90-22183

KAIZOJI, ALLYNE

- Analysis and testing of fiber-reinforced thermoplastic composite vertical stabilizer skins for an advanced attack helicopter p 441 A90-28193

KAJI, SHOJIRO

- Unsteady aerodynamic characteristics of oscillating cascade with tip clearance p 8 A90-11793

KAKUTA, YOSHIKI

- Evaluation of static and fatigue properties of thin sheets of 8090-T8 aluminum-lithium alloy and observation of its fracture surfaces [NAL-TR-1039] p 953 N90-29499

- Fractographic analysis of fatigue failures of airframe equipment parts: Examples of a rod end housing and a rod end cap [NAL-TR-1047] p 961 N90-29686

KALBURGI, VIJAY

- Goertler instability on an airfoil: Comparison of marching solution with experimental observations p 19 N90-10364

- Goertler instability on an airfoil p 91 N90-12517

KALDEICH, BRIGITTE

- Combustion Experiments During KC-135 Parabolic Flights [ESA-SP-1113] p 368 N90-16958

KALDELLIS, J.

- A secondary flow calculation method for one stage centrifugal compressor p 14 A90-12597
Secondary flow calculations for axial and radial compressors p 514 N90-21024

KALETKA, JUERGEN

- Identification of mathematical derivative models for the design of a model following control system p 56 A90-12764

- Time and frequency-domain identification and verification of BO-105 dynamic models [AD-A216828] p 415 N90-18389

KALIN, D. A.

- Design considerations for a compact table top hypersonic simulator of aero-optic effects p 525 A90-34585

- Table top experimental simulation of hypersonic aero-optical effects p 525 A90-34586

KALKANIS, P.

- The effect of rapid spoiler deployment on the transient forces on an aerofoil p 921 N90-28527

KALLERGIS, MICHAEL

- Possibility of active propeller-noise suppression in piston-engine aircraft by changing the phase relation between the propeller and exhaust signals p 218 A90-18450

KALLINDERIS, YANNIS

- Application of an adaptive algorithm to single and two-element airfoils in turbulent flow [AIAA PAPER 90-0698] p 169 A90-19983

KALLIS, JAMES M.

- Application of fracture mechanics to microscale phenomena in electronic assemblies p 684 A90-41334

KALSHOVEN-VAN TIJEN, EUGENIE L. M.

- Recent developments in EEC aviation law - 'The second phase' p 897 A90-46648

KALTSCHMIDT, HORST

- ROSAR (Helicopter-Rotor based Synthetic Aperture Radar) p 541 N90-21229

KALUMUCK, K. M.

- New concept for improved nonmetallic erosion protection systems p 407 A90-28188

KAMAL, M. A. Y.

- Aerostructural considerations for the power plant of overlapping wing configuration p 841 A90-49488

KAMATH, PRADEEP S.

- Numerical simulation of flow through the Langley parametric scramjet engine [SAE PAPER 892314] p 747 A90-45476

KAMIGAITO, OSAMI

- MRS International Meeting on Advanced Materials, 1st, Tokyo, Japan, May 31-June 3, 1988, Proceedings. Volume 5 - Structural ceramics/Fracture mechanics p 599 A90-35926

KAMINER, ISAAC

- Design of integrated pitch axis for autopilot/autothrottle and integrated lateral axis for autopilot/yaw damper for NASA TSRV airplane using integral LQG methodology [NASA-CR-4268] p 348 N90-16768

KAMIS, DONALD N.

- The new FFA T1500 transonic wind tunnel initial operation, calibration, and test results [AIAA PAPER 90-1420] p 596 A90-37957

KAN, V. L.

- Stability and controllability in proportional navigation p 725 A90-42990

- KANAI, K.**
Adaptive flight control of CCV aircraft with limiting zeros
[AIAA PAPER 90-3409] p 864 A90-47664
- KANARCHUK, VADIM E.**
Ground aviation equipment: Handbook
p 593 A90-36153
- KANDA, TAKESHI**
Cycle analysis of scramjet engines
[NAL-TR-1002] p 51 N90-10035
Analysis of scramjet engine characteristics
[NAL-TR-1041] p 933 N90-29398
- KANDEBO, STANLEY W.**
V-22 - The prospects now p 497 A90-34900
- KANDIL, OSAMA A.**
Prediction of steady and unsteady asymmetric vortical flows around cones
[AIAA PAPER 90-0598] p 168 A90-19940
Integral solution of unsteady full-potential equation for a transonic pitching airfoil p 232 A90-23280
Unsteady flow computation of oscillating flexible wings
[AIAA PAPER 90-0937] p 389 A90-29363
Unsteady inviscid and viscous computations for vortex-dominated flows p 553 A90-35752
Computational study for passive control of supersonic asymmetric vortical flows around cones
[AIAA PAPER 90-1581] p 566 A90-38718
Numerical simulation of steady and unsteady vortical flows around wings and bodies p 806 A90-46869
Analysis and mitigation of numerical dissipation in inviscid and viscous computation of vortex-dominated flows
[NASA-CR-186887] p 776 N90-26281
- KANE, J. H.**
Boundary-element shape optimization system for aircraft structural components p 680 A90-39786
- KANEKO, HISATERU**
Steady state performance of FJR 710/600S engine p 43 A90-12015
- KANEKO, R. S.**
Aluminum alloy 6013 sheet for new U.S. Navy aircraft p 599 A90-37442
- KANEVETS, GEORGII E.**
Handbook on heat exchangers p 273 A90-22743
- KANG, B.**
Comparison of 1-D and 2-D aircraft images p 927 A90-52884
- KANG, JICHANG**
The design and study of the information transfer mechanism for a distributed avionics system p 207 A90-16858
- KANG, P.**
A circular combustor configuration with multiple injection ports for mixing enhancement p 130 A90-15389
- KANG, SHUN**
A method for calculating axial turbomachine end wall turbulent boundary layers
[ASME PAPER 89-GT-15] p 287 A90-23759
An application of topological analysis to studying the three-dimensional flow in cascades. I - Topological rules for skin-friction lines and section streamlines p 908 A90-52607
- KANMURI, AKIO**
Analysis of scramjet engine characteristics
[NAL-TR-1041] p 933 N90-29398
- KANNINEN, MELVIN F.**
Application of fracture mechanics to microscale phenomena in electronic assemblies p 684 A90-41334
- KANNING, GERD**
Equations of motion of slung load systems with results for dual lift
[NASA-TM-102246] p 349 N90-17641
- KANNO, SHOKICHI**
Backside landing control of a STOL aircraft using approximate perfect servo p 934 A90-52801
- KAO, PI-JEN**
Comparison of equivalent plate and finite element analysis of a realistic aircraft structural configuration
[AIAA PAPER 90-3293] p 837 A90-48877
Efficient methods for integrated structural-aerodynamic wing optimum design p 184 N90-13376
- KAO, T. J.**
Application of a multiblock grid generation approach to aircraft configurations p 310 A90-26527
- KAO, YUNG-FU**
A two-dimensional unsteady analysis for transonic and supersonic cascade flows p 480 N90-20955
- KAPLAN, MICHAEL L.**
Mesoscale acid deposition modeling studies
[NASA-CR-4262] p 140 N90-13228
- KAPLITA, THADDEUS T.**
Helicopter simulation development by correlation with frequency sweep flight test data p 407 A90-28203
- KAPLUN, S. A.**
Optimal selection of the parameters to be measured during the identification of gas turbine engines. I - Problem statement p 255 A90-23410
Optimal choice of measured parameters during the identification of gas turbine engines. II - Combined confidence regions and intervals of the identification results p 850 A90-46493
- KAPOOR, K.**
Large-amplitude high-rate roll oscillation system for the measurement of non-linear airloads
[AIAA PAPER 90-1426] p 590 A90-37963
- KAPPLER, G.**
Experimental identification of helicopter engine dynamics from closed loop data p 855 N90-27627
- KARADIMAS, G.**
Mesh generation for flow computation in turbomachine p 588 N90-21981
- KARADIMAS, GEORGES**
Application of computational systems to aircraft engine components development p 188 A90-17448
- KARADIMITRIS, A.**
Regression and combustion characteristics of boron containing fuels for solid fuel ramjets p 858 N90-27928
- KARAGOZIAN, A. R.**
Modeling of liquid jets injected transversely into a supersonic crossflow p 153 A90-17985
- KARAMYSHEV, V. B.**
Numerical modeling of separated turbulent flows p 470 A90-32673
- KARANJIA, D. J.**
Optimization studies for the PW305 turbofan
[AIAA PAPER 90-2520] p 744 A90-42813
- KARAS, O. V.**
Application of the inverse method of three-dimensional boundary layer analysis to the problem of flow past a wing with allowance for the effect of viscosity p 804 A90-46548
Determination of the laminar-turbulent transition point for a turbulent layer on a yawing wing p 805 A90-46566
- KARATAEV, S. G.**
A numerical method for calculating supersonic flows of a viscous gas p 476 A90-34672
- KARAYAEV, E. A.**
Self-induced roll oscillations of lifting systems with thin delta wings p 860 A90-46570
- KARCZ, PETER J.**
GPS: Arrival in the fleet - A GPS AN/SRN-25 receiver assessment p 97 A90-13989
Global Positioning System: Arrival in the fleet - A GPS AN/SRN-25(V) receiver assessment p 331 A90-26338
- KARLOY, VALERII I.**
Optimization of the observations and control of aircraft p 60 A90-12468
- KARLSSON, JOAKIM**
Automatic speech recognition in air traffic control p 488 N90-20923
- KARMAN, STEVE L., JR.**
Benchmark calculations with an unstructured grid flow solver on a SIMD computer p 546 A90-34378
- KARON, DAVID M.**
Laser transit anemometry investigation of a high speed centrifugal compressor
[ASME PAPER 89-GT-155] p 360 A90-23843
- KARPEL, M.**
Sensitivity derivatives of flutter characteristics and stability margins for aeroservoelastic design p 433 A90-31287
Reduced-order aeroelastic models via dynamic residualization p 493 A90-33412
Reduced-order aeroelastic models via dynamic residualization p 579 A90-35762
- KARPEL, MORDECHAY**
Time-domain aeroservoelastic modeling using weighted unsteady aerodynamic forces p 195 A90-17698
Reduced size first-order subsonic and supersonic aeroelastic modeling
[AIAA PAPER 90-1154] p 390 A90-29366
Multi-disciplinary optimization of aeroservoelastic systems
[NASA-CR-185931] p 925 N90-29385
- KARPOV, E. V.**
Calculation of supersonic flow past a wing/fuselage combination with the resolution of a compression shock from the wing p 297 A90-24138
- KARPOVA, G. S.**
A study of the stability and thermal stability of complex reinforced structures p 880 A90-46541
- KARYAMPUDI, V. MOHAN**
Mesoscale acid deposition modeling studies
[NASA-CR-4262] p 140 N90-13228
- KAS'IANIKOV, VENIAMIN A.**
Coaxial helicopters - Current status and future developments p 838 A90-48951
- KASCAK, A. F.**
Test and theory for piezoelectric actuator-active vibration control of rotating machinery p 879 A90-46226
- KASCAK, ALBERT F.**
Vibration dampers for cryogenic turbomachinery
[AIAA PAPER 90-2740] p 882 A90-47228
- KASHIWA, T.**
Simulation of the reduction characteristics of scattering from an aircraft coated with a thin-type absorber by the spatial network method p 638 A90-39855
- KASHIWABARA, YASUSHIGE**
A study on surge and rotating stall in axial compressors - A summary of the measurement and fundamental analysis method p 87 A90-16105
- KASSAPOGLOU, CHRISTOS**
Design and analysis of composite structures with manufacturing flaws p 445 A90-28234
- KASSIES, A.**
Numerical interactive grid generation for 3D-flow calculations p 312 A90-26556
Boundary conditions for Euler equations at internal block faces of multi-block domains using local grid refinement
[AIAA PAPER 90-1590] p 607 A90-38725
Design and testing of a multiblock grid-generation procedure for aircraft design and research p 582 N90-21984
Informatics aspects of large flow calculations on the SX-2 supercomputer
[NLR-MP-88037-U] p 776 N90-26290
- KASTERINA, N. D.**
Computer-aided design of compressor rotor blade rings p 851 A90-46497
- KASTERSKII, S. M.**
Aviation equipment p 338 A90-24200
- KATHONG, M.**
Application of multiple grids topology to supersonic internal/external flow interactions p 308 A90-26135
- KATO, OSAMU**
Attitude projection method for analyzing large-amplitude airplane maneuvers p 197 A90-19555
- KATULEV, A. N.**
Generation of motion control for direction finders in a goniometer system p 187 A90-17137
- KATZ, ERIC S.**
Improved lighting of taxiway/taxiway intersections for Instrument Flight Rules (IFR) operations
[DOT/FAA/CT-TN89/64] p 243 N90-15089
- KATZ, JOSEPH**
Application of panel methods to wind-tunnel wall interference corrections
[AIAA PAPER 90-0007] p 200 A90-19629
Effect of vertical-ejector jet on the aerodynamics of delta wings p 553 A90-35755
Self-induced roll oscillations of low-aspect-ratio rectangular wings
[AIAA PAPER 90-2811] p 753 A90-45151
- KATZER, EDGAR**
On the lengthscales of laminar shock/boundary-layer interaction p 5 A90-11610
Numerical analysis of unsteady forces on oscillating ring airfoils and jet engines p 473 A90-33364
Steady and unsteady potential flow around thin annular wings and engines with simulation of jet engine flow
[DFVLR-FB-89-18] p 89 N90-11711
- KATZER, MICHAEL J.**
In-flight aircraft lightning surface current model p 819 A90-49844
- KAU, H. P.**
Numerical investigation of unsteady flow in oscillating turbine and compressor cascades p 426 N90-18407
- KAU, H.-P.**
Computation of aerodynamic blade loads due to wake influence and aerodynamic damping of turbine and compressor cascades p 7 A90-11791
- KAUFFMAN, H. G.**
System optimization for maximizing reconnaissance mission range of a hypersonic cruise vehicle
[AIAA PAPER 90-3292] p 837 A90-48876
- KAUFFMAN, R. E.**
Development of a remaining useful life of a lubricant evaluation technique. III - Cyclic voltammetric methods p 125 A90-15732
- KAUFMAN, A. E.**
Optimization of rotor performance in hover and axial flight using a free wake analysis p 407 A90-28175
- KAUKE, G. K.**
Experiments on the unsteady flow in a supersonic compressor stage p 427 N90-18422
- KAUSHAL, S. C.**
Unbalance response studies on a model rotor supported on uncentrally squeezed film dampers and the development experience of a jet engine p 69 A90-12579

KAUSHIK, S.

Performance improvement of an eroded axial flow compressor using water injection
[AIAA PAPER 90-2016] p 741 A90-42718

KAUTZ, E. F.

Certification testing methodology for fighter hybrid structure p 642 A90-40128

KAWACHI, K.

Noise prediction of a counter-rotation propfan p 218 A90-17861

KAWACHI, KEIJI

Analytical study of dynamic response of helicopter in autorotative flight p 670 A90-42469

KAWAHARA, HIROYASU

Flight simulator evaluation of a head-down display [NAL-TM-573] p 59 N90-10898

Flight simulation test facility: Function and specification of the simulator cockpit system [NAL-TM-577] p 59 N90-10899

KAWAI, NOBUHIRO

Investigation of ATP blades, part 2. Validation of two-dimensional viscous flow simulation codes around thin airfoils [NAL-TR-1046] p 912 N90-29326

A boundary-layer transition model for the Navier-Stokes computation for a natural-laminar-flow airfoil [NAL-TR-1038T] p 912 N90-29328

KAWAI, TATSUO

Improvement in turbine blade aerodynamic force in the tip region p 809 A90-47854

KAWAMURA, RYUMA

Computational and experimental analysis of transonic fanjet engine flow field using 3-D Euler code p 306 A90-25809

KAWAMURA, TETUYA

Numerical simulation of wing in ground effect p 307 A90-25863

KAWASHIMA, T.

Three dimensional photoelastic analysis of aeroengine parts p 270 A90-20077

KAWASHIMA, TOSHIHIRO

Mechanical rig test of FJR 710/600 engine components p 43 A90-12016

KAY, I. W.

Hydrocarbon-fueled scramjet combustor investigation [AIAA PAPER 90-2337] p 658 A90-40622

KAYA, M. ORHAN

Shock-wave/boundary-layer interaction at a swept compression corner p 16 A90-12850

KAYNES, I. V.

Interactions of active controls and structural loads p 517 A90-33404

KAYNES, IAN W.

The application of TSIM software to act design and analysis on flexible aircraft p 60 N90-10086

KAZAKIA, J. Y.

Embedded function methods for supersonic turbulent boundary layers [AIAA PAPER 90-0306] p 163 A90-19787

KAZAO, Y.

Dynamics of multi-spool gas turbines using the matrix transfer method - Applications p 509 A90-33594

Dynamics of multi-spool gas turbines using the matrix transfer method - Theory p 509 A90-33595

KAZEMPOUR, AMIR

Evaluation of critical speeds in high speed aircraft tires [SAE PAPER 892349] p 733 A90-45500

KAZNEVSKII, V. P.

Effect of the leading edge bluntness of a moderately swept wing on the aerodynamic characteristics of an aircraft model at subsonic and transonic velocities p 388 A90-29005

KEAGLE, C.

Categorization and performance analysis of advanced avionics algorithms on parallel processing architectures p 461 A90-30786

KEE, YEH

Initial flight test of half-scale unmanned air vehicle [AD-A219584] p 648 N90-23388

KEEL, BYRON M.

Adaptive clutter rejection filters for airborne Doppler weather radar applied to the detection of low altitude windshear [NASA-CR-186211] p 214 N90-14453

KEEL, G.

A test of airborne kinematic GPS positioning for aerial photography - Methodology p 97 A90-13982

KEENE, WILLIAM D.

Aerosol separator for use in aircraft [PB90-142217] p 611 N90-22155

KEESE, DAVID L.

Risk assessment and its application to flight safety analysis [DE90-004985] p 323 N90-16722

KEGARISE, R. J.

An aluminum quality breakthrough for aircraft structural reliability p 843 N90-26816

KEGELMAN, JEROME T.

An experimental investigation of sweep-angle influence on delta-wing flows [AIAA PAPER 90-0383] p 228 A90-22210

The flowfields of bursting vortices over moderately swept delta wings [AIAA PAPER 90-0599] p 314 A90-26969

The lateral spreading of finite-span instability waves in a laminar mixing layer [AIAA PAPER 90-1532] p 606 A90-38677

KEHOE, MICHAEL W.

Ground vibration test results of a JetStar airplane using impulsive sine excitation p 179 A90-16963

An in-flight interaction of the X-29A canard and flight control system [AIAA PAPER 90-1240] p 348 A90-26820

Flutter clearance of the F-14A variable-sweep transition flight experiment airplane, phase 2 [NASA-TM-101717] p 735 N90-25135

An in-flight interaction of the X-29A canard and flight control system [NASA-TM-101718] p 736 N90-25973

KEIRSEY, J. L.

Investigation of cowl vent slots for supercritical stability enhancement in dual-mode ramjet inlets p 507 A90-32951

KEITH, F. J.

Digital control of magnetic bearings supporting a multistage flexible rotor p 682 A90-40712

KEITH, T. G.

An LDA investigation of the normal shock wave boundary layer interaction p 908 A90-52618

KEITH, THEO G., JR.

Development of an anti-icing runback model [AIAA PAPER 90-0759] p 238 A90-22258

Time domain flutter analysis of cascades using a full-potential solver [AIAA PAPER 90-0984] p 391 A90-29374

KEITH, W. D.

Charging of aircraft - High-velocity collisions p 322 A90-26131

KEL'ZON, A. S.

Stability and controllability in proportional navigation p 725 A90-42990

KELAITA, PAUL

Supercomputer applications in gas turbine flowfield simulation p 620 A90-40495

KELDYSH, V. V.

Ideal propeller in compressible gas flow in a wind tunnel p 298 A90-24156

KELLACKEY, C. J.

Impact ice stresses in rotating airfoils [AIAA PAPER 90-0198] p 175 A90-19735

KELLER, DONALD F.

Experimental transonic flutter characteristics of supersonic cruise configurations [AIAA PAPER 90-0979] p 390 A90-29369

KELLERER, H.

Aerospace materials - Trends and potential p 529 A90-31902

KELLEY, HENRY L.

Aerodynamic performance of a 0.27-scale model of an AH-64 helicopter with baseline and alternate rotor blade sets [NASA-TM-4201] p 632 N90-24237

KELLY, A. P.

Production of jet fuels from coal-derived liquids. Volume 11: Production of advanced endothermic fuel blends from Great Plains Gasification Plant naphtha by-product stream [AD-A210251] p 65 N90-11184

KELLY, R. J.

MLS - A total system approach p 640 A90-41710

KEMMERLY, GUY T.

Dynamic ground-effect measurements on the F-15 STOL and Maneuver Technology Demonstrator (S/MTD) configuration [NASA-TP-3000] p 573 N90-22531

KEMP, R. A. W.

Description of the MARC measuring system [FEL-89-B170] p 963 N90-28887

KEMRY, M. M.

Geometrical factors influencing the flow field in a propulsive nozzle p 807 A90-46876

Study of the expansion of hydrocarbon-oxygen products through supersonic nozzle p 852 A90-46907

KENNEDY, ARTHUR E.

Flight testing and application of a Peripheral Vision Display p 652 A90-40381

KENTFIELD, J. A. C.

Numerical simulation of valveless pulsed combustors p 127 A90-13767

Small gas turbine using a second-generation pulse combustor p 421 A90-27972

KENTON, ARTHUR C.

Vision guidance update - Synthetic aperture radar (SAR) multiple image exploitation for position and velocity determination p 488 A90-34140

KENWORTHY, M. J.

Dynamic instability characteristics of aircraft turbine engine combustors p 53 N90-10195

KERELIUK, STAN

Flight test investigation of flight director and autopilot functions for helicopter decelerating instrument approaches [DOT/FAA/CT-TN89/54] p 869 N90-27724

KERN, DIETER

Effect of vertical-ejector jet on the aerodynamics of delta wings p 553 A90-35755

KERN, JOHN S.

The FAA gears up for Loran p 823 A90-49493

KERN, JONATHAN

The effect of windscreen bows and HUD pitch ladder on pilot performance during simulated flight p 420 A90-31333

KERN, LURA E.

Effects of simplifying assumptions on optimal trajectory estimation for a high-performance aircraft [NASA-TM-101721] p 757 N90-25142

KERR, ANDY

Integrally heated tooling for economical, nonautoclave production of thermoplastic parts p 956 A90-50200

KERRS, W.

Experimental investigation of the flow development of an airfoil at high angles of attack p 473 A90-33366

KERSCHEN, EDWARD J.

Boundary-layer receptivity and laminar-flow airfoil design p 91 N90-12516

KESACK, WILLIAM J.

Effects of damage on post-buckled skin-stiffener composite skin panels p 409 A90-28235

KESLER, S. B.

Comparison of 1-D and 2-D aircraft images p 927 A90-52884

KESSLER, EDWIN

Low-level windshear alert systems and Doppler radar in aircraft terminal operations p 574 A90-35758

KESSLER, H. R.

Implementation of integrated product development [AIAA PAPER 90-3194] p 786 A90-48829

KESSLER, T. C.

Development of process control procedure for ultrahigh-sensitivity fluorescent penetrant inspection systems p 771 A90-45225

KETTHAUS, B.

Direct measurement of laminar instability amplification factors in flight p 277 N90-16178

KEVENOGLU, M. F.

Testing facility and procedure of the ATTAS on-board data acquisition system p 39 A90-12202

KEYDEL, WOLFGANG

ROSAR (Helicopter-Rotor based Synthetic Aperture Radar) p 541 N90-21229

KEYES, DAVID E.

Modification and improvement of software for modeling multidimensional reacting fuel flows [AD-A217789] p 533 N90-20235

KEYVANI, ANOOSH

NASA/USRA high altitude reconnaissance aircraft - [NASA-CR-186685] p 650 N90-24266

KHADER, N.

Shaft flexibility effects on the forced response of a bladed-disk assembly p 744 A90-43218

KHADER, NAIM

Shaft flexibility effects on aeroelastic stability of a rotating bladed disk p 132 A90-16371

Blade mistuning coupled with shaft flexibility effects in rotor aeroelasticity [ASME PAPER 89-GT-330] p 343 A90-23896

KHADJAVI, F.

Low speed testing of a laminar flow airfoil in an adaptive wall wind tunnel [FFA-TN-1989-08] p 632 N90-23363

KHAIRULLIN, A. KH.

Design of computer-aided testing systems for aviation equipment. I p 222 A90-23416

Design of computer-aided aircraft testing systems. II p 785 A90-46498

KHALAF, A. S.

Combustion process in a gas turbine combustor when using H₂, NH₃ and LPG fuels p 873 A90-46882

KHALAFALLAH, M. G.

Study of various factors affecting secondary loss vortices downstream a straight turbine cascade [ASME PAPER 89-GT-12] p 287 A90-23757

- KHALID, M.**
Wind tunnel results and numerical computations for the NAE deHavilland series of natural laminar flow airfoils
p 628 A90-42403
- New transonic test sections for the NAE 5 ft x 5 ft trisonic wind tunnel
[AD-A220933] p 674 N90-24278
- KHALID, S. J.**
Propulsion system flight test analysis using modeling techniques
[AIAA PAPER 90-3288] p 853 A90-48874
- KHAN, M. M. S.**
Application of active noise control to model propeller noise
p 548 A90-34091
- KHAN, M. Z. SHAH**
A corrosion fatigue/stress corrosion testing facility at Materials Research Laboratory
[MRL-TN-568] p 527 N90-21044
- KHAN, S.**
Composites for aerospace application from Kevlar aramid reinforced PEKK thermoplastic
p 946 A90-50176
- KHAN, T.**
Recent and prospective developments in single-crystal superalloys for the blades of advanced turbines
p 355 A90-24288
- The anisotropy of the mechanical behaviour in nickel-based single crystal superalloys for turbine blades
[ONERA, TP NO. 1989-205] p 355 A90-25339
- Development of a new nickel based single crystal turbine blade alloy for very high temperatures
[ONERA, TP NO. 1989-206] p 356 A90-25340
- KHARAZIAN, L. G.**
Some aspects of the control system and power unit lead tests using in-flight simulator systems and flying test-beds
[AIAA PAPER 90-1323] p 580 A90-36031
- KHARITONOV, A. M.**
Aerodynamic interference of prismatic engine nacelles with the wing at supersonic velocities
p 294 A90-24078
- KHARRAZI, MELANIE M.**
Graphical interface tools for an avionics system
[AIAA PAPER 89-3130] p 75 A90-10606
- KHIZHNIK, ARNOLD N.**
The economics of the organization and the planning of civil aviation
p 897 A90-46629
- KHLEBNIKOV, V. S.**
Aerodynamic drag of a pair of bodies in transonic and supersonic flow
p 710 A90-44935
- KHODADADI, J. M.**
Effects of turbulence model constants on computation of confined swirling flows
p 444 A90-27999
- KHODADOUST, A.**
Measured aerodynamic performance of a swept wing with a simulated ice accretion
[AIAA PAPER 90-0490] p 557 A90-37063
- KHOSLA, P. K.**
A flux-split solution procedure for unsteady inlet flows
[AIAA PAPER 90-0585] p 314 A90-26967
- Transient behavior of supersonic flow through inlets
[AIAA PAPER 90-2130] p 704 A90-42734
- Composite reduced Navier Stokes procedures for flow problems with strong pressure interactions
[AD-A219621] p 689 N90-23687
- KHOSROVANEH, A. K.**
Simplified analysis of helicopter fatigue loading spectra
p 336 A90-26758
- Fatigue life estimates for helicopter loading spectra
p 772 A90-45324
- Fatigue life estimates for helicopter loading spectra
[NASA-CR-181941] p 279 N90-16294
- KHOSROVANEH, ABOLHASSAN KHOSROW**
Fatigue analysis and reconstruction of helicopter load spectra
p 206 N90-14304
- KHRABROV, A. N.**
Nonsymmetric vortex breakdown and aerodynamic hysteresis in flow past a low-aspect-ratio wing/fuselage configuration
p 294 A90-24076
- KHRAISHI, NASSER M.**
Propulsion system design specifications based on STOVL flight control requirements
[AIAA PAPER 90-3227] p 839 A90-49112
- KHUDENKO, B. G.**
Calculation of the efficiency of an active partial-admission gas turbine for counterpressures varying over a wide range
p 850 A90-46495
- KHUDIAKOV, G. E.**
Effect of incoming flow turbulence on the aerodynamic characteristics of a smooth symmetric body at large angles of attack
p 904 A90-50817
- KIBLER, D. F.**
Analytical and experimental study of runway runoff with wind effects
[PTI-8948] p 123 N90-12627
- KIDD, DAVID L.**
Evolution and test history of the V-22 0.2-scale aeroelastic model
p 831 A90-46954
- KIDD, JAMES A.**
Drag reduction by controlling flow separation using stepped afterbodies
p 622 A90-40690
- KIEFER, YALE F.**
Supersonic STOVL - The future is now
p 732 A90-44781
- KIERAS, JIM**
Helicopter surveillance - A look at current and proposed future programs
p 642 A90-39986
- KIERSZKO, ZBIGNIEW**
Laboratory analysis of antiwear properties of turbine-engine fuels
p 131 A90-15878
- KIESSLING, F.**
Recent results of numerical flutter studies in high performance gliders
[DGLR PAPER 88-038] p 934 A90-50249
- KIESSLING, FRITZ**
On simplified analytical flutter clearance procedures for light aircraft
[DLR-FB-89-56] p 672 N90-24276
- KIHARA, MASAHIKO**
Robust control system design synthesis with observers
p 375 A90-25994
- KIHM, K. D.**
Laser Doppler velocimetry investigation of swirler flowfields
p 682 A90-40929
- KIKER, R.**
JFS190 turbine engine performance optimized using Taguchi methods
[AIAA PAPER 90-2419] p 663 A90-42169
- KIKUCHI, KAZUO**
Flow dependent grid for aerodynamic designers
p 306 A90-25831
- KIKUNO, EIJI**
Investigation of ATP blades, part 2. Validation of two-dimensional viscous flow simulation codes around thin airfoils
[NAL-TR-1046] p 912 N90-29326
- KILCHERT, L.**
Four-dimensional navigation and Flight Management Systems
p 826 N90-27681
- KILFORD, R. I.**
A study of the technology required for advanced vertical take-off aircraft
[ETN-90-96786] p 650 N90-24268
- KILGORE, J. J.**
Test results for turbulent annular seals, using smooth rotors and helically grooved stators
[ASME PAPER 89-TRIB-11] p 537 A90-33556
- KILGORE, ROBERT A.**
Cryogenic wind tunnels in Japan
p 523 A90-34228
- Cryogenic wind tunnels
p 673 A90-41726
- Other cryogenic wind tunnel projects
p 263 N90-15948
- KILGORE, W. ALLEN**
Subsonic sting interference on the aerodynamic characteristics of a family of slanted-base ogive-cylinders
[NASA-CR-4299] p 633 N90-24242
- KILLEN, GARY A.**
Advanced technology MMW seeker testbed, a multi-technology demonstration sensor
p 488 A90-34143
- KILLINGSWORTH, E. C., JR.**
Requirements for business jet aircraft
[AIAA PAPER 90-2038] p 644 A90-41991
- KILLION, STEPHEN W.**
Flight tests of Adaptive Fuel Control and decoupled rotor speed control systems
p 422 A90-28183
- KILMER, FRANK**
Near-term applications of knowledge based systems to combat helicopters
[AIAA PAPER 90-3301] p 847 A90-48883
- KIM, A. IU.**
An experimental study of the combined effect of longitudinal riblets and vortex breakers on turbulent friction
p 805 A90-46565
- KIM, DOHOON**
Feasibility study for a microwave-powered ozone sniffer aircraft
[NASA-CR-186660] p 650 N90-23397
- KIM, E.**
Rotorcraft pursuit-evasion in nap-of-the-earth flight
[AIAA PAPER 90-3455] p 786 A90-47707
- KIM, H. T.**
Viscous flow around a propeller-shaft configuration with infinite-pitch rectangular blades
p 683 A90-40938
- KIM, HYOUNG-TAE**
Computation of viscous flow around a propeller-shaft configuration with infinite-pitch rectangular blades
p 481 N90-20958
- KIM, HYUN JIN**
Three-dimensional adaptive grid generation on a composite-block grid
p 374 A90-25289
- KIM, I.**
Navier-Stokes simulation of unsteady supersonic cavity flowfield with passive control
[AIAA PAPER 90-3101] p 796 A90-45913
- KIM, J.-J.**
Flow field measurements near a fighter model at high angles of attack
[AIAA PAPER 90-1431] p 559 A90-37968
- KIM, JONG SEONG**
Hot-wire measurements of near wakes behind an oscillating airfoil
p 154 A90-18138
- KIM, K. S.**
Elevated temperature crack growth
[NASA-CR-182247] p 777 N90-26355
- KIM, KI-CHUNG**
Aeroelastic analysis of helicopter rotor blades with advanced tip shapes
[AIAA PAPER 90-1118] p 392 A90-29390
- KIM, KWANG-SOO**
Skin friction measurements by laser interferometry in swept shock/boundary-layer interactions
p 154 A90-18153
- Skin friction measurements by laser interferometry in supersonic flows
p 317 N90-17557
- KIM, KYUN O.**
Analysis of aircraft tires via semianalytic finite elements
p 496 A90-34740
- Frictionless contact of aircraft tires
[SAE PAPER 892350] p 733 A90-45501
- KIM, S. J.**
Finite element analysis of the flow of a propeller on a slender body with a two-equation turbulence model
p 210 A90-18340
- KIM, WALTER S.**
Attachment of lead wires to thin film thermocouples mounted on high temperature materials using the parallel gap welding process
[NASA-TM-102442] p 543 N90-21361
- KIMBROUGH, A. J.**
UHB demonstrator interior noise control flight tests and analysis
[NASA-CR-181897] p 140 N90-13198
- KINAL, G. V.**
International satellite radionavigation and radiolocation - Choosing among the options
p 96 A90-13979
- KINAL, GEORGE**
An international civil integrity complement to GPS and GLONASS
p 821 A90-46392
- Time synchronization/distribution applications of navigation signals repeated by geostationary satellites
p 872 A90-46397
- KINARD, TOM A.**
Supersonic boundary layer stability analysis with and without suction on aircraft wings
p 148 A90-16792
- KIND, R. J.**
Flow in a centrifugal fan of the squirrel cage type
[ASME PAPER 89-GT-52] p 289 A90-23778
- KINDELSPIRE, DAVID W.**
Freestream turbulence effects on airfoil boundary-layer behavior at low Reynolds numbers
p 554 A90-35768
- KINDER, J. B.**
Commonality of MASA modules
p 462 A90-30816
- KINDRED, ERICK D.**
The Real Time Display Builder (RTDB)
p 546 N90-20656
- KING, ANDREW MARK**
Discretization and model reduction for a class of nonlinear systems
p 198 N90-13397
- KING, BRIAN W.**
Fluctuating wind forces measured on a bluff body extending from a cavity
[AD-A216414] p 371 N90-18020
- KING, E. W.**
Application of CFD to pitch/yaw thrust vectoring spherical convergent flap nozzles
[AIAA PAPER 90-2023] p 657 A90-40597
- KING, H. H. C.**
Rapid prediction of slender-wing-aircraft stability characteristics
[AIAA PAPER 90-0301] p 163 A90-19782
- Rapid prediction of slender-wing aircraft dynamics
[AIAA PAPER 90-3037] p 791 A90-45876
- KING, P. I.**
Aerodynamic testing of a new semi-prone ejection seat design
[AIAA PAPER 90-0234] p 182 A90-19748
- Electrical analog circuit for heat transfer measurements on a flat plate simulating turbine vane heat transfer in turbulent flow
[AIAA PAPER 90-2412] p 687 A90-42164
- Effect of riblets on flow separation in a subsonic diffuser
p 712 A90-45261

KING, PAUL A.

A computational model for thickening boundary layers with mass addition for hypersonic engine inlet testing [AIAA PAPER 90-2219] p 705 A90-42750

KING, PAUL I.

Effects of inlet turbulence scale on turbine blade surface heat transfer in a linear cascade [AIAA PAPER 90-2264] p 768 A90-42761

KINGCOMBE, R. C.

Aerodynamic and heat transfer measurements on blading for a high rim-speed transonic turbine [ASME PAPER 89-GT-228] p 293 A90-23883

Aerodynamic and heat transfer measurements on blading for a high rim-speed transonic turbine [RAE-TM-P-1151] p 256 N90-15920

KINGTON, H.

Development of impact design methods for ceramic gas turbine components [AIAA PAPER 90-2413] p 687 A90-42165

KINGTON, HARRY L.

Probabilistic design technology for ceramic components p 601 A90-35507

KINKEAD, E. R.

The acute, delayed neurotoxicity evaluation of two jet engine oil formulations [AD-A222018] p 875 N90-26972

KIRBY, M.

A proper orthogonal decomposition of a simulated supersonic shear layer p 904 A90-51009

KIRBY, MARK S.

Ultrasonic techniques for aircraft ice accretion measurement p 485 N90-20926

KIRBY, PETER J.

Fiber-optic turbine inlet temperature measurement system (FOTITMS) [AIAA PAPER 90-2033] p 657 A90-40603

KIRCHNER, MARK E.

Laminar flow: Challenge and potential p 90 N90-12504

KIRDEIKIS, JEFF

Evaluation of nonlinear motion-drive algorithms for flight simulators [UTIAS-TN-272] p 761 N90-25148

KIRILLOV, I. I.

An experimental study of the gasdynamic characteristics of annular nozzle cascades with small flow exit angles p 255 A90-23409

KIRK, G. E.

Material requirements for future aeroengines p 62 A90-12534

Material requirements for future aeroengines [PNR90595] p 116 N90-12610

Composite materials for future aeroengines [PNR90584] p 127 N90-12667

The impact and requirements of new materials on aeroengines [PNR90671] p 750 N90-26003

KIRK, R. G.

Advanced analysis of multi-ring liquid seals p 880 A90-46236

KIRK, R. GORDON

Analysis of thermal gradient effects in oil ring seals p 682 A90-40716

KIRKPATRICK, D. L. I.

Priorities for high-lift testing in the 1990s [AIAA PAPER 90-1413] p 596 A90-37950

KIRSTETTER, B.

PHARE: Concept and programme p 827 N90-27690

KIRZNER, R. A.

A minimal permissible radial clearance in a gas turbine p 110 A90-14569

KISELEV, V. I.

Multiple-step terminal control with parameter identification and prediction during flight vehicle descent p 872 A90-46484

KISHI, KAZUSHI

Hot-gas corrosion test of Si3N4 and SiC p 531 A90-33987

KISHI, TERUO

MRS International Meeting on Advanced Materials, 1st, Tokyo, Japan, May 31-June 3, 1988, Proceedings. Volume 5 - Structural ceramics/Fracture mechanics' p 599 A90-35926

KISHIMOTO, Y.

Adaptive flight control of CCV aircraft with limiting zeros [AIAA PAPER 90-3409] p 864 A90-47864

KISSINGER, R. DOHN

The challenge of demonstrating the X-30 p 659 A90-41162

KISSINGER, ROBERT D.

Powder metallurgy and oxide dispersion processing of superalloys p 531 A90-34158

KISSLINGER, ROBERT L.

Lessons learned in the development of a multivariable control system p 432 A90-30713

KITAGAWA, MASAKI

Life prediction and fatigue p 532 A90-34163

KITAGAWA, TETSUYA

Fast adaptive grid method for compressible flows p 445 A90-28006

KITANO, A.

Mechanical influences on crystallization in PEEK matrix/carbon fiber reinforced composites p 949 A90-50227

KITAPLIOGLU, CAMIT

Analysis of small-scale rotor hover performance data [NASA-TM-102271] p 540 A90-20325

KITTUR, MADAN G.

Finite element mesh refinement criteria for stress analysis p 273 A90-23013

KIVLIGHN, H. D., JR.

Grumman/FAA lightning study - A potential countermeasure for lightning induced flashblindness of aircrew members p 819 A90-49843

KJELGAARD, SCOTT O.

An embedded grid formulation applied to a delta wing [AIAA PAPER 90-0429] p 229 A90-22216

KLAASS, FRED

Advanced power system for 21st century fighter aircraft p 508 A90-33347

KLAASS, R. M.

Power system for 21st century fighter aircraft [SAE PAPER 892253] p 746 A90-45455

KLABOCH, LADISLAV

LDA processor TSI model 1990 analog input module reconstruction p 451 A90-29654

KLAUSING, HELMUT

ROSAR (Helicopter-Rotor based Synthetic Aperture Radar) p 541 A90-21229

KLEB, WILLIAM L.

Temporal-adaptive Euler/Navier-Stokes algorithm for unsteady aerodynamic analysis of airfoils using unstructured dynamic meshes [AIAA PAPER 90-1650] p 569 A90-38778

KLEIN, A. DAVID

Integrated navigation/flight control for future high performance aircraft p 917 N90-29362

KLEIN, H. L.

Benefits of advanced materials, structures, and aerodynamics in future high speed civil transport propulsion systems [AIAA PAPER 90-3285] p 853 A90-48872

KLEIN, HERMANN

General buckling tests with thin-walled shells [DLR-MITT-89-13] p 213 N90-13816

KLEIN, JOHN R.

Design and experimental verification of an equivalent forebody representation of flowing inlets p 152 A90-17863

KLEIN, K.

The evaluation of flight recorders p 653 A90-41729

KLEIN, KURT

Automation of the readout, transcription and evaluation of digital flight data at DLR p 893 N90-27645

KLEIN, MARK H.

Inertial navigation system simulator: Behavioral specification, revision [AD-A219294] p 578 N90-22554

KLEIN, VLADISLAV

Optimal input design for aircraft parameter estimation using dynamic programming principles [AIAA PAPER 90-2801] p 753 A90-45157

Aerodynamic parameters of High-Angle-of attack Research Vehicle (HARV) estimated from flight data [NASA-TM-102692] p 936 N90-28578

KLEINMEYER, JAMES D.

Applications of digital image processing in testing and evaluation of composite materials [AD-A222939] p 874 N90-26887

KLEISS, JAMES A.

Terrain visual cue analysis for simulating low-level flight: A multidimensional scaling approach [AD-A223564] p 938 N90-29407

KLEMBOWSKI, WIESLAW

Design of new Polish primary radars AVIA DM/CM p 638 A90-41035

KLEVENHUSEN, K. D.

The precise calculation of the inviscid leading edge flow on a laminar airfoil using simple methods and verification by measurements on the TLF pilot model p 277 N90-16180

KLEVENOW, F. T.

The Helicopter Antenna Radiation Prediction Code (HARP) [NASA-CR-186925] p 884 N90-27946

KLEWE, H.-J.

Testing facility and procedure of the ATTAS on-board data acquisition system p 39 A90-12202

KLIMETZEK, F.

Inverse computation of transonic internal flows with application for multi-point-design of supercritical compressor blades p 501 N90-20987

KLINE, TODD

High level language programming for avionic vector processors [AIAA PAPER 89-3107] p 74 A90-10589

KLINBERG, JOHN M.

Advances in computational design and analysis of airbreathing propulsion systems p 43 A90-12502

KLINGLE-WILSON, D.

Wind shear detection with pencil-beam radars p 279 A90-21386

KLISS, MARK HOLCOMBE

Neurocontrol systems and wing-fluid interactions underlying dragonfly flight p 434 N90-19240

KLOOP, R. W.

Influence of microstructure and microdamage processes on fracture at high loading rates [AD-A210307] p 65 N90-10253

KLOPPER, G. H.

High-resolution shock-capturing schemes for inviscid and viscous hypersonic flows p 476 A90-34545

KLOSE, A.

A comparison of flutter calculations based on eigenvalue and energy method p 425 N90-18406

KLUNOVER, A.

Application of a multiblock grid generation approach to aircraft configurations p 310 A90-26527

KLUWICK, A.

Marginal separation of laminar axisymmetric boundary layers p 1 A90-10074

KLUWICK, ALFRED

Asymptotic analysis of transonic flow through oscillating cascades p 427 N90-18421

KNAACK, MARCELLE S.

Encyclopedia of US Air Force aircraft and missile systems. Volume 2: Post-World War 2 bombers, 1945-1973 [AD-A209273] p 1 N90-10001

KNELLER, EDWARD W.

Model-based method for terrain-following display design [AD-A219302] p 583 N90-22563

KNEPPE, G.

Multicriteria optimal layouts of aircraft and spacecraft structures p 889 A90-46046

KNEPPE, GUENTER

Development and application of an optimization procedure for space and aircraft structures p 679 A90-39186

Development and application of an optimization procedure for space and aircraft structures [MBB-FW-522/S/PUB-383] p 779 N90-25078

KNAZEVE, V. V.

Fundamentals of turbine design for aircraft engines p 40 A90-10839

KNIP, GERALD, JR.

Advanced core technology - Key to subsonic propulsion benefits [ASME PAPER 89-GT-241] p 342 A90-23890

KNIPPRATH, GEORGE

Noise and sonic boom impact technology. Effects of aircraft noise and sonic booms on structures: An assessment of the current state-of-knowledge [AD-A213919] p 378 N90-17409

KNISKERN, MARC W.

Analysis of a six-component, flow-through, strain-gage, force balance used for hypersonic wind tunnel models with scramjet exhaust flow simulation [NASA-CR-186585] p 597 N90-21775

KNOBBE, EDWARD J.

Control and estimation for aerospace applications with system time delays p 918 N90-29367

KNOSPE, CARL R.

Adaptive control of helicopter vibrations via the impulse response method [AD-A213728] p 260 N90-15113

KNOSPE, CARL RICHARD

Adaptive control of a system with periodic dynamics: Application of an impulse response method to the helicopter vibration problem p 694 N90-23990

KNOTTS, LOUIS

Use of ground-based and in-flight simulation for flight control system development [AIAA PAPER 90-1286] p 519 A90-33907

KNOWLEN, C.

Operation of the ram accelerator in the transdetonative velocity regime [AIAA PAPER 90-1985] p 741 A90-42712

KNOWLES, G. E.

Fuel tank explosion protection p 251 N90-15914

KNOWLES, K.

Use of swirl for flow control in propulsion nozzles p 421 A90-27963

- Numerical modeling of an impinging jet in cross-flow
[AIAA PAPER 90-2246] p 686 A90-42093
Transonic flow computations in convergent propulsion
nozzles using the time-dependent mode p 708 A90-44459
- KNOX, CHARLES E.**
Description of the primary flight display and flight
guidance system logic in the NASA B-737 transport
systems research vehicle
[NASA-TM-102710] p 927 N90-28546
- KO, FRANK K.**
Engineering design of tough ceramic matrix composites
for turbine components
[ASME PAPER 89-GT-294] p 343 A90-23892
- KO, S. H.**
Power dissipation in smooth and honeycomb labyrinth
seals
[ASME PAPER 89-GT-220] p 362 A90-23881
- KO, TSE-HAO**
The changes of structures and properties in PAN-based
carbon fibers during heat treatment in carbon dioxide
p 945 A90-50145
- KO, W. L.**
Application of fracture mechanics and half-cycle method
to the prediction of fatigue life of B-52 aircraft pylon
components
[NASA-TM-88277] p 214 N90-13820
- KO, WILLIAM L.**
Optimum element density studies for finite-element
thermal analysis of hypersonic aircraft structures
[NASA-TM-4163] p 369 N90-17074
- KOBAYAKAWA, MAKOTO**
Application of a digital control theory for generating
adaptive grids p 366 A90-25734
Flow field around an oscillating cascade p 814 A90-49459
- KOBAYASHI, DOUGLAS N.**
CF 18 480 Gallon External Fuel Tank Stores Clearance
Program p 35 N90-10877
- KOBAYASHI, HIDEO**
Development of new segment carbon seal for use at
low sealing pressure region FJR710/600S turbo fan
engine p 69 A90-11950
The features of FJR 710 engine p 42 A90-12011
Start characteristics of FJR 710/600S engine p 42 A90-12013
Expert diagnosis system for FJR engine troubles p 587 A90-38597
- KOBAYASHI, HIROSHI**
Rotor-blades excitation due to differential interference
of vane wakes between upstream stator-rows in an axial
compressor p 6 A90-11784
Navier-Stokes simulations around a high-speed
propeller p 305 A90-25797
- KOBAYASHI, T.**
Influence of microstructure and microdamage processes
on fracture at high loading rates
[AD-A210307] p 65 N90-10253
- KOBELEV, V. V.**
Divergence of thin-walled composite rods of closed
profile in gas flow p 388 A90-29012
- KOBYLARZ, T.**
Flight controller design with nonlinear aerodynamics,
large parameter uncertainty, and pilot compensation
[AIAA PAPER 90-3478] p 866 A90-47728
- KOBZEV, V. I.**
Determination of the extreme values of the efficiency
criteria for a flight vehicle control system in the probable
scatter range of its characteristics p 859 A90-46569
- KOCH, A.**
Applications of LIF to high speed flows p 911 N90-29320
- KOCH, STEPHEN B.**
Thermoplastic composite fighter forward fuselage
p 81 A90-14659
- KOCHIN, V. A.**
Relationship between velocity circulation around a wing
profile and vorticity dispersion in a boundary layer p 620 A90-39539
- KOCUREK, J. DAVID**
Rotorwash flow fields - Flight test measurement,
prediction methodologies, and operational issues p 817 A90-46930
- KODAMA, H.**
Unsteady lifting surface theory for a rotating cascade
of swept blades
[ASME PAPER 89-GT-306] p 906 A90-51259
- KODRES, C. A.**
Experimental examination of the aerothermal
performance of a gas turbine engine test facility
[ASME PAPER 89-GT-94] p 341 A90-23810
- KOEHLER, H. DIETER**
On the occasion of the 100th birthday of Ernst
Heinkel
[MBB/LW/3015/S/PUB/321] p 141 N90-12494
- KOEHLER, M. G.**
Advanced fuel properties, phase 1
[AD-A219788] p 766 N90-25236
- KOEHLER, R.**
GRATE: A new flight test tool for flying qualities
evaluation p 34 N90-10868
- KOELMAN, H. J. W. M.**
COCOMAT: A Computer Aided Engineering (CAE)
system for composite structures design
[NLR-MP-87078-U] p 462 N90-19756
- KOENIG, H. G.**
A measurement window for a cryogenic windtunnel
p 523 A90-34233
- KOENIG, HERBERT**
OPST1 - An optical yaw control system for high
performance helicopters p 430 A90-28220
- KOENIG, KLAUS**
Gyroscopic matrices in computation of vibration
p 547 A90-33381
Short time Force and moment measurement System
for shock tubes (SFS) for measuring times less than 10
ms p 674 N90-24233
Short time-dynamometer system for shock wave
channels
[MBB-UT-115/89-PUB] p 773 N90-25084
- KOENIG, R.**
Monitoring and controlling flight in windshear
p 820 N90-27641
- KOENIG, REINHARD**
Aircraft response and pilot behaviour during a wake
vortex encounter perpendicular to the vortex axis
p 259 N90-15057
- KOEPP, F.**
Airborne CO2 Doppler lidar for wind shear detection
p 849 N90-27640
- KOERNER, H.**
Natural laminar flow research for subsonic transport
aircraft in the FRG p 2 A90-10137
- KOESTER, H.**
Design for a natural laminar flow glove for a transport
aircraft
[AIAA PAPER 90-3043] p 792 A90-45880
Determination of the N-factor in the Brunswick (Federal
Rep. of Germany) transonic wind tunnel using
measurements of pressure distributions and transition
points, and the Sally method p 276 N90-16177
Aerodynamic design techniques at DLR Institute for
Design Aerodynamics p 500 N90-20979
- KOGA, DENNIS J.**
Unsteady, separated flow behind an oscillating,
two-dimensional spoiler p 469 A90-32462
Active control of unsteady and separated flow
structures
[AD-A212109] p 89 N90-11707
- KOGAN, A.**
The calculation of incompressible separated turbulent
boundary layers p 905 A90-51025
- KOGLER, THOMAS R.**
Modeling the effects of the use of GPS (Global
Positioning System) derived altitude indication in the C-17A
airdrop system
[AD-A215366] p 333 N90-16748
- KOHYAR, F. A.**
Aerodynamics of store separation p 629 A90-42418
- KOHLI, DALIP K.**
Development of a high toughness heat resistant 177
C (350 F) curing film adhesive for aerospace bonding
applications - FM 377 adhesive p 955 A90-50126
- KOHN, STARR D.**
Development of a thickness design procedure for
stabilized layers under rigid airfield pavements
[DOT/FAA/RD-90/22] p 937 N90-28582
- KOKULUS, JAROSLAV**
Operating principles of a terrain-recognition air
navigation system p 403 A90-29655
- KOLAR, RAMESH**
An approach for analysis and design of composite rotor
blades
[AIAA PAPER 90-1005] p 449 A90-29276
- KOLARIK, ANN L.**
Strength substantiation of the all composite airframe (A
materials data base approach) p 490 A90-31519
- KOLDEN, J. J.**
A method of sizing multi-cycle engines for hypersonic
aircraft
[ASME PAPER 89-GT-281] p 507 A90-32261
- KOLEGAR, C. E.**
Design and test of a natural laminar flow/large Reynolds
number airfoil with a high design cruise lift coefficient
p 93 N90-12543
- KOLESHNIKOV, O. M.**
Effect of hydrogen combustion in a supersonic boundary
layer on friction coefficient p 355 A90-24116
- KOLESOV, A. N.**
An investigation of the flow characteristics of transonic
nozzle blades p 475 A90-33700
- KOLITZ, STEPHAN E.**
Real-time adaptive aircraft scheduling
[NASA-CR-177558] p 820 N90-27669
- KOLKMAN, H. J.**
Quench sensitivity of airframe aluminium alloys
p 765 A90-44348
Coatings for gas turbine compressors
[NLR-MP-88045-U] p 115 N90-11750
- KOLKMEIER, THOMAS J.**
Challenges of tomorrow - The future of secure
avionics p 419 A90-30723
- KOLLER, FRANZ**
Asymptotic analysis of transonic flow through oscillating
cascades p 427 N90-18421
- KOLODY, D.**
RAIM - An implementation study p 726 A90-43714
- KOLOTHNIKOV, M. E.**
Estimation of the safety factor of turbine blades under
thermal cycling and vibration loading p 958 A90-52356
- KOLTON, G. A.**
Irregular interaction of a strong shock wave with a thin
profile p 9 A90-12267
- KOMERATH, N. M.**
Measurement of the interaction between a rotor tip
vortex and a cylinder p 555 A90-36255
Flow field measurements near a fighter model at high
angles of attack p 559 A90-37968
Numerical simulation of the growth of instabilities in
supersonic free shear layers p 623 A90-40941
The Second ARO Workshop on Rotorcraft Interactional
Aerodynamics
[AD-A223310] p 911 N90-29304
- KOMERATH, NARAYANAN**
Prediction and measurement of the aerodynamic
interactions between a rotor and airframe in forward
flight p 384 A90-28176
- KOMET, Y.**
A multichannel wide FOV infrared radiometric system
p 67 A90-11410
- KOMOROWSKI, J. P.**
A technique for rapid impact damage detection with
implication for composite aircraft structures p 600 A90-37662
- KOMOROWSKI, JERZY P.**
A technique for rapid inspection of composite aircraft
structure for impact damage p 846 A90-28077
- KOMURO, T.**
Some governing parameters of plasma torch
igniter/flameholder in a scramjet combustor
[AIAA PAPER 90-2098] p 661 A90-42017
- KOMURO, TOMOYUKI**
Experimental study on autoignition in a scramjet
combustor p 46 A90-12559
- KONDO, K.**
CRL's mobile satellite communication experiments using
ETS-V
[AIAA PAPER 90-0775] p 366 A90-25602
- KONDO, Y.**
Application of the 'K-gage' to aircraft structural testing
p 926 A90-49891
- KONDRASHOV, A. A.**
A parametric optimization algorithm for the electrical
distribution circuits of civil aircraft p 255 A90-23417
- KONDRATEV, A. B.**
Stiffness of an aircraft pneumatic rudder drive
p 828 A90-46479
- KONDRATEV, I. A.**
A study of the laminar-turbulent boundary layer transition
on the windward side of a delta wing with a conical
surface p 298 A90-24144
- KONG, RELIAN**
The design of the series of blade flutter rotor and the
experimental investigation of flow-induced vibration
p 586 A90-37230
- KONG, ZUKAI**
Experimental investigation on composite cooling of a
turbine blade p 190 A90-17794
Experimental investigation of external heat transfer
coefficients on film-cooled turbine blade leading edge
p 585 A90-36787
- KONIUKHOV, B. M.**
A method for the computer-aided hydraulic analysis of
the turbine cooling systems of aviation gas turbine
engines p 255 A90-23430
- KONONOV, K. M.**
Strength of the guide vane components of gas
turbines p 266 A90-21318
- KONSTYONO, HARIANTO**
Development of airborne data reduction system in IPTN
flight test p 418 A90-28895
- KOONCE, JEFFERSON M.**
Another look at aircraft accident statistics
p 322 A90-26301

- KOOP, W. E.**
Metal matrix composites structural design experience
[AIAA PAPER 90-2175] p 677 A90-42059
Metal matrix composite fan blade development
[AIAA PAPER 90-2178] p 677 A90-42062
- KOPELEV, S. Z.**
Fundamentals of turbine design for aircraft engines
p 40 A90-10839
- KOPPA, RODGER J.**
Considerations of noise for the use of compressed
speech in a cockpit environment p 404 A90-31334
- KOPPAM, VIJAY**
Noise and sonic boom impact technology. Effects of
aircraft noise and sonic booms on structures: An
assessment of the current state-of-knowledge
[AD-A213919] p 378 N90-17409
- KOPPENWALLNER, G.**
Rarefied gas dynamics p 224 A90-21163
European research and testing facilities requested for
participation to SST/HST projects
[ONERA, TP NO. 1990-12] p 351 A90-25358
- KORABLEV, ALEKSANDR N.**
Radio deviation of airborne goniometers
p 242 A90-22733
- KORAKIANITIS, THEODOSIOS P.**
The effect of the magnitude of the inlet-boundary
disturbance on the unsteady forces on axial gas-turbine
blades p 6 A90-11781
- KORDIUK, V. N.**
Optimal blading density in axial-flow compressor stages
with a developed three-dimensional flow
p 851 A90-46505
- KORDULLA, W.**
Numerical simulation of hypersonic viscous continuum
flow p 707 A90-44407
European research on viscous flow (EuroVisc)
[NLR-TP-89077-U] p 609 N90-22014
- KOREN, BAREND**
Multigrid and defect correction for the steady
Navier-Stokes equations: Applications to aerodynamics
[ETN-90-96011] p 212 N90-13727
- KORENROMP, W.**
Fire safety in civil aviation p 325 N90-17586
- KORGEL, CLAYTON C.**
Advanced architecture for domestic and global aviation
systems p 822 A90-46398
- KORKAN, K. D.**
A study of ice shape prediction methodologies and
comparison with experimental data
[AIAA PAPER 90-0753] p 322 A90-26986
Ice induced aerodynamic performance degradation of
rotorcraft: An overview p 248 N90-15063
- KORKAN, KENNETH D.**
An approximation model for the performance and
acoustic predictions of counterrotating propeller
configurations
[AIAA PAPER 90-0282] p 378 A90-26931
- KORKOSZ, G.**
Plan, execute, and discuss vibration measurements and
correlations to evaluate a NASTRAN finite element model
of the AH-64 helicopter airframe
[NASA-CR-181973] p 960 N90-28866
- KORNBERGER, M.**
Development of two multi-sensor hot-film measuring
techniques for free-flight experiments
p 417 A90-28291
- KORNEEVA, T. V.**
Some problems on 'intelligence' of wind tunnel testing
p 436 A90-28282
- KORNIENKO, E. S.**
Effect of the inertial nature of injection and temperature
on the damping of body vibrations p 150 A90-17112
- KORNREICH, STUART**
The two level maintenance - I level dilemma
p 381 A90-28319
- KOROTKOV, IU. V.**
Some characteristics of interference between shock
waves and the aerodynamic wake behind a body
p 804 A90-46551
- KOROVIN, B. B.**
Some aspects of the control system and power unit
lead tests using in-flight simulator systems and flying
test-beds
[AIAA PAPER 90-1323] p 580 A90-36031
- KORS, DAVID L.**
The challenge of demonstrating the X-30
p 659 A90-41162
- KORSUNSKII, M. L.**
Aeroelastic vibrations of turbomachine blades and
propellers p 854 A90-49482
- KORTE, JOHN J.**
Numerical simulation of the actuation system for the
ALDF's propulsion control valve
[AIAA PAPER 90-0079] p 211 A90-19674

- KORTING, P. A. O. G.**
Ultrasonic regression rate measurement in solid fuel
ramjets
[AIAA PAPER 90-1963] p 656 A90-40573
Combustion of PMMA, PE, and PS in a ramjet
p 764 A90-43670
- KOSCHER, W.**
Solid fuel combustion chamber
[LR-634] p 939 N90-29433
- KOSCHEL, W.**
The in service multi-axial-stress situation in an uncooled
gas turbine blade p 423 A90-29880
Analysis of the rotor tip leakage flow with tip cooling
air ejection p 515 N90-21029
Past, present and future: Aircraft integrated monitoring
systems: An ever-developing technology p 848 N90-27618
- KOSCHEL, WULF**
Antenna and radar signature technology at Dornier
p 261 A90-21605
- KOSHINUMA, TAKESHI**
Noncontact measurement of rotating blade vibrations
[NAL-TR-1033] p 961 N90-29687
- KOSHORST, JOHANNES**
Point of view of a civil aircraft manufacturer on Al-Li
alloy p 268 N90-15200
- KOSINOV, A. D.**
Wave structure of artificial perturbations in a supersonic
boundary layer on a plate p 619 A90-39518
- KOSMATKA, J. B.**
Vibration analysis of composite turbopropellers using a
nonlinear beam-type finite-element approach
p 70 A90-12844
Analysis of composite rotor blades via Saint Venant's
solutions p 688 A90-42491
Extension-torsion coupling behavior of advanced
composite tilt-rotor blades p 651 N90-25057
Generalized Advanced Propeller Analysis System
(GAPAS). Volume 2: Computer program user manual
[NASA-CR-185277] p 933 N90-29394
- KOSS, D.**
Low Reynolds number airfoils evaluation program
p 151 A90-17692
Active flow control on low Reynolds number airfoils
[AIAA PAPER 90-3039] p 792 A90-45878
- KOSTEJE, V. K.**
Application of three-dimensional methods for the
calculation of gas dynamic and thermal processes at the
design of gas turbines for air breathing engines
p 46 A90-12552
- KOSTENKO, P. P.**
Estimation of the efficiency of a ramjet engine with a
thermocompressor using fuel conversion products
p 255 A90-23412
- KOSTENKO, V. S.**
An automatic system for the programmed control of the
parameters of the vibrational and thermal testing of the
blades of gas turbine engines p 343 A90-24216
- KOSTIN, G. V.**
Evaluation of the dynamic characteristics of a helicopter
instrument panel p 829 A90-46499
- KOSTIUK, V. I.**
Adaptive automatic control systems. Number 16
p 76 A90-10844
- KOSTRIKIN, V. N.**
Determination of the extreme values of the efficiency
criteria for a flight vehicle control system in the probable
scatter range of its characteristics p 859 A90-46569
- KOSTITSKII, A. S.**
Automation of flight safety control
p 589 A90-36157
- KOSYKH, A. P.**
A study of the laminar-turbulent boundary layer transition
on the windward side of a delta wing with a conical
surface p 298 A90-24144
Laminar separated flow on a biconical body at high
supersonic velocities p 387 A90-28992
- KOTEROV, V. N.**
A numerical method for calculating supersonic flows of
a viscous gas p 476 A90-34672
- KOTHARI, A. P.**
Unsteady hypersonic viscous flow in impulse facilities
[AIAA PAPER 90-0421] p 313 A90-26947
- KOTIUGA, P.**
Development of a robust calculation method for
transonic viscous blade-to-blade flows
p 703 A90-42671
- KOTOVSKII, VLADIMIR N.**
Mathematical modeling of plane parallel separated flows
past bodies p 619 A90-39475
- KOUBA, CARROLL CHARLES**
High temperature VSCF (Variable Speed Constant
Frequency) generator system
[AD-A210823] p 71 N90-10351

- KOUKOUSAKIS, COSTAS E.**
Detachment of turbulent boundary layers with varying
free-stream turbulence and lower Reynolds numbers
p 802 A90-46378
- KOURTA, A.**
Numerical simulation of the compressible flow in a
valve-cylinder assembly p 770 A90-44431
Numerical study of heat transfer for unsteady viscous
supersonic blunt body flows p 707 A90-44432
Development of turbulence models for the analysis of
compressible or incompressible unsteady flow
[ETN-90-97486] p 958 N90-28810
- KOURTIDES, DEMETRIUS A.**
The 1-((diorganooxyphosphonyl)-methyl)-2,4- and
-2,6-diamido benzenes p 532 N90-20133
Some 1-((diorganooxyphosphonyl)-methyl)-2,4- and
-2,6-dinitro-benzenes
[NASA-CASE-ARC-11425-3] p 678 N90-23475
- KOUSEN, KENNETH ARTHUR**
Nonlinear phenomena in computational transonic
aerelasticity p 235 N90-15070
- KOUTMOS, P.**
CFD predictions of lobed mixer flowfields
p 70 A90-12626
Isothermal velocity and turbulence measurements
downstream of a model multilobed turbofan mixer
p 365 A90-24353
Velocity and turbulence characteristics of isothermal
lobed mixer flows p 584 A90-35230
- KOVAL'NOGOV, S. A.**
Investigation of wall pressure pulsations during the
passive control of shock/boundary layer interaction
p 378 A90-24132
- KOVALENKO, T. D.**
Prediction of the strength-related reliability of structural
elements at the design stage p 274 A90-23402
- KOVALENKO, V. V.**
Numerical solution of the problem of supersonic flow
of an ideal gas past a trapezoidal wedge
p 386 A90-28980
- KOVALEV, V. E.**
Application of the inverse method of three-dimensional
boundary layer analysis to the problem of flow past a wing
with allowance for the effect of viscosity
p 804 A90-46548
Determination of the laminar-turbulent transition point
for a turbulent layer on a yawing wing
p 805 A90-46566
- KOVALEVA, N. A.**
Lee-side heating of a delta wing in supersonic flow
p 10 A90-12281
- KOVALEVSKII, A. K.**
Automation of the development of a finite element model
for shells of the wing type p 364 A90-24118
The use of automated parametric analysis for selecting
efficient structural schemes for wings
p 410 A90-29191
- KOVARTSEV, A. N.**
Estimation of the technical risk criterion in selecting the
operating parameters of aircraft gas turbine engines
p 110 A90-14570
- KOVENIA, V. M.**
Numerical modeling of a viscous separated flow in the
near wake p 159 A90-19236
- KOWALSKI, E. J.**
Study of advanced technology impact on cycle
characteristics and aircraft sizing (using multivariable
optimization techniques) p 29 A90-12612
- KOWALSKI, S.**
Automated prepreg tow placement for composite
structures p 954 A90-50113
- KOZEL, KAREL**
Numerical solution of 2D transonic flows in a turbine
cascade p 709 A90-44601
- KOZHEVNIKOV, IU. V.**
Design of a language for the testing of aircraft engines
p 137 A90-14573
Design of computer-aided testing systems for aviation
equipment. I p 222 A90-23416
Automatic testing in aircraft building
p 285 A90-24231
Design of computer-aided aircraft testing systems. II
p 785 A90-46498
- KOZLOV, ANATOLII I.**
Radar systems of aircraft p 26 A90-10841
- KOZLOV, L. F.**
Vortex theory for the screw propeller with a hub
p 620 A90-39538
Relationship between velocity circulation around a wing
profile and vorticity dispersion in a boundary layer
p 620 A90-39539
- KOZLOV, M. S.**
Aviation equipment p 338 A90-24200

- KOZLOV, V. V.**
Investigation of the flow structure behind the rotating blades in the elbow of a wind tunnel in the case of acoustic excitation p 297 A90-24124
Instability and susceptibility of a boundary layer in the vicinity of two-dimensional surface inhomogeneities p 535 A90-32675
A study of boundary layer stability in the case of an increased incoming stream turbulence in gradient flows p 555 A90-36065
Acoustic excitation of boundary layer oscillations on a yawing wing p 805 A90-46567
- KOZLOWSKI, MARC**
The DELTA MONSTER: An RPV designed to investigate the aerodynamics of a delta wing platform [NASA-CR-186226] p 924 A90-29381
- KOZOL, J.**
Al-Li alloys and ultrahigh-strength steels for U.S. Navy aircraft p 599 A90-37441
- KOZOL, JOSEPH**
Microstructural effects of plastic media blasting on graphite epoxy composites [SAE PAPER 890928] p 286 A90-24693
- KOZU, MASAO**
Reynolds number effects on the performance of a turbofan engine [ASME PAPER 89-GT-199] p 342 A90-23871
- KRAEMER, E.**
Euler procedure for calculation of the steady rotor flow with emphasis on wake evolution [AIAA PAPER 90-3007] p 789 A90-45857
Calculation of the flow field of a multiblade helicopter rotor using a Euler method including the wake p 278 A90-16189
- KRAEMER, EWALD**
A study of the influence of a helicopter rotor blade on the following blades using Euler equations p 630 A90-42435
- KRAIN, H.**
Verification of an impeller design by laser measurements and 3D-viscous flow calculations [ASME PAPER 89-GT-159] p 292 A90-23847
Centrifugal impeller geometry and its influence on secondary flows p 513 A90-21020
- KRAINER, A.**
Progress towards the development of an inviscid-viscous interaction method for unsteady flows in turbomachinery cascades p 8 A90-11806
- KRALLIS, G. A.**
Analytical and experimental study of runway runoff with wind effects [PTI-8948] p 123 A90-12627
- KRAMER, A.**
Improved thermal performance using allylnadec-imides p 946 A90-50175
- KRAMER, WILLIAM T. C.**
Effective use of Cray supercomputers p 546 A90-34436
- KRANBUEHL, D.**
In-situ measurement, modelling and control of the imidization reaction in PMR-15 p 941 A90-50066
- KRANTZ, TIMOTHY L.**
Efficiency study comparing two helicopter planetary reduction stages [AIAA PAPER 90-2156] p 956 A90-50644
Efficiency study comparing two helicopter planetary reduction stages [NASA-TM-103106] p 776 A90-26334
- KRANZ, WOLFGANG**
Target classification by vibration sensing p 1 A90-10170
- KRAPIVSKII, P. L.**
Jet flap theory p 298 A90-24154
- KRASHANITSA, I. A.**
The method of matched integral representations in viscous fluid dynamics p 129 A90-14565
- KRASHEINNIKOV, S. I.**
Determination of the effective areas of the mixing exhaust ducts of a bypass engine from autonomous test results p 102 A90-14584
Operation of a gas ejector in the pulsed regime p 850 A90-46488
- KRASIL'SHCHIKOV, MIKHAIL N.**
Optimization of the observations and control of aircraft p 60 A90-12468
- KRASNOWSKI, BOGDAN R.**
Designing rotorcraft dynamic components to reliability requirements p 641 A90-39978
- KRASNYKH, V. L.**
Automatic testing in aircraft building p 285 A90-24231
- KRAUSE, E.**
Numerical studies of incompressible flow around delta and double-delta wings p 150 A90-16845
- The effect of an oscillatory freestream-flow on a NACA-4412 profile at large relative amplitudes and low Reynolds-numbers p 560 A90-38495
- KRAUSZ, A. S.**
A rate theory investigation of cyclic loading and plastic deformation in the high stress and ambient temperature range p 954 A90-49884
- KRAUSZ, K.**
A rate theory investigation of cyclic loading and plastic deformation in the high stress and ambient temperature range p 954 A90-49884
- KRAVCHIK, N. I.**
Generalized relations for estimating the efficiency and basic dimensions of screw pumps and hydraulic turbines of pump units p 111 A90-14583
- KRAVETS, V. V.**
Numerical solution of the problem of supersonic flow of a viscous gas past a concave conical wing p 619 A90-39465
- KRAWCZYK, ANDRZEJ**
NMG - A system of numerical representation of aircraft geometry p 103 A90-15877
- KRAWCZYK, PETER A.**
Fatigue crack growth investigation of a Ti-6Al-4V forging under complex loading conditions: NATO/AGARD supplemental engine disk program [AD-A220239] p 678 A90-23538
- KRAZINSKI, J. L.**
Development of a computational fluid dynamics and chemistry model for the fouling of jet fuels [DE90-005664] p 608 A90-22003
- KRAZINSKI, JOHN L.**
Development of a mathematical model for the thermal decomposition of aviation fuels [AD-A221673] p 875 A90-26994
- KREBBEKK, J. A.**
Repair of composites by means of wet-lay-up [LR-551] p 205 A90-13617
- KREJSA, E. A.**
Mixer-ejector nozzle for jet noise suppression [AIAA PAPER 90-1909] p 894 A90-47202
- KREJSA, EUGENE A.**
Predicted and measured boundary layer refraction for advanced turboprop propeller noise [NASA-TM-102365] p 379 A90-17413
- KREKELER, GREGORY C., JR.**
High angle of attack flying qualities criteria [AIAA PAPER 90-0219] p 197 A90-19738
- KREPEC, T.**
Multivariable optimization scheme for tuning the controller of an electronic fuel control unit for small gas turbine engines p 745 A90-45301
- KREPEC, TADEUSZ**
Designing and tuning the digital controller of an electronic fuel control unit for small gas turbine engines [SAE PAPER 892255] p 747 A90-45457
- KREPLIN, H.-P.**
Experimental investigation of flowfield about a multi-element airfoil p 154 A90-18137
- KRESS, E. J.**
Multiple swirler dome combustor for high temperature rise applications [AIAA PAPER 90-2159] p 661 A90-42050
- KRESSE, JOHN**
An in-flight investigation of ground effect on a forward-swept wing airplane [NASA-TM-101708] p 175 A90-14202
An in-flight investigation of ground effect on a forward-swept wing airplane p 922 A90-28533
- KRETSCHMER, D.**
The performance of a small combustor operated over a wide range of conditions p 45 A90-12548
On the weak extinction of gas turbine combustors p 47 A90-12574
- KRIEGER, KENNETH W.**
Design and development of the Garrett F109 turbofan engine [SAE PAPER 891046] p 109 A90-14350
- KRIER, H.**
Investigation of supersonic mixing layers p 623 A90-40926
- KRIKORIAN, HAIG F.**
Real-time adaptive control of knowledge based avionics tasks p 460 A90-30764
- KRISHNAKUMAR, K.**
Synthesis of a simulator-based automated helicopter hover trainer [AIAA PAPER 90-3481] p 891 A90-47730
Genetic algorithms in control system optimization [AIAA PAPER 90-3488] p 867 A90-47736
A robust wind shear stochastic controller-estimator [AIAA PAPER 90-3489] p 867 A90-47737
- KRISHNAN, M. R.**
Gas turbine engine brush seal applications [AIAA PAPER 90-2142] p 685 A90-42041
- KRISHNAN, P. A.**
Response of orthogonally stiffened cylindrical shell panels p 603 A90-36285
- KRIST, SHERRIE L.**
An embedded grid formulation applied to a delta wing [AIAA PAPER 90-0429] p 229 A90-22216
- KRIST, SHERRIE TAYLOR**
Navier-Stokes computations of vortical flows over low-aspect-ratio wings p 232 A90-23103
- KRIUCHKOV, E. I.**
Wing design optimization under stress-strain constraints using full-strength and minimum mass criteria p 804 A90-46554
- KRIVENTSEV, V. I.**
A parametric optimization algorithm for the electrical distribution circuits of civil aircraft p 255 A90-23417
- KROGMANN, P.**
Applications of LIF to high speed flows p 911 A90-29320
- KROGMANN, UWE**
Integration and automation of navigation functions using Kalman filters p 915 A90-52615
- KROLL, N.**
Analysis of three-dimensional aerospace configurations using the Euler and Navier-Stokes equations p 305 A90-25798
- KROLL, NORBERT**
Computation of flow fields around propellers and hovering rotors based on the solution of the Euler equations [DLR-FB-89-37] p 170 A90-13333
- KRONE, NORRIS J., JR.**
X-wing experimental aircraft - Lessons learned [AIAA PAPER 90-3208] p 838 A90-49105
- KROO, ILAN**
A numerical method for relating two- and three-dimensional pressure distributions on transonic wings [AIAA PAPER 90-3211] p 812 A90-46837
A method for lifting surface design using nonlinear optimization [AIAA PAPER 90-3290] p 813 A90-49122
The aerodynamic design of the oblique flying wing supersonic transport [NASA-CR-177552] p 923 A90-28540
- KROO, ILAN M.**
Design synthesis and optimization of joined-wing transports [AIAA PAPER 90-3197] p 838 A90-49102
A closer look at the induced drag of crescent-shaped wings [AIAA PAPER 90-3063] p 903 A90-50638
- KROPFLI, R. A.**
Remote sensing techniques of the Wave Propagation Laboratory for the measurement of supercooled liquid water: Applications to aircraft icing [PB89-208102] p 24 A90-10842
- KROTHAPALLI, ANJANEYULU**
Basic studies of the unsteady flow past high angle of attack airfoils [AD-A210252] p 18 A90-10008
- KROTIL, PAVEL**
Digital servomechanism for the tachometer of the M 602 engine p 737 A90-44722
- KROTKOV, D. P.**
The local surface variation method in profile shape optimization problems p 297 A90-24136
Effect of the leading edge bluntness of a moderately swept wing on the aerodynamic characteristics of an aircraft model at subsonic and transonic velocities p 388 A90-29005
- KROTOVA, I. B.**
Determination of additive contents in aviation and turbine oils p 532 A90-34681
- KRUECKEBERG, C.-P.**
Direct measurement of laminar instability amplification factors in flight p 277 A90-16178
- KRUEGER, DAVE**
The new high Reynolds number Mach 8 capability in the NSWC Hypervelocity Wind Tunnel 9 [AIAA PAPER 90-1379] p 594 A90-37928
- KRUEGER, W. H.**
Composites for aerospace application from Kevlar aramid reinforced PEKK thermoplastic p 946 A90-50176
- KRUEGER, WILLIAM H.**
High performance thermoplastic composites with poly(etherketoneketone) matrix p 529 A90-31646
- KRUELLE, G.**
Recent advances in H₂/O₂ high pressure coaxial injector performance analysis [AIAA PAPER 90-1959] p 762 A90-42705
- KRUMNACK, T.**
Possibilities for improving traffic flows p 823 A90-49272

KRUT'KO, PETR D.

Inverse problems in controlled system dynamics:
Nonlinear models p 77 A90-12471

KRYLOV, B. A.

Effect of the radial clearance on the efficiency of a partial
microturbine p 111 A90-14586

KRYLOV, S. N.

Effect of pressure and temperature on residue formation
in aviation kerosenes p 203 A90-17281

KRYLOVA, L. A.

Lee-side heating of a delta wing in supersonic flow
p 10 A90-12281

KRYZHANOVSKII, GEORGII A.

Air traffic control p 638 A90-39581
Organization of air traffic control p 915 A90-52415

KTALKHERMAN, M. G.

Mean and pulse characteristics of supersonic flow in a
wind tunnel with a honeycomb nozzle p 231 A90-22421

Experimental investigation of GDL diffusers
[AIAA PAPER 90-1512] p 563 A90-38659

KU, CHIEH C.

Three dimensional full potential method for the
aeroelastic modeling of propfans p 393 A90-29392

KUBE, R.

Automatic vibration reduction at a four bladed hingeless
model rotor - A wind tunnel demonstration p 335 A90-25424

KUBINA, STANLEY J.

Measurement and computer simulation of antennas on
ships and aircraft for results of operational reliability p 370 N90-17936

KUBLER, TOMMY JACK

Design of a high angle of attack robotic sting mount
for tests in a low speed wind tunnel p 526 N90-20099

KUBO, SHOZO

Numerical simulation of wing in ground effect
p 307 A90-25863

KUBOMURA, K.

A study of filament wound high modulus carbon fiber
reinforced cylinders p 948 A90-50218

KUBOTA, HIROTOSHI

Topology of computed incompressible
three-dimensional separated flow field around
high-angle-of-attack cone-cylinders p 366 A90-25764

KUBOTA, TOSHI

The effect of walls on a spatially growing supersonic
shear layer p 393 A90-29591

KUCUK, SENOL

An adaptive human response mechanism controlling the
V/STOL aircraft. Appendix 3: The adaptive control model
of a pilot in V/STOL aircraft control loops p 598 N90-21777

KUCZEWSKI, STANISLAW

A calculation method for ducted propellers
p 226 A90-21626

KUDINOV, V. A.

The tape method for the automatic partitioning of an
arbitrary region when calculating temperature stresses p 138 A90-14587

KUDOU, K.

Some governing parameters of plasma torch
ignitor/flameholder in a scramjet combustor p 661 A90-42017

KUDOU, KENJI

Experimental study on autoignition in a scramjet
combustor p 46 A90-12559

KUDRIASHOV, A. B.

Application of the MARS system in aircraft-structure
design p 374 A90-24127

KUDRIAVTSEV, A. L.

Application of the finite element method to the problem
of rotational flow around wings p 156 A90-18305

KUGLER, ANDREW B.

Noise and sonic boom impact technology. Initial
development of an Assessment System for Aircraft Noise
(ASAN). Volume 1: Executive summary p 379 N90-17410

Assessment System for Aircraft Noise (ASAN) citation
database. Volume 3: New citation review procedures
[AD-A219177] p 615 N90-23190

KUGLER, B. ANDREW

Noise and sonic boom impact technology. Initial
development of an Assessment System for Aircraft Noise
(ASAN). Volume 2: System design strategy p 379 N90-17411

Noise and sonic boom impact technology. Initial
development of an Assessment System for Aircraft Noise
(ASAN). Volume 3: Technical description p 379 N90-17412

KUHL, MARK R.

Ridge regression processing p 489 N90-20931

KUHLMAN, JOHN M.

Computational design of low aspect ratio wing-winglet
configurations for transonic wind-tunnel tests p 316 N90-17539

KUHLMAN, M. R.

Characterization of chemicals on engine exhaust
particles p 256 N90-15106

KUHN, G. D.

Numerical simulation of a turbulent flow through a shock
wave p 608 A90-38769

KUHN, RICHARD E.

Low-speed wind-tunnel study of reaction control-jet
effectiveness for hover and transition of a STOVL fighter
concept p 119 N90-11751

KUHN, RODNEY

Ground and Obstacle Avoidance (GOA) concept of
operations p 28 N90-10855

National airspace system monitoring operational
concept p 178 N90-14214

National airspace system air-ground communications
operational concept p 542 N90-21249

KUIJVENHOVEN, J. L.

Numerical interactive grid generation for 3D-flow
calculations p 312 A90-26556

Validation of propeller slipstream calculations using a
multi-block Euler code p 791 A90-45874

KULL, A. E.

Operation of the ram accelerator in the transdetonative
velocity regime p 741 A90-42712

KUMAGAI, TAKAO

Cooling characteristics of a radial wafer blade
p 47 A90-12571

KUMAR, A.

Three-dimensional shock-shock interactions on the
scramjet inlet p 314 A90-26963

KUMAR, AJAY

A numerical study of the effects of reverse sweep on
a scramjet inlet performance p 705 A90-42749

KUMAR, ANAND

Euler solutions with a multi-block structured code
p 86 A90-15739

Flow-calculation over a delta-wing using the thin-layer
Navier-Stokes equations p 304 A90-25773

Solutions of two-dimensional Euler equations with
multigrad acceleration p 810 A90-48086

KUMAR, C. SURESH

Computational and experimental studies on ground
effect of a slender wing tailless delta aircraft p 810 A90-48083

KUNEGEL, JACQUES

The TVD 900 - A modern signal processing applied to
primary civilian ATC radar p 638 A90-41034

KUNTZ, H. L.

Interior noise in the untreated Gulfstream II Propfan Test
Assessment aircraft p 731 A90-44736

KUNTZ, TERRY

Autopilot flight test experience with BK 117 hingeless
rotor p 505 A90-33930

KUNZ, ROBERT F.

Calculation of internal flows using a single-pass,
parabolized Navier-Stokes analysis p 469 A90-32458

KUO, AN-YU

Stress intensity factors for cracking metal structures
under rapid thermal loading. Volume 2: Theoretical
background p 213 N90-13812

KUO, K. K.

Solid fuel ignition and combustion characteristics under
high-speed crossflows p 764 A90-42725

KUPAREV, V. A.

Determination of the laminar-turbulent transition point
for a turbulent layer on a yawing wing p 805 A90-46566

KUPRIANOV, O. E.

An experimental study of the gasdynamic characteristics
of annular nozzle cascades with small flow exit angles p 255 A90-23409

KURANAGA, SEISHI

Measurements of pressure fluctuations in the interaction
regions of shock waves and turbulent boundary layers
induced by blunt fins p 9 A90-12218

KURAS, C.

New materials for civil aircraft furnishing p 328 N90-17609

KURIBAYASHI, NOBUMITSU

Instrumentation and operation of NDA cryogenic wind
tunnel p 437 A90-28293

KURITA, N.

Turbulent plane jet excited mechanically by an oscillating
thin plate in the potential core p 553 A90-35262

KURIYAMA, MASUMICHI

Propulsive lift augmentation by side fences as applied
to Japan's experimental STOL aircraft, ASKA p 789 A90-45859

KUROSAKA, M.

Time-resolved measurements of total temperature and
pressure in the vortex street behind a cylinder p 557 A90-38522

KUROSAKA, TOSHIO

Total temperature separation in jets p 607 A90-38750

Thrust augmentation characteristics of jet reactions
[AIAA PAPER 90-0033] p 161 A90-19641

Multivariable control of jet engines p 507 A90-32421

KURTZ, J.

Categorization and performance analysis of advanced
avionics algorithms on parallel processing architectures p 461 A90-30786

KURYLOWICH, GEORGE

Correlation/validation of finite element code analyses
for vibration assessment of avionics equipment p 654 N90-23398

KURZIN, V. B.

Acoustic resonance in centrifugal compressors induced
by interaction between rotor and stator p 78 A90-11803

KURZROCK, JOHN W.

Experimental investigation of supersonic turbine
performance p 342 A90-23888

KUTINOV, V. F.

Ways of providing for the strength and service life of
aircraft structures made of polymer composites with
allowance for damage p 957 A90-50843

KUTLER, PAUL

Computational fluid dynamics - Current capabilities and
directions for the future p 540 A90-34385

KUWABARA, KOSEI

Calculation of flow over airfoil with slat and flap
p 149 A90-16797

KUWAHARA, KUNIO

Thrust augmentation characteristics of jet reactions
[AIAA PAPER 90-0033] p 161 A90-19641

KUZ'MICHEV, V. S.

A method for the matching of structural and geometric
parameters of the turbocompressors of small gas turbine
engines in computer-aided design p 850 A90-46491

KUZ'MIN, S. V.

Jet flap theory p 298 A90-24154

KUZ'MIN, V. V.

A study of the nonlinear deformation of a shell of
revolution with a surface bend p 129 A90-14574

KUZ'MINA, S. I.

Analytical studies of the transonic flutter of aircraft
p 860 A90-46577

KUZNETSOV, E. N.

Optimal nose shapes of bodies of revolution in transonic
flow p 299 A90-24165

KUZNETSOV, V. B.

Wall pressure fluctuation spectra in supersonic flow past
a forward facing step p 388 A90-29194

Wall pressure pulsation spectra ahead of internal
corners p 804 A90-46545

KUZNETSOV, V. I.

A study of the working process and losses in annular
turbine nozzle cascades with a low contraction ratio p 254 A90-23407

KUZNETSOVA, N. N.

Evaluation of the dynamic characteristics of a helicopter
instrument panel p 829 A90-46499

KVARDA, JIRI

Computer-aided simulation of aircraft motion including
nonlinearities in aerodynamic-coefficient relationships p 257 A90-23359

KVATERNIK, RAYMOND G.

Airframe structural dynamic considerations in rotor
design optimization p 134 N90-12057

Airframe design considerations: Overview p 106 N90-12586

KWA, T. S.

The design of a low Reynolds number RPV p 828 A90-46385

KWAK, DOCHAN

Upwind differencing scheme for the time-accurate
incompressible Navier-Stokes equations p 232 A90-23109

KWANTY, HARRY G.

Robust control design for relaxed static stability aircraft
[AIAA PAPER 90-3443] p 865 A90-47696

KWATNY, HAROLD G.

Robust control design for flight control
[AD-A211957] p 119 N90-11756

KWIECINSKI, JAMES ROBERT

High temperature VSCF (Variable Speed Constant Frequency) generator system
[AD-A210823] p 71 N90-10351

KWON, O.

Experimental evaluation of expendable supersonic nozzle concepts
[AIAA PAPER 90-1904] p 740 A90-42691

KWON, OH J.

Numerical study of the effects of icing on finite wing aerodynamics
[AIAA PAPER 90-0757] p 169 A90-20010

KWON, OH JOON

Stability of hingeless rotors in hover using three-dimensional unsteady aerodynamics
p 430 A90-28227

A technique for the prediction of aerodynamics and aeroelasticity of rotor blades
p 184 N90-13377

KYONG, NGUEN DYK

Induced drag of a wing of low aspect ratio
p 387 A90-28987
Calculation of the induced drag of a wing with arbitrary deformation
p 388 A90-29183

L**LA VALLE, LODOVICO**

Wind shear at Pantelleria airport p 692 A90-39702

LABARGE, W. L.

Transport composite fuselage technology: Impact dynamics and acoustic transmission
[NASA-CR-4035] p 126 N90-11821

LABARRE, CHRISTOPHER

Feasibility study for a microwave-powered ozone sniffer aircraft
[NASA-CR-186660] p 650 N90-23397

LABAUNE, G.

Experimental-theoretical comparison for current injection on an aircraft model
[ONERA, TP NO. 1989-133] p 22 A90-11157

Connection of structures by laboratory-generated electrical discharges
[ONERA, TP NO. 1989-147] p 58 A90-11169

Electrostatic description of a positive leader ignition from an aircraft
[ONERA, TP NO. 1989-149] p 23 A90-11171

LABEGORRE, B.

Numerical simulation of unsteady combustion in a dump combustor
p 54 N90-10203

LABERGE, E. F. C.

MLS - A total system approach p 640 A90-41710

LACAS, FRANCOIS

Three dimensional numerical simulation for an aircraft engine type combustion chamber
[ONERA, TP NO. 1989-120] p 49 A90-12591

LACHAPPELLE, G.

A test of airborne kinematic GPS positioning for aerial photography - Methodology p 97 A90-13982

LACOMME, PHILIPPE

Clutter rejection and transmitter-receiver requirements in an airborne radar p 738 A90-45354

LACOSTE, M.

Analysis and practical design of ceramic-matrix composite components p 445 A90-28135

LADDA, V.

The Operational Loads Monitoring System (OLMS)
p 926 A90-49879

LADDEN, R. M.

Large scale prop-fan structural design study. Volume 1: Initial concepts
[NASA-CR-174992] p 52 N90-10043

Large scale prop-fan structural design study. Volume 2: Preliminary design of SR-7
[NASA-CR-174993] p 52 N90-10044

LADSON, CHARLES L.

Facilities involved in adaptive wall research
p 871 N90-26840

LAFFERTY, JOHN F.

Aerodynamic heat transfer testing in hypersonic wind tunnels using an infrared imaging system
[AIAA PAPER 90-0189] p 350 A90-25027

LAFFRANCHI, D.

Direct drive servovalves: Why and how - The Magnaghi Milano answer p 688 A90-42484

LAFLAMME, J. C. G.

The effects of a compressor rebuild on gas turbine engine performance: Final results p 952 N90-28701

LAFFLE, J. H.

Elevated temperature crack growth
[NASA-CR-182247] p 777 N90-26355

LAFON, A.

Computation of the thin-layer Navier-Stokes equations for a 2D flow p 87 A90-16332

LAFON, P.

Influence of the control law on the performance of a helicopter model rotor
[ONERA, TP NO. 1989-136] p 4 A90-11158

LAFREY, R. R.

Parallel runway monitor p 241 A90-21382

LAFREY, RAYMOND R.

Development of common GPS and GLONASS avionics standards p 821 A90-46391

LAGACE, PAUL

Postbuckling behavior of laminated plates using a direct energy-minimization technique p 209 A90-17993

LAGRAFF, J. E.

Wake interaction effects on the transition process on turbine blades
[AD-A214492] p 343 N90-16759

LAGUTIN, V. G.

Optimization of the shape of a sealed shell and of the size and location of its reinforcements p 957 A90-50773

LAI, H. T.

Viscous three-dimensional analyses for nozzles for hypersonic propulsion
[NASA-CR-185197] p 344 N90-17635

LAIKHTMAN, V. I.

Variability characteristics of the meteorological optical range field in an optically inhomogeneous atmosphere p 962 A90-50784

LAITONE, E. V.

Comment on 'Drag reduction factor due to ground effect' p 159 A90-19396

LAITURI, TONY R.

A Monte Carlo simulation technique for low-altitude, wind-shear turbulence
[AIAA PAPER 90-0564] p 216 A90-19917

LAKE, E. A.

Focusing propulsion and lift system development for an evolving special operations aircraft
[AIAA PAPER 90-2277] p 730 A90-42768

LAKE, MAX L.

Vapor grown carbon fiber for space thermal management systems p 943 A90-50128

LAKIN, WILLIAM D.

A review of instability and noise propagation in supersonic flows
[NASA-CR-186800] p 717 N90-25112

LAKSHMANA GOWDA, B. H.

The characteristic decay region of a class of three-dimensional wall jets p 85 A90-15241

LAKSHMI, K. VASANTHA

Analytical evaluation of radiation patterns of a TACAN antenna p 404 A90-30695

LAKSHMINARASIMHA, A. N.

Simulation of compressor performance deterioration due to erosion
[ASME PAPER 89-GT-182] p 254 A90-22665

LDV measurements and the flow analysis in the vaneless region of a radial inflow turbine
[ASME PAPER 89-GT-157] p 292 A90-23845

Performance improvement of an eroded axial flow compressor using water injection
[AIAA PAPER 90-2016] p 741 A90-42718

LDV measurements and the flow analysis in the vortex region of a radial inflow turbine p 511 N90-21007

LAKSHMINARAYANA, B.

Computation of three dimensional turbulent boundary layers in internal flows, including turbomachinery rotor blades p 12 A90-12555

Three-dimensional separated flow field in the endwall region of an annular compressor cascade in the presence of rotor-stator interaction. I - Quasi-steady flow field and comparison with steady-state data
[ASME PAPER 89-GT-76] p 291 A90-23797

Three-dimensional separated flow field in the endwall region of an annular compressor cascade in the presence of rotor-stator interaction. II - Unsteady flow and pressure field
[ASME PAPER 89-GT-77] p 291 A90-23798

Computation of turbine flowfields with a Navier-Stokes code
[AIAA PAPER 90-2122] p 704 A90-42731

LALONDE, RICK J.

The determination of third order linear models from a seventh order nonlinear jet engine model p 964 A90-52881

LAM, CHUN-MING G.

Nonlinear aerodynamics of two-dimensional airfoils in severe maneuver p 301 A90-25276

LAMB, J. RICHARD

Advancements in rotor and airframe structural flight testing developed during the SH-60B G.W./C.G. expansion program
[AIAA PAPER 90-1281] p 495 A90-33902

LAMB, MARGARET W.

Colorado mountain flying - Crashes and weather
[AIAA PAPER 90-0369] p 175 A90-19818

LAMBERT, HEATHER H.

A preliminary evaluation of an F100 engine parameter estimation process using flight data
[AIAA PAPER 90-1921] p 656 A90-40559

LAMBETH, BENJAMIN S.

Pilot report - MiG-29 p 413 A90-29661

LAMBORN, LYNDON

Stress concentration factors - Comparison of theory with fatigue test data p 680 A90-39979

LAMBORN, LYNDON C.

Certification plan for an all-composite main rotor flexbeam p 642 A90-39992

LAMBOURION, J.

Tests of an ultra-light tunnel in the anechoic wind tunnel facility CEPRA 19
[ONERA-RF-20/7294-PH] p 872 N90-27729

LAMISCARRE, B.

Feasibility study of RADAC stereo optoelectronic model deformation measurement system for ETW p 539 A90-34239

LAMPARD, D.

Simulation of cooling film density ratios in a mass transfer technique
[ASME PAPER 89-GT-200] p 362 A90-23872

LAMPASOV, M. M.

Effect of pressure on the electrophysical properties of two-phase flows in nozzles p 110 A90-14572

LAM, C. EDWARD

Optimal control system design for departure prevention
[AIAA PAPER 90-2837] p 754 A90-45167

Aerodynamics of thrust vectoring
[NASA-CR-185074] p 172 N90-13354

Application of numerical optimization techniques to control system design for nonlinear dynamic models of aircraft p 593 N90-23032

Identification of aerodynamic models for maneuvering aircraft
[NASA-CR-186630] p 719 N90-25943

LAN, CHUAN-TAU EDWARD

Airplane aerodynamics and performance p 17 A90-12885

LAN, Q.

The development of an exact conservative scheme associated with the supersonic trailing edge separation modelling for the computation of the transonic 2D cascade p 12 A90-12551

LAN, ZHIFANG

The application and design of large integral panels for SH-5 aircraft p 211 A90-18632

LANCASTER, JEFFREY D.

USA - A system to represent airfoils throughout the product life cycle
[AIAA PAPER 89-2972] p 73 A90-10487

LANCE, M. B.

An experimental investigation of helicopter rotor hub fairing drag characteristics
[NASA-TM-102182] p 88 N90-11701

LANDAHL, MARTEN T.

Unsteady transonic flow p 716 A90-45760

LANDGREBE, ANTON J.

A comprehensive hover test of the airloads and airflow of an extensively instrumented model helicopter rotor p 407 A90-28173

LANDHERR, STEFAN F.

Inertial navigation system simulator: Behavioral specification, revision
[AD-A219294] p 578 N90-22554

LANDIS, DARIN

Flight test data processing, plotting and analysis at your finger tips - A flexible, automated, integrated approach
[AIAA PAPER 90-1322] p 545 A90-34150

LANDMANN, A. E.

Evaluation of analysis techniques for low frequency interior noise and vibration of commercial aircraft
[NASA-CR-181851] p 220 N90-14866

LANE, ALAN D.

Development of an advanced fan blade containment system
[DOT/FAA/CT-89/20] p 192 N90-13386

Aircraft crash survival design guide. Volume 3: Aircraft structural crash resistance
[AD-A218436] p 575 N90-22547

LANE, D. R.

From 1959-1989: 30 years of service experience with ramjets
[PNR90677] p 748 N90-25139

LANG, R. W.

Material development and second source qualification of carbon fiber/epoxy prepregs for primary and secondary Airbus structures p 948 A90-50225

LANGBEIN, D.

Parabolic flight experiments on fluid surfaces and wetting p 363 A90-23904

LANGE, H.-H.

ATTAS flight testing experiences p 34 N90-10862

LANGE, R.

An infrared camera system for detection of boundary layer transition in the ETW p 539 A90-34249

LANGE, ROY H.

Lockheed laminar-flow control systems development and applications p 90 N90-12506

LANGENFELD, C. A.

Nonaxisymmetric instabilities in a dump combustor with a swirling inlet flow p 253 A90-21228

LANGER, H.-J.

Helicopter rotor test rig (RoTeSt) in DNW: Application and results [RAE-TRANS-2171] p 201 N90-13408

LANGFORD, JOHN S., III

The NASA experience in aeronautical R and D: Three case studies with analysis [AD-A211486] p 82 N90-12496

LANGLEY, MARK J.

Air Force use of civil airworthiness criteria for testing and acceptance of military derivative transport aircraft [AIAA PAPER 90-3289] p 818 A90-48875

LANGLEY, R. S.

Application of the dynamic stiffness method to the free and forced vibrations of aircraft panels p 270 A90-20599

LANGSTON, L. S.

Research on cascade secondary and tip-leakage flows: Periodicity and surface flow visualization p 514 N90-21026

LANIUK, A. N.

Calculation of flows of an ideal gas in nozzles and jets by the relaxation method p 296 A90-24109

LANTIGUA, EDWARD A.

Rotordynamic analysis with shell elements for the transfer matrix method [AD-A217455] p 541 N90-20434

LANTZ, EDWARD

Accelerators and decelerators for large, hypersonic aircraft [AIAA PAPER 90-1986] p 674 A90-40582

LANZ, M.

Active flutter suppression for a wing model p 433 A90-31283

LAPIN, B. A.

The development result of SPEKTR automated air traffic control (ATC) system with extended grade of automation for terminal and hub areas p 639 A90-41058

LAPUCHA, RYSZARD

Predicting the CO, HC, and NO(x) emission and combustion efficiency of small turbine engines from the combustion chamber bench test results p 125 A90-15425

LAREDO, D.

A study of two-phase flow for a ramjet combustor p 45 A90-12532

LARICHEV, A. D.

Divergence of thin-walled composite rods of closed profile in gas flow p 388 A90-29012

LARIONOV, V. M.

Calculation of vibrational combustion limits in Helmholtz resonator-type chambers p 125 A90-14588

LARKIN, M. J.

Energy Efficient Engine exhaust mixer model technology report addendum; phase 3 test program [NASA-CR-174799] p 930 N90-28556

LARKIN, MICHAEL D.

Concept demonstration of the use of interactive fault diagnosis and isolation for TF30 engines p 617 A90-41177

LAROCCA, F.

Numerical method for designing 3D turbomachinery blade rows p 511 N90-20990

LAROCHE, P.

Electrostatic field conditions on an aircraft stricken by lightning [ONERA, TP NO. 1989-148] p 23 A90-11170

LAROSILIERE, L.

Unsteady loss in a low speed axial flow compressor during rotating stall p 12 A90-12527

LARROUTOUROU, B.

Upwind adaptive finite element investigations of the two-dimensional reactive interaction of supersonic gaseous jets p 209 A90-18264

LARSON, ERIC S.

Low-speed pressure distribution on semi-infinite two-dimensional bodies with elliptical noses p 553 A90-35766

LARSON, TERRY J.

Preliminary results from a subsonic high-angle-of-attack flush airdata sensing (HI-FADS) system - Design, calibration, algorithm development, and flight test evaluation [AIAA PAPER 90-0232] p 187 A90-19746

Preliminary results from a subsonic high angle-of-attack flush airdata sensing (HI-FADS) system: Design, calibration, and flight test evaluation [NASA-TM-101713] p 339 N90-16758

Wind-tunnel investigation of a flush airdata system at Mach numbers from 0.7 to 1.4 [NASA-TM-101697] p 421 N90-18395

LARSSON, FRITZ

Reinforcing fibers and technology development for resin composites. Consequences for aircraft structures [FOA-C-20777-2.5] p 876 N90-27883

LARWOOD, SCOTT

Aerodynamic design of the Cal Poly Da Vinci Human-Powered Helicopter p 830 A90-46950

LASCHET, GOTTFRIED

Postbuckling finite element analysis of composite panels p 365 A90-24377

LASCHKA, B.

On aerodynamic characteristics of canard in canard-forward-swept wing configuration p 709 A90-44833

LASCHKA, BORIS

SST/HST air traffic - Challenge for the future p 763 A90-44752

LASHINSKY, H.

Nonlinear mechanics of unstable plasmas as related to high altitude aerodynamics [AD-A215126] p 464 N90-19852

LASHKOV, I. A.

The effect of longitudinal fins on turbulent friction drag p 297 A90-24123

An experimental study of the combined effect of longitudinal riblets and vortex breakers on turbulent friction p 805 A90-46565

LASSOUDIERE, F.

Rotordynamics of the Vulcain LH2 Turbopump - Comparison between test results and non-linear dynamic analysis p 528 A90-33382

LASTER, J. P.

Proven dynamic modeling techniques for concurrent design and analysis of ECS controllers [SAE PAPER 901234] p 841 A90-49304

LATURELLE, F. G.

Thermostructural behavior of electromagnetic windows - Elaboration of a code package [ONERA, TP NO. 1989-145] p 76 A90-11167

LATYPOV, A. F.

Design of symmetric profiles with maximum critical flow Mach number under prescribed constraints p 295 A90-24095

LAUERMANN, H.-D.

Unsteady deformations of elastic rotor blades p 687 A90-42341

LAUGHREY, JAMES A.

Aerodynamic and propulsive control development of the STOL and maneuver technology demonstrator p 920 N90-28514

LAURENSEN, ROBERT M.

Chaotic response of aerosurfaces with structural nonlinearities (Status report) [AIAA PAPER 90-1034] p 392 A90-29378

LAURIE, EDWARD J.

An in-flight interaction of the X-29A canard and flight control system [AIAA PAPER 90-1240] p 348 A90-26820

An in-flight interaction of the X-29A canard and flight control system [NASA-TM-101718] p 736 N90-25973

LAUZON, M.

5DOF dynamic loads on a jet vane [AIAA PAPER 90-2382] p 675 A90-42147

LAVELLE, JAMES J.

Aeropropulsion facilities configuration control: Procedures manual [NASA-TM-102541] p 543 N90-21399

LAVERDANT, A.

Numerical simulation of unsteady combustion in a dump combustor p 54 N90-10203

LAVID, MOSHE

Photo-sensitized ignition of hydrogen/oxygen mixtures for hypersonic flight vehicles p 877 N90-27935

LAVIN, S. P.

Energy Efficient Engine acoustic supporting technology report [NASA-CR-174834] p 930 N90-28557

LAW, R. D.

Measurement of temperature gradients and assessment of balance performance using the RAE cryogenic test duct p 525 A90-34252

LAWING, PIERCE L.

Magnetic suspension - Today's marvel, tomorrow's tool p 262 A90-23697

Test techniques for cryogenic wind tunnels p 263 N90-15952

Models for cryogenic wind tunnels p 263 N90-15956

LAWLESS, ALAN R.

Flight testing for aircraft agility [AIAA PAPER 90-1308] p 519 A90-33918

LAWRENCE, ANTHONY

Providing an inexpensive gyro for the navigation mass market p 848 A90-49502

LAWRENCE, SCOTT L.

A three-dimensional upwind parabolized Navier-Stokes code for chemically reacting flows [AIAA PAPER 90-0394] p 165 A90-19831

Development of a three-dimensional upwind parabolized Navier-Stokes code p 802 A90-36253

Experimental and computational surface and flow-field results for an all-body hypersonic aircraft [AIAA PAPER 90-3067] p 793 A90-45893

LAWSON, S. M.

Design considerations for a compact table top hypersonic simulator of aero-optic effects p 525 A90-34585

LAWSON, TODD

Preliminary design of a supersonic Short Takeoff and Vertical Landing (STOVL) fighter aircraft [NASA-CR-186670] p 649 N90-23394

LAWTON, J.

Development of a heavy fuel engine for an unmanned air vehicle [AIAA PAPER 90-2170] p 662 A90-42056

LAZAREFF, M.

Development of the MZM numerical method for 3D boundary layer with interaction on complex configurations [ONERA, TP NO. 1989-174] p 223 A90-21036

LAZAREV, L. IA.

Calculation of an axial-flow birotary turbine p 880 A90-46492

LAZAREV, LEONID P.

Optoelectronic guidance sensors (5th revised and enlarged edition) p 881 A90-46620

LAZUTKIN, G. V.

Increasing the heat conductivity of elastic damping elements of MR material p 102 A90-14580

LE BALLEUR, J. C.

Unsteady viscous calculation of cascade flows with leading-edge-induced separation [ONERA, TP NO. 1989-116] p 3 A90-11148

Development of the MZM numerical method for 3D boundary layer with interaction on complex configurations [ONERA, TP NO. 1989-174] p 223 A90-21036

LE BLANC, M.

Development of a fibre optic damage detection system for an aircraft leading edge p 504 A90-32873

LE COURT DE BERU, H.

Electrostatic field conditions on an aircraft stricken by lightning [ONERA, TP NO. 1989-148] p 23 A90-11170

LE MEUR, ALAIN

Numerical simulation of three-dimensional unsteady flows in turbomachines [ONERA, TP NO. 1989-118] p 4 A90-11149

LE TOULLEC, LUC

Inviscid non equilibrium flow in ONERA F4 wind tunnel [ONERA, TP NO. 1989-161] p 223 A90-21029

LE HUACONG

Digital control experiment research on the engine JT15D-4 p 190 A90-18600

LE, T. H.

Numerical simulation of vortex breakdown via 3-D Euler equations [ONERA, TP NO. 1989-211] p 303 A90-25344

Numerical simulation of vortex breakdown by solving the Euler equations for an incompressible fluid p 476 A90-34323

LEA, ROBERT N.

Applications of fuzzy sets to rule-based expert system development p 216 A90-18050

LEA, T. C., III

AV-8B shipboard ski jump evaluation p 574 A90-38535

LEACH, B. W.

A precise flight reference system for evaluating airborne navigation aids p 27 A90-12752

LEARMOUNT, DAVID

After Habsheim p 401 A90-31388

LEASURE, STEVEN

Signal processing in a digital GPS receiver p 128 A90-14006

- LEAVITT, LAURENCE D.**
An experimental investigation of thrust vectoring two-dimensional convergent-divergent nozzles installed in a twin-engine fighter model at high angles of attack [NASA-TM-4155] p 237 N90-15884
- LEBACQZ, J. V.**
Ground-simulation investigations of VTOL airworthiness criteria for terminal-area operations [NASA-TM-102810] p 757 N90-25141
- LEBALLEUR, J. C.**
Unsteady viscous calculation method for cascades with leading edge induced separation p 426 N90-18408
- LEBED', I. V.**
A study of flow of a vibrationally nonequilibrium dissociated gas past a blunt body p 234 A90-23435
- LEBEDEV, A. S.**
Numerical modeling of a viscous separated flow in the near wake p 159 A90-19236
- LEBEDEV, I. M.**
Effect of the drag on the critical flutter velocity p 828 A90-46480
- LEBEDEVA, O. V.**
Optimization of the sound-absorption lining parameters of an ejector jet muffler p 378 A90-24117
- LEBIGA, V. A.**
Mean and pulse characteristics of supersonic flow in a wind tunnel with a honeycomb nozzle p 231 A90-22421
Experimental investigation of turbulence in a supersonic flow p 710 A90-44931
- LEBOEUF, F.**
Aerodynamics of cooling jets introduced in the secondary flow of a low speed turbine cascade [ASME PAPER 89-GT-192] p 362 A90-23868
Parabolized calculations of turbulent three dimensional flows in a turbine duct p 482 N90-21013
- LECCE, L.**
Aeroelastic analysis for a composite T-tailplane of a turboprop commuter aircraft p 492 A90-33390
- LECHT, M.**
Operating aspects of counter-rotating propfan and planetary-differential gear coupling p 50 A90-12615
- LEDERER, MELISSA A.**
Condensation in hypersonic nitrogen wind tunnels [AIAA PAPER 90-1392] p 558 A90-37937
High speed inlet testing in the NAVSWC wind tunnels [AIAA PAPER 90-1412] p 595 A90-37949
- LEDNICKER, DAVID**
A VSAERO analysis of several canard configured aircraft. II [SAE PAPER 892287] p 714 A90-45465
- LEE, ALFRED T.**
Air-ground information transfer in the National Airspace System p 380 A90-26235
- LEE, ALLAN Y.**
Optimal autorotational descent of a helicopter with control and state inequality constraints p 756 A90-45344
- LEE, B. H. K.**
Investigation of flow separation on a supercritical airfoil p 17 A90-13023
Oscillatory shock motion caused by transonic shock boundary-layer interaction p 470 A90-32478
Wind tunnel studies of F/A-18 tail buffet [AIAA PAPER 90-1432] p 559 A90-37969
Flow separation on a supercritical airfoil p 627 A90-42394
- LEE, BOO IL**
Hot-wire measurements of near wakes behind an oscillating airfoil p 154 A90-18138
- LEE, BRIAN P.**
Prediction methodologies for nonlinear aerodynamic characteristics of control surfaces [NIAF-90-17] p 718 N90-25937
- LEE, C. J.**
An airfoil theory of bifurcating laminar separation from thin obstacles p 702 A90-42639
- LEE, C. M.**
High speed commercial transport fuels considerations and research needs [NASA-TM-102535] p 600 N90-21869
- LEE, CHANG-LUN**
Chemical resistance of carbon fiber reinforced polyether ether ketone and polyphenylene sulfide composites p 944 A90-50142
- LEE, CHYANG S.**
A two dimensional study of rotor/airfoil interaction in hover [NASA-CR-183272] p 845 N90-27694
- LEE, CYNTHIA C.**
Flight-measured streamwise disturbance instabilities in laminar flow [AIAA PAPER 90-1283] p 495 A90-33904
- LEE, D.**
Numerical simulations of gas turbine combustor flows [AIAA PAPER 90-2305] p 686 A90-42116
- LEE, E. W.**
Al-Li alloys and ultrahigh-strength steels for U.S. Navy aircraft p 599 A90-37441
Aluminum alloy 6013 sheet for new U.S. Navy aircraft p 599 A90-37442
Aluminum lithium alloys for Navy aircraft p 267 N90-15193
- LEE, ELIZABETH M.**
Conical Euler solution for a highly-swept delta wing undergoing wing-rock motion [NASA-TM-102609] p 400 N90-19211
- LEE, FRANK**
High service temperature high compressive strength and tough prepreg system p 530 A90-33098
- LEE, FRANK W.**
High service temperature, damage tolerant prepreg systems based on cyanate chemistry p 941 A90-50069
- LEE, G.**
Airborne aerosol inlet passing efficiency measurement p 927 A90-52077
- LEE, GEORGE**
A two-dimensional adaptive-wall test section with ventilated walls in the Ames 2- by 2-foot transonic wind tunnel [NASA-TM-102207] p 201 N90-13407
- LEE, HENRY**
Methodology for estimating helicopter performance and weights using limited data p 829 A90-46936
- LEE, IN**
Flutter analysis of composite panels in supersonic flow [AIAA PAPER 90-1180] p 450 A90-29379
Static aeroelastic analysis for generic configuration aircraft [NASA-TM-89423] p 52 N90-10042
Static aeroelastic analysis of a three-dimensional generic wing [NASA-TM-102231] p 509 N90-20087
- LEE, J. T.**
Turbulence spectral widths view angle independence as observed by Doppler radar [DOT/FAA/SA-89/2] p 281 N90-15566
- LEE, J. Y.**
Unsteady hypersonic viscous flow in impulse facilities [AIAA PAPER 90-0421] p 313 A90-26947
- LEE, JAEWOO**
On optimal supersonic/hypersonic bodies [AIAA PAPER 90-3072] p 796 A90-45918
- LEE, JAMES S. J.**
Dual mode radar fusion based on morphological processing p 459 A90-30249
- LEE, K. C.**
Interfaces properties of high temperature polymer composite systems p 941 A90-50062
- LEE, K. P.**
Hypersonic viscous shock-layer solutions over long slender bodies. II - Low Reynolds number flows p 393 A90-29695
- LEE, K. T.**
Controlled vortical flow on delta wings through unsteady leading edge blowing [NASA-CR-186267] p 316 N90-16712
- LEE, KENNETH J.**
ARSR-4 long range radar will upgrade U.S. en-route surveillance p 403 A90-27925
An object-oriented solution example: A flight simulator electrical system [AD-A219190] p 761 N90-25145
- LEE, KUOK-MING**
Semi-implicit Navier-Stokes solver (SINSS) calculations of separated flows around blunt delta wings [AIAA PAPER 90-0590] p 168 A90-19936
- LEE, L. J.**
Finite element analysis of composite panel flutter p 681 A90-40032
- LEE, LUNG-CHENG**
Numerical simulation of transonic porous airfoil flows p 707 A90-44433
- LEE, MARIO**
Vortex dynamics of delta wings p 307 A90-26067
- LEE, MARK R.**
An alternative derivation for an integral equation for linearized subsonic flow over a wing [AD-A214140] p 236 N90-15079
- LEE, N. K. W.**
Effects of endwall suction and blowing on compressor stability enhancement [ASME PAPER 89-GT-64] p 290 A90-23787
- LEE, R. E.**
Tangential mass addition for the control of shock wave/boundary layer interactions in scramjet inlets p 13 A90-12586
- LEE, ROBERT A.**
Air Force Boom Event Analyzer Recorder (BEAR): System description [AD-A218048] p 548 N90-20800
BASEOPS default profiles for civil aircraft [AD-A223161] p 844 N90-26825
Air Force procedure for predicting aircraft noise around airbases: Airbase operations program (BASEOPS) description [AD-A223069] p 895 N90-27466
- LEE, S. A.**
A computer integrated approach to dimensional inspection [PNR90596] p 116 N90-12611
- LEE, SEUNGSOO**
Accelerated computation of viscous, steady incompressible flows [ASME PAPER 89-GT-45] p 288 A90-23771
- LEE, SUNG M.**
Improving snow roads and airstrips in Antarctica [AD-A211588] p 133 N90-11907
- LEE, WOON YUNG**
Optimal trajectories for hypervelocity flight p 918 N90-29378
- LEE, Y. J.**
A panel method for arbitrary moving boundaries problems p 302 A90-25284
- LEE, YU-TAI**
Flow coupling between a rotor and a stator in turbomachinery [AD-A223882] p 932 N90-28572
- LEEDY, DAVID H.**
A laser sheet flow visualization and aerodynamic force data evaluation of a 3 percent YF-17 fighter aircraft model at high angles of attack [AIAA PAPER 90-3019] p 792 A90-45886
- LEFEBVRE, A. H.**
Influence of fuel drop size and combustor operating conditions on pollutant emissions p 508 A90-33591
- LEFEBVRE, ARTHUR H.**
A novel method of atomization with potential gas turbine applications p 131 A90-16003
Influence of fuel composition on flame radiation in gas turbine combustors p 659 A90-40946
- LEFEBVRE, PIERRE**
High service temperature, damage tolerant prepreg systems based on cyanate chemistry p 941 A90-50069
- LEGER, A.**
Parachute opening shocks during high speed ejections: Normalization p 497 N90-20056
- LEGG, MARK**
Noise and sonic boom impact technology. Effects of aircraft noise and sonic booms on structures: An assessment of the current state-of-knowledge [AD-A213919] p 378 N90-17409
- LEGGETT, DAVID B.**
Low speed testing and simulation of the STOL and Maneuver Technology Demonstrator [AIAA PAPER 90-1820] p 334 A90-25169
The STOL maneuver technology demonstrator manned simulation test program p 439 A90-30716
Simulating turbulence and gusts for handling qualities evaluation [AIAA PAPER 90-2845] p 754 A90-45174
- LEGRAIN, I.**
New methods of buffeting prediction on civil aircraft p 908 A90-52620
- LEHMANN, G.**
Automatic vibration reduction at a four bladed hingeless model rotor - A wind tunnel demonstration p 335 A90-25424
Higher harmonic control of a helicopter model rotor to reduce blade/vortex interaction noise p 496 A90-34360
- LEHMANN, J.**
Multiple channel frequency demodulator p 69 A90-12190
- LEHNIG, T.**
An investigation of oblique shock/boundary layer bleed interaction [AIAA PAPER 90-1928] p 703 A90-42697
- LEHRA, HEINRICH**
Aerodynamic work for Hermes spaceplane p 675 A90-41115
- LEI, C. K.**
Augmented heat transfer in rectangular channels of narrow aspect ratios with rib turbulators p 70 A90-13091
- LEINGANG, JOHN L.**
ETO (Earth-To-Orbit): A trajectory program for aerospace vehicles [AD-A218157] p 528 N90-20103

LEISHMAN, D. K.

- Large scale prop-fan structural design study. Volume 1: Initial concepts [NASA-CR-174992] p 52 N90-10043
Large scale prop-fan structural design study. Volume 2: Preliminary design of SR-7 [NASA-CR-174993] p 52 N90-10044

LEISHMAN, J. G.

- Modeling of subsonic unsteady aerodynamics for rotary wing applications p 293 A90-23935
Investigation of aerodynamic interactions between a rotor and fuselage in forward flight p 385 A90-28198
State-space representation of unsteady airfoil behavior p 469 A90-32461
Dynamic stall experiments on the NACA 23012 airfoil p 552 A90-35140

LEISHMAN, J. GORDON

- Effects of unsteady blowing on the lift of a circulation controlled cylinder p 713 A90-45325

LEISTNER, R.

- Results of studies on a manipulator system for model handling in the ETW p 524 A90-34248

LEITH, D.

- Experience with multi-step test inputs for helicopter parameter identification p 56 A90-12775

LELE, SANJIVA K.

- Direct numerical simulation of aerodynamic noise [AD-A214122] p 379 N90-18225

LEMAN, JEAN-LUC

- The new Spheriflex tail rotor for the Super Puma Mark 2 p 408 A90-28213

LEMAY, S. P.

- Vortex dynamics on a pitching delta wing p 233 A90-23281

LEMAY, SCOTT P.

- Pneumatic vortex flow control on a 55-degree cropped delta wing with chined forebody [AIAA PAPER 90-1430] p 559 A90-37967

- Leading edge vortex dynamics on a pitching delta wing [NASA-CR-186327] p 398 N90-19198

LEMBLE, E. ROBERT

- DIGITAC - A unique digital flight control testbed aircraft [AIAA PAPER 90-1288] p 519 A90-33931

LEMMO, JOHN

- Two special cost-effective applications for electrochemical metallizing for improved brazing and bonding [SAE PAPER 890927] p 365 A90-24692

LEMER, A. C.

- Proceedings of a workshop on Future Airport Passenger Terminals [PB90-213620] p 937 N90-28580

LEMISTRE, M.

- Connection of structures by laboratory-generated electrical discharges [ONERA, TP NO. 1989-147] p 58 A90-11169

LEMMER, L.

- Design philosophy and construction techniques for integral fuselage fuel tanks p 250 N90-15913

LENNIOS, ANDREW Z.

- The servo flap - An advanced rotor control system p 860 A90-46934

LEMPEREUR, CH.

- Feasibility study of RADAC stereo optoelectronic model deformation measurement system for ETW p 539 A90-34239

LENORT, FRANCISZEK

- Discrete Fourier transform with high resolution for low frequencies applied to the modal analysis of aircraft vibration p 679 A90-38975

LENT, H.-M.

- Some processes of sound generation in a vortex-airfoil system with parallel axes p 218 A90-18448

LENTINI, D.

- Numerical simulation of nonpremixed turbulent flow in a dump combustor [AIAA PAPER 90-1858] p 768 A90-42685

LEONARD, J. T.

- Aviation Engine Test Facilities (AETF) fire protection study [AD-A211483] p 134 N90-12777

LEONARD, O.

- Subsonic and transonic blade design by means of analysis codes p 510 N90-20985

LEONDES, C. T.

- Analysis, Design and Synthesis Methods for Guidance and Control Systems [AGARD-AG-314] p 916 N90-29338

LEONDES, CORNELIUS T.

- Compensating for pneumatic distortion in pressure sensing devices [AIAA PAPER 90-0631] p 211 A90-19956

- Compensating for pneumatic distortion in pressure sensing devices [NASA-TM-101716] p 415 N90-19224

LEONE, B.

- Aeroelastic analysis for a composite T-tailplane of a turboprop commuter aircraft p 492 A90-33390

LEONG, SWEE HUNG

- A panel method computation for oscillating aerofoil in compressible flow p 906 A90-51483

LEONT'EV, A. I.

- Characteristics of turbulent separation flows on a porous surface under conditions of injection p 231 A90-22422

LEPICOVSKY, J.

- Total temperature effects on centerline Mach number characteristics of freejets p 302 A90-25290

LEQUETTE, LAURENT

- Three-dimensional modeling of turbulent transonic flow at the exit of a twin engine [AAAF PAPER NT 88-16] p 4 A90-11434

LEQUIME, M.

- Model attitude measurement system p 539 A90-34235

LERAT, A.

- Efficient solution of the steady Euler equations with a centered implicit method p 884 A90-27999

LERCH, BRAD

- Cyclic deformation, fatigue and fatigue crack propagation in Ni-base alloys p 531 A90-34162

LESAIN, ALAIN

- Numerical simulation of three-dimensional unsteady flows in turbomachines [ONERA, TP NO. 1989-118] p 4 A90-11149

LESCH, KLAUS

- Optimal periodic cruise with singular control [AIAA PAPER 90-3490] p 833 A90-47738

LESIEUTRE, DANIEL J.

- Prediction of subsonic vortex shedding from forebodies with chines [NASA-CR-4323] p 909 N90-28494

LESERISES, A. L.

- Acoustic characteristics of a research step combustor [AIAA PAPER 90-1851] p 655 A90-40530

LESTER, HAROLD C.

- Active control of propeller-induced noise fields inside a flexible cylinder p 833 A90-47306

- Mechanisms of active control in cylindrical fuselage structures p 862 A90-47309

LEUGERS, JOHN E.

- Development and extension of diagnostic techniques for advancing high speed aerodynamic research p 436 A90-28281

LEVAN, N.

- Control and stabilization of linear and nonlinear distributed systems [AD-A216446] p 462 N90-18908

LEVERSUICH, N. P.

- Aerodynamic and heat transfer measurements on blading for a high rim-speed transonic turbine [ASME PAPER 89-GT-228] p 293 A90-23883

- Aerodynamic and heat transfer measurements on blading for a high rim-speed transonic turbine [RAE-TM-P-1151] p 256 N90-15920

LEVERTON, J. W.

- Twenty-five years of rotorcraft aeroacoustics - Historical perspective and important issues p 78 A90-11878

LEVERTON, JOHN W.

- Advanced technology rotorcraft - Civil short haul transport of the future p 246 A90-21710

- EH101 Advance Technology Rotorcraft low detectability/good neighbor design p 579 A90-35774

- Multi-role advance technology rotorcraft - The EH101 [AIAA PAPER 90-3302] p 837 A90-48884

LEVI, KEITH R.

- Automating acquisition of plans for an intelligent assistant by observing user behavior p 459 A90-30230

LEVIN, D.

- Surface roughness effect on the aerodynamic characteristics of a blunt body p 16 A90-12740

LEVIN, DANIEL

- Self-induced roll oscillations of low-aspect-ratio rectangular wings [AIAA PAPER 90-2811] p 753 A90-45151

LEVIN, K.

- Damage tolerance of carbon fibre reinforced plastic sandwich panels p 675 A90-40047

LEVIN, M. P.

- Profiling of the supersonic components of three-dimensional corrugated nozzles p 804 A90-46563

LEVIN, V. M.

- Heat transfer in supersonic coaxial reacting jets p 601 A90-35394

LEVINE, M.

- Evaluation of current multiobjective optimization methods for aerodynamic problems using CFD codes [AIAA PAPER 90-0955] p 411 A90-29240

LEVINE, MICHAEL E.

- U.S. deregulation - Evidence from ten years of experience p 898 A90-49619

LEVINE, SEYMOUR

- Strapdown astro-inertial navigation (SAIN) utilizing the optical wide-angle lens startracker (OWLS) p 824 A90-49503

LEVINE, WILLIAM S.

- Digital controller design for the pitch axis of the F-14 using an H(infinity) method p 668 A90-40912

LEVIS, ALEXANDER H.

- On the generation of a variable structure airport surface traffic control system [AD-A211306] p 99 N90-11724

LEVY, Y.

- A study of two-phase flow for a ramjet combustor p 45 A90-12532

LEWANTOWICZ, ZDZISLAW H.

- Optimal selection of GRS sets to minimize emitter location errors p 97 A90-13992

- Dynamic interaction of separate INS/GPS Kalman filters (Filter-driving - Filter dynamics) p 124 A90-13996

- Estimation of atmospheric and transponder survey errors with a navigation Kalman filter p 459 A90-30689

LEWICKI, D. G.

- Effect of advanced component technology on helicopter transmissions p 271 A90-21115

- Transmission research activities at NASA Lewis Research Center [NASA-TM-103132] p 543 N90-21394

LEWIS, CLARK H.

- Parabolized Navier-Stokes predictions of three-dimensional hypersonic flows with strong crossflow effects p 223 A90-20508

LEWIS, E. T.

- The GMA 2100 and GMA 3007 engines for regional aircraft [AIAA PAPER 90-2523] p 744 A90-42815

LEWIS, G. M.

- XF40 - Rolls-Royce advanced fighter engine demonstrator p 112 A90-16002

LEWIS, J. S.

- Characteristics of combustion driven pressure oscillations in advanced turbo-fan engines with afterburner p 64 N90-10194

LEWIS, L. V.

- Flanged joints of aeroengines [PNR90594] p 116 N90-12609

LEWIS, LIANE C.

- Development of non-conventional control methods for high angle of attack flight using vortex manipulation p 935 N90-28522

LEWIS, M. C.

- The aims and history of adaptive wall wind tunnels p 871 N90-26839

LEWIS, MARK J.

- The effect of shock/shock interactions on the design of hypersonic inlets [AIAA PAPER 90-2217] p 705 A90-42748

LEWIS, NORRIS E.

- Fiber optic systems for mobile platforms II; Proceedings of the Meeting, Boston, MA, Sept. 6, 7, 1988 [SPIE-989] p 67 A90-11659

- Wavelength division multiplexed fiber optic sensors for aircraft applications p 38 A90-11663

- The performance of linear fiber optic data buses p 68 A90-11665

LEWIS, W.

- Engine testing of thermographic phosphors [DE90-013269] p 885 N90-28059

LEWIS, W. J.

- Propulsion systems for supersonic V/STOL aircraft [ASME PAPER 89-GT-309] p 507 A90-32259

- Future military powerplants [PNR90554] p 114 N90-11749

LEWIS, WILLIAM D.

- Airworthiness and flight characteristics test of the UH-60A Black Hawk helicopter equipped with the XM-139 multiple mine dispensing system (VOLCANO) [AD-A210271] p 32 N90-10025

LEWY, S.

- Directivity of the noise radiation emitted from the inlet duct of a turboshaft helicopter engine [ONERA, TP NO. 1990-26] p 695 A90-41205

- Noise-source measurements by thin-film pressure transducers in a subsonic turbofan model [ONERA, TP NO. 1990-36] p 659 A90-41212

- Tests of an ultra-light tunnel in the anechoic wind tunnel facility CEPRA 19 [ONERA-RF-20/7294-PH] p 872 N90-27729

- LEWY, SERGE**
Recent research on external helicopter noise at ONERA p 218 A90-16825
Characterization of helicopter turboshaft engine noise p 660 A90-41759
- LEYLAND, PENELOPE**
Fully vectorized implicit scheme for 2-D viscous hypersonic flow using adaptive finite element methods p 708 A90-44439
- LHYMN, C.**
Erosive wear of fibrous PEEK composites p 530 A90-33127
- LHYMN, Y. O.**
Erosive wear of fibrous PEEK composites p 530 A90-33127
- LI, BEI**
An improved version of LTRAN2 p 2 A90-10350
- LI, C.**
A numerical study of transverse jets into supersonic flows and influence of pressure waves [AIAA PAPER 90-0733] p 314 A90-26985
- LI, C.-C.**
Unsteady transonic cascade flow with in-passage shock wave p 556 A90-36281
- LI, CHENHAO**
Induced drag based on leading edge suction for a helicopter in forward flight p 232 A90-23102
- LI, CHIEN-PENG**
Computation of hypersonic flow fields p 225 A90-21169
- LI, FENGWEI**
Numerical method for solving the Euler equation for unsteady transonic flows over oscillating airfoils p 157 A90-18578
A numerical technique for computing the unsteady transonic flow around a wing profile in arbitrary oscillation p 906 A90-51530
- LI, HUIYING**
Exhaust emission performance of a vaporizer tube combustor as compared with a single tube combustor p 111 A90-14614
- LI, JIANPING**
Parameter sensitivity analysis of one kind of flight path reconstruction estimator p 779 A90-44832
- LI, JINGMEI**
The experiments for gas turbine plane cascade in a shock tunnel p 160 A90-19441
- LI, JINNIAN**
Experimental investigation on the performance of an annular nozzle cascade of a highly-loaded transonic turbine stage p 152 A90-17787
- LI, JUNSHAN**
An aerodynamical design and calculation method for gas turbine with cooling air mixing p 189 A90-17782
- LI, PING**
Mean loading effects on flutter of subsonic rotating annular cascade p 853 A90-49453
- LI, QING**
Experimental investigation on the interference effect of FL-23 wind tunnel wall on transonic flutter p 57 A90-10347
- LI, WENHUA**
Application of transformational ideas to automatic flight control design p 589 A90-36433
- LI, XIAN-PIN**
A finite element solution for transonic flow around lifting fuselage with arbitrary cross sections from the minimum pressure integral p 156 A90-18298
- LI, XIANPIN**
Finite element numerical analysis for transonic flows around lifting fuselages p 558 A90-37216
- LI, XIANPING**
A finite element method for solving lifting airfoil in transonic flow p 226 A90-21984
- LI, YANSHENG**
Variational principle with variable domain discontinuous finite element method for transonic flow and determining automatically the position and shape of the shock waves p 160 A90-19434
- LI, YOU-QIN**
Study on SPF and SPF/DB of the bulk-head structure with nonsymmetric shape p 132 A90-16619
- LI, YUANYE**
Digital control experiment research on the engine JT15D-4 p 190 A90-18600
- LI, YUCHUN**
Study of calculating an approximately constant reaction turbine stage with a tension spline streamline curvature method p 157 A90-18537
- LIAGUSHIN, B. E.**
Effect of the Mach number and shape of the front part of the obstacle on the separation zone length in supersonic flow p 903 A90-50816
- LIAKHOV, V. K.**
Operation of a gas ejector in the pulsed regime p 850 A90-46488
- LIAKHOV, VLADIMIR N.**
Effect of shock waves and jets on structural elements: Mathematical modeling in nonstationary gas dynamics p 806 A90-46621
- LIAN, Z. W.**
A rate theory investigation of cyclic loading and plastic deformation in the high stress and ambient temperature range p 954 A90-49884
- LIANG, D. F.**
The development of an airborne synthetic aperture radar motion compensation system p 333 A90-16745
- LIANG, FENG**
Application of transformational ideas to automatic flight control design p 589 A90-36433
- LIANG, X.**
Visualization of the turbulent trailing vortex behind a finite wing in steady and unsteady flows p 712 A90-45260
- LIAO, CHENG-WEI**
Analysis and numerical solution of flow over airfoil with control flap p 318 A90-17564
- LIAO, J. R.**
Navier Stokes simulation of waverider flowfields [AIAA PAPER 90-3066] p 793 A90-45892
- LIAO, SHU S.**
Aircraft modifications cost analysis. Volume 1: Overview of the study [AD-A220764] p 702 A90-25074
- LIAO, Y. T.**
Interfaces properties of high temperature polymer composite systems p 941 A90-50062
- LIAO, YUAN-SHIUAN**
Adaptive autopilot design via model expansion method p 55 A90-11124
- LIAPUNOV, S. V.**
Calculation of transonic axisymmetric flow past an engine nacelle with allowance for viscosity p 296 A90-24107
Effect of a jet on transonic flow past an airfoil p 388 A90-29181
- LIARDON, DARRELL L.**
V-22 ballistic vulnerability hardening program p 408 A90-28223
- LIASJO, KARE H.**
An aircraft noise study in Norway p 698 A90-24872
- LIBERIO, PATRICIA D.**
Micro separator and ball-on-cylinder lubricity evaluator tests or corrosion inhibitor/lubricity improver additives [AD-A221339] p 766 A90-25228
- LIBRESCU, L.**
The warping restraint effect in the critical and subcritical static aeroelastic behavior of swept forward composite wing structures [SAE PAPER 891056] p 129 A90-14358
The static aeroelastic behavior of sweptforward composite wing structures taking into account their warping restraint effect p 210 A90-18407
Supersonic flutter of shear deformable laminated composite flat panels p 683 A90-41104
- LICEAGA-CASTRO, E.**
Helicopter control design using feedback linearization techniques p 668 A90-40817
- LICHTENFELTS, FRED**
Ultrasonic techniques for aircraft ice accretion measurement p 485 A90-20926
- LIDSTONE, GARY L.**
Transverse fuel-injection model for a scramjet propulsion system p 659 A90-40927
- LIEBE, WOLFGANG**
The boundary-layer fence - Barrier against the separation process p 396 A90-31493
- LIEBECK, R. H.**
Calculation of low Reynolds number flows at high angles of attack [AIAA PAPER 90-0569] p 167 A90-19921
- LIEBECK, ROBERT H.**
Low Reynolds number airfoil design for subsonic compressible flow p 802 A90-46380
- LIEBIG, INGO**
Digital map for helicopter navigation and guidance p 252 A90-21609
- LIEFER, RANDALL K.**
Assessment of proposed fighter agility metrics [AIAA PAPER 90-2807] p 752 A90-45142
Fighter agility metrics, research, and test [NASA-CR-186118] p 648 A90-23386
Fighter agility metrics [NASA-CR-187289] p 925 A90-29389
- LIEPINS, GUNAR E.**
A preliminary sensitivity analysis of the Generalized Escape System Simulation (GESS) computer program [DE89-016891] p 24 A90-10844
- LIESE, HUBERT**
Technological preparations of civil aircraft programs p 617 A90-41110
- LIESE, KARL**
The applicability of simple helicopter models for flight mechanics studies [ETN-90-96962] p 736 A90-25975
- LIESNER, CH.**
Thin walled cast high-strength structural parts p 65 A90-10242
- LIFSHTS, I. U. B.**
Calculation of nonseparated flow past a wing profile at large Reynolds numbers p 706 A90-42995
The potential approximation in the theory of conical flows p 710 A90-44930
- LIGHT, JEFFREY S.**
Tip vortex geometry of a hovering helicopter rotor in ground effect p 407 A90-28196
Application of the wide-field shadowgraph technique to rotor wake visualization [NASA-TM-102222] p 88 A90-11700
- LIGON, JOHN B.**
Developments in mechanics. Volume 15 - Midwest Mechanics Conference, 21st, Michigan Technological University, Houghton, Aug. 13-16, 1989, Proceedings p 769 A90-42870
- LIGRANI, P. M.**
Effects of an embedded vortex on injectant from a single film-cooling hole in a turbulent boundary layer [ASME PAPER 89-GT-189] p 362 A90-23867
- LJEWski, LAWRENCE E.**
Transonic Euler solutions on mutually interfering finned bodies p 555 A90-36258
Transonic Euler solutions on mutually interfering finned bodies [AD-A213395] p 170 A90-13331
- LIKES, J. T.**
Fire hardening of aircraft through upgrades of materials and designs p 327 A90-17605
- LILJEGREN, TORSTEN**
Thermochemical calculations with inert compounds [FOA-C-20759-2.1] p 206 A90-13677
- LILLEY, ROBERT W.**
Demonstration of MLS advanced approach techniques p 640 A90-41711
- LIM, JOON W.**
Response and hub loads sensitivity analysis of a helicopter rotor p 181 A90-18145
Aeroelastic optimization of a helicopter rotor using an efficient sensitivity analysis [AIAA PAPER 90-0951] p 410 A90-29237
Stability sensitivity analysis of a helicopter rotor p 580 A90-36273
- LIN, C.**
Dual mode radar fusion based on morphological processing p 459 A90-30249
- LIN, C. J.**
Interfaces properties of high temperature polymer composite systems p 941 A90-50062
- LIN, CHIEN-CHANG**
A refined optimality criterion technique applied to aircraft wing structural design p 206 A90-16718
- LIN, CHUNG-HUA**
The changes of structures and properties in PAN-based carbon fibers during heat treatment in carbon dioxide p 945 A90-50145
- LIN, HUNG-HSI**
Influence of joint fixity on the structural static and dynamic response of a joined-wing aircraft. I - Static response [SAE PAPER 891060] p 100 A90-14361
Influence of joint fixity on the aeroelastic characteristics of a joined wing structure [AIAA PAPER 90-0980] p 390 A90-29370
- LIN, J. C.**
Investigation of several passive and active methods for turbulent flow separation control [AIAA PAPER 90-1598] p 607 A90-38730
- LIN, KUO-JIUN**
Flutter analysis of composite panels using high-precision finite elements p 207 A90-16725
- LIN, PINGJI**
Study of calculating an approximately constant reaction turbine stage with a tension spline streamline curvature method p 157 A90-18537
- LIN, R. R.**
Test and theory for piezoelectric actuator-active vibration control of rotating machinery p 879 A90-46226
- LIN, T. Y.**
Transient aeroelastic computations using multiple moving frames of reference [AIAA PAPER 90-3053] p 798 A90-45932
- LIN, W. F.**
3D transonic nacelle and winglet design [AIAA PAPER 90-3064] p 794 A90-45897
- LIN, Y. F.**
Measurements of turbulent dual-jet interaction [AIAA PAPER 90-2105] p 624 A90-42019

LIN, ZHAOFU

- Aeroengine condition monitoring and fault diagnosis system p 188 A90-16851
Main characteristic parameter model for jet engine fault diagnosis p 585 A90-37210
- LINCOLN, JOHN W.**
Damage tolerance for helicopters p 919 A90-49888
Proceedings of the 1988 Structural Integrity Program Conference [AD-A213545] p 275 N90-15486
Proceedings of the 1987 Aircraft/Engine Structural Integrity Program (ASIP/ENSIP) Conference [AD-A198037] p 842 N90-26807
- LIND, CHARLES A.**
The effect of shock/shock interactions on the design of hypersonic inlets [AIAA PAPER 90-2217] p 705 A90-42748
- LIND, ED**
Equipment feasibility study: Very high frequency communication equipment (136-137 megahertz) [DOT/FAA/CT-TN89/72] p 775 N90-26210
- LIND, H. O.**
Integration of intelligent avionics systems for crew decision aiding p 459 A90-30236
- LINDEN, STEFAN**
Multilevel optimization of large-scale structures in a parallel computing environment p 693 A90-39180
- LINDENBAUM, B.**
A status review of non-helicopter V/STOL aircraft development. II p 580 A90-38028
- LINDENBAUM, BERNARD**
A status review of non-helicopter V/STOL aircraft development. I p 413 A90-30117
- LINDHOLM, ULRIC S.**
Constitutive modeling for isotropic materials (HOST) [NASA-CR-179522] p 193 N90-13390
Constitutive modeling for isotropic materials (HOST) [NASA-CR-174718] p 193 N90-13391
- LINDHOUT, J.**
Development of a robust calculation method for transonic viscous blade-to-blade flows p 703 A90-42671
- LINDHOUT, J. P. F.**
VISTRAFS - A simulation method for strongly-interacting viscous transonic flow p 144 A90-16756
European research on viscous flow (EuroVisc) [NLR-TP-89077-U] p 609 N90-22014
- LINDLER, K. W.**
Computer aided analysis of gas turbine cycles p 779 A90-45289
- LINDLOHR, W.**
Processing of undifferenced GPS carrier beat phase measurements and adjustment computations [TR-5-1988] p 178 N90-13368
- LINDNER, M.**
Aerosol effects on jet-engine IR radiation p 40 A90-10152
- LINDSEY, NANCY**
The effect of windscreen bows and HUD pitch ladder on pilot performance during simulated flight p 420 A90-31333
- LINDSEY, STEVEN W.**
Prediction of longitudinal pilot induced oscillations using the optimal control model [AD-A220593] p 671 N90-23412
- LINDSEY, WILLIAM T.**
Experimental characterization of the effects of pneumatic tubing on unsteady pressure measurements [NASA-TM-4171] p 850 N90-27703
- LING, M. R.**
Fractographic analysis of fatigue crack growth under two-blocks loading on 2024-T351 sheet specimens [LR-628] p 961 N90-29680
Effects of blocks of overloads and underloads on fatigue crack growth in 2024-T351 sheet specimens: Fractographic analysis and crack closure predictions [LR-629] p 961 N90-29681
- LING, MAOFU**
The study of the theoretical calculation method for power stall dynamic characteristics of multiple-engine propeller airplane p 29 A90-10349
- LINK, JAMES E., II**
Placards, warning labels and operation manuals - An aircraft manufacturer's duty to warn p 79 A90-11396
- LINK, WESLEY B.**
Mode S system design and architecture p 330 A90-25569
- LINK, WILLIAM R.**
The IMIS F-16 interactive diagnostic demonstration p 383 A90-30768
- LINSE, DENNIS**
Neural networks for aircraft control p 521 N90-20937
- LINTERN, GAVAN**
Visual information for simulated landing approaches p 347 A90-26189

LIOSSI, ERNESTO

- Aircraft fuel tank construction and testing experience p 250 N90-15907
- LIU, S. G.**
Measurement of the interaction between a rotor tip vortex and a cylinder p 555 A90-36255
Flow field measurements near a fighter model at high angles of attack [AIAA PAPER 90-1431] p 559 A90-37968
- LIU, SHIUH-GUANG**
Prediction and measurement of the aerodynamic interactions between a rotor and airframe in forward flight p 384 A90-28176
Velocity measurements on a lifting rotor/airframe configuration in low speed forward flight p 815 N90-26790
- LIU, T.-M.**
Calculation of flowfields in side-inlet ramjet combustors with an algebraic Reynolds stress model p 87 A90-16367
Experimental and theoretical investigations of turbulent flow in a side-inlet rectangular combustor p 421 A90-27959
- LIPANOV, A. M.**
Stress-strain analysis of structural elements of incompressible or nearly incompressible materials by the finite element method p 129 A90-14557
Numerical calculation of turbulent separated flows in an abruptly expanding channel p 803 A90-46487
- LIPATOV, I. I.**
Effect of tangential injection on flow in a laminar boundary layer p 294 A90-24080
- LIPIN, E. K.**
Application of the MARS system in aircraft-structure design p 374 A90-24127
Determination of the torsion rigidity of a multiple-rib torsion box of an aircraft lifting surface p 364 A90-24134
Efficiency of using a multiple-wall torsion box in the load-bearing structures of lifting surfaces p 410 A90-29188
The use of automated parametric analysis for selecting efficient structural schemes for wings p 410 A90-29191
- LIPSITT, H. A.**
Intermetallic compounds for strong high-temperature materials - Status and potential p 125 A90-15022
- LISAGOR, W. BARRY**
Materials and structures for hypersonic vehicles p 31 A90-13015
- LISIN, EVGENII P.**
The economics of the organization and the planning of civil aviation p 897 A90-46629
- LISSAK, Z.**
A multichannel wide FOV infrared radiometric system p 67 A90-11410
- LISSAMAN, PETER B. S.**
The aims and history of adaptive wall wind tunnels p 871 N90-26839
- LITCHFORD, GEORGE B.**
Omega - A low-cost precision synchronizer p 727 A90-45233
- LITT, JONATHAN S.**
An expert system to perform on-line controller restructuring for abrupt model changes [NASA-TM-103609] p 964 N90-29121
- LITTLE, B. H.**
Proplan Test Assessment (PTA): Flight test report [NASA-CR-182278] p 113 N90-11738
Proplan Test Assessment (PTA) [NASA-CR-185138] p 113 N90-11739
- LITTLE, C. DALE**
Integrated product development (IPD) at General Dynamics Forth Worth [AIAA PAPER 90-3192] p 786 A90-48828
- LITTLE, FRANCIS**
Digital X-ray inspection p 445 A90-28162
- LITTLE, WILLIAM R.**
A review of fiber optic flight experience - Past problems, future direction p 38 A90-11661
- LIU, B.**
The turbulent near wake of a flat plate at low Reynolds number p 811 A90-48711
- LIU, C. H.**
Numerical studies of incompressible flow around delta and double-delta wings p 150 A90-16845
Prediction of steady and unsteady asymmetric vortical flows around cones [AIAA PAPER 90-0598] p 168 A90-19940
Prediction of vortical flows on wings using incompressible Navier-Stokes equations p 226 A90-21935
Navier-Stokes computation of flow around a round-edged double-delta wing p 555 A90-36251

- Computational study for passive control of supersonic asymmetric vortical flows around cones [AIAA PAPER 90-1581] p 566 A90-38718
Simulation of leading-edge vortex flows p 716 A90-45785
Numerical study of vortical flow over a sideslipping delta wing [AIAA PAPER 90-3001] p 798 A90-45936
High temperature behavior of the innovation carbon/CSPI composite p 941 A90-50067
- LIU, CHANG**
A study of the control technique for aircraft spin recovery p 590 A90-37226
- LIU, CHIN-FUNG**
Control of wall-separated flow by internal acoustic excitation p 809 A90-47314
- LIU, CUNLU**
Design and calculation of composite air-cooled blades in a highly-loaded transonic turbine p 189 A90-17790
Experimental investigation on composite air-cooled blades of highly-loaded transonic turbine p 189 A90-17793
- LIU, D. D.**
Unsteady transonic aerodynamics of oscillating airfoils in supersonic freestream p 232 A90-23277
Unsteady supersonic computations of arbitrary wing-body configurations including external stores p 232 A90-23278
Further studies of harmonic gradient method for supersonic aeroelastic applications p 473 A90-33410
- LIU, DAO-ZHI**
An efficient upwind relaxation-sweeping algorithm for three-dimensional Euler equations [AIAA PAPER 90-0129] p 162 A90-19895
- LIU, DENGYUN**
Research on film-cooling of turbine blade p 190 A90-17795
- LIU, DIQING**
The application of the engineering approach for analyzing crack tolerance of fuselage panels to a transport airplane p 272 A90-22014
- LIU, FANG**
A design of a twin variable control system for aero-turbojet engine p 423 A90-29917
- LIU, FENGJUN**
A method for calculating axial turbomachine end wall turbulent boundary layers [ASME PAPER 89-GT-15] p 287 A90-23759
- LIU, GAO-LIAN**
Variational formulation of 2-D unsteady transonic aerodynamics of oscillating cascades p 813 A90-49458
- LIU, H.**
High temperature behavior of the innovation carbon/CSPI composite p 941 A90-50067
- LIU, JIN-WEI**
A refined optimality criterion technique applied to aircraft wing structural design p 206 A90-16718
- LIU, J. L.**
Numerical investigation of airfoil/jet/fuselage-undersurface flowfields in ground effect [AIAA PAPER 90-0597] p 168 A90-19939
- LIU, LING**
Exhaust emission performance of a vaporizer tube combustor as compared with a single tube combustor p 111 A90-14614
- LIU, N.-S.**
Navier-Stokes study of rotating stall in compressor cascades p 302 A90-25292
- LIU, QIANGANG**
A unified approach to the overall body motion stability and flutter characteristics of elastic aircraft p 346 A90-25102
- LIU, QINGGUO**
Investigation and improvement of ground starting characteristics of a combustor with airblast nozzles p 45 A90-12546
- LIU, QIUSHENG**
A new method for high speed propeller flutter prediction p 854 A90-49454
- LIU, SANDY R.**
The acoustic results of a United Technologies scale model helicopter rotor tested at DNW [NASA-TM-101879] p 896 N90-27471
- LIU, SHAOBO**
The experimental study on the coaxial dump combustor with inner swirl inlet under the combustion condition p 585 A90-36786
- LIU, SHENG**
Calculation of two-dimensional transonic flow of Euler equations with multigrid method p 149 A90-16835
Hypersonic rarefied flow and its solution over the stagnation region [AIAA PAPER 90-0420] p 166 A90-19842

PERSONAL AUTHOR INDEX

LOUKIS, E.

- LIU, SHONGLING**
Calculation of two-dimensional transonic flow of Euler equations with multigrid method p 149 A90-16835
- LIU, SONGLING**
Prediction of heat transfer coefficient on turbine blade profiles p 423 A90-29904
- LIU, W. L.**
Interfaces properties of high temperature polymer composite systems p 941 A90-50062
- LIU, XIAO L.**
Unsteady streamlines near the trailing edge of NACA 0012 airfoil at a Reynolds number of 125,000 p 155 A90-18158
- LIU, XINGZHOU**
An experimental study on flowfields in a dual inlet swirl-dump combustor p 471 A90-33283
- LIU, YUFANG**
Design and calculation of composite air-cooled blades in a highly-loaded transonic turbine p 189 A90-17790
Calculation of coolant flow and heat transfer inside composite air-cooled turbine p 189 A90-17791
Experimental investigation on composite air-cooled blades of highly-loaded transonic turbine p 189 A90-17793
- LIU, ZHIGANG**
A study on spray characteristics down stream from a gutter-atomizer p 368 A90-26893
- LIU, ZHIMING**
The numerical method for solving the high Reynolds hypersonic viscous shock layer p 2 A90-10340
- LIU, ZHIZHONG**
Mach number effects on upstream influence in swept shock wave/turbulent boundary layer interactions p 556 A90-36415
- LIVINGS, JEFFREY G.**
Communications Interface Driver (CID) test plan [DOT/FAA/CT-TN89/35] p 958 A90-28762
- LIVNE, E.**
Exploratory design studies using an integrated multidisciplinary synthesis capability for actively controlled composite wings [AIAA PAPER 90-0953] p 411 A90-29238
- LIVNEH, RAFAEL**
Direct multivariable adaptive controller with application to wing flutter p 349 A90-17642
- LIZZA, CARL S.**
Pilot's Associate - A perspective on Demonstration 2 [AIAA PAPER 89-3023] p 36 A90-10524
- LJUNGREN, STEN**
Slipstream-induced pressure fluctuations on a wing panel p 77 A90-11004
- LLEWELYN-DAVIES, D. I. T. P.**
The effect of flow curvature on the aerodynamic characteristics of an ogive-cylinder body p 82 A90-13785
The determination of the aerodynamic characteristics of an ogive-cylinder body in subsonic, curved, incompressible flow, and an assessment of the effect of flow curvature [REPT-87-13] p 89 A90-11712
- LLORENTE, STEVEN**
Honeycomb sandwich primary structure applications on the Boeing Model 360 helicopter p 490 A90-31558
- LO, C. F.**
Investigation of adaptive-wall wind tunnels with two measured interfaces [AIAA PAPER 90-0186] p 200 A90-19728
Comparisons of one- and two- interface methods for tunnel wall interference calculation p 870 A90-48961
- LOBANOVSKI, I. I.**
Wing-fuselage interference regimes at supersonic flight velocities p 298 A90-24155
- LOC, TA PHUOC**
Vortex formation around an oscillating and translating airfoil at large incidences p 303 A90-25588
- LOCHOCKI, JOSEPH M.**
Smart Skins - A development roadmap p 504 A90-32860
- LOCK, R. C.**
Aerodynamic design methods for transonic wings p 293 A90-23978
- LOCKMAN, WILLIAM K.**
Experimental and computational surface and flow-field results for an all-body hypersonic aircraft [AIAA PAPER 90-3067] p 793 A90-45893
- LOCO, D.**
New metallic felts with improved resistance to high temperature oxidation [ONERA, TP NO. 1989-210] p 366 A90-25343
- LOEHR, K. F.**
Some processes of sound generation in a vortex-airfoil system with parallel axes p 218 A90-18448
- LOEVE, W.**
Flow simulation for aircraft [NLR-MP-87082-U] p 455 A90-19543
- The automation management to support research and development p 612 A90-22978
- LOEWENSTEIN, GEORGE**
An analysis of GPS as the sole means navigation system in US Navy aircraft p 917 A90-29350
- LOEWY, R. G.**
Nonlinear effects in helicopter rotor forward flight forced response p 347 A90-25420
Dynamic analysis of rotor blades with rotor retention design variations [AIAA PAPER 90-1159] p 412 A90-29394
A study of the influence of predeformations on the vibrations of blades p 585 A90-35673
Shaft flexibility effects on the forced response of a bladed-disk assembly p 744 A90-43218
- LOEWY, ROBERT**
Shaft flexibility effects on aeroelastic stability of a rotating bladed disk p 132 A90-16371
- LOEWY, ROBERT G.**
Blade mistuning coupled with shaft flexibility effects in rotor aeroelasticity [ASME PAPER 89-GT-330] p 343 A90-23896
Helicopter ground/air resonance including rotor shaft flexibility and control coupling p 406 A90-28153
- LOGAN, A. L.**
Classification and reduction of pilot error [NASA-CR-181867] p 24 A90-10014
- LOH, C. Y.**
A new Lagrangian method for steady supersonic flow computation. I - Godunov scheme p 631 A90-42506
- LOH, N. K.**
Guaranteed cost control via optimal parametric LQ design p 693 A90-40810
- LOH, ROBERT**
GPS monitor alarm limits for nonprecision approaches p 98 A90-15315
- LOHE, S. N.**
Nonflammable hydraulic power system for tactical aircraft. Volume 1: Aircraft system definition, design and analysis [AD-A218493] p 671 A90-23409
- LOHMANN, R. P.**
Energy efficient engine pin fin and ceramic composite segmented liner combustor sector rig test report [NASA-CR-179534] p 932 A90-28567
- LOHNER, R.**
A three-dimensional space marching algorithm for the solution of the Euler equations on unstructured grids [AIAA PAPER 90-0014] p 234 A90-23701
- LOHNER, RAINALD**
Interactive generation of unstructured grids for three dimensional problems p 310 A90-26537
Supersonic flow over an axisymmetric backward-facing step [AIAA PAPER 90-1580] p 566 A90-38717
Formation of shocks within axisymmetric nozzles [AIAA PAPER 90-1655] p 570 A90-38782
- LOHR, GARY W.**
Delivery performance of conventional aircraft by terminal-area, time-based air traffic control: A real-time simulation evaluation [NASA-TP-2978] p 404 A90-18378
- LOIKKANEN, MATTI J.**
Large-order modal analysis techniques in the Aeroelastic Design Optimization Program (ADOP) [SAE PAPER 892323] p 772 A90-45482
- LOKEN, HALVAR Y.**
Tradeoffs in honeycomb cored designs p 538 A90-33708
- LONG, C.**
Numerical investigations of heat transfer and flow rates in rotating cavities. Simulation of the movement generated by wall temperature gradients, by source-sink mass flows or by the differential rotation of the walls, under the influence of coriolis and centrifugal forces [ETN-90-96253] p 454 A90-18695
- LONG, DEAN F.**
An experimental evaluation of test section noise in transonic wind tunnels [AIAA PAPER 90-1419] p 614 A90-37956
- LONG, G. M.**
Enhanced bioreclamation of jet fuels: A full-scale test at Eglin AFB, Florida [AD-A222348] p 875 A90-26992
- LONG, LYLE N.**
Off-design performance of hypersonic waveriders p 763 A90-44735
- LONG, WEIHONG**
The design and study of the information transfer mechanism for a distributed avionics system p 207 A90-16858
- LONGLEY, J. P.**
Stability of flow through multistage axial compressors [ASME PAPER 89-GT-311] p 231 A90-22668
- LONGO, J. M. A.**
Numerical simulation of vortical flows over close-coupled canard-wing configuration [AIAA PAPER 90-3003] p 788 A90-45852
Research on three different Euler's schemes applied to a delta wing with vortical flows p 278 A90-16184
- LOOMIS, P. V. W.**
Guidance simulation and test support for differential GPS flight experiment [NASA-CR-177471] p 28 A90-10021
- LOOS, SCOTT**
Aerodynamic design considerations for aircraft radomes [AIAA PAPER 90-2843] p 711 A90-45163
- LOPATA, VINCE J.**
Radiation-curable prepreg composites [DE90-629740] p 951 A90-28674
- LOPER, BRENT**
High speed civil transport [NASA-CR-186661] p 649 A90-23396
- LOPES, STEVEN**
Developments in automation of flight test analysis and report generation [AIAA PAPER 90-1313] p 487 A90-33923
- LOPEZ, RAMON**
Turboshafts on tenterhooks p 188 A90-16703
- LORBER, PETER F.**
Computational and experimental studies of compressible dynamic stall p 146 A90-16776
A comprehensive hover test of the airloads and airflow of an extensively instrumented model helicopter rotor p 407 A90-28173
An unsteady helicopter rotor-fuselage aerodynamic interaction analysis p 712 A90-45323
- LORD, H. W.**
Developments in mechanics. Volume 15 - Midwestern Mechanics Conference, 21st, Michigan Technological University, Houghton, Aug. 13-16, 1989, Proceedings p 769 A90-42870
- LORD, MARGARET M.**
ARSR-4 long range radar will upgrade U.S. en-route surveillance p 403 A90-27925
- LORD, W. K.**
Navier-Stokes analysis of an ejector and mixer-ejector operating at pressure ratios in the range 2-4 [AIAA PAPER 90-2730] p 626 A90-42218
Mixer-ejector nozzle for jet noise suppression [AIAA PAPER 90-1909] p 894 A90-47202
- LORD, WESLEY K.**
Navier-Stokes analysis of a lobed mixer and nozzle [AIAA PAPER 90-0453] p 192 A90-19852
- LORELL, MARK A.**
The use of prototypes in selected foreign fighter aircraft development programs: Rafale, EAP, Lavi, and Gripen [AD-A214500] p 287 A90-16707
- LORENZ-MEYER, WOLFGANG**
Half model tests on an ONERA calibration model in the transonic wind tunnel Goettingen, Federal Republic of Germany [DLR-MITT-89-20] p 397 A90-18370
- LORIA, EDWARD A.**
Superalloy 718: Metallurgy and applications; Proceedings of the International Symposium, Pittsburgh, PA, June 12-14, 1989 p 266 A90-20775
- LOSIER, PAUL W.**
Airworthiness and flight characteristics test of the UH-60A Black Hawk helicopter equipped with the XM-139 multiple mine dispensing system (VOLCANO) [AD-A210271] p 32 A90-10025
- LOTH, ERIC**
Supersonic flow over an axisymmetric backward-facing step [AIAA PAPER 90-1580] p 566 A90-38717
Formation of shocks within axisymmetric nozzles [AIAA PAPER 90-1655] p 570 A90-38782
- LOTTER, K.**
Results of studies on a manipulator system for model handling in the ETW p 524 A90-34248
- LOTZE, A.**
The influence of mathematical optimization methods on the design of aircraft structures p 492 A90-33387
- LOU, WUJIANG**
Recent advancement in helicopter rotor wake study p 556 A90-36413
- LOUIE, CHECK M.**
Design and experimental verification of an equivalent forebody representation of flowing inlets p 152 A90-17863
- LOUKIS, E.**
Casing vibration and gas turbine operating conditions [ASME PAPER 89-GT-78] p 358 A90-23799
Computer modeling and data processing methods: An essential part of jet engine condition monitoring and fault diagnosis p 855 A90-27626

- LOUNDAGIN, J. A.**
Recent developments in Ramjet pressure oscillation technology p 53 N90-10199
- LOURENCO, LUIZ**
Basic studies of the unsteady flow past high angle of attack airfoils [AD-A210252] p 18 N90-10008
- LOW, W.**
Range determination in a multipath prone environment p 877 A90-45960
- LOW, EICHER**
Design of attitude and rate command systems for helicopters using eigenstructure assignment p 118 A90-14729
Design of flight control systems to meet rotorcraft handling qualities specifications [AIAA PAPER 90-2805] p 752 A90-45140
- LOWDEN, P.**
Development of erosion resistant coatings for compression airfoils p 443 A90-31120
- LOWE, ROBERT E.**
Estimating the relationships between the state of the art of technology and production cost for the US aircraft [AD-A212127] p 82 N90-12495
- LOWEY, H. E.**
GE's CF34 engine for business and regional jets [AIAA PAPER 90-2041] p 661 A90-41992
- LOWRIE, B. W.**
The next generation supersonic transport engine: Critical issues [PNR90576] p 115 N90-12605
- LOWRIE, R. B.**
An evaluation of Euler solvers for transonic flowfield computations on wing-fuselage geometries [AIAA PAPER 90-3015] p 798 A90-45935
- LOWSON, MARTIN V.**
Minimum induced drag for wings with spanwise camber p 709 A90-44733
The three-dimensional vortex sheet structure on delta wings p 19 N90-10367
Optimum spanwise camber for minimum induced drag [BU-403] p 397 N90-18369
- LOYD, BERNARD**
Semi-implicit Navier-Stokes solver (SINSS) calculations of separated flows around blunt delta wings [AIAA PAPER 90-0590] p 168 A90-19936
- LOZITO, SANDRA**
Air-ground information transfer in the National Airspace System p 380 A90-26235
- LU, BO**
Experimental investigation on the interference effect of FL-23 wind tunnel wall on transonic flutter p 57 A90-10347
- LU, F. K.**
Mach number effects on conical surface features of swept shock-wave/boundary-layer interactions p 154 A90-18147
Development of the UTA hypersonic shock tunnel [AIAA PAPER 90-0080] p 200 A90-19675
- LU, FRANK K.**
Upstream-influence scaling of fin-generated shock wave boundary-layer interactions [AIAA PAPER 90-0376] p 164 A90-19822
- LU, FUMEI**
The application of the engineering approach for analyzing crack tolerance of fuselage panels to a transport airplane p 272 A90-22014
- LU, H. Y.**
Fuselage boundary-layer effects on sound propagation and scattering p 695 A90-39781
- LU, PONG-JEU**
Flutter analysis of composite panels using high-precision finite elements p 207 A90-16725
Multigrid acceleration of TVD schemes in transonic Euler flow calculation p 908 A90-52030
- LU, QIZHENG**
Experimental investigation on the interference effect of FL-23 wind tunnel wall on transonic flutter p 57 A90-10347
- LU, YINGJIE**
Unsteady aerodynamics and aeroelasticity of turbomachines and propellers; Proceedings of the Fifth International Symposium, Beijing, People's Republic of China, Sept. 18-21, 1989 p 853 A90-49451
- LUCCHESINI, M.**
The use of simulation in support of the high AOA flight test program of the AM-X aircraft [AIAA PAPER 90-1289] p 495 A90-33909
Aerodynamic control design: Experience and results at Aermacchi p 935 N90-28518
- LUCKNER, ROBERT**
Simulation of transport aeroplanes [MBB-UT-007/89-PUB] p 723 N90-25089

- LUCKRING, JAMES M.**
Transonic Navier-Stokes solutions about a complex high-speed accelerator configuration [AIAA PAPER 90-0430] p 166 A90-19844
Connection between leading-edge sweep, vortex lift, and vortex strength for delta wings p 554 A90-35770
Stability characteristics of a conical aerospace plane concept [SAE PAPER 892313] p 757 A90-45475
- LUETKE, WILLIAM P.**
Wind tunnel tests of a 20-gore disk-gap-band parachute [AD-A221326] p 634 N90-24251
- LUDWIG, RAYMOND**
Solving compressible flow problems using adaptive finite quadtree and octree grids p 155 A90-18243
- LUECK, HELMUT**
Design and manufacture of a cryogenic wind tunnel model p 523 A90-34238
- LUECKING, P.**
Experimental and numerical study on basic phenomena of secondary flows in turbines p 512 N90-21014
- LUERS, JAMES K.**
Analyses of Arrow Air DC-8-63 accident of December 12, 1985 - Gander, Newfoundland p 635 A90-40687
- LUH, RAYMOND CHING-CHUNG**
Surface grid generation for complex three-dimensional geometries p 376 A90-26484
- LUH, YIH-PING**
Nonconvex polytope approximations of attracting basin boundaries for nonlinear systems [AIAA PAPER 90-3512] p 891 A90-47758
- LUISE, FEDERICA**
Expert system for pilot assistance - The challenge of an intensive prototyping p 693 A90-38909
Expert system for pilot assistance: The challenge of an intensive prototyping [ETN-90-97274] p 825 N90-27674
- LUKASHUK, S. A.**
Effect of vortex generators on the aerodynamic wing characteristics and body of revolution [AD-A22813] p 721 N90-25955
- LUKINYKH, I. G.**
A study of the stability of a wing aileron in supersonic flow p 222 A90-20442
- LUND, J.**
Internal rotor friction instability [NASA-CR-183942] p 543 N90-21395
- LUNDERSTAEDT, R.**
Knowledge based diagnosis of jet engines under consideration of model based methods p 855 N90-27631
- LUNDGREN, D. A.**
Design and calibration of an in-stack, low-pressure impactor [AD-A213531] p 255 N90-15105
- LUO, JIAN**
Parameter sensitivity analysis of one kind of flight path reconstruction estimator p 779 A90-44832
- LUO, MINGJUN**
Design and calculation of composite air-cooled blades in a highly-loaded transonic turbine p 189 A90-17790
Calculation of coolant flow and heat transfer inside composite air-cooled turbine p 189 A90-17791
Experimental investigation on composite air-cooled blades of highly-loaded transonic turbine p 189 A90-17793
- LUONG, TAI**
NASA/USRA high altitude reconnaissance aircraft [NASA-CR-186685] p 650 N90-24266
- LUSIGNEA, R.**
Effects of additives on the processing and properties of LARC-TPI polyimide p 942 A90-50070
- LUSSIER, WAYNE**
Preliminary design of a family of three close air support aircraft [NASA-CR-186070] p 336 N90-16751
- LUTIN, E. A.**
Radar systems of aircraft p 26 A90-10841
- LUTTGES, MARVIN W.**
Controlled three-dimensionality in unsteady separated flows about a sinusoidally oscillating flat plate [AIAA PAPER 90-0689] p 230 A90-22244
Unsteady aerodynamic loading produced by a sinusoidally oscillating delta wing [AIAA PAPER 90-1536] p 564 A90-38680
- LUTTON, MARK J.**
Comparison of C- and O-grid generation methods using a NACA 0012 airfoil [AD-A216375] p 479 N90-20948
- LUTZ, BRUCE L.**
Methods of safety analysis for Beech Model 2000 - Starship 1 [SAE PAPER 891064] p 101 A90-14364

- LUTZ, MARTIN**
Lightning testing and test analyses of the JAS39 aircraft p 842 A90-49836
- LUTZE, FREDERICK H.**
Toward a theory of aircraft agility [AIAA PAPER 90-2808] p 752 A90-45143
- LUU, T. S.**
The development of an exact conservative scheme associated with the supersonic trailing edge separation modelling for the computation of the transonic 2D cascade p 12 A90-12551
- LYCHIK, V. I.**
Ground aviation equipment: Handbook p 593 A90-36153
- LYNCH, B. G.**
The Helicopter Antenna Radiation Prediction Code (HARP) [NASA-CR-186925] p 884 N90-27946
- LYNN, PAUL A.**
Radar systems p 208 A90-17305
- LYNN, ROBERT R.**
The Bell Helicopter AH-1 Cobra - Past, present, and future [AIAA PAPER 90-3271] p 836 A90-48862
- LYONS, D. F.**
Flight test and numerical analysis of a half-scale Unmanned Air Vehicle [AIAA PAPER 90-1260] p 494 A90-33890
- LYONS, DANIEL F.**
Aerodynamic analysis of a US Navy and Marine Corps unmanned air vehicle [AD-A218282] p 498 N90-20077
- LYONS, T. J.**
Fog formation at Perth Airport p 611 A90-37748
- LYRINTZIS, CONSTANTINOS S.**
Random response and noise transmission of discretely stiffened composite panels p 283 A90-23288
Structure-borne noise transmission in cylindrical enclosures due to random excitation [AIAA PAPER 90-0990] p 463 A90-29402
- LYSENKO, A. I.**
An analysis of the possibility of expanding the information base of an adaptive control system for a flight vehicle surrounded by an ionized gas medium p 60 A90-10845
The discontinuity condition in the optimal control problem for a composite system p 76 A90-10848
- LYTLE, C. D.**
Airborne Doppler radar flight experiments for the detection of microbursts p 542 N90-21243

M

- MA, CHEN-CHI M.**
Chemical resistance of carbon fiber reinforced polyether ether ketone and polyphenylene sulfide composites p 944 A90-50142
- MA, DER-MING**
Optimal plane change by low aerodynamic forces [AIAA PAPER 90-2831] p 763 A90-45137
- MA, HUIYANG**
Vortex method modelling the unsteady motion of a thick airfoil p 396 A90-31489
- MA, JIAJU**
Effect of condensation in a diffuser on the flow field p 603 A90-36784
- MA, MEI**
The flutter characteristic analysis and optimization design of mistuning blade p 42 A90-11799
- MA, REI**
Digital control experiment research on the engine JT15D-4 p 190 A90-18600
- MA, SHENYI**
A study of ground vortex p 158 A90-18590
- MA, YANWEN**
On efficiency and accuracy of numerical methods for solving aerodynamic equations p 304 A90-25730
- MA, ZHIHENG**
A study on the application of controllability and observability concepts in the design of flight control systems p 693 A90-39303
- MAAHS, H. G.**
Performance evaluations of oxidation-resistant carbon-carbon composites in simulated hypersonic vehicle environments p 874 A90-48131
- MAAHS, HOWARD G.**
Carbon-carbon composites: Emerging materials for hypersonic flight [NASA-TM-103472] p 767 N90-26080
- MAARI, SAMI**
Robotic-aided system for inspection of aging aircraft [NIAR-90-9] p 777 N90-26346

- MAATOUCH, A.**
Aerodynamics of unsteady systems. Numerical study of potential flow/boundary layer coupling
[ETN-90-96257] p 396 N90-18367
- MABEE, DAVID S.**
Validation of GEMACS for prediction of lightning induced electromagnetic fields p 819 A90-49845
- MABEY, D. G.**
Alleviation of shock oscillations in transonic flow by passive controls
[AIAA PAPER 90-0046] p 161 A90-19648
Physical phenomena associated with unsteady transonic flows p 394 A90-29883
The development of leading-edge notches to improve the subsonic performance of wings of moderate sweep p 491 A90-33367
Wide angle diffusers with passive boundary-layer control
[AIAA PAPER 90-1600] p 567 A90-38732
Unsteady aerodynamics of controls p 935 N90-28525
The steady and time-dependent aerodynamic characteristics of a combat aircraft with a delta or swept canard p 921 N90-28526
- MACCAGNO, T. M.**
Processing of advanced ceramics which have potential for use in gas turbine aero engines
[AD-A220988] p 766 N90-25226
- MACCORMACK, ROBERT W.**
Modeling supersonic combustion using a fully-implicit numerical method
[AIAA PAPER 90-2307] p 677 A90-42117
- MACE, JAMES**
Integrated air vehicle/propulsion technology for a multirole fighter - A MCAIR perspective
[AIAA PAPER 90-2278] p 644 A90-42105
- MACEDO, MARIO**
The potential for an extra runway at Heathrow: A preliminary feasibility study
[TT-9007] p 938 N90-29403
- MACEDOMOURA, GERALDO A.**
An approach for design and analysis of composite rotor blades
[AD-A219257] p 734 N90-25125
- MACHA, J. M.**
Slotted-wall research with disk and parachute models in a low-speed wind tunnel
[AIAA PAPER 90-1407] p 595 A90-37946
Slotted-wall research with disk and parachute models in a low-speed wind tunnel
[DE90-002989] p 572 N90-21737
- MACHA, J. MICHAEL**
Wall-interference corrections for parachutes in a closed wind tunnel p 440 A90-31281
Preliminary characterization of parachute wake recontact p 622 A90-40681
An experimental investigation of wall-interference effects for parachutes in closed wind tunnels
[DE90-001802] p 236 N90-15076
- MACHEERS, FRANK**
Program plan: International aircraft operator data base
[IAR-90-1] p 783 N90-25697
- MACHEERS, FRANK H.**
Evaluation of existing aircraft operator data bases
[DOT/FAA/CT-90/18] p 898 N90-28463
International aircraft operator data base master requirements and implementation plan
[DOT/FAA/CT-90/17] p 967 N90-29247
- MACIA, JACQUELINE**
Improved Thermo-Oxidative-Deposition screening tests for turbine lubricants
[AD-A217795] p 533 N90-21188
- MACK, ROBERT J.**
A study of sonic boom overpressure trends with respect to weight, altitude, Mach number, and vehicle shaping
[AIAA PAPER 90-0367] p 164 A90-19816
- MACKALL, DALE A.**
A knowledge-based system design/information tool for aircraft flight control systems
[AIAA PAPER 89-2978] p 55 A90-10491
A knowledge-based system design/information tool for aircraft flight control systems
[NASA-TM-101704] p 217 N90-13990
- MACKAY, MICHAEL**
Chordwise loading and camber for two-dimensional thin sections
[AD-A213318] p 95 N90-12568
- MACKENZIE, FRANKLIN D.**
FAA Loran early implementation project
[AD-A221866] p 824 N90-26805
- MACKENZIE, P.**
Toughened cyanates for aerospace applications p 942 A90-50088
977 - Characterization of a family of new toughened epoxy resins p 943 A90-50089
- MACKIN, CLIFF**
MLS RNAV accuracy flight tests
[SAE PAPER 892218] p 728 A90-45435
- MACKIN, CLIFFORD W.**
An evaluation of the accuracy of a microwave landing system area navigation system at Miami/Tamiami Florida Airport
[DOT/FAA/CT-TN89/40] p 640 N90-23377
- MACKLER, STEVEN A.**
Robust hover control for a short takeoff/vertical landing aircraft
[AIAA PAPER 90-3333] p 862 A90-47593
- MACKUSE, FRANCES A.**
Flight service automation system, model 1 full capacity. NAS operational test and evaluation integration test plan
[DOT/FAA/CT-TN90/4] p 825 N90-27672
- MACLEAN, R.**
Hot gas environment around STOV aircraft in ground proximity. I - Experimental study
[AIAA PAPER 90-2269] p 742 A90-42765
- MACLEOD, J. D.**
The effects of a compressor rebuild on gas turbine engine performance: Final results p 952 N90-28701
- MACMINN, STEPHEN R.**
A very high speed switched-reluctance starter-generator for aircraft engine applications p 452 A90-30791
Control of a switched-reluctance aircraft engine starter-generator over a very wide speed range p 586 A90-38130
- MACPHAIL, J. D.**
Acoustic emission detection of crack presence and crack advance during flight p 886 N90-28082
- MACPHERSON, J. I.**
Adverse weather operations during the Canadian Atlantic storms program p 281 N90-15052
- MACROSSAN, M. N.**
Hypervelocity flow of dissociating nitrogen downstream of a blunt nose p 811 A90-48712
- MACY, WILLIAM W.**
Improved steel for landing gear design
[SAE PAPER 892335] p 765 A90-45490
Titanium matrix composite landing gear development
[SAE PAPER 892337] p 733 A90-45491
- MADABOOSI, S. R.**
Stochastic flutter of a panel subjected to random in-plane forces. I - Two mode interaction p 444 A90-27992
- MADAN, R. C.**
Subcomponent tests for composite fuselage technology readiness p 490 A90-33105
- MADAN, RAM C.**
Impact damage and residual strength analysis of composite panels with bonded stiffeners p 642 A90-40130
- MADAVAN, NATERI K.**
Supercomputer applications in gas turbine flowfield simulation p 620 A90-40495
Unsteady analysis of hot streak migration in a turbine stage
[AIAA PAPER 90-2354] p 769 A90-42782
- MADAYAG, A. F.**
Criteria for general aviation fuel systems crashworthiness
[SAE PAPER 891016] p 109 A90-14328
- MADDALON, D. V.**
Laminar flow control leading-edge systems in simulated airline service p 335 A90-26134
Measurement of crossflow vortices, attachment-line flow, and transition using microthin hot films
[AIAA PAPER 90-1636] p 607 A90-38765
- MADDALON, DAL V.**
Performance of laminar-flow leading-edge test articles in cloud encounters p 104 N90-12511
Simulated airline service experience with laminar-flow control leading-edge systems p 104 N90-12512
Simulated-airline-service flight tests of laminar-flow control with perforated-surface suction system
[NASA-TP-2966] p 338 N90-17627
- MADDUX, G. E.**
Modal characteristics of swept plate flutter models p 207 A90-16962
- MADHAVAN, N. S.**
Numerical solution of unsteady Navier-Stokes equations for laminar/turbulent flows past axis-symmetric bodies at angle of attack p 85 A90-15235
Numerical simulation of supersonic and hypersonic turbulent compression corner flows using PNS equations p 85 A90-15242
- MADISON, ROBIN M.**
An expert system for real-time aircraft monitoring
[AIAA PAPER 90-1311] p 545 A90-33921
- MAEDA, T.**
Development of ceramic components for high-temperature gas turbines p 602 A90-35951
- MAERTINS, HANS F.**
Design and development of the Garrett F109 turbofan engine
[SAE PAPER 891046] p 109 A90-14350
- MAESTRELLO, L.**
Optimum shape of a blunt forebody in hypersonic flow
[NASA-CR-181955] p 171 N90-13351
- MAESTRELLO, LUCIO**
Application of localized surface heating to actively control the boundary layer separation p 806 A90-46848
Application of sound and temperature to control boundary-layer transition p 92 N90-12537
- MAGILL, S. A. N.**
Computer-based tools for assisting air traffic controllers with arrivals flow management
[RSRE-88001] p 178 N90-13386
- MAGLIERI, D. J.**
Sonic boom signature data from cruciform microphone array experiments during the 1966-1967 EAFB national sonic boom evaluation program
[NASA-CR-182027] p 549 N90-21605
- MAGLIERI, DOMENIC J.**
Summary of sonic boom rise times observed during FAA community response studies over a 6-month period in the Oklahoma City area
[NASA-CR-4277] p 696 N90-24852
- MAGLIOZZI, BERNARD**
Acoustic test and analysis of a counterrotating prop-fan model
[NASA-CR-179590] p 79 N90-10683
- MAGNESS, C.**
Flow visualization via laser-induced reflection from bubble sheets p 680 A90-39784
- MAGNI, J. F.**
Design of a helicopter output feedback control law using modal and structured-robustness techniques p 282 A90-20557
- MAGNUSEN, P. E.**
The influence of material quality on airframe structural durability p 676 A90-41336
- MAGROGAN, MICHAEL**
MLS RNAV accuracy flight tests
[SAE PAPER 892218] p 728 A90-45435
- MAH, T.**
Processing and mechanical properties of Al2O3/Y3Al5O12 (YAG) eutectic composite p 951 A90-51966
- MAHAJAN, SAVITA**
Solutions of two-dimensional Euler equations with multigrid acceleration p 810 A90-48086
- MAHAPATRA, P. R.**
A powerful range-Doppler clutter rejection strategy for navigational radars p 403 A90-30688
- MAHAPATRA, PRAVAS R.**
Accurate ILS and MLS performance evaluation in presence of site errors p 404 A90-30693
- MAHMOOD, SOHAEL**
Aerodynamic losses in conventional fan blades of high by pass turbo engine p 854 A90-49487
- MAHMOUD, SAAD MUSTAFA**
Effective optimal control of a fighter aircraft engine p 928 N90-28548
- MAHONEY, WILLIAM P.**
The source region and evolution of a microburst downdraft p 456 A90-28612
- MAIDA, JAMES L.**
Prototype testing of an integrated Doppler/GPS navigation system p 577 A90-36926
- MAIER, THOMAS H.**
An examination of helicopter rotor load calculations p 833 A90-46972
An examination of helicopter rotor load calculations
[AD-A214295] p 249 N90-15098
- MAIKAPAR, G. I.**
Lee-side heating of a delta wing in supersonic flow p 10 A90-12281
Wave rider volume distribution p 388 A90-29006
- MAILAENDER, MARTIN**
Materials and structures for 2000 and beyond: An attempted forecast by the DLR Materials and Structures Department
[ESA-TT-1154-REV] p 775 N90-26173
- MAINARD, CURT W.**
An optically interfaced propulsion management system applied to a commercial transport aircraft p 424 A90-30811
- MAINE, TRINDEL A.**
A preliminary evaluation of an F100 engine parameter estimation process using flight data
[AIAA PAPER 90-1921] p 656 A90-40559
- MAINES, B. H.**
Impact of nose-probe chines on the vortex flows about the F-16C
[AIAA PAPER 90-0386] p 165 A90-19828

MAISEL, MARTIN D.

- Tilt rotor aircraft aeroacoustics p 409 A90-28238
- MAITA, MASATAKA**
Propulsive lift augmentation by side fences as applied to Japan's experimental STOL aircraft, ASKA [AIAA PAPER 90-3009] p 789 A90-45859
- MAJIDZADEH, KAMRAN**
Development of acceptance plans for airport pavement materials. Volume 1: Development [DOT/FAA/RD-80/15] p 937 N90-28581
- MAJJIGI, R. K.**
An investigation of counterrotating tip vortex interaction [NASA-CR-185135] p 79 N90-11549
- MAK, A.**
Reduction of the side force on pointed forebodies through add-on tip devices [AIAA PAPER 90-3005] p 788 A90-45854
- MAKIN, I. V.**
Asymptotic calculation of flow parameters in the problem of hypersonic flow past blunt axisymmetric bodies p 10 A90-12268
- MAKOWIEC, GEORGE M.**
Wind-tunnel and flight-test investigation of the exordone remotely piloted vehicle configuration [AIAA PAPER 90-1261] p 494 A90-33891
Static wind-tunnel and radio-controlled flight test investigation of a remotely piloted vehicle having a delta wing planform [NASA-TM-4200] p 632 N90-24238
- MAKSIMOVIC, STEVAN**
Some computational and experimental aspects of optimal design process of composite structures p 882 A90-48050
- MAKSYMUK, C. M.**
A comparison of two central difference schemes for solving the Navier-Stokes equations [NASA-TM-102815] p 816 N90-27654
- MAL'KOV, V. M.**
Mean and pulse characteristics of supersonic flow in a wind tunnel with a honeycomb nozzle p 231 A90-22421
Experimental investigation of GDL diffusers [AIAA PAPER 90-1512] p 563 A90-38659
- MAL'TSEV, I. N.**
Effect of the roughness of deposits in a compressor cascade on the flow lag angle p 84 A90-14578
- MALAEK, SEYYED**
Automated aircraft configuration design and analysis [SAE PAPER 891072] p 101 A90-14368
- MALAK, M. F.**
JFS190 turbine engine performance optimized using Taguchi methods [AIAA PAPER 90-2419] p 663 A90-42169
- MALANICHEV, V. A.**
An experimental study of a supersonic gas ejector p 851 A90-46546
- MALCOLM, G. N.**
Forebody vortex manipulation for aerodynamic control of aircraft at high angles of attack [SAE PAPER 892220] p 756 A90-45437
- MALCOLM, GERALD N.**
Aerodynamic control of aircraft by forebody vortex manipulation [AIAA PAPER 90-1827] p 301 A90-25167
Effect of leading edge roundness on a delta wing in wing-rock motion [AIAA PAPER 90-3080] p 795 A90-45911
Development of non-conventional control methods for high angle of attack flight using vortex manipulation p 935 N90-28522
- MALDONADO, JAIME J.**
Supersonic through-flow fan engine and aircraft mission performance [NASA-TM-102304] p 516 N90-21038
- MALECKI, R. E.**
Navier-Stokes analysis of an ejector and mixer-ejector operating at pressure ratios in the range 2-4 [AIAA PAPER 90-2730] p 626 A90-42218
- MALECKI, ROBERT E.**
Navier-Stokes analysis of a lobed mixer and nozzle [AIAA PAPER 90-0453] p 192 A90-19852
Calculation of internal flows using a single-pass, parabolized Navier-Stokes analysis p 469 A90-32458
- MALEK, A.**
New transonic test sections for the NAE 5 ft x 5 ft trisonic wind tunnel [AD-A220933] p 674 N90-24278
- MALHOTRA, R. C.**
Effect of downstream elements on the flow at the exit of centrifugal compressor rotor p 157 A90-18483
- MALHOTRA, V.**
Toughened cyanates for aerospace applications p 942 A90-50088
977 - Characterization of a family of new toughened epoxy resins p 943 A90-50089

MALIK, M. R.

- Goertler vortices in supersonic and hypersonic boundary layers p 83 A90-14091
Design and operational features of low-disturbance wind tunnels at NASA Langley for Mach numbers from 3.5 to 18 [AIAA PAPER 90-1391] p 594 A90-37936
- MALIK, MUJEEB R.**
Prediction and control of transition in supersonic and hypersonic boundary layers p 16 A90-12828
Effects of shock on the stability of hypersonic boundary layers [AIAA PAPER 90-1448] p 561 A90-38608
Advanced Mach 3.5 Axisymmetric Quiet Nozzle [AIAA PAPER 90-1592] p 566 A90-38727
Curvature effects on the stability of three-dimensional laminar boundary layers p 71 N90-10366
Supersonic laminar-flow control p 93 N90-12554
Design and fabrication requirements for low noise supersonic/hypersonic wind tunnels p 122 N90-12555
Experimental and theoretical investigation of boundary-layer instability mechanisms on a swept leading edge at Mach 3.5 p 94 N90-12557
- MALIK, S. N.**
Elevated temperature crack growth [NASA-CR-182247] p 777 N90-26355
- MALKIN, FRANK J.**
Counterair situation awareness display for Army aviation p 964 N90-28982
- MALKOV, V. A.**
The investigation of heat transfer in cooled blades of gas turbines [AIAA PAPER 90-2144] p 685 A90-42043
- MALLET, M.**
Development of finite element methods for compressible Navier-Stokes flow simulations in aerospace design [AIAA PAPER 90-0403] p 166 A90-19833
- MALONE, J. B.**
An efficient airfoil design method using the Navier-Stokes equations p 500 N90-20981
- MALONE, JOHN B.**
BELLTECH - A multipurpose Navier-Stokes code for rotor blade and fixed wing configurations p 384 A90-28174
- MALONEY, PAUL F.**
Strike tolerant main rotor blade tip p 409 A90-28232
- MALYSHEV, VENIAMIN V.**
Optimization of the observations and control of aircraft p 60 A90-12468
- MAMAEV, B. I.**
A minimal permissible radial clearance in a gas turbine p 110 A90-14569
- MANCUS, EDWARD**
Aircraft Reply and Interference Environment Simulator (ARIES) hardware principles of operation. Volume 2: Appendixes [DOT/FAA/CT-TN88/4-2] p 135 N90-12781
Aircraft Reply and Interference Environment Simulator (ARIES) hardware principles of operation, volume 1 [DOT/FAA/CT-TN88/4-1] p 135 N90-12782
- MANDERSCHIED, JANE M.**
Analysis of whisker-toughened ceramic components - A design engineer's viewpoint p 205 A90-19149
Noninteractive macroscopic reliability model for ceramic matrix composites with orthotropic material symmetry [ASME PAPER 89-GT-129] p 360 A90-23827
- MANFRIANI, L.**
Aerodynamic control design: Experience and results at Aermacchi p 935 N90-28518
- MANG, JOYCE M.**
Redesign of an electro-optical shroud in graphite/epoxy p 676 A90-40215
- MANGALAM, S. M.**
Measurement of crossflow vortices, attachment-line flow, and transition using microthin hot films [AIAA PAPER 90-1636] p 607 A90-38765
- MANGALAM, SIVA M.**
Goertler instability on an airfoil: Comparison of marching solution with experimental observations p 19 N90-10364
Simultaneous detection of separation and transition in surface shear layers p 72 N90-10368
Goertler instability on an airfoil p 91 N90-12517
Experimental studies on Goertler vortices p 91 N90-12529
- MANGALAM, SIVARAMAKRISHNAN M.**
Method and apparatus for detecting laminar flow separation and reattachment [NASA-CASE-LAR-13952-1-SB] p 455 N90-19534
- MANGANAS, A.**
Recursive real-time identification of step-response matrices of helicopters for adaptive digital flight control p 195 A90-17703

MANGIACASALE, L.

- Canard versus aft-tail ride qualities performance and pilot command response p 258 N90-15053
- MANGOLD, P.**
Inflight thrust vectoring: A further degree of freedom in the aerodynamic/flight mechanical design of modern fighter aircraft p 921 N90-28528
Aerodynamic interferences of in-flight thrust reversers in ground effect p 921 N90-28529
- MANGOLD, VERNON L., JR.**
Advanced software for turbine blade processing [SME PAPER MS89-330] p 274 A90-23694
- MANI, R.**
High speed turboprop aeroacoustic study (counterrotation). Volume 1: Model development [NASA-CR-185241] p 782 N90-26633
- MANI, RAMANI**
The radiation of sound from a propeller at angle of attack [NASA-CR-4264] p 548 N90-21602
- MANKBADI, REDA R.**
A study of unsteady rotor-stator interactions p 67 A90-11557
- MANN, D. L.**
A study of particle trajectories in a gas turbine intake p 48 A90-12583
A theoretical approach to particle separator design p 48 A90-12584
- MANN, J. Y.**
Fatigue of thick-section cold-expanded holes with and without cracks p 270 A90-20987
- MANN, MICHAEL J.**
Validation of a computer code for analysis of subsonic aerodynamic performance of wings with flaps in combination with a canard or horizontal tail and an application to optimization [NASA-TP-2961] p 173 N90-14187
- MANN, MICHAEL K.**
The US air traffic control system architecture p 330 A90-25561
- MANNANT, J. P.**
The question of the casting factor p 64 N90-10238
- MANNES, M. A.**
A technique for the tuning of helicopter flight control systems p 670 A90-42467
- MANNING, A. P.**
The development of a low cost data logging system for flight trials based on an IBM compatible PC [RAE-TM-FM-16] p 251 N90-15917
- MANNING, CLARKE O.**
Development of a least squares time response lower-order equivalent systems technique [AD-A220527] p 648 N90-23389
- MANNING, JAMES C.**
External nozzle flap dynamic load measurements on F-15 S/MTD model [AIAA PAPER 90-1910] p 740 A90-42692
- MANNING, S. D.**
Demonstration of probabilistic-based durability analysis method for metallic airframes p 273 A90-23287
Stochastic crack growth analysis methodologies for metallic structures [AIAA PAPER 90-1015] p 449 A90-29340
- MANOHARAN, L. C.**
A fiberoptic LAN for aircraft and other applications p 282 A90-23241
- MANOR, DAVID**
Static and dynamic water tunnel tests of slender wings and wing-body configurations at extreme angles of attack [AIAA PAPER 90-3021] p 869 A90-45888
- MANSER, R.**
Measurement of wind tunnel model deformation under airload p 522 A90-33370
Aeroelastic tailoring validation by windtunnel model testing p 492 A90-33389
- MANSFIELD, F. A.**
Numerical investigation of laminar separated viscous trailing-edge flow using triple-deck theory [AIAA PAPER 90-3046] p 792 A90-45883
- MANSINGH, VIVEK**
Effects of splitter plates on the wake flow behind a bluff body p 469 A90-32453
- MANSOUR, NAGI N.**
Direct numerical simulations of transition in a compressible wake p 553 A90-35212
The effect of Mach number on the stability of a plane supersonic wake p 557 A90-36524
- MANSUET, ANNE**
Toxicity of thermolysis products from the materials of airplane cockpits [CEAT-PV-M6/5924/02] p 876 N90-27895
- MANTAY, WAYNE R.**
Integrated multidisciplinary design optimization of rotorcraft [NASA-TM-101642] p 36 N90-10889

- Integrated multidisciplinary optimization of rotorcraft: A plan for development
[NASA-TM-101617] p 106 N90-12580
- General approach and scope p 106 N90-12581
- Rotor blade dynamic design p 106 N90-12583
- Validation of the procedures p 107 N90-12587
- MANTEGAZZA, CLAUDIO**
A fast collocation method for transonic airfoil design p 501 N90-20984
- MANTEGAZZA, P.**
Active flutter suppression for a wing model p 433 A90-31283
- MANUEL, G. S.**
Investigations of modifications to improve the spin resistance of a high-wing, single-engine, light airplane [SAE PAPER 891039] p 118 A90-14345
In-flight flow visualization using infrared imaging p 731 A90-44731
- MANUEL, GREGORY S.**
A flight test investigation of certification requirements for laminar-flow general aviation airplanes [AIAA PAPER 90-1310] p 496 A90-33920
- MANUILOVICH, S. V.**
Perturbations of a three-dimensional boundary layer produced by body irregularities p 150 A90-17107
Eigenvalue problem in the theory of flow past thin profiles at high supersonic velocity p 295 A90-24096
Response of a subsonic boundary layer to a pulsed oscillation of a localized region of the surface in the flow p 811 A90-48295
- MANWARING, S. R.**
Three-dimensional aerodynamics of an annular airfoil cascade including loading effects p 87 A90-15889
Inlet distortion generated periodic aerodynamic rotor response [ASME PAPER 89-GT-299] p 475 A90-33567
- MANWARING, STEVEN R.**
Forcing function effects on rotor row unsteady aerodynamic response in a multistage compressor p 573 N90-22536
- MAO, KE-JIU**
Simulation research on the afterburning dynamic characteristics of engine control system p 48 A90-12581
- MAO, KEJUI**
The establishment of mathematical model of engine control system and simulation research of afterburning dynamic characteristics p 190 A90-18613
Simulation research on the afterburning dynamic characteristics of engine control system p 585 A90-35708
- MAPES, D. E.**
Ultra high bypass turbofan technologies for the twenty-first century [AIAA PAPER 90-2397] p 662 A90-42158
- MAPHET, THOMAS ALLEN**
High temperature VSCF (Variable Speed Constant Frequency) generator system [AD-A210823] p 71 N90-10351
- MAPLE, RAYMOND C.**
An iterative solution to aeroelastic effects in potential flow [AD-A216291] p 320 N90-17580
- MARATHE, B. V.**
Comparative cascade studies of some high diffusion compressor bladings p 15 A90-12637
Comparison of NACA 65, CDA, and tandem bladed cascades p 190 A90-18484
- MARATHE, K. G.**
Unbalance response studies on a model rotor supported on uncentralised squeeze film dampers and the development experience of a jet engine p 69 A90-12579
- MARAWA, AMOS**
The potential for an extra runway at Heathrow: A preliminary feasibility study [TT-9007] p 938 N90-29403
- MARAZZI, R.**
A tool for automatic design of airfoils in different operating conditions p 502 N90-20994
- MARCH, ARTEMIS**
The future of the U.S. aircraft industry p 467 A90-32275
- MARCH, WILLIAM L.**
The role of expert systems in aircraft safety management p 375 A90-26225
- MARCHANT, R. D.**
Energy Efficient Engine: High-pressure compressor test hardware detailed design report [NASA-CR-180850] p 932 N90-28570
- MARCHBANK, IAN**
Automated R.T.M. for an airframe component p 534 A90-31881
- MARCHETTO, B.**
AM-X high incidence trials, development and results [ETN-90-97277] p 759 N90-26016
- MARCHIONNA, N.**
Controlled mixing and variable geometry combustor design effects on emissions and combustion characteristics p 45 A90-12547
- MARCHIONNI, M.**
Time dependent effects on high temperature low cycle fatigue and fatigue crack propagation on nickel base superalloys p 443 A90-29881
- MARCHITTI, M.**
Problems related to the acquisition, processing and utilization of the modal parameters measured in flight tests in order to obtain the full envelope for flutter [ETN-89-95210] p 103 N90-11735
- MARCOLINI, MICHAEL A.**
The acoustic results of a United Technologies scale model helicopter rotor tested at DNW [NASA-TM-101879] p 896 N90-27471
- MARCUM, D. L.**
A three-dimensional finite element Navier-Stokes solver with k-epsilon turbulence model for unstructured grids [AIAA PAPER 90-1652] p 570 A90-38780
- MARCUS, DANIEL L.**
The interaction between a counter-rotating vortex pair in vertical ascent and a free surface p 151 A90-17580
- MAREK, C. J.**
A planar reacting shear layer system for the study of fluid dynamics-combustion interaction [NASA-TM-102422] p 194 N90-13393
- MARESCA, CH.**
Experimental study of 2D/3D interactions between a vortical flow and a lifting surface p 86 A90-15849
- MARESH, JEFFERY L.**
Realtime graphic flight simulations using multiple minicomputers p 351 A90-26203
- MARGERIDIS, J.**
Extending the overhaul interval for gas turbine engines through the use of alternative coatings on first stage blades p 63 A90-12539
- MARIN, JEAN-YVES**
The application of infrared thermography to the nondestructive testing of composite materials p 886 N90-28084
- MARINI, MARTINO**
Axial flow compressor design optimization. II - Through-flow analysis [ASME PAPER 89-GT-202] p 342 A90-23874
- MARINICHENKO, S. K.**
Laminar separated flow on a biconical body at high supersonic velocities p 387 A90-28992
- MARION, PIERRE**
Breakage of fan blades in the S1 wind tunnel at Mondane-Avriex [ONERA, TP NO. 1989-104] p 57 A90-11138
- MARK, J. L.**
Research on a two-dimensional inlet for a supersonic V/STOL propulsion system. Appendix A [NASA-CR-174945] p 396 N90-18364
- MARK, W. D.**
Some implications of the isotropic momentarily frozen assumptions for the SPAN-MAT program [NASA-CR-181937] p 88 N90-11704
- MARKATOS, N. C.**
Forced and natural venting of aircraft cabin fires: A numerical simulation p 326 N90-17597
- MARKEWICZ, R.**
Theoretical and experimental analysis of a model rotor blade incorporating a swept tip p 151 A90-17586
- MARKIN, KELLY**
Design considerations for achieving MLS Category III requirements p 331 A90-25575
- MARKOPOULOS, NIKOS**
Thrust law effects on the longitudinal stability of hypersonic cruise [AIAA PAPER 90-2820] p 763 A90-45149
- MARKOV, V. G.**
Optimization of the shape of a sealed shell and of the size and location of its reinforcements p 957 A90-50773
- MARKS, BRET A.**
Innovative control concepts and component integration for a generic supercruise fighter p 935 N90-28521
- MARKS, JOHN E.**
Design and fabrication of a prototype resin matrix composite interceptor structure [AIAA PAPER 90-1004] p 442 A90-29275
- MARLEAU, A.**
Probabilistic approach to fleet management p 701 A90-42674
- MAROON, GARY N.**
Survivable penetration p 917 N90-29363
- MARQUIER, G.**
Characterization of the CP 214 T851. Dissection of a cast flat bar for a standard spar [CEAT-PV-M4/462200] p 876 N90-27905
- Characterization of the 7175 T7352. Dissection of a die casting standard spar [CEAT-PV-M5/528900] p 877 N90-27906
- Characterization of the 7175 T7352 101. Dissection of a die casting standard spar [CEAT-PV-M5/5288] p 877 N90-27907
- Characterization of the 7010 T73651. Dissection of a sheet billet for a standard spar [CEAT-PV-M5/521700] p 877 N90-27908
- MARQUIS, D.**
Modeling of the oil quench for Ni-based superalloy turbine disks p 957 A90-51525
- MARR, ROGER**
V-22 aerodynamic loads analysis and development of loads alleviation flight control system p 410 A90-28239
- MARRAFFA, LIONEL**
Inviscid non equilibrium flow in ONERA F4 wind tunnel [ONERA, TP NO. 1989-161] p 223 A90-21029
- MARRISON, CLAIRE**
Aircraft evacuations: The effect of passenger motivation and cabin configuration adjacent to the exit [CAA-PAPER-89019] p 913 N90-29336
- MARRONE, PAUL V.**
Blunt-nose inviscid airflows with coupled nonequilibrium processes p 171 N90-13336
- MARSH, GEORGE**
Developing aluminium p 204 A90-17924
Lose weight with Al-Li p 765 A90-44175
- MARSHAK, WILLIAM P.**
Strategic aircraft engineering design simulation p 439 A90-30729
- MARSHALL, R. J.**
Helicopter rotor test rig (RoTeSt) in DNW: Application and results [RAE-TRANS-2171] p 201 N90-13408
- MARSHALL, S. E.**
Evaluation of analysis techniques for low frequency interior noise and vibration of commercial aircraft [NASA-CR-181851] p 220 N90-14866
- MARSHALL, T. A.**
Spanwise properties of the unsteady separation shock in a Mach 5 unswept compression ramp interaction [AIAA PAPER 90-0377] p 228 A90-22208
- MARSILIO, R.**
Numerical method for designing 3D turbomachinery blade rows p 511 N90-20990
- MARSILIO, ROBERTO**
Shock-fitting method for two-dimensional inviscid, steady supersonic flows in ducts p 477 A90-34864
Shock-fitting in three space dimensions p 707 A90-44434
- MARSTON, R. K.**
Laser communication system design p 26 A90-11813
- MARSTON, S. E.**
Fly-by-light flight control system technology development plan [NASA-CR-181953] p 259 N90-15111
- MARTIANOVA, TATIANA S.**
Dynamics of aviation gas turbine engines p 113 A90-16049
- MARTELLI, FRANCESCO**
Viscous flow calculations in turbomachinery channels [ASME PAPER 89-GT-5] p 287 A90-23752
- MARTELLUCCI, A.**
The challenging process of validating CFD codes [AIAA PAPER 90-1402] p 558 A90-37943
- MARTENS, N. W.**
Effect of riblets on flow separation in a subsonic diffuser p 712 A90-45261
- MARTIN-CARRILLO DOMINGUEZ, ANTONIO**
The impact of composites on the aerospace industry p 221 A90-22649
- MARTIN-CARRILLO, A.**
Impact of composites in the aerospace industry [ETN-90-96231] p 443 N90-18527
- MARTIN, C. A.**
A flight dynamic model of aircraft spinning [AR-005-600] p 935 N90-28576
- MARTIN, C. L.**
Taguchi methods in conceptual design for life cycle cost [AIAA PAPER 90-3222] p 839 A90-49109
- MARTIN, CHARLES A.**
An advanced pneumatic impulse ice protection system (PIIP) for aircraft [AIAA PAPER 90-0492] p 182 A90-19875
- MARTIN, COLIN A.**
Measurements of pressures on the wing of an aircraft model during steady rotation [AIAA PAPER 90-2842] p 754 A90-45162
Measurements of pressures on the tail and aft fuselage of an airplane model during rotary motions at spin attitudes [NASA-TP-2939] p 20 N90-10829

- The spinning of aircraft: A discussion of spin prediction techniques including a chronological bibliography [ARL-AERO-R-177] p 36 N90-10888
- MARTIN, D. A.**
Fiber optic sensor systems for smart aerospace structures p 38 A90-11208
- MARTIN, DANIEL M.**
Analysis and design of sidestick controller systems for general aviation aircraft p 196 A90-19554
- MARTIN, DAVID J.**
Progress in certifying F402-RR-408 - The improved Pegasus engine for AV-8B and Harrier II Plus p 587 A90-38532
- MARTIN, J. F.**
Some considerations in ultra light aircraft design p 730 A90-42673
- MARTIN, JAMES L.**
Simulation, evaluation of transition and hover flying qualities of a mixed-flow, remote-lift STOVL aircraft [SAE PAPER 892284] p 757 A90-45464
- MARTIN, N. F., JR.**
Nonlinear finite-element analysis to predict fan-blade damage due to soft-body impact p 683 A90-40939
- MARTIN, R. H.**
Performance evaluations of oxidation-resistant carbon-carbon composites in simulated hypersonic vehicle environments p 874 A90-48131
- MARTIN, RUTH M.**
Rotor blade-vortex interaction impulsive noise source localization p 463 A90-27978
Acoustic design considerations: Review of rotor acoustic sources p 106 N90-12585
- MARTIN, STANLEY, JR.**
V-22 developmental status p 581 A90-38529
- MARTIN, WILLIAM P.**
Hypersonic waverider configurations for trans-atmospheric vehicles [AD-A217925] p 498 N90-20074
- MARTINEZ-VAL PENALOSA, RODRIGO**
Flight over the sea with twin or triple jet aircraft p 179 A90-17048
- MARTINEZ, FRANK**
Global Sentry: NASA/USRA high altitude reconnaissance aircraft design, volume 2 [NASA-CR-186820-VOL-2] p 736 N90-25971
- MARTINEZ, PATRICK**
Visualization of corona discharges p 819 A90-49839
- MARTINO, JOSEPH P.**
Study of bird ingestions into small inlet area, aircraft turbine engines (May 1987 to April 1988) [DOT/FAA/CT-89/17] p 402 N90-18375
- MARTINS, J. C. F.**
Empirical prediction of the blockage effect of a flat body on a rotor p 807 A90-46942
- MARTZ, STEVE**
Expert system - Conventional processing interface p 460 A90-30753
- MARULO, F.**
Aeroelastic analysis for a composite T-tailplane of a turboprop commuter aircraft p 492 A90-33390
- MARUSZEWSKI, J. P.**
Grid generation and its application to separated flows p 312 A90-26552
- MARVIN, JOSEPH G.**
CFD validation for aerodynamic flows - Challenge for the '90's [AIAA PAPER 90-2995] p 787 A90-45846
- MARX, ROBERT I.**
Air Force use of civil airworthiness criteria for testing and acceptance of military derivative transport aircraft [AIAA PAPER 90-3289] p 818 A90-48875
- MARX, Y.**
Multigrid acceleration of transonic flow computations p 147 A90-16783
- MASAD, J. A.**
Subharmonic instability of compressible boundary layers p 706 A90-44005
- MASAEIDA, H.**
Design and evaluation of graphite/epoxy truss core sandwich panels p 210 A90-18406
- MASCARELL, J. P.**
Three dimensional turbine blade analysis in thermo-viscoplasticity p 540 A90-34324
- MASCARELL, JEAN PIERRE**
Designing turbine blades for fatigue and creep p 112 A90-16007
- MASER, J. G.**
Parametric studies of advanced turboprops p 253 A90-21225
- MASKELL, R.**
Toughened cyanates for aerospace applications p 942 A90-50088
977 - Characterization of a family of new toughened epoxy resins p 943 A90-50089
- MASLOV, A. A.**
Wave structure of artificial perturbations in a supersonic boundary layer on a plate p 619 A90-39518
- MASON, MARY L.**
External nozzle flap dynamic load measurements on F-15 S/MTD model [AIAA PAPER 90-1910] p 740 A90-42692
An experimental investigation of thrust vectoring two-dimensional convergent-divergent nozzles installed in a twin-engine fighter model at high angles of attack [NASA-TM-4155] p 237 N90-15884
- MASON, W. H.**
2D vs. 3D - Selection of pressure distributions to delay separation on wings [AIAA PAPER 90-3026] p 790 A90-45868
On optimal supersonic/hypersonic bodies [AIAA PAPER 90-3072] p 796 A90-45918
Analytic models for technology integration in aircraft design [AIAA PAPER 90-3262] p 835 A90-48857
- MASSARDO, ARISTIDE**
Axial flow compressor design optimization. I - Pitchline analysis and multivariable objective function influence [ASME PAPER 89-GT-201] p 342 A90-23873
Axial flow compressor design optimization. II - Through-flow analysis [ASME PAPER 89-GT-202] p 342 A90-23874
- MASSARO, C.**
Co-development of CT7-6 engines - A continued tradition in technology and reliability p 665 A90-42485
- MASSOGLIA, PETER L.**
The use of satellite technology for oceanic air traffic control p 330 A90-25570
- MASSON, CHRISTIAN**
An integral method for transonic flows p 395 A90-31119
- MAST, H.-U.**
Neutron radiography: Applications and systems p 886 N90-28080
- MASTIN, C. W.**
Optimization methods applied to aerodynamic design problems in computational fluid dynamics p 156 A90-18308
Optimization of aerodynamic designs using computational fluid dynamics p 541 N90-20999
- MASUYA, G.**
Some governing parameters of plasma torch igniter/flammeholder in a scramjet combustor [AIAA PAPER 90-2098] p 661 A90-42017
- MASUYA, GORO**
Experimental study on autoignition in a scramjet combustor p 46 A90-12559
Cycle analysis of scramjet engines [NAL-TR-1002] p 51 N90-10035
Analysis of scramjet engine characteristics [NAL-TR-1041] p 933 N90-29398
- MATHEW, M. B.**
Nonlinear effects in helicopter rotor forward flight forced response p 347 A90-25420
Dynamic analysis of rotor blades with rotor retention design variations [AIAA PAPER 90-1159] p 412 A90-29394
A study of the influence of predeflections on the vibrations of blades p 585 A90-35673
- MATHIOUDAKIS, K.**
Jet engine fault detection with differential gas path analysis at discrete operating points p 50 A90-12633
Casing vibration and gas turbine operating conditions [ASME PAPER 89-GT-78] p 358 A90-23799
Computer modeling and data processing methods: An essential part of jet engine condition monitoring and fault diagnosis p 855 N90-27626
- MATHRE, JOHN MARK**
Computational investigation of incompressible airfoil flows at high angles of attack [AD-A205885] p 174 N90-14201
- MATHUR, G. P.**
UHB demonstrator interior noise control flight tests and analysis [NASA-CR-181897] p 140 N90-13198
- MATHUR, N. B.**
Axisymmetric afterbody flow separation at transonic speeds in presence of jet exhaust p 13 A90-12576
Underexpanded jet-freestream interactions on an axisymmetric afterbody configuration p 154 A90-18141
- MATOUSEK, OLDRICH**
Mathematical model of turboprop engine behaviour p 254 A90-23351
Modelling and simulation of turboprop engine behaviour p 424 A90-29946
Mathematical simulation model of an aircraft gas turbine p 745 A90-44721
- MATOV, VIKTOR I.**
Airborne digital computers and systems p 927 A90-52410
- MATSON, L. E.**
Processing and mechanical properties of Al2O3/Y3Al5O12 (YAG) eutectic composite p 951 A90-51966
- MATSUBARA, KAZUO**
Two effective methods of approach and landing by visual display [SAE PAPER 891054] p 108 A90-14356
- MATSUBARA, MASAOKI**
Study on application of ultrasonic wave measurement to creep-fatigue damage detection [DE89-782317] p 774 N90-25361
Development of creep-fatigue damage detection method of rotor steel by ultrasonic wave measurement [DE90-503792] p 777 N90-26365
- MATSUDA, S.**
Structure/control design synthesis of active flutter suppression system by goal programming [AIAA PAPER 90-3325] p 872 A90-47587
- MATSUDA, YUKIO**
Noncontact measurement of rotating blade vibrations [NAL-TR-1033] p 961 N90-29687
- MATSUI, TAKAO**
Studies on supersonic radial flow behavior in disk channel p 87 A90-16104
- MATSUI, TATSUYA**
Vorticity distribution of vortex street in the wake of a circular cylinder p 623 A90-41751
- MATSUKAWA, TATSUHIKO**
An electronic flight-recorder for a hang-glider p 39 A90-12234
- MATSUKI, MASAKATSU**
Cooling characteristics of a radial water blade p 47 A90-12571
- MATSUMOTO, Y.**
CRL's mobile satellite communication experiments using ETS-V [AIAA PAPER 90-0775] p 366 A90-25602
Air/water two-phase flow test tunnel for airfoil studies p 352 A90-26842
- MATSUMOTO, YOICHIRO**
Numerical calculation of bubbly two phase flow around an airfoil p 304 A90-25783
- MATSUMURA, HIROSHI**
Application of a digital control theory for generating adaptive grids p 366 A90-25734
- MATSUNAGA, K.**
Application of 3-D Navier-Stokes computation to bowed stacking turbine vane design [AIAA PAPER 90-2129] p 625 A90-42035
- MATSUNAKA, M.**
Development of ceramic components for high-temperature gas turbines p 602 A90-35951
- MATSUNO, KENICHI**
A high-order time-accurate scheme and its applications p 304 A90-25732
- MATSUO, YUICHI**
Navier-Stokes simulations around a high-speed propeller p 305 A90-25797
- MATSUSHIMA, KISA**
Navier-Stokes computations for the investigation of flowfields about a Space-Plane p 306 A90-25836
- MATSUSHITA, H.**
Multi-surface control law synthesis and wind tunnel test verification of active flutter suppression for a transport-type wing p 517 A90-33401
- MATSUURA, M.**
An experimental study of heat transfer and film cooling on low aspect ratio turbine nozzles [ASME PAPER 89-GT-187] p 361 A90-23865
- MATSUZAKI, Y.**
Response characteristics of a two-dimensional wing subjected to turbulence near the flutter boundary p 519 A90-34082
- MATTERN, DUANE L.**
H-infinity based integrated flight/propulsion control design for a STOVL aircraft in transition flight [AIAA PAPER 90-3335] p 862 A90-47595
H-infinity based integrated flight/propulsion control design for a STOVL aircraft in transition flight [NASA-TM-103198] p 758 N90-26011
- MATTES, L. A.**
Investigation of cowl vent slots for supercritical stability enhancement in dual-mode ramjet inlets p 507 A90-32951
- MATULICH, D.**
High-temperature bootstrap compared with F-15 growth air cycle air conditioning system [SAE PAPER 891436] p 336 A90-27407
- MATVEEVA, E. L.**
Nonstationary hypersonic flow past a thin wing of variable shape p 470 A90-32559
- MAUGHMER, MARK D.**
A computationally efficient modelling of laminar separation bubbles p 801 A90-46372

- The design of an airfoil for a high-altitude, long-endurance remotely piloted vehicle
p 104 N90-12545
- A computationally efficient modelling of laminar separation bubbles
[NASA-CR-185854] p 136 N90-12872
- Prediction of forces and moments for flight vehicle control effectors. Part 1: Validation of methods for predicting hypersonic vehicle controls forces and moments
[NASA-CR-186571] p 571 N90-21734
- Prediction of forces and moments for flight vehicle control effectors. Part 2: An analysis of delta wing aerodynamic control effectiveness in ground effect
[NASA-CR-186572] p 571 N90-21735
- A computational efficient modelling of laminar separation bubbles
[NASA-CR-186729] p 774 N90-25291
- MAULL, D. J.**
An investigation of the buffet excitation parameter
p 473 A90-33368
- An experimental and analytical investigation of the buffet excitation parameter
p 645 A90-42417
- MAURER, F.**
Applications of infra-red thermography in a hypersonic blowdown wind tunnel
p 438 A90-28300
- Infrared thermography at hypersonic channel H2K
p 674 N90-24235
- MAUTER, GEORGE A.**
Aircraft drawings index
p 618 N90-23340
- MAVRIPLIS, D. J.**
Euler and Navier-Stokes computations for airfoil geometries using unstructured meshes
p 630 A90-42425
- MAVRIPLIS, DIMITRI J.**
Adaptive mesh generation for viscous flows using Delaunay triangulation
p 310 A90-26531
- Algebraic turbulence modeling for unstructured and adaptive meshes
[AIAA PAPER 90-1653] p 608 A90-38781
- MAVRIS, DIMITRIS**
Prediction and measurement of the aerodynamic interactions between a rotor and airframe in forward flight
p 384 A90-28176
- MAVRIS, DIMITRIS N.**
GTPDP - A rotary wing aircraft preliminary design and performance estimation program including optimization and cost
p 830 A90-46944
- An analytical method for the prediction of unsteady rotor/airframe interactions in forward flight
p 186 N90-14223
- MAWHINNEY, WILLIAM A.**
Water test facilities for aviation life support equipment
p 200 A90-17431
- MAXSON, MYRON T.**
Fluorosilicone sealants for aircraft fuel containment
p 529 A90-31618
- MAXWELL, M. J.**
Proven dynamic modeling techniques for concurrent design and analysis of ECS controllers
[SAE PAPER 901234] p 841 A90-49304
- MAYA, T.**
Application of 3-D Navier-Stokes computation to bowed stacking turbine vane design
[AIAA PAPER 90-2129] p 625 A90-42035
- MAYBECK, PETER S.**
Reconfigurable flight controller for the STOL F-15 with sensor/actuator failures
p 432 A90-30707
- Multiple model adaptive controller for the STOL F-15 with sensor/actuator failures
p 668 A90-40878
- MAYER, W.**
Recent advances in H2/O2 high pressure coaxial injector performance analysis
[AIAA PAPER 90-1959] p 762 A90-42705
- MAYES, PAUL**
Australian experience in flight recorder readout and analysis
p 820 N90-27644
- MAYFIELD, WILLIAM**
AVION: A detailed report on the preliminary design of a 79-passenger, high-efficiency, commercial transport aircraft
[NASA-CR-186663] p 649 N90-23395
- MAYLE, R. E.**
Airfoil pressure measurements during a blade vortex interaction and a comparison with theory
p 232 A90-23105
- Pressure loss and heat transfer in channels roughened on two opposed walls
[ASME PAPER 89-GT-88] p 358 A90-23805
- Heat transfer in gas turbine engines; Proceedings of the Symposium, ASME Winter Annual Meeting, San Francisco, CA, Dec. 10-15, 1989
p 534 A90-32166
- MAYVILLE, W.**
Taguchi methods in conceptual design for life cycle cost
[AIAA PAPER 90-3222] p 639 A90-49109
- MAZUR, C. J.**
Air Force smart structures/skins program overview
p 38 A90-11205
- Experimental determination of the short crack effect for metals
p 265 A90-20064
- MAZUR, CHRISTOPHER J.**
Significance of the short crack effect on aerospace structures
p 269 A90-20065
- MAZUR, VLADISLAV**
Multistroke cloud-to-ground strike to the NASA F-106B airplane
p 482 A90-32304
- Cloud-to-ground strikes to the NASA F-106 airplane
p 574 A90-35767
- MAZUREK, DOUG**
Air Force Boom Event Analyzer Recorder (BEAR): System description
[AD-A218048] p 548 N90-20800
- Air Force Boom Event Analyzer Recorder (BEAR): System description
[AD-A218048] p 548 N90-20800
- MCCALLISTER, LAWRENCE E.**
The application of 'PT' resins to high temperature aerospace structures
p 949 A90-50230
- MCCARDLE, JACK G.**
Performance characteristics of a one-third-scale, vectorable ventral nozzle for SSTOVL aircraft
[AIAA PAPER 90-2271] p 586 A90-37562
- Analysis of internal flow in a ventral nozzle for STOVL aircraft
[AIAA PAPER 90-1899] p 739 A90-42688
- Performance characteristics of a one-third-scale, vectorable ventral nozzle for SSTOVL aircraft
[NASA-TM-103120] p 552 N90-21725
- Analysis of internal flow in a ventral nozzle for STOVL aircraft
[NASA-TM-103123] p 666 N90-23404
- Experimental and analytical study of close-coupled ventral nozzles for ASTOVL aircraft
[NASA-TM-103170] p 666 N90-24273
- MCCARTHUR, D. R.**
A comprehensive analysis of the viscous incompressible flow in quasi-three-dimensional aerofoil cascades
p 905 A90-51028
- MCCAULAY, ALASTAIR**
Neural networks for adaptive shape tracking
p 638 A90-39959
- MCCBRIDE, S. L.**
Acoustic emission detection of crack presence and crack advance during flight
p 886 N90-28082
- MCCBURNIE, PAUL W.**
Loran-aided GPS integrity
p 98 A90-14013
- MCCABRIA, JACK LEE**
High temperature VSCF (Variable Speed Constant Frequency) generator system
[AD-A210823] p 71 N90-10351
- MCCAMMOND, D.**
An ultrasonic fatigue facility for HCF/LCF interactive tests
p 363 A90-23900
- MCCANDLESS, RONALD S.**
High speed inlet testing in the NAVSWC wind tunnels
[AIAA PAPER 90-1412] p 595 A90-37949
- MCCANN, CATHERINE**
Reliability model generator specification
[NASA-CR-182005] p 780 N90-25638
- MCCANN, G. L.**
CFE738 - A case for joint engine development
[AIAA PAPER 90-2522] p 664 A90-42197
- MCCARRON, ROBERT G.**
Architecture options for GPS/Carousel IV integration
p 108 A90-13999
- MCCARTHY, D. K.**
The analysis and testing of composite panels subject to muzzle blast effects
p 675 A90-39991
- MCCARTHY, JOHN**
Advances in weather technology for the aviation system
p 373 A90-25572
- MCCARTNEY, TIMOTHY P.**
A test matrix sequencer for research test facility automation
[AIAA PAPER 90-2386] p 759 A90-42791
- MCCLAIR, JAMES ENNIS**
The interaction of chromostereopsis and stereopsis in stereoscopic CRT (Cathode Ray Tubes) displays
[AD-A217906] p 927 N90-28544
- MCCLAY, WILLIAM J.**
Harnessing detailed assembly process knowledge with CASE
p 535 A90-32504
- MCCLELLIN, C. R.**
A numerical study of mixing enhancement in a supersonic combustor
[AIAA PAPER 90-0203] p 272 A90-22182
- MCCLELLIN, CHARLES R.**
A computational investigation of flow losses in a supersonic combustor
[AIAA PAPER 90-2093] p 742 A90-42728
- Hypersonic CFD applications for the National Aero-Space Plane
[SAE PAPER 892310] p 714 A90-45473
- Numerical simulation of flow through the Langley parametric scramjet engine
[SAE PAPER 892314] p 747 A90-45476
- CFD support of NASP design
[AIAA PAPER 90-3252] p 872 A90-49120
- MCCLURE, ROBERT D.**
The Pointer - Test and evaluation of the tiltrotor UAV
p 406 A90-28170
- MCCOLLUM, MICHAEL A.**
The selection of actuation devices for aircraft pneumatic valves in systems under computer control
[SAE PAPER 891456] p 368 A90-27425
- MCCONKEY, E. D.**
Aeronautical decisionmaking for air ambulance program administrators
[DOT/FAA/DS-88/8] p 635 N90-23368
- MCCONNAUGHEY, H. V.**
Prediction of the aerodynamic environment and heat transfer for rotor-stator configurations
[ASME PAPER 89-GT-89] p 359 A90-23807
- Numerical prediction of axial turbine stage aerodynamics
p 426 N90-18416
- MCCONVILLE, JAMES B.**
Application of a general-purpose mechanical systems analysis code to rotorcraft dynamics problems
p 831 A90-46955
- MCCOOL, JOHN I.**
Life of concentrated contacts in the mixed EHD and boundary film regimes
[AD-A216673] p 454 N90-18738
- MCCORMACK, LISA**
Digital simulation of flight control systems for post-stall aircraft
p 431 A90-30704
- MCCORMICK, BARNES W.**
An iterative non-linear lifting line model for wings with unsymmetrical stall
[SAE PAPER 891020] p 83 A90-14332
- MCCORMICK, V. EDWARD**
Comparison of two- and three-dimensional Navier-Stokes solutions with NASA experimental data for CAST-10 airfoil
p 321 N90-17658
- MCCOWN-MCCLENTICK, BARBARA**
Unique methodology used in the Bell-Boeing V-22 main landing gear landing loads analysis and drop tests
p 409 A90-28236
- MCCOWN, PATRICIA M.**
Auxiliary power unit maintenance aid - Flight line engine diagnostics
p 382 A90-28348
- MCCOY, C. ELAINE**
General aviation pilot error in computer simulated adverse weather scenarios
p 322 A90-26254
- MCCROSKEY, W. J.**
Calculations of the flow past bluff bodies, including tilt-rotor wing sections at alpha = 90 deg
[AIAA PAPER 90-0032] p 227 A90-22156
- MCCROSSON, PAUL**
X-29A aircraft structural loads flight testing
[NASA-TM-101715] p 416 N90-19225
- MCCUNE, JAMES E.**
Nonlinear aerodynamics of two-dimensional airfoils in severe maneuver
p 301 A90-25276
- MCCURDY, DAVID A.**
En route noise annoyance laboratory test: Preliminary results
p 698 N90-24870
- Annoyance caused by advanced turboprop aircraft flyover noise: Counter-rotating-propeller configuration
[NASA-TP-3027] p 965 N90-29166
- MCDANIEL, JAMES C.**
Experimental investigation of a supersonic swept ramp injector using laser-induced iodine fluorescence
[AIAA PAPER 90-1518] p 606 A90-38663
- Injectant mole fraction measurements of transverse injection in constant area supersonic ducts
[AIAA PAPER 90-1632] p 587 A90-38761
- MCDANIEL, JOE W.**
Modeling strength data for CREW CHIEF
p 780 N90-25516
- MCDANIEL, OLIVER H.**
Free-field propagation of high intensity noise
[NASA-CR-186577] p 549 N90-21604
- MCDIVITT, T. K.**
A dynamic optical model attitude measurement system
p 539 A90-34236
- MCDIVITT, T. KEVIN**
An optical angle of attack sensor
p 446 A90-28263
- A two-dimensional adaptive-wall test section with ventilated walls in the Ames 2- by 2-foot transonic wind tunnel
[NASA-TM-102207] p 201 N90-13407
- MCDONALD, A. BLAIR**
Controllable propulsion for escape systems control
p 484 N90-20064

MCDONALD, BRIAN

The DELTA MONSTER: An RPV designed to investigate the aerodynamics of a delta wing platform
[NASA-CR-186226] p 924 N90-29381

MCDONALD, HENRY

Hypersonic flow calculations with a hybrid Navier-Stokes/Monte Carlo method
[AIAA PAPER 90-1691] p 560 A90-38394

MCDONALD, JEFFREY D.

Three dimensional Discrete Particle Simulation about the AFE geometry
[AIAA PAPER 90-1778] p 560 A90-38468

MCDONALD, KEITH D.

An analysis of GPS receiver performance capabilities and trends p 823 A90-49491

MCDONELL, V. G.

Influence of the continuous and dispersed phases on the symmetry of a gas turbine air-blast atomizer
[ASME PAPER 89-GT-303] p 273 A90-22651

MCDONNELL, V. G.

Symmetry assessment of an air-blast atomizer spray p 682 A90-40930

MCDUGALL, N. M.

A comparison between the design point and near-stall performance of an axial compressor
[ASME PAPER 89-GT-70] p 254 A90-22667

Stall inception in axial compressors
[ASME PAPER 89-GT-63] p 290 A90-23786

MCELREATH, K. W.

A reconfigurable integrated navigation and flight management system for military transport aircraft p 433 A90-30794

MCEWEN, C. D.

An array-fed reflector antenna with built-in calibration facility p 402 A90-27781

MCEWEN, K.

Development of a fibre optic damage detection system for an aircraft leading edge p 504 A90-32873

MC FARLAN, J. DONALD

Computational investigation of two-dimensional ejector nozzle flow fields
[AIAA PAPER 90-2148] p 768 A90-42739

MC FARLAND, R. E.

Quiet mode for nonlinear rotor models
[NASA-TM-102236] p 582 N90-21758

MC FARLAND, RICHARD H.

ILS - A safe bet for your future landings p 639 A90-41707

Weather data dissemination to aircraft p 486 N90-20934

MC FARLANE, C. W. R.

Measurement and calculation of the three-dimensional flow in axial compressor stators, with and without end-bends
[ASME PAPER 89-GT-6] p 287 A90-23753

MC FARLANE, DUNCAN C.

Robust controller design using normalized coprime factor plant descriptions p 457 A90-27645

MCGARRY, FRANK

Evolution of Ada technology in the flight dynamics area: Implementation/testing phase analysis
[NASA-TM-103310] p 546 N90-21539

MCGARRY, M. A.

Research on a two-dimensional inlet for a supersonic V/STOL propulsion system. Appendix A
[NASA-CR-174945] p 396 N90-18364

MCGHEE, ROBERT J.

Performance measurements of an airfoil at low Reynolds numbers p 800 A90-46369

Correlation of theory to wind-tunnel data at Reynolds numbers below 500,000 p 800 A90-46370

A study of high-lift airfoils at high Reynolds numbers in the Langley low-turbulence pressure tunnel
[NASA-TM-89125] p 1 N90-10002

Wind tunnel results of the low-speed NLF(1)-0414F airfoil p 93 N90-12541

Wind tunnel results of the high-speed NLF(1)-0213 airfoil p 93 N90-12542

MCGILL, D. P. M.

The EFA integrated monitoring and recording system: Requirements and concept for implementation p 848 N90-27620

MCGILL, JOHN

8 x 8-inch full color cockpit display p 927 A90-52953

MCGOWAN, JOSEPH

Hover position sensing system p 848 N90-27448

MCGRATH, J. E.

Poly(arylene ether ketone)/poly(aryl imide) homo- and polydimethylsiloxane segmented copolymer blends - Influence of chemical structure on miscibility and physical property behavior p 941 A90-50063

Effect of molecular weight and end group control on the adhesion behavior of thermoplastic polyimides and poly(imide siloxane) segmented copolymers p 947 A90-50199

MCGREEHAN, W. F.

Power dissipation in smooth and honeycomb labyrinth seals
[ASME PAPER 89-GT-220] p 362 A90-23881

MCGREW, JEAN A.

Douglas aging aircraft programs
[SAE PAPER 892208] p 732 A90-45425

MCGRORY, W. D.

A three-dimensional space marching algorithm for the solution of the Euler equations on unstructured grids
[AIAA PAPER 90-0014] p 234 A90-23701

MCGUIRK, J. J.

CFD predictions of lobed mixer flowfields p 70 A90-12626

Numerical study of single impinging jets through a crossflow p 17 A90-13020

Isothermal velocity and turbulence measurements downstream of a model multilobed turbofan mixer p 365 A90-24353

Velocity and turbulence characteristics of isothermal lobed mixer flows p 584 A90-35230

Subsonic combustor flow modeling: State of the art of CFD techniques for reacting and combustor flow p 749 N90-25991

MCGUIRK, JAMES J.

The calculation of under-expanded impinging jets p 147 A90-16782

MCHUGH, LISA A.

Process optimization of high temperature composite materials p 943 A90-50130

MCILVAINE, M.

Calculation of low Reynolds number flows at high angles of attack
[AIAA PAPER 90-0569] p 167 A90-19921

MCILVAINE, MARGARET

An interactive boundary-layer stability-transition approach for low Reynolds-number airfoils p 799 A90-46364

MCILWAIN, S. T.

Further investigations of transonic shock-wave boundary-layer interaction with passive control p 159 A90-19390

Wide angle diffusers with passive boundary-layer control
[AIAA PAPER 90-1600] p 567 A90-38732

MCINERNEY, S. A.

Pressure fluctuations in the tip region of a blunt-tipped airfoil p 154 A90-18136

MCINGVALE, PAT H.

Expert system technology applied to the automatic control of multiple unmanned aerial vehicles
[AIAA PAPER 90-3280] p 892 A90-48867

MCINTYRE, DAVID S.

Optimization of the effective GPS data rate p 489 N90-20932

MCINTYRE, MICHAEL E.

Direct lift STOVL engine integration
[AIAA PAPER 90-2274] p 644 A90-42103

MCKAIN, T. F.

Power transfer devices for V/STOL convertible engine systems p 587 A90-38539

The GMA 2100 and GMA 3007 engines for regional aircraft
[AIAA PAPER 90-2523] p 744 A90-42815

MCKAMEY, R. S.

Adjusting turbine engine transient performance for the effects of environmental variances
[AIAA PAPER 90-2501] p 658 A90-40639

MCKEEHEN, PHILLIP D.

A computer-aided control engineering environment for multi-disciplinary expert-aided analysis and design (MEAD) p 461 A90-30796

MCKEITHAN, CLIFFORD M.

Low speed maneuverability and agility design considerations for V/STOL aircraft p 581 A90-38536

MCKENNA, MATT

The DELTA MONSTER: An RPV designed to investigate the aerodynamics of a delta wing platform
[NASA-CR-186226] p 924 N90-29381

MCKENZIE, A. B.

Application of recess vaned casing treatment to axial flow fans
[ASME PAPER 89-GT-68] p 341 A90-23791

MCKENZIE, I. R. I.

Performance of a highly-loaded HP compressor
[RAE-TM-P-1149] p 256 N90-15919

MCKILLIP, R. M.

Free wake analysis of rotor configurations for reduced vibratory airloads p 833 A90-46975

MCKILLIP, R. M., JR.

Coupled rotor-body equations of motion hover flight
[NASA-CR-186710] p 717 N90-25111

MCKILLIP, ROBERT M., JR.

Helicopter flight control system design and evaluation for NOE operations using controller inversion techniques p 429 A90-28202

MCKNIGHT, R. L.

Application of HOST technology to the SSME HPFTP blade
[ASME PAPER 89-GT-130] p 360 A90-23828

MCLAUGHLIN, RICHARD J.

F/A-18 aileron smart servoactuator p 432 A90-30710

MCMAHON, H. M.

Measurement of the interaction between a rotor tip vortex and a cylinder p 555 A90-36255

Flow field measurements near a fighter model at high angles of attack
[AIAA PAPER 90-1431] p 559 A90-37968

MCMAHON, HOWARD

Prediction and measurement of the aerodynamic interactions between a rotor and airframe in forward flight p 384 A90-28176

MCMAHON, JOHN W.

Artificial intelligence (AI) based tactical guidance for fighter aircraft
[AIAA PAPER 90-3435] p 889 A90-47688

MCMASTERS, J. H.

The (airplane) design professor as shepherd - An industry role in enhancing engineering education
[AIAA PAPER 90-3259] p 897 A90-49121

MCMEKIN, ROBERT R.

Fire deaths in aircraft without the crashworthy fuel system p 22 A90-10266

MCMILLAN, J. C.

Fire hardening of aircraft through upgrades of materials and designs p 327 N90-17605

MCMLLEN, LARRY

Equipment feasibility study: Very high frequency communication equipment (136-137 megahertz)
[DOT/FAA/CT-TN89/72] p 775 N90-26210

MCMILLIN, S. E.

Helicopter wire strike accident and high voltage electrocution - A case report p 22 A90-10265

MCMILLIN, S. NAOMI

A computational study of incipient leading-edge separation on a 65-degree delta wing at M = 1.60
[AIAA PAPER 90-3029] p 791 A90-45871

MC MURRY, CARL B.

Computational investigation of two-dimensional ejector nozzle flow fields
[AIAA PAPER 90-2148] p 768 A90-42739

MCNALLY, B. D.

A flight-test methodology for identification of an aerodynamic model for a V/STOL aircraft p 413 A90-30107

MCNICHOLAS, K.

The remote sensing of temperature in gas turbine engine components using epithermal neutrons p 70 A90-12630

MCNULTY, MICHAEL J.

An experimental and analytical investigation of isolated rotor flap-lag stability in forward flight p 518 A90-33623

MCREE, GRIFFITH J.

Infrared imaging and tufts studies of boundary layer flow regimes on a NACA 0012 airfoil p 446 A90-28268

MCRUER, DUANE T.

Literat singular-value-based flight control system design techniques p 118 A90-14747

MCVANEY, GARY

Evaluation of the improved OV-ID anti-icing system, phase 2
[AD-A213928] p 239 N90-15083

MCWILLIAMS, IAN G.

FAA Loran early implementation project
[AD-A221866] p 824 N90-26805

MCWILLIAMS, LEO H.

A study of a propulsion control system for a VATOL aircraft (A direct design synthesis application) p 424 A90-30712

MEADOWS, D. E.

Fuel tank explosion protection p 251 N90-15914

MEALING, B. E.

Flow in a forward swept centrifugal fan, volumes 1 and 2 p 481 N90-20959

MEAR, MARK E.

Modeling growth of fatigue cracks which originate at rivet holes p 691 N90-25060

MEARS, MARK

Laboratory implementation of the Continuously Reconfiguring Multi-Microprocessor Flight Control System (CRMFCFS)
[AD-A217730] p 520 N90-20094

MEASE, KENNETH D.

Thrust law effects on the longitudinal stability of hypersonic cruise
[AIAA PAPER 90-2820] p 763 A90-45149

Trajectory optimization and guidance for an aerospace plane
[NASA-CR-185884] p 183 N90-13369

- MEASURES, R. M.**
Smart structures with nerves of glass p 444 A90-27951
- MEASURES, RAY M.**
Fiber optics smart structures program at UTIAS p 535 A90-32864
- MEAUZE, G.**
Numerical simulation of turbomachinery flows with a simple model of viscous effects - Comparison with experimental data [ONERA, TP NO. 1989-122] p 10 A90-12510
- MAUZE, GEORGES**
Numerical simulation of nonreactive flows in turbomachines p 908 A90-52621
- MEDEIROS, EDUARDO BAUZER**
An experimental study of the aeroelastic behaviour of two parallel interfering circular cylinders p 455 N90-19609
- MEDEIROS, MANUEL F.**
Advanced Traffic Management System automation p 330 A90-25565
- MEDIATE, BRUNO**
The MANTA: An RPV design to investigate forces and moments on a lifting surface [NASA-CR-186227] p 499 N90-20971
- MEDINA URBIZU, EDUARDO**
Insurance aspects of airline liability p 898 A90-49615
- MEDLEY, KATHRYN J.**
Automated measurement of aircraft-level electromagnetic interference p 404 A90-30752
- MEDVED, B.**
Wave cancellation properties of a splitter-plate porous wall configuration p 57 A90-11005
- MEDVED, B. L.**
An experimental investigation of pressure fluctuation mechanism for different transonic porous wall configurations [AIAA PAPER 90-1417] p 604 A90-37954
Broadband noise measurement in the transonic test section of the VTI T-38 wind tunnel [AIAA PAPER 90-1418] p 614 A90-37955
- MEE, BRIAN E.**
Rotorcraft low altitude CNS benefit/cost analysis: Rotorcraft operations data [DOT/FAA/DS-89/9] p 141 N90-12406
- MEECHAM, W. C.**
Pressure fluctuations in the tip region of a blunt-tipped airfoil p 154 A90-18136
- MEEKS, D. E.**
Flight test and numerical analysis of a half-scale Unmanned Air Vehicle [AIAA PAPER 90-1260] p 494 A90-33890
- MEGE, P.**
Numerical simulation of vortex breakdown via 3-D Euler equations [ONERA, TP NO. 1989-211] p 303 A90-25344
Numerical simulation of vortex breakdown by solving the Euler equations for an incompressible fluid p 476 A90-34323
- MEHALLI, MAHMOUD**
The potential for an extra runway at Heathrow: A preliminary feasibility study [TT-9007] p 938 N90-29403
- MEHDI, I. S.**
Electrical power systems for high Mach vehicles p 586 A90-38129
- MEHLMAN, B. P.**
An experimental investigation of film cooling effectiveness for slots of various exit geometries [AIAA PAPER 90-2266] p 768 A90-42763
- MEHTA, J. M.**
Dynamic instability characteristics of aircraft turbine engine combustors p 53 N90-10195
- MEHTA, JAYESH M.**
Fuel effects on gas turbine combustor dynamics [AIAA PAPER 90-1957] p 676 A90-40570
- MEHTA, RABINDRA D.**
Effects of streamwise vorticity injection on turbulent mixing layer development [AIAA PAPER 90-1459] p 561 A90-38616
- MEHTA, UNMEEL B.**
Multi-processing on supercomputers for computational aerodynamics [AIAA PAPER 90-0337] p 282 A90-22199
Computational requirements for hypersonic flight performance estimates p 440 A90-29686
- MEI, CHUH**
Finite element two-dimensional panel flutter at high supersonic speeds and elevated temperature [AIAA PAPER 90-0982] p 450 A90-29372
- MEI, ZHUANG**
The effect of walls on a spatially growing supersonic shear layer p 393 A90-29591
- MEIER, C. D.**
Integration of intelligent avionics systems for crew decision aiding p 459 A90-30236
- MEIER, G. E. A.**
Some processes of sound generation in a vortex-airfoil system with parallel axes p 218 A90-18448
Self-excited oscillations in internal transonic flows p 813 A90-49274
- MEIER, RON S.**
Development of a water-borne non-chromated primer and topcoat for aerospace applications p 956 A90-50213
- MEIJER, G.**
Applications of LIF to high speed flows p 911 N90-29320
- MEILANDER, W. C.**
Array processor supercomputers p 376 A90-26626
- MEISER, M. D.**
Development of monolithic and composite ceramics at Allied-Signal Aerospace Company p 599 A90-35950
- MEISTER, MARK A.**
ASR-9 weather channel test report [AD-A211749] p 133 N90-11934
- MEITNER, PETER L.**
Computer code for predicting coolant flow and heat transfer in turbomachinery [NASA-TP-2985] p 858 N90-27722
- MEKKES, G. L.**
A numerical study of mixing enhancement in a supersonic combustor [AIAA PAPER 90-0203] p 272 A90-22182
- MELANDER, BARBARA G.**
Comparison of four lightning simulation tests on a composite test bed aircraft p 818 A90-49831
- MELCONIAN, JERRY O.**
Introducing the VRT gas turbine combustor [AIAA PAPER 90-2452] p 743 A90-42808
Introducing the VRT gas turbine combustor [NASA-TM-103176] p 688 N90-23591
- MELIS, MATTHEW E.**
Thermal/structural analyses of several hydrogen-cooled leading-edge concepts for hypersonic flight vehicles [AIAA PAPER 90-0053] p 274 A90-23702
Thermal/structural analyses of several hydrogen-cooled leading-edge concepts for hypersonic flight vehicles [NASA-TM-102391] p 215 N90-14511
Finite element elastic-plastic-creep and cyclic life analysis of a cowl lip [NASA-TM-102342] p 610 N90-22808
- MELLOR, A. M.**
Turbine combustor preliminary design approach p 508 A90-32966
Engineering design models for ramjet efficiency and lean blowoff [AIAA PAPER 90-2453] p 663 A90-42176
- MELLOR, MALCOLM**
Airfields on antarctic glacier ice [AD-A217638] p 526 N90-20097
- MELSON, W. EDWARD, JR.**
Results of aerodynamic testing of large-scale wing sections in a simulated natural rain environment [AIAA PAPER 90-0486] p 167 A90-19874
Operational considerations for aerodynamic testing of large-scale wing sections in a simulated natural rain environment [AIAA PAPER 90-0485] p 313 A90-26956
- MELTON, JOHN E.**
An integrated CFD/experimental analysis of aerodynamic forces and moments [NASA-TM-102195] p 18 N90-10006
- MELVIN, W. W.**
Penetration landing guidance trajectories in the presence of windshear p 98 A90-14732
Acceleration, gamma, and theta guidance for abort landing in a windshear p 98 A90-14733
- MELZER, JAMES E.**
Holographic combiner design to obtain uniform symbol brightness at head-up display video camera p 652 A90-40394
- MENDENHALL, MICHAEL R.**
Prediction of subsonic vortex shedding from forebodies with chines [NASA-CR-4323] p 909 N90-28494
- MENDEZ, A. J.**
A fiber optic headset compatible with power-by-light p 504 A90-32906
- MENEES, GENE P.**
Numerical simulations of an oblique detonation wave engine p 508 A90-32964
- MENENDEZ, A. N.**
An asymptotic theory for the periodic turbulent boundary layer in zero mean-pressure gradient [AD-A228632] p 66 A90-10222
- MENON, S.**
Calculation of three-dimensional viscous and inviscid hypersonic flows using split-matrix marching methods [AIAA PAPER 90-3070] p 794 A90-45894
- MENON, P. K. A.**
Flight test of a trajectory controller using linearizing transformations with measurement feedback [AIAA PAPER 90-3373] p 864 A90-47631
Image based range determination [AIAA PAPER 90-3404] p 822 A90-47659
Rotorcraft pursuit-evasion in nap-of-the-earth flight [AIAA PAPER 90-3455] p 786 A90-47707
Nonlinear maneuver autopilot for the F-15 aircraft [NASA-CR-179442] p 77 N90-11487
Passive navigation using image irradiance tracking p 578 N90-22232
Time-optimal aircraft pursuit-evasion with a weapon envelope constraint [NASA-CR-186640] p 734 N90-25126
- MENON, S.**
A numerical study of mixing and chemical heat release in supersonic mixing layers [AIAA PAPER 90-0152] p 163 A90-19710
- MENON, SURESH**
Large-eddy simulations of pressure oscillations and combustion instability in a ramjet p 111 A90-15388
Large-eddy simulations of combustion instability in an axisymmetric ramjet combustor [AIAA PAPER 90-0267] p 191 A90-19764
Large-eddy simulations of flows in a ramjet combustor p 772 A90-45534
Numerical simulation of pressure oscillations in a ramjet combustor p 54 N90-10202
- MENRATH, M.**
Experimental identification of helicopter engine dynamics from closed loop data p 855 N90-27627
- MENSEN, H.**
Air traffic management in Europe: Structure, tasks, potential p 825 N90-27677
- MENSO, G.**
In flight reight tests on AM-X single engine fly-by-wire aircraft p 34 N90-10869
AM-X high incidence trials, development, and results [ETN-90-97277] p 759 N90-26016
- MERATI, PARVIZ**
Interaction of a plane shear layer with a downstream flat plate [AIAA PAPER 90-1460] p 561 A90-38617
- MERKEL, HAROLD S.**
A new method for measuring the transmissivity of aircraft transparencies [AD-A216953] p 464 N90-19842
- MERKLEY, DONALD J.**
MDHC technical assessment of advanced rotor and control concepts p 861 A90-46948
BHTI's technical assessment of advanced rotor and control concepts p 861 A90-46949
- MERRICK, V. K.**
Flight evaluations of several hover control and display combinations for precise blind vertical landings [AIAA PAPER 90-3479] p 867 A90-47764
- MERRICK, VERNON K.**
A head up display format for application to V/STOL aircraft approach and landing [NASA-TM-102216] p 340 N90-17632
- MERRIGAN, MICHAEL A.**
Design and demonstration of heat pipe cooling for NASP and evaluation of heating methods at high heating rates [DE89-016995] p 186 N90-14227
- MERRILL, B. J.**
Three-dimensional analysis on flow and temperature distributions for aircraft fuel thermal stability [AD-A219651] p 678 N90-23571
- MERRILL, WALTER C.**
A real time microcomputer implementation of sensor failure detection for turbofan engines p 745 A90-45414
Advanced detection, isolation, and accommodation of sensor failures in turbofan engines: Real-time microcomputer implementation [NASA-TP-2925] p 259 N90-15112
- MERRITT, M. W.**
Wind shear detection with pencil-beam radars p 279 A90-21386
- MERRITT, MARK W.**
Microburst divergence detection for terminal Doppler weather radar p 456 A90-28625
- MERRITT, NORMAN A.**
Aircraft crash survival design guide. Volume 1: Design criteria and checklists [AD-A218434] p 575 N90-22545
Aircraft crash survival design guide. Volume 3: Aircraft structural crash resistance [AD-A218436] p 575 N90-22547

- Aircraft crash survival design guide. Volume 4: Aircraft seats, restraints, litters, and cockpit/cabin deethalization [AD-A218437] p 575 N90-22548
- MERTENS, JOSEF**
Short time Force and moment measurement System for shock tubes (SFS) for measuring times less than 10 ms p 674 N90-24233
- MERTENS, JOSEPH**
Short time-dynamometer system for shock wave channels [MBB-UT-115/89-PUB] p 773 N90-25084
- MERZKIRCH, W.**
Practical systems for speckle velocimetry p 171 N90-13341
- MESSERSMITH, N. L.**
Investigation of supersonic mixing layers p 623 A90-40926
- MESSITER, A. F.**
Unsteady transonic cascade flow with in-passage shock wave p 556 A90-36281
- METCALF, JERRY**
Fatigue life assessment of a leaded electronic component under a combined thermal and random vibration environment p 770 A90-43734
- METCALFE, M. P.**
The BAe (commercial aircraft) LTD transport aircraft synthesis and optimisation program (TASOP) [AIAA PAPER 90-3295] p 837 A90-48879
- METRIKIN, V. S.**
Dynamic stiffness of a hydraulic damper in the system of a front landing gear strut p 102 A90-14555
- METWALLY, A.**
LDV measurements and the flow analysis in the vaneless region of a radial inflow turbine [ASME PAPER 89-GT-157] p 292 A90-23845
- METWALLY, OMAR M.**
The interaction of a supersonic streamwise vortex and a normal shock wave p 633 N90-24241
- METZGER, D. E.**
Local convection heat transfer on a plane wall in the vicinity of strong streamwise accelerations p 535 A90-32174
- MEUER, GARY D.**
Plastic media blast (PMB) paint removal from composites p 945 A90-50162
- MEVREL, REMY**
Effect of protective coatings on mechanical properties of superalloys [ONERA, TP NO. 1989-88] p 62 A90-11126
Effect of protective coatings on mechanical properties of superalloys p 952 N90-28707
- MEYENBERG, E.**
Tests of automatic dependent surveillance (ADS) in Western Europe - Possible future developments p 574 A90-35353
- MEYER-PIENING, H.-R.**
Buckling analysis of FRP faced cylindrical sandwich panel under combined loading p 365 A90-24376
- MEYER, F.-W.**
The influence of interactional aerodynamics of rotor-fuselage-interferences on the fuselage flow p 561 A90-38523
A method for calculating the rotor-fuselage interference in helicopters [DGLR PAPER 88-060] p 919 A90-50246
- MEYER, FRED H.**
Computerized corrosion forecasting model for C-5 aircraft p 843 N90-26815
- MEYER, FRIEDRICH**
Numerical simulation of transition in three-dimensional boundary layers [DLR-FB-89-12] p 212 N90-13728
- MEYER, H.-J.**
The Operational Loads Monitoring System (OLMS) p 926 A90-49879
- MEYER, H.-L.**
ATTAS flight testing experiences p 34 N90-10862
- MEYER, HORST**
The Modular Flighttest Instrumentation/MFI 90 - A helicopter measuring system p 418 A90-28850
- MEYER, J.**
Development of turbulence models for the analysis of compressible or incompressible unsteady flow [ETN-90-97486] p 958 N90-28810
- MEYER, R. T.**
Large aircraft flying qualities revisited [AIAA PAPER 90-2847] p 754 A90-45175
- MEYER, ROBERT R.**
F-14 VSTFE and results of the cleanup flight test program p 105 N90-12547
- MEYER, T. G.**
Constitutive modeling for isotropic materials (HOST) [NASA-CR-179522] p 193 N90-13390
- MEYER, THOMAS J.**
Additive evaluation criteria for aircraft noise p 698 N90-24867
- MEYERHOFF, MARK E.**
A reliable, maintenance-free oxygen sensor for aircraft using an oxygen-sensitive coating on potentiometric electrodes [AD-A222696] p 927 N90-28545
- MEYERS, JAMES F.**
Database for LDV signal processor performance analysis p 447 A90-28278
- MEYERS, JIM F.**
Experimental studies on Goertler vortices p 91 N90-12529
- MEYLER, KAREN L.**
Evaluation of various non-asbestos epoxy adhesives for aircraft repair p 529 A90-33078
- MEYN, LARRY A.**
Experimental studies of 90 deg corner cascades in the National Full-Scale Aerodynamic Complex [AIAA PAPER 90-1826] p 307 A90-25935
- MEZEIX, J. F.**
Maximum expected concentrations of hail in thunderstorm precipitation p 962 A90-52052
- MIAMEE, A. G.**
A new class of random processes with application to helicopter noise p 781 A90-42874
- MIANDOAB, FARID H.**
Effect of surface grooves on base pressure for a blunt trailing-edge airfoil p 556 A90-36280
- MICHAL, T. R.**
Supersonic/hypersonic Euler flowfield prediction method for aircraft configurations p 145 A90-16767
- MICHALAK, M.**
Monolithic CFC-Main Landing Gear Door for Tornado p 955 A90-50136
- MICHALSKY, DOUGLAS L.**
The Robotic Canopy Polishing System [SME PAPER MS89-134] p 222 A90-23680
- MICHARD, P. J.**
Test rig for the study of the flow in a rotor-stator system [ONERA, TP NO. 1989-124] p 58 A90-12634
- MICHELASSI, VITTORIO**
Viscous flow calculations in turbomachinery channels [ASME PAPER 89-GT-5] p 287 A90-23752
- MICKLOW, GERALD J.**
Viscous-inviscid interaction method for calculating the flow in compressor cascade blade passages and wake with separation [AIAA PAPER 90-2125] p 624 A90-42032
Effect of vane twist on the performance of dome swirlers for gas turbine airblast atomizers [AIAA PAPER 90-1955] p 881 A90-47203
Effect of vane twist on the performance of dome swirlers for gas turbine airblast atomizers [NASA-TM-103195] p 773 N90-25289
- MIDDLETON, DAVID B.**
Results of aircraft open-loop tests of an experimental magnetic leader cable system for guidance during roll-out and turnoff [NASA-TM-4135] p 348 N90-16767
Airplane takeoff and landing performance monitoring system [NASA-CASE-LAR-13734-1-CU] p 526 N90-20096
- MIDDLETON, GARY D.**
A review of the V-22 health monitoring system p 417 A90-28209
- MIELE, A.**
Penetration landing guidance trajectories in the presence of windshear p 98 A90-14732
Acceleration, gamma, and theta guidance for abort landing in a windshear p 98 A90-14733
Optimization and guidance of flight trajectories in the presence of windshear [NASA-CR-186163] p 574 N90-21747
- MIESS, JOSEPH C.**
Evaluation of the improved OV-ID anti-icing system, phase 2 [AD-A213928] p 239 N90-15083
Preliminary airworthiness evaluation of the RC-12K [AD-A219545] p 648 N90-23387
- MIGALIN, K. V.**
Operation of a gas ejector in the pulsed regime p 850 A90-46488
- MIGEMI, S.**
The calculation of incompressible separated turbulent boundary layers p 905 A90-51025
- MIGNOSI, A.**
T2 ability concerning model design and instrumentation in short run processing p 524 A90-34241
- MIGNOSI, ANDRE**
High productivity testing p 871 N90-26843
Limits of adaptation, residual interferences p 871 N90-26844
- MIHALISIN, J. R.**
Metallurgy of investment cast superalloy components p 531 A90-34154
- MIHALOEW, JAMES R.**
STOVL aircraft simulation for integrated flight and propulsion control research [NASA-TM-102419] p 193 N90-13389
- MIKHAILOV, P. D.**
Optimal nose shapes of bodies of revolution in transonic flow p 299 A90-24165
- MIKHAILOV, S. V.**
Calculation of supersonic flow past a wing/fuselage combination with the resolution of a compression shock from the wing p 297 A90-24138
Numerical solution of the problem of supersonic flow of an ideal gas past a trapezoidal wedge p 386 A90-28980
Calculation of three-dimensional flow past a plane supersonic air intake at angles of attack and sideslip p 805 A90-46573
- MIKHAILOV, V. V.**
Effect of surface riblets on the velocity profile of an incompressible boundary layer p 294 A90-24081
- MIKHEEV, R. A.**
Vibration equations for a helicopter rotor blade p 604 A90-37830
- MIKOYAN, STEPAN ANASTASOVICH**
Landing tests for Buran shuttle with jet engine-equipped mock-up p 61 N90-10904
- MIKROYANNIDIS, JOHN A.**
The 1-(diorganoxyphosphonyl)-methyl-2,4- and -2,6-diamido benzenes [NASA-CASE-ARC-11425-4] p 532 N90-20133
Some 1-(diorganoxyphosphonyl)-methyl-2,4- and -2,6-dinitro-benzenes [NASA-CASE-ARC-11425-3] p 678 N90-23475
- MILES, J. B.**
Navier Stokes simulation of waverider flowfields [AIAA PAPER 90-3066] p 793 A90-45892
- MILESHIN, L. S.**
Calculation of flows of an ideal gas in nozzles and jets by the relaxation method p 296 A90-24109
- MILEY, S. J.**
Direct measurement of laminar instability amplification factors in flight p 277 N90-16178
- MILHOLEN, VERNON W.**
Experimental evaluation of impedance control for robotic aircraft refueling [AD-A215532] p 337 N90-16755
- MILLER, B. A.**
Fighter escape system: The next step forward p 483 N90-20059
- MILLER, BRAD S.**
Benchmarking blackboards to support cockpit information management [AIAA PAPER 89-3095] p 37 A90-10580
- MILLER, BRIAN**
Advanced developments of the Turbo-Union RB199 p 745 A90-44595
- MILLER, C. G.**
Langley hypersonic aerodynamic/aerothermodynamic testing capabilities - Present and future [AIAA PAPER 90-1376] p 596 A90-38483
- MILLER, C. G., III**
Aerothermodynamics and transition in high-speed wind tunnels at NASA Langley p 386 A90-28555
- MILLER, CHRISTOPHER J.**
Euler analysis comparison with LDV data for an advanced counter-rotation propfan at cruise [AIAA PAPER 90-3033] p 903 A90-50637
Euler analysis comparison with LDV data for an advanced counter-rotation propfan at cruise [NASA-TM-103249] p 720 N90-25946
- MILLER, D. S.**
Supersonic boundary-layer transition on the LaRC F-106 and the DFRF F-15 aircraft. Part 1: Transition measurements and stability analysis p 94 N90-12558
Supersonic boundary-layer transition on the LaRC F-106 and the DFRF F-15 aircraft. Part 2: Aerodynamic predictions p 94 N90-12559
- MILLER, DAVID**
Very-high-performance data acquisition/analysis/display/control systems based on the APTEC I/O computer p 458 A90-28852
- MILLER, DAVID G.**
Active control of tiltrotor blade in-plane loads during maneuvers p 670 A90-42463
- MILLER, DAVID S.**
Design and experimental verification of an equivalent forebody representation of flowing inlets p 152 A90-17863
- MILLER, DEBORAH**
Use of Onboard Data Loaders [SAE PAPER 892327] p 738 A90-45485
- MILLER, DOUGLAS R.**
Significance of the short crack effect on aerospace structures p 269 A90-20065

- MILLER, GEORGE, JR.**
Rotary servohinge actuator
[SAE PAPER 892261] p 733 A90-45458
- MILLER, GLEN E.**
Fiber optic sensors for aircraft p 68 A90-11704
- MILLER, JOHN**
Evolution of Ada technology in the flight dynamics area: Implementation/testing phase analysis
[NASA-TM-103310] p 546 N90-21539
- MILLER, JUDITH**
Correlation of Puma airfoils - Evaluation of CFD prediction methods
[ONERA, TP NO. 1989-185] p 224 A90-21045
- MILLER, LAWRENCE**
The application of an expert maintenance and diagnostic tool to aircraft engines
[AIAA PAPER 90-2036] p 657 A90-40605
- MILLER, LEONARD**
Static and dynamic water tunnel tests of slender wings and wing-body configurations at extreme angles of attack
[AIAA PAPER 90-3021] p 869 A90-45888
- MILLER, M.**
Aging jet transport structural evaluation programs p 901 A90-49889
- MILLER, MICHAEL B.**
Wavelength division multiplexed fiber optic sensors for aircraft applications p 38 A90-11663
The performance of linear fiber optic data buses p 68 A90-11665
- MILLER, N.**
Advanced applications of BEM to gas turbine engine structures p 772 A90-45769
- MILLER, R. B.**
FPG2: A flight profile generator program
[AD-A212408] p 107 N90-12595
- MILLER, R. D.**
Garrett TPF351-20 turboprop fan engine development
[SAE PAPER 891047] p 109 A90-14351
- MILLER, R. F.**
A remote tip-driven fan powered supersonic fighter concept
[AIAA PAPER 90-2415] p 663 A90-42167
- MILLER, ROBERT A.**
TBCs for better engine efficiency p 203 A90-17294
Thermal barrier coatings for gas turbine and diesel engines
[NASA-TM-102408] p 205 N90-13636
- MILLER, ROBERT N.**
Computerized corrosion forecasting model for C-5 aircraft p 843 N90-26815
- MILLER, S. C.**
Cost effective technology p 188 A90-17447
Cost effective technology [PNR90664] p 883 N90-27002
- MILLER, THOMAS L.**
Icing Research Tunnel test of a model helicopter rotor p 400 A90-28179
- MILLER, W.**
Dynamic simulation of cross-shafted propulsion system for tilt nacelle application
[AIAA PAPER 90-0439] p 191 A90-19847
- MILLER, W. J.**
Development of an automated ultrasonic inspection system for composite structure on in-service aircraft p 885 N90-28079
- MILLER, WAYNE O.**
Efficient free wake calculations using Analytical/Numerical Matching and far-field linearization p 384 A90-28171
- MILLION, CLAUDE**
The use of onboard sensor data in aerial triangulation - GPS, pressure sensors, laser telemetry p 822 A90-47901
- MILLS, NIKOS**
Preliminary design of a family of three close air support aircraft
[NASA-CR-186070] p 336 N90-16751
- MILLS, S. D.**
Improved fiber reinforced polyphenylene sulfide thermoplastic composites p 947 A90-50180
- MILLWARD, J. A.**
Experimental investigation into the effects of rotating and static bolts on both windage heating and local heat transfer coefficients in a rotor/stator cavity
[ASME PAPER 89-GT-196] p 362 A90-23870
- MINECK, R. E.**
Wind tunnel wall interference investigations in NAE/NRC High Reynolds Number 2D Facility and NASA Langley 0.3m Transonic Cryogenic Tunnel p 628 A90-42404
- MINECK, RAYMOND E.**
Wall interference assessment/correction (WIAC) for transonic airfoil data from porous and shaped wall test sections
[AIAA PAPER 90-1406] p 595 A90-37945
- Comparison of NAE porous wall and NASA adaptive wall test results using the NAE CAST-10 airfoil model p 353 N90-17656
- MING, RUISEN**
Prediction of transmission loss through an aircraft sidewall using statistical energy analysis p 219 A90-18599
- MINGUET, PIERRE J.**
Postbuckling behavior of laminated plates using a direct energy-minimization technique p 209 A90-17993
- MININ, I. V.**
A study of three-dimensional supersonic flow of a real gas past axisymmetric bodies p 3 A90-10938
- MININ, O. V.**
A study of three-dimensional supersonic flow of a real gas past axisymmetric bodies p 3 A90-10938
- MINKE, DIERK**
General data processing support from project planning to workshop control
[MBB-UD-526/88-PUB] p 138 N90-12208
- MINKLER, G.**
Aerospace coordinate systems and transformations p 282 A90-23372
- MINKLER, J.**
Aerospace coordinate systems and transformations p 282 A90-23372
- MINOTT, GEORGE L.**
Spectral response of a UV flame sensor for a modern turbojet aircraft engine p 769 A90-43285
- MINTER, JANET**
The role of NDE in ceramic turbine engine component development p 601 A90-35508
- MINTO, K. DEAN**
An explicit model-matching approach to lateral-axis autopilot design p 756 A90-45413
- MINTZ, FRED**
When propfans cruise, will LDN 65 fly p 697 N90-24864
- MIQUEL, J.**
A formulation for the solution of Euler equations for compressible flow using finite elements p 708 A90-44447
- MIRONOV, S. G.**
An experimental study of fluctuations in the front separation zone at supersonic flow velocities p 10 A90-12282
- MIROW, P.**
Application of piezoelectric foils in experimental aerodynamics p 446 A90-28258
Detection of flow instabilities at airfoil profiles using piezoelectric arrays p 276 N90-16175
- MIRSKII, M. D.**
Determination of the effective areas of the mixing exhaust ducts of a bypass engine from autonomous test results p 102 A90-14584
- MIRZA-BAIG, F. S.**
On and off-design performance prediction of single spool turbojets using gasdynamics
[AIAA PAPER 90-2393] p 662 A90-42155
- MISHCHENKO, N. G.**
Prospects are good for using ATC radar to detect birds p 329 A90-25496
- MISIEWICZ, A.**
The solution of the unsteady transonic flow through a blade passage in an axial turbine p 5 A90-11777
- MISRA, PRATAP N.**
Development of common GPS and GLONASS avionics standards p 821 A90-46391
- MITCHELL, DAVID G.**
Reassessment and extensions of pilot ratings with new data
[AIAA PAPER 90-2823] p 753 A90-45158
Simulation investigation of multiple axis flying qualities
[AIAA PAPER 90-3480] p 866 A90-47729
- MITCHELL, JAMES J.**
The Uniform Engine Test Programme
[AGARD-AR-248] p 428 N90-19232
- MITCHELL, JAMES THOMAS**
High temperature VSCF (Variable Speed Constant Frequency) generator system
[AD-A210823] p 71 N90-10351
- MITCHELLTREE, ROBERT ALAN**
A one equation turbulence model for transonic airfoils p 174 N90-14199
- MITKUS, V. V.**
Composite-embedded optical fibers for communication links p 139 A90-13847
- MITRA, N. K.**
Computation of laminar mixed convection flow in a channel with wing type built-in obstacles p 67 A90-11114
Structure of velocity and temperature fields in laminar channel flows with longitudinal vortex generators p 273 A90-23207
- MITRA, NIMAI KUMAR**
Navier-Stokes computations of three-dimensional laminar flows with buoyancy in a channel with wing-type vortex generators p 772 A90-45728
- MITROFANOV, ALEKSANDR A.**
Monitoring of aircraft assembly: Optical and laser methods p 285 A90-24229
- MITSUODA, MASAHIKO**
Thrust augmentation characteristics of jet reactions
[AIAA PAPER 90-0033] p 161 A90-19641
- MITTAL, MANOJ**
Control of a twin lift helicopter system using nonlinear state feedback
[AIAA PAPER 90-3408] p 817 A90-47663
- MITYAS, S. J.**
Navier-Stokes analysis of an ejector and mixer-ejector operating at pressure ratios in the range 2-4
[AIAA PAPER 90-2730] p 626 A90-42218
- MIU, STEVE**
Design of a low cost short takeoff-vertical landing export fighter/attack aircraft
[NASA-CR-186658] p 734 N90-25132
- MIURA, H.**
Multiobjective decision making in a fuzzy environment with applications to helicopter design p 405 A90-27993
- MIURA, HIROKAZU**
Static aeroelastic analysis for generic configuration aircraft
[NASA-TM-89423] p 52 N90-10042
Static aeroelastic analysis of a three-dimensional generic wing
[NASA-TM-102231] p 509 N90-20087
- MIYAKE, S.**
Application of the 'K-gage' to aircraft structural testing p 926 A90-49891
- MIYAKE, TOSHIYA**
Thrust augmentation characteristics of jet reactions
[AIAA PAPER 90-0033] p 161 A90-19641
- MIYATA, M.**
Turbulent plane jet excited mechanically by an oscillating thin plate in the potential core p 553 A90-35262
- MIYATAKE, HIROKAZU**
The features of FJR 710 engine p 42 A90-12011
Endurance test of FJR 710/600S engine p 42 A90-12012
- MIYAZAKI, KENJI**
Hot-gas corrosion test of Si₃N₄ and SiC p 531 A90-33987
- MIYAZAWA, HIROAKI**
An adaptive flight control system design for non-minimum phase CCV by relative order reduction p 196 A90-19428
- MIYAZAWA, HIROSHI**
Evaluation and measurement of airplane flutter interference p 272 A90-22529
- MIYAZAWA, Y.**
Multi-surface control law synthesis and wind tunnel test verification of active flutter suppression for a transport-type wing p 517 A90-33401
- MIYAZAWA, YOSHIKAZU**
Robust flight control system design with multiple model approach
[AIAA PAPER 90-3411] p 865 A90-47666
- MIZRAHI, JOE**
Sizing up the Stealth p 247 A90-23200
- MKHITARYAN, A. M.**
Effect of vortex generators on the aerodynamic wing characteristics and body of revolution
[AD-A222813] p 721 N90-25955
- MO, JIADA**
The water tunnel test of delaying vortex breakdown over a delta wing using supplements p 2 A90-10346
- MOBARAK, A.**
Study of various factors affecting secondary loss vortices downstream a straight turbine cascade
[ASME PAPER 89-GT-12] p 287 A90-23757
- MOBARAK, A. M.**
Computation of the trailing edge flow downstream a flat plate with finite thickness p 151 A90-17464
- MOCHALOVA, I. U. A.**
Nonstationary motion of an elastic profile in subsonic incompressible flow p 300 A90-24741
- MOCKLER, THEODORE T.**
Thermal/structural analyses of several hydrogen-cooled leading-edge concepts for hypersonic flight vehicles
[AIAA PAPER 90-0053] p 274 A90-23702
Thermal/structural analyses of several hydrogen-cooled leading-edge concepts for hypersonic flight vehicles
[NASA-TM-102391] p 215 N90-14511
- MODARRESS, DARIUSH**
Remote detection of boundary-layer transition by an optical system p 139 N90-12524

MODGIL, M. S.

Computational and experimental studies on ground effect of a slender wing tailless delta aircraft
p 810 A90-48083

MODI, V. J.

Effect of moving surfaces on the airfoil boundary-layer control
p 159 A90-19388
Application of the moving surface boundary layer control to a two dimensional airfoil
p 628 A90-42405
Approach to side force alleviation through modification of the pointed forebody geometry
[AIAA PAPER 90-2834]
p 712 A90-45165
Reduction of the side force on pointed forebodies through add-on tip devices
[AIAA PAPER 90-3005]
p 788 A90-45854
On the drag reduction of bluff bodies through momentum injection
[AIAA PAPER 90-3076]
p 797 A90-45922

MODROW, MARLAN B.

High speed bus technology development
[AD-A224486]
p 960 N90-29565

MODRUSAN, MARTIN

Lightning testing and test analyses of the JAS39 aircraft
p 842 A90-49836

MOEBEST, R.

The interference of flightmechanical control laws with those of load alleviation and its influence on structural design
p 258 N90-15054

MOECKE, HEINZPETER P.

A comparison of emergency medical helicopter accident rates in the United States and the Federal Republic of Germany
p 722 A90-44640

MOELLER, M.

Computer-aided analysis of three-dimensional multiloop mechanisms
p 669 A90-42328

MOES, TIMOTHY R.

Preliminary results from a subsonic high-angle-of-attack flush airdata sensing (HI-FADS) system - Design, calibration, algorithm development, and flight test evaluation
[AIAA PAPER 90-0232]
p 187 A90-19746
Preliminary results from a subsonic high angle-of-attack flush airdata sensing (HI-FADS) system: Design, calibration, and flight test evaluation
[NASA-TM-101713]
p 339 N90-16758
Wind-tunnel investigation of a flush airdata system at Mach numbers from 0.7 to 1.4
[NASA-TM-101697]
p 421 N90-18395

MOFFATT, ALAN W.

Designing the V-22 'Osprey' tiltrotor V/Stol aircraft for maintenance and serviceability
[SAE PAPER 891075]
p 101 A90-14369

MOHLMAN, HENRY T.

Air Force procedure for predicting aircraft noise around airbases: Airbase operations program (BASEOPS) description
[AD-A223069]
p 895 N90-27466

MOHR, ROSS W.

Mach number effects on transonic aeroelastic forces and flutter characteristics
p 17 A90-13024

MOIN, PARVIZ

The instability of two-dimensional laminar separation
p 800 A90-46365
Direct numerical simulation of aerodynamic noise
[AD-A214122]
p 379 N90-18225

MOITRA, ANUTOSH

Quasi-three-dimensional grid generation by an algebraic homotopy procedure
p 376 A90-26481
Enthalpy damping for high Mach number Euler solutions
[AIAA PAPER 90-1585]
p 566 A90-38720
Two and three dimensional grid generation by an algebraic homotopy procedure
[AIAA PAPER 90-1603]
p 567 A90-38734

MOKHTARIAN, F.

Effect of moving surfaces on the airfoil boundary-layer control
p 159 A90-19388
Application of the moving surface boundary layer control to a two dimensional airfoil
p 628 A90-42405

MOKRY, M.

Complex variable boundary element method for external potential flows
[AIAA PAPER 90-0127]
p 162 A90-19694
New transonic test sections for the NAE 5 ft x 5 ft trisonic wind tunnel
[AD-A220933]
p 674 N90-24278

MOKRY, MIROSLAV

Finite volume solutions of two-dimensional Euler equations on adapted structured meshes
p 629 A90-42413
Residual interference and wind tunnel wall adaption
p 353 N90-17655
Limits of adaptation, residual interferences
p 871 N90-26844

MOLAVI, K.

Liquid fueled ramjet combustion instability: Acoustical and vortical interactions with burning sprays
[AD-A222752]
p 767 N90-26104

MOLCHANOV, A. M.

A numerical method for calculating supersonic nonisobaric jets
p 84 A90-14566

MOLDER, S.

The University of Toronto-Ryerson Polytechnical Institute hypersonic gun tunnel
p 673 A90-42432

MOLE, P. J.

Strain-gage applications in wind tunnel balances
p 957 A90-52037

MOLINERO, I.

Inspection system for in-situ inspection of aircraft composite structures
p 886 N90-28091

MOLINET, F. A.

GTU/UTD: Brief history of successive development of theory and recent advances. Applications to antennas on ships and aircraft
p 370 N90-17939

MOLLOY, W. J.

Investment-cast superalloys a good investment
p 949 A90-51198

MOLNAR, DANIEL O.

B-1B Doppler error compensation based on flight data analysis
p 404 A90-30790

MOLOCHKOV, EVGENII M.

The planning of air transportation on airlines
p 721 A90-42648

MOLTON, P.

Experimental study of incompressible flow on the upper surface of a delta wing
p 558 A90-37346

MOLZOW, M.

The interference of flightmechanical control laws with those of load alleviation and its influence on structural design
p 258 N90-15054

MONAHEMI, M. M.

Obtaining precise LTR with Luenberger type observer with arbitrary observer poles and finite gain
[AIAA PAPER 90-3228]
p 868 A90-49113

MONDRZYK, ROBERT J.

Boeing Transonic Windblast Generator System (BTWGS)
p 199 A90-17413

MONGIA, H. C.

Further validation of a semi-analytical approach for fuel injectors of different concepts
[AIAA PAPER 90-2190]
p 686 A90-42067

MONGIA, HUKAM C.

Composite matrix cooling scheme for small gas turbine combustors
[AIAA PAPER 90-2158]
p 852 A90-47210

MONNOYER, F.

Numerical simulation of transonic wing flows using a zonal Euler, boundary-layer, Navier-Stokes approach
p 225 A90-21596
Turbulence management: Application aspects
p 72 N90-10378

MONTAGNE, J.-L.

High-resolution shock-capturing schemes for inviscid and viscous hypersonic flows
p 476 A90-34545

MONTAGUE, J.

Test and theory for piezoelectric actuator-active vibration control of rotating machinery
p 879 A90-46226

MONTANES, J. L.

Non-iterative analytical methods for off-design turbofan calculations with or without mixed-flows
p 70 A90-12628

MONTEIL, F.

Applications of Mode S secondary surveillance radar to civil air traffic control - Studies, experiments, and policy of the French Direction de la Navigation-Aerienne
p 639 A90-41056

MONTI, G.

Eurofar - Status of the European tilt-rotor project
p 645 A90-42441

MONTI, GIULIANO

Advocating international cooperation: The Eurofar program - An example and a hope
p 785 A90-46929

MONTICONE, LEONE C.

ATC ground communications system optimization techniques
p 330 A90-25568

MOOIJEKIND, J. C. M.

Study improvement training facilities ground control air traffic controllers. Part 1: Alternative solutions and their consequences
[FEL-89-A257-PT-1]
p 919 N90-29380
Study improvement training facilities ground control air traffic controllers. Part 2: Functional analysis approach control trainer
[FEL-89-A280-PT-2]
p 939 N90-29409

MOOK, D. JOSEPH

Improved noise rejection in automatic carrier landing systems
[AIAA PAPER 90-3374]
p 864 A90-47632

A nonlinear aircraft tracking filter utilizing control variable estimation
[AIAA PAPER 90-3402]
p 822 A90-47657

MOOK, D. T.

Numerical simulation of wings in steady and unsteady ground effects
p 153 A90-17866
Flow over inclined finite length and width flat plates at low and high Reynolds numbers
[AIAA PAPER 90-1467]
p 562 A90-38624

MOOK, DEAN T.

Numerical model of unsteady subsonic aeroelastic behavior
p 535 A90-32471
Numerical simulation of wakes with application to blade-vortex interaction
p 807 A90-46881
Aerodynamic/dynamic interaction
[AD-A222263]
p 815 N90-26798

MOON, DARWIN

Towards a unified method of causing impact damage in thick laminated composites
p 946 A90-50168

MOON, R. N.

Modeling flexible aircraft for flight control design
[AD-A219123]
p 757 N90-25140

MOON, YOUNG JUNE

Interaction of an oblique shock wave with supersonic flow over a blunt body
p 398 N90-19197

MOONEY, L. W.

Analysis of hydraulic fluids and lubricating oils for the formation of Trimethylolpropane Phosphate (TMP-P)
[AD-A215188]
p 357 N90-16939

MOORE, EMERY L.

Fiber optic systems for mobile platforms II: Proceedings of the Meeting, Boston, MA, Sept. 6, 7, 1988
[SPIE-989]
p 67 A90-11659

MOORE, JOAN G.

Shock capturing and loss prediction for transonic turbine blades using a pressure correction method
p 11 A90-12518

MOORE, JOHN

Shock capturing and loss prediction for transonic turbine blades using a pressure correction method
p 11 A90-12518
Tip leakage losses in a linear turbine cascade
[ASME PAPER 89-GT-56]
p 290 A90-23782

MOORE, R. M.

C-grid generation for turbomachinery cascades
p 312 A90-26554

MOORHOUSE, DAVID J.

On the level 2 ratings of the Cooper-Harper scale
p 197 A90-19577
Lessons learned in the development of a multivariable control system
p 432 A90-30713
Simulating turbulence and gusts for handling qualities evaluation
[AIAA PAPER 90-2845]
p 754 A90-45174

Lessons learned from the S/MTD program for the Flying Qualities Specification
[AIAA PAPER 90-2849]
p 755 A90-45177
Status of the STOL and Maneuver Technology Demonstrator flight test program
[AIAA PAPER 90-3306]
p 838 A90-48887

Aerodynamic and propulsive control development of the STOL and maneuver technology demonstrator
p 920 N90-28514

MORAN, MARK S.

Supersonic low-density flow over airfoils
p 153 A90-17871

MORAWSKI, JANUSZ M.

Criteria for evaluating the flight dynamics model of flight simulators
p 121 A90-15422

MORCHIN, WILLIAM C.

Airborne early warning radar
p 727 A90-45200

MORCHOISNE, Y.

Numerical simulation of vortex breakdown via 3-D Euler equations
[ONERA, TP NO. 1989-211]
p 303 A90-25344
Numerical simulation of vortex breakdown by solving the Euler equations for an incompressible fluid
p 476 A90-34323

MOREAU, J. P.

Electromagnetic characterization of lightning on aircraft
[ONERA, TP NO. 1989-131]
p 22 A90-11155
Transall 88 - Lightning characterization program
[ONERA, TP NO. 1989-142]
p 22 A90-11164

Connection of structures by laboratory-generated electrical discharges
[ONERA, TP NO. 1989-147]
p 58 A90-11169

MOREAU, RICHARD

A test of kinematic GPS combined with aerial photography - Organization, logistics and results
p 97 A90-13983

MOREIRA, JOAO R.

A new method of aircraft motion error extraction from radar raw data for real-time motion compensation
p 824 A90-49675

- MORELLI, EUGENE A.**
Optimal input design for aircraft parameter estimation using dynamic programming principles [AIAA PAPER 90-2801] p 753 A90-45157
- MORETTI, GINO**
Shock-fitting method for two-dimensional inviscid, steady supersonic flows in ducts p 477 A90-34864
Shock-fitting in three space dimensions p 707 A90-44434
- MORGAN, DAVID**
Design of an aero-engine thrust reverser blocker door p 467 A90-31651
- MORGAN, H. L.**
Experimental investigation of flowfield about a multielement airfoil p 154 A90-18137
- MORGAN, HARRY L., JR.**
A study of high-lift airfoils at high Reynolds numbers in the Langley low-turbulence pressure tunnel [NASA-TM-89125] p 1 N90-10002
Theoretical methods and design studies for NLF and HLFC swept wings at subsonic and supersonic speeds p 92 N90-12535
Design of the low-speed NLF(1)-0414F and the high-speed HSNLF(1)-0213 airfoils with high-lift systems p 93 N90-12540
- MORGAN, J. MURRAY**
Control sensitivity, bandwidth and disturbance rejection concerns for advanced rotorcraft p 430 A90-28204
- MORGAN, K.**
Applications of an adaptive unstructured solution algorithm to the analysis of high speed flows [AIAA PAPER 90-0395] p 229 A90-22213
Unstructured finite element mesh generation and adaptive procedures for CFD p 608 N90-21993
- MORGAN, KEN**
Euler and Navier-Stokes solutions for hypersonic flows p 155 A90-18254
- MORGAN, R. E.**
Composite-embedded optical fibers for communication links p 139 A90-13847
- MORGAN, R. G.**
Hypersonic combustion of hydrogen in a shock tunnel p 46 A90-12560
- MORI, KENJI**
Flow dependent grid for aerodynamic designers p 306 A90-25831
- MORIMOTO, TOSHIKI**
Start characteristics of FJR 710/600S engine p 42 A90-12013
Expert diagnosis system for FJR engine troubles p 587 A90-38597
- MORINO, LUIGI**
Unsteady free-wake viscous aerodynamic analysis of helicopter rotors [AD-A217166] p 478 N90-20048
Analysis of dynamic transient response and postfluter behavior of super-maneuvering airplane [AD-A224126] p 925 N90-29386
- MORITA, MITSUO**
A study on the performance of the turbo-ramjet engines at high speed flight p 49 A90-12608
Restart characteristics of turbofan engines p 50 A90-12627
- MORIYA, KAZUMASA**
A study on flaw detection method for CFRP composite laminates. I - The measurement of crack extension in CFRP composites by electrical potential method p 441 A90-28003
- MORLEY, M.**
Cleaner superalloys via improved melting practices p 442 A90-29707
- MOROZOV, V. I.**
Modeling of the buffeting of flight vehicles p 803 A90-46500
- MORRELL, FREDERICK R.**
Joint University Program for Air Transportation Research, 1988-1989 [NASA-CP-3063] p 468 N90-20921
- MORRIS, DAVID L.**
Titanium matrix composite landing gear development [SAE PAPER 892337] p 733 A90-45491
- MORRIS, GUY V.**
Antenna sidelobe requirements for the medium PRF mode of an airborne radar p 37 A90-10985
- MORRIS, JOHN**
LFC: A maturing concept [DOUGLAS-PAPER-7878] p 90 N90-12505
- MORRIS, MARTIN J.**
Experimental investigation of terminal shock sensors in mixed-compression inlets [AIAA PAPER 90-1931] p 681 A90-40560
- MORRIS, P. M.**
Energy efficient engine pin fin and ceramic composite segmented liner combustor sector rig test report [NASA-CR-179534] p 932 N90-28567
- MORRIS, PATRICK M.**
Applications of flight control system methods to an advanced combat rotorcraft [NASA-TM-101054] p 119 N90-11752
- MORRIS, SHELBY J., JR.**
Performance potential of an advanced technology Mach 3 turbojet engine installed on a conceptual high-speed civil transport [NASA-TM-14144] p 51 N90-10034
- MORRIS, STEVEN LYNN**
A video-based experimental investigation of wing rock [AD-A218244] p 498 N90-20075
A video-based experimental investigation of wing rock p 592 N90-21771
- MORRIS, W. L.**
Fatigue crack initiation mechanics of metal aircraft structures [AD-A210567] p 65 N90-10255
- MORRISSETTE, E. LEON**
The effects of wall surface defects on boundary-layer transition in quiet and noisy supersonic flow p 94 N90-12556
- MORRISON, BILL**
Bubble memory applications for aircraft systems p 418 A90-30681
- MORRISON, JOSEPH H.**
Comparison between experimental and numerical results for a research hypersonic aircraft p 395 A90-31278
- MORRISON, MELVIN MARK**
Low cost QUBIK IMU for integration with GPS, Omega, Loran-C, and SDI systems p 577 A90-36929
- MORRISON, MICHAEL A.**
RSRA/X-Wing flight control system development - Lessons learned p 430 A90-28216
- MORROW, JOHN G.**
Heliport surface maneuvering test results [ACD-330] p 59 N90-10897
Analysis of heliport environmental data: Indianapolis downtown heliport, Wall Street heliport. Volume 2: Wall Street heliport data plots [DOT/FAA/CT-TN87/54-VOL-2] p 121 N90-11761
Analysis of heliport environmental data: Indianapolis downtown heliport, Wall Street heliport. Volume 3: Indianapolis downtown heliport data plots [AD-A217412] p 544 N90-20500
- MORROW, THOMAS H.**
Reliability and performance of friction measuring tires and friction equipment correlation [AD-A223694] p 939 N90-29408
- MORTCHELEWICZ, G. D.**
Solution of Euler equations with unstructured meshes p 558 A90-37343
- MORTON, SCOTT ANDREW**
Numerical simulation of compressible vortices [AD-A216221] p 371 N90-18017
- MOSBY, T. DEAN**
Interstitial materials for low thermal resistance joints in avionic equipment [SAE PAPER 891441] p 356 A90-27412
- MOSKALIK, L. M.**
A method for the active control of the boundary layer condition p 296 A90-24114
- MOSKOVITZ, CARY A.**
Experimental investigation of a new device to control the asymmetric flowfield on forebodies at large angles of attack [AIAA PAPER 90-0069] p 161 A90-19665
An experimental investigation of the physical mechanisms controlling the asymmetric flow past slender bodies at large angles of attack p 592 N90-21767
- MOSS, DAVID**
CFE738 - A case for joint engine development [AIAA PAPER 90-2522] p 664 A90-42197
- MOSS, J. B.**
Fire science and aircraft safety p 326 N90-17596
- MOSS, J. N.**
Hypersonic viscous shock-layer solutions over long slender bodies. II - Low Reynolds number flows p 393 A90-29695
- MOSS, JAMES N.**
Grid generation and adaptation for the direct simulation Monte Carlo method p 67 A90-11102
Direct simulation of three-dimensional hypersonic flow about intersecting blunt wedges p 16 A90-12835
Direct simulation of hypersonic rarefied flow about a delta wing [AIAA PAPER 90-0143] p 162 A90-19704
- MOSSER, P.-E.**
Modeling of the oil quench for Ni-based superalloy turbine disks p 957 A90-51525
- MOSTAFA, A.**
Viscous flow analysis for advanced inlet particle separators [AIAA PAPER 90-2136] p 661 A90-42038
- MOSTAFA, ABDU A.**
Introducing the VRT gas turbine combustor [AIAA PAPER 90-2452] p 743 A90-42808
Introducing the VRT gas turbine combustor [NASA-TM-103176] p 688 N90-23591
- MOSTAFA, SAMIR M.**
Numerical simulation of unsteady flow about cambered plates p 159 A90-19389
- MOSUNOV, V. A.**
Calculation of the vibrations of aircraft with elastic suspended loads p 345 A90-24171
- MOULD, V. H.**
Fabrication characteristics of 8090 alloy p 268 N90-15198
- MOULTON, BRYAN J.**
An in-flight investigation of ground effect on a forward-swept wing airplane [NASA-TM-101708] p 175 N90-14202
An in-flight investigation of ground effect on a forward-swept wing airplane p 922 N90-28533
- MOULTON, CAREY L.**
Air Force procedure for predicting aircraft noise around airbases: Noise Exposure Model (NOISEMAP). User's manual [AD-A223162] p 895 N90-27467
- MOURA, GERALDO A.**
An approach for analysis and design of composite rotor blades [AIAA PAPER 90-1005] p 449 A90-29276
- MOUSSEUX, MARC C.**
Experiments in swept-wing transition p 149 A90-16794
The development of crossflow vortices on a 45 degree swept wing [SAE PAPER 892245] p 713 A90-45452
- MOUSTAPHA, H.**
Application of 3-D flow analysis to the design of a high work transonic turbine p 628 A90-42395
- MOUSTAPHA, S. H.**
An experimental investigation of the effect of incidence on the two-dimensional performance of an axial turbine cascade p 11 A90-12520
An improved incidence losses prediction method for turbine airfoils [ASME PAPER 89-GT-284] p 475 A90-33563
- MOXON, JULIAN**
East coast Osprey flies p 246 A90-21713
- MOYER, SETH A.**
An integrated CFD/experimental analysis of aerodynamic forces and moments [NASA-TM-102195] p 18 N90-10006
- MOYLE, IAN N.**
Influence of the radial component of total pressure gradient on tip clearance secondary flow in axial compressors [ASME PAPER 89-GT-19] p 288 A90-23761
- MOYNES, JOHN F.**
Ride quality criteria for the B-2 bomber [AIAA PAPER 90-3256] p 835 A90-48852
- MOZUMDAR, S.**
Measurements in an annular combustor-diffuser system [AIAA PAPER 90-2162] p 768 A90-42740
- MOZZHEROVA, N. A.**
A method for determining equivalents during the fatigue testing of structures in an acoustic field p 364 A90-24153
- MOZZHILKIN, V. V.**
Multilevel method for calculating aerodynamic loads on a flight vehicle p 296 A90-24122
- MSHANA, J. S.**
A rate theory investigation of cyclic loading and plastic deformation in the high stress and ambient temperature range p 954 A90-49884
- MUELLER, B.**
Disturbance growth in an unstable three-dimensional boundary layer p 148 A90-16787
Numerical simulation of hypersonic viscous continuum flow p 707 A90-44407
Experiments on the laminar-turbulent transition on swept wings p 276 N90-16170
- MUELLER, ERIC**
Expert system - Conventional processing interface p 460 A90-30753
- MUELLER, K.**
Noise measurements of turboprop airplanes at different overflight elevations p 697 N90-24860
- MUELLER, R.**
A semiconductor laser-Doppler-anemometer for applications in aerodynamic research p 447 A90-28273
Determination of the N-factor in the Brunswick (Federal Rep. of Germany) transonic wind tunnel using measurements of pressure distributions and transition points, and the Sally method p 276 N90-16177

MUELLER, R. H. G.

Application of a new visualization method to helicopter rotor flow
[AIAA PAPER 90-3006] p 789 A90-45856

MUELLER, REINERT H. G.

Winglets on rotor blades in forward flight - A theoretical and experimental investigation p 303 A90-25422

MUELLER, T. J.

Transition phenomena on airfoils operating at low chord Reynolds numbers in steady and unsteady flow p 148 A90-16786

MUELLER, THOMAS J.

Measurements in a separation bubble on an airfoil using laser velocimetry p 384 A90-27977
An experimental study of a closely coupled tandem wing configuration at low Reynolds numbers p 797 A90-45923

[AIAA PAPER 90-3094]
Low Reynolds number aerodynamics; Proceedings of the Conference, University of Notre Dame, IN, June 5-7, 1989 p 799 A90-46358

Experimental measurements of the laminar separation bubble on an Eppler 387 airfoil at low Reynolds numbers [NASA-CR-186263] p 275 A90-15380

MUELLER, TYSEN

Reduced order INS/GPS guided unmanned air vehicle study p 726 A90-43707

MUELLER, U. R.

A strong viscous-inviscid interaction method for computing unsteady transonic airloads for use in aerodynamics p 471 A90-33355

MUENCH, F. X.

Natural laminar flow - A wind tunnel test campaign and comparison with flight test data [AIAA PAPER 90-3045] p 792 A90-45882

MUGAL, M. G.

Turbulent reacting flows and supersonic combustion [AD-A221793] p 875 A90-26933

MUGGLI, WOLFGANG

EUROFAR - European project for a commercial vertical-takeoff aircraft [MBB-UD-553/89] p 221 A90-22696

MUHS, J. D.

Engine testing of thermographic phosphors [DE90-013269] p 885 A90-28059

MUIR, HELEN

Aircraft evacuations: The effect of passenger motivation and cabin configuration adjacent to the exit [CAA-PAPER-89019] p 913 A90-29336

MUKHAMETOV, M. KH.

Numerical modeling of the combustion kinetics of hydrocarbon fuels in an annular combustion chamber with allowance for the formation of harmful impurities p 124 A90-14582

MUKHIN, V. S.

Design of the optimal hardening treatment for the metal surfaces of gas turbine engine components p 873 A90-46496

MUKHOPADHYAY, V.

Control law synthesis and optimization software for large order aeroservoelastic systems p 61 A90-10111

MUKHOPADHYAY, VIVEK

Digital-flutter-suppression-system investigations for the active flexible wing wind-tunnel model [AIAA PAPER 90-1074] p 430 A90-29382

Flutter suppression control law synthesis for the active flexible wing model p 517 A90-33403

Development and testing of methodology for evaluating the performance of multi-input/multi-output digital control systems [AIAA PAPER 90-3501] p 867 A90-47747

Digital-flutter-suppression-system investigations for the active flexible wing wind-tunnel model [NASA-TM-102618] p 520 A90-20093

Development and testing of methodology for evaluating the performance of multi-input/multi-output digital control systems [NASA-TM-102704] p 846 A90-27699

MUKUNDA, H. S.

Mixing and combustion enhancement in supersonic reacting flows p 744 A90-44410

Modeling of supersonic reacting flow fields p 855 A90-26898

MULAC, R. A.

The numerical simulation of multistage turbomachinery flows p 514 A90-21025

MULARZ, E. J.

A planar reacting shear layer system for the study of fluid dynamics-combustion interaction [NASA-TM-102422] p 194 A90-13393

MULDER, J. A.

Aircraft flight control system identification p 431 A90-30105

Stability and control derivatives of the De Havilland DHC-2 BEAVER aircraft [PB89-217525] p 119 A90-11754

Mathematical model identification for flight simulation, based on flight and taxi tests [LR-550] p 202 A90-13410

MULDON, PATRICIA L.

Ultra High Bypass (UHB) engine critical component technology [ASME PAPER 89-GT-229] p 342 A90-23884

MULLICAN, A.

WINCOF-I code for prediction of fan compressor unit with water ingestion [NASA-CR-185157] p 551 A90-21724

MUNDEN, RICHARD C.

New systems for helicopter and aircraft vibration monitoring p 653 A90-42477

MUNGAL, M. G.

Two- and three-dimensional effects in the supersonic mixing layer [AIAA PAPER 90-1978] p 703 A90-42708

MUNGUR, P.

Fuel effects on gas turbine combustor dynamics [AIAA PAPER 90-1957] p 676 A90-40570

Dynamic instability characteristics of aircraft turbine engine combustors p 53 A90-10195

MUNGUR, PARMA

Status report on a natural laminar-flow nacelle flight experiment p 105 A90-12550

Nacelle design p 105 A90-12551

MUNIN, A. G.

Calculation of the rotation noise of a single propeller with blades of arbitrary shape p 894 A90-46552

MUNJAL, ASHOK K.

Improvement in structural integrity and long term durability of aerospace composite components p 441 A90-28189

MUNSHTUKOV, D. A.

Estimation of the efficiency of a ramjet engine with a thermocompressor using fuel conversion products p 255 A90-23412

MUNTZ, A. H.

Software architecture concepts for avionics p 461 A90-30806

MUNZ, CLAUS-DIETER

The formation of vortex streets in supersonic flows p 907 A90-51539

MUNZ, PAUL D.

Numerical simulation of unsteady flow about cambered plates p 159 A90-19389

MURAKAMI, A.

Some governing parameters of plasma torch igniter/flameholder in a scramjet combustor [AIAA PAPER 90-2098] p 661 A90-42017

MURALI, B. K.

Simulation of separated flows using panel method p 308 A90-26349

MURAMOTO, KENNETH K.

A model for the electrohydrodynamic flow in a constricted arc heater p 131 A90-15393

MURAMOTO, KYLE M.

Optimum element density studies for finite-element thermal analysis of hypersonic aircraft structures [NASA-TM-4163] p 369 A90-17074

MURATA, HIDEYO

A calculation of the aerodynamic lift acting on cascade blades in a steady, viscous flow at high Reynolds number p 469 A90-32425

MURAYAMA, SHIGEKI

Multivariable control of jet engines p 507 A90-32421

MURCH, JERRY

Multifunction displays optimized for viewability p 652 A90-40398

MURMAN, EARL L.

Semi-implicit Navier-Stokes solver (SINSS) calculations of separated flows around blunt delta wings [AIAA PAPER 90-0590] p 168 A90-19936

MURNYACK, STEPHEN M.

STOL Maneuver Technology Demonstrator aeroservoelasticity [AIAA PAPER 90-3336] p 863 A90-47596

MUROTA, K.

A digital controller for active aeroelastic controls [NAL-TR-1014] p 936 A90-29402

MURPHY, BRIAN D.

A preliminary sensitivity analysis of the Generalized Escape System Simulation (GESS) computer program [DE89-016891] p 24 A90-10844

MURPHY, JOHN C.

Thermal nondestructive characterization of the integrity of protective coatings p 770 A90-44325

MURPHY, R. JAY

Database for LDV signal processor performance analysis p 447 A90-28278

MURPHY, RONALD D.

The North American Rockwell XFV-12A - Reflections and some lessons [AIAA PAPER 90-3240] p 839 A90-49118

MURPHY, T. J.

Antenna installation on aircraft: Theory and practice p 371 A90-17941

MURPHY, WILLIAM J.

Survivable penetration p 917 A90-29363

MURRAY-SMITH, D. J.

System identification strategies for helicopter rotor models incorporating induced flow p 30 A90-12768

A frequency-domain system identification approach to helicopter flight mechanics model validation p 56 A90-12772

Experience with multi-step test inputs for helicopter parameter identification p 56 A90-12775

A technique for the tuning of helicopter flight control systems p 670 A90-42467

MURRAY, DANIEL C.

The AVRO VZ-9 experimental aircraft - Lessons learned [AIAA PAPER 90-3237] p 835 A90-48847

MURRAY, J. E.

Flight testing a highly flexible aircraft - Case study on the MIT Light Eagle p 414 A90-31284

MURRAY, KENNETH D.

Automation and extension of LDV (Laser-Doppler Velocimetry) measurements of off-design flow in a subsonic cascade wind tunnel [AD-A216627] p 453 A90-18670

MURRAY, STEVE

Tilt rotor requirements on engine design and qualification p 587 A90-38534

MURRI, DANIEL G.

Wind tunnel results of the low-speed NLF(1)-0414F airfoil p 93 A90-12541

Actuated forebody strakes [NASA-CASE-LAR-13983-1] p 648 A90-23390

Development of non-conventional control methods for high angle of attack flight using vortex manipulation p 935 A90-28522

MURTHY, A. V.

Sidewall boundary-layer removal and wall adaptation studies p 672 A90-40680

Residual interference assessment in adaptive wall wind tunnels [NASA-CR-181896] p 123 A90-12625

Experience with some repeat tests on the 9 inch chord CAST-10-2/DOA 2 airfoil model in the Langley 0.3-m TCT adaptive wall test section p 321 A90-17657

MURTHY, DURBHA V.

Concurrent processing adaptation of aeroelastic analysis of propfans [AIAA PAPER 90-1036] p 450 A90-29380

Concurrent processing adaptation of aeroplastic analysis of propfans [NASA-TM-102455] p 215 A90-14656

MURTHY, MADHUSUDAN

Supersonic/hypersonic flow past wedge and plane ogive in oscillation p 85 A90-15231

MURTHY, S. N. B.

Water ingestion simulation - Test needs. p 23 A90-12620

Hot gas environment around STOVL aircraft in ground proximity. I - Experimental study [AIAA PAPER 90-2269] p 742 A90-42765

WINCOF-I code for prediction of fan compressor unit with water ingestion [NASA-CR-185157] p 551 A90-21724

MURTHY, SREEDHARA V.

Flow unsteadiness effects on boundary layers [NASA-CR-186067] p 690 A90-24557

MURTHY, T. SREEKANTA

Airframe structural dynamic considerations in rotor design optimization [NASA-TM-101646] p 134 A90-12057

Airframe design considerations: Overview p 106 A90-12586

MURTUGUDDE, R. G.

Development of the UTA hypersonic shock tunnel [AIAA PAPER 90-0080] p 200 A90-19675

MUSCH, GERHARD

Fibre reinforced thermoplastic integral constructions in modular build-up technology - The 'thermoplastic in-situ-technique' p 534 A90-31879

MUSSI, F.

EH101 development progress p 646 A90-42442

MUTHUVEL, S.

A fiberoptic LAN for aircraft and other applications p 282 A90-23241

MUYLAERT, JEAN

PETW testing results p 523 A90-34226

MYERS, JAMES W.

Forward canopy feasibility and Thru-The-Canopy (TTC) ejection system study [AD-A220360] p 637 A90-24258

MYERS, LAWRENCE P.

Propulsion system-flight control integration-flight evaluation and technology transition
[AIAA PAPER 90-2280] p 644 A90-42106

Propulsion system-flight control integration and optimization: Flight evaluation and technology transition
[NASA-TM-4207] p 929 N90-28551

MYERS, THOMAS T.

Literal singular-value-based flight control system design techniques p 118 A90-14747

MYLONAS, J.

Unsteady 2D flow calculation in turbomachinery cascades p 6 A90-11782

N**NAARDING, S. H. J.**

Experimental and numerical investigation of the vortex flow over a sharp edged delta wing; with and without sideslip
[PB90-167131] p 481 N90-20964

NAARDING, STEVEN H. J.

Experimental and numerical investigation of vortex flow over a sideslipping delta wing p 17 A90-13016

NAASERI, M.

Interaction between strong longitudinal vortices and turbulent boundary layers p 145 A90-16764

NABEEL, TARABISHY M.

Neural networks for detecting defects in aircraft structures
[IAR-90-4] p 777 N90-26345

NABITY, J. A.

Recent developments in Ramjet pressure oscillation technology p 53 N90-10199

NABITY, JAMES A.

Metalized fuel particle size study in a solid fuel ramjet [AD-A220079] p 679 N90-24451

NADVORSKY, A. S.

Heat transfer in supersonic coaxial reacting jets p 601 A90-35394

NAEEM, R. K.

Numerical solution of transonic flows on a streamfunction co-ordinate system p 17 A90-13238

NAEINI, ABBAS EMAMI

Propulsion system design specifications based on STOVL flight control requirements
[AIAA PAPER 90-3227] p 839 A90-49112

NAGABHUSHAN, B. L.

Control configured airship design
[AIAA PAPER 89-3170] p 244 A90-20585

NAGABHUSHANAM, J.

An experimental and analytical investigation of isolated rotor flap-lag stability in forward flight p 518 A90-33623

A study of symbolic processing and computational aspects in helicopter dynamics p 545 A90-34103

NAGAMATSU, F.

New features of JAL's ground station p 872 N90-27633

NAGAOKA, M.

A bearing error in the VHF omnirange due to sea surface reflection p 402 A90-27875

NAGAOKA, SAKAE

Evaluating the feasibility of a radar separation minimum for a long-range SSR p 25 A90-10240

NAGAR, ARVIND

Recent advances in fatigue life analysis methods for aerospace applications p 677 A90-41338

NAGASHIMA, T.

Radial swirl flows between parallel disks at critical flow rate p 14 A90-12596

NAGASHIMA, TOMOARI

Aeroelastic response characteristics of a rotor executing arbitrary harmonic blade pitch variations p 646 A90-42464

NAGATA, JOHN I.

Airworthiness and flight characteristics test of the UH-60A Black Hawk helicopter equipped with the XM-139 multiple mine dispensing system (VOLCANO)
[AD-A210271] p 32 N90-10025

NAGATI, M. G.

A low cost stall/spin simulator
[SAE PAPER 891022] p 117 A90-14334

Finite wing lift prediction at high angles of attack
[AIAA PAPER 90-3079] p 795 A90-45910

Stall/spin/flight simulation
[DOT/FAA/CT-88/28] p 122 N90-11765

NAGAYASU, MASAHICO

On the interactive computer program IPIS for aircraft parameter identification
[NAL-TR-1000] p 77 N90-10586

Short period control using angular acceleration feedback: Compensation for first lag servo
[NAL-TM-600] p 936 N90-29399

NAGEL, A. L.

Application of laminar flow control to supersonic transport configurations
[NASA-CR-181917] p 719 N90-25944

NAGENDRA, GOPAL K.

Sensitivity and optimization of composite structures in MSC/NASTRAN p 208 A90-17370

NAGID, GIORA

Efforts continue to increase airport/airspace capacity p 722 A90-44550

NAGLE-ESHLEMAN, JUDITH

The Shock and Vibration Digest, volume 21, no. 6 p 614 N90-22363

NAGPURWALA, Q. H.

Development of a software package for automatic data acquisition, analysis, and controls in an axial flow compressor test rig
[PD-PR-8910] p 965 N90-29926

NAGY, D.

Development of erosion resistant coatings for compression airfoils p 443 A90-31120

NAGY, EDWARD

Investigation of variation in fatigue life calculated using damage fraction p 537 A90-33624

NAGY, EDWARD G.

SH-2F airframe fatigue test program p 642 A90-39989

NAHON, MEYER A.

Simulator motion-drive algorithms - A designer's perspective p 375 A90-25997

NAIDU, D. S.

Guidance and Control strategies for aerospace vehicles
[NASA-CR-186195] p 199 N90-14243

NAIK, D. A.

Effects of nonplanar outboard wing forms on a wing p 232 A90-23279

NAIK, DINESH A.

3-D Euler calculations for aft-propfan integration
[AIAA PAPER 90-2147] p 625 A90-42044

NAKAGAWA, YUKIYA G.

Recrystallization behavior of nickel-base single crystal superalloys p 440 A90-27681

NAKAHASHI, KAZUHIRO

An automatic Euler solver using unstructured upwind method p 367 A90-25811

Investigation of ATP blades, part 2. Validation of two-dimensional viscous flow simulation codes around thin airfoils
[NAL-TR-1046] p 912 N90-29326

NAKAKI, DAVID

Noise and sonic boom impact technology. Effects of aircraft noise and sonic booms on structures: An assessment of the current state-of-knowledge
[AD-A213919] p 378 N90-17409

NAKAMICHI, JIRO

Calculations of unsteady aerodynamics over oscillating wings p 472 A90-33362

NAKAMURA, I.

Turbulent plane jet excited mechanically by an oscillating thin plate in the potential core p 553 A90-35262

NAKAMURA, IKUO

An experimental study of a turbulent jet impinging on a wedge p 553 A90-35274

NAKAMURA, MASAYOSHI

A numerical method for solving transonic flow past aircraft in Cartesian coordinates
[NAL-TR-1008] p 18 N90-10003

NAKAMURA, SHOICHIRO

A computational study of the impingement region of an unsteady subsonic jet
[AIAA PAPER 90-1657] p 570 A90-38784

NAKAMURA, Y.

Noise prediction of a counter-rotation propfan p 218 A90-17861

NAKAMURA, YOSHIKAKI

A flow around airfoil with slat and flap
[AIAA PAPER 90-1535] p 564 A90-38679

NAKAMURA, YOSIAKI

Calculation of flow over airfoil with slat and flap p 149 A90-16797

NAKANO, MICHIO

Application of Lomax-Bailey implicit scheme to reactive flows p 367 A90-25861

NAKATANI, IWAO

TW-58 tilt wing high speed commercial VTOL p 246 A90-21712

NAKAUCHI, YASUO

Instrumentation and operation of NDA cryogenic wind tunnel p 437 A90-28293

NAKAYAMA, A.

Experimental investigation of flowfield about a multielement airfoil p 154 A90-18137

The turbulent near wake of a flat plate at low Reynolds number p 811 A90-48711

NAKAZAWA, KIYOSHI

Start characteristics of FJR 710/600S engine p 42 A90-12013

NAKAZAWA, SHOHEI

The MHOST finite element program: 3-D inelastic analysis methods for hot section components. Volume 3: Systems' manual
[NASA-CR-182236] p 73 N90-10451

NALEPKA, JOSEPH P.

Significance of the short crack effect on aerospace structures p 269 A90-20065

NALLASAMY, M.

Unsteady Euler analysis of the flowfield of a propfan at an angle of attack
[AIAA PAPER 90-0339] p 300 A90-25028

Unsteady blade surface pressures on a large-scale advanced propeller - Prediction and data
[AIAA PAPER 90-2402] p 808 A90-47220

Prediction of unsteady blade surface pressures on an advanced propeller at an angle of attack
[NASA-TM-102374] p 94 N90-12560

Unsteady Euler analysis of the flow field of a propfan at an angle of attack
[NASA-TM-102426] p 380 N90-18229

NALLS, A. L.

AV-8B shipboard ski jump evaluation p 574 A90-38535

NAM, CHANGHO

Aeroservoelastic tailoring for lateral control enhancement p 516 A90-33060

NAMBA, M.

Improved double linearization method for prediction of mean loading effects on subsonic and supersonic cascade flutter p 41 A90-11795

Unsteady lifting surface theory for a rotating cascade of swept blades
[ASME PAPER 89-GT-306] p 906 A90-51259

NAMBA, MASANOBU

Finite element method for unsteady three-dimensional subsonic flows through a cascade oscillating with steady loading p 9 A90-11873

Numerical calculation of unsteady aerodynamic forces for three-dimensional subsonic oscillating cascades by a finite element method p 9 A90-12219

Numerical calculation of unsteady aerodynamic forces for two-dimensional supersonic oscillating cascades by finite element method p 9 A90-12238

Application of the double linearization theory to three-dimensional subsonic and supersonic cascade flutter p 50 A90-12638

Numerical study of interaction of a jet with a supersonic cross flow p 808 A90-47300

Mean loading effects on flutter of subsonic rotating annular cascade p 853 A90-49453

NANEVICZ, JOSEPH E.

An airborne instrument for characterizing the 10,000 electromagnetic signals generated by one lightning flash p 848 A90-49830

NANNONI, FABIO

Agusta methodology for pitch link loads prediction in preliminary design phase p 646 A90-42465

Agusta methodology for pitch link loads prediction in preliminary design phase
[ETN-90-97270] p 737 N90-25978

NAOR, YORAM

Angular feature mapping - An optical method p 377 A90-23974

NAPOLITANO, MARCELLO R.

An aircraft flight control reconfiguration algorithm p 432 A90-37078

NAQWI, A.

A semiconductor laser-Doppler-anemometer for applications in aerodynamic research p 447 A90-28273

NARASIMHAN, J. L.

Numerical prediction of wakes of different bodies p 308 A90-26341

NARBOROUGH-HALL, C. S.

Development and evaluation at ATCEU of executive and support operations, phase 4A/3D
[CAA-PAPER-88017] p 99 N90-12572

NARKIEWICZ, JANUSZ

Wind tunnel tests of models of helicopter rotors p 29 A90-10230

NARRAMORE, J. C.

BELLTECH - A multipurpose Navier-Stokes code for rotor blade and fixed wing configurations p 384 A90-28174

An efficient airfoil design method using the Navier-Stokes equations p 500 N90-20981

NASH, CAROLYN J.

Design criteria for helicopter night pilotage sensors p 417 A90-28221

NASTASE, ADRIANA

The design of supersonic aircraft and space vehicles by using global optimization techniques

p 353 A90-25781

Theoretical prediction of pressure distribution on wedged delta wing at higher supersonic Mach numbers and its agreement with experimental results

p 907 A90-51537

Prediction of pressure distribution on optimum-optimum delta wing at higher angles of attack in supersonic flow and its agreement with experimental results

p 907 A90-51538

NATAN, B.

Combustion characteristics of a boron-fueled SFRJ with aft-burner

p 62 A90-12514

NATARAJAN, R.

Experimental study of static pressure and mean velocity profiles inside a two-dimensional dump-type combustor model

p 45 A90-12530

NATARAJAN, V.

Local heat transfer on a flat surface roughened with broken ribs

p 534 A90-32169

NAUDIN, P.

New methods of buffeting prediction on civil aircraft

p 908 A90-52620

NAUMAN, CHRIS

High speed civil transport [NASA-CR-186661]

p 649 N90-23396

NAUMANN, K. W.

A novel technique for aerodynamic force measurement in shock tubes

p 438 A90-28302

Possible piloting techniques at hypersonic speeds [ISL-CO-216/88]

p 415 N90-18392

Maneuvering by means of lateral jets [ISL-CO-255/88]

p 758 N90-26015

NAUMENKO, Z. N.

Optimization of the sound-absorption lining parameters of an ejector jet muffler

p 378 A90-24117

NAUMOV, A. M.

Characteristics of temperature and pressure generation and retention in flow inside cryogenic wind tunnel T-04

p 869 A90-46576

NAVANEETHAN, RAMASAMY

Effect of an isolated shell on interior noise levels in a turboprop aircraft [SAE PAPER 891083]

p 102 A90-14375

NAWA, Y.

Application of the 'K-gage' to aircraft structural testing

p 926 A90-49891

NAYANI, SUDHEER N.

Low-density flow effects for hypervelocity vehicles, phase 2 [AD-A221034]

p 634 N90-24249

NAYFEH, A. H.

Subharmonic instability of compressible boundary layers

p 706 A90-44005

NAYFEH, ALI H.

Aerodynamic/dynamic interaction [AD-A222263]

p 815 N90-26798

NAYLER, A. W. L.

Modern technology in airship design [AIAA PAPER 89-3169]

p 244 A90-20584

NAZARI, A.

Impingement/effusion cooling - The influence of the number of impingement holes and pressure loss on the heat transfer coefficient [ASME PAPER 89-GT-188]

p 361 A90-23866

NEAGLE, BRAD D.

Electro-optics engineering support for the integrated launch and recovery television surveillance system [AD-A223450]

p 938 N90-29406

NEAL, BRADFORD

The implementation and operation of a variable-response electronic throttle control system for a TF-104G aircraft [NASA-TM-101696]

p 509 N90-20086

NEAL, D. F.

IMI 834 - A new high temperature capability titanium alloy for engine use

p 62 A90-12535

NEAL, GRAEME

Three-dimensional model testing in the transonic self-streamlining wind tunnel

p 938 N90-28583

NEBBACHE, A.

Numerical study of compressible nozzle flow

p 708 A90-44437

NEEDLEMAN, KATHY E.

A study of sonic boom overpressure trends with respect to weight, altitude, Mach number, and vehicle shaping [AIAA PAPER 90-0367]

p 164 A90-19816

NEGODA, V. V.

Calculation of flow past delta wings in the thin shock layer approximation

p 86 A90-15624

Aerodynamic characteristics of thin bodies moving in a gas with shock waves

p 297 A90-24140

NEGRIN, M.

Supplemented visual cues for helicopter hovering above a moving ship deck

p 195 A90-17704

NEIDZWECKI, R.

A circular combustor configuration with multiple injection ports for mixing enhancement

p 130 A90-15389

NEILAND, V. M.

A new quick method for integrating Euler equations for plane transonic flows

p 295 A90-24105

Permeability of the porous walls of a wind tunnel at transonic velocities

p 350 A90-24151

NEINER, GEORGE

Engine inlet distortion in a 9.2 percent scaled vectored thrust STOVL model in ground effect [AIAA PAPER 89-2910]

p 301 A90-25043

Engine inlet distortion in a 9.2 percent scale vectored thrust STOVL model in ground effect [NASA-TM-102358]

p 318 N90-17561

NEINER, GEORGE H.

Hot gas ingestion characteristics and flow visualization of a vectored thrust STOVL concept [NASA-TM-103212]

p 751 N90-26009

NEJAD, A. S.

An experimental investigation of isothermal swirling flow in a model of a dump combustor

p 47 A90-12572

Nonaxisymmetric instabilities in a dump combustor with a swirling inlet flow

p 253 A90-21228

NEJAD, R. S.

Inlet swirl effects on dump combustor flows [AIAA PAPER 90-0035]

p 312 A90-26904

NEKMOUCHE, L.

Subsonic and transonic blade design by means of analysis codes

p 510 N90-20985

NEKOHASHI, TOSHIFUMI

Aeroelastic response characteristics of a rotor executing arbitrary harmonic blade pitch variations

p 646 A90-42464

NELANDER, JAMES C.

Vision guidance update - Synthetic aperture radar (SAR) multiple image exploitation for position and velocity determination

p 488 A90-34140

NELSON, C. C.

An annular gas seal analysis using empirical entrance and exit region friction factors [ASME PAPER 89-TRIB-46]

p 537 A90-33555

NELSON, CURTIS F.

Unsteady, separated flow behind an oscillating, two-dimensional spoiler

p 469 A90-32462

NELSON, DAVID M.

The new FFA T1500 transonic wind tunnel initial operation, calibration, and test results [AIAA PAPER 90-1420]

p 596 A90-37957

NELSON, GARY G.

Real time winds data for flight management [AIAA PAPER 90-0565]

p 197 A90-19918

NELSON, P. A.

Experiments on the active control of the transmission of sound through a clamped rectangular plate

p 695 A90-41109

Active control of sound transmission through a cylindrical shell

p 893 A90-46192

Theoretical studies of the active control of propeller-induced cabin noise

p 893 A90-46351

In-flight experiments on the active control of propeller-induced cabin noise

p 893 A90-46352

NELSON, PAUL

Evaluation of brush seals for limited-life engines [AIAA PAPER 90-2140]

p 685 A90-42040

NELSON, PERRY

Escape system evolution

p 722 A90-44656

NELSON, R. C.

Unsteady surface pressure distributions on a delta wing undergoing large amplitude pitching motions [AIAA PAPER 90-0311]

p 164 A90-19790

Vortex dynamics on a pitching delta wing

p 233 A90-23281

An experimental study of the nonlinear dynamic phenomenon known as wing rock [AIAA PAPER 90-2812]

p 753 A90-45152

Delta wing surface pressures for high angle of attack maneuvers [AIAA PAPER 90-2813]

p 711 A90-45153

NELSON, ROBERT C.

Low speed, in-draft wind tunnels

p 351 A90-26061

NEMCHINOV, I. V.

Changes in supersonic flow past an obstacle due to the formation of a thin rarefaction channel ahead of the obstacle

p 150 A90-17108

NEMECEK, STEPHEN J.

V2500 turbofan engine [SAE PAPER 892363]

p 747 A90-45512

NEMOUCHI, ZOUBIR

The computation of turbulent thin shear flows associated with flow around multielement aerofoils

p 633 N90-24240

NERI, LARRY

The effect of aircraft size on cabin floor dynamic pulses [DOT/FAA/CT-88/15]

p 735 N90-25136

NERSESOV, G. G.

Laminar separated flow on a biconical body at high supersonic velocities

p 387 A90-28992

NERUDA, J.

Two-stage two-spool experimental centrifugal compressor investigation

p 49 A90-12593

NETTER, G.

Project Falke - Performance of free flight tests in the supersonic, transonic, and subsonic regimes from balloons [DGLR PAPER 88-018]

p 903 A90-50235

NETTLES, ALAN T.

Impact testing of glass/phenolic honeycomb panels with graphite/epoxy facesheets

p 946 A90-50166

NETZER, D.

Regression and combustion characteristics of boron containing fuels for solid fuel ramjets

p 858 N90-27928

An investigation of solid-fuel, dual-mode combustion ramjets

p 859 N90-27933

NEU, C. E.

Al-Li alloys and ultrahigh-strength steels for U.S. Navy aircraft

p 599 A90-37441

NEUBAUER, JAY C.

Why birds kill - Cross-sectional analysis of U.S. Air Force bird strike data

p 400 A90-30587

NEUBERT, R. J.

Application of sweep to improve the efficiency of a transonic fan. I - Design [AIAA PAPER 90-1915]

p 741 A90-42695

NEUHART, DAN H.

Water-tunnel investigation of concepts for alleviation of adverse inlet spillage interactions with external stores [NASA-TM-4181]

p 398 N90-19199

NEUMAN, FRANK

Analysis of sequencing and scheduling methods for arrival traffic [NASA-TM-102795]

p 636 N90-23373

NEUMAN, HARVEY E.

Laser-velocimeter-measured flow field around an advanced, swept, eight-blade propeller at Mach 0.8 [NASA-TP-2462]

p 468 N90-20942

NEUMANN, RICHARD D.

The integrated test vehicle, (I.T.V.) - A vehicle for cost-effective hypersonic testing [AIAA PAPER 90-0630]

p 352 A90-26974

Requirements in the 1990's for high enthalpy ground test facilities for CFD validation [AIAA PAPER 90-1401]

p 597 A90-38489

NEWBERG, I. L.

Reduced insertion loss of X-band RF fiber optic links

p 695 A90-41240

NEWCOMB, D. E.

Criteria for coal tar seal coats on airport pavements. Volume 2: Laboratory and field studies [AD-A220167]

p 674 N90-24277

NEWCOMER, ROBERT E.

Improved steel for landing gear design [SAE PAPER 892335]

p 765 A90-45490

NEWHOUSE, R. W.

What can we do after we've done it all? [AIAA PAPER 89-3209]

p 549 A90-31696

NEWMAN, BRETT

Multivariable flight control synthesis and literal robustness analysis for an aeroelastic vehicle [AIAA PAPER 90-3446]

p 890 A90-47699

NEWMAN, D. A.

The design and development of an acoustic test section for the ARA transonic wind tunnel [PNR90574]

p 140 N90-13202

NEWMAN, E. H.

A user's manual for the method of moments Aircraft Modeling Code (AMC) [NASA-CR-186371]

p 415 N90-18390

The Helicopter Antenna Radiation Prediction Code (HARP) [NASA-CR-186925]

p 884 N90-27946

NEWMAN, J. C., JR.

Fatigue crack initiation and small crack growth in several airframe alloys [NASA-TM-102598]

p 454 N90-18746

NEWMAN, JAMES C., JR.

An evaluation of the pressure proof test concept for thin sheet 2024-T3 [NASA-TM-101675]

p 543 N90-21424

NEWMAN, PARRY A.

Evaluation of transonic wall interference

NEWMAN, PERRY A.

- Nonlinear transonic Wall-Interference Assessment/Correction (WIA) procedures and application to cast-10 airfoil results from the NASA 0.3-m TCT 8- by 24-inch Slotted Wall Test Section (SWTS) p 352 N90-17648
- Limits of adaptation, residual interferences p 871 N90-26844

NEWMAN, RICHARD L.

- Design philosophy for a general aviation TCAS display [SAE PAPER 891052] p 108 A90-14354

NEWMAN, ROBERT B.

- Indianapolis Downtown Heliport: Operations analysis and marketing history [REPT-90RR-13] p 527 N90-21049

NEWSOME, RICHARD W.

- Navier-Stokes computations of lee-side flows over delta wings p 153 A90-17978

NEWTON, P. M.

- Aircraft testing in the electromagnetic environment p 248 N90-15066

NG, C. F.

- The prediction and measurement of thermoacoustic response of plate structures [AIAA PAPER 90-0988] p 451 A90-29400

NG, T. T.

- Aerodynamic control of NASP-type vehicles through vortex manipulation [AIAA PAPER 90-0594] p 203 A90-19938
- Aerodynamic control of aircraft by forebody vortex manipulation [AIAA PAPER 90-1827] p 301 A90-25167
- Forebody vortex manipulation for aerodynamic control of aircraft at high angles of attack [SAE PAPER 892220] p 756 A90-45437

NG, T. TERRY

- Effect of leading edge roundness on a delta wing in wing-rock motion [AIAA PAPER 90-3080] p 795 A90-45911
- Development of non-conventional control methods for high angle of attack flight using vortex manipulation p 935 N90-28522

NG, W. F.

- Turbulence measurements and noise generation in a transonic cryogenic wind tunnel [AIAA PAPER 88-2026] p 522 A90-32463
- Large-scale structure in a supersonic slot-injected flowfield p 602 A90-36265
- Time-resolved measurements of total temperature and pressure in the vortex street behind a cylinder p 557 A90-36522

NGHIEM, CUONG P.

- Design of axisymmetric bodies with minimum transonic drag p 154 A90-17997

NGUYEN, T. T.

- Modeling of liquid jets injected transversely into a supersonic crossflow p 153 A90-17985

NGUYEN, DUC T.

- A parallel-vector algorithm for rapid structural analysis on high-performance computers [AIAA PAPER 90-1149] p 458 A90-28293

NGUYEN, H. L.

- Critical evaluation of Jet-A spray combustion using propane chemical kinetics in gas turbine combustion simulated by KIVA-II [AIAA PAPER 90-2439] p 949 A90-50645

NGUYEN, H. LEE

- Effect of vane twist on the performance of dome swirlers for gas turbine airblast atomizers [AIAA PAPER 90-1955] p 881 A90-47203
- Two-dimensional analysis of two-phase reacting flow in a firing direct-injection diesel engine [NASA-TM-102069] p 194 N90-13392
- Effect of vane twist on the performance of dome swirlers for gas turbine airblast atomizers [NASA-TM-103195] p 773 N90-25289

NGUYEN, HAI N.

- Optimal solutions to flight mechanics problems using a Nonlinear Programming and Collocation technique [AIAA PAPER 90-3415] p 889 A90-47669

NGUYEN, HUNG LEE

- Introducing the VRT gas turbine combustor [AIAA PAPER 90-2452] p 743 A90-42808
- Introducing the VRT gas turbine combustor [NASA-TM-103176] p 688 N90-23591

NGUYEN, HUU LUAN

- Cyclic stress-strain behavior and low cycle fatigue of Ti 6242 p 530 A90-33523

NGUYEN, HUY X.

- Spectra composite enhances portability and survivability of electronic equipment p 947 A90-50189

NGUYEN, K. Q.

- State-space representation of unsteady airfoil behavior p 469 A90-32461

NGUYEN, KHANH

- Application of higher harmonic control (HHC) to rotors operating at high speed and maneuvering flight p 429 A90-28157

- Effects of higher harmonic control on rotor performance and control loads [AIAA PAPER 90-1158] p 412 A90-29467

NGUYEN, L. CATHY

- A review and update of the NASA aircraft noise prediction program propeller analysis system [SAE PAPER 891032] p 139 A90-14340

NGUYEN, LUAT T.

- Impact of emerging technologies on future combat aircraft agility [AIAA PAPER 90-1304] p 580 A90-36029
- Development of a preliminary high-angle-of-attack nose-down pitch control requirement for high-performance aircraft [NASA-TM-101684] p 399 N90-19206
- Control research in the NASA high-alpha technology program p 934 N90-28516

NI, R. H.

- Unsteady Euler analysis of the redistribution of an inlet temperature distortion in a turbine [AIAA PAPER 90-2262] p 768 A90-42759

NI, RON-HO

- Using 3D Euler flow simulations to assess effects of periodic unsteady flow through turbines [AIAA PAPER 90-2357] p 706 A90-42783

NI, SHIHONG

- Performance study of an integrated NAVSTAR GPS/SINS navigation system p 329 A90-24003

NICHOLAS, THEODORE

- Predicting crack growth under thermo-mechanical cycling p 209 A90-18169

NICHOLS, J. B.

- The Hiller X-18 experimental aircraft - Lessons learned [AIAA PAPER 90-3203] p 834 A90-48832

NICHOLSON, ROGER K.

- Testing of a highly integrated automatic flight system - The 747-400 Flight Management Computer System [AIAA PAPER 90-1302] p 505 A90-33916

- Onboard maintenance system testing - The Boeing 747-400 Central Maintenance Computer [AIAA PAPER 90-1303] p 505 A90-33917

NICOLAIDES, JOHN D.

- All fabric N-wing unmanned powered flight systems [AIAA PAPER 90-3282] p 836 A90-48869

NICOT, PH.

- Aeroelastic analysis using finite element models p 492 A90-33388

NICOUD, D.

- A methodology proposal to design and analyse counterrotating high speed propellers [ASME PAPER 89-GT-38] p 340 A90-23767

NIEDERSTRASSER, HELMUT

- Construction of a hybrid angular velocity reference system for investigation of the dynamic characteristics of strapdown gyros [ESA-TT-1181] p 774 N90-25332

NIEDZWIECKI, R. W.

- High speed commercial transport fuels considerations and research needs [NASA-TM-102535] p 600 N90-21869

NIEHUIS, R.

- Experimental and numerical study on basic phenomena of secondary flows in turbines p 512 N90-21014

NIELSON, JOHN T.

- Flight demonstration of two and three satellite navigation p 98 A90-13994

- A flight test comparison of two GPS/INS integration approaches p 726 A90-43708

NIEMANN, LUDWIG

- Structural optimization in view of aeroelastic constraints p 536 A90-33391

NIEMI, EUGENE E., JR.

- An improved canopy stiffness scaling law for determining opening time of flat circular parachutes [AIAA PAPER 90-3058] p 790 A90-45863

NIEUWPOORT, A. H. M.

- Mathematical model identification for flight simulation, based on flight and taxi tests [LR-550] p 202 N90-13410

NIGIM, H. H.

- Turbulent boundary layer development in the presence of small isolated two-dimensional surface discontinuities p 210 A90-18507

NIKIFORUK, P. N.

- Adaptive flight control of CCV aircraft with limiting zeros [AIAA PAPER 90-3409] p 864 A90-47664

NIKISHKOV, P. IA.

- Requirements for meteorological equipment designed for the acquisition of meteorological data essential for the takeoff and landing of aircraft at civil airports p 962 A90-50777

NIKODJEVIC, D.

- Generalized similarity solutions for three-dimensional laminar compressible wing boundary layers p 907 A90-51543

NIKOLAEV, A. V.

- Some characteristics of interference between shock waves and the aerodynamic wake behind a body p 804 A90-46551

NIKOLAEV, V. S.

- Effect of similarity parameters on the aerodynamic quality and moment characteristics of a supersonic wing with blunt edges p 298 A90-24150

NIKOLAIDIS, E.

- Design of aircraft wings subjected to gust loads - A system reliability approach p 958 A90-52044

NIKOLITSCH, D.

- A technique for calculating nonlinear normal-force and pitching-moment coefficients for slender delta wings, accounting for wing thickness p 476 A90-34356

NIKONOVA, IRINA A.

- Technical and economic efficiency of aviation gas turbine engines in service p 851 A90-46624

NINA, M. N. R.

- Suppression of 'Buzz' instability by geometrical design of the flameholder [AIAA PAPER 90-1966] p 741 A90-42706

NIPPRESS, K. R.

- Estimation of the flight dynamic characteristics of the YEZ-2A [AIAA PAPER 89-3173] p 245 A90-20590

NIRMALAN, V.

- An experimental study of turbine vane heat transfer with leading edge and downstream film cooling [ASME PAPER 89-GT-69] p 358 A90-23792

NISHI, MICHIOHITO

- Vortex generator jets - Means for flow separation control p 555 A90-36257

NISHIKAWA, HIDEJI

- Numerical calculation of bubbly two phase flow around an airfoil p 304 A90-25783

NISHIMURA, TAKAHIRO

- An adaptive flight control system design for non-minimum phase CCV by relative order reduction p 196 A90-19428

NISHIMURA, Y.

- Wind tunnel wall interference investigations in NAE/NRC High Reynolds Number 2D Facility and NASA Langley 0.3m Transonic Cryogenic Tunnel p 628 A90-42404

NISHIWAKI, T.

- The cycle evaluation of the advanced LACE performance [IAF PAPER 89-313] p 109 A90-13447

NISHIYAMA, T.

- Measurements of simulated wake/rotor interaction phenomena in turbomachinery p 814 A90-49475

NISHIZAWA, TOSHIO

- Numerical analysis of rotating stall by a vortex model p 13 A90-12590

NISHT, M. I.

- Numerical simulation of three-dimensional flow around parachute canopies p 84 A90-14438
- Induced drag of a wing of low aspect ratio p 387 A90-28987

NISHT, MIKHAIL I.

- Mathematical modeling of plane parallel separated flows past bodies p 619 A90-39475

NISSIM, E.

- Effect of control surface mass unbalance on the stability of a closed-loop active control system [NASA-TP-2952] p 134 N90-12042

NISSIM, ELI

- The effectiveness of vane-aileron excitation in the experimental determination of flutter speed by parameter identification [NASA-TP-2971] p 249 N90-15100

NITA, AKITO

- Study on application of ultrasonic wave measurement to creep-fatigue damage detection [DE89-782317] p 774 N90-25361

NITA, M. M.

- Rotary damping in aircraft motion due to jet propulsion system p 520 A90-34820

NITKA, EDWARD F., II

- Applications of fiber optic sensors in advanced engine controls p 68 A90-11703

NITSCHKE, W.

- Application of piezoelectric foils in experimental aerodynamics p 446 A90-28258
- Detection of flow instabilities at airfoil profiles using piezoelectric arrays p 276 N90-16175

- Test and Measurement Technique in Hypersonics
[ILR-MITT-225(1989)] p 618 N90-24225
- NITTA, AKIHITO**
Development of creep-fatigue damage detection method of rotor steel by ultrasonic wave measurement
[DE90-503792] p 777 N90-26365
- NITZSCHE, F.**
Whirl-flutter investigation on an advanced turboprop configuration p 40 A90-11008
Whirl flutter stability of a pusher configuration subject to a nonuniform flow
[AIAA PAPER 90-1162] p 393 A90-29397
- NIU, MICHAEL C. Y.**
Innovative design concepts for thermoplastic composite materials p 940 A90-50059
- NIU, MICHAEL CHUNG-YUNG**
Airframe structural design: Practical design information and data on aircraft structures p 103 A90-16624
- NIU, PEIYI**
The study of transient suppression techniques for multimode flight control system p 590 A90-37219
- NIXON, D.**
Numerical simulation of a turbulent flow through a shock wave
[AIAA PAPER 90-1641] p 608 A90-38769
- NIXON, DAVID**
Unsteady transonic aerodynamics p 393 A90-29882
Basic equations for unsteady transonic flow p 394 A90-29884
Alternative methods for modeling unsteady transonic flows p 394 A90-29889
Outflow boundary conditions using Duhamel's equation
[AIAA PAPER 90-3014] p 798 A90-45937
Prediction methods for store separation p 317 N90-17549
A study of supermaneuver aerodynamics
[AD-A218378] p 631 N90-23349
- NIXON, MARK W.**
Rotor blade structural design p 106 N90-12584
Appendix: Results obtained to date p 107 N90-12588
- NO, T. S.**
Dynamics and control of maneuverable towed flight vehicles
[AIAA PAPER 90-2841] p 754 A90-45161
- NOBACK, R.**
The S.D.G., P.S.D. and the nonlinear airplane
[NLR-MP-88018-U] p 183 N90-13371
- NOBIS, STEPHEN G.**
APG-70 radar test package development aid
[AIAA PAPER 89-3044] p 1 A90-10624
- NOCETTI, F. GARCIA**
Parallel processing implementation of a flight controller p 333 N90-16743
- NOEBE, R. D.**
Observations on the brittle to ductile transition temperatures of B2 nickel aluminides with and without zirconium p 205 A90-19153
- NOEL, B. W.**
Engine testing of thermographic phosphors
[DE90-013269] p 885 N90-28059
- NOETINGER, JACQUES**
The Airbus ... a challenge launched twenty years ago p 699 A90-41769
- NOLAN, S. A.**
Test results for turbulent annular seals, using smooth rotors and helically grooved stators
[ASME PAPER 89-TRIB-11] p 537 A90-33556
- NOLES, CHERIE J.**
A small inert gas generator p 180 A90-17405
- NOLL, STEVE**
The SKY SHARK: An RPV designed to investigate the pressure distribution on a lifting surface
[NASA-CR-186222] p 844 N90-26824
- NOLL, THOMAS**
Recent activities within the aeroservoelasticity branch at the NASA Langley Research Center p 492 A90-33400
Control law synthesis and optimization software for large order aeroservoelastic systems p 61 N90-10111
The active flexible wing aeroservoelastic wind-tunnel test program p 33 N90-10119
- NOLL, THOMAS E.**
Aeroservoelasticity
[AIAA PAPER 90-1073] p 411 A90-29381
Flutter suppression control law synthesis for the active flexible wing model p 517 A90-33403
Aeroservoelasticity
[NASA-TM-102620] p 416 N90-19227
- NOLLEN, D. A.**
Aircraft cabin interior systems meeting new FAA regulations p 482 A90-33710
- NOLLEN, DENNIS A.**
Flammability regulations affecting advanced composite materials p 947 A90-50190
- NOLTING, RICHARD F.**
Flight demonstration of two and three satellite navigation p 98 A90-13994
- NONAMI, K.**
Active vibration control for flexible rotor by optimal direct-output feedback control p 879 A90-46222
- NONWEILER, T. R. F.**
Forebody design for the aerospaceplane
[AIAA PAPER 90-2472] p 762 A90-42810
- NOONAN, KEVIN W.**
Rotor blade aerodynamic design p 106 N90-12582
Effect of blade planform variation on a small-scale hovering rotor
[NASA-TM-4146] p 173 N90-14186
Aerodynamic characteristics of two rotorcraft airfoils designed for application to the inboard region of a main rotor blade
[NASA-TP-3009] p 633 N90-24239
- NOOR, AHMED K.**
Computers boost structural technology p 138 A90-14799
Analysis of aircraft tires via semianalytic finite elements p 496 A90-34740
Frictionless contact of aircraft tires
[SAE PAPER 892350] p 733 A90-45501
- NORBY, WILLIAM P.**
Small-scale inlet testing for low cost screening applications
[AIAA PAPER 90-1926] p 741 A90-42696
- NORDQUIST, J.**
Visualization studies in rotating disk cavity flows p 475 A90-33568
- NORMAN, J. P.**
The application of cast SiC/Al to rotary engine components
[NASA-CR-179610] p 192 N90-13385
- NORMAN, SUSAN D.**
Flight deck automation: Promises and realities
[NASA-CP-10036] p 187 N90-13384
- NORMAN, THOMAS R.**
Application of the wide-field shadowgraph technique to rotor wake visualization
[NASA-TM-102222] p 88 N90-11700
- NORRIS, GUY**
Advantage Airbus? p 102 A90-15746
Jet futures p 190 A90-18526
Eurofighter fights back p 221 A90-21714
Wide chord fan club p 584 A90-35600
Power struggle p 851 A90-46650
Collision alert p 847 A90-48521
- NORRIS, JACK**
Drag and propulsive efficiency of a light aircraft based on a new flight test technique
[AIAA PAPER 90-0233] p 182 A90-19747
- NORSTRUD, HELGE**
Design of axisymmetric bodies with minimum transonic drag p 154 A90-17997
- NORTH, DAVID M.**
Aviation Week editor flies Soviet-based MiG-29 fighter p 334 A90-24964
Aviation Week editor flies top Soviet interceptor p 920 A90-52574
- NORTH, R. F.**
Institutional stepping stones for FANS p 403 A90-27923
- NORTHALL, J. D.**
Measurement and calculation of the three-dimensional flow in axial compressor stators, with and without end-bends
[ASME PAPER 89-GT-6] p 287 A90-23753
- NORTHAM, G. BURTON**
A validation study of the Spark Navier Stokes code for nonreacting scramjet combustor flowfields
[AIAA PAPER 90-2360] p 706 A90-42784
- NORTHSCOTT, A. J.**
VSTOL power plant control lessons from Harrier experience p 13 A90-12582
- NORTON, M. P.**
The receptivity of laminar boundary layer flow to leading edge vibrations p 815 A90-49800
- NORTON, R. L.**
Fly-by-light flight control system technology development plan
[NASA-CR-181953] p 259 N90-15111
- NORWINE, PHILIP C.**
The coming age of the tiltrotor. I p 246 A90-21711
The coming age of the tiltrotor. II p 413 A90-30119
- NOSKOV, A. P.**
Thermodynamic calculation of the compressors of gas turbine engines and powerplants at high air pressures p 130 A90-14585
- NOSOV, V. V.**
Combined effect of viscosity and bluntness on the aerodynamic efficiency of a delta wing in flow with a high supersonic velocity p 388 A90-29184
- NOSYREV, I. P.**
Investigation of the flow structure behind the rotating blades in the elbow of a wind tunnel in the case of acoustic excitation p 286 A90-24124
- NOTARO, JOSEPH**
Model designation of military aerospace vehicles
[PB90-206301] p 787 N90-27646
- NOUSE, HIROYUKI**
A study on the performance of the turbo-ramjet engines at high speed flight p 49 A90-12608
- NOVINSKI, EDWARD R.**
The selection and performance of thermal sprayed abrasible seal coatings for gas turbine engines
[SAE PAPER 890929] p 286 A90-24694
- NOWAK, ROBERT**
Experimental studies of shock wave/wall jet interaction in hypersonic flow
[AIAA PAPER 90-0607] p 231 A90-22449
- NOYES, T. A.**
Wind shear detection with airport surveillance radars p 241 A90-21387
- NUGMANOV, Z. KH.**
An approximate method for calculating flow past a wing profile with allowance for viscosity p 234 A90-23422
- NUHAIT, A. O.**
Numerical simulation of wings in steady and unsteady ground effects p 153 A90-17866
- NURICK, A.**
Empirical prediction of the blockage effect of a flat body on a rotor p 807 A90-46942
- NUSHTAEV, IU. P.**
A method for determining aileron efficiency and critical reversal and divergence rates at transonic velocities p 345 A90-24147
Some characteristics of changes in the nonstationary aerodynamic characteristics of a wing profile with an aileron in transonic flow p 387 A90-28989
- NUSHTAEV, P. D.**
A method for determining aileron efficiency and critical reversal and divergence rates at transonic velocities p 345 A90-24147
- NUTHALAPATI, C.**
High resolution spectrum analysis for airborne pulse Doppler radars p 339 A90-24329
- NUZZI, STEPHEN F.**
FAA Loran early implementation project
[AD-A221866] p 824 N90-26805
- NWOKAH, OSITA D. I.**
The integrated control of a propulsion-airframe system
[ASME PAPER 89-WA/DSC-12] p 751 A90-44847
- NYENHUIS, R.**
In-flight boundary-layer transition measurements on a swept wing p 17 A90-13017

O

- O'BLENES, M. J.**
Small gas turbine using a second-generation pulse combustor p 421 A90-27972
- O'BRIEN, E. W.**
Old lamps for new - A photoelastic design tool for weight and cost saving on aircraft structures p 878 A90-46039
- O'BRIEN, T. KEVIN**
Towards a damage tolerance philosophy for composite materials and structures p 675 A90-40127
- O'BRIEN, WALTER F.**
Stall cell blockage in a high-speed multistage axial-flow compressor
[AIAA PAPER 90-1913] p 740 A90-42693
- O'CALLAGHAN, PAT**
Structural and dynamic analysis of the A330/340 composite RAT blade p 942 A90-50083
- O'KEEFFE, BRIAN**
Our future air navigation system embodies a global concept p 402 A90-27922
- O'LONE, RICHARD G.**
STOVL wind tunnel tests demonstrate ejector viability p 245 A90-21000
- O'NEIL, P. J.**
Investigation of high angle of attack vortical flows over delta wings
[AIAA PAPER 90-0101] p 162 A90-19682
- O'PELLA, L. J.**
Laser communication system design p 26 A90-11813
- OAKLAND, SUSAN K.**
Convergence aloft as a precursor to microbursts p 456 A90-28620

- OATES, G. C.**
Throughflow theory for nonaxisymmetric turbomachinery flow. I - Formulation, II - Assessment
[ASME PAPER 89-GT-304] p 905 A90-51256
- OATES, GORDON C.**
Aircraft propulsion systems technology and design
p 188 A90-17308
- OBARA, CLIFFORD J.**
Flight-measured streamwise disturbance instabilities in laminar flow
[AIAA PAPER 90-1283] p 495 A90-33904
Status report on a natural laminar-flow nacelle flight experiment
p 105 N90-12550
Nacelle aerodynamic performance
p 105 N90-12552
- OBATA, M.**
Development of the jet-swirl high loading combustor
[AIAA PAPER 90-2451] p 658 A90-40633
- OBAYASHI, SHIGERU**
High-resolution upwind scheme for vortical-flow simulations
p 153 A90-17872
Application of a streamwise upwind algorithm for unsteady transonic computations over oscillating wings
[AIAA PAPER 90-3103] p 796 A90-45915
A streamwise upwind algorithm applied to vortical flow over a delta wing
[NASA-TM-102225] p 398 N90-19201
Extension of a streamwise upwind algorithm to a moving grid system
[NASA-TM-102800] p 572 N90-21739
- OBOLENSKII, EVGENII P.**
Durability of equipment assemblies and elements of life-support systems for flight vehicles
p 246 A90-21275
- OBRIEN, WALTER F.**
Stall and recovery in multistage axial flow compressors
p 428 N90-18429
- OGNEV, A. V.**
Optimization of complex data processing algorithms in multichannel radio direction finding
p 576 A90-36115
- ODABAS, ONUR**
Generalized Transition Finite-Boundary Elements for high speed flight structures
[AIAA PAPER 90-1105] p 449 A90-29286
- ODAM, G. A. M.**
Highlights of RAE lightning strike investigations
p 818 A90-49827
- ODGERS, J.**
The performance of a small combustor operated over a wide range of conditions
p 45 A90-12548
On the weak extinction of gas turbine combustors
p 47 A90-12574
- ODIN, ETHAN M.**
Feasibility study for a microwave-powered ozone sniffer aircraft
[NASA-CR-186660] p 650 N90-23397
- ODINOKOVA, G. B.**
Effect of pressure on the electrophysical properties of two-phase flows in nozzles
p 110 A90-14572
- OECKER, H.-CHR.**
Wind tunnel investigations on the configuration of the international vortex flow experiment
p 277 N90-16181
- OECKER, HANS-CHRISTOPH**
Effects of canard position on the aerodynamic characteristics of a close-coupled canard configuration at low speed
p 920 N90-28519
- OERTEL, HERBERT**
Numeric fluid mechanics
p 960 N90-29161
- OETTING, ROBERT B.**
Alternate table look-up routine for real-time digital flight simulation
p 611 A90-35769
Improving computer techniques for real-time digital flight simulation
[SAE PAPER 89-2354] p 760 A90-45505
- OFSTHUN, STAN**
Linking artificial intelligence (AI) and computer aided engineering (CAE) to analyze the testability of electronic designs
[AIAA PAPER 89-3070] p 74 A90-10559
- OGANA, W.**
Transonic integro-differential and integral equations with artificial viscosity
p 223 A90-20988
Analysis of transonic integral equations. I - Artificial viscosity
p 232 A90-23124
Analysis of transonic integral equations. II - Boundary element methods
p 302 A90-25301
Boundary element solution of the transonic integro-differential equation
p 383 A90-27947
- OGAWA, SATORU**
Turbulence models for 3D transonic viscous flows. II
p 306 A90-25820
- OGAWARA, A.**
The cycle evaluation of the advanced LACE performance
[IAF PAPER 89-313] p 109 A90-13447
- OGUSHI, MASAHICO**
Flow field around an oscillating cascade
p 814 A90-49459
- OH, BYEONG SOO**
Calculation of temperature distribution in various turbine blades using a boundary-fitted coordinate transformation method
p 929 N90-28550
- OH, C. H.**
Three-dimensional analysis on flow and temperature distributions for aircraft fuel thermal stability
[AD-A219651] p 678 N90-23571
- OH, TAE S.**
Finite element simulation of complex jets in a crossflow for V/STOL applications
p 585 A90-35753
- OHASHI, H.**
Air/water two-phase flow test tunnel for airfoil studies
p 352 A90-26842
- OHASHI, HIDEO**
Numerical calculation of bubbly two phase flow around an airfoil
p 304 A90-25783
- OHLHORST, C. W.**
Performance evaluations of oxidation-resistant carbon-carbon composites in simulated hypersonic vehicle environments
p 874 A90-48131
- OHLHORST, CRAIG W.**
NASA Langley Research Center National Aero-Space Plane Mission simulation profile sets
[NASA-TM-102670] p 924 N90-28541
- OHMAN, L. H.**
New transonic test sections for the NAE 5ftx5ft trisonic wind tunnel
p 630 A90-42431
New transonic test sections for the NAE 5 ft x 5 ft trisonic wind tunnel
[AD-A220933] p 674 N90-24278
- OHMI, KAZUO**
Vortex formation around an oscillating and translating airfoil at large incidences
p 303 A90-25588
- OHNISHI, HIROO**
Optimum design of rotational wheels under transient thermal and centrifugal loading
p 270 A90-20770
- OHNO, TAKAHARU**
Development of new segment carbon seal for use at low sealing pressure region FJR710/600S turbo fan engine
p 69 A90-11950
- OHNSORG, R. W.**
Injection molding development of ceramic turbine components
[ASME PAPER 89-GT-170] p 361 A90-23855
- OHNUKI, TAKESHI**
Transonic aerodynamics analysis of unconventional wing configurations by 3D-Euler code
p 306 A90-25835
- OHR, SANG Y.**
A preliminary sensitivity analysis of the Generalized Escape System Simulation (GESS) computer program
[DE89-016891] p 24 N90-10844
- OHTA, MASAHIRO**
Improved melt flow and physical properties of Mitsui Toatsu's LARC-TPI 1500 series polyimide
p 943 A90-50134
- OHTA, YOSHIO**
Recrystallization behavior of nickel-base single crystal superalloys
p 440 A90-27681
- OJALVO, I. U.**
Practical suggestions for modifying math models to correlate with actual modal test results
p 207 A90-16979
Dynamic structural correlation via nonlinear programming techniques
p 208 A90-17372
Application to a helicopter of a general method for modifying a finite-element model to correlate with modal test data
p 832 A90-46968
- OJIMA, H.**
Holographic interferometric study of shock wave propagation
p 66 A90-10732
- OKABE, MASANORI**
Flight simulation test facility: Function and specification of the simulator cockpit system
[NAL-TM-577] p 59 N90-10899
- OKADA, TOMONOBU**
Fatigue life prediction method for gas turbine rotor disk alloy FV535
p 440 A90-27679
- OKADA, TSUYOSHI**
Robust control system design synthesis with observers
p 375 A90-25994
- OKAMURA, HIROYUKI**
Development of creep-fatigue damage detection method of rotor steel by ultrasonic wave measurement
[DE90-503792] p 777 N90-26365
- OKIISHI, T. H.**
Boundary-layer transition and separation on a turbine blade in a plane cascade
[AIAA PAPER 90-2263] p 625 A90-42102
- OKIISHI, THEODORE H.**
Stall margin improvement in axial-flow compressors by circumferential variation of stationary blade setting angles
[AIAA PAPER 90-1912] p 656 A90-40554
- OKUDE, MUNESHIGE**
Vorticity distribution of vortex street in the wake of a circular cylinder
p 623 A90-41751
- OKULOV, V. L.**
Acoustic resonance in centrifugal compressors induced by interaction between rotor and stator
p 78 A90-11803
- OKUNIEFF, P.**
GPS Hover Position Sensing System
p 108 A90-13986
- OKUNO, YOSHINORI**
Analytical study of dynamic response of helicopter in autorotative flight
p 670 A90-42469
- OKUYAMA, MASAHIRO**
Wind tunnel test of CAD USB-STOL semi-borne prototype
[NAL-TM-566] p 88 N90-11696
- OLAN, EMMANUEL**
Vibration dampers for cryogenic turbomachinery
[AIAA PAPER 90-2740] p 882 A90-47228
- OLCOTT, JOHN W.**
Criteria for general aviation fuel systems crashworthiness
[SAE PAPER 891016] p 109 A90-14328
- OLDENBURG, J. R.**
Comparison of two droplet sizing systems in an icing wind tunnel
[NASA-TM-102456] p 215 N90-14617
- OLDENBURG, JOHN R.**
Comparison of two droplet sizing systems in an icing wind tunnel
[AIAA PAPER 90-0668] p 274 A90-23711
Spray nozzle investigation for the Improved Helicopter Icing Spray System (IHSS)
[AIAA PAPER 90-0666] p 350 A90-25040
- OLDFIELD, M. L. G.**
Temperature scaling of turbine blade heat transfer with and without shock wave passing
p 47 A90-12570
- OLEARY, C. O.**
The effects of foreplanes on the static and dynamic characteristics of a combat aircraft model
p 920 N90-28520
- OLEJNIK, A.**
Static and dynamic loss of stability of elements of a supersonic aeroplane covering - Numerical analysis
p 346 A90-25186
Analysis of self-excited vibrations of stiffened covering panels of an aeroplane wing
p 860 A90-46716
- OLESEN, K. A.**
Variations in impact test methods for tough composites
p 946 A90-50167
- OLIVA, RUDOLF**
Devices and procedures for the calibration of sensors and measurement: Systems of the flight test support system ATTAS
[DFVLR-MITT-89-06] p 134 N90-12007
- OLONA, TIMOTHY**
Optimum element density studies for finite-element thermal analysis of hypersonic aircraft structures
[NASA-TM-4163] p 369 N90-17074
- OLORUNMAIYE, J. A.**
Numerical simulation of valveless pulsed combustors
p 127 A90-13767
- OLSEN, GEORGE**
Experimental studies of shock wave/wall jet interaction in hypersonic flow
[AIAA PAPER 90-0607] p 231 A90-22449
- OLSEN, JAMES J.**
Finite element models of USAF aircraft structures
p 844 N90-26820
- OLSON, E. CARL**
The behavior of electric currents in graphite/epoxy structures
p 883 A90-49846
- OLSON, ERIC**
Very-high-performance data acquisition/analysis/display/control systems based on the APTEC I/O computer
p 458 A90-28852
- OLSON, JOHN R.**
Helicopter design optimization for maneuverability and agility
p 408 A90-28212
- OLSON, LAWRENCE**
NASA aerodynamics program
[NASA-TM-4175] p 373 N90-17235
- OLSON, M. E.**
Experience with scale effects in non-airplane wind tunnel testing
[AIAA PAPER 90-1822] p 350 A90-25165
- OLSSON, BENGT A.**
Lightning testing and test analyses of the JAS39 aircraft
p 842 A90-49836

OLSSON, MATS-OLOF

- Damage tolerance of the fighter aircraft 37 Viggen. Part 1: Analytical assessment
[FFA-TN-1990-12-PT-1] p 923 N90-28538
- Damage tolerance of the fighter aircraft 37 Viggen. Part 2: Experimental verification
[FFA-TN-1990-13-PT-2] p 923 N90-28539

OLTHOFF, JAAP

- Damage tolerance of a postbuckling soft skin hat stiffened compression panel p 534 A90-31647

OLYNICK, DAVID P.

- Grid generation and adaptation for the direct simulation Monte Carlo method p 67 A90-11102

OMAN, HENRY

- Extracting pulse power from batteries p 605 A90-38175
- Accelerating hypersonic airplanes with ground-power p 586 A90-38186
- Battery configurations for multi-megawatt pulse power p 873 A90-49763

OMAR, M. EMMETT

- Pressure and heat-transfer investigation of a hypersonic configuration p 598 A90-35757

OMASTA, R.

- Numerical analysis of vibrations of a helicopter tail boom p 31 A90-13224

OMINSKY, D.

- Evaluation of current multiobjective optimization methods for aerodynamic problems using CFD codes [AIAA PAPER 90-0955] p 411 A90-29240
- Simulation of static and dynamic aeroelastic behavior of a flexible wing with multiple control surfaces [AIAA PAPER 90-1075] p 392 A90-29383

ONATE, E.

- A formulation for the solution of Euler equations for compressible flow using finite elements p 708 A90-44447

ONDA, M.

- A new type of non-rigid airship system [AIAA PAPER 89-3175] p 244 A90-20583

ONEILL-ROOD, NORA

- An automated calibration laboratory for flight research instrumentation: Requirements and a proposed design approach [NASA-TM-101719] p 781 N90-26564

ONG, CHING-LONG

- Adhesive-bonded composite-patching repair of cracked aircraft structure p 467 A90-31576
- Chemical resistance of carbon fiber reinforced polyether ether ketone and polyphenylene sulfide composites p 944 A90-50142

ONISHCHENKO, V. M.

- Modeling of the buffeting of flight vehicles p 803 A90-46500

ONO, AKIO

- Numerical calculations of flows with shock waves by flux vector splitting method p 808 A90-47299

ONO, TAKATSUGU

- Evaluation for DLC-Flap Monitoring System of the VSRA [NAL-TM-607] p 928 N90-29391

ONODERA, O.

- Holographic interferometric study of shock wave propagation p 66 A90-10732

ONOFRIO, G.

- Time dependent effects on high temperature low cycle fatigue and fatigue crack propagation on nickel base superalloys p 443 A90-29881

ONSTOTT, ROBERT G.

- Synthetic aperture radar imagery of airports and surrounding areas: Archived SAR data [NASA-CR-4275] p 401 N90-18371
- Synthetic aperture radar imagery of airports and surrounding areas: Philadelphia Airport [NASA-CR-4280] p 401 N90-18372
- Synthetic aperture radar imagery of airports and surrounding areas: Denver Stapleton International Airport [NASA-CR-4305] p 637 N90-24257

ONVANI, A.

- Aerodynamics of cooling jets introduced in the secondary flow of a low speed turbine cascade [ASME PAPER 89-GT-192] p 362 A90-23868

OORE, M.

- Maritime environment airframe material fatigue testing p 764 A90-42675

OOSTHUIZEN, P. H.

- Effects of splitter plates on the wake flow behind a bluff body p 469 A90-32453
- The effect of secondary flow on the redistribution of the total temperature field downstream of a stationary turbine cascade p 515 N90-21033

ORAN, E. S.

- Numerical simulations of the structure of supersonic shear layers [AD-A224164] p 960 N90-29587

ORAN, ELAINE S.

- Acoustic-vortex-chemical interactions in an idealized ramjet p 54 N90-10206
- Numerical simulations of flowfields in a central-dump ramjet combustor. 3: Effects of chemistry [AD-A224145] p 933 N90-28573

ORLANDI, HARRY W.

- Flight deck automation: Promises and realities [NASA-CP-10036] p 187 N90-13384

ORLANDI, DIEGO

- Results of an A109 simulation validation and handling qualities study p 591 A90-38524

ORLANDO, V. A.

- The Mode S beacon radar system p 241 A90-21379

ORLANDO, VINCENT A.

- Mode S system design and architecture p 330 A90-25569

ORLOV, V. N.

- Experimental turbofan using liquid hydrogen and liquid natural gas as fuel [AIAA PAPER 90-2421] p 663 A90-42170

ORLOVA, T. I.

- Changes in supersonic flow past an obstacle due to the formation of a thin rarefaction channel ahead of the obstacle p 150 A90-17108

ORMISTON, ROBERT A.

- Fundamental dynamics issues for comprehensive rotorcraft analyses p 831 A90-46961
- Development of the Second Generation Comprehensive Helicopter Analysis System (2GCHAS) p 889 A90-46963

ORNGARD, G. M.

- A dynamic optical model attitude measurement system p 539 A90-34236

ORONO, P. O.

- Stochastic flutter of a panel subjected to random in-plane forces. I - Two mode interaction p 444 A90-27992
- Stochastic flutter of a panel subjected to random in-plane forces. II - Two and three mode non-Gaussian solutions [AIAA PAPER 90-0986] p 451 A90-29399

ORPHAN, V. J.

- Development of an X-ray backscatter densitometer for measurement of freestream density during hypersonic flight [AIAA PAPER 90-1384] p 604 A90-37933

ORTH, R. C.

- The use of pulse facilities for testing supersonic combustion ramjet (scramjet) combustors in simulated hypersonic flight conditions p 46 A90-12562

ORTIZ, MILTON

- Thermal barrier coating life prediction model development, phase 1 [NASA-CR-182230] p 193 N90-13388

OSBORN, A. R.

- A UK perspective on the uniform engine test programme [RAE-TM-P-1172] p 257 N90-15922

OSBORNE, G. W.

- The basis for facility comparison p 856 N90-27713

OSHIMA, K.

- Experience in developing an improved altitude test capability p 857 N90-27719

OSHIMA, SHUZO

- Avionics and electromagnetic compatibility (EMC) considerations on a helicopter with an advanced composite airframe p 417 A90-28217

OSHIMA, KOICHI

- Topological study of three-dimensional vortex interactions p 367 A90-25885

OSHIMA, SHUZO

- Some remarks on the Kutta condition p 716 A90-45738

OSHIMA, Y.

- Oscillation of circular shock wave p 557 A90-36465

OSIPOV, A. A.

- Topological study of three-dimensional vortex interactions p 367 A90-25885

OSKAM, B.

- Two- and three-dimensional problems of unsteady aerodynamics of low loaded turbomachinery blade rows stages p 813 A90-49452

OSMAN, A. M.

- Numerical flow simulation and supercomputers: More than a digital wind tunnel p 612 N90-22976

OSNAGHI, C.

- Study of various factors affecting secondary loss vortices downstream a straight turbine cascade [ASME PAPER 89-GT-12] p 287 A90-23757

OSOVSKII, A. E.

- Secondary flows in a transonic cascade - Comparison between experimental and numerical results p 157 A90-18501

OSOVSKII, A. E.

- Construction of a wing surface in a nonviscous transonic flow from a given pressure distribution p 298 A90-24149

- Calculation of the effect of the engine nacelle on transonic flow past a wing p 387 A90-28990

OSS, R. R.

- A hydrodynamic turbo-fan/shaft convertible engine p 665 A90-42487

OSSWALD, G.

- Study of low-Reynolds number separated flow past the Wortmann FX 63-137 airfoil p 799 A90-46363

OSTACHOWICZ, W.

- Analysis of high-incidence separated flow past airfoils p 147 A90-16781

OSTACHOWICZ, W.

- Simulation of high incidence unsteady flow past Joukowski airfoils p 156 A90-18301

OSTADT, F. R.

- Vibration of turbine blades damped by dry friction forces p 879 A90-46190

OSTADT, F. R.

- Compressor performance tests in the compressor research facility p 427 N90-18428

OSTLUND, RICHARD

- V-22 developmental status p 581 A90-38529

OSTOWARI, C.

- Effects of nonplanar outboard wing forms on a wing p 232 A90-23279

OSTROFF, AARON J.

- Application of variable-gain output feedback for high-alpha control [NASA-TM-102603] p 434 N90-18434

OSTROM, ROBERT B.

- Thermoplastic composite fighter forward fuselage p 81 A90-14659

OSWALD, FRED B.

- Experimental and analytical evaluation of dynamic load vibration of a 2240-kW (3000-hp) rotorcraft transmission p 127 A90-13750

OSWALD, FRED B.

- Gear noise, vibration, and diagnostic studies at NASA Lewis Research Center [NASA-TM-102435] p 372 N90-18041

OTRISHKO, L. I.

- Estimation of the efficiency of a ramjet engine with a thermocompressor using fuel conversion products p 255 A90-23412

OTT, GARY

- International aircraft operator data base master requirements and implementation plan [DOT/FAA/CT-90/17] p 967 N90-29247

OTT, JAMES

- HSCT research focuses on environmental issues p 143 A90-17780

OTT, P.

- Unsteady flow visualization in a vibrating annular turbine cascade operating in the transonic flow regime p 7 A90-11786

OTTEN, M. P. G.

- Aircraft SAR simulation Sargen 1.0 [FEL-1989-44] p 135 N90-12823

OTTENS, H. H.

- The use of supercomputers for the design and analysis of constructions p 612 N90-22977

OTTO, DIETER

- Devices and procedures for the calibration of sensors and measurement: Systems of the flight test support system ATTAS [DFVLR-MITT-89-06] p 134 N90-12007

OTTO, HORST

- Influence of wind tunnel circuit installations on test section flow quality p 436 A90-28287

OTTOCHIAN, S. P.

- Investigation of the vortex flow over a sharp-edged delta wing in the transonic speed regime [LR-594] p 717 N90-25115

OU, S.

- Augmented heat transfer in rectangular channels of narrow aspect ratios with rib turbulators p 70 A90-13091

OUTTERS, L.

- Numerical investigations of heat transfer and flow rates in rotating cavities. Simulation of the movement generated by wall temperature gradients, by source-sink mass flows or by the differential rotation of the walls, under the influence or coriolis and centrifugal forces [ETN-90-96253] p 454 N90-18695

OUTTIER, G.

- Half transport aircraft cryogenic model for T2 wind tunnel p 524 A90-34242

OUZTS, PETER

- H-infinity based integrated flight/propulsion control design for a STOVL aircraft in transition flight [AIAA PAPER 90-3335] p 862 A90-47595

OUZTS, PETER J.

- Real-time simulation of an F110/STOVL turbofan engine [NASA-TM-102409] p 117 N90-12618

OUZTS, PETER J.

- H-infinity based integrated flight/propulsion control design for a STOVL aircraft in transition flight [NASA-TM-103198] p 758 N90-26011

P

- OVCHARENKO, S. I.**
Development of a mathematical model of an adaptive antilutler system p 769 A90-42911
- OVCHINNIKOV, V. A.**
An approximate method for calculating flow past a wing profile with allowance for viscosity p 234 A90-23422
- OVERSTREET, MARK A.**
Lightweight fuel pump and metering component for advanced gas turbine engine control [AIAA PAPER 90-2032] p 657 A90-40602
- OVERTON, K. S.**
Automated aircraft engine costing using artificial intelligence [AIAA PAPER 90-1887] p 660 A90-41981
- OVSIANNIKOV, B. V.**
Calculation of the efficiency of an active partial-admission gas turbine for counterpressures varying over a wide range p 850 A90-46495
- OWEN, C. R.**
An aluminum quality breakthrough for aircraft structural reliability p 843 N90-26816
- OWEN, DAVID TUDOR**
Measurement and prediction of propeller blade surface pressure distributions p 481 N90-20961
- OWEN, F. K.**
Hot wire anemometry in transonic flows and cryogenic conditions p 539 A90-34229
A dynamic optical model attitude measurement system p 539 A90-34236
- OWEN, F. KEVIN**
An optical angle of attack sensor p 446 A90-28263
A laser fluorescence anemometer for water tunnel flowfield studies p 447 A90-28279
- OWEN, J. I. R.**
UK reference station for Navstar GPS p 725 A90-43681
- OWEN, J. M.**
Flow and heat transfer in rotating-disc systems. Volume I - Rotor-stator systems p 772 A90-45759
- OWENS, D. BRUCE**
Exploratory wind tunnel investigation of the stability and control characteristics of a three-surface, forward-swept wing advanced turboprop model [AIAA PAPER 90-3074] p 797 A90-45920
Low-speed wind-tunnel investigation of the flight dynamic characteristics of an advanced turboprop business/commuter aircraft configuration [NASA-TP-2982] p 434 N90-19239
- OWENS, R. E.**
Ultra high bypass turbofan technologies for the twenty-first century [AIAA PAPER 90-2397] p 662 A90-42158
- OWENS, SCOTT A.**
Automation of an RCS (Radar Cross Section) measurement system and its application to investigate the electromagnetic scattering from scale-model aircraft canopies [AD-A215741] p 371 N90-17970
- OXE, DALE R.**
Passive location accuracy via a general covariance error model p 914 A90-51060
- OXOKA, A. I.**
Modeling and analysis of airport and aircraft operations [PB90-222167] p 915 N90-28511
- OYIBO, GABRIEL A.**
Closed-form solutions for nonlinear quasi-unsteady transonic aerodynamics p 16 A90-12839
Exact solutions to the oscillations of composite aircraft wings with warping constraint and elastic coupling p 603 A90-36271
- OZCAN, OKTAY**
Shock-wave/boundary-layer interaction at a swept compression corner p 16 A90-12850
- OZOROSKI, L.**
Prediction of forces and moments for flight vehicle control effectors. Part 1: Validation of methods for predicting hypersonic vehicle controls forces and moments [NASA-CR-186571] p 571 N90-21734
Prediction of forces and moments for flight vehicle control effectors. Part 2: An analysis of delta wing aerodynamic control effectiveness in ground effect [NASA-CR-186572] p 571 N90-21735
- OZOROSKI, T.**
Prediction of forces and moments for flight vehicle control effectors. Part 1: Validation of methods for predicting hypersonic vehicle controls forces and moments [NASA-CR-186571] p 571 N90-21734
Prediction of forces and moments for flight vehicle control effectors. Part 2: An analysis of delta wing aerodynamic control effectiveness in ground effect [NASA-CR-186572] p 571 N90-21735
- PACE, K. K.**
Solid fuel ignition and combustion characteristics under high-speed crossflows [AIAA PAPER 90-2075] p 764 A90-42725
- PADFIELD, GARETH**
Estimation of rotor blade incidence and blade deformation from the measurement of pressures and strains in flight p 647 A90-42497
- PADGETT, JOHN**
The Stealth biplane: A proposal in response to a low Reynolds Number station keeping mission [NASA-CR-186680] p 734 N90-25127
- PADMADINATA, UTAMA HERAWAN**
Investigation of crack-closure prediction models for fatigue in aluminium alloy sheet under flight-simulation loading [LR-619] p 777 N90-26369
- PADMANABHAM, G.**
The characteristic decay region of a class of three-dimensional wall jets p 85 A90-15241
- PADMANABHAN, R.**
Photoelastic investigation of turbine rotor blade shrouds p 112 A90-16008
Computerised structural analysis for engine components p 190 A90-18486
A numerical three-dimensional thermal stress analysis for cooled blades [ASME PAPER 89-GT-168] p 341 A90-23853
- PADOVAN, J.**
Rub interactions of flexible casing rotor systems p 41 A90-11554
- PADOVAN, JOE**
Evaluation of critical speeds in high speed aircraft tires [SAE PAPER 892349] p 733 A90-45500
- PADOVANO, ERALDO**
A new test procedure for a wing made with carbon fiber composites [ETN-89-95220] p 126 N90-11820
- PAGAN, D.**
Experimental study of incompressible flow on the upper surface of a delta wing p 558 A90-37346
- PAGAN, G.**
Hypersonic (T-D) 'pinch' and aerospaceplane propulsion [AIAA PAPER 90-2474] p 675 A90-42189
- PAGE, A. G.**
AcSim: Aircraft simulation program with application to flight profile generation [AD-A212466] p 185 N90-14217
- PAGE, GARY J.**
The calculation of under-expanded impinging jets p 147 A90-16782
- PAGE, GREGORY W.**
An investigation of strake fence flaps on a canard-configured aircraft [AIAA PAPER 90-0762] p 230 A90-22259
- PAGE, JEFF**
High speed civil transport [NASA-CR-186661] p 649 N90-23396
- PAGE, RICHARD**
The wake vortex problem revisited p 817 A90-46395
- PAGGI, B.**
EH 101 Flight Test Program current status and future testing [AIAA PAPER 90-1296] p 495 A90-33912
- PAGNANO, GIUSEPPE**
Development of a method to design helicopter rotors [REPT-100-30-03] p 845 N90-26830
- PAHLE, JOSEPH W.**
Output model-following control synthesis for an oblique-wing aircraft [NASA-TM-100454] p 435 N90-19241
Validation of the F-18 high alpha research vehicle flight control and avionics systems modifications [NASA-TM-101723] p 924 N90-28542
- PAIGE, ALLAN B.**
Development of the stall warning/stick pusher system for the Boeing/de Havilland Dash 8 Series 300 p 645 A90-42420
- PAINE, CHARLES J.**
Dual pressure ratio compressor [ASME PAPER 89-GT-121] p 341 A90-23820
- PAISLEY, D. J.**
The aerodynamic assistant [AIAA PAPER 89-3132] p 75 A90-10608
- PAISLEY, M. F.**
Improvements in the formulations and numerical solution of the Euler problem for swept wings [RAE-TM-AERO-2139] p 95 N90-12562
- PALAZZOLO, A. B.**
Test and theory for piezoelectric actuator-active vibration control of rotating machinery p 879 A90-46226
- PALAZZOLO, ALAN B.**
Vibration dampers for cryogenic turbomachinery [AIAA PAPER 90-2740] p 882 A90-47228
- PALKO, JOSEPH L.**
Analysis of whisker-toughened ceramic components - A design engineer's viewpoint p 205 A90-19149
- PALMBERG, BJORN**
Damage tolerance of the fighter aircraft 37 Viggen. Part 1: Analytical assessment [FFA-TN-1990-12-PT-1] p 923 N90-28538
Damage tolerance of the fighter aircraft 37 Viggen. Part 2: Experimental verification [FFA-TN-1990-13-PT-2] p 923 N90-28539
- PALMER, BARBARA**
Air Force Boom Event Analyzer Recorder (BEAR): System description [AD-A218048] p 548 N90-20800
- PALMER, MICHAEL T.**
Display interface concepts for automated fault diagnosis [NASA-TM-101610] p 252 N90-15102
- PALMERIO, B.**
2-D and 3-D unstructured mesh adaption relying on physical analogy p 310 A90-26534
- PALUCH, B.**
Design, realization, and qualification of model composite rotor blades p 364 A90-24293
Sting design feasibility for E.T.W. cryogenic civil transport aircraft p 524 A90-34245
Design and manufacturing of composite materials blade models p 618 A90-42492
- PALUMBO, DANIEL L.**
Three approaches to reliability analysis p 452 A90-30706
- PALUMBO, G.**
Shock layer vacuum UV spectroscopy in an arc-jet wind tunnel [NASA-TM-102258] p 370 N90-17112
- PAN, JIAZHENG**
The water tunnel test of delaying vortex breakdown over a delta wing using supplements p 2 A90-10346
- PAN, SHUXUN**
A variable structure system (VSS) to robust control of aircraft p 257 A90-21987
- PAN, TIANMIN**
Unsteady aerodynamics and aeroelasticity of turbomachines and propellers; Proceedings of the Fifth International Symposium, Beijing, People's Republic of China, Sept. 18-21, 1989 p 853 A90-49451
- PANDALAI, KRISH**
Criteria for polymer concrete on airport pavements [DOT/FAA/DS-89/18] p 527 N90-21045
- PANDELIDIS, I. O.**
Obtaining precise LTR with Luenberger type observer with arbitrary observer poles and finite gain [AIAA PAPER 90-3228] p 868 A90-49113
- PANDOLFI, MAURIZIO**
Non-equilibrium hypersonic flows - Physics and numerics p 304 A90-25777
- PANDYA MAHAGNA, J.**
Design and off-design performance predictions of axial turbines p 45 A90-12540
- PANGLINAN, HAROLD**
The Stealth biplane: A proposal in response to a low Reynolds Number station keeping mission [NASA-CR-186680] p 734 N90-25127
- PANOV, IU. A.**
Effect of the Mach number and shape of the front part of the obstacle on the separation zone length in supersonic flow p 903 A90-50816
- PANTELEEV, I. M.**
Asymptotic solution of the optimal-deflection problem for a wing leading edge at subsonic flow velocities p 285 A90-24094
- PANTON, RONALD L.**
Effects of a contoured apex on vortex breakdown p 308 A90-26141
- PAO, JENN LOUH**
Study of vortex breakdown of F-106B by Euler code p 233 A90-23289
- PAO, S. PAUL**
Application of a new adaptive grid for aerodynamic analysis of shock containing single jets [AIAA PAPER 90-2025] p 624 A90-41988
- PAPADOPOULOS, DEMETRIOS S.**
Use of unbalanced laminates as a screening method for microcracking p 948 A90-50217
- PAPAGEORGIOU, D. T.**
Linear instability of the supersonic wake behind a flat plate aligned with a uniform stream p 716 A90-45783
Linear instability of supersonic plane wakes [NASA-CR-181911] p 20 N90-10833
- PAPAILIOU, K.**
Jet engine fault detection with differential gas path analysis at discrete operating points p 50 A90-12633

Computer modeling and data processing methods: An essential part of jet engine condition monitoring and fault diagnosis p 855 N90-27626

PAPAILIOU, K. D.

A secondary flow calculation method for one stage centrifugal compressor p 14 A90-12597
Calculation of axisymmetric flows in turbomachines, through an explicit time-splitting method p 14 A90-12622

Casing vibration and gas turbine operating conditions [ASME PAPER 89-GT-78] p 358 A90-23799
A two-dimensional unsteady potential solver in internal aerodynamics flow problems p 707 A90-44430
Development and application of a fractional-step method for the solution of transonic and supersonic flow problems p 709 A90-44461
Secondary flow calculations for axial and radial compressors p 514 N90-21024

PAPANICOLAPOULOS, ALECK

Aircraft applications of advanced composite fiber/metal pressure vessels [AIAA PAPER 90-2344] p 686 A90-42133

PAPKA, ROBERT J.

Modeling the wake as a continuous vortex sheet in a potential-flow solution using vortex panels [AD-A216220] p 371 N90-18016

PARAMESWARAN, V.

Flight path reconstruction using extended Kalman filtering techniques [PD-FC-9001] p 489 N90-20970

PARASCHIVOIU, I.

Finite element simulation of unsteady two-dimensional incompressible viscous flows p 629 A90-42423

PARASCHIVOIU, ION

An integral method for transonic flows p 395 A90-31119

PARCZEWSKI, J.

Aircraft program motion along a predetermined trajectory. I - Mathematical modelling p 345 A90-23979

PARDESSUS, TH.

The need for a common approach within AGARD p 425 N90-18404

PARHAM, THOMAS C., JR.

Tiltrotor aeroservoelastic design methodology at BHTI p 410 A90-28244

PARIKH, P. G.

Application of boundary layer control to HSCT low speed configuration [AIAA PAPER 90-3199] p 812 A90-49103
Application of laminar flow control to supersonic transport configurations [NASA-CR-181917] p 719 N90-25944

PARIKH, PARESH

Interactive generation of unstructured grids for three dimensional problems p 310 A90-26537
Application of sound and temperature to control boundary-layer transition p 92 N90-12537

PARK, B.

Development of a fibre optic damage detection system for an aircraft leading edge p 504 A90-32873

PARK, J. S.

Augmented heat transfer in rectangular channels of narrow aspect ratios with rib turbulators p 70 A90-13091

PARK, MYEONG KWAN

Oscillation of circular shock wave p 557 A90-36465

PARK, SEUNG O.

Hot-wire measurements of near wakes behind an oscillating airfoil p 154 A90-18138

PARK, SUNG-NAM

Flow visualization of the effect of pitch rate on the vortex development on the scale model of a F-18 fighter aircraft [AD-A214244] p 236 N90-15080

PARK, W. J.

An experimental investigation of the turbulent structure in a two-dimensional momentumless wake p 474 A90-33515

PARKER, CRAIG B.

Weather data dissemination to aircraft p 486 N90-20934

PARKER, DAVID HUW

Techniques for extreme attitude suspension of a wind tunnel model in a magnetic suspension and balance system [NASA-CR-181895] p 202 N90-14245

PARKER, E. ANN

Forebody design for the aerospaceplane [AIAA PAPER 90-2472] p 762 A90-42810

PARKER, ELLEN C.

Experimental transonic flutter characteristics of supersonic cruise configurations [AIAA PAPER 90-0979] p 390 A90-29369

Experimental transonic flutter characteristics of two 72 deg-sweep delta-wing models [NASA-TM-101659] p 175 N90-14205

PARKER, ELLEN M.

Success in tutoring electronic troubleshooting p 780 N90-25568

PARKER, IAN

Looking inside a structure p 209 A90-17920
The case for titanium p 204 A90-17922
Safer primers from 3M p 204 A90-17925
Glassy waters for Seastar p 382 A90-29637
Certificating the Speed Canard p 833 A90-48699

PARKER, JOHN

Peacekeeper IFSS - A TOM success story [AIAA PAPER 89-3218] p 549 A90-31702

PARKHOMOVSKII, IA. M.

Flutter and aileron reversal safety factors p 345 A90-24164

PARKINSON, B. W.

Autoland with GPS p 97 A90-13985

PARKINSON, E.

Parabolized calculations of turbulent three dimensional flows in a turbine duct p 482 N90-21013

PARKMAN, D. S.

Recovery concepts for propulsion and avionics components [AIAA PAPER 90-1810] p 353 A90-25172

PARKS, EDWIN K.

Sideslip-induced static pressure errors in flight-test measurements [AIAA PAPER 90-3082] p 794 A90-45898
Sideslip-induced static pressure errors in flight-test measurements [NASA-TM-102846] p 849 N90-27702

PARKS, GARY

Entrapment plating of abrasive particles for jet engine clearance control [SAE PAPER 890918] p 286 A90-24685

PARKS, MARK A.

Advanced transport operating system software upgrade: Flight management/flight controls software description [NASA-CR-181936] p 893 N90-28366

PARLETTE, EDWARD B.

Comparison between experimental and numerical results for a research hypersonic aircraft p 395 A90-31278

PARMENTER, K.

Transient response of leading-edge vortices to localized suction p 556 A90-36279
Applying qualitative knowledge to aircraft engine system design p 694 A90-41189

PARMET, ALLEN J.

Toxicology in aviation p 722 A90-44662

PAROBK, DANIEL M.

Development and extension of diagnostic techniques for advancing high speed aerodynamic research p 436 A90-28281

PARRAG, MICHAEL

Use of ground-based and in-flight simulation for flight control system development [AIAA PAPER 90-1286] p 519 A90-33907

PARRIS, RUSTY

High speed civil transport [NASA-CR-186661] p 649 N90-23396

PARRISH, C. J.

Dynamic tip clearance measurements in axial flow compressors [PNR90597] p 116 N90-12612

PARRISH, RUSSELL V.

Stereopsis cueing effects on hover-in-turbulence performance in a simulated rotorcraft [NASA-TP-2980] p 506 N90-21004
Simulator comparison of thumbball, thumb switch, and touch screen input concepts for interaction with a large screen cockpit display format [NASA-TM-102587] p 506 N90-21005

PARTHASARATHY, T. A.

Processing and mechanical properties of Al2O3/Y3Al5O12 (YAG) eutectic composite p 951 A90-51966

PARTL, O.

Reconstitution of crack growth from fractographic observations after flight simulation loading p 682 A90-40650

Fractographic observations on fatigue crack growth in 2024-T3 sheet material under flight-simulation loading [LR-592] p 689 N90-23760

PARTRIDGE, P. G.

Diffusion bonding of metals p 206 N90-14330

PARZYCH, DAVID

Acoustic test and analysis of a counterrotating prop-fan model [NASA-CR-179590] p 79 N90-10683

PASCAU, A.

Calculation of confined swirling flows with a second moment closure p 66 A90-10640

PASHINTSEV, V. T.

A study of approximately optimal cruising flight regimes of variable-mass aircraft p 430 A90-29187

PASHUTOV, A. V.

Characteristics of turbulent separation flows on a porous surface under conditions of injection p 231 A90-22422

PASIN, M.

Simulation of compressor performance deterioration due to erosion [ASME PAPER 89-GT-182] p 254 A90-22665

PASKIN, MARC D.

Composite matrix cooling scheme for small gas turbine combustors [AIAA PAPER 90-2158] p 852 A90-47210

PASQUALE, LINDA

MLS mathematical model validation study using airborne MLS data from Midway Airport engineering flight tests, August 1988 [DOT/FAA/CT-TN90/2] p 640 N90-23378

PASQUET, J. C.

Feasibility study of RADAC stereo optoelectronic model deformation measurement system for ETW p 539 A90-34239

PASTORE, CHRISTOPHER M.

Engineering design of tough ceramic matrix composites for turbine components [ASME PAPER 89-GT-294] p 343 A90-23892

PASTORIUS, WALTER J.

A technique for rapid inspection of composite aircraft structure for impact damage p 846 N90-28077

PASTRONE, D. M.

Blockage corrections at high angles of attack in a wind tunnel p 593 A90-35756

PATANKAR, S. V.

Studies of gas turbine heat transfer airfoil surfaces and end-wall cooling effects [AD-A212451] p 117 N90-12620

PATE, VICKI M.

The Shock and Vibration Digest, volume 21, no. 2 p 609 N90-22059

The Shock and Vibration Digest, volume 21, no. 3 p 609 N90-22064

PATEK, ZDENEK

Aerodynamic characteristics of an aircraft model at large angles of attack and large sideslip angles p 233 A90-23361

PATEL, B. R.

Turbulence model performance in V/STOL flow field simulation [AIAA PAPER 90-2248] p 625 A90-42094

PATEL, S. K.

Leading edge flap influence on aerodynamic efficiency p 85 A90-15240

PATEL, V. C.

The flow around wing-body junctions p 145 A90-16765

PATER, RUTH H.

Freeze drying for morphological control of inter-penetrating polymer networks p 948 A90-50214

PATIL, S. R.

Effectiveness of passive devices for axisymmetric base drag reduction at Mach 2 p 555 A90-36184

PATNAIK, P. C.

Braze repair of MA754 aero gas turbine engine nozzles [ASME PAPER 89-GT-235] p 342 A90-23886

Coatings for high temperature corrosion in aero and industrial gas turbines p 443 A90-30479

Life estimation of a gas turbine afterburner spraybar p 739 A90-42662

Evaluation of high temperature protective coatings for gas turbine engines under simulated service conditions p 952 N90-28712

Surface property improvement in titanium alloy gas turbine components through ion implantation p 953 N90-28713

PATRAULEA, R.

Rotary damping in aircraft motion due to jet propulsion system p 520 A90-34820

PATRICK, HOWARD VAN LIEW

Relating flow between counter-rotating propellers to aerodynamic interaction noise p 479 N90-20944

PATRICK, W. P.

Investigation of the near wake of a propfan p 622 A90-40686

PATTERSON, JAMES C., JR.

Preliminary flight test investigation of an airborne wake vortex detection concept [AIAA PAPER 90-1282] p 495 A90-33903

PATTERSON, JOHN

Compression pylon [NASA-CASE-LAR-13777-1] p 498 N90-20078

B-1B Doppler error compensation based on flight data analysis p 404 A90-30790

- PATTERSON, MICHAEL T.**
Computational and experimental studies of compressible dynamic stall p 146 A90-16776
- PATTON, R. J.**
Robust low norm output feedback design for flight control systems [AIAA PAPER 90-3505] p 891 A90-47751
- PATTON, RONALD J.**
Comparison of test signals for aircraft frequency domain identification p 490 A90-33057
- PATUREAU, PHILIPPE**
Magnetic recording on board aircraft p 39 A90-12195
- PATUREL, YVES**
Low air speed computation for helicopters: A new approach p 333 N90-16744
- PAUL, C. A.**
Some smart structures concepts p 503 A90-32858
- PAUL, CHRIS**
The Stealth biplane: A proposal in response to a low Reynolds Number station keeping mission [NASA-CR-186680] p 734 N90-25127
- PAUL, D. BRENTON**
Effect of temperature on the storage life of polysulfide aircraft sealants [MRL-TR-89-31] p 444 N90-19364
- PAUL, J.**
Evaluation of a damaged F/A-18 horizontal stabilizer [AD-A212573] p 107 N90-12597
- PAUL, LEE E.**
Dallas/Fort Worth simulation. Volume 2: Appendixes D, E, and F [AD-A216613] p 405 N90-18380
Dallas/Fort Worth simulation, volume 1 [DOT/FAA/CT-TN89/28-VOL-1] p 824 N90-26802
Atlanta tower simulation, volume 1 [DOT/FAA/CT-TN89/27-VOL-1] p 870 N90-26835
Atlanta tower simulation, Volume 2: Appendixes [DOT/FAA/CT-TN89/27-VOL-2] p 870 N90-26836
- PAUL, THOMAS C.**
Applied technology in gas turbine aircraft engine development p 112 A90-16001
- PAULAUSKAS, V. V.**
Durability characteristics of the LAK-12 Letuva glider made of composite materials at the stage of certification p 102 A90-15560
- PAULEY, LAURA L.**
The instability of two-dimensional laminar separation p 800 A90-46365
- PAULEY, WAYNE R.**
Boundary layer turbulence structure in the presence of embedded streamwise vortex pairs p 552 A90-35193
- PAULI, ROBERT**
Automated aircraft paint strip cell [SAE PAPER 890936] p 286 A90-24699
- PAULI, ROBERT A.**
Robotic dry stripping of airframes - Phase II [SAE PAPER 890926] p 365 A90-24691
- PAULON, J.**
Numerical simulation of turbomachinery flows with a simple model of viscous effects - Comparison with experimental data [ONERA, TP NO. 1989-122] p 10 A90-12510
- PAULON, JACQUES**
Numerical simulation of nonreactive flows in turbomachines p 908 A90-52621
- PAULSON, JOHN W., JR.**
Dynamic ground effects p 922 N90-28531
- PAUSDER, H.-J.**
A study of roll response required in a low altitude slalom task p 347 A90-25421
A highly maneuverable helicopter in-flight simulator - Aspects of realization [AIAA PAPER 88-4607] p 670 A90-42466
- PAUSDER, HEINZ-JUERGEN**
ATThES - A helicopter in-flight simulator for ACT testing p 643 A90-41727
- PAVIE, F.**
Numerical study of heat transfer for unsteady viscous supersonic blunt body flows p 707 A90-44432
- PAVLIUCHENKO, A. M.**
Characteristics of turbulent separation flows on a porous surface under conditions of injection p 231 A90-22422
- PAVLOV, L. S.**
An experimental study of instantaneous velocity perturbations over a rotor disk for low duty coefficients p 860 A90-46572
- PAVLOV, V. A.**
Effect of the drag on the critical flutter velocity p 828 A90-46480
- PAYNE, FRED R.**
Numerical aerodynamics via formal integration - Laplace, Euler, Prandtl, Navier-Stokes and Reynolds equations p 305 A90-25800
- PAYNE, R. C.**
Noise levels from a VSTOL aircraft measured at ground level and at 1.2 m above the ground [NPL-RSA(EXT)-009] p 464 N90-18999
- PAYRY, M. J.**
T2 ability concerning model design and instrumentation in short run processing p 524 A90-34241
- PEACOCK, R. E.**
Turbomachinery tip gap aerodynamics - A review p 13 A90-12557
- PEARCE, G.**
The performance of a small combustor operated over a wide range of conditions p 45 A90-12548
- PEARCE, J. A.**
Development of a computational fluid dynamics and chemistry model for the fouling of jet fuels [DE90-005664] p 608 N90-22003
- PEARCEY, H. H.**
The aims and history of adaptive wall wind tunnels p 871 A90-26839
- PEARSON, A.**
An array-fed reflector antenna with built-in calibration facility p 402 A90-27781
- PEARSON, P. K.**
Initiation of spalling in aircraft gas turbine bearings [AIAA PAPER 90-2291] p 686 A90-42110
- PECORA, M.**
Aeroelastic analysis for a composite T-tailplane of a turboprop commuter aircraft p 492 A90-33390
- PEDERSEN, J.**
NASA/GE Energy Efficient Engine low pressure turbine scaled test vehicle performance report [NASA-CR-168290] p 931 N90-28563
- PEDLEY, MIKE I.**
Airborne MSS for land cover classification II p 737 A90-43376
- PEEL, C. J.**
Analysis of failures in aircraft structures p 882 A90-48998
Royal Aerospace Establishment: No place for a castings factor p 64 N90-10235
Current status of the application of conventional aluminium-lithium alloys and the potential for future developments p 268 N90-15203
- PEETERS, M.**
Development of a robust calculation method for transonic viscous blade-to-blade flows p 703 A90-42671
- PEI, G.**
Transport composite fuselage technology: Impact dynamics and acoustic transmission [NASA-CR-4035] p 126 N90-11821
- PEIGIN, S. V.**
Supersonic nonuniform flow of a gas past oblong axisymmetric bodies p 159 A90-19237
- PEIRO, J.**
Applications of an adaptive unstructured solution algorithm to the analysis of high speed flows [AIAA PAPER 90-0395] p 229 A90-22213
Unstructured finite element mesh generation and adaptive procedures for CFD p 608 N90-21993
- PEISEL, M. A.**
Dynamic stiffness of a hydraulic damper in the system of a front landing gear strut p 102 A90-14555
- PEISEN, DEBORAH**
Rotorcraft low altitude CNS benefit/cost analysis: Rotorcraft operations data [DOT/FAA/OS-89/9] p 141 N90-12406
- PEISEN, DEBORAH J.**
Indianapolis Downtown Heliport: Operations analysis and marketing history [REPT-90RR-13] p 527 N90-21049
- PELANG, JAROSLAV**
Numerical method for the flow of an ideal fluid on a plane with subsonic and supersonic regions p 233 A90-23362
- PELL, R. A.**
Fatigue of thick-section cold-expanded holes with and without cracks p 270 A90-20987
- PELLETIER, DOMINIQUE**
Finite element simulation of turbulent propeller flowfields p 703 A90-42658
- PEN'KOV, V. F.**
The tape method for the automatic partitioning of an arbitrary region when calculating temperature stresses p 138 A90-14587
- PENCIL, ERIC**
Attachment of lead wires to thin film thermocouples mounted on high temperature materials using the parallel gap welding process [NASA-TM-102442] p 543 N90-21361
- PENDERGRAFT, ODIS C., JR.**
External nozzle flap dynamic load measurements on F-15 S/MTD model [AIAA PAPER 90-1910] p 740 A90-42692
- PENDLETON, EDMUND**
A review of aeroelasticity research at the flight dynamics laboratory p 493 A90-33409
- PENDLETON, PAUL O.**
Field experience with type certificated civil aircraft operated on motor gasolines and worldwide survey of motor gasoline characteristics p 912 A90-51619
- PENG, KEMAO**
The eigenvalue sensitivity analysis and design for integrated flight/propulsion control systems p 196 A90-18601
- PENG, QINGMING**
Design and calculation of composite air-cooled blades in a highly-loaded transonic turbine p 189 A90-17790
Calculation of coolant flow and heat transfer inside composite air-cooled turbine p 189 A90-17791
- PENG, ZEYAN**
A relaxation method for transonic potential flows through 2-D cascade with large camber angle p 152 A90-17786
- PENZIN, V. I.**
Pseudoshock and separated flow in rectangular ducts p 295 A90-24089
Effect of the cross-sectional shape of a straight duct on supersonic flow stagnation p 296 A90-24110
- PERAIRE, J.**
Applications of an adaptive unstructured solution algorithm to the analysis of high speed flows [AIAA PAPER 90-0395] p 229 A90-22213
Unstructured finite element mesh generation and adaptive procedures for CFD p 608 N90-21993
- PERAIRE, JAIME**
Euler and Navier-Stokes solutions for hypersonic flows p 155 A90-18254
- PERALA, R. A.**
Aircraft lightning protection handbook [AD-A222716] p 820 N90-27668
- PERDICHIZZI, A.**
Secondary flows in a transonic cascade - Comparison between experimental and numerical results p 157 A90-18501
- PERDICHIZZI, ANTONIO**
Mach number effects on secondary flow development downstream of a turbine cascade [ASME PAPER 89-GT-67] p 290 A90-23790
Secondary flows and Reynolds stress distributions downstream of a turbine cascade at different expansion ratios p 512 N90-21015
- PERDZOCK, JOHN M.**
Application of multifunction inertial reference systems to fighter aircraft p 332 N90-16740
Application of multifunction inertial reference systems to fighter aircraft p 916 N90-29341
- PERETTI, LINDA F.**
Asymptotic modal analysis and statistical energy analysis [NASA-CR-186732] p 782 N90-26634
- PEREZ COBO, EMILIO**
Flight over the sea with twin or triple jet aircraft p 179 A90-17048
- PEREZ, RIGOBERTO**
Improved steel for landing gear design [SAE PAPER 892335] p 765 A90-45490
- PEREZ, RONALD A.**
The integrated control of a propulsion-airframe system [ASME PAPER 89-WA/DSC-12] p 751 A90-44847
- PERIAUX, J.**
Development of finite element methods for compressible Navier-Stokes flow simulations in aerospace design [AIAA PAPER 90-0403] p 166 A90-19833
- PERIAUX, JACQUES**
Hypersonics. Volume 2 - Computation and measurement of hypersonic flows; Proceedings of the First Joint Europe/U.S. Short Course on Hypersonics, Paris, France, Dec. 7-11, 1987 p 224 A90-21164
- PERISON, J.**
Thermal stability of jet fuel [DE90-001160] p 206 N90-14385
- PERISON, JANICE**
Thermal stability of jet fuel [DE90-002760] p 269 N90-15288
- PERKINS, BRETT**
AVION: A detailed report on the preliminary design of a 79-passenger, high-efficiency, commercial transport aircraft [NASA-CR-186663] p 649 N90-23395
- PERKINS, JOHN N.**
Mach 6 testing of two generic three-dimensional sidewall compression scramjet inlets in tetrafluoromethane [AIAA PAPER 90-0530] p 192 A90-19895
Exploratory wind tunnel investigation of the stability and control characteristics of a three-surface, forward-swept wing advanced turboprop model [AIAA PAPER 90-3074] p 797 A90-45920

PEROV, S. N.

Prediction of the strength-related-reliability of structural elements at the design stage p 274 A90-23402

PERRELLA, ANDY P.

Designing aerospace structures with Du Pont's LDF thermoplastic composites p 530 A90-33126

PERRET-LIAUDET, J.

Theoretical studies carried out in 1988 on helicopter rotor noise under subsonic conditions [ONERA-RS-82/5094-PY] p 896 N90-28402

PERRI, TODD A.

Helicopter flight control system design and evaluation for NOE operations using controller inversion techniques p 429 A90-28202

PERRIN, R. H.

Identification of an adequate model for collective response dynamics of a Sea King helicopter in hover p 56 A90-12766

PERRON, MICHEL

A test of kinematic GPS combined with aerial photography - Organization, logistics and results p 97 A90-13983

PERRY, BOYD

The active flexible wing aeroservoelastic wind-tunnel test program p 33 N90-10119

PERRY, BOYD, III

Digital-flutter-suppression-system investigations for the active flexible wing wind-tunnel model [AIAA PAPER 90-1074] p 430 A90-29382

Recent activities within the aeroservoelasticity branch at the NASA Langley Research Center p 492 A90-33400

Flutter suppression control law synthesis for the active flexible wing model p 517 A90-33403

NASA investigation of a claimed 'overlap' between two gust response analysis methods p 771 A90-44730

Digital-flutter-suppression-system investigations for the active flexible wing wind-tunnel model [NASA-TM-102618] p 520 N90-20093

PERSCHBACHER, DAVID L.

Automating acquisition of plans for an intelligent assistant by observing user behavior p 459 A90-30230

PERSIANI, FRANCO

Design of helicopter components in metal matrix composites [REPT-100-20-55] p 874 N90-26894

PERSIN, S. M.

Measurement of wind characteristics at airports p 962 A90-50780

Variability characteristics of the meteorological optical range field in an optically inhomogeneous atmosphere p 962 A90-50784

PERSON, LEE H.

Airplane takeoff and landing performance monitoring system [NASA-CASE-LAR-13734-1-CU] p 526 N90-20096

PESCE, MATTHEW M.

Blade-vortex interaction experiments - Velocity and vorticity fields [AIAA PAPER 90-0030] p 312 A90-26903

PESCHKA, WALTER

Hydrogen in future energy and propulsion technology p 692 A90-41736

PESCHKE, W. T.

Hydrocarbon-fueled scramjet combustor investigation [AIAA PAPER 90-2337] p 658 A90-40622

PESCHKE, WILLIAM T.

Subsonic combustor testing p 749 N90-25997

PETERMAN, BRUCE E.

Laminar flow: The Cessna perspective p 91 N90-12507

PETERS, ASHISH

Global Sentry: NASA/USRA high altitude reconnaissance aircraft design, volume 2 [NASA-CR-186820-VOL-2] p 736 N90-25971

PETERS, D. A.

Helicopter stability and control modeling improvements and verification on two helicopters p 671 A90-42474

PETERS, D. T.

Acoustic emission detection of crack presence and crack advance during flight p 886 N90-28082

PETERS, DAVID A.

Comparison of measured induced velocities with results from a closed-form finite state wake model in forward flight p 385 A90-28195

The effect of an unsteady three-dimensional wake on elastic blade-flapping eigenvalues in hover p 385 A90-28228

Helicopter trim with flap-lag-torsion and stall by an optimized controller p 755 A90-45332

PETERS, M. E.

A user's manual for the method of moments Aircraft Modeling Code (AMC) [NASA-CR-186371] p 415 N90-18390

PETERS, N.

Higher-order effects in boundary-layer premixed combustion p 529 A90-32953

PETERS, S. E.

Impact of nose-probe chines on the vortex flows about the F-16C [AIAA PAPER 90-0386] p 165 A90-19828

PETERS, STEPHEN G.

Optimal selection of GPS sets to minimize emitter location errors p 97 A90-13992

PETERSEN, KEVIN L.

Real-time flight test analysis and display techniques for the X-29A aircraft p 34 N90-10866

PETERSON, ANDREW A.

Spray nozzle investigation for the Improved Helicopter Icing Spray System (IHSS) [AIAA PAPER 90-0666] p 350 A90-25040

Development of the improved helicopter icing spray system (IHSS) p 400 A90-28182

PETERSON, CARL W.

High-performance parachutes p 400 A90-29803

PETERSON, ERIC

Preliminary design of a supersonic Short Takeoff and Vertical Landing (STOVL) fighter aircraft [NASA-CR-186670] p 649 N90-23394

PETERSON, J. B., JR.

Turbulence measurements and noise generation in a transonic cryogenic wind tunnel [AIAA PAPER 88-2026] p 522 A90-32463

PETERSON, J. M.

Fire hardening of aircraft through upgrades of materials and designs p 327 N90-17605

PETIAU, C.

Aeroelastic analysis using finite element models p 492 A90-33388

PETITNOT, J. L.

Sting design feasibility for E.T.W. cryogenic civil transport aircraft p 524 A90-34245

PETLEY, DENNIS H.

Thermal management for a Mach 5 cruise aircraft using endothermic fuel [AIAA PAPER 90-3284] p 853 A90-48871

PETOT, D.

Differential equation modeling of dynamic stall p 476 A90-34325

Coupled aerodynamic forces due to unsteady stall on a high-aspect-ratio wing oscillating at high amplitude [ONERA, TP NO. 1990-24] p 623 A90-41203

PETRASEK, DONALD W.

Fiber reinforced superalloys p 532 A90-34169

PETRO, LAURA

Design of a low cost short takeoff-vertical landing export fighter/attack aircraft [NASA-CR-186658] p 734 N90-25132

PETROV, A. S.

Auxiliary hypotheses of the wave drag theory p 387 A90-29003

PETRUSHKA, EDWARD M.

Integrated product development (IPD) at General Dynamics Fort Worth [AIAA PAPER 90-3192] p 786 A90-48828

PETTINGILL, JAMES B.

A comparison of time-optimal interception trajectories for the F-8 and F-15 [NASA-CR-186300] p 581 N90-21753

PETTY, JAMES S.

Aircraft engine technology gets a second wind p 659 A90-41166

PETUKHOV, A. N.

Cyclic fracture toughness of VT3-1 and VT-25 titanium alloys p 873 A90-46514

PETZEL, H.

The gun tunnel of the Brunswick Institute for Fluid Mechanics: Current development status p 673 N90-24227

PEYRAN, RICHARD

Methodology for estimating helicopter performance and weights using limited data p 829 A90-46936

PEZZELLA, G.

High temperature solid lubricant requirements for advanced high performance gas turbine engines [AIAA PAPER 90-2042] p 661 A90-41993

PFAFFLE, E. E.

Effect of the angle of attack on the efficiency and thrust ratio of axial-flow microturbines with full admission p 111 A90-14590

Effect of the nozzle ring vane height on the efficiency of axial-flow full-admission microturbines p 851 A90-46509

PFENNINGER, W.

Design of low Reynolds number airfoils. I p 307 A90-26129

PFENNINGER, WERNER

Long-range LFC transport p 104 N90-12508

Design of the low-speed NLF(1)-0414F and the high-speed HSNLF(1)-0213 airfoils with high-lift systems p 93 N90-12540

PFITZNER, M.

Three-dimensional simulations of hypersonic flows p 306 A90-25823

PFOERTNER, H.

Advanced algorithms design and implementation in on-board microprocessor systems for engine life usage monitoring p 892 N90-27628

PHAM DUC, T.

The all glass helicopter cockpit p 653 A90-42447

PHAN, NAM D.

Effects of damage on post-buckled skin-stiffener composite skin panels p 409 A90-28235

PHAN, SIEU

Jet Engine Technical Advisor (JETA) p 693 A90-41184

PHANOS, JOHN

An analysis of GPS as the sole means navigation system in US Navy aircraft p 917 N90-29350

PHARES, W. J.

CFD applications in an aerospace engine test facility [AIAA PAPER 90-2003] p 681 A90-40590

PHILBIN, DENNIS J.

Modification and improvement of software for modeling multidimensional reacting fuel flows [AD-A217789] p 533 N90-20235

PHILIPPE, J. J.

Performance and aerodynamic development of the Super Puma Mk II main rotor with new SPB blade tip design [ONERA, TP NO. 1989-181] p 245 A90-21041

PHILLIPS, DANA

Data base correlation issues p 459 A90-30740

PHILLIPS, E. P.

Fatigue crack initiation and small crack growth in several airframe alloys [NASA-TM-102598] p 454 N90-18746

PHILLIPS, FREDERICK C.

The Canadair CL-84 experimental aircraft - Lessons learned [AIAA PAPER 90-3205] p 834 A90-48833

PHILLIPS, JAMES D.

Selected design issues of some high speed rotorcraft concepts [AIAA PAPER 90-3297] p 840 A90-49125

PHILLIPS, JOHN L.

Structural analysis and optimum design of geodesically stiffened composite panels [NASA-CR-186944] p 959 N90-28862

PHILLIPS, NOLAN B.

BHTI's technical assessment of advanced rotor and control concepts p 861 A90-46949

PHILLIPS, PAM S.

Design and test of an NLF wing glove for the variable-sweep transition flight experiment p 104 N90-12544

PHILLIPS, R. E.

Applying qualitative knowledge to aircraft engine system design p 694 A90-41189

PHILLIPS, RANDY E.

Embedded computer system integration support p 419 A90-30724

PHILLIPS, W. PELHAM

Stability characteristics of a conical aerospace plane concept [SAE PAPER 892313] p 757 A90-45475

PICARD, C. A.

Integral fuel tanks - design, production, aging, repair p 250 N90-15906

PICKERELL, THOMAS

Ground and Obstacle Avoidance (GOA) concept of operations [DOT/FAA/DS-89/08] p 28 N90-10855

National airspace system monitoring operational concept [NAS-SR-1330] p 178 N90-14214

National airspace system air-ground communications operational concept [DOT/FAA/DS-90/2] p 542 N90-21249

PIEPER, KEITH A.

In-line wear monitor [AD-A217799] p 510 N90-20091

PIERCE, C.

Integration of the LTN-72 INS with the DOD GPS 3A set p 728 A90-45236

PIERCE, N. J.

Nonflammable hydraulic power system for tactical aircraft. Volume 1: Aircraft system definition, design and analysis [AD-A218493] p 671 N90-23409

PIERCY, T. F.

The GMA 2100 and GMA 3007 engines for regional aircraft [AIAA PAPER 90-2523] p 744 A90-42815

- PIERONEK, JAMES V.**
ASR-9 weather channel test report
[AD-A211749] p 133 N90-11934
- PIKE, J.**
Forebody design for the aerospaceplane
[AIAA PAPER 90-2472] p 762 A90-42810
- PIKIELNY, JERZY**
Design of new Polish primary radars AVIA DM/CM
p 638 A90-41035
- PILIPENKO, A. A.**
A method for the active control of the boundary layer condition
p 296 A90-24114
- PILIUGIN, A. V.**
Aeroelastic deformation of a crescent-shaped rigid support in the diffuser chamber of a wind tunnel
p 364 A90-24112
Effect of a crescent-shaped rigid support on the aerodynamic characteristics of models in the presence of perforated boundaries p 869 A90-46537
- PILIUGIN, N. N.**
A study of the radiation of hydrogen-xenon mixtures near models flying at high supersonic velocities
p 470 A90-32509
- PILKEY, W. D.**
Adaptive control of helicopter vibrations via the impulse response method
[AD-A213728] p 260 N90-15113
- PILKEY, WALTER D.**
NASA-UVA light aerospace alloy and structures technology program
[NASA-CR-182607] p 601 N90-22651
Design of cryogenic tanks for launch vehicles
p 609 N90-22662
- PILON, D.**
Practical suggestions for modifying math models to correlate with actual modal test results
p 207 A90-16979
- PINCHUKOV, V. I.**
An implicit scheme with flow correction for the numerical solution of the Euler equation
p 477 A90-34674
- PINDERA, MAREK-JERZY**
NASA-UVA light aerospace alloy and structures technology program
[NASA-CR-182607] p 601 N90-22651
- PINTO DA FONSECA, WALDIR**
Financing of civil aircraft - Purchases and leasing
p 898 A90-49616
- PIOTROWSKI, JOSEPH L.**
Natural icing re-evaluation of the EH-60A Quick Fix helicopter
[AD-A214728] p 323 N90-16723
Preliminary airworthiness evaluation of the Woodward hydromechanical unit installed on T700-GE-700 engines in the UH-60A helicopter
[AD-A216751] p 428 N90-18430
- PIPERIAS, P.**
Flutter investigations on a Transavia PL12/T-400 aircraft
[AD-A219108] p 593 N90-22570
- PIPERNI, P.**
Application of the KTRAN transonic small disturbance code to the complete CF-18 aircraft with stores
p 629 A90-42416
- PIQUET, J.**
Multigrid acceleration of transonic flow computations
p 147 A90-16783
Navier-Stokes computations of vortical flows
[AIAA PAPER 90-1628] p 568 A90-38757
- PIRAT, JEAN LOUIS**
Applications of Mode S secondary surveillance radar to civil air traffic control - Studies, experiments, and policy of the French Direction de la Navigation Aérienne
p 639 A90-41056
- PIRZADEH, SHAHYAR**
Three-dimensional unsteady transonic viscous-inviscid interaction
p 18 N90-10005
- PIS'MENNYI, I. L.**
Dynamic characteristics of one-dimensional gas flow with friction
p 296 A90-24115
Relation between flow parameters of a gas turbine engine and rotor frequencies
p 851 A90-46539
- PISCATELLA, MICHAEL J.**
Total quality management and the transitioning company - The perfect fit
[AIAA PAPER 89-3211] p 549 A90-31698
- PISHVA, M. R.**
Surface property improvement in titanium alloy gas turbine components through ion implantation
p 953 N90-28713
- PIT, F.**
3D calculations of reacting flows within aircraft engine combustion chambers
[ONERA, TP NO. 1989-153] p 67 A90-11173
- PIT, FABIENNE**
Three dimensional numerical simulation for an aircraft engine type combustion chamber
[ONERA, TP NO. 1989-120] p 49 A90-12591
- PITA, G. P. A.**
Suppression of 'Buzz' instability by geometrical design of the flameholder
[AIAA PAPER 90-1966] p 741 A90-42706
- PITMAN, W. A.**
Transport composite fuselage technology: Impact dynamics and acoustic transmission
[NASA-CR-4035] p 126 N90-11821
- PITT, D. M.**
Applications of XTRAN3S and CAP-TSD to fighter aircraft
[AIAA PAPER 90-1035] p 389 A90-29360
- PITTMAN, JAMES L.**
Strike camber and thickness design procedure for low alpha supersonic flow
p 622 A90-40678
A Mach 6 external nozzle experiment with Argon-Freon exhaust simulation
[SAE PAPER 892315] p 714 A90-45477
A computational study of incipient leading-edge separation on a 65-deg delta wing at M = 1.60
[AIAA PAPER 90-3029] p 791 A90-45871
- PITTS, R. O.**
Fog formation at Perth Airport
p 611 A90-37748
- PITZ, ROBERT W.**
Raman scattering measurements using UV excimer lasers
p 874 N90-26902
Concentration, temperature, and density in a hydrogen-air flame by excimer-induced Raman scattering
p 875 N90-26903
- PITZL, W.**
Monolithic CFC-Main Landing Gear Door for Tornado
p 955 A90-50136
- PLAETSCHKE, E.**
Flight path reconstruction using extended Kalman filtering techniques
[PD-FC-9001] p 489 N90-20970
- PLAETSCHKE, ERMIN**
Identification of moderately nonlinear flight mechanics systems with additive process and measurement noise
p 347 A90-25987
- PLANEAUX, JAMES B.**
Bifurcation analysis of a model fighter aircraft with control augmentation
[AIAA PAPER 90-2836] p 934 A90-50640
- PLANO, MATT**
RADC fault tolerant system reliability evaluation facility
[AD-A215298] p 377 N90-17348
- PLATONOV, V. A.**
Effect of the inertial nature of injection and temperature on the damping of body vibrations
p 150 A90-17112
- PLATZ, K.**
R and D aspects of the future operational concept of the BFS
p 826 N90-27679
- PLATZ, S. J.**
Flight test data processing, plotting and analysis at your finger tips - A flexible, automated, integrated approach
[AIAA PAPER 90-1322] p 545 A90-34150
- PLATZER, M. F.**
Numerical investigation of unsteady compressible flow through nozzles and cascades
p 7 A90-11790
Progress towards the development of an inviscid-viscous interaction method for unsteady flows in turbomachinery cascades
p 8 A90-11806
Experimental and computational studies of dynamic stall
p 147 A90-16780
- PLAY, D.**
Preliminary design and load distributions of high performance mechanical systems
p 771 A90-45281
- PLAZANET, M.**
T2 ability concerning model design and instrumentation in short run processing
p 524 A90-34241
- PLEHN, N.**
Application of 3-D viscous code in the design of a high performance compressor
[AIAA PAPER 90-1914] p 740 A90-42694
- PLETCHER, R. H.**
A primitive variable, strongly implicit calculation procedure for viscous flows at all speeds
[AIAA PAPER 90-1521] p 563 A90-38666
Simulation of time-dependent viscous flows using central and upwind-biased finite-difference techniques
[AIAA PAPER 90-3012] p 790 A90-45864
- PLISSOV, N. B.**
Application of the finite element method to the problem of rotational flow around wings
p 156 A90-18305
- PLOTKIN, A.**
Comment on 'Improved thin-airfoil theory'
p 554 A90-35772
- PLUMBLEE, HARRY E., JR.**
Massively parallel computing
p 458 A90-29897
- PLUMER, J. A.**
Aircraft lightning protection handbook
[AD-A222716] p 820 N90-27668
- PLUMER, J. ANDERSON**
Final results of the NASA storm hazards program
p 819 A90-49834
The behavior of electric currents in graphite/epoxy structures
p 883 A90-49846
- PODBOY, GARY G.**
Euler analysis comparison with LDV data for an advanced counter-rotation propfan at cruise
[AIAA PAPER 90-3033] p 903 A90-50637
Euler analysis comparison with LDV data for an advanced counter-rotation propfan at cruise
[NASA-TM-103249] p 720 N90-25946
- PODDAR, K.**
A study of the unsteadiness of crossing shock wave turbulent boundary layer interactions
[AIAA PAPER 90-1456] p 606 A90-38614
- PODLUBNYI, VIKTOR V.**
Effect of shock waves and jets on structural elements: Mathematical modeling in nonstationary gas dynamics
p 806 A90-46621
- POE, C. C., JR.**
An evaluation of the pressure proof test concept for thin sheet 2024-T3
[NASA-TM-101675] p 543 N90-21424
- POENSGEN, C.**
Calculation of the aeroelastic blade stabilization with linearized process
[MITT-87-01] p 666 N90-24272
- POESTKOKE, R.**
Instrumentation requirements for laminar flow research in the NLR high speed wind tunnel HST
p 447 A90-28283
- POGODA, DONALD L.**
Reconfigurable flight controller for the STOL F-15 with sensor/actuator failures
p 432 A90-30707
Multiple model adaptive controller for the STOL F-15 with sensor/actuator failures
p 668 A90-40878
- POHLENZ, ERIC L.**
Critical inspection of high performance turbine engine components: The RFC concept
p 859 N90-28073
- POINDEXTER, THOMAS E.**
McDonnell Douglas Helicopter Company Factory of the Future Project
p 381 A90-28163
- POINSAITE, PHILIP E.**
Convective heat transfer measurements from a NACA 0012 airfoil in flight and in the NASA Lewis Icing Research Tunnel
[AIAA PAPER 90-0199] p 272 A90-22180
Convective heat transfer measurements from a NACA 0012 airfoil in flight and in the NASA Lewis Icing Research Tunnel
[NASA-TM-102448] p 213 N90-13750
Heat transfer measurements from a NACA 0012 airfoil in flight and in the NASA Lewis icing research tunnel
[NASA-CR-4278] p 399 N90-19203
- POISSON-QUINTON, PH.**
SST/HST air traffic - Challenge for the future
p 763 A90-44752
- POITZ, HERB A.**
History of aircraft piston engine oils - The last forty years
[SAE PAPER 891037] p 124 A90-14343
- POLAND, D. T.**
Propfan Test Assessment (PTA)
[NASA-CR-185138] p 113 N90-11739
- POLANSKI, L.**
Automatic calibration machine for cryogenic and conventional internal strain gage balances
[AIAA PAPER 90-1396] p 595 A90-37939
- POLANSKY, LUBOMIR**
Fully automatic calibration machine for internal 6-component wind tunnel balance including cryogenic balances
p 437 A90-28294
External 6-component wind tunnel balances for aerospace simulation facilities
p 438 A90-28296
- POLIAKOVA, E. V.**
Nonstationary motion of an elastic profile in subsonic incompressible flow
p 300 A90-24741
- POLING, DAVID**
Induced drag based on leading edge suction for a helicopter in forward flight
p 232 A90-23102
The prediction of loads on the Boeing Helicopters Model 360 rotor
p 410 A90-28240
- POLING, DAVID R.**
Blade-vortex interaction experiments - Velocity and vorticity fields
[AIAA PAPER 90-0030] p 312 A90-26903
- POLITOVICH, M. K.**
A program to improve aircraft icing forecasts
[AIAA PAPER 90-0196] p 216 A90-19733
- POLLARD, M. D.**
Acoustic emission detection of crack presence and crack advance during flight
p 886 A90-28082

- POLLOCK, W. J.**
Statistical treatment of slow strain rate data for assessment of hydrogen embrittlement in low alloy high strength steel [ARL-MAT-R-122] p 767 N90-26106
- POLOTZKY, ANTHONY S.**
Development and testing of methodology for evaluating the performance of multi-input/multi-output digital control systems [AIAA PAPER 90-3501] p 867 A90-47747
- POLTAVSKI, L. N.**
Convergence of the method of discrete vortices when applied to steady-state aerodynamics problems p 231 A90-22816
- POMERANTZ, ARTHUR**
Replication of NASPAC Dallas/Fort Worth study [DOT/FAA/CT-TN90/26] p 729 N90-25123
- POMEROY, BRUCE**
A blackboard approach for diagnosis in Pilot's Associate p 892 A90-49741
- POMINOV, V. I.**
Model problems of continuous control law optimization for a tensometric aerodynamic experiment p 295 A90-24086
- POMMEL, F.**
Parabolized calculations of turbulent three dimensional flows in a turbine duct p 482 N90-21013
- PONOMAREV, A. T.**
Development of a mathematical model of an adaptive antiflutter system p 769 A90-42911
Modeling of the buffeting of flight vehicles p 803 A90-46500
- PONOMAREV, I. A.**
Automation of flight safety control p 589 A90-36157
- PONTIKIS, Y. G.**
Experimental investigation of three-dimensional turbulent boundary layers on 'infinite' swept curved wings p 303 A90-25589
- PONTON, MICHAEL K.**
External nozzle flap dynamic load measurements on F-15 S/MTD model [AIAA PAPER 90-1910] p 740 A90-42692
- POOLE, MICHAEL R.**
The Canadian Aviation Safety Board's flight recorder facility p 849 N90-27643
- POOLE, WILLIAM L.**
Results of aircraft open-loop tests of an experimental magnetic leader cable system for guidance during roll-out and turnoff [NASA-TM-4135] p 348 N90-16767
- POON, C.**
A review of crashworthiness of composite aircraft structures [AD-A221555] p 846 N90-27697
- POPCHEV, IVAN P.**
Decentralized systems p 888 A90-46001
- POPELKA, DAVID A.**
A review of the V-22 dynamics validation program p 406 A90-28155
Prediction and alleviation of V-22 rotor dynamic loads p 833 A90-46974
- POPERNACK, THOMAS G., JR.**
National Transonic Facility model and model support vibration problems [AIAA PAPER 90-1416] p 596 A90-37953
Cryogenic temperature effects on sting-balance deflections in the National Transonic Facility [NASA-TM-4157] p 202 N90-14244
- POPHIN, DANNY RAYMOND**
Three-dimensional numerical study of thunderstorm downdrafts and associated outflow boundaries p 963 N90-29746
- POPOV, L. S.**
Flutter and aileron reversal safety factors p 345 A90-24164
- PORDAL, H. S.**
A flux-split solution procedure for unsteady inlet flows [AIAA PAPER 90-0585] p 314 A90-26967
Transient behavior of supersonic flow through inlets [AIAA PAPER 90-2130] p 704 A90-42734
- PORTER, A. J.**
Thermal management of closed computer modules utilizing high density circuitry [AIAA PAPER 90-1748] p 583 A90-38441
- PORTER, B.**
Recursive real-time identification of step-response matrices of helicopters for adaptive digital flight control p 195 A90-17703
Design of adaptive digital controllers incorporating dynamic pole-assignment compensators for high-performance aircraft p 432 A90-30714
Identification of multivariable models of jet engines [AIAA PAPER 90-1874] p 655 A90-40540
- Design of digital self-selecting multivariable controllers for jet engines [AIAA PAPER 90-1875] p 655 A90-40541
- PORTER, R.**
A proposed automatic calibration facility for cryogenic balances p 524 A90-34246
- PORTER, ROGER E.**
Flight test instrumentation and data processing at British Aerospace, Warton, U.K. p 59 N90-10887
- PORTNEY, JOE N.**
Multisensor Integrated Navigation System p 577 A90-36924
- PORTNOV, A. D.**
Determination of the effective areas of the mixing exhaust ducts of a bypass engine from autonomous test results p 102 A90-14584
- POSEY, D. M.**
Helicopter wire strike accident and high voltage electrocution - A case report p 22 A90-10265
- POSPELOV, I. I.**
Effect of creep on the load-bearing capacity of compressed panels p 364 A90-24102
- POSTANS, P. J.**
The future of non ferrous metals in aerospace engines [PNR90572] p 127 N90-12720
Application of high performance metals in gas turbine engines [PNR90640] p 750 N90-25999
- POSTLETHWAITE, ALAN**
Creditable commuter Yakovlev strikes back p 405 A90-27975
Commuter from Khodinka p 579 A90-35848
Commuter from Khodinka p 842 A90-49824
- POSTLETHWAITE, I.**
Improvement of helicopter handling qualities using H(infinity)-optimisation p 667 A90-38965
- POSTON, THURMAN R.**
Eshbach's handbook of engineering fundamentals / 4th edition/ p 448 A90-28825
- POTAPCZUK, M. G.**
Swept wing ice accretion modeling [AIAA PAPER 90-0756] p 300 A90-25042
The low frequency oscillation in the flow over a NACA0012 airfoil with an 'iced' leading edge p 801 A90-46377
Experimental investigation of multielement airfoil ice accretion and resulting performance degradation p 812 A90-48954
- POTAPCZUK, MARK**
Modeling of surface roughness effects on glaze ice accretion p 485 N90-20925
- POTAPCZUK, MARK G.**
Predictions of airfoil aerodynamic performance degradation due to icing p 144 A90-16753
Swept wing ice accretion modeling [NASA-TM-103114] p 570 N90-21727
- POTAPCZUK, MARK GREGORY**
Navier-Stokes analysis of airfoils with leading edge ice accretions p 174 N90-14196
- POTAPOV, G. P.**
Electrodynamic properties of engine exhaust jets p 265 A90-23428
- POTASHEV, A. V.**
Construction of a straight single-row airfoil lattice by the method of quasi-solutions for inverse boundary value problems p 84 A90-14564
Construction of wing profiles in subsonic gas flow by the method of quasi-solutions for inverse boundary value problems p 803 A90-46542
- POTEKHINA, E. A.**
Nonstationary hypersonic flow past a thin wing of variable shape p 470 A90-32559
- POTKANSKI, W.**
Design flutter calculations on PC p 545 A90-33379
- POTOTZKY, A.**
Control law synthesis and optimization software for large order aeroservoelastic systems p 61 N90-10111
- POTOTZKY, A. S.**
Further studies of harmonic gradient method for supersonic aeroelastic applications p 473 A90-33410
The application of active controls technology to a generic hypersonic aircraft configuration [NASA-TM-101689] p 497 N90-20071
- POTOTZKY, ANTHONY S.**
NASA investigation of a claimed 'overlap' between two gust response analysis methods p 771 A90-44730
Active control of aerothermoelastic effects for a conceptual hypersonic aircraft [AIAA PAPER 90-3337] p 863 A90-47597
Development and testing of methodology for evaluating the performance of multi-input/multi-output digital control systems [NASA-TM-102704] p 846 N90-27699
Active control of aerothermoelastic effects for a conceptual hypersonic aircraft [NASA-TM-102713] p 869 N90-27725
- POTSDAM, ERIC**
An analysis of feel system effects on lateral flying qualities [AIAA PAPER 90-1824] p 346 A90-25168
- POTTER, J. L.**
Array processor supercomputers p 376 A90-26626
- POTTER, J. LEITH**
Detachment of turbulent boundary layers with varying free-stream turbulence and lower Reynolds numbers p 802 A90-46378
- POTTER, JOHN M.**
Development of fatigue loading spectra [ASTM STP-1006] p 367 A90-26751
- POTTER, SCOTT S.**
General aviation pilot error in computer simulated adverse weather scenarios p 322 A90-26254
- POTTS, R.**
Microburst precursors observed with Doppler radar p 456 A90-28613
- POULOS, ARTHUR T.**
Photo-sensitized ignition of hydrogen/oxygen mixtures for hypersonic flight vehicles p 877 N90-27935
- POULOSE, M. M.**
Accurate ILS and MLS performance evaluation in presence of site errors p 404 A90-30693
- POVINELLI, LOUIS A.**
Advanced computational techniques for hypersonic propulsion p 69 A90-12606
CFD propels NASP propulsion progress p 683 A90-41163
- POWELL, ARTHUR G.**
Supersonic boundary layer stability analysis with and without suction on aircraft wings p 148 A90-16792
- POWELL, ARTHUR G.**
The right wing of the LEFT airplane p 91 N90-12510
- POWELL, CLEMANS A.**
FAA/NASA En Route Noise Symposium [NASA-CP-3067] p 696 N90-24853
- POWERS, DAVID A.**
Wind tunnel study of wake downwash behind A 6 percent scale model B1-B aircraft [DE90-011783] p 719 N90-25941
- POZESKY, MARTIN T.**
The US air traffic control system architecture p 330 A90-25561
The use of satellite technology for oceanic air traffic control p 330 A90-25570
- POZNYSHEV, S. D.**
Multicriterial optimization of lugs in hinge joints p 364 A90-24162
- PRABHU, R. K.**
Applications of an adaptive unstructured solution algorithm to the analysis of high speed flows [AIAA PAPER 90-0395] p 229 A90-22213
- PRABHU, RAMADAS K.**
Euler and Navier-Stokes solutions for hypersonic flows p 155 A90-18254
- PRAKASH, RAJIVA**
LQG/LTR controller design using a reduced order model p 964 A90-52877
- PRANDI, B.**
beta CEZ, a high performance titanium alloy for aerospace engines [ONERA, TP NO. 1990-8] p 356 A90-25356
- PRANDY, J.**
The effect of matrix toughness in the development of improved structural adhesives p 955 A90-50183
- PRASAD, CHUNCHU B.**
A Protection And Detection Surface (PADS) for damage tolerance [NASA-TP-3011] p 876 N90-27788
- PRASAD, J. V. B.**
A study of the effects of Rotating Frame Turbulence (RFT) on helicopter flight mechanics p 248 N90-15058
- PRASAD, J. V. R.**
Approximate loop transfer recovery method for designing fixed-order compensators p 375 A90-25989
Helicopter stability and control modeling improvements and verification on two helicopters p 671 A90-42474
Control of a twin lift helicopter system using nonlinear state feedback [AIAA PAPER 90-3408] p 817 A90-47663
- PRASAD, S. K.**
Analysis and design of symmetrical airfoils [PD-CF-8943] p 400 N90-19213
- PRASANTH, R. K.**
A robust wind shear stochastic controller-estimator [AIAA PAPER 90-3489] p 867 A90-47737
- PRATTE, J. F.**
Composites for aerospace application from Kevlar aramid reinforced PEKK thermoplastic p 946 A90-50176

- PRATTE, JAMES F.**
High performance thermoplastic composites with poly(etherketoneketone) matrix p 529 A90-31646
- PRECOURT, CHARLES J.**
Schleicher ASK-21 glider (TG-9) stall and spin [AD-A213513] p 249 N90-15096
- PREISSLER, HARALD**
Equation decoupling - A new approach to the aerodynamic identification of unstable aircraft [AIAA PAPER 90-1276] p 518 A90-33900
- PREL, PASCAL**
Theoretical analysis of an icing test apparatus for turbine engine air intakes [AAAF PAPER NT 88-20] p 23 A90-11437
- PREUSSER, TIMM**
Fully automatic calibration machine for internal 6-component wind tunnel balance including cryogenic balances p 437 A90-28294
External 6-component wind tunnel balances for aerospace simulation facilities p 438 A90-28296
- PRICE, DALE**
Air Force Boom Event Analyzer Recorder (BEAR): System description [AD-A218048] p 548 N90-20800
- PRICE, DONALD C.**
Use of ECS-conditioned air for FLIR avionics thermal control - Fighter aircraft [SAE PAPER 901219] p 840 A90-49294
- PRICE, J. O.**
Measurement and characterization of prepreg permeability with a modified bagging technique p 949 A90-50226
- PRICE, P. E.**
Mesoscale acid deposition modeling studies [NASA-CR-4262] p 140 N90-13228
- PRICE, TODD D.**
AV-8B composite repair program p 551 A90-38542
- PRIEUR, J.**
Wind-tunnel measurement of noise emitted by helicopter rotors at high speed [ONERA, TP NO. 1990-28] p 695 A90-41207
- PRINI, A.**
Large-amplitude high-rate roll oscillation system for the measurement of non-linear airloads [AIAA PAPER 90-1426] p 590 A90-37963
- PRINOS, P.**
Evaluation of two numerical techniques for the prediction of flow around blades p 10 A90-12512
- PRIOR, R. C.**
Engineering design models for ramjet efficiency and lean blowoff [AIAA PAPER 90-2453] p 663 A90-42176
- PRIOVOLOS, GEORGE J.**
Autonomous integrated GPS/INS navigation experiment for OMV. Phase 1: Feasibility study [NASA-CR-4267] p 489 N90-20969
- PRITCHARD, JOCELYN I.**
Optimal placement of tuning masses for vibration reduction in helicopter rotor blades p 247 A90-23117
Rotor blade dynamic design p 106 N90-12583
Appendix: Results obtained to date p 107 N90-12588
- PRITULO, T. M.**
A method for calculating the location and intensity of a conical head shock on the lower surface of a delta wing with supersonic edges p 297 A90-24139
- PROCTOR, F. H.**
Mesoscale acid deposition modeling studies [NASA-CR-4262] p 140 N90-13228
- PROKOPIUK, ANDRZEJ**
Application of mathematical modeling to the study of rigid helicopter rotors p 643 A90-41738
- PROSKAWETZ, KARL-OSKAR**
A contribution to the improvement of the accuracy in the parameter identification of nonlinear processes, by example of the aircraft motion [ETN-90-96961] p 736 N90-25974
- PROUTY, R. W.**
What's best to tilt - The rotor or the wing? p 580 A90-36850
- PROUTY, SCOTT**
Design of attitude and rate command systems for helicopters using eigenstructure assignment p 118 A90-14729
- PROVOTOROV, V. P.**
Hypersonic flow past blunt edges at low Reynolds numbers p 10 A90-12284
- PRUDHOMME, S.**
Design of a three dimensional Doppler anemometer for T2 transonic wind tunnel p 447 A90-28271
T2 ability concerning model design and instrumentation in short run processing p 524 A90-34241
- PRUDNIKOV, I. A.**
Comparison of calculated and experimental nonstationary aerodynamic characteristics of a delta wing pitching at large angles of attack p 387 A90-28988
- Self-induced roll oscillations of lifting systems with thin delta wings p 860 A90-46570
- PRUETT, STAN**
Laboratory implementation of the Continuously Reconfiguring Multi-Microprocessor Flight Control System (CRMMFCS) [AD-A217730] p 520 N90-20094
- PRUITT, M. O.**
SPF/DB takes off p 208 A90-17293
- PRUST, E. E.**
Independent Orbiter Assessment (IOA): Analysis of the displays and controls subsystem [NASA-CR-185563] p 124 N90-11774
- PRUVOST, J.**
Reduction of profile drag by modifying the structure next to the wake area [IMFL-88/35] p 172 N90-13356
- PRYDZ, R. A.**
Interior noise in the untreated Gulfstream II Propfan Test Assessment aircraft p 731 A90-44736
- PRZYBYLKO, STEPHEN J.**
High-temperature electronics for aircraft engines [AIAA PAPER 90-2035] p 657 A90-40604
- PRZYBYTKOWSKI, S.**
Development of a robust calculation method for transonic viscous blade-to-blade flows p 703 A90-42671
- PSIAKI, MARK L.**
Nonconvex polytope approximations of attracting basin boundaries for nonlinear systems [AIAA PAPER 90-3512] p 891 A90-47758
- PTACNIK, MICHAL**
LDA processor TSI model 1990 analog input module reconstruction p 451 A90-29654
- PUFFERT-MEISSNER, W.**
Observation and analysis of sidewall effect in a transonic airfoil test section p 436 A90-28257
Use of the film-of-oil technique for profile measurements in the Transonic Wind tunnel Brunswick (TWB) p 238 N90-16252
- PUFFETT, A. W.**
The assessment of visibility from automatic contrast Measurements p 242 N90-15061
- PUGLIESE, L.**
An ultrasonic system for in-service non-destructive inspection of composite structures p 885 N90-28076
- PULESTON, D. J.**
A laser obstacle avoidance and display system p 419 A90-30694
- PULLEY, D. F.**
Organic coatings - First line of defense p 204 A90-17300
- PULLIAM, T. H.**
A comparison of two central difference schemes for solving the Navier-Stokes equations [NASA-TM-102815] p 816 N90-27654
- PULLIAM, THOMAS H.**
An introduction to chaos theory in CFD [AIAA PAPER 90-1440] p 680 A90-39725
- PULSONETTI, MARIA V.**
Hypervelocity real gas capabilities of GASL's expansion tube (HYPULSE) facility [AIAA PAPER 90-1390] p 594 A90-37935
- PUMA, C. J.**
Development of a dual fuel injector for a gas turbine combustor [ASME PAPER 89-GT-25] p 340 A90-23764
- PUNDHIR, D. S.**
A study of flow structure in a contra-rotating axial compressor stage p 11 A90-12524
- PUR, RICHARD A.**
Airport pavement drainage [DOT/FAA/RD-90/24] p 872 N90-27728
- PURAM, C. K.**
Vortex control for tail buffet alleviation on a twin-tail fighter configuration [SAE PAPER 892221] p 756 A90-45438
- PURCELL, TIMOTHY W.**
CFD and transonic helicopter sound p 696 A90-42433
- PURVIS, BRADLEY D.**
Strategic aircraft engineering design simulation p 439 A90-30729
Model-based method for terrain-following display design [AD-A219302] p 583 N90-22563
- PUSEY, HENRY C.**
The 59th Shock and Vibration Symposium, volume 2 [AD-A214579] p 372 N90-18065
- PUSEY, SALLIE C.**
The 59th Shock and Vibration Symposium, volume 2 [AD-A214579] p 372 N90-18065
- PUSTER, RICHARD L.**
Device for quickly sensing the amount of O₂ in a combustion product gas [NASA-CASE-LAR-13816-1] p 609 N90-22025
- PUTATUNDA, SUSIL K.**
Quantitative methods in fractography; Proceedings of the Symposium on Evaluation and Techniques in Fractography, Atlanta, GA, Nov. 10, 1988 [ASTM STP-1085] p 949 A90-50551
- PUTT, JAMES C.**
An advanced pneumatic impulse ice protection system (PIIP) for aircraft [AIAA PAPER 90-0492] p 182 A90-19875
- PUZZO, DEAN C.**
ASR-9 weather channel test report [AD-A211749] p 133 N90-11834
- PYNE, C. R.**
The development of leading-edge notches to improve the subsonic performance of wings of moderate sweep p 491 A90-33367
The steady and time-dependent aerodynamic characteristics of a combat aircraft with a delta or swept canard p 921 N90-28526

Q

- QI, ZONGNENG**
Fracture morphology of toughened bismaleimide/carbon fiber composites p 948 A90-50205
- QIAN, BOSHUN**
Linear dynamics of supersonic ramjet p 655 A90-40519
- QIAO, XIN**
Aeroelastic tailoring of composite wing structures p 580 A90-37217
Optimum design of composite wing structures subjected to displacement constraints p 680 A90-39276
- QIAO, ZHIDE**
A transonic airfoil design method and examples p 627 A90-42351
- QIN, LISEN**
Analyses of full 3D S1-S2 iterative solution in CAS transonic compressor rotor and comparison with quasi-3D S1-S2m iterative solution and L2F measurement p 157 A90-18532
An approximate 3-D aerodynamic design method for centrifugal impeller blades [ASME PAPER 89-GT-73] p 291 A90-23794
- QIN, REN**
Boundary element method for solving direct aerodynamic problem of aerofoil cascades on an arbitrary stream surface of revolution p 554 A90-35830
- QIN, XIAOCHENG**
Boundary element method for solving direct aerodynamic problem of aerofoil cascades on an arbitrary stream surface of revolution p 554 A90-35830
- QIU, XINYU**
An experimental study on flowfields in a dual inlet swirl-dump combustor p 471 A90-33283
The experimental study on the coaxial dump combustor with inner swirl inlet under the combustion condition p 585 A90-36786
- QUACKENBUSH, T. R.**
Optimization of rotor performance in hover and axial flight using a free wake analysis p 407 A90-28175
Free wake analysis of rotor configurations for reduced vibratory airloads p 833 A90-46975
- QUACKENBUSH, TODD R.**
New free-wake analysis of rotorcraft hover performance using influence coefficients p 181 A90-17867
High resolution flow field prediction for tail rotor aeroacoustics p 463 A90-28158
- QUADIR, G. ABDUL**
Boundary layer growth on low aspect ratio compressor blades p 12 A90-12553
- QUAGLIOTTI, F. B.**
Blockage corrections at high angles of attack in a wind tunnel p 593 A90-35756
- QUARTERMAINE, R. W.**
Helicopter rotor test rig (RoTeSt) in DNW: Application and results [RAE-TRANS-2171] p 201 N90-13408
- QUAST, A.**
Flight and wind-tunnel investigations on boundary-layer transition p 233 A90-23283
Flight tests with a natural laminar flow glove on a transport aircraft [AIAA PAPER 90-3044] p 828 A90-45881
Natural laminar flow - A wind tunnel test campaign and comparison with flight test data [AIAA PAPER 90-3045] p 792 A90-45882
- QUAST, THOMAS**
The MANTA: An RPV design to investigate forces and moments on a lifting surface [NASA-CR-186227] p 499 N90-20971

QUEMARD, C.

Comparison of the results of tests on A300 aircraft in the RAE 5 metre and ONERA F1 wind tunnels
[RAE-TM-AERO-2130] p 122 N90-11768

QUEST, J.

Secondary flow in a turbine guide vane with low aspect ratio p 513 N90-21018

QUETS, JOHN M.

UCAR 2040, A novel wear resistant coating for aircraft structural components p 441 A90-28231

QUEUTEY, P.

Navier-Stokes computations of vortical flows
[AIAA PAPER 90-1628] p 568 A90-38757

QUICK, R. FRANK, JR.

Range Applications Joint Program Office GPS Range System data link p 725 A90-43686

QUIMBY, KELVIN L.

Evolution of Ada technology in the flight dynamics area: Implementation/testing phase analysis
[NASA-TM-103310] p 546 N90-21539

Evolution of Ada technology in the flight dynamics area: Design phase analysis
[NASA-TM-103307] p 547 N90-21542

QUIN, E.

A numerical technique for computing the unsteady transonic flow around a wing profile in arbitrary oscillation p 906 A90-51530

QUINOU, H.

Aircraft compressor flutter analysis p 41 A90-11797

QUINN, B. J.

Advanced technology in military gas turbine design and manufacture
[PNR90545] p 114 N90-11747

QUINN, R. D.

Turbomachinery blade vibration and dynamic stress measurements utilizing nonintrusive techniques p 41 A90-11558

QUINN, ROBERT D.

Real-time aerodynamic heating and surface temperature calculations for hypersonic flight simulation
[NASA-TM-4222] p 959 N90-28815

QUINTANA, F.

A formulation for the solution of Euler equations for compressible flow using finite elements p 708 A90-44447

QUINTO, P. FRANK

The Langley 14- by 22-foot subsonic tunnel: Description, flow characteristics, and guide for users
[NASA-TP-3008] p 816 N90-27649

QUIST, WILLIAM E.

The microstructure and properties of aluminum-lithium alloys p 267 N90-15187

QUOC-BUI, THANG

Cyclic stress-strain behavior and low cycle fatigue of Ti 6242 p 530 A90-33523

R

RABE, D. C.

Compressor performance tests in the compressor research facility p 427 N90-18428

RABIN, URI H.

Modeling and analysis tools for aircraft control system evaluations p 431 A90-30703
Maximum likelihood tuning of a vehicle motion filter p 755 A90-45334

RABINOWITZ, J.

Problems related to aircraft noise in Switzerland p 698 N90-24871

RACHOR, N.

Development of two multi-sensor hot-film measuring techniques for free-flight experiments p 417 A90-28291

RADESPIEL, R.

Analysis of three-dimensional aerospace configurations using the Euler and Navier-Stokes equations p 305 A90-25798
Geometric modelling of complex aerodynamic surfaces and three-dimensional grid generation p 311 A90-26545

Convergence speeding up in the calculation of the viscous flow about an airfoil p 279 N90-16194
Aerodynamic design techniques at DLR Institute for Design Aerodynamics p 500 N90-20979

RADESPIEL, ROLF

Advances in the efficient calculation of flows with friction p 225 A90-21475
Comparison of two- and three-dimensional Navier-Stokes solutions with NASA experimental data for CAST-10 airfoil p 321 N90-17658

RADFORD, LEANNA E.

AV-8B composite repair program p 551 A90-38542

RAETZER-SCHIEBE, H.-J.

Overview on hot gas tests and molten salt corrosion experiments at the DLR p 953 N90-28714

RAFAELIANTS, A. A.

Aerodynamic interference of prismatic engine nacelles with the wing at supersonic velocities p 294 A90-24078

RAGAB, SAAD A.

Instabilities of supersonic shear flows
[AIAA PAPER 90-0712] p 314 A90-26983

RAGEN, M.

Endurance of aircraft gas turbine mainshaft ball bearings-analysis using improved fatigue life theory. II - Application to a bearing operating under difficult lubrication conditions p 128 A90-13845

Endurance of aircraft gas turbine mainshaft ball bearings-analysis using improved fatigue life theory. I - Application to a long-life bearing p 537 A90-33557

RAGHAVAN, V.

Calculations of the flow past bluff bodies, including tilt-rotor wing sections at $\alpha = 90^\circ$
[AIAA PAPER 90-0032] p 227 A90-22156

RAGHUNATHAN, S.

Further investigations of transonic shock-wave boundary-layer interaction with passive control p 159 A90-19390

Alleviation of shock oscillations in transonic flow by passive controls
[AIAA PAPER 90-0046] p 161 A90-19648

RAGHUNATHANA, S.

Wide angle diffusers with passive boundary-layer control
[AIAA PAPER 90-1600] p 567 A90-38732

RAGNI, JAMES E.

Scientific justification and development plan for a mid-sized jet research aircraft
[PB89-208995] p 103 N90-11731

RAGSDALE, WILLIAM C.

Condensation in hypersonic nitrogen wind tunnels
[AIAA PAPER 90-1392] p 558 A90-37937

RAGSDELL, K. M.

Multilevel optimization of large-scale structures in a parallel computing environment p 693 A90-39180

RAHIER, G.

Tests of an ultra-light tunnel in the anechoic wind tunnel facility CEPRA 19
[ONERA-RF-20/7294-PH] p 872 N90-27729

RAHLFS, DIETRICH

Status and potential of GPS-receiver development p 265 A90-21717

RAHMANI, S.

An objective methodology for definition and evaluation of advanced avionics architectures
[AIAA PAPER 89-3035] p 36 A90-10535

RAI, MAN MOHAN

A kinematical/numerical analysis of rotor-stator interaction noise
[AIAA PAPER 90-0281] p 219 A90-19770

Navier-Stokes analyses of the redistribution of inlet temperature distortions in a turbine p 471 A90-32959
Temporally and spatially resolved flow in a two-stage axial compressor. Part 2: Computational assessment
[NASA-TM-102273] p 194 N90-14236

RAILLY, J. W.

A theoretical and experimental investigation of the Reynolds and apparent stresses in axial compressors p 12 A90-12554

RAINBIRD, W. J.

Wave cancellation properties of a splitter-plate porous wall configuration p 57 A90-11005

RAJ, A. ARUL

Integrated approach to design and manufacture of gas turbine components based on group theory p 113 A90-16010

RAJ, S. V.

Observations on the brittle to ductile transition temperatures of B2 nickel aluminides with and without zirconium p 205 A90-19153

RAJAGOPAL, P.

Aeroelastic analysis of a low aspect ratio wing p 619 A90-38915

RAJASEKAR, R.

Wake-boundary layer interaction p 85 A90-15238
Development of bluff body wake in a longitudinally curved stream p 86 A90-15745
Interaction between boundary layer and wakes of different bodies p 602 A90-36263

RAJENDRA, G.

Sting-support interference on afterbody drag at transonic speeds
[NAL-TM-EA-8902] p 909 N90-28492

RAJU, B. BASAVA

Nondestructive measurement of residual stresses in aircraft transparencies
[AD-A218680] p 689 N90-23762

RAKOTO, P.

Turbulence statistics in a shock wave boundary layer interaction p 552 A90-35205

RALEY, PAUL

Automated helicopter structural analysis data processing p 611 A90-38533

RAMACHANDRA, K.

Photoelastic investigation of turbine rotor blade shrouds p 112 A90-16008

RAMACHANDRAN, K.

Rotor hover performance prediction using a free-wake, computational fluid dynamics method p 153 A90-17869

Free-wake analysis of compressible rotor flows p 302 A90-25283

The prediction of loads on the Boeing Helicopters Model 360 rotor p 410 A90-28240

The free-wake computation of rotor-body flows
[AIAA PAPER 90-1540] p 565 A90-38684

RAMAKRISHNAN, S. V.

Versatility of an algebraic backflow turbulence model
[AIAA PAPER 90-1485] p 563 A90-38639

Supersonic flow computations for an ASTOVL aircraft configuration
[AIAA PAPER 90-2997] p 787 A90-45847

RAMAKRISHNAN, SEKARIPURAM V.

Supersonic flow computations for an ASTOVL aircraft configuration, phase 2, part 2
[NASA-CR-4284] p 610 N90-22746

RAMAMOORTHY, P.

Analysis and design of symmetrical airfoils
[PD-CF-8943] p 400 N90-19213

Design of a natural laminar flow airfoil for an unmanned aircraft
[PD-CF-9004] p 499 N90-20975

Flight testing of a natural laminar flow airfoil using gliders
[PD-CF-9005] p 718 N90-25936

RAMAMURTHY, T. S.

Recent studies on the behaviour of interference fit pins in composite plates p 132 A90-16320

RAMAMURTI, V.

Stress analysis of gas turbine bladed disc for structural integrity applying the concept of cyclic symmetry p 46 A90-12564

RAMANATHAN, R.

On-line temperature profile display system
[ASME PAPER 89-GT-10] p 374 A90-23755

RAMANI, T. S.

Aeroelastic analysis of a low aspect ratio wing p 619 A90-38915

RAMAPRIAN, B. R.

An asymptotic theory for the periodic turbulent boundary layer in zero mean-pressure gradient
[AD-A222832] p 66 A90-10222

Visualization of the turbulent trailing vortex behind a finite wing in steady and unsteady flows p 712 A90-45260

RAMASWAMY, M. A.

Computation of flow over airfoils under high lift separated flow condition p 86 A90-15741

Adaptive wall wind tunnels - Marriage between experiments and computations p 351 A90-26351

RAMAVAJJALA, M. S.

Controlled mixing and variable geometry combustor design effects on emissions and combustion characteristics p 45 A90-12547

RAMAZANOV, M. P.

A study of boundary layer stability in the case of an increased incoming stream turbulence in gradient flows p 555 A90-36065

RAMBONE, JAMES D.

ILS (Instrument Landing System) mathematical modeling study on the effects of proposed hangar construction west of runway 18R on localizer performance at Dallas-Fort Worth International Airport
[AD-A210631] p 27 N90-10019

ILS mathematical modeling study of the effects of proposed hangar construction at the Orlando International Airport, Runway 17R, Orlando, Florida
[DOT/FAA/CT-TN89/52] p 121 N90-11762

RAMESH, K.

Modelling free vortex flow on planar swept wing p 810 A90-48079

RAMESH, R.

A framework for the optimal design of instructor/operator stations in flight simulators p 779 A90-45373

RAMETTE, P.

Progress in airbreathing combined engines for future European launcher p 344 N90-16817

RAMJEE, V.

Wake-boundary layer interaction p 85 A90-15238
Development of bluff body wake in a longitudinally curved stream p 86 A90-15745

Numerical prediction of wakes of different bodies p 308 A90-26341

Interaction between boundary layer and wakes of different bodies p 602 A90-36263

- RAMMOHAN, K.**
Development of a software package for automatic data acquisition, analysis, and controls in an axial flow compressor test rig [PD-PR-8910] p 965 N90-29926
- RAMSBOTTOM, R. W.**
Development of an automated ultrasonic inspection system for composite structure on in-service aircraft p 885 N90-28079
- RANAUDO, RICHARD J.**
Initial results from the joint NASA-Lewis/U.S. Army icing flight research tests p 400 A90-28180
NASA's program on icing research and technology p 239 N90-15062
- RAND, O.**
Theoretical modelling of composite rotating beams p 208 A90-17684
Periodic response of thin-walled composite blades p 408 A90-28229
- RANDALL, C. C.**
Fuel tank explosion protection p 251 N90-15914
- RANDAZZO, PHILIP**
Feasibility of using frequency offset on very high frequency air/ground voice channels [DOT/FAA/CT-TN89/71] p 542 N90-21248
- RANDAZZO, SANTO**
Fuel resistant coatings for metal and composite fuel tanks p 269 N90-15911
- RANDLETT, JILL B.**
Control outside of independent surveillance coverage operational concept [AD-A214163] p 243 N90-15090
- RANDRIAMAMPANINA, A.**
Numerical predictions for the flow and the heat transfer in gas turbine cooling systems p 770 A90-44464
Numerical investigations of heat transfer and flow rates in rotating cavities. Simulation of the movement generated by wall temperature gradients, by source-sink mass flows or by the differential rotation of the walls, under the influence of Coriolis and centrifugal forces [ETN-90-96253] p 454 N90-18695
- RANGARAJAN, NAGARAJAN**
Development of a microcomputer based software system for use in crewmember ejection analysis [AD-A220398] p 723 N90-25117
- RANGARAJAN, R.**
Full-potential calculations using Cartesian grids p 86 A90-15740
Computation of flow over airfoils under high lift separated flow condition p 86 A90-15741
- RANGWALLA, AKIL A.**
A kinematical/numerical analysis of rotor-stator interaction noise [AIAA PAPER 90-0281] p 219 A90-19770
- RANKIN, C. C.**
Bulging cracks in pressurized fuselages - A procedure for computation p 880 A90-46301
- RAO, A. K.**
Acoustic emission and signal analysis p 781 A90-43782
- RAO, DHANVADA M.**
Vortex control for tail buffet alleviation on a twin-tail fighter configuration [SAE PAPER 892221] p 756 A90-45438
- RAO, J. S.**
The design of rotor blades taking into account the combined effects of vibratory and thermal loads p 40 A90-11553
Resonant stress determination of a turbine blade with modal damping as a function of rotor speed and vibrational amplitude [ASME PAPER 89-GT-27] p 340 A90-23765
- RAO, K. N.**
Security audit for embedded avionics systems p 957 A90-50649
- RAO, K. V.**
Simulation and analysis of a delta planform with multiple jets in ground effect [AIAA PAPER 90-0299] p 228 A90-22195
Investigation of unsteady flow through transonic turbine stage. I - Analysis [AIAA PAPER 90-2408] p 626 A90-42161
Investigation of unsteady flow through a transonic turbine stage. II - Data/prediction comparison for time-averaged and phase-resolved pressure data [AIAA PAPER 90-2409] p 626 A90-42162
- RAO, KOGANTI MOHANA**
Buckling analysis of FRP faced cylindrical sandwich panel under combined loading p 365 A90-24376
- RAO, NAGABHUSHAN**
Real time data collection and control in a distributed simulator system using Ethernet TCP/IP [SAE PAPER 892356] p 761 A90-45507
- RAO, S. S.**
Multiobjective decision making in a fuzzy environment with applications to helicopter design p 405 A90-27993
- RAO, S. VITTAL**
LOG/LTR controller design using a reduced order model p 964 A90-52877
- RAO, T. V. S.**
Human centrifuge controller [NAL-TM-SE-8901] p 527 N90-21043
- RASH, CLARENCE E.**
Cockpit lighting compatibility with image intensification night imaging systems: Issues and answers [AD-A210503] p 32 N90-10028
- RASMUSSEN, BRUCE A.**
Critical inspection of high performance turbine engine components: The RFC concept p 859 N90-28073
- RASMUSSEN, PAUL G.**
The influence of adjacent seating configurations on egress through a type 3 emergency exit [AD-A218393] p 636 N90-23371
- RASMUSSEN, R. M.**
A program to improve aircraft icing forecasts [AIAA PAPER 90-0196] p 216 A90-19733
- RASSOKHIN, V. A.**
An experimental study of the gasdynamic characteristics of annular nozzle cascades with small flow exit angles p 255 A90-23409
- RATVASKY, THOMAS R.**
Aerodynamic parameters of High-Angle-of-attack Research Vehicle (HARV) estimated from flight data [NASA-TM-102692] p 936 N90-28578
- RAUCH, WILLIAM D.**
Telemetry systems of the future p 458 A90-28829
- RAUNTEBERG, M.**
Estimation of losses in semi-open centrifugal impellers p 537 A90-33597
- RAUSCH, RUSS D.**
Euler flutter analysis of airfoils using unstructured dynamic meshes p 602 A90-35760
- RAUTENBERG, M.**
Mathematical formulation of blade surfaces in turbomachinery. I - Theoretical surface formulations [ASME PAPER 89-GT-160] p 360 A90-23848
Mathematical formulation of blade surfaces in turbomachinery. II - Practical examples of determined surfaces [ASME PAPER 89-GT-161] p 361 A90-23849
- RAVEN, ELIZABETH A.**
A study of a propulsion control system for a VATOL aircraft (A direct design synthesis application) p 424 A90-30712
- RAVENHALL, R.**
Metal matrix composite fan blade development [AIAA PAPER 90-2178] p 677 A90-42062
- RAVICHANDRAN, K. S.**
Full-potential calculations using Cartesian grids p 86 A90-15740
- RAVICHANDRAN, S.**
A study of symbolic processing and computational aspects in helicopter dynamics p 545 A90-34103
- RAW, M. J.**
A colocated finite volume method for solving the Navier-Stokes equations for incompressible and compressible flows in turbomachinery - Results and applications p 703 A90-42659
- RAWLINSON, E. G.**
Measurement of mean and fluctuating flow properties in hypersonic shear layers [AIAA PAPER 90-1409] p 560 A90-38488
- RAWLS, JOHN W., JR.**
Near-field noise predictions of an aircraft in cruise p 140 N90-12538
- RAY, E. J.**
Sidewall boundary-layer removal and wall adaptation studies p 672 A90-40680
- RAY, EDWARD J.**
The NASA Langley 0.3-meter transonic cryogenic tunnel p 262 N90-15941
Safety and cryogenic wind tunnels p 264 N90-15960
CAST-10-2/DOA 2 Airfoil Studies Workshop Results [NASA-CP-3052] p 352 N90-17647
High Reynolds number tests of the CAST-10-2/DOA 2 transonic airfoil at ambient and cryogenic temperature conditions p 320 N90-17650
Experience with some repeat tests on the 9 inch chord CAST-10-2/DOA 2 airfoil model in the Langley 0.3-m TCT adaptive wall test section p 321 N90-17657
- RAY, LAURA RYAN**
Stochastic performance robustness of aircraft control systems [AIAA PAPER 90-3410] p 865 A90-47665
- RAY, RONALD J.**
Development of a real-time aeroperformance analysis technique for the X-29A advanced technical demonstrator p 732 A90-44738
Preliminary development of an intelligent computer assistant for engine monitoring [NASA-TM-101702] p 612 N90-22322
Evaluation of various thrust calculation techniques on an F404 engine [NASA-TP-3001] p 735 N90-25134
- RAYMER, DANIEL P.**
Aircraft design: A conceptual approach p 179 A90-17307
Supersonic STOVL - The future is now p 732 A90-44781
- RAYMOND, ROBERT E.**
Propulsion control system designs for advanced Navy multimission aircraft [AIAA PAPER 90-2403] p 663 A90-42160
- RAYNAL, J. C.**
Wind-tunnel test of the air intake of an unducted fan [AAAF PAPER NT 88-19] p 4 A90-11436
- RAZZAQ, ZIA**
Flexural fatigue life prediction of closed hat-section using materially nonlinear axial fatigue characteristics p 691 N90-25062
- RE, R.**
Experimental evaluation of expendable supersonic nozzle concepts [AIAA PAPER 90-1904] p 740 A90-42691
- REA, CAROL**
In-flight evaluations of turbine fuel extenders [DOT/FAA/CT-89/33] p 444 N90-19387
- READER, KENNETH R.**
An unmanned air vehicle concept with tipjet drive p 830 A90-46951
- REAGAN, P. V.**
Research on a two-dimensional inlet for a supersonic V/STOL propulsion system. Appendix A [NASA-CR-174945] p 396 N90-18364
- REAGO, DONALD**
Helicopter obstacle avoidance system - The use of manned simulation to evaluate the contribution of key design parameters p 417 A90-28218
- READON, FREDERICK H.**
Heat Transfer and Fluid Mechanics Institute, 31st, California State University, Sacramento, June 1, 2, 1989, Proceedings p 130 A90-15387
Very-low-frequency oscillations in liquid-fueled ramjets p 54 N90-10204
Calculation of the combustion distribution in a liquid-fuel ramjet p 858 N90-27931
- REBBECCHI, BRIAN**
Aircraft engine vibration analysis p 46 A90-12568
- RECKER, H. G.**
Highly damage tolerant carbon fiber epoxy composites for primary aircraft structural applications p 125 A90-14660
Toughened thermosets for damage tolerant carbon fiber reinforced composites p 443 A90-29825
Rigidite 5255-3 - A highly damage tolerant prepreg resin system with a well balanced property profile p 944 A90-50139
- RECTOR, J. D.**
Domestic precursor technology - A unique route to current and future generation carbon fibers p 940 A90-50057
- REDA, D. C.**
Liquid crystal coatings for surface shear stress visualization in hypersonic flows [AIAA PAPER 90-1513] p 563 A90-38660
- REDDINGIUS, NICOLAAS H.**
Assessment System for Aircraft Noise (ASAN): Development of alpha-test prototype system software [AD-A223770] p 966 N90-30036
- REDDINGIUS, NICOLAAS**
Noise and sonic boom impact technology. Initial development of an Assessment System for Aircraft Noise (ASAN). Volume 1: Executive summary [AD-A214164] p 379 N90-17410
Noise and sonic boom impact technology. Initial development of an Assessment System for Aircraft Noise (ASAN). Volume 2: System design strategy [AD-A214454] p 379 N90-17411
Noise and sonic boom impact technology. Initial development of an Assessment System for Aircraft Noise (ASAN). Volume 3: Technical description [AD-A214455] p 379 N90-17412
Assessment System for Aircraft Noise (ASAN) citation database. Volume 1: User's manual [AD-A219175] p 615 N90-23188
Assessment System for Aircraft Noise (ASAN) citation database. Volume 2: Database update manual [AD-A219176] p 615 N90-23189

- Assessment System for Aircraft Noise (ASAN) citation database. Volume 3: New citation review procedures [AD-A219177] p 615 N90-23190
- REDDY, C. SUBBA**
Accumulated span loadings of an arrow wing having vortex flow p 17 A90-13025
- REDDY, D. R.**
Comparison of 3-D viscous flow computations of Mach 5 inlet with experimental data [AIAA PAPER 90-0600] p 314 A90-26970
Viscous three-dimensional analyses for nozzles for hypersonic propulsion p 344 N90-17635
Comparison of 3-D viscous flow computations of Mach 5 inlet with experimental data [NASA-TM-102518] p 510 N90-20090
- REDDY, K. C.**
A locally implicit scheme for 3-D compressible viscous flows [AIAA PAPER 90-1525] p 563 A90-38670
- REDDY, MAHESH**
Fault tolerant architecture for a fly-by-light flight control computer p 860 A90-46931
- REDDY, N. M.**
Viscous flow characteristics over a blunt cone at hypersonic Mach numbers by using a PNS code p 810 A90-48085
- REDDY, N. N.**
Propfan Test Assessment (PTA): Flight test report [NASA-CR-182278] p 113 N90-11738
- REDDY, T. S. R.**
Application of an efficient hybrid scheme for aeroelastic analysis of advanced propellers [AIAA PAPER 90-0028] p 226 A90-22153
Time domain flutter analysis of cascades using a full-potential solver [AIAA PAPER 90-0984] p 391 A90-29374
A study of symbolic processing and computational aspects in helicopter dynamics p 545 A90-34103
Application of an efficient hybrid scheme for aeroelastic analysis of advanced propellers [NASA-TM-102428] p 172 N90-13355
Numerical simulations of supersonic flow through oscillating cascade sections [NASA-TM-103100] p 478 N90-20051
- REDEKER, G.**
Flight and wind-tunnel investigations on boundary-layer transition p 233 A90-23283
Design for a natural laminar flow glove for a transport aircraft [AIAA PAPER 90-3043] p 792 A90-45880
Flight tests with a natural laminar flow glove on a transport aircraft [AIAA PAPER 90-3044] p 828 A90-45881
Development of transition criteria on the basis of e to the N power for three dimensional wing boundary layers p 277 N90-16179
- REDEKOPP, L. G.**
Nonlinear stability of subsonic mixing layers with symmetric temperature variations p 223 A90-20501
- REDINOTIS, O. K.**
Vortex shedding over delta wings p 470 A90-32479
- REED, HELEN**
Supersonic/hypersonic laminar/turbulent transition p 706 A90-42872
- REED, HELEN L.**
Stability limits for three-dimensional supersonic boundary layers [AIAA PAPER 90-1528] p 564 A90-38673
A method to determine the performance of low-Reynolds-number airfoils under off-design unsteady freestream conditions p 801 A90-46375
Stability and transition of three-dimensional boundary layers p 71 N90-10357
Navier-Stokes simulation of the crossflow instability in swept-wing flows [NASA-CR-186122] p 212 N90-13744
- REED, J. R.**
Analytical and experimental study of runway runoff with wind effects [PTI-8948] p 123 N90-12627
- REED, L. H. K.**
A full scale, VSTOL, ground environment test facility p 58 A90-12631
- REED, LEO H. K.**
Operation of the Rolls-Royce Pegasus Engine on low grade non-aviation fuels [SAE PAPER 892329] p 747 A90-45486
- REEDER, M. F.**
Pressure-based real-time measurements in compressible free shear layers [AIAA PAPER 90-1980] p 703 A90-42709
- REEDY, S. W.**
Advanced analysis of multi-ring liquid seals p 880 A90-46236

- REEDY, STEVEN W.**
Analysis of thermal gradient effects in oil ring seals p 682 A90-40716
- REENT, K. S.**
Two- and three-dimensional problems of unsteady aerodynamics of low loaded turbomachinery blade rows stages p 813 A90-49452
- REESE, WILHELM**
Procedure for calibrating fly-by-wire control chains of the flying testbed ATTAS [DLR-MITT-90-02] p 936 N90-29401
- REGENIE, VICTORIA A.**
Validation of the F-18 high alpha research vehicle flight control and avionics systems modifications [NASA-TM-101723] p 924 N90-28542
- REHMERT, HEINRICH**
Differential GPS (DGPS) as an approach and landing aid p 242 A90-21722
- REICH, G.**
Thermal protection systems for hypersonic transport vehicles [SAE PAPER 901306] p 882 A90-49358
- REICH, STANLEY**
The impact of fiber optics (photonics) on future aircraft p 504 A90-32863
- REICHERT, G.**
Optimization of helicopter takeoff and landing p 29 A90-11006
Influence of ground effect on helicopter takeoff and landing performance p 645 A90-42278
Helicopter ground and air resonance dynamics p 646 A90-42457
Influence of ground effect on helicopter takeoff and landing performance p 646 A90-42468
- REICHMUTH, J.**
On the structure of a future flight operations system p 826 N90-27682
- REID, ALEXANDER A.**
User's manual for the ride motion simulator [AD-A212855] p 201 N90-13402
- REID, LLOYD D.**
Simulator motion-drive algorithms - A designer's perspective p 375 A90-25997
Augmenting flight simulator motion response to turbulence p 440 A90-31279
Modeling of turbulence and downbursts for flight simulators p 870 A90-48956
- REILLY, THOMAS G.**
V-22 engine installation and removal tool - Designing support equipment with the aircraft, not after p 581 A90-38538
- REINA, FILIPPO**
EH101 design and development status p 407 A90-28211
- REINMANN, JOHN J.**
NASA's program on icing research and technology p 239 N90-15062
- REISING, JOHN M.**
Toward the panoramic cockpit, and 3-D cockpit displays p 419 A90-30682
- REISINGER, L.**
Production of Ti6Al4V-components for a new turbo-lan-engine p 132 A90-16618
- REK, BRON**
Caring for the elderly jet p 285 A90-24280
- REKSTIN, FELIKS S.**
Vortex-flow compressors p 69 A90-12479
- REMANDET, J.-N.**
New rotor test rig in the large Modane wind tunnel [ONERA, TP NO. 1989-137] p 58 A90-11159
- REMEEV, N. KH.**
Numerical solution of the problem of supersonic flow of an ideal gas past a trapezoidal wedge p 386 A90-28980
- REMONDI, BENJAMIN W.**
Kinematic and pseudo-kinematic GPS p 96 A90-13980
- REMY, L.**
An oxidation fatigue interaction damage model for thermal fatigue crack growth p 62 A90-11539
- REN, DA**
Investigation of a nonlinear Kalman filter for estimating aircraft state variables p 195 A90-16850
- REN, RUGEN**
An experimental study of tip clearance effects on the performance of an axial transonic turbine p 189 A90-17788
- REN, XINGMIN**
Gear vibration control with viscoelastic damping material in aeroengine p 451 A90-29911
- RENAUD, JEAN**
Advocating international cooperation: The Eurofar program - An example and a hope p 785 A90-46929
- RENAUDIE, J. F.**
Flight in adverse environmental conditions [AGARD-AR-277] p 185 N90-14218

- RENDIGS, K. H.**
Investigation on sheet material of 8090 and 2091 aluminium-lithium alloy p 267 N90-15192
- RENDIGS, KARL HEINZ**
Investigation on sheet material of 8090 and 2091 aluminium-lithium alloy [MBB-UT-122/89-PUB] p 766 N90-25090
- RENEAUX, J.**
Design and experimental investigation of a laminar horizontal tail [AIAA PAPER 90-3042] p 798 A90-45934
The use of numerical optimization for helicopter airfoil and blade design p 502 N90-20995
Numerical optimization of wings in transonic flow p 502 N90-20997
- RENIE, J. P.**
Investigation of supersonic mixing layers p 623 A90-40926
- RENKO, KARI**
Subsonic flutter analysis using MSC/NASTRAN [PB90-166786] p 522 N90-21041
- RENN, JAMES P.**
Improvements to the fatigue substantiation of the H-60 composite tail rotor blade p 642 A90-39985
- RENNER, A.**
Improved thermal performance using allyladiac-imides p 946 A90-50175
- RENO, CHARLES**
Interactive grid generation for turbomachinery flow field simulations p 312 A90-26553
- RENOUARD**
Electronic cartography - A new need for commercial aircraft p 576 A90-35351
- RENTON, MARGARET B.**
Rotorcraft low altitude CNS benefit/cost analysis: Rotorcraft operations data [DOT/FAA/DS-89/9] p 141 N90-12406
- RENZONI, P.**
Airfoil pressure measurements during a blade vortex interaction and a comparison with theory p 232 A90-23105
- REPACHOLI, N.**
The performance of a small combustor operated over a wide range of conditions p 45 A90-12548
- REPIK, E. U.**
Optimal conditions of flow turbulence suppression in the working section of a wind tunnel using screens located in the prechamber p 438 A90-29185
- RESHOTKO, ELI**
Interactive calculation procedures for mixed compression inlets [NASA-CR-186581] p 718 N90-25934
- RESNIK, C.**
Dynamic simulation of cross-shafted propulsion system for tilt nacelle application [AIAA PAPER 90-0439] p 191 A90-19847
- RESSIN, A. A.**
Estimation of the efficiency of various operational modes of a navigation complex p 725 A90-42924
- RESTALL, J. E.**
Properties and characterisation of novel thermal barrier systems for gas turbines p 62 A90-12538
- RESTIVO, A.**
Computer controlled test bench for axial turbines and propellers p 437 A90-28288
- REUBUSH, DAVID E.**
Pressure and heat-transfer investigation of a hypersonic configuration p 598 A90-35757
- REUSS, R. L.**
A hypersonic research vehicle to develop scramjet engines [AIAA PAPER 90-3232] p 839 A90-49115
- REUTHER, J.**
Subsonic and transonic low-Reynolds-number airfoils with reduced pitching moments [AIAA PAPER 90-3212] p 812 A90-48838
- REVELL, JOHN**
The EH101 electronic instrument system p 652 A90-40462
- REYHNER, T. A.**
Analytical methods for subsonic propulsion system integration p 29 A90-12613
- REYNOLDS, D. J.**
Harrier Information Management System (HIMS): The system and the approach p 884 A90-27630
- REYNOLDS, MICHAEL**
Operational evaluation of initial data link air traffic control services, volume 1 [DOT/FAA/CT-90/1-VOL-1] p 455 N90-19472
- REYNOLDS, MICHAEL C.**
Flight simulator evaluation of a dot-matrix display for presentation of approach map formats p 419 A90-30787
- REYNOLDS, PETE**
Ten years of stall testing [AIAA PAPER 90-1268] p 518 A90-33895

- REYNOLDS, W. C.**
Turbulent reacting flows and supersonic combustion
[AD-A221793] p 875 N90-26933
- REYNOLDS, WILLIAM C.**
The instability of two-dimensional laminar separation
p 800 A90-46365
- REZAI-ARIA, F.**
An oxidation fatigue interaction damage model for thermal fatigue crack growth p 62 A90-11539
- REZAI, K.**
Review of modelling methods to take account of material structure and defects p 425 N90-18402
Life management planning p 856 N90-27709
- REZNICHENKO, N. P.**
Transfer of the atomic ion energy of supersonic flow of a partially dissociated gas to a solid surface
p 234 A90-23432
- RHEA, JOHN**
The airborne supercomputer p 538 A90-33775
- RHEAUME, F.**
The performance of a small combustor operated over a wide range of conditions p 45 A90-12548
- RHEE, KENNETH J.**
A comparison of emergency medical helicopter accident rates in the United States and the Federal Republic of Germany p 722 A90-44640
- RHEW, RAY D.**
A fatigue study of electrical discharge machine (EDM) strain-gage balance materials p 448 A90-28295
- RHIE, CHAE M.**
Critical evaluation of three-dimensional supersonic combustor calculations
[AIAA PAPER 90-0207] p 272 A90-22265
Calculation of internal flows using a single-pass, parabolized Navier-Stokes analysis p 469 A90-32458
Computation of flow through a centrifugal impeller with tip leakage
[AIAA PAPER 90-2021] p 684 A90-41987
- RHODE, D. L.**
Tooth thickness effects on the performance of gas labyrinth seals p 771 A90-45300
- RHODE, MATTHEW N.**
Water-tunnel investigation of concepts for alleviation of adverse inlet spillage interactions with external stores
[NASA-TM-4181] p 398 N90-19199
- RHODEHAMEL, HARLEY**
Autonomous integrated GPS/INS navigation experiment for OMV. Phase 1: Feasibility study
[NASA-CR-4267] p 489 N90-20969
- RHODES, ALAN**
Technology update of early gas turbine designs
p 586 A90-38531
- RHODES, GRAHAM SCOTT**
Low-speed wind tunnel investigation of the static stability and control characteristics of an advanced turboprop configuration with the propellers placed over the tail
[NASA-CR-186900] p 759 N90-26017
- RHODES, J.**
Experimental study on the buckling and postbuckling of carbon fibre composite panels with and without interply disbonds p 130 A90-15355
- RHODES, J. A.**
Comparison of inviscid and viscous separated flows
p 302 A90-25277
- RHODES, R. P.**
Performance potential and technology issues of MHD augmented hypersonic simulation facilities
[AIAA PAPER 90-1380] p 598 A90-37929
- RHODES, TOM**
History of the airframe. IV p 30 A90-12791
- RIABOV, V. V.**
A study of flow of a vibrationally nonequilibrium dissociated gas past a blunt body p 234 A90-23435
- RIAPOSOV, V. B.**
Operation of a gas ejector in the pulsed regime
p 850 A90-46488
- RIBAUD, Y.**
Inverse cycle engine for hypersonic air-breathing propulsion
[ONERA, TP NO. 1989-121] p 50 A90-12611
- RICCARDELLA, PETER C.**
Stress intensity factors for cracking metal structures under rapid thermal loading. Volume 2: Theoretical background
[AD-A213297] p 213 N90-13812
- RICE, D.**
In-situ measurement, modelling and control of the imidization reaction in PMR-15 p 941 A90-50066
- RICE, EDWARD J.**
Control of flow separation and mixing by aerodynamic excitation
[NASA-TM-103131] p 571 N90-21733
- RICHARDS, DALE W.**
Intelligent built-in test and stress management
p 448 A90-28343
- RICHARDS, MARVIN KENT**
Operational effects on crashworthy seat attenuators
[AD-A221148] p 637 N90-24259
- RICHARDS, P. G.**
Extending the overhaul interval for gas turbine engines through the use of alternative coatings on first stage blades p 63 A90-12539
- RICHARDSON, DOUG**
Stealth - Deception, evasion, and concealment in the air p 285 A90-24265
- RICHARDSON, MARTIN D.**
Spray sealing: A breakthrough in integral fuel tank sealing technology p 276 N90-15912
A dynamicist's view of fuel tank skin durability p 251 N90-15915
Integral fuel tank certification and test methods p 251 N90-15916
- RICHARDSON, MICHAEL**
NASA/USRA high altitude reconnaissance aircraft
[NASA-CR-186685] p 650 N90-24266
- RICHARDSON, PAMELA F.**
Comparison between experimental and numerical results for a research hypersonic aircraft
p 395 A90-31278
Hypersonic CFD applications for the National Aero-Space Plane
[SAE PAPER 892310] p 714 A90-45473
- RICHARDSON, SCOTT M.**
Analysis of unsteady rotor-stator interactions using a viscous explicit method
[AIAA PAPER 90-0342] p 313 A90-26937
- RICHIE, JOSEPH**
Replication of NASPAC Dallas/Fort Worth study
[DOT/FAA/CT-TN90/26] p 729 N90-25123
- RICHMOND, M.**
Moisture absorption in graphite/epoxy laminates
p 951 A90-52799
- RICHTER, EIKE**
Application considerations for integral gas turbine electric starter/generator revisited
[SAE PAPER 892252] p 746 A90-45454
- RICHTER, G. P.**
Background, current status, and prognosis of the ongoing slush hydrogen technology development program for the NASP
[NASA-TM-103220] p 763 N90-26055
- RICHTER, G. PAUL**
Slush Hydrogen (SLH2) technology development for application to the National Aerospace Plane (NASP)
[NASA-TM-102315] p 203 N90-14268
- RICHTER, STEPHEN**
Integrated control-system design via generalized LQG (GLQG) theory p 613 N90-23023
- RICHWINE, DAVID M.**
In-flight flow visualization characteristics of the NASA F-18 high alpha research vehicle at high angles of attack
[SAE PAPER 892222] p 713 A90-45439
F-18 high alpha research vehicle surface pressures - Initial in-flight results and correlation with flow visualization and wind-tunnel data
[AIAA PAPER 90-3018] p 792 A90-45885
A smoke generator system for aerodynamic flight research
[NASA-TM-4137] p 183 N90-13372
- RICKETTS, RODNEY H.**
Experimental aeroelasticity - History, status and future in brief
[AIAA PAPER 90-0978] p 382 A90-29598
Experimental aeroelasticity history, status and future in brief
[NASA-TM-102651] p 527 N90-21047
- RICKLEY, E. J.**
En route noise: NASA proplan test aircraft (corrected data - simplified procedure)
[DOT-TSC-FA953-LR4] p 696 N90-24856
En route noise: NASA proplan test aircraft (calculated source noise)
[DOT-TSC-FA953-LR5] p 697 N90-24857
- RICKS, WENDELL R.**
Knowledge-based system for flight information management
[NASA-TM-102685] p 780 N90-26511
- RIDER, C. D.**
Flutter investigations on a Transavia PL12/T-400 aircraft
[AD-A219108] p 593 N90-22570
- RIEDELBAUCH, S.**
Numerical simulation of hypersonic viscous continuum flow p 707 A90-44407
- RIEGER, HERBERT**
Aerodynamic work for Hermes spaceplane
p 675 A90-41115
- RIESCO-CHUECA, P.**
Brownian motion far from equilibrium - A hypersonic approach p 555 A90-35917
- RIESTER, JOHN E., JR.**
A device for introducing helical perturbations into a trailing line vortex
[AIAA PAPER 90-1627] p 568 A90-38756
- RIFFEL, R. E.**
The GMA 2100 and GMA 3007 engines for regional aircraft
[AIAA PAPER 90-2523] p 744 A90-42815
- RIGAL, J.-F.**
Preliminary design and load distributions of high performance mechanical systems p 771 A90-45281
- RIGBY, M. J.**
Temperature scaling of turbine blade heat transfer with and without shock wave passing p 47 A90-12570
- RIGGINS, D. W.**
A numerical study of mixing enhancement in a supersonic combustor
[AIAA PAPER 90-0203] p 272 A90-22182
- RIGGINS, DAVID W.**
A computational investigation of flow losses in a supersonic combustor
[AIAA PAPER 90-2093] p 742 A90-42728
Supersonic combustor modeling p 749 N90-25992
- RIHA, BOHUSLAV**
The fast-response requirement of powerplant thrust in the set of engineering and economic criteria of an aircraft p 254 A90-23354
- RIKS, E.**
Bulging cracks in pressurized fuselages - A procedure for computation p 880 A90-46301
- RILEY, CHRISTOPHER J.**
An approximate method for calculating three-dimensional inviscid hypersonic flow fields
[NASA-TP-3018] p 883 N90-27066
- RILEY, D. R.**
Unified flying qualities criteria for longitudinal tracking
[AIAA PAPER 90-2806] p 752 A90-45141
- RILEY, DAVID R.**
High angle of attack flying qualities criteria
[AIAA PAPER 90-0219] p 197 A90-19738
Development of high angle of attack flying qualities criteria using ground-based manned simulators
p 433 A90-30717
An experimental investigation of roll agility in air-to-air combat
[AIAA PAPER 90-2809] p 752 A90-45144
- RILEY, DONALD R.**
Low-speed wind-tunnel study of reaction control-jet effectiveness for hover and transition of a STOVL fighter concept
[NASA-TM-4147] p 119 N90-11751
- RILEY, JAMES J.**
Numerical simulation of confined, spatially-developing mixing layers - Comparison to the temporal shear layer
[AIAA PAPER 90-1462] p 562 A90-38619
- RILEY, JOHN**
Estimation of rotor blade incidence and blade deformation from the measurement of pressures and strains in flight p 647 A90-42497
- RILEY, M. J.**
Correlation of Puma airloads: Lifting-line and wake calculation
[NASA-TM-102212] p 170 N90-13327
- RILEY, MICHAEL F.**
Application of formal optimization techniques in thermal/structural design of a heat-pipe-cooled panel for a hypersonic vehicle
[NASA-TM-89131] p 72 N90-10409
- RILEY, S. J.**
An investigation into the internal heat transfer characteristics of a thermally anti-iced aero-engine intake lipskin p 111 A90-15390
- RINK, K. K.**
Influence of fuel drop size and combustor operating conditions on pollutant emissions p 508 A90-33591
- RIOCHE, S.**
Main characteristics of an integrated flight and display system for AS MKII Super-Puma p 653 A90-42450
- RIPPI, M.**
Recent results of numerical flutter studies in high performance gliders
[DGLR PAPER 88-038] p 934 A90-50249
- RISH, EDWARD C.**
An analysis of GPS as the sole means navigation system in US Navy aircraft p 917 N90-29350
- RISSMAN, MICHAEL S.**
An object-oriented solution example: A flight simulator electrical system
[AD-A219190] p 761 N90-25145
- RISSMILLER, RALPH W., JR.**
Microwave landing system - A pilot's point of view
p 640 A90-41712
- RISTIC, M.**
A computer integrated approach to dimensional inspection
[PNR90596] p 116 N90-12611

RITTER, CHARLES

The impact of fiber optics (photonics) on future aircraft
p 504 A90-32863

RIVERA, JOE

X-29A aircraft structural loads flight testing
[NASA-TM-101715] p 416 N90-19225

RIVERA, JOSE A., JR.

A vapor generator for transonic flow visualization
[NASA-TM-101670] p 201 N90-13403
An experimental study of tip shape effects on the flutter
of aft-swept, flat-plate wings
[NASA-TM-4180] p 582 N90-22555

RIVET, G.

Model attitude measurement system
p 539 A90-34235

RIVETT, PAUL

High performance single-mode coupler for harsh
environments p 78 A90-11027

RIVLIN, R.

Simulation of helicopter landing on a ship deck
p 181 A90-17705

RIZK, M. H.

Aerodynamic optimization by simultaneously updating
flow variables and design parameters
p 501 N90-20991

RIZK, N. K.

Further validation of a semi-analytical approach for fuel
injectors of different concepts
[AIAA PAPER 90-2190] p 686 A90-42067

RIZK, YEHIA M.

Navier-Stokes predictions of the flowfield around the
F-18 (HARV) wing and fuselage at large incidence
[AIAA PAPER 90-0099] p 227 A90-22165
Numerical simulation of the viscous flow around a
simplified F/A-18 at high angles of attack
[AIAA PAPER 90-2999] p 787 A90-45849

RIZKALLA, OUSSAMA

Calculated chemical and vibrational nonequilibrium
effects in hypersonic nozzles p 253 A90-21224

RIZZETTA, D. P.

Results from a numerical simulation of an F-16A
configuration at a supersonic Mach number
p 146 A90-16769

RIZZI, A. W.

Development of supersonic and hypersonic Euler
solvers using shock fitting in two and three dimensions
p 707 A90-44426

RIZZI, ARTHUR

Numerical methods to solve the incompressible Euler
and Navier-Stokes equations in 3D with applications
p 209 A90-18302
Computations of hypersonic flow by finite-volume
methods p 224 A90-21168

ROACH, J. M.

Nonflammable hydraulic power system for tactical
aircraft. Volume 1: Aircraft system definition, design and
analysis
[AD-A218493] p 671 N90-23409

ROACH, W. RONALD

Polysilicon active-matrix liquid crystal displays for cockpit
applications p 481 A90-40393

ROACHE, PATRICK J.

The influence of sweep on dynamic stall produced by
a rapidly pitching wing
[AIAA PAPER 90-0581] p 230 A90-22231

ROBBINS, LIONEL

8 x 8-inch full color cockpit display
p 927 A90-52953

ROBBINS, ROBERT D.

Preliminary airworthiness evaluation of the RC-12K
[AD-A219545] p 648 N90-23387

ROBELEN, DAVID B.

Wind-tunnel and flight-test investigation of the exdrone
remotely piloted vehicle configuration
[AIAA PAPER 90-1261] p 494 A90-33891
Static wind-tunnel and radio-controlled flight test
investigation of a remotely piloted vehicle having a delta
wing planform
[NASA-TM-4200] p 632 N90-24238

ROBERT, MICHEL

Casting factors imposed by the French regulation for
foundry castings used in military aircraft
p 64 N90-10233

ROBERTS, A. SIDNEY, JR.

Infrared imaging and tufts studies of boundary layer flow
regimes on a NACA 0012 airfoil p 446 A90-28268

ROBERTS, BRADFORD J.

Maneuver performance comparison between the XV-15
and an advanced tiltrotor design p 518 A90-33622

ROBERTS, C. J.

A practical co-axial twin rotor model
p 335 A90-25423

ROBERTS, JACK C.

Redesign of an electro-optical shroud in
graphite/epoxy p 676 A90-40215

ROBERTS, L.

Control of asymmetric vortical flows over delta wings
at high angles of attack p 553 A90-35759
Control of vortex aerodynamics at high angles of
attack p 921 N90-28523

ROBERTS, LARRY A.

KC-135R low altitude air refueling flight test program
[AIAA PAPER 90-1265] p 494 A90-33893

ROBERTS, LEONARD

An investigation of asymmetric vortical flows over delta
wings with tangential leading-edge blowing at high angles
of attack
[AIAA PAPER 90-0103] p 227 A90-22167
A CFD study of tilt rotor flowfields
[NASA-CR-186116] p 171 N90-13349
Controlled vortical flow on delta wings through unsteady
leading edge blowing
[NASA-CR-186267] p 316 N90-16712
Transpiration cooling in hypersonic flight
[NASA-CR-186435] p 478 N90-20052

ROBERTS, PAUL W.

Development of a dual strain gage balance system for
measuring light loads p 437 A90-28289

ROBERTSON, DAVID D.

An integrated CFD/experimental analysis of
aerodynamic forces and moments
[NASA-TM-102195] p 18 N90-10006

ROBERTSON, S. H.

Aircraft crash survival design guide. Volume 5: Aircraft
postcrash survival
[AD-A218438] p 575 N90-22549

ROBINSON, BRIAN A.

Aeroelastic analysis of wings using the Euler equations
with a deforming mesh
[AIAA PAPER 90-1032] p 391 A90-29376

ROBINSON, C. J.

Measurement and calculation of the three-dimensional
flow in axial compressor stators, with and without
end-bends
[ASME PAPER 89-GT-6] p 287 A90-23753

ROBINSON, LAWSON H.

A study of fundamental issues in higher harmonic control
using aeroelastic simulation p 861 A90-46966

ROBINSON, LAWSON HAYES

Aeroelastic simulation of higher harmonic control
p 592 N90-21768

ROBINSON, MARTHA P.

Analysis of the National Transonic Facility mishap
[NASA-TM-101686] p 328 N90-17620

ROBINSON, MICHAEL C.

Unsteady aerodynamic loading produced by a
sinusoidally oscillating delta wing
[AIAA PAPER 90-1536] p 564 A90-38680

ROBINSON, P. H.

Experimental investigation into the effects of rotating
and static bolts on both windage heating and local heat
transfer coefficients in a rotor/stator cavity
[ASME PAPER 89-GT-196] p 362 A90-23870

ROBINSON, PAUL A.

Augmenting flight simulator motion response to
turbulence p 440 A90-31279
Modeling of turbulence and downbursts for flight
simulators p 870 A90-48956

ROBINSON, PETER J.

The influence of weather on flight operations at the
Atlanta Hartsfield International Airport p 279 A90-22688

ROBINSON, RANDY L.

Robustness evaluation of H2 and H(infinity) control
theory as applied to a transport aircraft
[AD-A222795] p 759 N90-26018

ROCK, J. L.

Modern strapdown system for helicopter
p 653 A90-42451

ROCKWELL, D.

Transient response of leading-edge vortices to localized
suction p 556 A90-36279
Flow visualization via laser-induced reflection from
bubble sheets p 680 A90-39784

ROCKWELL, DONALD

Leading-edge vortices due to low Reynolds number flow
past a pitching delta wing p 555 A90-36258
Flow structure generated by oscillating delta-wing
segments p 622 A90-40694

ROCKWELL, R. K.

Electrical analog circuit for heat transfer measurements
on a flat plate simulating turbine vane heat transfer in
turbulent flow
[AIAA PAPER 90-2412] p 687 A90-42164

ROCKWELL, THOMAS H.

General aviation pilot error in computer simulated
adverse weather scenarios p 322 A90-26254

RODDIGER, HENRY A.

Interstitial materials for low thermal resistance joints in
avionic equipment
[SAE PAPER 891441] p 356 A90-27412

RODELLAR, R.

Pressure surface trailing edge slot cooling
[ONERA, TP NO. 1989-123] p 47 A90-12569

RODGERS, C.

Review of mixed flow and radial turbine options
[AIAA PAPER 90-2414] p 687 A90-42166

RODGERS, COLIN

Fast start ceramic auxiliary power unit
[SAE PAPER 892254] p 747 A90-45456

RODI, ALFRED R.

The microphysical structure of severe downdrafts from
radar and aircraft observations in CINDE
p 455 A90-28582

RODI, PATRICK E.

Hyperbolic grid generation techniques for blunt body
configurations p 376 A90-26490

RODMAN, LAURA C.

A characterization and search technique for unsteady
flow control problems
[AIAA PAPER 90-3102] p 796 A90-45914
A study of supermaneuver aerodynamics
[AD-A218378] p 631 N90-23349

RODRIGUES, M. A.

Temperature insensitive fiber coil sensor for altimeters
p 339 A90-26374

RODRIGUES, A. H.

Computer controlled test bench for axial turbines and
propellers p 437 A90-28288

RODRIGUES, E. A.

Whirl flutter stability of a pusher configuration subject
to a nonuniform flow
[AIAA PAPER 90-1162] p 393 A90-29397

RODRIGUESPACHECO, RICARDO

The potential for an extra runway at Heathrow: A
preliminary feasibility study
[TT-9007] p 938 N90-29403

RODRIGUEZ LENCE, F.

Design and fabrication of the carbon fiber/epoxy A-320
horizontal tailplane p 286 A90-25221

RODRIGUEZ, C. G.

Flow over inclined finite length and width flat plates at
low and high Reynolds numbers
[AIAA PAPER 90-1467] p 562 A90-38624

RODRIGUEZ, E. S., III

Planet gear sleeve spinning analysis
[AIAA PAPER 90-2154] p 681 A90-40613

RODRIGUEZ, KATHLEEN M.

Experimental studies of shock wave/wall jet interaction
in hypersonic flow
[AIAA PAPER 90-0607] p 231 A90-22449

RODRIGUEZ, O.

Reduction of profile drag by modifying the structure next
to the wake area
[IMFL-88/35] p 172 N90-13356

ROELKE, RICHARD J.

Design of an air-cooled metallic high-temperature radial
turbine p 507 A90-32960

ROEMER, MICHAEL J.

Improved noise rejection in automatic carrier landing
systems
[AIAA PAPER 90-3374] p 864 A90-47632

ROEPCKE, FRANK

ILS - Past and present p 639 A90-41706

ROGAN, J. E.

Taguchi methods in conceptual design for life cycle
cost
[AIAA PAPER 90-3222] p 839 A90-49109
A efficient technique for multiobjective design
optimization
[AIAA PAPER 90-3291] p 892 A90-49123

ROGAN, WILLIAM

AVION: A detailed report on the preliminary design of
a 79-passenger, high-efficiency, commercial transport
aircraft
[NASA-CR-186663] p 649 N90-23395

ROGE, G.

Development of finite element methods for compressible
Navier-Stokes flow simulations in aerospace design
[AIAA PAPER 90-0403] p 166 A90-19833

ROGER, MICHEL

Prediction of the interaction noise emitted by helicopter
fenestrons p 218 A90-18449

ROGER, R. H.

Flow and heat transfer in rotating-disc systems. Volume
I - Rotor-stator systems p 772 A90-45759

ROGERS, E. W. E.

The aims and history of adaptive wall wind tunnels
p 871 N90-26839

ROGERS, ERNEST O.

An unmanned air vehicle concept with tipjet drive
p 830 A90-46951

ROGERS, J. D.

The remote sensing of temperature in gas turbine engine
components using epithermal neutrons p 70 A90-12630

- Helicopter flight vibration of large transportation containers: A case for testing tailoring [DE90-007429] p 402 N90-19215
- ROGERS, JONATHAN D.**
Sandia National Laboratories' new high level acoustic test facility [DE90-006810] p 464 N90-19820
- ROGERS, LAWRENCE W.**
Pneumatic vortex flow control on a 55-degree cropped delta wing with chined forebody [AIAA PAPER 90-1430] p 559 A90-37967
Canard-wing vortex interactions at subsonic through supersonic speeds [AIAA PAPER 90-2814] p 711 A90-45154
Multiple vortex and shock interactions at subsonic, transonic, and supersonic speeds [AIAA PAPER 90-3023] p 793 A90-45890
- ROGERS, MIKE**
VTOL military research aircraft p 828 A90-46002
- ROGERS, PHILIP J.**
Holographic head-up displays for air and ground applications p 108 A90-13885
- ROGERS, R. C.**
Flow establishment in a generic scramjet combustor [AIAA PAPER 90-2096] p 742 A90-42729
- ROGERS, RICHARD A.**
Artificial intelligence techniques applied to the non-cooperative identification (NCID) problem [AIAA PAPER 89-3005] p 75 A90-10619
- ROGERS, RUSSELL L.**
Dynamic testing of crashworthy fuel valves [SAE PAPER 891017] p 128 A90-14329
- ROGERS, STUART E.**
Upwind differencing scheme for the time-accurate incompressible Navier-Stokes equations p 232 A90-23109
- ROGERS, W. H.**
Classification and reduction of pilot error [NASA-CR-181867] p 24 N90-10014
- ROGERS, WALTER L.**
Applications of modern control theory synthesis to a super-augmented aircraft [AD-A215431] p 336 N90-16753
- ROHARDT, C.-H.**
Aerodynamic design techniques at DLR Institute for Design Aerodynamics p 500 N90-20979
- ROHLF, D.**
ATTAS flight testing experiences p 34 N90-10862
- ROHN, D. A.**
Efficiency testing of a helicopter transmission planetary reduction stage p 271 A90-21113
- ROHNE, P. B.**
Instrumentation requirements for laminar flow research in the NLR high speed wind tunnel HST p 447 A90-28283
- ROJAS, R. G.**
The Helicopter Antenna Radiation Prediction Code (HARP) [NASA-CR-186925] p 884 N90-27946
- ROKHSAN, KAMRAN**
Static stability and control characteristics of scissor wing configurations p 433 A90-31277
Some aerodynamic characteristics of the scissor wing configuration [SAE PAPER 892202] p 713 A90-45423
An aerodynamic tradeoff study of the scissor wing configuration [NASA-CR-186576] p 481 N90-20965
- ROKICKI, JACEK**
The inverse problem in the multielement airfoil theory p 906 A90-51531
- ROLF, R. L.**
The influence of material quality on airframe structural durability p 676 A90-41336
- ROLL, PHILLIP E.**
An apparatus to prepare composites for repair p 533 A90-31574
- ROLLISON, BILL**
Laboratory implementation of the Continuously Reconfiguring Multi-Microprocessor Flight Control System (CRMFCFS) [AD-A217730] p 520 N90-20094
- ROMANO, JAMES J.**
Inversion of nonlinear I-O map, zero dynamics and flight control system design [AIAA PAPER 90-3370] p 863 A90-47628
- ROMANOV, E. V.**
Semiautomatic coding of weather phenomenon groups in the meteorological reports of automatic airport stations p 962 A90-50783
- ROMBERG, H.-J.**
Two-dimensional wall adaption in the transonic windtunnel of the AIA p 597 A90-38497
- ROMERO, ANDREW**
Low speed testing and simulation of the STOL and Maneuver Technology Demonstrator [AIAA PAPER 90-1820] p 334 A90-25169
- ROMINE, B. M.**
High Mach exhaust system concept scale model test results [AIAA PAPER 90-1905] p 655 A90-40552
- RONALD, TERENCE M. F.**
Advanced materials to fly high in NASP p 203 A90-17297
- RONCHETTI, V.**
Aerodynamic study on forced vibrations on stator rows of axial compressors p 426 N90-18412
- RONCZ, JOHN G.**
Propeller development for the Rutan Voyager [SAE PAPER 891034] p 100 A90-14341
- RONTANI, B.**
Main characteristics of an integrated flight and display system for AS MKII Super-Puma p 653 A90-42450
- ROOKE, D. P.**
Numerical study of balanced patch repairs to cracked sheets p 210 A90-18442
- ROOS, FREDERICK W.**
An experimental investigation of sweep-angle influence on delta-wing flows [AIAA PAPER 90-0383] p 228 A90-22210
The flowfields of bursting vortices over moderately swept delta wings [AIAA PAPER 90-0599] p 314 A90-26969
The lateral spreading of finite-span instability waves in a laminar mixing layer [AIAA PAPER 90-1532] p 606 A90-38677
- ROQUEMORE, W. M.**
Development of a computational fluid dynamics and chemistry model for the fouling of jet fuels [DE90-005664] p 608 N90-22003
- ROSE, GAYLE E.**
Effect of reduced aft diameter and increased blade number on high-speed counterrotation propeller performance [NASA-TM-102077] p 172 N90-13352
- ROSE, OLLIE**
Supersonic aerodynamic characteristics of a Mach 3 high-speed civil transport configuration [AIAA PAPER 90-3210] p 811 A90-48836
- ROSE, OLLIE J.**
Supersonic boundary-layer transition on the LaRC F-106 and the DFRF F-15 aircraft. Part 1: Transition measurements and stability analysis p 94 N90-12558
Supersonic boundary-layer transition on the LaRC F-106 and the DFRF F-15 aircraft. Part 2: Aerodynamic predictions p 94 N90-12559
- ROSE, RAYMOND**
NASA aerodynamics program [NASA-TM-4175] p 373 N90-17235
- ROSE, T. L.**
Finite element analysis of the Twelve Foot Pressurized Wind Tunnel p 760 A90-45296
- ROSE, W. C.**
Measurement of mean and fluctuating flow properties in hypersonic shear layers [AIAA PAPER 90-1409] p 560 A90-38488
- ROSEBERRY, TOM**
Electromagnetic dent removal for aircraft repair [SAE PAPER 890923] p 286 A90-24689
- ROSEN, A.**
Supplemented visual cues for helicopter hovering above a moving ship deck p 195 A90-17704
Dynamic analysis of rotor blades with rotor retention design variations [AIAA PAPER 90-1159] p 412 A90-29394
A study of the influence of predeformations on the vibrations of blades p 585 A90-35673
- ROSEN, B. S.**
Numerical study of asymmetric air injection to control high angle-of-attack forebody vortices on the X-29 aircraft [AIAA PAPER 90-3004] p 788 A90-45853
- ROSEN, HILLARD A.**
Developments in automation of flight test analysis and report generation [AIAA PAPER 90-1313] p 487 A90-33923
- ROSEN, W. A.**
An analysis of reliability in fiber optic ring and star networks p 78 A90-11666
- ROSENBLAD, L. E.**
Evaluation of control techniques for aircraft propulsion systems p 507 A90-32262
- ROSENFELD, MOSHE**
A method for solving three-dimensional viscous incompressible flows over slender bodies p 558 A90-37890
- ROSETTI, CALIN**
An international civil integrity complement to GPS and GLONASS p 821 A90-46392
- ROSFJORD, T. J.**
Air and spray patterns produced by gas turbine high-shear nozzle/swirler assemblies [AIAA PAPER 90-0465] p 192 A90-19857
Influences on the uniformity of sprays produced by gas turbine high shear nozzle/swirler assemblies [AIAA PAPER 90-2193] p 686 A90-42068
- ROSKAM, JAN**
Airplane aerodynamics and performance p 17 A90-12865
Airplane design. Part 1 - Preliminary sizing of airplanes p 30 A90-12866
Airplane design. Part 2 - Preliminary configuration design and integration of the propulsion system p 30 A90-12867
Airplane design. Part 3 - Layout design of cockpit, fuselage, wing and empennage: Cutaways and inboard profiles p 30 A90-12868
Airplane design. Part 4 - Layout design of landing gear and systems p 31 A90-12869
Airplane design. Part 5 - Component weight estimation p 31 A90-12870
Airplane design. Part 6 - Preliminary calculation of aerodynamic, thrust and power characteristics p 31 A90-12871
Airplane design. Part 7 - Determination of stability, control and performance characteristics: Far and military requirements p 57 A90-12872
Automated aircraft configuration design and analysis [SAE PAPER 891072] p 101 A90-14368
Preliminary design of a supersonic short takeoff and vertical landing (STOVL) fighter aircraft [AIAA PAPER 90-3231] p 834 A90-48844
- ROSLOV, A. M.**
Numerical calculation of turbulent separated flows in an abruptly expanding channel p 803 A90-46487
- ROSS, GEORGE B.**
Spanwise distribution of lift and drag at high angles of attack [SAE PAPER 891019] p 83 A90-14331
- ROSS, J. C.**
Experience with scale effects in non-airplane wind tunnel testing [AIAA PAPER 90-1822] p 350 A90-25165
- ROSS, JAMES C.**
Theoretical and experimental study of flow-control devices for inlets of indraft wind tunnels [NASA-TM-100050] p 598 N90-21778
- ROSS, KEVIN**
A synergistic approach to logistics planning and engine design p 422 A90-28207
- ROSS, PHILLIP T.**
Composite matrix cooling scheme for small gas turbine combustors [AIAA PAPER 90-2158] p 852 A90-47210
- ROSS, TWEED, III**
Preliminary design of a supersonic Short Takeoff and Vertical Landing (STOVL) fighter aircraft [NASA-CR-186670] p 649 N90-23394
- ROSSI, GLENN T.**
Evaluation of 3-D reinforcements in commingled, thermoplastic structural elements p 441 A90-28192
- ROSSI, O.**
EH-101 main rotor hub application of thick carbon fiber unidirectional tension bands p 618 A90-42489
- ROSSI, R. J.**
Production of jet fuels from coal derived liquids. Volume 10: Jet fuels production by-products, utility, and sulfur emissions control integration study [AD-A213872] p 357 N90-16951
- ROSSOW, C.**
Convergence speeding up in the calculation of the viscous flow about an airfoil p 279 N90-16194
- ROSSOW, C. C.**
Analysis of three-dimensional aerospace configurations using the Euler and Navier-Stokes equations p 305 A90-25798
- ROSSOW, CORD-CHRISTIAN**
Advances in the efficient calculation of flows with friction p 225 A90-21475
- ROSSOW, VERNON J.**
Estimate of loads during wing-vortex interactions by Munk's transverse-flow method p 159 A90-19391
- ROSTAFINSKI, WOJCIECH**
Analysis of fully stalled compressor p 383 A90-27966
- ROTH, S.**
Simulation of airborne target imagery - Dependence on frequency and bistatic angle p 488 A90-34146
- ROTHMAN, PETER L.**
Evaluation of sensor management systems p 461 A90-30789
- ROTHWELL, A.**
WingDesign: Program for the structural design of a wing cross-section [LR-627] p 925 N90-29390

ROTTMAN, MICHAEL S.

The use of non-dedicated redundancy in the AMCAD fault tolerant control system p 461 A90-30793

ROUBERTIER, J.

Advanced parameter identification techniques for near real time flight flutter test analysis [AIAA PAPER 90-1275] p 494 A90-33899

ROUGIER, PIERRE

Full Authority Digital Engine Control for the AS 355 N TM 319 engines p 665 A90-42486

ROUSSAUD, A.

Numerical simulation of aeroplane response to a lightning injection [ETN-89-95271] p 96 N90-11716

ROUSSI, C.

Shadow-tracking algorithm for moving target detection p 488 A90-34137

ROUT, R. K.

Application of I-DEAS grid generator for three-dimensional transonic flow analysis p 311 A90-26542

Three dimensional transonic and supersonic flow prediction in axi-vented nozzles using a finite volume method [AIAA PAPER 90-2026] p 624 A90-41989

ROUX, B.

Numerical investigations of heat transfer and flow rates in rotating cavities. Simulation of the movement generated by wall temperature gradients, by source-sink mass flows or by the differential rotation of the walls, under the influence or coriolis and centrifugal forces [ETN-90-96253] p 454 N90-18695

ROVKOV, V. A.

An automatic system for the programmed control of the parameters of the vibrational and thermal testing of the blades of gas turbine engines p 343 A90-24216

ROWAN, S.

Composite electronic enclosures for engine-mounted environments [AIAA PAPER 90-2030] p 657 A90-40601

ROWE, DARRELL O., II

Payoffs in growth engines p 188 A90-16823

ROWE, R. K.

Three dimensional transonic and supersonic flow prediction in axi-vented nozzles using a finite volume method [AIAA PAPER 90-2026] p 624 A90-41989

ROWLAND, STEPHEN N., JR.

Inspection development for T-37 wing spar cap lug [AD-A214826] p 287 N90-16708

ROY-AIKINS, J. E. A.

A study of variable geometry in advanced gas turbines p 255 N90-15104

ROY, BHASKAR

Comparative cascade studies of some high diffusion compressor bladings p 15 A90-12637
Comparison of NACA 65, CDA, and tandem bladed cascades p 190 A90-18484

ROY, SCOTT D.

Equipment procurement - EH101 helicopter p 282 A90-22435

ROZANSKI, CHARLES S.

The new high Reynolds number Mach 8 capability in the NSWC Hypervelocity Wind Tunnel 9 [AIAA PAPER 90-1379] p 594 A90-37928

ROZENDAAL, ROGER A.

The 757 NLF glove flight test results p 104 N90-12546
Variable-Sweep Transition Flight Experiment (VSTFE): Stability code development and clean-up glove data analysis p 105 N90-12548

ROZENDAL, D.

Instrumentation requirements for laminar flow research in the NLR high speed wind tunnel HST p 447 A90-28283

ROZIN, N. IU.

Prospects are good for using ATC radar to detect birds p 329 A90-25496

RUBAN, N. A.

Mean and pulse characteristics of supersonic flow in a wind tunnel with a honeycomb nozzle p 231 A90-22421

Experimental investigation of GDL diffusers [AIAA PAPER 90-1512] p 563 A90-38659

RUBESIN, MORRIS W.

Turbulence modeling for aerodynamic flows [AIAA PAPER 89-0606] p 234 A90-23647

RUBIN, S. G.

Convergence properties of high-Reynolds-number separated flow calculations p 86 A90-15820
A flux-split solution procedure for unsteady inlet flows [AIAA PAPER 90-0585] p 314 A90-26967
Transient behavior of supersonic flow through inlets [AIAA PAPER 90-2130] p 704 A90-42734

Composite reduced Navier Stokes procedures for flow problems with strong pressure interactions [AD-A219621] p 689 N90-23687

RUBINShteIN, M. V.

An automated method for predicting the height of the lower cloud boundary p 888 A90-48359

RUBINSTEIN, MARY

Two special cost-effective applications for electrochemical metallizing for improved brazing and bonding [SAE PAPER 890927] p 365 A90-24692

RUBINSTEIN, ROBERT I.

Structural tailoring of select fiber composite structures [NASA-TM-102484] p 533 N90-21137

RUBLEVSKAIA, R. M.

Entry of a flexible airfoil into a vertical gust p 470 A90-32552

RUDD, J. L.

Experimental determination of the short crack effect for metals p 265 A90-20064

RUDIANU, CORNELIU

Theoretical prediction of pressure distribution on wedged delta wing at higher supersonic Mach numbers and its agreement with experimental results p 907 A90-51537

RUDNITSKI, D. M.

Comparison of ground-level test cells and ground-level to altitude test cells p 857 N90-27716

RUDDOFF, R.

Advanced instrumentation for aircraft icing research [NASA-CR-185225] p 506 N90-21006

RUDDOFF, R. C.

Development of a phase Doppler based probe for icing cloud droplet characterization [AIAA PAPER 90-0667] p 368 A90-26978

RUEHLE, C. J.

Helicopter wire strike accident and high voltage electrocution - A case report p 22 A90-10265

RUEHLE, CHARLES J.

Fire deaths in aircraft without the crashworthy fuel system p 22 A90-10266

RUFF, GARY A.

Users manual for the NASA Lewis Ice Accretion Prediction Code (LEWICE) [NASA-CR-185129] p 468 N90-20943

RUFFLES, P. C.

A vision of the future: The new engine technology [PNR90566] p 115 N90-12603

RUFLES, PHILIP

Wide-chord fan proved in nearly five years of service p 744 A90-44594

RUGAMA, JOSE A.

Applying AVIP to high voltage power supply designs p 605 A90-38132

RUIJGROK, G. J. J.

Noise data of four small propeller-driven airplanes [PB89-216980] p 139 N90-12291

RUIZ-CALAVERA, L. P.

A comparison between theoretical and experimental results for a 3-D wing with damped pitching oscillations p 472 A90-33361

RUIZ-CALAVERA, LUIS PABLO

A time-marching method to calculate unsteady airloads on three-dimensional wings. Part 1: Linearized formulation [DLR-FB-89-58] p 634 N90-24254

A time-marching method for calculating unsteady airloads on three-dimensional wings. Part 2: Full-potential formulation [DLR-FB-89-59] p 635 N90-24255

RUKAVINA, JOHN P.

Stall margin improvement in axial-flow compressors by circumferential variation of stationary blade setting angles [AIAA PAPER 90-1912] p 656 A90-40554

RUNNINGS, DAVID

Helmet mounted display systems for helicopter simulation p 420 A90-31344

RUNYAN, L. JAMES

Flight and wind tunnel investigation of aerodynamic effects of aircraft ground deicing/anticing fluids p 235 N90-15064

RUNYAN, L. JIM

The 757 NLF glove flight test results p 104 N90-12546

RUPKE, EDWARD J.

The behavior of electric currents in graphite/epoxy structures p 883 A90-49846

RUSAKOV, M. M.

Operation of a gas ejector in the pulsed regime p 850 A90-46488

RUSBARSKY, GREGORY J.

F-15 STOL and Maneuver Technology Demonstrator flight test progress report [AIAA PAPER 90-1269] p 494 A90-33896

RUSCHAU, JOHN J.

Fatigue crack growth investigation of a Ti-6Al-4V forging under complex loading conditions: NATO/AGARD supplemental engine disk program [AD-A220239] p 678 N90-23538

RUSSELL, D. A.

A numerical study of longitudinal vortex interaction with a boundary layer [AIAA PAPER 90-1630] p 568 A90-38759

RUSSELL, DAVID A.

HF shock tunnel facility for studying supersonic combustion [AIAA PAPER 90-1551] p 600 A90-38693

RUSSELL, JOHN D.

Comparison of processing techniques for Filmix unidirectional commingled fabric p 940 A90-50058

RUSSELL, L.

A laser based computer aided non-intrusive technique for full field flow characterization in macroscopic curved channels p 535 A90-32293

RUSSELL, L. T.

Maritime environment airframe material fatigue testing p 764 A90-42675

RUSSO, G. P.

Numerical simulation of an adaptive-wall wind-tunnel - A comparison of two different strategies p 439 A90-30251

RUSSO, GIUSEPPE P.

Limits of adaptation, residual interferences p 871 N90-26844

RUTKOWSKI, MICHAEL J.

Development of the Second Generation Comprehensive Helicopter Analysis System (2GCHAS) p 889 A90-46963

RUTLEDGE, GLYN S.

Successful performance development program for the T800-LHT-800 turboshaft engine [SAE PAPER 891048] p 110 A90-14352

RUTLEDGE, WALTER H.

Hyperbolic grid generation techniques for blunt body configurations p 376 A90-26490

RUZICKA, GENE C.

Fundamental dynamics issues for comprehensive rotorcraft analyses p 831 A90-46961

RYAN, LAURA E.

Application of stochastic robustness to aircraft control systems p 521 N90-20936

Stochastic robustness of linear control systems p 521 N90-20941

RYAN, ROBERT

X-29A aircraft structural loads flight testing [NASA-TM-101715] p 416 N90-19225

RYAN, SHARON K.

F-15 Environment Control System improvements [SAE PAPER 901235] p 841 A90-49305

RYBALKO, E. V.

Application of splines to the calculation of flow past a wing profile p 805 A90-46615

RYBERG, PI-YU

Future ATC automation aids based upon AI technology p 375 A90-25563

RYERSON, D. E.

Small multipurpose stored data acquisition system [DE90-010823] p 967 N90-30134

RYZHOV, IU. A.

Some problems on 'intelligence' of wind tunnel testing p 436 A90-28282

RYZHOV, O. S.

Boundary layer stability in the case of transonic external flow p 619 A90-39514

S

SAARIS, G. R.

Transonic analysis of complex configurations using TRANAIR program [SAE PAPER 892289] p 714 A90-45467

SABAH, D.

Finite element analysis of the Twelve Foot Pressurized Wind Tunnel p 760 A90-45296

SABEL'NIKOV, V. A.

A study of gas flow in hypersonic nozzles at large Reynolds numbers using simplified Navier-Stokes equations p 803 A90-46538

SABER, A. J.

A weighted residual formulation for finite element solutions of the steady Euler equations p 770 A90-44457

SABLA, P. E.

Energy Efficient Engine combustor test hardware detailed design report [NASA-CR-168301] p 929 N90-28554

Energy Efficient Engine (E3) combustion system component technology performance report [NASA-CR-168274] p 930 N90-28555

- SABNIS, JAYANT S.**
Hypersonic flow calculations with a hybrid Navier-Stokes/Monte Carlo method [AIAA PAPER 90-1691] p 560 A90-38394
- SABO, FRANCES E.**
Research in Natural Laminar Flow and Laminar-Flow Control, part 1 [NASA-CP-2487-PT-1] p 90 N90-12503
Research in Natural Laminar Flow and Laminar-Flow Control, part 2 [NASA-CP-2487-PT-2] p 91 N90-12519
Research in Natural Laminar Flow and Laminar-Flow Control, part 3 [NASA-CP-2487-PT-3] p 92 N90-12539
- SACHER, P. W.**
Design for hypersonic speed p 335 A90-26343
- SACHS, GOTTFRIED**
Flying qualities problems of aerospace craft [AIAA PAPER 90-2804] p 752 A90-45139
Optimal periodic cruise with singular control [AIAA PAPER 90-3490] p 833 A90-47738
- SADREHAGHIGHI, IDEEN**
Applications of Lagrangian blending functions for grid generation around airplane geometries [AIAA PAPER 90-0009] p 216 A90-19630
Application of Lagrangian blending functions for grid generation around airplane geometries [NASA-CR-186318] p 237 N90-15891
- SAEED, A.**
Practical techniques of modelling aeroelastic systems for active control applications p 545 A90-33402
- SAEED, MOHAMED**
The potential for an extra runway at Heathrow: A preliminary feasibility study [TT-9007] p 938 N90-29403
- SAFARIK, P.**
Experimental investigation of the transonic centrifugal compressor inducer straight cascades p 13 A90-12592
- SAFF, C. R.**
Damage tolerance analysis for manned hypervelocity vehicles. Volume 2: Software user's manual [AD-A222136] p 845 N90-26826
Damage tolerance analysis for manned hypervelocity vehicles. Volume 1: Final technical report [AD-A221970] p 887 N90-28106
- SAFF, CHARLES**
An expert system advisor for damage repair of composite wing skins (repairman) p 842 N90-26810
- SAFF, CHARLES R.**
Smart structures concept study p 504 A90-32876
- SAFONOV, MICHAEL G.**
Practical methods for robust multivariable control [AD-A216937] p 462 N90-18920
Algorithms for computing the multivariable stability margin p 612 N90-22999
- SAFONOV, V. P.**
Gasdynamic characteristics of a plane or axisymmetric nozzle with a rectilinear generatrix of the supersonic section p 805 A90-46575
- SAFRONOV, A. V.**
Conditions of the generation of autooscillations in aerodynamic control surfaces in nonseparated subsonic flow of a gas p 315 A90-27303
- SAGDEO, P. M.**
Conceptual design and feasibility study of very large passenger aircraft [AIAA PAPER 90-3220] p 834 A90-48841
- SAGIYA, YOSHIMASA**
Endurance test of FJR 710/600S engine p 42 A90-12012
Start characteristics of FJR 710/600S engine p 42 A90-12013
Oil migration of FJR 710/600S engine p 43 A90-12014
Steady state performance of FJR 710/600S engine p 43 A90-12015
Development study of air turbo-ramjet for future space plane [IAF PAPER 89-311] p 109 A90-13445
- SAGNES, PIERRE**
Three-dimensional modeling of turbulent transonic flow at the exit of a twin engine [AAAF PAPER NT 88-16] p 4 A90-11434
- SAGNIER, PHILIPPE**
Inviscid non equilibrium flow in ONERA F4 wind tunnel [ONERA, TP NO. 1989-161] p 223 A90-21029
- SAHA, S.**
Computation of transonic separated flow using the Euler equations p 85 A90-15233
- SAHU, JUBARAJ**
Numerical computations of transonic critical aerodynamic behavior p 469 A90-32457
Numerical simulation of three-dimensional transonic flows p 905 A90-51020
- SAIA, ROBERT J.**
The PW2000 - A mature engine with an eye to the future [SAE PAPER 892365] p 748 A90-45514
- SAID, FREDERIQUE**
Aircraft measurements of sea surface conditions and their relationship to marine boundary-layer dynamics p 888 A90-47572
- SAIGAL, SUNIL**
Boundary-element shape optimization system for aircraft structural components p 680 A90-39786
- SAIKI, NEAL**
Aerodynamic design of the Cal Poly Da Vinci Human-Powered Helicopter p 830 A90-46950
- SAIKI, YOSHIHARU**
An electronic flight-recorder for a hang-glider p 39 A90-12234
- SAIN, PATRICK M.**
A study of a propulsion control system for a VATOL aircraft (A direct design synthesis application) p 424 A90-30712
- SAINT CLAIR, T. L.**
Improved melt flow and physical properties of Mitsui Toatsu's LARC-TPI 1500 series polyimide p 943 A90-50134
- SAINZ, B.**
Pressure air tightness tests of laminated panels for wing leading edge heat shields [INFORME-I-377/89] p 357 N90-17873
- SAITO, KO-ICHI**
A new hybrid LTA vehicle, 'Heliship' - Its philosophy, outline [AIAA PAPER 89-3162] p 244 A90-20582
- SAITO, S.**
Application of the moving surface boundary layer control to a two dimensional airfoil p 628 A90-42405
- SAITO, SHIGERU**
Navier-Stokes simulations around a high-speed propeller p 305 A90-25797
Analytical study of dynamic response of helicopter in autorotative flight p 670 A90-42469
- SAITO, T.**
Hydrogen fueled subsonic-ram-combustor model tests for an air-turbo-ram engine p 44 A90-12529
- SAITO, YOSHINORI**
Studies on supersonic radial flow behavior in disk channel p 87 A90-16104
- SAJBEN, MIKLOS**
Experimental investigation of terminal shock sensors in mixed-compression inlets [AIAA PAPER 90-1931] p 681 A90-40560
- SAKAI, MOTOTSUGU**
MRS International Meeting on Advanced Materials, 1st, Tokyo, Japan, May 31-June 3, 1988, Proceedings. Volume 5 - Structural ceramics/Fracture mechanics p 599 A90-35926
- SAKAI, SHINSUKE**
Development of creep-fatigue damage detection method of rotor steel by ultrasonic wave measurement [DE90-503792] p 777 N90-26365
- SAKAMOTO, YUJIRO**
Thrust augmentation characteristics of jet reactions [AIAA PAPER 90-0033] p 161 A90-19641
- SAKHAROV, BORIS I.**
Durability of equipment assemblies and elements of life-support systems for flight vehicles p 246 A90-21275
- SAKOVICH, V. S.**
The potential approximation in the theory of conical flows p 710 A90-44930
- SALA, G.**
Understanding composite fatigue - New trends p 940 A90-49893
- SALAMA, E. E.**
Advanced gearbox technology [NASA-CR-179625] p 666 N90-24274
- SALARI, KAMBIZ**
The influence of the sweep on dynamic stall produced by a rapidly pitching wing [AIAA PAPER 90-0581] p 230 A90-22231
- SALAS, M. D.**
An abbreviated Reynolds stress turbulence model for airfoil flows [AIAA PAPER 90-1468] p 562 A90-38625
- SALAS, RIK**
Induction heating development for aircraft repair p 955 A90-50164
- SALCUDEAN, M.**
Film cooling of turbine blades - Two dimensional experiments and numerical simulations p 739 A90-42670
- SALGUERO, DAVID E.**
Hypersonic Arbitrary-Body Aerodynamics (HABA) for conceptual design [DE90-014750] p 910 N90-28495
- SALIBA, JOSEPH E.**
Elastic-viscoplastic finite-element program for modeling tire/soil interaction p 401 A90-31285
- SALIBA, SUSAN S.**
Aircraft battle damage repair of transparencies [AD-A224168] p 925 N90-29387
- SALIKUDDIN, M.**
Application of localized active control to reduce propeller noise transmitted through fuselage surface p 78 A90-11884
Application of active noise control to model propeller noise p 548 A90-34091
- SALIM, B.**
Effect of downstream elements on the flow at the exit of centrifugal compressor rotor p 157 A90-18483
- SALJNIKOV, V.**
Generalized similarity solutions for three-dimensional laminar compressible wing boundary layers p 907 A90-51543
- SALJNIKOV, VIKTOR**
Generalized similarity solutions for three dimensional, laminar, steady, compressible boundary layer flows on swept profile cylinders [DLR-FB-89-34] p 212 N90-13725
- SALKIND, MICHAEL**
Aerospace materials research opportunities p 267 A90-23177
- SALLEE, V. JAMES**
ADAM 2.0 - An ASE analysis code for aircraft with digital flight control systems [AIAA PAPER 90-1077] p 431 A90-29385
A review of aeroelasticity research at the flight dynamics laboratory p 493 A90-33409
- SALMAN, AHMED A.**
Unsteady flow computation of oscillating flexible wings [AIAA PAPER 90-0937] p 389 A90-29363
- SALVINO, J. T.**
Statistics on aircraft gas turbine engine rotor failures that occurred in US commercial aviation during 1986 [DOT/FAA/CT-89/30] p 511 N90-21008
- SAMAK, D. K.**
Investigation of aerodynamic interactions between a rotor and fuselage in forward flight p 385 A90-28198
Theoretical and experimental investigation of the aeroelastic stability of an advanced bearingless rotor in hover and forward flight p 831 A90-46958
- SAMARIN, V. G.**
Design of symmetric profiles with maximum critical flow Mach number under prescribed constraints p 295 A90-24095
- SAMIMY, M.**
Compressibility effects in free shear layers [AIAA PAPER 90-0705] p 212 A90-19984
Nonaxisymmetric instabilities in a dump combustor with a swirling inlet flow p 253 A90-21228
Effects of compressibility on the characteristics of free shear layers p 302 A90-25285
Structure of a reattaching supersonic shear layer p 555 A90-36252
Pressure-based real-time measurements in compressible free shear layers [AIAA PAPER 90-1980] p 703 A90-42709
- SAMOILOVA, N. V.**
The effect of longitudinal fins on turbulent friction drag p 297 A90-24123
- SAMPATH, PRASAD**
Wind tunnel testing of a helicopter model at HAL p 335 A90-26350
- SAMPH, SUZANNE**
Heliport visual approach surface high temperature and high altitude tests [DOT/FAA/CT-TN89/34] p 825 N90-27675
- SAMUELSEN, G. S.**
Active soot reduction in a spray-fired, axisymmetric model gas turbine combustor [AIAA PAPER 90-0039] p 191 A90-19644
Influence of the continuous and dispersed phases on the symmetry of a gas turbine air-blast atomizer [ASME PAPER 89-GT-303] p 273 A90-22651
A model gas turbine combustor with wall jets and optical access for turbulent mixing, fuel effects, and spray studies p 507 A90-32808
Symmetry assessment of an air-blast atomizer spray p 682 A90-40930
- SAMUELSSON, INGEMAR**
Slipstream-induced pressure fluctuations on a wing panel p 77 A90-11004
- SANCHEZ GOMEZ, J.**
Design and fabrication of the carbon fiber/epoxy A-320 horizontal tailplane p 286 A90-25221
- SANCHEZ, FELIX**
The National Aero-Space Plane, the guidance and control engineer's dream or nightmare? [AAS PAPER 89-040] p 264 A90-21546

SANCHO, MICHEL

Casting airworthiness joint European civil authorities view-point p 64 N90-10234

SAND, W. R.

A program to improve aircraft icing forecasts [AIAA PAPER 90-0196] p 216 A90-19733

SANDFORD, MAYNARD C.

Unsteady pressure and structural response measurements on an elastic supercritical wing p 159 A90-19392

SANDHU, J. S.

Torsional buckling and post-buckling of composite geodetic cylinders with special reference to joint flexibility p 878 A90-45971

SANDLER, SCOTT B.

Feasibility study for a microwave-powered ozone sniffer aircraft [NASA-CR-186660] p 650 N90-23397

SANDLIN, DORAL R.

A computer module used to calculate the horizontal control surface size of a conceptual aircraft design [NASA-CR-186872] p 780 N90-26515

SANDMAN, JULIE

Preliminary airworthiness evaluation of the Woodward hydromechanical unit installed on T700-GE-700 engines in the UH-60A helicopter [AD-A216751] p 428 N90-18430

SANDOR, P.

Parachute opening shocks during high speed ejections: Normalization p 497 N90-20056

SANDS, O. S.

Pattern representations and syntactic classification of radar measurements of commercial aircraft p 417 A90-28407

SANE, S. K.

Squeeze film damping for aircraft gas turbines p 113 A90-16009

SANGER, K. B.

Certification testing methodology for fighter hybrid structure p 642 A90-40128

SANGHA, K.

Correlation of AH-1G airframe flight vibration data with a coupled rotor-fuselage analysis [NASA-CR-181974] p 959 N90-28865

SANGHA, K. B.

Rotor/airframe aeroelastic analyses using the transfer matrix approach [AIAA PAPER 90-1119] p 392 A90-29391

SANGIOVANNI, J. J.

The role of hydrogen/air chemistry in nozzle performance for a hypersonic propulsion system [AIAA PAPER 90-2492] p 658 A90-40637

SANKAR, L. N.

Dynamic stall of circulation control airfoils [AIAA PAPER 90-0573] p 167 A90-19923

Euler solutions for self-generated rotor blade-vortex interactions [AIAA PAPER 90-1588] p 566 A90-38723

Numerical simulation of the growth of instabilities in supersonic free shear layers p 623 A90-40941

Numerical simulation of unsteady rotational flow over propfan configurations [NASA-CR-186037] p 90 N90-12500

Numerical simulation of supersonic free shear layers [AD-A216289] p 320 N90-17579

An efficient airfoil design method using the Navier-Stokes equations p 500 N90-20981

SANKAR, LAKSHMI N.

Numerical study of the effects of icing on finite wing aerodynamics [AIAA PAPER 90-0757] p 169 A90-20010

Stability of hingeless rotors in hover using three-dimensional unsteady aerodynamics p 430 A90-28227

SANKAR, N. L.

Application of an efficient hybrid scheme for aeroelastic analysis of advanced propellers [AIAA PAPER 90-0028] p 226 A90-22153

Application of an efficient hybrid scheme for aeroelastic analysis of advanced propellers [NASA-TM-102428] p 172 N90-13355

SANKARAN, L.

A numerical study of longitudinal vortex interaction with a boundary layer [AIAA PAPER 90-1630] p 568 A90-38759

SANKWITSCH, V.

Calculation of flight vibration levels of the AH-1G helicopter and correlation with existing flight vibration measurements [NASA-CR-181923] p 454 N90-18743

SANNE, D. W.

The effect of matrix toughness in the development of improved structural adhesives p 955 A90-50183

SANO, MASAOKI

Acoustic-thermal environment for USB flap structure. Report 1: Ground simulation test results [NAL-TM-567] p 88 N90-11697

SANTHAKUMAR, S.

Transonic flow over a single wedge p 85 A90-15237

SANTOLINI, C.

Comparison among modal analyses of axial compressor blade using experimental data of different measuring systems p 878 A90-46038

SAPORITO, JOSEPH

Sandwich structures on Aerospatiale helicopters p 467 A90-31657

SARANIERO, MICHAEL

An early overview of tiltrotor aircraft characteristics and pilot procedures in civil transport applications [DOT/FAA/DS-89/37] p 503 N90-21003

SARAVANAMUTTOO, H. I. H.

On and off-design performance prediction of single spool turbojets using gasdynamics [AIAA PAPER 90-2393] p 662 A90-42155

Recommended practices for measurement of gas path pressures and temperatures for performance assessment of aircraft turbine engines and components [AGARD-AR-245] p 933 N90-29393

SARH, BRANKO

Computer integrated quality assurance for robotic workcells in aerospace manufacturing [SME PAPER MS89-152] p 283 A90-23681

SARIC, W. S.

Measurement of crossflow vortices, attachment-line flow, and transition using microthin hot films [AIAA PAPER 90-1636] p 607 A90-38765

SARIC, WILLIAM S.

Experiments in swept-wing transition p 149 A90-16794

The development of crossflow vortices on a 45 degree swept wing [SAE PAPER 892245] p 713 A90-45452

Stability and transition of three-dimensional boundary layers p 71 N90-10357

SARIGUL-KLIJN, NESRIN

Generalized Transition Finite-Boundary Elements for high speed flight structures [AIAA PAPER 90-1105] p 449 A90-29286

SARKAR, S.

Kane's methods in rotorblade dynamics p 646 A90-42458

SARKOS, CONSTANTINE P.

Development of improved fire safety standards adopted by the Federal Aviation Administration p 324 N90-17585

Characteristics of transport, aircraft fires measured by full-scale tests p 325 N90-17591

SARNO, ROBERT L.

Experimental investigation to suppress flow-induced pressure oscillations in open cavities [AD-A216285] p 320 N90-17578

SARPKAYA, TURGUT

Numerical simulation of unsteady flow about cambered plates p 159 A90-19389

SARVARETDINOV, R. G.

Validation of the accelerated equivalent testing of gas turbine engines for multivariant applications p 110 A90-14568

SASA, SHUICHI

On the interactive computer program IPIS for aircraft parameter identification [NAL-TR-1000] p 77 N90-10586

Short period control using angular acceleration feedback: Compensation for first lag servo [NAL-TM-600] p 936 N90-29399

The function of the Interactive Model Assembly Program (IMAP) for a flight simulator [NAL-TR-1034] p 939 N90-29412

SASAKI, MAKOTO

Restart characteristics of turbofan engines p 50 A90-12627

SASSO, CHRISTIAN

System identification - Multibus acquisition and simulation equipment p 26 A90-12192

SATHEERATNAM, A. G.

On-line temperature profile display system [ASME PAPER 89-GT-10] p 374 A90-23755

SATO, JUNZO

Unsteady aerodynamic forces on rolling delta wings at high angle of attack p 159 A90-19426

SATO, T.

An experimental study of heat transfer and film cooling on low aspect ratio turbine nozzles [ASME PAPER 89-GT-187] p 361 A90-23865

SATO, YUKINORI

Experimental study on autoignition in a scramjet combustor p 46 A90-12559

SATOH, TATSUKI

Design of control amplifier for FJR 710 engine p 43 A90-12017

SATTA, ANTONIO

Axial flow compressor design optimization. I - Pitchline analysis and multivariable objective function influence [ASME PAPER 89-GT-201] p 342 A90-23873

Axial flow compressor design optimization. II - Through-flow analysis [ASME PAPER 89-GT-202] p 342 A90-23874

SAUER, GREGORY

A self-compensating aircraft recovery system (SCARS) [AIAA PAPER 90-3273] p 818 A90-48864

SAUNDERS, C. P. R.

Charging of aircraft - High-velocity collisions p 322 A90-26131

SAUNDERS, CHRIS B.

Radiation-curable prepreg composites [DE90-629740] p 951 N90-28674

SAUNDERS, D. S.

Moisture absorption in graphite/epoxy laminates p 951 A90-52799

SAUNDERS, T. B.

Combat aircraft control requirements p 934 N90-28515

SAURIN, V. V.

Efficient structural material distribution in the main frame of a light vehicle p 363 A90-24092

SAUVAIN, LARRY D.

Distribution of hardware and software elements in unmanned air vehicle systems p 251 N90-15933

SAUVEL, J.

Flow around a jet and thrust measurement bias from static tests [AAAF PAPER NT 88-11] p 40 A90-11431

SAVAGE, EDWARD

Omega - A low-cost precision synchronizer p 727 A90-45233

SAVAGLIO, CLARE

Six-degree-of-freedom aircraft simulation with mixed-data structure using the applied dynamics simulation language, ADSIM p 613 N90-23067

SAVENKOV, I. V.

Boundary layer stability in the case of transonic external flow p 619 A90-39514

SAVENKOV, MAKSIM V.

Monitoring and maintenance of automatic control systems in aviation p 778 A90-42524

SAVINI, M.

Secondary flows in a transonic cascade - Comparison between experimental and numerical results p 157 A90-18501

SAVINOV, K. G.

Equilibrium of an elastic porous shell in supersonic gas flow p 150 A90-17109

SAVITSKII, V. I.

Construction of a wing surface in a nonviscous transonic flow from a given pressure distribution p 298 A90-24149

SAWADA, HIDEO

Cryogenic wind tunnels p 199 A90-17346

SAWAL, D.

Synthesis of a simulator-based automated helicopter hover trainer [AIAA PAPER 90-3481] p 891 A90-47730

SAWYER, R. STEVEN

Lift development of delta wings undergoing constant acceleration from rest [AIAA PAPER 90-0310] p 164 A90-19789

Unsteady lift development on a constantly accelerated rectangular wing [AIAA PAPER 90-1633] p 569 A90-38762

Lift response of a rectangular wing undergoing a step change in forward speed p 620 A90-39801

SAWYER, RICHARD STEVEN

Measurement of lift development on rapidly-accelerated wings p 480 N90-20956

SAWYER, WALLACE C.

Overview of military technology at NASA Langley [SAE PAPER 892232] p 733 A90-45448

SAXER, ANDRE P.

Inlet radial temperature redistribution in a transonic turbine stage [AIAA PAPER 90-1543] p 565 A90-38687

SAYAMA, MASAMI

Experimental study on autoignition in a scramjet combustor p 46 A90-12559

SBUELZ, ANES

Mirach 100 flight control system p 260 N90-15926

SCAGGS, N. E.

The effect of separation on turbulent boundary layer characteristics over a smooth surface at Mach 6.0 [AIAA PAPER 90-3028] p 790 A90-45870

SCAGGS, NORMAN E.

High Reynolds number wedge-induced separation lengths at Mach 6 p 154 A90-18001

SCAGGS, W. FRANK

Computational investigation of two-dimensional ejector nozzle flow fields
[AIAA PAPER 90-2148] p 768 A90-42739

SCANLAN, ROBERT H.

A modern course in aeroelasticity (2nd revised and enlarged edition) p 497 A90-34968

SCARDINA, JOHN A.

Future ATC automation aids based upon AI technology p 375 A90-25563

SCAVUZZO, R. J.

Impact ice stresses in rotating airfoils
[AIAA PAPER 90-0198] p 175 A90-19735

SCENNA, R.

Co-development of CT7-6 engines - A continued tradition in technology and reliability p 665 A90-42485

SHADOW, K. C.

Flow and acoustic features of a supersonic tapered nozzle
[AIAA PAPER 90-1599] p 567 A90-38731

Supersonic rectangular isothermal shrouded jets
[AIAA PAPER 90-2028] p 621 A90-40599

Multistep dump combustor design to reduce combustion instabilities p 659 A90-40934

Suppression of 'Buzz' instability by geometrical design of the flameholder

[AIAA PAPER 90-1966] p 741 A90-42706

Active combustion control in a coaxial dump combustor

[AIAA PAPER 90-2447] p 743 A90-42806

SCHAEFER, CARL G., JR.

The effects of aerial combat on helicopter structural integrity p 406 A90-28166

SCHAEFER, H. J.

Experimental study of velocity fields and turbulence in a turbojet engine
[ISL-CO-231/88] p 344 N90-16766

SCHAEFER, HANS J.

Mean and turbulent velocity measurements in a turbojet exhaust p 423 A90-28272

SCHAEFER, RAINER

Fretting fatigue strength of Ti-6Al-4V at room and elevated temperatures and ways of improving it p 952 N90-28709

SCHAEFFER, GUY

The SEPR 844 reusable liquid rocket engine for Mirage combat aircraft

[AIAA PAPER 90-1835] p 655 A90-40526

SCHAEZNER, G.

Potential applications of satellite navigation p 264 A90-21716

Integrated system of differential Global Positioning System and inertial measurement unit - A position determination system for automatic landing

[AIAA PAPER 90-1300] p 487 A90-33914

Automatic landing with GPS - Design of the flight guidance and flight control system

[AIAA PAPER 90-1301] p 487 A90-33915

Integrated flight guidance system using differential-GPS for landing approach guidance p 332 N90-16735

SCHAEZNER, GUNTHER

Flight test results of a complex precise digital flight control system p 35 N90-10870

Influence of windshear, downdraft and turbulence on flight safety p 238 N90-15048

SCHAEUELE, HORST

Equation decoupling - A new approach to the aerodynamic identification of unstable aircraft

[AIAA PAPER 90-1276] p 518 A90-33900

SCHAFER, R. M.

Digital control of magnetic bearings supporting a multimass flexible rotor p 682 A90-40712

SCHAFFAR, M.

Aerodynamic loads and blade vortex interaction noise prediction p 614 A90-38520

Study of the blade/vortex interaction on a one-blade rotor during forward flight (incompressible, non viscous fluid)

[ISL-R-115/88] p 415 N90-18391

Aerodynamic loads and blade vortex interaction noise prediction

[ISL-PU-310/89] p 719 N90-25942

SCHAFFAR, MARTIN

Rotor loads computation using singularity methods and application to the noise prediction p 807 A90-46880

SCHAFRIK, ROBERT

Improved Thermo-Oxidative-Deposition screening tests for turbine lubricants

[AD-A217795] p 533 N90-21188

SCHAIRER, EDWARD

NASA aerodynamics program

[NASA-TM-4175] p 373 N90-17235

SCHAIRER, EDWARD T.

Nonlinear effects in the two-dimensional adaptive-wall outer-flow problem p 554 A90-35771

A two-dimensional adaptive-wall test section with ventilated walls in the Ames 2- by 2-foot transonic wind tunnel
[NASA-TM-102207] p 201 N90-13407

SCHALAU, B.

An interactive method for the flow calculation of airfoils with local separation regions p 278 N90-16190

SCHAMEL, GEORGE CUSHEN, II

Experimental and theoretical investigation of optimal control methods with model reduction p 521 N90-21039

SCHARPF, DANIEL F.

An experimental study of a closely coupled tandem wing configuration at low Reynolds numbers

[AIAA PAPER 90-3094] p 797 A90-45923

SCHAUWECKER, LUDWIG

Experimental windtunnel studies for EFA p 672 A90-41113

SCHICK, J. T.

The Helicopter Antenna Radiation Prediction Code (HARP)

[NASA-CR-186925] p 884 N90-27946

SCHIE, PAUL O.

A small inert gas generator p 180 A90-17405

SCHIEITL, H.

The use of a Laval nozzle and wall suction for blockage-free transonic wind-tunnel operation p 225 A90-21592

SHELL, B. E.

Helicopter wire strike accident and high voltage electrocution - A case report p 22 A90-10285

SHELL, R.

Autonomous automatic landing through computer vision p 332 N90-16734

SCHENCK, DAVID M.

The Dash 8 Series 400 regional airliner p 729 A90-42664

SCHENK, A.

Flutter analysis from ambient random responses p 491 A90-33374

SCHENK, H.-D.

Development of a COMPAS prototype for the ATC Centre at Frankfurt (Fed. Republic of Germany) p 826 N90-27684

SCHENKEN, KIMBERLY S.

Using goal programming to determine the optimal engine mix for UH-1 helicopters

[AD-A214893] p 343 N90-16762

SCHERRER, D.

Progress in airbreathing combined engines for future European launcher p 344 N90-16817

SCHETZ, J. A.

Finite element analysis of the flow of a propeller on a slender body with a two-equation turbulence model p 210 A90-18340

Effects of pressure mismatch on slot injection in supersonic flow

[AIAA PAPER 90-0092] p 227 A90-22161

Large-scale structure in a supersonic slot-injected flowfield p 602 A90-36265

Flow over inclined finite length and width flat plates at low and high Reynolds numbers

[AIAA PAPER 90-1467] p 562 A90-38624

Direct measurements of skin friction in a scramjet combustor

[AIAA PAPER 90-2342] p 626 A90-42132

SCHETZ, JOSEPH A.

Finite element simulation of complex jets in a crossflow for V/STOL applications p 585 A90-35753

SCHIEWE, G.

Examples of force measurements in a wind tunnel using multicomponent piezoelectric transducers p 540 A90-34352

SCHIANTARELI, ERNST F.

Core composites in Swissair aircraft p 493 A90-33709

SCHICK, FRED V.

Design and evaluation of the ATC interface - Planning system for approach flight p 937 A90-52617

SCHIERENBECK, DETLEF

Structural optimization in view of aeroelastic constraints p 536 A90-33391

SCHIERMAN, JOHN D.

Analysis of airframe/engine interactions - An integrated control perspective

[AIAA PAPER 90-1918] p 667 A90-40557

Extended implicit model following as applied to integrated flight and propulsion control

[AIAA PAPER 90-3444] p 890 A90-47697

SCHIEVELBUSCH, U.

Some processes of sound generation in a vortex-airfoil system with parallel axes p 218 A90-18448

SCHIFF, L. B.

An experimental study of the nonlinear dynamic phenomenon known as wing rock

[AIAA PAPER 90-2812] p 753 A90-45152

SCHIFF, LEWIS B.

Numerical simulation of separated and vortical flows on bodies at large angles of attack p 146 A90-16772

Pneumatic vortical flow control at high angles of attack

[AIAA PAPER 90-0098] p 227 A90-22164

Navier-Stokes predictions of the flowfield around the F-18 (HARV) wing and fuselage at large incidence

[AIAA PAPER 90-0099] p 227 A90-22165

Vortical flows over delta wings and numerical prediction of vortex breakdown

[AIAA PAPER 90-0102] p 227 A90-22166

Numerical simulation of the viscous flow around a simplified F/A-18 at high angles of attack

[AIAA PAPER 90-2999] p 787 A90-45849

Numerical simulation of the effects of variation of angle of attack and sweep angle on vortex breakdown over delta wings

[AIAA PAPER 90-3000] p 788 A90-45850

The effect of turbulence models on the numerical prediction of the flowfield about a prolate spheroid at high angle of attack

[AIAA PAPER 90-3106] p 789 A90-45855

SCHIJVE, J.

Reconstitution of crack growth from fractographic observations after flight simulation loading p 682 A90-40650

An evaluation of a fatigue crack growth prediction model for variable-amplitude loading (PREFFAS)

[LR-537] p 214 N90-13822

Crack stoppers and ARALL laminates

[PB90-166588] p 533 N90-21142

Fractographic observations on fatigue crack growth in 2024-T3 sheet material under flight-simulation loading

[LR-592] p 689 N90-23780

Fractographic analysis of fatigue crack growth under two-blocks loading on 2024-T351 sheet specimens

[LR-628] p 961 N90-29680

Effects of blocks of overloads and underloads on fatigue crack growth in 2024-T351 sheet specimens: Fractographic analysis and crack closure predictions

[LR-629] p 961 N90-29681

Fatigue, static tensile strength and stress corrosion of aircraft materials and structures. Part 1: Text

[LR-630-PT-1-REV] p 961 N90-29682

Fatigue, static tensile strength and stress corrosion of aircraft materials and structures. Part 2: Figures

[LR-630-PT-2] p 961 N90-29683

Fractographic observations on fatigue crack growth under miniTWIST flight-simulation loading (2024-T3 material)

[LR-631] p 961 N90-29684

SCHILLINGS, JOHN J.

Maneuver performance comparison between the XV-15 and an advanced tiltrotor design p 518 A90-33622

SCHIMANSKI, D.

Status of the development programme for instrumentation and test techniques of the European Transonic Windtunnel - ETW p 437 A90-28292

SCHINDLER, ZDENEK

Mathematical model of turboprop engine behaviour p 254 A90-23351

Modelling and simulation of turboprop engine behaviour p 424 A90-29946

Mathematical simulation model of an aircraft gas turbine p 745 A90-44721

SCHIPPERS, P.

Ground vibration testing of aeroplanes with a sequence of single-point excitations - Simple and effective p 522 A90-33371

SCHJELDERUP, HASSEL

International SAMPE Symposium and Exhibition, 35th, Anaheim, CA, Apr. 2-5, 1990, Proceedings. Books 1 & 2 p 940 A90-50056

SCHLACHTA, HENRY

Omega-GPS interoperability for the long haul p 577 A90-36927

SCHLAEFLI, D.

Unsteady flow visualization in a vibrating annular turbine cascade operating in the transonic flow regime p 7 A90-11786

Experimental investigation of the time-dependent flow in a vibrating annular cascade operating in the transonic flow regime p 7 A90-11787

SCHLEIN, B. C.

Development of a dual fuel injector for a gas turbine combustor

[ASME PAPER 89-GT-25] p 340 A90-23764

SCHLEY, C.-A.

Recent advances in H₂/O₂ high pressure coaxial injector performance analysis

[AIAA PAPER 90-1959] p 762 A90-42705

SCHLICKENMAIER, HERBERT W.

Windshear case study: Denver, Colorado, July 11, 1988

[DOT/FAA/DS-89/19] p 544 N90-21509

SCHLINKER, R. H.

- Rotor noise due to atmospheric turbulence ingestion. I
- Fluid mechanics p 219 A90-19385
Rotor noise due to atmospheric turbulence ingestion. II - Aeroacoustic results p 219 A90-19386

SCHMATZ, M. A.

- Numerical simulation of transonic wing flows using a zonal Euler, boundary-layer, Navier-Stokes approach p 225 A90-21596

- Grid patching approaches for complex three-dimensional configurations p 573 N90-21985

SCHMATZ, MANFRED A.

- Generalized fluxvectors for hypersonic shock-capturing [AIAA PAPER 90-0390] p 165 A90-19829

SCHMAUDER, JOACHIM

- Automotive gasoline - A fuel for modern aircraft piston engines p 950 A90-51620

SCHMID, R.

- Improved thermal performance using allylnadec-imides p 946 A90-50175

SCHMIDT, DAVID K.

- Cooperative synthesis of control and display augmentation in approach and landing p 516 A90-33061

- Analysis of airframe/engine interactions - An integrated control perspective [AIAA PAPER 90-1918] p 667 A90-40557

- Extended implicit model following as applied to integrated flight and propulsion control [AIAA PAPER 90-3444] p 890 A90-47697

- Multivariable flight control synthesis and literal robustness analysis for an aeroelastic vehicle [AIAA PAPER 90-3446] p 890 A90-47699

- Flexible aircraft dynamic modeling for dynamic analysis and control synthesis p 61 N90-10112

- Multivariable frequency weighted model order reduction for control synthesis [AIAA-89-3558] p 613 N90-23060

SCHMIDT, E.

- Inverse computation of transonic internal flows with application for multi-point-design of supercritical compressor blades p 501 N90-20987

SCHMIDT, H.

- Analysis of the rotor tip leakage flow with tip cooling air ejection p 515 N90-21029

SCHMIDT, LUTZ

- The formation of vortex streets in supersonic flows p 907 A90-51539

SCHMIT, L. A.

- Exploratory design studies using an integrated multidisciplinary synthesis capability for actively controlled composite wings [AIAA PAPER 90-0953] p 411 A90-29238

SCHMITMAN, CRAIG

- Building the B-2 p 701 A90-43826

SCHMITT, DIETER

- Airbus technologies - An evolutionary process p 902 A90-52699

SCHMITT, RON R.

- Viscoelastic relaxation in bolted thermoplastic composite joints p 945 A90-50158

SCHMITT, V.

- Design and experimental investigation of a laminar horizontal tail [AIAA PAPER 90-3042] p 798 A90-45934

SCHMITZ, F. H.

- Prediction and measurement of low-frequency harmonic noise of a hovering model helicopter rotor p 463 A90-28159

SCHMOLZ, PETER

- A contribution to the economic, optimal dimensioning, and shaping of aircraft structures using a design model [ETN-90-96966] p 737 N90-25976

SCHNEIDER, ALAN M.

- Observability of relative navigation using range-only measurements p 917 N90-29360

SCHNEIDER, EDWARD T.

- Piloted simulator assessments of agility [AIAA PAPER 90-1306] p 589 A90-36030

SCHNEIDER, GARRET L.

- Minimum-time turns using vectored thrust p 118 A90-14728

SCHNEIDER, GEORGE J.

- Application of damage tolerance p 843 N90-26817

SCHNEIDER, GUENTER

- Aeroelastic tailoring validation by windtunnel model testing p 492 A90-33389

SCHNEIDER, JOHN

- High-speed rotorcraft V/STOL - An initial assessment p 829 A90-46938

- The MH-60K - A special rotorcraft for special operations [AIAA PAPER 90-3266] p 835 A90-48860

Advanced rotorcraft V/STOL - Technology needs for

- high-speed rotorcraft [AIAA PAPER 90-3298] p 837 A90-48880

SCHNEIDER, K.

- Material development and second source qualification of carbon fiber/epoxy prepregs for primary and secondary Airbus structures p 948 A90-50225

SCHNEIDER, WILLIAM E.

- UV spectroradiometric output of an F404 turbojet aircraft engine p 552 A90-40195

- Spectral response of a UV flame sensor for a modern turbojet aircraft engine p 769 A90-43285

SCHNERR, G. H.

- Airfoils in supersonic source and sink flows p 149 A90-16844

- A straight attached shock wave at the profile tip at freestream Mach number greater than about 1 p 907 A90-51534

SCHNERR, GUENTER H.

- Transonic flow around airfoils with relaxation and energy supply by homogeneous condensation p 620 A90-39782

- The effect of energy input on the characteristics of profiles in compressible fluid media p 906 A90-51533

SCHOBELI, T.

- Optimum trailing edge ejection for cooled gas turbine blades p 41 A90-11562

SCHOBERT, H. H.

- Thermal stability of jet fuel [DE90-001160] p 206 N90-14385

SCHOBERT, HAROLD H.

- Thermal stability of jet fuel [DE90-002760] p 269 N90-15288

SCHODL, R.

- Laser two focus techniques p 212 N90-13348

SCHOEN, JAMES J.

- Potential role of avionics in escape systems p 483 N90-20060

SCHOENE, J.

- Analysis of three-dimensional aerospace configurations using the Euler and Navier-Stokes equations p 305 A90-25798

SCHOENE, JUERGEN

- Design of supersonic wings using an optimization strategy coupled with a solution scheme for the Euler equations [AIAA PAPER 90-3060] p 794 A90-45895

- A lifting surface method for the calculation of steady and unsteady, incompressible propeller aerodynamics [ESA-TT-1151] p 717 N90-25113

SCHOENSTER, JAMES A.

- Status report on a natural laminar-flow nacelle flight experiment p 105 N90-12550

- Effects of acoustic sources p 140 N90-12553

- A note on an acoustic response during an engine nacelle flight experiment [NASA-TM-102585] p 464 N90-19821

SCHOENTHAL, MARK

- Communications Interface Driver (CID) test plan [DOT/FAA/CT-TN89/35] p 958 N90-28762

SCHOLZ, D.

- A comparison between theoretical and experimental results for a 3-D wing with damped pitching oscillations p 472 A90-33361

- Coherent vortex structures in the wake of a sphere and a circular disk at rest and under forced vibrations p 623 A90-40749

SCHOMER, PAUL D.

- Human response research update p 699 N90-24873

SCHOOLCRAFT, R. J.

- Power transfer devices for V/STOL convertible engine systems p 587 A90-38539

SCHRA, L.

- Quench sensitivity of airframe aluminium alloys p 765 A90-44348

SCHRAEDER, KURT H.

- Automated analysis of MXU-553 flight data p 844 N90-26821

SCHRAG, R. L.

- Electro-impulse de-icing testing analysis and design [NASA-CR-4175] p 32 N90-10031

SCHRAGE, D. P.

- Time domain parameter identification techniques applied to the UH-60A Black Hawk Helicopter p 77 A90-12774

- Helicopter stability and control modeling improvements and verification on two helicopters p 671 A90-42474

- A study of the effects of Rotating Frame Turbulence (RFT) on helicopter flight mechanics p 248 N90-15058

SCHRAGE, DAN

- An investigation of aircraft maneuverability and agility [AIAA PAPER 90-3300] p 868 A90-48882

SCHRAGE, DANIEL P.

- Low speed maneuverability and agility design considerations for V/STOL aircraft p 581 A90-38536

- The impact of total quality management (TQM) and concurrent engineering on the aircraft design process p 785 A90-46927

- GTPDP - A rotary wing aircraft preliminary design and performance estimation program including optimization and cost p 830 A90-46944

- Helicopter individual blade control through optimal output feedback p 861 A90-46956

- Control of a twin lift helicopter system using nonlinear state feedback [AIAA PAPER 90-3408] p 817 A90-47663

SCHRAGER, C.

- An analysis of reliability in fiber optic ring and star networks p 78 A90-11666

SCHRAUF, GEZA

- An efficient solver of the Eigenvalue problem of the linear stability equations for three dimensional, compressible boundary-layer flows p 276 N90-16172

SCHREADLEY, HARRY W.

- Advanced actuation systems development, volume 1 [AD-A213334] p 121 N90-12624

- Advanced actuation systems development, volume 2 [AD-A213378] p 198 N90-13398

SCHRECK, SCOTT JEFFREY

- Experimental investigation of the mechanisms underlying vortex kinematics in unsteady separated flows [AD-A217889] p 540 N90-20346

SCHREINER, JOHN A.

- Canard-wing vortex interactions at subsonic through supersonic speeds [AIAA PAPER 90-2814] p 711 A90-45154

- Multiple vortex and shock interactions at subsonic, transonic, and supersonic speeds [AIAA PAPER 90-3023] p 793 A90-45890

SCHROEDER, G.

- Multiple channel frequency demodulator p 69 A90-12190

SCHROEDER, J. A.

- Flight evaluations of several hover control and display combinations for precise blind vertical landings [AIAA PAPER 90-3479] p 867 A90-47764

SCHROEDER, JEFFERY A.

- A pilot rating scale for evaluating failure transients in electronic flight control systems [AIAA PAPER 90-2827] p 754 A90-45159

- Effects of stick dynamics on helicopter flying qualities [AIAA PAPER 90-3477] p 866 A90-47727

SCHROERS, LAUREL G.

- Development of the XV-15 tiltrotor research aircraft - Lessons learned p 581 A90-38540

SCHUBERT, MARTIN

- The MANTA: An RPV design to investigate forces and moments on a lifting surface [NASA-CR-186227] p 499 N90-20971

SCHUCHMAN, LEONARD

- Applicability of an augmented GPS for navigation in the National Airspace System p 331 A90-25571

SCHUDT, JOE

- The SKY SHARK: An RPV designed to investigate the pressure distribution on a lifting surface [NASA-CR-186222] p 844 N90-26824

SCHUESSLER, RANDALL

- AVION: A detailed report on the preliminary design of a 79-passenger, high-efficiency, commercial transport aircraft [NASA-CR-186663] p 649 N90-23395

SCHUESSLER, WARREN, JR.

- V-22 aerodynamic loads analysis and development of loads alleviation flight control system p 410 A90-28239

SCHUETTE, HOLGER

- Unmanned helicopters for battlefield and maritime surveillance p 920 A90-51899

SCHUETZ, H.

- A semi-analytical procedure for the conformal mapping of arbitrary airfoil contours p 309 A90-26498

SCHUETZ, R.

- Neutron radiography: Applications and systems p 886 N90-28080

SCHUETZ, W.

- Methodology of variable amplitude fatigue tests p 451 A90-29866

SCHUETZ, WALTER

- Standardized stress-time histories - An overview p 368 A90-26752

- Fretting fatigue strength of Ti-6Al-4V at room and elevated temperatures and ways of improving it p 952 N90-28709

SCHULEIN, P.

- The comparison of the airbase simulation models airbase and sustained [FEL-1988-66] p 123 N90-12629

- SCHULTZ, J. L.**
Finite element simulation of compressible turbulent flows
- Validation and application to internal aerodynamic in gas-turbine engines p 210 A90-18343
- SCHULTZ, K. J.**
Rotor blade-vortex interaction impulsive noise source localization p 463 A90-27978
- SCHULTZ, KLAUS-J.**
Technical-scientific possibilities for helicopter noise research in the German-Dutch wind tunnel p 283 A90-21474
- SCHULTZ, T. A.**
Analysis of severe atmospheric disturbances from airline flight records p 280 N90-15045
- SCHULTZ, THOMAS A.**
Multiple vortex ring model of the DFW microburst p 280 A90-23286
- SCHULZ, H. D.**
Three-dimensional separated flow field in the endwall region of an annular compressor cascade in the presence of rotor-stator interaction. I - Quasi-steady flow field and comparison with steady-state data [ASME PAPER 89-GT-76] p 291 A90-23797
Three-dimensional separated flow field in the endwall region of an annular compressor cascade in the presence of rotor-stator interaction. II - Unsteady flow and pressure field [ASME PAPER 89-GT-77] p 291 A90-23798
Experimental investigation of the influence of rotor wakes on the development of the profile boundary layer and the performance of an annular compressor cascade p 427 N90-18425
- SCHULZ, UWE**
Digital electronic control unit for the European Fighter Aircraft (EFA) p 253 A90-21607
- SCHULZE, B.**
Comparison of two potential flow methods for transonic flutter analysis p 471 A90-33356
An infrared camera system for detection of boundary layer transition in the ETW p 539 A90-34249
- SCHUMM, M.**
Coherent vortex structures in the wake of a sphere and a circular disk at rest and under forced vibrations p 623 A90-40749
- SCHUSTER, DAVID M.**
Static aeroelastic analysis of fighter aircraft using a three-dimensional Navier-Stokes algorithm [AIAA PAPER 90-0435] p 166 A90-19845
- SCHUSTER, JOACHIM**
The signals of an ice warning device in dependence on total water content and normalized icing degree [ESA-TT-1207] p 963 N90-29692
- SCHUTTE, PAUL C.**
Real-time fault monitoring for aircraft applications using quantitative simulation and expert systems [AIAA PAPER 89-3103] p 37 A90-10586
- SCHWAB, R. R.**
Aspects of the design of a hypersonic engine system and the selection of the intake and tail [DGLR PAPER 88-040] p 928 A90-50233
- SCHWAB, RAINER R.**
Parametric assessment of propulsion system mass for airbreathing launcher configurations p 344 N90-16819
- SCHWAB, ROBERT W.**
Aircraft interface with the future ATC system p 331 A90-25574
- SCHWAMBORN, D.**
Computation of transonic turbine cascade flow using Navier-Stokes equations p 14 A90-12621
Some Navier-Stokes calculations for the CAST-10 airfoil p 320 N90-17651
- SCHWANE, R.**
On the computations of hypersonic viscous flows p 225 A90-21170
- SCHWARMANN, L.**
Investigation on sheet material of 8090 and 2091 aluminium-lithium alloy p 267 N90-15192
- SCHWARMANN, LUEDER**
Investigation on sheet material of 8090 and 2091 aluminium-lithium alloy [MBB-UT-122/89-PUB] p 766 N90-25090
- SCHWARTZ, ALAN L.**
An algebraic adaptive-grid technique for the solution of Navier-Stokes equations [AIAA PAPER 90-1605] p 567 A90-38736
- SCHWARTZ, ALAN W.**
An unmanned air vehicle concept with tipjet drive p 830 A90-46951
- SCHWARTZ, F.**
beta CEZ, a high performance titanium alloy for aerospace engines [ONERA, TP NO. 1990-8] p 356 A90-25356
- SCHWARTZ, H.**
RAIM - An implementation study p 726 A90-43714
- SCHWARTZ, R. J.**
Flow field measurements near a fighter model at high angles of attack [AIAA PAPER 90-1431] p 559 A90-37968
- SCHWARZ, M.**
Calculation of the side-wall boundary layer in axial turbomachines, accounting for the internal flow near the blades p 225 A90-21595
- SCHWARZ, W.**
Grid patching approaches for complex three-dimensional configurations p 573 N90-21985
- SCHWARZOTT, WALTER P.**
Experimental work station simulator at the test station of the Bundesanstalt fuer Flugsicherung p 937 A90-52616
- SCHWEIGER, F. A.**
Revolutionary opportunities for materials and structures study [NASA-CR-179642] p 63 N90-10184
- SCHWEIGER, J.**
The influence of mathematical optimization methods on the design of aircraft structures p 492 A90-33387
- SCHWEIKHARD, W. G.**
Flight test data processing, plotting and analysis at your finger tips - A flexible, automated, integrated approach [AIAA PAPER 90-1322] p 545 A90-34150
- SCHWEITZER, W.-B.**
The effect of an oscillatory freestream-flow on a NACA-4412 profile at large relative amplitudes and low Reynolds-numbers p 560 A90-38495
- SCHWEITZER, WILLI-BERT**
Carrier wing profile in nonstationary current [ETN-90-95368] p 399 N90-19208
- SCHWENKE, MICHAEL**
Aircraft condition monitoring system for future Airbus aircraft: New concept for programming and data recording p 848 N90-27619
- SCICCHITANO, EDWARD V.**
Considerations for successful application of integrated drive generators to aircraft [SAE PAPER 892226] p 746 A90-45442
- SCOLA, DANIEL A.**
The status of high temperature polymers for composites - Likely candidates p 528 A90-31516
- SCOLARIS, M.**
The evolution of light alloys in the aerospace industry [ETN-89-95216] p 126 N90-11872
An ultrasonic system for in-service non-destructive inspection of composite structures p 885 N90-28076
- SCOTSE, ARTHUR E.**
A low cost shadow moire device for the nondestructive evaluation of impact damage in composite laminates [AD-A223451] p 953 N90-29442
- SCOTT, B. C.**
Ground-simulation investigations of VTOL airworthiness criteria for terminal-area operations [NASA-TM-102810] p 757 N90-25141
- SCOTT, BARRY C.**
Simulator evaluation of 'basic' mode back azimuth issues in departure and missed approach usage [SAE PAPER 892216] p 728 A90-45433
Simulation of MLS-ATC procedures in the New York and San Francisco Terminal Control Areas [SAE PAPER 892217] p 728 A90-45434
- SCOTT, C. II**
Regression and combustion characteristics of boron containing fuels for solid fuel ramjets p 858 N90-27928
- SCOTT, CARL D.**
Effects of thermochemistry, nonequilibrium, and surface catalysis on the design of hypersonic vehicles p 224 A90-21159
- SCOTT, J. R.**
Analysis of nonuniform subsonic flows about a row of moving blades p 6 A90-11779
- SCOTT, JAMES N.**
Computation of ramjet internal flowfields [AD-A212001] p 114 N90-11743
- SCOTT, JAMES R.**
Numerical solutions of the linearized Euler equations for unsteady vortical flows around lifting airfoils [AIAA PAPER 90-0694] p 300 A90-25041
Numerical solutions of the linearized Euler equations for unsteady vortical flows around lifting airfoils p 394 A90-30264
Numerical solutions of the linearized Euler equations for unsteady vortical flows around lifting airfoils [NASA-TM-102466] p 318 N90-17562
- SCOTT, K. T.**
Properties and characterisation of novel thermal barrier systems for gas turbines p 62 A90-12538
- SCOTT, MARK W.**
Helicopter design optimization for maneuverability and agility p 408 A90-28212
- Mission performance comparison between tilt rotor, variable diameter tilt rotor and tilt wing aircraft p 830 A90-46940
- SCOTT, MATTHEW T.**
Nonlinear aerodynamics of two-dimensional airfoils in severe maneuver p 301 A90-25276
- SCOTT, PAUL T.**
Source emission test of gas turbine engine test facility, Kelly AFB, TX [AD-A223869] p 932 N90-28571
- SCOTT, STAN G.**
The Meteorological Measurement System on the NASA ER-2 aircraft p 926 A90-51658
- SCOTT, WILLIAM B.**
Rockwell's simulator emulates NASP flight characteristics p 60 A90-11650
YF-23A previews design features of future fighters p 643 A90-40344
- SCRUBY, C. B.**
Characterisation of fatigue of aluminium alloys by acoustic emission. Part 2: Discrimination between primary and other emissions [AERE-R-13303-PT-2] p 678 N90-23523
- SCURLOCK, R. G.**
Development of cryogenic instrumentation for ETW models p 525 A90-34251
- SEALS, J. DENNIS**
A heterogeneous parallel processing architecture for avionic and aerospace applications [AIAA PAPER 89-3108] p 74 A90-10590
- SEARS, W. R.**
Comment on 'Induced drag and the ideal wake of a lifting wing' p 233 A90-23291
- SEDDINI, A.**
Aerodynamics of cooling jets introduced in the secondary flow of a low speed turbine cascade [ASME PAPER 89-GT-192] p 362 A90-23868
- SEDDOUGUI, SHARON O.**
Wave interactions in a three-dimensional attachment-line boundary layer p 811 A90-48715
- SEETHARAM, S. M.**
Computational and experimental studies on ground effect of a slender wing tailless delta aircraft p 810 A90-48083
- SEFERIS, J. C.**
Measurement and characterization of prepreg permeability with a modified bagging technique p 949 A90-50226
Mechanical influences on crystallization in PEEK matrix/carbon fiber reinforced composites p 949 A90-50227
- SEGAERT, P.**
Secondary flows and radial mixing predictions in axial compressors p 512 N90-21010
- SEGURA, E.**
Numerical predictions for the flow and the heat transfer in gas turbine cooling systems p 770 A90-44464
Numerical investigations of heat transfer and flow rates in rotating cavities. Simulation of the movement generated by wall temperature gradients, by source-sink mass flows or by the differential rotation of the walls, under the influence of coriolis and centrifugal forces [ETN-90-96253] p 454 N90-18695
- SEHRA, A.**
Viscous flow analysis for advanced inlet particle separators [AIAA PAPER 90-2136] p 661 A90-42038
- SEIDEL, DAVID A.**
Unsteady pressure and structural response measurements on an elastic supercritical wing p 159 A90-19392
- SEIDMAN, ABRAHAM N.**
Applications of neural networks to avionics systems [AIAA PAPER 89-3093] p 76 A90-10627
- SEIFERT, A.**
Low Reynolds number airfoils evaluation program p 151 A90-17692
- SEIFUDDIN, LAMAR T.**
USCG HH-65A/SRR GPS integration and test results p 726 A90-43705
- SEIGLE, JEFFREY**
System testing of a production Ada (trademark) project: The GRODY study [NASA-TM-103308] p 546 N90-21541
- SEILER, WILLIAM, JR.**
Wide-range fuel flowmeter, phase 2 [AD-A210547] p 72 N90-10424
- SEINER, JOHN M.**
External nozzle flap dynamic load measurements on F-15 S/MTD model [AIAA PAPER 90-1910] p 740 A90-42692
- SEITELMAN, LEON H.**
USA - A system to represent airfoils throughout the product life cycle [AIAA PAPER 89-2972] p 73 A90-10487

SEKAR, B.

A numerical parametric study of a scramjet inlet in a Mach 6 arc heated test facility
[AIAA PAPER 90-0531] p 167 A90-19896

SELBERG, BRUCE P.

Static stability and control characteristics of scissor wing configurations p 433 A90-31277
Some aerodynamic characteristics of the scissor wing configuration

[SAE PAPER 892202] p 713 A90-45423
Improving computer techniques for real-time digital flight simulation

[SAE PAPER 892354] p 760 A90-45505
An aerodynamic tradeoff study of the scissor wing configuration

[NASA-CR-186576] p 481 N90-20965

SELBERT, BRUCE P.

Alternate table look-up routine for real-time digital flight simulation p 611 A90-35769

SELBY, D. A.

Enhanced bioreclamation of jet fuels: A full-scale test at Eglin AFB, Florida
[AD-A222348] p 875 N90-26992

SELBY, G. V.

Investigation of several passive and active methods for turbulent flow separation control
[AIAA PAPER 90-1598] p 607 A90-38730

SELBY, GREGORY V.

Effect of surface grooves on base pressure for a blunt trailing-edge airfoil p 556 A90-36280
Generation of circumferential velocity contours associated with pulsed point suction on a rotating disk p 691 N90-25065

SELEROWICZ, W. C.

Self-excited oscillations in internal transonic flows p 813 A90-49274

SELEZNEV, A. I.

A study of three-dimensional supersonic flow of a real gas past axisymmetric bodies p 3 A90-10938

SELIG, M. S.

Low Reynolds number airfoil design and wind tunnel testing at Princeton University p 799 A90-46362

SELIKHOV, A. F.

Ways of providing for the strength and service life of aircraft structures made of polymer composites with allowance for damage p 957 A90-50843

SELIVANOV, OLEG D.

Principles underlying the integration of an aircraft and its engine p 729 A90-42520

SELIVERSTOV, VLADIMIR M.

Handbook on heat exchangers p 273 A90-22743

SELLAR, RICH

The DELTA MONSTER: An RPV designed to investigate the aerodynamics of a delta wing platform
[NASA-CR-186226] p 924 N90-29381

SELLERS, WILLIAM L., III

An embedded grid formulation applied to a delta wing
[AIAA PAPER 90-0429] p 229 A90-22216

SELMIN, V.

A multistage method for the solution of the Euler equations on unstructured grids p 708 A90-44460

SELVAGGINI, R.

Conditional sampling
[ONERA, TP NO. 1989-187] p 261 A90-21047

SEMBER, JAMES W.

Control of a switched-plactance aircraft engine starter-generator over a very wide speed range p 586 A90-38130

SEME NOV, N. V.

Wave structure of artificial perturbations in a supersonic boundary layer on a plate p 619 A90-39518

SEME NOV, P. K.

Parametric synthesis of the decoupling filter in the manual control system of VTOL aircraft p 859 A90-46483

SEME NOV, V. N.

A study of the strength characteristics of a twin-fuselage aircraft with a trapezoid wing system p 410 A90-28993

SEME NOVA, O. K.

Effect of a crescent-shaped rigid support on the aerodynamic characteristics of models in the presence of perforated boundaries p 869 A90-46537

SEMMES, R. G.

Computational analysis of an open-nosed fighter/attack inlet
[AIAA PAPER 90-2145] p 704 A90-42737

SEN, J.

Modeling strategies for crashworthiness analysis of landing gears p 409 A90-28233

SENA, J. TOM

Design and demonstration of heat pipe cooling for NASP and evaluation of heating methods at high heating rates
[DE89-016995] p 186 N90-14227

SEND, W.

Unsteady lift and moment coefficients of an engine nacelle p 473 A90-33365

SENDECKYJ, G. P.

Air Force smart structures/skins program overview p 38 A90-11205
Some smart structures concepts p 503 A90-32858

SENF, CARY TAYLOR

Design of a low cost short takeoff-vertical landing export fighter/attack aircraft
[NASA-CR-186658] p 734 N90-25132

SENGE, HEINRICH

Application of vortex embedding to aircraft flows
[AIAA PAPER 90-1626] p 568 A90-38755

SENGER, R.

Static and dynamic characterization of the ATR 72 rods made of Ti 10.2.3 titanium alloy
[REPT-49-238] p 953 N90-28722

SENGUPTA, S.

Numerical grid generation in computational fluid mechanics '88; Proceedings of the Second International Conference, Miami Beach, FL, Dec. 5-8, 1988 p 376 A90-26476

SENGUPTA, UPAL

The implementation and operation of a variable-response electronic throttle control system for a TF-104G aircraft
[NASA-TM-101696] p 509 N90-20086

SENOO, Y.

Application of low-solidity cascade diffuser to transonic centrifugal compressor
[ASME PAPER 89-GT-66] p 290 A90-23789

SENOO, YASUTOSHI

Effect of blade tip configuration on tip clearance loss of a centrifugal impeller
[ASME PAPER 89-GT-80] p 358 A90-23801

Secondary flow due to the tip clearance at the exit of centrifugal impellers
[ASME PAPER 89-GT-81] p 358 A90-23802

SENSBURG, O.

The influence of mathematical optimization methods on the design of aircraft structures p 492 A90-33387

SENSBURG, OTTO

Review of active structural control systems and flight test techniques for dynamic stability investigations p 516 A90-33352

SENTOH, ETSUROH

A comparison of inverse control with optimal control
[AIAA PAPER 90-3484] p 866 A90-47733

SERAFINI, JOHN A.

Laser-velocimeter-measured flow field around an advanced, swept, eight-blade propeller at Mach 0.8
[NASA-TP-2462] p 468 N90-20942

SERAG-ELDIN, M. A.

Computation of the trailing edge flow downstream a flat plate with finite thickness p 151 A90-17464

SERAUDIE, A.

Design of a three dimensional Doppler anemometer for T2 transonic wind tunnel p 447 A90-28271

Flow quality in the T2 cryogenic wind-tunnel - Problems and solutions p 524 A90-34240
Main results of CAST-10 airfoil tested in T2 cryogenic wind tunnel p 321 N90-17652

SERGIENKO, A. A.

Dissipation thrust losses due to distortions of the jet nozzle profile p 254 A90-23405

SEROVY, G. K.

An off-design loss and deviation prediction study for transonic axial compressors
[ASME PAPER 89-GT-324] p 343 A90-23893

SERRANO, C.

Simple shear tests of the FMI 23.5.06 adhesive cured at low pressure (12 PSI)
[INFORME-I-298/88] p 357 N90-17871

SERRANO, M.

Numerical simulation of unsteady combustion in a dump combustor p 54 N90-10203

SERVATY, S.

Unsteady aerodynamics and aeroelasticity of turbomachines and propellers; Proceedings of the Fourth International Symposium, Aachen, Federal Republic of Germany, Sept. 6-10, 1987 p 5 A90-11776

Computation of aerodynamic blade loads due to wake influence and aerodynamic damping of turbine and compressor cascades p 7 A90-11791

Unsteady blade loads due to wake influence p 426 N90-18413

SERVOUZE, Y.

Pressure surface trailing edge slot cooling
[ONERA, TP NO. 1989-123] p 47 A90-12569

SETO, S. P.

Energy Efficient Engine combustor test hardware detailed design report
[NASA-CR-168301] p 929 N90-28554

Energy Efficient Engine (E3) combustion system component technology performance report
[NASA-CR-168274] p 930 N90-28555

SETTLE, T. BEN

Evolution and test history of the V-22 0.2-scale aeroelastic model p 831 A90-46954

SETTLES, G. S.

Mach number effects on conical surface features of swept shock-wave/boundary-layer interactions p 154 A90-18147

Swept shock/boundary-layer interactions - Tutorial and update
[AIAA PAPER 90-0375] p 228 A90-22207

Structure of swept shock wave/boundary-layer interactions using conical shadowgraphy
[AIAA PAPER 90-1644] p 569 A90-38772

SETTLES, GARY S.

Skin friction measurements by laser interferometry in swept shock/boundary-layer interactions p 154 A90-18153

Upstream-influence scaling of fin-generated shock wave boundary-layer interactions
[AIAA PAPER 90-0376] p 164 A90-19822

Experimental research on swept shock Wave/Boundary layer interactions
[AD-A211744] p 134 N90-11988

DURIP optical equipment for high-speed viscous-inviscid interaction research
[AD-A217772] p 540 N90-20345

SEVRAIN, A.

Development of turbulence models for the analysis of compressible or incompressible unsteady flow
[ETN-90-97486] p 958 N90-28810

SEWALL, W. G.

Simultaneous detection of separation and transition in surface shear layers p 72 N90-10368

SEWALL, WILLIAM G.

Wind tunnel results of the high-speed NLF(1)-0213 airfoil p 93 N90-12542

SEXTON, RALPH D.

Development of obstacle clearance criteria and standards for MLS and MLS/RNAV precision approaches and development of an MLS collision risk model
[SAE PAPER 892215] p 728 A90-45432

SEYFANG, GEORGE R.

Technology and evaluation of unmanned air vehicles p 252 N90-15934

SEYMOUR, JOHN G.

Aircraft performance enhancement with active compressor stabilization
[AD-A213652] p 249 N90-15097

SHA, BONAN

The anti-shimmy and break-proof study of nose landing gear p 178 A90-16856

SHABROV, N. N.

Finite element analysis of nonstationary temperature fields in gas turbine components p 271 A90-21324

SHAD, SHABBI

Teamwork for excellence
[AIAA PAPER 89-3195] p 549 A90-31686

SHADE, WAYNE A.

Vibration analysis for immediate assessment of battle-damaged gas turbine engines
[ASME PAPER 89-GT-96] p 341 A90-23811

SHADMON, G.

Real time estimation of aircraft angular attitude p 431 A90-30103

SHAFFER, J.

Reduced voltage and restart testing of the 1-watt integral cryogenic cooler (HD-1033B/C/D)
[AD-A215133] p 369 N90-16971

SHAFFER, PHILLIP L.

A multiprocessor implementation of real-time control for a turbojet engine p 746 A90-45415

SHAGAEV, A. A.

Application of Fedorenko's multigrid method for calculating transonic flow past a profile p 295 A90-24103

SHAGNEA, ANITA M.

Software verification plan for GCS
[NASA-TM-101668] p 372 N90-18057

SHAH, GAUTAM H.

Unsteady aerodynamic characteristics of a fighter model undergoing large-amplitude pitching motions at high angles of attack
[AIAA PAPER 90-0308] p 313 A90-26933

Vortex control for tail buffet alleviation on a twin-tail fighter configuration
[SAE PAPER 892221] p 756 A90-45438

Low-speed wind-tunnel study of reaction control-jet effectiveness for hover and transition of a STOVL fighter concept
[NASA-TM-4147] p 119 N90-11751

- SHAH, P. P.**
Production of jet fuels from coal-derived liquids. Volume 11: Production of advanced endothermic fuel blends from Great Plains Gasification Plant naphtha by-product stream
[AD-A210251] p 65 N90-11184
- SHAKHOV, V. G.**
Effect of the roughness of deposits in a compressor cascade on the flow lag angle p 84 A90-14578
- SHAKIR'IANOV, M. M.**
Classification of methods for eliminating surging in gas turbine engines p 111 A90-14591
- SHALIN, VALERIE L.**
Automating acquisition of plans for an intelligent assistant by observing user behavior p 459 A90-30230
- SHAMANSKY, H. T.**
The Helicopter Antenna Radiation Prediction Code (HARRP)
[NASA-CR-186925] p 884 N90-27946
- SHAMIE, J.**
Correlation of AH-1G airframe flight vibration data with a coupled rotor-fuselage analysis
[NASA-CR-181974] p 959 N90-28865
- SHAMIR, JOSEPH**
Angular feature mapping - An optical method p 377 A90-23974
- SHAMROTH, S. J.**
Navier-Stokes study of rotating stall in compressor cascades p 302 A90-25292
- SHAMROTH, STEPHEN J.**
Extension of a three-dimensional viscous wing flow analysis user's manual: VISTA 3-D code
[NASA-CR-182024] p 574 N90-22538
Extension of a three-dimensional viscous wing flow analysis
[NASA-CR-182023] p 631 N90-23348
- SHANG, J. J. S.**
Results from a numerical simulation of an F-16A configuration at a supersonic Mach number p 146 A90-16769
- SHANG, J. S.**
Numerical simulation of an F-16A at angle of attack
[AIAA PAPER 90-0100] p 313 A90-26911
- SHANG, JOSEPH S.**
Numerical simulation of reversed flow over a supersonic delta wing at high angle of attack p 8 A90-11849
Comparison between thin layer and full Navier-Stokes simulations over a supersonic delta wing
[AIAA PAPER 90-0589] p 314 A90-26968
- SHANG, YI**
The analysis and solution of the performance deterioration problem of WP7 engine under the full reheating condition p 191 A90-18624
- SHANKAR, VIJAYA**
Supersonic flow computations over aerospace configurations using an Euler marching solver
[NASA-CR-4085] p 19 N90-10012
- SHANKAR, VIJAYALAXMI**
Human centrifuge controller
[NAL-TM-SE-8901] p 527 N90-21043
- SHANYGIN, A. N.**
Application of the MARS system in aircraft-structure design p 374 A90-24127
- SHAPIRO, ALBERT J.**
The integration of multiple avionic sensors and technologies for future military helicopters p 916 N90-29344
- SHAPOVALOV, G. K.**
A method for the active control of the boundary layer condition p 296 A90-24114
Investigation of wall pressure pulsations during the passive control of shock/boundary layer interaction p 378 A90-24132
- SHARAN, A. M.**
The design of rotor blades taking into account the combined effects of vibratory and thermal loads p 40 A90-11553
- SHARMA, OM**
Using 3D Euler flow simulations to assess effects of periodic unsteady flow through turbines
[AIAA PAPER 90-2357] p 706 A90-42783
- SHARMA, P. B.**
A study of flow structure in a contra-rotating axial compressor stage p 11 A90-12524
- SHAU, Y. R.**
The detection of large scale structure in undisturbed and disturbed compressible turbulent free shear layers
[AIAA PAPER 90-0711] p 230 A90-22251
- SHAW, E. D.**
F/A-18 aileron smart servoactuator p 432 A90-30710
- SHAW, J. A.**
The construction of component-adaptive grids for aerodynamic geometries p 309 A90-26513
- A discussion on issues relating to multiblock grid generation p 608 N90-21991
- SHAW, LEONARD**
Twin-jet screech suppression p 894 A90-48957
- SHAW, ROBERT J.**
Predictions of airfoil aerodynamic performance degradation due to icing p 144 A90-16753
NASA's program on icing research and technology p 239 N90-15062
- SHCHEKIN, G. A.**
Calculation of nonseparated transonic flow past swept wings with allowance for viscosity p 294 A90-24079
- SHCHENNIKOV, S. A.**
Calculation of the drag of fuselage tail sections of different shapes in supersonic flow of a nonviscous gas p 388 A90-29182
- SHCHERBAKOV, S. A.**
Calculation of the front or rear part of a flat body in subsonic flow with the extremum value of the critical Mach number p 296 A90-24120
Gasdynamic characteristics of a plane or axisymmetric nozzle with a rectilinear generatrix of the supersonic section p 805 A90-46575
- SHCHERBAKOV, V. A.**
Instability and susceptibility of a boundary layer in the vicinity of two-dimensional surface inhomogeneities p 535 A90-32675
- SHEA, MARK A.**
Improved steel for landing gear design
[SAE PAPER 892335] p 765 A90-45490
Titanium matrix composite landing gear development
[SAE PAPER 892337] p 733 A90-45491
- SHEARON, ANDY**
The DELTA MONSTER: An RPV designed to investigate the aerodynamics of a delta wing platform
[NASA-CR-186226] p 924 N90-29381
- SHEEDY, K. P.**
Turbulent flow simulation of a three-dimensional turbine cascade
[AIAA PAPER 90-2124] p 704 A90-42732
- SHEFFLER, K. D.**
MATE (Materials for Advanced Turbine Engines) Program, Project 3. Volume 2: Design, fabrication and evaluation of an oxide dispersion strengthened sheet alloy combustor liner
[NASA-CR-180892] p 357 N90-17868
- SHEHAN, J. J.**
Nonflammable hydraulic power system for tactical aircraft. Volume 1: Aircraft system definition, design and analysis
[AD-A218493] p 671 N90-23409
- SHEKHOVTSOV, S. B.**
Formalization and solution of covering problems in the synthesis of control and monitoring systems p 76 A90-10963
- SHELLEY, LARRY**
Trends in real-time flight systems
[AIAA PAPER 89-3086] p 25 A90-10572
- SHEN, CHIH-PING**
Low-energy gamma ray attenuation characteristics of aviation fuels
[NASA-TP-2974] p 462 N90-18882
- SHEN, CHUNLIN**
A variable structure system (VSS) to robust control of aircraft p 257 A90-21987
- SHEN, GONGZHANG**
The eigenvalue sensitivity analysis and design for integrated flight/propulsion control systems p 196 A90-18601
- SHEN, HUILI**
Solution of Euler equations for fighter forebody-inlet combination at high angle of attack p 556 A90-36419
- SHEN, MENGYU**
Computation of transonic flow in a plane cascade with an unfactored flux splitting implicit method p 152 A90-17785
A new method for high speed propeller flutter prediction p 854 A90-49454
- SHEN, SHYAN**
Adhesive-bonded composite-patching repair of cracked aircraft structure p 467 A90-31576
- SHEN, TONY**
Damage tolerance analysis and testing of a welded cluster gear for the main transmission of the Advanced Attack Helicopter p 445 A90-28187
- SHEN, ZHEN-HUA**
Wall pressure fluctuations in the reattachment region of a supersonic free shear layer
[AIAA PAPER 90-1461] p 561 A90-38618
- SHEN, ZUDA**
Analyses of revising the inlet profile of a radial inflow turbine impeller p 602 A90-35831
- SHENBERGER, MICHAEL**
Automated helicopter structural analysis data processing p 611 A90-38533
- SHENDE, R. W.**
Squeeze film damping for aircraft gas turbines p 113 A90-16009
- SHENG, YUANSHENG**
An analysis of cavity resonance in the aeroengine casing during rig testing p 894 A90-49481
- SHENOY, RAJARAMA K.**
Aeroacoustic flowfield and acoustics of a model helicopter tail rotor at high advance ratio p 463 A90-28160
Emerging new technologies at Sikorsky aircraft p 382 A90-30114
- SHEPARD, RANDALL**
Advanced integrated avionics test support concepts
[AIAA PAPER 90-1259] p 504 A90-33889
- SHEPEL', VIACHESLAV T.**
Technical and economic efficiency of aviation gas turbine engines in service p 851 A90-46624
- SHEPHARD, MARK S.**
Solving compressible flow problems using adaptive finite quadtree and octree grids p 155 A90-18243
- SHEPHERD, JOHN T.**
The implications of using integrated software support environment for design of guidance and control systems software
[AGARD-AR-229] p 434 N90-18432
- SHEPSHELOVICH, M.**
Low Reynolds number airfoils evaluation program p 151 A90-17692
Active flow control on low Reynolds number airfoils
[AIAA PAPER 90-3039] p 792 A90-45878
- SHERIDAN, G. N.**
Integral fuel tank sealing practice at British Aerospace (Kingston) p 250 N90-15905
- SHERMAN, B. D.**
A fiber optic headset compatible with power-by-light p 504 A90-32906
- SHERMAN, DOUGLAS J.**
An examination of the fatigue meter records from the RAAF Orion P-3C fleet
[AD-A214000] p 338 N90-17628
- SHEU, M. J.**
Parameter effects on oscillatory aerofoil in transonic flows
[AIAA PAPER 90-1473] p 563 A90-38629
Measurements of turbulent dual-jet interaction
[AIAA PAPER 90-2105] p 624 A90-42019
Numerical solutions for unsteady aerofoil by internal singularity method p 716 A90-45536
- SHEU, MING-FA**
Chemical resistance of carbon fiber reinforced polyether ether ketone and polyphenylene sulfide composites p 944 A90-50142
- SHEVARE, G. R.**
Simulation of separated flows using panel method p 308 A90-26349
- SHEVCHENKO, IU. A.**
Application of the MARS system in aircraft-structure design p 374 A90-24127
- SHEVCHUK, L. A.**
A method for recalculating the temperature fields of aircraft structures for different experimental conditions p 448 A90-28994
- SHEVEL'KOV, S. G.**
Wave structure of artificial perturbations in a supersonic boundary layer on a plate p 619 A90-39518
- SHI, JING**
An aerodynamical design and calculation method for gas turbine with cooling air mixing p 189 A90-17782
Effect of vane and blade numbers on performance of transonic turbine stage p 189 A90-17789
- SHI, WANGXING**
Effect of condensation in a diffuser on the flow field p 603 A90-36784
- SHI, YING-LIANG**
System testing of a production Ada (trademark) project: The GRODY study
[NASA-TM-103308] p 546 N90-21541
- SHI, ZHONGKE**
A separated algorithm and applications to flight test p 216 A90-16857
- SHIAU, L. C.**
Finite element analysis of composite panel flutter p 681 A90-40032
- SHIAU, TING NUNG**
Optimum weight design of a rotor bearing system with dynamic behavior constraints
[ASME PAPER 89-GT-74] p 358 A90-23795
- SHIEN, L. S.**
A linear quadratic regulator approach to the stabilization of uncertain linear systems
[AIAA PAPER 90-3509] p 891 A90-47755
- SHIGEMATSU, JUNJI**
A numerical investigation of supersonic inlet using implicit TVD scheme
[AIAA PAPER 90-2135] p 621 A90-40612

SHIH, E.

On the drag reduction of bluff bodies through momentum injection
[AIAA PAPER 90-3076] p 797 A90-45922

SHIH, F. M.

Threshold performance optimization of a rotor-bearing system subjected to leakage excitation
[ASME PAPER 89-GT-126] p 360 A90-23825

SHIMADA, YUZO

An adaptive flight control system design for non-minimum phase CCV by relative order reduction
p 196 A90-19428

SHIMIZU, SHIN-ICHI

Endurance test of FJR 710/600S engine
p 42 A90-12012

SHIMODAIRA, K.

Hydrogen fueled subsonic-ram-combustor model tests for an air-turbo-ram engine
p 44 A90-12529

SHIMOKAWA, TOSHIYUKI

Evaluation of static and fatigue properties of thin sheets of 8090-T8 aluminum-lithium alloy and observation of its fracture surfaces
[NAL-TR-1039] p 953 N90-29499

Fractographic analysis of fatigue failures of airframe equipment parts: Examples of a rod end housing and a rod end cap
[NAL-TR-1047] p 961 N90-29686

SHIMOVETZ, RALPH

SARL noise measurements
[AIAA PAPER 90-0285] p 219 A90-19772

SHIMP, D. A.

New cyanate ester resin with low temperature (125-200 °C) cure capability
p 944 A90-50135

SHIN, JAIWON

Effective methods of controlling a junction vortex system in an incompressible, three-dimensional, turbulent flow
p 571 N90-21732

SHINBO, YUICHI

Unsteady aerodynamic forces on rolling delta wings at high angle of attack
p 159 A90-19426

SHINGLEDECKER, CLARK

Operational evaluation of initial data link air traffic control services, volume 1
[DOT/FAA/CT-90/1-VOL-1] p 455 N90-19472

SHINODA, PATRICK M.

Comparison of model- and full-scale wind-tunnel performance
[AIAA PAPER 88-2536] p 351 A90-26133

SHINOKI, SHUJI

Improvement in turbine blade aerodynamic force in the tip region
p 809 A90-47854

SHIODA, SUSUMU

Studies on supersonic radial flow behavior in disk channel
p 87 A90-16104

SHIOKAWA, TAKAYASU

Airborne array antennas for satellite communication
p 265 A90-23202

SHIPKOWSKI, MICHAEL S.

Realtime multi-plot graphics system
[NASA-CR-4304] p 965 N90-29919

SHIPMAN, RICHARD P.

Visual servoing for autonomous aircraft refueling
[AD-A216042] p 414 N90-18386

SHIRAIISHI, KAZUO

A numerical investigation of supersonic inlet using implicit TVD scheme
[AIAA PAPER 90-2135] p 621 A90-40612

SHITOVA, E. M.

Interchangeability of Soviet-made and foreign mineral oils for aviation gas turbine engines
p 873 A90-46525

SHIVAKUMARA SWAMY, M.

Wind tunnel testing of high blockage models
p 121 A90-15743

SHIVELY, C.

Rapsat - Application of onboard processing for communication and surveillance in air traffic control
[AIAA PAPER 90-0883] p 331 A90-25702

SHIVELY, JON H.

Towards a unified method of causing impact damage in thick laminated composites
p 946 A90-50168

SHKVAR, ANATOLII IA.

Vortex-flow compressors
p 69 A90-12479

SHMILOVICH, ARVIN

Calculation of transonic flows for novel engine-airframe installations
p 145 A90-16768

Calculation of transonic flows with separation past arbitrary inlets at incidence
p 384 A90-27979

SHNIDMAN, D. A.

Multipath modeling for simulating the performance of the microwave landing system
p 241 A90-21384

SHOCHET, EPHRAIM

Dallas/Fort Worth simulation, volume 1
[DOT/FAA/CT-TN89/28-VOL-1] p 824 N90-26802

Atlanta tower simulation, volume 1
[DOT/FAA/CT-TN89/27-VOL-1] p 870 N90-26835

Atlanta tower simulation, Volume 2: Appendixes
[DOT/FAA/CT-TN89/27-VOL-2] p 870 N90-26836

SHOCKET, EPHRAIM

Dallas/Fort Worth simulation, Volume 2: Appendixes D, E, and F
[AD-A216613] p 405 N90-18380

SHOCKEY, D. A.

Influence of microstructure and microdamage processes on fracture at high loading rates
[AD-A210307] p 65 N90-10253

SHOEMAKER, J. MICHAEL

Aerodynamic spike flowfields computed to select optimum configuration at Mach 2.5 with experimental validation
[AIAA PAPER 90-0414] p 166 A90-19837

SHOHADAE, AHMAD A.

Influence of bulk turbulence and entrance boundary layer thickness on the curved duct flow field
[AIAA PAPER 90-1502] p 606 A90-38651

SHOHET, K. N.

The survivability of centrifugal compressors in modern aircraft engines
p 928 A90-49883

SHOLLENBERGER, SCOTT

Helicopter Visual Segment Approach Lighting System (HALS)
[ACD-330] p 28 N90-10856

SHOOK, J. E.

Criteria for coal tar seal coats on airport pavements, Volume 2: Laboratory and field studies
[AD-A220167] p 674 N90-24277

SHORE, CHARLES P.

Finite element two-dimensional panel flutter at high supersonic speeds and elevated temperature
[AIAA PAPER 90-0982] p 450 A90-29372

SHORTLESS, DEBORAH L.

Comparison of four lightning simulation tests on a composite test bed aircraft
p 818 A90-49831

SHRAGAI, AVIAD

The effect of impact loading on residual strength of CFRP composite beams
p 208 A90-17683

SHREEVE, R. P.

Viscous flow in a controlled diffusion compressor cascade with increasing incidence
[ASME PAPER 89-GT-131] p 291 A90-23829

SHREWSBURY, GEORGE D.

Dynamic stall of circulation control airfoils
[AIAA PAPER 90-0573] p 167 A90-19923

SHRIVASTAVA, P. K. S.

A microprocessor-based system for monitoring gas turbines
p 350 A90-24359

SHU, M.

Numerical simulation of supersonic unsteady flow using Euler equations
[AIAA PAPER 90-0415] p 229 A90-22215

SHUART, MARK J.

Impact damage and residual strength analysis of composite panels with bonded stiffeners
p 642 A90-40130

A Protection And Detection Surface (PADS) for damage tolerance
[NASA-TP-3011] p 876 N90-27788

SHUBERT, M.

Taguchi methods in conceptual design for life cycle cost
[AIAA PAPER 90-3222] p 839 A90-49109

SHUCK, THOMAS L.

Flight-testing of the self-repairing flight control system using the F-15 highly integrated digital electronic control flight research facility
[AIAA PAPER 90-1321] p 520 A90-34149

Flight-testing of the self-repairing flight control system using the F-15 highly integrated digital electronic control flight research facility
[NASA-TM-101725] p 758 N90-25144

SHUEN, JIAN SHUN

Numerical study of chemically reacting flows using a lower-upper symmetric successive overrelaxation scheme
p 153 A90-17989

SHUKLA, JAY

Fabrication of aircraft structures from thermoplastic drapeable preforms
p 468 A90-33125

SHUMILKIN, V. G.

An experimental study of the combined effect of longitudinal ribs and vortex breakers on turbulent friction
p 805 A90-46565

SHUMILKINA, E. A.

The effect of longitudinal fins on turbulent friction drag
p 297 A90-24123

SHUMILOVA, I. N.

Optimization of the relative thicknesses of a high-aspect-ratio wing in a multicriterial formulation
p 334 A90-24133

SHUMSKII, G. M.

Comparison of calculated and experimental nonstationary aerodynamic characteristics of a delta wing pitching at large angles of attack
p 387 A90-28988

SHUSHIN, N. A.

Effect of the design of a diffuser with tangential injection on the starting and separation ratios of pressures
p 295 A90-24099

SHUSTOV, V. I.

Effect of a recess on the aerodynamic characteristics of very blunt bodies at supersonic velocities
p 299 A90-24167

SHUVALOV, V. A.

Transfer of the atomic ion energy of supersonic flow of a partially dissociated gas to a solid surface
p 234 A90-23432

SHVETS, A. I.

Aerodynamic characteristics of wave riders based on flows behind axisymmetric shock waves
p 395 A90-30342

SHVETS, ALEKSANDR I.

Supersonic flight vehicles
p 299 A90-24233

SHYU, IN-MING

A nonlinear aircraft tracking filter utilizing control variable estimation
[AIAA PAPER 90-3402] p 822 A90-47657

SHYU, JONG-YAW

Control of wall-separated flow by internal acoustic excitation
p 809 A90-47314

SHYY, WEI

A unified pressure correction algorithm for computing complex fluid flows
p 772 A90-45528

SIBILSKI, K.

Dynamics of spatial motion of an aeroplane after drop of loads
p 346 A90-25189

SICKLES, W. L.

Wall interference correction for three-dimensional transonic flows
[AIAA PAPER 90-1408] p 558 A90-37947

SICLARI, M. J.

Hybrid finite volume approach to Euler solutions for supersonic flows
p 154 A90-18144

Asymmetric separated flows at supersonic speeds
[AIAA PAPER 90-0595] p 230 A90-22233

SICLARI, MICHAEL J.

Strake camber and thickness design procedure for low alpha supersonic flow
p 622 A90-40678

SICRE, J. L.

The all glass helicopter cockpit
p 653 A90-42447

SIDDIQI, S.

The design of a low Reynolds number RPV
p 828 A90-46385

SIDEN, GUNNAR L. D.

A solution adaptive finite element method applied to two-dimensional unsteady viscous compressible cascade flow
p 15 A90-12624

SIDERIS, M. T.

Unsteady flow in centrifugal compressors due to downstream circumferential distortions
p 14 A90-12598

SIDERIS, M. TH.

Numerical study of centrifugal impeller response to an outlet pressure distortion
p 68 A90-11804

SIDES, J.

Euler equation solutions applied to a helicopter rotor in forward moving flight
[ONERA-RSF-32/1285-AY-346A] p 107 N90-12592

Efficient solution of the steady Euler equations with a centered implicit method
p 884 N90-27999

Solution of Euler equations applied to a rotor of a helicopter in steady flight
[ONERA-RSF-1/3731-AY-002A] p 910 N90-28500

SIDOROV, A. V.

Air traffic control
p 638 A90-39581

SIDOROV, O. P.

Calculation of cone drag
p 84 A90-14579

SIEBERT, RUEDIGER

Pressure measurement technique in the wind tunnel division of DFVLR
[ESA-TT-1145] p 264 N90-15963

SIEGEL, M. W.

Gas identification system using graded temperature sensor and neural net interpretation
[AD-A213359] p 205 N90-13627

SIEGL, J.

Fractographic observations on fatigue crack growth under miniTWIST flight-simulation loading (2024-T3 material)
[LR-631] p 961 N90-29684

SIEMERS, PAUL M., III

Wind-tunnel investigation of a flush airdata system at Mach numbers from 0.7 to 1.4
[NASA-TM-101697] p 421 N90-18395

SIEVERDING, C. H.

The influence of boundary layer state on vortex shedding from flat plates and turbine cascades
[ASME PAPER 89-GT-296] p 474 A90-33560

SIFERD, RAYMOND

Integrated circuits for avionics
[AD-A217964] p 540 N90-20312

- SIGAL, ASHER**
Wing-body mutual influence coefficients at angles-of-attack to 24 deg p 151 A90-17693
Aerodynamic effects of body roughness [AIAA PAPER 90-2850] p 712 A90-45168
- SIGALLA, LINDA A.**
Numerical simulation of confined, spatially-developing mixing layers - Comparison to the temporal shear layer [AIAA PAPER 90-1462] p 562 A90-38619
- SIGNORELLI, ROBERT A.**
Fiber reinforced superalloys p 532 A90-34169
- SIKONEN, TIMO**
Multigrid solution method for the Euler equations p 149 A90-16841
Solution of the thin-layer Navier-Stokes equations for laminar transonic flow [PB89-221600] p 136 N90-12879
Multigrid solution method for the Euler equations [PB89-219463] p 138 N90-13116
An evaluation of the two-dimensional Euler and Navier-Stokes calculations based on a flux-vector splitting [PB90-166778] p 481 N90-20963
- SIKAZAN, A. S.**
The shape assumed by a soft conical shell in fluid flow p 300 A90-24752
- SIKES, GREGORY D.**
Large-order modal analysis techniques in the Aeroelastic Design Optimization Program (ADOP) [SAE PAPER 892323] p 772 A90-45482
- SIKKA, DIGVIJAY I.**
A Distributed Artificial Intelligence approach to object identification and classification p 545 A90-34185
- SIKORA, SCOTT E.**
Model authoring system for fail safe analysis [NASA-CR-4317] p 964 N90-29142
A knowledge-based system design/information tool [NASA-CR-4316] p 965 N90-29143
- SILCOX, RICHARD J.**
Mechanisms of active control in cylindrical fuselage structures p 862 A90-47309
- SILVA, MARK**
The prediction of loads on the Boeing Helicopters Model 360 rotor p 410 A90-28240
- SILVA, WALTER A.**
Using transonic small disturbance theory for predicting the aeroelastic stability of a flexible wind-tunnel model [AIAA PAPER 90-1033] p 391 A90-29377
Experimental transonic flutter characteristics of two 72 deg-sweep delta-wing models [NASA-TM-101659] p 175 N90-14205
Using transonic small disturbance theory for predicting the aeroelastic stability of a flexible wind-tunnel model [NASA-TM-102617] p 478 N90-20047
- SILVER, W.**
A captive store flight vibration simulation project p 672 A90-40476
- SILVERMAN, J.**
Nonlinear mechanics of unstable plasmas as related to high altitude aerodynamics [AD-A215126] p 464 N90-19852
- SILVERTHORN, LOU**
HARP model rotor test at the DNW p 406 A90-28167
- SIM, DAVID**
Wing-body mutual influence coefficients at angles-of-attack to 24 deg p 151 A90-17693
- SIMANDIRAKIS, G.**
Calculation of axisymmetric flows in turbomachines, through an explicit time-splitting method p 14 A90-12622
Development and application of a fractional-step method for the solution of transonic and supersonic flow problems p 709 A90-44461
- SIMBIRSKII, D. F.**
Optimal selection of the parameters to be measured during the identification of gas turbine engines. I - Problem statement p 255 A90-23410
Optimal choice of measured parameters during the identification of gas turbine engines. II - Combined confidence regions and intervals of the identification results p 850 A90-46493
- SIMCOX, L. N.**
Software fault tolerance [RSRE-MEMO-4237] p 99 N90-12575
The application of Z to the specification of air traffic control systems. 1: An initial specification of the radar processing activity [RSRE-MEMO-4280] p 243 N90-15900
- SIMEONIDES, G.**
Infrared thermography in blowdown and intermittent hypersonic facilities p 440 A90-31302
- SIMMONS, J. R.**
A remote tip-driven fan powered supersonic fighter concept [AIAA PAPER 90-2415] p 663 A90-42167
- SIMMONS, M. J.**
A study of flows over highly-swept wings designed for maneuver at supersonic speeds [AD-A216837] p 399 N90-19202
- SIMMONS, WILLIAM E.**
Blade sweep for low-speed axial fans [ASME PAPER 89-GT-53] p 289 A90-23779
- SIMON, T. W.**
Studies of gas turbine heat transfer airfoil surfaces and end-wall cooling effects [AD-A212451] p 117 N90-12620
- SIMONCIC, ROBERT**
AIRNET: A real-time communications network for aircraft [NASA-CR-186140] p 690 N90-24514
- SIMONEAU, R. J.**
Progress towards the development of an inviscid-viscous interaction method for unsteady flows in turbomachinery cascades p 8 A90-11806
- SIMONICH, J. C.**
Rotor noise due to atmospheric turbulence ingestion. I - Fluid mechanics p 219 A90-19385
Rotor noise due to atmospheric turbulence ingestion. II - Aeroacoustic results p 219 A90-19386
- SIMONOV, O. A.**
Acoustic excitation of boundary layer oscillations on a yawing wing p 805 A90-46567
- SIMONS, J. W.**
Influence of microstructure and microdamage processes on fracture at high loading rates [AD-A210307] p 65 N90-10253
- SIMPSON, BRUCE**
Unsteady three-dimensional thin-layer Navier-Stokes solutions on dynamic blocked grids p 235 N90-15069
- SIMPSON, CAROL A.**
Evaluation of speech recognizers for use in advanced combat helicopter crew station research and development [NASA-CR-177547] p 650 N90-24265
Comparison of speech intelligibility in cockpit noise using SPH-4 flight helmet with and without active noise reduction [NASA-CR-177564] p 915 N90-28510
- SIMPSON, D.**
Development of an X-ray backscatter densitometer for measurement of freestream density during hypersonic flight [AIAA PAPER 90-1384] p 604 A90-37933
- SIMPSON, D. L.**
A technique for rapid impact damage detection with implication for composite aircraft structures p 600 A90-37662
- SIMPSON, DEAN W.**
Runaway rubber removal [AD-A218349] p 526 N90-20100
- SIMPSON, L. BRUCE**
Unsteady three-dimensional thin-layer Navier Stokes solutions on dynamic blocked grids [AD-A212377] p 136 N90-12899
- SIMPSON, M. A.**
UHB demonstrator interior noise control flight tests and analysis [NASA-CR-181897] p 140 N90-13198
- SIMPSON, MARK M.**
In-flight aircraft lightning surface current model p 819 A90-49844
- SIMPSON, ROBERT W.**
Investigation of air transportation technology at the Massachusetts Institute of Technology, 1988-1989 p 484 N90-20922
- SIMPSON, ROGER L.**
Time-dependent and time-averaged turbulence structure near the nose of a wing-body junction p 231 A90-23036
- SIMS, ROBERT**
X-29A aircraft structural loads flight testing [NASA-TM-101715] p 416 N90-19225
- SINCLAIR, A. N.**
An ultrasonic fatigue facility for HCF/LCF interactive tests p 363 A90-23900
- SINDEEV, IGOR' M.**
Power supply of aircraft p 43 A90-12474
- SINGER, S. FRED**
Avionic system based on global navigational satellite system p 97 A90-13984
- SINGH, AJIT**
Radiation-curable prepreg composites [DE90-629740] p 951 N90-28674
- SINGH, D. J.**
Three-dimensional shock-shock interactions on the scramjet inlet [AIAA PAPER 90-0529] p 314 A90-26963
A numerical study of the effects of reverse sweep on a scramjet inlet performance [AIAA PAPER 90-2218] p 705 A90-42749
- Effects of nose bluntness and shock-shock interactions on blunt bodies in viscous hypersonic flows [NASA-CR-186451] p 479 N90-20950
- SINGH, J. P.**
Full-potential calculations using Cartesian grids p 86 A90-15740
Computation of flow over airfoils under high lift separated flow condition p 86 A90-15741
Multigrid accelerated relaxation solution of transonic full potential flow equation [PD-CF-8942] p 480 N90-20951
- SINGH, JAG J.**
Low-energy gamma ray attenuation characteristics of aviation fuels [NASA-TP-2974] p 462 N90-18882
Device for quickly sensing the amount of O₂ in a combustion product gas [NASA-CASE-LAR-13816-1] p 609 N90-22025
- SINGH, JAI**
An international civil integrity complement to GPS and GLONASS p 821 A90-46392
- SINGH, JASBIR**
A microprocessor-based system for monitoring gas turbines p 350 A90-24359
- SINGH, N.**
Oscillating thin wings in inviscid incompressible flow p 2 A90-10224
Separated flow over slender wing, body and wing-body combination p 85 A90-15232
Potential flow calculation for three-dimensional wings and wing-body combination in oscillatory motion p 153 A90-17976
Incompressible potential flow about complete aircraft configurations p 156 A90-18443
Incompressible viscous flow about aircraft configurations p 233 A90-23290
Incompressible potential flow about three-dimensional configurations p 810 A90-48082
Aircraft passing through a sinusoidal gust p 811 A90-48090
- SINGH, RITI**
Combustion in the gas turbine. Part 1: Combustor types and design [CIT/SME/VKI/RS/1] p 748 N90-25986
Combustion in the gas turbine. Part 2: Preliminary design and performance [CIT/SME/VKI/RS/3] p 748 N90-25987
Combustion in the gas turbine. Part 3: Fuel injection, ignition and stability [CIT/SME/VKI/RS/4] p 748 N90-25988
Combustor cooling aspects [CIT/SME/VKI/RS/5] p 749 N90-25989
Pollutants: Production and methods of reduction [CIT/SME/VKI/RS/6] p 749 N90-25990
- SINGH, S. N.**
Effect of downstream elements on the flow at the exit of centrifugal compressor rotor p 157 A90-18483
- SINGH, SAHJENDRA N.**
Decoupled ultimate boundedness control of systems and large aircraft maneuver p 196 A90-19461
Ultimate boundedness control of uncertain systems with application to roll coupled aircraft maneuver p 668 A90-40886
Inversion of nonlinear I-O map, zero dynamics and flight control system design [AIAA PAPER 90-3370] p 863 A90-47628
- SINGLETON, JEFFREY D.**
Performance data from a wind-tunnel test of two main-rotor blade designs for a utility-class helicopter [NASA-TM-4183] p 499 N90-20974
- SINGLETON, MARK**
Entrapment plating of abrasive particles for jet engine clearance control [SAE PAPER 890918] p 286 A90-24685
- SINHA, A.**
Probabilistic method to compute the optimal slip load for a mistuned bladed disk assembly with friction dampers p 507 A90-32269
- SINHA, AGAM N.**
An operational perspective of potential benefits of microwave landing systems p 242 A90-23242
- SINHA, ALOK**
Analytical study of mistuning/friction/aerodynamics interaction in a bladed disk assembly [AD-A211139] p 55 N90-10893
- SINHA, P.**
Integrated navigation system design and performance with Phase III GPS user equipment p 98 A90-13997
- SINHAMAHAPATRA, K. P.**
Incompressible viscous flow about aircraft configurations p 233 A90-23290
Viscous corrections on wings in incompressible flow p 301 A90-25200
Multi-element aerofoils in viscous flow p 469 A90-32451

- Lift and pitching moment measurements on a swept tapered wing in oscillatory vertical gusts p 811 A90-48089
- SINIAEV, G. M.**
The tape method for the automatic partitioning of an arbitrary region when calculating temperature stresses p 138 A90-14587
- SINITISIN, D.**
Film cooling of turbine blades - Two dimensional experiments and numerical simulations p 739 A90-42670
- SINNETT, MICHAEL K.**
Alternate table look-up routine for real-time digital flight simulation p 611 A90-35769
Improving computer techniques for real-time digital flight simulation [SAE PAPER 892354] p 760 A90-45505
- SINNOTT, JOHN**
The MH-60K - A special rotorcraft for special operations [AIAA PAPER 90-3266] p 835 A90-48860
- SINNOTT, JOSEPH H.**
National Airspace System demand and capacity modeling p 330 A90-25562
- SINNOTT, M. J.**
Summary report of the Summer Conference of the DARPA-Materials Research Council [AD-A217380] p 532 N90-20143
- SIPIC, SLOBODAN**
Unsteady free-wake viscous aerodynamic analysis of helicopter rotors [AD-A217166] p 478 N90-20048
- SIPIC, SLOBODAN R.**
Analysis of dynamic transient response and postflutter behavior of super-maneuvering airplane [AD-A224126] p 925 N90-29386
- SIRAZETDINOV, T. K.**
Multiple-step terminal control with parameter identification and prediction during flight vehicle descent p 872 A90-46484
- SIRIGNANO, W. A.**
A one-dimensional model of ramjet combustion instability [AIAA PAPER 90-0271] p 266 A90-22192
Liquid fueled ramjet combustion instability: Acoustical and vortical interactions with burning sprays [AD-A222752] p 767 N90-26104
- SIROVICH, L.**
A proper orthogonal decomposition of a simulated supersonic shear layer p 904 A90-51009
- SISKIND, KENNETH S.**
Glass-ceramic matrix composites for advanced gas turbines [AIAA PAPER 90-2014] p 676 A90-40594
- SISLIAN, J. P.**
Aerodynamic and propulsive performance of hypersonic detonation wave ramjets p 49 A90-12609
On- and off-design performance analysis of hypersonic detonation wave ramjets [AIAA PAPER 90-2473] p 664 A90-42188
An experimental investigation of the velocity field in a reverse-flow combustor p 739 A90-42657
- SISTO, F.**
Computational prediction of stall flutter in cascaded airfoils [AIAA PAPER 90-1116] p 392 A90-29388
- SISTO, FERNANDO**
A modern course in aeroelasticity (2nd revised and enlarged edition) p 497 A90-34968
- SITARAM, N.**
Wake behaviour of a large deflection turbine rotor linear cascade p 157 A90-18481
- SITNIKOV, A. K.**
A study of the working process and losses in annular turbine nozzle cascades with a low contraction ratio p 254 A90-23407
- SITT, H.**
The effect of matrix toughness in the development of improved structural adhesives p 955 A90-50183
- SITZ, JOEL R.**
Initial flight qualification and operational maintenance of X-29A flight software [NASA-TM-101703] p 32 N90-10023
- SITZ, T. J.**
F-15E terrain following test results [AIAA PAPER 90-1299] p 504 A90-33913
- SIVAK, MIROSLAV**
Analysis of the mathematical modeling of an aircraft flight trajectory with consideration of engine thrust effect on the force ratio on the aircraft p 247 A90-23363
- SIVARAMAKRISHNAN, R.**
Rotor/fuselage vibration isolation studies by a Floquet-harmonic iteration technique p 182 A90-19393
- SIVASEGARAM, S.**
Combustion oscillations in ducts p 204 A90-19006
- SIVATI, L. A.**
Audibility and annoyance of en route noise of unducted fan engines [AD-A223687] p 966 N90-30035
- SIVTSOV, IU. M.**
A method for the matching of structural and geometric parameters of the turbocompressors of small gas turbine engines in computer-aided design p 850 A90-46491
- SIVY, GEORGE T.**
Rapid low-temperature cure patching system for field repair p 467 A90-31529
- SIZER, ANN M.**
Managing man-in-the-loop simulations [SAE PAPER 892355] p 761 A90-45506
- SJOBLOM, BJORN**
Full-scale liquid fuel ramjet combustor tests p 44 A90-12528
- SJOLANDER, S. A.**
An experimental investigation of the effect of incidence on the two-dimensional performance of an axial turbine cascade p 11 A90-12520
Development of the tip-leakage flow downstream of a planar cascade of turbine blades - Vorticity field [ASME PAPER 89-GT-55] p 289 A90-23781
Losses in the tip-leakage flow of a planar cascade of turbine blades p 514 A90-21027
- SKEEN, JAMES T., JR.**
Litigation and the National Weather Service [AIAA PAPER 90-0371] p 220 A90-19819
- SKIDMORE, F. W.**
The reduction of smoke emissions from Allison T56 engines [ARL-PROP-R-182] p 928 N90-28547
- SKINGLE, G. W.**
Sensitivity analysis using resonance and anti-resonance frequencies - A guide to structural modification p 536 A90-33396
- SKINN, DONALD A.**
Study of the engine bird ingestion experience of the Boeing 737 aircraft [DOT/FAA/CT-89/16] p 176 N90-13360
Study of bird ingestions into small inlet area, aircraft turbine engines (May 1987 to April 1988) [DOT/FAA/CT-89/17] p 402 N90-18375
Study of the engine bird ingestion experience of the Boeing 737 aircraft (October 1986 to September 1988) [DOT/FAA/CT-89/29] p 723 N90-25119
- SKIRA, CHARLES A.**
Aircraft propulsion control systems for the next century [AIAA PAPER 90-2034] p 742 A90-42720
- SKLUZAK, DELL F.**
Manufacturing and handling techniques used in the assembly of polished commercial aircraft [SAE PAPER 890925] p 286 A90-24690
Maintenance and economic benefits of non-painted aircraft operations [SAE PAPER 892208] p 732 A90-45427
- SKOUSEN, N.**
Boeing 727-100 test project (high energy radiated field tests) [DOT/FAA/CT-88/33] p 542 N90-21247
- SKOW, ANDREW M.**
Agility as a contribution to design balance [AIAA PAPER 90-1305] p 579 A90-35300
Combat aircraft control requirements for agility p 935 N90-28517
- SKRINJORICH, DONALD**
Air-to-Air Combat Test IV (AACT IV) and the AACT data base p 381 A90-28169
- SKUJINS, MARGARET B.**
Wright Research and Development Center test facilities handbook [AD-A222582] p 762 N90-26020
- SKURATOV, A. S.**
Laminar separated flow on a biconical body at high supersonic velocities p 387 A90-28992
- SLAUGHTER, J. K.**
Enhanced bioreclamation of jet fuels: A full-scale test at Eglin AFB, Florida [AD-A222348] p 875 N90-26992
- SLAVIK, SVATOMIR**
Measurement of propellers in the ARTI 3-meter wind tunnel p 262 A90-23364
- SLEEPER, ROBERT K.**
Spanwise measurements of vertical components of atmospheric turbulence [NASA-TP-2963] p 456 N90-19718
- SLOMINSKI, CHRISTOPHER J.**
Advanced transport operating system software upgrade: Flight management/flight controls software description [NASA-CR-181936] p 893 N90-28366
- SLONAKER, P.**
GPS Hover Position Sensing System p 108 A90-13986
- SLOOFF, J. W.**
Numerical flow simulation and supercomputers: More than a digital wind tunnel p 612 N90-22976
Technical evaluation report on the Fluid Dynamics Panel Symposium on Computational Methods for Aerodynamic Design (Inverse) and Optimization [AGARD-AR-267] p 720 N90-25947
- SMALLEY, A. J.**
Spray automated balancing of rotors - How process parameters influence performance p 879 A90-46228
- SMIALEK, J. L.**
Influence of alloying elements on the oxidation behavior of NbAl₃ p 355 A90-24861
- SMIALEK, JAMES L.**
Burner rig hot corrosion of silicon carbide and silicon nitride p 355 A90-25267
- SMIRNOV, GENNADI**
Multiple-power-path nonplanetary main gearbox of the Mi-26 heavy-lift transport helicopter p 452 A90-30115
- SMIRNOV, N. N.**
A study of three-dimensional supersonic flow of a real gas past axisymmetric bodies p 3 A90-10938
- SMIRNOV, V. A.**
Changes in supersonic flow past an obstacle due to the formation of a thin rarefaction channel ahead of the obstacle p 150 A90-17108
- SMIT, K. L.**
Transonic analysis of complex configurations using TRANAIR program [SAE PAPER 892289] p 714 A90-45467
- SMITH, A. F.**
Uses and properties of Al-Li on the new EH101 helicopter p 268 N90-15201
- SMITH, A. J. D.**
Liquid crystal thermography for aerodynamic heating measurements in short duration hypersonic facilities p 446 A90-28262
- SMITH, ALEXANDER J.**
Wall pressure fluctuations in the reattachment region of a supersonic free shear layer [AIAA PAPER 90-1461] p 561 A90-38618
- SMITH, BARBARA K.**
Evaluation of existing aircraft operator data bases [DOT/FAA/CT-90/18] p 898 N90-28463
- SMITH, BENJAMIN ROBERT**
Mean flow measurements of heated supersonic slot injection into a high Reynolds number supersonic stream [AIAA PAPER 90-0180] p 163 A90-19722
- SMITH, BERNARD**
Dual servo optical projection system (SOPS) - A solution for two crewmember and night vision goggle display needs [SAE PAPER 892353] p 760 A90-45504
- SMITH, BRIAN**
Fault tolerant architecture for a fly-by-light flight control computer p 860 A90-46931
- SMITH, BRIAN E.**
Comparison of model- and full-scale wind-tunnel performance [AIAA PAPER 88-2536] p 351 A90-26133
- SMITH, BRIAN R.**
The k-kl turbulence model and wall layer model for compressible flows [AIAA PAPER 90-1483] p 563 A90-38637
- SMITH, BRUCE A. W.**
The flow over a wing/nacelle combination in the presence of a propeller slipstream p 629 A90-42415
- SMITH, C.**
Dynamic simulation of cross-shafted propulsion system for tilt nacelle application [AIAA PAPER 90-0439] p 191 A90-19847
- SMITH, C. E.**
Mixing characteristics of dilution jets in small gas turbine combustors [AIAA PAPER 90-2728] p 664 A90-42217
- SMITH, C. F.**
Three-dimensional solutions for inviscid incompressible flow in turbomachines [ASME PAPER 89-GT-140] p 291 A90-23837
- SMITH, C. FREDERIC**
Analysis of internal flow in a ventral nozzle for STOVL aircraft [AIAA PAPER 90-1899] p 739 A90-42688
Analysis of internal flow in a ventral nozzle for STOVL aircraft [NASA-TM-103123] p 666 N90-23404
Experimental and analytical study of close-coupled ventral nozzles for ASTOVL aircraft [NASA-TM-103170] p 666 N90-24273
- SMITH, CHARLES**
HARP model rotor test at the DNW p 406 A90-28167
- SMITH, CHARLES A.**
Tilt rotor aircraft aeroacoustics p 409 A90-28238

- SMITH, CHRISTOPHER J.**
The promise of advanced materials for a 21st century UBE
[AIAA PAPER 90-2396] p 662 A90-42157
- SMITH, D. B.**
Engine testing of thermographic phosphors
[DE90-013269] p 885 N90-28059
- SMITH, D. R.**
Separation shock dynamics in Mach 5 turbulent interactions induced by cylinders p 153 A90-17981
- SMITH, DENNIS E.**
Reasoning from uncertain data - A BIT enhancement p 457 A90-28330
- SMITH, DONALD M.**
Advanced Automation System design p 375 A90-25566
- SMITH, DOUGLAS R.**
Wall pressure fluctuations in the reattachment region of a supersonic free shear layer
[AIAA PAPER 90-1461] p 561 A90-38618
- SMITH, FRANK T.**
Bursting in separating flow and in transition p 800 A90-46366
- SMITH, GAYLORD D.**
Thermal barrier characteristics of partially stabilized zirconia coatings on incoloy alloy 909 (A controlled expansion alloy)
[ASME PAPER 89-GT-146] p 354 A90-23839
- SMITH, GREGORY L.**
A two dimensional power spectral estimate for some nonstationary processes
[NASA-CR-186100] p 217 N90-14843
- SMITH, HERB, JR.**
Smart structures concept study p 504 A90-32876
Expert systems for design of battle damage repairs p 467 A90-33094
An expert system advisor for damage repair of composite wing skins (repairman) p 842 N90-26810
- SMITH, HOWARD R.**
The Battle Captain Expert System - A mission management decision support system for attack helicopter operations
[AIAA PAPER 89-3098] p 37 A90-10583
- SMITH, HOWARD WESLEY**
Aerospace structures supportability
[SAE PAPER 891058] p 129 A90-14360
- SMITH, J.**
Advanced instrumentation for aircraft icing research
[NASA-CR-185225] p 506 N90-21006
High productivity testing p 871 N90-26843
Limits of adaptation, residual interferences p 871 N90-26844
- SMITH, J. N.**
Development of a phase Doppler based probe for icing cloud droplet characterization
[AIAA PAPER 90-0667] p 368 A90-26978
- SMITH, JAMES D.**
An integrated diagnostics approach to embedded and flight-line support systems p 460 A90-30767
- SMITH, JANE**
Estimation of rotor blade incidence and blade deformation from the measurement of pressures and strains in flight p 647 A90-42497
- SMITH, JOHN A.**
Multi-level models for diagnosis of complex electro-mechanical systems p 693 A90-38888
- SMITH, LAURIE**
Evolution of Ada technology in the flight dynamics area: Implementation/testing phase analysis
[NASA-TM-103310] p 546 N90-21539
- SMITH, M. J. T.**
What should be done with those noisy old aircraft
[PNR90562] p 107 N90-12593
The commercial aircraft noise problem
[PNR90577] p 140 N90-13203
Stage 2 re-engining: The only way to achieve a real stage 3 aircraft
[PNR90636] p 737 N90-25977
Bringing aircraft noise testing down to Earth
[PNR90642] p 783 N90-26637
- SMITH, M. K. D.**
A comparison between engine test results and design predictions of turbine blade cooling performance
[ASME PAPER 89-GT-169] p 341 A90-23854
- SMITH, MARILYN J.**
Improvement to interactive two dimensional rotor section design p 808 A90-46943
- SMITH, MICHAEL J. T.**
Aircraft noise p 373 A90-24253
- SMITH, MICHAEL P.**
Improved toughness alloys based on titanium aluminides
[AD-A218149] p 533 N90-20208
- SMITH, MICHAEL R.**
Experiences in NASTRAN airframe vibration prediction at Bell Helicopter Textron p 832 A90-46964
- SMITH, ORVEL E.**
Analysis of extreme wind shear p 280 A90-23255
- SMITH, P. D.**
A viscous package for attached and separated flows on swept and tapered wings p 146 A90-16771
European research on viscous flow (EuroVisc)
[NLR-TP-89077-U] p 609 N90-22014
- SMITH, P. J.**
Development of pressure containment and damage tolerance technology for composite fuselage structures in large transport aircraft
[NASA-CR-3996] p 63 N90-10186
- SMITH, P. R.**
Input/output coupling in eigenstructure assignment
[AIAA PAPER 90-3476] p 865 A90-47726
- SMITH, R. A.**
Supersonic rectangular isothermal shrouded jets
[AIAA PAPER 90-2028] p 621 A90-40599
Multistep dump combustor design to reduce combustion instabilities p 659 A90-40934
- SMITH, R. E.**
Application of multiple grids topology to supersonic internal/external flow interactions p 308 A90-26135
- SMITH, R. K.**
Hypersonic test facility requirements for the 1990's
[AIAA PAPER 90-1389] p 594 A90-37934
- SMITH, R. V.**
Practical aspects of European collaboration p 785 A90-46928
- SMITH, RICHARD A.**
Methodology for developing an assessment expert system using a planning paradigm p 460 A90-30757
- SMITH, ROBERT D.**
FAA Rotorcraft Research, Engineering, and Development Bibliography 1962-1989
[AD-A224256] p 902 N90-29299
- SMITH, ROBERT E.**
Applications of Lagrangian blending functions for grid generation around airplane geometries
[AIAA PAPER 90-0009] p 216 A90-19630
Interactive grid generation for fighter aircraft geometries p 311 A90-26546
Multiple-block grid adaption for an airplane geometry p 311 A90-26547
- SMITH, ROBERT E., JR.**
Design of the UETP, experiment p 856 N90-27712
Comparison of altitude test cell results p 856 N90-27715
Experience in developing an improved design of experiment (lessons learned) p 857 N90-27718
General test plan p 857 N90-27721
- SMITH, ROGER L.**
An autopilot design methodology for bank-to-turn missiles
[AD-A213379] p 198 N90-13399
- SMITH, RON**
Aviation acoustical noise measurement
[AD-A222014] p 896 N90-27469
- SMITH, S. M.**
An analysis of reliability in fiber optic ring and star networks p 78 A90-11666
- SMITH, SAMUEL O.**
Thin film eddy current impulse deicer
[AIAA PAPER 90-0761] p 183 A90-20012
- SMITH, STEPHEN**
Visualization of three dimensional data p 782 N90-25553
- SMITH, STEPHEN C.**
Design synthesis and optimization of joined-wing transports
[AIAA PAPER 90-3197] p 838 A90-49102
A closer look at the induced drag of crescent-shaped wings
[AIAA PAPER 90-3063] p 903 A90-50638
- SMITH, STRETHER**
Very-high-performance data acquisition/analysis/display/control systems based on the APTEC I/O computer p 458 A90-28852
- SMITH, WAYNE D.**
Marshall Avionics Testbed System (MAST) p 421 N90-19417
- SMITS, A. J.**
Large-scale motions in a supersonic turbulent boundary layer on a curved surface
[AIAA PAPER 90-0019] p 160 A90-19636
- SMITS, ALEXANDER J.**
A supersonic turbulent boundary layer in an adverse pressure gradient p 303 A90-25592
- SMOL'IANINOVA, T. D.**
Vibration equations for a helicopter rotor blade p 604 A90-37830
- SMOOKE, MITCHELL D.**
Modification and improvement of software for modeling multidimensional reacting fuel flows
[AD-A217789] p 533 N90-20235
- SMULDERS, F. E. H. M.**
Rolling of ARALL laminates (an alternative method for post-stretching ARALL laminates)
[LR-560] p 135 N90-12778
- SMULLEN, R. R.**
Air Combat Environment Test and Evaluation Facility (ACETEF) p 58 N90-10883
- SMYTH, CHRISTOPHER C.**
Counterair situation awareness display for Army aviation p 964 N90-28982
- SMYTH, JOHN S.**
Assessment System for Aircraft Noise (ASAN): Development of alpha-test prototype system software
[AD-A223770] p 966 N90-30036
- SNAPE, D. M.**
Aircraft exhaust emissions: An engine manufacturer's perspective
[PNR90675] p 750 N90-26004
- SNELL, S. ANTONY**
Nonlinear inversion flight control for a supermaneuverable aircraft
[AIAA PAPER 90-3406] p 864 A90-47661
- SNIDLE, R. W.**
Wildhaber-Novikov circular arc gears - Some properties of relevance to their design p 70 A90-12999
- SNODGRASS, FARON BRITT**
Continued development and analysis of a new extended Kalman filter for the Completely Integrated Reference Instrumentation System (CIRIS)
[AD-A220106] p 654 N90-23400
- SNOW, WALTER L.**
Recent flow visualization studies in the 0.3-m TCT p 122 N90-12528
Video photographic considerations for measuring the proximity of a probe aircraft with a smoke seeded trailing vortex
[NASA-TM-102691] p 724 N90-25120
- SNYDER, CHRISTOPHER A.**
Advanced core technology - Key to subsonic propulsion benefits
[ASME PAPER 89-GT-241] p 342 A90-23890
- SNYDER, DEREK D.**
The generation of unstructured triangular meshes using Delaunay triangulation p 310 A90-26533
- SNYDER, J. H.**
Safety management in aircraft testing and certification p 180 A90-17421
- SNYDER, JAMES R.**
CFD needs in conceptual design
[AIAA PAPER 90-3209] p 813 A90-49106
- SNYDER, MELVIN H.**
Spanwise distribution of lift and drag at high angles of attack
[SAE PAPER 891019] p 83 A90-14331
Stall/spin aerodynamic data project
[DOT/FAA/CT-88/29] p 185 N90-14222
- SNYDER, PHILIP H.**
Design of an air-cooled metallic high-temperature radial turbine p 507 A90-32960
- SNYDER, STEVEN P.**
Exploration of concepts for multi-role fighters
[AIAA PAPER 90-2276] p 644 A90-42104
- SNYDER, T. S.**
Solid fuel ignition and combustion characteristics under high-speed crossflows
[AIAA PAPER 90-2075] p 764 A90-42725
- SNYDER, VIRGIL W.**
Developments in mechanics. Volume 15 - Midwestern Mechanics Conference, 21st, Michigan Technological University, Houghton, Aug. 13-16, 1989, Proceedings p 769 A90-42870
- SOARES, PAUL A.**
Development and testing of rapid repair methods for war damaged runways
[AD-A223970] p 938 N90-28586
- SOBEL, KENNETH M.**
Flight control application of eigenstructure assignment with optimization of robustness to structured state space uncertainty p 693 A90-40885
- SOBIECZKY, HELMUT**
Progress in inverse design and optimization in aerodynamics p 482 N90-20977
- SOBIERAJ, W.**
A discrete dynamic model of the crankshaft-airscrew assembly of an aircraft piston engine for the purpose of vibration analysis by the method of finite elements p 51 A90-13220
- SOBIESKI, IAN**
A theoretical and experimental investigation into the prerotation of aircraft tires
[AIAA PAPER 90-3272] p 836 A90-48863
- SOBOLEV, DMITRII A.**
The birth of the airplane: The first designs and constructions p 79 A90-12478
Aircraft of unconventional configuration (2nd revised and enlarged edition) p 247 A90-22734

SOCHOR, EUGENE

From the DC-3 to hypersonic flight - ICAO in a changing environment p 222 A90-23662

SODERMAN, P. T.

Pressure fluctuations in the tip region of a blunt-tipped airfoil p 154 A90-18136

SOETRISNO, MOELJO

Numerical simulation of confined, spatially-developing mixing layers - Comparison to the temporal shear layer [AIAA PAPER 90-1462] p 562 A90-38619

SOGA, YOSHIMITSU

Design of control amplifier for FJR 710 engine p 43 A90-12017

SOH, W. Y.

Computational analysis of the flowfield of a two-dimensional ejector nozzle [AIAA PAPER 90-1901] p 740 A90-42690

SOH, WOO-YUNG

Application of a lower-upper implicit scheme and an interactive grid generation for turbomachinery flow field simulations [ASME PAPER 89-GT-20] p 288 A90-23762

SOHN, MIN-SEOK

Electrostatic dry powder prepping of carbon fiber p 948 A90-50215

SOHONI, VIKRAM N.

A methodology for modeling, control design and simulation of aerospace mechanical systems [AIAA PAPER 89-3049] p 73 A90-10543

SOISTMANN, D. L.

The application of active controls technology to a generic hypersonic aircraft configuration [NASA-TM-101689] p 497 N90-20071

SOISTMANN, DAVID L.

Experimental transonic flutter characteristics of two 72 deg-sweep delta-wing models [NASA-TM-101659] p 175 N90-14205

SOIZE, C.

New approach to small transonic perturbations finite element numerical solving method. I - Numerical developments. II - Numerical applications p 16 A90-12783

SOKHEY, J. S.

Analysis of installed wind tunnel test results on large bypass ratio engine/nacelle installations [AIAA PAPER 90-2146] p 705 A90-42738

SOLIANNIKOV, V. A.

Estimation of the safety factor of turbine blades under thermal cycling and vibration loading p 958 A90-52356

SOLIES, U. P.

In flight flow angle measurements on the Ball-Bartoe Jetwing powered lift aircraft [AIAA PAPER 90-1284] p 495 A90-33905

SOLIGNAC, J.-L.

Experimental study of incompressible flow on the upper surface of a delta wing p 558 A90-37346

SOLOMON, JOSEPH K.

Estimation of atmospheric and transponder survey errors with a navigation Kalman filter p 459 A90-30689

SOLONIN, A. S.

Analysis and synthesis of meteorological support systems for airports p 914 A90-50778
Coordination strategies in a hierarchical air traffic control system with allowance for meteorological conditions p 914 A90-50779

SOLTANI, M. R.

Measurements on an oscillating 70-deg delta wing in subsonic flow p 307 A90-26130
Measured forces and moments on a delta wing during pitch-up p 308 A90-26137

SOMERS, DAN M.

The design of an airfoil for a high-altitude, long-endurance remotely piloted vehicle p 104 A90-12545

SOMERS, M. A. M.

VISTRAFS - A simulation method for strongly-interacting viscous transonic flow p 144 A90-16756

SOMERS, RICHARD D.

F-111/TF30 engine monitoring system - A fusion of past, present, and future technology p 425 A90-30817

SOMMER, ECKHART W.

Mean and turbulent velocity measurements in a turbojet exhaust p 423 A90-28272

SOMMER, G. S.

Airship survival - Damage avoidance and control for large ocean-going airships [AIAA PAPER 89-3166] p 238 A90-20588

SOMMERS, JOHN D.

Wind tunnel studies of support strut interference on a 3 percent YF-17 fighter aircraft model at high angles of attack [AIAA PAPER 90-3083] p 794 A90-45899

An experimental investigation of support strut interference on a three-percent fighter model at high angles of attack [AD-A219793] p 631 N90-23353

SONAR, TH.

Geometric modelling of complex aerodynamic surfaces and three-dimensional grid generation p 311 A90-26545

SONG, B.

Deicing of solids using radiant heating p 769 A90-43309

SONG, J.

Development of impact design methods for ceramic gas turbine components [AIAA PAPER 90-2413] p 687 A90-42165

SONG, QINGGUO

A fracture analysis using eight-node-isoparametric singular elements and its application in fuselage panels p 603 A90-36431

SONG, TAO

The flutter characteristic analysis and optimization design of mistuning blade p 42 A90-11799

SONG, ZHAN HONG

The effects of three centres of blade on flutter p 42 A90-11800

SONG, ZHAOHONG

The flutter characteristic analysis and optimization design of mistuning blade p 42 A90-11799

The design of the series of blade flutter rotor and the experimental investigation of flow-induced vibration p 586 A90-37230

SOPHER, R.

Calculation of flight vibration levels of the AH-1G helicopter and correlation with existing flight vibration measurements [NASA-CR-182031] p 775 N90-25375

SOPHER, ROBERT

Recent developments in rotor dynamics methodology in the U.S. industry p 889 A90-46960

SORENSEN, M.

Wind shear and hyperbolic distributions p 280 A90-23632

SOROKINA, L. A.

Generalized relations for estimating the efficiency and basic dimensions of screw pumps and hydraulic turbines of pump units p 111 A90-14583

SORRELLS, J. E.

Adaptive control law design for model uncertainty compensation [AD-A211712] p 120 N90-11758

SOSEDKO, I. U. P.

Optimal conditions of flow turbulence suppression in the working section of a wind tunnel using screens located in the prechamber p 438 A90-29185

SOSUNOV, V. A.

Experimental turboblow using liquid hydrogen and liquid natural gas as fuel [AIAA PAPER 90-2421] p 663 A90-42170

SOSUNOV, V. A.

The history of aviation engine development in the USSR and the 60th anniversary of CIAM [AIAA PAPER 90-2761] p 783 A90-42828

SOTHCOTT, VICTOR E.

Summary of sonic boom rise times observed during FAA community response studies over a 6-month period in the Oklahoma City area [NASA-CR-4277] p 696 N90-24852

SOTOZAKI, TOKUO

Estimation of power spectral density of runway roughness [NAL-TR-1037] p 939 N90-29411

SOULES, D. A.

Improved fiber reinforced polyphenylene sulfide thermoplastic composites p 947 A90-50180

SOUNDNAYAGAM, S.

Flow in compressor interstage ducts p 11 A90-12521

Boundary layer growth on low aspect ratio compressor blades p 12 A90-12553

SOUSA, A. C. M.

Time development of convection flow patterns in aircraft cabins under post-crash fire exposure p 327 N90-17598

SOUTAR, JOHN

The MANTA: An RPV design to investigate forces and moments on a lifting surface [NASA-CR-186227] p 499 N90-20971

SOUZA, J. W.

Advanced fuel properties, phase 1 [AD-A219788] p 766 N90-25236

SOWOOD, P. J.

Escape and survival following helicopter ditching - Training aspects p 722 A90-44658

SPABERG, GORDON H.

UV spectroradiometric output of an F404 turbojet aircraft engine p 652 A90-40195

SPADAFORA, S. J.

Organic coatings - First line of defense p 204 A90-17300

SPAID, FRANK W.

Experimental study of the turbulent boundary layer on a transport wing in subsonic flow p 709 A90-44728

SPAIN, C. V.

The application of active controls technology to a generic hypersonic aircraft configuration [NASA-TM-101689] p 497 N90-20071

SPAIN, CHARLES V.

Experimental transonic flutter characteristics of two 72 deg-sweep delta-wing models [NASA-TM-101659] p 175 N90-14205

SPALART, P. R.

Direct numerical study of leading-edge contamination p 19 N90-10361

SPALL, R. E.

Goertler vortices in supersonic and hypersonic boundary layers p 83 A90-14091

SPALL, ROBERT E.

A computational study of the taxonomy of vortex breakdown [AIAA PAPER 90-1624] p 568 A90-38753

SPANGLER, RONALD L. JR.

Piezoelectric actuators for helicopter rotor control [AIAA PAPER 90-1076] p 411 A90-29384

SPARA, KAREN M.

Aerodynamic detuning for control of supersonic rotor forced response [AIAA PAPER 90-2018] p 621 A90-40596

SPARKS, ANDREW

A mixed H2 and H(infinity) approach to an autopilot design problem [AIAA PAPER 90-3441] p 865 A90-47694

SPARROW, J. G.

Fatigue of thick-section cold-expanded holes with and without cracks p 270 A90-20987

SPEAKMAN, JERRY D.

Lateral attenuation of military aircraft flight noise [AD-A218041] p 548 N90-20799

SPEARMAN, M. LEROY

Design trends for Army/Air Force airplanes in the United States [NASA-TM-4179] p 615 N90-23338

SPECKER, LAWRENCE J.

Windblast protection for advanced ejection seats p 483 N90-20063

SPENCE, BRIAN R.

Compressive viscoelastic effects (creep) of a unidirectional glass/epoxy composite material p 946 A90-50170

SPENCER, D. A.

Experimental examination of the benefits of improved terminal air traffic control planning p 241 A90-21388

Applying artificial intelligence techniques to air traffic control automation p 282 A90-21389

SPENCER, NED A.

Development and operation of the Traffic Alert and Collision Avoidance System (TCAS) p 331 A90-25573

An update to the system safety study of TCAS 2 [DOT/FAA/SA-89/3] p 177 N90-13363

SPENCER, R. H.

Review and analysis of the DNW/Model 360 rotor acoustic data base [NASA-TM-102253] p 81 N90-11692

SPENNY, C. H.

Aerodynamic testing of a new semi-prone ejection seat design [AIAA PAPER 90-0234] p 182 A90-19748

SPERRY, GEORGE J.

Landing gear integrity - The bottom line of aircraft safety p 180 A90-17408

SPEYER, JASON L.

Robust hover control for a short takeoff/vertical landing aircraft [AIAA PAPER 90-3333] p 862 A90-47593

SPICER, JANE W. MACLACHLAN

Thermal nondestructive characterization of the integrity of protective coatings p 770 A90-44325

SPIEKHOUT, D. J.

Re-assessing the F-16 damage tolerance and durability life of the RNLAF F-16 aircraft p 901 A90-49881

SPIGEL, BARRY S.

Considerations of reliability design for rotorcraft p 680 A90-39977

SPILLMAN, W. B., JR.

Fiber optic sensors for composite monitoring p 37 A90-11203

SPINTZYK, JOHANNES

Euromart - The European aviation research and technology program p 617 A90-41112

SPIRO, IRVING J.

Infrared technology XIV; Proceedings of the Meeting, San Diego, CA, Aug. 15-17, 1988 [SPIE-972] p 66 A90-10138

- SPLETTSTOESSER, W. R.**
Rotor blade-vortex interaction impulsive noise source localization p 463 A90-27978
Higher harmonic control of a helicopter model rotor to reduce blade/vortex interaction noise p 496 A90-34360
- SPLETTSTOESSER, WOLF**
Technical-scientific possibilities for helicopter noise research in the German-Dutch wind tunnel p 283 A90-21474
- SPONAGLE, NEIL C.**
Noise from tip vortex and bubble cavitation [AD-A221962] p 896 A90-27468
- SPRATT, RANDOLPH W.**
STOVL fighter propulsion reliability, maintainability, and supportability characterization [AD-A224221] p 933 N90-28574
- SPRING, S. D.**
An experimental investigation of film cooling effectiveness for slots of various exit geometries [AIAA PAPER 90-2266] p 768 A90-42763
- SPRINGATE, CHARLES S.**
Fire deaths in aircraft without the crashworthy fuel system p 22 A90-10266
- SPRINGEN, A. LUCILLE**
National airspace system: Airport movement area control operational concept [WP-89W00181] p 243 N90-15086
- SPRINKLE, DANNY R.**
Low-energy gamma ray attenuation characteristics of aviation fuels [NASA-TP-2974] p 462 N90-18882
- SPURGEON, S. K.**
An investigation of the use of singular perturbation methods and modal control theory in the derivation of aircraft control schemes [MATHS-REPT-A-106] p 758 N90-26014
- SPURGEON, SARAH KATHERINE**
An assessment of robustness of flight control systems based on variable structure techniques p 57 N90-10895
- SPURWAY, S. P.**
The use of fibre reinforced thermoplastics for helicopter primary structures and their engineering substantiation p 441 A90-28191
- SPYROPOULOS, J. T.**
Application of a three-dimensional finite element grid generation scheme for an F-16 aircraft configuration p 336 A90-26541
Parallel computation of three-dimensional transonic flow problems with complex geometries [AIAA PAPER 90-0336] p 313 A90-26936
- SQUIRE, K. R.**
Advanced fuel properties, phase 1 [AD-A219788] p 766 N90-25236
- SQUIRE, L. C.**
A numerical study of supersonic flow over a compression corner with different incoming boundary-layer profiles [AIAA PAPER 90-1453] p 561 A90-38612
- SQUIRES, REBECCA L.**
An investigation of strake fence flaps on a canard-configured aircraft [AIAA PAPER 90-0762] p 230 A90-22259
- SREEDHAR, SREELAL**
Unbalance response studies on a model rotor supported on uncentrally squeeze film dampers and the development experience of a jet engine p 69 A90-12579
- SREEKANTH**
Viscous flow characteristics over a blunt cone at hypersonic Mach numbers by using a PNS code p 810 A90-48085
- SRI NAMACHCHIVAYA, N.**
Unfolding of double-zero eigenvalue bifurcations for supersonic flow past a pitching wedge p 347 A90-25995
- SRIDHAR, B.**
Image based range determination [AIAA PAPER 90-3404] p 822 A90-47659
- SRIDHAR, BANAVAR**
Kalman filter based range estimation for autonomous navigation using imaging sensors p 578 N90-22238
- SRILATHA, K. R.**
Design of a natural laminar flow airfoil for an unmanned aircraft [PD-CF-9004] p 499 N90-20975
- SRINIVASAN, GANAPATHI R.**
Numerical simulations of blade-vortex interactions and lifting hovering rotor flows [AD-A224238] p 911 N90-29302
- SRINIVASAN, J.**
A numerical three-dimensional thermal stress analysis for cooled blades [ASME PAPER 89-GT-168] p 341 A90-23853
- SRINIVASAN, R.**
Measurements in an annular combustor-diffuser system [AIAA PAPER 90-2162] p 768 A90-42740
Parametric evaluation of the aerodynamic performance of an annular combustor-diffuser system [AIAA PAPER 90-2163] p 742 A90-42741
- SRINIVASAN, R. S.**
Response of orthogonally stiffened cylindrical shell panels p 603 A90-36285
- SRINIVASAN, S.**
Experimental study of static pressure and mean velocity profiles inside a two-dimensional dump-type combustor model p 45 A90-12530
A numerical parametric study of a scramjet inlet in a Mach 6 arc heated test facility [AIAA PAPER 90-0531] p 167 A90-19896
- SRINIVASAN, SHIVAKUMAR**
Numerical simulation of flow through the Langley parametric scramjet engine [SAE PAPER 892314] p 747 A90-45476
- SRIVASTAVA, K. M.**
Studies on the influence of Mach number on profile losses of a reaction turbine cascade p 10 A90-12517
- SRIVASTAVA, R.**
Application of an efficient hybrid scheme for aeroelastic analysis of advanced propellers [AIAA PAPER 90-0028] p 226 A90-22153
Numerical simulation of unsteady rotational flow over propfan configurations [NASA-CR-186037] p 90 N90-12500
Application of an efficient hybrid scheme for aeroelastic analysis of advanced propellers [NASA-TM-102428] p 172 N90-13355
- SRIVATSAN, RAGHAVACHARI**
Airplane takeoff and landing performance monitoring system [NASA-CASE-LAR-13734-1-CU] p 526 N90-20096
- ST. JOHN, RALPH J.**
Model-based method for terrain-following display design [AD-A219302] p 583 N90-22563
- STABELLINI, ALESSANDRO**
Agusta methodology for pitch link loads prediction in preliminary design phase p 646 A90-42465
Agusta methodology for pitch link loads prediction in preliminary design phase [ETN-90-97270] p 737 N90-25978
- STACK, J. P.**
Simultaneous detection of separation and transition in surface shear layers p 72 N90-10368
- STACK, JOHN P.**
Predicted and hot-film measured Tollmien-Schlichting wave characteristics p 91 N90-12523
Method and apparatus for detecting laminar flow separation and reattachment [NASA-CASE-LAR-13952-1-SB] p 455 N90-19534
- STAGER, PAUL**
Underlying factors in air traffic control incidents p 401 A90-31335
- STAHL, WOLFGANG**
Suppression of vortex asymmetry behind circular cones p 556 A90-36282
- STAINBACK, P. C.**
Hot wire anemometry in transonic flows and cryogenic conditions p 539 A90-34229
- STAINBACK, P. CALVIN**
Hot-film system for transition detection in cryogenic wind tunnels p 122 N90-12522
Basic aerodynamic research facility for comparative studies of flow diagnostic techniques p 122 N90-12526
- STALEWSKI, WIENCZYSLAW**
Numerical analysis of flow of an ideal fluid past an airfoil p 2 A90-10228
- STALKER, R. J.**
Hypersonic combustion of hydrogen in a shock tunnel p 46 A90-12560
Approximations for nonequilibrium hypervelocity aerodynamics p 154 A90-17990
- STALLINGS, ROBERT L., JR.**
Passive venting technique for shallow cavities [NASA-CASE-LAR-14031-1] p 499 N90-20079
- STAMATIS, A.**
Jet engine fault detection with differential gas path analysis at discrete operating points p 50 A90-12633
Computer modeling and data processing methods: An essential part of jet engine condition monitoring and fault diagnosis p 855 N90-27626
- STANEWICH, B. J.**
Local convection heat transfer on a plane wall in the vicinity of strong streamwise accelerations p 535 A90-32174
- STANEWSKY, E.**
Comparison of conventional and adaptive wall wind tunnel results with regard to Reynolds number effects p 352 N90-17649
High Reynolds number tests of the CAST-10-2/DOA 2 transonic airfoil at ambient and cryogenic temperature conditions p 320 N90-17650
- STANISAV, EMIL**
Prediction of pressure distribution on optimum-optimorum delta wing at higher angles of attack in supersonic flow and its agreement with experimental results p 907 A90-51538
- STANKOV, B. B.**
Atmospheric conditions producing aircraft icing on 24-25 January 1989 - A case study utilizing combinations of surface and remote sensors [AIAA PAPER 90-0197] p 175 A90-19734
- STANLEY, ANNE M.**
An integrated diagnostics approach to embedded and flight-line support systems p 460 A90-30767
- STANWAY, R.**
Design and application of a finite element package for modelling turbomachinery vibrations p 70 A90-13011
- STAPLES, D. L.**
Finite wing lift prediction at high angles of attack [AIAA PAPER 90-3079] p 795 A90-45910
- STAPOUNTZIS, H.**
Hot wire measurements in the wake of an oscillating airfoil p 15 A90-12635
Vortex shedding over delta wings p 470 A90-32479
- STARIKOV, O. IU.**
Effect of a crescent-shaped rigid support on the aerodynamic characteristics of models in the presence of perforated boundaries p 869 A90-46537
- STARK, MIKE**
Evolution of Ada technology in the flight dynamics area: Implementation/testing phase analysis [NASA-TM-103310] p 546 N90-21539
- STARK, UDO**
Experimental investigations of effects of the stagger angle on secondary flows in plane compressor cascades p 83 A90-13787
- STARK, VALTER J. E.**
Canard-wing interaction in unsteady supersonic flow p 3 A90-11010
- STARKE, EDGAR A., JR.**
The microstructure and properties of aluminum-lithium alloys p 267 N90-15187
- STARKER, SIEGFRIED**
Time synchronization/distribution applications of navigation signals repeated by geostationary satellites p 872 A90-46397
- STAROPOLI, F.**
Fatigue behavior of specimens under compression load spectra [ETN-89-95207] p 137 N90-12954
- STARR, K. K.**
Failure analysis handbook [AD-A219747] p 689 N90-23752
- STAUFFER, B. L.**
Application of a design method for integrated control to a VTOL airplane in hover [AIAA PAPER 90-3334] p 862 A90-47594
- STAUTER, R. C.**
Three-dimensional aerodynamics of an annular airfoil cascade including loading effects p 87 A90-15889
- STAUTER, R. CHARLES**
A comprehensive hover test of the airloads and airflow of an extensively instrumented model helicopter rotor p 407 A90-28173
Temporally and spatially resolved flow in a two-stage axial compressor. Part 2: Computational assessment [NASA-TM-102273] p 194 N90-14236
- STEAD, DANIEL J.**
The organized nature of a turbulent trailing vortex [AIAA PAPER 90-1625] p 568 A90-38754
- STEAR, EDWIN B.**
The implications of using integrated software support environment for design of guidance and control systems software [AGARD-AR-229] p 434 N90-18432
- STEARMAN, RONALD**
Influence of joint fixity on the structural static and dynamic response of a joined-wing aircraft. I - Static response [SAE PAPER 891060] p 100 A90-14361
Influence of joint fixity on the aeroelastic characteristics of a joined wing structure [AIAA PAPER 90-0980] p 390 A90-29370
- STEARNS, E. MARSHALL**
Energy Efficient Engine: Flight propulsion system final design and analysis [NASA-CR-168219] p 930 N90-28558
Energy Efficient Engine core design and performance report [NASA-CR-168069] p 930 N90-28559

- Energy Efficient Engine integrated core/low spool design and performance report
[NASA-CR-168211] p 931 N90-28561
- STECCO, S. S.**
Inviscid cascade flow calculations using a multigrid method
[ASME PAPER 89-GT-22] p 288 A90-23763
- STECK, JAMES E.**
Alternate table look-up routine for real-time digital flight simulation p 611 A90-35769
- STECKEMETZ, BERND**
Force and moment measurements on delta wings in unsteady flow p 278 N90-16185
- STEEL, J.**
Aircraft cabin fire suppression by means of an interior water spray system
[CAA-PAPER-88014] p 96 N90-11719
- STEELE, MARK A.**
Design and development of the Garrett F109 turbofan engine
[SAE PAPER 891046] p 109 A90-14350
- STEELE, MONTGOMERIE C.**
Some issues in the growth of small gas turbine aircraft propulsion engines p 44 A90-12508
- STEGER, JOSEPH L.**
Basic numerical methods p 394 A90-29886
Numerical simulation of three-dimensional transonic flows p 905 A90-51020
- STEGEMPER, B.**
Application of a company data link at Lufthansa German Airlines p 827 N90-27689
- STEIN, BARRY A.**
A robust RAIM scheme using GPS/GLONASS systems p 726 A90-43713
- STEIN, EARL S.**
Parallel approach separation and controller performance: A study of the impact of two separation standards
[DOT/FAA/CT-TN89/50] p 99 N90-12574
- STEINBACH, GREG**
High speed civil transport
[NASA-CR-186661] p 649 N90-23396
- STEINBERG, B. D.**
Comparison of 1-D and 2-D aircraft images p 927 A90-52884
- STEINBERG, MARC**
Model reduction with a finite-interval $H(\infty)$ criterion
[AIAA PAPER 90-3473] p 890 A90-47723
- STEINER, A. L.**
Design and analysis of a large-plug inlet ADP nacelle and pylon
[AIAA PAPER 90-2015] p 673 A90-41986
- STEINHAUSER, REINHOLD**
Controller design for active vibration suppression of a helicopter
[DFVLR-FB-89-20] p 120 N90-11760
- STEINHILBER, H.**
Description and reconstitution of manoeuvre loadings p 919 A90-49878
- STEINHOFF, J.**
The free-wake computation of rotor-body flows
[AIAA PAPER 90-1540] p 565 A90-38684
- STEINHOFF, J. S.**
Application of a new visualization method to helicopter rotor flow
[AIAA PAPER 90-3006] p 789 A90-45856
- STEINHOFF, JOHN**
Free-wake analysis of compressible rotor flows p 302 A90-25283
Application of vortex embedding to aircraft flows
[AIAA PAPER 90-1626] p 568 A90-38755
- STEINKE, RONALD J.**
Application of a two-dimensional unsteady viscous analysis code to a supersonic throughflow fan stage
[NASA-TM-4141] p 192 N90-13387
- STEINMETZ, WARREN D.**
Aluminum surface preparation for aircraft field repair p 764 A90-43204
- STELLAR, FRED**
An investigation of aircraft maneuverability and agility
[AIAA PAPER 90-3300] p 868 A90-48882
- STELLAR, FREDERICK**
Low speed maneuverability and agility design considerations for V/STOL aircraft p 581 A90-38536
- STEMPLE, ALAN DOUGLAS**
Nonlinear static and dynamic modeling of composite rotor blades including warping effects p 924 N90-29382
- STEN'KIN, E. D.**
Operation of a compressor with intermediate air bleed p 111 A90-14589
- STENERSON, R. O.**
Integration of intelligent avionics systems for crew decision aiding p 459 A90-30236

- STENERSON, RICHARD**
Problem focus mechanisms for cockpit automation
[AIAA PAPER 89-3096] p 37 A90-10581
- STENGEL, ROBERT F.**
Restructurable control using proportional-integral implicit model following p 347 A90-25990
Stochastic performance robustness of aircraft control systems
[AIAA PAPER 90-3410] p 865 A90-47665
Probabilistic reasoning for intelligent wind shear avoidance
[AIAA PAPER 90-3437] p 890 A90-47690
Investigation of air transportation technology at Princeton University, 1988-1989 p 486 N90-20935
An expert system for wind shear avoidance p 486 N90-20938
Rule-based mechanisms of learning for intelligent adaptive flight control p 521 N90-20939
Perspectives on the use of rule-based control p 521 N90-20940
Stochastic robustness of linear control systems p 521 N90-20941
- STENGER, GREGORY J.**
Full-scale birdstrike testing of in-service aged F-111 ADBIT windshield transparencies
[AD-A218035] p 484 N90-20069
- STENNETT, PATRICK G.**
Investigation of variation in fatigue life calculated using damage fraction p 537 A90-33624
- STEPHENS, J. R.**
Influence of alloying elements on the oxidation behavior of NbAl₃ p 355 A90-24861
- STEPHENS, JOSEPH R.**
Composites boost 21st-century aircraft engines p 442 A90-29704
Resources - Supply and availability p 531 A90-34152
NASA's HITEMP program for UHBR engines
[AIAA PAPER 90-2395] p 852 A90-47218
- STEPHENS, WENDELL B.**
Development of the Second Generation Comprehensive Helicopter Analysis System (2GCHAS) p 889 A90-46963
- STEPHENSON, JACK D.**
Longitudinal stability and control characteristics of the Quiet Short-Haul Research Aircraft (QSRA)
[NASA-TP-2965] p 349 N90-17639
Lateral-directional stability and control characteristics of the Quiet Short-Haul Research Aircraft (QSRA)
[NASA-TM-102250] p 671 N90-23413
- STERN, A. M.**
Mixer-ejector nozzle for jet noise suppression
[AIAA PAPER 90-1909] p 894 A90-47202
- STERN, F.**
Viscous flow around a propeller-shaft configuration with infinite-pitch rectangular blades p 683 A90-40938
- STERN, G. J.**
Reduced insertion loss of X-band RF fiber optic links p 695 A90-41240
- STERNSTEIN, S. S.**
High temperature deformation studies on CVD silicon carbide fibers p 945 A90-50147
- STERRY, W. M.**
Boeing Transonic Windblast Generator System (BTWGS) p 199 A90-17413
- STETSON, KENNETH F.**
Comments on 'Effect of nose bluntness and cone angle on slender-vehicle transition' p 620 A90-39814
- STEVENS, D. M.**
Air Force smart structures/skins program overview p 38 A90-11205
- STEVENS, J. R.**
Investigation of cowl vent slots for supercritical stability enhancement in dual-mode ramjet inlets p 507 A90-32951
- STEVENS, JAMES R.**
Measured operating characteristics of a rectangular combustor/inlet isolator
[AIAA PAPER 90-2221] p 742 A90-42752
- STEVENS, JOHN G.**
Photo-sensitized ignition of hydrogen/oxygen mixtures for hypersonic flight vehicles p 877 N90-27935
- STEVENS, K. A.**
Torsional buckling and post-buckling of composite geodetic cylinders with special reference to joint flexibility p 878 A90-45971
- STEVENS, M. C.**
Mode S - A data link for future air traffic control p 576 A90-35684
- STEVENS, P. R.**
Software architecture concepts for avionics p 461 A90-30806
- STEVENS, S. J.**
Experimental studies of combustor dilution zone aerodynamics. I - Mean flowfields p 508 A90-32962

- Experimental studies of combustor dilution zone aerodynamics. II - Jet development p 559 A90-40947
The performance of a combustor pre-diffuser incorporating compressor outlet guide vanes
[AIAA PAPER 90-2165] p 661 A90-42053
- STEWART, A. C.**
Approach to side force alleviation through modification of the pointed forebody geometry
[AIAA PAPER 90-2834] p 712 A90-45165
- STEWART, JAMES F.**
Flight-testing of the self-repairing flight control system using the F-15 highly integrated digital electronic control flight research facility
[AIAA PAPER 90-1321] p 520 A90-34149
Flight-testing of the self-repairing flight control system using the F-15 highly integrated digital electronic control flight research facility
[NASA-TM-101725] p 758 N90-25144
- STEWART, JAMES R.**
Euler and Navier-Stokes solutions for hypersonic flows p 155 A90-18254
- STEWART, M. B.**
Experiments with unsteady, free surface, three-dimensional vortices in a thermally stable, stratified fluid
[AD-A222088] p 815 N90-26796
- STEWART, MARK E. M.**
A general decomposition algorithm applied to multi-element airfoil grids
[AIAA PAPER 90-1606] p 567 A90-38737
Automated generation of two-dimensional non-overlapping structured grids for multiple element airfoils with Euler solutions p 629 A90-42422
- STEWART, ROGER G.**
Polysilicon active-matrix liquid crystal displays for cockpit applications p 681 A90-40393
- STEWART, WILBER C.**
Polysilicon active-matrix liquid crystal displays for cockpit applications p 681 A90-40393
- STIELER, BERNHARD**
Measurement of angles and angle characteristics with accelerometers and gyroscopes p 653 A90-41730
- STIGLICH, STEPHEN WALTER, JR.**
Experimental investigation of a chemical laser cavity flowfield
[AD-A216398] p 372 N90-18038
- STILLMAN, G. E.**
The gas source molecular beam epitaxial growth of Al(x)Ga(1-x)P on (100) GaP p 894 A90-48657
- STIMPFING, A.**
Self compensation of rigid displacements in holographic interferometry
[ISL-CO-219/88] p 370 N90-17113
- STINE, L. R.**
Distributed control architecture for CNI preprocessors p 917 N90-29356
- STIPANOVICH, JOHN**
Fault tolerant architecture for a fly-by-light flight control computer p 860 A90-46931
- STIRLING, R.**
Implementation of comprehensive actuation system models in aerosemiviscous analysis p 517 A90-33406
- STITT, LEONARD E.**
Exhaust nozzles for propulsion systems with emphasis on supersonic cruise aircraft
[NASA-RP-1235] p 516 N90-21037
- STIVEN, JAMES F.**
Recent cases and developments in aviation law p 79 A90-11393
- STOCK, A. F.**
Design temperatures for flexible airfield pavement design
[AD-A214141] p 262 N90-15115
- STOCK, MICHAEL**
OPST1 - An optical yaw control system for high performance helicopters p 430 A90-28220
- STOCKER, BARRY P. W.**
Advancements in rotor and airframe structural flight testing developed during the SH-60B G.W./C.G. expansion program
[AIAA PAPER 90-1281] p 495 A90-33902
- STOCKERT, JOE**
AVION: A detailed report on the preliminary design of a 79-passenger, high-efficiency, commercial transport aircraft
[NASA-CR-186663] p 649 N90-23395
- STOCKINGER, F.**
Improved thermal performance using allylnadimides p 946 A90-50175
- STODOLSKY, NOREEN**
Flight deck modernization
[SAE PAPER 892231] p 732 A90-45447
- STOERMER, MATTHIAS**
NDI-concept for composites in future military aircraft p 877 N90-28070

- STOFFEL, BERND**
Experimental investigations on the spatial and time-dependent structure of part-load recirculations in centrifugal pumps p 83 A90-13788
- STOIANOV, FELIKS A.**
Optimal computer-aided design of the blading of axial-flow turbines p 452 A90-30268
- STOLLER, H. M.**
The application of cast SiC/Al to rotary engine components [NASA-CR-179610] p 192 N90-13385
- STOLLERY, J. L.**
Wing-section effects on the flight performance of a remotely piloted vehicle p 29 A90-11007
Hypersonics revisited (The First Leslie Bedford Lecture) p 60 A90-11458
Further work on aerofoils at Reynolds numbers between 3 x 10 to the 5th and 1 x 10 to the 6th p 145 A90-16758
- STOLLERY, JOHN L.**
Glancing shock-boundary layer interactions p 319 N90-17571
- STONE, GERALD**
Flight deck modernization [SAE PAPER 892231] p 732 A90-45447
- STONE, J.**
The potential for digital databases in flight planning and flight aiding for combat aircraft p 918 N90-29371
- STONE, J. E.**
Heat pipes for wing leading edges of hypersonic vehicles [NASA-CR-181922] p 369 N90-17055
- STONE, M. L.**
Advances in primary-radar technology p 241 A90-21380
- STONER, GLENN E.**
NASA-UVA light, aerospace alloy and structures technology program [NASA-CR-182607] p 601 N90-22651
- STOOKESBERRY, D. C.**
Supersonic/hypersonic Euler flowfield prediction method for aircraft configurations p 145 A90-16767
- STORAASLI, OLAF O.**
A parallel-vector algorithm for rapid structural analysis on high-performance computers [AIAA PAPER 90-1149] p 458 A90-29293
- STORER, J. A.**
The interaction between tip clearance flow and the passage flowfield in an axial compressor cascade p 11 A90-12525
- STORM, MICHELE E.**
Sequential design of experiments with physically based models 23 [AD-A211918] p 138 N90-12239
- STORMER, WILLIAM**
Airworthiness and flight characteristics evaluation of the McDonnell Douglas Helicopter Corporation (MDHC) 530FF helicopter [AD-A218253] p 498 N90-20076
- STORTZ, MICHAEL W.**
Flight/propulsion control integration for V/STOL fighter/attack aircraft p 591 A90-38530
Simulation, evaluation of transition and hover flying qualities of a mixed-flow, remote-lift STOVL aircraft [SAE PAPER 892284] p 757 A90-45464
- STOTHERS, I. M.**
In-flight experiments on the active control of propeller-induced cabin noise p 893 A90-46352
- STOTLER, C. L.**
PMR graphite engine duct development [NASA-CR-182228] p 51 N90-10037
- STOUFFLET, B.**
A class of implicit upwind schemes for Euler simulations with unstructured meshes p 5 A90-11597
- STOUGH, H. P., III**
Investigations of modifications to improve the spin resistance of a high-wing, single-engine, light airplane [SAE PAPER 891039] p 118 A90-14345
- STOUGH, H. PAUL, III**
A summary of spin-recovery parachute experience on light airplanes [AIAA PAPER 90-1317] p 519 A90-33926
- STOW, P.**
Navier-Stokes methods applied to turbomachinery blade design p 12 A90-12549
Simulation of inviscid blade-row interaction using a linearised potential code [AIAA PAPER 90-1916] p 621 A90-40555
Blading design for multi-storage HP compressor [PNR90602] p 116 N90-12616
- STRAHLEY, ERWIN H.**
Trends in telemetry front end architecture [AIAA PAPER 89-3085] p 25 A90-10571
- STRAHLE, WARREN C.**
Prediction of turbulent combustion flowfields behind a backward-facing step p 529 A90-32952
- STRAKA, W. A.**
Impact of nose-probe chines on the vortex flows about the F-16C [AIAA PAPER 90-0386] p 165 A90-19828
- STRASH, DANIEL J.**
A zonal flow analysis method for two-dimensional airfoils [AIAA PAPER 90-0571] p 230 A90-22230
Angle-of-attack validation of a new zonal CFD method for airfoil simulations [AIAA PAPER 90-3077] p 795 A90-45908
- STRATTON, A.**
Differential Omega/VLF as a world-wide navigation aid in the 21st century p 727 A90-45232
- STRATTON, D. ALEXANDER**
Probabilistic reasoning for intelligent wind shear avoidance [AIAA PAPER 90-3437] p 890 A90-47690
An expert system for wind shear avoidance p 486 N90-20938
- STRAUB, F.**
Plan, execute, and discuss vibration measurements and correlations to evaluate a NASTRAN finite element model of the AH-64 helicopter airframe [NASA-CR-181973] p 960 N90-28866
- STRAUB, F. K.**
Rotor/airframe aeroelastic analyses using the transfer matrix approach [AIAA PAPER 90-1119] p 392 A90-29391
- STRAUB, FRIEDRICH K.**
MDHC technical assessment of advanced rotor and control concepts p 861 A90-46948
- STRAUS, J.**
Airfoil pressure measurements during a blade vortex interaction and a comparison with theory p 232 A90-23105
- STRAUSS, BERNARD M.**
Quantitative methods in fractography; Proceedings of the Symposium on Evaluation and Techniques in Fractography, Atlanta, GA, Nov. 10, 1988 [ASTM STP-1085] p 949 A90-50551
- STRAUSS, JACK L.**
Challenges of tomorrow - The future of secure avionics p 419 A90-30723
- STRAUSS, KURT H.**
Future fuels for general aviation; Proceedings of the Symposium on Future Fuels for General Aviation Intermittent Combustion, Baltimore, MD, June 29, 1988 [ASTM STP-1048] p 950 A90-51616
- STRAUSSFOGEL, D.**
Prediction of forces and moments for flight vehicle control effectors. Part 1: Validation of methods for predicting hypersonic vehicle controls forces and moments [NASA-CR-186571] p 571 N90-21734
Prediction of forces and moments for flight vehicle control effectors. Part 2: An analysis of delta wing aerodynamic control effectiveness in ground effect [NASA-CR-186572] p 571 N90-21735
- STRAWA, ANTHONY W.**
Streamtube analysis of supersonic combustion in an in-tube-scrumjet [AIAA PAPER 90-2339] p 762 A90-42776
- STRAWN, ROGER C.**
Correlation of Puma airfoils - Evaluation of CFD prediction methods [ONERA, TP NO. 1989-185] p 224 A90-21045
Advanced rotor computations with a corrected potential method p 385 A90-28197
- STRAZISAR, A. J.**
An LDA investigation of the normal shock wave boundary layer interaction p 908 A90-52618
- STRAZISAR, ANTHONY J.**
Laser anemometer measurements in a transonic axial-flow fan rotor [NASA-TP-2879] p 73 N90-11245
- STREET, K. N.**
Repair of thermoplastic composite structures by fusion bonding p 941 A90-50060
- STREKOZOV, NIKOLAI P.**
Durability of equipment assemblies and elements of life-support systems for flight vehicles p 246 A90-21275
- STRGANAC, THOMAS W.**
Numerical model of unsteady subsonic aeroelastic behavior p 535 A90-32471
- STRICKLAND, JAMES H.**
Preliminary characterization of parachute wake recontact p 622 A90-40681
Wind tunnel study of wake downwash behind A 6 percent scale model B1-B aircraft [DE90-011783] p 719 N90-25941
- STRIZ, ALFRED G.**
Influence of structural and aerodynamic modeling on flutter analysis [AIAA PAPER 90-0954] p 411 A90-29239
- STROCK, T. W.**
Engine inlet distortion in a 9.2 percent scaled vectored thrust STOVL model in ground effect [AIAA PAPER 89-2910] p 301 A90-25043
Engine inlet distortion in a 9.2 percent scale vectored thrust STOVL model in ground effect [NASA-TM-102358] p 318 N90-17561
- STROCK, THOMAS W.**
Hot gas ingestion characteristics and flow visualization of a vectored thrust STOVL concept [NASA-TM-103212] p 751 N90-26009
- STROH, S.**
Semi-empirical transition criteria for the design of laminar profiles p 276 N90-16174
- STROUB, R. H.**
An experimental investigation of helicopter rotor hub fairing drag characteristics [NASA-TM-102182] p 88 N90-11701
- STRIJNS, R.**
Solution of the Euler equations using unstructured polygonal meshes p 708 A90-44435
- STUBERT, B.**
Experimental and numerical study on basic phenomena of secondary flows in turbines p 512 N90-21014
- STUCKERT, GREGORY**
Supersonic/hypersonic laminar/turbulent transition p 706 A90-42872
- STUESSY, W. S.**
Development of the UTA hypersonic shock tunnel [AIAA PAPER 90-0080] p 200 A90-19675
- STUETTGEN, W.**
Higher-order effects in boundary-layer premixed combustion p 529 A90-32953
- STUEVER, R. A.**
Investigations of modifications to improve the spin resistance of a high-wing, single-engine, light airplane [SAE PAPER 891039] p 118 A90-14345
Application of a design method for integrated control to a VTOL airplane in hover [AIAA PAPER 90-3334] p 862 A90-47594
- STUMPF, W. F.**
Helicopter stability and control modeling improvements and verification on two helicopters p 671 A90-42474
- STUREK, WALTER B.**
Navier-Stokes predictions of pitch damping for finned projectiles using steady coning motion [AIAA PAPER 90-3088] p 795 A90-45902
- STURGESS, G. J.**
Acoustic characteristics of a research step combustor [AIAA PAPER 90-1851] p 655 A90-40530
- STURM, G. P., JR.**
Production of jet fuels from coal-derived liquids. Volume 13: Evaluation of storage and thermal stability of jet fuels derived from coal liquids [AD-A224576] p 954 N90-29527
- STURROCK, W. R.**
Development of an automated ultrasonic inspection system for composite structure on in-service aircraft p 885 N90-28079
- STURZA, MARK A.**
Fault Detection and Isolation (FDI) techniques for guidance and control systems p 918 N90-29366
- SU, AY**
The effect of an unsteady three-dimensional wake on elastic blade-flapping eigenvalues in hover p 385 A90-28228
- SU, CHANG SHAN**
China-built airborne synchronous laser ranger the new L-8 jet trainer aircraft [AD-A213835] p 275 N90-15422
- SU, JICHAO**
Computations of unsteady transonic flows about thin airfoils by integral equation method p 158 A90-18609
Calculation of the complete transonic unsteady small disturbance equation by ADI method p 627 A90-42353
- SU, YAOXI**
Mechanism of sidewall effect studied with oil flow visualization p 154 A90-18002
Observation and analysis of sidewall effect in a transonic airfoil test section p 436 A90-28257
- SUBBOTIN, ALEKSANDR N.**
The planning of air transportation on airlines p 721 A90-42648
- SUBRAHMANYAM, M. B.**
Model reduction with a finite-interval H(infinity) criterion [AIAA PAPER 90-3473] p 890 A90-47723
- SUBRAMANYAN, V. R.**
Distributed control architecture for CNI preprocessors p 917 N90-29356
- SUDAKOV, A. G.**
Numerical simulation of three-dimensional flow around parachute canopies p 84 A90-14438

SUDAKOV, G. G.

Flow past a wing/fuselage combination with separation from the side edges of the wing p 295 A90-24088
Local convergence of the solution in the discrete vortex method p 803 A90-46534

SUDDHO, A.

Simulation of inviscid blade-row interaction using a linearised potential code
[AIAA PAPER 90-1916] p 621 A90-40555

SUDDUTH, R.

Start-up built-in test for the DISCUS fault tolerant, fly-by-wire computer system p 869 N90-27625

SUDER, KENNETH L.

Laser anemometer measurements in a transonic axial-flow fan rotor
[NASA-TP-2879] p 73 N90-11245

SUDHARMONO, F. X.

Development of airborne data reduction system in IPTN flight test p 418 A90-28895

SUGIYAMA, NANAHAISA

Noncontact measurement of rotating blade vibrations [NAL-TR-1033] p 961 N90-29687

SUGIYAMA, YOSHIYUKI

An application of the surface-singularity method to wing-body-tail configurations p 9 A90-12229
Prediction of tip-clearance effects on a wing by the panel method p 307 A90-25871

SUH, YOUNG B.

Takeoff characteristics of turbofan engines p 585 A90-35764

SULARSO

Systematic study of flutter characteristics of two-dimensional cascades in incompressible flow p 41 A90-11796

SULLEREY, R. K.

Design and off-design performance predictions of axial turbines p 45 A90-12540

SULLINS, G. A.

Investigation of the mixing of parallel supersonic streams p 69 A90-12561

SULLIVAN, J.

Hot gas environment around STOVL aircraft in ground proximity. I - Experimental study
[AIAA PAPER 90-2269] p 742 A90-42765

SULLIVAN, J. P.

Propeller wakes and their interaction with wings p 14 A90-12614

Design and performance of a small, high speed axial compressor
[AIAA PAPER 90-1911] p 624 A90-41983

SULLIVAN, JOHN P.

Lift development of delta wings undergoing constant acceleration from rest
[AIAA PAPER 90-0310] p 164 A90-19789

Propeller tip vortex interactions
[AIAA PAPER 90-0437] p 166 A90-19846

Unsteady lift development on a constantly accelerated rectangular wing
[AIAA PAPER 90-1633] p 569 A90-38762

Lift response of a rectangular wing undergoing a step change in forward speed p 620 A90-39801

SULLIVAN, P. A.

The University of Toronto-Ryerson Polytechnical Institute hypersonic gun tunnel p 673 A90-42432

SULLIVAN, THOMAS

HTTB - Industry's first STOL test bed p 414 A90-31246

SULZER, J. F.

Prospects of onboard magnetic tape recording during flight tests p 39 A90-12198

SUMMA, J. MICHAEL

A zonal flow analysis method for two-dimensional airfoils
[AIAA PAPER 90-0571] p 230 A90-22230

Angle-of-attack validation of a new zonal CFD method for airfoil simulations
[AIAA PAPER 90-3077] p 795 A90-45908

SUMMERS, GILBERT L.

Scientific justification and development plan for a mid-sized jet research aircraft
[PB89-208995] p 103 N90-11731

SUN, CHUNLIN

Aeroengine condition monitoring and fault diagnosis system p 188 A90-16851

Main characteristic parameter model for jet engine fault diagnosis p 585 A90-37210

SUN, FRANK

Laser Doppler velocimetry investigation of swirler flowfields p 682 A90-40929

SUN, HONGWEI

Complementary field method for interferometric tomographic reconstruction of high speed aerodynamic flows
[AD-A219698] p 131 A90-15900

SUN, HUIXIAN

Numerical calculation of gaseous reacting flows in a model of gas turbine combustors p 271 A90-21979

SUN, JINCAI

Prediction of transmission loss through an aircraft sidewall using statistical energy analysis p 219 A90-18599

SUN, MAO

Method for calculating the unsteady flow of an elliptical circulation-control airfoil p 3 A90-11003

An experiment study of rotor aerodynamic in ground effect at low speed p 149 A90-16826

The influence of the helicopter fuselage on its rotor p 301 A90-25101

SUN, SHULING

Analysis methods of tie-down loads and airframe stress for shipboard-helicopters p 199 A90-16855

SUN, XIAO-FENG

On the unsteady loading noise of counter-rotating propeller p 895 A90-49484

On numerical prediction of sound field generated by propeller p 895 A90-49485

SUN, XIAOFENG

Noise generation by swept cascade p 895 A90-49486

SUN, ZHONGKANG

Passive location and tracking using DOA and TOA measurements of single nonmaneuvering observer p 576 A90-35709

SUNANDA, K. SATYA

Analytical evaluation of radiation patterns of a TACAN antenna p 404 A90-30695

SUNDARARAJAN, S.

Finite-element analysis of large spur and helical gear systems p 683 A90-40940

SUNDBERG, GALE R.

Civil air transport: A fresh look at power-by-wire and fly-by-light
[NASA-TM-102574] p 542 N90-21283

SUNDER, R.

Compilation of procedures for fatigue crack propagation testing under complex load sequences p 368 A90-26759

Estimation of fatigue crack growth in patched cracked panels p 684 A90-41335

SUNDERRAMAN, RAJ

International aircraft operator data base master requirements and implementation plan
[DOT/FAA/CT-90/17] p 967 N90-29247

SUNG, D. Y.

An experimental investigation of helicopter rotor hub fairing drag characteristics
[NASA-TM-102182] p 88 N90-11701

SUNKEL, J. W.

A linear quadratic regulator approach to the stabilization of uncertain linear systems
[AIAA PAPER 90-3509] p 891 A90-47755

SUPPLEE, FRANK H., JR.

High temperature skin friction measurement p 448 A90-28306

SUPRUNENKO, S. N.

Mean-square approximation by an even nonnegative polynomial p 374 A90-24101

Determination of the extreme values of the efficiency criteria for a flight vehicle control system in the probable scatter range of its characteristics p 859 A90-46569

SURESH, A.

The propagation of a normal shock in a varying area duct p 130 A90-15045

SUTHERLAND, LOUIS C.

Sound propagation elements in evaluation of en route noise of advanced turbofan aircraft p 697 N90-24861

SUWAL, K. R.

Singular, periodic solutions in aircraft cruise-dash optimization
[AIAA PAPER 90-3369] p 863 A90-47627

SUZUKI, KOJIRO

Topology of computed incompressible three-dimensional separated flow field around high-angle-of-attack cone-cylinders p 366 A90-25764

SUZUKI, R.

CRL's mobile satellite communication experiments using ETS-V
[AIAA PAPER 90-0775] p 366 A90-25602

SUZUKI, S.

Multi-surface control law synthesis and wind tunnel test verification of active flutter suppression for a transport-type wing p 517 A90-33401

Structure/control design synthesis of active flutter suppression system by goal programming
[AIAA PAPER 90-3325] p 872 A90-47587

SUZUKI, SHINJI

Calculation of stability derivatives for slender bodies using boundary element method p 620 A90-40181

SVIATYSHEV, K. G.

Estimation of the safety factor of turbine blades under thermal cycling and vibration loading p 958 A90-52356

SVIRIDENKO, IU. N.

Using the method of symmetric singularities for calculating flow past subsonic flight vehicles p 386 A90-28979

Calculation of the effect of the engine nacelle on transonic flow past a wing p 387 A90-28990

SWAIM, ROBERT L.

An aircraft flight control reconfiguration algorithm p 432 A90-30708

Turbulence effects of aircraft flight dynamics and control p 258 N90-15055

SWAIN, M. H.

Fatigue crack initiation and small crack growth in several airframe alloys
[NASA-TM-102598] p 454 N90-18746

SWAMINADHAM, M.

Structural testing and analytical research of turbine components
[AD-A223516] p 933 N90-29396

SWAMINATHAN, V.

Numerical solution of unsteady Navier-Stokes equations for laminar/turbulent flows past axis-symmetric bodies at angle of attack p 85 A90-15235

Numerical simulation of supersonic and hypersonic turbulent compression corner flows using PNS equations p 85 A90-15242

SWANGIM, JOANN

Challenges of tomorrow - The future of secure avionics p 419 A90-30723

SWANGWANNA, SULLYUTH

Real-time decision making for autonomous flight control
[SAE PAPER 891053] p 118 A90-14355

SWANN, MADELINE

The prediction of middle distillate fuel properties using liquid chromatography-proton nuclear magnetic resonance spectroscopy data
[AD-A211879] p 126 N90-11899

SWANSON, DOUGLAS A.

Improved noise rejection in automatic carrier landing systems
[AIAA PAPER 90-3374] p 864 A90-47632

SWANSON, E. R.

Omega coverage - Analytical and empirical methods and solutions p 728 A90-45234

SWANSON, R. C.

On central-difference and upwind schemes
[NASA-CR-182061] p 781 N90-26595

A comparison of two central difference schemes for solving the Navier-Stokes equations
[NASA-TM-102815] p 816 N90-27654

SWANSON, R. CHARLES

Comparison of two- and three-dimensional Navier-Stokes solutions with NASA experimental data for CAST-10 airfoil p 321 N90-17658

SWANSON, ROBERT E.

NASA-UVA light aerospace alloy and structures technology program
[NASA-CR-182607] p 601 N90-22651

SWANSON, STEPHEN MARK

A computer module used to calculate the horizontal control surface size of a conceptual aircraft design
[NASA-CR-186872] p 780 N90-26515

SWARTLING, FRED

Two special cost-effective applications for electrochemical metallizing for improved brazing and bonding
[SAE PAPER 890927] p 365 A90-24692

SWEENEY, PATRICK C.

Fiber-optic turbine inlet temperature measurement system (FOTITMS)
[AIAA PAPER 90-2033] p 657 A90-40603

SWEET, DAVID H.

Flight testing of the Chandler Evans adaptive fuel control on the S-76A helicopter p 422 A90-28178

SWEETMAN, BILL

Sharing power and profit p 188 A90-16701

IHPET spawns engines for 21st century p 188 A90-16702

Turboshafts on tenterhooks p 188 A90-16703

Civil supersonics - A less distant thunder p 731 A90-44223

Military navigation - The fourth generation p 914 A90-50775

SWERN, FREDERIC L.

A methodology for validating software reliability
[AIAA PAPER 89-3081] p 74 A90-10567

Hardware and software reliability estimation using simulations
[NASA-CR-186637] p 780 N90-25580

SWIATECKI, ANTONI

- The FAA technical classification of aircraft and airports p 96 A90-15876
ICAO airfield reference code p 261 A90-21628

SWIFT, G.

- Propan Test Assessment (PTA): Flight test report [NASA-CR-182278] p 113 N90-11738

SWIGART, R. J.

- Generalized Advanced Propeller Analysis System (GAPAS). Volume 2: Computer program user manual [NASA-CR-185277] p 933 N90-29394

SWINFORD, SCOTT S.

- Aerodynamic heat transfer testing in hypersonic wind tunnels using an infrared imaging system [AIAA PAPER 90-0189] p 350 A90-25027

SWINNEY, DAVID V.

- A fractional calculus model of aeroelasticity [AD-A216244] p 377 N90-18212

SWIRYDCZUK, J.

- A visualization study of the interaction of a free vortex with the wake behind an airfoil p 623 A90-41119

SWITHINBANK, CHARLES

- Ice runways near the South Pole [AD-A211606] p 133 N90-11908

- Airfields on antarctic glacier ice [AD-A217638] p 526 N90-20097

SWITZER, GEORGE F.

- Comparison between experimental and numerical results for a research hypersonic aircraft p 395 A90-31278

SWOLINSKY, MANFRED

- Wind shear models for aircraft hazard investigation p 280 N90-15044

SWORSKI, THOMAS J.

- A preliminary sensitivity analysis of the Generalized Escape System Simulation (GESS) computer program [DE89-016891] p 24 N90-10844

SYED, S. A.

- Application of CFD to pitch/yaw thrust vectoring spherical convergent flap nozzles [AIAA PAPER 90-2023] p 657 A90-40597

- The role of hydrogen/air chemistry in nozzle performance for a hypersonic propulsion system [AIAA PAPER 90-2492] p 658 A90-40637

SYED, SAADAT A.

- Critical evaluation of three-dimensional supersonic combustor calculations [AIAA PAPER 90-0207] p 272 A90-22265

SYERS, G.

- The application of engineering ceramics in gas turbines [PNR90676] p 750 N90-26005

SYLLA, CHEICKNA

- A framework for the optimal design of instructor/operator stations in flight simulators p 779 A90-45373

SYMONDS, C. H.

- A friendly alloy p 764 A90-44173

SYMONDS, M. D.

- The Radarsat system p 873 A90-49671

SYNSTELIEN, LARRY D.

- Phase III GPS Manpack receiver operation and navigation performance p 823 A90-49497

SZE, K. Y.

- The Helicopter Antenna Radiation Prediction Code (HARP) [NASA-CR-186925] p 884 N90-27946

SZEMA, K. Y.

- Supersonic flow computations for an ASTOVL aircraft configuration [AIAA PAPER 90-2997] p 787 A90-45847

SZEMA, KUO-YEN

- Supersonic flow computations over aerospace configurations using an Euler marching solver [NASA-CR-4085] p 19 N90-10012

- Supersonic flow computations for an ASTOVL aircraft configuration, phase 2, part 2 [NASA-CR-4284] p 610 N90-22746

SZEWCZYK, V. M.

- What should be done with those noisy old aircraft [PNR90562] p 107 N90-12593

- Re-engine with the Rolls-Royce Tay 670, the route to significant noise reduction [PNR90585] p 115 N90-12606

SZODRUCH, J.

- Design for a natural laminar flow glove for a transport aircraft [AIAA PAPER 90-3043] p 792 A90-45880

- Test and Measurement Technique in Hypersonics [ILR-MITT-225(1989)] p 618 N90-24225

- Aerodynamic development perspective for traffic aeroplanes [DGLR-89-141] p 637 N90-24260

SZUMANSKI, KAZIMIERZ

- A multifunctional system of helicopter dynamics simulations p 28 A90-10226

- Some unconventional cases of the dynamical testing of helicopters p 28 A90-10227

SZUMOWSKI, A. P.

- Self-excited oscillations in internal transonic flows p 813 A90-49274

SZYMKOWIAK, E. A.

- A captive store flight vibration simulation project p 672 A90-40476

T

T HART, W. G. J.

- Quench sensitivity of airframe aluminium alloys p 765 A90-44348

TABADDOR, FARHAD

- Evaluation of critical speeds in high speed aircraft tires [SAE PAPER 892349] p 733 A90-45500

TABAKOFF, W.

- Effect of environmental particles on a radial compressor p 113 A90-16373

- Effect of inlet flow angle on the erosion of radial turbine guide vanes [ASME PAPER 89-GT-208] p 254 A90-22664

- Simulation of compressor performance deterioration due to erosion [ASME PAPER 89-GT-182] p 254 A90-22665

- LDV measurements and the flow analysis in the vaneless region of a radial inflow turbine [ASME PAPER 89-GT-157] p 292 A90-23845

- Performance improvement of an eroded axial flow compressor using water injection [AIAA PAPER 90-2016] p 741 A90-42718

- Jet engines performance deterioration p 852 A90-46871

TACINA, ROBERT R.

- Low NO(x) potential of gas turbine engines [AIAA PAPER 90-0550] p 343 A90-25036

- Combustor technology for future aircraft [AIAA PAPER 90-2400] p 852 A90-47219

- Low NO(x) potential of gas turbine engines [NASA-TM-102452] p 345 N90-17636

TADGHIGHI, HORMOZ

- Circulation control tail boom aerodynamic prediction and validation p 385 A90-28243

TADIOS, EDEN L.

- Wind tunnel study of wake downwash behind A 6 percent scale model B1-B aircraft [DE90-011783] p 719 N90-25941

TADROS, R. N.

- Fracture mechanics assessment of EB-welded blisked rotors p 453 A90-31117

- The survivability of centrifugal compressors in modern aircraft engines p 928 A90-49883

- Review of modelling methods to take account of material structure and defects p 425 N90-18402

- Life management planning p 856 N90-27709

TADROS, REDA N.

- Cyclic stress-strain behavior and low cycle fatigue of Ti 6242 p 530 A90-33523

TAFTI, D. K.

- Hot gas environment around STOVL aircraft in ground proximity. II - Numerical study [AIAA PAPER 90-2270] p 743 A90-42766

TAGANOV, G. I.

- Flow past bodies within a narrow class of cross-sectional shapes with stationary separation zones at large Reynolds numbers p 805 A90-46568

TAGIROV, R. K.

- Determination of the specific thrust in open regimes and design of a nonseparating convergent nozzle profile p 395 A90-30339

TAGORI, TETSUO

- Development of a new low-Reynolds-number type Reynolds stress model and its application to a lobe mixer flow p 584 A90-35229

TAI, TSZE C.

- Supersonic low-density flow over airfoils p 153 A90-17871

- Direct simulation of low-density flow over airfoils [AIAA PAPER 90-1539] p 564 A90-38683

TAILBY, ANDREW J.

- Natural icing re-evaluation of the EH-60A Quick Fix helicopter [AD-A214728] p 323 N90-16723

TAIURSKAIA, G. R.

- Construction of a straight single-row airfoil lattice by the method of quasi-solutions for inverse boundary value problems p 84 A90-14564

TAKAHASHI, HITOSHI

- Wind tunnel test of CAD USB-STOL semi-borne prototype [NAL-TM-566] p 88 N90-11696

TAKAHASHI, M. D.

- A simple active controller to suppress helicopter air resonance in hover and forward flight p 119 A90-16521

- A model for active control of helicopter air resonance in hover and forward flight p 670 A90-42462

TAKAHASHI, R. K.

- Unsteady Euler analysis of the redistribution of an inlet temperature distortion in a turbine [AIAA PAPER 90-2262] p 768 A90-42759

TAKAHASHI, YOSHIKI

- Supersonic viscous shear layers p 367 A90-25873

TAKAKURA, YOKO

- Turbulence models for 3D transonic viscous flows. II p 306 A90-25820

TAKALLU, M. A.

- A hybrid method for prediction of propeller performance [AIAA PAPER 90-0440] p 229 A90-22219

- Effect of pylon wake with and without pylon blowing on propeller thrust [NASA-TM-4162] p 173 N90-14190

- Unsteady potential flow past a propeller blade section [NASA-CR-4307] p 634 N90-24246

TAKAMI, HIDEO

- Effect of ground on wake roll-up behind a lifting surface p 160 A90-19436

TAKANASHI, SUSUMU

- Navier-Stokes computations for the investigation of flowfields about a Space-Plane p 306 A90-25836

- Grid generation procedure using the integral equation method [NAL-TR-1009] p 77 N90-10630

- Some topics in computational transonic aerodynamics: Revision [NAL-TR-1018T] p 912 N90-29332

TAKANO, MASANORI

- Numerical simulations of unsteady shock reflections by ramps p 305 A90-25795

TAKATA, HIROYUKI

- Numerical analysis of rotating stall by a vortex model p 13 A90-12590

TAKAYAMA, K.

- Holographic interferometric study of shock wave propagation p 66 A90-10732

TAKEDA, KATSUMI

- Propulsive lift augmentation by side fences as applied to Japan's experimental STOL aircraft, ASKA [AIAA PAPER 90-3009] p 789 A90-45859

- Parametric studies of acoustic duct attenuation perforated-plate-on-honeycomb absorber [NAL-TM-603] p 966 N90-30030

TAKEISHI, K.

- An experimental study of heat transfer and film cooling on low aspect ratio turbine nozzles [ASME PAPER 89-GT-187] p 361 A90-23865

TAKEMORI, TOSHIKAZU

- Gas identification system using graded temperature sensor and neural net interpretation [AD-A213359] p 205 N90-13627

TAKEUCHI, H.

- Application of 3-D Navier-Stokes computation to bowed stacking turbine vane design [AIAA PAPER 90-2129] p 625 A90-42035

TALBOT, PETER D.

- Identification of rotor flapping equation of motion from flight measurements with the RSRA compound helicopter p 56 A90-12769

- Selected design issues of some high speed rotorcraft concepts [AIAA PAPER 90-3297] p 840 A90-49125

- Synthesis of individual rotor blade control system for gust alleviation [NASA-TM-101886] p 736 N90-25972

TALIA, JORGE E.

- Mechanical paint removal techniques for aircraft structures [NIAR-90-12] p 775 N90-26166

TALLEY, WILLIAM G.

- Advanced actuation systems development, volume 1 [AD-A213334] p 121 N90-12624

- Advanced actuation systems development, volume 2 [AD-A213378] p 198 N90-13398

TALOTTA, NICHOLAS J.

- Operational evaluation of initial data link air traffic control services, volume 1 [DOT/FAA/CT-90/1-VOL-1] p 455 N90-19472

TALYZIN, V. A.

- The problem of aircraft test flight correction p 828 A90-46485

TAM, H.

- Endurance of aircraft gas turbine mainshaft ball bearings-analysis using improved fatigue life theory. II - Application to a bearing operating under difficult lubrication conditions p 128 A90-13845

TAMAGNO, JOSE

- Hypervelocity real gas capabilities of GASL's expansion tube (HYPULSE) facility [AIAA PAPER 90-1390] p 594 A90-37935

TAMAI, SHOJI

- Improved melt flow and physical properties of Mitsui Toatsu's LARC-TPI 1500 series polyimide p 943 A90-50134

TAMAKI, H.

- A study of filament wound high modulus carbon fiber reinforced cylinders p 948 A90-50218

TAMAMIDIS, P.

- Evaluation of two numerical techniques for the prediction of flow around blades p 10 A90-12512

TAMANINI, FRANCO

- Ignitability of jet-A fuel vapors in aircraft fuel tanks p 326 N90-17594

TAMARU, T.

- Hydrogen fueled subsonic-ram-combustor model tests for an air-turbo-ram engine p 44 A90-12529

TAMURA, MASATO

- Application of Lomax-Bailey implicit scheme to reactive flows p 367 A90-25861

TAMURA, YOSHIKAI

- Capability of current supercomputers for the computational fluid dynamics p 546 A90-34382

TAN, ANZHONG

- Measurements of pressure fluctuations in the interaction regions of shock waves and turbulent boundary layers induced by blunt fins p 9 A90-12218

- Aerodynamic heating in the interaction regions of shock waves and turbulent boundary layers induced by sharp fins p 9 A90-12220

- Aerodynamic heating in shock wave/turbulent boundary layer interaction regions induced by blunt fins p 82 A90-13775

- Numerical simulations of unsteady shock reflections by ramps p 305 A90-25795

TAN, CARINA M.

- Development of the Second Generation Comprehensive Helicopter Analysis System (2GCHAS) p 889 A90-46963

TAN, FENGXIANG

- Digital electronic control for WJ6G4A engine p 424 A90-29919

TAN, S. C.

- A study of particle trajectories in a gas turbine intake p 48 A90-12583

- A theoretical approach to particle separator design p 48 A90-12584

TAN, T. M.

- Engineering design of tough ceramic matrix composites for turbine components [ASME PAPER 89-GT-294] p 343 A90-23892

TANABE, GIICHI

- Airline productivity relating to the fuel cost. (2): Fuel consumption values and fuel efficiency [NAL-TM-604-2] p 913 N90-29333

TANAKA, A.

- Application of 3-D Navier-Stokes computation to bowed stacking turbine vane design [AIAA PAPER 90-2129] p 625 A90-42035

TANAKA, ATSUSHIGE

- Flow dependent grid for aerodynamic designers p 306 A90-25831

- A numerical investigation of supersonic inlet using implicit TVD scheme [AIAA PAPER 90-2135] p 621 A90-40612

TANAKA, HIDEO

- Flutter of cascade blades composed of blades having arbitrarily different natural frequencies p 42 A90-11798

TANAKA, KEIJI

- Flight simulator evaluation of a head-down display [NAL-TM-573] p 59 N90-10898

TANAKA, T.

- Three dimensional photoelastic analysis of aeroengine parts p 270 A90-20077

TANAKA, YASUYUKI

- Mechanical rig rest of FJR 710/600 engine components p 43 A90-12016

TANATSUGU, NOBUHIRO

- Development study of air turbo-ramjet for future space plane [IAF PAPER 89-311] p 109 A90-13445

TANG, CHIA-PIN

- Aging and antioxidant surveillance studies on turbine fuel JP-5 and JP-10 p 442 A90-29492

TANG, DENGBIN

- An investigation of unsteady leading edge separation of rapidly pitched airfoils p 157 A90-18587

TANG, DENNIS

- Air Force application of injection molding technology [SME PAPER EM89-103] p 274 A90-23686

TANG, GUO CAI

- An investigation of artificial compressor surge p 11 A90-12526

TANG, JICHEN

- Investigation on the determination of airplane tail loads by flight tests p 178 A90-16853

TANG, MING

- Exhaust emission performance of a vaporizer tube combustor as compared with a single tube combustor p 111 A90-14614

- Numerical calculation of gaseous reacting flows in a model of gas turbine combustors p 271 A90-21979

TANG, N.

- New transonic test sections for the NAE 5 ft x 5 ft trisonic wind tunnel [AD-A220933] p 674 N90-24278

TANG, SHU S.

- Stress intensity factors for cracking metal structures under rapid thermal loading. Volume 2: Theoretical background [AD-A213297] p 213 N90-13812

TANG, W.

- Numerical simulation of the growth of instabilities in supersonic free shear layers p 623 A90-40941

TANG, ZHIMING

- A semi-actuator disk theory for prediction of stall flutter in axial flow compressors p 301 A90-25105

TANI, K.

- Some governing parameters of plasma torch igniter/flameholder in a scramjet combustor [AIAA PAPER 90-2098] p 661 A90-42017

TANIDA, Y.

- Self-excited oscillation of shock waves on an airfoil in two-dimensional transonic channel flow p 8 A90-11808

TANIDA, YOSHIMICHI

- Self-excited oscillation of transonic flow around an airfoil in two-dimensional channel [ASME PAPER 89-GT-58] p 290 A90-23784

TANNA, H. K.

- Application of active noise control to model propeller noise p 548 A90-34091

TANNEHILL, J. C.

- Numerical prediction of turbulent flow over airfoil sections with a new nonequilibrium turbulence model [AIAA PAPER 90-1469] p 562 A90-38626

TANNEHILL, JOHN C.

- A three-dimensional upwind parabolized Navier-Stokes code for chemically reacting flows [AIAA PAPER 90-0394] p 165 A90-19831

- Development of a three-dimensional upwind parabolized Navier-Stokes code p 602 A90-36253

TANNER, J. C.

- Flight test and numerical analysis of a half-scale Unmanned Air Vehicle [AIAA PAPER 90-1260] p 494 A90-33890

TANNER, JOHN A.

- Analysis of aircraft tires via semianalytic finite elements p 496 A90-34740

- Frictionless contact of aircraft tires [SAE PAPER 892350] p 733 A90-45501

TANRIKUT, S.

- Energy efficient engine pin fin and ceramic composite segmented liner combustor sector rig test report [NASA-CR-179534] p 932 N90-28567

TAO, ALBERT C. C.

- Structure analysis of burning liquid-fueled spray in a confined combustor [AIAA PAPER 90-2444] p 677 A90-42174

TAO, D. P.

- A method for predicting stall flutter under variable interblade phase angle along rotating direction p 813 A90-49455

TAPE, ROBERT F.

- Direct lift STOV engine integration [AIAA PAPER 90-2274] p 644 A90-42103

- Advanced material applications for direct lift engines [AIAA PAPER 90-2753] p 664 A90-42226

TAPLEY, BYRON D.

- Eshbach's handbook of engineering fundamentals /4th edition/ p 448 A90-28825

TAPPAN, D. V.

- Analysis of hydraulic fluids and lubricating oils for the formation of Trimethylolpropane Phosphate (TMP-P) [AD-A215188] p 357 N90-16939

TARABRIN, I. G.

- Multicriterial optimization of lugs in hinge joints p 364 A90-24162

TARN, JIANN-QUO

- Flutter analysis of composite panels using high-precision finite elements p 207 A90-16725

TARR, LARRY E.

- Chromate free electrolytic deoxidizer for aluminum p 956 A90-50216

TARTTELIN, P. C.

- Theoretical and experimental correlation of helicopter aeromechanics in hover p 429 A90-28200

TARVIN, CHRISTINA

- High Voltage Design Guide summary p 605 A90-38097

TASK, HARRY L.

- A new method for measuring the transmissivity of aircraft transparencies [AD-A216953] p 464 N90-19842

TASKER, FREDERICK A.

- Multi-output implementation of a modified sparse time domain technique for rotor stability testing [AIAA PAPER 90-0946] p 412 A90-29405

TASLIM, M. E.

- An experimental investigation of film cooling effectiveness for slots of various exit geometries [AIAA PAPER 90-2266] p 768 A90-42763

TAUBER, M. E.

- A brief review of some mechanisms causing boundary layer transition at high speeds [NASA-TM-102834] p 720 N90-25945

TAUBER, MICHAEL E.

- Hypervelocity, minimum-radii, coordinated turns p 667 A90-40691

- A review of high-speed, convective, heat-transfer computation methods p 316 N90-17548

TAVELLA, DOMINGO

- Transpiration cooling in hypersonic flight [NASA-CR-186435] p 478 N90-20052

TAVELLA, DOMINGO A.

- Pneumatic vortical flow control at high angles of attack [AIAA PAPER 90-0098] p 227 A90-22164

TAY, ANDREW

- Design and fabrication considerations for composite structures with embedded fiber optic sensors p 536 A90-32871

TAYLOR, A. F.

- Aircraft fires: A study of transport accidents from 1975 to the present p 324 N90-17583

TAYLOR, CRAIG

- Noise and sonic boom impact technology. Effects of aircraft noise and sonic booms on structures: An assessment of the current state-of-knowledge [AD-A213919] p 378 N90-17409

TAYLOR, IVOR J.

- In-line wear monitor [AD-A217799] p 510 N90-20091

TAYLOR, J. R.

- Multiple swirler dome combustor for high temperature rise applications [AIAA PAPER 90-2159] p 661 A90-42050

- Energy Efficient Engine combustor test hardware detailed design report [NASA-CR-168301] p 929 N90-28554

- Energy Efficient Engine (E3) combustion system component technology performance report [NASA-CR-168274] p 930 N90-28555

TAYLOR, JAMES

- Multidisciplinary Expert-aided Analysis and Design (MEAD) p 613 N90-23050

TAYLOR, JAMES H.

- A computer-aided control engineering environment for multi-disciplinary expert-aided analysis and design (MEAD) p 461 A90-30796

TAYLOR, JOHN G.

- Static investigation of a two-dimensional convergent-divergent exhaust nozzle with multiaxis thrust-vectoring capability [NASA-TP-2973] p 397 N90-19193

TAYLOR, L. O.

- A reconfigurable integrated navigation and flight management system for military transport aircraft p 433 A90-30794

TAYLOR, MICHAEL ROBINSON

- Studies in automatic speech recognition and its application in aerospace p 958 N90-28759

TAYLOR, N. J.

- An aerofoil testing technique for low supersonic speeds in an adaptive flexible-walled wind tunnel [AIAA PAPER 90-3086] p 795 A90-45900

TAYLOR, NORMA F.

- Solution of potential flow past an elastic body using the boundary element technique [AD-A213843] p 275 N90-15390

TAYLOR, R. G.

- NDT in aerospace: The next decade (1990's) [PNR90628] p 777 N90-26348

- The role of NDI in the certification of turbine engine components [PNR90629] p 777 N90-26349

- The role of NDI in the certification of turbine engine components p 859 N90-28069

TAYLOR, R. P.

- Surface roughness measurements on gas turbine blades [ASME PAPER 89-GT-285] p 508 A90-33559

TAYLOR, RICHARD W.

- Twin-engine transports - A look at the future [AIAA PAPER 90-3215] p 818 A90-49107

- TAYLOR, RODNEY S.**
CTR-1000 civil tiltrotor concept p 829 A90-46939
- TAYLOR, SCOTT**
The MANTA: An RPV design to investigate forces and moments on a lifting surface [NASA-CR-186227] p 499 N90-20971
- TCHENG, PING**
High temperature skin friction measurement p 448 A90-28306
- TCHON, K. F.**
Finite element simulation of unsteady two-dimensional incompressible viscous flows p 629 A90-42423
- TEAGUE, CHARLES J.**
Lightweight fuel pump and metering component for advanced gas turbine engine control [AIAA PAPER 90-2032] p 657 A90-40602
- TEARE, D. A.**
Time domain parameter identification techniques applied to the UH-60A Black Hawk Helicopter p 77 A90-12774
- TEETER, DARRIN**
Elevator tab assembly producibility study [IAR-89-16] p 734 N90-25133
- TEGTMEIER, A.**
Project Falke - Performance of free flight tests in the supersonic, transonic, and subsonic regimes from balloons [DGLR PAPER 88-018] p 903 A90-50235
- TEIPEL, I.**
Two-dimensional transonic flow field analysis with different turbulence models p 150 A90-16846
- TEKAWY, JONATHAN A.**
Algorithms for computing the multivariable stability margin p 612 N90-22999
- TELIONIS, D. P.**
The hemisphere-cylinder at an angle of attack [AIAA PAPER 90-0050] p 313 A90-26907
Vortex shedding over delta wings p 470 A90-32479
- TELIONIS, DEMETRI P.**
Blade-vortex interaction experiments - Velocity and vorticity fields [AIAA PAPER 90-0030] p 312 A90-26903
- TEMNENKO, V. A.**
The shape assumed by a soft conical shell in fluid flow p 300 A90-24752
Analytical solution of the problem of nonaxisymmetric potential flow past a spherical canopy - A summary of the principal asymptotic formulas and qualitative analysis p 300 A90-24753
- TEN EYCK, M. O.**
Injection molding development of ceramic turbine components [ASME PAPER 89-GT-170] p 361 A90-23855
- TEN HAVE, A. A.**
Usage monitoring of military helicopters p 651 A90-39984
- TENCH, KENNETH A.**
A microcomputer-based airspace control simulation and prototype human-machine interface p 461 A90-30800
GPSNOTAM - A demonstration system for GPS status notification p 728 A90-45238
- TENG, N. G.**
Progress towards the development of an inviscid-viscous interaction method for unsteady flows in turbomachinery cascades p 8 A90-11806
- TENIAEVA, V. E.**
Determination of the torsion rigidity of a multiple-rib torsion box of an aircraft lifting surface p 364 A90-24134
Efficiency of using a multiple-wall torsion box in the load-bearing structures of lifting surfaces p 410 A90-29188
- TENISON, G.**
A comparison of a droplet impingement code to icing tunnel results [AIAA PAPER 90-0670] p 352 A90-26979
- TENNEY, DARREL R.**
Materials and structures for hypersonic vehicles p 31 A90-13015
- TERADA, T.**
Evaluation of high temperature protective coatings for gas turbine engines under simulated service conditions p 952 N90-28712
- TERAMAE, TETSUO**
Reliability evaluation system for ceramic gas turbine components p 444 A90-27678
- TEREKHOVA, N. M.**
Perturbations of higher modes in a supersonic jet p 619 A90-39516
- TERENT'EV, S. A.**
Synthesis of locally optimal aircraft control in the presence of delay p 137 A90-14561
- TERRAB, MOSTAFA**
Real-time adaptive aircraft scheduling [NASA-CR-177558] p 820 N90-27669
- TERRY, JOEL L., JR.**
The Advanced Digital-Optical Control System (ADOCS) user demonstration program [AD-A215984] p 349 N90-17644
- TESCH, H.**
Rigidite S255-3 - A highly damage tolerant prepreg resin system with a well balanced property profile p 944 A90-50139
- TEWARI, A.**
A reduced cost rational-function approximation for unsteady aerodynamics [AIAA PAPER 90-1155] p 390 A90-29367
- TEWARSON, A.**
Flammability testing of aircraft cabin materials p 328 N90-17611
- THAIN, J.**
New transonic test sections for the NAE 5 ft x 5 ft trisonic wind tunnel [AD-A220933] p 674 N90-24278
- THALIB, ARDJUNA**
Development of airborne data reduction system in IPTN flight test p 418 A90-28895
- THAMBURAJ, R.**
Braze repair of MA754 aero gas turbine engine nozzles [ASME PAPER 89-GT-235] p 342 A90-23886
Life estimation of a gas turbine afterburner spraybar p 739 A90-42662
Surface property improvement in titanium alloy gas turbine components through ion implantation p 953 N90-28713
- THANGAM, S.**
Computational prediction of stall flutter in cascaded airfoils [AIAA PAPER 90-1116] p 392 A90-29388
- THANGITHAM, S.**
The warping restraint effect in the critical and subcritical static aeroelastic behavior of swept forward composite wing structures [SAE PAPER 891056] p 129 A90-14358
The static aeroelastic behavior of sweptforward composite wing structures taking into account their warping restraint effect p 210 A90-18407
- THAREJA, R. R.**
Applications of an adaptive unstructured solution algorithm to the analysis of high speed flows [AIAA PAPER 90-0395] p 229 A90-22213
- THAREJA, RAJIV R.**
Euler and Navier-Stokes solutions for hypersonic flows p 155 A90-18254
- THAYER, JEFFREY S.**
An airborne instrument for characterizing the 10,000 electromagnetic signals generated by one lightning flash p 848 A90-49830
- THEN, MICHAEL J.**
The future of aircraft paint removal methods [AD-A214946] p 356 N90-16936
- THERIAULT, Y.**
Probabilistic approach to fleet management p 701 A90-42674
- THEUNISSEN, E. A. M.**
The comparison of the airbase simulation models airbase and sustained [FEL-1988-66] p 123 N90-12629
- THIBERT, J. J.**
Design and experimental investigation of a laminar horizontal tail [AIAA PAPER 90-3042] p 798 A90-45934
- THIEDE, P.**
Computation of multi-element airfoil flows including confluence effects p 144 A90-16755
Design for a natural laminar flow glove for a transport aircraft [AIAA PAPER 90-3043] p 792 A90-45880
Turbulence management: Application aspects p 72 N90-10378
Semi-empirical transition criteria for the design of laminar profiles p 276 N90-16174
Transonic wing charge improvements by passive shock boundary layer interference control: Development status and prospects [ETN-90-96463] p 650 N90-24267
- THIELE, F.**
Computation of multi-element airfoil flows including confluence effects p 144 A90-16755
A semi-analytical procedure for the conformal mapping of arbitrary airfoil contours p 309 A90-26498
An interactive method for the flow calculation of airfoils with local separation regions p 278 N90-16190
- THINH, DINH**
Heat Transfer and Fluid Mechanics Institute, 31st, California State University, Sacramento, June 1, 2, 1989, Proceedings p 130 A90-15387
- THOE, D. W.**
Analysis of three-dimensional turbomachinery flows on C-type grids using an implicit Euler solver [SAE PAPER 89-GT-85] p 905 A90-51258
- THOM, JIM**
New power system architecture for the 747-400 p 508 A90-33349
Design features of the 747-400 Electric Power System [SAE PAPER 892227] p 746 A90-45443
- THOMAN, DAVID C.**
Advanced technology ATE for fuel accessory testing p 439 A90-30770
- THOMAN, STEVEN**
Microstructural effects of plastic media blasting on graphite epoxy composites [SAE PAPER 890928] p 286 A90-24693
- THOMAS, D. R.**
Experiments on the active control of the transmission of sound through a clamped rectangular plate p 695 A90-41109
Active control of sound transmission through a cylindrical shell p 893 A90-46192
- THOMAS, FRANK O.**
A comparison of emergency medical helicopter accident rates in the United States and the Federal Republic of Germany p 722 A90-44640
- THOMAS, JAMES**
Signal processing in a digital GPS receiver p 128 A90-14006
- THOMAS, JAMES L.**
Navier-Stokes computations of a prolate spheroid at angle of attack p 17 A90-13018
Navier-Stokes computations of lee-side flows over delta wings p 153 A90-17978
Transonic Navier-Stokes solutions about a complex high-speed accelerator configuration [AIAA PAPER 90-0430] p 166 A90-19844
An embedded grid formulation applied to a delta wing [AIAA PAPER 90-0429] p 229 A90-22216
Navier-Stokes computations of vortical flows over low-aspect-ratio wings p 232 A90-23103
Implicit flux-split schemes for the Euler equations p 602 A90-36254
A computational study of incipient leading-edge separation on a 65-deg delta wing at $M = 1.60$ [AIAA PAPER 90-3029] p 791 A90-45871
- THOMAS, K.**
Turbulence spectral widths view angle independence as observed by Doppler radar [DOT/FAA/SA-89/2] p 281 N90-15566
- THOMAS, M.**
beta CEZ, a high performance titanium alloy for aerospace engines [ONERA, TP NO. 1990-8] p 356 A90-25356
- THOMAS, RICHARD W.**
Aerodynamic and propulsive control development of the STOL and maneuver technology demonstrator p 920 N90-28514
- THOMAS, S.**
A numerical parametric study of a scramjet inlet in a Mach 6 arc heated test facility [AIAA PAPER 90-0531] p 167 A90-19896
- THOMAS, SCOTT R.**
Scramjet testing from Mach 4 to 20 - Present capability and needs for the nineties [AIAA PAPER 90-1388] p 597 A90-38485
- THOMAS, WILLIAM T.**
Flying qualities lessons learned - 1988 p 431 A90-30705
- THOMASON, A.**
Investigation of model rigging limitations on a high speed wind tunnel model at cryogenic temperature p 523 A90-34232
A feasibility study for a combat aircraft model sting for the European transonic wind tunnel p 524 A90-34243
- THOMASON, T. H.**
The Bell Helicopter XV-3 and XV-15 experimental aircraft - Lessons learned [AIAA PAPER 90-3265] p 835 A90-48859
- THOMPSON, W. T., JR.**
Experimental and theoretical investigations of flowfields and heat transfer in modern gas turbines [AD-A217663] p 429 N90-19237
- THOMPSON, B. E.**
Fluorescence spectroscopy and thermometry for hypersonic flight research [AIAA PAPER 90-1272] p 538 A90-33897
- THOMPSON, B. S.**
A new generation of innovative ultra-advanced intelligent composite materials featuring electro-rheological fluids - An experimental investigation p 204 A90-17962
- THOMPSON, BRIAN G.**
Toward a theory of aircraft agility [AIAA PAPER 90-2808] p 752 A90-45143

THOMPSON, DAN

Laboratory implementation of the Continuously Reconfiguring Multi-Microprocessor Flight Control System (CRMFCFS) [AD-A217730] p 520 N90-20094

THOMPSON, DANIEL B.

The use of non-dedicated redundancy in the AMCAD fault tolerant control system p 461 A90-30793

THOMPSON, G. E.

The surface pretreatment of aluminum-lithium alloys for structural bonding p 881 A90-47118

THOMPSON, H. A.

Implementation of a transputer-based flight controller p 667 A90-38966

Fault-tolerant transputer-based controller configurations for gas-turbine engines p 852 A90-48529

Parallel processing implementation of a flight controller p 333 N90-16743

THOMPSON, H. DOYLE

Swirling flow in thrust nozzles p 421 A90-27962

THOMPSON, JOE F.

Grid generation with the 1988 EAGLE code p 156 A90-18310

Three-dimensional solution-adaptive grid generation on composite configurations [AIAA PAPER 90-0329] p 164 A90-19799

Three-dimensional adaptive grid generation on a composite-block grid p 374 A90-25289

Numerical grid generation in computational fluid mechanics '88: Proceedings of the Second International Conference, Miami Beach, FL, Dec. 5-8, 1988 p 376 A90-26476

Computation of transonic flow about stores [AD-A210402] p 18 N90-10009

THOMPSON, JOHN A.

Harnessing detailed assembly process knowledge with CASE p 535 A90-32504

THOMPSON, KEVIN

Fault tolerant architecture for a fly-by-light flight control computer p 860 A90-46931

THOMPSON, M. W.

Tangential mass addition for the control of shock wave/boundary layer interactions in scramjet inlets p 13 A90-12586

Measured operating characteristics of a rectangular combustor/inlet isolator [AIAA PAPER 90-2221] p 742 A90-42752

THOMPSON, PETER M.

Literal singular-value-based flight control system design techniques p 118 A90-14747

THOMPSON, RICHARD A.

Application of the LAURA code for slender-vehicle aerothermodynamics [AIAA PAPER 90-1714] p 560 A90-38416

THOMPSON, S. A.

Unsteady surface pressure distributions on a delta wing undergoing large amplitude pitching motions [AIAA PAPER 90-0311] p 164 A90-19790

Delta wing surface pressures for high angle of attack maneuvers [AIAA PAPER 90-2813] p 711 A90-45153

THOMPSON, SCOTT A.

Surface pressure distributions on a delta wing undergoing large amplitude pitching oscillations [NASA-CR-186326] p 317 N90-17558

THOMPSON, THOMAS L.

Circulation control tail boom aerodynamic prediction and validation p 385 A90-28243

THOMSON, D. G.

Development and verification of an algorithm for helicopter inverse simulations p 591 A90-38522

THOMSON, L. W.

Development of pressure containment and damage tolerance technology for composite fuselage structures in large transport aircraft [NASA-CR-3996] p 63 N90-10186

THOREN, S. J.

Navier-Stokes study of rotating stall in compressor cascades p 302 A90-25292

THOREN, STEPHEN J.

Extension of a three-dimensional viscous wing flow analysis user's manual: VISTA 3-D code [NASA-CR-182024] p 574 N90-22538

Extension of a three-dimensional viscous wing flow analysis [NASA-CR-182023] p 631 N90-23348

THORESON, SHARILYN A.

The automated software development project at McDonnell Aircraft Company (The Software Factory) p 460 A90-30782

THORN, R. I.

A study of particle trajectories in a gas turbine intake p 48 A90-12583

THORNTON, EARL A.

Thermal structures - Four decades of progress [AIAA PAPER 90-0971] p 411 A90-29305

NASA-UVA light aerospace alloy and structures technology program [NASA-CR-182607] p 601 N90-22651

Thermal structures: Four decades of progress [NASA-CR-186898] p 887 N90-28105

THORPE, CHRISTOPHER J.

Structural mode significance using INCA [AIAA PAPER 90-3346] p 889 A90-47606

THRONE, JAMES L.

Electrostatic dry powder prepregging of carbon fiber p 948 A90-50215

THUKRAL, A.

Dynamics and control of maneuverable towed flight vehicles [AIAA PAPER 90-2841] p 754 A90-45161

THULLEN, MARK J.

Embedded computer system integration support p 419 A90-30724

TIAN, SHILIN

Analysis methods of tie-down loads and airframe stress for shipboard-helicopters p 199 A90-16855

TIARN, W. N.

Surface grid generation through elliptic PDEs p 309 A90-26496

TIBERIA, LOUIS M.

The Mast Mounted Sight 771 processor upgrade program p 926 A90-51058

TICHTINSKY, H.

3D calculations of reacting flows within aircraft engine combustion chambers [ONERA, TP NO. 1989-153] p 67 A90-11173

TICHTINSKY, HELENE

Three dimensional numerical simulation for an aircraft engine type combustion chamber [ONERA, TP NO. 1989-120] p 49 A90-12581

TIDWELL, EUGENE D.

Development and operating experience on a zinc-sulfide window for the Infrared Instrumentation System (IRIS) p 505 A90-34584

TIDWELL, REED P.

Stereopsis as a visual cue in flight simulation p 870 A90-48960

TIEDERMAN, WILLIAM G.

Comparison of steady and unsteady secondary flows in a turbine stator cascade [ASME PAPER 89-GT-79] p 291 A90-23800

TIELKING, JOHN T.

Aircraft tire/pavement pressure distributions [SAE PAPER 892351] p 734 A90-45502

TIE, JOHN K.

Powder metallurgy and oxide dispersion processing of superalloys p 531 A90-34158

TIEZ, MANFRED

New aspects in aircraft inspection using eddy current methods p 886 N90-28085

TIGHE, THOMAS

SARL noise measurements [AIAA PAPER 90-0285] p 219 A90-19772

TIKHONOV, N. T.

Effect of the angle of attack on the efficiency and thrust ratio of axial-flow microturbines with full admission p 111 A90-14590

Effect of the nozzle ring vane height on the efficiency of axial-flow full-admission microturbines p 851 A90-46509

TIKHONOV, VLADIMIR M.

Air transportation in COMECON countries p 785 A90-46616

TILLEMA, H. F.

Evaluation of analysis techniques for low frequency interior noise and vibration of commercial aircraft [NASA-CR-181851] p 220 N90-14866

TILLOTSON, DANIEL H.

TCAS for commuter aircraft p 487 A90-33348

TILSTON, J. R.

The stability of fuel fires p 327 N90-17601

TIMAR, T.

Application of boundary layer control to HSCT low speed configuration [AIAA PAPER 90-3199] p 812 A90-49103

TIMCHENKO, S. V.

Supersonic nonuniform flow of a gas past oblong axisymmetric bodies p 159 A90-19237

TIMKO, L. P.

Energy Efficient Engine high pressure turbine component test performance report [NASA-CR-168289] p 929 N90-28553

TIMMER, W. A.

Experimental aerodynamic characteristics of the airfoils LA 5055 and DU 86-084/18 at low Reynolds numbers p 800 A90-46368

TIMNAT, Y. M.

A study of two-phase flow for a ramjet combustor p 45 A90-12532

TIMOFEEV, E. V.

Determination of pressure and heat flow on the front surface of smooth blunt bodies p 299 A90-24166

Numerical modeling of transverse flow past a cylinder using Euler equations p 709 A90-44922

TIMOFEYVA, T. A.

Using third-fourth order compact schemes for calculating gas flows in nozzles with high supersonic M numbers on the basis of simplified Navier-Stokes equations p 299 A90-24157

A study of gas flow in hypersonic nozzles at large Reynolds numbers using simplified Navier-Stokes equations p 803 A90-46538

TIMOSHENKO, V. I.

Effect of the nonuniformity of external supersonic flow and nozzle deflection angle on the base pressure behind an axisymmetric body with a single supersonic jet p 802 A90-46486

TIMOSHIN, S. N.

Interaction between a vibrating compression shock and a boundary layer p 298 A90-24143

TING, L.

Optimum shape of a blunt forebody in hypersonic flow [NASA-CR-181955] p 171 A90-13351

TING, T.

Practical suggestions for modifying math models to correlate with actual modal test results p 207 A90-16979

Dynamic structural correlation via nonlinear programming techniques p 208 A90-17372

Application to a helicopter of a general method for modifying a finite-element model to correlate with modal test data p 832 A90-46968

TINOCO, E. N.

Transonic analysis of complex configurations using TRANAIR program [SAE PAPER 892289] p 714 A90-45467

3D transonic nacelle and winglet design [AIAA PAPER 90-3064] p 794 A90-45897

TRANAIR applications to engine/airframe integration p 838 A90-48958

TINOCO, EDWARD N.

The role of computational fluid dynamics (CFD) in aircraft design [AIAA PAPER 90-1801] p 335 A90-25175

TIRSKII, G. A.

Comparison of thin and full viscous shock layer models in the problem of supersonic flow of a viscous gas past blunt cones p 231 A90-22396

The effect of vibration-dissociation interaction on heat transfer and drag during the hypersonic flow past bodies p 710 A90-44934

TISCHLER, MARK B.

Advancements in frequency-domain methods for rotorcraft system identification p 56 A90-12771

System identification requirements for high-bandwidth rotorcraft flight control system design p 755 A90-45333

Applications of flight control system methods to an advanced combat rotorcraft [NASA-TM-101054] p 119 N90-11752

Time and frequency-domain identification and verification of BO-105 dynamic models [AD-A216828] p 415 N90-18389

Identification of XV-15 aeroelastic modes using frequency-domain methods [NASA-TM-101021] p 582 N90-21756

TISHCHENKO, MARAT N.

Helicopter or tiltrotor - A Soviet view p 838 A90-48952

TITARENKO, VIKTOR V.

Effect of shock waves and jets on structural elements: Mathematical modeling in nonstationary gas dynamics p 806 A90-46621

TIWARI, S. N.

Application of multiple grids topology to supersonic internal/external flow interactions p 308 A90-26135

Three-dimensional shock-shock interactions on the scramjet inlet [AIAA PAPER 90-0529] p 314 A90-26963

Goertler instability on an airfoil p 91 N90-12517

Effects of nose bluntness and shock-shock interactions on blunt bodies in viscous hypersonic flows [NASA-CR-186451] p 479 N90-20950

TIWARI, SURENDRA N.

Applications of Lagrangian blending functions for grid generation around airplane geometries [AIAA PAPER 90-0009] p 216 A90-19630

Application of Lagrangian blending functions for grid generation around airplane geometries [NASA-CR-186318] p 237 N90-15891

TJEE, R. T. H.

Stability and control derivatives of the De Havilland DHC-2 BEAVER aircraft [PB89-217525] p 119 N90-11754

- TJONNELAND, E.**
Study of advanced technology impact on cycle characteristics and aircraft sizing (using multivariable optimization techniques) p 29 A90-12612
- TO, W. M.**
The numerical simulation of multistage turbomachinery flows p 514 A90-21025
- TOBAK, MURRAY**
Analytical study of the origin and behavior of asymmetric vortices
[NASA-TM-102796] p 573 A90-21746
- TOBIN, K. W.**
Engine testing of thermographic phosphors
[DE90-013269] p 885 A90-28059
- TOBIN, M. G.**
Flow in a centrifugal fan of the squirrel cage type
[ASME PAPER 89-GT-52] p 289 A90-23778
- TODD, JOHN R.**
Toward fly-by-light aircraft p 39 A90-11664
- TODD, ROBERT E.**
Realtime graphic flight simulations using multiple minicomputers p 351 A90-26203
- TOFFOLETTO, R.**
Development of a VSAERO (Vortex Separation Aerodynamics) model of the F/A-18
[AD-A212442] p 95 A90-12566
- TOGNACCINI, R.**
Boundary conditions for Euler equations at internal block faces of multi-block domains using local grid refinement
[AIAA PAPER 90-1590] p 607 A90-38725
Design and testing of a multiblock grid-generation procedure for aircraft design and research p 582 A90-21984
- TOH, H.**
Development of the jet-swirl high loading combustor
[AIAA PAPER 90-2451] p 658 A90-40633
- TOI, Y.**
Unique features and innovative application of advanced composites to the MD-11
[AIAA PAPER 90-3217] p 838 A90-49108
- TOLL, KENNETH R.**
An integrated diagnostics approach to embedded and flight-line support systems p 460 A90-30767
- TOLOFARI, S.**
The cost of air service fragmentation
[TT-9010] p 913 A90-29334
- TOLSTYKH, A. I.**
Using third-fourth order compact schemes for calculating gas flows in nozzles with high supersonic M numbers on the basis of simplified Navier-Stokes equations p 299 A90-24157
- TOMA, BURT A.**
Winds aloft measurement and airspeed calibration using Loran
[AIAA PAPER 90-3331] p 847 A90-47592
- TOMASINI, E. P.**
Comparison among modal analyses of axial compressor blade using experimental data of different measuring systems p 878 A90-46038
- TOMASZEWICZ, PIOTR**
Evaluation of the dynamic properties of the auto-pilot servo of a single-rotor helicopter through laboratory testing p 118 A90-15424
- TOMCZYK, ANDRZEJ**
An analysis of the possibility of using direct control of the lifting force for modifying the flying qualities of aircraft p 118 A90-15423
Digital autopilot for light aircraft p 653 A90-41741
Onboard digital recording system for flight tests p 653 A90-41742
- TOMS, R. DAVID, JR.**
The LHTEC T800-LHT-800 engine integration into the Agusta A129 helicopter p 422 A90-28177
- TOMSIK, T. M.**
Background, current status, and prognosis of the ongoing slush hydrogen technology development program for the NASP
[NASA-TM-103220] p 763 A90-26055
- TONG, MIKE**
Thermal/structural analyses of several hydrogen-cooled leading-edge concepts for hypersonic flight vehicles
[AIAA PAPER 90-0053] p 274 A90-23702
Thermal/structural analyses of several hydrogen-cooled leading-edge concepts for hypersonic flight vehicles
[NASA-TM-102391] p 215 A90-14511
- TONG, MINBO**
A study on initial fatigue quality of typical aircraft structures (fastener holes) p 272 A90-22004
- TONGUE, B. H.**
Time domain parameter identification techniques applied to the UH-60A Black Hawk Helicopter p 77 A90-12774
- TONGUE, BENSON H.**
Experimental study of the effects of nonlinearities on ground resonance p 643 A90-40172
- TOOSI, M.**
Plan, execute, and discuss vibration measurements and correlations to evaluate a NASTRAN finite element model of the AH-64 helicopter airframe
[NASA-CR-181973] p 960 A90-28866
- TOOT, PEGGY L.**
Flight testing of the Low Altitude/Airspeed Unmanned Research Aircraft (LAURA)
[AIAA PAPER 90-1262] p 579 A90-36026
Summary of experimental testing of a transonic low Reynolds number airfoil p 802 A90-46384
Flight testing Navy low Reynolds Number (LRN) unmanned aircraft p 828 A90-46387
- TOPPEL, BETH A.**
A method to determine the performance of low-Reynolds-number airfoils under off-design unsteady freestream conditions p 801 A90-46375
- TORELLA, G.**
Numerical simulation of the behaviour of internal combustion supercharged engines
[AIAA PAPER 90-1873] p 655 A90-40539
Trend analysis and diagnostics codes for training purposes
[AIAA PAPER 90-2394] p 617 A90-42156
- TORII, H.**
Response characteristics of a two-dimensional wing subjected to turbulence near the flutter boundary p 519 A90-34082
- TORISAKI, TADAO**
Restart characteristics of turbofan engines p 50 A90-12627
Parametric studies of acoustic duct attenuation of perforated-plate-on-honeycomb absorber
[NAL-TM-603] p 966 A90-30030
- TORKELSON, THOMAS C.**
IAPSA 2 small-scale system specification
[NASA-CR-182006] p 695 A90-24103
- TORNABENE, ROBERT**
Lightweight fuel pump and metering component for advanced gas turbine engine control
[AIAA PAPER 90-2032] p 657 A90-40602
- TORNGREN, LARS**
The new FFA T1500 transonic wind tunnel initial operation, calibration, and test results
[AIAA PAPER 90-1420] p 596 A90-37957
- TOROK, MICHAEL S.**
Rotor loads validation utilizing a coupled aeroelastic analysis with refined aerodynamic modeling p 408 A90-28226
- TORRES, M.**
Improving helicopter aerodynamics - A step ahead p 631 A90-42443
- TOSHIMITSU, K.**
Improved double linearization method for prediction of mean loading effects on subsonic and supersonic cascade flutter p 41 A90-11795
- TOSHIMITSU, KAZUHIKO**
Application of the double linearization theory to three-dimensional subsonic and supersonic cascade flutter p 50 A90-12638
Mean loading effects on flutter of subsonic rotating annular cascade p 853 A90-49453
- TOTAH, JOSEPH**
Helicopter Airborne Laser Positioning System (HALPS)
[NASA-TM-102814] p 654 A90-23399
- TOTAH, JOSEPH J.**
Selected design issues of some high speed rotorcraft concepts
[AIAA PAPER 90-3297] p 840 A90-49125
- TOTTON, W. W.**
Application of fracture mechanics and half-cycle method to the prediction of fatigue life of B-52 aircraft pylon components
[NASA-TM-88277] p 214 A90-13820
- TOUMER, SAID**
Dual cross-polarization planar arrays in the C and X bands p 638 A90-40979
- TOULMAY, FRANCOIS**
Turbulent mixing in helicopter jet diluters - Navier-Stokes calculations and correlations
[AAAF PAPER NT 88-13] p 40 A90-11432
Correlation of Puma airloads: Lifting-line and wake calculation
[NASA-TM-102212] p 170 A90-13327
- TOVSTIK, P. E.**
Stability and vibrations of mechanical systems p 270 A90-20426
- TOWELL, T. W.**
Improved melt flow and physical properties of Mitsui Toatsu's LARC-TPI 1500 series polyimide p 943 A90-50134
- TOWNE, MATTHEW C.**
A matrix-free locally-implicit scheme for Navier-Stokes equations
[AD-A218298] p 541 A90-20349
- TOWNEND, C. K.**
The 1987 survey of track keeping and altitudes on Heathrow and Gatwick standard instrument departure routes (DAY)
[CAA-PAPER-88010] p 99 A90-11729
- TOWNEND, L. H.**
Hypersonic (T-D) 'pinch' and aerospaceplane propulsion
[AIAA PAPER 90-2474] p 675 A90-42189
Forebody design for the aerospaceplane
[AIAA PAPER 90-2472] p 762 A90-42810
- TOWNSEND, D. P.**
Effect of advanced component technology on helicopter transmissions p 271 A90-21115
- TOWNSEND, DENNIS P.**
Experimental and analytical evaluation of dynamic load vibration of a 2240-kW (3000-hp) rotorcraft transmission p 127 A90-13750
Gear noise, vibration, and diagnostic studies at NASA Lewis Research Center
[NASA-TM-102435] p 372 A90-18041
- TOWNSEND, JOHN**
ILS/MLS comparison tests at Miami/Tamiami, Florida Airport
[ACD-330] p 27 A90-10018
- TOYODA, TATSUZO**
Mechanical rig rest of FJR 710/600 engine components p 43 A90-12016
- TRABOCCO, R. E.**
Materials pace aerospace technology p 203 A90-17298
- TRACY, GENE V.**
A smoke generator system for aerodynamic flight research
[NASA-TM-4137] p 183 A90-13372
- TRACY, NOEL A.**
In-service inspection of composite components on aircraft at depot and field levels p 885 A90-28078
- TRAHAN, W. H.**
Independent Orbiter Assessment (IOA): Analysis of the displays and controls subsystem
[NASA-CR-185563] p 124 A90-11774
- TRAINI, E.**
P-180 AVANTI: Project and flight test program comprehensive overview p 34 A90-10863
- TRAINOR, JOHN W.**
A wind tunnel study of a sting-mounted circulation control wing
[AD-A216248] p 319 A90-17577
- TRAN, ANTHONY T.**
Yaw fin deployment apparatus for ejection seat
[AD-D014512] p 723 A90-25118
- TRAN, B. N.**
UHB demonstrator interior noise control flight tests and analysis
[NASA-CR-181897] p 140 A90-13198
- TRAN, C. B.**
Aircraft modal suppression system: Existing design approach and its shortcomings p 33 A90-10115
- TRAN, DUC**
Sideslip-induced static pressure errors in flight-test measurements
[AIAA PAPER 90-3082] p 794 A90-45898
Sideslip-induced static pressure errors in flight-test measurements
[NASA-TM-102846] p 849 A90-27702
- TRAN, LUC P.**
An adaptive-learning expert system for maintenance diagnostics p 460 A90-30754
- TRANKLE, THOMAS L.**
Maximum likelihood tuning of a vehicle motion filter p 755 A90-45334
- TREFNY, CHARLES J.**
On the use of external burning to reduce aerospace vehicle transonic drag
[AIAA PAPER 90-1935] p 656 A90-40562
On the use of external burning to reduce aerospace vehicle transonic drag
[NASA-TM-103107] p 588 A90-21762
- TREGO, LINDA E.**
Computers and the aerospace engineer p 375 A90-25719
- TRELOAR, G. J.**
Fire hardening of an aircraft passenger cabin p 328 A90-17606
- TREMBLAY, B.**
An improved incidence losses prediction method for turbine airfoils
[ASME PAPER 89-GT-284] p 475 A90-33563
- TREMBLAY, M.**
Helicopter store separation - Predictive techniques and flight testing p 647 A90-42495
- TRENT, WILLIAM**
Ground and Obstacle Avoidance (GOA) concept of operations
[DOT/FAA/DS-89/08] p 28 A90-10855

- National airspace system monitoring operational concept
[NAS-SR-1330] p 178 N90-14214
- National airspace system air-ground communications operational concept
[DOT/FAA/DS-90/2] p 542 N90-21249
- TRESSSET, JACQUES**
Lessons learned from the integration of flight systems
p 35 N90-10874
- TRETOUT, HERVE**
The application of infrared thermography to the nondestructive testing of composite materials
p 886 N90-28084
- TREVINO, C.**
Higher-order effects in boundary-layer, premixed combustion
p 529 A90-32953
- TREVINO, GEORGE**
A Monte Carlo simulation technique for low-altitude, wind-shear turbulence
[AIAA PAPER 90-0564] p 216 A90-19917
- Developments in mechanics. Volume 15 - Midwest Mechanics Conference, 21st, Michigan Technological University, Houghton, Aug. 13-16, 1989, Proceedings
p 769 A90-42870
- TREXLER, CARL A.**
A numerical study of the effects of reverse sweep on a scramjet inlet performance
[AIAA PAPER 90-2218] p 705 A90-42749
- TRIEBSTEIN, H.**
A comparison between theoretical and experimental results for a 3-D wing with damped pitching oscillations
p 472 A90-33361
- TRIPATHI, SATISH K.**
Integrated approach fault tolerance-current state and future requirements
[AD-A214402] p 275 N90-15465
- TRIPLETT, T. E.**
Lightning strike protection concepts for composite materials
p 528 A90-31617
- TRIPP, DAVID E.**
A review of failure models for ceramic matrix composite laminates under monotonic loads
[ASME PAPER 89-GT-153] p 354 A90-23842
- TRITES, D.**
Fiber optic sensor systems for smart aerospace structures
p 38 A90-11208
- TROCHALIDIS, V.**
The performance and longitudinal stability and control of large receiver aircraft during air to air refueling
p 346 A90-24338
- TROCHALIDIS, VASSILIOS**
Large receiver aircraft - The performance and longitudinal stability and control during air to air refueling
p 669 A90-41767
- TROESCH, A. W.**
Experiments with unsteady, free surface, three-dimensional vortices in a thermally stable, stratified fluid
[AD-A22088] p 815 N90-26796
- TROIANOVSKII, A. D.**
Estimation of the efficiency of various operational modes of a navigation complex
p 725 A90-42924
- TROLL, N. L.**
Assessment of voice coders for ATC/pilot voice communications via satellite digital communication channels
[CAA-PAPER-89004] p 135 N90-12807
- TROMP, JEFFREY C.**
A Volterra kernel identification scheme applied to aerodynamic reactions
[AIAA PAPER 90-2803] p 712 A90-45178
- TROSHCHENKO, V. T.**
An automatic system for the programmed control of the parameters of the vibrational and thermal testing of the blades of gas turbine engines
p 343 A90-24216
- TROXEL, SETH W.**
ASR-9 weather channel test report
[AD-A211749] p 133 N90-11934
- TRUBENOK, V. D.**
Effect of vortex generators on the aerodynamic wing characteristics and body of revolution
[AD-A222813] p 721 N90-25955
- TRUJILLO, BIANCA M.**
F-14 VSTFE and results of the cleanup flight test program
p 105 N90-12547
- TRUJILLO, EDWARD**
Modular avionic architectures
p 453 A90-30819
- TRUONG, KHIEM VAN**
Modeling of vortex-induced oscillations based on indicial response approach
[NASA-CR-186560] p 572 N90-21736
- TRYBUS, JEROME C.**
The SKY SHARK: An RPV designed to investigate the pressure distribution on a lifting surface
[NASA-CR-186222] p 844 N90-26824
- TRZASKOS, WILLIAM J.**
Aluminum surface preparation for aircraft field repair
p 764 A90-43204
- TSABOURAKIS, N.**
A computer integrated approach to dimensional inspection
[PNR90596] p 116 N90-12611
- TSANG, WAI L.**
A robust RAIM scheme using GPS/GLONASS systems
p 726 A90-43713
- TSANGARIS, S.**
Multigrid scheme for the compressible Euler-equations
p 907 A90-51559
- TSAU, FANG H.**
Prediction of turbulent combustion flowfields behind a backward-facing step
p 529 A90-32952
- TSAY, D. H.**
Finite element analysis of composite panel flutter
p 681 A90-40032
- TSAY, S. B.**
The influence of swirl on velocity, temperature and species characteristics in a can combustor
[AIAA PAPER 90-2454] p 664 A90-42177
- TSE, D. G. N.**
Combustion characteristics of a model can-type combustor
p 676 A90-40479
- TSENG, J. B.**
Aerodynamics of thrust vectoring
[NASA-CR-185074] p 172 N90-13354
- TSEPLIAEV, I. F.**
Air traffic control
p 638 A90-39581
- TSIL'KER, B. I. A.**
Estimation of the efficiency of various operational modes of a navigation complex
p 725 A90-42924
- TSOU, JIM**
Global Sentry: NASA/USRA high altitude reconnaissance aircraft design, volume 2
[NASA-CR-186820-VOL-2] p 736 N90-25971
- TSUBAKISHITA, YASUJI**
Simulation of sound propagation in axisymmetric jet
p 378 A90-25872
- Fast adaptive grid method for compressible flows
p 445 A90-28006
- TSUCHIYA, YOSHIO**
Heat release rate measurement for evaluating the flammability of aircraft materials
p 328 N90-17610
- TSUEI, Y. G.**
A component modal synthesis technique for the lateral vibration analysis of aircraft engine systems
p 179 A90-16983
- TSUEI, Y. M.**
Numerical simulations of gas turbine combustor flows
[AIAA PAPER 90-2305] p 686 A90-42116
- TSUI, CHIH-YA**
Varying specific heat gasdynamic function formulae simplification and analytical solution of normal shock waves
p 908 A90-52776
- TSUI, CHIH-YA**
Study of calculating an approximately constant reaction turbine stage with a tension spline streamline curvature method
p 157 A90-18537
- TSUJI, JUNJI**
Recrystallization behavior of nickel-base single crystal superalloys
p 440 A90-27681
- TSUKANO, YUKICHI**
Evaluation for DLC-Flap Monitoring System of the VSRA
[NAL-TM-607] p 928 N90-29391
- TSUKIYAMA, T.**
Air/water two-phase flow test tunnel for airfoil studies
p 352 A90-26842
- TSUNENARI, TOSHIYASU**
Fatigue life prediction method for gas turbine rotor disk alloy FV535
p 440 A90-27679
- TU, XING**
Experimental investigation of trailing-edge and near wake flow of a symmetric airfoil
p 160 A90-19449
- The application of concentric vortex simulation to calculating the aerodynamic characteristics of bodies of revolution at high angles of attack
p 627 A90-42357
- TU, YEN**
Three-dimensional solution-adaptive grid generation on composite configurations
[AIAA PAPER 90-0329] p 164 A90-19799
- TUCCILLO, RAFFAELE**
A proposal for optimized design of multistage compressors
[ASME PAPER 89-GT-34] p 288 A90-23766
- TUCKER, GEORGE T.**
Applications of flight control system methods to an advanced combat rotorcraft
[NASA-TM-101054] p 119 N90-11752
- TUCKER, J. H.**
Combat aircraft control requirements
p 934 N90-28515
- TUCKER, W. T.**
Aircraft fire safety: Learning from past accidents
p 324 N90-17584
- TUEGEL, E. J.**
SPFF/DB takes off
p 208 A90-17293
- TUKHVATULIN, V. V.**
Generation of motion control for direction finders in a goniometer system
p 187 A90-17137
- TULAPURKARA, E. G.**
Wake-boundary layer interaction
p 85 A90-15238
- Development of bluff body wake in a longitudinally curved stream
p 86 A90-15745
- Interaction between boundary layer and wakes of different bodies
p 602 A90-36263
- TUNCER, I.**
Numerical simulation of supersonic free shear layers
[AD-A216289] p 320 N90-17579
- TUNCER, ISMAIL HAKKI**
Unsteady aerodynamics of oscillating and rapidly pitched airfoils
p 235 N90-15074
- TUNG, C.**
Rotor hover performance prediction using a free-wake, computational fluid dynamics method
p 153 A90-17869
- A numerical study of general viscous flows around multi-element airfoils
[AIAA PAPER 90-0572] p 167 A90-19922
- Euler solutions for self-generated rotor blade-vortex interactions
[AIAA PAPER 90-1588] p 566 A90-38723
- TUNG, CHEE**
Model tilt-rotor hover performance and surface pressure measurement
[AD-A222535] p 845 N90-26827
- TUNG, CHI R.**
Yaw fin deployment apparatus for ejection seat
[AD-D014512] p 723 N90-25118
- TUNIK, A. A.**
Synthesis of optimal multidimensional digital systems for the simulation of the angular motions of a flight vehicle under random loading
p 669 A90-41957
- TURCICH, ELIZABETH**
Plan for the FAA air traffic operational evaluation of the Automated Surface Observing System (ASOS)
[DOT/FAA/CT-TN89/56] p 489 N90-20968
- TURISHCHEV, A. I.**
Heat transfer in supersonic coaxial reacting jets
p 601 A90-35394
- TURKEL, ELI**
On central-difference and upwind schemes
[NASA-CR-182061] p 781 N90-26595
- TURLEY, W. D.**
Engine testing of thermographic phosphors
[DE90-013269] p 885 N90-28059
- TURNBERG, J. E.**
Large scale prop-fan structural design study. Volume 1: Initial concepts
[NASA-CR-174992] p 52 N90-10043
- Large scale prop-fan structural design study. Volume 2: Preliminary design of SR-7
[NASA-CR-174993] p 52 N90-10044
- TURNBERG, JAY E.**
Large-scale Advanced Prop-fan (LAP) static rotor test report
[NASA-CR-180848] p 117 N90-12617
- TURNBULL, DONALD**
Development of an automated windshear detection system using Doppler weather radar
p 373 A90-25567
- TURNER, STEVEN G.**
Low-speed wind-tunnel investigation of the flight dynamic characteristics of an advanced turboprop business/commuter aircraft configuration
[NASA-TP-2982] p 434 N90-19239
- TURNOCK, STEPHEN R.**
Investigation of surface water behavior during glaze ice accretion
p 485 N90-20927
- TURPIN, RUSSELL L.**
Improved damage tolerance by controlling thermoplastic solubility in thermoset composites
p 944 A90-50138
- TURVEY, JON PAUL**
Installation and implementation of an extrusion cell in aircraft industry utilizing group technology
[SAE PAPER 891025] p 81 A90-14336
- TUTTLE, D. G.**
Design and operational features of low-disturbance wind tunnels at NASA Langley for Mach numbers from 3.5 to 18
[AIAA PAPER 90-1391] p 594 A90-37936
- TWOMEY, DANIEL**
The Stealth biplane: A proposal in response to a low Reynolds Number station keeping mission
[NASA-CR-186680] p 734 N90-25127

- TWOMEY, W. J.**
Application to a helicopter of a general method for modifying a finite-element model to correlate with modal test data p 832 A90-46968
Plan, formulate, and discuss a NASTRAN finite element model of the UH-60A helicopter airframe [NASA-CR-181975] p 541 N90-20439
Ground shake test of the UH-60A helicopter airframe and comparison with NASTRAN finite element model predictions [NASA-CR-181993] p 758 N90-25143
Calculation of flight vibration levels of the AH-1G helicopter and correlation with existing flight vibration measurements [NASA-CR-182031] p 775 N90-25375
- TWOMEY, WILLIAM**
Practical suggestions for modifying math models to correlate with actual modal test results p 207 A90-16979
- TYLER, A. C. F.**
Computer-based tools for assisting air traffic controllers with arrivals flow management [RSRE-88001] p 178 N90-13366
- TYNER, T. M.**
Design and performance of a small, high speed axial compressor [AIAA PAPER 90-1911] p 624 A90-41983
- TYNOR, STEPHEN D.**
Reflexive navigation for autonomous aircraft [AIAA PAPER 89-2991] p 25 A90-10502
- TZENG, CHING-YAW**
Windshear estimation along the trajectory of an aircraft p 963 N90-29745
- TZONG, TSAIR-JYH**
Large-order modal analysis techniques in the Aeroelastic Design Optimization Program (ADOP) [SAE PAPER 892323] p 772 A90-45482
- U**
- UBALDI, MARINA**
Secondary flows and Reynolds stress distributions downstream of a turbine cascade at different expansion ratios p 512 N90-21015
- UCER, A. S.**
An off-design loss and deviation prediction study for transonic axial compressors [ASME PAPER 89-GT-324] p 343 A90-23893
- UCER, AHMET S.**
A computational design method for shock free transonic cascades and airfoils p 501 N90-20986
A study on secondary flow and spanwise mixing in axial flow compressors p 512 N90-21012
- UDD, ERIC**
Fiber optic smart structures and skins: Proceedings of the Meeting, Boston, MA, Sept. 8, 9, 1988 [SPIE-986] p 37 A90-11201
Overview of fiber optic smart structures for aerospace applications p 37 A90-11202
- UDUPA, K. M.**
Hierarchical finite element method for rotating beams p 605 A90-38353
- UEDA, T.**
Multi-surface control law synthesis and wind tunnel test verification of active flutter suppression for a transport-type wing p 517 A90-33401
A digital controller for active aeroelastic controls [NAL-TR-1014] p 936 N90-29402
- UEKI, HIRONOBU**
Effect of blade tip configuration on tip clearance loss of a centrifugal impeller [ASME PAPER 89-GT-80] p 358 A90-23801
Secondary flow due to the tip clearance at the exit of centrifugal impellers [ASME PAPER 89-GT-81] p 358 A90-23802
- UENISHI, K.**
An investigation of counterrotating tip vortex interaction... [NASA-CR-185135] p 79 N90-11549
- UENO, SEIYA**
Minimum fuel cruise by periodic optimization p 182 A90-19429
- UGOLINI, B.**
Aerodynamics of store separation p 629 A90-42418
- UHL, BERND**
The new light weight, high performance reconnaissance camera KRb 8/24 F p 847 A90-48607
- ULBRICH, HEINZ**
Elements of active vibration control for rotating machinery [NASA-TM-102368] p 610 N90-22703
- ULBRICH, N.**
Comparisons of one- and two- interface methods for tunnel wall interference calculation p 870 A90-48961
- UMEBAYASHI, SEIKI**
Hot-gas corrosion test of Si3N4 and SiC p 531 A90-33987
- UMEKAGE, TOSHIHIKO**
Development process of turbulence in a round-nozzle air jet p 87 A90-16101
- UMENE, KOJIRO**
An application of expert system to jet engine diagnostic procedures p 587 A90-38596
- UNGER, GEORGE**
NASA aerodynamics program [NASA-TM-4175] p 373 N90-17235
- UNGER, W. H.**
A dynamicist's view of fuel tank skin durability p 251 N90-15915
- UNRUH, J. F.**
Installation effects on propeller wake/vortex-induced structure-borne noise transmissions p 579 A90-35761
- UNRUH, JAMES F.**
Structure-borne noise estimates for the PTA aircraft [NASA-CR-4315] p 896 N90-28396
- UPADHYAY, TRIVENI N.**
Autonomous integrated GPS/INS navigation experiment for OMV. Phase 1: Feasibility study [NASA-CR-4267] p 489 N90-20969
- UPHAUS, JAMES A., JR.**
Flight simulator evaluation of a dot-matrix display for presentation of approach map formats p 419 A90-30787
- URAL, ERDEM A.**
Ignitability of jet-A fuel vapors in aircraft fuel tanks p 326 N90-17594
- URINOVSKII, BORIS D.**
Technical means and methods of flight safety assurance p 238 A90-22735
- USHAKOV, A. E.**
Durability characteristics of the LAK-12 Letuva glider made of composite materials at the stage of certification p 102 A90-15560
Ways of providing for the strength and service life of aircraft structures made of polymer composites with allowance for damage p 957 A90-50843
- USOV, A. T.**
A method for recalculating the temperature fields of aircraft structures for different experimental conditions p 448 A90-28994
- UTIUZHNIKOV, S. V.**
Comparison of thin and full viscous shock layer models in the problem of supersonic flow of a viscous gas past blunt cones p 231 A90-22396
- UTREJA, L. R.**
Aerodynamic breakup of liquid jets - A review [AIAA PAPER 90-1616] p 607 A90-38746
- UTSCH, T.**
Flow visualization via laser-induced reflection from bubble sheets p 680 A90-39784
- UTSCH, THOMAS**
Flow structure generated by oscillating delta-wing segments p 622 A90-40694
- UTSUNOMIYA, K.**
Application of low-solidity cascade diffuser to transonic centrifugal compressor [ASME PAPER 89-GT-66] p 290 A90-23789
- UVAROV, S. E.**
Calculation of the efficiency of an active partial-admission gas turbine for counterpressures varying over a wide range p 850 A90-46495
- UVAROV, VIKTOR S.**
Radar systems of aircraft p 26 A90-10841
- V**
- VABLE, MADHUKAR**
Developments in mechanics. Volume 15 - Midwestern Mechanics Conference, 21st, Michigan Technological University, Houghton, Aug. 13-16, 1989, Proceedings p 769 A90-42870
- VADYAK, JOSEPH**
Static aeroelastic analysis of fighter aircraft using a three-dimensional Navier-Stokes algorithm [AIAA PAPER 90-0435] p 166 A90-19845
- VAESSEN, G. J. H.**
Fabrication of test-articles from Al-Li 2091 for Fokker 100 p 267 N90-15196
- VAICAITIS, RIMAS**
Random response and noise transmission of discretely stiffened composite panels p 283 A90-23288
Nonlinear response and fatigue of stiffened panels p 363 A90-23953
- VAIL, GORDON T.**
Design for maintainability [SAE PAPER 891079] p 81 A90-14371
- VAINTRUB, ALEKSANDR P.**
Helicopter dynamics: Limiting flight conditions p 55 A90-12481
- VAISSIERE, A.**
The Super Puma MKII automatic flight control system p 669 A90-42449
- VAKILI, AHMAD D.**
Review of vortical flow utilization [AIAA PAPER 90-1429] p 605 A90-37966
- VALAREZO, WALTER O.**
Computation of subsonic shrouded propeller flows [AIAA PAPER 90-0029] p 226 A90-22154
Subsonic calculation of propeller/wing interference [AIAA PAPER 90-0031] p 226 A90-22155
- VALASEK, JOHN**
Assessment of proposed fighter agility metrics [AIAA PAPER 90-2807] p 752 A90-45142
Fighter agility metrics, research, and test [NASA-CR-186118] p 648 N90-23386
- VALAVANI, L.**
Active stabilization of aeromechanical systems [AD-A216629] p 454 N90-18672
- VALDES, L.-C.**
Interaction between a high-level steady acoustic field and a ducted turbulent flow [ONERA, TP NO. 1990-27] p 695 A90-41206
- VALENTINO, GEORGE J.**
The integrated support station (ISS) - A modular Ada-based test system to support AN/ALE-47 countermeasure dispenser system testing, evaluation, and reprogramming p 457 A90-28323
- VALETT, JON**
Software Management Environment (SME) concepts and architecture [NASA-TM-103306] p 547 N90-21543
- VALKOV, THEODORE V.**
Aerodynamic loads computation on coaxial hingeless helicopter rotors [AIAA PAPER 90-0070] p 161 A90-19666
- VALLONE, VINCENZO**
A new test procedure for a wing made with carbon fiber composites [ETN-89-95220] p 126 N90-11820
- VALTORTA, E.**
The use of simulation in support of the high AOA flight test program of the AM-X aircraft [AIAA PAPER 90-1289] p 495 A90-33909
Aerodynamic control design: Experience and results at Aermacchi p 935 N90-28518
- VALVADE, A. P.**
Leading edge flap influence on aerodynamic efficiency p 85 A90-15240
- VAN AKEN, JOHANNES M.**
Experimental investigation of wingtip aerodynamic loading p 808 A90-46945
- VAN BLARICUM, T. J.**
Moisture absorption in graphite/epoxy laminates p 951 A90-52799
- VAN BODEGRAVEN, GEORGE W.**
Commercial aircraft DOC methods [AIAA PAPER 90-3224] p 897 A90-48843
- VAN DALSEM, W. R.**
Calculations of the flow past bluff bodies, including tilt-rotor wing sections at alpha = 90 deg [AIAA PAPER 90-0032] p 227 A90-22156
Simulation and analysis of a delta platform with multiple jets in ground effect [AIAA PAPER 90-0299] p 228 A90-22195
Thermal interaction between an impinging hot jet and a conducting solid surface [AIAA PAPER 90-3010] p 956 A90-50636
- VAN DALSEM, WILLIAM R.**
Computation of viscous transonic flow over porous airfoils p 153 A90-17864
Basic numerical methods p 394 A90-29886
A computational study of the impingement region of an unsteady subsonic jet [AIAA PAPER 90-1657] p 570 A90-38784
- VAN DAM, C. P.**
Wind-tunnel investigation on the effect of a crescent platform on drag [AIAA PAPER 90-0300] p 228 A90-22196
Wind-tunnel investigations of wings with serrated sharp trailing edges p 802 A90-46379
Subsonic and transonic low-Reynolds-number airfoils with reduced pitching moments [AIAA PAPER 90-3212] p 812 A90-48838
Parametric analysis of swept-wing geometry with sheared wing tips [AIAA PAPER 90-3196] p 812 A90-49101
- VAN DE VOORDE, M.**
High-temperature corrosion and mechanical properties of some silicon nitride ceramics p 531 A90-33985
- VAN DEN BERG, R. P.**
Ultrasonic regression rate measurement in solid fuel ramjets [AIAA PAPER 90-1963] p 656 A90-40573

VAN DEN BORNE, P. C. M.

Investigation of propeller slipstream effects on the Fokker 50 through in-flight pressure measurements
[AIAA PAPER 90-3084] p 806 A90-46645

VAN DEN BRAEMBUSSCHE, R. A.

Unsteady flow in centrifugal compressors due to downstream circumferential distortions
p 14 A90-12598

Experimental and theoretical study of the swirling flow in centrifugal compressor volutes
[ASME PAPER 89-GT-183] p 273 A90-22663

VAN DER GELD, C. W. M.

Combustion of PMMA, PE, and PS in a ramjet
p 764 A90-43670

VAN DER SCHRAAF, A.

Initial service experience with the Fokker 100
[SAE PAPER 892238] p 733 A90-45450

VAN DER STICHELE, S.

Infrared thermography in blowdown and intermittent hypersonic facilities
p 440 A90-31302

VAN DER VELDEN, ALEXANDER J. M.

A numerical method for relating two- and three-dimensional pressure distributions on transonic wings
[AIAA PAPER 90-3211] p 812 A90-48837

VAN DER VOOREN, J.

Inviscid drag prediction for transonic transport wings using a full-potential method
[AIAA PAPER 90-0576] p 168 A90-19926

VAN DER WALL, B.

Higher harmonic control of a helicopter model rotor to reduce blade/vortex interaction noise
p 496 A90-34360

VAN DER WEES, A. J.

Inviscid drag prediction for transonic transport wings using a full-potential method
[AIAA PAPER 90-0576] p 168 A90-19926
Impact of multigrad smoothing analysis on three-dimensional potential flow calculations
p 449 A90-29147

VAN DER WESTHUIZEN, B. J.

Atomization of synthetic jet fuel
p 63 A90-12602

VAN DIERENDONCK, A. J.

Applicability of an augmented GPS for navigation in the National Airspace System
p 331 A90-25571

VAN DOREN, RICHARD E.

Airborne telemetry trends for the 1990's
p 418 A90-28874

VAN DYKE, KAREN L.

GPSNOTAM - A demonstration system for GPS status notification
p 728 A90-45238

VAN EGMOND, J. A.

Computation of viscous aerodynamic characteristics of 2-D airfoils for helicopter applications
p 631 A90-42440

VAN EVERY, D.

Slotted-wall research with disk and parachute models in a low-speed wind tunnel
[AIAA PAPER 90-1407] p 595 A90-37946

VAN FOSSEN, G. JAMES

Convective heat transfer measurements from a NACA 0012 airfoil in flight and in the NASA Lewis Icing Research Tunnel
[AIAA PAPER 90-0199] p 272 A90-22180

VAN GELDER, P. A.

Computation of viscous aerodynamic characteristics of 2-D airfoils for helicopter applications
p 631 A90-42440

VAN HENGST, J.

Investigation of propeller slipstream effects on the Fokker 50 through in-flight pressure measurements
[AIAA PAPER 90-3084] p 806 A90-46645

VAN INGEN, J. L.

Experimental aerodynamic characteristics of the airfoils LA 5055 and DU 86-084/18 at low Reynolds numbers
p 800 A90-46368

VAN LEER, B.

Unsteady transonic cascade flow with in-passage shock wave
p 556 A90-36281

VAN LEER, BRAM

Implicit flux-split schemes for the Euler equations
p 602 A90-36254

VAN LIERDE, P.

Infrared thermography in blowdown and intermittent hypersonic facilities
p 440 A90-31302

VAN NIEKERK, J. E.

Atomization of synthetic jet fuel
p 63 A90-12602

VAN NOCKER, R. C.

Electric controls for a high-performance EHA using an interior permanent magnet motor drive
p 452 A90-30711

VAN NOCKER, RICHARD C.

High-performance EHA controls using an interior permanent magnet motor
p 730 A90-43152
EHA loading on the 270-Vdc bus
[SAE PAPER 892225] p 746 A90-45441

VAN PELT, S. G.

Initiation of spalling in aircraft gas turbine bearings
[AIAA PAPER 90-2291] p 686 A90-42110

VAN RANSBEECK, PETER R. O.

Experimental and numerical investigation of the flow in the core of a leading edge vortex
[AIAA PAPER 90-0384] p 165 A90-19826

VAN ROESSEL, H. J.

Unfolding of double-zero eigenvalue bifurcations for supersonic flow past a pitching wedge
p 347 A90-25995

VAN SCHALKWYK, J. J.

Range determination in a multipath prone environment
p 877 A90-45960

VAN WECHER, ROBERT J.

Accuracy considerations for GPS TSP1 system design
p 98 A90-14001

VAN WIE, D. M.

Investigation of cowl vent slots for supercritical stability enhancement in dual-mode ramjet inlets
p 507 A90-32951

VAN WILLIGAN, DURK

Eurofix
p 25 A90-10239

VANAGS, ANDREJS A.

A head up display format for application to V/STOL aircraft approach and landing
[NASA-TM-102216] p 340 N90-17632

VANBUREN, MARK A.

Trajectory optimization and guidance for an aerospace plane
[NASA-CR-185884] p 183 N90-13369

VANDEBRAEMBUSSCHE, R. A.

Subsonic and transonic blade design by means of analysis codes
p 510 N90-20985

VANDEDAM, R. F.

Constrained spanload optimization for minimum drag of multi-lifting-surface configurations
p 501 N90-20992

VANDENBERG, B.

A European collaborative investigation of the three-dimensional turbulent shear layers of a swept wing
p 20 N90-10380

VANDERHEIJDE, M. A. D.

Tests for aircraft interior materials in fire accident
[LR-622] p 914 N90-29337

VANDERPLAATS, G. N.

Optimum design of composite structures
p 272 A90-22135

VANDERPOOL, R. W.

Design and calibration of an in-stack, low-pressure impactor
[AD-A213531] p 255 N90-15105

VANDERVEEN, G.

Study improvement training facilities ground control air traffic controllers. Part 1: Alternative solutions and their consequences
[FEL-89-A257-PT-1] p 919 N90-29380

VANDERVEEN, M.

Aircraft technology management and the related significance of the supercomputer
p 612 N90-22975

VANDERVELDE, R. L.

Flight testing in the Netherlands: An overview
p 36 N90-10884

VANDERVELDEN, ALEXANDER J. M.

The aerodynamic design of the oblique flying wing supersonic transport
[NASA-CR-177552] p 923 N90-28540

VANDERVOOREN, J.

Flow simulation for aircraft
[NLR-MP-87082-U] p 455 N90-19543

VANDOMMELEN, LEON

Basic studies of the unsteady flow past high angle of attack airfoils
[AD-A210252] p 18 N90-10008

VANDONGEN, JOHN

Data link test and analysis system/ATCRBS transponder test system technical reference
[DOT/FAA/CT-TN90/7] p 824 N90-26803

VANDOORN, J. T. M.

Flight testing in the Netherlands: An overview
p 36 N90-10884

VANDROMME, D.

Numerical simulation of the compressible flow in a valve-cylinder assembly
p 770 A90-44431

VANEGMOND, J. A.

Numerical optimization of target pressure distributions for subsonic and transonic airfoil design
p 502 N90-20993

Computation of viscous aerodynamic characteristics of 2-D airfoils for helicopter applications
[NLR-MP-88052-U] p 720 N90-25951

VANEK, V.

Two-stage two-spool experimental centrifugal compressor investigation
p 49 A90-12593

VANEVRY, D.

Slotted-wall research with disk and parachute models in a low-speed wind tunnel
[DE90-002989] p 572 N90-21737

VANFOSSEN, G. JAMES

Convective heat transfer measurements from a NACA 0012 airfoil in flight and in the NASA Lewis Icing Research Tunnel
[NASA-TM-102448] p 213 N90-13750

VANGELDER, P. A.

Computation of viscous aerodynamic characteristics of 2-D airfoils for helicopter applications
[NLR-MP-88052-U] p 720 N90-25951

VANGRAAS, FRANK

Sole means navigation and integrity through hybrid Loran-C and NAVSTAR GPS
p 489 N90-20933

VANGSNES, M. D.

Acoustic characteristics of a research step combustor
[AIAA PAPER 90-1851] p 655 A90-40530

VANIN, V. A.

Calculation of nonstationary forces in a three-row compressor cascade
p 803 A90-46502
Numerical simulation of transonic flow through oscillating and multi-row two-dimensional airfoil cascades
p 814 A90-49460

VANKA, S. P.

Hot gas environment around STOVL aircraft in ground proximity. II - Numerical study
[AIAA PAPER 90-2270] p 743 A90-42766

Development of a computational fluid dynamics and chemistry model for the fouling of jet fuels
[DE90-005664] p 608 N90-22003

Development of a mathematical model for the thermal decomposition of aviation fuels
[AD-A221673] p 875 N90-26994

VANKA, S. PRATAP

Analytical studies of three-dimensional combustion processes
[AD-A211903] p 126 N90-11837

VANKIERSBILCK, P.

Solution of the Euler equations using unstructured polygonal meshes
p 708 A90-44435

VANLEEUWEN, H. P.

The use of supercomputers for the design and analysis of constructions
p 612 N90-22977

VANNICOLA, VINCENT C.

A Distributed Artificial Intelligence approach to object identification and classification
p 545 A90-34185

VANOOIJEN, W. H.

Test network Delft
[ETN-90-96009] p 177 N90-13365

VANOVERBEKE, THOMAS J.

Three-dimensional turbulent flow code calculations of hot gas ingestion
p 745 A90-44726

VANPAASSEN, D. M.

Noise data of four small propeller-driven airplanes
[PB89-216980] p 139 N90-12291

VANROOIJEN, H. W.

Fabrication of test-articles from Al-Li 2091 for Fokker 100
p 267 N90-15196

VANSTONE, R. H.

Elevated temperature crack growth
[NASA-CR-182247] p 777 N90-26355

VANTHOURNUT, MIKE

The SKY SHARK: An RPV designed to investigate the pressure distribution on a lifting surface
[NASA-CR-186222] p 844 N90-26824

VANTILBORGH, C.

Fabrication of test-articles from Al-Li 2091 for Fokker 100
p 267 N90-15196

VANWANDERHAM, M. C.

Retirement for cause of the F100 engine
p 843 N90-26813

VARADAN, T. K.

Rotor/fuselage vibration isolation studies by a Floquet-harmonic iteration technique
p 182 A90-19393

Hierarchical finite element method for rotating beams
p 605 A90-38353

VARSNEY, PRAMOD K.

A Distributed Artificial Intelligence approach to object identification and classification
p 545 A90-34185

VARSNEYA, D.

Optic multiplex for aircraft sensors - Issues and options
p 38 A90-11660

VASIL'EV, A. A.

Analysis and prediction of weather for aviation
p 888 A90-48351

VASIL'EV, V. I.

Determination of the effective areas of the mixing exhaust ducts of a bypass engine from autonomous test results
p 102 A90-14584

VASQUEZ ROCHA, ERNESTO

The integration of Latin American transport - Realities and perspectives
p 898 A90-49618

- VASSBERG, JOHN C.**
An Euler method for wing-body-winglet flows
[AIAA PAPER 90-0436] p 229 A90-22218
AIRPLANE - Experiences, benchmarks and improvements
[AIAA PAPER 90-2998] p 787 A90-45848
An unstructured-mesh Euler method for multielement airfoil geometries
[AIAA PAPER 90-3051] p 797 A90-45930
- VATSA, VEER N.**
Navier-Stokes computations of a prolate spheroid at angle of attack p 17 A90-13018
Evaluation of transonic wall interference assessment and correction for semi-span wing data
[AIAA PAPER 90-1433] p 597 A90-38487
Prediction of separated transonic wing flows with nonequilibrium algebraic turbulence model p 809 A90-47312
- VAUGHAN, C.**
Numerical investigations of heat transfer and flow rates in rotating cavities. Simulation of the movement generated by wall temperature gradients, by source-sink mass flows or by the differential rotation of the walls, under the influence or coriolis and centrifugal forces
[ETN-90-96253] p 454 N90-18695
- VAUGHN, RONALD W.**
Source emission test of gas turbine engine test facility, Kelly AFB, TX
[AD-A223869] p 932 N90-28571
- VAUGHN, W. L.**
Performance evaluations of oxidation-resistant carbon-carbon composites in simulated hypersonic vehicle environments p 874 A90-48131
- VAUGHN, WALLACE L.**
NASA Langley Research Center National Aero-Space Plane Mission simulation profile sets
[NASA-TM-102670] p 924 N90-28541
- VAUGHT, C.**
An investigation of solid-fuel, dual-mode combustion ramjets p 859 N90-27933
- VAVRINCOVA, MIRKA**
Numerical solution of 2D transonic flows in a turbine cascade p 709 A90-44601
- VEERBECK, H. W.**
COCOMAT: A Computer Aided Engineering (CAE) system for composite structures design
[NLR-MP-87078-U] p 462 N90-19756
- VELDMAN, A.**
Development of a robust calculation method for transonic viscous blade-to-blade flows p 703 A90-42671
- VELDMAN, A. E. P.**
VISTRAFS - A simulation method for strongly-interacting viscous transonic flow p 144 A90-16756
- VELICHKO, S. A.**
Calculation of nonseparated flow past a wing profile at large Reynolds numbers p 706 A90-42995
- MEMURU, C. S.**
Design of low Reynolds number airfoils. I p 307 A90-26129
- VENART, J. E. E.**
Time development of convection flow patterns in aircraft cabins under post-crash fire exposure p 327 N90-17598
- VENEDIKTOV, V. D.**
An investigation of the flow characteristics of transonic nozzle blades p 475 A90-33700
- VENINGER, ALBERT**
Operation of the Rolls-Royce Pegasus Engine on low grade non-aviation fuels
[SAE PAPER 892329] p 747 A90-45486
- VENIS, A. C. J.**
An experimental and theoretical investigation of the flow over plane delta wings with supersonic leading edges [LR-588] p 717 N90-25114
- VENKATKRISHNAN, V.**
Viscous computations using a direct solver p 315 A90-27133
- VENKATAPATHY, E.**
Application of a self-adaptive grid method to complex flows
[NASA-TM-102223] p 143 N90-13324
- VENKATARAJU, K.**
On-line temperature profile display system
[ASME PAPER 89-GT-10] p 374 A90-23755
- VENKATRAYULU, N.**
Wake behaviour of a large deflection turbine rotor linear cascade p 157 A90-18481
- VENKATESAN, C.**
Rotor/fuselage vibration isolation studies by a Floquet-harmonic iteration technique p 182 A90-19393
- VENKATRAYULU, N.**
Studies on the influence of Mach number on profile losses of a reaction turbine cascade p 10 A90-12517
- VENKAYYA, VIPPERLA B.**
Influence of structural and aerodynamic modeling on flutter analysis
[AIAA PAPER 90-0954] p 411 A90-29239
Finite element models of USAF aircraft structures p 844 N90-26820
- VENN, G. J.**
EH101 vibration control p 647 A90-42496
- VENN, GEOFFROY**
Advocating international cooperation: The Eurofar program - An example and a hope p 785 A90-46929
- VENNER, J. G.**
Domestic precursor technology - A unique route to current and future generation carbon fibers p 940 A90-50057
- VENNERI, SAMUEL L.**
Computers boost structural technology p 138 A90-14799
- VEPA, R.**
Practical techniques of modelling aeroelastic systems for active control applications p 545 A90-33402
- VERBINSKI, V. V.**
Development of an X-ray backscatter densitometer for measurement of freestream density during hypersonic flight
[AIAA PAPER 90-1384] p 604 A90-37933
- VERBRUGGE, R.**
Study of ground effects on flying scaled models p 922 N90-28532
- VERBRUGGEN, MARC**
Metal laminates for aerospace applications p 874 A90-48997
- VERDON, JOSEPH M.**
Theoretical prediction of high Reynolds number viscid/inviscid interaction phenomena in cascades p 145 A90-16759
Unsteady aerodynamics for turbomachinery aeroelastic applications p 394 A90-29888
Linearized unsteady aerodynamics for turbomachinery aeroelastic applications
[AIAA PAPER 90-2355] p 626 A90-42137
Development of a linearized unsteady aerodynamic analysis for cascade gust response predictions
[NASA-CR-4308] p 816 N90-27655
- VERHAAGEN, N. G.**
Experimental and numerical investigation of the vortex flow over a sharp edged delta wing; with and without sideslip
[PB90-167131] p 481 N90-20964
- VERHAAGEN, NICK G.**
Experimental and numerical investigation of vortex flow over a sideslipping delta wing p 17 A90-13016
Experimental and numerical investigation of the flow in the core of a leading edge vortex
[AIAA PAPER 90-0384] p 165 A90-19826
- VERHOFF, A.**
Supersonic/hypersonic Euler flowfield prediction method for aircraft configurations p 145 A90-16767
- VERHOFF, VINCENT G.**
An applicational process for dynamic balancing of turbomachinery shafting
[NASA-TM-102537] p 541 N90-20392
- VERNIGOR, V. N.**
Effect of the nonuniform rotation of the gas turbine rotor on blade vibrations p 253 A90-20431
- VERNOVSKII, L. S.**
Effect of the fluid level of a hydraulic shock absorber on the characteristics of the gas supply system p 851 A90-46504
- VERONA, ROBERT W.**
Cockpit lighting compatibility with image intensification night imaging systems: Issues and answers
[AD-A210503] p 32 N90-10028
- VERRIEST, E. I.**
Estimation and control of nonlinear and hybrid systems with applications to air-to-air guidance
[AD-A214542] p 348 N90-16770
- VERSHININ, MIKHAIL P.**
Identification and diagnostics in the data processing and control systems of aerospace powerplants p 611 A90-36151
- VERSTYNEN, HARRY A.**
Preliminary flight test investigation of an airborne wake vortex detection concept
[AIAA PAPER 90-1282] p 495 A90-33903
- VERTZBERGER, M.**
Blade surface pressure measurement on a pusher propeller in flight
[SAE PAPER 891040] p 139 A90-14346
- VEUILLOT, J. P.**
Recent developments in calculation methods for internal flows by solution of Euler or Navier-Stokes equations
[ONERA, TP NO. 1989-167] p 223 A90-21033
- VEUILLOT, J.-P.**
Quasi-3D viscous flow computations in subsonic and transonic turbomachinery bladings
[AIAA PAPER 90-2126] p 625 A90-42033
- VEYRET, J. B.**
High-temperature corrosion and mechanical properties of some silicon nitride ceramics p 531 A90-33985
- VEYS, JEAN-MARIE**
Effect of protective coatings on mechanical properties of superalloys
[ONERA, TP NO. 1989-88] p 62 A90-11126
Effect of protective coatings on mechanical properties of superalloys p 952 N90-28707
- VIAN, J. L.**
Application of a design method for integrated control to a VTOL airplane in hover
[AIAA PAPER 90-3334] p 862 A90-47594
- VIDAL, GEORGES**
Study of the ground effects in the CEAT aerohydrodynamic tunnel: Using the results p 922 N90-28530
- VIDAL, JACQUES J.**
Real-time support for high performance aircraft operation
[NASA-CR-185475] p 57 N90-10075
- VIDELA ESCALADA, FEDERICO**
Considerations on the legal regulation of air transport in the near future p 897 A90-46649
- VIDLICH, MICHAEL A.**
The benefits and costs of automation in advanced helicopters - An empirical study p 348 A90-26258
- VIENWEGGER, G.**
The Kryo-Kanal Koeln, KKK: Description of tunnel conversion - Results of calibration tests under ambient and cryogenic conditions p 523 A90-34230
- VIETS, K.**
Rapsat - Application of onboard processing for communication and surveillance in air traffic control
[AIAA PAPER 90-0883] p 331 A90-25702
- VIETS, KAREN J.**
Independent ground monitor coverage of Global Positioning System (GPS) satellites for use by civil aviation p 918 N90-29364
- VIGNATI, G.**
EH101 vibration control p 647 A90-42496
- VIGNAU, F.**
Transition in surface boundary layers
[CERT-RSF-OA-43/5018-AYD] p 136 N90-12897
- VIGNERON, DIDIER**
Design, fabrication and experimental test of hi-temperature CFRP stiffened structures p 534 A90-31892
- VIGUIER, P.**
Measurement of wind tunnel model deformation under airload p 522 A90-33370
- VIJAN, MEERA**
8 x 8-inch full color cockpit display p 927 A90-52953
- VIJGEN, P. M. H. W.**
Wind-tunnel investigation on the effect of a crescent planform on drag
[AIAA PAPER 90-0300] p 228 A90-22196
Wind-tunnel investigations of wings with serrated sharp trailing edges p 802 A90-46379
Parametric analysis of swept-wing geometry with sheared wing tips
[AIAA PAPER 90-3196] p 812 A90-49101
- VIJGEN, PAUL M. H. W.**
Experimental and numerical analyses of laminar boundary-layer flow stability over an aircraft fuselage forebody p 93 N90-12549
Serrated trailing edges for improving lift and drag characteristics of lifting surfaces
[NASA-CASE-LAR-13870-1] p 248 N90-15094
- VIKEN, JEFFREY K.**
Design of the low-speed NLF(1)-0414F and the high-speed HSNLF(1)-0213 airfoils with high-lift systems p 93 N90-12540
Wind tunnel results of the low-speed NLF(1)-0414F airfoil p 93 N90-12541
- VINCENT, B.**
Aeroelastic instabilities in aircraft engines - Application to a SNECMA fan stage p 584 A90-35174
Full span analysis for flutter prediction of slender blade assemblies p 879 A90-46188
- VINCENT, JAMES H.**
Modeling and analysis tools for aircraft control system evaluations p 431 A90-30703
Flight control design considerations for STOVL powered-lift flight
[AIAA PAPER 90-3225] p 868 A90-49110
Propulsion system design specifications based on STOVL flight control requirements
[AIAA PAPER 90-3227] p 839 A90-49112

VINH, NGUYEN X.

- Optimal plane change by low aerodynamic forces
[AIAA PAPER 90-2831] p 763 A90-45137

VINING, SUSAN J.

- Considerations in using broad specification fuels for aircraft propulsion
[SAE PAPER 892330] p 765 A90-45487
Modelling of fuel effects on naval aircraft operations
[SAE PAPER 892331] p 765 A90-45488

VINNEMEIER, F. M.

- Heat transfer in a solid fuel ramjet combustor
[AIAA PAPER 90-1783] p 586 A90-38472

VINOGRADOV, I. A.

- Effect of the Mach number and shape of the front part of the obstacle on the separation zone length in supersonic flow
p 903 A90-50816

VINSON, T. S.

- Definition of research needs to address airport pavement distress in cold regions
[DOT/FAA/DS-89/13] p 59 N90-10896

VIRNIG, JOHN C.

- The implementation of STOV task-tailored control modes in a fighter cockpit
[AIAA PAPER 90-3229] p 839 A90-49114

VIRSHUPSKII, IGOR' M.

- Vortex-flow compressors p 69 A90-12479

VISBAL, MIGUEL R.

- Dynamic stall of a constant-rate pitching airfoil
p 553 A90-35754
Unsteady Navier-Stokes solutions for a low aspect ratio delta wing
[AIAA PAPER 90-1538] p 564 A90-38682

VISKANTA, R.

- Deicing of solids using radiant heating
p 769 A90-43309

VISSER, H. G.

- First-order weight corrections for real-time flight path management
[LR-580] p 578 N90-21751
An approach to on-board optimization of cruise at constant altitude
[LR-581] p 578 N90-21752

VISWANATH, P. R.

- Effectiveness of passive devices for axisymmetric base drag reduction at Mach 2 p 555 A90-36184
Sting-support interference on afterbody drag at transonic speeds
[NAL-TM-EA-8902] p 909 N90-28492

VITAGLIANO, P. L.

- Design and testing of a multiblock grid-generation procedure for aircraft design and research
p 582 N90-21984

VITALONE, G.

- Decommutation techniques and their integration into post flight analysis system p 26 A90-12191

VITIC, A.

- Broadband noise measurement in the transonic test section of the VTI T-38 wind tunnel
[AIAA PAPER 90-1418] p 614 A90-37955

VITIELLO, DOMENICO

- Prediction of post-stall flows on airfoils
p 145 A90-16757

VITIELLO, P.

- Aeroelastic analysis for a composite T-tailplane of a turboprop commuter aircraft p 492 A90-33390

VITTAL, B.

- Experimental evaluation of expendable supersonic nozzle concepts
[AIAA PAPER 90-1904] p 740 A90-42691

VITTALA, N. G. V.

- Aeroelastic analysis of a low aspect ratio wing
p 619 A90-38915

VIZZINI, RUSSELL W.

- Propulsion control system designs for advanced Navy multimission aircraft
[AIAA PAPER 90-2403] p 663 A90-42160

VLACHOS, N. S.

- Effects of turbulence model constants on computation of confined swirling flows p 444 A90-27999

VLACHYNSKY, JOSEF

- Fatigue damage of an aircraft due to movement on the airfield p 247 A90-23352

VLADIMIROVA, N. A.

- Calculation of nonseparated transonic flow past swept wings with allowance for viscosity p 294 A90-24079

VLAMINCK, ROBERT R.

- V-22 MSC/NASTRAN airframe vibration analysis and correlation p 832 A90-46969

VLIEGER, H.

- Static strength and damage tolerance tests on the Fokker 100 airframe
[NLR-MP-88023-U] p 416 N90-19228

VOELCKERS, U.

- Approach towards a future integrated airport surface traffic management p 827 N90-27686

VOERSMANN, PETER

- Meteopod, an airborne system for measurements of mean wind, turbulence, and other meteorological parameters p 418 A90-29943
Systems for airborne wind and turbulence measurement p 281 N90-15046

VOEVODENKO, N. V.

- Calculation of flow past flight vehicles of complex configurations at high supersonic Mach numbers using the hypersonic theory of small perturbations p 299 A90-24158

VOEVODIN, A. V.

- Flow past a wing/fuselage combination with separation from the side edges of the wing p 295 A90-24088

VOGEL, S.

- Comparison of two potential flow methods for transonic flutter analysis p 471 A90-33356

VOGELESANG, L. B.

- Rolling of ARALL laminates (an alternative method for post-stretching ARALL laminates)
[LR-560] p 135 N90-12778

VOGELESANG, LAURENS B.

- Aerospace Arall - The advancement in aircraft materials p 947 A90-50186

VOGES, H.

- Applications of LIF to high speed flows p 911 N90-29320

VOGLER, WILLIAM A.

- Current status of Joint FAA/NASA Runway Friction Program
[SAE PAPER 892340] p 760 A90-45494
Evaluation of two transport aircraft and several ground test vehicle friction measurements obtained for various runway surface types and conditions. A summary of test results from joint FAA/NASA Runway Friction Program
[NASA-TP-2917] p 249 N90-15902

VOGLSINGER, M.

- Design philosophy and construction techniques for integral fuselage fuel tanks p 250 N90-15913

VOIGT, J.

- Airline requirements for a future air traffic management system p 825 N90-27678

VOINOVICH, P. A.

- Numerical modeling of transverse flow past a cylinder using Euler equations p 709 A90-44922

VOITYSHEN, V. S.

- A method for calculating the stiffness characteristics of large-aspect-ratio wings with anisotropic panels in accordance with strength and aileron efficiency requirements p 334 A90-24161

VOLAND, RANDALL T.

- Methods for determining the internal thrust of scramjet engine modules from experimental data
[AIAA PAPER 90-2340] p 743 A90-42777

VOLCHKOV, V. M.

- Multicriterial optimization of lugs in hinge joints p 364 A90-24162

VOLGIN, VIKTOR V.

- Fundamentals of the design and development of parts and mechanisms for flight vehicles p 414 A90-30275

VOLGMANN, W.

- Calculation of the side-wall boundary layer in axial turbomachines, accounting for the internal flow near the blades p 225 A90-21595

VOLKOV, V. S.

- Dynamic properties of a system for the roll control of a model electromagnetically suspended in a wind tunnel p 262 A90-22762

VOLLMERHAUSEN, RICHARD H.

- Design criteria for helicopter night pilotage sensors p 417 A90-28221

VOLODKO, A. M.

- Tail rotor dynamics during the translational turn maneuver of a helicopter p 334 A90-24148

VOLODKO, ALEKSANDR M.

- Aerodynamic and dynamic principles of helicopter flight p 55 A90-12473

VOLOSHCHENKO, A. P.

- An automatic system for the programmed control of the parameters of the vibrational and thermal testing of the blades of gas turbine engines p 343 A90-24216

VOLPE, G.

- Efficient method for computing transonic and supersonic flows about aircraft p 307 A90-26132
Inverse design of airfoil contours: Constraints, numerical method, and applications p 500 N90-20980

VON ELLENRIEDER, KARL D.

- Active control of gust- and interference-induced vibration of tilt-rotor aircraft p 429 A90-28201

VON FLOTOW, A. H.

- Flight testing a highly flexible aircraft - Case study on the MIT Light Eagle p 414 A90-31284

VON GERSDORFF, M.

- Autopilot flight test experience with BK 117 hingeless rotor
[AIAA PAPER 90-1267] p 505 A90-33930

VON GRUENHAGEN, W.

- A highly maneuverable helicopter in-flight simulator - Aspects of realization
[AIAA PAPER 88-4607] p 670 A90-42466

VON GRUENHAGEN, WOLFGANG

- Identification of mathematical derivative models for the design of a model following control system p 56 A90-12764

ATTHeS - A helicopter in-flight simulator for ACT testing

- p 643 A90-41727

VON HARDENBERG, P. C.

- Developments in ground vibration test and data analysis techniques for airframe structures p 832 A90-46970

VON LAVANTE, E.

- Comparison of inviscid and viscous separated flows p 302 A90-25277

VON RETH, R. D.

- EUROFAR - European project for a commercial vertical-takeoff aircraft
[MBB-UD-553/89] p 221 A90-22696

VON TEIN, VOLKER

- Modern dynamic components for helicopters
[MBB-UD-556-89-PUB] p 29 A90-12253
Development of military helicopters p 181 A90-18488

Scenario 2000

- [MBB-UD-560/89] p 222 A90-22698

The revolution continuous

- [MBB-UD-557-89-PUB] p 381 A90-28242

VONTEIN, VOLKER

- Scenario 2000
[MBB-UD-500/89-PUB] p 734 N90-25092

VOORHEES, KENT J.

- The use of soot analysis as an investigative tool in aircraft fires p 22 A90-10269

VORACEK, DAVID F.

- Ground vibration test results of a JetStar airplane using impulsive sine excitation p 179 A90-16963

VORNBERGER, A.

- Analysis of the rotor tip leakage flow with tip cooling air ejection p 515 N90-10209

VOROB'EV, I. U. S.

- Aeroelastic vibrations of turbomachine blades and propellers p 854 A90-49482

VOROB'EV, N. F.

- The problem of supersonic flow past a thin wing of finite span with fully subsonic leading edges p 620 A90-39519

VOROB'EV, VLADIMIR G.

- Technical means and methods of flight safety assurance p 238 A90-22735

VORONIN, V. I.

- Aerodynamic characteristics of wave riders based on flows behind axisymmetric shock waves p 395 A90-30342

VORONTSOVA, N. B.

- Effect of a jet on transonic flow past an airfoil p 388 A90-29181

- Some possibilities of the vortex layer method for calculating the aerodynamic characteristics of an augmented airfoil interacting with the engine jet p 804 A90-46564

VORRES, C. L.

- Advanced fuel properties, phase 1
[AD-A219788] p 766 N90-25236

VOS, J. B.

- Development of supersonic and hypersonic Euler solvers using shock fitting in two and three dimensions p 707 A90-44426

VOSKRESENSKII, G. P.

- Some aspects of the numerical modeling of supersonic flow past flight vehicles p 293 A90-24048

VOSKRESENSKII, IURII E.

- Aviation equipment p 338 A90-24200

VOSS, NORBERT

- Saenger propulsion system options p 344 N90-16818

VOSS, R.

- Computation of unsteady transonic flows around oscillating airfoils using full potential and Euler equations p 472 A90-33357

- Adaptation for unsteady flow p 871 N90-26845

VU, KHAI TRAN

- Advances in optimal active control techniques for aerospace systems; application to aircraft active landing gear p 592 N90-21769

VUILLET, A.

- Performance and aerodynamic development of the Super Puma Mk II main rotor with new SPP8 blade tip design
[ONERA, TP NO. 1989-181] p 245 A90-21041

VUILLEZ, C.

- Quasi-3D viscous flow computations in subsonic and transonic turbomachinery bladings
[AIAA PAPER 90-2126] p 625 A90-42033

VUILLOT, A. M.

- A multi-domain 3D Euler solver for flows in turbomachines
[ONERA, TP NO. 1989-119] p 15 A90-12623
- Recent developments in calculation methods for internal flows by solution of Euler or Navier-Stokes equations
[ONERA, TP NO. 1989-167] p 223 A90-21033

VUKELICH, SHARON I.

- The role of NDI in the certification of turbine engine components
[PNR90629] p 777 N90-26349
- The role of NDI in the certification of turbine engine components
p 859 N90-28069
- VULIKH, B. E.**
Effect of the fluid level of a hydraulic shock absorber on the characteristics of the gas supply system
p 851 A90-46504

VYAS, N. S.

- Resonant stress determination of a turbine blade with modal damping as a function of rotor speed and vibrational amplitude
[ASME PAPER 89-GT-27] p 340 A90-23765

VYRIOTES, P.

- Preliminary design and analysis of propellers
p 645 A90-42407

VYSHINSKII, V. V.

- Calculation of nonseparated transonic flow past swept wings with allowance for viscosity p 294 A90-24079
- Calculation of transonic axisymmetric flow past an engine nacelle with allowance for viscosity
p 296 A90-24107
- Optimal nose shapes of bodies of revolution in transonic flow
p 299 A90-24165

W**WACHSPRESS, D. A.**

- Optimization of rotor performance in hover and axial flight using a free wake analysis p 407 A90-28175
- Free wake analysis of rotor configurations for reduced vibratory airloads p 833 A90-46975

WACHSPRESS, DANIEL A.

- New free-wake analysis of rotorcraft hover performance using influence coefficients p 181 A90-17867

WADIA, A. R.

- Three-dimensional relief in turbomachinery blading
[ASME PAPER 89-GT-151] p 292 A90-23840

WADIA, ASPI R.

- Advanced combustor liner cooling technology for gas turbines p 112 A90-16004

WADKINS, R. P.

- Three-dimensional analysis on flow and temperature distributions for aircraft fuel thermal stability
[AD-A219651] p 678 N90-23571

WADSWORTH, MARK

- Resin transfer molding of composite aircraft structures
[SAE PAPER 89-1042] p 128 A90-14347
- Elevator tab assembly producibility study
[IAR-89-16] p 734 N90-25133

WAGENER, J.

- A comparison between theoretical and experimental results for a 3-D wing with damped pitching oscillations
p 472 A90-33361

WAGGONER, ED G.

- Design and test of an NLF wing glove for the variable-sweep transition flight experiment
p 104 N90-12544

WAGNER, BARBARA AGNES

- Optimum hypersonic airfoils with attached shocks
p 481 N90-20960

WAGNER, BERNHARD

- Aerodynamic work for Hermes spaceplane
p 675 A90-41115

WAGNER, D. A.

- Hypersonic test facility requirements for the 1990's
[AIAA PAPER 90-1389] p 594 A90-37934
- Power transfer devices for V/STOL convertible engine systems
p 587 A90-38539
- Advanced gearbox technology
[NASA-CR-179625] p 666 N90-24274

WAGNER, G. N.

- Helicopter wire strike accident and high voltage electrocution - A case report p 22 A90-10265

WAGNER, MATTHEW J.

- Development and extension of diagnostic techniques for advancing high speed aerodynamic research
p 436 A90-28281

WAGNER, R.

- Full scale study of a cabin fire in an A300 fuselage section
p 326 N90-17592

WAGNER, R. D.

- Curvature effects on the stability of laminar boundary layers on swept wings p 148 A90-16788
- Laminar flow control leading-edge systems in simulated airline service p 335 A90-26134

WAGNER, RICHARD D.

- Performance of laminar-flow leading-edge test articles in cloud encounters p 104 N90-12511

WAGNER, S.

- The use of a Laval nozzle and wall suction for blockage-free transonic wind-tunnel operation
p 225 A90-21592
- Euler procedure for calculation of the steady rotor flow with emphasis on wake evolution
[AIAA PAPER 90-3007] p 789 A90-45857
- A nonlinear vortex-lattice method for the calculation of interference effects between free vortex sheets and wings p 277 N90-16183
- Calculation of the flow field of a multiblade helicopter rotor using a Euler method including the wake
p 278 N90-16189

WAGNER, SIEGFRIED

- A study of the influence of a helicopter rotor blade on the following blades using Euler equations
p 630 A90-42435

WAGNER, THEODORE O.

- Future use of automotive gasoline in light aircraft
p 951 A90-51624

WAGURI, TOSHIHARU

- An application of expert system to jet engine diagnostic procedures p 587 A90-38596

WAHLGREN, BO I.

- Lightning testing and test analyses of the JAS39 aircraft p 842 A90-49836

WAIDMANN, W.

- Numerical calculation of the jet-interaction induced separation with respect to thrust vector control
p 584 A90-35228

WAILES, W. K.

- Advanced recovery systems wind tunnel test report
[NASA-CR-177563] p 816 N90-27653

WAINAUSKI, HAROLD S.

- Large-scale Advanced Prop-fan (LAP) high speed wind tunnel test report
[NASA-CR-182125] p 52 N90-10045

WAINAUSKI, HARRY S.

- Large-scale Advanced Prop-fan (LAP) static rotor test report
[NASA-CR-180848] p 117 N90-12617

WAINFAN, BARNABY

- Application of the joined wing to tiltrotor aircraft
[NASA-CR-177543] p 248 N90-15093

WAKAIRO, KAORU

- Flight simulation test facility: Function and specification of the simulator cockpit system
[NAL-TM-577] p 59 N90-10899
- The function of the Interactive Model Assembly Program (IMAP) for a flight simulator
[NAL-TR-1034] p 939 N90-29412

WAKAMATSU, YOSHIO

- Cycle analysis of scramjet engines
[NAL-TR-1002] p 51 N90-10035
- Analysis of scramjet engine characteristics
[NAL-TR-1041] p 933 N90-29398

WAKAYAMA, SEAN

- A method for lifting surface design using nonlinear optimization
[AIAA PAPER 90-3290] p 813 A90-49122

WAKE, BRIAN E.

- Application of a rotary-wing viscous flow solver on a massively parallel computer
[AIAA PAPER 90-0334] p 164 A90-19802

WALCHLI, LAWRENCE A.

- A look at tomorrow today p 921 N90-28524

WALCOTT, BRUCE L.

- Yaw rate control of an air bearing vehicle
p 435 N90-19420

WALDER, A.

- New metallic felts with improved resistance to high temperature oxidation
[ONERA, TP NO. 1989-210] p 366 A90-25343

WALDMAN, J.

- Materials pace aerospace technology
p 203 A90-17298
- Aluminum lithium alloys for Navy aircraft
p 267 N90-15193

WALKER, BETTY S.

- Performance measurements of an airfoil at low Reynolds numbers p 800 A90-46369
- Correlation of theory to wind-tunnel data at Reynolds numbers below 500,000 p 800 A90-46370

WALKER, C. R.

- Failure analysis handbook
[AD-A219747] p 689 N90-23752

WALKER, D. A.

- Large-scale structure in a supersonic slot-injected flowfield p 602 A90-36265

WALKER, J. D. A.

- Embedded function methods for supersonic turbulent boundary layers
[AIAA PAPER 90-0306] p 163 A90-19787

WALKER, JOE L.

- Dual servo optical projection system (SOPS) - A solution for two crewmember and night vision goggle display needs
[SAE PAPER 892353] p 760 A90-45504

WALKER, K.

- The effect on fatigue crack growth under spectrum loading of an imposed placard 'G' limit
p 643 A90-41339

WALKER, K. P.

- Constitutive modeling for isotropic materials (HOST)
[NASA-CR-174718] p 193 N90-13391

WALKER, MICHAEL

- Visual information for simulated landing approaches
p 347 A90-26189

WALKER, P. J.

- The extension and application of three-dimensional time marching analyses to incompressible turbomachinery flows
[ASME PAPER 89-GT-212] p 293 A90-23878

WALKER, R. A.

- Nonlinear maneuver autopilot for the F-15 aircraft
[NASA-CR-174442] p 77 N90-11487

WALKER, S. H.

- Twin jet screech suppression concepts tested for 4.7 percent axisymmetric and two-dimensional nozzle configurations
[AIAA PAPER 90-2150] p 696 A90-42046

WALKER, S. H.

- Computation of vectoring nozzle performance
[AIAA PAPER 90-2752] p 627 A90-42225

WALL, H. G.

- The acute, delayed neurotoxicity evaluation of two jet engine oil formulations
[AD-A222018] p 875 N90-26972

WALLACE, J.

- Aerosol effects on jet-engine IR radiation
p 40 A90-10152

WALLACE, MICHAEL G.

- Logistics support planning for standardized avionics
p 383 A90-30809

WALLE, GERARDO

- Tests for integrating measurement of gas pressures in flight propellers
[ETN-90-96498] p 634 N90-24253

WALLER, PETER

- Replay and transmission of AIMS-data to mainframe computer using remote transcribers p 892 N90-27634

WALLIS, R.

- Effects of additives on the processing and properties of LARC-TPI polyimide p 942 A90-50070

WALLS, JOHN E.

- ILS (Instrument Landing System) mathematical modeling study on the effects of proposed hangar construction west of runway 18R on localizer performance at Dallas-Fort Worth International Airport
[AD-A210631] p 27 N90-10019

WALLS, JOHN E.

- ILS mathematical modeling study of the effects of proposed hangar construction at the Orlando International Airport, Runway 17R, Orlando, Florida
[DOT/FAA/CT-TN89/52] p 121 N90-11762

WALSH, DAVID M.

- Mission effectiveness testing of an adaptive electronic fuel control on an S-76A p 422 A90-28199

WALSH, J. A.

- Inlet skew and the growth of secondary losses and vorticity in a turbine cascade
[ASME PAPER 89-GT-65] p 290 A90-23788

WALSH, J. L.

- Application of optimization methods to helicopter rotor blade design p 604 A90-37337

WALSH, JOANNE L.

- Minimum weight design of helicopter rotor blades with frequency constraints p 180 A90-17313
- Minimum weight design of rotorcraft blades with multiple frequency and stress constraints p 335 A90-25304
- Rotor blade aerodynamic design p 106 N90-12582
- Appendix: Results obtained to date p 107 N90-12588

WALSH, MICHAEL J.

- Effect of detailed surface geometry on riblet drag reduction performance p 622 A90-40693

WALSH, THOMAS P.

- Preliminary airworthiness evaluation of the Woodward hydromechanical unit installed on T700-GE-700 engines in the UH-60A helicopter
[AD-A216751] p 428 N90-18430

WALSH, TIMOTHY E.

- The Stealth biplane: A proposal in response to a low Reynolds Number station keeping mission
[NASA-CR-186680] p 734 N90-25127

WALTERS, N. M.

- Investigation of high angle of attack vortical flows over delta wings
[AIAA PAPER 90-0101] p 162 A90-19682

WALTERS, R. W.

A three-dimensional space marching algorithm for the solution of the Euler equations on unstructured grids
[AIAA PAPER 90-0014] p 234 A90-23701

WALTERS, ROBERT W.

Implicit flux-split schemes for the Euler equations
Compressible flow algorithms on structured/unstructured grids
p 602 A90-36254
p 779 A90-44855

WALTON, J.

Internal rotor friction instability
[NASA-CR-183942] p 543 N90-21395

WALTON, J. F.

High temperature powder lubricated dampers for gas turbine engines
[AIAA PAPER 90-2048] p 684 A90-41999

WANDER, STEPHEN

NASA aerodynamics program
[NASA-TM-4175] p 373 N90-17235

WANDERT, H.

Direct measurement of laminar instability amplification factors in flight
p 277 N90-16178

WANG, A.

Injectable bismaleimide systems p 943 A90-50132

WANG, BAIPENG

A quadratic programming method for solving three dimensional elastic-plastic contact problems
p 603 A90-36417

WANG, BAO-GUO

An improved SIP scheme for numerical solutions of transonic streamfunction equations p 904 A90-51014

WANG, BAOGUAN

Experimental investigation on composite cooling of a turbine blade p 190 A90-17794

WANG, BAOGUO

A new implicit hybrid schemes for the Euler equation of transonic flow p 158 A90-18608
The prediction of boundary layers with rotation and variation of stream filament thickness
[ASME PAPER 89-GT-227] p 362 A90-23882
Stability analysis and numerical experiments for viscous-inviscid interaction in transonic flow
p 293 A90-24009
Numerical analysis of viscous-inviscid interaction in transonic flow p 627 A90-42363

WANG, BAOREN

Application investigation on superplastic forming/diffusion bonding combined technology of titanium alloy TC4 p 204 A90-18603

WANG, BIN

The application of the engineering approach for analyzing crack tolerance of fuselage panels to a transport airplane p 272 A90-22014

WANG, C. H.

Unsteady transonic aerodynamics of oscillating airfoils in supersonic freestream p 232 A90-23277

WANG, C. M.

A numerical study of general viscous flows around multi-element airfoils
[AIAA PAPER 90-0572] p 167 A90-19922

A numerical method for three-dimensional viscous flows
[AIAA PAPER 90-0236] p 228 A90-22186

WANG, GARY S.

An Euler method for wing-body-winglet flows
[AIAA PAPER 90-0436] p 229 A90-22218

WANG, HONGJI

Exhaust emission performance of a vaporizer tube combustor as compared with a single tube combustor p 111 A90-14614

WANG, J. H.

Threshold performance optimization of a rotor-bearing system subjected to leakage excitation
[ASME PAPER 89-GT-126] p 360 A90-23825

WANG, JAMES M.

Air resonance stability of hingeless rotors in forward flight p 590 A90-38519

Theoretical and experimental investigation of the aeroelastic stability of an advanced bearingless rotor in hover and forward flight p 831 A90-46958

WANG, JI C.

Identification of rotor flapping equation of motion from flight measurements with the RSRA compound helicopter p 56 A90-12769

Synthesis of individual rotor blade control system for gust alleviation
[NASA-TM-101886] p 736 N90-25972

WANG, JIAHUA

A study on spray characteristics down stream from a gutter-atomizer p 368 A90-26893

WANG, JINXIAN

A quadratic programming method for solving three dimensional elastic-plastic contact problems
p 603 A90-36417

WANG, JUNYANG

A study on initial fatigue quality of typical aircraft structures (fastener holes) p 272 A90-22004

WANG, JYH-CHYANG ALEX

A scalar/vector potential solution for aerodynamic coefficients in wind shear p 21 N90-10838

WANG, LI CHENG

PCISM method for two dimensional compressible viscous cascade flow calculation p 15 A90-12625

WANG, M. R.

The influence of swirl on velocity, temperature and species characteristics in a can combustor
[AIAA PAPER 90-2454] p 664 A90-42177

WANG, P. K. C.

Control and stabilization of linear and nonlinear distributed systems
[AD-A218446] p 462 N90-18908

WANG, PEIDE

A separated algorithm and applications to flight test p 216 A90-16857

WANG, PEISHEN

A transonic airfoil design method and examples p 627 A90-42351

WANG, PINGQIA

An approach for calculating steady subsonic and transonic blade to blade flows p 152 A90-17784

WANG, PIYQIA

An aerodynamical design and calculation method for gas turbine with cooling air mixing p 189 A90-17782

WANG, QINGHUAN

A new design method for centrifugal compressor vaned diffusers
[ASME PAPER 89-GT-156] p 292 A90-23844

WANG, S. J.

Investigation of adaptive-wall wind tunnels with two measured interfaces
[AIAA PAPER 90-0186] p 200 A90-19728

WANG, SHANGWEN

Dynamic analysis of airport pavement p 593 A90-36418

WANG, SHERMAN

A component modal synthesis technique for the lateral vibration analysis of aircraft engine systems p 179 A90-16983

WANG, SHI-CUN

Analytical approach to the induced flow of a helicopter rotor in vertical descent p 293 A90-23938

WANG, SHICUN

Recent advancement in helicopter rotor wake study p 556 A90-36413

WANG, T.

Penetration landing guidance trajectories in the presence of windshear p 98 A90-14732
Acceleration, gamma, and theta guidance for abort landing in a windshear p 98 A90-14733

WANG, TONGQING

An analysis of cavity resonance in the aeroengine casing during rig testing p 894 A90-49481

WANG, WEI

Method for calculating the unsteady flow of an elliptical circulation-control airfoil p 3 A90-11003

WANG, X.

Theoretical and experimental determination of natural frequencies of laced blading p 878 A90-46037
Vibration analysis of laced blades p 878 A90-46186

WANG, XU

Simulation research on the afterburning dynamic characteristics of engine control system p 48 A90-12581

The establishment of mathematical model of engine control system and simulation research of afterburning dynamic characteristics p 190 A90-18613

Simulation research on the afterburning dynamic characteristics of engine control system p 585 A90-35708

WANG, XUEYU

Partial similarity and a real-time model of twin-spool gas turbine p 654 A90-40512

WANG, Y. J.

A linear quadratic regulator approach to the stabilization of uncertain linear systems
[AIAA PAPER 90-3509] p 891 A90-47755

WANG, Y. W.

The acoustic phenomena of the stalling flutter p 78 A90-11801

WANG, Y.-J.

A modal parameter identification technique and its application to large complex structures with multiple steady sinusoidal excitation p 602 A90-35670

WANG, YANZHONG

The analysis and solution of the performance deterioration problem of WP7 engine under the full reheating condition p 191 A90-18624

WANG, YAWEI

Special essays for the 40th anniversary of the revolution: The chief designer discusses the F-8 2 and future fighter planes
[AD-A221587] p 845 N90-26829

WANG, YI

The design and study of the information transfer mechanism for a distributed avionics system p 207 A90-16858

WANG, YUEQI

A method for aerodynamic design calculation of axial gas turbine stages with cooling air mixing p 152 A90-17781

An experimental study of tip clearance effects on the performance of an axial transonic turbine p 189 A90-17788

Effect of vane and blade numbers on performance of transonic turbine stage p 189 A90-17789

WANG, YUWEI

The design of the series of blade flutter rotor and the experimental investigation of flow-induced vibration p 586 A90-37230

WANG, ZHENG

New progress in airframe durability requirements p 246 A90-22001

WANG, ZHENGMIN

A quasi-3D design method of transonic compressor blade with the function of improving velocity distribution p 49 A90-12589

WANG, ZHONGQI

Influence of blade leaning on the flow field behind turbine rectangular cascades with different incidences and aspect ratios p 11 A90-12519

A method for calculating axial turbomachine end wall turbulent boundary layers
[ASME PAPER 89-GT-15] p 287 A90-23759

WANIE, K. M.

Numerical simulation of transonic wing flows using a zonal Euler, boundary-layer, Navier-Stokes approach p 225 A90-21596

WANKE, CRAIG

Cockpit display of hazardous wind shear information p 484 N90-20924

Cockpit display of hazardous weather information p 485 N90-20929

WANSTALL, BRIAN

Air combat beyond the stall p 589 A90-35888

WANTUCK, PAUL J.

Radio frequency (RF) heated supersonic flow laboratory
[AIAA PAPER 90-2469] p 673 A90-42186

WARD, B. D.

Advanced airbreathing powerplant for hypersonic vehicles p 49 A90-12607

WARD, RICHARD D.

Fighter design from the Soviet perspective
[AIAA PAPER 89-2074] p 181 A90-18135

WARD, T. C.

Poly(arylene ether ketone)/poly(aryl imide) homo- and polydimethylsiloxane segmented copolymer blends - Influence of chemical structure on miscibility and physical property behavior p 941 A90-50063

WARD, WILLIAM CARL

An investigation of the generation and radiation of aerodynamic noise in real piping systems p 614 N90-22368

WARE, BRUCE E.

Plan for the FAA air traffic operational evaluation of the Automated Surface Observing System (ASOS)
[DOT/FAA/CT-TN89/56] p 489 N90-20968

Meteorologist Weather Processor (MWP) integration test plan
[DOT/FAA/CT-TN89/62] p 544 N90-21500

WARE, GEORGE M.

Supersonic aerodynamic characteristics of a proposed Assured Crew Return Capability (ACRC) lifting-body configuration
[NASA-TM-4136] p 317 N90-17560

WAREHAM, J. R.

Improved fiber reinforced polyphenylene sulfide thermoplastic composites p 947 A90-50180

WARES, RICHARD

The performance of alternate fuels in general aviation aircraft p 950 A90-51621

WARGENAU, UDO

Fire prevention in transport airplane passenger cabins p 325 N90-17590

WARNATZ, J.

Chemistry of combustion processes p 749 N90-25994

WARNECKE, G.

On the coupling of finite elements and boundary elements for transonic potential flows p 155 A90-18297

- WARNER, GORDON E.**
A preliminary sensitivity analysis of the Generalized Escape System Simulation (GESS) computer program [DE89-016891] p 24 N90-10844
- WARNER, J. V.**
Digital control of local sound fields in an aircraft passenger compartment p 247 A90-23113
- WARNER, PAUL A.**
High temperature solid lubricant requirements for advanced high performance gas turbine engines [AIAA PAPER 90-2042] p 661 A90-41993
- WARREN, ANTHONY**
Application of energy turn g-limiting for aircraft high performance turns [AIAA PAPER 90-3328] p 862 A90-47590
- WARREN, GARY P.**
Adaptive grid embedding for the two-dimensional Euler equations [AIAA PAPER 90-3049] p 797 A90-45929
- WARREN, GARY PATRICK**
Adaptive grid embedding for the two-dimensional flux-split Euler equations [NASA-CR-186533] p 547 N90-21571
- WARREN, H. R.**
The Radarsat system p 873 A90-49671
- WARREN, J. R.**
Thermal mechanical fatigue of coated blade materials [AD-A214258] p 256 N90-15107
- WARREN, R. E.**
Supersonic combustion of hydrogen jets behind a backward-facing step [AIAA PAPER 90-0204] p 266 A90-22183
- WARREN, W. L.**
Airborne aerosol inlet passing efficiency measurement p 927 A90-52077
- WARRICK, JAMES C.**
Aircraft crash survival design guide. Volume 3: Aircraft structural crash resistance [AD-A218436] p 575 N90-22547
- WARS, SAIF A.**
User's guide to PMESH: A grid-generation program for single-rotation and counterrotation advanced turboprops [NASA-CR-185156] p 217 N90-14783
- WARS, Z. U. A.**
Surface grid generation through elliptic PDEs p 309 A90-26496
- WARWICK, GRAHAM**
Material progress p 221 A90-21715
Building the B-2 p 701 A90-43826
- WASHUTA, KEVIN W.**
Advancements in rotor and airframe structural flight testing developed during the SH-60B G.W./C.G. expansion program [AIAA PAPER 90-1281] p 495 A90-33902
- WASIKOWSKI, MARK**
Low speed maneuverability and agility design considerations for V/STOL aircraft p 581 A90-38536
GTPDP - A rotary wing aircraft preliminary design and performance estimation program including optimization and cost p 830 A90-46944
- WASIKOWSKI, MARK E.**
Helicopter individual blade control through optimal output feedback p 861 A90-46956
- WASSENBERGH, H. A.**
Anatomy of airline regulation - Towards a pluriform, plurilateral, pluralistic, flexible world-wide regulatory framework for air transport p 898 A90-49620
- WASSERMAN, M.**
Next-generation automatic test equipment for military support p 767 A90-42667
- WASYL, JOSEPH**
Optimization of glides for constant wind fields and course headings p 731 A90-44734
- WATANABE, AKIRA**
Flight simulation test facility: Function and specification of the simulator cockpit system [NAL-TM-577] p 59 N90-10899
The function of the Interactive Model Assembly Program (IMAP) for a flight simulator [NAL-TR-1034] p 939 N90-29412
- WATANABE, FUMIO**
Airborne array antennas for satellite communication p 265 A90-23202
- WATANABE, HARRY H.**
Radio frequency (RF) heated supersonic flow laboratory [AIAA PAPER 90-2469] p 673 A90-42186
- WATANABE, MINORU**
Parametric studies of acoustic duct attenuation of perforated-plate-on-honeycomb absorber [NAL-TM-603] p 966 N90-30030
- WATANABE, MITUNORI**
Space plane model for visual measurement of aerodynamic heating [DE90-505514] p 720 N90-25949
- WATANABE, ROY T.**
Development of fatigue loading spectra [ASTM STP-1006] p 367 A90-26751
Development of jet transport airframe fatigue test spectra p 351 A90-26753
- WATANABE, T.**
Noise prediction of a counter-rotation propfan p 218 A90-17861
- WATANABE, TOSHINORI**
Unsteady aerodynamic characteristics of oscillating cascade with tip clearance p 8 A90-11793
- WATANABE, YASUO**
Evaluating the feasibility of a radar separation minimum for a long-range SSR p 25 A90-10240
- WATKINS, WILLIAM B.**
Noninterference blade-vibration measurement system for gas turbine engines p 132 A90-16372
- WATSON-VIKEN, SALLY A.**
Design of the low-speed NLF(1)-0414F and the high-speed HSNLF(1)-0213 airfoils with high-lift systems p 93 N90-12540
- WATSON, DOUGLAS C.**
Effects of stick dynamics on helicopter flying qualities [AIAA PAPER 90-3477] p 866 A90-47727
- WATSON, KENNETH A.**
ETO (Earth-To-Orbit): A trajectory program for aerospace vehicles [AD-A218157] p 528 N90-20103
- WATT, GEORGE W.**
Minimum-time turns using vectored thrust p 118 A90-14728
- WATTS, C. B., JR.**
Applications of slotted cable antennas in the instrument landing system p 639 A90-41708
- WATTS, G. A.**
Modeling flexible aircraft for flight control design [AD-A219123] p 757 N90-25140
- WATTS, NORMAN W.**
Data Link Processor (DLP) operational test and evaluation/integration test plan [DOT/FAA/CT-TN89/32] p 214 N90-14404
- WAWNER, FRANKLIN E., JR.**
NASA-UVA light aerospace alloy and structures technology program [NASA-CR-182607] p 601 N90-22651
- WAY, D. J.**
Performance of a highly-loaded HP compressor [RAE-TM-P-1149] p 256 N90-15919
- WAY, THOMAS C.**
3-D in pictorial formats for aircraft cockpits p 420 A90-31331
- WEATHERILL, N. P.**
The construction of component-adaptive grids for aerodynamic geometries p 309 A90-26513
On the combination of structured-unstructured meshes p 311 A90-26540
- WEAVER, ALFRED C.**
AIRNET: A real-time communications network for aircraft [NASA-CR-186140] p 690 N90-24514
- WEAVER, M. J.**
IMI 834 - A new high temperature capability titanium alloy for engine use p 62 A90-12535
- WEBB, R.**
An array-fed reflector antenna with built-in calibration facility p 402 A90-27781
Development of cryogenic instrumentation for ETW models p 525 A90-34251
- WEBER, JOHN H.**
Mechanical alloying spreads its wings p 950 A90-51200
- WEBER, K. F.**
Analysis of three-dimensional turbomachinery flows on C-type grids using an implicit Euler solver [ASME PAPER 89-GT-85] p 905 A90-51258
- WEBER, M. E.**
Wind shear detection with airport surveillance radars p 241 A90-21387
- WEBER, MARK E.**
ASR-9 weather channel test report [AD-A211749] p 133 N90-11934
- WEBER, R. M.**
Constitutive modeling for isotropic materials (HOST) [NASA-CR-179522] p 193 N90-13390
Constitutive modeling for isotropic materials (HOST) [NASA-CR-174718] p 193 N90-13391
- WEBER, T.**
Rigidite 5255-3 - A highly damage tolerant prepreg resin system with a well balanced property profile p 944 A90-50139
- WEBER, TIM L.**
Inclusion of nonlinear aerodynamics in the FLAP code [DE89-009507] p 281 N90-15519
- WEBRE, JAMES L.**
Airworthiness and flight characteristics evaluation of the McDonnell Douglas Helicopter Corporation (MDHC) 530FF helicopter [AD-A218253] p 498 N90-20076
- WEBSTER, DONALD**
Tough(er) aluminum-lithium alloys p 62 A90-11575
- WEBSTER, HARRY**
Full-scale air transport category fuselage burnthrough tests [DOT/FAA/CT-TN89/65] p 486 N90-20967
- WEBSTER, W. PHILLIP**
Numerical simulation of reversed flow over a supersonic delta wing at high angle of attack [AIAA PAPER 89-1802] p 8 A90-11849
Comparison between thin layer and full Navier-Stokes simulations over a supersonic delta wing [AIAA PAPER 90-0589] p 314 A90-26968
- WECHKIN, J.**
Visualization studies in rotating disk cavity flows p 475 A90-33568
- WEDAN, BRUCE W.**
Navier-Stokes computations of a prolate spheroid at angle of attack p 17 A90-13018
Prediction of separated transonic wing flows with nonequilibrium algebraic turbulence model p 809 A90-47312
- WEDEKIND, G.**
Inflight thrust vectoring: A further degree of freedom in the aerodynamic/flight mechanical design of modern fighter aircraft p 921 N90-28528
Aerodynamic interferences of in-flight thrust reversers in ground effect p 921 N90-28529
- WEDEMAYER, ERICH H.**
High productivity testing p 871 N90-26843
Limits of adaptation, residual interferences p 871 N90-26844
- WEDLAKE, E. T.**
Aerodynamic and heat transfer measurements on blading for a high rim-speed transonic turbine [ASME PAPER 89-GT-228] p 293 A90-23883
Aerodynamic and heat transfer measurements on blading for a high rim-speed transonic turbine [RAE-TM-P-1151] p 256 N90-15920
- WEGENER, D.**
Secondary flow in a turbine guide vane with low aspect ratio p 513 N90-21018
- WEGRZYN, EMIL**
Some aspects of the erosive wear of components of aircraft turbine engines p 253 A90-21627
- WEHRMEYER, JOSEPH A.**
Raman scattering measurements using UV excimer lasers p 874 N90-26902
Concentration, temperature, and density in a hydrogen-air flame by excimer-induced Raman scattering p 875 N90-26903
- WEI, FU-SHANG**
Vibration reduction on servo flap controlled rotor using HHC p 861 A90-46967
- WEI, LIXIN**
An improvement on upwinding technique used in the Galerkin finite element method for the computation of inviscid transonic flow with shock waves p 627 A90-42361
- WEI, X. I.**
A numerical method solving 2-D unsteady flow field around cascade of oscillating airfoils with arbitrary camber and thickness p 7 A90-11788
- WEI, X. L.**
Analysis of the effect of rotor-angular-acceleration on the features of gas flow in turbomachinery p 6 A90-11780
- WEI, XING-LU**
Some explorations on the mechanism of blade flutter suppression by porous wall casing p 854 A90-49470
- WEIDNER, E. H.**
Flow establishment in a generic scramjet combustor [AIAA PAPER 90-2096] p 742 A90-42729
- WEILAND, C.**
Three-dimensional simulations of hypersonic flows p 306 A90-25823
Calculation of three-dimensional viscous and inviscid hypersonic flows using split-matrix marching methods [AIAA PAPER 90-3070] p 794 A90-45894
- WEILKE, J.**
Investigation on sheet material of 8090 and 2091 aluminum-lithium alloy p 267 N90-15192
- WEILKE, JUERGEN**
Investigation on sheet material of 8090 and 2091 aluminum-lithium alloy [MBB-UT-122/89-PUB] p 766 N90-25090
- WEIMER, M. M.**
An experimental investigation of turbine rotor wakes for the development of a fiber optic pressure sensor [AIAA PAPER 90-2411] p 687 A90-42163

- WEIN, J. A.**
Development of process control procedure for ultrahigh-sensitivity fluorescent penetrant inspection systems p 771 A90-45225
- WEINACHT, PAUL**
Navier-Stokes predictions of pitch damping for finned projectiles using steady coning motion [AIAA PAPER 90-3088] p 795 A90-45902
- WEINBERG, BERNARD C.**
Extension of a three-dimensional viscous wing flow analysis user's manual: VISTA 3-D code [NASA-CR-182024] p 574 A90-22538
Extension of a three-dimensional viscous wing flow analysis [NASA-CR-182023] p 631 A90-23348
- WEINBERG, P.**
US Navy aircraft fire protection technology p 327 A90-17603
- WEINGARTEN, NORMAN**
Use of ground-based and in-flight simulation for flight control system development [AIAA PAPER 90-1286] p 519 A90-33907
- WEINGOLD, H. D.**
Application of sweep to improve the efficiency of a transonic fan. I - Design [AIAA PAPER 90-1915] p 741 A90-42695
- WEINREICH, H.-L.**
Aspects of the design of a hypersonic engine system and the selection of the intake and tail [DGLR PAPER 88-040] p 928 A90-50233
- WEIR, B.**
The effects of foreplanes on the static and dynamic characteristics of a combat aircraft model p 920 A90-28520
- WEIR, DONALD S.**
The prediction of the noise generating mechanisms of an Aerospatiale 365N-1 Dauphin helicopter p 463 A90-28161
The ROTONET prediction system and initial comparisons with far-field acoustics measurements for the XV-15 tilt-rotor aircraft p 894 A90-46947
- WEIR, L. J.**
Comparison of 3-D viscous flow computations of Mach 5 inlet with experimental data [AIAA PAPER 90-0600] p 314 A90-26970
Comparison of 3-D viscous flow computations of Mach 5 inlet with experimental data [NASA-TM-102518] p 510 A90-20090
- WEISENBURGER, R.**
Plan, execute, and discuss vibration measurements and correlations to evaluate a NASTRAN finite element model of the AH-64 helicopter airframe [NASA-CR-181973] p 960 A90-28866
- WEISENBURGER, R. K.**
Rotor/airframe aeroelastic analyses using the transfer matrix approach [AIAA PAPER 90-1119] p 392 A90-29391
- WEISEND, NORBERT A., JR.**
Design of an advanced pneumatic deicer for the composite rotor blade p 29 A90-11009
- WEISROSE, S. A.**
Aerosol effects on jet-engine IR radiation p 40 A90-10152
- WEISS, ROSANNE M.**
Helicopter surface maneuvering test results [ACD-330] p 59 A90-10897
Analysis of heliport environmental data: Indianapolis downtown heliport, Wall Street heliport. Volume 2: Wall Street heliport data plots [DOT/FAA/CT-TN87/54-VOL-2] p 121 A90-11761
Analysis of heliport environmental data: Indianapolis downtown heliport, Wall Street heliport. Volume 3: Indianapolis downtown heliport data plots [AD-A217412] p 544 A90-20500
Heliport visual approach surface high temperature and high altitude tests [DOT/FAA/CT-TN89/34] p 825 A90-27675
Analysis of heliport environmental data, Infracoastal City [DOT/FAA/CT-TN89/43] p 938 A90-28584
- WEISSHAAR, T. A.**
Optimum design of composite structures p 272 A90-22135
Time domain simulations of a flexible wing in subsonic, compressible flow [AIAA PAPER 90-1153] p 390 A90-29365
Static aeroelastic behavior of an adaptive laminated piezoelectric composite wing [AIAA PAPER 90-1078] p 412 A90-29386
- WEISSHAAR, TERRENCE A.**
Integrated structure/control concepts for oblique wing roll control and trim p 433 A90-31282
Aeroseuroelastic tailoring for lateral control enhancement p 516 A90-33060
Static aeroelastic tailoring for oblique wing lateral trim p 667 A90-40689
- Parametric aeroelastic stability analysis of a generic X-wing aircraft p 731 A90-44737
Design of a spanloader cargo aircraft [NASA-CR-186046] p 184 A90-14216
- WEISSMAN, DAVID**
Representation of two-dimensional hypersonic inlet flows for one-dimensional scramjet cycle analysis [AIAA PAPER 90-0527] p 229 A90-22226
- WELCH, J. D.**
Experimental examination of the benefits of improved terminal air traffic control planning p 241 A90-21388
Using aircraft radar tracks to estimate wind aloft p 241 A90-21390
- WELCH, JERRY D.**
The mythology of first-come-first-serve landing order p 821 A90-46394
- WELL, KLAUS H.**
Toward a theory of aircraft agility [AIAA PAPER 90-2808] p 752 A90-45143
- WELLEN, H.**
Computer-aided structural optimisation of aircraft structures [BR112837] p 499 A90-20973
- WELLER, WILLIAM H.**
Relative aeromechanical stability characteristics for hingeless and bearingless rotors p 409 A90-28230
- WELLMAN, DENNIS L.**
Aerosol separator for use in aircraft [PB90-142217] p 611 A90-22155
- WELLS, L. J.**
The 1987 survey of track keeping and altitudes on Heathrow and Gatwick standard instrument departure routes (DAY) [CAA-PAPER-88010] p 99 A90-11729
- WELLS, R. G.**
The design and test of a two stage transonic axial flow compressor [ASME PAPER 89-GT-164] p 341 A90-23852
- WELLS, VALANA L.**
Analysis of a propeller in compressible, steady flow p 814 A90-49778
- WELSH, B. L.**
The development of leading-edge notches to improve the subsonic performance of wings of moderate sweep p 491 A90-33367
The steady and time-dependent aerodynamic characteristics of a combat aircraft with a delta or swept canard p 921 A90-28526
- WELSH, W. A.**
Higher harmonic and trim control of the X-wing circulation control wind tunnel model rotor p 435 A90-28156
- WELZ, JOSEPH P.**
Free-field propagation of high intensity noise [NASA-CR-186577] p 549 A90-21604
- WEN, WEIDONG**
A combined Riccati transfer matrix-direct integration method with its applications p 611 A90-37218
- WENDLAND, W.**
On the coupling of finite elements and boundary elements for transonic potential flows p 155 A90-18297
- WENDT, J. F.**
Infrared thermography in blowdown and intermittent hypersonic facilities p 440 A90-31302
- WENIGWIESER, C.**
Structural-acoustic analysis of aircraft fuselage structures using general purpose finite element codes p 492 A90-33385
- WENNEKERS, ROLAND**
Rotor concepts for the European Future Advanced Rotorcraft (Eurofar) [MBB-UD-0551-89-PUB] p 29 A90-12258
- WENNERSTROM, A. J.**
Highly loaded axial flow compressors - History and current developments p 44 A90-12503
- WENNERSTROM, ARTHUR J.**
Stall margin improvement in axial-flow compressors by circumferential variation of stationary blade setting angles [AIAA PAPER 90-1912] p 656 A90-40554
- WENTZ, K. R.**
The prediction and measurement of thermoacoustic response of plate structures [AIAA PAPER 90-0988] p 451 A90-29400
- WENTZ, WILLIAM H.**
In-flight boundary-layer transition measurements on a swept wing p 17 A90-13017
- WENTZ, WILLIAM H., JR.**
Static and dynamic water tunnel tests of slender wings and wing-body configurations at extreme angles of attack [AIAA PAPER 90-3021] p 869 A90-45888
- WENTZEL, CYRIL M.**
The application of the finite element method to an aerodynamic problem specific to propeller design [LR-614] p 718 A90-25116
- WERELEY, NORMAN M.**
Active control of gust- and interference-induced vibration of tilt-rotor aircraft p 429 A90-28201
Linear control issues in the higher harmonic control of helicopter vibrations p 430 A90-28225
- WERLE, H.**
Hydrodynamic visualization of the flow around a high-speed aircraft propeller [ONERA, TP NO. 1989-108] p 3 A90-11141
Vortex interactions in fixed and oscillating delta wings (water tunnel visualizations) p 16 A90-12784
Hydrodynamic visualization of organized structures and turbulences in boundary layers, wakes, jets or propeller flows [ONERA, TP NO. 1989-158] p 223 A90-21026
- WERLEY, CRAIG J.**
Fatigue evaluation of C/MH-53E main rotor damper threaded joints p 642 A90-39988
- WERNER, WINFRIED**
Structural components of fiber-reinforced thermoplastics p 676 A90-41111
- WERNESS, S.**
Shadow-tracking algorithm for moving target detection p 488 A90-34137
- WERNICKE, KENNETH G.**
Maneuver performance comparison between the XV-15 and an advanced tiltrotor design p 518 A90-33622
- WERT, JOHN A.**
NASA-UVA light aerospace alloy and structures technology program [NASA-CR-182607] p 601 A90-22651
- WESKAMP, K.**
Computational prediction and measurement of the flow in axial turbine cascades and stages p 514 A90-21028
- WESLER, JOHN**
Sound propagation elements in evaluation of en route noise of advanced turbofan aircraft p 697 A90-24861
- WESSELENG, P.**
Multigrid methods in computational fluid dynamics p 906 A90-51526
- WEST, BLAINE S.**
Full-scale birdstrike testing of in-service aged F-111 ADBIRT windshield transparencies [AD-A218035] p 484 A90-20069
Nondestructive measurement of residual stresses in aircraft transparencies [AD-A218680] p 689 A90-23762
- WEST, MICHAEL**
Iterative algorithm for correlation of strain gauge data with aerodynamic load p 709 A90-44739
- WESTERMAN, EVERETT A.**
An apparatus to prepare composites for repair p 533 A90-31574
- WESTON, K. C.**
Turbofan engine analysis and optimization using spreadsheets p 779 A90-45290
- WESTRAY, M. S.**
Enhanced bioreclamation of jet fuels: A full-scale test at Eglin AFB, Florida [AD-A222348] p 875 A90-26992
- WESTWATER, E. R.**
Remote sensing techniques of the Wave Propagation Laboratory for the measurement of supercooled liquid water: Applications to aircraft icing [PB89-208102] p 24 A90-10842
- WEY, C.**
A planar reacting shear layer system for the study of fluid dynamics-combustion interaction [NASA-TM-102422] p 194 A90-13393
- WEY, C. C.**
A planar reacting shear layer system for the study of fluid dynamics-combustion interaction [NASA-TM-102422] p 194 A90-13393
- WEY, P.**
Measurements, visualization and interpretation of 3-D flows - Application within base flows p 386 A90-28252
- WEYER, R. M.**
Computational analysis of an open-nosed fighter/attack inlet [AIAA PAPER 90-2145] p 704 A90-42737
- WHALEN, M. V.**
Background, current status, and prognosis of the ongoing slush hydrogen technology development program for the NASP [NASA-TM-103220] p 763 A90-26055
- WHALEN, MARGARET V.**
Slush Hydrogen (SLH2) technology development for application to the National Aerospace Plane (NASP) [NASA-TM-102315] p 203 A90-14268
- WHALEN, THOMAS J.**
Improved silicon carbide for advanced heat engines [NASA-CR-180831] p 65 A90-10293

- WHATLEY, DAVID W.**
The implementation of STOVl task-tailored control modes in a fighter cockpit
[AIAA PAPER 90-3229] p 839 A90-49114
- WHEELER, C. F.**
Modeling and analysis of airport and aircraft operations
[PB90-222167] p 915 N90-28511
- WHEELER, ED**
The multi-function RLG system comes of age - A technical update p 578 A90-36931
- WHEELER, EDWARD**
Air Force manufacturing technology NDE programs supporting manufacturing and maintenance p 452 A90-30779
- WHEELER, JOYCE A.**
An algebraic adaptive-grid technique for the solution of Navier-Stokes equations
[AIAA PAPER 90-1605] p 567 A90-38736
- WHELESS, K.**
JFS190 turbine engine performance optimized using Taguchi methods
[AIAA PAPER 90-2419] p 663 A90-42169
- WHICKER, JERRY T.**
Manufacturing and handling techniques used in the assembly of polished commercial aircraft
[SAE PAPER 890925] p 286 A90-24690
- WHIPPLE, DANIEL Y.**
Laser-velocimeter-measured flow field around an advanced, swept, eight-blade propeller at Mach 0.8
[NASA-TX-2462] p 468 N90-20942
- WHITAKER, KEVIN W.**
The influence of a wall function on turbine blade heat transfer prediction p 429 N90-19421
- WHITBY, DAVID G.**
Wind tunnel support system effects on a fighter aircraft model at Mach numbers from 0.6 to 2.0
[AD-A210614] p 19 N90-10010
- WHITE, ALLAN P.**
Real-time test data processing system p 458 A90-28860
- WHITE, C. H.**
Cleaner superalloys via improved melting practices p 442 A90-29707
- WHITE, G. THOMAS**
Air-to-Air Combat Test IV (AACT IV) and the AACT data base p 381 A90-28169
- WHITE, GEORGE O.**
Correlation between vibration and computer operator response onboard a UH-1H helicopter p 737 A90-43727
- WHITE, M. E.**
Tangential mass addition for the control of shock wave/boundary layer interactions in scramjet inlets p 13 A90-12586
Investigation of cowl vent slots for supercritical stability enhancement in dual-mode ramjet inlets p 507 A90-32951
- WHITE, MICHAEL**
Airworthiness and flight characteristics evaluation of the McDonnell Douglas Helicopter Corporation (MDHC) 530FF helicopter
[AD-A218253] p 498 N90-20076
- WHITE, R. G.**
Developments in the acoustic fatigue design process for composite aircraft structures p 882 A90-48047
- WHITE, RICHARD P., JR.**
Landing gear integrity - The bottom line of aircraft safety p 180 A90-17408
- WHITE, ROLAND J.**
Effect of wind shear on the airspeed during the airplane landing approach
[AIAA PAPER 90-2838] p 754 A90-45160
- WHITEHEAD, D. S.**
Flutter of turbine blades p 41 A90-11794
A finite element solution of unsteady two-dimensional flow in cascades p 226 A90-21946
- WHITELAW, J. H.**
Experiments are telling you something (Stewartson Memorial Lecture) p 144 A90-16752
Instrumentation for combustion and flow in engines; Proceedings of the NATO Advanced Study Institute, Vimeiro, Portugal, Sept. 13-26, 1987 p 211 A90-19004
Combustion oscillations in ducts p 204 A90-19006
Combustion characteristics of a model can-type combustor p 676 A90-40479
- WHITFIELD, C. E.**
High speed turboprop aeroacoustic study (counterrotation). Volume 1: Model development
[NASA-CR-185241] p 782 N90-26633
- WHITFIELD, DAVID L.**
Counterrotating prop-fan simulations which feature a relative-motion multiblock grid decomposition enabling arbitrary time-steps
[AIAA PAPER 90-0687] p 169 A90-19978
- Computation of transonic flow about stores
[AD-A210402] p 18 N90-10009
- WHITFIELD, KENNETH W.**
Onboard maintenance system testing - The Boeing 747-400 Central Maintenance Computer
[AIAA PAPER 90-1303] p 505 A90-33917
- WHITFIELD, R. T.**
Aircraft cabin fire suppression by means of an interior water spray system
[CAA-PAPER-88014] p 96 N90-11719
- WHITFORD, RAY**
Design of a close-support aircraft
[AIAA PAPER 90-3241] p 835 A90-48849
- WHITMORE, STEPHEN A.**
Preliminary results from a subsonic high-angle-of-attack flush airdata sensing (HI-FADS) system - Design, calibration, algorithm development, and flight test evaluation
[AIAA PAPER 90-0232] p 187 A90-19746
Compensating for pneumatic distortion in pressure sensing devices
[AIAA PAPER 90-0631] p 211 A90-19956
Preliminary results from a subsonic high angle-of-attack flush airdata sensing (HI-FADS) system: Design, calibration, and flight test evaluation
[NASA-TM-101713] p 339 N90-16758
Compensating for pneumatic distortion in pressure sensing devices
[NASA-TM-101716] p 415 N90-19224
Experimental characterization of the effects of pneumatic tubing on unsteady pressure measurements
[NASA-TM-4171] p 850 N90-27703
- WHITMORE, STEPHEN ANTHONY**
Formulation and verification of a technique for compensation of pneumatic attenuation errors in airborne pressure sensing devices p 369 N90-17084
- WHITTAKER, R. W.**
High Mach exhaust system concept scale model test results
[AIAA PAPER 90-1905] p 655 A90-40552
- WHORTON, MARK S.**
UH-60 flight data replay and replay system state estimator analysis
[AIAA PAPER 90-0181] p 197 A90-19723
- WICHMANN, G. R.**
The aerodynamic assistant
[AIAA PAPER 89-3132] p 75 A90-10608
- WIDDER, PATRICIA A.**
Data base correlation issues p 459 A90-30740
- WIDIG, KURT**
Slipstream-induced pressure fluctuations on a wing panel p 77 A90-11004
- WIE, YONG-SUN**
Numerical solution of the boundary-layer equations for a general aviation fuselage
[AIAA PAPER 90-0305] p 163 A90-19786
- WIECK, TIMOTHY D.**
Effect of riblets on flow separation from a cylinder and an airfoil in subsonic flow
[AD-A216197] p 319 N90-17574
- WIEDERMANN, A.**
Two-dimensional transonic flow field analysis with different turbulence models p 150 A90-16846
- WIEDERMANN, ALEXANDER**
The aerodynamic design of the contraction for a subsonic wind tunnel p 907 A90-51545
- WIEGERS, F. A.**
Safety management in aircraft testing and certification p 180 A90-17421
- WIELDT, J. A.**
Nonflammable hydraulic power system for tactical aircraft. Volume 1: Aircraft system definition, design and analysis
[AD-A218493] p 671 N90-23409
- WIERCINSKI, Z.**
The influence of the wake structure on the dynamic blade load p 6 A90-11785
- WIESEMAN, CAROL**
Development and testing of methodology for evaluating the performance of multi-input/multi-output digital control systems
[AIAA PAPER 90-3501] p 867 A90-47747
- WIESEMAN, CAROL D.**
Development and testing of methodology for evaluating the performance of multi-input/multi-output digital control systems
[NASA-TM-102704] p 846 N90-27699
- WIETING, ALLAN R.**
The critical role of aerodynamic heating effects in the design of hypersonic vehicles p 155 A90-18249
- WIJCHERS, T.**
Combustion of PMMA, PE, and PS in a ramjet p 764 A90-43670
Solid fuel combustion chamber
[LR-634] p 939 N90-29433
- WIKOFF, DENNIS**
Drag reduction by controlling flow separation using stepped afterbodies p 622 A90-40690
- WILBER, GEORGE F.**
Embedded knowledge based avionics
[AIAA PAPER 89-3141] p 75 A90-10615
- WILBUR, MATTHEW L.**
Reduction of blade-vortex interaction noise through higher harmonic pitch control p 377 A90-23937
Performance data from a wind-tunnel test of two main-rotor blade designs for a utility-class helicopter
[NASA-TM-4183] p 499 N90-20974
- WILBY, J. F.**
Noise transmission into propeller-driven airplanes p 614 N90-22364
- WILCOX, FLOYD J., JR.**
Passive venting technique for shallow cavities
[NASA-CASE-LAR-14031-1] p 499 N90-20079
- WILDER, MICHAEL C.**
Blade-vortex interaction experiments - Velocity and vorticity fields
[AIAA PAPER 90-0030] p 312 A90-26903
- WILFORD, S. P.**
The effect of primer age on adhesion of polysulphide sealant p 269 N90-15909
- WILGUS, J.**
Categorization and performance analysis of advanced avionics algorithms on parallel processing architectures p 461 A90-30786
- WILKEN, IRIS E.**
The North American Rockwell XFV-12A - Reflections and some lessons
[AIAA PAPER 90-3240] p 839 A90-49118
- WILKERSON, DAVE**
NASA/USRA high altitude reconnaissance aircraft
[NASA-CR-186685] p 650 N90-24266
- WILKERSON, JOSEPH**
High-speed rotorcraft V/STOL - An initial assessment p 829 A90-46938
Advanced rotorcraft V/STOL - Technology needs for high-speed rotorcraft
[AIAA PAPER 90-3298] p 837 A90-48880
- WILKIE, W. KEATS**
Experimental transonic flutter characteristics of supersonic cruise configurations
[AIAA PAPER 90-0979] p 390 A90-29369
- WILKINSON, E. T.**
Computer-based tools for assisting air traffic controllers with arrivals flow management
[RSRE-88001] p 178 N90-13366
- WILKINSON, S. P.**
Design and operational features of low-disturbance wind tunnels at NASA Langley for Mach numbers from 3.5 to 18
[AIAA PAPER 90-1391] p 594 A90-37936
- WILL, DAVID**
Comparison of active control on a servo flap rotor using fixed system and rotating system parameters p 862 A90-46976
- WILLAN, U.**
Knowledge based diagnosis of jet engines under consideration of model based methods p 855 N90-27631
- WILLIAMS-STUBER, K.**
Transition from order to chaos in the wake of an airfoil p 474 A90-33506
- WILLIAMS, B. R.**
Further work on aerofoils at Reynolds numbers between 3 x 10 to the 5th and 1 x 10 to the 6th p 145 A90-16758
- WILLIAMS, BEN R.**
Hot gas ingestion characteristics and flow visualization of a vectored thrust STOVl concept
[NASA-TM-103212] p 751 N90-26009
- WILLIAMS, D. R.**
Proportional control of asymmetric forebody vortices with the unsteady bleed technique
[AIAA PAPER 90-1629] p 591 A90-38758
- WILLIAMS, DENA G.**
Critical inspection of high performance turbine engine components: The RFC concept p 859 N90-28073
- WILLIAMS, F. H.**
An interfacing solution for real-time avionics development
[SAE PAPER 892357] p 738 A90-45508
- WILLIAMS, J. C.**
Titanium aluminides for advanced aircraft engines p 874 A90-49000
- WILLIAMS, M.**
An analysis methodology for internal swirling flow systems with a rotating wall
[ASME PAPER 89-GT-185] p 361 A90-23863
- WILLIAMS, M. H.**
Time domain simulations of a flexible wing in subsonic, compressible flow
[AIAA PAPER 90-1153] p 390 A90-29365

WILLIAMS, M. SUSAN

Experience with strain-gage balances for cryogenic wind tunnels p 264 N90-15958

WILLIAMS, MARC H.

Propeller-wing interaction using a frequency domain panel method p 307 A90-26128

Three dimensional full potential method for the aeroelastic modeling of propfans [AIAA PAPER 90-1120] p 393 A90-29392

Temporal-adaptive Euler/Navier-Stokes algorithm for unsteady aerodynamic analysis of airfoils using unstructured dynamic meshes [AIAA PAPER 90-1650] p 569 A90-38778

Counter-rotating propellant analysis using a frequency domain panel method p 623 A90-40937

An alternative derivation for an integral equation for linearized subsonic flow over a wing [AD-A214140] p 236 N90-15079

An unsteady lifting surface method for single rotation propellers [NASA-CR-4302] p 719 N90-25940

WILLIAMS, MARK
Rotary servohinge actuator [SAE PAPER 89-2261] p 733 A90-45458

WILLIAMS, P. M.
Cleaner superalloys via improved practices p 442 A90-29707

WILLIAMS, R. D.
Digital control of magnetic bearings supporting a multimass flexible rotor p 682 A90-40712

WILLIAMS, R. J.
Prediction and measurement of rotor blade/stator vane dynamic characteristics of a modern aero-engine axial compressor p 878 A90-46036

Prediction and measurement of rotor blade/stator vane dynamic characteristics of a modern aero-engine axial compressor [PNR90667] p 750 N90-26002

WILLIAMS, S. L.
Navier-Stokes methods to predict circulation control airfoil performance [AIAA PAPER 90-0574] p 167 A90-19924

WILLIAMS, STEVEN P.
Stereopsis cueing effects on hover-in-turbulence performance in a simulated rotorcraft [NASA-TP-2980] p 506 N90-21004

WILLIAMS, W.
Effects of an embedded vortex on injectant from a single film-cooling hole in a turbulent boundary layer [ASME PAPER 89-GT-189] p 362 A90-23867

WILLIAMSON, A.
In-situ measurement, modelling and control of the imidization reaction in PMR-15 p 941 A90-50066

WILLIAMSON, THOMAS
Development and operation of the Traffic Alert and Collision Avoidance System (TCAS) p 331 A90-25573

WILLIAMSON, WALTON E., JR.
Hypersonic flight testing p 245 A90-21171

WILLIFORD, R. E.
Stochastic propagation of an array of parallel cracks: Exploratory work on matrix fatigue damage in composite laminates [DE89-017837] p 126 N90-11813

WILLIS, EDWARD A.
Performance of a supercharged direct-injection stratified-charge rotary combustion engine [NASA-TM-103105] p 748 N90-25982

WILLSHIRE, WILLIAM L., JR.
PTA en route noise measurements p 696 N90-24855

WILMS, H. R.
Multichannel on-board load and fatigue monitoring p 849 N90-27621

WILSON, ALAN J.
The safety analysis approach for the EH101 p 635 A90-42456

WILSON, ANTHONY
Floor pull test of a transport airframe section [DOT/FAA/CT-TN88/14] p 497 N90-20072

WILSON, D. J.
Unified flying qualities criteria for longitudinal tracking [AIAA PAPER 90-2806] p 752 A90-45141

WILSON, D. R.
Development of the UTA hypersonic shock tunnel [AIAA PAPER 90-0080] p 200 A90-19675

WILSON, D. W.
Domestic precursor technology - A unique route to current and future generation carbon fibers p 940 A90-50057

WILSON, DALE A.
Design and fabrication considerations for composite structures with embedded fiber optic sensors p 536 A90-32871

WILSON, DAVID GORDON

The effect of the magnitude of the inlet-boundary disturbance on the unsteady forces on axial gas-turbine blades p 6 A90-11781

WILSON, DAVID J.

High angle of attack flying qualities criteria [AIAA PAPER 90-0219] p 197 A90-19738

Development of high angle of attack flying qualities criteria using ground-based manned simulators p 433 A90-30717

WILSON, DONALD E.
Contamination of cabin air by synthetic oil and breakdown products [SAE PAPER 891455] p 323 A90-27424

WILSON, DONALD R.
Development and calibration of a continuous-flow arc-heated hypersonic wind tunnel [AIAA PAPER 90-1381] p 594 A90-37930

WILSON, GREGORY J.
Modeling supersonic combustion using a fully-implicit numerical method [AIAA PAPER 90-2307] p 677 A90-42117

WILSON, J. R.
Caring for the elderly jet p 285 A90-24280

Air combat beyond the stall p 589 A90-35888

WILSON, JAMES
Aviation meteorology - Panel report p 692 A90-39403

WILSON, K. J.
Supersonic rectangular isothermal shrouded jets [AIAA PAPER 90-2028] p 621 A90-40599

Multistep dump combustor design to reduce combustion instabilities p 659 A90-40934

Active combustion control in a coaxial dump combustor [AIAA PAPER 90-2447] p 743 A90-42806

WILSON, R. B.
Advanced applications of BEM to gas turbine engine structures p 772 A90-45769

WILSON, R. D.
Development of pressure containment and damage tolerance technology for composite fuselage structures in large transport aircraft [NASA-CR-3996] p 63 N90-10186

WILSON, W. W.
Applying qualitative knowledge to aircraft engine system design p 694 A90-41189

WILTON, STEPHEN A.
Gearbox system design for ultra-high bypass engines [AIAA PAPER 90-2152] p 685 A90-42048

WINDECK, THEO
Experimental windtunnel studies for EFA p 672 A90-41113

WINDLEY, R. O.
Gas turbine combustion - A personal perspective p 283 A90-20604

WINFIELD, JAMES
Simple marching-vortex model for two-dimensional unsteady aerodynamics p 395 A90-31288

WINFREE, WILLIAM P.
Advanced NDE techniques for quantitative characterization of aircraft p 886 N90-28088

WINGROVE, R. C.
Analysis of severe atmospheric disturbances from airline flight records p 280 N90-15045

WINKEL, J.
Description of the MARC measuring system [FEL-89-B170] p 963 N90-28887

WINKEL, J. D.
Improved fiber reinforced polyphenylene sulfide thermoplastic composites p 947 A90-50180

WINKELMANN, ALLEN E.
Design of a three-component wall-mounted balance [AIAA PAPER 90-1397] p 595 A90-37940

Flow field studies behind a wing at low Reynolds numbers [AIAA PAPER 90-1471] p 563 A90-38628

WINKLER, JOHANNES
The jet engine: 1932 [ISBN-3-922010-49-0] p 763 N90-25189

WINKLER, P.-J.
Production of Ti6Al4V-components for a new turbo-fan engine p 132 A90-16618

WINN, ALLAN
Water borne again p 579 A90-35846

WINTER, CARL-JOCHEN
Hydrogen propulsion and the next century - A challenge that raises questions and problems p 266 A90-21774

Materials and structures for 2000 and beyond: An attempted forecast by the DLR Materials and Structures Department [ESA-TT-1154-REV] p 775 N90-26173

WINTER, FRANK H.
'Black Betsy' - The 6000C-4 rocket engine, 1945-1989. [IAF PAPER 89-726] p 141 A90-13700

WINTER, HEINZ

Flight test engineering with the ATTAS p 902 N90-29160

WINTER, JOACHIM

Active control system for gust load alleviation and structural damping p 259 N90-15056

WINTERMANTEL, ERICH

Fibre reinforced thermoplastic integral constructions in modular build-up technology - The 'thermoplastic in-situ-technique' p 534 A90-31879

WINZELL, B.

Applications of the unsteady full potential equation for wings p 472 A90-33358

WIRKANDER, SVEN-LENNART

A study of terrain following systems and the creation of flight paths for terrain following vehicles [FOA-C-20774-2.5] p 827 N90-27691

WIRZ-SAFRANEK, DEBRA L.

Thermoplastic composite fighter forward fuselage p 81 A90-14659

WISE, GLENN L.

Safety and health trends in aerospace composite materials p 947 A90-50188

WISLER, D. C.

Boundary-layer transition and separation on a turbine blade in a plane cascade [AIAA PAPER 90-2263] p 625 A90-42102

WISSER, THOMAS

LOLAN C stability integrity assurance [AD-A212663] p 177 N90-13364

WITHERELL, CHARLES E.

Analysis of damaged components from DOE security helicopter N7EG [DE90-004488] p 324 N90-16729

WITHERS, C. C.

Proplan Test Assessment (PTA): Flight test report [NASA-CR-182278] p 113 N90-11738

Proplan Test Assessment (PTA) [NASA-CR-185138] p 113 N90-11739

WITKOWSKI, D.

Propeller wakes and their interaction with wings p 14 A90-12614

WITT, M.

An investigation of solid-fuel, dual-mode combustion ramjets p 859 N90-27933

WITTE, D. W.

Aerodynamic heat transfer testing in hypersonic wind tunnels using an infrared imaging system [AIAA PAPER 90-0189] p 350 A90-25027

WITTE, J.

Fast calculation of root loci of aeroelastic systems and of gust response in time domain p 517 A90-33413

WITTEKINDT, W.

Mathematical formulation of blade surfaces in turbomachinery. I - Theoretical surface formulations [ASME PAPER 89-GT-160] p 360 A90-23848

Mathematical formulation of blade surfaces in turbomachinery. II - Practical examples of determined surfaces [ASME PAPER 89-GT-161] p 361 A90-23849

WITTENBERG, ART M.

Robotic dry stripping of airframes - Phase II [SAE PAPER 890926] p 365 A90-24691

WITTENBERG, ARTHUR M.

New aircraft cabin and cargo flammability standards for transport category aircraft p 325 N90-17589

WITTENBERG, H.

Aircraft propulsion: Leading the way in aviation [LR-532] p 194 N90-13395

Solid fuel combustion chamber [LR-634] p 939 N90-29433

WITTLIN, G.

Transport composite fuselage technology: Impact dynamics and acoustic transmission [NASA-CR-4035] p 126 N90-11821

WITTLIN, GIL

The effect of aircraft size on cabin floor dynamic pulses [DOT/FAA/CT-88/15] p 735 N90-25136

WITTLÖV, ARNE

Swedish philosophy in aeroengine development p 44 A90-12504

WITTMANN, MANFRED

Objectives and results of cabin fire research in Germany p 325 N90-17588

WITTY, PETER

The MANTA: An RPV design to investigate forces and moments on a lifting surface [NASA-CR-186227] p 499 N90-20971

WITZE, P. O.

Instrumentation for combustion and flow in engines; Proceedings of the NATO Advanced Study Institute, Vimeiro, Portugal, Sept. 13-26, 1987 p 211 A90-19004

- WIXTED, JOHN J.**
Applications of digital image processing in testing and evaluation of composite materials
[AD-A22939] p 874 N90-26887
- WLEZIEN, R. W.**
Supersonic jet noise reduction by a porous single expansion ramp nozzle
[AIAA PAPER 90-0366] p 219 A90-19815
- WLEZIEN, RICHARD W.**
The sensitivity of near-field acoustics to the orientation of twin two-dimensional supersonic nozzles
[AIAA PAPER 90-2149] p 625 A90-42045
- WO, ANDREW**
Unsteady streamlines near the trailing edge of NACA 0012 airfoil at a Reynolds number of 125,000
p 155 A90-18158
- WO, ANDREW M.**
On the effects of wind tunnel turbulence on steady and unsteady airfoil characteristics p 147 A90-16777
Unsteady aerodynamics of Wortmann FX63-137 airfoil at low Reynolds numbers p 801 A90-46374
- WOCHHOLZ, H. F.**
The evolution of design/development requirements for avionics/mission equipment (MEP) insertion
p 846 A90-46932
- WOELTJEN, DONALD**
Design of a low cost short takeoff-vertical landing export fighter/attack aircraft
[NASA-CR-186658] p 734 N90-25132
- WOHL, ROBERT A.**
Developing the Canadair Regional Jet airliner
p 729 A90-42656
- WOJCIK, LEONARD A.**
Probabilistic risk assessment and aviation system safety p 322 A90-26231
- WOLF, CHRIS**
Analytical studies for computed center line operations
[SAE PAPER 892219] p 729 A90-45436
- WOLF, CHRISTOPHER J.**
Helicopter surface maneuvering test results
[ACD-330] p 59 N90-10897
Analysis of distributions of Visual Meteorological Conditions (VMC) helicopter data
[DOT/FAA/CT-TN89/67] p 544 N90-21508
Position computation without elevation information for computed centerline operations
[DOT/FAA/CT-TN89/42] p 640 N90-23379
Helicopter visual approach surface high temperature and high altitude tests
[DOT/FAA/CT-TN89/34] p 825 N90-27675
- WOLF, STEPHEN**
An experimental AWTs process and comparisons of ONERA T2 and 0.3-m TCT AWTs data for the ONERA CAST-10 aerofoil p 321 N90-17653
- WOLF, STEPHEN W. D.**
Supersonic wind tunnel nozzles: A selected, annotated bibliography to aid in the development of quiet wind tunnel technology
[NASA-CR-4294] p 762 N90-26019
- WOLF, T.**
On the possibilities for improvement and modernization of subsonic wind tunnels
[AIAA PAPER 90-1423] p 596 A90-37960
- WOLFE, R. E.**
The acute, delayed neurotoxicity evaluation of two jet engine oil formulations
[AD-A222018] p 875 N90-26972
- WOLFF, JAMES M.**
Viscous oscillating cascade aerodynamics and flutter by a locally analytical method
[AIAA PAPER 90-0579] p 168 A90-19929
- WOLFRUM, H.**
Applications of LIF to high speed flows
p 911 N90-29320
- WOLFSHTEIN, MICHA**
A method for solving three-dimensional viscous incompressible flows over slender bodies
p 558 A90-37890
- WOLKOVITCH, JULIAN**
Application of the joined wing to tiltrotor aircraft
[NASA-CR-177543] p 248 N90-15093
- WOLVERTON, DAVID A.**
Advanced transport operating system software upgrade: Flight management/flight controls software description
[NASA-CR-181936] p 893 N90-28366
- WOLZ, R. R.**
Requirements for business jet aircraft
[AIAA PAPER 90-2038] p 644 A90-41991
- WONACOTT, G. D.**
Design and fabrication of a prototype resin matrix composite interceptor structure
[AIAA PAPER 90-1004] p 442 A90-29275
- WONG, E. W.**
Generalized Advanced Propeller Analysis System (GAPAS). Volume 2: Computer program user manual
[NASA-CR-185277] p 933 N90-29394
- WONG, JAMES M. H.**
RISC lifting off in avionics
[AIAA PAPER 89-2967] p 73 A90-10483
- WONG, LANWAI**
Gas identification system using graded temperature sensor and neural net interpretation
[AD-A213359] p 205 N90-13627
- WONG, RICHARD**
Durability and damage tolerance of graphite/epoxy honeycomb structures p 942 A90-50085
- WONG, TIN-CHEE**
Prediction of steady and unsteady asymmetric vortical flows around cones p 168 A90-19940
Computational study for passive control of supersonic asymmetric vortical flows around cones
[AIAA PAPER 90-1581] p 566 A90-38718
- WOOD, G. R.**
The design and test of a two stage transonic axial flow compressor
[ASME PAPER 89-GT-164] p 341 A90-23852
- WOOD, JERRY R.**
Laser anemometer measurements in a transonic axial-flow fan rotor
[NASA-TP-2879] p 73 N90-11245
- WOOD, M. E.**
The design and development of an acoustic test section for the ARA transonic wind tunnel
[PNR90574] p 140 N90-13202
- WOOD, M. L.**
Propagation of Mode S beacon signals on the airport surface p 241 A90-21381
- WOOD, MARYLYN E.**
Application of experimental techniques to store release problems p 316 N90-17545
- WOOD, N. J.**
An investigation of asymmetric vortical flows over delta wings with tangential leading-edge blowing at high angles of attack
[AIAA PAPER 90-0103] p 227 A90-22167
Control of asymmetric vortical flows over delta wings at high angles of attack p 553 A90-35759
Control of vortex aerodynamics at high angles of attack p 921 N90-28523
- WOOD, R. LEE**
Design and fabrication considerations for composite structures with embedded fiber optic sensors
p 536 A90-32871
- WOOD, RICHARD M.**
Leading- and trailing-edge flaps on supersonic delta wings p 233 A90-23285
- WOOD, TOMMIE L.**
Maneuver performance comparison between the XV-15 and an advanced tiltrotor design p 518 A90-33622
- WOODFIELD, A. A.**
Classification of windshear severity p 281 N90-15049
- WOODS, E. J.**
Electrical power systems for high Mach vehicles
p 586 A90-38129
- WOODS, JESSICA A.**
NASA investigation of a claimed 'overlap' between two gust response analysis methods p 771 A90-44730
Parametric aeroelastic stability analysis of a generic X-wing aircraft p 731 A90-44737
- WOODWARD, D. S.**
Priorities for high-lift testing in the 1990s
[AIAA PAPER 90-1413] p 596 A90-37950
- WOODWARD, DONALD E.**
An AEW metalclad airship
[AIAA PAPER 89-3158] p 244 A90-20579
- WOODWARD, RICHARD P.**
Noise of a simulated installed model counterrotation propeller at angle-of-attack and takeoff/approach conditions
[AIAA PAPER 90-0283] p 547 A90-32505
Comparison between design and installed acoustic characteristics of NASA Lewis 9- by 15-foot low-speed wind tunnel acoustic treatment
[NASA-TP-2996] p 440 N90-19242
Noise of a simulated installed model counterrotation propeller at angle-of-attack and takeoff/approach conditions
[NASA-TM-102440] p 548 N90-20794
- WORDEHOFF, J.**
Onboard fire- and explosion suppression for fighter aircraft p 327 N90-17602
- WORNOM, STEPHEN F.**
Relative efficiency and accuracy of two Navier-Stokes codes for simulating attached transonic flow over wings
[AIAA PAPER 90-3078] p 795 A90-45909
- WORSLEY, M. F.**
A real-time wind model using digital data from aircraft
[RSRE-MEMO-4309] p 137 N90-13005
- WORTH, E.**
Application of 3-D viscous code in the design of a high performance compressor
[AIAA PAPER 90-1914] p 740 A90-42694
- WRAY, A. P.**
The performance of a combustor pre-diffuser incorporating compressor outlet guide vanes
[AIAA PAPER 90-2165] p 661 A90-42053
- WRENN, GREGORY A.**
Comparison of equivalent plate and finite element analysis of a realistic aircraft structural configuration
[AIAA PAPER 90-3293] p 837 A90-48877
Multilevel decomposition approach to the preliminary sizing of a transport aircraft wing
[NASA-CR-4296] p 583 N90-22557
Aircraft design for mission performance using nonlinear multiobjective optimization methods
[NASA-CR-4328] p 925 N90-29384
- WRIGHT, H.**
National aero-spaceplane status and plans
p 337 N90-16801
- WRIGHT, J. R.**
Application of time domain decomposition techniques to aircraft ground and flutter test data
p 491 A90-33373
- WRIGHT, JAMES A.**
Vision guidance update - Synthetic aperture radar (SAR) multiple image exploitation for position and velocity determination p 488 A90-34140
- WRIGHT, JOSEPH**
Full-scale air transport category fuselage burnthrough tests
[DOT/FAA/CT-TN89/65] p 486 N90-20967
- WRIGHT, KENNETH E.**
Computer integrated quality assurance for robotic workcells in aerospace manufacturing
[SME PAPER MS89-152] p 283 A90-23681
- WRIGHT, P. K.**
Application of advanced materials to aircraft gas turbine engines
[AIAA PAPER 90-2281] p 764 A90-42769
- WRIGHT, R. E., JR.**
In-flight flow visualization using infrared imaging
p 731 A90-44731
- WRIGHT, TERRY**
Blade sweep for low-speed axial fans
[ASME PAPER 89-GT-53] p 289 A90-23779
- WROBLEWSKI, PETER**
Design considerations for achieving MLS Category III requirements p 331 A90-25575
- WROBLEWSKI, W.**
The solution of the unsteady transonic flow through a blade passage in an axial turbine p 5 A90-11777
- WROBLEWSKI, WLODZIMIERZ**
Numerical solution of 2-D transonic flow through an axial turbine stage p 814 A90-49464
- WU, CHIHUA**
Study on process control of aeroengine using microcomputer p 586 A90-37239
- WU, CHUNG-HUA**
Analyses of full 3D S1-S2 iterative solution in CAS transonic compressor rotor and comparison with quasi-3D S1-S2m iterative solution and L2F measurement
p 157 A90-18532
- WU, DAVID**
Induced drag based on leading edge suction for a helicopter in forward flight p 232 A90-23102
- WU, DINGYI**
Prediction of heat transfer coefficient on turbine blade profiles p 423 A90-29904
- WU, DONG-NAN**
Algorithm for simultaneous stabilization of single-input systems via dynamic feedback p 462 A90-31108
- WU, ERPING**
Exhaust emission performance of a vaporizer tube combustor as compared with a single tube combustor
p 111 A90-14614
- WU, GIIN YUAN**
Structure analysis of burning liquid-fueled spray in a confined combustor
[AIAA PAPER 90-2444] p 677 A90-42174
- WU, GUOHUA**
A relaxation method for transonic potential flows through 2-D cascade with large camber angle
p 152 A90-17786
- WU, J. C.**
A numerical study of general viscous flows around multi-element airfoils
[AIAA PAPER 90-0572] p 167 A90-19922
A numerical method for three-dimensional viscous flows
[AIAA PAPER 90-0236] p 228 A90-22186
- WU, J. L.**
Instabilities of supersonic shear flows
[AIAA PAPER 90-0712] p 314 A90-26983

WU, J. M.

The water tunnel test of delaying vortex breakdown over a delta wing using supplements p 2 A90-10346
Vortical sources of aerodynamic force and moment [SAE PAPER 892346] p 715 A90-45498

WU, J. Z.

Vortical sources of aerodynamic force and moment [SAE PAPER 892346] p 715 A90-45498

WU, KUEN-CHUAN

Multigrid acceleration of TVD schemes in transonic Euler flow calculation p 908 A90-52030

WU, LIYI

Computations of unsteady transonic flows about thin airfoils by integral equation method p 158 A90-18609

WU, QIFEN

The numerical method for solving the high Reynolds hypersonic viscous shock layer p 2 A90-10340

WU, S.-M.

Experimental and theoretical investigations of turbulent flow in a side-inlet rectangular combustor p 421 A90-27959

WU, WENQUAN

Analysis and calculation for interaction between shock wave and laminar boundary layer p 909 A90-52778

WU, XIAOLU

Unsteady aerodynamics and aeroelasticity of turbomachines and propellers; Proceedings of the Fifth International Symposium, Beijing, People's Republic of China, Sept. 18-21, 1989 p 853 A90-49451

WU, XUANZHANG

Fracture morphology of toughened bismaleimide/carbon fiber composites p 948 A90-50205

WU, YAOHUA

An orthogonal algorithm to the maximum likelihood estimation using an efficient method for computing sensitivities [AIAA PAPER 90-3507] p 891 A90-47753

WU, YIZHAO

Galerkin finite element method for transonic flow about airfoils and wings p 396 A90-31486

WU, ZIZHONG

The analysis and solution of the performance deterioration problem of WP7 engine under the full reheating condition p 191 A90-18624

WUNSCHER, ALFRED J., JR.

Final results of the NASA storm hazards program p 819 A90-49834

WUORI, ALBERT F.

Improving snow roads and airstrips in Antarctica [AD-A211588] p 133 N90-11907

WUSK, MICHAEL S.

Flight-measured streamwise disturbance instabilities in laminar flow [AIAA PAPER 90-1283] p 495 A90-33904

WYATT, G. H.

Application of boundary layer control to HSCT low speed configuration [AIAA PAPER 90-3199] p 812 A90-49103

WYBIERALA, MICHEL

Performances and new surveillance possibilities in SSR - Mode S p 639 A90-41036

WYGNANSKI, I.

Low Reynolds number airfoils evaluation program p 151 A90-17692

WYNDHAM, B. A.

Fine resolution errors in secondary surveillance radar altitude reporting amongst aircraft transmitting the conspicuity codes 4321 and 4322 [RSRE-88004] p 135 N90-12816

WYNDHAM, BRIAN A.

The automatic detection of anti-collision lights [RSRE-MEMO-4272] p 240 N90-15896

WYNOSKY, T. A.

Energy Efficient Engine program advanced turbofan nacelle definition study [NASA-CR-174942] p 930 N90-28560

X

XERICOS, J.

Measurement of mean and fluctuating flow properties in hypersonic shear layers [AIAA PAPER 90-1409] p 560 A90-38488

XIANG, YANSUN

The numerical simulation of the low speed aerodynamic characteristics of a set of close-coupled canard configurations p 396 A90-31485

XIAO, SHUNDA

The research of cubic spline optimal terrain following system p 186 A90-18584
Concise design of aircraft longitudinal model reference adaptive command augmentation system p 345 A90-24002

XIAO, X. R.

Repair of thermoplastic composite structures by fusion bonding p 941 A90-50060

XIAO, YELUN

Digital generation of two-dimensional field of turbulence for flight simulation p 611 A90-36427

XIE, YONGHUA

The investigation of stress at an enter-gas nozzle of main landing gears for fighter aeroplanes p 181 A90-18606

XU, EJUN

An analysis of cavity resonance in the aeroengine casing during rig testing p 894 A90-49481

XU, GENE

Iterative algorithm for correlation of strain gauge data with aerodynamic load p 709 A90-44739

XU, JINFENG

Analyses of revising the inlet profile of a radial inflow turbine impeller p 602 A90-35831

XU, JINGZHONG

Research on film-cooling of turbine blade p 190 A90-17795

XU, L.

The trailing edge loss of transonic turbine blades [ASME PAPER 89-GT-278] p 475 A90-33564

XU, LIPING

The influence of the inlet Mach number on the boundary layer development on turbomachinery blade surfaces p 621 A90-40504

XU, MING

Gear vibration control with viscoelastic damping material in aeroengine p 451 A90-29911

XU, RUIJUAN

Longitudinal stability analysis for deformable aircraft p 867 A90-48514

XU, WENYUAN

Influence of blade leaning on the flow field behind turbine rectangular cascades with different incidences and aspect ratios p 11 A90-12519

XU, XIN YU

The response of helicopter to dispersed gust p 670 A90-42470

XU, XIN-YU

The influence of the inertia coupling on the stability and control of the helicopter and the response of helicopter gust p 671 A90-42472

XU, XINYU

The induced velocity distribution and the flap-pitch-torsion coupling on the stability and control of the helicopter in flight condition with lateral velocity p 196 A90-18633

XU, YONGLIN

Reflection by defective diffusion bonds [AD-A212995] p 206 N90-13638

XUE, DAVID Y.

Finite element two-dimensional panel flutter at high supersonic speeds and elevated temperature [AIAA PAPER 90-0982] p 450 A90-29372

Y

YADLIN, YORAM

Block multigrid implicit solution of the Euler equations of compressible fluid flow [AIAA PAPER 90-0106] p 162 A90-19684

YAGER, THOMAS J.

Aircraft and ground vehicle friction measurements obtained under winter runway conditions [SAE PAPER 891070] p 95 A90-14367

YAGER, THOMAS J.

Current status of Joint FAA/NASA Runway Friction Program [SAE PAPER 892340] p 760 A90-45494

Evaluation of two transport aircraft and several ground test vehicle friction measurements obtained for various runway surface types and conditions. A summary of test results from joint FAA/NASA Runway Friction Program [NASA-TP-2917] p 249 N90-15902

An overview of the joint FAA/NASA aircraft/ground runway friction program [NASA-TM-103486] p 724 N90-25957

YAJNIK, K. S.

Axisymmetric afterbody flow separation at transonic speeds in presence of jet exhaust p 13 A90-12576
Underexpanded jet-freestream interactions on an axisymmetric afterbody configuration p 154 A90-18141

YAMADA, H.

Hydrogen fueled subsonic-ram-combustor model tests for an air-turbo-ram engine p 44 A90-12529

YAMADA, HIROYA

An experimental study of a turbulent jet impinging on a wedge p 553 A90-35274

YAMADA, YUKIO

Current status of ceramic gas turbine R&D in Japan [ASME PAPER 89-GT-114] p 359 A90-23818

YAMAGISHI, KIICHIRO

Current status of ceramic gas turbine R&D in Japan [ASME PAPER 89-GT-114] p 359 A90-23818

YAMAGUCHI, KEIKO

Modeling of surface roughness effects on glaze ice accretion p 485 N90-20925

YAMAGUCHI, NOBUYUKI

Rotor-blades excitation due to differential interference of vane wakes between upstream stator-rows in an axial compressor p 6 A90-11784

YAMAGUCHI, YUTAKA

Instrumentation and operation of NDA cryogenic wind tunnel p 437 A90-28293

YAMAKAWA, GEORGE M.

Preliminary airworthiness evaluation of the RC-12K [AD-A219545] p 648 N90-23387

YAMAMOTO, K.

Self-excited oscillation of shock waves on an airfoil in two-dimensional transonic channel flow p 8 A90-11808

A bearing error in the VHF omnirange due to sea surface reflection p 402 A90-27875

YAMAMOTO, K. J.

Supersonic jet noise reduction by a porous single expansion ramp nozzle [AIAA PAPER 90-0366] p 219 A90-19815

YAMAMOTO, KAZUOMI

Self-excited oscillation of transonic flow around an airfoil in two-dimensional channel [ASME PAPER 89-GT-58] p 290 A90-23784

A numerical investigation of supersonic inlet using implicit TVD scheme [AIAA PAPER 90-2135] p 621 A90-40612

YAMAMOTO, MAKOTO

Calculation of tip leakage flow with three-dimensional Euler code p 304 A90-25772

Development of a new low-Reynolds-number type Reynolds stress model and its application to a lobe mixer flow p 584 A90-35229

YAMAMOTO, S.

Numerical methods for transonic cascade flow problems p 305 A90-25796

A numerical method for solving the unsteady compressible Navier-Stokes equations p 306 A90-25827

YAMAMOTO, T.

Advanced joint of 3-D composite materials for space structure p 944 A90-50137

YAMAMOTO, YUKIMITSU

Numerical simulation of hypersonic flow around a space plane. Part 2: Application to high angles of attack flow [NAL-TR-1011T] p 570 N90-21726

YAMANAKA, KUNIASU

Development of new segment carbon seal for use at low sealing pressure region FJR710/600S turbo fan engine p 69 A90-11950

Expert diagnosis system for FJR engine troubles p 587 A90-38597

YAMANAKA, SHIGERU

Transonic flow in throat region of supersonic nozzles p 149 A90-16799

YAMANE, KOSABURO

Estimation of power spectral density of runway roughness [NAL-TR-1037] p 939 N90-29411

YAMANE, RYUICHIRO

Oscillation of circular shock wave p 557 A90-36465

YAMANE, TAKASHI

Aeroelastic tailoring analysis for preliminary design of advanced turbo propellers with composite blades p 412 A90-29395

YAMASAKI, HIROYUKI

Studies on supersonic radial flow behavior in disk channel p 87 A90-16104

YAMASAKI, NOBUHIKO

Finite element method for unsteady three-dimensional subsonic flows through a cascade oscillating with steady loading p 9 A90-11873

Numerical calculation of unsteady aerodynamic forces for three-dimensional subsonic oscillating cascades by a finite element method p 9 A90-12219

Numerical study of interaction of a jet with a supersonic cross flow p 808 A90-47300

YAMASHITA, SHINTARO

An experimental study of a turbulent jet impinging on a wedge p 553 A90-35274

YAMAUCHI, GLORIA K.

Hub loads analysis of the SA349/2 helicopter p 333 A90-23936

YAMOMOTO, O.

Structural and aerodynamic analysis of a large scale advanced propeller blade [AIAA PAPER 90-2401] p 743 A90-42793

YAN, CHUANJUN

Numerical calculation of gaseous reacting flows in a model of gas turbine combustors p 271 A90-21979

YAN, LITANG

Study on travelling wave vibration of bladed disks in turbomachinery p 423 A90-29908

YAN, WENXUAN

Unsteady aerodynamics and aeroelasticity of turbomachines and propellers: Proceedings of the Fifth International Symposium, Beijing, People's Republic of China, Sept. 18-21, 1989 p 853 A90-49451

YANAGIHARA, MASAOKI

On the interactive computer program IPIS for aircraft parameter identification [NAL-TR-1000] p 77 N90-10586

Short period control using angular acceleration feedback: Compensation for first lag servo [NAL-TM-600] p 936 N90-29399

YANASE, M.

Design and evaluation of graphite/epoxy truss core sandwich panels p 210 A90-48406

YANG, DI

An orthogonal algorithm to the maximum likelihood estimation using an efficient method for computing sensitivities [AIAA PAPER 90-3507] p 891 A90-47753

YANG, H. S.

Integration of the LTN-72 INS with the DOD GPS-3A set p 728 A90-45236

YANG, HENRY T. Y.

Mach number effects on transonic aeroelastic forces and flutter characteristics p 17 A90-13024

Aeroelastic analysis of wings using the Euler equations with a deforming mesh [AIAA PAPER 90-1032] p 391 A90-29376

Euler flutter analysis of airfoils using unstructured dynamic meshes p 602 A90-35760

YANG, J. N.

Demonstration of probabilistic-based durability analysis method for metallic airframes p 273 A90-23287

Stochastic crack growth analysis methodologies for metallic structures [AIAA PAPER 90-1015] p 449 A90-29340

YANG, J. S.

Design of aircraft wings subjected to gust loads - A system reliability approach p 958 A90-52044

YANG, J. Y.

A panel method for arbitrary moving boundaries problems p 302 A90-25284

YANG, JIANN-SHIOW

Digital controller design for the pitch axis of the F-14 using an H(infinity) method p 668 A90-40912

YANG, JINFU

A method for aerodynamic design calculation of axial gas turbine stages with cooling air mixing p 152 A90-17781

YANG, JINGFU

An experimental study of tip clearance effects on the performance of an axial transonic turbine p 189 A90-17788

YANG, JU-SUNG

System reliability optimization of aircraft wings p 923 N90-28536

YANG, KAITIAN

Numerical approaches for solving parametric vibration problems in helicopter dynamics p 182 A90-18607

YANG, KUO-CHENG

Finite element method for unsteady three-dimensional subsonic flows through a cascade oscillating with steady loading p 9 A90-11873

Numerical calculation of unsteady aerodynamic forces for three-dimensional subsonic oscillating cascades by a finite element method p 9 A90-12219

Numerical calculation of unsteady aerodynamic forces for two-dimensional supersonic oscillating cascades by finite element method p 9 A90-12238

YANG, S. Y.

Numerical investigation of airfoil/jet/fuselage-undersurface flowfields in ground effect [AIAA PAPER 90-0597] p 168 A90-19939

YANG, X. D.

A method for predicting stall flutter under variable interblade phase angle along rotating direction p 813 A90-49455

The interaction between distortion of inlet flow and blade stall flutter in axial-flow compressor p 854 A90-49466

YANG, XIAODONG

A semi-actuator disk theory for prediction of stall flutter in axial flow compressors p 301 A90-25105

YANG, XUEZHEN

Experimental investigation on the performance of an annular nozzle cascade of a highly-loaded transonic turbine stage p 152 A90-17787

YANG, YIDONG

The study of transient suppression techniques for multimode flight control system p 590 A90-37219

YANG, YONGNIAN

A numerical method for computing the aerodynamic loads on wings with sharp-edge separations at large angles of attack in subcritical transonic flows p 150 A90-16852

A unified approach to the overall body motion stability and flutter characteristics of elastic aircraft p 346 A90-25102

A numerical method in aeroelasticity for wings with separation at large angle of attack p 557 A90-37209

YANG, ZUO-SHENG

Boundary integral equations method for compressible Navier-Stokes equations p 209 A90-18262

YANG, ZUOSHENG

Galerkin finite element method for transonic flow about airfoils and wings p 396 A90-31486

Boundary integral formulation for compressible nonlinear potential and Navier-Stokes equations p 706 A90-44406

YANIK, THOMAS D.

Considerations for successful application of integrated drive generators to aircraft [SAE PAPER 892226] p 746 A90-45442

YANIV, ZVI

Performance of full color active-matrix-LCD in the cockpit environment p 681 A90-40392

YANO, HARUHISA

An experimental study of a turbulent jet impinging on a wedge p 553 A90-35274

YANTA, W. J.

Tangential mass addition for the control of shock wave/boundary layer interactions in scramjet inlets p 13 A90-12586

YANTA, WILLIAM J.

Condensation in hypersonic nitrogen wind tunnels [AIAA PAPER 90-1392] p 558 A90-37937

High speed inlet testing in the NAVSWC wind tunnels [AIAA PAPER 90-1412] p 595 A90-37949

YAO, CHENG-FAN

Analysis of blade loadings in centrifugal compressors p 158 A90-18591

YAO, FURU

Calculations of transonic flows over wing-body combinations p 395 A90-31479

YAO, Q.-H.

A modal parameter identification technique and its application to large complex structures with multiple steady sinusoidal excitation p 602 A90-35670

YAO, T.-C.

A fiber optic headset compatible with power-by-light p 504 A90-32906

YAO, YONGQING

Research on film-cooling of turbine blade p 190 A90-17795

YARAS, M.

Development of the tip-leakage flow downstream of a planar cascade of turbine blades - Vorticity field [ASME PAPER 89-GT-55] p 289 A90-23781

YARAS, M. I.

Losses in the tip-leakage flow of a planar cascade of turbine blades p 514 A90-21027

YARROW, MAURICE

Multi-processing on supercomputers for computational aerodynamics [AIAA PAPER 90-0337] p 282 A90-22199

YASHIMA, SATOSHI

Reynolds number effects on the performance of a turbofan engine [ASME PAPER 89-GT-199] p 342 A90-23871

YASUHARA, MICHIRU

Calculation of flow over airfoil with slat and flap p 149 A90-16797

A flow around airfoil with slat and flap [AIAA PAPER 90-1535] p 564 A90-38679

YASUNAGA, MASAYUKI

Airborne array antennas for satellite communication p 265 A90-23202

YATES, E. CARSON, JR.

Boundary-integral method for calculating aerodynamic sensitivities with illustration for lifting-surface theory p 806 A90-46841

Integral-equation methods in steady and unsteady subsonic, transonic and supersonic aerodynamics for interdisciplinary design [NASA-TM-102677] p 716 N90-25110

YATES, IVAN R.

Innovation and investment for survival and prosperity - The new Battle of Britain [AIAA PAPER 90-3189] p 786 A90-48826

YATES, JAMES H.

Development of obstacle clearance criteria and standards for MLS and MLS/RNAV precision approaches and development of an MLS collision risk model [SAE PAPER 892215] p 728 A90-45432

YBARRONDO, L. J.

Boeing 727-100 test project (high energy radiated field tests) [DOT/FAA/CT-88/33] p 542 N90-21247

YE, ZHENGYIN

Aeroelastic characteristics of wings in subsonic flow p 102 A90-14615

A numerical method for computing the aerodynamic loads on wings with sharp-edge separations at large angles of attack in subcritical transonic flows p 150 A90-16852

A numerical method in aeroelasticity for wings with separation at large angle of attack p 557 A90-37209

YE, ZHONG-YUAN

Preliminary analysis of methodology for assessment of propulsion system for aerospace plane [IAF PAPER 89-307] p 123 A90-13442

YEAGER, WILLIAM T., JR.

Reduction of blade-vortex interaction noise through higher harmonic pitch control p 377 A90-23937

Performance data from a wind-tunnel test of two main-rotor blade designs for a utility-class helicopter [NASA-TM-4183] p 499 N90-20974

YEATON, ROBERT B.

Predicted and hot-film measured Tollmien-Schlichting wave characteristics p 91 N90-12523

YEE, ERIC K. L.

A component modal synthesis technique for the lateral vibration analysis of aircraft engine systems p 179 A90-16983

YEE, H. C.

High-resolution shock-capturing schemes for inviscid and viscous hypersonic flows p 476 A90-34545

YEH, C. L.

Numerical simulations of gas turbine combustor flows [AIAA PAPER 90-2305] p 686 A90-42116

YEH, HSI-HAN

A mixed H2 and H(infinity)-approach to an autopilot design problem [AIAA PAPER 90-3441] p 865 A90-47694

YEH, HSING C.

Lessons learned from the T-46A durability and damage tolerance program p 842 N90-26812

YEN, MIKE

Adapting an AI-based application from its LISP environment into a real-time embedded system [AIAA PAPER 89-3142] p 75 A90-10616

YENNI, KENNETH R.

Flight tests of a helmet-mounted display synthetic visibility system [AIAA PAPER 90-1279] p 579 A90-36027

YEOW, KIM F.

Two dimensional post stall maneuver of a NACA 0015 airfoil at high pitching rates [AIAA PAPER 90-2810] p 710 A90-45150

YEUNG, C.

An ultrasonic fatigue facility for HCF/LCF interactive tests p 363 A90-23900

YI, FENGMING

Boundary element method for solving direct aerodynamic problem of aerofoil cascades on an arbitrary stream surface of revolution p 554 A90-35830

YIH, CHIA-SHUN

Wave formation on a liquid layer for de-icing airplane wings p 445 A90-28137

YILLIKCI, YILDIRIM KEMAL

Finite difference techniques and rotor blade aeroelastic partial differential equations with quasisteady aerodynamics p 236 N90-15075

YIM, B.

Trajectories of vortex lines beneath a free surface or above a plane p 716 A90-45740

YING, S.-J.

Critical evaluation of Jet-A spray combustion using propane chemical kinetics in gas turbine combustion simulated by KIVA-II [AIAA PAPER 90-2439] p 949 A90-50645

YING, WENJIANG

The optimum control and adaptive control for airplane cabin pressure p 182 A90-18627

YIP, LONG P.

Wind-tunnel and flight-test investigation of the exdrome remotely piloted vehicle configuration [AIAA PAPER 90-1261] p 494 A90-33891

Static wind-tunnel and radio-controlled flight test investigation of a remotely piloted vehicle having a delta wing planform [NASA-TM-4200] p 632 N90-24238

YIP, T. GARY

Streamtube analysis of supersonic combustion in an in-tube-scamjet [AIAA PAPER 90-2339] p 762 A90-42776

YOAV, Y.

A multichannel wide FOV infrared radiometric system p 67 A90-11410

YODA, MINAMI

Three-dimensional measurement, display, and interpretation of fluid flow datasets p 679 A90-38854

YOGAI, TOSHIROH

Cloud features suggesting low level wind shear and turbulence p 778 A90-44545

YOKEL, S. A.

PMR graphite engine duct development [NASA-CR-182228] p 51 N90-10037

YOKOI, RENZO

Two effective methods of approach and landing by visual display [SAE PAPER 891054] p 108 A90-14356

YOKOMIZO, T.

Effect of moving surfaces on the airfoil boundary-layer control p 159 A90-19388

Application of the moving surface boundary layer control to a two dimensional airfoil p 628 A90-42405

Reduction of the side force on pointed forebodies through add-on tip devices [AIAA PAPER 90-3005] p 788 A90-45854

On the drag reduction of bluff bodies through momentum injection [AIAA PAPER 90-3076] p 797 A90-45922

YOKOTA, JEFFREY W.

Multigrid calculations of 3-D turbulent viscous flows [NASA-CR-185154] p 143 N90-13323

YONEZAWA, Y.

Development of the jet-swirl high loading combustor [AIAA PAPER 90-2451] p 658 A90-40633

YONG, WANG

Spanwise distribution of lift and drag at high angles of attack [SAE PAPER 891019] p 83 A90-14331

YOO, SUNGYUL

A zonal flow analysis method for two-dimensional airfoils [AIAA PAPER 90-0571] p 230 A90-22230

Angle-of-attack validation of a new zonal CFD method for airfoil simulations [AIAA PAPER 90-3077] p 795 A90-45908

YOON, SEOKKWAN

Numerical study of chemically reacting flows using a lower-upper symmetric successive overrelaxation scheme p 153 A90-17989

Application of a lower-upper implicit scheme and an interactive grid generation for turbomachinery flow field simulations [ASME PAPER 89-GT-20] p 288 A90-23762

YOON, T. H.

Effect of molecular weight and end group control on the adhesion behavior of thermoplastic polyimides and poly(imide siloxane) segmented copolymers p 947 A90-50199

YORK, ROGER L.

Fatigue spectra development for airborne stores p 336 A90-26757

YOSHIDA, N.

Simulation of the reduction characteristics of scattering from an aircraft coated with a thin-type absorber by the spatial network method p 638 A90-39855

YOSHIDA, SHIZUYUKI

Instrumentation and operation of NDA cryogenic wind tunnel p 437 A90-28293

YOSHIDA, TOYOAKI

Cooling characteristics of a radial wafer blade p 47 A90-12571

YOSHIHARA, H.

Recent Navier/Stokes calculations in applications p 85 A90-15227

YOSHIHARA, HIDEO

Problem areas in applied computational fluid dynamics p 366 A90-25770

Current Japanese supercomputers for computational fluid dynamics applications p 610 N90-23172

YOSHIKAWA, NORIHIKO

Application of Lomax-Bailey implicit scheme to reactive flows p 367 A90-25861

YOSHIKAWA, TAKAO

Simulation of sound propagation in axisymmetric jet p 378 A90-25872

Fast adaptive grid method for compressible flows p 445 A90-28006

YOSHIMURA, SHIN-JI

Endurance test of FJR 710/600S engine p 42 A90-12012

Steady state performance of FJR 710/600S engine p 43 A90-12015

YOST, PETER W.

Yaw fin deployment apparatus for ejection seat [AD-D014512] p 723 N90-25118

YOUNG, A.

Numerical study of balanced patch repairs to cracked sheets p 210 A90-18442

YOUNG, B. G.

Finite-element analysis of large spur and helical gear systems p 683 A90-40940

YOUNG, C. C.

Domestic precursor technology - A unique route to current and future generation carbon fibers p 940 A90-50057

YOUNG, CHRISTOPHER J.

Airworthiness and flight characteristics test of the UH-60A Black Hawk helicopter equipped with the XM-139 multiple mine dispensing system (VOLCANO) [AD-A210271] p 32 N90-10025

Preliminary airworthiness evaluation of the Woodward hydromechanical unit installed on T700-GE-700 engines in the UH-60A helicopter [AD-A216751] p 428 N90-18430

YOUNG, CLARENCE P., JR.

National Transonic Facility model and model support vibration problems [AIAA PAPER 90-1416] p 596 A90-37953

YOUNG, COLIN

Correlation of Puma airloads: Lifting-line and wake calculation [NASA-TM-102212] p 170 N90-13327

YOUNG, DAVID

Intelligent situation assessment and response aiding in flight emergencies [AIAA PAPER 89-2999] p 36 A90-10507

YOUNG, JAMES W., III

Controlled three-dimensionality in unsteady separated flows about a sinusoidally oscillating flat plate [AIAA PAPER 90-0689] p 230 A90-22244

YOUNG, K. G.

An investigation on the coiled-up of vortices on a double delta wing [AIAA PAPER 90-0382] p 165 A90-19825

YOUNG, L. A.

An experimental investigation of helicopter rotor hub fairing drag characteristics [NASA-TM-102182] p 88 N90-11701

YOUNG, M. I.

On dynamic stability boundaries for binary systems p 538 A90-33698

YOUNG, PETER

Comparison of test signals for aircraft frequency domain identification p 490 A90-33057

YOUNG, R.

Automated prepreg tow placement for composite structures p 954 A90-50113

YOUNG, STANLEY D.

The Robotic Canopy Polishing System [SME PAPER MS89-134] p 222 A90-23680

YOUNGHANS, JAMES L.

The next AIAA engine design competition - A commercial engine [AIAA PAPER 89-2258] p 550 A90-33675

YOUSEFFOR, MARDUKE

Analyzing the flared landing task with pitch-rate flight control systems [AIAA PAPER 90-3483] p 866 A90-47732

YOUSSEF, A. M.

Simulation of a turbocompound two-stroke diesel engine [SAE PAPER 891066] p 110 A90-14366

YOUSSEF, ALI M.

A simulation code for turbocompound diesel engines [IAR-89-26] p 774 N90-25348

YOUSSEF, HUSSEIN

A new methodology for model order reduction with application to eigenstructure controllers [AIAA PAPER 90-3475] p 891 A90-47725

YU, F. M.

An investigation on the coiled-up of vortices on a double delta wing [AIAA PAPER 90-0382] p 165 A90-19825

Hydraulic analogy application in the study of a two-phase mixture combustion flow [AIAA PAPER 90-0451] p 211 A90-19850

YU, HUA

A quadratic programming method for solving three dimensional elastic-plastic contact problems p 603 A90-36417

YU, KIM

An Euler method for wing-body-winglet flows [AIAA PAPER 90-0436] p 229 A90-22218

YU, KIN C.

A grid generation method for an aft-fuselage mounted capped-nacelle/pylon configuration with an actuator disk [AIAA PAPER 90-1564] p 565 A90-38703

YU, LINING

Concise design of aircraft longitudinal model reference adaptive command augmentation system p 345 A90-24002

YU, N. J.

Application of a multiblock grid generation approach to aircraft configurations p 310 A90-26527

Application of boundary layer control to HSCT low speed configuration [AIAA PAPER 90-3199] p 812 A90-49103

YU, QIANG

The experimental study on the coaxial dump combustor with inner swirl inlet under the combustion condition p 585 A90-36786

YU, SHOUQIN

An improvement on unwinding technique used in the Galerkin finite element method for the computation of inviscid transonic flow with shock waves p 627 A90-42361

YU, WANGLING

Flight control application of eigenstructure assignment with optimization of robustness to structured state space uncertainty p 693 A90-40885

YU, YE

Global Sentry: NASA/USRA high altitude reconnaissance aircraft design, volume 2 [NASA-CR-186820-VOL-2] p 736 N90-25971

YUAN, XIN

An investigation of characteristics of transonic and viscous flows for turbine cascades p 909 A90-52779

YUE, A.

Improvement of helicopter handling qualities using H(infinity)-optimisation p 667 A90-38965

YUHAS, J. S.

Spray automated balancing of rotors - How process parameters influence performance p 879 A90-46228

YUU, SHINICHI

Development process of turbulence in a round-nozzle air jet p 87 A90-16101

Z

ZABRODIN, A. V.

Some aspects of the numerical modeling of supersonic flow past flight vehicles p 293 A90-24048

ZACH, A.

ATTAS flight testing experiences p 34 N90-10862

ZACH, ADOLF

Procedure for calibrating fly-by-wire control chains of the flying testbed ATTAS [DLR-MITT-90-02] p 936 N90-29401

ZACHARIAS, GREG L.

Model-based method for terrain-following display design [AD-A219302] p 583 N90-22563

ZACK, JOHN W.

Mesoscale acid deposition modeling studies [NASA-CR-4262] p 140 N90-13228

ZACKRO, W. C.

Production of jet fuels from coal-derived liquids. Volume 11: Production of advanced endothermic fuel blends from Great Plains Gasification Plant naphtha by-product stream [AD-A210251] p 65 N90-11184

ZADARNOWSKI, J. H.

Spray sealing: A breakthrough in integral fuel tank sealing technology p 276 N90-15912

ZADOROZHNI, A. I.

Nonsymmetric vortex breakdown and aerodynamic hysteresis in flow past a low-aspect-ratio wing/fuselage configuration p 294 A90-24076

ZADOROZHNYI, ALEKSEI I.

Monitoring and maintenance of automatic control systems in aviation p 778 A90-42524

ZAEFFEL, KLAUS P.

The 1985 and 1986 direct strike lightning data, part 1 [NASA-TM-100533-PT-1] p 374 N90-18125

The 1985 and 1986 direct strike lightning data, part 2 [NASA-TM-100533-PT-2] p 374 N90-18126

ZAIDI, Z. H.

Wind tunnel testing of a helicopter model at HAL p 335 A90-26350

ZAISER, STEPHEN M.

Stability characteristics of a combat aircraft with control surface failure [AD-A216196] p 350 N90-17646

ZAITSEV, I. I.

Some aspects of the control system and power unit lead tests using in-flight simulator systems and flying test-beds [AIAA PAPER 90-1323] p 580 A90-36031

ZAKEM, STEVEN B.

Lightweight fuel pump and metering component for advanced gas turbine engine control [AIAA PAPER 90-2032] p 657 A90-40602

ZAKHAROV, I. U. K.

An automatic system for the programmed control of the parameters of the vibrational and thermal testing of the blades of gas turbine engines p 343 A90-24216

ZAKHAROV, S. B.

An experimental study of separated flow past a low-aspect-ratio delta wing p 294 A90-24077

- ZAKHAROV, V. D.**
The principle of jet engine thrust generation
p 110 A90-14571
- ZAKIROV, RAFAEL' A.**
Monitoring and maintenance of automatic control systems in aviation
p 778 A90-42524
- ZAKRAJSEK, JAMES J.**
Gear noise, vibration, and diagnostic studies at NASA Lewis Research Center [NASA-TM-102435]
p 372 N90-18041
- ZALESKI, P.**
Static and dynamic loss of stability of elements of a supersonic aeroplane covering - Numerical analysis
p 346 A90-25186
- ZALIAEV, I. A.**
Design of a language for the testing of aircraft engines
p 137 A90-14573
- ZALIAEV, IL'DUS A.**
Automatic testing in aircraft building
p 285 A90-24231
- ZALOOSH, ROBERT G.**
Ignitability of jet-A fuel vapors in aircraft fuel tanks
p 326 N90-17594
- ZALOSH, R. G.**
Flammability testing of aircraft cabin materials
p 328 N90-17611
- ZAMAN, K. B. M. Q.**
The low frequency oscillation in the flow over a NACA0012 airfoil with an 'iced' leading edge
p 801 A90-46377
Some observations on transitory stall in conical diffusers
[NASA-TM-102387]
p 94 N90-12561
- ZAMANZADEH, MEHROUZ**
Chemical vapor deposition of Hf/Si compounds as a high temperature coating for carbon/carbon composites
p 855 A90-50159
- ZAMULA, G. N.**
A study of the stability and thermal stability of complex reinforced structures
p 880 A90-46541
A method for reducing a buckled skin under combined loading
p 860 A90-46571
- ZAN, S. J.**
An investigation of the buffet excitation parameter
p 473 A90-33368
An experimental and analytical investigation of the buffet excitation parameter
p 645 A90-42417
- ZANDBERGEN, B. T. C.**
Experimental and computational flammability limits in a solid fuel ramjet
[AIAA PAPER 90-1964]
p 676 A90-40574
Solid fuel combustion chamber
[LR-634]
p 939 N90-29433
- ZANG, LINGQIAN**
An investigation on boron used as a component of solid propellant
p 765 A90-45708
- ZANNETTI, L.**
Numerical method for designing 3D turbomachinery blade rows
p 511 N90-20990
- ZAPOROZHETS, VLADIMIR V.**
Ground aviation equipment: Handbook
p 593 A90-36153
- ZAPOROZHSKAIA, O. A.**
Interchangeability of Soviet-made and foreign mineral oils for aviation gas turbine engines
p 873 A90-46525
- ZAPRIAGAEV, V. I.**
An experimental study of fluctuations in the front separation zone at supersonic flow velocities
p 10 A90-12282
- ZARUBIN, V. A.**
Sensitivity analysis in the design of composite structures
p 880 A90-46478
- ZATONSKII, VIKTOR M.**
Air traffic control
p 638 A90-39581
- ZAVERTAILO, V. IA.**
A generalized relation for the aerodynamic efficiency of plane bodies
p 804 A90-46559
- ZAVRACKY, PAUL M.**
Smart microsensors for high temperature applications, phase 1
[AD-A224151]
p 959 N90-28828
- ZEBROWSKI, ANTHONY E.**
The GE solid state air defence/ATC radar
p 639 A90-41062
- ZEDAN, M.**
Viscous flow analysis for advanced inlet particle separators
[AIAA PAPER 90-2136]
p 661 A90-42038
- ZEI, JAMES M.**
The STOL maneuver technology demonstrator manned simulation test program
p 439 A90-30716
Simulating turbulence and gusts for handling qualities evaluation
[AIAA PAPER 90-2845]
p 754 A90-45174
- ZEILER, THOMAS A.**
Simulation model-building procedure for dynamic systems integration
p 138 A90-14744
- ZEIS, JOE**
Flight testing the F-15E terrain following system
p 334 A90-24272
- ZEISLOFT, HARRY C.**
Aircraft field experience with automotive gasoline in the United States
p 912 A90-51618
- ZEITOUN, D.**
Numerical study of compressible nozzle flow
p 708 A90-44437
- ZELENKOV, IU. A.**
Effect of the nonuniform rotation of the gas turbine rotor on blade vibrations
p 253 A90-20431
- ZELL, PETER T.**
Comparison of model- and full-scale wind-tunnel performance
[AIAA PAPER 88-2536]
p 351 A90-26133
- ZELLER, SIEGFRIED**
OPST1 - An optical yaw control system for high performance helicopters
p 430 A90-28220
- ZELTSEY, MELVIN**
Design considerations for achieving MLS Category III requirements
p 331 A90-25575
- ZEMNUKHOV, I. V.**
Determination of the effective areas of the mixing exhaust ducts of a bypass engine from autonomous test results
p 102 A90-14584
- ZEMSKAIA, A. S.**
Optimal conditions of flow turbulence suppression in the working section of a wind tunnel using screens located in the prechamber
p 438 A90-29185
- ZENG, QINGFU**
Linear dynamics of supersonic ramjet
p 655 A90-40519
- ZENSES, B.**
Full scale study of a cabin fire in an A300 fuselage section
p 326 N90-17592
- ZERWECKH, S. H.**
Flight testing a highly flexible aircraft - Case study on the MIT Light Eagle
p 414 A90-31284
- ZESCHKY, J.**
Computational prediction and measurement of the flow in axial turbine cascades and stages
p 514 N90-21028
- ZGELA, MIRKO B.**
CF 18 480 Gallon External Fuel Tank Stores Clearance Program
p 35 N90-10877
- ZHA, GE-CHENG**
An efficient upwind relaxation-sweeping algorithm for three-dimensional Euler equations
[AIAA PAPER 90-0129]
p 162 A90-19695
- ZHANG, BINQIAN**
On aerodynamic characteristics of canard in canard-forward-swept wing configuration
p 709 A90-44833
- ZHANG, CHAO**
A new design method for centrifugal compressor vaned diffusers
[ASME PAPER 89-GT-156]
p 292 A90-23844
- ZHANG, CHENG SHENG**
The effects of three centres of blade on flutter
p 42 A90-11800
- ZHANG, DENGGAO**
Fracture morphology of toughened bismaleimide/carbon fiber composites
p 948 A90-50205
- ZHANG, GUO-FU**
A finite element solution for transonic flow around lifting fuselage with arbitrary cross sections from the minimum pressure integral
p 156 A90-18298
- ZHANG, GUOFU**
A finite element method for solving lifting airfoil in transonic flow
p 226 A90-21984
Finite element numerical analysis for transonic flows around lifting fuselages
p 558 A90-37216
- ZHANG, HANGUO**
Modified fault tolerant inertial navigation system
p 578 A90-37211
- ZHANG, HONG**
Studies of predicting departure characteristics of aircraft
p 433 A90-31480
- ZHANG, HONGYUE**
Modified fault tolerant inertial navigation system
p 578 A90-37211
- ZHANG, HUI MIN**
PCISM method for two dimensional compressible viscous cascade flow calculation
p 15 A90-12625
- ZHANG, HUI MING**
An investigation of artificial compressor surge
p 11 A90-12526
- ZHANG, HUI-LIU**
Boundary integral equations method for compressible Navier-Stokes equations
p 209 A90-18262
- ZHANG, J.**
Computation of three dimensional turbulent boundary layers in internal flows, including turbomachinery rotor blades
p 12 A90-12555
- ZHANG, JIALIN**
Computation and analysis of the shapes of S1 and S2 streamsurfaces in a transonic compressor rotor
p 160 A90-19446
Improvement of 3D full-potential method and computation of flowfield of CAS compressor rotor
[ASME PAPER 89-GT-17]
p 288 A90-23760
Numerical solution of 3-D hybrid problems in turbomachinery
p 621 A90-40501
- ZHANG, JIAZHENG**
A design of a twin variable control system for aero-turbojet engine
p 423 A90-29917
- ZHANG, LINGUAN**
A numerical solution for instruction tracing problem
p 424 A90-29918
- ZHANG, MENGPIING**
Vortex method modelling the unsteady motion of a thick airfoil
p 396 A90-31489
- ZHANG, MING**
Passive location and tracking using DOA and TOA measurements of single nonmaneuvering observer
p 576 A90-35709
- ZHANG, P.**
Effect of rib-angle orientation on local mass transfer distribution in a three-pass rib-roughened channel
[ASME PAPER 89-GT-98]
p 359 A90-23812
- ZHANG, QINGBING**
An improvement on upwinding technique used in the Galerkin finite element method for the computation of inviscid transonic flow with shock waves
p 627 A90-42361
- ZHANG, QINGFAN**
Infrared sources of jet propulsion system and their suppression
p 252 A90-22614
- ZHANG, QIONG**
A new method for high speed propeller flutter prediction
p 854 A90-49454
- ZHANG, SHI-LING**
Study on SPF and SPF/DB of the bulk-head structure with nonsymmetric shape
p 132 A90-16619
- ZHANG, TIANSONG**
Experimental investigation on the performance of an annular nozzle cascade of a highly-loaded transonic turbine stage
p 152 A90-17787
- ZHANG, WEI**
Parameter sensitivity analysis of one kind of flight path reconstruction estimator
p 779 A90-44832
- ZHANG, WENHUA**
Wall interference correction of high-lift multi-component airfoils
p 158 A90-18604
A wall pressure correction method for half-model experiment in closed subsonic wind tunnel test section
p 593 A90-36437
- ZHANG, XIMING**
A ground simulation-inspection system for avionic devices
p 594 A90-37232
- ZHANG, XIN**
Surface flow on a flat plate induced by a supersonic jet exhausting normally into a low speed crossflow
[AIAA PAPER 90-3011]
p 789 A90-45860
An experimental investigation of supersonic flow over two cavities in tandem
[AIAA PAPER 90-3087]
p 795 A90-45901
- ZHANG, XUEREN**
An experimental study on flowfields in a dual inlet swirl-dump combustor
p 471 A90-33283
- ZHANG, YAOKE**
Computation of transonic flow in a plane cascade with an unfactored flux splitting implicit method
p 152 A90-17785
- ZHANG, YULUN**
Calculations of transonic flows over wing-body combinations
p 395 A90-31479
- ZHANG, ZHONGYIN**
A transonic airfoil design method and examples
p 627 A90-42351
- ZHAO, LINGCHENG**
Aeroelastic characteristics of wings in subsonic flow
p 102 A90-14615
A numerical method for computing the aerodynamic loads on wings with sharp-edge separations at large angles of attack in subcritical transonic flows
p 150 A90-16852
A numerical method in aeroelasticity for wings with separation at large angle of attack
p 557 A90-37209
- ZHAO, MINSHENG**
Analysis and improvement of cabin temperature control system
p 580 A90-37241
- ZHAO, QUSEN**
Fracture morphology of toughened bismaleimide/carbon fiber composites
p 948 A90-50205

ZHAO, RENMIN

ZHAO, RENMIN

The experiments for gas turbine plane cascade in a shock tunnel p 160 A90-19441

ZHAO, X. H.

The acoustic phenomena of the stalling flutter p 78 A90-11801

ZHAO, XIAOLU

A quasi-3D design method of transonic compressor blade with the function of improving velocity distribution p 49 A90-12589

Analyses of full 3D S1-S2 iterative solution in CAS transonic compressor rotor and comparison with quasi-3D S1-S2m iterative solution and L2F measurement p 157 A90-18532

Full 3D iterative solution of transonic flow for a swept wing test channel p 160 A90-19431

An approximate 3-D aerodynamic design method for centrifugal impeller blades [ASME PAPER 89-GT-73] p 291 A90-23794

ZHAO, YI YUAN

Optimal control of an aircraft flying through a downburst p 591 N90-21765

ZHAO, YIYUAN

Simple analyses of paths through windshears and downdrafts [AIAA PAPER 90-0222] p 197 A90-19740

Optimal paths through downbursts p 755 A90-45330

Control of an aircraft in downbursts p 755 A90-45331

ZHAO, YONG

The computer aided weight engineering of aircraft - (CAWE) system p 179 A90-16860

ZHELEZNOV, L. P.

Identification of a stress-strain computation model and planning of tensometry points in strength and stability studies p 880 A90-46482

ZHELTUKHIN, N. A.

Perturbations of higher modes in a supersonic jet p 619 A90-39516

ZHENG, E.

Performance study of an integrated NAVSTAR GPS/SINS navigation system p 329 A90-24003

ZHENG, JIE

The analysis of entry into and recovery from a spin for the J6 aircraft p 195 A90-16854

ZHENG, JIRUI

Experimental investigation on composite cooling of a turbine blade p 190 A90-17794

Experimental investigation of external heat transfer coefficients on film-cooled turbine blade leading edge p 585 A90-36787

ZHENG, MINZHONG

A study on initial fatigue quality of typical aircraft structures (fastener holes) p 272 A90-22004

ZHENG, SITAO

The investigation of stress at an enter-gas nozzle of main landing gears for fighter aeroplanes p 181 A90-18606

ZHENG, SUIJIANG

A variable structure system (VSS) to robust control of aircraft p 257 A90-21987

ZHENG, XIAOPING

Dynamic analysis of airport pavement p 593 A90-36418

ZHENG, XIAOQING

Solution of Euler equations for fighter forebody-inlet combination at high angle of attack p 556 A90-36419

ZHIZHKIN, A. M.

Increasing the heat conductivity of elastic damping elements of MR material p 102 A90-14580

ZHLUKTOV, S. V.

The effect of vibration-dissociation interaction on heat transfer and drag during the hypersonic flow past bodies p 710 A90-44934

ZHONG, KE

Aeroelastic tailoring applied to composite wing p 211 A90-18580

Aeroelastic tailoring of a wing with composite skin p 366 A90-25108

ZHOU, RENLIANG

The distribution of normal-wash for minimum induced drag of non-planar wings p 226 A90-21983

ZHOU, S.

A numerical method solving 2-D unsteady flow field around cascade of oscillating airfoils with arbitrary camber and thickness p 7 A90-11788

A method for predicting stall flutter under variable interblade phase angle along rotating direction p 813 A90-49455

ZHOU, SHENG

Numerical Euler solution for the interaction between oscillating cascade and forced inlet unsteadiness p 8 A90-11792

Computation of unsteady compressible turbulent boundary layers in cascade flow with controlled inlet perturbation p 8 A90-11807

A semi-actuator disk theory for prediction of stall flutter in axial flow compressors p 301 A90-25105

A model of small-disturbance wave in large-scale separation zone associated with stall flutter p 883 A90-49469

Some explorations on the mechanism of blade flutter suppression by porous wall casing p 854 A90-49470

On the unsteady loading noise of counter-rotating propeller p 895 A90-49484

On numerical prediction of sound field generated by propeller p 895 A90-49485

Noise generation by swept cascade p 895 A90-49486

ZHOU, SHIYING

Experimental investigation on the performance of an annular nozzle cascade of a highly-loaded transonic turbine stage p 152 A90-17787

Effect of vane and blade numbers on performance of transonic turbine stage p 189 A90-17789

ZHU, FANGYUAN

Throughflow numerical calculations including influence of spanwise mixing in a multistage axial flow compressor p 157 A90-18534

ZHU, HUILING

Numerical calculation of gaseous reacting flows in a model of gas turbine combustors p 271 A90-21979

ZHU, KEQIN

Effect of ground on wake roll-up behind a lifting surface p 160 A90-19436

ZHU, NIANGUO

The influence of the inlet Mach number on the boundary layer development on turbomachinery blade surfaces p 621 A90-40504

ZHU, XINGJIAN

Partial similarity and a real-time model of twin-spool gas turbine p 654 A90-40512

ZHU, YINGKANG

Analysis of blade loadings in centrifugal compressors p 158 A90-18591

ZHU, ZHIGUO

Variational principle with variable domain discontinuous finite element method for transonic flow and determining automatically the position and shape of the shock waves p 160 A90-19434

ZHU, ZI-QIANG

The transonic nonisentropic potential calculation p 304 A90-25739

ZHU, ZIQIANG

An improved version of LTRAN2 p 2 A90-10350

ZHUANG, ZHONGLIANG

A simple prediction method for low-cycle fatigue life of structures p 604 A90-37240

ZHURAVLEV, V. A.

Effect of the leading edge bluntness of a moderately swept wing on the aerodynamic characteristics of an aircraft model at subsonic and transonic velocities p 388 A90-29005

ZHURAVLEV, VLADIMIR A.

Fundamentals of turbine design for aircraft engines p 40 A90-10839

ZIEGLER, DAVID W.

Tracking a hypersonic aircraft from a space platform [AD-A216399] p 371 A90-17984

ZIEGLER, FRANK

The disturbance processes on the data links of the mode-S air traffic control system [ETN-90-96960] p 729 A90-25965

ZIEMBA, ROB

The SKY SHARK: An RPV designed to investigate the pressure distribution on a lifting surface [NASA-CR-186222] p 844 A90-26824

ZIEREP, J.

Airfoils in supersonic source and sink flows p 149 A90-16844

A straight attached shock wave at the profile tip at freestream Mach number greater than about 1 p 907 A90-51534

ZIERTEN, THOMAS A.

Flight and wind tunnel investigation of aerodynamic effects of aircraft ground deicing/antiicing fluids p 235 A90-15064

ZIEVE, PETER B.

Thin film eddy current impulse deicer [AIAA PAPER 90-0761] p 183 A90-20012

ZIKEEV, VLADIMIR V.

Fundamentals of turbine design for aircraft engines p 40 A90-10839

ZILLIAC, G. G.

Experimental study of nonsteady asymmetric flow around an ogive-cylinder at incidence p 384 A90-27985

ZILLIAC, GREGORY G.

Analytical study of the origin and behavior of asymmetric vortices [NASA-TM-102796] p 573 N90-21746

ZILZ, DAVID E.

The sensitivity of near-field acoustics to the orientation of twin two-dimensional supersonic nozzles [AIAA PAPER 90-2149] p 625 A90-42045

ZIMBRICK, R. A.

Investigation of very high bypass ratio engines for subsonic transports p 659 A90-40945

ZIMMERMAN, RICHARD E.

Aircraft crash survival design guide. Volume 1: Design criteria and checklists [AD-A218434] p 575 N90-22545

Aircraft crash survival design guide. Volume 2: Aircraft design crash impact conditions and human tolerance [AD-A218435] p 575 N90-22546

Aircraft crash survival design guide. Volume 3: Aircraft structural crash resistance [AD-A218436] p 575 N90-22547

Aircraft crash survival design guide. Volume 4: Aircraft seats, restraints, litters, and cockpit/cabin dealthalization [AD-A218437] p 575 N90-22548

ZIMMERMANN, GEORG

Development and application of an optimization procedure for space and aircraft structures p 679 A90-39186

Development and application of an optimization procedure for space and aircraft structures [MBB-FW-522/S/PUB-383] p 779 N90-25078

ZIMMERMANN, H.

Computation of transonic turbine cascade flow using Navier-Stokes equations p 14 A90-12621

Calculation of two- and three-dimensional flow in a transonic turbine cascade with particular regard to the losses [AIAA PAPER 90-1542] p 565 A90-38686

ZINGEL, H.

On the prediction of the aeroelastic behaviour of lifting systems due to flow separation p 491 A90-33369

ZINGG, D. W.

Interactive airfoil calculations with higher-order viscous-flow equations [AIAA PAPER 90-1533] p 564 A90-38678

Higher-order boundary-layer approximations in interactive airfoil calculations p 628 A90-42402

Nonlinear unsteady airfoil response studies p 628 A90-42406

ZINK, W.

Investigation on sheet material of 8090 and 2091 aluminum-lithium alloy p 267 A90-15192

ZINK, WALTER

Investigation on sheet material of 8090 and 2091 aluminum-lithium alloy [MBB-UT-122/89-PUB] p 766 A90-25090

ZINN, R. J.

Safety management in aircraft testing and certification p 180 A90-17421

ZINNER, R. A.

Review and analysis of the DNW/Model 360 rotor acoustic data base [NASA-TM-102253] p 81 A90-11692

ZINOV'EV, V. N.

Mean and pulse characteristics of supersonic flow in a wind tunnel with a honeycomb nozzle p 231 A90-22421

ZIPF, MARK E.

The insertion of human dynamics models in the flight control loops of V/STOL research aircraft. Appendix 2: The optimal control model of a pilot in V/STOL aircraft control loops [NASA-CR-186598] p 598 A90-21776

ZNATY, ELIE

Three-dimensional modeling of turbulent transonic flow at the exit of a twin engine [AAAF PAPER NT 88-16] p 4 A90-11434

ZOBY, E. V.

Hypersonic viscous shock-layer solutions over long slender bodies. II - Low Reynolds number flows p 393 A90-29695

ZOMERMAN, I.

Definition of research needs to address airport pavement distress in cold regions [DOT/FAA/DS-89/13] p 59 A90-10896

ZONTOV, V. M.

Aviation equipment p 338 A90-24200

ZOONTJES, R. P. G.

WingDesign: Program for the structural design of a wing cross-section [LR-627] p 925 A90-29390

ZORZI, E.

Internal rotor friction instability [NASA-CR-183942] p 543 A90-21395

ZOTTO, M.

Dynamic analysis of rotor blades with rotor retention design variations
[AIAA PAPER 90-1159] p 412 A90-29394

ZOTTO, MARK

Helicopter ground/air resonance including rotor shaft flexibility and control coupling p 406 A90-28153

ZOU, CHONGQING

The mechanisms and benefits of aeroelastic tailoring p 641 A90-39286

ZRUBEK, M. NORMAN

Scientific justification and development plan for a mid-sized jet research aircraft
[PB89-208995] p 103 N90-11731

ZUBKIOV, BORIS V.

Technical means and methods of flight safety assurance p 238 A90-22735

ZUBKOV, A. I.

Effect of the Mach number and shape of the front part of the obstacle on the separation zone length in supersonic flow p 903 A90-50816

ZUBTSOV, A. V.

An experimental study of separated flow past a low-aspect-ratio delta wing p 294 A90-24077

ZUCKER, M. S.

An image analysis method for vehicle stabilization p 668 A90-40914

ZUMBRUM, M. A.

Poly(arylene ether ketone)/poly(aryl imide) homo- and polydimethylsiloxane segmented copolymer blends - Influence of chemical structure on miscibility and physical property behavior p 941 A90-50063

ZUMWALT, G. W.

Fatigue and electromagnetic interference test for Electro-Impulse De-Icing
[SAE PAPER 891062] p 100 A90-14362
Electro-impulse de-icing testing analysis and design
[NASA-CR-4175] p 32 N90-10031

ZUMWALT, GLEN W.

A NASA/university/industry consortium for research on aircraft ice protection
[IAR-89-18] p 736 N90-25969

ZUNIGA, FANNY A.

In-flight flow field analysis on the NASA F-18 high alpha research vehicle with comparisons to ground facility data
[AIAA PAPER 90-0231] p 163 A90-19745
In-flight flow visualization with pressure measurements at low speeds on the NASA F-18 high alpha research vehicle
[NASA-TM-101726] p 910 N90-28505

ZUNINO, PIETRO

Secondary flows and Reynolds stress distributions downstream of a turbine cascade at different expansion ratios p 512 N90-21015

ZUPPARDI, G.

Numerical simulation of an adaptive-wall wind-tunnel - A comparison of two different strategies p 439 A90-30251

ZURKOWSKI, S.

Balance model of the perfectly stirred reactor with the discontinuity surface p 125 A90-14652

ZVEREV, O. V.

A study of the radiation of hydrogen-xenon mixtures near models flying at high supersonic velocities p 470 A90-32509

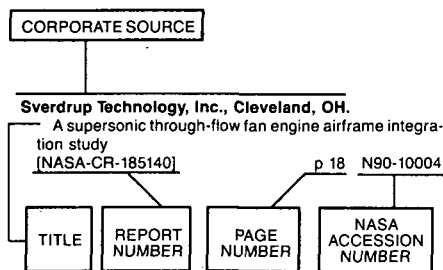
ZWILLENBERG, PETER

Tiltrotor aeroservoelastic design methodology at BHTI p 410 A90-28244

ZYTEKOW, JAN M.

Real-time decision making for autonomous flight control
[SAE PAPER 891053] p 118 A90-14355

Typical Corporate Source Index Listing



Listings in this index are arranged alphabetically by corporate source. The title of the document is used to provide a brief description of the subject matter. The page number and the accession number are included in each entry to assist the user in locating the abstract in the abstract section. If applicable, a report number is also included as an aid in identifying the document.

A

- ACA Industries, Inc., Rancho Palos Verdes, CA.**
Application of the joined wing to tiltrotor aircraft
[NASA-CR-177543] p 248 N90-10393
- Advanced Rotorcraft Technology, Inc., Mountain View, CA.**
Identification of a coupled flapping/inflow model for the PUMA helicopter from flight test data p 56 A90-12767
Parameter identification of aeroelastic modes of rotary wings from transient time histories p 642 A90-40166
- Advanced Structures Technology, Inc., Phoenix, AZ.**
Development of an advanced fan blade containment system
[DOT/FAA/CT-89/20] p 192 N90-13386
- Advisory Group for Aerospace Research and Development, Neuilly-Sur-Seine (France).**
Combustion Instabilities in Liquid-Fuelled Propulsion Systems
[AGARD-CP-450] p 63 N90-10191
Castings Airworthiness
[AGARD-R-762] p 64 N90-10231
Fluid Dynamics of Three-Dimensional Turbulent Shear Flows and Transition
[AGARD-CP-438] p 71 N90-10356
Kalman Filter Integration of Modern Guidance and Navigation Systems
[AGARD-LS-166] p 28 N90-10847
Flight Test Techniques
[AGARD-CP-452] p 33 N90-10860
The human factors relating to escape and survival from helicopters ditching in water
[AGARD-AG-305(E)] p 176 N90-13358
Flight in adverse environmental conditions
[AGARD-AR-277] p 185 N90-14218
Flight in Adverse Environmental Conditions
[AGARD-CP-470] p 222 N90-15041
New Light Alloys
[AGARD-CP-444] p 267 N90-15185

- Advances in techniques and technologies for air vehicle navigation and guidance
[AGARD-AR-276] p 243 N90-15899
Fuel Tank Technology
[AGARD-R-771] p 250 N90-15904
Guidance and Control of Unmanned Air Vehicles
[AGARD-CP-436] p 260 N90-15924
Advances in Techniques and Technologies for Air Vehicle Navigation and Guidance
[AGARD-CP-455] p 332 N90-16731
Aircraft Fire Safety
[AGARD-CP-467] p 324 N90-17581
AGARD/SMP Review: Damage Tolerance for Engine Structures. 2: Defects and Quantitative Materials Behaviour
[AGARD-R-769] p 425 N90-18396
Unsteady Aerodynamic Phenomena in Turbomachines
[AGARD-CP-468] p 425 N90-18405
The implications of using integrated software support environment for design of guidance and control systems software
[AGARD-AR-229] p 434 N90-18432
Calendar of selected aeronautical and space meetings
[AGARD-CAL-90/1] p 464 N90-19060
The Uniform Engine Test Programme
[AGARD-AR-248] p 428 N90-19232
Implications of Advanced Technologies for Air and Spacecraft Escape
[AGARD-CP-472] p 483 N90-20054
Computational Methods for Aerodynamic Design (Inverse) and Optimization
[AGARD-CP-463] p 500 N90-20976
Secondary Flows in Turbomachines
[AGARD-CP-469] p 511 N90-21009
Technical evaluation report on the Fluid Dynamics Panel Symposium on Computational Methods for Aerodynamic Design (Inverse) and Optimization
[AGARD-AR-267] p 720 N90-25947
Technical evaluation report on the Guidance and Control Panel 49th Symposium on Fault Tolerant Design Concepts for Highly Integrated Flight Critical Guidance and Control Systems
[AGARD-AR-281] p 758 N90-26012
Report of the Fluid Dynamics Panel Working Group 10 on calculation of 3D separate turbulent flows in boundary layer limit
[AGARD-AR-255] p 776 N90-26280
AGARD highlights 90/1 p 783 N90-26788
Fluid Dynamics Panel Working Group 12 on Adaptive Wind Tunnel Walls: Technology and Applications
[AGARD-AR-269] p 870 N90-26838
AGARD/SMP Review Damage Tolerance for Engine Structures. 3: Component Behaviour and Life Management
[AGARD-R-770] p 855 N90-27704
Comparative Engine Performance Measurements
[AGARD-LS-169] p 856 N90-27711
Impact of Emerging NDE-NDI Methods on Aircraft Design, Manufacture, and Maintenance
[AGARD-CP-462] p 885 N90-28068
Aerodynamics of Combat Aircraft Controls and of Ground Effects
[AGARD-CP-465] p 920 N90-28513
High Temperature Surface Interactions
[AGARD-CP-461] p 951 N90-28698
Analysis, Design and Synthesis Methods for Guidance and Control Systems
[AGARD-AG-314] p 916 N90-29338
Recommended practices for measurement of gas path pressures and temperatures for performance assessment of aircraft turbine engines and components
[AGARD-AR-245] p 933 N90-29393
- Aeritalia S.p.A., Caselle Torinese (Italy).**
In flight reflight tests on AM-X single engine fly-by-wire aircraft p 34 N90-10869
- Aeritalia S.p.A., Turin (Italy).**
Problems related to the acquisition, processing and utilization of the modal parameters measured in flight tests in order to obtain the full envelope for flutter
[ETN-89-95210] p 103 N90-11735
Evolution of flight commands in Aeritalia design
[ETN-89-95211] p 120 N90-11759

- The aerodynamic experimental center of Aeritalia: Combat aircraft group
[ETN-89-95213] p 122 N90-11766
Choice and characterization of new materials for aerospace applications
[ETN-89-95219] p 126 N90-11819
A new test procedure for a wing made with carbon fiber composites
[ETN-89-95220] p 126 N90-11820
The evolution of light alloys in the aerospace industry
[ETN-89-95216] p 126 N90-11872
In service life monitoring system using g-meter readings and mass configuration control
[ETN-89-95218] p 134 N90-12035
Development and applications of reliability and maintainability design criteria in military aircraft
[ETN-89-95208] p 107 N90-12591
Acquisition and recording an AMX A/C. Aeritalia experience and present trends
[ETN-89-95217] p 109 N90-12598
Project, implementation, and utilization of composite structures
[ETN-89-95209] p 127 N90-12665
Fatigue behavior of specimens under compression load spectra
[ETN-89-95207] p 137 N90-12954
Aircraft fuel tank construction and testing experience p 250 N90-15907
AM-X high incidence trials, development and results
[ETN-90-97277] p 759 N90-26016
New inflight experiments to measure aerodynamics loads
[ETN-90-97276] p 868 N90-26834
Estimation of defective rate of mechanic-hydraulic components
[ETN-90-97275] p 884 N90-27120
Expert system for pilot assistance: The challenge of an intensive prototyping
[ETN-90-97274] p 825 N90-27674
An ultrasonic system for in-service non-destructive inspection of composite structures p 885 N90-28076
- Aerodata Flugmesstechnik G.m.b.H., Brunswick (Germany, F.R.).**
Systems for airborne wind and turbulence measurement p 281 N90-15046
- Aerolift, Inc., Tillamook, OR.**
X.2 limited flight test plan
[AD-A214412] p 249 N90-15099
- Aerometrics, Inc., Sunnyvale, CA.**
Development of a phase Doppler based probe for icing cloud droplet characterization
[AIAA PAPER 90-0667] p 368 A90-26978
The development of a 3-D laser velocimeter for the NASA Langley low turbulence pressure wind tunnel
[AIAA PAPER 90-1385] p 597 A90-38484
Advanced instrumentation for aircraft icing research
[NASA-CR-185225] p 506 N90-21006
- Aeronautica Macchi S.p.A., Varese (Italy).**
Canard versus aft-tail ride qualities performance and pilot command response p 258 N90-15053
A tool for automatic design of airfoils in different operating conditions p 502 N90-20994
Aerodynamic control design: Experience and results at Aeromacchi p 935 N90-28518
- Aeronautica Militare Italiana, Rome.**
Results of an A109 simulation validation and handling qualities study p 591 A90-38524
- Aeronautical Research Inst. of Sweden, Stockholm.**
Low speed testing of a laminar flow airfoil in an adaptive wall wind tunnel
[FFA-TN-1989-08] p 632 N90-23363
Euler code predicted separation at the airfoil trailing edge
[FFA-TN-1989-30] p 632 N90-23364
Damage tolerance of the fighter aircraft 37 Viggen. Part 1: Analytical assessment
[FFA-TN-1990-12-PT-1] p 923 N90-28538
Damage tolerance of the fighter aircraft 37 Viggen. Part 2: Experimental verification
[FFA-TN-1990-13-PT-2] p 923 N90-28539

Aeronautical Research Labs., Melbourne (Australia).

- Measurements of pressures on the wing of an aircraft model during steady rotation
[AIAA PAPER 90-2642] p 754 N90-45162
- A review of Australian and New Zealand investigations on aeronautical fatigue during the period April 1987 to March 1989
[AD-A210373] p 32 N90-10026
- Report on an overseas visit, June 1988
[AD-A210374] p 52 N90-10040
- An appraisal of a number of power assessment procedures being proposed for use in Chinook-Lycoming T55 engine
[AD-A210482] p 52 N90-10041
- The spinning of aircraft: A discussion of spin prediction techniques including a chronological bibliography
[ARL-AERO-R-177] p 36 N90-10888
- An open-loop transient thermodynamic model of the Cougar turbojet
[AD-A211774] p 114 N90-11745
- Additions and corrections to SUPER: A program for calculating steady and oscillatory supersonic flow over a thin wing, tail plane and fin
[AD-A211771] p 90 N90-12501
- Development of a VSAERO (Vortex Separation Aerodynamics) model of the F/A-18
[AD-A212442] p 95 N90-12566
- FGP2: A flight profile generator program
[AD-A212408] p 107 N90-12595
- RAN (Royal Australian Navy) vibration analysis system operator's guide
[AD-A212441] p 107 N90-12596
- Evaluation of a damaged F/A-18 horizontal stabilizer
[AD-A212573] p 107 N90-12597
- AcSim: Aircraft simulation program with application to flight profile generation
[AD-A212466] p 185 N90-14217
- RAAF Orion aircraft A9-300 oxygen fire
[AD-A215496] p 323 N90-16725
- An examination of the fatigue meter records from the RAAF Orion P-3C fleet
[AD-A214000] p 338 N90-17628
- A data acquisition parallel bus for wind tunnels at ARL (Aeronautical Research Laboratory)
[AD-A218052] p 526 N90-20098
- Flutter investigations on a Transavia PL12/T-400 aircraft
[AD-A219108] p 593 N90-22570
- Application of optimal tracking methods to aircraft terrain following
[AD-A221099] p 641 N90-24264
- Statistical treatment of slow strain rate data for assessment of hydrogen embrittlement in low alloy high strength steel
[ARL-MAT-R-122] p 767 N90-26106
- ARLSUPER version 1.0, program users guide
[AD-A222693] p 815 N90-26793
- Comparative evaluation of Allison T56 engine chip detectors
[AD-A221864] p 855 N90-26832
- The reduction of smoke emissions from Allison T56 engines
[ARL-PROP-R-182] p 928 N90-28547
- A flight dynamic model of aircraft spinning
[AR-005-600] p 935 N90-28576
- Aeroplane and Armament Experimental Establishment, Boscombe Down (England).**
- Aircraft testing in the electromagnetic environment
p 248 N90-15066
- Aerospace Engineering Test Establishment, Cold Lake (Alberta).**
- CF 18 480 Gallon External Fuel Tank Stores Clearance Program
p 35 N90-10877
- Aerospace Medical Research Labs., Wright-Patterson AFB, OH.**
- A new method for measuring the transmissivity of aircraft transparencies
[AD-A216953] p 464 N90-19842
- Windblast protection for advanced ejection seats
p 483 N90-20063
- Lateral attenuation of military aircraft flight noise
[AD-A218041] p 548 N90-20799
- Air Force Boom Event Analyzer Recorder (BEAR): System description
[AD-A218048] p 548 N90-20800
- CREW CHIEF: A computer graphics simulation of an aircraft maintenance technician
p 779 N90-25515
- Modeling strength data for CREW CHIEF
p 780 N90-25516
- BASEOPS default profiles for civil aircraft
[AD-A223161] p 844 N90-26825
- Air Force procedure for predicting aircraft noise around airbases: Airbase operations program (BASEOPS) description
[AD-A223069] p 895 N90-27466

Aerospatiale, Marignane (France).

- Hub loads analysis of the SA349/2 helicopter
p 333 N90-23936

Aerospatiale, Suresnes (France).

- Inspection system for in-situ inspection of aircraft composite structures
p 886 N90-28091
- Static and dynamic characterization of the ATR 72 rods made of Ti 10.2.3 titanium alloy
[REPT-49-238] p 953 N90-28722

Aerospatiale, Toulouse (France).

- How to fly windshear using the fly-by-wire concept
p 258 N90-15050
- New materials for civil aircraft furnishing
p 328 N90-17609
- Determination of the ground effect on the characteristics of the A320 aircraft
p 922 N90-28534

Aerostructures, Inc., Arlington, VA.

- Finite element mesh refinement criteria for stress analysis
p 273 N90-23013

Air Canada, Montreal (Quebec).

- New aircraft cabin and cargo flammability standards for transport category aircraft
p 325 N90-17589

Air Force Aero Propulsion Lab., Wright-Patterson AFB, OH.

- Hot surface ignition studies of aviation fluids
p 327 N90-17600

Air Force Armament Lab., Eglin AFB, FL.

- Unsteady three-dimensional thin-layer Navier Stokes solutions on dynamic blocked grids
[AD-A212377] p 136 N90-12899
- An autopilot design methodology for bank-to-turn missiles
[AD-A213379] p 198 N90-13399

Air Force Avionics Lab., Wright-Patterson AFB, OH.

- Transonic Euler solutions on mutually interfering finned bodies
[AD-A213395] p 170 N90-13331

Air Force Flight Dynamics Lab., Wright-Patterson AFB, OH.

- Multidisciplinary Expert-aided Analysis and Design (MEAD)
p 613 N90-23050

Air Force Flight Test Center, Edwards AFB, CA.

- The Air Force Flight Test Center Flight Test Safety Program
p 35 N90-10872
- Schleicher ASK-21 glider (TG-9) stall and spin
[AD-A213513] p 249 N90-15096

Air Force Geophysics Lab., Hanscom AFB, MA.

- A comparison of lightning network data with surface weather observations
[AD-A220003] p 692 N90-23832

Air Force Human Resources Lab., Brooks AFB, TX.

- Success in tutoring electronic troubleshooting
p 780 N90-25568

Air Force Inst. of Tech., Wright-Patterson AFB, OH.

- Source emission test of gas turbine engine test facility, Kelly AFB, TX
[AD-A223869] p 932 N90-28571

Air Force Inst. of Tech., Wright-Patterson AFB, OH.

- Aircraft performance enhancement with active compressor stabilization
[AD-A213652] p 249 N90-15097

Air Force Inst. of Tech., Wright-Patterson AFB, OH.

- Solution of potential flow past an elastic body using the boundary element technique
[AD-A213843] p 275 N90-15390

Air Force Inst. of Tech., Wright-Patterson AFB, OH.

- Modeling the effects of the use of GPS (Global Positioning System) derived altitude indication in the C-17A airdrop system
[AD-A215366] p 333 N90-16748

Air Force Inst. of Tech., Wright-Patterson AFB, OH.

- Experimental evaluation of impedance control for robotic aircraft refueling
[AD-A215532] p 337 N90-16755

Air Force Inst. of Tech., Wright-Patterson AFB, OH.

- The future of aircraft paint removal methods
[AD-A214946] p 356 N90-16936

Air Force Inst. of Tech., Wright-Patterson AFB, OH.

- Effect of riblets on flow separation from a cylinder and an airfoil in subsonic flow
[AD-A216197] p 319 N90-17574

Air Force Inst. of Tech., Wright-Patterson AFB, OH.

- Hypersonic nozzle/afterbody performance at low Mach numbers
[AD-A216223] p 319 N90-17575

Air Force Inst. of Tech., Wright-Patterson AFB, OH.

- A computational model for thickening boundary layers with mass addition for hypersonic engine inlet testing
[AD-A216246] p 319 N90-17576

Air Force Inst. of Tech., Wright-Patterson AFB, OH.

- A wind tunnel study of a sting-mounted circulation control wing
[AD-A216248] p 319 N90-17577

Air Force Inst. of Tech., Wright-Patterson AFB, OH.

- Experimental investigation to suppress flow-induced pressure oscillations in open cavities
[AD-A216285] p 320 N90-17578

Air Force Inst. of Tech., Wright-Patterson AFB, OH.

- An iterative solution to aeroelastic effects in potential flow
[AD-A216291] p 320 N90-17580

Reducing C130E Hercules operating costs in the Royal Australian Air Force and the United States Air Force by increasing cruise speeds
[AD-A215747] p 338 N90-17629

The technology challenge of the advanced tactical fighter: A study of the technology transition process
[AD-A216109] p 338 N90-17630

Cost effectiveness of composite materials on the F-15 and F-16 aircraft
[AD-A216353] p 338 N90-17631

Stability characteristics of a combat aircraft with control surface failure
[AD-A216196] p 350 N90-17646

Investigation of the failure modes in a metal matrix composite under thermal cycling
[AD-A216195] p 357 N90-17825

Automation of an RCS (Radar Cross Section) measurement system and its application to investigate the electromagnetic scattering from scale model aircraft canopies
[AD-A215741] p 371 N90-17970

Tracking a hypersonic aircraft from a space platform
[AD-A216399] p 371 N90-17984

Modeling the wake as a continuous vortex sheet in a potential-flow solution using vortex panels
[AD-A216220] p 371 N90-18016

Numerical simulation of compressible vortices
[AD-A216221] p 371 N90-18017

Fluctuating wind forces measured on a bluff body extending from a cavity
[AD-A216414] p 371 N90-18020

Analysis and test of a wide angle spectrometer
[AD-A215819] p 372 N90-18030

Experimental investigation of a chemical laser cavity flowfield
[AD-A216398] p 372 N90-18038

Hypercube expert system shell-applying production parallelism
[AD-A215762] p 377 N90-18173

A fractional calculus model of aeroelasticity
[AD-A216244] p 377 N90-18212

Visual servicing for autonomous aircraft refueling
[AD-A216042] p 414 N90-18386

Discrete proportional Plus Integral (PI) multivariable control laws for the Control Reconfigurable Combat Aircraft (CRCA)
[AD-A215664] p 433 N90-18431

F-15B high angle-of-attack phenomena and spin prediction using bifurcation analysis
[AD-A217366] p 498 N90-20073

Design of a high angle of attack robotic sting mount for tests in a low speed wind tunnel
[AD-A218105] p 526 N90-20099

Runaway rubber removal
[AD-A218349] p 526 N90-20100

A matrix-free locally-implicit scheme for Navier-Stokes equations
[AD-A218298] p 541 N90-20349

Rotordynamic analysis with shell elements for the transfer matrix method
[AD-A217455] p 541 N90-20434

Comparison of C- and O-grid generation methods using a NACA 0012 airfoil
[AD-A216375] p 479 N90-20948

Development of a least squares time response lower-order equivalent systems technique
[AD-A220527] p 648 N90-23389

Continued development and analysis of a new extended Kalman filter for the Completely Integrated Reference Instrumentation System (CIRIS)
[AD-A220106] p 654 N90-23400

Prediction of longitudinal pilot induced oscillations using the optimal control model
[AD-A220593] p 671 N90-23412

Throughput and delay characteristics for a slow-frequency hopped aircraft-to-aircraft packet radio network
[AD-A220525] p 688 N90-23609

Robustness evaluation of H2 and H(infinity) control theory as applied to a transport aircraft
[AD-A222795] p 759 N90-26018

Air Force Medical Center, Wright-Patterson AFB, OH.

The benefits and costs of automation in advanced helicopters - An empirical study
p 348 N90-26258

Air Force Occupational and Environmental Health Lab., Brooks AFB, TX.

A/F32T-9 large turbo fan engine enclosed noise suppressor system (T-9 NSS), exterior far-field and interior noise, McConnell AFB, Kansas
[AD-A220535] p 665 N90-23402

Air Force Systems Command, Hanscom AFB, MA.

Final results of the NASA storm hazards program
p 819 N90-49834

Air Force Systems Command, Wright-Patterson AFB, OH.

- Pilotless airplanes
[AD-A211719] p 103 N90-11734
- China-built airborne synchronous laser ranger the new L-8 jet trainer aircraft
[AD-A213835] p 275 N90-15422
- National aero-spaceplane status and plans
p 337 N90-16801
- Effect of vortex generators on the aerodynamic wing characteristics and body of revolution
[AD-A222813] p 721 N90-25955
- Lessons learned from the T-46A durability and damage tolerance program
p 842 N90-26812
- Special essays for the 40th anniversary of the revolution: The chief designer discusses the F-8 2 and future fighter planes
[AD-A221587] p 845 N90-26829
- The role of C(sub n beta.dyn) in the aircraft stability at high angles of attack
[AD-A221586] p 868 N90-26833
- Critical inspection of high performance turbine engine components: The RFC concept
p 859 N90-28073

Air Force Wright Aeronautical Labs., Langley AFB, VA.

- Proceedings of the 1987 Aircraft/Engine Structural Integrity Program (ASIP/ENSIP) Conference
[AD-A198037] p 842 N90-26807

Air Force Wright Aeronautical Labs., Wright-Patterson AFB, OH.

- Navier-Stokes computations of lee-side flows over delta wings
p 153 A90-17978
- Spray sealing: A breakthrough in integral fuel tank sealing technology
p 276 N90-15912
- Finite element models of USAF aircraft structures
p 844 N90-26820
- The interaction of chromostereopsis and stereopsis in stereoscopic CRT (Cathode Ray Tubes) displays
[AD-A217906] p 927 N90-28544

Air Force Wright Research and Development Center, Wright-Patterson AFB, OH.

- Vortex dynamics on a pitching delta wing
p 233 A90-23281
- Numerical simulation of an F-16A at angle of attack
[AIAA PAPER 90-0100] p 313 A90-26911
- Multiple vortex and shock interactions at subsonic, transonic, and supersonic speeds
[AIAA PAPER 90-3023] p 793 A90-45890
- An alternative derivation for an integral equation for linearized subsonic flow over a wing
[AD-A214140] p 236 N90-15079
- Proceedings of the 1988 Structural Integrity Program Conference
[AD-A213545] p 275 N90-15486
- Integral fuel tank certification and test methods
p 251 N90-15916
- Application of multifunction inertial reference systems to fighter aircraft
p 332 N90-16740
- ETO (Earth-To-Orbit): A trajectory program for aerospace vehicles
[AD-A218157] p 528 N90-20103

Air War Coll., Maxwell AFB, AL.

- Interoperability issues in the use of satellite-based navigation systems for civil aviation purposes
[AD-A217279] p 405 N90-19223

Airbus Industrie, Blagnac (France).

- A320 flight tests: Particularities and innovations
p 34 N90-10864
- Point of view of a civil aircraft manufacturer on Al-Li alloy
p 268 N90-15200

Aircraft Research Association Ltd., Bedford (England).

- Application of experimental techniques to store release problems
p 316 N90-17545
- Aerofoil design techniques
p 500 N90-20978
- A discussion on issues relating to multiblock grid generation
p 608 N90-21991

Aix-Marseille Univ. (France).

- Laser applications in supersonic unsteady flow
p 212 N90-13344
- Aerodynamics of unsteady systems. Numerical study of potential flow/boundary layer coupling
[ETN-90-96257] p 396 N90-18367
- Device for the dilution of hot exhaust jets
[ETN-90-97435] p 858 N90-27723

Akron Univ., OH.

- Experimental and analytical evaluation of dynamic load vibration of a 2240-kW (3000-hp) rotorcraft transmission
p 127 A90-13750
- Impact ice stresses in rotating airfoils
[AIAA PAPER 90-0198] p 175 A90-19735
- Parametric studies of advanced turboprops
p 253 A90-21225
- A laser based computer aided non-intrusive technique for full field flow characterization in macroscopic curved channels
p 535 A90-32293

The determination of third order linear models from a seventh order nonlinear jet engine model
p 964 A90-52881

- Navier-Stokes analysis of airfoils with leading edge ice accretions
p 174 N90-14196

Alabama Univ., Huntsville.

- The influence of a wall function on turbine blade heat transfer prediction
p 429 N90-19421

Allied-Signal Aerospace Co., Des Plaines, IL.

- Production of jet fuels from coal-derived liquids. Volume 11: Production of advanced endothermic fuel blends from Great Plains Gasification Plant naphtha by-product stream
[AD-A210251] p 65 N90-11184

Allied-Signal Aerospace Co., Phoenix, AZ.

- The role of NDE in ceramic turbine engine component development
p 601 A90-35508
- Development of impact design methods for ceramic gas turbine components
[AIAA PAPER 90-2413] p 687 A90-42165
- Measurements in an annular combustor-diffuser system
[AIAA PAPER 90-2162] p 768 A90-42740
- Parametric evaluation of the aerodynamic performance of an annular combustor-diffuser system
[AIAA PAPER 90-2163] p 742 A90-42741
- Advanced Turbine Technology Applications Project (ATTAP)
[NASA-CR-185109] p 220 N90-14153

Allied-Signal Aerospace Co., Torrance, CA.

- Development and fabrication of structural components for a scramjet engine
[NASA-CR-181945] p 510 N90-20088

Allied-Signal Corp., Des Plaines, IL.

- Advanced fuel properties, phase 1
[AD-A219788] p 766 N90-25236

Aluminum Co. of America, Davenport, IA.

- An aluminum quality breakthrough for aircraft structural reliability
p 843 N90-26816

Amdahl Corp., Sunnyvale, CA.

- Supercomputer applications in gas turbine flowfield simulation
p 620 A90-40495

Analog, Inc., San Jose, CA.

- Numerical simulations of an oblique detonation wave engine
p 508 A90-32964

Analytical Mechanics Associates, Inc., Hampton, VA.

- Preliminary results from a subsonic high-angle-of-attack flush airdata sensing (HI-FADS) system - Design, calibration, algorithm development, and flight test evaluation
[AIAA PAPER 90-0232] p 187 A90-19746

Analytical Methods, Inc., Redmond, WA.

- A zonal flow analysis method for two-dimensional airfoils
[AIAA PAPER 90-0571] p 230 A90-22230
- Angle-of-attack validation of a new zonal CFD method for airfoil simulations
[AIAA PAPER 90-3077] p 795 A90-45908

Analytical Sciences Corp., Research Triangle Park, NC.

- Comparison of equivalent plate and finite element analysis of a realistic aircraft structural configuration
[AIAA PAPER 90-3293] p 837 A90-48877

Analytical Services and Materials, Inc., Hampton, VA.

- Minimum weight design of helicopter rotor blades with frequency constraints
p 180 A90-17313

A numerical study of mixing enhancement in a supersonic combustor

- [AIAA PAPER 90-0203] p 272 A90-22182
- Minimum weight design of rotorcraft blades with multiple frequency and stress constraints
p 335 A90-25304
- Design of low Reynolds number airfoils. I
p 307 A90-26129

Viscous computations using a direct solver

- p 315 A90-27133

Comparison between experimental and numerical results for a research hypersonic aircraft

- p 395 A90-31278

Flight-measured streamwise disturbance instabilities in laminar flow

- [AIAA PAPER 90-1283] p 495 A90-33904

Application of optimization methods to helicopter rotor blade design

- p 604 A90-37337

Application of a new adaptive grid for aerodynamic analysis of shock containing single jets

- [AIAA PAPER 90-2025] p 624 A90-41988

A computational investigation of flow losses in a supersonic combustor

- [AIAA PAPER 90-2093] p 742 A90-42728

Flow establishment in a generic scramjet combustor

- [AIAA PAPER 90-2096] p 742 A90-42729

A numerical study of the effects of reverse sweep on a scramjet inlet performance

- [AIAA PAPER 90-2218] p 705 A90-42749

Hypersonic CFD applications for the National Aero-Space Plane

- [SAE PAPER 892310] p 714 A90-45473

Numerical simulation of flow through the Langley parametric scramjet engine

- [SAE PAPER 892314] p 747 A90-45476

Navier-Stokes simulation of transonic afterbody flows with jet exhaust

- [AIAA PAPER 90-3057] p 790 A90-45862

Correlation of theory to wind-tunnel data at Reynolds numbers below 500,000

- p 800 A90-46370

Application of localized surface heating to actively control the boundary layer separation

- p 806 A90-46848

Performance of an optimized rotor blade at off-design flight conditions

- p 830 A90-46946

Long-range LFC transport

- p 104 N90-12508

Performance of an optimized rotor blade at off-design flight conditions

- [NASA-CR-4288] p 416 N90-19226

An enhanced integrated aerodynamic load/dynamic optimization procedure for helicopter rotor blades

- [NASA-CR-4326] p 924 N90-29383

Applied Dynamics International, Ann Arbor, MI.

- Six-degree-of-freedom aircraft simulation with mixed-data structure using the applied dynamics simulation language, ADSIM
p 613 N90-23067

Applied Sciences Corp., Yellow Springs, OH.

- Vapor grown carbon fiber for space thermal management systems
p 943 A90-50128

Aquanautics Corp., Alameda, CA.

- A reliable, maintenance-free oxygen sensor for aircraft using an oxygen-sensitive coating on potentiometric electrodes
[AD-A222696] p 927 N90-28545

ARE, Inc., Riverdale, MD.

- Criteria for coal tar seal coats on airport pavements. Volume 2: Laboratory and field studies
[AD-A220167] p 674 N90-24277

Argonne National Lab., IL.

- Analytical studies of three-dimensional combustion processes
[AD-A211903] p 126 N90-11837

Development of a computational fluid dynamics and chemistry model for the fouling of jet fuels

- [DE90-005664] p 608 N90-22003

Development of a mathematical model for the thermal decomposition of aviation fuels

- [AD-A221673] p 875 N90-26994

Arizona State Univ., Tempe.

- Experiments in swept-wing transition
p 149 A90-16794

Measurement of crossflow vortices, attachment-line flow, and transition using microthin hot films

- [AIAA PAPER 90-1636] p 607 A90-38765

Analysis of airframe/engine interactions - An integrated control perspective

- [AIAA PAPER 90-1918] p 667 A90-40557

The development of crossflow vortices on a 45 degree swept wing

- [SAE PAPER 892245] p 713 A90-45452

Extended implicit model following as applied to integrated flight and propulsion control

- [AIAA PAPER 90-3444] p 890 A90-47697

Multivariable flight control synthesis and literal robustness analysis for an aeroelastic vehicle

- [AIAA PAPER 90-3446] p 890 A90-47699

Stability and transition of three-dimensional boundary layers

- p 71 N90-10357

Navier-Stokes simulation of the crossflow instability in swept-wing flows

- [NASA-CR-186122] p 212 N90-13744

Multivariable frequency weighted model order reduction for control synthesis

- [AIAA-89-3558] p 613 N90-23060

Arizona Univ., Tucson.

- On the instabilities of supersonic mixing layers - A high-Mach-number asymptotic theory
p 702 A90-42644

Sideslip-induced static pressure errors in flight-test measurements

- [AIAA PAPER 90-3082] p 794 A90-45898

Boundary-layer receptivity and laminar-flow airfoil design

- p 91 N90-12516

Influence of vane sweep on rotor-stator interaction noise

- p 169 N90-13325

Aerodynamics of bodies in shear flow

- p 910 N90-28496

ARMCON, Inc., Shallmar, FL.

- The integration of stores on modern tactical aircraft: Where we have been, and what we should do for the future
p 337 N90-17552

Army Aeromedical Research Lab., Fort Rucker, AL.

- Cockpit lighting compatibility with image intensification night imaging systems: Issues and answers
[AD-A210503] p 32 N90-10028

Army Aerostructures Directorate, Hampton, VA.

- Towards a damage tolerance philosophy for composite materials and structures
p 675 A90-40127

Performance of an optimized rotor blade at off-design flight conditions p 830 A90-46946
Effect of blade planform variation on a small-scale hovering rotor
[NASA-TM-4146] p 173 N90-14186

Army Air Mobility Research and Development Lab., Cleveland, OH.

Test and theory for piezoelectric actuator-active vibration control of rotating machinery p 879 A90-46226

Army Aviation Development Test Activity, Fort Rucker, AL

Aviation acoustical noise measurement
[AD-A222014] p 896 N90-27469

Army Aviation Engineering Flight Activity, Edwards AFB, CA.

Initial results from the joint NASA-Lewis/U.S. Army icing flight research tests p 400 A90-28180
Airworthiness and flight characteristics test of the UH-60A Black Hawk helicopter equipped with the XM-139 multiple mine dispensing system (VOLCANO)
[AD-A210271] p 32 N90-10025

Evaluation of the improved OV-ID anti-icing system, phase 2
[AD-A213928] p 239 N90-15083

Natural icing re-evaluation of the EH-60A Quick Fix helicopter
[AD-A214728] p 323 N90-16723

Preliminary airworthiness evaluation of the Woodward hydromechanical unit installed on T700-GE-700 engines in the UH-60A helicopter
[AD-A216751] p 428 N90-18430

Airworthiness and flight characteristics evaluation of the McDonnell Douglas Helicopter Corporation (MDHC) 530FF helicopter
[AD-A218253] p 498 N90-20076

Preliminary airworthiness evaluation of the RC-12K
[AD-A219545] p 648 N90-23387

Army Aviation Research and Development Command, Cleveland, OH.

A planar reacting shear layer system for the study of fluid dynamics-combustion interaction
[NASA-TM-102422] p 194 N90-13393

Liquid water content and droplet size calibration of the NASA Lewis Icing Research Tunnel
[NASA-TM-102447] p 213 N90-13797

Army Aviation Research and Development Command, Fort Eustis, VA.

Force determination sensitivities study for full-scale helicopter ground vibration testing
[AD-A215983] p 349 N90-17643

The Advanced Digital-Optical Control System (ADOCS) user demonstration program
[AD-A215984] p 349 N90-17644

Army Aviation Research and Development Command, Hampton, VA.

Scaling effects in the impact response of graphite-epoxy composite beams
[SAE PAPER 891014] p 128 A90-14326

Impact evaluation of composite floor sections
[SAE PAPER 891018] p 100 A90-14330

Army Aviation Research and Development Command, Moffett Field, CA.

A numerical study of general viscous flows around multi-element airfoils
[AIAA PAPER 90-0572] p 167 A90-19922

Calculations of the flow past bluff bodies, including tilt-rotor wing sections at $\alpha = 90$ deg
[AIAA PAPER 90-0032] p 227 A90-22156

An examination of helicopter rotor load calculations
[AD-A214295] p 249 N90-15098

The response of helicopter rotors to vibratory airload
[AD-A215678] p 337 N90-16756

Time and frequency-domain identification and verification of BO-105 dynamic models
[AD-A216828] p 415 N90-18389

Identification of XV-15 aeroelastic modes using frequency-domain methods
[NASA-TM-101021] p 582 N90-21756

Army Aviation Systems Command, Cleveland, OH.

Efficiency testing of a helicopter transmission planetary reduction stage
p 271 A90-21113

Effect of advanced component technology on helicopter transmissions
p 271 A90-21115

Liquid water content and droplet size calibration of the NASA Lewis Icing Research Tunnel
[AIAA PAPER 90-0669] p 261 A90-22242

Comparison of two droplet sizing systems in an icing wind tunnel
[AIAA PAPER 90-0668] p 274 A90-23711

Composite matrix cooling scheme for small gas turbine combustors
[AIAA PAPER 90-2158] p 852 A90-47210

Efficiency study comparing two helicopter planetary reduction stages
[AIAA PAPER 90-2156] p 956 A90-50644

Assessment of worm gearing for helicopter transmissions
[NASA-TM-102441] p 257 N90-15923

Transmission research activities at NASA Lewis Research Center
[NASA-TM-103132] p 543 N90-21394

Efficiency study comparing two helicopter planetary reduction stages
[NASA-TM-103106] p 776 N90-26334

Computer code for predicting coolant flow and heat transfer in turbomachinery
[NASA-TP-2985] p 858 N90-27722

An expert system to perform on-line controller restructuring for abrupt model changes
[NASA-TM-103609] p 964 N90-29121

Army Aviation Systems Command, Corpus Christi, TX.

Analysis of the T63-A-700 engine used in alcohol turbine fuel extender test
[DOT/FAA/CT-TN90/18] p 928 N90-28549

Army Aviation Systems Command, Hampton, VA.

Reduction of blade-vortex interaction noise through higher harmonic pitch control
p 377 A90-23937

Experimental transonic flutter characteristics of supersonic cruise configurations
[AIAA PAPER 90-0979] p 390 A90-29369

Rotor blade structural design
p 106 N90-12584

Validation of the procedures
p 107 N90-12587

Performance data from a wind-tunnel test of two main-rotor blade designs for a utility-class helicopter
[NASA-TM-4183] p 499 N90-20974

Army Aviation Systems Command, Moffett Field, CA.

Advancements in frequency-domain methods for rotorcraft system identification
p 56 A90-12771

Experimental and computational studies of dynamic stall
p 147 A90-16780

Correlation of Puma airfoils - Evaluation of CFD prediction methods
[ONERA, TP NO. 1989-185] p 224 A90-21045

Comparison of model- and full-scale wind-tunnel performance
[AIAA PAPER 88-2536] p 351 A90-26133

Prediction and measurement of low-frequency harmonic noise of a hovering model helicopter rotor
p 463 A90-28159

HARP model rotor test at the DNW
p 406 A90-28167

A numerical analysis of the British Experimental Rotor Program blade
p 384 A90-28194

Advanced rotor computations with a corrected potential method
p 385 A90-28197

Tilt rotor aircraft aeroacoustics
p 409 A90-28238

The prediction of loads on the Boeing Helicopters Model 360 rotor
p 410 A90-28240

Design and development of a facility for compressible dynamic stall studies of a rapidly pitching airfoil
p 436 A90-28255

Application of transonic flow analysis to helicopter rotor problems
p 394 A90-29887

Helmet mounted display systems for helicopter simulation
p 420 A90-31344

An experimental and analytical investigation of isolated rotor flap-lag stability in forward flight
p 518 A90-33623

Results of an A109 simulation validation and handling qualities study
p 591 A90-38524

Development of the XV-15 tiltrotor research aircraft - Lessons learned
p 581 A90-38540

The free-wake computation of rotor-body flows
[AIAA PAPER 90-1540] p 565 A90-38684

Euler solutions for self-generated rotor blade-vortex interactions
[AIAA PAPER 90-1588] p 566 A90-38723

CFD and transonic helicopter sound
p 696 A90-42433

System identification requirements for high-bandwidth rotorcraft flight control system design
p 755 A90-45333

Experimental and numerical study of the British Experimental Rotor Programme blade
[AIAA PAPER 90-3008] p 789 A90-45858

Schlieren studies of compressibility effects on dynamic stall of airfoils in transient pitching motion
[AIAA PAPER 90-3038] p 791 A90-45877

Methodology for estimating helicopter performance and weights using limited data
p 829 A90-46936

The response of helicopter rotors to vibratory airload
p 832 A90-46971

Evaluation of speech recognizers for use in advanced combat helicopter crew station research and development
[NASA-CR-177547] p 650 N90-24265

Obtaining consistent models of helicopter flight-data measurement errors using kinematic-compatibility and state-reconstruction methods
[AD-A222533] p 815 N90-26799

Rotorcraft aeromechanical stability-methodology assessment, Phase 2: Workshop
[NASA-TM-102272] p 816 N90-26800

Model tilt-rotor hover performance and surface pressure measurement
[AD-A222535] p 845 N90-26827

The effects of structural flap-lag and pitch-lag coupling on soft inplane hingeless rotor stability in hover
[NASA-TP-3002] p 910 N90-28503

Comparison of speech intelligibility in cockpit noise using SPH-4 flight helmet with and without active noise reduction
[NASA-CR-177564] p 915 N90-28510

Army Aviation Systems Command, Saint Louis, MO.

Development of the improved helicopter icing spray system (IHSS)
p 400 A90-28182

Using goal programming to determine the optimal engine mix for UH-1 helicopters
[AD-A214893] p 343 N90-16762

Peacetime replacement and crash damage factors for army aircraft
[AD-A218544] p 636 N90-23372

Army Avionics Lab., Fort Monmouth, NJ.

Hover position sensing system
p 848 N90-27448

Army Belvoir Research and Development Center, Fort Belvoir, VA.

The prediction of middle distillate fuel properties using liquid chromatography-proton nuclear magnetic resonance spectroscopy data
[AD-A211879] p 126 N90-11899

Army Cold Regions Research and Engineering Lab., Hanover, NH.

Definition of research needs to address airport pavement distress in cold regions
[DOT/FAA/DS-89/13] p 59 N90-10896

Ice runways near the South Pole
[AD-A211606] p 133 N90-11908

Airfields on antarctic glacier ice
[AD-A217638] p 526 N90-20097

Army Construction Engineering Research Lab., Champaign, IL.

Human response research update
p 699 N90-24873

Army Materials Technology Lab., Watertown, MA.

HPLC analysis of helicopter rotor blade materials
[AD-A221121] p 650 N90-24270

Applications of digital image processing in testing and evaluation of composite materials
[AD-A229399] p 874 N90-26887

Army Propulsion Lab., Cleveland, OH.

Spray automated balancing of rotors - How process parameters influence performance
p 879 A90-46228

Army Tank-Automotive Command, Warren, MI.

User's manual for the ride motion simulator
[AD-A212855] p 201 N90-13402

Army War Coll., Carlisle Barracks, PA.

Flight testing and flight research: From the age of the tower jumper to the age of the astronaut
p 35 N90-10882

Arnold Engineering Development Center, Arnold Air Force Station, TN.

Wind tunnel support system effects on a fighter aircraft model at Mach numbers from 0.6 to 2.0
[AD-A210614] p 19 N90-10010

The effects of wind tunnel data uncertainty on aircraft point performance predictions
[AD-A216091] p 414 N90-18387

Optimization of aerodynamic designs using computational fluid dynamics
p 541 N90-20999

AS&M, Inc., Hampton, VA.

A numerical parametric study of a scramjet inlet in a Mach 6 arc heated test facility
[AIAA PAPER 90-0531] p 167 A90-19896

Measurement of crossflow vortices, attachment-line flow, and transition using microthin hot films
[AIAA PAPER 90-1636] p 607 A90-38765

The design of a low Reynolds number RPV
p 828 A90-46385

Assistant Secretary of Defense (Production and Logistics), Washington, DC.

Model designation of military aerospace vehicles
[PB90-206301] p 787 N90-27646

Atlantic Applied Research Corp., Van Nuys, CA.

Noise transmission into propeller-driven airplanes
p 614 N90-22364

Atomic Energy of Canada Ltd., Pinawa (Manitoba).

Radiation-curable prepreg composites
[DE90-629740] p 951 N90-28674

Auburn Univ., AL

- AVION:** A detailed report on the preliminary design of a 79-passenger, high-efficiency, commercial transport aircraft
[NASA-CR-186663] p 649 N90-23395
- High speed civil transport
[NASA-CR-186661] p 649 N90-23396
- Design of a low cost short takeoff-vertical landing export fighter/attack aircraft
[NASA-CR-186658] p 734 N90-25132

Aviation Advanced Technology Applications, Orlando, FL

- The design of a low Reynolds number RPV
p 828 A90-46385

Avions Marcel Dassault, Saint-Cloud (France).

- Integral fuel tanks - design, production, aging, repair
p 250 N90-15906

Avions Marcel Dassault-Breguet Aviation, Istres (France).

- Flight test techniques adopted by Avions Marcel Dassault-Breguet Aviation p 34 N90-10867

Avions Marcel Dassault-Breguet Aviation, Saint-Cloud (France).

- Putting alloy 2091 to work p 268 N90-15197
- Automatic grid generation in complex three-dimensional configurations using a frontal system p 608 N90-21992
- The application of infrared thermography to the nondestructive testing of composite materials p 886 N90-28084

B**Ballistic Research Labs., Aberdeen Proving Ground, MD.**

- Numerical simulation of three-dimensional transonic flows p 905 A90-51020
- External flow computations for a finned 60mm ramjet in steady supersonic flight
[AD-A216998] p 428 N90-19233

Battelle Columbus Labs., OH.

- Characterization of chemicals on engine exhaust particles
[AD-A213566] p 256 N90-15106

BBN Systems and Technologies Corp., Canoga Park, CA.

- Noise and sonic boom impact technology. Effects of aircraft noise and sonic booms on structures: An assessment of the current state-of-knowledge
[AD-A213919] p 378 N90-17409
- Noise and sonic boom impact technology. Initial development of an Assessment System for Aircraft Noise (ASAN). Volume 1: Executive summary
[AD-A214164] p 379 N90-17410
- Noise and sonic boom impact technology. Initial development of an Assessment System for Aircraft Noise (ASAN). Volume 2: System design strategy
[AD-A214454] p 379 N90-17411
- Noise and sonic boom impact technology. Initial development of an Assessment System for Aircraft Noise (ASAN). Volume 3: Technical description
[AD-A214455] p 379 N90-17412
- Assessment System for Aircraft Noise (ASAN) citation database. Volume 1: User's manual
[AD-A219175] p 615 N90-23188
- Assessment System for Aircraft Noise (ASAN) citation database. Volume 2: Database update manual
[AD-A219176] p 615 N90-23189
- Assessment System for Aircraft Noise (ASAN) citation database. Volume 3: New citation review procedures
[AD-A219177] p 615 N90-23190
- Audibility and annoyance of en route noise of unducted fan engines
[AD-A223687] p 966 N90-30035
- Assessment System for Aircraft Noise (ASAN): Development of alpha-test prototype system software
[AD-A223770] p 966 N90-30036

Berkeley Research Association, Springfield, VA.

- Interactive generation of unstructured grids for three dimensional problems p 310 A90-26537

Bihrie Applied Research, Inc., Jericho, NY.

- Measurements of pressures on the wing of an aircraft model during steady rotation
[AIAA PAPER 90-2842] p 754 A90-45162
- Influence of forebody geometry on aerodynamic characteristics and a design guide for defining departure/spin resistant forebody configurations
[AD-A216714] p 414 N90-18388

Boeing Advanced Systems Co., Seattle, WA.

- Pressure and heat-transfer investigation of a hypersonic configuration p 598 A90-35757
- Compatibility of fuel system components with high density fuel
[AD-A210381] p 32 N90-10027

- IAPSA 2 small-scale system specification
[NASA-CR-182006] p 695 N90-24103
- Reliability model generator specification
[NASA-CR-182005] p 780 N90-25638

Boeing Aerospace Co., Seattle, WA.

- Development of pressure containment and damage tolerance technology for composite fuselage structures in large transport aircraft
[NASA-CR-3996] p 63 N90-10186

Boeing Co., Seattle, WA.

- Modifying high-order aeroelastic math model of a jet transport using maximum likelihood estimation p 61 N90-10106
- Aircraft modal suppression system: Existing design approach and its shortcomings p 33 N90-10115
- Boeing/NASA composite components flight service evaluation
[NASA-CR-181898] p 601 N90-22609
- Boeing Commercial Airplane Co., Renton, WA.**
- Flight and wind tunnel investigation of aerodynamic effects of aircraft ground deicing/antiicing fluids p 235 N90-15064

Boeing Commercial Airplane Co., Seattle, WA.

- Laminar flow test installation in the Boeing Research Wind Tunnel
[AIAA PAPER 90-1425] p 559 A90-37962
- Transonic analysis of complex configurations using TRANAIR program
[SAE PAPER 892289] p 714 A90-45467
- TRANAIR applications to engine/airframe integration p 838 A90-48958
- Application of boundary layer control to HSCT low speed configuration
[AIAA PAPER 90-3199] p 812 A90-49103
- Classification and reduction of pilot error
[NASA-CR-181867] p 24 N90-10014
- Structural stability augmentation system design using BODEDIRECT: A quick and accurate approach p 33 N90-10116
- Laminar flow: Challenge and potential p 90 N90-12504
- The 757 NLF glove flight test results p 104 N90-12546

- Variable-Sweep Transition Flight Experiment (VSTFE): Stability code development and clean-up glove data analysis p 105 N90-12548
- Evaluation of analysis techniques for low frequency interior noise and vibration of commercial aircraft
[NASA-CR-181851] p 220 N90-14866

- Fly-by-light flight control system technology development plan
[NASA-CR-181953] p 259 N90-15111

- Design of integrated pitch axis for autopilot/autothrottle and integrated lateral axis for autopilot/yaw damper for NASA TSRV airplane using integral LQG methodology
[NASA-CR-4268] p 348 N90-16768

- Fire hardening of aircraft through upgrades of materials and designs p 327 N90-17605

- Flight survey of the 757 wing noise field and its effects on laminar boundary layer transition. Volume 3: Extended data analysis
[NASA-CR-178419] p 380 N90-18233

- A conflict analysis of 4D descent strategies in a metered, multiple-arrival route environment
[NASA-CR-182019] p 593 N90-21772

- Application of laminar flow control to supersonic transport configurations
[NASA-CR-181917] p 719 N90-25944

- World jet airplane inventory at year-end 1989
[PB90-207218] p 902 N90-28489

- High-speed civil transport study: Special factors
[NASA-CR-181881] p 923 N90-28537

Boeing Helicopter Co., Philadelphia, PA.

- Spray nozzle investigation for the Improved Helicopter Icing Spray System (IHSS)
[AIAA PAPER 90-0666] p 350 A90-25040

- Blade-vortex interaction experiments - Velocity and vorticity fields
[AIAA PAPER 90-0030] p 312 A90-26903

- Development of the improved helicopter icing spray system (IHSS) p 400 A90-26182

- The prediction of loads on the Boeing Helicopters Model 360 rotor p 410 A90-28240

- Active control of tiltrotor blade in-plane loads during maneuvers p 670 A90-42463

- Calculation of flight vibration levels of the AH-1G helicopter and correlation with existing flight vibration measurements
[NASA-CR-181923] p 454 N90-18743

Boeing Military Airplane Development, Seattle, WA.

- Design and test of a natural laminar flow/large Reynolds number airfoil with a high design cruise lift coefficient p 93 N90-12543

Bolt, Beranek, and Newman, Inc., Cambridge, MA.

- Intelligent situation assessment and response aiding in flight emergencies
[AIAA PAPER 89-2999] p 36 A90-10507
- Some implications of the isotropic momentarily frozen assumptions for the SPAN-MAT program
[NASA-CR-181937] p 88 N90-11704

Boston Univ., MA.

- Unsteady free-wake viscous aerodynamic analysis of helicopter rotors
[AD-A217166] p 478 N90-20048
- Analysis of dynamic transient response and postflutter behavior of super-maneuvering airplane
[AD-A224126] p 925 N90-29386

Brescia Univ. (Italy).

- Secondary flows and Reynolds stress distributions downstream of a turbine cascade at different expansion ratios p 512 N90-21015

Bristol Univ. (England).

- The three-dimensional vortex sheet structure on delta wings p 19 N90-10367
- The active control of an unstable canard aircraft p 57 N90-10894

- Optimum spanwise camber for minimum induced drag [BU-403] p 397 N90-18369

Bristow Helicopters Ltd., Redhill (England).

- AIMS for helicopters p 820 N90-27639

British Aerospace Aircraft Group, Brough (England).

- Performance assessment of MIL-STD-1553B on the avionics systems demonstrator rig of British Aerospace p 849 N90-27624

British Aerospace Dynamics Group, Bristol (England).

- Antenna installation on aircraft: Theory and practice p 371 N90-17941

British Aerospace Public Ltd. Co., Bristol (England).

- Fabrication characteristics of 8090 alloy p 268 N90-15198

British Aerospace Public Ltd. Co., Hatfield (England).

- Multiblock topology specification and grid generation for complete aircraft configurations p 582 N90-21986

British Aerospace Public Ltd. Co., Kingston-upon-Thames (England).

- Integral fuel tank sealing practice at British Aerospace (Kingston) p 250 N90-15905

British Aerospace Public Ltd. Co., Lancashire (England).

- Technology and evaluation of unmanned air vehicles p 252 N90-15934

- Combat aircraft control requirements p 934 N90-28515

British Aerospace Public Ltd. Co., Preston (England).

- The Experimental Aircraft Flight Test Programme p 34 N90-10865

- Flight test instrumentation and data processing at British Aerospace, Warton, U.K. p 59 N90-10887

- Aerodynamic and structural design challenges of a reusable single stage to orbit air-breathing launch vehicle p 354 N90-16814

British Aerospace Public Ltd. Co., Stevenage (England).

- HOTOL: A future launcher for Europe p 353 N90-16800

British Aerospace Public Ltd. Co., Woodford (England).

- Fire hardening of an aircraft passenger cabin p 328 N90-17606

Bundesanstalt fuer Flugsicherung, Frankfurt am Main (Germany, F.R.).

- R and D aspects of the future operational concept of the BFS p 826 N90-27679

Bureau of Air Safety Investigation, Canberra (Australia).

- Australian experience in flight recorder readout and analysis p 820 N90-27644

Burns and Roe Services Corp., Pittsburgh, PA.

- Production of jet fuels from coal derived liquids. Volume 10: Jet fuels production by-products, utility, and sulfur emissions control integration study
[AD-A213872] p 357 N90-16951

C**CAE Electronics Ltd., Montreal (Quebec).**

- Helmet mounted display systems for helicopter simulation p 420 A90-31344

California Inst. of Tech., Pasadena.

- Application of dynamical systems theory to the high angle of attack dynamics of the F-14
[AIAA PAPER 90-0221] p 257 A90-22184

- Combustion instabilities in liquid-fueled propulsion systems: An overview p 63 N90-10192

California Polytechnic State Univ., San Luis Obispo.

- Aerodynamic design of the Cal Poly Da Vinci Human-Powered Helicopter p 830 A90-46950

- California air transportation study: A transportation system for the California Corridor of the year 2010 [NASA-CR-186219] p 176 N90-14212
- Preliminary design of four aircraft to service the California Corridor in the year 2010: The California Corridor, California Sky-Hopper, high capacity short range transport tilt rotor aircraft needed to simplify intercity transportation [NASA-CR-186232] p 186 N90-14226
- A computer module used to calculate the horizontal control surface size of a conceptual aircraft design [NASA-CR-186872] p 780 N90-26515
- Economical graphics display system for flight simulation avionics [NASA-CR-186886] p 849 N90-27701
- California State Polytechnic Univ., Pomona.**
- NASA/USRA high altitude reconnaissance aircraft [NASA-CR-186685] p 650 N90-24266
- Global Sentry: NASA/USRA high altitude reconnaissance aircraft design, volume 2 [NASA-CR-186820-VOL-2] p 736 N90-25971
- California State Univ., Long Beach.**
- Progress towards the development of an inviscid-viscous interaction method for unsteady flows in turbomachinery cascades p 8 A90-11806
- Fortified LEWICE with viscous effects [AIAA PAPER 90-0754] p 176 A90-20009
- A three-dimensional linear stability approach to transition on wings at incidence p 20 N90-10373
- California State Univ., Sacramento.**
- Very-low-frequency oscillations in liquid-fueled ramjets p 54 N90-10204
- Calculation of the combustion distribution in a liquid-fuel ramjet p 858 N90-27931
- Entropy wave instability in compact ramjets p 858 N90-27932
- California Univ., Berkeley.**
- Streamtube analysis of supersonic combustion in an in-tube scramjet [AIAA PAPER 90-2339] p 762 A90-42776
- Interaction of an oblique shock wave with supersonic flow over a blunt body p 398 N90-19197
- Liquid fueled ramjet combustion instability: Acoustical and vortical interactions with burning sprays [AD-A222752] p 767 N90-26104
- California Univ., Davis.**
- Wind-tunnel investigation on the effect of a crescent planform on drag [AIAA PAPER 90-0300] p 228 A90-22196
- An application of generalized predictive control to rotorcraft terrain-following flight p 257 A90-23478
- Generalized Transition Finite-Boundary Elements for high speed flight structures [AIAA PAPER 90-1105] p 449 A90-29286
- Design and evaluation of a cockpit display for hovering flight p 490 A90-33059
- Wind-tunnel investigations of wings with serrated sharp trailing edges p 802 A90-46379
- Analyzing the flared landing task with pitch-rate flight control systems [AIAA PAPER 90-3483] p 866 A90-47732
- Subsonic and transonic low-Reynolds-number airfoils with reduced pitching moments [AIAA PAPER 90-3212] p 812 A90-48838
- Parametric analysis of swept-wing geometry with sheared wing tips [AIAA PAPER 90-3196] p 812 A90-49101
- Convergence acceleration of hypersonic flow calculations: A nonlinear relaxation factor p 480 N90-20957
- California Univ., Irvine.**
- Influence of the continuous and dispersed phases on the symmetry of a gas turbine air-blast atomizer [ASME PAPER 89-GT-303] p 273 A90-22651
- Symmetry assessment of an air-blast atomizer spray p 682 A90-40930
- California Univ., Los Angeles.**
- A simple active controller to suppress helicopter air resonance in hover and forward flight p 119 A90-16521
- Modeling of liquid jets injected transversely into a supersonic crossflow p 153 A90-17985
- Pressure fluctuations in the tip region of a blunt-tipped airfoil p 154 A90-18136
- Compensating for pneumatic distortion in pressure sensing devices [AIAA PAPER 90-0631] p 211 A90-19956
- Helicopter rotor dynamics and aeroelasticity - Some key ideas and insights p 335 A90-25425
- Rotary-wing aeroelasticity with application to VTOL vehicles [AIAA PAPER 90-1115] p 392 A90-29387
- Aeroelastic problems in turbomachines [AIAA PAPER 90-1157] p 393 A90-29393
- Structural optimization with aeroelastic constraints of rotor blades with straight and swept tips p 535 A90-32475
- A model for active control of helicopter air resonance in hover and forward flight p 670 A90-42462
- A study of fundamental issues in higher harmonic control using aeroelastic simulation p 861 A90-46966
- Real-time support for high performance aircraft operation [NASA-CR-185475] p 57 N90-10075
- Formulation and verification of a technique for compensation of pneumatic attenuation errors in airborne pressure sensing devices p 369 N90-17084
- Control and stabilization of linear and nonlinear distributed systems [AD-A216446] p 462 N90-18908
- Aeroelastic simulation of higher harmonic control p 592 N90-21768
- Advances in optimal active control techniques for aerospace systems; application to aircraft active landing gear p 592 N90-21769
- California Univ., San Diego, La Jolla.**
- Observability of relative navigation using range-only measurements p 917 N90-29360
- Calspan-Buffalo Univ. Research Center, NY.**
- Experimental studies of shock wave/wall jet interaction in hypersonic flow [AIAA PAPER 90-0607] p 231 A90-22449
- Shock-shock boundary layer interactions p 318 N90-17569
- Calspan Corp., Arnold AFS, TN.**
- Wind tunnel support system effects on a fighter aircraft model at Mach numbers from 0.6 to 2.0 [AD-A210614] p 19 N90-10010
- Cavity aerodynamics [AD-A223853] p 911 N90-29307
- Cambridge Collaborative, Inc., MA.**
- Evaluation of analysis techniques for low frequency interior noise and vibration of commercial aircraft [NASA-CR-181851] p 220 N90-14866
- Cambridge Univ. (England).**
- A method for the prediction of supersonic compressor blade performance [CUED/A-TURBO/TR-126] p 344 N90-17634
- Modelling unsteady transition and its effects on profile loss p 427 N90-18423
- Canadian Aviation Safety Board, Ottawa (Ontario).**
- Aircraft fire safety: Learning from past accidents p 324 N90-17584
- The Canadian Aviation Safety Board's flight recorder facility p 849 N90-27643
- Carleton Univ., Ottawa (Ontario).**
- Losses in the tip-leakage flow of a planar cascade of turbine blades p 514 N90-21027
- Carnegie-Mellon Univ., Pittsburgh, PA.**
- Gas identification system using graded temperature sensor and neural net interpretation [AD-A213359] p 205 N90-13627
- Inertial navigation system simulator: Behavioral specification, revision [AD-A219294] p 578 N90-22554
- An object-oriented solution example: A flight simulator electrical system [AD-A219190] p 761 N90-25145
- Case Inst. of Tech., Cleveland, OH.**
- Interactive calculation procedures for mixed compression inlets [NASA-CR-186581] p 718 N90-25934
- Case Western Reserve Univ., Cleveland, OH.**
- Use of unbalanced laminates as a screening method for microcracking p 948 A90-50217
- Catholic Univ. of America, Washington, DC.**
- An experimental investigation of viscous aspects of propeller blade flow p 315 N90-16711
- Center for Night Vision and Electro-Optics, Fort Belvoir, VA.**
- Reduced voltage and restart testing of the 1-watt integral cryogenic cooler (HD-1033B/C/D) [AD-A215133] p 369 N90-16971
- Central Research Inst. of Electric Power Industry, Tokyo (Japan).**
- Study on application of ultrasonic wave measurement to creep-fatigue damage detection [DE89-782317] p 774 N90-25361
- Development of creep-fatigue damage detection method of rotor steel by ultrasonic wave measurement [DE90-503792] p 777 N90-26365
- Centre Aeroport de Toulouse (France).**
- Performance and quality of a wing type parachute: Parametric analysis [REPT-88-19] p 89 N90-11710
- Centre d'Essais Aeronautique Toulouse (France).**
- Nondestructive analysis of aileron fatigue and aging in a Mirage F1 [REPT-M6-594000] p 184 N90-13378
- Analysis of indirect effects of lightning on a metallic A 300 wing: Test report [REPT-E87/645800] p 323 N90-16726
- Bird impact tests on asymmetric sandwich structures made in Kevlar 49 [CEAT-NT-10/S/83-5] p 323 N90-16727
- Bird impact tests on curved structures of the type Sandwich-Kevlar-Nida for normal and angular shooting [CEAT-NT-10/S/83-4] p 324 N90-16728
- Bird impact tests on a Kevlar 49 structure: Monolithic plates: Oblique-angled impact [REPT-S3-4273] p 402 N90-18376
- The need for a common approach within AGARD p 425 N90-18404
- Toxicity of thermolysis products from the materials of airplane cockpits [CEAT-PV-M6/5924/02] p 876 N90-27895
- Characterization of the CP 214 T851. Dissection of a cast flat bar for a standard spar [CEAT-PV-M4/462200] p 876 N90-27905
- Characterization of the 7175 T7352. Dissection of a die casting standard spar [CEAT-PV-M5/528900] p 877 N90-27906
- Characterization of the 7175 T7352 101. Dissection of a die casting standard spar [CEAT-PV-M5/5288] p 877 N90-27907
- Characterization of the 7010 T73651. Dissection of a sheet billet for a standard spar [CEAT-PV-M5/521700] p 877 N90-27908
- Study of the ground effects in the CEAT aerohydrodynamic tunnel: Using the results p 922 N90-28530
- Centre d'Essais en Vol, Bretigny-sur-Orge (France).**
- Lessons learned from the integration of flight systems p 35 N90-10874
- Centre d'Etudes et de Recherches, Toulouse (France).**
- Reduction of turbulent drag: Boundary layer manipulators [CERT-RSF-OA-74/2259-AYD] p 136 N90-12889
- Transition in surface boundary layers [CERT-RSF-OA-43/5018-AYD] p 136 N90-12897
- Main results of CAST-10 airfoil tested in T2 cryogenic wind tunnel p 321 N90-17652
- Study of the flow around the prototype of A300: Results of the third test campaign at F2 and comparison with calculations [CERT-33/5025-29-DERAT] p 817 N90-27663
- Centre National de la Recherche Scientifique, Ecullly (France).**
- Parabolized calculations of turbulent three dimensional flows in a turbine duct p 482 N90-21013
- Centro Italiano Ricerche Aerospaziali, Naples.**
- A computer code for the prediction of aerodynamic characteristics of lifting airfoils at transonic speed [DLC-EST-TN-030] p 632 N90-23359
- Prediction of aerodynamic performance of airfoils in low Reynolds number flows [DLC-EST-TN-031] p 632 N90-23360
- Problems of internal acoustics in two and three dimensional cavities with deformable walls using the MSC/Nastran code [DLC/STR-INT-TN-004] p 699 N90-24876
- Cessna Aircraft Co., Wichita, KS.**
- In-flight boundary-layer transition measurements on a swept wing p 17 A90-13017
- A flight test investigation of certification requirements for laminar-flow general aviation airplanes [AIAA PAPER 90-1310] p 496 A90-33920
- Laminar flow: The Cessna perspective p 91 N90-12507
- Flight test investigation of certification issues pertaining to general-aviation-type aircraft with natural laminar flow [NASA-CR-181967] p 480 N90-20952
- Charles River Analytics, Inc., Cambridge, MA.**
- An experimental investigation of fault tolerant software structures in an avionics application [AIAA PAPER 89-3082] p 74 A90-10568
- Hierarchical damage tolerant controllers for smart structures [AD-A209422] p 31 N90-10022
- Model-based method for terrain-following display design [AD-A219302] p 583 N90-22563
- Chung Shan Inst. of Science and Technology, Lung Tan (China).**
- Optimal plane change by low aerodynamic forces [AIAA PAPER 90-2831] p 763 A90-45137
- Cincinnati Univ., OH.**
- Analysis of high-incidence separated flow past airfoils p 147 A90-16781
- Finite element mesh refinement criteria for stress analysis p 273 A90-23013
- A flux-split solution procedure for unsteady inlet flows [AIAA PAPER 90-0585] p 314 A90-26967
- Transient behavior of supersonic flow through inlets [AIAA PAPER 90-2130] p 704 A90-42734
- Flow separation in oblique shock wave turbulent boundary layer interactions p 807 A90-46872

- Analysis and numerical solution of flow over airfoil with control flap p 318 N90-17564
- Direct multivariable adaptive controller with application to wing flutter p 349 N90-17642
- LDV measurements and the flow analysis in the vortex region of a radial inflow turbine p 511 N90-21007
- Composite reduced Navier Stokes procedures for flow problems with strong pressure interactions [AD-A219621] p 689 N90-23687
- City Coll. of the City Univ. of New York, NY.**
- Linear instability of the supersonic wake behind a flat plate aligned with a uniform stream p 716 A90-45783
- Civil Aeromedical Inst., Oklahoma City, OK.**
- The influence of adjacent seating configurations on egress through a type 3 emergency exit [AD-A218393] p 636 N90-23371
- Civil Aviation Authority, Gatwick (England).**
- Aircraft internal fires p 326 N90-17593
- Civil Aviation Authority, London (England).**
- UK airmisses involving commercial air transport, May-August 1988 [ISSN-0951-6301] p 96 N90-11717
- UK airmisses involving commercial air transport [CAA-2/88] p 96 N90-11718
- Aircraft cabin fire suppression by means of an interior water spray system [CAA-PAPER-88014] p 96 N90-11719
- The 1987 survey of track keeping and altitudes on Heathrow and Gatwick standard instrument departure routes (DAY) [CAA-PAPER-88010] p 99 N90-11729
- Development and evaluation at ATCEU of executive and support operations, phase 4A/3D [CAA-PAPER-88017] p 99 N90-12572
- Operational trial of effect of raising minimum stack level in Heathrow stacks [CAA-PAPER-89003] p 99 N90-12573
- Assessment of voice coders for ATC/pilot voice communications via satellite digital communication channels [CAA-PAPER-89004] p 135 N90-12807
- UK airmisses involving commercial air transport, September to December 1988 [ISSN-0951-6301] p 240 N90-15897
- A review of UK civil aviation fire and cabin safety research p 325 N90-17587
- UK airmisses involving commercial air transport, January - April 1989 [ISSN-0951-6301] p 575 N90-22544
- UK airmisses involving commercial air transport: May - August 1989 [ISSN-0951-6301] p 913 N90-29335
- Aircraft evacuations: The effect of passenger motivation and cabin configuration adjacent to the exit [CAA-PAPER-89019] p 913 N90-29336
- Clemson Univ., SC.**
- Adaptive clutter rejection filters for airborne Doppler weather radar applied to the detection of low altitude windshear [NASA-CR-186211] p 214 N90-14453
- Cleveland State Univ., OH.**
- Analysis of whisker-toughened ceramic components - A design engineer's viewpoint p 205 A90-19149
- Noninteractive macroscopic reliability model for ceramic matrix composites with orthotropic material symmetry [ASME PAPER 89-GT-129] p 360 A90-23827
- A review of failure models for ceramic matrix composite laminates under monotonic loads [ASME PAPER 89-GT-153] p 354 A90-23842
- College of William and Mary, Williamsburg, VA.**
- In-situ measurement, modelling and control of the imidization reaction in PMR-15 p 941 A90-50066
- Colorado Univ., Boulder.**
- Computation of viscous transonic flow over porous airfoils p 153 A90-17864
- Computational simulation of flows about hypersonic geometries with sharp leading edges [AIAA PAPER 90-3065] p 793 A90-45891
- Thermal interaction between an impinging hot jet and a conducting solid surface [AIAA PAPER 90-3010] p 956 A90-50636
- Neurocontrol systems and wing-fluid interactions underlying dragonfly flight p 434 N90-19240
- Experimental investigation of the mechanisms underlying vortex kinematics in unsteady separated flows [AD-A217889] p 540 N90-20346
- Dynamic separation: Search for the cause of dynamic stall and search for its control [AD-A223412] p 911 N90-29305
- Columbia Univ., New York, NY.**
- Numerical grid generation in computational fluid mechanics '88; Proceedings of the Second International Conference, Miami Beach, FL, Dec. 5-8, 1988 p 376 A90-26476

- Interactive grid generation for turbomachinery flow field simulations p 312 A90-26553
- Fiber reinforced superalloys p 532 A90-34169
- Committee on Science, Space and Technology (U.S. House).**
- Review of the Aerospace Safety Advisory Panel report for NASA fiscal year 1990 authorization [GPO-24-234] p 177 N90-14213
- Computational Mechanics Co., Austin, TX.**
- Analysis of flow-, thermal-, and structural-interaction of hypersonic structures subjected to severe aerodynamic heating [AD-A217882] p 478 N90-20053
- Computer Resource Management, Inc., Vienna, VA.**
- Ground and Obstacle Avoidance (GOA) concept of operations [DOT/FAA/DS-89/08] p 28 N90-10855
- National airspace system monitoring operational concept [NAS-SR-1330] p 178 N90-14214
- National airspace system air-ground communications operational concept [DOT/FAA/DS-90/2] p 542 N90-21249
- Computer Sciences Corp., Hampton, VA.**
- Advanced transport operating system software upgrade: Flight management/flight controls software description [NASA-CR-181936] p 893 N90-28366
- Computer Sciences Corp., Huntsville, AL.**
- Analysis of extreme wind shear p 280 A90-23255
- Computer Technology Associates, Inc., Colorado Springs, CO.**
- FAA air traffic control operations concepts, Volume 7: ATCT (Airport Traffic Control Towers) tower controllers [AD-A210455] p 332 N90-16730
- Computer-Technology Associates, Inc., McKee City, NJ.**
- Dallas/Forth Worth simulation, Phase 2: Triple simultaneous parallel Instrument Landing System (ILS) approaches (turbojets) [DOT/FAA/CT-90/2] p 915 N90-28509
- Computing Devices Co., Ottawa (Ontario).**
- Development of a real-time aeroperformance analysis technique for the X-29A advanced technical demonstrator p 732 A90-44738
- Concordia Univ., Montreal (Quebec).**
- Measurement and computer simulation of antennas on ships and aircraft for results of operational reliability p 370 N90-17936
- Connecticut Univ., Storrs.**
- Research on cascade secondary and tip-leakage flows: Periodicity and surface flow visualization p 514 N90-21026
- Construcciones Aeronauticas S.A., Madrid (Spain).**
- Simple shear tests of the FMI 23.5.06 adhesive cured at low pressure (12 PSI) [INFORME-I-298/88] p 357 N90-17871
- Pressure air tightness tests of laminated panels for wing leading edge heat shields [INFORME-I-377/89] p 357 N90-17873
- Impact of composites in the aerospace industry [ETN-90-96231] p 443 N90-18527
- Continuum Dynamics, Inc., Princeton, NJ.**
- New free-wake analysis of rotorcraft hover performance using influence coefficients p 181 A90-17867
- High resolution flow field prediction for tail rotor aerodynamics p 463 A90-28158
- Optimization of rotor performance in hover and axial flight using a free wake analysis p 407 A90-28175
- Cornell Univ., Ithaca, NY.**
- Tilt rotor aircraft aerodynamics p 409 A90-28238
- Costruzioni Aeronautiche Giovanni Agusta S.p.A., Cascina Costa (Italy).**
- Results of an A109 simulation validation and handling qualities study p 591 A90-38524
- Agusta methodology for pitch link loads prediction in preliminary design phase [ETN-90-97270] p 737 N90-25978
- Development of a method to design helicopter rotors [REPT-100-30-03] p 845 N90-26830
- Design of helicopter components in metal matrix composites [REPT-100-20-55] p 874 N90-26894
- Council for National Academic Awards (England).**
- A study of variable geometry in advanced gas turbines p 255 N90-15104
- Flow in a forward swept centrifugal fan, volumes 1 and 2 p 481 N90-20959
- Supersonic nozzle design of arbitrary cross-section p 515 N90-21035
- Studies in automatic speech recognition and its application in aerospace p 958 N90-28759

- Cranfield Inst. of Tech., Bedford (England).**
- The determination of the aerodynamic characteristics of an ogive-cylinder body in subsonic, curved, incompressible flow, and an assessment of the effect of flow curvature p 89 N90-11712
- Incompressible flow about ellipsoids of revolution [REPT-88-02] p 90 N90-11713
- On the application of modified stepwise regression for the estimation of aircraft stability and control parameters [REPT-8905] p 198 N90-13400
- Glancing shock-boundary layer interactions p 319 N90-17571
- Aircraft fires: A study of transport accidents from 1975 to the present p 324 N90-17583
- Combustion in the gas turbine. Part 1: Combustor types and design [CIT/SME/VKI/RS/1] p 748 N90-25986
- Combustion in the gas turbine. Part 2: Preliminary design and performance [CIT/SME/VKI/RS/3] p 748 N90-25987
- Combustion in the gas turbine. Part 3: Fuel injection, ignition and stability [CIT/SME/VKI/RS/4] p 748 N90-25988
- Combustor cooling aspects [CIT/SME/VKI/RS/5] p 749 N90-25989
- Pollutants: Production and methods of reduction [CIT/SME/VKI/RS/6] p 749 N90-25990
- Aircraft evacuations: The effect of passenger motivation and cabin configuration adjacent to the exit [CAA-PAPER-89019] p 913 N90-29336

D

- Dayton Univ., OH.**
- Fatigue life estimates for helicopter loading spectra p 772 A90-45324
- Computation of ramjet internal flowfields [AD-A212001] p 114 N90-11743
- Study of the engine bird ingestion experience of the Boeing 737 aircraft [DOT/FAA/CT-89/16] p 176 N90-13360
- Stress intensity factors for cracking metal structures under rapid thermal loading. Volume 2: Theoretical background [AD-A213297] p 213 N90-13812
- The collection of non-conus aircraft icing data along with an identification of the geographical areas of potential severe icing and a study of a method of remote determining atmospheric icing data [AD-A215055] p 323 N90-16724
- Study of bird ingestions into small inlet area, aircraft turbine engines (May 1987 to April 1988) [DOT/FAA/CT-89/17] p 402 N90-18375
- Full-scale birdstrike testing of in-service aged F-111 ADBIRT windshield transparencies [AD-A218035] p 484 N90-20069
- Fatigue crack growth investigation of a Ti-6Al-4V forging under complex loading conditions: NATO/AGARD supplemental engine disk program [AD-A220239] p 678 N90-23538
- Nondestructive measurement of residual stresses in aircraft transparencies [AD-A218680] p 689 N90-23762
- Study of the engine bird ingestion experience of the Boeing 737 aircraft (October 1986 to September 1988) [DOT/FAA/CT-89/29] p 723 N90-25119
- B-1B improved windshield development. Volume 2: Magna analysis: Baseline and parametric [AD-A221501] p 845 N90-26828
- Aircraft battle damage repair of transparencies [AD-A224168] p 925 N90-29387
- Structural testing and analytical research of turbine components p 933 N90-29396
- Terrain visual cue analysis for simulating low-level flight: A multidimensional scaling approach [AD-A223564] p 938 N90-29407
- Defence and Civil Inst. of Environmental Medicine, Downsview (Ontario).**
- The application of queuing theory to the modelling of CP-140 aircraft communications [AD-A213479] p 274 N90-15310
- Defence Research Establishment Atlantic, Dartmouth (Nova Scotia).**
- Chordwise loading and camber for two-dimensional thin sections [AD-A213318] p 95 N90-12568
- Noise from tip vortex and bubble cavitation [AD-A221962] p 896 N90-27468
- Defence Research Establishment, Ottawa (Ontario).**
- The development of an airborne synthetic aperture radar motion compensation system p 333 N90-16745

Defence Research Establishment Pacific, Victoria (British Columbia).
Development of an automated ultrasonic inspection system for composite structure on in-service aircraft p 885 N90-28079

Defence Research Establishment Suffield, Ralston (Alberta).
A sensor stabilization/tracking system for unmanned air vehicles [AD-A224008] p 936 N90-28579

Delta Air Lines, Inc., Atlanta, GA.
Penetration landing guidance trajectories in the presence of windshear p 98 A90-14732
Acceleration, gamma, and theta guidance for abort landing in a windshear p 98 A90-14733

Department of Civil Aviation, An Hoofddorp (Netherlands).
Fire safety in civil aviation p 325 N90-17586

Department of Energy, Washington, DC.
Relative merits of reactive and forward-looking detection for wind-shear encounters during landing approach for various microburst escape strategies [NASA-TM-4158] p 259 N90-15108

Department of the Air Force, Washington, DC.
Externally vaporizing system for turbine combustor [AD-D014284] p 256 N90-15918

Department of the Navy, Washington, DC.
Apparatus for cooling electronic components in aircraft [AD-D014207] p 183 N90-13373
Inflatable fuel tank buffer [AD-D014446] p 503 N90-21002
Yaw fin deployment apparatus for ejection seat [AD-D014512] p 723 N90-25118

Detroit Diesel Allison, Indianapolis, IN.
Advanced Turbine Technology Applications Project (ATTAP) [NASA-CR-185133] p 51 N90-10036

Deutsche Forschungs- und Versuchsanstalt fuer Luft- und Raumfahrt, Brunswick (Germany, F.R.).
Rotor blade-vortex interaction impulsive noise source localization p 463 A90-27978
ATTAS flight testing experiences p 34 N90-10862
GRATE: A new flight test tool for flying qualities evaluation p 34 N90-10868
Devices and procedures for the calibration of sensors and measurement: Systems of the flight test support system ATTAS [DFVLR-MITT-89-06] p 134 N90-12007
Aircraft response and pilot behaviour during a wake vortex encounter perpendicular to the vortex axis p 259 N90-15057
Determination of the N-factor in the Brunswick (Federal Rep. of Germany) transonic wind tunnel using measurements of pressure distributions and transition points, and the Sally method p 276 N90-16177
Direct measurement of laminar instability amplification factors in flight p 277 N90-16178
Research on three different Euler's schemes applied to a delta wing with vortical flows p 278 N90-16184
Use of the film-of-oil technique for profile measurements in the Transonic Wind tunnel Brunswick (TWB) p 238 N90-16252
Aerodynamic design techniques at DLR Institute for Design Aerodynamics p 500 N90-20979

Deutsche Forschungs- und Versuchsanstalt fuer Luft- und Raumfahrt, Cologne (Germany, F.R.).
Laser two focus techniques p 212 N90-13348
Full scale study of a cabin fire in an A300 fuselage section p 326 N90-17592

Deutsche Forschungs- und Versuchsanstalt fuer Luft- und Raumfahrt, Goettingen (Germany, F.R.).
Experimental investigation of flowfield about a multielement airfoil p 154 A90-18137
Steady and unsteady potential flow around thin annular wings and engines with simulation of jet engine flow [DFVLR-FB-89-18] p 89 N90-11711
Flow field visualization study on a 65 deg delta wing at $M = 0.85$ p 277 N90-16182
Numerical simulation of the laminar and turbulent three dimensional flow on a delta wing with sharp leading edge p 278 N90-16186
Comparison of conventional and adaptive wall wind tunnel results with regard to Reynolds number effects p 352 N90-17649
Progress in inverse design and optimization in aerodynamics p 482 N90-20977
Adaptation for unsteady flow p 871 N90-26845

Deutsche Forschungs- und Versuchsanstalt fuer Luft- und Raumfahrt, Oberpfaffenhofen (Germany, F.R.).
Controller design for active vibration suppression of a helicopter [DFVLR-FB-89-20] p 120 N90-11760

Deutsche Forschungsanstalt fuer Luft- und Raumfahrt, Brunswick (Germany, F.R.).
Automatic processing of images from the GRATE flight test tool [DLR-FB-89-28] p 109 N90-12599
Computation of flow fields around propellers and hovering rotors based on the solution of the Euler equations [DLR-FB-89-37] p 170 N90-13333
General buckling tests with thin-walled shells [DLR-MITT-89-13] p 213 N90-13816
Hermes training aircraft p 354 N90-16827
En route noise of two turboprop aircraft [DLR-MITT-89-18] p 697 N90-24859
Aircraft Integrated Monitoring Systems [DLR-MITT-90-04] p 786 N90-27617
Past, present and future: Aircraft integrated monitoring systems: An ever-developing technology p 848 N90-27618
Start-up built-in test for the DISCUS fault tolerant, fly-by-wire computer system p 869 N90-27625
Monitoring and controlling flight in windshear p 820 N90-27641
Automation of the readout, transcription and evaluation of digital flight data at DLR p 893 N90-27645
Position finding and ground target direction finding by an aircraft with a gimbal video camera [DLR-FB-89-62] p 825 N90-27673
Integrated Air Traffic Management [DLR-MITT-89-23] p 825 N90-27676
On-board planning and control of 4D-trajectories in the TMA p 826 N90-27680
On the structure of a future flight operations system p 826 N90-27682
Four-dimensional planner: A ground based planning system for time accurate approach guidance p 826 N90-27683
Development of a COMPAS prototype for the ATC Centre at Frankfurt (Fed. Republic of Germany) p 826 N90-27684
Approach towards a future integrated airport surface traffic management p 827 N90-27686
Experimental study towards a future airport ground movement simulator p 827 N90-27687
Aspects of data link applications for ATC purposes p 827 N90-27688
Procedure for calibrating fly-by-wire control chains of the flying testbed ATTAS [DLR-MITT-90-02] p 936 N90-29401

Deutsche Forschungsanstalt fuer Luft- und Raumfahrt, Cologne (Germany, F.R.).
Activities report in German aerospace [ISSN-0070-3966] p 465 N90-19189
Secondary flow in a turbine guide vane with low aspect ratio p 513 N90-21018
Centrifugal impeller geometry and its influence on secondary flows p 513 N90-21020
Infrared thermography at hypersonic channel H2K p 674 N90-24235
Overview on hot gas tests and molten salt corrosion experiments at the DLR p 953 N90-28714

Deutsche Forschungsanstalt fuer Luft- und Raumfahrt, Goettingen (Germany, F.R.).
Generalized similarity solutions for three dimensional, laminar, steady, compressible boundary layer flows on swept profile cylinders [DLR-FB-89-34] p 212 N90-13725
Numerical simulation of transition in three-dimensional boundary layers p 212 N90-13728
The cryogenic Ludwig tube tunnel at Goettingen p 263 N90-15947
Half model tests on an ONERA calibration model in the transonic wind tunnel Goettingen, Federal Republic of Germany [DLR-MITT-89-20] p 397 N90-18370
Measurement of the flow field in the blade passage and side-wall region of a plane turbine cascade p 513 N90-21019
A time-marching method to calculate unsteady airloads on three-dimensional wings. Part 1: Linearized formulation [DLR-FB-89-58] p 634 N90-24254
A time-marching method for calculating unsteady airloads on three-dimensional wings. Part 2: Full-potential formulation [DLR-FB-89-59] p 635 N90-24255
On simplified analytical flutter clearance procedures for light aircraft [DLR-FB-89-56] p 672 N90-24276
Design of an axisymmetric, contoured nozzle for the HEG [DLR-FB-90-04] p 959 N90-28812
Applications of LIF to high speed flows p 911 N90-29320

Deutsche Forschungsanstalt fuer Luft- und Raumfahrt, Hamburg (Germany, F.R.).
Four-dimensional navigation and Flight Management Systems p 826 N90-27681

Deutsche Forschungsanstalt fuer Luft- und Raumfahrt, Oberpfaffenhofen (Germany, F.R.).
Airborne CO2 Doppler lidar for wind shear detection p 849 N90-27640

Deutsche Gesellschaft fuer Luft- und Raumfahrt, Bonn (Germany, F.R.).
Flows with Separation [DGLR-PAPERS-88-05] p 276 N90-16169
Experiments on the laminar-turbulent transition on swept wings p 276 N90-16170
The jet engine: 1932 [ISBN-3-922010-49-0] p 763 N90-25189

Deutsche Lufthansa A.G., Hamburg (Germany, F.R.).
The 30th Airlines International Electronics Meeting Proceedings [ETN-90-96973] p 637 N90-24261
Airline requirements for a future air traffic management system p 825 N90-27678
Application of a company data link at Lufthansa German Airlines p 827 N90-27689

Dornier System G.m.b.H., Friedrichshafen (Germany, F.R.).
Periodically unsteady effects on profiles, induced by separation p 279 N90-16196

Dornier-Werke G.m.b.H., Friedrichshafen (Germany, F.R.).
Active control system for gust load alleviation and structural damping p 259 N90-15056
Dynamic derivatives of missiles and fighter-type configurations at high angles of attack p 337 N90-17554
Aerodynamic design by optimization p 502 N90-20996
Inflight thrust vectoring: A further degree of freedom in the aerodynamic/light mechanical design of modern fighter aircraft p 921 N90-28528
Aerodynamic interferences of in-flight thrust reversers in ground effect p 921 N90-28529

Douglas Aircraft Co., Inc., Long Beach, CA.
Supersonic boundary layer stability analysis with and without suction on aircraft wings p 148 A90-16792
Experimental investigation of flowfield about a multielement airfoil p 154 A90-18137
Subcomponent tests for composite fuselage technology readiness p 490 A90-33105
Impact damage and residual strength analysis of composite panels with bonded stiffeners p 642 A90-40130
LFC: A maturing concept [DOUGLAS-PAPER-7878] p 90 N90-12505
The right wing of the LEFT airplane p 91 N90-12510
UHB demonstrator interior noise control flight tests and analysis [NASA-CR-181897] p 140 N90-13198
Study of high-speed civil transports [NASA-CR-4235] p 183 N90-13370
Potential role of avionics in escape systems p 483 N90-20060
Controllable propulsion for escape systems control p 484 N90-20064
An interactive boundary-layer method for unsteady airfoil flows. Part 1: Quasi-steady-state model [AD-A221220] p 634 N90-24250
Study of high-speed civil transports. Summary [NASA-CR-4236] p 735 N90-25966

Draper (Charles Stark) Lab., Inc., Cambridge, MA.
A knowledge-based system design/information tool for aircraft flight control systems [AIAA PAPER 89-2978] p 55 A90-10491
Real-time adaptive aircraft scheduling [NASA-CR-177558] p 820 N90-27669
Model authoring system for fail safe analysis [NASA-CR-4317] p 964 N90-29142
A knowledge-based system design/information tool [NASA-CR-4316] p 965 N90-29143

Dual and Associates, Houston, TX.
The Real Time Display Builder (RTDB) p 546 N90-20656

Duke Univ., Durham, NC.
New free-wake analysis of rotorcraft hover performance using influence coefficients p 181 A90-17867
High resolution flow field prediction for tail rotor aerodynamics p 463 A90-28158
Optimization of rotor performance in hover and axial flight using a free wake analysis p 407 A90-28175
Asymptotic modal analysis and statistical energy analysis [NASA-CR-186732] p 782 N90-26634

- Dundee Univ. (Scotland).**
Design temperatures for flexible airfield pavement design
[AD-A214141] p 262 N90-15115
- Durham Univ. (England).**
An investigation of secondary flows in nozzle guide vanes
p 512 N90-21016
- Dynamic Controls, Inc., Dayton, OH.**
Advanced actuation systems development, volume 1
[AD-A213334] p 121 N90-12624
Advanced actuation systems development, volume 2
[AD-A213378] p 198 N90-13398
- Dynetics, Inc., Huntsville, AL.**
Adaptive control law design for model uncertainty compensation
[AD-A211712] p 120 N90-11758

E

- EA Engineering Science and Technology, Inc., Lafayette, CA.**
Enhanced bioreclamation of jet fuels: A full-scale test at Eglin AFB, Florida
[AD-A22348] p 875 N90-26992
- Eagle Engineering, Inc., Hampton, VA.**
The NASA digital VGH program: Exploration of methods and final results. Volume 2: L 1011 data 1978-1979: 1619 hours
[NASA-CR-181909-VOL-2] p 505 N90-20080
The NASA digital VGH program: Exploration of methods and final results. Volume 1: Development of methods
[NASA-CR-181909-VOL-1] p 505 N90-20081
The NASA digital VGH program: Exploration of methods and final results. Volume 3: B 727 data 1978-1980: 1765 hours
[NASA-CR-181909-VOL-3] p 505 N90-20082
The NASA digital VGH program: Exploration of methods and final results. Volume 4: B 747 data 1978-1980, 1689 hours
[NASA-CR-181909-VOL-4] p 506 N90-20083
The NASA digital VGH program: Exploration of methods and final results. Volume 5: DC 10 data 1981-1982, 129 hours
[NASA-CR-181909-VOL-5] p 506 N90-20084
Summary of sonic boom rise times observed during FAA community response studies over a 6-month period in the Oklahoma City area
[NASA-CR-4277] p 696 N90-24852
- Ecole Centrale de Lyon (France).**
A model suitable for predicting the noise associated with the ducted tail rotor of a helicopter
[ECL-88-09] p 220 N90-14074
- Ecole Nationale de l'Aeronautique et de l'Espace, Toulouse (France).**
Synthesis of control law, on a RPV, in order to minimize the number of sensors
p 260 N90-15925
- Ecole Nationale Supérieure d'Arts et Metiers, Paris (France).**
Efficient solution of the steady Euler equations with a centered implicit method
p 884 N90-27999
- Edgerton, Germeshausen and Grier, Inc., Idaho Falls, ID.**
Three-dimensional analysis on flow and temperature distributions for aircraft fuel thermal stability
[AD-A219651] p 678 N90-23571
- Eldetics International, Inc., Torrance, CA.**
Effect of leading edge roundness on a delta wing in wing-rock motion
[AIAA PAPER 90-3080] p 795 A90-45911
Combat aircraft control requirements for agility
p 935 N90-28517
- Electroimpact, Inc., Seattle, WA.**
Thin film eddy current impulse deicer
[AIAA PAPER 90-0761] p 183 A90-20012
- Eloret Corp., Palo Alto, CA.**
Three dimensional Discrete Particle Simulation about the AFE geometry
[AIAA PAPER 90-1778] p 560 A90-38468
Experimental aerothermodynamic research of hypersonic aircraft
[NASA-CR-186903] p 721 N90-25954
- Eloret Corp., Sunnyvale, CA.**
Experimental and computational surface and flow-field results for an all-body hypersonic aircraft
[AIAA PAPER 90-3067] p 793 A90-45893
Shock layer vacuum UV spectroscopy in an arc-jet wind tunnel
[NASA-TM-102258] p 370 N90-17112
Modeling of vortex-induced oscillations based on indicial response approach
[NASA-CR-186560] p 572 N90-21736
- Embraer S.A., Sao Jose dos Campos (Brazil).**
Analysis of aircraft performance during lateral maneuvering for microburst avoidance
[AIAA PAPER 90-0568] p 197 A90-19920

- Engineering Analysis, Inc., Ames, IA.**
A three-dimensional upwind parabolized Navier-Stokes code for chemically reacting flows
[AIAA PAPER 90-0394] p 165 A90-19831
- Environmental Protection Agency, Washington, DC.**
When propfans cruise, will LDN 65 fly
p 697 N90-24864
- Environmental Research Inst. of Michigan, Ann Arbor.**
Synthetic aperture radar imagery of airports and surrounding areas: Archived SAR data
[NASA-CR-4275] p 401 N90-18371
Synthetic aperture radar imagery of airports and surrounding areas: Philadelphia Airport
[NASA-CR-4280] p 401 N90-18372
Synthetic aperture radar imagery of airports and surrounding areas: Denver Stapleton International Airport
[NASA-CR-4305] p 637 N90-24257
Electro-optics engineering support for the integrated launch and recovery television surveillance system
[AD-A223450] p 938 N90-29406
- ESDU International Ltd., London (England).**
Normal-force-curve and pitching-moment-curve slopes of forebody-cylinder combinations at zero angle of attack for Mach numbers up to 5
[ESDU-89008] p 89 N90-11709
Normal force, pitching moment, and side force of forebody-cylinder combinations for angles of attack up to 90 degrees and Mach numbers up to 5
[ESDU-89014] p 173 N90-14192
Introduction to data items on flight path optimisation
[ESDU-89015] p 185 N90-14221
Hinge moment coefficient derivatives for trailing-edge controls on wings at subsonic speeds
[ESDU-89009] p 198 N90-14239
Example of procedure in calculation of control hinge moments
[ESDU-89010] p 199 N90-14240
Installed tailplane lift-curve slope at subsonic speeds
[ESDU-89029] p 236 N90-15081
The maximum lift coefficient of plain wings at subsonic speeds
[ESDU-89034] p 236 N90-15082
In-plane forces and moments on installed inclined propellers at low forward speeds
[ESDU-89047] p 316 N90-16720
Estimation of subsonic far-field jet-mixing noise from single-stream circular nozzles
[ESDU-89041] p 316 N90-16721
Body effect on wing angle of attack and pitching moment at zero lift at low speeds
[ESDU-89042] p 337 N90-16757
Fatigue of aluminium alloy joints with various fastener systems. Low load transfer
[ESDU-89046] p 370 N90-17193
Calculation of excrescence drag magnification due to pressure gradient at high subsonic speeds
[ESDU-87004] p 397 N90-19195
- Essen Univ. (Germany, F.R.).**
Practical systems for speckle velocimetry
p 171 N90-13341
- ETW G.m.b.H., Cologne (Germany, F.R.).**
The European Transonic Windtunnel (ETW)
p 262 N90-15945
- Eurocontrol Agency, Brussels (Belgium).**
PHARE: Concept and programme
p 827 N90-27690
- European Office of Aerospace Research and Development, London (England).**
HOTOL structures and materials at British Aerospace, Warton, UK
[EOARD-LR-90-001] p 503 N90-21001
Proceedings of the 13th International Congress on Instrumentation in Aerospace Simulation Facilities
[EOARD-LR-89-069] p 527 N90-21046
- European Space Agency, Paris (France).**
A robust digital model following controller for helicopters
[ESA-TT-1041] p 120 N90-12621
Wind tunnel tests of the influence of aerotail thickness on the normal force and pitching moment of two slender wings at transonic and supersonic Mach numbers
[ESA-TT-1129] p 237 N90-15889
Pressure measurement technique in the wind tunnel division of DFVLR
[ESA-TT-1145] p 264 N90-15963
Combustion Experiments During KC-135 Parabolic Flights
[ESA-SP-1113] p 368 N90-16958
Contribution to the study of three-dimensional separation in turbulent incompressible flow
[ESA-TT-1169] p 454 N90-18697
A lifting surface method for the calculation of steady and unsteady, incompressible propeller aerodynamics
[ESA-TT-1151] p 717 N90-25113

- A decision-making aid for multi-layer radar absorbent coverings
[ESA-TT-1173] p 773 N90-25267
Construction of a hybrid angular velocity reference system for investigation of the dynamic characteristics of strapdown gyros
[ESA-TT-1181] p 774 N90-25332
Materials and structures for 2000 and beyond: An attempted forecast by the DLR Materials and Structures Department
[ESA-TT-1154-REV] p 775 N90-26173
Experimental investigations on the stability and vorticity of the vortex breakdown phenomenon above delta wings, measured by the ultrasonic laser method
[ESA-TT-1079] p 910 N90-28498
Flight test engineering with the ATTAS
p 902 N90-29160
Numeric fluid mechanics
p 960 N90-29161
The signals of an ice warning device in dependence on total water content and normalized icing degree
[ESA-TT-1207] p 963 N90-29692
- European Space Agency, European Space Research and Technology Center, ESTEC, Noordwijk (Netherlands).**
Numerical grid generation in computational fluid mechanics '88: Proceedings of the Second International Conference, Miami Beach, FL, Dec. 5-8, 1988
p 376 A90-26476
- Exeter Univ. (England).**
On the Goertler vortex instability mechanism at hypersonic speeds
p 158 A90-18886
Non-axisymmetric viscous lower-branch modes in axisymmetric supersonic flows
p 474 A90-33509
On the instability of hypersonic flow past a wedge
p 554 A90-35902
Wave interactions in a three-dimensional attachment-line boundary layer
p 811 A90-48715

F

- Factory Mutual Research Corp., Norwood, MA.**
Ignitability of jet-A fuel vapors in aircraft fuel tanks
p 326 N90-17594
Flammability testing of aircraft cabin materials
p 328 N90-17611
- Fairchild Space Co., Germantown, MD.**
Structural model significance using INCA
[AIAA PAPER 90-3346] p 889 A90-47606
- Federal Aviation Administration, Atlantic City, NJ.**
ILS/MLS comparison tests at Miami/Tamiami, Florida Airport
[ACD-330] p 27 N90-10018
ILS (Instrument Landing System) mathematical modeling study on the effects of proposed hangar construction west of runway 18R on localizer performance at Dallas-Fort Worth International Airport
[AD-A210631] p 27 N90-10019
The addition of Bendix MLS (Microwave Landing System) antenna patterns to MLS mathematical model
[AD-A210633] p 27 N90-10020
Helicopter Visual Segment Approach Lighting System (HALS)
[ACD-330] p 28 N90-10856
Helicopter surface maneuvering test results
[ACD-330] p 59 N90-10897
Analysis of heliport environmental data: Indianapolis downtown heliport, Wall Street heliport. Volume 2: Wall Street heliport data plots
[DOT/FAA/CT-TN87/54-VOL-2] p 121 N90-11761
ILS mathematical modeling study of the effects of proposed hangar construction at the Orlando International Airport, Runway 17R, Orlando, Florida
[DOT/FAA/CT-TN89/52] p 121 N90-11762
Parallel approach separation and controller performance: A study of the impact of two separation standards
[DOT/FAA/CT-TN89/50] p 99 N90-12574
Aircraft Reply and Interference Environment Simulator (ARIES) hardware principles of operation. Volume 2: Appendixes
[DOT/FAA/CT-TN88/4-2] p 135 N90-12781
Aircraft Reply and Interference Environment Simulator (ARIES) hardware principles of operation, volume 1
[DOT/FAA/CT-TN88/4-1] p 135 N90-12782
Study of the engine bird ingestion experience of the Boeing 737 aircraft
[DOT/FAA/CT-89/16] p 176 N90-13360
LORAN C stability integrity assurance
[AD-A212663] p 177 N90-13364
Data Link Processor (DLP) operational test and evaluation/integration test plan
[DOT/FAA/CT-TN89/32] p 214 N90-14404
Improved lighting of taxiway/taxiway intersections for Instrument Flight Rules (IFR) operations
[DOT/FAA/CT-TN89/64] p 243 N90-15089

Investigation and characteristics of major fire-related accidents in civil air transports over the past ten years p 324 N90-17582

Development of improved fire safety standards adopted by the Federal Aviation Administration p 324 N90-17585

Characteristics of transport, aircraft fires measured by full-scale tests p 325 N90-17591

Preliminary fire extinguishing tests with handheld bottles: A comparison of extinguishing compounds [DOT/FAA/CT-TN89/60] p 370 N90-17930

Dallas/Fort Worth simulation. Volume 2: Appendices D, E, and F [AD-A216613] p 405 N90-18380

In-flight evaluations of turbine fuel extenders [DOT/FAA/CT-89/33] p 444 N90-19387

Operational evaluation of initial data link air traffic control services, volume 1 [DOT/FAA/CT-90/1-VOL-1] p 455 N90-19472

Floor pull test of a transport airframe section [DOT/FAA/CT-TN88/14] p 497 N90-20072

Analysis of heliport environmental data: Indianapolis downtown heliport, Wall Street heliport. Volume 3: Indianapolis downtown heliport data plots [AD-A217412] p 544 N90-20500

Full-scale air transport category fuselage burnthrough tests [DOT/FAA/CT-TN89/65] p 486 N90-20967

Plan for the FAA air traffic operational evaluation of the Automated Surface Observing System (ASOS) [DOT/FAA/CT-TN89/56] p 489 N90-20968

Statistics on aircraft gas turbine engine rotor failures that occurred in US commercial aviation during 1986 [DOT/FAA/CT-89/30] p 511 N90-21008

Modified touchdown zone lighting [DOT/FAA/CT-TN89/70] p 526 N90-21042

Feasibility of using frequency offset on very high frequency air/ground voice channels [DOT/FAA/CT-TN89/71] p 542 N90-21248

Meteorologist Weather Processor (MWP) integration test plan [DOT/FAA/CT-TN89/62] p 544 N90-21500

Analysis of distributions of Visual Meteorological Conditions (VMC) heliport data [DOT/FAA/CT-TN89/67] p 544 N90-21508

Enhanced Low Level Wind Shear (LLWAS) 6-sensor improvement user's manual for data processing of field data [DOT/FAA/CT-TN90/8] p 583 N90-21759

Turbine fuel alternatives (near term) [AD-A219405] p 601 N90-22695

Fire hazards of aerosol cans in aircraft cargo compartments [DOT/FAA/CT-89/32] p 636 N90-23369

An evaluation of the accuracy of a microwave landing system area navigation system at Miami/Tamiami Florida Airport [DOT/FAA/CT-TN89/40] p 640 N90-23377

MLS mathematical model validation study using airborne MLS data from Midway Airport engineering flight tests, August 1988 [DOT/FAA/CT-TN90/2] p 640 N90-23378

Position computation without elevation information for computed centerline operations [DOT/FAA/CT-TN89/42] p 640 N90-23379

Study of the engine bird ingestion experience of the Boeing 737 aircraft (October 1986 to September 1988) [DOT/FAA/CT-89/29] p 723 N90-25119

Replication of NASPAC Dallas/Fort Worth study [DOT/FAA/CT-TN90/26] p 729 N90-25123

The effect of aircraft size on cabin floor dynamic pulses [DOT/FAA/CT-88/15] p 735 N90-25136

Taxiway sign effectiveness under reduced visibility conditions [DOT/FAA/CT-TN90/20] p 761 N90-25150

Flammability of fire resistant, aircraft hydraulic fluid [DOT/FAA/CT-TN90/19] p 766 N90-25222

Equipment feasibility study: Very high frequency communication equipment (136-137 megahertz) [DOT/FAA/CT-TN89/72] p 775 N90-26210

Dallas/Fort Worth simulation, volume 1 [DOT/FAA/CT-TN89/28-VOL-1] p 824 N90-26802

Data link test and analysis system/ATCRBS transponder test system technical reference [DOT/FAA/CT-TN90/7] p 824 N90-26803

Atlanta tower simulation, volume 1 [DOT/FAA/CT-TN89/27-VOL-1] p 870 N90-26835

Atlanta tower simulation. Volume 2: Appendices [DOT/FAA/CT-TN89/27-VOL-2] p 870 N90-26836

Flight service automation system, model 1 full capacity, NAS operational test and evaluation integration test plan [DOT/FAA/CT-TN90/4] p 825 N90-27672

Heliport visual approach surface high temperature and high altitude tests [DOT/FAA/CT-TN89/34] p 825 N90-27675

Dallas/Fort Worth simulation. Phase 2: Triple simultaneous parallel Instrument Landing System (ILS) approaches (turbojets) [DOT/FAA/CT-90/2] p 915 N90-28509

Analysis of heliport environmental data, Intracoastal City [DOT/FAA/CT-TN89/43] p 938 N90-28584

Communications Interface Driver (CID) test plan [DOT/FAA/CT-TN89/35] p 958 N90-28762

A glossary of terms, definitions, acronyms, and abbreviations related to the National Airspace System [DOT/FAA/CT-TN89/53] p 967 N90-29249

Federal Aviation Administration, Washington, DC.

FAA air traffic activity: Fiscal year 1988 [AD-A211338] p 99 N90-12570

National airspace system plan: Facilities, equipment, associated development and other capital needs [AD-A215882] p 402 N90-18373

Census of US civil aircraft [PB90-120296] p 468 N90-20920

An early overview of tiltrotor aircraft characteristics and pilot procedures in civil transport applications [DOT/FAA/DS-89/37] p 503 N90-21003

Criteria for polymer concrete on airport pavements [DOT/FAA/DS-89/18] p 527 N90-21045

Windshear case study: Denver, Colorado, July 11, 1988 [DOT/FAA/DS-89/19] p 544 N90-21509

FAA (Federal Aviation Administration) aviation forecasts, fiscal years 1990-2001 [AD-A219165] p 552 N90-22530

IFR aircraft handled forecast by air route traffic control center: Fiscal years 1990 to 2005 [AD-A220312] p 641 N90-24263

The Federal Aviation Administration plan for research, engineering and development. Volume 1: Program plan [AD-A221263] p 783 N90-25930

The Federal Aviation Administration plan for research, engineering and development. Volume 2: Project descriptions [AD-A221264] p 783 N90-25931

Development of acceptance plans for airport pavement materials. Volume 1: Development [DOT/FAA/RD-90/15] p 937 N90-28581

FAA Rotorcraft Research, Engineering, and Development Bibliography 1962-1989 [AD-A224256] p 902 N90-29299

Reliability and performance of friction measuring tires and friction equipment correlation [AD-A223694] p 939 N90-29408

Federal Ministry of Transport, Bonn (Germany, F.R.).

Objectives and results of cabin fire research in Germany p 325 N90-17588

Fields (James M.), Silver Spring, MD.

Social survey findings on en route noise annoyance issues p 698 N90-24868

Fire Research Station, Borehamwood (England).

Fire science and aircraft safety p 326 N90-17596

Flight Data Co., London (England).

Replay and transmission of AIMS-data to mainframe computer using remote transcribers p 892 N90-27634

Flight Safety Foundation, Inc., Arlington, VA.

The human element: The key to safe, civil operations in adverse weather p 248 N90-15042

International Aircraft Occupant Safety Conference and Workshop proceedings [AD-A214452] p 239 N90-15085

Second Annual International Conference on Aging Aircraft [AD-A222715] p 724 N90-25961

Florida Agricultural and Mechanical Univ., Tallahassee.

Basic studies of the unsteady flow past high angle of attack airfoils [AD-A210252] p 18 N90-10008

Florida Atlantic Univ., Boca Raton.

Sound radiation from an airfoil encountering an oblique gust in its plane of motion p 218 N90-17998

An experimental and analytical investigation of isolated rotor flap-lag stability in forward flight p 518 N90-33623

Mobility power flow analysis of an L-shaped plate structure subjected to acoustic excitation [NASA-CR-186130] p 214 N90-13817

Florida Univ., Gainesville.

Wave formation on a liquid layer for de-icing airplane wings p 445 N90-28137

Effect of vane twist on the performance of dome swirlers for gas turbine airblast atomizers [AIAA PAPER 90-1955] p 881 N90-47203

Design and calibration of an in-stack, low-pressure impactor [AD-A213531] p 255 N90-15105

On total variation diminishing schemes for transonic turbulent flow computation p 479 N90-20945

Flow Analysis, Inc., Mountain View, CA.

Rotor hover performance prediction using a free-wake, computational fluid dynamics method p 153 A90-17869

The prediction of loads on the Boeing Helicopters Model 360 rotor p 410 A90-28240

Flow Analysis, Inc., Tullahoma, TN.

The free-wake computation of rotor-body flows [AIAA PAPER 90-1540] p 565 A90-38684

Flow Research, Inc., Kent, WA.

Numerical simulation of pressure oscillations in a ramjet combustor p 54 N90-10202

Fokker B.V., Schiphol-Oost (Netherlands).

Fabrication of test-articles from Al-Li 2091 for Fokker 100 p 267 N90-15196

Aircraft technology management and the related significance of the supercomputer p 612 N90-22975

Ford Motor Co., Dearborn, MI.

A Monte Carlo simulation technique for low-altitude, wind-shear turbulence [AIAA PAPER 90-0564] p 216 A90-19917

Improved silicon carbide for advanced heat engines [NASA-CR-180831] p 65 N90-10293

Forest Service, San Dimas, CA.

Preliminary thoughts on an acoustic metric for the wilderness aircraft overflight study p 697 N90-24862

Foster-Miller Associates, Inc., Waltham, MA.

Effects of additives on the processing and properties of LARC-TPI polyimide p 942 A90-50070

G

GEC Avionics Ltd., Rochester (England).

The potential for digital databases in flight planning and flight aiding for combat aircraft p 918 N90-29371

General Accounting Office, Washington, DC.

Test and evaluation: Reducing risks to military aircraft from bird collisions. Report to the Chairman, Legislation, and National Security Subcommittee, Committee on Government Operations, House of Representatives [AD-A210670] p 25 N90-10845

Aviation security: Corrective actions underway, but better inspection guidance still needed. Report to the Chairwoman, Government Activities and Transportation Subcommittee, Committee on Government Operations, House of Representatives [GAO/RCED-88-160] p 635 N90-23367

Aviation safety: Conditions within the air traffic control work force. Fact sheet for congressional requesters [GAO/RCED-89-113FS] p 724 N90-25958

Aviation safety: Serious problems continue to trouble the air traffic control work force. Report to congressional requesters [GAO/RCED-89-112] p 724 N90-25959

General Applied Science Labs., Inc., Ronkonkoma, NY.

Hypervelocity real gas capabilities of GASL's expansion tube (HYPULSE) facility [AIAA PAPER 90-1390] p 594 A90-37935

General Dynamics Corp., Fort Worth, TX.

Impact of nose-probe chines on the vortex flows about the F-16C [AIAA PAPER 90-0386] p 165 A90-19828

General Dynamics/Fort Worth, TX.

The implementation of STOVL task-tailored control modes in a fighter cockpit [AIAA PAPER 90-3229] p 839 A90-49114

General Electric Co., Cincinnati, OH.

Application of HOST technology to the SSME HPFTP blade [ASME PAPER 89-GT-130] p 360 A90-23828

PMR graphite engine duct development [NASA-CR-182228] p 51 N90-10037

Full scale technology demonstration of a modern counterrotating unducted fan engine concept: Component test [NASA-CR-180868] p 53 N90-10047

Full scale technology demonstration of a modern counterrotating unducted fan engine concept. Design report [NASA-CR-180867] p 53 N90-10048

Full scale technology demonstration of a modern counterrotating unducted fan engine concept. Engine test [NASA-CR-180869] p 53 N90-10049

Revolutionary opportunities for materials and structures study [NASA-CR-179642] p 63 N90-10184

Dynamic instability characteristics of aircraft turbine engine combustors p 53 N90-10195

An investigation of counterrotating tip vortex interaction [NASA-CR-185135] p 79 N90-11549

Nacelle design p 105 N90-12551

Altitude testing of the 2D V/STOL ADEN demonstrator, on an F404 engine
[NASA-CR-174824] p 345 N90-17638

Experimental performance and acoustic investigation of modern, counterrotating blade concepts
[NASA-CR-185158] p 649 N90-23393

Elevated temperature crack growth
[NASA-CR-182247] p 777 N90-26355

High speed turboprop aeroacoustic study (counterrotation). Volume 1: Model development
[NASA-CR-185241] p 782 N90-26633

Energy Efficient Engine high pressure turbine component test performance report
[NASA-CR-168289] p 929 N90-28553

Energy Efficient Engine combustor test hardware detailed design report
[NASA-CR-168301] p 929 N90-28554

Energy Efficient Engine (E3) combustion system component technology performance report
[NASA-CR-168274] p 930 N90-28555

Energy Efficient Engine acoustic supporting technology report
[NASA-CR-174834] p 930 N90-28557

Energy Efficient Engine core design and performance report
[NASA-CR-168069] p 930 N90-28559

NASA/GE Energy Efficient Engine low pressure turbine scaled test vehicle performance report
[NASA-CR-168290] p 931 N90-28563

General Electric Co., Evendale, OH.

Energy Efficient Engine: Flight propulsion system final design and analysis
[NASA-CR-168219] p 930 N90-28558

Energy Efficient Engine integrated core/low spool design and performance report
[NASA-CR-168211] p 931 N90-28561

Energy Efficient Engine: Control system component performance report
[NASA-CR-174651] p 931 N90-28562

General Electric Co., Lynn, MA.

Convertible engine system for high speed rotorcraft
[AIAA PAPER 90-2512] p 658 A90-40643

General Electric Co., Schenectady, NY.

Generation and decay of secondary flows and their impact on aerodynamic performance of modern turbomachinery components p 514 N90-21023

The radiation of sound from a propeller at angle of attack
[NASA-CR-4264] p 548 N90-21602

Flame extinction in compressible flow
p 883 N90-26899

General Engineering and Systems Analysis Co., Inc., Silver Spring, MD.

Development of a microcomputer based software system for use in crewmember ejection analysis
[AD-A220398] p 723 N90-25117

General Motors Corp., Indianapolis, IN.

An experimental study of turbine vane heat transfer with leading edge and downstream film cooling
[ASME PAPER 89-GT-69] p 358 A90-23792

Design of an air-cooled metallic high-temperature radial turbine p 507 A90-32960

Experimental evaluation of expendable supersonic nozzle concepts
[AIAA PAPER 90-1904] p 740 A90-42691

3D Euler analysis of ducted propfan flowfields
[AIAA PAPER 90-3034] p 791 A90-45873

Composite matrix cooling scheme for small gas turbine combustors
[AIAA PAPER 90-2158] p 852 A90-47210

In-line wear monitor
[AD-A217799] p 510 N90-20091

Advanced gearbox technology
[NASA-CR-179625] p 666 N90-24274

Geneva Univ. (Switzerland).

Problems related to aircraft noise in Switzerland p 698 N90-24871

George Washington Univ., Hampton, VA.

Impact of nose-probe chines on the vortex flows about the F-16C
[AIAA PAPER 90-0386] p 165 A90-19828

Analysis of aircraft tires via semianalytic finite elements p 496 A90-34740

Advanced Mach 3.5 Axisymmetric Quiet Nozzle
[AIAA PAPER 90-1592] p 566 A90-38727

Optimal input design for aircraft parameter estimation using dynamic programming principles
[AIAA PAPER 90-2801] p 753 A90-45157

Frictionless contact of aircraft tires p 733 A90-45501

[SAE PAPER 892350]

George Washington Univ., Washington, DC.

Rotating primary flow induction using jet-flapped blades p 48 A90-12585

Computers boost structural technology p 138 A90-14799

A three-dimensional space marching algorithm for the solution of the Euler equations on unstructured grids
[AIAA PAPER 90-0014] p 234 A90-23701

Rotary-Jet thrust augmentor with jet-flapped blades p 633 N90-24243

Georgia Inst. of Tech., Atlanta.

A numerical study of general viscous flows around multi-element airfoils
[AIAA PAPER 90-0572] p 167 A90-19922

Numerical study of the effects of icing on finite wing aerodynamics
[AIAA PAPER 90-0757] p 169 A90-20010

Application of an efficient hybrid scheme for aeroelastic analysis of advanced propellers
[AIAA PAPER 90-0028] p 226 A90-22153

Approximate loop transfer recovery method for designing fixed-order compensators p 375 A90-25989

Comparison of measured induced velocities with results from a closed-form finite state wake model in forward flight p 385 A90-28195

The effect of an unsteady three-dimensional wake on elastic blade-flapping eigenvalues in hover p 385 A90-28228

Cyclic deformation, fatigue and fatigue crack propagation in Ni-base alloys p 531 A90-34162

Euler solutions for self-generated rotor blade-vortex interactions
[AIAA PAPER 90-1588] p 566 A90-38723

Helicopter stability and control modeling improvements and verification on two helicopters p 671 A90-42474

Helicopter trim with flap-lag-torsion and stall by an optimized controller p 755 A90-45332

Flight test of a trajectory controller using linearizing transformations with measurement feedback
[AIAA PAPER 90-3373] p 864 A90-47631

Numerical simulation of unsteady rotational flow over propfan configurations
[NASA-CR-186037] p 90 N90-12500

A technique for the prediction of aerodynamics and aeroelasticity of rotor blades p 184 N90-13377

Dynamic testing techniques and applications for an aeroelastic rotor test facility p 201 N90-13406

An experimental investigation of the interaction between a model rotor and airframe in forward flight p 185 N90-14219

An analytical method for the prediction of unsteady rotor/airframe interactions in forward flight p 186 N90-14223

Acoustic-vortical-combustion interaction in a solid fuel ramjet simulator p 194 N90-14234

A helicopter flight path controller design via a nonlinear transformation technique p 199 N90-14242

A study of the effects of Rotating Frame Turbulence (RFT) on helicopter flight mechanics p 248 N90-15058

Unsteady aerodynamics of oscillating and rapidly pitched airfoils p 235 N90-15074

Finite difference techniques and rotor blade aeroelastic partial differential equations with quasisteady aerodynamics p 236 N90-15075

Estimation and control of nonlinear and hybrid systems with applications to air-to-air guidance
[AD-A214542] p 348 N90-16770

Numerical simulation of supersonic free shear layers
[AD-A216289] p 320 N90-17579

Design of a helicopter automatic flight control system using adaptive control p 522 N90-21040

Development and application of a generalized dynamic wake theory for lifting rotors p 570 N90-21731

A comparison of time-optimal interception trajectories for the F-8 and F-15
[NASA-CR-186300] p 581 N90-21753

Passive navigation using image irradiance tracking p 578 N90-22232

Application of a dynamic stall model to rotor trim and aeroelastic response p 583 N90-22556

Time-optimal aircraft pursuit-evasion with a weapon envelope constraint
[NASA-CR-186640] p 734 N90-25126

Velocity measurements on a lifting rotor/airframe configuration in low speed forward flight p 815 N90-26790

The Second ARO Workshop on Rotorcraft Interactional Aerodynamics
[AD-A223310] p 911 N90-29304

German Air Force, Cologne (Germany, F.R.).

NDI-concept for composites in future military aircraft p 877 N90-28070

Getti Speciali S.p.A., Turin (Italy).

Combined advanced foundry and quality control techniques to enhance reliability of castings for the aerospace industry p 64 N90-10240

Grumman Aerospace Corp., Bethpage, NY.

An in-flight interaction of the X-29A canard and flight control system p 348 A90-26820

Strake camber and thickness design procedure for low alpha supersonic flow p 622 A90-40678

Hypersonic forebody lift-induced drag
[SAE PAPER 892345] p 715 A90-45497

Inverse design of airfoil contours: Constraints, numerical method, and applications p 500 N90-20980

H

Hamilton Standard, Windsor Locks, CT.

Large scale prop-fan structural design study. Volume 1: Initial concepts
[NASA-CR-174992] p 52 N90-10043

Large scale prop-fan structural design study. Volume 2: Preliminary design of SR-7
[NASA-CR-174993] p 52 N90-10044

Large-scale Advanced Prop-fan (LAP) high speed wind tunnel test report
[NASA-CR-182125] p 52 N90-10045

Large-scale Advanced Prop-fan (LAP) technology assessment report
[NASA-CR-182142] p 53 N90-10046

Acoustic test and analysis of a counterrotating prop-fan model
[NASA-CR-179590] p 79 N90-10683

Measurement of the steady surface pressure distribution on a single rotation large scale advanced prop-fan blade at Mach numbers from 0.03 to 0.78
[NASA-CR-182124] p 929 N90-28552

Hamilton Standard Div., United Aircraft Corp., Windsor Locks, CT.

Large-scale Advanced Prop-fan (LAP) static rotor test report
[NASA-CR-180848] p 117 N90-12617

Hampton Univ., VA.

A new class of random processes with application to helicopter noise p 781 A90-42874

A two dimensional power spectral estimate for some nonstationary processes
[NASA-CR-186100] p 217 N90-14843

Automatic speech recognition in air-ground data link p 690 N90-25037

Harris Corp., Melbourne, FL.

Integrated control-system design via generalized LQG (GLQG) theory p 613 N90-23023

Hawker Siddeley Canada Ltd., Toronto (Ontario).

Surface property improvement in titanium alloy gas turbine components through ion implantation p 953 N90-28713

Helicopter Aeronautics and Noise Associates, Mountain View, CA.

Prediction and measurement of low-frequency harmonic noise of a hovering model helicopter rotor p 463 A90-28159

Helsinki Univ. of Technology, Espoo (Finland).

Solution of the thin-layer Navier-Stokes equations for laminar transonic flow
[PB89-221600] p 136 N90-12879

Multigrid solution method for the Euler equations
[PB89-219463] p 138 N90-13116

An evaluation of the two-dimensional Euler and Navier-Stokes calculations based on a flux-vector splitting
[PB90-166778] p 481 N90-20963

Subsonic flutter analysis using MSC/NASTRAN
[PB90-166786] p 522 N90-21041

Hessian Ministry for Economics and Technology, Frankfurt (Germany, F.R.).

En route noise of turboprop aircraft and their acceptability: Report of tests p 697 N90-24858

High Technology Corp., Hampton, VA.

Prediction and control of transition in supersonic and hypersonic boundary layers p 16 A90-12828

Goertler vortices in supersonic and hypersonic boundary layers p 83 A90-14091

Curvature effects on the stability of laminar boundary layers on swept wings p 148 A90-16788

Numerical solution of the boundary-layer equations for a general aviation fuselage
[AIAA PAPER 90-0305] p 163 A90-19786

Wind-tunnel investigation on the effect of a crescent planform on drag
[AIAA PAPER 90-0300] p 228 A90-22196

Effects of shock on the stability of hypersonic boundary layers
[AIAA PAPER 90-1448] p 561 A90-38608

Advanced Mach 3.5 Axisymmetric Quiet Nozzle
[AIAA PAPER 90-1592] p 566 A90-38727

Two and three dimensional grid generation by an algebraic homotopy procedure
[AIAA PAPER 90-1603] p 567 A90-38734

A computational study of the taxonomy of vortex breakdown
[AIAA PAPER 90-1624] p 568 A90-38753

- Wind-tunnel investigations of wings with serrated sharp trailing edges p 802 A90-46379
- Parametric analysis of swept-wing geometry with sheared wing tips p 812 A90-49101
- [AIAA PAPER 90-3196] p 812 A90-49101
- Curvature effects on the stability of three-dimensional laminar boundary layers p 71 N90-10366
- Hochschule der Bundeswehr, Munich (Germany, F.R.).**
- Autonomous automatic landing through computer vision p 332 N90-16734
- Honeywell, Inc., Minneapolis, MN.**
- Nonlinear inversion flight control for a supermaneuverable aircraft p 864 A90-47661
- [AIAA PAPER 90-3406] p 864 A90-47661
- Houston Univ., TX.**
- A linear quadratic regulator approach to the stabilization of uncertain linear systems p 891 A90-47755
- [AIAA PAPER 90-3509] p 891 A90-47755
- Human Engineering Labs., Aberdeen Proving Ground, MD.**
- Software and hardware description of the helicopter motion equations for VAX computers p 184 N90-13375
- [AD-A213248] p 184 N90-13375
- Interaction of switch actuation on tracking with a four-axis flight control (cross-coupling) p 520 N90-20095
- [AD-A217981] p 520 N90-20095
- Counterair situation awareness display for Army aviation p 964 N90-28982

I

- I.A.M. Rinaldo Piaggio, Finale Ligure (Italy).**
- P-180 AVANTI: Project and flight test program comprehensive overview p 34 N90-10863
- IIT Research Inst., Bartlesville, OK.**
- Production of jet fuels from coal-derived liquids. Volume 13: Evaluation of storage and thermal stability of jet fuels derived from coal liquids p 954 N90-29527
- [AD-A224576] p 954 N90-29527
- Illinois Univ., Champaign.**
- Cognitive perspectives on map displays for helicopter flight p 419 A90-31329
- Illinois Univ., Urbana.**
- Hot gas environment around STOL aircraft in ground proximity. II - Numerical study p 743 A90-42766
- [AIAA PAPER 90-2270] p 743 A90-42766
- Airport pavement drainage p 872 N90-27728
- [DOT/FAA/RD-90/24] p 872 N90-27728
- Illinois Univ., Urbana-Champaign.**
- An improvement of convection fidelity in Euler calculations p 315 N90-16709
- An experimental study of fault propagation in a jet-engine controller p 665 N90-23401
- [NASA-CR-181335] p 665 N90-23401
- Cognitive requirements for aircraft navigation p 824 N90-26804
- [NASA-CR-186933] p 824 N90-26804
- Illinois Univ. at Urbana-Champaign, Savoy.**
- Numerical simulation of leading-edge vortex rollup and bursting p 20 N90-10831
- Imperial Coll. of Science and Technology, London (England).**
- Interaction between strong longitudinal vortices and turbulent boundary layers p 145 A90-16764
- Applications of an adaptive unstructured solution algorithm to the analysis of high speed flows p 229 A90-22213
- [AIAA PAPER 90-0395] p 229 A90-22213
- On the instability of hypersonic flow past a wedge p 554 A90-35902
- Subsonic combustor flow modeling: State of the art of CFD techniques for reacting and combusting flow p 749 N90-25991
- The effect of rapid spoiler deployment on the transient forces on an airfoil p 921 N90-28527
- Indian Inst. of Science, Bangalore.**
- An experimental and analytical investigation of isolated rotor flap-lag stability in forward flight p 518 A90-33623
- Indiana Univ.-Purdue Univ., Indianapolis.**
- Block-structured solution of three-dimensional transonic flows using parallel processing p 170 N90-13330
- [AD-A212851] p 170 N90-13330
- Industrieanlagen-Betriebsgesellschaft m.b.H., Ottobrunn (Germany, F.R.).**
- Neutron radiography: Applications and systems p 886 N90-28080
- Fretting fatigue strength of Ti-6Al-4V at room and elevated temperatures and ways of improving it p 952 N90-28709
- Ingemansson Anstalt A.B., Askim (Sweden).**
- Viscoelastic tuned dampers for control of structural dynamics p 73 N90-10999
- Institut de Mecanique des Fluides de Lille (France).**
- Reduction of profile drag by modifying the structure next to the wake area p 172 N90-13356
- [IMFL-88/35] p 172 N90-13356

- Study of ground effects on flying scaled models p 922 N90-28532
- Institut de Mecanique des Fluides de Marseille (France).**
- Numerical investigations of heat transfer and flow rates in rotating cavities. Simulation of the movement generated by wall temperature gradients, by source-sink mass flows or by the differential rotation of the walls, under the influence of coriolis and centrifugal forces [ETN-90-96253] p 454 N90-18695
- Institut de Mecanique des Fluides de Toulouse (France).**
- Development of turbulence models for the analysis of compressible or incompressible unsteady flow [ETN-90-97486] p 958 N90-28810
- Institut Foerster G.m.b.H. und Co. K.G., Reutlingen (Germany, F.R.).**
- New aspects in aircraft inspection using eddy current methods p 886 N90-28085
- Institut Franco-Allemand de Recherches, Saint-Louis (France).**
- Volumetric analysis by spontaneous Raman diffusion in a supersonic wind tunnel p 95 N90-12564
- [ISL-R-109/88] p 95 N90-12564
- Experimental study of velocity fields and turbulence in a turbojet engine p 344 N90-16766
- [ISL-CO-231/88] p 344 N90-16766
- Self compensation of rigid displacements in holographic interferometry p 370 N90-17113
- [ISL-CO-219/88] p 370 N90-17113
- Prediction of rotor blade-vortex interaction noise from 2-D aerodynamic calculations and measurements p 396 N90-18365
- [ISL-CO-243/88] p 396 N90-18365
- Study of the blade/vortex interaction on a one-blade rotor during forward flight (incompressible, non viscous fluid) p 415 N90-18391
- [ISL-R-115/88] p 415 N90-18391
- Possible piloting techniques at hypersonic speeds p 415 N90-18392
- [ISL-CO-216/88] p 415 N90-18392
- Aerodynamic loads and blade vortex interaction noise prediction p 719 N90-25942
- [ISL-PU-310/89] p 719 N90-25942
- Maneuvering by means of lateral jets p 758 N90-26015
- [ISL-CO-255/88] p 758 N90-26015
- Institut fuer Theoretische Stromungsmechanik, Goettingen (Germany, F.R.).**
- Some Navier-Stokes calculations for the CAST-10 airfoil p 320 N90-17651
- Institute for Computer Applications in Science and Engineering, Hampton, VA.**
- Linear instability of supersonic plane wakes p 20 N90-10833
- [NASA-CR-181911] p 20 N90-10833
- Optimum shape of a blunt forebody in hypersonic flow p 171 N90-13351
- [NASA-CR-181955] p 171 N90-13351
- Spectral simulation of unsteady compressible flow past a circular cylinder p 478 N90-20050
- [NASA-CR-182030] p 478 N90-20050
- On central-difference and upwind schemes p 781 N90-26595
- [NASA-CR-182061] p 781 N90-26595
- Institute for Defense Analyses, Alexandria, VA.**
- The NASA experience in aeronautical R and D: Three case studies with analysis p 82 N90-12496
- [AD-A211486] p 82 N90-12496
- Institute of Aviation Medicine, Farnborough (England).**
- Development of an ejection seat specification for a new fighter aircraft p 483 N90-20057
- Instituto Superior Tecnico, Lisbon (Portugal).**
- A pitch control law for compensation of the phugoid mode induced by windshears p 258 N90-15051
- Application of an inverse method to the design of a radial inflow turbine p 511 N90-20989
- Integrated Systems, Inc., Palo Alto, CA.**
- Nonlinear maneuver autopilot for the F-15 aircraft p 77 N90-11487
- [NASA-CR-179442] p 77 N90-11487
- Iowa State Univ. of Science and Technology, Ames.**
- Development of a three-dimensional upwind parabolized Navier-Stokes code p 602 A90-36253
- Numerical prediction of turbulent flow over airfoil sections with a new nonequilibrium turbulence model [AIAA PAPER 90-1469] p 562 A90-38626
- [AIAA PAPER 90-1469] p 562 A90-38626
- Navier-Stokes solutions of 2-D transonic flow over unconventional airfoils p 173 N90-14195
- Iowa Univ., Iowa City.**
- Stage effects on stalling and recovery of a high-speed 10-stage axial-flow compressor p 115 N90-12600
- Computation of viscous flow around a propeller-shaft configuration with infinite-pitch rectangular blades p 481 N90-20958
- JAI Associates, Inc., Mountain View, CA.**
- Numerical simulations of blade-vortex interactions and lifting hovering rotor flows p 911 N90-29302
- [AD-A224238] p 911 N90-29302

J

- Japan Air Lines Co. Ltd., Tokyo.**
- New features of JAL's ground station p 872 N90-27633
- Daily flight operation monitoring in JAL p 820 N90-27636
- Jet Propulsion Lab., California Inst. of Tech., Pasadena.**
- Optimal autorotational descent of a helicopter with control and state inequality constraints p 756 A90-45344
- Johnson Aeronautics, Palo Alto, CA.**
- Hub loads analysis of the SA349/2 helicopter p 333 A90-23936
- Airloads, wakes, and aeroelasticity p 572 N90-21738
- [NASA-CR-177551] p 572 N90-21738
- Joint Publications Research Service, Arlington, VA.**
- Landing tests for Buran shuttle with jet engine-equipped mock-up p 61 N90-10904
- Jordan Univ. of Science and Technology, Irbid.**
- Shaft flexibility effects on aeroelastic stability of a rotating bladed disk p 132 A90-16371
- Blade mistuning coupled with shaft flexibility effects in rotor aeroelasticity p 343 A90-23896
- [ASME PAPER 89-GT-330] p 343 A90-23896
- Shaft flexibility effects on the forced response of a bladed-disk assembly p 744 A90-43218
- Kansas Univ., Lawrence.**
- Blade surface pressure measurement on a pusher propeller in flight p 139 A90-14346
- [SAE PAPER 891040] p 139 A90-14346
- Assessment of proposed fighter agility metrics p 752 A90-45142
- [AIAA PAPER 90-2807] p 752 A90-45142
- Computation of unsteady transonic flow about airfoils in frequency domain using the full-potential equation p 174 N90-14198
- Preliminary design of a family of three close air support aircraft p 336 N90-16751
- [NASA-CR-186070] p 336 N90-16751
- Airplane takeoff and landing performance monitoring system p 526 N90-20096
- [NASA-CASE-LAR-13734-1-CU] p 526 N90-20096
- Application of numerical optimization techniques to control system design for nonlinear dynamic models of aircraft p 593 N90-23032
- Preliminary design of a supersonic Short Takeoff and Vertical Landing (STOVL) fighter aircraft p 649 N90-23394
- [NASA-CR-186670] p 649 N90-23394
- Life cycle cost in the conceptual design of subsonic commercial aircraft, volumes 1 and 2 p 923 N90-28535
- Fighter agility metrics p 925 N90-29389
- [NASA-CR-187289] p 925 N90-29389
- Kansas Univ. Center for Research, Inc., Lawrence.**
- Analysis and design of sidestick controller systems for general aviation aircraft p 196 A90-19554
- Experimental investigation of wingtip aerodynamic loading p 808 A90-46945
- Aerodynamics of thrust vectoring p 172 N90-13354
- [NASA-CR-185074] p 172 N90-13354
- Fighter agility metrics, research, and test p 648 N90-23386
- [NASA-CR-186118] p 648 N90-23386
- Identification of aerodynamic models for maneuvering aircraft p 719 N90-25943
- [NASA-CR-186630] p 719 N90-25943
- Karlsruhe Univ. (Germany, F.R.).**
- Wind tunnel design of heat island turbulent boundary layer p 455 N90-19542
- [IHW-ET/50] p 455 N90-19542
- Kentucky Univ., Lexington.**
- Yaw rate control of an air bearing vehicle p 435 N90-19420
- Kopin Corp., Taunton, MA.**
- Smart microsensors for high temperature applications, phase 1 p 959 N90-28828
- [AD-A224151] p 959 N90-28828
- Laboratoire Central Aeronautique, Suresnes Cedex (France).**
- Properties of Al-Li alloys p 267 N90-15191
- Laboratoire de Medecine Aeronautique, Bretigny-sur-Orge (France).**
- Parachute opening shocks during high speed ejections: Normalization p 497 N90-20056
- Landesanstalt fuer Umweltschutz, Baden-Wuerttemberg (Germany, F.R.).**
- Noise measurements of turboprop airplanes at different overflight elevations p 697 N90-24860

L

Lawrence Livermore National Lab., CA.

Analysis of damaged components from DOE security helicopter N7EG
[DE90-004488] p 324 N90-16729

Lehigh Univ., Bethlehem, PA.

Embedded function methods for supersonic turbulent boundary layers
[AIAA PAPER 90-0306] p 163 A90-19787

Lightning Technologies, Inc., Pittsfield, MA.

Final results of the NASA storm hazards program
p 819 A90-49834
Aircraft lightning protection handbook
[AD-A22716] p 820 N90-27668

Limoges Univ. (France).

Numerical simulation of aeroplane response to a lightning injection
[ETN-89-95271] p 96 N90-11716

Litton Guidance and Control Systems, Woodland Hills, CA.

Integrated navigation/flight control for future high performance aircraft p 917 N90-29362
Fault Detection and Isolation (FDI) techniques for guidance and control systems p 918 N90-29366

Lockheed Aeronautical Systems Co., Burbank, CA.

Interior noise in the untreated Gulfstream II Proplan Test Assessment aircraft p 731 A90-44736
Modeling flexible aircraft for flight control design
[AD-A219123] p 757 N90-25140

Lockheed Aeronautical Systems Co., Marietta, GA.

Total temperature effects on centerline Mach number characteristics of freejets p 302 A90-25290
Evaluation of transonic wall interference assessment and correction for semi-span wing data
[AIAA PAPER 90-1433] p 597 A90-38487
Proplan Test Assessment (PTA): Flight test report
[NASA-CR-182278] p 113 N90-11738
Proplan Test Assessment (PTA)
[NASA-CR-185138] p 113 N90-11739
Fuel tank explosion protection p 251 N90-15914

Lockheed-California Co., Burbank.

Transport composite fuselage technology: Impact dynamics and acoustic transmission
[NASA-CR-4035] p 126 N90-11821

Lockheed Engineering and Sciences Co., Hampton, VA.

Applications of an adaptive unstructured solution algorithm to the analysis of high speed flows
[AIAA PAPER 90-0395] p 229 A90-22213
A hybrid method for prediction of propeller performance
[AIAA PAPER 90-0440] p 229 A90-22219
Experimental transonic flutter characteristics of supersonic cruise configurations
[AIAA PAPER 90-0979] p 390 A90-29369
Using transonic small disturbance theory for predicting the aeroelastic stability of a flexible wind-tunnel model
[AIAA PAPER 90-1033] p 391 A90-29377
Flight-measured streamwise disturbance instabilities in laminar flow
[AIAA PAPER 90-1283] p 495 A90-33904
Comparison of high-angle-of-attack slender-body theory and exact solutions for potential flow over an ellipsoid
p 622 A90-40692
The ROTONET prediction system and initial comparisons with far-field acoustics measurements for the XV-15 tilt-rotor aircraft p 894 A90-46947
Development and testing of methodology for evaluating the performance of multi-input/multi-output digital control systems
[AIAA PAPER 90-3501] p 867 A90-47747
Supersonic aerodynamic characteristics of a Mach 3 high-speed civil transport configuration
[AIAA PAPER 90-3210] p 811 A90-48836
Thermal management for a Mach 5 cruise aircraft using endothermic fuel
[AIAA PAPER 90-3284] p 853 A90-48871
Comparison of equivalent plate and finite element analysis of a realistic aircraft structural configuration
[AIAA PAPER 90-3293] p 837 A90-48877
Characterization of LaRC-TPI 1500 powders - A new version with controlled molecular weight
p 946 A90-50177

Sonic boom signature data from cruciform microphone array experiments during the 1966-1967 EAFB national sonic boom evaluation program
[NASA-CR-182027] p 549 N90-21605
Multilevel decomposition approach to the preliminary sizing of a transport aircraft wing
[NASA-CR-4296] p 583 N90-22557
Unsteady potential flow past a propeller blade section
[NASA-CR-4307] p 634 N90-24246
Vibration responses of two house structures during the Edwards Air Force Base phase of the national sonic boom program
[NASA-CR-182089] p 966 N90-29169

Aircraft design for mission performance using nonlinear multiobjective optimization methods
[NASA-CR-4328] p 925 N90-29384

Lockheed Engineering and Sciences Co., Houston, TX.

Active control of aerothermoelastic effects for a conceptual hypersonic aircraft
[AIAA PAPER 90-3337] p 863 A90-47597
Parametric analysis of swept-wing geometry with sheared wing tips
[AIAA PAPER 90-3196] p 812 A90-49101

Lockheed-Georgia Co., Marietta.

Lockheed laminar-flow control systems development and applications p 90 N90-12506
An experimental evaluation of slots versus porous strips for laminar-flow applications p 92 N90-12530
Computerized corrosion forecasting model for C-5 aircraft p 843 N90-26815

Lockheed Missiles and Space Co., Austin, TX.

Unmanned air vehicles payloads and sensors p 251 N90-15930
Distribution of hardware and software elements in unmanned air vehicle systems p 251 N90-15933

London Univ. (England).

Unsteady aerodynamics of controls p 935 N90-28525

Los Alamos National Lab., NM.

Design and demonstration of heat pipe cooling for NASP and evaluation of heating methods at high heating rates
[DE89-016995] p 186 N90-14227

Loughborough Univ. of Technology (England).

Aircraft/airport compatibility: Some strategic, tactical, and operational issues
[TT-8902] p 202 N90-13409
An investigation of the use of singular perturbation methods and modal control theory in the derivation of aircraft control schemes
[MATHS-REPT-A-106] p 758 N90-26014
The cost of air service fragmentation
[TT-9010] p 913 N90-29334
The potential for an extra runway at Heathrow: A preliminary feasibility study
[TT-9007] p 938 N90-29403

Lufthansa German Airlines, Frankfurt (Germany, F.R.).

Fire prevention in transport airplane passenger cabins p 325 N90-17590

M**M L Energia, Inc., Princeton, NJ.**

Photo-sensitized ignition of hydrogen/oxygen mixtures for hypersonic flight vehicles p 877 N90-27935

Macrodyne, Inc., Schenectady, NY.

Database for LDV signal processor performance analysis p 447 A90-28278

MAG Consultants, Inc., San Francisco, CA.

Proposed definition of the term en route in en route aircraft noise p 696 N90-24854
The effect of noise-abatement profiles on noise immissions and human annoyance underneath a subsequent climbpath p 698 N90-24865

Maine Univ., Orono.

An analytic study of nonsteady two-phase laminar boundary layer around an airfoil p 691 N90-25051

Manchester Univ. (England).

Non-axisymmetric viscous lower-branch modes in axisymmetric supersonic flows p 474 A90-33509
The inviscid axisymmetric stability of the supersonic flow along a circular cylinder p 554 A90-35916
Study of forces and moments on wing-bodies at high incidence, volumes 1 and 2 p 171 N90-13350
The computation of turbulent thin shear flows associated with flow around multielement aerofoils p 633 N90-24240

Manitoba Univ., Winnipeg.

Use of acoustic emission for continuous surveillance of aircraft structures p 887 N90-28092

MARC Analysis Research Corp., Palo Alto, CA.

The MHOIST finite element program: 3-D inelastic analysis methods for hot section components. Volume 3: Systems' manual
[NASA-CR-182236] p 73 N90-10451

Martin-Baker Aircraft Co. Ltd., Denham (England).

Fighter escape system: The next step forward p 483 N90-20059

Maryland Univ., College Park.

Response and hub loads sensitivity analysis of a helicopter rotor p 181 A90-18145
Aeroelastic optimization of a helicopter rotor using an efficient sensitivity analysis
[AIAA PAPER 90-0951] p 410 A90-29237
Effects of higher harmonic control on rotor performance and control loads
[AIAA PAPER 90-1158] p 412 A90-29467

Structural optimization with aeroelastic constraints of rotor blades with straight and swept tips p 535 A90-32475

Stability sensitivity analysis of a helicopter rotor

p 580 A90-36273
Design of a three-component wall-mounted balance
[AIAA PAPER 90-1397] p 595 A90-37940

Aeroelastic effects on stability and control of hingeless rotor helicopters p 647 A90-42473

Theoretical and experimental investigation of the aeroelastic stability of an advanced bearingless rotor in hover and forward flight p 831 A90-46958

Hypersonic aerodynamics p 171 N90-13335
Integrated approach fault tolerance-current state and future requirements
[AD-A214402] p 275 N90-15465

Computation of hypersonic unsteady viscous flow over a cylinder p 397 N90-19194

Nonlinear mechanics of unstable plasmas as related to high altitude aerodynamics
[AD-A215126] p 464 N90-19852

Aeroelastic characteristics of aircraft with circulation control wings p 497 N90-20070

Nonlinear static and dynamic modeling of composite rotor blades including warping effects p 924 N90-29382

Massachusetts Inst. of Tech., Cambridge.

Calculation of unsteady Euler flows in turbomachinery using the linearized Euler equations p 5 A90-11778

Rotor noise due to atmospheric turbulence ingestion. I - Fluid mechanics p 219 A90-19385

Analysis of aircraft performance during lateral maneuvering for microburst avoidance
[AIAA PAPER 90-0568] p 197 A90-19920

Nonlinear aerodynamics of two-dimensional airfoils in severe maneuver p 301 A90-25276

Active control of gust- and interference-induced vibration of tilt-rotor aircraft p 429 A90-28201

Flight testing a highly flexible aircraft - Case study on the MIT Light Eagle p 414 A90-31284

Active control of tiltrotor blade in-plane loads during maneuvers p 670 A90-42463

On the generation of a variable structure airport surface traffic control system p 99 N90-11724

Sequential design of experiments with physically based models 23 p 138 N90-12239

Active stabilization of aeromechanical systems
[AD-A216629] p 454 N90-18672

Experimental and theoretical investigations of flowfields and heat transfer in modern gas turbines
[AD-A217663] p 429 N90-19237

Investigation of air transportation technology at the Massachusetts Institute of Technology, 1988-1989 p 484 N90-20922

Automatic speech recognition in air traffic control p 488 N90-20923

Cockpit display of hazardous wind shear information p 484 N90-20924

Ultrasonic techniques for aircraft ice accretion measurement p 485 N90-20926

Investigation of surface water behavior during glaze ice accretion p 485 N90-20927

The influence of ice accretion physics on the forecasting of aircraft icing conditions p 485 N90-20928

Cockpit display of hazardous weather information p 485 N90-20929

Massachusetts Inst. of Tech., Lexington.

ASR-9 weather channel test report
[AD-A211749] p 133 N90-11934

Materials Research Labs., Ascot Vale (Australia).

Effect of temperature on the storage life of polysulfide aircraft sealants
[MRL-TR-89-31] p 444 N90-19364

Materials Research Labs., Maribymong (Australia).

A corrosion fatigue/stress corrosion testing facility at Materials Research Laboratory
[MRL-TN-568] p 527 N90-21044

Mauter (George A.), Huntington Station, NY.

Aircraft drawings index p 618 N90-23340

Mayflower Communications Co., Inc., Reading, MA.

Autonomous integrated GPS/INS navigation experiment for OMV. Phase 1: Feasibility study
[NASA-CR-4267] p 489 N90-20969

MCAT Inst., Moffett Field, CA.

Application of a lower-upper implicit scheme and an interactive grid generation for turbomachinery flow field simulations
[ASME PAPER 89-GT-20] p 288 A90-23762

Supersonic wind tunnel nozzles: A selected, annotated bibliography to aid in the development of quiet wind tunnel technology
[NASA-CR-4294] p 762 N90-26019

McDonnell Aircraft Co., Houston, TX.

Research on a two-dimensional inlet for a supersonic V/STOL propulsion system. Appendix A
[NASA-CR-174945] p 396 N90-18364

McDonnell Aircraft Co., Saint Louis, MO.

Supersonic boundary layer stability analysis with and without suction on aircraft wings p 148 A90-16792
Design and experimental verification of an equivalent forebody representation of flowing inlets p 152 A90-17863

Engine inlet distortion in a 9.2 percent scaled vectored thrust STOL model in ground effect
[AIAA PAPER 89-2910] p 301 A90-25043

Aeroelastic analysis of wings using the Euler equations with a deforming mesh
[AIAA PAPER 90-1032] p 391 A90-29376

Aluminum-lithium: Application of plate and sheet to fighter aircraft p 268 N90-15202
A dynamicist's view of fuel tank skin durability p 251 N90-15915

Heat pipes for wing leading edges of hypersonic vehicles
[NASA-CR-181922] p 369 N90-17055

Exhaust environment measurements of a turbofan engine equipped with an afterburner and 2D nozzle
[NASA-CR-4289] p 588 N90-21760

Nonflammable hydraulic power system for tactical aircraft. Volume 1: Aircraft system definition, design and analysis
[AD-A218493] p 671 N90-23409

Damage tolerance analysis for manned hypervelocity vehicles. Volume 2: Software user's manual
[AD-A22136] p 845 N90-26826

Damage tolerance analysis for manned hypervelocity vehicles. Volume 1: Final technical report
[AD-A221970] p 887 N90-28106

Application of multifunction inertial reference systems to fighter aircraft p 916 N90-29341
Survivable penetration p 917 N90-29363

McDonnell-Douglas Astronautics Co., Houston, TX.

Independent Orbiter Assessment (IOA): Analysis of the displays and controls subsystem
[NASA-CR-185563] p 124 N90-11774

McDonnell-Douglas Corp., Long Beach, CA.

Laminar flow control perforated wing panel development
[NASA-CR-178166] p 63 N90-10187

McDonnell-Douglas Corp., Saint Louis, MO.

An expert system advisor for damage repair of composite wing skins (repairman) p 842 N90-26810

McDonnell-Douglas Helicopter Co., Mesa, AZ.

HARP model rotor test at the DNW p 406 A90-28167

Euler solutions for self-generated rotor blade-vortex interactions
[AIAA PAPER 90-1588] p 566 A90-38723

Numerical simulations of three-dimensional rotor blade-vortex interactions p 807 A90-46879
A study of fundamental issues in higher harmonic control using aeroelastic simulation p 861 A90-46966

Correlation of AH-1G airframe flight vibration data with a coupled rotor-fuselage analysis
[NASA-CR-181974] p 959 N90-28865

Plan, execute, and discuss vibration measurements and correlations to evaluate a NASTRAN finite element model of the AH-64 helicopter airframe
[NASA-CR-181973] p 960 N90-28866

McDonnell-Douglas Research Labs., Saint Louis, MO.

Experimental investigation of terminal shock sensors in mixed-compression inlets
[AIAA PAPER 90-1931] p 681 A90-40560

Mechanical Technology, Inc., Latham, NY.

Internal rotor friction instability
[NASA-CR-183942] p 543 N90-21395

Mesoscale Environmental Simulations and Operations, Inc., Hampton, VA.

Mesoscale acid deposition modeling studies
[NASA-CR-4262] p 140 N90-13228

Messerschmitt-Boelkow-Blohm G.m.b.H., Bremen (Germany, F.R.).

Investigation on sheet material of 8090 and 2091 aluminum-lithium alloy p 267 N90-15192
An efficient solver of the Eigenvalue problem of the linear stability equations for three dimensional, compressible boundary-layer flows p 276 N90-16172

Development of transition criteria on the basis of ϵ to the N power for three dimensional wing boundary layers p 277 N90-16179

The precise calculation of the inviscid leading edge flow on a laminar airfoil using simple methods and verification by measurements on the TLF pilot model p 277 N90-16180

Research on three different Euler's schemes applied to a delta wing with vortical flows p 278 N90-16184

An interactive method for the flow calculation of airfoils with local separation regions p 278 N90-16190

Calculation of the flap profile flows with separation based on coupled potential and boundary layer solutions p 278 N90-16191

Inverse solutions for boundary layers with separation or close to separation under locally infinite swept wing conditions p 279 N90-16192

Advanced materials for interior and equipment related to fire safety in aviation p 328 N90-17608

Short time Force and moment measurement System for shock tubes (SFS) for measuring times less than 10 ms p 674 N90-24233

Aerodynamic development perspective for traffic aeroplanes
[DGLR-89-141] p 637 N90-24260

Transonic wing charge improvements by passive shock boundary layer interference control: Development status and prospects
[ETN-90-96463] p 650 N90-24267

Short time-dynamometer system for shock wave channels
[MBB-UT-115/89-PUB] p 773 N90-25084

Messerschmitt-Boelkow-Blohm G.m.b.H., Hamburg (Germany, F.R.).

The interference of flightmechanical control laws with those of load alleviation and its influence on structural design p 258 N90-15054

Simulation of transport aeroplanes
[MBB-UT-007/89-PUB] p 723 N90-25089

Damage tolerance demonstration for A310-300 CFPR components
[MBB-UT-012/89-PUB] p 766 N90-25091

Aircraft condition monitoring system for future Airbus aircraft: New concept for programming and data recording p 848 N90-27619

Messerschmitt-Boelkow-Blohm G.m.b.H., Munich (Germany, F.R.).

Turbulence management: Application aspects p 72 N90-10378

Flight testing of the Tornado Terrain Following System p 35 N90-10875

On the occasion of the 100th birthday of Ernst Heinkel
[MBB/LW/3015/S/PUB/321] p 141 N90-12494

Design philosophy and construction techniques for integral fuselage fuel tanks p 250 N90-15913

Saenger propulsion system options p 344 N90-16818

Verification of aerothermodynamic codes by means of a winged experimental re-entry vehicle p 354 N90-16842

Onboard fire- and explosion suppression for fighter aircraft p 327 N90-17602

An intensive procedure for the design of pressure-specified three-dimensional configurations at subsonic and supersonic speeds by means of a higher-order panel method p 500 N90-20982

Grid patching approaches for complex three-dimensional configurations p 573 N90-21985

Investigation on sheet material of 8090 and 2091 aluminum-lithium alloy
[MBB-UT-122/89-PUB] p 766 N90-25090

Messerschmitt-Boelkow-Blohm G.m.b.H., Ottobrunn (Germany, F.R.).

General data processing support from project planning to workshop control
[MBB-UD-526/88-PUB] p 138 N90-12208

ROSAR (Helicopter-Rotor based Synthetic Aperture Radar) p 541 N90-21229

Development and application of an optimization procedure for space and aircraft structures
[MBB-FW-522/S/PUB-383] p 779 N90-25078

Scenario 2000
[MBB-UD-500/89-PUB] p 734 N90-25092

Development and test of software by safety critical aircraft systems
[MBB-FE-363/S/PUB-384] p 723 N90-25103

Calculation of thick wall fiber binders for rotor components of modern helicopters
[MBB-UD-554/84-PUB] p 735 N90-25137

Messier Fonderie, Arudy (France).

The question of the casting factor p 64 N90-10238

METEOR Costruzioni Aeronautiche ed Elettroniche S.p.A., Ronchi del Legionari (Italy).

Mirach 100 flight control system p 260 N90-15926

Meyer (Thomas J.), Hamburg (Germany, F.R.).

Additive evaluation criteria for aircraft noise p 698 N90-24867

Michigan Technological Univ., Houghton.

A Monte Carlo simulation technique for low-altitude, wind-shear turbulence
[AIAA PAPER 90-0564] p 216 A90-19917

Improving snow roads and airstrips in Antarctica
[AD-A211588] p 133 N90-11907

Michigan Univ., Ann Arbor.

Implicit flux-split schemes for the Euler equations p 602 A90-36254

Optimal plane change by low aerodynamic forces
[AIAA PAPER 90-2831] p 763 A90-45137

Summary report of the Summer Conference of the DARPA-Materials Research Council
[AD-A217380] p 532 N90-20143

MicroNet, Celle (Germany, F.R.).

AIMS test and simulation equipment p 892 N90-27623

Middle East Technical Univ., Ankara (Turkey).

A computational design method for shock free transonic cascades and airfoils p 501 N90-20986

A study on secondary flow and spanwise mixing in axial flow compressors p 512 N90-21012

Midwest Research Inst., Golden, CO.

Inclusion of nonlinear aerodynamics in the FLAP code
[DE89-009507] p 281 N90-15519

Minnesota Univ., Minneapolis.

Simple analyses of paths through windshears and downdrafts
[AIAA PAPER 90-0222] p 197 A90-19740

Optimal paths through downbursts p 755 A90-45330

Control of an aircraft in downbursts p 755 A90-45331

Nonlinear inversion flight control for a supermaneuverable aircraft
[AIAA PAPER 90-3406] p 864 A90-47661

Studies of gas turbine heat transfer airfoil surfaces and end-wall cooling effects
[AD-A212451] p 117 N90-12620

Mississippi State Univ., Mississippi State.

Counterrotating prop-fan simulations which feature a relative-motion multiblock grid decomposition enabling arbitrary time-steps
[AIAA PAPER 90-0687] p 169 A90-19978

Numerical grid generation in computational fluid mechanics '88; Proceedings of the Second International Conference, Miami Beach, FL, Dec. 5-8, 1988 p 376 A90-26476

Computation of transonic flow about stores
[AD-A210402] p 18 N90-10009

Marshall Avionics Testbed System (MAST) p 421 N90-19417

Adaptive grid embedding for the two-dimensional flux-split Euler equations
[NASA-CR-186533] p 547 N90-21571

Mississippi State Univ., State College.

Three-dimensional unsteady transonic viscous-inviscid interaction p 18 N90-10005

A dynamic multiblock approach to solving the unsteady Euler equations about complex configurations p 214 N90-14497

Unsteady three-dimensional thin-layer Navier-Stokes solutions on dynamic blocked grids p 235 N90-15069

Missouri Univ., Rolla.

Some aerodynamic characteristics of the scissor wing configuration
[SAE PAPER 892202] p 713 A90-45423

An aerodynamic tradeoff study of the scissor wing configuration
[NASA-CR-186576] p 481 N90-20965

Mitre Corp., McLean, VA.

National airspace system approach and departure sequencing operational concept
[NAS-SR-1322] p 27 N90-10017

National Airspace System airspace management operational concept
[DOT/FAA/DS-89/29] p 177 N90-13361

National Airspace System flight planning operational concept
[DOT/FAA/DS-89/30] p 177 N90-13362

An update to the system safety study of TCAS 2
[DOT/FAA/SA-89/3] p 177 N90-13363

National airspace system: Airport movement area control operational concept
[WP-89W00181] p 243 N90-15086

Control outside of independent surveillance coverage operational concept
[AD-A214163] p 243 N90-15090

Independent ground monitor coverage of Global Positioning System (GPS) satellites for use by civil aviation p 918 N90-29364

Mitsui Toatsu Chemicals, Inc., Yokohama (Japan).

Improved melt flow and physical properties of Mitsui Toatsu's LARC-TPI 1500 series polyimide p 943 A90-50134

Motoren- und Turbinen-Union Muenchen G.m.b.H. (Germany, F.R.).

A comparison of flutter calculations based on eigenvalue and energy method p 425 N90-18406

Unsteady blade loads due to wake influence p 426 N90-18413

Experimental and numerical study on basic phenomena of secondary flows in turbines p 512 N90-21014

Advanced algorithms design and implementation in on-board microprocessor systems for engine life usage monitoring p 892 N90-27628

MRC Bearings-SKF Aerospace, Jamestown, NY.
Life of concentrated contacts in the mixed EHD and boundary film regimes
[AD-A216673] p 454 N90-18738

N

Naples Univ. (Italy).
Infrared thermography p 911 N90-29325

National Academy of Sciences - National Research Council, Hampton, VA.
A validation study of the Spark Navier Stokes code for nonreacting scramjet combustor flowfields
[AIAA PAPER 90-2360] p 706 A90-42784

National Academy of Sciences - National Research Council, Washington, DC.
Proceedings of a workshop on Future Airport Passenger Terminals
[PB90-213620] p 937 N90-28580

National Aeronautical Establishment, Ottawa (Ontario).
Wind tunnel wall interference investigations in NAE/NRC High Reynolds Number 2D Facility and NASA Langley 0.3m Transonic Cryogenic Tunnel p 628 A90-42404
Analysis of experimental data for CAST 10-2/DOA 2 supercritical airfoil at low Reynolds numbers and application to high Reynolds number flow
[AD-A211654] p 170 N90-13326
Adverse weather operations during the Canadian Atlantic storms program p 281 N90-15052
Investigation of CAST-10-2/DOA 2 airfoil in NAE high Reynolds number two-dimensional test facility p 321 N90-17654
Residual interference and wind tunnel wall adaption p 353 N90-17655
New transonic test sections for the NAE 5 ft x 5 ft trisonic wind tunnel
[AD-A220933] p 674 N90-24278
An accurate numerical technique for determining flight test rate gyroscope biases prior to takeoff
[AD-A220987] p 739 N90-25138
Processing of advanced ceramics which have potential for use in gas turbine aero engines
[AD-A220988] p 766 N90-25226
A review of crashworthiness of composite aircraft structures
[AD-A221555] p 846 N90-27697
A review of research and development in crashworthiness of general aviation aircraft: Seats, restraints and floor structures
[AD-A221557] p 846 N90-27698
A technique for rapid inspection of composite aircraft structure for impact damage p 846 N90-28077
Evaluation of high temperature protective coatings for gas turbine engines under simulated service conditions p 952 N90-28712

National Aeronautical Lab., Bangalore (India).
Analysis and design of symmetrical airfoils
[PD-CF-8943] p 400 N90-19213
Multigrid accelerated relaxation solution of transonic full potential flow equation
[PD-CF-8942] p 480 N90-20951
Flight path reconstruction using extended Kalman filtering techniques
[PD-FC-9001] p 489 N90-20970
Design of a natural laminar flow airfoil for an unmanned aircraft
[PD-CF-9004] p 499 N90-20975
Human centrifuge controller p 527 N90-21043
Flight testing of a natural laminar flow airfoil using gliders
[PD-CF-9005] p 718 N90-25936
Model following control system design: Preliminary ATTAS in-flight simulation test results
[PD-FC-9003] p 758 N90-26010
Do inviscid vortex sheets roll-up
[PD-CF-9010] p 909 N90-28491
Sting-support interference on afterbody drag at transonic speeds
[NAL-TM-EA-8902] p 909 N90-28492
A conceptual framework for fighter flight control systems
[PD-CF-9009] p 936 N90-28577
Development of a software package for automatic data acquisition, analysis, and controls in an axial flow compressor test rig
[PD-PR-8910] p 965 N90-29926

National Aeronautics and Space Administration, Washington, DC.
Recent results and major activities in the NASA Balloon Program
[IAF PAPER 89-468] p 81 A90-13557

Computers boost structural technology p 138 A90-14799
Tilt rotor aircraft aeroacoustics p 409 A90-28238
Aeronautical facility requirements into the 2,000's
[AIAA PAPER 90-1375] p 594 A90-37926
The Meteorological Measurement System on the NASA ER-2 aircraft p 926 A90-51658
NASA aerodynamics program
[NASA-TM-4175] p 373 N90-17235

National Aeronautics and Space Administration, Ames Research Center, Moffett Field, CA.
Turbulent separated flow over and downstream of a two-element airfoil p 16 A90-12738
Identification of rotor flapping equation of motion from flight measurements with the RSRA compound helicopter p 56 A90-12769
Advancements in frequency-domain methods for rotorcraft system identification p 56 A90-12771
Numerical simulation of separated and vortical flows on bodies at large angles of attack p 146 A90-16772
Experimental and computational studies of dynamic stall p 147 A90-16780
Computation of viscous transonic flow over porous airfoils p 153 A90-17864
Rotor hover performance prediction using a free-wake, computational fluid dynamics method p 153 A90-17869
High-resolution upwind scheme for vortical-flow simulations p 153 A90-17872
Numerical study of chemically reacting flows using a lower-upper symmetric successive overrelaxation scheme p 153 A90-17989
Pressure fluctuations in the tip region of a blunt-tipped airfoil p 154 A90-18136
Mach number effects on conical surface features of swept shock-wave/boundary-layer interactions p 154 A90-18147
Estimate of loads during wing-vortex interactions by Munk's transverse-flow method p 159 A90-19391
A kinematical/numerical analysis of rotor-stator interaction noise p 159 A90-19391
[AIAA PAPER 90-0281] p 219 A90-19770
A three-dimensional upwind parabolized Navier-Stokes code for chemically reacting flows
[AIAA PAPER 90-0394] p 165 A90-19831
A numerical study of general viscous flows around multi-element airfoils
[AIAA PAPER 90-0572] p 167 A90-19922
Amplitude effects on dynamic stall of an oscillating airfoil
[AIAA PAPER 90-0575] p 167 A90-19925
Correlation of Puma airfoils - Evaluation of CFD prediction methods
[ONERA, TP NO. 1989-185] p 224 A90-21045
Calculations of the flow past bluff bodies, including tilt-rotor wing sections at $\alpha = 90$ deg
[AIAA PAPER 90-0032] p 227 A90-22156
Pneumatic vortical flow control at high angles of attack
[AIAA PAPER 90-0098] p 227 A90-22164
Navier-Stokes predictions of the flowfield around the F-18 (HARV) wing and fuselage at large incidence
[AIAA PAPER 90-0099] p 227 A90-22165
Vortical flows over delta wings and numerical prediction of vortex breakdown
[AIAA PAPER 90-0102] p 227 A90-22166
Simulation and analysis of a delta planform with multiple jets in ground effect
[AIAA PAPER 90-0299] p 228 A90-22195
Unsteady transonic Navier-Stokes computations for an oscillating wing using single and multiple zones
[AIAA PAPER 90-0313] p 228 A90-22197
Multi-processing on supercomputers for computational aerodynamics
[AIAA PAPER 90-0337] p 282 A90-22199
Upwind differencing scheme for the time-accurate incompressible Navier-Stokes equations p 232 A90-23109
Multiple vortex ring model of the DFW microburst p 280 A90-23286
Turbulence modeling for aerodynamic flows
[AIAA PAPER 89-0606] p 234 A90-23647
Application of a lower-upper implicit scheme and an interactive grid generation for turbomachinery flow field simulations
[ASME PAPER 89-GT-20] p 288 A90-23762
Hub loads analysis of the SA349/2 helicopter p 333 A90-23936
Experience with scale effects in non-airplane wind tunnel testing
[AIAA PAPER 90-1822] p 350 A90-25165
Unsteady aerodynamic and aeroelastic calculations for wings using Euler equations p 302 A90-25288
Experimental studies of 90 deg corner cascades in the National Full-Scale Aerodynamic Complex
[AIAA PAPER 90-1826] p 307 A90-25935

Comparison of model- and full-scale wind-tunnel performance
[AIAA PAPER 88-2536] p 351 A90-26133
Toward a human-centered aircraft automation philosophy p 347 A90-26177
Avoiding a maneuvering aircraft with TCAS p 347 A90-26222
Air-ground information transfer in the National Airspace System p 380 A90-26235
Knowledge-based flow field zoning p 308 A90-26478
Surface grid generation for complex three-dimensional geometries p 376 A90-26484
Navier-Stokes computations useful in aircraft design
[AIAA PAPER 90-1800] p 315 A90-27311
Experimental study of nonsteady asymmetric flow around an ogive-cylinder at incidence p 384 A90-27985
Multiobjective decision making in a fuzzy environment with applications to helicopter design p 405 A90-27993
Prediction and measurement of low-frequency harmonic noise of a hovering model helicopter rotor p 463 A90-28159
HARP model rotor test at the DNW p 406 A90-28167
A numerical analysis of the British Experimental Rotor Program blade p 384 A90-28194
Tip vortex geometry of a hovering helicopter rotor in ground effect p 407 A90-28196
Advanced rotor computations with a corrected potential method p 385 A90-28197
RSRA/X-Flow flight control system development - Lessons learned p 430 A90-28216
Tilt rotor aircraft aeroacoustics p 409 A90-28238
The prediction of loads on the Boeing Helicopters Model 360 rotor p 410 A90-28240
Design and development of a facility for compressible dynamic stall studies of a rapidly pitching airfoil p 436 A90-28255
Navier-Stokes computations on swept-tapered wings, including flexibility
[AIAA PAPER 90-1152] p 389 A90-29364
Effects of higher harmonic control on rotor performance and control loads p 412 A90-29467
Computational requirements for hypersonic flight performance estimates p 440 A90-29686
Basic numerical methods p 394 A90-29886
Application of transonic flow analysis to helicopter rotor problems p 394 A90-29887
A flight-test methodology for identification of an aerodynamic model for a V/STOL aircraft p 413 A90-30107
Flight testing a highly flexible aircraft - Case study on the MIT Light Eagle p 414 A90-31284
Helmet mounted display systems for helicopter simulation p 420 A90-31344
Navier-Stokes analyses of the redistribution of inlet temperature distortions in a turbine p 471 A90-32959
Numerical simulations of an oblique detonation wave engine p 508 A90-32964
Computational aerothermodynamics p 476 A90-34380
Computational fluid dynamics - Current capabilities and directions for the future p 540 A90-34385
Effective use of Cray supercomputers p 546 A90-34436
High-resolution shock-capturing schemes for inviscid and viscous hypersonic flows p 476 A90-34545
Direct numerical simulations of transition in a compressible wake p 553 A90-35212
Nonlinear effects in the two-dimensional adaptive-wall outer-flow problem p 554 A90-35771
Development of a three-dimensional upwind parabolized Navier-Stokes code p 602 A90-36253
The effect of Mach number on the stability of a plane supersonic wake p 557 A90-36524
Three dimensional Discrete Particle Simulation about the AFE geometry
[AIAA PAPER 90-1778] p 560 A90-38468
A survey of nonuniform inflow models for rotorcraft flight dynamics and control applications p 590 A90-38521
Results of an A109 simulation validation and handling qualities study p 591 A90-38524
Flight/propulsion control integration for V/STOL fighter/attack aircraft p 591 A90-38530
Development of the XV-15 tiltrotor research aircraft - Lessons learned p 581 A90-38540
Effects of streamwise vorticity injection on turbulent mixing layer development
[AIAA PAPER 90-1459] p 561 A90-38616
The free-wake computation of rotor-body flows
[AIAA PAPER 90-1540] p 565 A90-38684

- Euler solutions for self-generated rotor blade-vortex interactions
[AIAA PAPER 90-1588] p 566 A90-38723
- A computational study of the impingement region of an unsteady subsonic jet
[AIAA PAPER 90-1657] p 570 A90-38784
- Calculation of hypersonic forebody/inlet flow fields
[AIAA PAPER 90-1493] p 619 A90-39049
- An introduction to chaos theory in CFD
[AIAA PAPER 90-1440] p 680 A90-39725
- Supercomputer applications in gas turbine flowfield simulation
p 620 A90-40495
- Flow visualization studies of the Mach number effects on dynamic stall of an oscillating airfoil
p 622 A90-40683
- Hypervelocity, minimum-radius, coordinated turns
p 667 A90-40691
- CFD propels NASP propulsion progress
p 683 A90-41163
- Concept development of automatic guidance for rotorcraft obstacle avoidance
p 669 A90-41632
- CFD and transonic helicopter sound
p 696 A90-42433
- A review of tilt rotor download research
p 630 A90-42437
- Evolution of engine cycles for STOVL propulsion concepts
[AIAA PAPER 90-2272] p 743 A90-42767
- Streamtube analysis of supersonic combustion in an in-tube-scamjet
[AIAA PAPER 90-2339] p 762 A90-42776
- Unsteady analysis of hot streak migration in a turbine stage
[AIAA PAPER 90-2354] p 769 A90-42782
- A validation study of the Spark Navier Stokes code for nonreacting scramjet combustor flowfields
[AIAA PAPER 90-2360] p 706 A90-42784
- Airborne MSS for land cover classification II
p 737 A90-43376
- Zonal Navier-Stokes methodology for flow simulation about a complete aircraft
p 709 A90-44727
- Self-induced roll oscillations of low-aspect-ratio rectangular wings
[AIAA PAPER 90-2811] p 753 A90-45151
- An experimental study of the nonlinear dynamic phenomenon known as wing rock
[AIAA PAPER 90-2812] p 753 A90-45152
- Canard-wing vortex interactions at subsonic through supersonic speeds
[AIAA PAPER 90-2814] p 711 A90-45154
- A pilot rating scale for evaluating failure transients in electronic flight control systems
[AIAA PAPER 90-2827] p 754 A90-45159
- System identification requirements for high-bandwidth rotorcraft flight control system design
p 755 A90-45333
- Effects of turbulence models on the prediction of transonic wing flows
[SAE PAPER 892224] p 713 A90-45440
- Simulation evaluation of transition and hover flying qualities of a mixed-flow, remote-lift STOVL aircraft
[SAE PAPER 892284] p 757 A90-45464
- Helmet-mounted display systems for flight simulation
[SAE PAPER 892352] p 760 A90-45503
- CFD validation for aerodynamic flows - Challenge for the '90's
[AIAA PAPER 90-2995] p 787 A90-45846
- Numerical simulation of the viscous flow around a simplified F/A-18 at high angles of attack
[AIAA PAPER 90-2999] p 787 A90-45849
- Numerical simulation of the effects of variation of angle of attack and sweep angle on vortex breakdown over delta wings
[AIAA PAPER 90-3000] p 788 A90-45850
- The effect of turbulence models on the numerical prediction of the flowfield about a prolate spheroid at high angle of attack
[AIAA PAPER 90-3106] p 789 A90-45855
- Experimental and numerical study of the British Experimental Rotor Programme blade
[AIAA PAPER 90-3008] p 789 A90-45858
- Schlieren studies of compressibility effects on dynamic stall of airfoils in transient pitching motion
[AIAA PAPER 90-3038] p 791 A90-45877
- Multiple vortex and shock interactions at subsonic, transonic, and supersonic speeds
[AIAA PAPER 90-3023] p 793 A90-45890
- Experimental and computational surface and flow-field results for an all-body hypersonic aircraft
[AIAA PAPER 90-3067] p 793 A90-45893
- Sideslip-induced static pressure errors in flight-test measurements
[AIAA PAPER 90-3082] p 794 A90-45898
- An upwind approach to unsteady flowfield simulation
[AIAA PAPER 90-3100] p 796 A90-45912
- Application of a streamwise upwind algorithm for unsteady transonic computations over oscillating wings
[AIAA PAPER 90-3103] p 796 A90-45915
- Methodology for estimating helicopter performance and weights using limited data
p 829 A90-46936
- Aerodynamic design of the Cal Poly Da Vinci Human-Powered Helicopter
p 830 A90-46950
- Theoretical and experimental investigation of the aeroelastic stability of an advanced bearingless rotor in hover and forward flight
p 831 A90-46958
- The response of helicopter rotors to vibratory airload
p 832 A90-46971
- Prediction of separated transonic wing flows with nonequilibrium algebraic turbulence model
p 809 A90-47312
- Real-time piloted simulation of fully automatic guidance and control for rotorcraft nap-of-the-earth (NOE) flight following planned profiles
[AIAA PAPER 90-3372] p 864 A90-47630
- Image based range determination
[AIAA PAPER 90-3404] p 822 A90-47659
- Rotorcraft pursuit-evasion in nap-of-the-earth flight
[AIAA PAPER 90-3455] p 786 A90-47707
- Effects of stick dynamics on helicopter flying qualities
[AIAA PAPER 90-3477] p 866 A90-47727
- Flight investigation of variations in rotorcraft control and display dynamics for hover
[AIAA PAPER 90-3482] p 866 A90-47731
- Flight evaluations of several hover control and display combinations for precise blind vertical landings
[AIAA PAPER 90-3479] p 867 A90-47764
- Subsonic and transonic low-Reynolds-number airfoils with reduced pitching moments
[AIAA PAPER 90-3212] p 812 A90-48838
- Design synthesis and optimization of joined-wing transports
[AIAA PAPER 90-3197] p 838 A90-49102
- Selected design issues of some high speed rotorcraft concepts
[AIAA PAPER 90-3297] p 840 A90-49125
- Thermal interaction between an impinging hot jet and a conducting solid surface
[AIAA PAPER 90-3010] p 956 A90-50636
- A closer look at the induced drag of crescent-shaped wings
[AIAA PAPER 90-3063] p 903 A90-50638
- Numerical simulation of three-dimensional transonic flows
p 905 A90-51020
- An integrated CFD/experimental analysis of aerodynamic forces and moments
[NASA-TM-102195] p 18 A90-10006
- Static aeroelastic analysis for generic configuration aircraft
[NASA-TM-89423] p 52 A90-10042
- Direct numerical study of leading-edge contamination
p 19 A90-10361
- Design of a final approach spacing tool for TRACON air traffic control
[NASA-TM-102229] p 24 A90-10841
- Real-time flight test analysis and display techniques for the X-29A aircraft
p 34 A90-10866
- Review and analysis of the DNW/Model 360 rotor acoustic data base
[NASA-TM-102253] p 81 A90-11692
- Computer simulation of aircraft aerodynamics
[NASA-TM-102221] p 88 A90-11699
- Application of the wide-field shadowgraph technique to rotor wake visualization
[NASA-TM-102222] p 88 A90-11700
- An experimental investigation of helicopter rotor hub fairing drag characteristics
[NASA-TM-102182] p 88 A90-11701
- Applications of flight control system methods to an advanced combat rotorcraft
[NASA-TM-101054] p 119 A90-11752
- Simulation of glancing shock wave and boundary layer interaction
[NASA-TM-102233] p 133 A90-11970
- Powered-lift aircraft technology
[NASA-SP-501] p 107 A90-12589
- Application of a self-adaptive grid method to complex flows
[NASA-TM-102223] p 143 A90-13324
- Study of the integration of wind tunnel and computational methods for aerodynamic configurations
[NASA-TM-102196] p 170 A90-13332
- Computation of Navier-Stokes equations for three-dimensional flow separation
[NASA-TM-102266] p 172 A90-13353
- Flight deck automation: Promises and realities
[NASA-CP-10036] p 187 A90-13384
- A two-dimensional adaptive-wall test section with ventilated walls in the Ames 2- by 2-foot transonic wind tunnel
[NASA-TM-102207] p 201 A90-13407
- Global stratospheric change: Requirements for a Very-High-Altitude Aircraft for Atmospheric Research
[NASA-CP-10041] p 185 A90-14220
- Airdata calibration of a high-performance aircraft for measuring atmospheric wind profiles
[NASA-TM-101714] p 186 A90-14228
- Temporally and spatially resolved flow in a two-stage axial compressor. Part 2: Computational assessment
[NASA-TM-102273] p 194 A90-14236
- Analysis of severe atmospheric disturbances from airline flight records
p 280 A90-15045
- The effectiveness of vane-aileron excitation in the experimental determination of flutter speed by parameter identification
[NASA-TP-2971] p 249 A90-15100
- Piloted simulation of a ground-based time-control concept for air traffic control
[NASA-TM-101085] p 240 A90-15898
- A survey of nonuniform inflow models for rotorcraft flight dynamics and control applications
[NASA-TM-102219] p 260 A90-15938
- Optimum element density studies for finite-element thermal analysis of hypersonic aircraft structures
[NASA-TM-4163] p 369 A90-17074
- A review of high-speed, convective, heat-transfer computation methods
p 316 A90-17548
- A head up display format for application to V/STOL aircraft approach and landing
[NASA-TM-102216] p 340 A90-17632
- Longitudinal stability and control characteristics of the Quiet Short-Haul Research Aircraft (QsRA)
[NASA-TP-2965] p 349 A90-17639
- Equations of motion of slung load systems with results for dual lift
[NASA-TM-102246] p 349 A90-17641
- A streamwise upwind algorithm applied to vortical flow over a delta wing
[NASA-TM-102225] p 398 A90-19201
- Three-dimensional viscous rotor flow calculations using a viscous-inviscid interaction approach
[NASA-TM-102235] p 399 A90-19204
- Static aeroelastic analysis of a three-dimensional generic wing
[NASA-TM-102231] p 509 A90-20087
- The 1-((diorganoxyphosphonyl)methyl)-2,4- and -2,6-diamido benzenes
[NASA-CASE-ARC-11425-4] p 532 A90-20133
- Analysis of small-scale rotor hover performance data
[NASA-TM-102271] p 540 A90-20325
- Extension of a streamwise upwind algorithm to a moving grid system
[NASA-TM-102800] p 572 A90-21739
- Analytical study of the origin and behavior of asymmetric vortices
[NASA-TM-102796] p 573 A90-21746
- Identification of XV-15 aeroelastic modes using frequency-domain methods
[NASA-TM-101021] p 582 A90-21756
- Quiet mode for nonlinear rotor models
[NASA-TM-102236] p 582 A90-21758
- Theoretical and experimental study of flow-control devices for inlets of indraft wind tunnels
[NASA-TM-100050] p 598 A90-21778
- Kalman filter based range estimation for autonomous navigation using imaging sensors
p 578 A90-22238
- Preliminary development of an intelligent computer assistant for engine monitoring
[NASA-TM-101702] p 612 A90-22322
- Analysis of sequencing and scheduling methods for arrival traffic
[NASA-TM-102795] p 636 A90-23373
- Simulator evaluation of the final approach spacing tool
[NASA-TM-102807] p 636 A90-23374
- Helicopter Airborne Laser Positioning System (HALPS)
[NASA-TM-102814] p 654 A90-23399
- Lateral-directional stability and control characteristics of the Quiet Short-Haul Research Aircraft (QsRA)
[NASA-TM-102250] p 671 A90-23413
- Some 1-((diorganoxyphosphonyl)methyl)-2,4- and -2,6-dinitro-benzenes
[NASA-CASE-ARC-11425-3] p 678 A90-23475
- Ground-simulation investigations of VTOL airworthiness criteria for terminal-area operations
[NASA-TM-102810] p 757 A90-25141
- TRENDS: The aeronautical's post-test database management system
[NASA-TM-101025] p 761 A90-25149
- Visualization of three dimensional data
p 782 A90-25553
- Research at NASA's NFAC wind tunnels
[NASA-TM-102827] p 702 A90-25933
- A brief review of some mechanisms causing boundary layer transition at high speeds
[NASA-TM-102834] p 720 A90-25945

- Synthesis of individual rotor blade control system for gust alleviation
[NASA-TM-101886] p 736 N90-25972
- Rotorcraft aeromechanical stability-methodology assessment. Phase 2: Workshop
[NASA-TM-102272] p 816 N90-26800
- The validation and application of a rotor acoustic prediction computer program
[NASA-TM-101794] p 895 N90-27465
- A comparison of two central difference schemes for solving the Navier-Stokes equations
[NASA-TM-102815] p 816 N90-27654
- Sideslip-induced static pressure errors in flight-test measurements
[NASA-TM-102846] p 849 N90-27702
- The effects of structural flap-lag and pitch-lag coupling on soft inplane hingeless rotor stability in hover
[NASA-TP-3002] p 910 N90-28503
- Velocity filtering applied to optical flow calculations
[NASA-TM-102802] p 916 N90-28512
- National Aeronautics and Space Administration. Flight Research Center, Edwards, CA.**
- Propulsion system-flight control integration-flight evaluation and technology transition
[AIAA PAPER 90-2280] p 644 A90-42106
- National Aeronautics and Space Administration. Goddard Space Flight Center, Greenbelt, MD.**
- Structural mode significance using INCA
[AIAA PAPER 90-3346] p 889 A90-47606
- Evolution of Ada technology in the flight dynamics area: Implementation/testing phase analysis
[NASA-TM-103310] p 546 N90-21539
- System testing of a production Ada (trademark) project: The GRODY study
[NASA-TM-103308] p 546 N90-21541
- Evolution of Ada technology in the flight dynamics area: Design phase analysis
[NASA-TM-103307] p 547 N90-21542
- Software Management Environment (SME) concepts and architecture
[NASA-TM-103306] p 547 N90-21543
- Implementation of a production Ada project: The GRODY study
[NASA-TM-103305] p 547 N90-21544
- National Aeronautics and Space Administration. Hugh L. Dryden Flight Research Center, Edwards, CA.**
- Preliminary results from a subsonic high angle-of-attack flush airdata sensing (HI-FADS) system: Design, calibration, and flight test evaluation
[NASA-TM-101713] p 339 N90-16758
- Output model-following control synthesis for an oblique-wing aircraft
[NASA-TM-100454] p 435 N90-19241
- Water-tunnel study results of a TF/A-18 and F/A-18 canopy flow visualization
[NASA-TM-101705] p 573 N90-22532
- National Aeronautics and Space Administration. Hugh L. Dryden Flight Research Facility, Edwards, CA.**
- A knowledge-based system design/information tool for aircraft flight control systems
[AIAA PAPER 89-2978] p 55 A90-10491
- Ground vibration test results of a JetStar airplane using impulsive sine excitation
p 179 A90-16963
- In-flight flow field analysis on the NASA F-18 high alpha research vehicle with comparisons to ground facility data
[AIAA PAPER 90-0231] p 163 A90-19745
- Preliminary results from a subsonic high-angle-of-attack flush airdata sensing (HI-FADS) system - Design, calibration, algorithm development, and flight test evaluation
[AIAA PAPER 90-0232] p 187 A90-19746
- Compensating for pneumatic distortion in pressure sensing devices
[AIAA PAPER 90-0631] p 211 A90-19956
- Laminar flow control leading-edge systems in simulated airline service
p 335 A90-26134
- An in-flight interaction of the X-29A canard and flight control system
[AIAA PAPER 90-1240] p 348 A90-26820
- An American knowledge base in England - Alternate implementations of an expert system flight status monitor
p 459 A90-30719
- Estimating short-period dynamics using an extended Kalman filter
[AIAA PAPER 90-1277] p 518 A90-33901
- Flight-testing of the self-repairing flight control system using the F-15 highly integrated digital electronic control flight research facility
[AIAA PAPER 90-1321] p 520 A90-34149
- Piloted simulator assessments of agility
[AIAA PAPER 90-1306] p 589 A90-36030
- A proposed Kalman filter algorithm for estimation of unmeasured output variables for an F100 turbofan engine
[AIAA PAPER 90-1920] p 656 A90-40558
- A preliminary evaluation of an F100 engine parameter estimation process using flight data
[AIAA PAPER 90-1921] p 656 A90-40559
- A simple dynamic engine model for use in a real-time aircraft simulation with thrust vectoring
[AIAA PAPER 90-2166] p 662 A90-42054
- Development of a real-time aeroperformance analysis technique for the X-29A advanced technical demonstrator
p 732 A90-44738
- In-flight flow visualization characteristics of the NASA F-18 high alpha research vehicle at high angles of attack
[SAE PAPER 892222] p 713 A90-45439
- F-18 high alpha research vehicle surface pressures - Initial in-flight results and correlation with flow visualization and wind-tunnel data
[AIAA PAPER 90-3018] p 792 A90-45885
- Flight test of a trajectory controller using linearizing transformations with measurement feedback
[AIAA PAPER 90-3373] p 864 A90-47631
- Initial flight qualification and operational maintenance of X-29A flight software
[NASA-TM-101703] p 32 N90-10023
- Flutter clearance of the F-18 high-angle-of-attack research vehicle with experimental wingtip instrumentation pods
[NASA-TM-4148] p 103 N90-11732
- Measurement effects on the calculation of in-flight thrust for an F404 turbofan engine
[NASA-TM-4140] p 114 N90-11741
- A design procedure for the handling qualities optimization of the X-29A aircraft
[NASA-TM-4142] p 119 N90-11753
- Effect of control surface mass unbalance on the stability of a closed-loop active control system
[NASA-TP-2952] p 134 N90-12042
- Development flight tests of JetStar LFC leading-edge flight test experiment
p 104 N90-12509
- F-14 VSTFE and results of the cleanup flight test program
p 105 N90-12547
- A smoke generator system for aerodynamic flight research
[NASA-TM-4137] p 183 N90-13372
- Application of fracture mechanics and half-cycle method to the prediction of fatigue life of B-52 aircraft pylon components
[NASA-TM-88277] p 214 N90-13820
- A knowledge-based system design/information tool for aircraft flight control systems
[NASA-TM-101704] p 217 N90-13990
- A knowledge-based flight status monitor for real-time application in digital avionics systems
[NASA-TM-101710] p 217 N90-13995
- An in-flight investigation of ground effect on a forward-swept wing airplane
[NASA-TM-101708] p 175 N90-14202
- Flight evaluation of a pneumatic system for unsteady pressure measurements using conventional sensors
[NASA-TM-4131] p 186 N90-14225
- Wind-tunnel investigation of a flush airdata system at Mach numbers from 0.7 to 1.4
[NASA-TM-101697] p 421 N90-18395
- Compensating for pneumatic distortion in pressure sensing devices
[NASA-TM-101716] p 415 N90-19224
- X-29A aircraft structural loads flight testing
[NASA-TM-101715] p 416 N90-19225
- The implementation and operation of a variable-response electronic throttle control system for a TF-104G aircraft
[NASA-TM-101696] p 509 N90-20086
- Estimating short-period dynamics using an extended Kalman filter
[NASA-TM-101722] p 648 N90-23392
- STARS: An integrated general-purpose finite element structural, aeroelastic, and aeroservoelastic analysis computer program
[NASA-TM-101709] p 689 N90-23768
- Evaluation of various thrust calculation techniques on an F404 engine
[NASA-TP-3001] p 735 N90-25134
- Flutter clearance of the F-14A variable-sweep transition flight experiment airplane, phase 2
[NASA-TM-101717] p 735 N90-25135
- Effects of simplifying assumptions on optimal trajectory estimation for a high-performance aircraft
[NASA-TM-101721] p 757 N90-25142
- Flight-testing of the self-repairing flight control system using the F-15 highly integrated digital electronic control flight research facility
[NASA-TM-101725] p 758 N90-25144
- An in-flight interaction of the X-29A canard and flight control system
[NASA-TM-101718] p 736 N90-25973
- An automated calibration laboratory for flight research instrumentation: Requirements and a proposed design approach
[NASA-TM-101719] p 781 N90-26564
- Experimental characterization of the effects of pneumatic tubing on unsteady pressure measurements
[NASA-TM-4171] p 850 N90-27703
- In-flight flow visualization with pressure measurements at low speeds on the NASA F-18 high alpha research vehicle
[NASA-TM-101726] p 910 N90-28505
- An in-flight investigation of ground effect on a forward-swept wing airplane
p 922 N90-28533
- Validation of the F-18 high alpha research vehicle flight control and avionics systems modifications
[NASA-TM-101723] p 924 N90-28542
- Propulsion system-flight control integration and optimization: Flight evaluation and technology transition
[NASA-TM-4207] p 929 N90-28551
- Real-time aerodynamic heating and surface temperature calculations for hypersonic flight simulation
[NASA-TM-4222] p 959 N90-28815
- National Aeronautics and Space Administration. Lyndon B. Johnson Space Center, Houston, TX.**
- Applications of fuzzy sets to rule-based expert system development
p 216 A90-18050
- Effects of thermochemistry, nonequilibrium, and surface catalysis on the design of hypersonic vehicles
p 224 A90-21159
- Computation of hypersonic flow fields
p 225 A90-21169
- A linear quadratic regulator approach to the stabilization of uncertain linear systems
[AIAA PAPER 90-3509] p 891 A90-47755
- National Aeronautics and Space Administration. Langley Research Center, Hampton, VA.**
- An experimental investigation of fault tolerant software structures in an avionics application
[AIAA PAPER 89-3082] p 74 A90-10568
- Real-time fault monitoring for aircraft applications using quantitative simulation and expert systems
[AIAA PAPER 89-3103] p 37 A90-10586
- Grid generation and adaptation for the direct simulation Monte Carlo method
p 67 A90-11102
- Direct simulation of three-dimensional hypersonic flow about intersecting blunt wedges
p 16 A90-12835
- Materials and structures for hypersonic vehicles
p 31 A90-13015
- Navier-Stokes computations of a prolate spheroid at angle of attack
p 17 A90-13018
- Mach number effects on transonic aeroelastic forces and flutter characteristics
p 17 A90-13024
- Scaling effects in the impact response of graphite-epoxy composite beams
[SAE PAPER 891014] p 128 A90-14326
- Impact evaluation of composite floor sections
[SAE PAPER 891018] p 100 A90-14330
- A review and update of the NASA aircraft noise prediction program propeller analysis system
[SAE PAPER 891032] p 139 A90-14340
- Investigations of modifications to improve the spin resistance of a high-wing, single-engine, light airplane
[SAE PAPER 891039] p 118 A90-14345
- Aircraft and ground vehicle friction measurements obtained under winter runway conditions
[SAE PAPER 891070] p 95 A90-14367
- Acceleration, gamma, and theta guidance for abort landing in a windshear
p 98 A90-14733
- Simulation model-building procedure for dynamic systems integration
p 138 A90-14744
- Curvature effects on the stability of laminar boundary layers on swept wings
p 148 A90-16788
- Experimental transition and boundary-layer stability analysis for a slotted swept laminar flow control airfoil
p 148 A90-16793
- Numerical studies of incompressible flow around delta and double-delta wings
p 150 A90-16845
- Minimum weight design of helicopter rotor blades with frequency constraints
p 180 A90-17313
- Design and experimental verification of an equivalent forebody representation of flowing inlets
p 152 A90-17863
- Navier-Stokes computations of lee-side flows over delta wings
p 153 A90-17978
- Experimental investigation of flowfield about a multielement airfoil
p 154 A90-18137
- The critical role of aerodynamic heating effects in the design of hypersonic vehicles
p 155 A90-18249
- Unsteady pressure and structural response measurements on an elastic supercritical wing
p 159 A90-19392
- Applications of Lagrangian blending functions for grid generation around airplane geometries
[AIAA PAPER 90-0009] p 216 A90-19630

Experimental investigation of a new device to control the asymmetric flowfield on forebodies at large angles of attack

[AIAA PAPER 90-0069] p 161 A90-19665

Numerical simulation of the actuation system for the ALDF's propulsion control valve

[AIAA PAPER 90-0079] p 211 A90-19674

Direct simulation of hypersonic rarefied flow about a delta wing

[AIAA PAPER 90-0143] p 162 A90-19704

Numerical solution of the boundary-layer equations for a general aviation fuselage

[AIAA PAPER 90-0305] p 163 A90-19786

A study of sonic boom overpressure trends with respect to weight, altitude, Mach number, and vehicle shaping

[AIAA PAPER 90-0367] p 164 A90-19816

A study of the limitations of linear theory methods as applied to sonic boom calculations

[AIAA PAPER 90-0368] p 219 A90-19817

Impact of nose-probe chines on the vortex flows about the F-16C

[AIAA PAPER 90-0386] p 165 A90-19828

Transonic Navier-Stokes solutions about a complex high-speed accelerator configuration

[AIAA PAPER 90-0430] p 166 A90-19844

Results of aerodynamic testing of large-scale wing sections in a simulated natural rain environment

[AIAA PAPER 90-0486] p 167 A90-19874

A numerical parametric study of a scramjet inlet in a Mach 6 arc heated test facility

[AIAA PAPER 90-0531] p 167 A90-19896

A Monte Carlo simulation technique for low-altitude, wind-shear turbulence

[AIAA PAPER 90-0564] p 216 A90-19917

Prediction of steady and unsteady asymmetric vortical flows around cones

[AIAA PAPER 90-0598] p 168 A90-19940

Hypersonic airbreathing vehicle design - Focus on aero-space plane

[AIAA PAPER 90-0598] p 245 A90-21156

Prediction of vortical flows on wings using incompressible Navier-Stokes equations

[AIAA PAPER 90-0598] p 226 A90-21935

A numerical study of mixing enhancement in a supersonic combustor

[AIAA PAPER 90-0203] p 272 A90-22182

Wind-tunnel investigation on the effect of a crescent planform on drag

[AIAA PAPER 90-0300] p 228 A90-22196

An embedded grid formulation applied to a delta wing

[AIAA PAPER 90-0429] p 229 A90-22216

A hybrid method for prediction of propeller performance

[AIAA PAPER 90-0440] p 229 A90-22219

Experimental studies of shock wave/wall jet interaction in hypersonic flow

[AIAA PAPER 90-0607] p 231 A90-22449

Navier-Stokes computations of vortical flows over low-aspect-ratio wings

[AIAA PAPER 90-0607] p 232 A90-23103

Optimal placement of tuning masses for vibration reduction in helicopter rotor blades

[AIAA PAPER 90-0607] p 247 A90-23117

Minimizing life cycle cost for subsonic commercial aircraft

[AIAA PAPER 90-0607] p 283 A90-23282

Airborne Doppler radar detection of low-altitude wind shear

[AIAA PAPER 90-0607] p 252 A90-23284

Leading- and trailing-edge flaps on supersonic delta wings

[AIAA PAPER 90-0607] p 233 A90-23285

Magnetic suspension - Today's marvel, tomorrow's tool

[AIAA PAPER 90-0607] p 262 A90-23697

Reduction of blade-vortex interaction noise through higher harmonic pitch control

[AIAA PAPER 90-0607] p 377 A90-23937

Minimum weight design of rotorcraft blades with multiple frequency and stress constraints

[AIAA PAPER 90-0607] p 335 A90-25304

Measurements on an oscillating 70-deg delta wing in subsonic flow

[AIAA PAPER 90-0607] p 307 A90-26130

Laminar flow control leading-edge systems in simulated airline service

[AIAA PAPER 90-0607] p 335 A90-26134

Application of multiple grids topology to supersonic internal/external flow interactions

[AIAA PAPER 90-0607] p 308 A90-26135

Fourth-order accurate three-dimensional compressible boundary-layer calculations

[AIAA PAPER 90-0607] p 308 A90-26136

Adaptive mesh generation for viscous flows using Delaunay triangulation

[AIAA PAPER 90-0607] p 310 A90-26531

Interactive generation of unstructured grids for three dimensional problems

[AIAA PAPER 90-0607] p 310 A90-26537

Interactive grid generation for fighter aircraft geometries

[AIAA PAPER 90-0607] p 311 A90-26546

Multiple-block grid adaption for an airplane geometry

[AIAA PAPER 90-0607] p 311 A90-26547

The hemisphere-cylinder at an angle of attack

[AIAA PAPER 90-0050] p 313 A90-26907

Unsteady aerodynamic characteristics of a fighter model undergoing large-amplitude pitching motions at high angles of attack

[AIAA PAPER 90-0309] p 313 A90-26933

Operational considerations for aerodynamic testing of large-scale wing sections in a simulated natural rain environment

[AIAA PAPER 90-0485] p 313 A90-26956

Three-dimensional shock-shock interactions on the scramjet inlet

[AIAA PAPER 90-0529] p 314 A90-26963

Rotor blade-vortex interaction impulsive noise source localization

[AIAA PAPER 90-0529] p 463 A90-27978

The prediction of the noise generating mechanisms of an Aerospatiale 365N-1 Dauphin helicopter

[AIAA PAPER 90-0529] p 463 A90-28161

A transition detection study at Mach 1.5, 2.0, and 2.5 using a micro-thin hot-film system

[AIAA PAPER 90-0529] p 386 A90-28260

Database for LDV signal processor performance analysis

[AIAA PAPER 90-0529] p 447 A90-28278

Development of a dual strain gage balance system for measuring light loads

[AIAA PAPER 90-0529] p 437 A90-28289

A fatigue study of electrical discharge machine (EDM) strain-gage balance materials

[AIAA PAPER 90-0529] p 448 A90-28295

High temperature skin friction measurement

[AIAA PAPER 90-0529] p 448 A90-28306

Aerothermodynamics and transition in high-speed wind tunnels at NASA Langley

[AIAA PAPER 90-0529] p 386 A90-28555

A parallel-vector algorithm for rapid structural analysis on high-performance computers

[AIAA PAPER 90-1149] p 458 A90-29293

Implicit flux-split Euler schemes for unsteady aerodynamic analysis involving unstructured dynamic meshes

[AIAA PAPER 90-0936] p 389 A90-29362

Experimental transonic flutter characteristics of supersonic cruise configurations

[AIAA PAPER 90-0979] p 390 A90-29369

Effects of spoiler surfaces on the aeroelastic behavior of a low-aspect-ratio rectangular wing

[AIAA PAPER 90-0981] p 391 A90-29371

Finite element two-dimensional panel flutter at high supersonic speeds and elevated temperature

[AIAA PAPER 90-0982] p 450 A90-29372

Aeroelastic analysis of wings using the Euler equations with a deforming mesh

[AIAA PAPER 90-1032] p 391 A90-29376

Using transonic small disturbance theory for predicting the aeroelastic stability of a flexible wind-tunnel model

[AIAA PAPER 90-1033] p 391 A90-29377

Aeroservoelasticity

[AIAA PAPER 90-1073] p 411 A90-29381

Digital flutter-suppression-system investigations for the active flexible wing wind-tunnel model

[AIAA PAPER 90-1074] p 430 A90-29382

Experimental aeroelasticity - History, status and future in brief

[AIAA PAPER 90-0978] p 382 A90-29598

Hypersonic viscous shock-layer solutions over long slender bodies. II - Low Reynolds number flows

[AIAA PAPER 90-0978] p 393 A90-29695

Comparison between experimental and numerical results for a research hypersonic aircraft

[AIAA PAPER 90-0978] p 395 A90-31278

Multistroke cloud-to-ground strike to the NASA F-106B airplane

[AIAA PAPER 90-0978] p 482 A90-32304

Turbulence measurements and noise generation in a transonic cryogenic wind tunnel

[AIAA PAPER 88-2026] p 522 A90-32463

Numerical model of unsteady subsonic aeroelastic behavior

[AIAA PAPER 90-1073] p 535 A90-32471

Unsteady airloads due to separated flow on airfoils and wings

[AIAA PAPER 90-1073] p 471 A90-33311

Unsteady aerodynamics methods for transonic aeroelastic analysis

[AIAA PAPER 90-1073] p 471 A90-33353

Application of the CAP-TSD unsteady transonic small disturbance program to wing flutter

[AIAA PAPER 90-1073] p 491 A90-33354

Recent activities within the aeroservoelasticity branch at the NASA Langley Research Center

[AIAA PAPER 90-1073] p 492 A90-33400

Flutter suppression control law synthesis for the active flexible wing model

[AIAA PAPER 90-1073] p 517 A90-33403

An analytical sensitivity method for use in integrated aeroservoelastic aircraft design

[AIAA PAPER 90-1073] p 517 A90-33405

Wind-tunnel and flight-test investigation of the extruder remotely piloted vehicle configuration

[AIAA PAPER 90-1261] p 494 A90-33891

Preliminary flight test investigation of an airborne wake vortex detection concept

[AIAA PAPER 90-1282] p 495 A90-33903

Flight-measured streamwise disturbance instabilities in laminar flow

[AIAA PAPER 90-1283] p 495 A90-33904

A flight test investigation of certification requirements for laminar-flow general aviation airplanes

[AIAA PAPER 90-1310] p 496 A90-33920

A summary of spin-recovery parachute experience on light airplanes

[AIAA PAPER 90-1317] p 519 A90-33926

The vortex flap F-106B, overcoming safety and data problems in flight testing

[AIAA PAPER 90-1280] p 496 A90-34725

Analysis of aircraft tires via semianalytic finite elements

[AIAA PAPER 90-1280] p 496 A90-34740

Pressure and heat-transfer investigation of a hypersonic configuration

[AIAA PAPER 90-1280] p 598 A90-35757

Euler flutter analysis of airfoils using unstructured dynamic meshes

[AIAA PAPER 90-1280] p 602 A90-35760

Cloud-to-ground strikes to the NASA F-106 airplane

[AIAA PAPER 90-1280] p 574 A90-35767

Connection between leading-edge sweep, vortex lift, and vortex strength for delta wings

[AIAA PAPER 90-1279] p 579 A90-36027

Flight tests of a helmet-mounted display synthetic visibility system

[AIAA PAPER 90-1279] p 579 A90-36027

Impact of emerging technologies on future combat aircraft agility

[AIAA PAPER 90-1304] p 580 A90-36029

Navier-Stokes computation of flow around a round-edged double-delta wing

[AIAA PAPER 90-1304] p 555 A90-36251

Implicit flux-split schemes for the Euler equations

[AIAA PAPER 90-1304] p 602 A90-36254

Application of optimization methods to helicopter rotor blade design

[AIAA PAPER 90-1375] p 604 A90-37337

Aeronautical facility requirements into the 2,000's

[AIAA PAPER 90-1375] p 594 A90-37926

Design and operational features of low-disturbance wind tunnels at NASA Langley for Mach numbers from 3.5 to 18

[AIAA PAPER 90-1391] p 594 A90-37936

Wall interference assessment/correction (WIIAC) for transonic airfoil data from porous and shaped wall test sections

[AIAA PAPER 90-1406] p 595 A90-37945

Evaluation of equilibrium turbulence for a naturally developing hypersonic boundary layer at nonadiabatic wall conditions

[AIAA PAPER 90-1410] p 559 A90-37948

National Transonic Facility model and model support vibration problems

[AIAA PAPER 90-1416] p 596 A90-37953

A numerical study on the use of sulfur hexafluoride as a test gas for wind tunnels

[AIAA PAPER 90-1421] p 605 A90-37958

Application of the LAURA code for slender-vehicle aerothermodynamics

[AIAA PAPER 90-1714] p 560 A90-38416

Langley hypersonic aerodynamic/aerothermodynamic testing capabilities - Present and future

[AIAA PAPER 90-1376] p 596 A90-38483

The development of a 3-D laser velocimeter for the NASA Langley low turbulence pressure wind tunnel

[AIAA PAPER 90-1385] p 597 A90-38484

Scramjet testing from Mach 4 to 20 - Present capability and needs for the nineties

[AIAA PAPER 90-1388] p 597 A90-38485

Evaluation of transonic wall interference assessment and correction for semi-span wing data

[AIAA PAPER 90-1433] p 597 A90-38487

Effects of shock on the stability of hypersonic boundary layers

[AIAA PAPER 90-1448] p 561 A90-38608

An abbreviated Reynolds stress turbulence model for airfoil flows

[AIAA PAPER 90-1468] p 562 A90-38625

A hybrid Reynolds averaged/PDF closure model for supersonic turbulent combustion

[AIAA PAPER 90-1573] p 600 A90-38711

Computational study for passive control of supersonic asymmetric vortical flows around cones

[AIAA PAPER 90-1581] p 566 A90-38718

Enthalpy damping for high Mach number Euler solutions

[AIAA PAPER 90-1585] p 566 A90-38720

Advanced Mach 3.5 Axisymmetric Quiet Nozzle

[AIAA PAPER 90-1592] p 566 A90-38727

Supersonic aircraft drag reduction

[AIAA PAPER 90-1596] p 567 A90-38729

Two and three dimensional grid generation by an algebraic homotopy procedure

[AIAA PAPER 90-1603] p 567 A90-38734

A computational study of the taxonomy of vortex breakdown

[AIAA PAPER 90-1624] p 568 A90-38753

The organized nature of a turbulent trailing vortex

[AIAA PAPER 90-1625] p 568 A90-38754

A device for introducing helical perturbations into a trailing line vortex

[AIAA PAPER 90-1627] p 568 A90-38756

Measurement of crossflow vortices, attachment-line flow, and transition using microthin hot films

[AIAA PAPER 90-1636] p 607 A90-38765

- Temporal-adaptive Euler/Navier-Stokes algorithm for unsteady aerodynamic analysis of airfoils using unstructured dynamic meshes
[AIAA PAPER 90-1650] p 569 A90-38778
- Algebraic turbulence modeling for unstructured and adaptive meshes
[AIAA PAPER 90-1653] p 608 A90-38781
- Navier-Stokes solutions for vortical flows over a tangent-ogive cylinder p 620 A90-39780
- Towards a damage tolerance philosophy for composite materials and structures p 675 A90-40127
- Impact damage and residual strength analysis of composite panels with bonded stiffeners p 642 A90-40130
- Strake camber and thickness design procedure for low alpha supersonic flow p 622 A90-40678
- Sidewall boundary-layer removal and wall adaptation studies p 672 A90-40680
- Drag measurements on a modified prolate spheroid using a magnetic suspension and balance system p 672 A90-40684
- Static aeroelastic tailoring for oblique wing lateral trim p 667 A90-40689
- Effect of detailed surface geometry on riblet drag reduction performance p 622 A90-40693
- CFD propels NASP propulsion progress p 683 A90-41163
- Cryogenic wind tunnels p 673 A90-41726
- Application of a new adaptive grid for aerodynamic analysis of shock containing single jets
[AIAA PAPER 90-2025] p 624 A90-41988
- Direct measurements of skin friction in a scramjet combustor
[AIAA PAPER 90-2342] p 626 A90-42132
- Wind tunnel wall interference investigations in NAE/NRC High Reynolds Number 2D Facility and NASA Langley 0.3m Transonic Cryogenic Tunnel p 628 A90-42404
- Euler and Navier-Stokes computations for airfoil geometries using unstructured meshes p 630 A90-42425
- Experimental evaluation of expendable supersonic nozzle concepts
[AIAA PAPER 90-1904] p 740 A90-42691
- External nozzle flap dynamic load measurements on F-15 S/MTD model p 740 A90-42692
- A computational investigation of flow losses in a supersonic combustor
[AIAA PAPER 90-2093] p 742 A90-42728
- Flow establishment in a generic scramjet combustor
[AIAA PAPER 90-2096] p 742 A90-42729
- A numerical study of the effects of reverse sweep on a scramjet inlet performance
[AIAA PAPER 90-2218] p 705 A90-42749
- Methods for determining the internal thrust of scramjet engine modules from experimental data
[AIAA PAPER 90-2340] p 743 A90-42777
- A validation study of the Spark Navier Stokes code for nonreacting scramjet combustor flowfields
[AIAA PAPER 90-2360] p 706 A90-42784
- A new class of random processes with application to helicopter noise p 781 A90-42874
- Aerodynamic applications of infrared thermography p 770 A90-44147
- Mixing and combustion enhancement in supersonic reacting flows p 744 A90-44410
- NASA investigation of a claimed 'overlap' between two gust response analysis methods p 771 A90-44730
- In-flight flow visualization using infrared imaging p 731 A90-44731
- Parametric aeroelastic stability analysis of a generic X-wing aircraft p 731 A90-44737
- Canard-wing vortex interactions at subsonic through supersonic speeds p 711 A90-45154
- Optimal input design for aircraft parameter estimation using dynamic programming principles
[AIAA PAPER 90-2801] p 753 A90-45157
- Measurements of pressures on the wing of an aircraft model during steady rotation
[AIAA PAPER 90-2842] p 754 A90-45162
- Technology issues for high-speed civil transports
[SAE PAPER 892201] p 778 A90-45422
- The effect of solidity on propeller normal force
[SAE PAPER 892205] p 713 A90-45424
- Vortex control for tail buffet alleviation on a twin-tail fighter configuration
[SAE PAPER 892221] p 756 A90-45438
- Task-oriented display design - Concept and example
[SAE PAPER 892230] p 738 A90-45446
- Overview of military technology at NASA Langley
[SAE PAPER 892232] p 733 A90-45448
- Propulsion integration for military aircraft
[SAE PAPER 892234] p 733 A90-45449
- The development of crossflow vortices on a 45 degree swept wing
[SAE PAPER 892245] p 713 A90-45452
- Hypersonic CFD applications for the National Aero-Space Plane
[SAE PAPER 892310] p 714 A90-45473
- Low-speed aerodynamic characteristics of a powered NASP-like configuration in ground effect
[SAE PAPER 892312] p 714 A90-45474
- Stability characteristics of a conical aerospace plane concept
[SAE PAPER 892313] p 757 A90-45475
- Numerical simulation of flow through the Langley parametric scramjet engine
[SAE PAPER 892314] p 747 A90-45476
- A Mach 6 external nozzle experiment with Argon-Freon exhaust simulation
[SAE PAPER 892315] p 714 A90-45477
- Current status of Joint FAA/NASA Runway Friction Program
[SAE PAPER 892340] p 760 A90-45494
- Induced drag - Historical perspective
[SAE PAPER 892341] p 715 A90-45495
- An entropy method for induced drag minimization
[SAE PAPER 892344] p 715 A90-45496
- Frictionless contact of aircraft tires
[SAE PAPER 892350] p 733 A90-45501
- Computational results for the effects of external disturbances on transition location of bodies of revolution from subsonic to supersonic speeds and comparisons with experimental data
[SAE PAPER 892381] p 715 A90-45522
- Simulation of leading-edge vortex flows p 716 A90-45785
- Navier-Stokes simulation of transonic afterbody flows with jet exhaust
[AIAA PAPER 90-3057] p 790 A90-45862
- A computational study of incipient leading-edge separation on a 65-deg delta wing at $M = 1.60$
[AIAA PAPER 90-3029] p 791 A90-45871
- F-18 high alpha research vehicle surface pressures - Initial in-flight results and correlation with flow visualization and wind-tunnel data
[AIAA PAPER 90-3018] p 792 A90-45885
- Multiple vortex and shock interactions at subsonic, transonic, and supersonic speeds
[AIAA PAPER 90-3023] p 793 A90-45890
- Relative efficiency and accuracy of two Navier-Stokes codes for simulating attached transonic flow over wings
[AIAA PAPER 90-3078] p 795 A90-45909
- Exploratory wind tunnel investigation of the stability and control characteristics of a three-surface, forward-swept wing advanced turboprop model
[AIAA PAPER 90-3074] p 797 A90-45920
- Adaptive grid embedding for the two-dimensional Euler equations
[AIAA PAPER 90-3049] p 797 A90-45929
- Numerical study of vortical flow over a sideslipping delta wing
[AIAA PAPER 90-3001] p 798 A90-45936
- Performance measurements of an airfoil at low Reynolds numbers p 800 A90-46369
- Correlation of theory to wind-tunnel data at Reynolds numbers below 500,000 p 800 A90-46370
- Wind-tunnel investigations of wings with serrated sharp trailing edges p 802 A90-46379
- Boundary-integral method for calculating aerodynamic sensitivities with illustration for lifting-surface theory p 806 A90-46841
- Unsteady aerodynamics - Physical issues and numerical predictions p 806 A90-46843
- Application of localized surface heating to actively control the boundary layer separation p 806 A90-46848
- Interactive grid adaption p 806 A90-46850
- Performance of an optimized rotor blade at off-design flight conditions p 830 A90-46946
- The ROTONET prediction system and initial comparisons with far-field acoustics measurements for the XV-15 tilt-rotor aircraft p 894 A90-46947
- Experimental observations of two-dimensional blade-vortex interaction p 809 A90-47303
- Active control of propeller-induced noise fields inside a flexible cylinder p 833 A90-47306
- Unsteady Euler airfoil solutions using unstructured dynamic meshes p 809 A90-47307
- Mechanisms of active control in cylindrical fuselage structures p 862 A90-47309
- Prediction of separated transonic wing flows with nonequilibrium algebraic turbulence model p 809 A90-47312
- Active control of aerothermoelastic effects for a conceptual hypersonic aircraft
[AIAA PAPER 90-3337] p 863 A90-47597
- Artificial intelligence (AI) based tactical guidance for fighter aircraft
[AIAA PAPER 90-3435] p 889 A90-47688
- Development and testing of methodology for evaluating the performance of multi-input/multi-output digital control systems
[AIAA PAPER 90-3501] p 867 A90-47747
- Performance evaluations of oxidation-resistant carbon-carbon composites in simulated hypersonic vehicle environments p 874 A90-48131
- Wave interactions in a three-dimensional attachment-line boundary layer p 811 A90-48715
- Supersonic aerodynamic characteristics of a Mach 3 high-speed civil transport configuration
[AIAA PAPER 90-3210] p 811 A90-48836
- Thermal management for a Mach 5 cruise aircraft using endothermic fuel
[AIAA PAPER 90-3284] p 853 A90-48871
- Comparison of equivalent plate and finite element analysis of a realistic aircraft structural configuration
[AIAA PAPER 90-3293] p 837 A90-48877
- CFD support of NASP design
[AIAA PAPER 90-3252] p 872 A90-49120
- Final results of the NASA storm hazards program p 819 A90-49834
- Improved melt flow and physical properties of Mitsui Toatsu's LARC-TPI 1500 series polyimide p 943 A90-50134
- Freeze drying for morphological control of inter-penetrating polymer networks p 948 A90-50214
- A study of high-lift airfoils at high Reynolds numbers in the Langley low-turbulence pressure tunnel
[NASA-TM-89125] p 1 N90-10002
- Performance potential of an advanced technology Mach 3 turbojet engine installed on a conceptual high-speed civil transport
[NASA-TM-4144] p 51 N90-10034
- Control law synthesis and optimization software for large order aeroservoelastic systems p 61 N90-10111
- The active flexible wing aeroservoelastic wind-tunnel test program p 33 N90-10119
- Goertler instability on an airfoil: Comparison of marching solution with experimental observations p 19 N90-10364
- Simultaneous detection of separation and transition in surface shear layers p 72 N90-10368
- Application of formal optimization techniques in thermal/structural design of a heat-pipe-cooled panel for a hypersonic vehicle
[NASA-TM-89131] p 72 N90-10409
- Measurement resolution of noise directivity patterns from acoustic flight tests
[NASA-TM-4134] p 79 N90-10679
- Measurements of pressures on the tail and aft fuselage of an airplane model during rotary motions at spin attitudes
[NASA-TP-2939] p 20 N90-10829
- Low-speed, high-lift aerodynamic characteristics of slender, hypersonic accelerator-type configurations
[NASA-TP-2945] p 20 N90-10830
- Design of a final approach spacing tool for TRACON air traffic control
[NASA-TM-102229] p 24 N90-10841
- Integrated multidisciplinary design optimization of rotorcraft
[NASA-TM-101642] p 36 N90-10889
- Low-speed wind-tunnel study of reaction control-jet effectiveness for hover and transition of a STOVL fighter concept
[NASA-TM-4147] p 119 N90-11751
- Comparison of flying qualities derived from in-flight and ground-based simulators for a jet-transport airplane for the approach and landing pilot tasks
[NASA-TP-2962] p 120 N90-11757
- Airframe structural dynamic considerations in rotor design optimization
[NASA-TM-101646] p 134 N90-12057
- Research in Natural Laminar Flow and Laminar-Flow Control, part 1 p 90 N90-12503
- Performance of laminar-flow leading-edge test articles in cloud encounters p 104 N90-12511
- Simulated airline service experience with laminar-flow control leading-edge systems p 104 N90-12512
- Goertler instability on an airfoil p 91 N90-12517
- Research in Natural Laminar Flow and Laminar-Flow Control, part 2 p 91 N90-12519
- Hot-film system for transition detection in cryogenic wind tunnels p 122 N90-12522
- Predicted and hot-film measured Tollmien-Schlichting wave characteristics p 91 N90-12523
- Remote detection of boundary-layer transition by an optical system p 139 N90-12524

Basic aerodynamic research facility for comparative studies of flow diagnostic techniques

p 122 N90-12526

Recent flow visualization studies in the 0.3-m TCT

p 122 N90-12528

Experimental studies on Goertler vortices

p 91 N90-12529

Results of LFC experiment on slotted swept supercritical airfoil in Langley's 8-foot transonic pressure tunnel

p 92 N90-12531

Boundary-layer stability analysis of Langley Research Center 8-foot LFC experimental data

p 92 N90-12532

Theoretical methods and design studies for NLF and HLF swept wings at subsonic and supersonic speeds

p 92 N90-12535

Application of sound and temperature to control boundary-layer transition

p 92 N90-12537

Research in Natural Laminar Flow and Laminar-Flow Control, part 3

[NASA-CP-2487-PT-3] p 92 N90-12539

Design of the low-speed NLF(1)-0414F and the high-speed HSNLF(1)-0213 airfoils with high-lift systems

p 93 N90-12540

Wind tunnel results of the low-speed NLF(1)-0414F airfoil

p 93 N90-12541

Wind tunnel results of the high-speed NLF(1)-0213 airfoil

p 93 N90-12542

Design and test of an NLF wing glove for the variable-sweep transition flight experiment

p 104 N90-12544

The design of an airfoil for a high-altitude, long-endurance remotely piloted vehicle

p 104 N90-12545

Experimental and numerical analyses of laminar boundary-layer flow stability over an aircraft fuselage forebody

p 93 N90-12549

Status report on a natural laminar-flow nacelle flight experiment

p 105 N90-12550

Effects of acoustic sources

p 140 N90-12553

Supersonic laminar-flow control

p 93 N90-12554

Design and fabrication requirements for low noise supersonic/hypersonic wind tunnels

p 122 N90-12555

The effects of wall surface defects on boundary-layer transition in quiet and noisy supersonic flow

p 94 N90-12556

Experimental and theoretical investigation of boundary-layer instability mechanisms on a swept leading edge at Mach 3.5

p 94 N90-12557

Supersonic boundary-layer transition on the LaRC F-106 and the DFRF F-15 aircraft. Part 1: Transition measurements and stability analysis

p 94 N90-12558

Supersonic boundary-layer transition on the LaRC F-106 and the DFRF F-15 aircraft. Part 2: Aerodynamic predictions

p 94 N90-12559

Integrated multidisciplinary optimization of rotorcraft: A plan for development

[NASA-TM-101617] p 106 N90-12580

General approach and scope

p 106 N90-12581

Rotor blade aerodynamic design

p 106 N90-12582

Rotor blade dynamic design

p 106 N90-12583

Acoustic design considerations: Review of rotor acoustic sources

p 106 N90-12585

Airframe design considerations: Overview

p 106 N90-12586

Appendix: Results obtained to date

p 107 N90-12588

A vapor generator for transonic flow visualization

[NASA-TM-101670] p 201 N90-13403

Laboratory test methodology for evaluating the effects of electromagnetic disturbances on fault-tolerant control systems

[NASA-TM-101665] p 217 N90-14061

Effect of blade planform variation on a small-scale hovering rotor

[NASA-TM-4146] p 173 N90-14186

Validation of a computer code for analysis of subsonic aerodynamic performance of wings with flaps in combination with a canard or horizontal tail and an application to optimization

[NASA-TP-2961] p 173 N90-14187

Effect of pylon wake with and without pylon blowing on propeller thrust

[NASA-TM-4162] p 173 N90-14190

Experimental transonic flutter characteristics of two 72 deg-sweep delta-wing models

[NASA-TM-101659] p 175 N90-14205

A candidate concept for display of forward-looking wind shear information

[NASA-TM-101585] p 187 N90-14232

Cryogenic temperature effects on sting-balance deflections in the National Transonic Facility

[NASA-TM-4157] p 202 N90-14244

Effects of lightning on operations of aerospace vehicles

p 239 N90-15065

Serrated trailing edges for improving lift and drag characteristics of lifting surfaces

[NASA-CASE-LAR-13870-1] p 248 N90-15094

Display interface concepts for automated fault diagnosis

[NASA-TM-101610] p 252 N90-15102

Relative merits of reactive and forward-look detection for wind-shear encounters during landing approach for various microburst escape strategies

[NASA-TM-4158] p 259 N90-15108

Guidance analysis of the aeroglide plane change maneuver as a turning point problem

[NASA-TM-101639] p 259 N90-15110

Rotor induced-inflow-ratio measurements and CAMRAD calculations

[NASA-TP-2946] p 237 N90-15882

An experimental investigation of thrust vectoring two-dimensional convergent-divergent nozzles installed in a twin-engine fighter model at high angles of attack

[NASA-TM-4155] p 237 N90-15884

Assessment of computational prediction of tail buffeting

[NASA-TM-101613] p 237 N90-15886

Evaluation of two transport aircraft and several ground test vehicle friction measurements obtained for various runway surface types and conditions. A summary of test results from joint FAA/NASA Runway Friction Program

[NASA-TP-2917] p 249 N90-15902

The NASA Langley 0.3-meter transonic cryogenic tunnel

p 262 N90-15941

The US National Transonic Facility, NTF

p 262 N90-15942

Other cryogenic wind tunnel projects

p 263 N90-15948

Test techniques for cryogenic wind tunnels

p 263 N90-15952

Models for cryogenic wind tunnels

p 263 N90-15956

Automatic control of cryogenic wind tunnels

p 263 N90-15957

Experience with strain-gage balances for cryogenic wind tunnels

p 264 N90-15958

Cryogenic balances for the US NTF

p 264 N90-15959

Safety and cryogenic wind tunnels

p 264 N90-15960

Convergence speeding up in the calculation of the viscous flow about an airfoil

p 279 N90-16194

NASA supercritical airfoils: A matrix of family-related airfoils

[NASA-TP-2969] p 315 N90-16710

Results of aircraft open-loop tests of an experimental magnetic leader cable system for guidance during roll-out and turnoff

[NASA-TM-4135] p 348 N90-16767

Supersonic aerodynamic characteristics of a proposed Assured Crew Return Capability (ACRC) lifting-body configuration

[NASA-TM-4136] p 317 N90-17560

Opportunities for improved understanding of supersonic and hypersonic flows

p 318 N90-17566

Analysis of the National Transonic Facility mishap

[NASA-TM-101686] p 328 N90-17620

Simulated-airline-service flight tests of laminar-flow control with perforated-surface suction system

[NASA-TP-2966] p 338 N90-17627

CAST-10-2/DOA 2 Airfoil Studies Workshop Results

[NASA-CP-3052] p 352 N90-17647

Nonlinear transonic Wall-Interference Assessment/Correction (WIAC) procedures and application to cast-10 airfoil results from the NASA 0.3-m TCT 8- by 24-inch Slotted Wall Test Section (SWTS)

p 352 N90-17648

High Reynolds number tests of the CAST-10-2/DOA 2 transonic airfoil at ambient and cryogenic temperature conditions

p 320 N90-17650

An experimental AWTS process and comparisons of ONERA T2 and 0.3-m TCT AWTS data for the ONERA CAST-10 airfoil

p 321 N90-17653

Comparison of NAE porous wall and NASA adaptive wall test results using the NAE CAST-10 airfoil model

p 353 N90-17656

Experience with some repeat tests on the 9 inch chord CAST-10-2/DOA 2 airfoil model in the Langley 0.3-m TCT adaptive wall test section

p 321 N90-17657

Comparison of two- and three-dimensional Navier-Stokes solutions with NASA experimental data for CAST-10 airfoil

p 321 N90-17658

Software verification plan for GCS

[NASA-TM-101668] p 372 N90-18057

A study of the structural efficiency of fluted core graphite-epoxy panels

[NASA-TM-101681] p 373 N90-18070

The 1985 and 1986 direct strike lightning data, part 1

[NASA-TM-100533-PT-1] p 374 N90-18125

The 1985 and 1986 direct strike lightning data, part 2

[NASA-TM-100533-PT-2] p 374 N90-18126

Delivery performance of conventional aircraft by terminal-area, time-based air traffic control: A real-time simulation evaluation

[NASA-TP-2978] p 404 N90-18378

Fuselage design for a specified Mach-sliced area distribution

[NASA-TP-2975] p 414 N90-18385

A simulation evaluation of the engine monitoring and control system display

[NASA-TP-2960] p 420 N90-18393

Three input concepts for flight crew interaction with information presented on a large-screen electronic cockpit display

[NASA-TM-4173] p 420 N90-18394

Application of variable-gain output feedback for high-alpha control

[NASA-TM-102603] p 434 N90-18434

Fatigue crack initiation and small crack growth in several airframe alloys

[NASA-TM-102598] p 454 N90-18746

Low-energy gamma ray attenuation characteristics of aviation fuels

[NASA-TP-2974] p 462 N90-18882

Static investigation of a two-dimensional convergent-divergent exhaust nozzle with multiaxis thrust-vectoring capability

[NASA-TP-2973] p 397 N90-19193

Water-tunnel investigation of concepts for alleviation of adverse inlet spillage interactions with external stores

[NASA-TM-4181] p 398 N90-19199

Development of a preliminary high-angle-of-attack nose-down pitch control requirement for high-performance aircraft

[NASA-TM-101684] p 399 N90-19206

Conical Euler solution for a highly-swept delta wing undergoing wing-rock motion

[NASA-TM-102609] p 400 N90-19211

Aeroservoelasticity

[NASA-TM-102620] p 416 N90-19227

Low-speed wind-tunnel investigation of the flight dynamic characteristics of an advanced turboprop business/commuter aircraft configuration

[NASA-TP-2982] p 434 N90-19239

Method and apparatus for detecting laminar flow separation and reattachment

[NASA-CASE-LAR-13952-1-SB] p 455 N90-19534

Spanwise measurements of vertical components of atmospheric turbulence

[NASA-TP-2963] p 456 N90-19718

A note on an acoustic response during an engine nacelle flight experiment

[NASA-TM-102585] p 464 N90-19821

Experimental and theoretical aerodynamic characteristics of a high-lift semispan wing model

[NASA-TP-2990] p 477 N90-20046

Using transonic small disturbance theory for predicting the aeroelastic stability of a flexible wind-tunnel model

[NASA-TM-102617] p 478 N90-20047

A review of the analytical simulation of aircraft crash dynamics

[NASA-TM-102595] p 484 N90-20068

The application of active controls technology to a generic hypersonic aircraft configuration

[NASA-TM-101689] p 497 N90-20071

Compression pylon

[NASA-CASE-LAR-13777-1] p 498 N90-20078

Passive venting technique for shallow cavities

[NASA-CASE-LAR-14031-1] p 499 N90-20079

Digital-flutter-suppression-system investigations for the active flexible wing wind-tunnel model

[NASA-TM-102618] p 520 N90-20093

Airplane takeoff and landing performance monitoring system

[NASA-CASE-LAR-13734-1-CU] p 526 N90-20096

Joint University Program for Air Transportation Research, 1988-1989

[NASA-CP-3063] p 468 N90-20921

Performance data from a wind-tunnel test of two main-rotor blade designs for a utility-class helicopter

[NASA-TM-4183] p 499 N90-20974

Stereopsis cueing effects on hover-in-turbulence performance in a simulated rotorcraft

[NASA-TP-2980] p 506 N90-21004

Simulator comparison of thumbball, thumb switch, and touch screen input concepts for interaction with a large screen cockpit display format

[NASA-TM-102587] p 506 N90-21005

Experimental aeroelasticity history, status and future in brief

[NASA-TM-102651] p 527 N90-21047

Airborne Doppler radar flight experiments for the detection of microbursts

p 542 N90-21243

NASA airframe structural integrity program

[NASA-TM-102637] p 543 N90-21422

- An evaluation of the pressure proof test concept for thin sheet 2024-T3
[NASA-TM-101675] p 543 N90-21424
- Device for quickly sensing the amount of O₂ in a combustion product gas
[NASA-CASE-LAR-13816-1] p 609 N90-22025
- Dynamic ground-effect measurements on the F-15 STOL and Maneuver Technology Demonstrator (S/MTD) configuration
[NASA-TP-3000] p 573 N90-22531
- An experimental study of tip shape effects on the flutter of aft-swept, flat-plate wings
[NASA-TM-4180] p 582 N90-22555
- Thermal/structural analysis of the shaft-disk region of a fan drive system
[NASA-TM-101687] p 610 N90-22807
- Real-time closed-loop simulation and upset evaluation of control systems in harsh electromagnetic environments
p 613 N90-23069
- Design trends for Army/Air Force airplanes in the United States
[NASA-TM-4179] p 615 N90-23338
- Actuated forebody strakes
[NASA-CASE-LAR-13983-1] p 648 N90-23390
- Miniaturization of flight deflection measurement system
[NASA-CASE-LAR-13628-1] p 689 N90-23707
- Real-time simulation clock
[NASA-CASE-LAR-14056-1] p 689 N90-23713
- Langley aerospace test highlights, 1989
[NASA-TM-102631] p 699 N90-24221
- Aerodynamic performance of a 0.27-scale model of an AH-64 helicopter with baseline and alternate rotor blade sets
[NASA-TM-4201] p 632 N90-24237
- Static wind-tunnel and radio-controlled flight test investigation of a remotely piloted vehicle having a delta wing planform
[NASA-TM-4200] p 632 N90-24238
- Aerodynamic characteristics of two rotorcraft airfoils designed for application to the inboard region of a main rotor blade
[NASA-TP-3009] p 633 N90-24239
- Unique failure behavior of metal/composite aircraft structural components under crash type loads
[NASA-TM-102679] p 690 N90-24660
- FAA/NASA En Route Noise Symposium
[NASA-CP-3067] p 696 N90-24853
- PTA en route noise measurements
p 696 N90-24855
- En route noise annoyance laboratory test: Preliminary results
p 698 N90-24870
- Integral-equation methods in steady and unsteady subsonic, transonic and supersonic aerodynamics for interdisciplinary design
[NASA-TM-102677] p 716 N90-25110
- Video/photographic considerations for measuring the proximity of a probe aircraft with a smoke seeded trailing vortex
[NASA-TM-102691] p 724 N90-25120
- Behavior of composite/metal aircraft structural elements and components under crash type loads: What are they telling us
[NASA-TM-102681] p 774 N90-25368
- Effect of tail size reductions on longitudinal aerodynamic characteristics of a three surface F-15 model with nonaxisymmetric nozzles
[NASA-TP-3036] p 718 N90-25938
- An overview of the joint FAA/NASA aircraft/ground runway friction program
[NASA-TM-103486] p 724 N90-25957
- Qualitative evaluation of a conformational velocity vector display for use at high angles-of-attack in fighter aircraft
[NASA-TM-102629] p 739 N90-25981
- Supersonic combustor modeling
p 749 N90-25992
- Carbon-carbon composites: Emerging materials for hypersonic flight
[NASA-TM-103472] p 767 N90-26080
- Supersonic reacting internal flow fields
[NASA-TM-103480] p 767 N90-26094
- Knowledge-based system for flight information management
[NASA-TM-102685] p 780 N90-26511
- Facilities involved in adaptive wall research
p 871 N90-26840
- Limits of adaptation, residual interferences
p 871 N90-26844
- Modeling of supersonic reacting flow fields
p 855 N90-26898
- An approximate method for calculating three-dimensional inviscid hypersonic flow fields
[NASA-TP-3018] p 883 N90-27066
- The acoustic results of a United Technologies scale model helicopter rotor tested at DNW
[NASA-TM-101879] p 896 N90-27471
- The Langley 14-by 22-foot subsonic tunnel: Description, flow characteristics, and guide for users
[NASA-TP-3008] p 816 N90-27649
- Development and testing of methodology for evaluating the performance of multi-input/multi-output digital control systems
[NASA-TM-102704] p 846 N90-27699
- Effects of spoiler surfaces on the aeroelastic behavior of a low-aspect-ratio rectangular wing
[NASA-TM-102622] p 846 N90-27700
- Active control of aerothermoelastic effects for a conceptual hypersonic aircraft
[NASA-TM-102713] p 869 N90-27725
- Evaluation of composite components on the Bell 206L and Sikorsky S-76 helicopters
[NASA-TM-4195] p 876 N90-27787
- A Protection And Detection Surface (PADS) for damage tolerance
[NASA-TP-3011] p 876 N90-27788
- Advanced NDE techniques for quantitative characterization of aircraft
p 886 N90-28088
- Control of submersible vortex flows
[NASA-TM-102693] p 909 N90-28493
- Control research in the NASA high-alpha technology program
p 934 N90-28516
- Innovative control concepts and component integration for a generic supercruise fighter
p 935 N90-28521
- Development of non-conventional control methods for high angle of attack flight using vortex manipulation
p 935 N90-28522
- Dynamic ground effects
p 922 N90-28531
- NASA Langley Research Center National Aero-Space Plane Mission simulation profile sets
[NASA-TM-102670] p 924 N90-28541
- Description of the primary flight display and flight guidance system logic in the NASA B-737 transport systems research vehicle
[NASA-TM-102710] p 927 N90-28546
- Aerodynamic parameters of High-Angle-of attack Research Vehicle (HARV) estimated from flight data
[NASA-TM-102692] p 936 N90-28578
- Annoyance caused by advanced turboprop aircraft flyover noise: Counter-rotating-propeller configuration
[NASA-TP-3027] p 965 N90-29166
- Formal design and verification of a reliable computing platform for real-time control. Phase 1: Results
[NASA-TM-102716] p 965 N90-29965
- National Aeronautics and Space Administration, Lewis Research Center, Cleveland, OH.**
- Fiber optics for advanced aircraft
p 68 N90-11702
- Analysis of nonuniform subsonic flows about a row of moving blades
p 6 N90-11779
- The unsteady aerodynamics of an oscillating cascade in a compressible flow field
p 7 N90-11789
- Progress towards the development of an inviscid-viscous interaction method for unsteady flows in turbomachinery cascades
p 8 N90-11806
- Advances in computational design and analysis of airbreathing propulsion systems
p 43 N90-12502
- Advanced computational techniques for hypersonic propulsion
p 69 N90-12606
- Experimental and analytical evaluation of dynamic load vibration of a 2240-kW (3000-hp) rotorcraft transmission
p 127 N90-13750
- A circular combustor configuration with multiple injection ports for mixing enhancement
p 130 N90-15389
- Predictions of airfoil aerodynamic performance degradation due to icing
p 144 N90-16753
- TBCs for better engine efficiency
p 203 N90-17294
- Aeroelastic detuning for stability enhancement of unstalled supersonic flutter
p 189 N90-17462
- Numerical study of chemically reacting flows using a lower-upper symmetric successive overrelaxation scheme
p 153 N90-17989
- Analysis of whisker-toughened ceramic components - A design engineer's viewpoint
p 205 N90-19149
- Observations on the brittle to ductile transition temperatures of B2 nickel aluminides with and without zirconium
p 205 N90-19153
- Efficiency testing of a helicopter transmission planetary reduction stage
p 271 N90-21113
- Effect of advanced component technology on helicopter transmissions
p 271 N90-21115
- Parametric studies of advanced turboprops
p 253 N90-21225
- Application of an efficient hybrid scheme for aeroelastic analysis of advanced propellers
[AIAA PAPER 90-0028] p 226 N90-22153
- Convective heat transfer measurements from a NACA 0012 airfoil in flight and in the NASA Lewis Icing Research Tunnel
[AIAA PAPER 90-0199] p 272 N90-22180
- Liquid water content and droplet size calibration of the NASA Lewis Icing Research Tunnel
[AIAA PAPER 90-0669] p 261 N90-22242
- Hypersonic aerospace sizing analysis for the preliminary design of aerospace vehicles
p 247 N90-23276
- Effect of reduced aft diameter and increased blade number of high-speed counterrotation propeller performance
[AIAA PAPER 89-0438] p 234 N90-23650
- Thermal/structural analyses of several hydrogen-cooled leading-edge concepts for hypersonic flight vehicles
[AIAA PAPER 90-0053] p 274 N90-23702
- Comparison of two droplet sizing systems in an icing wind tunnel
[AIAA PAPER 90-0668] p 274 N90-23711
- Application of a lower-upper implicit scheme and an interactive grid generation for turbomachinery flow field simulations
[ASME PAPER 89-GT-20] p 288 N90-23762
- Noninteractive macroscopic reliability model for ceramic matrix composites with orthotropic material symmetry
[ASME PAPER 89-GT-129] p 360 N90-23827
- Simulation of three-dimensional viscous flow within a multistage turbine
[ASME PAPER 89-GT-152] p 292 N90-23841
- A review of failure models for ceramic matrix composite laminates under monotonic loads
[ASME PAPER 89-GT-153] p 354 N90-23842
- Advanced core technology - Key to subsonic propulsion benefits
[ASME PAPER 89-GT-241] p 342 N90-23890
- Influence of alloying elements on the oxidation behavior of NbAl₃
p 355 N90-24861
- Unsteady Euler analysis of the flowfield of a propfan at an angle of attack
[AIAA PAPER 90-0339] p 300 N90-25028
- Low NO(x) potential of gas turbine engines
[AIAA PAPER 90-0550] p 343 N90-25036
- Spray nozzle investigation for the Improved Helicopter Icing Spray System (IHSS)
[AIAA PAPER 90-0666] p 350 N90-25040
- Numerical solutions of the linearized Euler equations for unsteady vortical flows around lifting airfoils
[AIAA PAPER 90-0694] p 300 N90-25041
- Swept wing ice accretion modeling
[AIAA PAPER 90-0756] p 300 N90-25042
- Engine inlet distortion in a 9.2 percent scaled vectored thrust STOVL model in ground effect
[AIAA PAPER 89-2910] p 301 N90-25043
- Burner rig hot corrosion of silicon carbide and silicon nitride
p 355 N90-25267
- Interactive grid generation for turbomachinery flow field simulations
p 312 N90-26553
- Comparison of 3-D viscous flow computations of Mach 5 inlet with experimental data
[AIAA PAPER 90-0600] p 314 N90-26970
- Analysis of fully stalled compressor
p 383 N90-27966
- Icing Research Tunnel test of a model helicopter rotor
p 400 N90-28179
- Initial results from the joint NASA-Lewis/U.S. Army icing flight research tests
p 400 N90-28180
- Advanced technology's impact on compressor design and development - A perspective
[SAE SP-800] p 423 N90-28571
- Concurrent processing adaptation of aeroelastic analysis of propfans
[AIAA PAPER 90-1036] p 450 N90-29380
- Composites boost 21st-century aircraft engines
p 442 N90-29704
- Numerical solutions of the linearized Euler equations for unsteady vortical flows around lifting airfoils
p 394 N90-30264
- Three approaches to reliability analysis
p 452 N90-30706
- A laser based computer aided non-intrusive technique for full field flow characterization in macroscopic curved channels
p 535 N90-32293
- Noise of a simulated installed model counterrotation propeller at angle-of-attack and takeoff/approach conditions
[AIAA PAPER 90-0283] p 547 N90-32505
- Design of an air-cooled metallic high-temperature radial turbine
p 507 N90-32960
- Cooperative synthesis of control and display augmentation in approach and landing
p 516 N90-33061
- Resources - Supply and availability
p 531 N90-34152
- Cyclic deformation, fatigue and fatigue crack propagation in Ni-base alloys
p 531 N90-34162
- Fiber reinforced superalloys
p 532 N90-34169
- Performance characteristics of a one-third-scale, vectorable ventral nozzle for SSTOVL aircraft
[AIAA PAPER 90-2271] p 586 N90-37562
- Analysis of airframe/engine interactions - An integrated control perspective
[AIAA PAPER 90-1918] p 667 N90-40557

On the use of external burning to reduce aerospace vehicle transonic drag
[AIAA PAPER 90-1935] p 656 A90-40562

CFD propels NASP propulsion progress
p 683 A90-41163

A modeling technique for STOVL ejector and volume dynamics
[AIAA PAPER 90-2417] p 663 A90-42168

On the instabilities of supersonic mixing layers - A high-Mach-number asymptotic theory
p 702 A90-42644

Analysis of internal flow in a ventral nozzle for STOVL aircraft
[AIAA PAPER 90-1899] p 739 A90-42688

Computational analysis of the flowfield of a two-dimensional ejector nozzle
[AIAA PAPER 90-1901] p 740 A90-42690

A test matrix sequencer for research test facility automation
[AIAA PAPER 90-2386] p 759 A90-42791

Introducing the VRT gas turbine combustor
[AIAA PAPER 90-2452] p 743 A90-42808

Three-dimensional turbulent flow code calculations of hot gas ingestion
p 745 A90-44726

A real time microcomputer implementation of sensor failure detection for turbofan engines
p 745 A90-45414

Active vibration control for flexible rotor by optimal direct-output feedback control
p 879 A90-46222

Test and theory for piezoelectric actuator-active vibration control of rotating machinery
p 879 A90-46226

Spray automated balancing of rotors - How process parameters influence performance
p 879 A90-46228

The low frequency oscillation in the flow over a NACA0012 airfoil with an 'iced' leading edge
p 801 A90-46377

The selection of convertible engines with current gas generator technology for high speed rotorcraft
p 852 A90-46933

Mixer-ejector nozzle for jet noise suppression
[AIAA PAPER 90-1909] p 894 A90-47202

Effect of vane twist on the performance of dome swirlers for gas turbine airblast atomizers
[AIAA PAPER 90-1955] p 881 A90-47203

Composite matrix cooling scheme for small gas turbine combustors
[AIAA PAPER 90-2158] p 852 A90-47210

NASA's HITEMP program for UHBR engines
[AIAA PAPER 90-2395] p 852 A90-47218

Combustor technology for future aircraft
[AIAA PAPER 90-2400] p 852 A90-47219

Unsteady blade surface pressures on a large-scale advanced propeller - Prediction and data
[AIAA PAPER 90-2402] p 808 A90-47220

Vibration dampers for cryogenic turbomachinery
[AIAA PAPER 90-2740] p 882 A90-47228

H-infinity based integrated flight/propulsion control design for a STOVL aircraft in transition flight
[AIAA PAPER 90-3335] p 862 A90-47595

Experimental investigation of multielement airfoil ice accretion and resulting performance degradation
p 812 A90-48954

Thermo-oxidative stability studies of PMR-15 polymer matrix composites reinforced with various continuous fibers
p 941 A90-50068

Use of unbalanced laminates as a screening method for microcracking
p 948 A90-50217

Euler analysis comparison with LDV data for an advanced counter-rotation propfan at cruise
[AIAA PAPER 90-3033] p 903 A90-50637

Efficiency study comparing two helicopter planetary reduction stages
[AIAA PAPER 90-2156] p 956 A90-50644

Critical evaluation of Jet-A spray combustion using propane chemical kinetics in gas turbine combustion simulated by KIVA-II
[AIAA PAPER 90-2439] p 949 A90-50645

Least-squares finite element methods for compressible Euler equations
p 904 A90-51013

An LDA investigation of the normal shock wave boundary layer interaction
p 908 A90-52618

Advanced technologies impact on compressor design and development: A perspective
[NASA-TM-102341] p 54 A90-10891

Laser anemometer measurements in a transonic axial-flow fan rotor
[NASA-TP-2879] p 73 A90-11245

STOVL propulsion system volume dynamics approximations
[NASA-TM-102397] p 114 A90-11740

Prediction of unsteady blade surface pressures on an advanced propeller at an angle of attack
[NASA-TM-102374] p 94 A90-12560

Some observations on transitory stall in conical diffusers
[NASA-TM-102387] p 94 A90-12561

Real-time simulation of an F110/STOVL turbofan engine
[NASA-TM-102409] p 117 A90-12618

Effect of reduced aft diameter and increased blade number on high-speed counterrotation propeller performance
[NASA-TM-102077] p 172 A90-13352

Application of an efficient hybrid scheme for aeroelastic analysis of advanced propellers
[NASA-TM-102428] p 172 A90-13355

Silicon-etalon fiber-optic temperature sensor
[NASA-TM-102389] p 187 A90-13381

Application of a two-dimensional unsteady viscous analysis code to a supersonic throughflow fan stage
[NASA-TM-4141] p 192 A90-13387

STOVL aircraft simulation for integrated flight and propulsion control research
[NASA-TM-102419] p 193 A90-13389

Two-dimensional analysis of two-phase reacting flow in a firing direct-injection diesel engine
[NASA-TM-102069] p 194 A90-13392

A planar reacting shear layer system for the study of fluid dynamics-combustion interaction
[NASA-TM-102422] p 194 A90-13393

Recent progress in research pertaining to estimates of gas-side heat transfer in an aircraft gas turbine
[NASA-TM-102460] p 194 A90-13394

Thermal barrier coatings for gas turbine and diesel engines
[NASA-TM-102408] p 205 A90-13636

Convective heat transfer measurements from a NACA 0012 airfoil in flight and in the NASA Lewis Icing Research Tunnel
[NASA-TM-102448] p 213 A90-13750

Liquid water content and droplet size calibration of the NASA Lewis Icing Research Tunnel
[NASA-TM-102447] p 213 A90-13797

RAMSCRAM: A flexible ramjet/scramjet engine simulation program
[NASA-TM-102451] p 194 A90-14235

Slush Hydrogen (SLH2) technology development for application to the National Aerospace Plane (NASP)
[NASA-TM-102315] p 203 A90-14268

Thermal/structural analyses of several hydrogen-cooled leading-edge concepts for hypersonic flight vehicles
[NASA-TM-102391] p 215 A90-14511

Comparison of two droplet sizing systems in an icing wind tunnel
[NASA-TM-102456] p 215 A90-14617

Thermal fatigue durability for advanced propulsion materials
[NASA-TM-102348] p 215 A90-14641

Concurrent processing adaptation of aeroplastic analysis of propfans
[NASA-TM-102455] p 215 A90-14656

NASA's program on icing research and technology
p 239 A90-15062

Advanced detection, isolation, and accommodation of sensor failures in turbofan engines: Real-time microcomputer implementation
[NASA-TP-2925] p 259 A90-15112

Assessment of worm gearing for helicopter transmissions
[NASA-TM-102441] p 257 A90-15923

Predicted and measured boundary layer refraction for advanced turboprop propeller noise
[NASA-TM-102365] p 379 A90-17413

Engine inlet distortion in a 9.2 percent scale vectored thrust STOVL model in ground effect
[NASA-TM-102358] p 318 A90-17561

Numerical solutions of the linearized Euler equations for unsteady vortical flows around lifting airfoils
[NASA-TM-102466] p 318 A90-17562

Low NO(x) potential of gas turbine engines
[NASA-TM-102452] p 345 A90-17636

Gear noise, vibration, and diagnostic studies at NASA Lewis Research Center
[NASA-TM-102435] p 372 A90-18041

Unsteady Euler analysis of the flow field of a propfan at an angle of attack
[NASA-TM-102426] p 380 A90-18229

Comparison between design and installed acoustic characteristics of NASA Lewis 9- by 15-foot low-speed wind tunnel acoustic treatment
[NASA-TP-2996] p 440 A90-19242

Numerical simulations of supersonic flow through oscillating cascade sections
[NASA-TM-103100] p 478 A90-20051

Aerospace induction motor actuators driven from a 20-kHz power link
[NASA-TM-102482] p 509 A90-20085

Comparison of 3-D viscous flow computations of Mach 5 inlet with experimental data
[NASA-TM-102518] p 510 A90-20090

An applicational process for dynamic balancing of turbomachinery shafting
[NASA-TM-102537] p 541 A90-20392

Noise of a simulated installed model counterrotation propeller at angle-of-attack and takeoff/approach conditions
[NASA-TM-102440] p 548 A90-20794

Modeling of surface roughness effects on glaze ice accretion
p 485 A90-20925

Laser-velocimeter-measured flow field around an advanced, swept, eight-blade propeller at Mach 0.8
[NASA-TP-2462] p 468 A90-20942

The numerical simulation of multistage turbomachinery flows
p 514 A90-21025

Probabilistic modeling for simulation of aerodynamic uncertainties in propulsion systems
[NASA-TM-102472] p 515 A90-21036

Supersonic through-flow fan engine and aircraft mission performance
[NASA-TM-102304] p 516 A90-21038

Structural tailoring of select fiber composite structures
[NASA-TM-102484] p 533 A90-21137

Civil air transport: A fresh look at power-by-wire and fly-by-light
[NASA-TM-102574] p 542 A90-21283

Navier-Stokes analysis of turbine blade heat transfer
[NASA-TM-102496] p 542 A90-21300

Attachment of lead wires to thin film thermocouples mounted on high temperature materials using the parallel gap welding process
[NASA-TM-102442] p 543 A90-21361

Transmission research activities at NASA Lewis Research Center
[NASA-TM-103132] p 543 A90-21394

Aeropropulsion facilities configuration control: Procedures manual
[NASA-TM-102541] p 543 A90-21399

Performance characteristics of a one-third-scale, vectorable ventral nozzle for SSTOVL aircraft
[NASA-TM-103120] p 552 A90-21725

Swept wing ice accretion modeling
[NASA-TM-103114] p 570 A90-21727

Control of flow separation and mixing by aerodynamic excitation
[NASA-TM-103131] p 571 A90-21733

On the use of external burning to reduce aerospace vehicle transonic drag
[NASA-TM-103107] p 588 A90-21762

High speed commercial transport fuels considerations and research needs
[NASA-TM-102535] p 600 A90-21869

A modeling technique for STOVL ejector and volume dynamics
[NASA-TM-103167] p 589 A90-22566

Elements of active vibration control for rotating machinery
[NASA-TM-102368] p 610 A90-22703

Finite element elastic-plastic-creep and cyclic life analysis of a cowl lip
[NASA-TM-102342] p 610 A90-22808

Experimental evaluation of a tuned electromagnetic damper for vibration control of cryogenic turbopump rotors
[NASA-TP-3005] p 665 A90-23403

Analysis of internal flow in a ventral nozzle for STOVL aircraft
[NASA-TM-103123] p 666 A90-23404

Introducing the VRT gas turbine combustor
[NASA-TM-103176] p 688 A90-23591

Experimental and analytical study of close-coupled ventral nozzles for ASTOVL aircraft
[NASA-TM-103170] p 666 A90-24273

Effect of vane twist on the performance of dome swirlers for gas turbine airblast atomizers
[NASA-TM-103195] p 773 A90-25289

Euler analysis comparison with LDV data for an advanced counter-rotation propfan at cruise
[NASA-TM-103249] p 720 A90-25946

Two-dimensional Euler and Navier-Stokes Time accurate simulations of fan rotor flows
[NASA-TM-102402] p 720 A90-25948

Performance of a supercharged direct-injection stratified-charge rotary combustion engine
[NASA-TM-103105] p 748 A90-25982

Hot gas ingestion characteristics and flow visualization of a vectored thrust STOVL concept
[NASA-TM-103212] p 751 A90-26009

H-infinity based integrated flight-propulsion control design for a STOVL aircraft in transition flight
[NASA-TM-103198] p 758 A90-26011

Background, current status, and prognosis of the ongoing slush hydrogen technology development program for the NASP
[NASA-TM-103220] p 763 A90-26055

- Structural dynamics branch research and accomplishments
[NASA-TM-102488] p 778 N90-26373
- Aeroacoustics of advanced propellers
[NASA-TM-103137] p 782 N90-26635
- Aerodynamics of a linear oscillating cascade
[NASA-TM-103250] p 817 N90-27657
- Computer code for predicting coolant flow and heat transfer in turbomachinery
[NASA-TP-2985] p 858 N90-27722
- An expert system to perform on-line controller restructuring for abrupt model changes
[NASA-TM-103609] p 964 N90-29121
- National Aeronautics and Space Administration.**
Marshall Space Flight Center, Huntsville, AL.
Prediction of the aerodynamic environment and heat transfer for rotor-stator configurations
[ASME PAPER 89-GT-89] p 359 A90-23807
- Impact testing of glass/phenolic honeycomb panels with graphite/epoxy facesheets
p 946 A90-50166
- Numerical prediction of axial turbine stage aerodynamics
p 426 N90-18416
- National Aeronautics and Space Administration.**
Wallops Flight Facility, Wallops Island, VA.
Results of aerodynamic testing of large-scale wing sections in a simulated natural rain environment
[AIAA PAPER 90-0486] p 167 A90-19874
- Operational considerations for aerodynamic testing of large-scale wing sections in a simulated natural rain environment
[AIAA PAPER 90-0485] p 313 A90-26956
- National Aerospace Lab., Amsterdam (Netherlands).**
A European collaborative investigation of the three-dimensional turbulent shear layers of a swept wing
p 20 N90-10380
- Flight testing in the Netherlands: An overview
p 36 N90-10884
- Coatings for gas turbine compressors
[NLR-MP-88045-U] p 115 N90-11750
- Development of a multi-component internal strain-gauge balance for model tests in a cryogenic wind tunnel
[NLR-TR-88157-U] p 123 N90-12628
- The S.D.G., P.S.D. and the nonlinear airplane
[NLR-MP-88018-U] p 183 N90-13371
- Static strength and damage tolerance tests on the Fokker 100 airframe
[NLR-MP-88023-U] p 416 N90-19228
- Flow simulation for aircraft
[NLR-MP-87082-U] p 455 N90-19543
- COCOMAT: A Computer Aided Engineering (CAE) system for composite structures design
[NLR-MP-87078-U] p 462 N90-19756
- A system for transonic wing design with geometric constraints based on an inverse method
p 501 N90-20983
- Constrained spanload optimization for minimum drag of multi-lifting-surface configurations
p 501 N90-20992
- Numerical optimization of target pressure distributions for subsonic and transonic airfoil design
p 502 N90-20993
- Design and testing of a multiblock grid-generation procedure for aircraft design and research
p 582 N90-21984
- European research on viscous flow (EuroVisc)
[NLR-TP-89077-U] p 609 N90-22014
- Numerical flow simulation and supercomputers: More than a digital wind tunnel
p 612 N90-22976
- The use of supercomputers for the design and analysis of constructions
p 612 N90-22977
- The automation management to support research and development
p 612 N90-22978
- The development of a system for the numerical simulation of Euler flows
p 612 N90-22980
- Activities report in aerospace and aerodynamics
[ETN-90-96774] p 699 N90-24224
- Experimental study on vortex and shock wave development on a 65 deg delta wing
[NLR-MP-88033-U] p 720 N90-25950
- Computation of viscous aerodynamic characteristics of 2-D airfoils for helicopter applications
[NLR-MP-88052-U] p 720 N90-25951
- Mobile satellite communications for civil aviation
[NLR-MP-88066-U] p 775 N90-26238
- Development of a system for the numerical simulation of Euler flows, with results of preliminary 3-D propeller-slipstream/exhaust-jet calculations
[NLR-TR-88008-U] p 776 N90-26285
- Informatics aspects of large flow calculations on the SX-2 supercomputer
[NLR-MP-88037-U] p 776 N90-26290
- High productivity testing
p 871 N90-26843
- National Aerospace Lab., Tokyo (Japan).**
A numerical method for solving transonic flow past aircraft in Cartesian coordinates
[NAL-TR-1008] p 18 N90-10003
- Cycle analysis of scramjet engines
[NAL-TR-1002] p 51 N90-10035
- On the interactive computer program IPIS for aircraft parameter identification
[NAL-TR-1000] p 77 N90-10586
- Grid generation procedure using the integral equation method
[NAL-TR-1009] p 77 N90-10630
- Flight simulator evaluation of a head-down display
[NAL-TR-573] p 59 N90-10898
- Flight simulation test facility: Function and specification of the simulator cockpit system
[NAL-TM-577] p 59 N90-10899
- Wind tunnel test of CAD USB-STOL semi-borne prototype
[NAL-TM-566] p 88 N90-11696
- Acoustic-thermal environment for USB flap structure. Report 1: Ground simulation test results
[NAL-TM-567] p 88 N90-11697
- Effects of a heat cycle on material strength
[NAL-TM-562] p 113 N90-11737
- Development of the triplex digital flight control system of the STOL research aircraft ASKA
[NAL-TR-1013] p 349 N90-17640
- Numerical simulation of hypersonic flow around a space plane. Part 2: Application to high angles of attack flow
[NAL-TR-1011T] p 570 N90-21726
- Space plane model for visual measurement of aerodynamic heating
[DE90-505514] p 720 N90-25949
- Research and development of advanced gas turbine
[DE90-503377] p 776 N90-26335
- Investigation of ATP blades, part 2. Validation of two-dimensional viscous flow simulation codes around thin airfoils
[NAL-TR-1046] p 912 N90-29326
- Transonic 3-D Euler analysis of flows around fanjet engine and TPS (Turbine Powered Simulator). Comparison with wind tunnel experiment, evaluation of TPS testing method and 3-D flow
[NAL-TR-1045] p 912 N90-29327
- A boundary-layer transition model for the Navier-Stokes computation for a natural-laminar-flow airfoil
[NAL-TR-1038T] p 912 N90-29328
- Some topics in computational transonic aerodynamics: Revision
[NAL-TR-1018T] p 912 N90-29332
- Airline productivity relating on the fuel cost. (2): Fuel consumption values and fuel efficiency
[NAL-TM-604-2] p 913 N90-29333
- Evaluation for DLC-Flap Monitoring System of the VSRA
[NAL-TM-607] p 928 N90-29391
- Analysis of scramjet engine characteristics
[NAL-TR-1041] p 933 N90-29398
- Short period control using angular acceleration feedback: Compensation for first lag servo
[NAL-TM-600] p 936 N90-29399
- A digital controller for active aeroelastic controls
[NAL-TR-1014] p 936 N90-29402
- Estimation of power spectral density of runway roughness
[NAL-TR-1037] p 939 N90-29411
- The function of the Interactive Model Assembly Program (IMAP) for a flight simulator
[NAL-TR-1034] p 939 N90-29412
- Evaluation of static and fatigue properties of thin sheets of 8090-T8 aluminum-lithium alloy and observation of its fracture surfaces
[NAL-TR-1039] p 953 N90-29499
- Fractographic analysis of fatigue failures of airframe equipment parts: Examples of a rod end housing and a rod end cap
[NAL-TR-1047] p 961 N90-29686
- Noncontact measurement of rotating blade vibrations
[NAL-TR-1033] p 961 N90-29687
- Parametric studies of acoustic duct attenuation of perforated-plate-on-honeycomb absorber
[NAL-TM-603] p 966 N90-30030
- National Center for Atmospheric Research, Boulder, CO.**
Meeting Review: Workshop on Airborne Instrumentation
[PB89-174775] p 39 N90-10032
- Scientific justification and development plan for a mid-sized jet research aircraft
[PB89-208995] p 103 N90-11731
- Meeting review: The Second NCAR (National Center for Atmospheric Research) Research Aircraft Fleet Workshop
[PB89-200901] p 137 N90-12113
- National Defence Headquarters, Ottawa (Ontario).**
Aircraft fire safety in the Canadian Forces
p 327 N90-17604
- National Oceanic and Atmospheric Administration, Boulder, CO.**
Remote sensing techniques of the Wave Propagation Laboratory for the measurement of supercooled liquid water: Applications to aircraft icing
[PB89-208102] p 24 N90-10842
- National Oceanic and Atmospheric Administration, Norman, OK.**
Multistroke cloud-to-ground strike to the NASA F-106B airplane
p 482 A90-32304
- Cloud-to-ground strikes to the NASA F-106 airplane
p 574 A90-35767
- National Oceanic and Atmospheric Administration, Silver Spring, MD.**
Aerosol separator for use in aircraft
[PB90-142217] p 611 N90-22155
- National Physical Lab., Teddington (England).**
Noise levels from a VSTOL aircraft measured at ground level and at 1.2 m above the ground
[NPL-RSA(EXT)-009] p 464 N90-18999
- National Research Council of Canada, Ottawa (Ontario).**
Heat release rate measurement for evaluating the flammability of aircraft materials
p 328 N90-17610
- The effect of secondary flow on the redistribution of the total temperature field downstream of a stationary turbine cascade
p 515 N90-21033
- Comparison of ground-level test cells and ground-level to altitude test cells
p 857 N90-27716
- The effects of a compressor rebuild on gas turbine engine performance: Final results
p 952 N90-28701
- National Science Foundation, Washington, DC.**
Profiles-aeronautical/astronautical engineering: Human resources and funding
[PB90-103888] p 369 N90-16969
- National Technical Univ., Athens (Greece).**
Forced and natural venting of aircraft cabin fires: A numerical simulation
p 326 N90-17597
- Secondary flow calculations for axial and radial compressors
p 514 N90-21024
- Computer modeling and data processing methods: An essential part of jet engine condition monitoring and fault diagnosis
p 855 N90-27626
- National Transportation Safety Board, Washington, DC.**
Aircraft accident report: Aloha Airlines, Flight 243, Boeing 737-200, N73711, near Maui, Hawaii, April 28, 1988
[PB89-910404] p 24 N90-10013
- Aircraft accident report: Delta Air Lines, Inc., Boeing 727-232, N473DA, Dallas-Fort Worth International Airport, Texas, August 31, 1988
[PB89-910406] p 240 N90-15895
- Annual review of aircraft accident data: US general aviation calendar year 1987
[PB90-138066] p 486 N90-20966
- Brake performance of the McDonnell Douglas DC-10-30/40 during high speed, high energy rejected takeoffs
[PB90-917004] p 503 N90-21000
- Aircraft accident report, United Airlines Flight 811, Boeing 747-122, N4713U, Honolulu, Hawaii, February 24, 1989
[PB90-910401] p 574 N90-21748
- The new US flight recorder regulations
p 849 N90-27642
- Annual review of aircraft accident data: US general aviation, calendar year 1987
[PB90-138066] p 820 N90-27666
- NATO European Fighter Management Agency, Munich (Germany, F.R.).**
The EFA integrated monitoring and recording system: Requirements and concept for implementation
p 848 N90-27620
- Naval Air Development Center, Warminster, PA.**
Aluminum lithium alloys for Navy aircraft
p 267 N90-15193
- An analysis of GPS as the sole means navigation system in US Navy aircraft
p 917 N90-29350
- A low cost shadow moire device for the nondestructive evaluation of impact damage in composite laminates
[AD-A223451] p 953 N90-29442
- Naval Air Engineering Center, Lakehurst, NJ.**
Analytical and experimental study of runway runoff with wind effects
[PTI-8948] p 123 N90-12627
- Naval Air Systems Command, Washington, DC.**
US Navy aircraft fire protection technology
p 327 N90-17603
- Naval Air Test Center, Patuxent River, MD.**
US Navy principal site testing concept and the F-18
p 33 N90-10861
- Air Combat Environment Test and Evaluation Facility (ACETEF)
p 58 N90-10883

Naval Ocean Systems Center, San Diego, CA.

Observability of relative navigation using range-only measurements p 917 N90-29360

Naval Postgraduate School, Monterey, CA.

Progress towards the development of an inviscid-viscous interaction method for unsteady flows in turbomachinery cascades p 8 A90-11806

Experimental and computational studies of dynamic stall p 147 A90-16780

Amplitude effects on dynamic stall of an oscillating airfoil

[AIAA PAPER 90-0575] p 167 A90-19925

Vortical flows over delta wings and numerical prediction of vortex breakdown

[AIAA PAPER 90-0102] p 227 A90-22166

Design and development of a facility for compressible dynamic stall studies of a rapidly pitching airfoil

p 436 A90-28255

Flow visualization studies of the Mach number effects on dynamic stall of an oscillating airfoil

p 622 A90-40683

Numerical simulation of the effects of variation of angle of attack and sweep angle on vortex breakdown over delta wings

[AIAA PAPER 90-3000] p 788 A90-45850

Schlieren studies of compressibility effects on dynamic stall of airfoils in transient pitching motion

[AIAA PAPER 90-3038] p 791 A90-45877

Post crash flight analysis: Visualizing flight recorder data

[AD-A212063] p 96 N90-11715

Estimating the relationships between the state of the art of technology and production cost for the US aircraft

[AD-A212127] p 82 N90-12495

Computational investigation of incompressible airfoil flows at high angles of attack

[AD-A205885] p 174 N90-14201

Flow visualization of the effect of pitch rate on the vortex development on the scale model of a F-18 fighter aircraft

[AD-A214244] p 236 N90-15080

Applications of modern control theory synthesis to a super-augmented aircraft

[AD-A215431] p 336 N90-16753

Automation and extension of LDV (Laser-Doppler Velocimetry) measurements of off-design flow in a subsonic cascade wind tunnel

[AD-A216627] p 453 N90-18670

Aerodynamic analysis of a US Navy and Marine Corps unmanned air vehicle

[AD-A218282] p 498 N90-20077

An experimental investigation of support strut interference on a three-percent fighter model at high angles of attack

[AD-A219793] p 631 N90-23353

Initial flight test of half-scale unmanned air vehicle

[AD-A219584] p 648 N90-23388

Application of neural networks to the F/A-18 engine condition monitoring system

[AD-A219820] p 666 N90-24271

Helicopter controllability

[AD-A220078] p 672 N90-24275

Metalized fuel particle size study in a solid fuel ramjet

[AD-A220079] p 679 N90-24451

Aircraft modifications cost analysis. Volume 1: Overview of the study

[AD-A220764] p 702 N90-25074

An approach for design and analysis of composite rotor blades

[AD-A219257] p 734 N90-25125

Flow visualization of dynamic stall on an oscillating airfoil

[AD-A222202] p 815 N90-26797

Regression and combustion characteristics of boron containing fuels for solid fuel ramjets

p 858 N90-27928

An investigation of solid-fuel, dual-mode combustion ramjets

p 859 N90-27933

Development and testing of rapid repair methods for war damaged runways

[AD-A223970] p 938 N90-28586

The stress and temperature dependence of creep in an Al-2.0 wt percent Li alloy

[AD-A223676] p 953 N90-29480

Further studies of turbulence structure resulting from interactions between embedded vortices and wall jets at high blowing ratios

[AD-A223296] p 960 N90-29593

Naval Research Lab., Washington, DC.

Interactive generation of unstructured grids for three dimensional problems

p 310 A90-26537

Acoustic-vortex-chemical interactions in an idealized ramjet

p 54 N90-10206

Aviation Engine Test Facilities (AETF) fire protection study

[AD-A211483] p 134 N90-12777

Experiments with unsteady, free surface, three-dimensional vortices in a thermally stable, stratified fluid

[AD-A222088] p 815 N90-26796

Numerical simulations of flowfields in a central-dump ramjet combustor. 3: Effects of chemistry

[AD-A224145] p 933 N90-28573

Numerical simulations of the structure of supersonic shear layers

[AD-A224164] p 960 N90-29587

Naval Ship Research and Development Center, Bethesda, MD.

Flow coupling between a rotor and a stator in turbomachinery

[AD-A223882] p 932 N90-28572

Naval Submarine Medical Research Lab., Groton, CT.

Analysis of hydraulic fluids and lubricating oils for the formation of Trimethylpropane Phosphate (TMP-P)

[AD-A215188] p 357 N90-16939

Naval Surface Warfare Center, Silver Spring, MD.

Condensation in hypersonic nitrogen wind tunnels

[AIAA PAPER 90-1392] p 558 A90-37937

Wind tunnel tests of a 20-gore disk-gap-band parachute

[AD-A221326] p 634 N90-24251

Naval Weapons Center, China Lake, CA.

Recent developments in Ramjet pressure oscillation technology

p 53 N90-10199

Navistar International Transportation Corp., Fort Wayne, IN.

Experience with scale effects in non-airplane wind tunnel testing

[AIAA PAPER 90-1822] p 350 A90-25165

Navstar Systems Development, Monument, CO.

GPS integrity requirements for use by civil aviation

p 916 N90-29339

New Brunswick Univ., Fredericton.

Time development of convection flow patterns in aircraft cabins under post-crash fire exposure

p 327 N90-17598

Nielsen Engineering and Research, Inc., Mountain View, CA.

Development of an unstructured mesh/Navier-Stokes method for aerodynamics of aircraft with ice accretions

[AIAA PAPER 90-0758] p 169 A90-20011

Chemically reacting supersonic flow calculation using an assumed PDF model

[AIAA PAPER 90-0731] p 230 A90-22256

High-resolution shock-capturing schemes for inviscid and viscous hypersonic flows

p 476 A90-34545

Prediction methods for store separation

p 317 N90-17549

A study of supermaneuver aerodynamics

[AD-A218378] p 631 N90-23349

Prediction of subsonic vortex shedding from forebodies with chines

[NASA-CR-4323] p 909 N90-28494

Norfolk State Univ., VA.

Ground evaluation of seeding an in-flight wingtip vortex using infrared imaging flow visualization technique

p 635 N90-25035

Norges Tekniske Høgskole, Trondheim.

An aircraft noise study in Norway

p 698 N90-24872

North American Aircraft Operations, Los Angeles, CA.

Conceptual design optimization study

[NASA-CR-4298] p 582 N90-21755

North Carolina State Univ., Raleigh.

Grid generation and adaptation for the direct simulation Monte Carlo method

p 67 A90-11102

Experimental investigation of a new device to control the asymmetric flowfield on forebodies at large angles of attack

[AIAA PAPER 90-0069] p 161 A90-19665

Mach 6 testing of two generic three-dimensional sidewall compression scramjet inlets in tetrafluoromethane

[AIAA PAPER 90-0530] p 192 A90-19895

Condensation in hypersonic nitrogen wind tunnels

[AIAA PAPER 90-1392] p 558 A90-37937

An abbreviated Reynolds stress turbulence model for airfoil flows

[AIAA PAPER 90-1468] p 562 A90-38625

A hybrid Reynolds averaged/PDF closure model for supersonic turbulent combustion

[AIAA PAPER 90-1573] p 600 A90-38711

Exploratory wind tunnel investigation of the stability and control characteristics of a three-surface, forward-swept wing advanced turboprop model

[AIAA PAPER 90-3074] p 797 A90-45920

Numerical modeling of supersonic turbulent reacting free shear layers

p 174 N90-14197

A one equation turbulence model for transonic airfoils

p 174 N90-14199

Relating flow between counter-rotating propellers to aerodynamic interaction noise

p 479 N90-20944

An approximate viscous shock layer method for calculating the hypersonic flow over blunt-nosed bodies

p 479 N90-20947

An experimental investigation of the physical mechanisms controlling the asymmetric flow past slender bodies at large angles of attack

p 592 N90-21767

Analysis of a six-component, flow-through, strain-gage, force balance used for hypersonic wind tunnel models with scramjet exhaust flow simulation

[NASA-CR-186585] p 597 N90-21775

Low-speed wind tunnel investigation of the static stability and control characteristics of an advanced turboprop configuration with the propellers placed over the tail

[NASA-CR-186900] p 759 N90-26017

Northrop Corp., Hawthorne, CA.

Algorithms for computing the multivariable stability margin

p 612 N90-22999

Lessons learned for composite aircraft structures qualification

p 842 N90-26808

Control and estimation for aerospace applications with system time delays

p 918 N90-29367

Northwestern Univ., Evanston, IL.

Reflection by defective diffusion bonds

[AD-A212995] p 206 N90-13638

Notre Dame Univ., IN.

Analysis of nonuniform subsonic flows about a row of moving blades

p 6 A90-11779

Unsteady surface pressure distributions on a delta wing undergoing large amplitude pitching motions

[AIAA PAPER 90-0311] p 164 A90-19790

Vortex dynamics on a pitching delta wing

p 233 A90-23281

Numerical solutions of the linearized Euler equations for unsteady vortical flows around lifting airfoils

[AIAA PAPER 90-0694] p 300 A90-25041

Measurements in a separation bubble on an airfoil using laser velocimetry

p 384 A90-27977

Numerical solutions of the linearized Euler equations for unsteady vortical flows around lifting airfoils

p 394 A90-30264

An experimental study of the nonlinear dynamic phenomenon known as wing rock

[AIAA PAPER 90-2812] p 753 A90-45152

Delta wing surface pressures for high angle of attack maneuvers

[AIAA PAPER 90-2813] p 711 A90-45153

The structure of separated flow regions occurring near the leading edge of airfoils - including transition

[NASA-CR-185853] p 87 N90-11695

Experimental measurements of the laminar separation bubble on an Eppler 387 airfoil at low Reynolds numbers

[NASA-CR-186263] p 275 N90-15380

Surface pressure distributions on a delta wing undergoing large amplitude pitching oscillations

[NASA-CR-186326] p 317 N90-17558

Leading edge vortex dynamics on a pitching delta wing

[NASA-CR-186327] p 398 N90-19198

The MANTA: An RPV design to investigate forces and moments on a lifting surface

[NASA-CR-186227] p 499 N90-20971

The Stealth biplane: A proposal in response to a low Reynolds Number station keeping mission

[NASA-CR-186680] p 734 N90-25127

The SKY SHARK: An RPV designed to investigate the pressure distribution on a lifting surface

[NASA-CR-186222] p 844 N90-26824

The DELTA MONSTER: An RPV designed to investigate the aerodynamics of a delta wing platform

[NASA-CR-186226] p 924 N90-29381

NSI Technology Services Corp., Dayton, OH.

The acute, delayed neurotoxicity evaluation of two jet engine oil formulations

[AD-A22018] p 875 N90-26972



Oak Ridge National Lab., TN.

A preliminary sensitivity analysis of the Generalized Escape System Simulation (GESS) computer program

[DE89-016891] p 24 N90-10844

Robots for aircraft coatings removal: Parameters and requirements

[DE90-009429] p 609 N90-22048

Engine testing of thermographic phosphors

[DE90-013269] p 885 N90-28059

Office National d'Etudes et de Recherches

Aerospaciales, Paris (France).

Correlation of Puma airfoils - Evaluation of CFD prediction methods

[ONERA, TP NO. 1989-185] p 224 A90-21045

High-resolution shock-capturing schemes for inviscid and viscous hypersonic flows

p 476 A90-34545

Numerical simulation of unsteady combustion in a dump combustor

p 54 N90-10203

- Euler equation solutions applied to a helicopter rotor in forward moving flight
[ONERA-RSF-32/1285-AY-346A] p 107 N90-12592
- Studies of the European transonic wind tunnel
[ONERA-RSF-12/0694-GV] p 141 N90-13278
- Description of atmospheric turbulence
p 280 N90-15043
- Principal characteristics of lightning on aircraft
p 239 N90-15067
- Unsteady viscous calculation method for cascades with leading edge induced separation
p 426 N90-18408
- An inverse method for the design of turbomachine blades
p 511 N90-20988
- The use of numerical optimization for helicopter airfoil and blade design
p 502 N90-20995
- Numerical optimization of wings in transonic flow
p 502 N90-20997
- Calculation of the three dimensional turbulent flow in a linear turbine blade
p 513 N90-21021
- Tests of an ultra-light tunnel in the anechoic wind tunnel facility CEPRA 19
[ONERA-RF-20/7294-PH] p 872 N90-27729
- Theoretical studies carried out in 1988 on helicopter rotor noise under subsonic conditions
[ONERA-RS-82/5094-PY] p 896 N90-28402
- Solution of Euler equations applied to a rotor of a helicopter in steady flight
[ONERA-RSF-1/3731-AY-002A] p 910 N90-28500
- Molten salt induced high temperature degradation of thermal barrier coatings
p 952 N90-28704
- Effect of protective coatings on mechanical properties of superalloys
p 952 N90-28707
- Office National d'Etudes et de Recherches Aérospatiales, Toulouse (France).**
- Experimental study of transition and leading edge contamination on swept wings
p 71 N90-10362
- Control and modification of turbulence
p 72 N90-10377
- High enthalpy hypersonic wind tunnel F4: General description and associated instrumentation
p 673 N90-24228
- Office of Air Force History, Washington, DC.**
- Encyclopedia of US Air Force aircraft and missile systems. Volume 2: Post-World War 2 bombers, 1945-1973
[AD-A209273] p 1 N90-10001
- Office of Naval Research Liaison Office, Far East, APO San Francisco, CA.**
- Current Japanese supercomputers for computational fluid dynamics applications
p 610 N90-23172
- Office of Technology Assessment, Washington, DC.**
- Safer skies with TCAS: Traffic Alert and Collision Avoidance System
[PB89-169221] p 27 N90-10016
- Ohio State Univ., Columbus.**
- Compressibility effects in free shear layers
[AIAA PAPER 90-0705] p 212 A90-19984
- Effects of compressibility on the characteristics of free shear layers
p 302 A90-25285
- Measurements on an oscillating 70-deg delta wing in subsonic flow
p 307 A90-26130
- Measured forces and moments on a delta wing during pitch-up
p 308 A90-26137
- Generalized Transition Finite-Boundary Elements for high speed flight structures
[AIAA PAPER 90-1105] p 449 A90-29286
- Structure of a reattaching supersonic shear layer
p 555 A90-36252
- Measured aerodynamic performance of a swept wing with a simulated ice accretion
[AIAA PAPER 90-0490] p 557 A90-37063
- A computational study of the impingement region of an unsteady subsonic jet
[AIAA PAPER 90-1657] p 570 A90-38784
- Pressure-based real-time measurements in compressible free shear layers
[AIAA PAPER 90-1980] p 703 A90-42709
- Aeroelastic control of composite lifting surfaces: Integrated aeroelastic control optimization
p 198 N90-13396
- A user's manual for the method of moments Aircraft Modeling Code (AMC)
[NASA-CR-186371] p 415 N90-18390
- A heat transfer analysis for rough turbine airfoils
[AD-A221942] p 854 N90-26831
- The Helicopter Antenna Radiation Prediction Code (HARP)
[NASA-CR-186925] p 884 N90-27946
- Ohio Univ., Athens.**
- Ridge regression processing
p 489 N90-20931
- Optimization of the effective GPS data rate
p 489 N90-20932
- Sole means navigation and integrity through hybrid Loran-C and NAVSTAR GPS
p 489 N90-20933
- Weather data dissemination to aircraft
p 486 N90-20934

- Oklahoma State Univ., Stillwater.**
- Turbulence effects of aircraft flight dynamics and control
p 258 N90-15055
- Oklahoma Univ., Norman.**
- A computational analysis of the transonic flow field of two-dimensional minimum length nozzles
p 173 N90-14194
- Turbulence spectral widths view angle independence as observed by Doppler radar
[DOT/FAA/SA-89/2] p 281 N90-15566
- Hypersonic waverider configurations for trans-atmospheric vehicles
[AD-A217925] p 498 N90-20074
- Performance of an aero-space plane propulsion nozzle
p 515 N90-21034
- Old Dominion Univ., Norfolk, VA.**
- Applications of Lagrangian blending functions for grid generation around airplane geometries
[AIAA PAPER 90-0009] p 216 A90-19630
- Prediction of steady and unsteady asymmetric vortical flows around cones
[AIAA PAPER 90-0598] p 168 A90-19940
- Integral solution of unsteady full-potential equation for a transonic pitching airfoil
p 232 A90-23280
- Application of multiple grids topology to supersonic internal/external flow interactions
p 308 A90-26135
- Multiple-block grid adaption for an airplane geometry
p 311 A90-26547
- Three-dimensional shock-shock interactions on the scramjet inlet
[AIAA PAPER 90-0529] p 314 A90-26963
- Infrared imaging and tufts studies of boundary layer flow regimes on a NACA 0012 airfoil
p 446 A90-28268
- A parallel-vector algorithm for rapid structural analysis on high-performance computers
[AIAA PAPER 90-1149] p 458 A90-29293
- Unsteady flow computation of oscillating flexible wings
[AIAA PAPER 90-0937] p 389 A90-29363
- Finite element two-dimensional panel flutter at high supersonic speeds and elevated temperature
[AIAA PAPER 90-0982] p 450 A90-29372
- Vibrations of rectangular plates with moderately large initial deflections at elevated temperatures using finite element method
[AIAA PAPER 90-1125] p 451 A90-29429
- Unsteady inviscid and viscous computations for vortex-dominated flows
p 553 A90-35752
- Evaluation of equilibrium turbulence for a naturally developing hypersonic boundary layer at nonadiabatic wall conditions
[AIAA PAPER 90-1410] p 559 A90-37948
- Computational study for passive control of supersonic asymmetric vortical flows around cones
[AIAA PAPER 90-1581] p 566 A90-38718
- The organized nature of a turbulent trailing vortex
[AIAA PAPER 90-1625] p 568 A90-38754
- A device for introducing helical perturbations into a trailing line vortex
[AIAA PAPER 90-1627] p 568 A90-38756
- Recent aerodynamic measurements with Magnetic Suspension Systems
p 759 A90-44399
- Interactive grid adaption
p 806 A90-46850
- Characterization of LaRC-TPI 1500 powders - A new version with controlled molecular weight
p 946 A90-50177
- Optimal integral controller with sensor failure accommodation
p 61 N90-10123
- An experimental investigation of the aerodynamic characteristics of slanted base ogive cylinders using magnetic suspension technology
[NASA-CR-181708] p 21 N90-10834
- Guidance and Control strategies for aerospace vehicles
[NASA-CR-186195] p 199 N90-14243
- Application of Lagrangian blending functions for grid generation around airplane geometries
[NASA-CR-186318] p 237 N90-15891
- Low speed flowfield characterization by infrared measurements of surface temperatures
p 317 N90-17556
- Effects of nose bluntness and shock-shock interactions on blunt bodies in viscous hypersonic flows
[NASA-CR-186451] p 479 N90-20950
- Subsonic sting interference on the aerodynamic characteristics of a family of slanted-base ogive-cylinders
[NASA-CR-4299] p 633 N90-24242
- Flexural fatigue life prediction of closed hat-section using materially nonlinear axial fatigue characteristics
p 691 N90-25062
- Generation of circumferential velocity contours associated with pulsed point suction on a rotating disk
p 691 N90-25065
- A review of instability and noise propagation in supersonic flows
[NASA-CR-186800] p 717 N90-25112

- Analysis and mitigation of numerical dissipation in inviscid and viscous computation of vortex-dominated flows
[NASA-CR-186887] p 776 N90-26281
- Thermal structures: Four decades of progress
[NASA-CR-186898] p 887 N90-28105
- Oxford Univ. (England).**
- Data acquisition in aerodynamic research
p 171 N90-13340
- Wake interaction effects on the transition process on turbine blades
[AD-A214492] p 343 N90-16759
- Heat transfer near the entrance to a film cooling hole in a gas turbine blade
[AD-A217396] p 510 N90-20089

P

Pacific Northwest Lab., Richland, WA.

- Stochastic propagation of an array of parallel cracks: Exploratory work on matrix fatigue damage in composite laminates
[DE89-017837] p 126 N90-11813

PDA Engineering, Santa Ana, CA.

- The application of cast SiC/Al to rotary engine components
[NASA-CR-179610] p 192 N90-13385

Pennsylvania State Univ., State College.

- Free-field propagation of high intensity noise
[NASA-CR-186577] p 549 N90-21604

Pennsylvania State Univ., University Park.

- Computation of three dimensional turbulent boundary layers in internal flows, including turbomachinery rotor blades
p 12 A90-12555
- Mach number effects on conical surface features of swept shock-wave/boundary-layer interactions
p 154 A90-18147
- Skin friction measurements by laser interferometry in swept shock/boundary-layer interactions
p 154 A90-18153
- Upstream-influence scaling of fin-generated shock wave boundary-layer interactions
[AIAA PAPER 90-0376] p 164 A90-19822
- Computation of turbine flowfields with a Navier-Stokes code
[AIAA PAPER 90-2122] p 704 A90-42731
- A computationally efficient modelling of laminar separation bubbles
p 801 A90-46372
- Analytical study of mistuning/friction/aerodynamics interaction in a bladed disk assembly
[AD-A211139] p 55 N90-10893
- An investigation of end-wall vortex cavitation in a high Reynolds number axial-flow pump
[AD-A211426] p 133 N90-11982
- Experimental research on swept shock Wave/Boundary layer interactions
[AD-A211744] p 134 N90-11988
- A computationally efficient modelling of laminar separation bubbles
[NASA-CR-185854] p 136 N90-12872
- Thermal stability of jet fuel
[DE90-001160] p 206 N90-14385
- Thermal stability of jet fuel
[DE90-002760] p 269 N90-15288
- Skin friction measurements by laser interferometry in supersonic flows
p 317 N90-17557
- Design guidance to minimize unsteady forces in turbomachines
p 426 N90-18411
- DURIP optical equipment for high-speed viscous-inviscid interaction research
[AD-A217772] p 540 N90-20345
- Prediction of forces and moments for flight vehicle control effectors. Part 1: Validation of methods for predicting hypersonic vehicle controls forces and moments
[NASA-CR-186571] p 571 N90-21734
- Prediction of forces and moments for flight vehicle control effectors. Part 2: An analysis of delta wing aerodynamic control effectiveness in ground effect
[NASA-CR-186572] p 571 N90-21735
- An investigation of the generation and radiation of aerodynamic noise in real piping systems
p 614 N90-22368
- The interaction of a supersonic streamwise vortex and a normal shock wave
p 633 N90-24241
- A computational efficient modelling of laminar separation bubbles
[NASA-CR-186729] p 774 N90-25291
- Pennsylvania Transportation Inst., University Park.**
- Analytical and experimental study of runway runoff with wind effects
[PTI-8948] p 123 N90-12627
- Penny and Giles Data Recorders Ltd. (England).**
- Flight data replay and analysis system
p 893 N90-27635

PhotoStrain, Dallas, TX.

Photoelasticity: A cost effective design tool
p 883 N90-26819

Physical Sciences, Inc., Andover, MA.

Laser induced fluorescence: Practical applications
p 911 N90-29323

Physics and Electronics Lab. TNO, The Hague (Netherlands).

The comparison of the airbase simulation models airbase and sustained
[FEL-1988-66] p 123 N90-12629

Aircraft SAR simulation Sargen 1.0
[FEL-1989-44] p 135 N90-12823

Description of the MARC measuring system
[FEL-89-B170] p 963 N90-28887

Study improvement training facilities ground control air traffic controllers. Part 1: Alternative solutions and their consequences
[FEL-89-A257-PT-1] p 919 N90-29380

Study improvement training facilities ground control air traffic controllers. Part 2: Functional analysis approach control trainer
[FEL-89-A280-PT-2] p 939 N90-29409

Pioneer Aerospace Corp., Melbourne, FL.

Advanced recovery systems wind tunnel test report
[NASA-CR-177563] p 816 N90-27653

Pittsburgh Univ., PA.

The insertion of human dynamics models in the flight control loops of V/STOL research aircraft. Appendix 2: The optimal control model of a pilot in V/STOL aircraft control loops
[NASA-CR-186598] p 598 N90-21776

An adaptive human response mechanism controlling the V/STOL aircraft. Appendix 3: The adaptive control model of a pilot in V/STOL aircraft control loops
[NASA-CR-186599] p 598 N90-21777

Planning Research Corp., Hampton, VA.

Scaling effects in the impact response of graphite-epoxy composite beams
[SAE PAPER 891014] p 128 A90-14326

Impact evaluation of composite floor sections
[SAE PAPER 891018] p 100 A90-14330

A review and update of the NASA aircraft noise prediction program propeller analysis system
[SAE PAPER 891032] p 139 A90-14340

Simulation model-building procedure for dynamic systems integration
p 138 A90-14744

Euler and Navier-Stokes solutions for hypersonic flows
p 155 A90-18254

Leading- and trailing-edge flaps on supersonic delta wings
p 233 A90-23285

Reduction of blade-vortex interaction noise through higher harmonic pitch control
p 377 A90-23937

The prediction of the noise generating mechanisms of an Aerospatiale 365N-1 Dauphin helicopter
p 463 A90-28161

Flutter suppression control law synthesis for the active flexible wing model
p 517 A90-33403

NASA investigation of a claimed 'overlap' between two gust response analysis methods
p 771 A90-44730

Performance evaluations of oxidation-resistant carbon-carbon composites in simulated hypersonic vehicle environments
p 874 A90-48131

Planning Research Corp., McLean, VA.

Current status of Joint FAA/NASA Runway Friction Program
[SAE PAPER 892340] p 760 A90-45494

Poitiers Univ. (France).

Study of the compressibility effects on the turbulence of supersonic drags
[ETN-90-97448] p 817 N90-27661

Politecnico di Milano (Italy).

A fast collocation method for transonic airfoil design
p 501 N90-20984

Politecnico di Torino (Italy).

Numerical method for designing 3D turbomachinery blade rows
p 511 N90-20990

PPG Industries, Inc., Huntsville, AL.

Forward canopy feasibility and Thru-The-Canopy (TTC) ejection system study
[AD-A220360] p 637 N90-24258

Pratt and Whitney Aircraft, East Hartford, CT.

Thermal barrier coating life prediction model development, phase 1
[NASA-CR-182230] p 193 N90-13388

MATE (Materials for Advanced Turbine Engines) Program, Project 3. Volume 2: Design, fabrication and evaluation of an oxide dispersion strengthened sheet alloy combustor liner
[NASA-CR-180892] p 357 N90-17868

Energy Efficient Engine exhaust mixer model technology report addendum; phase 3 test program
[NASA-CR-174799] p 930 N90-28556

Energy Efficient Engine program advanced turbofan nacelle definition study
[NASA-CR-174942] p 930 N90-28560

Energy efficient engine program technology benefit/cost study. Volume 1: Executive summary
[NASA-CR-174766-VOL-1] p 931 N90-28564

Energy efficient engine program technology benefit/cost study, volume 2
[NASA-CR-174766-VOL-2] p 931 N90-28565

Energy Efficient Engine integrated core/low spool test hardware design report
[NASA-CR-168137] p 931 N90-28566

Energy efficient engine pin fin and ceramic composite segmented liner combustor sector rig test report
[NASA-CR-179534] p 932 N90-28567

Energy Efficient Engine: Control system preliminary definition report
[NASA-CR-179578] p 932 N90-28569

Energy Efficient Engine: High-pressure compressor test hardware detailed design report
[NASA-CR-180850] p 932 N90-28570

Pratt and Whitney Aircraft, West Palm Beach, FL.

Evolution of engine cycles for STOVL propulsion concepts
[AIAA PAPER 90-2272] p 743 A90-42767

Combustor influence on fighter engine operability
p 64 N90-10193

Thermal mechanical fatigue of coated blade materials
[AD-A214258] p 256 N90-15107

Improved toughness alloys based on titanium aluminides
[AD-A218149] p 533 N90-20208

Assessment of High Temperature Superconducting (HTS) electric motors for rotorcraft propulsion
[NASA-CR-185222] p 588 N90-21761

Failure analysis handbook
[AD-A219747] p 689 N90-23752

Retirement for cause of the F100 engine
p 843 N90-26813

Pratt and Whitney Aircraft Group, East Hartford, CT.

Mixer-ejector nozzle for jet noise suppression
[AIAA PAPER 90-1909] p 894 A90-47202

Pratt and Whitney Aircraft of Canada Ltd., Longueuil (Quebec).

Review of modelling methods to take account of material structure and defects
p 425 N90-18402

Life management planning
p 856 N90-27709

PRC Kentron, Inc., Hampton, VA.

Connection between leading-edge sweep, vortex lift, and vortex strength for delta wings
p 554 A90-35770

Near-field noise predictions of an aircraft in cruise
p 140 N90-12538

Nacelle aerodynamic performance
p 105 N90-12552

PRC Systems Services Co., Edwards, CA.

An American knowledge base in England - Alternate implementations of an expert system flight status monitor
p 459 A90-30719

A proposed Kalman filter algorithm for estimation of unmeasured output variables for an F100 turbofan engine
[AIAA PAPER 90-1920] p 656 A90-40558

In-flight flow visualization characteristics of the NASA F-18 high alpha research vehicle at high angles of attack
[SAE PAPER 892222] p 713 A90-45439

F-18 high alpha research vehicle surface pressures - Initial in-flight results and correlation with flow visualization and wind-tunnel data
[AIAA PAPER 90-3018] p 792 A90-45885

Princeton Univ., NJ.

Large-scale motions in a supersonic turbulent boundary layer on a curved surface
[AIAA PAPER 90-0019] p 160 A90-19636

Hypersonic propulsion
p 253 A90-21949

Helicopter flight control system design and evaluation for NOE operations using controller inversion techniques
p 429 A90-28202

A study of the unsteadiness of crossing shock wave turbulent boundary layer interactions
[AIAA PAPER 90-1456] p 606 A90-38614

Wall pressure fluctuations in the reattachment region of a supersonic free shear layer
[AIAA PAPER 90-1461] p 561 A90-38618

Thrust law effects on the longitudinal stability of hypersonic cruise
[AIAA PAPER 90-2820] p 763 A90-45149

Stochastic performance robustness of aircraft control systems
[AIAA PAPER 90-3410] p 865 A90-47665

Probabilistic reasoning for intelligent wind shear avoidance
[AIAA PAPER 90-3437] p 890 A90-47690

Trajectory optimization and guidance for an aerospace plane
[NASA-CR-185884] p 183 N90-13369

Nonlinear phenomena in computational transonic aeroelasticity
p 235 N90-15070

A rule-based paradigm for intelligent adaptive flight control
p 434 N90-19238

Investigation of air transportation technology at Princeton University, 1988-1989
p 486 N90-20935

Application of stochastic robustness to aircraft control systems
p 521 N90-20936

Neural networks for aircraft control
p 521 N90-20937

An expert system for wind shear avoidance
p 486 N90-20938

Rule-based mechanisms of learning for intelligent adaptive flight control
p 521 N90-20939

Perspectives on the use of rule-based control
p 521 N90-20940

Stochastic robustness of linear control systems
p 521 N90-20941

Aerodynamic design via control theory
p 546 N90-20998

A methodology for knowledge-based restructurable control to accommodate system failures
p 609 N90-22058

Coupled rotor-body equations of motion hover flight
[NASA-CR-186710] p 717 N90-25111

Prins Maurits Lab. TNO, Rijswijk (Netherlands).

Solid fuel combustion chamber
[LR-634] p 939 N90-29433

Products Research and Chemical Corp., Glendale, CA.

Fuel resistant coatings for metal and composite fuel tanks
p 269 N90-15911

Psycho-Linguistic Research Associates, Woodside, CA.

Evaluation of speech recognizers for use in advanced combat helicopter crew station research and development
[NASA-CR-177547] p 650 N90-24265

Purdue Univ., West Lafayette, IN.

The unsteady aerodynamics of an oscillating cascade in a compressible flow field
p 7 A90-11789

Mach number effects on transonic aeroelastic forces and flutter characteristics
p 17 A90-13024

Three-dimensional aerodynamics of an annular airfoil cascade including loading effects
p 87 A90-15889

Aeroelastic detuning for stability enhancement of unstalled supersonic flutter
p 189 A90-17462

Unsteady incompressible aerodynamics and forced response of detuned blade rows
[AIAA PAPER 90-0340] p 191 A90-19805

Propeller tip vortex interactions
[AIAA PAPER 90-0437] p 166 A90-19846

Comparison of steady and unsteady secondary flows in a turbine stator cascade
[ASME PAPER 89-GT-79] p 291 A90-23800

Propeller-wing interaction using a frequency domain panel method
p 307 A90-26128

Multiobjective decision making in a fuzzy environment with applications to helicopter design
p 405 A90-27993

Aeroelastic analysis of wings using the Euler equations with a deforming mesh
[AIAA PAPER 90-1032] p 391 A90-29376

Static aeroelastic behavior of an adaptive laminated piezoelectric composite wing
[AIAA PAPER 90-1078] p 412 A90-29386

Three dimensional full potential method for the aeroelastic modeling of propfans
[AIAA PAPER 90-1120] p 393 A90-29392

Aeroservoelastic tailoring for lateral control enhancement
p 516 A90-33060

Cooperative synthesis of control and display augmentation in approach and landing
p 516 A90-33061

Estimating short-period dynamics using an extended Kalman filter
[AIAA PAPER 90-1277] p 518 A90-33901

Euler flutter analysis of airfoils using unstructured dynamic meshes
p 602 A90-35760

Temporal-adaptive Euler/Navier-Stokes algorithm for unsteady aerodynamic analysis of airfoils using unstructured dynamic meshes
[AIAA PAPER 90-1650] p 569 A90-38778

Static aeroelastic tailoring for oblique wing lateral trim
p 667 A90-40689

Counter-rotating propellant analysis using a frequency domain panel method
p 623 A90-40937

Flow induced forced response of an incompressible radial cascade including profile and incidence effects
[AIAA PAPER 90-2352] p 626 A90-42136

Parametric aeroelastic stability analysis of a generic X-wing aircraft
p 731 A90-44737

Cascade aerodynamic gust response including steady loading effects
p 904 A90-51006

Flexible aircraft dynamic modeling for dynamic analysis and control synthesis
p 61 N90-10112

Frequency domain aerodynamic analysis of interacting rotating systems
p 21 N90-10837

- Discretization and model reduction for a class of nonlinear systems p 198 N90-13397
- Design of a spanloader cargo aircraft [NASA-CR-186046] p 184 N90-14216
- A two-dimensional unsteady analysis for transonic and supersonic cascade flows p 480 N90-20955
- Measurement of lift development on rapidly-accelerated wings p 480 N90-20956
- WINCOF-I code for prediction of fan compressor unit with water ingestion p 551 N90-21724
- Forcing function effects on rotor row unsteady aerodynamic response in a multistage compressor p 573 N90-22536
- An unsteady lifting surface method for single rotation propellers [NASA-CR-4302] p 719 N90-25940

Q

- Queensland Univ., Brisbane (Australia).**
- Hypersonic combustion of hydrogen in a shock tunnel p 46 A90-12560
- Questek, Inc., Centerport, NY.**
- See and avoid/cockpit visibility [DOT/FAA/CT-TN89/18] p 24 N90-10843
- See and avoid/cockpit visibility [AD-A214214] p 239 N90-15084

R

- RAND Corp., Santa Monica, CA.**
- The use of prototypes in selected foreign fighter aircraft development programs: Rafale, EAP, Lavi, and Gripen [AD-A214500] p 287 N90-16707
- Range Commanders Council, White Sands Missile Range, NM.**
- Flight termination system battery guidelines [AD-A217310] p 520 N90-20092
- Raytheon Co., Waltham, MA.**
- History and status of beamed power technology and applications at 2.45 Gigahertz p 61 N90-10150
- Rensselaer Polytechnic Inst., Troy, NY.**
- Shaft flexibility effects on aeroelastic stability of a rotating bladed disk p 132 A90-16371
- Blade mistuning coupled with shaft flexibility effects in rotor aeroelasticity [ASME PAPER 89-GT-330] p 343 A90-23896
- Shaft flexibility effects on the forced response of a bladed-disk assembly p 744 A90-43218
- Compendium of abstracts and viewgraphs [AD-A217189] p 532 N90-20140
- Optimum hypersonic airfoils with attached shocks p 481 N90-20960
- Research Inst. of National Defence, Stockholm (Sweden).**
- Thermochemical calculations with inert compounds [FOA-C-20759-2.1] p 206 N90-13677
- A study of terrain following systems and the creation of flight paths for terrain following vehicles [FOA-C-20774-2.5] p 827 N90-27691
- Reinforcing fibers and technology development for resin composites. Consequences for aircraft structures [FOA-C-20777-2.5] p 876 N90-27883
- Research Triangle Inst., Hampton, VA.**
- Airborne Doppler radar detection of low-altitude wind shear p 252 A90-23284
- Rice Univ., Houston, TX.**
- Penetration landing guidance trajectories in the presence of windshear p 98 A90-14732
- Acceleration, gamma, and theta guidance for abort landing in a windshear p 98 A90-14733
- Optimization and guidance of flight trajectories in the presence of windshear [NASA-CR-186163] p 574 N90-21747
- Optimal trajectories for hypervelocity flight p 918 N90-29378
- Windshear estimation along the trajectory of an aircraft p 963 N90-29745
- Rockwell International Corp., Cedar Rapids, IA.**
- High speed bus technology development [AD-A224486] p 960 N90-29565
- Rockwell International Science Center, Thousand Oaks, CA.**
- Supersonic flow computations over aerospace configurations using an Euler marching solver [NASA-CR-4085] p 19 N90-10012
- Fatigue crack initiation mechanics of metal aircraft structures [AD-A210567] p 65 N90-10255
- Supersonic flow computations for an ASTOVL aircraft configuration, phase 2, part 2 [NASA-CR-4284] p 610 N90-22746

- Rolls-Royce Ltd., Bristol (England).**
- Characteristics of combustion driven pressure oscillations in advanced turbo-fan engines with afterburner p 64 N90-10194
- Parametric assessment of propulsion system mass for airbreathing launcher configurations p 344 N90-16819
- Rolls-Royce Ltd., Derby (England).**
- The RB199: An in-service success [PNR90544] p 114 N90-11746
- Advanced technology in military gas turbine design and manufacture [PNR90545] p 114 N90-11747
- Engine controls for the 1990's [PNR90546] p 114 N90-11748
- Future military powerplants [PNR90554] p 114 N90-11749
- Aluminium alloy development for aero engines [PNR90548] p 126 N90-11874
- What should be done with those noisy old aircraft [PNR90562] p 107 N90-12593
- A vision of the future: The new engine technology [PNR90566] p 115 N90-12603
- Designing for reliable and low maintenance cost aero engines [PNR90570] p 115 N90-12604
- The next generation supersonic transport engine: Critical issues [PNR90576] p 115 N90-12605
- Re-engine with the Rolls-Royce Tay 670, the route to significant noise reduction [PNR90585] p 115 N90-12606
- The role of component testing [PNR90589] p 115 N90-12608
- Flanged joints of aeroengines [PNR90594] p 116 N90-12609
- Material requirements for future aeroengines [PNR90595] p 116 N90-12610
- A computer integrated approach to dimensional inspection [PNR90596] p 116 N90-12611
- Dynamic tip clearance measurements in axial flow compressors [PNR90597] p 116 N90-12612
- The development of a high response aerodynamic wedge probe and use on a high-speed research compressor [PNR90598] p 116 N90-12613
- Gas turbine performance analysis [PNR90599] p 116 N90-12614
- Blading design for multi-storage HP compressor [PNR90602] p 116 N90-12616
- Composite materials for future aeroengines [PNR90584] p 127 N90-12667
- The future of non ferrous metals in aerospace engines [PNR90572] p 127 N90-12720
- The nature and control of skidding in lightly loaded intershaft bearings [PNR90591] p 136 N90-12933
- The design and development of an acoustic test section for the ARA transonic wind tunnel [PNR90574] p 140 N90-13202
- The commercial aircraft noise problem [PNR90577] p 140 N90-13203
- Development of a mass averaging temperature probe p 427 N90-18418
- From 1959-1989: 30 years of service experience with ramjets [PNR90677] p 748 N90-25139
- Stage 2 re-engining: The only way to achieve a real stage 3 aircraft [PNR90636] p 737 N90-25977
- Application of high performance metals in gas turbine engines [PNR90640] p 750 N90-25999
- Towards 2000: The composite engine [PNR90646] p 750 N90-26000
- Prediction of rotating disc flow and heat transfer in gas turbine engines [PNR90650] p 750 N90-26001
- Prediction and measurement of rotor blade/stator vane dynamic characteristics of a modern aero-engine axial compressor [PNR90667] p 750 N90-26002
- The impact and requirements of new materials on aeroengines [PNR90671] p 750 N90-26003
- Aircraft exhaust emissions: An engine manufacturer's perspective [PNR90675] p 750 N90-26004
- The application of engineering ceramics in gas turbines [PNR90676] p 750 N90-26005
- Metal matrix composites and powder processing for aero-engine applications [PNR90617] p 767 N90-26087

- NDT in aerospace: The next decade (1990's) [PNR90628] p 777 N90-26348
- The role of NDI in the certification of turbine engine components [PNR90629] p 777 N90-26349
- Bringing aircraft noise testing down to Earth [PNR90642] p 783 N90-26637
- Cost effective technology [PNR90664] p 883 N90-27002
- AGARD damage tolerance concepts for engine structures Workshop 3, Component Behaviour and Life Management p 855 N90-27705
- The role of NDI in the certification of turbine engine components p 859 N90-28069
- Rome Air Development Center, Griffiss AFB, NY.**
- RADC fault tolerant system reliability evaluation facility [AD-A215298] p 377 N90-17348
- Rouen Univ. (France).**
- Turbulent combustion modeling for turbo-jet combustion chambers p 749 N90-25993
- Royal Aerospace Establishment, Bedford (England).**
- The need for platform motion in modern piloted flight training simulators [AD-A221720] p 871 N90-26847
- The effects of foreplanes on the static and dynamic characteristics of a combat aircraft model p 920 N90-28520
- The steady and time-dependent aerodynamic characteristics of a combat aircraft with a delta or swept canard p 921 N90-28526
- Royal Aerospace Establishment, Farnborough (England).**
- Correlation of Puma airfoils - Evaluation of CFD prediction methods [ONERA, TP NO. 1989-185] p 224 A90-21045
- An American knowledge base in England - Alternate implementations of an expert system flight status monitor p 459 A90-30719
- The application of TSIM software to act design and analysis on flexible aircraft p 60 N90-10086
- Comparison of the results of tests on A300 aircraft in the RAE 5 metre and ONERA F1 wind tunnels [RAE-TM-AERO-2130] p 122 N90-11768
- Improvements in the formulations and numerical solution of the Euler problem for swept wings [RAE-TM-AERO-2139] p 95 N90-12562
- CFD methods for drag prediction and analysis currently in use in UK [RAE-TM-AERO-2146] p 95 N90-12563
- Preliminary experience with high response pressure measurements in a multistage, high speed compressor [RAE-TM-P-1141] p 117 N90-12619
- Acoustic recording systems for use in military aircraft [RAE-TM-MM-11] p 140 N90-13207
- Current status of the application of conventional aluminium-lithium alloys and the potential for future developments p 268 N90-15203
- The development of a low cost data logging system for flight trials based on an IBM compatible PC [RAE-TM-FM-16] p 251 N90-15917
- Performance of a highly-loaded HP compressor [RAE-TM-P-1149] p 256 N90-15919
- Aerodynamic and heat transfer measurements on blading for a high rim-speed transonic turbine [RAE-TM-P-1151] p 256 N90-15920
- Cycle analysis for helicopter gas turbine engines [RAE-TM-P-1154] p 256 N90-15921
- A UK perspective on the uniform engine test programme [RAE-TM-P-1172] p 257 N90-15922
- The stability of fuel fires p 327 N90-17601
- A study of flows over highly-swept wings designed for maneuver at supersonic speeds [AD-A216837] p 399 N90-19202
- Escape systems research at RAE p 483 N90-20058
- Secondary flow predictions for a transonic nozzle guide vane p 513 N90-21017
- Feature-associated mesh embedding for complex configurations p 608 N90-21988
- Formation of design envelope criterion in terms of deterministic spectral procedure [RAE-TM-SS-9] p 721 N90-25953
- Handbook of uncertainty methodology for engine testing at Pyestock (England) [RAE-TM-P-1179] p 751 N90-26007
- Integration of flight management and air traffic management systems [RAE-TM-FM-41] p 827 N90-27693
- The basis for facility comparison p 856 N90-27713
- Experience in developing an improved altitude test capability p 857 N90-27719
- Inspection reliability p 885 N90-28072
- Use of liquid crystals for qualitative and quantitative 2-D studies of transition and skin friction [RAE-TM-AERO-2159] p 958 N90-28800

Royal Air Force, Dereham (England).

The repair of aircraft integral fuel tanks in the RAF: A user's view of fuel tank technology p 250 N90-15908

Royal Air Force Coll., Cranwell (England).

A study of the technology required for advanced vertical take-off aircraft [ETN-90-96786] p 650 N90-24268

Royal Aircraft Establishment, Bedford (England).

Classification of windshear severity p 281 N90-15049

The assessment of visibility from automatic contrast measurements p 242 N90-15061

Royal Aircraft Establishment, Farnborough (England).

Royal Aerospace Establishment: No place for a castings factor p 64 N90-10235

Experimental investigation of attachment-line transition in low-speed, high-lift wind-tunnel testing p 71 N90-10358

Helicopter rotor test rig (RoTeSt) in DNW: Application and results [RAE-TRANS-2171] p 201 N90-13408

Evaluation of the indirect effects of lightning on a system: Double transfer function method [RAE-TRANS-2172] p 176 N90-14211

Diffusion bonding of metals p 206 N90-14330

The effect of primer age on adhesion of polysulphide sealant p 269 N90-15909

The role of structural analysis in airworthiness certification [BR112064] p 499 N90-20972

Computer-aided structural optimisation of aircraft structures [BR112837] p 499 N90-20973

Component behaviour and life management: The need for common AGARD approaches and actions p 856 N90-27710

The experimental investigation of flow in the core of a vortex structure [BR114893] p 960 N90-29597

Royal Military Coll. of Canada, Kingston (Ontario).

Acoustic emission detection of crack presence and crack advance during flight p 886 N90-28082

Royal Signals and Radar Establishment, Malvern (England).

A simulation study of landing time allocation procedures for use in computer-assisted air traffic management systems [AD-A212159] p 99 N90-11722

Software fault tolerance [RSRE-MEMO-4237] p 99 N90-12575

Fine resolution errors in secondary surveillance radar altitude reporting amongst aircraft transmitting the conspicuity codes 4321 and 4322 [RSRE-88004] p 135 N90-12816

A real-time wind model using digital data from aircraft [RSRE-MEMO-4309] p 137 N90-13005

Computer-based tools for assisting air traffic controllers with arrivals flow management [RSRE-88001] p 178 N90-13366

The automatic detection of anti-collision lights [RSRE-MEMO-4272] p 240 N90-15896

The application of Z to the specification of air traffic control systems. 1: An initial specification of the radar processing activity [RSRE-MEMO-4280] p 243 N90-15900

Rutgers Univ., New Brunswick, NJ.

Numerical investigation of some control methods for 3-D turbulent interactions due to sharp fins p 591 N90-21764

S

Salford Univ. (England).

An experimental study of the aeroelastic behaviour of two parallel interfering circular cylinders p 455 N90-19609

San Diego State Univ., CA.

Application of panel methods to wind-tunnel wall interference corrections [AIAA PAPER 90-0007] p 200 A90-19629

Effect of vertical-ejector jet on the aerodynamics of delta wings p 553 A90-35755

Self-induced roll oscillations of low-aspect-ratio rectangular wings [AIAA PAPER 90-2811] p 753 A90-45151

San Jose State Univ., CA.

Identification of rotor flapping equation of motion from flight measurements with the RSRA compound helicopter p 56 A90-12769

Air-ground information transfer in the National Airspace System p 380 A90-26235

The Meteorological Measurement System on the NASA ER-2 aircraft p 926 A90-51658

Sandia National Labs., Albuquerque, NM.

An experimental investigation of wall-interference effects for parachutes in closed wind tunnels [DE90-001802] p 236 N90-15076

Risk assessment and its application to flight safety analysis [DE90-004985] p 323 N90-16722

The 59th Shock and Vibration Symposium, volume 2 [AD-A214579] p 372 N90-18065

Helicopter flight vibration of large transportation containers: A case for testing tailoring [DE90-007429] p 402 N90-19215

Heli/SITAN: A terrain referenced navigation algorithm for helicopters [DE90-005193] p 405 N90-19217

Sandia National Laboratories' new high level acoustic test facility [DE90-006810] p 464 N90-19820

Slotted-wall research with disk and parachute models in a low-speed wind tunnel [DE90-002989] p 572 N90-21737

Equilibrium swelling of elastomeric materials in solvent environments [DE90-010184] p 678 N90-24430

Wind tunnel study of wake downwash behind A 6 percent scale model B1-B aircraft [DE90-011783] p 719 N90-25941

Hypersonic Arbitrary-Body Aerodynamics (HABA) for conceptual design [DE90-014750] p 910 N90-28495

Small multipurpose stored data acquisition system [DE90-010823] p 967 N90-30134

Santa Clara Univ., CA.

Streamtube analysis of supersonic combustion in an in-tube-scamjet [AIAA PAPER 90-2339] p 762 A90-42776

Scicon Consultancy International Ltd., London (England).

Harrier Information Management System (HIMS): The system and the approach p 884 N90-27630

Scientech, Inc., Idaho Falls, ID.

Boeing 727-100 test project (high energy radiated field tests) [DOT/FAA/CT-88/33] p 542 N90-21247

Scientific Computing Associates, Inc., New Haven, CT.

Modification and improvement of software for modeling multidimensional reacting fuel flows [AD-A217789] p 533 N90-20235

Scientific Research and Technology, Inc., Hampton, VA.

Hypersonic viscous shock-layer solutions over long slender bodies. II - Low Reynolds number flows p 393 A90-29695

Low-density flow effects for hypervelocity vehicles, phase 2 [AD-A221034] p 634 N90-24249

Scientific Research Associates, Inc., Glastonbury, CT.

Fluorescence spectroscopy and thermometry for hypersonic flight research [AIAA PAPER 90-1272] p 538 A90-33897

Extension of a three-dimensional viscous wing flow analysis user's manual: VISTA 3-D code [NASA-CR-182024] p 574 N90-22538

Extension of a three-dimensional viscous wing flow analysis [NASA-CR-182023] p 631 N90-23348

Search Technology, Inc., Norcross, GA.

Designers as users - Design supports based on crew system design practices p 457 A90-28184

Service Technique des Programmes Aeronautiques, Paris (France).

Casting factors imposed by the French regulation for foundry castings used in military aircraft p 64 N90-10233

Casting airworthiness joint European civil authorities view-point p 64 N90-10234

Sheffield Univ. (England).

Airborne MSS for land cover classification II p 737 A90-43376

Sikorsky Aircraft, Stratford, CT.

Aeroacoustic flowfield and acoustics of a model helicopter tail rotor at high advance ratio p 463 A90-28160

Plan, formulate, and discuss a NASTRAN finite element model of the UH-60A helicopter airframe [NASA-CR-181975] p 541 N90-20439

Ground shake test of the UH-60A helicopter airframe and comparison with NASTRAN finite element model predictions [NASA-CR-181993] p 758 N90-25143

Calculation of flight vibration levels of the AH-1G helicopter and correlation with existing flight vibration measurements [NASA-CR-182031] p 775 N90-25375

Application of damage tolerance p 843 N90-26817

Individual Helicopter Tracking Program (IHTP) for the MH-53J helicopter p 843 N90-26818

Simula, Inc., Phoenix, AZ.

Aircraft crash survival design guide. Volume 1: Design criteria and checklists [AD-A218434] p 575 N90-22545

Aircraft crash survival design guide. Volume 2: Aircraft design crash impact conditions and human tolerance [AD-A218435] p 575 N90-22546

Aircraft crash survival design guide. Volume 3: Aircraft structural crash resistance [AD-A218436] p 575 N90-22547

Aircraft crash survival design guide. Volume 4: Aircraft seats, restraints, litters, and cockpit/cabin dehalization [AD-A218437] p 575 N90-22548

Aircraft crash survival design guide. Volume 5: Aircraft postcrash survival [AD-A218438] p 575 N90-22549

Operational effects on crashworthy seat attenuators [AD-A221148] p 637 N90-24259

Singer Co., Wayne, NJ.

The integration of multiple avionic sensors and technologies for future military helicopters p 916 N90-29344

Societe de Fabrication d'Instruments de Mesure, Massy (France).

Low air speed computation for helicopters: A new approach p 333 N90-16744

Societe Mothesim, Le Plessis-Robinson (France).

GTD/UTD: Brief history of successive development of theory and recent advances. Applications to antennas on ships and aircraft p 370 N90-17939

Societe Nationale d'Etude et de Construction de Moteurs d'Aviation, Corbeil (France).

Progress in airbreathing combined engines for future European launcher p 344 N90-16817

Societe Nationale d'Etude et de Construction de Moteurs d'Aviation, Moissy-Cramayel (France).

Aerodynamic study on forced vibrations on stator rows of axial compressors p 426 N90-18412

Calculation of the secondary flow in an axial turbine p 513 N90-21022

Mesh generation for flow computation in turbomachine p 588 N90-21981

Soil and Materials Engineers, Inc., Ann Arbor, MI.

Development of a thickness design procedure for stabilized layers under rigid airfield pavements [DOT/FAA/RD-90/22] p 937 N90-28582

SOL-3 Resources, Inc., Reading, MA.

Introducing the VRT gas turbine combustor [AIAA PAPER 90-2452] p 743 A90-42808

Southampton Univ. (England).

Surface flow visualization in the cryogenic wind tunnel p 539 A90-34234

Techniques for extreme attitude suspension of a wind tunnel model in a magnetic suspension and balance system [NASA-CR-181895] p 202 N90-14245

Measurement and prediction of propeller blade surface pressure distributions p 481 N90-20961

The aims and history of adaptive wall wind tunnels p 871 N90-26839

Three-dimensional model testing in the transonic self-streamlining wind tunnel p 938 N90-28583

Southwest Research Inst., San Antonio, TX.

Installation effects on propeller wake/vortex-induced structure-borne noise transmissions p 579 A90-35761

Spray automated balancing of rotors - How process parameters influence performance p 879 A90-46228

NDI (Nondestructive Inspection) oriented corrosion control for Army aircraft. Phase 1: Inspection methods [AD-A213368] p 176 N90-13359

Constitutive modeling for isotropic materials (HOST) [NASA-CR-179522] p 193 N90-13390

Constitutive modeling for isotropic materials (HOST) [NASA-CR-174718] p 193 N90-13391

Inspection development for T-37 wing spar cap lug [AD-A214826] p 287 N90-16708

Cumulative airport noise exposure metrics: An assessment of evidence for time-of-day weightings, revision [AD-A214878] p 352 N90-16773

Automated analysis of MXU-553 flight data p 844 N90-26821

Structure-borne noise estimates for the PTA aircraft [NASA-CR-4315] p 896 N90-28396

Spectralab, Kilchberg (Switzerland).

Multichannel on-board load and fatigue monitoring p 849 N90-27621

SRI International Corp., Menlo Park, CA.

Influence of microstructure and microdamage processes on fracture at high loading rates [AD-A210307] p 65 N90-10253

Stanford Univ., CA.

- Simple analyses of paths through windshears and downdrafts
[AIAA PAPER 90-0222] p 197 A90-19740
- Pneumatic vortical flow control at high angles of attack
[AIAA PAPER 90-0098] p 227 A90-22164
- Direct numerical simulations of transition in a compressible wake p 553 A90-35212
- The effect of Mach number on the stability of a plane supersonic wake p 557 A90-36524
- Three dimensional Discrete Particle Simulation about the AFE geometry
[AIAA PAPER 90-1778] p 560 A90-38468
- Effects of streamwise vorticity injection on turbulent mixing layer development
[AIAA PAPER 90-1459] p 561 A90-38616
- Modeling supersonic combustion using a fully-implicit numerical method
[AIAA PAPER 90-2307] p 677 A90-42117
- Two- and three-dimensional effects in the supersonic mixing layer
[AIAA PAPER 90-1978] p 703 A90-42708
- Parameter identification of linear systems based on smoothing
[AIAA PAPER 90-2800] p 753 A90-45156
- Optimal paths through downbursts p 755 A90-45330
- Control of an aircraft in downbursts p 755 A90-45331
- A numerical method for relating two- and three-dimensional pressure distributions on transonic wings
[AIAA PAPER 90-3211] p 812 A90-48837
- Design synthesis and optimization of joined-wing transports
[AIAA PAPER 90-3197] p 838 A90-49102
- A closer look at the induced drag of crescent-shaped wings
[AIAA PAPER 90-3063] p 903 A90-50638
- Unsteady aerodynamics with applications to flight mechanics
[AD-A211944] p 89 N90-11706
- Active control of unsteady and separated flow structures
[AD-A212109] p 89 N90-11707
- A CFD study of tilt rotor flowfields
[NASA-CR-186116] p 171 N90-13349
- Controlled vortical flow on delta wings through unsteady leading edge blowing
[NASA-CR-186267] p 316 N90-16712
- An experimental study of the effect of streamwise vortices on unsteady turbulent boundary-layer separation p 369 N90-17045
- Direct numerical simulation of aerodynamic noise
[AD-A214122] p 379 N90-18225
- Unsteady aerodynamics of delta wings performing maneuvers to high angle of attack p 398 N90-19196
- Computation of hypersonic low density flows with thermochemical nonequilibrium p 477 N90-20044
- Transpiration cooling in hypersonic flight
[NASA-CR-186435] p 478 N90-20052
- Optimal control of an aircraft flying through a downburst p 591 N90-21765
- Turbulent reacting flows and supersonic combustion
[AD-A221793] p 875 N90-26933
- A two dimensional study of rotor/airfoil interaction in hover
[NASA-CR-183272] p 845 N90-27694
- Control of vortex aerodynamics at high angles of attack p 921 N90-28523
- The aerodynamic design of the oblique flying wing supersonic transport
[NASA-CR-177552] p 923 N90-28540
- The computation and analysis of acoustic waves in transonic airfoil-vortex interactions p 966 N90-30031
- Starmark Corp., Arlington, VA.**
- An early overview of tiltrotor aircraft characteristics and pilot procedures in civil transport applications
[DOT/FAA/DS-89/37] p 503 N90-21003
- State Univ. of New York, Brockport.**
- A quantitative technique to estimate microburst wind shear hazard to aircraft p 692 N90-25040
- State Univ. of New York, Buffalo.**
- Blunt-nose inviscid airflows with coupled nonequilibrium processes p 171 N90-13336
- State Univ. of New York, Stony Brook.**
- Calculation of temperature distribution in various turbine blades using a boundary-fitted coordinate transformation method p 929 N90-28550
- Sterling Federal Systems, Inc., Moffett Field, CA.**
- Supercomputer applications in gas turbine flowfield simulation p 620 A90-40495

Sterling Federal Systems, Inc., Palo Alto, CA.

- Upwind differencing scheme for the time-accurate incompressible Navier-Stokes equations p 232 A90-23109
- Sterling Software, Moffett Field, CA.**
- Multi-processing on supercomputers for computational aerodynamics
[AIAA PAPER 90-0337] p 282 A90-22199
- Sterling Software, Palo Alto, CA.**
- Calculations of the flow past bluff bodies, including tilt-rotor wing sections at $\alpha = 90$ deg
[AIAA PAPER 90-0032] p 227 A90-22156
- Stevens Inst. of Tech., Hoboken, NJ.**
- A methodology for validating software reliability
[AIAA PAPER 89-3081] p 74 A90-10567
- Computational and experimental investigations of rotating stall in compressor cascades p 588 N90-22565
- Hardware and software reliability estimation using simulations
[NASA-CR-186637] p 780 N90-25580
- Structural Integrity Associates, Inc., San Jose, CA.**
- Stress intensity factors for cracking metal structures under rapid thermal loading. Volume 2: Theoretical background
[AD-A213297] p 213 N90-13812
- Stuttgart Univ. (Germany, F.R.).**
- Geodetic network adjustment using GPS triple difference observations and a priori stochastic information
[TR-1-1987] p 178 N90-13367
- Processing of undifferenced GPS carrier beat phase measurements and adjustment computations
[TR-5-1988] p 178 N90-13368
- Inverse computation of transonic internal flows with application for multi-point-design of supercritical compressor blades p 501 N90-20987
- A contribution to the economic, optimal dimensioning, and shaping of aircraft structures using a design model
[ETN-90-96966] p 737 N90-25976
- Chemistry of combustion processes p 749 N90-25994
- Sverdrup Technology, Inc., Arnold AFS, TN.**
- Optimization of aerodynamic designs using computational fluid dynamics p 541 N90-20999
- Design of the UETP experiment p 856 N90-27712
- Comparison of altitude test cell results p 856 N90-27715
- Experience in developing an improved design of experiment (lessons learned) p 857 N90-27718
- General test plan p 857 N90-27721
- Sverdrup Technology, Inc., Brook Park, OH.**
- Preliminary design of a long-endurance Mars aircraft
[AIAA PAPER 90-2000] p 674 A90-40587
- Analysis of internal flow in a ventral nozzle for STOVL aircraft
[AIAA PAPER 90-1899] p 739 A90-42688
- Computational analysis of the flowfield of a two-dimensional ejector nozzle
[AIAA PAPER 90-1901] p 740 A90-42690
- Unsteady blade surface pressures on a large-scale advanced propeller - Prediction and data
[AIAA PAPER 90-2402] p 808 A90-47220
- Experimental investigation of multielement airfoil ice accretion and resulting performance degradation p 812 A90-48954
- Preliminary design of a long-endurance Mars aircraft
[NASA-CR-185243] p 588 N90-21763
- Sverdrup Technology, Inc., Eglin AFB, FL.**
- Aerodynamic optimization by simultaneously updating flow variables and design parameters p 501 N90-20991
- Sverdrup Technology, Inc., Cleveland, OH.**
- Hypersonic aerospace sizing analysis for the preliminary design of aerospace vehicles p 247 A90-23276
- Application of a lower-upper implicit scheme and an interactive grid generation for turbomachinery flow field simulations
[ASME PAPER 89-GT-20] p 288 A90-23762
- Simulation of three-dimensional viscous flow within a multistage turbine
[ASME PAPER 89-GT-152] p 292 A90-23841
- Influence of alloying elements on the oxidation behavior of NbAl₃ p 355 A90-24861
- Unsteady Euler analysis of the flowfield of a propfan at an angle of attack
[AIAA PAPER 90-0339] p 300 A90-25028
- Comparison of 3-D viscous flow computations of Mach 5 inlet with experimental data
[AIAA PAPER 90-0600] p 314 A90-26970
- Cooperative synthesis of control and display augmentation in approach and landing p 516 A90-33061
- Analysis of airframe/engine interactions - An integrated control perspective
[AIAA PAPER 90-1918] p 667 A90-40557

- H-infinity based integrated flight/propulsion control design for a STOVL aircraft in transition flight
[AIAA PAPER 90-3335] p 862 A90-47595
- A supersonic through-flow fan engine airframe integration study
[NASA-CR-185140] p 18 N90-10004
- Multigrid calculations of 3-D turbulent viscous flows
[NASA-CR-185154] p 143 N90-13323
- User's guide to PMESH: A grid-generation program for single-rotation and counterrotation advanced turboprops
[NASA-CR-185156] p 217 N90-14783
- Viscous three-dimensional analyses for nozzles for hypersonic propulsion
[NASA-CR-185197] p 344 N90-17635
- Users manual for the NASA Lewis Ice Accretion Prediction Code (LEWICE)
[NASA-CR-185129] p 468 N90-20943
- Exhaust nozzles for propulsion systems with emphasis on supersonic cruise aircraft
[NASA-RP-1235] p 516 N90-21037
- Sverdrup Technology, Inc., Middleburg Heights, OH.**
- Test and theory for piezoelectric actuator-active vibration control of rotating machinery p 879 A90-46226
- Sydney Univ. (Australia).**
- Direct simulation of three-dimensional hypersonic flow about intersecting blunt wedges p 16 A90-12835
- Systemes et Audio Frequences, Paris (France).**
- Integration of a centralized multiplexed control unit into the cockpit of an aircraft
[F6150-DT410-1-88329] p 120 N90-12622
- Systems Control Technology, Inc., Arlington, VA.**
- Rotorcraft low altitude CNS benefit/cost analysis: Rotorcraft operations data
[DOT/FAA/DS-89/9] p 141 N90-12406
- Indianapolis Downtown Heliport: Operations analysis and marketing history
[REPT-90RR-13] p 527 N90-21049
- Aeronautical decisionmaking for air ambulance program administrators
[DOT/FAA/DS-88/8] p 635 N90-23368
- Flight test investigation of flight director and autopilot functions for helicopter decelerating instrument approaches
[DOT/FAA/CT-TN89/54] p 869 N90-27724
- Systems Control Technology, Inc., Palo Alto, CA.**
- Maximum likelihood tuning of a vehicle motion filter p 755 A90-45334
- Flight control design considerations for STOVL powered-lift flight
[AIAA PAPER 90-3225] p 868 A90-49110
- Expert system diagnostics and parts life tracking as applied to the AV-8B aircraft for the USMC p 884 N90-27629
- Systems Technology, Inc., Hawthorne, CA.**
- Literal singular-value-based flight control system design techniques p 118 A90-14747
- Flight test investigation of flight director and autopilot functions for helicopter decelerating instrument approaches
[DOT/FAA/CT-TN89/54] p 869 N90-27724
- Systems Technology, Inc., Mountain View, CA.**
- Fully automatic guidance for rotorcraft nap-of-the-earth (NOE) flight following planned profiles p 403 A90-28219
- Real-time piloted simulation of fully automatic guidance and control for rotorcraft nap-of-the-earth (NOE) flight following planned profiles
[AIAA PAPER 90-3372] p 864 A90-47630
- T**
- Technion - Israel Inst. of Tech., Haifa.**
- Reduced size first-order subsonic and supersonic aerodynamic modeling
[AIAA PAPER 90-1154] p 390 A90-29366
- Convex models of malfunction diagnosis in high performance aircraft
[AD-A218514] p 702 N90-25073
- Technion Research and Development Foundation Ltd., Haifa (Israel).**
- Multi-disciplinary optimization of aeroservoelastic systems
[NASA-CR-185931] p 925 N90-29385
- Technische Hochschule, Aachen (Germany, F.R.).**
- Force and moment measurements on delta wings in unsteady flow p 278 N90-16185
- Numerical investigation of unsteady flow in oscillating turbine and compressor cascades p 426 N90-18407
- Experiments on the unsteady flow in a supersonic compressor stage p 427 N90-18422
- Experimental investigation of the influence of rotor wakes on the development of the profile boundary layer and the performance of an annular compressor cascade p 427 N90-18425

- A panel process for the calculation of the flow around a wing with front angle damping
[ETN-90-95367] p 399 N90-19207
Carrier wing profile in nonstationary current
[ETN-90-95368] p 399 N90-19208
Influence of friction and separation phenomena on the dynamic blade loading of transonic turbine cascades
[MITT-88-04] p 428 N90-19235
Computational prediction and measurement of the flow in axial turbine cascades and stages
p 514 N90-21028
Analysis of the rotor tip leakage flow with tip cooling air ejection
p 515 N90-21029
Calculation of the aeroelastic blade stabilization with linearized process
[MITT-87-01] p 666 N90-24272
- Technische Hochschule, Darmstadt (Germany, F.R.).**
Semi-empirical transition criteria for the design of laminar profiles
p 276 N90-16174
The discretization of the three dimensional boundary layer equations
[ETN-90-97292] p 884 N90-27987
- Technische Hogeschool, Delft (Netherlands).**
Stability and control derivatives of the De Havilland DHC-2 BEAVER aircraft
[PB89-217525] p 119 N90-11754
Noise data of four small propeller-driven airplanes
[PB89-216980] p 139 N90-12291
Experimental and numerical investigation of the vortex flow over a sharp edged delta wing: with and without sideslip
[PB90-167131] p 481 N90-20964
Crack stoppers and ARALL laminates
[PB90-166588] p 533 N90-21142
- Technische Univ., Aachen (Germany, F.R.).**
Numerical studies of incompressible flow around delta and double-delta wings
p 150 A90-16845
- Technische Univ., Berlin (Germany, F.R.).**
Detection of flow instabilities at airfoil profiles using piezoelectric arrays
p 276 N90-16175
Test and Measurement Technique in Hypersonics
[ILR-MITT-225(1989)] p 618 N90-24225
Air traffic management in Europe: Structure, tasks, potential
p 825 N90-27677
A process for analysis, evaluation, and development of aerial servicing noise reduction measures in civil aircraft
[ETN-90-97300] p 896 N90-28398
- Technische Univ., Brunswick (Germany, F.R.).**
Flight test results of a complex precise digital flight control system
p 35 N90-10870
Wind shear models for aircraft hazard investigation
p 280 N90-15044
Influence of windshear, downdraft and turbulence on flight safety
p 238 N90-15048
Wind tunnel investigations on the configuration of the international vortex flow experiment
p 277 N90-16181
Integrated flight guidance system using differential-GPS for landing approach guidance
p 332 N90-16735
Calculation and optimization of rotor start process
[ETN-90-95894] p 416 N90-19229
Results of TCAS-2 simulations in reconstructed dangerous encounters (Jul. 1986 to Jun. 1989)
[ETN-90-96474] p 636 N90-23375
The gun tunnel of the Brunswick Institute for Fluid Mechanics: Current development status
p 673 N90-24227
Tests for integrating measurement of gas pressures in flight propellers
[ETN-90-96498] p 634 N90-24253
The disturbance processes on the data links of the mode-S air traffic control system
[ETN-90-96960] p 729 N90-25965
A contribution to the improvement of the accuracy in the parameter identification of nonlinear processes, by example of the aircraft motion
[ETN-90-96961] p 736 N90-25974
The applicability of simple helicopter models for flight mechanics studies
[ETN-90-96962] p 736 N90-25975
Safety net functions
p 826 N90-27685
Effects of canard position on the aerodynamic characteristics of a close-coupled canard configuration at low speed
p 920 N90-28519
- Technische Univ., Delft (Netherlands).**
Rolling of ARALL laminates (an alternative method for post-stretching ARALL laminates)
[LR-560] p 135 N90-12778
An investigation on combined extension and bending of thin sheets with a central crack
[LR-561] p 137 N90-12958
Induced drag for non-planar wings
[LR-521] p 172 N90-13357
Test network Delft
[ETN-90-96009] p 177 N90-13365
Some new techniques for aircraft fuselage skin tests
[LR-547] p 184 N90-13379
- Aircraft propulsion: Leading the way in aviation
[LR-532] p 194 N90-13395
Mathematical model identification for flight simulation, based on flight and taxi tests
[LR-550] p 202 N90-13410
Repair of composites by means of wet-lay-up
[LR-551] p 205 N90-13617
Multigrid and defect correction for the steady Navier-Stokes equations: Applications to aerodynamics
[ETN-90-96011] p 212 N90-13727
An evaluation of a fatigue crack growth prediction model for variable-amplitude loading (PREFFAS)
[LR-537] p 214 N90-13822
A computer program for the prediction of nozzle-propeller performance
[LR-578] p 572 N90-21740
Theory and numerical analysis of single and multi-element nozzle propellers
[LR-579] p 572 N90-21741
Recent improvements in the scope and accuracy of the performance prediction of nozzle propellers
[LR-598] p 572 N90-21742
First-order weight corrections for real-time flight path management
[LR-580] p 578 N90-21751
An approach to on-board optimization of cruise at constant altitude
[LR-581] p 578 N90-21752
Fractographic observations on fatigue crack growth in 2024-T3 sheet material under flight-simulation loading
[LR-592] p 689 N90-23760
An experimental and theoretical investigation of the flow over plane delta wings with supersonic leading edges
[LR-588] p 717 N90-25114
Investigation of the vortex flow over a sharp-edged delta wing in the transonic speed regime
[LR-594] p 717 N90-25115
The application of the finite element method to an aerodynamic problem specific to propeller design
[LR-614] p 718 N90-25116
Lecture notes on flight simulation techniques
[LR-596] p 762 N90-25153
Investigation of crack-closure prediction models for fatigue in aluminium alloy sheet under flight-simulation loading
[LR-619] p 777 N90-26369
Tests for aircraft interior materials in fire accident
[LR-622] p 914 N90-29337
WingDesign: Program for the structural design of a wing cross-section
[LR-627] p 925 N90-29390
Solid fuel combustion chamber
[LR-634] p 939 N90-29433
Fractographic analysis of fatigue crack growth under two-blocks loading on 2024-T351 sheet specimens
[LR-628] p 961 N90-29680
Effects of blocks of overloads and underloads on fatigue crack growth in 2024-T351 sheet specimens: Fractographic analysis and crack closure predictions
[LR-629] p 961 N90-29681
Fatigue, static tensile strength and stress corrosion of aircraft materials and structures. Part 1: Text
[LR-630-PT-1-REV] p 961 N90-29682
Fatigue, static tensile strength and stress corrosion of aircraft materials and structures. Part 2: Figures
[LR-630-PT-2] p 961 N90-29683
Fractographic observations on fatigue crack growth under miniTWIST flight-simulation loading (2024-T3 material)
[LR-631] p 961 N90-29684
- Technische Univ., Munich (Germany, F.R.).**
Experimental identification of helicopter engine dynamics from closed loop data
p 855 N90-27627
- Techno-Sciences, Inc., Greenbelt, MD.**
Robust control design for flight control
[AD-A211957] p 119 N90-11756
- Technology Assessment and Transfer, Inc., Annapolis, MD.**
Improved Thermo-Oxidative-Deposition screening tests for turbine lubricants
[AD-A217795] p 533 N90-21188
- Technology Planning, Inc., Rockville, MD.**
National Airspace System (NAS) software life cycle management study
[AD-A221180] p 729 N90-25122
- Tel-Aviv Univ. (Israel).**
On central-difference and upwind schemes
[NASA-CR-182061] p 781 N90-26595
- Tennessee Univ., Knoxville.**
Freeze drying for morphological control of inter-penetrating polymer networks
p 948 A90-50214
A scalar/vector potential solution for aerodynamic coefficients in wind shear
p 21 N90-10838
- Tennessee Univ., Tullahoma.**
Investigation of adaptive-wall wind tunnels with two measured interfaces
[AIAA PAPER 90-0186] p 200 A90-19728
Influence of bulk turbulence and entrance boundary layer thickness on the curved duct flow field
[AIAA PAPER 90-1502] p 606 A90-38651
Application of vortex embedding to aircraft flows
[AIAA PAPER 90-1626] p 568 A90-38755
A wall interference assessment/correction interface measurement system for the NASA/ARC 12-ft PWT
[NASA-CR-185474] p 200 N90-13401
- Tennessee Univ. Space Inst., Tullahoma.**
Vortical sources of aerodynamic force and moment
[SAE PAPER 892346] p 715 A90-45498
Comparisons of one- and two- interface methods for tunnel wall interference calculation
p 870 A90-48961
- Test Group (6585th), Holloman AFB, NM.**
The Fourteenth Biennial Guidance Test Symposium, volume 1
[AD-A216925] p 405 N90-18383
- Texas A&M Univ., College Station.**
In-flight boundary-layer transition measurements on a swept wing
p 17 A90-13017
Augmented heat transfer in rectangular channels of narrow aspect ratios with rib turbulators
p 70 A90-13091
Effects of nonplanar outboard wing forms on a wing
p 232 A90-23279
A study of ice shape prediction methodologies and comparison with experimental data
[AIAA PAPER 90-0753] p 322 A90-26986
An annular gas seal analysis using empirical entrance and exit region friction factors
[ASME PAPER 89-TRIB-46] p 537 A90-33555
Determination of aerodynamic sensitivity coefficients based on the transonic small perturbation formulation
p 622 A90-40682
Aircraft tire/pavement pressure distributions
[SAE PAPER 892351] p 734 A90-45502
Test and theory for piezoelectric actuator-active vibration control of rotating machinery
p 879 A90-46226
Vibration dampers for cryogenic turbomachinery
[AIAA PAPER 90-2740] p 882 A90-47228
Development of direct-inverse 3-D methods for applied transonic aerodynamic wing design and analysis
[NASA-CR-186036] p 103 N90-11733
Ice induced aerodynamic performance degradation of rotorcraft: An overview
p 248 N90-15063
A direct-inverse method for transonic and separated flows about airfoils
[NASA-CR-4270] p 235 N90-15072
An approximate model for the performance and acoustic predictions of counterrotating propeller configurations
[NASA-CR-180667] p 379 N90-18228
A video-based experimental investigation of wing rock
[AD-A218244] p 498 N90-20075
A video-based experimental investigation of wing rock
p 592 N90-21771
Three-dimensional numerical study of thunderstorm downdrafts and associated outflow boundaries
p 963 N90-29746
- Texas Univ., Arlington.**
Upstream-influence scaling of fin-generated shock wave boundary-layer interactions
[AIAA PAPER 90-0376] p 164 A90-19822
- Texas Univ., Austin.**
Separation shock dynamics in Mach 5 turbulent interactions induced by cylinders
p 153 A90-17981
Dynamics of the outgoing turbulent boundary layer in a Mach 5 unswept compression ramp interaction
[AIAA PAPER 90-1645] p 569 A90-38773
Least-squares finite element methods for compressible Euler equations
p 904 A90-51013
Computation of nonequilibrium chemically reacting flows in hypersonic flow field
p 480 N90-20954
Modeling growth of fatigue cracks which originate at rivet holes
p 691 N90-25060
- Textron Bell Helicopter, Fort Worth, TX.**
Nonlinear aerodynamics of two-dimensional airfoils in severe maneuver
p 301 A90-25276
Tilt rotor aircraft aeroacoustics
p 409 A90-28238
Investigation of difficult component effects on finite element model vibration prediction for the Bell AH-1G helicopter. Volume 1: Ground vibration test results
[NASA-CR-181916-VOL-1] p 134 N90-12058
Investigation of difficult component effects on finite element model vibration prediction for the Bell AG-1G helicopter. Volume 2: Correlation results
[NASA-CR-181916-VOL-2] p 213 N90-13814
An efficient airfoil design method using the Navier-Stokes equations
p 500 N90-20981
- Textron Lycoming, Stratford, CT.**
Introducing the VRT gas turbine combustor
[AIAA PAPER 90-2452] p 743 A90-42808

- Thames Polytechnic, London (England).**
Forced and natural venting of aircraft cabin fires: A numerical simulation p 326 N90-17597
- Theory and Applications Unlimited Corp., Los Gatos, CA.**
Guidance simulation and test support for differential GPS flight experiment [NASA-CR-177471] p 28 N90-10021
- Thermacore, Inc., Lancaster, PA.**
Flexible heat pipe cold plate [AD-A216053] p 434 N90-18433
- Thiokol Corp., Brigham City, UT.**
Systems tunnel linear shaped charge lightning strike [NASA-CR-183832] p 201 N90-13404
- Titan-Aluminum-Feinguss G.m.b.H., Bestwig (Germany, F.R.).**
Thin walled cast high-strength structural parts p 65 N90-10242
- TMA/Norcal, Richmond, CA.**
The optimum control and adaptive control for airplane cabin pressure p 182 A90-18627
- Tokyo Univ., Sagami-hara (Japan).**
High-resolution upwind scheme for vortical-flow simulations p 153 A90-17872
- Toledo Univ., OH.**
Application of an efficient hybrid scheme for aeroelastic analysis of advanced propellers [AIAA PAPER 90-0028] p 226 A90-22153
Convective heat transfer measurements from a NACA 0012 airfoil in flight and in the NASA Lewis Icing Research Tunnel [AIAA PAPER 90-0199] p 272 A90-22180
Time domain flutter analysis of cascades using a full-potential solver [AIAA PAPER 90-0984] p 391 A90-29374
Concurrent processing adaptation of aeroelastic analysis of propellers [AIAA PAPER 90-1036] p 450 A90-29380
An LDA investigation of the normal shock wave boundary layer interaction p 908 A90-52618
Heat transfer measurements from a NACA 0012 airfoil in flight and in the NASA Lewis icing research tunnel [NASA-CR-4278] p 399 N90-19203
Finite element analysis of structural components using viscoplastic models with application to a cowl lip problem [NASA-CR-185189] p 690 N90-23769
- Toronto Univ., Downsview (Ontario).**
Evaluation of nonlinear motion-drive algorithms for flight simulators [UTIAS-TN-272] p 761 N90-25148
- Toronto Univ. (Ontario).**
Prediction of two-dimensional time-dependent gasdynamic flows for hypersonic studies [UTIAS-335] p 718 N90-25935
- Transportation Research Board, Washington, DC.**
Public-sector aviation issues, 1987 to 1988 graduate research award papers [PB90-191206] p 820 N90-27667
Modeling and analysis of airport and aircraft operations [PB90-222167] p 915 N90-28511
- Transportation Systems Center, Cambridge, MA.**
En route noise: NASA propfan test aircraft (corrected data - simplified procedure) [DOT-TSC-FA953-LR4] p 696 N90-24856
En route noise: NASA propfan test aircraft (calculated source noise) [DOT-TSC-FA953-LR5] p 697 N90-24857
FAA Loran early implementation project [AD-A221866] p 824 N90-26805
Airport capacity enhancement plan 1989 [PB90-197997] p 913 N90-28507
- TRW Defense and Space Systems Group, Redondo Beach, CA.**
Generalized Advanced Propeller Analysis System (GAPAS). Volume 2: Computer program user manual [NASA-CR-185277] p 933 N90-29394
- TRW Defense and Space Systems Group, San Diego, CA.**
Distributed control architecture for CNI preprocessors p 917 N90-29356
- Turbomeca S.A. - Brevets Szydlowski, Bzanos (France).**
Defects in monoblock cast turbine wheels p 443 N90-18400

U

- Union Coll., Schenectady, NY.**
Accumulated span loadings of an arrow wing having vortex flow p 17 A90-13025

- United Kingdom Atomic Energy Authority, Harwell (England).**
Characterisation of fatigue of aluminium alloys by acoustic emission. Part 2: Discrimination between primary and other emissions [AERE-R-13303-PT-2] p 678 N90-23523
- United Technologies Corp., Windsor Locks, CT.**
Investigation of the near wake of a propfan p 622 A90-40686
- United Technologies Research Center, East Hartford, CT.**
Calculation of unsteady Euler flows in turbomachinery using the linearized Euler equations p 5 A90-11778
Rotor noise due to atmospheric turbulence ingestion. I - Fluid mechanics p 219 A90-19385
Rotor noise due to atmospheric turbulence ingestion. II - Aeroacoustic results p 219 A90-19386
Simulation of three-dimensional viscous flow within a multistage turbine [ASME PAPER 89-GT-152] p 292 A90-23841
Unsteady aerodynamics for turbomachinery aeroelastic applications p 394 A90-29888
Navier-Stokes analyses of the redistribution of inlet temperature distortions in a turbine p 471 A90-32959
Hydrocarbon-fueled scramjet combustor investigation [AIAA PAPER 90-2337] p 658 A90-40622
Investigation of the near wake of a propfan p 622 A90-40686
Linearized unsteady aerodynamics for turbomachinery aeroelastic applications [AIAA PAPER 90-2355] p 626 A90-42137
Unsteady analysis of hot streak migration in a turbine stage [AIAA PAPER 90-2354] p 769 A90-42782
An unsteady helicopter rotor-fuselage aerodynamic interaction analysis p 712 A90-45323
Investigation of advanced mixer-ejector exhaust system [AD-A211943] p 89 N90-11705
The effects of compressor endwall flow on airfoil incidence and deviation p 512 N90-21011
Subsonic combustor testing p 749 N90-25997
Development of a linearized unsteady aerodynamic analysis for cascade gust response predictions [NASA-CR-4308] p 816 N90-27655
- Universal Energy Systems, Inc., Dayton, OH.**
Self-lubricating surfaces by ion beam processing [AD-A222489] p 884 N90-27118
- Universal Technology Corp., Dayton, OH.**
In-service inspection of composite components on aircraft at depot and field levels p 885 N90-28078
STOVL fighter propulsion reliability, maintainability, and supportability characterization [AD-A224221] p 933 N90-28574
- Universitaet der Bundeswehr, Hamburg (Germany, F.R.).**
Knowledge based diagnosis of jet engines under consideration of model based methods p 855 N90-27631
- Universitaet der Bundeswehr Muenchen, Neubiberg (Germany, F.R.).**
A nonlinear vortex-lattice method for the calculation of interference effects between free vortex sheets and wings p 277 N90-16183
Calculation of the flow field of a multiblade helicopter rotor using a Euler method including the wake p 278 N90-16189
- Universite de Technologie de Compiègne (France).**
Study of the microstructure of a titanium alloy (6246) for turbomachine compressors [ETN-90-97450] p 876 N90-27900
- University Coll., London (England).**
Impact of NDE-NDI methods on aircraft design, manufacture, and maintenance, from the fundamental point of view p 887 N90-28093
- University Coll. of North Wales, Bangor.**
Parallel processing implementation of a flight controller p 333 N90-16743
- University Coll. of Swansea (Wales).**
Airborne MSS for land cover classification II p 737 A90-43376
Unstructured finite element mesh generation and adaptive procedures for CFD p 608 N90-21993
- University of South Florida, Tampa.**
Critical evaluation of Jet-A spray combustion using propane chemical kinetics in gas turbine combustion simulated by KIVA-II [AIAA PAPER 90-2439] p 949 A90-50645
- University of Southern California, Los Angeles.**
Dynamics and control of turbulent shear flows [AD-A210396] p 72 N90-10402
Practical methods for robust multivariable control [AD-A216937] p 462 N90-18920
- University of Southern Colorado, Pueblo.**
RSRA/X-Wing flight control system development - Lessons learned p 430 A90-28216

- University of Technology, Loughborough (England).**
Effective optimal control of a fighter aircraft engine p 928 N90-28548
- University of the Pacific, Stockton, CA.**
Flow unsteadiness effects on boundary layers [NASA-CR-186067] p 690 N90-24557
- University of Wales, Swansea.**
Euler and Navier-Stokes solutions for hypersonic flows p 155 A90-18254
- University of Western Michigan, Kalamazoo.**
Thermal management of closed computer modules utilizing high density circuitry [AIAA PAPER 90-1748] p 583 A90-38441
- UOP, Inc., Des Plaines, IL.**
Advanced fuel properties, phase I [AD-A219788] p 766 N90-25236
- Utah Univ., Salt Lake City.**
Production of high density aviation fuels via novel zeolite catalyst routes [AD-A216444] p 443 N90-18601
- Vanderbilt Univ., Nashville, TN.**
Detachment of turbulent boundary layers with varying free-stream turbulence and lower Reynolds numbers p 802 A90-46378
Raman scattering measurements using UV excimer lasers p 874 N90-26902
Concentration, temperature, and density in a hydrogen-air flame by excimer-induced Raman scattering p 875 N90-26903
- Vibration Inst., Clarendon Hills, IL.**
The Shock and Vibration Digest, volume 21, no. 2 p 609 N90-22059
The Shock and Vibration Digest, volume 21, no. 3 p 609 N90-22064
The Shock and Vibration Digest, volume 21, no. 6 p 614 N90-22363
- Vigyan Research Associates, Inc., Hampton, VA.**
Direct simulation of three-dimensional hypersonic flow about intersecting blunt wedges p 16 A90-12835
Navier-Stokes computations of a prolate spheroid at angle of attack p 17 A90-13018
Fresh look at floating shock fitting [AIAA PAPER 90-0108] p 162 A90-19686
Direct simulation of hypersonic rarefied flow about a delta wing [AIAA PAPER 90-0143] p 182 A90-19704
Design optimization of natural laminar flow fuselages in compressible flow [AIAA PAPER 90-0303] p 182 A90-19784
Transonic Navier-Stokes solutions about a complex high-speed accelerator configuration [AIAA PAPER 90-0430] p 166 A90-19844
A numerical parametric study of a scramjet inlet in a Mach 6 arc heated test facility [AIAA PAPER 90-0531] p 167 A90-19896
Prediction of vortical flows on wings using incompressible Navier-Stokes equations p 226 A90-21935
An embedded grid formulation applied to a delta wing [AIAA PAPER 90-0429] p 229 A90-22216
Navier-Stokes computations of vortical flows over low-aspect-ratio wings p 232 A90-23103
Effects of nonplanar outboard wing forms on a wing p 232 A90-23279
Study of vortex breakdown of F-106B by Euler code p 233 A90-23289
Fourth-order accurate three-dimensional compressible boundary-layer calculations p 308 A90-26136
Interactive generation of unstructured grids for three dimensional problems p 310 A90-26537
Comparison between experimental and numerical results for a research hypersonic aircraft p 395 A90-31278
On dynamic stability boundaries for binary systems p 538 A90-33698
Wind-tunnel and flight-test investigation of the exordone remotely piloted vehicle configuration [AIAA PAPER 90-1261] p 494 A90-33891
Preliminary flight test investigation of an airborne wake vortex detection concept [AIAA PAPER 90-1282] p 495 A90-33903
Navier-Stokes computation of flow around a round-edged double-delta wing p 555 A90-36251
Evaluation of transonic wall interference assessment and correction for semi-span wing data [AIAA PAPER 90-1433] p 597 A90-38487
Navier-Stokes solutions for vortical flows over a tangent-ogive cylinder p 620 A90-39780
Sidewall boundary-layer removal and wall adaptation studies p 672 A90-40680
3-D Euler calculations for aft-propfan integration [AIAA PAPER 90-2147] p 625 A90-42044

Vortex control for tail buffet alleviation on a twin-tail fighter configuration
[SAE PAPER 892221] p 756 A90-45438
Effects of turbulence models on the prediction of transonic wing flows
[SAE PAPER 892224] p 713 A90-45440
Simulation of leading-edge vortex flows p 716 A90-45785

Numerical study of vortical flow over a sideslipping delta wing
[AIAA PAPER 90-3001] p 798 A90-45936
Prediction of separated transonic wing flows with nonequilibrium algebraic turbulence model p 809 A90-47312

Residual interference assessment in adaptive wall wind tunnels
[NASA-CR-181896] p 123 N90-12625
Effects of forebody geometry on subsonic boundary-layer stability
[NASA-CR-4314] p 718 N90-25939

Virginia Polytechnic Inst. and State Univ., Blacksburg.
Free-field correction factor for spherical acoustic waves impinging on cylinders p 218 A90-17984
Experimental investigation of a new device to control the asymmetric flowfield on forebodies at large angles of attack

[AIAA PAPER 90-0069] p 161 A90-19665
A three-dimensional space marching algorithm for the solution of the Euler equations on unstructured grids
[AIAA PAPER 90-0014] p 234 A90-23701
Blade-vortex interaction experiments - Velocity and vorticity fields

[AIAA PAPER 90-0030] p 312 A90-26903
The hemisphere-cylinder at an angle of attack
[AIAA PAPER 90-0050] p 313 A90-26907
Turbulence measurements and noise generation in a transonic cryogenic wind tunnel

[AIAA PAPER 88-2026] p 522 A90-32463
Numerical model of unsteady subsonic aeroelastic behavior p 535 A90-32471
An annular gas seal analysis using empirical entrance and exit region friction factors

[ASME PAPER 89-TRIB-46] p 537 A90-33555
Implicit flux-split schemes for the Euler equations p 602 A90-36254

Large-scale structure in a supersonic slot-injected flowfield p 602 A90-36265
Direct measurements of skin friction in a scramjet combustor

[AIAA PAPER 90-2342] p 626 A90-42132
Fatigue life estimates for helicopter loading spectra p 772 A90-45324

Active control of propeller-induced noise fields inside a flexible cylinder p 833 A90-47306
Mechanisms of active control in cylindrical fuselage structures p 862 A90-47309

Design of aircraft wings subjected to gust loads - A system reliability approach p 958 A90-52044
Efficient methods for integrated structural-aerodynamic wing optimum design p 184 N90-13376

Fatigue analysis and reconstruction of helicopter load spectra p 206 N90-14304
Fatigue life estimates for helicopter loading spectra [NASA-CR-181941] p 279 N90-16294

Stall and recovery in multistage axial flow compressors p 428 N90-18429
Experimental and theoretical investigation of optimal control methods with model reduction

p 521 N90-21039
Effective methods of controlling a junction vortex system in an incompressible, three-dimensional, turbulent flow

p 571 N90-21732
Extension-torsion coupling behavior of advanced composite tilt-rotor blades p 651 N90-25057

Aerodynamic/dynamic interaction
[AD-A222263] p 815 N90-26798
System reliability optimization of aircraft wings

p 923 N90-28536
Structural analysis and optimum design of geodesically stiffened composite panels

[NASA-CR-186944] p 959 N90-28862
Virginia Univ., Charlottesville.

Thermal structures - Four decades of progress
[AIAA PAPER 90-0971] p 411 A90-29305

Experimental investigation of a supersonic swept ramp injector using laser-induced iodine fluorescence
[AIAA PAPER 90-1518] p 606 A90-38663

Injectant mole fraction measurements of transverse injection in constant area supersonic ducts
[AIAA PAPER 90-1632] p 587 A90-38761

Effects of aeroelastic tailoring on anisotropic composite material beam models of helicopter blades
[AD-A213478] p 249 N90-15095

Adaptive control of helicopter vibrations via the impulse response method
[AD-A213728] p 260 N90-15113

The microstructure and properties of aluminum-lithium alloys p 267 N90-15187
NASA-UVA light aerospace alloy and structures technology program
[NASA-CR-182607] p 601 N90-22651

Design of cryogenic tanks for launch vehicles p 609 N90-22662
Adaptive control of a system with periodic dynamics:

Application of an impulse response method to the helicopter vibration problem p 694 N90-23990
AIRNET: A real-time communications network for aircraft

[NASA-CR-186140] p 690 N90-24514
Von Karman Inst. for Fluid Dynamics, Rhode-Saint-Genese (Belgium).

Subsonic and transonic blade design by means of analysis codes p 510 N90-20985
Gas Turbine Combustion, volume 1

[VKI-LS-1990-02-VOL-1] p 748 N90-25985
Gas Turbine Combustion, volume 2
[VKI-LS-1990-02-VOL-2] p 749 N90-25995

Vrije Univ., Amsterdam (Netherlands).
Secondary flows and radial mixing predictions in axial compressors p 512 N90-21010

Vrije Univ., Brussels (Belgium).
Measurement of velocity profiles and Reynolds stresses on an oscillating airfoil p 397 N90-18427

W

Walters Software, Inc., Blacksburg, VA.

A three-dimensional space marching algorithm for the solution of the Euler equations on unstructured grids
[AIAA PAPER 90-0014] p 234 A90-23701

Washington Univ., Seattle.

A numerical study of longitudinal vortex interaction with a boundary layer
[AIAA PAPER 90-1630] p 568 A90-38759

Numerical algorithms for parallel computers
[AD-A216812] p 377 N90-18181
Conceptual design for aerospace vehicles p 651 N90-25043

Waucho Controls Corp., Chatsworth, CA.

Wide-range fuel flowmeter, phase 2
[AD-A210547] p 72 N90-10424

West Virginia Univ., Morgantown.

Computational design of low aspect ratio wing-winglet configurations for transonic wind-tunnel tests
[NASA-CR-181939] p 316 N90-17539

Western Aerospace Labs., Inc., Moffett Field, CA.
The benefits and costs of automation in advanced helicopters - An empirical study p 348 A90-26258

Westinghouse Electric Corp., Lima, OH.
High temperature VSCF (Variable Speed Constant Frequency) generator system

[AD-A210823] p 71 N90-10351

Westland Helicopters Ltd., Yeovil (England).

Experimental and numerical study of the British Experimental Rotor Programme blade
[AIAA PAPER 90-3008] p 789 A90-45858

Uses and properties of Al-Li on the new EH101 helicopter p 268 N90-15201

Wichita State Univ., KS.

In-flight boundary-layer transition measurements on a swept wing p 17 A90-13017
Electro-impulse de-icing testing analysis and design [NASA-CR-4175] p 32 N90-10031

Stall/spin/flight simulation

[DOT/FAA/CT-88/28] p 122 N90-11765
Stall/spin aerodynamic data project

[DOT/FAA/CT-88/29] p 185 N90-14222
Development of a finite element based delamination analysis for laminates subject to extension, bending, and torsion

p 679 N90-25049
Elevator tab assembly producibility study

[IAR-89-16] p 734 N90-25133

Mechanical paint removal techniques for aircraft structures
[IAR-89-23] p 773 N90-25254

A simulation code for turbocompound diesel engines
[IAR-89-26] p 774 N90-25348

Program plan: International aircraft operator data base
[IAR-90-1] p 783 N90-25697

Prediction methodologies for nonlinear aerodynamic characteristics of control surfaces

[NIAR-90-17] p 718 N90-25937

Computational crash dynamics. Project 1.2:

Computational crash dynamics analysis

[IAR-89-19] p 724 N90-25956

A NASA/university/industry consortium for research on aircraft ice protection

[IAR-89-18] p 736 N90-25969

Mechanical paint removal techniques for aircraft structures

[NIAR-90-12] p 775 N90-26166

Numerical analysis of three-dimensional particle-laden flow equations

[IAR-90-2] p 775 N90-26268

Neural networks for detecting defects in aircraft structures

[IAR-90-4] p 777 N90-26345

Robotic-aided system for inspection of aging aircraft

[NIAR-90-9] p 777 N90-26346

Evaluation of existing aircraft operator data bases

[DOT/FAA/CT-90/18] p 898 N90-28463

International aircraft operator data base master requirements and implementation plan

[DOT/FAA/CT-90/17] p 967 N90-29247

Wien Univ. (Austria).

Asymptotic analysis of transonic flow through oscillating cascades p 427 N90-18421

Woodside Summit Group, Inc., Mountain View, CA.

Advanced rotor computations with a corrected potential method p 385 A90-28197

Worcester Polytechnic Inst., MA.

Feasibility study for a microwave-powered ozone sniffer aircraft

[NASA-CR-186660] p 650 N90-23397

Feasibility study for a microwave-powered ozone sniffer aircraft, volume 2

[NASA-CR-186676] p 735 N90-25967

Wright Research Development Center,

Wright-Patterson AFB, OH.

Compressor performance tests in the compressor research facility p 427 N90-18428

Laboratory implementation of the Continuously Reconfiguring Multi-Microprocessor Flight Control System (CRMFCFS)

[AD-A217730] p 520 N90-20094

Correlation/validation of finite element code analyses for vibration assessment of avionic equipment

[AD-A220393] p 654 N90-23398

Micro separator and ball-on-cylinder lubricity evaluator tests or corrosion inhibitor/lubricity improver additives

[AD-A221339] p 766 N90-25228

Wright Research and Development Center test facilities handbook

[AD-A222582] p 762 N90-26020

Aerodynamic and propulsive control development of the STOL and maneuver technology demonstrator

p 920 N90-28514

A look at tomorrow today

Proceedings of damping '89. Volume 1: Pages AAB-1 through DCD-11

[AD-A223431] p 960 N90-29664

Wright State Univ., Dayton, OH.

Integrated circuits for avionics

[AD-A217964] p 540 N90-20312

Wyle Labs., Inc., El Segundo, CA.

Sound propagation elements in evaluation of en route noise of advanced turboprop aircraft p 697 N90-24861

Air Force procedure for predicting aircraft noise around airbases: Noise Exposure Model (NOISEMAP). User's manual

[AD-A223162] p 895 N90-27467

Wyle Labs., Inc., Hampton, VA.

Realtime multi-plot graphics system

[NASA-CR-4304] p 965 N90-29919

Y

York Univ. (England).

An assessment of robustness of flight control systems based on variable structure techniques

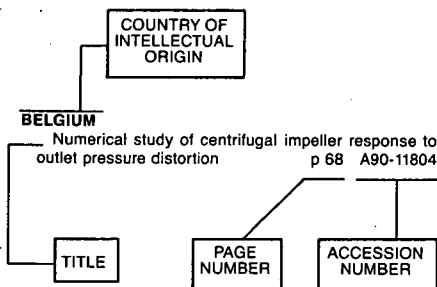
p 57 N90-10895

FOREIGN TECHNOLOGY INDEX

AERONAUTICAL ENGINEERING / A Continuing Bibliography
1990 Cumulative Index

February 1991

Typical Foreign Technology Index Listing



Listings in this index are arranged alphabetically by country of intellectual origin. The title of the document is used to provide a brief description of the subject matter. The page number and the accession number are included in each entry to assist the user in locating the citation in the abstract section. If applicable, a report number is also included as an aid in identifying the document.

A

ARGENTINA

- An asymptotic theory for the periodic turbulent boundary layer in zero mean-pressure gradient [AD-A222832] p 66 A90-10222
- Considerations on the legal regulation of air transport in the near future p 897 A90-46649

AUSTRALIA

- Extending the overhaul interval for gas turbine engines through the use of alternative coatings on first stage blades p 63 A90-12539
- Hypersonic combustion of hydrogen in a shock tunnel p 46 A90-12560
- Aircraft engine vibration analysis p 46 A90-12568
- Engine diagnostics - An application for expert system concepts p 50 A90-12632
- Adverse pressure gradient effects on boundary layer transition in a turbulent free stream p 15 A90-12639
- Identification of an adequate model for collective response dynamics of a Sea King helicopter in hover p 56 A90-12766
- Approximations for nonequilibrium hypervelocity aerodynamics p 154 A90-17990
- Fatigue of thick-section cold-expanded holes with and without cracks p 270 A90-20987
- Robust controller design using normalized coprime factor plant descriptions p 457 A90-27645
- Our future air navigation system embodies a global concept p 402 A90-27922
- Microburst precursors observed with Doppler radar p 456 A90-28613
- Fog formation at Perth Airport p 611 A90-37748
- Concept demonstration of the use of interactive fault diagnosis and isolation for TF30 engines p 617 A90-41177
- The effect on fatigue crack growth under spectrum loading of an imposed placard 'G' limit p 643 A90-41339

- Measurements of pressures on the wing of an aircraft model during steady rotation [AIAA PAPER 90-2842] p 754 A90-45162
- Hypervelocity flow of dissociating nitrogen downstream of a blunt nose p 811 A90-48712
- The receptivity of laminar boundary layer flow to leading edge vibrations p 815 A90-49800
- Fractographic techniques for the assessment of aircraft component cracking p 954 A90-49885
- Analysis and interpretation of aircraft component defects using quantitative fractography p 956 A90-50555
- Moisture absorption in graphite/epoxy laminates p 951 A90-52799
- A review of Australian and New Zealand investigations on aeronautical fatigue during the period April 1987 to March 1989 [AD-A210373] p 32 N90-10026
- Report on an overseas visit, June 1988 [AD-A210374] p 52 N90-10040
- An appraisal of a number of power assessment procedures being proposed for use in Chinook-Lycoming T55 engine [AD-A210482] p 52 N90-10041
- The spinning of aircraft: A discussion of spin prediction techniques including a chronological bibliography [ARL-AERO-R-177] p 36 N90-10888
- An open-loop transient thermodynamic model of the Cougar turbojet [AD-A211774] p 114 N90-11745
- Additions and corrections to SUPER: A program for calculating steady and oscillatory supersonic flow over a thin wing, tail plane and fin [AD-A211771] p 90 N90-12501
- Development of a VSAERO (Vortex Separation Aerodynamics) model of the F/A-18 [AD-A212442] p 95 N90-12566
- FFG2: A flight profile generator program [AD-A212408] p 107 N90-12595
- RAN (Royal Australian Navy) vibration analysis system operator's guide [AD-A212441] p 107 N90-12596
- Evaluation of a damaged F/A-18 horizontal stabilizer [AD-A212573] p 107 N90-12597
- AcSim: Aircraft simulation program with application to flight profile generation [AD-A212466] p 185 N90-14217
- RAAF Orion aircraft A9-300 oxygen fire [AD-A215496] p 323 N90-16725
- An examination of the fatigue meter records from the RAAF Orion P-3C fleet [AD-A214000] p 338 N90-17628
- Effect of temperature on the storage life of polysulfide aircraft sealants [MRL-TR-89-31] p 444 N90-19364
- A data acquisition parallel bus for wind tunnels at ARL (Aeronautical Research Laboratory) [AD-A218052] p 526 N90-20098
- A corrosion fatigue/stress corrosion testing facility at Materials Research Laboratory [MRL-TN-568] p 527 N90-21044
- Flutter investigations on a Transavia PL12/T-400 aircraft [AD-A219108] p 593 N90-22570
- Application of optimal tracking methods to aircraft terrain following [AD-A221099] p 641 N90-24264
- Statistical treatment of slow strain rate data for assessment of hydrogen embrittlement in low alloy high strength steel [ARL-MAT-R-122] p 787 N90-26106
- ARLSUPER version 1.0, program users guide [AD-A222693] p 815 N90-26793
- Comparative evaluation of Allison T56 engine chip detectors [AD-A221864] p 855 N90-26832
- Australian experience in flight recorder readout and analysis p 820 N90-27644
- The reduction of smoke emissions from Allison T56 engines [ARL-PROP-R-182] p 928 N90-28547
- A flight dynamic model of aircraft spinning [AR-005-600] p 935 N90-28576

AUSTRIA

- Marginal separation of laminar axisymmetric boundary layers p 1 A90-10074
- Asymptotic analysis of transonic flow through oscillating cascades p 427 N90-18421

B

BELGIUM

- Numerical study of centrifugal impeller response to an outlet pressure distortion p 68 A90-11804
- Postbuckling finite element analysis of composite panels p 365 A90-24377
- Three dimensional turbine blade analysis in thermo-viscoplasticity p 540 A90-34324
- Measurement of velocity profiles and Reynolds stresses on an oscillating airfoil p 397 N90-18427
- Subsonic and transonic blade design by means of analysis codes p 510 N90-20985
- Gas Turbine Combustion, volume 1 [VKI-LS-1990-02-VOL-1] p 748 N90-25985
- Gas Turbine Combustion, volume 2 [VKI-LS-1990-02-VOL-2] p 749 N90-25995
- PHARE: Concept and programme p 827 N90-27690

BRAZIL

- Whirl-flutter investigation on an advanced turboprop configuration p 40 A90-11008
- Analysis of aircraft performance during lateral maneuvering for microburst avoidance [AIAA PAPER 90-0568] p 197 A90-19920
- Whirl flutter stability of a pusher configuration subject to a nonuniform flow [AIAA PAPER 90-1162] p 393 A90-29397
- Financing of civil aircraft - Purchases and leasing p 898 A90-49616

BULGARIA

- Decentralized systems p 888 A90-46001

C

CANADA

- Wave cancellation properties of a splitter-plate porous wall configuration p 57 A90-11005
- High performance single-mode coupler for harsh environments p 78 A90-11027
- The design of rotor blades taking into account the combined effects of vibratory and thermal loads p 40 A90-11553
- An experimental investigation of the effect of incidence on the two-dimensional performance of an axial turbine cascade p 11 A90-12520
- The performance of a small combustor operated over a wide range of conditions p 45 A90-12548
- On the weak extinction of gas turbine combustors p 47 A90-12574
- Calculation of unsteady boundary layer development on axial-flow turbomachinery blading p 48 A90-12588
- Aerodynamic and propulsive performance of hypersonic detonation wave ramjets p 49 A90-12609
- A precise flight reference system for evaluating airborne navigation aids p 27 A90-12752
- The application of linear maximum likelihood estimation of aerodynamic derivatives for the Bell-205 and Bell-206 p 30 A90-12773
- Investigation of flow separation on a supercritical airfoil p 17 A90-13023
- Numerical solution of transonic flows on a streamfunction co-ordinate system p 17 A90-13238
- A test of airborne kinematic GPS positioning for aerial photography - Methodology p 97 A90-13982
- A test of kinematic GPS combined with aerial photography - Organization, logistics and results p 97 A90-13983
- Designing the next generation flying test bed [SAE PAPER 891049] p 100 A90-14353
- Effect of moving surfaces on the airfoil boundary-layer control p 159 A90-19388
- Aerodynamic loads computation on coaxial hingeless helicopter rotors [AIAA PAPER 90-0070] p 161 A90-19666

- Complex variable boundary element method for external potential flows
[AIAA PAPER 90-0127] p 162 A90-19694
- Large-amplitude high-rate roll experiments on a delta and double delta wing
[AIAA PAPER 90-0224] p 163 A90-19742
- Fuel molecular structure and flame temperature effects on soot formation in gas turbine combustors
[ASME PAPER 89-GT-286] p 253 A90-22652
- Flow in a centrifugal fan of the squirrel cage type
[ASME PAPER 89-GT-52] p 289 A90-23778
- Development of the tip-leakage flow downstream of a planar cascade of turbine blades - Vorticity field
[ASME PAPER 89-GT-55] p 289 A90-23781
- Characteristics of partial length circular pin fins as heat transfer augmentors for airfoil internal cooling passages
[ASME PAPER 89-GT-87] p 359 A90-23806
- Braze repair of MA754 aero gas turbine engine nozzles
[ASME PAPER 89-GT-235] p 342 A90-23886
- An ultrasonic fatigue facility for HCF/LCF interactive tests
p 363 A90-23900
- Simulator motion-drive algorithms - A designer's perspective
p 375 A90-25997
- Temperature insensitive fiber coil sensor for altimeters
p 339 A90-26374
- A waveform alignment approach to positioning airborne radar-sounding data
p 332 A90-26651
- Institutional stepping stones for FANS
p 403 A90-27923
- Smart structures with nerves of glass
p 444 A90-27951
- Small gas turbine using a second-generation pulse combustor
p 421 A90-27972
- Control sensitivity, bandwidth and disturbance rejection concerns for advanced rotorcraft
p 430 A90-28204
- Coatings for high temperature corrosion in aero and industrial gas turbines
p 443 A90-30479
- Fracture mechanics assessment of EB-welded blisk rotors
p 453 A90-31117
- An integral method for transonic flows
p 395 A90-31119
- Development of erosion resistant coatings for compression airfoils
p 443 A90-31120
- Augmenting flight simulator motion response to turbulence
p 440 A90-31279
- Simple marching-vortex model for two-dimensional unsteady aerodynamics
p 395 A90-31288
- Underlying factors in air traffic control incidents
p 401 A90-31335
- Oscillatory shock motion caused by transonic shock boundary-layer interaction
p 470 A90-32478
- Fiber optics smart structures program at UTIAS
p 535 A90-32864
- Development of a fibre optic damage detection system for an aircraft leading edge
p 504 A90-32873
- Sliding and abrasive wear behaviour of an aluminum (2014)-SiC particle reinforced composite
p 530 A90-33344
- Cyclic stress-strain behavior and low cycle fatigue of Ti 6242
p 530 A90-33523
- An improved incidence losses prediction method for turbine airfoils
[ASME PAPER 89-GT-284] p 475 A90-33563
- Omega-GPS interoperability for the long haul
p 577 A90-36927
- A technique for rapid impact damage detection with implication for composite aircraft structures
p 600 A90-37662
- An experimental investigation of pressure fluctuation mechanism for different transonic porous wall configurations
[AIAA PAPER 90-1417] p 604 A90-37954
- Broadband noise measurement in the transonic test section of the VTI T-38 wind tunnel
[AIAA PAPER 90-1418] p 614 A90-37955
- Large-amplitude high-rate roll oscillation system for the measurement of non-linear airloads
[AIAA PAPER 90-1426] p 590 A90-37963
- Wind tunnel studies of F/A-18 tail buffet
[AIAA PAPER 90-1432] p 559 A90-37969
- Interactive airfoil calculations with higher-order viscous-flow equations
[AIAA PAPER 90-1533] p 564 A90-38678
- Flight testing and application of a Peripheral Vision Display
p 652 A90-40381
- Planet gear sleeve spinning analysis
[AIAA PAPER 90-2154] p 681 A90-40613
- Finite-element analysis of large spur and helical gear systems
p 683 A90-40940
- Jet Engine Technical Advisor (JETA)
p 693 A90-41184
- Fracture control via DRM-Algorithm
p 694 A90-41343
- Computation of flow through a centrifugal impeller with tip leakage
[AIAA PAPER 90-2021] p 684 A90-41987
- 5DOF dynamic loads on a jet vane
[AIAA PAPER 90-2382] p 675 A90-42147
- On and off-design performance prediction of single spool turbojets using gasdynamics
[AIAA PAPER 90-2393] p 662 A90-42155
- On- and off-design performance analysis of hypersonic detonation wave ramjets
[AIAA PAPER 90-2473] p 664 A90-42188
- Flow separation on a supercritical airfoil
p 627 A90-42394
- Application of 3-D flow analysis to the design of a high work transonic turbine
p 628 A90-42395
- Higher-order boundary-layer approximations in interactive airfoil calculations
p 628 A90-42402
- Wind tunnel results and numerical computations for the NAE deHavilland series of natural laminar flow airfoils
p 628 A90-42403
- Wind tunnel wall interference investigations in NAE/NRC High Reynolds Number 2D Facility and NASA Langley 0.3m Transonic Cryogenic Tunnel
p 628 A90-42404
- Application of the moving surface boundary layer control to a two dimensional airfoil
p 628 A90-42405
- Nonlinear unsteady airfoil response studies
p 628 A90-42406
- Preliminary design and analysis of propellers
p 645 A90-42407
- Modelling of boundary layer and trailing edge thickness effects for the Euler equations using surface transpiration
p 629 A90-42412
- Finite volume solutions of two-dimensional Euler equations on adapted structured meshes
p 629 A90-42413
- The flow over a wing/nacelle combination in the presence of a propeller slipstream
p 629 A90-42415
- Application of the KTRAN transonic small disturbance code to the complete CF-18 aircraft with stores
p 629 A90-42416
- An experimental and analytical investigation of the buffet excitation parameter
p 645 A90-42417
- Aerodynamics of store separation
p 629 A90-42418
- Measurements of aerodynamic forces on aircraft external stores in the NAE trisonic blowdown wind-tunnel
p 629 A90-42419
- Development of the stall warning/stick pusher system for the Boeing/de Havilland Dash 8 Series 300
p 645 A90-42420
- Finite element simulation of unsteady two-dimensional incompressible viscous flows
p 629 A90-42423
- New transonic test sections for the NAE 5ftx5ft trisonic wind tunnel
p 630 A90-42431
- The University of Toronto-Ryerson Polytechnical Institute hypersonic gun tunnel
p 673 A90-42432
- Helicopter store separation - Predictive techniques and flight testing
p 647 A90-42495
- A new Lagrangian method for steady supersonic flow computation. I - Godunov scheme
p 631 A90-42506
- Flow over a leading edge with distributed roughness
p 703 A90-42646
- Annual General Meeting of the Canadian Aeronautics and Space Institute, 36th, Ottawa, Canada, May 15, 16, 1989, Proceedings
p 701 A90-42652
- The Canadian Airspace Systems Plan - Maintaining the safety and efficiency of the air navigation system
p 725 A90-42655
- Developing the Canadair Regional Jet airliner
p 729 A90-42656
- An experimental investigation of the velocity field in a reverse-flow combustor
p 739 A90-42657
- Finite element simulation of turbulent propeller flowfields
p 703 A90-42658
- A colocated finite volume method for solving the Navier-Stokes equations for incompressible and compressible flows in turbomachinery - Results and applications
p 703 A90-42659
- Life estimation of a gas turbine afterburner spraybar
p 739 A90-42662
- The Dash 8 Series 400 regional airliner
p 729 A90-42664
- Next-generation automatic test equipment for military support
p 767 A90-42667
- Film cooling of turbine blades - Two dimensional experiments and numerical simulations
p 739 A90-42670
- Development of a robust calculation method for transonic viscous blade-to-blade flows
p 703 A90-42671
- Some considerations in ultra light aircraft design
p 730 A90-42673
- Probabilistic approach to fleet management
p 701 A90-42674
- Maritime environment airframe material fatigue testing
p 764 A90-42675
- Optimization studies for the PW305 turbofan
[AIAA PAPER 90-2520] p 744 A90-42813
- Embedded GPS - The Canadian Marconi approach
p 725 A90-43700
- RAIM - An implementation study
p 726 A90-43714
- Prompt identification of a troubled engine can help avoid catastrophe
p 721 A90-44222
- A weighted residual formulation for finite element solutions of the steady Euler equations
p 770 A90-44457
- More cruising levels expected at higher altitudes
p 721 A90-44548
- Improved guidance and control of vehicles and personnel on the ground will benefit airport traffic capacity
p 760 A90-44549
- Efforts continue to increase airport/airspace capacity
p 722 A90-44550
- Approach to side force alleviation through modification of the pointed forebody geometry
[AIAA PAPER 90-2834] p 712 A90-45165
- Handling qualities research at the Flight Research Laboratory, NAE/NRC, 1980 - 1990 and beyond
[AIAA PAPER 90-2848] p 755 A90-45176
- Multivariable optimization scheme for tuning the controller of an electronic fuel control unit for small gas turbine engines
p 745 A90-45301
- Designing and tuning the digital controller of an electronic fuel control unit for small gas turbine engines
[SAE PAPER 892255] p 747 A90-45457
- Reduction of the side force on pointed forebodies through add-on tip devices
[AIAA PAPER 90-3005] p 788 A90-45854
- On the drag reduction of bluff bodies through momentum injection
[AIAA PAPER 90-3076] p 797 A90-45922
- An experimental study of low-speed single-surface airfoils withaired leading edges
p 801 A90-46371
- Iterative preliminary design tools for composite structures
p 882 A90-48045
- Modelling of turbulence and downbursts for flight simulators
p 870 A90-48956
- The Radarsat system
p 873 A90-49671
- The survivability of centrifugal compressors in modern aircraft engines
p 928 A90-49883
- A rate theory investigation of cyclic loading and plastic deformation in the high stress and ambient temperature range
p 954 A90-49884
- Repair of thermoplastic composite structures by fusion bonding
p 941 A90-50060
- A design method for turbomachinery blading in three-dimensional flow
p 904 A90-51003
- A parametric study of radial turbomachinery blade design in three-dimensional subsonic flow
[ASME PAPER 89-GT-84] p 905 A90-51257
- CF 18 480 Gallon External Fuel Tank Stores Clearance Program
p 35 N90-10877
- Chordwise loading and camber for two-dimensional thin sections
[AD-A213318] p 95 N90-12568
- Analysis of experimental data for CAST 10-2/DOA 2 supercritical airfoil at low Reynolds numbers and application to high Reynolds number flow
[AD-A211654] p 170 N90-13326
- Adverse weather operations during the Canadian Atlantic storms program
p 281 N90-15052
- The application of queueing theory to the modelling of CP-140 aircraft communications
[AD-A213479] p 274 N90-15310
- The development of an airborne synthetic aperture radar motion compensation system
p 333 N90-16745
- Aircraft fire safety: Learning from past accidents
p 324 N90-17584
- New aircraft cabin and cargo flammability standards for transport category aircraft
p 325 N90-17589
- Time development of convection flow patterns in aircraft cabins under post-crash fire exposure
p 327 N90-17598
- Aircraft fire safety in the Canadian Forces
p 327 N90-17604
- Heat release rate measurement for evaluating the flammability of aircraft materials
p 328 N90-17610
- Investigation of CAST-10-2/DOA 2 airfoil in NAE high Reynolds number two-dimensional test facility
p 321 N90-17654
- Residual interference and wind tunnel wall adaption
p 353 N90-17655
- Measurement and computer simulation of antennas on ships and aircraft for results of operational reliability
p 370 N90-17936
- Review of modelling methods to take account of material structure and defects
p 425 N90-18402
- Losses in the tip-leakage flow of a planar cascade of turbine blades
p 514 N90-21027
- The effect of secondary flow on the redistribution of the total temperature field downstream of a stationary turbine cascade
p 515 N90-21033

- New transonic test sections for the NAE 5 ft x 5 ft trisonic wind tunnel
[AD-A220933] p 674 A90-24278
- An accurate numerical technique for determining flight test rate gyroscopes biases prior to takeoff
[AD-A220987] p 739 A90-25138
- Evaluation of nonlinear motion-drive algorithms for flight simulators
[UTIAS-TN-272] p 761 A90-25148
- Processing of advanced ceramics which have potential for use in gas turbine aero engines
[AD-A220988] p 766 A90-25226
- Prediction of two-dimensional time-dependent gasdynamic flows for hypersonic studies
[UTIAS-335] p 718 A90-25935
- Noise from tip vortex and bubble cavitation
[AD-A221962] p 896 A90-27468
- The Canadian Aviation Safety Board's flight recorder facility
p 849 A90-27643
- A review of crashworthiness of composite aircraft structures
[AD-A221555] p 846 A90-27697
- A review of research and development in crashworthiness of general aviation aircraft: Seats, restraints and floor structures
[AD-A221557] p 846 A90-27698
- Life management planning
p 856 A90-27709
- Comparison of ground-level test cells and ground-level to altitude test cells
p 857 A90-27716
- A technique for rapid inspection of composite aircraft structure for impact damage
p 846 A90-28077
- Development of an automated ultrasonic inspection system for composite structure on in-service aircraft
p 885 A90-28079
- Acoustic emission detection of crack presence and crack advance during flight
p 886 A90-28082
- A sensor stabilization/tracking system for unmanned air vehicles
[AD-A224008] p 936 A90-28579
- Radiation-curable prepreg composites
[DE90-629740] p 951 A90-28674
- The effects of a compressor rebuild on gas turbine engine performance: Final results
p 952 A90-28701
- Evaluation of high temperature protective coatings for gas turbine engines under simulated service conditions
p 952 A90-28712
- Surface property improvement in titanium alloy gas turbine components through ion implantation
p 953 A90-28713
- CHINA, PEOPLE'S REPUBLIC OF**
- The numerical method for solving the high Reynolds hypersonic viscous shock layer
p 2 A90-10340
- The water tunnel test of delaying vortex breakdown over a delta wing using supplements
p 2 A90-10346
- Experimental investigation on the interference effect of FL-23 wind tunnel wall on transonic flutter
p 57 A90-10347
- The study of the theoretical calculation method for power stall dynamic characteristics of multiple-engine propeller airplane
p 29 A90-10349
- An improved version of LTRAN2
p 2 A90-10350
- Color schlieren system using square color filter and its application to aerofoil test in transonics
p 66 A90-10748
- Method for calculating the unsteady flow of an elliptical circulation-control airfoil
p 3 A90-11003
- Analysis of the effect of rotor-angular-acceleration on the features of gas flow in turbomachinery
p 6 A90-11780
- A numerical method solving 2-D unsteady flow field around cascade of oscillating airfoils with arbitrary camber and thickness
p 7 A90-11788
- Numerical Euler solution for the interaction between oscillating cascade and forced inlet unsteadiness
p 8 A90-11792
- The flutter characteristic analysis and optimization design of mistuning blade
p 42 A90-11799
- The effects of three centres of blade on flutter
p 42 A90-11800
- The acoustic phenomena of the stalling flutter
p 78 A90-11801
- Computation of unsteady compressible turbulent boundary layers in cascade flow with controlled inlet perturbation
p 8 A90-11807
- Research on transmission quality of telemetry system in flight test
p 26 A90-12189
- Influence of blade leaning on the flow field behind turbine rectangular cascades with different incidences and aspect ratios
p 11 A90-12519
- An investigation of artificial compressor surge
p 11 A90-12526
- Investigation and improvement of ground starting characteristics of a combustor with airblast nozzles
p 45 A90-12546

- Simulation research on the afterburning dynamic characteristics of engine control system
p 48 A90-12581
- A quasi-3D design method of transonic compressor blade with the function of improving velocity distribution
p 49 A90-12589
- PCISM method for two dimensional compressible viscous cascade flow calculation
p 15 A90-12625
- Preliminary analysis of methodology for assessment of propulsion system for aerospace plane
[IAF PAPER 89-307] p 123 A90-13442
- Exhaust emission performance of a vaporizer tube combustor as compared with a single tube combustor
p 111 A90-14614
- Aeroelastic characteristics of wings in subsonic flow
p 102 A90-14615
- Wing boundary layer calculation and its application to aircraft design
p 84 A90-15151
- Study on SPF and SPF/DB of the bulk-head structure with nonsymmetric shape
p 132 A90-16619
- An experiment study of rotor aerodynamic in ground effect at low speed
p 149 A90-16826
- A synthetic research for aircraft active flutter suppression
p 195 A90-16827
- Calculation of two-dimensional transonic flow of Euler equations with multigrid method
p 149 A90-16835
- Investigation of a nonlinear Kalman filter for estimating aircraft state variables
p 195 A90-16850
- Aeroengine condition monitoring and fault diagnosis system
p 188 A90-16851
- A numerical method for computing the aerodynamic loads on wings with sharp-edge separations at large angles of attack in subcritical transonic flows
p 150 A90-16852
- Investigation on the determination of airplane tail loads by flight tests
p 178 A90-16853
- The analysis of entry into and recovery from a spin for the JJJ aircraft
p 195 A90-16854
- Analysis methods of tie-down loads and airframe stress for shipboard-helicopters
p 199 A90-16855
- The anti-shimmy and break-proof study of nose landing gear
p 178 A90-16856
- A separated algorithm and applications to flight test
p 216 A90-16857
- The design and study of the information transfer mechanism for a distributed avionics system
p 207 A90-16858
- The computer aided weight engineering of aircraft - (CAWE) system
p 179 A90-16860
- Vibration analysis of aircraft panels
p 207 A90-17026
- A method for aerodynamic design calculation of axial gas turbine stages with cooling air mixing
p 152 A90-17781
- An aerodynamical design and calculation method for gas turbine with cooling air mixing
p 189 A90-17782
- An approach for calculating steady subsonic and transonic blade to blade flows
p 152 A90-17784
- Computation of transonic flow in a plane cascade with an unfactored flux splitting implicit method
p 152 A90-17785
- A relaxation method for transonic potential flows through 2-D cascade with large camber angle
p 152 A90-17786
- Experimental investigation on the performance of an annular nozzle cascade of a highly-loaded transonic turbine stage
p 152 A90-17787
- An experimental study of tip clearance effects on the performance of an axial transonic turbine
p 189 A90-17788
- Effect of vane and blade numbers on performance of transonic turbine stage
p 189 A90-17789
- Design and calculation of composite air-cooled blades in a highly-loaded transonic turbine
p 189 A90-17790
- Calculation of coolant flow and heat transfer inside composite air-cooled turbine
p 189 A90-17791
- Experimental investigation on composite air-cooled blades of highly-loaded transonic turbine
p 189 A90-17793
- Experimental investigation on composite cooling of a turbine blade
p 190 A90-17794
- Research on film-cooling of turbine blade
p 190 A90-17795
- Mechanism of sidewall effect studied with oil flow visualization
p 154 A90-18002
- Boundary integral equations method for compressible Navier-Stokes equations
p 209 A90-18262
- A finite element solution for transonic flow around lifting fuselage with arbitrary cross sections from the minimum pressure integral
p 156 A90-18298
- Analyses of full 3D S1-S2 iterative solution in CAS transonic compressor rotor and comparison with quasi-3D S1-S2m iterative solution and L2F measurement
p 157 A90-18532

- Throughflow numerical calculations including influence of spanwise mixing in a multistage axial flow compressor
p 157 A90-18534
- Study of calculating an approximately constant reaction turbine stage with a tension spline streamline curvature method
p 157 A90-18537
- Numerical method for solving the Euler equation for unsteady transonic flows over oscillating airfoils
p 157 A90-18578
- Aeroelastic tailoring applied to composite wing
p 211 A90-18580
- The research of cubic spline optimal terrain following system
p 196 A90-18584
- An investigation of unsteady leading edge separation of rapidly pitched airfoils
p 157 A90-18587
- A study of ground vortex
p 158 A90-18590
- Analysis of blade loadings in centrifugal compressors
p 158 A90-18591
- Design of direct lift control systems against vertical gust
p 196 A90-18592
- Gas turbine engine condition monitoring and fault diagnostics
p 190 A90-18594
- Modal aggregation and its application in flight mechanics
p 196 A90-18595
- Prediction of transmission loss through an aircraft sidewall using statistical energy analysis
p 219 A90-18599
- Digital control experiment research on the engine JT15D-4
p 190 A90-18600
- The eigenvalue sensitivity analysis and design for integrated flight/propulsion control systems
p 196 A90-18601
- Application investigation on superplastic forming/diffusion bonding combined technology of titanium alloy TC4
p 204 A90-18603
- Wall interference correction of high-lift multi-component airfoils
p 158 A90-18604
- The investigation of stress at an enter-gas nozzle of main landing gears for fighter aeroplanes
p 181 A90-18606
- Numerical approaches for solving parametric vibration problems in helicopter dynamics
p 182 A90-18607
- A new implicit hybrid schemes for the Euler equation of transonic flow
p 158 A90-18608
- Computations of unsteady transonic flows about thin airfoils by integral equation method
p 158 A90-18609
- The establishment of mathematical model of engine control system and simulation research of afterburning dynamic characteristics
p 190 A90-18613
- The aerodynamic behaviours of vortices for slender-wing
p 158 A90-18623
- The analysis and solution of the performance deterioration problem of WP7 engine under the full reheating condition
p 191 A90-18624
- The optimum control and adaptive control for airplane cabin pressure
p 182 A90-18627
- The application and design of large integral panels for SH-5 aircraft
p 211 A90-18632
- The induced velocity distribution and the flap-pitch-torsion coupling on the stability and control of the helicopter in flight condition with lateral velocity
p 196 A90-18633
- Basic principles of measuring thrust through exhaust to inlet total pressure ratio - Engine Pressure Ratio (EPR)
p 191 A90-18635
- Full 3D iterative solution of transonic flow for a swept wing test channel
p 160 A90-19431
- Variational principle with variable domain discontinuous finite element method for transonic flow and determining automatically the position and shape of the shock waves
p 160 A90-19434
- Effect of ground on wake roll-up behind a lifting surface
p 160 A90-19436
- The computational method for the transonic wing design
p 160 A90-19438
- The experiments for gas turbine plane cascade in a shock tunnel
p 160 A90-19441
- Computation and analysis of the shapes of S1 and S2 streamsurfaces in a transonic compressor rotor
p 160 A90-19446
- Experimental investigation of trailing-edge and near wake flow of a symmetric airfoil
p 160 A90-19449
- An efficient upwind relaxation-sweeping algorithm for three-dimensional Euler equations
[AIAA PAPER 90-0129] p 162 A90-19695
- Numerical calculation of gaseous reacting flows in a model of gas turbine combustors
p 271 A90-19799
- The distribution of normal-wash for minimum induced drag of non-planar wings
p 226 A90-19793
- A finite element method for solving lifting airfoil in transonic flow
p 226 A90-19894
- A variable structure system (VSS) to robust control of aircraft
p 257 A90-19897
- New progress in airframe durability requirements
p 246 A90-22001

- A study on initial fatigue quality of typical aircraft structures (fastener holes) p 272 A90-22004
- The application of the engineering approach for analyzing crack tolerance of fuselage panels to a transport airplane p 272 A90-22014
- Infrared sources of jet propulsion system and their suppression p 252 A90-22614
- A method for calculating axial turbomachine end wall turbulent boundary layers [ASME PAPER 89-GT-15] p 287 A90-23759
- Improvement of 3D full-potential method and computation of flowfield of CAS compressor rotor [ASME PAPER 89-GT-17] p 288 A90-23760
- 3D Mean-Stream-Line Method - A new engineering approach to the inverse problem of 3D cascade [ASME PAPER 89-GT-48] p 289 A90-23774
- An approximate 3-D aerodynamic design method for centrifugal impeller blades [ASME PAPER 89-GT-73] p 291 A90-23794
- A new design method for centrifugal compressor vaned diffusers [ASME PAPER 89-GT-156] p 292 A90-23844
- A method of predicting the energy losses in vaneless diffusers of centrifugal compressors [ASME PAPER 89-GT-158] p 292 A90-23846
- The prediction of boundary layers with rotation and variation of stream filament thickness [ASME PAPER 89-GT-227] p 362 A90-23882
- A simplified model for unstable temperature field calculation of gas turbine rotor [ASME PAPER 89-GT-234] p 363 A90-23885
- Concise design of aircraft longitudinal model reference adaptive command augmentation system p 345 A90-24002
- Performance study of an integrated NAVSTAR GPS/SINS navigation system p 329 A90-24003
- Stability analysis and numerical experiments for viscous-inviscid interaction in transonic flow p 293 A90-24009
- The influence of the helicopter fuselage on its rotor p 301 A90-25101
- A unified approach to the overall body motion stability and flutter characteristics of elastic aircraft p 346 A90-25102
- A semi-actuator disk theory for prediction of stall flutter in axial flow compressors p 301 A90-25105
- Aeroelastic tailoring of a wing with composite skin p 366 A90-25108
- On efficiency and accuracy of numerical methods for solving aerodynamic equations p 304 A90-25730
- The transonic nonisentropic potential calculation p 304 A90-25739
- Unified optimal criterion method - Combination of direction of gradient and ejection line p 367 A90-26077
- A study on spray characteristics down stream from a gutter-atomizer p 368 A90-26893
- Observation and analysis of sidewall effect in a transonic airfoil test section p 436 A90-28257
- Prediction of heat transfer coefficient on turbine blade profiles p 423 A90-29904
- The effect of swirl on short reversal-flow annular combustor p 423 A90-29906
- Study on travelling wave vibration of bladed disks in turbomachinery p 423 A90-29908
- Gear vibration control with viscoelastic damping material in aeroengine p 451 A90-29911
- A design of a twin variable control system for aero-turbojet engine p 423 A90-29917
- A numerical solution for instruction tracing problem p 424 A90-29918
- Digital electronic control for WJ6G4A engine p 424 A90-29919
- Algorithm for simultaneous stabilization of single-input systems via dynamic feedback p 462 A90-31108
- Calculations of transonic flows over wing-body combinations p 395 A90-31479
- Studies of predicting departure characteristics of aircraft p 433 A90-31480
- The numerical simulation of the low speed aerodynamic characteristics of a set of close-coupled canard configurations p 396 A90-31485
- Galerkin finite element method for transonic flow about airfoils and wings p 396 A90-31486
- Vortex method modelling the unsteady motion of a thick airfoil p 396 A90-31489
- An experimental study on flowfields in a dual inlet swirl-dump combustor p 471 A90-33283
- An experimental investigation on control of flow dynamic distortions downstream under strong shock-boundary layer interaction in the two-dimensional flow field p 471 A90-33288
- Unsteady aerodynamic forces of oscillating supersonic/hypersonic wings with attached shock waves p 473 A90-33363
- A modal parameter identification technique and its application to large complex structures with multiple steady sinusoidal excitation p 602 A90-35670
- Simulation research on the afterburning dynamic characteristics of engine control system p 585 A90-35708
- Passive location and tracking using DOA and TOA measurements of single nonmaneuvering observer p 576 A90-35709
- Boundary element method for solving direct aerodynamic problem of aerofoil cascades on an arbitrary stream surface of revolution p 554 A90-35830
- Analyses of revising the inlet profile of a radial inflow turbine impeller p 602 A90-35831
- The TSP methods applied to the calculation of transonic flow about wing/body/nacelle/pylon-configurations p 554 A90-35868
- Recent advancement in helicopter rotor wake study p 556 A90-36413
- Mach number effects on upstream influence in swept shock wave/turbulent boundary layer interactions p 556 A90-36415
- A quadratic programming method for solving three dimensional elastic-plastic contact problems p 603 A90-36417
- Dynamic analysis of airport pavement p 593 A90-36418
- Solution of Euler equations for fighter forebody-inlet combination at high angle of attack p 556 A90-36419
- A study on mechanical model of the helicopter 'ground resonance' p 580 A90-36423
- Digital generation of two-dimensional field of turbulence for flight simulation p 611 A90-36427
- A fracture analysis using eight-node-isoparametric singular elements and its application in fuselage panels p 603 A90-36431
- Application of transformational ideas to automatic flight control design p 589 A90-36433
- A design method for real-time computer control hydraulic force system p 590 A90-36434
- A wall pressure correction method for half-model experiment in closed subsonic wind tunnel test section p 593 A90-36437
- Analysis of serious mechanical trouble in a retractable main landing gear of a jet fighter p 580 A90-36438
- Effect of condensation in a diffuser on the flow field p 603 A90-36784
- The experimental study on the coaxial dump combustor with inner swirl inlet under the combustion condition p 585 A90-36786
- Experimental investigation of external heat transfer coefficients on film-cooled turbine blade leading edge p 585 A90-36787
- An efficient finite-difference algorithm for computing axisymmetric transonic nacelle flow fields p 557 A90-37205
- A numerical method in aeroelasticity for wings with separation at large angle of attack p 557 A90-37209
- Main characteristic parameter model for jet engine fault diagnosis p 585 A90-37210
- Modified fault tolerant inertial navigation system p 578 A90-37211
- Finite element numerical analysis for transonic flows around lifting fuselages p 558 A90-37216
- Aeroelastic tailoring of composite wing structures p 580 A90-37217
- A combined Riccati transfer matrix-direct integration method with its applications p 611 A90-37218
- The study of transient suppression techniques for multimode flight control system p 590 A90-37219
- The method of random variable structure optimal control for aircraft p 590 A90-37220
- A study of the control technique for aircraft spin recovery p 590 A90-37226
- The design of the series of blade flutter rotor and the experimental investigation of flow-induced vibration p 586 A90-37230
- A ground simulation-inspection system for avionic devices p 594 A90-37232
- Study on process control of aeroengine using microcomputer p 586 A90-37239
- A simple prediction method for low-cycle fatigue life of structures p 604 A90-37240
- Analysis and improvement of cabin temperature control system p 580 A90-37241
- An analytic solution on hypersonic flow over an arbitrary slender body with near power-law profile p 558 A90-37736
- Wind tunnel testing techniques on aerodynamic effects with small asymmetry [AIAA PAPER 90-1400] p 560 A90-38490
- Optimum design of composite wing structures subjected to displacement constraints p 680 A90-39276
- The mechanisms and benefits of aeroelastic tailoring p 641 A90-39286
- Analysis of aeroelastic divergence for the slender flight vehicles p 680 A90-39298
- A study on the application of controllability and observability concepts in the design of flight control systems p 693 A90-39303
- Numerical solution of 3-D hybrid problems in turbomachinery p 621 A90-40501
- Application of leaned blades to an aeroengine p 654 A90-40503
- The influence of the inlet Mach number on the boundary layer development on turbomachinery blade surfaces p 621 A90-40504
- Partial similarity and a real-time model of twin-spool gas turbine p 654 A90-40512
- An experimental investigation of rotating stall in a centrifugal compressor with vaneless diffuser p 621 A90-40513
- Linear dynamics of supersonic ramjet p 655 A90-40519
- Influence of fuel composition on flame radiation in gas turbine combustors p 659 A90-40946
- A transonic airfoil design method and examples p 627 A90-42351
- Calculation of the complete transonic unsteady small disturbance equation by ADI method p 627 A90-42353
- A novel synthetic method for studying nonlinear flight stability p 645 A90-42355
- The application of concentric vortex simulation to calculating the aerodynamic characteristics of bodies of revolution at high angles of attack p 627 A90-42357
- An improvement on unwinding technique used in the Galerkin finite element method for the computation of inviscid transonic flow with shock waves p 627 A90-42361
- Numerical analysis of viscous-inviscid interaction in transonic flow p 627 A90-42363
- Calculation of viscous-inviscid strong interaction for transonic flows over aerofoils p 627 A90-42364
- A new simplification method for analysing the rapid rolling stability of aircraft p 669 A90-42367
- The response of helicopter to dispersed gust p 670 A90-42470
- The influence of the inertia coupling on the stability and control of the helicopter and the response of helicopter gust p 671 A90-42472
- Boundary integral formulation for compressible nonlinear potential and Navier-Stokes equations p 706 A90-44406
- Parameter sensitivity analysis of one kind of flight path reconstruction estimator p 779 A90-44832
- On aerodynamic characteristics of canard in canard-forward-swept wing configuration p 709 A90-44833
- Visualization of the turbulent trailing vortex behind a finite wing in steady and unsteady flows p 712 A90-45260
- An investigation on boron used as a component of solid propellant p 765 A90-45708
- An orthogonal algorithm to the maximum likelihood estimation using an efficient method for computing sensitivities [AIAA PAPER 90-3507] p 891 A90-47753
- Aerospace - Collected translations of selected papers p 786 A90-48510
- Longitudinal stability analysis for deformable aircraft p 867 A90-48514
- Exceptions to the C(n beta, dyn) criterion for aircraft stability at high angles of attack p 867 A90-48515
- Unsteady aerodynamics and aeroelasticity of turbomachines and propellers: Proceedings of the Fifth International Symposium, Beijing, People's Republic of China, Sept. 18-21, 1989 p 853 A90-49451
- A new method for high speed propeller flutter prediction p 854 A90-49454
- A method for predicting stall flutter under variable interblade phase angle along rotating direction p 813 A90-49455
- Variational formulation of 2-D unsteady transonic aerodynamics of oscillating cascades p 813 A90-49458
- The interaction between distortion of inlet flow and blade stall flutter in axial-flow compressor p 854 A90-49466
- A model of small-disturbance wave in large-scale separation zone associated with stall flutter p 883 A90-49469
- Some explorations on the mechanism of blade flutter suppression by porous wall casing p 854 A90-49470
- An analysis of cavity resonance in the aeroengine casing during rig testing p 894 A90-49481
- On the unsteady loading noise of counter-rotating propeller p 895 A90-49484
- On numerical prediction of sound field generated by propeller p 895 A90-49485
- Noise generation by swept cascade p 895 A90-49486

Fracture morphology of toughened bismaleimide/carbon fiber composites

p 948 A90-50205

An improved SIP scheme for numerical solutions of transonic streamfunction equations

p 904 A90-51014

A numerical technique for computing the unsteady transonic flow around a wing profile in arbitrary oscillation

p 906 A90-51530

An application of topological analysis to studying the three-dimensional flow in cascades. I - Topological rules for skin-friction lines and section streamlines

p 908 A90-52607

Varying specific heat gasdynamic function formulae simplification and analytical solution of normal shock waves

p 908 A90-52776

A method of predicting 3-D compressible boundary layer on the rotating blade of turbomachinery

p 908 A90-52777

An investigation of characteristics of transonic and viscous flows for turbine cascades

p 909 A90-52779

Pilotless airplanes

p 103 N90-11734

China-built airborne synchronous laser ranger the new L-8 jet trainer aircraft

p 275 N90-15422

Special essays for the 40th anniversary of the revolution: The chief designer discusses the F-8 2 and future fighter planes

p 845 N90-26829

The role of $C_{sub} n \beta_{dyn}$ in the aircraft stability at high angles of attack

p 868 N90-26833

CZECHOSLOVAKIA

Experimental investigation of the transonic centrifugal compressor inducer straight cascades

p 13 A90-12592

Two-stage two-spool experimental centrifugal compressor investigation

p 49 A90-12593

Mathematical model of turboprop engine behaviour

p 254 A90-23351

Fatigue damage of an aircraft due to movement on the airfield

p 247 A90-23352

Fatigue tests of samples of flanged joints of wings

p 274 A90-23353

The fast-response requirement of powerplant thrust in the set of engineering and economic criteria of an aircraft

p 254 A90-23354

Measurements and calculations of the aerodynamic characteristics of the propeller sections series V3

p 233 A90-23355

Unconventional leading edges of airfoils

p 233 A90-23356

The application of the discrete vortex method in aircraft design

p 257 A90-23357

Flight-mechanics tasks in solving problems of active control

p 257 A90-23358

Computer-aided simulation of aircraft motion including nonlinearities in aerodynamic-coefficient relationships

p 257 A90-23359

Aerodynamic characteristics of an aircraft model at large angles of attack and large sideslip angles

p 233 A90-23361

Numerical method for the flow of an ideal fluid on a plane with subsonic and supersonic regions

p 233 A90-23362

Analysis of the mathematical modeling of an aircraft flight trajectory with consideration of engine thrust effect on the force ratio on the aircraft

p 247 A90-23363

Measurement of propellers in the ARTI 3-meter wind tunnel

p 262 A90-23364

LDA processor TSI model 1990 analog input module reconstruction

p 451 A90-29654

Operating principles of a terrain-recognition air navigation system

p 403 A90-29655

Modelling and simulation of turboprop engine behaviour

p 424 A90-29946

Reconstitution of crack growth from fractographic observations after flight simulation loading

p 682 A90-40650

Numerical solution of 2D transonic flows in a turbine cascade

p 709 A90-44601

Mathematical simulation model of an aircraft gas turbine

p 745 A90-44721

Digital servomechanism for the tachometer of the M 602 engine

p 737 A90-44722

Problems in the synthesis of advanced aircraft control systems

p 751 A90-44723

D

DENMARK

Wind shear and hyperbolic distributions

p 280 A90-23632

E

EGYPT

A study of unsteady rotor-stator interactions

p 67 A90-11557

Effect of primary air swirl on emissions formations in gas turbine combustors

p 47 A90-12573

Computation of the trailing edge flow downstream a flat plate with finite thickness

p 151 A90-17464

Study of various factors affecting secondary loss vortices downstream a straight turbine cascade

p 287 A90-23757

Leading-edge vortices due to low Reynolds number flow past a pitching delta wing

p 555 A90-36258

Geometrical factors influencing the flow field in a propulsive nozzle

p 807 A90-46876

Combustion process in a gas turbine combustor when using H₂, NH₃ and LPG fuels

p 873 A90-46882

Two-dimensional convergent-divergent nozzle flow with wall velocity slip and temperature jump

p 807 A90-46884

Computation of complex flows in gas turbine combustors with a multi-level additive correction technique

p 881 A90-46899

Study of the expansion of hydrocarbon-oxygen products through supersonic nozzle

p 852 A90-46907

F

FINLAND

Multigrid solution method for the Euler equations

p 149 A90-16841

Solution of the thin-layer Navier-Stokes equations for laminar transonic flow

p 136 A90-12879

Multigrid solution method for the Euler equations

p 138 A90-13116

An evaluation of the two-dimensional Euler and Navier-Stokes calculations based on a flux-vector splitting

p 481 A90-20963

Subsonic flutter analysis using MSC/NASTRAN

p 522 A90-21041

FRANCE

Effect of protective coatings on mechanical properties of superalloys

p 62 A90-11126

Several problems posed by aerothermal calculations in machines

p 67 A90-11136

Breakage of fan blades in the S1 wind tunnel at Mondane-Avrieux

p 57 A90-11138

Application of the hydrogen bubble visualization method to the water tunnels of ONERA

p 58 A90-11140

Hydrodynamic visualization of the flow around a high-speed aircraft propeller

p 3 A90-11141

Ceramic heat exchangers in gas turbine

p 40 A90-11142

Calculation of three-dimensional turbulent flow in a linear turbine cascade

p 3 A90-11147

Unsteady viscous calculation of cascade flows with leading-edge-induced separation

p 3 A90-11148

Numerical simulation of three-dimensional unsteady flows in turbomachines

p 4 A90-11149

Electromagnetic characterization of lightning on aircraft

p 22 A90-11155

Experimental-theoretical comparison for current injection on an aircraft model

p 22 A90-11157

Influence of the control law on the performance of a helicopter model rotor

p 4 A90-11158

New rotor test rig in the large Modane wind tunnel

p 58 A90-11159

Transall 88 - Lightning characterization program

p 22 A90-11164

Thermostructural behavior of electromagnetic windows

p 76 A90-11167

Elaboration of a code package

p 58 A90-11169

Connection of structures by laboratory-generated electrical discharges

p 23 A90-11170

Electrostatic field conditions on an aircraft stricken by lightning

p 23 A90-11171

Electrostatic description of a positive leader ignition from an aircraft

p 23 A90-11171

3D calculations of reacting flows within aircraft engine combustion chambers

p 67 A90-11173

[ONERA, TP NO. 1989-153]

An improved method for the computation of unsteady transonic potential flow - Application for airfoil and blade performance prediction

p 4 A90-11175

[ONERA, TP NO. 1989-154]

Flow around a jet and thrust measurement bias from static tests

p 40 A90-11431

[AAAF PAPER NT 88-11]

Turbulent mixing in helicopter jet diluters - Navier-Stokes calculations and correlations

p 40 A90-11432

[AAAF PAPER NT 88-13]

Three-dimensional modeling of turbulent transonic flow at the exit of a twin engine

p 4 A90-11434

[AAAF PAPER NT 88-16]

The inclusion of a similarity representation of compressor rotation in the modeling of the interaction of cannon firing with air intakes at incidence

p 4 A90-11435

[AAAF PAPER NT 88-18]

Wind-tunnel test of the air intake of an unducted fan

p 4 A90-11436

[AAAF PAPER NT 88-19]

Theoretical analysis of an icing test apparatus for turbine engine air intakes

p 23 A90-11437

[AAAF PAPER NT 88-20]

An oxidation fatigue interaction damage model for thermal fatigue crack growth

p 62 A90-11539

A class of implicit upwind schemes for Euler simulations with unstructured meshes

p 5 A90-11597

Aircraft compressor flutter analysis

p 41 A90-11797

Collocation methods and lifting-surfaces

p 9 A90-12023

System identification - Multibus acquisition and simulation equipment

p 26 A90-12192

Magnetic recording on board aircraft

p 39 A90-12195

Prospects of onboard magnetic tape recording during flight tests

p 39 A90-12198

NAVSTAR-GPS: An evolution or a revolution, Ecole Supérieure d'Electricité, Gif-sur-Yvette, France, Feb. 11, 1987, Workshop

p 27 A90-12250

Numerical simulation of turbomachinery flows with a simple model of viscous effects - Comparison with experimental data

p 10 A90-12510

[ONERA, TP NO. 1989-122]

The development of an exact conservative scheme associated with the supersonic trailing edge separation modelling for the computation of the transonic 2D cascade

p 12 A90-12551

Pressure surface trailing edge slot cooling

p 47 A90-12569

[ONERA, TP NO. 1989-123]

Three dimensional numerical simulation for an aircraft engine type combustion chamber

p 49 A90-12591

[ONERA, TP NO. 1989-120]

Inverse cycle engine for hypersonic air-breathing propulsion

p 50 A90-12611

[ONERA, TP NO. 1989-121]

Icing test techniques for air intake screens on helicopters functioning in temperatures around 0 C

p 23 A90-12619

A multi-domain 3D Euler solver for flows in turbomachines

p 15 A90-12623

[ONERA, TP NO. 1989-119]

Test rig for the study of the flow in a rotor-stator system

p 58 A90-12634

[ONERA, TP NO. 1989-124]

New approach to small transonic perturbations finite element numerical solving method. I - Numerical developments. II - Numerical applications

p 16 A90-12783

Vortex interactions in fixed and oscillating delta wings (water tunnel visualizations)

p 16 A90-12784

Experimental study of 2D/3D interactions between a vortical flow and a lifting surface

p 86 A90-15849

Designing turbine blades for fatigue and creep

p 112 A90-16007

Airfoil noise in a uniform flow

p 139 A90-16330

Computation of the thin-layer Navier-Stokes equations for a 2D flow

p 87 A90-16332

Synthetic holography applied to head-up displays

p 218 A90-16692

The VSCF system has arrived - The way in which a new constant-frequency electrical generation system in aeronautics has been developed

p 187 A90-16696

Calculation of three-dimensional boundary layers including hypersonic flows

p 146 A90-16773

Multigrid acceleration of transonic flow computations

p 147 A90-16783

Leading edge contamination and relaminarisation on a swept wing at incidence

p 148 A90-16789

Aerospatiale's military helicopter programs

p 143 A90-16824

Recent research on external helicopter noise at ONERA

p 218 A90-16825

Application of computational systems to aircraft engine components development

p 188 A90-17448

Upwind adaptive finite element investigations of the two-dimensional reactive interaction, of supersonic gaseous jets p 209 A90-18264

Computation of hypersonic flows by a finite element least-squares method p 155 A90-18296

Finite element simulation of compressible turbulent flows - Validation and application to internal aerodynamic in gas-turbine engines p 210 A90-18343

Prediction of the interaction noise emitted by helicopter fenestrons p 218 A90-18449

Aerodynamic design of an HP compressor stage using advanced computation codes p 156 A90-18479

Future test rigs p 200 A90-19012

Development of finite element methods for compressible Navier-Stokes flow simulations in aerospace design [AIAA PAPER 90-0403] p 166 A90-19833

Design of a helicopter output feedback control law using modal and structured-robustness-techniques p 282 A90-20557

Hydrodynamic visualization of organized structures and turbulences in boundary layers, wakes, jets or propeller flows

[ONERA, TP NO. 1989-158] p 223 A90-21026

Inviscid non equilibrium flow in ONERA F4 wind tunnel [ONERA, TP NO. 1989-161] p 223 A90-21029

Thermodynamics and the future turbine engines [ONERA, TP NO. 1989-165] p 253 A90-21031

Recent developments in calculation methods for internal flows by solution of Euler or Navier-Stokes equations [ONERA, TP NO. 1989-167] p 223 A90-21033

Preliminary tests of a gust generator in the ONERA S3Ch transonic wind tunnel [ONERA, TP NO. 1989-171] p 261 A90-21035

Development of the MZM numerical method for 3D boundary layer with interaction on complex configurations [ONERA, TP NO. 1989-174] p 223 A90-21036

Chemical and vibrational non-equilibrium nozzle flow calculation by an implicit upwind method [ONERA, TP NO. 1989-175] p 223 A90-21037

Performance and aerodynamic development of the Super Puma Mk II main rotor with new SPP8 blade tip design [ONERA, TP NO. 1989-181] p 245 A90-21041

Conditional sampling [ONERA, TP NO. 1989-187] p 261 A90-21047

Determination of the ground effect on the characteristics of the A320 aircraft [ONERA, TP NO. 1989-188] p 245 A90-21048

Instrumentation being developed for the ONERA F4 wind tunnel [ONERA, TP NO. 1989-189] p 261 A90-21049

The application of infrared thermography to the measurement of heat fluxes in a wind tunnel [ONERA, TP NO. 1989-192] p 261 A90-21051

Leading edge transition in hypersonic flows p 224 A90-21167

New high-speed air transport system and stratospheric pollution [ONERA, TP NO. 1989-202] p 279 A90-22445

A methodology proposal to design and analyse counterrotating high speed propellers [ASME PAPER 89-GT-38] p 340 A90-23767

Aerodynamics of cooling jets introduced in the secondary flow of a low speed turbine cascade [ASME PAPER 89-GT-192] p 362 A90-23868

The disadvantages of GPS - Comparative study of solutions adapted to civil aviation p 329 A90-23994

Recent and prospective developments in single-crystal superalloys for the blades of advanced turbines p 355 A90-24288

Composites for aeronautical structures p 286 A90-24291

Design, realization, and qualification of model composite rotor blades p 364 A90-24293

The anisotropy of the mechanical behaviour in nickel-based single crystal superalloys for turbine blades [ONERA, TP NO. 1989-205] p 355 A90-25339

Development of a new nickel based single crystal turbine blade alloy for very high temperatures [ONERA, TP NO. 1989-206] p 356 A90-25340

New metallic felts with improved resistance to high temperature oxidation [ONERA, TP NO. 1989-210] p 366 A90-25343

Numerical simulation of vortex breakdown via 3-D Euler equations [ONERA, TP NO. 1989-211] p 303 A90-25344

Determination of convective transfer coefficients on a wind-tunnel model by stimulated infrared thermography [ONERA, TP NO. 1989-218] p 351 A90-25351

beta CEZ, a high performance titanium alloy for aerospace engines [ONERA, TP NO. 1990-8] p 356 A90-25356

A generalized lifting-line theory for curved and swept wings p 303 A90-25597

2-D and 3-D unstructured mesh adaption relying on physical analogy p 310 A90-26534

Hypersonic reactive flow computations p 315 A90-27131

Analysis and practical design of ceramic-matrix composite components p 445 A90-28135

Design, evaluation and proof-of-concept flights of a main rotor interblade viscoelastic damping system p 406 A90-28152

The new Spheriflex tail rotor for the Super Puma Mark 2 p 408 A90-28213

Design of a three dimensional Doppler anemometer for T2 transonic wind tunnel p 447 A90-28271

Aerodynamic, thermal and mechanical problems in the aerospace field p 382 A90-29921

Aerothermomechanical design of turbine-engine combustion chambers p 424 A90-29922

A test facility for high-pressure high-temperature combustion chambers p 438 A90-29924

Sandwich structures on Aerospatiale helicopters p 467 A90-31657

Design, fabrication and experimental test of hi-temperature CFRP stiffened structures p 534 A90-31892

Rotordynamics of the Vulcain LH2 Turbopump - Comparison between test results and non-linear dynamic analysis p 528 A90-33382

Aeroelastic analysis using finite element models p 492 A90-33388

Calculation of flow on a flat plate at angle of attack by numerical solution of Navier-Stokes equations p 537 A90-33424

Advanced parameter identification techniques for near real time flight flutter test analysis [AIAA PAPER 90-1275] p 494 A90-33899

Model attitude measurement system p 539 A90-34235

Feasibility study of RADAC stereo optoelectronic model deformation measurement system for ETW p 539 A90-34239

Flow quality in the T2 cryogenic wind-tunnel - Problems and solutions p 524 A90-34240

T2 ability concerning model design and instrumentation in short run processing p 524 A90-34241

Half transport aircraft cryogenic model for T2 wind tunnel p 524 A90-34242

Sting design feasibility for E.T.W. cryogenic civil transport aircraft p 524 A90-34245

Numerical simulation of vortex breakdown by solving the Euler equations for an incompressible fluid p 476 A90-34323

Differential equation modeling of dynamic stall p 476 A90-34325

Aeroelastic instabilities in aircraft engines - Application to a SNECMA fan stage p 584 A90-35174

Turbulence statistics in a shock wave boundary layer interaction p 552 A90-35205

Electronic cartography - A new need for commercial aircraft p 576 A90-35351

Mode S - A data link for future air traffic control p 576 A90-35684

Solution of Euler equations with unstructured meshes p 558 A90-37343

Experimental study of incompressible flow on the upper surface of a delta wing p 558 A90-37346

Aerodynamic loads and blade vortex interaction noise prediction p 614 A90-38520

Navier-Stokes computations of vortical flows [AIAA PAPER 90-1628] p 568 A90-38757

The SEP8 844 reusable liquid rocket engine for Mirage combat aircraft [AIAA PAPER 90-1835] p 655 A90-40526

Dual cross-polarization planar arrays in the C and X bands p 638 A90-40979

The TVD 900 - A modern signal processing applied to primary civilian ATC radar p 638 A90-41034

Performances and new surveillance possibilities in SSR - Mode S p 639 A90-41036

Applications of Mode S secondary surveillance radar to civil air traffic control - Studies, experiments, and policy of the French Direction de la Navigation Aérienne p 639 A90-41056

Experiments on Mode S secondary surveillance radar - The participation of the French Direction de la Navigation Aérienne in the European effort p 639 A90-41057

Recent propeller development and studies conducted at ONERA [ONERA, TP NO. 1990-16] p 683 A90-41201

Coupled aerodynamic forces due to unsteady stall on a high-aspect-ratio wing oscillating at high amplitude [ONERA, TP NO. 1990-24] p 623 A90-41203

Directivity of the noise radiation emitted from the inlet duct of a turboshaft helicopter engine [ONERA, TP NO. 1990-26] p 695 A90-41205

Interaction between a high-level steady acoustic field and a ducted turbulent flow [ONERA, TP NO. 1990-27] p 695 A90-41206

Wind-tunnel measurement of noise emitted by helicopter rotors at high speed [ONERA, TP NO. 1990-28] p 695 A90-41207

Noise-source measurements by thin-film pressure transducers in a subsonic turbofan model [ONERA, TP NO. 1990-36] p 659 A90-41212

Military engines - Cradle of technology p 660 A90-41758

Characterization of helicopter turboshaft engine noise p 660 A90-41759

Starter systems and auxiliary power units p 660 A90-41760

Developmental tests on the M 88 engine are on track p 660 A90-41761

Toward total quality in industry p 684 A90-41768

The Airbus... a challenge launched twenty years ago p 699 A90-41769

Quasi-3D viscous flow computations in subsonic and transonic turbomachinery bladings [AIAA PAPER 90-2126] p 625 A90-42033

Experimental study of the flow around an helicopter fuselage - Comparison with three-dimensional boundary layer calculations p 630 A90-42438

Eurofar - Status of the European tilt-rotor project p 645 A90-42441

Improving helicopter aerodynamics - A step ahead p 631 A90-42443

The all glass helicopter cockpit p 653 A90-42447

Digital map reader for helicopters p 653 A90-42448

The Super Puma MKII automatic flight control system p 669 A90-42449

Main characteristics of an integrated flight and display system for AS MKII Super-Puma p 653 A90-42450

Modern strapdown system for helicopter p 653 A90-42451

Full Authority Digital Engine Control for the AS 355 N TM 319 engines p 665 A90-42486

Design and manufacturing of composite materials blade models p 618 A90-42492

Preliminary flight evaluation of the SA 365 Panther helicopter in air-to-air combat manoeuvres p 647 A90-42494

Numerical study of heat transfer for unsteady viscous supersonic blunt body flows p 707 A90-44432

Numerical study of compressible nozzle flow p 708 A90-44437

Fully vectorized implicit scheme for 2-D viscous hypersonic flow using adaptive finite element methods p 708 A90-44439

Numerical predictions for the flow and the heat transfer in gas turbine cooling systems p 770 A90-44464

Preliminary design and load distributions of high performance mechanical systems p 771 A90-45281

Clutter rejection and transmitter-receiver requirements in an airborne radar p 738 A90-45354

Software maintenance on the Airbus family [SAE PAPER 892326] p 738 A90-45484

Design and experimental investigation of a laminar horizontal tail [AIAA PAPER 90-3042] p 798 A90-45934

Homogenization of composite beams in dynamical flexure p 878 A90-46184

Full span analysis for flutter prediction of slender blade assemblies p 879 A90-46188

The airborne synthetic cartographic indicator p 822 A90-46671

Advocating international cooperation: The Eurofar program - An example and a hope p 785 A90-46929

Aircraft measurements of sea surface conditions and their relationship to marine boundary-layer dynamics p 888 A90-47572

The use of onboard sensor data in aerial triangulation - GPS, pressure sensors, laser telemetry p 822 A90-47901

Computerized MLS flight inspection system developed p 823 A90-48983

Visualization of corona discharges p 819 A90-49839

A probabilistic approach for the establishment of an aircraft structure inspection program p 902 A90-49892

High temperature adhesives commercially available to be used for extended time with PMR15 laminates p 943 A90-50125

Modeling of the oil quench for Ni-based superalloy turbine disks p 957 A90-51525

Maximum expected concentrations of hail in thunderstorm precipitation p 962 A90-52052

Prediction of transition on a swept wing p 908 A90-52592

New methods of buffeting prediction on civil aircraft p 908 A90-52620

- Numerical simulation of nonreactive flows in turbomachines p 908 N90-52621
- Combustion Instabilities in Liquid-Fueled Propulsion Systems [AGARD-CP-450] p 63 N90-10191
- Numerical simulation of unsteady combustion in a dump combustor p 54 N90-10203
- Castings Airworthiness [AGARD-R-762] p 64 N90-10231
- Casting factors imposed by the French regulation for foundry castings used in military aircraft p 64 N90-10233
- Casting airworthiness joint European civil authorities view-point p 64 N90-10234
- The question of the casting factor p 64 N90-10238
- Fluid Dynamics of Three-Dimensional Turbulent Shear Flows and Transition [AGARD-CP-438] p 71 N90-10356
- Experimental study of transition and leading edge contamination on swept wings p 71 N90-10362
- Control and modification of turbulence p 72 N90-10377
- Kalman Filter Integration of Modern Guidance and Navigation Systems [AGARD-LS-166] p 28 N90-10847
- Flight Test Techniques [AGARD-CP-452] p 33 N90-10860
- A320 flight tests: Particularities and innovations p 34 N90-10864
- Flight test techniques adopted by Avions Marcel Dassault-Breguet Aviation p 34 N90-10867
- Lessons learned from the integration of flight systems p 35 N90-10874
- Performance and quality of a wing type parachute: Parametric analysis [REPT-88-19] p 89 N90-11710
- Numerical simulation of aeroplane response to a lightning injection [ETN-89-95271] p 96 N90-11716
- Volumetric analysis by spontaneous Raman diffusion in a supersonic wind tunnel [ISL-R-109/88] p 95 N90-12564
- Euler equation solutions applied to a helicopter rotor in forward moving flight [ONERA-RSF-32/1285-AY-346A] p 107 N90-12592
- Integration of a centralized multiplexed control unit into the cockpit of an aircraft [F6150-DT410-1-88329] p 120 N90-12622
- Reduction of turbulent drag: Boundary layer manipulators [CERT-RSF-OA-74/2259-AYD] p 136 N90-12889
- Transition in surface boundary layers [CERT-RSF-OA-43/5018-AYD] p 136 N90-12897
- Studies of the European transonic wind tunnel [ONERA-RSF-12/0694-GY] p 141 N90-13278
- Laser applications in supersonic unsteady flow p 212 N90-13344
- Reduction of profile drag by modifying the structure next to the wake area [IMFL-88/35] p 172 N90-13356
- The human factors relating to escape and survival from helicopters ditching in water [AGARD-AG-305(E)] p 176 N90-13358
- Nondestructive analysis of aileron fatigue and aging in a Mirage F1 [REPT-M6-594000] p 184 N90-13378
- A model suitable for predicting the noise associated with the ducted tail rotor of a helicopter [ECL-88-09] p 220 N90-14074
- Evaluation of the indirect effects of lightning on a system: Double transfer function method [RAE-TRANS-2172] p 176 N90-14211
- Flight in adverse environmental conditions [AGARD-AR-277] p 185 N90-14218
- Flight in Adverse Environmental Conditions [AGARD-CP-470] p 222 N90-15041
- Description of atmospheric turbulence p 280 N90-15043
- How to fly windshear using the fly-by-wire concept p 258 N90-15050
- Principal characteristics of lightning on aircraft p 239 N90-15067
- New Light Alloys [AGARD-CP-444] p 267 N90-15185
- Properties of Al-Li alloys p 267 N90-15191
- Putting alloy 2091 to work p 268 N90-15197
- Point of view of a civil aircraft manufacturer on Al-Li alloy p 268 N90-15200
- Fuel Tank Technology [AGARD-R-771] p 250 N90-15904
- Integral fuel tanks - design, production, aging, repair p 250 N90-15906
- Guidance and Control of Unmanned Air Vehicles [AGARD-CP-436] p 260 N90-15924
- Synthesis of control law, on a RPV, in order to minimize the number of sensors p 260 N90-15925
- Analysis of indirect effects of lightning on a metallic A 300 wing: Test report [REPT-E87/645800] p 323 N90-16726
- Bird impact tests on asymmetric sandwich structures made in Kevlar 49 [CEAT-NT-10/S/83-5] p 323 N90-16727
- Bird impact tests on curved structures of the type Sandwich-Kevlar-Nida for normal and angular shooting [CEAT-NT-10/S/83-4] p 324 N90-16728
- Advances in Techniques and Technologies for Air Vehicle Navigation and Guidance [AGARD-CP-455] p 332 N90-16731
- Low air speed computation for helicopters: A new approach p 333 N90-16744
- Experimental study of velocity fields and turbulence in a turbojet engine [ISL-CO-231/88] p 344 N90-16766
- Progress in airbreathing combined engines for future European launcher p 344 N90-16817
- Combustion Experiments During KC-135 Parabolic Flights [ESA-SP-1113] p 368 N90-16958
- Self compensation of rigid displacements in holographic interferometry [ISL-CO-219/88] p 370 N90-17113
- Aircraft Fire Safety [AGARD-CP-467] p 324 N90-17581
- New materials for civil aircraft furnishing p 328 N90-17609
- Main results of CAST-10 airfoil tested in T2 cryogenic wind tunnel p 321 N90-17652
- GTD/UTD: Brief history of successive development of theory and recent advances. Applications to antennas on ships and aircraft p 370 N90-17939
- Prediction of rotor blade-vortex interaction noise from 2-D aerodynamic calculations and measurements [ISL-CO-243/88] p 396 N90-18365
- Aerodynamics of unsteady systems: Numerical study of potential flow/boundary layer coupling [ETN-90-96257] p 396 N90-18367
- Bird impact tests on a Kevlar 49 structure. Monolithic plates. Oblique-angled impact [REPT-S3-4273] p 402 N90-18376
- Study of the blade/vortex interaction on a one-blade rotor during forward flight (incompressible, non viscous fluid) [ISL-R-115/88] p 415 N90-18391
- Possible piloting techniques at hypersonic speeds [ISL-CO-216/88] p 415 N90-18392
- AGARD/SMP Review: Damage Tolerance for Engine Structures. 2: Defects and Quantitative Materials Behaviour [AGARD-R-769] p 425 N90-18396
- Defects in monoblock cast turbine wheels p 443 N90-18400
- The need for a common approach within AGARD p 425 N90-18404
- Unsteady Aerodynamic Phenomena in Turbomachines [AGARD-CP-468] p 425 N90-18405
- Unsteady viscous calculation method for cascades with leading edge induced separation p 426 N90-18408
- Aerodynamic study on forced vibrations on stator rows of axial compressors p 426 N90-18412
- The implications of using integrated software support environment for design of guidance and control systems software [AGARD-AR-229] p 434 N90-18432
- Numerical investigations of heat transfer and flow rates in rotating cavities. Simulation of the movement generated by wall temperature gradients, by source-sink mass flows or by the differential rotation of the walls, under the influence of Coriolis and centrifugal forces [ETN-90-96253] p 454 N90-18695
- Contribution to the study of three-dimensional separation in turbulent incompressible flow [ESA-TT-1169] p 454 N90-18697
- Calendar of selected aeronautical and space meetings [AGARD-CAL-90/1] p 464 N90-19060
- The Uniform Engine Test Programme [AGARD-AR-248] p 428 N90-19232
- Implications of Advanced Technologies for Air and Spacecraft Escape [AGARD-CP-472] p 483 N90-20054
- Parachute opening shocks during high speed ejections: Normalization p 497 N90-20056
- Computational Methods for Aerodynamic Design (Inverse) and Optimization [AGARD-CP-463] p 500 N90-20976
- An inverse method for the design of turbomachine blades p 511 N90-20988
- The use of numerical optimization for helicopter airfoil and blade design p 502 N90-20995
- Numerical optimization of wings in transonic flow p 502 N90-20997
- Secondary Flows in Turbomachines [AGARD-CP-469] p 511 N90-21009
- Parabolized calculations of turbulent three dimensional flows in a turbine duct p 482 N90-21013
- Calculation of the three dimensional turbulent flow in a linear turbine blade p 513 N90-21021
- Calculation of the secondary flow in an axial turbine p 513 N90-21022
- Mesh generation for flow computation in turbomachine p 588 N90-21981
- Automatic grid generation in complex three-dimensional configurations using a frontal system p 608 N90-21992
- A decision-making aid for multi-layer radar absorbent coverings [ESA-TT-1173] p 773 N90-25267
- Aerodynamic loads and blade vortex interaction noise prediction [ISL-PU-310/89] p 719 N90-25942
- Technical evaluation report on the Fluid Dynamics Panel Symposium on Computational Methods for Aerodynamic Design (Inverse) and Optimization [AGARD-AR-267] p 720 N90-25947
- Turbulent combustion modeling for turbo-jet combustion chambers p 749 N90-25993
- Technical evaluation report on the Guidance and Control Panel 49th Symposium on Fault Tolerant Design Concepts for Highly Integrated Flight Critical Guidance and Control Systems [AGARD-AR-281] p 758 N90-26012
- Report of the Fluid Dynamics Panel Working Group 10 on calculation of 3D separate turbulent flows in boundary layer limit [AGARD-AR-255] p 776 N90-26280
- AGARD highlights 90/1 p 783 N90-26788
- Fluid Dynamics Panel Working Group 12 on Adaptive Wind Tunnel Walls: Technology and Applications [AGARD-AR-269] p 870 N90-26838
- Study of the compressibility effects on the turbulence of supersonic drags [ETN-90-97448] p 817 N90-27661
- Study of the flow around the prototype of A300: Results of the third test campaign at F2 and comparison with calculations [CERT-33/5025-29-DERAT] p 817 N90-27663
- AGARD/SMP Review Damage Tolerance for Engine Structures. 3: Component Behaviour and Life Management [AGARD-R-770] p 855 N90-27704
- Comparative Engine Performance Measurements [AGARD-LS-169] p 856 N90-27711
- Device for the dilution of hot exhaust jets [ETN-90-97435] p 858 N90-27723
- Tests of an ultra-light tunnel in the anechoic wind tunnel facility CEPRA 19 [ONERA-RF-20/7294-PH] p 872 N90-27729
- Toxicity of thermolysis products from the materials of airplane cockpits [CEAT-PV-M6/5924/02] p 876 N90-27895
- Study of the microstructure of a titanium alloy (6246) for turbomachine compressors [ETN-90-97450] p 876 N90-27900
- Characterization of the CP 214 T851. Dissection of a cast flat bar for a standard spar [CEAT-PV-M4/462200] p 876 N90-27905
- Characterization of the 7175 T7352. Dissection of a die casting standard spar [CEAT-PV-M5/528900] p 877 N90-27906
- Characterization of the 7175 T7352 101. Dissection of a die casting standard spar [CEAT-PV-M5/5288] p 877 N90-27907
- Characterization of the 7010 T73651. Dissection of a sheet billet for a standard spar [CEAT-PV-M5/521700] p 877 N90-27908
- Efficient solution of the steady Euler equations with a centered implicit method p 884 N90-27999
- Impact of Emerging NDE-NDI Methods on Aircraft Design, Manufacture, and Maintenance [AGARD-CP-462] p 885 N90-28068
- The application of infrared thermography to the nondestructive testing of composite materials p 886 N90-28084
- Inspection system for in-situ inspection of aircraft composite structures p 886 N90-28091
- Use of acoustic emission for continuous surveillance of aircraft structures p 887 N90-28092
- Theoretical studies carried out in 1988 on helicopter rotor noise under subsonic conditions [ONERA-RS-82/5094-PY] p 896 N90-28402
- Solution of Euler equations applied to a rotor of a helicopter in steady flight [ONERA-RSF-1/3731-AY-002A] p 910 N90-28500
- Aerodynamics of Combat Aircraft Controls and of Ground Effects [AGARD-CP-465] p 920 N90-28513
- Study of the ground effects in the CEAT aerohydrodynamic tunnel: Using the results p 922 N90-28530

- Study of ground effects on flying scaled models
p 922 N90-28532
- Determination of the ground effect on the characteristics of the A320 aircraft
p 922 N90-28534
- High Temperature Surface Interactions
[AGARD-CP-461] p 951 N90-28698
- Molten salt induced high temperature degradation of thermal barrier coatings
p 952 N90-28704
- Effect of protective coatings on mechanical properties of superalloys
p 952 N90-28707
- Static and dynamic characterization of the ATR 72 rods made of Ti 10.2.3 titanium alloy
[REPT-49-238] p 953 N90-28722
- Development of turbulence models for the analysis of compressible or incompressible unsteady flow
[ETN-90-97486] p 958 N90-28810
- Analysis, Design and Synthesis Methods for Guidance and Control Systems
[AGARD-AG-314] p 916 N90-29338
- Recommended practices for measurement of gas path pressures and temperatures for performance assessment of aircraft turbine engines and components
[AGARD-AR-245] p 933 N90-29393

G

GERMANY DEMOCRATIC REPUBLIC

- The European Transonic Windtunnel (ETW)
p 262 N90-15945

GERMANY, FEDERAL REPUBLIC OF

- Natural laminar flow research for subsonic transport aircraft in the FRG
p 2 A90-10137
- Infrared radiation model for aircraft and reentry vehicle
p 77 A90-10169
- Target classification by vibration sensing
p 1 A90-10170
- Optimization of helicopter takeoff and landing
p 29 A90-11006
- Comparison of three concepts for a long stroke displacement transducer
p 66 A90-11041
- Computation of laminar mixed convection flow in a channel with wing type built-in obstacles
p 67 A90-11114
- On the length scales of laminar shock/boundary-layer interaction
p 5 A90-11610
- Unsteady aerodynamics and aeroelasticity of turbomachines and propellers: Proceedings of the Fourth International Symposium, Aachen, Federal Republic of Germany, Sept. 6-10, 1987
p 5 A90-11776
- Unsteady 2D flow calculation in turbomachinery cascades
p 6 A90-11782
- Computation of aerodynamic blade loads due to wake influence and aerodynamic damping of turbine and compressor cascades
p 7 A90-11791
- Testing facility and procedure of the ATTAS on-board data acquisition system
p 39 A90-12202
- A comfortable and universal data-acquisition-system for flight research
p 39 A90-12204
- Modern dynamic components for helicopters
[MBB-UD-556-89-PUB] p 29 A90-12253
- Rotor concepts for the European Future Advanced Rotorcraft (Eurofar)
[MBB-UD-0551-89-PUB] p 29 A90-12258
- Investigation of some effects on the compressor characteristics of an advanced bleed air compressor design
p 49 A90-12594
- Operating aspects of counter-rotating propfan and planetary-differential gear coupling
p 50 A90-12615
- Gearless crank - The logical step to economic engines for high thrust
p 50 A90-12616
- Computation of transonic turbine cascade flow using Navier-Stokes equations
p 14 A90-12621
- System identification collaboration - The role of AGARD
p 1 A90-12763
- Identification of mathematical derivative models for the design of a model following control system
p 56 A90-12764
- Experimental investigations of effects of the stagger angle on secondary flows in plane compressor cascades
p 83 A90-13787
- Experimental investigations on the spatial and time-dependent structure of part-load recirculations in centrifugal pumps
p 83 A90-13788
- Smoothing the way to future designs - A new technique for wind-tunnel measurements
p 121 A90-15873
- Production of Ti6Al4V-components for a new turbo-fan-engine
p 132 A90-16618
- DB/SPF cooler outlet duct for aircraft application
p 132 A90-16620
- Computation of multi-element airfoil flows including confluence effects
p 144 A90-16755
- Disturbance growth in an unstable three-dimensional boundary layer
p 148 A90-16787
- Airfoils in supersonic source and sink flows
p 149 A90-16844

- Numerical studies of incompressible flow around delta and double-delta wings
p 150 A90-16845
- Two-dimensional transonic flow field analysis with different turbulence models
p 150 A90-16846
- Effect of wind shear on flight safety
p 175 A90-17973
- Unsteady streamlines near the trailing edge of NACA 0012 airfoil at a Reynolds number of 125,000
p 155 A90-18158
- On the coupling of finite elements and boundary elements for transonic potential flows
p 155 A90-18297
- Some processes of sound generation in a vortex-airfoil system with parallel axes
p 218 A90-18448
- Possibility of active propeller-noise suppression in piston-engine aircraft by changing the phase relation between the propeller and exhaust signals
p 218 A90-18450
- Development of military helicopters
p 181 A90-18488
- Generalized fluxvectors for hypersonic shock-capturing
[AIAA PAPER 90-0390] p 165 A90-19829
- Development status of epicyclic gears
p 271 A90-21141
- Rarefied gas dynamics
p 224 A90-21163
- On the computations of hypersonic viscous flows
p 225 A90-21170
- Oils for flight turbine engines - Research and development in the 90s
p 266 A90-21473
- Technical-scientific possibilities for helicopter noise research in the German-Dutch wind tunnel
p 283 A90-21474
- Advances in the efficient calculation of flows with friction
p 225 A90-21475
- The use of a Laval nozzle and wall suction for blockage-free transonic wind-tunnel operation
p 225 A90-21592
- A parametric study of the flutter stability of two-dimensional turbine and compressor cascades in incompressible flow
p 225 A90-21593
- Calculation of the side-wall boundary layer in axial turbomachines, accounting for the internal flow near the blades
p 225 A90-21595
- Numerical simulation of transonic wing flows using a zonal Euler, boundary-layer, Navier-Stokes approach
p 225 A90-21596
- Antenna and radar signature technology at Dornier
p 261 A90-21605
- Digital electronic control unit for the European Fighter Aircraft (EFA)
p 253 A90-21607
- Digital map for helicopter navigation and guidance
p 252 A90-21609
- Design criteria, constructions, and materials for the Dornier 328 airframe
p 246 A90-21610
- Low- and high-speed tests with the Dornier 328 wind-tunnel model
p 246 A90-21611
- Potential applications of satellite navigation
p 264 A90-21716
- Status and potential of GPS-receiver development
p 265 A90-21717
- A GPS-based flight-control concept
p 242 A90-21719
- Precision navigation using an integrated GPS-IMU system
p 242 A90-21720
- Flight-path measurement
p 242 A90-21721
- Differential GPS (DGPS) as an approach and landing aid
p 242 A90-21722
- Ground navigation in airport traffic
p 242 A90-21725
- Hydrogen propulsion and the next century - A challenge that raises questions and problems
p 266 A90-21774
- High-performance composite materials in air and space travel - State of the art and future perspectives
[MBB-Z-0279/89] p 266 A90-22595
- EUROFAR - European project for a commercial vertical-takeoff aircraft
[MBB-UD-553/89] p 221 A90-22696
- Scenario 2000
[MBB-UD-560/89] p 222 A90-22698
- Structure of velocity and temperature fields in laminar channel flows with longitudinal vortex generators
p 273 A90-23207
- Trends in avionics - From analog black boxes to integrated digital avionics systems
p 252 A90-23245
- Flight and wind-tunnel investigations on boundary-layer transition
p 233 A90-23283
- Overview on test cases for computation of internal flows in turbomachines
[ASME PAPER 89-GT-46] p 288 A90-23772
- Three-dimensional separated flow field in the endwall region of an annular compressor cascade in the presence of rotor-stator interaction. I - Quasi-steady flow field and comparison with steady-state data
[ASME PAPER 89-GT-76] p 291 A90-23797

- Three-dimensional separated flow field in the endwall region of an annular compressor cascade in the presence of rotor-stator interaction. II - Unsteady flow and pressure field
[ASME PAPER 89-GT-77] p 291 A90-23798
- Verification of an impeller design by laser measurements and 3D-viscous flow calculations
[ASME PAPER 89-GT-159] p 292 A90-23847
- Mathematical formulation of blade surfaces in turbomachinery. I - Theoretical surface formulations
[ASME PAPER 89-GT-160] p 360 A90-23848
- Mathematical formulation of blade surfaces in turbomachinery. II - Practical examples of determined surfaces
[ASME PAPER 89-GT-161] p 361 A90-23849
- Parabolic flight experiments on fluid surfaces and wetting
p 363 A90-23904
- Unsteady transonic flow around double-wedge profiles
p 299 A90-24354
- European research and testing facilities requested for participation to SST/HST projects
[ONERA, TP NO. 1990-12] p 351 A90-25358
- A study of roll response required in a low altitude slalom task
p 347 A90-25421
- Winglets on rotor blades in forward flight - A theoretical and experimental investigation
p 303 A90-25422
- Automatic vibration reduction at a four bladed hingeless model rotor - A wind tunnel demonstration
p 335 A90-25424
- The design of supersonic aircraft and space vehicles by using global optimization techniques
p 353 A90-25781
- Analysis of three-dimensional aerospace configurations using the Euler and Navier-Stokes equations
p 305 A90-25798
- Three-dimensional simulations of hypersonic flows
p 306 A90-25823
- Identification of moderately nonlinear flight mechanics systems with additive process and measurement noise
p 347 A90-25987
- Design for hypersonic speed
p 335 A90-26343
- A semi-analytical procedure for the conformal mapping of arbitrary airfoil contours
p 309 A90-26498
- Geometric modelling of complex aerodynamic surfaces and three-dimensional grid generation
p 311 A90-26545
- Standardized stress-time histories - An overview
p 368 A90-26752
- Basic approach in the development of TURBISTAN, a loading standard for fighter aircraft engine disks
p 368 A90-26754
- OPST1 - An optical yaw control system for high performance helicopters
p 430 A90-28220
- The revolution continues
[MBB-UD-557-89-PUB] p 381 A90-28242
- Application of piezoelectric foils in experimental aerodynamics
p 446 A90-28258
- A semiconductor laser-Doppler-anemometer for applications in aerodynamic research
p 447 A90-28273
- Influence of wind tunnel circuit installations on test section flow quality
p 436 A90-28287
- Development of two multi-sensor hot-film measuring techniques for free-flight experiments
p 417 A90-28291
- Status of the development programme for instrumentation and test techniques of the European Transonic Windtunnel - ETW
p 437 A90-28292
- Fully automatic calibration machine for internal 6-component wind tunnel balance including cryogenic balances
p 437 A90-28294
- External 6-component wind tunnel balances for aerospace simulation facilities
p 438 A90-28296
- Applications of infra-red thermography in a hypersonic blowdown wind tunnel
p 438 A90-28300
- The rotor-signal-module of MF190
p 418 A90-28849
- The Modular Flighttest Instrumentation/MFI 90 - A helicopter measuring system
p 418 A90-28850
- Fast calculation of root loci for aeroelastic systems and of response in time domain
[AIAA PAPER 90-1156] p 390 A90-29368
- Methodology of variable amplitude fatigue tests
p 451 A90-29866
- The in service multi-axial-stress situation in an uncooled gas turbine blade
p 423 A90-29880
- Meteopod, an airborne system for measurements of mean wind, turbulence, and other meteorological parameters
p 418 A90-29943
- The boundary-layer fence - Barrier against the separation process
p 396 A90-31493
- Aerospace materials - Trends and potential
p 529 A90-31902
- Higher-order effects in boundary-layer premixed combustion
p 529 A90-32953

- European Forum on Aeroelasticity and Structural Dynamics, Aachen, Federal Republic of Germany, Apr. 17-19, 1989, Proceedings [DGLR BERICHT 89-01] p 468 A90-33351
- Review of active structural control systems and flight test techniques for dynamic stability investigations p 516 A90-33352
- A strong viscous-inviscid interaction method for computing unsteady transonic airloads for use in aeroelastics p 471 A90-33355
- Comparison of two potential flow methods for transonic flutter analysis p 471 A90-33356
- Computation of unsteady transonic flows around oscillating airfoils using full potential and Euler equations p 472 A90-33357
- Numerical analysis of unsteady forces on oscillating ring airfoils and jet engines p 473 A90-33364
- Unsteady lift and moment coefficients of an engine nacelle p 473 A90-33365
- Experimental investigation of the flow development of an airfoil at high angles of attack p 473 A90-33366
- On the prediction of the aeroelastic behaviour of lifting systems due to flow separation p 491 A90-33369
- Measurement of wind tunnel model deformation under airload p 522 A90-33370
- Flutter analysis from ambient random responses p 491 A90-33374
- Gyroscopic matrices in computation of vibration p 547 A90-33381
- Structural-acoustic analysis of aircraft fuselage structures using general purpose finite element codes p 492 A90-33385
- Hydroelastic problems in space flight vehicles p 536 A90-33386
- The influence of mathematical optimization methods on the design of aircraft structures p 492 A90-33387
- Aeroelastic tailoring validation by windtunnel model testing p 492 A90-33389
- Structural optimization in view of aeroelastic constraints p 536 A90-33391
- The effect of winglets on aircraft wing flutter p 473 A90-33411
- Fast calculation of root loci of aeroelastic systems and of gust response in time domain p 517 A90-33413
- Estimation of losses in semi-open centrifugal impellers p 537 A90-33597
- Honeycomb quality requirements - A user's perspective p 538 A90-33705
- Airbus A320 CFRP-rudder structural requirements p 493 A90-33707
- Equation decoupling - A new approach to the aerodynamic identification of unstable aircraft [AIAA PAPER 90-1276] p 518 A90-33900
- Integrated system of differential Global Positioning System and inertial measurement unit - A position determination system for automatic landing [AIAA PAPER 90-1300] p 487 A90-33914
- Automatic landing with GPS - Design of the flight guidance and flight control system [AIAA PAPER 90-1301] p 487 A90-33915
- Autopilot flight test experience with BK 117 hingeless rotor [AIAA PAPER 90-1267] p 505 A90-33930
- The Kryo-Kanal Koeln, KKK: Description of tunnel conversion - Results of calibration tests under ambient and cryogenic conditions p 523 A90-34230
- A measurement window for a cryogenic windtunnel p 523 A90-34233
- Balance calibration and evaluation software p 523 A90-34237
- Design and manufacture of a cryogenic wind tunnel model p 523 A90-34238
- Automatic calibration machine for internal cryogenic balances p 524 A90-34247
- An infrared camera system for detection of boundary layer transition in the ETW p 539 A90-34249
- Examples of force measurements in a wind tunnel using multicomponent piezoelectric transducers p 540 A90-34352
- A technique for calculating nonlinear normal-force and pitching-moment coefficients for slender delta wings, accounting for wing thickness p 476 A90-34356
- Higher harmonic control of a helicopter model rotor to reduce blade/vortex interaction noise p 496 A90-34360
- Numerical calculation of the jet-interaction induced separation with respect to thrust vector control p 584 A90-35228
- Suppression of vortex asymmetry behind circular cones p 556 A90-36282
- Research department fluid mechanics - Scientific report (1988) p 603 A90-36538
- Computational methods in design aerodynamics p 557 A90-36539
- Configuration aerodynamics p 557 A90-36540
- Acoustics p 614 A90-36541
- Automatic calibration machine for cryogenic and conventional internal strain gage balances [AIAA PAPER 90-1396] p 595 A90-37939
- On the possibilities for improvement and modernization of subsonic wind tunnels [AIAA PAPER 90-1423] p 596 A90-37960
- Results of wind tunnel ground effect measurements on Airbus A320 using turbine power simulation and moving tunnel floor techniques [AIAA PAPER 90-1427] p 559 A90-37964
- Heat transfer in a solid fuel ramjet combustor [AIAA PAPER 90-1783] p 586 A90-38472
- The effect of an oscillatory freestream-flow on a NACA-4412 profile at large relative amplitudes and low Reynolds-numbers p 560 A90-38495
- Two-dimensional wall adaption in the transonic windtunnel of the AIA p 597 A90-38497
- The influence of interactional aerodynamics of rotor-fuselage-interferences on the fuselage flow p 561 A90-38523
- Calculation of two- and three-dimensional flow in a transonic turbine cascade with particular regard to the losses [AIAA PAPER 90-1542] p 565 A90-38686
- Multilevel optimization of large-scale structures in a parallel computing environment p 693 A90-39180
- Development and application of an optimization procedure for space and aircraft structures p 679 A90-39186
- Transonic flow around airfoils with relaxation and energy supply by homogeneous condensation p 620 A90-39782
- Acoustics of ultralight airplanes p 643 A90-40685
- Coherent vortex structures in the wake of a sphere and a circular disk at rest and under forced vibrations p 623 A90-40749
- Technological preparations of civil aircraft programs p 617 A90-41110
- Structural components of fiber-reinforced thermoplastics p 676 A90-41111
- Euromart - The European aviation research and technology program p 617 A90-41112
- Experimental windtunnel studies for EFA p 672 A90-41113
- Obstacle warning system for helicopters p 653 A90-41114
- Aerodynamic work for Hermes spaceplane p 675 A90-41115
- ATTHes - A helicopter in-flight simulator for ACT testing p 643 A90-41727
- A new noise certification method for 'light propeller aircraft' in testing p 635 A90-41728
- The evaluation of flight recorders p 653 A90-41729
- Measurement of angles and angle characteristics with accelerometers and gyroscopes p 653 A90-41730
- Hydrogen in future energy and propulsion technology p 692 A90-41736
- Inviscid and viscous flows in transonic and supersonic cascades using an implicit upwind relaxation algorithm [AIAA PAPER 90-2128] p 625 A90-42034
- Influence of ground effect on helicopter takeoff and landing performance p 645 A90-42278
- Computer-aided analysis of three-dimensional multiloop mechanisms p 669 A90-42328
- Model of a labyrinth seal with flow p 687 A90-42334
- Unsteady deformations of elastic rotor blades p 687 A90-42341
- A study of the influence of a helicopter rotor blade on the following blades using Euler equations p 630 A90-42435
- Comparison with experiment of various computational methods of airflow on three helicopter fuselages p 630 A90-42436
- System concept and performance criteria of modern helicopter navigation p 640 A90-42452
- Development and verification of software for flight safety critical strapdown systems p 694 A90-42454
- Helicopter ground and air resonance dynamics p 646 A90-42457
- A highly maneuverable helicopter in-flight simulator - Aspects of realization [AIAA PAPER 88-4607] p 670 A90-42466
- Influence of ground effect on helicopter takeoff and landing performance p 646 A90-42468
- The Franco-German helicopter programme HAP, PAH-2/HAC p 618 A90-42478
- Eight years of flight operations with composite rotorblades p 635 A90-42481
- Analytical evaluation of helicopter true air speed and associated flight tests p 647 A90-42499
- Recent advances in H₂/O₂ high pressure coaxial injector performance analysis [AIAA PAPER 90-1959] p 762 A90-42705
- Nozzle design optimization by method-of-characteristics [AIAA PAPER 90-2024] p 741 A90-42719
- Numerical simulation of hypersonic viscous continuum flow p 707 A90-44407
- Dornier Composite Aircraft - Economical and faultless p 732 A90-44751
- SST/HST air traffic - Challenge for the future p 763 A90-44752
- Slip-cast hot isostatically pressed silicon nitride gas turbine components p 765 A90-44816
- Flying qualities problems of aerospace craft [AIAA PAPER 90-2804] p 752 A90-45139
- Numerical simulation of vortical flows over close-coupled canard-wing configuration [AIAA PAPER 90-3003] p 788 A90-45852
- Euler procedure for calculation of the steady rotor flow with emphasis on wake evolution [AIAA PAPER 90-3007] p 789 A90-45857
- Design for a natural laminar flow glove for a transport aircraft [AIAA PAPER 90-3043] p 792 A90-45880
- Flight tests with a natural laminar flow glove on a transport aircraft [AIAA PAPER 90-3044] p 828 A90-45881
- Natural laminar flow - A wind tunnel test campaign and comparison with flight test data [AIAA PAPER 90-3045] p 792 A90-45882
- Calculation of three-dimensional viscous and inviscid hypersonic flows using split-matrix marching methods [AIAA PAPER 90-3070] p 794 A90-45894
- Design of supersonic wings using an optimization strategy coupled with a solution scheme for the Euler equations [AIAA PAPER 90-3060] p 794 A90-45895
- Multicriteria optimal layouts of aircraft and spacecraft structures p 889 A90-46046
- One wing for two airliners - Computer screens are technical trailblazers for a unique wing p 785 A90-46719
- A leap forward in aircraft construction technology - High-speed cutting sets new production standards p 881 A90-46720
- Airfoil design and data p 809 A90-47608
- Optimal periodic cruise with singular control [AIAA PAPER 90-3490] p 833 A90-47738
- The new light weight, high performance reconnaissance camera KRb 8/24 F p 847 A90-48607
- Possibilities for improving traffic flows p 823 A90-49272
- Self-excited oscillations in internal transonic flows p 813 A90-49274
- Thermal protection systems for hypersonic transport vehicles [SAE PAPER 901306] p 882 A90-49358
- A new method of aircraft motion error extraction from radar raw data for real-time motion compensation p 824 A90-49675
- Description and reconstitution of manoeuvre loadings p 919 A90-49878
- The Operational Loads Monitoring System (OLMS) p 926 A90-49879
- Damage tolerance demonstration for A310-300 CFRP-components p 919 A90-49894
- Monolithic CFC-Main Landing Gear Door for Tornado p 955 A90-50136
- Material development and second source qualification of carbon fiber/epoxy prepregs for primary and secondary Airbus structures p 948 A90-50225
- Assuring the future of civil aircraft industry in Germany [DGLR PAPER 88-004] p 902 A90-50232
- Aspects of the design of a hypersonic engine system and the selection of the intake and tail [DGLR PAPER 88-040] p 928 A90-50233
- Project Falke - Performance of free flight tests in the supersonic, transonic, and subsonic regimes from balloons [DGLR PAPER 88-018] p 903 A90-50235
- A method for calculating the rotor-fuselage interference in helicopters [DGLR PAPER 88-060] p 919 A90-50246
- Recent results of numerical flutter studies in high performance gliders [DGLR PAPER 88-038] p 934 A90-50249
- New experimental results on the origin and structure of Ferri and Dailey instabilities ('buzz') p 906 A90-51507
- The effect of energy input on the characteristics of profiles in compressible fluid media p 906 A90-51533
- A straight attached shock wave at the profile tip at freestream Mach number greater than about 1 p 907 A90-51534
- Theoretical prediction of pressure distribution on wedged delta wing at higher supersonic Mach numbers and its agreement with experimental results p 907 A90-51537

- Prediction of pressure distribution on optimum-optimum delta wing at higher angles of attack in supersonic flow and its agreement with experimental results p 907 N90-51538
- The formation of vortex streets in supersonic flows p 907 N90-51539
- The aerodynamic design of the contraction for a subsonic wind tunnel p 907 N90-51545
- Automotive gasoline - A fuel for modern aircraft piston engines p 950 N90-51620
- Unmanned helicopters for battlefield and maritime surveillance p 920 N90-51899
- A supplement to GPS/Navstar for civil use p 915 N90-52613
- Inspection of instrument landing systems p 915 N90-52614
- Integration and automation of navigation functions using Kalman filters p 915 N90-52615
- Experimental work station simulator at the test station of the Bundesanstalt fuer Flugsicherung p 937 N90-52616
- Design and evaluation of the ATC interface - Planning system for approach flight p 937 N90-52617
- At a depth of 500 meters - The TU Dresden supersonic wind tunnel p 937 N90-52700
- Thin walled cast high-strength structural parts p 65 N90-10242
- Turbulence management: Application aspects p 72 N90-10378
- ATTAS flight testing experiences p 34 N90-10862
- GRATE: A new flight test tool for flying qualities evaluation p 34 N90-10868
- Flight test results of a complex precise digital flight control system p 35 N90-10870
- Flight testing of the Tornado Terrain Following System p 35 N90-10875
- Steady and unsteady potential flow around thin annular wings and engines with simulation of jet engine flow [DFVLR-FB-89-18] p 89 N90-11711
- Controller design for active vibration suppression of a helicopter [DFVLR-FB-89-20] p 120 N90-11760
- Devices and procedures for the calibration of sensors and measurement: Systems of the flight test support system ATTAS [DFVLR-MITT-89-06] p 134 N90-12007
- General data processing support from project planning to workshop control [MBB-UD-526/88-PUB] p 138 N90-12208
- On the occasion of the 100th birthday of Ernst Heinkel [MBB/LW/3015/S/PUB/321] p 141 N90-12494
- Automatic processing of images from the GRATE flight test tool [DLR-FB-89-28] p 109 N90-12599
- A robust digital model following controller for helicopters [ESA-TT-1041] p 120 N90-12621
- Computation of flow fields around propellers and hovering rotors based on the solution of the Euler equations p 170 N90-13333
- Practical systems for speckle velocimetry p 171 N90-13341
- Laser two focus techniques p 212 N90-13348
- Geodetic network adjustment using GPS triple difference observations and a priori stochastic information [TR-1-1987] p 178 N90-13367
- Processing of undifferenced GPS carrier beat phase measurements and adjustment computations [TR-5-1988] p 178 N90-13368
- Generalized similarity solutions for three dimensional, laminar, steady, compressible boundary layer flows on swept profile cylinders [DLR-FB-89-34] p 212 N90-13725
- Numerical simulation of transition in three-dimensional boundary layers p 212 N90-13728
- General buckling tests with thin-walled shells [DLR-MITT-89-13] p 213 N90-13816
- Wind shear models for aircraft hazard investigation p 280 N90-15044
- Systems for airborne wind and turbulence measurement p 281 N90-15046
- Influence of windshear, downdraft and turbulence on flight safety p 238 N90-15048
- The interference of flightmechanical control laws with those of load alleviation and its influence on structural design p 258 N90-15054
- Active control system for gust load alleviation and structural damping p 259 N90-15056
- Aircraft response and pilot behaviour during a wake vortex encounter perpendicular to the vortex axis p 259 N90-15057
- Investigation on sheet material of 8090 and 2091 aluminium-lithium alloy p 267 N90-15192
- Wind tunnel tests of the influence of aerofoil thickness on the normal force and pitching moment of two slender wings at transonic and supersonic Mach numbers [ESA-TT-1129] p 237 N90-15889
- Design philosophy and construction techniques for integral fuselage fuel tanks p 250 N90-15913
- The cryogenic Ludwig tube tunnel at Goettingen p 263 N90-15947
- Pressure measurement technique in the wind tunnel division of DFVLR [ESA-TT-1145] p 264 N90-15963
- Flows with Separation [DGLR-PAPERS-88-05] p 276 N90-16169
- Experiments on the laminar-turbulent transition on swept wings p 276 N90-16170
- An efficient solver of the Eigenvalue problem of the linear stability equations for three dimensional, compressible boundary-layer flows p 276 N90-16172
- Semi-empirical transition criteria for the design of laminar profiles p 276 N90-16174
- Detection of flow instabilities at airfoil profiles using piezoelectric arrays p 276 N90-16175
- Determination of the N-factor in the Brunswick (Federal Rep. of Germany) transonic wind tunnel using measurements of pressure distributions and transition points, and the Sally method p 276 N90-16177
- Direct measurement of laminar instability amplification factors in flight p 277 N90-16178
- Development of transition criteria on the basis of e to the N power for three dimensional wing boundary layers p 277 N90-16179
- The precise calculation of the inviscid leading edge flow on a laminar airfoil using simple methods and verification by measurements on the TLF pilot model p 277 N90-16180
- Wind tunnel investigations on the configuration of the international vortex flow experiment p 277 N90-16181
- Flow field visualization study on a 65 deg delta wing at $M = 0.85$, p 277 N90-16182
- A nonlinear vortex-lattice method for the calculation of interference effects between free vortex sheets and wings p 277 N90-16183
- Research on three different Euler's schemes applied to a delta wing with vortical flows p 278 N90-16184
- Force and moment measurements on delta wings in unsteady flow p 278 N90-16185
- Numerical simulation of the laminar and turbulent three dimensional flow on a delta wing with sharp leading edge p 278 N90-16186
- Calculation of the flow field of a multiblade helicopter rotor using a Euler method including the wake p 278 N90-16189
- An interactive method for the flow calculation of airfoils with local separation regions p 278 N90-16190
- Calculation of the flap profile flows with separation based on coupled potential and boundary layer solutions p 278 N90-16191
- Inverse solutions for boundary layers with separation or close to separation under locally infinite swept wing conditions p 279 N90-16192
- Convergence speeding up in the calculation of the viscous flow about an airfoil p 279 N90-16194
- Periodically unsteady effects on profiles, induced by separation p 279 N90-16196
- Use of the film-of-oil technique for profile measurements in the Transonic Wind tunnel Brunswick (TWB) p 238 N90-16252
- Autonomous automatic landing through computer vision p 332 N90-16734
- Integrated flight guidance system using differential-GPS for landing approach guidance p 332 N90-16735
- Saenger propulsion system options p 344 N90-16818
- Hermes training aircraft p 354 N90-16827
- Verification of aerothermodynamic codes by means of a winged experimental re-entry vehicle p 354 N90-16842
- Dynamic derivatives of missiles and fighter-type configurations at high angles of attack p 337 N90-17554
- Objectives and results of cabin fire research in Germany p 325 N90-17588
- Fire prevention in transport airplane passenger cabins p 325 N90-17590
- Full scale study of a cabin fire in an A300 fuselage section p 326 N90-17592
- Onboard fire- and explosion suppression for fighter aircraft p 327 N90-17602
- Advanced materials for interior and equipment related to fire safety in aviation p 328 N90-17608
- Comparison of conventional and adaptive wall wind tunnel results with regard to Reynolds number effects p 352 N90-17649
- Some Navier-Stokes calculations for the CAST-10 airfoil p 320 N90-17651
- Half model tests on an ONERA calibration model in the transonic wind tunnel Goettingen, Federal Republic of Germany [DLR-MITT-89-20] p 397 N90-18370
- A comparison of flutter calculations based on eigenvalue and energy method p 425 N90-18406
- Numerical investigation of unsteady flow in oscillating turbine and compressor cascades p 426 N90-18407
- Unsteady blade loads due to wake influence p 426 N90-18413
- Experiments on the unsteady flow in a supersonic compressor stage p 427 N90-18422
- Experimental investigation of the influence of rotor wakes on the development of the profile boundary layer and the performance of an annular compressor cascade p 427 N90-18425
- Activities report in German aerospace [ISSN-0070-3966] p 465 N90-19189
- A panel process for the calculation of the flow around a wing with front angle damping [ETN-90-95367] p 399 N90-19207
- Carrier wing profile in nonstationary current [ETN-90-95368] p 399 N90-19208
- Calculation and optimization of rotor start process [ETN-90-95894] p 416 N90-19229
- Influence of friction and separation phenomena on the dynamic blade loading of transonic turbine cascades [MITT-88-04] p 428 N90-19235
- Wind tunnel design of heat island turbulent boundary layer [IHW-ET/50] p 455 N90-19542
- Progress in inverse design and optimization in aerodynamics p 482 N90-20977
- Aerodynamic design techniques at DLR Institute for Design Aerodynamics p 500 N90-20979
- An intensive procedure for the design of pressure-specified three-dimensional configurations at subsonic and supersonic speeds by means of a higher-order panel method p 500 N90-20982
- Inverse computation of transonic internal flows with application for multi-point-design of supercritical compressor blades p 501 N90-20987
- Aerodynamic design by optimization p 502 N90-20996
- Experimental and numerical study on basic phenomena of secondary flows in turbines p 512 N90-21014
- Secondary flow in a turbine guide vane with low aspect ratio p 513 N90-21018
- Measurement of the flow field in the blade passage and side-wall region of a plane turbine cascade p 513 N90-21019
- Centrifugal impeller geometry and its influence on secondary flows p 513 N90-21020
- Computational prediction and measurement of the flow in axial turbine cascades and stages p 514 N90-21028
- Analysis of the rotor tip leakage flow with tip cooling air ejection p 515 N90-21029
- Proceedings of the 13th International Congress on Instrumentation in Aerospace Simulation Facilities [EOADR-LR-89-069] p 527 N90-21046
- ROSAR (Helicopter-Rotor based Synthetic Aperture Radar) p 541 N90-21229
- Grid patching approaches for complex three-dimensional configurations p 573 N90-21985
- Results of TCAS-2 simulations in reconstructed dangerous encounters (Jul. 1986 to Jun. 1989) [ETN-90-96474] p 636 N90-23375
- Test and Measurement Technique in Hypersonics [ILR-MITT-225(1989)] p 618 N90-24225
- The gun tunnel of the Brunswick Institute for Fluid Mechanics: Current development status p 673 N90-24227
- High enthalpy hypersonic wind tunnel F4: General description and associated instrumentation p 673 N90-24228
- Short time Force and moment measurement System for shock tubes (SFS) for measuring times less than 10 ms p 674 N90-24233
- Infrared thermography at hypersonic channel H2K p 674 N90-24235
- Tests for integrating measurement of gas pressures in flight propellers [ETN-90-96498] p 634 N90-24253
- A time-marching method to calculate unsteady airloads on three-dimensional wings. Part 1: Linearized formulation [DLR-FB-89-58] p 634 N90-24254
- A time-marching method for calculating unsteady airloads on three-dimensional wings. Part 2: Full-potential formulation [DLR-FB-89-59] p 635 N90-24255
- Aerodynamic development perspective for traffic aeroplanes [DGLR-89-141] p 637 N90-24260

The 30th Airlines International Electronics Meeting Proceedings
[ETN-90-96973] p 637 N90-24261

Transonic wing charge improvements by passive shock boundary layer interference control: Development status and prospects
[ETN-90-96463] p 650 N90-24267

Calculation of the aeroelastic blade stabilization with linearized process
[MITT-87-01] p 666 N90-24272

On simplified analytical flutter clearance procedures for light aircraft
[DLR-FB-89-56] p 672 N90-24276

En route noise of turboprop aircraft and their acceptability: Report of tests
p 697 N90-24858

En route noise of two turboprop aircraft
[DLR-MITT-89-18] p 697 N90-24859

Noise measurements of turboprop airplanes at different overflight elevations
p 697 N90-24860

Additive evaluation criteria for aircraft noise
p 698 N90-24867

Development and application of an optimization procedure for space and aircraft structures
[MBB-FW-522/S/PUB-383] p 779 N90-25078

Short time-dynamometer system for shock wave channels
[MBB-UT-115/89-PUB] p 773 N90-25084

Simulation of transport aeroplanes
[MBB-UD-007/89-PUB] p 723 N90-25089

Investigation on sheet material of 8090 and 2091 aluminium-lithium alloy
[MBB-UD-122/89-PUB] p 766 N90-25090

Damage tolerance demonstration for A310-300 CFPR components
[MBB-UT-012/89-PUB] p 766 N90-25091

Scenario 2000
[MBB-UD-500/89-PUB] p 734 N90-25092

Development and test of software by safety critical aircraft systems
[MBB-FE-363/S/PUB-384] p 723 N90-25103

A lifting surface method for the calculation of steady and unsteady, incompressible propeller aerodynamics
[ESA-TT-1151] p 717 N90-25113

Calculation of thick wall fiber binders for rotor components of modern helicopters
[MBB-UD-554/84-PUB] p 735 N90-25137

The jet engine: 1932
[ISBN-3-922010-49-0] p 763 N90-25189

Construction of a hybrid angular velocity reference system for investigation of the dynamic characteristics of strapdown gyros
[ESA-TT-1181] p 774 N90-25332

The disturbance processes on the data links of the mode-S air traffic control system
[ETN-90-96960] p 729 N90-25965

A contribution to the improvement of the accuracy in the parameter identification of nonlinear processes, by example of the aircraft motion
[ETN-90-96961] p 736 N90-25974

The applicability of simple helicopter models for flight mechanics studies
[ETN-90-96962] p 736 N90-25975

A contribution to the economic, optimal dimensioning, and shaping of aircraft structures using a design model
[ETN-90-96966] p 737 N90-25976

Chemistry of combustion processes
p 749 N90-25994

Maneuvering by means of lateral jets
[ISL-CO-255/88] p 758 N90-26015

Materials and structures for 2000 and beyond: An attempted forecast by the DLR Materials and Structures Department
[ESA-TT-1154-REV] p 775 N90-26173

Adaptation for unsteady flow
p 871 N90-26845

Aircraft Integrated Monitoring Systems
[DLR-MITT-90-04] p 786 N90-27617

Past, present and future: Aircraft integrated monitoring systems: An ever-developing technology
p 848 N90-27618

Aircraft condition monitoring system for future Airbus aircraft: New concept for programming and data recording
p 848 N90-27619

The EFA integrated monitoring and recording system: Requirements and concept for implementation
p 848 N90-27620

AIMS test and simulation equipment
p 892 N90-27623

Start-up built-in test for the DISCUS fault tolerant, fly-by-wire computer system
p 869 N90-27625

Experimental identification of helicopter engine dynamics from closed loop data
p 855 N90-27627

Advanced algorithms design and implementation in on-board microprocessor systems for engine life usage monitoring
p 892 N90-27628

Knowledge based diagnosis of jet engines under consideration of model based methods
p 855 N90-27631

Airborne CO₂ Doppler lidar for wind shear detection
p 849 N90-27640

Monitoring and controlling flight in windshear
p 820 N90-27641

Automation of the readout, transcription and evaluation of digital flight data at DLR
p 893 N90-27645

Position finding and ground target direction finding by an aircraft with a gimbaled video camera
[DLR-FB-89-62] p 825 N90-27673

Integrated Air Traffic Management
[DLR-MITT-89-23] p 825 N90-27676

Air traffic management in Europe: Structure, tasks, potential
p 825 N90-27677

Airline requirements for a future air traffic management system
p 825 N90-27678

R and D aspects of the future operational concept of the BFS
p 826 N90-27679

On-board planning and control of 4D-trajectories in the TMA
p 826 N90-27680

Four-dimensional navigation and Flight Management Systems
p 826 N90-27681

On the structure of a future flight operations system
p 826 N90-27682

Four-dimensional planner: A ground based planning system for time accurate approach guidance
p 826 N90-27683

Development of a COMPAS prototype for the ATC Centre at Frankfurt (Fed. Republic of Germany)
p 826 N90-27684

Safety net functions
p 826 N90-27685

Approach towards a future integrated airport surface traffic management
p 827 N90-27686

Experimental study towards a future airport ground movement simulator
p 827 N90-27687

Aspects of data link applications for ATC purposes
p 827 N90-27688

Application of a company data link at Lufthansa German Airlines
p 827 N90-27689

The discretization of the three dimensional boundary layer equations
[ETN-90-97292] p 884 N90-27987

NDI-concept for composites in future military aircraft
p 877 N90-28070

Neutron radiography: Applications and systems
p 886 N90-28080

New aspects in aircraft inspection using eddy current methods
p 886 N90-28085

A process for analysis, evaluation, and development of aerial servicing noise reduction measures in civil aircraft
[ETN-90-97300] p 896 N90-28398

Experimental investigations on the stability and vorticity of the vortex breakdown phenomenon above delta wings, measured by the ultrasonic laser method
[ESA-TT-1079] p 910 N90-28498

Effects of canard position on the aerodynamic characteristics of a close-coupled canard configuration at low speed
p 920 N90-28519

Inflight thrust vectoring: A further degree of freedom in the aerodynamic/light mechanical design of modern fighter aircraft
p 921 N90-28528

Aerodynamic interferences of in-flight thrust reversers in ground effect
p 921 N90-28529

Fretting fatigue strength of Ti-6Al-4V at room and elevated temperatures and ways of improving it
p 952 N90-28709

Overview on hot gas tests and molten salt corrosion experiments at the DLR
p 953 N90-28714

Design of an axisymmetric, contoured nozzle for the HEG
[DLR-FB-90-04] p 959 N90-28812

Flight test engineering with the ATTAS
p 902 N90-29160

Numeric fluid mechanics
p 960 N90-29161

Applications of LIF to high speed flows
p 911 N90-29320

Procedure for calibrating fly-by-wire control chains of the flying testbed ATTAS
[DLR-MITT-90-02] p 936 N90-29401

The signals of an ice warning device in dependence on total water content and normalized icing degree
[ESA-TT-1207] p 963 N90-29692

GREECE

Evaluation of two numerical techniques for the prediction of flow around blades
p 10 A90-12512

A secondary flow calculation method for one stage centrifugal compressor
p 14 A90-12597

Calculation of axisymmetric flows in turbomachines, through an explicit time-splitting method
p 14 A90-12622

Jet engine fault detection with differential gas path analysis at discrete operating points
p 50 A90-12633

Hot wire measurements in the wake of an oscillating airfoil
p 15 A90-12635

Casing vibration and gas turbine operating conditions [ASME PAPER 89-GT-78] p 358 A90-23799

A two-dimensional unsteady potential solver in internal aerodynamics flow problems
p 707 A90-44430

Development and application of a fractional-step method for the solution of transonic and supersonic flow problems
p 709 A90-44461

Multigrid scheme for the compressible Euler-equations
p 907 A90-51559

Secondary flow calculations for axial and radial compressors
p 514 A90-21024

Computer modeling and data processing methods: An essential part of jet engine condition monitoring and fault diagnosis
p 855 N90-27626

INDIA

Oscillating thin wings in inviscid incompressible flow
p 2 A90-10224

Studies on the influence of Mach number on profile losses of a reaction turbine cascade
p 10 A90-12517

Flow in compressor interstage ducts
p 11 A90-12521

A study of flow structure in a contra-rotating axial compressor stage
p 11 A90-12524

Experimental study of static pressure and mean velocity profiles inside a two-dimensional dump-type combustor model
p 45 A90-12530

Design and off-design performance predictions of axial turbines
p 45 A90-12540

Boundary layer growth on low aspect ratio compressor blades
p 12 A90-12553

Stress analysis of gas turbine bladed disc for structural integrity applying the concept of cyclic symmetry
p 46 A90-12564

Axisymmetric afterbody flow separation at transonic speeds in presence of jet exhaust
p 13 A90-12576

Unbalance response studies on a model rotor supported on uncentralised squeeze film dampers and the development experience of a jet engine
p 69 A90-12579

Comparative cascade studies of some high diffusion compressor bladings
p 15 A90-12637

Unified super/hypersonic similitude for steady and oscillating cones and ogives
p 82 A90-13786

Supersonic/hypersonic flow past wedge and plane ogive in oscillation
p 85 A90-15231

Separated flow over slender wing, body and wing-body combination
p 85 A90-15232

Computation of transonic separated flow using the Euler equations
p 85 A90-15233

Numerical solution of unsteady Navier-Stokes equations for laminar/turbulent flows past axis-symmetric bodies at angle of attack
p 85 A90-15235

Transonic flow over a single wedge
p 85 A90-15237

Wake-boundary layer interaction
p 85 A90-15238

Leading edge flap influence on aerodynamic efficiency
p 85 A90-15240

The characteristic decay region of a class of three-dimensional wall jets
p 85 A90-15241

Numerical simulation of supersonic and hypersonic turbulent compression corner flows using PNS equations
p 85 A90-15242

Euler solutions with a multi-block structured code
p 86 A90-15739

Full-potential calculations using Cartesian grids
p 86 A90-15740

Computation of flow over airfoils under high lift separated flow condition
p 86 A90-15741

Wind tunnel testing of high blockage models
p 121 A90-15743

Development of bluff body wake in a longitudinally curved stream
p 86 A90-15745

Selection of a suitable combustion system for a small gas turbine engine
p 112 A90-16005

Photoelastic investigation of turbine rotor blade shrouds
p 112 A90-16008

Squeeze film damping for aircraft gas turbines
p 113 A90-16009

Integrated approach to design and manufacture of gas turbine components based on group theory
p 113 A90-16010

Creep-fatigue interactions of gas turbine materials
p 131 A90-16011

Potential flow calculation for three-dimensional wings and wing-body combination in oscillatory motion
p 153 A90-17976

Underexpanded jet-freestream interactions on an axisymmetric afterbody configuration
p 154 A90-18141

Incompressible potential flow about complete aircraft configurations
p 156 A90-18443

Wake behaviour of a large deflection turbine rotor linear cascade p 157 A90-18481

Effect of downstream elements on the flow at the exit of centrifugal compressor rotor p 157 A90-18483

Comparison of NACA 65, CDA, and tandem bladed cascades p 190 A90-18484

Computerised structural analysis for engine components p 190 A90-18486

In process failure investigations in aeronautics p 181 A90-18489

Rotor/fuselage vibration isolation studies by a Floquet-harmonic iteration technique p 182 A90-19393

Investigation of oscillating airfoil shock phenomena [AIAA PAPER 90-0695] p 169 A90-19981

A fiberoptic LAN for aircraft and other applications p 282 A90-23241

Incompressible viscous flow about aircraft configurations p 233 A90-23290

On-line temperature profile display system [ASME PAPER 89-GT-10] p 374 A90-23755

Resonant stress determination of a turbine blade with modal damping as a function of rotor speed and vibrational amplitude [ASME PAPER 89-GT-27] p 340 A90-23765

A numerical three-dimensional thermal stress analysis for cooled blades [ASME PAPER 89-GT-168] p 341 A90-23853

A microprocessor-based system for monitoring gas turbines p 350 A90-24359

Buckling analysis of FRP faced cylindrical sandwich panel under combined loading p 365 A90-24376

Viscous corrections on wings in incompressible flow p 301 A90-25200

Flow-calculation over a delta-wing using the thin-layer Navier-Stokes equations p 304 A90-25773

Computation of 2D Navier-Stokes equations p 367 A90-25801

Numerical prediction of wakes of different bodies p 308 A90-26341

Design priorities for an air-superiority fighter p 335 A90-26344

Optimal reflex camber p 308 A90-26347

Simulation of separated flows using panel method p 308 A90-26349

Wind tunnel testing of a helicopter model at HAL p 335 A90-26350

Adaptive wall wind tunnels - Marriage between experiments and computations p 351 A90-26351

A powerful range-Doppler clutter rejection strategy for navigational radars p 403 A90-30688

Accurate ILS and MLS performance evaluation in presence of site errors p 404 A90-30693

Analytical evaluation of radiation patterns of a TACAN antenna p 404 A90-30695

Multi-element aerofoils in viscous flow p 469 A90-32451

Effectiveness of passive devices for axisymmetric base drag reduction at Mach 2 p 555 A90-36184

Interaction between boundary layer and wakes of different bodies p 602 A90-36263

Response of orthogonally stiffened cylindrical shell panels p 603 A90-36285

Hierarchical finite element method for rotating beams p 605 A90-38353

Flutter of shaft-supported low aspect-ratio control surfaces p 667 A90-38912

Aeroelastic analysis of a low aspect ratio wing p 619 A90-38915

Estimation of fatigue crack growth in patched cracked panels p 684 A90-41335

Acoustic emission and signal analysis p 781 A90-43782

Aerodynamic characteristics of forward sweep [AIAA PAPER 90-3041] p 792 A90-45879

National Conference on Aerodynamics, 5th, Poona, India, May 24, 25, 1990, Proceedings p 809 A90-48076

Winger - Computer code for aerodynamic analysis of wings p 810 A90-48077

Optimal camber distributions with multiple constraints p 810 A90-48078

Modelling free vortex flow on planar swept wing p 810 A90-48079

Vertical tail design for base-line configuration of military combat aircraft p 810 A90-48080

Airbrake design for base-line configuration of advanced jet trainers/light attack airplanes and military combat airplanes p 810 A90-48081

Incompressible potential flow about three-dimensional configurations p 810 A90-48082

Computational and experimental studies on ground effect of a slender wing tailless delta aircraft p 810 A90-48083

Viscous flow characteristics over a blunt cone at hypersonic Mach numbers by using a PNS code p 810 A90-48085

Solutions of two-dimensional Euler equations with multigrid acceleration p 810 A90-48086

Lift and pitching moment measurements on a swept tapered wing in oscillatory vertical gusts p 811 A90-48089

Aircraft passing through a sinusoidal gust p 811 A90-48090

Application of a vortex lattice numerical model in the calculation of inviscid incompressible flow around delta wings p 904 A90-51017

Analysis and design of symmetrical airfoils [PD-CF-8943] p 400 N90-19213

Multigrid accelerated relaxation solution of transonic full potential flow equation [PD-CF-8942] p 480 N90-20951

Flight path reconstruction using extended Kalman filtering techniques [PD-CF-9001] p 489 N90-20970

Design of a natural laminar flow airfoil for an unmanned aircraft [PD-CF-9004] p 499 N90-20975

Human centrifuge controller [NAL-TM-SE-8901] p 527 N90-21043

Flight testing of a natural laminar flow airfoil using gliders [PD-CF-9005] p 718 N90-25936

Model following control system design: Preliminary ATTS in-flight simulation test results [PD-CF-9003] p 758 N90-26010

Do inviscid vortex sheets roll-up [PD-CF-9010] p 909 N90-28491

Sting-support interference on afterbody drag at transonic speeds [NAL-TM-EA-8902] p 909 N90-28492

A conceptual framework for fighter flight control systems [PD-CF-9009] p 936 N90-28577

Development of a software package for automatic data acquisition, analysis, and controls in an axial flow compressor test rig [PD-PR-8910] p 965 N90-29926

INDONESIA

Systematic study of flutter characteristics of two-dimensional cascades in incompressible flow p 41 A90-11796

Development of airborne data reduction system in IPTN flight test p 418 A90-28895

INTERNATIONAL ORGANIZATION

Unsteady loss in a low speed axial flow compressor during rotating stall p 12 A90-12527

Unsteady flow in centrifugal compressors due to downstream circumferential distortions p 14 A90-12598

Aviation Security (Avsec) p 23 A90-12782

International satellite radionavigation and radiolocation - Choosing among the options p 96 A90-13979

MAVIS flight load simulation p 202 A90-17003

Cockpit evolution in Airbus p 247 A90-22434

Experimental and theoretical study of the swirling flow in centrifugal compressor volutes [ASME PAPER 89-GT-183] p 273 A90-22663

Measurements, visualization and interpretation of 3-D flows - Application within base flows p 386 A90-28252

Mean and turbulent velocity measurements in a turbojet exhaust p 423 A90-28272

A novel technique for aerodynamic force measurement in shock tubes p 438 A90-28302

Infrared thermography in blowdown and intermittent hypersonic facilities p 440 A90-31302

The influence of boundary layer state on vortex shedding from flat plates and turbine cascades [ASME PAPER 89-GT-296] p 474 A90-33560

High-temperature corrosion and mechanical properties of some silicon nitride ceramics p 531 A90-33985

PETW testing results p 523 A90-34226

Results of studies on a manipulator system for model handling in the ETW p 524 A90-34248

Tests of automatic dependent surveillance (ADS) in Western Europe - Possible future developments p 574 A90-35353

Development of supersonic and hypersonic Euler solvers using shock fitting in two and three dimensions p 707 A90-44426

Numerical simulation of the compressible flow in a valve-cylinder assembly p 770 A90-44431

Solution of the Euler equations using unstructured polygonal meshes p 708 A90-44435

V2500 turbofan engine [SAE PAPER 892363] p 747 A90-45512

Compressible Navier-Stokes solutions over low Reynolds number airfoils p 802 A90-46382

An international civil integrity complement to GPS and GLONASS p 821 A90-46392

Time synchronization/distribution applications of navigation signals repeated by geostationary satellites p 872 A90-46397

Rotor loads computation using singularity methods and application to the noise prediction p 807 A90-46880

Latin American Conference on International Air Transport and Activities in Outer Space, Mexico City, Mexico, Aug. 14-18, 1988, Proceedings p 897 A90-49613

The integration of Latin American transport - Realities and perspectives p 898 A90-49618

Airbus technologies - An evolutionary process p 902 A90-52699

IRAN

Algebraic boundary-conforming grid generation around wing/tail-body configurations p 308 A90-26480

IRAQ

A computer aided manufacturing procedure for experimental two-dimensional aerofoils p 270 A90-20609

ISRAEL

Aerosol effects on jet-engine IR radiation p 40 A90-10152

A multichannel wide FOV infrared radiometric system p 67 A90-11410

Similarity and scale effects in solid fuel ramjet combustors p 60 A90-12513

Combustion characteristics of a boron-fueled SFRJ with aft-burner p 62 A90-12514

A study of two-phase flow for a ramjet combustor p 45 A90-12532

Surface roughness effect on the aerodynamic characteristics of a blunt body p 16 A90-12740

The fundamentals of vectored propulsion p 180 A90-17461

The effect of impact loading on residual strength of CFRP composite beams p 208 A90-17683

Theoretical modelling of composite rotating beams p 208 A90-17684

Low Reynolds number airfoils evaluation program p 151 A90-17692

Wing-body mutual influence coefficients at angles-of-attack to 24 deg p 151 A90-17693

Time-domain aeroservoelastic modeling using weighted unsteady aerodynamic forces p 195 A90-17698

Supplemented visual cues for helicopter hovering above a moving ship deck p 195 A90-17704

Simulation of helicopter landing on a ship deck p 181 A90-17705

Angular feature mapping - An optical method p 377 A90-23974

Periodic response of thin-walled composite blades p 408 A90-28229

Reduced size first-order subsonic and supersonic aeroelastic modeling [AIAA PAPER 90-1154] p 390 A90-29366

Real time estimation of aircraft angular attitude p 431 A90-30103

Sensitivity derivatives of flutter characteristics and stability margins for aeroservoelastic design p 433 A90-31287

Reduced-order aeroelastic models via dynamic residualization p 493 A90-33412

Reduced-order aeroelastic models via dynamic residualization p 579 A90-35762

A method for solving three-dimensional viscous incompressible flows over slender bodies p 558 A90-37890

Aerodynamic effects of body roughness [AIAA PAPER 90-2850] p 712 A90-45168

Active flow control on low Reynolds number airfoils [AIAA PAPER 90-3039] p 792 A90-45878

Speed-up of the strongly implicit procedure with application to subsonic/transonic potential flows p 809 A90-47301

Aeronautical fatigue in the electronic era; Proceedings of the Fifteenth ICAF Symposium, Jerusalem, Israel, June 21-23, 1989 p 901 A90-49876

Acoustic fatigue analysis by the finite element method p 954 A90-49886

The calculation of incompressible separated turbulent boundary layers p 905 A90-51025

Convex models of malfunction diagnosis in high performance aircraft [AD-A218514] p 702 N90-25073

Multi-disciplinary optimization of aeroservoelastic systems [NASA-CR-185931] p 925 N90-29385

ITALY

Effects of random initial conditions and deterministic winds on simulated parachute motion p 22 A90-11002

Decommutation techniques and their integration into post flight analysis system p 26 A90-12191

- Acquisition and recording of AMX A/C Aeritalia experience and present trends p 26 A90-12194
- Turbomachinery tip gap aerodynamics - A review p 13 A90-12557
- Flutter analysis on a non-linear wing model p 207 A90-17009
- Secondary flows in a transonic cascade - Comparison between experimental and numerical results p 157 A90-18501
- New approach for Doppler ambiguities resolution in medium pulse repetition frequency radars p 240 A90-20937
- Viscous flow calculations in turbomachinery channels [ASME PAPER 89-GT-5] p 287 A90-23752
- Inviscid cascade flow calculations using a multigrid method [ASME PAPER 89-GT-22] p 288 A90-23763
- A proposal for optimized design of multistage compressors [ASME PAPER 89-GT-34] p 288 A90-23766
- Mach number effects on secondary flow development downstream of a turbine cascade [ASME PAPER 89-GT-67] p 290 A90-23790
- Axial flow compressor design optimization. I - Pitchline analysis and multivariable objective function influence [ASME PAPER 89-GT-201] p 342 A90-23873
- Axial flow compressor design optimization. II - Through-flow analysis [ASME PAPER 89-GT-202] p 342 A90-23874
- Computation of steady three dimensional transonic internal flows p 304 A90-25771
- Non-equilibrium hypersonic flows - Physics and numerics p 304 A90-25777
- Time dependent effects on high temperature low cycle fatigue and fatigue crack propagation on nickel base superalloys p 443 A90-29881
- Numerical simulation of an adaptive-wall wind-tunnel - A comparison of two different strategies p 439 A90-30251
- Active flutter suppression for a wing model p 433 A90-31283
- Aeroelastic analysis for a composite T-tailplane of a turboprop commuter aircraft p 492 A90-33390
- The use of simulation in support of the high AOA flight test program of the AM-X aircraft [AIAA PAPER 90-1289] p 495 A90-33909
- EH 101 Flight Test Program current status and future testing [AIAA PAPER 90-1296] p 495 A90-33912
- Flight test safety and 'high risk' tests - The Aeritalia approach [AIAA PAPER 90-1315] p 483 A90-33924
- Doppler-rate filtering for detecting moving targets with synthetic aperture radars p 488 A90-34138
- Shock-fitting method for two-dimensional inviscid, steady supersonic flows in ducts p 477 A90-34864
- Blockage corrections at high angles of attack in a wind tunnel p 593 A90-35756
- Boundary layer diagnostics by means of an infrared scanning radiometer p 605 A90-38493
- Numerical prediction of transonic viscous flows around airfoils through an Euler/boundary layer interaction method [AIAA PAPER 90-1537] p 564 A90-38681
- Expert system for pilot assistance - The challenge of an intensive prototyping p 693 A90-38909
- Wind shear at Pantelleria airport p 692 A90-39702
- Numerical simulation of the behaviour of internal combustion supercharged engines [AIAA PAPER 90-1873] p 655 A90-40539
- Trend analysis and diagnostics codes for training purposes [AIAA PAPER 90-2394] p 617 A90-42156
- Agusta methodology for pitch link loads prediction in preliminary design phase p 646 A90-42465
- Use of smart actuators for the tail rotor collective pitch control p 688 A90-42483
- Direct drive servovalves: Why and how - The Magnaghi Milano answer p 688 A90-42484
- Co-development of CT7-6 engines - A continued tradition in technology and reliability p 665 A90-42485
- Contribution of engine improvement on next future rotorcraft p 665 A90-42488
- EH-101 main rotor hub application of thick carbon fiber unidirectional tension bands p 618 A90-42489
- Hydraulic accumulators and high pressure bottles in composite material p 688 A90-42493
- Numerical simulation of nonpremixed turbulent flow in a dump combustor [AIAA PAPER 90-1858] p 768 A90-42685
- A multistage method for the solution of the Euler equations on unstructured grids p 708 A90-44460
- Wake effects on the prediction of transonic viscous flows around airfoils with an Euler/boundary layer interaction approach [AIAA PAPER 90-3061] p 798 A90-45933
- Comparison among modal analyses of axial compressor blade using experimental data of different measuring systems p 878 A90-46038
- Prediction of aerodynamic performance of airfoils in low Reynolds number flows p 799 A90-46360
- Understanding composite fatigue - New trends p 940 A90-49893
- Combined advanced foundry and quality control techniques to enhance reliability of castings for the aerospace industry p 64 A90-10240
- P-180 AVANTI: Project and flight test program comprehensive overview p 34 A90-10863
- In flight reflight tests on AM-X single engine fly-by-wire aircraft p 34 A90-10869
- Problems related to the acquisition, processing and utilization of the modal parameters measured in flight tests in order to obtain the full envelope for flutter [ETN-89-95210] p 103 A90-11735
- Evolution of flight commands in Aeritalia design [ETN-89-95211] p 120 A90-11759
- The aerodynamic experimental center of Aeritalia: Combat aircraft group [ETN-89-95213] p 122 A90-11766
- Choice and characterization of new materials for aerospace applications [ETN-89-95219] p 126 A90-11819
- A new test procedure for a wing made with carbon fiber composites [ETN-89-95220] p 126 A90-11820
- The evolution of light alloys in the aerospace industry [ETN-89-95216] p 126 A90-11872
- In service life monitoring system using g-meter readings and mass configuration control [ETN-89-95218] p 134 A90-12035
- Development and applications of reliability and maintainability design criteria in military aircraft [ETN-89-95208] p 107 A90-12591
- Acquisition and recording of an AMX A/C Aeritalia experience and present trends [ETN-89-95217] p 109 A90-12598
- Project, implementation, and utilization of composite structures [ETN-89-95209] p 127 A90-12665
- Fatigue behavior of specimens under compression load spectra [ETN-89-95207] p 137 A90-12954
- Canard versus aft-tail ride qualities performance and pilot command response p 258 A90-15053
- Aircraft fuel tank construction and testing experience p 250 A90-15907
- Mirach 100 flight control system p 260 A90-15926
- A fast collocation method for transonic airfoil design p 501 A90-20984
- Numerical method for designing 3D turbomachinery blade rows p 511 A90-20990
- A tool for automatic design of airfoils in different operating conditions p 502 A90-20994
- Secondary flows and Reynolds stress distributions downstream of a turbine cascade at different expansion ratios p 512 A90-21015
- A computer code for the prediction of aerodynamic characteristics of lifting airfoils at transonic speed [DLC-EST-TN-030] p 632 A90-23359
- Prediction of aerodynamic performance of airfoils in low Reynolds number flows [DLC-EST-TN-031] p 632 A90-23360
- Problems of internal acoustics in two and three dimensional cavities with deformable walls using the MSC/Nastran code [DLC/STR-INT-TN-004] p 699 A90-24876
- Agusta methodology for pitch link loads prediction in preliminary design phase [ETN-90-97270] p 737 A90-25978
- AM-X high incidence trials, development and results [ETN-90-97277] p 759 A90-26016
- Development of a method to design helicopter rotors [REPT-100-30-03] p 845 A90-26830
- New inflight experiments to measure aerodynamics loads [ETN-90-97276] p 868 A90-26834
- Design of helicopter components in metal matrix composites [REPT-100-20-55] p 874 A90-26894
- Estimation of defective rate of mechanic-hydraulic components [ETN-90-97275] p 884 A90-27120
- Expert system for pilot assistance: The challenge of an intensive prototyping [ETN-90-97274] p 825 A90-27674
- An ultrasonic system for in-service non-destructive inspection of composite structures p 885 A90-28076
- Aerodynamic control design: Experience and results at Aermacchi p 935 A90-28518
- Infrared thermography p 911 A90-29325
- JAPAN**
- Evaluating the feasibility of a radar separation minimum for a long-range SSR p 25 A90-10240
- Holographic interferometric study of shock wave propagation p 66 A90-10732
- Rotor-blades excitation due to differential interference of vane wakes between upstream stator-rows in an axial compressor p 6 A90-11784
- Unsteady aerodynamic characteristics of oscillating cascade with tip clearance p 8 A90-11793
- Improved double linearization method for prediction of mean loading effects on subsonic and supersonic cascade flutter p 41 A90-11795
- Flutter of cascade blades composed of blades having arbitrarily different natural frequencies p 42 A90-11798
- Self-excited oscillation of shock waves on an airfoil in two-dimensional transonic channel flow p 8 A90-11808
- Finite element method for unsteady three-dimensional subsonic flows through a cascade oscillating with steady loading p 9 A90-11873
- A new hybrid 'airship' ('Heliship') for commuter transport p 29 A90-11875
- Development of new segment carbon seal for use at low sealing pressure region FJR710/600S turbo fan engine p 69 A90-11950
- The features of FJR 710 engine p 42 A90-12011
- Endurance test of FJR 710/600S engine p 42 A90-12012
- Start characteristics of FJR 710/600S engine p 42 A90-12013
- Oil migration of FJR 710/600S engine p 43 A90-12014
- Steady state performance of FJR 710/600S engine p 43 A90-12015
- Mechanical rig rest of FJR 710/600 engine components p 43 A90-12016
- Design of control amplifier for FJR 710 engine p 43 A90-12017
- Measurements of pressure fluctuations in the interaction regions of shock waves and turbulent boundary layers induced by blunt fins p 9 A90-12218
- Numerical calculation of unsteady aerodynamic forces for three-dimensional subsonic oscillating cascades by a finite element method p 9 A90-12219
- Aerodynamic heating in the interaction regions of shock waves and turbulent boundary layers induced by sharp fins p 9 A90-12220
- An application of the surface-singularity method to wing-body-tail configurations p 9 A90-12229
- An electronic flight-recorder for a hang-glider p 39 A90-12234
- Numerical calculation of unsteady aerodynamic forces for two-dimensional supersonic oscillating cascades by finite element method p 9 A90-12238
- Hydrogen fueled subsonic-ram-combustor model tests for an air-turbo-ram engine p 44 A90-12529
- Experimental study on autoignition in a scramjet combustor p 46 A90-12559
- Cooling characteristics of a radial water blade p 47 A90-12571
- Numerical analysis of rotating stall by a vortex model p 13 A90-12590
- Radial swirl flows between parallel disks at critical flow rate p 14 A90-12596
- A study on the performance of the turbo-ramjet engines at high speed flight p 49 A90-12608
- Restart characteristics of turbofan engines p 50 A90-12627
- Application of the double linearization theory to three-dimensional subsonic and supersonic cascade flutter p 50 A90-12638
- Development study of air turbo-ramjet for future space plane [IAF PAPER 89-311] p 109 A90-13445
- The cycle evaluation of the advanced LACE performance [IAF PAPER 89-313] p 109 A90-13447
- Aerodynamic heating in shock wave/turbulent boundary layer interaction regions induced by blunt fins p 82 A90-13775
- Two effective methods of approach and landing by visual display [SAE PAPER 891054] p 108 A90-14356
- Recent Navier/Stokes calculations in applications p 85 A90-15227
- Development process of turbulence in a round-nozzle air jet p 87 A90-16101
- Studies on supersonic radial flow behavior in disk channel p 87 A90-16104
- A study on surge and rotating stall in axial compressors - A summary of the measurement and fundamental analysis method p 87 A90-16105

- Calculation of flow over airfoil with slat and flap p 149 A90-16797
- Transonic flow in throat region of supersonic nozzles p 149 A90-16799
- Cryogenic wind tunnels p 199 A90-17346
- Noise prediction of a counter-rotation propfan p 218 A90-17861
- Direct search method to aeroelastic tailoring of a composite wing under multiple constraints p 208 A90-17865
- High-resolution upwind scheme for vortical-flow simulations p 153 A90-17872
- Design and evaluation of graphite/epoxy truss core sandwich panels p 210 A90-18406
- Unsteady aerodynamic forces on rolling delta wings at high angle of attack p 159 A90-19426
- An adaptive flight control system design for non-minimum phase CCV by relative order reduction p 196 A90-19428
- Minimum fuel cruise by periodic optimization p 182 A90-19429
- Attitude projection method for analyzing large-amplitude airplane maneuvers p 197 A90-19555
- Thrust augmentation characteristics of jet reactions [AIAA PAPER 90-0033] p 161 A90-19641
- Three dimensional photoelastic analysis of aeroengine parts p 270 A90-20077
- Preliminary feasibility study for a new hybrid airship (Heliship) p 244 A90-20581
- A new hybrid LTA vehicle, 'Heliship' - its philosophy, outline [AIAA PAPER 89-3162] p 244 A90-20582
- A new type of non-rigid airship system [AIAA PAPER 89-3175] p 244 A90-20583
- Optimum design of rotational wheels under transient thermal and centrifugal loading p 270 A90-20770
- Evaluation and measurement of airplane flutter interference p 272 A90-22529
- Airborne array antennas for satellite communication p 265 A90-23202
- Self-excited oscillation of transonic flow around an airfoil in two-dimensional channel [ASME PAPER 89-GT-58] p 290 A90-23784
- Application of low-solidity cascade diffuser to transonic centrifugal compressor [ASME PAPER 89-GT-66] p 290 A90-23789
- Effect of blade tip configuration on tip clearance loss of a centrifugal impeller [ASME PAPER 89-GT-80] p 358 A90-23801
- Secondary flow due to the tip clearance at the exit of centrifugal impellers [ASME PAPER 89-GT-81] p 358 A90-23802
- Current status of ceramic gas turbine R&D in Japan [ASME PAPER 89-GT-114] p 359 A90-23818
- An experimental study of heat transfer and film cooling on low aspect ratio turbine nozzles [ASME PAPER 89-GT-187] p 361 A90-23865
- Reynolds number effects on the performance of a turbofan engine [ASME PAPER 89-GT-199] p 342 A90-23871
- Vortex formation around an oscillating and translating airfoil at large incidences p 303 A90-25588
- CRL's mobile satellite communication experiments using ETS-V [AIAA PAPER 90-0775] p 366 A90-25602
- A high-order time-accurate scheme and its applications p 304 A90-25732
- Application of a digital control theory for generating adaptive grids p 366 A90-25734
- Topology of computed incompressible three-dimensional separated flow field around high-angle-of-attack cone-cylinders p 366 A90-25764
- Problem areas in applied computational fluid dynamics p 366 A90-25770
- Calculation of tip leakage flow with three-dimensional Euler code p 304 A90-25772
- Numerical calculation of bubbly two phase flow around an airfoil p 304 A90-25783
- Numerical simulations of unsteady shock reflections by ramps p 305 A90-25795
- Numerical methods for transonic cascade flow problems p 305 A90-25796
- Navier-Stokes simulations around a high-speed propeller p 305 A90-25797
- Computational and experimental analysis of transonic fanjet engine flow field using 3-D Euler code p 306 A90-25809
- An automatic Euler solver using unstructured upwind method p 367 A90-25811
- Turbulence models for 3D transonic viscous flows. II p 306 A90-25820
- A numerical method for solving the unsteady compressible Navier-Stokes equations p 306 A90-25827
- Flow dependent grid for aerodynamic designers p 306 A90-25831
- Transonic aerodynamics analysis of unconventional wing configurations by 3D-Euler code p 306 A90-25835
- Navier-Stokes computations for the investigation of flowfields about a Space-Plane p 306 A90-25836
- Numerical simulation of separated flows around a wing section by a discrete vortex method p 307 A90-25846
- Application of Lomax-Bailey implicit scheme to reactive flows p 367 A90-25861
- Numerical simulation of wing in ground effect p 307 A90-25863
- Prediction of tip-clearance effects on a wing by the panel method p 307 A90-25871
- Simulation of sound propagation in axisymmetric jet p 378 A90-25872
- Supersonic viscous shear layers p 367 A90-25873
- Topological study of three-dimensional, vortex interactions p 367 A90-25885
- Robust control system, design synthesis with observers p 375 A90-25994
- Air/water two-phase flow test tunnel for airfoil studies p 352 A90-26842
- Reliability evaluation system for ceramic gas turbine components p 444 A90-27678
- Fatigue life prediction method for gas turbine rotor disk alloy FV535 p 440 A90-27679
- Recrystallization behavior of nickel-base single crystal superalloys p 440 A90-27681
- A bearing error in the VHF omnirange due to sea surface reflection p 402 A90-27875
- A study on flaw detection method for CFRP composite laminates. I - The measurement of crack extension in CFRP composites by electrical potential method p 441 A90-28003
- Fast adaptive grid method for compressible flows p 445 A90-28006
- A practical flight path for microwave-powered airplanes p 429 A90-28007
- Instrumentation and operation of NDA cryogenic wind tunnel p 437 A90-28293
- Aeroelastic tailoring analysis for preliminary design of advanced turbo propellers with composite blades p 412 A90-29395
- Numerical simulation of separated flow around two-dimensional wing section by a discrete vortex method p 469 A90-32067
- Multivariable control of jet engines p 507 A90-32421
- A calculation of the aerodynamic lift acting on cascade blades in a steady, viscous flow at high Reynolds number p 469 A90-32425
- Calculations of unsteady aerodynamics over oscillating wings p 472 A90-33362
- Multi-surface control law synthesis and wind tunnel test verification of active flutter suppression for a transport-type wing p 517 A90-33401
- Dynamics of multi-spool gas turbines using the matrix transfer method - Applications p 509 A90-33594
- Dynamics of multi-spool gas turbines using the matrix transfer method - Theory p 509 A90-33595
- Numerical simulation of separated flows around a wing section at pitching motion by a discrete vortex method p 475 A90-33753
- Hot-gas corrosion test of Si3N4 and SiC p 531 A90-33987
- Response characteristics of a two-dimensional wing subjected to turbulence near the flutter boundary p 519 A90-34082
- Life prediction and fatigue p 532 A90-34163
- Capability of current supercomputers for the computational fluid dynamics p 546 A90-34382
- Development of a new low-Reynolds-number type Reynolds stress model and its application to a lobe mixer flow p 584 A90-35229
- Turbulent plane jet excited mechanically by an oscillating thin plate in the potential core p 553 A90-35262
- An experimental study of a turbulent jet impinging on a wedge p 553 A90-35274
- MRS International Meeting on Advanced Materials, 1st, Tokyo, Japan, May 31-June 3, 1988, Proceedings. Volume 5 - Structural ceramics/Fracture mechanics p 599 A90-35926
- Development of ceramic components for high-temperature gas turbines p 602 A90-35951
- Oscillation of circular shock wave p 557 A90-36465
- An application of expert system to jet engine diagnostic procedures p 587 A90-38596
- Expert diagnosis system for FJR engine troubles p 587 A90-38597
- Study of compressibility effects in mixing layer by numerical simulation [AIAA PAPER 90-1464] p 562 A90-38621
- A flow around airfoil with slat and flap [AIAA PAPER 90-1535] p 564 A90-38679
- Simulation of the reduction characteristics of scattering from an aircraft coated with a thin-type absorber by the spatial network method p 638 A90-39855
- Calculation of stability derivatives for slender bodies using boundary element method p 620 A90-40181
- The cryogenic wind tunnel as a testing tool for airframe/propulsion systems p 672 A90-40400
- A numerical investigation of supersonic inlet using implicit TVD scheme [AIAA PAPER 90-2135] p 621 A90-40612
- Development of the jet-swirl high loading combustor [AIAA PAPER 90-2451] p 658 A90-40633
- Vorticity distribution of vortex street in the wake of a circular cylinder p 623 A90-41751
- Critical review of design philosophies for recent transport WIG effect vehicles p 684 A90-41753
- Some governing parameters of plasma torch igniter/flameholder in a scramjet combustor [AIAA PAPER 90-2098] p 661 A90-42017
- Application of 3-D Navier-Stokes computation to bowed stacking turbine vane design [AIAA PAPER 90-2129] p 625 A90-42035
- Aeroelastic response characteristics of a rotor executing arbitrary harmonic blade pitch variations p 646 A90-42464
- Analytical study of dynamic response of helicopter in autorotative flight p 670 A90-42469
- Cloud features suggesting low level wind shear and turbulence p 778 A90-44545
- Propulsive lift augmentation by side fences as applied to Japan's experimental STOL aircraft, ASKA [AIAA PAPER 90-3009] p 789 A90-45859
- Numerical calculations of flows with shock waves by flux vector splitting method p 808 A90-47299
- Numerical study of interaction of a jet with a supersonic cross flow p 808 A90-47300
- Structure/control design synthesis of active flutter suppression system by goal programming [AIAA PAPER 90-3325] p 872 A90-47587
- Adaptive flight control of CCV aircraft with limiting zeros [AIAA PAPER 90-3409] p 864 A90-47664
- Robust flight control system design with multiple model approach [AIAA PAPER 90-3411] p 865 A90-47666
- Improvement in turbine blade aerodynamic force in the tip region p 809 A90-47854
- Mean loading effects on flutter of subsonic rotating annular cascade p 853 A90-49453
- Flow field around an oscillating cascade p 814 A90-49459
- Measurements of simulated wake/rotor interaction phenomena in turbomachinery p 814 A90-49475
- Application of the 'K-gage' to aircraft structural testing p 926 A90-49891
- Improved melt flow and physical properties of Mitsui Toatsu's LARC-TPI 1500 series polyimide p 943 A90-50134
- Advanced joint of 3-D composite materials for space structure p 944 A90-50137
- A study of filament wound high modulus carbon fiber reinforced cylinders p 948 A90-50218
- Unsteady lifting surface theory for a rotating cascade of swept blades [ASME PAPER 89-GT-306] p 906 A90-51259
- Backside landing control of a STOL aircraft using approximate perfect servo p 934 A90-52801
- A numerical method for solving transonic flow past aircraft in Cartesian coordinates [NAL-TR-1008] p 18 N90-10003
- Cycle analysis of scramjet engines [NAL-TR-1002] p 51 N90-10035
- On the interactive computer program IPIS for aircraft parameter identification [NAL-TR-1000] p 77 N90-10586
- Grid generation procedure using the integral equation method [NAL-TR-1009] p 77 N90-10630
- Fight simulator evaluation of a head-down display [NAL-TM-573] p 59 N90-10898
- Fight simulation test facility: Function and specification of the simulator cockpit system [NAL-TM-577] p 59 N90-10899
- Wind tunnel test of CAD USB-STOL semi-borne prototype [NAL-TM-566] p 88 N90-11696
- Acoustic-thermal environment for USB flap structure. Report 1: Ground simulation test results [NAL-TM-567] p 88 N90-11697
- Effects of a heat cycle on material strength [NAL-TM-562] p 113 N90-11737
- Development of the triplex digital flight control system of the STOL research aircraft ASKA [NAL-TR-1013] p 349 N90-17640

- Numerical simulation of hypersonic flow around a space plane. Part 2: Application to high angles of attack flow [NAL-TR-1011T] p 570 N90-21726
- Study on application of ultrasonic wave measurement to creep-fatigue damage detection [DE89-782317] p 774 N90-25361
- Space plane model for visual measurement of aerodynamic heating [DE90-505514] p 720 N90-25949
- Research and development of advanced gas turbine [DE90-503377] p 776 N90-26335
- Development of creep-fatigue damage detection method of rotor steel by ultrasonic wave measurement [DE90-503792] p 777 N90-26365
- New features of JAL's ground station p 872 N90-27633
- Daily flight operation monitoring in JAL p 820 N90-27636
- Investigation of ATP blades, part 2. Validation of two-dimensional viscous flow simulation codes around thin airfoils [NAL-TR-1046] p 912 N90-29326
- Transonic 3-D Euler analysis of flows around fanjet engine and TPS (Turbine Powered Simulator). Comparison with wind tunnel experiment, evaluation of TPS testing method and 3-D flow [NAL-TR-1045] p 912 N90-29327
- A boundary-layer transition model for the Navier-Stokes computation for a natural-laminar-flow airfoil [NAL-TR-1038T] p 912 N90-29328
- Some topics in computational transonic aerodynamics: Revision [NAL-TR-1018T] p 912 N90-29332
- Airline productivity relating on the fuel cost. (2): Fuel consumption values and fuel efficiency [NAL-TM-604-2] p 913 N90-29333
- Evaluation for DLC-Flap Monitoring System of the VSRA [NAL-TM-607] p 928 N90-29391
- Analysis of scramjet engine characteristics [NAL-TR-1041] p 933 N90-29398
- Short period control using angular acceleration feedback: Compensation for first lag servo [NAL-TM-600] p 936 N90-29399
- A digital controller for active aeroelastic controls [NAL-TR-1014] p 936 N90-29402
- Estimation of power spectral density of runway roughness [NAL-TR-1037] p 939 N90-29411
- The function of the Interactive Model Assembly Program (IMAP) for a flight simulator [NAL-TR-1034] p 939 N90-29412
- Evaluation of static and fatigue properties of thin sheets of 8090-T8 aluminum-lithium alloy and observation of its fracture surfaces [NAL-TR-1039] p 953 N90-29499
- Fractographic analysis of fatigue failures of airframe equipment parts: Examples of a rod end housing and a rod end cap [NAL-TR-1047] p 961 N90-29686
- Noncontact measurement of rotating blade vibrations [NAL-TR-1033] p 961 N90-29687
- Parametric studies of acoustic duct attenuation of perforated-plate-on-honeycomb absorber [NAL-TM-603] p 966 N90-30030
- JORDAN**
- Shaft flexibility effects on aeroelastic stability of a rotating bladed disk p 132 A90-16371
- Blade mistuning coupled with shaft flexibility effects in rotor aeroelasticity [ASME PAPER 89-GT-330] p 343 A90-23896
- Shaft flexibility effects on the forced response of a bladed-disk assembly p 744 A90-43218

K

KENYA

- Transonic integro-differential and integral equations with artificial viscosity p 223 A90-20988
- Analysis of transonic integral equations. I - Artificial viscosity p 232 A90-23124
- Analysis of transonic integral equations. II - Boundary element methods p 302 A90-25301
- Boundary element solution of the transonic integro-differential equation p 383 A90-27947

KOREA(SOUTH)

- Hot-wire measurements of near wakes behind an oscillating airfoil p 154 A90-18138
- Finite element analysis of the flow of a propeller on a slender body with a two-equation turbulence model p 210 A90-18340
- Three-dimensional adaptive grid generation on a composite-block grid p 374 A90-25289

- Flutter analysis of composite panels in supersonic flow [AIAA PAPER 90-1180] p 450 A90-29379

L

LATVIA

- Estimation of the efficiency of various operational modes of a navigation complex p 725 A90-42924

LITHUANIA

- Durability characteristics of the LAK-12 Letuva glider made of composite materials at the stage of certification p 102 A90-15560

M

MEXICO

- Helicopter control design using feedback linearization techniques p 668 A90-40817
- A review of regulations - The Chicago Convention and the bilateral network p 898 A90-49614
- Insurance aspects of airline liability p 898 A90-49615

N

NETHERLANDS

- Eurofix p 25 A90-10239
- Review of fiber optic methods for strain monitoring and non-destructive testing p 67 A90-11042
- Development and application of a computer-based system for conceptual aircraft design p 30 A90-12860
- Experimental and numerical investigation of vortex flow over a sideslipping delta wing p 17 A90-13016
- VISTRAFS - A simulation method for strongly-interacting viscous transonic flow p 144 A90-16756
- Low-speed unsteady aerodynamics of a pitching straked wing at high incidence. I - Test program. II - Harmonic analysis p 159 A90-19387
- Experimental and numerical investigation of the flow in the core of a leading edge vortex [AIAA PAPER 90-0384] p 165 A90-19826
- Inviscid drag prediction for transonic transport wings using a full-potential method [AIAA PAPER 90-0576] p 168 A90-19926
- Interference detection and suppression in Loran-C receivers p 240 A90-20504
- Numerical interactive grid generation for 3D-flow calculations p 312 A90-26556
- A review of flight simulation techniques p 435 A90-27953
- Model incidence measurement using the SAAB Elopotos system p 446 A90-28264
- Instrumentation requirements for laminar flow research in the NLR high speed wind tunnel HST p 447 A90-28283
- Impact of multigrid smoothing analysis on three-dimensional potential flow calculations p 449 A90-29147
- Aircraft flight control system identification p 431 A90-30105
- Damage tolerance of a postbuckling soft skin hat stiffened compression panel p 534 A90-31647
- Calculation of unsteady subsonic and supersonic flow about oscillating wings and bodies by new panel methods p 472 A90-33359
- Ground vibration testing of aeroplanes with a sequence of single-point excitations - Simple and effective p 522 A90-33371
- Endurance of aircraft gas turbine mainshaft ball bearings-analysis using improved fatigue life theory. I - Application to a long-life bearing p 537 A90-33557
- Boundary conditions for Euler equations at internal block faces of multi-block domains using local grid refinement [AIAA PAPER 90-1590] p 607 A90-38725
- Usage monitoring of military helicopters p 651 A90-39984
- Ultrasonic regression rate measurement in solid fuel ramjets [AIAA PAPER 90-1963] p 656 A90-40573
- Experimental and computational flammability limits in a solid fuel ramjet [AIAA PAPER 90-1964] p 676 A90-40574
- Computation of viscous aerodynamic characteristics of 2-D airfoils for helicopter applications p 631 A90-42440
- Combustion of PMMA, PE, and PS in a ramjet p 764 A90-43670
- Quench sensitivity of airframe aluminium alloys p 765 A90-44348
- Validation of propeller slipstream calculations using a multi-block Euler code [AIAA PAPER 90-3035] p 791 A90-45874

- Bulging cracks in pressurized fuselages - A procedure for computation p 880 A90-46301
- Experimental aerodynamic characteristics of the airfoils LA 5055 and DU 86-084/18 at low Reynolds numbers p 800 A90-46368
- Investigation of propeller slipstream effects on the Fokker 50 through in-flight pressure measurements [AIAA PAPER 90-3084] p 806 A90-46645
- Recent developments in EEC aviation law - 'The second phase' p 897 A90-46648
- Metal laminates for aerospace applications p 874 A90-48997
- Anatomy of airline regulation - Towards a pluriform, plurilateral, pluralistic, flexible world-wide regulatory framework for air transport p 898 A90-49620
- Assessment of service load experience p 901 A90-49877
- Re-assessing the F-16 damage tolerance and durability life of the RNLAF F-16 aircraft p 901 A90-49881
- Aerospace - Arall - The advancement in aircraft materials p 947 A90-50186
- Multigrid methods in computational fluid dynamics p 906 A90-51526
- A European collaborative investigation of the three-dimensional turbulent shear layers of a swept wing p 20 N90-10380
- Flight testing in the Netherlands: An overview p 36 N90-10884
- Coatings for gas turbine compressors [NLR-MP-88045-U] p 115 N90-11750
- Stability and control derivatives of the De Havilland DHC-2 BEAVER aircraft [PB89-217525] p 119 N90-11754
- Noise data of four small propeller-driven airplanes [PB89-216980] p 139 N90-12291
- Development of a multi-component internal strain-gauge balance for model tests in a cryogenic wind tunnel [NLR-TR-88157-U] p 123 N90-12628
- The comparison of the airbase simulation models airbase and sustained [FEL-1988-66] p 123 N90-12629
- Rolling of ARALL laminates (an alternative method for post-stretching ARALL laminates) [LR-560] p 135 N90-12778
- Aircraft SAR simulation Sargen 1.0 [FEL-1989-44] p 135 N90-12823
- An investigation on combined extension and bending of thin sheets with a central crack [LR-561] p 137 N90-12958
- Induced drag for non-planar wings [LR-521] p 172 N90-13357
- Test network Delft [ETN-90-96009] p 177 N90-13365
- The S.D.G., P.S.D. and the nonlinear airplane [NLR-MP-88018-U] p 183 N90-13371
- Some new techniques for aircraft fuselage skin tests [LR-547] p 184 N90-13379
- Aircraft propulsion: Leading the way in aviation [LR-532] p 194 N90-13395
- Mathematical model identification for flight simulation, based on flight and taxi tests [LR-550] p 202 N90-13410
- Repair of composites by means of wet-lay-up [LR-551] p 205 N90-13617
- Multigrid and defect correction for the steady Navier-Stokes equations: Applications to aerodynamics [ETN-90-96011] p 212 N90-13727
- An evaluation of a fatigue crack growth prediction model for variable-amplitude loading (PREFFAS) [LR-537] p 214 N90-13822
- Fabrication of test-articles from Al-Li 2091 for Fokker 100 p 267 N90-15196
- Fire safety in civil aviation p 325 N90-17586
- Static strength and damage tolerance tests on the Fokker 100 airframe [NLR-MP-88023-U] p 416 N90-19228
- Flow simulation for aircraft [NLR-MP-87082-U] p 455 N90-19543
- COCOMAT: A Computer Aided Engineering (CAE) system for composite structures design [NLR-MP-87078-U] p 462 N90-19756
- Experimental and numerical investigation of the vortex flow over a sharp edged delta wing: with and without sideslip [PB90-167131] p 481 N90-20964
- A system for transonic wing design with geometric constraints based on an inverse method p 501 N90-20983
- Constrained spanload optimization for minimum drag of multi-lifting-surface configurations p 501 N90-20992
- Numerical optimization of target pressure distributions for subsonic and transonic airfoil design p 502 N90-20993
- Secondary flows and radial mixing predictions in axial compressors p 512 N90-21010

- Crack stoppers and ARALL laminates
[PB90-166588] p 533 N90-21142
- A computer program for the prediction of
nozzle-propeller performance
[LR-578] p 572 N90-21740
- Theory and numerical analysis of single and
multi-element nozzle propellers
[LR-579] p 572 N90-21741
- Recent improvements in the scope and accuracy of the
performance prediction of nozzle propellers
[LR-598] p 572 N90-21742
- First-order weight corrections for real-time flight path
management
[LR-580] p 578 N90-21751
- An approach to on-board optimization of cruise at
constant altitude
[LR-581] p 578 N90-21752
- Design and testing of a multiblock grid-generation
procedure for aircraft design and research
p 582 N90-21984
- European research on viscous flow (EuroVisc)
[NLR-TP-89077-U] p 609 N90-22014
- Aircraft technology management and the related
significance of the supercomputer p 612 N90-22975
- Numerical flow simulation and supercomputers: More
than a digital wind tunnel p 612 N90-22976
- The use of supercomputers for the design and analysis
of constructions p 612 N90-22977
- The automation management to support research and
development p 612 N90-22978
- The development of a system for the numerical
simulation of Euler flows p 612 N90-22980
- Fractographic observations on fatigue crack growth in
2024-T3 sheet material under flight-simulation loading
[LR-592] p 689 N90-23760
- Activities report in aerospace and aerodynamics
[ETN-90-96774] p 699 N90-24224
- An experimental and theoretical investigation of the flow
over plane delta wings with supersonic leading edges
[LR-588] p 717 N90-25114
- Investigation of the vortex flow over a sharp-edged delta
wing in the transonic speed regime
[LR-594] p 717 N90-25115
- The application of the finite element method to an
aerodynamic problem specific to propeller design
[LR-614] p 718 N90-25116
- Lecture notes on flight simulation techniques
[LR-596] p 762 N90-25153
- Experimental study on vortex and shock wave
development on a 65 deg delta wing
[NLR-MP-88033-U] p 720 N90-25950
- Computation of viscous aerodynamic characteristics of
2-D airfoils for helicopter applications
[NLR-MP-88052-U] p 720 N90-25951
- Mobile satellite communications for civil aviation
[NLR-MP-88066-U] p 775 N90-26238
- Development of a system for the numerical simulation
of Euler flows, with results of preliminary 3-D
propeller-slipstream/exhaust-jet calculations
[NLR-TR-88008-U] p 776 N90-26285
- Informatics aspects of large flow calculations on the
SX-2 supercomputer
[NLR-MP-88037-U] p 776 N90-26290
- Investigation of crack-closure prediction models for
fatigue in aluminium alloy sheet under flight-simulation
loading
[LR-619] p 777 N90-26369
- High productivity testing p 871 N90-26843
- Description of the MARC measuring system
[FEL-89-B170] p 963 N90-28887
- Tests for aircraft interior materials in fire accident
[LR-622] p 914 N90-29337
- Study improvement training facilities ground control air
traffic controllers. Part 1: Alternative solutions and their
consequences p 919 N90-29380
- WingDesign: Program for the structural design of a wing
cross-section
[LR-627] p 925 N90-29390
- Study improvement training facilities ground control air
traffic controllers. Part 2: Functional analysis approach
control trainer
[FEL-89-A280-PT-2] p 939 N90-29409
- Solid fuel combustion chamber
[LR-634] p 939 N90-29433
- Fractographic analysis of fatigue crack growth under
two-blocks loading on 2024-T351 sheet specimens
[LR-628] p 961 N90-29680
- Effects of blocks of overloads and underloads on fatigue
crack growth in 2024-T351 sheet specimens:
Fractographic analysis and crack closure predictions
[LR-629] p 961 N90-29681
- Fatigue, static tensile strength and stress corrosion of
aircraft materials and structures. Part 1: Text
[LR-630-PT-1-REV] p 961 N90-29682

- Fatigue, static tensile strength and stress corrosion of
aircraft materials and structures. Part 2: Figures
[LR-630-PT-2] p 961 N90-29683
- Fractographic observations on fatigue crack growth
under miniTWTST flight-simulation loading (2024-T3
material)
[LR-631] p 961 N90-29684

NIGERIA

- Numerical simulation of valveless pulsed combustors
p 127 A90-13767

NORWAY

- Design of axisymmetric bodies with minimum transonic
drag p 154 A90-17997
- An aircraft noise study in Norway p 698 N90-24872

O

OTHER

- Air combat beyond the stall p.589 A90-35888

P

PAKISTAN

- Aerodynamic losses in conventional fan blades of high
by pass turbo engine p 854 A90-49487
- Aerostructural considerations for the power plant of
overlapping wing configuration p 841 A90-49488

POLAND

- A multifunctional system of helicopter dynamics
simulations p 28 A90-10226
- Some unconventional cases of the dynamical testing
of helicopters p 28 A90-10227
- Numerical analysis of flow of an ideal fluid past an
airfoil p 2 A90-10228
- A statistical model of helicopter noise
p 77 A90-10229
- Wind tunnel tests of models of helicopter rotors
p 29 A90-10230
- The solution of the unsteady transonic flow through a
blade passage in an axial turbine p 5 A90-11777
- The influence of the wake structure on the dynamic blade
load p 6 A90-11785
- A discrete dynamic model of the crankshaft-airscrew
assembly of an aircraft piston engine for the purpose of
vibration analysis by the method of finite elements
p 51 A90-13220
- Numerical analysis of vibrations of a helicopter tail
boom p 31 A90-13224
- Balance model of the perfectly stirred reactor with the
discontinuity surface p 125 A90-14652
- Criteria for evaluating the flight dynamics model of flight
simulators p 121 A90-15422
- An analysis of the possibility of using direct control of
the lifting force for modifying the flying qualities of
aircraft p 118 A90-15423
- Evaluation of the dynamic properties of the auto-pilot
servo of a single-rotor helicopter through laboratory
testing p 118 A90-15424
- Predicting the CO, HC, and NO(x) emission and
combustion efficiency of small turbine engines from the
combustion chamber bench test results p 125 A90-15425
- The FAA technical classification of aircraft and
airports p 96 A90-15876
- NMG - A system of numerical representation of aircraft
geometry p 103 A90-15877
- Laboratory analysis of antiwear properties of
turbine-engine fuels p 131 A90-15878
- A calculation method for ducted propellers
p 226 A90-21626
- Some aspects of the erosive wear of components of
aircraft turbine engines p 253 A90-21627
- ICAO airfield reference code p 261 A90-21628
- Aircraft program motion along a predetermined
trajectory. I - Mathematical modelling p 345 A90-23979
- The influence of selected geometrical and mass
parameters on the structural dynamics of an aircraft with
a variable-geometry airfoil p 346 A90-24284
- Damping of the inlet vortex in a turbojet engine
p 301 A90-25185
- Static and dynamic loss of stability of elements of a
supersonic aeroplane covering - Numerical analysis
p 346 A90-25186
- Dynamics of spatial motion of an aeroplane after drop
of loads p 346 A90-25189
- Aircraft program motion along a predetermined
trajectory. II - Numerical simulation with application of
spline functions to trajectory definitions p 347 A90-25199
- Design flutter calculations on PC p 545 A90-33379
- Discrete Fourier transform with high resolution for low
frequencies applied to the modal analysis of aircraft
vibration p 679 A90-38975

- Design of new Polish primary radars AVIA DM/CM
p 638 A90-41035
- A visualization study of the interaction of a free vortex
with the wake behind an airfoil p 623 A90-41119
- The influence of control-surface compensation
parameters on the hinge moment characteristics
p 643 A90-41737
- Application of mathematical modeling to the study of
rigid helicopter rotors p 643 A90-41738
- Influence of some geometrical and design parameters
on the hinge moment characteristics of rudders
p 643 A90-41739
- Investigations of the influence of slot blowing from the
upper wing surface on the flow around the wing and its
aerodynamic characteristics p 623 A90-41740
- Digital autopilot for light aircraft p 653 A90-41741
- Onboard digital recording system for flight tests
p 653 A90-41742
- Vibration of turbine blades damped by dry friction
forces p 879 A90-46190
- Numerical analysis of natural vibrations of an aeroplane
with symmetrically variable geometry wing p 860 A90-46715
- Analysis of self-excited vibrations of stiffened covering
panels of an aeroplane wing p 860 A90-46716
- Numerical solution of 2-D transonic flow through an axial
turbine stage p 814 A90-49464
- The inverse problem in the multielement airfoil theory
p 906 A90-51531

PORTUGAL

- On the 'inverse phugoid problem' as an instance of
non-linear stability in pitch p 55 A90-10221
- Numerical study of single impinging jets through a
crossflow p 17 A90-13020
- On a pitch control law for a constant glide slope through
windshears p 117 A90-13784
- Instrumentation for combustion and flow in engines;
Proceedings of the NATO Advanced Study Institute,
Vimeiro, Portugal, Sept. 13-26, 1987 p 211 A90-19004
- Velocity and scalar measurements in model and real
gas turbine combustors p 191 A90-19005
- A three dimensional inverse method in turbomachinery.
II - Experimental verification p 360 A90-23834
- [ASME PAPER 89-GT-137] p 360 A90-23834
- Computer controlled test bench for axial turbines and
propellers p 437 A90-28288
- A pitch control law for compensation of the phugoid
mode induced by windshears p 258 A90-15051
- Application of an inverse method to the design of a
radial inflow turbine p 511 A90-20989

R

ROMANIA (RUMANIA)

- On a lifting line theory for supersonic flow. I - The velocity
field due to a vortex line in supersonic flow p 143 A90-16735
- On steady subsonic flow past slender bodies of
revolution p 144 A90-16736
- On a lifting line theory for supersonic flow. II - A
supersonic lifting line theory for wings p 477 A90-34817
- On an extension of the Kutta-Joukowski theorem to the
supersonic regime p 477 A90-34819
- Rotary damping in aircraft motion due to jet propulsion
system p 520 A90-34820
- A verification of the supersonic lifting line theory for the
case of infinite yawed wings p 477 A90-34821
- Analysis of perturbed longitudinal dynamics of an aircraft
taking into consideration the stationary aeroelastic effects
and the atmospheric perturbances p 520 A90-34822

S

SAUDI ARABIA

- Newtonian flow over oscillating two-dimensional airfoils
at moderate or large incidence p 383 A90-27976

SINGAPORE

- A panel method computation for oscillating aerofoil in
compressible flow p 906 A90-51483

SOUTH AFRICA, REPUBLIC OF

- Atomization of synthetic jet fuel p 63 A90-12602
- Range determination in a multipath prone environment
p 877 A90-45960
- Empirical prediction of the blockage effect of a flat body
on a rotor p 807 A90-46942

SPAIN

- Non-iterative analytical methods for off-design turbofan
calculations with or without mixed-flows p 70 A90-12628
- Flight over the sea with twin or triple jet aircraft
p 179 A90-17048

- The impact of composites on the aerospace industry p 221 A90-22649
- Design and fabrication of the carbon fiber/epoxy A-320 horizontal tailplane p 286 A90-25221
- Two-dimensional compressible unsteady aerodynamics in the Laplace domain p 472 A90-33360
- A comparison between theoretical and experimental results for a 3-D wing with damped pitching oscillations p 472 A90-33361
- Gas turbine engines for combat aviation - Current realities and perspectives for the near future p 584 A90-35513
- Use of pulse radars for helicopters detection - Design constraints p 583 A90-41073
- A formulation for the solution of Euler equations for compressible flow using finite elements p 708 A90-44447
- Simple shear tests of the FMI 23.5.06 adhesive cured at low pressure (12 PSI) [INFORME-I-298/88] p 357 N90-17871
- Pressure air tightness tests of laminated panels for wing leading edge heat shields [INFORME-I-377/89] p 357 N90-17873
- Impact of composites in the aerospace industry [ETN-90-96231] p 443 N90-18527
- SWEDEN**
- Slipstream-induced pressure fluctuations on a wing panel p 77 A90-11004
- Canard-wing interaction in unsteady supersonic flow p 3 A90-11010
- Swedish philosophy in aeroengine development p 44 A90-12504
- Full-scale liquid fuel ramjet combustor tests p 44 A90-12528
- A solution adaptive finite element method applied to two-dimensional unsteady viscous compressible cascade flow p 15 A90-12624
- Interior noise control of the Saab 340 aircraft [SAE PAPER 891080] p 101 A90-14372
- Finite element calculations of the interior noise of the Saab 340 aircraft [SAE PAPER 891081] p 101 A90-14373
- Numerical methods to solve the incompressible Euler and Navier-Stokes equations in 3D with applications p 209 A90-18302
- Computations of hypersonic flow by finite-volume methods p 224 A90-21168
- A new type of calibration rig for wind tunnel balances p 438 A90-28305
- Applications of the unsteady full potential equation for wings p 472 A90-33358
- Low-speed pressure distribution on semi-infinite two-dimensional bodies with elliptical noses p 553 A90-35766
- The new FFA T1500 transonic wind tunnel initial operation, calibration, and test results [AIAA PAPER 90-1420] p 596 A90-37957
- Damage tolerance of carbon fibre reinforced plastic sandwich panels p 675 A90-40047
- Lightning testing and test analyses of the JAS39 aircraft p 842 A90-49836
- Viscoelastic tuned dampers for control of structural dynamics p 73 N90-10999
- Thermochemical calculations with inert compounds [FOA-C-20759-2.1] p 206 N90-13677
- Low speed testing of a laminar flow airfoil in an adaptive wall wind tunnel [FFA-TN-1989-08] p 632 N90-23363
- Euler code predicted separation at the airfoil trailing edge [FFA-TN-1989-30] p 632 N90-23364
- A study of terrain following systems and the creation of flight paths for terrain following vehicles [FOA-C-20774-2.5] p 827 N90-27691
- Reinforcing fibers and technology development for resin composites. Consequences for aircraft structures [FOA-C-20777-2.5] p 876 N90-27883
- Damage tolerance of the fighter aircraft 37 Viggen. Part 1: Analytical assessment [FFA-TN-1990-12-PT-1] p 923 N90-28538
- Damage tolerance of the fighter aircraft 37 Viggen. Part 2: Experimental verification [FFA-TN-1990-13-PT-2] p 923 N90-28539
- SWITZERLAND**
- Unsteady flow visualization in a vibrating annular turbine cascade operating in the transonic flow regime p 7 A90-11786
- Experimental investigation of the time-dependent flow in a vibrating annular cascade operating in the transonic flow regime p 7 A90-11787
- Numerical investigation of unsteady compressible flow through nozzles and cascades p 7 A90-11790
- Flutter of mistuned cascades with structural coupling p 42 A90-11802
- Sharing power and profit p 188 A90-16701

- IHPDET spawns engines for 21st century p 188 A90-16702
- Turboshafts on tenterhooks p 188 A90-16703
- Caring for the elderly jet p 285 A90-24280
- Fibre reinforced thermoplastic integral constructions in modular build-up technology - The 'thermoplastic in-situ-technique' p 534 A90-31879
- Core composites in Swissair aircraft p 493 A90-33709
- Civil supersonics - A less distant thunder p 731 A90-44223
- Initial service experience with the Fokker 100 [SAE PAPER 892238] p 733 A90-45450
- Application possibilities of expert systems in modern maintenance for increasing operational security p 892 A90-49271
- Eight years of experience with small computerized retrofit load monitoring systems p 926 A90-49882
- Improved thermal performance using allylnadac-imides p 946 A90-50175
- Military navigation - The fourth generation p 914 A90-50775
- Inversions and associated wind-shear warnings must be related to airport characteristics p 962 A90-52051
- Problems related to aircraft noise in Switzerland p 698 N90-24871
- Multichannel on-board load and fatigue monitoring p 849 N90-27621

T

TAIWAN

- Adaptive autopilot design via model expansion method p 55 A90-11124
- Numerical simulation of an impinging jet on a flat plate p 86 A90-15821
- Calculation of flowfields in side-inlet ramjet combustors with an algebraic Reynolds stress model p 87 A90-16367
- A refined optimality criterion technique applied to aircraft wing structural design p 206 A90-16718
- Flutter analysis of composite panels using high-precision finite elements p 207 A90-16725
- An investigation on the coiled-up of vortices on a double delta wing [AIAA PAPER 90-0382] p 165 A90-19825
- Hydraulic analogy application in the study of a two-phase mixture combustion flow [AIAA PAPER 90-0451] p 211 A90-19850
- Numerical investigation of airfoil/jet/fuselage-undersurface flowfields in ground effect [AIAA PAPER 90-0597] p 168 A90-19939
- Optimum weight design of a rotor bearing system with dynamic behavior constraints [ASME PAPER 89-GT-74] p 358 A90-23795
- Threshold performance optimization of a rotor-bearing system subjected to leakage excitation [ASME PAPER 89-GT-126] p 360 A90-23825
- A panel method for arbitrary moving boundaries problems p 302 A90-25284
- Comparisons among grid generation using elliptic partial differential equations p 374 A90-25478
- Experimental and theoretical investigations of turbulent flow in a side-inlet rectangular combustor p 421 A90-27959
- Aging and antioxidant surveillance studies on turbine fuel JP-5 and JP-10 p 442 A90-29492
- Adhesive-bonded composite-patching repair of cracked aircraft structure p 467 A90-31576
- Unsteady transonic cascade flow with in-passage shock wave p 556 A90-36281
- Non-conservative stability of a cracked thick rotating blade p 606 A90-38544
- Parameter effects on oscillatory aerofoil in transonic flows [AIAA PAPER 90-1473] p 563 A90-38629
- Finite element analysis of composite panel flutter p 681 A90-40032
- Measurements of turbulent dual-jet interaction [AIAA PAPER 90-2105] p 624 A90-42019
- Numerical simulations of gas turbine combustor flows [AIAA PAPER 90-2305] p 686 A90-42116
- Structure analysis of burning liquid-fueled spray in a confined combustor [AIAA PAPER 90-2444] p 677 A90-42174
- The influence of swirl on velocity, temperature and species characteristics in a can combustor [AIAA PAPER 90-2454] p 664 A90-42177
- Numerical simulation of transonic porous airfoil flows p 707 A90-44433
- Numerical solutions for unsteady aerofoil by internal singularity method p 716 A90-45536
- Control of wall-separated flow by internal acoustic excitation p 809 A90-47314

- Interfaces properties of high temperature polymer composite systems p 941 A90-50062
- High temperature behavior of the innovation carbon/CSPI composite p 941 A90-50067
- Chemical resistance of carbon fiber reinforced polyether ether ketone and polyphenylene sulfide composites p 944 A90-50142
- The changes of structures and properties in PAN-based carbon fibers during heat treatment in carbon dioxide p 945 A90-50145
- Multigrid acceleration of TVD schemes in transonic Euler flow calculation p 908 A90-52030
- TURKEY**
- Simulation and second law analysis of the unsteady combustion of a non-ideal pulsating ramjet p 44 A90-12516
- Shock-wave/boundary-layer interaction at a swept compression corner p 16 A90-12850
- An off-design loss and deviation prediction study for transonic axial compressors [ASME PAPER 89-GT-324] p 343 A90-23893
- A computational design method for shock free transonic cascades and airfoils p 501 N90-20986
- A study on secondary flow and spanwise mixing in axial flow compressors p 512 N90-21012

U

U.S.S.R.

- Computer-aided design of flight vehicle instrument bays p 76 A90-10837
- Fundamentals of turbine design for aircraft engines p 40 A90-10839
- Radar systems of aircraft p 26 A90-10841
- Adaptive automatic control systems. Number 16 p 76 A90-10844
- An analysis of the possibility of expanding the information base of an adaptive control system for a flight vehicle surrounded by an ionized gas medium p 60 A90-10845
- The discontinuity condition in the optimal control problem for a composite system p 76 A90-10848
- A study of three-dimensional supersonic flow of a real gas past axisymmetric bodies p 3 A90-10938
- Formalization and solution of covering problems in the synthesis of control and monitoring systems p 76 A90-10963
- Acoustic resonance in centrifugal compressors induced by interaction between rotor and stator p 78 A90-11803
- Irregular interaction of a strong shock wave with a thin profile p 9 A90-12267
- Asymptotic calculation of flow parameters in the problem of hypersonic flow past blunt axisymmetric bodies p 10 A90-12268
- Pressure pulsation in a cavity in the path of subsonic and supersonic gas flow p 10 A90-12279
- Lee-side heating of a delta wing in supersonic flow p 10 A90-12281
- An experimental study of fluctuations in the front separation zone at supersonic flow velocities p 10 A90-12282
- Hypersonic flow past blunt edges at low Reynolds numbers p 10 A90-12284
- Optimization of the observations and control of aircraft p 60 A90-12468
- Inverse problems in controlled system dynamics: Nonlinear models p 77 A90-12471
- Aerodynamic and dynamic principles of helicopter flight p 55 A90-12473
- Power supply of aircraft p 43 A90-12474
- The birth of the airplane: The first designs and constructions p 79 A90-12478
- Vortex-flow compressors p 69 A90-12479
- Helicopter dynamics: Limiting flight conditions p 55 A90-12481
- Application of three-dimensional methods for the calculation of gas dynamic and thermal processes at the design of gas turbines for air breathing engines p 46 A90-12552
- Numerical simulation of three-dimensional flow around parachute canopies p 84 A90-14438
- Dynamic stiffness of a hydraulic damper in the system of a front landing gear strut p 102 A90-14555
- Structural analysis of the horizontal tail surfaces of subsonic transport aircraft p 102 A90-14556
- Stress-strain analysis of structural elements of incompressible or nearly incompressible materials by the finite element method p 129 A90-14557
- Nonlinear transverse oscillations of a composite dynamic system p 129 A90-14558
- Dynamic analysis of lifting surfaces of small relative thickness in the case of finite displacements p 129 A90-14560

Synthesis of locally optimal aircraft control in the presence of delay p 137 A90-14561

Variable-velocity flow at the initial mixing section in a diffuser channel p 84 A90-14563

Construction of a straight single-row airfoil lattice by the method of quasi-solutions for inverse boundary value problems p 84 A90-14564

The method of matched integral representations in viscous fluid dynamics p 129 A90-14565

A numerical method for calculating supersonic nonisobaric jets p 84 A90-14566

Validation of the accelerated equivalent testing of gas turbine engines for multivariant applications p 110 A90-14568

A minimal permissible radial clearance in a gas turbine p 110 A90-14569

Estimation of the technical risk criterion in selecting the operating parameters of aircraft gas turbine engines p 110 A90-14570

The principle of jet engine thrust generation p 110 A90-14571

Effect of pressure on the electrophysical properties of two-phase flows in nozzles p 110 A90-14572

Design of a language for the testing of aircraft engines p 137 A90-14573

A study of the nonlinear deformation of a shell of revolution with a surface bend p 129 A90-14574

Parametric synthesis of piecewise constant locally optimal aircraft control under conditions of indeterminacy p 137 A90-14576

Effect of the inlet diameter and neck edge radius on the flow coefficient of straight-generator nozzles p 84 A90-14577

Effect of the roughness of deposits in a compressor cascade on the flow lag angle p 84 A90-14578

Calculation of cone drag p 84 A90-14579

Increasing the heat conductivity of elastic damping elements of MR material p 102 A90-14580

Numerical modeling of the combustion kinetics of hydrocarbon fuels in an annular combustion chamber with allowance for the formation of harmful impurities p 124 A90-14582

Generalized relations for estimating the efficiency and basic dimensions of screw pumps and hydraulic turbines of pump units p 111 A90-14583

Determination of the effective areas of the mixing exhaust ducts of a bypass engine from autonomous test results p 102 A90-14584

Thermodynamic calculation of the compressors of gas turbine engines and powerplants at high air pressures p 130 A90-14585

Effect of the radial clearance on the efficiency of a partial microturbine p 111 A90-14586

The tape method for the automatic partitioning of an arbitrary region when calculating temperature stresses p 138 A90-14587

Calculation of vibrational combustion limits in Helmholtz resonator-type chambers p 125 A90-14588

Operation of a compressor with intermediate air bleed p 111 A90-14589

Effect of the angle of attack on the efficiency and thrust ratio of axial-flow microturbines with full admission p 111 A90-14590

Classification of methods for eliminating surging in gas turbine engines p 111 A90-14591

Dynamic damping of vibrations in mechanical systems by means of elastic links with distributed parameters p 139 A90-15568

Calculation of flow past delta wings in the thin shock layer approximation p 86 A90-15624

Dynamics of aviation gas turbine engines p 113 A90-16049

Perturbations of a three-dimensional boundary layer produced by body irregularities p 150 A90-17107

Changes in supersonic flow past an obstacle due to the formation of a thin rarefaction channel ahead of the obstacle p 150 A90-17108

Equilibrium of an elastic porous shell in supersonic gas flow p 150 A90-17109

Effect of the inertial nature of injection and temperature on the damping of body vibrations p 150 A90-17112

Generation of motion control for direction finders in a goniometer system p 187 A90-17137

Jets, vortices, and turbulence p 207 A90-17175

Effect of pressure and temperature on residue formation in aviation kerosenes p 203 A90-17281

Application of the finite element method to the problem of rotational flow around wings p 156 A90-18305

Numerical modeling of a viscous separated flow in the near wake p 159 A90-19236

Supersonic nonuniform flow of a gas past oblong axisymmetric bodies p 159 A90-19237

Stability and vibrations of mechanical systems p 270 A90-20426

Effect of the nonuniform rotation of the gas turbine rotor on blade vibrations p 253 A90-20431

Vibration of a wing of nonzero thickness in supersonic flow p 222 A90-20432

A study of the stability of a wing aileron in supersonic flow p 222 A90-20442

Durability of equipment assemblies and elements of life-support systems for flight vehicles p 246 A90-21275

Strength of the guide vane components of gas turbines p 266 A90-21318

Finite element analysis of nonstationary temperature fields in gas turbine components p 271 A90-21324

Comparison of thin and full viscous shock layer models in the problem of supersonic flow of a viscous gas past blunt cones p 231 A90-22396

Mean and pulse characteristics of supersonic flow in a wind tunnel with a honeycomb nozzle p 231 A90-22421

Characteristics of turbulent separation flows on a porous surface under conditions of injection p 231 A90-22422

Radio deviation of airborne goniometers p 242 A90-22733

Aircraft of unconventional configuration (2nd revised and enlarged edition) p 247 A90-22734

Technical means and methods of flight safety assurance p 238 A90-22735

Handbook on heat exchangers p 273 A90-22743

Dynamic properties of a system for the roll control of a model electromagnetically suspended in a wind tunnel p 262 A90-22762

Convergence of the method of discrete vortices when applied to steady-state aerodynamics problems p 231 A90-22816

Selection of the blended wing configuration for light aircraft p 234 A90-23401

Prediction of the strength-related reliability of structural elements at the design stage p 274 A90-23402

Dissipation thrust losses due to distortions of the jet nozzle profile p 254 A90-23405

A study of the working process and losses in annular turbine nozzle cascades with a low contraction ratio p 254 A90-23407

An experimental study of the gasdynamic characteristics of annular nozzle cascades with small flow exit angles p 255 A90-23409

Optimal selection of the parameters to be measured during the identification of gas turbine engines. I - Problem statement p 255 A90-23410

Estimation of the efficiency of a ramjet engine with a thermocompressor using fuel conversion products p 255 A90-23412

Design of computer-aided testing systems for aviation equipment. I p 222 A90-23416

A parametric optimization algorithm for the electrical distribution circuits of civil aircraft p 255 A90-23417

An approximate method for calculating flow past a wing profile with allowance for viscosity p 234 A90-23422

Effect of the control of turbocompressor guide vanes on the throttle characteristics of a bypass engine p 255 A90-23425

Electrodynamic properties of engine exhaust jets p 265 A90-23428

A method for the computer-aided hydraulic analysis of the turbine cooling systems of aviation gas turbine engines p 255 A90-23430

Transfer of the atomic ion energy of supersonic flow of a partially dissociated gas to a solid surface p 234 A90-23432

A study of flow of a vibrationally nonequilibrium dissociated gas past a blunt body p 234 A90-23435

Some aspects of the numerical modeling of supersonic flow past flight vehicles p 293 A90-24048

Nonsymmetric vortex breakdown and aerodynamic hysteresis in flow past a low-aspect-ratio wing/fuselage configuration p 294 A90-24076

An experimental study of separated flow past a low-aspect-ratio delta wing p 294 A90-24077

Aerodynamic interference of prismatic engine nacelles with the wing at supersonic velocities p 294 A90-24078

Calculation of nonseparated transonic flow past swept wings with allowance for viscosity p 294 A90-24079

Effect of tangential injection on flow in a laminar boundary layer p 294 A90-24080

Effect of surface riblets on the velocity profile of an incompressible boundary layer p 294 A90-24081

An experimental study of the effect of the Reynolds number on flow past a swept wing at transonic velocities p 294 A90-24082

Model problems of continuous control law optimization for a tensometric aerodynamic experiment p 295 A90-24086

Testing of statistical hypotheses and derivation of confidence intervals from inspection data samples p 363 A90-24087

Flow past a wing/fuselage combination with separation from the side edges of the wing p 295 A90-24088

Pseudoshock and separated flow in rectangular ducts p 295 A90-24089

Efficient structural material distribution in the main frame of a flight vehicle p 363 A90-24092

Asymptotic solution of the optimal-deflection problem for a wing leading edge at subsonic flow velocities p 295 A90-24094

Design of symmetric profiles with maximum critical flow Mach number under prescribed constraints p 295 A90-24095

Eigenvalue problem in the theory of flow past thin profiles at high supersonic velocity p 295 A90-24096

Effect of the design of a diffuser with tangential injection on the starting and separation ratios of pressures p 295 A90-24099

Mean-square approximation by an even nonnegative polynomial p 374 A90-24101

Effect of creep on the load-bearing capacity of compressed panels p 364 A90-24102

Application of Fedorenko's multigrid method for calculating transonic flow past a profile p 295 A90-24103

A new quick method for integrating Euler equations for plane transonic flows p 295 A90-24105

Calculation of transonic axisymmetric flow past an engine nacelle with allowance for viscosity p 296 A90-24107

Calculation of flows of an ideal gas in nozzles and jets by the relaxation method p 296 A90-24109

Effect of the cross-sectional shape of a straight duct on supersonic flow stagnation p 296 A90-24110

Aeroelastic deformation of a crescent-shaped rigid support in the diffuser chamber of a wind tunnel p 364 A90-24112

Nonstationary liquid flow of a fluid in the core of a conical vortex sheet p 296 A90-24113

A method for the active control of the boundary layer condition p 296 A90-24114

Dynamic characteristics of one-dimensional gas flow with friction p 296 A90-24115

Effect of hydrogen combustion in a supersonic boundary layer on friction coefficient p 355 A90-24116

Optimization of the sound-absorption lining parameters of an ejector jet muffler p 378 A90-24117

Automation of the development of a finite element model for shells of the wing type p 364 A90-24118

Calculation of the front or rear part of a flat body in subsonic flow with the extremum value of the critical Mach number p 296 A90-24120

Multilevel method for calculating aerodynamic loads on a flight vehicle p 296 A90-24122

The effect of longitudinal fins on turbulent friction drag p 297 A90-24123

Investigation of the flow structure behind the rotating blades in the elbow of a wind tunnel in the case of acoustic excitation p 297 A90-24124

Acoustic noise emitted from vessels in an impulse-type wind tunnel p 378 A90-24125

Application of the MARS system in aircraft-structure design p 374 A90-24127

An investigation of fillets in wing-fuselage joints at subsonic velocities p 297 A90-24131

Investigation of wall pressure pulsations during the passive control of shock/boundary layer interaction p 378 A90-24132

Optimization of the relative thicknesses of a high-aspect-ratio wing in a multicriterial formulation p 334 A90-24133

Determination of the torsion rigidity of a multiple-rib torsion box of an aircraft lifting surface p 364 A90-24134

The local surface variation method in profile shape optimization problems p 297 A90-24136

Calculation of supersonic flow past a wing/fuselage combination with the resolution of a compression shock from the wing p 297 A90-24138

A method for calculating the location and intensity of a conical head shock on the lower surface of a delta wing with supersonic edges p 297 A90-24139

Aerodynamic characteristics of thin bodies moving in a gas with shock waves p 297 A90-24140

Separation development and its effect on the aerodynamics of supercritical profiles at transonic velocities p 297 A90-24142

Interaction between a vibrating compression shock and a boundary layer p 298 A90-24143

A study of the laminar-turbulent boundary layer transition on the windward side of a delta wing with a conical surface p 298 A90-24144

Advantages of flow variables in thin viscous shock layer problems p 364 A90-24145

A method for determining aileron efficiency and critical reversal and divergence rates at transonic velocities p 345 A90-24147

- Tail rotor dynamics during the translational turn maneuver of a helicopter p 334 A90-24148
- Construction of a wing surface in a nonviscous transonic flow from a given pressure distribution p 298 A90-24149
- Effect of similarity parameters on the aerodynamic quality and moment characteristics of a supersonic wing with blunt edges p 298 A90-24150
- Permeability of the porous walls of a wind tunnel at transonic velocities p 350 A90-24151
- A method for determining equivalents during the fatigue testing of structures in an acoustic field p 364 A90-24153
- Jet flap theory p 298 A90-24154
- Wing-fuselage interference regimes at supersonic flight velocities p 298 A90-24155
- Ideal propeller in compressible gas flow in a wind tunnel p 298 A90-24156
- Using third-fourth order compact schemes for calculating gas flows in nozzles with high supersonic M numbers on the basis of simplified Navier-Stokes equations p 299 A90-24157
- Calculation of flow past flight vehicles of complex configurations at high supersonic Mach numbers using the hypersonic theory of small perturbations p 299 A90-24158
- A method for calculating the stiffness characteristics of large-aspect-ratio wings with anisotropic panels in accordance with strength and aileron efficiency requirements p 334 A90-24161
- Multicriterial optimization of lugs in hinge joints p 364 A90-24162
- Flutter and aileron reversal safety factors p 345 A90-24164
- Optimal nose shapes of bodies of revolution in transonic flow p 299 A90-24165
- Determination of pressure and heat flow on the front surface of smooth blunt bodies p 299 A90-24166
- Effect of a recess on the aerodynamic characteristics of very blunt bodies at supersonic velocities p 299 A90-24167
- Interference between the pitot-static tube and the model in wind tunnel studies of flow parameters p 350 A90-24169
- Calculation of the vibrations of aircraft with elastic suspended loads p 345 A90-24171
- Aviation equipment p 338 A90-24200
- An automatic system for the programmed control of the parameters of the vibrational and thermal testing of the blades of gas turbine engines p 343 A90-24216
- Practical aerodynamics of the Yak-42 aircraft p 334 A90-24218
- Monitoring of aircraft assembly: Optical and laser methods p 285 A90-24229
- Automatic testing in aircraft building p 285 A90-24231
- Supersonic flight vehicles p 299 A90-24233
- Nonstationary motion of an elastic profile in subsonic incompressible flow p 300 A90-24741
- The shape assumed by a soft conical shell in fluid flow p 300 A90-24752
- Analytical solution of the problem of nonaxisymmetric potential flow past a spherical canopy - A summary of the principal asymptotic formulas and qualitative analysis p 300 A90-24753
- Prospects are good for using ATC radar to detect birds p 329 A90-25496
- Conditions of the generation of autooscillations in aerodynamic control surfaces in nonseparated subsonic flow of a gas p 315 A90-27303
- Prospects are very good for using satellites for aeronautical navigation p 403 A90-27924
- Some problems on 'intelligence' of wind tunnel testing p 436 A90-28282
- Using the method of symmetric singularities for calculating flow past subsonic flight vehicles p 386 A90-28979
- Numerical solution of the problem of supersonic flow of an ideal gas past a trapezoidal wedge p 386 A90-28980
- Calculation of flow characteristics in the core of a vortex sheet p 386 A90-28981
- Effect of structural anisotropy on the dynamic characteristics of the wing and critical flutter speed p 386 A90-28985
- Induced drag of a wing of low aspect ratio p 387 A90-28987
- Comparison of calculated and experimental nonstationary aerodynamic characteristics of a delta wing pitching at large angles of attack p 387 A90-28988
- Some characteristics of changes in the nonstationary aerodynamic characteristics of a wing profile with an aileron in transonic flow p 387 A90-28989
- Calculation of the effect of the engine nacelle on transonic flow past a wing p 387 A90-28990
- Aerodynamic quality of a plane delta wing with blunted edges at large supersonic flow velocities p 387 A90-28991
- Laminar separated flow on a biconical body at high supersonic velocities p 387 A90-28992
- A study of the strength characteristics of a twin-fuselage aircraft with a trapezoid wing system p 410 A90-28993
- A method for recalculating the temperature fields of aircraft structures for different experimental conditions p 448 A90-28994
- Approximation of frequency characteristics using identification with a complex mass matrix p 448 A90-29001
- Auxiliary hypotheses of the wave drag theory p 387 A90-29003
- Using the lifting line theory for calculating straight wings of arbitrary profile p 387 A90-29004
- Effect of the leading edge bluntness of a moderately swept wing on the aerodynamic characteristics of an aircraft model at subsonic and transonic velocities p 388 A90-29005
- Wave rider volume distribution p 388 A90-29006
- Divergence of thin-walled composite rods of closed profile in gas flow p 388 A90-29012
- Effect of a jet on transonic flow past an airfoil p 388 A90-29181
- Calculation of the drag of fuselage tail sections of different shapes in supersonic flow of a nonviscous gas p 388 A90-29182
- Calculation of the induced drag of a wing with arbitrary deformation p 388 A90-29183
- Combined effect of viscosity and bluntness on the aerodynamic efficiency of a delta wing in flow with a high supersonic velocity p 388 A90-29184
- Optimal conditions of flow turbulence suppression in the working section of a wind tunnel using screens located in the prechamber p 438 A90-29185
- A study of approximately optimal cruising flight regimes of variable-mass aircraft p 430 A90-29187
- Efficiency of using a multiple-wall torsion box in the load-bearing structures of lifting surfaces p 410 A90-29188
- The use of automated parametric analysis for selecting efficient structural schemes for wings p 410 A90-29191
- Wall pressure fluctuation spectra in supersonic flow past a forward facing step p 388 A90-29194
- Multiple-power-path nonplanetary main gearbox of the Mi-26 heavy-lift transport helicopter p 452 A90-30115
- Optimal computer-aided design of the blading of axial-flow turbines p 452 A90-30268
- Fundamentals of the design and development of parts and mechanisms for flight vehicles p 414 A90-30275
- Skin effect in flow of a disperse fluid past a wing profile p 395 A90-30334
- Determination of the specific thrust in open regimes and design of a nonseparating convergent nozzle profile p 395 A90-30339
- Aerodynamic characteristics of wave riders based on flows behind axisymmetric shock waves p 395 A90-30342
- Flow rate and thrust coefficients for biaxial flows in a convergent nozzle p 395 A90-30344
- A study of the radiation of hydrogen-xenon mixtures near models flying at high supersonic velocities p 470 A90-32509
- Entry of a flexible airfoil into a vertical gust p 470 A90-32552
- Nonstationary hypersonic flow past a thin wing of variable shape p 470 A90-32559
- Control point selection in the discrete vortex method p 470 A90-32567
- Numerical modeling of separated turbulent flows p 470 A90-32673
- Instability and susceptibility of a boundary layer in the vicinity of two-dimensional surface inhomogeneities p 535 A90-32675
- Solution of sonic flow problems p 470 A90-32712
- An investigation of the flow characteristics of transonic nozzle blades p 475 A90-33700
- A numerical method for calculating supersonic flows of a viscous gas p 476 A90-34672
- An implicit scheme with flow correction for the numerical solution of the Euler equation p 477 A90-34674
- Determination of additive contents in aviation and turbine oils p 532 A90-34681
- Heat transfer in supersonic coaxial reacting jets p 601 A90-35394
- Basic areas of research in the development of a future ATM system p 551 A90-35685
- Some aspects of the control system and power unit lead tests using in-flight simulator systems and flying test-beds p 580 A90-36031
- A study of boundary layer stability in the case of an increased incoming stream turbulence in gradient flows p 555 A90-36065
- Optimization of complex data processing algorithms in multichannel radio direction finding p 576 A90-36115
- Identification and diagnostics in the data processing and control systems of aerospace powerplants p 611 A90-36151
- Ground aviation equipment: Handbook p 593 A90-36153
- Automation of flight safety control p 589 A90-36157
- Vibration equations for a helicopter rotor blade p 604 A90-37830
- Experimental investigation of GDL diffusers [AIAA PAPER 90-1512] p 563 A90-38659
- Numerical solution of the problem of supersonic flow of a viscous gas past a concave conical wing p 619 A90-39465
- Mathematical modeling of plane parallel separated flows past bodies p 619 A90-39475
- Boundary layer stability in the case of transonic external flow p 619 A90-39514
- Perturbations of higher modes in a supersonic jet p 619 A90-39516
- Wave structure of artificial perturbations in a supersonic boundary layer on a plate p 619 A90-39518
- The problem of supersonic flow past a thin wing of finite span with fully subsonic leading edges p 620 A90-39519
- Vortex theory for the screw propeller with a hub p 620 A90-39538
- Relationship between velocity circulation around a wing profile and vorticity dispersion in a boundary layer p 620 A90-39539
- Air traffic control p 638 A90-39581
- Differential-geometrical technique of signal transformation and estimation of position, rate and acceleration parameters using supplementary data sources p 638 A90-41004
- The development result of SPEKTR automated air traffic control (ATC) system with extended grade of automation for terminal and hub areas p 639 A90-41058
- Synthesis of optimal multidimensional digital systems for the simulation of the angular motions of a flight vehicle under random loading p 669 A90-41957
- The investigation of heat transfer in cooled blades of gas turbines p 685 A90-42043
- [AIAA PAPER 90-2144] p 685 A90-42043
- Experimental turbofan using liquid hydrogen and liquid natural gas as fuel p 663 A90-42170
- [AIAA PAPER 90-2421] p 663 A90-42170
- Principles underlying the integration of an aircraft and its engine p 729 A90-42520
- Monitoring and maintenance of automatic control systems in aviation p 778 A90-42524
- The planning of air transportation on airlines p 721 A90-42648
- The history of aviation engine development in the USSR and the 60th anniversary of CIAM p 783 A90-42828
- [AIAA PAPER 90-2761] p 783 A90-42828
- Development of a mathematical model of an adaptive antiflutter system p 769 A90-42911
- Stability and controllability in proportional navigation p 725 A90-42990
- Calculation of nonseparated flow past a wing profile at large Reynolds numbers p 706 A90-42995
- Some technological errors in the use of capillary inspection in gas turbine engine repair p 769 A90-43039
- Numerical modeling of transverse flow past a cylinder using Euler equations p 709 A90-44922
- Excitation and development of unstable perturbations in a supersonic boundary layer p 710 A90-44928
- The potential approximation in the theory of conical flows p 710 A90-44930
- Experimental investigation of turbulence in a supersonic flow p 710 A90-44931
- The effect of vibration-dissociation interaction on heat transfer and drag during the hypersonic flow past bodies p 710 A90-44934
- Aerodynamic drag of a pair of bodies in transonic and supersonic flow p 710 A90-44935
- Design of wing profiles for application in nonstall conditions in a given angle-of-attack range p 710 A90-44936
- A study of the electrophysical phenomena in the combustion chambers of jet engines p 765 A90-45028
- A study of the errors of a gyroscopic instrument for measuring linear accelerations p 771 A90-45133
- Sensitivity analysis in the design of composite structures p 880 A90-46478
- Stiffness of an aircraft pneumatic rudder drive p 828 A90-46479

- Effect of the drag on the critical flutter velocity
p 828 A90-46480
- Identification of a stress-strain computation model and planning of tensometry points in strength and stability studies
p 880 A90-46482
- Parametric synthesis of the decoupling filter in the manual control system of VTOL aircraft
p 859 A90-46483
- Multiple-step terminal control with parameter identification and prediction during flight vehicle descent
p 872 A90-46484
- The problem of aircraft test flight correction
p 828 A90-46485
- Effect of the nonuniformity of external supersonic flow and nozzle deflection angle on the base pressure behind an axisymmetric body with a single supersonic jet
p 802 A90-46486
- Numerical calculation of turbulent separated flows in an abruptly expanding channel
p 803 A90-46487
- Operation of a gas ejector in the pulsed regime
p 850 A90-46488
- A method for the matching of structural and geometric parameters of the turbocompressors of small gas turbine engines in computer-aided design
p 850 A90-46491
- Calculation of an axial-flow birotary turbine
p 880 A90-46492
- Optimal choice of measured parameters during the identification of gas turbine engines. II - Combined confidence regions and intervals of the identification results
p 850 A90-46493
- Calculation of the efficiency of an active partial-admission gas turbine for counterpressures varying over a wide range
p 850 A90-46495
- Design of the optimal hardening treatment for the metal surfaces of gas turbine engine components
p 873 A90-46496
- Computer-aided design of compressor rotor blade rings
p 851 A90-46497
- Design of computer-aided aircraft testing systems. II
p 785 A90-46498
- Evaluation of the dynamic characteristics of a helicopter instrument panel
p 829 A90-46499
- Modeling of the buffeting of flight vehicles
p 803 A90-46500
- Calculation of nonstationary forces in a three-row compressor cascade
p 803 A90-46502
- A problem in the theory of optimal aerodynamic shapes
p 803 A90-46503
- Effect of the fluid level of a hydraulic shock absorber on the characteristics of the gas supply system
p 851 A90-46504
- Optimal blading density in axial-flow compressor stages with a developed three-dimensional flow
p 851 A90-46505
- A source of discrete noise components in the flow path of gas turbines and fans
p 894 A90-46506
- Effect of the nozzle ring vane height on the efficiency of axial-flow full-admission microturbines
p 851 A90-46509
- Cyclic fracture toughness of VT-31 and VT-25 titanium alloys
p 873 A90-46514
- Interchangeability of Soviet-made and foreign mineral oils for aviation gas turbine engines
p 873 A90-46525
- Local convergence of the solution in the discrete vortex method
p 803 A90-46534
- Calculation of the heat flux at a three-dimensional critical point in supersonic flow past a body
p 803 A90-46536
- Effect of a crescent-shaped rigid support on the aerodynamic characteristics of models in the presence of perforated boundaries
p 869 A90-46537
- A study of gas flow in hypersonic nozzles at large Reynolds numbers using simplified Navier-Stokes equations
p 803 A90-46538
- Relation between flow parameters of a gas turbine engine and rotor frequencies
p 851 A90-46539
- A study of the stability and thermal stability of complex reinforced structures
p 880 A90-46541
- Construction of wing profiles in subsonic gas flow by the method of quasi-solutions for inverse boundary value problems
p 803 A90-46542
- Wall pressure pulsation spectra ahead of internal corners
p 804 A90-46545
- An experimental study of a supersonic gas ejector
p 851 A90-46546
- Application of the inverse method of three-dimensional boundary layer analysis to the problem of flow past a wing with allowance for the effect of viscosity
p 804 A90-46548
- Interference between a vortex filament and shock waves in free flow and in nonisobaric jets
p 804 A90-46550
- Some characteristics of interference between shock waves and the aerodynamic wake behind a body
p 804 A90-46551
- Calculation of the rotation noise of a single propeller with blades of arbitrary shape
p 894 A90-46552
- Wing design optimization under stress-strain constraints using full-strength and minimum mass criteria
p 804 A90-46554
- A generalized relation for the aerodynamic efficiency of plane bodies
p 804 A90-46559
- Using the smoking-wire visualization method in the study of wing models at large angles of attack in subsonic wind tunnels
p 881 A90-46561
- Profiling of the supersonic components of three-dimensional corrugated nozzles
p 804 A90-46563
- Some possibilities of the vortex layer method for calculating the aerodynamic characteristics of an augmented airfoil interacting with the engine jet
p 804 A90-46564
- An experimental study of the combined effect of longitudinal riblets and vortex breakers on turbulent friction
p 805 A90-46565
- Determination of the laminar-turbulent transition point for a turbulent layer on a yawing wing
p 805 A90-46566
- Acoustic excitation of boundary layer oscillations on a yawing wing
p 805 A90-46567
- Flow past bodies within a narrow class of cross-sectional shapes with stationary separation zones at large Reynolds numbers
p 805 A90-46568
- Determination of the extreme values of the efficiency criteria for a flight vehicle control system in the probable scatter range of its characteristics
p 859 A90-46569
- Self-induced roll oscillations of lifting systems with thin delta wings
p 860 A90-46570
- A method for reducing a buckled skin under combined loading
p 860 A90-46571
- An experimental study of instantaneous velocity perturbations over a rotor disk for low duty coefficients
p 860 A90-46572
- Calculation of three-dimensional flow past a plane supersonic air intake at angles of attack and sideslip
p 805 A90-46573
- Gasdynamic characteristics of a plane or axisymmetric nozzle with a rectilinear generatrix of the supersonic section
p 805 A90-46575
- Characteristics of temperature and pressure generation and retention in flow inside cryogenic wind tunnel T-04
p 869 A90-46576
- Analytical studies of the transonic flutter of aircraft
p 860 A90-46577
- Application of splines to the calculation of flow past a wing profile
p 805 A90-46615
- Air transportation in COMECON countries
p 785 A90-46616
- Optimum aircraft design: Multipurpose approach
p 829 A90-46618
- Optoelectronic guidance sensors (5th revised and enlarged edition)
p 881 A90-46620
- Effect of shock waves and jets on structural elements: Mathematical modeling in nonstationary gas dynamics
p 806 A90-46621
- Technical and economic efficiency of aviation gas turbine engines in service
p 851 A90-46624
- The economics of the organization and the planning of civil aviation
p 897 A90-46629
- Response of a subsonic boundary layer to a pulsed oscillation of a localized region of the surface in the flow
p 811 A90-46295
- Analysis and prediction of weather for aviation
p 888 A90-48351
- Using cloud moisture calculations for estimating aircraft icing
p 888 A90-48358
- An automated method for predicting the height of the lower cloud boundary
p 888 A90-48359
- Vertical wind shears in lower-level jet stream over some airfields in the Urals and Siberia
p 888 A90-48362
- Some characteristics of the meteorological conditions of low cloud formation around the Baku airport
p 888 A90-48364
- Coaxial helicopters - Current status and future developments
p 838 A90-48951
- Helicopter or tiltrotor - A Soviet view
p 838 A90-48952
- Two- and three-dimensional problems of unsteady aerodynamics of low loaded turbomachinery blade rows stages
p 813 A90-49452
- Numerical simulation of transonic flow through oscillating and multi-row two-dimensional airfoil cascades
p 814 A90-49460
- Numerical simulation of three-dimensional nonstationary flows and variable aerodynamic forces in turbomachine stages
p 814 A90-49465
- Aeroelastic vibrations of turbomachine blades and propellers
p 854 A90-49482
- Operation of aviation radio and electronic equipment (Handbook)
p 914 A90-50747
- Optimization of the shape of a sealed shell and of the size and location of its reinforcements
p 957 A90-50773
- Requirements for meteorological equipment designed for the acquisition of meteorological data essential for the takeoff and landing of aircraft at civil airports
p 962 A90-50777
- Analysis and synthesis of meteorological support systems for airports
p 914 A90-50778
- Coordination strategies in a hierarchical air traffic control system with allowance for meteorological conditions
p 914 A90-50779
- Measurement of wind characteristics at airports
p 962 A90-50780
- Semiautomatic coding of weather phenomenon groups in the meteorological reports of automatic airport stations
p 962 A90-50783
- Variability characteristics of the meteorological optical range field in an optically inhomogeneous atmosphere
p 962 A90-50784
- Flow past two cylinders and two spheres
p 903 A90-50815
- Effect of the Mach number and shape of the front part of the obstacle on the separation zone length in supersonic flow
p 903 A90-50816
- Effect of incoming flow turbulence on the aerodynamic characteristics of a smooth symmetric body at large angles of attack
p 904 A90-50817
- Ways of providing for the strength and service life of aircraft structures made of polymer composites with allowance for damage
p 957 A90-50843
- Acoustic wave excitation during the aerodynamic interaction between a fan blade and a bluff obstacle
p 965 A90-52289
- Estimation of the safety factor of turbine blades under thermal cycling and vibration loading
p 958 A90-52356
- Airborne digital computers and systems
p 927 A90-52410
- Organization of air traffic control
p 915 A90-52415
- Landing tests for Buran shuttle with jet engine-equipped mock-up
p 61 A90-10904
- Effect of vortex generators on the aerodynamic wing characteristics and body of revolution
p 721 A90-25955
- UNITED KINGDOM**
- Calculation of confined swirling flows with a second moment closure
p 66 A90-10640
- Wing-section effects on the flight performance of a remotely piloted vehicle
p 29 A90-11007
- Hypersonics revisited (The First Leslie Bedford Lecture)
p 60 A90-11458
- Flutter of turbine blades
p 41 A90-11794
- The active control of engine instabilities
p 44 A90-12505
- The interaction between tip clearance flow and the passage flowfield in an axial compressor cascade
p 11 A90-12525
- Material requirements for future aeroengines
p 62 A90-12534
- IMI 834 - A new high temperature capability titanium alloy for engine use
p 62 A90-12535
- Properties and characterisation of novel thermal barrier systems for gas turbines
p 62 A90-12538
- Navier-Stokes methods applied to turbomachinery blade design
p 12 A90-12549
- A theoretical and experimental investigation of the Reynolds and apparent stresses in axial compressors
p 12 A90-12554
- Temperature scaling of turbine blade heat transfer with and without shock wave passing
p 47 A90-12570
- VSTOL power plant control lessons from Harrier experience
p 13 A90-12582
- A study of particle trajectories in a gas turbine intake
p 48 A90-12583
- A theoretical approach to particle separator design
p 48 A90-12584
- Advanced airbreathing powerplant for hypersonic vehicles
p 49 A90-12607
- The development of a high response aerodynamic wedge probe and use on a high-speed research compressor
p 69 A90-12618
- CFD predictions of lobed mixer flowfields
p 70 A90-12626
- The remote sensing of temperature in gas turbine engine components using epithermal neutrons
p 70 A90-12630
- A full scale, VSTOL, ground environment test facility
p 58 A90-12631
- Identification of a coupled body/coning/inflow model of Puma vertical response in the hover
p 56 A90-12765
- System identification strategies for helicopter rotor models incorporating induced flow
p 30 A90-12768
- A frequency-domain system identification approach to helicopter flight mechanics model validation
p 56 A90-12772
- Experience with multi-step test inputs for helicopter parameter identification
p 56 A90-12775

- Wildhaber-Novikov circular arc gears - Some properties of relevance to their design p 70 A90-12999
- Design and application of a finite element package for modelling turbomachinery vibrations p 70 A90-13011
- The effect of trailing edge extensions on the performance of the Goettingen 797 and the Wortmann FX 63-137 aerofoil section at Reynolds numbers between 3×10 to the 5th and 1×10 to the 6th p 82 A90-13783
- The effect of flow curvature on the aerodynamic characteristics of an ogive-cylinder body p 82 A90-13785
- General Dynamics F-16 p 100 A90-13791
- Holographic head-up displays for air and ground applications p 108 A90-13885
- The role of adaptive antenna systems when used with GPS p 128 A90-13995
- Signal processing in a digital GPS receiver p 128 A90-14006
- Carbon fibre composite bolted joints p 130 A90-15354
- Experimental study on the buckling and postbuckling of carbon fibre composite panels with and without interply disbands p 130 A90-15355
- The advantages of automation in aerospace production p 130 A90-15357
- An investigation into the internal heat transfer characteristics of a thermally anti-iced aero-engine intake lipskin p 111 A90-15390
- Advantage Airbus? p 102 A90-15746
- The production of uniformly sheared streams by means of double gauzes in wind tunnels - A mathematical analysis p 131 A90-15887
- YG40 - Rolls-Royce advanced fighter engine demonstrator p 112 A90-16002
- Diffusion bonding aeroengine components p 131 A90-16012
- The manufacture of SPF military aircraft doors in aluminium alloy p 132 A90-16616
- Experiments are telling you something (Stewartson Memorial Lecture) p 144 A90-16752
- An interactive boundary layer method for subsonic airfoil flows p 144 A90-16754
- Further work on aerofoils at Reynolds numbers between 3×10 to the 5th and 1×10 to the 6th p 145 A90-16758
- Interaction between strong longitudinal vortices and turbulent boundary layers p 145 A90-16764
- A viscous package for attached and separated flows on swept and tapered wings p 146 A90-16771
- The calculation of under-expanded impinging jets p 147 A90-16782
- Radar systems p 208 A90-17305
- Cost effective technology p 188 A90-17447
- An experimental investigation of the downwash beneath a lifting rotor and low advance ratios p 151 A90-17585
- Theoretical and experimental analysis of a model rotor blade incorporating a swept tip p 151 A90-17586
- The strength and weakness of carbon composite structures p 180 A90-17679
- Recursive real-time identification of step-response matrices of helicopters for adaptive digital flight control p 195 A90-17703
- Cooking an aeroplane p 209 A90-17918
- Stronger starlifter p 143 A90-17919
- Looking inside a structure p 209 A90-17920
- The case for titanium p 204 A90-17922
- Developing aluminium p 204 A90-17924
- Safer primers from 3M p 204 A90-17925
- Numerical study of balanced patch repairs to cracked sheets p 210 A90-18442
- An application of SQP and Ada to the structural optimisation of aircraft wings p 216 A90-18444
- Turbulent boundary layer development in the presence of small isolated two-dimensional surface discontinuities p 210 A90-18507
- Jet futures p 190 A90-18526
- On the Goertler vortex instability mechanism at hypersonic speeds p 158 A90-18886
- Combustion oscillations in ducts p 204 A90-19006
- Further investigations of transonic shock-wave boundary-layer interaction with passive control p 159 A90-19390
- Alleviation of shock oscillations in transonic flow by passive controls [AIAA PAPER 90-0046] p 161 A90-19648
- Modern technology in airship design [AIAA PAPER 89-3169] p 244 A90-20584
- An analytical technique for addressing airship ditching behavior [AIAA PAPER 89-3167] p 238 A90-20589
- Estimation of the flight dynamic characteristics of the YEZ-2A [AIAA PAPER 89-3173] p 245 A90-20590
- Application of the dynamic stiffness method to the free and forced vibrations of aircraft panels p 270 A90-20599
- Gas turbine combustion - A personal perspective p 283 A90-20604
- Repair of composite aircraft parts - An operator's viewpoint p 221 A90-20606
- Gear steels for future helicopter transmissions p 265 A90-20607
- Helicopter transmissions - Design for safety and reliability p 270 A90-20608
- Eurofighter fights back p 221 A90-21714
- Material progress p 221 A90-21715
- A finite element solution of unsteady two-dimensional flow in cascades p 226 A90-21946
- Applications of an adaptive unstructured solution algorithm to the analysis of high speed flows [AIAA PAPER 90-0395] p 229 A90-22213
- Equipment procurement - EH101 helicopter p 282 A90-22435
- A comparison between the design point and near-stall performance of an axial compressor [ASME PAPER 89-GT-70] p 254 A90-22667
- Stability of flow through multistage axial compressors [ASME PAPER 89-GT-311] p 231 A90-22668
- Measurement and calculation of the three-dimensional flow in axial compressor stators, with and without end-bends [ASME PAPER 89-GT-6] p 287 A90-23753
- Secondary loss generation in a linear cascade of high-turning turbine blades [ASME PAPER 89-GT-47] p 289 A90-23773
- Compressor blade boundary layers. II - Measurements with incident wakes [ASME PAPER 89-GT-51] p 289 A90-23777
- Stall inception in axial compressors [ASME PAPER 89-GT-63] p 290 A90-23786
- Inlet skew and the growth of secondary losses and vorticity in a turbine cascade [ASME PAPER 89-GT-65] p 290 A90-23788
- Application of recess vane casing treatment to axial flow fans [ASME PAPER 89-GT-68] p 341 A90-23791
- The influence of diffuser vane leading edge geometry on the performance of a centrifugal compressor [ASME PAPER 89-GT-163] p 292 A90-23851
- The design and test of a two stage transonic axial flow compressor [ASME PAPER 89-GT-164] p 341 A90-23852
- A comparison between engine test results and design predictions of turbine blade cooling performance [ASME PAPER 89-GT-169] p 341 A90-23854
- A theoretical study of ingress for shrouded rotating disc systems with radial outflow [ASME PAPER 89-GT-178] p 361 A90-23859
- Impingement/effusion cooling - The influence of the number of impingement holes and pressure loss on the heat transfer coefficient [ASME PAPER 89-GT-188] p 361 A90-23866
- Experimental investigation into the effects of rotating and static bolts on both windage heating and local heat transfer coefficients in a rotor/stator cavity [ASME PAPER 89-GT-196] p 362 A90-23870
- Simulation of cooling film density ratios in a mass transfer technique [ASME PAPER 89-GT-200] p 362 A90-23872
- The extension and application of three-dimensional time marching analyses to incompressible turbomachinery flows [ASME PAPER 89-GT-212] p 293 A90-23878
- Aerodynamic and heat transfer measurements on blading for a high rim-speed transonic turbine [ASME PAPER 89-GT-228] p 293 A90-23883
- Holographic flow visualisation of turbofan by-pass and core nozzle streams [ASME PAPER 89-GT-260] p 363 A90-23891
- Aerodynamic design methods for transonic wings p 293 A90-23978
- The effect of uniform spanwise vorticity on the two-dimensional flow through cascades p 293 A90-23996
- Aircraft noise p 373 A90-24253
- Pay-offs and pitfalls of fly-by-wire p 346 A90-24281
- The performance and longitudinal stability and control of large receiver aircraft during air to air refueling p 346 A90-24338
- Reductions in induced drag by the use of aft swept wing tips p 299 A90-24342
- Isothermal velocity and turbulence measurements downstream of a model multilobed turbofan mixer p 365 A90-24353
- A practical co-axial twin rotor model p 335 A90-25423
- Experimental investigation of three-dimensional turbulent boundary layers on 'infinite' swept curved wings p 303 A90-25589
- An analysis of factors impeding passenger escape from aircraft fires p 322 A90-26018
- Charging of aircraft - High-velocity collisions p 322 A90-26131
- Numerical grid generation in computational fluid mechanics '88; Proceedings of the Second International Conference, Miami Beach, FL, Dec. 5-8, 1988 p 376 A90-26476
- Solution-adaptive grids for transonic flows p 309 A90-26508
- The construction of component-adaptive grids for aerodynamic geometries p 309 A90-26513
- Techniques in multiblock domain decomposition and surface grid generation p 309 A90-26526
- On the combination of structured-unstructured meshes p 311 A90-26540
- Metal matrix composites - Ready for take-off? p 356 A90-26865
- An array-fed reflector antenna with built-in calibration facility p 402 A90-27781
- Use of swirl for flow control in propulsion nozzles p 421 A90-27963
- Creditable commuter p 405 A90-27975
- Identification of retreating blade stall mechanisms using flight test pressure measurements p 384 A90-28172
- The use of fibre reinforced thermoplastics for helicopter primary structures and their engineering substantiation p 441 A90-28191
- Theoretical and experimental correlation of helicopter aeromechanics in hover p 429 A90-28200
- EH101 design and development status p 407 A90-28211
- A new data acquisition, display and control system for the ARA transonic wind tunnel p 436 A90-28256
- Use of liquid crystals for qualitative and quantitative 2-D studies of transition and skin friction p 446 A90-28259
- Liquid crystal thermography for aerodynamic heating measurements in short duration hypersonic facilities p 446 A90-28262
- An automated vorticity surveying system using a rotating hot-wire probe p 447 A90-28284
- Glassy waters for Seastar p 382 A90-29637
- The challenge of LHX p 382 A90-29641
- Natural honeycomb p 442 A90-29643
- Cleaner superalloys via improved melting practices p 442 A90-29707
- Physical phenomena associated with unsteady transonic flows p 394 A90-29883
- A laser obstacle avoidance and display system p 419 A90-30694
- Design of adaptive digital controllers incorporating dynamic pole-assignment compensators for high-performance aircraft p 432 A90-30714
- An American knowledge base in England - Alternate implementations of an expert system flight status monitor p 459 A90-30719
- After Habsheim p 401 A90-31388
- Design of an aero-engine thrust reverser blocker door p 467 A90-31651
- Automated R.T.M. for an airframe component p 534 A90-31881
- Thermoplastic composites, past, present and future p 529 A90-31882
- Cycle analysis for helicopter gas turbine engines [ASME PAPER 89-GT-328] p 506 A90-32258
- Propulsion systems for supersonic V/STOL aircraft [ASME PAPER 89-GT-309] p 507 A90-32259
- Experimental studies of combustor dilution zone aerodynamics. I - Mean flowfields p 508 A90-32962
- Comparison of test signals for aircraft frequency domain identification p 490 A90-33057
- In the shadow of Aloha p 468 A90-33174
- The development of leading-edge notches to improve the subsonic performance of wings of moderate sweep p 491 A90-33367
- An investigation of the buffet excitation parameter p 473 A90-33368
- Application of time domain decomposition techniques to aircraft ground and flutter test data p 491 A90-33373
- Identification of time varying modal parameters p 536 A90-33375
- Whole helicopter aeroelasticity - Experience with a new approach p 492 A90-33380
- Sensitivity analysis using resonance and anti-resonance frequencies - A guide to structural modification p 536 A90-33396
- Practical techniques of modelling aeroelastic systems for active control applications p 545 A90-33402
- Interactions of active controls and structural loads p 517 A90-33404
- Implementation of comprehensive actuation system models in aeroservoelastic analysis p 517 A90-33406

- Effects of tailplane aerodynamics and fuselage flexibility on the flutter of high aspect ratio, low speed aircraft p 493 A90-33414
- Non-axisymmetric viscous lower-branch modes in axisymmetric supersonic flows p 474 A90-33509
- Unsteady transition in an axial-flow turbine. I - Measurements on the turbine rotor. II - Cascade measurements and modeling p 474 A90-33562 [ASME PAPER 89-GT-289]
- The trailing edge loss of transonic turbine blades [ASME PAPER 89-GT-278] p 475 A90-33564
- The use of circumferentially varying stagger guide vanes in an axial flow pump or compressor p 537 A90-33566
- The story of sandwich construction p 538 A90-33702
- Repairing the damage p 530 A90-33712
- Force balance errors due to temperature changes in ETW p 539 A90-34231
- Investigation of model rigging limitations on a high speed wind tunnel model at cryogenic temperature p 523 A90-34232
- Surface flow visualization in the cryogenic wind tunnel p 539 A90-34234
- A feasibility study for a combat aircraft model sting for the European transonic wind tunnel p 524 A90-34243
- A proposed automatic calibration facility for cryogenic balances p 524 A90-34246
- Development of cryogenic instrumentation for ETW models p 525 A90-34251
- Measurement of temperature gradients and assessment of balance performance using the RAE cryogenic test duct p 525 A90-34252
- Multiple impact jet apparatus (MIJA) - Application to rain erosion studies p 525 A90-34580
- Dynamic stall experiments on the NACA 23012 aerofoil p 552 A90-35140
- Velocity and turbulence characteristics of isothermal lobed mixer flows p 584 A90-35230
- Wide chord fan club p 584 A90-35600
- Water borne again p 579 A90-35846
- Flight beyond normal limits p 589 A90-35847
- Yakovlev strikes back p 579 A90-35848
- On the instability of hypersonic flow past a wedge p 554 A90-35902
- The inviscid axisymmetric stability of the supersonic flow along a circular cylinder p 554 A90-35916
- Carbon-carbon for NASP p 599 A90-36672
- Applications of fiber optic sensors in the aerospace and marine industries p 603 A90-36782
- Priorities for high-lift testing in the 1990s [AIAA PAPER 90-1413] p 596 A90-37950
- Experience in the use of a viscous simulation methodology for tests in transonic tunnels [AIAA PAPER 90-1414] p 559 A90-37951
- Development and verification of an algorithm for helicopter inverse simulations p 591 A90-38522
- Technology update of early gas turbine designs p 586 A90-38531
- Progress in certifying F402-RR-408 - The improved Pegasus engine for AV-8B and Harrier II Plus p 587 A90-38532
- A numerical study of supersonic flow over a compression corner with different incoming boundary-layer profiles [AIAA PAPER 90-1453] p 561 A90-38612
- Wide angle diffusers with passive boundary-layer control [AIAA PAPER 90-1600] p 567 A90-38732
- Improvement of helicopter handling qualities using H(infinity)-optimisation p 667 A90-38965
- Implementation of a transputer-based flight controller p 667 A90-38966
- The EH101 electronic instrument system p 652 A90-40462
- Combustion characteristics of a model can-type combustor p 676 A90-40479
- Identification of multivariable models of jet engines [AIAA PAPER 90-1874] p 655 A90-40540
- Design of digital self-selecting multivariable controllers for jet engines [AIAA PAPER 90-1875] p 655 A90-40541
- Simulation of inviscid blade-row interaction using a linearised potential code [AIAA PAPER 90-1916] p 621 A90-40555
- An image analysis method for vehicle stabilization p 668 A90-40914
- Experimental studies of combustor dilution zone aerodynamics. II - Jet development p 659 A90-40947
- Experiments on the active control of the transmission of sound through a clamped rectangular plate p 695 A90-41109
- SMAS - An expert system for configuring a research flight simulator p 694 A90-41191
- The effects of toughening stresses on liquid impact induced fracture p 692 A90-41315
- The six component magnetic suspension system for wind tunnel testing p 673 A90-41725
- Large receiver aircraft - The performance and longitudinal stability and control during air to air refuelling p 669 A90-41767
- The performance of a combustor pre-diffuser incorporating compressor outlet guide vanes [AIAA PAPER 90-2165] p 661 A90-42053
- Numerical modeling of an impinging jet in cross-flow [AIAA PAPER 90-2246] p 686 A90-42093
- Hypersonic (T-D) 'pinch' and aerospaceplane propulsion [AIAA PAPER 90-2474] p 675 A90-42189
- Active control of helicopter cabin noise p 645 A90-42434
- EH101 development progress p 646 A90-42442
- The safety analysis approach for the EH101 p 635 A90-42456
- A comprehensive approach to coupled rotor-fuselage dynamics p 646 A90-42460
- A technique for the tuning of helicopter flight control systems p 670 A90-42467
- The place of knowledge based systems in helicopter dynamic system condition prognosis p 618 A90-42475
- The modular HUM system p 618 A90-42476
- New systems for helicopter and aircraft vibration monitoring p 653 A90-42477
- EH101 vibration control p 647 A90-42496
- Estimation of rotor blade incidence and blade deformation from the measurement of pressures and strains in flight p 647 A90-42497
- Flight tests to explore tail rotor limitations in the low speed envelope p 647 A90-42498
- Sound generation by a supersonic aerofoil cutting through a steady jet flow p 781 A90-42638
- Design of aeroengines in a low-fuel price scenario p 739 A90-42653
- Forebody design for the aerospaceplane [AIAA PAPER 90-2472] p 762 A90-42810
- UK reference station for Navstar GPS p 725 A90-43681
- The propan... What future now? p 744 A90-43763
- The standard-setting Hornet p 730 A90-43764
- Mi-14 - The Soviet Sea King p 730 A90-43765
- The McDonnell Douglas MD-11... or, how the DC-10 grew bigger p 730 A90-43766
- Demonstrating technologies for enhanced fighter manoeuvrability - The Rockwell/MBB X-31 p 731 A90-43767
- Mirage 2000 - A French success that is no illusion p 731 A90-43768
- Support backbone for the Soviet air forces... The Ilyushin 'Candid' family p 731 A90-43769
- Building the B-2 p 701 A90-43826
- A comparison of honeycomb-core and foam-core carbon-fibre/epoxy sandwich panels p 764 A90-43855
- Compressor aerodynamics p 706 A90-44052
- A friendly alloy p 764 A90-44173
- Loss weight with Al-Li p 765 A90-44175
- Transonic flow computations in convergent propulsion nozzles using the time-dependent mode p 708 A90-44459
- Wide-chord fan proved in nearly five years of service p 744 A90-44594
- Advanced developments of the Turbo-Union RB199 p 745 A90-44595
- Future development of the 535E4 engine p 745 A90-44596
- More power for the Harrier p 745 A90-44597
- Escape and survival following helicopter ditching - Training aspects p 722 A90-44658
- Escape and survival following helicopter ditching - Research aspects p 722 A90-44659
- Minimum induced drag for wings with spanwise camber p 709 A90-44733
- Differential Omega/VLF as a world-wide navigation aid in the 21st century p 727 A90-45232
- Flow and heat transfer in rotating-disc systems. Volume I - Rotor-stator systems p 772 A90-45759
- Experimental and numerical study of the British Experimental Rotor Programme blade [AIAA PAPER 90-3008] p 789 A90-45858
- Surface flow on a flat plate induced by a supersonic jet exhausting normally into a low speed crossflow [AIAA PAPER 90-3011] p 789 A90-45860
- An aerofoil testing technique for low supersonic speeds in an adaptive flexible-walled wind tunnel [AIAA PAPER 90-3086] p 795 A90-45900
- An experimental investigation of supersonic flow over two cavities in tandem [AIAA PAPER 90-3087] p 795 A90-45901
- Torsional buckling and post-buckling of composite geodetic cylinders with special reference to joint flexibility p 878 A90-45971
- Prediction and measurement of rotor blade/stator vane dynamic characteristics of a modern aero-engine axial compressor p 878 A90-46036
- Theoretical and experimental determination of natural frequencies of laced blading p 878 A90-46037
- Old lamps for new - A photoelastic design tool for weight and cost saving on aircraft structures p 878 A90-46039
- Vibration analysis of laced blades p 878 A90-46186
- Active control of sound transmission through a cylindrical shell p 893 A90-46192
- Theoretical studies of the active control of propeller-induced cabin noise p 893 A90-46351
- In-flight experiments on the active control of propeller-induced cabin noise p 893 A90-46352
- Bursting in separating flow and in transition p 800 A90-46366
- A review of low Reynolds number aerodynamic research at the University of Glasgow p 800 A90-46367
- Power struggle p 851 A90-46650
- Practical aspects of European collaboration p 785 A90-46928
- Modelling aspects for the synthesis and performance assessment of some future advanced helicopters p 829 A90-46937
- Application of the Westland CRFD program to total helicopter dynamics p 832 A90-46965
- Two and three dimensional indicial methods for rotor dynamic airloads p 808 A90-46973
- The surface pretreatment of aluminium-lithium alloys for structural bonding p 881 A90-47118
- Input/output coupling in eigenstructure assignment [AIAA PAPER 90-3476] p 865 A90-47726
- Robust low norm output feedback design for flight control systems [AIAA PAPER 90-3505] p 891 A90-47751
- Developments in the acoustic fatigue design process for composite aircraft structures p 882 A90-48047
- Fault-tolerant transputer-based controller configurations for gas-turbine engines p 852 A90-48529
- Certificating the Speed Canard p 833 A90-48699
- Wave interactions in a three-dimensional attachment-line boundary layer p 811 A90-48715
- Innovation and investment for survival and prosperity - The new Battle of Britain [AIAA PAPER 90-3189] p 786 A90-48826
- Design of a close-support aircraft [AIAA PAPER 90-3241] p 835 A90-48849
- The BAe (commercial aircraft) LTD transport aircraft synthesis and optimisation program (TASOP) [AIAA PAPER 90-3295] p 837 A90-48879
- Analysis of failures in aircraft structures p 882 A90-48998
- 1990-1995, a period of international decision making for the navigation community - Is our planning as good as it should be? p 823 A90-49490
- Towards a quantitative assessment of benefits which INS/GPS integration can offer to civil aviation operating in a non-jamming environment p 823 A90-49496
- Gripen wins its wings p 842 A90-49823
- Commuter from Khodinka p 842 A90-49824
- Starship sails through p 842 A90-49825
- Highlights of RAE lightning strike investigations p 818 A90-49827
- Investment-cast superalloys a good investment p 949 A90-51198
- The absorption of sound by perforated linings p 965 A90-51994
- Airport technology international 1989/1990 p 937 A90-52857
- The application of TSIM software to act design and analysis on flexible aircraft p 60 A90-10086
- Characteristics of combustion driven pressure oscillations in advanced turbo-fan engines with afterburner p 64 A90-10194
- Royal Aerospace Establishment: No place for a castings factor p 64 A90-10235
- Experimental investigation of attachment-line transition in low-speed, high-lift wind-tunnel testing p 71 A90-10358
- The three-dimensional vortex sheet structure on delta wings p 19 A90-10367
- The Experimental Aircraft Flight Test Programme p 34 A90-10865
- Flight test instrumentation and data processing at British Aerospace, Warton, U.K. p 59 A90-10887
- The active control of an unstable canard aircraft p 57 A90-10894
- An assessment of robustness of flight control systems based on variable structure techniques p 57 A90-10895

- Normal-force-curve and pitching-moment-curve slopes of forebody-cylinder combinations at zero angle of attack for Mach numbers up to 5
[ESDU-89008] p 89 N90-11709
- The determination of the aerodynamic characteristics of an ogive-cylinder body in subsonic, curved, incompressible flow, and an assessment of the effect of flow curvature
[REPT-87-13] p 89 N90-11712
- Incompressible flow about ellipsoids of revolution
[REPT-88-02] p 90 N90-11713
- UK airmisses involving commercial air transport, May-August 1988
[ISSN-0951-6301] p 96 N90-11717
- UK airmisses involving commercial air transport
[CAA-2/88] p 96 N90-11718
- Aircraft cabin fire suppression by means of an interior water spray system
[CAA-PAPER-88014] p 96 N90-11719
- A simulation study of landing time allocation procedures for use in computer-assisted air traffic management systems
[AD-A212159] p 99 N90-11722
- The 1987 survey of track keeping and altitudes on Heathrow and Gatwick standard instrument departure routes (DAY)
[CAA-PAPER-88010] p 99 N90-11729
- The RB199: An in-service success
[PNR90544] p 114 N90-11746
- Advanced technology in military gas turbine design and manufacture
[PNR90545] p 114 N90-11747
- Engine controls for the 1990's
[PNR90546] p 114 N90-11748
- Future military powerplants
[PNR90554] p 114 N90-11749
- Comparison of the results of tests on A300 aircraft in the RAE 5 metre and ONERA F1 wind tunnels
[RAE-TM-AERO-2130] p 122 N90-11768
- Aluminium alloy development for aero engines
[PNR90548] p 126 N90-11874
- Improvements in the formulations and numerical solution of the Euler problem for swept wings
[RAE-TM-AERO-2139] p 95 N90-12562
- CFD methods for drag prediction and analysis currently in use in UK
[RAE-TM-AERO-2146] p 95 N90-12563
- Development and evaluation at ATCEU of executive and support operations, phase 4A/3D
[CAA-PAPER-88017] p 99 N90-12572
- Operational trial of effect of raising minimum stack level in Heathrow stacks
[CAA-PAPER-89003] p 99 N90-12573
- Software fault tolerance
[RSRE-MEMO-4237] p 99 N90-12575
- What should be done with those noisy old aircraft
[PNR90562] p 107 N90-12593
- A vision of the future: The new engine technology
[PNR90566] p 115 N90-12603
- Designing for reliable and low maintenance cost aero engines
[PNR90570] p 115 N90-12604
- The next generation supersonic transport engine: Critical issues
[PNR90576] p 115 N90-12605
- Re-engine with the Rolls-Royce Tay 670, the route to significant noise reduction
[PNR90585] p 115 N90-12606
- The role of component testing
[PNR90589] p 115 N90-12608
- Flanged joints of aeroengines
[PNR90594] p 116 N90-12609
- Material requirements for future aeroengines
[PNR90595] p 116 N90-12610
- A computer integrated approach to dimensional inspection
[PNR90596] p 116 N90-12611
- Dynamic tip clearance measurements in axial flow compressors
[PNR90597] p 116 N90-12612
- The development of a high response aerodynamic wedge probe and use on a high-speed research compressor
[PNR90598] p 116 N90-12613
- Gas turbine performance analysis
[PNR90599] p 116 N90-12614
- Blading design for multi-storage HP compressor
[PNR90602] p 116 N90-12616
- Preliminary experience with high response pressure measurements in a multistage, high speed compressor
[RAE-TM-P-1141] p 117 N90-12619
- Composite materials for future aeroengines
[PNR90584] p 127 N90-12667
- The future of non ferrous metals in aerospace engines
[PNR90572] p 127 N90-12720
- Assessment of voice coders for ATC/pilot voice communications via satellite digital communication channels
[CAA-PAPER-89004] p 135 N90-12807
- Fine resolution errors in secondary surveillance radar altitude reporting amongst aircraft transmitting the conspicuity codes 4321 and 4322
[RSRE-88004] p 135 N90-12816
- The nature and control of skidding in lightly loaded intershaft bearings
[PNR90591] p 136 N90-12933
- A real-time wind model using digital data from aircraft
[RSRE-MEMO-4309] p 137 N90-13005
- The design and development of an acoustic test section for the ARA transonic wind tunnel
[PNR90574] p 140 N90-13202
- The commercial aircraft noise problem
[PNR90577] p 140 N90-13203
- Acoustic recording systems for use in military aircraft
[RAE-TM-MM-11] p 140 N90-13207
- Data acquisition in aerodynamic research
p 171 N90-13340
- Study of forces and moments on wing-bodies at high incidence, volumes 1 and 2
p 171 N90-13350
- Computer-based tools for assisting air traffic controllers with arrivals flow management
[RSRE-88001] p 178 N90-13366
- On the application of modified stepwise regression for the estimation of aircraft stability and control parameters
[REPT-8905] p 198 N90-13400
- Helicopter rotor test rig (RoTeSt) in DNW: Application and results
[RAE-TRANS-2171] p 201 N90-13408
- Aircraft/airport compatibility: Some strategic, tactical, and operational issues
[TT-8902] p 202 N90-13409
- Normal force, pitching moment, and side force of forebody-cylinder combinations for angles of attack up to 90 degrees and Mach numbers up to 5
[ESDU-89014] p 173 N90-14192
- Introduction to data items on flight path optimisation
[ESDU-89015] p 185 N90-14221
- Hinge moment coefficient derivatives for trailing-edge controls on wings at subsonic speeds
[ESDU-89009] p 198 N90-14239
- Example of procedure in calculation of control hinge moments
[ESDU-89010] p 199 N90-14240
- Techniques for extreme attitude suspension of a wind tunnel model in a magnetic suspension and balance system
[NASA-CR-181895] p 202 N90-14245
- Diffusion bonding of metals
p 206 N90-14330
- Classification of windshear severity
p 281 N90-15049
- The assessment of visibility from automatic contrast Measurements
p 242 N90-15061
- Aircraft testing in the electromagnetic environment
p 248 N90-15066
- Installed tailplane lift-curve slope at subsonic speeds
[ESDU-89029] p 236 N90-15081
- The maximum lift coefficient of plain wings at subsonic speeds
[ESDU-89034] p 236 N90-15082
- A study of variable geometry in advanced gas turbines
p 255 N90-15104
- Design temperatures for flexible airfield pavement design
[AD-A214141] p 262 N90-15115
- Fabrication characteristics of 8090 alloy
p 268 N90-15198
- Uses and properties of Al-Li on the new EH101 helicopter
p 268 N90-15201
- Current status of the application of conventional aluminium-lithium alloys and the potential for future developments
p 268 N90-15203
- The automatic detection of anti-collision lights
[RSRE-MEMO-4272] p 240 N90-15896
- UK airmisses involving commercial air transport, September to December 1988
[ISSN-0951-6301] p 240 N90-15897
- The application of Z to the specification of air traffic control systems. 1: An initial specification of the radar processing activity
[RSRE-MEMO-4280] p 243 N90-15900
- Integral fuel tank seating practice at British Aerospace (Kingston)
p 250 N90-15905
- The repair of aircraft integral fuel tanks in the RAF: A user's view of fuel tank technology
p 250 N90-15908
- The effect of primer age on adhesion of polysulphide sealant
p 269 N90-15909
- The development of a low cost data logging system for flight trials based on an IBM compatible PC
[RAE-TM-FM-16] p 251 N90-15917
- Performance of a highly-loaded HP compressor
[RAE-TM-P-1149] p 256 N90-15919
- Aerodynamic and heat transfer measurements on blading for a high rim-speed transonic turbine
[RAE-TM-P-1151] p 256 N90-15920
- Cycle analysis for helicopter gas turbine engines
[RAE-TM-P-1154] p 256 N90-15921
- A UK perspective on the uniform engine test programme
[RAE-TM-P-1172] p 257 N90-15922
- Technology and evaluation of unmanned air vehicles
p 252 N90-15934
- In-plane forces and moments on installed inclined propellers at low forward speeds
[ESDU-89047] p 316 N90-16720
- Estimation of subsonic far-field jet-mixing noise from single-stream circular nozzles
[ESDU-89041] p 316 N90-16721
- Parallel processing implementation of a flight controller
p 333 N90-16743
- Body effect on wing angle of attack and pitching moment at zero lift at low speeds
[ESDU-89042] p 337 N90-16757
- Wake interaction effects on the transition process on turbine blades
[AD-A214492] p 343 N90-16759
- HOTOL: A future launcher for Europe
p 353 N90-16800
- Aerodynamic and structural design challenges of a reusable single stage to orbit air-breathing launch vehicle
p 354 N90-16814
- Parametric assessment of propulsion system mass for airbreathing launcher configurations
p 344 N90-16819
- Fatigue of aluminium alloy joints with various fastener systems. Low load transfer
[ESDU-89046] p 370 N90-17193
- Application of experimental techniques to store release problems
p 316 N90-17545
- Glancing shock-boundary layer interactions
p 319 N90-17571
- Aircraft fires: A study of transport accidents from 1975 to the present
p 324 N90-17583
- A review of UK civil aviation fire and cabin safety research
p 325 N90-17587
- Aircraft internal fires
p 326 N90-17593
- Fire science and aircraft safety
p 326 N90-17596
- Forced and natural venting of aircraft cabin fires: A numerical simulation
p 326 N90-17597
- The stability of fuel fires
p 327 N90-17601
- Fire hardening of an aircraft passenger cabin
p 328 N90-17606
- A method for the prediction of supersonic compressor blade performance
[CUE/A-TURBO/TR-126] p 344 N90-17634
- Antenna installation on aircraft: Theory and practice
p 371 N90-17941
- Optimum spanwise camber for minimum induced drag
[BU-403] p 397 N90-18369
- Development of a mass averaging temperature probe
p 427 N90-18418
- Modelling unsteady transition and its effects on profile loss
p 427 N90-18423
- Noise levels from a VSTOL aircraft measured at ground level and at 1.2 m above the ground
[NPL-RSA(EXT)-009] p 464 N90-18999
- Calculation of excrescence drag magnification due to pressure gradient at high subsonic speeds
[ESDU-87004] p 397 N90-19195
- A study of flows over highly-swept wings designed for maneuver at supersonic speeds
[AD-A216837] p 399 N90-19202
- An experimental study of the aeroelastic behaviour of two parallel interfering circular cylinders
p 455 N90-19609
- Development of an ejection seat specification for a new fighter aircraft
p 483 N90-20057
- Escape systems research at RAE
p 483 N90-20058
- Fighter escape system: The next step forward
p 483 N90-20059
- Heat transfer near the entrance to a film cooling hole in a gas turbine blade
[AD-A217396] p 510 N90-20089
- Flow in a forward swept centrifugal fan, volumes 1 and 2
p 481 N90-20959
- Measurement and prediction of propeller blade surface pressure distributions
p 481 N90-20961
- The role of structural analysis in airworthiness certification
[BR112064] p 499 N90-20972
- Computer-aided structural optimisation of aircraft structures
[BR112837] p 499 N90-20973
- Aerofoil design techniques
p 500 N90-20978
- HOTOL structures and materials at British Aerospace, Warton, UK
[EOARD-LR-90-001] p 503 N90-21001

An investigation of secondary flows in nozzle guide vanes p 512 N90-21016

Secondary flow predictions for a transonic nozzle guide vane p 513 N90-21017

Supersonic nozzle design of arbitrary cross-section p 515 N90-21035

Multiblock topology specification and grid generation for complete aircraft configurations p 582 N90-21986

Feature-associated mesh embedding for complex configurations p 608 N90-21988

A discussion on issues relating to multiblock grid generation p 608 N90-21991

Unstructured finite element mesh generation and adaptive procedures for CFD p 608 N90-21993

UK airmisses involving commercial air transport, January - April 1989 p 575 N90-22544

[ISSN-0951-6301]

Characterisation of fatigue of aluminium alloys by acoustic emission. Part 2: Discrimination between primary and other emissions p 678 N90-23523

[AERE-R-13303-PT-2]

The computation of turbulent thin shear flows associated with flow around multielement aerofoils p 633 N90-24240

A study of the technology required for advanced vertical take-off aircraft p 650 N90-24268

[ETN-90-96786]

From 1959-1989: 30 years of service experience with ramjets p 748 N90-25139

[PNR90677]

Formation of design envelope criterion in terms of deterministic spectral procedure p 721 N90-25953

[RAE-TM-SS-9]

Stage 2 re-engining: The only way to achieve a real stage 3 aircraft p 737 N90-25977

[PNR90636]

Combustion in the gas turbine. Part 1: Combustor types and design p 748 N90-25986

[CIT/SME/VKI/RS/1]

Combustion in the gas turbine. Part 2: Preliminary design and performance p 748 N90-25987

[CIT/SME/VKI/RS/3]

Combustion in the gas turbine. Part 3: Fuel injection, ignition and stability p 748 N90-25988

[CIT/SME/VKI/RS/4]

Combustor cooling aspects p 749 N90-25989

[CIT/SME/VKI/RS/5]

Pollutants: Production and methods of reduction p 749 N90-25990

[CIT/SME/VKI/RS/6]

Subsonic combustor flow modeling: State of the art of CFD techniques for reacting and combustor flow p 749 N90-25991

Application of high performance metals in gas turbine engines p 750 N90-25999

[PNR90640]

Towards 2000: The composite engine p 750 N90-26000

[PNR90646]

Prediction of rotating disc flow and heat transfer in gas turbine engines p 750 N90-26001

[PNR90650]

Prediction and measurement of rotor blade/stator vane dynamic characteristics of a modern aero-engine axial compressor p 750 N90-26002

[PNR90667]

The impact and requirements of new materials on aeroengines p 750 N90-26003

[PNR90671]

Aircraft exhaust emissions: An engine manufacturer's perspective p 750 N90-26004

[PNR90675]

The application of engineering ceramics in gas turbines p 750 N90-26005

[PNR90676]

Handbook of uncertainty methodology for engine testing at Pyestock (England) p 751 N90-26007

[RAE-TM-P-1179]

An investigation of the use of singular perturbation methods and modal control theory in the derivation of aircraft control schemes p 758 N90-26014

[MATHS-REPT-A-106]

Metal matrix composites and powder processing for aero-engine applications p 767 N90-26087

[PNR90617]

NDT in aerospace: The next decade (1990's) p 777 N90-26348

[PNR90628]

The role of NDI in the certification of turbine engine components p 777 N90-26349

[PNR90629]

Bringing aircraft noise testing down to Earth p 783 N90-26637

[PNR90642]

The aims and history of adaptive wall wind tunnels p 871 N90-26839

The need for platform motion in modern piloted flight training simulators p 871 N90-26847

[AD-A221720]

Cost effective technology p 883 N90-27002

[PNR90664]

Performance assessment of MIL-STD-1553B on the avionic systems demonstrator rig of British Aerospace p 849 N90-27624

Harrier Information Management System (HIMS): The system and the approach p 884 N90-27630

Replay and transmission of AIMS-data to mainframe computer using remote transcribers p 892 N90-27634

Flight data replay and analysis system p 893 N90-27635

AIMS for helicopters p 820 N90-27639

Integration of flight management and air traffic management systems p 827 N90-27693

[RAE-TM-FM-41]

AGARD damage tolerance concepts for engine structures Workshop 3, Component Behaviour and Life Management p 855 N90-27705

Component behaviour and life management: The need for common AGARD approaches and actions p 856 N90-27710

The basis for facility comparison p 856 N90-27713

Experience in developing an improved altitude test capability p 857 N90-27719

The role of NDI in the certification of turbine engine components p 859 N90-28069

Inspection reliability p 885 N90-28072

Impact of NDE-NDI methods on aircraft design, manufacture, and maintenance, from the fundamental point of view p 887 N90-28093

Combat aircraft control requirements p 934 N90-28515

The effects of foreplanes on the static and dynamic characteristics of a combat aircraft model p 920 N90-28520

Unsteady aerodynamics of controls p 935 N90-28525

The steady and time-dependent aerodynamic characteristics of a combat aircraft with a delta or swept canard p 921 N90-28526

The effect of rapid spoiler deployment on the transient forces on an aerofoil p 921 N90-28527

Effective optimal control of a fighter aircraft engine p 928 N90-28548

Three-dimensional model testing in the transonic self-streamlining wind tunnel p 938 N90-28583

Studies in automatic speech recognition and its application in aerospace p 958 N90-28759

Use of liquid crystals for qualitative and quantitative 2-D studies of transition and skin friction p 958 N90-28800

[RAE-TM-AERO-2159]

The cost of air service fragmentation p 913 N90-29334

[TT-9010]

UK airmisses involving commercial air transport: May - August 1989 p 913 N90-29335

[ISSN-0951-6301]

Aircraft evacuations: The effect of passenger motivation and cabin configuration adjacent to the exit p 913 N90-29336

[CAA-PAPER-89019]

The potential for digital databases in flight planning and flight aiding for combat aircraft p 918 N90-29371

The potential for an extra runway at Heathrow: A preliminary feasibility study p 938 N90-29403

[TT-9007]

The experimental investigation of flow in the core of a vortex structure p 960 N90-29597

[BR114893]

Y

YUGOSLAVIA

Nonlinear stability of subsonic mixing layers with symmetric temperature variations p 223 A90-20501

Some computational and experimental aspects of optimal design process of composite structures p 882 A90-48050

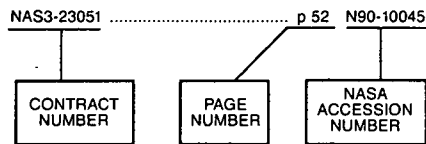
Generalized similarity solutions for three-dimensional laminar compressible wing boundary layers p 907 A90-51543

CONTRACT NUMBER INDEX

AERONAUTICAL ENGINEERING / A Continuing Bibliography
1990 Cumulative Index

February 1991

Typical Contract Number Index Listing



Listings in this index are arranged alphanumerically by contract number. Under each contract number, the accession numbers denoting documents that have been produced as a result of research done under the contract are arranged in ascending order with the AIAA accession numbers appearing first. The accession number denotes the number by which the citation is identified in the abstract section. Preceding the accession number is the page number on which the citation may be found.

AF PROJ. 1900	p 256	N90-15106
AF PROJ. 1926	p 484	N90-20069
	p 689	N90-23762
	p 637	N90-24258
	p 845	N90-26828
AF PROJ. 2103	p 875	N90-26992
AF PROJ. 2302	p 55	N90-10893
	p 478	N90-20053
	p 925	N90-29386
AF PROJ. 2304	p 348	N90-16770
	p 377	N90-18181
	p 462	N90-18908
	p 462	N90-18920
AF PROJ. 2307	p 18	N90-10008
	p 18	N90-10009
	p 89	N90-11706
	p 89	N90-11707
	p 134	N90-11988
	p 170	N90-13330
	p 343	N90-16759
	p 454	N90-18672
	p 464	N90-19852
	p 540	N90-20345
	p 689	N90-23687
	p 634	N90-24250
	p 815	N90-26798
AF PROJ. 2308	p 126	N90-11837
AF PROJ. 2401	p 845	N90-26826
	p 887	N90-28106
AF PROJ. 2402	p 654	N90-23398
AF PROJ. 2403	p 198	N90-13398
	p 757	N90-25140
AF PROJ. 2418	p 275	N90-15486
	p 678	N90-23538
	p 689	N90-23752
	p 842	N90-26807
	p 925	N90-29387
AF PROJ. 2480	p 32	N90-10027
	p 357	N90-16951
	p 678	N90-23571
	p 875	N90-26994
	p 954	N90-29527
AF PROJ. 2567	p 911	N90-29307
AF PROJ. 2688	p 692	N90-23832
AF PROJ. 2734	p 960	N90-29565
AF PROJ. 3005	p 120	N90-11758
	p 631	N90-23349
	p 634	N90-24249
	p 884	N90-27118
AF PROJ. 3035	p 671	N90-23409
AF PROJ. 3037	p 378	N90-17409

AF PROJ. 3048	p 379	N90-17411
	p 379	N90-17412
	p 548	N90-20800
	p 615	N90-23188
	p 615	N90-23189
	p 615	N90-23190
	p 966	N90-30036
	p 443	N90-18601
	p 766	N90-25228
	p 854	N90-26831
	p 933	N90-28574
	p 933	N90-29396
AF PROJ. 3145	p 71	N90-10351
AF PROJ. 3484	p 875	N90-26933
AF PROJ. 486U	p 960	N90-29664
AF PROJ. 6302	p 875	N90-26972
AF PROJ. 7184	p 464	N90-19842
AF PROJ. 7231	p 548	N90-20799
	p 548	N90-20800
	p 723	N90-25117
	p 844	N90-26825
	p 895	N90-27466
	p 895	N90-27467
	p 540	N90-20312
AF PROJ. 7662	p 927	N90-28545
AF PROJ. 7930	p 355	A90-24865
AF PROJECT 2302P101	p 209	A90-18169
AF PROJECT 2302P1	p 171	N90-13336
AF 49(638)-792	p 134	N90-11988
AF-AFOSR-0082-86	p 89	N90-11706
AF-AFOSR-0099-84	p 462	N90-18908
AF-AFOSR-0132-86	p 540	N90-20345
AF-AFOSR-0140-89	p 55	N90-10893
AF-AFOSR-0142-87	p 377	N90-18181
AF-AFOSR-0154-86	p 815	N90-26798
AF-AFOSR-0158-85	p 89	N90-11707
AF-AFOSR-0159-86	p 170	N90-13330
AF-AFOSR-0184-87	p 702	N90-25073
AF-AFOSR-0209-88	p 911	N90-29305
AF-AFOSR-0241-88	p 18	N90-10008
AF-AFOSR-0243-86	p 462	N90-18920
AF-AFOSR-0282-88	p 343	N90-16759
AF-AFOSR-0295-85	p 478	N90-20050
AF-AFOSR-0303-85	p 348	N90-16770
AF-AFOSR-0308-87	p 454	N90-18672
AF-AFOSR-0398-87	p 464	N90-19852
AF-AFOSR-3129-76	p 336	A90-26541
AF-AFOSR-80-0258	p 313	A90-26936
	p 169	A90-19983
AF-AFOSR-82-0136	p 557	A90-36522
AF-AFOSR-83-0049	p 529	A90-32952
AF-AFOSR-83-0356	p 444	A90-27992
AF-AFOSR-85-0008	p 451	A90-29399
	p 303	A90-25582
AF-AFOSR-85-0126	p 309	A90-26496
AF-AFOSR-85-0143	p 153	A90-17866
AF-AFOSR-85-0158	p 195	A90-17703
AF-AFOSR-85-0208	p 567	A90-38753
AF-AFOSR-85-0273	p 154	A90-18153
AF-AFOSR-86-0082	p 164	A90-19822
	p 154	A90-18147
AF-AFOSR-86-0092	p 153	A90-17981
AF-AFOSR-86-0112	p 162	A90-19670
	p 228	A90-22208
	p 569	A90-38773
	p 569	A90-38774
AF-AFOSR-86-0159	p 469	A90-32462
AF-AFOSR-86-157	p 301	A90-25276
AF-AFOSR-87-0029	p 791	A90-45877
AF-AFOSR-87-0032	p 608	A90-38769
AF-AFOSR-87-0074	p 147	A90-16781
	p 799	A90-46363
AF-AFOSR-87-0121	p 288	A90-23771
AF-AFOSR-87-0218	p 169	A90-19983
AF-AFOSR-87-0312	p 710	A90-45150
AF-AFOSR-87-0366	p 167	A90-19876
AF-AFOSR-88-0007	p 608	A90-38769
AF-AFOSR-88-0010	p 436	A90-28255
	p 791	A90-45877
AF-AFOSR-88-0120	p 160	A90-19636
	p 303	A90-25592
AF-AFOSR-88-0155	p 393	A90-29591
AF-AFOSR-88-0233	p 347	A90-25995
AF-AFOSR-89-0033	p 606	A90-38614
AF-AFOSR-89-0042	p 158	A90-18886
AF-AFOSR-89-0055	p 16	A90-12839
	p 603	A90-36271
AF-AFOSR-89-0315	p 569	A90-38772
AF-AFOSR-89-0403	p 563	A90-38666
AF-AFOSR-89-0422	p 798	A90-45932
ARO PROJ. P-24025-EG	p 478	N90-20048
AVRADA PROJ. 5620112DA	p 405	N90-19217
A84/KLU/046	p 123	N90-12629
A88/KLU/621	p 919	N90-29380
	p 939	N90-29409
BARR-10-119	p 485	N90-20929
BMFT-LFF-84318	p 646	A90-42457
BMFT-QV-8723	p 363	A90-23904
BMFT-13-AS-0038/3	p 66	A90-11041
BMFT-514-8891-LFF-8440	p 278	N90-16189
CNR-86,00758,59	p 157	A90-18501
CNR-86,00865,59	p 433	A90-31283
CNR-87,02280,59	p 342	A90-23873
	p 342	A90-23874
CNR-88-03287-07	p 884	N90-27120
DA PROJ. 1L1-2211-A-47-A	p 543	N90-21394
DA PROJ. 1L1-61102-AH-45-A	p 173	N90-14186
DA PROJ. 1L1-61102-AH-45	p 194	N90-13393
	p 257	N90-15923
	p 506	N90-21004
	p 858	N90-27722
	p 964	N90-29121
DA PROJ. 1L1-62105-AH-84	p 650	N90-24270
	p 874	N90-26887
DA PROJ. 1L1-62209-A4-7A	p 215	N90-14617
	p 372	N90-18041
DA PROJ. 1L1-62209-A47-A	p 213	N90-13797
DA PROJ. 1L1-62211-A-47-AA	p 237	N90-15882
	p 633	N90-24239
DA PROJ. 1L1-62211-A-47-AB	p 876	N90-27787
DA PROJ. 1L1-62211-A-47-A	p 776	N90-26334
DA PROJ. 1L1-62211-AH-7-AA	p 632	N90-24237
DA PROJ. 1L1-62618-AH-80	p 428	N90-19233
DA PROJ. 1L1-62716-AH-70	p 520	N90-20095
DA PROJ. 1L1-63211-D-436	p 349	N90-17644
DA PROJ. 2480	p 65	N90-11184
DAAB07-87-D-H020	p 108	A90-13986
DAAD05-87-ML-584	p 457	A90-28184
DAAG29-79-G-0017	p 66	A90-10222
DAAG29-82-K-0029	p 852	A90-46871
DAAG29-82-K-0084	p 384	A90-28176
	p 555	A90-36255
DAAG29-82-K-0093	p 347	A90-25420
	p 406	A90-28153
	p 585	A90-35673
DAAG29-82-K-0094	p 430	A90-28227
DAAG29-83-K-0002	p 293	A90-23935
	p 518	A90-33625
	p 831	A90-46958
DAAG29-83-K-0004	p 66	A90-10222
DAAG29-84-K-0048	p 347	A90-25990
	p 521	N90-20939
	p 521	N90-20940
DAAG29-92-K-0093	p 232	A90-23105
DAAH01-87-D-0035	p 891	A90-47730
DAAJ02-85-C-0048	p 537	A90-33624
DAAJ02-85-C-0049	p 409	A90-28233
DAAJ02-86-C-0013	p 422	A90-28183
DAAJ02-86-C-0014	p 421	A90-28168
	p 422	A90-28178
DAAJ02-86-C-0028	p 575	N90-22545
	p 575	N90-22546
	p 575	N90-22547
	p 575	N90-22548
	p 575	N90-22549
DAAJ02-87-C-0022	p 637	N90-24259
DAAJ09-88-C-A003	p 832	A90-46968
DAAK51-81-C-0017	p 445	A90-28234
DAAK51-82-C-0002	p 349	N90-17644
DAAK51-83-C-0045	p 407	A90-28173
DAAL03-36-K-0056	p 752	A90-45140
DAAL03-86-G-0043	p 260	N90-15113
DAAL03-86-K-0056	p 118	A90-14729
	p 516	A90-33058
DAAL03-87-G-0003	p 118	A90-14355
DAAL03-87-G-0004	p 668	A90-40886

DAAL03-87-G-0011

CONTRACT NUMBER INDEX

DAAL03-87-G-0011	p 863	A90-47628	DRET-87-034	p 817	N90-27661	F33615-82-C-3406	p 819	A90-49844
DAAL03-87-K-0001	p 712	A90-45260	DRET-87-068	p 95	N90-12564	F33615-83-C-1036	p 960	N90-29565
DAAL03-87-K-0022	p 891	A90-47755	DRET-87-131	p 958	N90-28810	F33615-83-C-2331	p 361	A90-23858
DAAL03-87-K-0037	p 478	N90-20048	DRET-87-34-083-00-470-75-01	p 454	N90-18695	F33615-83-C-2339	p 626	A90-42161
DAAL03-88-C-0002	p 518	A90-33623	DRET-87-1497/DS/SR2	p 96	N90-11716		p 626	A90-42162
	p 429	A90-28157	DRET-88-001-58	p 896	N90-28402	F33615-83-C-3600	p 121	N90-12624
	p 385	A90-28198	DRET-88-045	p 858	N90-27723		p 198	N90-13398
	p 408	A90-28226	DRET-88-103	p 166	A90-19833	F33615-84-C-2427	p 768	A90-42740
	p 590	A90-38519	DRET-88-1156	p 876	N90-27900		p 742	A90-42741
DAAL03-88-C-0003	p 366	A90-25303	DRET-88-34-001	p 107	N90-12592	F33615-84-C-2432	p 661	A90-42051
	p 430	A90-28227	DRET-88-34432	p 957	A90-51525	F33615-84-C-2475	p 47	A90-12570
	p 861	A90-46956	DRET-88-817	p 141	N90-13278	F33615-84-C-2567	p 302	A90-25292
DAAL03-88-C-0004	p 585	A90-35673	DRET-89-34-001	p 910	N90-28500	F33615-84-C-3005	p 763	A90-44735
DAAL03-88-C-0006	p 911	N90-29302	DTFA01-86-Y-01015	p 527	N90-21045	F33615-84-C-3404	p 484	N90-20069
DAAL03-88-C-0028	p 560	A90-38394	DTFA01-80-Y-10524	p 456	A90-28620		p 689	N90-23762
DAAL03-88-C-002	p 412	A90-29389		p 281	N90-15566		p 845	N90-26828
	p 392	A90-29390	DTFA01-80-Y-10546	p 133	N90-11934	F33615-84-C-5027	p 256	N90-15107
	p 412	A90-29405	DTFA01-81-Y-10555	p 937	N90-28582	F33615-85-C-0532	p 875	N90-26972
DAAL03-88-C-004	p 412	A90-29394	DTFA01-82-Y-10553	p 373	A90-25572	F33615-85-C-1718	p 540	N90-20312
DAAL03-88-K-0163	p 204	A90-17962		p 456	A90-28612	F33615-85-C-2515	p 192	A90-19857
DAAL03-89-C-0024	p 959	N90-28828	DTFA01-84-C-00001	p 242	A90-23242		p 686	A90-42068
DAAL03-89-G-0003	p 532	N90-20140		p 918	N90-29364	F33615-85-C-2537	p 510	N90-20091
DAAL03-89-K-0092	p 865	A90-47665	DTFA01-84-Z-02038	p 59	N90-10896	F33615-85-C-2551	p 71	N90-10351
DAAL03-90-G-0037	p 911	N90-29304	DTFA01-85-Y-010304	p 332	N90-16730	F33615-85-C-2567	p 443	N90-18601
DAJA45-85-C-0039	p 397	N90-18427	DTFA01-86-C-00023	p 674	N90-24277	F33615-85-C-2575	p 683	A90-40943
DAJA45-87-M-0484	p 262	N90-15115	DTFA01-86-Y-01046	p 937	N90-28581	F33615-85-C-2585	p 933	N90-29396
DARPA ORDER 6029	p 532	N90-20143	DTFA01-87-C-00014	p 141	N90-12406	F33615-85-C-3013	p 147	N90-16779
DASG60-85-C-0053	p 123	A90-13993		p 527	N90-21049		p 159	A90-19387
DASG60-85-C-0122	p 624	A90-42018		p 635	N90-23368	F33615-85-C-3610	p 866	A90-47729
DASG60-86-C-0013	p 560	A90-38488		p 869	N90-27724	F33615-85-C-3611	p 461	A90-30796
DASG60-87-C-0042	p 476	A90-34583	DTFA01-88-C-00059	p 641	N90-24263	F33615-85-C-3804	p 418	A90-30238
	p 525	A90-34586	DTFA01-88-C-0020	p 239	N90-15085		p 892	A90-49741
DDAJ02-77-C-0031	p 507	A90-32960	DTFA01-88-Y-01073	p 178	N90-14214	F33615-85-C-5030	p 533	N90-20208
DE-AC02-83CH-10093	p 281	N90-15519		p 542	N90-21249	F33615-85-C-5058	p 843	N90-26815
DE-AC03-87ER-80532	p 74	A90-10599	DTFA01-88-Y-10173	p 28	N90-10855	F33615-86-C-0530	p 378	N90-17409
DE-AC03-88ER-80663	p 75	A90-10614	DTFA01-89-C-00001	p 27	N90-10017		p 379	N90-17410
DE-AC04-76DP-P00789	p 557	A90-36524		p 177	N90-13361		p 379	N90-17411
DE-AC04-76DP-00789	p 146	A90-16774		p 177	N90-13362		p 379	N90-17412
	p 393	A90-29687		p 177	N90-13363		p 615	N90-23188
	p 440	A90-31281		p 243	N90-15086		p 615	N90-23189
	p 595	A90-37946	DTFA01-89-C-0001	p 243	N90-15090		p 615	N90-23190
	p 563	A90-38660	DTFA01-89-P-01074	p 503	N90-21003		p 966	N90-30035
	p 622	A90-40681	DTFA03-83-A-00328	p 551	N90-21724	F33615-86-C-0542	p 457	A90-28184
	p 236	N90-15076	DTFA03-84-C-00004	p 735	N90-25136	F33615-86-C-0551	p 583	N90-22563
	p 323	N90-16722	DTFA03-85-C-00009	p 323	N90-16724	F33615-86-C-2600	p 671	N90-23409
	p 372	N90-18065	DTFA03-86-C-00041	p 122	N90-11765	F33615-86-C-2615	p 114	N90-11743
	p 402	N90-19215	DTFA03-86-C-00049	p 820	N90-27668	F33615-86-C-2616	p 661	A90-42050
	p 405	N90-19217	DTFA03-88-A-00027	p 542	N90-21247	F33615-86-C-2623	p 684	A90-41997
	p 464	N90-19820	DTFA03-88-C-00024	p 176	N90-13360	F33615-86-C-2668	p 68	A90-11703
	p 572	N90-21737		p 402	N90-18375	F33615-86-C-2694	p 533	N90-20235
	p 678	N90-24430		p 723	N90-25119	F33615-86-C-2695	p 205	N90-19713
	p 719	N90-25941	DTFA03-89-C-00023	p 915	N90-28509	F33615-86-C-2697	p 533	N90-21188
	p 910	N90-28495	DTFA03-89-C-00057	p 783	N90-25697	F33615-86-C-3208	p 845	N90-26826
	p 967	N90-30134		p 898	N90-28463		p 887	N90-28106
DE-AC05-84OR-21400	p 946	A90-50179	DTFA03-890-A-00019	p 967	N90-29247	F33615-86-C-3601	p 420	A90-31331
	p 24	N90-10844	DTFA03-96-C-00041	p 505	N90-20080	F33615-86-C-3615	p 516	A90-33061
	p 609	N90-22048	DTOS59-88-C-00064	p 724	N90-25956	F33615-86-C-3623	p 301	A90-25167
	p 885	N90-28059	DTRS-57-88-C-00117	p 729	N90-25122		p 756	A90-45437
DE-AC06-76RL-01830	p 126	N90-11813	DTRS-573-86-C-00131	p 192	N90-13386		p 935	N90-28522
DE-AC22-87PC-79810	p 65	N90-11184	DTRS57L-85-C-00101	p 375	A90-25563	F33615-86-C-3624	p 414	N90-18388
DE-AC22-88PC-88827	p 206	N90-14385	ESA-H-ST-13-01-AS	p 322	A90-26254	F33615-86-C-3625	p 757	N90-25140
	p 269	N90-15288	FAA-T0804-L	p 354	N90-16842	F33615-86-C-5007	p 689	N90-23752
DE-AI01-85CE-50111	p 51	N90-10036	FAA-T0701-R	p 27	N90-10018	F33615-86-C-5031	p 925	N90-29387
DE-FC22-83FE-60149	p 954	N90-29527	FAA-T0701-U	p 59	N90-10897	F33615-86-C-5044	p 286	A90-24699
DE-FG02-87ER-14550	p 555	A90-35917	FAA-T2001-F	p 28	N90-10856	F33615-86-K-2621	p 854	N90-26831
DE-FG03-86ER-13608	p 552	A90-35193	FMV-82260-88-061-73-001	p 938	N90-28584	F33615-87-C-0012	p 938	N90-29407
DE-FG03-88ER-13910	p 153	A90-17985	FY1455-86-N-0657	p 824	N90-26803	F33615-87-C-1550	p 837	A90-48876
DEN3-335	p 601	A90-35508		p 632	N90-23364	F33615-87-C-2709	p 766	N90-25236
	p 687	A90-42165		p 357	N90-16951	F33615-87-C-2711	p 32	N90-10027
	p 220	N90-14153	FY1455-88-N0617	p 678	N90-23571	F33615-87-C-2739	p 656	A90-40554
DEN3-336	p 51	N90-10036	FY1457-85-O-5036	p 126	N90-11837	F33615-87-C-2767	p 655	A90-40530
DEPE(CNA)-PROJ. EU650	p 135	N90-12807	F08635-83-C-0136	p 286	A90-24699	F33615-87-C-2807	p 746	A90-45455
DFG-BE-343/17	p 623	A90-40749	F08635-84-C-02281	p 255	N90-15105	F33615-87-C-2822	p 655	A90-40530
DFG-HU-254/8	p 920	N90-28519		p 156	A90-18310	F33615-87-C-3020	p 634	N90-24249
DFG-SFB-212	p 29	A90-11006		p 374	A90-25289	F33615-87-C-3209	p 166	A90-19845
	p 645	A90-42278	F08635-84-C-0228	p 18	N90-10009	F33615-87-C-3212	p 389	A90-29360
DFG-SFB-25	p 646	A90-42468	F08635-85-C-0122	p 256	N90-15106	F33615-87-C-3250	p 213	N90-13812
	p 150	A90-16845	F08635-86-C-0309	p 507	A90-32808	F33615-87-C-3403	p 684	A90-41334
DFG-WA-424/3	p 473	A90-33366		p 682	A90-40930	F33615-87-C-3607	p 153	A90-17868
DLG-ZI-18-31	p 277	N90-16183	F08635-86-C-0341	p 875	N90-26992		p 711	A90-45164
DLA900-84-C-0910	p 620	A90-39782	F08635-87-C-0003	p 560	A90-38394		p 712	A90-45166
	p 176	N90-13359	F08635-89-C-0196	p 741	A90-42712	F33615-87-C-5221	p 770	A90-44325
	p 287	N90-16708	F19628-85-C-0002	p 133	N90-11934	F33615-88-C-0544	p 723	N90-25117
DLA900-88-D-0392	p 938	N90-29406	F19628-85-C-0003	p 578	N90-22554	F33615-88-C-0638	p 927	N90-28545
DOT-FA01-89-Z-02062	p 216	A90-19733		p 761	N90-25145	F33615-88-C-1712	p 461	A90-30786
DOT-FA03-86-R-60039	p 117	A90-14334	F19628-87-C-0268	p 583	A90-37088	F33615-88-C-1739	p 459	A90-30230
DOT-FA74WAI-432	p 123	N90-12627	F2006C	p 824	N90-26802	F33615-88-C-2823	p 933	N90-28574
DOT-MA91-85-C-50114	p 48	A90-12585		p 870	N90-26835	F33615-88-C-2836	p 685	A90-42040
DRET-82-272	p 396	N90-18367	F2006D	p 870	N90-26836	F33615-88-C-2846	p 685	A90-42041
DRET-84-002	p 136	N90-12897	F2006E	p 99	N90-12574	F33615-88-C-2904	p 163	A90-19710
DRET-84-014	p 5	A90-11597	F33615-78-C-5346	p 729	N90-25123	F33615-88-C-3204	p 127	A90-13770
DRET-84-34-481-00-470-75-01	p 120	N90-12622	F33615-80-C-3234	p 951	A90-51966	F33615-88-C-3212	p 31	N90-10022
DRET-86-1031-01	p 876	N90-27895	F33615-81-C-2078	p 901	A90-49890	F33615-88-C-3606	p 865	A90-47696
DRET-86-104	p 568	A90-38757	F33615-81-C-3403	p 54	N90-10204		p 119	N90-11756
DRET-86-107	p 147	A90-16783	F33615-81-C-5002	p 637	N90-24258	F33615-88-C-3609	p 120	N90-11758
DRET-87-003	p 172	N90-13356		p 859	N90-28073	F33615-88-C-5437	p 678	N90-23538

CONTRACT NUMBER INDEX

NASW-4435

F33615-89-C-0531	p 895	N90-27467	p 667	A90-40689	p 335	A90-25425
F33615-89-C-2944	p 884	N90-27118	p 218	A90-17984	p 670	A90-42462
F33615-89-C-5604	p 951	A90-51966	p 71	N90-10357	p 257	A90-23478
F33615-94-C-3208	p 273	A90-23287	p 479	N90-20950	p 535	A90-32475
F33615086-C-0530	p 966	N90-30036	p 802	A90-46378	p 429	A90-28202
F33657-79-C-0730	p 132	A90-16372	p 549	N90-21604	p 568	A90-38759
F33657-83-C-0100	p 362	A90-23881	p 98	A90-14732	p 57	N90-10075
F33657-84-C-2014	p 853	A90-48874	p 98	A90-14733	p 419	A90-31329
F33657-88-C-0026	p 457	A90-28323	p 574	N90-21747	p 824	N90-26804
F34601-87-C-1655	p 108	A90-13999	p 568	A90-38754	p 849	N90-27701
F40600-86-C-0003	p 72	N90-10424	p 568	A90-38756	p 831	A90-46958
F49620-84-C-0065	p 230	A90-22244	p 160	A90-19636	p 385	A90-28195
	p 552	A90-35137	p 946	A90-50177	p 385	A90-28228
	p 564	A90-38680	p 74	A90-10567	p 786	A90-47707
F49620-84-C-0082	p 146	A90-16776	p 780	N90-25580	p 578	N90-22232
F49620-85-C-0027	p 314	A90-26967	p 665	N90-23401	p 119	A90-16521
	p 704	A90-42734	p 103	N90-11733	p 335	A90-25425
	p 689	N90-23687	p 316	N90-17539	p 392	A90-29387
F49620-85-C-0049	p 117	N90-12620	p 307	A90-26130	p 670	A90-42462
F49620-85-C-0080	p 223	A90-20501	p 308	A90-26137	p 861	A90-46966
	p 307	A90-26067	p 959	N90-28862	p 886	A90-47732
	p 474	A90-33514	p 562	A90-38626	p 200	A90-19728
F49620-85-C-0090	p 603	A90-36271	p 232	A90-23280	p 870	A90-48961
F49620-85-C-0111	p 2	A90-10699	p 553	A90-35752	p 200	N90-13401
F49620-86-C-0040	p 925	N90-29386	p 301	A90-25276	p 409	A90-28238
F49620-86-C-0066	p 450	A90-29373	p 595	A90-37940	p 717	N90-25111
F49620-86-C-0090	p 606	A90-38677	p 214	N90-13817	p 743	A90-42766
F49620-86-C-0033	p 591	A90-38758	p 197	A90-19920	p 949	A90-50645
F49620-86-K-0010	p 65	N90-10253	p 485	N90-20929	p 718	N90-25934
F49620-86-K-0020	p 553	A90-35759	p 478	N90-20050	p 537	A90-33555
	p 679	A90-38854	p 782	N90-26634	p 32	N90-10031
F49620-86-K-0022	p 875	N90-26933	p 755	A90-45332	p 393	A90-29393
F49620-86-10-0020	p 921	N90-28523	p 218	A90-17998	p 790	A90-13091
F49620-87-C-0016	p 752	A90-45143	p 759	A90-44399	p 379	N90-18228
	p 863	A90-47627	p 21	N90-10834	p 132	A90-16371
	p 867	A90-47734	p 633	N90-24242	p 343	A90-23896
F49620-87-C-0046	p 16	A90-12839	p 164	A90-19790	p 744	A90-43218
	p 603	A90-36271	p 233	A90-23281	p 175	A90-19735
F49620-87-C-0069	p 498	N90-20075	p 711	A90-45153	p 551	N90-21724
F49620-87-K-0003	p 411	A90-29238	p 317	N90-17558	p 307	A90-26128
F49620-88-C-0006	p 796	A90-45914	p 398	N90-19198	p 393	A90-29392
	p 798	A90-45937	p 71	N90-10357	p 623	A90-40937
	p 631	N90-23349	p 228	A90-22196	p 719	N90-25940
F49620-88-C-0020	p 812	A90-48953	p 446	A90-28268	p 154	A90-18153
	p 634	N90-24250	p 199	N90-14243	p 606	A90-38651
F49620-88-C-0022	p 168	A90-19929	p 181	A90-18145	p 690	N90-24514
	p 475	A90-33567	p 410	A90-29237	p 485	N90-20925
F49620-88-C-0041	p 607	A90-38750	p 580	A90-36273	p 485	N90-20926
F49620-88-C-0047	p 392	A90-29378	p 601	N90-22651	p 485	N90-20927
F49620-88-C-0053	p 693	A90-40885	p 147	A90-16781	p 485	N90-20928
	p 703	A90-42697	p 890	A90-47699	p 314	A90-26967
	p 793	A90-45887	p 217	N90-14843	p 704	A90-42734
F49620-88-C-0076	p 564	A90-38673	p 875	N90-26903	p 598	N90-21776
F49620-88-CK-0001	p 478	N90-20053	p 234	A90-23701	p 598	N90-21777
JPL-956416	p 763	A90-45137	p 801	A90-46372	p 399	N90-19203
MCAIR PROJ. 7-220	p 268	N90-15202	p 136	N90-12872	p 226	A90-22153
MDA903-85-C-0030	p 287	N90-16707	p 774	N90-25291	p 90	N90-12500
MDA903-86-C-0169	p 347	A90-26189	p 948	A90-50215	p 6	A90-11779
MDA972-88-C-0058	p 249	N90-15099	p 231	A90-22449	p 215	N90-14656
MDA972-88-K-0008	p 138	N90-12239	p 622	A90-40682	p 879	A90-46226
MIPR-CRREL-89-12	p 133	N90-11908	p 606	A90-38663	p 212	A90-19984
MIPR-FY1455-86-N0655	p 65	N90-11184	p 587	A90-38761	p 302	A90-25285
MIPR-FY1455-86-N0657	p 875	N90-26994	p 149	A90-16794	p 555	A90-36252
	p 954	N90-29527	p 607	A90-38765	p 703	A90-42709
MOD-ER/2170/090/XR	p 508	A90-32962	p 713	A90-45452	p 169	A90-19978
MOD-2048/39/XR/FS	p 591	A90-38522	p 772	A90-45324	p 169	A90-20010
MOD-2082/192	p 198	N90-13400	p 279	N90-16294	p 964	A90-52881
NAGW-1022	p 562	A90-38625	p 163	A90-19787	p 48	A90-12585
NAGW-1072	p 67	A90-11102	p 392	A90-29387	p 169	A90-19978
	p 192	A90-19895	p 890	A90-47690	p 606	A90-38614
	p 558	A90-37937	p 486	N90-20938	p 176	A90-20009
	p 600	A90-38711	p 172	N90-13354	p 667	A90-40557
NAGW-1331	p 562	A90-38625	p 451	A90-29429	p 890	A90-47697
	p 600	A90-38711	p 715	A90-45498	p 516	A90-33061
NAGW-1708	p 390	A90-29366	p 776	N90-26281	p 891	A90-47755
	p 925	N90-29385	p 571	N90-21734	p 891	A90-47755
NAGW-1809	p 229	A90-22213	p 571	N90-21735	p 718	N90-25936
NAGW-478	p 155	A90-18254	p 496	A90-34740	p 515	N90-21036
NAGW-581	p 145	A90-16764	p 458	A90-29293	p 720	N90-25948
NAGW-964	p 569	A90-38773	p 139	A90-14346	p 373	N90-17235
NAGW-965	p 677	A90-42117	p 212	N90-13744	p 505	N90-20080
NAG1-104	p 17	A90-13017	p 793	A90-45891	p 505	N90-20081
NAG1-1058	p 884	N90-27946	p 717	N90-25112	p 505	N90-20082
NAG1-1072	p 561	A90-38618	p 164	A90-19822	p 506	N90-20083
NAG1-1087	p 719	N90-25943	p 568	A90-38755	p 506	N90-20084
NAG1-168	p 958	A90-52044	p 763	A90-45149	p 176	N90-14212
NAG1-243	p 375	A90-25989	p 183	N90-13369	p 184	N90-14216
NAG1-244	p 600	A90-38711	p 214	N90-14453	p 186	N90-14226
NAG1-280	p 71	N90-10357	p 607	A90-38765	p 499	N90-20971
NAG1-321	p 864	A90-47661	p 713	A90-45452	p 649	N90-23394
NAG1-324	p 196	A90-19554	p 713	A90-45423	p 649	N90-23395
NAG1-345	p 802	A90-46379	p 481	N90-20965	p 649	N90-23396
NAG1-372	p 17	A90-13024	p 197	A90-19740	p 650	N90-23397
	p 391	A90-29376	p 755	A90-45330	p 650	N90-24266
	p 602	A90-35760	p 755	A90-45331	p 734	N90-25127
	p 569	A90-38778	p 119	A90-16521	p 734	N90-25132
		NAG1-390				
		NAG1-402				
		NAG1-423				
		NAG1-483				
		NAG1-4				
		NAG1-516				
		NAG1-530				
		NAG1-545				
		NAG1-569				
		NAG1-587				
		NAG1-602				
		NAG1-619				
		NAG1-625				
		NAG1-641				
		NAG1-643				
		NAG1-645				
		NAG1-648				
		NAG1-658				
		NAG1-681				
		NAG1-685				
		NAG1-690				
		NAG1-703				
		NAG1-709				
		NAG1-710				
		NAG1-715				
		NAG1-716				
		NAG1-727				
		NAG1-731				
		NAG1-732				
		NAG1-735				
		NAG1-736				
		NAG1-739				
		NAG1-745				
		NAG1-753				
		NAG1-758				
		NAG1-768				
		NAG1-770				
		NAG1-776				
		NAG1-778				
		NAG1-779				
		NAG1-790				
		NAG1-793				
		NAG1-795				
		NAG1-805				
		NAG1-822				
		NAG1-832				
		NAG1-833				
		NAG1-834				
		NAG1-837				
		NAG1-838				
		NAG1-844				
		NAG1-846				
		NAG1-849				
		NAG1-852				
		NAG1-858				
		NAG1-867				
		NAG1-874				
		NAG1-880				
		NAG1-881				
		NAG1-891				
		NAG1-898				
		NAG1-907				
		NAG1-928				
		NAG1-937				
		NAG1-975				
		NAG2-191				
		NAG2-209				
		NAG2-221				
		NAG2-226				
		NAG2-244				
		NAG2-283				
		NAG2-302				
		NAG2-308				
		NAG2-375				
		NAG2-409				
		NAG2-462				
		NAG2-463				
		NAG2-477				
		NAG2-490				
		NAG2-551				
		NAG2-554				
		NAG2-561				
		NAG3-1026				
		NAG3-1112				
		NAG3-140				
		NAG3-181				
		NAG3-284				
		NAG3-308				
		NAG3-311				
		NAG3-354				
		NAG3-37				
		NAG3-479				
		NAG3-481				
		NAG3-499				
		NAG3-527				
		NAG3-617				
		NAG3-630				
		NAG3-666				
		NAG3-716				
		NAG3-729				
</						

NAS1-11668

CONTRACT NUMBER INDEX

NAS1-11668	p 601	N90-22609	NAS1-18585	p 150	A90-16845	p 193	N90-13391
NAS1-14193	p 17	A90-13025		p 162	A90-19686	p 777	N90-26355
NAS1-14630	p 559	A90-37962		p 182	A90-19784	NAS3-23940	p 193
NAS1-15325	p 380	N90-18233		p 166	A90-19844	NAS3-23944	N90-13388
	p 719	N90-25944		p 167	A90-19896	NAS3-24080	p 79
NAS1-15820	p 19	N90-10012		p 538	A90-33698		N90-11549
NAS1-16097	p 510	N90-20088		p 715	A90-45522	NAS3-24105	p 649
NAS1-16521	p 88	N90-11704		p 716	A90-45785		N90-23276
NAS1-17077	p 909	N90-28494		p 798	A90-45936		p 217
NAS1-17096	p 219	A90-19385		p 123	N90-12625	NAS3-24210	N90-17635
	p 219	A90-19386	NAS1-18599	p 568	A90-38754		p 53
NAS1-17145	p 807	A90-46879		p 568	A90-38756	NAS3-24222	N90-10048
NAS1-17146	p 463	A90-28160		p 607	A90-38765	NAS3-24227	p 53
NAS1-17234	p 253	A90-21949		p 828	A90-46385	NAS3-24230	N90-10049
NAS1-17469	p 712	A90-45323		p 416	N90-19226	NAS3-24339	p 79
NAS1-17492	p 787	A90-45847	NAS1-18605	p 924	N90-29383		N90-10683
	p 610	N90-22746		p 158	A90-18886		p 70
NAS1-17496	p 134	N90-12058		p 554	A90-35916	NAS3-24341	N90-13091
	p 213	N90-13814		p 561	A90-38608	NAS3-24350	p 507
NAS1-17497	p 454	N90-18743		p 716	A90-45783		A90-32960
NAS1-17498	p 959	N90-28865		p 20	N90-10833	NAS3-24384	p 731
	p 960	N90-28866	NAS1-18607	p 171	N90-13351	NAS3-24619	A90-44736
NAS1-17499	p 541	N90-20439	NAS1-18788	p 478	N90-20050	NAS3-24622	p 113
	p 758	N90-25143	NAS1-18804	p 781	N90-26595	NAS3-24847	N90-11738
	p 775	N90-25375	NAS1-19000	p 463	A90-28158	NAS3-24855	p 113
NAS1-17506	p 63	N90-10187		p 36	A90-10507	NAS3-24861	N90-1739
NAS1-17698	p 126	N90-11821		p 538	A90-33897	NAS3-25117	p 666
NAS1-17701	p 490	A90-33105		p 229	A90-22213	NAS3-25193	N90-24274
NAS1-17703	p 819	A90-49834		p 946	A90-50177		p 273
NAS1-17705	p 74	A90-10568		p 549	N90-21605	NAS3-25266	A90-22651
NAS1-17740	p 63	N90-10186		p 583	N90-22557		p 682
NAS1-17794	p 658	A90-40622		p 634	N90-24246	NAS3-24384	A90-40930
NAS1-17919	p 150	A90-16845	NAS1-19471	p 966	N90-29169	NAS3-24619	p 65
	p 233	A90-23289	NAS1-648	p 924	N90-29383	NAS3-24622	N90-10293
	p 308	A90-26136	NAS2-11391	p 925	N90-29384	NAS3-24847	p 358
	p 539	A90-34234	NAS2-11555	p 313	A90-26907	NAS3-24855	N90-23792
	p 555	A90-36251	NAS2-11877	p 389	A90-29363	NAS3-24861	p 63
	p 620	A90-39780	NAS2-12148	p 755	A90-45334	NAS3-25117	N90-10184
	p 625	A90-42044	NAS2-12157	p 572	N90-21738	NAS3-25193	p 192
	p 718	N90-25939	NAS2-12378	p 77	N90-11487		N90-13385
NAS1-17921	p 579	A90-35761	NAS2-12419	p 501	N90-20991		p 501
	p 896	N90-28396	NAS2-12425	p 28	N90-10021	NAS3-25270	N90-20991
NAS1-17970	p 642	A90-40130		p 820	N90-27669	NAS3-25317	p 360
NAS1-17987	p 118	A90-14747	NAS2-12451	p 650	N90-24265	NAS3-25425	A90-23828
NAS1-17999	p 893	N90-28366		p 915	N90-28510	NAS3-25446	p 588
NAS1-18000	p 229	A90-22213	NAS2-12513	p 964	N90-29142	NAS3-25460	N90-21761
	p 554	A90-35770		p 965	N90-29143	NAS3-25470	p 868
	p 622	A90-40692	NAS2-12518	p 714	A90-45467	NAS3-25555	A90-49110
NAS1-18015	p 582	N90-21755	NAS2-12640	p 838	A90-48958	NAS3-25574	p 839
NAS1-18027	p 24	N90-10014		p 642	A90-40166	NAS3-25601	A90-49114
	p 220	N90-14866	NAS2-12782	p 403	N90-28219	NAS3-25633	p 314
	p 259	N90-15111	NAS2-12787	p 864	A90-47630	NAS3-25653	A90-26970
	p 348	N90-16768	NAS2-12789	p 877	N90-27935	NAS3-25836	p 674
	p 593	N90-21772	NAS2-12861	p 795	A90-45911	NAS8-30490	A90-42688
NAS1-18037	p 148	A90-16792	NAS2-12962	p 407	A90-28175	NAS8-35601	p 740
	p 140	N90-13198		p 165	A90-19831	NAS8-36284	N90-42690
NAS1-18099	p 695	N90-24103	NAS2-12988	p 230	A90-22230	NAS8-36631	p 18
	p 780	N90-25638	NAS2-13188	p 795	A90-45908	NAS8-38031	N90-10004
NAS1-18107	p 158	A90-18886	NAS2-13194	p 248	N90-15093	NAS9-17650	p 94
	p 474	A90-33509	NAS3-20072	p 915	N90-28510	NAS9-17900	N90-13323
	p 554	A90-35902	NAS3-20643	p 795	A90-45908		p 344
	p 554	A90-35916		p 357	N90-17868	NCA2-IR-340-501	N90-17635
	p 811	A90-48715		p 929	N90-28553	NCA2-IR-589-502	p 468
	p 478	N90-20050		p 929	N90-28554		N90-20943
NAS1-18140	p 574	N90-22539		p 930	N90-28555	NCA2-223	p 516
	p 631	N90-23348		p 930	N90-28557	NCA2-266	N90-21037
NAS1-18144	p 369	N90-17055		p 930	N90-28558	NCA2-298	p 588
NAS1-18235	p 307	A90-26129		p 930	N90-28559	NCA2-310	N90-21763
NAS1-18240	p 16	A90-12828		p 931	N90-28561	NCA2-343	p 666
	p 83	A90-14091	NAS3-20646	p 931	N90-28562		N90-23404
	p 163	A90-19786		p 931	N90-28563	NCA2-397	p 791
	p 228	A90-22196		p 930	N90-28564		A90-45873
	p 561	A90-38608		p 930	N90-28565	NCA2-406	p 506
	p 566	A90-38727		p 931	N90-28566	NCA2-455	N90-21006
	p 802	A90-46379		p 932	N90-28567	NCC1-112	p 816
	p 812	A90-49101		p 932	N90-28569	NCC1-123	N90-27655
	p 71	N90-10366		p 932	N90-28570	NCC1-129	p 658
NAS1-18304	p 965	N90-29919	NAS3-21854	p 51	N90-10037	NCC1-22	A90-50128
NAS1-18336	p 140	N90-13228	NAS3-22158	p 396	N90-18364	NCC1-29	N90-20012
NAS1-18377	p 812	A90-49103	NAS3-22251	p 933	N90-29394	NCC1-47	p 393
	p 923	N90-28537	NAS3-22394	p 52	N90-10043	NCC1-68	A90-20011
NAS1-18378	p 183	N90-13370		p 52	N90-10044		p 169
	p 735	N90-25966	NAS3-23042	p 345	N90-17638	NCA2-298	N90-20011
NAS1-18458	p 807	A90-46872	NAS3-23051	p 52	N90-10045	NCA2-310	p 230
NAS1-18465	p 401	N90-18371		p 53	N90-10046	NCA2-343	A90-22256
	p 401	N90-18372		p 117	N90-12617		p 368
	p 637	N90-24257		p 929	N90-28552	NCA2-397	N90-20012
NAS1-18527	p 942	A90-50070	NAS3-23697	p 73	N90-10451		p 201
NAS1-18561	p 480	N90-20952	NAS3-23708	p 302	A90-25290	NCA2-406	N90-13404
NAS1-18584	p 168	A90-19940	NAS3-23720	p 622	A90-40686	NCA2-455	p 543
	p 450	A90-29372	NAS3-23721	p 548	N90-21602	NCC1-112	N90-21395
	p 566	A90-38718		p 782	N90-26633	NCC1-123	p 359
	p 237	N90-15891	NAS3-23925	p 193	N90-13390	NCC1-129	A90-23807
						NCC1-22	p 816
						NCC1-29	N90-27653
						NCC1-47	p 489
						NCC1-68	N90-20969
							p 124
							N90-11774
							p 549
							N90-21605
							p 696
							N90-24852
							p 602
							A90-36253
							p 154
							A90-18147
							p 164
							A90-19822
							p 405
							A90-27993
							p 248
							N90-15058
							p 570
							A90-38784
							p 647
							A90-42473
							p 812
							A90-48837
							p 923
							N90-28540
							p 228
							A90-22196
							p 812
							A90-49101
							p 753
							A90-45152
							p 677
							A90-42117
							p 67
							A90-11102
							p 759
							N90-26017
							p 597
							N90-21775
							p 562
							A90-38625
							p 753
							A90-45157
							p 812
							A90-49101
							p 216
							A90-19630
							p 308
							A90-26135
							p 806
							A90-46850
							p 756
							A90-45344
							p 808
							A90-46945
							p 780
							N90-26515
							p 56
							A90-12769
							p 736
							N90-25972
							p 430
							A90-28216
							p 153
							A90-17864
							p 690
							N90-24557
							p 518
							A90-33623
							p 670
							A90-42463
							p 153
							A90-17985
							p 490
							A90-33059
							p 721
							N90-25954

CONTRACT NUMBER INDEX

505-62-21

NCC2-417	p 808	A90-46945	NSG-1419	p 384	A90-27977	STPA-86-91-021-00-471-75-86	p 953	N90-28722
NCC2-447	p 429	A90-28201		p 87	N90-11695	SWRI PROJ. 06:7576	p 193	N90-13390
NCC2-458	p 200	A90-19629		p 275	N90-15380		p 193	N90-13391
	p 553	A90-35755	NSG-1498	p 415	N90-18390	SWRI PROJ. 17-7958-843	p 176	N90-13359
	p 753	A90-45151	NSG-3079	p 5	A90-11778	T/RF-41/E0010/E14	p 500	N90-20982
NCC2-486	p 348	A90-26258	NSG-3139	p 391	A90-29374	TAMRF PROJ. RF-5373	p 103	N90-11733
NCC2-493	p 583	A90-38441	NSG-3188	p 273	A90-23013	T06-038	p 640	N90-23378
NCC2-506	p 581	N90-21753	NSG-3266	p 12	A90-12555	T0604L	p 640	N90-23377
	p 734	N90-25126		p 704	A90-42731	T0707A	p 640	N90-23379
NCC2-540	p 796	A90-45912	NSG-7523	p 202	N90-14245	W-31-109-ENG-38	p 608	N90-22003
NCC2-543	p 478	N90-20052	N00014-81-K-0024	p 429	N90-19237	W-7405-ENG-36	p 186	N90-14227
NCC2-55	p 561	A90-38616	N00014-82-C-0451	p 558	A90-37890	W-7405-ENG-48	p 324	N90-16729
	p 316	N90-16712	N00014-82-K-0315	p 702	A90-42639	141-20-10-10	p 462	N90-18882
NCC2-564	p 789	A90-45855	N00014-83-K-0239	p 148	A90-16786	146-90-04-52	p 140	N90-13228
NCC2-575	p 822	A90-47659		p 797	A90-45923	147-14-12	p 185	N90-14220
NCC2-588	p 752	A90-45142	N00014-84-C-0359	p 772	A90-45534	307-07-00	p 509	N90-20086
	p 648	N90-23386		p 54	N90-10202	505-43-01	p 107	N90-12589
NCC2-604	p 762	N90-26019	N00014-84-G-0185	p 204	A90-19006	505-43-02	p 777	N90-26355
NCC2-634	p 572	N90-21736	N00014-84-K-0232	p 800	A90-46365	505-43-22	p 345	N90-17638
NCC3-120	p 690	N90-23769	N00014-84-K-0519	p 99	N90-11724	505-43-31	p 214	N90-13820
NCC3-626	p 322	A90-26986	N00014-85-K-0011	p 706	A90-44005	505-45-23-53	p 724	N90-25957
NCC3-81	p 360	A90-23827	N00014-85-K-0346	p 153	A90-17979	505-45-33-64	p 480	N90-20952
	p 354	A90-23842	N00014-85-K-0347	p 683	A90-40938	505-45-58	p 468	N90-20942
NCC3-93	p 535	A90-32293	N00014-85-K-0509	p 151	A90-17580	505-60-00	p 194	N90-14236
NGL-22-009-640	p 197	A90-19920	N00014-85-K-0513	p 147	A90-16777		p 398	N90-19201
	p 485	N90-20925		p 801	A90-46374		p 572	N90-21739
	p 485	N90-20926	N00014-85-K-0658	p 266	A90-22192		p 816	N90-27654
	p 485	N90-20927		p 767	N90-26104	505-60-01-01	p 923	N90-28540
	p 485	N90-20928	N00014-86-K-0066	p 801	A90-46375	505-60-01-02	p 893	N90-28366
NGL-31-001-252	p 485	N90-20929	N00014-86-K-0202	p 417	A90-28407		p 414	N90-18385
	p 865	A90-47685	N00014-86-K-0288	p 168	A90-19936		p 610	N90-22746
	p 521	N90-20941	N00014-86-K-0434	p 623	A90-40926		p 767	N90-26094
NGR-009-017	p 489	N90-20933	N00014-86-K-0468	p 764	A90-42725		p 909	N90-28493
NGT-01-008-021	p 421	N90-19417	N00014-86-K-0679	p 223	A90-20501	505-60-01	p 88	N90-11699
	p 435	N90-19420		p 72	N90-10402	505-60-21-01	p 1	N90-10002
	p 429	N90-19421	N00014-86-K-0754	p 904	A90-51009	505-60-21	p 175	N90-14202
NGT-21-002-800	p 736	N90-25971	N00014-86-K-0758	p 474	A90-33506		p 421	N90-18395
NGT-50123	p 312	A90-26903	N00014-86-K-0759	p 558	A90-37890		p 598	N90-21778
NGT-50144	p 313	A90-26907	N00014-87-C-0483	p 608	A90-38769		p 850	N90-27703
NGT-70090	p 595	A90-37940	N00014-87-C-9901	p 676	A90-40570	505-60-31-01	p 63	N90-10187
NIVR-01604N	p 776	N90-26285	N00014-87-G-0040	p 291	A90-23800	505-60-31-06	p 90	N90-12503
NIVR-03506N	p 462	N90-19756	N00014-87-G-0217	p 532	N90-20143		p 91	N90-12519
NIVR-06501N	p 416	N90-19228	N00014-87-K-0132	p 623	A90-40941		p 92	N90-12539
NSC-CS76-0210-D005-01	p 206	A90-16718	N00014-87-K-0168	p 555	A90-36252	505-60-31	p 735	N90-25135
NSC-CS77-0210-D006-14	p 207	A90-16725	N00014-87-K-0169	p 212	A90-19984	505-60-41-01	p 338	N90-17627
NSC-76-0401-E006-21	p 809	A90-47314		p 302	A90-25285		p 380	N90-18233
NSC-77-0210-D006-16	p 677	A90-42174	N00014-87-K-0174	p 562	A90-38619		p 719	N90-25944
NSC-77-0210-D006-20	p 681	A90-40032	N00014-87-K-0874	p 118	A90-14355	505-60-61	p 762	N90-26019
NSC-77-0401-E007-17	p 360	A90-23825	N00014-88-C-0654	p 89	N90-11705	505-61-01-01	p 965	N90-29919
NSC-78-0210-D006-01	p 686	A90-42116	N00014-88-K-0001	p 145	A90-16765	505-61-01-02	p 202	N90-14245
NSC-78-0401-E008-04	p 374	A90-25478	N00014-88-K-0592	p 379	N90-18225	505-61-01-09	p 123	N90-12625
NSERC-A-1671	p 289	A90-23781	N00014-89-J-1319	p 320	N90-17579		p 352	N90-17647
NSERC-A-2181	p 159	A90-19388	N00014-89-J-1342	p 683	A90-40938	505-61-01	p 201	N90-13407
	p 712	A90-45165	N00014-89-J-1362	p 206	N90-13638	505-61-21-03	p 235	N90-15072
	p 788	A90-45854	N00014-89-J-1544	p 314	A90-26983		p 315	N90-16710
NSERC-A-4604	p 530	A90-33523	N00014-89-J-1867	p 275	N90-15465		p 316	N90-17539
NSERC-A-5549	p 40	A90-11553	N00014-90-J-1270	p 894	A90-48657	505-61-41-02	p 718	N90-25939
NSERC-A-7928	p 127	A90-13767	N00014-90-J-1730	p 703	A90-42709	505-61-51-10	p 173	N90-14186
	p 421	A90-27972	N00019-84-G-0203	p 495	A90-33902		p 237	N90-15882
NSERC-A1671	p 514	N90-21027	N00019-85-C-0090	p 209	A90-17993		p 632	N90-24237
NSERC-G-2016	p 739	A90-42657	N00019-87-C-0016	p 245	A90-20587	505-61-51	p 88	N90-11700
NSF ATM 86-13121	p 927	A90-52077	N00019-88-C-0290	p 111	A90-15388		p 88	N90-11701
NSF ATM-82-05468	p 913	A90-52093		p 191	A90-19764		p 119	N90-11752
NSF ATM-82-18621	p 913	A90-52093	N00024-80-C-5375	p 755	A90-45334		p 248	N90-15093
NSF ATM-84-03049	p 927	A90-52077	N0014-86-K-0513	p 155	A90-18158		p 260	N90-15938
NSF ATM-87-02993	p 455	A90-28582	N00140-82-CH-532	p 741	A90-42695	505-61-59-76	p 399	N90-19204
NSF ATM-87-09659	p 39	N90-10032	N00140-83-C-7149	p 454	N90-18738	505-61-71-02	p 540	N90-20325
	p 103	N90-11731	N00140-86-C-9069	p 765	A90-45488	505-61-71-07	p 572	N90-21738
	p 137	N90-12113	N00140-86-C-9070	p 765	A90-45488		p 654	N90-23399
NSF ATM-88-09795	p 927	A90-52077	N00140-86-C-9415	p 657	A90-40603		p 650	N90-24265
NSF ATM-89-19697	p 913	A90-52093	N00140-87-C-9902	p 661	A90-42051		p 757	N90-25141
NSF CBT-82-11713	p 790	A90-45864	N00140-88-C-RE04	p 685	A90-42041		p 761	N90-25149
NSF CBT-86-12151	p 555	A90-35917	N00167-85-K-0164	p 232	A90-23277		p 702	N90-25933
NSF CBT-87-13833	p 359	A90-23812	N00167-87-C-0021	p 547	A90-34090		p 915	N90-28510
NSF CDR-88-03012	p 668	A90-40912	N00406-87-C-0790	p 148	A90-16790		p 633	N90-24239
NSF CTS-84-51610	p 867	A90-47736	N00421-85-D-0155	p 755	A90-45334	505-61-71-02	p 573	N90-22531
NSF DMC-86-03025	p 155	A90-18243	N60530-87-WR-30009	p 858	N90-27928	505-61-71-07	p 119	N90-11751
NSF DMS-88-10150	p 478	N90-20050		p 859	N90-27933		p 399	N90-19206
NSF DPP-87-001	p 526	N90-20097	N60921-83-GA-165B02	p 231	A90-23036	505-61-71-69	p 632	N90-24238
NSF ECD-89-43168	p 894	A90-48657	N62269-85-C-0268	p 433	A90-31282	505-61-71	p 20	N90-10829
NSF ENG-87-12997	p 508	A90-32966	N62269-86-C-0261	p 65	N90-10255		p 340	N90-17632
NSF INT-87-02083	p 12	A90-12555	N62269-86-C-0284	p 228	A90-22210		p 349	N90-17639
NSF ISI-88-61052	p 234	A90-23701		p 314	A90-26969		p 573	N90-21746
NSF MEA-80-18565	p 811	A90-48711	N62269-88-C-0210	p 434	N90-18433	505-61-85-01	p 671	N90-23413
NSF MEA-83-51417	p 475	A90-33568	N62271-86-M-0272	p 905	A90-51256	505-61-91-03	p 202	N90-14244
NSF MSM-85-04579	p 507	A90-32269	N62271-87-M-0187	p 145	A90-16759	505-61-91	p 633	N90-24242
NSF MSM-85-05834	p 247	A90-23113	N62271-87-M-0200	p 905	A90-51256		p 18	N90-10006
NSF MSM-85-19116	p 556	A90-36280	ONERA-3423-AN-131-D	p 817	N90-27663	505-62-OK	p 257	N90-15923
NSF MSM-87-07653	p 474	A90-33515	OV/RDL-837	p 183	N90-13371	505-62-OK	p 372	N90-18041
NSF MSM-88-09132	p 688	A90-42491	PROJ. MSG-89A1	p 650	N90-23397		p 858	N90-27722
NSF 85-52702	p 485	N90-20925	RAE-2028/131-XRAW	p 89	N90-11712		p 964	N90-29121
	p 485	N90-20927	SERC-GR/D/53029	p 361	A90-23866	505-62-01	p 187	N90-13381
NSG-1157	p 412	A90-29388	STPA-82-96042	p 876	N90-27905		p 259	N90-15112
	p 518	A90-33060	STPA-83-96013	p 877	N90-27908		p 758	N90-26011
NSG-1174	p 235	N90-15072	STPA-83-96024	p 877	N90-27906	505-62-11	p 748	N90-25982
NSG-1321	p 887	N90-28105		p 877	N90-27907	505-62-21	p 94	N90-12561

505-62-3B

CONTRACT NUMBER INDEX

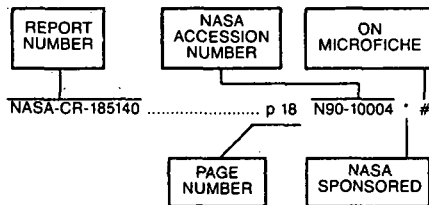
505-62-3B	p 143 N90-13323	505-66-01-02	p 120 N90-11757	532-06-00	p 582 N90-21756
505-62-4D	p 192 N90-13387		p 259 N90-15110	532-09-01	p 369 N90-17074
	p 194 N90-13393		p 434 N90-18434	533-02-01	p 573 N90-22532
	p 213 N90-13750	505-66-01	p 468 N90-20921		p 781 N90-26564
	p 318 N90-17562	505-66-11-02	p 349 N90-17641		p 929 N90-28551
	p 440 N90-19242		p 506 N90-21004	533-02-21	p 758 N90-25144
	p 510 N90-20090	505-66-11	p 506 N90-21005	533-02-51	p 32 N90-10023
	p 515 N90-21036		p 28 N90-10021		p 114 N90-11741
	p 542 N90-21300		p 820 N90-27669		p 119 N90-11753
	p 551 N90-21724	505-66-21-01	p 965 N90-29965		p 416 N90-19225
	p 571 N90-21733	505-66-21-03	p 372 N90-18057		p 648 N90-23392
	p 720 N90-25948	505-66-21-04	p 217 N90-14061		p 735 N90-25134
	p 541 N90-20392		p 374 N90-18125		p 736 N90-25973
	p 478 N90-20051	505-66-29	p 374 N90-18126	533-02-71	p 103 N90-11732
	p 719 N90-25940	505-66-41-01	p 582 N90-21758	533-02-91	p 186 N90-14225
505-62-41-03	p 696 N90-24853		p 404 N90-18378	533-04-1A	p 193 N90-13390
505-62-41-07	p 434 N90-19239	505-66-41-04	p 593 N90-21772		p 193 N90-13391
505-62-61	p 73 N90-11245		p 348 N90-16767	533-04-11	p 73 N90-10451
	p 194 N90-13392	505-66-41-41	p 348 N90-16768	533-06-01	p 52 N90-10042
	p 345 N90-17636	505-66-41-42	p 259 N90-15108		p 435 N90-19241
505-62-71-01	p 237 N90-15884	505-66-41-43	p 187 N90-14232		p 509 N90-20087
	p 397 N90-19193	505-66-41	p 259 N90-15111	534-06-23-10	p 63 N90-10186
	p 398 N90-19199		p 849 N90-27702	534-06-23	p 126 N90-11821
	p 718 N90-25938	505-66-51	p 927 N90-28546	535-03-01-02	p 173 N90-14190
505-62-71	p 114 N90-11740	505-66-71-02	p 916 N90-28512		p 477 N90-20046
	p 117 N90-12618		p 695 N90-24103		p 634 N90-24246
	p 193 N90-13389	505-66-71	p 780 N90-25638		p 816 N90-27649
	p 318 N90-17561		p 770 N90-11487	535-03-01-03	p 724 N90-25120
	p 552 N90-21725		p 134 N90-12042	535-03-01	p 52 N90-10045
	p 589 N90-22566		p 217 N90-13995		p 53 N90-10046
	p 666 N90-23404		p 249 N90-15100		p 53 N90-10047
	p 666 N90-24273		p 612 N90-22322		p 53 N90-10048
	p 751 N90-26009		p 689 N90-23768		p 53 N90-10049
505-62-81-05	p 72 N90-10409		p 757 N90-25142		p 79 N90-11549
505-62-91	p 588 N90-21760	505-67-01-02	p 739 N90-25981		p 113 N90-11739
505-63-01-05	p 279 N90-16294		p 420 N90-18393		p 94 N90-12560
	p 454 N90-18746	505-67-21-07	p 420 N90-18394		p 172 N90-13352
	p 505 N90-20080	505-67-21	p 780 N90-26511		p 379 N90-17413
	p 505 N90-20081		p 24 N90-10841		p 380 N90-18229
	p 505 N90-20082		p 187 N90-13384		p 548 N90-20794
	p 506 N90-20083		p 252 N90-15102		p 548 N90-21602
	p 506 N90-20084		p 240 N90-15898		p 649 N90-23393
	p 543 N90-21422		p 636 N90-23373		p 720 N90-25946
	p 543 N90-21424	505-67-41-57	p 636 N90-23374		p 782 N90-26635
505-63-01-07	p 583 N90-22557		p 401 N90-18371		p 929 N90-28552
505-63-01-09	p 373 N90-18070		p 401 N90-18372	535-03-11-03	p 140 N90-13198
	p 876 N90-27787	505-68-11	p 637 N90-24257		p 220 N90-14866
505-63-01-11	p 484 N90-20068		p 32 N90-10031		p 896 N90-28396
	p 690 N90-24660		p 213 N90-13797		p 966 N90-29169
	p 774 N90-25368		p 215 N90-14617	535-03-22	p 666 N90-24274
505-63-01	p 716 N90-25110		p 468 N90-20943	535-05-01	p 217 N90-14783
	p 925 N90-29384		p 506 N90-21006		p 600 N90-21869
505-63-1A	p 205 N90-13636	505-68-27	p 570 N90-21727		p 782 N90-26633
505-63-1B	p 172 N90-13355		p 217 N90-13990		p 817 N90-27657
	p 215 N90-14656	505-68-31	p 964 N90-29142	535-505-01	p 54 N90-10891
	p 610 N90-22703	505-68-71-03	p 186 N90-14228	537-01-11	p 688 N90-23591
	p 778 N90-26373	505-68-71	p 909 N90-28494		p 773 N90-25289
505-63-11	p 533 N90-21137		p 170 N90-13332	537-01-31-01	p 735 N90-25966
505-63-21-01	p 237 N90-15886		p 183 N90-13372	537-01-37-01	p 923 N90-28537
	p 400 N90-19211		p 339 N90-16758	537-03-21-03	p 549 N90-21605
	p 574 N90-22538		p 415 N90-19224		p 696 N90-24852
	p 631 N90-23348		p 910 N90-28505	553-13-00	p 215 N90-14641
505-63-21-02	p 846 N90-27700		p 924 N90-28542		p 610 N90-22808
505-63-21-04	p 88 N90-11704	505-68-91-02	p 936 N90-28578	582-01-31	p 665 N90-23403
	p 416 N90-19227		p 19 N90-10012	583-01-01	p 370 N90-17112
	p 456 N90-19718		p 173 N90-14187	590-21-31	p 816 N90-27655
	p 478 N90-20047	505-69-01-01	p 183 N90-13370	591-11-31	p 588 N90-21763
	p 497 N90-20071	505-69-31	p 194 N90-14235	591-42-11	p 720 N90-25945
	p 520 N90-20093	505-69-41-01	p 615 N90-23338	763-01-21	p 203 N90-14268
	p 846 N90-27699	505-69-61	p 18 N90-10004		p 344 N90-17635
	p 869 N90-27725		p 516 N90-21037		p 588 N90-21762
505-63-21-09	p 201 N90-13403		p 516 N90-21038		p 763 N90-26055
	p 582 N90-22555	505-69-71-03	p 588 N90-21761	763-01-31-22	p 20 N90-10830
505-63-21	p 527 N90-21047	505-80-31-01	p 51 N90-10034	763-01-41-17	p 924 N90-28541
505-63-31	p 959 N90-28815	505-80-31	p 510 N90-20088	906-65-43	p 816 N90-27653
505-63-41-02	p 249 N90-15902	505-90-21-01	p 215 N90-14511	992-21-01	p 170 N90-13327
	p 328 N90-17620		p 20 N90-10833		p 910 N90-28503
505-63-5A	p 372 N90-18041		p 171 N90-13351		
505-63-51-01	p 134 N90-12057	506-40-11	p 478 N90-20050		
	p 134 N90-12058	506-40-41-01	p 781 N90-26595		
	p 213 N90-13814	506-40-91-01	p 143 N90-13324		
	p 454 N90-18743	506-41-41	p 317 N90-17560		
	p 541 N90-20439		p 883 N90-27066		
	p 758 N90-25143	506-43-41-01	p 509 N90-20085		
	p 775 N90-25375	506-43-41-02	p 542 N90-21283		
	p 959 N90-28865	506-43-71	p 582 N90-21755		
	p 960 N90-28866	506-49-11-05	p 610 N90-22807		
505-63-51-03	p 499 N90-20974	506-68-11	p 767 N90-26080		
505-63-51-07	p 79 N90-10679	506-80-31-03	p 369 N90-17055		
505-63-51-09	p 965 N90-29166	506-80-31-06	p 399 N90-19203		
505-63-51-10	p 36 N90-10889	510-01-0A	p 175 N90-14205		
	p 106 N90-12580		p 464 N90-19821		
	p 416 N90-19226	510-01-01	p 51 N90-10037		
	p 924 N90-29383	510-02-21-01	p 543 N90-21361		
505-63-51	p 543 N90-21394		p 690 N90-23769		
	p 776 N90-26334		p 876 N90-27788		

REPORT NUMBER INDEX

AERONAUTICAL ENGINEERING / A Continuing Bibliography
1990 Cumulative Index

February 1991

Typical Report Number Index Listing



Listings in this index are arranged alphanumerically by report number. The page number indicates the page on which the citation is located. The accession number denotes the number by which the citation is identified. An asterisk (*) indicates that the item is a NASA report. A pound sign (#) indicates that the item is available on microfiche.

A-87091 p 52 N90-10042 * #
A-88040 p 598 N90-21778 * #
A-88225 p 761 N90-25149 * #
A-88268 p 582 N90-21756 * #
A-89006 p 119 N90-11752 * #
A-89085 p 240 N90-15898 * #
A-89093 p 910 N90-28503 * #
A-89096 p 88 N90-11701 * #
A-89133 p 349 N90-17639 * #
A-89145 p 18 N90-10006 * #
A-89148 p 170 N90-13332 * #
A-89172 p 143 N90-13324 * #
A-89195 p 201 N90-13407 * #
A-89196 p 187 N90-13384 * #
A-89209 p 170 N90-13327 * #
A-89213 p 81 N90-11692 * #
A-89215 p 340 N90-17632 * #
A-89220 p 260 N90-15938 * #
A-89227 p 88 N90-11699 * #
A-89229 p 88 N90-11700 * #
A-89230 p 398 N90-18201 * #
A-89235 p 24 N90-10841 * #
A-89239 p 509 N90-20087 * #
A-89241 p 133 N90-11970 * #
A-89243 p 185 N90-14220 * #
A-89246 p 399 N90-19204 * #
A-89247 p 582 N90-21758 * #
A-89270 p 349 N90-17641 * #
A-90007 p 671 N90-23413 * #
A-90017 p 370 N90-17112 * #
A-90036 p 172 N90-13353 * #
A-90046 p 540 N90-20325 * #
A-90048 p 194 N90-14236 * #
A-90086 p 636 N90-23373 * #
A-90089 p 573 N90-21746 * #
A-90090 p 650 N90-24265 * #
A-90101 p 572 N90-21739 * #
A-90108 p 916 N90-28512 * #
A-90122 p 636 N90-23374 * #
A-90129 p 757 N90-25141 * #
A-90139 p 654 N90-23399 * #
A-90141 p 816 N90-27654 * #
A-90163 p 762 N90-26019 * #
A-90165 p 572 N90-21738 * #
A-90168 p 923 N90-28540 * #
A-90170 p 702 N90-25933 * #
A-90186 p 720 N90-25945 * #
A-90198 p 820 N90-27669 * #
A-90229 p 849 N90-27702 * #
A-90259 p 816 N90-27653 * #
A-90264 p 915 N90-28510 * #

AAAF PAPER NT 88-11 p 40 A90-11431
AAAF PAPER NT 88-13 p 40 A90-11432
AAAF PAPER NT 88-16 p 4 A90-11434

AAAF PAPER NT 88-18 p 4 A90-11435
AAAF PAPER NT 88-19 p 4 A90-11436
AAAF PAPER NT 88-20 p 23 A90-11437
AAMRL-SR-89-501 p 723 N90-25117 #
AAMRL-TR-89-034 p 548 N90-20799 #
AAMRL-TR-89-035 p 548 N90-20800 #
AAMRL-TR-89-039 p 583 N90-22563 #
AAMRL-TR-89-044 p 464 N90-19842 #
AAMRL-TR-90-009 p 844 N90-26825 #
AAMRL-TR-90-011 p 895 N90-27467 #
AAMRL-TR-90-012 p 895 N90-27466 #
AAMRL-TR-90-018 p 875 N90-26972 #

AAR-244 p 574 N90-21747 * #

AAS PAPER 89-040 p 264 A90-21546

ACD-330 p 27 N90-10018 #
ACD-330 p 28 N90-10856 #
ACD-330 p 59 N90-10897 #

AD-A198037 p 842 N90-26807 #
AD-A203518 p 95 N90-12562 #
AD-A205885 p 174 N90-14201 #
AD-A209273 p 1 N90-10001 #
AD-A209422 p 31 N90-10022 #
AD-A210251 p 65 N90-11184 #
AD-A210252 p 18 N90-10008 #
AD-A210271 p 32 N90-10025 #
AD-A210307 p 65 N90-10253 #
AD-A210373 p 32 N90-10026 #
AD-A210374 p 52 N90-10040 #
AD-A210381 p 32 N90-10027 #
AD-A210396 p 72 N90-10402 #
AD-A210402 p 18 N90-10009 #
AD-A210455 p 332 N90-16730 #
AD-A210482 p 52 N90-10041 #
AD-A210503 p 32 N90-10028 #
AD-A210547 p 72 N90-10424 #
AD-A210567 p 65 N90-10255 #
AD-A210614 p 19 N90-10010 #
AD-A210631 p 27 N90-10019 #
AD-A210633 p 27 N90-10020 #
AD-A210670 p 25 N90-10845 #
AD-A210823 p 71 N90-10351 #
AD-A211101 p 71 N90-10356 #
AD-A211109 p 63 N90-10191 #
AD-A211111 p 64 N90-10231 #
AD-A211139 p 55 N90-10893 #
AD-A211306 p 99 N90-11724 #
AD-A211338 p 99 N90-12570 #
AD-A211426 p 133 N90-11982 #
AD-A211483 p 134 N90-12777 #
AD-A211486 p 82 N90-12496 #
AD-A211588 p 133 N90-11907 #
AD-A211606 p 133 N90-11908 #
AD-A211654 p 170 N90-13326 #
AD-A211712 p 120 N90-11758 #
AD-A211719 p 103 N90-11734 #
AD-A211744 p 134 N90-11988 #
AD-A211749 p 133 N90-11934 #
AD-A211771 p 90 N90-12501 #
AD-A211774 p 114 N90-11745 #
AD-A211879 p 126 N90-11899 #
AD-A211903 p 126 N90-11837 #
AD-A211906 p 119 N90-11752 #
AD-A211918 p 138 N90-12239 #
AD-A211943 p 89 N90-11705 #
AD-A211944 p 89 N90-11706 #
AD-A211957 p 119 N90-11756 #
AD-A212001 p 114 N90-11743 #
AD-A212063 p 96 N90-11715 #
AD-A212109 p 89 N90-11707 #
AD-A212127 p 82 N90-12495 #
AD-A212159 p 99 N90-11722 #
AD-A212209 p 256 N90-15921 #
AD-A212238 p 59 N90-10896 #
AD-A212377 p 136 N90-12899 #
AD-A212402 p 243 N90-15900 #
AD-A212408 p 107 N90-12595 #
AD-A212441 p 107 N90-12596 #

AD-A212442 p 95 N90-12566 #
AD-A212451 p 117 N90-12620 #
AD-A212466 p 185 N90-14217 #
AD-A212573 p 107 N90-12597 #
AD-A212582 p 251 N90-15917 #
AD-A212663 p 177 N90-13364 #
AD-A212851 p 170 N90-13330 #
AD-A212855 p 201 N90-13402 #
AD-A212995 p 206 N90-13638 #
AD-A213248 p 184 N90-13375 #
AD-A213297 p 213 N90-13812 #
AD-A213318 p 95 N90-12568 #
AD-A213334 p 121 N90-12624 #
AD-A213359 p 205 N90-13627 #
AD-A213368 p 176 N90-13359 #
AD-A213378 p 198 N90-13398 #
AD-A213379 p 198 N90-13399 #
AD-A213395 p 170 N90-13331 #
AD-A213478 p 249 N90-15095 #
AD-A213479 p 274 N90-15310 #
AD-A213513 p 249 N90-15098 #
AD-A213531 p 255 N90-15105 #
AD-A213545 p 275 N90-15486 #
AD-A213566 p 256 N90-15106 #
AD-A213652 p 249 N90-15097 #
AD-A213728 p 260 N90-15113 #
AD-A213795 p 33 N90-10860 #
AD-A213835 p 275 N90-15422 #
AD-A213843 p 275 N90-15390 #
AD-A213872 p 357 N90-16951 #
AD-A213919 p 378 N90-17409 #
AD-A213928 p 239 N90-15083 #
AD-A214000 p 338 N90-17628 #
AD-A214085 p 28 N90-10856 #
AD-A214091 p 135 N90-12781 #
AD-A214113 p 141 N90-12406 #
AD-A214116 p 59 N90-10897 #
AD-A214122 p 379 N90-18225 #
AD-A214140 p 236 N90-15079 #
AD-A214141 p 262 N90-15115 #
AD-A214163 p 243 N90-15090 #
AD-A214164 p 379 N90-17410 #
AD-A214214 p 239 N90-15084 #
AD-A214244 p 236 N90-15080 #
AD-A214258 p 256 N90-15107 #
AD-A214284 p 28 N90-10847 #
AD-A214295 p 249 N90-15098 #
AD-A214377 p 137 N90-13005 #
AD-A214402 p 275 N90-15465 #
AD-A214412 p 249 N90-15099 #
AD-A214452 p 239 N90-15085 #
AD-A214454 p 379 N90-17411 #
AD-A214455 p 379 N90-17412 #
AD-A214492 p 343 N90-16759 #
AD-A214500 p 287 N90-16707 #
AD-A214542 p 348 N90-16770 #
AD-A214579 p 372 N90-18065 #
AD-A214728 p 323 N90-16723 #
AD-A214826 p 287 N90-16708 #
AD-A214865 p 81 N90-11692 #
AD-A214878 p 352 N90-16773 #
AD-A214893 p 343 N90-16762 #
AD-A214946 p 356 N90-16936 #
AD-A215006 p 260 N90-15924 #
AD-A215055 p 323 N90-16724 #
AD-A215126 p 464 N90-19852 #
AD-A215133 p 369 N90-16971 #
AD-A215188 p 357 N90-16939 #
AD-A215298 p 377 N90-17348 #
AD-A215366 p 333 N90-16748 #
AD-A215431 p 336 N90-16753 #
AD-A215494 p 170 N90-13327 #
AD-A215496 p 323 N90-16725 #
AD-A215532 p 337 N90-16755 #
AD-A215664 p 433 N90-18431 #
AD-A215678 p 337 N90-16756 #
AD-A215741 p 371 N90-17970 #
AD-A215747 p 338 N90-17629 #
AD-A215755 p 176 N90-13358 #
AD-A215762 p 377 N90-18173 #
AD-A215819 p 372 N90-18030 #
AD-A215832 p 267 N90-15185 #
AD-A215876 p 185 N90-14218 #

AD-A215882	p 402	N90-18373	#	AD-A219101	p 434	N90-18432	#	AD-A222832	p 66	A90-10222	#
AD-A215983	p 349	N90-17643	#	AD-A219108	p 593	N90-22570	#	AD-A222939	p 874	N90-26887	#
AD-A215984	p 349	N90-17644	#	AD-A219123	p 757	N90-25140	#	AD-A223069	p 895	N90-27466	#
AD-A216014	p 79	N90-10679	#	AD-A219165	p 552	N90-22530	#	AD-A223161	p 844	N90-26825	#
AD-A216042	p 414	N90-18386	#	AD-A219168	p 527	N90-21045	#	AD-A223162	p 895	N90-27467	#
AD-A216053	p 434	N90-18433	#	AD-A219175	p 615	N90-23188	#	AD-A223296	p 960	N90-29593	#
AD-A216091	p 414	N90-18387	#	AD-A219176	p 615	N90-23189	#	AD-A223310	p 911	N90-29304	#
AD-A216109	p 338	N90-17630	#	AD-A219177	p 615	N90-23190	#	AD-A223412	p 911	N90-29305	#
AD-A216195	p 357	N90-17825	#	AD-A219190	p 761	N90-25145	#	AD-A223431	p 960	N90-29664	#
AD-A216196	p 350	N90-17646	#	AD-A219223	p 483	N90-20054	#	AD-A223450	p 938	N90-29406	#
AD-A216197	p 319	N90-17574	#	AD-A219257	p 734	N90-25125	#	AD-A223451	p 953	N90-29442	#
AD-A216200	p 36	N90-10888	#	AD-A219294	p 578	N90-22554	#	AD-A223516	p 933	N90-29396	#
AD-A216220	p 371	N90-18016	#	AD-A219296	p 237	N90-15882	#	AD-A223564	p 938	N90-29407	#
AD-A216221	p 371	N90-18017	#	AD-A219302	p 583	N90-22563	#	AD-A223602	p 552	A90-35137	#
AD-A216223	p 319	N90-17575	#	AD-A219405	p 601	N90-22695	#	AD-A223676	p 953	N90-29480	#
AD-A216244	p 377	N90-18212	#	AD-A219545	p 648	N90-23387	#	AD-A223680	p 920	N90-28513	#
AD-A216246	p 319	N90-17576	#	AD-A219563	p 167	A90-19925	#	AD-A223687	p 966	N90-30035	#
AD-A216247	p 329	N90-17621	#	AD-A219584	p 648	N90-23388	#	AD-A223694	p 939	N90-29408	#
AD-A216248	p 319	N90-17577	#	AD-A219621	p 689	N90-23687	#	AD-A223770	p 966	N90-30036	#
AD-A216285	p 320	N90-17578	#	AD-A219651	p 678	N90-23571	#	AD-A223853	p 911	N90-29307	#
AD-A216289	p 320	N90-17579	#	AD-A219698	p 131	A90-15900	#	AD-A223869	p 932	N90-28571	#
AD-A216291	p 320	N90-17580	#	AD-A219741	p 425	N90-18405	#	AD-A223882	p 932	N90-28572	#
AD-A216353	p 338	N90-17631	#	AD-A219747	p 689	N90-23752	#	AD-A223935	p 720	N90-25947	#
AD-A216375	p 479	N90-20948	#	AD-A219788	p 766	N90-25236	#	AD-A223936	p 776	N90-26280	#
AD-A216398	p 372	N90-18038	#	AD-A219793	p 631	N90-23353	#	AD-A223937	p 870	N90-26838	#
AD-A216399	p 371	N90-17984	#	AD-A219820	p 666	N90-24271	#	AD-A223970	p 938	N90-28586	#
AD-A216414	p 371	N90-18020	#	AD-A220003	p 692	N90-23832	#	AD-A224008	p 936	N90-28579	#
AD-A216444	p 443	N90-18601	#	AD-A220078	p 672	N90-24275	#	AD-A224126	p 925	N90-29386	#
AD-A216446	p 462	N90-18908	#	AD-A220079	p 679	N90-24451	#	AD-A224145	p 933	N90-28573	#
AD-A216601	p 201	N90-13408	#	AD-A220106	p 654	N90-23400	#	AD-A224151	p 959	N90-28828	#
AD-A216613	p 405	N90-18380	#	AD-A220167	p 674	N90-24277	#	AD-A224164	p 960	N90-29587	#
AD-A216627	p 453	N90-18670	#	AD-A220239	p 678	N90-23538	#	AD-A224168	p 925	N90-29387	#
AD-A216629	p 454	N90-18672	#	AD-A220312	p 641	N90-24263	#	AD-A224221	p 933	N90-28574	#
AD-A216673	p 454	N90-18738	#	AD-A220360	p 637	N90-24258	#	AD-A224238	p 911	N90-29302	#
AD-A216714	p 414	N90-18388	#	AD-A220393	p 654	N90-23398	#	AD-A224256	p 902	N90-29299	#
AD-A216751	p 428	N90-18430	#	AD-A220398	p 723	N90-25117	#	AD-A224477	p 925	N90-29389	#
AD-A216812	p 377	N90-18181	#	AD-A220525	p 688	N90-23609	#	AD-A224484	p 506	N90-21004	#
AD-A216828	p 415	N90-18389	#	AD-A220527	p 648	N90-23389	#	AD-A224486	p 960	N90-29565	#
AD-A216837	p 399	N90-19202	#	AD-A220535	p 665	N90-23402	#	AD-A224493	p 632	N90-24237	#
AD-A216925	p 405	N90-18383	#	AD-A220593	p 671	N90-23412	#	AD-A224576	p 954	N90-29527	#
AD-A216937	p 462	N90-18920	#	AD-A220764	p 702	N90-25074	#				
AD-A216953	p 464	N90-19842	#	AD-A220870	p 500	N90-20976	#	AD-B133616L	p 115	N90-11750	#
AD-A216998	p 428	N90-19233	#	AD-A220901	p 511	N90-21009	#	AD-B134983L	p 134	N90-12007	#
AD-A217166	p 478	N90-20048	#	AD-A220933	p 674	N90-24278	#	AD-B135295L	p 120	N90-11760	#
AD-A217189	p 532	N90-20140	#	AD-A220987	p 739	N90-25138	#	AD-B136274L	p 89	N90-11711	#
AD-A217279	p 405	N90-19223	#	AD-A220988	p 766	N90-25226	#	AD-B136809L	p 213	N90-13816	#
AD-A217310	p 520	N90-20092	#	AD-A220997	p 347	A90-25990	#	AD-B136837L	p 109	N90-12599	#
AD-A217366	p 498	N90-20073	#	AD-A221034	p 634	N90-24249	#	AD-B138729L	p 170	N90-13333	#
AD-A217380	p 532	N90-20143	#	AD-A221099	p 641	N90-24264	#	AD-B138754L	p 212	N90-13725	#
AD-A217396	p 510	N90-20089	#	AD-A221121	p 650	N90-24270	#	AD-B140130L	p 212	N90-13728	#
AD-A217412	p 544	N90-20500	#	AD-A221148	p 637	N90-24259	#	AD-B140818L	p 776	N90-26290	#
AD-A217455	p 541	N90-20434	#	AD-A221180	p 729	N90-25122	#	AD-B140819L	p 720	N90-25950	#
AD-A217461	p 951	N90-28698	#	AD-A221220	p 634	N90-24250	#	AD-B142845L	p 775	N90-26238	#
AD-A217512	p 332	N90-16731	#	AD-A221263	p 783	N90-25930	#	AD-B142974L	p 720	N90-25951	#
AD-A217575	p 324	N90-17581	#	AD-A221264	p 783	N90-25931	#	AD-B144415L	p 634	N90-24254	#
AD-A217606	p 222	N90-15041	#	AD-A221326	p 634	N90-24251	#	AD-B144569L	p 672	N90-24276	#
AD-A217638	p 526	N90-20097	#	AD-A221339	p 766	N90-25228	#	AD-B145082L	p 635	N90-24255	#
AD-A217663	p 429	N90-19237	#	AD-A221501	p 845	N90-26828	#				
AD-A217730	p 520	N90-20094	#	AD-A221541	p 444	N90-19387	#	AD-D014207	p 183	N90-13373	#
AD-A217772	p 540	N90-20345	#	AD-A221555	p 846	N90-27697	#	AD-D014284	p 256	N90-15918	#
AD-A217789	p 533	N90-20235	#	AD-A221557	p 846	N90-27698	#	AD-D014446	p 503	N90-21002	#
AD-A217795	p 533	N90-21188	#	AD-A221586	p 868	N90-26833	#	AD-D014512	p 723	N90-25118	#
AD-A217799	p 510	N90-20091	#	AD-A221587	p 845	N90-26829	#				
AD-A217832	p 250	N90-15904	#	AD-A221591	p 544	N90-21508	#	AD-E501144	p 82	N90-12496	#
AD-A217873	p 173	N90-14186	#	AD-A221673	p 875	N90-26994	#	AD-E501191	p 498	N90-20075	#
AD-A217882	p 478	N90-20053	#	AD-A221696	p 827	N90-27693	#	AD-E501239	p 824	N90-26804	#
AD-A217889	p 540	N90-20346	#	AD-A221720	p 871	N90-26847	#	AD-E801954	p 18	N90-10009	#
AD-A217906	p 927	N90-28544	#	AD-A221793	p 875	N90-26933	#	AD-E801979	p 198	N90-13399	#
AD-A217925	p 498	N90-20074	#	AD-A221864	p 855	N90-26832	#	AD-E951478	p 762	N90-26020	#
AD-A217964	p 540	N90-20312	#	AD-A221866	p 824	N90-26805	#				
AD-A217981	p 520	N90-20095	#	AD-A221942	p 854	N90-26831	#	AD-F800085	p 349	N90-17644	#
AD-A218035	p 484	N90-20069	#	AD-A221962	p 896	N90-27468	#	AD-F800086	p 349	N90-17643	#
AD-A218041	p 548	N90-20799	#	AD-A221970	p 887	N90-28106	#				
AD-A218048	p 548	N90-20800	#	AD-A222014	p 896	N90-27469	#	AECL-9560	p 951	N90-28674	#
AD-A218052	p 526	N90-20098	#	AD-A222018	p 875	N90-26972	#				
AD-A218105	p 526	N90-20099	#	AD-A222088	p 815	N90-26796	#	AEDC-TR-89-14	p 414	N90-18387	#
AD-A218149	p 533	N90-20208	#	AD-A222136	p 845	N90-26826	#	AEDC-TR-89-4	p 19	N90-10010	#
AD-A218157	p 528	N90-20103	#	AD-A222202	p 815	N90-26797	#	AEDC-TR-89-6	p 72	N90-10424	#
AD-A218227	p 958	N90-28800	#	AD-A222263	p 815	N90-26798	#				
AD-A218244	p 498	N90-20075	#	AD-A222348	p 875	N90-26992	#	AEFA-89-14	p 428	N90-18430	#
AD-A218253	p 498	N90-20076	#	AD-A222489	p 884	N90-27118	#				
AD-A218282	p 498	N90-20077	#	AD-A222532	p 896	N90-27471	#	AERE-R-13303-PT-2	p 678	N90-23523	#
AD-A218298	p 541	N90-20349	#	AD-A222533	p 815	N90-26799	#				
AD-A218349	p 526	N90-20100	#	AD-A222535	p 845	N90-26827	#	AFATL-TP-89-18	p 170	N90-13331	#
AD-A218378	p 631	N90-23349	#	AD-A222543	p 816	N90-26800	#	AFATL-TP-90-08	p 911	N90-29307	#
AD-A218393	p 636	N90-23371	#	AD-A222582	p 762	N90-26020	#				
AD-A218434	p 575	N90-22545	#	AD-A222693	p 815	N90-26793	#	AFATL-TR-89-19	p 136	N90-12899	#
AD-A218435	p 575	N90-22546	#	AD-A222696	p 927	N90-28545	#	AFATL-TR-89-20	p 18	N90-10009	#
AD-A218436	p 575	N90-22547	#	AD-A222715	p 724	N90-25961	#	AFATL-TR-89-49	p 198	N90-13399	#
AD-A218437	p 575	N90-22548	#	AD-A222716	p 820	N90-27668	#				
AD-A218438	p 575	N90-22549	#	AD-A222725	p 895	N90-27465	#				
AD-A218493	p 671	N90-23409	#	AD-A222732	p 767	N90-26106	#	AFESC/ESL-TR-88-31	p 255	N90-15105	#
AD-A218514	p 702	N90-25073	#	AD-A222736	p 824	N90-26804	#	AFESC/ESL-TR-88-50	p 256	N90-15106	#
AD-A218544	p 636	N90-23372	#	AD-A222752	p 767	N90-26104	#	AFESC/ESL-TR-88-78	p 875	N90-26992	#
AD-A218680	p 689	N90-23762	#	AD-A222795	p 759	N90-26018	#				
AD-A218764	p 428	N90-19232	#	AD-A222813	p 721	N90-25955	#	AFFTC-TR-89-27	p 249	N90-15096	#

AIAA PAPER 90-0392

F-3

AIAA PAPER 90-0394

REPORT NUMBER INDEX

AIAA PAPER 90-0394	p 165	A90-19831	#	AIAA PAPER 90-0984	p 391	A90-29374	#	AIAA PAPER 90-1390	p 594	A90-37935	#
AIAA PAPER 90-0395	p 229	A90-22213	#	AIAA PAPER 90-0986	p 451	A90-29399	#	AIAA PAPER 90-1391	p 594	A90-37936	#
AIAA PAPER 90-0403	p 166	A90-19833	#	AIAA PAPER 90-0988	p 451	A90-29400	#	AIAA PAPER 90-1392	p 558	A90-37937	#
AIAA PAPER 90-0414	p 166	A90-19837	#	AIAA PAPER 90-0990	p 463	A90-29402	#	AIAA PAPER 90-1396	p 595	A90-37939	#
AIAA PAPER 90-0415	p 229	A90-22215	#	AIAA PAPER 90-1004	p 442	A90-29275	#	AIAA PAPER 90-1397	p 595	A90-37940	#
AIAA PAPER 90-0419	p 166	A90-19841	#	AIAA PAPER 90-1005	p 449	A90-29276	#	AIAA PAPER 90-1400	p 560	A90-38490	#
AIAA PAPER 90-0420	p 166	A90-19842	#	AIAA PAPER 90-1015	p 449	A90-29340	#	AIAA PAPER 90-1401	p 597	A90-38489	#
AIAA PAPER 90-0421	p 313	A90-26947	#	AIAA PAPER 90-1031	p 391	A90-29375	#	AIAA PAPER 90-1402	p 558	A90-37943	#
AIAA PAPER 90-0429	p 229	A90-22216	#	AIAA PAPER 90-1032	p 391	A90-29376	#	AIAA PAPER 90-1405	p 595	A90-37944	#
AIAA PAPER 90-0430	p 166	A90-19844	#	AIAA PAPER 90-1033	p 391	A90-29377	#	AIAA PAPER 90-1406	p 595	A90-37945	#
AIAA PAPER 90-0435	p 166	A90-19845	#	AIAA PAPER 90-1034	p 392	A90-29378	#	AIAA PAPER 90-1407	p 595	A90-37946	#
AIAA PAPER 90-0436	p 229	A90-22218	#	AIAA PAPER 90-1035	p 389	A90-29360	#	AIAA PAPER 90-1408	p 558	A90-37947	#
AIAA PAPER 90-0437	p 166	A90-19846	#	AIAA PAPER 90-1036	p 450	A90-29380	#	AIAA PAPER 90-1409	p 560	A90-38488	#
AIAA PAPER 90-0439	p 191	A90-19847	#	AIAA PAPER 90-1073	p 411	A90-29381	#	AIAA PAPER 90-1410	p 559	A90-37948	#
AIAA PAPER 90-0440	p 229	A90-22219	#	AIAA PAPER 90-1074	p 430	A90-29382	#	AIAA PAPER 90-1412	p 595	A90-37949	#
AIAA PAPER 90-0451	p 211	A90-19850	#	AIAA PAPER 90-1075	p 392	A90-29383	#	AIAA PAPER 90-1413	p 596	A90-37950	#
AIAA PAPER 90-0453	p 192	A90-19852	#	AIAA PAPER 90-1076	p 411	A90-29384	#	AIAA PAPER 90-1414	p 559	A90-37951	#
AIAA PAPER 90-0465	p 192	A90-19857	#	AIAA PAPER 90-1077	p 431	A90-29385	#	AIAA PAPER 90-1416	p 596	A90-37953	#
AIAA PAPER 90-0485	p 313	A90-26956	#	AIAA PAPER 90-1078	p 412	A90-29386	#	AIAA PAPER 90-1417	p 604	A90-37954	#
AIAA PAPER 90-0486	p 167	A90-19874	#	AIAA PAPER 90-1105	p 449	A90-29286	#	AIAA PAPER 90-1418	p 614	A90-37955	#
AIAA PAPER 90-0490	p 557	A90-37063	#	AIAA PAPER 90-1115	p 392	A90-29387	#	AIAA PAPER 90-1419	p 614	A90-37956	#
AIAA PAPER 90-0492	p 182	A90-19875	#	AIAA PAPER 90-1116	p 392	A90-29388	#	AIAA PAPER 90-1420	p 596	A90-37957	#
AIAA PAPER 90-0495	p 167	A90-19876	#	AIAA PAPER 90-1117	p 412	A90-29389	#	AIAA PAPER 90-1421	p 605	A90-37958	#
AIAA PAPER 90-0527	p 229	A90-22226	#	AIAA PAPER 90-1118	p 392	A90-29390	#	AIAA PAPER 90-1423	p 596	A90-37960	#
AIAA PAPER 90-0529	p 314	A90-26963	#	AIAA PAPER 90-1119	p 392	A90-29391	#	AIAA PAPER 90-1424	p 596	A90-37961	#
AIAA PAPER 90-0530	p 192	A90-19895	#	AIAA PAPER 90-1120	p 393	A90-29392	#	AIAA PAPER 90-1425	p 559	A90-37962	#
AIAA PAPER 90-0531	p 167	A90-19896	#	AIAA PAPER 90-1125	p 451	A90-29429	#	AIAA PAPER 90-1426	p 590	A90-37963	#
AIAA PAPER 90-0550	p 343	A90-25036	#	AIAA PAPER 90-1149	p 458	A90-29293	#	AIAA PAPER 90-1427	p 559	A90-37964	#
AIAA PAPER 90-0564	p 216	A90-19917	#	AIAA PAPER 90-1152	p 389	A90-29364	#	AIAA PAPER 90-1429	p 605	A90-37966	#
AIAA PAPER 90-0565	p 197	A90-19918	#	AIAA PAPER 90-1153	p 390	A90-29365	#	AIAA PAPER 90-1430	p 559	A90-37967	#
AIAA PAPER 90-0568	p 197	A90-19920	#	AIAA PAPER 90-1154	p 390	A90-29366	#	AIAA PAPER 90-1431	p 559	A90-37968	#
AIAA PAPER 90-0569	p 167	A90-19921	#	AIAA PAPER 90-1155	p 390	A90-29367	#	AIAA PAPER 90-1432	p 559	A90-37969	#
AIAA PAPER 90-0571	p 230	A90-22230	#	AIAA PAPER 90-1156	p 390	A90-29368	#	AIAA PAPER 90-1433	p 597	A90-38487	#
AIAA PAPER 90-0572	p 167	A90-19922	#	AIAA PAPER 90-1157	p 393	A90-29393	#	AIAA PAPER 90-1440	p 680	A90-39725	#
AIAA PAPER 90-0573	p 167	A90-19923	#	AIAA PAPER 90-1158	p 412	A90-29467	#	AIAA PAPER 90-1448	p 561	A90-38608	#
AIAA PAPER 90-0574	p 167	A90-19924	#	AIAA PAPER 90-1159	p 412	A90-29394	#	AIAA PAPER 90-1450	p 606	A90-38610	#
AIAA PAPER 90-0575	p 167	A90-19925	#	AIAA PAPER 90-1161	p 450	A90-29396	#	AIAA PAPER 90-1453	p 561	A90-38612	#
AIAA PAPER 90-0576	p 168	A90-19926	#	AIAA PAPER 90-1162	p 393	A90-29397	#	AIAA PAPER 90-1456	p 606	A90-38614	#
AIAA PAPER 90-0579	p 168	A90-19929	#	AIAA PAPER 90-1180	p 450	A90-29379	#	AIAA PAPER 90-1459	p 561	A90-38616	#
AIAA PAPER 90-0581	p 230	A90-22231	#	AIAA PAPER 90-1240	p 348	A90-26820	#	AIAA PAPER 90-1460	p 561	A90-38617	#
AIAA PAPER 90-0583	p 168	A90-19932	#	AIAA PAPER 90-1259	p 504	A90-33889	#	AIAA PAPER 90-1461	p 561	A90-38618	#
AIAA PAPER 90-0585	p 314	A90-26967	#	AIAA PAPER 90-1260	p 494	A90-33890	#	AIAA PAPER 90-1462	p 562	A90-38619	#
AIAA PAPER 90-0589	p 314	A90-26968	#	AIAA PAPER 90-1261	p 494	A90-33891	#	AIAA PAPER 90-1464	p 562	A90-38621	#
AIAA PAPER 90-0590	p 168	A90-19936	#	AIAA PAPER 90-1262	p 579	A90-36026	#	AIAA PAPER 90-1467	p 562	A90-38624	#
AIAA PAPER 90-0594	p 203	A90-19938	#	AIAA PAPER 90-1263	p 494	A90-33892	#	AIAA PAPER 90-1468	p 562	A90-38625	#
AIAA PAPER 90-0595	p 230	A90-22233	#	AIAA PAPER 90-1265	p 494	A90-33893	#	AIAA PAPER 90-1469	p 562	A90-38626	#
AIAA PAPER 90-0597	p 168	A90-19939	#	AIAA PAPER 90-1266	p 509	A90-33894	#	AIAA PAPER 90-1470	p 562	A90-38627	#
AIAA PAPER 90-0598	p 168	A90-19940	#	AIAA PAPER 90-1267	p 505	A90-33930	#	AIAA PAPER 90-1471	p 563	A90-38628	#
AIAA PAPER 90-0599	p 314	A90-26969	#	AIAA PAPER 90-1268	p 518	A90-33895	#	AIAA PAPER 90-1473	p 563	A90-38629	#
AIAA PAPER 90-0600	p 314	A90-26970	#	AIAA PAPER 90-1269	p 494	A90-33896	#	AIAA PAPER 90-1483	p 563	A90-38637	#
AIAA PAPER 90-0607	p 231	A90-22449	#	AIAA PAPER 90-1272	p 538	A90-33897	#	AIAA PAPER 90-1485	p 563	A90-38639	#
AIAA PAPER 90-0630	p 352	A90-26974	#	AIAA PAPER 90-1273	p 496	A90-34148	#	AIAA PAPER 90-1493	p 619	A90-39049	#
AIAA PAPER 90-0631	p 211	A90-19956	#	AIAA PAPER 90-1274	p 504	A90-33898	#	AIAA PAPER 90-1502	p 606	A90-38651	#
AIAA PAPER 90-0647	p 205	A90-19966	#	AIAA PAPER 90-1275	p 494	A90-33899	#	AIAA PAPER 90-1512	p 563	A90-38659	#
AIAA PAPER 90-0665	p 322	A90-26977	#	AIAA PAPER 90-1276	p 518	A90-33900	#	AIAA PAPER 90-1513	p 563	A90-38660	#
AIAA PAPER 90-0666	p 350	A90-25040	#	AIAA PAPER 90-1277	p 518	A90-33901	#	AIAA PAPER 90-1518	p 606	A90-38663	#
AIAA PAPER 90-0667	p 368	A90-26978	#	AIAA PAPER 90-1279	p 579	A90-36027	#	AIAA PAPER 90-1521	p 563	A90-38666	#
AIAA PAPER 90-0668	p 274	A90-23711	#	AIAA PAPER 90-1280	p 496	A90-34725	#	AIAA PAPER 90-1525	p 563	A90-38670	#
AIAA PAPER 90-0669	p 261	A90-22242	#	AIAA PAPER 90-1281	p 495	A90-33902	#	AIAA PAPER 90-1528	p 564	A90-38673	#
AIAA PAPER 90-0670	p 352	A90-26979	#	AIAA PAPER 90-1282	p 495	A90-33903	#	AIAA PAPER 90-1532	p 606	A90-38677	#
AIAA PAPER 90-0687	p 169	A90-19978	#	AIAA PAPER 90-1283	p 495	A90-33904	#	AIAA PAPER 90-1533	p 564	A90-38678	#
AIAA PAPER 90-0689	p 230	A90-22244	#	AIAA PAPER 90-1284	p 495	A90-33905	#	AIAA PAPER 90-1535	p 564	A90-38679	#
AIAA PAPER 90-0694	p 300	A90-25041	#	AIAA PAPER 90-1285	p 519	A90-33906	#	AIAA PAPER 90-1536	p 564	A90-38680	#
AIAA PAPER 90-0695	p 169	A90-19981	#	AIAA PAPER 90-1286	p 519	A90-33907	#	AIAA PAPER 90-1537	p 564	A90-38681	#
AIAA PAPER 90-0698	p 169	A90-19983	#	AIAA PAPER 90-1288	p 519	A90-33931	#	AIAA PAPER 90-1538	p 564	A90-38682	#
AIAA PAPER 90-0705	p 212	A90-19984	#	AIAA PAPER 90-1289	p 495	A90-33909	#	AIAA PAPER 90-1539	p 564	A90-38683	#
AIAA PAPER 90-0711	p 230	A90-22251	#	AIAA PAPER 90-1290	p 522	A90-33910	#	AIAA PAPER 90-1540	p 565	A90-38684	#
AIAA PAPER 90-0712	p 314	A90-26983	#	AIAA PAPER 90-1296	p 495	A90-33912	#	AIAA PAPER 90-1542	p 565	A90-38686	#
AIAA PAPER 90-0731	p 230	A90-22256	#	AIAA PAPER 90-1299	p 504	A90-33913	#	AIAA PAPER 90-1543	p 565	A90-38687	#
AIAA PAPER 90-0733	p 314	A90-26985	#	AIAA PAPER 90-1300	p 487	A90-33914	#	AIAA PAPER 90-1544	p 565	A90-38688	#
AIAA PAPER 90-0753	p 322	A90-26986	#	AIAA PAPER 90-1301	p 487	A90-33915	#	AIAA PAPER 90-1551	p 600	A90-38693	#
AIAA PAPER 90-0754	p 176	A90-20009	#	AIAA PAPER 90-1302	p 505	A90-33916	#	AIAA PAPER 90-1564	p 565	A90-38703	#
AIAA PAPER 90-0756	p 300	A90-25042	#	AIAA PAPER 90-1303	p 505	A90-33917	#	AIAA PAPER 90-1565	p 565	A90-38704	#
AIAA PAPER 90-0757	p 169	A90-20010	#	AIAA PAPER 90-1304	p 580	A90-36029	#	AIAA PAPER 90-1573	p 600	A90-38711	#
AIAA PAPER 90-0758	p 169	A90-20011	#	AIAA PAPER 90-1305	p 579	A90-35300	#	AIAA PAPER 90-1580	p 566	A90-38717	#
AIAA PAPER 90-0759	p 238	A90-22258	#	AIAA PAPER 90-1306	p 589	A90-36030	#	AIAA PAPER 90-1581	p 566	A90-38718	#
AIAA PAPER 90-0761	p 183	A90-20012	#	AIAA PAPER 90-1308	p 519	A90-33918	#	AIAA PAPER 90-1585	p 566	A90-38720	#
AIAA PAPER 90-0762	p 230	A90-22259	#	AIAA PAPER 90-1309	p 523	A90-33919	#	AIAA PAPER 90-1586	p 566	A90-38721	#
AIAA PAPER 90-0775	p 366	A90-25602	#	AIAA PAPER 90-1310	p 496	A90-33920	#	AIAA PAPER 90-1588	p 566	A90-38723	#
AIAA PAPER 90-0883	p 331	A90-25702	#	AIAA PAPER 90-1311	p 545	A90-33921	#	AIAA PAPER 90-1590	p 607	A90-38725	#
AIAA PAPER 90-0935	p 389	A90-29361	#	AIAA PAPER 90-1313	p 487	A90-33923	#	AIAA PAPER 90-1592	p 566	A90-38727	#
AIAA PAPER 90-0936	p 389	A90-29362	#	AIAA PAPER 90-1315	p 483	A90-33924	#	AIAA PAPER 90-1596	p 567	A90-38729	#
AIAA PAPER 90-0937	p 389	A90-29363	#	AIAA PAPER 90-1316	p 488	A90-33925	#	AIAA PAPER 90-1598	p 607	A90-38730	#
AIAA PAPER 90-0946	p 412	A90-29405	#	AIAA PAPER 90-1317	p 519	A90-33926	#	AIAA PAPER 90-1599	p 567	A90-38731	#
AIAA PAPER 90-0951	p 410	A90-29237	#	AIAA PAPER 90-1321	p 520	A90-34149	#	AIAA PAPER 90-1600	p 567	A90-38732	#
AIAA PAPER 90-0953	p 411	A90-29238	#	AIAA PAPER 90-1322	p 545	A90-34150	#	AIAA PAPER 90-1603	p 567	A90-38734	#
AIAA PAPER 90-0954	p 411	A90-29239	#	AIAA PAPER 90-1323	p 580	A90-36031	#	AIAA PAPER 90-1605	p 567	A90-38736	#
AIAA PAPER 90-0955	p 411	A90-29240	#	AIAA PAPER 90-1375	p 594	A90-37926	#	AIAA PAPER 90-1606	p 567	A90-38737	#
AIAA PAPER 90-0956	p 438	A90-29241	#	AIAA PAPER 90-1376	p 596	A90-38483	#	AIAA PAPER 90-1607	p 612	A90-38738	#
AIAA PAPER 90-0971	p 411	A90-29305	#	AIAA PAPER 90-1379	p 594	A90-37928	#</				

AIAA PAPER 90-1627	p 568	A90-38756	#	AIAA PAPER 90-2042	p 661	A90-41993	#	AIAA PAPER 90-2401	p 743	A90-42793	#
AIAA PAPER 90-1628	p 568	A90-38757	#	AIAA PAPER 90-2046	p 684	A90-41997	#	AIAA PAPER 90-2402	p 808	A90-47220	#
AIAA PAPER 90-1629	p 591	A90-38758	#	AIAA PAPER 90-2048	p 684	A90-41999	#	AIAA PAPER 90-2403	p 663	A90-42160	#
AIAA PAPER 90-1630	p 568	A90-38759	#	AIAA PAPER 90-2075	p 764	A90-42725	#	AIAA PAPER 90-2404	p 701	A90-42794	#
AIAA PAPER 90-1632	p 587	A90-38761	#	AIAA PAPER 90-2093	p 742	A90-42728	#	AIAA PAPER 90-2408	p 626	A90-42161	#
AIAA PAPER 90-1633	p 569	A90-38762	#	AIAA PAPER 90-2096	p 742	A90-42729	#	AIAA PAPER 90-2409	p 626	A90-42162	#
AIAA PAPER 90-1636	p 607	A90-38765	#	AIAA PAPER 90-2098	p 661	A90-42017	#	AIAA PAPER 90-2411	p 687	A90-42163	#
AIAA PAPER 90-1641	p 608	A90-38769	#	AIAA PAPER 90-2099	p 624	A90-42018	#	AIAA PAPER 90-2412	p 687	A90-42164	#
AIAA PAPER 90-1644	p 569	A90-38772	#	AIAA PAPER 90-2105	p 624	A90-42019	#	AIAA PAPER 90-2413	p 687	A90-42165	#
AIAA PAPER 90-1645	p 569	A90-38773	#	AIAA PAPER 90-2107	p 684	A90-42020	#	AIAA PAPER 90-2414	p 687	A90-42166	#
AIAA PAPER 90-1646	p 569	A90-38774	#	AIAA PAPER 90-2122	p 704	A90-42731	#	AIAA PAPER 90-2415	p 663	A90-42167	#
AIAA PAPER 90-1649	p 569	A90-38777	#	AIAA PAPER 90-2124	p 704	A90-42732	#	AIAA PAPER 90-2417	p 663	A90-42168	#
AIAA PAPER 90-1650	p 569	A90-38778	#	AIAA PAPER 90-2125	p 624	A90-42032	#	AIAA PAPER 90-2419	p 663	A90-42169	#
AIAA PAPER 90-1652	p 570	A90-38780	#	AIAA PAPER 90-2126	p 625	A90-42033	#	AIAA PAPER 90-2421	p 663	A90-42170	#
AIAA PAPER 90-1653	p 608	A90-38781	#	AIAA PAPER 90-2127	p 704	A90-42733	#	AIAA PAPER 90-2439	p 949	A90-50645	#
AIAA PAPER 90-1655	p 570	A90-38782	#	AIAA PAPER 90-2128	p 625	A90-42034	#	AIAA PAPER 90-2444	p 677	A90-42174	#
AIAA PAPER 90-1657	p 570	A90-38784	#	AIAA PAPER 90-2129	p 625	A90-42035	#	AIAA PAPER 90-2447	p 743	A90-42806	#
AIAA PAPER 90-1691	p 560	A90-38394	#	AIAA PAPER 90-2130	p 704	A90-42734	#	AIAA PAPER 90-2451	p 658	A90-40633	#
AIAA PAPER 90-1714	p 560	A90-38416	#	AIAA PAPER 90-2132	p 704	A90-42735	#	AIAA PAPER 90-2452	p 743	A90-42808	#
AIAA PAPER 90-1748	p 583	A90-38441	#	AIAA PAPER 90-2133	p 685	A90-42037	#	AIAA PAPER 90-2453	p 663	A90-42176	#
AIAA PAPER 90-1778	p 560	A90-38468	#	AIAA PAPER 90-2135	p 621	A90-40612	#	AIAA PAPER 90-2454	p 664	A90-42177	#
AIAA PAPER 90-1783	p 568	A90-38472	#	AIAA PAPER 90-2136	p 661	A90-42038	#	AIAA PAPER 90-2469	p 673	A90-42186	#
AIAA PAPER 90-1800	p 315	A90-27311	#	AIAA PAPER 90-2140	p 685	A90-42040	#	AIAA PAPER 90-2472	p 762	A90-42810	#
AIAA PAPER 90-1801	p 335	A90-25175	#	AIAA PAPER 90-2142	p 685	A90-42041	#	AIAA PAPER 90-2473	p 664	A90-42188	#
AIAA PAPER 90-1802	p 334	A90-25174	#	AIAA PAPER 90-2144	p 685	A90-42043	#	AIAA PAPER 90-2474	p 675	A90-42189	#
AIAA PAPER 90-1810	p 353	A90-25172	#	AIAA PAPER 90-2145	p 704	A90-42737	#	AIAA PAPER 90-2486	p 658	A90-40636	#
AIAA PAPER 90-1814	p 919	A90-51450	#	AIAA PAPER 90-2146	p 705	A90-42738	#	AIAA PAPER 90-2492	p 658	A90-40637	#
AIAA PAPER 90-1820	p 334	A90-25169	#	AIAA PAPER 90-2147	p 625	A90-42044	#	AIAA PAPER 90-2501	p 658	A90-40639	#
AIAA PAPER 90-1822	p 350	A90-25165	#	AIAA PAPER 90-2148	p 768	A90-42739	#	AIAA PAPER 90-2508	p 682	A90-40641	#
AIAA PAPER 90-1824	p 346	A90-25168	#	AIAA PAPER 90-2149	p 625	A90-42045	#	AIAA PAPER 90-2512	p 658	A90-40643	#
AIAA PAPER 90-1826	p 307	A90-25935	#	AIAA PAPER 90-2150	p 696	A90-42046	#	AIAA PAPER 90-2520	p 744	A90-42813	#
AIAA PAPER 90-1827	p 301	A90-25167	#	AIAA PAPER 90-2151	p 644	A90-42047	#	AIAA PAPER 90-2521	p 744	A90-42814	#
AIAA PAPER 90-1835	p 655	A90-40526	#	AIAA PAPER 90-2152	p 685	A90-42048	#	AIAA PAPER 90-2522	p 664	A90-42197	#
AIAA PAPER 90-1851	p 655	A90-40530	#	AIAA PAPER 90-2154	p 681	A90-40613	#	AIAA PAPER 90-2523	p 744	A90-42815	#
AIAA PAPER 90-1858	p 768	A90-42685	#	AIAA PAPER 90-2156	p 956	A90-50644	#	AIAA PAPER 90-2728	p 664	A90-42217	#
AIAA PAPER 90-1860	p 655	A90-40533	#	AIAA PAPER 90-2158	p 852	A90-47210	#	AIAA PAPER 90-2730	p 626	A90-42218	#
AIAA PAPER 90-1873	p 655	A90-40539	#	AIAA PAPER 90-2159	p 661	A90-42050	#	AIAA PAPER 90-2739	p 664	A90-42221	#
AIAA PAPER 90-1874	p 655	A90-40540	#	AIAA PAPER 90-2161	p 661	A90-42051	#	AIAA PAPER 90-2740	p 882	A90-47228	#
AIAA PAPER 90-1875	p 655	A90-40541	#	AIAA PAPER 90-2162	p 768	A90-42740	#	AIAA PAPER 90-2752	p 627	A90-42225	#
AIAA PAPER 90-1887	p 660	A90-41981	#	AIAA PAPER 90-2163	p 742	A90-42741	#	AIAA PAPER 90-2753	p 664	A90-42226	#
AIAA PAPER 90-1899	p 739	A90-42688	#	AIAA PAPER 90-2164	p 685	A90-42052	#	AIAA PAPER 90-2754	p 617	A90-40648	#
AIAA PAPER 90-1901	p 740	A90-42690	#	AIAA PAPER 90-2165	p 661	A90-42053	#	AIAA PAPER 90-2761	p 783	A90-42828	#
AIAA PAPER 90-1904	p 740	A90-42691	#	AIAA PAPER 90-2166	p 662	A90-42054	#	AIAA PAPER 90-2800	p 753	A90-45156	#
AIAA PAPER 90-1905	p 655	A90-40552	#	AIAA PAPER 90-2169	p 662	A90-42055	#	AIAA PAPER 90-2801	p 753	A90-45157	#
AIAA PAPER 90-1906	p 660	A90-41982	#	AIAA PAPER 90-2170	p 662	A90-42056	#	AIAA PAPER 90-2803	p 712	A90-45178	#
AIAA PAPER 90-1909	p 894	A90-47202	#	AIAA PAPER 90-2175	p 677	A90-42059	#	AIAA PAPER 90-2804	p 752	A90-45139	#
AIAA PAPER 90-1910	p 740	A90-42692	#	AIAA PAPER 90-2176	p 662	A90-42060	#	AIAA PAPER 90-2805	p 752	A90-45140	#
AIAA PAPER 90-1911	p 624	A90-41983	#	AIAA PAPER 90-2177	p 686	A90-42061	#	AIAA PAPER 90-2806	p 752	A90-45141	#
AIAA PAPER 90-1912	p 656	A90-40554	#	AIAA PAPER 90-2178	p 677	A90-42062	#	AIAA PAPER 90-2807	p 752	A90-45142	#
AIAA PAPER 90-1913	p 740	A90-42693	#	AIAA PAPER 90-2190	p 686	A90-42067	#	AIAA PAPER 90-2808	p 752	A90-45143	#
AIAA PAPER 90-1914	p 740	A90-42694	#	AIAA PAPER 90-2193	p 686	A90-42068	#	AIAA PAPER 90-2809	p 752	A90-45144	#
AIAA PAPER 90-1915	p 741	A90-42695	#	AIAA PAPER 90-2217	p 705	A90-42748	#	AIAA PAPER 90-2810	p 710	A90-45150	#
AIAA PAPER 90-1916	p 621	A90-40555	#	AIAA PAPER 90-2218	p 705	A90-42749	#	AIAA PAPER 90-2811	p 753	A90-45151	#
AIAA PAPER 90-1917	p 656	A90-40556	#	AIAA PAPER 90-2219	p 705	A90-42750	#	AIAA PAPER 90-2812	p 753	A90-45152	#
AIAA PAPER 90-1918	p 667	A90-40557	#	AIAA PAPER 90-2220	p 705	A90-42751	#	AIAA PAPER 90-2813	p 711	A90-45153	#
AIAA PAPER 90-1920	p 656	A90-40558	#	AIAA PAPER 90-2221	p 742	A90-42752	#	AIAA PAPER 90-2814	p 711	A90-45154	#
AIAA PAPER 90-1921	p 656	A90-40559	#	AIAA PAPER 90-2246	p 686	A90-42093	#	AIAA PAPER 90-2815	p 711	A90-45155	#
AIAA PAPER 90-1926	p 741	A90-42696	#	AIAA PAPER 90-2248	p 625	A90-42094	#	AIAA PAPER 90-2820	p 763	A90-45149	#
AIAA PAPER 90-1928	p 703	A90-42697	#	AIAA PAPER 90-2262	p 768	A90-42759	#	AIAA PAPER 90-2823	p 753	A90-45158	#
AIAA PAPER 90-1930	p 759	A90-42698	#	AIAA PAPER 90-2263	p 625	A90-42102	#	AIAA PAPER 90-2827	p 754	A90-45159	#
AIAA PAPER 90-1931	p 681	A90-40560	#	AIAA PAPER 90-2264	p 768	A90-42761	#	AIAA PAPER 90-2828	p 763	A90-45135	#
AIAA PAPER 90-1935	p 656	A90-40562	#	AIAA PAPER 90-2266	p 768	A90-42763	#	AIAA PAPER 90-2831	p 763	A90-45137	#
AIAA PAPER 90-1955	p 881	A90-47203	#	AIAA PAPER 90-2269	p 742	A90-42765	#	AIAA PAPER 90-2833	p 711	A90-45164	#
AIAA PAPER 90-1957	p 676	A90-40570	#	AIAA PAPER 90-2270	p 743	A90-42766	#	AIAA PAPER 90-2834	p 712	A90-45165	#
AIAA PAPER 90-1959	p 762	A90-42705	#	AIAA PAPER 90-2271	p 586	A90-37562	#	AIAA PAPER 90-2835	p 712	A90-45166	#
AIAA PAPER 90-1963	p 656	A90-40573	#	AIAA PAPER 90-2272	p 743	A90-42767	#	AIAA PAPER 90-2836	p 934	A90-50640	#
AIAA PAPER 90-1964	p 676	A90-40574	#	AIAA PAPER 90-2274	p 644	A90-42103	#	AIAA PAPER 90-2837	p 754	A90-45167	#
AIAA PAPER 90-1966	p 741	A90-42706	#	AIAA PAPER 90-2276	p 644	A90-42104	#	AIAA PAPER 90-2838	p 754	A90-45160	#
AIAA PAPER 90-1978	p 703	A90-42708	#	AIAA PAPER 90-2277	p 730	A90-42768	#	AIAA PAPER 90-2841	p 754	A90-45161	#
AIAA PAPER 90-1980	p 703	A90-42709	#	AIAA PAPER 90-2278	p 644	A90-42105	#	AIAA PAPER 90-2842	p 754	A90-45162	#
AIAA PAPER 90-1985	p 741	A90-42712	#	AIAA PAPER 90-2280	p 644	A90-42106	#	AIAA PAPER 90-2843	p 711	A90-45163	#
AIAA PAPER 90-1986	p 674	A90-40582	#	AIAA PAPER 90-2281	p 764	A90-42769	#	AIAA PAPER 90-2845	p 754	A90-45174	#
AIAA PAPER 90-2000	p 674	A90-40587	#	AIAA PAPER 90-2291	p 686	A90-42110	#	AIAA PAPER 90-2847	p 754	A90-45175	#
AIAA PAPER 90-2003	p 681	A90-40590	#	AIAA PAPER 90-2305	p 686	A90-42116	#	AIAA PAPER 90-2848	p 755	A90-45176	#
AIAA PAPER 90-2005	p 621	A90-40592	#	AIAA PAPER 90-2307	p 677	A90-42117	#	AIAA PAPER 90-2849	p 755	A90-45177	#
AIAA PAPER 90-2014	p 676	A90-40594	#	AIAA PAPER 90-2309	p 769	A90-42773	#	AIAA PAPER 90-2850	p 712	A90-45168	#
AIAA PAPER 90-2015	p 673	A90-41986	#	AIAA PAPER 90-2337	p 658	A90-40622	#	AIAA PAPER 90-2995	p 787	A90-45846	#
AIAA PAPER 90-2016	p 741	A90-42718	#	AIAA PAPER 90-2339	p 762	A90-42776	#	AIAA PAPER 90-2997	p 787	A90-45847	#
AIAA PAPER 90-2018	p 621	A90-40596	#	AIAA PAPER 90-2340	p 743	A90-42777	#	AIAA PAPER 90-2998	p 787	A90-45848	#
AIAA PAPER 90-2021	p 684	A90-41987	#	AIAA PAPER 90-2342	p 626	A90-42132	#	AIAA PAPER 90-2999	p 787	A90-45849	#
AIAA PAPER 90-2023	p 657	A90-40597	#	AIAA PAPER 90-2344	p 686	A90-42133	#	AIAA PAPER 90-3000	p 788	A90-45850	#
AIAA PAPER 90-2024	p 741	A90-42719	#	AIAA PAPER 90-2352	p 626	A90-42136	#	AIAA PAPER 90-3001	p 798	A90-45936	#
AIAA PAPER 90-2025	p 624	A90-41988	#	AIAA PAPER 90-2353	p 705	A90-42781	#	AIAA PAPER 90-3002	p 788	A90-45851	#
AIAA PAPER 90-2026	p 624	A90-41989	#	AIAA PAPER 90-2354	p 769	A90-42782	#	AIAA PAPER 90-3003	p 788	A90-45852	#
AIAA PAPER 90-2027	p 657	A90-40598	#	AIAA PAPER 90-2355	p 626	A90-42137	#	AIAA PAPER 90-3004	p 788	A90-45853	#
AIAA PAPER 90-2028	p 621	A90-40599	#	AIAA PAPER 90-2357	p 706	A90-42783	#	AIAA PAPER 90-3005	p 788	A90-45854	#
AIAA PAPER 90-2030	p 657	A90-40601	#	AIAA PAPER 90-2360	p 706	A90-42784	#	AIAA PAPER 90-3006	p 789	A90-45856	#
AIAA PAPER 90-2031	p 660	A90-41990	#	AIAA PAPER 90-2382	p 675	A90-42147	#	AIAA PAPER 90-3007	p 789	A90-45857	#
AIAA PAPER 90-2032	p 657	A90-40602	#	AIAA PAPER 90-2386	p 759	A90-42791	#	AIAA PAPER 90-3008	p 789	A90-45858	#
AIAA PAPER 90-2033	p 657	A90-40603	#	AIAA PAPER 90-2393	p 662	A90-42155	#</				

AIAA PAPER 90-3019

REPORT NUMBER INDEX

AIAA PAPER 90-3019	p 792	A90-45886	#	AIAA PAPER 90-3265	p 835	A90-48859	#	AIAA-89-3596	p 32	N90-10023	* #
AIAA PAPER 90-3020	p 793	A90-45887	#	AIAA PAPER 90-3266	p 835	A90-48860	#	AIAA-90-0028	p 172	N90-13355	* #
AIAA PAPER 90-3021	p 869	A90-45888	#	AIAA PAPER 90-3268	p 836	A90-48861	#	AIAA-90-0048	p 94	N90-12561	* #
AIAA PAPER 90-3023	p 793	A90-45890	#	AIAA PAPER 90-3271	p 836	A90-48862	#	AIAA-90-0053	p 215	N90-14511	* #
AIAA PAPER 90-3025	p 790	A90-45867	#	AIAA PAPER 90-3272	p 836	A90-48863	#	AIAA-90-0230	p 186	N90-14228	* #
AIAA PAPER 90-3026	p 790	A90-45868	#	AIAA PAPER 90-3273	p 818	A90-48864	#	AIAA-90-0232	p 339	N90-16758	* #
AIAA PAPER 90-3028	p 790	A90-45870	#	AIAA PAPER 90-3274	p 836	A90-48865	#	AIAA-90-0283	p 548	N90-20794	* #
AIAA PAPER 90-3029	p 791	A90-45871	* #	AIAA PAPER 90-3279	p 836	A90-48866	#	AIAA-90-0339	p 380	N90-18229	* #
AIAA PAPER 90-3033	p 903	A90-50637	#	AIAA PAPER 90-3280	p 892	A90-48867	#	AIAA-90-0438	p 720	N90-25946	* #
AIAA PAPER 90-3034	p 791	A90-45873	* #	AIAA PAPER 90-3282	p 836	A90-48869	#	AIAA-90-0550	p 345	N90-17636	* #
AIAA PAPER 90-3035	p 791	A90-45874	#	AIAA PAPER 90-3284	p 853	A90-48871	* #	AIAA-90-0668	p 215	N90-14617	* #
AIAA PAPER 90-3036	p 791	A90-45875	#	AIAA PAPER 90-3285	p 853	A90-48872	#	AIAA-90-0669	p 213	N90-13797	* #
AIAA PAPER 90-3037	p 791	A90-45876	#	AIAA PAPER 90-3286	p 812	A90-48873	#	AIAA-90-0694	p 318	N90-17562	* #
AIAA PAPER 90-3038	p 791	A90-45877	* #	AIAA PAPER 90-3288	p 853	A90-48874	#	AIAA-90-0756	p 570	N90-21727	* #
AIAA PAPER 90-3039	p 792	A90-45878	#	AIAA PAPER 90-3289	p 818	A90-48875	#	AIAA-90-0978	p 527	N90-21047	* #
AIAA PAPER 90-3041	p 792	A90-45879	#	AIAA PAPER 90-3290	p 813	A90-49122	#	AIAA-90-1321	p 758	N90-25144	* #
AIAA PAPER 90-3042	p 798	A90-45934	#	AIAA PAPER 90-3291	p 892	A90-49123	#	AIAA-90-1899	p 666	N90-23404	* #
AIAA PAPER 90-3043	p 792	A90-45880	#	AIAA PAPER 90-3292	p 837	A90-48876	#	AIAA-90-1935	p 588	N90-21762	* #
AIAA PAPER 90-3044	p 828	A90-45881	#	AIAA PAPER 90-3293	p 837	A90-48877	* #	AIAA-90-1955	p 773	N90-25289	* #
AIAA PAPER 90-3045	p 792	A90-45882	#	AIAA PAPER 90-3295	p 837	A90-48879	#	AIAA-90-2000	p 588	N90-21763	* #
AIAA PAPER 90-3046	p 792	A90-45883	#	AIAA PAPER 90-3296	p 840	A90-49124	#	AIAA-90-2271	p 552	N90-21725	* #
AIAA PAPER 90-3049	p 797	A90-45929	* #	AIAA PAPER 90-3297	p 840	A90-49125	* #	AIAA-90-2417	p 589	N90-22566	* #
AIAA PAPER 90-3051	p 797	A90-45930	#	AIAA PAPER 90-3298	p 837	A90-48880	#	AIAA-90-2452	p 688	N90-23591	* #
AIAA PAPER 90-3053	p 798	A90-45932	#	AIAA PAPER 90-3299	p 853	A90-48881	#	ALLISON-EDR-14074	p 510	N90-20091	#
AIAA PAPER 90-3057	p 790	A90-45862	* #	AIAA PAPER 90-3300	p 868	A90-48882	#	AMS-420	p 468	N90-20920	#
AIAA PAPER 90-3058	p 790	A90-45863	#	AIAA PAPER 90-3301	p 847	A90-48883	#	AMSEL-NV-TR-0085	p 369	N90-16971	#
AIAA PAPER 90-3060	p 794	A90-45895	#	AIAA PAPER 90-3302	p 837	A90-48884	#	AR-005-530	p 36	N90-10888	#
AIAA PAPER 90-3061	p 798	A90-45933	#	AIAA PAPER 90-3303	p 837	A90-48885	#	AR-005-600	p 935	N90-28576	#
AIAA PAPER 90-3062	p 794	A90-45896	#	AIAA PAPER 90-3305	p 837	A90-48886	#	AR-005-730	p 444	N90-19364	#
AIAA PAPER 90-3063	p 903	A90-50638	* #	AIAA PAPER 90-3306	p 838	A90-48887	#	AR-006-055	p 928	N90-28547	* #
AIAA PAPER 90-3064	p 794	A90-45897	#	AIAA PAPER 90-3307	p 868	A90-48888	#	AR-006-084	p 767	N90-26106	#
AIAA PAPER 90-3065	p 793	A90-45891	* #	AIAA PAPER 90-3325	p 872	A90-47587	#	AR-006-288	p 527	N90-21044	#
AIAA PAPER 90-3066	p 793	A90-45892	#	AIAA PAPER 90-3328	p 862	A90-47590	#	ARL-AERO-R-177	p 36	N90-10888	#
AIAA PAPER 90-3067	p 793	A90-45893	* #	AIAA PAPER 90-3331	p 847	A90-47592	#	ARL-APP-R-84	p 323	N90-16725	#
AIAA PAPER 90-3070	p 794	A90-45894	#	AIAA PAPER 90-3333	p 862	A90-47593	#	ARL-FLIGHT-MECH-R-180	p 935	N90-28576	#
AIAA PAPER 90-3071	p 796	A90-45917	#	AIAA PAPER 90-3334	p 862	A90-47594	#	ARL-FLIGHT-MECH-TM-404	p 95	N90-12566	#
AIAA PAPER 90-3072	p 796	A90-45918	#	AIAA PAPER 90-3335	p 862	A90-47595	* #	ARL-FLIGHT-MECH-TM-412	p 526	N90-20098	#
AIAA PAPER 90-3074	p 797	A90-45920	* #	AIAA PAPER 90-3336	p 863	A90-47596	#	ARL-MAT-R-122	p 767	N90-26106	#
AIAA PAPER 90-3076	p 797	A90-45922	#	AIAA PAPER 90-3337	p 863	A90-47597	* #	ARL-PROP-R-182	p 928	N90-28547	#
AIAA PAPER 90-3077	p 795	A90-45908	* #	AIAA PAPER 90-3338	p 863	A90-47598	#	ARL-PROP-TM-441	p 107	N90-12596	#
AIAA PAPER 90-3078	p 795	A90-45909	* #	AIAA PAPER 90-3346	p 889	A90-47606	* #	ARL-PROP-TM-454	p 52	N90-10041	#
AIAA PAPER 90-3079	p 795	A90-45910	#	AIAA PAPER 90-3369	p 863	A90-47627	#	ARL-PROP-TM-455	p 52	N90-10040	#
AIAA PAPER 90-3080	p 795	A90-45911	* #	AIAA PAPER 90-3370	p 863	A90-47628	#	ARL-PROP-TM-457	p 114	N90-11745	#
AIAA PAPER 90-3082	p 794	A90-45898	* #	AIAA PAPER 90-3371	p 863	A90-47629	#	ARL-PROP-TM-469	p 855	N90-26832	#
AIAA PAPER 90-3083	p 794	A90-45899	#	AIAA PAPER 90-3372	p 864	A90-47630	* #	ARL-STRUC-TM-503	p 107	N90-12597	#
AIAA PAPER 90-3084	p 806	A90-46645	#	AIAA PAPER 90-3373	p 864	A90-47631	* #	ARL-STRUC-TM-504	p 90	N90-12501	#
AIAA PAPER 90-3086	p 795	A90-45900	#	AIAA PAPER 90-3374	p 864	A90-47632	#	ARL-STRUC-TM-505	p 338	N90-17628	#
AIAA PAPER 90-3087	p 795	A90-45901	#	AIAA PAPER 90-3375	p 847	A90-47633	#	ARL-STRUC-TM-506	p 32	N90-10026	#
AIAA PAPER 90-3088	p 795	A90-45902	#	AIAA PAPER 90-3402	p 822	A90-47657	#	ARL-STRUC-TM-515	p 593	N90-22570	#
AIAA PAPER 90-3094	p 797	A90-45923	#	AIAA PAPER 90-3404	p 822	A90-47659	* #	ARL-STRUC-TM-526	p 815	N90-26793	#
AIAA PAPER 90-3100	p 796	A90-45912	* #	AIAA PAPER 90-3406	p 864	A90-47661	* #	ARL-SYS-TM-106	p 185	N90-14217	#
AIAA PAPER 90-3101	p 796	A90-45913	#	AIAA PAPER 90-3407	p 864	A90-47662	#	ARL-SYS-TM-133	p 641	N90-24264	#
AIAA PAPER 90-3102	p 796	A90-45914	#	AIAA PAPER 90-3408	p 817	A90-47663	#	ARL-SYS-TM-98	p 107	N90-12595	#
AIAA PAPER 90-3103	p 796	A90-45915	* #	AIAA PAPER 90-3409	p 864	A90-47664	#	ARL/PSU/TR-89-004	p 133	N90-11982	#
AIAA PAPER 90-3106	p 789	A90-45855	* #	AIAA PAPER 90-3410	p 865	A90-47665	* #	ARO-23761.2-EG-F	p 260	N90-15113	#
AIAA PAPER 90-3189	p 786	A90-48826	#	AIAA PAPER 90-3411	p 865	A90-47666	#	ARO-24025.12-EG	p 478	N90-20048	#
AIAA PAPER 90-3192	p 786	A90-48828	#	AIAA PAPER 90-3415	p 889	A90-47669	#	ARO-25575.7-EG	p 911	N90-29302	#
AIAA PAPER 90-3194	p 786	A90-48829	#	AIAA PAPER 90-3435	p 889	A90-47688	* #	ARO-26588.1-EG-CF	p 532	N90-20140	#
AIAA PAPER 90-3196	p 812	A90-49101	* #	AIAA PAPER 90-3437	p 890	A90-47690	* #	ARO-27323.1-SBI	p 959	N90-28828	#
AIAA PAPER 90-3197	p 838	A90-49102	* #	AIAA PAPER 90-3441	p 865	A90-47694	#	ARO-27619.1-EG-CF	p 911	N90-29304	#
AIAA PAPER 90-3198	p 834	A90-48831	#	AIAA PAPER 90-3442	p 865	A90-47695	#	ARO-446	p 736	N90-25971	* #
AIAA PAPER 90-3199	p 812	A90-49103	* #	AIAA PAPER 90-3443	p 865	A90-47696	#	ARO-463	p 736	N90-25971	* #
AIAA PAPER 90-3203	p 834	A90-48832	#	AIAA PAPER 90-3444	p 890	A90-47697	* #	ASME PAPER 89-GT-10	p 374	A90-23755	#
AIAA PAPER 90-3204	p 838	A90-49104	#	AIAA PAPER 90-3445	p 890	A90-47698	#	ASME PAPER 89-GT-114	p 359	A90-23818	#
AIAA PAPER 90-3205	p 834	A90-48833	#	AIAA PAPER 90-3446	p 890	A90-47699	* #	ASME PAPER 89-GT-118	p 360	A90-23819	#
AIAA PAPER 90-3206	p 834	A90-48834	#	AIAA PAPER 90-3453	p 890	A90-47706	#	ASME PAPER 89-GT-121	p 341	A90-23820	#
AIAA PAPER 90-3207	p 834	A90-48835	#	AIAA PAPER 90-3455	p 786	A90-47707	* #	ASME PAPER 89-GT-126	p 360	A90-23825	#
AIAA PAPER 90-3208	p 838	A90-49105	#	AIAA PAPER 90-3473	p 890	A90-47723	#	ASME PAPER 89-GT-129	p 360	A90-23827	* #
AIAA PAPER 90-3209	p 813	A90-49106	#	AIAA PAPER 90-3475	p 891	A90-47725	* #	ASME PAPER 89-GT-131	p 287	A90-23757	#
AIAA PAPER 90-3210	p 811	A90-48836	* #	AIAA PAPER 90-3476	p 865	A90-47726	#	ASME PAPER 89-GT-130	p 360	A90-23828	* #
AIAA PAPER 90-3211	p 812	A90-48837	* #	AIAA PAPER 90-3477	p 866	A90-47727	* #	ASME PAPER 89-GT-131	p 291	A90-23829	#
AIAA PAPER 90-3212	p 812	A90-48838	* #	AIAA PAPER 90-3478	p 866	A90-47728	* #	ASME PAPER 89-GT-137	p 360	A90-23834	#
AIAA PAPER 90-3215	p 818	A90-49107	#	AIAA PAPER 90-3479	p 867	A90-47764	* #	ASME PAPER 89-GT-140	p 291	A90-23837	#
AIAA PAPER 90-3217	p 838	A90-49108	#	AIAA PAPER 90-3480	p 866	A90-47729	#	ASME PAPER 89-GT-146	p 354	A90-23839	#
AIAA PAPER 90-3219	p 786	A90-48840	#	AIAA PAPER 90-3481	p 891	A90-47730	#	ASME PAPER 89-GT-148	p 340	A90-23758	#
AIAA PAPER 90-3220	p 834	A90-48841	#	AIAA PAPER 90-3482	p 866	A90-47731	* #	ASME PAPER 89-GT-151	p 292	A90-23840	#
AIAA PAPER 90-3222	p 839	A90-49109	#	AIAA PAPER 90-3483	p 866	A90-47732	* #	ASME PAPER 89-GT-152	p 292	A90-23841	* #
AIAA PAPER 90-3223	p 897	A90-48842	#	AIAA PAPER 90-3484	p 866	A90-47733	#	ASME PAPER 89-GT-153	p 354	A90-23842	* #
AIAA PAPER 90-3224	p 897	A90-48843	#	AIAA PAPER 90-3485	p 867	A90-47734	#	ASME PAPER 89-GT-155	p 360	A90-23843	#
AIAA PAPER 90-3225	p 868	A90-49110	* #	AIAA PAPER 90-3488	p 867	A90-47736	#	ASME PAPER 89-GT-156	p 292	A90-23844	#
AIAA PAPER 90-3226	p 868	A90-49111	#	AIAA PAPER 90-3489	p 867	A90-47737	#				
AIAA PAPER 90-3227	p 839	A90-49112	#	AIAA PAPER 90-3490	p 833	A90-47738	#				
AIAA PAPER 90-3228	p 868	A90-49113	#	AIAA PAPER 90-3501	p 867	A90-47747	* #				
AIAA PAPER 90-3229	p 839	A90-49114	* #	AIAA PAPER 90-3505	p 891	A90-47751	#				
AIAA PAPER 90-3231	p 834	A90-48844	#	AIAA PAPER 90-3507	p 891	A90-47753	#				
AIAA PAPER 90-3232	p 839	A90-49115	#	AIAA PAPER 90-3509	p 891	A90-47755	* #				
AIAA PAPER 90-3236	p 834	A90-48846	#	AIAA PAPER 90-3512	p 891	A90-47758	#				
AIAA PAPER 90-3237	p 835	A90-48847	#								
AIAA PAPER 90-3238	p 835	A90-48848	#	AIAA-89-0438	p 172	N90-13352	* #				
AIAA PAPER 90-3240	p 839	A90-49118	#	AIAA-89-1060	p 94	N90-12560	* #				
AIAA PAPER 90-3241	p 835	A90-48849	#	AIAA-89-2139	p 516	N90-21038	* #				
AIAA PAPER 90-3244	p 839	A90-49119	#	AIAA-89-2140	p 118	N90-10004	* #				
AIAA PAPER 90-3252	p 872	A90-49120	* #	AIAA-89-2364	p 114	N90-11741	* #				
AIAA PAPER 90-3256	p 835	A90-48852	#	AIAA-89-2910	p 318</						

REPORT NUMBER INDEX

DFVLR-FB-89-25

ASME PAPER 89-GT-157	p 292	A90-23845	#	ASME PAPER 89-GT-84	p 905	A90-51257	#	CAA-PAPER-89004	p 135	N90-12807	#
ASME PAPER 89-GT-158	p 292	A90-23846	#	ASME PAPER 89-GT-85	p 905	A90-51258	#	CAA-PAPER-89019	p 913	N90-29336	#
ASME PAPER 89-GT-159	p 292	A90-23847	#	ASME PAPER 89-GT-86	p 358	A90-23805	#				
ASME PAPER 89-GT-15	p 287	A90-23759	#	ASME PAPER 89-GT-87	p 359	A90-23806	#	CAA-2/88	p 96	N90-11718	#
ASME PAPER 89-GT-160	p 360	A90-23848	#	ASME PAPER 89-GT-89	p 359	A90-23807	#				
ASME PAPER 89-GT-161	p 361	A90-23849	#	ASME PAPER 89-GT-94	p 341	A90-23810	#	CCMS-90-05	p 959	N90-28862	#
ASME PAPER 89-GT-163	p 292	A90-23851	#	ASME PAPER 89-GT-96	p 341	A90-23811	#				
ASME PAPER 89-GT-164	p 341	A90-23852	#	ASME PAPER 89-GT-98	p 359	A90-23812	#	CEAT-NT-10/S/83-4	p 324	N90-16728	#
ASME PAPER 89-GT-168	p 341	A90-23853	#	ASME PAPER 89-GT-99	p 359	A90-23813	#	CEAT-NT-10/S/83-5	p 323	N90-16727	#
ASME PAPER 89-GT-169	p 341	A90-23854	#	ASME PAPER 89-TRIB-11	p 537	A90-33556	#	CEAT-NT-10/S/83	p 402	N90-18376	#
ASME PAPER 89-GT-170	p 361	A90-23855	#	ASME PAPER 89-TRIB-46	p 537	A90-33555	#				
ASME PAPER 89-GT-177	p 361	A90-23858	#	ASME PAPER 89-WA/DSC-12	p 751	A90-44847	#	CEAT-PV-M4/462200	p 876	N90-27905	#
ASME PAPER 89-GT-178	p 361	A90-23859	#					CEAT-PV-M5/521700	p 877	N90-27908	#
ASME PAPER 89-GT-17	p 288	A90-23760	#	AST-89-004	p 192	N90-13386	#	CEAT-PV-M5/5288	p 877	N90-27907	#
ASME PAPER 89-GT-182	p 254	A90-22665	#					CEAT-PV-M5/528900	p 877	N90-27906	#
ASME PAPER 89-GT-183	p 273	A90-22663	#	ASTM STP-1006	p 367	A90-26751	#	CEAT-PV-M6/5924/02	p 876	N90-27895	#
ASME PAPER 89-GT-185	p 361	A90-23863	#	ASTM STP-1048	p 950	A90-51616	#				
ASME PAPER 89-GT-187	p 361	A90-23865	#	ASTM STP-1085	p 949	A90-50551	#	CERT-RSF-OA-43/5018-AYD	p 136	N90-12897	#
ASME PAPER 89-GT-188	p 361	A90-23866	#					CERT-RSF-OA-74/2259-AYD	p 136	N90-12889	#
ASME PAPER 89-GT-189	p 362	A90-23867	#	ATC-165	p 133	N90-11934	#				
ASME PAPER 89-GT-192	p 362	A90-23868	#					CERT-33/5025-29-DERAT	p 817	N90-27663	#
ASME PAPER 89-GT-196	p 362	A90-23870	#	AVSCOM-TM-89-B-004	p 106	N90-12580	#				
ASME PAPER 89-GT-199	p 342	A90-23871	#	AVSCOM-TM-89-B-008	p 36	N90-10889	#	CIT/SME/VKI/RS/1	p 748	N90-25986	#
ASME PAPER 89-GT-19	p 288	A90-23761	#	AVSCOM-TM-89-B-009	p 173	N90-14186	#	CIT/SME/VKI/RS/3	p 748	N90-25987	#
ASME PAPER 89-GT-200	p 362	A90-23872	#	AVSCOM-TM-89-B-010	p 237	N90-15882	#	CIT/SME/VKI/RS/4	p 748	N90-25988	#
ASME PAPER 89-GT-201	p 342	A90-23873	#	AVSCOM-TM-89-C-010	p 257	N90-15923	#	CIT/SME/VKI/RS/5	p 749	N90-25989	#
ASME PAPER 89-GT-202	p 342	A90-23874	#	AVSCOM-TM-89-C-014	p 213	N90-13797	#	CIT/SME/VKI/RS/6	p 749	N90-25990	#
ASME PAPER 89-GT-208	p 254	A90-22664	#	AVSCOM-TM-89-C-015	p 215	N90-14617	#				
ASME PAPER 89-GT-20	p 288	A90-23762	#	AVSCOM-TM-90-B-001	p 454	N90-18746	#	CMU-RI-TR-89-20	p 205	N90-13627	#
ASME PAPER 89-GT-212	p 293	A90-23878	#	AVSCOM-TM-90-B-004	p 499	N90-20974	#				
ASME PAPER 89-GT-220	p 362	A90-23881	#	AVSCOM-TM-90-B-015	p 632	N90-24237	#	CMU/SEI-89-TR-35-REV	p 578	N90-22554	#
ASME PAPER 89-GT-227	p 362	A90-23882	#	AVSCOM-TM-90-C-005	p 776	N90-26334	#	CMU/SEI-89-TR-5	p 761	N90-25145	#
ASME PAPER 89-GT-228	p 293	A90-23883	#	AVSCOM-TM-90-C-006	p 543	N90-21394	#				
ASME PAPER 89-GT-229	p 342	A90-23884	#					CONF-8910203-1	p 186	N90-14227	#
ASME PAPER 89-GT-22	p 288	A90-23763	#	AVSCOM-TR-89-A-002	p 910	N90-28503	#	CONF-900136-5	p 281	N90-15519	#
ASME PAPER 89-GT-234	p 363	A90-23885	#	AVSCOM-TR-89-B-004	p 79	N90-10679	#	CONF-900372-1	p 405	N90-19217	#
ASME PAPER 89-GT-235	p 342	A90-23886	#	AVSCOM-TR-89-C-008	p 858	N90-27722	#	CONF-900479-1	p 464	N90-19820	#
ASME PAPER 89-GT-238	p 342	A90-23888	#	AVSCOM-TR-89-C-013	p 194	N90-13393	#	CONF-900479-4	p 402	N90-19215	#
ASME PAPER 89-GT-241	p 342	A90-23890	#	AVSCOM-TR-89-C-020	p 372	N90-18041	#	CONF-9005155-1	p 609	N90-22048	#
ASME PAPER 89-GT-25	p 340	A90-23764	#	AVSCOM-TR-90-B-002	p 506	N90-21004	#	CONF-900615-1	p 608	N90-22003	#
ASME PAPER 89-GT-260	p 363	A90-23891	#	AVSCOM-TR-90-B-004	p 876	N90-27787	#	CONF-900672-1	p 572	N90-21737	#
ASME PAPER 89-GT-275	p 535	A90-32263	#	AVSCOM-TR-90-B-005	p 633	N90-24239	#	CONF-901074-1	p 967	N90-30134	#
ASME PAPER 89-GT-278	p 475	A90-33564	#	AVSCOM-TR-90-C-018	p 964	N90-29121	#				
ASME PAPER 89-GT-27	p 340	A90-23765	#					CRIE-T-87046	p 774	N90-25361	#
ASME PAPER 89-GT-281	p 507	A90-32261	#	B-222217	p 724	N90-25958	#	CRIE-T-88078	p 777	N90-26365	#
ASME PAPER 89-GT-284	p 475	A90-33563	#	B-222217	p 724	N90-25959	#				
ASME PAPER 89-GT-285	p 508	A90-33559	#					CRREL-SP-89-22	p 133	N90-11907	#
ASME PAPER 89-GT-288	p 253	A90-22652	#	BAR-89-3	p 414	N90-18388	#				
ASME PAPER 89-GT-289	p 474	A90-33562	#					CRREL-SR-89-19	p 133	N90-11908	#
ASME PAPER 89-GT-290	p 474	A90-33562	#	BBN-TM-938	p 88	N90-11704	#				
ASME PAPER 89-GT-294	p 343	A90-23892	#					CRREL-89-10	p 59	N90-10896	#
ASME PAPER 89-GT-296	p 474	A90-33560	#	BBN-6624-VOL-1	p 379	N90-17410	#	CRREL-89-21	p 526	N90-20097	#
ASME PAPER 89-GT-299	p 475	A90-33567	#	BBN-6830	p 378	N90-17409	#				
ASME PAPER 89-GT-303	p 273	A90-22651	#	BBN-6832-VOL-1	p 615	N90-23188	#	CSG-124	p 665	N90-23401	#
ASME PAPER 89-GT-304	p 905	A90-51256	#	BBN-6833-VOL-2	p 615	N90-23189	#				
ASME PAPER 89-GT-305	p 905	A90-51256	#	BBN-6953-VOL-3	p 615	N90-23190	#	CUED/A-TURBO/TR-126	p 344	N90-17634	#
ASME PAPER 89-GT-306	p 906	A90-51259	#	BBN-7212	p 966	N90-30035	#				
ASME PAPER 89-GT-308	p 490	A90-32260	#					DCIEM-89-TR-23	p 274	N90-15310	#
ASME PAPER 89-GT-309	p 507	A90-32259	#	BHT-699-099-251-VOL-2	p 213	N90-13814	#				
ASME PAPER 89-GT-310	p 490	A90-32257	#					DERAT-43/5018.29	p 136	N90-12897	#
ASME PAPER 89-GT-311	p 231	A90-22668	#	BRDEC-2478	p 126	N90-11899	#	DERAT-43/5018.30	p 136	N90-12897	#
ASME PAPER 89-GT-324	p 343	A90-23893	#					DERAT-59/5004.25	p 136	N90-12889	#
ASME PAPER 89-GT-328	p 506	A90-32258	#	BRL-MR-3801	p 428	N90-19233	#				
ASME PAPER 89-GT-330	p 343	A90-23896	#					DE89-009507	p 281	N90-15519	#
ASME PAPER 89-GT-34	p 288	A90-23766	#	BR108113	p 122	N90-11768	#	DE89-016891	p 24	N90-10844	#
ASME PAPER 89-GT-38	p 340	A90-23767	#	BR108362	p 95	N90-12562	#	DE89-016995	p 186	N90-14227	#
ASME PAPER 89-GT-42	p 340	A90-23769	#	BR108480	p 178	N90-13366	#	DE89-017837	p 126	N90-11813	#
ASME PAPER 89-GT-45	p 288	A90-23771	#	BR108489	p 117	N90-12619	#	DE89-782317	p 774	N90-25361	#
ASME PAPER 89-GT-46	p 288	A90-23772	#	BR108878	p 99	N90-12575	#	DE90-001160	p 206	N90-14385	#
ASME PAPER 89-GT-47	p 289	A90-23773	#	BR108924	p 135	N90-12816	#	DE90-001802	p 236	N90-15076	#
ASME PAPER 89-GT-48	p 289	A90-23774	#	BR109026	p 140	N90-13207	#	DE90-002760	p 269	N90-15288	#
ASME PAPER 89-GT-4	p 354	A90-23751	#	BR109770	p 95	N90-12563	#	DE90-002989	p 572	N90-21737	#
ASME PAPER 89-GT-51	p 289	A90-23777	#	BR110168	p 240	N90-15896	#	DE90-004488	p 324	N90-16729	#
ASME PAPER 89-GT-52	p 289	A90-23778	#	BR110400	p 256	N90-15920	#	DE90-004985	p 323	N90-16722	#
ASME PAPER 89-GT-53	p 289	A90-23779	#	BR110401	p 256	N90-15919	#	DE90-005193	p 405	N90-19217	#
ASME PAPER 89-GT-55	p 289	A90-23781	#	BR110402	p 256	N90-15921	#	DE90-005664	p 608	N90-22003	#
ASME PAPER 89-GT-56	p 290	A90-23782	#	BR110742	p 251	N90-15917	#	DE90-006810	p 464	N90-19820	#
ASME PAPER 89-GT-58	p 290	A90-23784	#	BR110949	p 257	N90-15922	#	DE90-007429	p 402	N90-19215	#
ASME PAPER 89-GT-5	p 287	A90-23752	#	BR111060	p 243	N90-15900	#	DE90-009429	p 609	N90-22048	#
ASME PAPER 89-GT-63	p 290	A90-23786	#	BR111413	p 176	N90-14211	#	DE90-010164	p 678	N90-24430	#
ASME PAPER 89-GT-64	p 290	A90-23787	#	BR111666	p 137	N90-13005	#	DE90-010823	p 967	N90-30134	#
ASME PAPER 89-GT-65	p 290	A90-23788	#	BR112013	p 201	N90-13408	#	DE90-011783	p 719	N90-25941	#
ASME PAPER 89-GT-66	p 290	A90-23789	#	BR112064	p 499	N90-20972	#	DE90-013269	p 885	N90-28059	#
ASME PAPER 89-GT-67	p 290	A90-23790	#	BR112416	p 958	N90-28800	#	DE90-014750	p 910	N90-28495	#
ASME PAPER 89-GT-68	p 341	A90-23791	#	BR112837	p 499	N90-20973	#	DE90-503377	p 776	N90-26335	#
ASME PAPER 89-GT-69	p 358	A90-23792	#	BR112839	p 751	N90-26007	#	DE90-503792	p 777	N90-26365	#
ASME PAPER 89-GT-6	p 287	A90-23753	#	BR113195	p 721	N90-25953	#	DE90-505514	p 720	N90-25949	#
ASME PAPER 89-GT-70	p 254	A90-22667	#	BR113246	p 827	N90-27693	#	DE90-629740	p 951	N90-28674	#
ASME PAPER 89-GT-73	p 291	A90-23794	#	BR114893	p 960	N90-29597	#				
ASME PAPER 89-GT-74	p 358	A90-23795	#					DFVLR-FB-87-06	p 910	N90-28498	#
ASME PAPER 89-GT-76	p 291	A90-23797	#	BU-403	p 397	N90-18369	#	DFVLR-FB-88-07	p 120	N90-12621	#
ASME PAPER 89-GT-77	p 291	A90-23798	#					DFVLR-FB-88-17	p 237	N90-15889	#
ASME PAPER 89-GT-78	p 358	A90-23799	#	CAA-PAPER-88010	p 99	N90-11729	#	DFVLR-FB-89-04	p 717	N90-25113	#
ASME PAPER 89-GT-79	p 291	A90-23800	#	CAA-PAPER-88014	p 96	N90-11719	#	DFVLR-FB-89-18	p 89	N90-11711	#
ASME PAPER 89-GT-80	p 358	A90-23801	#	CAA-PAPER-88017	p 99	N90-12572	#	DFVLR-FB-89-20	p 120	N90-11760	#
ASME PAPER 89-GT-81	p 358	A90-23802	#	CAA-PAPER-89003	p 99	N90-12573	#	DFVLR-FB-89-25	p 774	N90-25332	#

DFVLR-FB-89-52

REPORT NUMBER INDEX

DFVLR-FB-89-52	p 963	N90-29692	#	DOT/FAA/CT-TN89/18	p 24	N90-10843	#	DOT/FAA/SA-89/2	p 281	N90-15566	#
DFVLR-MITT-88-11	p 264	N90-15963	#	DOT/FAA/CT-TN89/21	p 28	N90-10856	#	DOT/FAA/SA-89/3	p 177	N90-13363	#
DFVLR-MITT-89-02-REV	p 775	N90-26173	#	DOT/FAA/CT-TN89/26	p 27	N90-10020	#	DOT/FAA/SA-90/4	p 824	N90-26805	#
DFVLR-MITT-89-06	p 134	N90-12007	#	DOT/FAA/CT-TN89/27-VOL-1	p 870	N90-26835	#	DOT/FAA/SE-90/1	p 729	N90-25122	#
DGLR BERICHT 89-01	p 468	A90-33351	#	DOT/FAA/CT-TN89/27-VOL-2	p 870	N90-26836	#	DOUGLAS-PAPER-7878	p 90	N90-12505	#
DGLR PAPER 88-004	p 902	A90-50232	#	DOT/FAA/CT-TN89/28-VOL-1	p 824	N90-26802	#	DREA-TM-89/219	p 95	N90-12568	#
DGLR PAPER 88-018	p 903	A90-50235	#	DOT/FAA/CT-TN89/28-VOL-2	p 405	N90-18380	#	DREA-TM-90/202	p 896	N90-27468	#
DGLR PAPER 88-038	p 934	A90-50249	#	DOT/FAA/CT-TN89/29	p 27	N90-10019	#	DRES-SM-1321	p 936	N90-28579	#
DGLR PAPER 88-040	p 928	A90-50233	#	DOT/FAA/CT-TN89/32	p 214	N90-14404	#	DRIC-BR-110739	p 99	N90-11722	#
DGLR PAPER 88-060	p 919	A90-50246	#	DOT/FAA/CT-TN89/34	p 825	N90-27675	#	DRIC-BR-112012	p 399	N90-19202	#
DGLR-PAPER-85-113	p 201	N90-13408	#	DOT/FAA/CT-TN89/35	p 958	N90-28762	#	DRIC-BR-113553	p 871	N90-26847	#
DGLR-PAPERS-88-05	p 276	N90-16169	#	DOT/FAA/CT-TN89/39	p 27	N90-10018	#	DTRC/PAS-90/15	p 932	N90-28572	#
DGLR-89-127	p 735	N90-25137	#	DOT/FAA/CT-TN89/40	p 640	N90-23377	#	D6-53196-3-VOL-3	p 380	N90-18233	#
DGLR-89-141	p 637	N90-24260	#	DOT/FAA/CT-TN89/42	p 640	N90-23379	#	E-2429	p 468	N90-20942	#
DLC-EST-TN-030	p 632	N90-23359	#	DOT/FAA/CT-TN89/43	p 638	N90-28584	#	E-4137	p 929	N90-28552	#
DLC-EST-TN-031	p 632	N90-23360	#	DOT/FAA/CT-TN89/50	p 99	N90-12574	#	E-4279	p 32	N90-10031	#
DLC/STR-INT-TN-004	p 699	N90-24876	#	DOT/FAA/CT-TN89/52	p 121	N90-11762	#	E-4391	p 259	N90-15112	#
DLR-FB-89-12	p 212	N90-13728	#	DOT/FAA/CT-TN89/53	p 967	N90-29249	#	E-4480	p 73	N90-11245	#
DLR-FB-89-28	p 109	N90-12599	#	DOT/FAA/CT-TN89/54	p 869	N90-27724	#	E-4768	p 541	N90-20392	#
DLR-FB-89-34	p 212	N90-13725	#	DOT/FAA/CT-TN89/56	p 489	N90-20968	#	E-4788	p 215	N90-14511	#
DLR-FB-89-37	p 170	N90-13333	#	DOT/FAA/CT-TN89/59	p 123	N90-12627	#	E-4789	p 516	N90-21037	#
DLR-FB-89-56	p 672	N90-24276	#	DOT/FAA/CT-TN89/60	p 370	N90-17930	#	E-4826	p 194	N90-13392	#
DLR-FB-89-58	p 634	N90-24254	#	DOT/FAA/CT-TN89/62	p 544	N90-21500	#	E-4837	p 172	N90-13352	#
DLR-FB-89-59	p 635	N90-24255	#	DOT/FAA/CT-TN89/63	p 551	N90-21724	#	E-4848	p 192	N90-13387	#
DLR-FB-89-62	p 825	N90-27673	#	DOT/FAA/CT-TN89/64	p 243	N90-15089	#	E-4920	p 690	N90-23769	#
DLR-FB-90-04	p 959	N90-28812	#	DOT/FAA/CT-TN89/65	p 486	N90-20967	#	E-4981	p 440	N90-19242	#
DLR-MITT-89-13	p 213	N90-13816	#	DOT/FAA/CT-TN89/67	p 544	N90-21508	#	E-4991	p 516	N90-21038	#
DLR-MITT-89-18	p 697	N90-24859	#	DOT/FAA/CT-TN89/70	p 526	N90-21042	#	E-5001	p 203	N90-14268	#
DLR-MITT-89-20	p 397	N90-18370	#	DOT/FAA/CT-TN89/71	p 542	N90-21248	#	E-5012	p 685	N90-23403	#
DLR-MITT-89-23	p 825	N90-27676	#	DOT/FAA/CT-TN89/72	p 775	N90-26210	#	E-5036	p 610	N90-22703	#
DLR-MITT-90-02	p 936	N90-29401	#	DOT/FAA/CT-TN90/01	p 729	N90-25122	#	E-5039	p 54	N90-10891	#
DLR-MITT-90-04	p 786	N90-27617	#	DOT/FAA/CT-TN90/18	p 928	N90-28549	#	E-5050	p 610	N90-22808	#
DOD-4120.15-L	p 787	N90-27646	#	DOT/FAA/CT-TN90/19	p 766	N90-25122	#	E-5057	p 215	N90-14641	#
DODA-AR-004-525	p 107	N90-12596	#	DOT/FAA/CT-TN90/20	p 761	N90-25150	#	E-5063	p 194	N90-13393	#
DODA-AR-004-535	p 323	N90-16725	#	DOT/FAA/CT-TN90/26	p 729	N90-25123	#	E-5068	p 18	N90-10004	#
DODA-AR-004-574	p 107	N90-12595	#	DOT/FAA/CT-TN90/2	p 640	N90-23378	#	E-5072	p 318	N90-17561	#
DODA-AR-005-512	p 185	N90-14217	#	DOT/FAA/CT-TN90/4	p 825	N90-27672	#	E-5081	p 379	N90-17413	#
DODA-AR-005-543	p 95	N90-12566	#	DOT/FAA/CT-TN90/7	p 824	N90-26803	#	E-5105	p 215	N90-14656	#
DODA-AR-005-574	p 52	N90-10041	#	DOT/FAA/CT-TN90/8	p 583	N90-21759	#	E-5108	p 94	N90-12560	#
DODA-AR-005-575	p 52	N90-10040	#	DOT/FAA/CT-88/15	p 735	N90-25136	#	E-5116	p 143	N90-13323	#
DODA-AR-005-582	p 114	N90-11745	#	DOT/FAA/CT-88/28	p 122	N90-11765	#	E-5128	p 94	N90-12561	#
DODA-AR-005-591	p 90	N90-12501	#	DOT/FAA/CT-88/29	p 185	N90-14222	#	E-5130	p 187	N90-13381	#
DODA-AR-005-602	p 338	N90-17628	#	DOT/FAA/CT-88/33	p 542	N90-21247	#	E-5137	p 318	N90-17562	#
DODA-AR-005-604	p 32	N90-10026	#	DOT/FAA/CT-89/16	p 176	N90-13360	#	E-5139	p 548	N90-21602	#
DODA-AR-005-626	p 593	N90-22570	#	DOT/FAA/CT-89/17	p 402	N90-18375	#	E-5147	p 114	N90-11740	#
DODA-AR-005-629	p 526	N90-20098	#	DOT/FAA/CT-89/18	p 239	N90-15084	#	E-5152	p 217	N90-14783	#
DODA-AR-005-644	p 641	N90-24264	#	DOT/FAA/CT-89/20	p 192	N90-13386	#	E-5155	p 720	N90-25948	#
DODA-AR-005590	p 107	N90-12597	#	DOT/FAA/CT-89/22	p 820	N90-27668	#	E-5160	p 205	N90-13636	#
DODA-AR-006-054	p 855	N90-26832	#	DOT/FAA/CT-89/23	p 601	N90-22695	#	E-5162	p 117	N90-12618	#
DODA-AR-006-090	p 815	N90-26793	#	DOT/FAA/CT-89/29	p 723	N90-25119	#	E-5185	p 193	N90-13389	#
DOE/NASA/0335-1	p 220	N90-14153	#	DOT/FAA/CT-89/30	p 511	N90-21008	#	E-5186	p 858	N90-27722	#
DOE/NASA/0336-1	p 51	N90-10036	#	DOT/FAA/CT-89/32	p 636	N90-23369	#	E-5191	p 380	N90-18229	#
DOE/PC-88827/T3	p 206	N90-14385	#	DOT/FAA/CT-89/33	p 444	N90-19387	#	E-5196	p 172	N90-13355	#
DOE/PC-88827/T4	p 269	N90-15288	#	DOT/FAA/CT-89/34	p 783	N90-25697	#	E-5204	p 372	N90-18041	#
DOT-TSC-FAA-89-1	p 913	N90-28507	#	DOT/FAA/CT-89/35	p 724	N90-25961	#	E-5210	p 548	N90-20794	#
DOT-TSC-FAA-90-1	p 824	N90-26805	#	DOT/FAA/CT-90/1-VOL-1	p 455	N90-19472	#	E-5212	p 257	N90-15923	#
DOT-TSC-FA953-LR4	p 696	N90-24856	#	DOT/FAA/CT-90/17	p 967	N90-29247	#	E-5218	p 543	N90-21361	#
DOT-TSC-FA953-LR5	p 697	N90-24857	#	DOT/FAA/CT-90/18	p 898	N90-28463	#	E-5219	p 542	N90-21300	#
DOT/FAA-CT-89/36-1	p 505	N90-20081	#	DOT/FAA/CT-90/2	p 915	N90-28509	#	E-5228	p 399	N90-19203	#
DOT/FAA-CT-89/36-2	p 505	N90-20080	#	DOT/FAA/DS-88/8	p 635	N90-23368	#	E-5231	p 213	N90-13797	#
DOT/FAA-CT-89/36-3	p 505	N90-20082	#	DOT/FAA/DS-89/08	p 28	N90-10855	#	E-5232	p 213	N90-13750	#
DOT/FAA-CT-89/36-4	p 506	N90-20083	#	DOT/FAA/DS-89/13	p 59	N90-10896	#	E-5236	p 194	N90-14235	#
DOT/FAA-CT-89/36-5	p 506	N90-20084	#	DOT/FAA/DS-89/14	p 401	N90-18371	#	E-5237	p 345	N90-17636	#
DOT/FAA/AM-89/14	p 636	N90-23371	#	DOT/FAA/DS-89/15	p 401	N90-18372	#	E-5238	p 570	N90-21727	#
DOT/FAA/AP-87/01-VOL-7	p 332	N90-16730	#	DOT/FAA/DS-89/16	p 637	N90-24257	#	E-5240	p 215	N90-14617	#
DOT/FAA/AS-90/1	p 939	N90-29408	#	DOT/FAA/DS-89/18	p 527	N90-21045	#	E-5247	p 194	N90-13394	#
DOT/FAA/CP-89-4	p 913	N90-28507	#	DOT/FAA/DS-89/19	p 544	N90-21509	#	E-5260	p 515	N90-21036	#
DOT/FAA/CT-TN87/54-VOL-2	p 121	N90-11761	#	DOT/FAA/DS-89/23	p 187	N90-14232	#	E-5267	p 344	N90-17635	#
DOT/FAA/CT-TN87/54-VOL-3	p 544	N90-20500	#	DOT/FAA/DS-89/24	p 24	N90-10014	#	E-5272	p 509	N90-20085	#
DOT/FAA/CT-TN88/13	p 177	N90-13364	#	DOT/FAA/DS-89/25	p 27	N90-10017	#	E-5273	p 533	N90-21137	#
DOT/FAA/CT-TN88/14	p 497	N90-20072	#	DOT/FAA/DS-89/26	p 243	N90-15090	#	E-5279	p 778	N90-26373	#
DOT/FAA/CT-TN88/30	p 59	N90-10897	#	DOT/FAA/DS-89/29	p 177	N90-13361	#	E-5302	p 588	N90-21760	#
DOT/FAA/CT-TN88/4-1	p 135	N90-12782	#	DOT/FAA/DS-89/30	p 177	N90-13362	#	E-5322	p 510	N90-20090	#
DOT/FAA/CT-TN88/4-2	p 135	N90-12781	#	DOT/FAA/DS-89/31	p 178	N90-14214	#	E-5345	p 600	N90-21869	#
DOT/FAA/CT-TN88/4-2	p 135	N90-12781	#	DOT/FAA/DS-89/32	p 243	N90-21049	#	E-5351	p 543	N90-21399	#
DOT/FAA/CT-TN88/4-2	p 135	N90-12781	#	DOT/FAA/DS-89/33	p 527	N90-21048	#	E-5402	p 542	N90-21283	#
DOT/FAA/CT-TN88/4-2	p 135	N90-12781	#	DOT/FAA/DS-89/35	p 259	N90-15108	#	E-5405	p 776	N90-26334	#
DOT/FAA/CT-TN88/4-2	p 135	N90-12781	#	DOT/FAA/DS-89/37	p 503	N90-21003	#	E-5421	p 478	N90-20051	#
DOT/FAA/CT-TN88/4-2	p 135	N90-12781	#	DOT/FAA/DS-89/9	p 141	N90-12406	#	E-5428	p 719	N90-25940	#
DOT/FAA/CT-TN88/4-2	p 135	N90-12781	#	DOT/FAA/DS-90/2	p 542	N90-21249	#	E-5430	p 748	N90-25982	#
DOT/FAA/CT-TN88/4-2	p 135	N90-12781	#	DOT/FAA/EE-86/10-REV	p 352	N90-16773	#	E-5431	p 588	N90-21762	#
DOT/FAA/CT-TN88/4-2	p 135	N90-12781	#	DOT/FAA/EE-90-03	p 966	N90-30035	#	E-5446	p 782	N90-26635	#
DOT/FAA/CT-TN88/4-2	p 135	N90-12781	#	DOT/FAA/OV-89/2	p 239	N90-15085	#	E-5448	p 552	N90-21725	#
DOT/FAA/CT-TN88/4-2	p 135	N90-12781	#	DOT/FAA/PM-87/9-VOL-2	p 674	N90-24277	#	E-5451	p 666	N90-23404	#
DOT/FAA/CT-TN88/4-2	p 135	N90-12781	#	DOT/FAA/PS-89-3	p 133	N90-11934	#	E-5462	p 571	N90-21733	#
DOT/FAA/CT-TN88/4-2	p 135	N90-12781	#	DOT/FAA/RD-90/15	p 937	N90-28581	#	E-5469	p 543	N90-21394	#
DOT/FAA/CT-TN88/4-2	p 135	N90-12781	#	DOT/FAA/RD-90/1	p 902	N90-29299	#	E-5475	p 588	N90-21763	#
DOT/FAA/CT-TN88/4-2	p 135	N90-12781	#	DOT/FAA/RD-90/22	p 937	N90-28582	#	E-5499	p 666	N90-24273	#
DOT/FAA/CT-TN88/4-2	p 135	N90-12781	#	DOT/FAA/RD-90/24	p 872	N90-27728	#				

REPORT NUMBER INDEX

ETN-90-97481

E-5533	p 816	N90-27655 *	#	ETN-89-95248	p 135	N90-12807	ETN-90-96275	p 397	N90-18370	#
E-5539	p 589	N90-22566 *	#	ETN-89-95249	p 96	N90-11717	ETN-90-96280	p 465	N90-19189	#
E-5554	p 688	N90-23591 *	#	ETN-89-95276	p 96	N90-11716	ETN-90-96286	p 397	N90-18369	#
E-5589	p 773	N90-25289 *	#	ETN-89-95279	p 120	N90-12622	ETN-90-96287	p 464	N90-18999	#
E-5594	p 758	N90-26011 *	#	ETN-89-95279	p 136	N90-12897	ETN-90-96331	p 454	N90-18697	#
E-5623	p 751	N90-26009 *	#	ETN-89-95286	p 107	N90-12592	ETN-90-96342	p 572	N90-21740	#
E-5634	p 763	N90-26055 *	#	ETN-89-95297	p 134	N90-12007	ETN-90-96343	p 572	N90-21741	#
E-5676	p 720	N90-25946 *	#	ETN-89-95313	p 89	N90-11711	ETN-90-96344	p 578	N90-21751	#
E-5677	p 817	N90-27657 *	#	ETN-89-95315	p 120	N90-11760	ETN-90-96345	p 578	N90-21752	#
E-5761	p 964	N90-29121 *	#	ETN-89-95389	p 120	N90-12621	ETN-90-96350	p 689	N90-23760	#
				ETN-89-95533	p 96	N90-11718	ETN-90-96353	p 572	N90-21742	#
E/BLO/163	p 115	N90-12605	#	ETN-89-95534	p 99	N90-11729	ETN-90-96399	p 609	N90-22014	#
				ETN-89-95535	p 96	N90-11719	ETN-90-96445	p 575	N90-22544	#
ECL-88-09	p 220	N90-14074	#	ETN-89-95542	p 114	N90-11746	ETN-90-96463	p 650	N90-24267	#
				ETN-89-95543	p 114	N90-11747	ETN-90-96474	p 636	N90-23375	#
EDR-12909	p 666	N90-24274 *	#	ETN-89-95544	p 114	N90-11748	ETN-90-96475	p 666	N90-24272	#
EDR-14232	p 51	N90-10036 *	#	ETN-89-95545	p 126	N90-11874	ETN-90-96480	p 618	N90-24225	#
				ETN-89-95547	p 114	N90-11749	ETN-90-96498	p 634	N90-24253	#
EOARD-LR-89-069	p 527	N90-21046	#	ETN-89-95549	p 107	N90-12593	ETN-90-96560	p 632	N90-23359	#
EOARD-LR-90-001	p 503	N90-21001	#	ETN-89-95551	p 115	N90-12603	ETN-90-96561	p 632	N90-23360	#
				ETN-89-95553	p 115	N90-12604	ETN-90-96565	p 699	N90-24876	#
ERIM-213400-54-F	p 938	N90-29406	#	ETN-89-95554	p 127	N90-12720	ETN-90-96599	p 632	N90-23363	#
				ETN-89-95555	p 140	N90-13202	ETN-90-96601	p 632	N90-23364	#
ERP-1031	p 692	N90-23832	#	ETN-89-95556	p 115	N90-12605	ETN-90-96774	p 699	N90-24224	#
				ETN-89-95557	p 140	N90-13203	ETN-90-96779	p 735	N90-25137	#
ESA-SP-1113	p 368	N90-16958	#	ETN-89-95559	p 127	N90-12667	ETN-90-96781	p 637	N90-24260	#
				ETN-89-95560	p 115	N90-12606	ETN-90-96784	p 763	N90-25189	#
ESA-TT-1041	p 120	N90-12621	#	ETN-89-95562	p 115	N90-12608	ETN-90-96786	p 650	N90-24268	#
ESA-TT-1079	p 910	N90-28498	#	ETN-89-95563	p 136	N90-12933	ETN-90-96960	p 729	N90-25965	#
ESA-TT-1129	p 237	N90-15889	#	ETN-89-95565	p 116	N90-12609	ETN-90-96961	p 736	N90-25974	#
ESA-TT-1145	p 264	N90-15963	#	ETN-89-95566	p 116	N90-12610	ETN-90-96962	p 736	N90-25975	#
ESA-TT-1151	p 717	N90-25113	#	ETN-89-95567	p 116	N90-12611	ETN-90-96966	p 737	N90-25976	#
ESA-TT-1154-REV	p 775	N90-26173	#	ETN-89-95568	p 116	N90-12612	ETN-90-96973	p 637	N90-24261	#
ESA-TT-1169	p 454	N90-18697	#	ETN-89-95569	p 116	N90-12613	ETN-90-97001	p 748	N90-25985	#
ESA-TT-1173	p 773	N90-25267	#	ETN-89-95570	p 116	N90-12614	ETN-90-97002	p 749	N90-25995	#
ESA-TT-1181	p 774	N90-25332	#	ETN-89-95573	p 116	N90-12616	ETN-90-97006	p 672	N90-24276	#
ESA-TT-1195	p 397	N90-18370	#	ETN-89-95575	p 89	N90-11712	ETN-90-97008	p 634	N90-24254	#
ESA-TT-1207	p 963	N90-29692	#	ETN-89-95576	p 90	N90-11713	ETN-90-97009	p 635	N90-24255	#
				ETN-89-95606	p 135	N90-12778	ETN-90-97011	p 825	N90-27673	#
ESD-TR-89-46-REV	p 578	N90-22554	#	ETN-89-95607	p 137	N90-12958	ETN-90-97021	p 758	N90-26015	#
ESD-TR-89-5	p 761	N90-25145	#	ETN-89-95714	p 136	N90-12889	ETN-90-97024	p 719	N90-25942	#
				ETN-89-95837	p 109	N90-12599	ETN-90-97063	p 958	N90-28800	#
ESDU-AERO-C.04.01.00	p 198	N90-14239	#	ETN-90-94833	p 178	N90-13366	ETN-90-97066	p 721	N90-25953	#
ESDU-AERO-C.04.01.05	p 198	N90-14239	#	ETN-90-95008	p 276	N90-16169	ETN-90-97068	p 751	N90-26007	#
ESDU-AERO-C.04.01.09	p 199	N90-14240	#	ETN-90-95051	p 170	N90-13333	ETN-90-97075	p 717	N90-25113	#
				ETN-90-95269	p 172	N90-13356	ETN-90-97078	p 773	N90-25267	#
ESDU-74002	p 316	N90-16721	#	ETN-90-95324	p 428	N90-19235	ETN-90-97081	p 774	N90-25332	#
ESDU-83039	p 173	N90-14192	#	ETN-90-95367	p 399	N90-19207	ETN-90-97095	p 827	N90-27691	#
ESDU-85025	p 173	N90-14192	#	ETN-90-95368	p 399	N90-19208	ETN-90-97097	p 876	N90-27883	#
ESDU-86009	p 173	N90-14192	#	ETN-90-95372	p 455	N90-19542	ETN-90-97122	p 758	N90-26014	#
ESDU-86029	p 89	N90-11709	#	ETN-90-95413	p 455	N90-19543	ETN-90-97135	p 767	N90-26087	#
ESDU-87004	p 397	N90-19195	#	ETN-90-95419	p 416	N90-19228	ETN-90-97139	p 777	N90-26348	#
ESDU-88026	p 89	N90-11709	#	ETN-90-95523	p 206	N90-13677	ETN-90-97140	p 777	N90-26349	#
ESDU-89008	p 89	N90-11709	#	ETN-90-95715	p 184	N90-13378	ETN-90-97143	p 737	N90-25977	#
ESDU-89009	p 198	N90-14239	#	ETN-90-95765	p 220	N90-14074	ETN-90-97145	p 750	N90-25999	#
ESDU-89010	p 199	N90-14240	#	ETN-90-95843	p 212	N90-13725	ETN-90-97146	p 783	N90-26637	#
ESDU-89014	p 173	N90-14192	#	ETN-90-95847	p 213	N90-13816	ETN-90-97147	p 750	N90-26000	#
ESDU-89015	p 185	N90-14221	#	ETN-90-95861	p 178	N90-13367	ETN-90-97148	p 750	N90-26001	#
ESDU-89029	p 236	N90-15081	#	ETN-90-95863	p 178	N90-13368	ETN-90-97150	p 883	N90-27002	#
ESDU-89034	p 236	N90-15082	#	ETN-90-95894	p 416	N90-19229	ETN-90-97152	p 750	N90-26002	#
ESDU-89041	p 316	N90-16721	#	ETN-90-95932	p 198	N90-13400	ETN-90-97155	p 750	N90-26003	#
ESDU-89042	p 337	N90-16757	#	ETN-90-95935	p 202	N90-13409	ETN-90-97156	p 750	N90-26004	#
ESDU-89046	p 370	N90-17193	#	ETN-90-95980	p 172	N90-13357	ETN-90-97157	p 750	N90-26005	#
ESDU-89047	p 316	N90-16720	#	ETN-90-95981	p 194	N90-13395	ETN-90-97158	p 748	N90-25139	#
				ETN-90-95984	p 214	N90-13822	ETN-90-97162	p 717	N90-25114	#
ETN-89-94047	p 462	N90-19756	#	ETN-90-95990	p 184	N90-13379	ETN-90-97164	p 717	N90-25115	#
ETN-89-94334	p 122	N90-11768	#	ETN-90-95993	p 202	N90-13410	ETN-90-97165	p 762	N90-25153	#
ETN-89-94470	p 123	N90-12629	#	ETN-90-95994	p 205	N90-13617	ETN-90-97177	p 718	N90-25116	#
ETN-89-94614	p 141	N90-12494	#	ETN-90-96009	p 177	N90-13365	ETN-90-97181	p 777	N90-26369	#
ETN-89-94619	p 138	N90-12208	#	ETN-90-96011	p 212	N90-13727	ETN-90-97183	p 776	N90-26285	#
ETN-89-94829	p 95	N90-12562	#	ETN-90-96049	p 212	N90-13728	ETN-90-97186	p 720	N90-25950	#
ETN-89-94834	p 135	N90-12816	#	ETN-90-96078	p 323	N90-16726	ETN-90-97187	p 776	N90-26290	#
ETN-89-94842	p 99	N90-12575	#	ETN-90-96079	p 323	N90-16727	ETN-90-97189	p 720	N90-25951	#
ETN-89-94869	p 137	N90-13005	#	ETN-90-96080	p 324	N90-16728	ETN-90-97192	p 775	N90-26238	#
ETN-89-94994	p 135	N90-12823	#	ETN-90-96086	p 370	N90-17113	ETN-90-97268	p 874	N90-26894	#
ETN-89-94999	p 117	N90-12619	#	ETN-90-96090	p 344	N90-16766	ETN-90-97270	p 737	N90-25978	#
ETN-89-95001	p 95	N90-12563	#	ETN-90-96116	p 240	N90-15896	ETN-90-97271	p 845	N90-26830	#
ETN-89-95002	p 140	N90-13207	#	ETN-90-96119	p 243	N90-15900	ETN-90-97274	p 825	N90-27674	#
ETN-89-95019	p 141	N90-13278	#	ETN-90-96126	p 256	N90-15919	ETN-90-97275	p 884	N90-27120	#
ETN-89-95024	p 89	N90-11710	#	ETN-90-96127	p 256	N90-15920	ETN-90-97276	p 868	N90-26834	#
ETN-89-95028	p 95	N90-12564	#	ETN-90-96128	p 256	N90-15921	ETN-90-97277	p 759	N90-26016	#
ETN-89-95053	p 183	N90-13371	#	ETN-90-96129	p 257	N90-15922	ETN-90-97292	p 884	N90-27987	#
ETN-89-95057	p 115	N90-11750	#	ETN-90-96130	p 251	N90-15917	ETN-90-97300	p 896	N90-28398	#
ETN-89-95207	p 137	N90-12954	#	ETN-90-96148	p 240	N90-15897	ETN-90-97357	p 775	N90-26173	#
ETN-89-95208	p 107	N90-12591	#	ETN-90-96183	p 357	N90-17871	ETN-90-97408	p 963	N90-28887	#
ETN-89-95209	p 127	N90-12665	#	ETN-90-96187	p 357	N90-17873	ETN-90-97413	p 919	N90-29380	#
ETN-89-95210	p 103	N90-11735	#	ETN-90-96189	p 237	N90-15889	ETN-90-97414	p 939	N90-29409	#
ETN-89-95211	p 120	N90-11759	#	ETN-90-96190	p 264	N90-15963	ETN-90-97435	p 858	N90-27723	#
ETN-89-95213	p 122	N90-11766	#	ETN-90-96197	p 368	N90-16958	ETN-90-97441	p 876	N90-27905	#
ETN-89-95216	p 126	N90-11872	#	ETN-90-96231	p 443	N90-18527	ETN-90-97442	p 876	N90-27895	#
ETN-89-95217	p 109	N90-12598	#	ETN-90-96237	p 415	N90-18391	ETN-90-97443	p 877	N90-27906	#
ETN-89-95218	p 134	N90-12035	#	ETN-90-96244	p 415	N90-18392	ETN-90-97444	p 877	N90-27907	#
ETN-89-95219	p 126	N90-11819	#	ETN-90-96247	p 396	N90-18365	ETN-90-97445	p 877	N90-27908	#
ETN-89-95220	p 126	N90-11820	#	ETN-90-96253	p 454	N90-18695	ETN-90-97448	p 817	N90-27661	#
ETN-89-95246	p 99	N90-12572	#	ETN-90-96257	p 396	N90-18367	ETN-90-97450	p 876	N90-27900	#
ETN-89-95247	p 99	N90-12573	#	ETN-90-96258	p 402	N90-18376	ETN-90-97481	p 817	N90-27663	#

ETN-90-97484	p 953	N90-28722	#	H-1573	p 175	N90-14202	* #	ISBN-0-85679-720-0	p 370	N90-17193	#
ETN-90-97486	p 958	N90-28810	#	H-1574	p 416	N90-19225	* #	ISBN-0-85679-721-9	p 316	N90-16720	#
ETN-90-97495	p 896	N90-28402	#	H-1580	p 186	N90-14228	* #	ISBN-0-86039-406-9	p 913	N90-29336	#
ETN-90-97496	p 872	N90-27729	#	H-1582	p 689	N90-23768	* #	ISBN-0-904947-14-9	p 202	N90-13409	#
ETN-90-97502	p 910	N90-28500	#	H-1583	p 339	N90-16758	* #	ISBN-0-904947-21-1	p 938	N90-29403	#
ETN-90-97510	p 923	N90-28538	#	H-1586	p 415	N90-19224	* #	ISBN-0-904947-25-4	p 913	N90-29334	#
ETN-90-97511	p 923	N90-28539	#	H-1590	p 736	N90-25973	* #	ISBN-0-947767-86-X	p 90	N90-11713	#
ETN-90-97527	p 827	N90-27693	#	H-1594	p 781	N90-26564	* #	ISBN-0-947767-90-8	p 89	N90-11712	#
ETN-90-97535	p 825	N90-27676	#	H-1597	p 757	N90-25142	* #	ISBN-1-871315-03-4	p 198	N90-13400	#
ETN-90-97537	p 936	N90-29401	#	H-1602	p 959	N90-28815	* #	ISBN-3-922010-42-3	p 276	N90-16169	#
ETN-90-97539	p 786	N90-27617	#	H-1603	p 929	N90-28551	* #	ISBN-3-922010-49-0	p 763	N90-25189	#
ETN-90-97543	p 959	N90-28812	#	H-1620	p 964	N90-29142	* #	ISBN-92-835-0499-2	p 933	N90-29393	#
ETN-90-97552	p 910	N90-28498	#	H-1621	p 965	N90-29143	* #	ISBN-92-835-0501-8	p 428	N90-19232	#
ETN-90-97598	p 963	N90-29692	#	H-1625	p 648	N90-23392	* #	ISBN-92-835-0502-6	p 71	N90-10356	#
ETN-90-97613	p 913	N90-29335	#	H-1632	p 924	N90-28542	* #	ISBN-92-835-0503-4	p 63	N90-10191	#
ETN-90-97614	p 913	N90-29336	#	H-1635	p 758	N90-25144	* #	ISBN-92-835-0507-7	p 64	N90-10231	#
ETN-90-97635	p 914	N90-29337	#	H-1651	p 910	N90-28505	* #	ISBN-92-835-0509-3	p 33	N90-10860	#
ETN-90-97638	p 925	N90-29390	#					ISBN-92-835-0514-X	p 28	N90-10847	#
ETN-90-97639	p 961	N90-29680	#	HEL-TM-17-89	p 520	N90-20095	#	ISBN-92-835-0518-2	p 425	N90-18396	#
ETN-90-97640	p 961	N90-29681	#					ISBN-92-835-0519-0	p 267	N90-15185	#
ETN-90-97641	p 961	N90-29682	#	HEL-TN-8-89	p 184	N90-13375	#	ISBN-92-835-0522-0	p 176	N90-13358	#
ETN-90-97642	p 961	N90-29683	#					ISBN-92-835-0523-9	p 260	N90-15924	#
ETN-90-97643	p 961	N90-29684	#	HSD-TP-89-011-VOL-1	p 615	N90-23188	#	ISBN-92-835-0527-1	p 222	N90-15041	#
ETN-90-97645	p 939	N90-29433	#	HSD-TP-89-011-VOL-2	p 615	N90-23189	#	ISBN-92-835-0528-X	p 243	N90-15899	#
				HSD-TP-89-011-VOL-3	p 615	N90-23190	#	ISBN-92-835-0529-8	p 324	N90-17581	#
EU404	p 99	N90-12572						ISBN-92-835-0531-X	p 185	N90-14218	#
EU619	p 99	N90-11729		HSD-TR-89-002	p 378	N90-17409	#	ISBN-92-835-0533-6	p 951	N90-28698	#
EU656	p 99	N90-12573		HSD-TR-89-010-VOL-1	p 379	N90-17410	#	ISBN-92-835-0534-4	p 250	N90-15904	#
				HSD-TR-89-010-VOL-2	p 379	N90-17411	#	ISBN-92-835-0535-2	p 332	N90-16731	#
FAA-APO-90-3	p 641	N90-24263	#	HSD-TR-89-010-VOL-3	p 379	N90-17412	#	ISBN-92-835-0536-0	p 464	N90-19060	#
				HSD-TR-90-005	p 966	N90-30036	#	ISBN-92-835-0538-7	p 434	N90-18432	#
FAA-APO-90-1	p 552	N90-22530	#					ISBN-92-835-0539-5	p 483	N90-20054	#
FEF/PD/1102/89-VOL-3	p 73	N90-10451	* #	HSER-11518-VOL-1	p 52	N90-10043	* #	ISBN-92-835-0542-5	p 500	N90-20976	#
				HSER-11518-VOL-2	p 52	N90-10044	* #	ISBN-92-835-0543-3	p 425	N90-18405	#
FEL-1988-66	p 123	N90-12629	#	HSER-116227	p 117	N90-12617	* #	ISBN-92-835-0544-1	p 511	N90-21009	#
FEL-1989-44	p 135	N90-12823	#	HSER-11804	p 53	N90-10046	* #	ISBN-92-835-0545-X	p 855	N90-27704	#
FEL-89-A257-PT-1	p 919	N90-29380	#	HSER-11894	p 52	N90-10045	* #	ISBN-92-835-0546-8	p 885	N90-28068	#
FEL-89-A280-PT-2	p 939	N90-29409	#					ISBN-92-835-0555-7	p 920	N90-28513	#
FEL-89-B170	p 963	N90-28887	#	IAF PAPER 89-307	p 123	A90-13442	#	ISBN-92-835-0557-3	p 720	N90-25947	#
				IAF PAPER 89-311	p 109	A90-13445	#	ISBN-92-835-0558-1	p 870	N90-26838	#
FFA-TN-1989-08	p 632	N90-23363	#	IAF PAPER 89-313	p 109	A90-13447	#	ISBN-92-835-0559-X	p 758	N90-26012	#
FFA-TN-1989-30	p 632	N90-23364	#	IAF PAPER 89-468	p 81	A90-13557	* #	ISBN-92-835-0560-3	p 776	N90-26280	#
FFA-TN-1990-12-PT-1	p 923	N90-28538	#	IAF PAPER 89-726	p 141	A90-13700	#	ISBN-92-835-0565-4	p 856	N90-27711	#
FFA-TN-1990-13-PT-2	p 923	N90-28539	#					ISBN-92-835-0566-2	p 916	N90-29338	#
FOA-C-20759-2.1	p 206	N90-13677	#	IAR-89-16	p 734	N90-25133	#	ISBN-92-9092-008-4	p 368	N90-16958	#
FOA-C-20774-2.5	p 827	N90-27691	#	IAR-89-18	p 736	N90-25969	#	ISBN-951-22-0040-6	p 481	N90-20963	#
FOA-C-20777-2.5	p 876	N90-27883	#	IAR-89-19	p 724	N90-25956	#	ISBN-951-754-766-8	p 138	N90-13116	#
				IAR-89-23	p 773	N90-25254	#	ISBN-951-754-855-9	p 136	N90-12879	#
				IAR-89-26	p 774	N90-25348	#	ISBN-951-754-951-2	p 522	N90-21041	#
FR-716199-14	p 415	N90-18390	* #	IAR-90-1	p 783	N90-25697	#				
FR-722792-1	p 884	N90-27946	* #	IAR-90-2	p 775	N90-26268	#	ISL-CO-216/88	p 415	N90-18392	#
				IAR-90-4	p 777	N90-26345	#	ISL-CO-219/88	p 370	N90-17113	#
FTD-ID(RS)T-0221-89	p 275	N90-15422	#					ISL-CO-231/88	p 344	N90-16766	#
FTD-ID(RS)T-0266-90	p 721	N90-25955	#	ICASE-89-51	p 171	N90-13351	* #	ISL-CO-243/88	p 396	N90-18365	#
FTD-ID(RS)T-0392-89	p 103	N90-11734	#	ICASE-89-66	p 20	N90-10833	* #	ISL-CO-255/88	p 758	N90-26015	#
FTD-ID(RS)T-1187-89	p 868	N90-26833	#	ICASE-90-29	p 478	N90-20050	* #				
FTD-ID(RS)T-1296-89	p 845	N90-26829	#	ICASE-90-44	p 781	N90-26595	* #	ISL-PU-310/89	p 719	N90-25942	#
F6150-DT410-1-88329	p 120	N90-12622	#	ICOMP-89-29	p 720	N90-25948	* #	ISL-R-109/88	p 95	N90-12564	#
				ICOMP-89-32	p 515	N90-21036	* #	ISL-R-115/88	p 415	N90-18391	#
GAO/NSIAD-89-127	p 25	N90-10845	#	IDA-R-319	p 82	N90-12496	#				
GAO/RCED-88-160	p 635	N90-23367	#	IDA/HQ-87-32596	p 82	N90-12496	#	ISSN-0067-0367	p 951	N90-28674	#
GAO/RCED-89-112	p 724	N90-25959	#					ISSN-0070-3966	p 465	N90-19189	#
GAO/RCED-89-113FS	p 724	N90-25958	#	IHW-ET/50	p 455	N90-19542	#	ISSN-0082-5255	p 718	N90-25935	#
GARRETT-31-8071(1)	p 220	N90-14153	* #	ILR-MITT-225(1989)	p 618	N90-24225	#	ISSN-0082-5263	p 761	N90-25148	#
GIT/AER-90-1	p 911	N90-29304	#					ISSN-0141-397X	p 89	N90-11709	#
GL-TR-89-0129	p 692	N90-23832	#	IMFL-88/35	p 172	N90-13356	#	ISSN-0141-397X	p 173	N90-14192	#
GPO-24-234	p 177	N90-14213	#					ISSN-0141-397X	p 198	N90-14239	#
				INFORME-I-298/88	p 357	N90-17871	#	ISSN-0141-397X	p 199	N90-14240	#
				INFORME-I-377/89	p 357	N90-17873	#	ISSN-0141-397X	p 236	N90-15081	#
								ISSN-0141-397X	p 236	N90-15082	#
H-1383	p 214	N90-13820	* #	INR90259	p 140	N90-13202	#	ISSN-0141-4054	p 185	N90-14221	#
H-1505	p 735	N90-25134	* #					ISSN-0141-4356	p 397	N90-19195	#
H-1508	p 186	N90-14225	* #	INT-PATENT-CLASS-B64C-9/02	p 648	N90-23390	* #	ISSN-0171-1342	p 89	N90-11711	#
H-1515	p 183	N90-13372	* #	INT-PATENT-CLASS-B64C-9/08	p 648	N90-23390	* #	ISSN-0171-1342	p 120	N90-11760	#
H-1516	p 249	N90-15100	* #					ISSN-0171-1342	p 109	N90-12599	#
H-1519	p 369	N90-17074	* #	INT-PATENT-CLASS-C07S-9/40	p 678	N90-23475	* #	ISSN-0171-1342	p 170	N90-13333	#
H-1522	p 435	N90-19241	* #					ISSN-0171-1342	p 212	N90-13725	#
H-1528	p 103	N90-11732	* #	INT-PATENT-CLASS-G01M-9/00	p 689	N90-23707	* #	ISSN-0171-1342	p 212	N90-13728	#
H-1534	p 134	N90-12042	* #					ISSN-0171-1342	p 634	N90-24254	#
H-1538	p 850	N90-27703	* #	ISBN-0-309-04813-3	p 820	N90-27667	#	ISSN-0171-1342	p 635	N90-24255	#
H-1541	p 77	N90-11487	* #	ISBN-0-309-04817-6	p 915	N90-28511	#	ISSN-0171-1342	p 672	N90-24276	#
H-1542	p 509	N90-20086	* #	ISBN-0-8330-0970-2	p 287	N90-16707	#	ISSN-0171-1342	p 825	N90-27673	#
H-1544	p 421	N90-18395	* #	ISBN-0-85679-597-6	p 397	N90-19195	#	ISSN-0176-7739	p 959	N90-28812	#
H-1546	p 735	N90-25135	* #	ISBN-0-85679-679-4	p 89	N90-11709	#	ISSN-0176-7739	p 134	N90-12007	#
H-1548	p 217	N90-13990	* #	ISBN-0-85679-680-8	p 198	N90-14239	#	ISSN-0176-7739	p 213	N90-13816	#
H-1548	p 119	N90-11753	* #	ISBN-0-85679-681-6	p 199	N90-14240	#	ISSN-0176-7739	p 397	N90-18370	#
H-1553	p 612	N90-22322	* #	ISBN-0-85679-686-7	p 173	N90-14192	#	ISSN-0176-7739	p 786	N90-27617	#
H-1556	p 114	N90-11741	* #	ISBN-0-85679-687-5	p 185	N90-14221	#	ISSN-0176-7739	p 825	N90-27676	#
H-1558	p 32	N90-10023	* #	ISBN-0-85679-701-4	p 236	N90-15081	#	ISSN-0307-0115	p 936	N90-29401	#
H-1568	p 217	N90-13995	* #	ISBN-0-85679-707-3	p 236	N90-15082	#	ISSN-0307-0115	p 316	N90-16721	#
				ISBN-0-85679-714-6	p 316	N90-16721	#	ISSN-0309-6521	p 344	N90-17634	#
H-1570	p 573	N90-22532	* #	ISBN-0-85679-715-4	p 337	N90-16757	#	ISSN-0347-3694	p 206	N90-13677	#
								ISSN-0347-3694	p 827	N90-27691	#

REPORT NUMBER INDEX

NAS 1.15:101715

ISSN-0347-3694	p 876	N90-27883	#	L-16725	p 632	N90-24237 *	#	MSD-TR-89-21-VOL-1	p 405	N90-18383	#
ISSN-0358-2620	p 481	N90-20963	#	L-16731	p 816	N90-27649 *	#				
ISSN-0377-8312	p 748	N90-25985	#	L-16736	p 499	N90-20974 *	#	MTI-88TR39	p 543	N90-21395 *	#
ISSN-0377-8312	p 749	N90-25995	#	L-16737	p 633	N90-24239 *	#				
ISSN-0389-4010	p 18	N90-10003	#	L-16740	p 468	N90-20921 *	#	MTL-TR-90-12	p 650	N90-24270	#
ISSN-0389-4010	p 51	N90-10035	#	L-16742	p 632	N90-24238 *	#	MTL-TR-90-24	p 874	N90-26887	#
ISSN-0389-4010	p 77	N90-10586	#	L-16745	p 883	N90-27066 *	#				
ISSN-0389-4010	p 77	N90-10630	#	L-16763	p 696	N90-24853 *	#	MTR-88W115	p 177	N90-13363	#
ISSN-0389-4010	p 349	N90-17640	#	L-16775	p 876	N90-27788 *	#				
ISSN-0389-4010	p 570	N90-21726	#	L-16776	p 876	N90-27787 *	#	NA-88-1877	p 582	N90-21755 *	#
ISSN-0389-4010	p 912	N90-29326	#	L-16780	p 965	N90-29166 *	#				
ISSN-0389-4010	p 912	N90-29327	#	L-16800	p 718	N90-25938 *	#	NADC-89044-60	p 65	N90-10255	#
ISSN-0389-4010	p 912	N90-29328	#					NADC-89067-60	p 434	N90-18433	#
ISSN-0389-4010	p 912	N90-29332	#	LA-UR-89-2876	p 186	N90-14227	#	NADC-90011-60	p 953	N90-29442	#
ISSN-0389-4010	p 933	N90-29398	#								
ISSN-0389-4010	p 936	N90-29402	#	LC-86-23	p 932	N90-28567 *	#	NAE-AN-58	p 766	N90-25226	#
ISSN-0389-4010	p 939	N90-29411	#	LC-89-39482	p 107	N90-12589 *	#	NAE-AN-59	p 739	N90-25138	#
ISSN-0389-4010	p 939	N90-29412	#	LC-89-600725	p 27	N90-10016	#	NAE-AN-60	p 170	N90-13326	#
ISSN-0389-4010	p 953	N90-29499	#	LC-90-31527	p 915	N90-28511	#	NAE-AN-62	p 674	N90-24278	#
ISSN-0389-4010	p 961	N90-29686	#	LC-90-5426	p 820	N90-27667	#	NAE-AN-63	p 846	N90-27697	#
ISSN-0389-4010	p 961	N90-29687	#					NAE-AN-64	p 846	N90-27698	#
ISSN-0452-2982	p 59	N90-10898	#	LG89ER0026	p 113	N90-11738 *	#				
ISSN-0452-2982	p 59	N90-10899	#	LG89ER0064	p 113	N90-11739 *	#	NAL-TM-EA-8902	p 909	N90-28492	#
ISSN-0452-2982	p 88	N90-11696	#								
ISSN-0452-2982	p 88	N90-11697	#	LIDS-P-1899	p 99	N90-11724	#	NAL-TM-SE-8901	p 527	N90-21043	#
ISSN-0452-2982	p 113	N90-11737	#								
ISSN-0452-2982	p 720	N90-25949	#	LR-31038	p 126	N90-11821 *	#	NAL-TM-562	p 113	N90-11737	#
ISSN-0452-2982	p 913	N90-29333	#	LR-31426	p 735	N90-25136	#	NAL-TM-566	p 88	N90-11696	#
ISSN-0452-2982	p 928	N90-29391	#	LR-521	p 172	N90-13357	#	NAL-TM-567	p 88	N90-11697	#
ISSN-0452-2982	p 936	N90-29399	#	LR-532	p 194	N90-13395	#	NAL-TM-573	p 59	N90-10898	#
ISSN-0452-2982	p 966	N90-30030	#	LR-537	p 214	N90-13822	#	NAL-TM-577	p 59	N90-10899	#
ISSN-0933-2839	p 178	N90-13367	#	LR-544	p 139	N90-12291	#	NAL-TM-600	p 936	N90-29399	#
ISSN-0933-2839	p 178	N90-13368	#	LR-547	p 184	N90-13379	#	NAL-TM-603	p 966	N90-30030	#
ISSN-0951-6301	p 96	N90-11717	#	LR-550	p 202	N90-13410	#	NAL-TM-604-2	p 913	N90-29333	#
ISSN-0951-6301	p 96	N90-11718	#	LR-551	p 205	N90-13617	#	NAL-TM-607	p 928	N90-29391	#
ISSN-0951-6301	p 240	N90-15897	#	LR-556	p 119	N90-11754	#	NAL-TM-608	p 720	N90-25949	#
ISSN-0951-6301	p 575	N90-22544	#	LR-560	p 135	N90-12778	#				
ISSN-0951-6301	p 913	N90-29335	#	LR-561	p 137	N90-12958	#	NAL-TR-1000	p 77	N90-10586	#
ISSN-0955-9655	p 464	N90-18999	#	LR-573	p 481	N90-20964	#	NAL-TR-1002	p 51	N90-10035	#
ISSN-0958-0379	p 370	N90-17193	#	LR-578	p 572	N90-21740	#	NAL-TR-1008	p 18	N90-10003	#
				LR-579	p 572	N90-21741	#	NAL-TR-1009	p 77	N90-10630	#
JAIA-TR-90-1	p 911	N90-29302	#	LR-580	p 578	N90-21751	#	NAL-TR-1011T	p 570	N90-21726	#
				LR-581	p 578	N90-21752	#	NAL-TR-1013	p 349	N90-17640	#
JIAA-TR-96	p 171	N90-13349 *	#	LR-588	p 717	N90-25114	#	NAL-TR-1014	p 936	N90-29402	#
				LR-589	p 533	N90-21142	#	NAL-TR-1018T	p 912	N90-29332	#
JTN-88-80057	p 113	N90-11737	#	LR-592	p 689	N90-23760	#	NAL-TR-1023	p 776	N90-26335	#
JTN-88-80061	p 88	N90-11696	#	LR-594	p 717	N90-25115	#	NAL-TR-1033	p 961	N90-29687	#
JTN-88-80062	p 88	N90-11697	#	LR-596	p 762	N90-25153	#	NAL-TR-1034	p 939	N90-29412	#
JTN-88-80068	p 59	N90-10898	#	LR-598	p 572	N90-21742	#	NAL-TR-1037	p 939	N90-29411	#
JTN-88-80069	p 59	N90-10899	#	LR-614	p 718	N90-25116	#	NAL-TR-1038T	p 912	N90-29328	#
JTN-90-80188	p 936	N90-29399	#	LR-619	p 777	N90-26369	#	NAL-TR-1039	p 953	N90-29499	#
JTN-90-80190	p 966	N90-30030	#	LR-622	p 914	N90-29337	#	NAL-TR-1041	p 933	N90-29398	#
JTN-90-80191	p 913	N90-29333	#	LR-627	p 925	N90-29390	#	NAL-TR-1045	p 912	N90-29327	#
JTN-90-80192	p 928	N90-29391	#	LR-628	p 961	N90-29680	#	NAL-TR-1046	p 912	N90-29326	#
				LR-629	p 961	N90-29681	#	NAL-TR-1047	p 961	N90-29686	#
KU-FRL-831-2	p 648	N90-23386 *	#	LR-630-PT-1-REV	p 961	N90-29682	#				
KU-FRL-872-1	p 719	N90-25943 *	#	LR-630-PT-2	p 961	N90-29683	#	NAPC-PE-188	p 511	N90-21008	#
				LR-631	p 961	N90-29684	#	NAPC-PE-204C	p 454	N90-18738	#
				LR-634	p 939	N90-29433	#				
L-16134	p 72	N90-10409 *	#					NAS 1.15:100050	p 598	N90-21778 *	#
L-16266	p 1	N90-10002 *	#	M/NAFA/89-1	p 551	N90-21724 *	#	NAS 1.15:100454	p 435	N90-19241 *	#
L-16350-PT-1	p 90	N90-12503 *	#					NAS 1.15:100533-PT-1	p 374	N90-18125 *	#
L-16350-PT-2	p 91	N90-12519 *	#	MATHS-REPT-A-106	p 758	N90-26014	#	NAS 1.15:100533-PT-2	p 374	N90-18126 *	#
L-16350-PT-3	p 92	N90-12539 *	#					NAS 1.15:101021	p 582	N90-21756 *	#
L-16441	p 477	N90-20046 *	#	MBB-FE-363/S/PUB-384	p 723	N90-25103	#	NAS 1.15:101025	p 761	N90-25149 *	#
L-16456	p 79	N90-10679 *	#					NAS 1.15:101054	p 119	N90-11752 *	#
L-16531	p 51	N90-10034 *	#	MBB-FW-522/S/PUB-383	p 779	N90-25078	#	NAS 1.15:101085	p 240	N90-15898 *	#
L-16536	p 249	N90-15902 *	#					NAS 1.15:101585	p 187	N90-14232 *	#
L-16537	p 20	N90-10830 *	#	MBB-UD-0551-89-PUB	p 29	A90-12258	#	NAS 1.15:101610	p 252	N90-15102 *	#
L-16550	p 456	N90-19718 *	#	MBB-UD-500/89-PUB	p 734	N90-25092	#	NAS 1.15:101613	p 237	N90-15886 *	#
L-16555	p 573	N90-22531 *	#	MBB-UD-526/88-PUB	p 138	N90-12208	#	NAS 1.15:101617	p 106	N90-12580 *	#
L-16563	p 237	N90-15884 *	#	MBB-UD-553/89	p 221	A90-22696	#	NAS 1.15:101639	p 259	N90-15110 *	#
L-16570	p 20	N90-10829 *	#	MBB-UD-554/84-PUB	p 735	N90-25137	#	NAS 1.15:101642	p 36	N90-10889 *	#
L-16574	p 348	N90-16767 *	#	MBB-UD-556-89-PUB	p 29	A90-12253	#	NAS 1.15:101646	p 134	N90-12057 *	#
L-16589	p 338	N90-17627 *	#	MBB-UD-557-89-PUB	p 381	A90-28242	#	NAS 1.15:101659	p 175	N90-14205 *	#
L-16594	p 237	N90-15882 *	#	MBB-UD-560/89	p 222	A90-22698	#	NAS 1.15:101665	p 217	N90-14061 *	#
L-16608	p 173	N90-14186 *	#					NAS 1.15:101668	p 372	N90-18057 *	#
L-16609	p 120	N90-11757 *	#	MBB-UT-007/89-PUB	p 723	N90-25089	#	NAS 1.15:101670	p 201	N90-13403 *	#
L-16611	p 173	N90-14187 *	#	MBB-UT-012/89-PUB	p 766	N90-25091	#	NAS 1.15:101675	p 543	N90-21424 *	#
L-16615	p 404	N90-18378 *	#	MBB-UT-115/89-PUB	p 773	N90-25084	#	NAS 1.15:101681	p 373	N90-18070 *	#
L-16616	p 119	N90-11751 *	#	MBB-UT-122/89-PUB	p 766	N90-25090	#	NAS 1.15:101684	p 399	N90-19206 *	#
L-16622	p 259	N90-15108 *	#					NAS 1.15:101686	p 328	N90-17620 *	#
L-16625	p 315	N90-16710 *	#	MBB-Z-0279/89	p 266	A90-22595	#	NAS 1.15:101687	p 610	N90-22807 *	#
L-16626	p 202	N90-14244 *	#					NAS 1.15:101689	p 497	N90-20071 *	#
L-16627	p 317	N90-17560 *	#	MBB/LW/3015/S/PUB/321	p 141	N90-12494	#	NAS 1.15:101696	p 509	N90-20086 *	#
L-16632	p 397	N90-19193 *	#					NAS 1.15:101697	p 421	N90-18395 *	#
L-16633	p 352	N90-17647 *	#	MDC-K4856	p 634	N90-24250	#	NAS 1.15:101702	p 612	N90-22322 *	#
L-16636	p 615	N90-23338 *	#					NAS 1.15:101703	p 32	N90-10023 *	#
L-16637	p 420	N90-18393 *	#	MISS-2144	p 115	N90-12604	#	NAS 1.15:101704	p 217	N90-13990 *	#
L-16638	p 582	N90-22555 *	#					NAS 1.15:101705	p 573	N90-22532 *	#
L-16642	p 420	N90-18394 *	#	MITT-87-01	p 666	N90-24272	#	NAS 1.15:101708	p 175	N90-14202 *	#
L-16645	p 173	N90-14190 *	#	MITT-88-04	p 428	N90-19235	#	NAS 1.15:101709	p 689	N90-23768 *	#
L-16651	p 414	N90-18385 *	#					NAS 1.15:101710	p 217	N90-13995 *	#
L-16652	p 506	N90-21004 *	#	MRL-TN-568	p 527	N90-21044	#	NAS 1.15:101713	p 339	N90-16758 *	#
L-16664	p 434	N90-19239 *	#					NAS 1.15:101714	p 186	N90-14228 *	#
L-16710	p 398	N90-19199 *	#	MRL-TR-89-31	p 444	N90-19364	#	NAS 1.15:101715	p 416	N90-19225 *	#
L-16719	p 462	N90-18882 *	#								

NAS 1.15:101716	p 415	N90-19224 *	#	NAS 1.15:102679	p 690	N90-24660 *	#	NAS 1.26:174824	p 345	N90-17638 *	#
NAS 1.15:101717	p 735	N90-25135 *	#	NAS 1.15:102681	p 774	N90-25368 *	#	NAS 1.26:174834	p 930	N90-28557 *	#
NAS 1.15:101718	p 736	N90-25973 *	#	NAS 1.15:102685	p 780	N90-26511 *	#	NAS 1.26:174942	p 930	N90-28560 *	#
NAS 1.15:101719	p 781	N90-26564 *	#	NAS 1.15:102691	p 724	N90-25120 *	#	NAS 1.26:174945	p 396	N90-18364 *	#
NAS 1.15:101721	p 757	N90-25142 *	#	NAS 1.15:102692	p 936	N90-28578 *	#	NAS 1.26:174992	p 52	N90-10043 *	#
NAS 1.15:101722	p 648	N90-23392 *	#	NAS 1.15:102693	p 909	N90-28493 *	#	NAS 1.26:174993	p 52	N90-10044 *	#
NAS 1.15:101723	p 924	N90-28542 *	#	NAS 1.15:102704	p 846	N90-27699 *	#	NAS 1.26:177471	p 28	N90-10021 *	#
NAS 1.15:101725	p 758	N90-25144 *	#	NAS 1.15:102710	p 927	N90-28546 *	#	NAS 1.26:177543	p 248	N90-15093 *	#
NAS 1.15:101726	p 910	N90-28505 *	#	NAS 1.15:102713	p 869	N90-27725 *	#	NAS 1.26:177547	p 650	N90-24265 *	#
NAS 1.15:101794	p 895	N90-27465 *	#	NAS 1.15:102716	p 965	N90-29965 *	#	NAS 1.26:177551	p 572	N90-21738 *	#
NAS 1.15:101879	p 896	N90-27471 *	#	NAS 1.15:102795	p 636	N90-23373 *	#	NAS 1.26:177552	p 923	N90-28540 *	#
NAS 1.15:101886	p 736	N90-25972 *	#	NAS 1.15:102796	p 573	N90-21746 *	#	NAS 1.26:177558	p 820	N90-27669 *	#
NAS 1.15:102069	p 194	N90-13392 *	#	NAS 1.15:102800	p 572	N90-21739 *	#	NAS 1.26:177563	p 816	N90-27653 *	#
NAS 1.15:102077	p 172	N90-13352 *	#	NAS 1.15:102802	p 916	N90-28512 *	#	NAS 1.26:177564	p 915	N90-28510 *	#
NAS 1.15:102182	p 88	N90-11701 *	#	NAS 1.15:102807	p 636	N90-23374 *	#	NAS 1.26:178166	p 63	N90-10187 *	#
NAS 1.15:102195	p 18	N90-10006 *	#	NAS 1.15:102810	p 757	N90-25141 *	#	NAS 1.26:178419	p 380	N90-18233 *	#
NAS 1.15:102196	p 170	N90-13332 *	#	NAS 1.15:102814	p 654	N90-23399 *	#	NAS 1.26:179442	p 77	N90-11487 *	#
NAS 1.15:102207	p 201	N90-13407 *	#	NAS 1.15:102815	p 816	N90-27654 *	#	NAS 1.26:179522	p 193	N90-13390 *	#
NAS 1.15:102212	p 170	N90-13327 *	#	NAS 1.15:102827	p 702	N90-25933 *	#	NAS 1.26:179534	p 932	N90-28567 *	#
NAS 1.15:102216	p 340	N90-17632 *	#	NAS 1.15:102834	p 720	N90-25945 *	#	NAS 1.26:179578	p 932	N90-28569 *	#
NAS 1.15:102219	p 260	N90-15938 *	#	NAS 1.15:102846	p 849	N90-27702 *	#	NAS 1.26:179590	p 79	N90-10683 *	#
NAS 1.15:102221	p 88	N90-11699 *	#	NAS 1.15:103100	p 478	N90-20051 *	#	NAS 1.26:179610	p 192	N90-13385 *	#
NAS 1.15:102222	p 88	N90-11700 *	#	NAS 1.15:103105	p 748	N90-25982 *	#	NAS 1.26:179625	p 666	N90-24274 *	#
NAS 1.15:102223	p 143	N90-13324 *	#	NAS 1.15:103106	p 776	N90-26334 *	#	NAS 1.26:179642	p 63	N90-10184 *	#
NAS 1.15:102225	p 398	N90-19201 *	#	NAS 1.15:103107	p 588	N90-21762 *	#	NAS 1.26:180667	p 379	N90-18228 *	#
NAS 1.15:102229	p 24	N90-10841 *	#	NAS 1.15:103114	p 570	N90-21727 *	#	NAS 1.26:180831	p 65	N90-10293 *	#
NAS 1.15:102231	p 509	N90-20087 *	#	NAS 1.15:103120	p 552	N90-21725 *	#	NAS 1.26:180848	p 117	N90-12617 *	#
NAS 1.15:102233	p 133	N90-11970 *	#	NAS 1.15:103123	p 666	N90-23404 *	#	NAS 1.26:180850	p 932	N90-28570 *	#
NAS 1.15:102235	p 399	N90-19204 *	#	NAS 1.15:103131	p 571	N90-21733 *	#	NAS 1.26:180867	p 53	N90-10048 *	#
NAS 1.15:102236	p 582	N90-21758 *	#	NAS 1.15:103132	p 543	N90-21394 *	#	NAS 1.26:180868	p 53	N90-10047 *	#
NAS 1.15:102246	p 349	N90-17641 *	#	NAS 1.15:103137	p 782	N90-26635 *	#	NAS 1.26:180869	p 53	N90-10049 *	#
NAS 1.15:102250	p 671	N90-23413 *	#	NAS 1.15:103167	p 589	N90-22566 *	#	NAS 1.26:180892	p 357	N90-17868 *	#
NAS 1.15:102253	p 81	N90-11692 *	#	NAS 1.15:103170	p 666	N90-24273 *	#	NAS 1.26:181335	p 665	N90-23401 *	#
NAS 1.15:102258	p 370	N90-17112 *	#	NAS 1.15:103176	p 688	N90-23591 *	#	NAS 1.26:181708	p 21	N90-10834 *	#
NAS 1.15:102266	p 172	N90-13353 *	#	NAS 1.15:103195	p 773	N90-25289 *	#	NAS 1.26:181851	p 220	N90-14866 *	#
NAS 1.15:102271	p 540	N90-20325 *	#	NAS 1.15:103198	p 758	N90-26011 *	#	NAS 1.26:181867	p 24	N90-10014 *	#
NAS 1.15:102272	p 816	N90-26800 *	#	NAS 1.15:103212	p 751	N90-26009 *	#	NAS 1.26:181881	p 923	N90-28537 *	#
NAS 1.15:102273	p 194	N90-14236 *	#	NAS 1.15:103220	p 763	N90-26055 *	#	NAS 1.26:181895	p 202	N90-14245 *	#
NAS 1.15:102304	p 516	N90-21038 *	#	NAS 1.15:103249	p 720	N90-25946 *	#	NAS 1.26:181896	p 123	N90-12625 *	#
NAS 1.15:102315	p 203	N90-14268 *	#	NAS 1.15:103250	p 817	N90-27657 *	#	NAS 1.26:181897	p 140	N90-13198 *	#
NAS 1.15:102341	p 54	N90-10891 *	#	NAS 1.15:103305	p 547	N90-21544 *	#	NAS 1.26:181898	p 601	N90-22609 *	#
NAS 1.15:102342	p 610	N90-22808 *	#	NAS 1.15:103306	p 547	N90-21543 *	#	NAS 1.26:181909-VOL-1	p 505	N90-20081 *	#
NAS 1.15:102348	p 215	N90-14641 *	#	NAS 1.15:103307	p 547	N90-21542 *	#	NAS 1.26:181909-VOL-2	p 505	N90-20080 *	#
NAS 1.15:102358	p 318	N90-17561 *	#	NAS 1.15:103308	p 546	N90-21541 *	#	NAS 1.26:181909-VOL-3	p 505	N90-20082 *	#
NAS 1.15:102365	p 379	N90-17413 *	#	NAS 1.15:103310	p 546	N90-21539 *	#	NAS 1.26:181909-VOL-4	p 506	N90-20083 *	#
NAS 1.15:102368	p 610	N90-22703 *	#	NAS 1.15:103347	p 767	N90-26080 *	#	NAS 1.26:181909-VOL-5	p 506	N90-20084 *	#
NAS 1.15:102374	p 94	N90-12560 *	#	NAS 1.15:103480	p 767	N90-26094 *	#	NAS 1.26:181911	p 20	N90-10833 *	#
NAS 1.15:102387	p 94	N90-12561 *	#	NAS 1.15:103486	p 724	N90-25957 *	#	NAS 1.26:181916-VOL-1	p 134	N90-12058 *	#
NAS 1.15:102389	p 187	N90-13381 *	#	NAS 1.15:103609	p 964	N90-29121 *	#	NAS 1.26:181916-VOL-2	p 213	N90-13814 *	#
NAS 1.15:102391	p 215	N90-14511 *	#	NAS 1.15:4131	p 186	N90-14225 *	#	NAS 1.26:181917	p 719	N90-25944 *	#
NAS 1.15:102397	p 114	N90-11740 *	#	NAS 1.15:4134	p 79	N90-10679 *	#	NAS 1.26:181922	p 369	N90-17055 *	#
NAS 1.15:102402	p 720	N90-25948 *	#	NAS 1.15:4135	p 348	N90-16767 *	#	NAS 1.26:181923	p 454	N90-18743 *	#
NAS 1.15:102408	p 205	N90-13636 *	#	NAS 1.15:4136	p 317	N90-17560 *	#	NAS 1.26:181936	p 893	N90-28366 *	#
NAS 1.15:102409	p 117	N90-12618 *	#	NAS 1.15:4137	p 183	N90-13372 *	#	NAS 1.26:181937	p 88	N90-11704 *	#
NAS 1.15:102419	p 193	N90-13389 *	#	NAS 1.15:4140	p 114	N90-11741 *	#	NAS 1.26:181939	p 316	N90-17539 *	#
NAS 1.15:102422	p 194	N90-13393 *	#	NAS 1.15:4141	p 192	N90-13387 *	#	NAS 1.26:181941	p 279	N90-16294 *	#
NAS 1.15:102426	p 380	N90-18229 *	#	NAS 1.15:4142	p 119	N90-11753 *	#	NAS 1.26:181945	p 510	N90-20088 *	#
NAS 1.15:102428	p 172	N90-13355 *	#	NAS 1.15:4144	p 51	N90-10034 *	#	NAS 1.26:181953	p 259	N90-15111 *	#
NAS 1.15:102435	p 372	N90-18041 *	#	NAS 1.15:4146	p 173	N90-14186 *	#	NAS 1.26:181955	p 171	N90-13351 *	#
NAS 1.15:102440	p 548	N90-20794 *	#	NAS 1.15:4147	p 119	N90-11751 *	#	NAS 1.26:181967	p 480	N90-20952 *	#
NAS 1.15:102441	p 257	N90-15923 *	#	NAS 1.15:4148	p 103	N90-11732 *	#	NAS 1.26:181973	p 960	N90-28866 *	#
NAS 1.15:102442	p 543	N90-21361 *	#	NAS 1.15:4155	p 237	N90-15884 *	#	NAS 1.26:181974	p 959	N90-28865 *	#
NAS 1.15:102447	p 213	N90-13797 *	#	NAS 1.15:4157	p 202	N90-14244 *	#	NAS 1.26:181975	p 541	N90-20439 *	#
NAS 1.15:102448	p 213	N90-13750 *	#	NAS 1.15:4158	p 259	N90-15108 *	#	NAS 1.26:181993	p 758	N90-25143 *	#
NAS 1.15:102451	p 194	N90-14235 *	#	NAS 1.15:4162	p 173	N90-14190 *	#	NAS 1.26:182005	p 780	N90-25638 *	#
NAS 1.15:102452	p 345	N90-17636 *	#	NAS 1.15:4163	p 369	N90-17074 *	#	NAS 1.26:182006	p 695	N90-24103 *	#
NAS 1.15:102455	p 215	N90-14656 *	#	NAS 1.15:4171	p 850	N90-27703 *	#	NAS 1.26:182019	p 593	N90-21772 *	#
NAS 1.15:102456	p 215	N90-14617 *	#	NAS 1.15:4173	p 420	N90-18394 *	#	NAS 1.26:182023	p 631	N90-23348 *	#
NAS 1.15:102460	p 194	N90-13394 *	#	NAS 1.15:4175	p 373	N90-17235 *	#	NAS 1.26:182024	p 574	N90-22538 *	#
NAS 1.15:102466	p 318	N90-17562 *	#	NAS 1.15:4179	p 615	N90-23338 *	#	NAS 1.26:182027	p 549	N90-21605 *	#
NAS 1.15:102472	p 515	N90-21036 *	#	NAS 1.15:4180	p 582	N90-22555 *	#	NAS 1.26:182030	p 478	N90-20050 *	#
NAS 1.15:102482	p 509	N90-20085 *	#	NAS 1.15:4181	p 398	N90-19199 *	#	NAS 1.26:182031	p 775	N90-25375 *	#
NAS 1.15:102484	p 533	N90-21137 *	#	NAS 1.15:4183	p 499	N90-20974 *	#	NAS 1.26:182061	p 781	N90-26595 *	#
NAS 1.15:102488	p 778	N90-26373 *	#	NAS 1.15:4195	p 876	N90-27787 *	#	NAS 1.26:182089	p 966	N90-29169 *	#
NAS 1.15:102496	p 542	N90-21300 *	#	NAS 1.15:4200	p 632	N90-24238 *	#	NAS 1.26:182124	p 929	N90-28552 *	#
NAS 1.15:102518	p 510	N90-20090 *	#	NAS 1.15:4201	p 632	N90-24237 *	#	NAS 1.26:182125	p 52	N90-10045 *	#
NAS 1.15:102535	p 600	N90-21869 *	#	NAS 1.15:4207	p 929	N90-28551 *	#	NAS 1.26:182142	p 53	N90-10046 *	#
NAS 1.15:102537	p 541	N90-20392 *	#	NAS 1.15:4222	p 959	N90-28815 *	#	NAS 1.26:182228	p 51	N90-10037 *	#
NAS 1.15:102541	p 543	N90-21399 *	#	NAS 1.15:88277	p 214	N90-13820 *	#	NAS 1.26:182230	p 193	N90-13388 *	#
NAS 1.15:102574	p 542	N90-21283 *	#	NAS 1.15:89125	p 1	N90-10002 *	#	NAS 1.26:182236	p 73	N90-10451 *	#
NAS 1.15:102585	p 464	N90-19821 *	#	NAS 1.15:89131	p 72	N90-10409 *	#	NAS 1.26:182247	p 777	N90-26355 *	#
NAS 1.15:102587	p 506	N90-21005 *	#	NAS 1.15:89423	p 52	N90-10042 *	#	NAS 1.26:182278	p 113	N90-11738 *	#
NAS 1.15:102595	p 484	N90-20068 *	#	NAS 1.21:501	p 107	N90-12589 *	#	NAS 1.26:182607	p 601	N90-22651 *	#
NAS 1.15:102598	p 454	N90-18746 *	#	NAS 1.26:168069	p 930	N90-28559 *	#	NAS 1.26:183272	p 845	N90-27694 *	#
NAS 1.15:102603	p 434	N90-18434 *	#	NAS 1.26:168137	p 931	N90-28566 *	#	NAS 1.26:183832	p 201	N90-13404 *	#
NAS 1.15:102609	p 400	N90-19211 *	#	NAS 1.26:168211	p 931	N90-28561 *	#	NAS 1.26:183942	p 543	N90-21395 *	#
NAS 1.15:102617	p 478	N90-20047 *	#	NAS 1.26:168219	p 930	N90-28558 *	#	NAS 1.26:185074	p 172	N90-13354 *	#
NAS 1.15:102618	p 520	N90-20093 *	#	NAS 1.26:168274	p 930	N90-28555 *	#	NAS 1.26:185109	p 220	N90-14153 *	#
NAS 1.15:102620	p 416	N90-19227 *	#	NAS 1.26:168289	p 929	N90-28553 *	#	NAS 1.26:185129	p 468	N90-	

REPORT NUMBER INDEX

NASA-CR-183942

NAS 1.26:185158	p 649	N90-23393 *	NAS 1.26:4289	p 588	N90-21760 *	NASA-CR-168219	p 930	N90-28558 *
NAS 1.26:185189	p 690	N90-23769 *	NAS 1.26:4294	p 762	N90-26019 *	NASA-CR-168274	p 930	N90-28555 *
NAS 1.26:185197	p 344	N90-17635 *	NAS 1.26:4296	p 583	N90-22557 *	NASA-CR-168289	p 929	N90-28553 *
NAS 1.26:185222	p 588	N90-21761 *	NAS 1.26:4298	p 582	N90-21755 *	NASA-CR-168290	p 931	N90-28563 *
NAS 1.26:185225	p 506	N90-21006 *	NAS 1.26:4299	p 633	N90-24242 *	NASA-CR-168301	p 929	N90-28554 *
NAS 1.26:185241	p 782	N90-26633 *	NAS 1.26:4302	p 719	N90-25940 *	NASA-CR-174651	p 931	N90-28562 *
NAS 1.26:185243	p 588	N90-21763 *	NAS 1.26:4304	p 965	N90-29919 *	NASA-CR-174718	p 193	N90-13391 *
NAS 1.26:185277	p 933	N90-29394 *	NAS 1.26:4305	p 637	N90-24257 *	NASA-CR-174766-VOL-1	p 931	N90-28564 *
NAS 1.26:185474	p 200	N90-13401 *	NAS 1.26:4307	p 634	N90-24246 *	NASA-CR-174766-VOL-2	p 931	N90-28565 *
NAS 1.26:185475	p 57	N90-10075 *	NAS 1.26:4308	p 816	N90-27655 *	NASA-CR-174799	p 930	N90-28556 *
NAS 1.26:185563	p 124	N90-11774 *	NAS 1.26:4314	p 718	N90-25939 *	NASA-CR-174824	p 345	N90-17638 *
NAS 1.26:185583	p 87	N90-11695 *	NAS 1.26:4315	p 896	N90-28396 *	NASA-CR-174834	p 930	N90-28557 *
NAS 1.26:185854	p 136	N90-12872 *	NAS 1.26:4316	p 965	N90-29143 *	NASA-CR-174942	p 930	N90-28560 *
NAS 1.26:185884	p 183	N90-13369 *	NAS 1.26:4317	p 964	N90-29142 *	NASA-CR-174945	p 396	N90-18364 *
NAS 1.26:185931	p 925	N90-29385 *	NAS 1.26:4323	p 909	N90-28494 *	NASA-CR-174992	p 52	N90-10043 *
NAS 1.26:186036	p 103	N90-11733 *	NAS 1.26:4326	p 924	N90-29383 *	NASA-CR-174993	p 52	N90-10044 *
NAS 1.26:186037	p 90	N90-12500 *	NAS 1.26:4328	p 925	N90-29384 *	NASA-CR-177471	p 28	N90-10021 *
NAS 1.26:186046	p 184	N90-14216 *	NAS 1.55:10036	p 187	N90-13384 *	NASA-CR-177543	p 248	N90-15093 *
NAS 1.26:186067	p 690	N90-24557 *	NAS 1.55:10041	p 185	N90-14220 *	NASA-CR-177547	p 650	N90-24265 *
NAS 1.26:186070	p 336	N90-16751 *	NAS 1.55:2487-PT-1	p 90	N90-12503 *	NASA-CR-177551	p 572	N90-21738 *
NAS 1.26:186100	p 217	N90-14843 *	NAS 1.55:2487-PT-2	p 91	N90-12519 *	NASA-CR-177552	p 923	N90-28540 *
NAS 1.26:186116	p 171	N90-13349 *	NAS 1.55:2487-PT-3	p 92	N90-12539 *	NASA-CR-177558	p 820	N90-27669 *
NAS 1.26:186118	p 648	N90-23386 *	NAS 1.55:3052	p 352	N90-17647 *	NASA-CR-177563	p 816	N90-27653 *
NAS 1.26:186122	p 212	N90-13744 *	NAS 1.55:3063	p 468	N90-20921 *	NASA-CR-177564	p 915	N90-28510 *
NAS 1.26:186130	p 214	N90-13817 *	NAS 1.55:3067	p 696	N90-24853 *	NASA-CR-178166	p 63	N90-10187 *
NAS 1.26:186140	p 690	N90-24514 *	NAS 1.60:2462	p 468	N90-20942 *	NASA-CR-178419	p 380	N90-18233 *
NAS 1.26:186163	p 574	N90-21747 *	NAS 1.60:2879	p 73	N90-11245 *	NASA-CR-179442	p 77	N90-11487 *
NAS 1.26:186195	p 199	N90-14243 *	NAS 1.60:2917	p 249	N90-15902 *	NASA-CR-179522	p 193	N90-13390 *
NAS 1.26:186211	p 214	N90-14453 *	NAS 1.60:2925	p 259	N90-15112 *	NASA-CR-179534	p 932	N90-28567 *
NAS 1.26:186219	p 176	N90-14212 *	NAS 1.60:2939	p 20	N90-10829 *	NASA-CR-179578	p 932	N90-28569 *
NAS 1.26:186222	p 844	N90-26824 *	NAS 1.60:2945	p 20	N90-10830 *	NASA-CR-179590	p 79	N90-10683 *
NAS 1.26:186226	p 924	N90-29381 *	NAS 1.60:2946	p 237	N90-15882 *	NASA-CR-179610	p 192	N90-13385 *
NAS 1.26:186227	p 499	N90-20971 *	NAS 1.60:2952	p 134	N90-12042 *	NASA-CR-179625	p 666	N90-24274 *
NAS 1.26:186232	p 186	N90-14226 *	NAS 1.60:2960	p 420	N90-18393 *	NASA-CR-179642	p 63	N90-10184 *
NAS 1.26:186263	p 275	N90-15380 *	NAS 1.60:2961	p 173	N90-14187 *	NASA-CR-180667	p 379	N90-18228 *
NAS 1.26:186267	p 316	N90-16712 *	NAS 1.60:2962	p 120	N90-11757 *	NASA-CR-180831	p 65	N90-10293 *
NAS 1.26:186300	p 581	N90-21753 *	NAS 1.60:2963	p 456	N90-19718 *	NASA-CR-180848	p 117	N90-12617 *
NAS 1.26:186318	p 237	N90-15891 *	NAS 1.60:2965	p 349	N90-17639 *	NASA-CR-180850	p 932	N90-28570 *
NAS 1.26:186326	p 317	N90-17558 *	NAS 1.60:2966	p 338	N90-17627 *	NASA-CR-180867	p 53	N90-10048 *
NAS 1.26:186327	p 398	N90-19198 *	NAS 1.60:2969	p 315	N90-16710 *	NASA-CR-180868	p 53	N90-10047 *
NAS 1.26:186371	p 415	N90-18390 *	NAS 1.60:2971	p 249	N90-15100 *	NASA-CR-180869	p 53	N90-10049 *
NAS 1.26:186435	p 478	N90-20052 *	NAS 1.60:2973	p 397	N90-19193 *	NASA-CR-180892	p 357	N90-17668 *
NAS 1.26:186451	p 479	N90-20950 *	NAS 1.60:2974	p 462	N90-18882 *	NASA-CR-181335	p 665	N90-23401 *
NAS 1.26:186533	p 547	N90-21571 *	NAS 1.60:2975	p 414	N90-18385 *	NASA-CR-181708	p 21	N90-10834 *
NAS 1.26:186560	p 572	N90-21736 *	NAS 1.60:2978	p 404	N90-18378 *	NASA-CR-181851	p 220	N90-14866 *
NAS 1.26:186571	p 571	N90-21734 *	NAS 1.60:2980	p 506	N90-21004 *	NASA-CR-181867	p 24	N90-10014 *
NAS 1.26:186572	p 571	N90-21735 *	NAS 1.60:2982	p 434	N90-19239 *	NASA-CR-181881	p 923	N90-28537 *
NAS 1.26:186576	p 481	N90-20965 *	NAS 1.60:2985	p 858	N90-27722 *	NASA-CR-181895	p 202	N90-14245 *
NAS 1.26:186577	p 549	N90-21604 *	NAS 1.60:2990	p 477	N90-20046 *	NASA-CR-181896	p 123	N90-12625 *
NAS 1.26:186581	p 718	N90-25934 *	NAS 1.60:2996	p 440	N90-19242 *	NASA-CR-181897	p 140	N90-13198 *
NAS 1.26:186585	p 597	N90-21775 *	NAS 1.60:3000	p 573	N90-22531 *	NASA-CR-181898	p 601	N90-22609 *
NAS 1.26:186598	p 598	N90-21776 *	NAS 1.60:3001	p 735	N90-25134 *	NASA-CR-181909-VOL-1	p 505	N90-20081 *
NAS 1.26:186599	p 598	N90-21777 *	NAS 1.60:3002	p 910	N90-28503 *	NASA-CR-181909-VOL-2	p 505	N90-20080 *
NAS 1.26:186630	p 719	N90-25943 *	NAS 1.60:3005	p 665	N90-23403 *	NASA-CR-181909-VOL-3	p 505	N90-20082 *
NAS 1.26:186637	p 780	N90-25580 *	NAS 1.60:3008	p 816	N90-27649 *	NASA-CR-181909-VOL-4	p 506	N90-20083 *
NAS 1.26:186640	p 734	N90-25126 *	NAS 1.60:3009	p 633	N90-24239 *	NASA-CR-181909-VOL-5	p 506	N90-20084 *
NAS 1.26:186658	p 734	N90-25132 *	NAS 1.60:3011	p 876	N90-27788 *	NASA-CR-181911	p 20	N90-10833 *
NAS 1.26:186660	p 650	N90-23397 *	NAS 1.60:3018	p 883	N90-27066 *	NASA-CR-181916-VOL-1	p 134	N90-12058 *
NAS 1.26:186661	p 649	N90-23396 *	NAS 1.60:3027	p 965	N90-29166 *	NASA-CR-181916-VOL-2	p 213	N90-13814 *
NAS 1.26:186663	p 649	N90-23395 *	NAS 1.60:3036	p 718	N90-25938 *	NASA-CR-181917	p 719	N90-25944 *
NAS 1.26:186670	p 649	N90-23394 *	NAS 1.61:1235	p 516	N90-21037 *	NASA-CR-181922	p 369	N90-17055 *
NAS 1.26:186676	p 735	N90-25967 *	NAS 1.71:1387-13870-1	p 248	N90-15094 *	NASA-CR-181923	p 454	N90-18743 *
NAS 1.26:186680	p 734	N90-25127 *				NASA-CR-181936	p 893	N90-28366 *
NAS 1.26:186685	p 650	N90-24266 *	NAS-SR-1310	p 177	N90-13362 *	NASA-CR-181937	p 88	N90-11704 *
NAS 1.26:186710	p 717	N90-25111 *	NAS-SR-1321	p 243	N90-15086 *	NASA-CR-181939	p 316	N90-17539 *
NAS 1.26:186729	p 774	N90-25291 *	NAS-SR-1321	p 177	N90-13361 *	NASA-CR-181941	p 279	N90-16294 *
NAS 1.26:186732	p 782	N90-26634 *	NAS-SR-1322	p 27	N90-10017 *	NASA-CR-181945	p 510	N90-20088 *
NAS 1.26:186800	p 717	N90-25112 *	NAS-SR-1324	p 243	N90-15090 *	NASA-CR-181953	p 259	N90-15111 *
NAS 1.26:186820-VOL-2	p 736	N90-25971 *	NAS-SR-1330	p 178	N90-14214 *	NASA-CR-181955	p 171	N90-13351 *
NAS 1.26:186872	p 780	N90-26515 *	NAS-SR-1361	p 542	N90-21249 *	NASA-CR-181967	p 480	N90-20952 *
NAS 1.26:186886	p 849	N90-27701 *				NASA-CR-181973	p 960	N90-28866 *
NAS 1.26:186887	p 776	N90-26281 *	NASA-CASE-ARC-11425-3	p 678	N90-23475 *	NASA-CR-181974	p 959	N90-28865 *
NAS 1.26:186898	p 887	N90-28105 *	NASA-CASE-ARC-11425-4	p 532	N90-20133 *	NASA-CR-181975	p 541	N90-20439 *
NAS 1.26:186900	p 759	N90-26017 *				NASA-CR-181993	p 758	N90-25143 *
NAS 1.26:186903	p 721	N90-25954 *	NASA-CASE-LAR-13628-1	p 689	N90-23707 *	NASA-CR-182005	p 780	N90-25638 *
NAS 1.26:186925	p 884	N90-27946 *	NASA-CASE-LAR-13734-1-CU	p 526	N90-20096 *	NASA-CR-182006	p 695	N90-24103 *
NAS 1.26:186933	p 824	N90-26804 *	NASA-CASE-LAR-13777-1	p 498	N90-20078 *	NASA-CR-182019	p 593	N90-21772 *
NAS 1.26:186944	p 959	N90-28862 *	NASA-CASE-LAR-13816-1	p 609	N90-22025 *	NASA-CR-182023	p 631	N90-23348 *
NAS 1.26:187289	p 925	N90-29389 *	NASA-CASE-LAR-13870-1	p 248	N90-15094 *	NASA-CR-182024	p 574	N90-22538 *
NAS 1.26:3996	p 63	N90-10186 *	NASA-CASE-LAR-13952-1-SB	p 455	N90-19534 *	NASA-CR-182027	p 549	N90-21605 *
NAS 1.26:4035	p 126	N90-11821 *	NASA-CASE-LAR-13983-1	p 648	N90-23390 *	NASA-CR-182030	p 478	N90-20050 *
NAS 1.26:4085	p 19	N90-10012 *	NASA-CASE-LAR-14031-1	p 499	N90-20079 *	NASA-CR-182031	p 775	N90-25375 *
NAS 1.26:4175	p 32	N90-10031 *	NASA-CASE-LAR-14056-1	p 689	N90-23713 *	NASA-CR-182061	p 781	N90-26595 *
NAS 1.26:4235	p 183	N90-13370 *				NASA-CR-182089	p 966	N90-29169 *
NAS 1.26:4236	p 735	N90-25966 *	NASA-CP-10036	p 187	N90-13384 *	NASA-CR-182124	p 929	N90-28552 *
NAS 1.26:4262	p 140	N90-13228 *	NASA-CP-10041	p 185	N90-14220 *	NASA-CR-182125	p 52	N90-10045 *
NAS 1.26:4264	p 548	N90-21602 *	NASA-CP-2487-PT-1	p 90	N90-12503 *	NASA-CR-182142	p 53	N90-10046 *
NAS 1.26:4267	p 489	N90-20969 *	NASA-CP-2487-PT-2	p 91	N90-12519 *	NASA-CR-182228	p 51	N90-10037 *
NAS 1.26:4268	p 348	N90-16768 *	NASA-CP-2487-PT-3	p 92	N90-12539 *	NASA-CR-182230	p 193	N90-13388 *
NAS 1.26:4270	p 235	N90-15072 *	NASA-CP-3052	p 352	N90-17647 *	NASA-CR-182236	p 73	N90-10451 *
NAS 1.26:4275	p 401	N90-18371 *	NASA-CP-3063	p 468	N90-20921 *	NASA-CR-182247	p 777	N90-26355 *
NAS 1.26:4277	p 696	N90-24852 *	NASA-CP-3067	p 696	N90-24853 *	NASA-CR-182278	p 113	N90-11738 *
NAS 1.26:4278	p 399	N90-19203 *				NASA-CR-182607	p 601	N90-22651 *
NAS 1.26:4280	p 401	N90-18372 *	NASA-CR-168069	p 930	N90-28559 *	NASA-CR-183272	p 845	N90-27694 *
NAS 1.26:4284	p 610	N90-22746 *	NASA-CR-168137	p 931	N90-28566 *	NASA-CR-183832	p 201	N90-13404 *
NAS 1.26:4288	p 416	N90-19226 *	NASA-CR-168211	p 931	N90-28561 *	NASA-CR-183942	p 543	N90-21395 *

NASA-CR-185074	p 172	N90-13354 *	#	NASA-CR-4264	p 548	N90-21602 *	#	NASA-TM-102233	p 133	N90-11970 *	#
NASA-CR-185109	p 220	N90-14153 *	#	NASA-CR-4267	p 489	N90-20969 *	#	NASA-TM-102235	p 399	N90-19204 *	#
NASA-CR-185129	p 468	N90-20943 *	#	NASA-CR-4268	p 348	N90-16768 *	#	NASA-TM-102236	p 582	N90-21758 *	#
NASA-CR-185133	p 51	N90-10036 *	#	NASA-CR-4270	p 235	N90-15072 *	#	NASA-TM-102246	p 349	N90-17641 *	#
NASA-CR-185135	p 79	N90-11549 *	#	NASA-CR-4275	p 401	N90-18371 *	#	NASA-TM-102250	p 671	N90-23413 *	#
NASA-CR-185138	p 113	N90-11739 *	#	NASA-CR-4277	p 696	N90-24852 *	#	NASA-TM-102253	p 81	N90-11692 *	#
NASA-CR-185140	p 18	N90-10004 *	#	NASA-CR-4278	p 399	N90-19203 *	#	NASA-TM-102258	p 370	N90-17112 *	#
NASA-CR-185154	p 143	N90-13323 *	#	NASA-CR-4280	p 401	N90-18372 *	#	NASA-TM-102266	p 172	N90-13353 *	#
NASA-CR-185156	p 217	N90-14783 *	#	NASA-CR-4284	p 610	N90-22746 *	#	NASA-TM-102271	p 540	N90-20325 *	#
NASA-CR-185157	p 551	N90-21724 *	#	NASA-CR-4288	p 416	N90-19226 *	#	NASA-TM-102272	p 816	N90-26800 *	#
NASA-CR-185158	p 649	N90-23393 *	#	NASA-CR-4289	p 588	N90-21760 *	#	NASA-TM-102273	p 194	N90-14236 *	#
NASA-CR-185189	p 690	N90-23769 *	#	NASA-CR-4294	p 762	N90-26019 *	#	NASA-TM-102304	p 516	N90-21038 *	#
NASA-CR-185197	p 344	N90-17635 *	#	NASA-CR-4296	p 583	N90-22557 *	#	NASA-TM-102315	p 203	N90-14268 *	#
NASA-CR-185222	p 588	N90-21761 *	#	NASA-CR-4298	p 582	N90-21755 *	#	NASA-TM-102341	p 54	N90-10891 *	#
NASA-CR-185225	p 506	N90-21006 *	#	NASA-CR-4299	p 633	N90-24242 *	#	NASA-TM-102342	p 610	N90-22808 *	#
NASA-CR-185241	p 782	N90-26633 *	#	NASA-CR-4302	p 719	N90-25940 *	#	NASA-TM-102348	p 215	N90-14641 *	#
NASA-CR-185243	p 588	N90-21763 *	#	NASA-CR-4304	p 965	N90-29919 *	#	NASA-TM-102358	p 318	N90-17561 *	#
NASA-CR-185277	p 933	N90-29394 *	#	NASA-CR-4305	p 637	N90-24257 *	#	NASA-TM-102365	p 379	N90-17413 *	#
NASA-CR-185474	p 200	N90-13401 *	#	NASA-CR-4307	p 634	N90-24246 *	#	NASA-TM-102368	p 610	N90-22703 *	#
NASA-CR-185475	p 57	N90-10075 *	#	NASA-CR-4308	p 816	N90-27655 *	#	NASA-TM-102374	p 84	N90-12560 *	#
NASA-CR-185563	p 124	N90-11774 *	#	NASA-CR-4314	p 718	N90-25939 *	#	NASA-TM-102387	p 94	N90-12561 *	#
NASA-CR-185853	p 87	N90-11695 *	#	NASA-CR-4315	p 896	N90-28396 *	#	NASA-TM-102389	p 187	N90-13381 *	#
NASA-CR-185854	p 136	N90-12872 *	#	NASA-CR-4316	p 965	N90-29143 *	#	NASA-TM-102391	p 215	N90-14511 *	#
NASA-CR-185884	p 183	N90-13369 *	#	NASA-CR-4317	p 964	N90-29142 *	#	NASA-TM-102397	p 114	N90-11740 *	#
NASA-CR-185931	p 925	N90-29385 *	#	NASA-CR-4323	p 909	N90-28494 *	#	NASA-TM-102402	p 720	N90-25948 *	#
NASA-CR-186036	p 103	N90-11733 *	#	NASA-CR-4326	p 924	N90-29383 *	#	NASA-TM-102408	p 205	N90-13636 *	#
NASA-CR-186037	p 90	N90-12500 *	#	NASA-CR-4328	p 925	N90-29384 *	#	NASA-TM-102409	p 197	N90-12618 *	#
NASA-CR-186046	p 184	N90-14216 *	#					NASA-TM-102419	p 113	N90-13389 *	#
NASA-CR-186067	p 690	N90-24557 *	#	NASA-RP-1235	p 516	N90-21037 *	#	NASA-TM-102422	p 194	N90-13393 *	#
NASA-CR-186070	p 336	N90-16751 *	#					NASA-TM-102426	p 380	N90-18229 *	#
NASA-CR-186100	p 217	N90-14843 *	#	NASA-SP-501	p 107	N90-12589 *	#	NASA-TM-102428	p 172	N90-13355 *	#
NASA-CR-186116	p 171	N90-13349 *	#					NASA-TM-102435	p 372	N90-18041 *	#
NASA-CR-186118	p 648	N90-23386 *	#	NASA-TM-100050	p 598	N90-21778 *	#	NASA-TM-102440	p 548	N90-20794 *	#
NASA-CR-186122	p 212	N90-13744 *	#	NASA-TM-100454	p 435	N90-19241 *	#	NASA-TM-102441	p 257	N90-15923 *	#
NASA-CR-186130	p 214	N90-13817 *	#	NASA-TM-100533-PT-1	p 374	N90-18125 *	#	NASA-TM-102442	p 543	N90-21361 *	#
NASA-CR-186140	p 690	N90-24514 *	#	NASA-TM-100533-PT-2	p 374	N90-18126 *	#	NASA-TM-102447	p 213	N90-13797 *	#
NASA-CR-186163	p 574	N90-21747 *	#	NASA-TM-101021	p 582	N90-21756 *	#	NASA-TM-102448	p 213	N90-13750 *	#
NASA-CR-186195	p 199	N90-14243 *	#	NASA-TM-101025	p 761	N90-25149 *	#	NASA-TM-102451	p 194	N90-14235 *	#
NASA-CR-186211	p 214	N90-14453 *	#	NASA-TM-101054	p 119	N90-11752 *	#	NASA-TM-102452	p 345	N90-17636 *	#
NASA-CR-186219	p 176	N90-14212 *	#	NASA-TM-101085	p 240	N90-15898 *	#	NASA-TM-102455	p 215	N90-14656 *	#
NASA-CR-186222	p 844	N90-26824 *	#	NASA-TM-101585	p 187	N90-14232 *	#	NASA-TM-102456	p 215	N90-14617 *	#
NASA-CR-186226	p 924	N90-29381 *	#	NASA-TM-101610	p 252	N90-15102 *	#	NASA-TM-102460	p 194	N90-13394 *	#
NASA-CR-186227	p 499	N90-20971 *	#	NASA-TM-101613	p 237	N90-15886 *	#	NASA-TM-102466	p 318	N90-17562 *	#
NASA-CR-186232	p 186	N90-14226 *	#	NASA-TM-101617	p 106	N90-12580 *	#	NASA-TM-102472	p 515	N90-21036 *	#
NASA-CR-186263	p 275	N90-15380 *	#	NASA-TM-101639	p 259	N90-15110 *	#	NASA-TM-102482	p 509	N90-20085 *	#
NASA-CR-186267	p 316	N90-16712 *	#	NASA-TM-101642	p 36	N90-10889 *	#	NASA-TM-102484	p 533	N90-21137 *	#
NASA-CR-186300	p 581	N90-21753 *	#	NASA-TM-101646	p 134	N90-12057 *	#	NASA-TM-102488	p 778	N90-26373 *	#
NASA-CR-186318	p 237	N90-15891 *	#	NASA-TM-101659	p 175	N90-14205 *	#	NASA-TM-102496	p 542	N90-21300 *	#
NASA-CR-186326	p 317	N90-17558 *	#	NASA-TM-101665	p 217	N90-14061 *	#	NASA-TM-102518	p 510	N90-20090 *	#
NASA-CR-186327	p 398	N90-19198 *	#	NASA-TM-101668	p 372	N90-18057 *	#	NASA-TM-102535	p 600	N90-21869 *	#
NASA-CR-186371	p 415	N90-18390 *	#	NASA-TM-101670	p 201	N90-13403 *	#	NASA-TM-102537	p 541	N90-20392 *	#
NASA-CR-186435	p 478	N90-20052 *	#	NASA-TM-101675	p 543	N90-21424 *	#	NASA-TM-102541	p 543	N90-21399 *	#
NASA-CR-186451	p 479	N90-20950 *	#	NASA-TM-101681	p 373	N90-18070 *	#	NASA-TM-102574	p 542	N90-21283 *	#
NASA-CR-186533	p 547	N90-21571 *	#	NASA-TM-101684	p 399	N90-19206 *	#	NASA-TM-102585	p 464	N90-19821 *	#
NASA-CR-186560	p 572	N90-21736 *	#	NASA-TM-101686	p 328	N90-17620 *	#	NASA-TM-102587	p 506	N90-21005 *	#
NASA-CR-186571	p 571	N90-21734 *	#	NASA-TM-101687	p 610	N90-22807 *	#	NASA-TM-102595	p 484	N90-20068 *	#
NASA-CR-186572	p 571	N90-21735 *	#	NASA-TM-101689	p 497	N90-20071 *	#	NASA-TM-102598	p 454	N90-18746 *	#
NASA-CR-186576	p 481	N90-20965 *	#	NASA-TM-101696	p 509	N90-20086 *	#	NASA-TM-102603	p 434	N90-18434 *	#
NASA-CR-186577	p 549	N90-21604 *	#	NASA-TM-101697	p 421	N90-18395 *	#	NASA-TM-102609	p 400	N90-19211 *	#
NASA-CR-186581	p 718	N90-25934 *	#	NASA-TM-101702	p 612	N90-22322 *	#	NASA-TM-102617	p 478	N90-20047 *	#
NASA-CR-186585	p 597	N90-21775 *	#	NASA-TM-101703	p 32	N90-10023 *	#	NASA-TM-102618	p 520	N90-20093 *	#
NASA-CR-186598	p 598	N90-21776 *	#	NASA-TM-101704	p 217	N90-13990 *	#	NASA-TM-102620	p 416	N90-19227 *	#
NASA-CR-186599	p 598	N90-21777 *	#	NASA-TM-101705	p 573	N90-22532 *	#	NASA-TM-102622	p 846	N90-22700 *	#
NASA-CR-186630	p 719	N90-25943 *	#	NASA-TM-101708	p 175	N90-14202 *	#	NASA-TM-102629	p 739	N90-25981 *	#
NASA-CR-186637	p 780	N90-25580 *	#	NASA-TM-101709	p 689	N90-23768 *	#	NASA-TM-102631	p 699	N90-24221 *	#
NASA-CR-186640	p 734	N90-25126 *	#	NASA-TM-101710	p 217	N90-13995 *	#	NASA-TM-102637	p 543	N90-21422 *	#
NASA-CR-186658	p 734	N90-25132 *	#	NASA-TM-101713	p 339	N90-16758 *	#	NASA-TM-102651	p 527	N90-21047 *	#
NASA-CR-186660	p 650	N90-23397 *	#	NASA-TM-101714	p 186	N90-14228 *	#	NASA-TM-102670	p 924	N90-28541 *	#
NASA-CR-186661	p 649	N90-23396 *	#	NASA-TM-101715	p 416	N90-19225 *	#	NASA-TM-102677	p 716	N90-25110 *	#
NASA-CR-186663	p 649	N90-23395 *	#	NASA-TM-101716	p 415	N90-19224 *	#	NASA-TM-102679	p 690	N90-24660 *	#
NASA-CR-186670	p 649	N90-23394 *	#	NASA-TM-101717	p 735	N90-25135 *	#	NASA-TM-102681	p 774	N90-25368 *	#
NASA-CR-186676	p 735	N90-25967 *	#	NASA-TM-101718	p 736	N90-25973 *	#	NASA-TM-102685	p 780	N90-26511 *	#
NASA-CR-186680	p 734	N90-25127 *	#	NASA-TM-101719	p 781	N90-26564 *	#	NASA-TM-102691	p 724	N90-25120 *	#
NASA-CR-186685	p 650	N90-24266 *	#	NASA-TM-101721	p 757	N90-25142 *	#	NASA-TM-102692	p 936	N90-28578 *	#
NASA-CR-186710	p 717	N90-25111 *	#	NASA-TM-101722	p 648	N90-23392 *	#	NASA-TM-102693	p 909	N90-28493 *	#
NASA-CR-186729	p 774	N90-25291 *	#	NASA-TM-101723	p 924	N90-28542 *	#	NASA-TM-102704	p 846	N90-27699 *	#
NASA-CR-186732	p 782	N90-26634 *	#	NASA-TM-101725	p 758	N90-25144 *	#	NASA-TM-102710	p 927	N90-28546 *	#
NASA-CR-186800	p 717	N90-25112 *	#	NASA-TM-101726	p 910	N90-28505 *	#	NASA-TM-102713	p 869	N90-27725 *	#
NASA-CR-186820-VOL-2	p 736	N90-25971 *	#	NASA-TM-101794	p 895	N90-27465 *	#	NASA-TM-102716	p 965	N90-29965 *	#
NASA-CR-186872	p 780	N90-26515 *	#	NASA-TM-101879	p 896	N90-27471 *	#	NASA-TM-102795	p 636	N90-23373 *	#
NASA-CR-186886	p 849	N90-27701 *	#	NASA-TM-101886	p 736	N90-25872 *	#	NASA-TM-102796	p 573	N90-21746 *	#
NASA-CR-186887	p 776	N90-26281 *	#	NASA-TM-102069	p 194	N90-13392 *	#	NASA-TM-102800	p 572	N90-21739 *	#
NASA-CR-186898	p 887	N90-28105 *	#	NASA-TM-102077	p 172	N90-13352 *	#	NASA-TM-102802	p 916	N90-28512 *	#
NASA-CR-186900	p 759	N90-26017 *	#	NASA-TM-102182	p 88	N90-11701 *	#	NASA-TM-102807	p 636	N90-23374 *	#
NASA-CR-186903	p 721	N90-25954 *	#	NASA-TM-102195	p 18	N90-10006 *	#	NASA-TM-102810	p 757	N90-25141 *	#
NASA-CR-186925	p 884	N90-27946 *	#	NASA-TM-102206	p 170	N90-13332 *	#	NASA-TM-102814	p 654	N90-23399 *	#
NASA-CR-186933	p 824	N90-26804 *	#	NASA-TM-102207	p 201	N90-13407 *	#	NASA-TM-102815	p 816	N90-27654 *	#
NASA-CR-186944	p 959	N90-28862 *	#	NASA-TM-102212	p 170	N90-13327 *	#	NASA-TM-102827	p 702	N90-25933 *	#
NASA-CR-187289	p 925	N90-29389 *	#	NASA-TM-102216	p 340	N90-17632 *	#	NASA-TM-102834	p 720	N90-25945 *	#
NASA-CR-3996	p 63	N90-10186 *	#	NASA-TM-102219	p 260	N90-15938 *	#	NASA-TM-102846	p 849	N90-27702 *	#
NASA-CR-4035	p 126	N90-11821 *	#	NASA-TM-102221	p 88	N90-11699 *	#	NASA-TM-103100	p 478	N90-20051 *	#
NASA-CR-4085	p 19	N90-10012 *	#	NASA-TM-102222	p 88	N90-11700 *	#	NASA-TM-103105	p 748	N90-25982 *	#
NASA-CR-4175	p 32	N90-10031 *	#	NASA-TM-102223	p 143	N90-13324 *	#	NASA-TM-103106	p 776	N90-26334 *	#
NASA-CR-4235	p 183	N90-13370 *	#	NASA-TM-102225	p 398	N90-19201 *	#	NASA-TM-103107	p 588	N90-21762 *	#
NASA-CR-4238	p 735	N90-									

REPORT NUMBER INDEX

PNR90570

NASA-TM-103123	p 666	N90-23404 *	#	NCAR/TN-337-EDD	p 103	N90-11731	#	ONERA, TP NO. 1989-154	p 4	A90-11175	#
NASA-TM-103131	p 571	N90-21733 *	#					ONERA, TP NO. 1989-158	p 223	A90-21026	#
NASA-TM-103132	p 543	N90-21394 *	#	NIAR-90-12	p 775	N90-26166	#	ONERA, TP NO. 1989-161	p 223	A90-21029	#
NASA-TM-103137	p 782	N90-26635 *	#	NIAR-90-17	p 718	N90-25937	#	ONERA, TP NO. 1989-165	p 253	A90-21031	#
NASA-TM-103167	p 589	N90-22566 *	#	NIAR-90-9	p 777	N90-26346	#	ONERA, TP NO. 1989-167	p 223	A90-21033	#
NASA-TM-103170	p 666	N90-24273 *	#					ONERA, TP NO. 1989-171	p 261	A90-21035	#
NASA-TM-103176	p 688	N90-23591 *	#	NLR-MP-87078-U	p 462	N90-19756	#	ONERA, TP NO. 1989-174	p 223	A90-21036	#
NASA-TM-103195	p 773	N90-25289 *	#	NLR-MP-87082-U	p 455	N90-19543	#	ONERA, TP NO. 1989-175	p 223	A90-21037	#
NASA-TM-103198	p 758	N90-26011 *	#	NLR-MP-88018-U	p 183	N90-13371	#	ONERA, TP NO. 1989-181	p 245	A90-21041	#
NASA-TM-103212	p 751	N90-26009 *	#	NLR-MP-88023-U	p 416	N90-19228	#	ONERA, TP NO. 1989-185	p 224	A90-21045 *	#
NASA-TM-103220	p 763	N90-26055 *	#	NLR-MP-88033-U	p 720	N90-25950	#	ONERA, TP NO. 1989-187	p 261	A90-21047	#
NASA-TM-103249	p 720	N90-25946 *	#	NLR-MP-88037-U	p 776	N90-26290	#	ONERA, TP NO. 1989-188	p 245	A90-21048	#
NASA-TM-103250	p 817	N90-27657 *	#	NLR-MP-88045-U	p 115	N90-11750	#	ONERA, TP NO. 1989-189	p 261	A90-21049	#
NASA-TM-103305	p 547	N90-21544 *	#	NLR-MP-88052-U	p 720	N90-25951	#	ONERA, TP NO. 1989-192	p 261	A90-21051	#
NASA-TM-103306	p 547	N90-21543 *	#	NLR-MP-88066-U	p 775	N90-26238	#	ONERA, TP NO. 1989-202	p 279	A90-22445	#
NASA-TM-103307	p 547	N90-21542 *	#					ONERA, TP NO. 1989-205	p 355	A90-25339	#
NASA-TM-103308	p 546	N90-21541 *	#	NLR-TP-89077-U	p 609	N90-22014	#	ONERA, TP NO. 1989-206	p 356	A90-25340	#
NASA-TM-103310	p 546	N90-21539 *	#					ONERA, TP NO. 1989-210	p 366	A90-25343	#
NASA-TM-103472	p 767	N90-26080 *	#	NLR-TR-88008-U	p 776	N90-26285	#	ONERA, TP NO. 1989-211	p 303	A90-25344	#
NASA-TM-103480	p 767	N90-26094 *	#	NLR-TR-88157-U	p 123	N90-12628	#	ONERA, TP NO. 1989-218	p 351	A90-25351	#
NASA-TM-103486	p 724	N90-25957 *	#					ONERA, TP NO. 1989-88	p 62	A90-11126	#
NASA-TM-103609	p 964	N90-29121 *	#	NMRI-90-16	p 875	N90-26972	#	ONERA, TP NO. 1990-12	p 351	A90-25358	#
NASA-TM-4131	p 186	N90-14225 *	#					ONERA, TP NO. 1990-151	p 798	A90-45934	#
NASA-TM-4134	p 79	N90-10679 *	#	NOAA-TM-ERL-ARL-179	p 811	N90-22155	#	ONERA, TP NO. 1990-16	p 683	A90-41201	#
NASA-TM-4135	p 348	N90-16767 *	#					ONERA, TP NO. 1990-24	p 623	A90-41203	#
NASA-TM-4136	p 317	N90-17560 *	#	NOAA-TM-ERL-WPL-163	p 24	N90-10842	#	ONERA, TP NO. 1990-26	p 695	A90-41205	#
NASA-TM-4137	p 183	N90-13372 *	#					ONERA, TP NO. 1990-27	p 695	A90-41206	#
NASA-TM-4140	p 114	N90-11741 *	#	NPL-RSA(EXT)-009	p 464	N90-18999	#	ONERA, TP NO. 1990-28	p 695	A90-41207	#
NASA-TM-4141	p 192	N90-13387 *	#					ONERA, TP NO. 1990-36	p 659	A90-41212	#
NASA-TM-4142	p 119	N90-11753 *	#	NPS-54-90-005	p 702	N90-25074	#	ONERA, TP NO. 1990-8	p 356	A90-25356	#
NASA-TM-4144	p 51	N90-10034 *	#								
NASA-TM-4146	p 173	N90-14186 *	#	NRC-30057	p 766	N90-25226	#	ORNL/ATD-31	p 885	N90-28059	#
NASA-TM-4147	p 119	N90-11751 *	#	NRC-30116	p 739	N90-25138	#				
NASA-TM-4148	p 103	N90-11732 *	#	NRC-30268	p 170	N90-13326	#	ORNL/CSD/TM-250	p 24	N90-10844	#
NASA-TM-4155	p 237	N90-15884 *	#	NRC-31216	p 674	N90-24278	#				
NASA-TM-4157	p 202	N90-14244 *	#	NRC-31276	p 846	N90-27697	#	OTA-SET-431	p 27	N90-10016	#
NASA-TM-4158	p 259	N90-15108 *	#	NRC-31334	p 846	N90-27698	#				
NASA-TM-4162	p 173	N90-14190 *	#					PB89-169221	p 27	N90-10016	#
NASA-TM-4163	p 369	N90-17074 *	#	NRL-MR-6505	p 134	N90-12777	#	PB89-174775	p 39	N90-10032	#
NASA-TM-4171	p 850	N90-27703 *	#	NRL-MR-6630	p 815	N90-26796	#	PB89-200901	p 137	N90-12113	#
NASA-TM-4173	p 420	N90-18394 *	#	NRL-MR-6667	p 960	N90-29587	#	PB89-208102	p 24	N90-10842	#
NASA-TM-4175	p 373	N90-17235 *	#	NRL-MR-6682	p 933	N90-28573	#	PB89-208995	p 103	N90-11731	#
NASA-TM-4179	p 615	N90-23338 *	#					PB89-216980	p 139	N90-12291	#
NASA-TM-4180	p 582	N90-22555 *	#	NSF-89-314	p 369	N90-16969	#	PB89-217525	p 119	N90-11754	#
NASA-TM-4181	p 398	N90-19199 *	#					PB89-219463	p 138	N90-13116	#
NASA-TM-4183	p 499	N90-20974 *	#	NSMRL-SP89-5	p 357	N90-16939	#	PB89-221600	p 136	N90-12879	#
NASA-TM-4195	p 876	N90-27787 *	#					PB89-910404	p 24	N90-10013	#
NASA-TM-4200	p 632	N90-24238 *	#	NSWC/TR-89-180	p 634	N90-24251	#	PB89-910406	p 240	N90-15895	#
NASA-TM-4201	p 632	N90-24237 *	#					PB90-103888	p 369	N90-16969	#
NASA-TM-4207	p 929	N90-28551 *	#	NTSB-ARG-89/01	p 820	N90-27666	#	PB90-120296	p 468	N90-20920	#
NASA-TM-4222	p 959	N90-28815 *	#					PB90-125113	p 141	N90-12406	#
NASA-TM-88277	p 214	N90-13820 *	#	NTSB/AAR-89/03	p 24	N90-10013	#	PB90-138066	p 486	N90-20966	#
NASA-TM-89125	p 1	N90-10002 *	#	NTSB/AAR-89/04	p 240	N90-15895	#	PB90-138066	p 820	N90-27666	#
NASA-TM-89131	p 72	N90-10409 *	#	NTSB/AAR-90/01	p 574	N90-21748	#	PB90-142217	p 611	N90-22155	#
NASA-TM-89423	p 52	N90-10042 *	#					PB90-166588	p 533	N90-21142	#
				NTSB/ARG-89/01	p 486	N90-20966	#	PB90-166778	p 481	N90-20963	#
								PB90-166786	p 522	N90-21041	#
NASA-TP-2462	p 468	N90-20942 *	#	NTSB/SIR-90/01	p 503	N90-21000	#	PB90-167131	p 481	N90-20964	#
NASA-TP-2879	p 73	N90-11245 *	#					PB90-167883	p 578	N90-21751	#
NASA-TP-2917	p 249	N90-15902 *	#	NU-CENTER-QEFP-1989-3	p 206	N90-13638	#	PB90-167891	p 578	N90-21752	#
NASA-TP-2925	p 259	N90-15112 *	#					PB90-191206	p 820	N90-27667	#
NASA-TP-2939	p 20	N90-10829 *	#	ONERA-NT-1988-6	p 454	N90-18697	#	PB90-197997	p 913	N90-28507	#
NASA-TP-2945	p 20	N90-10830 *	#	ONERA-NT-1989-2	p 773	N90-25267	#	PB90-206301	p 787	N90-27646	#
NASA-TP-2946	p 237	N90-15882 *	#					PB90-207218	p 902	N90-28489	#
NASA-TP-2952	p 134	N90-12042 *	#	ONERA-RF-20/7294-PH	p 872	N90-27729	#	PB90-211061	p 503	N90-21003	#
NASA-TP-2960	p 420	N90-18393 *	#					PB90-213620	p 937	N90-28580	#
NASA-TP-2961	p 173	N90-14187 *	#	ONERA-RS-82/5094-PY	p 896	N90-28402	#	PB90-222167	p 915	N90-28511	#
NASA-TP-2962	p 120	N90-11757 *	#					PB90-910401	p 574	N90-21748	#
NASA-TP-2963	p 456	N90-19718 *	#	ONERA-RSF-1/3731-AY-002A	p 910	N90-28500	#	PB90-917004	p 503	N90-21000	#
NASA-TP-2965	p 349	N90-17639 *	#	ONERA-RSF-12/0694-GY	p 141	N90-13278	#				
NASA-TP-2966	p 338	N90-17627 *	#	ONERA-RSF-32/1285-AY-346A	p 107	N90-12592	#	PD-CF-8942	p 480	N90-20951	#
NASA-TP-2969	p 315	N90-16710 *	#					PD-CF-8943	p 400	N90-19213	#
NASA-TP-2971	p 249	N90-15100 *	#	ONERA, TP NO. 1989-102	p 67	A90-11136	#	PD-CF-9004	p 499	N90-20975	#
NASA-TP-2973	p 397	N90-19193 *	#	ONERA, TP NO. 1989-104	p 57	A90-11138	#	PD-CF-9005	p 718	N90-25936	#
NASA-TP-2974	p 462	N90-18882 *	#	ONERA, TP NO. 1989-107	p 58	A90-11140	#	PD-CF-9009	p 936	N90-28577	#
NASA-TP-2975	p 414	N90-18385 *	#	ONERA, TP NO. 1989-108	p 3	A90-11141	#	PD-CF-9010	p 909	N90-28491	#
NASA-TP-2978	p 404	N90-18378 *	#	ONERA, TP NO. 1989-109	p 40	A90-11142	#				
NASA-TP-2980	p 506	N90-21004 *	#	ONERA, TP NO. 1989-115	p 3	A90-11147	#	PD-FC-9001	p 489	N90-20970	#
NASA-TP-2982	p 434	N90-19239 *	#	ONERA, TP NO. 1989-116	p 3	A90-11148	#	PD-FC-9003	p 758	N90-26010	#
NASA-TP-2985	p 858	N90-27722 *	#	ONERA, TP NO. 1989-118	p 4	A90-11149	#				
NASA-TP-2990	p 477	N90-20046 *	#	ONERA, TP NO. 1989-119	p 15	A90-12623	#	PD-PR-8910	p 965	N90-29926	#
NASA-TP-2996	p 440	N90-19242 *	#	ONERA, TP NO. 1989-120	p 49	A90-12591	#				
NASA-TP-3000	p 573	N90-22531 *	#	ONERA, TP NO. 1989-121	p 50	A90-12611	#	PDA-86-FR-5333-00-06	p 192	N90-13385 *	#
NASA-TP-3001	p 735	N90-25134 *	#	ONERA, TP NO. 1989-122	p 10	A90-12510	#				
NASA-TP-3002	p 910	N90-28503 *	#	ONERA, TP NO. 1989-123	p 47	A90-12569	#	PML-1990-C50	p 939	N90-29433	#
NASA-TP-3005	p 665	N90-23403 *	#	ONERA, TP NO. 1989-124	p 58	A90-12634	#				
NASA-TP-3008	p 816	N90-27649 *	#	ONERA, TP NO. 1989-131	p 22	A90-11155	#	PNL-6903	p 126	N90-11813	#
NASA-TP-3009	p 633	N90-24239 *	#	ONERA, TP NO. 1989-133	p 22	A90-11157	#				
NASA-TP-3011	p 876	N90-27788 *	#	ONERA, TP NO. 1989-136	p 4	A90-11158	#	PNR90544	p 114	N90-11746	#
NASA-TP-3018	p 883	N90-27066 *	#	ONERA, TP NO. 1989-137	p 58	A90-11159	#	PNR90545	p 114	N90-11747	#
NASA-TP-3027	p 965	N90-29166 *	#	ONERA, TP NO. 1989-142	p 22	A90-11164	#	PNR90546	p 114	N90-11748	#
NASA-TP-3036	p 718	N90-25938 *	#	ONERA, TP NO. 1989-145	p 76	A90-11167	#	PNR90548	p 126	N90-11874	#
				ONERA, TP NO. 1989-147	p 58	A90-11169	#	PNR90554	p 114	N90-11749	#
NASA-992-21-01-PHASE-2	p 816	N90-26800 *	#	ONERA, TP NO. 1989-148	p 23	A90-11170	#	PNR90562	p 107	N90-12593	#
				ONERA, TP NO. 1989-149	p 23	A90-11171	#	PNR90566	p 115	N90-12603	#
NCAR/TN-330+PROC	p 39	N90-10032	#	ONERA, TP NO. 1989-153	p 67	A90-11173	#	PNR90570	p 115	N90-12604	#
NCAR/TN-332-PROC	p 137	N90-12113	#								

PNR90572	p 127	N90-12720	#	REPT-S3-4273-5	p 323	N90-16727	#	SAE PAPER 891081	p 101	A90-14373
PNR90574	p 140	N90-13202	#	REPT-S3-4273	p 402	N90-18376	#	SAE PAPER 891082	p 101	A90-14374
PNR90576	p 115	N90-12605	#	REPT-S3-4274-4	p 324	N90-16728	#	SAE PAPER 891083	p 102	A90-14375
PNR90577	p 140	N90-13203	#					SAE PAPER 891436	p 336	A90-27407
PNR90584	p 127	N90-12667	#	REPT-1.0-WP-VA87001-06	p 124	N90-11774	#	SAE PAPER 891438	p 339	A90-27409
PNR90585	p 115	N90-12606	#	REPT-100-20-55	p 874	N90-26894	#	SAE PAPER 891441	p 356	A90-27412
PNR90589	p 115	N90-12608	#	REPT-100-30-03	p 845	N90-26830	#	SAE PAPER 891455	p 323	A90-27424
PNR90591	p 136	N90-12933	#	REPT-49-238	p 953	N90-28722	#	SAE PAPER 891456	p 368	A90-27425
PNR90594	p 116	N90-12609	#	REPT-508	p 99	N90-12572	#	SAE PAPER 891457	p 339	A90-27426
PNR90595	p 116	N90-12610	#	REPT-542	p 99	N90-11729	#	SAE PAPER 892201	p 778	A90-45422
PNR90596	p 116	N90-12611	#	REPT-549	p 99	N90-12573	#	SAE PAPER 892202	p 713	A90-45423
PNR90597	p 116	N90-12612	#	REPT-550	p 135	N90-12807	#	SAE PAPER 892205	p 713	A90-45424
PNR90598	p 116	N90-12613	#	REPT-7227	p 966	N90-30036	#	SAE PAPER 892206	p 732	A90-45425
PNR90599	p 116	N90-12614	#	REPT-87-13	p 89	N90-11712	#	SAE PAPER 892207	p 701	A90-45426
PNR90602	p 116	N90-12616	#	REPT-88-02	p 90	N90-11713	#	SAE PAPER 892208	p 732	A90-45427
PNR90617	p 767	N90-26087	#	REPT-88-19	p 89	N90-11710	#	SAE PAPER 892209	p 701	A90-45428
PNR90628	p 777	N90-26348	#	REPT-89-GT-326	p 344	N90-17634	#	SAE PAPER 892210	p 732	A90-45429
PNR90629	p 777	N90-26349	#	REPT-89-62543	p 510	N90-20088	#	SAE PAPER 892212	p 772	A90-45430
PNR90636	p 737	N90-25977	#	REPT-8905	p 198	N90-13400	#	SAE PAPER 892213	p 423	A90-28571
PNR90640	p 750	N90-25999	#	REPT-90RR-13	p 527	N90-21049	#	SAE PAPER 892214	p 732	A90-45431
PNR90642	p 783	N90-26637	#					SAE PAPER 892215	p 728	A90-45432
PNR90646	p 750	N90-26000	#	RSRE-MEMO-4132	p 99	N90-11722	#	SAE PAPER 892216	p 728	A90-45433
PNR90650	p 750	N90-26001	#	RSRE-MEMO-4237	p 99	N90-12575	#	SAE PAPER 892217	p 728	A90-45434
PNR90664	p 883	N90-27002	#	RSRE-MEMO-4272	p 240	N90-15896	#	SAE PAPER 892218	p 728	A90-45435
PNR90667	p 750	N90-26002	#	RSRE-MEMO-4280	p 243	N90-15900	#	SAE PAPER 892219	p 729	A90-45436
PNR90671	p 750	N90-26003	#	RSRE-MEMO-4309	p 137	N90-13005	#	SAE PAPER 892220	p 756	A90-45437
PNR90675	p 750	N90-26004	#					SAE PAPER 892221	p 756	A90-45438
PNR90676	p 750	N90-26005	#	RSRE-88001	p 178	N90-13366	#	SAE PAPER 892222	p 713	A90-45439
PNR90677	p 748	N90-25139	#	RSRE-88004	p 135	N90-12816	#	SAE PAPER 892224	p 713	A90-45440
								SAE PAPER 892225	p 746	A90-45441
PPG-CDRL-6	p 637	N90-24258	#	R82AEB401	p 930	N90-28555	#	SAE PAPER 892226	p 746	A90-45442
PSU-ME-R-88/89-0068	p 134	N90-11988	#	R82AEB406	p 929	N90-28553	#	SAE PAPER 892227	p 746	A90-45443
PTI-8948	p 123	N90-12627	#	R82AEB470	p 930	N90-28559	#	SAE PAPER 892228	p 746	A90-45444
PU-TR-1894T	p 717	N90-25111	#	R82AEB472	p 929	N90-28554	#	SAE PAPER 892229	p 723	A90-45445
PW-FR-20668	p 588	N90-21761	#	R83AEB143	p 931	N90-28563	#	SAE PAPER 892230	p 738	A90-45446
PW-FR-20760	p 533	N90-20208	#	R83AEB488	p 930	N90-28558	#	SAE PAPER 892231	p 732	A90-45447
				R83AEB503	p 931	N90-28561	#	SAE PAPER 892232	p 733	A90-45448
PW/ED/FR-20820	p 689	N90-23752	#	R83AEB623	p 931	N90-28562	#	SAE PAPER 892234	p 733	A90-45449
				R84AEB246	p 930	N90-28557	#	SAE PAPER 892238	p 733	A90-45450
PW/FL/FR-20505	p 256	N90-15107	#	R89AEB-325	p 777	N90-26355	#	SAE PAPER 892245	p 713	A90-45452
				R90-957907-2	p 816	N90-27655	#	SAE PAPER 892252	p 746	A90-45454
								SAE PAPER 892253	p 746	A90-45455
				SAALC/MMEP-88-02	p 287	N90-16708	#	SAE PAPER 892254	p 747	A90-45456
								SAE PAPER 892255	p 747	A90-45457
				SAE P-217	p 817	A90-46004		SAE PAPER 892261	p 733	A90-45458
								SAE PAPER 892264	p 733	A90-45459
PWA-5394-315	p 930	N90-28560	#	SAE PAPER 890913	p 365	A90-24681		SAE PAPER 892284	p 757	A90-45464
PWA-5574-223-VOL-2	p 357	N90-17868	#	SAE PAPER 890918	p 286	A90-24685		SAE PAPER 892287	p 714	A90-45465
PWA-5594-231	p 931	N90-28566	#	SAE PAPER 890923	p 286	A90-24689		SAE PAPER 892288	p 714	A90-45466
PWA-5594-251-VOL-2	p 931	N90-28565	#	SAE PAPER 890925	p 286	A90-24690		SAE PAPER 892289	p 714	A90-45467
PWA-5594-258-VOL-1	p 931	N90-28564	#	SAE PAPER 890926	p 365	A90-24691		SAE PAPER 892292	p 723	A90-45468
PWA-5594-271-ADD	p 930	N90-28556	#	SAE PAPER 890927	p 365	A90-24692		SAE PAPER 892293	p 778	A90-45469
PWA-5594-287	p 932	N90-28570	#	SAE PAPER 890928	p 286	A90-24693		SAE PAPER 892310	p 714	A90-45473
PWA-5594-331	p 932	N90-28569	#	SAE PAPER 890929	p 286	A90-24694		SAE PAPER 892312	p 714	A90-45474
PWA-5594-333	p 932	N90-28567	#	SAE PAPER 890936	p 286	A90-24699		SAE PAPER 892313	p 757	A90-45475
PWA-5970-40	p 193	N90-13388	#	SAE PAPER 890939	p 365	A90-24702		SAE PAPER 892314	p 747	A90-45476
				SAE PAPER 891014	p 128	A90-14326		SAE PAPER 892315	p 714	A90-45477
R/D-5852-EN-01	p 262	N90-15115	#	SAE PAPER 891015	p 100	A90-14327		SAE PAPER 892322	p 715	A90-45481
RADC-TR-89-165	p 377	N90-17348	#	SAE PAPER 891016	p 109	A90-14328		SAE PAPER 892323	p 772	A90-45482
				SAE PAPER 891017	p 128	A90-14329		SAE PAPER 892326	p 738	A90-45484
RAE-TM-AERO-2130	p 122	N90-11768	#	SAE PAPER 891018	p 100	A90-14330		SAE PAPER 892327	p 738	A90-45485
RAE-TM-AERO-2139	p 95	N90-12562	#	SAE PAPER 891019	p 83	A90-14331		SAE PAPER 892329	p 747	A90-45486
RAE-TM-AERO-2146	p 95	N90-12563	#	SAE PAPER 891020	p 83	A90-14332		SAE PAPER 892330	p 765	A90-45487
RAE-TM-AERO-2147	p 399	N90-19202	#	SAE PAPER 891021	p 83	A90-14333		SAE PAPER 892331	p 765	A90-45488
RAE-TM-AERO-2159	p 958	N90-28800	#	SAE PAPER 891022	p 117	A90-14334		SAE PAPER 892335	p 765	A90-45490
				SAE PAPER 891025	p 81	A90-14336		SAE PAPER 892337	p 733	A90-45491
RAE-TM-FM-16	p 251	N90-15917	#	SAE PAPER 891031	p 128	A90-14339		SAE PAPER 892340	p 760	A90-45494
RAE-TM-FM-35	p 871	N90-26847	#	SAE PAPER 891032	p 139	A90-14340		SAE PAPER 892341	p 715	A90-45495
RAE-TM-FM-41	p 827	N90-27693	#	SAE PAPER 891034	p 100	A90-14341		SAE PAPER 892344	p 715	A90-45496
				SAE PAPER 891037	p 124	A90-14343		SAE PAPER 892345	p 715	A90-45497
RAE-TM-MAT-STR-1138	p 499	N90-20973	#	SAE PAPER 891038	p 124	A90-14344		SAE PAPER 892346	p 715	A90-45498
				SAE PAPER 891039	p 118	A90-14345		SAE PAPER 892349	p 733	A90-45500
RAE-TM-MM-11	p 140	N90-13207	#	SAE PAPER 891040	p 139	A90-14346		SAE PAPER 892350	p 733	A90-45501
				SAE PAPER 891042	p 128	A90-14347		SAE PAPER 892351	p 734	A90-45502
RAE-TM-MS-1129	p 499	N90-20972	#	SAE PAPER 891046	p 109	A90-14350		SAE PAPER 892352	p 760	A90-45503
				SAE PAPER 891047	p 109	A90-14351		SAE PAPER 892353	p 760	A90-45504
RAE-TM-P-1141	p 117	N90-12619	#	SAE PAPER 891048	p 110	A90-14352		SAE PAPER 892354	p 760	A90-45505
RAE-TM-P-1149	p 256	N90-15919	#	SAE PAPER 891049	p 100	A90-14353		SAE PAPER 892355	p 761	A90-45506
RAE-TM-P-1151	p 256	N90-15920	#	SAE PAPER 891052	p 108	A90-14354		SAE PAPER 892356	p 761	A90-45507
RAE-TM-P-1154	p 256	N90-15921	#	SAE PAPER 891053	p 118	A90-14355		SAE PAPER 892357	p 738	A90-45508
RAE-TM-P-1172	p 257	N90-15922	#	SAE PAPER 891054	p 108	A90-14356		SAE PAPER 892359	p 738	A90-45509
RAE-TM-P-1179	p 751	N90-26007	#	SAE PAPER 891055	p 98	A90-14357		SAE PAPER 892362	p 747	A90-45511
				SAE PAPER 891056	p 129	A90-14358		SAE PAPER 892363	p 747	A90-45512
RAE-TM-SS-9	p 721	N90-25953	#	SAE PAPER 891058	p 129	A90-14360		SAE PAPER 892364	p 748	A90-45513
				SAE PAPER 891060	p 100	A90-14361		SAE PAPER 892365	p 748	A90-45514
RAE-TRANS-2171	p 201	N90-13408	#	SAE PAPER 891062	p 100	A90-14362		SAE PAPER 892372	p 782	A90-45519
RAE-TRANS-2172	p 176	N90-14211	#	SAE PAPER 891063	p 129	A90-14363		SAE PAPER 892381	p 715	A90-45522
RAE-TRANS-2176	p 960	N90-29597	#	SAE PAPER 891064	p 101	A90-14364		SAE PAPER 901217	p 840	A90-49292
				SAE PAPER 891065	p 110	A90-14365		SAE PAPER 901218	p 840	A90-49293
RAND/R-3687-P/L	p 287	N90-16707	#	SAE PAPER 891066	p 110	A90-14366		SAE PAPER 901219	p 840	A90-49294
				SAE PAPER 891070	p 95	A90-14367		SAE PAPER 901221	p 840	A90-49295
RCC/RSG-318-89	p 520	N90-20092	#	SAE PAPER 891072	p 101	A90-14368		SAE PAPER 901234	p 841	A90-49304
				SAE PAPER 891075	p 101	A90-14369		SAE PAPER 901235	p 841	A90-49305
REPT-E87/645800	p 323	N90-16726	#	SAE PAPER 891078	p 101	A90-14370		SAE PAPER 901236	p 841	A90-49306
				SAE PAPER 891079	p 81	A90-14371		SAE PAPER 901237	p 841	A90-49307
REPT-M6-594000	p 184	N90-13378	#	SAE PAPER 891080	p 101	A90-14372		SAE PAPER 901238	p 841	A90-49308

WRDC-20

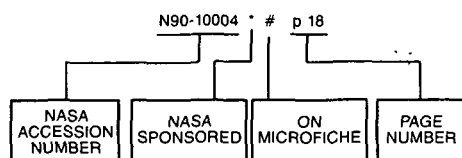
SAE PAPER 901306	p 882	A90-49358	TSI-89-04-06-WB	p 119	N90-11756	#	USAAEFA-87-25-1-PHASE-2	p 239	N90-15083	#
SAE SP-800	p 423	A90-28571 *	TT-8902	p 202	N90-13409	#	USAAEFA-88-03	p 648	N90-23387	#
			TT-9007	p 938	N90-29403		USAAEFA-88-06-1	p 323	N90-16723	#
			TT-9010	p 913	N90-29334	#	USAAEFA-88-06-1	p 323	N90-16723	#
SAND-88-2473C-VOL-2	p 372	N90-18065					USAAEFA-88-06-1	p 323	N90-16723	#
SAND-89-1485	p 236	N90-15076	TWR-19872	p 201	N90-13404 *	#	USAAEFA-88-06-1	p 323	N90-16723	#
SAND-89-1972C	p 405	N90-19217					USAAEFA-88-06-1	p 323	N90-16723	#
SAND-89-1982	p 323	N90-16722	UC-13-VOL-2	p 372	N90-18065	#	USAAEFA-88-06-1	p 323	N90-16723	#
SAND-89-2140C	p 402	N90-19215					USAAEFA-88-06-1	p 323	N90-16723	#
SAND-89-2666C	p 572	N90-21737	UCID-21898	p 324	N90-16729	#	USAAEFA-88-06-1	p 323	N90-16723	#
SAND-89-2867C	p 464	N90-19820					USAAEFA-88-06-1	p 323	N90-16723	#
SAND-90-0008	p 719	N90-25941	UDR-TR-88-10	p 323	N90-16724	#	USAAEFA-88-06-1	p 323	N90-16723	#
SAND-90-0078	p 910	N90-28495	UDR-TR-88-129-VOL-2	p 845	N90-26828	#	USAAEFA-88-06-1	p 323	N90-16723	#
SAND-90-0421	p 678	N90-24430	UDR-TR-88-137	p 176	N90-13360	#	USAAEFA-88-06-1	p 323	N90-16723	#
SAND-90-0985C	p 967	N90-30134	UDR-TR-88-39	p 484	N90-20069	#	USAAEFA-88-06-1	p 323	N90-16723	#
			UDR-TR-88-65	p 689	N90-23762	#	USAAEFA-88-06-1	p 323	N90-16723	#
SCA-142	p 533	N90-20235	UDR-TR-89-03	p 402	N90-18375	#	USAAEFA-88-06-1	p 323	N90-16723	#
			UDR-TR-89-114	p 678	N90-23538	#	USAAEFA-88-06-1	p 323	N90-16723	#
SCT-89RRR-47	p 141	N90-12406	UDR-TR-89-60	p 933	N90-29396	#	USAAEFA-88-06-1	p 323	N90-16723	#
			UDR-TR-89-65	p 723	N90-25119	#	USAAEFA-88-06-1	p 323	N90-16723	#
SEL-88-001	p 546	N90-21541 *	UILU-ENG-90-2216	p 665	N90-23401 *	#	USAAEFA-88-06-1	p 323	N90-16723	#
SEL-88-003	p 547	N90-21542 *					USAAEFA-88-06-1	p 323	N90-16723	#
SEL-89-002	p 547	N90-21544 *	UNDAS-1419-FR	p 275	N90-15380 *	#	USAAEFA-88-06-1	p 323	N90-16723	#
SEL-89-003	p 547	N90-21543 *					USAAEFA-88-06-1	p 323	N90-16723	#
SEL-89-004	p 546	N90-21539 *					USAAEFA-88-06-1	p 323	N90-16723	#
SER-A-89-A10	p 138	N90-13116	US-PATENT-APPL-SN-010949	p 689	N90-23713 *		USAAEFA-88-06-1	p 323	N90-16723	#
SER-A-89-A11	p 136	N90-12879	US-PATENT-APPL-SN-054982	p 678	N90-23475 *		USAAEFA-88-06-1	p 323	N90-16723	#
			US-PATENT-APPL-SN-054985	p 532	N90-20133 *		USAAEFA-88-06-1	p 323	N90-16723	#
SER-B-89-B16	p 522	N90-21041	US-PATENT-APPL-SN-082766	p 526	N90-20096 *		USAAEFA-88-06-1	p 323	N90-16723	#
SER-B-89-B18	p 481	N90-20963	US-PATENT-APPL-SN-165945	p 609	N90-22025 *		USAAEFA-88-06-1	p 323	N90-16723	#
			US-PATENT-APPL-SN-192563	p 648	N90-23390 *		USAAEFA-88-06-1	p 323	N90-16723	#
SERI/TP-257-3558	p 281	N90-15519	US-PATENT-APPL-SN-203178	p 455	N90-19534 *		USAAEFA-88-06-1	p 323	N90-16723	#
SFCC-59	p 939	N90-29433	US-PATENT-APPL-SN-201480	p 498	N90-20078 *		USAAEFA-88-06-1	p 323	N90-16723	#
			US-PATENT-APPL-SN-215139	p 723	N90-25118 *		USAAEFA-88-06-1	p 323	N90-16723	#
SIR-89-023-VOL-2	p 213	N90-13812	US-PATENT-APPL-SN-251073	p 689	N90-23713 *		USAAEFA-88-06-1	p 323	N90-16723	#
			US-PATENT-APPL-SN-251438	p 689	N90-23707 *		USAAEFA-88-06-1	p 323	N90-16723	#
SME PAPER EM89-103	p 274	A90-23686	US-PATENT-APPL-SN-252081	p 499	N90-20079 *		USAAEFA-88-06-1	p 323	N90-16723	#
			US-PATENT-APPL-SN-304048	p 183	N90-13373	#	USAAEFA-88-06-1	p 323	N90-16723	#
SME PAPER MS89-134	p 222	A90-23680	US-PATENT-APPL-SN-429516	p 248	N90-15094 *	#	USAAEFA-88-06-1	p 323	N90-16723	#
SME PAPER MS89-152	p 283	A90-23681	US-PATENT-APPL-SN-493864	p 532	N90-20133 *		USAAEFA-88-06-1	p 323	N90-16723	#
SME PAPER MS89-158	p 222	A90-23683	US-PATENT-APPL-SN-501667	p 503	N90-21002		USAAEFA-88-06-1	p 323	N90-16723	#
SME PAPER MS89-330	p 274	A90-23694	US-PATENT-APPL-SN-522629	p 532	N90-20133 *		USAAEFA-88-06-1	p 323	N90-16723	#
			US-PATENT-APPL-SN-522629	p 678	N90-23475 *		USAAEFA-88-06-1	p 323	N90-16723	#
SPIE-972	p 66	A90-10138	US-PATENT-APPL-SN-641152	p 678	N90-23475 *		USAAEFA-88-06-1	p 323	N90-16723	#
SPIE-986	p 37	A90-11201	US-PATENT-APPL-SN-905439	p 256	N90-15918	#	USAAEFA-88-06-1	p 323	N90-16723	#
SPIE-989	p 67	A90-11659					USAAEFA-88-06-1	p 323	N90-16723	#
SRA-900049-UM	p 574	N90-22538 *	US-PATENT-CLASS-244-122	p 723	N90-25118		USAAEFA-88-06-1	p 323	N90-16723	#
SRA-900049F	p 631	N90-23348 *	US-PATENT-CLASS-244-130	p 498	N90-20078 *		USAAEFA-88-06-1	p 323	N90-16723	#
			US-PATENT-CLASS-244-130	p 499	N90-20079 *		USAAEFA-88-06-1	p 323	N90-16723	#
SRI-04-8542-2	p 896	N90-28396 *	US-PATENT-CLASS-244-135	p 503	N90-21002		USAAEFA-88-06-1	p 323	N90-16723	#
SRI-17-7958-851	p 287	N90-16708	US-PATENT-CLASS-244-137.4	p 499	N90-20079 *		USAAEFA-88-06-1	p 323	N90-16723	#
			US-PATENT-CLASS-244-450A	p 648	N90-23390 *		USAAEFA-88-06-1	p 323	N90-16723	#
SU-JIAA-TR-88	p 845	N90-27694 *	US-PATENT-CLASS-244-46	p 648	N90-23390 *		USAAEFA-88-06-1	p 323	N90-16723	#
SU-JIAA-TR-92	p 478	N90-20052 *	US-PATENT-CLASS-244-54	p 498	N90-20078 *		USAAEFA-88-06-1	p 323	N90-16723	#
SU-JIAA-TR-97	p 316	N90-16712 *	US-PATENT-CLASS-244-55	p 498	N90-20078 *		USAAEFA-88-06-1	p 323	N90-16723	#
			US-PATENT-CLASS-244-75R	p 648	N90-23390 *		USAAEFA-88-06-1	p 323	N90-16723	#
SWRI-06-7576/13	p 193	N90-13391 *	US-PATENT-CLASS-244-90R	p 648	N90-23390 *		USAAEFA-88-06-1	p 323	N90-16723	#
SWRI-7576/45	p 193	N90-13390 *	US-PATENT-CLASS-340-825.69	p 689	N90-23707 *		USAAEFA-88-06-1	p 323	N90-16723	#
			US-PATENT-CLASS-364-427	p 526	N90-20096 *		USAAEFA-88-06-1	p 323	N90-16723	#
S3912A	p 434	N90-18433	US-PATENT-CLASS-364-578	p 689	N90-23713 *		USAAEFA-88-06-1	p 323	N90-16723	#
			US-PATENT-CLASS-364-900	p 689	N90-23713 *		USAAEFA-88-06-1	p 323	N90-16723	#
TABES PAPER 89-1203	p 238	A90-20390	US-PATENT-CLASS-364-924.4	p 689	N90-23713 *		USAAEFA-88-06-1	p 323	N90-16723	#
			US-PATENT-CLASS-364-925.1	p 689	N90-23713 *		USAAEFA-88-06-1	p 323	N90-16723	#
TACOM-TR-13464	p 201	N90-13402	US-PATENT-CLASS-364-933.8	p 689	N90-23713 *		USAAEFA-88-06-1	p 323	N90-16723	#
			US-PATENT-CLASS-364-934	p 689	N90-23713 *		USAAEFA-88-06-1	p 323	N90-16723	#
TAMRF-3224-85-12	p 235	N90-15072 *	US-PATENT-CLASS-422-111	p 609	N90-22025 *		USAAEFA-88-06-1	p 323	N90-16723	#
TAMRF-5373-8903	p 103	N90-11733 *	US-PATENT-CLASS-422-126	p 609	N90-22025 *		USAAEFA-88-06-1	p 323	N90-16723	#
			US-PATENT-CLASS-422-62	p 609	N90-22025 *		USAAEFA-88-06-1	p 323	N90-16723	#
TAO-50277	p 893	N90-28366 *	US-PATENT-CLASS-422-98	p 609	N90-22025 *		USAAEFA-88-06-1	p 323	N90-16723	#
			US-PATENT-CLASS-436-137	p 609	N90-22025 *		USAAEFA-88-06-1	p 323	N90-16723	#
TD-89-3865-PT-2	p 939	N90-29409	US-PATENT-CLASS-436-143	p 609	N90-22025 *		USAAEFA-88-06-1	p 323	N90-16723	#
TD-89-3873	p 963	N90-28887	US-PATENT-CLASS-436-55	p 609	N90-22025 *		USAAEFA-88-06-1	p 323	N90-16723	#
TD-89-3874-PT-1	p 919	N90-29380	US-PATENT-CLASS-558-190	p 532	N90-20133 *		USAAEFA-88-06-1	p 323	N90-16723	#
			US-PATENT-CLASS-558-193	p 678	N90-23475 *		USAAEFA-88-06-1	p 323	N90-16723	#
TD88-1107	p 123	N90-12629	US-PATENT-CLASS-73-147	p 689	N90-23707 *		USAAEFA-88-06-1	p 323	N90-16723	#
TD89-0953	p 135	N90-12823	US-PATENT-CLASS-73-178-T	p 526	N90-20096 *		USAAEFA-88-06-1	p 323	N90-16723	#
			US-PATENT-CLASS-73-432.1	p 455	N90-19534 *		USAAEFA-88-06-1	p 323	N90-16723	#
TECOM-7-CO-R89-AVO-004	p 896	N90-27469	US-PATENT-4,838,029	p 256	N90-15918	#	USAAEFA-88-06-1	p 323	N90-16723	#
			US-PATENT-4,843,554	p 526	N90-20096 *		USAAEFA-88-06-1	p 323	N90-16723	#
TR-1-1987	p 178	N90-13367	US-PATENT-4,848,153	p 455	N90-19534 *		USAAEFA-88-06-1	p 323	N90-16723	#
TR-11	p 214	N90-14453 *	US-PATENT-4,863,118	p 499	N90-20079 *		USAAEFA-88-06-1	p 323	N90-16723	#
TR-391	p 909	N90-28494 *	US-PATENT-4,864,050	p 532	N90-20133 *		USAAEFA-88-06-1	p 323	N90-16723	#
TR-5-1988	p 178	N90-13368	US-PATENT-4,867,394	p 498	N90-20078 *		USAAEFA-88-06-1	p 323	N90-16723	#
TR-89-WPAFB-3609-033	p 120	N90-11758	US-PATENT-4,886,896	p 678	N90-23475 *		USAAEFA-88-06-1	p 323	N90-16723	#
TR-89-15	p 478	N90-20053	US-PATENT-4,896,533	p 689	N90-23707 *		USAAEFA-88-06-1	p 323	N90-16723	#
TR-90	p 65	N90-10253	US-PATENT-4,901,951	p 723	N90-25118		USAAEFA-88-06-1	p 323	N90-16723	#
			US-PATENT-4,911,890	p 609	N90-22025 *		USAAEFA-88-06-1	p 323	N90-16723	#
TRB/TRR-1214	p 915	N90-28511	US-PATENT-4,917,333	p 648	N90-23390 *		USAAEFA-88-06-1	p 323	N90-16723	#
TRB/TRR-1218	p 820	N90-27667	US-PATENT-4,918,652	p 689	N90-23713 *		USAAEFA-88-06-1	p 323	N90-16723	#
TSG0428	p 116	N90-12616	USAAEFA-86-12	p 32	N90-10025	#	USAAEFA-88-06-1	p 323	N90-16723	#
TSG0478	p 750	N90-26001	USAAEFA-86-15	p 498	N90-20076	#	USAAEFA-88-06-1	p 323	N90-16723	#

ACCESSION NUMBER INDEX

AERONAUTICAL ENGINEERING / A Continuing Bibliography
1990 Cumulative Index

February 1991

Typical Accession Number Index Listing



Listings in this index are arranged alphanumerically by accession number. The page number listed to the right indicates the page on which the citation is located. An asterisk (*) indicates that the item is a NASA report. A pound sign (#) indicates that the item is available on microfiche.

A90-10074	p 1	A90-10624	# p 1	A90-11208	p 38	A90-12189	p 26	A90-12576	# p 13
A90-10137	# p 2	A90-10627	# p 76	A90-11210	p 38	A90-12190	p 69	A90-12577	# p 48
A90-10138	p 66	A90-10640	# p 66	A90-11221	p 38	A90-12191	p 26	A90-12579	# p 69
A90-10152	p 40	A90-10641	# p 2	A90-11393	p 79	A90-12192	p 26	A90-12581	# p 48
A90-10169	p 77	A90-10699	p 2	A90-11396	p 79	A90-12194	p 26	A90-12582	# p 13
A90-10170	p 1	A90-10732	p 66	A90-11410	p 67	A90-12195	p 39	A90-12583	# p 48
A90-10221	p 55	A90-10748	p 66	A90-11431	p 40	A90-12198	p 39	A90-12584	# p 48
A90-10222	p 66	A90-10837	p 76	A90-11432	p 40	A90-12202	p 39	A90-12585	# p 48
A90-10224	p 2	A90-10839	p 40	A90-11434	p 4	A90-12204	p 39	A90-12586	# p 13
A90-10226	# p 28	A90-10841	p 26	A90-11435	p 4	A90-12209	p 60	A90-12587	# p 13
A90-10227	# p 28	A90-10844	p 76	A90-11436	p 4	A90-12218	# p 9	A90-12588	# p 48
A90-10228	# p 2	A90-10848	p 76	A90-11437	p 23	A90-12219	# p 9	A90-12589	# p 49
A90-10229	# p 77	A90-10938	p 3	A90-11458	p 60	A90-12220	# p 9	A90-12590	# p 13
A90-10230	# p 29	A90-10963	p 76	A90-11539	p 62	A90-12229	# p 9	A90-12591	# p 49
A90-10239	p 25	A90-10985	p 37	A90-11553	# p 40	A90-12234	# p 39	A90-12592	# p 13
A90-10240	p 25	A90-11002	# p 22	A90-11554	# p 41	A90-12238	# p 9	A90-12593	# p 49
A90-10264	p 21	A90-11003	# p 3	A90-11557	# p 67	A90-12250	p 27	A90-12594	# p 49
A90-10265	p 22	A90-11004	# p 77	A90-11558	# p 41	A90-12253	p 29	A90-12595	# p 14
A90-10266	p 22	A90-11005	# p 57	A90-11562	# p 41	A90-12258	# p 29	A90-12596	# p 14
A90-10269	p 22	A90-11006	# p 29	A90-11575	# p 62	A90-12267	p 9	A90-12597	# p 14
A90-10340	# p 2	A90-11007	# p 29	A90-11597	p 5	A90-12268	p 10	A90-12598	# p 14
A90-10346	# p 2	A90-11008	# p 40	A90-11604	p 5	A90-12279	p 10	A90-12602	# p 63
A90-10347	# p 57	A90-11009	# p 29	A90-11610	p 5	A90-12281	p 10	A90-12606	# p 69
A90-10349	# p 29	A90-11010	# p 3	A90-11650	p 60	A90-12282	p 10	A90-12607	# p 49
A90-10350	# p 2	A90-11027	p 78	A90-11659	p 67	A90-12284	p 10	A90-12608	# p 49
A90-10462	p 25	A90-11041	p 66	A90-11660	p 38	A90-12468	p 60	A90-12609	# p 49
A90-10483	# p 73	A90-11042	p 67	A90-11661	p 38	A90-12471	p 77	A90-12611	# p 50
A90-10487	# p 73	A90-11102	# p 67	A90-11662	p 68	A90-12473	p 55	A90-12612	# p 29
A90-10491	# p 55	A90-11114	# p 67	A90-11663	p 38	A90-12474	p 43	A90-12613	# p 29
A90-10502	# p 25	A90-11124	# p 55	A90-11664	p 39	A90-12478	p 79	A90-12614	# p 14
A90-10507	# p 36	A90-11126	# p 62	A90-11665	p 68	A90-12479	p 69	A90-12615	# p 50
A90-10524	# p 36	A90-11136	# p 67	A90-11666	p 78	A90-12481	p 55	A90-12616	# p 50
A90-10529	# p 73	A90-11138	# p 57	A90-11696	p 26	A90-12501	p 43	A90-12618	# p 69
A90-10535	# p 36	A90-11140	# p 58	A90-11702	p 68	A90-12502	# p 43	A90-12619	# p 23
A90-10543	# p 73	A90-11141	# p 3	A90-11703	p 68	A90-12503	# p 44	A90-12620	# p 23
A90-10559	# p 74	A90-11142	# p 40	A90-11704	p 68	A90-12504	# p 44	A90-12621	# p 14
A90-10567	# p 74	A90-11147	# p 3	A90-11776	p 5	A90-12505	# p 44	A90-12622	# p 14
A90-10568	# p 74	A90-11148	# p 3	A90-11777	# p 5	A90-12508	# p 44	A90-12623	# p 15
A90-10571	# p 25	A90-11149	# p 4	A90-11778	# p 5	A90-12510	# p 10	A90-12624	# p 15
A90-10572	# p 25	A90-11155	# p 22	A90-11779	# p 6	A90-12512	# p 10	A90-12625	# p 15
A90-10580	# p 37	A90-11157	# p 22	A90-11780	# p 6	A90-12513	# p 60	A90-12626	# p 70
A90-10581	# p 37	A90-11158	# p 4	A90-11781	# p 6	A90-12514	# p 62	A90-12627	# p 50
A90-10583	# p 37	A90-11159	# p 58	A90-11782	# p 6	A90-12516	# p 44	A90-12628	# p 70
A90-10586	# p 37	A90-11164	# p 22	A90-11783	# p 6	A90-12517	# p 10	A90-12630	# p 70
A90-10589	# p 74	A90-11167	# p 76	A90-11784	# p 6	A90-12518	# p 11	A90-12631	# p 58
A90-10590	# p 74	A90-11169	# p 58	A90-11785	# p 6	A90-12519	# p 11	A90-12632	# p 50
A90-10599	# p 74	A90-11170	# p 23	A90-11786	# p 7	A90-12520	# p 11	A90-12633	# p 50
A90-10600	# p 75	A90-11171	# p 23	A90-11787	# p 7	A90-12521	# p 11	A90-12634	# p 58
A90-10606	# p 75	A90-11173	# p 67	A90-11788	# p 7	A90-12524	# p 11	A90-12635	# p 15
A90-10608	# p 75	A90-11175	# p 4	A90-11789	# p 7	A90-12525	# p 11	A90-12637	# p 15
A90-10614	# p 75	A90-11201	p 37	A90-11790	# p 7	A90-12526	# p 11	A90-12638	# p 50
A90-10615	# p 75	A90-11202	p 37	A90-11791	# p 7	A90-12527	# p 12	A90-12639	# p 15
A90-10616	# p 75	A90-11203	p 37	A90-11792	# p 8	A90-12528	# p 44	A90-12738	# p 16
A90-10619	# p 75	A90-11205	p 38	A90-11793	# p 8	A90-12529	# p 44	A90-12740	p 16
A90-10620	# p 76			A90-11794	# p 41	A90-12530	# p 45	A90-12752	# p 27
				A90-11795	# p 41	A90-12533	# p 62	A90-12763	# p 1
				A90-11796	# p 41	A90-12534	# p 62	A90-12764	p 56
				A90-11797	# p 41	A90-12535	# p 62	A90-12765	p 56
				A90-11798	# p 42	A90-12538	# p 62	A90-12766	p 56
				A90-11799	# p 42	A90-12539	# p 63	A90-12767	# p 56
				A90-11800	# p 42	A90-12540	# p 45	A90-12768	p 30
				A90-11801	# p 78	A90-12546	# p 45	A90-12769	# p 56
				A90-11802	# p 42	A90-12547	# p 45	A90-12770	p 30
				A90-11803	# p 78	A90-12548	# p 45	A90-12771	# p 56
				A90-11804	# p 68	A90-12549	# p 12	A90-12772	# p 56
				A90-11806	# p 8	A90-12551	# p 12	A90-12773	p 30
				A90-11807	# p 8	A90-12552	# p 46	A90-12774	# p 77
				A90-11808	# p 8	A90-12553	# p 12	A90-12775	p 56
				A90-11813	# p 26	A90-12554	# p 12	A90-12781	p 23
				A90-11849	# p 8	A90-12555	# p 12	A90-12782	# p 23
				A90-11873	# p 9	A90-12557	# p 13	A90-12783	# p 16
				A90-11875	# p 29	A90-12559	# p 46	A90-12784	# p 16
				A90-11878	# p 78	A90-12560	# p 46	A90-12791	p 30
				A90-11884	# p 78	A90-12561	# p 69	A90-12828	# p 16
				A90-11950	# p 69	A90-12562	# p 46	A90-12835	# p 16
				A90-12011	# p 42	A90-12564	# p 46	A90-12838	# p 16
				A90-12012	# p 42	A90-12568	# p 46	A90-12839	# p 16
				A90-12013	# p 42	A90-12569	# p 47	A90-12844	# p 70
				A90-12014	# p 43	A90-12570	# p 47	A90-12850	# p 16
				A90-12015	# p 43	A90-12571	# p 47	A90-12851	# p 17
				A90-12016	# p 43	A90-12572	# p 47	A90-12860	p 30
				A90-12017	# p 43	A90-12573	# p 47	A90-12865	p 17
				A90-12023	p 9	A90-12574	# p 47	A90-12866	p 30

A90-12867

ACCESSION NUMBER INDEX

A90-12867	p 30	A90-14367	p 95	A90-15849	p 86	A90-16853	# p 178	A90-17925	p 204
A90-12868	p 30	A90-14368	p 101	A90-15873	p 121	A90-16854	# p 195	A90-17962	p 204
A90-12869	p 31	A90-14369	p 101	A90-15876	# p 96	A90-16855	# p 199	A90-17973	p 175
A90-12870	p 31	A90-14370	p 101	A90-15877	# p 103	A90-16856	# p 178	A90-17976	# p 153
A90-12871	p 31	A90-14371	p 81	A90-15878	# p 131	A90-16857	# p 216	A90-17978	# p 153
A90-12872	p 57	A90-14372	p 101	A90-15887	p 131	A90-16858	# p 207	A90-17979	# p 153
A90-12999	p 70	A90-14373	p 101	A90-15889	# p 87	A90-16860	# p 179	A90-17981	# p 153
A90-13011	p 70	A90-14374	p 101	A90-15900	p 131	A90-16862	# p 207	A90-17984	# p 218
A90-13015	# p 31	A90-14375	p 102	A90-16001	# p 112	A90-16962	# p 179	A90-17985	# p 153
A90-13016	# p 17	A90-14438	p 84	A90-16002	# p 112	A90-16979	p 207	A90-17989	# p 153
A90-13017	# p 17	A90-14555	p 102	A90-16003	# p 131	A90-16983	p 179	A90-17990	# p 154
A90-13018	# p 17	A90-14556	p 102	A90-16004	# p 112	A90-16986	p 207	A90-17993	# p 209
A90-13019	# p 31	A90-14557	p 129	A90-16005	# p 112	A90-17003	p 202	A90-17997	# p 154
A90-13020	# p 17	A90-14558	p 129	A90-16006	# p 112	A90-17009	p 207	A90-17998	# p 218
A90-13023	# p 17	A90-14560	p 129	A90-16007	# p 112	A90-17026	p 207	A90-18001	# p 154
A90-13024	# p 17	A90-14561	p 137	A90-16008	# p 112	A90-17048	p 179	A90-18002	# p 154
A90-13025	# p 17	A90-14563	p 84	A90-16009	# p 113	A90-17107	p 150	A90-18050	# p 216
A90-13091	# p 70	A90-14564	p 84	A90-16010	# p 113	A90-17108	p 150	A90-18135	# p 181
A90-13220	p 51	A90-14565	p 129	A90-16011	# p 131	A90-17109	p 150	A90-18136	# p 154
A90-13224	p 31	A90-14566	p 84	A90-16012	# p 131	A90-17112	p 150	A90-18137	# p 154
A90-13238	p 17	A90-14568	p 110	A90-16049	p 113	A90-17137	p 187	A90-18138	# p 154
A90-13442	# p 123	A90-14569	p 110	A90-16101	p 87	A90-17175	p 207	A90-18141	# p 154
A90-13445	# p 109	A90-14570	p 110	A90-16104	p 87	A90-17281	p 203	A90-18144	# p 154
A90-13447	# p 109	A90-14571	p 110	A90-16105	p 87	A90-17291	p 203	A90-18145	# p 181
A90-13557	# p 81	A90-14572	p 110	A90-16300	p 141	A90-17293	p 208	A90-18147	# p 154
A90-13700	# p 141	A90-14573	p 137	A90-16320	p 132	A90-17294	p 203	A90-18153	# p 154
A90-13750	# p 127	A90-14574	p 129	A90-16330	# p 139	A90-17297	p 203	A90-18158	# p 155
A90-13767	p 127	A90-14576	p 137	A90-16332	# p 87	A90-17298	p 203	A90-18169	p 209
A90-13770	p 127	A90-14577	p 84	A90-16367	# p 87	A90-17300	p 204	A90-18243	p 155
A90-13775	# p 82	A90-14578	p 84	A90-16371	# p 132	A90-17305	p 208	A90-18249	# p 155
A90-13783	p 82	A90-14579	p 84	A90-16372	# p 132	A90-17307	# p 179	A90-18254	# p 155
A90-13784	p 117	A90-14580	p 102	A90-16373	# p 113	A90-17308	p 188	A90-18262	# p 209
A90-13785	p 82	A90-14582	p 124	A90-16521	# p 119	A90-17309	p 179	A90-18264	# p 209
A90-13786	p 82	A90-14583	p 111	A90-16616	p 132	A90-17312	p 151	A90-18296	p 155
A90-13787	p 83	A90-14584	p 102	A90-16618	p 132	A90-17313	p 179	A90-18297	p 155
A90-13788	p 83	A90-14585	p 130	A90-16619	p 132	A90-17314	p 180	A90-18298	p 156
A90-13791	p 100	A90-14586	p 111	A90-16620	p 132	A90-17346	p 199	A90-18301	p 156
A90-13845	# p 128	A90-14587	p 138	A90-16624	p 103	A90-17370	p 208	A90-18302	p 209
A90-13847	p 139	A90-14588	p 125	A90-16692	p 218	A90-17372	p 208	A90-18305	p 156
A90-13885	p 108	A90-14589	p 111	A90-16696	p 187	A90-17405	p 180	A90-18308	p 156
A90-13976	p 123	A90-14590	p 111	A90-16701	p 188	A90-17408	p 180	A90-18310	p 156
A90-13979	# p 96	A90-14591	p 111	A90-16702	p 188	A90-17413	p 199	A90-18340	p 210
A90-13980	# p 96	A90-14614	# p 111	A90-16703	p 188	A90-17416	p 175	A90-18343	p 210
A90-13982	# p 97	A90-14615	# p 102	A90-16718	p 206	A90-17417	p 180	A90-18406	p 210
A90-13983	# p 97	A90-14652	# p 125	A90-16725	p 207	A90-17421	p 180	A90-18407	p 210
A90-13984	# p 97	A90-14659	p 81	A90-16735	# p 143	A90-17426	p 200	A90-18442	p 210
A90-13985	# p 97	A90-14660	p 125	A90-16736	# p 144	A90-17431	p 200	A90-18443	p 156
A90-13986	# p 108	A90-14728	# p 118	A90-16751	# p 144	A90-17447	p 188	A90-18444	p 216
A90-13989	# p 97	A90-14729	# p 118	A90-16752	# p 144	A90-17448	# p 188	A90-18448	p 218
A90-13990	# p 97	A90-14730	# p 118	A90-16753	# p 144	A90-17461	p 180	A90-18449	p 218
A90-13992	# p 97	A90-14732	# p 98	A90-16754	# p 144	A90-17462	# p 189	A90-18450	p 218
A90-13993	# p 123	A90-14733	# p 98	A90-16755	# p 144	A90-17464	p 151	A90-18479	# p 156
A90-13994	# p 98	A90-14744	# p 138	A90-16756	# p 144	A90-17580	p 151	A90-18481	# p 157
A90-13995	# p 128	A90-14747	# p 118	A90-16757	# p 145	A90-17585	p 151	A90-18483	# p 157
A90-13996	# p 124	A90-14799	# p 138	A90-16758	# p 145	A90-17586	p 151	A90-18484	# p 190
A90-13997	# p 98	A90-14800	# p 81	A90-16759	# p 145	A90-17678	# p 180	A90-18486	# p 190
A90-13999	# p 108	A90-14997	# p 81	A90-16764	# p 145	A90-17679	# p 180	A90-18488	# p 181
A90-14001	# p 98	A90-15022	p 125	A90-16765	# p 145	A90-17683	# p 208	A90-18489	# p 181
A90-14006	# p 128	A90-15045	p 130	A90-16767	# p 145	A90-17684	# p 208	A90-18501	# p 157
A90-14012	# p 108	A90-15151	p 84	A90-16768	# p 145	A90-17688	# p 189	A90-18507	# p 210
A90-14013	# p 98	A90-15214	p 125	A90-16769	# p 146	A90-17692	# p 151	A90-18526	# p 190
A90-14091	p 83	A90-15227	# p 85	A90-16771	p 146	A90-17693	# p 151	A90-18532	# p 157
A90-14326	# p 128	A90-15231	# p 85	A90-16772	# p 146	A90-17698	# p 195	A90-18534	# p 157
A90-14327	p 100	A90-15232	# p 85	A90-16773	# p 146	A90-17703	# p 195	A90-18537	# p 157
A90-14328	p 109	A90-15233	# p 85	A90-16774	# p 146	A90-17705	# p 195	A90-18578	# p 157
A90-14329	p 128	A90-15235	# p 85	A90-16775	# p 146	A90-17707	# p 181	A90-18580	# p 211
A90-14330	p 100	A90-15237	# p 85	A90-16776	# p 146	A90-17780	p 143	A90-18584	# p 196
A90-14331	p 83	A90-15238	# p 85	A90-16777	# p 147	A90-17781	# p 152	A90-18587	# p 157
A90-14332	p 83	A90-15240	# p 85	A90-16779	# p 147	A90-17782	# p 189	A90-18590	# p 158
A90-14333	p 83	A90-15241	# p 85	A90-16780	# p 147	A90-17784	# p 152	A90-18591	# p 158
A90-14334	p 117	A90-15242	# p 85	A90-16781	# p 147	A90-17785	# p 152	A90-18592	# p 196
A90-14336	p 81	A90-15315	p 98	A90-16782	# p 147	A90-17786	# p 152	A90-18594	# p 190
A90-14339	p 128	A90-15354	p 130	A90-16783	# p 147	A90-17787	# p 152	A90-18595	# p 196
A90-14340	p 139	A90-15355	p 130	A90-16786	# p 148	A90-17788	# p 189	A90-18599	# p 219
A90-14341	p 100	A90-15357	p 130	A90-16787	# p 148	A90-17789	# p 189	A90-18600	# p 190
A90-14343	p 124	A90-15387	p 130	A90-16788	# p 148	A90-17790	# p 189	A90-18601	# p 196
A90-14344	p 124	A90-15388	p 111	A90-16789	# p 148	A90-17791	# p 189	A90-18603	# p 204
A90-14345	p 118	A90-15389	p 130	A90-16790	# p 148	A90-17793	# p 189	A90-18604	# p 158
A90-14346	p 139	A90-15390	p 111	A90-16792	# p 148	A90-17795	# p 190	A90-18606	# p 181
A90-14347	p 128	A90-15393	p 131	A90-16793	# p 148	A90-17851	# p 218	A90-18607	# p 182
A90-14350	p 109	A90-15422	# p 121	A90-16794	# p 149	A90-17862	# p 152	A90-18608	# p 158
A90-14351	p 109	A90-15423	# p 118	A90-16797	# p 149	A90-17863	# p 152	A90-18609	# p 158
A90-14352	p 110	A90-15424	# p 118	A90-16799	# p 149	A90-17864	# p 153	A90-18613	# p 190
A90-14353	p 100	A90-15425	# p 125	A90-16823	p 188	A90-17865	# p 208	A90-18623	# p 158
A90-14354	p 108	A90-15560	p 102	A90-16824	p 143	A90-17866	# p 153	A90-18624	# p 191
A90-14355	p 118	A90-15568	p 139	A90-16825	p 218	A90-17867	# p 181	A90-18627	# p 182
A90-14356	p 108	A90-15624	p 86	A90-16826	# p 149	A90-17868	# p 153	A90-18632	# p 211
A90-14357	p 98	A90-15732	p 125	A90-16827	# p 195	A90-17869	# p 153	A90-18633	# p 196
A90-14358	p 129	A90-15739	# p 86	A90-16835	# p 149	A90-17871	# p 153	A90-18635	# p 191
A90-14360	p 129	A90-15740	# p 86	A90-16841	# p 149	A90-17872	# p 153	A90-18886	# p 158
A90-14361	p 100	A90-15741	# p 86	A90-16844	p 149	A90-17918	p 209	A90-19004	p 211
A90-14362	p 100	A90-15743	# p 121	A90-16845	# p 150	A90-17919	p 143	A90-19005	p 191
A90-14363	p 129	A90-15745	# p 86	A90-16846	p 150	A90-17920	p 209	A90-19006	p 204
A90-14364	p 101	A90-15746	p 102	A90-16850	p 195	A90-17922	p 204	A90-19012	p 200
A90-14365	p 110	A90-15820	p 86	A90-16851	# p 188	A90-17924	p 204	A90-19149	# p 205
A90-14366	p 110	A90-15821	p 86	A90-16852	# p 150			A90-19153	# p 205

ACCESSION NUMBER INDEX

A90-23867

A90-19236	p 159	A90-19850	# p 211	A90-21167	p 224	A90-22231	# p 230	A90-23430	p 255
A90-19237	p 159	A90-19852	# p 192	A90-21168	p 224	A90-22233	# p 230	A90-23432	p 234
A90-19385	* # p 219	A90-19857	# p 192	A90-21169	p 225	A90-22242	# p 261	A90-23435	p 234
A90-19386	* # p 219	A90-19874	# p 167	A90-21170	p 225	A90-22244	# p 230	A90-23478	p 257
A90-19387	# p 159	A90-19875	# p 182	A90-21171	p 245	A90-22251	# p 230	A90-23632	p 280
A90-19388	# p 159	A90-19876	# p 167	A90-21172	# p 253	A90-22256	# p 230	A90-23647	* # p 234
A90-19389	# p 159	A90-19895	# p 192	A90-21225	* # p 253	A90-22258	# p 238	A90-23650	* # p 234
A90-19390	# p 159	A90-19896	# p 167	A90-21228	# p 253	A90-22259	# p 230	A90-23662	p 222
A90-19391	# p 159	A90-19917	# p 216	A90-21275	p 246	A90-22265	# p 272	A90-23680	p 222
A90-19392	# p 159	A90-19918	# p 197	A90-21318	p 266	A90-22396	p 231	A90-23681	p 283
A90-19393	# p 182	A90-19920	# p 197	A90-21324	p 271	A90-22421	p 231	A90-23683	p 222
A90-19396	# p 159	A90-19921	# p 167	A90-21378	p 240	A90-22422	p 231	A90-23686	p 274
A90-19426	# p 159	A90-19922	# p 167	A90-21379	p 241	A90-22434	p 247	A90-23694	p 274
A90-19428	# p 196	A90-19923	# p 167	A90-21380	p 241	A90-22435	p 282	A90-23697	* # p 262
A90-19429	# p 182	A90-19924	# p 167	A90-21381	p 241	A90-22445	# p 279	A90-23701	* # p 234
A90-19431	# p 160	A90-19925	# p 167	A90-21382	p 241	A90-22449	# p 231	A90-23702	* # p 274
A90-19434	# p 160	A90-19926	# p 168	A90-21383	p 252	A90-22529	# p 272	A90-23711	* # p 274
A90-19436	# p 160	A90-19929	# p 168	A90-21384	p 241	A90-22595	# p 266	A90-23751	# p 354
A90-19438	# p 160	A90-19932	# p 168	A90-21385	p 282	A90-22614	# p 252	A90-23752	# p 287
A90-19441	# p 160	A90-19936	# p 168	A90-21386	p 279	A90-22649	# p 221	A90-23753	# p 287
A90-19446	# p 160	A90-19938	# p 203	A90-21387	p 241	A90-22651	# p 273	A90-23755	# p 374
A90-19449	# p 160	A90-19939	# p 168	A90-21388	p 241	A90-22652	# p 253	A90-23757	# p 287
A90-19461	# p 196	A90-19940	# p 168	A90-21389	p 282	A90-22663	# p 273	A90-23758	# p 340
A90-19554	* # p 196	A90-19956	* # p 211	A90-21390	p 241	A90-22664	# p 254	A90-23759	# p 287
A90-19555	# p 197	A90-19966	# p 205	A90-21473	p 266	A90-22665	# p 254	A90-23760	# p 288
A90-19577	# p 197	A90-19978	# p 169	A90-21474	p 283	A90-22667	# p 254	A90-23761	# p 288
A90-19629	# p 200	A90-19981	# p 169	A90-21475	p 225	A90-22668	# p 231	A90-23762	* # p 288
A90-19630	* # p 216	A90-19983	# p 169	A90-21546	p 264	A90-22688	# p 279	A90-23763	# p 288
A90-19636	# p 160	A90-19984	* # p 212	A90-21592	p 225	A90-22689	# p 280	A90-23764	# p 340
A90-19639	# p 211	A90-20009	* # p 176	A90-21593	p 225	A90-22696	# p 221	A90-23765	# p 340
A90-19641	# p 161	A90-20010	# p 169	A90-21595	p 225	A90-22698	# p 222	A90-23766	# p 288
A90-19644	# p 191	A90-20011	# p 169	A90-21596	p 225	A90-22733	p 242	A90-23767	# p 340
A90-19648	# p 181	A90-20012	* # p 183	A90-21605	# p 261	A90-22734	p 247	A90-23769	# p 340
A90-19652	# p 161	A90-20064	p 265	A90-21607	# p 253	A90-22735	p 238	A90-23771	# p 288
A90-19663	# p 161	A90-20065	p 269	A90-21609	# p 252	A90-22743	p 273	A90-23772	# p 288
A90-19664	# p 161	A90-20077	p 270	A90-21610	# p 246	A90-22762	p 262	A90-23773	# p 289
A90-19665	* # p 161	A90-20259	# p 265	A90-21611	# p 246	A90-22816	p 231	A90-23774	# p 289
A90-19666	# p 161	A90-20261	p 243	A90-21626	# p 226	A90-23013	# p 273	A90-23777	# p 289
A90-19670	# p 162	A90-20262	p 244	A90-21627	# p 253	A90-23036	p 231	A90-23778	# p 289
A90-19674	* # p 211	A90-20263	p 265	A90-21628	# p 261	A90-23102	# p 232	A90-23779	# p 289
A90-19675	# p 200	A90-20264	p 270	A90-21702	p 221	A90-23103	# p 232	A90-23781	# p 289
A90-19682	# p 162	A90-20380	p 282	A90-21703	p 246	A90-23105	# p 232	A90-23782	# p 290
A90-19684	# p 162	A90-20390	p 238	A90-21710	p 246	A90-23109	# p 232	A90-23784	# p 290
A90-19686	# p 162	A90-20426	p 270	A90-21711	p 246	A90-23113	# p 247	A90-23786	# p 290
A90-19694	# p 162	A90-20431	p 253	A90-21712	p 246	A90-23117	# p 247	A90-23787	# p 290
A90-19695	# p 162	A90-20432	p 222	A90-21713	p 246	A90-23124	# p 232	A90-23788	# p 290
A90-19704	* # p 162	A90-20442	p 222	A90-21714	p 221	A90-23177	p 267	A90-23789	# p 290
A90-19710	# p 163	A90-20501	p 223	A90-21715	p 221	A90-23200	p 247	A90-23790	# p 290
A90-19713	# p 205	A90-20504	p 240	A90-21716	# p 264	A90-23202	p 265	A90-23791	# p 341
A90-19722	# p 163	A90-20508	# p 223	A90-21717	# p 265	A90-23207	p 273	A90-23792	* # p 358
A90-19723	# p 197	A90-20557	p 282	A90-21719	# p 242	A90-23241	# p 282	A90-23794	# p 291
A90-19728	* # p 200	A90-20576	p 221	A90-21720	# p 242	A90-23242	# p 242	A90-23795	# p 358
A90-19733	# p 216	A90-20579	# p 244	A90-21721	# p 242	A90-23245	# p 252	A90-23797	# p 291
A90-19734	# p 175	A90-20581	# p 244	A90-21722	# p 242	A90-23255	* # p 280	A90-23798	# p 291
A90-19735	* # p 175	A90-20582	# p 244	A90-21725	# p 242	A90-23276	# p 247	A90-23799	# p 358
A90-19738	# p 197	A90-20583	# p 244	A90-21774	p 266	A90-23277	# p 232	A90-23800	* # p 291
A90-19740	* # p 197	A90-20584	# p 244	A90-21935	* # p 226	A90-23278	# p 232	A90-23801	# p 358
A90-19742	* # p 163	A90-20585	# p 244	A90-21946	p 226	A90-23279	* # p 232	A90-23802	# p 358
A90-19745	* # p 163	A90-20586	# p 244	A90-21949	* p 253	A90-23280	# p 232	A90-23805	# p 358
A90-19746	# p 187	A90-20587	# p 245	A90-21979	# p 271	A90-23281	# p 233	A90-23806	# p 359
A90-19747	# p 182	A90-20588	# p 238	A90-21983	# p 226	A90-23282	* # p 283	A90-23807	* # p 359
A90-19748	# p 182	A90-20589	# p 238	A90-21984	# p 226	A90-23283	# p 233	A90-23810	# p 341
A90-19764	# p 191	A90-20590	# p 245	A90-21987	# p 257	A90-23284	* # p 252	A90-23811	# p 341
A90-19770	* # p 219	A90-20599	p 270	A90-22001	# p 246	A90-23285	* # p 233	A90-23812	# p 359
A90-19772	# p 219	A90-20604	p 283	A90-22004	# p 272	A90-23286	# p 280	A90-23813	# p 359
A90-19782	# p 163	A90-20606	p 221	A90-22014	# p 272	A90-23287	# p 273	A90-23818	# p 359
A90-19784	* # p 182	A90-20607	p 265	A90-22135	# p 272	A90-23288	# p 283	A90-23819	# p 360
A90-19786	# p 163	A90-20608	p 270	A90-22153	* # p 226	A90-23289	* # p 233	A90-23820	# p 341
A90-19787	# p 163	A90-20609	p 270	A90-22154	# p 226	A90-23290	# p 233	A90-23825	# p 360
A90-19789	# p 164	A90-20770	p 270	A90-22155	# p 226	A90-23291	# p 233	A90-23827	* # p 360
A90-19790	* # p 164	A90-20775	p 266	A90-22156	* # p 227	A90-23351	# p 254	A90-23828	* # p 360
A90-19799	# p 164	A90-20937	p 240	A90-22161	# p 227	A90-23352	p 247	A90-23829	# p 291
A90-19802	# p 164	A90-20987	p 270	A90-22164	* # p 227	A90-23353	p 274	A90-23834	# p 360
A90-19805	* # p 191	A90-20988	p 223	A90-22165	* # p 227	A90-23354	p 254	A90-23837	# p 291
A90-19815	# p 219	A90-21000	p 245	A90-22166	* # p 227	A90-23355	p 233	A90-23839	# p 354
A90-19816	* # p 164	A90-21026	# p 223	A90-22167	# p 227	A90-23356	p 233	A90-23840	# p 292
A90-19817	* # p 219	A90-21029	# p 223	A90-22180	* # p 272	A90-23357	p 257	A90-23841	* # p 292
A90-19818	# p 175	A90-21031	# p 253	A90-22182	* # p 272	A90-23358	p 257	A90-23842	* # p 354
A90-19819	# p 220	A90-21033	p 223	A90-22183	# p 266	A90-23359	p 257	A90-23843	# p 360
A90-19820	# p 175	A90-21035	# p 261	A90-22184	* # p 257	A90-23361	p 233	A90-23844	# p 292
A90-19821	# p 216	A90-21036	# p 223	A90-22186	# p 228	A90-23362	p 233	A90-23845	# p 292
A90-19822	* # p 164	A90-21037	# p 223	A90-22192	# p 266	A90-23363	p 247	A90-23846	# p 292
A90-19825	# p 165	A90-21041	# p 245	A90-22195	* # p 228	A90-23364	p 262	A90-23847	# p 292
A90-19826	# p 165	A90-21045	* # p 224	A90-22196	* # p 228	A90-23372	p 282	A90-23848	# p 360
A90-19828	* # p 165	A90-21047	# p 261	A90-22197	* # p 228	A90-23401	p 234	A90-23849	# p 361
A90-19829	# p 165	A90-21048	# p 245	A90-22199	* # p 282	A90-23402	p 274	A90-23851	# p 292
A90-19830	# p 165	A90-21049	# p 261	A90-22207	# p 228	A90-23405	p 254	A90-23852	# p 341
A90-19831	* # p 165	A90-21051	# p 261	A90-22208	# p 228	A90-23407	p 254	A90-23853	# p 341
A90-19833	# p 166	A90-21113	* # p 271	A90-22210	# p 228	A90-23409	p 255	A90-23854	# p 341
A90-19837	# p 166	A90-21115	* # p 271	A90-22211	# p 229	A90-23410	p 255	A90-23855	# p 361
A90-19841	# p 166	A90-21129	# p 271	A90-22215	# p 229	A90-23412	p 255	A90-23858	# p 361
A90-19842	# p 166	A90-21141	# p 271	A90-22216	* # p 229	A90-23416	p 222	A90-23859	# p 361
A90-19844	* # p 166	A90-21156	p 245	A90-22218	# p 229	A90-23417	p 255	A90-23863	# p 361
A90-19845	# p 166	A90-21159	p 224	A90-22219	* # p 229	A90-23422	p 234	A90-23865	# p 361
A90-19846	* # p 166	A90-21163	p 224	A90-22226	# p 229	A90-23425	p 255	A90-23866	# p 361
A90-19847	# p 191	A90-21164	p 224	A90-22230	* # p 230	A90-23428	p 265	A90-23867	# p 362

A90-23868

A90-23868 # p 362
 A90-23870 # p 362
 A90-23871 # p 342
 A90-23872 # p 362
 A90-23873 # p 342
 A90-23874 # p 342
 A90-23878 # p 293
 A90-23881 # p 362
 A90-23882 # p 362
 A90-23883 # p 293
 A90-23884 # p 342
 A90-23885 # p 363
 A90-23886 # p 342
 A90-23888 # p 342
 A90-23890 * # p 342
 A90-23891 # p 363
 A90-23892 # p 343
 A90-23893 # p 343
 A90-23896 * # p 343
 A90-23900 # p 363
 A90-23904 # p 363
 A90-23917 # p 285
 A90-23922 # p 333
 A90-23924 # p 321
 A90-23934 # p 285
 A90-23935 # p 293
 A90-23936 # p 333
 A90-23937 # p 377
 A90-23938 # p 293
 A90-23953 # p 363
 A90-23974 # p 377
 A90-23978 # p 293
 A90-23979 # p 345
 A90-23994 # p 329
 A90-23995 # p 329
 A90-23996 # p 293
 A90-24002 # p 345
 A90-24003 # p 329
 A90-24009 # p 293
 A90-24048 # p 293
 A90-24076 # p 294
 A90-24077 # p 294
 A90-24078 # p 294
 A90-24079 # p 294
 A90-24080 # p 294
 A90-24081 # p 294
 A90-24082 # p 294
 A90-24086 # p 295
 A90-24087 # p 363
 A90-24088 # p 295
 A90-24089 # p 295
 A90-24092 # p 363
 A90-24094 # p 295
 A90-24095 # p 295
 A90-24096 # p 295
 A90-24099 # p 295
 A90-24101 # p 374
 A90-24102 # p 364
 A90-24103 # p 295
 A90-24105 # p 295
 A90-24107 # p 296
 A90-24109 # p 296
 A90-24110 # p 296
 A90-24112 # p 364
 A90-24113 # p 296
 A90-24114 # p 296
 A90-24115 # p 296
 A90-24116 # p 355
 A90-24117 # p 378
 A90-24118 # p 364
 A90-24120 # p 296
 A90-24122 # p 296
 A90-24123 # p 297
 A90-24124 # p 297
 A90-24125 # p 378
 A90-24127 # p 374
 A90-24131 # p 297
 A90-24132 # p 378
 A90-24133 # p 334
 A90-24134 # p 364
 A90-24136 # p 297
 A90-24138 # p 297
 A90-24139 # p 297
 A90-24140 # p 297
 A90-24142 # p 297
 A90-24143 # p 298
 A90-24144 # p 298
 A90-24145 # p 364
 A90-24147 # p 345
 A90-24148 # p 334
 A90-24149 # p 298
 A90-24150 # p 298
 A90-24151 # p 350
 A90-24153 # p 364
 A90-24154 # p 298
 A90-24155 # p 298

A90-24156 # p 298
 A90-24157 # p 299
 A90-24158 # p 299
 A90-24161 # p 334
 A90-24162 # p 364
 A90-24164 # p 345
 A90-24165 # p 299
 A90-24166 # p 299
 A90-24167 # p 299
 A90-24169 # p 350
 A90-24171 # p 345
 A90-24200 # p 338
 A90-24216 # p 343
 A90-24218 # p 334
 A90-24229 # p 285
 A90-24231 # p 285
 A90-24233 # p 299
 A90-24253 # p 373
 A90-24265 # p 285
 A90-24272 # p 334
 A90-24280 # p 285
 A90-24281 # p 346
 A90-24284 # p 346
 A90-24288 # p 355
 A90-24291 # p 286
 A90-24293 # p 364
 A90-24329 # p 339
 A90-24338 # p 346
 A90-24342 # p 299
 A90-24353 # p 365
 A90-24354 # p 299
 A90-24359 # p 350
 A90-24376 # p 365
 A90-24377 # p 365
 A90-24681 # p 365
 A90-24685 # p 286
 A90-24689 # p 286
 A90-24690 # p 286
 A90-24691 # p 365
 A90-24692 # p 365
 A90-24693 # p 286
 A90-24694 # p 286
 A90-24699 # p 286
 A90-24702 # p 365
 A90-24741 # p 300
 A90-24752 # p 300
 A90-24753 # p 300
 A90-24825 # p 300
 A90-24861 # p 355
 A90-24865 # p 355
 A90-24964 # p 334
 A90-25027 # p 350
 A90-25028 # p 300
 A90-25036 # p 343
 A90-25040 # p 350
 A90-25041 # p 300
 A90-25042 # p 300
 A90-25043 # p 301
 A90-25101 # p 301
 A90-25102 # p 346
 A90-25105 # p 301
 A90-25108 # p 366
 A90-25165 # p 350
 A90-25167 # p 301
 A90-25168 # p 346
 A90-25169 # p 334
 A90-25172 # p 353
 A90-25174 # p 334
 A90-25175 # p 335
 A90-25185 # p 301
 A90-25186 # p 346
 A90-25189 # p 346
 A90-25199 # p 347
 A90-25200 # p 301
 A90-25221 # p 286
 A90-25267 # p 355
 A90-25276 # p 301
 A90-25277 # p 302
 A90-25280 # p 302
 A90-25283 # p 302
 A90-25284 # p 302
 A90-25285 # p 302
 A90-25288 # p 302
 A90-25289 # p 374
 A90-25290 # p 302
 A90-25292 # p 302
 A90-25301 # p 302
 A90-25303 # p 366
 A90-25304 # p 335
 A90-25339 # p 355
 A90-25340 # p 356
 A90-25343 # p 366
 A90-25344 # p 303
 A90-25351 # p 351
 A90-25356 # p 356
 A90-25358 # p 351

A90-25420 # p 347
 A90-25421 # p 347
 A90-25422 # p 303
 A90-25423 # p 335
 A90-25424 # p 335
 A90-25425 # p 335
 A90-25478 # p 374
 A90-25494 # p 339
 A90-25495 # p 329
 A90-25496 # p 329
 A90-25561 # p 330
 A90-25562 # p 330
 A90-25563 # p 375
 A90-25565 # p 330
 A90-25566 # p 375
 A90-25567 # p 373
 A90-25568 # p 330
 A90-25569 # p 330
 A90-25570 # p 330
 A90-25571 # p 331
 A90-25572 # p 373
 A90-25573 # p 331
 A90-25574 # p 331
 A90-25575 # p 331
 A90-25588 # p 303
 A90-25589 # p 303
 A90-25592 # p 303
 A90-25597 # p 303
 A90-25602 # p 366
 A90-25702 # p 331
 A90-25719 # p 375
 A90-25730 # p 304
 A90-25732 # p 304
 A90-25734 # p 366
 A90-25739 # p 304
 A90-25764 # p 366
 A90-25770 # p 366
 A90-25771 # p 304
 A90-25772 # p 304
 A90-25773 # p 304
 A90-25777 # p 304
 A90-25781 # p 353
 A90-25783 # p 304
 A90-25795 # p 305
 A90-25796 # p 305
 A90-25797 # p 305
 A90-25798 # p 305
 A90-25800 # p 305
 A90-25801 # p 367
 A90-25804 # p 305
 A90-25809 # p 306
 A90-25811 # p 367
 A90-25820 # p 306
 A90-25823 # p 306
 A90-25827 # p 306
 A90-25831 # p 306
 A90-25835 # p 306
 A90-25836 # p 306
 A90-25846 # p 307
 A90-25861 # p 367
 A90-25863 # p 307
 A90-25871 # p 307
 A90-25872 # p 378
 A90-25873 # p 367
 A90-25885 # p 367
 A90-25935 # p 307
 A90-25987 # p 347
 A90-25989 # p 375
 A90-25990 # p 347
 A90-25994 # p 375
 A90-25995 # p 347
 A90-25997 # p 375
 A90-26018 # p 322
 A90-26022 # p 375
 A90-26059 # p 367
 A90-26061 # p 351
 A90-26067 # p 307
 A90-26077 # p 367
 A90-26128 # p 307
 A90-26129 # p 307
 A90-26130 # p 307
 A90-26131 # p 322
 A90-26132 # p 307
 A90-26133 # p 351
 A90-26134 # p 335
 A90-26135 # p 308
 A90-26136 # p 308
 A90-26137 # p 308
 A90-26138 # p 378
 A90-26141 # p 308
 A90-26177 # p 347
 A90-26189 # p 347
 A90-26203 # p 351
 A90-26222 # p 347
 A90-26225 # p 375
 A90-26231 # p 322

A90-26235 * # p 380
 A90-26254 # p 322
 A90-26258 * # p 348
 A90-26301 # p 322
 A90-26338 # p 331
 A90-26341 # p 308
 A90-26343 # p 335
 A90-26344 # p 335
 A90-26347 # p 308
 A90-26349 # p 308
 A90-26350 # p 335
 A90-26351 # p 351
 A90-26374 # p 339
 A90-26476 # p 376
 A90-26478 # p 308
 A90-26480 # p 308
 A90-26481 # p 376
 A90-26484 # p 376
 A90-26490 # p 376
 A90-26494 # p 309
 A90-26496 # p 309
 A90-26498 # p 309
 A90-26507 # p 309
 A90-26508 # p 309
 A90-26513 # p 309
 A90-26526 # p 309
 A90-26527 # p 310
 A90-26528 # p 310
 A90-26531 # p 310
 A90-26533 # p 310
 A90-26534 # p 310
 A90-26536 # p 310
 A90-26537 # p 310
 A90-26540 # p 311
 A90-26541 # p 336
 A90-26542 # p 311
 A90-26543 # p 311
 A90-26544 # p 311
 A90-26545 # p 311
 A90-26546 # p 311
 A90-26547 # p 311
 A90-26552 # p 312
 A90-26553 # p 312
 A90-26554 # p 312
 A90-26556 # p 312
 A90-26562 # p 376
 A90-26651 # p 332
 A90-26751 # p 367
 A90-26752 # p 368
 A90-26753 # p 351
 A90-26754 # p 368
 A90-26755 # p 376
 A90-26757 # p 336
 A90-26758 # p 336
 A90-26759 # p 368
 A90-26820 # p 348
 A90-26842 # p 352
 A90-26865 # p 356
 A90-26893 # p 368
 A90-26903 # p 312
 A90-26904 # p 312
 A90-26907 # p 313
 A90-26911 # p 313
 A90-26931 # p 378
 A90-26933 # p 313
 A90-26936 # p 313
 A90-26937 # p 313
 A90-26947 # p 313
 A90-26956 # p 313
 A90-26963 # p 314
 A90-26967 # p 314
 A90-26968 # p 314
 A90-26969 # p 314
 A90-26970 # p 314
 A90-26974 # p 352
 A90-26977 # p 322
 A90-26978 # p 368
 A90-26979 # p 352
 A90-26983 # p 314
 A90-26985 # p 314
 A90-26986 # p 322
 A90-27131 # p 315
 A90-27133 # p 315
 A90-27303 # p 315
 A90-27311 # p 315
 A90-27407 # p 336
 A90-27409 # p 339
 A90-27412 # p 356
 A90-27424 # p 323
 A90-27425 # p 368
 A90-27426 # p 339
 A90-27596 # p 336
 A90-27597 # p 356
 A90-27598 # p 356
 A90-27645 # p 457
 A90-27678 # p 444

A90-27679 # p 440
 A90-27681 # p 440
 A90-27781 # p 402
 A90-27875 # p 402
 A90-27922 # p 402
 A90-27923 # p 403
 A90-27924 # p 403
 A90-27925 # p 403
 A90-27947 # p 383
 A90-27951 # p 444
 A90-27953 # p 435
 A90-27959 # p 421
 A90-27962 # p 421
 A90-27963 # p 421
 A90-27966 # p 383
 A90-27972 # p 421
 A90-27975 # p 405
 A90-27976 # p 383
 A90-27977 # p 384
 A90-27978 # p 463
 A90-27979 # p 384
 A90-27985 # p 384
 A90-27986 # p 400
 A90-27992 # p 444
 A90-27993 # p 405
 A90-27999 # p 444
 A90-28003 # p 441
 A90-28006 # p 445
 A90-28007 # p 429
 A90-28135 # p 445
 A90-28137 # p 445
 A90-28151 # p 381
 A90-28152 # p 406
 A90-28153 # p 406
 A90-28154 # p 406
 A90-28155 # p 406
 A90-28156 # p 435
 A90-28157 # p 429
 A90-28158 # p 463
 A90-28159 # p 463
 A90-28160 # p 463
 A90-28161 # p 463
 A90-28162 # p 445
 A90-28163 # p 381
 A90-28164 # p 381
 A90-28165 # p 445
 A90-28166 # p 406
 A90-28167 # p 406
 A90-28168 # p 421
 A90-28169 # p 381
 A90-28170 # p 406
 A90-28171 # p 384
 A90-28172 # p 384
 A90-28173 # p 407
 A90-28174 # p 384
 A90-28175 # p 407
 A90-28176 # p 384
 A90-28177 # p 422
 A90-28178 # p 422
 A90-28179 # p 400
 A90-28180 # p 400
 A90-28181 # p 422
 A90-28182 # p 400
 A90-28183 # p 422
 A90-28184 # p 457
 A90-28187 # p 445
 A90-28188 # p 407
 A90-28189 # p 441
 A90-28191 # p 441
 A90-28192 # p 441
 A90-28193 # p 441
 A90-28194 # p 384
 A90-28195 # p 385
 A90-28196 # p 407
 A90-28197 # p 385
 A90-28198 # p 385
 A90-28199 # p 422
 A90-28200 # p 429
 A90-28201 # p 429
 A90-28202 # p 429
 A90-28203 # p 407
 A90-28204 # p 430
 A90-28207 # p 422
 A90-28209 # p 417
 A90-28211 # p 407
 A90-28212 # p 408
 A90-28213 # p 408
 A90-28214 # p 408
 A90-28215 # p 408
 A90-28216 # p 430
 A90-28217 # p 417
 A90-28218 # p 417
 A90-28219 # p 403
 A90-28220 # p 430
 A90-28221 # p 417
 A90-28223 # p 408

ACCESSION NUMBER INDEX

A90-28225	p 430	A90-29005	p 388	A90-29888	# p 394	A90-30813	p 453	A90-32559	p 470
A90-28226	p 408	A90-29006	p 388	A90-29889	# p 394	A90-30816	p 462	A90-32567	p 470
A90-28227	p 430	A90-29012	p 388	A90-29890	p 413	A90-30817	p 425	A90-32673	p 470
A90-28228	p 385	A90-29147	p 449	A90-29891	p 451	A90-30819	p 453	A90-32675	p 535
A90-28229	p 408	A90-29181	p 388	A90-29892	p 382	A90-31028	p 453	A90-32712	p 470
A90-28230	p 409	A90-29182	p 388	A90-29893	p 451	A90-31108	p 462	A90-32808	p 507
A90-28231	p 441	A90-29183	p 388	A90-29894	p 458	A90-31117	# p 453	A90-32858	p 503
A90-28232	p 409	A90-29184	p 388	A90-29904	# p 423	A90-31119	# p 395	A90-32860	p 504
A90-28233	p 409	A90-29185	p 438	A90-29906	# p 423	A90-31120	# p 443	A90-32863	p 504
A90-28234	p 445	A90-29187	p 430	A90-29908	# p 423	A90-31246	# p 414	A90-32864	p 535
A90-28235	p 409	A90-29188	p 410	A90-29911	# p 451	A90-31247	# p 383	A90-32871	p 536
A90-28236	p 409	A90-29191	p 410	A90-29917	# p 423	A90-31248	# p 439	A90-32873	p 504
A90-28238	p 409	A90-29194	p 388	A90-29918	# p 424	A90-31276	# p 395	A90-32876	p 504
A90-28239	p 410	A90-29226	p 449	A90-29919	# p 424	A90-31277	# p 433	A90-32885	p 536
A90-28240	p 410	A90-29237	# p 410	A90-29921	p 382	A90-31278	# p 395	A90-32906	p 504
A90-28241	p 385	A90-29238	# p 411	A90-29922	p 424	A90-31279	# p 440	A90-32951	# p 507
A90-28242	p 381	A90-29239	# p 411	A90-29924	p 438	A90-31281	# p 440	A90-32952	# p 529
A90-28243	p 385	A90-29240	# p 411	A90-29943	p 418	A90-31282	# p 433	A90-32953	# p 529
A90-28244	p 410	A90-29241	# p 438	A90-29946	p 424	A90-31283	# p 433	A90-32959	# p 471
A90-28252	p 386	A90-29275	# p 442	A90-29977	p 452	A90-31284	# p 414	A90-32960	# p 507
A90-28254	# p 435	A90-29276	# p 449	A90-30103	p 431	A90-31285	# p 401	A90-32961	# p 508
A90-28255	# p 436	A90-29286	# p 449	A90-30105	p 431	A90-31287	# p 433	A90-32962	# p 508
A90-28256	p 436	A90-29293	# p 458	A90-30107	p 413	A90-31288	# p 395	A90-32964	# p 508
A90-28257	p 436	A90-29305	# p 411	A90-30114	p 382	A90-31302	# p 440	A90-32966	# p 508
A90-28258	p 446	A90-29340	# p 449	A90-30115	p 452	A90-31329	# p 419	A90-33057	# p 490
A90-28259	p 446	A90-29359	p 449	A90-30117	p 413	A90-31331	p 420	A90-33058	# p 516
A90-28260	p 436	A90-29360	# p 389	A90-30118	p 413	A90-31333	p 420	A90-33059	# p 490
A90-28262	p 446	A90-29361	# p 389	A90-30119	p 413	A90-31334	p 404	A90-33060	# p 516
A90-28263	p 446	A90-29362	# p 389	A90-30222	p 413	A90-31335	p 401	A90-33061	# p 516
A90-28264	p 446	A90-29363	# p 389	A90-30226	p 458	A90-31344	# p 420	A90-33078	p 529
A90-28268	p 446	A90-29364	# p 389	A90-30230	# p 459	A90-31388	p 401	A90-33094	p 467
A90-28271	p 447	A90-29365	# p 390	A90-30236	# p 459	A90-31479	# p 395	A90-33098	p 530
A90-28272	p 423	A90-29366	# p 390	A90-30238	# p 418	A90-31480	# p 433	A90-33105	# p 490
A90-28273	p 447	A90-29367	# p 390	A90-30249	# p 459	A90-31485	# p 396	A90-33125	p 468
A90-28278	p 447	A90-29368	# p 390	A90-30251	p 439	A90-31486	# p 396	A90-33126	p 530
A90-28279	p 447	A90-29369	# p 390	A90-30264	# p 394	A90-31489	# p 396	A90-33127	p 530
A90-28281	# p 436	A90-29370	# p 390	A90-30268	p 452	A90-31493	p 396	A90-33174	p 468
A90-28282	p 436	A90-29371	# p 391	A90-30275	p 414	A90-31516	p 528	A90-33283	# p 471
A90-28283	p 447	A90-29372	# p 450	A90-30334	p 395	A90-31519	p 490	A90-33288	# p 471
A90-28284	p 447	A90-29373	# p 450	A90-30339	p 395	A90-31529	p 467	A90-33311	# p 471
A90-28287	p 436	A90-29374	# p 391	A90-30342	p 395	A90-31558	p 490	A90-33344	p 530
A90-28288	p 437	A90-29375	# p 391	A90-30344	p 395	A90-31574	p 533	A90-33347	p 508
A90-28289	# p 437	A90-29376	# p 391	A90-30479	p 443	A90-31575	p 528	A90-33348	p 487
A90-28291	p 417	A90-29377	# p 391	A90-30587	p 400	A90-31576	p 467	A90-33349	p 508
A90-28292	p 437	A90-29378	# p 392	A90-30681	p 418	A90-31617	p 528	A90-33351	p 468
A90-28293	p 437	A90-29379	# p 450	A90-30682	# p 419	A90-31618	p 529	A90-33352	# p 516
A90-28294	p 437	A90-29380	# p 450	A90-30688	p 403	A90-31619	p 529	A90-33353	# p 471
A90-28295	# p 448	A90-29381	# p 411	A90-30689	# p 459	A90-31646	p 529	A90-33354	# p 491
A90-28296	p 438	A90-29382	# p 430	A90-30693	p 404	A90-31647	p 534	A90-33355	# p 471
A90-28300	p 438	A90-29383	# p 392	A90-30694	p 419	A90-31651	p 467	A90-33356	# p 471
A90-28302	p 438	A90-29384	# p 411	A90-30695	p 404	A90-31657	p 467	A90-33357	# p 472
A90-28305	p 438	A90-29385	# p 431	A90-30699	p 424	A90-31686	# p 549	A90-33358	# p 472
A90-28306	# p 448	A90-29386	# p 412	A90-30703	p 431	A90-31696	# p 549	A90-33359	# p 472
A90-28310	p 457	A90-29387	# p 392	A90-30704	# p 431	A90-31698	# p 549	A90-33360	# p 472
A90-28319	p 381	A90-29388	# p 392	A90-30705	# p 431	A90-31702	# p 549	A90-33361	# p 472
A90-28321	p 457	A90-29389	# p 412	A90-30706	# p 452	A90-31703	# p 482	A90-33362	# p 472
A90-28323	p 457	A90-29390	# p 392	A90-30707	# p 432	A90-31879	p 534	A90-33363	# p 473
A90-28330	p 457	A90-29391	# p 392	A90-30708	p 432	A90-31881	p 534	A90-33364	# p 473
A90-28337	p 448	A90-29392	# p 393	A90-30710	p 432	A90-31882	p 529	A90-33365	# p 473
A90-28342	p 458	A90-29393	# p 393	A90-30711	p 452	A90-31892	p 534	A90-33366	# p 473
A90-28343	p 448	A90-29394	# p 412	A90-30712	p 424	A90-31902	p 529	A90-33367	# p 491
A90-28348	p 382	A90-29395	# p 412	A90-30713	# p 432	A90-31938	p 487	A90-33368	# p 473
A90-28407	p 417	A90-29396	# p 450	A90-30714	p 432	A90-32028	p 503	A90-33369	# p 491
A90-28552	p 386	A90-29397	# p 393	A90-30715	# p 432	A90-32067	# p 469	A90-33370	# p 522
A90-28555	p 386	A90-29399	# p 451	A90-30716	# p 439	A90-32166	p 534	A90-33371	# p 522
A90-28571	p 423	A90-29400	# p 451	A90-30717	p 433	A90-32169	p 534	A90-33373	# p 491
A90-28582	p 455	A90-29402	# p 463	A90-30719	# p 459	A90-32174	p 535	A90-33374	# p 491
A90-28612	p 456	A90-29405	# p 412	A90-30723	p 419	A90-32257	# p 490	A90-33375	# p 536
A90-28613	p 456	A90-29429	# p 451	A90-30724	p 419	A90-32258	# p 506	A90-33379	# p 545
A90-28617	p 456	A90-29467	# p 412	A90-30729	# p 439	A90-32259	# p 507	A90-33380	# p 492
A90-28620	p 456	A90-29492	# p 442	A90-30730	# p 419	A90-32260	# p 490	A90-33381	# p 547
A90-28625	p 456	A90-29591	p 393	A90-30734	# p 439	A90-32261	# p 507	A90-33382	# p 528
A90-28825	p 448	A90-29598	# p 382	A90-30740	p 459	A90-32262	# p 507	A90-33385	# p 492
A90-28829	p 458	A90-29637	p 382	A90-30752	# p 404	A90-32263	# p 535	A90-33386	# p 536
A90-28839	p 403	A90-29638	p 442	A90-30754	p 460	A90-32269	# p 507	A90-33387	# p 492
A90-28849	p 418	A90-29641	p 382	A90-30755	p 460	A90-32275	p 467	A90-33388	# p 492
A90-28850	p 418	A90-29643	p 442	A90-30757	p 460	A90-32293	# p 535	A90-33389	# p 492
A90-28852	p 458	A90-29654	p 451	A90-30760	# p 383	A90-32304	# p 482	A90-33390	# p 492
A90-28860	p 458	A90-29655	p 403	A90-30764	p 460	A90-32421	# p 507	A90-33391	# p 536
A90-28874	p 418	A90-29661	p 413	A90-30767	p 460	A90-32425	# p 469	A90-33396	p 536
A90-28895	p 418	A90-29686	# p 440	A90-30768	# p 383	A90-32451	# p 469	A90-33400	# p 492
A90-28979	p 386	A90-29687	# p 393	A90-30770	p 439	A90-32452	# p 490	A90-33401	# p 517
A90-28980	p 386	A90-29695	# p 393	A90-30779	# p 452	A90-32453	# p 469	A90-33402	# p 545
A90-28981	p 386	A90-29704	# p 442	A90-30782	p 460	A90-32457	# p 469	A90-33403	# p 517
A90-28985	p 386	A90-29707	p 442	A90-30786	p 461	A90-32458	# p 469	A90-33404	# p 517
A90-28987	p 387	A90-29803	p 400	A90-30787	p 419	A90-32461	# p 469	A90-33405	# p 517
A90-28988	p 387	A90-29825	p 443	A90-30789	p 461	A90-32462	# p 469	A90-33406	# p 517
A90-28989	p 387	A90-29866	p 451	A90-30790	p 404	A90-32463	# p 522	A90-33409	# p 493
A90-28990	p 387	A90-29880	p 423	A90-30791	p 452	A90-32471	# p 535	A90-33410	# p 473
A90-28991	p 387	A90-29881	p 443	A90-30793	# p 461	A90-32475	# p 535	A90-33411	# p 473
A90-28992	p 387	A90-29882	p 393	A90-30794	p 433	A90-32478	# p 470	A90-33412	# p 493
A90-28993	p 410	A90-29883	# p 394	A90-30796	p 461	A90-32479	# p 470	A90-33413	# p 517
A90-28994	p 448	A90-29884	# p 394	A90-30800	p 461	A90-32504	p 535	A90-33414	# p 493
A90-29001	p 448	A90-29885	# p 394	A90-30806	p 461	A90-32505	# p 547	A90-33424	p 537
A90-29003	p 387	A90-29886	# p 394	A90-30809	p 383	A90-32509	p 470	A90-33506	p 474
A90-29004	p 387	A90-29887	# p 394	A90-30811	p 424	A90-32552	p 470	A90-33509	p 474

A90-33514.

A90-33514 p 474
A90-33515 p 474
A90-33523 p 530
A90-33555 # p 537
A90-33556 # p 537
A90-33557 # p 537
A90-33559 # p 508
A90-33560 # p 474
A90-33562 # p 474
A90-33563 # p 475
A90-33564 # p 475
A90-33566 # p 537
A90-33567 # p 475
A90-33568 # p 475
A90-33591 p 508
A90-33594 p 509
A90-33595 p 509
A90-33597 p 537
A90-33613 p 487
A90-33622 p 518
A90-33623 p 518
A90-33624 p 537
A90-33625 p 518
A90-33675 # p 550
A90-33698 p 538
A90-33700 p 475
A90-33701 p 530
A90-33702 # p 538
A90-33704 # p 538
A90-33705 # p 538
A90-33706 # p 538
A90-33707 # p 493
A90-33708 # p 538
A90-33709 # p 493
A90-33710 # p 482
A90-33712 # p 530
A90-33714 # p 493
A90-33753 # p 475
A90-33775 p 538
A90-33886 p 493
A90-33889 # p 504
A90-33890 # p 494
A90-33891 # p 494
A90-33892 # p 494
A90-33893 # p 494
A90-33894 # p 509
A90-33895 # p 518
A90-33896 # p 494
A90-33897 # p 538
A90-33898 # p 504
A90-33899 # p 494
A90-33900 # p 518
A90-33901 # p 518
A90-33902 # p 495
A90-33903 # p 495
A90-33904 # p 495
A90-33905 # p 495
A90-33906 # p 519
A90-33907 # p 519
A90-33909 # p 495
A90-33910 # p 522
A90-33912 # p 495
A90-33913 # p 504
A90-33914 # p 487
A90-33915 # p 487
A90-33916 # p 505
A90-33917 # p 505
A90-33918 # p 519
A90-33919 # p 523
A90-33920 # p 496
A90-33921 # p 545
A90-33923 # p 487
A90-33924 # p 483
A90-33925 # p 488
A90-33926 # p 519
A90-33930 # p 505
A90-33931 # p 519
A90-33985 p 531
A90-33987 p 531
A90-34028 p 496
A90-34082 p 519
A90-34090 p 547
A90-34091 p 548
A90-34103 p 545
A90-34137 p 488
A90-34138 p 488
A90-34140 p 488
A90-34143 p 488
A90-34146 p 488
A90-34148 # p 496
A90-34149 # p 520
A90-34150 # p 545
A90-34152 # p 531
A90-34154 p 531
A90-34156 p 531
A90-34158 p 531

A90-34162 # p 531
A90-34163 p 532
A90-34169 # p 532
A90-34185 p 545
A90-34226 # p 523
A90-34228 # p 523
A90-34229 # p 539
A90-34230 # p 523
A90-34231 # p 539
A90-34232 # p 523
A90-34233 # p 523
A90-34234 # p 539
A90-34235 # p 539
A90-34236 # p 539
A90-34237 # p 523
A90-34238 # p 523
A90-34239 # p 539
A90-34240 # p 524
A90-34241 # p 524
A90-34242 # p 524
A90-34243 # p 524
A90-34245 # p 524
A90-34246 # p 524
A90-34247 # p 524
A90-34248 # p 524
A90-34249 # p 539
A90-34251 # p 525
A90-34252 p 525
A90-34323 # p 476
A90-34324 # p 540
A90-34325 # p 476
A90-34352 # p 540
A90-34356 p 476
A90-34360 p 496
A90-34378 p 546
A90-34380 p 476
A90-34382 p 546
A90-34385 p 540
A90-34436 p 546
A90-34545 p 476
A90-34578 p 525
A90-34580 p 525
A90-34581 p 496
A90-34583 p 476
A90-34584 p 505
A90-34585 p 525
A90-34586 p 525
A90-34672 p 476
A90-34674 p 477
A90-34681 p 532
A90-34725 # p 496
A90-34740 p 496
A90-34817 # p 477
A90-34819 # p 477
A90-34820 # p 520
A90-34821 # p 477
A90-34822 # p 520
A90-34864 p 477
A90-34900 p 497
A90-34968 p 497
A90-34990 p 532
A90-35137 p 552
A90-35140 p 552
A90-35174 p 584
A90-35193 # p 552
A90-35205 # p 552
A90-35212 # p 553
A90-35228 # p 584
A90-35229 # p 584
A90-35230 # p 584
A90-35262 # p 553
A90-35274 # p 553
A90-35300 # p 579
A90-35351 p 576
A90-35353 p 574
A90-35394 p 601
A90-35507 p 601
A90-35508 # p 601
A90-35513 p 584
A90-35600 p 584
A90-35670 p 602
A90-35673 p 585
A90-35684 p 576
A90-35685 p 551
A90-35708 p 585
A90-35709 p 576
A90-35752 # p 553
A90-35753 # p 585
A90-35754 # p 553
A90-35755 # p 553
A90-35756 # p 593
A90-35757 # p 598
A90-35758 # p 574
A90-35759 # p 553
A90-35760 # p 602
A90-35761 # p 579

A90-35762 # p 579
A90-35764 # p 585
A90-35766 # p 553
A90-35767 # p 574
A90-35768 # p 554
A90-35769 # p 611
A90-35770 # p 554
A90-35771 # p 554
A90-35772 # p 554
A90-35773 # p 585
A90-35774 p 579
A90-35830 # p 554
A90-35831 # p 602
A90-35846 p 579
A90-35847 p 589
A90-35848 p 579
A90-35868 # p 554
A90-35888 p 589
A90-35902 # p 554
A90-35916 # p 554
A90-35917 p 555
A90-35926 p 599
A90-35950 p 599
A90-35951 p 602
A90-36026 # p 579
A90-36027 # p 579
A90-36029 # p 580
A90-36030 # p 589
A90-36031 # p 580
A90-36065 p 555
A90-36115 p 576
A90-36151 p 611
A90-36153 p 593
A90-36157 p 589
A90-36184 # p 555
A90-36251 # p 555
A90-36252 # p 555
A90-36253 # p 602
A90-36254 # p 602
A90-36255 # p 555
A90-36256 # p 555
A90-36257 # p 555
A90-36258 # p 555
A90-36262 # p 556
A90-36263 # p 602
A90-36265 # p 602
A90-36271 # p 603
A90-36273 # p 580
A90-36277 # p 603
A90-36279 # p 556
A90-36280 # p 556
A90-36281 # p 556
A90-36282 # p 556
A90-36285 # p 603
A90-36300 # p 551
A90-36413 # p 556
A90-36415 # p 556
A90-36417 # p 603
A90-36418 # p 593
A90-36419 # p 556
A90-36423 # p 580
A90-36427 # p 611
A90-36431 # p 603
A90-36433 # p 589
A90-36434 # p 590
A90-36437 # p 593
A90-36438 # p 580
A90-36465 p 557
A90-36522 p 557
A90-36524 # p 557
A90-36538 p 603
A90-36539 # p 557
A90-36540 # p 557
A90-36541 # p 614
A90-36672 p 599
A90-36782 p 603
A90-36784 # p 603
A90-36786 # p 585
A90-36787 # p 585
A90-36850 p 580
A90-36916 # p 576
A90-36917 # p 576
A90-36918 # p 576
A90-36921 # p 577
A90-36922 # p 577
A90-36924 # p 577
A90-36926 # p 577
A90-36927 # p 577
A90-36929 # p 577
A90-36931 # p 578
A90-37063 # p 557
A90-37088 p 583
A90-37205 # p 557
A90-37209 # p 557
A90-37210 # p 585
A90-37211 # p 578

A90-37216 # p 558
A90-37217 # p 580
A90-37218 # p 611
A90-37219 # p 590
A90-37220 # p 590
A90-37226 # p 590
A90-37230 # p 586
A90-37232 # p 594
A90-37239 # p 586
A90-37240 # p 604
A90-37241 # p 580
A90-37337 # p 604
A90-37343 # p 558
A90-37346 # p 558
A90-37441 p 599
A90-37442 p 599
A90-37443 p 599
A90-37444 p 600
A90-37562 # p 586
A90-37662 p 600
A90-37736 # p 558
A90-37748 p 611
A90-37830 p 604
A90-37881 p 604
A90-37890 p 558
A90-37899 p 551
A90-37901 p 604
A90-37902 p 600
A90-37926 # p 594
A90-37928 # p 594
A90-37929 # p 598
A90-37930 # p 594
A90-37933 # p 604
A90-37934 # p 594
A90-37935 # p 594
A90-37936 # p 594
A90-37937 # p 558
A90-37939 # p 595
A90-37940 # p 595
A90-37943 # p 558
A90-37944 # p 595
A90-37945 # p 595
A90-37946 # p 595
A90-37947 # p 558
A90-37948 # p 559
A90-37949 # p 595
A90-37950 # p 596
A90-37951 # p 559
A90-37953 # p 596
A90-37954 # p 604
A90-37955 # p 614
A90-37956 # p 614
A90-37957 # p 596
A90-37958 # p 605
A90-37960 # p 596
A90-37961 # p 596
A90-37962 # p 559
A90-37963 # p 590
A90-37964 # p 559
A90-37966 # p 605
A90-37967 # p 559
A90-37968 # p 559
A90-37969 # p 559
A90-38028 p 580
A90-38097 p 605
A90-38129 p 586
A90-38130 p 586
A90-38132 p 605
A90-38175 p 605
A90-38186 p 586
A90-38353 p 605
A90-38394 # p 560
A90-38416 # p 560
A90-38441 # p 583
A90-38468 # p 560
A90-38472 # p 586
A90-38483 # p 596
A90-38484 # p 597
A90-38485 # p 597
A90-38487 # p 597
A90-38488 # p 560
A90-38489 # p 597
A90-38490 # p 560
A90-38493 p 605
A90-38495 p 560
A90-38497 p 597
A90-38519 p 590
A90-38520 p 614
A90-38521 # p 590
A90-38522 p 591
A90-38523 p 561
A90-38524 # p 591
A90-38525 p 581
A90-38526 p 551
A90-38529 # p 581
A90-38530 # p 591

A90-38531 # p 586
A90-38532 # p 587
A90-38533 # p 611
A90-38534 # p 587
A90-38535 # p 574
A90-38536 # p 581
A90-38538 # p 581
A90-38539 # p 587
A90-38540 # p 581
A90-38542 # p 551
A90-38544 p 606
A90-38596 # p 587
A90-38597 # p 587
A90-38608 # p 561
A90-38610 # p 606
A90-38612 # p 561
A90-38614 # p 606
A90-38616 # p 561
A90-38617 # p 561
A90-38618 # p 561
A90-38619 # p 562
A90-38621 # p 562
A90-38624 # p 562
A90-38625 # p 562
A90-38626 # p 562
A90-38627 # p 562
A90-38628 # p 563
A90-38629 # p 563
A90-38637 # p 563
A90-38639 # p 563
A90-38651 # p 606
A90-38659 # p 563
A90-38660 # p 563
A90-38663 # p 606
A90-38666 # p 563
A90-38670 # p 563
A90-38673 # p 564
A90-38677 # p 606
A90-38678 # p 564
A90-38679 # p 564
A90-38680 # p 564
A90-38681 # p 564
A90-38682 # p 564
A90-38683 # p 564
A90-38684 # p 565
A90-38686 # p 565
A90-38687 # p 565
A90-38688 # p 565
A90-38693 # p 600
A90-38703 # p 565
A90-38704 # p 565
A90-38711 # p 600
A90-38717 # p 566
A90-38718 # p 566
A90-38720 # p 566
A90-38721 # p 566
A90-38723 # p 566
A90-38727 # p 566
A90-38729 # p 567
A90-38730 # p 607
A90-38731 # p 567
A90-38732 # p 567
A90-38734 # p 567
A90-38736 # p 567
A90-38737 # p 567
A90-38738 # p 612
A90-38746 # p 607
A90-38750 # p 607
A90-38751 # p 567
A90-38752 # p 607
A90-38753 # p 568
A90-38754 # p 568
A90-38755 # p 568
A90-38756 # p 568
A90-38757 # p 568
A90-38758 # p 591
A90-38759 # p 568
A90-38761 # p 587
A90-38762 # p 569
A90-38765 # p 607
A90-38769 # p 608
A90-38772 # p 569
A90-38773 # p 569
A90-38774 # p 569
A90-38777 # p 569
A90-38778 # p 569
A90-38780 # p 570
A90-38781 # p 608
A90-38782 # p 570
A90-38784 # p 570
A90-38854 p 679
A90-38888 p 693
A90-38908 p 667
A90-38909 # p 693
A90-38912 # p 667

ACCESSION NUMBER INDEX

ACCESSION NUMBER INDEX

A90-38915 # p 619
A90-38965 # p 667
A90-38966 # p 667
A90-38975 # p 679
A90-39002 # p 637
A90-39049 # p 619
A90-39180 # p 693
A90-39186 # p 679
A90-39276 # p 680
A90-39286 # p 641
A90-39298 # p 680
A90-39303 # p 693
A90-39403 # p 692
A90-39465 # p 619
A90-39475 # p 619
A90-39514 # p 619
A90-39516 # p 619
A90-39518 # p 619
A90-39519 # p 620
A90-39538 # p 620
A90-39539 # p 620
A90-39581 # p 638
A90-39702 # p 692
A90-39725 # p 680
A90-39780 # p 620
A90-39781 # p 695
A90-39782 # p 620
A90-39784 # p 680
A90-39786 # p 680
A90-39801 # p 620
A90-39814 # p 620
A90-39855 # p 638
A90-39859 # p 638
A90-39976 # p 641
A90-39977 # p 680
A90-39978 # p 641
A90-39979 # p 680
A90-39980 # p 680
A90-39982 # p 651
A90-39983 # p 651
A90-39984 # p 651
A90-39985 # p 642
A90-39986 # p 642
A90-39987 # p 681
A90-39988 # p 642
A90-39989 # p 642
A90-39991 # p 675
A90-39992 # p 642
A90-40032 # p 681
A90-40047 # p 675
A90-40109 # p 681
A90-40127 # p 675
A90-40128 # p 642
A90-40130 # p 642
A90-40166 # p 642
A90-40172 # p 643
A90-40181 # p 620
A90-40195 # p 652
A90-40215 # p 676
A90-40344 # p 643
A90-40345 # p 617
A90-40381 # p 652
A90-40382 # p 652
A90-40392 # p 681
A90-40393 # p 681
A90-40394 # p 652
A90-40398 # p 652
A90-40399 # p 652
A90-40400 # p 672
A90-40462 # p 652
A90-40476 # p 672
A90-40479 # p 676
A90-40495 # p 620
A90-40501 # p 621
A90-40503 # p 654
A90-40504 # p 621
A90-40512 # p 654
A90-40513 # p 621
A90-40519 # p 655
A90-40526 # p 655
A90-40530 # p 655
A90-40533 # p 655
A90-40539 # p 655
A90-40540 # p 655
A90-40541 # p 655
A90-40552 # p 655
A90-40554 # p 656
A90-40555 # p 621
A90-40556 # p 656
A90-40557 # p 667
A90-40558 # p 656
A90-40559 # p 656
A90-40560 # p 681
A90-40562 # p 656
A90-40570 # p 676
A90-40573 # p 656

A90-40574 # p 676
A90-40582 # p 674
A90-40587 # p 674
A90-40590 # p 681
A90-40592 # p 621
A90-40594 # p 676
A90-40596 # p 621
A90-40597 # p 657
A90-40598 # p 657
A90-40599 # p 621
A90-40601 # p 657
A90-40602 # p 657
A90-40603 # p 657
A90-40604 # p 657
A90-40605 # p 657
A90-40606 # p 658
A90-40612 # p 621
A90-40613 # p 681
A90-40622 # p 658
A90-40633 # p 658
A90-40636 # p 658
A90-40637 # p 658
A90-40639 # p 658
A90-40641 # p 682
A90-40643 # p 658
A90-40648 # p 617
A90-40650 # p 682
A90-40678 # p 622
A90-40679 # p 622
A90-40680 # p 672
A90-40681 # p 622
A90-40682 # p 622
A90-40683 # p 622
A90-40684 # p 672
A90-40685 # p 643
A90-40686 # p 622
A90-40687 # p 635
A90-40689 # p 667
A90-40690 # p 622
A90-40691 # p 667
A90-40692 # p 622
A90-40693 # p 622
A90-40694 # p 622
A90-40712 # p 682
A90-40716 # p 682
A90-40749 # p 623
A90-40810 # p 693
A90-40817 # p 668
A90-40833 # p 668
A90-40878 # p 668
A90-40885 # p 693
A90-40886 # p 668
A90-40912 # p 668
A90-40914 # p 668
A90-40926 # p 623
A90-40927 # p 659
A90-40929 # p 682
A90-40930 # p 682
A90-40934 # p 659
A90-40937 # p 623
A90-40938 # p 683
A90-40939 # p 683
A90-40940 # p 683
A90-40941 # p 623
A90-40942 # p 623
A90-40943 # p 683
A90-40945 # p 659
A90-40946 # p 659
A90-40947 # p 659
A90-40979 # p 638
A90-41004 # p 638
A90-41034 # p 638
A90-41035 # p 638
A90-41036 # p 639
A90-41056 # p 639
A90-41057 # p 639
A90-41058 # p 639
A90-41062 # p 639
A90-41073 # p 683
A90-41104 # p 683
A90-41109 # p 695
A90-41110 # p 617
A90-41111 # p 676
A90-41112 # p 617
A90-41113 # p 672
A90-41114 # p 653
A90-41115 # p 675
A90-41119 # p 623
A90-41162 # p 659
A90-41163 # p 683
A90-41165 # p 659
A90-41166 # p 659
A90-41177 # p 617
A90-41184 # p 693
A90-41188 # p 694
A90-41189 # p 694

A90-41191 # p 694
A90-41201 # p 683
A90-41203 # p 623
A90-41205 # p 695
A90-41206 # p 695
A90-41207 # p 695
A90-41212 # p 659
A90-41240 # p 695
A90-41315 # p 692
A90-41334 # p 684
A90-41335 # p 684
A90-41336 # p 676
A90-41338 # p 677
A90-41339 # p 643
A90-41343 # p 694
A90-41632 # p 669
A90-41705 # p 639
A90-41706 # p 639
A90-41707 # p 639
A90-41708 # p 639
A90-41709 # p 640
A90-41710 # p 640
A90-41711 # p 640
A90-41712 # p 640
A90-41725 # p 673
A90-41726 # p 673
A90-41727 # p 643
A90-41728 # p 635
A90-41729 # p 653
A90-41730 # p 653
A90-41736 # p 692
A90-41737 # p 643
A90-41738 # p 643
A90-41739 # p 643
A90-41740 # p 623
A90-41741 # p 653
A90-41742 # p 653
A90-41751 # p 623
A90-41753 # p 684
A90-41758 # p 660
A90-41759 # p 660
A90-41760 # p 660
A90-41761 # p 660
A90-41767 # p 669
A90-41768 # p 684
A90-41769 # p 699
A90-41899 # p 644
A90-41900 # p 677
A90-41957 # p 669
A90-41981 # p 660
A90-41982 # p 660
A90-41983 # p 624
A90-41986 # p 673
A90-41987 # p 684
A90-41988 # p 624
A90-41989 # p 624
A90-41990 # p 660
A90-41991 # p 644
A90-41992 # p 661
A90-41993 # p 661
A90-41997 # p 684
A90-41999 # p 684
A90-42017 # p 661
A90-42018 # p 624
A90-42019 # p 624
A90-42020 # p 684
A90-42032 # p 624
A90-42033 # p 625
A90-42034 # p 625
A90-42035 # p 625
A90-42037 # p 685
A90-42038 # p 661
A90-42040 # p 685
A90-42041 # p 685
A90-42043 # p 685
A90-42044 # p 625
A90-42045 # p 625
A90-42046 # p 696
A90-42047 # p 644
A90-42048 # p 685
A90-42050 # p 661
A90-42051 # p 661
A90-42052 # p 685
A90-42053 # p 661
A90-42054 # p 662
A90-42055 # p 662
A90-42056 # p 662
A90-42059 # p 677
A90-42060 # p 662
A90-42061 # p 686
A90-42062 # p 677
A90-42067 # p 686
A90-42068 # p 686
A90-42093 # p 686
A90-42094 # p 625
A90-42102 # p 625

A90-42103 # p 644
A90-42104 # p 644
A90-42105 # p 644
A90-42106 # p 644
A90-42110 # p 686
A90-42116 # p 686
A90-42117 # p 677
A90-42132 # p 626
A90-42133 # p 686
A90-42136 # p 626
A90-42137 # p 626
A90-42147 # p 675
A90-42155 # p 662
A90-42156 # p 617
A90-42157 # p 662
A90-42158 # p 662
A90-42159 # p 663
A90-42160 # p 663
A90-42161 # p 626
A90-42162 # p 626
A90-42163 # p 687
A90-42164 # p 687
A90-42165 # p 687
A90-42166 # p 687
A90-42167 # p 663
A90-42168 # p 663
A90-42169 # p 663
A90-42170 # p 663
A90-42174 # p 677
A90-42176 # p 663
A90-42177 # p 664
A90-42186 # p 673
A90-42188 # p 664
A90-42189 # p 675
A90-42197 # p 664
A90-42217 # p 664
A90-42218 # p 626
A90-42221 # p 664
A90-42225 # p 627
A90-42226 # p 664
A90-42278 # p 645
A90-42328 # p 669
A90-42334 # p 687
A90-42341 # p 687
A90-42351 # p 627
A90-42353 # p 627
A90-42355 # p 645
A90-42357 # p 627
A90-42361 # p 627
A90-42363 # p 627
A90-42364 # p 627
A90-42367 # p 669
A90-42372 # p 678
A90-42394 # p 627
A90-42395 # p 628
A90-42402 # p 628
A90-42403 # p 628
A90-42404 # p 628
A90-42405 # p 628
A90-42406 # p 628
A90-42407 # p 645
A90-42412 # p 629
A90-42413 # p 629
A90-42415 # p 629
A90-42416 # p 629
A90-42417 # p 645
A90-42418 # p 629
A90-42419 # p 629
A90-42420 # p 645
A90-42422 # p 629
A90-42423 # p 629
A90-42425 # p 630
A90-42431 # p 630
A90-42432 # p 673
A90-42433 # p 696
A90-42434 # p 645
A90-42435 # p 630
A90-42436 # p 630
A90-42437 # p 630
A90-42438 # p 630
A90-42439 # p 630
A90-42440 # p 631
A90-42441 # p 645
A90-42442 # p 646
A90-42443 # p 631
A90-42445 # p 646
A90-42447 # p 653
A90-42448 # p 653
A90-42449 # p 669
A90-42450 # p 653
A90-42451 # p 653
A90-42452 # p 640
A90-42454 # p 694
A90-42456 # p 635
A90-42457 # p 646
A90-42458 # p 646

A90-42750

A90-42460 # p 646
A90-42461 # p 669
A90-42462 # p 670
A90-42463 # p 670
A90-42464 # p 646
A90-42465 # p 646
A90-42466 # p 670
A90-42467 # p 670
A90-42468 # p 646
A90-42469 # p 670
A90-42470 # p 670
A90-42471 # p 670
A90-42472 # p 671
A90-42473 # p 647
A90-42474 # p 671
A90-42475 # p 618
A90-42476 # p 618
A90-42477 # p 653
A90-42478 # p 618
A90-42481 # p 635
A90-42483 # p 688
A90-42484 # p 688
A90-42485 # p 665
A90-42486 # p 665
A90-42487 # p 665
A90-42488 # p 665
A90-42489 # p 618
A90-42490 # p 688
A90-42491 # p 688
A90-42492 # p 618
A90-42493 # p 688
A90-42494 # p 647
A90-42495 # p 647
A90-42496 # p 647
A90-42497 # p 647
A90-42498 # p 647
A90-42499 # p 647
A90-42506 # p 631
A90-42520 # p 729
A90-42524 # p 778
A90-42638 # p 781
A90-42639 # p 702
A90-42644 # p 702
A90-42646 # p 703
A90-42648 # p 721
A90-42652 # p 701
A90-42653 # p 739
A90-42655 # p 725
A90-42656 # p 729
A90-42657 # p 739
A90-42658 # p 703
A90-42659 # p 703
A90-42662 # p 739
A90-42664 # p 729
A90-42667 # p 767
A90-42670 # p 739
A90-42671 # p 703
A90-42672 # p 730
A90-42673 # p 730
A90-42674 # p 701
A90-42675 # p 764
A90-42685 # p 768
A90-42688 # p 739
A90-42690 # p 740
A90-42691 # p 740
A90-42692 # p 740
A90-42693 # p 740
A90-42694 # p 740
A90-42695 # p 741
A90-42696 # p 741
A90-42697 # p 703
A90-42698 # p 759
A90-42705 # p 762
A90-42706 # p 741
A90-42708 # p 703
A90-42709 # p 703
A90-42712 # p 741
A90-42718 # p 741
A90-42719 # p 741
A90-42720 # p 742
A90-42725 # p 764
A90-42728 # p 742
A90-42729 # p 742
A90-42731 # p 704
A90-42732 # p 704
A90-42733 # p 704
A90-42734 # p 704
A90-42735 # p 704
A90-42737 # p 704
A90-42738 # p 705
A90-42739 # p 768
A90-42740 # p 768
A90-42741 # p 742
A90-42748 # p 705
A90-42749 # p 705
A90-42750 # p 705

A90-42751

A90-42751 # p 705
 A90-42752 # p 742
 A90-42759 # p 768
 A90-42761 # p 768
 A90-42763 # p 768
 A90-42765 # p 742
 A90-42766 # p 743
 A90-42767 # p 743
 A90-42768 # p 730
 A90-42769 # p 764
 A90-42773 # p 769
 A90-42776 # p 762
 A90-42777 # p 743
 A90-42781 # p 705
 A90-42782 # p 769
 A90-42783 # p 706
 A90-42784 # p 706
 A90-42791 # p 759
 A90-42793 # p 743
 A90-42794 # p 701
 A90-42806 # p 743
 A90-42808 # p 743
 A90-42810 # p 762
 A90-42813 # p 744
 A90-42814 # p 744
 A90-42815 # p 744
 A90-42828 # p 783
 A90-42870 # p 769
 A90-42872 # p 706
 A90-42874 # p 781
 A90-42911 # p 769
 A90-42924 # p 725
 A90-42990 # p 725
 A90-42995 # p 706
 A90-43039 # p 769
 A90-43152 # p 730
 A90-43204 # p 764
 A90-43218 # p 744
 A90-43230 # p 725
 A90-43285 # p 769
 A90-43309 # p 769
 A90-43376 # p 737
 A90-43460 # p 762
 A90-43670 # p 764
 A90-43681 # p 725
 A90-43686 # p 725
 A90-43700 # p 725
 A90-43701 # p 726
 A90-43705 # p 726
 A90-43706 # p 751
 A90-43707 # p 726
 A90-43708 # p 726
 A90-43710 # p 726
 A90-43713 # p 726
 A90-43714 # p 726
 A90-43724 # p 727
 A90-43727 # p 737
 A90-43729 # p 770
 A90-43734 # p 770
 A90-43763 # p 744
 A90-43764 # p 730
 A90-43765 # p 730
 A90-43766 # p 730
 A90-43767 # p 731
 A90-43768 # p 731
 A90-43769 # p 731
 A90-43782 # p 781
 A90-43826 # p 701
 A90-43855 # p 764
 A90-44005 # p 706
 A90-44052 # p 706
 A90-44147 # p 770
 A90-44173 # p 764
 A90-44175 # p 765
 A90-44222 # p 721
 A90-44223 # p 731
 A90-44325 # p 770
 A90-44348 # p 765
 A90-44399 # p 759
 A90-44406 # p 706
 A90-44407 # p 707
 A90-44410 # p 744
 A90-44426 # p 707
 A90-44430 # p 707
 A90-44431 # p 770
 A90-44432 # p 707
 A90-44433 # p 707
 A90-44434 # p 707
 A90-44435 # p 708
 A90-44437 # p 708
 A90-44439 # p 708
 A90-44447 # p 708
 A90-44457 # p 770
 A90-44459 # p 708
 A90-44460 # p 708
 A90-44461 # p 709

A90-44464 # p 770
 A90-44545 # p 778
 A90-44548 # p 721
 A90-44549 # p 760
 A90-44550 # p 722
 A90-44594 # p 744
 A90-44595 # p 745
 A90-44596 # p 745
 A90-44597 # p 745
 A90-44601 # p 709
 A90-44605 # p 745
 A90-44606 # p 771
 A90-44640 # p 722
 A90-44644 # p 778
 A90-44656 # p 722
 A90-44658 # p 722
 A90-44659 # p 722
 A90-44662 # p 722
 A90-44721 # p 745
 A90-44722 # p 737
 A90-44723 # p 751
 A90-44726 # p 745
 A90-44727 # p 709
 A90-44728 # p 709
 A90-44730 # p 771
 A90-44731 # p 731
 A90-44733 # p 709
 A90-44734 # p 731
 A90-44735 # p 763
 A90-44736 # p 731
 A90-44737 # p 731
 A90-44738 # p 732
 A90-44739 # p 709
 A90-44740 # p 709
 A90-44751 # p 732
 A90-44752 # p 763
 A90-44755 # p 771
 A90-44781 # p 732
 A90-44816 # p 765
 A90-44832 # p 779
 A90-44833 # p 709
 A90-44847 # p 751
 A90-44855 # p 779
 A90-44922 # p 709
 A90-44928 # p 710
 A90-44930 # p 710
 A90-44931 # p 710
 A90-44934 # p 710
 A90-44935 # p 710
 A90-44936 # p 710
 A90-45028 # p 765
 A90-45133 # p 771
 A90-45134 # p 751
 A90-45135 # p 763
 A90-45137 # p 763
 A90-45139 # p 752
 A90-45140 # p 752
 A90-45141 # p 752
 A90-45142 # p 752
 A90-45143 # p 752
 A90-45144 # p 752
 A90-45149 # p 763
 A90-45150 # p 710
 A90-45151 # p 753
 A90-45152 # p 753
 A90-45153 # p 711
 A90-45154 # p 711
 A90-45155 # p 711
 A90-45156 # p 753
 A90-45157 # p 753
 A90-45158 # p 753
 A90-45159 # p 754
 A90-45160 # p 754
 A90-45161 # p 754
 A90-45162 # p 754
 A90-45163 # p 711
 A90-45164 # p 711
 A90-45165 # p 712
 A90-45166 # p 712
 A90-45167 # p 754
 A90-45168 # p 712
 A90-45174 # p 754
 A90-45175 # p 754
 A90-45176 # p 755
 A90-45177 # p 755
 A90-45178 # p 712
 A90-45200 # p 727
 A90-45225 # p 771
 A90-45226 # p 727
 A90-45227 # p 727
 A90-45232 # p 727
 A90-45233 # p 727
 A90-45234 # p 728
 A90-45236 # p 728
 A90-45238 # p 728
 A90-45239 # p 737

A90-45260 # p 712
 A90-45261 # p 712
 A90-45281 # p 771
 A90-45289 # p 779
 A90-45290 # p 779
 A90-45296 # p 760
 A90-45300 # p 771
 A90-45301 # p 745
 A90-45323 # p 712
 A90-45324 # p 772
 A90-45325 # p 713
 A90-45330 # p 755
 A90-45331 # p 755
 A90-45332 # p 755
 A90-45333 # p 755
 A90-45334 # p 755
 A90-45335 # p 756
 A90-45344 # p 756
 A90-45354 # p 738
 A90-45373 # p 779
 A90-45413 # p 756
 A90-45414 # p 745
 A90-45415 # p 746
 A90-45422 # p 778
 A90-45423 # p 713
 A90-45424 # p 713
 A90-45425 # p 732
 A90-45426 # p 701
 A90-45427 # p 732
 A90-45428 # p 701
 A90-45429 # p 732
 A90-45430 # p 772
 A90-45431 # p 732
 A90-45432 # p 728
 A90-45433 # p 728
 A90-45434 # p 728
 A90-45435 # p 728
 A90-45436 # p 729
 A90-45437 # p 756
 A90-45438 # p 756
 A90-45439 # p 713
 A90-45440 # p 713
 A90-45441 # p 746
 A90-45442 # p 746
 A90-45443 # p 746
 A90-45444 # p 746
 A90-45445 # p 723
 A90-45446 # p 738
 A90-45447 # p 732
 A90-45448 # p 733
 A90-45449 # p 733
 A90-45450 # p 733
 A90-45452 # p 713
 A90-45454 # p 746
 A90-45455 # p 746
 A90-45456 # p 747
 A90-45457 # p 747
 A90-45458 # p 733
 A90-45459 # p 733
 A90-45464 # p 757
 A90-45465 # p 714
 A90-45466 # p 714
 A90-45467 # p 714
 A90-45468 # p 723
 A90-45469 # p 778
 A90-45473 # p 714
 A90-45474 # p 714
 A90-45475 # p 757
 A90-45476 # p 747
 A90-45477 # p 714
 A90-45481 # p 715
 A90-45482 # p 772
 A90-45484 # p 738
 A90-45485 # p 738
 A90-45486 # p 747
 A90-45487 # p 765
 A90-45488 # p 765
 A90-45489 # p 765
 A90-45491 # p 733
 A90-45494 # p 760
 A90-45495 # p 715
 A90-45496 # p 715
 A90-45497 # p 715
 A90-45498 # p 715
 A90-45500 # p 733
 A90-45501 # p 733
 A90-45502 # p 734
 A90-45503 # p 760
 A90-45504 # p 760
 A90-45505 # p 760
 A90-45506 # p 761
 A90-45507 # p 761
 A90-45508 # p 738
 A90-45509 # p 738
 A90-45511 # p 747
 A90-45512 # p 747

A90-45513 # p 748
 A90-45514 # p 748
 A90-45519 # p 782
 A90-45522 # p 715
 A90-45528 # p 772
 A90-45534 # p 772
 A90-45536 # p 716
 A90-45708 # p 765
 A90-45727 # p 716
 A90-45728 # p 772
 A90-45738 # p 716
 A90-45740 # p 716
 A90-45759 # p 772
 A90-45760 # p 716
 A90-45769 # p 772
 A90-45783 # p 716
 A90-45785 # p 716
 A90-45788 # p 773
 A90-45845 # p 787
 A90-45846 # p 787
 A90-45847 # p 787
 A90-45848 # p 787
 A90-45849 # p 787
 A90-45850 # p 788
 A90-45851 # p 788
 A90-45852 # p 788
 A90-45853 # p 788
 A90-45854 # p 788
 A90-45855 # p 789
 A90-45856 # p 789
 A90-45857 # p 789
 A90-45858 # p 789
 A90-45859 # p 789
 A90-45860 # p 789
 A90-45862 # p 790
 A90-45863 # p 790
 A90-45864 # p 790
 A90-45867 # p 790
 A90-45868 # p 790
 A90-45870 # p 790
 A90-45871 # p 791
 A90-45873 # p 791
 A90-45874 # p 791
 A90-45875 # p 791
 A90-45876 # p 791
 A90-45877 # p 791
 A90-45878 # p 792
 A90-45879 # p 792
 A90-45880 # p 792
 A90-45881 # p 828
 A90-45882 # p 792
 A90-45883 # p 792
 A90-45885 # p 792
 A90-45886 # p 792
 A90-45887 # p 793
 A90-45888 # p 869
 A90-45890 # p 793
 A90-45891 # p 793
 A90-45892 # p 793
 A90-45893 # p 793
 A90-45894 # p 794
 A90-45895 # p 794
 A90-45896 # p 794
 A90-45897 # p 794
 A90-45898 # p 794
 A90-45899 # p 794
 A90-45900 # p 795
 A90-45901 # p 795
 A90-45902 # p 795
 A90-45908 # p 795
 A90-45909 # p 795
 A90-45910 # p 795
 A90-45911 # p 795
 A90-45912 # p 796
 A90-45913 # p 796
 A90-45914 # p 796
 A90-45915 # p 796
 A90-45917 # p 796
 A90-45918 # p 796
 A90-45920 # p 797
 A90-45922 # p 797
 A90-45923 # p 797
 A90-45929 # p 797
 A90-45930 # p 797
 A90-45932 # p 798
 A90-45933 # p 798
 A90-45934 # p 798
 A90-45935 # p 798
 A90-45936 # p 798
 A90-45937 # p 798
 A90-45960 # p 877
 A90-45971 # p 878
 A90-46001 # p 888
 A90-46002 # p 828
 A90-46004 # p 817
 A90-46036 # p 878

A90-46037 # p 878
 A90-46038 # p 878
 A90-46039 # p 878
 A90-46046 # p 889
 A90-46150 # p 850
 A90-46184 # p 878
 A90-46186 # p 878
 A90-46188 # p 879
 A90-46190 # p 879
 A90-46192 # p 893
 A90-46215 # p 879
 A90-46222 # p 879
 A90-46226 # p 879
 A90-46228 # p 879
 A90-46236 # p 880
 A90-46237 # p 880
 A90-46301 # p 880
 A90-46351 # p 893
 A90-46352 # p 893
 A90-46358 # p 799
 A90-46359 # p 799
 A90-46360 # p 799
 A90-46361 # p 799
 A90-46362 # p 799
 A90-46363 # p 799
 A90-46364 # p 799
 A90-46365 # p 800
 A90-46366 # p 800
 A90-46367 # p 800
 A90-46368 # p 800
 A90-46369 # p 800
 A90-46370 # p 800
 A90-46371 # p 801
 A90-46372 # p 801
 A90-46374 # p 801
 A90-46375 # p 801
 A90-46376 # p 801
 A90-46377 # p 801
 A90-46378 # p 802
 A90-46379 # p 802
 A90-46380 # p 802
 A90-46382 # p 802
 A90-46383 # p 802
 A90-46384 # p 802
 A90-46385 # p 828
 A90-46386 # p 828
 A90-46387 # p 828
 A90-46390 # p 821
 A90-46391 # p 821
 A90-46392 # p 821
 A90-46393 # p 821
 A90-46394 # p 821
 A90-46395 # p 817
 A90-46396 # p 821
 A90-46397 # p 872
 A90-46398 # p 822
 A90-46479 # p 880
 A90-46480 # p 828
 A90-46482 # p 880
 A90-46483 # p 859
 A90-46484 # p 872
 A90-46485 # p 828
 A90-46486 # p 802
 A90-46487 # p 803
 A90-46488 # p 850
 A90-46491 # p 850
 A90-46492 # p 880
 A90-46493 # p 850
 A90-46495 # p 850
 A90-46496 # p 873
 A90-46497 # p 851
 A90-46498 # p 785
 A90-46499 # p 829
 A90-46500 # p 803
 A90-46502 # p 803
 A90-46503 # p 803
 A90-46504 # p 851
 A90-46505 # p 851
 A90-46506 # p 894
 A90-46509 # p 851
 A90-46514 # p 873
 A90-46525 # p 873
 A90-46534 # p 803
 A90-46536 # p 803
 A90-46537 # p 869
 A90-46538 # p 803
 A90-46539 # p 851
 A90-46541 # p 880
 A90-46542 # p 803
 A90-46545 # p 804
 A90-46546 # p 851
 A90-46548 # p 804
 A90-46550 # p 804
 A90-46551 # p 804
 A90-46552 # p 894

ACCESSION NUMBER INDEX

ACCESSION NUMBER INDEX

A90-50638

A90-46554	p 804	A90-46976	# p 862	A90-48090	# p 811	A90-49109	# p 839	A90-49881	p 901
A90-46559	p 804	A90-47021	p 881	A90-48131	p 874	A90-49110	# p 868	A90-49882	p 926
A90-46561	p 881	A90-47118	p 881	A90-48295	p 811	A90-49111	# p 868	A90-49883	p 928
A90-46563	p 804	A90-47202	# p 894	A90-48351	p 888	A90-49112	# p 839	A90-49884	p 954
A90-46564	p 804	A90-47203	# p 881	A90-48358	p 888	A90-49113	# p 868	A90-49885	p 954
A90-46565	p 805	A90-47210	# p 852	A90-48359	p 888	A90-49114	# p 839	A90-49886	p 954
A90-46566	p 805	A90-47218	# p 852	A90-48362	p 888	A90-49115	# p 839	A90-49888	p 919
A90-46567	p 805	A90-47219	# p 852	A90-48364	p 888	A90-49118	# p 839	A90-49889	p 901
A90-46568	p 805	A90-47220	# p 808	A90-48510	p 786	A90-49119	# p 839	A90-49890	p 901
A90-46569	p 859	A90-47228	# p 882	A90-48514	# p 867	A90-49120	# p 872	A90-49891	p 926
A90-46570	p 860	A90-47299	# p 808	A90-48515	# p 867	A90-49121	# p 897	A90-49892	p 902
A90-46571	p 860	A90-47300	# p 808	A90-48521	p 847	A90-49122	# p 813	A90-49893	p 940
A90-46572	p 860	A90-47301	# p 809	A90-48522	p 833	A90-49123	# p 892	A90-49894	p 919
A90-46573	p 805	A90-47303	# p 809	A90-48529	p 852	A90-49124	# p 840	A90-50056	p 940
A90-46575	p 805	A90-47306	# p 833	A90-48607	p 847	A90-49125	# p 840	A90-50057	p 940
A90-46576	p 869	A90-47307	# p 809	A90-48620	p 847	A90-49271	# p 892	A90-50058	p 940
A90-46577	p 860	A90-47309	# p 862	A90-48629	p 882	A90-49272	# p 823	A90-50059	p 940
A90-46615	p 805	A90-47312	# p 809	A90-48657	p 894	A90-49273	p 870	A90-50060	p 941
A90-46616	p 785	A90-47314	# p 809	A90-48699	p 833	A90-49274	p 813	A90-50062	p 941
A90-46618	p 829	A90-47572	p 888	A90-48711	p 811	A90-49292	p 840	A90-50063	p 941
A90-46620	p 881	A90-47576	p 862	A90-48712	p 811	A90-49293	p 840	A90-50066	p 941
A90-46621	p 806	A90-47587	# p 872	A90-48715	p 811	A90-49294	p 840	A90-50067	p 941
A90-46624	p 851	A90-47590	# p 862	A90-48826	# p 786	A90-49295	p 840	A90-50068	p 941
A90-46629	p 897	A90-47592	# p 847	A90-48828	# p 786	A90-49304	p 841	A90-50069	p 941
A90-46645	# p 806	A90-47593	# p 862	A90-48829	# p 786	A90-49305	p 841	A90-50070	p 942
A90-46648	p 897	A90-47594	# p 862	A90-48831	# p 834	A90-49306	p 841	A90-50071	p 942
A90-46649	p 897	A90-47595	# p 862	A90-48832	# p 834	A90-49307	p 841	A90-50082	p 942
A90-46650	p 851	A90-47596	# p 863	A90-48833	# p 834	A90-49308	p 841	A90-50083	p 942
A90-46671	p 822	A90-47597	# p 863	A90-48834	# p 834	A90-49358	p 882	A90-50085	p 942
A90-46715	p 860	A90-47598	# p 863	A90-48835	# p 834	A90-49451	p 853	A90-50088	p 942
A90-46716	p 860	A90-47606	# p 889	A90-48836	# p 811	A90-49452	p 813	A90-50089	p 943
A90-46719	# p 785	A90-47608	p 809	A90-48837	# p 812	A90-49453	p 853	A90-50111	p 954
A90-46720	# p 881	A90-47627	# p 863	A90-48838	# p 812	A90-49454	p 854	A90-50113	p 954
A90-46841	# p 806	A90-47628	# p 863	A90-48840	# p 786	A90-49455	p 813	A90-50125	p 943
A90-46843	# p 806	A90-47629	# p 863	A90-48841	# p 834	A90-49458	p 813	A90-50126	p 955
A90-46848	# p 806	A90-47630	# p 864	A90-48842	# p 897	A90-49459	p 814	A90-50128	p 943
A90-46850	# p 806	A90-47631	# p 864	A90-48843	# p 897	A90-49460	p 814	A90-50130	p 943
A90-46857	# p 806	A90-47632	# p 864	A90-48844	# p 834	A90-49464	p 814	A90-50131	p 943
A90-46869	# p 806	A90-47637	# p 822	A90-48846	# p 834	A90-49465	p 814	A90-50132	p 943
A90-46871	# p 852	A90-47659	# p 822	A90-48847	# p 835	A90-49466	p 854	A90-50134	p 943
A90-46872	# p 807	A90-47661	# p 864	A90-48848	# p 835	A90-49469	p 883	A90-50135	p 944
A90-46876	# p 807	A90-47662	# p 864	A90-48849	# p 835	A90-49470	p 854	A90-50136	p 955
A90-46879	# p 807	A90-47663	# p 817	A90-48852	# p 835	A90-49475	p 814	A90-50137	p 944
A90-46880	# p 807	A90-47664	# p 864	A90-48857	# p 835	A90-49477	p 841	A90-50138	p 944
A90-46881	# p 807	A90-47665	# p 865	A90-48859	# p 835	A90-49481	p 894	A90-50139	p 944
A90-46882	# p 873	A90-47666	# p 865	A90-48860	# p 835	A90-49482	p 854	A90-50140	p 944
A90-46884	# p 807	A90-47669	# p 889	A90-48861	# p 836	A90-49484	p 895	A90-50142	p 944
A90-46889	# p 881	A90-47688	# p 889	A90-48862	# p 836	A90-49485	p 895	A90-50145	p 945
A90-46907	# p 852	A90-47690	# p 890	A90-48863	# p 836	A90-49486	p 895	A90-50147	p 945
A90-46926	p 829	A90-47694	# p 865	A90-48864	# p 818	A90-49487	p 854	A90-50155	p 945
A90-46927	# p 785	A90-47695	# p 865	A90-48865	# p 836	A90-49488	p 841	A90-50158	p 945
A90-46928	# p 785	A90-47696	# p 865	A90-48866	# p 836	A90-49490	p 823	A90-50159	p 955
A90-46929	# p 785	A90-47697	# p 890	A90-48867	# p 892	A90-49491	# p 823	A90-50162	p 945
A90-46930	# p 817	A90-47698	# p 890	A90-48869	# p 836	A90-49493	# p 823	A90-50163	p 945
A90-46931	# p 860	A90-47699	# p 890	A90-48871	# p 853	A90-49494	# p 823	A90-50164	p 955
A90-46932	# p 846	A90-47700	p 809	A90-48872	# p 853	A90-49496	p 823	A90-50166	p 946
A90-46933	# p 852	A90-47706	# p 890	A90-48873	# p 812	A90-49497	# p 823	A90-50167	p 946
A90-46934	# p 860	A90-47707	# p 786	A90-48874	# p 853	A90-49501	# p 824	A90-50168	p 946
A90-46935	# p 829	A90-47723	# p 890	A90-48875	# p 818	A90-49502	# p 848	A90-50170	p 946
A90-46936	# p 829	A90-47725	# p 891	A90-48876	# p 837	A90-49503	# p 824	A90-50173	p 955
A90-46937	# p 829	A90-47726	# p 865	A90-48877	# p 837	A90-49613	p 897	A90-50175	p 946
A90-46938	# p 829	A90-47727	# p 866	A90-48879	# p 837	A90-49614	p 898	A90-50176	p 946
A90-46939	# p 829	A90-47728	# p 866	A90-48880	# p 837	A90-49615	p 898	A90-50177	p 946
A90-46940	# p 830	A90-47729	# p 866	A90-48881	# p 853	A90-49616	p 898	A90-50179	p 946
A90-46942	# p 807	A90-47730	# p 891	A90-48882	# p 868	A90-49618	p 898	A90-50180	p 947
A90-46943	# p 808	A90-47731	# p 866	A90-48883	# p 847	A90-49619	p 898	A90-50183	p 955
A90-46944	# p 830	A90-47732	# p 866	A90-48884	# p 837	A90-49620	p 898	A90-50186	p 947
A90-46945	# p 808	A90-47733	# p 866	A90-48885	# p 837	A90-49675	p 873	A90-50187	p 956
A90-46946	# p 830	A90-47734	# p 867	A90-48886	# p 837	A90-49741	p 892	A90-50188	p 947
A90-46947	# p 894	A90-47736	# p 867	A90-48887	# p 838	A90-49763	p 873	A90-50189	p 947
A90-46948	# p 861	A90-47737	# p 867	A90-48888	# p 868	A90-49776	# p 814	A90-50190	p 947
A90-46949	# p 861	A90-47738	# p 833	A90-48891	p 838	A90-49778	# p 814	A90-50199	p 947
A90-46950	# p 830	A90-47747	# p 867	A90-48952	p 838	A90-49800	p 815	A90-50200	p 956
A90-46951	# p 830	A90-47751	# p 891	A90-48953	# p 812	A90-49823	p 842	A90-50205	p 948
A90-46952	# p 830	A90-47753	# p 891	A90-48954	# p 812	A90-49824	p 842	A90-50212	p 948
A90-46953	# p 831	A90-47755	# p 891	A90-48955	# p 838	A90-49825	p 842	A90-50213	p 956
A90-46954	# p 831	A90-47758	# p 891	A90-48956	# p 838	A90-49826	p 888	A90-50214	p 948
A90-46955	# p 831	A90-47763	# p 847	A90-48957	# p 894	A90-49827	# p 818	A90-50215	p 948
A90-46956	# p 861	A90-47764	# p 867	A90-48958	# p 838	A90-49830	# p 848	A90-50216	p 956
A90-46958	# p 831	A90-47854	p 809	A90-48959	# p 870	A90-49831	# p 818	A90-50217	p 948
A90-46960	# p 889	A90-47901	p 822	A90-48961	# p 870	A90-49832	# p 818	A90-50218	p 948
A90-46961	# p 831	A90-47909	p 822	A90-48982	p 847	A90-49833	# p 818	A90-50225	p 948
A90-46962	# p 831	A90-48045	p 882	A90-48983	p 823	A90-49834	# p 819	A90-50226	p 949
A90-46963	# p 889	A90-48047	p 882	A90-48984	p 874	A90-49835	# p 819	A90-50227	p 949
A90-46964	# p 832	A90-48050	p 882	A90-48985	p 848	A90-49836	# p 842	A90-50230	p 949
A90-46965	# p 832	A90-48076	p 809	A90-48987	p 874	A90-49839	# p 819	A90-50232	p 902
A90-46966	# p 861	A90-48077	# p 810	A90-48988	p 882	A90-49843	# p 819	A90-50233	p 928
A90-46967	# p 861	A90-48078	# p 810	A90-49000	p 874	A90-49844	# p 819	A90-50235	p 903
A90-46968	# p 832	A90-48079	# p 810	A90-49101	# p 812	A90-49845	# p 819	A90-50246	p 919
A90-46969	# p 832	A90-48080	# p 810	A90-49102	# p 838	A90-49846	# p 883	A90-50249	p 934
A90-46970	# p 832	A90-48081	# p 810	A90-49103	# p 812	A90-49876	p 901	A90-50544	p 902
A90-46971	# p 832	A90-48082	# p 810	A90-49104	# p 838	A90-49877	p 901	A90-50551	p 949
A90-46972	# p 833	A90-48083	# p 810	A90-49105	# p 838	A90-49878	p 919	A90-50555	p 956
A90-46973	# p 808	A90-48085	# p 810	A90-49106	# p 813	A90-49879	p 926	A90-50636	# p 956
A90-46974	# p 833	A90-48086	# p 810	A90-49107	# p 818	A90-49880	p 926	A90-50637	# p 903
A90-46975	# p 833	A90-48089	# p 811	A90-49108	# p 838			A90-50638	# p 903

A90-50640

ACCESSION NUMBER INDEX

A90-50640 #	p 934	A90-52801 #	p 934	N90-10409 *	p 72	N90-11749 #	p 114	N90-12564 #	p 95
A90-50644 *	p 956	A90-52857	p 937	N90-10424 *	p 72	N90-11750 #	p 115	N90-12566 #	p 95
A90-50645 *	p 949	A90-52877	p 964	N90-10451 *	p 73	N90-11751 *	p 119	N90-12568 #	p 95
A90-50649	p 957	A90-52881 *	p 964	N90-10586 #	p 77	N90-11752 *	p 119	N90-12570 #	p 99
A90-50747	p 914	A90-52884	p 927	N90-10630 #	p 77	N90-11753 *	p 119	N90-12572	p 99
A90-50773	p 957	A90-52953	p 927	N90-10679 *	p 79	N90-11754 #	p 119	N90-12573	p 99
A90-50775	p 914	A90-52954	p 958	N90-10683 *	p 79	N90-11756 #	p 119	N90-12574 #	p 99
A90-50777	p 962			N90-10829 *	p 20	N90-11757 *	p 120	N90-12575 #	p 99
A90-50778	p 914	N90-10001 #	p 1	N90-10830 *	p 20	N90-11758 *	p 120	N90-12580 *	p 106
A90-50779	p 914	N90-10002 #	p 1	N90-10831	p 20	N90-11759 #	p 120	N90-12581 #	p 106
A90-50780	p 962	N90-10003 #	p 18	N90-10833 *	p 20	N90-11760 #	p 120	N90-12582 *	p 106
A90-50783	p 962	N90-10004 #	p 18	N90-10834 *	p 21	N90-11761	p 121	N90-12583 *	p 106
A90-50784	p 962	N90-10005	p 18	N90-10837	p 21	N90-11762 #	p 121	N90-12584 *	p 106
A90-50815	p 903	N90-10006 *	p 18	N90-10838	p 21	N90-11765 #	p 122	N90-12585 *	p 106
A90-50816	p 903	N90-10008 #	p 18	N90-10841 *	p 24	N90-11766 #	p 122	N90-12586 *	p 106
A90-50817	p 904	N90-10009 #	p 18	N90-10842 #	p 24	N90-11768 #	p 122	N90-12587 *	p 107
A90-50843	p 957	N90-10010 #	p 19	N90-10843 #	p 24	N90-11774 *	p 124	N90-12588 *	p 107
A90-51003	p 904	N90-10011 #	p 19	N90-10844 #	p 24	N90-11813 #	p 126	N90-12589 *	p 107
A90-51006	p 904	N90-10012 #	p 19	N90-10845 #	p 25	N90-11819 #	p 126	N90-12591 #	p 107
A90-51009	p 904	N90-10013 #	p 24	N90-10847 #	p 28	N90-11820 #	p 126	N90-12592 #	p 107
A90-51013	p 904	N90-10014 #	p 24	N90-10855 #	p 28	N90-11821 #	p 126	N90-12593 #	p 107
A90-51014	p 904	N90-10016 #	p 27	N90-10856 #	p 28	N90-11837 #	p 126	N90-12595 #	p 107
A90-51017	p 904	N90-10017 #	p 27	N90-10860 #	p 33	N90-11872 #	p 126	N90-12596 #	p 107
A90-51020	p 905	N90-10018 #	p 27	N90-10861 #	p 33	N90-11874 #	p 126	N90-12597 #	p 107
A90-51025	p 905	N90-10019 #	p 27	N90-10862 #	p 34	N90-11899 #	p 126	N90-12598 #	p 109
A90-51028	p 905	N90-10020 #	p 27	N90-10863 #	p 34	N90-11907 #	p 133	N90-12599 #	p 109
A90-51058	p 926	N90-10021 #	p 28	N90-10864 #	p 34	N90-11908 #	p 133	N90-12600	p 115
A90-51060	p 914	N90-10022 #	p 31	N90-10865 #	p 34	N90-11934 #	p 133	N90-12603 #	p 115
A90-51154	p 934	N90-10023 #	p 32	N90-10866 #	p 34	N90-11970 #	p 133	N90-12604 #	p 115
A90-51198	p 949	N90-10025 #	p 32	N90-10867 #	p 34	N90-11982 #	p 133	N90-12605 #	p 115
A90-51200	p 950	N90-10026 #	p 32	N90-10868 #	p 34	N90-11988 #	p 134	N90-12606 #	p 115
A90-51256 #	p 905	N90-10027 #	p 32	N90-10869 #	p 34	N90-12007 #	p 134	N90-12608 #	p 115
A90-51257 #	p 905	N90-10028 #	p 32	N90-10870 #	p 35	N90-12035 #	p 134	N90-12609 #	p 116
A90-51258 #	p 905	N90-10031 #	p 32	N90-10872 #	p 35	N90-12042 #	p 134	N90-12610 #	p 116
A90-51259 #	p 906	N90-10032 #	p 39	N90-10874 #	p 35	N90-12057 *	p 134	N90-12611 #	p 116
A90-51261 #	p 957	N90-10034 #	p 51	N90-10875 #	p 35	N90-12058 *	p 134	N90-12612 #	p 116
A90-51339	p 914	N90-10035 #	p 51	N90-10877 #	p 35	N90-12113 #	p 137	N90-12613 #	p 116
A90-51450 #	p 919	N90-10036 #	p 51	N90-10882 #	p 35	N90-12208 #	p 138	N90-12614 #	p 116
A90-51483	p 906	N90-10037 #	p 51	N90-10883 #	p 58	N90-12239 #	p 138	N90-12616 #	p 116
A90-51507	p 906	N90-10040 #	p 52	N90-10884 #	p 36	N90-12291 #	p 139	N90-12617 #	p 117
A90-51525	p 957	N90-10041 #	p 52	N90-10887 #	p 59	N90-12406 #	p 141	N90-12618 #	p 117
A90-51526	p 906	N90-10042 #	p 52	N90-10888 #	p 36	N90-12494 #	p 141	N90-12619 #	p 117
A90-51530	p 906	N90-10043 #	p 52	N90-10889 #	p 36	N90-12495 #	p 82	N90-12620 #	p 117
A90-51531	p 906	N90-10044 #	p 52	N90-10891 #	p 54	N90-12496 #	p 82	N90-12621 #	p 120
A90-51533	p 906	N90-10045 #	p 52	N90-10893 #	p 55	N90-12500 #	p 90	N90-12622 #	p 120
A90-51534	p 907	N90-10046 #	p 53	N90-10894	p 57	N90-12501 #	p 90	N90-12624 #	p 121
A90-51537	p 907	N90-10047 #	p 53	N90-10895 #	p 57	N90-12503 #	p 90	N90-12625 #	p 123
A90-51538	p 907	N90-10048 #	p 53	N90-10896 #	p 59	N90-12504 #	p 90	N90-12627 #	p 123
A90-51539	p 907	N90-10049 #	p 53	N90-10897 #	p 59	N90-12505 #	p 90	N90-12628 #	p 123
A90-51543	p 907	N90-10075 #	p 57	N90-10898 #	p 59	N90-12506 *	p 90	N90-12629 #	p 123
A90-51545	p 907	N90-10086 #	p 60	N90-10899 #	p 59	N90-12507 #	p 91	N90-12665 #	p 127
A90-51559	p 907	N90-10106 #	p 61	N90-10904 #	p 61	N90-12508 #	p 104	N90-12667 #	p 127
A90-51616	p 950	N90-10111 #	p 61	N90-10909 #	p 73	N90-12509 #	p 104	N90-12720 #	p 127
A90-51617	p 950	N90-10112 #	p 61	N90-11184 #	p 65	N90-12510 #	p 91	N90-12777 #	p 134
A90-51618	p 912	N90-10115 #	p 33	N90-11245 #	p 73	N90-12511 #	p 104	N90-12778 #	p 135
A90-51619	p 912	N90-10116 #	p 33	N90-11487 #	p 77	N90-12512 #	p 104	N90-12781 #	p 135
A90-51620	p 950	N90-10119 #	p 33	N90-11549 #	p 79	N90-12516 #	p 91	N90-12782 #	p 135
A90-51621	p 950	N90-10123 #	p 61	N90-11692 #	p 81	N90-12517 #	p 91	N90-12807	p 135
A90-51622	p 950	N90-10150 #	p 61	N90-11695 #	p 87	N90-12519 #	p 91	N90-12816 #	p 135
A90-51623	p 950	N90-10184 #	p 63	N90-11696 #	p 88	N90-12522 #	p 122	N90-12823	p 135
A90-51624	p 951	N90-10186 #	p 63	N90-11697 #	p 88	N90-12523 #	p 91	N90-12872 #	p 136
A90-51625	p 951	N90-10187 #	p 63	N90-11699 #	p 88	N90-12524 #	p 139	N90-12879 #	p 136
A90-51658	p 926	N90-10191 #	p 63	N90-11700 #	p 88	N90-12526 #	p 122	N90-12889 #	p 136
A90-51899 #	p 920	N90-10192 #	p 63	N90-11701 #	p 88	N90-12528 #	p 122	N90-12897 #	p 136
A90-51966	p 951	N90-10193 #	p 64	N90-11704 #	p 88	N90-12529 #	p 91	N90-12899 #	p 136
A90-51984	p 965	N90-10194 #	p 64	N90-11705 #	p 89	N90-12530 #	p 92	N90-12933 #	p 136
A90-52030 #	p 908	N90-10195 #	p 53	N90-11706 #	p 89	N90-12531 #	p 92	N90-12954 #	p 137
A90-52037	p 957	N90-10199 #	p 53	N90-11707 #	p 89	N90-12532 #	p 92	N90-12958 #	p 137
A90-52044	p 958	N90-10202 #	p 54	N90-11709 #	p 89	N90-12535 #	p 92	N90-13005 #	p 137
A90-52051	p 962	N90-10203 #	p 54	N90-11710 #	p 89	N90-12537 #	p 92	N90-13116 #	p 138
A90-52052	p 962	N90-10204 #	p 54	N90-11711 #	p 89	N90-12538 #	p 140	N90-13198 #	p 140
A90-52077	p 927	N90-10206 #	p 54	N90-11712 #	p 89	N90-12539 #	p 92	N90-13202 #	p 140
A90-52093	p 913	N90-10231 #	p 64	N90-11713 #	p 90	N90-12540 #	p 93	N90-13203 #	p 140
A90-52289	p 965	N90-10233 #	p 64	N90-11715 #	p 96	N90-12541 #	p 93	N90-13207 #	p 140
A90-52356	p 958	N90-10234 #	p 64	N90-11716 #	p 96	N90-12542 #	p 93	N90-13228 #	p 140
A90-52410	p 927	N90-10235 #	p 64	N90-11717 #	p 96	N90-12543 #	p 93	N90-13278 #	p 141
A90-52415	p 915	N90-10238 #	p 64	N90-11718 #	p 96	N90-12544 #	p 104	N90-13323 #	p 143
A90-52574	p 920	N90-10240 #	p 64	N90-11719 #	p 96	N90-12545 #	p 104	N90-13324 #	p 143
A90-52575	p 902	N90-10242 #	p 65	N90-11722 #	p 99	N90-12546 #	p 104	N90-13325 #	p 169
A90-52592 #	p 908	N90-10253 #	p 65	N90-11724 #	p 99	N90-12547 #	p 105	N90-13326 #	p 170
A90-52607 #	p 908	N90-10255 #	p 65	N90-11729 #	p 99	N90-12548 #	p 105	N90-13327 #	p 170
A90-52613 #	p 915	N90-10293 #	p 65	N90-11731 #	p 103	N90-12549 #	p 105	N90-13330 #	p 170
A90-52614 #	p 915	N90-10351 #	p 71	N90-11732 #	p 103	N90-12551 #	p 105	N90-13331 #	p 170
A90-52615 #	p 915	N90-10356 #	p 71	N90-11733 #	p 103	N90-12552 #	p 105	N90-13332 #	p 170
A90-52616 #	p 937	N90-10357 #	p 71	N90-11735 #	p 103	N90-12553 #	p 140	N90-13333 #	p 171
A90-52617 #	p 937	N90-10358 #	p 71	N90-11737 #	p 113	N90-12554 #	p 93	N90-13334 #	p 171
A90-52618 #	p 908	N90-10361 #	p 19	N90-11738 #	p 113	N90-12555 #	p 122	N90-13341 #	p 171
A90-52620 #	p 908	N90-10362 #	p 71	N90-11739 #	p 113	N90-12556 #	p 94	N90-13344 #	p 212
A90-52621 #	p 908	N90-10364 #	p 19	N90-11740 #	p 114	N90-12557 #	p 94	N90-13348 #	p 212
A90-52699	p 902	N90-10366 #	p 71	N90-11741 #	p 114	N90-12558 #	p 94	N90-13349 #	p 171
A90-52700	p 937	N90-10367 #	p 19	N90-11743 #	p 114	N90-12559 #	p 94	N90-13350 #	p 171
A90-52776 #	p 908	N90-10368 #	p 72	N90-11745 #	p 114	N90-12560 #	p 94	N90-13351 #	p 171
A90-52777 #	p 908	N90-10373 #	p 20	N90-11746 #	p 114	N90-12562 #	p 95	N90-13352 #	p 172
A90-52778 #	p 909	N90-10377 #	p 72	N90-11747 #	p 114	N90-12563 #	p 95	N90-13353 #	p 172
A90-52779 #	p 909	N90-10378 #	p 72	N90-11748 #	p 114				
A90-52799	p 951	N90-10380 #	p 20						
		N90-10402 #	p 72						

ACCESSION NUMBER INDEX

N90-13354 * # p 172
N90-13355 * # p 172
N90-13356 # # p 172
N90-13357 # # p 172
N90-13358 # # p 176
N90-13359 # # p 176
N90-13360 # # p 176
N90-13361 # # p 177
N90-13362 # # p 177
N90-13363 # # p 177
N90-13364 # # p 177
N90-13365 # # p 177
N90-13366 # # p 178
N90-13367 # # p 178
N90-13368 # # p 178
N90-13369 * # p 183
N90-13370 * # p 183
N90-13371 # # p 183
N90-13372 * # p 183
N90-13373 # # p 183
N90-13375 # # p 184
N90-13376 # # p 184
N90-13377 # # p 184
N90-13378 # # p 184
N90-13379 # # p 184
N90-13381 * # p 187
N90-13384 * # p 187
N90-13385 * # p 192
N90-13386 # # p 192
N90-13387 * # p 192
N90-13388 * # p 193
N90-13389 * # p 193
N90-13390 * # p 193
N90-13391 * # p 193
N90-13392 * # p 194
N90-13393 * # p 194
N90-13394 * # p 194
N90-13395 - # p 194
N90-13396 # # p 198
N90-13397 # # p 198
N90-13398 # # p 198
N90-13399 # # p 198
N90-13400 # # p 198
N90-13401 * # p 200
N90-13402 # # p 201
N90-13403 * # p 201
N90-13404 * # p 201
N90-13406 # # p 201
N90-13407 * # p 201
N90-13408 # # p 201
N90-13409 # # p 202
N90-13410 # # p 202
N90-13617 # # p 205
N90-13627 # # p 205
N90-13636 # # p 206
N90-13638 # # p 206
N90-13677 # # p 206
N90-13725 # # p 212
N90-13727 # # p 212
N90-13728 # # p 212
N90-13744 * # p 213
N90-13750 * # p 213
N90-13797 * # # p 213
N90-13812 # # p 213
N90-13814 * # p 213
N90-13816 * # p 213
N90-13817 * # p 214
N90-13820 * # p 214
N90-13822 # # p 214
N90-13990 * # p 217
N90-13995 * # p 217
N90-14061 * # p 217
N90-14074 # # p 220
N90-14153 * # p 220
N90-14186 * # p 173
N90-14187 * # p 173
N90-14190 * # p 173
N90-14192 # # p 173
N90-14194 # # p 173
N90-14195 # # p 173
N90-14196 # # p 174
N90-14197 # # p 174
N90-14198 # # p 174
N90-14199 # # p 174
N90-14201 # # p 174
N90-14202 * # # p 175
N90-14205 * # # p 175
N90-14211 # # p 176
N90-14212 * # # p 176
N90-14213 # # p 177
N90-14214 # # p 178
N90-14216 * # # p 184
N90-14217 # # p 185
N90-14218 # # p 185
N90-14219 # # p 185
N90-14220 * # # p 185

N90-14221 # p 185
N90-14222 # p 185
N90-14223 # p 186
N90-14225 # p 186
N90-14226 # p 186
N90-14227 # p 186
N90-14228 # p 186
N90-14232 # p 187
N90-14234 # p 194
N90-14235 # p 194
N90-14236 # p 194
N90-14239 # p 198
N90-14240 # p 199
N90-14242 # p 199
N90-14243 # p 199
N90-14244 # p 202
N90-14245 # p 202
N90-14268 # p 203
N90-14304 # p 206
N90-14330 # p 206
N90-14385 # p 206
N90-14404 # p 212
N90-14453 # p 214
N90-14497 # p 214
N90-14511 # p 215
N90-14617 # p 215
N90-14641 # p 215
N90-14656 # p 215
N90-14783 # p 217
N90-14843 # p 217
N90-14866 # p 220
N90-15041 # p 222
N90-15042 # p 248
N90-15043 # p 280
N90-15044 # p 280
N90-15045 # p 280
N90-15046 # p 281
N90-15048 # p 238
N90-15049 # p 281
N90-15050 # p 258
N90-15051 # p 258
N90-15052 # p 281
N90-15053 # p 258
N90-15054 # p 258
N90-15055 # p 258
N90-15056 # p 259
N90-15057 # p 259
N90-15058 # p 248
N90-15061 # p 242
N90-15062 # p 248
N90-15063 # p 239
N90-15064 # p 235
N90-15065 # p 239
N90-15066 # p 248
N90-15067 # p 239
N90-15069 # p 235
N90-15070 # p 235
N90-15072 # p 235
N90-15074 # p 235
N90-15075 # p 236
N90-15076 # p 236
N90-15079 # p 236
N90-15080 # p 236
N90-15081 # p 236
N90-15082 # p 236
N90-15083 # p 239
N90-15084 # p 239
N90-15085 # p 239
N90-15086 # p 243
N90-15089 # p 243
N90-15090 # p 243
N90-15093 # p 248
N90-15094 # p 248
N90-15095 # p 249
N90-15096 # p 249
N90-15097 # p 249
N90-15098 # p 249
N90-15099 # p 249
N90-15100 # p 249
N90-15102 # p 252
N90-15104 # p 255
N90-15105 # p 255
N90-15106 # p 256
N90-15107 # p 256
N90-15108 # p 259
N90-15110 # p 259
N90-15111 # p 259
N90-15112 # p 259
N90-15113 # p 280
N90-15115 # p 262
N90-15185 # p 267
N90-15187 # p 267
N90-15191 # p 267
N90-15192 # p 267
N90-15193 # p 267
N90-15196 # p 267

N90-15197 # p 268
N90-15198 # p 268
N90-15200 # p 268
N90-15201 # p 268
N90-15202 # p 268
N90-15203 # p 268
N90-15288 # p 269
N90-15310 # p 274
N90-15380 * # p 275
N90-15390 # p 275
N90-15422 # p 275
N90-15465 # p 275
N90-15486 # p 275
N90-15519 # p 281
N90-15566 # p 287
N90-15882 * # p 237
N90-15884 * # p 237
N90-15886 * # p 237
N90-15889 # p 237
N90-15891 * # p 237
N90-15895 # p 240
N90-15896 # p 240
N90-15897 # p 240
N90-15898 * # p 240
N90-15899 # p 243
N90-15900 # p 243
N90-15902 * # p 249
N90-15904 # p 250
N90-15905 # p 250
N90-15906 # p 250
N90-15907 # p 250
N90-15908 # p 250
N90-15909 # p 269
N90-15911 # p 269
N90-15912 # p 276
N90-15913 # p 250
N90-15914 # p 251
N90-15915 # p 251
N90-15916 # p 251
N90-15917 # p 251
N90-15918 # p 256
N90-15919 # p 256
N90-15920 # p 256
N90-15921 # p 256
N90-15922 # p 257
N90-15923 * # p 257
N90-15924 # p 257
N90-15925 # p 260
N90-15926 # p 260
N90-15930 # p 251
N90-15933 # p 251
N90-15934 # p 252
N90-15938 * # p 260
N90-15941 * # p 262
N90-15942 * # p 262
N90-15945 # p 262
N90-15947 # p 263
N90-15948 * # p 263
N90-15952 * # p 263
N90-15956 * # p 263
N90-15957 * # p 263
N90-15958 * # p 264
N90-15959 * # p 264
N90-15960 * # p 264
N90-15963 # p 264
N90-16169 # p 276
N90-16170 # p 276
N90-16172 * # p 276
N90-16174 # p 276
N90-16175 # p 276
N90-16177 # p 276
N90-16178 # p 277
N90-16179 # p 277
N90-16180 # p 277
N90-16181 # p 277
N90-16182 # p 277
N90-16183 # p 277
N90-16184 # p 278
N90-16185 # p 278
N90-16186 # p 278
N90-16189 # p 278
N90-16190 # p 278
N90-16191 # p 278
N90-16192 # p 279
N90-16194 * # p 279
N90-16196 # p 279
N90-16252 # p 238
N90-16294 * # p 279
N90-16707 # p 287
N90-16708 # p 287
N90-16709 # p 315
N90-16710 * # p 315
N90-16711 # p 315
N90-16712 * # p 316
N90-16720 # p 316
N90-16721 # p 316

N90-16722 # p 323
N90-16723 # p 323
N90-16724 # # p 323
N90-16725 # p 323
N90-16726 # p 323
N90-16727 # p 323
N90-16728 # p 324
N90-16729 # p 324
N90-16730 # p 332
N90-16731 # p 332
N90-16734 # p 332
N90-16735 # p 332
N90-16740 # p 332
N90-16743 # p 333
N90-16744 # p 333
N90-16745 # p 333
N90-16748 # p 333
N90-16751 # p 336
N90-16753 # p 336
N90-16755 # p 337
N90-16756 # p 337
N90-16757 # p 337
N90-16758 # p 339
N90-16759 # p 343
N90-16762 # p 343
N90-16766 # p 344
N90-16767 # p 348
N90-16768 # p 348
N90-16770 # p 348
N90-16773 # p 352
N90-16800 # p 353
N90-16801 # p 337
N90-16814 # p 354
N90-16817 # p 344
N90-16818 # p 344
N90-16819 # p 344
N90-16827 # p 354
N90-16842 # p 354
N90-16936 # p 356
N90-16939 # p 357
N90-16951 # p 357
N90-16958 # p 368
N90-16969 # p 369
N90-16971 # p 369
N90-17045 # p 369
N90-17055 # p 369
N90-17074 # p 369
N90-17084 # p 369
N90-17112 # p 370
N90-17113 # p 370
N90-17193 # p 370
N90-17235 # p 373
N90-17348 # p 377
N90-17409 # p 378
N90-17410 # p 379
N90-17411 # p 379
N90-17412 # p 379
N90-17413 # p 379
N90-17539 # p 316
N90-17545 # p 316
N90-17548 # p 317
N90-17552 # p 337
N90-17554 # p 337
N90-17556 # p 317
N90-17557 # p 317
N90-17558 # p 317
N90-17560 # p 317
N90-17561 # p 318
N90-17562 # p 318
N90-17564 # p 318
N90-17566 # p 318
N90-17569 # p 318
N90-17571 # p 319
N90-17574 # p 319
N90-17575 # p 319
N90-17576 # p 319
N90-17577 # p 319
N90-17578 # p 320
N90-17579 # p 320
N90-17580 # p 320
N90-17581 # p 324
N90-17582 # p 324
N90-17583 # p 324
N90-17584 # p 324
N90-17585 # p 324
N90-17586 # p 325
N90-17587 # p 325
N90-17588 # p 325
N90-17589 # p 325
N90-17590 # p 325
N90-17591 # p 325
N90-17592 # p 326
N90-17593 # p 326
N90-17594 # p 326
N90-17596 # p 326

N90-18395

N90-17597	#	p 326
N90-17598	#	p 327
N90-17600	#	p 327
N90-17601	#	p 327
N90-17602	#	p 327
N90-17603	#	p 327
N90-17604	#	p 327
N90-17605	#	p 327
N90-17606	#	p 328
N90-17608	#	p 328
N90-17609	#	p 328
N90-17610	#	p 328
N90-17611	#	p 328
N90-17620 *	#	p 328
N90-17621	#	p 329
N90-17627 *	#	p 338
N90-17628	#	p 338
N90-17629	#	p 338
N90-17630	#	p 338
N90-17631	#	p 338
N90-17632 *	#	p 340
N90-17634	#	p 344
N90-17635 *	#	p 344
N90-17636 *	#	p 345
N90-17638 *	#	p 345
N90-17639 *	#	p 349
N90-17640	#	p 349
N90-17641 *	#	p 349
N90-17642 *	#	p 349
N90-17643	#	p 349
N90-17644	#	p 349
N90-17646	#	p 350
N90-17647 *	#	p 352
N90-17648 *	#	p 352
N90-17649 *	#	p 352
N90-17650 *	#	p 320
N90-17651 *	#	p 320
N90-17652 *	#	p 321
N90-17653 *	#	p 321
N90-17654 *	#	p 321
N90-17655 *	#	p 353
N90-17656 *	#	p 353
N90-17657 *	#	p 321
N90-17658 *	#	p 321
N90-17825	#	p 357
N90-17868 *	#	p 357
N90-17871 *	#	p 357
N90-17873	#	p 357
N90-17930	#	p 370
N90-17936	#	p 370
N90-17939	#	p 370
N90-17941	#	p 371
N90-17970	#	p 371
N90-17984	#	p 371
N90-18016	#	p 371
N90-18017	#	p 371
N90-18020	#	p 371
N90-18030	#	p 372
N90-18038	#	p 372
N90-18041 *	#	p 372
N90-18057 *	#	p 372
N90-18065	#	p 372
N90-18070 *	#	p 373
N90-18125 *	#	p 374
N90-18126 *	#	p 374
N90-18173	#	p 377
N90-18181	#	p 377
N90-18212	#	p 377
N90-18225	#	p 379
N90-18228 *	#	p 379
N90-18229 *	#	p 380
N90-18233 *	#	p 380
N90-18364 *	#	p 396
N90-18365	#	p 396
N90-18367	#	p 396
N90-18369	#	p 397
N90-18370	#	p 397
N90-18371 *	#	p 401
N90-18372 *	#	p 401
N90-18373	#	p 402
N90-18375	#	p 402
N90-18376	#	p 402
N90-18378 *	#	p 404
N90-18380	#	p 405
N90-18383	#	p 405
N90-18385 *	#	p 414
N90-18386	#	p 414
N90-18387	#	p 414
N90-18388	#	p 414
N90-18389	#	p 415
N90-18390 *	#	p 415
N90-18391	#	p 415
N90-18392	#	p 415
N90-18393 *	#	p 420
N90-18394 *	#	p 420
N90-18395 *	#	p 421

N90-18396

N90-18396 # p 425
 N90-18400 # p 443
 N90-18402 # p 425
 N90-18404 # p 425
 N90-18405 # p 425
 N90-18406 # p 425
 N90-18407 # p 426
 N90-18408 # p 426
 N90-18411 # p 426
 N90-18412 # p 426
 N90-18413 # p 426
 N90-18416 # p 426
 N90-18418 # p 427
 N90-18421 # p 427
 N90-18422 # p 427
 N90-18423 # p 427
 N90-18425 # p 427
 N90-18427 # p 397
 N90-18428 # p 427
 N90-18429 # p 428
 N90-18430 # p 428
 N90-18431 # p 433
 N90-18432 # p 434
 N90-18433 # p 434
 N90-18434 # p 434
 N90-18527 # p 443
 N90-18601 # p 443
 N90-18670 # p 453
 N90-18672 # p 454
 N90-18695 # p 454
 N90-18697 # p 454
 N90-18738 # p 454
 N90-18743 # p 454
 N90-18746 # p 454
 N90-18882 # p 462
 N90-18908 # p 462
 N90-18920 # p 462
 N90-18999 # p 464
 N90-19060 # p 464
 N90-19189 # p 465
 N90-19193 # p 397
 N90-19194 # p 397
 N90-19195 # p 397
 N90-19196 # p 398
 N90-19197 # p 398
 N90-19198 # p 398
 N90-19199 # p 398
 N90-19201 # p 398
 N90-19202 # p 399
 N90-19203 # p 399
 N90-19204 # p 399
 N90-19206 # p 399
 N90-19207 # p 399
 N90-19208 # p 399
 N90-19211 # p 400
 N90-19213 # p 400
 N90-19215 # p 402
 N90-19217 # p 405
 N90-19223 # p 405
 N90-19224 # p 415
 N90-19225 # p 416
 N90-19226 # p 416
 N90-19227 # p 416
 N90-19228 # p 416
 N90-19229 # p 416
 N90-19232 # p 428
 N90-19233 # p 428
 N90-19235 # p 428
 N90-19237 # p 429
 N90-19238 # p 434
 N90-19239 # p 434
 N90-19240 # p 434
 N90-19241 # p 435
 N90-19242 # p 440
 N90-19364 # p 444
 N90-19387 # p 444
 N90-19417 # p 421
 N90-19420 # p 435
 N90-19421 # p 429
 N90-19472 # p 455
 N90-19534 # p 455
 N90-19542 # p 455
 N90-19543 # p 455
 N90-19609 # p 455
 N90-19718 # p 456
 N90-19756 # p 462
 N90-19820 # p 464
 N90-19821 # p 464
 N90-19842 # p 464
 N90-19852 # p 464
 N90-20044 # p 477
 N90-20046 # p 477
 N90-20047 # p 478
 N90-20048 # p 478
 N90-20050 # p 478
 N90-20051 # p 478

N90-20052 # p 478
 N90-20053 # p 478
 N90-20054 # p 483
 N90-20056 # p 497
 N90-20057 # p 483
 N90-20058 # p 483
 N90-20059 # p 483
 N90-20060 # p 483
 N90-20063 # p 483
 N90-20064 # p 484
 N90-20068 # p 484
 N90-20069 # p 484
 N90-20070 # p 497
 N90-20071 # p 497
 N90-20072 # p 497
 N90-20073 # p 498
 N90-20074 # p 498
 N90-20075 # p 498
 N90-20076 # p 498
 N90-20077 # p 498
 N90-20078 # p 498
 N90-20079 # p 499
 N90-20080 # p 505
 N90-20081 # p 505
 N90-20082 # p 505
 N90-20083 # p 506
 N90-20084 # p 506
 N90-20085 # p 509
 N90-20086 # p 509
 N90-20087 # p 509
 N90-20088 # p 510
 N90-20089 # p 510
 N90-20090 # p 510
 N90-20091 # p 510
 N90-20092 # p 520
 N90-20093 # p 520
 N90-20094 # p 520
 N90-20095 # p 520
 N90-20096 # p 526
 N90-20097 # p 526
 N90-20098 # p 526
 N90-20099 # p 526
 N90-20100 # p 526
 N90-20103 # p 528
 N90-20133 # p 532
 N90-20140 # p 532
 N90-20143 # p 532
 N90-20208 # p 533
 N90-20235 # p 533
 N90-20312 # p 540
 N90-20325 # p 540
 N90-20345 # p 540
 N90-20346 # p 540
 N90-20349 # p 541
 N90-20392 # p 541
 N90-20434 # p 541
 N90-20439 # p 541
 N90-20500 # p 544
 N90-20656 # p 546
 N90-20794 # p 548
 N90-20799 # p 548
 N90-20800 # p 548
 N90-20920 # p 468
 N90-20921 # p 468
 N90-20922 # p 484
 N90-20923 # p 488
 N90-20924 # p 484
 N90-20925 # p 485
 N90-20926 # p 485
 N90-20927 # p 485
 N90-20928 # p 485
 N90-20929 # p 485
 N90-20931 # p 489
 N90-20932 # p 489
 N90-20933 # p 489
 N90-20934 # p 486
 N90-20935 # p 486
 N90-20936 # p 521
 N90-20937 # p 521
 N90-20938 # p 486
 N90-20939 # p 521
 N90-20940 # p 521
 N90-20941 # p 521
 N90-20942 # p 468
 N90-20943 # p 468
 N90-20944 # p 479
 N90-20945 # p 479
 N90-20947 # p 479
 N90-20948 # p 479
 N90-20950 # p 479
 N90-20951 # p 480
 N90-20952 # p 480
 N90-20954 # p 480
 N90-20955 # p 480
 N90-20956 # p 480
 N90-20957 # p 480

N90-20958 # p 481
 N90-20959 # p 481
 N90-20960 # p 481
 N90-20961 # p 481
 N90-20963 # p 481
 N90-20964 # p 481
 N90-20965 # p 481
 N90-20966 # p 486
 N90-20967 # p 486
 N90-20968 # p 489
 N90-20969 # p 489
 N90-20970 # p 489
 N90-20971 # p 499
 N90-20972 # p 499
 N90-20973 # p 499
 N90-20974 # p 499
 N90-20975 # p 499
 N90-20976 # p 500
 N90-20977 # p 482
 N90-20978 # p 500
 N90-20979 # p 500
 N90-20980 # p 500
 N90-20981 # p 500
 N90-20982 # p 500
 N90-20983 # p 501
 N90-20984 # p 501
 N90-20985 # p 510
 N90-20986 # p 501
 N90-20987 # p 501
 N90-20988 # p 511
 N90-20989 # p 511
 N90-20990 # p 511
 N90-20991 # p 501
 N90-20992 # p 501
 N90-20993 # p 502
 N90-20994 # p 502
 N90-20995 # p 502
 N90-20996 # p 502
 N90-20997 # p 502
 N90-20998 # p 546
 N90-20999 # p 541
 N90-21000 # p 503
 N90-21001 # p 503
 N90-21002 # p 503
 N90-21003 # p 503
 N90-21004 # p 506
 N90-21005 # p 506
 N90-21006 # p 506
 N90-21007 # p 511
 N90-21008 # p 511
 N90-21009 # p 511
 N90-21010 # p 512
 N90-21011 # p 512
 N90-21012 # p 512
 N90-21013 # p 482
 N90-21014 # p 512
 N90-21015 # p 512
 N90-21016 # p 512
 N90-21017 # p 513
 N90-21018 # p 513
 N90-21019 # p 513
 N90-21020 # p 513
 N90-21021 # p 513
 N90-21022 # p 513
 N90-21023 # p 514
 N90-21024 # p 514
 N90-21025 # p 514
 N90-21026 # p 514
 N90-21027 # p 514
 N90-21028 # p 514
 N90-21029 # p 515
 N90-21033 # p 515
 N90-21034 # p 515
 N90-21035 # p 515
 N90-21036 # p 515
 N90-21037 # p 516
 N90-21038 # p 516
 N90-21039 # p 521
 N90-21040 # p 522
 N90-21041 # p 522
 N90-21042 # p 526
 N90-21043 # p 527
 N90-21044 # p 527
 N90-21045 # p 527
 N90-21046 # p 527
 N90-21047 # p 527
 N90-21049 # p 527
 N90-21137 # p 533
 N90-21142 # p 533
 N90-21188 # p 533
 N90-21229 # p 541
 N90-21243 # p 542
 N90-21247 # p 542
 N90-21248 # p 542
 N90-21249 # p 542
 N90-21283 # p 542

N90-21300 # p 542
 N90-21361 # p 543
 N90-21394 # p 543
 N90-21395 # p 543
 N90-21399 # p 543
 N90-21422 # p 543
 N90-21424 # p 543
 N90-21500 # p 544
 N90-21508 # p 544
 N90-21509 # p 544
 N90-21539 # p 546
 N90-21541 # p 546
 N90-21542 # p 547
 N90-21543 # p 547
 N90-21544 # p 547
 N90-21571 # p 547
 N90-21602 # p 548
 N90-21604 # p 549
 N90-21605 # p 549
 N90-21724 # p 551
 N90-21725 # p 552
 N90-21726 # p 570
 N90-21727 # p 570
 N90-21731 # p 570
 N90-21732 # p 571
 N90-21733 # p 571
 N90-21734 # p 571
 N90-21735 # p 571
 N90-21736 # p 572
 N90-21737 # p 572
 N90-21738 # p 572
 N90-21739 # p 572
 N90-21740 # p 572
 N90-21741 # p 572
 N90-21742 # p 572
 N90-21746 # p 573
 N90-21747 # p 574
 N90-21748 # p 574
 N90-21751 # p 578
 N90-21752 # p 578
 N90-21753 # p 581
 N90-21755 # p 582
 N90-21756 # p 582
 N90-21758 # p 582
 N90-21759 # p 583
 N90-21760 # p 588
 N90-21761 # p 588
 N90-21762 # p 588
 N90-21763 # p 588
 N90-21764 # p 591
 N90-21765 # p 591
 N90-21767 # p 592
 N90-21768 # p 592
 N90-21769 # p 592
 N90-21771 # p 592
 N90-21772 # p 593
 N90-21775 # p 597
 N90-21776 # p 598
 N90-21777 # p 598
 N90-21778 # p 598
 N90-21869 # p 600
 N90-21981 # p 588
 N90-21984 # p 582
 N90-21985 # p 573
 N90-21986 # p 582
 N90-21988 # p 608
 N90-21991 # p 608
 N90-21992 # p 608
 N90-21993 # p 608
 N90-22003 # p 608
 N90-22014 # p 609
 N90-22025 # p 609
 N90-22048 # p 609
 N90-22058 # p 609
 N90-22059 # p 609
 N90-22064 # p 609
 N90-22155 # p 611
 N90-22232 # p 578
 N90-22238 # p 578
 N90-22322 # p 612
 N90-22363 # p 614
 N90-22364 # p 614
 N90-22368 # p 614
 N90-22530 # p 552
 N90-22531 # p 573
 N90-22532 # p 573
 N90-22536 # p 573
 N90-22538 # p 574
 N90-22544 # p 575
 N90-22545 # p 575
 N90-22546 # p 575
 N90-22547 # p 575
 N90-22548 # p 575
 N90-22554 # p 578
 N90-22555 # p 582

N90-22556 # p 583
 N90-22557 # p 583
 N90-22563 # p 583
 N90-22565 # p 588
 N90-22566 # p 589
 N90-22570 # p 593
 N90-22609 # p 601
 N90-22651 # p 601
 N90-22662 # p 609
 N90-22695 # p 601
 N90-22703 # p 610
 N90-22746 # p 610
 N90-22807 # p 610
 N90-22808 # p 610
 N90-22975 # p 612
 N90-22976 # p 612
 N90-22977 # p 612
 N90-22978 # p 612
 N90-22980 # p 612
 N90-22999 # p 612
 N90-23023 # p 613
 N90-23032 # p 593
 N90-23050 # p 613
 N90-23060 # p 613
 N90-23067 # p 613
 N90-23069 # p 613
 N90-23172 # p 610
 N90-23188 # p 615
 N90-23189 # p 615
 N90-23190 # p 615
 N90-23338 # p 615
 N90-23340 # p 618
 N90-23348 # p 631
 N90-23349 # p 631
 N90-23353 # p 631
 N90-23359 # p 632
 N90-23360 # p 632
 N90-23363 # p 632
 N90-23364 # p 632
 N90-23367 # p 635
 N90-23368 # p 635
 N90-23369 # p 636
 N90-23371 # p 636
 N90-23372 # p 636
 N90-23373 # p 636
 N90-23374 # p 636
 N90-23375 # p 636
 N90-23377 # p 640
 N90-23378 # p 640
 N90-23379 # p 640
 N90-23386 # p 648
 N90-23387 # p 648
 N90-23388 # p 648
 N90-23389 # p 648
 N90-23390 # p 648
 N90-23392 # p 648
 N90-23393 # p 649
 N90-23394 # p 649
 N90-23395 # p 649
 N90-23396 # p 649
 N90-23397 # p 650
 N90-23398 # p 654
 N90-23399 # p 654
 N90-23400 # p 654
 N90-23401 # p 665
 N90-23402 # p 665
 N90-23403 # p 665
 N90-23404 # p 666
 N90-23409 # p 671
 N90-23412 # p 671
 N90-23413 # p 671
 N90-23475 # p 678
 N90-23523 # p 678
 N90-23538 # p 678
 N90-23571 # p 678
 N90-23591 # p 688
 N90-23609 # p 688
 N90-23687 # p 689
 N90-23707 # p 689
 N90-23713 # p 689
 N90-23752 # p 689
 N90-23760 # p 689
 N90-23762 # p 689
 N90-23768 # p 689
 N90-23769 # p 690
 N90-23832 # p 692
 N90-23990 # p 694
 N90-24103 # p 695
 N90-24221 # p 699
 N90-24224 # p 699
 N90-24225 # p 618
 N90-24227 # p 673
 N90-24228 # p 673
 N90-24233 # p 674
 N90-24235 # p 674
 N90-24237 # p 632

ACCESSION NUMBER INDEX

ACCESSION NUMBER INDEX

N90-28546

N90-24238 * #	p 632	N90-25135 * #	p 735	N90-26004 #	p 750	N90-26902 #	p 874	N90-27723 #	p 858
N90-24239 * #	p 633	N90-25136 #	p 735	N90-26005 #	p 750	N90-26903 * #	p 875	N90-27724 #	p 869
N90-24240 #	p 633	N90-25137 #	p 735	N90-26007 #	p 751	N90-26933 #	p 875	N90-27725 * #	p 869
N90-24241 #	p 633	N90-25138 #	p 739	N90-26009 #	p 751	N90-26972 #	p 875	N90-27728 #	p 872
N90-24242 * #	p 633	N90-25139 #	p 748	N90-26010 #	p 758	N90-26992 #	p 875	N90-27729 #	p 872
N90-24243 #	p 633	N90-25140 #	p 757	N90-26011 #	p 758	N90-26994 #	p 875	N90-27787 * #	p 876
N90-24246 #	p 634	N90-25141 * #	p 757	N90-26012 #	p 758	N90-27002 #	p 883	N90-27788 * #	p 876
N90-24249 #	p 634	N90-25142 * #	p 757	N90-26014 #	p 758	N90-27066 * #	p 883	N90-27883 #	p 876
N90-24250 #	p 634	N90-25143 #	p 758	N90-26015 #	p 758	N90-27118 #	p 884	N90-27895 #	p 876
N90-24251 #	p 634	N90-25144 #	p 758	N90-26016 #	p 759	N90-27120 #	p 884	N90-27900 #	p 876
N90-24253 #	p 634	N90-25145 #	p 761	N90-26017 #	p 759	N90-27448 #	p 848	N90-27905 #	p 876
N90-24254 #	p 634	N90-25148 #	p 761	N90-26018 #	p 759	N90-27465 * #	p 895	N90-27906 #	p 877
N90-24255 #	p 635	N90-25149 * #	p 761	N90-26019 #	p 762	N90-27466 #	p 895	N90-27907 #	p 877
N90-24257 #	p 637	N90-25150 #	p 761	N90-26020 #	p 762	N90-27467 #	p 895	N90-27908 #	p 877
N90-24258 #	p 637	N90-25153 #	p 762	N90-26055 * #	p 763	N90-27468 #	p 896	N90-27928 #	p 858
N90-24259 #	p 637	N90-25189 #	p 763	N90-26080 * #	p 767	N90-27469 #	p 896	N90-27931 #	p 858
N90-24260 #	p 637	N90-25222 #	p 766	N90-26087 #	p 767	N90-27471 * #	p 896	N90-27932 #	p 858
N90-24261 #	p 637	N90-25226 #	p 766	N90-26094 #	p 767	N90-27617 #	p 786	N90-27933 #	p 859
N90-24263 #	p 641	N90-25228 #	p 766	N90-26104 #	p 767	N90-27618 #	p 848	N90-27935 * #	p 877
N90-24264 #	p 641	N90-25236 #	p 766	N90-26106 #	p 767	N90-27619 #	p 848	N90-27946 * #	p 884
N90-24265 * #	p 650	N90-25254 #	p 773	N90-26166 #	p 775	N90-27620 #	p 848	N90-27987 #	p 884
N90-24266 * #	p 650	N90-25267 #	p 773	N90-26173 #	p 775	N90-27621 #	p 849	N90-27999 #	p 884
N90-24267 #	p 650	N90-25289 #	p 773	N90-26210 #	p 775	N90-27623 #	p 892	N90-28059 #	p 885
N90-24268 #	p 650	N90-25291 * #	p 774	N90-26238 #	p 775	N90-27624 #	p 849	N90-28068 #	p 885
N90-24270 #	p 650	N90-25332 #	p 774	N90-26268 #	p 775	N90-27625 #	p 869	N90-28069 #	p 859
N90-24271 #	p 666	N90-25348 #	p 774	N90-26280 #	p 776	N90-27626 #	p 855	N90-28070 #	p 877
N90-24272 #	p 666	N90-25361 #	p 774	N90-26281 #	p 776	N90-27627 #	p 855	N90-28072 #	p 885
N90-24273 * #	p 666	N90-25368 #	p 774	N90-26285 #	p 776	N90-27628 #	p 892	N90-28073 #	p 859
N90-24274 * #	p 666	N90-25375 #	p 775	N90-26290 #	p 776	N90-27629 #	p 884	N90-28076 #	p 885
N90-24275 #	p 672	N90-25515 * #	p 779	N90-26334 #	p 776	N90-27630 #	p 884	N90-28077 #	p 846
N90-24276 #	p 672	N90-25516 * #	p 780	N90-26335 #	p 776	N90-27631 #	p 855	N90-28078 #	p 885
N90-24277 #	p 674	N90-25553 #	p 782	N90-26345 #	p 777	N90-27633 #	p 872	N90-28079 #	p 885
N90-24278 #	p 674	N90-25568 #	p 780	N90-26346 #	p 777	N90-27634 #	p 892	N90-28080 #	p 886
N90-24430 #	p 678	N90-25580 #	p 780	N90-26348 #	p 777	N90-27635 #	p 893	N90-28082 #	p 886
N90-24451 #	p 679	N90-25638 * #	p 780	N90-26349 #	p 777	N90-27636 #	p 820	N90-28084 #	p 886
N90-24514 * #	p 690	N90-25697 #	p 783	N90-26355 #	p 777	N90-27639 #	p 820	N90-28085 #	p 886
N90-24557 * #	p 690	N90-25930 #	p 783	N90-26365 #	p 777	N90-27640 #	p 849	N90-28088 * #	p 886
N90-24660 #	p 690	N90-25931 #	p 783	N90-26369 #	p 777	N90-27641 #	p 820	N90-28091 #	p 886
N90-24852 * #	p 696	N90-25933 #	p 702	N90-26373 #	p 778	N90-27642 #	p 849	N90-28092 #	p 887
N90-24853 * #	p 696	N90-25934 * #	p 718	N90-26511 #	p 780	N90-27643 #	p 849	N90-28093 #	p 887
N90-24854 * #	p 696	N90-25935 #	p 718	N90-26515 * #	p 780	N90-27644 #	p 820	N90-28105 * #	p 887
N90-24855 * #	p 696	N90-25936 #	p 718	N90-26564 #	p 781	N90-27645 #	p 893	N90-28106 #	p 887
N90-24856 * #	p 696	N90-25937 #	p 718	N90-26595 #	p 781	N90-27646 #	p 787	N90-28366 * #	p 893
N90-24857 * #	p 697	N90-25938 #	p 718	N90-26633 #	p 782	N90-27649 #	p 816	N90-28396 * #	p 896
N90-24858 * #	p 697	N90-25939 #	p 718	N90-26634 #	p 782	N90-27653 #	p 816	N90-28398 #	p 896
N90-24859 * #	p 697	N90-25940 #	p 719	N90-26635 #	p 782	N90-27654 #	p 816	N90-28402 #	p 896
N90-24860 #	p 697	N90-25941 #	p 719	N90-26637 #	p 783	N90-27655 #	p 816	N90-28463 #	p 898
N90-24861 #	p 697	N90-25942 #	p 719	N90-26788 #	p 783	N90-27657 * #	p 817	N90-28489 #	p 902
N90-24862 * #	p 697	N90-25943 #	p 719	N90-26790 #	p 815	N90-27661 #	p 817	N90-28491 #	p 909
N90-24864 #	p 697	N90-25944 #	p 719	N90-26793 #	p 815	N90-27663 #	p 817	N90-28492 #	p 909
N90-24865 #	p 698	N90-25945 #	p 720	N90-26796 #	p 815	N90-27666 #	p 820	N90-28493 * #	p 909
N90-24867 * #	p 698	N90-25946 #	p 720	N90-26797 #	p 815	N90-27667 #	p 820	N90-28494 * #	p 909
N90-24868 #	p 698	N90-25947 #	p 720	N90-26798 #	p 815	N90-27668 #	p 820	N90-28495 #	p 910
N90-24870 #	p 698	N90-25948 #	p 720	N90-26799 #	p 815	N90-27669 * #	p 820	N90-28496 #	p 910
N90-24871 #	p 698	N90-25949 #	p 720	N90-26800 #	p 816	N90-27672 #	p 825	N90-28498 #	p 910
N90-24872 * #	p 698	N90-25950 #	p 720	N90-26802 #	p 824	N90-27673 #	p 825	N90-28500 #	p 910
N90-24873 * #	p 699	N90-25951 #	p 720	N90-26803 #	p 824	N90-27674 #	p 825	N90-28503 * #	p 910
N90-24876 #	p 699	N90-25953 #	p 721	N90-26804 #	p 824	N90-27675 #	p 825	N90-28505 #	p 910
N90-25035 #	p 635	N90-25954 * #	p 721	N90-26805 #	p 824	N90-27676 #	p 825	N90-28507 #	p 913
N90-25037 * #	p 690	N90-25955 #	p 721	N90-26807 #	p 842	N90-27677 #	p 825	N90-28509 #	p 915
N90-25040 #	p 692	N90-25956 #	p 724	N90-26808 #	p 842	N90-27678 * #	p 825	N90-28510 * #	p 915
N90-25043 #	p 651	N90-25957 * #	p 724	N90-26810 #	p 842	N90-27679 #	p 826	N90-28511 #	p 915
N90-25049 #	p 679	N90-25958 #	p 724	N90-26812 #	p 842	N90-27680 #	p 826	N90-28512 * #	p 916
N90-25051 #	p 691	N90-25959 #	p 724	N90-26813 #	p 843	N90-27681 #	p 826	N90-28513 #	p 920
N90-25057 * #	p 651	N90-25961 #	p 724	N90-26815 #	p 843	N90-27682 #	p 826	N90-28514 #	p 920
N90-25060 #	p 691	N90-25965 #	p 729	N90-26816 #	p 843	N90-27683 #	p 826	N90-28515 #	p 934
N90-25062 #	p 691	N90-25966 #	p 735	N90-26817 #	p 843	N90-27684 #	p 826	N90-28516 * #	p 934
N90-25065 #	p 691	N90-25967 * #	p 735	N90-26818 #	p 843	N90-27685 #	p 826	N90-28517 #	p 935
N90-25073 #	p 702	N90-25969 #	p 736	N90-26819 #	p 883	N90-27686 #	p 827	N90-28518 #	p 935
N90-25074 #	p 702	N90-25971 #	p 736	N90-26820 #	p 844	N90-27687 #	p 827	N90-28519 #	p 920
N90-25078 #	p 779	N90-25972 * #	p 736	N90-26821 #	p 844	N90-27688 #	p 827	N90-28520 #	p 920
N90-25084 #	p 773	N90-25973 #	p 736	N90-26822 #	p 844	N90-27689 #	p 827	N90-28521 * #	p 935
N90-25089 #	p 723	N90-25974 #	p 736	N90-26824 #	p 844	N90-27690 #	p 827	N90-28522 #	p 935
N90-25090 #	p 766	N90-25975 #	p 736	N90-26825 #	p 844	N90-27691 #	p 827	N90-28523 #	p 921
N90-25091 #	p 766	N90-25976 #	p 737	N90-26826 #	p 845	N90-27693 #	p 827	N90-28524 #	p 921
N90-25092 #	p 734	N90-25977 #	p 737	N90-26827 #	p 845	N90-27694 #	p 845	N90-28525 #	p 935
N90-25103 #	p 723	N90-25978 #	p 737	N90-26828 #	p 845	N90-27697 #	p 846	N90-28526 #	p 921
N90-25110 #	p 716	N90-25981 * #	p 739	N90-26829 #	p 845	N90-27698 #	p 846	N90-28527 #	p 921
N90-25111 * #	p 717	N90-25982 * #	p 748	N90-26830 #	p 845	N90-27699 * #	p 846	N90-28528 #	p 921
N90-25112 * #	p 717	N90-25985 #	p 748	N90-26831 #	p 854	N90-27700 * #	p 846	N90-28529 #	p 921
N90-25113 #	p 717	N90-25986 #	p 748	N90-26832 #	p 855	N90-27701 #	p 849	N90-28530 #	p 922
N90-25114 #	p 717	N90-25987 #	p 748	N90-26833 #	p 868	N90-27702 #	p 849	N90-28531 #	p 922
N90-25115 #	p 717	N90-25988 #	p 748	N90-26834 #	p 868	N90-27703 * #	p 850	N90-28532 #	p 922
N90-25116 #	p 718	N90-25989 #	p 749	N90-26835 #	p 870	N90-27704 #	p 855	N90-28533 #	p 922
N90-25117 #	p 723	N90-25990 #	p 749	N90-26836 #	p 870	N90-27705 #	p 855	N90-28534 #	p 922
N90-25118 #	p 723	N90-25991 #	p 749	N90-26838 #	p 870	N90-27709 #	p 856	N90-28535 #	p 923
N90-25119 #	p 723	N90-25992 #	p 749	N90-26839 #	p 871	N90-27710 #	p 856	N90-28536 #	p 923
N90-25120 * #	p 724	N90-25993 #	p 749	N90-26840 #	p 871	N90-27711 #	p 856	N90-28537 * #	p 923
N90-25122 #	p 729	N90-25994 #	p 749	N90-26843 #	p 871	N90-27712 #	p 856	N90-28538 #	p 923
N90-25123 #	p 729	N90-25995 #	p 749	N90-26844 * #	p 871	N90-27713 #	p 856	N90-28539 #	p 923
N90-25125 #	p 734	N90-25997 #	p 749	N90-26845 #	p 871	N90-27715 #	p 856	N90-28540 * #	p 923
N90-25126 * #	p 734	N90-25999 #	p 750	N90-26847 #	p 871	N90-27716 #	p 857	N90-28541 * #	p 924
N90-25127 * #	p 734	N90-26000 #	p 750	N90-26848 #	p 874	N90-27718 #	p 857	N90-28542 * #	p 924
N90-25132 * #	p 734	N90-26001 #	p 750	N90-26887 #	p 874	N90-27719 #	p 857	N90-28544 #	p 927
N90-25133 #	p 734	N90-26002 #	p 750	N90-26889 #	p 855	N90-27721 #	p 857	N90-28545 #	p 927
N90-25134 * #	p 735	N90-26003 #	p 750	N90-26899 #	p 883	N90-27722 * #	p 858	N90-28546 * #	p 927

N90-28547

ACCESSION NUMBER INDEX

N90-28547	#	p 928	N90-29367	#	p 918
N90-28548	#	p 928	N90-29371	#	p 918
N90-28549	#	p 928	N90-29378	#	p 918
N90-28550	#	p 929	N90-29380	#	p 919
N90-28551	* #	p 929	N90-29381	* #	p 924
N90-28552	* #	p 929	N90-29382	#	p 924
N90-28553	* #	p 929	N90-29383	* #	p 924
N90-28554	* #	p 929	N90-29384	* #	p 925
N90-28555	* #	p 930	N90-29385	* #	p 925
N90-28556	* #	p 930	N90-29386	* #	p 925
N90-28557	* #	p 930	N90-29387	* #	p 925
N90-28558	* #	p 930	N90-29389	* #	p 925
N90-28559	* #	p 930	N90-29390	#	p 925
N90-28560	* #	p 930	N90-29391	#	p 928
N90-28561	* #	p 931	N90-29393	#	p 933
N90-28562	* #	p 931	N90-29394	* #	p 933
N90-28563	* #	p 931	N90-29396	#	p 933
N90-28564	* #	p 931	N90-29398	#	p 933
N90-28565	* #	p 931	N90-29399	#	p 936
N90-28566	* #	p 931	N90-29401	#	p 936
N90-28567	* #	p 932	N90-29402	#	p 936
N90-28569	* #	p 932	N90-29403	#	p 938
N90-28570	* #	p 932	N90-29406	#	p 938
N90-28571	#	p 932	N90-29407	#	p 938
N90-28572	#	p 932	N90-29408	#	p 939
N90-28573	#	p 933	N90-29409	#	p 939
N90-28574	#	p 933	N90-29411	#	p 939
N90-28576	#	p 935	N90-29412	#	p 939
N90-28577	#	p 936	N90-29433	#	p 939
N90-28578	* #	p 936	N90-29442	#	p 953
N90-28579	#	p 936	N90-29480	#	p 953
N90-28580	#	p 937	N90-29499	#	p 953
N90-28581	#	p 937	N90-29527	#	p 954
N90-28582	#	p 937	N90-29565	#	p 960
N90-28583	#	p 938	N90-29587	#	p 960
N90-28584	#	p 938	N90-29593	#	p 960
N90-28586	#	p 938	N90-29597	#	p 960
N90-28674	#	p 951	N90-29664	#	p 960
N90-28698	#	p 951	N90-29680	#	p 961
N90-28701	#	p 952	N90-29681	#	p 961
N90-28704	#	p 952	N90-29682	#	p 961
N90-28707	#	p 952	N90-29683	#	p 961
N90-28709	#	p 952	N90-29684	#	p 961
N90-28712	#	p 952	N90-29686	#	p 961
N90-28713	#	p 953	N90-29687	#	p 961
N90-28714	#	p 953	N90-29692	#	p 963
N90-28722	#	p 953	N90-29745	#	p 963
N90-28759	#	p 958	N90-29746	#	p 963
N90-28762	#	p 958	N90-29919	* #	p 965
N90-28800	#	p 958	N90-29926	#	p 965
N90-28810	#	p 958	N90-29965	* #	p 965
N90-28812	#	p 959	N90-30030	#	p 966
N90-28815	* #	p 959	N90-30031	#	p 966
N90-28828	#	p 959	N90-30035	#	p 966
N90-28862	* #	p 959	N90-30036	#	p 966
N90-28865	* #	p 959	N90-30134	#	p 967
N90-28866	* #	p 960			
N90-28887	#	p 963			
N90-28982	#	p 964			
N90-29121	* #	p 964			
N90-29142	* #	p 964			
N90-29143	* #	p 965			
N90-29160	#	p 902			
N90-29161	#	p 960			
N90-29166	* #	p 965			
N90-29169	* #	p 966			
N90-29247	#	p 967			
N90-29249	#	p 967			
N90-29299	#	p 902			
N90-29302	#	p 911			
N90-29304	#	p 911			
N90-29305	#	p 911			
N90-29307	#	p 911			
N90-29320	#	p 911			
N90-29323	#	p 911			
N90-29325	#	p 911			
N90-29326	#	p 912			
N90-29327	#	p 912			
N90-29328	#	p 912			
N90-29332	#	p 912			
N90-29333	#	p 913			
N90-29334	#	p 913			
N90-29335	#	p 913			
N90-29336	#	p 913			
N90-29337	#	p 914			
N90-29338	#	p 916			
N90-29339	#	p 916			
N90-29341	#	p 916			
N90-29344	#	p 916			
N90-29350	#	p 917			
N90-29356	#	p 917			
N90-29360	#	p 917			
N90-29362	#	p 917			
N90-29363	#	p 917			
N90-29364	#	p 918			
N90-29366	#	p 918			

SPECIAL NOTICE

The abstract sections of the monthly supplements of *Aeronautical Engineering* can be bound separately. Individual abstracts can be located readily by means of the page numbers given at each entry, e.g., p 654 N90-23399. To assist the user in binding Supplements SP-7037(249) through SP-7037(260), a title page is included in this Cumulative Index.

AERONAUTICAL ENGINEERING

A CONTINUING BIBLIOGRAPHY

Abstracts
January — December 1990

TABLE OF CONTENTS

<i>SP-7037 Supplement</i>	<i>Page</i>
249	1
250	81
251	143
252	221
253	285
254	381
255	467
256	551
257	617
258	701
259	785
260	901

1. Report No. NASA SP-7037 (261)		2. Government Accession No.		3. Recipient's Catalog No.	
4. Title and Subtitle AERONAUTICAL ENGINEERING A Cumulative Index to the 1990 Issues				5. Report Date February 1991	
				6. Performing Organization Code NTT	
7. Author(s)				8. Performing Organization Report No.	
9. Performing Organization Name and Address NASA Scientific and Technical Information Division				10. Work Unit No.	
				11. Contract or Grant No.	
12. Sponsoring Agency Name and Address National Aeronautics and Space Administration Washington, DC 20546				13. Type of Report and Period Covered Special Publication	
				14. Sponsoring Agency Code	
15. Supplementary Notes					
16. Abstract This is a cumulative index to the abstracts contained in NASA SP-7037 (249) through NASA SP-7037 (260) of Aeronautical Engineering: A Continuing Bibliography. NASA SP-7037 and its supplements have been compiled through the cooperative efforts of the American Institute of Aeronautics and Astronautics (AIAA) and the National Aeronautics and Space Administration (NASA). This cumulative index includes subject, personal author, corporate source, foreign technology, contract number, report number, and accession number indexes.					
17. Key Words (Suggested by Authors(s)) Aerodynamics Aeronautical Engineering Aeronautics Bibliographies			18. Distribution Statement Unclassified - Unlimited Subject Category - 01		
19. Security Classif. (of this report) Unclassified		20. Security Classif. (of this page) Unclassified		22. Price * A24 HC	
				21. No. of Pages 564	

* For sale by the National Technical Information Service, Springfield, Virginia 22161

FEDERAL REGIONAL DEPOSITORY LIBRARIES

ALABAMA

AUBURN UNIV. AT MONTGOMERY
LIBRARY
Documents Department
Montgomery, AL 36193
(205) 279-9110 ext.253

UNIV. OF ALABAMA LIBRARY
Reference Department/Documents
Box S
Tuscaloosa, AL 35486
(205) 348-6046

ARIZONA

DEPT. OF LIBRARY, ARCHIVES,
AND PUBLIC RECORDS
Third Floor State Capitol
1700 West Washington
Phoenix, AZ 85007
(602) 255-4121

ARKANSAS

ARKANSAS STATE LIBRARY
Documents Service Section
One Capitol Mall
Little Rock, AR 72201
(501) 371-2090

CALIFORNIA

CALIFORNIA STATE LIBRARY
Govt. Publications Section
914 Capitol Mall
Sacramento, CA 95814
(916) 322-4572

COLORADO

UNIV. OF COLORADO
North Library
Government Publications Division
Campus Box 184
Boulder, CO 80309
(303) 492-8834

DENVER PUBLIC LIBRARY
Govt. Pub. Department
1357 Broadway
Denver, CO 80203
(303) 571-2346

CONNECTICUT

CONNECTICUT STATE LIBRARY
231 Capitol Avenue
Hartford, CT 06105
(203) 566-4971

FLORIDA

UNIV. OF FLORIDA LIBRARIES
Documents Department
Library West
Gainesville, FL 32611
(804) 392-0367

GEORGIA

UNIV. OF GEORGIA LIBRARIES
Government Documents Dept.
Athens, GA 30602
(404) 542-8948

ILLINOIS

UNIV. OF ILLINOIS
Hamilton Library
Government Documents Collection
2550 Yeo Hall
Urbana, IL 61802
(800) 940-3260

INDIANA

UNIV. OF INDIANA LIBRARY
Documents Section
Vasco, IN 43083
(203) 885-8344

MISSISSIPPI

MISSISSIPPI STATE LIBRARY
Federal Documents
Centennial Building
Springfield, IL 62756
(217) 782-5012

INDIANA

INDIANA STATE LIBRARY
Serials Section
140 North Senate Avenue
Indianapolis, IN 46204
(317) 232-3686

IOWA

UNIV. OF IOWA LIBRARIES
Government Publications Dept.
Iowa City, IA 52242
(319) 335-5926

KANSAS

UNIVERSITY OF KANSAS
Spencer Research Library
Government Documents
Lawrence, KS 66045
(913) 864-4362

KENTUCKY

UNIV. OF KENTUCKY LIBRARIES
Government Publications/Maps Dept.
Lexington, KY 40505
(606) 257-8400

LOUISIANA

LOUISIANA STATE UNIVERSITY
Middleton Library
Government Documents Dept.
Baton Rouge, LA 70803
(504) 388-2570

LOUISIANA TECHNICAL UNIV.

Prescott Memorial Library
Government Documents Dept.
Ruston, LA 71272
(318) 257-4962

MAINE

UNIVERSITY OF MAINE
Raymond H. Fogler Library
Govt. Documents & Microforms Dept.
Orono, ME 04469
(207) 581-1680

MARYLAND

UNIVERSITY OF MARYLAND
McKeldin Library
Documents/Maps Room
College Park, MD 20742
(301) 454-3034

MASSACHUSETTS

BOSTON PUBLIC LIBRARY
Government Documents Dept.
666 Boylston Street
Boston, MA 02117
(617) 536-5400 ext.226

MICHIGAN

DETROIT PUBLIC LIBRARY
5201 Woodward Avenue
Detroit, MI 48202
(313) 333-1408

MICHIGAN OF MICHIGAN

Government Documents
P.O. Box 30007
735 E. Michigan Avenue
Lansing, MI 48909
(517) 573-5583

MINNESOTA

UNIVERSITY OF MINNESOTA
Wilson Library
Government Publications
309 Nineteenth Avenue South
Minneapolis, MN 55455
(612) 373-7813

MISSISSIPPI

UNIV. OF MISSISSIPPI LIB.
Government Documents Dept.
103 Old Gym Bldg.
University, MS 38677
(601) 232-5857

MISSOURI

University of Missouri at
Columbia Library
Government Documents
Columbia, MO 65201
(314) 882-6733

MONTANA

UNIV. OF MONTANA
Mansfield Library
Documents Division
Missoula, MT 59812
(406) 243-6700

NEBRASKA

UNIVERSITY OF NEBRASKA -
LINCOLN
Love Memorial Library
Documents Department
Lincoln, NE 68588
(402) 472-2562

NEVADA

UNIV. OF NEVADA-RENO LIB.
Govt. Pub. Department
Reno, NV 89557
(702) 784-6579

NEW JERSEY

NEWARK PUBLIC LIBRARY
U.S. Documents Division
5 Washington Street
P.O. Box 630
Newark, NJ 07101
(201) 733-7812

NEW MEXICO

UNIVERSITY OF NEW MEXICO
General Library
Government Publications/Maps Dept.
Albuquerque, NM 87131
(505) 277-5441

NEW MEXICO STATE LIBRARY

325 Don Gaspar Avenue
Santa Fe, NM 87501
(505) 827-3826

NEW YORK

NEW YORK STATE LIBRARY
Documents Sect. Cultural Educ. Ctr.
Empire State Plaza
Albany, NY 12230
(518) 474-5563

NORTH CAROLINA

UNIVERSITY OF NORTH CAROLINA
AT CHAPEL HILL
Davis Library 080A
BA SS Department Documents
Chapel Hill, NC 27514
(919) 932-1151

NORTH DAKOTA

NORTH DAKOTA STATE
UNIVERSITY LIBRARY
Government Documents Dept.
Fargo, ND 58105
(701) 237-6352

In cooperation with Univ. of North
Dakota, Chester Fritz Library
Grand Forks

OHIO

STATE LIBRARY OF OHIO
Documents Section
65 South Front Street
Columbus, OH 43266
(614) 844-7051

OKLAHOMA

OKLAHOMA DEPT. OF LIBRARIES
Government Documents
200 NE 18th Street
Oklahoma City, OK 73105
(405) 521-2502, ext. 252

OKLAHOMA STATE UNIV. LIB.

Documents Department
Stillwater, OK 74078
(405) 624-0489

OREGON

PORTLAND STATE UNIV.
Miller Library
934 SW Harrison - P.O. Box 1151
Portland, OR 97207
(503) 229-3673

PENNSYLVANIA

STATE LIBRARY OF PENN.
Government Publications Section
Box 1601
Walnut St. & Commonwealth Ave.
Harrisburg, PA 17105
(717) 787-3752

SOUTH CAROLINA

CLEMSON UNIV. COOPER LIB.
Documents Department
Clemson, SC 29634
(803) 656-5174
In cooperation with Univ. of South
Carolina, Thomas Cooper Library,
Columbia

TEXAS

TEXAS STATE LIBRARY
Public Services Department
P.O. Box 12927 - 1201 Brazos
Austin, TX 78711
(512) 463-5455

TEXAS TECH. UNIV. LIBRARY

Documents Department
Lubbock, TX 79409
(806) 742-2268

UTAH

UTAH STATE UNIVERSITY
Merrill Library & Learning Resources
Center, UMC-30
Documents Department
Logan, UT 84322
(801) 750-2682

VIRGINIA

UNIVERSITY OF VIRGINIA
Alderman Library
Government Documents
Charlottesville, VA 22903
(804) 924-3133

WASHINGTON

WASHINGTON STATE LIBRARY
Document Section
Olympia, WA 98504
(206) 753-4027

WEST VIRGINIA

WEST VIRGINIA UNIV. LIB.
Government Documents Section
P.O. Box 6069
Martinsburg, WV 26005
(304) 293-3640

WISCONSIN

ST. MARY'S OF WISCONSIN LIB.
Government Pub. Section
310 State Street
Madison, WI 53705
(608) 262-2781
In cooperation with Univ. of Wisconsin-
Madison, Memorial Library

WISCONSIN STATE LIBRARY

Documents Division
814 West Wisconsin Avenue
Madison, WI 53733
(414) 278-3065

WYOMING

WYOMING STATE LIBRARY
Supreme Court & Library Bldg.
Cheyenne, WY 82002
(307) 777-5919

National Aeronautics and
Space Administration
Code NTT-4

Washington, D.C.
20546-0001

Official Business
Penalty for Private Use, \$300



National Aeronautics and
Space Administration

Washington, D.C.
20546

**SPECIAL FOURTH CLASS MAIL
BOOK**

Postage and Fees Paid
National Aeronautics and
Space Administration
NASA-451

Official Business
Penalty for Private Use \$300



L3 001 SP7037-261910221S000903D
DEPT OF THE AIR FORCE
WL/SUL TECHNICAL PROCESSING
ATTN : DOROTHY GORDAN
KIRTLAND AFB NM 871176008



POSTMASTER: If Undeliverable (Section 158
Postal Manual) Do Not Return
